Sandra J. Shin
Yunn-Yi Chen
Paula S. Ginter
Editors

A Comprehensive Guide to Core Needle Biopsies of the Breast

Second Edition

Springer

A Comprehensive Guide to Core Needle Biopsies of the Breast

Sandra J. Shin • Yunn-Yi Chen • Paula S. Ginter
Editors

A Comprehensive Guide to Core Needle Biopsies of the Breast

Second Edition

Springer

Editors
Sandra J. Shin
Department of Pathology
and Laboratory Medicine
Albany Medical College
Albany, NY, USA

Yunn-Yi Chen
Department of Pathology
University of California San Francisco
San Francisco, CA, USA

Paula S. Ginter
Pathology and Laboratory Medicine
Weill Cornell Medicine
New York, NY, USA

ISBN 978-3-031-05531-7 ISBN 978-3-031-05532-4 (eBook)
https://doi.org/10.1007/978-3-031-05532-4

© The Editor(s) (if applicable) and The Author(s), under exclusive license to Springer Nature Switzerland AG 2022
This work is subject to copyright. All rights are solely and exclusively licensed by the Publisher, whether the whole or part of the material is concerned, specifically the rights of translation, reprinting, reuse of illustrations, recitation, broadcasting, reproduction on microfilms or in any other physical way, and transmission or information storage and retrieval, electronic adaptation, computer software, or by similar or dissimilar methodology now known or hereafter developed.
The use of general descriptive names, registered names, trademarks, service marks, etc. in this publication does not imply, even in the absence of a specific statement, that such names are exempt from the relevant protective laws and regulations and therefore free for general use.
The publisher, the authors, and the editors are safe to assume that the advice and information in this book are believed to be true and accurate at the date of publication. Neither the publisher nor the authors or the editors give a warranty, expressed or implied, with respect to the material contained herein or for any errors or omissions that may have been made. The publisher remains neutral with regard to jurisdictional claims in published maps and institutional affiliations.

This Springer imprint is published by the registered company Springer Nature Switzerland AG
The registered company address is: Gewerbestrasse 11, 6330 Cham, Switzerland

To my mother, Young Soon Suh, MD and in loving memory of my father, Ki Ha Shin (Sandra J. Shin, MD)

In loving memory of my mother, Hwan-May Lee, and my father, Yuan-Chang Chen (Yunn-Yi Chen, MD, PhD)

In loving memory of my mother, Carole F. Ginter (Paula S. Ginter, MD)

Preface (Reprinted from the First Edition)

The Elephant and the Blind Men
A long time ago, there lived in a small village several men who had been born blind. One sunny day, there was an announcement that an elephant was in town, and that the King wanted to extend a special invitation to the blind men to come and pay it a visit. The blind men were very excited as they had never seen an elephant before.
They agreed to visit the animal even though they could not see it. They reasoned that they could at least feel the elephant and get a sense of what it was like.
When the elephant was brought before them, the blind men who stroked the elephant's leg gasped "The elephant is like a pillar!"
The blind men who were touching the elephant's tail were quick to disagree, insisting "Oh, no! It is like a vine."
Other of the blind men had their own opinion about the animal and protested, "Not like a pillar or vine, this elephant is like a tree branch," as they felt its trunk.
"No, this elephant is clearly like a handheld fan" said the blind men who were stroking the ear of the elephant with their palms.
The blind men touching the animal's broad underside remarked "It is like a wall," while others said "It is like a pipe," as their fingers slid down the tusk of the elephant.
Those who had felt the head of the elephant said "an elephant is like a large round jar."
It wasn't long until all of the men were quarreling about who was right. The King intervened, telling them, "You are all correct. The reason why you are saying different things is because each of you had felt a different part of the elephant's body. If you could see, you would realize that the animal possesses all of the traits you described."

This parable which originated in the Indian subcontinent has crossed many religious traditions and is part of Jain, Buddhist, Sufi, Hindu, and Bahá'í lore, and in Europe, the story became well known when the nineteenth-century American poet John Godfrey Saxe created his own version as a poem [1].

Generally speaking, the tale illustrates how one's (limited) perspective may be true yet, simultaneously, not represent the complete truth. I employ this metaphor when describing the pitfalls of rendering diagnoses on breast core biopsy material to my residents and fellows.

The random sampling of a targeted breast abnormality can contain all, some or none, of the diagnostic features necessary for accurate diagnosis. As pathologists we try to compensate for this inherent disadvantage by further correlating with clinical and imaging findings, utilizing adjunctive tools such as immunohistochemistry, and extracting as much histologic information from the limited sampling to the extent that we are at risk of "overdiagnosing" subtle changes. This challenge is further compounded by the unfortunate phenomenon of even commonly encountered lesions morphologically mimicking other processes or entities when evaluated in a fragmented state.

I was given a wonderful opportunity when Springer Publishing approached me about writing a textbook on breast pathology. While very excited, the notion of authoring a textbook was daunting to say the least. However, I was compelled to commit to such an endeavor for several reasons. First, I strongly believed (and still do) that due to the inherent fragmented and randomly sampled nature of breast core biopsies, practicing pathologists could benefit from learning alternative or supplementary diagnostic approaches. While pattern-based diagnosis has been introduced in other surgical pathology subspecialty fields, I believed this was a particularly useful approach in breast core biopsy specimens which had not been previously

emphasized. It seemed logical that initially assessing core biopsy material by the overall histologic pattern as a way to formulate an inclusive differential diagnosis incorporating benign and malignant as well as common and uncommon entities was diagnostically very powerful. I first lectured on the topic of pattern-based diagnosis of breast lesions at the breast pathology subspecialty evening session at the United States and Canadian Academy of Pathology 99th Annual Meeting in 2010. My lecture was entitled "Small glandular proliferations of the breast." The following year, I was invited to speak on the topic at the Harvard continuing medical education course "Breast Pathology: Current Concepts and Controversies" directed by Drs. Stuart J. Schnitt and Laura C. Collins. More recently, I have been directing a course with my colleagues, Drs. Timothy M. D'Alfonso and Sonal Varma, on the topic of pattern-based diagnosis in breast core biopsies at the American Society of Clinical Pathologists (ASCP) annual meetings.

Second, while several breast pathology textbooks exclusively dedicated to core biopsies were already on the market, I was personally frustrated when I had to refer to a larger reference book after initially opening a core biopsy book to read more in depth about a particular entity at hand. As an end user, I desired a breast core biopsy textbook that was in-depth and comprehensive in nature. Last, I found this as a wonderful opportunity to promote our junior and soon to be future leaders of academic breast pathology in the coming decades.

For readers, my hope is that this will provide a comprehensive and in-depth resource on the topic of breast core biopsies. Rendering diagnoses in this subset of breast specimens can be challenging, and yet little is written about how best to handle them in daily practice. The use of a pattern-based approach in these specimens can be highly complementary to one's existing practicing style and, at the very least, will encourage pathologists to consider less commonly encountered entities in the differential diagnosis. Due to the important clinical junction at which the core biopsy is performed in the management of patients with breast disease, it is critical that pathologists draw from every possible source of information to avoid misdiagnosis and subsequent mistreatment.

This book is organized into four sections. The first section provides an overview of the fundamentals of a successful breast core biopsy program. The second section is dedicated to instructive topics toward the diagnosis of breast core biopsies including the utilization of a pattern-based approach. The third and largest section is an in-depth discussion of entities that are commonly encountered in the breast core biopsy setting. The last section encompasses special considerations in core biopsies of the breast including special clinical scenarios, role of molecular profiling in small breast samples and personalized medicine, and dermatologic mimickers of breast lesions. Together, I hope that you will find this book to be a valuable addition to your pathology library and assist you in navigating through the occasionally treacherous waters of breast core biopsy diagnosis.

Reference

1. Blind men and an elephant. Wikipedia. https://en.wikipedia.org/wiki/Blind_men_and_an_elephant. Retrieved 7 Nov 2015.

New York, NY, USA Sandra J. Shin

Acknowledgments

It is with sincere gratitude that we thank numerous individuals who were instrumental in the creation of this book. First and foremost, we are indebted to the contributors, already renowned experts in the field, who graciously and without hesitation accepted to participate in the second edition of the first multi-institutional-authored breast pathology textbook dedicated to core needle biopsies. For readers, this is an unprecedented opportunity to glean the cumulative knowledge and expertise of leading breast pathologists (and radiologists) from top institutions in a single resource. We are also pleased to bring to attention that many of these contributors used this opportunity to help promote their junior colleagues with the hope that many will continue on their paths in becoming the future leaders of breast pathology. We also thank Ms. Patricia Kuharic who skillfully optimized every image in this highly illustrated book.

Dr. Shin thanks her beloved family, John P. Nabagiez, MD, husband of 26 years, and their two daughters, Melisande (age 17) and Avelene (age 14), who ultimately make it possible for her to pursue such meaningful professional endeavors. Dr. Chen thanks her husband of 31 years, Hung-Ming Chu, MD, PhD, for his love and unwavering support, and their three sons, Tianlee Chu (age 29), Tianrae Chu (age 27), and Tianming Chu (age 20) for the inspiration and in making everything worthwhile. Dr. Ginter thanks her father, Paul G. Ginter, brother, Robert D. Ginter, and husband, Kevin M. Learn for their unwavering support.

Sandra J. Shin, MD
Yunn-Yi Chen, MD, PhD
Paula S. Ginter, MD

Contents

1 **Essential Components of a Successful Breast Core Needle Biopsy Program: Imaging Modalities, Sampling Techniques, Specimen Processing, Radiologic/Pathologic Correlation, and Appropriate Follow-Up** 1
Christine M. Denison and Susan C. Lester

2 **Pattern-Based Evaluation of Breast Core Needle Biopsies** 47
Sandra J. Shin and Paula S. Ginter

3 **Multiples in Core Needle Biopsy Samples** 97
Sandra J. Shin and Paula S. Ginter

4 **Inflammatory, Reactive, and Infectious Conditions of the Breast** 131
Anne Grabenstetter and Timothy M. D'Alfonso

5 **Adenosis, Sclerosing Lesions, Microglandular Adenosis, and Mucocele-Like Lesions** 165
Beth T. Harrison and Deborah A. Dillon

6 **Papillary and Epithelial–Myoepithelial Tumors** 205
Paula S. Ginter and Timothy M. D'Alfonso

7 **Fibroepithelial Lesions** 253
Gregor Krings and Yunn-Yi Chen

8 **Columnar Cell Lesions and Flat Epithelial Atypia** 331
Beth T. Harrison, Timothy M. D'Alfonso, and Stuart J. Schnitt

9 **Intraductal Proliferations (DCIS, ADH, and UDH)** 351
Kimberly H. Allison and Kristin C. Jensen

10 **Invasive Breast Carcinoma of No Special Type, Microinvasive Carcinoma, Tubular Carcinoma, and Cribriform Carcinoma** 391
Helena Hwang, Karan Saluja, and Sunati Sahoo

11 **Triple-Negative/Basal-Like Breast Carcinomas** 445
Yaileen D. Guzmán-Arocho, Benjamin C. Calhoun, and Laura C. Collins

12 **Less Common Triple-Negative Breast Cancers** 463
Poonam Vohra, Yunn-Yi Chen, and Gregor Krings

13 **Special Histologic Types and Special Morphologic Patterns of Invasive Ductal Carcinoma of No Special Type: Mucinous, Micropapillary, Mucinous Cystadenocarcinoma, Neuroendocrine Neoplasm, Cystic Hypersecretory, Glycogen-Rich Clear Cell, Carcinoma with Osteoclast-Like Giant Cells** 575
Yun Wu, Sandra J. Shin, and Aysegul A. Sahin

14 Atypical Lobular Hyperplasia and Lobular Carcinoma In Situ 615
Gregor Krings, Helena Hwang, and Yunn-Yi Chen

15 Invasive Lobular Carcinoma 655
Eliah R. Shamir, Helena Hwang, and Yunn-Yi Chen

16 Benign and Malignant Mesenchymal Tumors 691
Ashley Cimino-Mathews, Emily B. Ambinder, Pedram Argani, and Marissa J. White

17 Vascular Lesions of the Breast 737
Melinda E. Sanders and Justin M. Cates

18 Breast Tumors in Adolescents/Children and Males 759
Melinda E. Sanders

19 Lesions of the Nipple 787
Nicole B. Johnson and Laura C. Collins

20 Lymphoid and Hematopoietic Tumors of the Breast 805
Julia Turbiner Geyer

21 Special Clinical Settings: Tumors Arising in Pregnancy, Pregnancy-Like (Pseudolactational) Proliferations, Breast Carcinoma in the Pre-neoadjuvant Chemotherapy Setting, Recurrent Breast Carcinoma, and Inflammatory Breast Carcinoma 825
Paula S. Ginter and Timothy M. D'Alfonso

22 Current Standard Clinical Predictive Markers 873
Kimberly H. Allison

23 Future Role of Molecular Profiling in Small Breast Samples and Personalised Medicine 895
Samuel Y. F. Foong, Peter T. Simpson, Margaret C. Cummings, and Sunil R. Lakhani

24 Metastases to the Breast 917
Ashley Cimino-Mathews, Emily B. Ambinder, Pedram Argani, and Marissa J. White

25 Dermatologic Mimickers of Breast Lesions Arising in the Breast Skin, Subcutis, or Axilla 949
Garrett Desman, Lurmag Y. Orta, and Sandra J. Shin

Index 1007

Editors and Contributors

About the Editors

Sandra J. Shin is a tenured professor at Albany Medical College and serves as department chair of Pathology and Laboratory Medicine. Previously, she served as Chief of Breast Pathology at the New York-Presbyterian Hospital-Weill Cornell Medicine (NYPH-WMC) in New York, NY. Dr. Shin has earned a national and international reputation as an expert breast pathologist and translational researcher focused on breast disease. Dr. Shin is a graduate of Albany Medical College. She completed her training in anatomic and clinical pathology at the NYPH-WMC; completed a 1-year breast pathology fellowship with Dr. Paul Peter Rosen, a world-renowned breast pathologist; and subsequently joined the faculty where she practiced for 16 years prior to her chairmanship at Albany Medical College in 2017. She also holds a Master's in Business Administration from the New York University Stern School of Business.

Yunn-Yi Chen is a Professor of Pathology at the University of California, San Francisco, and Director of Immunohistochemistry Laboratory, Department of Pathology at the UCSF Medical Center. After completing medical school training from National Taiwan University and PhD in Immunology from Tufts University, she attended Beth Israel Deaconess Medical Center for pathology residency where she learned breast pathology from Dr. James Connolly and Dr. Stuart Schnitt, two world-renowned breast pathologists, followed by surgical pathology fellowship at UCSF, and subsequently joined the faculty. Dr. Chen has contributed many articles and book chapters in breast pathology, including the fifth edition of *WHO Classification of Tumours of the Breast*. In addition to teaching medical students, residents, and fellows and lecturing in multiple national/international meetings and continuing medical education courses, Dr. Chen directs her research interests in the areas of lobular carcinoma, special subtypes of breast cancer, fibroepithelial lesions, and the pathology of breast cancers in the neoadjuvant settings. She has served in the Breast Cancer Subcommittee of the College of American Pathologists, the Executive Committee of International Association of Chinese Pathologists (including president for 2014–2015), and expert breast pathology committee for The Cancer Genome Atlas (TCGA).

Paula S. Ginter is an Associate Professor of Clinical Pathology and Laboratory Medicine at New York-Presbyterian Hospital-Weill Cornell Medicine (NYPH-WCM). She is a graduate of Chicago Medical School—Rosalind Franklin University. Prior to her faculty appointment at NYPH-WCM, Dr. Ginter completed residency training at NYPH-WCM, where she served as Chief Resident. She subsequently pursued subspecialty fellowship training in breast pathology at Weill Cornell under leading breast pathologists Drs. Syed A. Hoda and Sandra J. Shin. Dr. Ginter is a board-certified Anatomic and Clinical pathologist with a subspecialty interest in breast pathology. Her academic pursuits have focused on the pathogenesis, diagnosis, and treatment of breast malignancies which have led to 30+ publications in peer-reviewed journals. Dr. Ginter is actively involved in resident and medical student education and has conducted regional, national, and international educational courses focused on breast pathology.

Contributors

Kimberly H. Allison Department of Pathology, Stanford University School of Medicine, Stanford, CA, USA

Emily B. Ambinder The Russell H. Morgan Department of Radiology and Radiologic Science, The Johns Hopkins Hospital, Baltimore, MD, USA

Pedram Argani Departments of Pathology and Oncology, The Johns Hopkins Hospital, Baltimore, MD, USA

Benjamin C. Calhoun Department of Pathology and Laboratory Medicine, University of North Carolina at Chapel Hill, Chapel Hill, NC, USA

Justin M. Cates Department of Pathology, Microbiology and Immunology, Vanderbilt University Medical Center, Nashville, TN, USA

Yunn-Yi Chen Department of Pathology, University of California San Francisco, San Francisco, CA, USA

Ashley Cimino-Mathews Departments of Pathology and Oncology, The Johns Hopkins Hospital, Baltimore, MD, USA

Laura C. Collins Department of Pathology, Beth Israel Deaconess Medical Center and Harvard Medical School, Boston, MA, USA

Margaret C. Cummings UQ Centre for Clinical Research, Faculty of Medicine, The University of Queensland, Brisbane, QLD, Australia

Pathology Queensland, The Royal Brisbane and Women's Hospital, Brisbane, QLD, Australia

Timothy M. D'Alfonso Department of Pathology, Memorial Sloan Kettering Cancer Center, New York, NY, USA

Christine M. Denison Department of Radiology, Brigham and Women's Hospital and Harvard Medical School, Boston, MA, USA

Garrett Desman Department of Pathology, Icahn School of Medicine at Mount Sinai, New York, NY, USA

Department of Dermatology, Icahn School of Medicine at Mount Sinai, New York, NY, USA
Dermatopathology Division, Optum Care, New Hyde Park, NY, USA

Deborah A. Dillon Department of Pathology, Brigham and Women's Hospital and Harvard Medical School, Boston, MA, USA

Samuel Y. F. Foong UQ Centre for Clinical Research, Faculty of Medicine, The University of Queensland, Brisbane, QLD, Australia
Pathology Queensland, The Royal Brisbane and Women's Hospital, Brisbane, QLD, Australia

Julia Turbiner Geyer Department of Pathology and Laboratory Medicine, Weill Cornell Medicine, New York, NY, USA

Paula S. Ginter Department of Pathology and Laboratory Medicine, Weill Cornell Medicine, New York, NY, USA

Anne Grabenstetter Department of Pathology, Memorial Sloan Kettering Cancer Center, New York, NY, USA

Yaileen D. Guzmán-Arocho Department of Pathology, Beth Israel Deaconess Medical Center and Harvard Medical School, Boston, MA, USA

Beth T. Harrison Department of Pathology, Brigham and Women's Hospital and Harvard Medical School, Boston, MA, USA

Helena Hwang Department of Pathology, UT Southwestern Medical Center, Dallas, TX, USA

Kristin C. Jensen Department of Pathology, Stanford University School of Medicine, Stanford, CA, USA
Pathology and Laboratory Medicine Service, Veteran Affairs Palo Alto Health Care System, Palo Alto, CA, USA

Nicole B. Johnson Presbyterian Pathology Group, Novant Health Presbyterian Medical Center, Charlotte, NC, USA

Gregor Krings Department of Pathology, University of California San Francisco, San Francisco, CA, USA

Sunil R. Lakhani UQ Centre for Clinical Research, Faculty of Medicine, The University of Queensland, Brisbane, QLD, Australia
Pathology Queensland, The Royal Brisbane and Women's Hospital, Brisbane, QLD, Australia

Susan C. Lester Department of Pathology, Brigham and Women's Hospital and Harvard Medical School, Boston, MA, USA

Lurmag Y. Orta Integrated Pathology Services, Trujillo Alto, Puerto Rico
Hospital Auxilio Mutuo, San Juan, Puerto Rico

Aysegul A. Sahin Department of Pathology, The University of Texas MD Anderson Cancer Center, Houston, TX, USA

Sunati Sahoo Department of Pathology, UT Southwestern Medical Center, Dallas, TX, USA

Karan Saluja Department of Pathology, UT Health Science Center at Houston, Houston, TX, USA

Melinda E. Sanders Department of Pathology, Microbiology and Immunology, Vanderbilt University Medical Center, Nashville, TN, USA

Stuart J. Schnitt Department of Pathology, Brigham and Women's Hospital and Harvard Medical School, Boston, MA, USA

Eliah R. Shamir Department of Pathology, University of California San Francisco, San Francisco, CA, USA

Sandra J. Shin Department of Pathology and Laboratory Medicine, Albany Medical College, Albany, NY, USA

Peter T. Simpson UQ Centre for Clinical Research, Faculty of Medicine, The University of Queensland, Brisbane, QLD, Australia

Poonam Vohra Department of Pathology, University of California San Francisco (UCSF), San Francisco, CA, USA

Marissa J. White Department of Pathology, The Johns Hopkins Hospital, Baltimore, MD, USA

Yun Wu Department of Pathology, The University of Texas MD Anderson Cancer Center, Houston, TX, USA

1 Essential Components of a Successful Breast Core Needle Biopsy Program: Imaging Modalities, Sampling Techniques, Specimen Processing, Radiologic/Pathologic Correlation, and Appropriate Follow-Up

Christine M. Denison and Susan C. Lester

Introduction

The development of image-guided core needle biopsies (CNBs) by Steve Parker and colleagues in 1990 shifted diagnosis away from surgical breast biopsies and led to profound changes in the treatment of breast disease in the following decades [1]. Currently, over 95% of breast lesions are first diagnosed by needle biopsy [2]. CNBs have major advantages for patients, radiologists, pathologists, surgeons, biomedical research, and the healthcare system.

Benefits to Patients

- The amount of tissue removed is minimized.
- The morbidity is less than that of a surgical excision.
- Fewer biopsy-related changes (e.g., scarring) are created that could complicate imaging follow-up.
- The time to biopsy and a definitive diagnosis is shortened which can reduce anxiety.
- Women with benign findings are spared surgery.
- Women with malignant findings have additional choices for systemic treatment and have improved surgical outcomes.
- Germline mutation testing can be performed in select women to determine the value of bilateral mastectomy.
- Multiple areas in both breasts can be sampled to determine optimal surgery.
- Surgery after CNB is more likely to achieve definitive excision of the breast cancer with improved cosmesis and nodal evaluation in one procedure.
- Patients also have the option to undergo treatment first (i.e., presurgical or neoadjuvant therapy).
- CNBs obtained without the use of heating or freezing tissue and with minimal cold ischemic time optimally preserve biomolecules for assays to determine therapy and prognosis.
- Women with lymphoma or metastases to the breast are spared unnecessary surgery.

Benefits to Radiologists

- Radiologists have an expanded role in clinical care by both detecting and biopsying lesions followed by counseling patients and making referrals for subsequent treatment.
- Lesions identified by imaging are directly sampled resulting in optimal correlation with pathologic diagnosis.
- A specific benign diagnosis can aid in following patients with imaging over time.
- The need for radiologic/pathologic correlation has led to greater collaboration and cross-training between the two imaging specialties.

Benefits to Pathologists

- Core needle specimens are easier to process and evaluate compared to excisions.
- There is greater certainty that the tissue being examined contains the lesion detected by imaging. In contrast, small lesions can be very difficult to identify in excisions and mastectomies.
- Pathologists have become adept at recognizing portions of lesions in CNBs.

C. M. Denison
Department of Radiology, Brigham and Women's Hospital and Harvard Medical School, Boston, MA, USA
e-mail: cdenison@bwh.harvard.edu

S. C. Lester (✉)
Department of Pathology, Brigham and Women's Hospital and Harvard Medical School, Boston, MA, USA
e-mail: slester@bwh.harvard.edu

© The Author(s), under exclusive license to Springer Nature Switzerland AG 2022
S. J. Shin et al. (eds.), *A Comprehensive Guide to Core Needle Biopsies of the Breast*,
https://doi.org/10.1007/978-3-031-05532-4_1

- Pathologists identified a group of benign lesions that when present in a CNB predict for adjacent cancer and, thus, require excision.
- The need for radiologic/pathologic correlation has led to greater collaboration and cross-training between the two imaging specialties.

Benefits to Surgeons

- The proportion of surgeries performed for cancer has increased from 20–30% to 80–90% because women with benign disease are now diagnosed by CNB.
- Surgical planning is facilitated by the ability to evaluate multiple lesions by CNB.
- The likelihood that surgery for cancer will be successful in one procedure is increased.
- Better cosmesis is achieved when fewer surgeries need to be performed.
- Surgeons have become adept at using techniques to identify localization devices for targeted removal of breast lesions (e.g., radioactive seeds and reflector devices).
- More women become eligible for breast conserving therapy with the use of neoadjuvant therapy.
- The removal of previously positive lymph nodes after neoadjuvant therapy is facilitated by the placement of clips and localization devices.

Benefits for Biomedical Research

- A CNB provides tissue with optimal preservation of biomolecules due to minimal ischemic time and the absence of damage due to heating or freezing of the tissue.
- A definitive diagnosis of invasive carcinoma with determination of tumor markers on CNB provides sufficient information to evaluate patients for enrollment in clinical trials.
- Tumors can be sampled at multiple time points during treatment.

Benefits to the Medical Care System

- CNBs reduce the cost of investigating breast lesions found by imaging.
- Women with benign findings do not require surgery or surgical follow-up.

A successful CNB program requires close communication among radiologists, pathologists, and surgeons and a basic understanding of the principles of all three disciplines by everyone involved [3–6]. Cross-training across specialties creates a safety net to ensure that all cancers are detected, diagnosed, and surgically excised and that patients receive optimal care. Lack of knowledge outside one's own specialty, and the failure of members of the team to communicate effectively, can result in a diminished capacity to determine if imaging and pathologic features correlate and can allow errors to escape detection (Fig. 1.1). In this chapter the information that pathologists need to know about breast imaging, specimen processing, radiologic/pathologic correlation, findings present in surgical excision after CNB, missing cancers after CNB, and recurrences after CNB will be discussed, as well as the critical role of the pathologist in a CNB program.

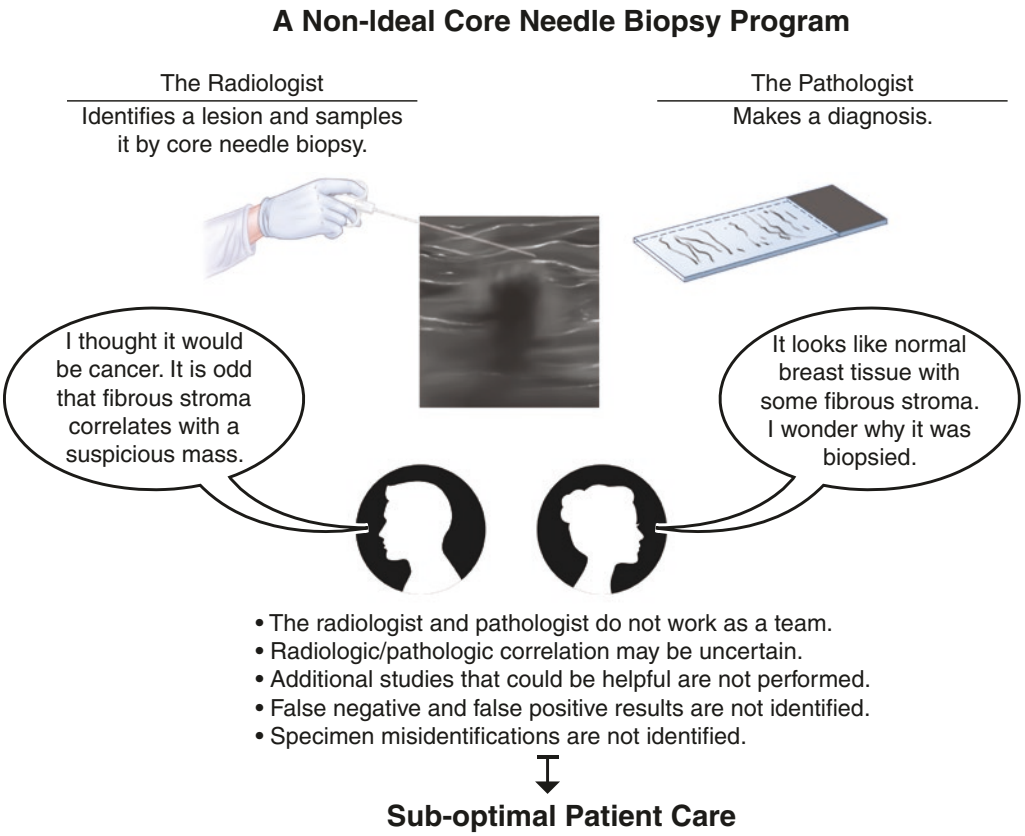

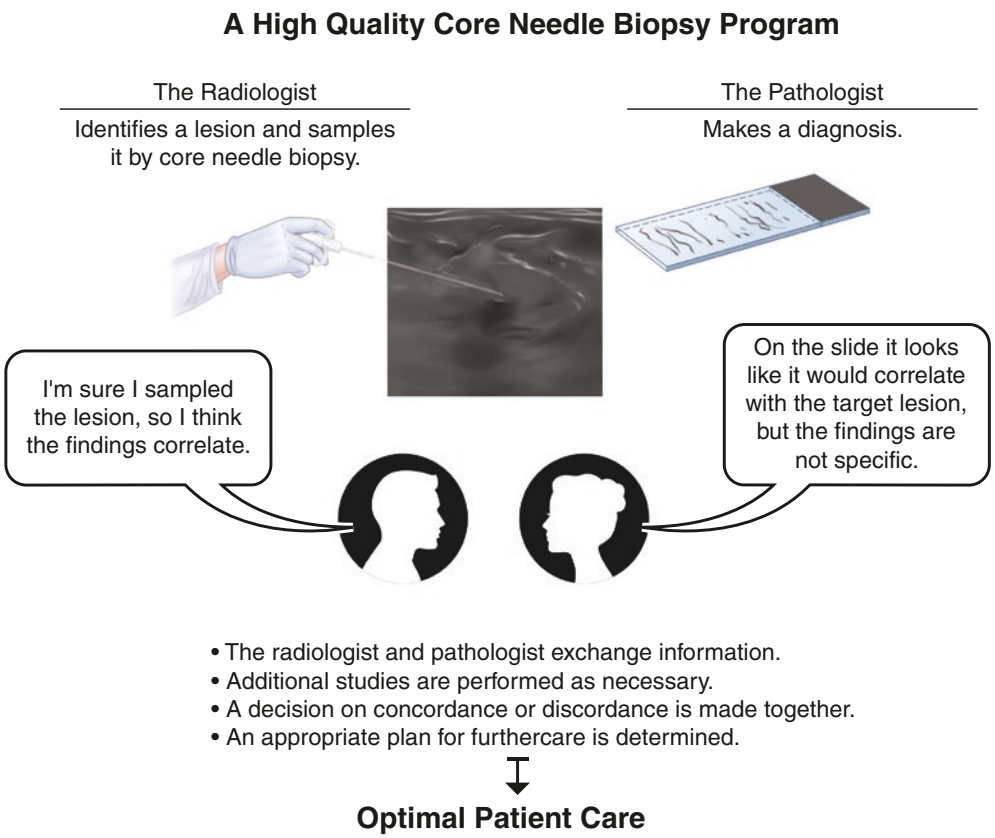

Fig. 1.1 In an ideal CNB program, the radiologist and pathologist discuss the imaging and pathologic findings and come to a mutual decision about whether or not there is concordance. This ensures patients receive the best care. In a non-ideal program, there is no communication, creating the opportunity for errors in misinterpreting findings and potentially causing harm to patients

Breast Imaging Modalities

The three modalities commonly used to evaluate the breast are mammography, ultrasound, and magnetic resonance imaging (MRI). The modalities provide information about lesions that are both confirmatory and complementary. Each has its own advantages and disadvantages compared to the other modalities, which will be discussed below.

Breast Imaging Reporting and Data System (BI-RADS)

The American College of Radiologists issues standardized terminology for reporting imaging findings (the Breast Imaging Reporting and Data System or BI-RADS, currently the 5th edition, 2013) (Table 1.1). A BI-RADS category is assigned to a breast imaging report to indicate an overall concern for malignancy [7]. The majority of lesions undergoing biopsy are in the BI-RADS three to five categories.

BI-RADS recommends describing masses according to the shape of the lesion (Table 1.2, Fig. 1.2) and the margin (edge or border) of the lesion (Table 1.3, Fig. 1.2). The margin (i.e., the relationship of the mass to the surrounding tissue) is more important than the shape of the lesion in determining the most likely underlying biologic process (Table 1.4). For example, the same types of lesions form masses with spiculated margins regardless of whether or not the overall shape is round, oval, or irregular. Unfortunately, the terms used to describe shape and margins overlap in common usage (e.g., irregular may be used to describe a margin whereas spiculated is the recommended term) and it may not be clear on a requisition form how a term is being used. Information about a mass would be clearer for pathologists if only the margin description was provided.

While a BI-RADS assessment category indicates the likelihood of malignancy, it does not provide sufficient information to determine if there is correlation between the radiologic finding and the pathologic diagnosis. In addition, terms such as "occult lesion," "abnormality," or "area of interest" are unhelpful for correlation. The specific lesion must be described in sufficient detail in the radiology report and on the requisition form to determine if the pathologic findings could be responsible for the imaging finding. This can generally be accomplished in a few words and appropriate terminology will be discussed below.

Table 1.1 BI-RADS risk assessment categories

Assessment category	Clinical management	Likelihood of cancer
0: Incomplete	Additional imaging or comparison to prior images	Not applicable
1: Negative	Routine screening	~0%
2: Benign	Routine screening	~0%
3: Probably benign	Short-interval follow-up or continued surveillance	>0% but ≤2%
4: Suspicious	Biopsy	>2% but <95%
4A: Low suspicion		>2% but ≤10%
4B: Moderate suspicion		>10% but ≤50%
4C: High suspicion		>50% but <95%
5: Highly suggestive of malignancy	Biopsy Note: If core biopsy shows benign findings, in general an excision would be recommended	≥95%
6: Known biopsy proven malignancy	Depends on clinical situation	Not applicable

Table 1.2 BI-RADS descriptive terms for shapes

Type	Definition
Round	Spherical, ball-shaped, circular, or globular-shaped
Oval	Elliptical or egg-shaped (may include two or three undulations). If >3 undulations, classify as irregular
Irregular	Neither round nor oval

Mammography

Mammography is the standard modality for cancer screening. Screening utilizes two views with the breast under compression. The craniocaudal (CC) view is in a horizontal plane. A portion of the pectoralis muscle should be seen at the posterior edge of the image. The medial–lateral–oblique (MLO) view compresses the breast in a diagonal plane extending upwards towards the axilla. This angled image is superior to a medial–lateral (ML) or vertical view because it visualizes more breast tissue in the upper outer quadrant (the most common location of breast carcinomas) as well as the axillary contents. The use of the two orthogonal views helps to distinguish a true mass from mass-like density created by focally overlapping breast tissues. The two views also aid in localizing lesions to a specific site in the breast.

Digital breast tomosynthesis (DBT) is a technique that acquires multiple images as the X-ray tube moves in an arc across the breast. The images are processed into a volume rendering and displayed as 1-mm-thin high-resolution slices. This reduces the interference from tissue overlap and reveals certain findings to better advantage. The types of lesions most likely to be evident on DBT but not visible on routine mammography are lesions causing subtle changes in breast parenchymal texture that are often described as architectural

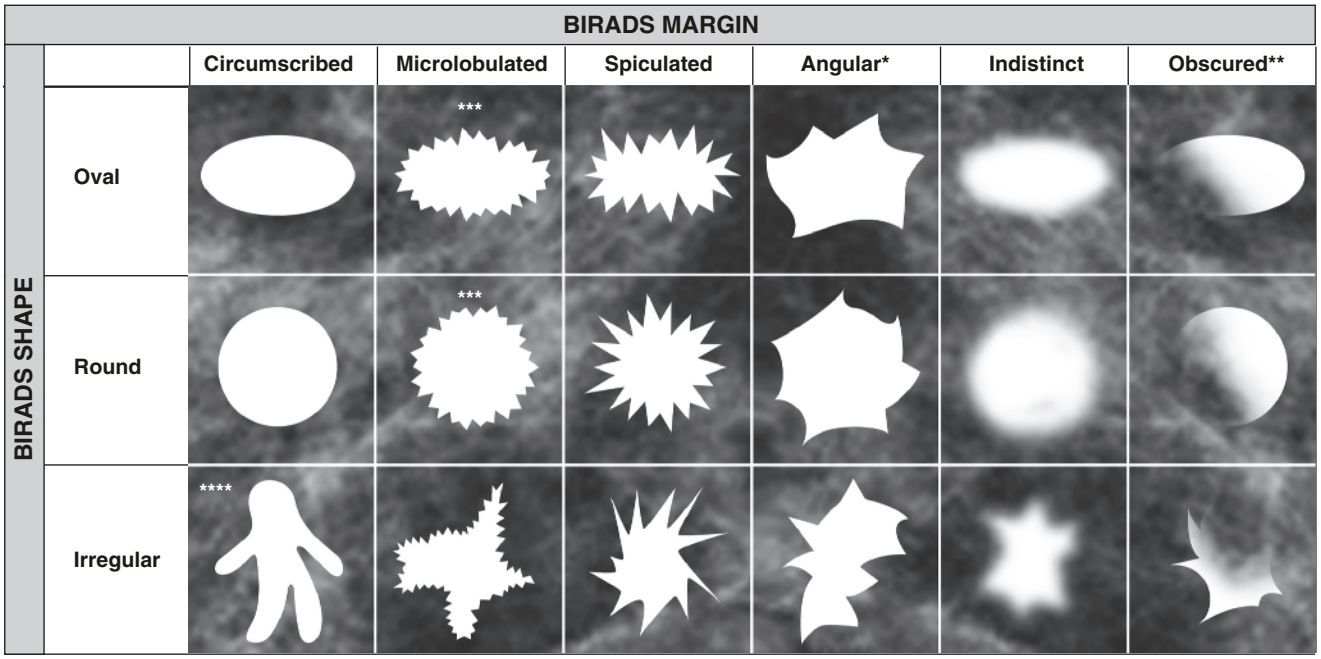

Fig. 1.2 Radiologists describe masses according to both overall shape and margins. The type of margin is more important for correlation with pathologic lesions. *Angular is only used to describe masses evaluated by ultrasound. **"Obscured" is only used to describe masses evaluated by mammography. ***The 5th (current) edition of the American College of Radiology BIRADS Atlas utilizes "microlobulated" to describe both border ("short cycle undulations") and shape (>3 undulations are classified as an irregular shape). Using these criteria, an oval mass with microlobulated margins ("short cycle undulations") cannot exist and is required to be reported as an irregular mass with microlobulated margins. Note, however, that not all radiologists follow these recommendations given that this terminology was not in place for BIRADS Atlas editions 1–4 and given that similar restrictions were not placed on round or irregular masses. "Spiculated" describes lines radiating from a mass. Thus, there can be an oval or round mass with spiculated margins. ****An irregular mass with circumscribed margins would be quite unusual but could theoretically exist—just like the Yeti!

Table 1.3 BI-RADS descriptive terms for margins

Type	Definition
Circumscribed	Sharply demarcated with an abrupt transition between the lesion and the surrounding tissue
Microlobulated	Short-cycle undulations
Spiculated	Characterized by lines radiating from the mass
Angular (only ultrasound)	Some or all of the margins have sharp corners, often forming acute angles
Indistinct	No clear demarcation of the entire margin, or any portion of the margin, from the surrounding tissue. Not used when it appears this is due to adjacent breast tissue (this is "obscured")
Obscured (only mammography)	Hidden by superimposed or adjacent fibroglandular tissue

distortion or asymmetry. Although DBT is sometimes referred to as 3D mammography, the image is not truly three dimensional and this term is not recommended [7].

X-rays variably penetrate into the breast depending on the tissue type, resulting in exposures ranging in shades from black to white:

- Adipose tissue—well penetrated—dark gray to black
- Fibrous tissue—poorly penetrated—white
- Calcifications—not penetrated—very white
- Metal—not penetrated—whiter than calcifications

Table 1.4 Margins of masses—radiologic/pathologic correlation

Margin	Pathologic correlate
Circumscribed	~60% fibroadenomas
	~20% other benign lesions (clusters of cysts, papillomas, lipomas, myofibroblastomas, hamartomas, fat necrosis)
	10% invasive carcinomas (mucinous carcinomas, high-grade "triple negative" carcinomas, often with a medullary pattern) <1% encapsulated papillary carcinoma, solid papillary carcinoma
	<5% DCIS (DCIS involving other benign lesions such as fibroadenomas or papillomas, high-grade DCIS with periductal fibrosis)
Spiculated, microlobulated, angular	~95% invasive carcinomas
	~3% inflammatory lesions (e.g., surgical sites, trauma)
	~2% benign lesions (complex sclerosing lesions/radial sclerosing lesions (radial scars), fibromatosis, granular cell tumors)
Indistinct	~30% normal breast
	~30% benign nonneoplastic lesions (often pseudoangiomatous stromal hyperplasia (PASH) or fibroadenomatoid change)
	~30% carcinomas (diffusely infiltrative without a desmoplastic response (often lobular in type) or DCIS)
Obscured	Specific correlations cannot be made because the margins are not seen due to the surrounding tissue

Normal breast tissue is a mixture of adipose tissue and fibroglandular tissue and has a variable appearance from gray to white.

There are three major types of mammographic lesions associated with malignancy:

- Masses: ~45% of lesions
- Architectural distortion or asymmetry: ~10% of lesions
- Calcifications: ~45% of lesions

Masses

The most important features of masses needed for radiologic correlation are size, margins, and density.

Size

The size of a mass by imaging is very helpful when determining if the pathology results are concordant. For example, a ~0.4 cm cluster of apocrine cysts on the biopsy could correlate with a 0.8 cm mass but would be very unlikely to correlate with a ~1.5 cm mass. In some cases, the size of a carcinoma cannot be determined by pathologic examination and the size by imaging will need to be used (discussed later under the section "Carcinomas with Indeterminant Size by Pathology").

Size is also helpful in determining the reliability of negative results for hormone receptors or HER2 on the CNB. For example, a negative result on a 0.8 cm area of carcinoma on a core biopsy from a 1 cm carcinoma is highly likely to be a true result, whereas a negative result on a 0.2 cm area of carcinoma on a core biopsy from a 4 cm carcinoma could be falsely negative if heterogeneity in expression is present.

Margin

The type of margin is an important indication of how lesional cells interact with the surrounding tissue (Tables 1.3 and 1.4). Benign lesions generally have an expansile growth pattern and push against the surrounding tissue (Fig. 1.3a). Thus, the majority of masses with circumscribed margins are benign (Table 1.4). The most common solid benign lesion of the breast is the fibroadenoma (Fig. 1.3b). However, some malignancies have circumscribed margins and thus the majority of these lesions require biopsy for diagnosis. Invasive carcinomas can have circumscribed margins due to the production of extensive extracellular matrix (e.g., mucinous carcinomas), when the cells grow as solid masses of cells and/or are surrounded by a lymphocytic infiltrate (often "triple negative" carcinomas), or carcinomas associated with hemorrhage (carcinomas with osteoclast like giant cells) (Fig. 1.3c). Encapsulated papillary carcinomas and solid papillary carcinomas grow as circumscribed masses. DCIS is usually only associated with a circumscribed mass when it involves a benign circumscribed lesion such as a fibroadenoma. Rarely, clusters of expanded ducts involved by high-grade DCIS associated with periductal fibrosis form small (~1 cm) lobulated masses.

A spiculated, microlobulated, or angular margin indicates that the lesional cells have penetrated into the surrounding tissue (Fig. 1.3d). It should be noted that "spiculated" refers to the appearance of the margin and is not related to "bone spicules" or calcifications. The great majority of lesions with this appearance are invasive carcinomas (Table 1.4 and Fig. 1.3f). The most common benign lesion with this appearance is the radial sclerosing lesion (RSL; also termed radial scar) (Fig. 1.3e). An RSL consists of a small densely collagenized central nidus that appears to be an area of collapsed stroma that pulls in or tethers the surrounding breast parenchyma to create the radiating arms. The central "mass" is small relative to the length of the arms, when compared to spicules formed by invasive carcinomas. The radiologist should inform the pathologist when the imaging findings are suggestive of an RSL. An alert pathologist will be aware of the imaging appearance and not fall into the possible pitfall of confusing the central nidus of an RSL for a tubular carcinoma or, vice versa, confusing a tubular carcinoma for an RSL.

Other benign lesions that are associated with this growth pattern are surgical scars, scarring due to other types of trauma, inflammatory lesions, fibromatosis, and occasionally granular cell tumors.

Indistinct margins may indicate a lesion that is due to a focal tissue change but is not a discrete neoplasm or specific pathologic process (Table 1.4 and Fig. 1.3g). For example, the prominent myofibroblasts of pseudoangiomatous stromal hyperplasia (PASH) can form nodular areas without specific borders (Fig. 1.3h). Fibroadenomatoid changes can also form a vague area of tissue density. Alternatively, some carcinomas invade with little or no desmoplastic response and, thus, a specific border with the surrounding tissue is not present. Invasive lobular carcinoma is the most common malignancy with this growth pattern (Fig. 1.3i). Cancers with this growth pattern can also have the imaging appearance of architectural distortion or asymmetry (discussed below). When evaluating core needle biopsies performed for masses with indistinct margins, architectural distortion, or asymmetry, pathologists should be alert to subtle changes in increased stromal cellularity that could be due to dispersed malignant cells. For example, the cells of grade 1 and 2 lobular carcinomas often mimic lymphocytes or histiocytes at low power. In some cases, immunohistochemical studies for cytokeratin may be necessary to identify the tumor cells.

An obscured margin signifies that a portion of the margin cannot be determined due to overlap of surrounding equal or greater density tissue and, therefore, pathologic correlation can only be assessed from the portions of the margin that are visible. The BI-RADS lexicon recommends that this term be

MAMMOGRAPHIC MASSES – RADIOLOGIC/PATHOLOGIC CORRELATION		
Radiologic Appearance of Margins	**Most Common Benign Lesion**	**Most Common Malignant Lesion**
a. Circumscribed	**b.** Fibroadenoma	**c.** Carcinoma with Medullary Features
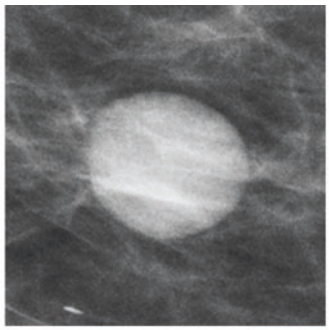	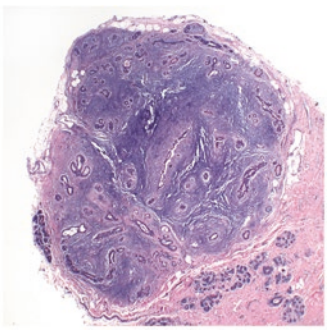	
d. Spiculated	**e.** Radial sclerosing lesion	**f.** Invasive carcinoma
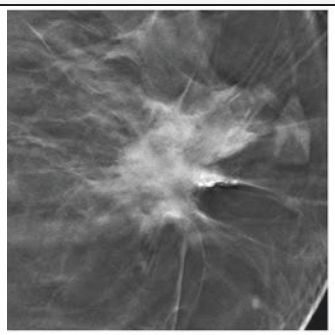	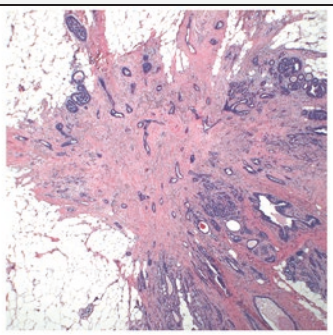	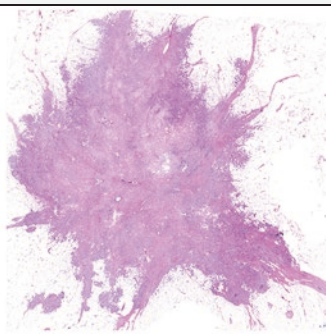
g. Indistinct	**h.** PASH	**i.** Invasive carcinoma
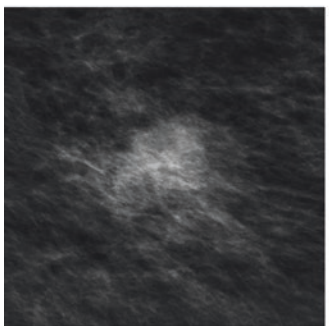	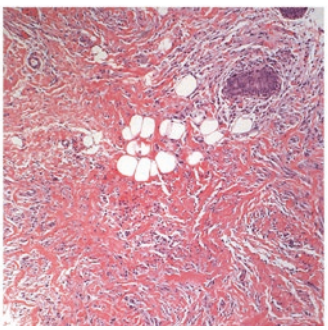	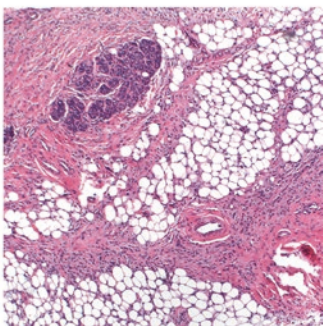

Fig. 1.3 The margin of masses correlates with the growth pattern of the lesion. (**a**) This radiograph shows a round mass with circumscribed margins. (**b**) Benign lesions, such as this fibroadenoma, have an expansile growth pattern and typically grow as masses with pushing smoothly contoured margins. (**c**) A minority of invasive carcinomas, such as this carcinoma with medullary features, form rounded or ovoid masses with smooth borders. (**d**) This radiograph shows an irregular mass with spiculated margins. Lesions with spiculated, microlobulated, or angular margins either invade into adjacent stroma or appear to do so. (**e**) This radial sclerosing lesion has a central sclerotic focus associated with radiating arms and forms an irregular mass. This and fat necrosis are the only common benign lesions associated with spiculated margins. (**f**) The majority of lesions with spiculated, microlobulated, or angular margins will be invasive carcinomas that invade into surrounding stroma, such as this invasive ductal carcinoma. (**g**) This is a mass with an irregular shape and indistinct margins by imaging. (**h**) Pseudoangiomatous stromal hyperplasia (PASH) is a focal accentuation of normal stromal myofibroblasts and, thus, can form an area of density but may not have a defined margin. (**i**) Carcinomas without a desmoplastic response, such as this invasive lobular carcinoma, can form areas of increased density but have ill-defined margins due to the intermingling of tumor cells with adipose tissue

used when all margins of a circumscribed lesion cannot be seen. Thus, masses with obscured margins are more likely to correlate pathologically with those lesions previously described with circumscribed margins.

Density

The majority of mass-forming breast lesions are of equal or greater density (as determined by the degree of whiteness) to fibroglandular tissue because they usually do not include adipose tissue. Thus, they appear as solid white lesions on a gray background. The majority of malignancies are very dense because these tumors grow as solid masses. In contrast, lesions that consist partly or completely of adipose tissue are usually benign (e.g., hamartoma, lipoma, fat necrosis, and lipomatous variants of myofibroblastomas).

Architectural Distortion

Architectural distortion is a localized alteration in the typical uniform texture of the breast characterized by lines radiating from a central point (Fig. 1.4a). Unlike a mass with spiculated margins, a definable central area of solid density is not seen. These lesions are more frequently detected with the use of tomosynthesis, as this technique is capable of detecting very subtle changes in stromal texture.

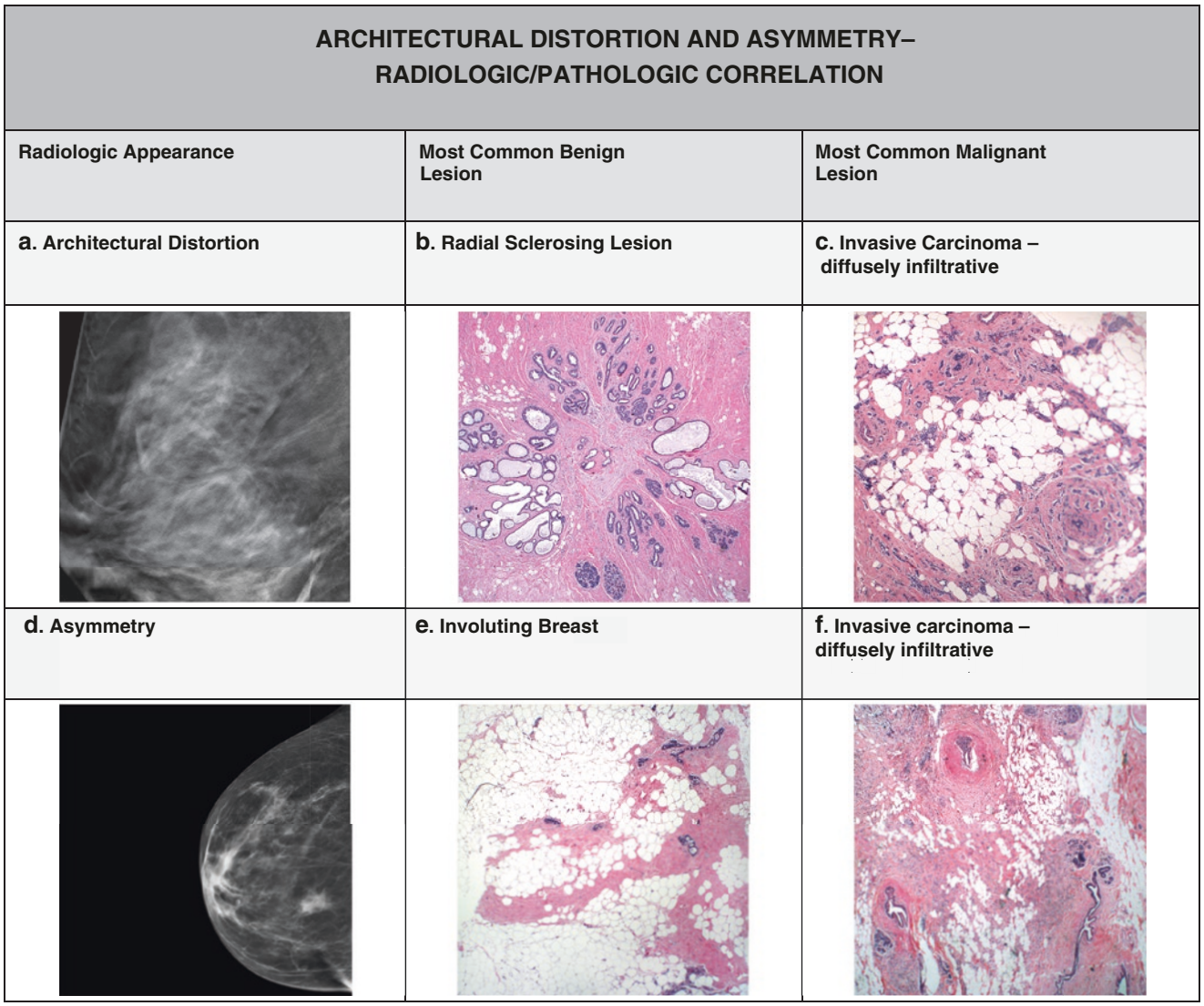

Fig. 1.4 (**a**) This architectural distortion is seen on tomosynthesis as an area of lines radiating from a central focus. (**b**) A common benign lesion forming architectural distortion is a radial sclerosing lesion. (**c**) This invasive ductal carcinoma invades in adipose tissue with little desmoplastic response. This type of carcinoma can cause an area of distortion without forming an obvious mass. (**d**) This focal asymmetry consists of a patchy area of increased density. A definite mass with definable margins is not present. (**e**) As the breast undergoes normal involution, fibrous stroma turns into adipose tissue. Residual islands of fibrous tissue can create areas of increased tissue density in comparison to surrounding breast tissues. (**f**) Invasive lobular carcinoma is the most common type of carcinoma that may not form a mammographic mass. This tumor infiltrates in both fibrous tissue and adipose tissue with little stromal response

About one-third of lesions causing architectural distortion are carcinomas, one-third specific types of benign lesions, and one-third a variety of non-specific benign findings [8–10].

The majority of malignancies (>95%) are invasive carcinomas that have a diffuse infiltrative pattern in fibroadipose tissue with little or no desmoplastic response (Fig. 1.4c). Many (30–60%) are either lobular carcinomas or have lobular features. DCIS rarely results in architectural distortion but this pattern can be seen when the tumor cells involve a sclerosing lesion or are associated with dense periductal fibrosis.

Benign lesions that result in architectural distortion include sclerosing lesions (RSLs, complex sclerosing lesions, and sclerosing adenosis), surgical scars, fat necrosis, and cysts with rupture and adjacent inflammation [8, 10]. An RSL can present as architectural distortion rather than a mass with spiculated margins because the central nidus is small, or the entire lesion is small, or because of dense surrounding tissue (Fig. 1.4b).

The final third of cores show benign changes that do not clearly correlate with architectural distortion. When these lesions undergo excision, about 10% are missed cancers and 50% are specific benign lesions that were either missed or could not be diagnosed on the CNB [10]. However, in ~40% of cases a specific cause of the architectural distortion cannot be identified.

Focal Asymmetry

A focal asymmetry is an area of denser tissue, as compared to the contralateral breast, that is seen in both mammographic CC and MLO views (Fig. 1.4d) [11, 12]. While masses have distinct borders and convex contours, focal asymmetries do not have definable borders and often include interspersed adipose tissue. If the area is only seen in one projection, it is described as "asymmetry" rather than "focal asymmetry."

Subtle changes in breast parenchyma can arise during the normal aging process with involution typically beginning in the fourth decade. Lobules regress and the normal fibrous interlobular tissue is replaced by adipose tissue. This process may occur at different rates at different sites and create the impression of an area of focal density (Fig. 1.4e). In such cases, a specific pathologic process cannot be identified to correlate with the imaging-identified asymmetry because it in fact represents residual fibroglandular tissue. Benign lesions such as PASH or postsurgical changes can also cause an area of focal density.

The likelihood of malignancy is low unless other features are present such as a palpable mass, calcifications, or architectural distortion, or the area is increasing in size or density [13, 14]. The most common malignancy is a diffusely infiltrative invasive carcinoma with little or no desmoplastic response (Fig. 1.4f).

Calcifications

Mammography is the best and most sensitive modality for the detection of calcifications. Although larger calcifications can sometimes be detected by U/S or MRI, these are not the preferred modalities for the identification of the smaller calcifications associated with malignancies. Calcifications detected by U/S are likely at least 1–2 mm in size and are typically only seen when numerous and grouped. Only large (>5 mm) calcifications are seen on MRI as areas of signal void.

Calcium and phosphate are minerals normally present in solution in extracellular fluid. Oxalate is an organic acid that is an end product of metabolism. The formation of calcium salts into crystalline structures requires a regular repeating structure. Fragments of the phospholipid membranes of breast epithelial cells (either due to apocrine secretion or cell death and necrosis) or dense hyalinized collagen (in hyalinized fibroadenomas, hyalinized fibrovascular cores of papillomas, or collagen placed after CNB), are the most common substrates for calcification (Table 1.5).

The majority of calcifications are composed of calcium and phosphate. They are purple in color and have a granular appearance. Very large calcifications associated with secretory/lactational changes can have a psammoma-body appearance with concentric rings. Calcium phosphate crystals form on membrane fragments from secretions and necrosis and on hyalinized stroma.

The formation of calcium oxalate crystals is only associated with secretory material in cysts and cystic structures, usually lined by cells with apocrine metaplasia. Interestingly, the only sites where calcium oxalate crystals form in normal tissue are in breast cysts and in colloid in thyroid follicles. The crystals are plate-like (rhomboid) to needle-shaped and translucent to yellow and can be difficult to detect in secretory material. However, they are strongly birefringent and

Table 1.5 Calcifications

Substrate for crystallization	Microscopic appearance	Most common benign lesions	Most common malignant lesions
Membranes—secretion	Apocrine snouts leave membrane fragments in cysts or lumens	Apocrine cysts	Low-grade DCIS, tubular carcinoma
Membranes—necrosis	Dead cells result in membrane fragments	Fat necrosis	High-grade DCIS, high-grade invasive carcinoma
Collagen	Regular repeating hyalinized collagen	Hyalinized fibroadenoma, fibrotic papillary cores, blood vessels	Rare—stroma of invasive carcinomas

are easily seen as bright objects under polarized light. When extruded from cysts, they are found in the adjacent tissue associated with a giant cell response. Calcium oxalate crystals are not associated with malignancy [15].

Many calcifications are detected by screening mammograms but only a few patterns are of sufficient risk for underlying malignancy to warrant biopsy. The most important features are number, size, distribution, and change over time:

- *Number*: At least five calcifications are necessary to be classified as a "group." The larger the number of calcifications in a localized area, the greater the likelihood that they are being formed by an area of DCIS or (less commonly) an invasive carcinoma with calcifications in secretions, mucin, or necrosis.
- *Size*: Calcifications must be at least 50–100 μm (0.05–0.1 mm) in size in order to be detected by mammography. Very small incidental calcifications below the resolution of imaging are often present in tissue sections.
- Very large calcifications (>1 mm or >1000 μm) require a long time to form and are unlikely to be due to malignancy. Large multilobated calcifications are termed "popcorn-like" and are typically associated with hyalinized fibroadenomas (Table 1.6). These calcifications would not be targeted for biopsy.

Small to mid-range calcifications (0.05–1 mm or 50–1000 μm) can be associated with either benign lesions or malignancy.

- *Distribution*: Widely scattered single calcifications are common and are not associated with malignancy. Other patterns are often indicative of the underlying pathologic lesion (Table 1.6).
- *Grouped*: This is the most common pattern undergoing biopsy (Fig. 1.5a). Multiple calcifications in the same area indicate the presence of multiple substrates for crystallization. The substrate could be multiple membrane fragments in a cluster of cysts (Fig. 1.5b) or a ductal system involved by DCIS with necrosis (Fig. 1.5c).
- *Linear*: Calcifications in a linear distribution are present in ducts or blood vessels. Vascular calcifications are described below. The term "casting" describes the appearance of a substance having been formed in a mold. "Casting" has been used to refer to calcifications in a linear distribution but is not a current recommended descriptive term in the BI-RADS lexicon. Numerous small uneven calcifications following the underlying branching ducts is the pattern with the highest association with malignancy (Fig. 1.5d). This is most commonly due to high-grade DCIS with central necrosis involving ducts (Fig. 1.5f). Large rod-like smooth ("secretory") calcifications filling a duct or ducts are associated with duct ectasia with inspissated secretions and/or calcification of the duct wall (Fig. 1.5e). This is a low suspicion pattern and would not typically undergo biopsy.
- *Vascular*: Calcifications of vascular walls form parallel linear patterns that are usually easily identifiable on mammography. Radiologists would not intentionally biopsy such calcifications, but they may be present as an incidental finding. Thus, they are not a good correlate for targeted calcifications. If only vascular calcifications are seen in the initial slides, the pathologist should perform deeper levels to search for another source.
- *Milk of calcium*: This term is used to describe calcifications that change in appearance when CC (horizontal) and ML (vertical) views are compared (Table 1.6, Fig. 1.6). Gravity influences the spatial distribution when the calcifications are floating in fluid in a cystic space. The most common associated lesions are large apocrine cysts with calcifications and secretions. In the ML view, the calcifications are viewed from the side, and due to the influence

Table 1.6 Calcifications—radiologic terms and pathologic correlation

Term	Description	Pathologic correlate
Grouped	Localized group of at least five calcifications	Clusters of cysts, fibroadenoma, DCIS
Linear and branching	A pattern that follows the structure of the ductal system	Majority are DCIS, less common hyalinized ducts
Rod-like	Solid or discontinuous rods radiating from the nipple	Ectatic lactiferous sinuses (rarely biopsied)
Vascular	Parallel tracks or linear tubular pattern ("train tracks")	Hyalinized blood vessels (not intentionally biopsied)
Popcorn-like	Coarse and large (>2–3 mm)	Hyalinized fibroadenoma (usually not biopsied)
Egg-shell	Calcifications surrounding a circumscribed lucent mass	Fat necrosis or cyst wall (usually not biopsied)
Dystrophic	Large irregular calcifications >1 mm (1000 μm), often with lucent centers	Prior surgical sites or other trauma and/or after radiation (usually not biopsied)
Coarse heterogeneous	Irregular calcifications that are >0.5 mm (500 μm) but smaller than dystrophic calcifications. Vary in size and shape	Can be associated with malignancy and may be biopsied
Fine pleomorphic	Small calcifications varying in size and shape	Very suspicious for malignancy (usually biopsied)
Amorphous	Too small to determine the morphologic appearance	Usually benign if scattered, can be malignant if in groups or linear
Milk of calcium	Calcifications that change in position with respect to gravity	Cysts with calcifications (usually not biopsied)

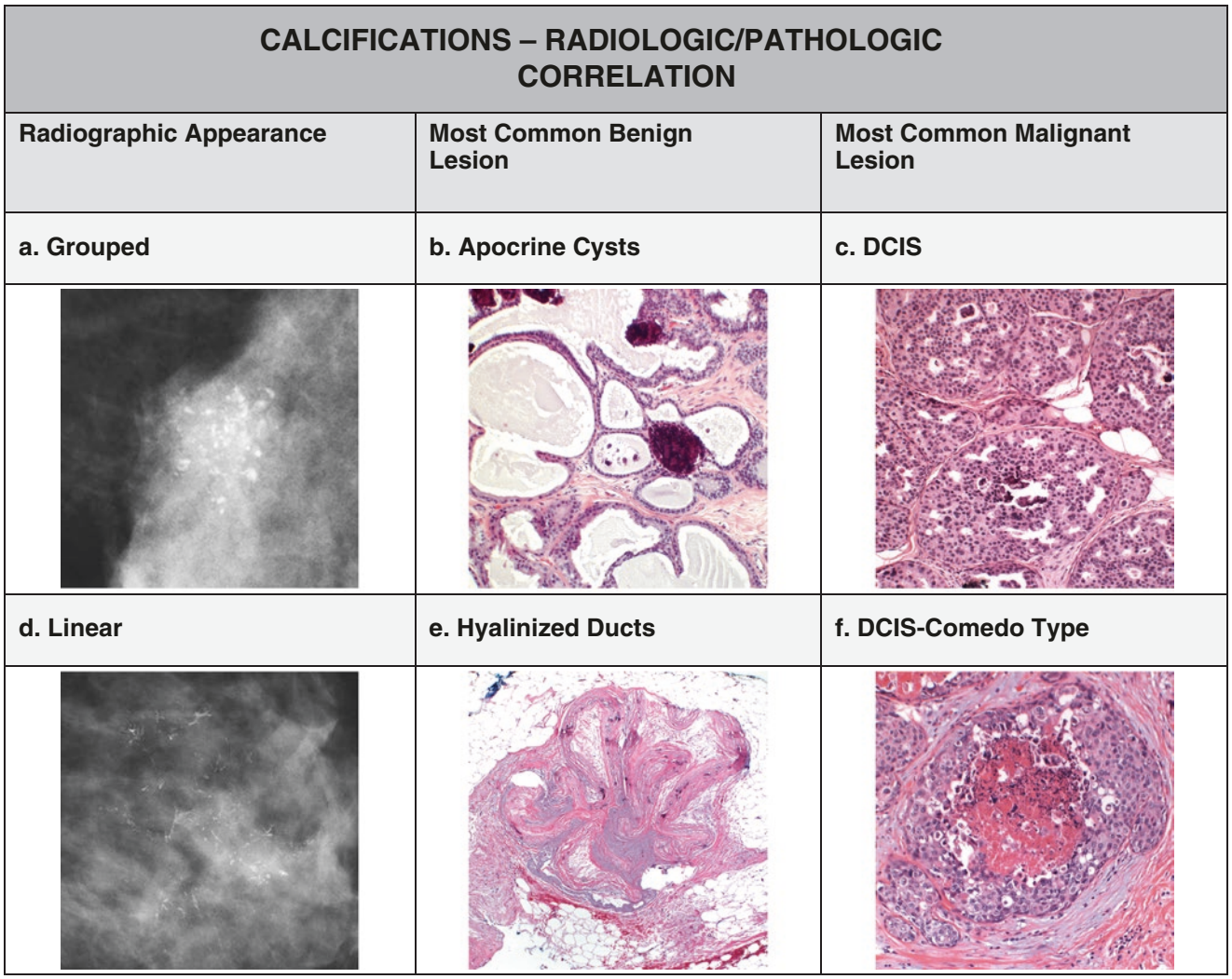

Fig. 1.5 (**a**) This radiograph shows a group of heterogeneous morphology calcifications. (**b**) Calcium phosphate (*granular purple deposits*) and calcium oxalate (*smaller pale crystals*) have formed on secretions in this cluster of apocrine cysts. (**c**) This low-grade DCIS is associated with calcium phosphate crystals forming on secretions in cribriform spaces. (**d**) This radiograph shows linear and branching heterogeneous morphology calcifications. This pattern of calcifications follows the ductal system and is often associated with malignancy. In contrast, larger linear calcifications that appear to fill the ducts are typically due to ectatic ducts. (**e**) This duct has a thick calcified hyalinized wall. This finding would correlate with large tubular calcifications in multiple large ducts radiating from the nipple. (**f**) Multiple fine calcifications tracing the pattern of ducts are most often associated with high-grade DCIS. The calcifications form on membrane fragments in the central area of necrosis

of gravity, are seen at the bottom of the cysts as a semilunar or curvilinear line (a "teacup" shape). In the CC view, the calcifications layered at the bottom of the cyst are viewed from above and appear as indistinct round groups. The appearance in the MLO (semi-vertical) view is intermediate between these views. This pattern of calcification is not associated with malignancy and is typically not biopsied.

- *Change in calcifications over time*: Calcifications associated with benign lesions are typically stable over time in multiple sequential mammographic examinations. In rare cases, benign calcifications decrease in number—particularly those associated with cysts or dystrophic calcifications. Benign calcifications can also diminish in number after radiation therapy. In contrast, calcifications associated with a malignant process usually increase over time and persist after treatment.

Radiologists judge the likelihood of calcifications being associated with carcinoma by considering all of these features in aggregate. A biopsy for calcifications reveals carcinoma in approximately 20–30% of cases and the majority are DCIS. The detection of DCIS due to calcifications on screening mammography has led to the marked increase in the number of cases diagnosed since the 1980s [16].

A specimen radiograph of the cores is performed by the radiologist to demonstrate that the targeted calcifications

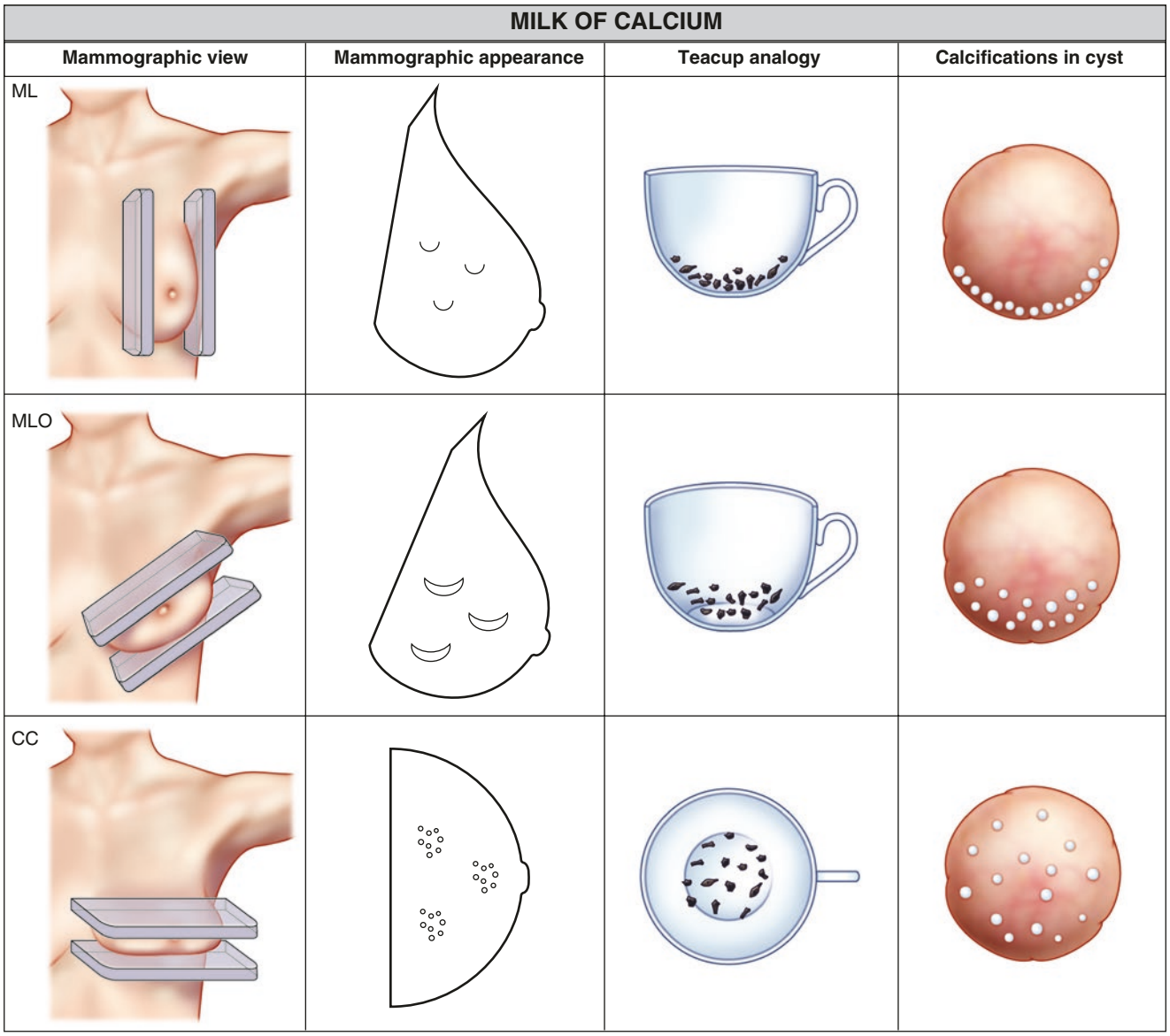

Fig. 1.6 Milk of calcium is the term used by radiologists to refer to calcifications that change in shape in the different mammographic views. In the medial–lateral (ML; *vertical*) view, gravity acts on calcifications in cysts so that they are seen as layering at the bottom forming a crescent shape. This is analogous to looking at tea leaves in a teacup from the side. In the craniocaudal (CC; *horizontal*) view, the calcifications are distributed over the entire cyst. This is analogous to looking at tea leaves in a cup from above. In the medial–lateral–oblique (MLO; *angled*) view, intermediate features are seen

were removed. The radiograph also provides helpful information for the pathologist in order to directly see the number and distribution of calcifications by imaging (Fig. 1.7a). If the targeted calcifications are not removed, or if only rare faint calcifications are present, this must be communicated to the pathologist. If the targeted calcifications were not sampled, there is no need to perform additional levels to look for incidental calcifications.

If the calcifications are removed from the breast using a vacuum-assisted technique, but not evident on the specimen radiograph, the radiologist should consider the possibility that the tissue-bearing calcifications have been suctioned into the tubing and/or debris canister. This tissue can be retrieved for pathologic analysis [17, 18].

Correlation of the size and number of mammographic calcifications with histologic calcifications is often imperfect for many reasons:

1. *Calcifications more numerous on imaging than on histology*: The radiograph shows all the calcifications in three dimensions within a larger volume of tissue than that present on the glass slide which is (essentially) two-dimensional and shows only a subset of the calcifications. Thus, fewer calcifications are generally present on a tissue section.

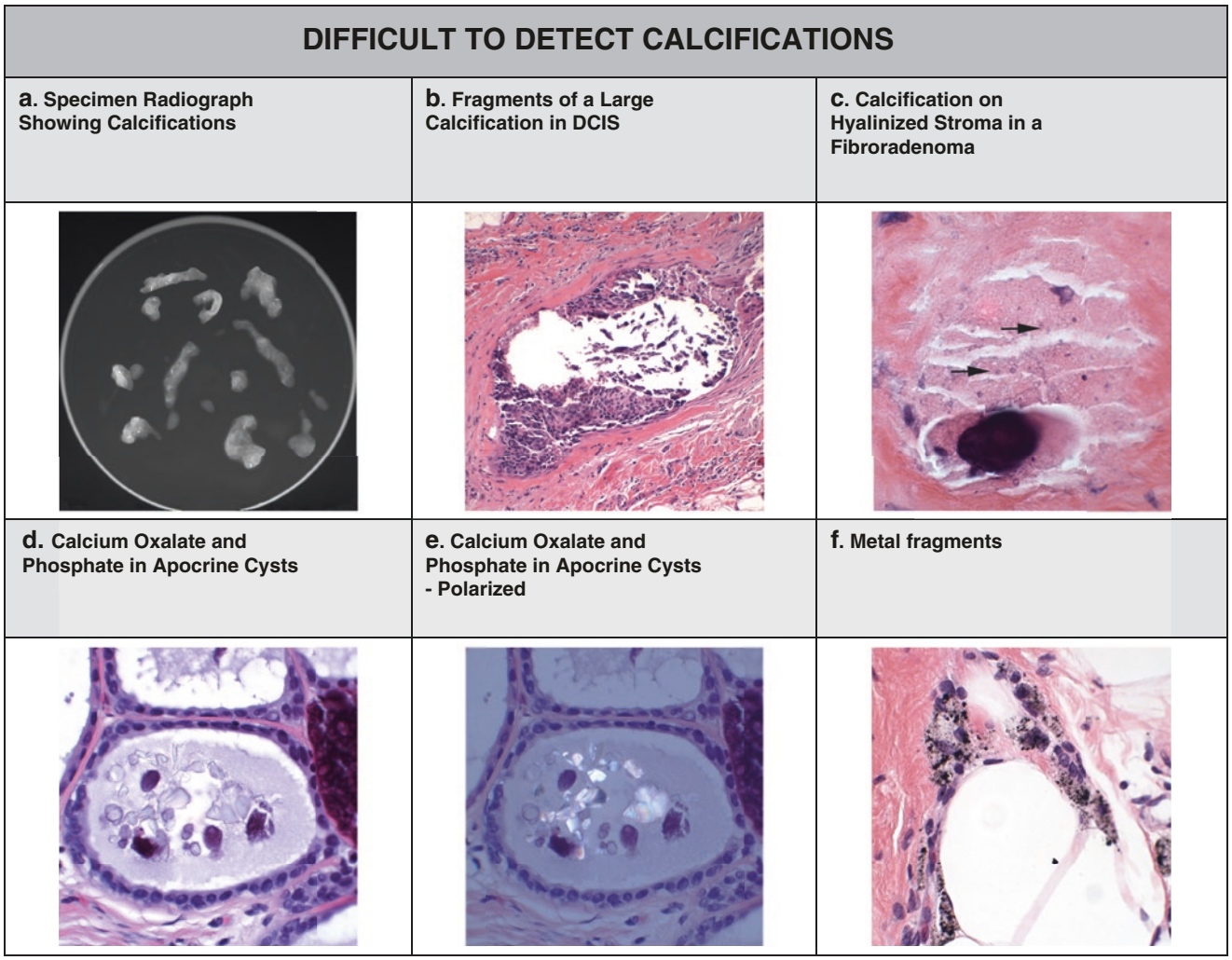

Fig. 1.7 (**a**) The radiologist performs a specimen radiograph to confirm the presence of calcifications in the cores. Calcifications that are faint or few in number may be difficult to detect in tissue sections. The numerous calcifications in this radiograph should be readily apparent in the histologic sections. (**b**) Large calcifications can chip out of the specimen rather than be sectioned. Only fragments of a calcification may be present, as seen in this case of DCIS. (**c**) Direct crystallization of calcium phosphate onto dense collagen, most commonly seen in hyalinized fibroadenomas, can appear as subtle small spherical "bubbles." In this case a large calcification is present next to numerous smaller difficult to see calcifications (*arrows*). (**d**) Calcium phosphate is generally readily seen because it forms granular purple crystals, as seen in the cyst at the right of the photograph. The calcium oxalate crystals in the center of the photograph are more difficult to see because the crystals are translucent. (**e**) Under polarized light, the calcium oxalate crystals are birefringent, but the calcium phosphate deposits are not. (**f**) These metallic fragments are present as small sharply angulated black structures in histiocytes at a prior excisional site. Metal can resemble calcifications on mammography but may be recognizable due to the shape and increased density

2. *Calcifications more numerous on histology than on imaging*: Very small calcifications (<50 μm) not evident on mammography can be seen in tissue sections. If only scattered small calcifications are present, this is unlikely to correlate with a group of imaging calcifications and additional deeper levels should be obtained. Alternatively, in some cases when only small calcifications are seen, it is possible that the "larger" calcifications seen in the radiograph consist of multiple small overlapping calcifications.

Ultimately, the most important factor to help determine if the results are concordant is to ensure that the radiologist and the pathologist are looking at the same tissue containing the calcifications. Placing the cores with the radiologic calcifications in a separate cassette is one method to do this. If the correlation is poor after complete evaluation of the tissue with multiple levels and comparison to the specimen radiograph, the following possible reasons for the missing calcifications should be considered.

Reasons for Absent Calcifications

1. *Deeper in the paraffin block*

   Identification of the cores with calcifications followed by careful attention to embedding all cores at the same level in the block during processing is helpful to ensure all tissue is seen in the initial sections. The first section should be shallow with a minimum of tissue wastage.

However, if calcifications are not seen on the initial levels, radiography of the block (flat and on edge) can sometimes document calcifications remaining deeper in the block [19, 20]. Deeper levels should be obtained to search for the calcifications.

2. *Lost from the block during slide preparation*

   The presence of relatively large calcifications (e.g., 400 μm) in the shavings discarded during the preparation of slides demonstrates that the microtome blade can push calcified particles out of the block rather than cutting through them [21]. This most commonly occurs when calcifications are present in adipose tissue, such as occurs in fat necrosis or heterotopic bone formation. Difficult to see partial residual fragments of the calcifications may be seen on only some levels of the slides (Fig. 1.7b).

3. *Present but difficult to see*

   The only stroma that commonly calcifies is the hyalinized stroma of a fibroadenoma or fibrovascular cores in papillomas. These calcifications can look like tiny blue bubbles and are easily missed (Fig. 1.7c).

   Calcium oxalate crystals are translucent and can be difficult to see (Fig. 1.7d). The contents of cysts should be examined under polarized light which makes the crystals easy to see (Fig. 1.7e). Crystals can also be extruded from cysts and be present in the tissue adjacent to the cysts associated with a multinucleated giant cell response. Crystals free floating on the glass slide unassociated with tissue must be interpreted with caution as debris introduced during processing can also be birefringent.

4. *Dissolved in fixative*

   Prolonged time in formalin over several days can result in the disappearance of radiologic calcifications [22]. This should never happen with routine processing occurring within 1–2 days. Formalin must be properly buffered as acidic solutions cause leaching of calcium. Other types of fixatives, such as Bouin's, that are acidic and cause decalcification should not be used.

5. *Fallen out of the specimen*

   If the calcifications are in cystic spaces, they can disperse into the formalin after cysts have been punctured by the needle biopsy. This possibility can be minimized by enclosing the cores in paper or a nylon bag (discussed later under specimen processing). Evaluation of the formalin for crystals (e.g., by preparation of a cell block) is not recommended as crystal-like material can be present as an artifact.

6. *Foreign material mimicking calcifications*

   On mammography, metal is very white in appearance and its presence may be suspected by the radiologist. Metallic fragments may be introduced due to prior surgical procedures or rarely from prior trauma [23–26]. Microscopically, metallic fragments can look like very small black inter- or intracellular particles (Fig. 1.7f).

   Gold from injections for rheumatoid arthritis is sometimes seen in intramammary or axillary lymph nodes [27]. The node can appear on mammography as an oval mass-containing calcifications. The gold forms black granular masses that resemble anthracotic pigment.

   Tattoo pigment can migrate from the skin to lymph nodes and mimic calcifications [28–30]. The particles usually look black but occasionally colors can be seen.

7. *The specimen has been misidentified*

   If definitive calcifications are present in the specimen radiograph but not identified in the specimen, the possibility that two specimens have been misidentified should be considered.

Ultrasound

The majority (around 65%) of image-guided core needle biopsies are performed using ultrasound (U/S) as it requires the least amount of equipment and is the easiest to perform [2]. Its greatest role is for the further definition of masses detected by mammography or MRI. U/S also may be useful in detecting lesions in particularly dense breasts of patients when mammography does not reveal a definite lesion. It is the best modality for distinguishing fluid filled from solid masses. Calcifications are not generally visible unless large and numerous.

- *Size*: U/S is generally accurate for determining tumor size but tends to slightly underestimate it. An echogenic halo can be formed by tumor cells infiltrating into adipose tissue at the periphery [31].
- *Margins*: The contours of masses are described as being circumscribed or non-circumscribed (indistinct, angular, microlobulated, or spiculated) (Table 1.4). The differential diagnosis for lesions with these categories of margins is the same as that for mammography.
- *Shape*: The terms for shape are the same as for mammography (oval, round, or irregular). Malignant lesions are often non-parallel to the skin surface or "taller than wide" because the tumor cells grow across tissue planes. In contrast, benign lesions tend to be oriented parallel to the skin surface ("wider than tall").
- *Echogenicity*: Sound waves rebound from tissue and fluids in different patterns. The echo pattern provides information about the type of lesion (Table 1.7). U/S is the best modality to determine if masses are solid or cystic. A simple cyst has circumscribed margins and lacks internal echoes ("anechoic") (Fig. 1.8a). Cysts can be observed when small or drained to completion when large under U/S guidance. Lesions with solid and cystic areas can be cysts containing debris, papillary lesions, phyllodes tumors, or invasive carcinomas with areas of necrosis (Fig. 1.8b). Biopsies from such lesions are often fragmented.
- *Posterior shadowing*: The pattern of echoes behind the lesion also provides information. Sound waves pass easily

Table 1.7 Ultrasound —echo patterns

Echo pattern	Definition	Pathologic correlation
Anechoic	No internal echoes (appears black)	Fluid-filled cyst
Hyperechoic	Increased echoes relative to fat (appears light)	Angiolipoma, fat necrosis, some lactating adenomas and galactoceles, hilum of lymph nodes—almost all benign Rare malignancies usually contain areas of fat (e.g., lobular carcinoma), tubules containing fluid (e.g., some ductal carcinomas), or blood vessels (e.g., angiosarcoma)
Complex cystic and solid	Both anechoic (fluid) and hypoechoic areas	Cysts with debris or hyperplasia, hematomas, abscess, fat necrosis, galactocele, papillary lesions, carcinomas with central necrosis, phyllodes tumor
Hypoechoic	Low level internal echoes compared to subcutaneous fat (appears dark)	Majority of solid benign and malignant masses
Isoechoic	Same echogenicity as subcutaneous fat (appears gray)	Fat-containing lesions such as lipomas—almost always benign

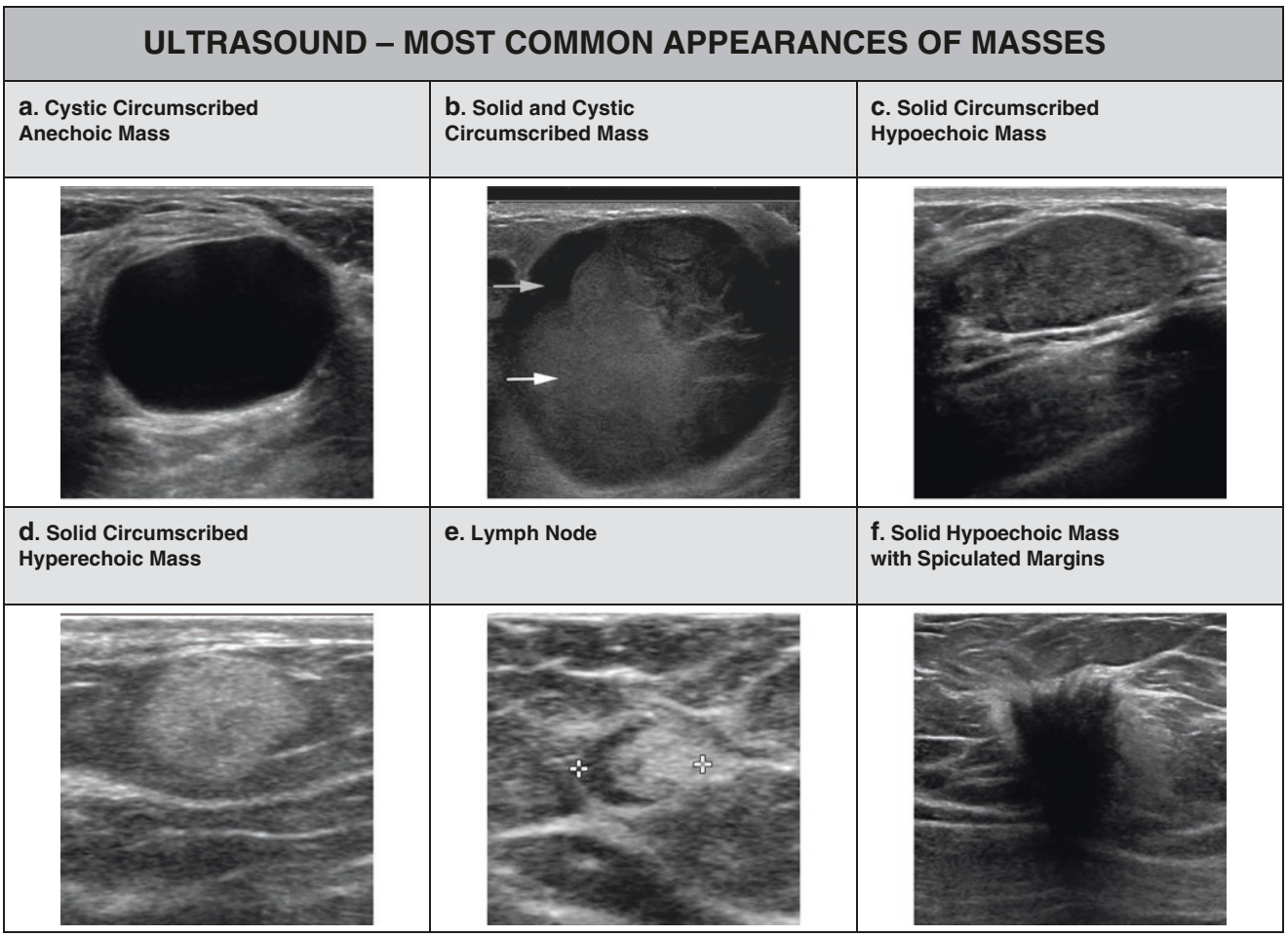

Fig. 1.8 (**a**) This circumscribed lesion with no internal echoes (anechoic) and posterior acoustic enhancement has the diagnostic features of a fluid-filled cyst. A simple cyst can be observed or completely drained by aspiration. (**b**) This mass has both solid (*white arrow*) and cystic (*gray arrow*) areas. Pathologic lesions with this appearance include papillary lesions, cysts with debris, phyllodes tumors, and invasive carcinomas with necrosis. Biopsies from such lesions are often fragmented. (**c**) This solid mass has circumscribed margins and is less echogenic than subcutaneous fat ("hypoechoic"). The orientation is parallel to the skin ("wider than tall"). This is most likely a benign lesion such as a fibroadenoma. (**d**) This solid circumscribed mass has an increased number of internal echoes and is brighter than fat. This appearance is termed "hyperechoic." The majority of lesions with this appearance are fat-containing and benign, such as angiolipoma, fat necrosis, and galactocele. (**e**) Lymph nodes are usually easily recognized due to the hypoechoic lunate-shaped mass, with a fatty hyperechoic hilum. (**f**) This mass has spiculated margins, is "taller than wide," and shows posterior acoustic shadowing. The most likely diagnosis is an invasive carcinoma

through homogeneous lesions and fluids, creating an area of white echoes behind the lesion called acoustic enhancement. It is more difficult for sound waves to pass through heterogeneous lesions and many are reflected back. This creates a dark area behind the lesion termed acoustic shadowing. Malignant lesions are more likely to show shadowing.

All of these features are used to determine the likelihood of malignancy. For example, solid masses with circumscribed margins that are "wider than tall," hypoechoic, and with posterior acoustic enhancement are very likely to be benign (Fig. 1.8c). If the mass is hyperechoic (suggesting fat content) and has circumscribed margins, it is almost always benign (Fig. 1.8d). Typical lesions with this appearance are angiolipomas, fat necrosis, and galactoceles. Rare malignancies consisting of closely interposed elements of differing echogenicity (i.e., tumor cells, dense stroma, adipose tissue, and fluid in tubules, vessels, or stromal clefts) can be hyperechoic but do not have circumscribed margins [31]. An intramammary lymph node can be recognized as it forms a hypoechoic lunate-shaped mass with a fatty hyperechoic hilum (Fig. 1.8e).

In contrast, masses with spiculated, microlobulated, or angular margins that are hypoechoic, "taller than wide," and associated with posterior acoustic shadowing are usually invasive carcinomas (Fig. 1.8f).

Magnetic Resonance Imaging

MRI is used for fewer than 5% of image-guided core needle biopsies as this is the modality most difficult to perform and requires patients to be injected with a contrast agent [2]. Other modalities are used to biopsy MRI-detected lesions when possible.

Contrast-enhanced MRI detects breast lesions due to increased blood flow visualized as increased enhancement after injection of gadolinium. There is high sensitivity for malignancies (as most are associated with angiogenesis and increased blood flow) but low specificity (as many benign lesions are also vascular). MRI may be used in the following situations:

1. *Screening of women at increased risk for carcinoma*: This group includes women with germline mutations, a history of chest radiation between the ages of 10 and 30, and women with a recent diagnosis of cancer in the contralateral breast. Women of average risk generally are not screened by MRI because of the large number of false-positive results requiring biopsy in this population compared to the small number of cancers found only by MRI and missed by routine screening.
2. *Evaluation of the extent of disease in women with known breast cancer*: In some cases, MRI can better define the size of a cancer, the presence of additional areas of cancer, and whether or not there is invasion into the chest wall. This can aid in surgical planning.
3. *Evaluation of tumor response in women undergoing neoadjuvant chemotherapy*: If no response occurs during treatment, the type of therapy may be changed or the patient may undergo surgery before the cancer becomes unresectable. When carcinomas do respond to treatment, one of the earliest changes seen is decreased enhancement, presumably due to diminished vascular flow in the tumor bed. However, substantial residual carcinoma can be present even when enhancement is reduced or absent. Alternatively, persistent enhancement can be due to DCIS in cases where there has been a complete or almost complete obliteration of the invasive carcinoma. CNB assessment of the tumor bed is being investigated to determine if surgery can be avoided in patients with pathologic complete responses [32].
4. *Detection of occult primaries responsible for known metastases*: Rare women are found to have an axillary or distant metastasis, but no breast lesion can be detected by mammography or U/S. MRI can identify the primary carcinoma in some cases.
5. *Follow-up of women with a history of cancer*: Recent surgical sites show enhancement due to tissue disruption with granulation tissue, but these changes should resolve within 1–2 years after the completion of treatment. New nodular areas of peripheral enhancement are more suspicious for a local recurrence.
6. *Problem-solving in difficult cases*: Patients may have symptoms or findings by other modalities of unclear etiology. MRI can provide additional information.

CNB can be difficult to perform using MRI and the procedure requires special non-ferromagnetic equipment. In addition, patients must undergo intravascular injection of a contrast agent (gadolinium). The majority of lesions detected by MRI can be detected and biopsied by mammography or U/S. For example, subsequent U/S can identify about 60% of lesions first detected by MRI.

The subset of lesions only seen by MRI, and therefore requiring a biopsy guided by MRI, are typically small in size if mass-forming (<1 cm). However, because lesions must be over a certain size (usually >0.5 cm) to be detected by MRI, diagnostic tissue is generally present on the first H&E level [33].

The overall incidence of carcinoma is 20–30%—about 60% invasive carcinoma and 40% DCIS [34, 35]. The invasive carcinomas that are detected are most commonly of low grade and estrogen receptor positive. More poorly differentiated carcinomas typically grow rapidly and are less likely to be detected when still small in size. In contrast, the DCIS detected by MRI is often high grade, possibly due to periductal angiogenesis, which could result in MRI enhancement.

BI-RADS defines three types of enhancement: focus, mass-like, and non-mass like.

Focus of Enhancement

A focus is a <5 mm dot like area with an indeterminant shape and margins. Although very small, about 18% are due to malignancies, the majority invasive carcinomas [36].

Mass-Like Enhancement

A mass is defined as an area of space occupying enhancement that can be characterized as to shape and margin. Shapes are the same as those used for mammography and U/S. Margins are described as circumscribed (smooth and sharply demarcated from the surrounding tissue), irregular (uneven or jagged), or spiculated (lines radiate from the mass into the surrounding tissue) (Fig. 1.9a, b). There is lower correlation between the MRI morphology and the actual biologic shape of masses as compared to masses detected by mammography or U/S, and this is particularly true for the small masses only seen by MRI. This is likely because the vascularity of the lesion has a greater impact on appearance with MRI than with the other two modalities. The internal pattern of enhancement (homogeneous, heterogeneous, or rim) as well as the rate at which the contrast enters and leaves the lesion (enhancement kinetics) are important predictors of malignancy in combination with shape and margins. Size of the lesion also influences the likelihood of malignancy, with higher rates of malignancy in lesions larger than 1 cm [37, 38]. In terms of shape and margin, it is generally true that irregular shape and irregular or spiculated margins are more frequently associated with malignancy than round and oval shapes with circumscribed margins, but the likelihood of malignancy is best determined in combination with enhancement characteristics [37, 38].

Non-mass Enhancement

Non-mass enhancement (NME) describes an area of enhancement that cannot be categorized as a focus or a mass. It may involve a small or large area, but the internal enhancement characteristics (homogeneous, heterogeneous, clumped, or clustered ring) are different from that typical of normal background parenchyma. There is often normal enhancing parenchyma or fat interspersed between the area or areas of abnormal enhancement. There are six different patterns of NME:

- *Focal*: occupies less than one quadrant and has fat or normal glandular tissue interspersed.
- *Linear*: arrayed in a line that may or may not branch.
- *Segmental*: triangular or cone-shaped with the apex towards the nipple.
- *Regional:* occupies more than a single duct system and a large portion of the breast, at minimum, a breast quadrant.
- *Multiple regions*: involves at least two large areas not conforming to a ductal distribution and separated by normal tissue.
- *Diffuse*: distributed throughout the breast.

The patterns of NME correlate poorly with specific pathologic lesions [38]. The highest correlation is with linear clumped enhancement as about 20% of these cases are due to DCIS (Fig. 1.9c).

Because MRI patterns of enhancement do not have a strong correlation with pathologic findings, it is the radiologist's task to ensure the targeted lesion was sampled when the biopsy shows benign results.

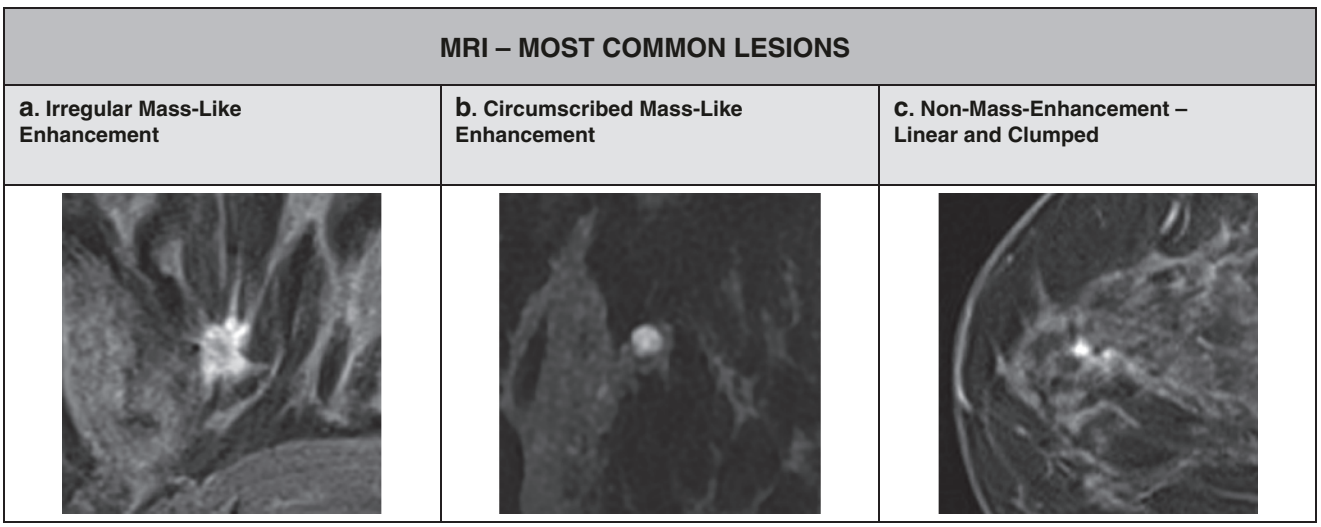

Fig. 1.9 MRI detects lesions due to increased vascular flow, resulting in enhancement after injection of a contrast agent. (**a**) This is an irregular enhancing mass with spiculated margins. (**b**) This is a round enhancing mass with circumscribed margins. (**c**) This is an area of linear clumped non-mass enhancement

Types of Needle Biopsies

The type of biopsy performed to sample a lesion will depend on the means of detecting the lesion, the type of lesion, and the technology available to the radiologist. Each technique has advantages and disadvantages (Fig. 1.10). Pathologists should be aware of the types of biopsies performed at their institution and radiologists should inform pathologists when a new device or technique is introduced.

In all techniques, the needle should penetrate the breast parallel to the chest wall. Skeletal muscle should not be present and should be reported when seen—as this is an indica-

Fig. 1.10 Many types of needle biopsies are available to radiologists for sampling lesions. Pathologists must be aware of the types of biopsies being utilized at their institution and the advantages and limitations of each type of biopsy

TYPES OF NEEDLE BIOPSIES

Type of needle biopsy	Shape of specimen	Comments
Fine needle aspiration	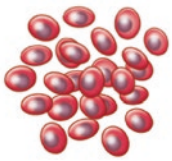	Single cell aspiration does not distinguish in situ carcinoma from invasive carcinoma. Best technique to document lymph node metastases prior to neoadjuvant treatment.
Core 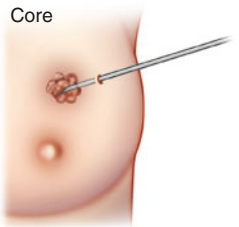		Standard cutting technique for breast lesions. Requires multiple passes.
Cryobiopsy 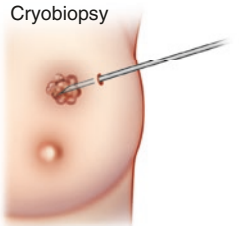	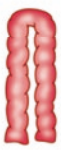	Freezes tissue potentially introducing morphologic artifacts and altering biomolecules.
Vacuum-assisted core 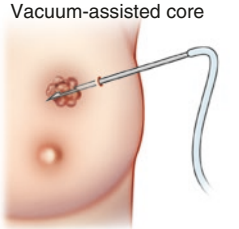		Removes large cores of tissue with only one needle insertion.
Intact 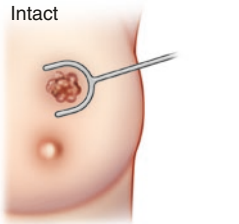		Heats tissue potentially introducing morphologic artifacts and potentially altering biomolecules.
Very large core 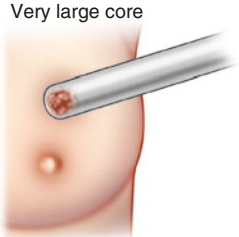		Removes a large amount of benign tissue including subcutaneous tissue – cosmetic results may be poor and complication rate higher.

tion of suboptimal positioning of the needle. Small fragments of skin may be present and are generally not of importance to report unless the lesion is in the same fragment as the skin, as this indicates that the lesion is very superficial.

Needle Size

The goal for needle biopsies is to adequately sample lesions but to not completely remove them. Gauge is inversely related to size such that smaller values correspond to larger bore needles (Table 1.8). Smaller gauge needles result in minimal tissue damage but are more likely to fragment and be difficult to interpret due to scant lesional tissue. Larger gauge needles provide more diagnostic material but may be more likely to cause complications (e.g., bleeding) and to create problems in pathologic interpretation after excision due to removal of the majority of a lesion in a piecemeal fashion. A good compromise is generally attained with needle gauges ranging from 9 to 14. The needle size is largely dependent on the modality chosen (mammography, U/S, or MRI) and the specific manufacturer of the device used. When the radiologist has a choice of needles, lesion and patient factors are taken into consideration. For example, a larger needle may be used for partially cystic and partially solid masses to ensure adequate sampling. A smaller needle may be chosen if there is a concern about potential bleeding.

Fine Needle Aspiration

Fine needle aspiration (FNA) is generally performed with 22-gauge or smaller needles. The needle typically removes samples of individual cells but generally not intact tissue fragments. The aspirate is used to make smears and the syringe can be rinsed and the fluid used to make a cell block. Cell blocks are fixed and sectioned like solid tissue and can be used for ancillary studies such as immunohistochemistry.

Table 1.8 Needle gauge and size of cores

Gauge	~Diameter size, mm
22 or smaller	0.7 (single cells)
14	1.6
12	2
11	2.3
9[a]	2.9
8	3.2
7	3.5

[a]9G petite—a needle with a shorter sampling bowl and rounded tip. This type of needle is used for sampling breasts that are thinner than 3 cm when compressed. The resulting cores are shorter and rounder in shape

Advantages

- Best technique to drain and evaluate presumably benign cysts.
- Fluid need not be examined unless bloody or associated with a residual palpable mass or unresolved cyst.
- A large area of involved tissue can be sampled using multiple passes (e.g., architectural distortion or calcifications).
- Smears can be immediately evaluated for sufficiency and diagnosis.
- An FNA minimally alters the sampled lesion. FNA is very helpful to confirm metastasis to a lymph node prior to neoadjuvant therapy as the metastasis is left in place and response to treatment can be evaluated.

Disadvantages

- Invasive carcinoma is not reliably distinguished from in situ carcinoma.
- Subsequent CNB may be necessary to confirm invasion to allow planning for lymph node sampling and/or neoadjuvant chemotherapy.
- Requires special training for interpretation.
- Immunoperoxidase studies are best performed on routinely fixed paraffin sections (although cell blocks can be used if other specimens are not available).

In general, positive results for malignancy by FNA should be confirmed by CNB or excision prior to definitive treatment due to the risk (albeit very small) of a false-positive diagnosis.

Core Needle Biopsies: Non-vacuum-Assisted

"Core" needle biopsies remove an intact tubular fragment of tissue, as opposed to the single cells removed by a fine needle biopsy. "Core needle" biopsies, "needle core" biopsies, and "core" biopsies are synonyms for the same type of biopsy.

A manual device (e.g., Tru-Cut type) or spring-loaded biopsy gun may be used. The needle is advanced to the periphery of the lesion. The lesion is sampled by either manually advancing the needle or firing the gun of a spring-loaded device. Multiple passes (typically 4–5) must be made to sample a larger area. This technique is usually performed with 14-gauge needles.

Advantages

- Removes a core of tissue.
- Core site is generally small and does not distort lesion.
- The device is relatively inexpensive, widely available, and simple to use.

Disadvantages

- Cores are generally small and may be fragmented.
- Multiple insertions are necessary to sample lesions.
- If a mass is sampled multiple times, the cores may be designated as 3:00, 6:00, 9:00, 12:00, and center. It should be clear that these are areas within the same lesion and that the clock designations do not indicate the location in the breast with respect to the nipple.

Core Needle Biopsies: Vacuum-Assisted

Use of vacuum allows more tissue to be sampled using only one puncture. A needle is inserted into the target or directly next to the target. Vacuum draws tissue into the needle trough (sampling chamber). An inner rotating cutting cannula is advanced and cuts the core. The tissue is then delivered by vacuum through the barrel of the probe into a collection chamber. Multiple additional biopsies can be taken by rotating the needle without the need for multiple insertions. Small eddies of tissue are sometimes seen in these biopsies but they do not interfere with interpretation. 14-, 12-, 10-, 9-, 8-, or 7-gauge needles may be used.

Advantages

- Removes multiple cores with a single insertion.
- Cores are generally larger.
- Lesions are more completely sampled.
- The gross detection of the core site is more obvious than non-vacuum-assisted sites.

Disadvantages

- Removing too much tissue can make subsequent pathologic evaluation difficult.
- The device is relatively expensive compared to non-vacuum-assisted biopsies and more complicated to use.

Vacuum-assisted excision (the complete removal of a lesion using this technique) is used in some centers as an alternative to surgery for benign lesions [39].

Core Needle Biopsy: Cryobiopsy

Freezing of tissue is used in some devices on the theory that the freezing will stabilize the lesion (particularly if close to the skin or chest wall) and make it easier to perform the biopsy. A thin 19-gauge solid needle is introduced into the middle of the lesion. The tip is then cooled to −10 °C with a CO_2 cartridge in order to freeze the tissue to the needle. An outer rotating cutting 10-gauge cannula is advanced over the first needle. The device is removed from the breast for a single pass. Additional passes must be made for additional sampling.

Disadvantages

- Tissue artifacts associated with freezing can cause distortion of tissue architecture, cell shrinkage, and loss of nuclear detail [40].
- Freezing can diminish immunoreactivity [40]. Possible detrimental effects on the preservation of other biomolecules have not been studied.
- A central needle track (from the first needle) appearing as a fracture may be present [41].
- Multiple passes are required for additional sampling which will introduce additional repeated freezing and thawing of tissue.

Freezing of the lesion remaining in the patient also occurs. Therefore, artifact will also be present in the excisional specimen.

Freezing and thawing tissue to uncontrolled temperatures over uncontrolled times could have effects on biomolecules which may or may not be detectable morphologically. It will be impossible to validate the results of immunoperoxidase studies for estrogen receptor, progesterone receptor, and HER2 as the conditions will vary in each patient. This is also relevant for assays based on mRNA levels. The possible effects on other biomolecules have not been studied.

The disadvantages of this technique far outweigh the minimal theoretical benefits over biopsy techniques that do not introduce freezing artifacts.

Very Large Core Needle Biopsies

Large (1, 1.5, or 2 cm) core needle biopsies use an oscillating circular knife to cut through tissues (e.g., the Advanced Breast Biopsy Instrument or ABBI). A 1–2.5 cm skin incision is necessary to introduce the cannula and must be sutured after the procedure. A cautery snare cuts the tissue at the tip of the biopsy specimen.

Advantage

- Requires less precise targeting as a large area of tissue is removed.

Disadvantages

- The amount of tissue removed is extensive compared to other techniques.
- The majority of the tissue removed is not lesional.
- Removes subcutaneous tissue, which may result in a poor cosmetic outcome.
- A surgeon must be available in case of bleeding complications.

- The size of the biopsy is insufficient to obtain adequate margins in the majority of cases—most patients diagnosed with carcinoma require additional surgery.
- The use of cautery may introduce artifacts if the lesion is too close to the heated area.

Because this type of biopsy combines disadvantages of CNBs with disadvantages of surgical excisions, alternative techniques are preferred.

"Intact" Biopsies

Multiple methods have been devised to remove a single fragment of tissue rather than multiple separate cores using a needle.

- *Intact Breast Lesion Excision System* (BLES™) (Medtronic Inc., Dublin): Uses radiofrequency to remove a spheroidal-shaped fragment of tissue measuring from 1 × 1.4 to 2 × 2.5 cm.
- *Ovation* (Rubicor Medical, Inc., Redwood City, CA): Uses cautery with a cutting wire loop to remove a spheroidal-shaped fragment of tissue. A plastic bag encircles the specimen in order to remove it.

Advantages

- The tissue is removed in one fragment, possibly aiding in pathologic interpretation.
- For highly selected small lesions, some patients may not require additional excision.

Disadvantages

- Thermal damage occurs at the edge of the biopsy from 0.1 up to 1.9 mm [42].
- Heating tissue can interfere with histologic diagnosis and biomolecule preservation.
- Does not replace surgical excision for the majority of women [42].

Techniques introducing heat into or near carcinomas create the possibility that histologic evaluation and biomolecule assays will be compromised. Because many carcinomas are not completely excised, the residual carcinoma in the breast is also exposed to heat. Heat is known to reduce antigenicity for hormone receptors and likely has deleterious effects on other biomolecules. Studies have not evaluated the possible effects of these biopsies on the expression of hormone receptors, HER2, and RNA transcripts used for multigene expression assays. The likely disadvantages of these techniques far outweigh the minimal theoretical benefits over biopsy techniques that do not introduce heating artifacts.

Tru-Cut Core Needle Biopsies for Palpable Masses

Free-hand ("tru-cut") CNBs can be performed for palpable masses without imaging guidance. However, masses may be pushed rather than penetrated due to the pliability of the surrounding breast tissue. There is a high rate of false-negative results. In one study, 2/3 of the false-negative CNBs had been performed without image guidance, although this type of biopsy accounted for only half of the cases [43]. Unless a definitive mass-forming lesion is diagnosed in a free-hand biopsy, the possibility that the lesion was missed should be considered. It is preferable to sample palpable lesions with U/S guidance as the needle can be seen penetrating the mass.

Clips and Bio-absorbable Carrier Material

After a CNB is performed, a clip is usually introduced through the needle to mark the site of the biopsy. Additional bio-absorbable carrier material (BCM) is sometimes introduced with the clip.

Clips

Clips are useful to mark the site of a CNB in case the pathologic findings require excision and to mark primary carcinomas or lymph node metastases prior to neoadjuvant therapy. CNBs (particularly vacuum-assisted biopsies) can completely remove the lesion seen by imaging or significantly alter it, making later identification difficult in the absence of a clip.

Clips are typically very small (0.2–1.2 cm) and often difficult to see grossly. They can be composed of titanium, stainless steel, ceramic, or other compounds. Over 35 different shapes are available (Fig. 1.11). It is preferable to use clips of different shapes when more than one biopsy is performed in the same breast in order to be able to easily identify each site. The specific name assigned by the manufacturer to the clip should be documented in the radiology report. Using non-official descriptive terms to describe a clip may create uncertainty in identification of the clip by other radiologists [44]. Providing only the name of the manufacturer is also insufficient because each company markets multiple clip shapes. Identification of clips can also be difficult as clips can have different appearances at some angles or when viewed on end [44, 45]. When identification is critical in a surgical specimen, additional radiographs can be taken. Rectangular, rod-shaped, or V-shaped clips may be difficult to distinguish from surgical staples (Fig. 1.11). However surgical clips are generally larger in size (0.6 × 0.1 cm). Clips must also be distinguished from localization devices that are

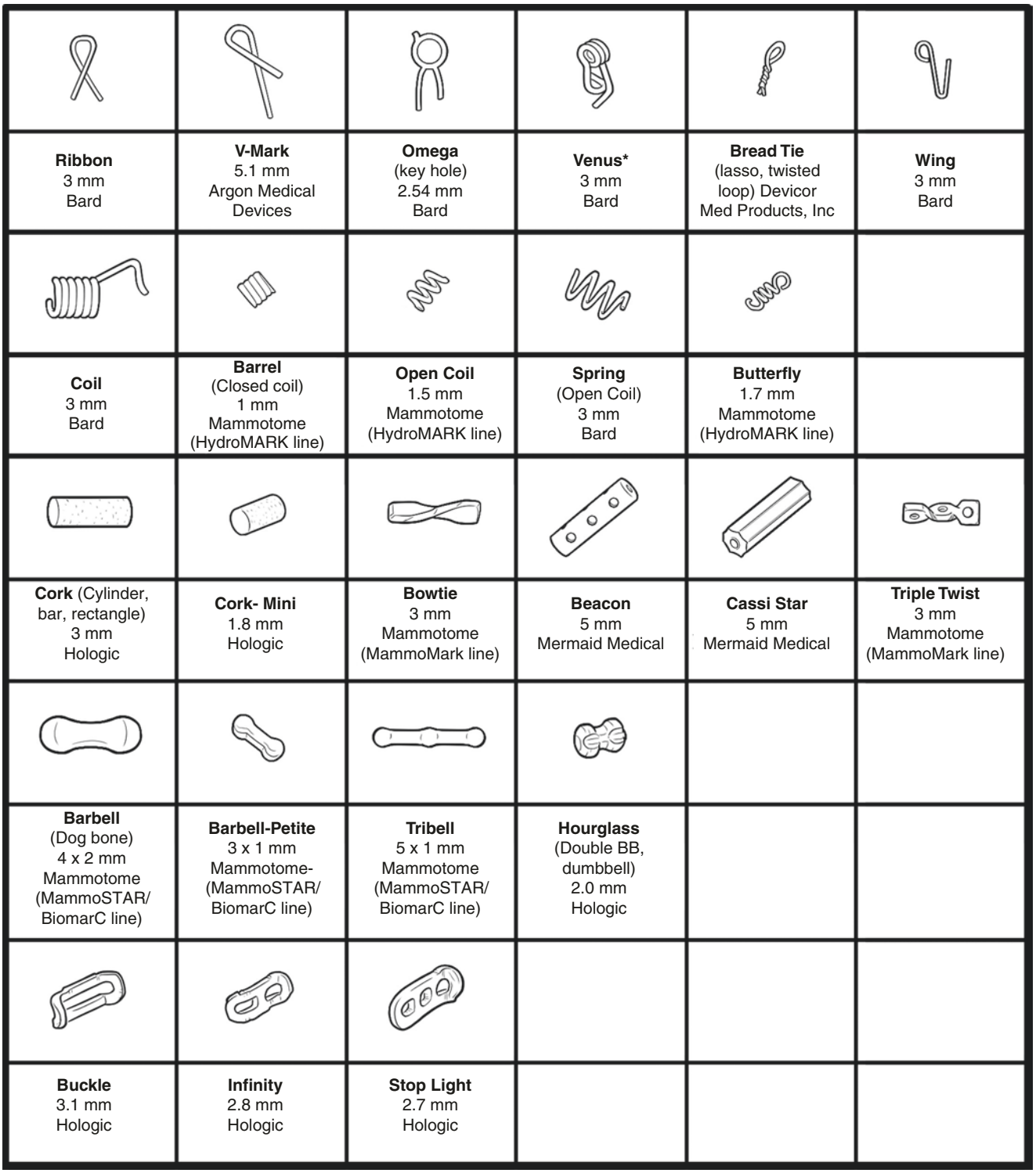

Ribbon 3 mm Bard	**V-Mark** 5.1 mm Argon Medical Devices	**Omega** (key hole) 2.54 mm Bard	**Venus*** 3 mm Bard	**Bread Tie** (lasso, twisted loop) Devicor Med Products, Inc	**Wing** 3 mm Bard
Coil 3 mm Bard	**Barrel** (Closed coil) 1 mm Mammotome (HydroMARK line)	**Open Coil** 1.5 mm Mammotome (HydroMARK line)	**Spring** (Open Coil) 3 mm Bard	**Butterfly** 1.7 mm Mammotome (HydroMARK line)	
Cork (Cylinder, bar, rectangle) 3 mm Hologic	**Cork- Mini** 1.8 mm Hologic	**Bowtie** 3 mm Mammotome (MammoMark line)	**Beacon** 5 mm Mermaid Medical	**Cassi Star** 5 mm Mermaid Medical	**Triple Twist** 3 mm Mammotome (MammoMark line)
Barbell (Dog bone) 4 x 2 mm Mammotome (MammoSTAR/ BiomarC line)	**Barbell-Petite** 3 x 1 mm Mammotome- (MammoSTAR/ BiomarC line)	**Tribell** 5 x 1 mm Mammotome (MammoSTAR/ BiomarC line)	**Hourglass** (Double BB, dumbbell) 2.0 mm Hologic		
Buckle 3.1 mm Hologic	**Infinity** 2.8 mm Hologic	**Stop Light** 2.7 mm Hologic			

Fig. 1.11 Numerous clips in different shapes are available to mark CNB sites. Each manufacturer assigns a clip name and it is recommended that this name be used to standardize terminology. Alternative names that are used are provided in parentheses but are not recommended. The longest dimension of the clip and the manufacturer are provided. Clips with similar shapes are displayed together (rows 1–7) and clips with unique shapes in row 8. Localization devices are generally larger than clips (row 9). Surgical clips and large calcifications can mimic clips marking core sites (row 9)

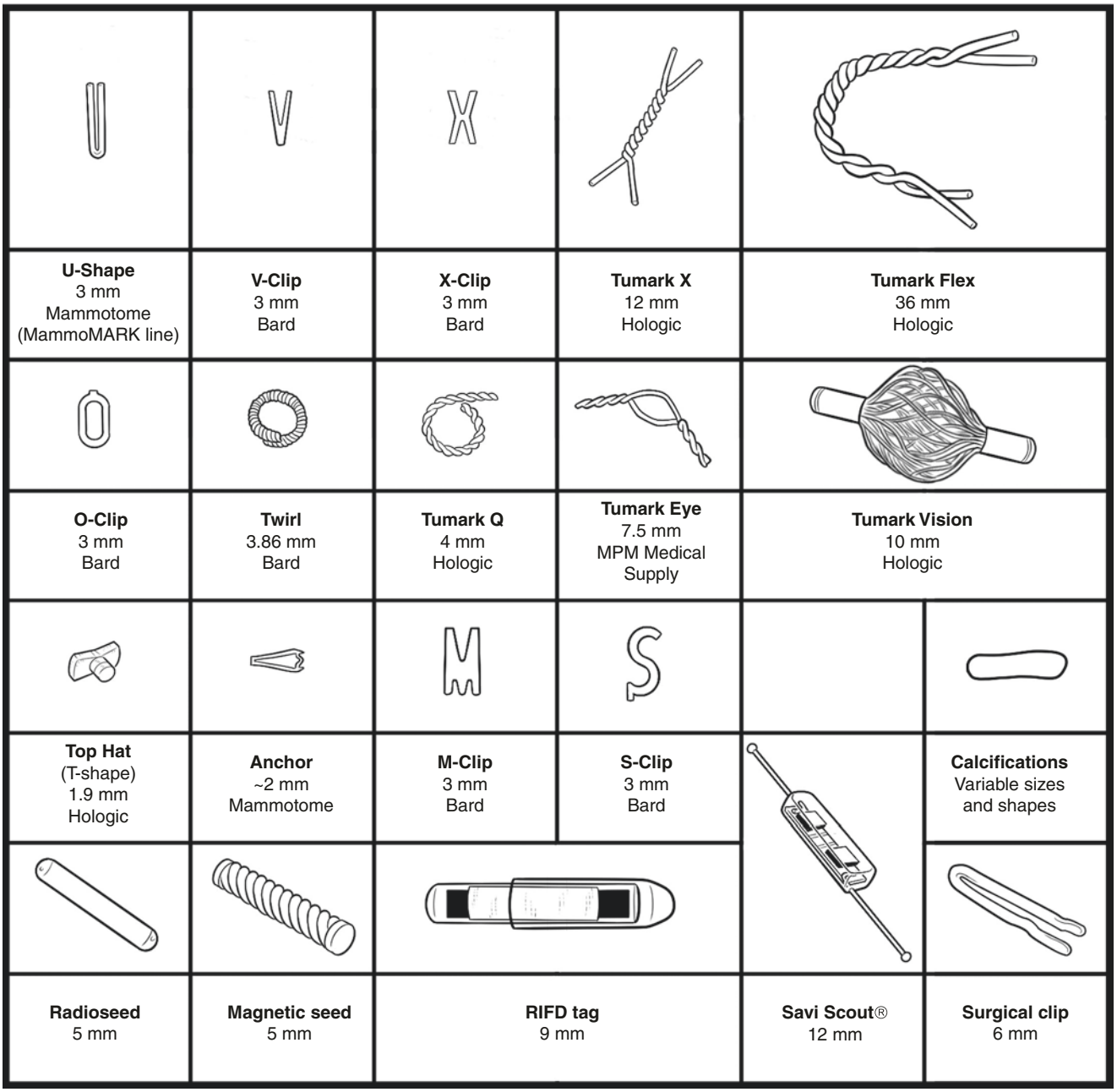

Fig. 1.11 (continued)

placed hours to days prior to excisional biopsy (Fig. 1.11). Occasionally large calcifications can resemble a clip or a clip can be mistaken for a calcification.

Bio-absorbable Carrier Material (BCM)

A number of different types of materials may be introduced into the biopsy site along with the clip using either a vacuum-assisted device or by direct deployment. These materials absorb water quickly and completely fill the cavity. The primary reasons for introducing BCM are to increase visibility on subsequent ultrasound examination, to decrease the risk of clip migration, and/or to improve hemostasis [44, 46]. BCM is gradually resorbed at differing rates ranging from 2 weeks to several months. The material fills the empty space left by the biopsy and does not obscure the remaining breast tissue.

BCM is composed of a variety of different substances:

- Polyethylene glycol (PEG)-based hydrogel
- Polyvinyl alcohol (PVA) polymer
- Polylactic acid-PGA pellets
- PGA microfiber-PVA polymer combinations
- Polyglycolic acid (PGA) microfiber pad

- Starch pellets
- Beta glucan
- Suture-like netting
- Bovine collagen

These substances have different appearances grossly in biopsy sites:

- *Pellets*: Pellets comprised of synthetic material measure about 0.5 × 0.15 cm and several are used for each biopsy. They resemble grains of rice in color and shape. Pellets can be mistaken grossly for calcifications or portions of a papillary lesion.
- *Plugs*: These consist of a single lozenge-shaped mass of synthetic material measuring about 2 × 0.2 cm. When in place, they have an amorphous gelatinous appearance. If they fall out of the tissue after excision they leave a single empty space. This cystic cavity can collapse and be difficult to recognize grossly or microscopically.
- *Collagen or suture-like netting*: These materials form a solid mass of finely pink granular amorphous material grossly.

Core Needle Biopsy Specimen Processing

A long series of complex events are required to transform a core of tissue from a patient into a slide that the pathologist views under a microscope. Each step requires optimal handling to ensure the best care for patients. At each stage in the process, tips for quality assurance (QA) to enhance communication and to minimize the likelihood of a specimen misidentification are highlighted.

Specimen Requisition Form

Communication between the radiologist and pathologist is essential for a successful CNB program and this conversation starts with the requisition form. Specifically designed forms with checklists are helpful to ensure the relevant information is transferred [41, 47]. The contents of the form should be discussed and optimized for each institution (Table 1.9). Multiple choices that can be circled or checked facilitate the completion of the form by radiologists and also ensure that all the relevant information is provided.

QA tip: Biopsies are optimally evaluated in the context of the patient and the characteristics of the imaging lesion. This information is also essential to detect rare specimen mix-ups.

Specimen Preparation in the Radiology Department

The following steps are recommended for the processing of CNBs after the biopsy is performed.

Table 1.9 Requisition form

Information requested	Importance for patient care
Patient identification: name, medical record number, date of birth	Specimen identification
Radiologist name and other clinicians who should receive report	Ensures continuity of care
Relevant clinical history:	
Symptoms (nipple discharge, palpable mass, skin erythema or retraction, pain)	Correlation with pathologic findings
Prior malignancy and/or treatment for malignancy (endocrine, chemotherapy, radiation)	Correlation with current findings, distinguishing changes due to treatment from malignancy
Current pregnancy and/or lactation	Distinguishing changes due to pregnancy (nucleolar enlargement, mitoses, necrosis) from malignancy
Imaging modality (stereotactic (mammography), ultrasound, MRI)	Sometimes helpful for radiologic/pathologic correlation
Gauge of needle	Can be helpful for determining the adequacy of tissue on the slides and the likelihood of a lesion being completely removed by the biopsy
Location in breast (quadrant, clock designation, distance from nipple)	Very important for correlating results with prior or subsequent biopsies and locating sites in mastectomies
Distance between current biopsy and another lesion (e.g., a second CNB, a known lesion, a prior excision site)	Often important for determining the likely relationship between lesions and for locating lesions in excisions
Type of lesion: Mass (size, margin) Calcifications (results of specimen radiograph) Architectural distortion MRI enhancement (mass, non-mass, focus)	Essential for correlating the pathologic findings with the radiologic lesion If calcifications are the target and were not removed, it is not necessary to take extra efforts to identify incidental calcifications in the specimen
Changes in lesion after biopsy (e.g., lesion disappeared, mass completely removed, removal of calcifications)	If a mass disappears, this is highly suggestive of a cystic lesion
Time cores are placed in formalin	Necessary to ensure that the cores fix in formalin for at least 6 h prior to processing

1. *Transferring the cores*: If the cores must be removed from a needle or other device, this must be done very carefully with a second needle or by flushing with saline. Crushing with forceps must be avoided. The cores must be kept moist in saline or fixative. Allowing the cores to dry, placing the cores on dry gauze, or exposure to water can introduce significant artifacts.
2. *Radiographing cores*: Radiographs demonstrate that the targeted calcifications have been removed (Fig. 1.7a). It is helpful to identify cores with and without calcifications and submit them separately, as malignancy is more likely to be found in cores with calcifications [48]. If histologic calcifications are not seen on the initial slides, additional levels to find calcifications can be directed towards the blocks with radiologic calcifications. However, significant lesions can also be present in the cores without calcifications and, thus, all cores must be examined microscopically [49].

   The cores may be radiographed in a simple Petri dish or a commercial Petri dish type device with compartments. The compartments may be prelabelled with clock designations or quadrants. However, it should be clear on the requisition form that the clock designations do not correlate with the actual site of the core needle biopsies in the breast with respect to the nipple.
3. *Securing cores in paper or a nylon specimen bag*: Cores often fragment if the lesion is papillary or consists predominantly of adipose tissue. If the cores are placed directly in formalin, small fragments of tissue and calcifications may not be recovered from the fluid and/or cores can adhere to the lid and be missed by the prosector. Placing the cores in paper or a nylon specimen bag optimizes the recovery of all tissue and calcifications for microscopic evaluation.

   The paper must be thin (lens cleaning paper works well) and should measure approximately 2 in. × 4 in. (or about 8 × 5 cm; a typical 4 × 6 in. sheet cut into thirds). The paper must be dampened with saline or formalin. The cores should be aligned in parallel in the central third portion of the paper. The two sides are folded over in thirds such that the cores remain aligned and not overlapping. The ends are then folded over and the entire flat packet placed in a cassette (Fig. 1.12).

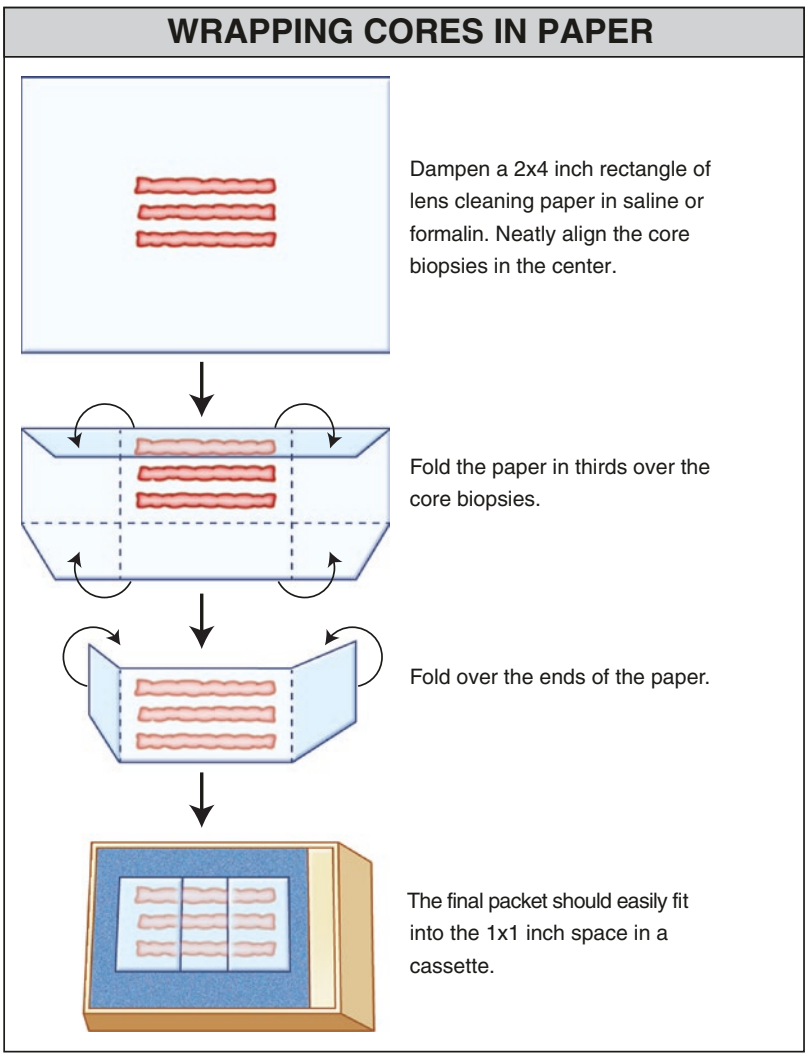

Fig. 1.12 Wrapping cores before placing them in fixative ensures the greatest recovery of tissue and calcifications for pathologic processing. It is important that enough paper is used to allow the cores to be placed in a nonoverlapping linear array, but not so much that the paper distorts the tissue and/or prevents adequate fixation. Lens paper cut into approximately 4 × 2 in. is a typical size used

If too large a sheet of paper is used, the formalin will not penetrate well and the cores will not undergo adequate fixation. If too small a sheet of paper is used, the cores may overlap and/or the packet may open resulting in possible loss of tissue.

4. *Placing the cores into a tissue processing cassette*: The cores should fit easily into a cassette as a single layer with at least 1–2 mm of space between the cores and the edges of the cassette. Formalin must be able to freely flow around the cores for proper fixation.

   If cores are large and/or many CNBs are performed, they must be distributed into multiple cassettes.

   The cassettes can be labeled to identify cores with and without calcifications or cores from more than one site in the same patient. Multiple cassettes from the same patient can be placed in the one formalin container.

   QA tip: A different color cassette can be used for each patient on a given day. This is an added method to distinguish cores from different patients. If this method is used, the color of the cassette is recorded on the requisition form.

5. *Placing the cores or cassette into a labeled formalin container*: The cores or cassettes are placed into a container of formalin labeled with the patient name and other identifiers. It is important to record the time the specimen is placed into formalin on the requisition form.

   QA tip: To avoid specimen mix-ups, it is preferable to only have one patient's specimen containers labeled at any given time. The time the specimen is placed in fixation is needed to ensure optimal fixation.

   Cold ischemic time: The cold ischemic time (the time from cessation of blood flow to the tissue to exposure of the lesion to formalin) is generally much less than 5 min making the preservation of biomolecules optimal in these specimens. The absence of freezing and heating (except for devices that utilize these techniques) also makes core biopsies ideal specimens for molecular testing. Estrogen receptor, progesterone receptor, and HER2 can diminish after 2 h of ischemic time at room temperature and after 4 h with refrigeration [50, 51]. Detrimental effects on phosphorylated proteins and mRNA are likely greater and occur sooner but have not been well studied. Conversely, increased expression of genes associated with hypoxia is associated with prolonged ischemic time [51].

   Fixation time: Cores need to fix in formalin for at least 6 h for optimal performance of receptor assays [52]. The time the cores are placed in fixative can be used to ensure that this requirement is met during processing in the pathology department.

Touch Preparations from Cores

It is possible to make a cytologic touch preparation of a CNB prior to fixation in formalin [53]. Although the preparations can be used to provide a preliminary diagnosis, they do not add additional information. The performance of the touch imprint could potentially cause crush artifact or loss of tissue from the core. The disadvantages outweigh any advantage.

Specimen Processing in the Pathology Department

Standard pathology specimen processing procedures are used for CNBs.

1. *Specimen identification*: The container label must be correlated with the patient name and unit number on the requisition form. The color, number, and labeling of cassettes is verified if this method is used. The specimen is then accessioned and assigned a pathology number.

   QA tip: If there are any discrepancies between the requisition form and the specimen, the case should be held until the radiologist is contacted. The use of cassettes color coded to different patients provides an additional visual method of specimen identification.

2. *Gross evaluation and transfer of cores to a labeled cassette*: If the cores are received loose in formalin, the container must be carefully searched for all tissue fragments which are then transferred to a nylon specimen bag or wrapped in paper. The inside of the lid must also be examined.

   If the cores are received wrapped in paper or in a nylon bag, they can be transferred intact to a new cassette.

   The cores can be grossly described by observing the number and aggregate size of the cores through the paper packet or bag.

3. *Inking cores*: Cores can be inked different colors coded to each patient on a given day. Ink can be applied directly to the cores or through a paper packet or nylon specimen bag.

   QA tip: The ink color identifies the cores from tissue embedding, to slide preparation, to diagnosis. This procedure can aid in detecting errors due to mislabeling and help detect extraneous tissue introduced during processing [54]. The color can also assist the histotechnologist when embedding the cores in paraffin.

4. *Transferring cassettes to a specimen processor*: A minimum 6-h formalin fixation time is recommended by the College of American Pathologists to ensure optimal epitope preservation for ancillary studies [52].

   QA tip: Adequate fixation is necessary to ensure accurate results for immunohistochemical markers for breast cancer. If the time recorded on the requisition form to the time the specimen processor starts is less than 6 h, the specimen should be held in formalin until the next day.

Specimen Processing: Histology

1. *Embedding*: The cores should be embedded as closely as possible in the same plane such that all levels will be representative of all the cores. Telfa pads or sponges can be used to hold the cores in a single plane for optimal embedding but should not directly touch the tissue [55].
2. *Cores with radiologic calcifications*: The cassettes with cores containing calcifications should be identified for the histotechnologist. These should have an initial very shallow level cut in order not to miss any calcifications, followed by additional deeper levels. Otherwise, calcifications may be lost when the block is faced.
3. *Slide preparation*: Three slides are typically prepared from each block, but the number varies from 1 to 20 in different institutions [56].

   If a 0.2 cm in width core biopsy is sectioned at 4 μm per each slide (the typical thickness of a tissue section), 500 glass slides could be prepared from each block, provided no re-facing of the block is performed. Several studies of the value of different sectioning protocols have been undertaken [33, 56–59]. Although the number of levels is stated in these studies, the depth into the block is not. The depth of sectioning is more important than the actual number of glass slides examined.

   Three H&E levels spaced such that the deepest level is about halfway through the block provides a good sampling of the tissue but also leaves sufficient tissue for additional studies when necessary. Few additional lesions are detected when at least half the depth of the core is examined initially [57].

   Unstained slides between the H&E levels can be made and reserved for possible additional studies when a block is first cut. This may be preferable when a known or highly suspected malignancy is biopsied. However, because the majority of cores do not require additional studies, this results in additional work for the histology laboratory that is most often unnecessary. Although there is a risk of losing diagnostic tissue when re-facing a block to cut it a second time, ordering additional levels as needed is a better option in the majority of cases.

   For mass-forming lesions, diagnostic tissue is present in the first level in about 98% of cases [59]. Lesions associated with calcifications are typically smaller than mass-forming lesions and usually require more levels [56, 59]. It is important to identify the lesion that is forming the calcifications. About 15% of diagnoses require two additional deeper levels and about 10% require even deeper levels in the block to identify calcifications and lesional tissue.

   Only the first H&E level was required for diagnosis of MR lesions in 95% of biopsies [33]. Because these lesions must be large enough to be seen by a change in vascularity, the size should be large enough to be seen in all sections of the core.

Procedure-Related Tissue Changes in Core Needle Biopsies

Changes introduced into tissue during the acquisition of CNBs can create artifacts that may complicate interpretation.

- "*Swirlies*": Eddies of small fragments of tissue may be seen in vacuum-assisted biopsies (Fig. 1.13a) [60]. This change only affects a small portion of the entire specimen and does not alter the pathologic evaluation.
- *Gauze artifact*: Dry gauze can impress a hatch-mark pattern into the tissue (Fig. 1.13b). This tissue defect adversely affects the pathologic evaluation of the specimen. Gauze or paper must be moistened with saline or formalin before coming into contact with cores.
- *Crush artifact:* Tissue can be crushed when being removed from a needle or when handled by forceps. Great care must be taken to not compress the tissue. Marked crush artifact can preclude definitive evaluation of the biopsy (Fig. 1.13c). Crushing can also result in loss of cohesion of cells. This artifact makes invasive carcinomas take on a "lobular appearance" and makes it difficult to distinguish epithelial hyperplasia or DCIS from lobular carcinoma in situ.
- *Cautery or freezing artifact*: These artifacts can be seen in needle biopsy systems using heat or freezing and will also affect the residual lesion in the breast [40]. Such artifacts can preclude diagnosis or make diagnosis more difficult. Changes in temperature can also alter biomolecules used for prognostic and predictive assays.
- *Artifactual displacement of epithelium into vascular spaces*: A CNB can disrupt tissue and occasionally push epithelial cells into vascular spaces within the cores [61]. If invasive carcinoma is present, it may not be possible to determine with certainty if the tumor in lymphatics is true lymphovascular invasion (LVI) or artifact. This artifact may be more common in biopsies in which the needle is deployed through the lesion for multiple passes rather than in vacuum-assisted biopsies in which the needle is deployed adjacent to the lesion. Diagnosing LVI on a CNB in the absence of invasive carcinoma should only be made when the diagnosis is certain and, preferably, when more than one lymphatic space is involved.
- Detached epithelium in ductal spaces, due to disruption from the biopsy, can also mimic LVI. Immunohistochemical studies for myoepithelial cells can be helpful to distinguish ducts lined by myo-

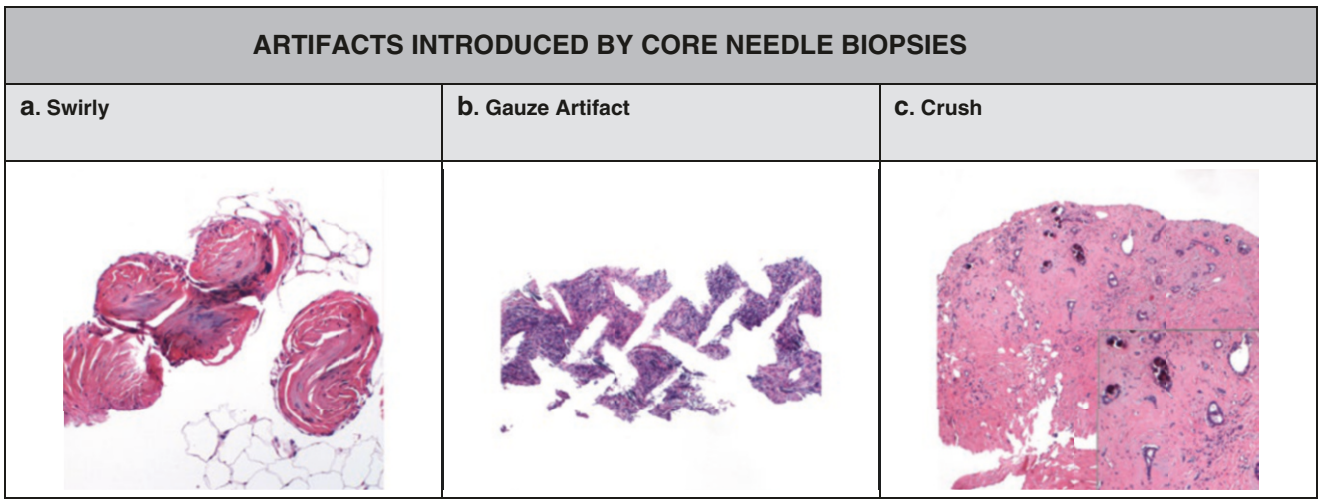

Fig. 1.13 (**a**) Small fragments of tissue from vacuum-assisted biopsies have a swirled appearance. This artifact affects only a small portion of the entire specimen and does not interfere with interpretation. (**b**) Tissue placed directly on gauze, particularly if dry, will have the weave of the fabric imprinted in the tissue. This artifact can preclude optimal evaluation and should be prevented by appropriate specimen processing. (**c**) Crush artifact can occur if the tissue is pinched with forceps. This small acinar proliferation is difficult to interpret due to crush artifact. The distorted acini were falsely interpreted as invasive carcinoma (*inset*). Subsequent immunohistochemical studies confirmed the presence of myoepithelial cells

epithelial cells from vascular spaces lined by endothelial cells.

- *Pseudo-micropapillary structures*: The lining of cysts, particularly when associated with columnar cell changes, can be artifactually pulled into the center of the cyst to create papillary-like structures [62]. These formations can be recognized by an adjacent denuded cyst wall and the presence of myoepithelial cells, supporting that these are infoldings rather than true architectural atypia.

Radiologic/Pathologic Correlation

A successful CNB program is highly dependent upon a team approach. The primary essential members are radiologists and pathologists [1, 3, 63]. Surgeons join the team when it is determined that the results may require excision. After each CNB an assessment must be made as to whether or not the results are concordant in order to determine appropriate subsequent management (Table 1.10). A biopsy is defined as concordant when the pathologic findings provide a reasonable explanation for the imaging lesion [64].

Role of Pathologist

When making a diagnosis on a CNB, the pathologist should assess whether or not the results are concordant with the imaging findings. However to do this, the pathologist must know what type of lesion was sampled. In a Q-Probes study, pathologists were informed of the general category of lesion in all cases (i.e., mass, calcifications, or distortion) [64]. However, the type of margin was not provided for 70% of masses. In clinical practice, many pathologists are not provided with imaging information. In this situation, it is impossible for the pathologist to determine if the findings are concordant or to determine if additional studies would be helpful (e.g., deeper levels to look for calcifications or DNA testing if a specimen misidentification is suspected).

In the majority of biopsies, the pathologic findings correlate well with the imaging findings (Table 1.10). In a smaller group of cases, the pathologic findings may correlate with the imaging findings, but the findings are such that the pathologist cannot be sure. These include biopsies of masses with circumscribed, obscured, or indistinct margins that could be hamartomas, lipomas, or PASH, as well as many MRI-guided biopsies for non-mass enhancement or a focus. For these biopsies, the pathologist can note that the findings could be concordant but that the radiologist must be sure that the biopsy sampled the targeted lesion.

Rarely, the pathologic findings appear to be discordant with the imaging findings. The following possibilities should be considered:

1. *Diagnostic tissue is deeper in the block*: Additional deeper levels may be performed to attempt to identify lesional tissue. This most commonly occurs when the

Table 1.10 Radiologic/pathology correlation—examples of concordant and discordant findings

Imaging lesion	Pathologic diagnosis
Highly likely to be concordant	
BI-RADS 4 or 5	Malignancy
Mass with microlobulated or spiculated margins	Invasive carcinoma
Mass with circumscribed margins	Definite mass-forming lesion
Multiple calcifications in cores	Multiple calcifications present in tissue
Possibly concordant	
Mass with circumscribed margins	Stromal changes replacing adipose tissue that could form a mass (e.g., PASH, fibroadenomatoid changes)
Mass with indistinct or obscured margins	Benign changes
Multiple calcifications in cores	Few calcifications present
MRI non-mass-like enhancement	Benign findings
Highly likely to be discordant	
Mass with microlobulated or spiculated margins	Benign findings
Mass with circumscribed margins	Normal breast tissue
Highly suspicious lesion	Benign findings
Linear and branching calcifications	Benign findings
Low suspicion lesion	Malignancy–especially if not associated with imaging finding

imaging lesion is for calcifications but the initial slides do not show calcifications or only rare calcifications.

2. *The targeted lesion was missed by the biopsy*: The radiologist should review the images of the procedure and the location of the clip.
3. *There has been a misidentification of the slides*: The tissue on the slides should be compared to the tissue in the block to ensure the labeling is correct and the slides correspond to the correct patient.
4. *There has been a misidentification of the blocks*: Other CNBs processed the same day should be compared to determine if there are two likely cases that could have been mixed-up (see section below on specimen identification). In some cases, DNA testing may be required to resolve a possible discordance.
5. *There has been a patient misidentification*: If the slides and blocks are shown to correspond to the patient named on the specimen container, the possibility there was a labeling misidentification at the time of the biopsy should be considered. Again, DNA testing may be required to resolve the provenance of the biopsy.

The radiologist can make a determination of radiologic/pathologic correlation in the majority of cases from the pathology report. However, in the Q-Probes study, of cases considered to have no correlation by the pathologist, information about the lack of correlation was included in the pathology report in only about half of cases [64]. It is important for there to be good communication between the radiologist and pathologist for all cases that may be discordant or are discordant. When the pathologist is provided with the information necessary (i.e., the type of targeted lesion), it is helpful to add a statement in the report when concordance is uncertain.

Role of Radiologist

After the radiologist receives the pathologic diagnosis, he or she must make the final decision as to whether or not there is concordance in order to make a recommendation for follow-up. Radiology departments are required by the Mammography Quality Standards Act (MQSA Regulatios Subpart B—Quality Standards and Certification, Section 900.12(f)) to have a system to correlate pathology results with the mammography report (Policy Guidance Help System—Medical Outcomes Audit Program (fda.gov)). For cases considered concordant, recommendations are made depending on the nature of the lesion.

With good radiologic and pathologic communication, only 1–8% of biopsies are typically considered discordant or potentially discordant after the steps outlined above have been followed and specimen misidentification has been excluded [63, 65–67]. Possible management choices are short-term imaging follow-up, repeat CNB (especially if the first core is known to have missed the lesion), or excision. The number of malignancies found after excision of discordant cases varies widely from <10% to over 50% [66, 68]. In more recent studies, with the use of larger vacuum-assisted biopsies, fewer than 10% of patients with discordant findings are likely to have missed malignancies [67, 69].

Role of a Core Correlation Conference

Pathologists and radiologists can do much of the process of determining whether or not a biopsy is concordant via the requisition form and the pathology report. This, however, requires that the requisition form provides sufficient information about the targeted lesion and that the pathologist has knowledge of the pathologic correlates of imaging lesions and includes information about the certainty of concordance in the pathology report. In turn, the radiologist must have familiarity with pathologic lesions and their appearances.

Some institutions have devised data forms completed by radiologists and pathologists that aid in making this assessment without the need for direct communication. Although this may be adequate or necessary in some practice settings in which practitioners are not physically in the same location, there are many advantages to having correlation conferences to meet in person in order to discuss difficult cases [1, 41, 47, 64]. Features of an efficacious correlation conference include the following components:

1. *Multidisciplinary*: Radiologists, pathologists, and surgeons attend and suggest cases for review. These conferences are most effective when multiple members of each specialty attend in order to provide multiple opinions.
2. *Radiology and pathology reviewed*: Radiologic and pathologic images are presented. This is an excellent opportunity for cross-training in both disciplines.
3. *Timely*: Cases are reviewed within a timeframe such that the discussion can be used to inform the management of patients.
4. *Action plan*: A plan for the next appropriate steps for each patient is developed.
5. *Follow-up of cases*: Subsequent excisions are reviewed for select cases. For example, if it is suspected that the needle biopsy missed a lesion, it is helpful to review the excision to identify the targeted lesion and how close the biopsy came to sampling it.

   Excisions that do not show residual lesional tissue should always be reviewed, especially when the lesion was a malignancy. There are six possible reasons for the absence of a cancer and each one should be carefully considered (discussed in the section "Missing Cancers After Core Needle Biopsy").

Cases of interest due to unusual findings or with important teaching points should also be reviewed. These cases are helpful to emphasize best practices and expand knowledge about breast lesions—especially for fellows in training and junior faculty.

Excisions and Mastectomies After Core Needle Biopsies

About one-third of patients will undergo excision after CNB due to the presence of malignancy, "high risk" lesions with a likelihood of malignancy on excision, or in cases of possible or suspected missed lesions.

Close cooperation among radiologists, surgeons, and pathologists is necessary to ensure the lesion is located, excised, and examined microscopically in the excisional specimen [70, 71]. A study performed in 1997 reported that in only 45% of cases was the type of radiologic lesion communicated to the pathologist and in only 62% of pathology reports was there a correlation between the radiologic lesion and the microscopic findings [72]. Ideally, pathologists should always be aware of the radiologic findings and always correlate the pathologic findings with the targeted lesion.

Clips

In the majority of cases the clip placed at the time of CNB will mark the site or be within 1 cm. Residual lesional tissue (mass or calcifications) may also be present. However, in about 10–20% of cases the clip is one cm or more away from the target immediately after placement [73–75]. It is less common for clips to migrate over time.

Causes of Clip Migration

- Changes in conformation of breast when released from compression
- Clip pulled along needle track
- Clip present within a hematoma
- Dislodgement of clip by a second biopsy
- Migration through tissue over time—in rare cases the clip can be extruded through the skin

If the clip has migrated, the core site can be identified by residual lesional tissue (if present), a hematoma (if present—but often resolves within a month), or by use of the distance of the biopsy site from the clip or other landmarks.

If the clip is not at the site of the targeted lesion, this is documented by the radiologist and the pathologist should be informed at the time of excision. The pathologist should know that the clip may not be present or, if present, may not be at the site of the lesion that was biopsied. In these cases it is essential for the pathologist to identify that the core site and/or residual lesional tissue has been removed to ensure the adequacy of the excision.

Localization Devices

For breast conserving excisions of nonpalpable lesions, the radiologist places a localization device via a needle to mark the core site for the surgeon. There are currently five methods used: wires, radioactive seeds, magnetic seeds, radar reflectors, and radiofrequency identification (RFID) tags (Fig. 1.11) [46]. The principal advantage of non-wire devices is that they can be placed by the radiologist via needle days before the surgery, thus making scheduling easier and reducing operating room time [76]. Wires can also be uncomfortable for patients. The main disadvantages of non-wire devices are additional cost, the need for specialized equipment, and the inability to use MRI for localization. All of these devices show similar efficacy in identifying lesions and biopsy sites for surgeons.

- *Wire*: A wire with a hook to secure it in the tissue was the first type of localization device to be used and is the least expensive. Specimens can be bisected along the plane of the wire to identify the lesion, which should be located just proximal to the hook.
- ^{125}I *Radioactive seed*: The main disadvantage of radioactive seeds is that their use requires licensure and training for the use of radioactive materials and they must be removed within a set period of time. The seed must be identified during specimen processing, documented, and returned for safe disposal [77, 78]. The prosector should have access to a gamma probe to precisely locate the seed in the specimen. If the seed is damaged, the site must be treated as a radioactive spill [79].
- *Magnetic seed*: The main clinical disadvantage of this device is distortion limiting the use of MRI after placement. Pathologists can use the specimen radiograph to identify the device in the specimen. They are the same size as radioactive seeds (5 mm) but do not need to be retrieved for safety reasons.
- *RIFD tag*: These tags are 9 mm in size. Although they transmit a signal that can be used to identify different tags, this feature is unlikely to be necessary for pathologic evaluation. The specimen radiograph can be used to localize the device in the specimen.
- *Radar reflector* (e.g., Savi Scout®, Cianna Medical Inc.): This is the largest of the devices (12 mm) and the one with the most distinctive shape. Due to the size, this device is likely the easiest to identify grossly.

Intraoperative U/S to identify clips can be used as an alternative to a localization device. Special clips are manufactured to be highly visible by U/S and can be combined with BCM to increase their visibility. A limitation to this technique is that if the core site is transected during surgery, both the clip and the BCM can be extruded from the specimen [80]. In these cases, the specimen radiograph is not helpful in identifying the site of the lesion and the prosector will need to rely on finding gross biopsy site changes or residual lesion.

Specimen Radiography of Excisions

It is standard practice for excisions performed for lesions identified by imaging to undergo radiographic examination after excision (Fig. 1.14a, b). A radiologist issues a report confirming that the targeted lesion or lesions were removed or alerts the surgeon if a target is missing. It is essential for the pathologist to have access to the specimen radiograph as well as the interpretation to use as a map showing important findings. This is very important to ensure that all lesions identified by imaging (including clips and localization devices) are sampled and correlated with the corresponding image finding.

- *Identifying the margins*: Four of the six margins can be identified on the specimen radiograph. Using the shape of the specimen and a grid or wire (if present), the specimen can generally be oriented in the same plane as the radiograph. It is very helpful to note the proximity of radiologic lesions close to or at a specific margin for correlation with microscopic findings. For example, the identification of a margin marked by an ink color is more obvious grossly than microscopically. In 4-μm-thick sections, any smearing of ink colors, as well as ink leakage into tissue clefts, can result in uncertain margin identification.
- *Identifying lesions*: After serial sectioning the specimen, lesions, the core site, clips, and localization devices are identified and recorded in the gross description. The tissue at the site of these lesions is placed in designated cassettes.
- If more than one localization device is present, they either mark multiple lesions or bracket an area of abnormality (usually calcifications or architectural distortion). In the latter case, it is often necessary to sample the entire area.

Mastectomies

Mastectomies performed after CNB (or often multiple CNBs) are very challenging specimens to evaluate. Specimen radiography is not routinely requested by the surgeon as the intent is to remove all breast tissue and, thus, a radiograph is not required. Ideally, all specimens with lesions by imaging are radiographed prior to sectioning either in the radiology

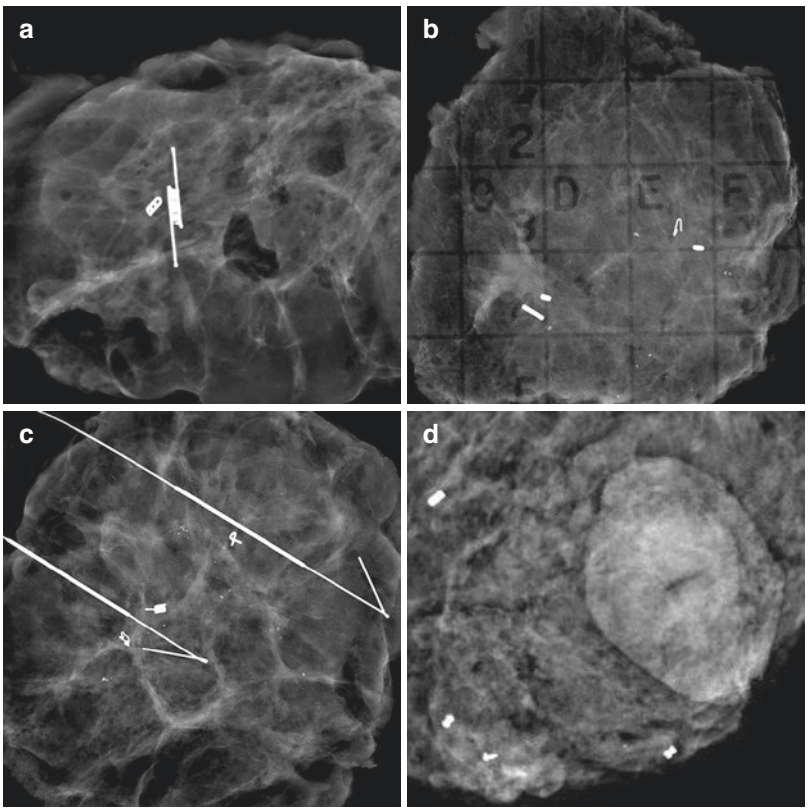

Fig. 1.14 Specimen radiography. (**a**) A Savi Scout® marks a buckle clip adjacent to an area of calcifications that had been biopsied and showed DCIS. (**b**) Two radioactive seeds and two clips bracket two masses with surrounding calcifications. Both sites showed invasive carcinoma and DCIS on CNB. (**c**) Three clips and an area of calcifications bracketed by two hookwires mark the site of a tumor bed after neoadjuvant therapy. A radiograph assists in identifying the tumor bed in this setting which can be difficult to see grossly. (**d**) This radiograph of a mastectomy was obtained by the surgeon to ensure that a very superficial hourglass clip marking a cancer had been removed. In addition, there is a mass with associated calcifications suspicious for carcinoma marked by two adjacent clips. A fourth cork clip is present marking a site of prior biopsy that showed benign findings. This specimen would have been very difficult to sample and evaluate without the aid of the radiograph. (*Courtesy of Dr. Esther Rhei*, Brigham and Women's Hospital)

department or the pathology department (Fig. 1.14c) [20, 81]. Radiographing mastectomies after sectioning raises the possibility that clips will be lost or it will be difficult to identify a mass or cluster of calcifications if they are transected.

In rare cases a core site and/or cancer may not be removed by mastectomy due to an unusual superficial, high upper outer quadrant, subareolar (in nipple sparing mastectomies), or far lateral location. In a study of skin and nipple sparing mastectomies, 0.7% of the surgeries failed to remove the cancer [82]. In such cases, additional surgery is necessary to remove the cancer. The best way to demonstrate the absence of a targeted lesion is by radiography of the intact specimen.

If a radiograph was not performed on the intact specimen, and the biopsy site is not grossly apparent, slices of the mastectomy should be radiographed. If the target cannot be identified, extensive sampling may be necessary to identify the core site. In such cases, it is essential to know the location of the core site (e.g., quadrant or clock position and distance from the nipple).

Core Sites in Excisions and Mastectomies

Gross Appearance

If only a clip was placed, the core site often forms a small stellate area of fibrosis with fat necrosis (Fig. 1.15a). There may be an associated small seroma or hematoma with a fibrous wall. The area may heal quickly and not be apparent after a month. The clip is often very difficult to identify due to its small size. A clip is sometimes felt rather than seen and may be encountered as a hard fragment that cannot be cut with the scalpel. If located, a clip should be removed from the tissue as it could potentially damage the blade of a microtome. A localization device may be present marking the clip.

Core sites filled with BCM are more easily identified grossly [83]. BCM shaped like pellets look like white grains of rice and can fall out of the specimen. They are sometimes mistaken for large calcifications or papillary lesions. BCM consisting of a single large fragment has a white or pale gray appearance (Fig. 1.15b). If the BCM falls out of the speci-

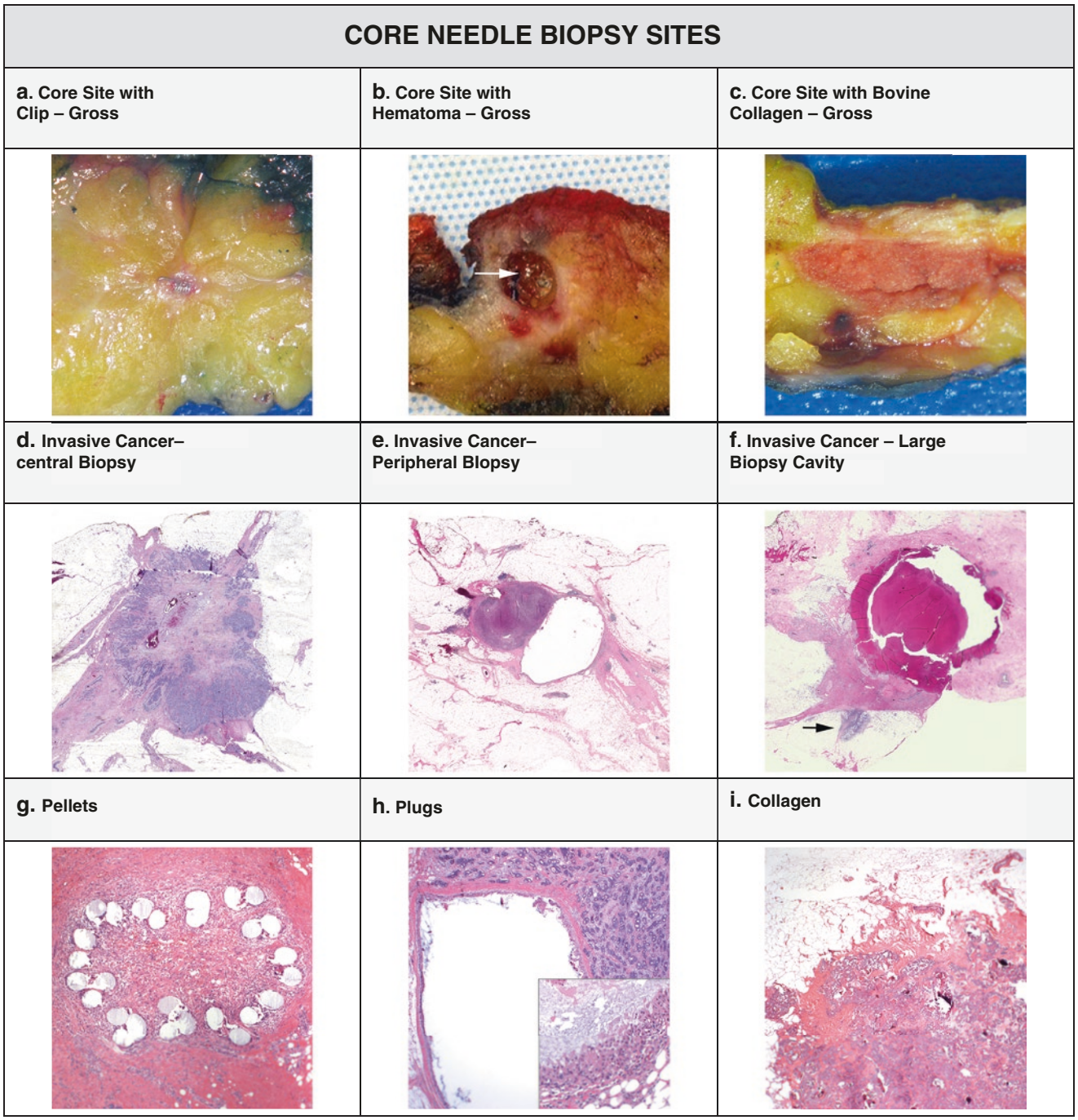

Fig. 1.15 (**a**) The clip marking the core site can sometimes be identified grossly as in this case of a coil-shaped clip with a hook (photograph courtesy of Dr. S. Shin). Very little reaction to the biopsy is seen. (**b**) Some biopsy techniques fill the biopsy cavity with plugs or pellets. This biopsy site consists of a cavity filled with gel (photograph courtesy of Dr. S. Sahoo). A gray metallic clip is present (*arrow*). (**c**) This core site was filled with bovine collagen, which has a pink granular appearance (photograph courtesy of Dr. S. Shin). (**d**) A well-placed CNB samples the center of a mass as seen in this case of an invasive carcinoma. The size of the carcinoma can be determined, and the adjacent tissue can be examined for lymphovascular invasion. (**e**) If the core site is located to the side of an invasive carcinoma, as in this case, the size may be impossible to determine. It may be necessary to consider the size of the lesion on imaging prior to the biopsy and the size of the carcinoma in the needle biopsy to determine the best AJCC T classification. The pellet was dissolved in processing leaving an empty hole in the tissue. (**f**) Very large core sites can result in hematomas and/or seromas. In this case, only a small focus of invasive carcinoma is located at the periphery. The intent of CNB is to sample and not remove the entire lesion. The size of this carcinoma prior to biopsy cannot be determined. (**g**) Multiple pellets introduced along with a clip look like individual white to pink ovoid objects embedded deeply in the tissue. They will eventually be resorbed by chronic inflammation and giant cells. (**h**) Plugs consist of a single large object and often either fall out of the tissue or dissolve during processing leaving an empty hole, as seen in this core site. The resulting empty space is lined by a pseudosynovial reaction (*inset*). These core sites can be difficult to identify if the cystic space collapses. (**i**) Collagen used to mark a biopsy site consists of dense amorphous eosinophilic material that can rarely calcify over time

men during or after excision and the space collapses, the core site can be difficult to recognize. If the BCM consists of bovine collagen or suture-like material, it has a pink granular appearance (Fig. 1.15c).

Acute Biopsy Site Changes and Biodegradable Carrier Material (BCM)

The earliest reaction (hours to days) to the CNB site is stromal fibrosis, fat necrosis, and hemorrhage [84, 85]. Over time, chronic inflammatory cells and hemosiderin-laden macrophages are seen. If a seroma or hematoma forms, the fluid is surrounded by a fibrotic rim. Squamous metaplasia can form around a seroma and can often appear quite atypical [86].

BCM injected with the clip fills the cavity left by the biopsy and, therefore, generally does not interfere with interpretation of the findings in the adjacent tissue. A variety of different materials are used and each has a different microscopic appearance. Pellet-shaped BCM consists of separate white ovoid objects embedded in the tissue, typically in a circular array, and surrounded by chronic inflammatory infiltrate and multinucleated giant cells (Fig. 1.15g). Plug BCM consisting of a single fragment fills an entire space. The space is lined by a pseudosynovial lining consisting of histiocytes [87–89]. The material can either fall out of the tissue or be dissolved during processing leaving an empty hole (Fig. 1.15h). If the space collapses, the site of the CNB can be very difficult to identify in tissue sections. Bovine collagen consists of coarse eosinophilic bands of tissue with a pink amorphous appearance and may contain blood vessels (Fig. 1.15i) [90]. Suture-like material has the appearance of tangled sutures within a cavity. BCM may be completely degraded in 2 weeks to several months. However, in some patients collagen plugs can undergo calcification within a few months and this can prompt a second biopsy [91].

If the core site is transected during surgery, the clip can be lost in the suction device and will not be present in the specimen radiograph or in subsequent patient mammograms [92]. It is important for the pathologist to note if a core site has been transected, particularly if malignancy was present on the CNB. If tissue completely surrounding the core site is not excised, the entire area of the targeted lesion cannot be evaluated.

In contrast to the core site, which ideally is completely excised with a rim of surrounding tissue, the needle track will cross a margin of the specimen unless the entire core needle track including skin is removed. The needle track is usually linear in configuration and does not contain BCM. In some cases it may not be possible to distinguish a needle track from a core site, especially over prolonged lengths of time.

Carcinomas with Indeterminant Size by Pathology

The intent of CNB, in general, is to sample the targeted lesion but to not entirely remove it [92–95]. Ideally, carcinomas will have a core site in the center of the mass allowing the size to be determined (Fig. 1.15d).

In some cases it may be difficult or impossible to determine the size of the cancer. For example, a core site at the edge of a cancer may have removed the largest dimension (Fig. 1.15e). Size can also not be determined if the carcinoma has been extensively sampled leaving only small fragments of tumor adjacent to a large biopsy cavity (Fig. 1.15f). If this is a common occurrence at an institution, the radiologists should reconsider the size and/or number of core biopsies they are using to sample small (<1 cm) lesions [93]. In these cases, the size of the lesion by imaging prior to biopsy, and the maximum size of the cancer in the prior CNB, also should be considered when determining the best T category for American Joint Committee for Cancer/Union for International Cancer Control (AJCC/UICC) tumor staging [96]. Other cases which require considering the size by imaging include cases in which an invasive carcinoma is removed in more than one specimen and after neoadjuvant therapy.

Using pathologic size as the gold standard, all three imaging modalities give good determinations of size (within 1–3 mm) for the majority of cancers [97]. The size of an invasive carcinoma presenting as a mass with spiculated margins is in general quite accurate by mammography except in women with surrounding dense breast tissue. In such cases, U/S usually gives a better estimate of size. MRI can be very accurate unless there is surrounding DCIS. DCIS can also cause enhancement which can lead to the size being overestimated. The size of invasive carcinomas presenting as calcifications is typically quite small—on average 0.6 cm. These cancers may be completely removed by CNB. The size of invasive carcinomas presenting as architectural distortion can be difficult to determine by imaging because of a diffuse infiltrative pattern without the formation of a mass. About a third (34%) are ≤1 cm in size and could be removed by CNB [10].

Effects on Molecular Assays

Correlation of the results of hormone receptor testing and multigene assays for paired core biopsies and excisions is quite good [98]. However, it is important to note that core sites can alter the results of assays—especially when the carcinoma is small (<1 cm) and/or of low cellularity and the core site is relatively large [99–101]. Ideally, a block will be chosen for testing that does not include biopsy site changes. If a block with the core site is used for testing, molecular markers associated with the tumor cells will be reduced (e.g., hormone receptors) and molecules associated with reactive

stroma will be increased (e.g., mRNA and proteins increased due to proliferation). This could lead to an erroneous result. Core sites often appear dark and are difficult to distinguish from cancer when slides are viewed macroscopically. The slide should always be examined under the microscope when choosing the best block for additional studies. Selective retesting of excisions when a result was negative on the CNB should be considered when only a relatively small portion of the cancer was sampled.

Epithelial Displacement

Epithelial displacement refers to the iatrogenic pushing of benign or malignant epithelial cells into stroma, vascular spaces, or lymph nodes, usually by needling procedures [84, 85, 101–116]. This phenomenon is typically an incidental finding and is most commonly observed in association with papillary lesions [104].

Epithelial displacement is reported in 42% of excisions in the first 2 weeks after CNB, but in only 15% of excisions performed after 28 days [109]. The decrease in incidence may be due to disruption of the normal vascular supply to the displaced epithelial cells resulting in the inability for these cells to survive. However, the actual biologic potential of malignant cells pushed into stroma cannot be determined with certainty.

Multiple histologic features aid in the recognition of epithelial displacement (Table 1.11). Dislodgement of cells into a needle track can often be suspected due to the linear array along the course of the biopsy (Fig. 1.16a). The number of epithelial cells is sparse relative to the surrounding reactive stroma (Fig. 1.16b). In contrast, desmoplasia associated with invasive carcinoma generally only extends for a few millimeters beyond the malignant cells. There may be clearing around the cells, although stromal retraction is also associated with some invasive carcinomas. Reactive stroma can be recognized by the presence of a mixed population of inflammatory cells including lymphocytes, histiocytes, and occasionally polymorphonuclear leukocytes, hemorrhage, hemosiderin, and fat necrosis. In contrast, desmoplastic stroma may include lymphocytes, but the other components are generally absent. Lastly, displaced epithelium should not demonstrate an invasive growth pattern.

Table 1.11 Epithelial displacement vs. invasive carcinoma

Histologic feature	Epithelial displacement	Invasive carcinoma
Distribution	Linear—along core track	Radiates in all directions from a central area
Stromal response	Extensive relative to number of epithelial cells	Stromal changes only surround tumor cells
Other stromal changes	Fat necrosis, hemorrhage, hemosiderin-laden macrophages, neutrophils	Usually absent except at the core site
Lymphocytic response	May be present	May be present
Epithelial cells	Usually small dispersed clusters; may show squamous metaplasia	Larger clusters of tumor cells, possibly forming tubules; squamous features are uncommon
Myoepithelial cells	May be absent; if present, do not form a complete layer; may require immunohistochemical studies	Absent

Displacement of benign epithelium can closely mimic invasive carcinoma. The nuclei can be hyperchromatic with larger nucleoli and there may be a high nucleus-to-cytoplasm ratio. In addition, the epithelial cells may show squamous metaplasia which, to the unaware, can add to the appearance of malignancy due to a perceived higher nuclear grade. Although a complete myoepithelial layer may not be present, at least some myoepithelial cells usually can be documented using immunohistochemistry (Fig. 1.16c). Heterogeneity for cytokeratin 5/6 and estrogen receptor may also be helpful to support that the cells are benign.

It is important to not overinterpret epithelial displacement as invasive carcinoma. In general, a diagnosis of invasive carcinoma should never be made if the only areas of epithelial cells in stroma are within biopsy site changes and no other areas of carcinoma are present.

Epithelial cells can also be displaced into stroma during the surgical excision or during processing of the specimen. In these cases, no tissue reaction will be present. Artifactual smearing of tumors is a particular problem with friable lesions such as DCIS with necrosis and papillary lesions. The displaced cells may be present along the edges of the specimen or within cracks in the tissue (Fig. 1.16d). The cells are typically seen in adipose tissue and not fibrous tissue. Displacement should be suspected when the cells are only seen in large solid clusters in adipose tissue.

Epithelial cells also can be pushed into vascular spaces (Fig. 1.16e) [101, 105–107]. Although it may not be possible to distinguish this finding from true vascular invasion associated with an invasive carcinoma, the association with a biopsy site or needle track should be noted. If no invasive carcinoma is present, the possibility that epithelial cells in vascular spaces is an artifact of the procedure should be strongly considered.

Benign or malignant cells can be pushed into lymph nodes (Fig. 1.16f) [84, 104, 110, 111]. It has been suggested that an association with hemosiderin-laden macrophages and giant cells supports that the tumor cells arrived in the node via "benign transport." The report should note these findings and discuss the possibility of epithelial displacement. The

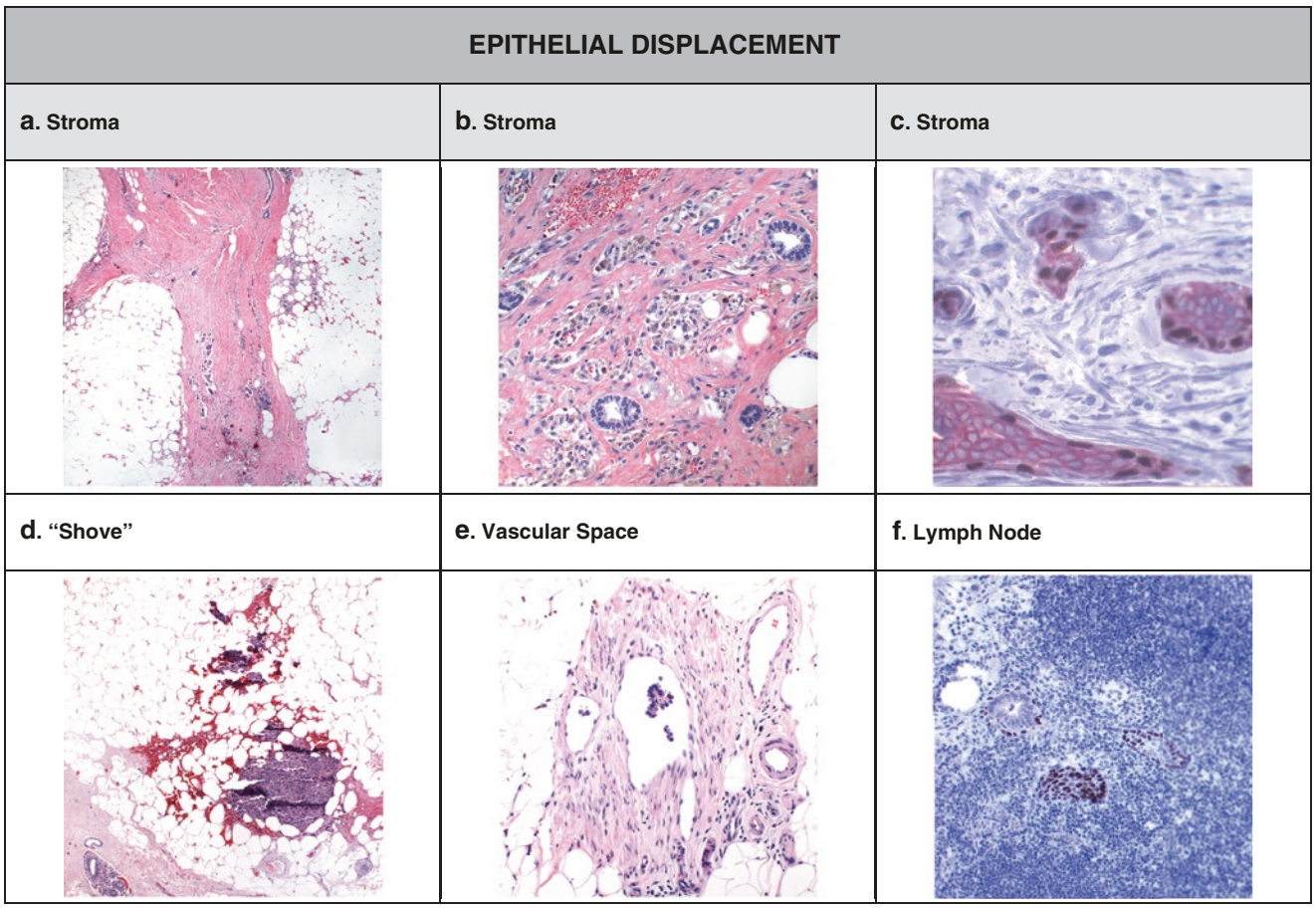

Fig. 1.16 (**a**) Epithelial displacement into the stroma is a common phenomenon, occurring in about 22% of needle tracks soon after the procedure. A needle track is generally recognized as it is linear in shape. (**b**) Displaced epithelial cells can be present singly or in small nests. The amount of reactive stroma is extensive compared to the amount of desmoplastic stroma associated with true invasion. In addition, the reactive stroma includes hemorrhage, hemosiderin, fat necrosis, and a mixed inflammatory infiltrate. (**c**) If no carcinoma is present, immunohistochemical studies for p63 may be helpful. In some epithelial clusters, a peripheral rim of myoepithelial cells may be identifiable. In other clusters, positive cells may be intermingled with negative cells either due to displacement of myoepithelial cells or due to squamous metaplasia. However, the absence of myoepithelial cells is not definitive evidence of malignancy. (**d**) Epithelial cells can also be pushed into stroma during surgery or later during specimen processing. In these cases, there is no stromal reaction. Tumor cells can appear to be in clefts of tissue, along tissue edges, or in adipose tissue. The cells are often in large irregular clumps. (**e**) Both benign and malignant epithelial cells can be pushed into lymphatic spaces. These small papillary fragments appear to be in lymphatic spaces. The patient did not have cancer. (**f**) Benign cells can be pushed into lymph nodes by prior biopsy procedures. The cells can be demonstrated to be benign if myoepithelial cells are present. This immunoperoxidase study for p63 shows two tubules with myoepithelial cells and another cluster of cells that may be benign metaplastic squamous cells. Cells that may have been displaced into nodes are often accompanied by hemosiderin-laden macrophages and giant cells

biologic potential of malignant cells pushed into nodes is not known. The number of cells is usually small and most cases would be classified as "isolated tumor cells."

True Needle Track Seeding by Malignant Cells

True needle track seeding is defined by the detection of new imaging findings of masses or calcifications in a linear distribution from a cancer to the skin after CNB but before surgical excision. The subsequent excision confirms malignancy in the needle track in continuity with the invasive carcinoma [117–119]. This finding is distinguished from epithelial displacement by the evidence that the tumor is proliferating, rather than having just been pushed into the track. In the single large series, true needle track seeding was observed in 0.17% of patients, which is much lower than rates of epithelial displacement [119]. Recurrent carcinoma arising in the needle track after surgery and an interval of time will be discussed later.

Squamous Cells at Core Sites

Keratin producing squamous cells of the skin can be pushed deep into the breast by the CNB [120]. The continued production of keratin can result in cyst formation (Fig. 1.17a). Alternatively, breast epithelial cells traumatized by the biopsy

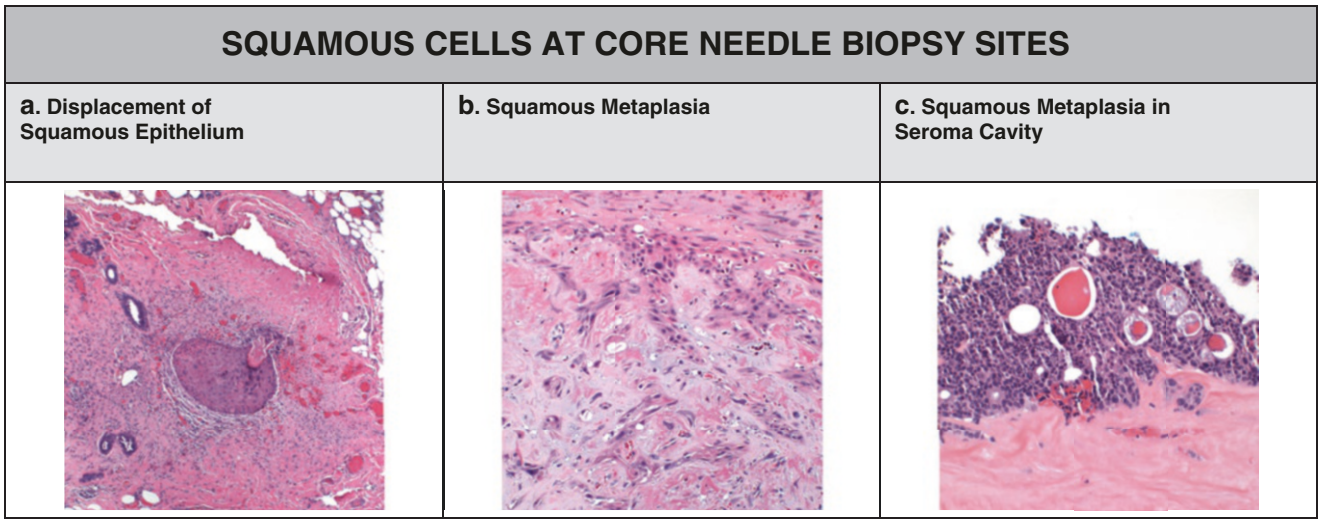

Fig. 1.17 (**a**) Squamous epithelium of the skin can be displaced into core sites by the needle. If keratin accumulates, a keratin-filled cyst may be produced. (**b**) Squamous metaplasia is a frequent epithelial reaction to the trauma of a biopsy. This change should not be mistaken for malignancy. (**c**) The cells lining seroma cavities can undergo squamous metaplasia and may appear atypical in some cases

often undergo squamous metaplasia (Fig. 1.17b). Atypical appearing squamous cells can also be found lining seroma cavities (Fig. 1.17c). The finding of squamous cells at a core site must be distinguished from primary keratin producing lesions of the breast such as an adenosquamous or squamous carcinoma. If the lesion in the prior CNB was not squamous in nature, the findings in the excision are likely to be reactive.

If the primary lesion was squamous in nature, such as an epithelial inclusion cyst, dislodgement of keratin into stroma can result in an intense foreign body reaction. This reaction after the CNB can closely mimic infection.

Reactive Spindle Cell Nodule

An exuberant stromal reaction can occur after fine needle aspiration or CNB (Fig. 1.18a) [87, 121, 122]. This reaction can also occur in lymph nodes [123]. The interval from biopsy to observation is generally 2–4 weeks. It often occurs when the original lesion biopsied is associated with sclerotic stroma with myofibroblasts (e.g., a papilloma or complex sclerosing lesion).

The size of reactive spindle cell nodules ranges from 0.1 to 1 cm. Evidence of the CNB site should be present (Fig. 1.18a). The lesion may have pushing borders but more commonly the borders are irregular. The cells can appear to infiltrate around adjacent breast epithelium and closely simulate malignant invasive behavior.

The spindle cells are plump with mild to moderate nuclear pleomorphism (Fig. 1.18b). Rare mitoses may be present but should not be atypical. Delicate collagen fibrils may be present along with thin-walled blood vessels. There is typically a mixed inflammatory infiltrate including macrophages, lymphocytes, and plasma cells. Hemosiderin-laden macrophages and multinucleated giant cells may be seen (Fig. 1.18c). Displacement of cells into lymphatic spaces can also complicate the histologic appearance.

Immunoperoxidase studies support a myofibroblastic origin for the cells as they are generally positive for smooth muscle actin and muscle-specific actin. The cells should be negative for keratins (including high molecular weight "basal" keratins) and p63.

The differential diagnosis includes sarcoma, spindle cell metaplastic carcinoma, and other spindle cell lesions such as fibromatosis. All of these lesions are highly unlikely to be found incidentally at the site of a CNB performed to evaluate a different lesion. The absence of a spindle cell lesion present in the prior CNB strongly supports that the lesion in the excision is a reaction to this prior procedure.

In rare cases, a spindle cell carcinoma can arise from squamous metaplasia in a cystic lesion, which could potentially be due to a seroma cavity associated with a biopsy site. Thus, it is important to determine if an adjacent spindle cell proliferation is epithelial or fibroblastic (Fig. 1.18d). The majority of spindle cell metaplastic carcinomas show marked nuclear atypia and often have areas of necrosis (Fig. 1.18e). However, low-grade fibromatosis-like metaplastic carcinomas have minimal nuclear changes. Immunohistochemical studies for multiple keratins (including high molecular weight "basal" keratins) and p63 may be required to exclude a spindle cell carcinoma (Fig. 1.18f).

Infarction

CNBs rarely cause infarction of masses which can make interpretation difficult [124]. Benign lesions can be mistaken for malignancy due to necrosis especially when complicated

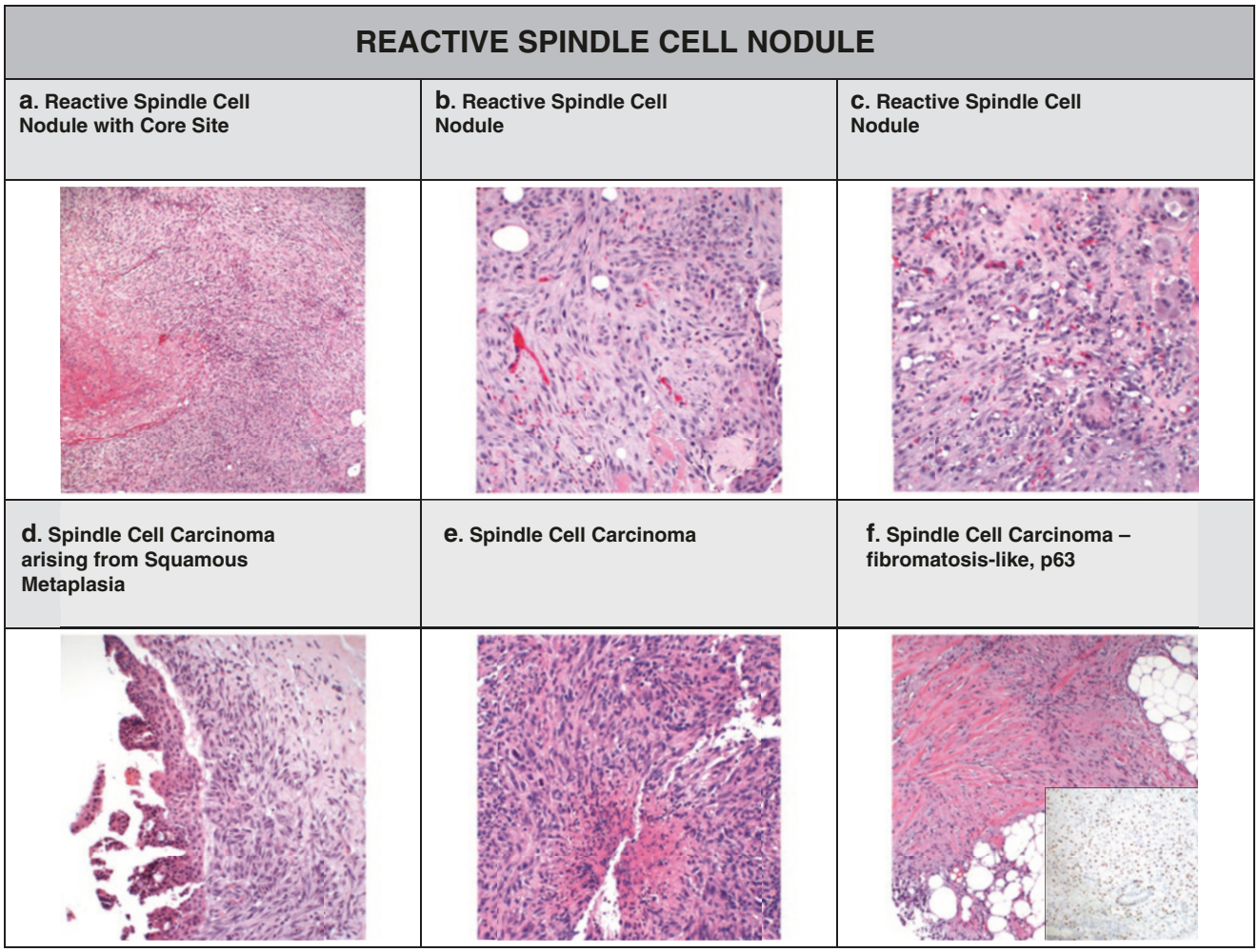

Fig. 1.18 (**a**) The stromal reaction around a CNB site can be so extensive to sometimes form a distinct nodule. The CNB site is seen to the left. (**b**) The reactive stromal cells can have moderate nuclear pleomorphism and occasional mitoses. (**c**) The presence of hemorrhage, hemosiderin-laden macrophages, inflammatory cells, and giant cells helps to identify the cells as reactive fibroblasts. (**d**) This is a spindle cell carcinoma arising from metaplastic squamous cells lining a cyst. In the majority of cases, the carcinoma would have also been seen on the CNB. (**e**) The majority of spindle cell carcinomas show marked nuclear pleomorphism and often have areas of necrosis. (**f**) A minority of spindle cell carcinomas closely resemble fibromatosis or other benign stromal lesions. Immunohistochemical studies for high molecular keratins and p63 (shown here in the *inset*) can identify the spindle cells as epithelial

by squamous cell metaplasia and reactive stromal cells [125]. In turn, malignant lesions can be mistaken for benign lesions due to loss of cellularity and difficulty in interpreting necrotic cells.

The results on the prior CNB should always be taken into consideration. If necrosis associated with malignant cells was present on the core, then the lesion is likely a high-grade malignancy. However, if there was no necrosis present in the core biopsy, and the findings were benign, then the necrosis is likely due to the procedure.

Hemorrhage

Extensive hemorrhage into tissue can occur after CNB if large vessels are disrupted. Blood in stroma and in the lumens of ducts and lobules may be seen in excisions. Hematomas may take weeks or months to resolve, eventually leaving only hemosiderin-laden macrophages.

Cautery or Freezing Artifact

Some types of CNBs use heating or freezing to remove an intact piece of tissue. These methods can cause artifacts in the CNB as well as in the surrounding tissue in the excision [40]. This is of particular concern because artifacts may be introduced directly into the targeted lesion. These methods should be avoided due to potential problems in histologic interpretation and possible changes in biomolecules (e.g., hormone receptors, HER2, as well as other proteins, and mRNA). If negative results are obtained on tissue tested after the use of one of these devices, the possibility of the results being due to tissue damage should be considered.

Healed Core Needle Biopsy Sites

The majority of core needle sites heal without a trace within weeks to months. However, in some patients a core site may be recognizable as an area of scarring. Vacuum-assisted excision (VAE), defined as complete removal of a benign lesion by CNB, has been reported to create a scar that mimicked carcinoma [126].

Missing Cancers After Core Needle Biopsy

The majority (>95%) of malignant lesions diagnosed on CNB are also present in the excisional specimen [127, 128]. There are six possible reasons for why a cancer might be absent, only two of them acceptable. The other four indicate a significant error has occurred. Therefore, when a cancer is missing each of the possible causes should be considered and the most likely reason determined. This investigation usually requires the collaboration of radiologists, pathologists, and surgeons (Table 1.12).

Complete Removal of Cancer by Core Needle Biopsy

Studies from two institutions found that in the majority of cases when no residual cancer was present in the excision (70 and 93% of cases), the entire malignancy had been removed by the CNB [127, 128]. The likelihood of complete pathologic removal depends on the size of the lesion, the number and size of the CNBS, the use of vacuum-assisted biopsy, and whether or not the entire imaging lesion was removed [93, 95, 128, 129]. However, even when the entire imaging lesion is removed by CNB, in the majority of cases carcinoma will be found in the excision [93–95].

Table 1.12 Reasons for a cancer being present in a CNB and absent in the excision

	Reason for a cancer being absent in an excision	% of cases
1	The cancer was completely removed by the core needle biopsy	>70%
2	The cancer completely responded to neoadjuvant therapy	Variable[a]
3	The surgery did not remove the cancer	~10%
4	The original diagnosis of cancer was incorrect	~10%
5	The cancer was not found in the specimen	Rare[b]
6	There has been a specimen misidentification	~1%

[a] The likelihood of a pathologic complete response varies from >60% to <10% depending on the biologic type of breast cancer and the type of therapy

[b] It is highly unlikely for the pathologic examination to not identify a cancer in an excision as many of these specimens are completely evaluated microscopically. However, cancers can be missed in mastectomies. These specimens rarely undergo specimen radiography making small cancers difficult to find

In one study, about 70% of malignancies completely removed by CNB presented as calcifications, 20% as small (<1 cm) masses, and 10% as architectural distortion [128]. The average size of lesions completely removed by CNB was 0.6 cm. If the imaging lesion was larger than 1 cm, complete removal was unlikely. The most common malignancy completely removed by CNB was DCIS. The possibility of complete removal should only be accepted when other alternative explanations have been excluded and the core biopsy site has definitely been identified.

Neoadjuvant Therapy

Ideally, the pathologist will always be alerted that there has been prior neoadjuvant therapy, but this is not always the case. A major goal of this treatment strategy is to achieve a pathologic complete response (pCR). Treated cancers and tumor beds are often very difficult to identify grossly. Therefore, pretreatment clip placement is essential to document the site of the cancer. A patient cannot be determined to have had a pCR unless the clip marking the prior tumor site is identified and the area thoroughly sampled. This should be documented in the pathology report [130]. It would be highly unusual for breast tissue at the site of a treated cancer to look histologically normal.

If there is no residual cancer, and the tumor bed is not clearly identified, it should be determined whether or not the clip marking the tumor was identified in the specimen and that the clip was at the correct site (i.e., the clip had not migrated).

The Surgery Did Not Remove the Cancer

In the two studies of cancers absent after CNB, in 2–16% of the cases the core site was not removed in the surgical excision [127, 128]. In the majority of localized excisions, the clip marks the cancer and a specimen radiograph documents the clip has been removed, making the likelihood of not removing the site very small (Fig. 1.14a, b). However, this can occur if a clip was not placed, if the clip did not deploy, or if the clip migrated away from the lesion. In these cases, the surgeon may not be able to locate the site of the cancer. Another rare cause of a cancer not being excised is if a surgeon removes a palpable lesion that is incorrectly thought to be the same as the image detected lesion that was biopsied.

In rare cases, more than one clip can be present and the wrong clip may be removed (Fig. 1.19a, b). The shape of the clip associated with each biopsy should be recorded and different shapes should be used when possible.

Mastectomies generally remove all breast tissue, including any prior CNB sites. In rare cases, carcinomas may not

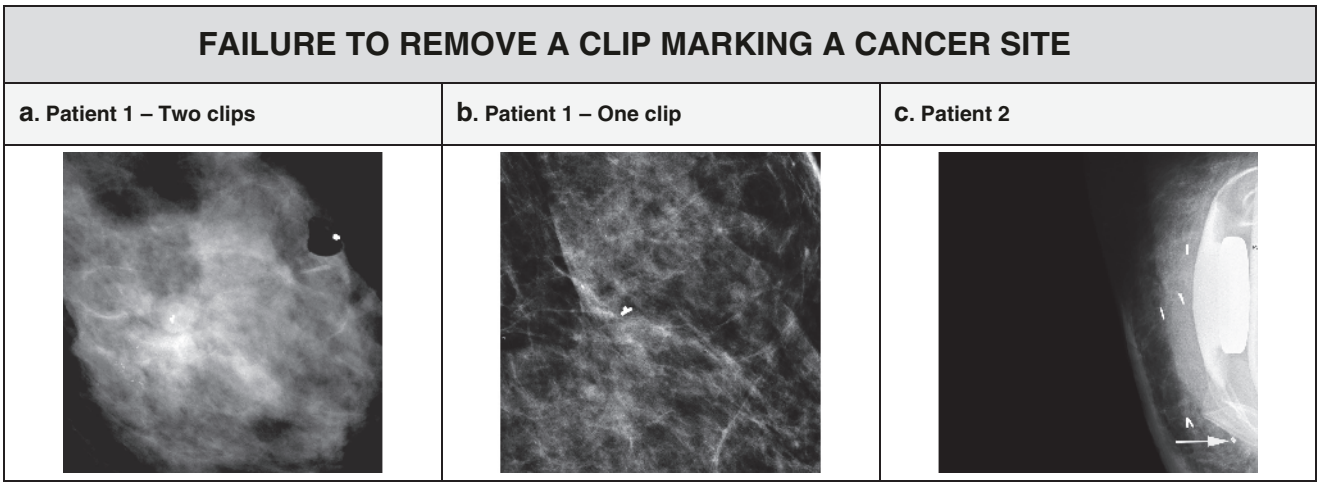

Fig. 1.19 *Patient 1*: A CNB performed for calcifications showed poorly differentiated invasive carcinoma and DCIS. She subsequently underwent an MRI study and a CNB for enhancement showed only benign tissue. (**a**) In this mammogram, the top hat clip marking the calcifications associated with the cancer is to the left and the bowtie clip from the MRI biopsy is to the right. The patient subsequently underwent a wire-localized excision and a clip and faint calcifications were removed. No carcinoma was present in the specimen. The patient was thought to have had a successful operation and received adjuvant treatment. (**b**) On a follow-up mammogram a year later it can be seen that the top hat clip and the calcifications at the site of the cancer are still present. By mistake, the MRI clip and calcifications unrelated to the cancer had been removed. The patient subsequently underwent mastectomy to excise the cancer. *Patient 2*: This patient underwent mastectomy for an invasive carcinoma diagnosed by CNB. The site was marked by a coil clip. No carcinoma could be identified in the specimen despite extensive sampling. Although the clip was not identified, a specimen radiograph had not been performed prior to processing and it was thought the clip might have been lost after slicing the specimen. Two years later she developed a mass in the chest wall next to the implant used for reconstruction. (**c**) This radiograph shows the original cancer marked by the coil clip (*arrow*). Several surgical clips are also present. The cancer was located very superficially and was left in the patient in the skin flap

be removed if they are in a superficial location (within the skin flap), very lateral (near the junction with chest wall skin), retroareolar (if the procedure is nipple sparing), or high in the upper outer quadrant/axilla [82]. Radiography of the intact specimen is very helpful to document that cancers and clips have been removed (Fig. 1.14c). If the cancer and clip cannot be identified, follow-up imaging may identify the clip and the cancer still in the patient (Fig. 1.19c).

The Original Core Needle Biopsy Diagnosis Was Incorrect

The two studies of missing cancers reported that in 5% and 13% of cases the original lesion was determined to not be cancer on second review [127, 128]. The majority of such cases were originally diagnosed as DCIS detected in a core biopsy for calcifications. These cases were re-classified as atypical ductal hyperplasia (ADH), columnar cell change with atypia, atypia associated with lactational/secretory change, or pleomorphic lobular carcinoma in situ [128]. Distinguishing between very small foci of DCIS and ADH can be difficult and for some lesions subjective [131]. Excision would likely have been advised for all of these lesions. However, the subsequent treatment may be altered, such as radiation therapy, if it is determined that the lesion should not have been diagnosed as DCIS.

False-positive diagnoses of invasive carcinoma are rare, reported to be <1% in multiple studies [128, 132]. Sclerosing adenosis, particularly if involved by carcinoma in situ or apocrine metaplasia, can easily be mistaken for invasive carcinoma in small biopsies. Crushed small acinar proliferations can look like invasive carcinoma, as can the central sclerosed area of an RSL (Fig. 1.13c). A second review of the diagnosis occurs when additional assays are performed on cancers and this is an opportunity to detect this type of error [133].

The Cancer Was Not Found in the Specimen

It is highly unlikely that a cancer removed by a typical excision would not be identified by the pathologist. The specimen radiograph shows the clip and any residual lesion. Many of these specimens are completely evaluated microscopically. If the core site is not identified, and not all tissue has been examined, then additional tissue should be submitted for evaluation.

Mastectomies after CNB are much more difficult to evaluate for core sites marking small cancers. It is essential that the pathologist be aware of the number of lesions, the types

of lesions, and the locations of lesions prior to specimen processing. In some cases, radiographing the intact specimen may be the only technique that will reliably identify small lesions (Fig. 1.14c).

If a specimen radiograph has not been performed, and the core site and cancer are not identified grossly after sectioning, radiographing the tissue slices may identify the lesion(s). However, clips can be dislodged during sectioning. Calcification groups may be difficult to identify if present in multiple slices. Masses are especially difficult to identify because variation in tissue thickness and density can mask true masses. If the imaging does not reveal a clip or residual lesion, extensive sampling may be required to identify the cancer. If no cancer can be identified, the possibility that the cancer was not removed by the mastectomy due to an unusual location must be considered (Fig 1.19c) [82].

The Specimen Has Been Misidentified

The possibility that a specimen has been misidentified should be considered if the core site is identified, the patient has not been treated with neoadjuvant therapy, and the lesion did not appear to be completely removed by the CNB. Other breast core biopsies processed on the same day should be reviewed to determine if there is another case that could have been involved in a specimen mix-up. If cassette color and/or inking of cores are used, colors should be compared and confirmed to be concordant. DNA testing can be used to resolve difficult cases by comparing the tissue in the CNB to the excisional specimen [134].

A study performed DNA testing on 3545 breast core needle biopsies showing cancer and compared the results to cheek swabs from the same patients and found that the results did not match for 6 patients (0.1%), implying that the specimens had been misidentified [135]. This study also implies that additional cases of misidentification would have been found had all CNBs been tested. This study highlights the need to employ methods to prevent specimen misidentification and quality measures to detect possible cases.

Recurrent Cancers After Core Needle Biopsy

Carcinoma at a Prior Core Site Showing Carcinoma

Carcinomas identified by CNB undergo excision and additional treatment to reduce the likelihood of local recurrence. However, about 10% of women will have an ipsilateral recurrence within 10 years. In 50–80% of cases, cancers recur with the same imaging finding that resulted in the primary diagnosis [136, 137].

True recurrences should be distinguished from new primary carcinomas arising in the same region of the breast when possible. Recurrence of the same invasive carcinoma at the excisional site confers a poor prognosis because the carcinoma has proven it is treatment-resistant [138–141].

An educated guess can be made as to whether a cancer is a true recurrence or a new primary by comparison of histologic type, grade, marker expression, and location (i.e., at or away from the prior excisional site). If a recurrent cancer is of a different type and located far from the previous cancer, it is highly likely to be a new primary. However, many breast cancers are similar in type and commonly occur in the upper outer quadrant. Molecular studies have shown that comparing pathologic features and location results in an incorrect determination in about 40% of cases [140–142].

Carcinoma at the Site of the Needle Track

There are 19 reported cases of clinically evident recurrences in a needle track after definitive surgery and a disease-free interval [119, 143–154]. Fourteen of the original cancers were invasive carcinoma, four were DCIS (two of these with microinvasion), and one was not specified. The time to recurrence ranged from 1 to 6 years (average 2.5 years). Of six patients treated with breast conservation, three recurred as invasive carcinoma in the breast and three in skin and subcutaneous tissue. Thirteen patients underwent mastectomy and the majority (9 patients) recurred as invasive carcinoma involving the skin and subcutaneous tissue. Two patients with HER2 positive DCIS with microinvasion recurred as Paget disease of the skin without an invasive component [152, 153]. One patient recurred in skeletal muscle and this was attributed to the core needle possibly penetrating the muscle [146]. The site of recurrence was not stated for one patient [145]. Only two of the patients had received radiation therapy, suggesting that this treatment may be effective at eliminating any residual tumor cells when the needle track is not excised.

It is likely this type of recurrence is underreported because for most patients the skin puncture site can no longer be identified years later. The site of the puncture is determined by the modality and location of the lesion and cannot be determined with certainty once the skin has healed. It could be prudent for the needle puncture site on the skin to be recorded with either a diagram or with a photograph in the patient's record, as the majority of recurrences (14 of 19) have been in the skin and subcutaneous tissue. In some of the cases, diagnosis was delayed because the relationship to the core site was not appreciated and the skin lesion was thought to be inflammatory in nature. If the site was recorded, any subcutaneous mass or skin change arising at the site could be investigated promptly and recognized as a needle track recur-

rence. Although follow-up information is very limited, all of the 19 reported patients were treated successfully locally and no distant metastasis has been reported. Therefore, a needle track recurrence may not have the same dire prognosis generally associated with recurrent invasive carcinoma elsewhere in the chest wall [155].

Carcinoma at a Prior Core Site Showing Benign Results

When a cancer is found at the site of a prior CNB site with benign findings, there are three possibilities. Either a cancer was missed by the biopsy, the pathologist misdiagnosed a malignant lesion as benign, or the cancer is unrelated to the prior biopsy. Good quality practices require a review of the case to determine if an error occurred and, if so, how to avoid such errors in the future [156].

A large study of CNBs showing benign results found there were false-negative results in 22 of 988 cases because subsequent imaging studies confirmed the presence of a malignancy at the same site (2%) [157]. In 8 cases, it was decided that the CNB had not sampled the lesion. In the remaining 14 cases, review of the pathology slides showed missed malignancies in 2 (invasive lobular carcinoma and DCIS) and missed atypia in the remaining 12.

With good communication between radiologists and pathologists and identification of discordant cases, the number of core needle biopsies that fail to sample a targeted malignancy is reported to be <5–8% [63, 65, 67, 156]. About half of missed malignancies are DCIS [67, 157]. The majority of these cases are detected immediately by the radiologist, by noting that the lesion was not adequately sampled during the procedure, or on short-term follow-up because the original imaging lesion progresses (i.e., masses become larger or additional calcifications form) [156–158].

False-negative pathologic diagnoses are rare but can occur. Examples are mistaking a tubular carcinoma for sclerosing adenosis, invasive lobular carcinoma for inflammatory cells, papillary carcinoma for a papilloma, or micropapillary DCIS for usual ductal hyperplasia. A radiologist should request a second review of the slides or presentation at a radiology/pathology concordance conference if the imaging findings are highly suggestive of malignancy.

In some cases, a cancer may be unrelated to a nearby benign lesion that previously underwent biopsy. In the excisional specimen, the relationship of the cancer to the prior clip marking the benign biopsy site should be determined. If the prior biopsy was performed for a benign lesion that can be identified (e.g., the clip is in a fibroadenoma adjacent to the cancer), then the cancer most likely arose in the same area but was not the original imaging lesion.

References

1. Lester SC. How image-guided core needle biopsies altered the treatment of breast disease: challenges accepted and opportunities taken. Breast J. 2020;26:1156–9.
2. Teberian I, Kaufman T, Shames J, Rao VM, Liao L, Leven DC. Trends in the use of percutaneous versus open surgical breast biopsy: an update. J Am Coll Radiol. 2020;17:1004–10.
3. Bleiweiss IJ, Drossman S, Hermann G. Accuracy in mammographically directed breast biopsies: communication is key. Arch Pathol Lab Med. 1997;121:11–8.
4. Sorace J, Aberle DR, Eliman D, Lawvere S, Tawfik O, Wallace WD. Integrating pathology and radiology disciplines: an emerging opportunity? BMC Med. 2012;10:100–7.
5. Lieu D. Breast imaging for interventional pathologists. Arch Pathol Lab Med. 2013;137:100–19.
6. DeSimone MS, DeSimone AK, Sun EX, Laur O, Miskin NP, Brock JE, Matalon SA. Cross-residency radiologic/pathologic correlation curriculum: teaching correlation of surgical specimens with imaging. Acad Pathol. 2020; https://doi.org/10.1177/2374289520939258.
7. American College of Radiology. BI-RADS mammography; 2014.
8. Shaheen R, Schimmelpenninck CA, Stoddart L, Raymond H, Slanetz PJ. Spectrum of diseases presenting as architectural distortion on mammography: multimodality radiologic imaging with pathologic correlation. Semin Ultrasound CT MRI. 2011;32:351–62.
9. Choudhery S, Johnson M, Larson NB, Anderson T. Malignant outcomes of architectural distortion on tomosynthesis: a systematic review and meta-analysis. AJR Am J Roentgenol. 2020; https://doi.org/10.2214/AJR.20.23935.
10. Bachert E, Jen A, Denison DM, Chikarmane S, Karimova J, Kwait D, Hong X, Rhei E, Lester SC. Pathologic lesions correlating with mammographic architectural distortion: a study of 558 core needle biopsies. In: Abstract presented at the United States and Canadian Academy of Pathology annual meeting, 2021, submitted for publication.
11. Samardar P, Shaw de Paredes E, Grimes MM, Wilson JD. Focal asymmetric densities seen at mammography: US and pathologic correlation. Radiographics. 2002;22:19–33.
12. Cheseboro AL, Winkler NS, Birdwell RL, Giess CS. Developing asymmetries at mammography: a multimodality approach to assessment and management. Radiographics. 2016;36:322–34.
13. Sperber F, Metser U, Gat A, Shalmon A, Yaal-Hahoshen N. Focal asymmetric breast density: mammographic, sonographic and pathological correlation in 97 lesions—a call to restrain biopsies. Isr Med Assoc J. 2007;9:720–3.
14. Leung JWT, Sickles EA. Developing asymmetry identified on mammography: correlation with imaging outcome and pathologic findings. AJR Am J Roentgenol. 2007;188:667–75.
15. Haghayeghi K, Najibi M, Wang H, Donegan L, Wany Y. Clinicopathologic update of calcium oxalate in breast: a 15-year retrospective. Breast J. 2020;26:1736–41.
16. Gagnon RE, Sprague BL, Stout NK, Alagoz O, Weedon-Fekjaer H, Holford TR, Trentham-Dietz A. The contribution of mammography screening to breast cancer incidence trends in the United States: an updated age-period-cohort model. Cancer Epidemiol Biomark Prev. 2015;24(6):905–12.
17. Friedman PD, Sanders LM, Menendez C, Kalisher L, Petrillo G. Retrieval of lost microcalcifications during stereotactic vacuum-assisted core biopsy. AJR Am J Roentgenol. 2003;180:275–80.
18. El Khoury M, Mesurolle B, Omeroglu A, Aldis A, Kao E. Values of pathological analysis of lost tissue fragments in the vacuum canister during a vacuum-assisted stereotactic biopsy of the

breast. Br J Radiol. 2013;86:20120270. https://doi.org/10.1259/bjr.20120270.
19. Guinebretiere JM, Becette V, Hagay C, Belichard C, Tardivon A, Vanel D. Use of radiology for the pathologist in the management of breast lesions. Eur J Radiol. 2005;54:15–25.
20. Aruda SKC, Garvey LC, Hagemann IS. In-laboratory breast specimen radiography reduces tissue block utilization and improves turnaround time of pathologic examination. BMC Med Imaging. 2021;21:59–65.
21. Winston JS, Geradts J, Liu DF, Stomper PC. Microtome shaving radiography: demonstration of loss of mammographic microcalcifications during histologic sectioning. Breast J. 2004;10:200–3.
22. Moritz JD, Luftner-Nagel S, Westerhof JP, Oestmann J-W, Grabbe E. Microcalcifications in breast core biopsy specimens: disappearance at radiography after storage in formaldehyde. Radiology. 1996;200:361–3.
23. Bertrand AF, Dubois-Toussaint S, Lorimier G, Basle MF, Bertrand G. Breast micro-opacities of lead origin mimicking microcalcifications [Article in French]. J Radiol. 1995;76:213–5.
24. Korbin CD, Denison CM, Lester S. Metallic particles on mammography after wire localization. AJR Am J Roentgenol. 1997;169:1637–8.
25. Katz JF, Homer MJ, Graham RA, Rothschild JG. Metallic fragments on mammography after intraoperative deployment of radiopaque clips. AJR Am J Roentgenol. 2000;175:1591–3.
26. Bamford L, Lioe TF, O'Rourke DM, Buckley MR. Barium sulphate particles in breast mimicking malignant type microcalcification. Breast J. 2009;15:305–6.
27. Bruwer A, Nelson GW, Spark RP. Punctate intranodal gold deposits simulating microcalcifications on mammograms. Radiology. 1987;163:87–8.
28. Litton TP, Ghate SV. Tatto pigment mimicking axillary lymph node calcifications on mammography. Radiol Case Rep. 2020;15:1194–6.
29. Aguillar VLN, de Mello Tuncunduva TC, Carvalho FM, Mazucato MB, Viana MP, Torres US, de Mello GGN. Breast J. 2020;26:764–6.
30. Lane EG, Eisen CS, Ginter PS, Drotman MB. Ink on the move: tattoo pigment resembling axillary lymph node calcifications. Clin Imaging. 2021;79:154–7.
31. Kuba MG, Giess CS, Wieczorek TJ, Lester SC. Hyperechoic malignancies of the breast: underlying pathologic features correlating with this unusual appearance on ultrasound. Breast J. 2020;26:643–52.
32. Tasoulis MK, Lee H-B, Yang W, et al. Accuracy of post-neoadjuvant chemotherapy image-guided breast biopsy to predict residual cancer. JAMA Surg. 2020;155:e204103. https://doi.org/10.1001/jamasurg.2020.4103.
33. Cornea V, Jaffer S, Bleiweiss IJ, Nagi C. Adequate histologic sampling of breast magnetic resonance imaging-guided core needle biopsy. Arch Pathol Lab Med. 2009;133:1961–4.
34. Manion E, Brock JE, Raza S, Reisenbichler ES. MRI-guided breast core needle biopsies: pathologic features of newly diagnosed malignancies. Breast J. 2014;20:453–60.
35. Lilly AJ, Johnson M, Kuzmiak CM, Ollila DW, O'Connor SM, Hertel JD, Calhoun BC. MRI-guided core needle biopsy of the breast: radiology-pathology correlation and impact on clinical management. Ann Diagn Pathol. 2020;48:151563. https://doi.org/10.1016/j.anndiagpath.2020.151563.
36. Myers KS, Oluyemi ET, Mullen LA, Ambinder EB, Kamel IR, Harvey SC. Outcomes of foci on breast MRI: features associated with malignancy. AJR Am J Roentgenol. 2020;215:1012–9.
37. Gutierrez RL, DeMartini WB, Eby PR, Kurland BF, Peacock S, Lehman CD. BI-RADS lesion characteristics predict likelihood of malignancy in breast MRI for masses but not for nonmasslike enhancement. AJR Am J Roentgenol. 2009;193:994–1000.
38. Baltzer PA, Benndorf M, Dietzel M, Gajda M, Runnebaum IB, Kaiser WA. False-positive findings at contrast-enhanced breast MRI: a BI-RADS descriptor study. AJR Am J Roentgenol. 2010;194:1658–63.
39. Bennett IC, Saboo A. The evolving role of vacuum assisted biopsy of the breast: a progression from fine-needle aspiration biopsy. World J Surg. 2019;43:1054–61.
40. Sahoo S, Talwalker SS, Martin AW, Chagpar AB. Pathologic evaluation of cryoprobe-assisted lumpectomy for breast cancer. Am J Clin Pathol. 2007;128:239–44.
41. Rogers LW. Breast biopsy: a pathologist's perspective on biopsy acquisition techniques and devices with mammographic-pathologic correlation. Semin Breast Dis. 2005;8:127–37.
42. Sanderink WBG, Laarhuis BI, Strobbe LJA, Sechopoulos I, Bult P, Karssemeijer N, Mann RM. A systematic review on the use of the breast lesion excision system in breast disease. Insights Imaging. 2019;10:49–60.
43. Shah VI, Raju U, Chitale D, Deshpande V, Gregory N, Strand V. False-negative core needle biopsies of the breast: an analysis of clinical, radiologic, and pathologic findings in 27 consecutive cases of missed breast cancer. Cancer. 2003;97:1824–31.
44. Portnow LH, Thornton CM, Milch HS, Mango VL, Morris EA, Saphier NB. Biopsy marker standardization: what's in a name? AJR Am J Roentgenol. 2019;212:1400–5.
45. Seow JH, Phillips M, Taylor D. Sonographic visibility of breast tissue markers: a tissue phantom comparison study. Australas J Ultrasound Med. 2012;15:1490157.
46. Kapoor MM, Patel MM, Scoggins ME. The wire and beyond: recent advances in breast imaging preoperative needle localization. Radiographics. 2019;39:1–21.
47. Bassett LW, Mahoney MC, Apple SK. Interventional breast imaging: current procedures and assessing for concordance with pathology. Radiol Clin N Am. 2007;45:881–94.
48. Margolin FR, Kaufman L, Jacobs RP, Denny SR, Schrumpf JD. Stereotactic core breast biopsy of malignant calcifications: diagnostic yield of cores with and cores without calcifications on specimen radiographs. Radiology. 2004;233:252–4.
49. Easley S, Abdul-Karim FW, Klein N, Wang N. Segregation of radiographic calcifications in stereotactic core biopsies of breast: is it necessary? Breast J. 2007;13:486–9.
50. Neumeister VM, Anagnostou V, Siddiqui S, England AM, Zarrella ER, Vassilakopoulou M, Parisi F, Kluger Y, Hicks DG, Rimm DL. Quantitative assessment of effect of preanalytic cold ischemic time on protein expression in breast cancer tissues. J Natl Cancer Inst. 2012;104:1815–24.
51. Yildiz-Aktas IZ, Dabbs DJ, Bhargava R. The effect of cold ischemic time on the immunohistochemical evaluation of estrogen receptor, progesterone receptor, and HER2 expression in invasive breast carcinoma. Mod Pathol. 2012;25:1098–105.
52. College of American Pathologists. Estrogen and progesterone receptor testing in breast cancer guideline update, 13 Jan 2020. www.cap.org. Accessed 2 May 2021.
53. Green RS, Mathew S. The contribution of cytologic imprints of stereotactically guided core needle biopsies of the breast in the management of patients with mammographic abnormalities. Breast J. 2001;7:214–8.
54. Renshaw A, Kish R, Gould EW. The value of inking breast cores to reduce specimen mix-up. Am J Clin Pathol. 2007;127:271–2.
55. Gala I, Fisher P, Hermann GA. Usefulness of Telfa pads in the histologic assessment of stereotactic-guided breast biopsy specimens. Mod Pathol. 1999;12:553–7.
56. Grimes MM, Karageorge LS, Hogge JP. Does exhaustive search for microcalcifications improve diagnostic yield in stereotactic core needle breast biopsies? Mod Pathol. 2001;14:350–3.
57. Renshaw AA. Adequate histologic sampling of breast core needle biopsies. Arch Pathol Lab Med. 2001;125:1055–7.

58. Kumaraswamy V, Carder PJ. Examination of breast needle core biopsy specimens performed for screen-detected microcalcification. J Clin Pathol. 2007;60:681–4.
59. Lee AHS, Salinas NMVS, Hodi Z, Rakha EA, Ellis IO. The value of examination of multiple levels of mammary needle core biopsy specimens taken for investigation of lesions other than calcification. J Clin Pathol. 2012;65:1097–9.
60. Crisi GM, Pantanowitz L, Otis CN. Mammotome footprints: histologic artifacts in the era of stereotactic vacuum mammotome biopsy. Int J Surg Pathol. 2006;14:221–2.
61. Koo JS, Jung W-H, Kim H. Epithelial displacement into the lymphovascular space can be seen in breast core needle biopsy specimens. Am J Clin Pathol. 2010;133:781–7.
62. Ichihara S, Moritani S, Hasegawa M, Morita T, Oiwa M, Endo T, Hayashi T, Kato A, Sato Y, Sugie S. Pseudo-micropapillary structures associated with columnar cell lesions of the breast are an artifact due to traumatic epithelial detachment: a potential pitfall which can lead to overtreatment. Virchows Arch. 2013;463:93–5.
63. Parikh J, Tickman R. Image-guided tissue sampling: where radiology meets pathology. Breast J. 2005;11:403–9.
64. Idowu M, Hardy LB, Souers RJ, Nakhleh RE. Pathology diagnostic correlation with breast imaging findings: a College of American Pathologists Q-probes study of 48 institutions. Arch Pathol Lab Med. 2012;136:53–60.
65. Verkooijen HM. Diagnostic accuracy of stereotactic large-core needle biopsy for nonpalpable breast disease: results of a multicenter prospective study with 95% surgical confirmation. Int J Cancer. 2002;99:853–9.
66. Son EJ, Kim E-K, Youk JH, Kim MJ, Kwak JY, Choi SH. Imaging-histologic discordance after sonographically guided percutaneous breast biopsy: a prospective observational study. Ultrasound Med Biol. 2011;37(11):1771–8.
67. Poole BB, Wecsler JS, Sheth P, Sener SF, Wang L, Larsen L, Tripathy D, Lang JE. Malignancy rates after surgical excision of discordant breast biopsies. J Surg Res. 2014;14:1–6.
68. Liberman L, Drotman M, Morris EA, LaTrenta LR, Abramson AF, Zakowski MF, Dershaw DD. Imaging-histologic discordance at percutaneous breast biopsy. Cancer. 2000;89:2538–46.
69. Sohn Y-M, Yoon JH, Kim E-K, Moon HJ, Kim MJ. Percutaneous ultrasound-guided vacuum assisted removal versus surgery for breast lesions showing imaging-histology discordance after ultrasound-guided core-needle biopsy. Korean J Radiol. 2014;15:697–703.
70. Lester SC, editor. Breast, manual of surgical pathology. 3rd ed. Philadelphia: Elsevier; 2010.
71. Lester SC, Bose S, Chen YY, Connolly JL, de Baca ME, Fitzgibbons PL, Hayes DF, Kleer C, O'Malley FP, Page DL, Smith BL, Weaver DL, Winer E, Members of the Cancer Committee, College of American Pathologists. Protocol for the examination of specimen from patients with ductal carcinoma in situ of the breast. Arch Pathol Lab Med. 2009;133:15–25.
72. Nakhleh RE, Jones B, Zarbo RJ. Mammographically directed breast biopsies: a College of American Pathologists Q-Probes study of clinical physician expectations and of specimen handling and reporting characteristics in 434 institutions. Arch Pathol Lab Med. 1997;121:11–8.
73. Kass R, Kumar G, Klimberg VS, Kass L, Henry-Tillman R, Johnson A, Colvert M, Lane S, Harshfield D, Korourian S, Parrish R, Mancino A. Clip migration in stereotactic biopsy. Am J Surg. 2002;184:325–31.
74. Esserman LE, Cura MA, DaCosta D. Recognizing pitfalls in early and late migration of clip markers after imaging-guided directional vacuum-assisted biopsy. Radiographics. 2004;24:147–56.
75. Teichgraeber DC, Martaindale S, Omofoye TS, Hess KR, Parikh JR, Whitman GJ. Immediate migration of biopsy clip markers after upright digital breast tomosynthesis-guided vacuum-assisted core biopsy. Acad Radiol. 2020;27:204–9.
76. Srour MK, Kim S, Amersi F, Giuliano AE, Chung A. Comparison of wire localization, radioactive seed, and Savi Scout® radar for management of surgical breast disease. Breast J. 2020;26:406–13.
77. Graham RP, Jakub JW, Brunette JJ, Reynolds C. Handling of radioactive seed localization breast specimens in the pathology laboratory. Am J Surg Pathol. 2012;36:1718–23.
78. Harrison BT. Radioactive seed identification. In: Lester SC, editor. Diagnostic pathology: intraoperative consultation. 2nd ed. Amsterdam: Elsevier; 2018. (Also available on ExpertPath.com; video available with the ebook edition).
79. Gilcrease MZ, Dogan BE, Black DM, Contreras A, Dryden MJ, Jimenez SM. Transection of radioactive seeds on breast specimens. Am J Surg Pathol. 2016;40:1375–9.
80. Klein RL, Mook JA, Euhus DM, Rao R, Wynn RT, Eastman AB, Leitch AM. Evaluation of a hydrogel based breast biopsy marker (HydroMARK→) as an alternative to wire and radioactive seed localization for non-palpable breast lesions. J Surg Oncol. 2012;105:591–4.
81. Kallen ME, Sim MS, Radosavcev BL, Humphries RM, Ward DC, Apple SK. A quality initiative of postoperative radiographic imaging performed on mastectomy specimens to reduce histology cost and pathology report turnaround time. Ann Diagn Pathol. 2015;19:353–8.
82. Zeng J, Mercado C, Axelrod D, Guth A, Darvishian F. Missing targets after nipple-sparing mastectomy: a multi-disciplinary approach to avoid an undesirable outcome. Breast J. 2018;24:678–9.
83. Guarda LA, Tran TA. The pathology of breast biopsy site marking devices. Am J Surg Pathol. 2005;29:814–9.
84. Bleiweiss IJ, Nayak A. Iatrogenic issues in breast pathology. Breast J. 2019;26:1179–84.
85. Provenzano E, Pinder SE. Modern therapies and iatrogenic changes in breast pathology. Histopathology. 2017;70:40–55.
86. Saad RS, Silverman JF, Julian T, Clary KM, Sturgis CD. Atypical squamous metaplasia of seromas in breast needle aspirates from irradiated lumpectomy sites: a potential for false-positive diagnoses of carcinoma. Diagn Cytopathol. 2002;26:104–8.
87. Layfield LJ, Frazier S, Schanzmeyer E. Histomorphologic features of biopsy sites following excisional and core needle biopsies of the breast. Breast J. 2015;1:1–7.
88. Carmon M, Zilber S, Gekhtman D, Osha O, Hadar T, Golomb E. Hygroscopic sonographically detectable clips form characteristic breast and lymph node pseudocysts. Mod Pathol. 2018;31:62–7.
89. Pinilla-Pagnon I, Perez-Mies B, Reguero ME, et al. Histological changes secondary to wire coil placement in breast tissue and lymph nodes. Virchows Arch. 2018;473:285–91.
90. Alatassi H, Pile NS, Chagbar AB, Sahoo S. Breast biopsy marker masquerading as a mass lesion. Breast J. 2005;11:504–5.
91. Trop I, David J, El Khoury M, Gautier N, Gaboury L, Lalonde L. Microcalcifications around a collagen-based breast biopsy marker: complication of biopsy with a percutaneous marking system. AJR Am J Roentgenol. 2011;197:W353–7.
92. Calhoun K, Giuliano A, Brenner RJ. Intraoperative loss of core biopsy clips: clinical implications. AJR Am J Roentgenol. 2008;190:W196–200.
93. Liberman L, Kaplan JB, Morris EA, Abramson AF, Menell JH, Dershaw DD. To excise or to sample the mammographic target: what is the goal of stereotactic 11-guage vacuum-assisted breast biopsy? AJR Am J Roentgenol. 2002;179:679–83.
94. Liberman L, Zakowski MF, Avery S, Hudis C, Morris EA, Abramson AF, LaTrenta LR, Glassman JR, Dershaw DD. Complete percutaneous excision of infiltrating carcinoma at stereotactic breast biopsy: how can tumor size be assessed? AJR Am J Roentgenol. 1999;173:1315–22.

95. Lee J-M, Kaplan JB, Murray MB, Liberman L. Complete excision of the MRI target lesion at MRI-guided vacuum-assisted biopsy of breast cancer. AJR Am J Roentgenol. 2008;191:1198–202.
96. Hortobagyi GN, Connolly JL, D'Orsi CJ, et al. Chapter 48. Breast. In: Amin, MB, Edge S, Greene F, Byrd DR, et al., American Joint Commission on Cancer, editors. AJCC cancer staging manual. New York: Springer; 2017 (Corrected edition published in 2018; also available at https://cancerstaging.org/references-tools/deskreferences/Pages/Breast-Cancer-Staging.aspx. Accessed 21 May 2021).
97. Leddy R, Irshad A, Metcalfe A, Mabalam P, Abid A, Ackerman S, Lewis M. Comparative accuracy of preoperative tumor size assessment on mammography, sonography, and MRI: is the accuracy affected by breast density or cancer subtype? J Clin Ultrasound. 2016;44:17–25.
98. Qi P, Yang Y, Bai Q, Xue T, Ren M, Yao Q, Yang W, Zhou X. Concordance of the 21-gene assay between core needle biopsy and resection specimens in early breast cancer patients. Breast Cancer Res Treat. 2021;186:327–42.
99. Baehner FL, Quale C, Pomeroy C, Cherbavaz D, Shak S. Biopsy cavities in breast cancer specimens: their impact on quantitative RT-PCR gene expression profiles and recurrence risk assessment (abstract). Mod Pathol. 2008;22:28A–9A.
100. Acs G, Esposito NN, Kiluk J, Loftus L, Laronga C. A mitotically active, cellular tumor stroma and/or inflammatory cells associated with tumor cells may contribute to intermediate or high Oncotype DX recurrence scores in low-grade invasive breast carcinomas. Mod Pathol. 2012;25:556–66.
101. Bonneau C, Lebas P, Michenet P. Histologic changes after stereotactic 11-gauge directional vacuum assisted breast biopsy for mammary calcification: experience in 31 surgical specimens. Ann Pathol. 2002;22:441–7.
102. Douglas-Jones AG, Verghese A. Diagnostic difficulty arising from displaced epithelium after core biopsy in intracystic papillary lesions of the breast. J Clin Pathol. 2002;55:780–3.
103. Liberman L, Vuolo M, Dershaw DD, Morris EA, Abramson AF, LaTrenta LR, Polini NM, Rosen PP. Epithelial displacement after stereotactic 11-gauge directional vacuum-assisted breast biopsy. AJR Am J Roentgenol. 1999;172:677–81.
104. Nagi C, Bleiweiss I, Jaffer S. Epithelial displacement in breast lesions: a papillary phenomenon. Arch Pathol Lab Med. 2005;129:1465–9.
105. Phelan S, O'Doherty A, Hill A, Quinn CM. Epithelial displacement during breast core biopsy causes diagnostic difficulties in subsequent surgical excision specimens. J Clin Pathol. 2007;60:373–6.
106. Tardivon AA, Guinebretiere JM, Dromain C, Deghaye M, Caillet H, Georgin V. Histological findings in surgical specimens after core biopsy of the breast. Eur J Radiol. 2002;41:40–51.
107. Youngson BJ, Cranor M, Rosen PP. Epithelial displacement in surgical breast specimens following needling procedures. Am J Surg Pathol. 1994;18:896–903.
108. Youngson BJ, Liberman L, Rosen PP. Displacement of carcinomatous epithelium in surgical breast specimens following stereotaxic core biopsy. Am J Clin Pathol. 1995;103:598–602.
109. Diaz LK, Wiley EI, Venta LA. Are malignant cells displaced by large-gauge needle core biopsy of the breast? AJR Am J Roentgenol. 1999;173:1303–13.
110. Carter BA, Jensen RA, Simpson JF, Page DL. Benign transport of breast epithelium into axillary nodes after biopsy. Am J Clin Pathol. 2000;113:259–65.
111. Nayak A, Bleiweiss IJ. Iatrogenically false positive sentinel lymph nodes in breast cancer: methods of recognition and evaluation. Semin Diagn Pathol. 2018;35:228–35.
112. Grabau DA, Andersen JA, Graverson HP, Dyreborg U. Needle biopsy of breast cancer: appearance of tumor cells along the needle track. Eur J Surg Oncol. 1993;19:192–4.
113. Harter LP, Curtis JS, Ponto G, Craig PH. Malignant seeding of the needle track during stereotaxic core needle breast biopsy. Radiology. 1991;185:713–4.
114. Hoorntje LE, Schipper MEI, Kaya A, Verkooijen H, Klinkenbijl JG, Borel Rinkes IH. Tumour cell displacement after 14G breast biopsy. Eur J Surg Oncol. 2004;30:520–5.
115. Liebens F, Carly B, Cusumano P, Van Beveren M, Beier B, Fastrez M, Rozenberg S. Breast cancer seeding associated with core needle biopsies: a systematic review. Maturitas. 2009;62:113–23.
116. Uematsu T, Kasami M. The use of positive core wash cytology to estimate potential risk of needle tract seeding of breast cancer: directional vacuum-assisted biopsy versus automated core needle biopsy. Breast Cancer. 2010;17:61–7.
117. Ishizuna K, Ota D, Okamoto J, Fukuuchi A, Tanaka R, Fujii A, Mori M, Nishi T. A case of mucinous carcinoma of the breast in which needle tract seeding was diagnosed by preoperative diagnostic imaging. Breast Cancer. 2011;18:324–7.
118. Brenner RJ, Gordon LM. Malignant seeding following percutaneous breast biopsy: documentation with comprehensive imaging and clinical implications. Breast J. 2011;17:651–6.
119. Santiago L, Adrada BE, Huang ML, Wei W, Candelaria RP. Breast cancer neoplastic seeding in the setting of image-guided needle biopsies of the breast. Breast Cancer Res Treat. 2017;166:29–39.
120. Davies JD, Nonni A, D'Costa HF. Mammary epidermoid inclusion cysts after wide-core needle biopsies. Histopathology. 1997;31:549–51.
121. Garijo MF, Val-Bernal JF, Vega A, Val D. Postoperative spindle cell nodule of the breast: pseudosarcomatous myofibroblastic proliferation following endo-surgery. Pathol Int. 2008;58:787–91.
122. Gobbi H, Tse G, Page DL, Olson SJ, Jensen RA, Simpson JF. Reactive cell nodules of the breast after core biopsy or fine-needle aspiration. Am J Clin Pathol. 2000;113:288–94.
123. Tsang WY, Chan JK. Spectrum of morphologic changes in lymph nodes attributable to fine needle aspiration. Hum Pathol. 1992;23:562–5.
124. Pinto RG, Couto F, Mandreker S. Infarction after fine needle aspiration: a report of four cases. Acta Cytol. 1996;40:739–41.
125. Flint A, Oberman HA. Infarction and squamous metaplasia of intraductal papilloma: a benign breast lesion that may simulate carcinoma. Hum Pathol. 1984;15:764–7.
126. Murphy MC, Quinn CM, Prichard RS, Pender S, McNally S. A mimic of breast carcinoma 1-year post vacuum-assisted excision of a benign breast lesion. BMJ Case Rep. 2019;12:e230237. https://doi.org/10.1136/bcr-2019-230237.
127. Cheurfa N, Giard S. Non-palpable breast cancer malignant on needle core biopsy and no malignancy in surgical excision: how to manage? [Article in French]. Gynecol Obstet Fertil. 2015;43:18–24.
128. Rakha EA, El-Sayed ME, Reed J, Lee AHS, Evans AJ, Ellis IO. Screen-detected breast lesions with malignant needle core biopsy diagnoses and no malignancy identified in subsequent surgical excision specimens (potential false-positive diagnosis). Eur J Cancer. 2009;45:1162–7.
129. Gajdos C, Levy M, Herman Z, Herman G, Bleiweiss IJ, Tartter PI. Complete removal of nonpalpable breast malignancies with a stereotactic percutaneous vacuum-assisted biopsy instrument. J Am Coll Surg. 1999;189:237–40.
130. Bossuyt V, Spring L. Pathologic evaluation of response to neoadjuvant therapy drives treatment changes and improves long-term outcomes for breast cancer patients. Breast J. 2020;26:1189–98.
131. Elmore JG, Longton GM, Carney PA, Geller BM, Onega T, Tosteson AN, Nelson HD, Pepe MS, Allison KH, Schnitt SJ, O'Malley FP, Weaver DL. Diagnostic concordance among pathologists interpreting breast biopsy specimens. JAMA. 2015;313:1122–32.

132. Segnan N, Minozzi S, Ponti A, et al. Estimate of false-positive breast cancer diagnoses from accuracy studies: a systematic review. J Clin Pathol. 2017;70:282–94.
133. Harrison BT, Dillon DA, Richardson AL, Brock JE, Guidi AJ, Lester SC. Quality assurance in breast pathology: lessons learned from a review of amended reports. Arch Pathol Lab Med. 2017;141:260–6.
134. Pfeifer JD, Liu J. Rate of occult specimen provenance complications in routine clinical practice. Am J Clin Pathol. 2013;139:93–100.
135. Lerner AG, Bush AL, Kenler AS, Dorfman DD, Morgan TA, Boyd B, Burak WE, Fine RE. Incidence of misattributed specimen provenance among surgical breast biopsies. In: San Antonio Breast Cancer symposium publication number P5-02-08; 2014.
136. Giess CS, Keating DM, Osborne MP, Rosenblatt R. Local tumor recurrence following breast-conservation therapy: correlation of histopathologic findings with detection method and mammographic findings. Radiology. 1999;212:829–35.
137. Gunhan-Bilgen I, Oktay A. Mammographic features of local recurrence after conservative surgery and radiation therapy: comparison with that of the primary tumor. Acta Radiol. 2007;48:390–7.
138. Alexandrova E, Sergieva S, Kostova P, Mihaylova I, Katzarov D, Milev A. Ipsilateral-in breast tumor recurrence after breast conserving therapy: true recurrence versus new primary tumor. J BUON. 2015;20:1001–8.
139. Laird J, Lok B, Siu C, et al. Impact of an in situ component on outcome after in-breast tumor recurrence in patients treated with breast-conserving therapy. Ann Surg Oncol. 2018;25:154–63.
140. Bollet MA, Servant N, Neuvial P, Decraene C, Lebigot I, Meyniel FP, De Rycke Y, Savignoni A, Rigaill G, Hupe P, Fourquet A, Sigal-Zafrani B, Barillot E, Thiery JP. High-resolution mapping of DNA breakpoints to define true recurrences among ipsilateral breast cancers. J Natl Cancer Inst. 2008;100:48–58.
141. McGrath S, Antonucci J, Goldstein N, Wallace M, Mitchell C, Grills I, Jolly S, Kestin L, Vicini F. Long-term patterns of in-breast failure in patients with early stage breast cancer treated with breast-conserving therapy: a molecular based clonality evaluation. Am J Clin Oncol. 2010;33:17–22.
142. Goldstein NS, Vicini FA, Hunter S, Odish E, Forbes S, Kraus D, Kestin LL. Molecular clonality determination of ipsilateral recurrence of invasive breast carcinomas after breast-conserving therapy: comparison with clinical and biological factors. Am J Clin Pathol. 2005;123:679–89.
143. Stolier A, Skinner J, Levine E. A prospective study of seeding of the skin after core biopsy of the breast. Am J Surg. 2000;180:104–7.
144. Brouwer OR, Donker M, Woerdman LA, Vrancken Peeters MJ. Local recurrence after skin-sparing mastectomy [Article in Dutch]. Ned Tijdschr Geneeskd. 2012;156:1256–9.
145. Chao C, Torosian MH, Boraas MC, Sigurdson ER, Hoffman JP, Eisenberg BL, Fowble B. Local recurrence of breast cancer in the stereotactic core needle biopsy site: case reports and review of the literature. Breast J. 2001;7:124–7.
146. Intra M, Mazzarol G, Rietjens M, Diaz Brito JA, Gennari R, Sotelo J, Rodriguez J, Bassani G, Bassi F. Extramammary recurrence of DCIS after total mastectomy: an iatrogenic displacement following needling procedures? [Letter to the editor]. Breast J. 2005;11:297–300.
147. Kawasaki T, Ishida M, Tada T, Matsuya H, Saitoh M, Sato A, Suzuki M, Sugimoto R, Mue Y, Uesugi N, Ishida K, Ishida K, Ariga H, Ichihara S, Sugai T, Sapino A. Well-differentiated neuroendocrine tumor of the breast with recurrence due to needle tract seeding. Virchows Arch. 2015;466:479–81.
148. Kwo S, Grotting JC. Does stereotactic core needle biopsy increase the risk of local recurrence of invasive breast cancer? [Editorial]. Breast J. 2006;12:191–3.
149. Thurfjell MG, Jansson T, Nordgren H, Bergh J, Lindgren A, Thurfjell E. Local breast cancer recurrence caused by mammographically guided punctures. Acta Radiol. 2000;41:435–40.
150. Uriburu JL, Vuoto HD, Cogorno L, Isetta JA, Candas G, Imach GC, Bernabo OS. Local recurrence of breast cancer after skin-sparing mastectomy following core needle biopsy: case reports and review of the literature. Breast J. 2006;12:194–8.
151. Cho E, Kim MH, Cha SH, Cho SH, Oh SJ, Lee JD. Breast cancer cutaneous metastasis at core needle biopsy site. Ann Dermatol. 2010;2:238–40.
152. Calvillo KZ, Guo L, Brostrom V, Schnitt SJ, Hong X, Raza S, Lester SC. Recurrence of breast carcinoma as Paget disease of the skin at a prior core needle biopsy site: case report and review of the literature. Int J Surg Case Rep. 2015;15:152–6.
153. Choi S, Kim EK, Kong J, Gong G, Shin HJ, Lee YJ, Son BH, Ahn SH, Lee JW. Recurrence of breast carcinoma as Paget's disease of the skin along the core needle biopsy tract after skin-sparing mastectomy. Breast Cancer. 2020;23:224–9.
154. Yoneyama K, Nakagawa M, Hara A. Local recurrence of breast cancer caused by core needle biopsy: case report and review of the literature. Int J Surg Case Rep. 2020;72:318–21.
155. Wapnir IL, Khan A. Current strategies for the management of locoregional breast cancer recurrence. Oncology. 2019;33:19–25.
156. Peter D, Grunhagen J, Wenke R, Shafer FKW, Schreer I. False-negative results after stereotactically guided vacuum biopsy. Eur Radiol. 2008;18:177–82.
157. Jackman RJ, Marzoni FA Jr, Rosenberg J. False-negative diagnoses at stereotactic vacuum-assisted needle breast biopsy: long-term follow-up of 1,280 lesions and review of the literature. AJR Am J Roentgenol. 2009;192:341–51.
158. Boba M, Koltun U, Bobek-Billewicz B, Chmielik E, Eksner B, Olejnik T. False-negative results of breast core needle biopsies—retrospective analysis of 988 biopsies. Pol J Radiol. 2011;76:25–9.

Pattern-Based Evaluation of Breast Core Needle Biopsies

2

Sandra J. Shin and Paula S. Ginter

Introduction

In this era of widespread screening protocols, greater understanding of the complexities of breast disease by both professionals and patients, and the high demand to fully (and accurately) characterize malignancies for optimal treatment management, it is imperative that pathologists who sign out breast specimens are equipped with as much knowledge and have access to as many resources as possible.

Core needle biopsies (CNBs) as mere samplings of a larger lesion can be likened to pieces of a jigsaw puzzle. Out of context, observers can easily conclude that the picture of the assembled puzzle is one entity based on very limited information gleaned from a single puzzle piece when in fact, represents something entirely different had all the pieces been available. Fortunately, most core needle samples are both representative of the abnormality identified clinically or radiologically and contain the necessary histologic features to allow for a straightforward diagnosis. This is particularly reassuring as the CNB stage has become a critical juncture in the clinical management of the patient. The pathologist bears a tremendous amount of responsibility in a patient's care as his/her diagnosis will directly and immediately determine the next steps of clinical management. An incorrect diagnosis rendered by the pathologist can lead to lack of proper treatment allowing the condition to progress and conceivably worsen or alternatively subject the patient to unnecessary treatment such as an excisional biopsy, sentinel lymph node biopsy, and theoretically even neoadjuvant chemotherapy. Although largely unspoken, most clinicians expect that a correct and complete diagnosis should be attainable whether the specimen is an excisional specimen where the entire lesion is available for evaluation or a fraction of it such as in a CNB sample. For these reasons, practicing pathologists find breast CNBs to be challenging in some cases.

S. J. Shin (✉)
Department of Pathology and Laboratory Medicine, Albany Medical College, Albany, NY, USA
e-mail: shins1@amc.edu

P. S. Ginter
Department of Pathology and Laboratory Medicine, Weill Cornell Medicine, New York, NY, USA
e-mail: psg9003@med.cornell.edu

Pattern-Based Approach to Core Needle Biopsies

Over time, practicing pathologists develop internal "diagnostic" algorithms when evaluating breast CNBs. In teaching hospitals, attending pathologists may share their personal approach in evaluating certain types of cases to trainees. Some pathologists evaluate a given case using a strictly analytical approach while others may scan for certain familiar key findings that will confirm their "gestalt" feeling about the case. Most pathologists likely practice with a style somewhere in between these two extremes. While any variation of practicing styles are compatible with rendering diagnoses on excised material, these approaches may not be the most effective when evaluating limited samplings where the diagnostic findings can be either present, partially present, or absent.

All pathologists are innately (or learn to be) adept at pattern recognition. This is our forté as pathologists and we utilize it with every case that passes under our microscopes. However, what may not be as obvious is *when* this skill should be employed during the initial morphologic evaluation. Beginning the evaluation by first subcategorizing based on the overall pattern can be advantageous, particularly in CNB samples, for several reasons.

The discipline of taking a moment to take stock of the overall picture (pattern) can provide an unbiased first assessment of a breast CNB case. The advantage of using this approach is that it automatically encompasses all diagnostic possibilities, benign and malignant entities as well as common and rare diagnoses. As mentioned, most diagnoses can

© The Author(s), under exclusive license to Springer Nature Switzerland AG 2022
S. J. Shin et al. (eds.), *A Comprehensive Guide to Core Needle Biopsies of the Breast*,
https://doi.org/10.1007/978-3-031-05532-4_2

be rendered with ease but to define the minority of cases that elude us, supplementing our evaluative process with another approach may be the difference between a correct diagnosis and a misdiagnosis.

Pathologic findings in breast CNBs can be grouped into several categories of overall morphologic pattern and encompass many but not all entities encountered in this setting. Learning and applying a pattern-based approach to diagnosis may prove useful as an adjunctive tool if a given case falls into one of these groups. The three that will be discussed in this chapter are small glandular proliferations, spindle cell proliferations, and cystically dominant lesions. Other patterns including vascular, fibroepithelial, and papillary are discussed in their respective chapters elsewhere in this book.

The predominant pattern of any case should be evident at the time of initial histologic perusal at low-power magnification. This should generate a list of entities in the differential diagnosis which can be further narrowed by closer scrutiny of more subtle morphologic features that may be present in the given sample. After appropriate correlation with clinical and radiologic information, the remaining diagnostic possibilities should be further narrowed after interrogation with a targeted panel of immunohistochemical (IHC) stains and/or evaluation by additional H&E levels until the correct diagnosis is reached. As any seasoned pathologist is well aware, this seemingly simple process can be wrought with pitfalls. Nonetheless, such difficulties outweigh the opportunity to formulate a robust differential diagnosis by employing this diagnostic approach. While this strategy is not intended for the evaluation of all breast specimens, it is undeniably a worthwhile alternative approach in the CNB setting that can serve either as a primary or adjunctive role in diagnosis.

Small Glandular Proliferations

Among dominant patterns, this is the most commonly encountered one as many mammary entities that fall under this group are commonly mass forming or associated with calcifications, the two most common targets of CNBs [1]. It should be emphasized that all of the entities in this differential diagnosis are low grade (cytologically bland) with rare exception despite the fact that both benign and malignant entities constitute the differential diagnosis. As a general rule, any degree of cytologic atypia in a small glandular proliferation expands the differential diagnosis to include atypical microglandular adenosis (MGA), atypical apocrine adenosis, post-radiation atypia, or degenerative atypia. It is also important to be able to distinguish cytologic atypia of lesional glands from secondary involvement of benign glands by a neoplastic proliferation (discussed in Chap. 3).

A lesion that constitutes a *small glandular proliferation* is one that consists of an aggregate of epithelial lined glands growing in concert where a defined spatial arrangement among individual glands is evident (Fig. 2.1). In the broadest of terms, the differential diagnosis encompasses common

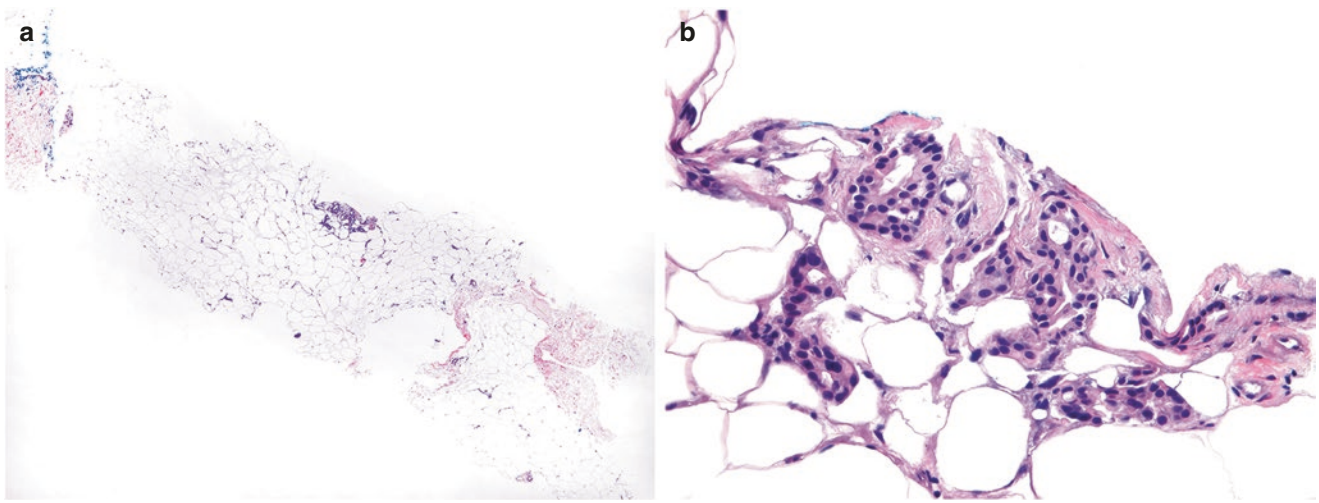

Fig. 2.1 Example of a small glandular proliferation in a CNB sample. (**a**) Low magnification of a cluster of small glands in breast adipose tissue. (**b**) On high-power view, the proliferation consists of round to angulated glands lined by cytologically bland cells and with open lumina. The glands are haphazardly arranged. (**c**) Smooth muscle myosin heavy chain (SMM) and (**d**) p63 immunostains demonstrate lack of myoepithelium around glands confirming the diagnosis of invasive tubular carcinoma. Adjacent capillaries serve as an internal positive control for SMM

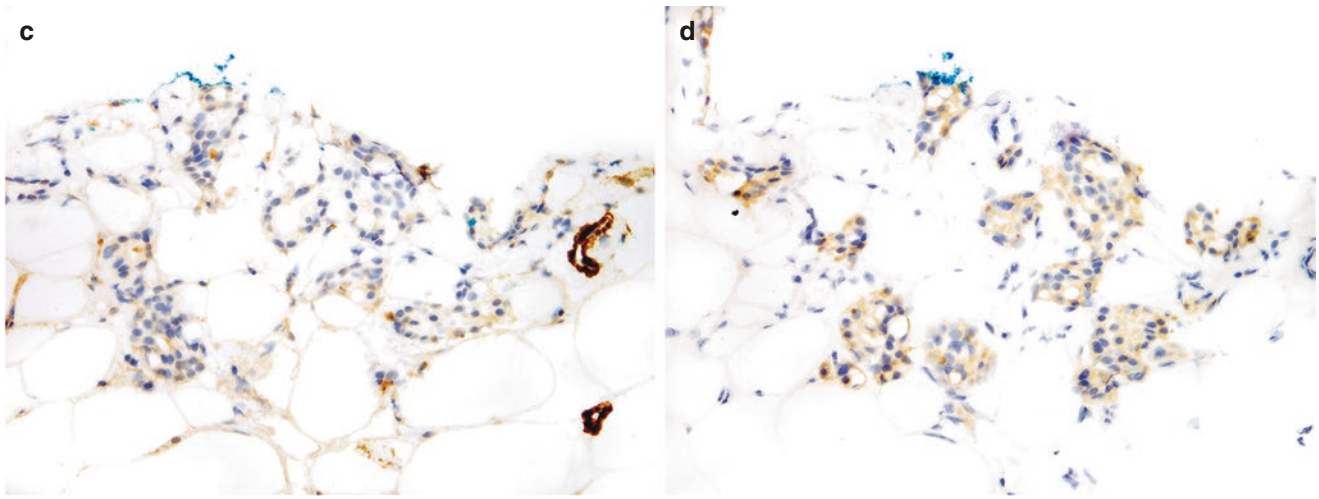

Fig. 2.1 (continued)

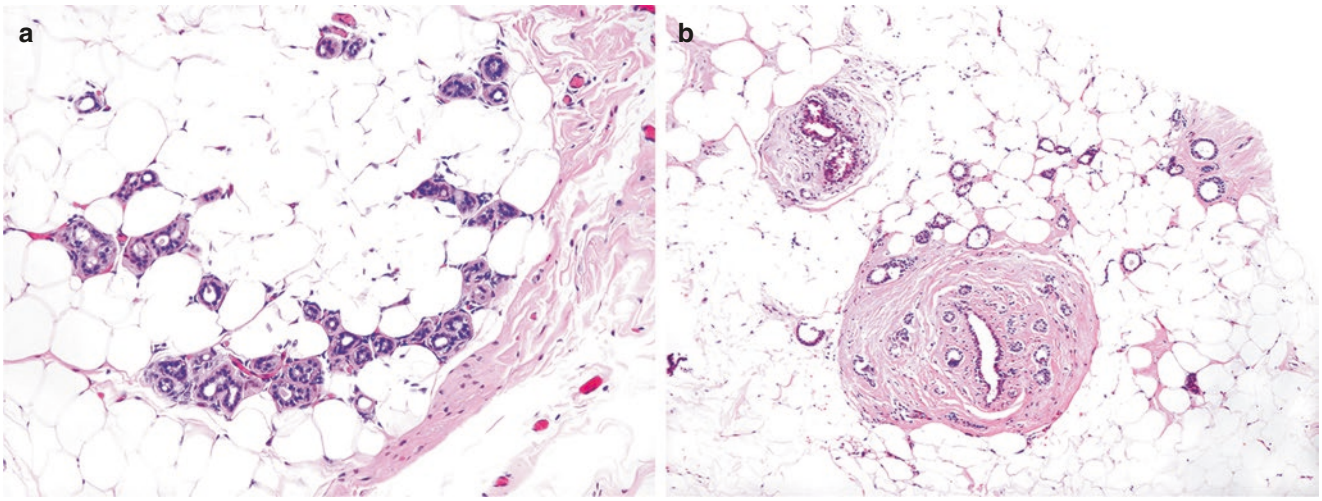

Fig. 2.2 Two examples of a small glandular proliferation in adipose tissue. (**a**) Adenosis consisting of scattered but largely non-infiltrative arrangement of round lobular glands in adipose tissue. (**b**) Invasive tubular carcinoma as round glands encircling a benign duct as well as in the adjacent adipose tissue

entities such as invasive well-differentiated ductal carcinoma (commonly tubular type), radial scar/complex sclerosing lesion, and sclerosing adenosis; and less common ones such as microglandular adenosis (MGA), low-grade adenosquamous carcinoma (LGASC), and syringomatous tumor. More common small glandular proliferations (invasive well-differentiated ductal carcinoma, radial scar, and sclerosing adenosis) are estrogen receptor (ER)-positive while the less common ones (MGA, LGASC, and syringomatous tumor) are ER-negative (in addition to PR and HER2, i.e., triple negative). For this reason, it may be helpful to include ER as part of one's initial round of IHC workup when evaluating a small glandular proliferation that exhibits morphologic features common to both subgroups. In most cases, the glands in question possess an infiltrative growth pattern; however, it should be noted here that a noninvasive growth pattern can be equally misleading. The presence of glands within mammary adipose tissue usually is indicative of invasion; however, adenosis and even benign glands can be found admixed in adipose tissue as well. While adenosis should not exhibit an infiltrating appearance in fat, some examples of invasive tubular carcinoma can demonstrate a convincingly innocuous, noninvasive arrangement (Fig. 2.2).

ER-Positive Small Glandular Proliferations

While invasive ductal carcinoma (tubular type) can be mistaken for ER-negative small glandular proliferations such as MGA, the morphologic features of this entity are more fre-

quently confused with other ER-positive small glandular proliferations. Particularly in core biopsy material, the distinction between invasive tubular carcinoma and radial scar is most challenging. Invasive tubular carcinoma and radial scar share many common characteristics beginning with their similar clinical presentation. While both entities can form a palpable mass, in recent times they are largely detected by screening mammogram. Particularly in larger examples, both entities are radiologically suspicious as they characteristically appear as a stellate mass. Not surprisingly, these entities are similarly described as a firm mass with irregular tumor borders by gross examination and the suspicion of invasive carcinoma remains high until histologic evaluation is performed. Microscopically, both invasive tubular carcinoma and radial scar comprise a proliferation of cytologically bland glands that are angulated or teardrop shaped with open lumina (Fig. 2.3). The tumor-associated stroma can be elastotic (Fig. 2.4) or sclerotic (Fig. 2.5) in both, but additionally invasive tubular carcinoma can also demonstrate desmoplastic stroma which is more cellular in appearance. The arrangement of the glands in examples of invasive tubular carcinoma is haphazard (Fig. 2.6); however, this telltale sign may not be fully appreciated in a partially sampled tumor. On the other hand, glands comprising a radial scar generally maintain uniformity in their spatial arrangement with each other as they emanate away from the nidus in an orderly centrifugal fashion (Figs. 2.3a, b and 2.7a–c). It is important to recognize that the glands in the center of a radial scar tend to be more disorganized than those more peripheral, and therefore if the sampling is that of

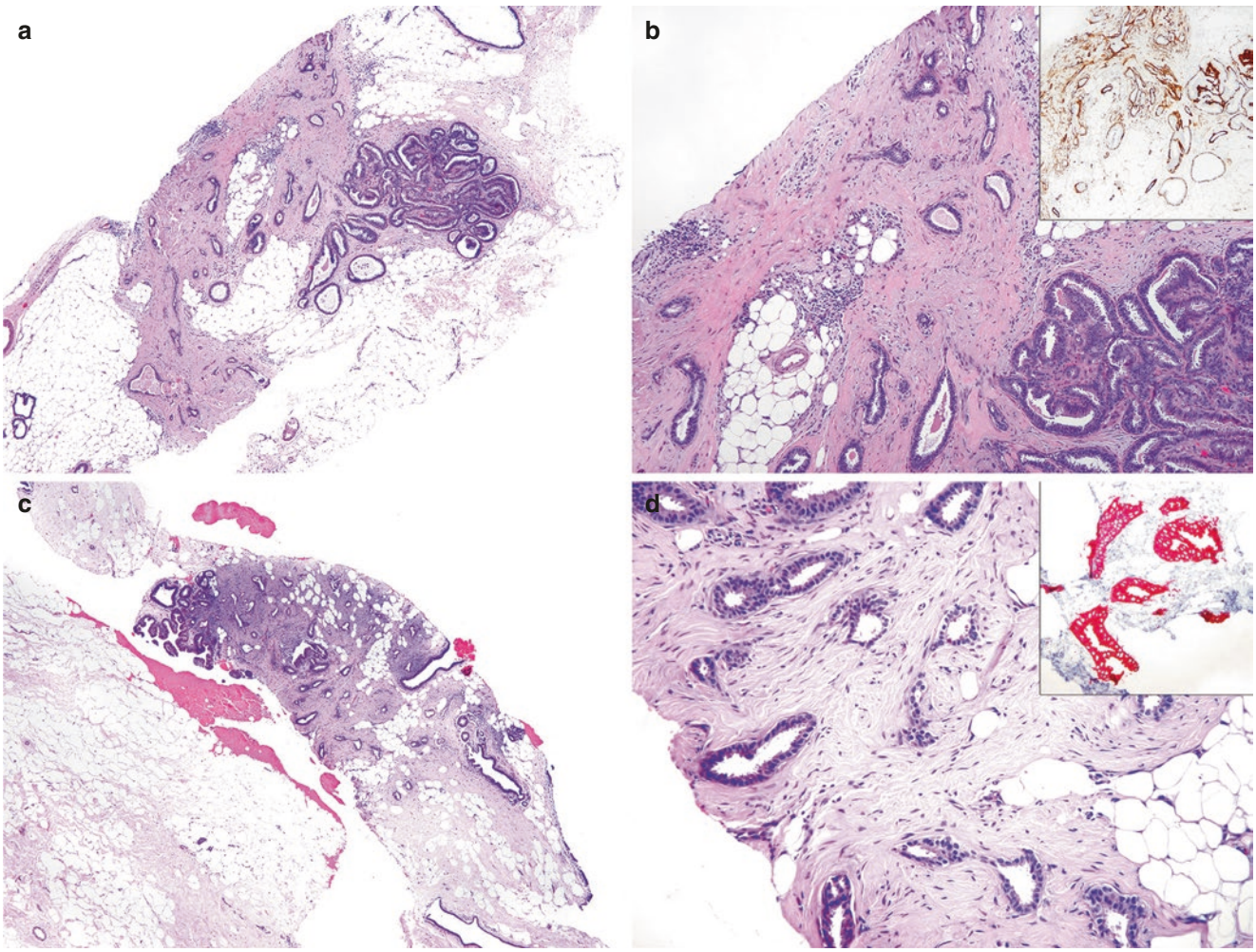

Fig. 2.3 Radial growth pattern of small glandular proliferations. (**a**) Glands of this complex sclerosing lesion grow partly in a radial configuration which appear pseudoinvasive. (**b**) Higher magnification shows lesional glands are compressed and angulated due to surrounding stromal sclerosis. A SMM immunostain highlights the presence of investing myoepithelial cells around the compressed glands (*inset*). (**c**) Invasive tubular carcinoma composed of glands in a partly radiating configuration. (**d**) On higher view, the glands are angulated and embedded in fibrotic stroma. A multiplex immunostain (composed of CK8/18, CK 5/6, and p63) confirms the absence of myoepithelial cells in the neoplastic glands (*inset*)

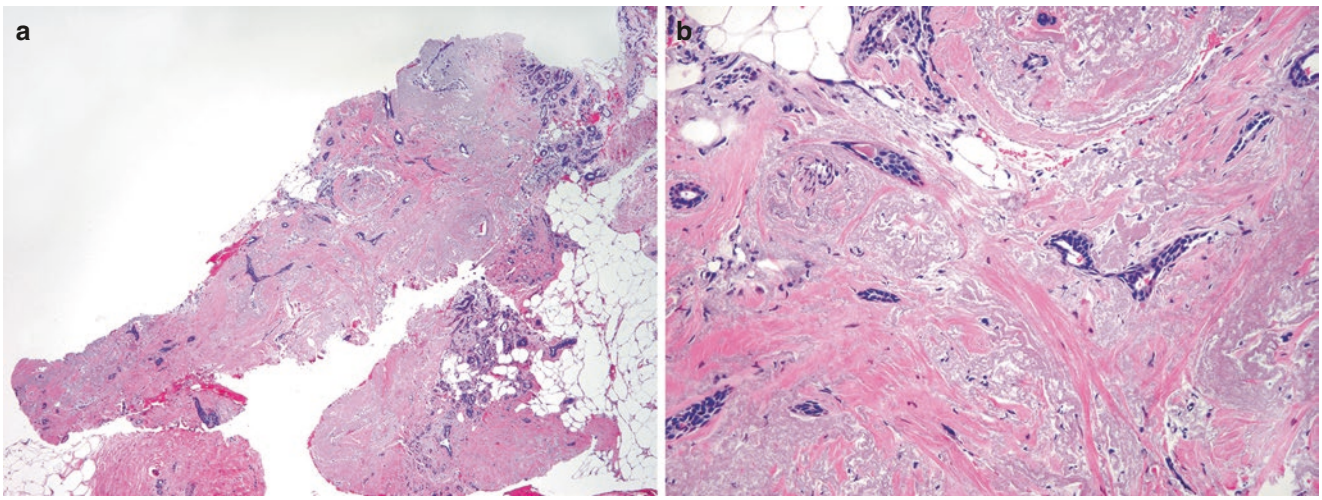

Fig. 2.4 Elastotic stroma associated with a small glandular proliferation. (**a**, **b**) Low- and high-power magnifications showing angulated and compressed glands embedded in paucicellular, blue-gray elastotic stroma of this radial scar

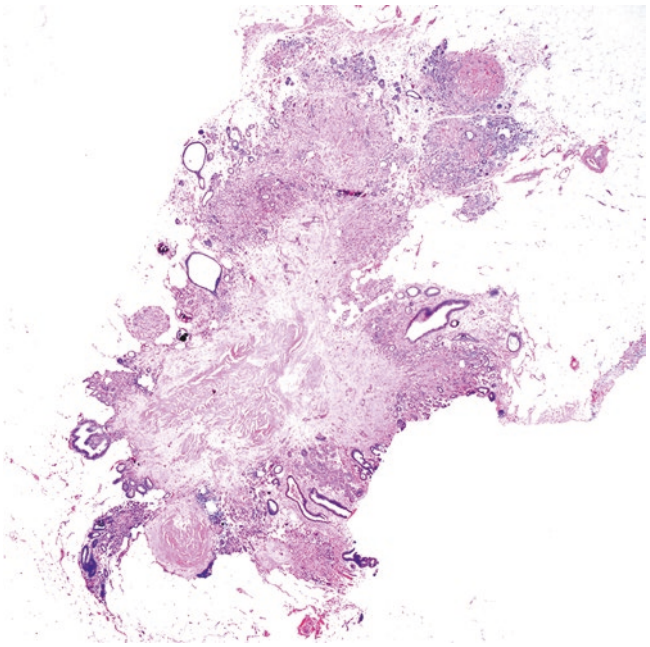

Fig. 2.5 Sclerotic stroma associated with this small glandular proliferation (radial scar)

the former, the difficulty in discerning from invasive tubular carcinoma is increased (Fig. 2.8).

Mitoses are absent in both and, as mentioned previously, the nuclear grade is low (cytologically bland). Subtle differences include the presence of apical snouts in some cases of invasive tubular carcinoma (Fig. 2.9) as well as the presence of proliferative (and non-proliferative) elements including squamous metaplasia (or eddies) comprising other parts of a radial scar (Fig. 2.10). Chronic inflammation may occasionally accompany a radial scar where this is not characteristically seen in cases of invasive tubular carcinoma. Often concomitant ductal carcinoma in situ (DCIS) is not seen in examples of invasive tubular carcinoma and when present is low grade. More commonly, rare foci of atypical ductal hyperplasia (sometimes morphologically bordering on low-grade DCIS) are the only finding (Fig. 2.11). As part of the low-grade breast neoplasia family, invasive tubular carcinomas are not uncommonly found together with other members such as columnar cell change/hyperplasia, flat epithelial atypia, atypical ductal hyperplasia/low-grade DCIS, and lobular lesions (Fig. 2.12). Identifying one or more of these entities in the surrounding breast tissue should lead the pathologist to consider invasive tubular carcinoma more strongly over radial scar in challenging cases. Lastly, some radial scars will have mildly cellular stroma around participating elements and/or squamous eddies that could raise concern for an ER-negative small glandular proliferations such as LGASC (Fig. 2.10). Unlike invasive tubular carcinomas, radial scars can be secondarily involved by atypical proliferations such as LCIS, DCIS, or even invasive carcinoma (Fig. 2.13). Invasive tubular carcinoma arising in a preexisting radial scar can occur but are exceptional. Needless to say, characteristic features are helpful in rendering the diagnosis only if they are *present* which is not always true in CNB specimens. Once the differential diagnosis of a small glandular proliferation has been narrowed to these two entities, the next step is to further characterize by IHC. A panel of myoepithelial markers (±ER) should suffice. It should be noted that focal attenuation or absence of myoepithelial staining may occur in some radial scars that are centrally more sclerotic (Fig. 2.14). ER can be helpful in some cases as it tends to stain diffusely but heterogeneously intense in a radial scar which is distinct from the diffuse and evenly strong immunoreactivity observed in invasive well-

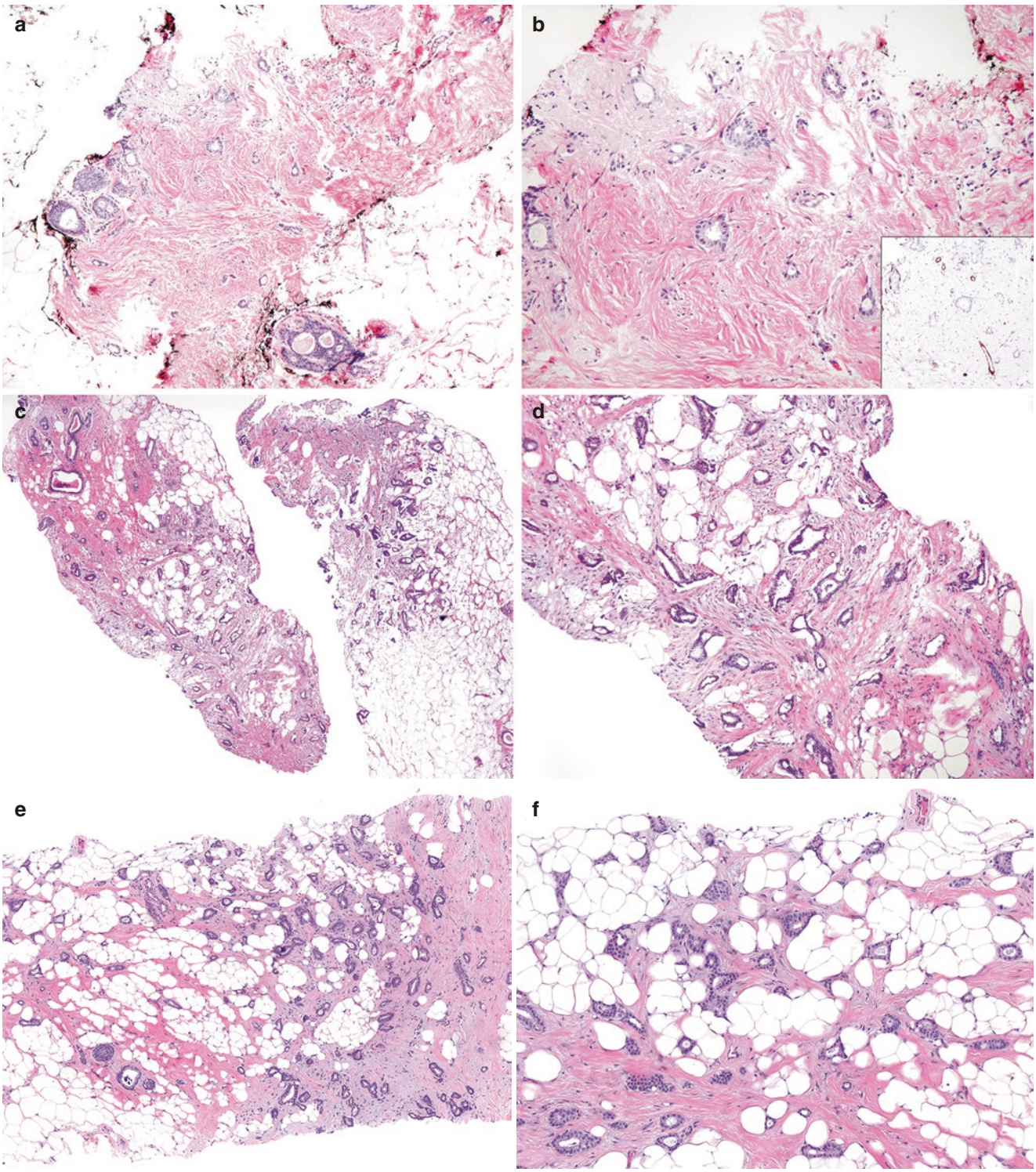

Fig. 2.6 Haphazard arrangement of glands in invasive tubular carcinoma. (**a**) Invasive tubular carcinoma with infiltrating growth pattern and nearby foci of atypical cribriform ductal hyperplasia. (**b**) Each neoplastic gland "points" in a different direction imparting an overall haphazard appearance. Glands are devoid of myoepithelial cells as demonstrated by a non-reactive SMM immunostain (*inset*). (**c**, **d**) Low- and high-power magnifications of another example of invasive tubular carcinoma demonstrating the disorganized arrangement of angulated or teardrop-shaped neoplastic glands in a CNB sample. (**e**, **f**) Another example of low- and high-power magnifications of invasive tubular carcinoma. Angulated and haphazardly arranged glands infiltrate through fibrous stroma and adipose tissue

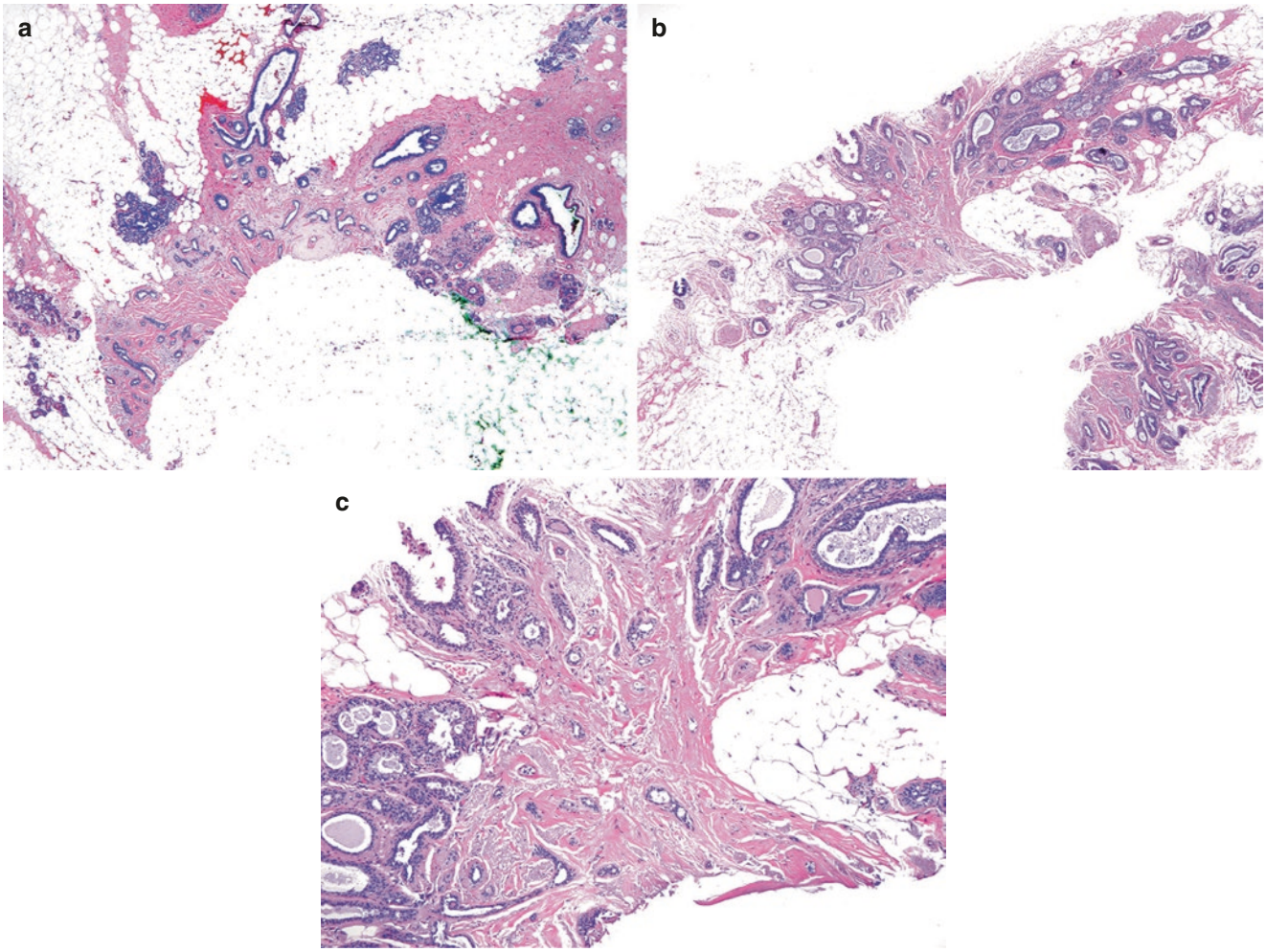

Fig. 2.7 (**a**–**c**) Examples of radial scars illustrating centrifugal glands emanating from a central nidus (not always sampled)

differentiated ductal carcinoma (Fig. 2.15). However, it should be emphasized here that ER for this diagnostic purpose should not be utilized in isolation.

Sclerosing adenosis is another ER-positive small glandular proliferation which is most often targeted due to its association with calcifications but sometimes can become confluent and mass forming (adenosis tumor or nodular adenosis) (Fig. 2.16). Sclerosing adenosis is a lobulocentric proliferation which may be difficult to appreciate in CNB material and largely depends on the degree of sclerosis in a given example (Fig. 2.17). If the sclerosing process is fairly uniform, the expansion of the intralobular stroma will lead to a nodular configuration (Fig. 2.18). In these instances, distinguishing from invasive examples of small glandular proliferations is easy. However, if the sclerosis is uneven, then the affected lobular glands will become compressed, distorted, and slit-like, which in turn can appear pseudoinvasive (Fig. 2.19). The latter scenario is considerably treacherous in the CNB setting. Sclerosing adenosis can exhibit apocrine change; however, if cytologic atypia is also evident, a diagnosis of atypical apocrine adenosis should be considered (Fig. 2.20). Other types of differentiation such as squamous, mucin, and neuroendocrine are not seen in typical sclerosing adenosis, and the finding of such traits should alert the pathologist to consider other diagnostic possibilities.

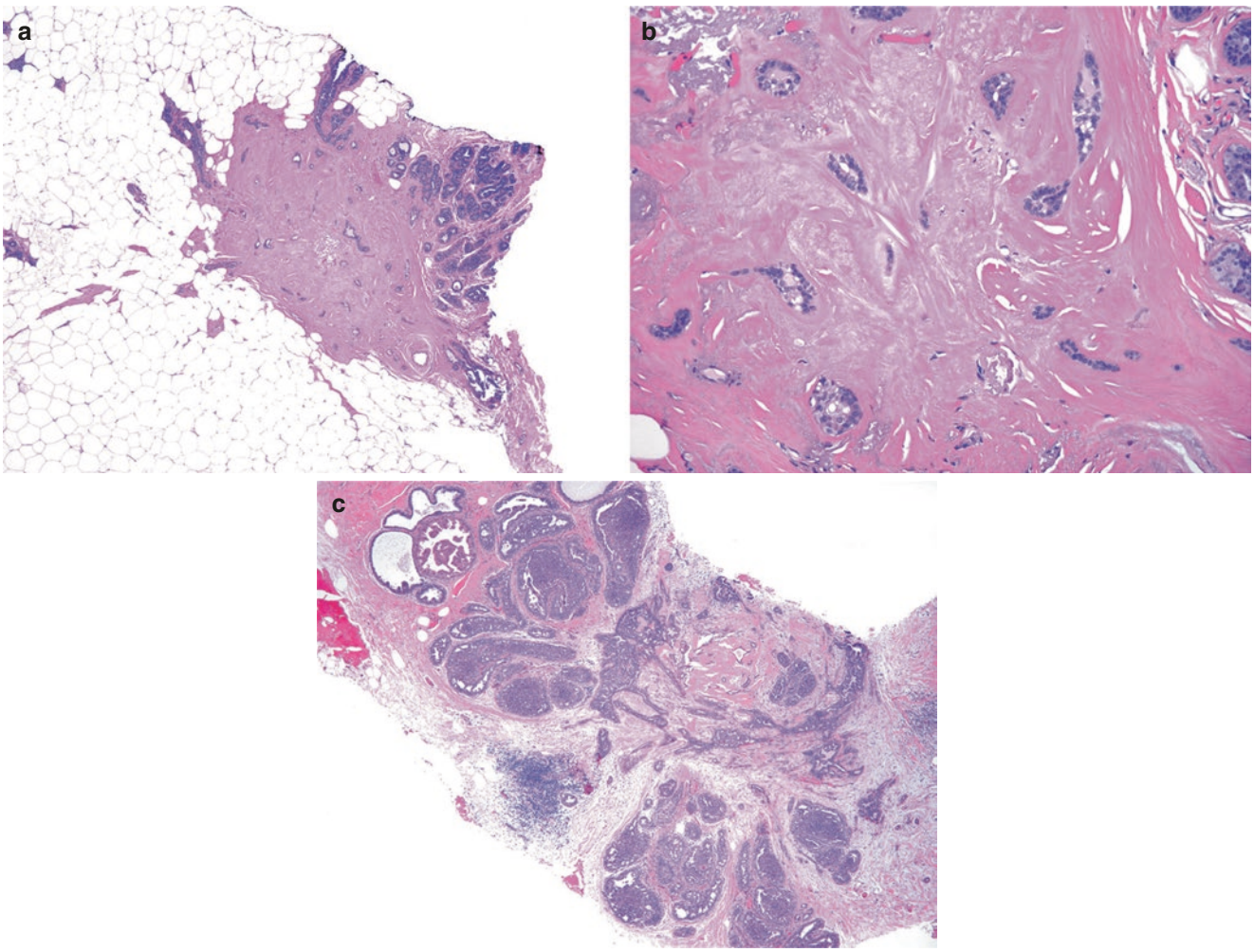

Fig. 2.8 Disorganized glands in the nidus of a radial scar. (**a**) Significant central sclerosis of this radial scar leads to compression and disarray of lesional glands imparting a haphazard appearance. (**b**) This increased disorganization of glands imparts a pseudoinvasive appearance concerning for malignancy. (**c**) Low magnification of a radial scar. Note the angulated and compressed glands in the sclerotic nidus of this lesion

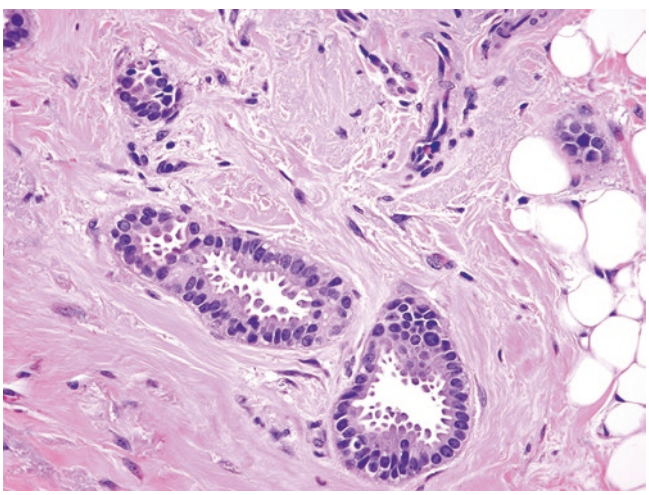

Fig. 2.9 Luminal cytoplasmic snouts of neoplastic glands constituting this invasive tubular carcinoma

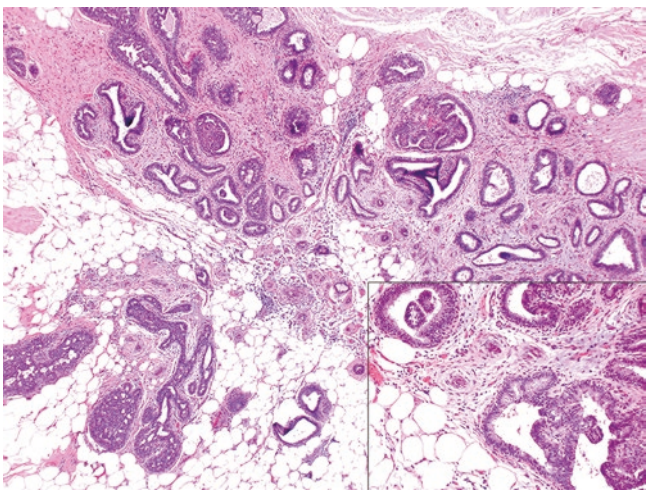

Fig. 2.10 Radial scar with prominent squamous eddies in the stroma. These structures should not be mistaken for low-grade adenosquamous carcinoma (*inset*)

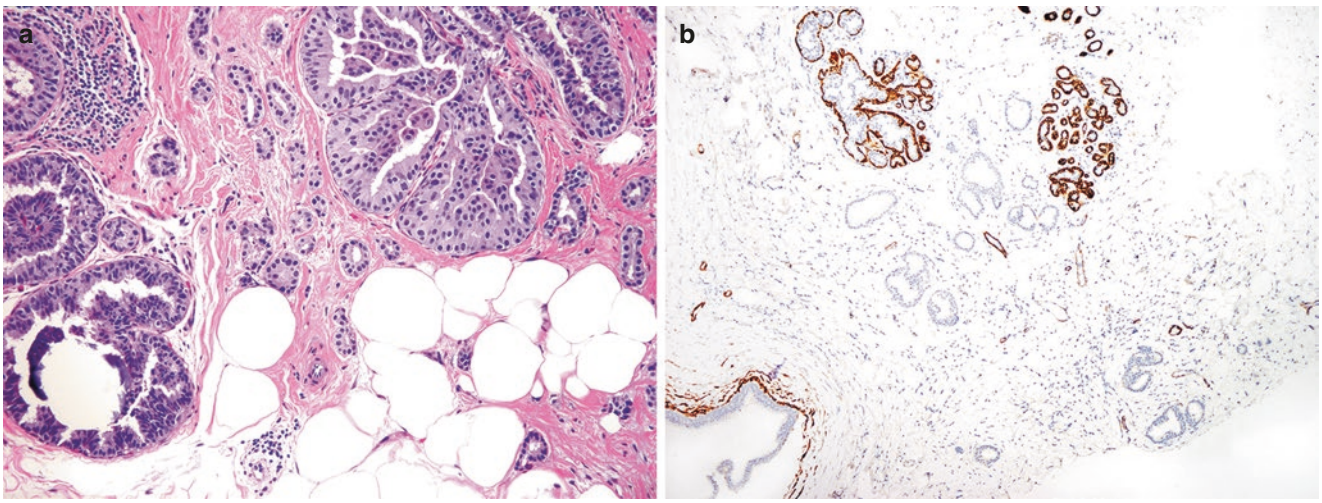

Fig. 2.11 Atypical ductal hyperplasia/low-grade ductal DCIS adjacent to invasive tubular carcinoma. (**a**) Foci of atypical ductal hyperplasia/low-grade DCIS flanking invasive tubular carcinoma. (**b**) Myoepithelial cells are absent around neoplastic glands, as seen in this SMM immunostain, thus confirming the presence of invasive carcinoma

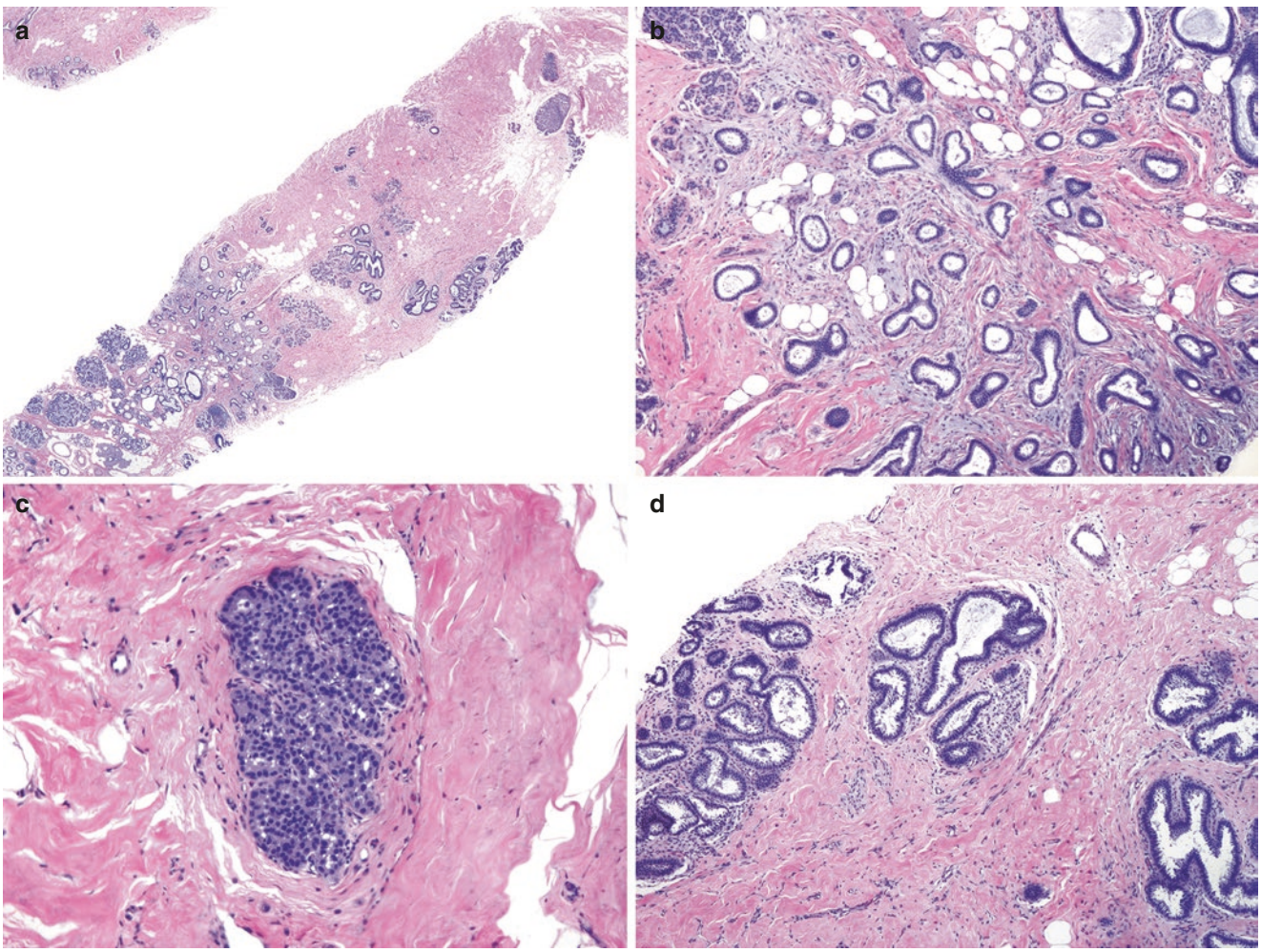

Fig. 2.12 Core biopsy showing all three components of the columnar cell triad. (**a**) Low-power magnification of a core biopsy shows a small glandular proliferation (*lower left*) amid columnar cell change and expansion of several terminal duct lobular units (TDLUs). (**b**) High-power view reveals that the small glandular proliferation represents invasive tubular carcinoma seen here as angulated glands arranged haphazardly in a cellular desmoplastic stroma. (**c**) Higher magnification reveals that the expansion of TDLUs is due to involvement by atypical lobular hyperplasia. (**d**) Columnar cell change was associated with calcifications (not shown) and represented the biopsy target in this case

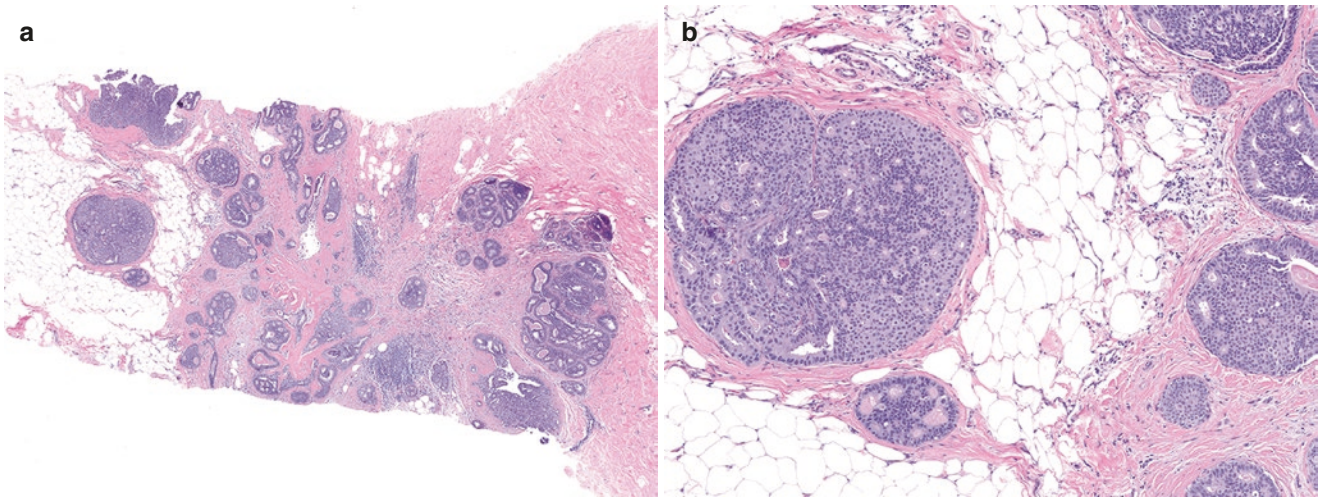

Fig. 2.13 (**a**) Radial scar partly involved by DCIS. (**b**) Higher view shows DCIS to be solid and cribriform types with intermediate nuclear grade and minute calcifications

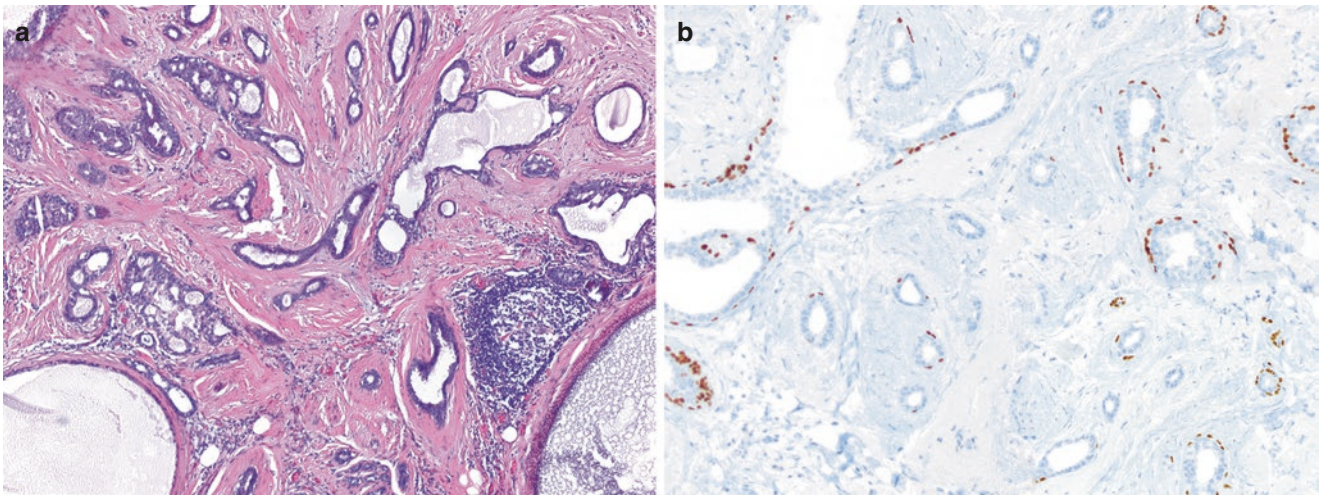

Fig. 2.14 Radial scar with attenuated/focally absent myoepithelial immunoreactivity. (**a**) H&E image of a radial scar. (**b**) Corresponding p63 immunostain shows complete, discontinuous, and focally absent reactivity of investing myoepithelium in participating benign glands

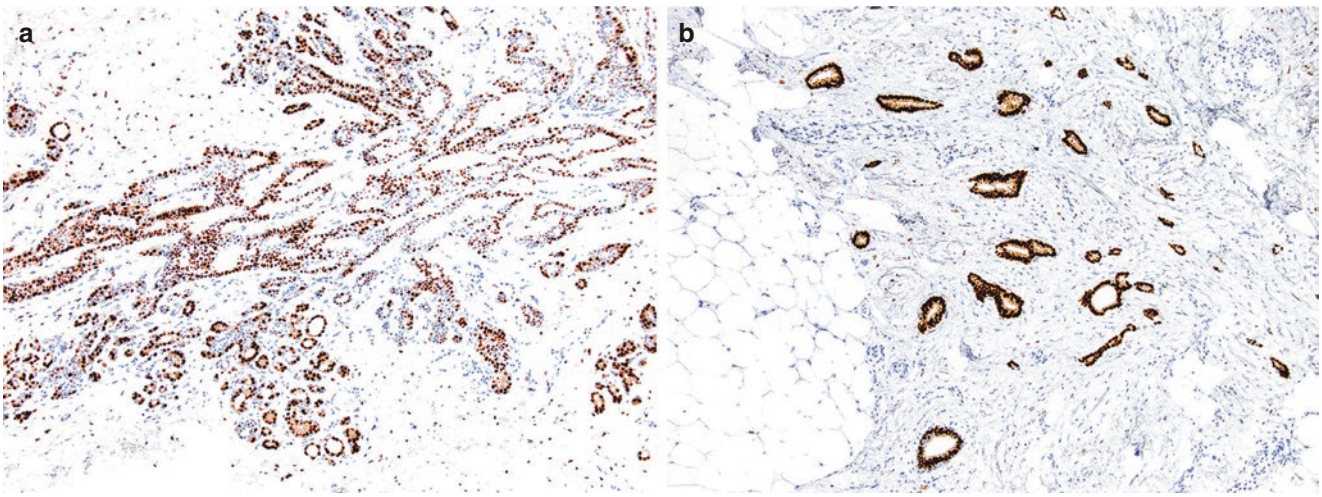

Fig. 2.15 Comparison of ER staining patterns in radial scar versus invasive well-differentiated ductal carcinoma. (**a**) Positivity is diffuse but heterogeneously intense in this radial scar. (**b**) In contrast, every neoplastic cell of this invasive well-differentiated ductal carcinoma demonstrates equally strong immunoreactivity for this stain

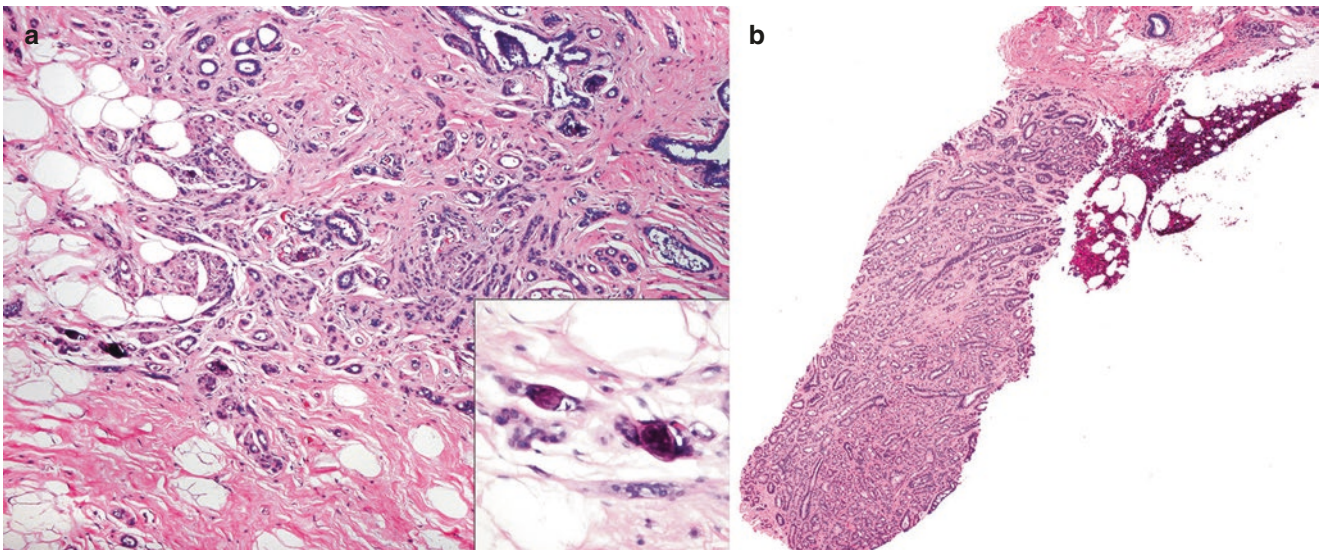

Fig. 2.16 Sclerosing adenosis. (**a**) Calcifications (*inset*) were detected by screening mammogram and biopsy revealed their association with sclerosing adenosis. (**b**) Confluent examples of sclerosing adenosis can present as a breast mass such as this one sampled by core needle biopsy

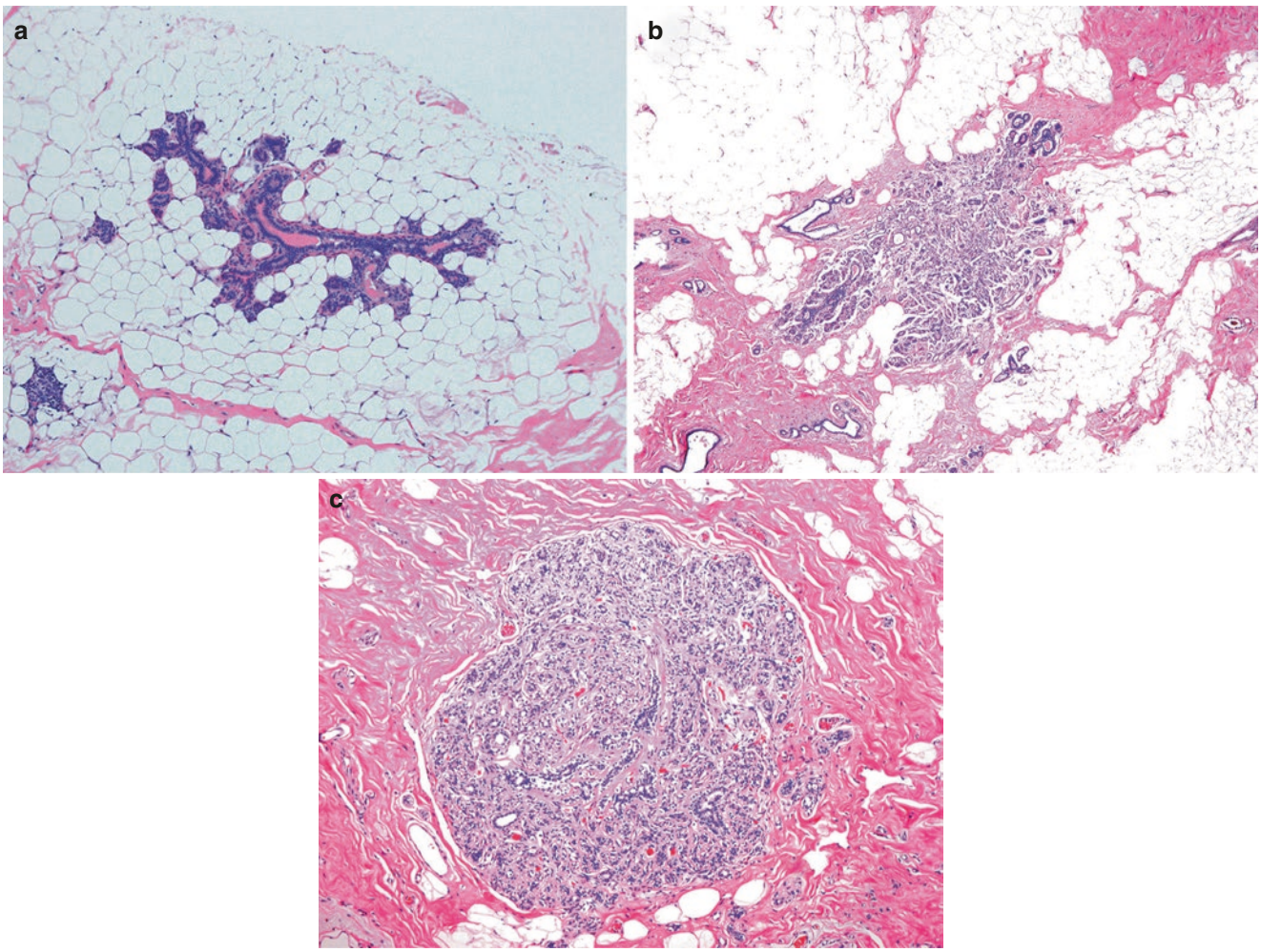

Fig. 2.17 Sclerosing adenosis. (**a**) Image of a benign terminal duct lobular unit (TDLU). (**b**) A TDLU involved by sclerosing adenosis with uneven compression of lobular glands by intralobular stromal sclerosis. (**c**) Another TDLU with uniform involvement by sclerosing adenosis resulting in a nodular appearance

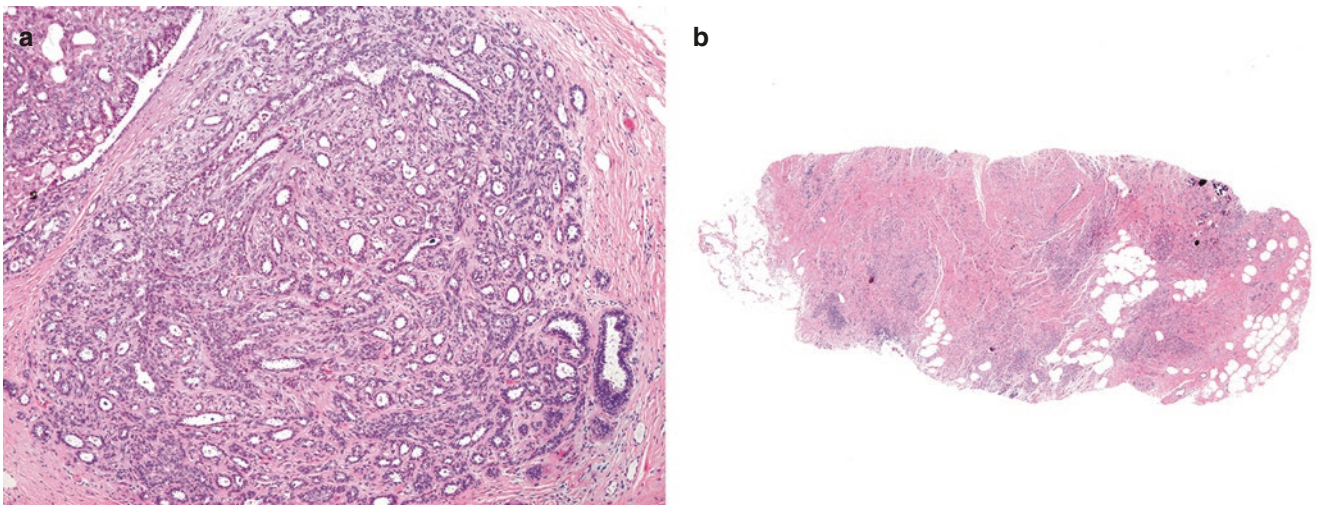

Fig. 2.18 Nodular configuration of sclerosing adenosis. (**a**) Compressed glands of sclerosing adenosis are arranged with similar directionality akin to a "school of fish." (**b**) Multifocal sclerosing adenosis gives rise to a multinodular appearance on low-power view. Associated calcifications are also present

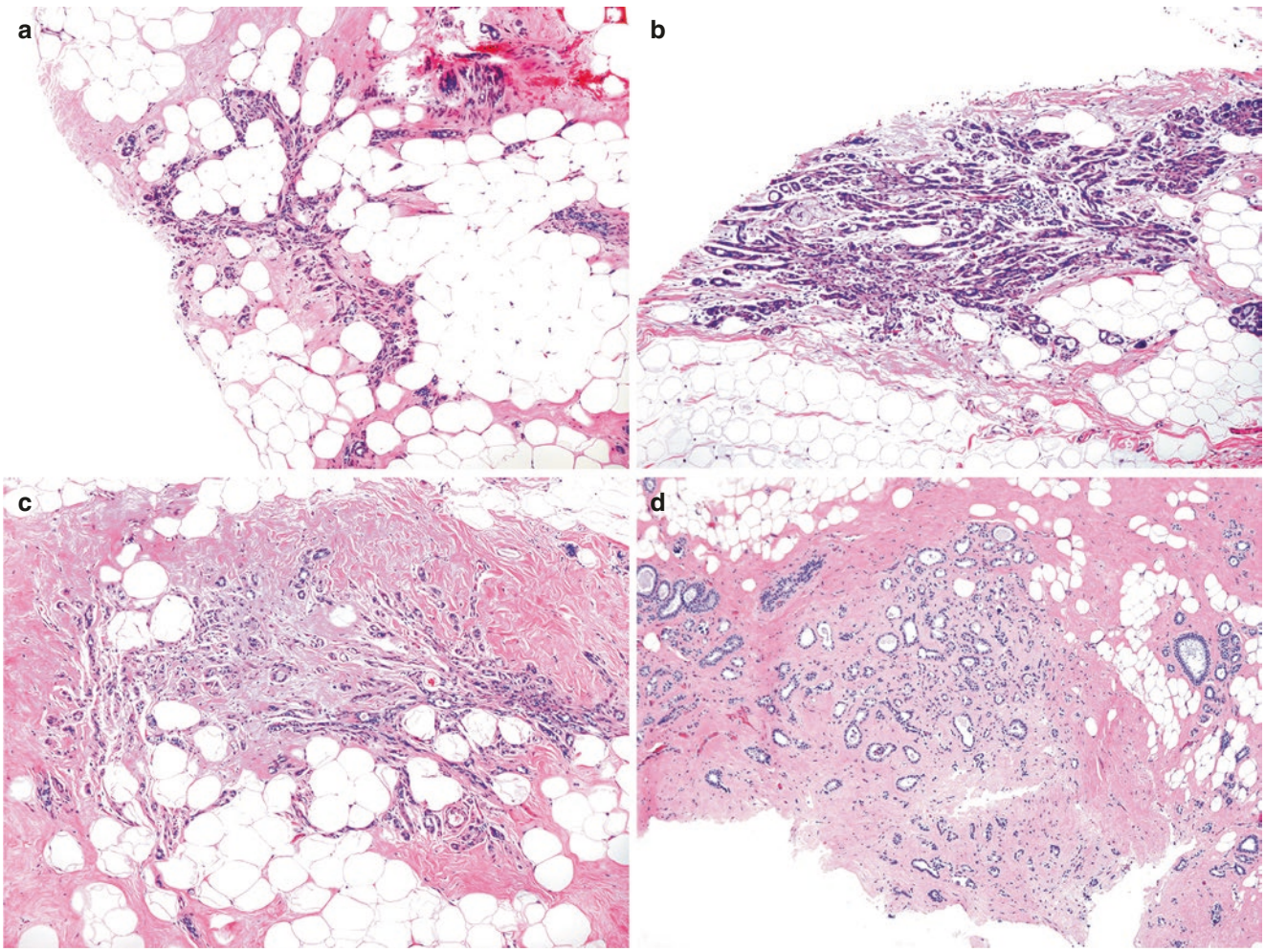

Fig. 2.19 Sclerosing adenosis. (**a**–**c**) When intralobular stromal fibrosis is significant, glands of sclerosing adenosis become compressed, slit-like, and distorted. The lobulocentric appearance is no longer apparent, and in some cases participating glands impart a pseudoinfiltrative appearance that can be confused with invasive carcinoma, a diagnostic pitfall in CNBs. (**d**, **e**) In other instances, the degree of sclerosis is less but the resulting rounder glands can also mimic invasive well-differentiated ductal carcinoma

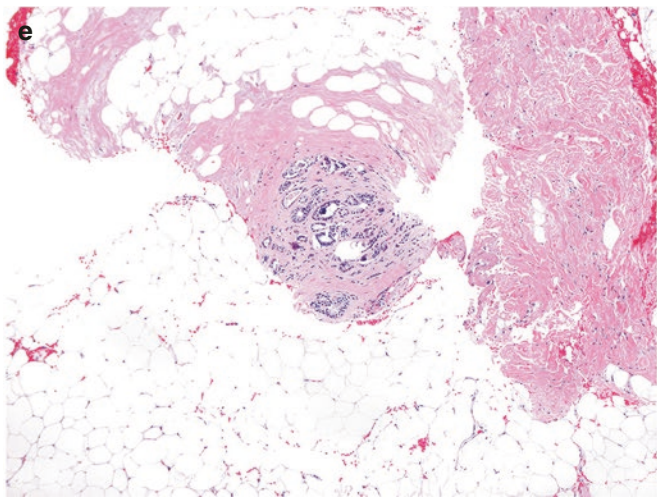

Fig. 2.19 (continued)

In addition, sclerosing adenosis is not uncommonly occupied by a second proliferation, particularly atypical lobular hyperplasia/LCIS and less frequently DCIS. The cytologic atypia of these secondary proliferations gives rise to the appearance of an atypical infiltrative lesion, worrisome for invasive carcinoma. Confirmation of the diagnosis should be performed by IHC for myoepithelial markers and additionally E-cadherin if LCIS is suspected (Fig. 2.21). An ER immunohistochemical stain can be useful as positivity is heterogeneous in appearance in sclerosing adenosis as concomitant myoepithelial hyperplasia is non-reactive, whereas invasive well-differentiated ductal carcinoma is strongly and diffusely immunoreactive (Fig. 2.22). As in the distinction between radial scar and invasive well-differentiated ductal carcinoma, ER utilized in this diagnostic setting should not be performed in isolation.

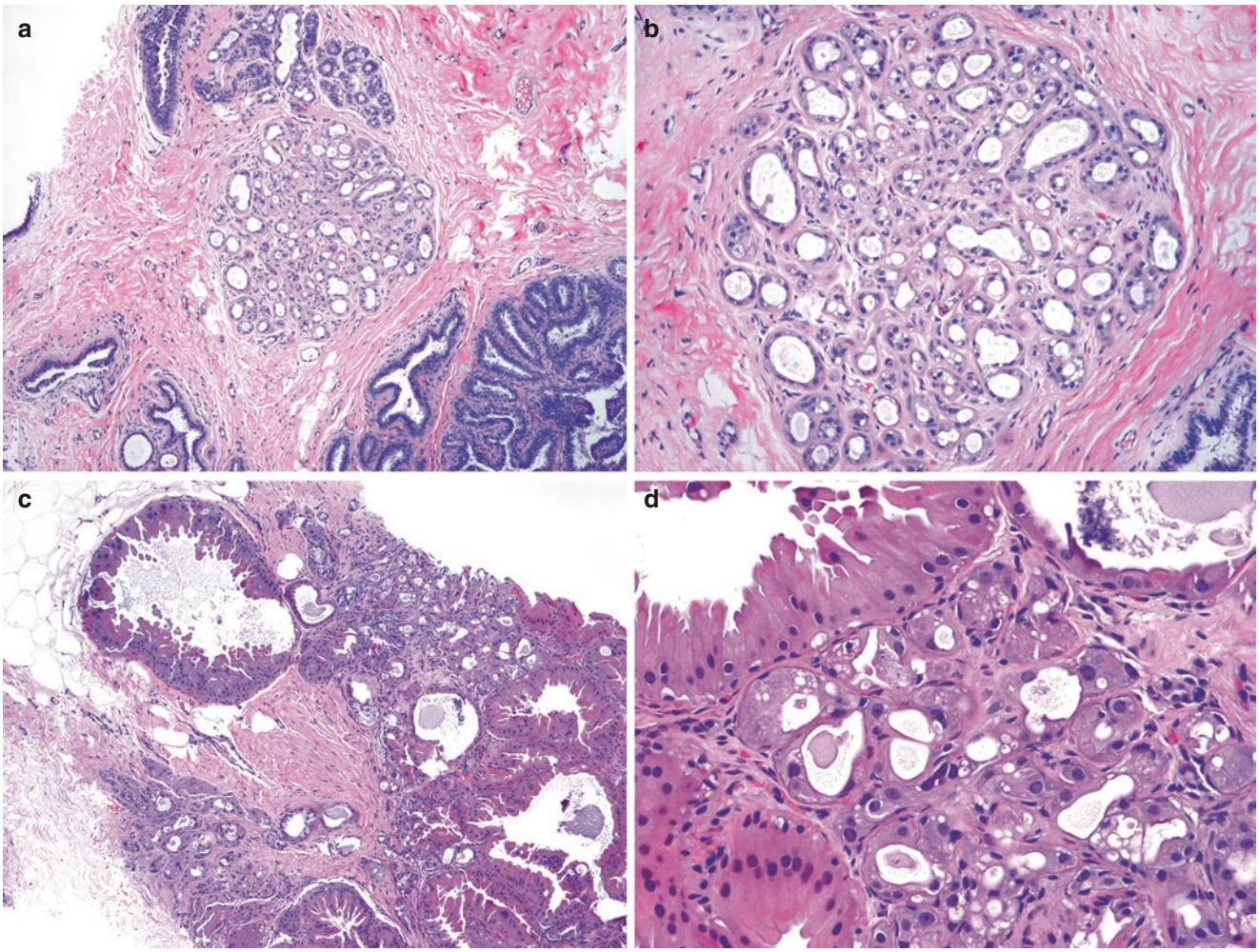

Fig. 2.20 Usual and atypical apocrine adenosis. (**a**, **b**) Focus of usual apocrine adenosis comprises cells with eosinophilic cytoplasm. Cytologic atypia is not appreciated. (**c**) Usual cystic apocrine papillary hyperplasia and atypical apocrine adenosis. (**d**) Usual cystic apocrine papillary hyperplasia (*upper left*) is composed of cells with bland nuclei and eosinophilic cytoplasm. In contrast, cells of this exceptional case of atypical apocrine adenosis (*bottom right*) show markedly exaggerated, degenerative appearing nuclear atypia and cytoplasmic vacuolization. However, no mitoses are present

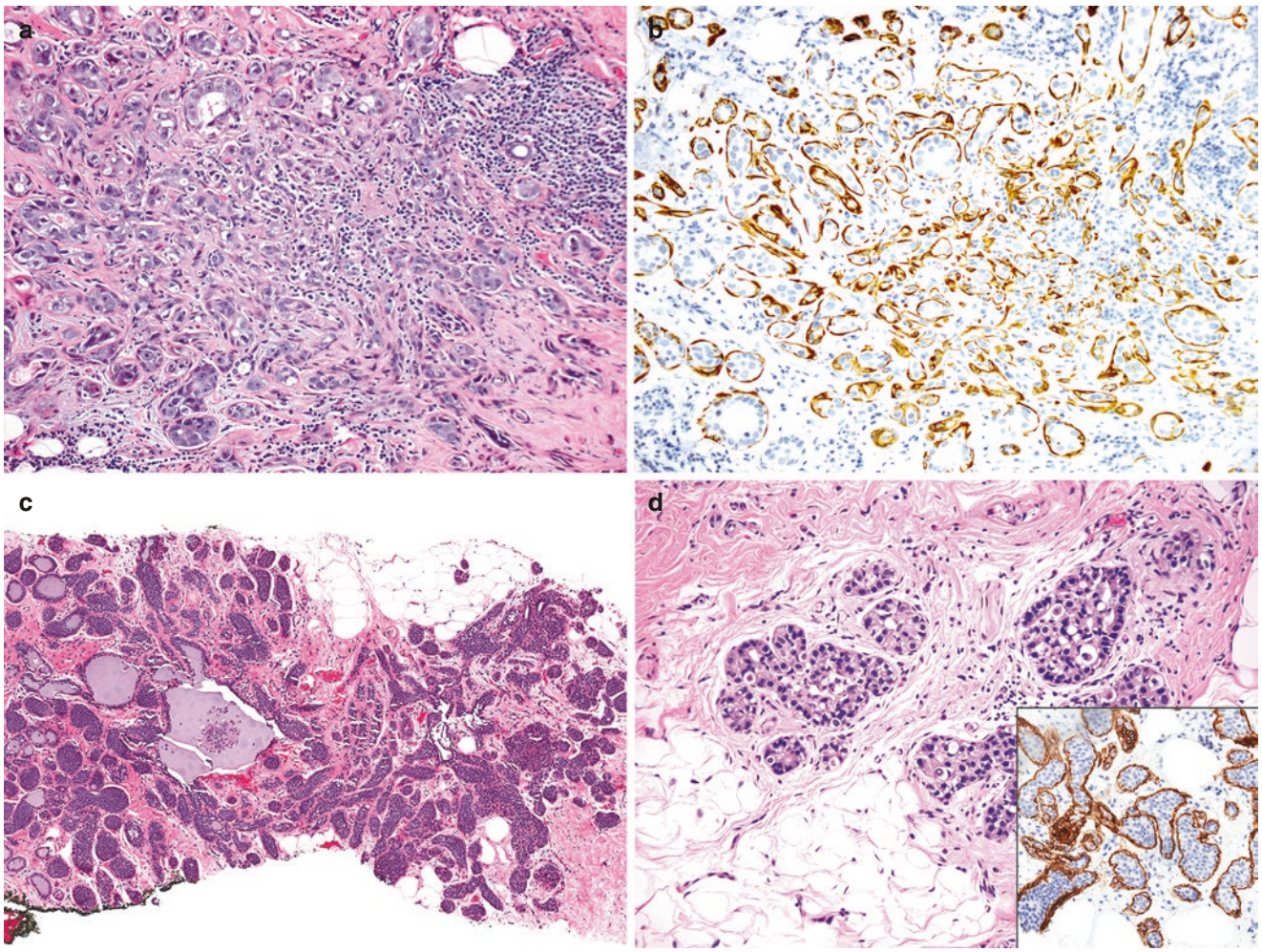

Fig. 2.21 In situ carcinoma secondarily involving sclerosing adenosis. (**a**) Ductal carcinoma in situ (DCIS) involving sclerosing adenosis. This example can be easily misdiagnosed as invasive ductal carcinoma. (**b**) SMM immunostain confirms its noninvasive nature. (**c**) Lobular carcinoma in situ (LCIS) secondarily involving sclerosing adenosis. (**d**) Morphologically similar LCIS is present in adjacent lobules. E-cadherin immunostain confirms the lobular nature of LCIS (*inset*)

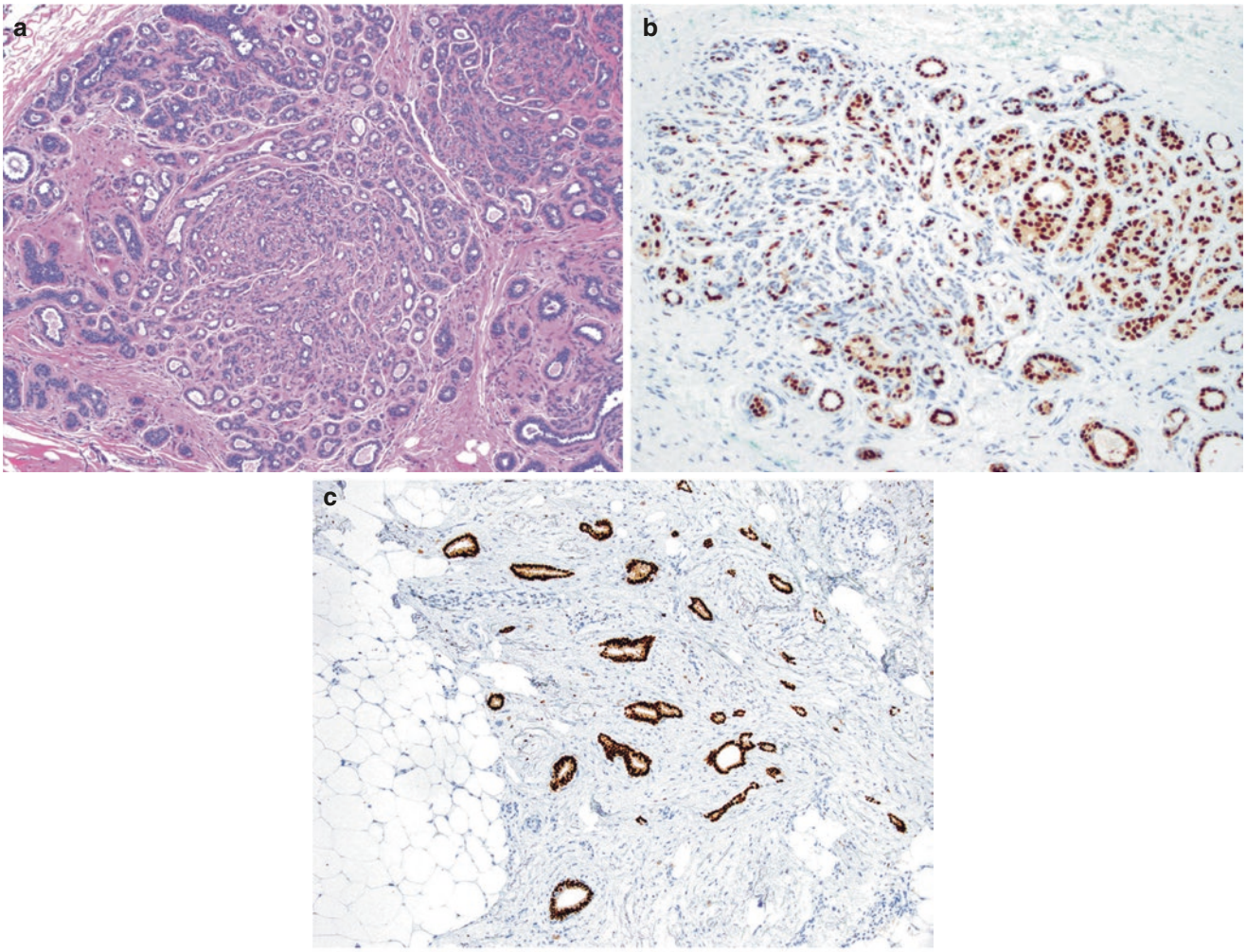

Fig. 2.22 Comparison of ER staining patterns in sclerosing adenosis and invasive well-differentiated ductal carcinoma. (**a**) Sclerosing adenosis comprises a proliferation of lobular glands consisting of epithelium and myoepithelium. (**b**) Corresponding ER immunostain only stains the epithelium, thus imparting a heterogeneous staining pattern as compared to (**c**) invasive well-differentiated ductal carcinoma composed exclusively of neoplastic epithelial cells which is strongly and diffusely positive

ER-Negative (Triple-Negative) Small Glandular Proliferations

Among ER-negative or triple-negative small glandular proliferations, MGA is most easily confused with invasive tubular carcinoma because the latter, on occasion, forms round (less-angulated) neoplastic glands (Figs. 2.2b and 2.23). Clinically, both entities can form a breast mass and additionally invasive tubular carcinoma is more frequently associated with calcifications. In CNB specimens, the number of lesional glands to evaluate is limited, and therefore the full range of gland shape and size is difficult to assess. Also, the pathognomonic finding of bright, dense eosinophilic luminal secretions is typically not present in every lesional gland and therefore can be absent or infrequent in core biopsies simply due to sampling error (Fig. 2.24). Both invasive tubular carcinoma and MGA can grow in a highly infiltrative manner and furthermore are not invested in myoepithelium. The unwary pathologist may initially sign out a case of MGA as invasive tubular carcinoma after confirming the absence of myoepithelium by IHC. Hopefully, these will be considered "near misses" (and not misdiagnoses) when the biomarkers (ER, PR) stains are found to be negative, thus alerting the pathologist that the diagnosis should be reconsidered since the majority of invasive, well-differentiated ductal carcinomas are ER-positive and variably PR-positive. Triple negativity is also seen in LGASC which in CNBs can be misconstrued as invasive ductal carcinoma (IDC) or radial scar. LGASC resembles IDC due to its invasive glandular growth pattern, mild cytologic atypia, and cellular (desmoplastic-appearing) stroma (Fig. 2.25). However, the presence of squamous differentiation should be a clue that the lesion in question is not a garden variety example of IDC, as among breast malignancies, this feature is largely limited

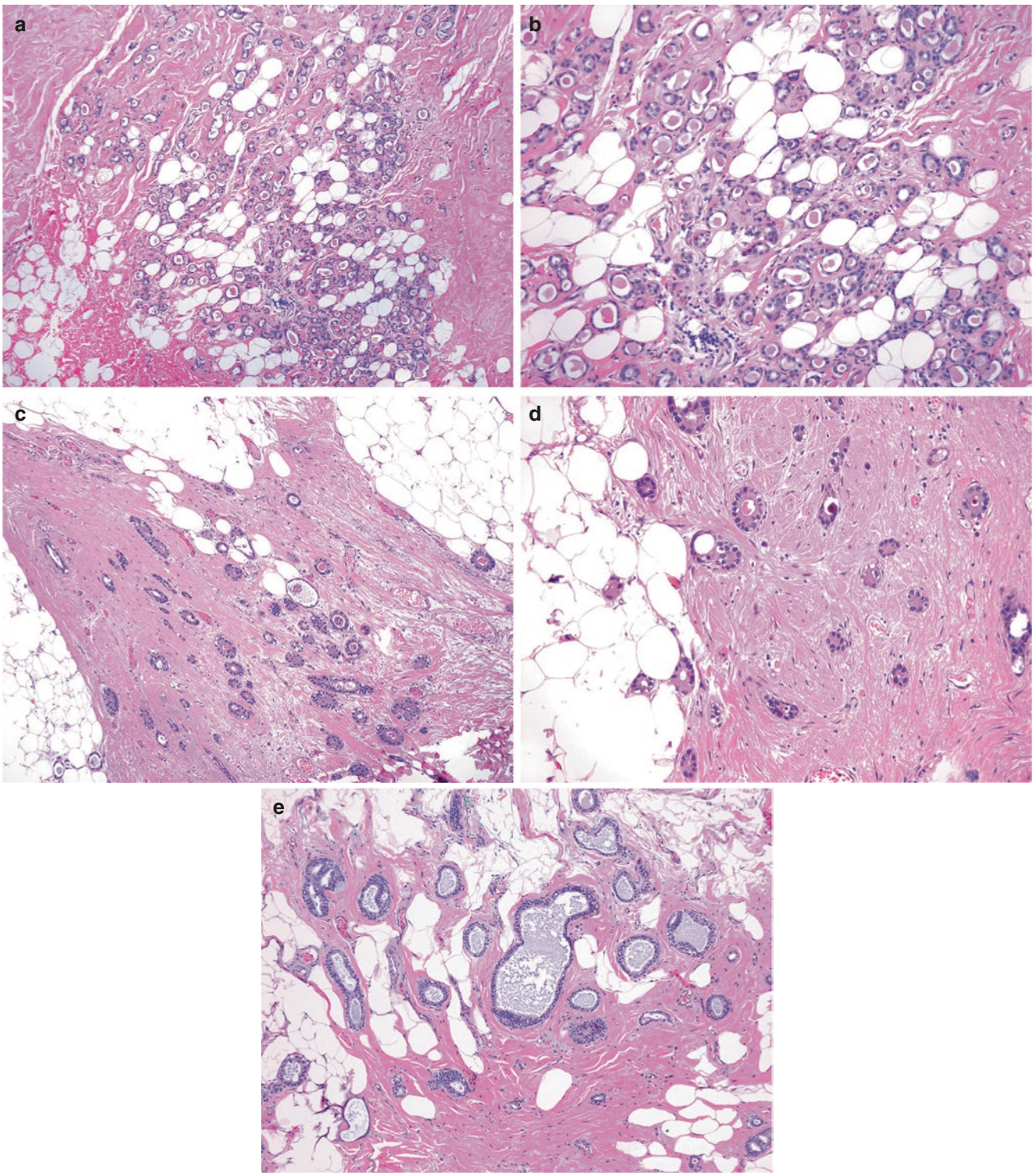

Fig. 2.23 Small glandular proliferations comprising round glands with eosinophilic luminal secretions. (**a**) A focus of MGA with round glands infiltrating through mammary stroma and adipose tissue. (**b**) The round cytologically bland glands contain bright eosinophilic luminal secretions. (**c**) Invasive tubular carcinoma predominantly composed of round glands. (**d**) Rarely, eosinophilic luminal secretions can be seen, thus mimicking MGA. (**e**) Another example of invasive tubular carcinoma with particularly rounded neoplastic glands

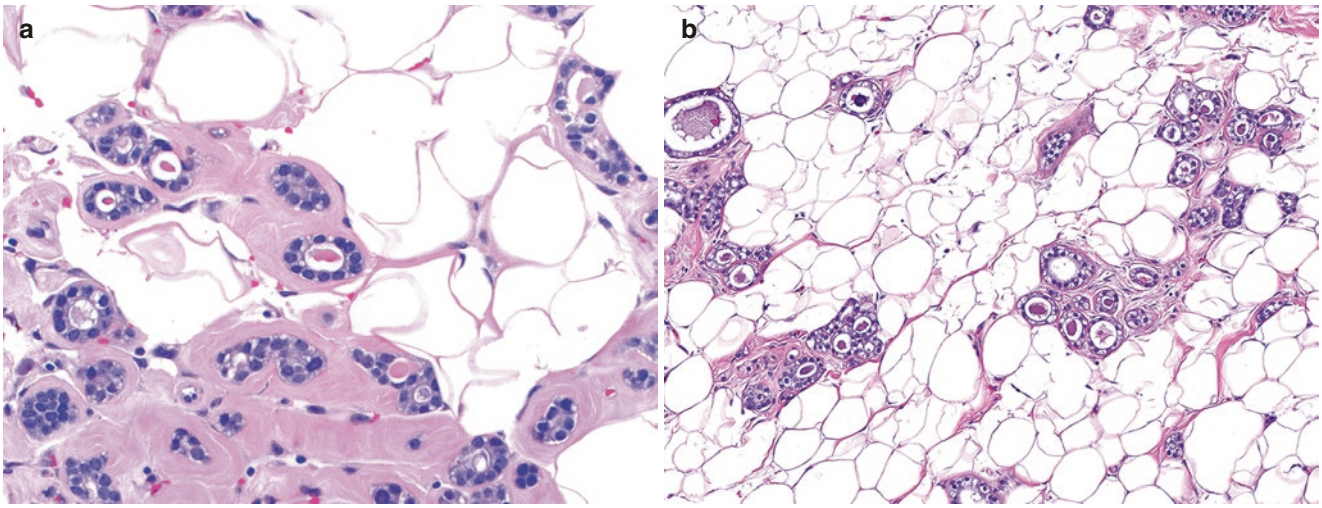

Fig. 2.24 Luminal secretions in microglandular adenosis. (**a**, **b**) Bright eosinophilic secretions within glandular lumina of microglandular adenosis

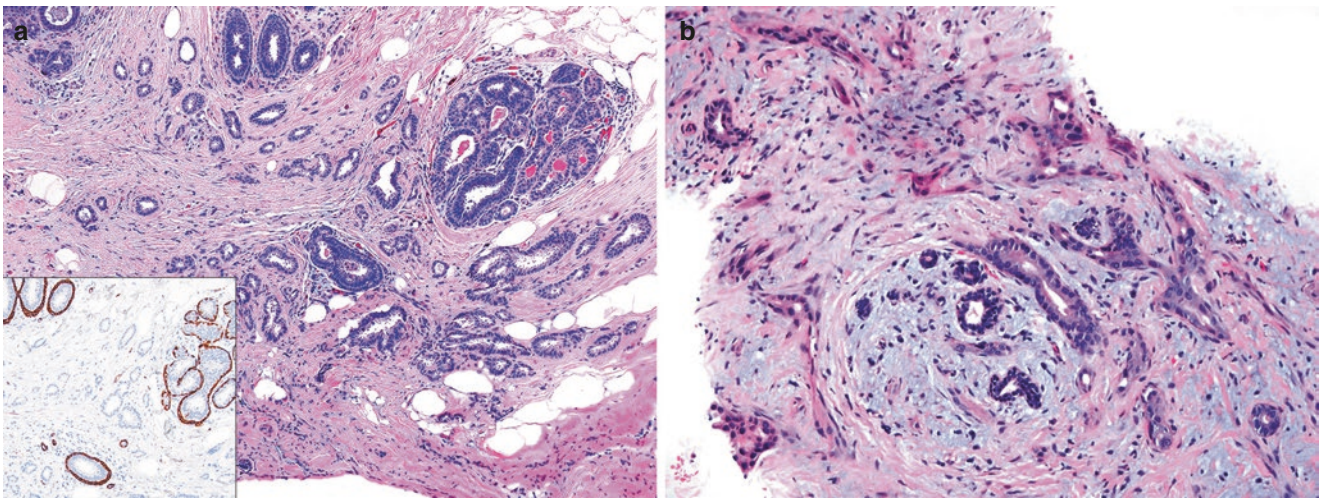

Fig. 2.25 Morphologic similarities of invasive tubular carcinoma and low-grade adenosquamous carcinoma (LGASC). (**a**) Invasive tubular carcinoma infiltrating around and between benign ducts and terminal duct lobular units (TDLUs). The glands are angulated and growing in cellular, desmoplastic stroma. The glands lack myoepithelial cells as seen in this SMM immunostain (*inset*). (**b**) Similarly angulated neoplastic glands of LGASC infiltrating around benign ducts in cellular stroma, however, additionally exhibit squamous differentiation on closer inspection

to metaplastic carcinomas. The degree of squamous differentiation varies not only from gland to gland in a given case of LGASC but also among different examples of this entity (Figs. 2.25b and 2.26). A diagnosis of "invasive ductal carcinoma with squamous features/differentiation" should always be re-evaluated for an alternate diagnosis. Branching glands can be seen in LGASC as is true in invasive well-differentiated ductal carcinoma (non-tubular type). Chronic inflammation is often present as peripherally located aggregates in LGASC whereas invasive tubular carcinoma typically shows no associated inflammation (Figs. 2.26c and 2.27). Both entities can arise in hyalinized stroma. Radial scars and LGASCs share morphologic similarities including centrifugal growth (Fig. 2.28) and squamous differentiation (in the form of eddies in occasional radial scars).

Syringomatous tumor of the nipple is the rarest of all small glandular proliferations and the only other one besides LGASC that demonstrates prominent squamous differentiation. While there is some debate as to the possible kinship of these two lesions, there are definite histologic differences which help discern them. For instance, the variability of glands in their shape, size, and complexity is greater in LGASC (Figs. 2.25b and 2.26) than syringomatous tumor. In the latter, the neoplastic glands are seen as either tadpole-

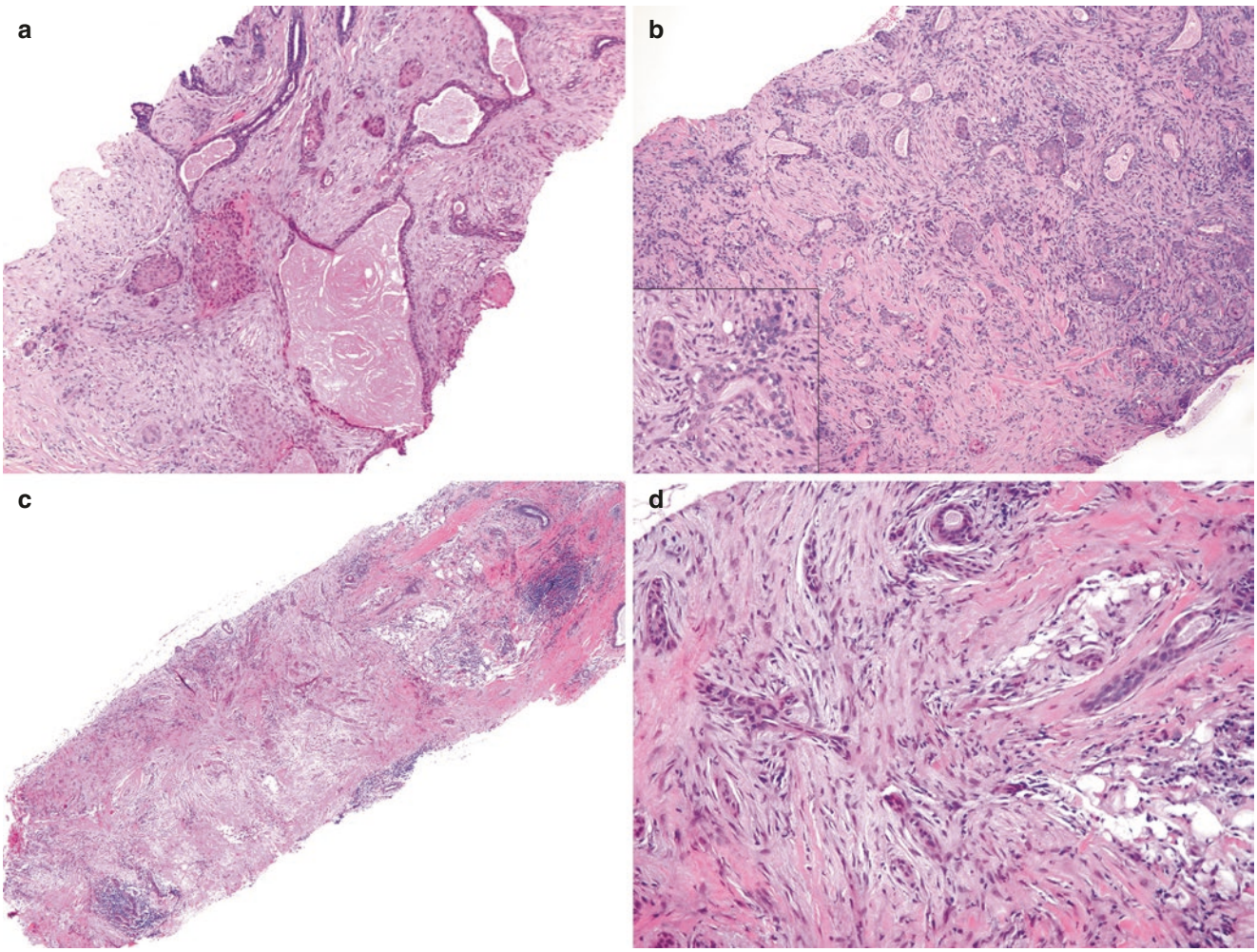

Fig. 2.26 Varying degrees of squamous differentiation and size/shape of glands in low-grade adenosquamous carcinoma (LGASC). (**a**) An example with marked squamous differentiation and luminal keratin formation. (**b**) Another case showing a moderate degree of squamous differentiation. A high-power view of a neoplastic gland (*inset*). (**c**, **d**) Neoplastic glands of this LGASC are more compressed and squamous differentiation is less conspicuous. Note characteristic lymphoid aggregates in (**c**)

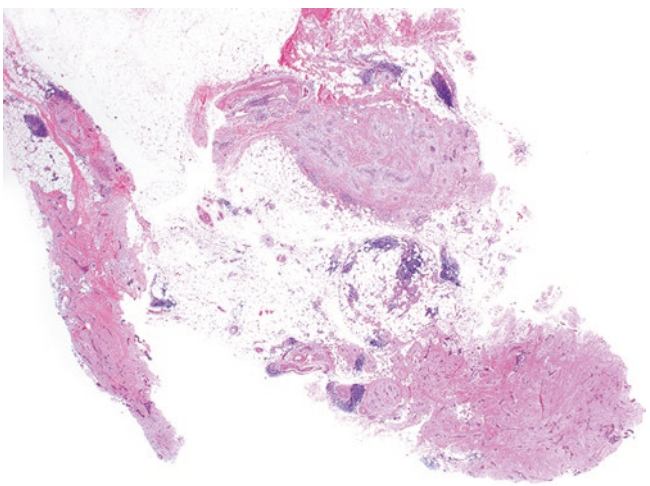

Fig. 2.27 Chronic inflammation in low-grade adenosquamous carcinoma (LGASC). Low-power view of this CNB shows peripherally located lymphoid aggregates characteristic of LGASC

shaped ductules with comma-like tails, stratified cysts (with or without luminal keratin), or small cords or nests of cells. These structures are either single or double layered (Fig. 2.29).

While LGASC has been rarely reported to arise in the nipple, the vast majority of syringomatous tumors come to clinical attention in this location. Both entities are diffusely infiltrative with some glands additionally showing periglandular stromal cellularity (Fig. 2.30). By IHC, these entities appear to have similarly inconsistent staining patterns with myoepithelial markers and frequently are ER, PR, and HER2-negative. Chronic inflammatory infiltrates can be seen in both; however, in syringomatous tumor, they occur in association with foreign body giant cells secondary to a ruptured squamous cyst (Fig. 2.31). As mentioned previously, lymphoid aggregates can be appreciated at the periphery of LGASCs. Common features and discriminating IHC stains among small glandular proliferations are provided in Figs. 2.32 and 2.33.

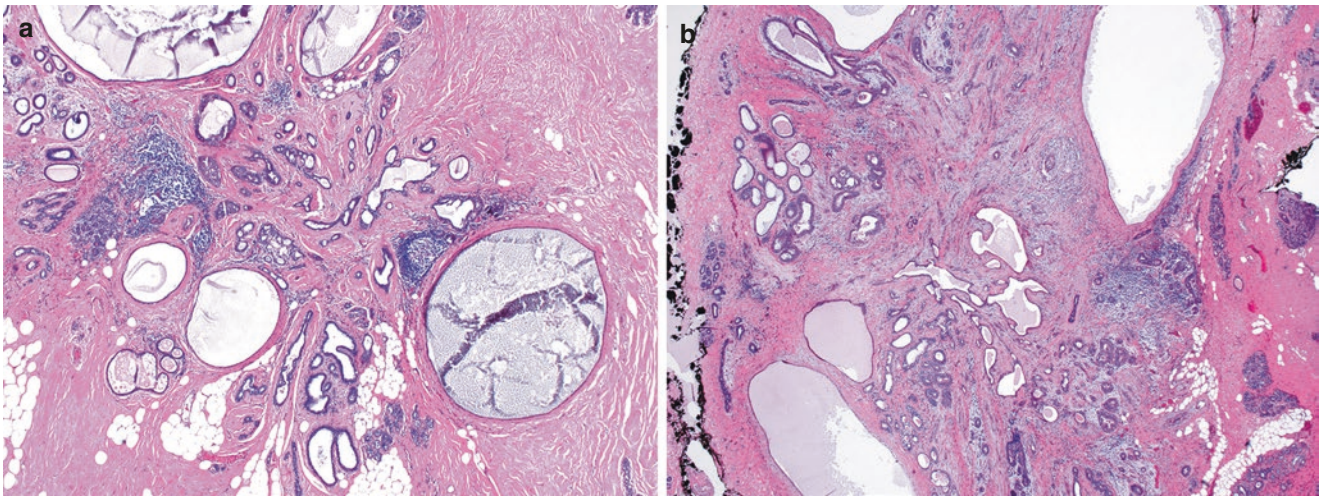

Fig. 2.28 Radial growth pattern of radial scar and low-grade adenosquamous carcinoma (LGASC). (**a**) Radial scar and (**b**) LGASC which are virtually identical at low-power magnification illustrates an important diagnostic pitfall

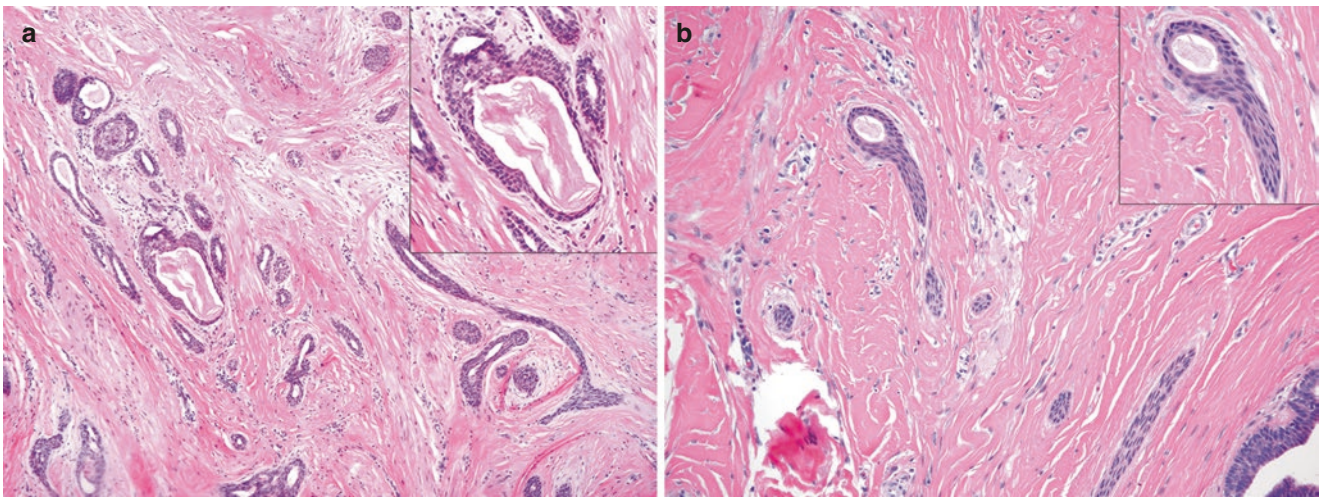

Fig. 2.29 Glands of syringomatous tumor. (**a**, **b**) Lesional glands are typically seen in the form of tadpole-shaped ductules, stratified cysts, or small cords/nests of cells

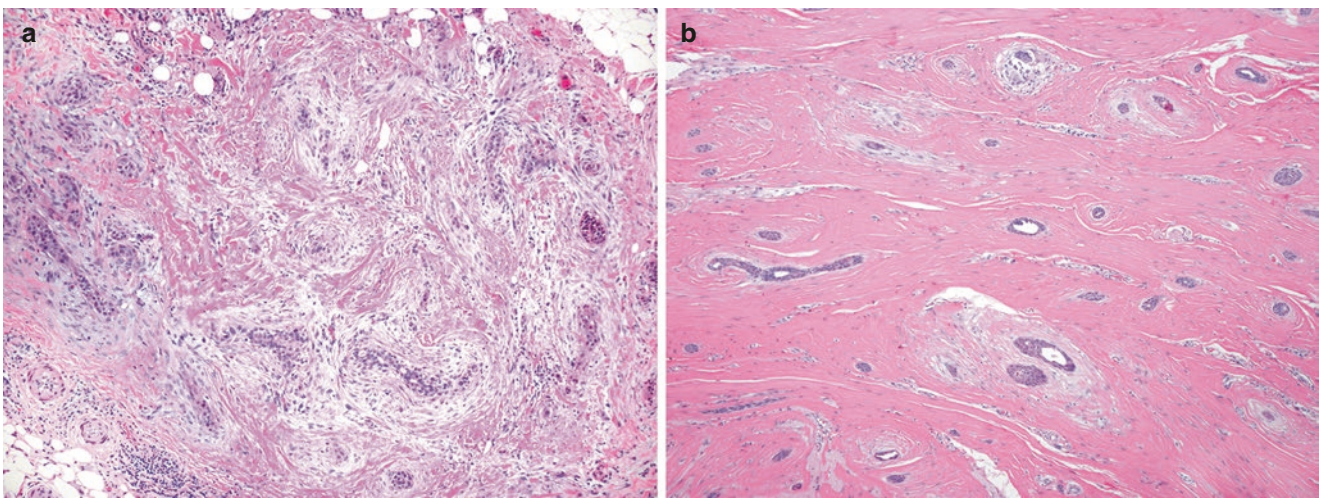

Fig. 2.30 Stromal cellularity in low-grade adenosquamous carcinoma (LGASC) and syringomatous tumor. (**a**) This example of LGASC with notable periductal stromal cellularity. (**b**) Similar stromal cellularity can be seen around lesional glands of syringomatous tumor

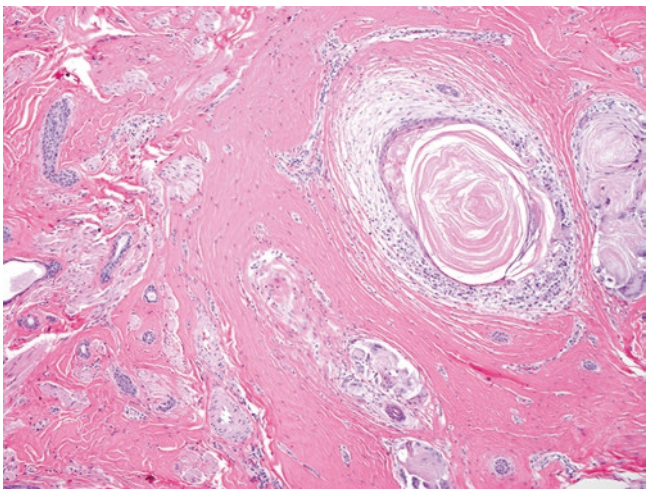

Fig. 2.31 Chronic inflammation in syringomatous tumor. Chronic inflammation and multinucleated giant cells can be seen in syringomatous tumor secondary to a ruptured squamous cyst

IHC STAIN	MGA	IBC-NST	SCLEROSING ADENOSIS
MYOEPITHELIAL	-	-	+
BASEMENT MEMBRANE	+	-	+
HORMONE RECEPTORS	-	+	+* *heterogenously
S100 PROTEIN	+	-	+ (myoepithelium)

Fig. 2.33 Immunohistochemical profiles of small glandular proliferations in the breast

Fig. 2.32 Common morphologic features seen in small glandular proliferations in the breast

MORPHOLOGIC FEATURES OF SMALL GLANDULAR PROLIFERATIONS IN THE BREAST

ARRANGEMENT OF GLANDS

- HAPHAZARD (INVASIVE TUBULAR CARCINOMA, LGASC, MGA)
- CENTRIFUGAL (RADIAL SCAR, LGASC)
- LOBULOCENTRIC (SCLEROSING ADENOSIS-SA)

ELASTOTIC OR HYALINIZED STROMA

- INVASIVE TUBULAR CARCINOMA
- RADIAL SCAR
- LOW GRADE ADENOSQUAMOUS CARCINOMA (LGASC)
- SYRINGOMATOUS TUMOR

CO-EXISTING PROLIFERATIONS

- COLUMNAR CELL LESIONS/FLAT EPITHELIAL ATYPIA, ADH/DCIS, INVASIVE TUBULAR CARCINOMA, LOBULAR LESIONS (ALH, LCIS, INVASIVE LOBULAR CARCINOMA)
- PARTICIPATING FIBROCYSTIC CHANGES (IN RADIAL SCARS)
- SECONDARY INVOLVEMENT BY ALH/LCIS or ADH/DCIS (IN SCLEROSING ADENOSIS, RADIAL SCARS)

PERIGLANDULAR CELLULAR STROMA

- LGASC
- SYRINGOMATOUS TUMOR
- RADIAL SCAR (LIMITED EXTENT)

SQUAMOUS DIFFERENTIATION

- RADIAL SCAR (OCCASIONALLY)
- LGASC
- SYRINGOMATOUS TUMOR

LYMPHOID AGGREGATES/INFILTRATES

- LGASC
- SYRINGOMATOUS TUMOR (IN ASSOCIATION WITH RUPTURED KERATIN CYSTS)

IN-SITU CARCINOMA

- ABSENT OR ADH (INVASIVE TUBULAR CARCINOMA)
- ABSENT (MICROGLANDULAR ADENOSIS -MGA, LGASC)

CALCIFICATIONS

- INVASIVE TUBULAR CARCINOMA
- RADIAL SCAR
- SCLEROSING ADENOSIS

LUMINAL SECRETIONS

- EOSINOPHILIC (MGA)

Spindle Cell Proliferations

Entities composed of cells with a spindled shape constitute a broad spectrum of entities of different histologic lineages, biologic aggressiveness, and prevalence. As a group, spindle cell lesions arising in the breast are not a favorite among pathologists owing to several reasons. First, the differential diagnosis is replete with uncommon entities including the most commonly encountered one of spindle cell metaplastic carcinoma, a malignancy that constitutes <5% of all breast cancers. Second, to render the diagnosis, additional workup with IHC is invariably necessary, and even after such studies are performed, a definitive diagnosis may not be attainable on CNB material. Third, due to the outcome of some cases as lacking a final diagnosis despite extensive workup, the whole process can be quite unsatisfying for the pathologist.

For such cases, an algorithmic approach in assessing these lesions may be a welcomed tool as it provides structure and direction in an otherwise daunting task (Figs. 2.34 and 2.35) [2]. Like small glandular proliferations, entities consti-

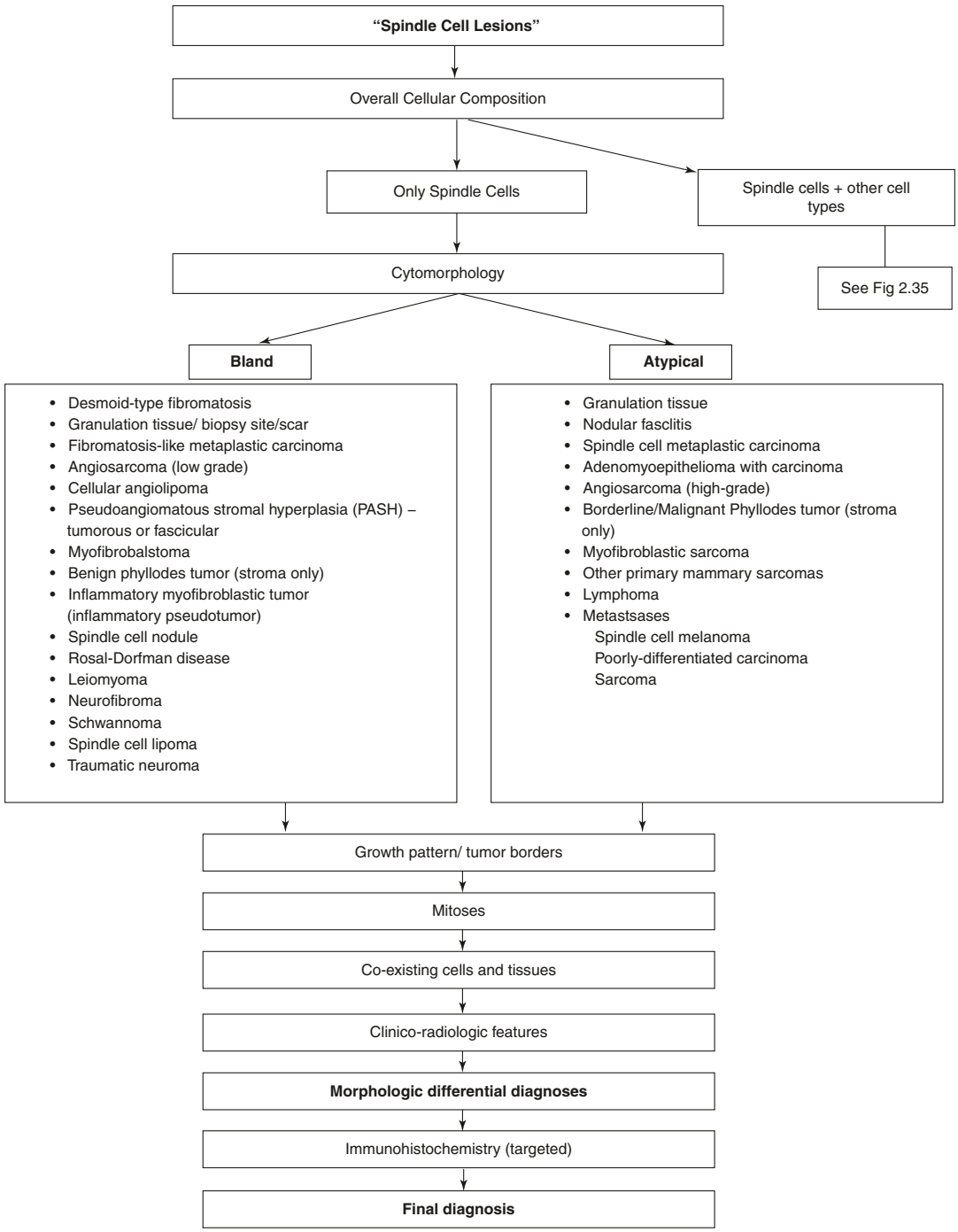

Fig. 2.34 Flowchart outlining the workup of a spindle cell proliferation arising in the breast

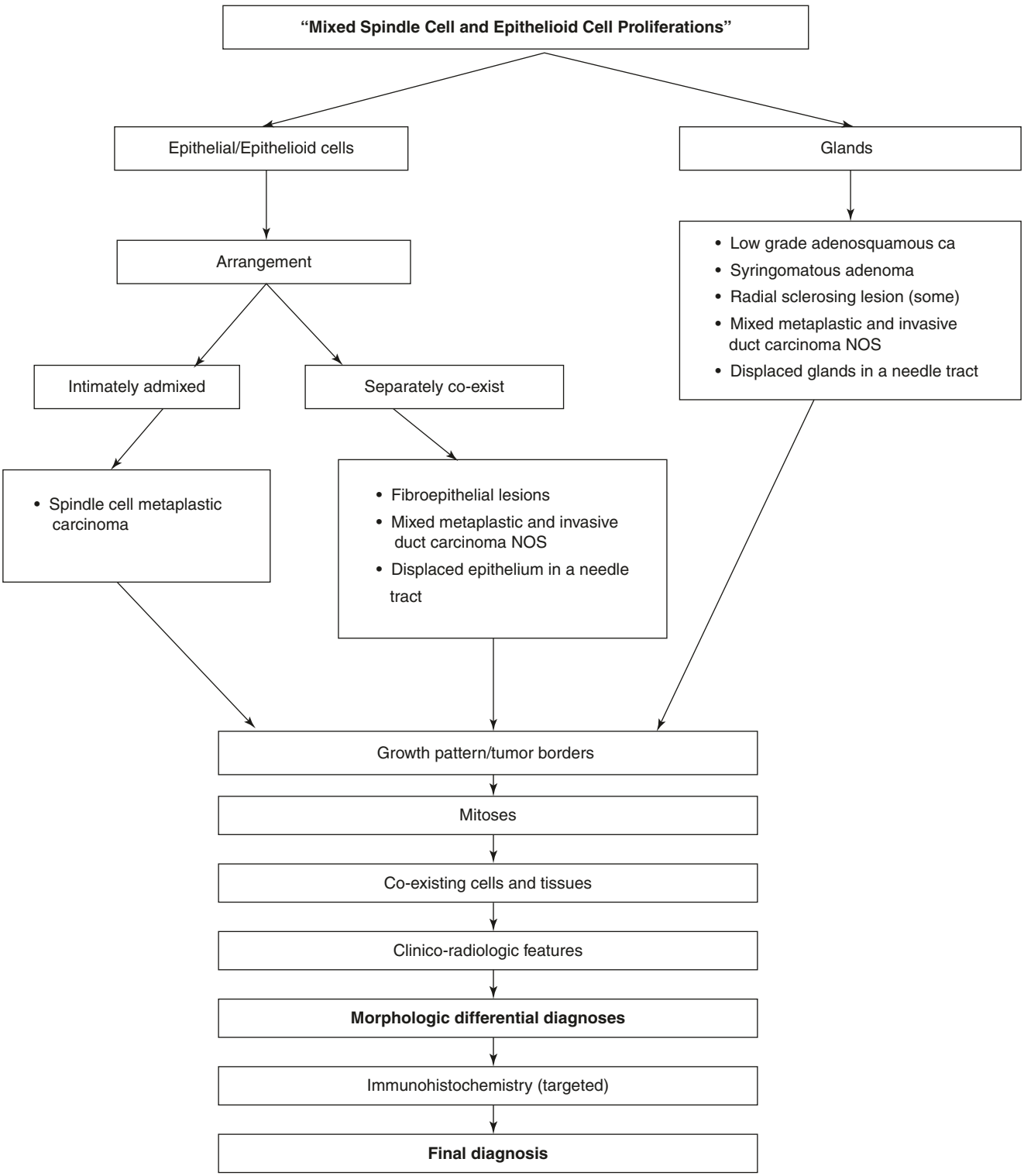

Fig. 2.35 Flowchart outlining the workup of a spindle cell proliferation arising in the breast

tuting this pattern are both benign and malignant with considerable morphologic overlap. Furthermore, conventional measures of atypia or malignancy such as nuclear pleomorphism and mitotic activity are less reliable in spindle cell proliferations.

Once a given case has been determined to represent a spindle cell proliferation, additional morphologic features are assessed to further narrow the differential diagnosis. The reflexive tendency is to next assess the degree of cytologic atypia but this step is better performed later in the evaluation. It is prudent to first evaluate the growth pattern of the lesional spindle cells. The vast majority of cases will fall into one (or rarely more) of four broad growth patterns: long fascicles, short-medium fascicles, histiocytic, and vascular. Histiocytic and vascular lesions are discussed in greater detail in Chaps. 4 and 17, respectively, and only briefly mentioned here in the context of spindle cell growth patterns. It should be noted that these growth patterns do not correlate with cell lineage in all cases. For instance, spindle cell metaplastic carcinoma can fall into either the long- or short-medium fascicle groups but its cell lineage is epithelial (Fig. 2.36).

Tumor border is an important part of analyzing growth pattern. While the opportunity to do this in a CNB is not always available since this entirely depends on the actual sampling, it can provide reliable diagnostic information towards rendering the diagnosis when present. While descriptors of tumor border characteristics are readily used in textbooks, it is valuable to see examples of the entire spectrum within each type of spindle cell lesion. An invasive tumor front is easiest to recognize, but in CNBs, this finding may be subtle or only focally present in one of several tissue cores. Fibromatosis is a spindle cell tumor that reliably demonstrates an invasive tumor border by its characteristic "tentacles" or "finger-like" projections infiltrating mammary stroma, fat or skeletal muscle (Fig. 2.37). However, even in this entity focal non-infiltrative tumoral edges can exist and under the most unfortunate circumstances may be the only tumor-normal interface seen in the CNB sampling (Fig. 2.38). Scar formed in a prior biopsy site can be easily mistaken for fibromatosis due to its irregular borders (Fig. 2.39), and therefore pertinent clinical history should be confirmed in such cases. The presence of hemosiderin pigments, foamy macrophages, and/or foreign body-type giant cell reaction would favor scar (unless it is a recurrent spindle cell lesion). Overtly invasive tumor borders are different from minimally infiltrative ones, the latter pattern more commonly seen in some spindle cell tumors like pseudoangiomatous stromal hyperplasia (PASH) tumors than others. Minimal infiltration is best appreciated when seen in the background of fat as lesional cells are seen insinuating themselves in between and around individual adipocytes or engulfing skeletal muscle fibers (Fig. 2.40). In general, spindle cell proliferations in the breast tend *not* to infiltrate into lobules (but rather push them aside) with the exception of angiosarcomas. While the malignant nature of high-grade examples is evident due to other morphologic features, angiosarcomas of low grade can be

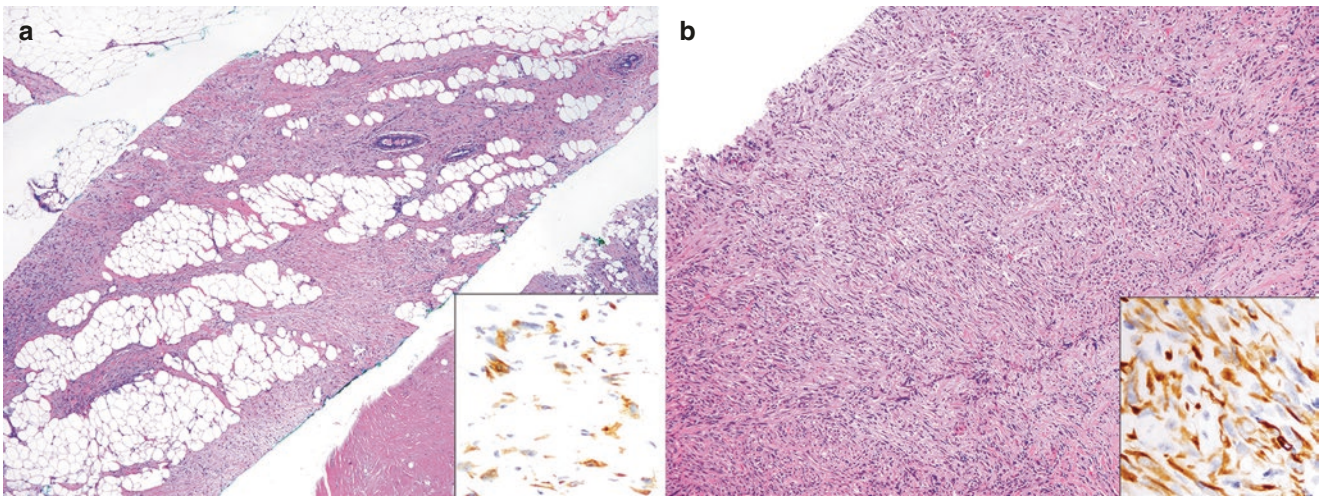

Fig. 2.36 Growth patterns of spindle cell metaplastic carcinoma. (**a**) This example of spindle cell metaplastic carcinoma is seen growing in long fascicles. The epithelial histogenesis is confirmed by positivity for high molecular weight cytokeratin (34ßE12) (*inset*). (**b**) Other examples of spindle cell metaplastic carcinoma have growth patterns composed of short to -medium-sized fascicles. A Cam 5.2 immunostain (*inset*) confirms the epithelial nature of the neoplastic cells

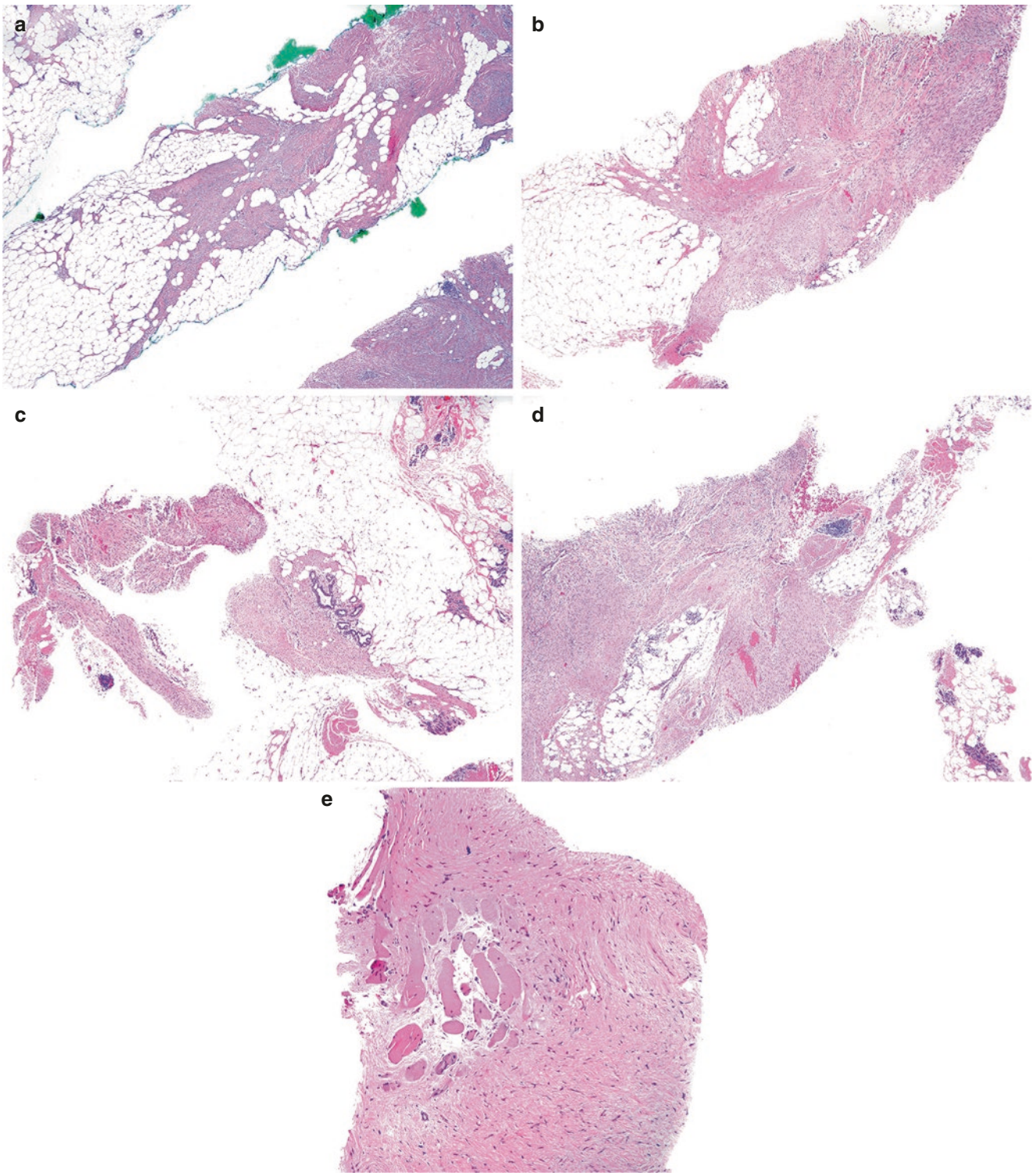

Fig. 2.37 The tumor border of mammary fibromatosis. (**a**–**c**) Fibromatosis often demonstrates an invasive tumor border. "Finger-like" projections or "tongues" of fibromatosis permeate adipose tissue. However, the invasive growth of fibromatosis is not always evident in all sampled tissue cores. (**d**) Fibromatosis infiltrating around and encasing adipose tissue. (**e**) Fibromatosis growing into skeletal muscle

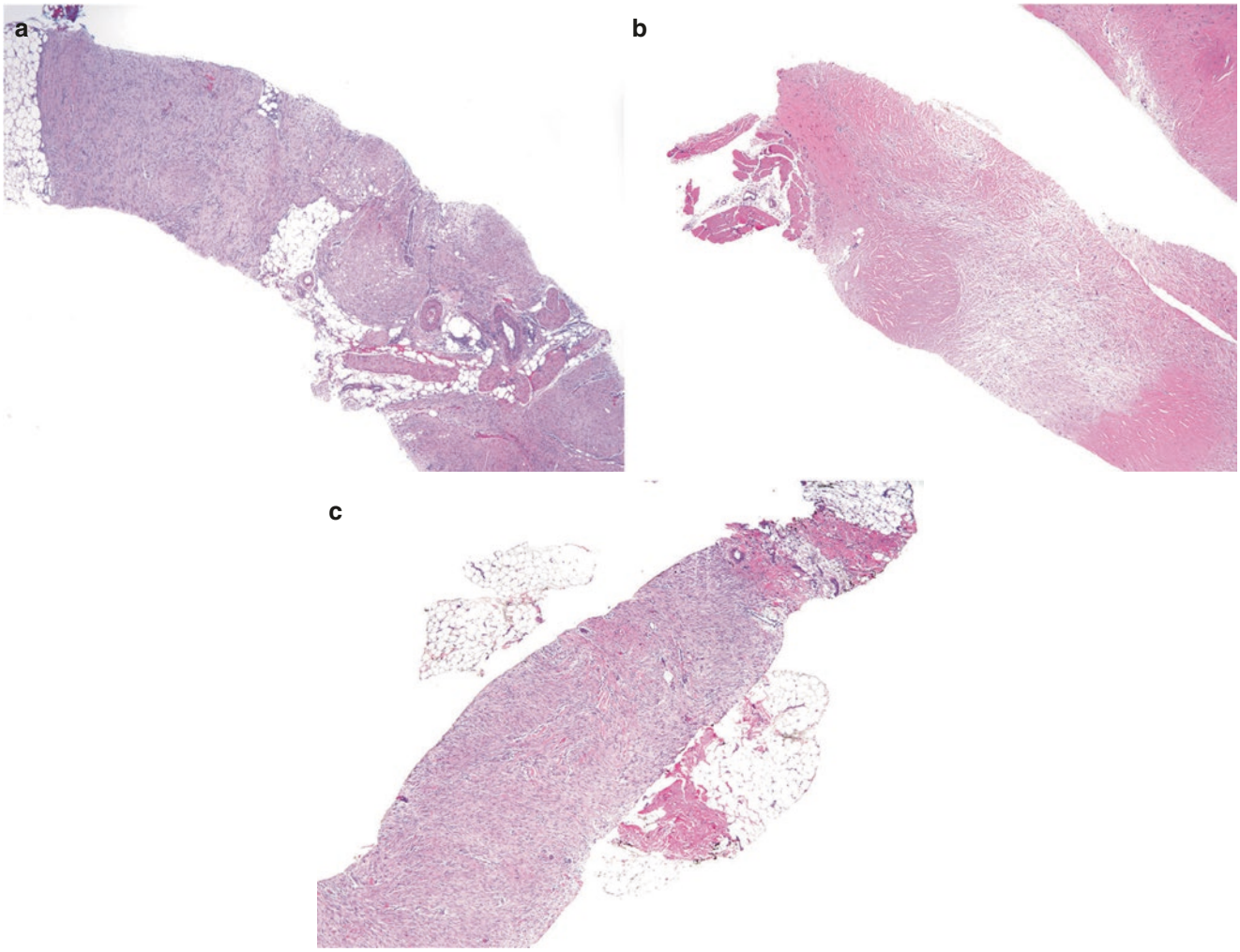

Fig. 2.38 Mammary fibromatosis. (**a–c**) Examples in CNB samples showing only noninvasive tumor borders

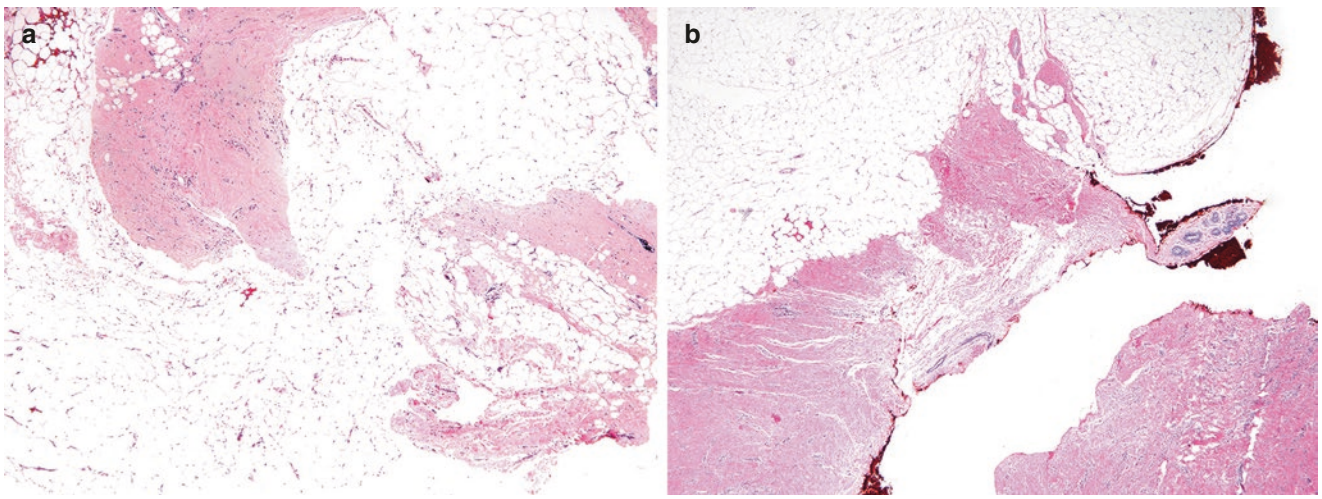

Fig. 2.39 Scar mimicking fibromatosis. (**a**) Example of a scar with "tentacle-like" projections infiltrating adipose tissue. (**b**) Example of dense fibrous scar with irregular tumor borders. Clinical history of prior surgical procedure was confirmed in this case

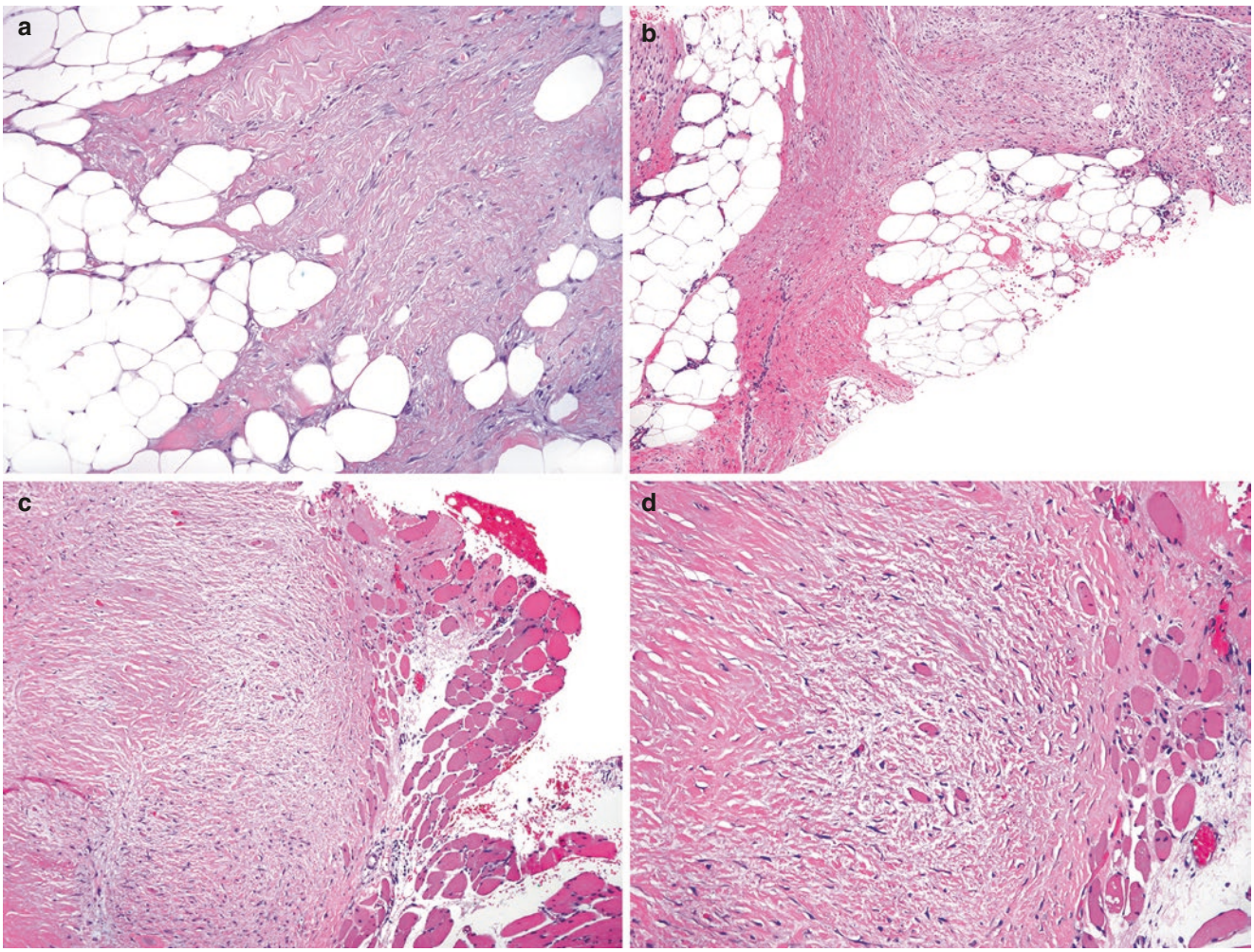

Fig. 2.40 Fibromatosis with subtle but definite invasion into adjacent tissue. (**a**, **b**) The tumor border appears irregular, but engulfment of adipocytes confirms the infiltrative nature of this example. (**c**, **d**) Fibromatosis appears to grow and abut skeletal muscle on low-power magnification. However closer inspection reveals engulfment of muscle fibers confirming the invasive nature of the tumor

mistaken for benign vascular lesions and the identification of infiltration (and splaying apart) of lobules and their glands can be pivotal to the diagnosis (Fig. 2.41). Low-grade angiosarcomas involving adipose tissue has a pattern of involvement distinct from the noninvasive, orderly arrangement of capillary vessels and adipose tissue seen in an angiolipoma. In the former, the growth pattern is diffuse and broad, while the latter is circumscribed. Unfortunately, the circumscription of the lesion may not be fully appreciated in the latter, which is why this differential is particularly problematic in limited material (Fig. 2.42). In mammary stroma, low-grade angiosarcomas can superficially resemble perilobular hemangiomas, but the former will invariably be much more extensive and infiltrate well beyond the affected lobule

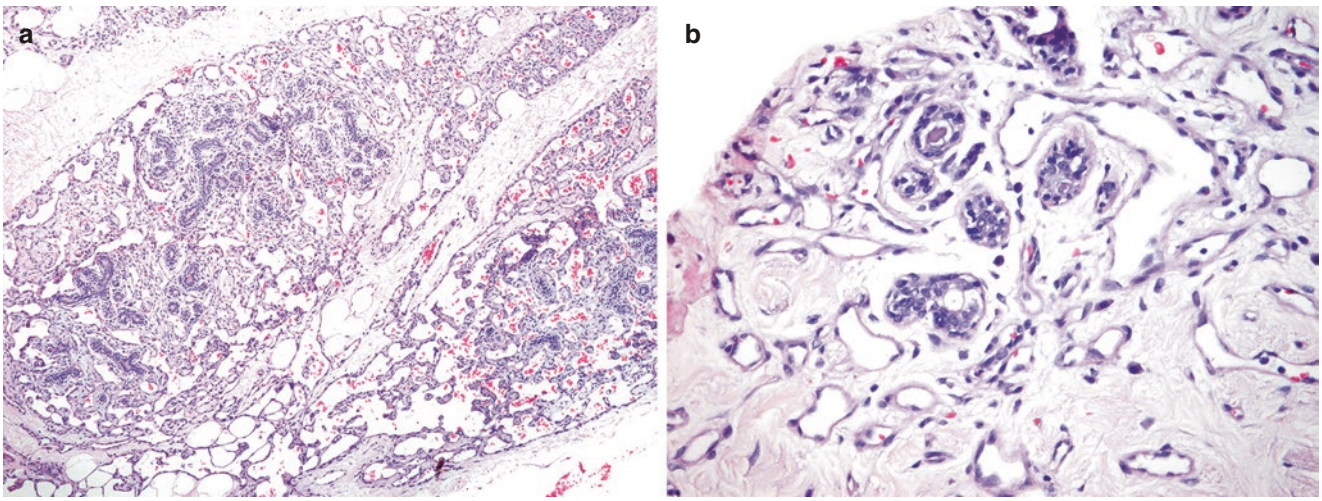

Fig. 2.41 Angiosarcoma invading into mammary lobules. (**a**, **b**) Examples of low-grade angiosarcoma composed of well-formed vascular channels dissecting into lobules and splaying apart lobular glands

(Fig. 2.43). The identification of a minimally infiltrative growing front is not an indication of malignancy in all cases as benign spindle cell tumors such as myofibroblastoma or pseudoangiomatous stromal hyperplasia (PASH) tumors can occasionally show this feature (Fig. 2.44). Spindle cell metaplastic carcinomas including the fibromatosis-like variant can show the entire spectrum of tumor border characteristics from circumscribed, minimally infiltrative, and overtly invasive; therefore, the assessment of this trait may not be particularly helpful in ruling in or out this entity (Fig. 2.45). Morphologic variants of some spindle cell tumors have differing tumor border characteristics. For example, variants of myofibroblastoma can have infiltrating tumor borders while others are well circumscribed. It would be critical for cases of possible myofibroblastomas of infiltrative variant to correlate with radiologic findings as if found to be well circumscribed, the limited findings in the CNB may simply represent the admixing of adipose tissue which is readily seen in conventional myofibroblastomas (Fig. 2.46). In general, information gleaned from inspecting the tumor border is less useful if the spindle cell tumor is fundamentally histiocytic appearing as entities in this category often exhibit a localized rather than a distinct tumoral outline.

Next, the cytomorphology of the spindle cells should be determined as either bland or atypical. The most diagnostically problematic subgroup of spindle cell proliferations is those that have a cytologically bland appearance, regardless of growth pattern. More malignant tumors masquerade as benign ones than the converse and this is largely due to their bland cytomorphologic features than any other morphologic trait. The biggest culprits in this regard are spindle cell metaplastic carcinoma and low-grade angiosarcomas (Fig. 2.47).

The reverse scenario also occurs as nodular fasciitis or exuberant granulation tissue may appear cytologically alarming despite their benignity (Fig. 2.48). These benign entities are also mitotically active which further augments their atypical appearance. Caution should be exercised when utilizing the presence of mitotic activity as a diagnostic clue in spindle cell tumors as several entities in the differential diagnosis are paradoxically (mitotically) active or inert (Fig. 2.49).

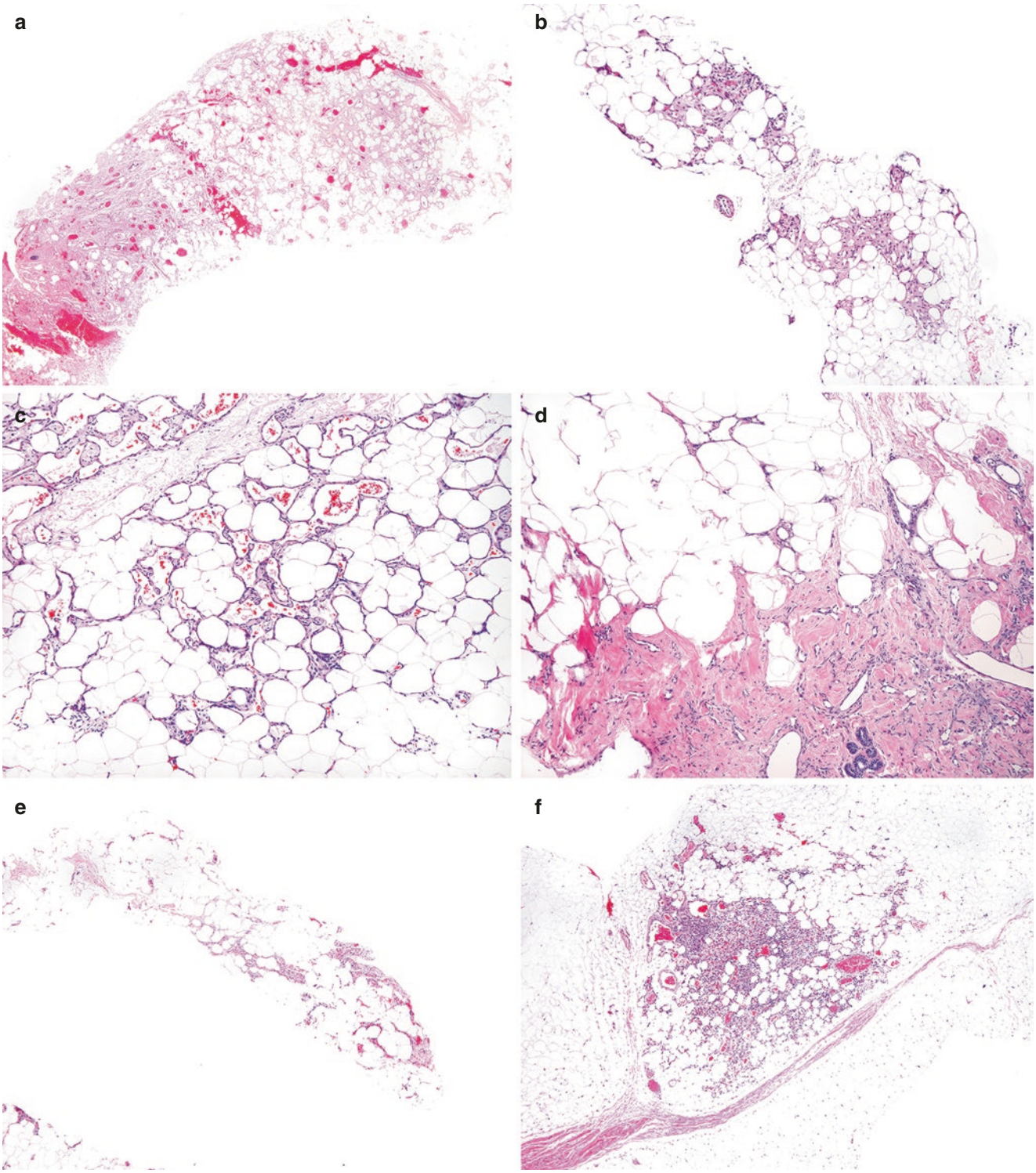

Fig. 2.42 Low-grade angiosarcoma infiltrating adipose tissue versus benign vascular tumors. (**a**) Vessels in this low-grade angiosarcoma infiltrate adipose tissue as a broad front. (**b**) Capillaries of this angiolipoma cluster unevenly around lesional adipose tissue which can give the illusion of an infiltrative vascular proliferation in CNBs. (**c**) Lesional vessels of this low-grade angiosarcoma diffusely infiltrate adipose tissue. (**d**) In some examples of low-grade angiosarcoma, the invasive growth pattern can be subtle where single vessels can be seen infiltrating into the adjacent adipose tissue or mammary stroma. (**e**) This CNB of an angiolipoma only partially reveals its circumscribed border. (**f**) A more generous CNB sampling demonstrates the well-delineated border of this capillary hemangioma

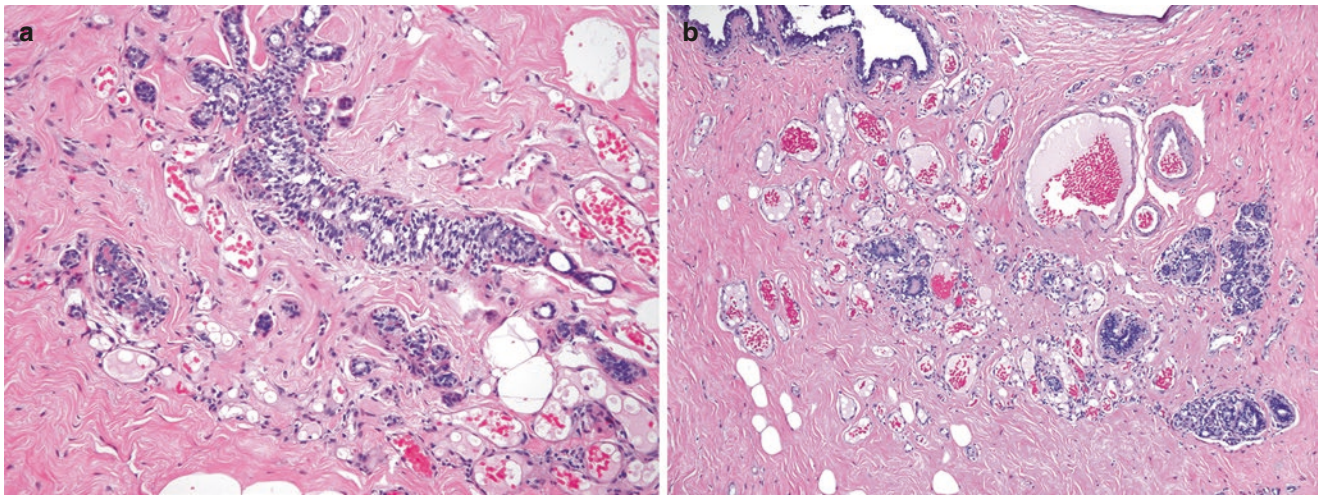

Fig. 2.43 Vascular lesions in mammary stroma (**a**) Angiosarcoma. Vessels of low-grade angiosarcoma insinuating between ducts and lobules while otherwise resembling a perilobular hemangioma. (**b**) An example of perilobular hemangioma. Note the noninvasive localized arrangement of vessels at low magnification

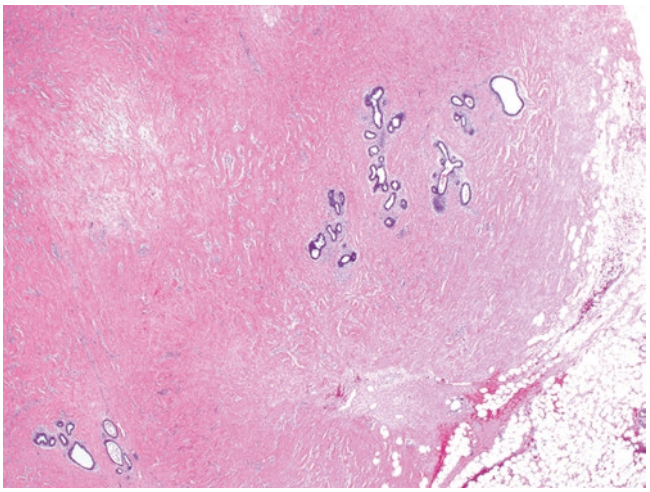

Fig. 2.44 Pseudoangiomatous stromal hyperplasia (PASH) tumor with a minimally infiltrative tumor border

Clinical and radiologic correlation is very important when evaluating spindle cell tumors as a history of prior biopsy in that area will confirm a diagnosis of scar over fibromatosis for example. Knowing the size of the lesion can be pivotal in rendering the diagnosis as a large mass (>3 cm) would make the diagnosis of nodular fasciitis or angiolipoma unlikely. Invariably with most cases belonging to this pattern group, IHC is employed to pinpoint the histogenesis of the lesion. IHC stains are most useful in cytologically bland spindle cell lesions with a fascicular growth pattern. Spindle cell metaplastic carcinoma, myofibroblastoma, and fibromatosis are examples that would entail pertinent positive and negative findings by IHC. The IHC profiles of these entities can be found in their respective chapters.

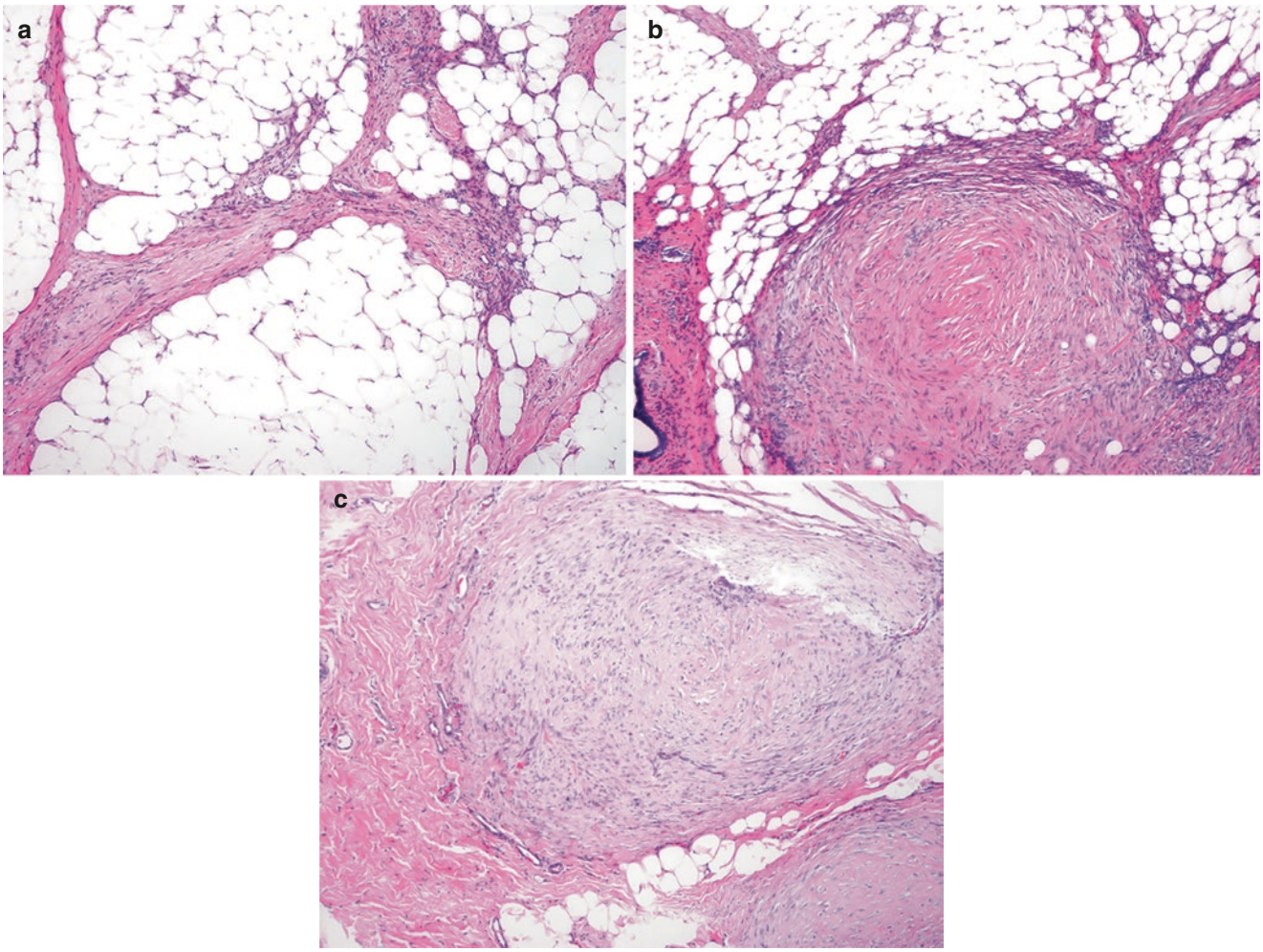

Fig. 2.45 Spectrum of tumor border characteristics in spindle cell metaplastic carcinoma (fibromatosis-like variant). Two examples of spindle cell metaplastic carcinoma of the fibromatosis-like variant showing (**a**) infiltrative, (**b**) minimally infiltrative, and (**c**) circumscribed tumor borders

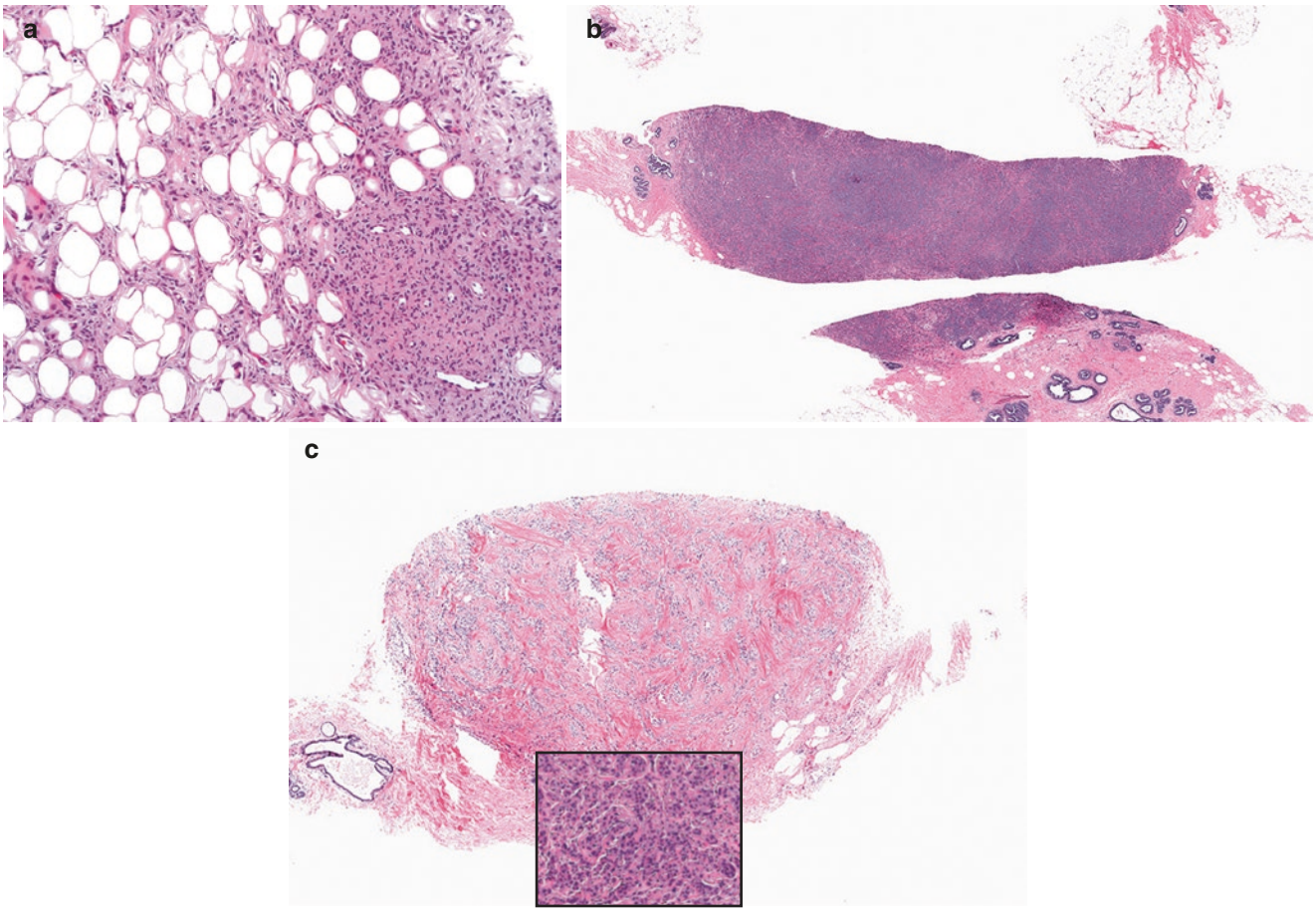

Fig. 2.46 Tumor borders of myofibroblastomas. (**a**) Myofibroblastoma with infiltrative tumor borders into adjacent adipose tissue (infiltrative variant) and other examples (**b**, **c**) with circumscribed borders (cellular and epithelioid variants shown, respectively)

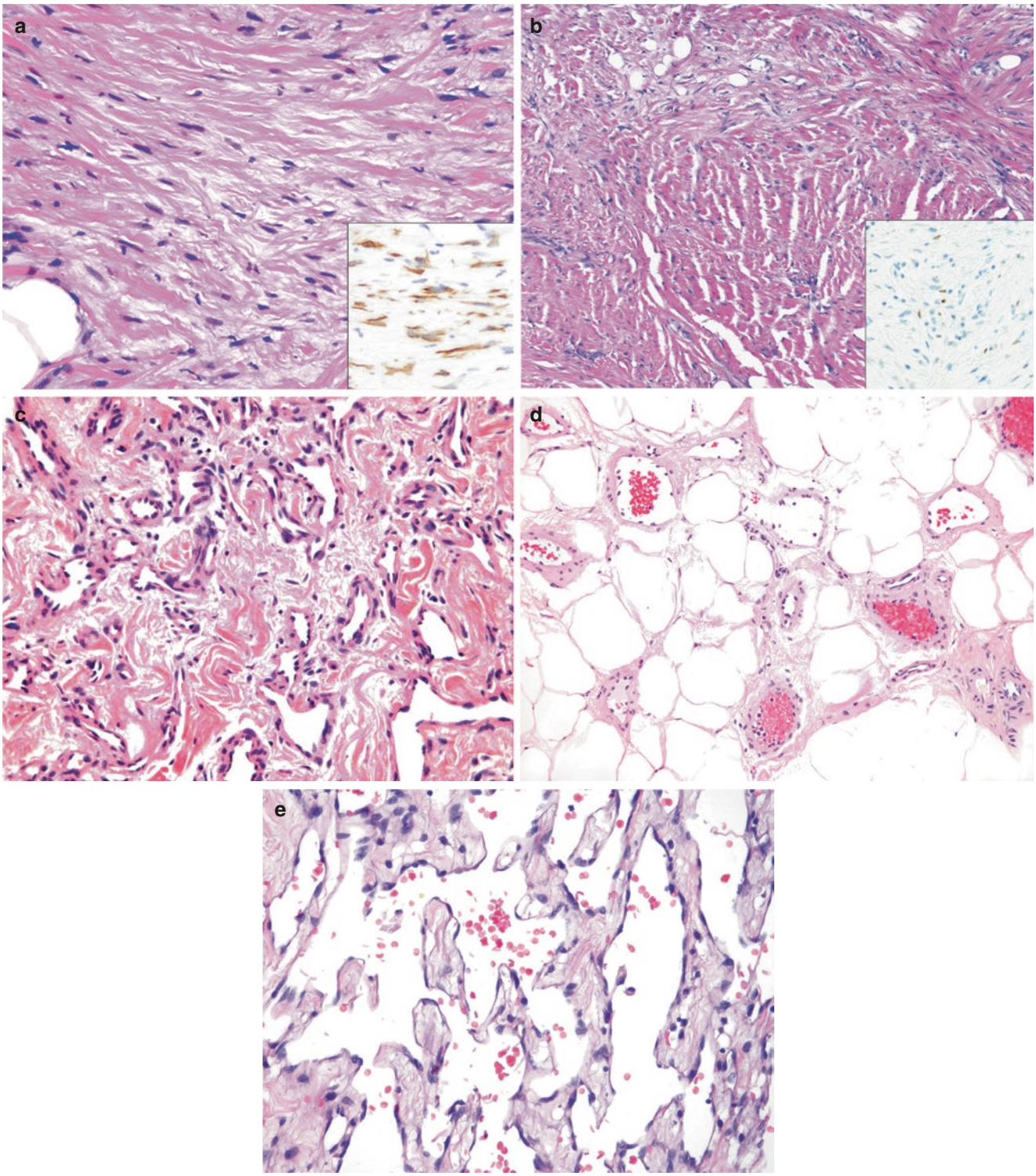

Fig. 2.47 Malignant but cytologically bland spindle cell proliferations of the breast. (**a**) Spindle cell metaplastic carcinoma with bland cytomorphology. The spindle cells are positive for high molecular weight cytokeratin (34ßE12) (*inset*). (**b**) Another example of spindle cell metaplastic carcinoma with low-grade cytomorphology. The tumor cells are positive for p63 (*inset*). (**c**–**e**) Examples of low-grade angiosarcoma composed of cytologically bland or inconspicuous endothelial cells which can be confused with benign vascular lesions

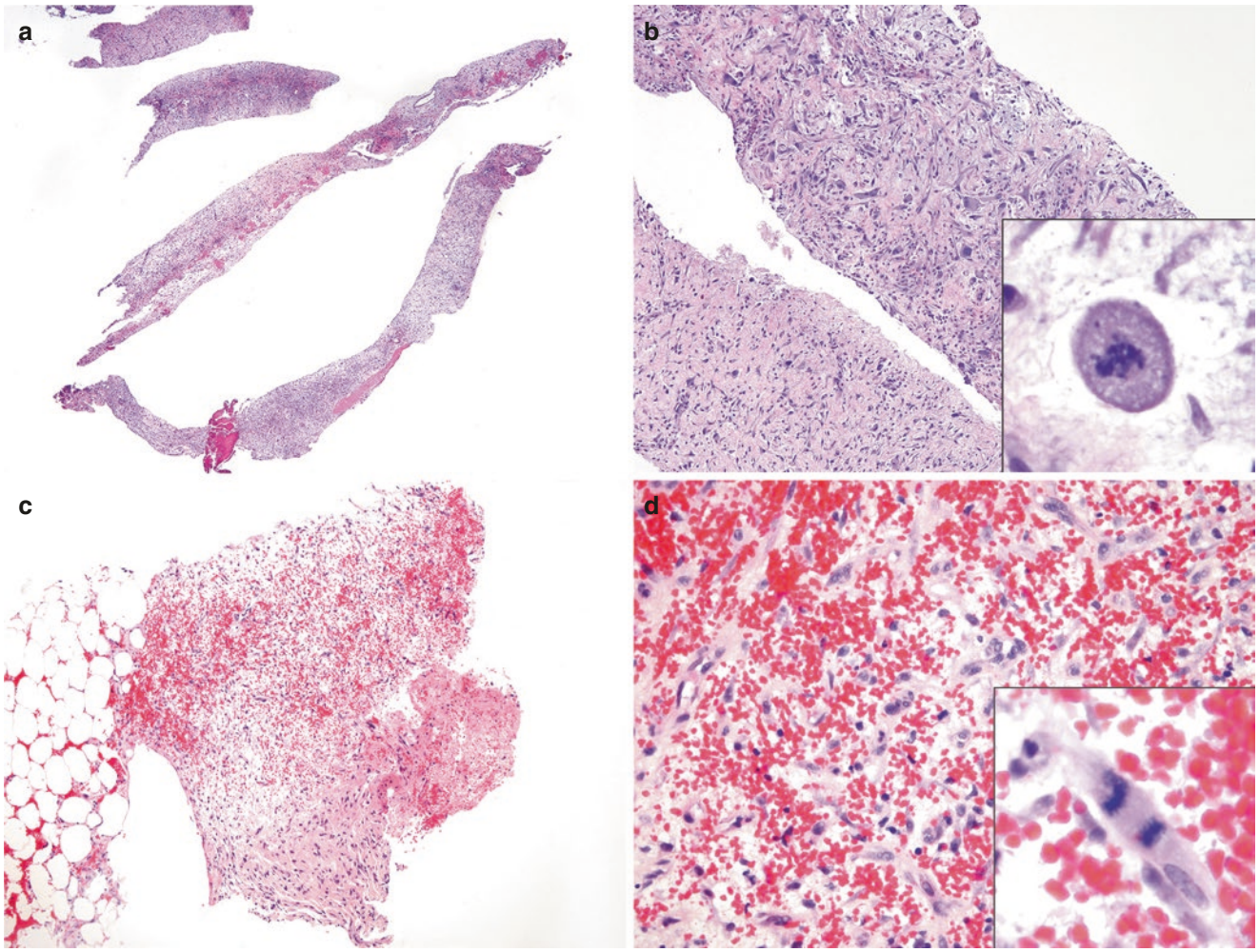

Fig. 2.48 Cytologic atypia in benign spindle cell proliferations. (**a**) CNB of nodular fasciitis shows a cellular spindle cell proliferation. (**b**) On higher magnification, the atypical spindle cells have a "tissue culture" appearance. Nuclear pleomorphism and hyperchromasia are evident. Mitoses are also seen (*inset*). (**c**) CNB shows exuberant granulation tissue in an area of prior biopsy. (**d**) Cytologic atypia including nuclear pleomorphism are present in the lesional cells. Rare mitotic figures are also identified (*inset*)

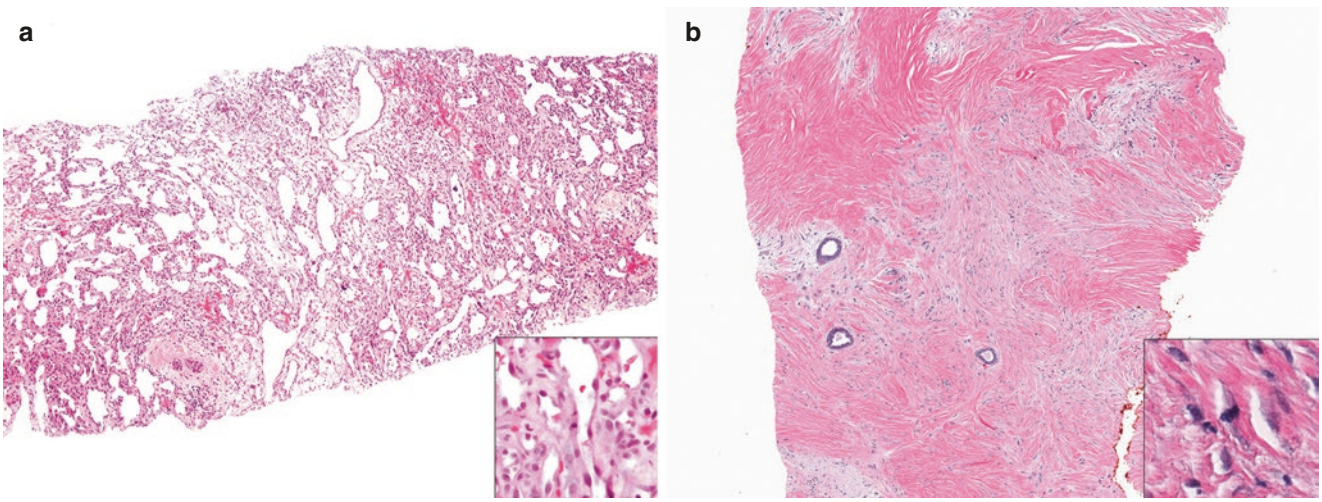

Fig. 2.49 Malignant spindle cell tumors with low mitotic activity. (**a**) Low-grade angiosarcoma composed of well-formed capillary-like vessels. On high magnification, only rare mitotic figures are identified (*inset*). (**b**) Spindle cell metaplastic carcinoma composed of cytologically bland spindle cells. Mitotic figures are difficult to locate (*inset*)

Cystically Dominant Lesions of the Breast

Mammary entities that appear as an aggregate of cystic structures at initial scanning magnification should conjure a list of possibilities in the pathologist's mind. It is natural that the more common entities come to mind first such as benign cysts in the context of fibrocystic disease and as such, a fibrocystic change is often the "go to" diagnosis when one encounters cystic structures on low magnification. However, in some instances, closer scrutiny of the epithelial lining of these cystic structures is critical for accurate diagnosis, particularly in less common entities that also have atypical and malignant counterparts.

Once the predominantly cystic nature of the lesion is recognized, it is important to assess the extent and origin of the proliferation within the normal breast tissue, characteristics of luminal (and stromal) secretions as well as associated calcifications if any, and the presence of other proliferative or inflammatory findings.

The arrangement of the cystic structures to one another can provide useful information. For instance, pregnancy-like change is strictly a lobulocentric process and therefore should not be considered as a possible diagnosis if the process is arising within large ducts. Regardless of the degree of cystic dilation seen in pregnancy-like change, the overall contour of the affected lobule is preserved and should be evident, even in partial samplings of CNBs (Fig. 2.50). Cystic processes that typically arise in larger caliber ducts include benign cysts in the context of fibrocystic changes, duct ectasia/duct stasis, juvenile papillomatosis, cystic hypersecretory lesions, and some mucocele-like lesions (MLLs) (Fig. 2.51). In CNBs, cystic changes in larger ducts are more difficult to evaluate since a greater proportion of the lesion is unsampled as compared to more discrete, smaller lobulocentric cystic lesions such as pregnancy-like change, columnar cell change, and extension of a MLL into lobules. Consequently, there is a greater probability of a definitive diagnosis rendered in CNB material in the latter, whereas in the former, a short differential diagnosis may be more appropriate to include in the pathology report (Fig. 2.52).

Since both processes arise in lobules among other similarities, the distinction between columnar cell lesions and MLLs is particularly difficult. In fact, it has been suggested that they may represent different components of the same morphologic spectrum [3]. Both are characterized by dilated lobular glands lined by a monolayer of benign epithelium (Fig. 2.53). The presence of epithelial atypia broadens the differential diagnosis to include atypical columnar cell change (flat epithelial atypia) (Fig. 2.54) and atypical ductal hyperplasia or DCIS arising in a MLL. Both columnar cell lesions and MLLs contain similarly appearing lightly basophilic luminal secretions, the finer details of which and their associated calcifications are described below.

Another diagnostic pitfall which largely occurs at scanning magnification is mistaking cystic hypersecretory hyperplasia for cysts of fibrocystic disease. Cysts from both processes can cluster and can contain eosinophilic secretions. However, eosinophilic secretions of cystic hypersecretory hyperplasia are distinctly opaque with cracks or pock marks whereas those in fibrocystic changes are thin and flocculent (described in detail below). The danger of overlooking a case of cystic hypersecretory lesion lies in the risk of

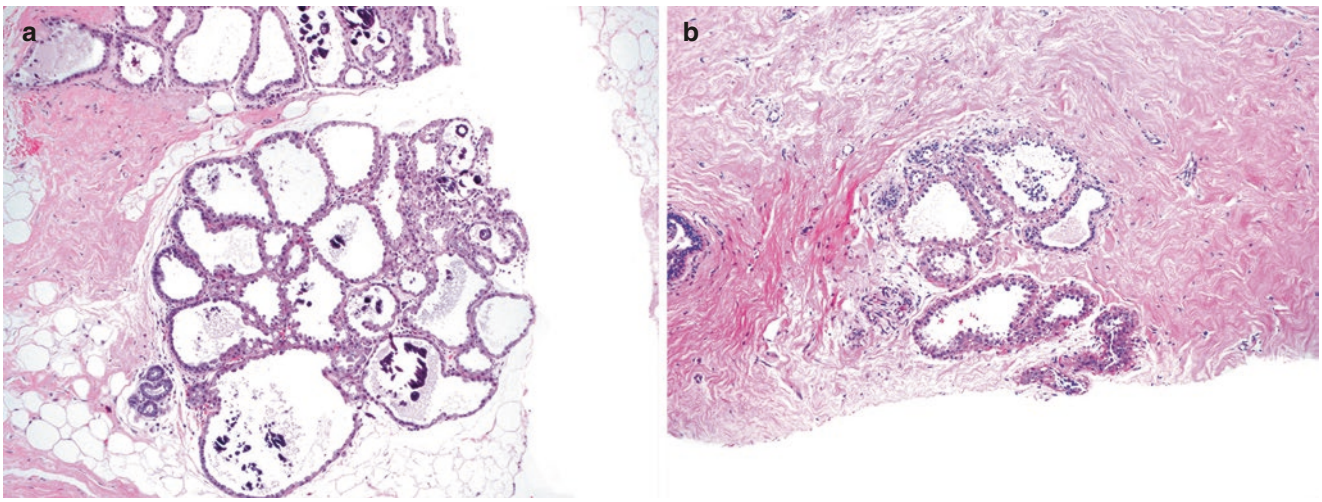

Fig. 2.50 Cystic dilatation of lobules exhibiting pregnancy-like change. (**a**) The contour of this lobule is still evident despite undergoing pregnancy-like change. (*Courtesy of Dr. Timothy M. D'Alfonso, Department of Pathology, Memorial Sloan Kettering Cancer Center, with permission*). (**b**) Another example of pregnancy-like change where the lobular contour can be appreciated

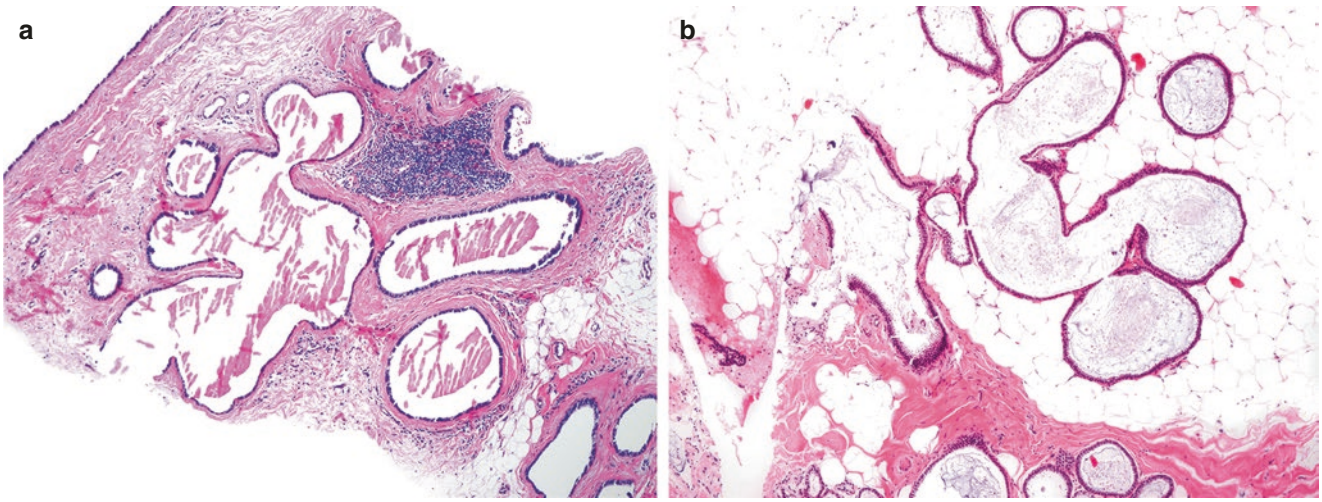

Fig. 2.51 Cystic lesions arising in ducts encountered in CNBs. (**a**) Cystic hypersecretory hyperplasia consisting of several cystically dilated ducts lined by flat epithelium and filled with bright colloid-like luminal secretions with parallel cracks. Note the lymphocytic infiltrate in the adjacent stroma, a not-uncommon finding in this lesion. (**b**) Mucocele-like change comprising cystically dilated ducts lined by flat epithelium and filled with viscous appearing mucinous secretion. Focal extravasation of mucin in the adjacent stroma is also present

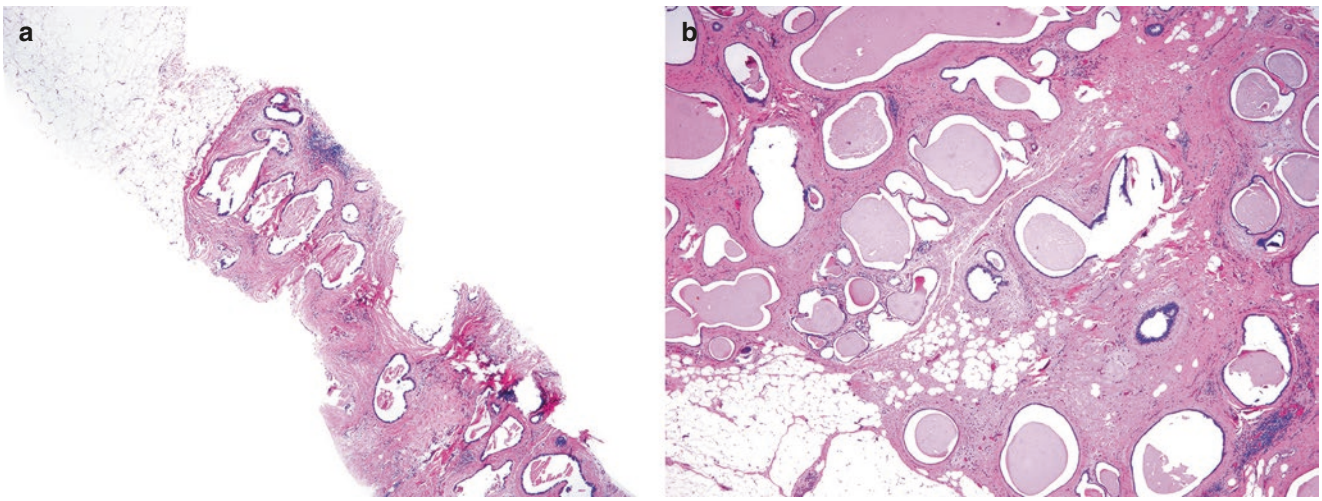

Fig. 2.52 Cystic hypersecretory lesion in CNB and subsequent excisional biopsy specimen. (**a**) CNB shows histologic findings consistent with cystic hypersecretory hyperplasia; however, the extent of the lesion is difficult to assess in this limited sampling. (**b**) Examination of the subsequent excisional biopsy confirms the diagnosis of cystic hypersecretory hyperplasia and additionally reveals rare foci of atypical cystic hypersecretory hyperplasia not sampled in the prior CNB (lower left field). This underscores the importance of excising all cases of cystic hypersecretory hyperplasia when seen in CNB material

missing a more atypical form of this entity, namely atypical cystic hypersecretory hyperplasia or cystic hypersecretory in situ carcinoma (Fig. 2.55). Both of these entities are minimally proliferative and therefore can look identical to usual cystic hypersecretory hyperplasia or benign cysts of other processes at low magnification. On CNBs in particular, all cases of cystic hypersecretory lesions regardless of whether they are benign or not should be excised. Foci of atypical cystic hypersecretory hyperplasia or cystic hypersecretory in situ carcinoma characteristically arise in a sporadic fashion in between cysts of cystic hypersecretory hyperplasia and may easily go unsampled in a CNB.

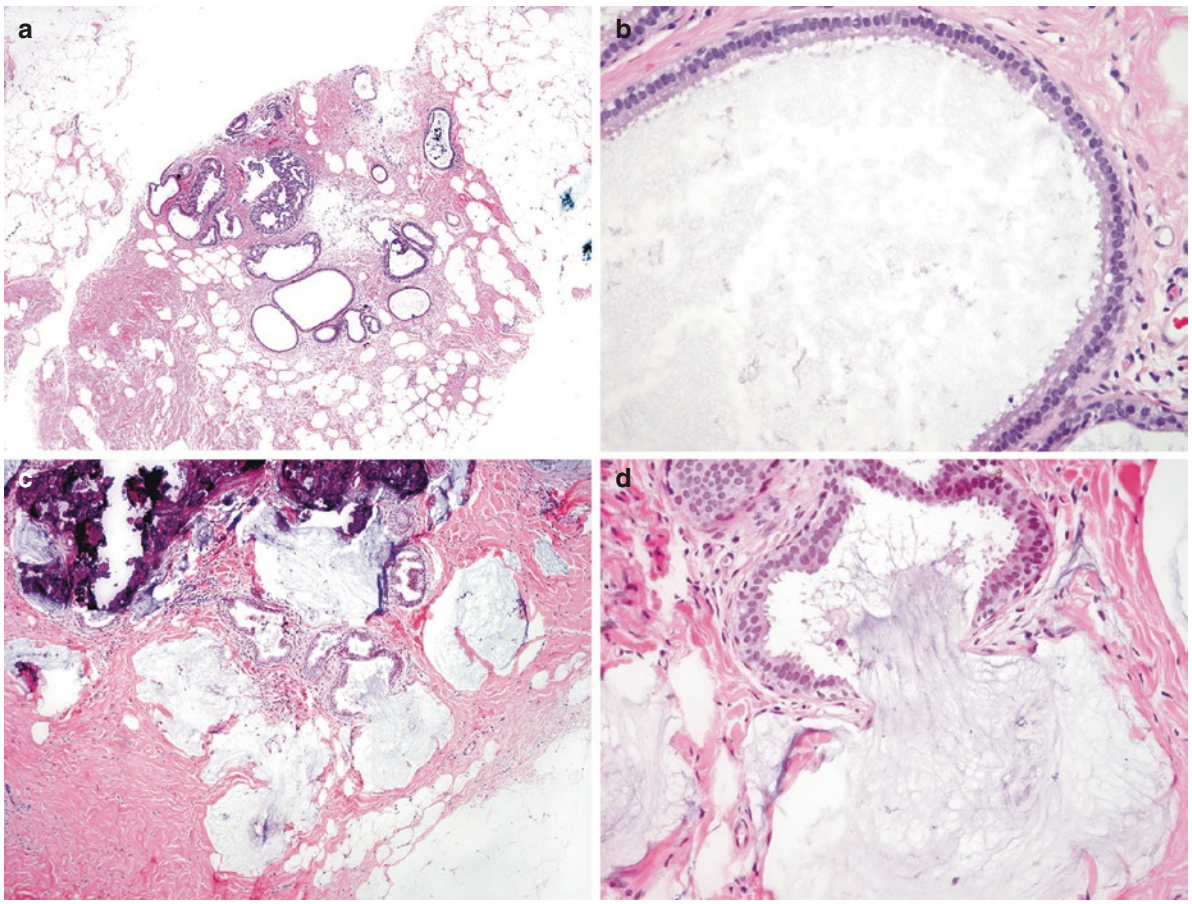

Fig. 2.53 Features of columnar cell lesion and mucocele-like lesion (MLL). (**a**) CNB performed for microcalcifications show columnar cell proliferation with luminal secretions and calcifications. (**b**) On higher magnification, luminal secretions commonly seen in this entity are appreciated. The secretions are often lightly basophilic, semitransparent, and sometimes flocculent in appearance. (**c**) MLL with significant extravasation of mucin in the adjacent stroma and abundant associated calcifications. (**d**) On higher magnification, the characteristics of the mucin are better appreciated including its lightly basophilic hue and viscous, wrinkled texture

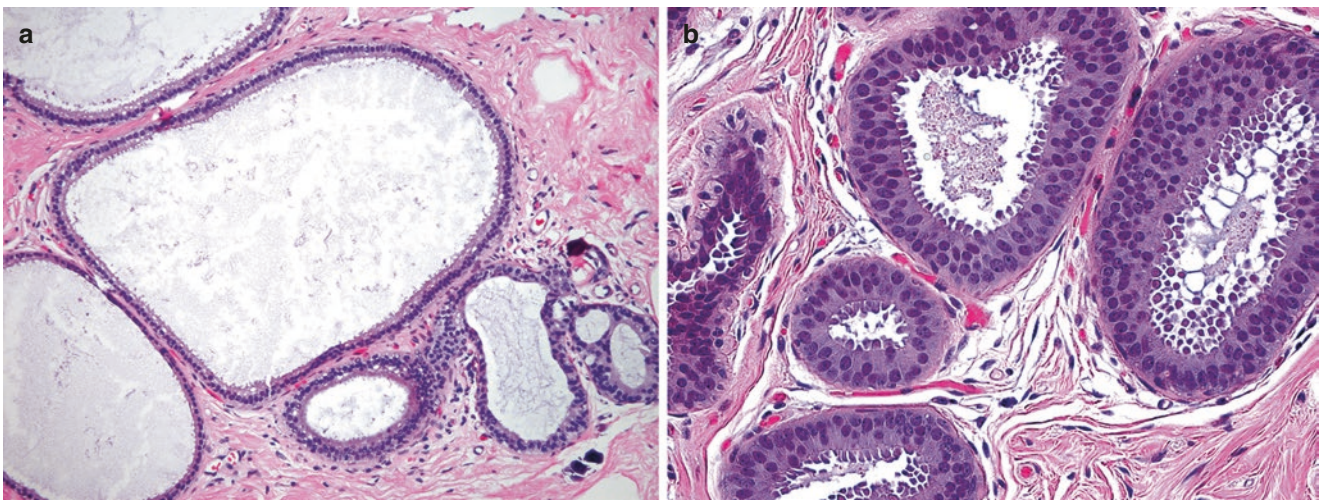

Fig. 2.54 Comparison of usual and atypical columnar cell change (flat epithelial atypia). (**a**) Columnar cell change lined by cytologically bland columnar or cuboidal-shaped epithelial cells with apical snouts and basally aligned nuclei. (**b**) Atypical columnar cell change (flat epithelial atypia) with pseudostratification of cytologically atypical cells and apical snouts. Basal orientation of the nuclei is lost. (*Image* ***(b)*** *courtesy of Dr. Stuart J. Schnitt, with permission*)

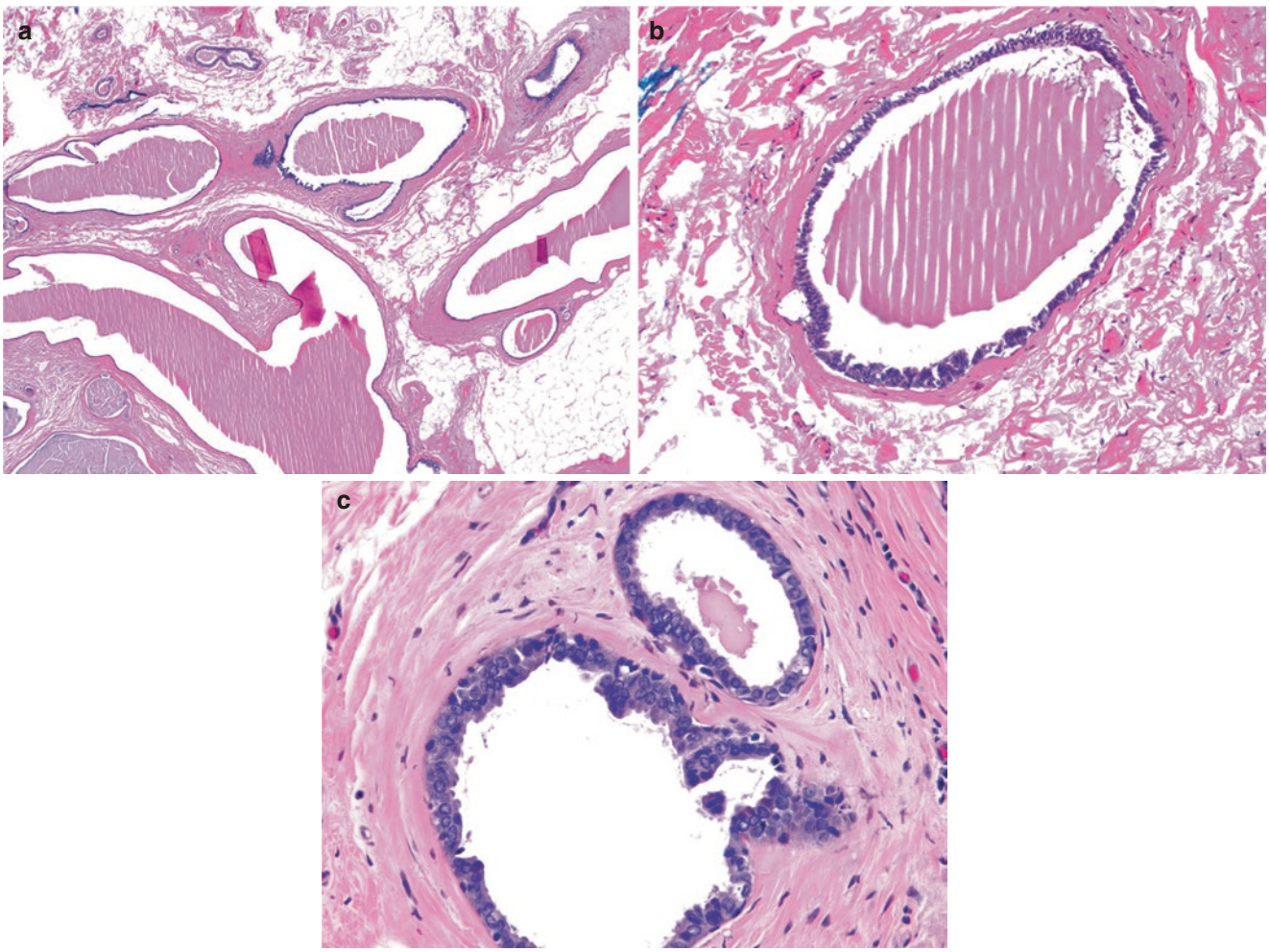

Fig. 2.55 Usual and atypical cystic hypersecretory lesions. (**a, b**) Cystic hypersecretory hyperplasia with densely eosinophilic (thyroidal colloid-like) secretions that commonly show parallel linear cracks and retraction from the luminal epithelium. (**c**) An example of atypical cystic hypersecretory hyperplasia characterized by cytologic atypia (enlarged, hyperchromatic and pleomorphic nuclei) and diminished luminal secretions

Juvenile papillomatosis is a difficult diagnosis to render in CNB material owing to the fact that examination of the entire lesion is necessary for diagnosis. In limited samplings, this entity is most often confused with fibrocystic changes or less frequently a radial scar with proliferative elements (Fig. 2.56). In such cases, the localized arrangement and spectrum of morphologic findings including cysts filled with macrophages and ductal hyperplasia are findings that more strongly suggest juvenile papillomatosis from others in the differential diagnosis. It would be important to correlate with radiologic and clinical findings as juvenile papillomatosis is characteristically a mass forming lesion. While this can be suggested in the CNB report, the diagnosis of juvenile papillomatosis should be rendered only after the entire lesion has been assessed (i.e., excisional biopsy).

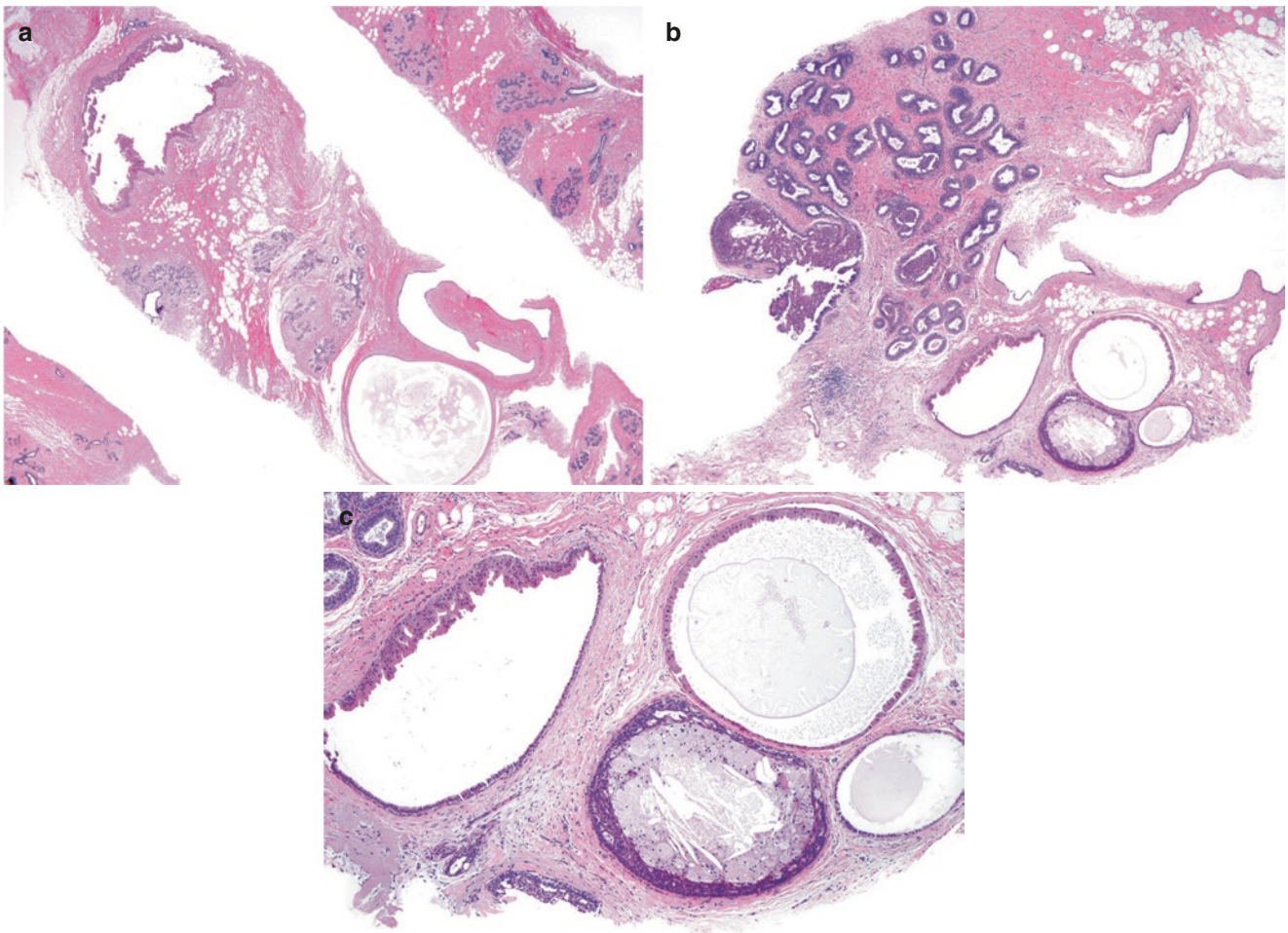

Fig. 2.56 Juvenile papillomatosis. (**a**, **b**) CNB of a cystic mass lesion shows closely approximated benign changes including cystic apocrine metaplasia, cysts filled with histiocytes, and ductal hyperplasia. While the findings were insufficient for diagnosis in this limited sampling, juvenile papillomatosis was confirmed on the subsequent excisional biopsy specimen. (**c**) Some cysts of juvenile papillomatosis contain translucent eosinophilic secretions while others are filled with histiocytes

Characteristics of Luminal Secretions and Calcifications in Cystically Dominant Lesions

Assessing the histologic nuances of microcalcifications and luminal secretions is undervalued in their ability to provide useful diagnostic information of certain breast lesions. In CNBs where histologic findings are already limited, extracting as much information from what is available for study including the particular features of luminal secretions and/or calcifications is essential. When evaluating cystic lesions, the probability of coexisting luminal secretions and calcifications is high.

Luminal secretions show differences in color, consistency (degree of translucency and textural quality), location within glandular lumina, and extent/pattern of involvement in glands. Columnar cell change and columnar cell hyperplasia not uncommonly contain semitranslucent, lightly basophilic, and flocculent secretions which are distinct from more opaque, wrinkled secretions seen in mucocele-like change (Fig. 2.57). MLL-associated secretions also tend to fill the entire glandular lumen and likely the cause of the ductal dilatation. In contrast, secretions within columnar cell alterations tend to show retraction from the luminal epithelium with scalloped, indistinct edges. Basophilic secretions can also be seen in histologically unremarkable glands but are

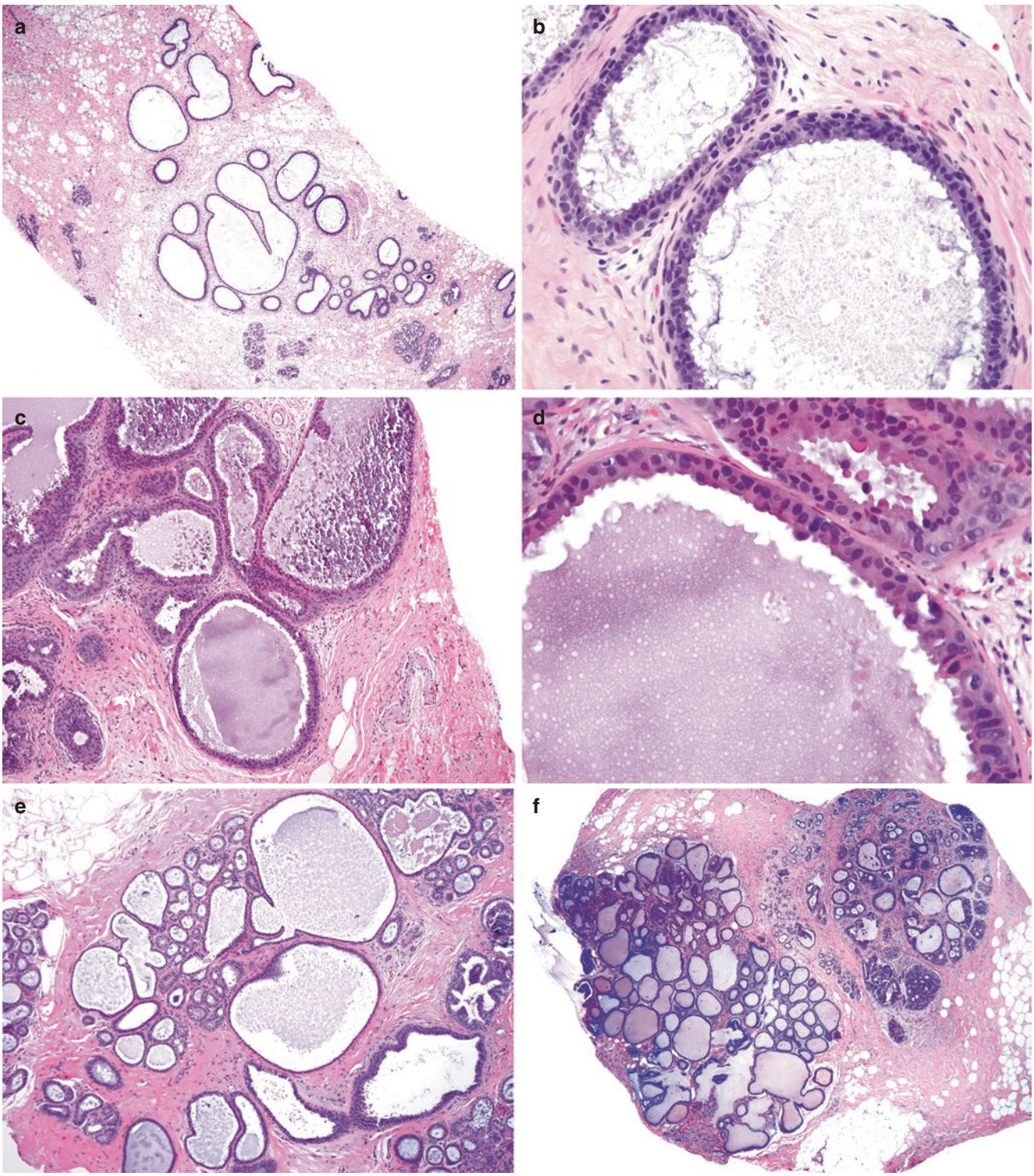

Fig. 2.57 Luminal secretions in columnar cell lesions and mucocele-like lesions. (**a**) Columnar cell change in a CNB sample. (**b**) On higher magnification, the luminal secretions are lightly basophilic and flocculent. (**c**) An example of columnar cell change and columnar cell hyperplasia with basophilic secretions and abundant calcifications. (**d**) Higher magnification shows the luminal secretions to be more deeply basophilic but still flocculent in appearance. (**e**) Another example of columnar cell change with lightly basophilic, flocculent luminal secretions. (**f**) Mucocele-like change involving terminal duct lobular units (TDLUs) is uncommon. In this example, lightly basophilic secretions fill dilated lobular glands where they have a flat opaque appearance. (**g**) The viscous texture and semi-opaque appearance of the secretions are more evident in areas of extravasation

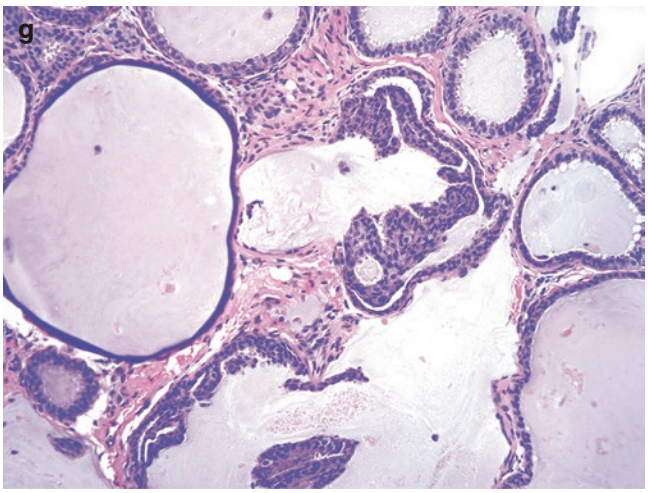

Fig. 2.57 (continued)

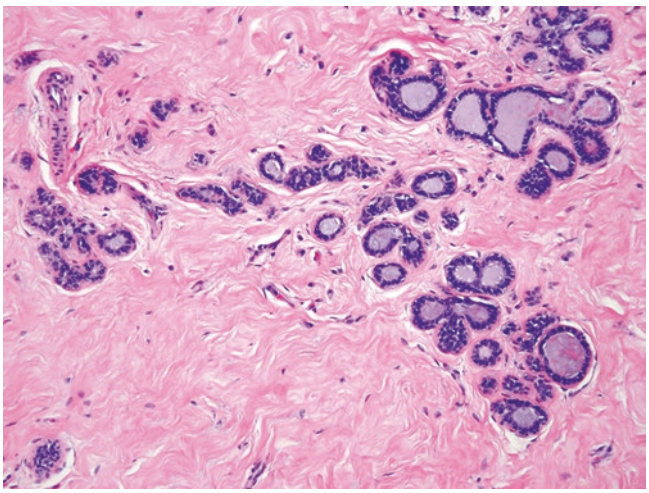

Fig. 2.58 Luminal secretions in histologically unremarkable lobular glands. TDLUs containing basophilic secretions

scanty in amount with irregular-scalloped edges retracted minimally from the luminal epithelium (Fig. 2.58). In some instances of MLLs, secondary cyst/duct rupture will result in mucin extravasation into the adjacent stroma. While this is not surprising and in itself not considered an atypical finding, care should be taken to exclude the possibility of an invasive mucinous carcinoma, a malignancy known to arise in a subset of these lesions. Extravasated acellular mucin can pool with rounded contours or show a dissecting pattern through stroma, the latter occasionally mistaken for edematous change (Fig. 2.59). Invasive mucinous carcinoma tend to grow with an advancing broad but contoured front (Fig. 2.60). One should also be cognizant that in some cases, ruptured, dislodged, or "shed" epithelium can collect in glandular lumina and should not be mistaken for invasive mucinous carcinoma.

Eosinophilic or pink luminal secretions can be seen in a variety of lesions and processes. Most commonly, semi-translucent, flocculent, and pink secretions are seen within benign cysts in the background of other fibrocystic changes or in cysts comprising juvenile papillomatosis (Figs. 2.56 and 2.61). Similarly appearing secretions can also be seen in growths that result in a cystic or partially cystic space such as an intraductal papilloma or in pregnancy-like change (Fig. 2.62). In contrast, opaque eosinophilic luminal secretions are characteristic of MGA and cystic hypersecretory lesions but with differences. In MGA, luminal secretions are typically round, brightly pink, and retracted from the luminal edges (Fig. 2.63). It is important to recognize that these secretions, although characteristic, may not be seen in limited samplings as they are not uniformly present in all lesional glands. Moreover, they are less frequently seen in atypical and carcinomatous forms of MGA. Like in MGA, the pink luminal secretions in cystic hypersecretory lesions are also opaque but of a darker hue (sometimes, reddish) and can resemble thyroidal colloid (Fig. 2.64). These typically fill the markedly dilated glands of cystic hypersecretory lesions but often show uneven degrees of retraction from the luminal edges. The edges of the secretions can be smoothly contoured or scalloped. Linear parallel cracks (likened to Venetian blinds) and pock marks with macrophages within the secretions themselves are also hallmarks of this entity (Fig. 2.65). These secretions diminish in quantity and extent when associated with atypical and carcinomatous forms of this lesion, a trait also found in atypical forms of MGA (Fig. 2.66).

Recently described, the histologically combined lesion of pregnancy-like change and cystic hypersecretory hyperplasia can be the target of core needle biopsy due to their association with calcifications [4]. The eosinophilic secretions seen in these hybrid lesions can either be flocculent like those seen in pregnancy-like change or dense like those characteristic of cystic hypersecretory lesions (Fig. 2.67).

Like luminal secretions, calcifications can offer clues particularly in limited samplings when diagnostic findings are already sparse. While the mammographic characteristics of calcifications have been well characterized and used to assess the need for further evaluation via biopsy, such traits as appreciated in routine H&E slides have largely gone unappreciated for their diagnostic value.

Beyond simply identifying targeted calcifications histologically, pathologists can use their observations that calcifications associated with certain processes can have, in and of themselves, distinctive qualities. While this correlation is not 100% specific, when observed, such a positive association can be affirming of the rendered diagnosis. For instance, calcifications associated with usual and atypical columnar cell lesions are deeply purple (hematoxylin-rich) with smooth contours and sometimes additionally psammomatous in appearance (Fig. 2.68). They are usually single or in small clusters of two or three. Often times the calcifications can be fragmented but the pieces remain closely approximated and their smooth borders remain intact. Columnar cell lesion-

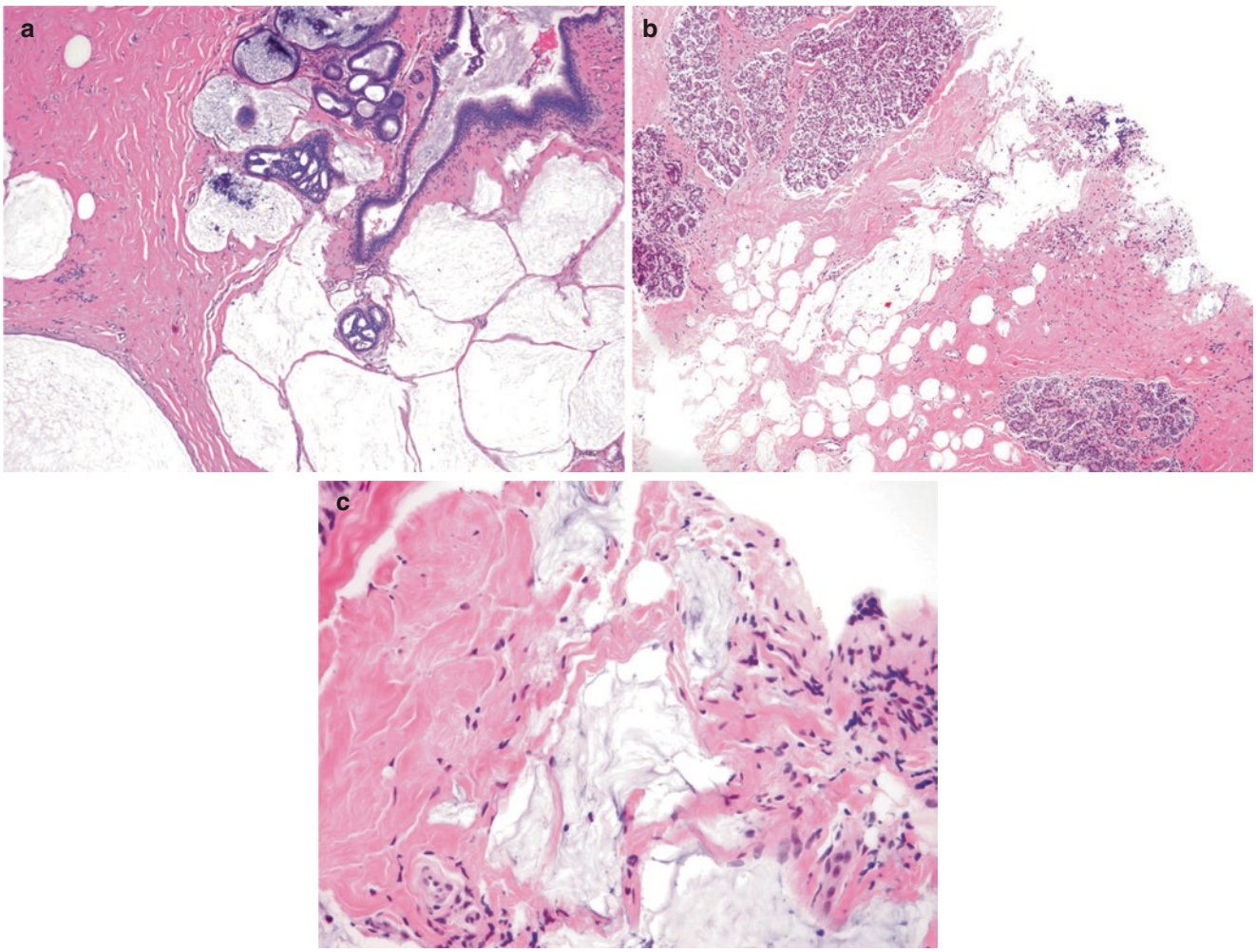

Fig. 2.59 Stromal mucin pools in mucocele-like lesions (MLLs). (**a**) In some cases of MLLs, extravasated mucin pools are abundantly present and show a smooth rounded interface with the adjacent stroma. It is important in these situations to exclude invasive mucinous carcinoma which can arise in a subset of these lesions and exhibits a similarly smooth contour. (**b**) Other cases of MLLs show extravasated stromal mucin with jagged irregular edges and in some cases can be mistaken for edematous stromal change on scanning magnification. (**c**) On closer inspection, the lightly basophilic hue and wrinkled texture of the mucin can be better appreciated

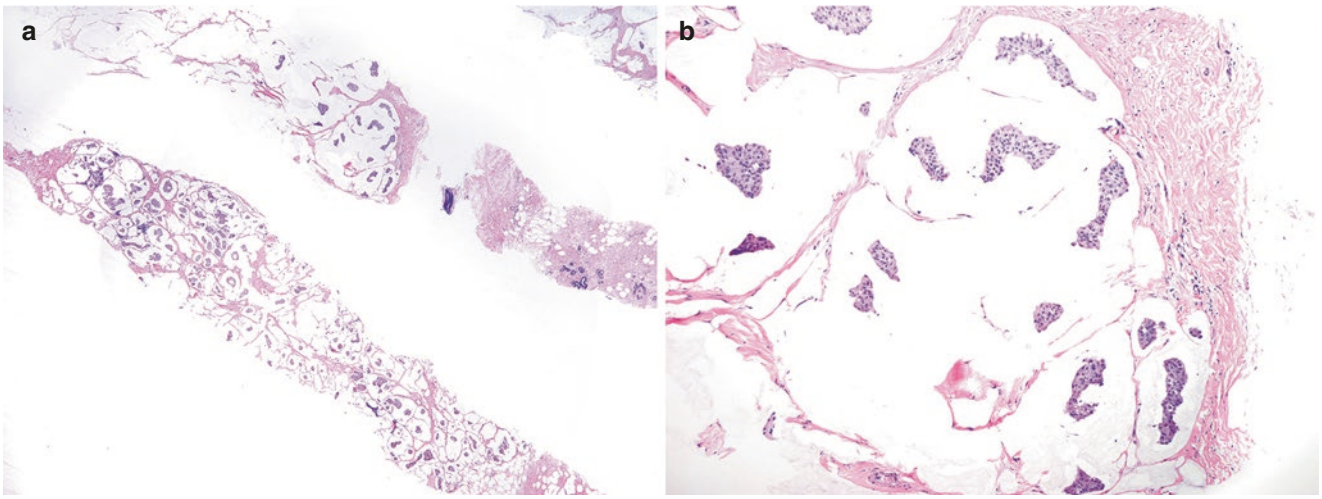

Fig. 2.60 Mucin pools in invasive mucinous carcinoma. (**a**) Invasive mucinous carcinoma seen here as clusters of carcinoma cells floating in pools of mucin. (**b**) The leading edge of invasive mucinous carcinomas typically grows as a pushing front and exhibits a smooth bulbous contour similar to extravasated mucin pools of MLLs

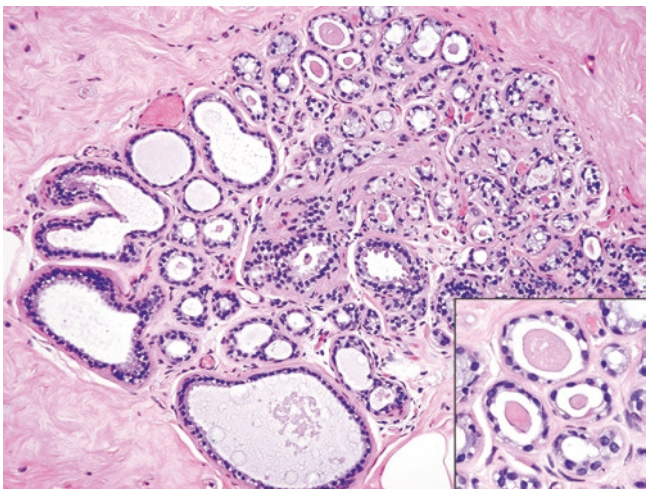

Fig. 2.61 Eosinophilic luminal secretions in a benign lobule. Semitranslucent eosinophilic secretions within glandular lumens of a lobule showing intralobular stromal sclerosis. When viewed in isolation, these can resemble secretions seen in microglandular adenosis (*inset*)

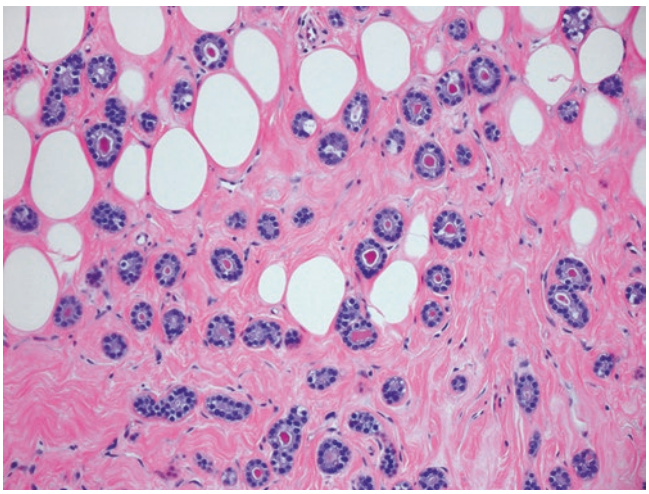

Fig. 2.63 Luminal secretions in microglandular adenosis. Opaque, bright, and sometimes glassy-appearing pink secretions in glandular lumens. These secretions are typically rounded with smooth contours and retracted from the glandular walls

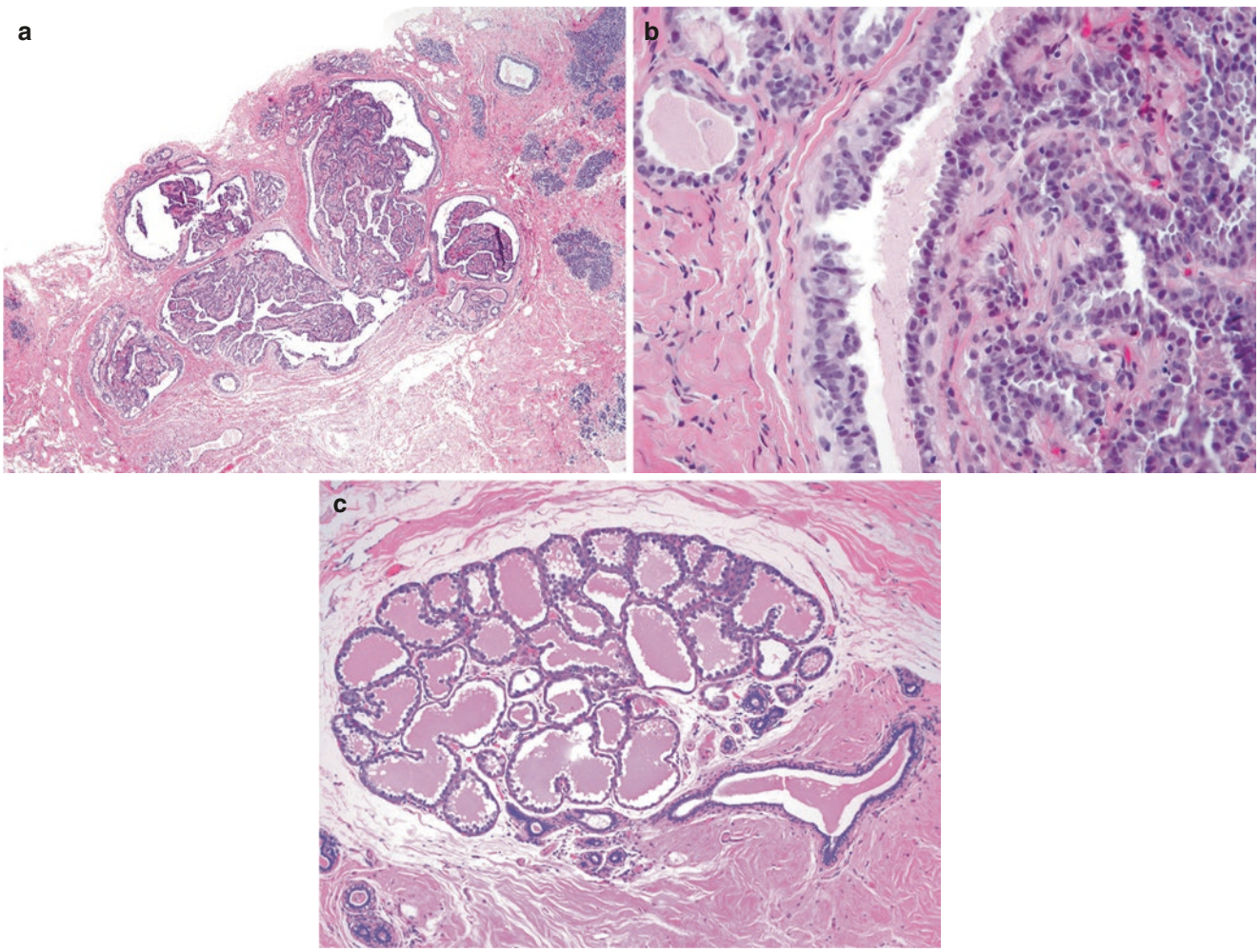

Fig. 2.62 Eosinophilic luminal secretions in other benign lesions. (**a**, **b**) Occasionally, the cystic space that develops in some intraductal papillomas contain eosinophilic secretions which are thin and flocculent. (**c**) In most examples of pregnancy-like change, the ectatic lobular glands contain eosinophilic secretions that are thin and flocculent or slightly more opaque than those in fibrocystic changes. This example shows both appearances. Also note that the secretions show scalloped edges and are variably retracted from the glandular walls. (*Courtesy of Dr. Timothy M. D'Alfonso, with permission*)

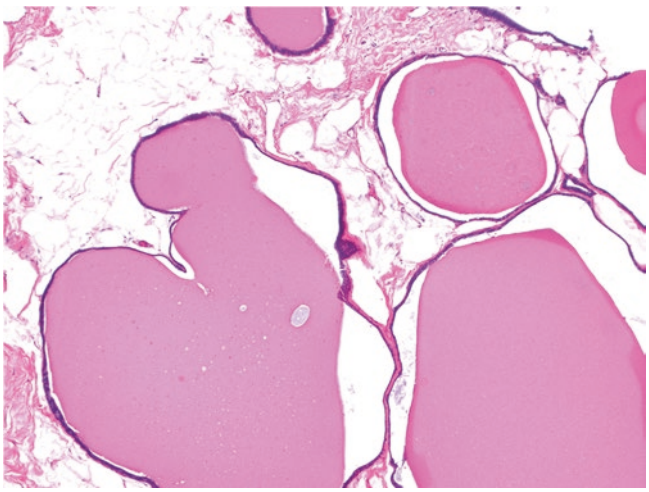

Fig. 2.64 Cystic hypersecretory hyperplasia containing abundant opaque and deeply eosinophilic luminal secretions with smooth contours and characteristically retracted from the cyst wall

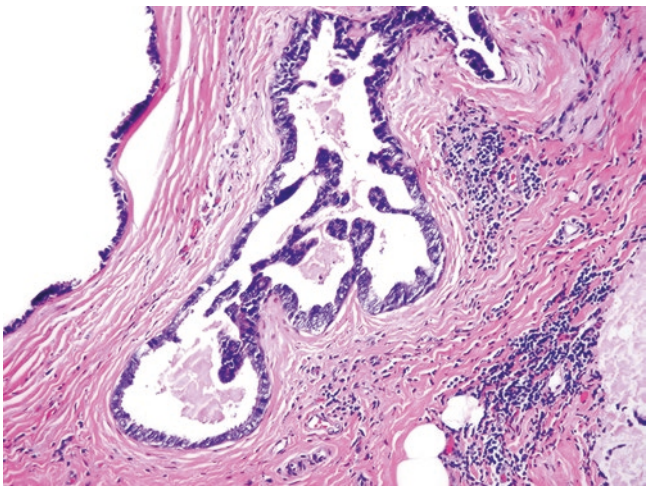

Fig. 2.66 Diminished secretions in atypical and carcinomatous forms of cystic hypersecretory lesions. In contrast to its benign counterpart, the volume of secretion is markedly decreased in examples of atypical cystic hypersecretory hyperplasia and cystic hypersecretory in situ carcinoma

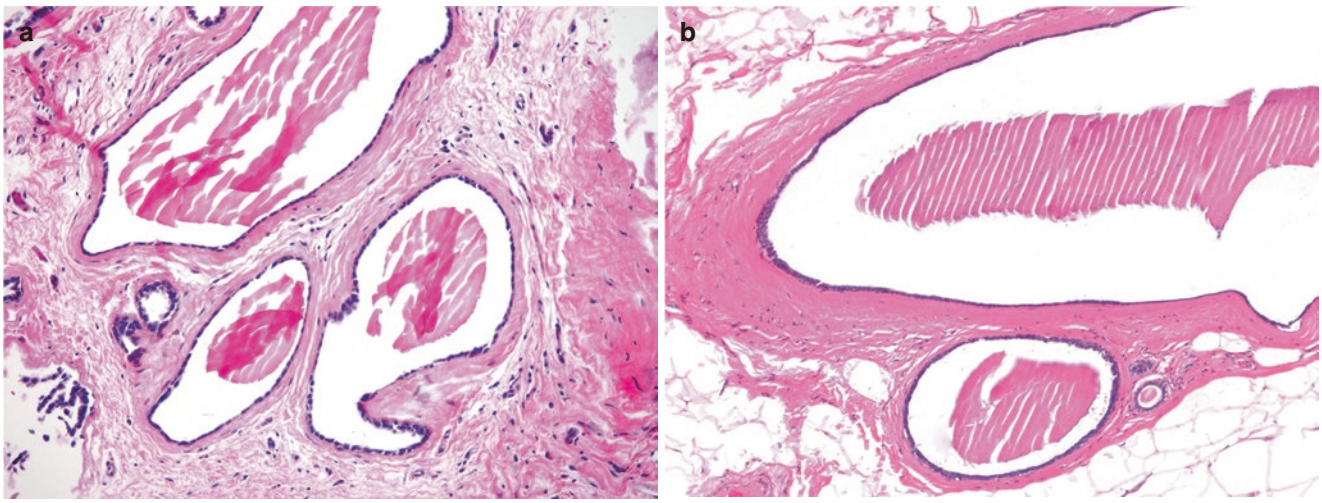

Fig. 2.65 Characteristics of secretions in cystic hypersecretory hyperplasia. (**a**, **b**) Secretions associated with cystic hypersecretory lesions are densely eosinophilic (thyroidal colloid-like) and commonly show parallel linear cracks and retraction from the cyst walls

associated calcifications can be lined by epithelium and seen either arising from the columnar cell epithelium within a duct or free floating in the ductal lumen (Fig. 2.69). Occasionally, the calcifications are encased in a thick pink rind and these have been referred to as the "ossifying type" of calcifications (Fig. 2.70).

Deeply basophilic calcifications are also seen in association with MLLs. While some calcifications are nondescript in their appearance, others are characteristically small and numerous imparting a granular, gritty, or powdery appearance, and tend to aggregate to one side of the cyst's lumen. Again, while not pathognomonic for MLLs, calcifications with this appearance help to support the diagnosis (Fig. 2.71).

Calcifications in pregnancy-like change and pregnancy-like hyperplasia are characteristically solitary (one per lumen) with smooth, lobulated borders and concentric, irregularly spaced laminations. Most examples are deeply purple while occasional calcifications are rimmed (or entirely) lighter purple or pink in color (Fig. 2.72).

Apocrine cysts (and apocrine metaplasia) are commonly the target of CNBs due to their association with calcium oxalate crystals. These are clear to pale yellow in color, translucent and irregular-shaped crystals that can be difficult to identify in tissue sections and also have a tendency to dislodge and displace far from its original location during tissue processing. Polarization of the slide is helpful for identifica-

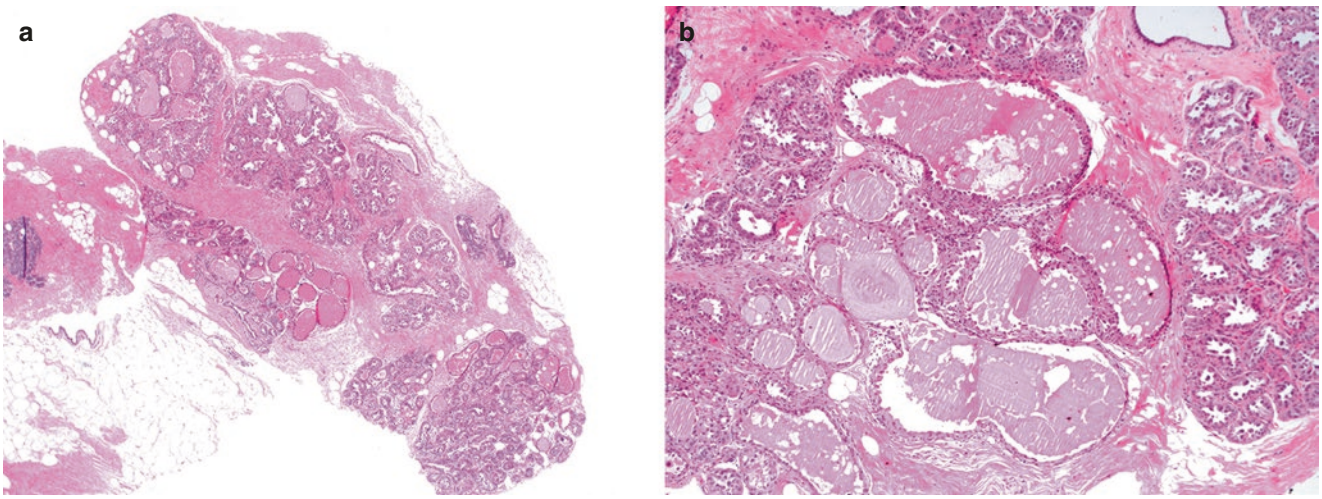

Fig. 2.67 Histologically combined pregnancy-like change and cystic hypersecretory hyperplasia. (**a**) On low magnification, this CNB performed for mammographically detected calcifications shows multiple enlarged and ectatic terminal duct lobular units (TDLUs) with epithelial proliferation and eosinophilic luminal secretions. (**b**) Higher magnification reveals the characteristic luminal secretions seen in cystic hypersecretory hyperplasia including the presence of parallel cracks and pock marks. (*Courtesy of Dr. Timothy M. D'Alfonso, with permission*)

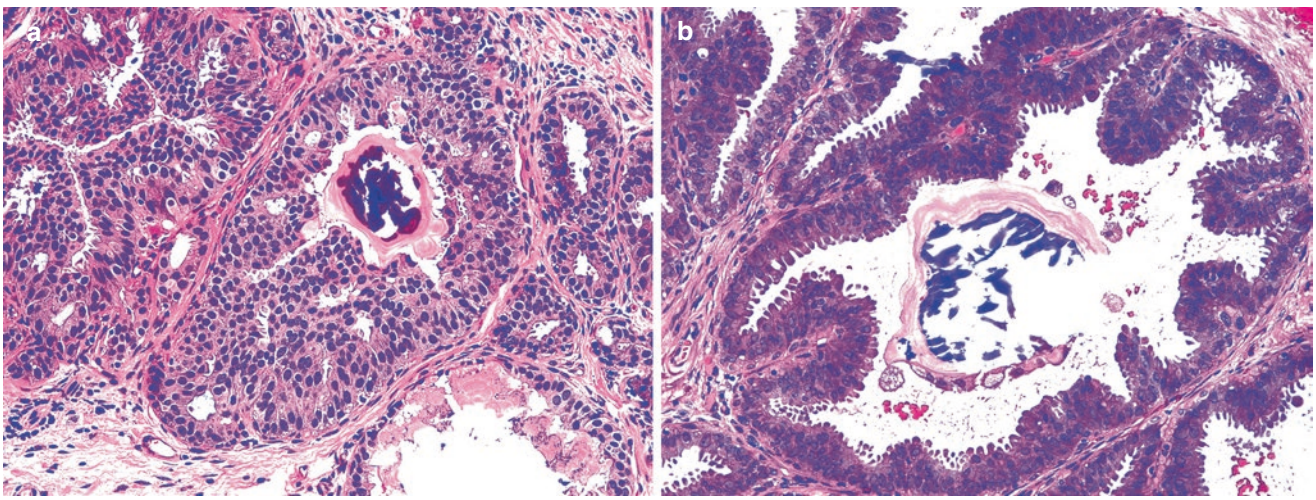

Fig. 2.68 Psammomatous calcifications in atypical columnar cell hyperplasia (flat epithelial atypia). (**a**, **b**) Concentric laminated calcifications can be seen in entities other than pregnancy-like change and pregnancy-like hyperplasia such as in this example of flat epithelial atypia. (*Courtesy of Dr. Stuart J. Schnitt, with permission*)

tion in these instances. In some cases, the calcium oxalate crystals become embedded in fibrous stroma and elicit a multinucleated giant cell reaction (Fig. 2.73). Also, note tracks left behind from calcifications dragged across tissue during tissue block cutting. This is a useful clue that calcifications are present in the sample even if not immediately visible.

Other cystically dominated lesions such as duct ectasia, duct stasis, and cystic hypersecretory lesions are not accompanied by calcifications and calcifications are only seen in juvenile papillomatosis to the extent that one or more of its proliferative components may be associated with them (e.g., papillomas).

Calcifications seen in other benign and malignant changes are largely nondescript (Fig. 2.74) with the exception of radiologically pleomorphic appearing calcifications typically seen in high-grade, comedo-type DCIS. Histologically, these are numerous, granular to coarse, and invariably associated with necrosis.

Needless to say, calcifications (and secretions) are not limited to cystically dominant breast lesions and can be seen in a host of other entities. However, being cognizant of the characteristics of calcifications and secretions associated with certain lesions commonly targeted and sampled by CNB can be helpful to further support one's morphologic impression.

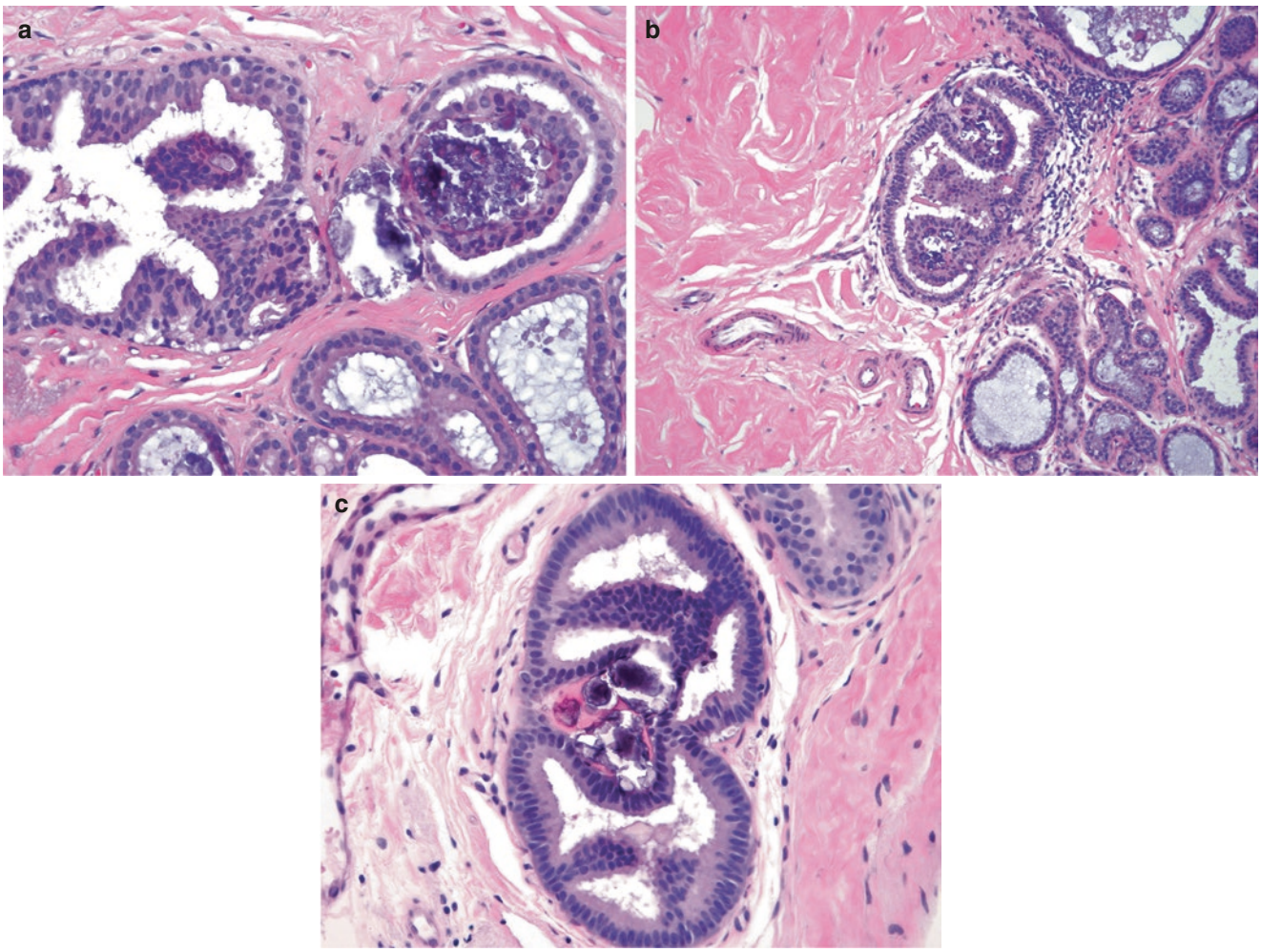

Fig. 2.69 Calcifications associated with columnar cell hyperplasia. (**a**, **b**) Epithelial rimmed calcifications in columnar cell hyperplasia which can be seen either arising from/connected to the ductal epithelium or are free floating within the lumen. In this example, the calcifications are small, round, and numerous and rimmed by epithelium as a single cluster. (**c**) Another example where the calcifications are partially encased in a pink rind referred to as the "ossifying type" of calcifications

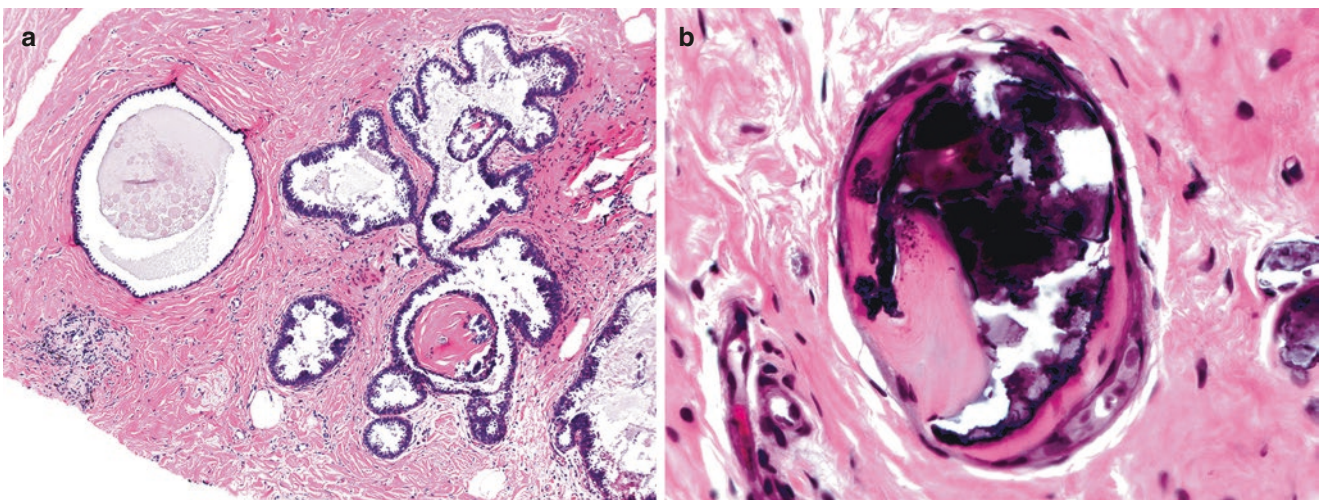

Fig. 2.70 "Ossifying type" calcifications in columnar cell lesions. (**a**, **b**) Associated calcifications in some examples of columnar cell change or columnar cell hyperplasia harbor a distinctive pink rind with hematoxylin-rich, purple calcifications in the center. While not pathognomonic for a columnar cell lesion, the distinct appearance of these calcifications is strongly associated with this entity

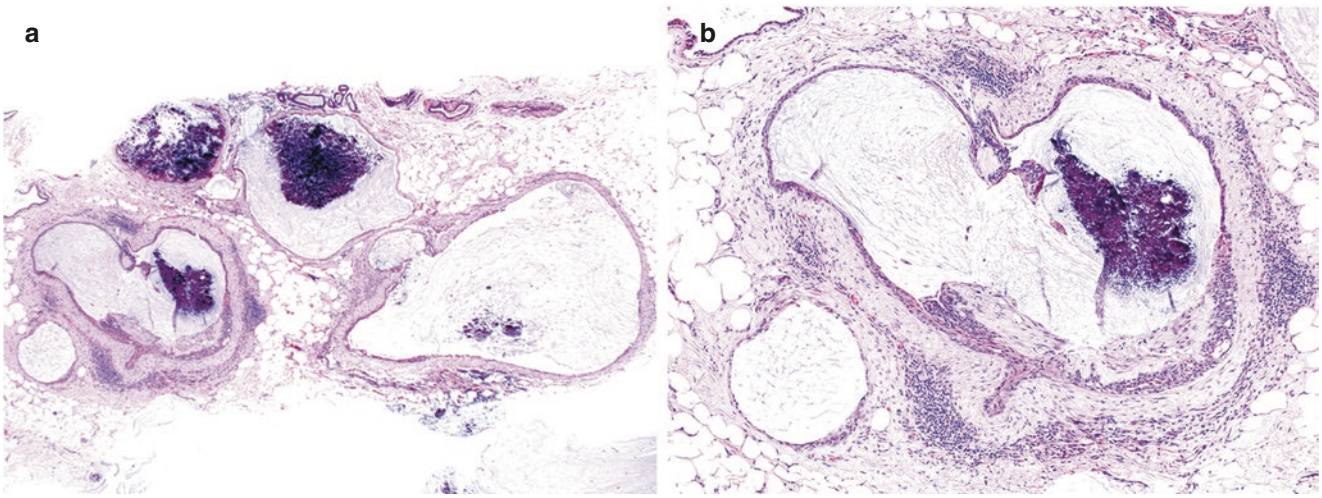

Fig. 2.71 Calcifications in mucocele-like lesion (MLL). (**a**, **b**) This example of MLL is associated with calcifications. MLL-associated calcifications are small and numerous and impart a granular or gritty appearance. They tend to cluster and localize to one area within the cyst's lumen. Note the viscous and wrinkled appearance of the luminal mucin

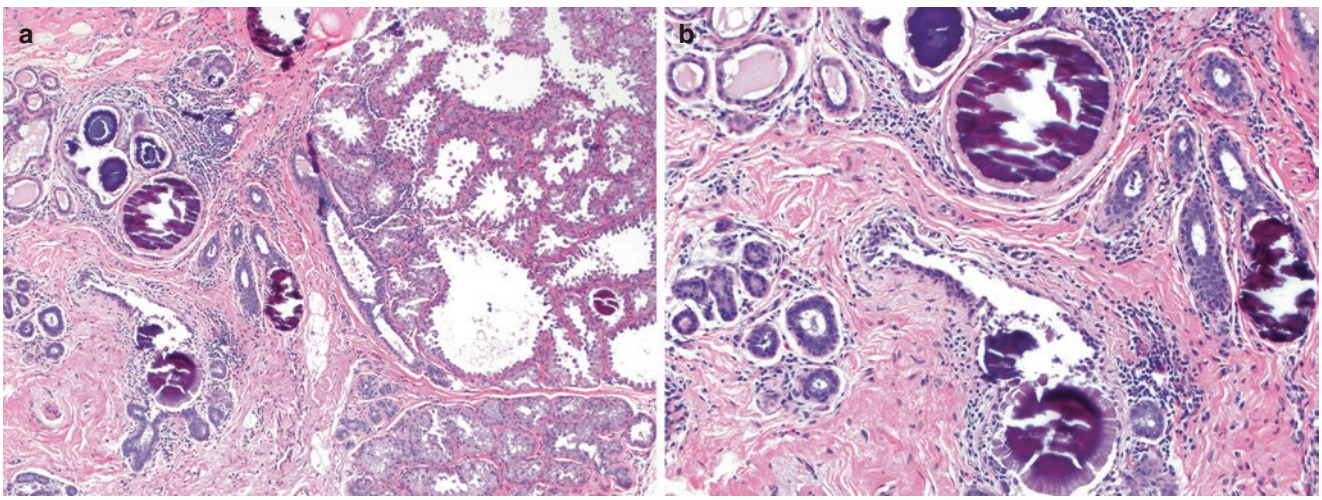

Fig. 2.72 Laminated calcifications in pregnancy-like change and pregnancy-like hyperplasia. (**a**) Pregnancy-like change and pregnancy-like hyperplasia typified by enlarged terminal duct lobular units (TDLUs) with ectatic lobular glands lined by epithelium with secretory changes. Round, sometimes shattered calcifications are commonly found within glandular lumens. (**b**) On closer inspection the calcifications have irregularly spaced concentric laminations (psammomatous) and in some examples additionally show a lighter purple or pink rim. (*Courtesy of Dr. Timothy M. D'Alfonso, with permission*)

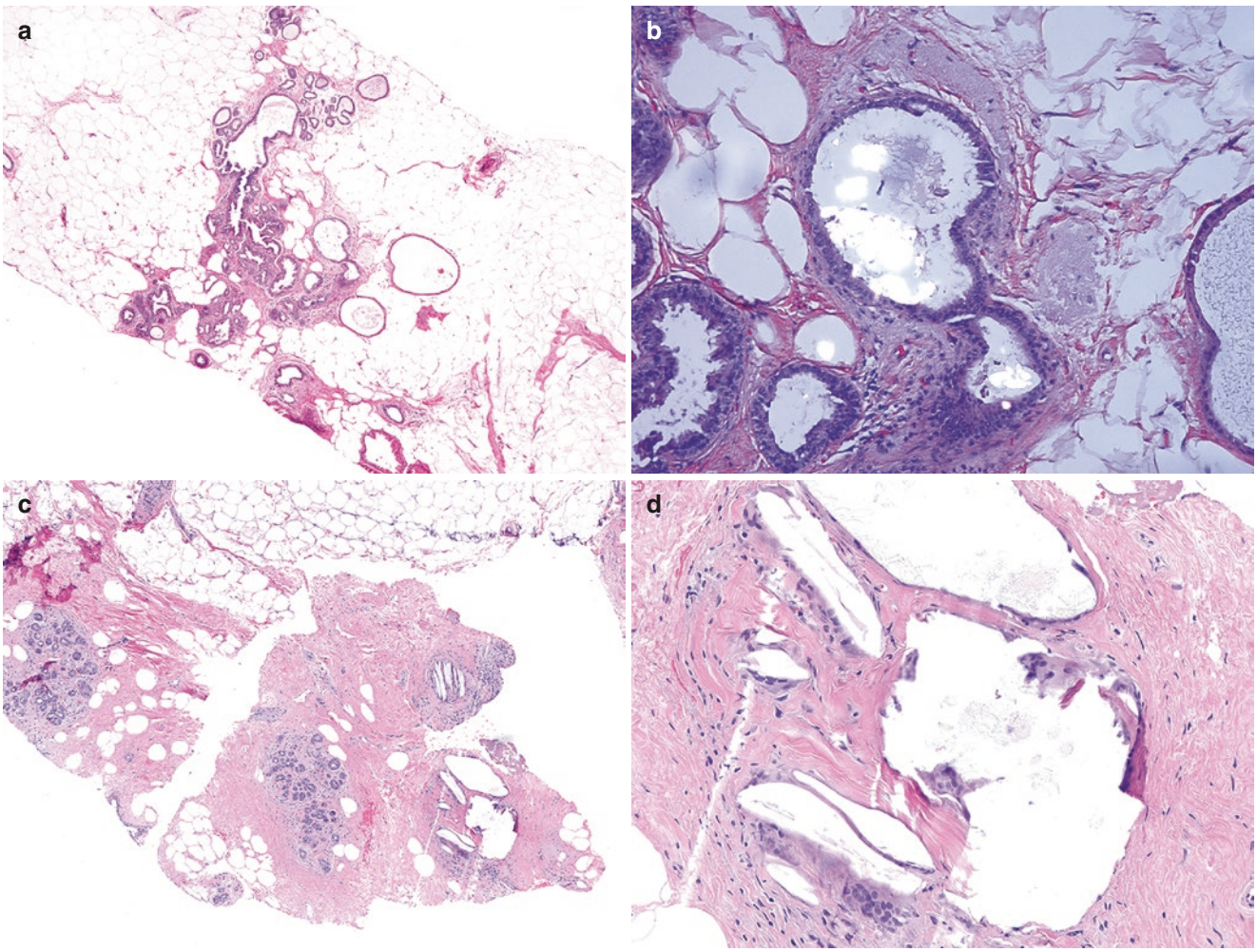

Fig. 2.73 Calcifications associated with apocrine metaplasia. (**a**, **b**) Luminal calcium oxalate crystals present in cystic apocrine metaplasia may be difficult to detect at low magnification; however, they are evident at higher magnification under polarized light. (**c**, **d**) Calcium oxalate embedded in fibrous stroma with multinucleated giant cell reaction. Apocrine metaplasia is present in the surrounding breast tissue

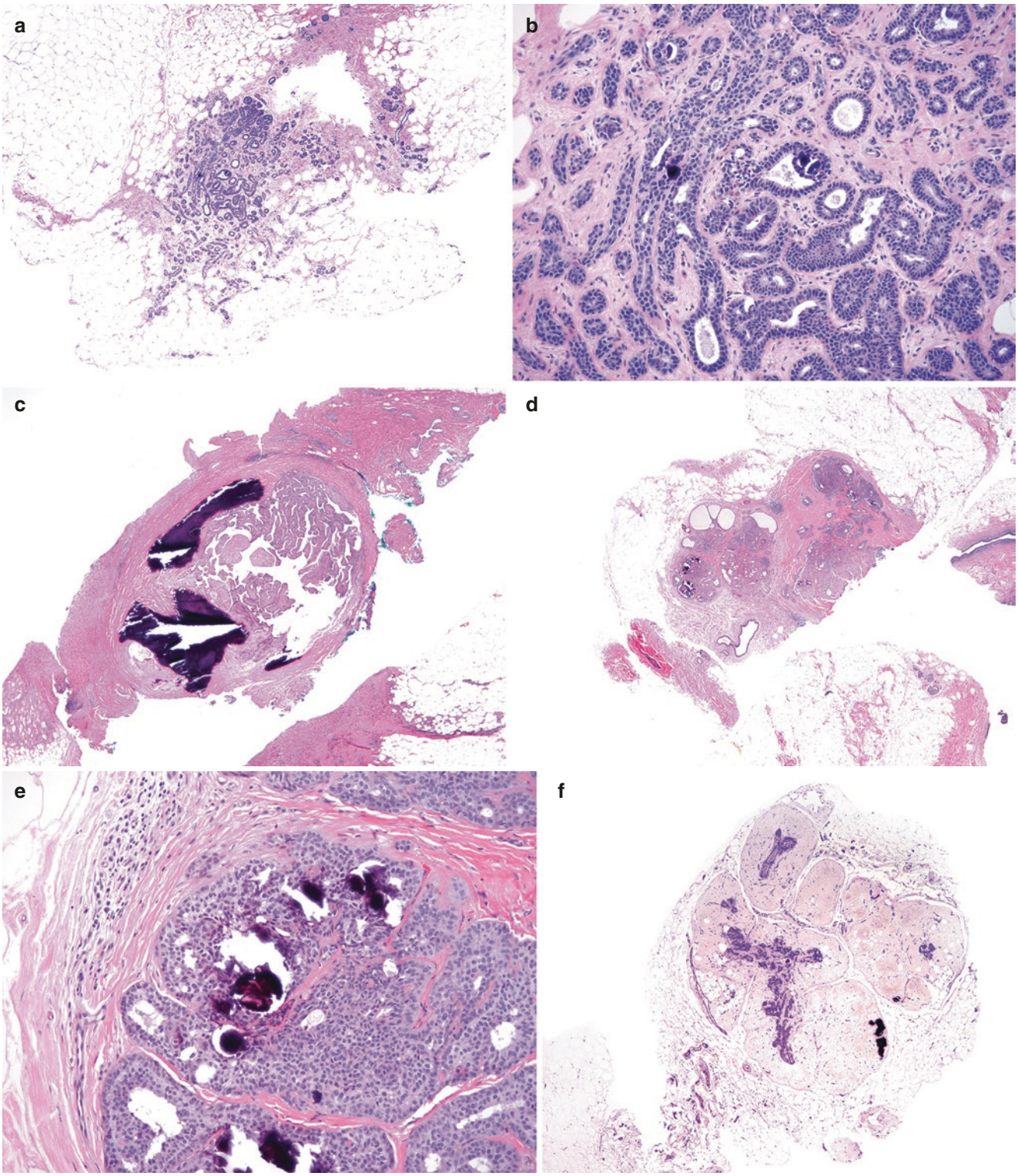

Fig. 2.74 CNBs targeted for calcifications and their associated benign entities. (**a**, **b**) Epithelial calcifications are present in a focus of sclerosing adenosis. (**c**) Coarse stromal calcifications are associated with a sclerosing papilloma. (**d**, **e**) Epithelial calcifications are present in florid ductal hyperplasia associated with a sclerosing papilloma. (**f, g**) Coarse calcifications identified in hyalinized fibroadenomatoid stroma

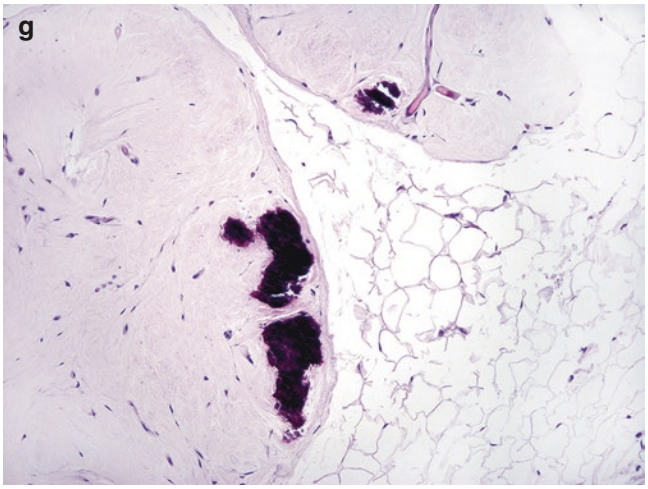

Fig. 2.74 (continued)

References

1. D'Alfonso TM, Shin SJ. Small glandular proliferations of the breast. In: Schnitt SJ, Shin SJ, guest editors. Breast pathology: diagnosis and insights. Surgical pathology clinics. Philadelphia, PA: W.B. Saunders; 2012.
2. Varma S, Shin SJ. An algorithmic approach to spindle cell lesions of the breast. Adv Anat Pathol. 2013;20(2):95–109.
3. Fadare O, Mariappan MR. Mucocele-like tumor and columnar cell hyperplasia of the breast occurring in a morphologic continuum. J Med Case Rep. 2008;2:138.
4. Shin SJ, Rosen PP. Pregnancy-like (pseudolactational) hyperplasia: a primary diagnosis in mammographically detected lesions of the breast and its relationship to cystic hypersecretory hyperplasia. Am J Surg Pathol. 2000;24(12):1670–4.

Multiples in Core Needle Biopsy Samples

3

Sandra J. Shin and Paula S. Ginter

Introduction

Unlike larger resection specimens, the limited material available for study in core needle biopsy (CNB) samples impacts the way in which we approach these cases diagnostically. If the diagnosis is not straightforward, the steps taken to work up the case must be carefully considered as the risk of exhausting lesional tissue is always present. Seasoned pathologists who have largely learned from past experience develop the ability to choose the best method of working up any individual case whether that entails obtaining additional H&E slides, ordering immunohistochemistry/immunohistochemical (IHC) or special stains, or a combination thereof. Moreover, a diagnosis rendered in a CNB directly impacts the next step of clinical management which only further underscores the importance of working up diagnostically challenging cases in a wise and efficient manner for the betterment of patient care.

In this era of CNB evaluation, pathologists are required more than ever to "do more with less." This chapter is dedicated to highlighting specific aspects of pathologic evaluation that are particularly relevant in the setting of CNB samples.

The Value of H&E Levels

While examining additional hematoxylin and eosin (H&E) levels is routinely employed for problematic cases in all specimens, this strategy is particularly valuable when evaluating CNB samples. Evaluating areas of concern in small tissue samples can be very challenging as the risk of exhausting lesional tissue from the paraffin block is high, and in many instances the pathologist is limited to choosing one plan of action to work up a case while cognizant of the strong possibility that there will be insufficient lesional tissue to conduct another round of investigation using an alternate approach. When faced with a small focus of concern, pathologists find themselves at a juncture where workup can either entail obtaining additional H&E levels or performing IHC stains. It is difficult to convey to a newly minted pathologist when one approach is better than the other as it all depends on the focus of concern and the differential diagnosis at hand. With that said, it is helpful to be cognizant of several diagnostic scenarios that are not uncommonly encountered in breast CNBs which will be reviewed here.

Scenario 1: Seemingly Nondiagnostic Findings on Initial H&E Levels

Radiographically suspicious calcifications constitute a large if not the majority of mammographically detected abnormalities sampled by CNB. While benign appearing calcifications are managed by surveillance, other mammographically detected calcifications with indeterminate or suspicious imaging characteristics are biopsied for definitive diagnosis. As discussed in Chap. 1, radiologic–pathologic concordance should be performed in all cases. At times, targeted calcifications may not be evident in the initially prepared slides and it is imperative that pathologists do their due diligence to locate them by further working up the case.

The number of initial H&E sections and/or slides prepared from a breast CNB is determined by the individual laboratory, and factors such as specimen volume, resources, and pathologists' preferences invariably contribute to such decisions. While a handful of studies have shown that approximately three slides from each paraffin block prepared in cases of targeted calcifications is sufficient for histologic evaluation [1, 2], the number (if

S. J. Shin (✉)
Department of Pathology and Laboratory Medicine, Albany Medical College, Albany, NY, USA
e-mail: shins1@amc.edu

P. S. Ginter
Department of Pathology and Laboratory Medicine, Weill Cornell Medicine, New York, NY, USA
e-mail: psg9003@med.cornell.edu

© The Author(s), under exclusive license to Springer Nature Switzerland AG 2022
S. J. Shin et al. (eds.), *A Comprehensive Guide to Core Needle Biopsies of the Breast*,
https://doi.org/10.1007/978-3-031-05532-4_3

any) and thickness of intervening sections between slides is not explicitly stated. At some institutions, two slides are prepared after five intervening 5-μm thick sections are discarded. Each slide contains 1–3 sections from the tissue ribbon depending on the size of the specimen. While a formal study has not been conducted, this method has been found to be sufficient to render a diagnosis in the majority of cases while conserving enough tissue for cases that require additional studies.

When calcifications are not present in the initial slides or much smaller in caliber than what is seen on the accompanying specimen radiograph, a few options can be exercised. If a faxitron is accessible, it is helpful to X-ray the paraffin blocks to identify the ones that contain the targeted calcifications. This step will bypass unnecessary labor and costs to prepare additional H&E levels from tissue blocks that do not contain calcifications. Once blocks most likely to contain calcifications are selected, a number of H&E levels should be prepared from each of them. As previously mentioned, the number of slides prepared is contingent upon a number of factors including whether (and to what degree) of trimming or tissue discarding is performed between slides, individual skill level of the histotechnician which impacts the extent of trimming, and personal preference of the pathologist. At some institutions, there are stringent criteria about different sections that can be requested. "Serial" sections refer to consecutive tissue sections without intervening trimming while "levels" refer to sections where five 4-μm thick tissue sections are discarded between prepared slides (Figs. 3.1 and 3.2). "Deepers" refer to sections where four 10-μm thick tissue sections are discarded between prepared slides (Fig. 3.3). When hunting for microcalcifications in breast CNBs, 5–7 additional H&E levels are

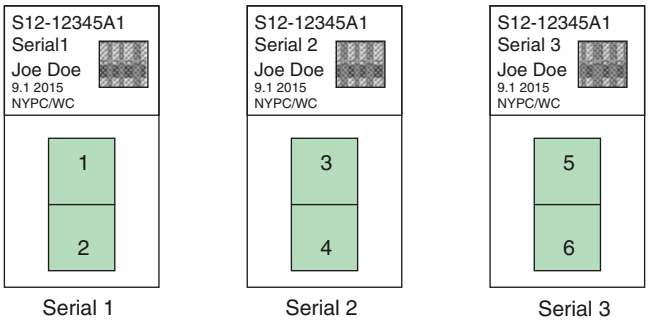

Fig. 3.1 Serial sections. Tissue sections are cut from the block in sequential order without discarding any intervening sections between prepared slides. (*Courtesy of Ms. Lilian Antonio*, New York Presbyterian Hospital, with permission)

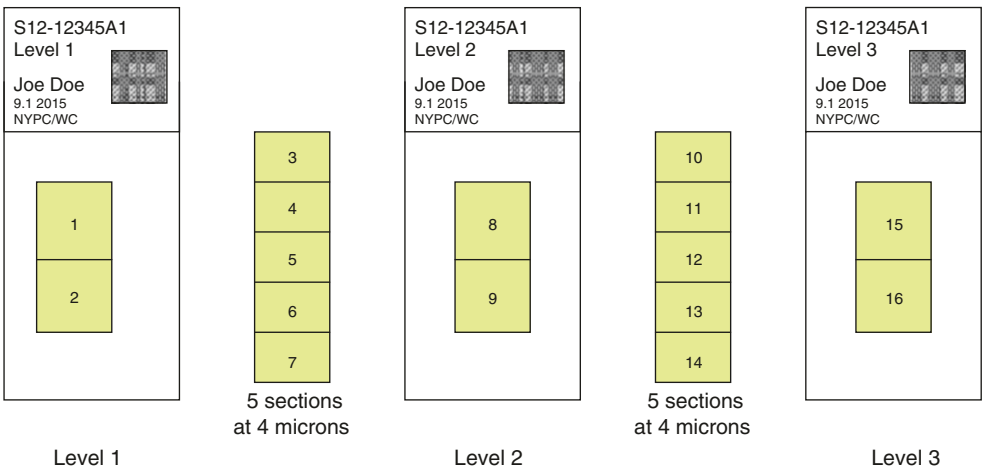

Fig. 3.2 Level sections. Tissue sections are cut from the block in sequential order but four 5 μm-thick sections are discarded in between prepared slides. (*Courtesy of Ms. Lilian Antonio*, New York Presbyterian Hospital, with permission)

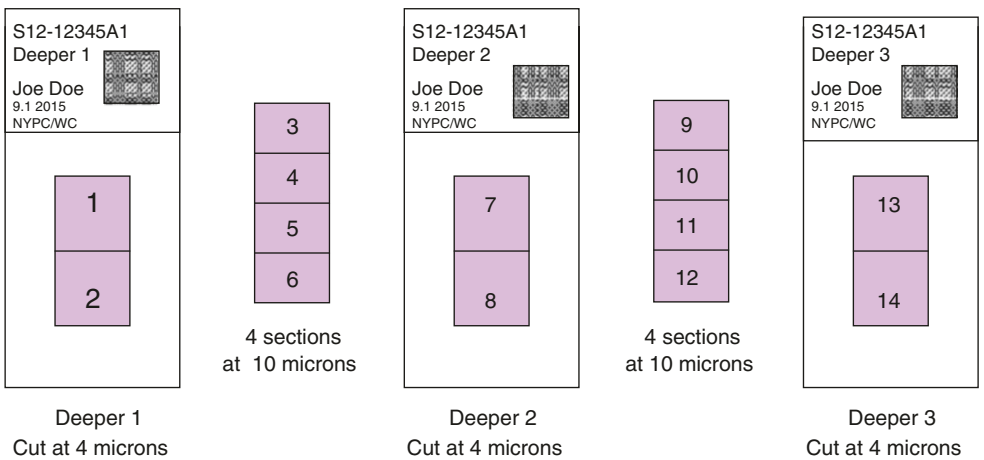

Fig. 3.3 Deeper sections. Sections cut from the block in sequential order but four 10-μm thick sections are discarded in between prepared slides. (*Courtesy of Ms. Lilian Antonio*, New York Presbyterian Hospital, with permission)

sufficient to locate targeted calcifications in most cases. It is also advisable to assign an experienced histology technician adept at handling small biopsy material and able to recognize larger caliber calcifications in the tissue block as to avoid exhausting lesional tissue from aggressive trimming.

Radiologists who routinely perform CNBs become highly skilled at sampling their target. However, even when the mammographic abnormality is biopsied, missing the most clinically relevant finding can still occur (Fig. 3.4). It is difficult for the pathologist to assess the probability of this occur-

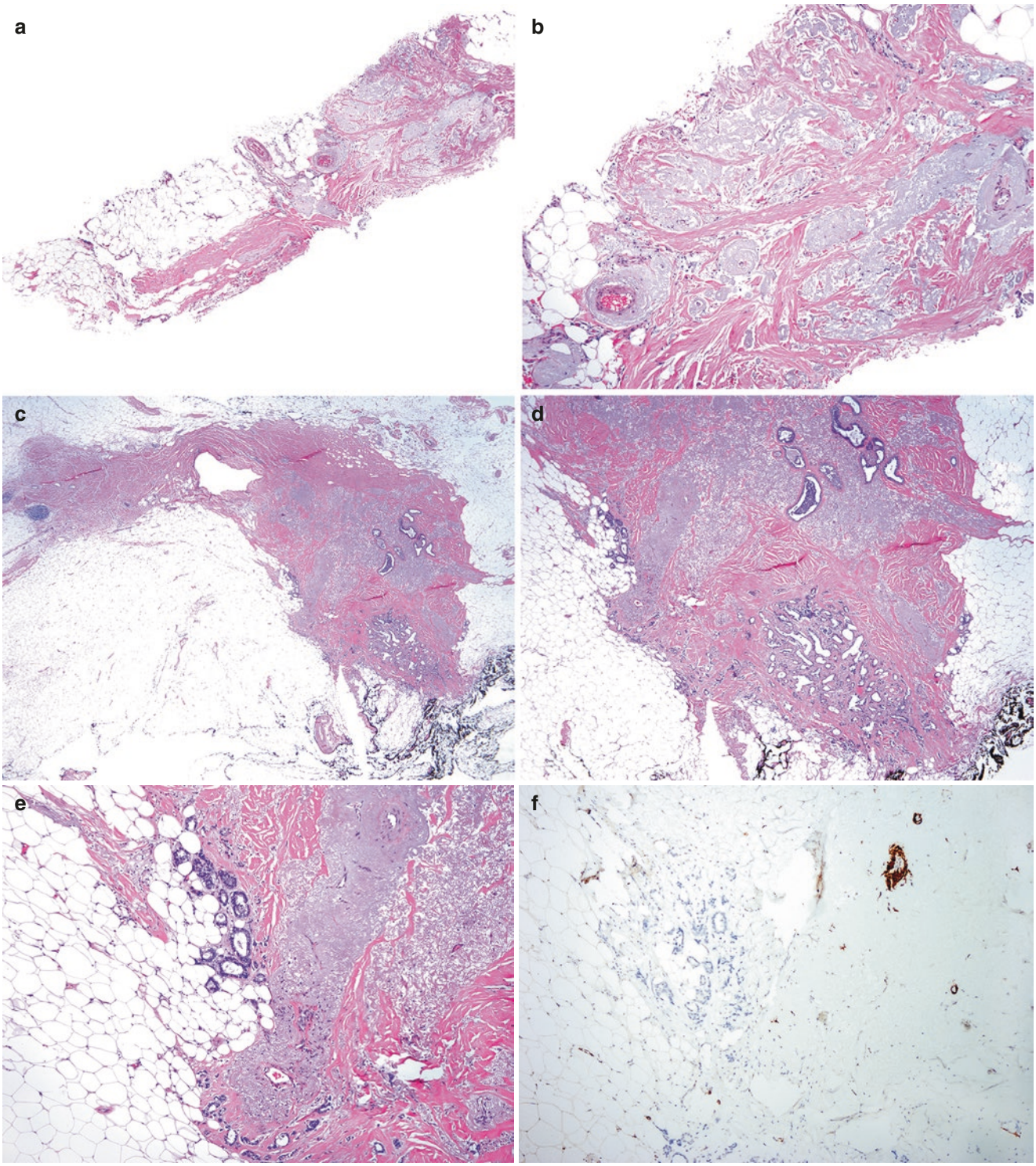

Fig. 3.4 The most clinically relevant finding goes unsampled despite pathologic–radiologic concordance. (**a**, **b**) CNB shows localized stromal fibrosis and elastosis in a case targeted for a focal breast density. (**c**) Low-power magnification of the subsequent excisional biopsy specimen shows a biopsy site (*upper field*) and invasive ductal carcinoma (*lower right*) both within the targeted focus of stromal fibrosis and elastosis. (**d**, **e**) Higher magnification of unsampled invasive, well-differentiated ductal carcinoma characterized by infiltrating well-formed neoplastic glands. (**f**, **g**) SMM and p63 IHC stains, respectively, are negative and (**h**) estrogen receptor is diffusely positive in neoplastic glands

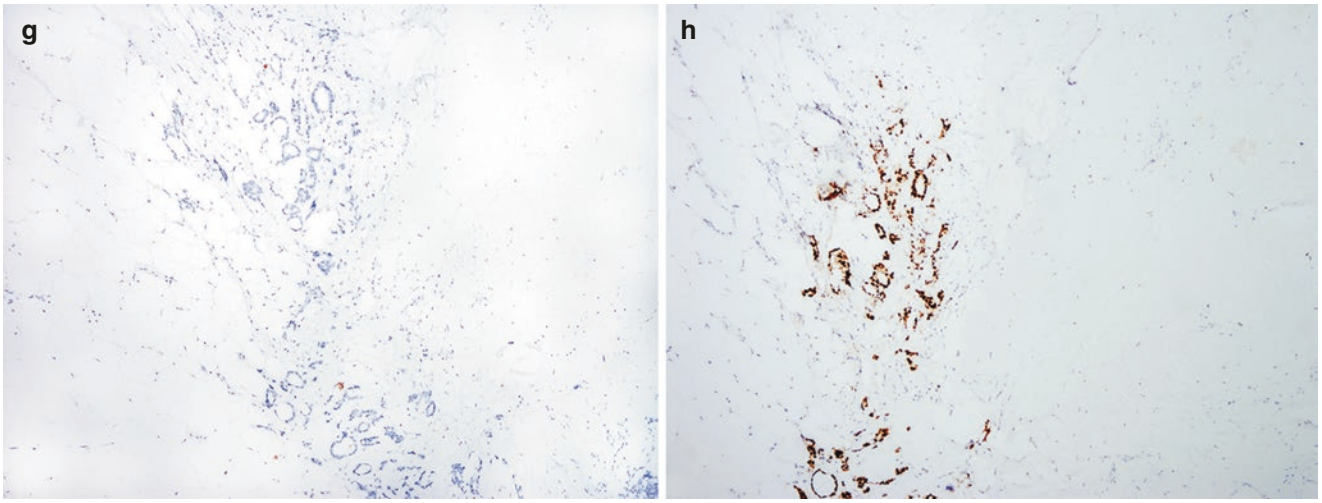

Fig. 3.4 (continued)

rence in any given case due to the limited clinical information that often accompanies the specimen. After a reasonable effort to identify histologic changes that would correlate with the radiologic findings, an active dialogue with the radiologist is always best practice. Pathologic–radiologic correlation is critically important and should be routinely performed. Even still, in some instances, uncertainty lingers and excisional biopsy may be necessary for definitive diagnosis.

Ductal carcinoma in situ (DCIS) is often detected mammographically due to its association with calcifications. Occasionally, the initial H&E slides prepared from the CNB specimen can show nonspecific changes such as foci of chronic inflammation or reactive appearing stroma without evidence of calcifications or a diagnostic lesion. In other instances, only foci of necrosis with or without calcifications in stroma are seen. Even if calcifications are identified and appear concordant with the radiologic impression, the nonspecific diagnosis of "stromal calcifications" should not be rendered until the specimen has been thoroughly evaluated on multiple deeper H&E levels, particularly if the calcifications are multiple and coarse. In some instances, these additional H&E levels reveal the association of these calcifications with DCIS. Extensive luminal necrosis can obliterate carcinomatous epithelium and such examples of DCIS have been described as ones with "necrosis to the wall." It is good practice to obtain an H&E level that shows a section where the epithelium, however attenuated, is diagnostic for carcinoma (Figs. 3.5 and 3.6).

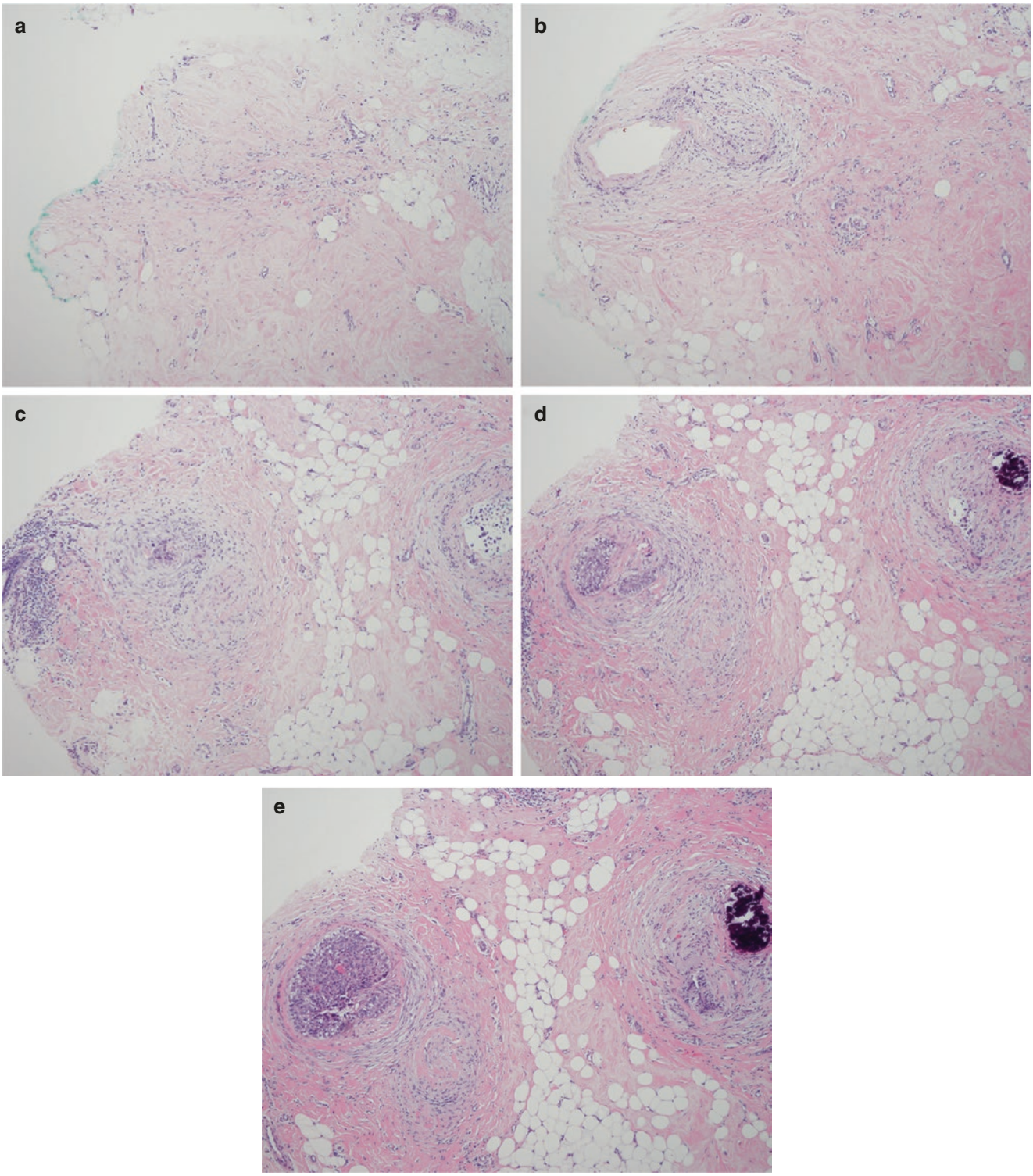

Fig. 3.5 Consecutive H&E sections of a CNB performed for microcalcifications. (**a**, **b**) Initial levels only reveal altered stroma with scattered lymphocytic infiltrates. (**c**, **d**) An epithelial proliferation surfaces (*left*) but histologically insufficient for diagnosis while stromal calcifications appear nearby (*right*). (**e**) Deepest H&E level reveals DCIS (*left*) and likely an additional focus of DCIS (*right*) associated with calcifications

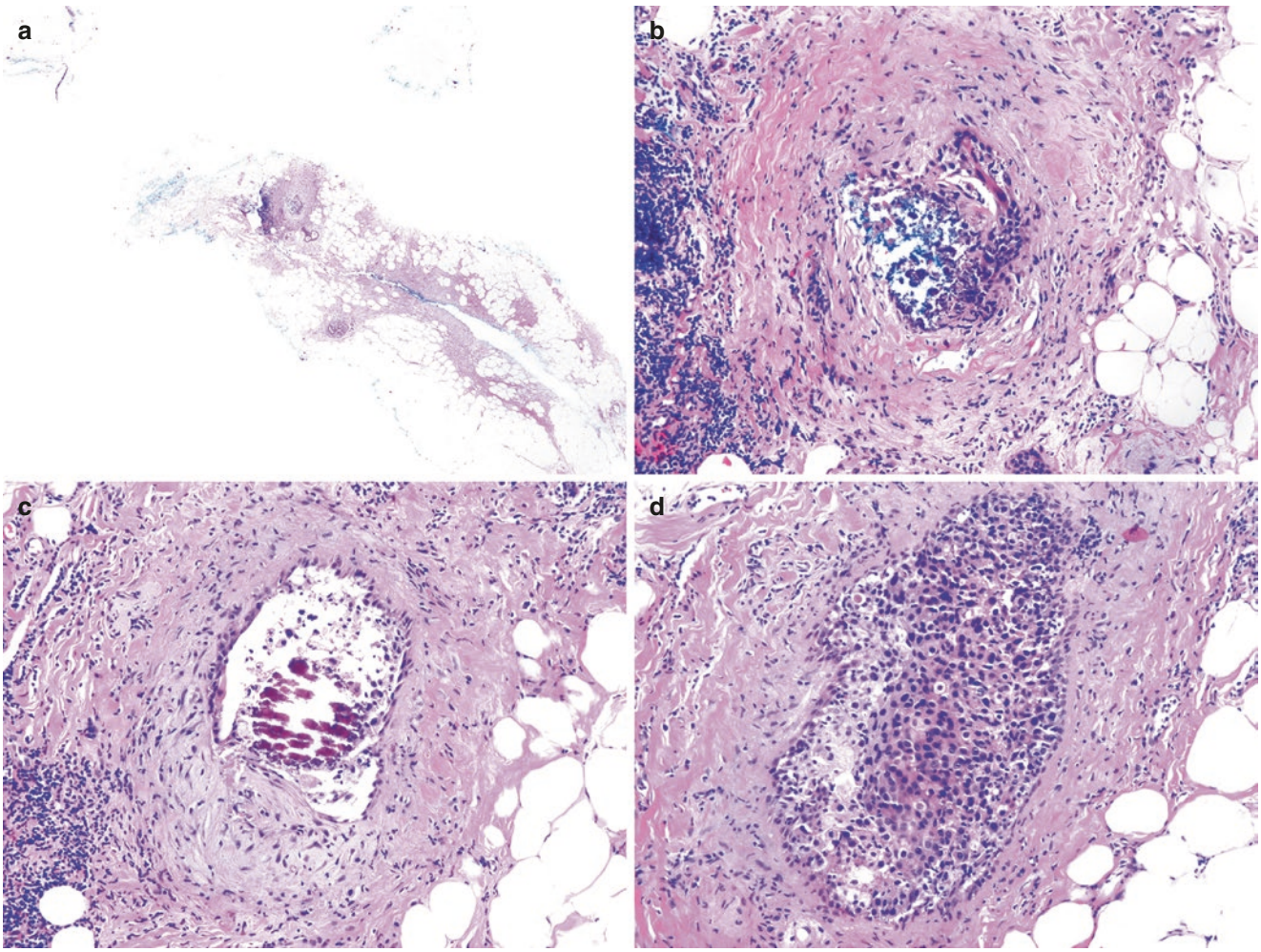

Fig. 3.6 CNB performed for mammographically detected calcifications. (**a**, **b**) Initial H&E level reveals stromal calcifications associated with minimal, distorted epithelium. (**c**, **d**) Deeper sections show a duct completely involved by an atypical epithelial proliferation diagnostic for DCIS

Scenario 2: Excluding Concomitant Microinvasive Carcinoma

Microinvasive carcinoma arising in a background of DCIS is a common pathologic finding and is a diagnosis that can be rendered in CNB material. Areas suspicious for microinvasive carcinoma can be further evaluated by either examining additional H&E levels or by IHC stains, ideally cytokeratin and myoepithelial markers.

Another but less commonly encountered diagnostic scenario is that of a mucocele-like lesion (MLL) with extravasated acellular mucin in the adjacent stroma. MLL encountered in the CNB setting is typically due to its association with calcifications or less frequently its ability to form a mass. Not uncommonly, there are pools of acellular mucin in the stroma adjacent to the MLL, a finding that is not entirely unexpected, particularly after local tissue disruption secondary to the biopsy procedure. However, pathologists should know to investigate such a finding further to exclude the possibility of invasive mucinous carcinoma as a subset of MLLs gives rise to them. The optimal approach is to obtain several H&E levels to identify, if any, carcinomatous epithelium suspended in these mucin pools. Benign epithelium lining the MLL can sometimes detach/shed and become free-floating within the luminal mucin and this should not be mistaken for invasive mucinous carcinoma (see Chap. 5). As the finding of invasive mucinous carcinoma would greatly alter clinical management, pathologists should remain vigilant of this possibility when encountering a MLL in core samples.

Scenario 3: Incomplete or Tangential Sections

Incomplete sections can lead to foci mimicking other processes, the most concerning of which resemble clinically more significant lesions. For instance, incomplete sectioning

of DCIS can give rise to an appearance that can be mistaken for another process. While it is excessive and unnecessary to obtain additional H&E levels to "further confirm" each finding/diagnosis, more evaluation is warranted when the findings collectively do not make clinical sense (Fig. 3.7).

The more common scenario is encountering tangential sections of benign mammary ducts that may or may not show epithelial hyperplasia. Trainees learn to identify tangential sections of benign ducts and these are quickly dismissed in excisional or resection specimens. However, in CNB samples where the amount of tissue available for evaluation is far less, pathologists may be tempted to overly scrutinize such foci and more quickly raise the possibility of atypia.

If the duct in question contains ductal hyperplasia, a tangential section can mimic atypical ductal hyperplasia (ADH), most commonly of the cribriform pattern (Fig. 3.8). Morphologic clues that would favor a tangential section of usual ductal hyperplasia include microlumens arranged in a parallel fashion across the span of the duct lumen as well as the appearance of "stretched" ductal epithelial cells in the center of the duct lumen (Figs. 3.9, 3.10, and 3.11). When in doubt, evaluating additional deeper H&E levels can be helpful as the duct in question tends to "straighten out" and lose its initial atypical appearing features. In some instances, the duct is tangentially sectioned in such a way that causes the myoepithelial layer to appear proliferative mimicking an atypical lobular proliferation (i.e., atypical lobular hyperplasia [ALH] or lobular carcinoma in situ [LCIS]) growing in a pagetoid distribution (Fig. 3.12). In such cases, obtaining IHC stains specific to myoepithelium (p63) and lobular lesions (E-cadherin, p120) can provide clarity. It should be noted that myoepithelial cells are weakly immunoreactive for E-cadherin and thus can be misinterpreted as fragmented membranous staining of lobular proliferations if utilized in isolation. Therefore, a myoepithelial marker that localizes to a separate cellular compartment such as the nucleus (i.e., p63) would be prudent to evaluate in tandem with E-cadherin to clearly discern between myoepithelial and lobular cells.

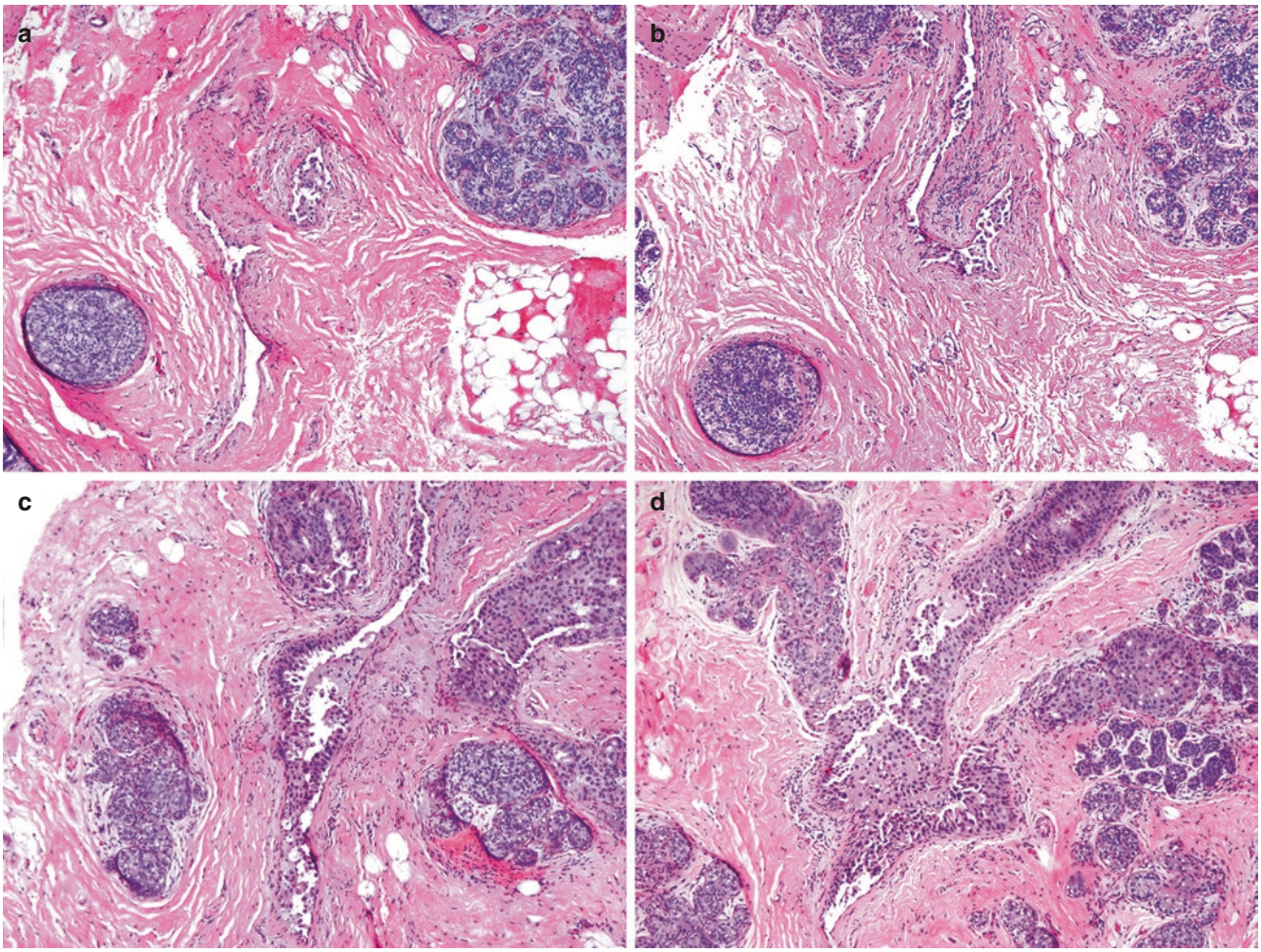

Fig. 3.7 A focus suspicious for lymphovascular invasion. (**a**) Initial H&E section shows a focus resembling lymphovascular invasion amidst surrounding DCIS in a case without concurrent invasive carcinoma. (**b**–**d**) Deeper levels reveal this focus to represent an additional focus of DCIS

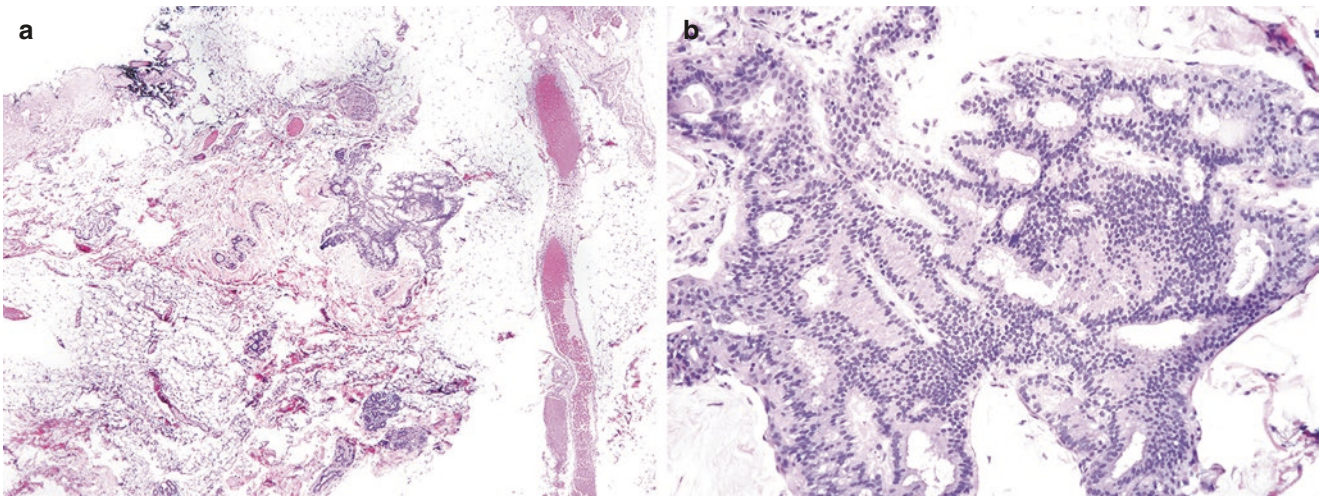

Fig. 3.8 Tangential sectioning of ductal hyperplasia mimicking ADH. (**a**) A tangential section of a duct involved by usual ductal hyperplasia forming pseudo-bridges and microlumens. (**b**) On close inspection, bridging cells appear attenuated (stretched) across the span of the duct—a finding characteristic of a tangential section. Evaluation of additional deeper H&E levels can be performed which typically "corrects" the effects of tangential sectioning

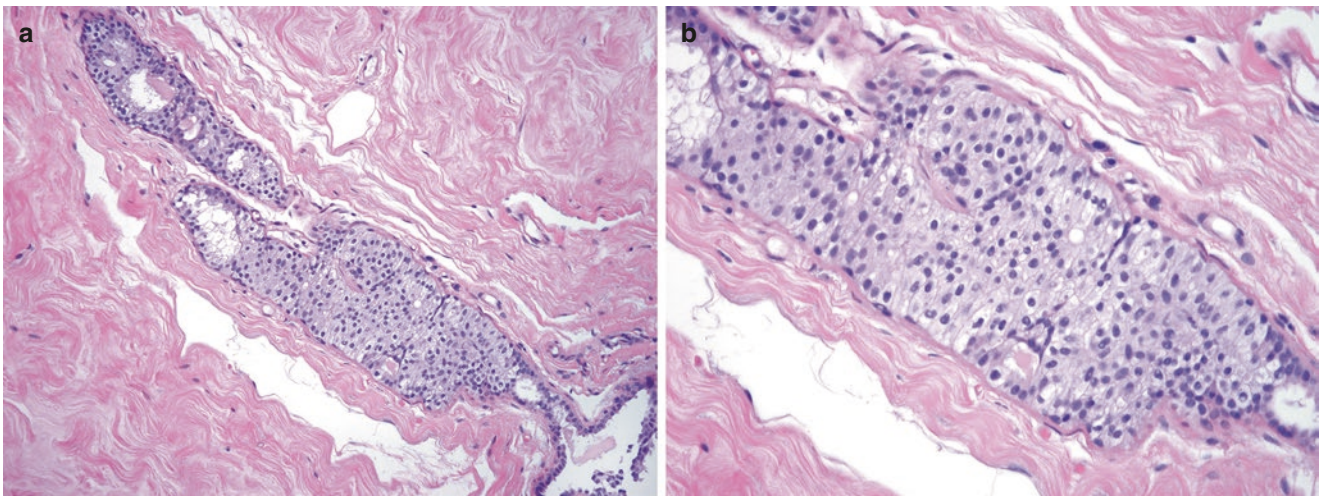

Fig. 3.9 A tangential section of the myoepithelial layer of this benign duct mimics an atypical lobular proliferation. (**a**, **b**) Occasionally, tangential sectioning through the myoepithelium can lead to the mistaken appearance of LCIS due to the clear appearance of these cells

While evaluating a focus of interest in additional sections of H&E or immunostained slides, it is important to be aware of the possibility that additional, incidental but clinically significant findings can surface or alternatively, a separate atypical focus becomes diagnostic for a clinically more significant lesion. If discovered on an immunostained slide, a histologic diagnosis should only be rendered on a subsequently prepared H&E-stained slide from the same block. At some institutions, an H&E slide is prepared concurrently with IHC stains to avoid losing small foci of interest from re-facing the block a second time. Above all, formulating a histologic diagnosis on an immunostained slide should be avoided in all but the most exceptional circumstances (Fig. 3.13).

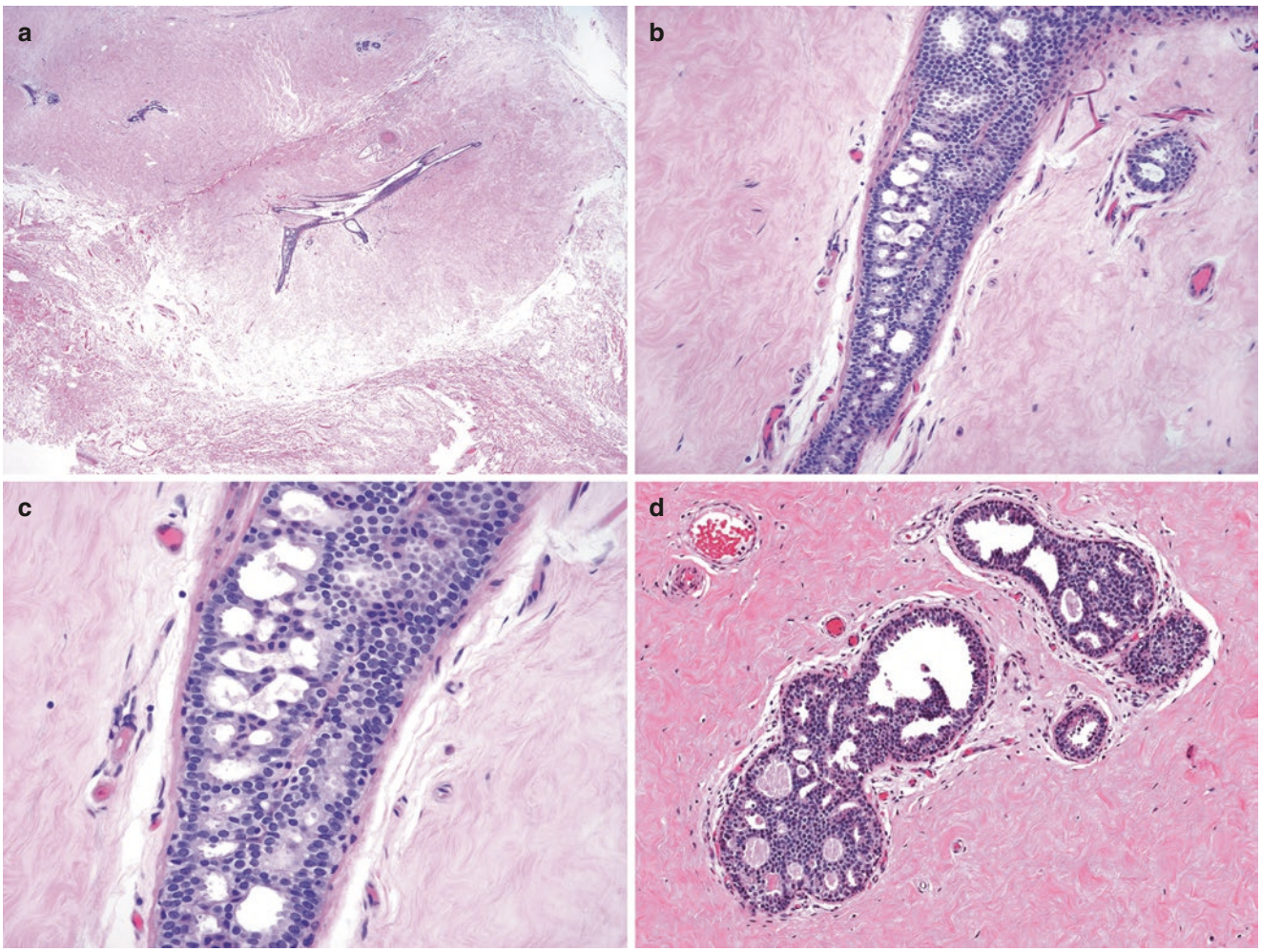

Fig. 3.10 A tangential section of a benign duct in male breast tissue. (**a**, **b**) Histologic changes of gynecomastia with a rare duct showing partial epithelial proliferation. (**c**) On closer inspection, the microlumens are formed by stretched bridging cells characteristic of tangential sectioning. (**d**) Medium power view of ADH from another male patient for comparison

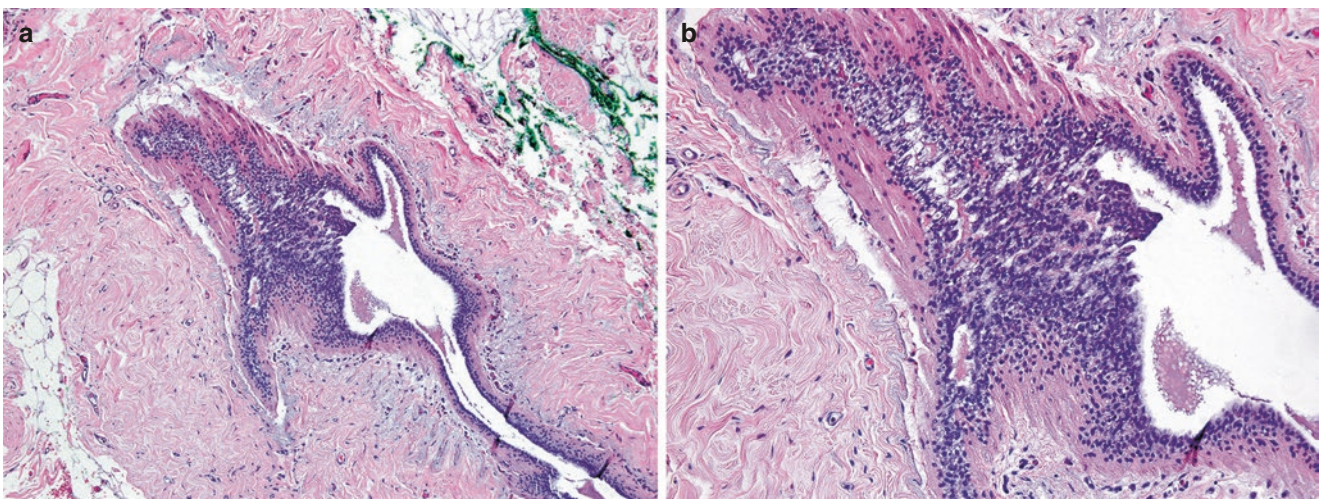

Fig. 3.11 A tangential section of a duct mimicking ADH. (**a**, **b**) This example of tangential sectioning resembles atypical ductal hyperplasia with micropapillary pattern

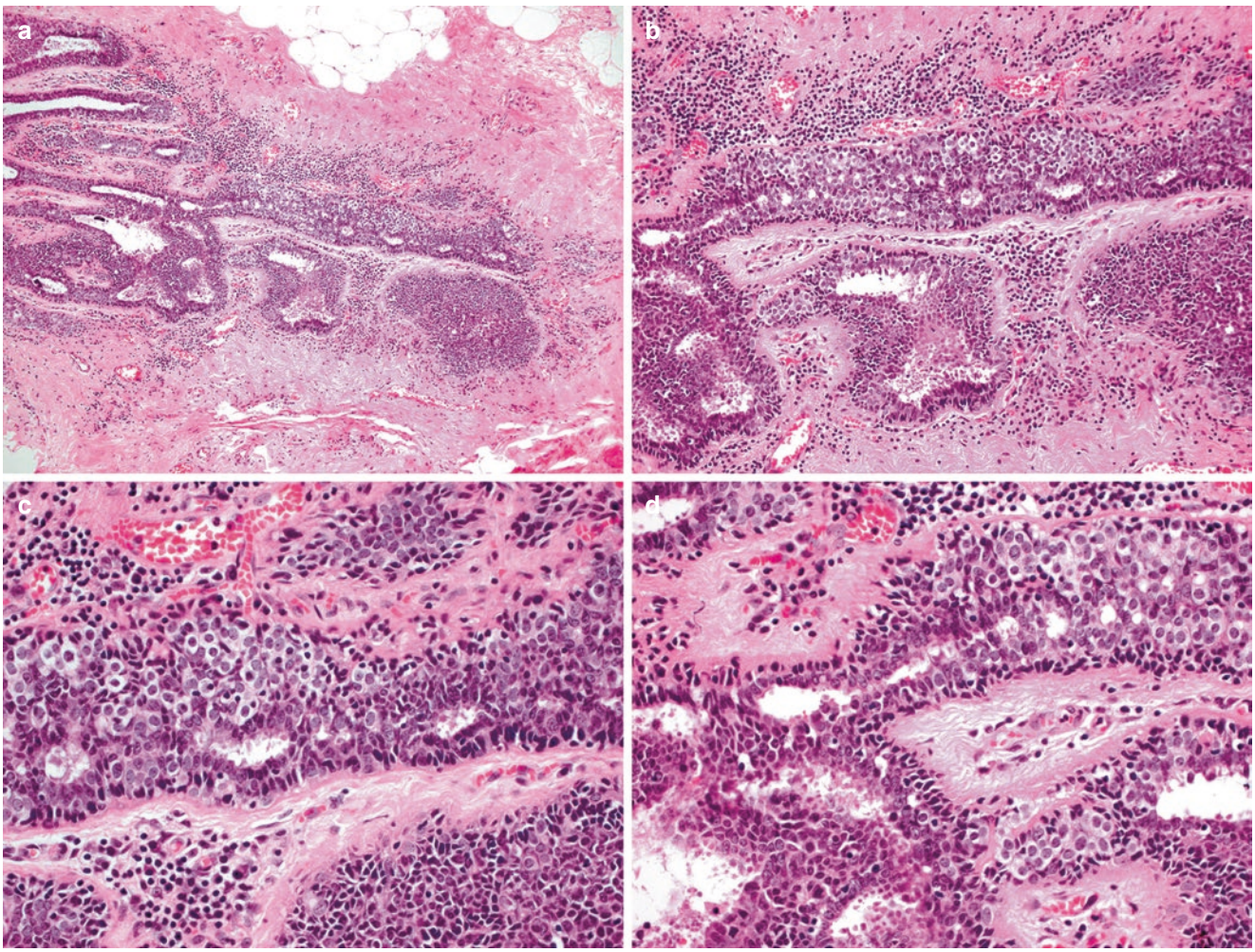

Fig. 3.12 A tangential section of a duct mimicking LCIS. (**a**, **b**) On low and medium magnification, respectively, the localized population of clear cells is eye-catching. (**c**, **d**) Higher magnifications show attenuated bridging cells indicating that this is a tangentially sectioned duct. Consequently, the clear cells of question most likely represent tangentially sectioned myoepithelium. Immunostains p63 and E-cadherin confirmed the myoepithelial origin of these cells (not shown)

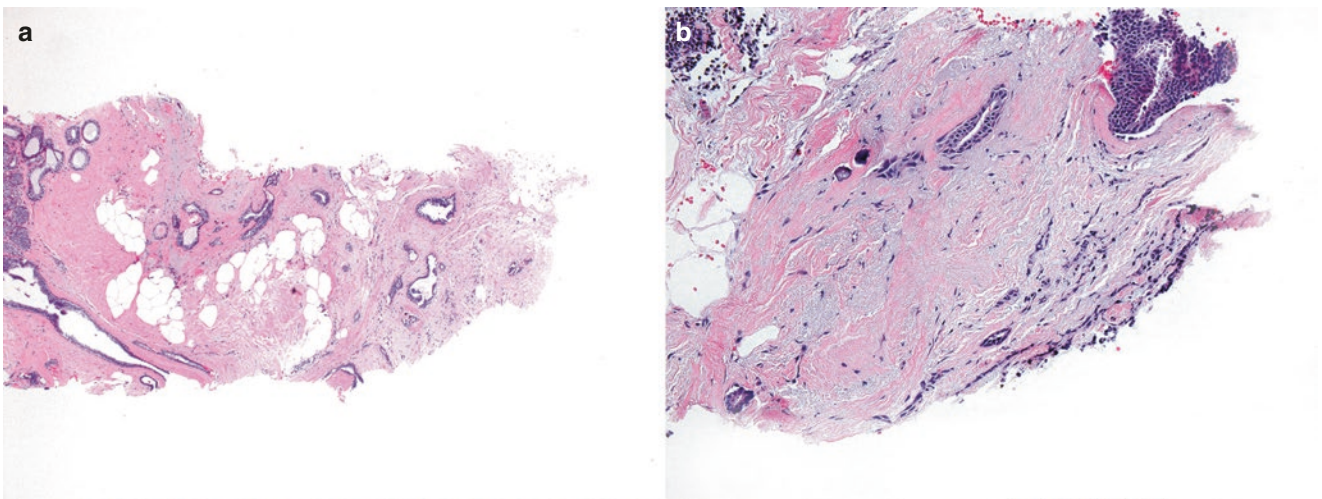

Fig. 3.13 CNB containing an incidental focus of invasive carcinoma diagnostic only on deeper tissue sections. (**a**–**c**) H&E images show small, darkly staining crushed cells in an infiltrative pattern. The morphologic features are severely compromised preventing a definitive diagnosis. (**d**, **e**) IHC stains CKAE1/AE3 and smooth muscle myosin are positive and negative, respectively. (**f**, **g**) An H&E stained slide was subsequently prepared from the block which demonstrated sufficient morphologic features to render a diagnosis of invasive carcinoma

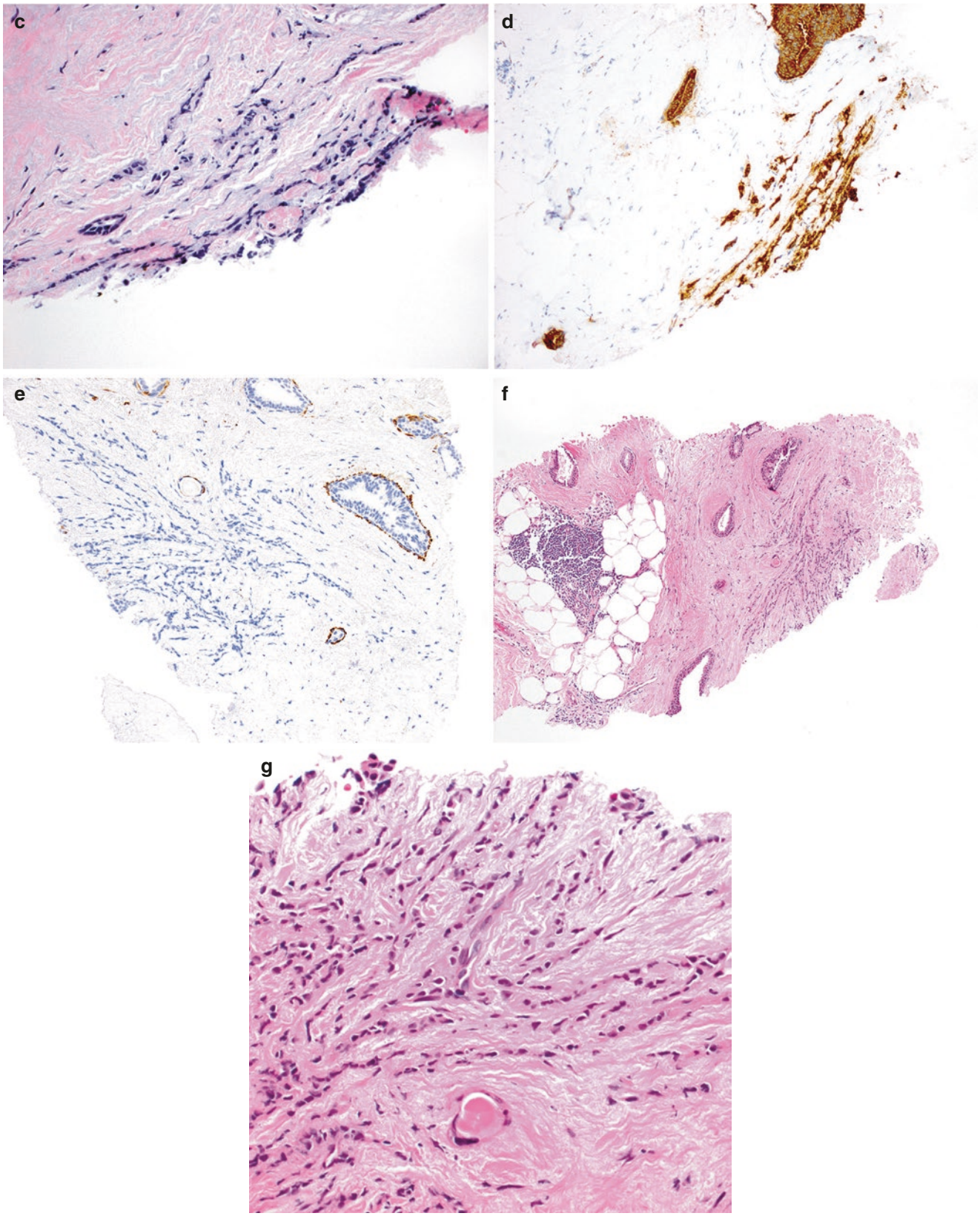

Fig. 3.13 (continued)

Multiple Diagnoses in Core Needle Biopsy Samples

Small tissue samples do not necessarily mean fewer diagnoses and achieving pathologic–radiologic concordance, albeit important, does not ensure that all clinically significant findings have been uncovered. CNB samples can harbor more than one diagnosis and identifying all of them is important since one but not all of them could alter clinical management at this stage of a patient's care. Maintaining a healthy index of suspicion is essential in this regard, and moreover knowing lesions that commonly coexist or secondarily involve one another is helpful. In other instances, a combination of two proliferations can be morphologically misconstrued as a single (usually atypical or malignant) process.

A prototypical example of coexisting proliferations is the low-grade breast neoplasia pathway and its members. Columnar cell lesions have become a commonly rendered diagnosis, particularly in the context of CNBs, due to their frequent association with calcifications. It is in these encounters that an observation was made regarding the not infrequent finding of lobular lesions and tubular carcinoma in these biopsies [3]. While morphologically distinct from each other, these entities were found to be closely related at the molecular level, specifically in their shared loss of 16q and gain of 1q. This fascinating revelation led way to the concept of the low-grade breast neoplasia pathway which includes columnar cell lesions including flat epithelial atypia, ADH/low-grade DCIS, invasive well-differentiated ductal carcinoma including tubular carcinoma, invasive tubulolobular carcinoma and lobular lesions (ALH, LCIS, invasive lobular carcinoma) [4]. Practically speaking, awareness of this increased tendency to see one or more members of this pathway in a single specimen can encourage pathologists to more closely scrutinize CNBs where one or more of these members have been identified (Figs. 3.14 and 3.15). Subsequent

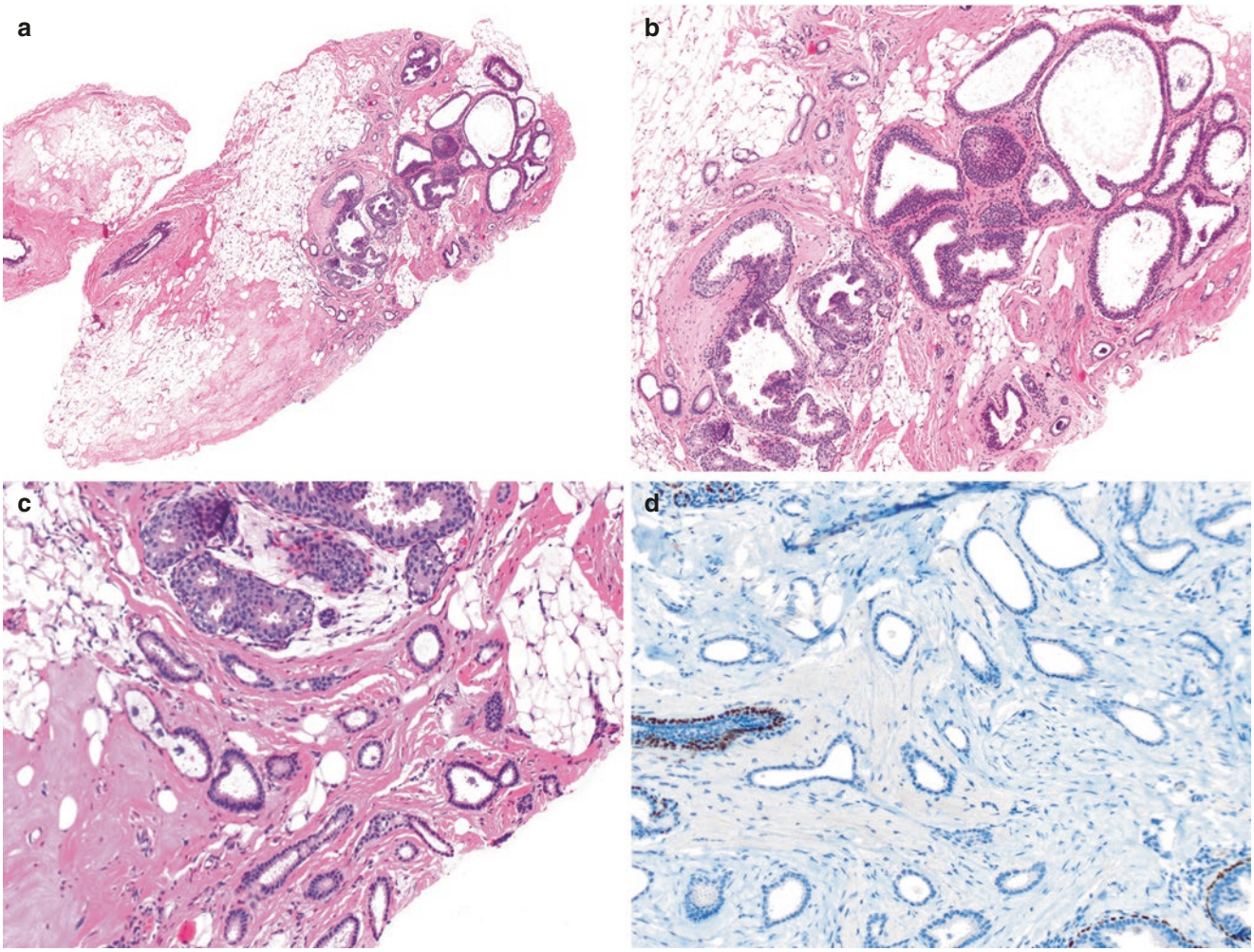

Fig. 3.14 CNB performed for mammographically targeted calcifications. (**a**, **b**) Larger calcifications are associated with columnar cell lesions while smaller ones are present in lumens of a small glandular proliferation in the adjacent stroma (*upper left* and *lower right* in figure **b**). (**c**) Higher magnification shows this small glandular proliferation to represent invasive tubular carcinoma. (**d**) The invasive nature of this carcinoma is confirmed by lack of expression for p63

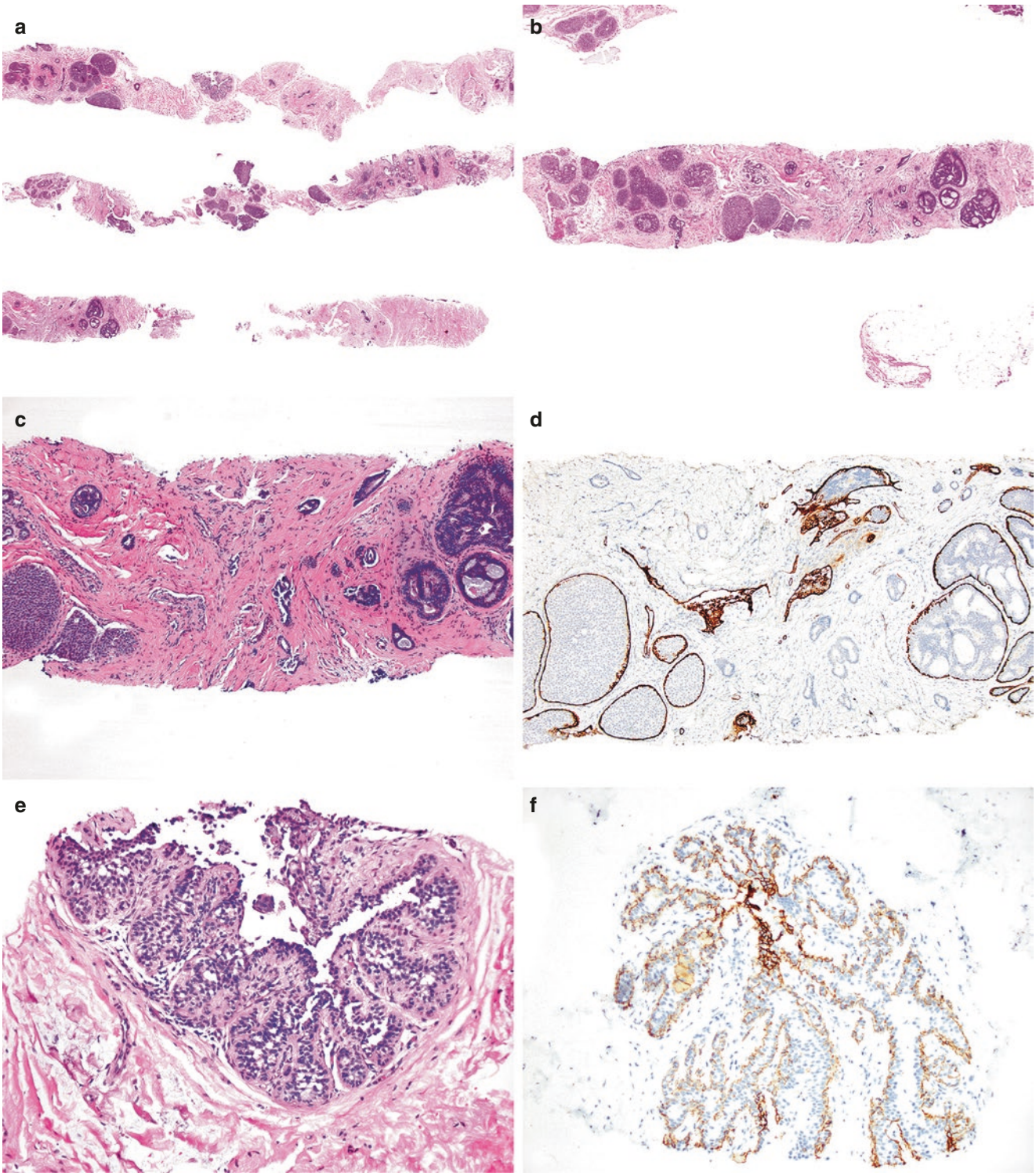

Fig. 3.15 CNB performed for mammographic calcifications. (**a**) The targeted lesion was DCIS which was associated with calcifications. (**b**, **c**) However, a small glandular proliferation was identified infiltrating between foci of DCIS. (**d**) Absence of SMM reactivity around these glands confirmed the diagnosis of invasive, well-differentiated ductal carcinoma. (**e**, **f**) In addition, a focus of lobular neoplasia was identified and confirmed by negative staining for E-cadherin. Note investing myoepithelium is positive

identification of a clinically more significant lesion (i.e., invasive carcinoma) will invariably alter management for the patient despite achieving pathologic–radiologic concordance (i.e., columnar cell hyperplasia associated with calcifications).

In other instances, benign lesions can be secondarily occupied by another, sometimes malignant, proliferation. The most commonly afflicted entities are sclerosing adenosis, radial scar, and papilloma, and these are often seen in CNB material due to their association with calcifications or the ability to cause a mammographic abnormality (i.e., mass). Less commonly, fibroepithelial lesions and collagenous spherulosis targeted for a mass or calcifications, respectively, can be involved by other proliferations such as LCIS. Needless to say, the clinically more significant lesions that would alter subsequent clinical management are the most important to identify in these scenarios. In some instances, the additional finding will not alter management (i.e., radial scar may warrant excisional biopsy by its presence alone); however, in other cases only the "secondary" diagnosis (i.e., DCIS found to involve sclerosing adenosis biopsied for calcifications associated with the latter) would justify more aggressive management (i.e., excisional biopsy). LCIS, ADH, DCIS, and invasive carcinomas commonly represent such "secondary" but clinically more significant diagnoses in the CNB samples performed for calcifications or a mass (Figs. 3.16, 3.17, 3.18, 3.19, 3.20, 3.21, 3.22, 3.23, 3.24, 3.25, 3.26, 3.27, 3.28, and 3.29). Instances of microscopic findings that do not typically coexist can also raise the possibility of two distinct lesions or processes (Fig. 3.30).

Another diagnostic pitfall is misinterpreting the appearance of two coexisting and possibly co-mingling lesions

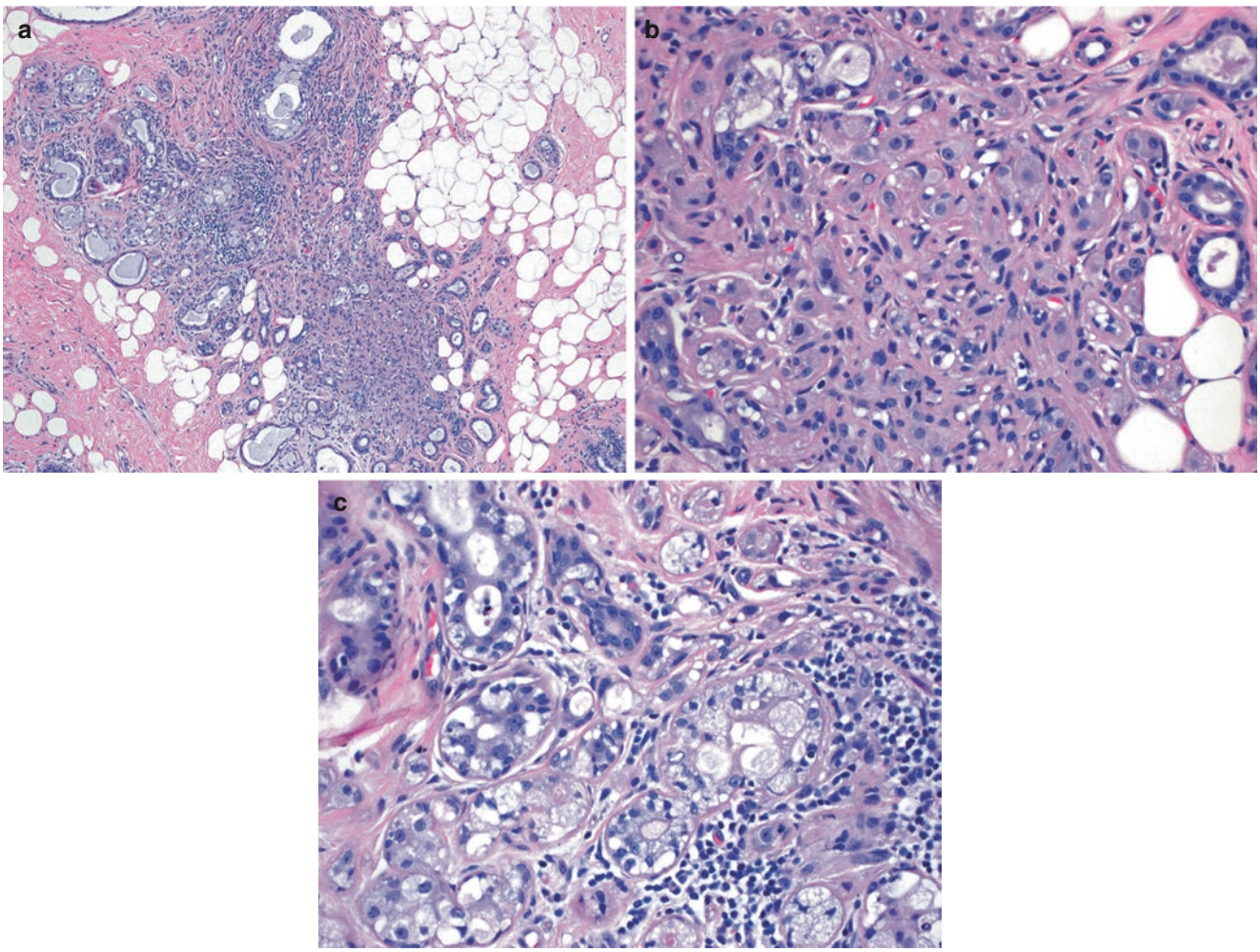

Fig. 3.16 Atypical apocrine adenosis. (**a**, **b**) This finding can be concerning when encountered in a core needle biopsy and in some cases represent apocrine DCIS secondarily involving sclerosing adenosis. (**c**) On occasion, the apocrine features can appear more clear in appearance

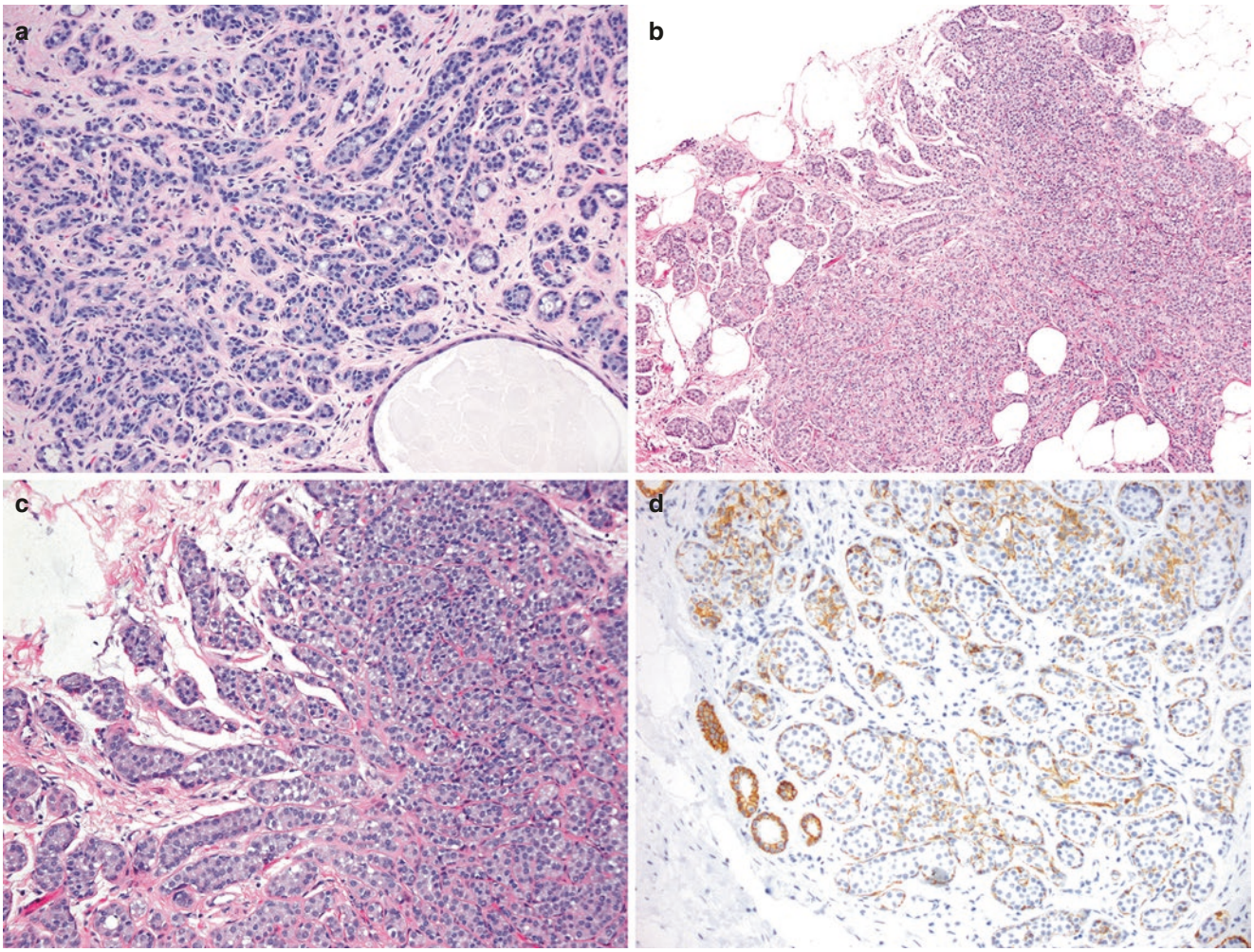

Fig. 3.17 Sclerosing adenosis secondarily involved by LCIS. (**a**) Usual sclerosing adenosis. (**b**, **c**) Sclerosing adenosis completely involved by LCIS, classic type. (**d**) E-cadherin immunostain is nonreactive in LCIS, thus confirming the diagnosis

for another distinct entity. For instance, sclerosing adenosis when secondarily involved by DCIS can morphologically resemble invasive ductal carcinoma (Fig. 3.31). In the CNB setting, the clinical ramifications of such a misdiagnosis can include subjecting the patient to unnecessary procedures (i.e., sentinel lymph node biopsy; more extensive resection). Collagenous spherulosis is another benign entity that is the target of CNB due to its association with calcifications. While collagenous spherulosis can, itself, mimic atypical cribriform ductal hyperplasia or cribriform DCIS, secondary involvement by LCIS can further lead to an erroneous diagnosis of a clinically more significant lesion due to its cytology monotonous features (Figs. 3.32, 3.33, and 3.34).

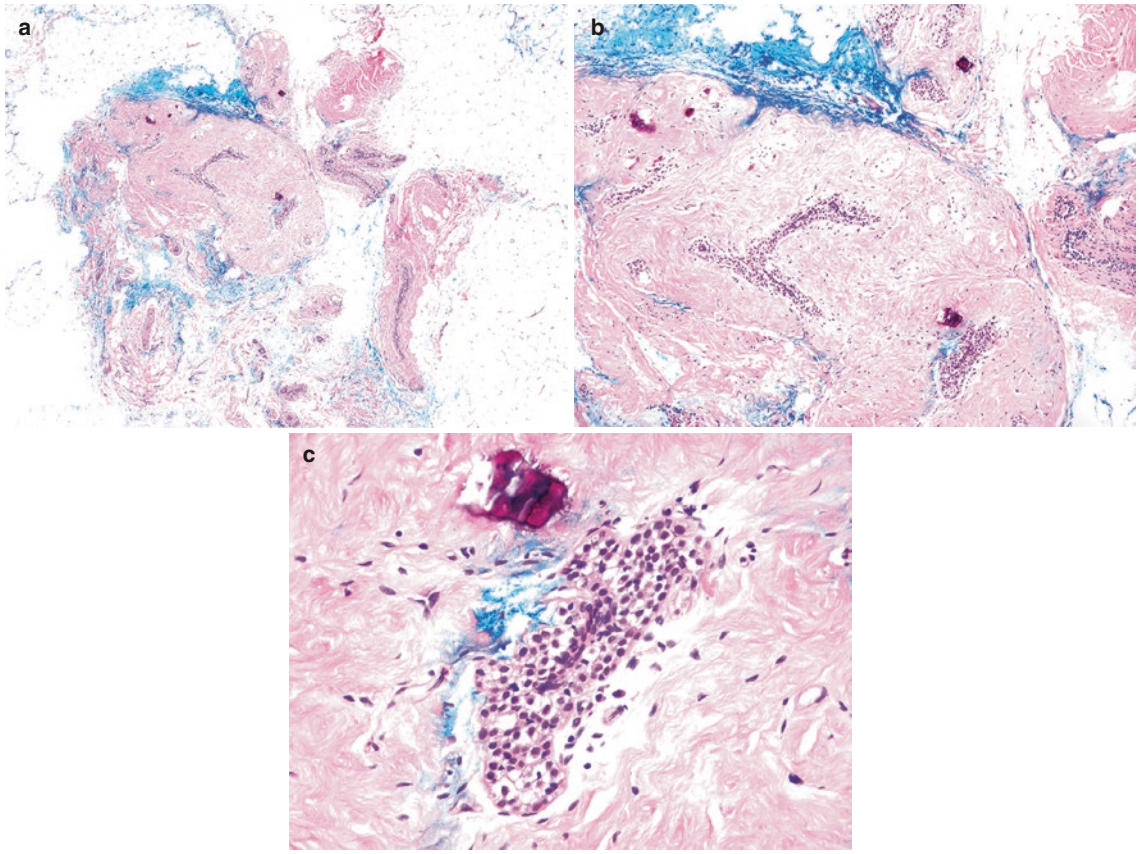

Fig. 3.18 CNB performed for calcifications yield fibroadenomatoid change and incidental atypical lobular hyperplasia (ALH). (**a**, **b**) Coarse calcifications are identified in the stroma of fibroadenomatoid change. (**c**) ALH is present both within fibroadenomatoid change and in the surrounding breast tissue, shown here in high magnification. E-cadherin immunostain was nonreactive in ALH (not shown)

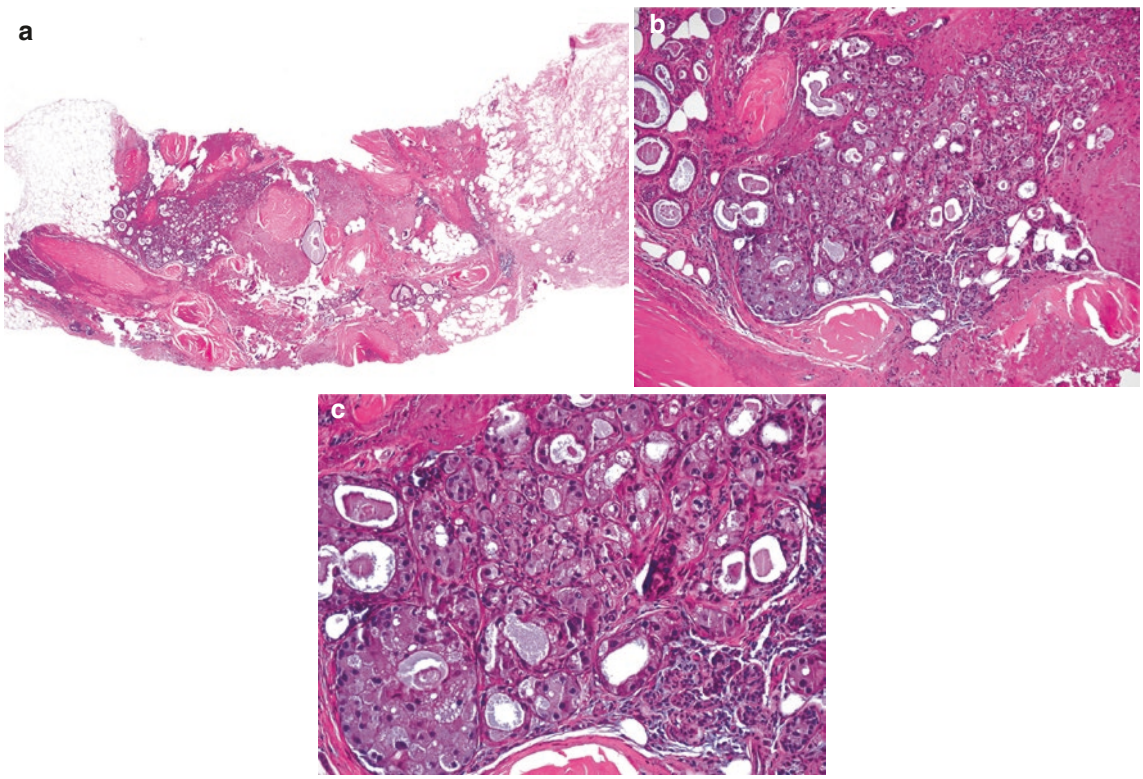

Fig. 3.19 Radial scar containing DCIS in a CNB. (**a**) Low-power magnification shows a portion of a radial scar in a CNB performed for a mammographically detected mass. (**b**, **c**) Higher magnification shows a focus of apocrine DCIS which was an unexpected finding

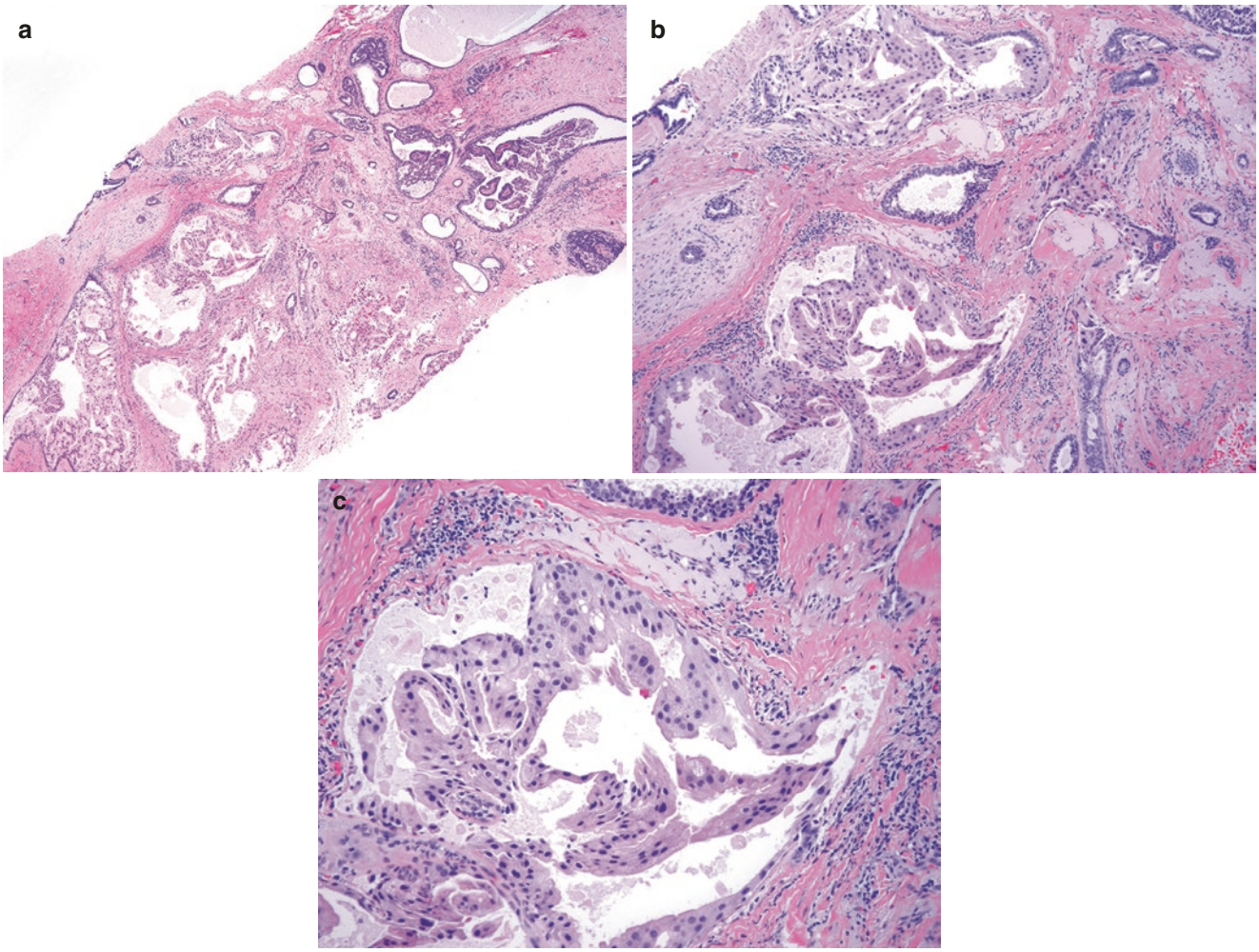

Fig. 3.20 Radial scar containing DCIS in a CNB. (**a**) Low-power magnification shows a portion of a radial scar consisting of proliferative and nonproliferative elements. (**b**, **c**) Part of the radial scar is involved by DCIS which can be mistaken for invasive ductal carcinoma in some instances

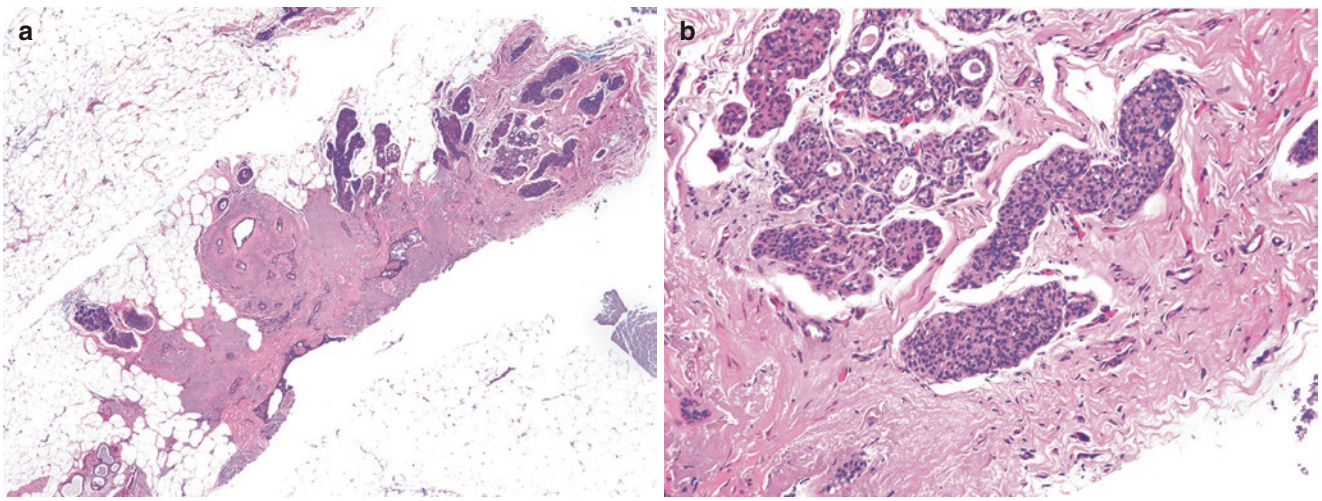

Fig. 3.21 Radial scar containing lobular neoplasia in a CNB. (**a**) Low-power magnification shows a transected radial scar with marked stromal elastosis. Peripheral lobules participating in the radial scar appear expanded by an epithelial proliferation. (**b**) Closer examination of these lobules shows the presence of an atypical lobular proliferation. (**c**) The lobular nature of this proliferation is confirmed by an E-cadherin immunostain. Note residual ductal epithelium focally in some lobules shows positive staining

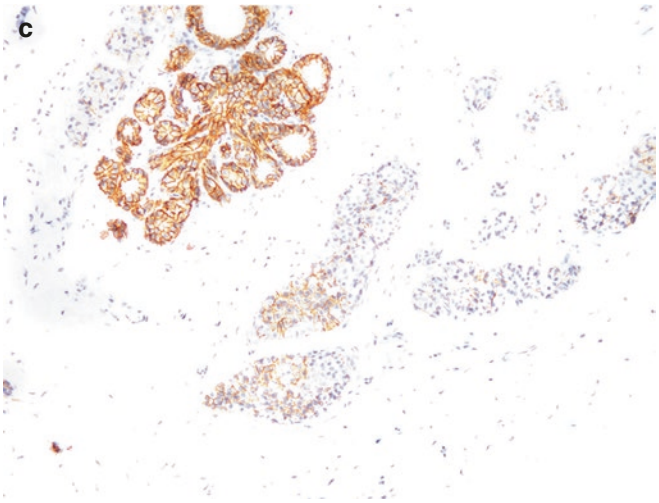

Fig. 3.21 (continued)

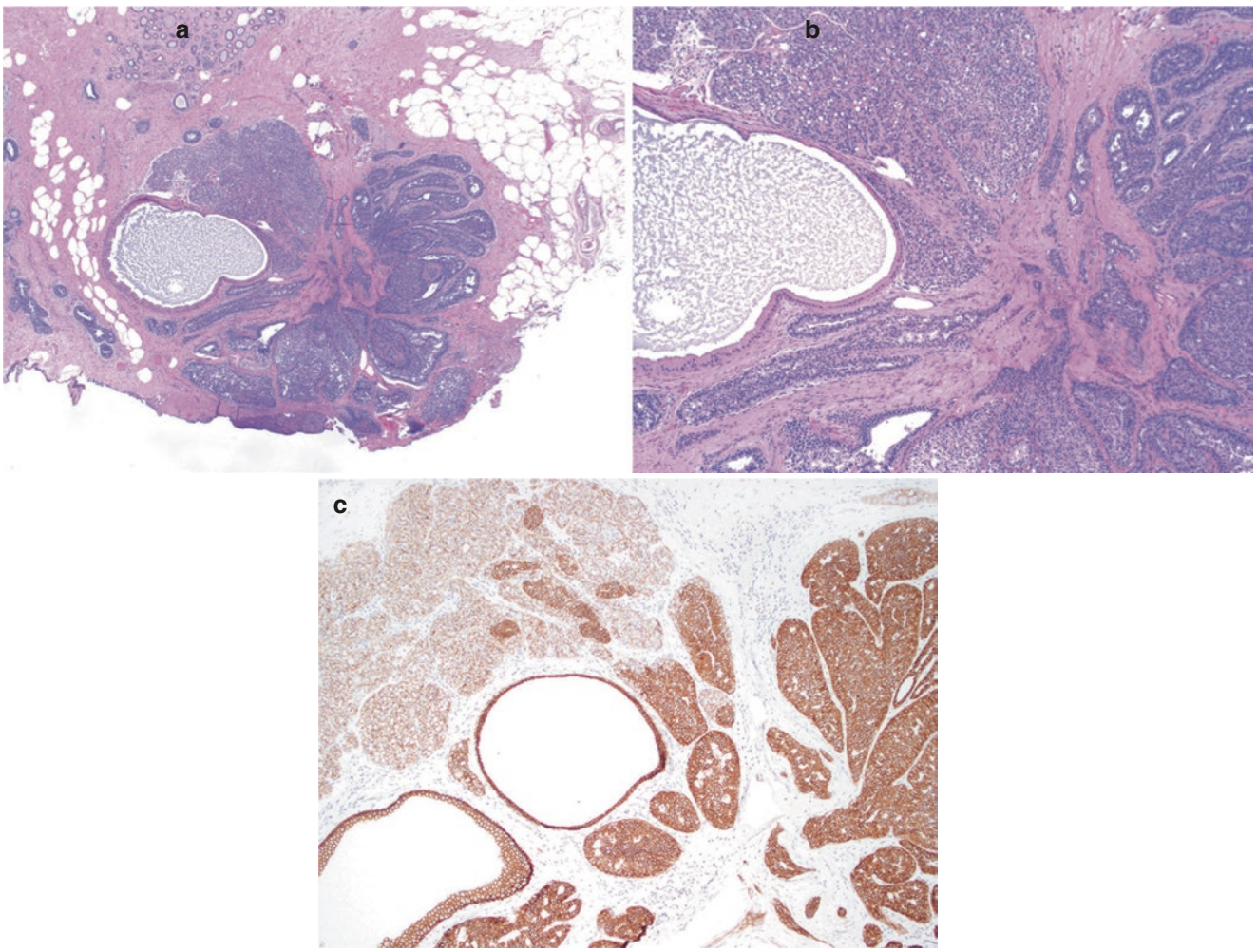

Fig. 3.22 Radial scar containing LCIS and usual ductal hyperplasia in a CNB. (**a**) Low-power view shows a radial scar predominantly comprising proliferative elements. (**b**) Higher magnification reveals that the epithelial proliferation may consist of a dual population. (**c**) This suspicion is confirmed by an E-cadherin immunostain which demonstrates strong membranous staining in usual ductal hyperplasia (*center*, *bottom*, and *right*) and weak, fragmented membranous staining in LCIS (*upper left*)

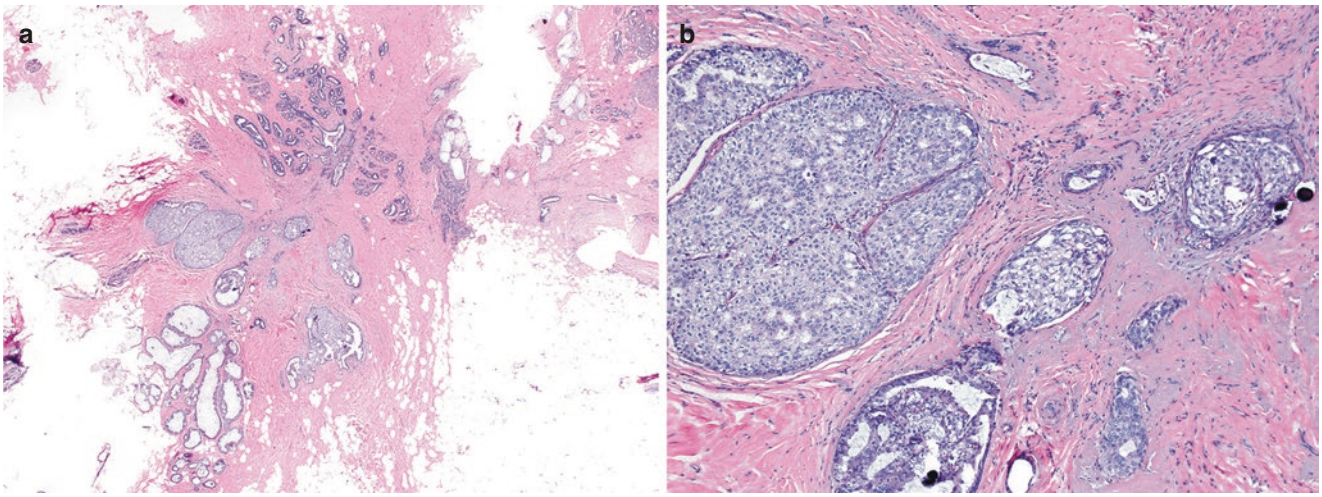

Fig. 3.23 Radial scar containing DCIS in an excisional biopsy specimen. (**a**) Low-power magnification shows that roughly half of the radial scar is involved by a secondary population of atypical epithelial cells. Biopsy site changes are seen in the upper right-hand corner. (**b**) High-power view shows DCIS with intermediate nuclear grade and calcifications

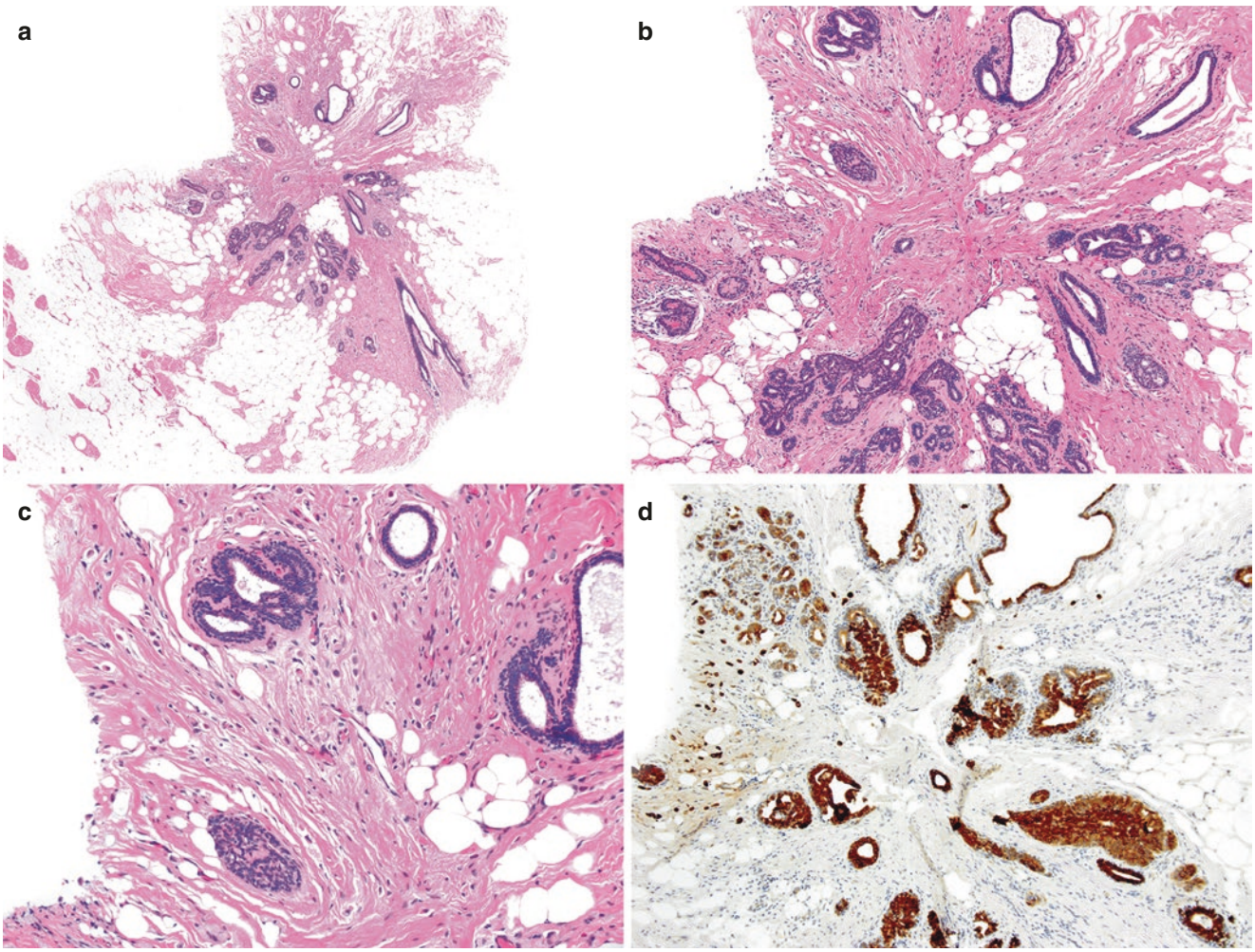

Fig. 3.24 Radial scar secondarily involved by invasive lobular carcinoma in a CNB. (**a**) Low-power magnification shows a radial scar with proliferative and nonproliferative elements. (**b**, **c**) However, on medium- and high-power views, a population of cells arranged in an invasive pattern is seen in the intervening stroma. (**d**) A corresponding CKAE1/AE3 immunostain confirms the suspicion of invasive carcinoma which highlights tumor cells singly or in small clusters (*best seen on left*)

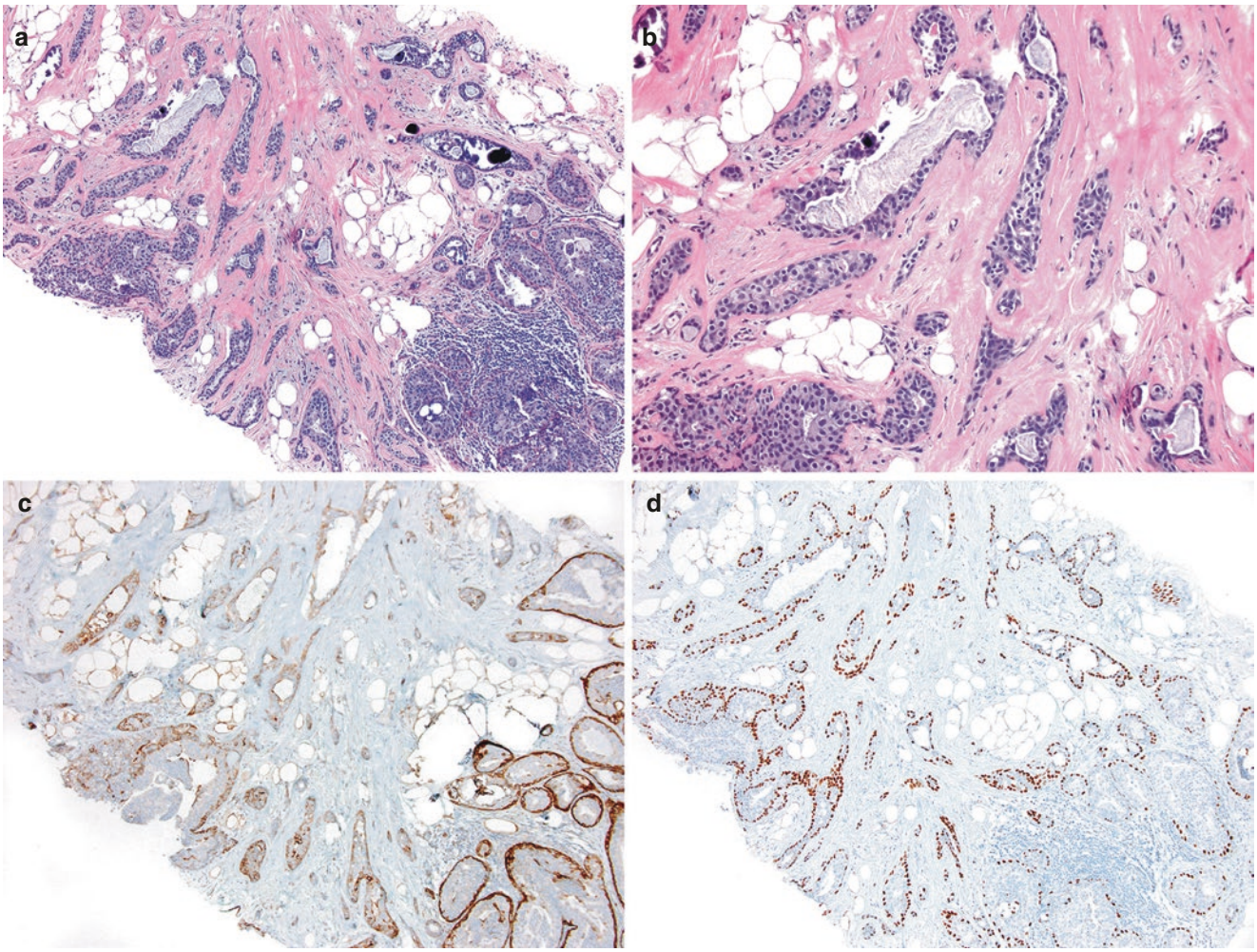

Fig. 3.25 DCIS in a radial sclerosing pattern resembling invasive ductal carcinoma. (**a**, **b**) Incomplete samplings of targeted lesions in core biopsies accentuate the difficulties of excluding invasive carcinoma in some cases. (**c**) To compound the problem, the SMM immunostain demonstrated aberrant loss of immunoreactivity in some glands suggesting the presence of invasive ductal carcinoma. (**d**) However, p63 immunostain performed in tandem and demonstrated intact myoepithelium throughout the entire lesion

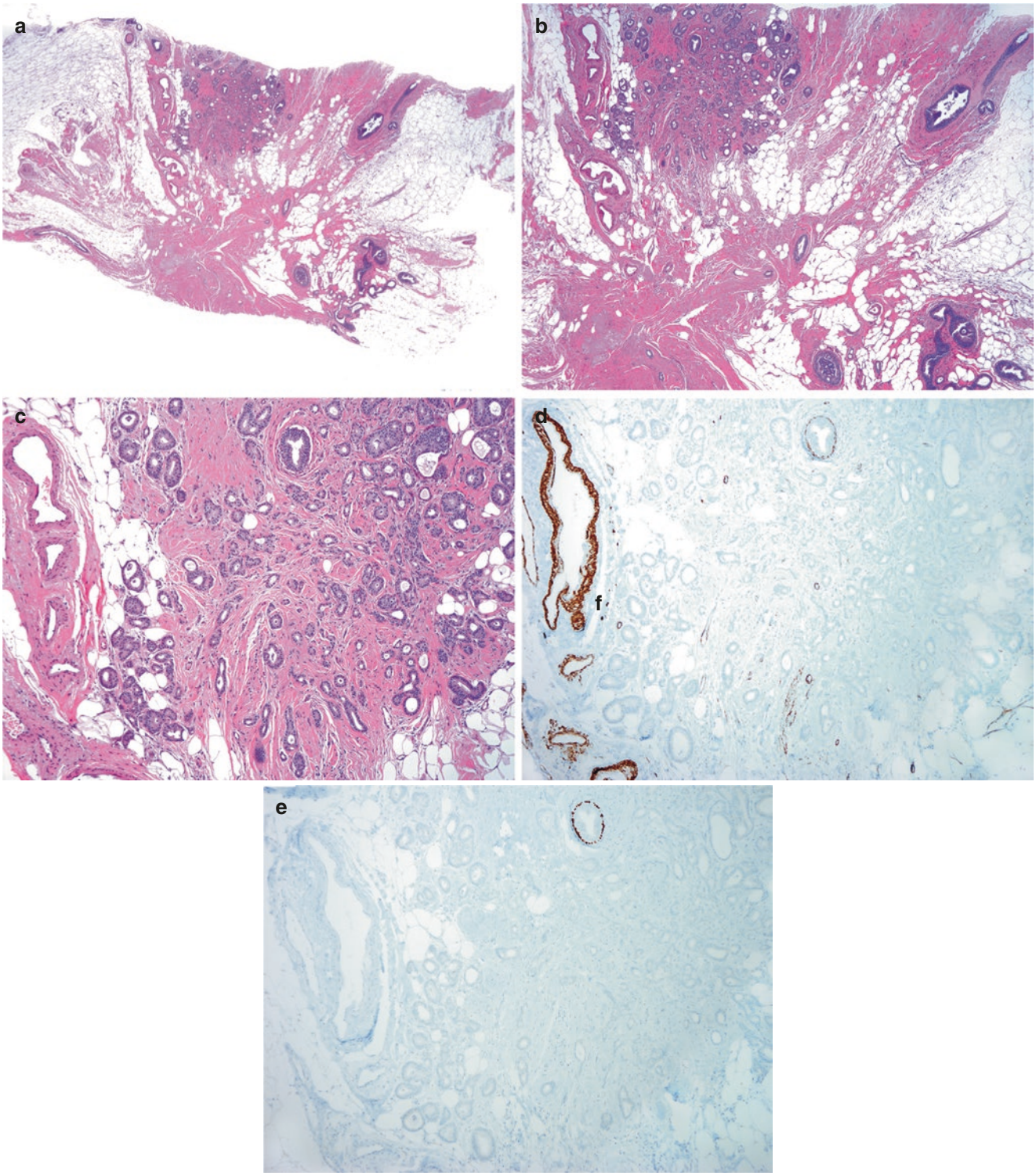

Fig. 3.26 CNB showing the nidus of a radial scar and adjacent invasive ductal carcinoma. (**a**, **b**) Low-power magnification showing the nidus of the radial scar consisting of elastotic and hyalinized stroma and several benign glands (*right*) and a distinct, separate focus of small glands (*top*). (**c**) Higher magnification shows a small glandular proliferation with an invasive growth pattern highly suspicious for invasive, well-differentiated ductal carcinoma. (**d**, **e**) The diagnosis is confirmed by the absence of myoepithelial staining in glands by SMM and p63, respectively

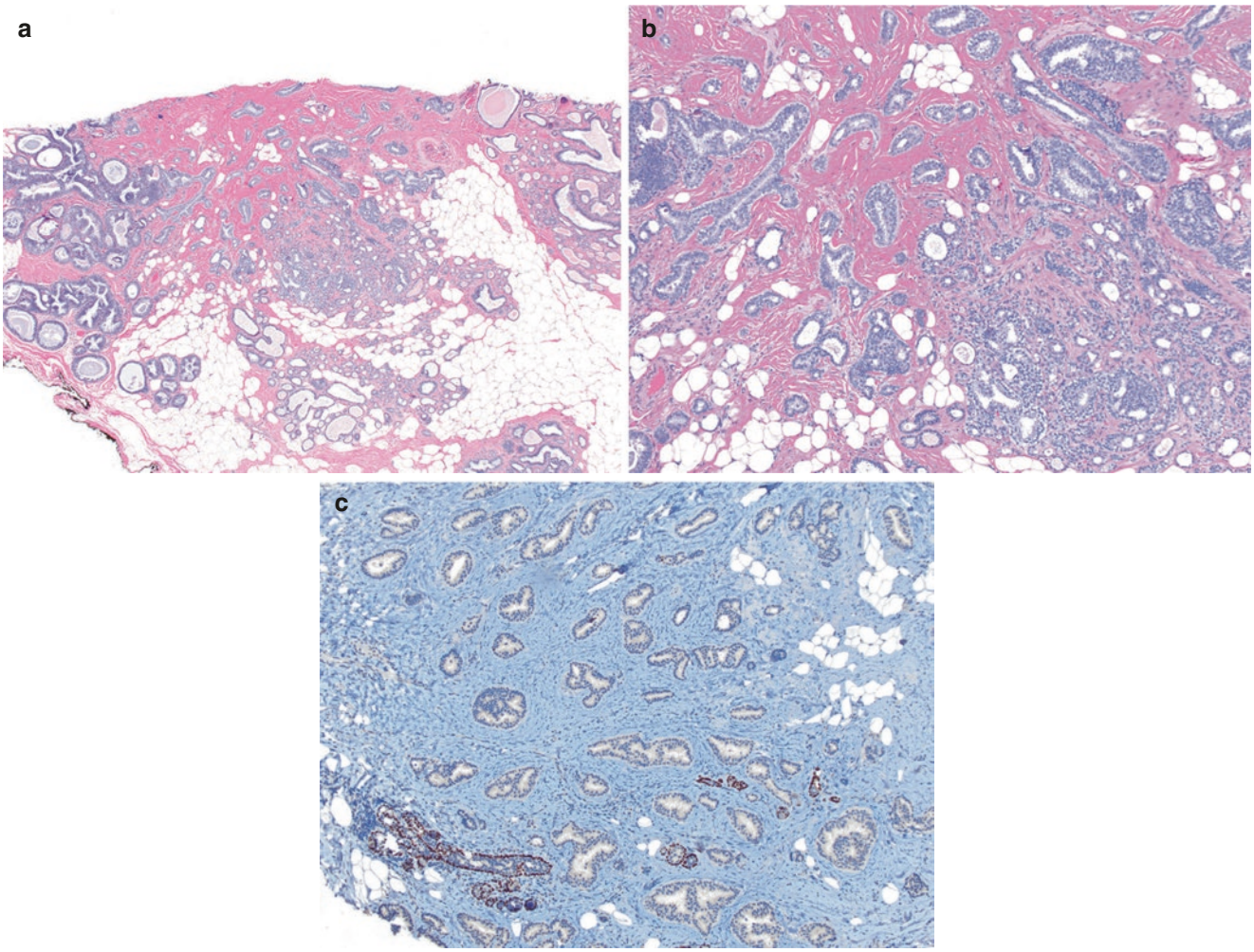

Fig. 3.27 A transected glandular proliferation resembling a radial scar but representing invasive ductal carcinoma. (**a**, **b**) Low- and high-power magnifications depict a proliferation of well-formed glands in a radiating configuration. The presence of neighboring benign proliferative changes gives this lesion the overall appearance of a radial scar. (**c**) However, a p63 immunostain demonstrates loss of myoepithelial cells around the glands in question, thus supporting the diagnosis of invasive, well-differentiated ductal carcinoma

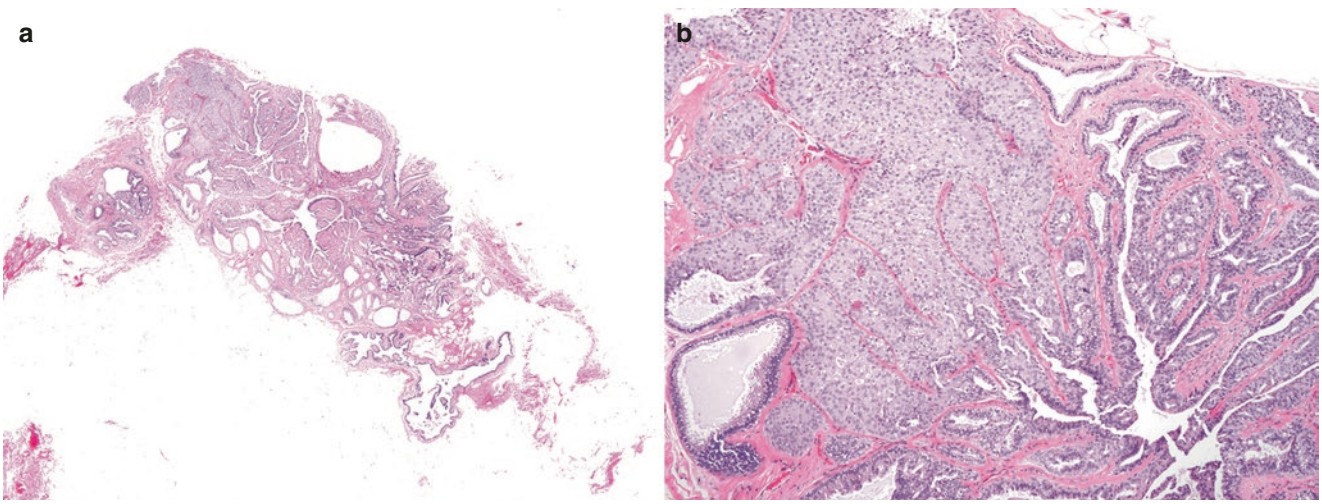

Fig. 3.28 DCIS arising in a sclerosing papillary adenotic lesion on CNB. (**a**–**c**) H&E views of DCIS, solid type with intermediate nuclear grade arising in a sclerosing papillary adenotic lesion. (**d**, **e**) CK5/6 shows absence of staining in DCIS (**f**) while E-cadherin demonstrates strong membranous positivity. (**g**, **h**) Estrogen receptor is strongly and diffusely positive throughout and of little utility in differentiating DCIS from the benign lesion it occupies

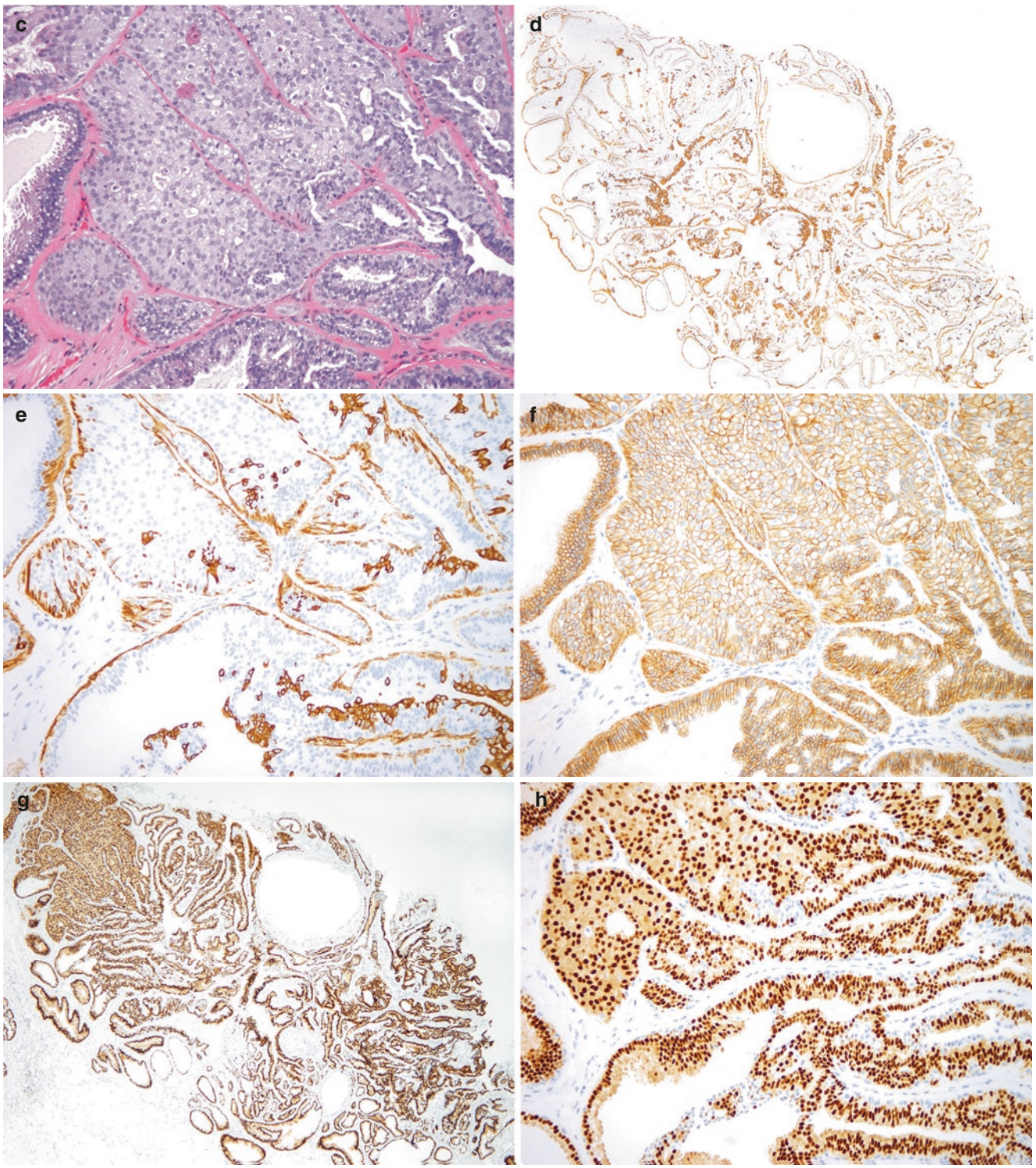

Fig. 3.28 (continued)

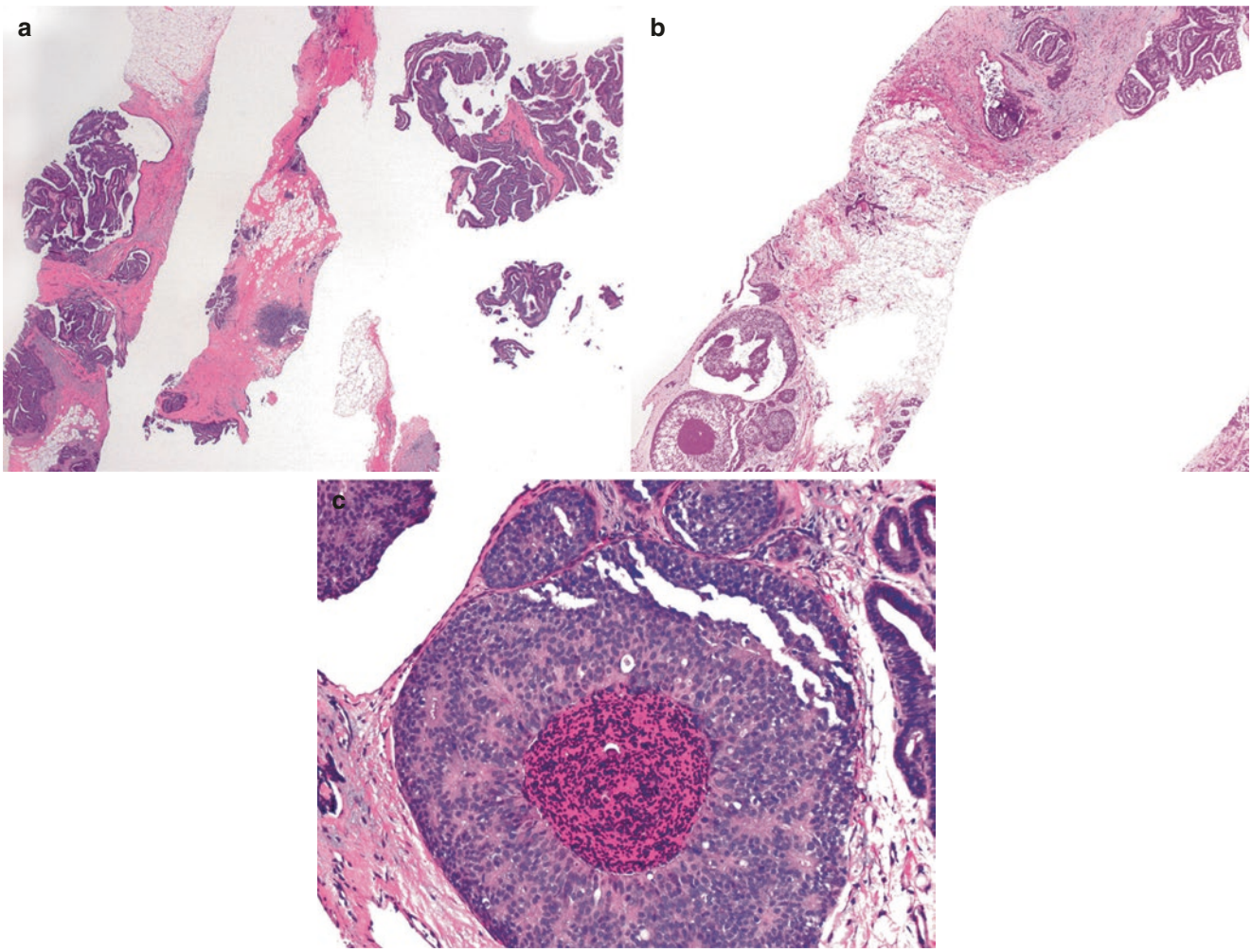

Fig. 3.29 CNB performed for a breast mass. (**a**) The targeted lesion was a papilloma. (**b**, **c**) However, an incidental focus of DCIS with central necrosis was also included in the sampling

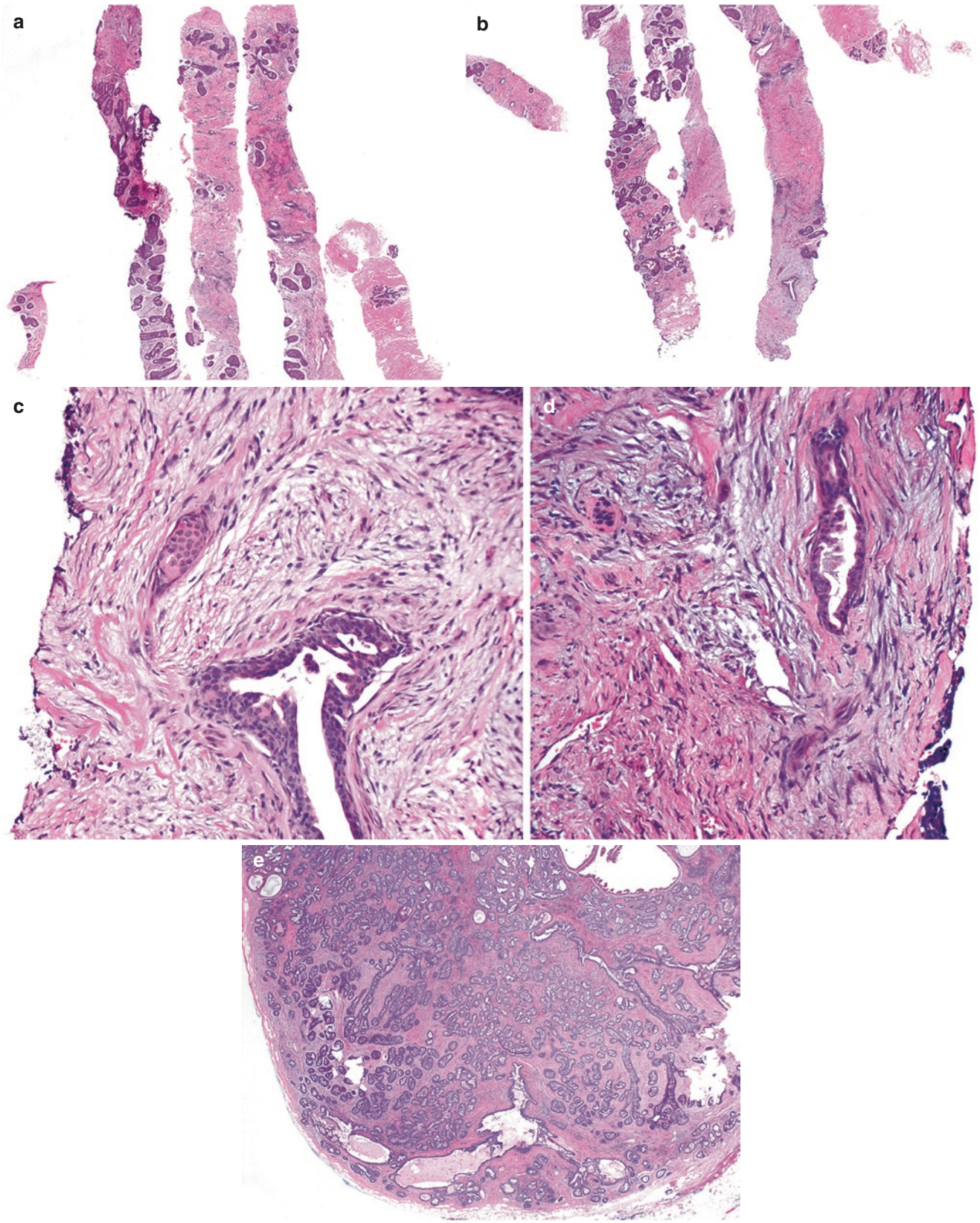

Fig. 3.30 CNB performed for a mass reveals benign fibroepithelial lesion involved by low-grade adenosquamous carcinoma in the subsequent excisional biopsy. (**a**, **b**) Core biopsies contained portions of a benign fibroepithelial lesion with cellular and mitotically active stroma. (**c**, **d**) On closer inspection, rare squamous glands are identified within the stroma. (**e**) The subsequent excisional biopsy shows a benign phyllodes tumor with a prominent glandular component. (**f**, **g**) Low-grade adenosquamous carcinoma is seen arising within this tumor. (**h**, **i**) High-molecular-weight cytokeratin and p63 immunostains demonstrate characteristic staining patterns for this entity

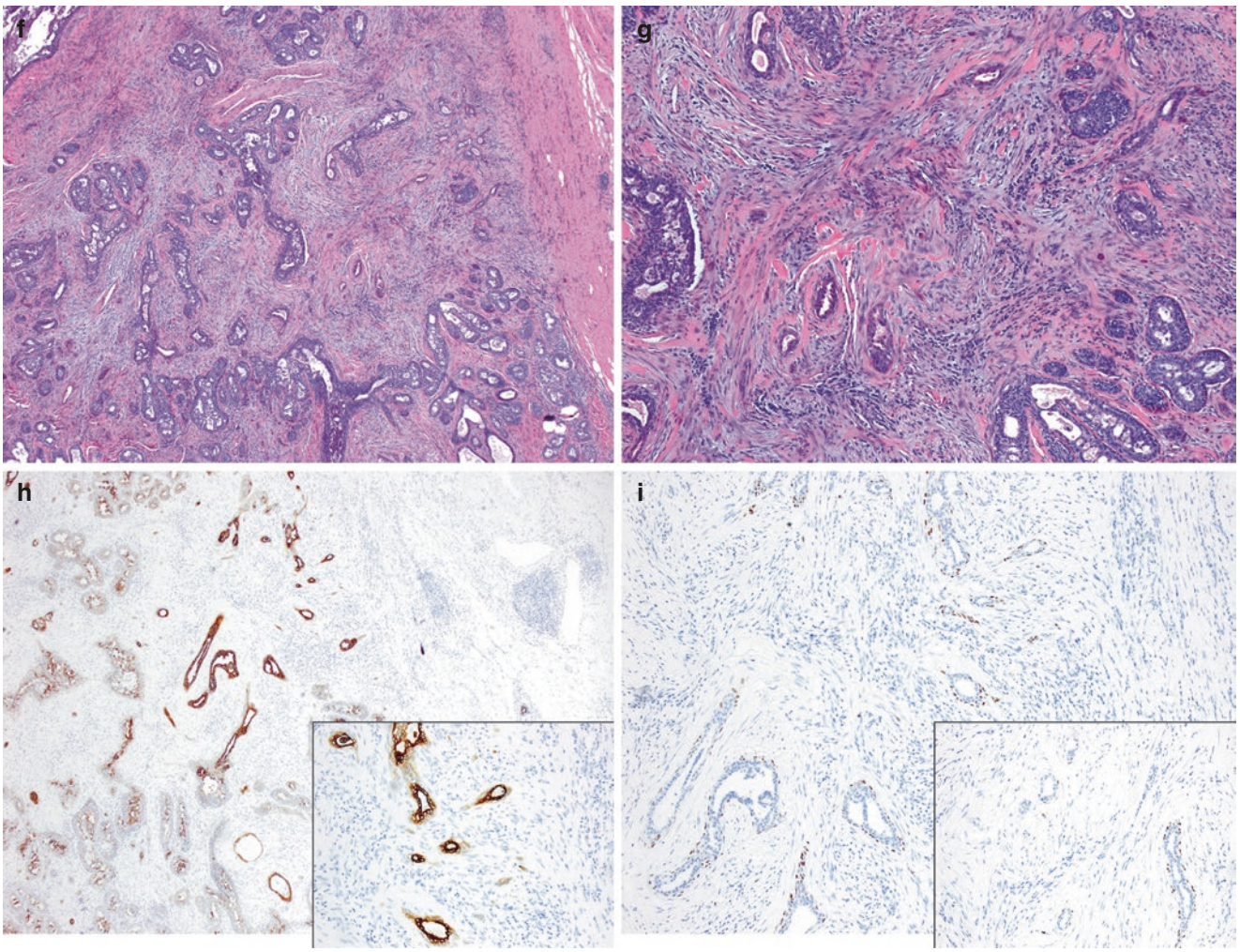

Fig. 3.30 (continued)

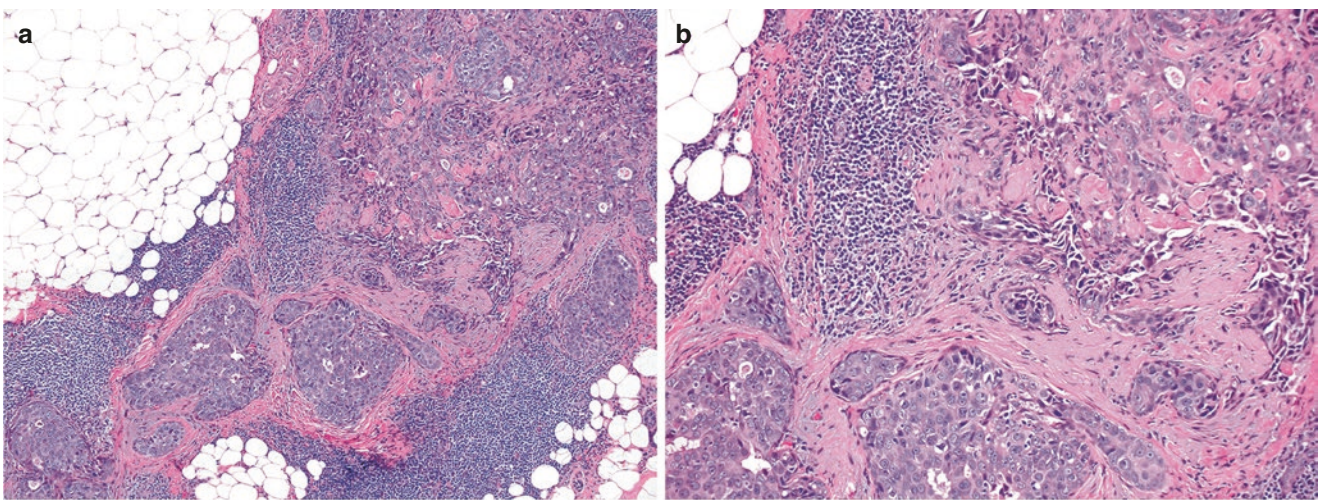

Fig. 3.31 Sclerosing adenosis secondarily involved by DCIS. (**a**, **b**) Extensive sclerosing adenosis is seen in the background of this example of DCIS. The degree of sclerosis is particularly severe and its involvement by DCIS mimics invasive ductal carcinoma. (**c**, **d**) Myoepithelial stains SMM and p63 show retention of myoepithelium, thus confirming the presence of DCIS only. (**e**, **f**) Another example of DCIS involving sclerosing adenosis and its resemblance to invasive ductal carcinoma. (**g**) SMM demonstrates retention of myoepithelium in this focus

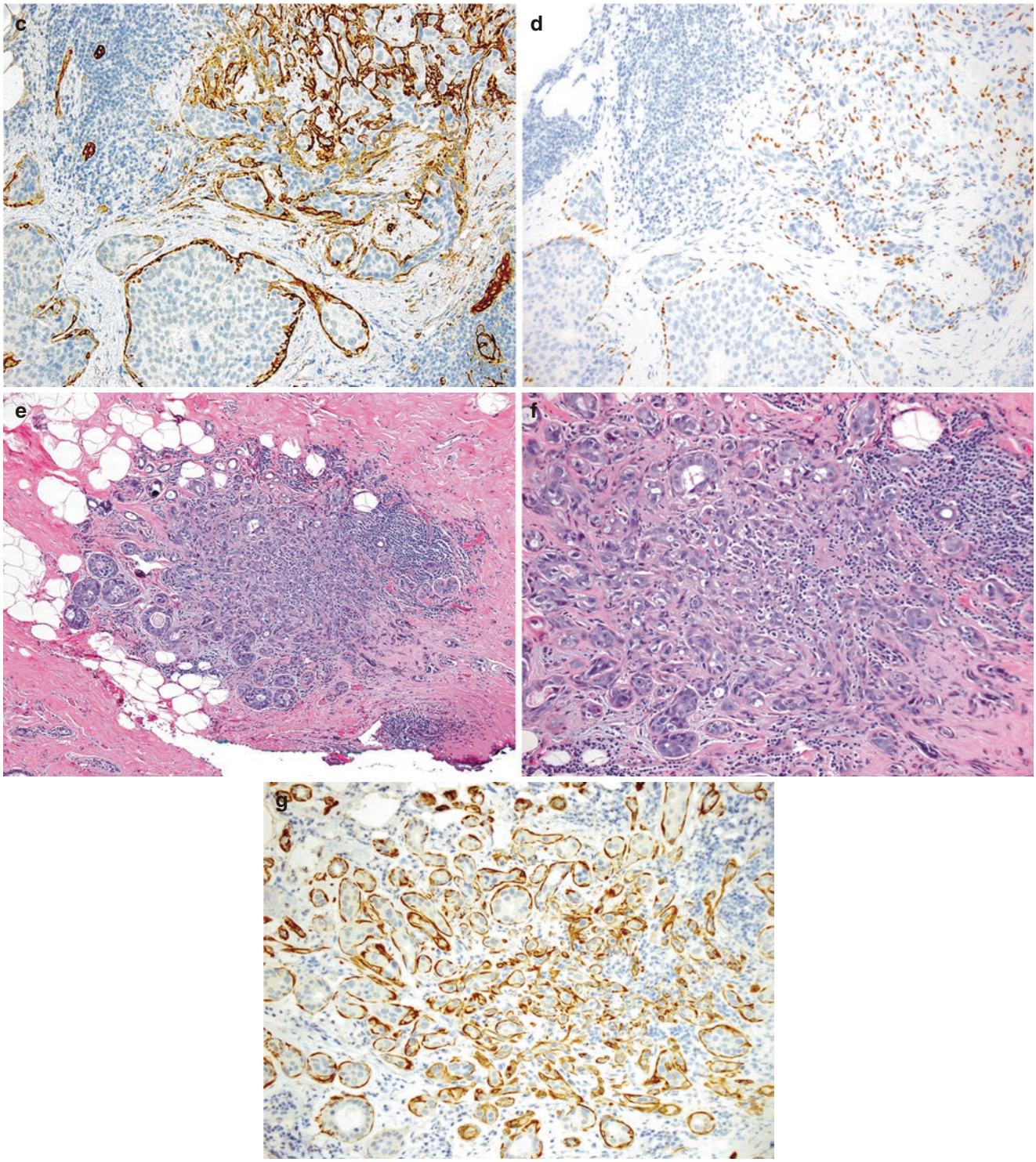

Fig. 3.31 (continued)

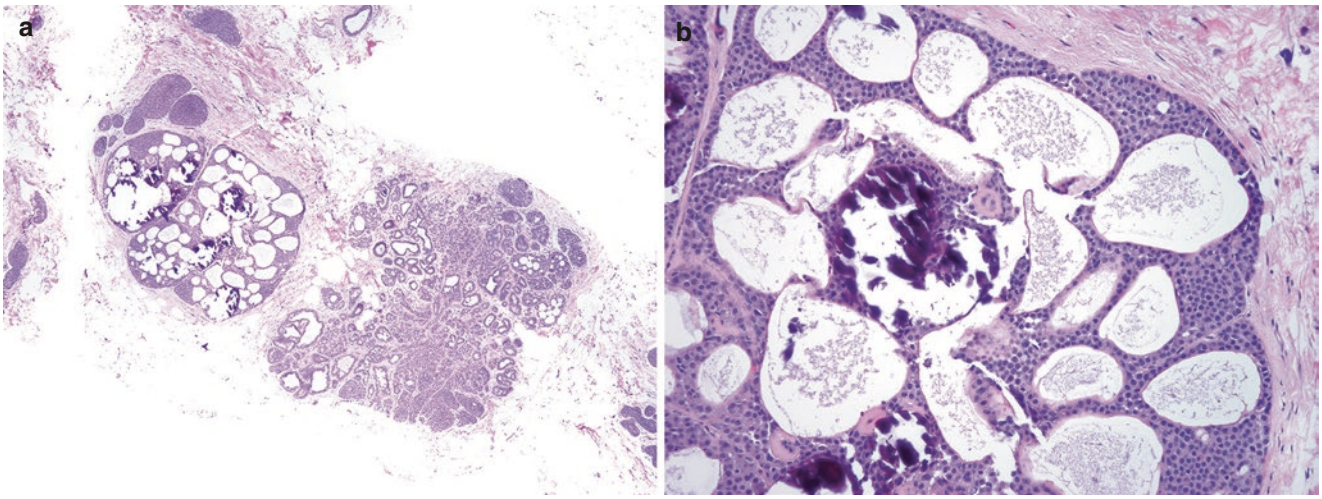

Fig. 3.32 Targeted calcifications associated with collagenous spherulosis. (**a**) Low magnification of a CNB sample showing prominent calcifications in collagenous spherulosis. **(b**) Higher magnification reveals secondary involvement by LCIS. LCIS is also present in the surrounding breast tissue (not shown)

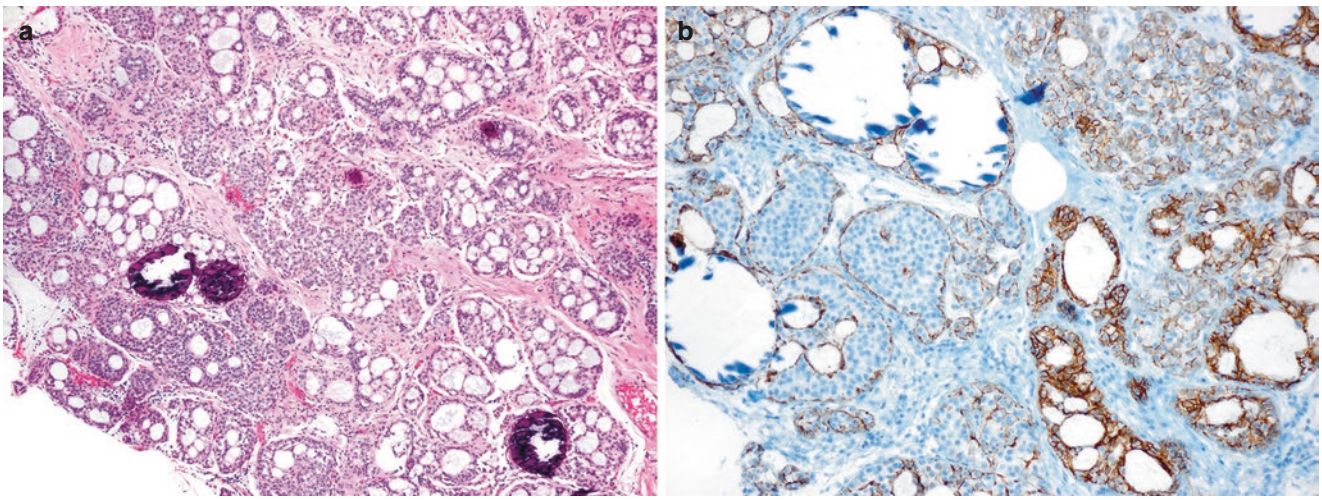

Fig. 3.33 Collagenous spherulosis calcifications and LCIS. (**a**) LCIS is less obvious in this example than in Fig. 3.32. (**b**) However, the corresponding E-cadherin immunostain confirms the presence of LCIS as it is nonreactive in these cells compared to adjacent ductal cells (*lower right*)

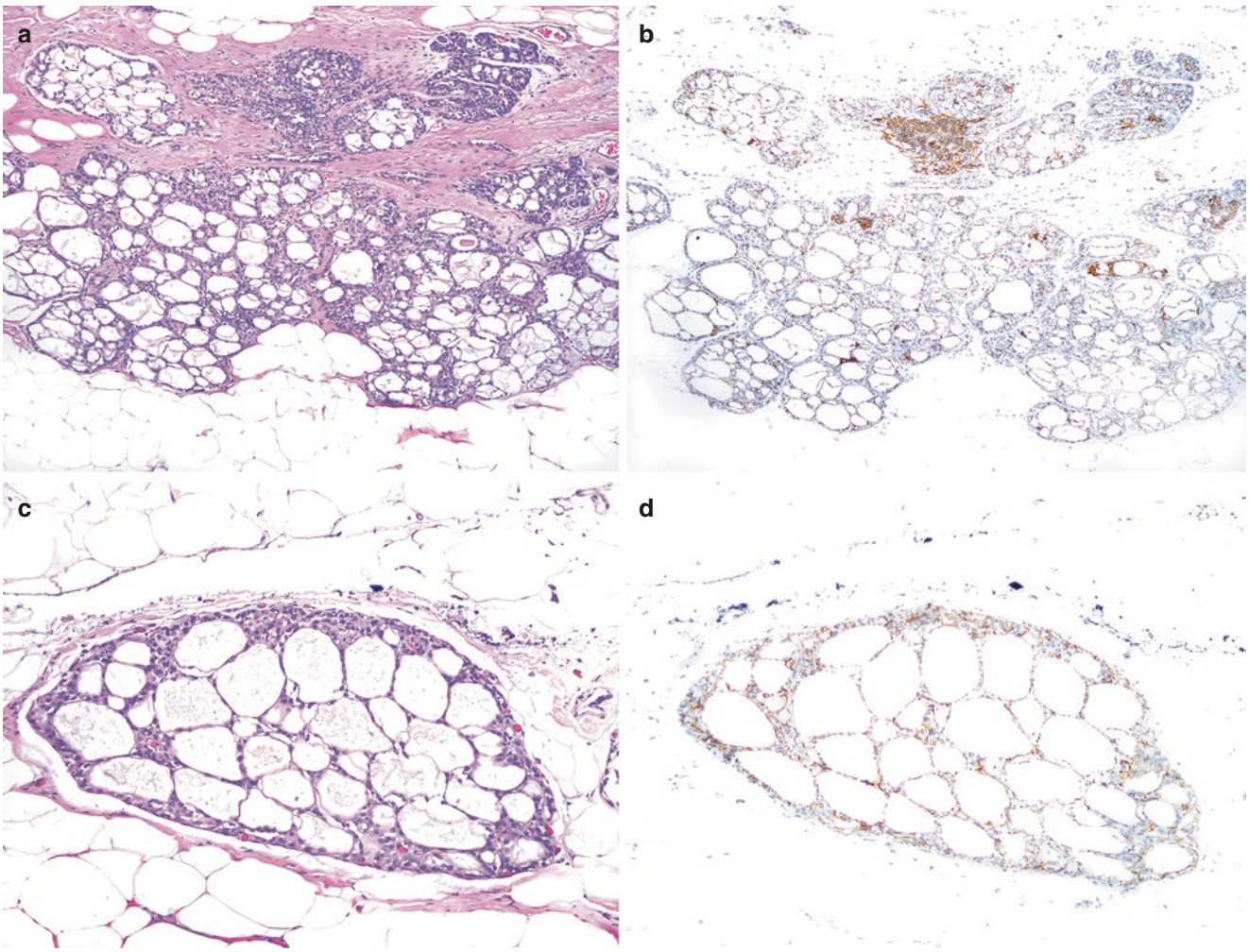

Fig. 3.34 Collagenous with degenerative changes involved by LCIS. (**a**, **b**) Low magnification on H&E and E-cadherin immunostain, respectively. (**c**, **d**) High-power magnification on H&E and E-cadherin, the latter shows weak, fragmented membranous staining in LCIS cells. Note collapsed basement membrane in several luminal spaces in the H&E image

Multiplex Immunohistochemistry

While in larger specimens, multiplex IHC may not be warranted with rare exception such as evaluating a focus near a surgical margin, its utility is enhanced in the context of small biopsy samples where tissue conservation is a priority.

Multiplex IHC allows visualization of more than one antigen at a time, but can suffer from antibody cross talk, signal overlap, and procedural complexities [5]. Nonetheless, the development and use of multiplex IHC stains is growing in popularity for diagnostic pathology. While homegrown antibody cocktails have been developed and studied to serve as reliable adjunctive diagnostic tools in breast pathology [6–8], there are increasing numbers of commercially available multiplex IHC stains for purchase (Fig. 3.35) including the Breast Triple Stain (BTS) (NeoGenomics Laboratories, Fort Myers, FL), p120 + E-cadherin (Biocare Medical, Concord, CA), CK5/14 + p63 + CK7/18 Multiplex IHC™ (aka, ADH-5, Breast Marker Cocktail) (Biocare, Concord, CA), Breast Cocktail (CK HMW/p63 + CK7/8/18) (Biocare Medical, Concord, CA), and Gross cystic disease fluid protein-15 (GCDFP-15) + Mammaglobin (Biocare Medical, Concord, CA) (Table 3.1).

The BTS is a cocktail of antibodies against CK5, p63, and CK8/18 using two chromogens (brown and red) and is intended to clarify the presence (and extent) of invasive carcinoma from in situ carcinoma. The p120 + E-cadherin breast cocktail is also a dual-color chromogen immunostain localizing to antibodies against E-cadherin and p120. This stain is used to discern between ductal and lobular epithelial proliferations in the breast (Fig. 3.36). The ADH-5 stain is composed of antibodies against CK5, CK14, p63, CK7, and CK18 using two chromogens: brown for CK5/CK14/p63 and red for CK7/CK18. The benefit of employing this cocktail stain is to discriminate between usual ductal hyperplasia and ADH/low-grade DCIS as polyclonal cells of the former will stain for either basal cytokeratins CK5/CK14 (brown) or

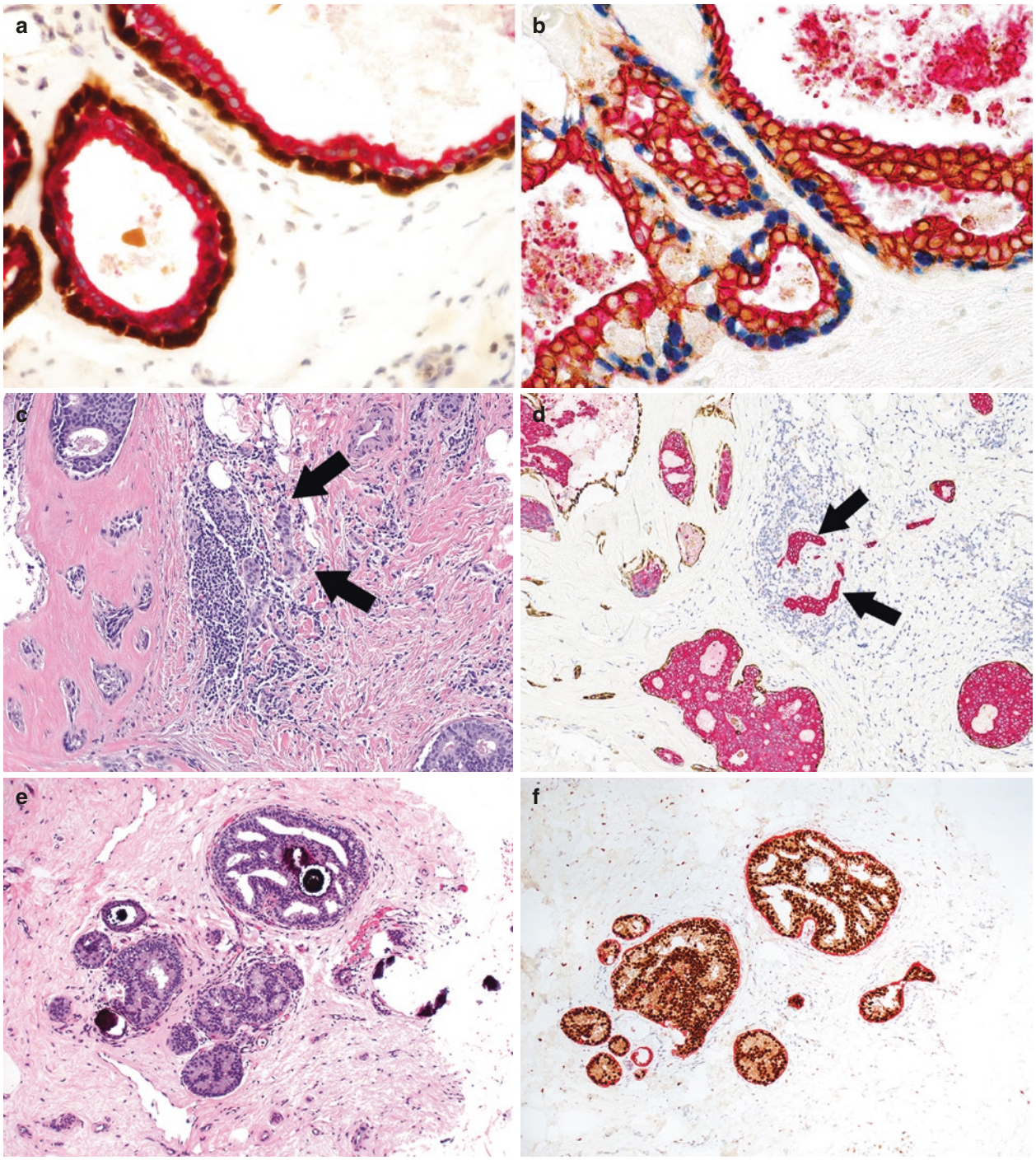

Fig. 3.35 Multiplex IHC stains. (**a**) The dual-color chromogen Breast Triple stain consists of antibodies against CK5/6, p63, and CK8/18 which localizes to the myoepithelial cytoplasm (*brown*), myoepithelial nucleus (*brown*), and the epithelial cytoplasm (*red*), respectively. This stain is utilized to distinguish invasive from in situ carcinoma. (**b**) The Minimal Carcinoma Triple stain (developed in the Department of Pathology and Laboratory Medicine, Weill Cornell Medicine) is a tricolor antibody cocktail against p63, E-cadherin, and CK7 which localizes to the myoepithelial nucleus (*blue*), epithelial cytoplasmic membrane (*brown*), and epithelial cytoplasm (*red*), respectively. This stain is utilized to distinguish invasive from in situ carcinoma as well as ductal from lobular proliferations. (**c**) A focus suspicious for microinvasive carcinoma (*arrows*) is identified on H&E stained slide from a CNB. (**d**) The dual-color chromogen ADH-5 consists of antibodies against CK5/14, p63, and CK7/18 which localizes to the basal/myoepithelial cytoplasm (*brown*), myoepithelial nucleus (*brown*), and the luminal epithelial cytoplasm (*red*), respectively. In this example, the presence of microinvasive carcinoma is confirmed by the lack of myoepithelial cell staining around the invasive tumor nests (*arrows*). A diagnosis of low-grade DCIS is confirmed in the surrounding expanded by the lack of CK5/14 basal cell staining and retention of CK5/14 and p63 myoepithelial cell staining. (**e**) This CNB shows a focus of ductal epithelial hyperplasia with cribriform growth and calcifications suspicious for ADH. (**f**) A homegrown dual-color chromogen antibody against CK5 (red, membranous) and ER (brown, nuclear) shows negative and positive (diffuse, strong) staining in epithelial cells, respectively, while investing myoepithelium is highlighted by CK5. These results support the diagnosis of ADH. (*Courtesy of Ankur Sangoi, MD*, El Camino Hospital, with permission)

luminal cytokeratins CK7/CK18 (red) while the cells of the latter exclusively express luminal cytokeratins CK7/CK18 (red). It is also used to distinguish between in situ and invasive carcinoma as the former will express both chromogens (red localizing to carcinoma cells and brown localizing to investing myoepithelial cells) and the latter will only express the red chromogen localizing to carcinoma cells. Similarly, the Breast Cocktail is a dual-color chromogen immunostain localizing to antibodies against CKHMW/p63 (cytoplasmic and nuclear staining, respectively; brown chromogen) and CK7, CK8, and CK18 (red chromogen) and is intended to both clarify the presence (and extent) of invasive carcinoma from in situ carcinoma as well as differentiated cases of usual ductal hyperplasia from ADH and low-grade DCIS. Some of these commercially available multiplex IHC stains have been evaluated and shown to improve interobserver and intraobserver variability among pathologists rendering these diagnoses [9]. Others have compared several multiplex IHC stains against each other such as one study which found a homegrown cocktail stain to perform better

Table 3.1 Summary of commercially available multiplex IHC stains

Stain	Component (chromogen color, cellular target, stain localization/pattern)		
Breast triple stain	CK5 (brown, myoepithelial cells, cytoplasmic)	p63 (brown, myoepithelial cells, nuclear)	CK8/18 (red, epithelial cells, cytoplasmic)
p120 + E-cadherin	p120 (red, ductal = membranous, lobular = cytoplasmic)	E-cadherin (brown, ductal = membranous, lobular = lost and/or fragmented)	
CK5/14 + p63 + CK7/18 Multiplex IHC™ (aka, ADH-5, Breast Marker Cocktail)	CK5/14 (brown, basal cells/ myoepithelial cells, cytoplasmic)	p63 (brown, myoepithelial cells, nuclear)	CK7/8/18 (red, luminal cells, cytoplasmic)
Breast Cocktail (CKHMW/ p63 + CK7/8/18)	CKHWM (brown, basal cells/ myoepithelial cells, cytoplasmic)	p63 (brown, myoepithelial cells, nuclear)	CK7/8/18 (red, luminal cells, cytoplasmic)
GCDFP-15 + Mammaglobin	GCDFP-15 (brown, cytoplasmic)	Mammaglobin (red, cytoplasmic)	

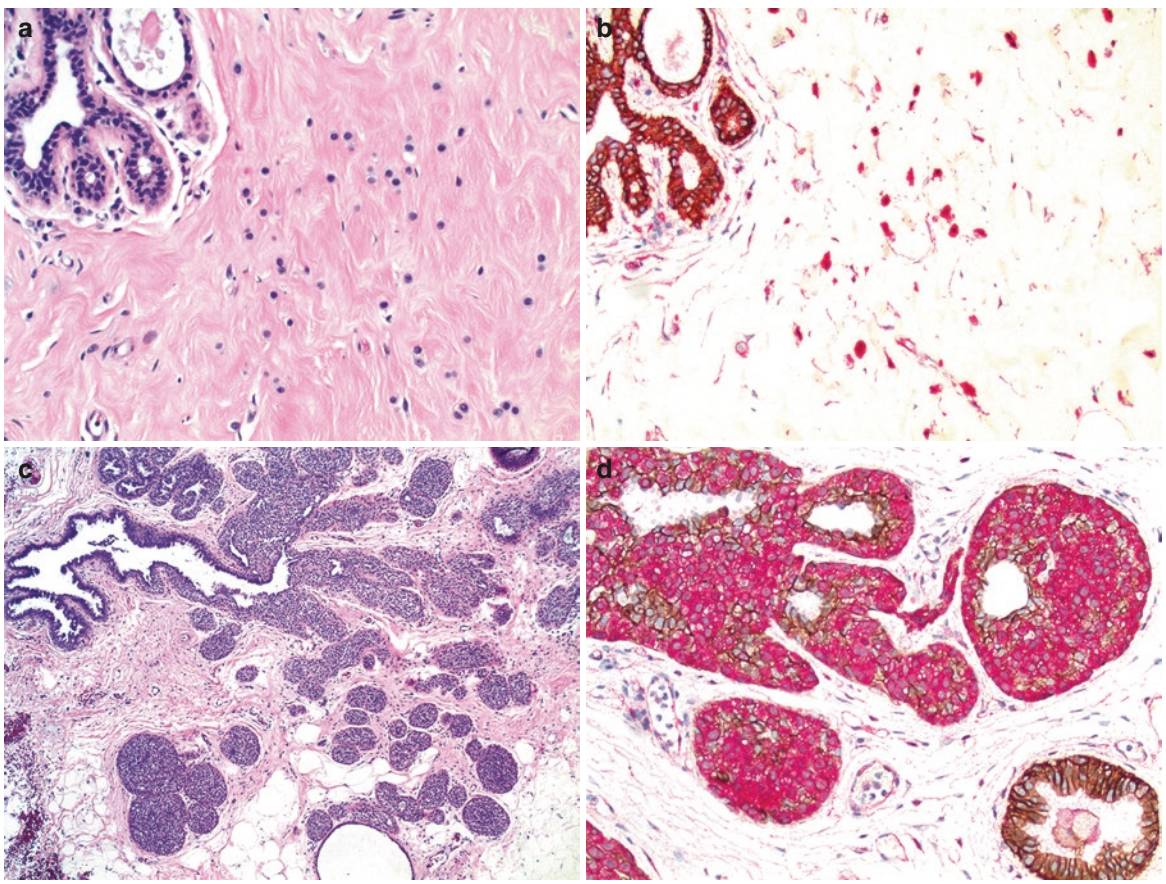

Fig. 3.36 Diagnostic utility of the p120 + E-cadherin stain. (**a**) H&E image scattered bland cells in the stroma are suspicious for invasive lobular carcinoma. (**b**) The p120 + E-cadherin stain confirms diagnosis of invasive lobular carcinoma through the loss of E-cadherin expression (brown) and the presence of cytoplasmic p120 expression (*red*). A benign duct (*upper left*) demonstrates complete membranous expression for both p120 and E-cadherin. (**c**) An example of a solid epithelial proliferation confined to terminal duct lobular units which may represent LCIS or DCIS. (**d**) The p120 + E-cadherin stain confirm a diagnosis of LCIS through the loss of E-cadherin expression and the presence of cytoplasmic p120 expression (*red*). (*Courtesy of Ankur Sangoi, MD*, El Camino Hospital, with permission)

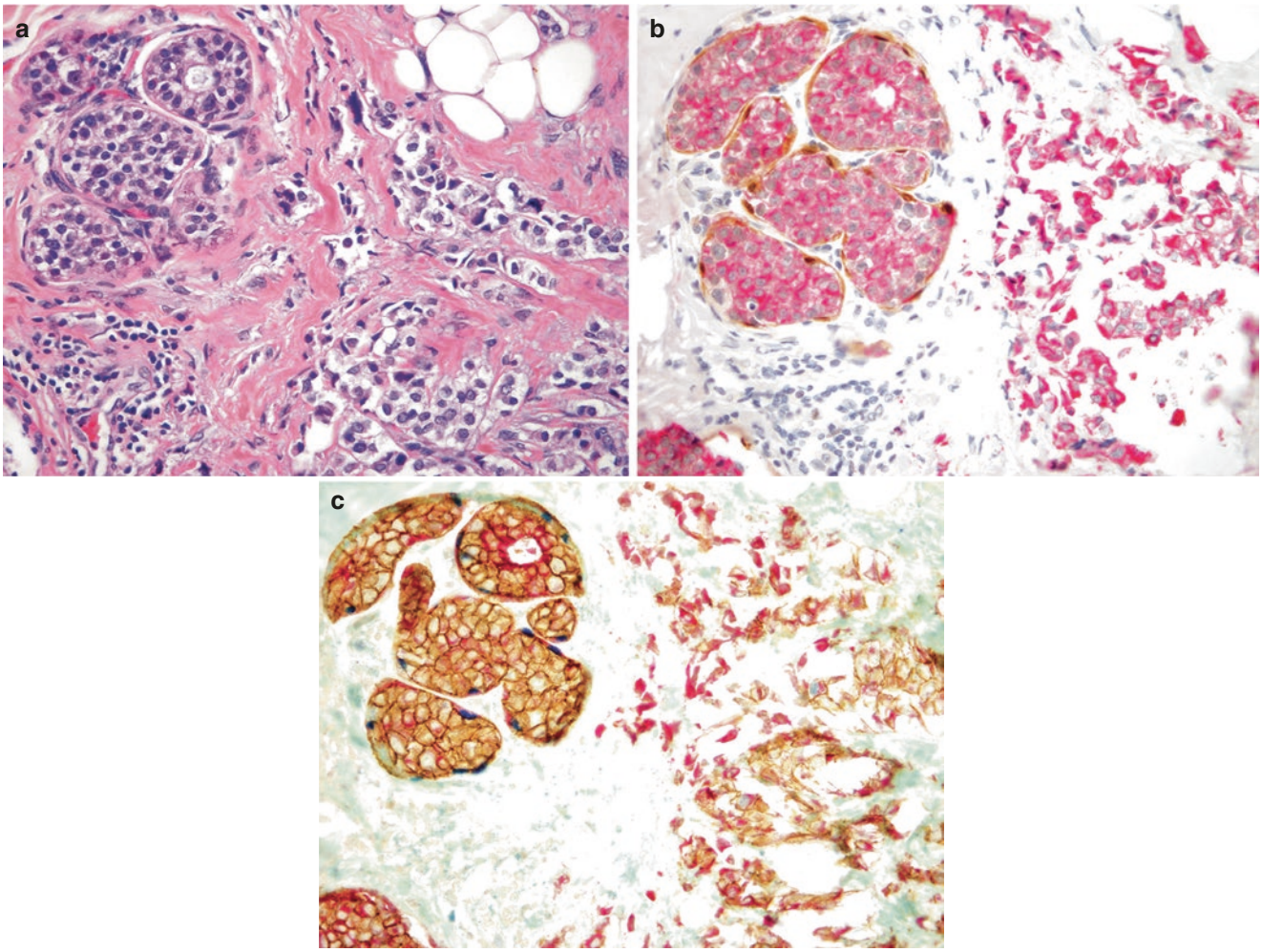

Fig. 3.37 Diagnostic utility of the Breast Triple stain and the Minimal Carcinoma Triple stain. (**a**) H&E image of in situ and invasive mammary carcinoma. (**b**) The Breast Triple stain confirms the epithelial nature of both the in situ and invasive components (*red*) and additionally distinguishes the in situ carcinoma (invested in *brown*) from invasive carcinoma. (**c**) The Minimal Carcinoma Triple stain similarly confirms the epithelial nature of both components (*red*) as well as distinguishes in situ carcinoma (*blue*) from invasive carcinoma. In addition, the retention of E-cadherin expression in both components (*brown*) indicate that this is a carcinoma of ductal type

than two commercially available multiplex IHC stains [10] (Fig. 3.37). The GCDFP-15 + Mammaglobin multiplex immunostain may help to establish the correct interpretation of metastatic breast carcinoma as mammaglobin is a more sensitive marker than GCDFP-15 for breast carcinoma; however, it lacks the specificity of GCDFP-15. More recently, a new immunostain TRPS1 has shown potential as a breast marker in cases of metastatic disease.

Similar to the phenomenon observed in prostate biopsy reporting where the use of PIN4, a cocktail antibody against high-molecular-weight keratin and antibodies to p63 and p504s, is virtually routine, the use of multiplex IHC stains in breast core biopsies will likely increase and serve as an effective way to answer diagnostic questions while optimally conserving tissue.

References

1. Lee AHS, Salinas NMV, Hodi Z, et al. The value of examination of multiple levels of mammary needle core biopsy specimens taken for investigation of lesions other than calcification. J Clin Pathol. 2012;65:1097–9.
2. Grimes MM, Karageorge LS, Hogge JP. Does exhaustive search for microcalcifications improve diagnostic yield in stereotactic core needle breast biopsies? Mod Pathol. 2001;1494:350–3.
3. Rosen PP. Columnar cell hyperplasia is associated with lobular carcinoma in situ and tubular carcinoma. Am J Surg Pathol. 1999;23(12):1561.
4. Abdel-Fatah TM, Powe DG, Hodi Z, et al. High frequency of coexistence of columnar cell lesions, lobular neoplasia, and low grade ductal carcinoma in situ with invasive tubular carcinoma and invasive lobular carcinoma. Am J Surg Pathol. 2007;31(3):417–26.

5. Dixon AR, Bathany C, Tsuei M, et al. Recent developments in multiplexing techniques for immunohistochemistry. Expert Rev Mol Diagn. 2015;15(9):1171–86.
6. Ross DS, Liu YF, Pipa J, Shin SJ. The diagnostic utility of the minimal carcinoma triple stain in breast carcinomas. Am J Clin Pathol. 2013;139:62–70.
7. Reisenbichler ES, Balmer NN, Adams AL, et al. Luminal cytokeratin expression profiles of breast papillomas and papillary carcinomas and the utility of a cytokeratin 5/p63/cytokeratin 8/18 antibody in their distinction. Mod Pathol. 2011;139:62–70.
8. Reisenbichler ES, Ross JR, Hameed O. The clinical use of a p63/cytokeratin 7/18/cytokeratin 5/14 antibody cocktail in diagnostic breast pathology. Ann Diagn Pathol. 2014;18:313–8.
9. Jain RK, Mehta R, Dimitrov R, et al. Atypical ductal hyperplasia: interobserver and intraobserver variability. Mod Pathol. 2011;2497:917–23.
10. Ginter PS, Varma S, Liu YF, Shin SJ. The minimal carcinoma triple stain is superior to commercially available multiplex immunohistochemical stains breast triple stain and LC/DC breast cocktail. Am J Clin Pathol. 2015;144:869–79.

Inflammatory, Reactive, and Infectious Conditions of the Breast

4

Anne Grabenstetter and Timothy M. D'Alfonso

Fat Necrosis

Overview

Fat necrosis, a relatively common finding in breast core biopsy specimens, is most often seen in breast tissue that has undergone some type of trauma and is typically a component of post-surgical or post-biopsy reactive changes. Radiation therapy can induce the development of fat necrosis, and fat necrosis can develop following all types of radiation, including external beam, accelerated partial breast irradiation (Mammosite®), and intraoperative radiotherapy [1–3]. Less commonly, fat necrosis occurs when there is no history of prior trauma. Fat necrosis can present as a palpable abnormality in an area of prior surgery or trauma. In some cases, skin and/or nipple retraction may be present and can simulate invasive carcinoma [4]. Fat necrosis may also come to attention on screening mammography or follow-up imaging as a mass or calcifications and may be suspicious enough to warrant biopsy.

A histologic diagnosis of fat necrosis is relatively straightforward, especially in the appropriate clinical context. It is necessary for the pathologist to have information about the patient's clinical history (surgery, trauma, radiation) as well as imaging findings. If the patient has a history of carcinoma in the site being biopsied, information about the type of carcinoma should be known, either from prior reports or preferably from review of prior slides. Some uncommon types of mammary carcinoma show similar morphologic features to fat necrosis (discussed below) and should be kept in mind. Fat necrosis is benign and does not need to be excised when diagnosed in a core biopsy sample, provided there is radiologic-pathologic concordance.

Gross and Radiologic features

Grossly, fat necrosis is firm and shows a gritty or chalky yellow cut surface that may contain areas of cystic degeneration and hemorrhage. Calcifications can be grossly appreciated in some cases. Fat necrosis can be seen on mammography as a spiculated mass, asymmetric density, lipid or oil cyst, or due to the presence of calcifications [5, 6]. Lipid cysts are a pathognomonic finding of fat necrosis [5, 7, 8]. They appear as round radiolucent masses with a fibrous rim and frequently calcify (Fig. 4.1). In other instances, calcifications in fat necrosis appear clustered, pleomorphic, and linear and may simulate malignancy [5, 6]. On ultrasonography, fat necrosis has a variable appearance and may be identified as a solid well-circumscribed mass, a stellate mass with infiltrative margins, a complex cyst, or as lipid cysts [9–11]. Fat

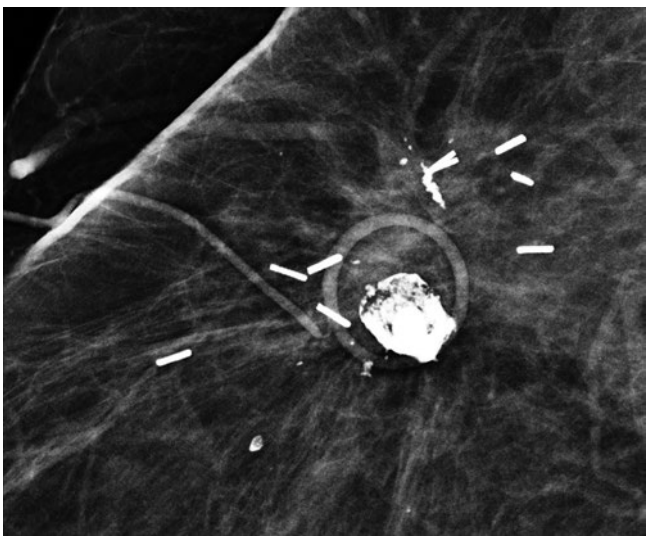

Fig. 4.1 Mammography of fat necrosis shows a lipid cyst with well-defined borders and coarse calcification. Surgical clips from a prior resection are present in the vicinity of fat necrosis. (*Courtesy of Janine Katzen, MD*, Weill Cornell Medicine, with permission)

A. Grabenstetter · T. M. D'Alfonso (✉)
Department of Pathology, Memorial Sloan Kettering Cancer Center, New York, NY, USA
e-mail: grabensa@mskcc.org; dalfonst@mskcc.org

© The Author(s), under exclusive license to Springer Nature Switzerland AG 2022
S. J. Shin et al. (eds.), *A Comprehensive Guide to Core Needle Biopsies of the Breast*,
https://doi.org/10.1007/978-3-031-05532-4_4

necrosis may show a variable pattern of enhancement on magnetic resonance imaging (MRI) and can mimic invasive carcinoma [6].

Microscopic Features

The appearance of fat necrosis is variable and depends on the degree of fibrosis and inflammation within the lesion. In areas of recent trauma, fat necrosis shows more inflammation and less fibrosis, while in older lesions, scarring and calcification are present and less inflammation is seen. Fat necrosis is easily recognized due to the presence of foamy histocytes and foreign body type giant cells surrounding lipid vacuoles and anucleate necrotic adipocytes (Fig. 4.2). Cysts are formed containing saponified lipids and are surrounded by foamy histiocytes and giant cells (Fig. 4.3). Lymphocytes, plasma cells, and in some cases eosinophils are present to a variable degree (Fig. 4.4). Neutrophils are seen in the first few days of the process and are not abundant. Evidence of prior hemorrhage is seen as hemosiderin-laden macrophages or hematoidin pigment (Fig. 4.5). Fibrosis progressively develops around necrotic fat and can form fibrous walled cysts that undergo calcification (Fig. 4.6). Breast glandular tissue is often not present in core biopsies of fat necrosis, particularly in prior surgical sites.

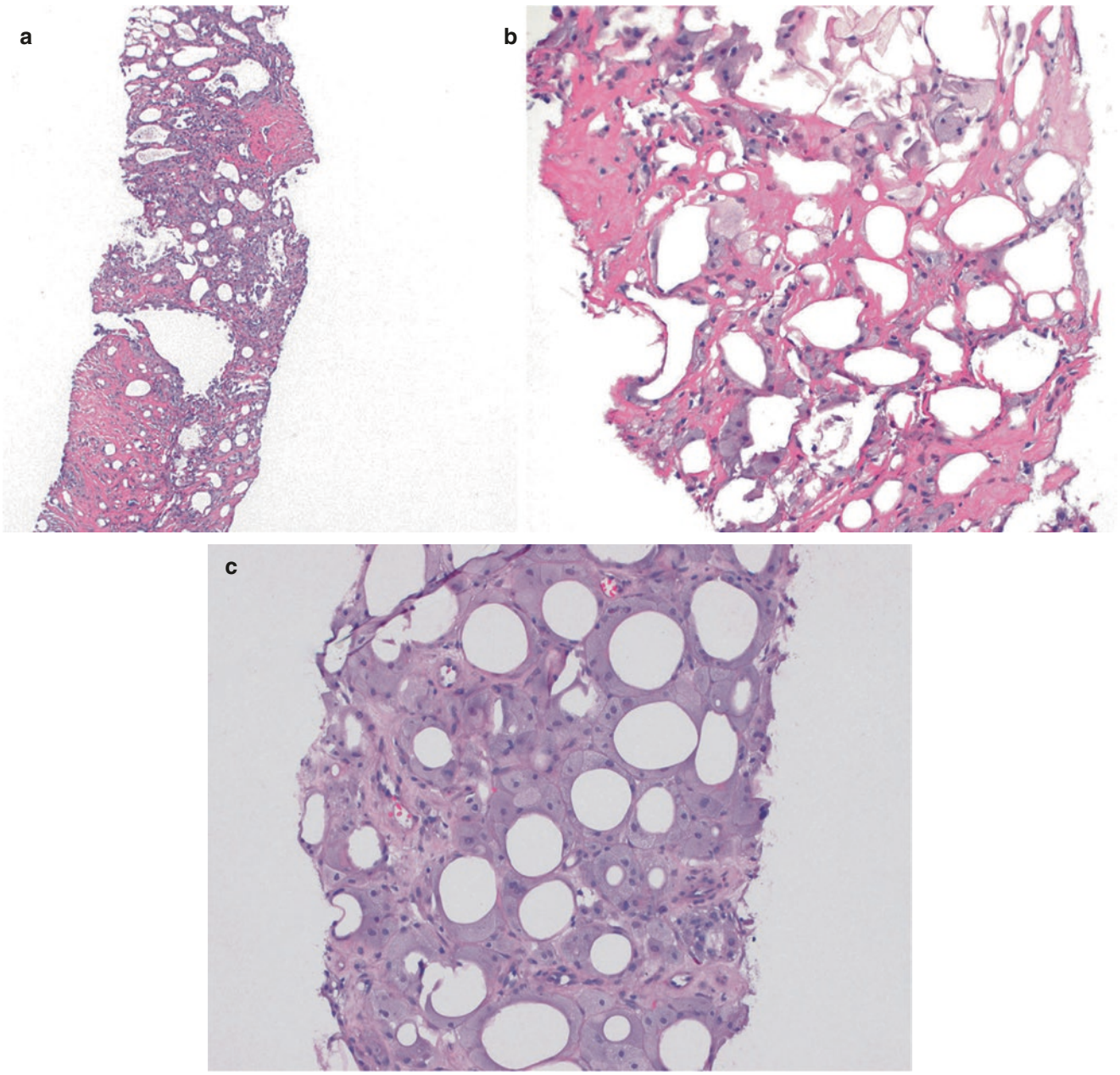

Fig. 4.2 Fat necrosis in core biopsy samples. (**a**, **b**) Core biopsy showing fibrosis and foamy histiocytes surrounding necrotic adipocytes. (**c**) Another case of fat necrosis in a core biopsy sample

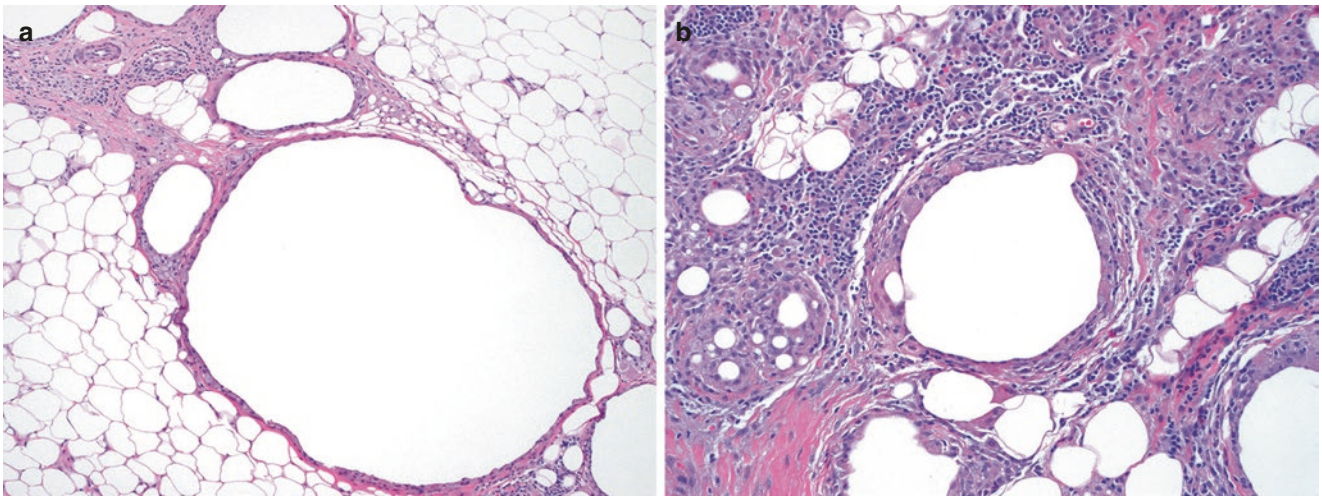

Fig. 4.3 Cysts formed by histiocytes lining lipid pools (**a**, **b**)

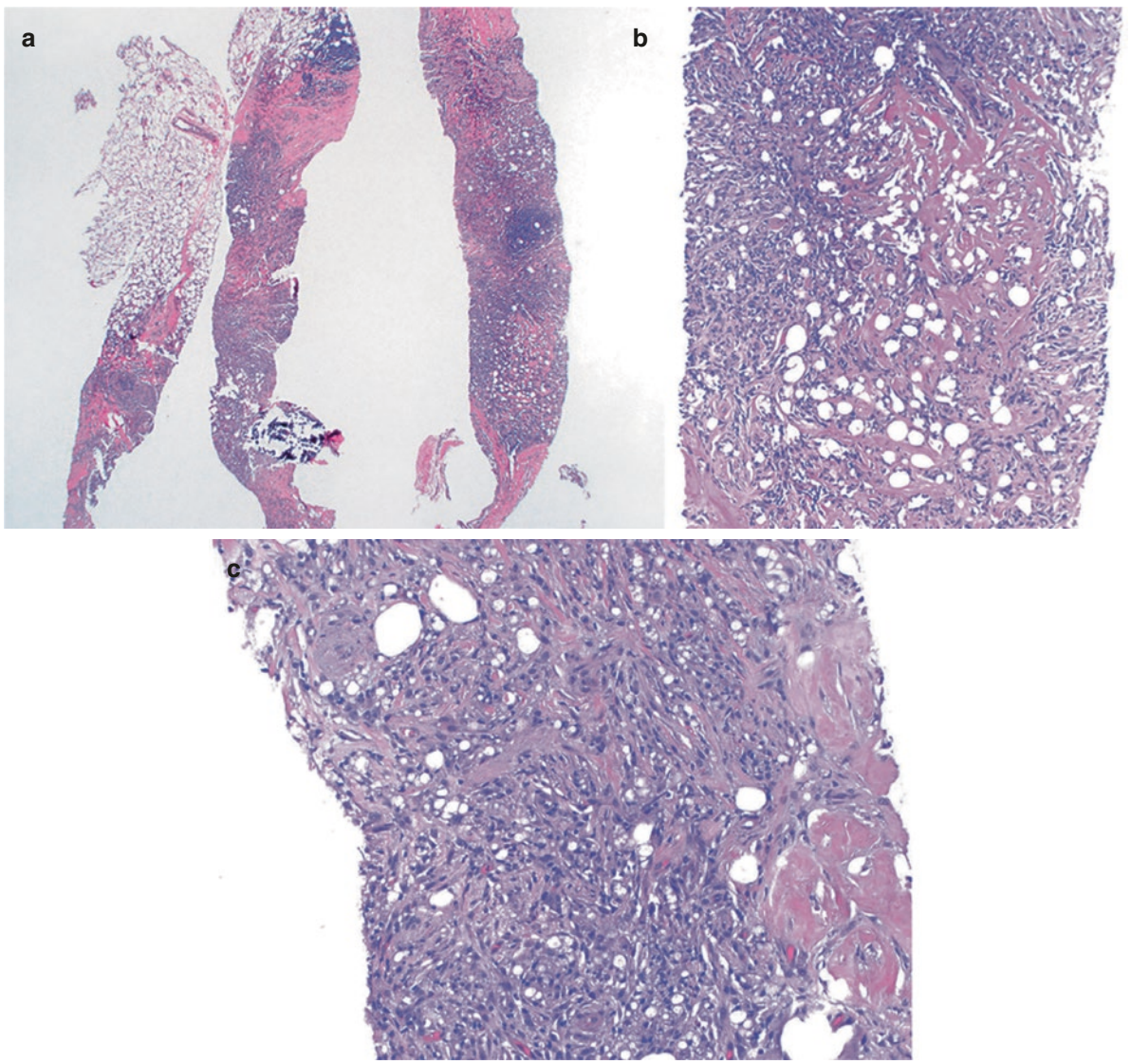

Fig. 4.4 Fat necrosis in a core biopsy performed for a mass in the site of prior lumpectomy. (**a**) A cellular proliferation of inflammatory cells is seen in fibroadipose tissue. (**b**) The inflammatory component is mostly composed of lymphocytes and histiocytes. (**c**) Cellular focus of spindled histiocytes. A cytokeratin (AE1/AE3) immunostain (not shown) was performed in this case to rule out recurrent carcinoma and was negative

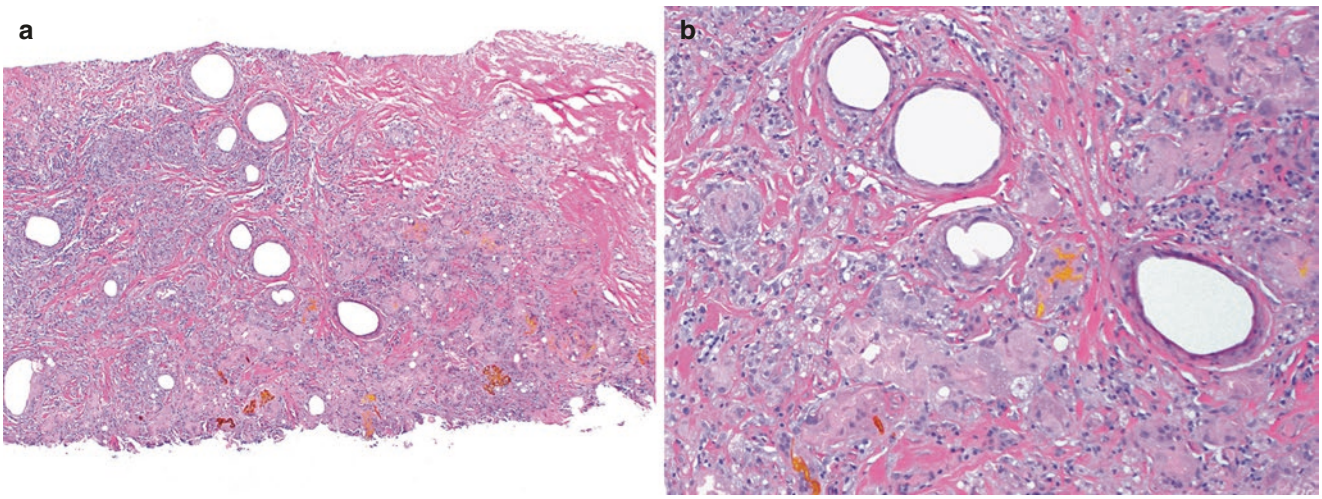

Fig. 4.5 (**a**) Fibrosis, mixed inflammation, and cysts lined by histiocytes are present. Yellow-brown hematoidin pigment is also seen (*bottom* of image). (**b**) The pigment is surrounded by foreign body type giant cells

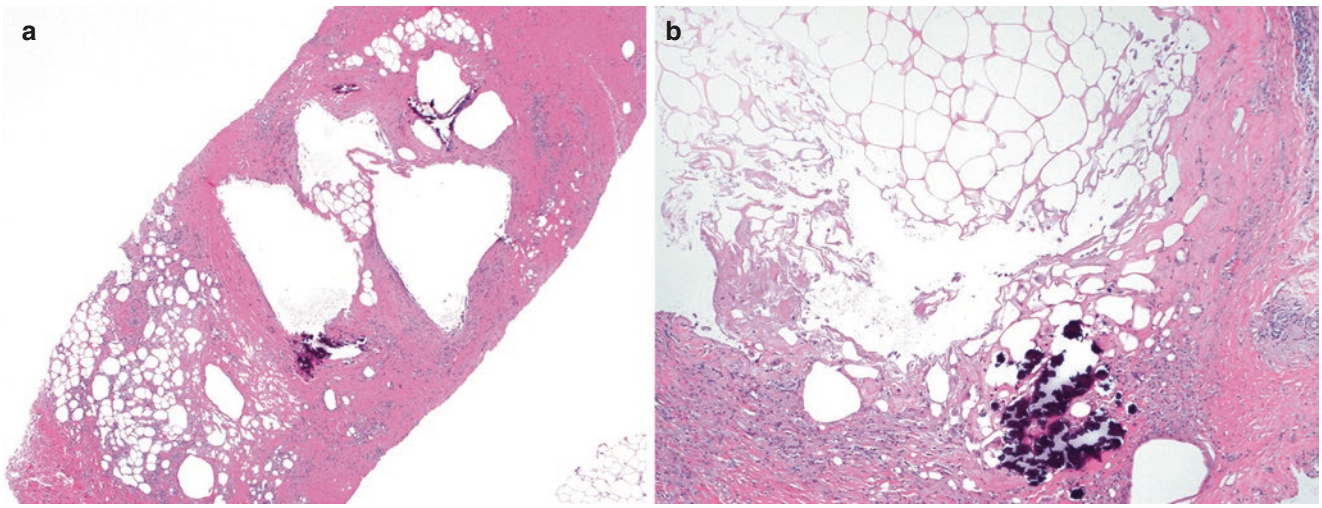

Fig. 4.6 Calcification can be identified in the fibrotic cyst walls surrounding necrotic fat, as seen in these two cases (**a**, **b**)

Differential Diagnosis

Fat necrosis is often biopsied in areas of prior surgery to rule out recurrent carcinoma. In most instances, fat necrosis is diagnosed based on its classic morphologic appearance. If there is a cellular inflammatory component, and there is any doubt to the diagnosis of fat necrosis, a broad-spectrum cytokeratin or CK7 immunostain may be performed to help rule out carcinoma. This is important if there is history of classical type invasive lobular carcinoma, in which the cells can mimic lymphocytes. Other less common types of invasive carcinoma show cells with abundant cytoplasm that can mimic histiocytes. These include "histiocytoid" invasive lobular carcinoma (Fig. 4.7), apocrine carcinoma with histiocytoid morphology, and lipid-rich carcinoma [12–14]. A cytokeratin immunostain will highlight these.

Less common histiocytic proliferations may also be included in the differential diagnosis of fat necrosis, provided the clinical and radiographic features support their consideration. Rosai–Dorfman disease, also known as sinus histiocytosis with massive lymphadenopathy, is a rare, self-limited histiocytic disorder that most commonly occurs in children and young adults. The disease can occur in nodal and extranodal sites, and virtually all sites in the body have been affected [15]. Involvement of the breast is uncommon but has been reported in both males and females. The disease

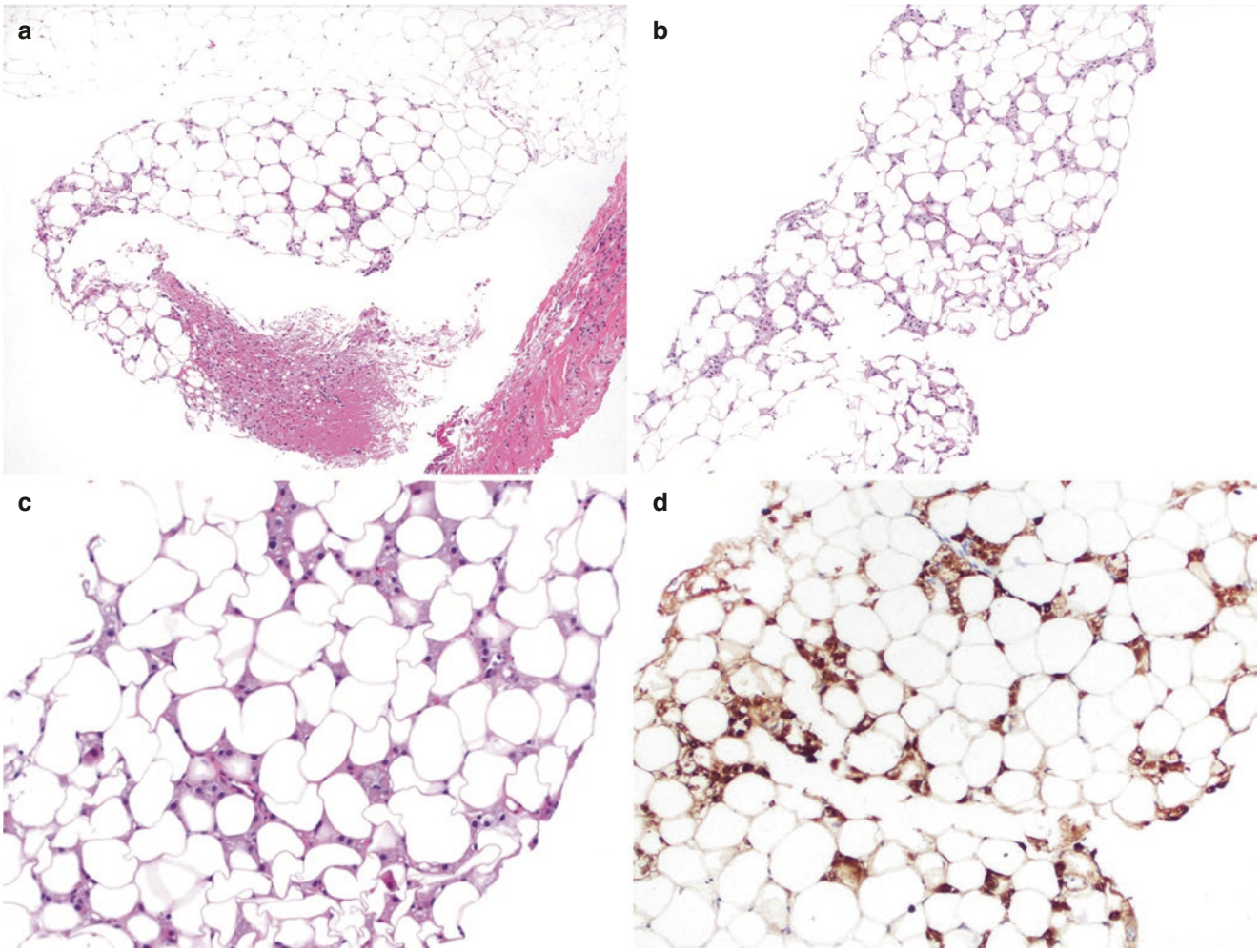

Fig. 4.7 Invasive lobular carcinoma with histiocytoid features in a core biopsy performed for a spiculated mass. (**a**, **b**) Carcinoma cells infiltrating fat mimic fat necrosis on low-power magnification. (**c**) Neoplastic cells have small uniform nuclei and abundant pink cytoplasm. (**d**) Carcinoma cells are highlighted by cytokeratin (AE1/AE3). E-cadherin (not shown) was negative, supporting lobular differentiation. (*Courtesy of Paula Ginter*, *MD*, Weill Cornell Medicine, with permission)

presents in the breast as a mass that is either palpable or detected on screening imaging [15–17]. Axillary lymph nodes may also be involved, leading to the clinical impression of malignancy. Microscopically, a diffuse multinodular infiltrate composed of histiocytes and accompanying lymphocytes and plasma cells is seen in the breast tissue or deep dermis/subcutaneous tissue (Fig. 4.8). Histiocytes have abundant eosinophilic cytoplasm and round nuclei with a single central nucleolus. A diagnostic feature seen in Rosai–Dorfman disease is emperipolesis, in which histiocytes contain lymphocytes in their cytoplasm, and occasionally, plasma cells, neutrophils, and erythrocytes. Emperipolesis may be more difficult to identify in extranodal locations such as the breast. Histiocytes in Rosai–Dorfman disease show positive immunostaining with S100 protein and macrophage-associated antigens (CD68, CD163), and are negative for CD1a and langerin.

Erdheim–Chester is an uncommon histiocytosis composed of foamy histiocytes that is extremely rare in the breast and occurs in the setting of multisystem disease in all cases [18]. Sheets of foamy histiocytes, lymphocytes, plasma cells, and Touton-type giant cells are seen in breast tissue. Histiocytes are positive for CD68 and negative for S100 protein and CD1a.

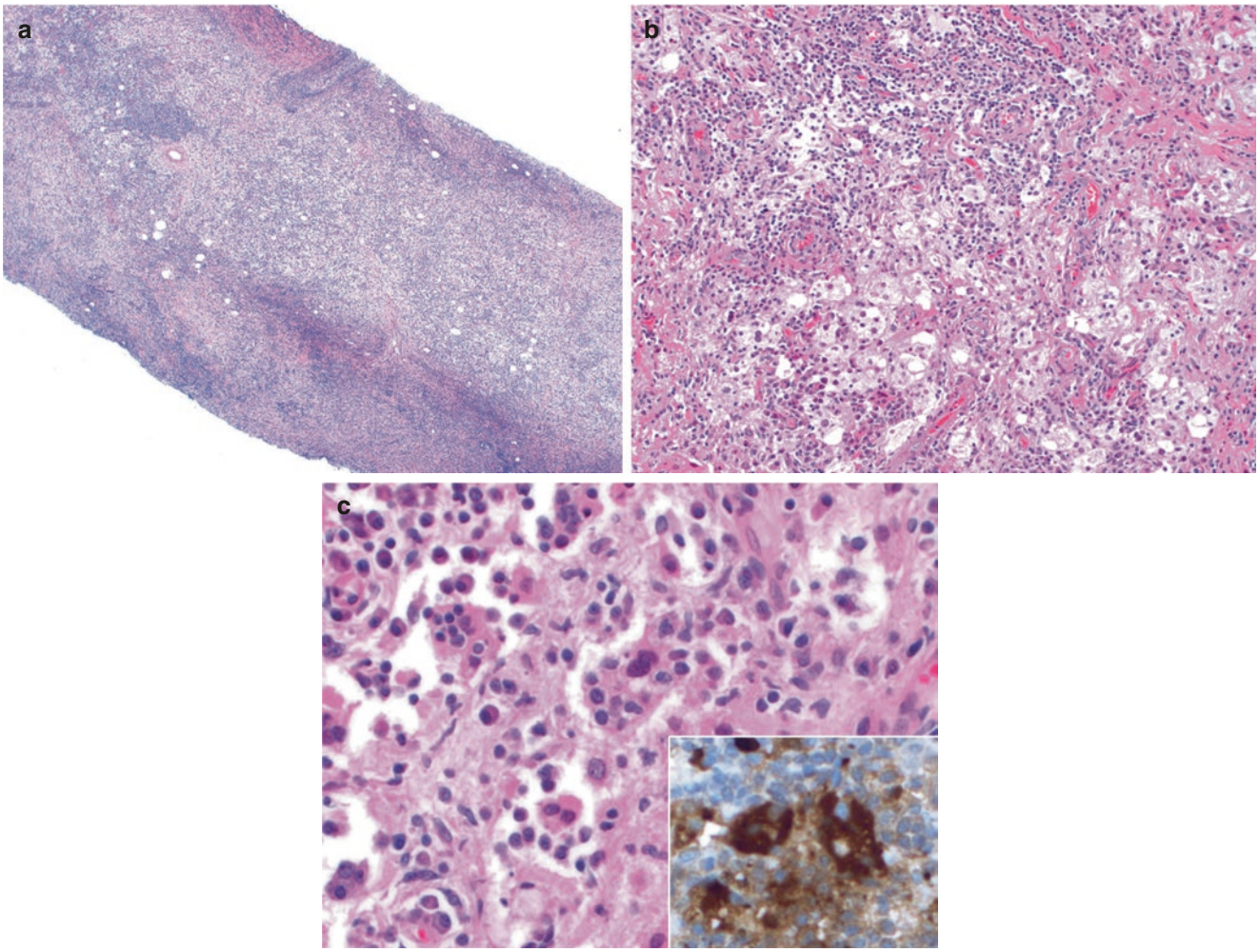

Fig. 4.8 Rosai–Dorfman disease involving the breast. (**a**) Core biopsy shows a diffuse infiltrate of histiocytes, lymphocytes, and plasma cells. (**b**, **c**) The lesion is composed of histiocytes with abundant eosinophilic cytoplasm that show emperipolesis of lymphocytes and plasma cells. Histiocytes are highlighted by an S100 protein immunostain (*inset*, **c**)

Prognosis

Fat necrosis is benign and does not need to be excised when diagnosed in a core biopsy.

Mammary Duct Ectasia

Overview

Mammary duct ectasia is an inflammatory process characterized by dilatation of the central ducts of the breast with variable degrees of fibrosis and inflammation. There are some overlapping clinical and pathologic features with periductal mastitis, squamous metaplasia of lactiferous ducts, and subareolar abscess and these processes can coexist. Minor degrees of ductal dilatation with associated inflammation are not uncommon and are often seen in breast surgical specimens as incidental findings. The discussion of duct ectasia in this chapter will focus on duct ectasia as the pathologic manifestation an inflammatory condition with characteristic clinical and radiographic features [19].

Duct ectasia occurs in adult women in their 30s–60s [20–22]. Rare cases have been reported in males and in children [23–25]. Duct ectasia can be unilateral or bilateral. Clinically, duct ectasia presents as nipple discharge, nipple or skin retraction, or as a subareolar mass. Pain is often present in association with these signs and symptoms or may be the only symptom [26]. Nipple discharge, when present, is yellow, brown, or green in color. Discharge can be spontaneous, intermittent, and can occur over long periods of time (months to years) [26]. Rare cases of duct ectasia reported in infants and children of both sexes have come to clinical attention due to bloody nipple discharge [23, 24]. It has been suggested that cigarette smoking is associated with the development of duct ectasia; however, smoking appears to be related

to periductal inflammation/mastitis, but not ductal dilatation [20, 27, 28]. Duct ectasia has been reported in patients with hyperprolactinemia secondary to pituitary adenomas and phenothiazine therapy [29].

Gross and Radiologic Features

Grossly, duct ectasia shows dilated ducts with thick fibrous walls. The dilated ducts may contain a pasty, yellow-brown secretion, similar to that seen in ductal carcinoma in situ (DCIS) with "comedonecrosis." Features of duct ectasia on imaging can mimic malignancy and are often suspicious enough to warrant a biopsy. On mammography, duct ectasia shows intraductal or periductal branching calcifications, ductal dilatation, or a stellate mass [30]. Periductal calcifications form rings of dense calcification with a central lucency and converge on the nipple [30]. In some cases of duct ectasia, there may be no mammographic findings and abnormalities are only seen on ultrasound. Ultrasound shows dilated subareolar ducts or a mass-like lesion filled with echogenic material [31].

Microscopic Features

Duct ectasia is characterized by dilated ducts with luminal foamy histiocytes and variable degrees of fibrosis and periductal chronic inflammation (Fig. 4.9). The morphology varies depending on the stage in evolution of the process. Early lesions show mild ductal dilatation with luminal histiocytes and minimal or no fibrosis of the ducts. The epithelium of involved ducts is either attenuated or absent and is not hyperplastic. Sloughed epithelium can be seen in duct lumens in

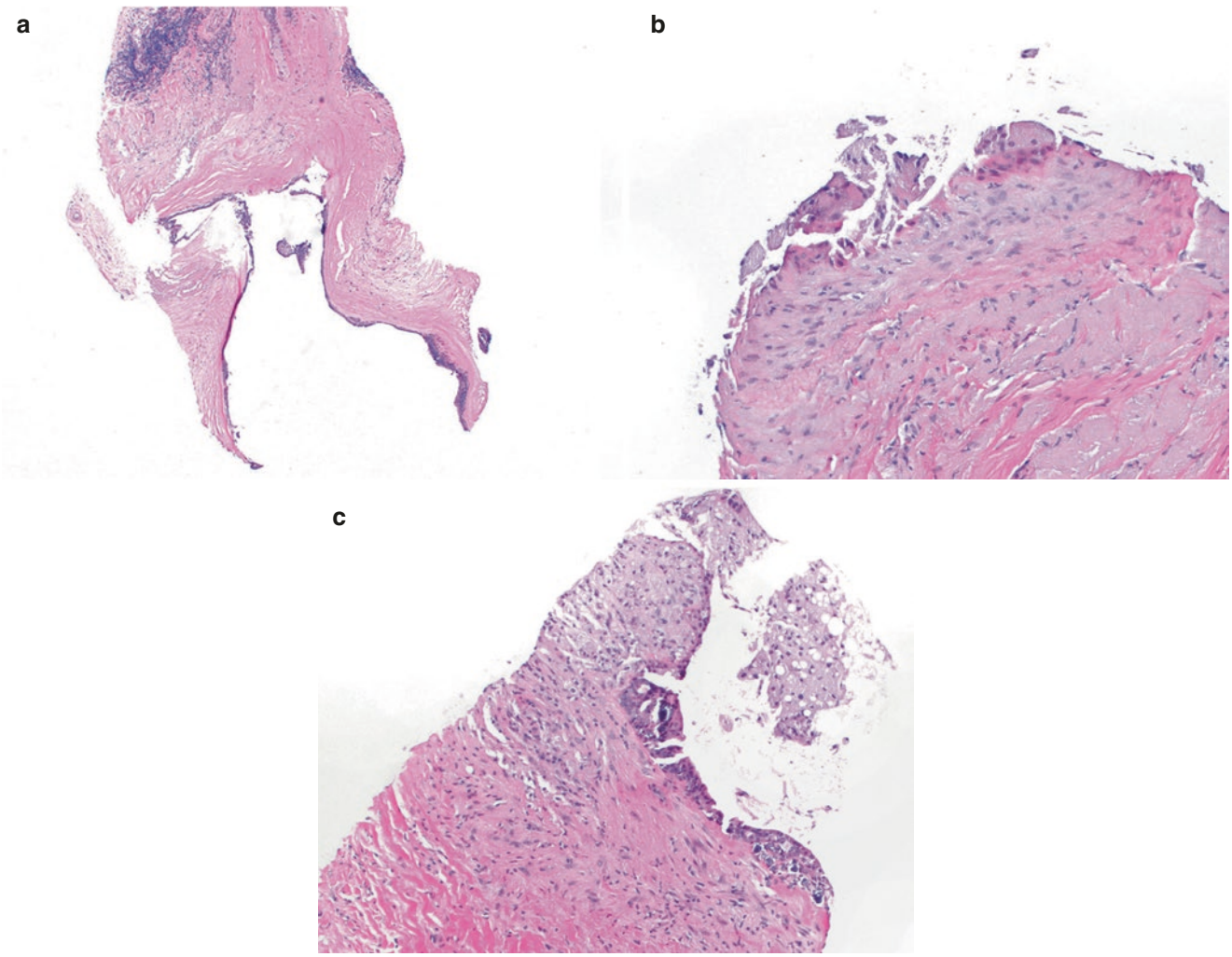

Fig. 4.9 Duct ectasia in core biopsy samples. (**a**) The duct is fibrotic with a flattened epithelial lining. Periductal lymphocytic inflammation is present. (**b**) The duct wall in this case is fibrotic and shows elastosis. The lining is composed of histiocytes only. (**c**) Flatted ductal epithelium and luminal foamy histiocytes are seen

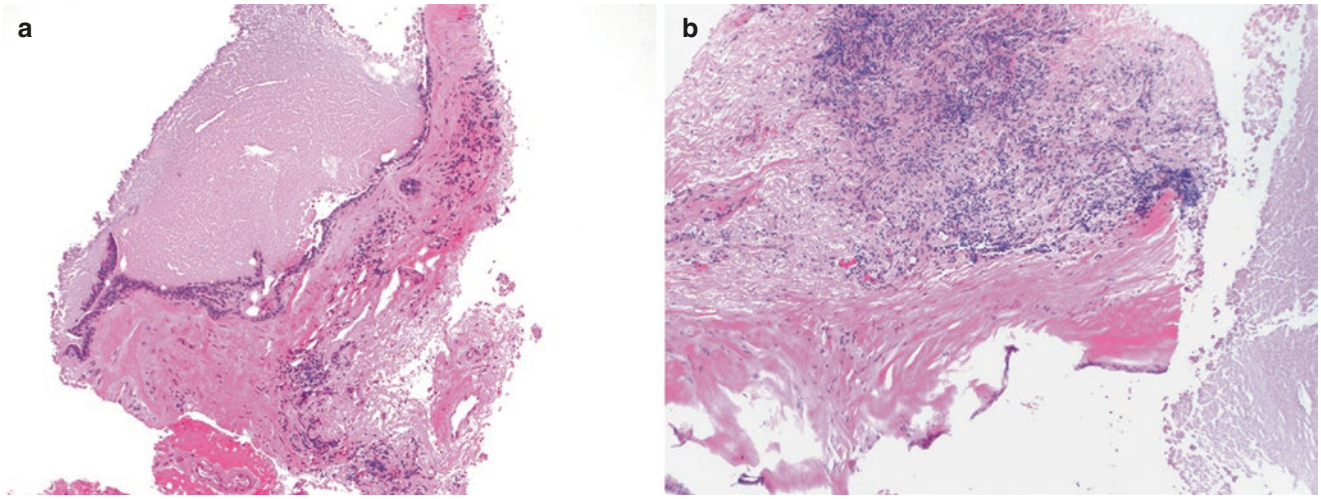

Fig. 4.10 Duct ectasia in a core biopsy sample. (**a**) Amorphous pink secretion is present in the lumen of a dilated duct. (**b**) The duct wall is fibrotic and is associated with periductal chronic inflammation

some cases. The luminal debris is composed of lipid-laden foamy histiocytes, amorphous pink secretion, and sometimes foreign body type giant cells (Fig. 4.10). Intraepithelial foamy histiocytes may be seen (Fig. 4.11). Histiocytes containing brown pigment, referred to as "ochrocytes," may be present in a periductal location (Fig. 4.12) [32]. Periductal chronic inflammation is composed mainly of lymphocytes and plasma cells.

As duct ectasia evolves, duct walls become thickened and fibrotic and are more likely to cause symptoms and become apparent on imaging. Fibrosis is often accompanied by elastosis in the duct walls. Calcification can be present in the lumen of the duct or within the duct wall (Fig. 4.13). A core biopsy of duct ectasia at this stage may only reveal a small portion of a fibrotic duct wall with minimal inflammation. In the late stages of duct ectasia, ducts may become ruptured and obliterated (Fig. 4.14). Rupture of the duct wall with spilling of contents into the surrounding breast tissue can lead to the formation of abscess. Cholesterol granulomas, "cholesterolomas," may form within fibrotic ducts and can manifest as a mass or calcifications on imaging (Fig. 4.15) [33]. "Mastitis obliterans" refers to the histologic finding of fibrosis completely filling the duct lumen that occurs in the later stages of duct ectasia (Fig. 4.16).

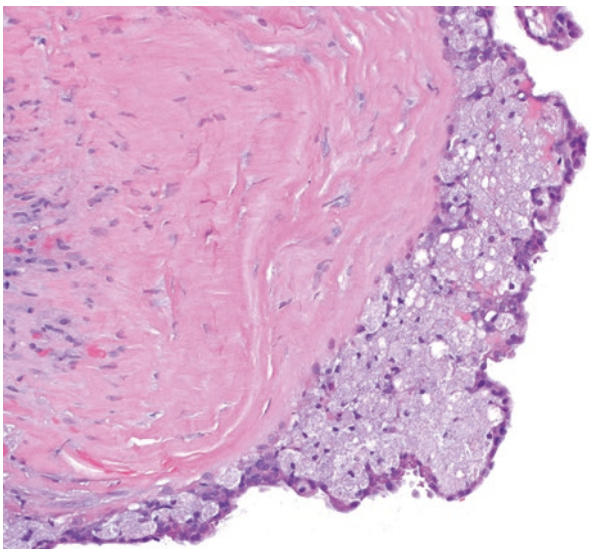

Fig. 4.11 Duct ectasia with intraepithelial histiocytes

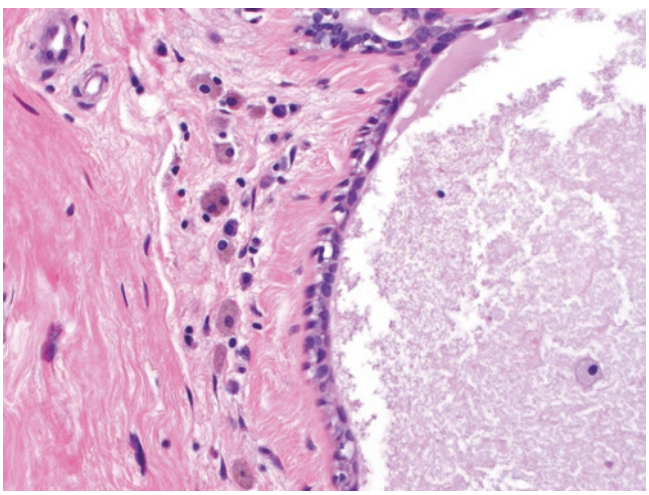

Fig. 4.12 Periductal histiocytes containing brown pigment, so-called "ochrocytes"

Differential Diagnosis

By clinical, imaging, and gross findings, duct ectasia mimics high-grade DCIS with central necrosis ("comedonecrosis"). In cases that show fibrotic ducts without epithelium, it is important to rule out the presence of DCIS. Clues to the presence of DCIS include necrosis and luminal calcifications. Periductal inflammation will be present in DCIS, but typically does not contain foamy histiocytes. Additional deeper hematoxylin and eosin (H&E) levels should be obtained in

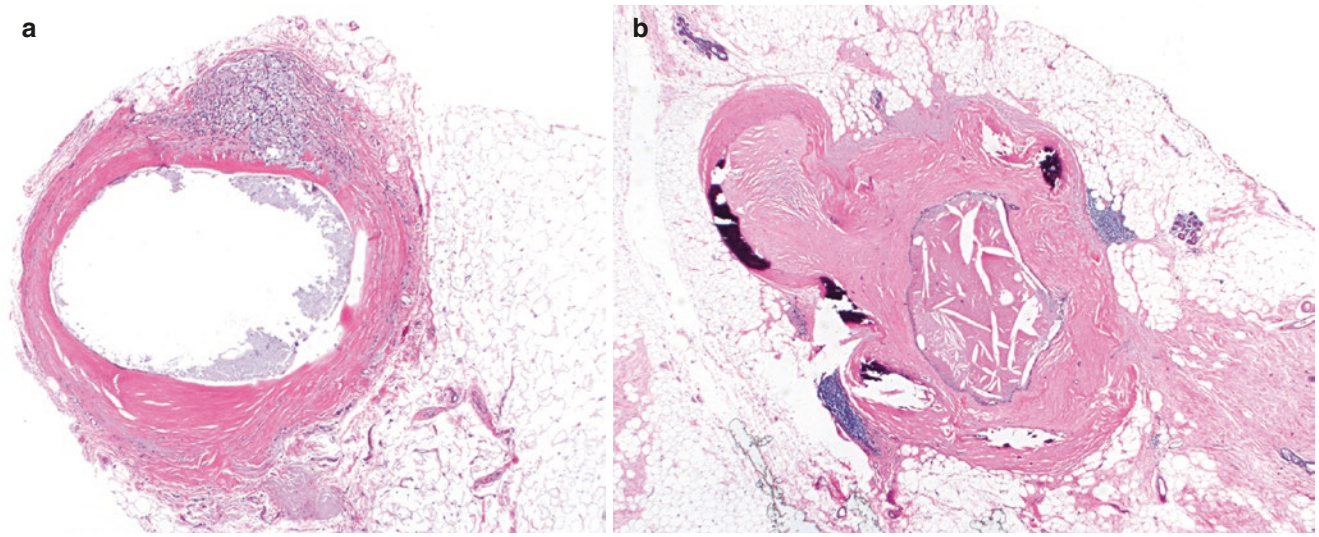

Fig. 4.13 Duct ectasia in stereotactic biopsies performed for mammographic calcifications. (**a**) Luminal calcifications are present in this biopsy. (**b**) Calcifications are present within the fibrotic duct wall

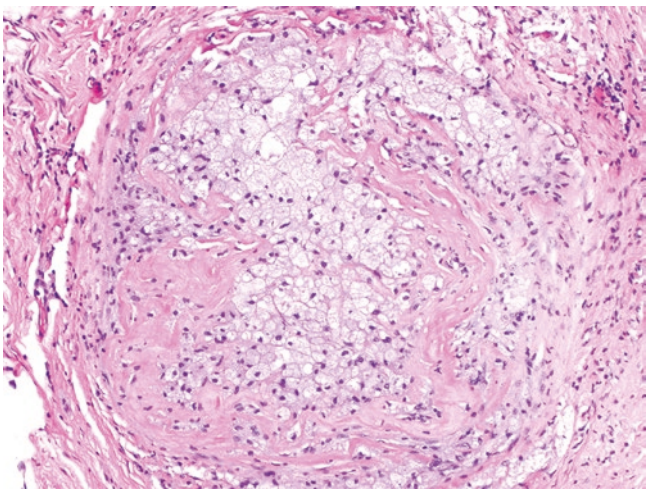

Fig. 4.14 Duct ectasia showing obliteration of duct wall

uncertain cases. Intraepithelial histiocytes can mimic pagetoid spread of carcinoma, either ductal or lobular. A broad-spectrum cytokeratin stain can be used to rule out carcinoma, if necessary. Ductal dilatation can occur distal to an intraductal lesion such as a papilloma. If dilated ducts are present in a core biopsy for an intraductal mass, correlation with imaging findings is necessary to determine whether the targeted lesion has been sampled.

Cysts associated with fibrocystic changes can show fibrosis and inflammation of the cyst wall. Cysts are formed in the terminal duct lobular units, while duct ectasia involves subareolar ducts. Proximity to the nipple favors duct ectasia. Making the distinction between cysts and duct ectasia in a core biopsy is not critically important as these are managed similarly.

Immunohistochemistry

Duct ectasia is usually diagnosed without immunohistochemical stains. CD68 may be used to highlight histiocytes in uncertain cases. A broad-spectrum cytokeratin stain can be used to rule out pagetoid spread of carcinoma when intraepithelial histiocytes appear atypical, especially in cases with coexisting DCIS in the breast.

Pathogenesis

Duct ectasia may be a result of stasis and accumulation of debris in ducts, which leads to an inflammatory response and duct fibrosis. Squamous metaplasia of lactiferous ducts is the cause of duct stasis in some cases. Alternatively, the process may begin with periductal inflammation which leads to fibrosis and duct dilatation [34].

Prognosis

Duct ectasia may be treated by excision of the involved duct(s) in symptomatic cases. Re-excision and/or incision and drainage may be necessary in cases complicated by abscess or sinus formation. In most cases, if duct ectasia is diagnosed in a core biopsy of a radiographically detected lesion in an asymptomatic patient, the lesion does not need to be excised, provided there is radiologic-pathologic concordance. Patients with duct ectasia are not at increased risk for the development of breast carcinoma.

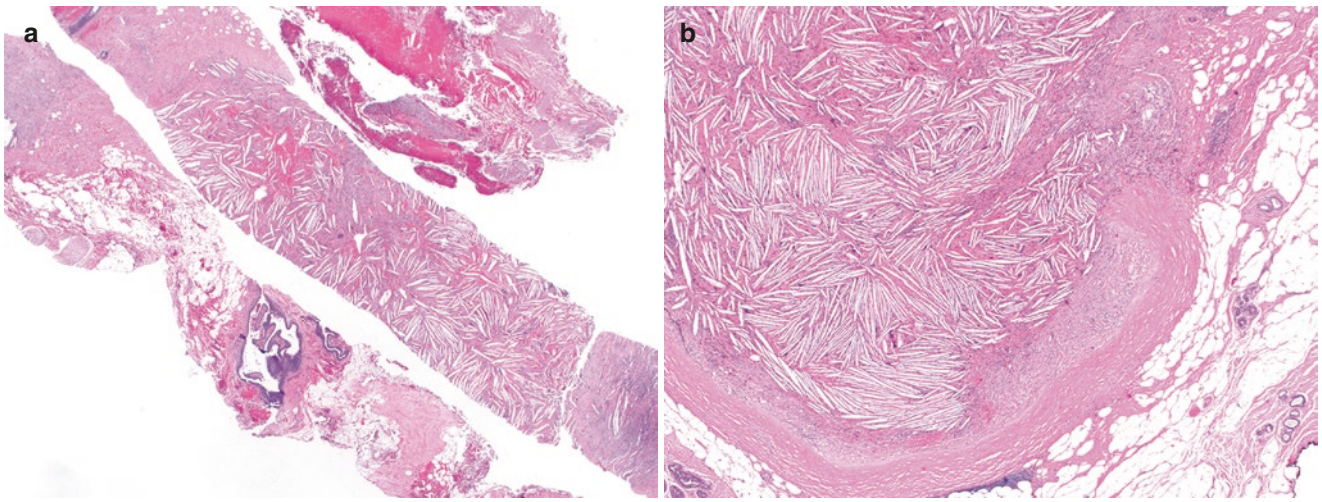

Fig. 4.15 "Cholesteroloma" in duct ectasia. (**a**) Core biopsy and (**b**) excision shows cholesterol clefts associated with histiocytes within a fibrotic duct

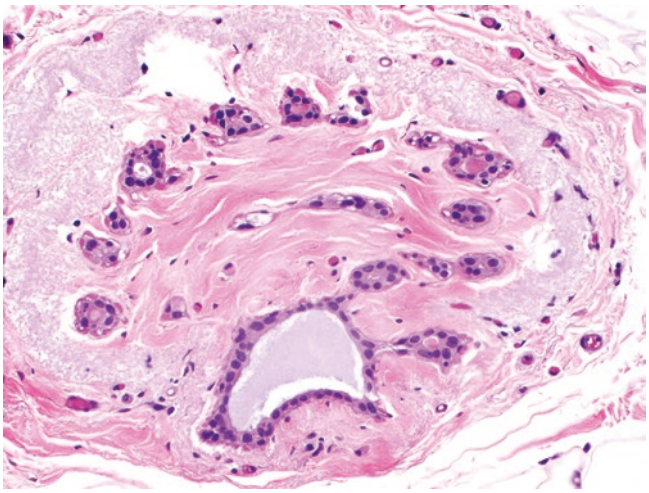

Fig. 4.16 Mastitis obliterans shows fibrosis completely filling the duct lumen and a garland pattern of epithelium at periphery of the duct

Granulomatous Lobular Mastitis

Overview

Granulomatous inflammation involving breast tissue is uncommon and can occur as a result of various infectious and inflammatory processes. Non-necrotizing granulomatous mastitis that is idiopathic is referred to as granulomatous lobular mastitis. The clinical and imaging features of granulomatous lobular mastitis are often suggestive of malignancy and core biopsy is necessary to rule out a malignant process.

Granulomatous lobular mastitis typically occurs in parous women of reproductive age (20s–40s) [35–38]. Some studies have noted a demographic trend of the development of granulomatous mastitis in Hispanic patients and patients born outside of the United States [38–40]. Clinical features can mimic malignancy or an inflammatory process. Most cases are unilateral. Less than 5% of patients present with bilateral disease [38, 41]. Patients present most often with a palpable mass or ill-defined firmness in the breast that may be accompanied by overlying skin erythema and nipple retraction. Masses are often large (over 3 cm in size) and may be associated with pain and tenderness. Nipple discharge can be the presenting symptom in some cases. Palpable ipsilateral axillary lymphadenopathy is reported in about one-quarter of cases [36, 37, 41]. Patients report a history of prior trauma to the affected breast in rare cases [42–44]. Many cases of granulomatous lobular mastitis become complicated by the development of abscesses and draining skin sinuses. Granulomatous lobular mastitis is difficult to treat, and patients often experience persistent and/or recurrent disease. In recent years, infection with *Corynebacterium* bacteria has been implicated in the development of granulomatous lobular mastitis. "Cystic neutrophilic granulomatous mastitis" is a distinctive histologic pattern of granulomatous mastitis characterized by suppurative lipogranulomas in which *Corynebacterium* bacteria may be identified on a Gram stain [44].

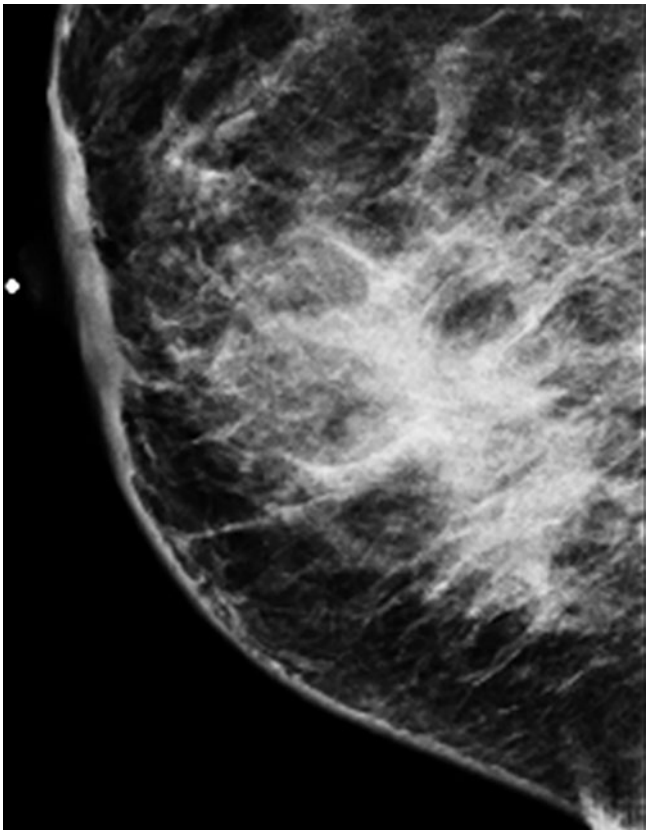

Fig. 4.17 Granulomatous lobular mastitis on mammography. Mammography shows an ill-defined spiculated mass in this case. (*Courtesy of Elizabeth Arleo*, *MD*, Weill Cornell Medicine, with permission)

When granulomatous lobular mastitis is identified in a core biopsy sample, obtaining clinical history is important to exclude other causes of granulomatous information. Special stains for fungi and acid-fast bacilli (AFB) should be performed to rule out these as infectious causes. Review of clinical, imaging, and pathologic findings in an interdisciplinary setting such as tumor board is helpful for establishing an effective treatment plan for these uncommon cases.

Gross and Radiologic Features

Grossly, granulomatous lobular mastitis is characterized by one or multiple ill-defined firm masses or nodules. Granulomatous lobular mastitis can appear on mammography as an ill-defined mass which with spiculated contours (Fig. 4.17) or heterogeneous parenchyma without a discrete mass [37, 45, 46]. Multiple masses or nodules may be identified. Microcalcifications are not a feature of granulomatous lobular mastitis. Ultrasound may show an irregular hypoechoic mass with shadowing, fluid collection, tubular structures, or parenchymal mixed echogenicity [36, 37, 45–47].

Microscopic Features

Granulomatous lobular mastitis is characterized by non-necrotizing granulomatous inflammation that is centered on lobules (Fig. 4.18). Granulomas are composed of epithelioid histiocytes, Langhans giant cells, and variable numbers of lymphocytes, plasma cells, and neutrophils. Eosinophils can be identified in some cases. Microabscesses can be present within or outside lobules (Fig. 4.19). Granulomatous inflammation can involve few lobules or can diffusely involve the breast. Lobules may appear confluent with destruction of the lobules by the granulomatous inflammation. Frank abscesses can develop in some cases. Core biopsy samples are often taken at the time an abscess develops. In these samples, rare breast glands may be present in the biopsy that show granulomatous lobular mastitis.

"Cystic neutrophilic granulomatous mastitis" refers to a histologic pattern of granulomatous lobular mastitis characterized by granulomas containing cystic vacuoles lined by neutrophils [42–44]. The empty vacuoles represent dissolved lipid and contain Gram-positive bacilli (described below) (Fig. 4.20). The cystic neutrophilic pattern may be identified within lobules and may also be formed within an abscess without any identified glands (Fig. 4.21).

Differential Diagnosis

The differential diagnosis includes other causes of lobular granulomatous inflammation. Granulomas seen in tuberculosis are necrotizing, while those of granulomatous lobular mastitis are non-necrotizing, suppurative granulomas containing neutrophils. Clinical and laboratory findings help to exclude sarcoidosis as a cause of granulomatous mastitis. Sarcoidosis rarely involves the breast without evidence of disease in other sites. Asteroid bodies and Schaumann bodies can be seen in sarcoidosis but are not seen in granulomatous lobular mastitis. Rosai–Dorfman disease (discussed above under differential diagnosis for fat necrosis) is characterized by sheets of large S100 protein-positive histiocytes accompanied by lymphocytes and plasma cells, which can mimic granulomatous lobular mastitis histologically. Langhans giant cells are not seen in Rosai–Dorfman disease.

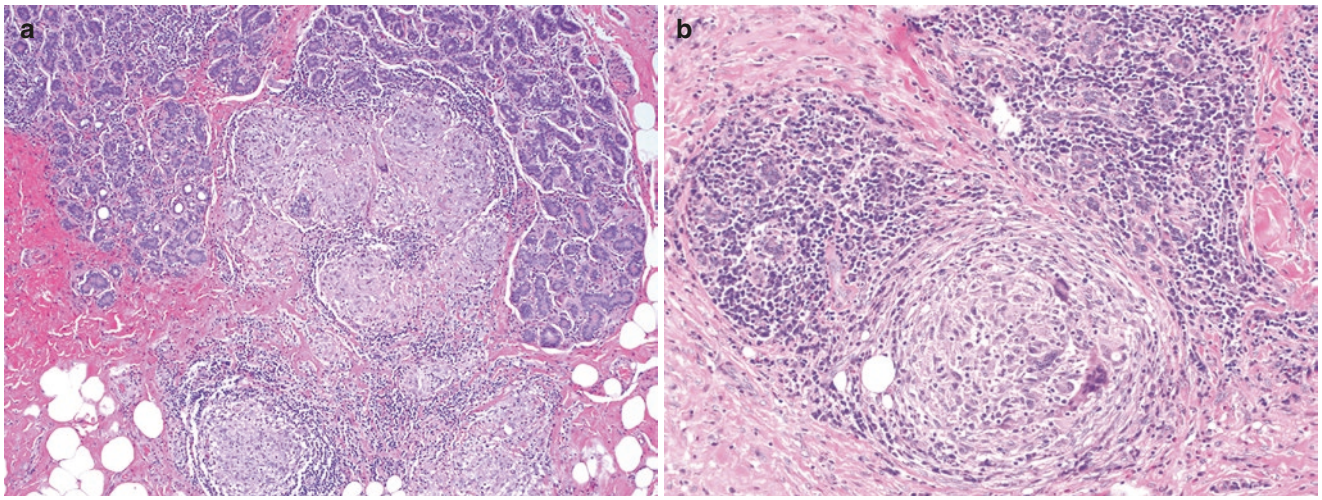

Fig. 4.18 Granulomatous lobular mastitis. (**a**) Non-necrotizing granulomatous inflammation centered on lobules. (**b**) Granulomas are composed of epithelioid histiocytes, Langhans giant cells, lymphocytes, and plasma cells

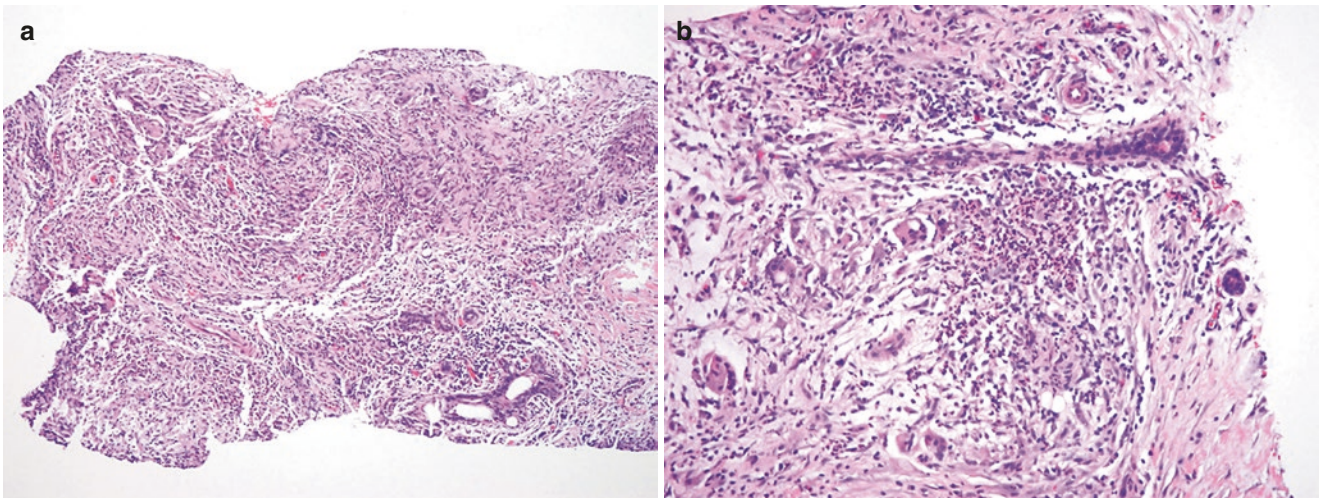

Fig. 4.19 Granulomatous lobular mastitis in a core biopsy. (**a**) Granulomas have destroyed the lobules. (**b**) Microabscesses are evident

Special Histochemical Stains and Methods to Identify Bacteria

Special stains for AFB and fungal organisms (Periodic acid–Schiff or Grocott-Gomori's [or Gömöri] methenamine silver) help to rule out mycobacterial and fungal infection as the cause of granulomatous mastitis. A Gram stain may allow identification of bacteria in cases that show cystic neutrophilic granulomatous mastitis (Fig. 4.19c, d). In most cases, only rare bacteria will be evident on the Gram-stained section and will only be present in 1–2 vacuoles. One study reported that performing Gram stains on 6 μm "thick sections" resulted in increased detection and easier identification of bacteria compared with 4 μm sections [48]. Coryneform features such as grouping of bacteria into "V" shapes and palisade arrangement may be seen in cases with more abundant bacteria. These bacteria are not usually evident on H&E examination.

Corynebacterium species can be difficult to isolate by routine culture and may require a special medium containing 1% polysorbate (Tween) 80 that may more easily grow lipophilic bacteria [42, 49]. Other methods such as matrix assisted later desorption ionization-time of flight mass spectrometry and 16S rRNA sequencing have been employed successfully to identify *Corynebacterium* in granulomatous mastitis specimens and these tests can be performed on paraffin-embedded tissue [39, 40, 50].

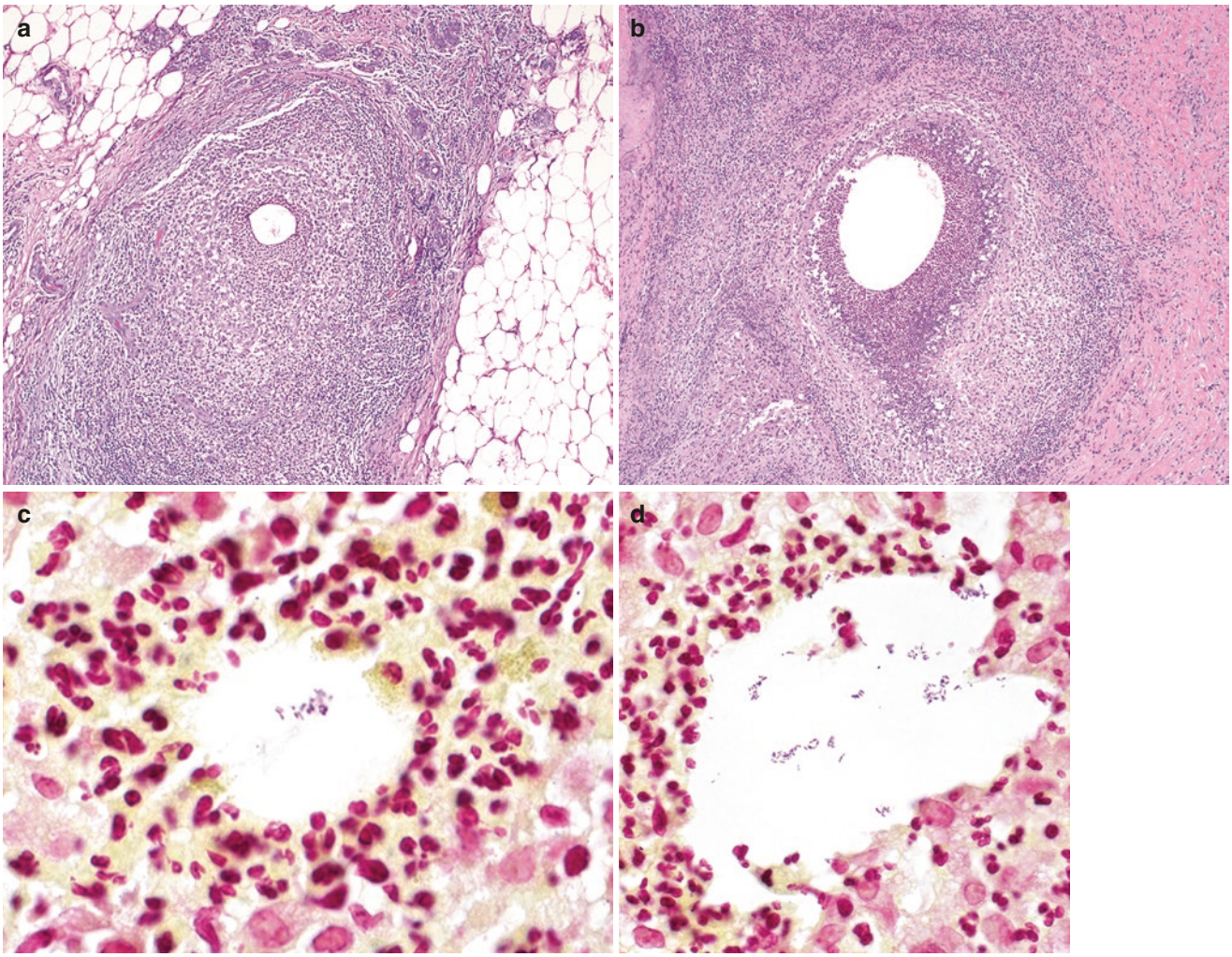

Fig. 4.20 Cystic neutrophilic granulomatous mastitis. (**a**) Suppurative granuloma centered on a lobule with a central clear vacuole surrounded by neutrophils. (**b**) Cystic neutrophilic granuloma showing more abundant neutrophils. (**c**, **d**) Gram-positive coryneform bacilli within cystic vacuoles

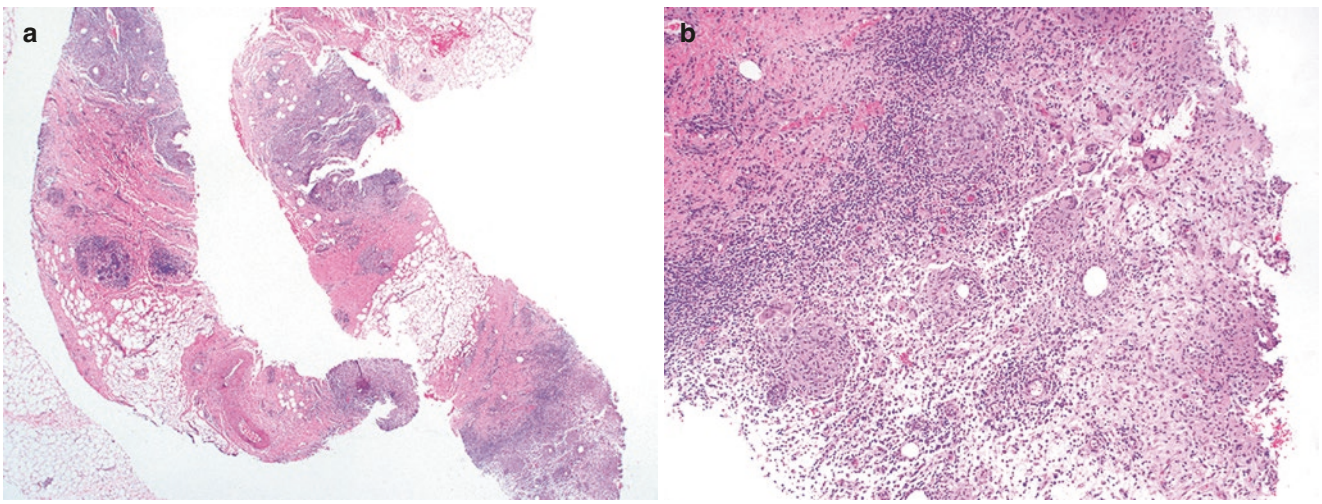

Fig. 4.21 Core biopsy of granulomatous lobular mastitis with abscess. (**a**, **b**) Core biopsy shows abscess containing non-necrotizing granulomas, some of which contain neutrophil-lined cystic vacuoles

Pathogenesis

The etiology of granulomatous lobular mastitis is unclear, which is why the disease is also called "idiopathic granulomatous mastitis." It is thought that prior pregnancy and breastfeeding leads to stasis of secretion and predisposes ducts rupture, which can lead to granulomatous lobular mastitis [36, 42]. There are some overlapping features with duct ectasia and these processes can coexist [42]. Oral contraceptive use, smoking, and autoimmune disease do not appear to be directly related to the development of granulomatous lobular mastitis [41].

Corynebacterium bacteria, which are typically non-pathogenic skin microbiota, are associated with cystic neutrophilic granulomatous mastitis and appear to be pathogenic in this disease. Evidence for pathogenicity include its pure growth in culture, association with acute inflammatory cells, and the presence of bacteria in clinical specimens (i.e., histologic slides) [42, 49, 51]. Species of *Corynebacterium* that are most frequently isolated are lipophilic bacteria, which is consistent with their presence in lipid vacuoles [42].

Prognosis

There is no standard approach for treating patients with granulomatous lobular mastitis. The use of steroids alone or in combination with surgery or antibiotics has been shown to be effective in multiple reports [37–39, 42, 52, 53]. Surgery includes wide excision or abscess drainage, and patients may require multiple procedures to manage persistent disease. Antibiotics appear to be less effective but may be beneficial if granulomatous mastitis is complicated by abscess formation. Tetracycline was effective in resolving the process in all 3 patients with cystic neutrophilic granulomatous mastitis in one study [44]. Microbial cultures should be taken to help guide therapy.

Sarcoidosis

Overview

Sarcoidosis is a systemic inflammatory condition that rarely involves the breast and can mimic malignancy based on clinical and imaging features. Women in their 20s–40s are most often affected. Breast sarcoidosis is not usually the primary manifestation of the disease and most patients have been diagnosed with sarcoidosis prior to the time of presentation. Patients present with a unilateral non-tender palpable mobile mass in most cases [54]. Rare patients have been reported to have bilateral disease [54]. In some cases, the mass can become fixed to the skin, clinically mimicking involvement by invasive carcinoma [55].

Gross and Radiologic Features

Sarcoidosis grossly shows firm nodules with well-defined or ill-defined borders. Mammography may show a spiculated mass, architectural distortion, or asymmetry, and can be suggestive of malignancy [54, 56, 57]. The most common finding on ultrasound is an ill-defined hypoechoic mass [58]. Enlarged axillary or intramammary lymph nodes may be seen if also involved by sarcoidosis. MRI shows an irregular enhancing mass, similar to an invasive carcinoma [58]. Core biopsy may be performed to rule out malignancy because of the worrisome imaging features.

Microscopic Features

Sarcoidosis is characterized by non-necrotizing granulomas with variable numbers of Langhans giant cells (Fig. 4.22). Schaumann bodies and asteroid bodies may be identified. Granulomas are present within lobules and are

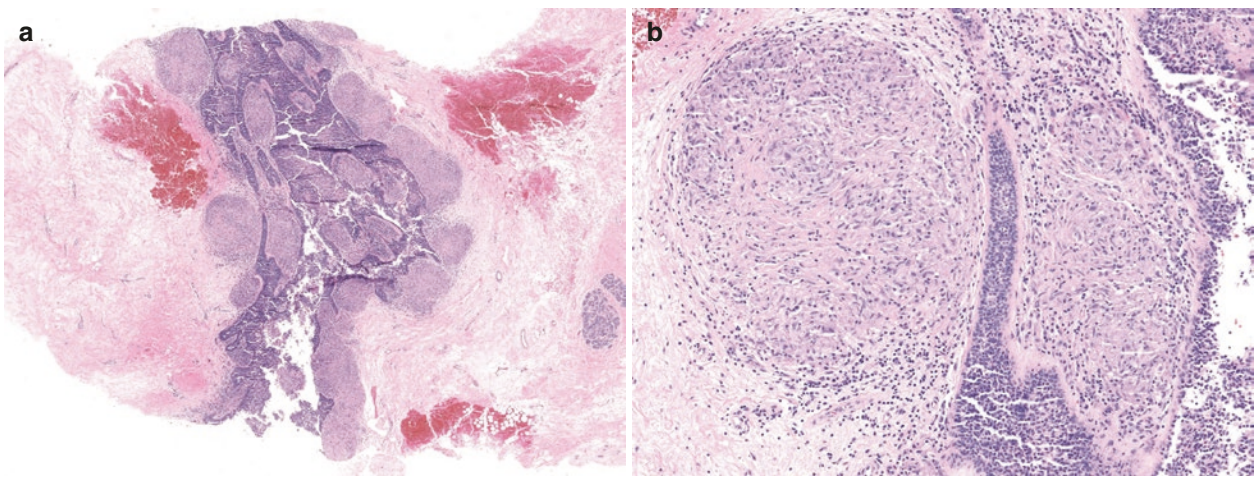

Fig. 4.22 Sarcoidosis in an MRI-guided biopsy for suspicious enhancement in a patient with known systemic sarcoidosis. (**a**) Low-power examination of the biopsy shows a duct extensively involved by granulomatous inflammation. (**b**) Higher power shows periductal non-necrotizing granulomas associated with minimal chronic inflammation

also seen in the interlobular stroma. Microabscess formation and suppurative granulomas are not typical features of sarcoidosis.

Differential Diagnosis

The differential diagnosis of sarcoidosis includes other causes of granulomatous inflammation such as granulomatous lobular mastitis and mycobacterial and fungal infections. As such special stains should be performed to rule out infectious processes. Sarcoid-like granulomas can be present in association with invasive carcinoma in rare cases [59]. Granulomas are present within the tumor and circumferentially around the tumor, so they are unlikely to be the sole finding in a core biopsy.

Prognosis

Treatment may include excisional biopsy of the lesion if imaging features are suspicious, and it is necessary to exclude the possibility of coexisting carcinoma. Recurrence of sarcoidosis can occur in the ipsilateral or contralateral breast following excision [54].

Diabetic Mastopathy

Overview

Diabetic mastopathy refers to a mass-forming fibrous proliferation of the breast occurring in patients with diabetes mellitus. The histologic changes of diabetic mastopathy are most often seen in patients with long-standing insulin-dependent (type 1) diabetes mellitus with secondary complications including retinopathy, nephropathy, and neuropathy [60–62]. Identical histologic changes can be seen in breast tissue from patients with non-insulin-dependent (type 2) diabetes mellitus, autoimmune and/or endocrine diseases (particularly thyroid disease), and in nondiabetic patients with no evidence of autoimmune disease [62, 63].

Diabetic mastopathy typically occurs in women in their 20s–40s, with rare cases occurring in men [60, 62–64]. Patients most often present with a non-painful palpable mass, multiple masses, or diffuse nodularity. The mass or masses may be localized to the subareolar region [63]. In other instances, an abnormality is detected on screening mammography. The disease can be unilateral or bilateral. Logan and Hoffman reported 36 patients with diabetic mastopathy who all presented with palpable abnormalities, 24 (67%) of which presented with multiple nodules [64]. In a series of 19 patients with diabetic mastopathy (17 women, 2 men) reported by Ely et al., 15 patients presented with a unifocal lesion and 4 patients presented with bilateral disease [63].

Gross and Radiologic Features

Grossly, diabetic mastopathy most often shows fibrous breast parenchyma or an ill-defined firm area but does not usually show a discrete mass. Diabetic mastopathy has a variable radiographic appearance which in some cases may be suggestive of malignancy. Mammography shows an ill-defined mass, architectural distortion, or indeterminate fibrous tissue without a discrete mass [65]. On sonography, diabetic mastopathy has been reported to appear as an irregular hypoechoic solid mass with posterior shadowing [65–67]. In some cases, ultrasound may not show a mass to correlate with an area of palpable concern [61]. Findings on MRI are nonspecific and can show patchy or diffuse homogeneous low enhancement or may not reveal any abnormality [67–69].

Microscopic and Immunohistochemical Features

Diabetic mastopathy is characterized by a constellation of findings including stromal fibrosis, epithelioid fibroblasts, and lymphocytic infiltrates in a periductal, perilobular, and perivascular distribution (Fig. 4.23). The fibrous stroma is dense with keloidal features and a glassy appearance (Fig. 4.24). Plump epithelioid stromal fibroblasts are characteristic and show round to ovoid vesicular nuclei and abundant eosinophilic cytoplasm. Their distribution is scattered within the stromal and they may be sparse or absent. Ely et al. reported epithelioid fibroblasts in 14 of 19 (74%) of cases, including three cases in nondiabetic patients [63]. These cells were not seen in the two cases occurring in men in their study. Lymphoid infiltrates are well defined and are prominent around ducts and lobules, while variably present around small vessels. Infiltrates are composed of small mature lymphocytes that are mostly B cells by immunohistochemistry and a smaller population of admixed T cells [70]. Plasma cells may be associated with the lymphocytic infiltrates. Germinal centers are not usually present.

Fine-needle aspiration cytology is difficult to perform in cases of diabetic mastopathy due to dense stroma and will be non-diagnostic in most cases due to the small quantity of tissue withdrawn [64]. Smears are hypocellular and scant and may consist of benign ductal cells, scattered fibroblasts, and fragments of collagen [71].

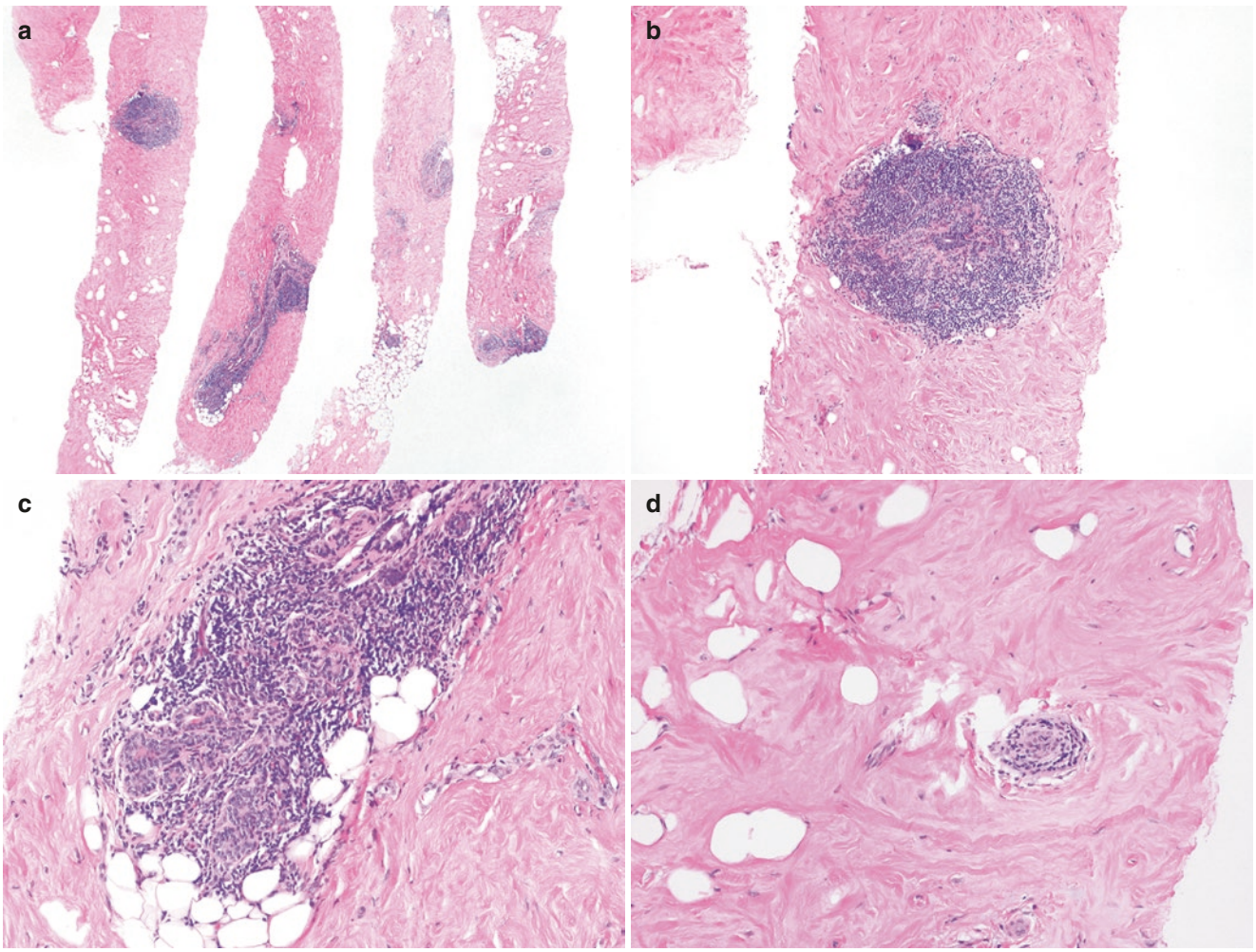

Fig. 4.23 Inflammation in diabetic mastopathy. Core biopsy in this case was performed due to the presence of an asymmetric density on ultrasound. (**a**) Low-power examination reveals lymphoid infiltrates within a fibrous stroma. (**b**, **c**) Lymphocytes are seen surrounding ducts and lobules. (**d**) Perivascular (capillary) lymphocytic inflammation is also present. The stroma shows dense fibrosis

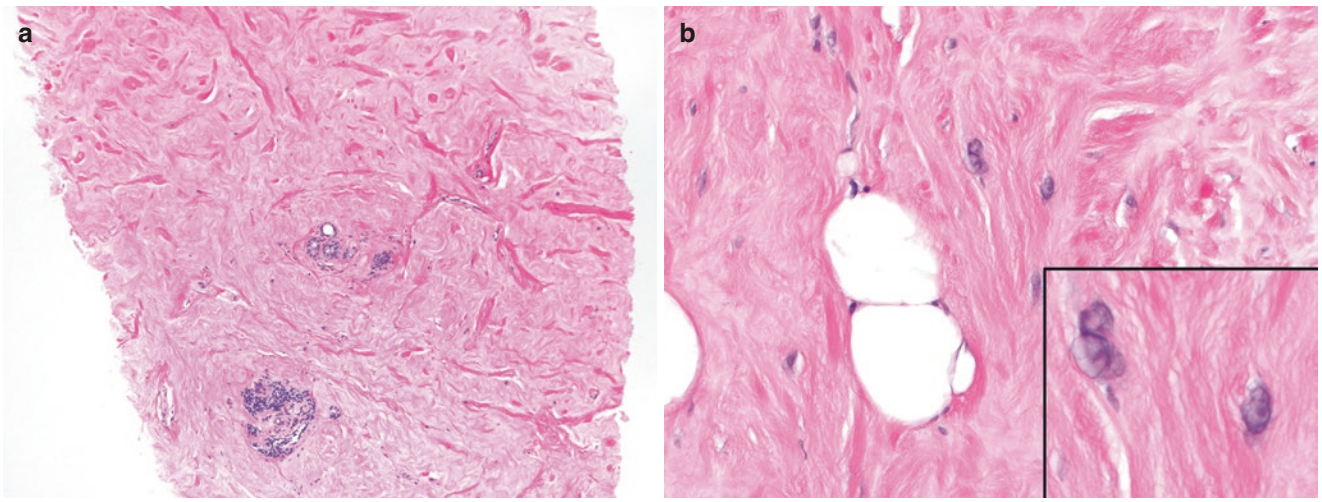

Fig. 4.24 Stromal changes in diabetic mastopathy. (**a**) Dense hypocellular fibrous tissue with broad bands of keloidal-like collagen without characteristic epithelioid fibroblasts. (**b**, **c**) Epithelioid fibroblasts are present within the hyalinized "glassy" stroma. (**d**, **e**) Case of diabetic mastopathy with cellular proliferation of fibroblasts with abundant pink cytoplasm

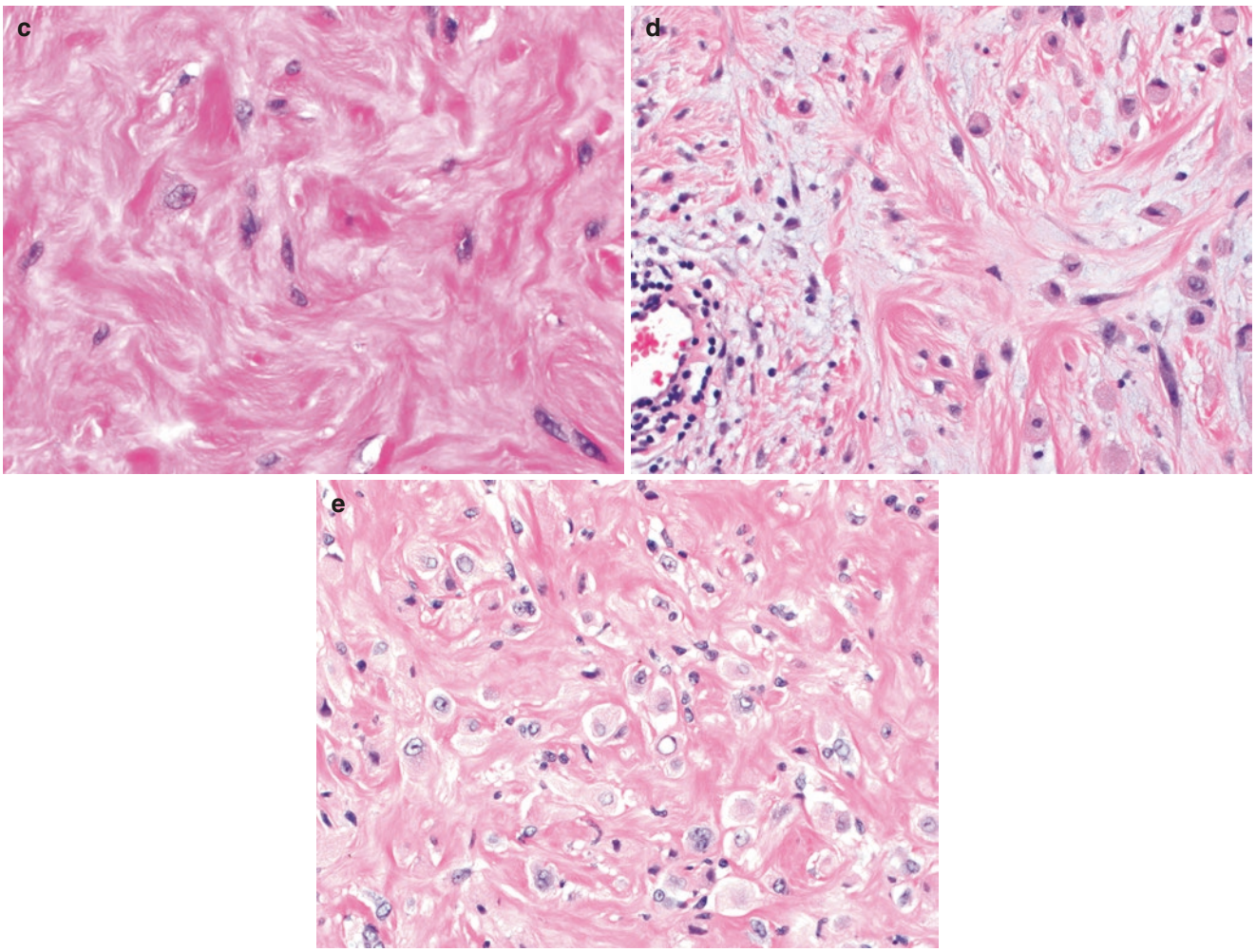

Fig. 4.24 (continued)

Differential Diagnosis

The entire constellation of findings of diabetic mastopathy may not be present, particularly in a small core biopsy sample (Fig. 4.25). When diabetic mastopathy is suspected in a core biopsy, knowing whether the patient is diabetic or has an autoimmune disease is helpful in establishing a diagnosis. Epithelioid fibroblasts with abundant cytoplasm can mimic invasive carcinoma and in suspicious cases, a cytokeratin immunostain can be performed to rule out carcinoma. Granular cell tumor can have a similar appearance to these cells in some cases and can be distinguished from diabetic mastopathy due to its granular cytoplasm and immunoreactivity with S100 protein and CD68. Multinucleated stromal giant cells can also be present within a fibrotic stroma and can mimic epithelioid fibroblasts in diabetic mastopathy. Stromal fibrosis as a component of fibrocystic changes can have a similar clinical and radiographic appearance as diabetic mastopathy and can show similar stromal changes on histology; however, epithelioid fibroblasts are not a feature of stromal fibrosis. Periductal, perilobular, and perivascular lymphoid infiltrates are not usually present in the aforementioned lesions in the differential diagnosis.

Lymphoid infiltrates/aggregates can be seen in a variety of reactive and neoplastic breast lesions, but do not show the same distribution as diabetic mastopathy and are not associated with stromal findings discussed above. Lymphoma involving the breast, for example, does not form well-defined infiltrates of cells, but rather shows diffuse infiltration of glands and stroma by neoplastic lymphoid cells. Immunostains and/or molecular studies show a clonal population of cells in lymphoma, which is not seen in diabetic mastopathy.

Pathogenesis

Multiple factors may be involved in the pathogenesis of diabetic mastopathy. One theory is that the fibrous stroma seen in diabetic mastopathy is due to glycosylation of col-

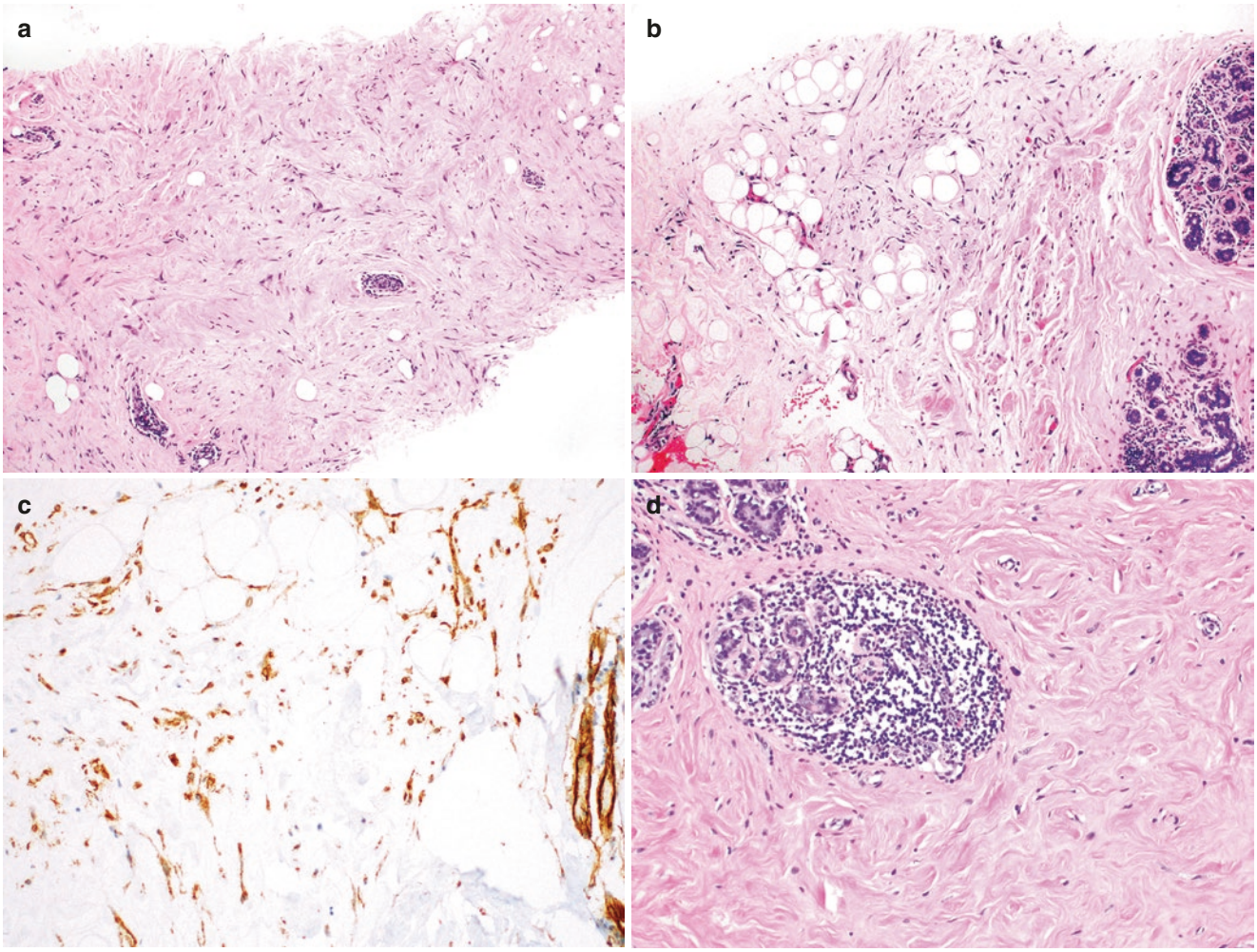

Fig. 4.25 Diabetic mastopathy appearing as a spindle cell lesion in a core biopsy. (**a**) Dense fibrous tissue containing stellate spindle cells with lymphocytes surrounding capillaries. (**b**) Spindle cells appear to infiltrate fat. Benign lobules (right) show scant inflammatory cells. (**c**) A beta-catenin immunostain was performed because fibromatosis was considered. Beta-catenin shows nonspecific cytoplasmic staining. (**d**) Excision of the lesion revealed more classic features of diabetic mastopathy with dense perilobular lymphoid aggregates and epithelioid fibroblasts

lagen, making it more resistant to degradation [62]. Seidman et al. suggested that diabetic mastopathy develops as a result of an immunologic response to exogenous insulin, its vehicle, or a contaminant in the vehicle [72]. Tomaszewski et al. hypothesized a sequence of events to explain the development of diabetic mastopathy, which included stromal matrix expansion due to hyperglycemia, accumulation of advanced glycosylation end products that possibly act as neoantigens, which lead to a B cell autoimmune lymphocytic response. This results in cytokine release and further matrix expansion [60].

Autoimmunity has been suggested to play a role because of the association between diabetic mastopathy and autoimmune diseases, in both diabetics and nondiabetics [62, 73]. As seen in autoimmune diseases, the lymphocytic infiltrates in diabetic mastopathy are predominantly composed of B lymphocytes, while other types of mastitis are composed mainly of T lymphocytes [60, 70, 73]. The lymphocytes in diabetic mastopathy have not shown evidence of clonality by immunoglobulin heavy chain gene rearrangement studies [70].

Prognosis

Diabetic mastopathy is a benign condition, and affected patients do not appear to have an increased risk for the development of carcinoma or lymphoma [64, 70, 74]. Unilateral and/or bilateral recurrences of diabetic mastopathy may occur following surgical excision. Ely et al. reported recurrences in 6 of 19 (32%) patients, including 3 patients that had multiple recurrences [63]. Five of 34 (15%) cases of diabetic mastopathy recurred (2 ipsilateral, 3 bilateral) in another report [67]. When identified in a core biopsy, surgical excision is not recommended unless findings are clinically or radiographically suspicious for malignancy or if histologic findings do not correlate with imaging.

Amyloidosis

Overview

Amyloidosis is a heterogeneous group of diseases that cause tissue damage by extracellular deposition of abnormal fibrous proteins called amyloid. Breast amyloidosis is rare and can be part of systemic disease, where amyloid is present in multiple organs, or localized without extramammary involvement. Most reported cases have been identified in postmenopausal women with a mean age at diagnosis of 63 years, ranging from 43 to 86 [75, 76]. The clinical and radiologic findings are nonspecific, commonly presenting as painless, solitary mass or multiple breast masses with or without associated calcifications [77]. Typically breast biopsies are done to exclude malignancy. Recognition of amyloid deposits is essential to exclude an association with a significant underlying disease as approximately 50% of patients have a hematologic disorder, predominantly malignant B cell neoplasms, including extranodal marginal zone lymphoma, diffuse B cell lymphoma, or plasma cell proliferations [78]. Diagnosis can only be made through histologic examination where the presence of pink, amorphous amyloid deposits can be confirmed with Congo red staining which shows a characteristic green birefringence under polarized light. The prognosis depends on whether the disease is localized or systemic.

Pathogenesis

To date 36 different types of amyloid protein structures have been described in humans. The most common types are primary immunoglobulin light-chain amyloidosis (AL) and secondary (AA) amyloidosis. AL amyloidosis is associated with plasma cell dyscrasias or multiple myeloma whereas AA amyloidosis is associated with chronic inflammatory conditions, including autoimmune disease such as rheumatoid arthritis [77]. Most commonly amyloid diffusely involves the breast in the systemic form of AL type amyloidosis [75]. The pathogenesis of localized AL amyloidosis in the breast without a concomitant hematolymphoid disorder is unknown though may be related to immunoglobulins secreted by plasma cells along with other undetermined factors [78]. Sjogren syndrome, an autoimmune disease of unknown etiology, has been associated with breast amyloidosis in 7 reported cases [79].

Gross and Radiologic Findings

There are no specific gross features of amyloidosis. The most common mammographic presentation is single or multiple masses with or without grouped calcifications [75–77]. Infrequently, breast amyloidosis can present as a spiculated density or pleomorphic calcifications without an associated mass. Rarely, in systemic amyloidosis, there may be diffuse involvement with skin thickening mimicking an inflammatory carcinoma [80]. Ultrasound features are nonspecific and include an ill-defined hypoechoic mass or heterogeneous masses with posterior acoustic shadowing [81]. Amyloidosis demonstrates low signal intensity on T1 and high signal on T2-weighted MRI [82].

Microscopic Features

Amyloid has a uniform, pink, waxy appearance and forms nodular deposits around ducts and lobules and the epithelial basement membranes can be markedly thickened (Fig. 4.26). Deposition can also be seen in fibrous and adipose tissue

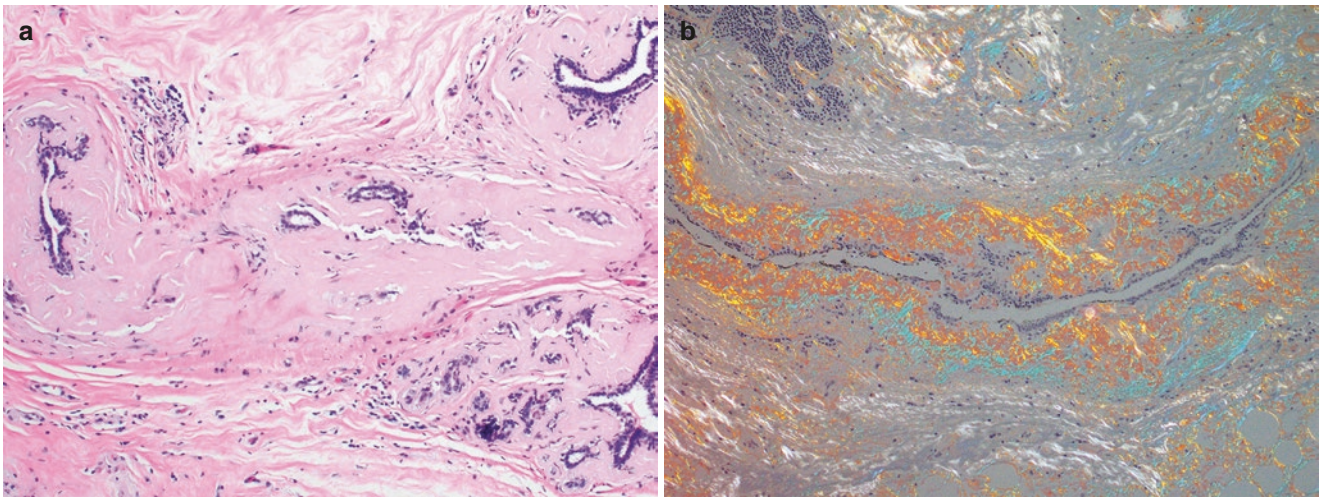

Fig. 4.26 Amyloidosis in the breast (**a**) Amyloidosis in a periductal distribution. (**b**) Congo red shows apple green birefringence of amyloid

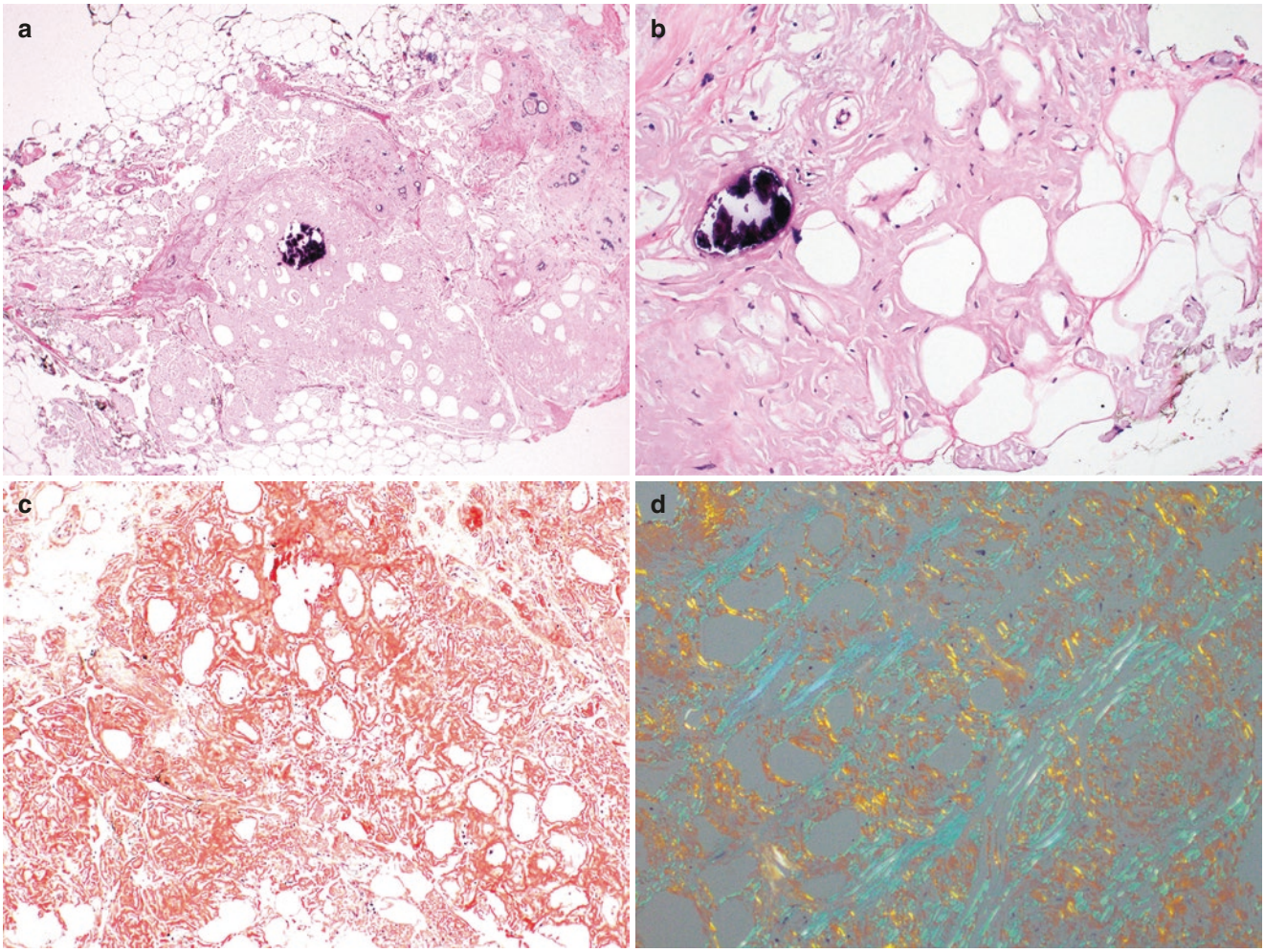

Fig. 4.27 Amyloidosis in a stereotactic biopsy performed for mammographic calcifications. (**a**) Eosinophilic material is present in association with fat and is calcified. (**b**) Higher power reveals waxy amorphous amyloid and calcification. (**c**) A Congo red special histochemical stain shows deep orange-red staining. (**d**) The Congo red stain shows apple green birefringence under polarized light

(Fig. 4.27) and along vascular channels, in the form of small nodules. Scattered multinucleated giant cells and calcifications are frequently present with amyloid. Amyloid in axillary lymph nodes has been described as sheet-like patchy deposits intermixed with lymphocytic proliferations with plasmacytic differentiation [77]. Amyloid stained with Congo red will show an orange-red color on light microscopy and will reveal characteristic apple green birefringence under polarized light (Figs. 4.26b and 4.27d). Because at least 50% of patients have a concurrent B cell lymphoma, most commonly extranodal marginal zone lymphoma, this diagnosis should be excluded through appropriate pathologic and clinical evaluation in any patient with mammary amyloidosis. Further, Congo red stains are recommended in patients with extranodal marginal zone lymphoma on breast core needle biopsy to exclude coexistent amyloidosis [78].

Differential Diagnosis

Due to the significant association of amyloidosis with hematologic disorders, lymphoma should be suspected and must be ruled out in cases where amyloid is identified, especially in the presence of a lymphocytic infiltrate. Amorphous amyloid deposits in fibroadipose tissue can resemble fat necrosis; a complete clinical history could be helpful in making this distinction. Densely collagenized tissue or elastosis can have the appearance of amyloid and large nodular deposits may mimic fibroadenomatoid changes; however, the small nodular deposits along basement membranes and vascular channels typical of amyloid would not be seen. Likewise, diabetic mastopathy shows a keloidal-like hyalinized stroma but amyloid lacks the dense lymphocytic infiltrates characteristically seen around lobules and blood vessels.

Prognosis

Localized primary breast amyloidosis is benign and has a good prognosis. The main treatment is surgical excision [76]. In contrast, patients with systemic amyloidosis have systemic disease with abnormal amyloid proteins causing organ dysfunction or failure. These patients have a generally poor prognosis and are managed medically [80].

IgG4-Related Sclerosing Mastitis

Overview

Immunoglobulin G4-related disease (IgG4-RD) is a chronic fibroinflammatory condition whose exact cause is unknown but is likely due to an autoimmune response to an inciting antigen which has yet to be elucidated. First identified in the pancreas as autoimmune pancreatitis, IgG4-RD has now been described in almost every organ of the body. Multiple organ sites can be affected, each showing a similar triad of histologic findings characteristic of the disease: a dense lymphoplasmacytic infiltrate rich in IgG4-positive plasma cells, fibrosis, and obliterative phlebitis. Serum concentrations of IgG4 are often elevated; however, 5% of the normal population can have elevated IgG4 levels and further up to 40% of patients with histomorphologic and immunhistochemical findings of IgG4-RD can have normal immunoglobulin concentrations [83, 84].

Breast involvement, presenting as IgG4-related sclerosing mastitis (IgG4-SM), is rare, with less than 50 cases described to date [85]. Affected patients range in age from 40 to 69 years old and all but two reported cases have been in women, in contrast to extramammary sites where males outnumber females 3 to 1 [84, 86]. Patients typically present with a discrete painless breast mass along with suspicious imaging findings, which can be concerning for malignancy. The recognition of this rare entity is important as the clinical features mimic carcinoma while the clinical course appears to be benign and in many cases the condition responds to steroid therapy [87].

Gross and Radiologic Features

Grossly the lesions of IgG4-SM are firm, tan, yellow masses. Necrosis and hemorrhage are not seen. Radiographic images demonstrate an ill-defined, asymmetric density [86].

Microscopic Features

An international symposium held in Boston in 2011 released consensus guidelines for the diagnosis of IgG4-RD, stating that two of three major histologic features are required along with either increased IgG4-positive plasma cells or an elevated IgG4/IgG plasma cell ratio. However, these guidelines allowed for site-specific criteria to be introduced as certain features may be inconspicuous or absent in some organs [83]. The first, and most consistent, major histologic feature is a dense lymphoplasmacytic infiltrate composed of small lymphocytes, predominantly T cells with admixed B cells, forming diffuse sheets or nodular aggregates with interspersed germinal centers along with a prominent plasma cell component (Fig. 4.28). An increase in the number of eosinophils is a minor supporting feature. The second feature is stromal fibrosis, arranged at least focally in a storiform pattern in which fibroblasts resemble a cartwheel or pinwheel in that spindle cells radiate around a common point. The final major criterion is obliterative phlebitis where veins are obliterated by a dense lymphoplasmacytic infiltrate; elastin stains may be helpful to identify venous walls. Phlebitis without obliteration of the lumen is a minor supporting feature. While it may be difficult to identify these features due to the inherent limitations of small core needle biopsy samples, it should be noted that in the breast, storiform fibrosis and obliterative phlebitis are reported to be infrequently identified and are often absent compared to other sites involved by IgG4-RD [86, 88, 89]. In IgG4-SM, breast lobules are lost in areas with heavy infiltrate and lymphoepithelial lesions are not seen [90]. Large aggregates of macrophages, especially foamy histiocytes and multinucleate giant cells, are inconsistent with IgG4-RD. Likewise, granulomas, prominent neutrophilic infiltrate and necrosis argue strongly against the diagnosis [84]. While histopathologic evaluation is the best method for detecting IgG4-SM, the diagnosis cannot be established without an immunohistochemical stain for IgG4.

An increased IgG4-positive plasma cell count or an IgG4/IgG plasma cell ratio is needed to meet the second consensus requirement (Fig. 4.29). An absolute IgG4-positive plasma cell count of >50 per high-power field is highly specific; however, in biopsy samples the presence of >10 IgG4-positive plasma cells could be sufficient, depending on the organ [83]. Therefore the IgG4/IgG plasma cell ratio is a better way to establish elevated IgG4 levels than absolute counts. A ratio of >40% is considered to be high in any organ.

Differential Diagnosis

Despite the worrisome clinical impression of IgG4-SM for mammary carcinoma these two diagnoses can be easily distinguished by the lack of neoplastic epithelial cells. However, it is important to not mistake benign ductal cells which may become entrapped in the lesion as malignant epithelium. The diffuse proliferation of lymphoid cells may give an initial low magnification impression of a lymphoma, but closer

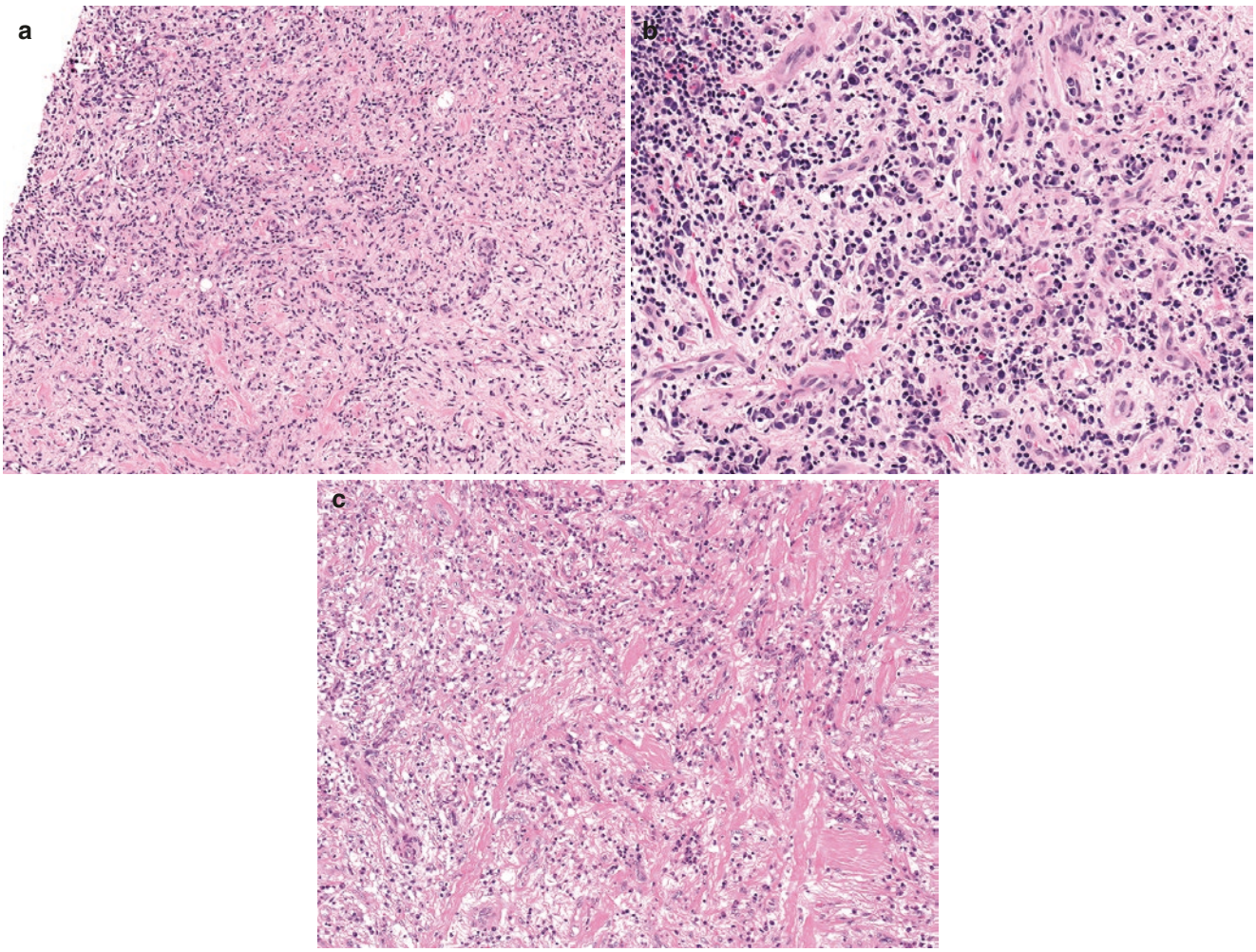

Fig. 4.28 IgG4-related sclerosing mastitis in a core biopsy of a breast mass. (**a**) A mixed inflammatory infiltrate associated with fibrosis is evident. (**b**) Higher power shows an abundance of plasma cells, scattered lymphocytes, and rare eosinophils. (**c**) Fibrosis is seen as broad bands of collagen. (*Images courtesy of Gulisa Turashvili, MD, PhD*, Mount Sinai Hospital, University of Toronto, with permission)

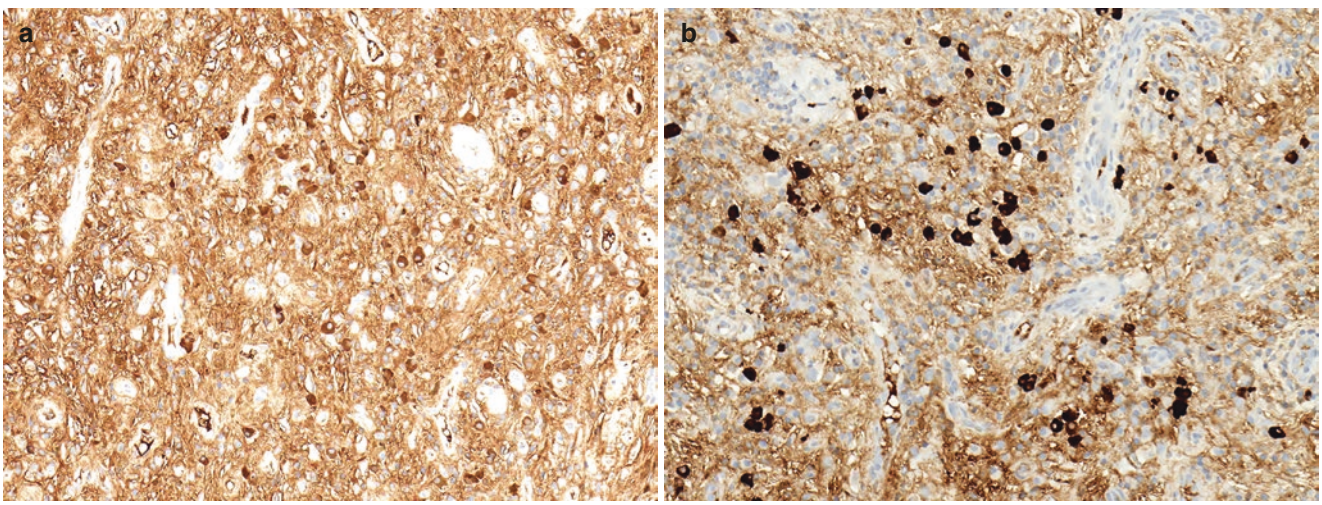

Fig. 4.29 IgG and IgG4 immunohistochemistry in IgG4-related sclerosing mastitis. (**a**) An IgG immunostain highlights IgG-positive plasma cells. (**b**) An IgG4 immunostain shows that a high proportion of IgG-positive plasma cells express IgG4. (*Images courtesy of Gulisa Turashvili, MD, PhD*, Mount Sinai Hospital, University of Toronto, with permission)

examination will reveal a polymorphous population of inflammatory cells, including plasma cells, T and B lymphocytes, and eosinophils. Plasma cell mastitis presents acutely as a painful or tender breast mass and the histologic appearance is one of extravasated secretions inciting an inflammatory reaction composed of histiocytes, giant cells and a periductal plasma cell infiltrate. Thus, the clinical and histologic features are discordant with IgG4-SM. Granulomatous lobular mastitis is characterized by lobulocentric, non-necrotizing granulomas composed of giant cells, epithelioid histiocytes, neutrophils, and plasma cells. IgG4-SM lacks a lobulocentric pattern, granulomas, and neutrophils. Diabetic mastopathy, like IgG4-SM, is characterized by stromal fibrosis and a lymphocytic infiltrate; however, the fibrosis in diabetic mastopathy is keloidal-like and tends to predominate over the lymphocytic infiltrates, comprised predominantly of B cells with scant plasma cells, which are well defined and tightly circumscribed around the lobules and blood vessels. More commonly seen in lymph nodes, Rosai–Dorfman disease shows atypical S100 protein-positive histiocytes with prominent nucleoli, abundant cytoplasm and engulfed neutrophils and erythrocytes, known as emperipolesis. Elevated levels of IgG4-positive plasma cells have been identified in cases of Rosai–Dorfman disease; however, none met the criteria defined for IgG4-SM [91]. Inflammatory myofibroblastic tumor is a bland spindle cell proliferation with an associated lymphoplasmacytic infiltrate. These lesions lack lymphoid aggregates and obliterative phlebitis and approximately half are positive for anaplastic lymphoma kinase (ALK) by immunohistochemistry. A caveat is that a small subset has been observed to have increased numbers of IgG4-positive plasma cells and an elevated IgG4/IgG ratio with half also being negative for ALK and so could be classified as IgG4-SM [92].

Prognosis

The clinical course is benign, and IgG4-SM responds to and improves with steroid therapy [87]. In 15 reported cases with available outcome information, all showed complete resolution and no recurrence after a median of 12 months following either surgical excision or steroid therapy [86].

Inflammatory Myofibroblastic Tumor

Overview

Inflammatory myofibroblastic tumors (IMT) are low-grade neoplasms composed of myofibroblastic and fibroblastic spindle cells with prominent admixed inflammatory cells which can occur at any anatomic site with the most common presentation being in the lung or soft tissues of children and young adults. IMT is rare in the breast, with only 31 reported cases to date since its initial description [93, 94]. The etiology is unclear but approximately half of cases harbor a clonal chromosomal rearrangement that activates the *ALK* receptor tyrosine kinase gene, leading to the formation of a fusion protein that can be detected by immunohistochemistry or fluorescence in situ hybridization [95].

Affected patients present with nonspecific signs and symptoms such as fever, weight loss, anemia, or hyperproteinemia, seen in 15–30% of cases [96, 97]. Most patients with IMT are children or young adults; however, the tumor can occur at any age. Of the reported breast IMT cases, the average patient age is 44, ranging between 13 and 86 years, with approximately 1/3 of cases occurring in women less than 30 years old [93]. Patients generally present with a palpable, slightly tender breast mass that may be adherent to the skin. IMTs can be concerning for malignancy based on clinical and imaging findings. IMTs in the breast typically follow a benign course following complete surgical resection [98].

Gross and Radiologic Features

Gross examination reveals firm, circumscribed nodules ranging in size from 1 to more than 20 cm, with a mean size of 6 cm [96]. The cut surface is gray-white to yellow, fleshy, or gelatinous. The radiologic findings are nonspecific with ultrasound showing ill-defined or well-defined hypoechoic masses, with an average lesion diameter of 29 mm [93].

Microscopic Features

The morphology is characterized by a proliferation of bland myofibroblasts admixed with an inflammatory infiltrate (Fig. 4.30). The spindle cells of IMT are uniform in appearance with ovoid to tapered nuclei, small nucleoli, pale to eosinophilic cytoplasm, and are arranged in one of three patterns. These include a myxoid/granulation-tissue type (fasciitis-like) pattern, a compact spindle cell pattern, and a fibromatosis or scar-like pattern. Combinations of these patterns often occur in the same tumor. The myxoid/granulation tissue pattern has a nodular fasciitis-like appearance consisting of plump spindle cells loosely arranged in a myxoid or edematous stroma with a prominent inflammatory infiltrate, composed of plasma cells, neutrophils, and eosinophils. A conspicuous vasculature can also be appreciated. The second pattern shows a compact, solid, and confluent spindle cell proliferation with fascicular growth and numerous plasma cells and lymphocytes. The fibromatosis-like pattern is paucicellular with elongated spindle cells in a background of abundant hyalinized collagen, resembling scar tissue, and

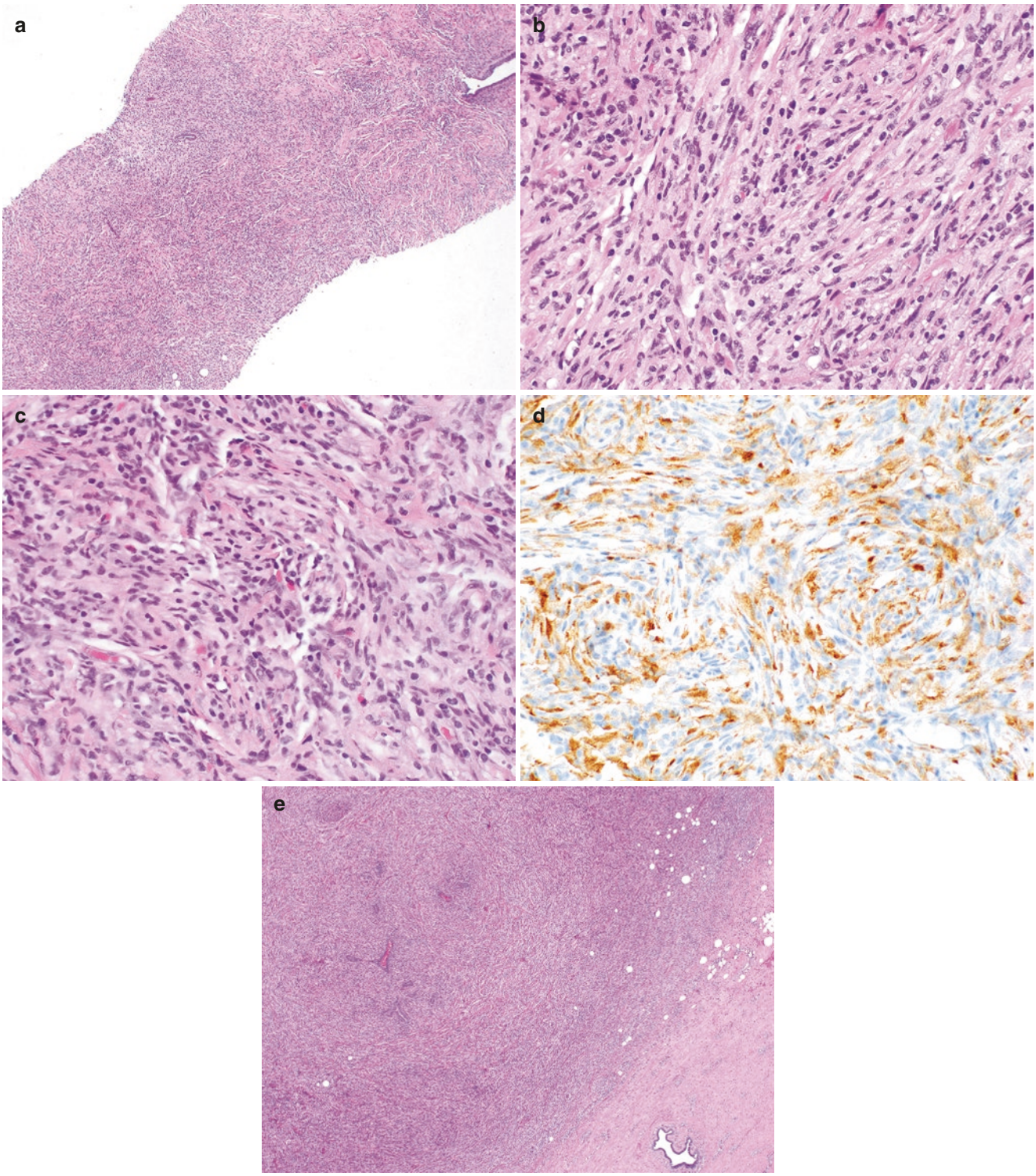

Fig. 4.30 Inflammatory myofibroblastic tumor of the breast. (**a**) Core biopsy shows a cellular proliferation with rare benign ducts. (**b**) Higher power shows fascicles of spindle cells with scattered lymphocytes. (**c**) Spindled myofibroblasts growing in a vaguely storiform patterns with scattered lymphocytes and eosinophils. (**d**) ALK immunohistochemistry shows diffuse staining in spindle cells. (**e**) Low-power view of excision specimen for IMT seen in **a-d**

contains scattered inflammatory cells. High-grade cytologic features, mitotic activity, and necrosis are uncommon features of IMT.

Immunohistochemistry

The spindle cells of IMT are myofibroblasts that show strong positivity for smooth muscle actin, desmin, and calponin in the majority of cases, although expression can be focal. Approximately 1/3 co-express cytokeratin, which can show focal reactivity [94]. The plasma cell infiltrate is polyclonal. Roughly half of IMTs are positive for ALK by immunohistochemistry (Fig. 4.30d); this expression has been reported to be more common in younger patients [96]. It should be noted that in one study, up to 24% of fusion-positive IMTs did not express ALK and thus it is recommended to perform fluorescence in situ hybridization testing on those ALK-negative tumors with morphologic features highly suggestive of IMT [95].

Differential Diagnosis

An important differentiating feature of IMT is ALK positivity, which when present aids in the diagnosis. Yet around half of IMTs are negative for ALK staining making the distinction from other spindle cell neoplasms more challenging. The most consequential differential diagnosis is metaplastic spindle cell carcinoma which can be confused for the compact spindle cell pattern, especially in those tumors which show keratin positivity. However, large aggregates of plasma cells are uncommon in metaplastic carcinomas and the carcinomas will often show at least focal nuclear hyperchromasia, brisk mitotic activity, or necrosis which are not typically identified in IMT. Similarly, fibromyxoid sarcomas are exceedingly rare in the breast and as with carcinoma would show spindled cells with marked nuclear pleomorphism and higher mitotic rates, features unusual in IMT. The hypocellular fibromatosis-like patterned IMTs raise the differential of fibromatosis which shows long, sweeping fascicles of bland spindle cells without atypia or mitoses in a background of variable stromal collagenization with irregular infiltrating margins. The associated lymphocytic infiltrate is often located peripherally and typically does not show abundant plasma cells. Like IMT, the spindle cells of fibromatosis are positive for smooth muscle actin and/or desmin while in contrast to IMT are negative for cytokeratin and characteristically show nuclear beta-catenin expression. Nodular fasciitis is rare in the breast, presenting typically as a small nodule, generally less than 2 cm, with rapid onset, pain and tenderness, contrary to the usually large painless mass associated with IMT. Histologically, it can mimic the myxoid/granulation-tissue type pattern showing a spindle cell proliferation with so-called tissue-culture like growth in a loose myxoid stroma. Mitotic activity is high and extravasated red blood cells can be seen scattered throughout while lacking the prominent inflammatory infiltrate of IMT. Biopsy site or surgical scarring with extensive granulation tissue can be excluded with the appropriate clinical history and/or the presence of fat necrosis in the adjacent soft tissues. Given the plasma cell rich infiltrate of IMT, it may be confused with IgG4-SM; however, IgG4-SM does not show plump, ovoid spindled cells or ALK positivity. Additionally, IgG4-RD is normally seen in adults, and it is important to remember IMT is uncommon in middle-aged or elderly patients. Evaluation with IgG4 immunohistochemistry is advised as this could identify IgG4-SM and prevent unnecessary surgery.

Prognosis

IMTs have different outcomes based on the tissue of origin, but most frequently follow a benign course. Surgical resection is considered the treatment of choice. Recurrence rates vary by location and completeness of resection, occurring in less than 2% for tumors in the lung and up to 25% in extrapulmonary sites. Distant metastases are observed in less than 5% of cases [96]. There have been at least two cases of distant metastases of breast IMT to date [99]. Rare malignant transformation has been reported [96]. It has been shown that a subgroup of ALK-fusion proteins are sensitive to ALK-inhibition, which suggests targeted kinase inhibition is a therapeutic option in these more aggressive forms of IMT [100].

Abscess and Infectious Conditions of the Breast

Overview

Infections in the breast (infectious mastitis) is uncommon. Infectious mastitis is most often bacterial and is seen in the setting of lactational mastitis and abscess. Much less frequently, other infectious processes including mycobacterial, fungal, and parasitic infections occur in the breast and can sometimes be the source of the mammographic abnormality leading to core biopsy.

Recognition of certain infections in the breast is important in the core biopsy setting so that appropriate medical therapy can be initiated, and unnecessary surgery can be avoided. This chapter will mainly focus on abscess, which is the most common infectious process encountered in a core biopsy. Other less common infectious processes will also be discussed.

Abscess

Overview

Abscess in the breast occurs most commonly during breastfeeding (lactational/puerperal abscess) or in the non-lactating breast as a subareolar (non-puerperal) abscess. In both settings, abscesses develop as a result of duct stasis. Core biopsy may be performed in cases of abscess to rule out malignancy because of suspicious clinical and radiographic features.

Lactational (puerperal) mastitis occurs in approximately 1–10% of lactating women and may be complicated by the development of abscess if not adequately treated [101–103]. Mastitis and abscess most often occur during the first 6 weeks of breastfeeding, but may also occur during the time of weaning, when milk stagnates within engorged ducts [104]. Patients with mastitis present with redness, warmth, swelling, tenderness, and sometimes fever. An abscess will show a tender fluctuant mass in addition to these findings [103]. Cracking of the nipple skin of the affected breast may serve as a point of entry for bacteria [103]. Other risk factors for the development of mastitis and abscess include primiparity, mastitis with a previous infant, poor hygiene, and improper nursing technique [101–103].

Non-puerperal abscesses are typically subareolar in location, and most often develop as consequence of squamous metaplasia of lactiferous ducts (described below under pathogenesis). The resulting clinical picture of recurring subareolar abscesses and fistula formation has been referred to as Zuska's disease and periductal mastitis [105]. Patients with subareolar abscesses are typically premenopausal women, but older women and males may also be affected [106, 107]. Patients present with a painful subareolar or periareolar mass that may be accompanied by a draining sinus. Nipple retraction can be seen [108]. Nipple discharge, if present, may have a pasty consistency. Bilateral disease is not uncommon. In a series of 152 patients reported by Habif et al., 40 (26%) presented with bilateral abscesses [106]. Cigarette smoking is strongly associated with the development of subareolar abscesses, and a history of smoking has been elicited in approximately 70–90% of patients [109–111]. In some reports, subareolar abscesses have developed following nipple piercing [111, 112]. Diabetes and obesity are other risk factors for the development of subareolar abscesses [111].

Radiologic Features

Ultrasound is the most effective imaging abnormality for evaluation of suspected abscess. Abscess appears as a hypoechoic mass or a hypoechoic collection that is often multiloculated and with a thick echogenic periphery [102, 108]. Mammography is not specific and can show an asymmetric density, mass, distortion, or skin thickening [101, 102]. Calcifications are not a feature of abscess [101].

Microscopic Features

A mixed inflammatory infiltrate mainly composed of neutrophils is seen involving breast tissue (Fig. 4.31). Glands may show lactational changes in lactational abscess (Fig. 4.32). Granulation tissue and chronic inflammation are seen as the abscess resolves. In a core biopsy of a subareolar abscess, dilated ducts may be identified, but squamous metaplasia is not always evident. Keratin material may be seen within the abscess with an associated foreign body giant cell reaction (Fig. 4.33). Bacteria may be identified and, in most cases, will be Gram-positive cocci in clusters (*Staphylococcus aureus*).

Differential Diagnosis

Clinically, the most important differential diagnosis for abscess is invasive carcinoma, particularly inflammatory carcinoma. In the pregnant or lactating patient, galactocele, nodular lactational hyperplasia (lactating adenoma), and fibroadenoma should be included in the differential diagnosis of a new mass. Infarcts may also occur during pregnancy and can present as a palpable tender mass [104]. Subareolar abscesses can clinically mimic malignancy, duct ectasia, and granulomatous mastitis. The histologic diagnosis of abscess is fairly straightforward based on the characteristic inflammatory and reactive findings. Granulomatous lobular mastitis and duct ectasia can be associated with the development of abscesses.

Pathogenesis

Abscess is the result of duct stasis in both lactational and non-lactational abscesses. With lactation, milk stasis within engorged ducts provides a lactose-rich environment for bacteria that enter through duct openings or cracks and fissures in the nipple. Subareolar abscesses develop when keratin debris accumulates in lactiferous ducts undergoing squamous metaplasia. This leads to duct rupture with spillage of contents into the stroma. A mixed inflammatory response is elicited with bacterial invasion, resulting in abscess formation [106, 108]. The abscess may eventually rupture spontaneously with the formation of a draining sinus. The

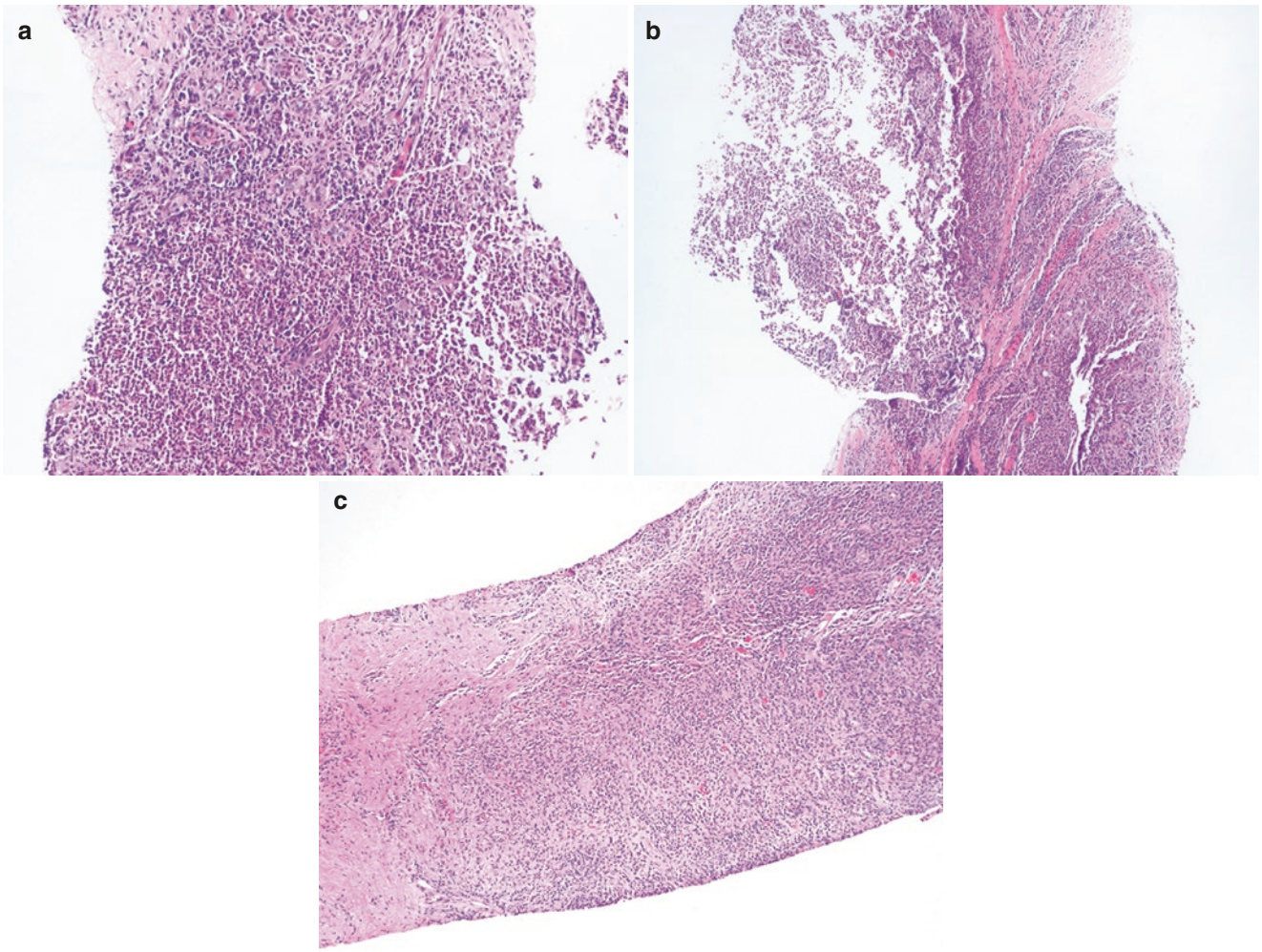

Fig. 4.31 Abscess in non-lactating breast. (**a**, **b**) Abscess centered on lobules with abundant neutrophils and plasma cells. (**c**) Core biopsy of resolving abscess with granulation tissue and plasma cells

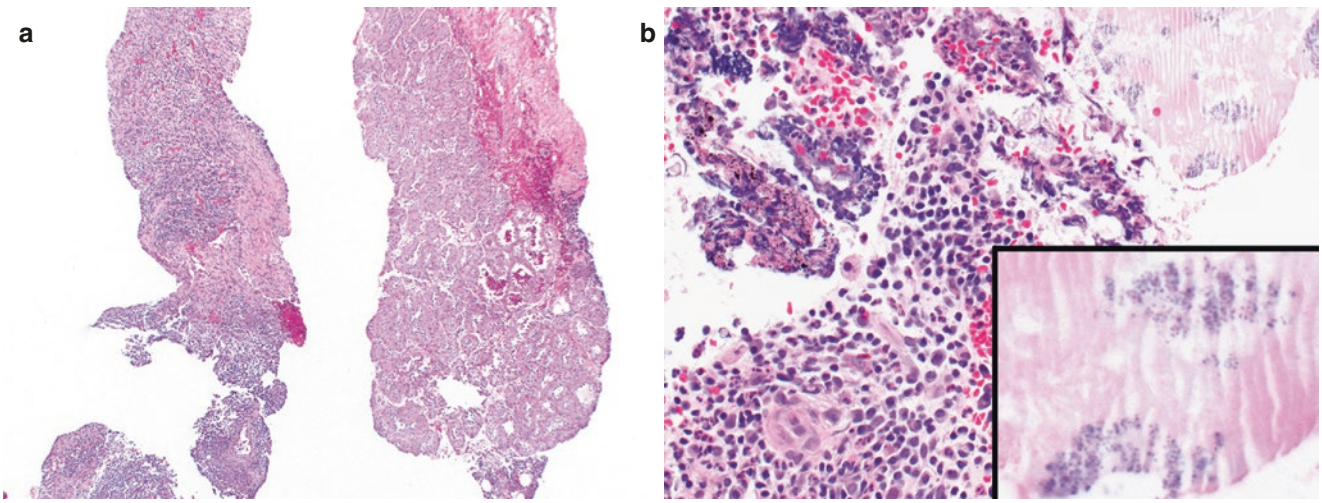

Fig. 4.32 Lactational abscess. (**a**) Core biopsy reveals and abscess with associated fibrosis (*left*) involving lactational breast tissue (*right*). (**b**) A mixed inflammatory infiltrate with plasma cells and neutrophils constitutes the abscess. Clusters of cocci bacteria (*top right* and high-power inset) are visible on H&E examination and are present within secretion (not necrosis)

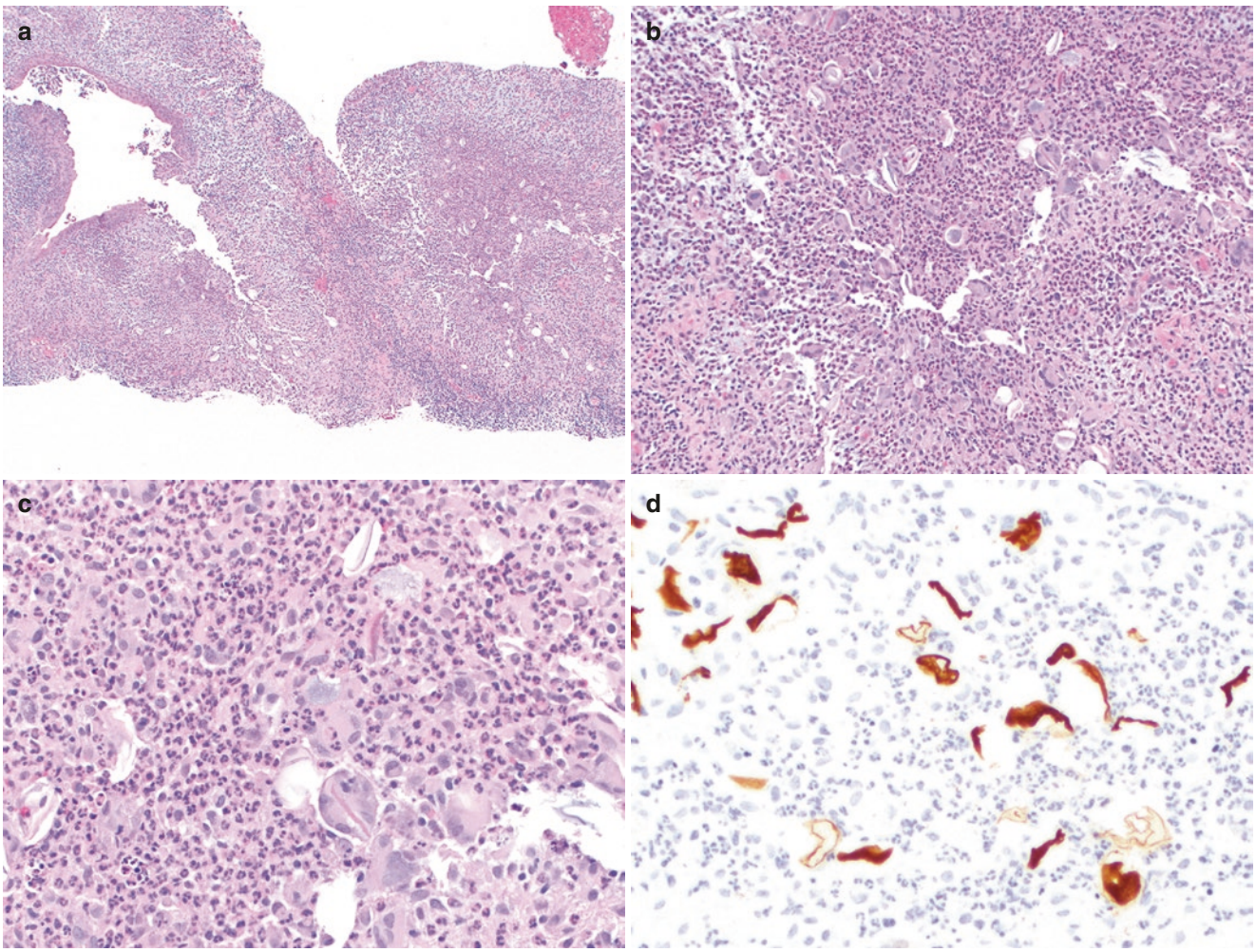

Fig. 4.33 Subareolar abscess in a core biopsy. (**a**) Core biopsy shows a mixed inflammatory infiltrate composed mainly of neutrophils. A duct with squamous metaplasia is seen on the left part of the image. (**b**, **c**) Keratin material is present within the abscess and is associated with a foreign body giant cell reaction. (**d**) A cytokeratin (AE1/AE3) immunostain highlights keratin material in the abscess

association of smoking with subareolar abscesses may be due to vitamin A deficiency, low blood levels of β-carotene, direct toxic effects, or hormonal stimulation [110, 111].

The most common organism isolated from breast abscesses is *S. aureus*, identified in approximately 50% of cases [103, 106, 109, 113]. In a series of 189 patients with breast abscess, *S. aureus* was isolated in 51.3% of positive cultures overall and in 67.7% of lactational abscesses (vs. 30.5% of non-lactational abscesses) [113]. Seven (8.6%) isolates were methicillin-resistant *S. aureus*. Subareolar abscesses tend to show mixed flora [111]. In a series of non-puerperal breast abscesses reported by Walker et al., most cultures showed a mixed flora of predominantly anaerobes, with coagulase-negative staphylococci being the most common aerobic organism isolated [114]. Other organisms that may be isolated from breast abscesses include mixed anaerobes, anaerobic cocci, Group D streptococci, and *Bacteroides* [113]. Cultures are negative in some cases, which may be a result of previous antibiotic therapy.

Prognosis

Lactational mastitis usually responds to antibiotics. Abscesses require surgical drainage along with antibiotics for the process to resolve and do not typically recur [115]. Nursing should be continued during treatment for most cases of mastitis and abscess and may help in resolving the process.

Subareolar abscess is a chronic and recurring condition with longer times to resolution and higher rates of recurrence compared with lactational abscesses [102, 109, 115]. Treatment involves a combination of antibiotics and surgery which includes excision of the abscess, sinus tract (if present), and

involved lactiferous duct. Significantly lower rates of recurrence are seen when the involved duct is excised compared with surgery that does not include duct excision [109, 110].

Other Infectious Conditions

Bacterial Infections

S. aureus, described above, is the most common bacteria isolated from mastitis and breast abscesses (described above). Granulomatous lobular mastitis with a "cystic neutrophilic granulomatous mastitis" pattern has been associated with *Corynebacterium* species [44].

Tuberculous Mastitis

Tuberculous mastitis is rare and occurs most often in patients with established infection with *Mycobacterium tuberculosis*. Patients present with palpable mass or masses in the breast that may be painful [116]. Most cases are unilateral [116, 117]. Aggressive cases can show skin ulceration and draining sinuses [118]. Nipple discharge may be present and AFB may be identified in smears from nipple discharge using a Ziehl–Neelsen stain [119]. Ipsilateral axillary lymph node involvement is seen in most cases and enlarged lymph nodes can be seen on mammography and ultrasound [117]. Imaging findings in the breast may be suggestive of abscess or can mimic malignancy if tuberculosis is unexpected [118]. In older lesions, calcified healed granulomas can be evident on mammogram [117].

Tuberculous granulomas are seen within lobules, surrounding ducts, and are present in the interlobular stroma. Granulomas are typically composed of epithelioid histiocytes and Langhans giant cells surrounding "caseous"-type necrosis. Acid-fast bacilli may not be detected in histologic sections. The gold standard for diagnosis is detection of *M. tuberculosis* by culture [120].

Fungal Infections

Histoplasmosis is caused by infection of *Histoplasma capsulatum*, a thermally dimorphic fungus common in river valleys in the United States [121]. Infection occurs via inhalation of spores, and most people infected are asymptomatic [121, 122]. Involvement of the breast is rare and histologically shows necrotizing granulomatous inflammation involving lobules. Narrow-based budding and non-budding yeast forms 2 to 4 μm in size can be demonstrated within histiocytes with a Grocott-Gomori's (or Gömöri) methenamine silver stain [122].

Mastitis or abscesses caused by Cryptococcus (*C. neoformans*) have been reported in immunocompetent and immunosuppressed patients and in the setting of disseminated cryptococcal infection [123, 124]. Budding yeast forms can be seen within sheets of foamy histiocytes on H&E (Fig. 4.34) and Periodic acid–Schiff or Grocott-Gomori's (or Gömöri) methenamine silver stains. Mucicarmine stains the polysaccharide capsule of the yeast.

Blastomycosis (*Blastomyces dermatitidis* or *B. gilchristii*) can occur in immunocompetent patients and may present as a breast mass in the setting of disseminated disease [125]. Infection occurs by inhalation of lung spores. Wooded areas and river valleys in the central United States are common areas of infection [126]. Infection can spread from the lungs to the skin and other organs. Necrotizing granulomas and abscesses are evident that may contain broad-based budding yeast that can be seen with a GMS stain [127].

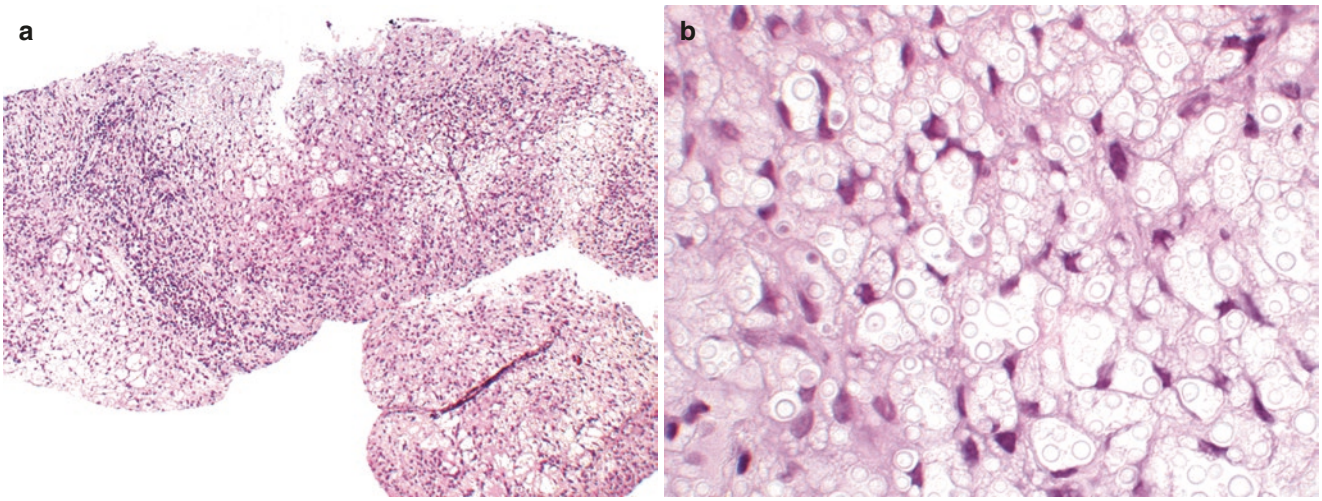

Fig. 4.34 Cryptococcus in a core biopsy. (**a**) Sheets of foamy histiocytes and lymphocytes are present in the biopsy. (**b**) Round yeast forms are present within the histiocytes. (*Courtesy of Susan Lester, MD*, Brigham and Women's Hospital, with permission)

Parasitic Infections

Schistosomiasis is a parasitic fluke that is uncommon in the United States but may be seen in patients from South East Asia, South America, and the Caribbean. Involvement of the breast by schistosomiasis comes to attention due to the presence of mammographic calcifications. Calcifications can show a segmental or clustered distribution that can mimic DCIS on mammography [128–130]. On histology, calcified ova are present around lobules and in the stroma, but not within ducts (Fig. 4.35). It is not possible to discern the species of schistosomiasis in most cases. *Schistosoma japonicum* is endemic to southeast Asia, while patients from the Caribbean and South America will likely be infected with *S. mansoni*, which is also endemic in parts of Africa. *S. haematobium* is found in Africa and the Middle East [131, 132].

Sparganosis, which usually occurs in Southeast Asia, is caused by infection with larvae of the tapeworm of the genus *Spirometra* [133]. Infection may be the result of drinking water contaminated with copepods containing *Spirometra* larvae. Consumption of raw snakes and frogs, the parasite's second intermediate host, is another way humans acquire the larvae [134]. Larvae migrate to subcutaneous tissue and the reported cases involving the breast typically occur in subcutaneous tissue, rather than breast glandular tissue. Patients present with a palpable mass that may be associated with pain or itching [133]. Biopsies of sparganosis show granulomatous inflammation with eosinophils associated with the body of the worm. The worm is lined by an eosinophilic tegument and has a myxoid appearing matrix that contains smooth muscle fibers and calcospherules (Fig. 4.36).

Cysticercosis can be distinguished from sparganosis by its scolex, hooks, and fluid-filled "bladder" surrounding the worm (Fig. 4.37) [135]. Cysticercosis is caused by infection of the larval form of *Taenia solium*. Larvae penetrate the intestinal mucosa and migrate to sites such as skeletal muscle, skin, and brain, and form cysts. Breast involvement has been reported in rare cases in which cystic lesions are formed [136, 137].

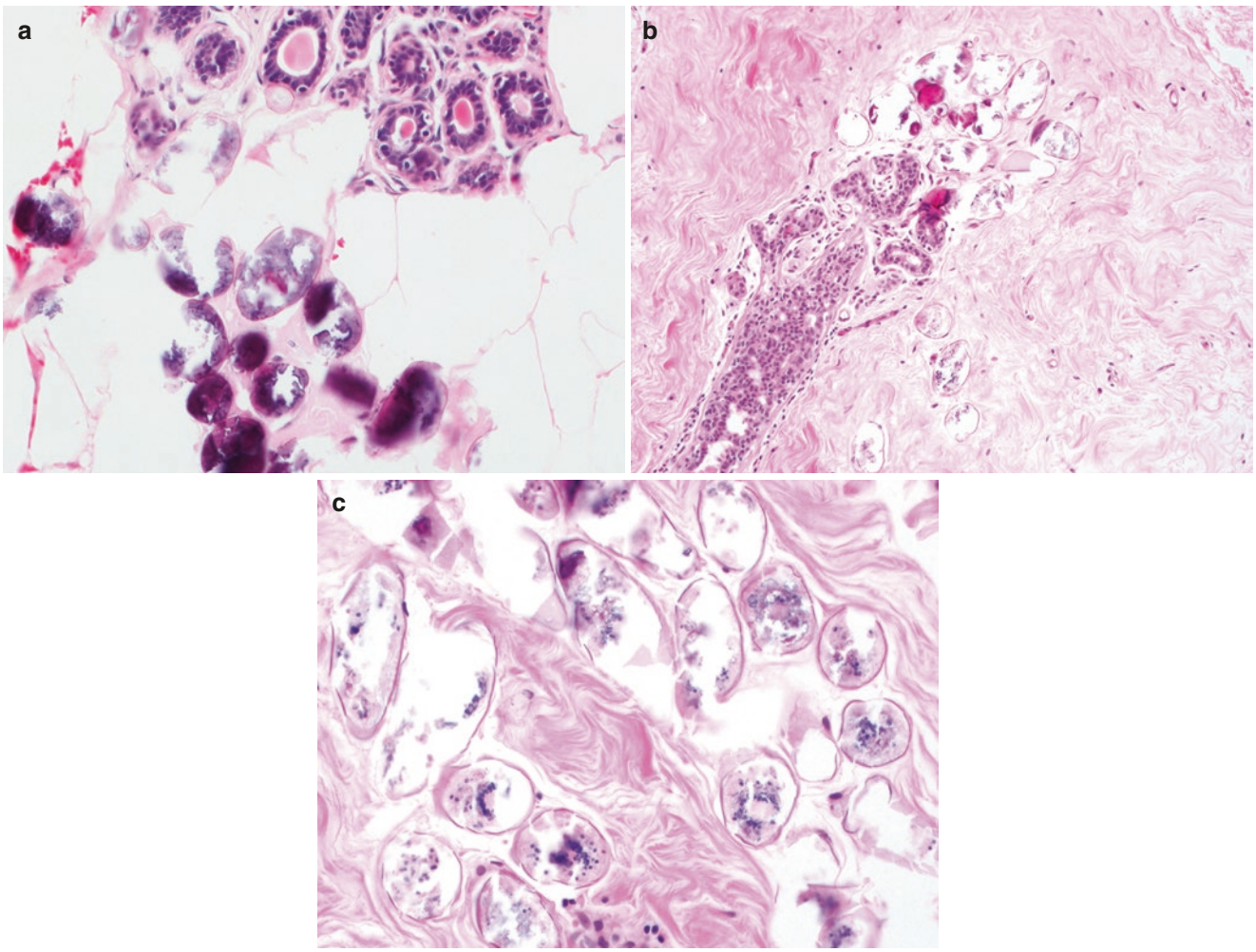

Fig. 4.35 Schistosomiasis in stereotactic biopsies performed for mammographic microcalcifications. (**a**–**c**) Calcified ova are present in perilobular stroma. ((**b**, **c**) *Courtesy of Adam Gersten, MD*, Albert Einstein College of Medicine, with permission)

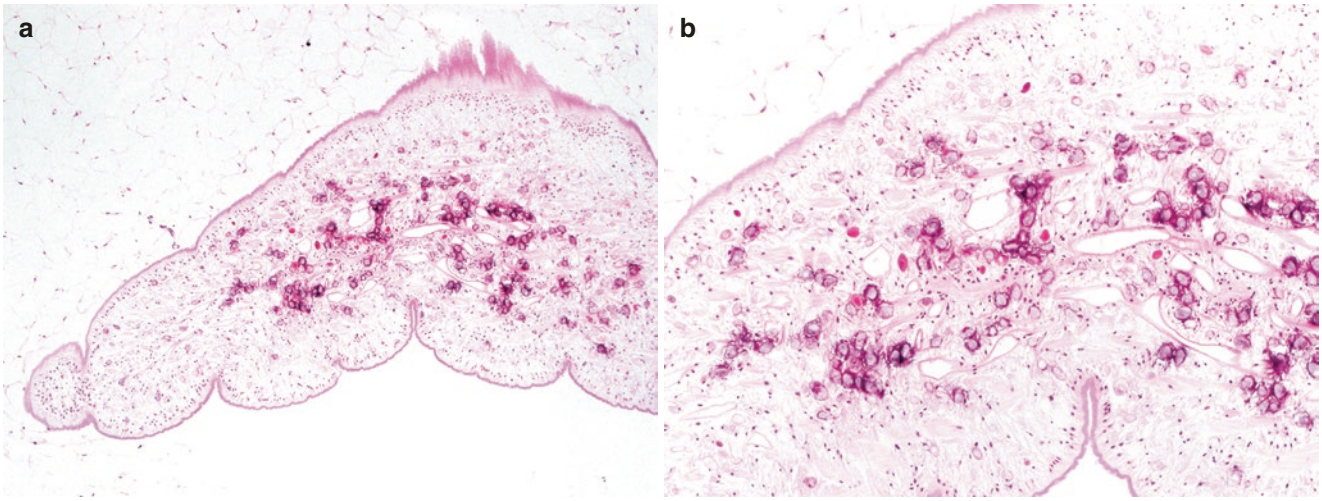

Fig. 4.36 Sparganosis. (**a**) The larva shows a myxoid matrix and contains calcified spherules. (**b**) Smooth muscle fibers can be seen on higher power

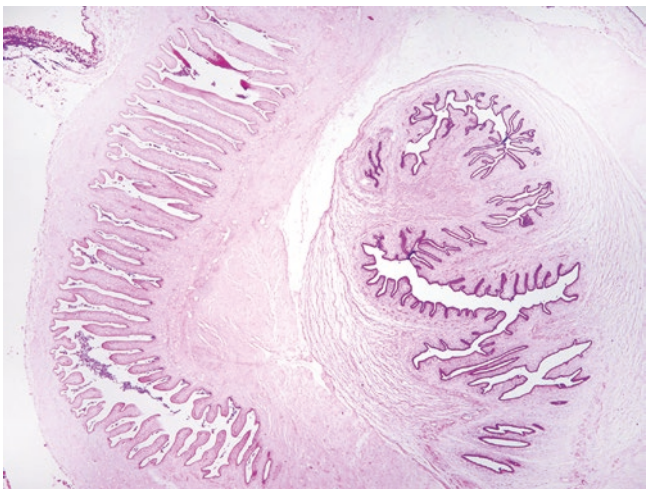

Fig. 4.37 Cysticercosis. The body of the larva is seen inside a fluid-filled "bladder"

References

1. Clarke D, Curtis JL, Martinez A, Fajardo L, Goffinet D. Fat necrosis of the breast simulating recurrent carcinoma after primary radiotherapy in the management of early stage breast carcinoma. Cancer. 1983;52(3):442–5.
2. Rivera R, Smith-Bronstein V, Villegas-Mendez S, Rayhanabad J, Sheth P, Rashtian A, et al. Mammographic findings after intraoperative radiotherapy of the breast. Radiol Res Pract. 2012;2012:758371.
3. Shah C, Badiyan S, Ben Wilkinson J, Vicini F, Beitsch P, Keisch M, et al. Treatment efficacy with accelerated partial breast irradiation (APBI): final analysis of the American Society of Breast Surgeons MammoSite((R)) breast brachytherapy registry trial. Ann Surg Oncol. 2013;20(10):3279–85.
4. Aqel NM, Howard A, Collier DS. Fat necrosis of the breast: a cytological and clinical study. Breast. 2001;10(4):342–5.
5. Hogge JP, Robinson RE, Magnant CM, Zuurbier RA. The mammographic spectrum of fat necrosis of the breast. Radiographics. 1995;15(6):1347–56.
6. Taboada JL, Stephens TW, Krishnamurthy S, Brandt KR, Whitman GJ. The many faces of fat necrosis in the breast. AJR Am J Roentgenol. 2009;192(3):815–25.
7. Bassett LW, Gold RH, Mirra JM. Nonneoplastic breast calcifications in lipid cysts: development after excision and primary irradiation. AJR Am J Roentgenol. 1982;138(2):335–8.
8. Evers K, Troupin RH. Lipid cyst: classic and atypical appearances. AJR Am J Roentgenol. 1991;157(2):271–3.
9. Bilgen IG, Ustun EE, Memis A. Fat necrosis of the breast: clinical, mammographic and sonographic features. Eur J Radiol. 2001;39(2):92–9.
10. Atasoy MM, Oren NC, Ilica AT, Guvenc I, Gunal A, Mossa-Basha M. Sonography of fat necrosis of the breast: correlation with mammography and MR imaging. J Clin Ultrasound. 2013;41(7):415–23.
11. Soo MS, Kornguth PJ, Hertzberg BS. Fat necrosis in the breast: sonographic features. Radiology. 1998;206(1):261–9.
12. Tan PH, Harada O, Thike AA, Tse GM. Histiocytoid breast carcinoma: an enigmatic lobular entity. J Clin Pathol. 2011;64(8):654–9.
13. Ramos CV, Taylor HB. Lipid-rich carcinoma of the breast. A clinicopathologic analysis of 13 examples. Cancer. 1974;33(3):812–9.
14. Reis-Filho JS, Fulford LG, Lakhani SR, Schmitt FC. Pathologic quiz case: a 62-year-old woman with a 4.5-cm nodule in the right breast. Lipid-rich breast carcinoma. Arch Pathol Lab Med. 2003;127(9):e396–8.
15. Tenny SO, McGinness M, Zhang D, Damjanov I, Fan F. Rosai-Dorfman disease presenting as a breast mass and enlarged axillary lymph node mimicking malignancy: a case report and review of the literature. Breast J. 2011;17(5):516–20.
16. Green I, Dorfman RF, Rosai J. Breast involvement by extranodal Rosai-Dorfman disease: report of seven cases. Am J Surg Pathol. 1997;21(6):664–8.
17. Morkowski JJ, Nguyen CV, Lin P, Farr M, Abraham SC, Gilcrease MZ, et al. Rosai-Dorfman disease confined to the breast. Ann Diagn Pathol. 2010;14(2):81–7.
18. Guo S, Yan Q, Rohr J, Wang Y, Fan L, Wang Z. Erdheim-Chester disease involving the breast—a rare but important differential diagnosis. Hum Pathol. 2015;46(1):159–64.
19. Haagensen CD. Mammary-duct ectasia; a disease that may simulate carcinoma. Cancer. 1951;4(4):749–61.
20. Rahal RM, de Freitas-Junior R, Paulinelli RR. Risk factors for duct ectasia. Breast J. 2005;11(4):262–5.
21. Thomas WG, Williamson RC, Davies JD, Webb AJ. The clinical syndrome of mammary duct ectasia. Br J Surg. 1982;69(7):423–5.

22. Dixon JM. Periductal mastitis/duct ectasia. World J Surg. 1989;13(6):715–20.
23. Bober E, Ozer E, Akgur F, Buyukgebiz A. Bilateral breast masses and bloody nipple discharge in a two year-old boy. J Pediatr Endocrinol Metab. 1996;9(3):419–21.
24. Leung AK, Kao CP. Mammary duct ectasia: a cause of bloody nipple discharge. J Natl Med Assoc. 2004;96(4):543–5.
25. Ashworth MT, Corcoran GD, Haqqani MT. Periductal mastitis and mammary duct ectasia in a male. Postgrad Med J. 1985;61(717):621–3.
26. Abramson DJ. Mammary duct ectasia, mammillary fistula and subareolar sinuses. Ann Surg. 1969;169(2):217–26.
27. Furlong AJ, Al-Nakib L, Knox WF, Parry A, Bundred NJ. Periductal inflammation and cigarette smoke. J Am Coll Surg. 1994;179(4):417–20.
28. Dixon JM, Ravisekar O, Chetty U, Anderson TJ. Periductal mastitis and duct ectasia: different conditions with different aetiologies. Br J Surg. 1996;83(6):820–2.
29. Shousha S, Backhouse CM, Dawson PM, Alaghband-Zadeh J, Burn I. Mammary duct ectasia and pituitary adenomas. Am J Surg Pathol. 1988;12(2):130–3.
30. Sweeney DJ, Wylie EJ. Mammographic appearances of mammary duct ectasia that mimic carcinoma in a screening programme. Australas Radiol. 1995;39(1):18–23.
31. An HY, Kim KS, Yu IK, Kim KW, Kim HH. Image presentation. The nipple-areolar complex: a pictorial review of common and uncommon conditions. J Ultrasound Med. 2010;29(6):949–62.
32. Davies JD. Pigmented periductal cells (ochrocytes) in mammary dysplasias: their nature and significance. J Pathol. 1974;114(4):205–16.
33. Seidman MA, Scognamiglio T, Hoda SA. "Cholesteroloma": a rare cause of "indeterminate" microcalcifications on mammography. Breast J. 2009;15(3):303–4.
34. Rahal RM, de Freitas-Junior R, Carlos da Cunha L, Moreira MA, Rosa VD, Conde DM. Mammary duct ectasia: an overview. Breast J. 2011;17(6):694–5.
35. Going JJ, Anderson TJ, Wilkinson S, Chetty U. Granulomatous lobular mastitis. J Clin Pathol. 1987;40(5):535–40.
36. Ocal K, Dag A, Turkmenoglu O, Kara T, Seyit H, Konca K. Granulomatous mastitis: clinical, pathological features, and management. Breast J. 2010;16(2):176–82.
37. Hovanessian Larsen LJ, Peyvandi B, Klipfel N, Grant E, Iyengar G. Granulomatous lobular mastitis: imaging, diagnosis, and treatment. AJR Am J Roentgenol. 2009;193(2):574–81.
38. Pandey TS, Mackinnon JC, Bressler L, Millar A, Marcus EE, Ganschow PS. Idiopathic granulomatous mastitis—a prospective study of 49 women and treatment outcomes with steroid therapy. Breast J. 2014;20(3):258–66.
39. Troxell ML, Gordon NT, Doggett JS, Ballard M, Vetto JT, Pommier RF, et al. Cystic neutrophilic granulomatous mastitis: association with gram-positive bacilli and Corynebacterium. Am J Clin Pathol. 2016;145(5):635–45.
40. Shoyele O, Vidhun R, Dodge J, Cheng Z, Margules R, Nee P, et al. Cystic neutrophilic granulomatous mastitis: a clinicopathologic study of a distinct entity with supporting evidence of a role for Corynebacterium-targeted therapy. Ann Diagn Pathol. 2018;37:51–6.
41. Oran ES, Gurdal SO, Yankol Y, Oznur M, Calay Z, Tunaci M, et al. Management of idiopathic granulomatous mastitis diagnosed by core biopsy: a retrospective multicenter study. Breast J. 2013;19(4):411–8.
42. Taylor GB, Paviour SD, Musaad S, Jones WO, Holland DJ. A clinicopathological review of 34 cases of inflammatory breast disease showing an association between corynebacteria infection and granulomatous mastitis. Pathology. 2003;35(2):109–19.
43. D'Alfonso TM, Moo TA, Arleo EK, Cheng E, Antonio LB, Hoda SA. Cystic neutrophilic granulomatous mastitis: further clinical and pathological characterization of an under-recognized entity based on eleven cases. Mod Pathol. 2015;28(Suppl 2):40A–1A.
44. Renshaw AA, Derhagopian RP, Gould EW. Cystic neutrophilic granulomatous mastitis: an underappreciated pattern strongly associated with gram-positive bacilli. Am J Clin Pathol. 2011;136(3):424–7.
45. Ozturk M, Mavili E, Kahriman G, Akcan AC, Ozturk F. Granulomatous mastitis: radiological findings. Acta Radiol. 2007;48(2):150–5.
46. Al-Khawari HA, Al-Manfouhi HA, Madda JP, Kovacs A, Sheikh M, Roberts O. Radiologic features of granulomatous mastitis. Breast J. 2011;17(6):645–50.
47. Joseph KA, Luu X, Mor A. Granulomatous mastitis: a New York public hospital experience. Ann Surg Oncol. 2014;21(13):4159–63.
48. Sangoi AR. "Thick section" gram stain yields improved detection of organisms in tissue sections of cystic neutrophilic granulomatous mastitis. Am J Clin Pathol. 2020;153(5):593–7.
49. Paviour S, Musaad S, Roberts S, Taylor G, Taylor S, Shore K, et al. Corynebacterium species isolated from patients with mastitis. Clin Infect Dis. 2002;35(11):1434–40.
50. Johnstone KJ, Robson J, Cherian SG, Wan Sai Cheong J, Kerr K, Bligh JF. Cystic neutrophilic granulomatous mastitis associated with Corynebacterium including Corynebacterium kroppenstedtii. Pathology. 2017;49(4):405–12.
51. Funke G, von Graevenitz A, Clarridge JE 3rd, Bernard KA. Clinical microbiology of coryneform bacteria. Clin Microbiol Rev. 1997;10(1):125–59.
52. Jorgensen MB, Nielsen DM. Diagnosis and treatment of granulomatous mastitis. Am J Med. 1992;93(1):97–101.
53. Akbulut S, Yilmaz D, Bakir S. Methotrexate in the management of idiopathic granulomatous mastitis: review of 108 published cases and report of four cases. Breast J. 2011;17(6):661–8.
54. Ojeda H, Sardi A, Totoonchie A. Sarcoidosis of the breast: implications for the general surgeon. Am Surg. 2000;66(12):1144–8.
55. Fitzgibbons PL, Smiley DF, Kern WH. Sarcoidosis presenting initially as breast mass: report of two cases. Hum Pathol. 1985;16(8):851–2.
56. Dilaveri CA, Mac Bride MB, Sandhu NP, Neal L, Ghosh K, Wahner-Roedler DL. Breast manifestations of systemic diseases. Int J Womens Health. 2012;4:35–43.
57. Gisvold JJ, Crotty TB, Johnson RE. Sarcoidosis presenting as spiculated breast masses. Mayo Clin Proc. 2000;75(3):293–5.
58. Isley LM, Cluver AR, Leddy RJ, Baker MK. Primary sarcoid of the breast with incidental malignancy. J Clin Imaging Sci. 2012;2:46.
59. Bassler R, Birke F. Histopathology of tumour associated sarcoid-like stromal reaction in breast cancer. An analysis of 5 cases with immunohistochemical investigations. Virchows Arch A Pathol Anat Histopathol. 1988;412(3):231–9.
60. Tomaszewski JE, Brooks JS, Hicks D, Livolsi VA. Diabetic mastopathy: a distinctive clinicopathologic entity. Hum Pathol. 1992;23(7):780–6.
61. Camuto PM, Zetrenne E, Ponn T. Diabetic mastopathy: a report of 5 cases and a review of the literature. Arch Surg. 2000;135(10):1190–3.
62. Soler NG, Khardori R. Fibrous disease of the breast, thyroiditis, and cheiroarthropathy in type I diabetes mellitus. Lancet. 1984;1(8370):193–5.
63. Ely KA, Tse G, Simpson JF, Clarfeld R, Page DL. Diabetic mastopathy. A clinicopathologic review. Am J Clin Pathol. 2000;113(4):541–5.
64. Logan WW, Hoffman NY. Diabetic fibrous breast disease. Radiology. 1989;172(3):667–70.

65. Moschetta M, Telegrafo M, Triggiani V, Rella L, Cornacchia I, Serio G, et al. Diabetic mastopathy: a diagnostic challenge in breast sonography. J Clin Ultrasound. 2015;43(2):113–7.
66. Chan CL, Ho RS, Shek TW, Kwong A. Diabetic mastopathy. Breast J. 2013;19(5):533–8.
67. Dorokhova O, Fineberg S, Koenigsberg T, Wang Y. Diabetic mastopathy, a clinicopathological correlation of 34 cases. Pathol Int. 2012;62(10):660–4.
68. Tuncbilek N, Karakas HM, Okten O. Diabetic fibrous mastopathy: dynamic contrast-enhanced magnetic resonance imaging findings. Breast J. 2004;10(4):359–62.
69. Wong KT, Tse GM, Yang WT. Ultrasound and MR imaging of diabetic mastopathy. Clin Radiol. 2002;57(8):730–5.
70. Valdez R, Thorson J, Finn WG, Schnitzer B, Kleer CG. Lymphocytic mastitis and diabetic mastopathy: a molecular, immunophenotypic, and clinicopathologic evaluation of 11 cases. Mod Pathol. 2003;16(3):223–8.
71. Chhieng DC, Cangiarella JF, Waisman J, Fernandez G, Cohen JM. Fine-needle aspiration cytology of spindle cell lesions of the breast. Cancer. 1999;87(6):359–71.
72. Seidman JD, Schnaper LA, Phillips LE. Mastopathy in insulin-requiring diabetes mellitus. Hum Pathol. 1994;25(8):819–24.
73. Lammie GA, Bobrow LG, Staunton MD, Levison DA, Page G, Millis RR. Sclerosing lymphocytic lobulitis of the breast—evidence for an autoimmune pathogenesis. Histopathology. 1991;19(1):13–20.
74. Kudva YC, Reynolds C, O'Brien T, Powell C, Oberg AL, Crotty TB. "Diabetic mastopathy," or sclerosing lymphocytic lobulitis, is strongly associated with type 1 diabetes. Diabetes Care. 2002;25(1):121–6.
75. Rocken C, Kronsbein H, Sletten K, Roessner A, Bassler R. Amyloidosis of the breast. Virchows Arch. 2002;440(5):527–35.
76. Tsuji W, Takeuchi E, Oka S, Yamashita T, Yotsumoto F. Localized primary amyloidosis of the breast: a case report and review of the literature. BMC Surg. 2016;16(1):62.
77. Lytle A, Darvishian F, Ozerdem U. Localized amyloidosis: a diagnostic pitfall in breast pathology. Pathol Res Pract. 2019;215(12):152699.
78. Said SM, Reynolds C, Jimenez RE, Chen B, Vrana JA, Theis JD, et al. Amyloidosis of the breast: predominantly AL type and over half have concurrent breast hematologic disorders. Mod Pathol. 2013;26(2):232–8.
79. Fischer EG. Localized breast amyloidosis associated with Sjorgren syndrome. Case Rep Pathol. 2020;2020:8828263.
80. Jawahar A, Nagamine A, Gamez R. Breast plasmacytoma with associated amyloidosis mimicking breast carcinoma. Breast J. 2018;24(6):1071–3.
81. Eghtedari M, Dogan BE, Gilcrease M, Roberts J, Cook ED, Yang WT. Imaging and pathologic characteristics of breast amyloidosis. Breast J. 2015;21(2):197–9.
82. O'Brien J, Aherne S, McCormack O, Jeffers M, McInerney D. MRI features of bilateral amyloidosis of breast. Breast J. 2013;19(3):338–9.
83. Deshpande V, Zen Y, Chan JK, Yi EE, Sato Y, Yoshino T, et al. Consensus statement on the pathology of IgG4-related disease. Mod Pathol. 2012;25(9):1181–92.
84. Mahajan VS, Mattoo H, Deshpande V, Pillai SS, Stone JH. IgG4-related disease. Annu Rev Pathol. 2014;9:315–47.
85. Goulabchand R, Hafidi A, Van de Perre P, Millet I, Maria ATJ, Morel J, et al. Mastitis in autoimmune diseases: review of the literature, diagnostic pathway, and pathophysiological key players. J Clin Med. 2020;9(4):958.
86. Erivwo P, Turashvili G. Pathology of IgG4-related sclerosing mastitis. J Clin Pathol. 2020; https://doi.org/10.1136/jclinpath-2020-207029.
87. Ogiya A, Tanaka K, Tadokoro Y, Kikutani M, Uematsu T, Kashiwagi H, et al. IgG4-related sclerosing disease of the breast successfully treated by steroid therapy. Breast Cancer. 2014;21(2):231–5.
88. Erivwo P, Bharatwal V, Huang M, Godra A, Turashvili G. Classic IgG4-related sclerosing mastitis is not so classic. Breast J. 2020;26(6):1245–8.
89. Kriegsmann M, Gomez C, Heil J, Schafgen B, Gutjahr E, Kommoss FKF, et al. IgG4-related sclerosing mastitis in a 49-year-old patient with multiple, tumor-like nodules-diagnostic accuracy of core needle biopsy. Breast J. 2019;25(6):1251–3.
90. Cheuk W, Chan AC, Lam WL, Chow SM, Crowley P, Lloydd R, et al. IgG4-related sclerosing mastitis: description of a new member of the IgG4-related sclerosing diseases. Am J Surg Pathol. 2009;33(7):1058–64.
91. Hoffmann JC, Lin CY, Bhattacharyya S, Weinberg OK, Chisholm KM, Bayerl M, et al. Rosai-Dorfman disease of the breast with variable IgG4+ plasma cells: a diagnostic mimicker of other malignant and reactive entities. Am J Surg Pathol. 2019;43(12):1653–60.
92. Deshpande V. The pathology of IgG4-related disease: critical issues and challenges. Semin Diagn Pathol. 2012;29(4):191–6.
93. Inoue M, Ohta T, Shioya H, Sato S, Takahashi H, Nakata N, et al. Inflammatory myofibroblastic tumors of the breast with simultaneous intracranial, lung, and pancreas involvement: ultrasonographic findings and a review of the literature. J Med Ultrason (2001). 2018;45(2):331–5.
94. Khanafshar E, Phillipson J, Schammel DP, Minobe L, Cymerman J, Weidner N. Inflammatory myofibroblastic tumor of the breast. Ann Diagn Pathol. 2005;9(3):123–9.
95. Antonescu CR, Suurmeijer AJ, Zhang L, Sung YS, Jungbluth AA, Travis WD, et al. Molecular characterization of inflammatory myofibroblastic tumors with frequent ALK and ROS1 gene fusions and rare novel RET rearrangement. Am J Surg Pathol. 2015;39(7):957–67.
96. Gleason BC, Hornick JL. Inflammatory myofibroblastic tumours: where are we now? J Clin Pathol. 2008;61(4):428–37.
97. Sastre-Garau X, Couturier J, Derre J, Aurias A, Klijanienko J, Lagace R. Inflammatory myofibroblastic tumour (inflammatory pseudotumour) of the breast. Clinicopathological and genetic analysis of a case with evidence for clonality. J Pathol. 2002;196(1):97–102.
98. Siraj F, Kaur M, Dalal V, Sonam J. Inflammatory myofibroblastic tumor of the breast mimicking malignancy in an elderly male. Ochsner J. 2017;17(3):277–9.
99. Choi EJ, Jin GY, Chung MJ, Moon WS, Youn HJ. Primary inflammatory myofibroblastic tumors of the breast with metastasis: radiographic and histopathologic predictive factors. J Breast Cancer. 2015;18(2):200–5.
100. Butrynski JE, D'Adamo DR, Hornick JL, Dal Cin P, Antonescu CR, Jhanwar SC, et al. Crizotinib in ALK-rearranged inflammatory myofibroblastic tumor. N Engl J Med. 2010;363(18):1727–33.
101. Mahoney MC, Ingram AD. Breast emergencies: types, imaging features, and management. AJR Am J Roentgenol. 2014;202(4):W390–9.
102. Trop I, Dugas A, David J, El Khoury M, Boileau JF, Larouche N, et al. Breast abscesses: evidence-based algorithms for diagnosis, management, and follow-up. Radiographics. 2011;31(6):1683–99.
103. Dener C, Inan A. Breast abscesses in lactating women. World J Surg. 2003;27(2):130–3.
104. Scott-Conner CE, Schorr SJ. The diagnosis and management of breast problems during pregnancy and lactation. Am J Surg. 1995;170(4):401–5.
105. Zuska JJ, Crile G Jr, Ayres WW. Fistulas of lactifierous ducts. Am J Surg. 1951;81(3):312–7.

106. Habif DV, Perzin KH, Lipton R, Lattes R. Subareolar abscess associated with squamous metaplasia of lactiferous ducts. Am J Surg. 1970;119(5):523–6.
107. Johnson SP, Kaoutzanis C, Schaub GA. Male Zuska's disease. BMJ Case Rep. 2014;2014. https://doi.org/10.1136/bcr-2013-201922.
108. Lo G, Dessauvagie B, Sterrett G, Bourke AG. Squamous metaplasia of lactiferous ducts (SMOLD). Clin Radiol. 2012;67(11):e42–6.
109. Versluijs-Ossewaarde FN, Roumen RM, Goris RJ. Subareolar breast abscesses: characteristics and results of surgical treatment. Breast J. 2005;11(3):179–82.
110. Meguid MM, Oler A, Numann PJ, Khan S. Pathogenesis-based treatment of recurring subareolar breast abscesses. Surgery. 1995;118(4):775–82.
111. Gollapalli V, Liao J, Dudakovic A, Sugg SL, Scott-Conner CE, Weigel RJ. Risk factors for development and recurrence of primary breast abscesses. J Am Coll Surg. 2010;211(1):41–8.
112. Leibman AJ, Misra M, Castaldi M. Breast abscess after nipple piercing: sonographic findings with clinical correlation. J Ultrasound Med. 2011;30(9):1303–8.
113. Dabbas N, Chand M, Pallett A, Royle GT, Sainsbury R. Have the organisms that cause breast abscess changed with time?—Implications for appropriate antibiotic usage in primary and secondary care. Breast J. 2010;16(4):412–5.
114. Walker AP, Edmiston CE Jr, Krepel CJ, Condon RE. A prospective study of the microflora of nonpuerperal breast abscess. Arch Surg. 1988;123(7):908–11.
115. Kasales CJ, Han B, Smith JS Jr, Chetlen AL, Kaneda HJ, Shereef S. Nonpuerperal mastitis and subareolar abscess of the breast. AJR Am J Roentgenol. 2014;202(2):W133–9.
116. Khodabakhshi B, Mehravar F. Breast tuberculosis in northeast Iran: review of 22 cases. BMC Womens Health. 2014;14:72.
117. Meerkotter D, Spiegel K, Page-Shipp LS. Imaging of tuberculosis of the breast: 21 cases and a review of the literature. J Med Imaging Radiat Oncol. 2011;55(5):453–60.
118. Khandelwal R, Jain I. Breast tuberculosis mimicking a malignancy: a rare case report with review of literature. Breast Dis. 2013;34(2):53–5.
119. Mandal S, Jain S. Purulent nipple discharge—a presenting manifestation in tuberculous mastitis. Breast J. 2007;13(2):205.
120. Tewari M, Shukla HS. Breast tuberculosis: diagnosis, clinical features & management. Indian J Med Res. 2005;122(2):103–10.
121. Adenis AA, Aznar C, Couppie P. Histoplasmosis in HIV-infected patients: a review of new developments and remaining gaps. Curr Trop Med Rep. 2014;1:119–28.
122. Payne S, Kim S, Das K, Mirani N. A 36-year-old woman with a unilateral breast mass. Necrotizing granulomatous mastitis secondary to budding yeast forms morphologically consistent with Histoplasma capsulatum. Arch Pathol Lab Med. 2006;130(1):e1–2.
123. Haddow LJ, Sahid F, Moosa MY. Cryptococcal breast abscess in an HIV-positive patient: arguments for reviewing the definition of immune reconstitution inflammatory syndrome. J Infect. 2008;57(1):82–4.
124. Goldman M, Pottage JC Jr. Cryptococcal infection of the breast. Clin Infect Dis. 1995;21(5):1166–9.
125. Seymour EQ. Blastomycosis of the breast. AJR Am J Roentgenol. 1982;139(4):822–3.
126. Bradsher RW Jr. The endemic mimic: blastomycosis an illness often misdiagnosed. Trans Am Clin Climatol Assoc. 2014;125:188–202; discussion 202–203.
127. Salfelder K, Schwarz J. Mycotic "pseudotumors" of the breast. Report of four cases. Arch Surg. 1975;110(6):751–4.
128. Kawasaki T, Tsunoda-Shimizu H, Inoue S, Kondo T, Yuminamochi T, Nakazawa T, et al. Breast schistosomiasis japonica—a report of four Japanese cases. Histopathology. 2009;54(2):263–6.
129. Varin CR, Eisenberg BL, Ladd WA. Mammographic microcalcifications associated with schistosomiasis. South Med J. 1989;82(8):1060–1.
130. Gorman JD, Champaign JL, Sumida FK, Canavan L. Schistosomiasis involving the breast. Radiology. 1992;185(2):423–4.
131. Gryseels B, Polman K, Clerinx J, Kestens L. Human schistosomiasis. Lancet. 2006;368(9541):1106–18.
132. Makunike RT, Muronda C. Breast schistosomiasis: a case report. Histopathology. 2002;41(2):175–6.
133. Koo M, Kim JH, Kim JS, Lee JE, Nam SJ, Yang JH. Cases and literature review of breast sparganosis. World J Surg. 2011;35(3):573–9.
134. Chan AB, Wan SK, Leung SL, Law BK, Lai DP, Ip M, et al. Sparganosis of the breast. Histopathology. 2004;44(5):510–1.
135. Graham RP, Pritt BS, Glazebrook KN, Shah S. Sparganosis presenting as a mammographic abnormality. Breast J. 2014;20(1):92–4.
136. Gupta NK, Panchonia A, Jain D. Cysticercosis of breast. Trop Parasitol. 2013;3(2):148–50.
137. Sah SP, Jha PC, Gupta AK, Raj GA. An incidental case of breast cysticercosis associated with fibroadenoma. Indian J Pathol Microbiol. 2001;44(1):59–61.

5 Adenosis, Sclerosing Lesions, Microglandular Adenosis, and Mucocele-Like Lesions

Beth T. Harrison and Deborah A. Dillon

Adenosis

Overview

Adenosis represents a group of benign proliferative lesions of the breast that feature an increased number of glands in the terminal duct lobular units. Sclerosing adenosis, the most common type, is characterized by coexistent stromal sclerosis that compresses the glands and distorts the architecture of involved lobules. In 1940, Ewing briefly described the entity of "fibrosing adenomatosis." Foote and Stewart [1] provided one of the first detailed histopathologic studies of "sclerosing adenosis." Subsequently, Urban and Adair [2] and Heller and Fleming [3] published early clinicopathologic studies of this lesion. A common emphasis by the authors of these early reports is the potential to misinterpret this benign small glandular proliferation as invasive carcinoma. Today, although experienced pathologists are well aware of this entity and its diagnostic pitfalls, various histopathologic variants continue to pose challenges, especially in the limited sample on core needle biopsy (CNB).

Clinical, Radiologic, and Gross Features

Sclerosing adenosis is a common lesion of the breast, most prevalent in women of reproductive or perimenopausal age, especially those in the third and fourth decades. It is present in over one quarter of all benign breast biopsies, frequently in association with other proliferative and nonproliferative fibrocystic changes [4]. Sclerosing adenosis limited to isolated lobules is often an incidental microscopic finding; however, lesions involved by microcalcifications may manifest mammographically. Confluent and florid lobules of adenosis, termed "nodular adenosis" or "adenosis tumor," may present as a palpable or radiologically detectable mass. Clinical examination reveals a firm, mobile mass with or without associated tenderness.

Sclerosing adenosis most frequently presents as microcalcifications or masses and less frequently as atypical densities or architectural distortion [5–9]. On mammography, microcalcifications tend to be clustered in distribution and show amorphous, pleomorphic, or punctate morphologies [5, 6]. Sclerosing adenosis also correlates with scattered mammographic calcifications, but these radiologic lesions are seldom biopsied due to their benign appearance. Masses may be visualized on mammogram and/or ultrasound and range from an oval shape and circumscribed or indistinct margins to an irregular shape with irregular margins [5–9]. Sclerosing adenosis is associated with spiculated masses in few cases [5, 6]. Ultrasonography may also reveal heterogeneously echogenic areas or focal acoustic shadowing [5, 7, 10].

Gross pathology of excised adenosis varies depending on the histologic patterns of the lesion. Nodular adenosis appears as a mass with relatively circumscribed or lobulated borders, a firm consistency, and a grayish-white or pale tan cut surface. Sclerotic lesions tend to form multinodular masses with more irregular borders. Masses usually measure less than 3 cm. A gritty texture is observed if the adenosis is involved by numerous calcifications. Chalky streaks characteristic of invasive carcinoma are absent. Sclerosing adenosis involving scattered lobules is not apparent on gross examination.

Microscopic Features

Adenosis may be a focal, diffuse, or tumor-like process (Fig. 5.1). At low magnification, it is characterized by a small glandular proliferation with a lobulocentric pattern of growth (Fig. 5.1c). Lesions range from sclerotic to florid. Myoepithelial cells are retained throughout the lesion,

B. T. Harrison (✉) · D. A. Dillon
Department of Pathology, Brigham and Women's Hospital and Harvard Medical School, Boston, MA, USA
e-mail: bharrison3@bwh.harvard.edu; ddillon@bwh.harvard.edu

© The Author(s), under exclusive license to Springer Nature Switzerland AG 2022
S. J. Shin et al. (eds.), *A Comprehensive Guide to Core Needle Biopsies of the Breast*,
https://doi.org/10.1007/978-3-031-05532-4_5

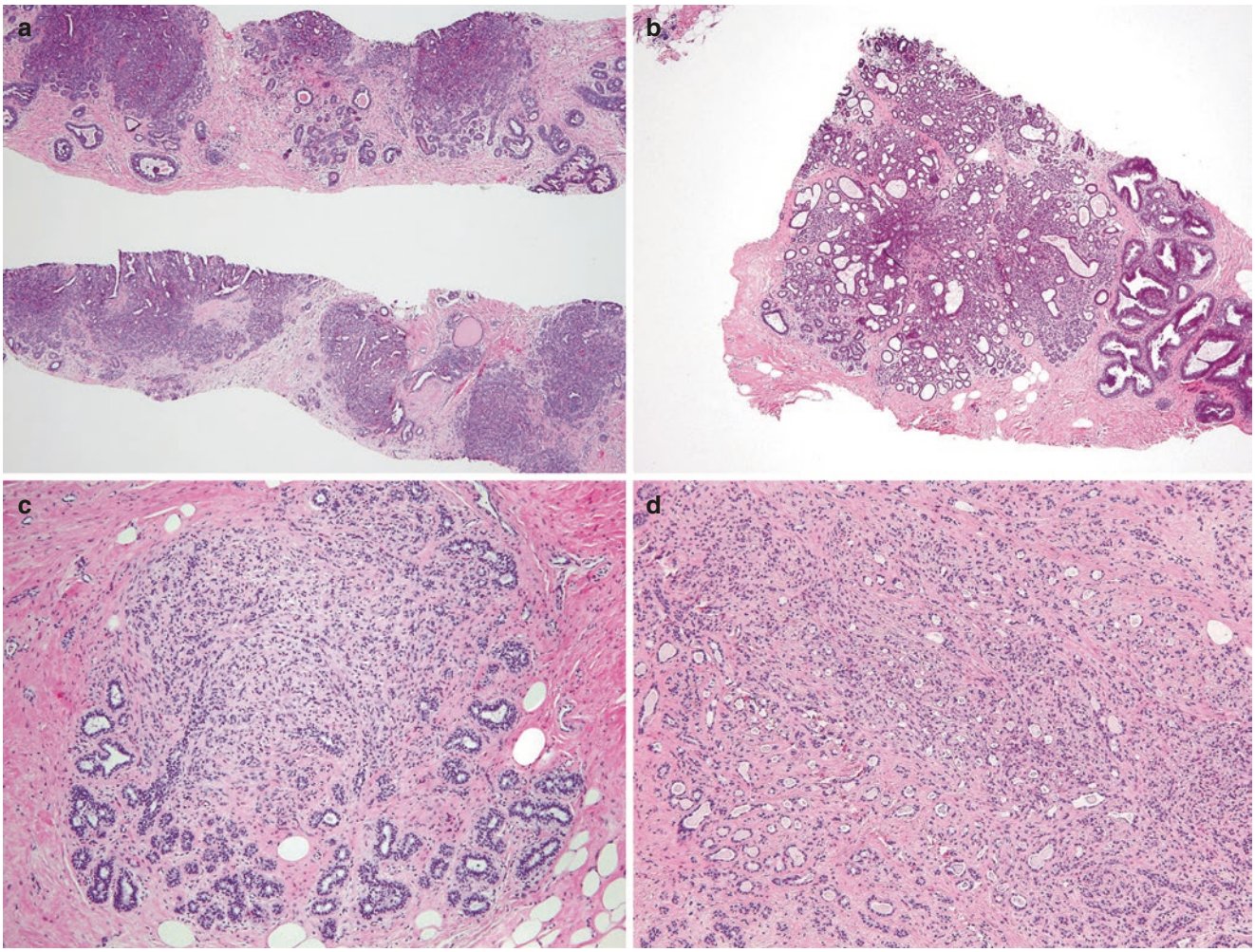

Fig. 5.1 Sclerosing adenosis, diffuse (**a**), nodular (**b**), and incidental (**c**). It commonly features a lobulocentric pattern of growth with compressed glands centrally and retained tubules peripherally (**c**); however, this may be difficult to discern in some examples (**d**)

although it can be challenging to identify two cell layers in very florid or sclerotic lesions by hematoxylin and eosin (H&E) morphology alone.

Sclerosing adenosis displays swirling lobules of compressed and distorted glands in fibrotic stroma. Sclerosis is often accentuated in the central portion of the lobule. Areas with less sclerosis contain round glands with open lumens and elongated glands with compressed lumens (Fig. 5.1c). Eosinophilic secretions may be present within the open lumens. The luminal epithelium consists of variably attenuated cuboidal to columnar cells with bland cytomorphology. The myoepithelium is typically flattened and rather inconspicuous. With increasing sclerosis, compressed glands with obliterated lumens appear as small nests or cords of epithelioid or spindled myoepithelial cells. Atrophic epithelial cells may be barely perceptible or absent. The glands are surrounded by a thickened basement membrane and variably expanded dense fibrotic to hyalinized stroma. Scattered stromal and intraluminal microcalcifications are common (Fig. 5.2). Stromal elastosis may be seen and may be a clue that the adenosis is part of a larger sclerosing lesion. Sclerosing adenosis is often associated with other fibrocystic changes, such as columnar cell and apocrine change (Fig. 5.3), usual epithelial hyperplasia, radial sclerosing lesions, papillomas, and fibroadenomas (Fig. 5.4a, b), as well as atypical epithelial hyperplasia (especially atypical lobular hyperplasia) and carcinoma in situ (CIS).

Florid adenosis consists of enlarged or coalescent lobules of densely packed ductules and glands (Fig. 5.4c, d). The hyperplastic ductules are elongated, tortuous, and entwined. Transversely sectioned glands are round with patent lumens and tangentially or longitudinally sectioned glands are more elongated. The glands are lined by cuboidal to columnar epithelial cells. Mitoses are infrequent. "Adenosis tumor" and "nodular adenosis" refer to confluent areas of florid or sclerosing adenosis that form a mass. The mass may have cir-

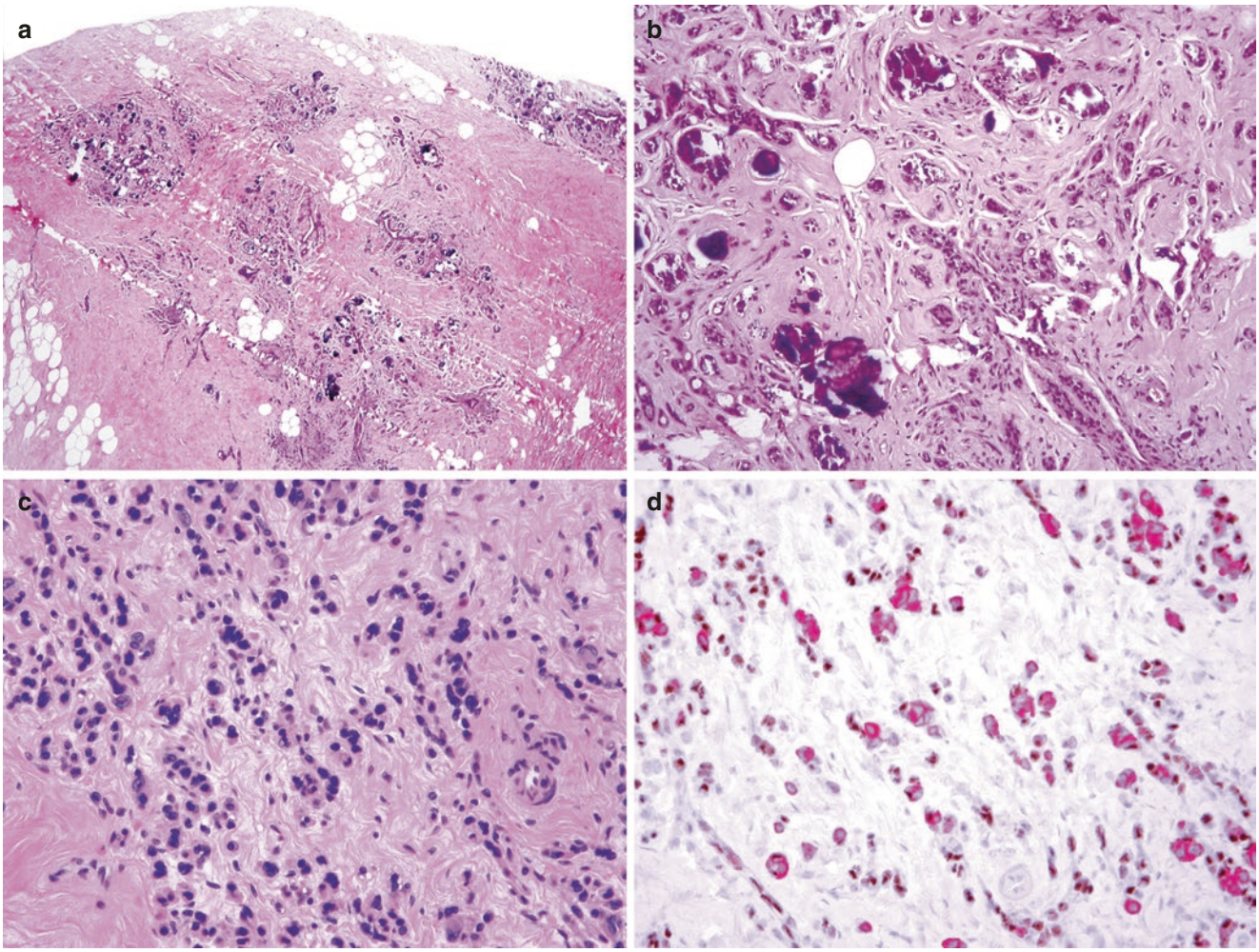

Fig. 5.2 Sclerosing adenosis with marked stromal sclerosis. Calcifications may be numerous (**a**, **b**). In some examples, myoepithelial cells predominate as cords of cells and single cells, mimicking invasive lobular carcinoma (**c**), as highlighted by this p63/keratin immunostain (**d**)

cumscribed or lobulated margins. On CNB, recognition of a well-demarcated border is helpful in determining the benign nature of particularly florid cases of adenosis.

Rare cases of florid or sclerosing adenosis have an infiltrative appearance. Sclerosing adenosis may contain benign glands that extend into adjacent adipose tissue, simulating stromal invasion, or that surround nerves or lie within the epineurium of nerve fibers. Taylor and Norris [11] and Davies [12] identified the phenomenon of perineural invasion in approximately 2–4% of their cases and showed that it was not associated with the development of invasive carcinoma. In a series of 10,000 breast consult cases, Gobbi et al. [13] found 13 cases of sclerosing adenosis (4 cases) and complex sclerosing lesions (9 cases) that were involved by florid usual hyperplasia, atypical ductal hyperplasia (ADH), or ductal carcinoma in situ (DCIS) and associated with perineural invasion. In these lesions, the glands involving nerves showed cytologic and architectural features of the adjacent usual or atypical hyperplasia. Additionally, Eusebi and Azzopardi [14] reported a small series of cases with infiltration of blood vessel walls by benign glands (Fig. 5.5).

Adenosis may be partially or completely involved by other pathologic entities, including typical and atypical apocrine change (see below for separate discussion of apocrine adenosis), atypical epithelial hyperplasia, and CIS [15–19]. Sclerosing adenosis involved by CIS warrants special attention for its ability to mimic invasive carcinoma. Lobular carcinoma in situ (LCIS) more commonly involves sclerosing adenosis than DCIS. LCIS involving adenosis may fill and expand glands with a solid proliferation of small uniform cells with eccentric nuclei and scant pale cytoplasm, or less commonly spread through the lesion in a pagetoid fashion [16] (Fig. 5.6). In contrast, DCIS involving adenosis is characterized by a solid or cribriform proliferation of more cohesive cells with increased cytologic atypia and necrosis [15, 17–19] (Figs. 5.7 and 5.8). The overall impression of CIS

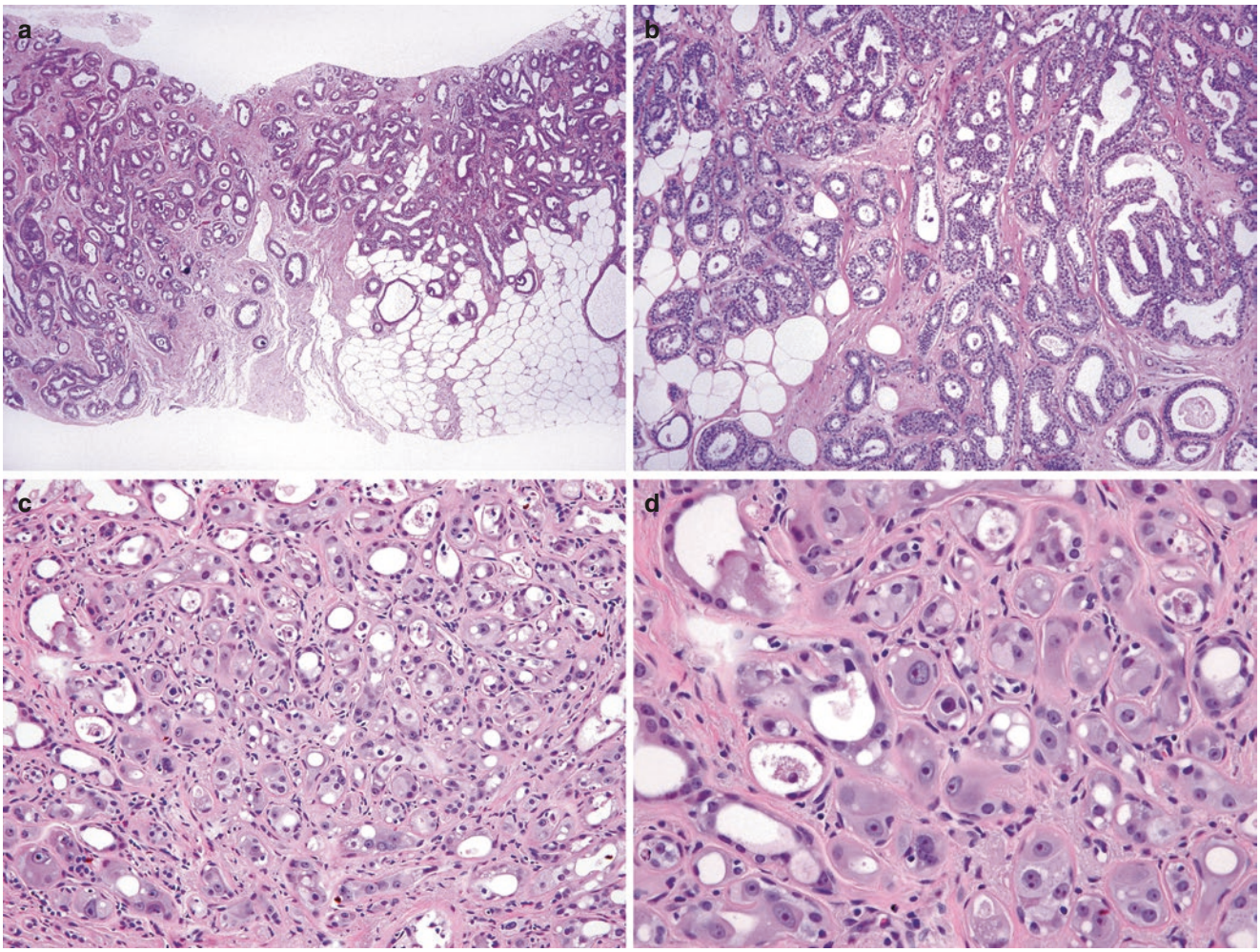

Fig. 5.3 Sclerosing adenosis involved by columnar cell change and focal ADH (**a**, **b**) and sclerosing adenosis involved by apocrine metaplasia (**c**, **d**). Apocrine adenosis has distinct cytologic features including abundant eosinophilic cytoplasm and large round/oval nuclei with prominent nucleoli (**d**)

within sclerosing adenosis is one of glands, nests, or cords of neoplastic epithelial cells in a fibrotic stroma—a diagnostic dilemma in some cases.

Differential Diagnosis

Invasive carcinoma of tubular, lobular, or ductal types is the primary consideration in the differential diagnosis of sclerosing adenosis and its histopathologic variants. It must be emphasized that the key to the diagnosis of sclerosing adenosis is recognition of the lobulocentric pattern at low magnification. This approach may be limited by a small or fragmented sample on CNB. If this pattern cannot be appreciated, immunohistochemistry (IHC) should be employed to confirm the presence of myoepithelial cells in sclerosing adenosis and definitively distinguish it from invasive carcinoma.

Sclerosing adenosis with less sclerosis and retention of glandular tubules—especially those examples with extension into adipose tissue or perineural invasion—is a well-known mimic of tubular carcinoma and well-differentiated invasive ductal carcinoma. Because tubular carcinoma is composed almost exclusively of well-formed glands with bland cytology, it is in the differential diagnosis of most types of adenosis and sclerosing lesions. It is characterized by a haphazard proliferation of tubules with sharply angulated contours, tapering ends, and open lumens, which stands in contrast to the lobulocentric proliferation of rounded and compressed tubules of adenosis. The surrounding stroma is typically desmoplastic rather than fibrotic or hyalinized. At high magnification, the tubules consist solely of columnar epithelial cells with apical snouts and little epithelial attenuation. Tubular carcinoma lacks a basal lamina by ultrastructural studies and Periodic acid–Schiff (PAS) staining, and myoepithelial cells by IHC, in contrast to retention of these

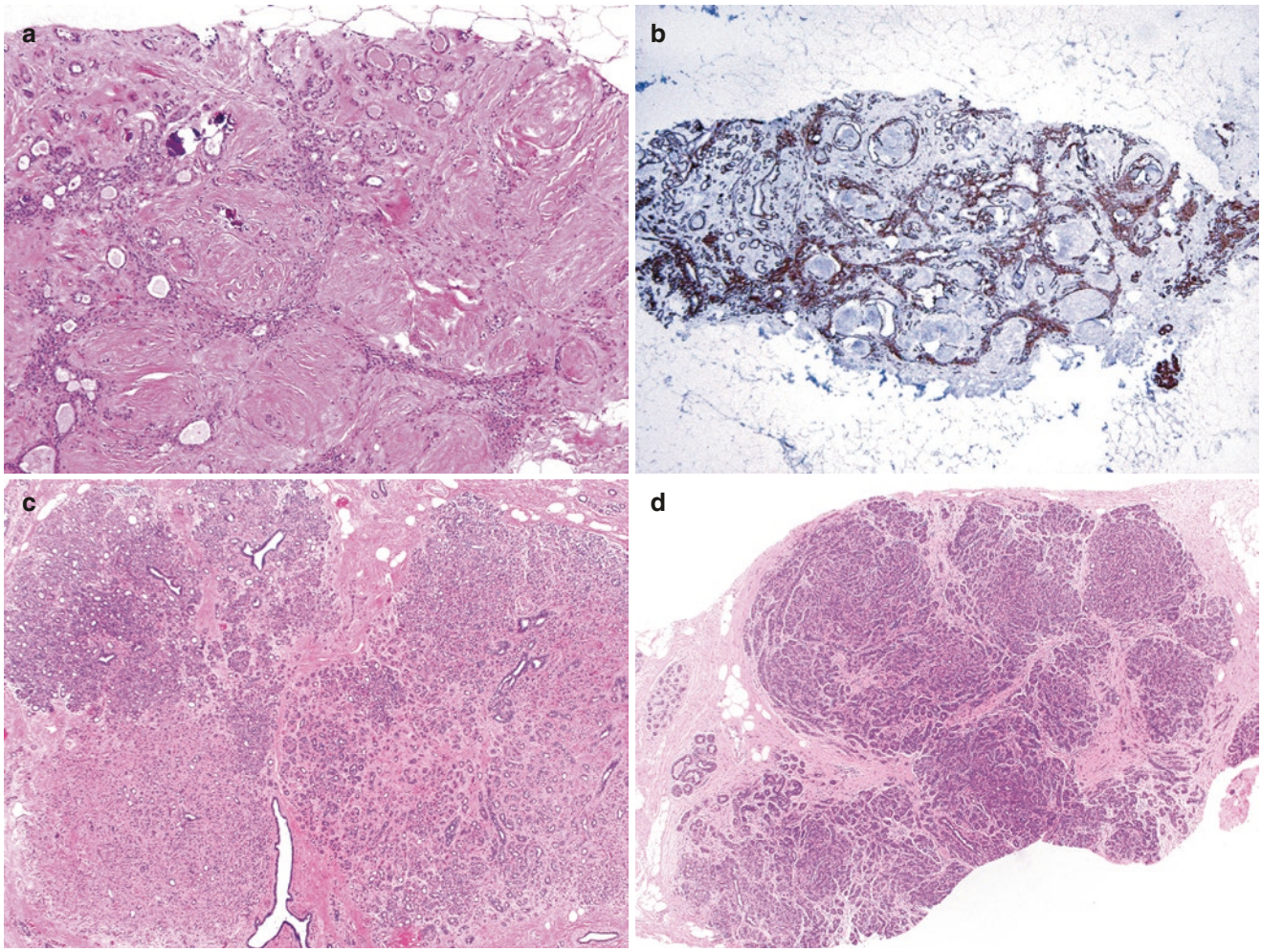

Fig. 5.4 Sclerosing adenosis involving a fibroadenoma (**a**, **b**). A SMM stain highlights the myoepithelial cell layer in this lesion (**b**). Nodular sclerosing adenosis (**c**, **d**)

elements in sclerosing adenosis [20–22]. Sclerosing adenosis with marked sclerosis and glandular atrophy simulates invasive lobular carcinoma with classic morphology (Fig. 5.2c, d) or variant tubulolobular morphology. In these cases, most of the glands are reduced to myoepithelial cells arranged as cords and single cells and their lobulocentric distribution is distorted by the expanded stroma. Invasive lobular carcinoma, in contrast, is usually a more cellular and infiltrative lesion composed of cells with a more prominent epithelioid morphology. However, it tends to form scattered foci of more dispersed cells, and it is this pattern that most resembles sclerosing adenosis. Invasive lobular carcinoma may show focal formation of small tubules, which could further complicate this distinction.

Perhaps one of the greatest diagnostic pitfalls is confusing adenosis involved by CIS with an invasive ductal carcinoma growing in a predominantly nested pattern. We recently reported that misinterpretation of DCIS involving sclerosing adenosis as invasive ductal carcinoma was responsible for 3 of 14 major diagnostic changes (2 patients, 3 cases) in a study of revised pathology reports specific to breast pathology over a 5-year period at our institution [23]. Both cases were especially challenging. One case was a quite florid example of adenosis involved by high nuclear grade apocrine DCIS for which the lobulocentric configuration could not be fully appreciated on CNB. Another case was a CNB of a particularly infiltrative example of sclerosing adenosis and an associated sclerosing lesion partially involved by intermediate nuclear grade DCIS. Atypical glands and nests of tumor cells were present in a haphazard distribution, including freely permeating adipose tissue, which defied recognition of a lobulocentric pattern in the limited sample (Fig. 5.7). In general, it is difficult to distinguish sclerosing adenosis involved by CIS from invasive carcinoma due to the pattern of glands, nests, or cords of neoplastic epithelial cells in a fibrotic stroma. Features that favor sclerosing adenosis involved by CIS include lobular configuration, at least focally identifiable myoepithelial cells on H&E-stained sec-

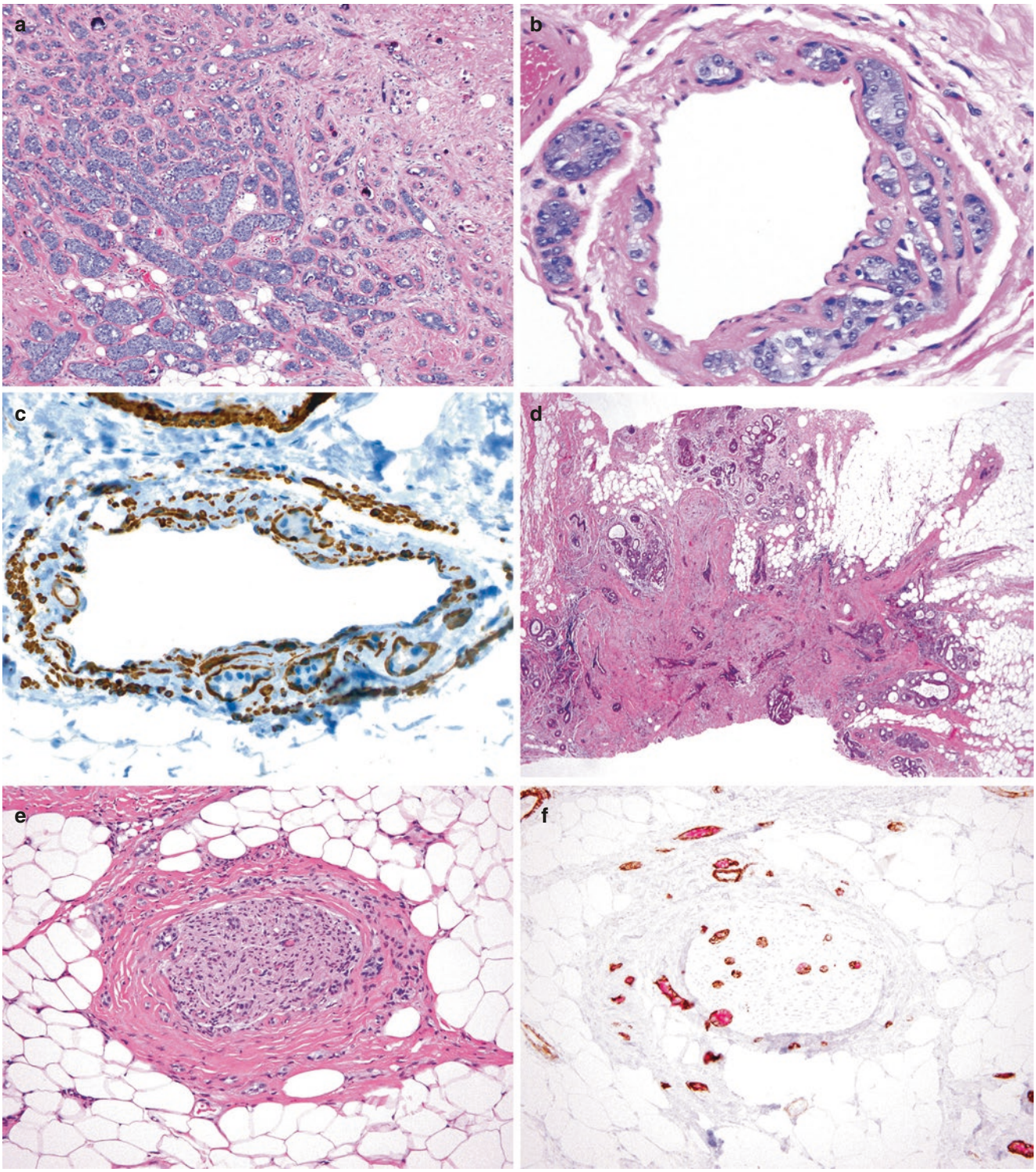

Fig. 5.5 Sclerosing lesions with neural and vascular infiltration. Sclerosing adenosis involved by DCIS infiltrates the wall of a lymphatic vessel (**a**–**c**). SMM confirms the presence of myoepithelial cells in this lesion (**c**). A benign sclerosing lesion shows perineural invasion (**d**–**f**). A multiplex immunostain with SMM (brown) confirms the presence of myoepithelial cells in this lesion (**f**)

tions, hyaline basement membrane surrounding tumor cell nests, uninvolved sclerosing adenosis in neighboring tissue, and separate foci of CIS [23, 24]. It is helpful to maintain a low threshold for the consideration of CIS involving sclerosing adenosis prior to making a diagnosis of invasive carcinoma on CNB.

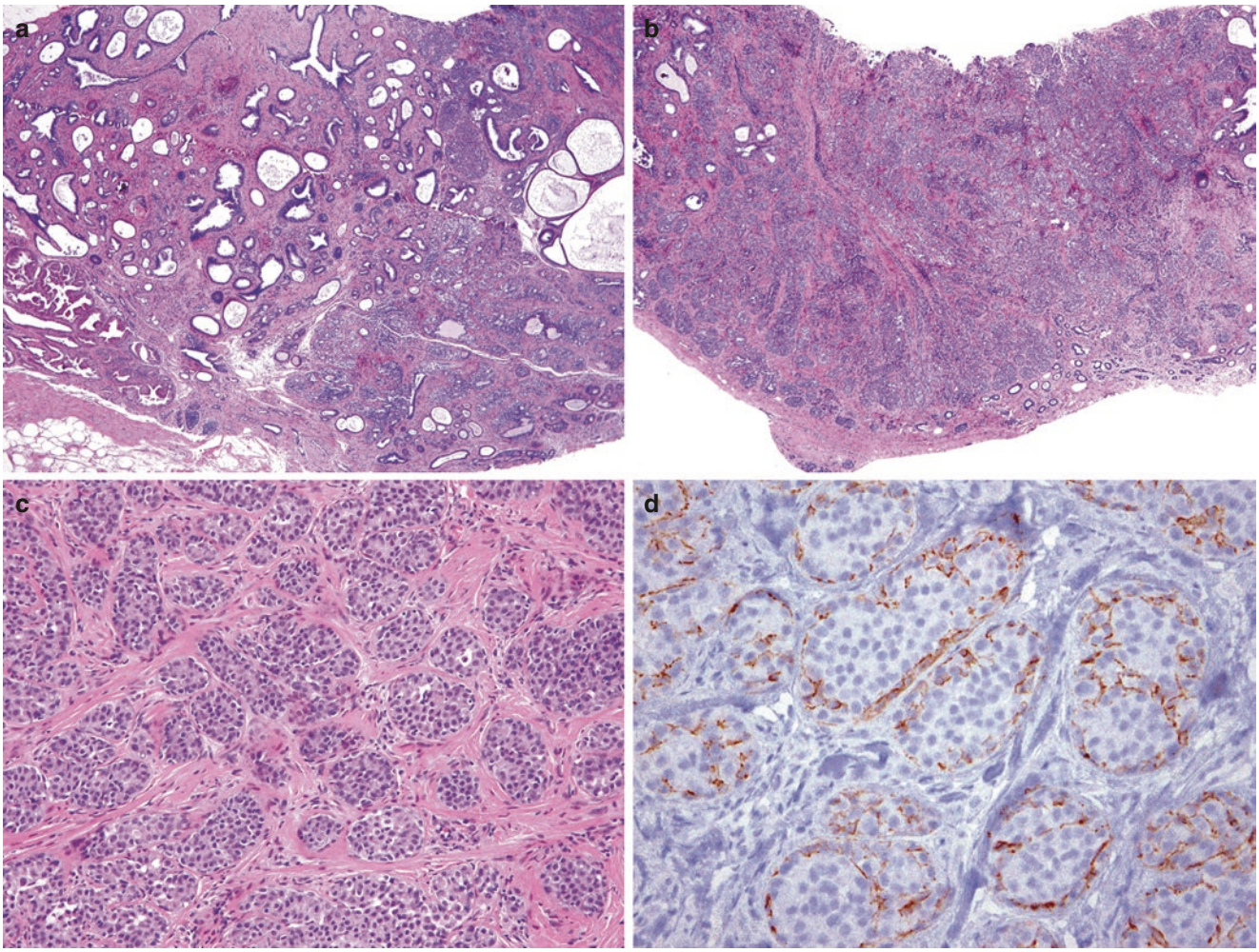

Fig. 5.6 Florid adenosis involved by apocrine metaplasia, columnar cell change, and lobular carcinoma in situ (**a**–**d**). In this case, LCIS involving adenosis simulates an invasive carcinoma with a nested growth pattern (**b**, **c**). Loss of membranous staining for E-cadherin supports lobular morphology (**d**)

Immunohistochemical Workup

Immunohistochemical studies to confirm the presence of the myoepithelial cell layer are useful for cases of sclerosing adenosis that cannot be easily distinguished from invasive carcinoma on routine histology. Although numerous myoepithelial markers are available (p63, smooth muscle myosin heavy chain (SMM), calponin, smooth muscle actin (SMA), S100 protein, CD10, and basal cytokeratins, et cetera), they differ in their sensitivity, specificity, and ease of interpretation, which may be attributed in part to the variable immunoreactivity of these markers in stromal cells, vessels, luminal epithelial cells, and tumor cells. The myoepithelial markers with the best combination of sensitivity and specificity are p63 (nuclear staining) and SMM (cytoplasmic staining). An immunostain for p63 is easy to interpret due to its nuclear staining pattern and its lack of immunoreactivity in myofibroblasts and blood vessels. An immunostain for SMM is preferable to those for other contractile proteins, calponin and SMA, because it shows only limited staining of myofibroblasts (Fig. 5.7i). All three of these markers stain blood vessels [25, 26]. It is often best to use immunostains for p63 and SMM, or one of the other markers, in a complementary approach. In addition, it is useful to note that sclerosing adenosis and other sclerosing lesions may be distinguished from invasive carcinoma by the pattern of expression of estrogen receptor (ER). Sclerosing adenosis typically shows heterogeneous immunoreactivity in contrast to the strong diffuse pattern of staining in well-differentiated invasive carcinomas.

Pathogenesis

Although the exact etiology and pathogenesis remain unknown, it is hypothesized that estrogen-stimulated prolif-

eration plays a role in the development of sclerosing adenosis and other types of proliferative fibrocystic change. Epidemiologic studies have shown that proliferative fibrocystic change, including sclerosing adenosis, is more common in reproductive age, parous, and obese women and those receiving hormone replacement therapy [4]. Shoker

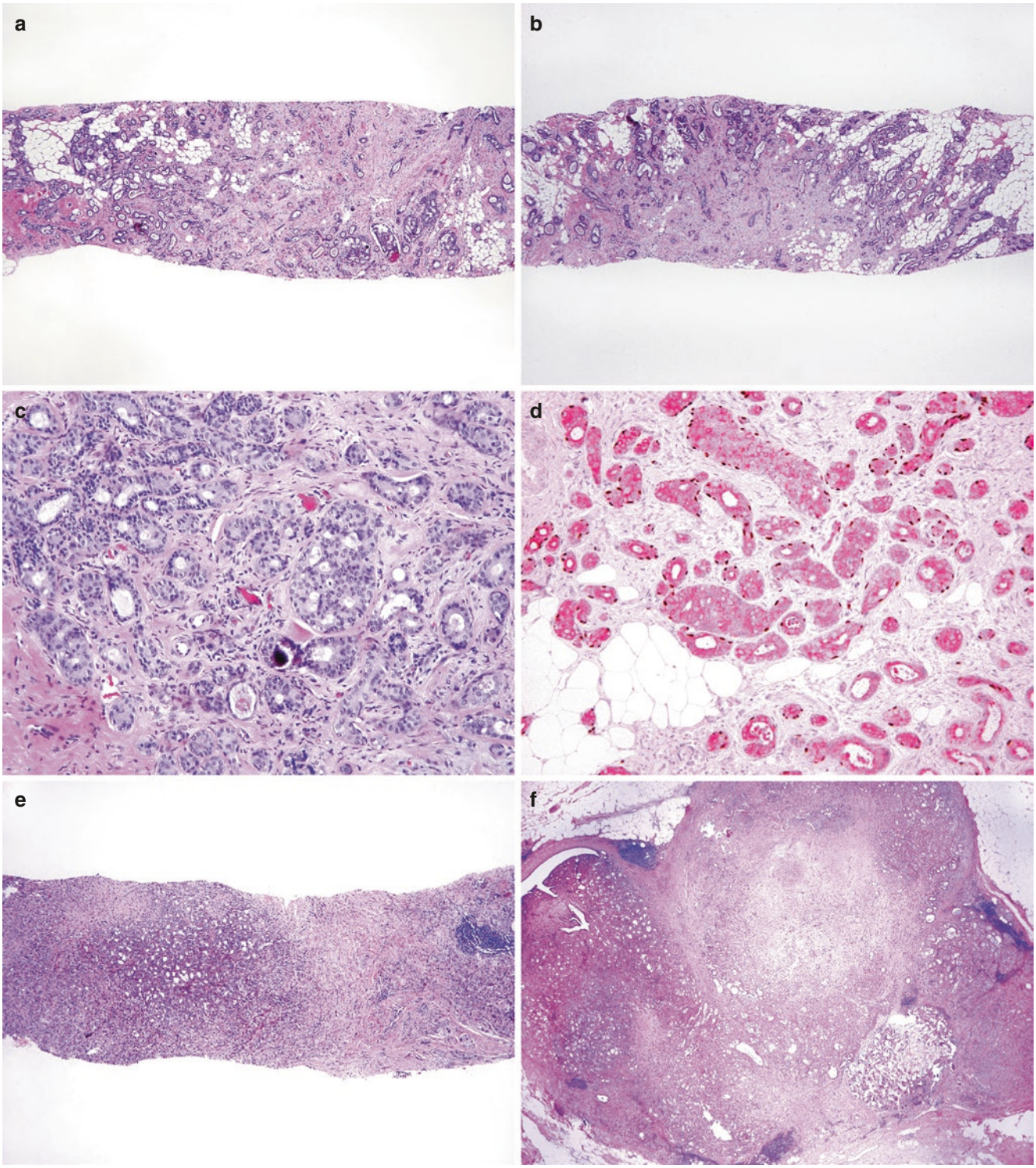

Fig. 5.7 Two cases of DCIS involving adenosis that mimicked invasive ductal carcinoma on core biopsy. One case is characterized by an atypical small glandular proliferation with an infiltrative appearance (**a**–**d**), whereas the other represents a nodular and florid proliferation for which the circumscribed margin is only apparent on excision (**e**–**h**). A myoepithelial cell layer is confirmed in both lesions by a p63/keratin dual stain (**d**) and a SMM/keratin dual stain (**h**). SMA is not as useful in distinguishing DCIS involving adenosis from invasive tubular carcinoma (**i**) due to high background staining of myofibroblasts

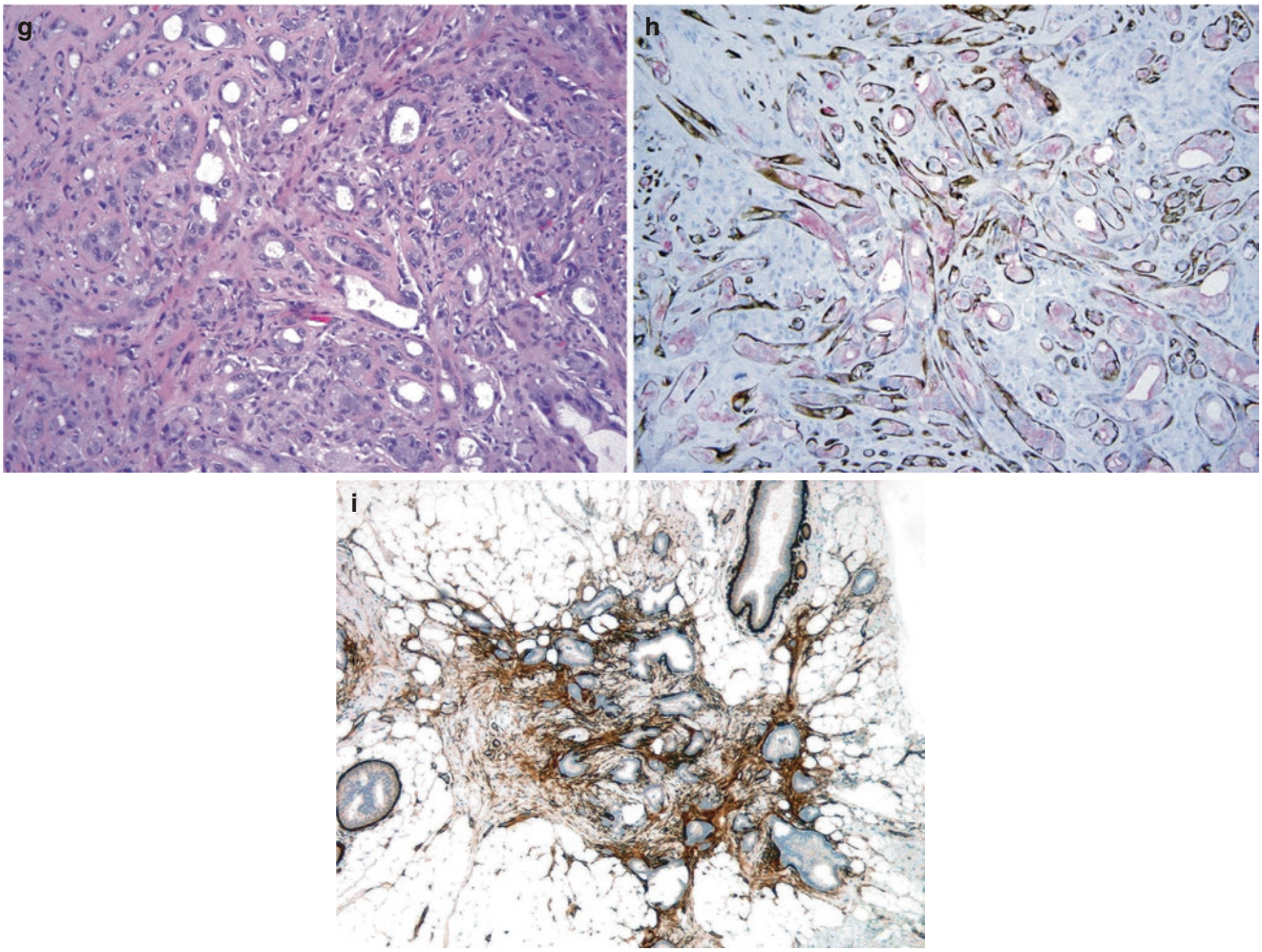

Fig. 5.7 (continued)

et al. [27] demonstrated increased ER expression and Ki-67 proliferation index in sclerosing adenosis, radial scars, papillomas, and fibroepithelial lesions, suggesting ER dysregulation in these lesions. These authors suggested that the degree of dysregulation correlates with the risk of developing breast cancer.

Clinical Management and Prognosis

A diagnosis of sclerosing adenosis on CNB is safely managed by observation if it is concordant with the radiologic findings and if it is not associated with another lesion requiring excision. Gill et al. [6] showed that sclerosing adenosis provided sufficient correlation for clustered microcalcifications and well-circumscribed or indistinctly marginated masses on CNB. Sclerosing adenosis was accurately sampled in all but one case with adequate follow-up. In retrospect, on CNB of the only spiculated mass, a radial sclerosing lesion was present in association with sclerosing adenosis, and on excision, this lesion was involved by several small foci of invasive carcinoma with tubular and lobular features. This study highlights the point that a diagnosis of sclerosing adenosis should not be accepted as concordant for spiculated masses. Although spiculated masses sometimes represent sclerosing adenosis, the radiologic differential diagnosis includes several benign and malignant entities, including post-surgical scar, radial sclerosing lesion, and invasive carcinoma. These entities cannot reliably be distinguished by radiologic features alone [28]. Moreover, radial sclerosing lesions commonly coexist with sclerosing adenosis and their recognition at CNB may be difficult if the overall architecture is not apparent. It is important to recognize these lesions as a nontrivial number of cases are associated with in situ or invasive carcinoma [29]. Surgical excision is generally recommended for spiculated masses.

Multiple studies have demonstrated that sclerosing adenosis is associated with a modestly increased risk of breast cancer. Jensen et al. [30] found that sclerosing adenosis is an independent risk factor for breast cancer, and the relative

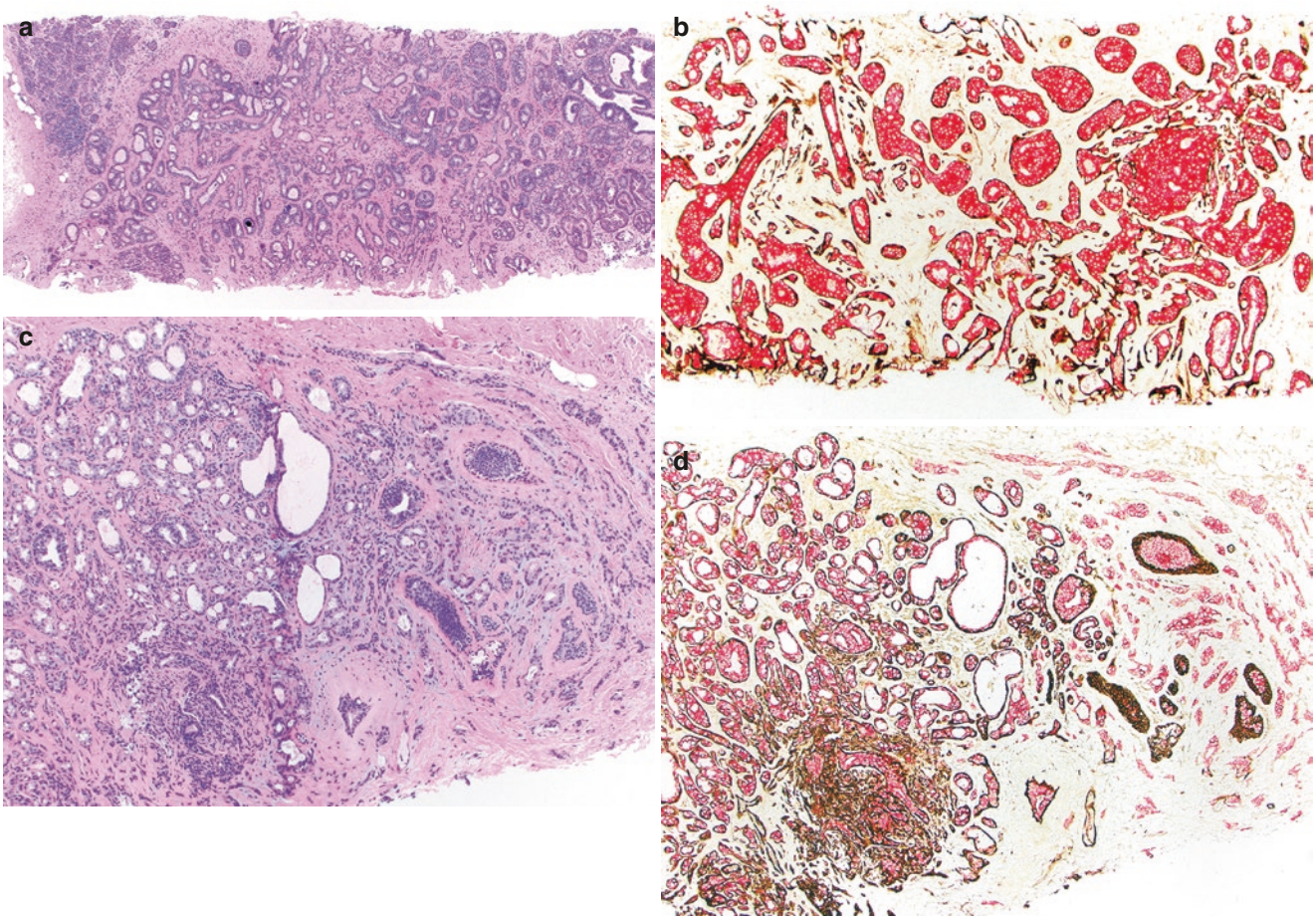

Fig. 5.8 Challenging core biopsy with extensive sclerosing adenosis involved by DCIS (**a**–**d**) and a small focus of invasion (**c**, **d**). Dual staining for SMM and keratin highlights the myoepithelial cell layer throughout the adenosis (**b**, **d**) as well as confirms its absence in the small invasive focus (**d**)

risk was approximately 1.7, in a study of 547 cases of sclerosing adenosis with long-term follow-up identified from over 10,000 benign breast biopsies from the Nashville Breast Cohort. More recently, Visscher et al. [4] investigated the risk of breast cancer in women diagnosed with sclerosing adenosis who had been followed long term as part of the Mayo Benign Breast Disease Cohort. Breast cancer risk was assessed using standardized incidence ratios (SIRs) relative to the Iowa Surveillance, Epidemiology, and End Results (SEER) registry. Sclerosing adenosis was present in 3733 women (27.8%) out of a cohort of over 13,000 women followed for a median of 15.7 years. Across the entire cohort, women with sclerosing adenosis had a higher risk of developing breast cancer (SIR 2.10, 95% confidence interval [CI] 1.91–2.30) than those without it (SIR 1.52, 95% CI 1.42–1.63). In general, sclerosing adenosis is associated with a 1.5–2-fold increased risk of breast cancer and should be classified with other types of proliferative breast disease without atypia showing similar risk [31, 32].

Apocrine Adenosis

"Apocrine adenosis," apocrine metaplasia of the epithelium comprising sclerosing adenosis, is present in 3% of benign breast biopsies [33]. Apocrine adenosis occurs in an older population than sclerosing adenosis, with an average age of almost 60 years at diagnosis [33–35]. Apocrine adenosis and atypical apocrine adenosis belong to a spectrum of apocrine lesions of the breast, ranging from benign apocrine change to apocrine CIS to invasive carcinoma with apocrine features. Apocrine cytologic features include cellular enlargement, abundant eosinophilic granular cytoplasm, round central nuclei, and prominent nucleoli (Fig. 5.3c, d). Atypical apocrine adenosis is generally diagnosed in the presence of greater than threefold variation in nuclear size (1.73-fold increase in nuclear diameter) and nucleolar enlargement [36]. Because cells with apocrine features are enlarged, nuclear enlargement must be assessed using cells with normal apocrine cytology as a reference point. Mitoses are rare and necrosis is absent in these lesions [34].

The differential diagnosis of atypical apocrine adenosis includes apocrine DCIS and invasive ductal carcinoma with apocrine features. The distinction between atypical apocrine adenosis and apocrine DCIS involving sclerosing adenosis can be extremely difficult. Although no consensus criteria exist, features suggestive of apocrine DCIS include considerable cytologic atypia, characteristic patterns of architectural atypia, necrosis, and greater extent of the lesion [37, 38]. As noted for sclerosing adenosis involved by other atypical lesions, it is also possible to confuse atypical apocrine adenosis for invasive carcinoma, especially in particularly florid or sclerotic cases without an obvious lobulocentric pattern of growth (Fig. 5.7e–h). In a study of the reproducibility of diagnoses in breast biopsies, 4 of 12 pathologists rendered a diagnosis of invasive carcinoma in a case of apocrine adenosis [39].

Immunohistochemical studies show that apocrine lesions of the breast are characterized by lack of expression of estrogen and progesterone receptors in addition to expression of androgen receptor and gross cystic disease fluid protein-15 (GCDFP-15) [40]. Some cases of apocrine metaplasia and apocrine adenosis exhibit abnormal oncoprotein and apoptosis-related protein expression and a higher proliferation rate. By IHC, apocrine adenosis shows expression of human epidermal growth factor 2 (HER2) in over 50% of cases [41–43]; however, it is not accompanied by gene amplification on fluorescence in situ hybridization [42]. In one study, Selim et al. [41] detected membranous HER2 expression of variable intensity in 55.6% of apocrine adenosis cases and 10.9% of apocrine metaplasia cases as well as nuclear p53 expression in 27.8% of apocrine adenosis cases and 1.6% of apocrine metaplasia cases. All cases of apocrine adenosis and apocrine metaplasia were positive for the oncoprotein c-Myc and negative for the anti-apoptotic protein BCL2. The Ki-67 proliferation index was higher in apocrine adenosis (3.6%) than in apocrine metaplasia (1.3%) and normal breast epithelium (0.9%). The authors hypothesized that cases of apocrine adenosis with these molecular changes may represent precursor lesions to in situ and invasive apocrine carcinomas. An important implication of this study is that the expression of HER2 or p53 by IHC cannot distinguish atypical apocrine adenosis from apocrine DCIS, although studies have not directly compared markers in these two entities.

Much less data is available to inform the clinical management of atypical apocrine adenosis compared to other atypical breast lesions. In the largest study to date on atypical apocrine adenosis diagnosed on CNB, Chang Sen et al. [44] found that 4 of 20 (20%) surgically excised cases were upgraded to malignancy, including three with DCIS and one with invasive carcinoma. All four malignancies were masses on ultrasound, while three of them were associated with calcifications. In contrast, in other recent studies by Calhoun and Booth [33] and Hou et al. [45], there were no upgrades to DCIS or invasive carcinoma on surgical excision of apocrine adenosis and atypical apocrine adenosis without coexisting atypical hyperplasia or carcinoma in 7 and 10 cases, respectively. The findings raise the possibility that atypical apocrine adenosis diagnosed on CNB may not require surgical excision. However, given the limited data, as well as the difficulty in morphologically and immunohistochemically distinguishing atypical apocrine adenosis from apocrine DCIS, it would be prudent to carefully consider surgical excision of most cases of atypical apocrine adenosis on CNB. A diagnosis of non-atypical apocrine adenosis on CNB does not require further intervention.

The few long-term follow-up studies regarding the risk of breast cancer associated with atypical apocrine adenosis show conflicting results. In a series of 51 cases of atypical apocrine adenosis by Carter and Rosen [46], none of the patients developed carcinoma after an average follow-up period of approximately 3 years. Likewise, Fuehrer et al. [34] showed that the rate of breast cancer diagnosis in patients with atypical apocrine adenosis (8.1%) after an average follow-up period of 14 years did not significantly differ from that of the remainder in the Mayo Benign Breast Disease cohort (7.8%). In contrast, Seidman et al. [35] found that 4 of 37 patients diagnosed with atypical apocrine adenosis at the Armed Forces Institute of Pathology developed breast cancer after a mean follow-up of 8.7 years. This study demonstrated an overall risk of 5.5 relative to the reference population from the SEER registry, a relative risk similar to that of other atypical lesions of the breast. The authors suggested that atypical apocrine adenosis is associated with an increased risk of breast cancer, either because it is a true atypical proliferation of apocrine-type epithelium, or because some cases represent apocrine DCIS involving sclerosing adenosis with insufficient architectural features to make this diagnosis.

Radial Scars and Complex Sclerosing Lesions

Overview

Radial scars are benign lesions characterized by a central fibroelastotic core surrounded by radiating ducts and lobules with cysts and proliferative changes. In 1928, Semb [47] provided the first description of this lesion, referring to it as "rosette like lesion" and "proliferative centre." Subsequently, radial scars have been reported by several different authors using several different terms, including sclerosing papillary proliferation [48], benign sclerosing ductal proliferation [49], nonencapsulated sclerosing lesions [50], infiltrating epitheliosis [51], and indurative mastopathy [52], amongst others. In 1975, Hamperl [53] named this same entity in German as "strahlige narben," which was translated into "radial scar."

Some authors have recommended use of the term "radial scar" for lesions measuring up to 1 cm and "complex sclerosing lesion" for larger lesions [54]. Others reserve the term "complex sclerosing lesion" for lesions composed of several closely contiguous fibroelastotic areas or lesions with a less organized appearance [55]. Both terms are recommended in the most recent World Health Organization Classification of Breast Tumours [56].

As with the other small glandular proliferations in this chapter, it is well known that radial scar/complex sclerosing lesions (RS/CSLs) mimic invasive carcinoma on both radiologic and pathologic examination. Several early authors even hypothesized that these lesions represented direct precursors to breast cancer, noting "transitional features" of tubular carcinoma [57], and referring to them as "incipient tubular carcinomas" [50]. Although RS/CSLs are regarded as benign, a small proportion of lesions are associated with in situ and invasive carcinoma, posing a number of diagnostic and clinical management challenges.

Clinical, Radiologic, and Gross Features

The incidence of radial scar is 3–9 per 1000 mammograms in the screened population [58, 59]. Studies of population-based large cohorts such as the Mayo Benign Breast Disease cohort, the Nurses' Health Study, and the Nashville cohort report incidences of radial scars in benign breast biopsies in the range of 5–10% [60–62]. Radial scars most frequently occur in women between 40 and 60 years of age [60–62]. An association with menopausal status, parity, or contraceptive use has not been identified [60]. Radial scars are often incidental microscopic findings; however, larger lesions are clinically detected on screening mammography. Radial scars form palpable and freely mobile masses in a minority of cases. Multicentric and bilateral lesions are common.

Radial scars are well-known mimics of invasive carcinoma on mammography. Radial scars may appear as stellate densities, spiculated masses, or architectural distortions. Rare cases present as isolated microcalcifications. Taber and Dean [63] proposed criteria to favor an interpretation of radial scars over invasive carcinoma based on certain mammographic features. According to these authors, radial scars are characterized by a radiolucent central core, long and thin radiating spicules, radiolucent projections parallel to the spicules, varying appearances in different projections, and an absence of a palpable mass or skin changes. In contrast, invasive carcinoma typically has a dense central zone and short spicules.

Several studies have shown that these features are not specific for radial scars. In a retrospective review of 255 stellate lesions, Mitnick et al. [64] concluded that the criteria of Tabar and Dean could not reliably distinguish radial scars and invasive carcinomas. Of 73 nonpalpable carcinomas, 14 (19%) had features attributed to radial scars, including radiolucent centers and radiating elongated spicules. Conversely, 4 (44%) of 9 radial scars had a dense central region. In this study, microcalcifications constituted the only mammographic finding capable of differentiating between the lesions with overlapping features, more common in invasive carcinomas (9 of 14 cases) than radial scars (1 of 4 cases). Subsequent studies by Hassell et al. [65] and Boute et al. [66] found that radial scars only displayed all of the classic criteria in 71.6% (48 of 67) and 48% (54 of 133) cases, respectively. Contrary to the study by Mitnick et al. [67], both studies identified microcalcifications in approximately half of the lesions, arguing against microcalcifications as a discriminating feature.

On ultrasound, a radial scar most often appears as an irregular hypoechoic mass with ill-defined borders and posterior acoustic shadowing. Parenchymal distortion may be seen in the absence of a mass. It has been claimed that an echogenic halo, peripheral cysts, and complex echotexture represent other features more commonly seen with radial scars than invasive carcinomas [66]. However, there is a significant overlap in the appearance of radial scar and invasive carcinoma on this imaging modality as well.

Most radial scars cannot be identified on gross examination. If the radial scar is large enough to be appreciated grossly, usually greater than 1 cm, it appears as a stellate mass, quite similar in appearance to invasive carcinoma. It is a firm lesion with central puckering and an irregular edge that infiltrates into the surrounding fatty breast tissue. Creamy white or yellow streaks of elastosis emanate from a pale gray central core. Dilated cysts may be visible at the periphery of the lesion. Some radial scars appear as vague masses without distinct features.

Microscopic Features

A radial scar features a central zone of sclerosis and elastosis with radiating ducts and lobules (Fig. 5.9), giving it a stellate appearance on low magnification. Obliterated ducts and smaller angulated glands are entrapped within the fibroelastotic stroma of the central zone. The entrapped glands are lined by one or more inner layers of benign epithelium and an outer layer of inconspicuous myoepithelium. The epithelium may appear separated from the underlying myoepithelium and stroma in some areas as a result of retraction artifact. It is important to note that myoepithelial cells may be reduced in numbers or absent at the periphery of some entrapped glands due to plane of sectioning. The entrapped glands are invested in a paucicellular stroma with a mixture of bright pink hyalinized collagenous tissue and pale pink or pale blue elastosis. Ducts and lobules radiate from the scle-

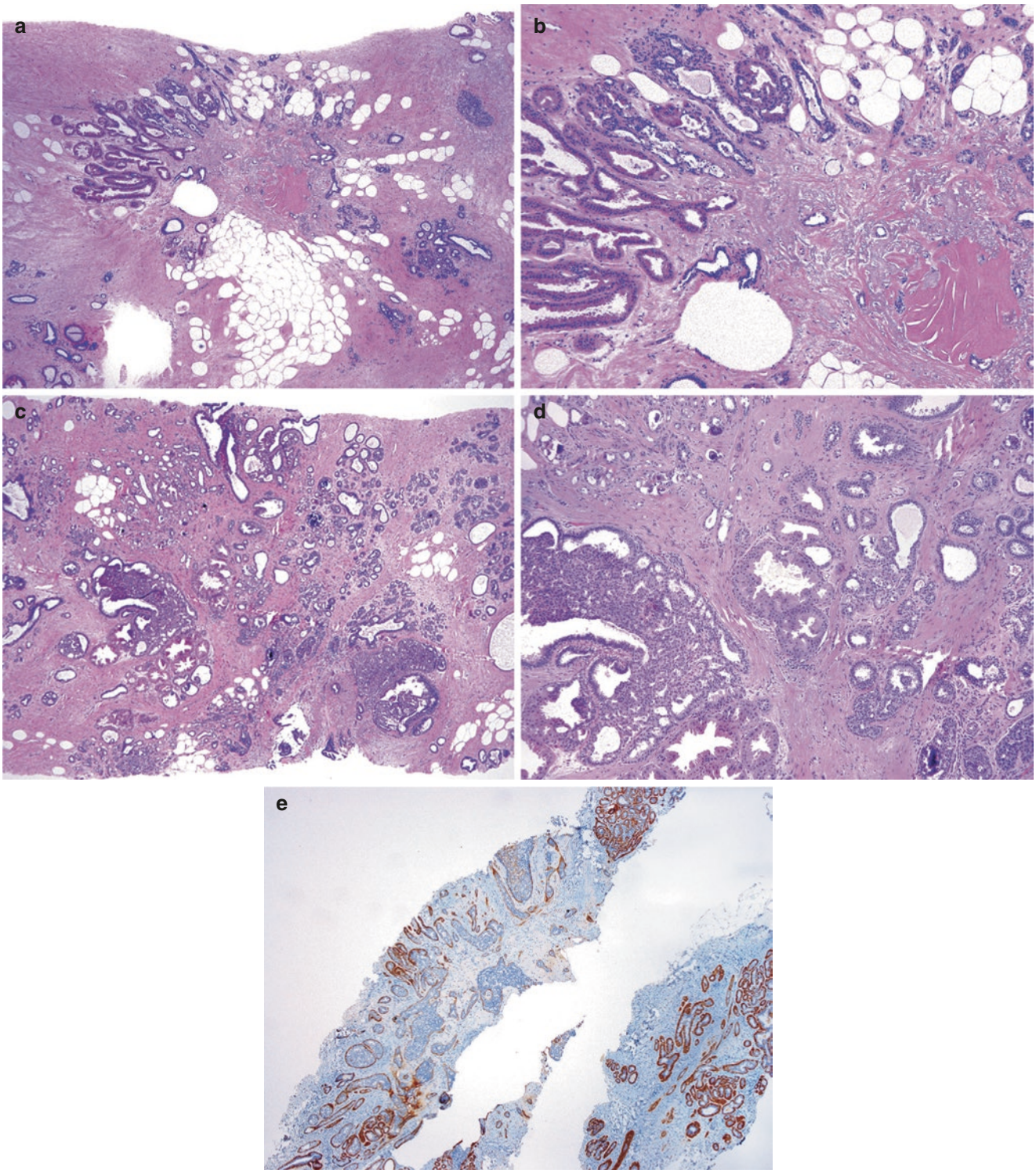

Fig. 5.9 Radial scar and complex sclerosing lesions. Radial scars may be discrete lesions with a single central sclerotic focus and radiating epithelial elements (**a**, **b**), possibly removed in large part by the biopsy. CSLs may have a more disorganized architecture with multiple sclerotic foci, often involved by various types of fibrocystic change (**c**, **d**). Myoepithelial markers aid in the distinction from invasive carcinoma, but must be interpreted with caution. For lesions that mimic invasive carcinoma, it is best to perform immunohistochemistry for multiple myoepithelial cell markers, as a sclerosing lesion with attenuated staining may be confused for invasive carcinoma (SMM, **e**)

rotic center along with interdigitating bands of fibrous tissue and interspersed adipose tissue and appear to expand in a centrifugal manner. The ducts and lobules are involved by cysts, apocrine metaplasia, and proliferative changes, such as sclerosing adenosis, usual and atypical epithelial hyperplasia, and papillomatosis (Fig. 5.9). Calcifications are often associated with the lesion. As with sclerosing adenosis, a minority of sclerosing lesions may demonstrate perineural invasion by benign ducts (Fig. 5.5d–f) [11, 13]. Complex sclerosing lesions (CSLs) are characterized by the same elements—fibroelastotic core(s), entrapped glands, and ducts and lobules with fibrocystic changes (Figs. 5.10, 5.11, and 5.12). However, some authors would use this designation if the lesion is larger and does not have the radial configuration of a radial scar [55]. CSLs with intraductal papillomatosis show considerable overlap in histologic features with sclerosing intraductal papillomas and the classification of lesion may be best performed based on the predominant finding (Fig. 5.13).

Radial scars may be involved by CIS and invasive carcinoma as evidenced by the numerous studies on the incidence of upgrade to malignancy on surgical excision of these lesions. LCIS and DCIS tend to involve the peripheral ducts and lobules with characteristic patterns of growth and cytomorphologies. However, it is possible for CIS to extend into the distorted glands of the fibroelastotic core, and in these instances the lesion bears resemblance to invasive carcinoma. Low to intermediate nuclear grade DCIS is most common. Invasive carcinoma is typically ductal or tubular in histology, well to moderately differentiated, small (less than 2 cm), and limited to the periphery of the lesion [29].

Metaplastic carcinomas, including low-grade adenosquamous carcinomas (LGASC) and spindle cell carcinomas, may also arise in association with complex sclerosing lesions and sclerosing papillomas [68, 69] (Fig. 5.14). Such tumors may be related to adenosquamous proliferation (ASP) of the breast, which is recognized by some pathologists as a common finding in sclerosing breast lesions and a hallmark of

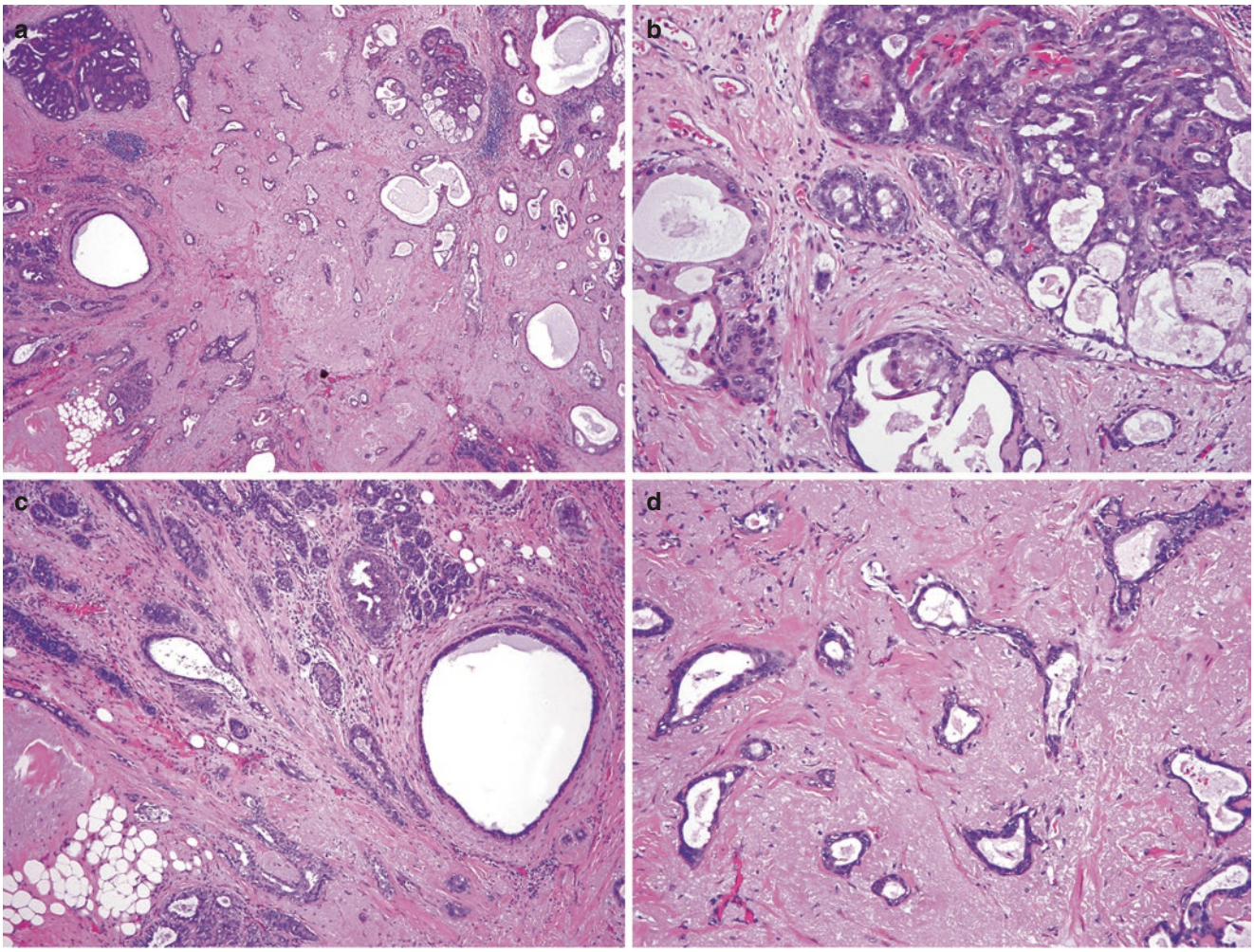

Fig. 5.10 Complex sclerosing lesion (**a**) with cysts, papillomas, and metaplastic or hyperplastic epithelial elements (**b**, **c**) radiating from a central fibroelastotic core with entrapped glands (**d**)

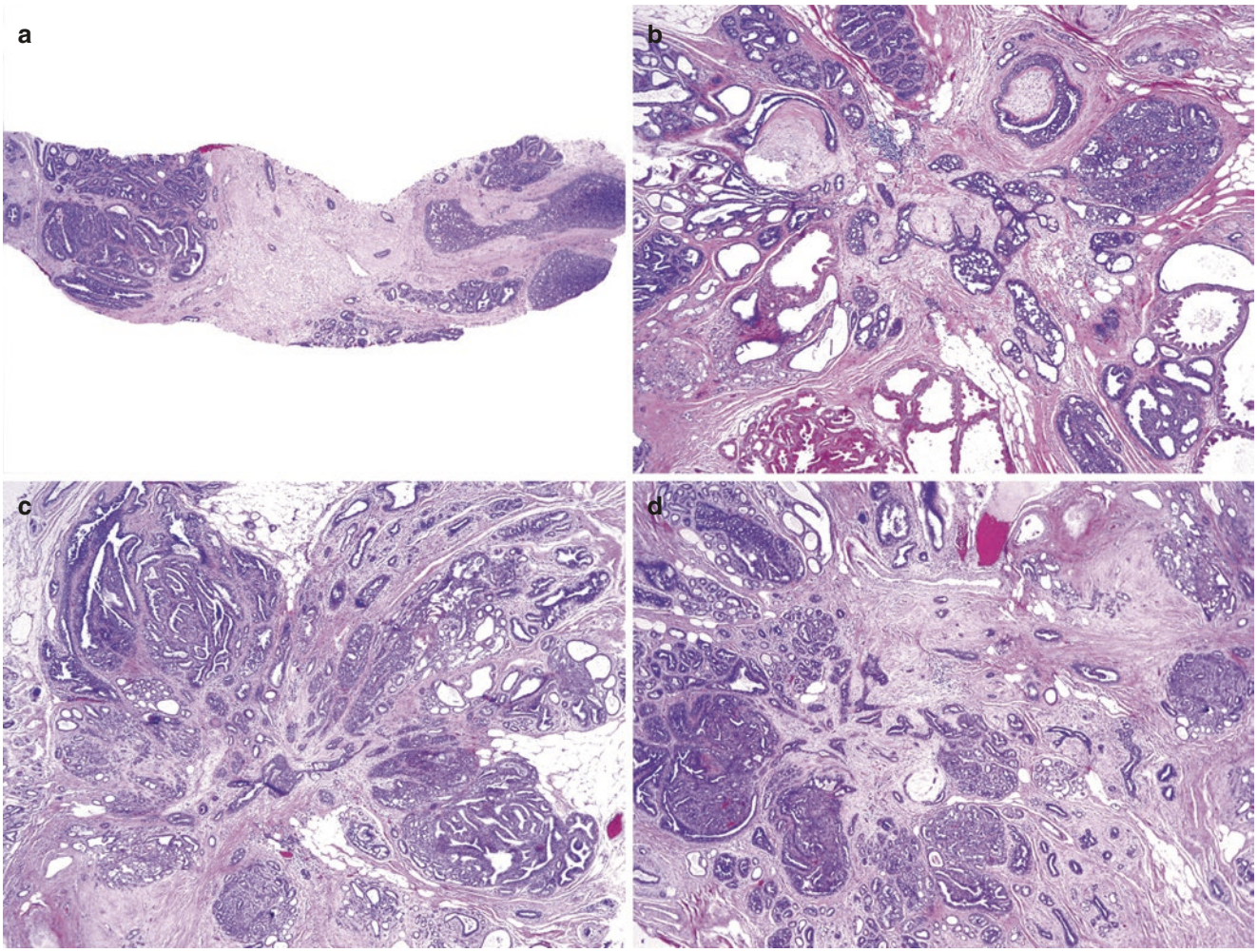

Fig. 5.11 Complex sclerosing lesion with both central and peripheral elements on core biopsy (**a**). Subsequent excision showed multiple large CSLs with papillomas, hyperplasia, and cysts (**b–d**)

these lesions. ASP consists of compact ducts with both glandular and squamous features within spindle cell stroma in the nidus of the lesion. It is similar in appearance and immunophenotype to LGASC, but limited in extent and lacking infiltration into the surrounding breast tissue [70, 71].

Infiltrating epitheliosis, a controversial entity, is considered by most pathologists to represent a RS/CSL involved by florid usual ductal hyperplasia (UDH) ("epitheliosis"). Other pathologists have argued that it should be classified as a separate entity due to its distinctive histologic features, including (1) a florid epithelial proliferation comprising the bulk of the lesion, involving ducts with jagged edges, and "flowing out" into the adjacent breast tissue, (2) scleroelastotic stromal changes present throughout the lesion rather than confined to the central nidus, (3) frequent desmoplastic stroma and keloid-like fibrous bands, and (4) a discontinuous-to-absent myoepithelial cell layer. However, the epithelial proliferation is reminiscent of florid UDH with a solid growth pattern, frequent intranuclear inclusions, and heterogeneous CK5 and ER expression [72]. Moreover, reduced staining for myoepithelial cells is a recognized phenomenon in RS/CSLs [73]. As such, optimal classification of infiltrating epitheliosis remains a matter of debate.

Differential Diagnosis

RS/CSLs are well-recognized mammographic, gross, and histologic mimics of invasive carcinoma, especially tubular carcinomas. Both entities may appear as spiculated lesions on imaging and stellate lesions on gross examination. Histologically, the glands entrapped within the fibroelastotic core of the RS/CSLs are most worrisome for invasion. This is a pitfall encountered particularly in CNBs in which recognition of the overall architecture may be difficult. Again, as with other small glandular proliferations, it is important to have a high degree of suspicion for these lesions on core biopsy. Although these glands may be distorted and haphaz-

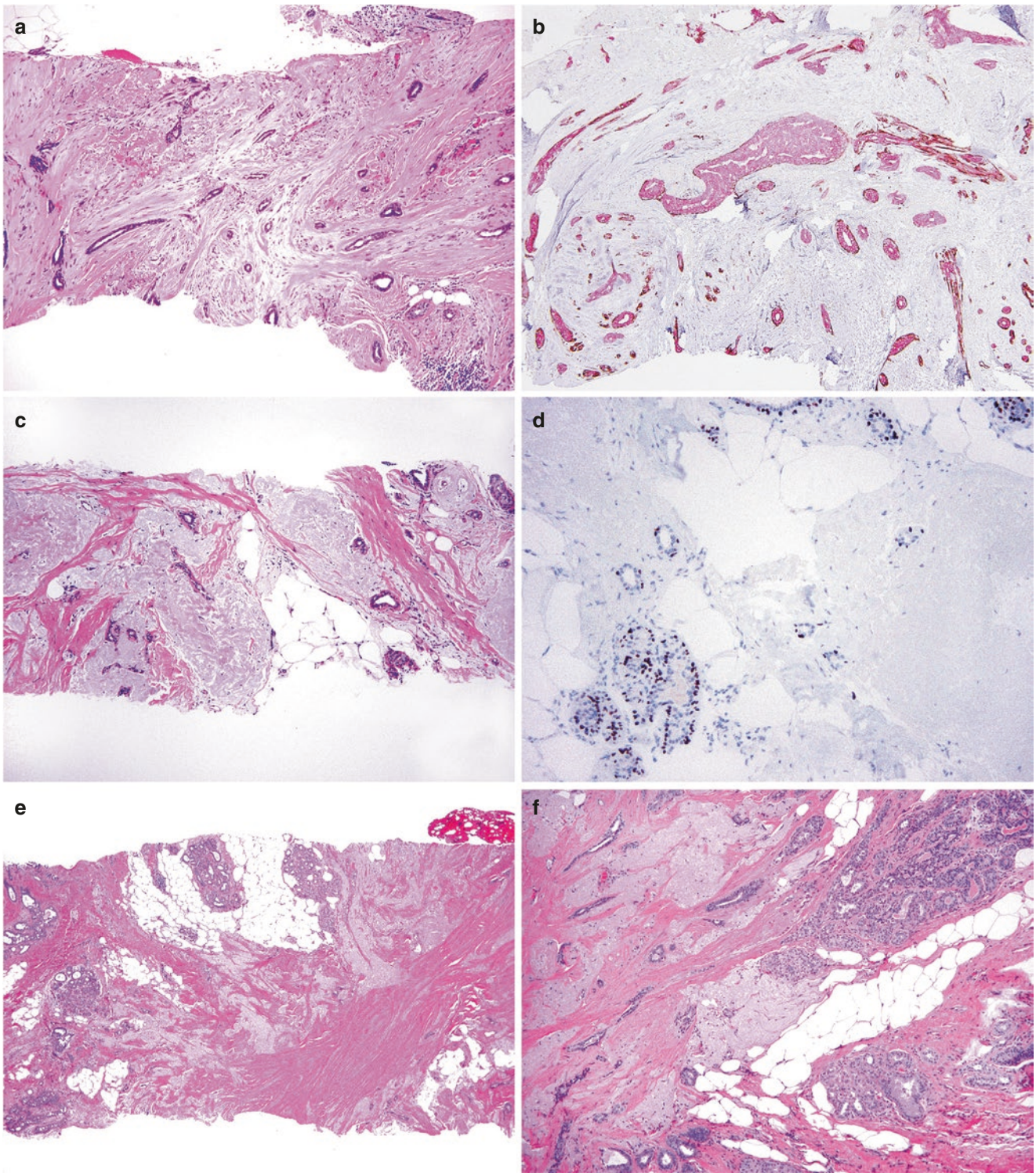

Fig. 5.12 Fibroelastotic core of sclerosing lesion on core biopsy (**a**–**f**). Fibrotic (**a**, **b**), elastotic (**c**, **d**), and mixture (**e**, **f**). Entrapped glands within the core may simulate invasive tubular carcinoma, but IHC confirms a myoepithelial cell layer (p63/keratin, **b**; p63,**d**)

ardly arranged, they are confined to the central portion of the lesion and encircled by benign elements, typically with hyperplasia present at the periphery. Moreover, on high magnification, at least some, if not all, of the glands contain an outer layer of myoepithelial cells. In contrast, tubular carcinoma contains angulated tubules that are typically embedded in a desmoplastic stroma throughout the entire lesion; however, some tumors may have areas of fibrotic or elastotic

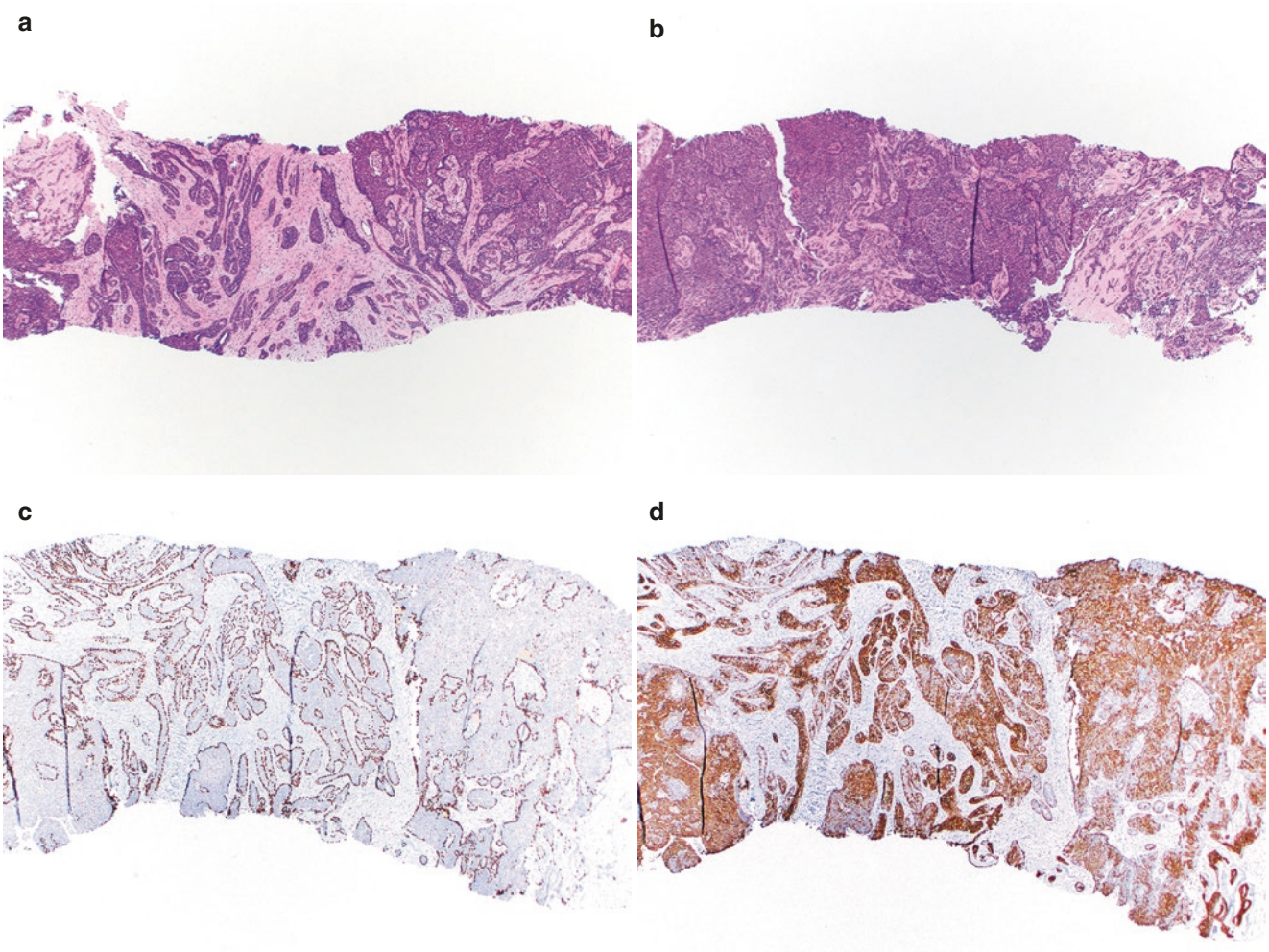

Fig. 5.13 Sclerosing papillary lesion involved by florid usual ductal hyperplasia (**a**–**d**). SMM demonstrates the myoepithelial cell layer throughout the lesion (**c**), while CK5 is positive in the epithelial hyperplasia (**d**)

stroma similar to that of sclerosing lesions. The tubules infiltrate into the breast parenchyma and adipose tissue at the periphery of the tumor. Myoepithelial cells are completely absent. It is particularly challenging to distinguish RS/CSLs from tubular carcinoma on CNB, especially if only the fibroelastotic core of the lesion has been sampled (Fig. 5.12).

LGASC is another carcinoma in the differential diagnosis of RS/CSLs, which may be rather subtle and difficult to recognize when it arises in the background of these lesions [68]. LGASC is characterized by well-formed glandular structures and solid nests of squamous cells within reactive cellular stroma [74]. RS/CSLs are often associated with an adenosquamous proliferation within the nidus of the lesion; however, LGASC extends beyond the sclerosing lesion into the surrounding breast parenchyma [70]. At scanning magnification, the tumor may have a spiculated appearance resembling the configuration of a RS/CSL, while adenosquamous elements of the central nidus may be mistaken for entrapped benign glands. Clues to the diagnosis of LGASC include the squamoid and syringoid features of tumor cell nests, the lamellar arrangement of the spindled stroma around glandular structures, and frequent peripheral lymphoid aggregates. LGASC is characterized by variable immunohistochemical staining at the periphery of lesional glands for myoepithelial markers (p63, SMM, SMA, CD10, and calponin), with complete circumferential staining in a minority of cases, which may further complicate the distinction from RS/CSLs. In contrast to benign RS/CSLs, in our experience, LGASC is more likely to display loss of myoepithelial markers, dual p63 and cytokeratin staining of tumor cells in squamoid nests, and variable staining of stromal cells with cytokeratins (CKAE1/AE3, CK5/6, CK7, CK 34βE12, and Cam5.2) [74]. Immunoreactivity for p63 is rare in the stromal cells of both RS/CSLs and LGASC [74, 75] and should prompt consideration for spindle cell carcinoma, which may arise in association with either of these lesions.

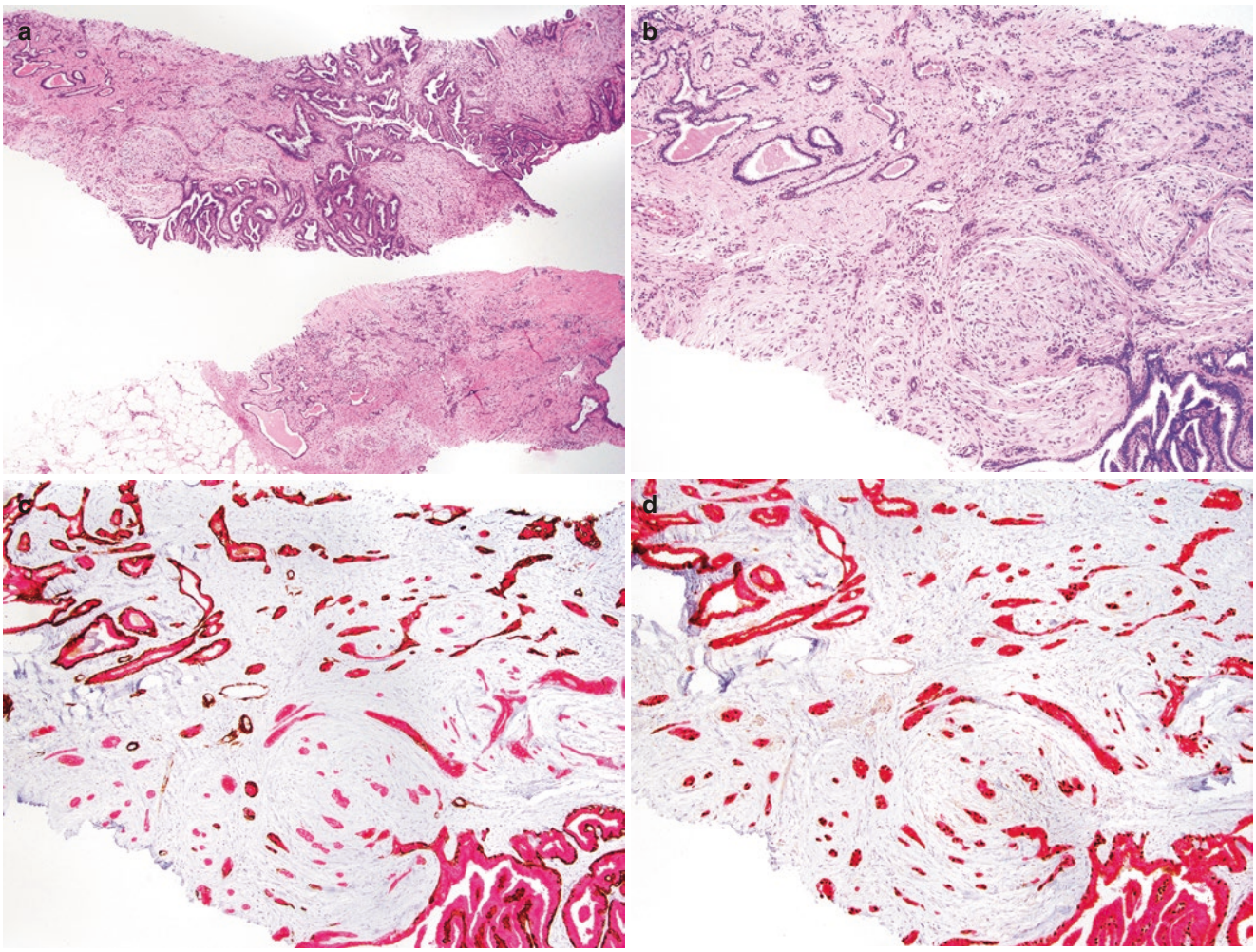

Fig. 5.14 Sclerosing papillary lesion associated with a subtle atypical adenosquamous proliferation worrisome for LGASC (**a**–**d**). Small nests and tubules are present in the background spindled stroma. This focus lacks evidence of a surrounding myoepithelial cell layer on a SMM and keratin double stain (**c**), and lesional cells display dual positivity for p63 and keratin (**d**). LGASC was confirmed on excision (not shown)

Immunohistochemical Workup

As with other small glandular proliferations, immunohistochemical staining for myoepithelial cells aids in the differential diagnosis of radial scars versus invasive carcinoma. A study by Hilson et al. [73] revealed that myoepithelial cells in benign sclerosing lesions demonstrate immunophenotypic differences from myoepithelial cells surrounding normal mammary ducts and lobules. Almost half of the cases of sclerosing lesions in their study showed reduced expression of at least one of seven myoepithelial cell markers. Expression of CK5/6 was reduced in approximately one third of cases. Expression of SMM, CD10, p63, and calponin was reduced in 21%, 15%, 9%, and 6%, respectively. A failure to confirm the presence of myoepithelial cells in sclerosing lesions could lead to the erroneous classification of these benign lesions as invasive cancer. This study highlights the importance of using two or more myoepithelial cell markers in combination (Fig. 5.9e). Most benign sclerosing lesions show no staining for p63 or cytokeratins in stromal cells, which helps in ruling out metaplastic carcinoma, although stromal positivity for CK MNF116 is a diagnostic pitfall [75]. Like sclerosing adenosis, sclerosing lesions show a heterogeneous pattern of estrogen receptor expression, which aids in the distinction of this lesion from strongly and diffusely staining well-differentiated invasive carcinoma and triple-negative LGASC.

Pathogenesis

The exact pathogenesis of radial scars is unknown. It has been hypothesized that these lesions result from an unknown injury that leads to fibrosis, possibly related to duct ectasia and obliteration [76], chronic inflammation [77], or vascular compromise [78], or that they result from an abnormal

epithelial/stromal interaction. Radial scars are characterized by a cellular phase with abundant central myofibroblasts and a mature phase with few myofibroblasts and prominent collagen and elastin fibers [77]. A number of factors involved in vascular stroma formation, such as collagen type 1, fibronectin, thrombospondin 1, and vascular endothelial growth factor, are expressed [78]. Like other proliferative lesions of the breast, the epithelium shows evidence of estrogen receptor dysregulation [27, 79].

PIK3CA-activating point mutations have been detected in over 60% of RS/CSLs [80], over three quarters of ASPs microdissected from the nidus of early cellular RS/CSLs [71], and most cases of so-called infiltrating epitheliosis [72]. Given recurrent *PIK3CA* mutations in carcinomas of the breast (TCGA), including a high rate of these mutations in LGASC [81], some authors have suggested that RS/CSLs and related lesions may represent clonal proliferations and precursors to invasive carcinoma, although this has not been clearly supported by evidence of shared molecular alterations between coexistent RS/CSLs and carcinoma [71, 72]. However, PIK3CA-AKT pathway mutations have also been found in several other benign proliferative lesions, such as UDH (50%) [82], papillomas (over 60%) [83], and columnar cell lesions (over 50%) [84], some of which harbored a different mutation than coexistent carcinoma [84], and therefore it is postulated that *PIK3CA* mutations may play a greater role in epithelial proliferation than malignant transformation [80].

Clinical Management and Prognosis

A diagnosis of RS/CSL on CNB is routinely managed by surgical excision. Surgical excision is a consensus recommendation for RS/CSL involved by atypical hyperplasia, as a significant fraction of cases (24–37%) will be upgraded to malignancy (DCIS or invasive carcinoma) [29]. On the other hand, clinical management of RS/CSLs without associated atypical hyperplasia has been a matter of debate over the years. Bianchi et al. [29] conducted one of the largest single center studies on the surgical outcomes of radial scars without atypical hyperplasia diagnosed on CNB revealing that 8.2% (4 of 49 cases) of lesions were upgraded to malignancy. The same authors found a similar mean upgrade rate of 8.3% in a review of the literature to date, which included 21 prior series with a total of 899 cases of radial sclerosing lesions without atypia diagnosed at CNB [59, 85–104]. The upgrade rate differed widely among series, ranging from 0% to 40%, with most in the range of 4% to 16%. This most likely reflects variability in study design, inconsistent radiologic-pathologic concordance and small sample sizes. In a large multi-institutional study of radiologic lesions of uncertain malignant potential (Breast Imaging-Reporting and Data System 3), Rahka et al. [105] also found that 8.9% (25 of 278 cases) of radial sclerosing lesions without atypical hyperplasia were upgraded to malignancy on excision (14 DCIS, 6 invasive carcinoma). Although it can be argued based on this data that the risk of malignancy is sufficiently high to warrant routine surgical excision for RS/CSLs.

Recent studies suggest that a reliable diagnosis can be made on CNB if the lesion has been sufficiently sampled. In a study of 80 cases at MD Anderson Cancer Center, Resetkova et al. [106] argued that extensive sampling by 9- and 11-gauge needles in conjunction with radiologic-pathologic correlation may eliminate the need for surgical excision in a majority of patients. Similarly, in a multi-institutional study, Brenner et al. [93] showed that missed carcinomas are less likely with larger gauge (11-gauge) vacuum-assisted biopsy devices than with 14-gauge automated biopsy devices (0% and 9% upgrade rates, respectively), especially if at least 12 cores are examined. Some authors have proposed complete excision of radial scars without atypical hyperplasia by vacuum-assisted mammotomy as a way to avoid surgery and some centers have adopted this practice [104].

Other studies suggest that smaller radial scars can be managed conservatively with close follow-up rather than surgical excision. Sloane and Mayers [107] examined 126 radial scars and CSLs and noted that carcinoma was very uncommon in lesions smaller than 0.6–0.7 cm. More recently, in a series of 77 small radial scars (all measuring less than 0.5 cm), Matrai et al. [108] did not find any malignancy on surgical excision. Similarly, Lee et al. [109] found no upgrade to malignancy for incidental or "microscopic" radial scars diagnosed during the evaluation of another target lesion, while Park et al. [110] noted the same for mammographically occult asymptomatic RS/CSLs detected on ultrasound guided CNB. Consistent with this, a recent meta-analysis of 49 studies that included 3163 radial scars with surgical outcomes revealed a pooled estimate for upgrade to malignancy for RS without atypia of 5%, which dropped to 1% for the subgroup diagnosed on 8–11-gauge vacuum-assisted biopsies, with an upgrade of 0% for special case scenarios of small or incidental lesions [111].

While management of RS/CSLs remains controversial and institution-dependent, this newer data suggests that radiological-pathological concordant lesions without atypia may not require surgical excision, especially those that are small and well sampled by larger bore needles. It may be prudent to make management decisions on a case-by-case basis through careful radiologic-pathologic correlation and multidisciplinary discussion.

In the past, radial sclerosing lesions were hypothesized to be direct precursors of invasive carcinoma due to the morphologic similarities to invasive carcinoma and the coexistence with it in a fraction of cases [50, 57]. Currently, radial scars are regarded as benign proliferative lesions and risk

factors for breast cancer. Like sclerosing adenosis, much of the data regarding the risk of breast cancer associated with radial scars comes from the three large cohorts of benign breast disease in the United States. In a nested case control study of 1396 women followed for a median of 12 years in the Nurses' Health Study, Jacobs et al. [61] reported an incidence of 7.1% and a relative risk of 1.8. The risk of breast cancer was independent of the histologic category of benign breast disease and additive to the risk associated with other well-established pre-malignant lesions such as ADH. The risk increased with larger lesions and multiple lesions. There was no significant difference in the number of cases with subsequent development of ipsilateral or contralateral breast cancer. In contrast, Sanders et al. [62] showed that radial scars were associated with only a minimally increased risk of breast cancer (relative risk = 1.11) in women followed for a mean of 20.5 years in the Nashville Breast Cohort. Radial scars were almost always associated with proliferative breast disease and their risk was dependent on the category of proliferative breast disease present. Similarly, radial scars did not increase the risk of breast cancer above the presence of other proliferative breast disease in women with a mean follow-up of 14 years in the Mayo Benign Breast Disease cohort [60]. Overall, a diagnosis of radial scar places a patient into the same risk category as proliferative breast disease.

Microglandular Adenosis

Overview

Microglandular adenosis (MGA) is a small glandular proliferation with a lack of myoepithelial cells and an infiltrative growth pattern that may be confused with invasive carcinoma. It was initially illustrated by McDivitt et al. [112] in 1968 and subsequently characterized in greater detail in clinicopathologic studies by Clement and Azzopardi [113], Rosen [114], and Tavassoli and Norris [115] in 1983.

Clinical, Radiologic, and Gross Features

MGA is a rare lesion that has only been reported in women. Although it affects patients across a broad range of ages, the majority of patients are 45–55 years of age. MGA may present as an incidental microscopic finding or as a palpable mass or thickening in the breast. Some cases are associated with pain or tenderness [113–119]. On mammography, MGA may correlate with various findings, including a density, a mass, parenchymal distortion, or calcifications [120]. Sebate et al. described the radiologic features of MGA in a single case found at surveillance screening in a 22-year-old *BRCA1* germline mutation carrier. Although mammography revealed dense breast tissue with no abnormality, sonography demonstrated a hypoechoic mass with an irregular border, and magnetic resonance imaging showed a small non-circumscribed mass with moderate early and delayed enhancement [121].

Grossly, MGA forms an ill-defined and infiltrative induration, plaque-like lesion, or mass with a firm or rubbery consistency. Masses typically measure 3–4 cm, but lesions as large as 20 cm have been reported [122]. Many cases of MGA cannot be appreciated grossly.

Microscopic Features

MGA is characterized by a haphazard proliferation of small uniform round glands in mammary stroma or fat. The glands are lined by a single layer of cuboidal epithelial cells completely invested by basement membrane. The epithelial cells contain a round nucleus and clear to slightly eosinophilic vacuolated cytoplasm. In a minority of cases, the cytoplasm contains coarse, eosinophilic granules that express alpha-1-antitrypsin and alpha-1-antichymotrypsin reminiscent of serous-type salivary glands. Rarely, chondromyxoid metaplasia can be found in association with MGA. Inspissated secretion is present as brightly eosinophilic globules within the glands, highlighted on PAS, mucicarmine, and Alcian blue special stains. Calcification of the secretions is occasionally observed. Mitotic figures are uncommon. Myoepithelial cells are absent throughout the lesion. A discrete basement membrane is present on reticulin and PAS special stains and ultrastructural studies (Fig. 5.15). Immunohistochemical stains for collagen type IV and laminin can also be utilized. The glands are embedded in a hypocellular dense collagenous stroma and freely permeate the mammary adipose tissue. There is no particular orientation of the glands relative to normal ducts and lobules. The glands may be crowded, but each gland remains distinct from its neighbor [113–115, 123].

MGA encompasses a spectrum of lesions ranging from uncomplicated MGA, as described above, to atypical MGA and MGA associated with in situ and invasive carcinoma. Atypical MGA is composed of typical elements as well as foci with more complicated architecture and mild to moderate cytologic atypia. It consists of a pleomorphic mixture of small and large glands that are more closely packed together, sometimes in a "back-to-back" configuration. The glands are irregularly shaped and can be interconnected. Cellular proliferation within the lumen results in cribriform glands and solid nests. Intraluminal secretions are reduced or absent. The epithelial cells display enlarged hyperchromatic or vesicular nuclei with coarse chromatin and prominent nucleoli. Mitotic activity is increased (Fig. 5.16). A diagnosis of CIS involving MGA is rendered when MGA contains glands with an expansile solid proliferation obliterating the lumen,

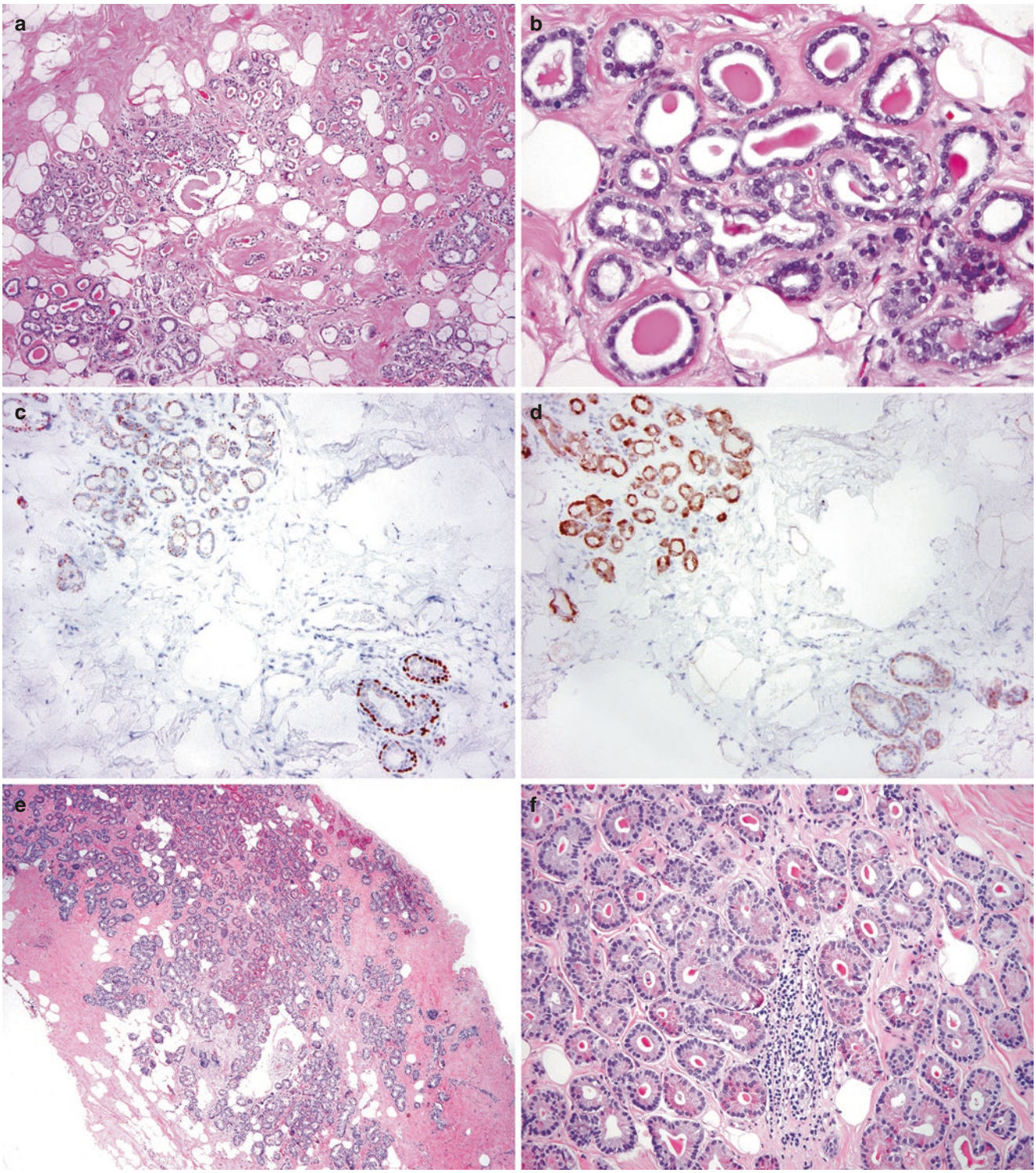

Fig. 5.15 Microglandular adenosis, typical (**a**–**h**). MGA consists of a haphazard proliferation of round glands with attenuated epithelium and bright pink secretions (**a**, **b**). Occasional cases feature cuboidal cells with bright eosinophilic granules (**e**, **f**). It simulates invasive carcinoma due to this growth pattern and lack of a myoepithelial cell layer (p63, **c**), but it is distinguished by intense staining for S100 protein (**d**) and retention of the basement membrane (reticulin, **g**; type IV collagen, **h**)

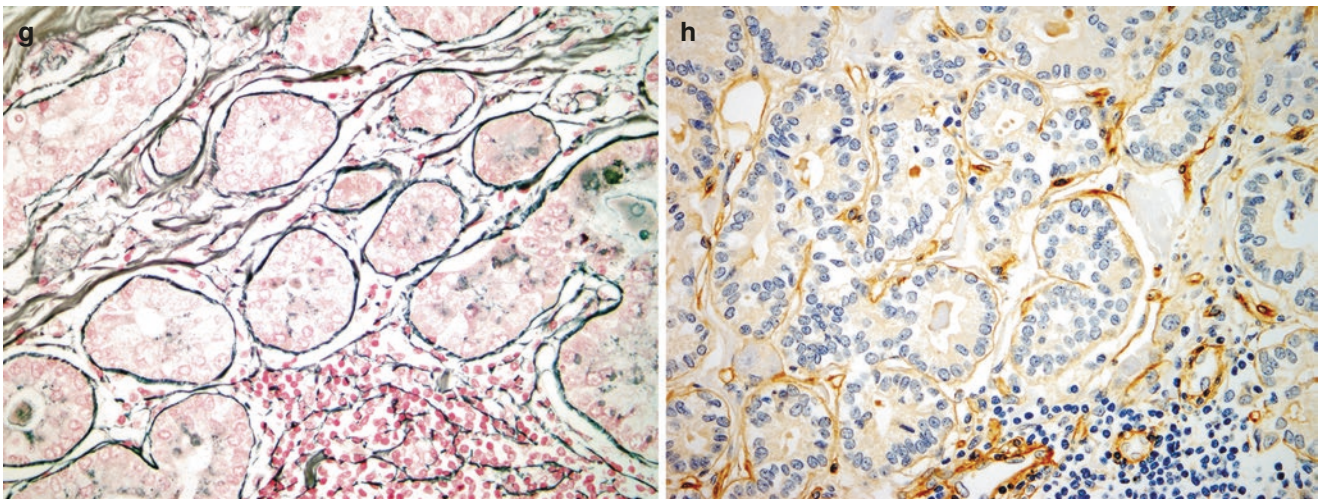

Fig. 5.15 (continued)

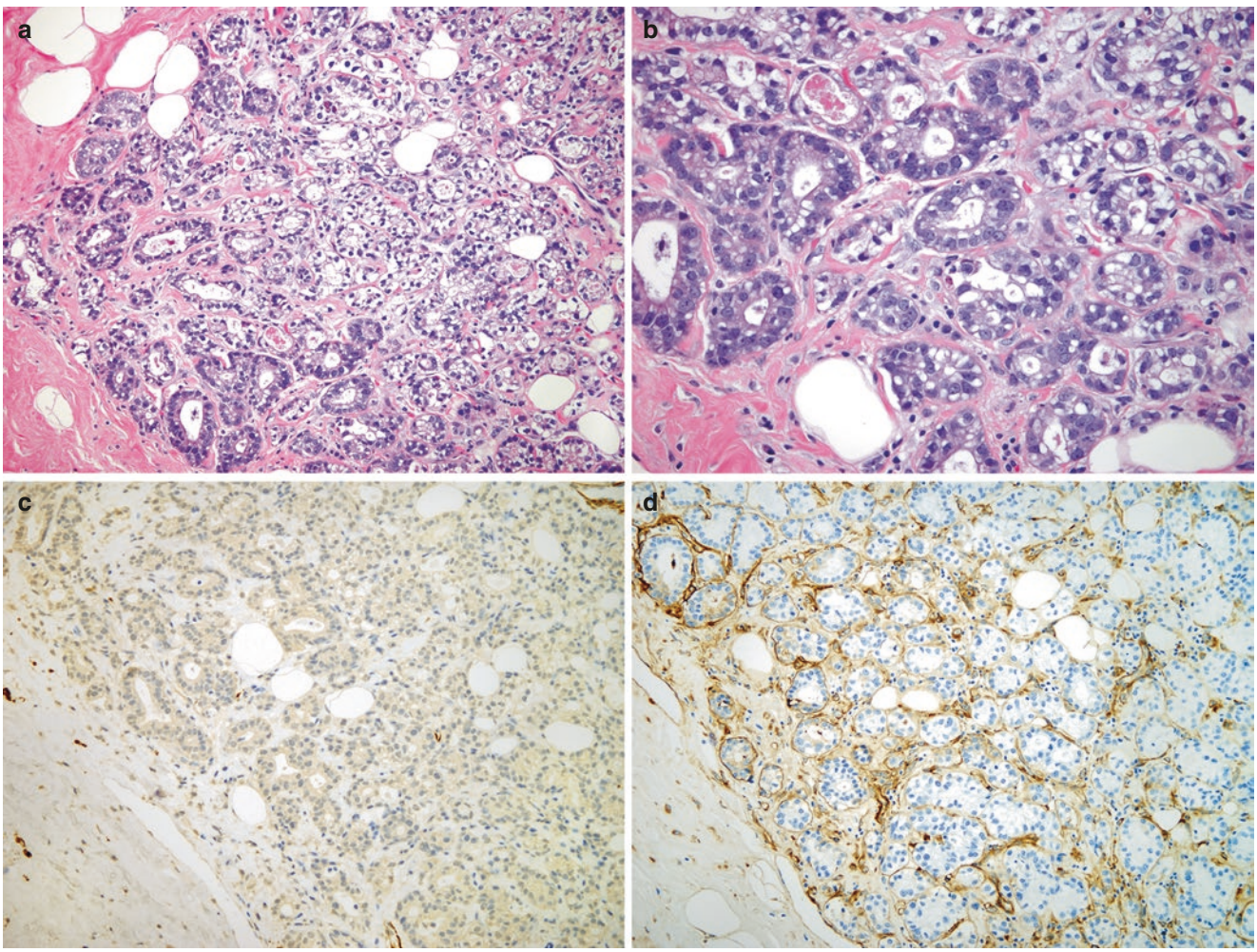

Fig. 5.16 Microglandular adenosis, atypical (**a**–**d**). Atypical MGA consists of irregular glands with cytologic atypia (**a**, **b**). The glands lack a myoepithelial cell layer (SMM, **c**) but retain a basement membrane (laminin, **d**)

severe cytologic atypia, and frequent mitotic or apoptotic figures. It tends to retain the underlying alveolar growth pattern of MGA (Fig. 5.17) [116, 124].

Invasive carcinoma arises in a background of atypical MGA and CIS as a coalescent growth of the CIS or as infiltrating cords and single tumor cells within a desmoplastic stroma (Fig. 5.18). It may be difficult to determine the extent of invasive carcinoma due to the disorderly growth pattern and lack of myoepithelial cells throughout the entire lesion. One distinguishing feature is that the basement membrane, which is preserved in MGA and atypical MGA, is disrupted in invasive carcinoma. Several case series have reported that the invasive carcinomas associated with MGA are frequently high grade and display various growth patterns and histologic subtypes. Although a solid growth pattern (Fig. 5.18) is most common, cribriform, glandular, and trabecular growth patterns may be seen. Invasive carcinoma with acinic cell differentiation, secretory differentiation, basaloid features, or metaplastic elements (chondromyxoid metaplasia, squamous metaplasia, spindle cell carcinoma) have been reported [116–119, 124–131] (Fig. 5.19). Moreover, Acs et al. described 17 cases of adenoid cystic carcinoma transitioning from MGA.

Differential Diagnosis

MGA may be confused with other types of adenosis. Khalifeh et al. [116] retrospectively identified 65 cases diagnosed as MGA at MD Anderson Cancer Center from 1983 to 2007 and found that 54 (83%) of these cases contained myoepithelial cells and 48 (70%) would be better classified as adenosis. Most of these cases were diagnosed before 1990 and before the routine use of immunohistochemical studies to aid in this diagnosis. In general, most cases of adenosis are easily distinguished from MGA by their lobulocentric pattern of growth and variable glandular contours in contrast to the haphazard and infiltrative pattern and uniform round glands

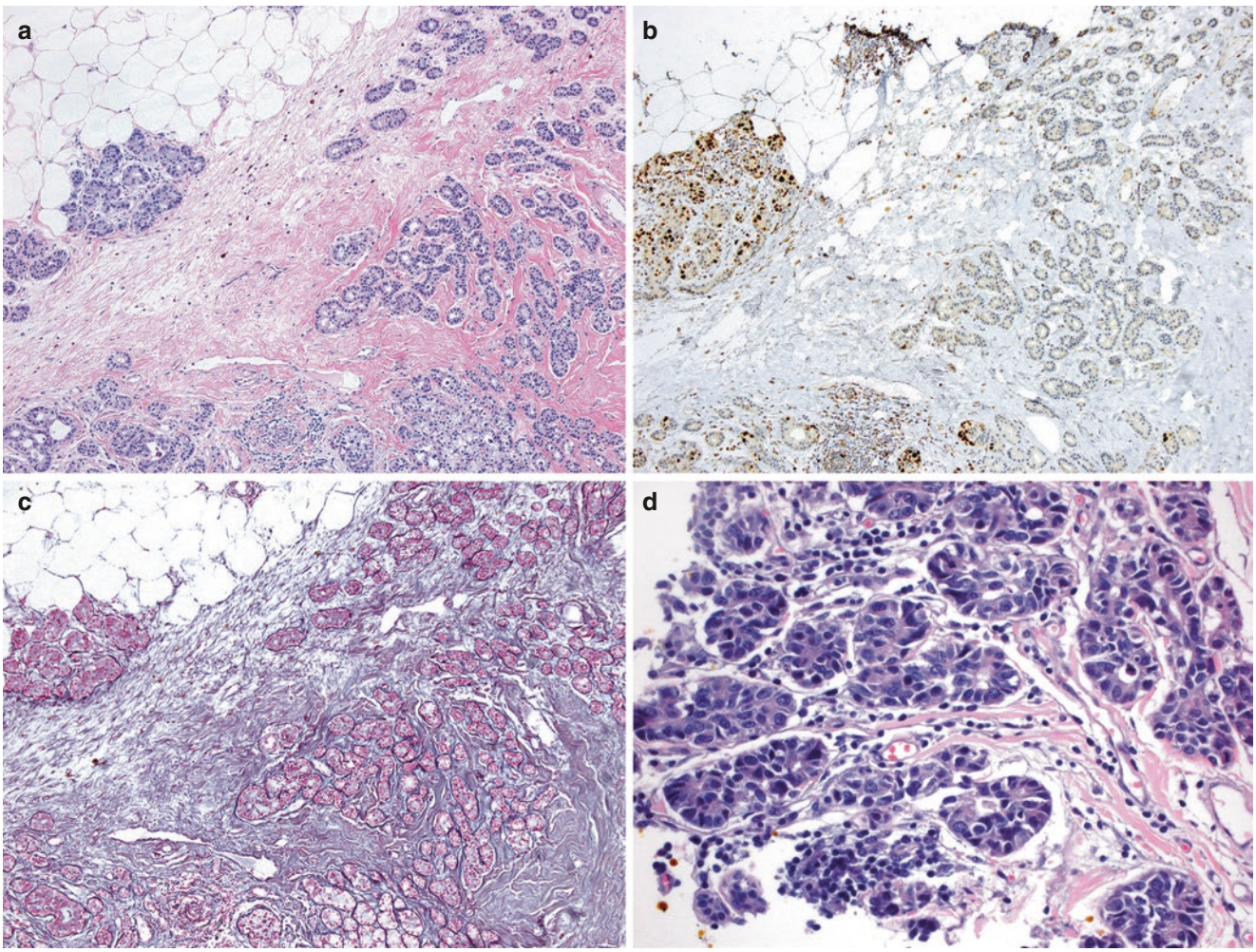

Fig. 5.17 Microglandular adenosis, typical, associated with CIS (**a**–**d**). A highly atypical proliferation of cells (**a**, **d**) with increased mitotic activity (Ki67, **b**) remains confined within basement membrane (reticulin, **c**)

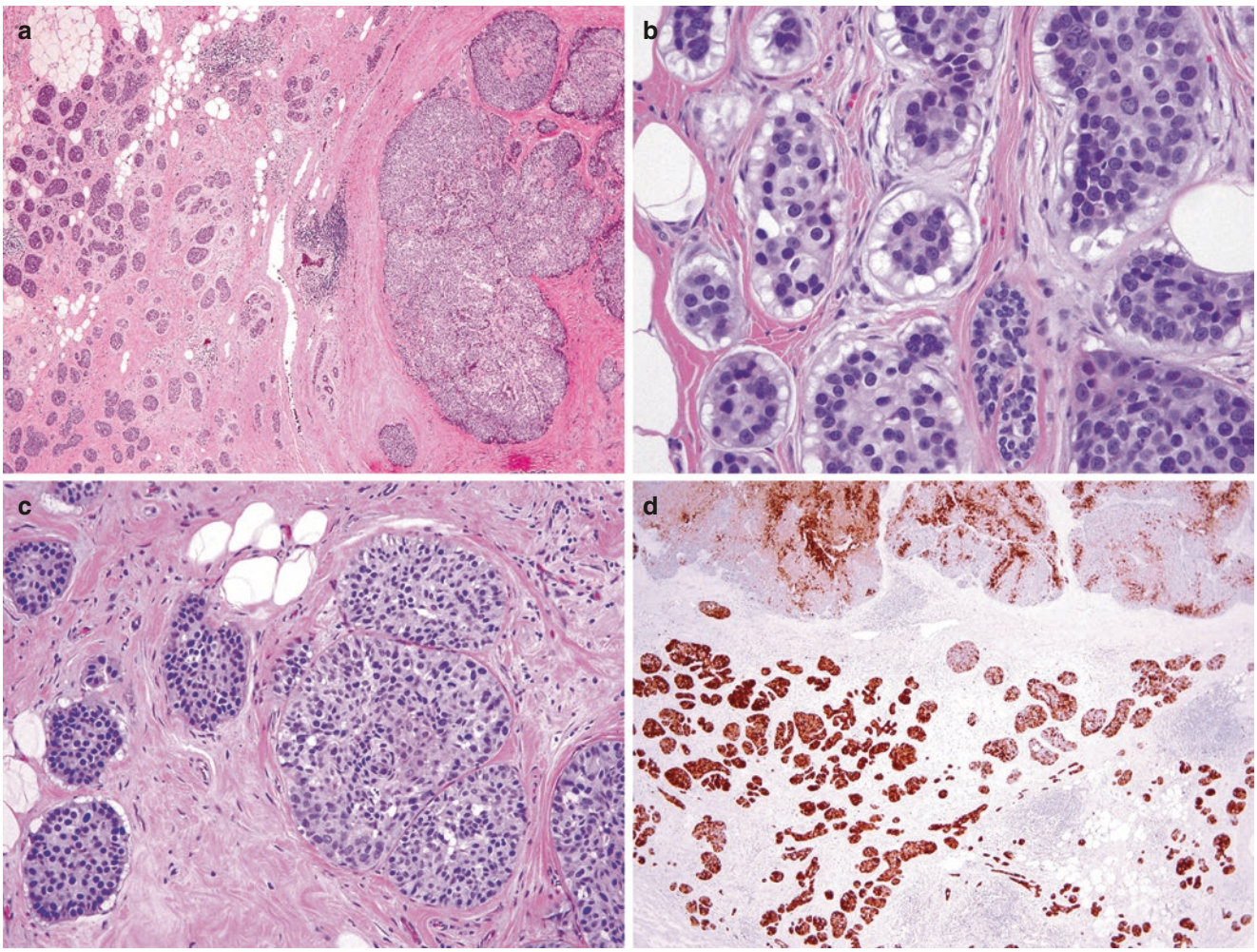

Fig. 5.18 Poorly differentiated carcinoma arising from atypical MGA and CIS (**a**–**d**). Atypical MGA features irregular glands with lumens obliterated by a solid proliferation of atypical cells (**b**). CIS is characterized by expanded solid nests of tumor cells that retain the alveolar growth pattern (**c**). Invasive carcinoma frequently manifests as a solid nodule arising from coalescent CIS (**a**). All components stain for S100 protein, although it may be reduced in atypical MGA and carcinoma (**d**)

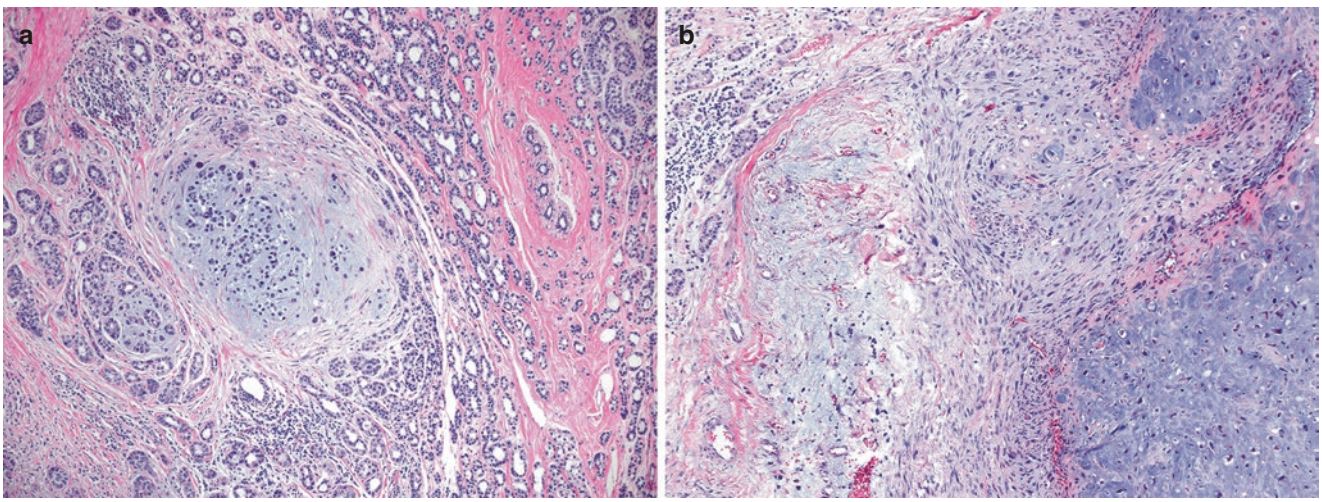

Fig. 5.19 Microglandular adenosis associated with chondromyxoid metaplasia (**a**) and spindle cell carcinoma and heterologous chondrosarcomatous elements ("metaplastic carcinoma," **b**)

of MGA. The cases of adenosis that may be misdiagnosed as MGA exhibit clear cell change, thick eosinophilic luminal secretions, and/or an infiltrative growth pattern. These cases can be identified as adenosis by confirmation of a myoepithelial cell layer on IHC.

MGA is notorious for the potential to be mistaken for well-differentiated invasive ductal or tubular carcinoma, especially on CNB, due to the infiltrative growth pattern of its glands and their lack of myoepithelial cells (Fig. 5.20). Tubular carcinoma features variably sized angulated glands lined by columnar epithelium with apical snouts in contrast to the uniform round glands with cuboidal epithelium characteristic of MGA. The glands of both tubular carcinoma and MGA lack myoepithelial cells, but those of tubular carcinoma lack basement membrane as well. Although tubular carcinoma commonly has a desmoplastic stroma, MGA does not elicit a stromal reaction. Instead, MGA has a hypocellular and hyalinized fibrous stroma. Despite these differences, this differential diagnosis is often challenging and requires immunohistochemical studies to definitively distinguish the two entities [132].

MGA, in particular atypical forms, may demonstrate significant overlap with acinic cell carcinoma (ACCa) in clinicopathologic, immunohistochemical, and molecular features and may represent part of the same spectrum of lesions. Like MGA, ACCa may display an infiltrative proliferation of small glands lacking myoepithelial cells, strong expression of S100 protein, and a triple-negative immunophenotype. ACCa is characterized by diffuse serous differentiation with the presence of intracytoplasmic zymogen-type granules and the expression of immunohistochemical markers of acinar differentiation, such as lysozyme and amylase; however, MGA can also exhibit these features (Fig. 5.21). ACCa may show greater architectural heterogeneity than MGA, with well-differentiated microglandular and less-differentiated solid areas [133, 134], although this may also be observed in cases of MGA transitioning to carcinoma. In fact, it has been argued that primary ACCa of the breast represents an example of carcinoma arising in MGA with acinic cell differentiation [131], while others contend that MGA and ACCa are distinct entities [134]. Recently, Geyer et al. [133] provided molecular evidence that MGA and ACCa are related lesions that belong to a low-grade triple-negative breast neoplasia family, as they harbor similar genomic profiles including recurrent *TP53* mutations. While this may be true, only ACCa is currently considered an indolent form of triple-negative breast cancer (TNBC). Both entities may be associated with high-grade TNBC.

Immunohistochemical Workup

MGA, atypical MGA, and carcinoma arising in MGA have common immunohistochemical profiles, negative for ER, PR, and HER2 (i.e., triple negative) and positive for S100 protein and cathepsin D [116, 125, 126, 135]. Staining for S100 protein is characterized by an intense "chocolate brown" quality in MGA (Fig. 5.15d) but may be decreased in intensity in atypical and carcinomatous forms. The epithelial cells stain for CKAE1/AE3 and Cam5.2, but neither for epithelial membrane antigen nor GCDFP-15 [135]. Myoepithelial cell markers, such as p63 (Fig. 5.15c), SMM (Fig. 5.16c), and calponin, are negative throughout this spectrum of lesions. In contrast, immunohistochemical studies for collagen type IV (Fig. 5.15h) and laminin (Fig. 5.16d) demonstrate the presence of basement membrane in MGA and atypical MGA, distinguishing these components from coexistent invasive carcinoma. In a study of 11 cases of MGA with transition into in situ and invasive carcinoma, Khalifeh et al. [116] showed that the Ki-67 and p53 labeling indices varied in uncomplicated MGA (<3%), atypical MGA (5–10%), and carcinoma associated with MGA (>30%). All of the components expressed both CK8/18 and EGFR, including MGA-associated invasive carcinoma, suggesting that these lesions are characterized by a dual luminal and basal-like phenotype.

Uncomplicated MGA may be confused with well-differentiated invasive ductal carcinoma or tubular carcinoma when immunohistochemical studies reveal a lack of myoepithelial cells. However, the studies for ER, PR, and HER2 provide a clue to the correct diagnosis since a triple-negative phenotype would be highly unusual for these types of invasive carcinoma. A diagnosis of MGA over invasive carcinoma is supported by the demonstration of staining for S100 protein and lack of staining for epithelial membrane antigen [135].

Pathogenesis

As the only benign epithelial entity of the breast in which a myoepithelial cell layer is completely absent, the true nature of MGA has long been a matter of controversy. It has been argued that this lesion is a benign lesion [115], a precursor of invasive breast cancer [116–119, 124], or a form of ER-negative invasive breast cancer with indolent clinical behavior. Accumulating evidence suggests that it represents a nonobligate precursor lesion of TNBC. Rosenblum et al. [124] provided the first compelling morphologic evidence that MGA is a precancerous lesion. The authors described seven cases of invasive carcinoma arising in MGA in which there was progressive architectural and cytologic atypia in the transition from uncomplicated and atypical MGA to invasive carcinoma as well as unusual histologic features shared by these components. Since then, several case series of MGA have been published, with an incidence of invasive carcinoma ranging from 23% to 64% of cases [116–119, 125–130]. A rate of 64% may be an overestimation due to

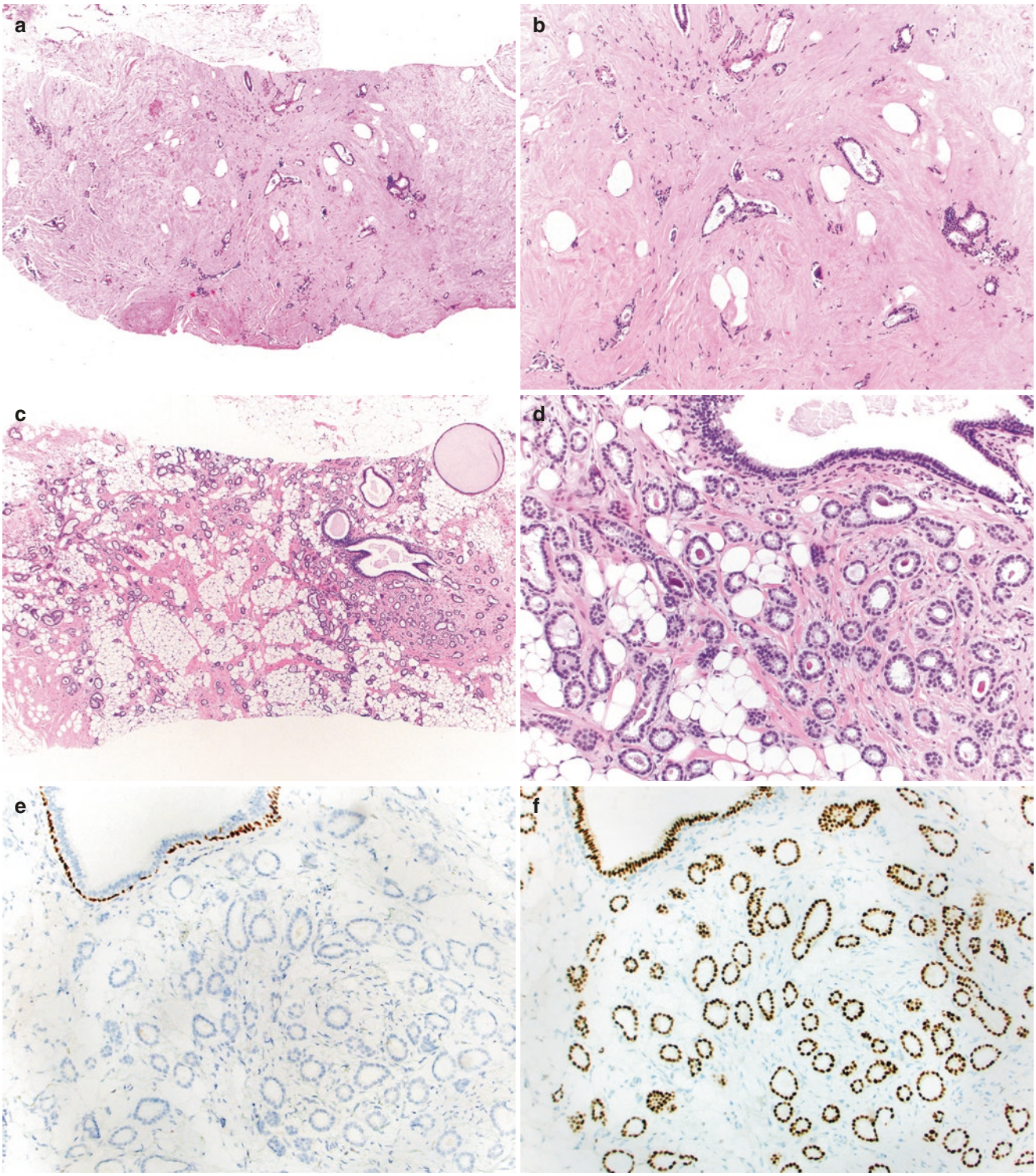

Fig. 5.20 Well-differentiated invasive ductal carcinoma is an important consideration in the diagnosis of sclerosing lesions, adenosis, and MGA (**a**–**f**). This paucicellular tubule-forming carcinoma in sclerotic stroma is difficult to distinguish from a sclerosing lesion on core biopsy (**a**, **b**). This carcinoma composed of round tubules with intraluminal eosinophilic secretions bears striking resemblance to MGA (**c**–**f**). Lack of p63-positive myoepithelial cells (**e**) may be seen with invasive carcinoma and MGA, but strong and diffuse ER expression (**f**) supports the diagnosis of well-differentiated invasive ductal carcinoma

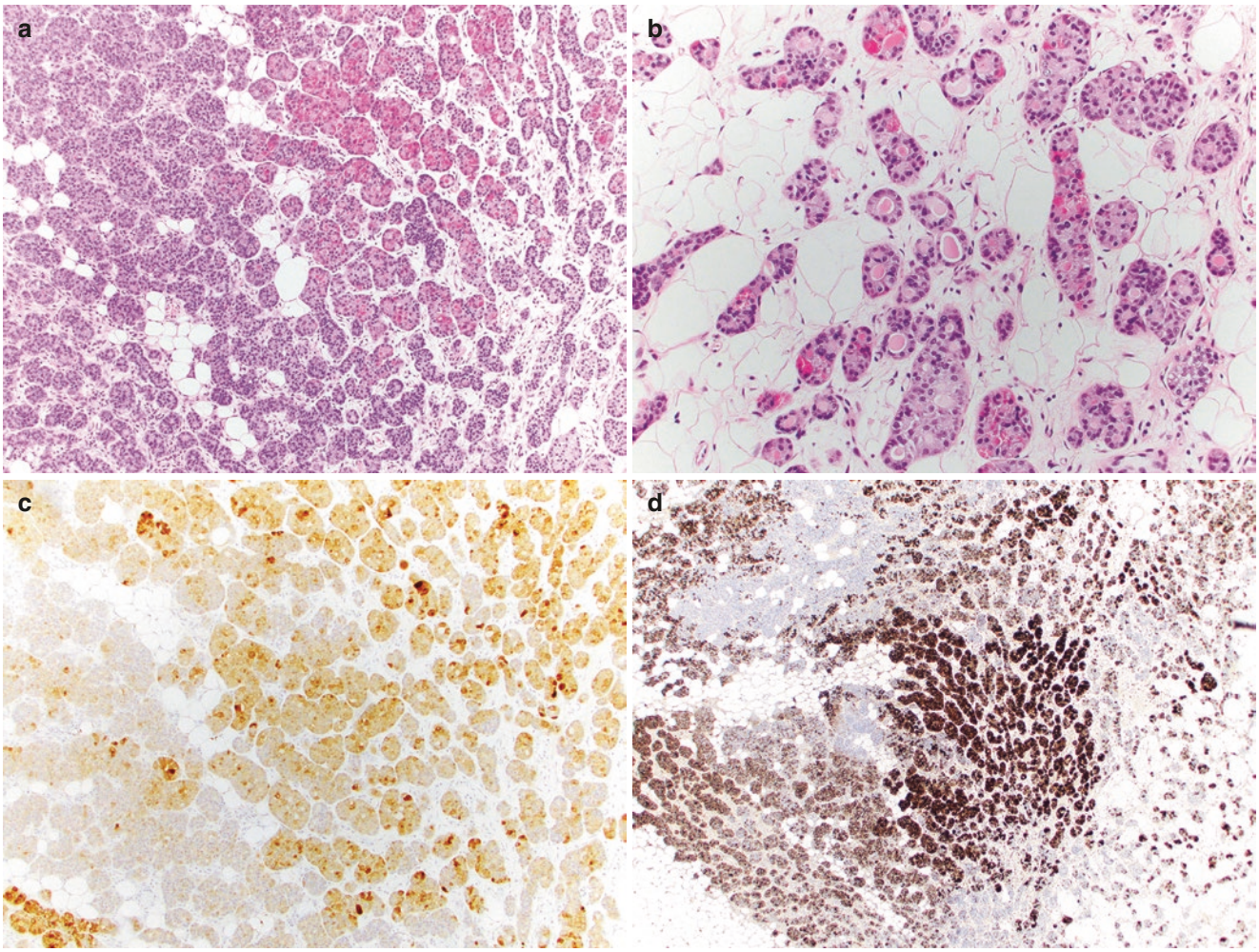

Fig. 5.21 Acinic cell carcinoma (**a**–**d**). ACCa may have a microglandular and nested growth pattern that resembles atypical MGA, while the presence of eosinophilic zymogen granules is usually more prominent than seen in MGA (**a**, **b**). ACCa stains for S100 protein like MGA (**c**); however, it also shows strong and diffuse expression of lysozyme (**d**) corresponding to diffuse serous differentiation

referral bias in one study [116]. As mentioned above, immunohistochemical studies of cases with morphologic transitions from MGA to atypical MGA to invasive carcinoma have shown that all components are "triple negative" and positive for S100 protein, basal markers, and CK8/18 (luminal marker) [116, 125, 126, 135].

Recent molecular genetic studies provide further support that MGA represents a precancerous lesion. Shin et al. [119] and Geyer et al. [118] identified DNA copy number alterations (CNAs) in a subset of MGA cases employing high-resolution chromosomal and microarray comparative genomic hybridization, respectively, supporting that at least some cases are clonal and neoplastic rather than hyperplastic. Recurrent alterations included gains of 1q, 2q, 7p, 7q, and 8q and losses of 1p, 8p, 14q, 16q, and 17q. Microdissected components of MGA, atypical MGA, and invasive carcinoma displayed similar genomic alterations. In few cases, there was acquisition of additional alterations in the progression from MGA to the invasive component, consistent with clonal evolution. Some cases of MGA had complex patterns of CNAs similar to those seen in high-grade TNBC, while others lacked any CNAs. Utilizing massively parallel sequencing, Guerini-Rocco et al. [136] found limited CNAs and an absence of clonal non-synonymous somatic mutations in pure MGA (2 cases), but identical *TP53* mutations and similar patterns of CNAs in the microdissected components of MGA (7 cases) and atypical MGA (3 cases) associated with TNBC. Another recent effort to comprehensively profile MGA suggested epigenetic inactivation of *GATA3* via aberrant hypermethylation of CpG sites within the gene may play a role in pathogenesis [137].

TNBC is a heterogeneous group with varying morphology, genomic alterations, and clinical behavior. It is associated with MGA in only very rare cases. One hypothesis is that MGA exists in a transient stage in which its progression to invasive carcinoma happens rapidly before it is ever detected. Another more likely possibility is that MGA serves as a nonobligate precursor to only a subset of TNBCs.

Clinical Management and Prognosis

Complete excision of uncomplicated and atypical MGA is recommended. Because MGA does not elicit a stromal response, and therefore forms a grossly ill-defined lesion, it may be challenging for the surgeon to achieve clear margins. If incompletely excised, local recurrence of MGA has been reported [114, 123]. Limited data are available regarding cases treated by breast conservation. Resetkova et al. [127] reported the case of a patient who developed recurrent carcinoma 10 years after breast conservation surgery with incomplete resection of MGA. The clinical and pathologic findings of this case suggested that the MGA gave rise to two metachronous primary mammary carcinomas, with the second carcinoma arising in residual MGA. Of note, this patient demonstrated a rather indolent course following a diagnosis of TNBC. If invasive carcinoma associated with MGA is managed conservatively, it is prudent to completely excise the MGA in addition to the invasive component.

It is not known whether carcinomas arising in MGA have unusual clinical behavior and outcome in comparison to other TNBCs. A study by James et al. [126] suggested that carcinomas arising in MGA have a relatively favorable prognosis. Fourteen cases of invasive carcinoma, mostly triple negative (11 cases), were identified from 60 cases of MGA. Ten patients treated by mastectomy were recurrence-free after a median follow-up period of approximately 5 years. Of the three patients treated by breast conservation, two were recurrence-free 12 and 105 months after treatment and the third was still alive at 98 months after developing bone metastases at 51 months. In another study, however, 2 of 6 patients had distant metastases at presentation and died of disease within 2 years [116].

Mucocele-Like Lesions

Overview

Mucocele-like lesions (MLLs) of the breast were first described by Rosen [138] in 1986 as benign lesions analogous to mucoceles of the salivary glands. Rosen defined these lesions as mucin-containing cysts lined by flat or low cuboidal epithelium with or without extravasated mucin. Subsequent series revealed that MLLs encompass a spectrum of pathologic changes, including completely benign lesions, ADH, DCIS, and mucinous carcinoma [139, 140]. Therefore, the terms "mucocele-like lesion" and "mucocele-like tumor" are descriptive terms for mucin-filled cysts that may contain associated extravasated mucin, but they do not provide a diagnosis of the pathologic process at hand. A major focus of the literature is whether radiologic or pathologic features can discriminate benign from malignant MLLs in order to inform the clinical management of these lesions.

Clinical, Radiologic, and Gross Features

MLLs are identified in 0.5–1% of breast CNBs [141, 142]. MLLs have been reported in patients who ranged from the third to eighth decade in age. The majority of MLLs are detected by mammography, most frequently as indeterminate calcifications, and less frequently as a mass lesion [143–145]. Trends in the literature suggest that screen-detected benign MLLs tend to present in postmenopausal women, whereas those that present as palpable masses tend to present in premenopausal women. Mucinous carcinoma, in contrast, presents as masses in an older age group.

In a recent study, Park and Kim [143] described the imaging findings for 27 cases diagnosed as pure MLLs on CNB. Microcalcifications were the most common mammographic feature (48%), and most of them had a round shape (50%) and grouped distribution (70%). Few (21%) cases presented as asymmetries or masses without calcifications. The ultrasound features included oval shape (95%), circumscribed margin (76%), parallel orientation (91%), complex cystic and solid echo pattern (95%), and no posterior feature (76%).

Other studies have compared the radiologic features of both benign and malignant MLLs. Kim et al. [144] reviewed 15 benign and 10 malignant (9 DCIS, 1 mucinous carcinoma) cases of MLL. At mammography, all of the MLLs showed calcifications and 5 cases (2 benign and 3 malignant) appeared as either a single round mass or multiple "rosary-like" masses. Pleomorphic calcifications were characteristic of the majority of both benign (73%) and malignant (80%) MLLs, often admixed with large coarse eggshell-shaped calcifications or fine linear or granular calcifications. Of note, in this study, the distribution of calcifications differed between benign and malignant lesions. Benign MLLs were associated with grouped calcifications (73% of cases), whereas in malignant MLLs, calcifications displayed a segmental or diffuse distribution (80% of cases) and extended over a wider area. At sonography, benign and malignant MLLs showed similar features, most commonly presenting as complex cysts associated with calcified or noncalcified mural nodules.

In a series of 47 cases of MLLs with benign features, ADH and DCIS, Carkaci et al. [145] found that many (61%) of these lesions were associated with calcifications on mammography, likewise either grouped coarse heterogeneous or fine pleomorphic calcifications in most instances. A small subset of MLLs from each pathologic category presented as masses, characterized by round/oval, lobular, or irregular shapes and circumscribed, indistinct, or irregular margins. At

sonography, MLLs appeared as complex cysts and solid hypoechoic masses with varying shapes and margins as well. Neither the features of the calcifications nor the masses could reliably differentiate between benign, atypical, and malignant MLLs. Consistent with these findings, other smaller studies have demonstrated that the predominant radiologic lesions are clustered pleomorphic calcifications or well-defined nodules on mammogram and complex cysts or hypoechoic nodules on ultrasound. Each of these studies included too few cases to draw conclusions regarding the distinguishing characteristics of benign and malignant lesions [146, 147]. Although some features overlap with mucinous adenocarcinoma, it is useful to note that mucinous adenocarcinoma is much more likely to present as a mass and less likely to contain calcifications [148].

Grossly, MLLs may be well-defined multiloculated cystic nodules or ill-defined shiny areas with a gelatinous or mucoid cut surface. If prominent calcifications are present, yellow flecks may be apparent on the cut surface and a gritty texture may be appreciated near the lesion. Lesions ranging in size from 0.5 to 10 cm have been reported. One study showed that the average size of malignant lesions is greater (2.8 versus 1.8 cm) [139].

Microscopic Features

MLLs are characterized by aggregates of mucin-containing cysts that may be associated with mucin extravasation. Benign MLLs consist of cysts partially or completely lined by flat to cuboidal epithelium. Ruptured cysts show strips of benign epithelium that have lifted from the ductal wall and that are floating within the mucin. Benign MLLs may show clusters of epithelial cells in the luminal or extravasated mucin, but these clusters must be rare and must lack cytologic atypia. Extravasated mucin is present as pools of various shapes and sizes with a pushing border or with dissection through the fibrous stroma (Fig. 5.22). The mucin elicits little to no inflammatory response. Rarely, multinucleated giant cells are present within or surrounding the extravasated mucin. Mucicarmine and PAS special stains highlight the mucin. The mucin is frequently associated with characteristic coarse calcifications with distinct areas of finer granularity (Fig. 5.23). The epithelium may exhibit columnar cell metaplasia or proliferative changes ranging from UDH to ADH (Fig. 5.24).

Rare case reports have described a unique lesion with hybrid features of columnar cell change and mucocele-like lesion (Fig. 5.25). Coyne [149] noted a single enlarged lobular unit consisting of cystically dilated glands lined by columnar cells with basally oriented nuclei, abundant eosinophilic cytoplasm, and prominent apical snouts. Foci of columnar cell hyperplasia were present. Alcian blue-positive mucin was observed within the dilated glands and as small lakes within the stroma. The glands contained large round basophilic calcifications and numerous crystalloids. Areas of conventional MLL with attenuated epithelium were not seen. Fadare and Mariappan [150] reported a mucocele-lesion with large cysts lined by attenuated epithelium admixed with tubules with columnar cell change and hyperplasia. There was a gradual morphologic transition between columnar cell areas and conventional MLL areas in some cysts. Both reported cases showed diffuse positivity for estrogen and progesterone receptors. The findings suggest that the pathogenesis of MLLs may be linked to columnar cell lesions in some cases.

Malignant MLLs include those with intraductal carcinoma and those with foci of invasion (Figs. 5.26 and 5.27). Intraductal carcinoma typically displays papillary, micropapillary, or cribriform patterns of growth. Lesions with the cytological and architectural features of low-grade DCIS, but measuring less than 0.2 cm or involving only a single duct space, should be categorized as ADH. Also, if it is difficult to assess the true extent of the lesion due to significant dilatation of multiple duct spaces, a diagnosis of DCIS should be rendered only when at least two duct spaces or lobules are completely involved by the atypical proliferation. Invasive carcinoma can be diagnosed on a background of MLL when there are foci of detached clusters of cytologically malignant epithelial cells within separate pools of extravasated mucin. Adjacent intraductal carcinoma is usually present. Hamele-Bena et al. [139] noted that large, coarse calcifications within the cysts and the extravasated mucin were a striking characteristic of MLLs, more often identified in malignant cases (71%) than benign cases (46%). Moreover, ADH was present in 7 of the 11 benign cases with these calcifications. It can be argued that identification of large, coarse calcifications in a MLL should prompt careful examination of the tissue to rule out involvement by atypia or malignancy.

Differential Diagnosis

The primary consideration in the differential diagnosis of MLLs is mucinous (or "colloid") carcinoma of the breast. Mucinous carcinoma features tumor cells that grow as clusters, trabeculae, festoons, micropapillae, or cribriform structures within pools of extracellular mucin. The tumor cells usually show low to intermediate grade nuclear atypia. The cellularity of the tumor varies from case to case. Multiple sections may be necessary to detect carcinoma cells if the carcinoma is composed almost entirely of mucin or if only pools of acellular mucin are seen. Intraductal carcinoma is associated with 75% of these tumors, generally located at the periphery, and occasionally there are morphologic transitions from intraductal to invasive components. MLLs in

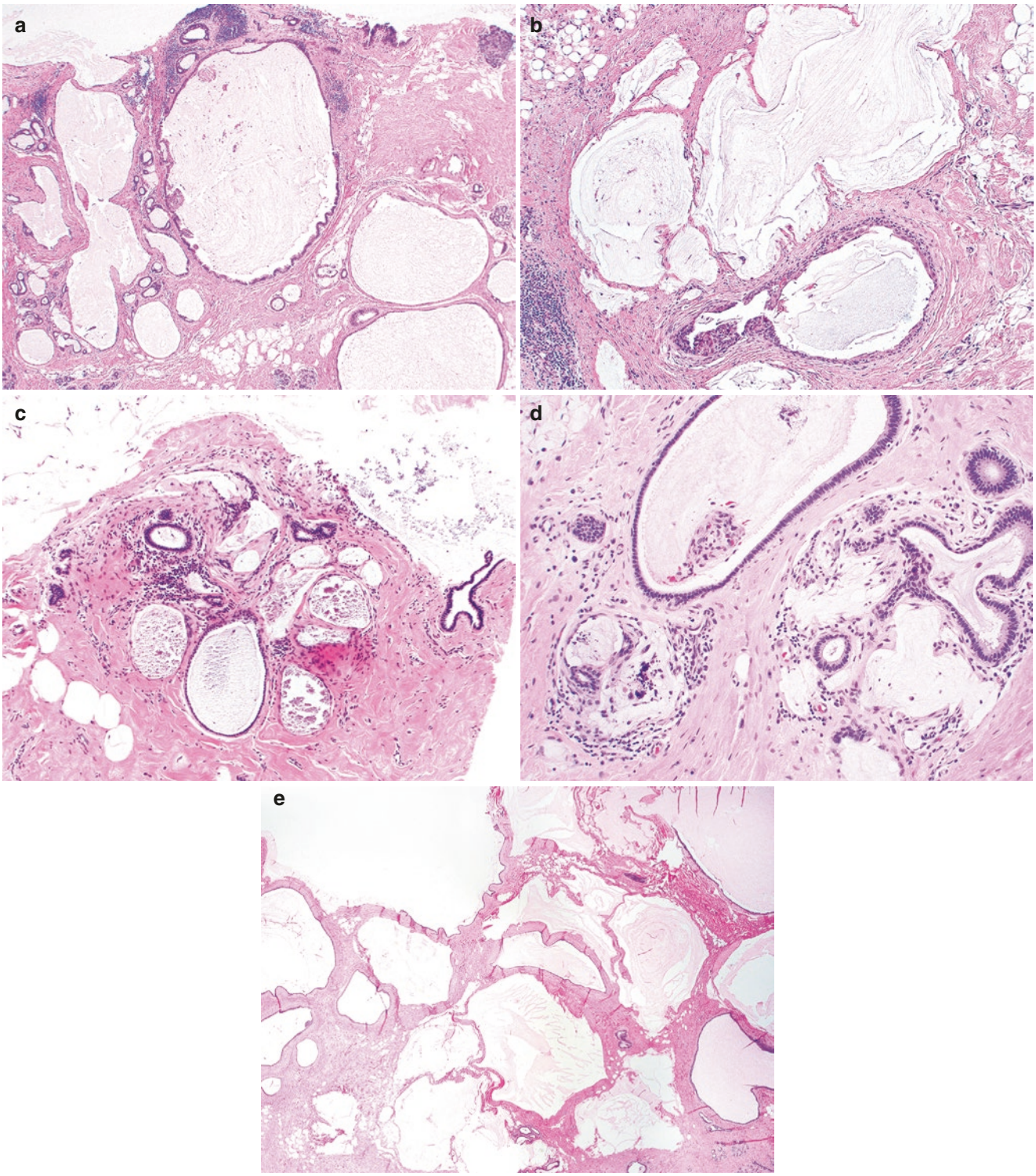

Fig. 5.22 Mucocele-like lesions without atypia (**a**–**e**). Benign mucinous cysts with focal rupture and extravasated mucin in stroma (**a**). Pools of extravasated mucin adjacent to a duct with epithelial hyperplasia and mucin production (**b**). Small MLL with associated calcifications (**c**). Small, incidental MLL (**d**). Large, mass forming MLL on excision (**e**)

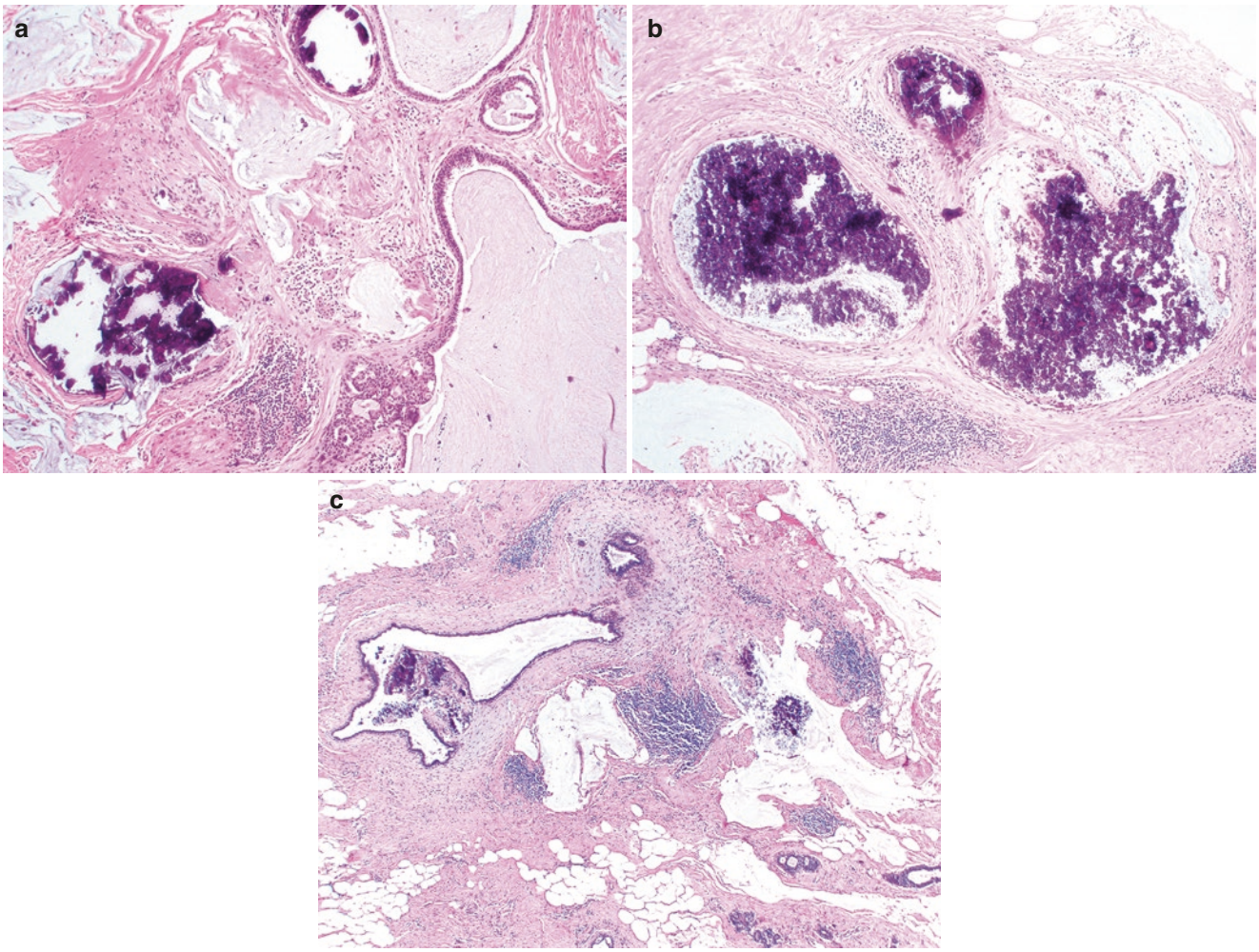

Fig. 5.23 Calcifications typically associated with MLL (**a**–**c**). Coarse calcifications with distinct areas of finer granularity are characteristically associated with extracellular mucin

which small fragments of epithelium have dislodged into the extracellular mucin raise the greatest suspicion for mucinous carcinoma. It is particularly problematic if DCIS is associated with the MLL and the free-floating clusters of cells are clearly neoplastic; in this setting, focal invasion is a possibility [151].

Careful evaluation of the epithelial elements of the MLL will aid in determining the true nature of the free-floating epithelium (Fig. 5.28). If a well-sampled MLL is devoid of significant atypia or CIS, it is unlikely that small epithelial fragments floating within the mucin represent a malignant process. In cases of MLL associated with DCIS, a diagnosis of displaced epithelium is favored when the floating clusters of tumor cells are few and focal; when they are associated with myoepithelial cells; or when they are contiguous with the ductal epithelium and appear to have lifted off of the duct wall (Fig. 5.29). It may be nearly impossible to determine the significance of floating epithelial clusters in some cases. In this situation, it would be appropriate to express uncertainty and to acknowledge the possibility of a small focus of invasion.

Immunohistochemical Workup

Immunohistochemistry for myoepithelial cell markers may aid in the distinction of epithelial displacement from focal invasion in cases of MLLs associated with DCIS. A diagnosis of epithelial displacement is suggested by the identification of preserved myoepithelial cells within the floating clusters of tumor cells [151]. A myoepithelial cell layer is confirmed beneath the epithelium of the cysts and distended ducts of MLLs on these studies.

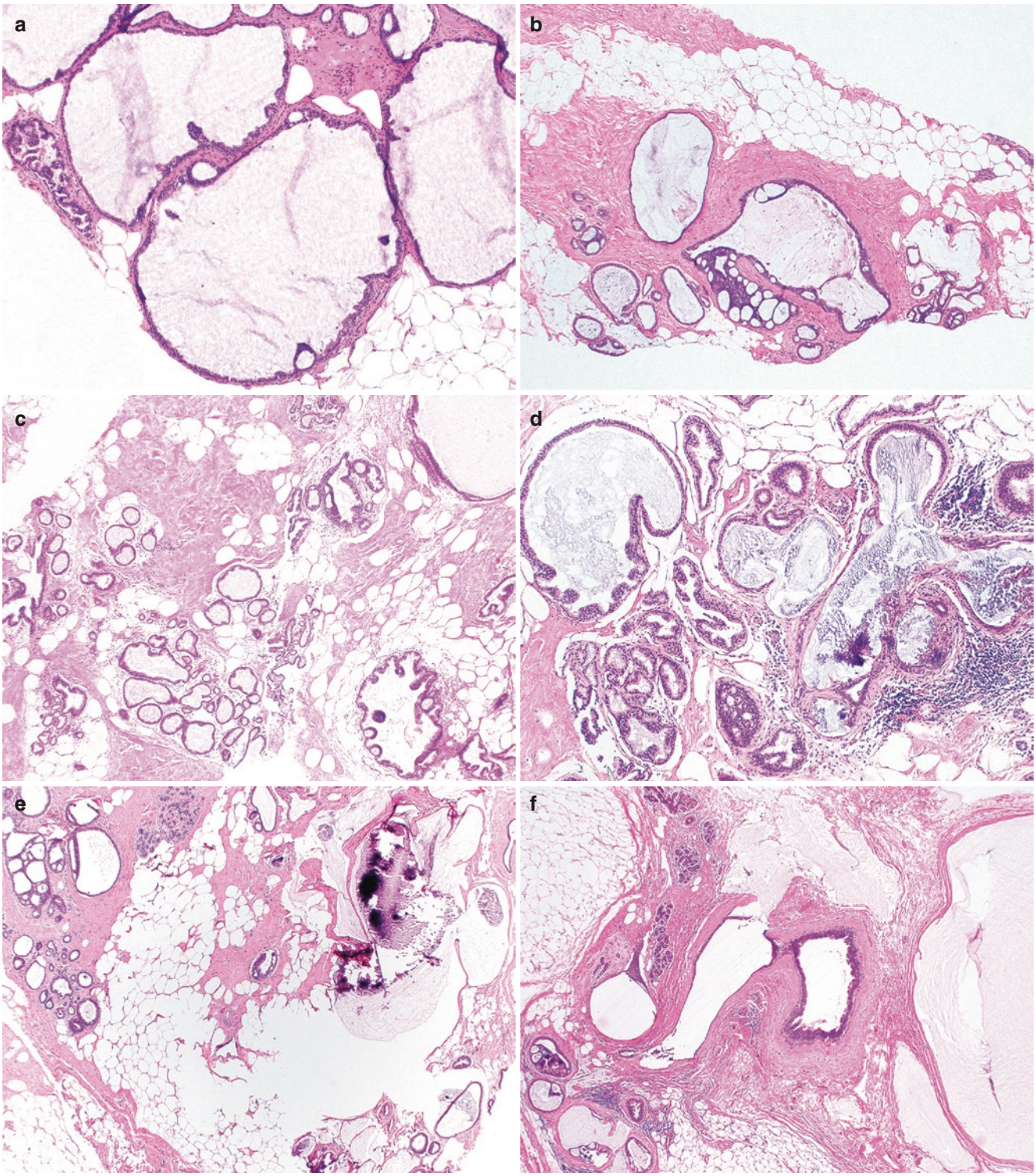

Fig. 5.24 Mucocele-like lesions with atypia (**a**–**f**). ADH with cribriform and micropapillary growth pattern and small foci of extravasated mucin (**a**–**d**). Pools of extravasated mucin with foci of ADH in the background parenchyma (**e**, **f**)

Pathogenesis

MLLs most likely result from excess production of mucinous secretions or ductal obstruction, which lead to ductal distention, rupture, and extravasation of mucin. Minor trauma may contribute to the rupture of the cysts. Some authors have suggested that MLLs with DCIS may be a precursor of mucinous carcinoma of the breast. Kryvenko et al.

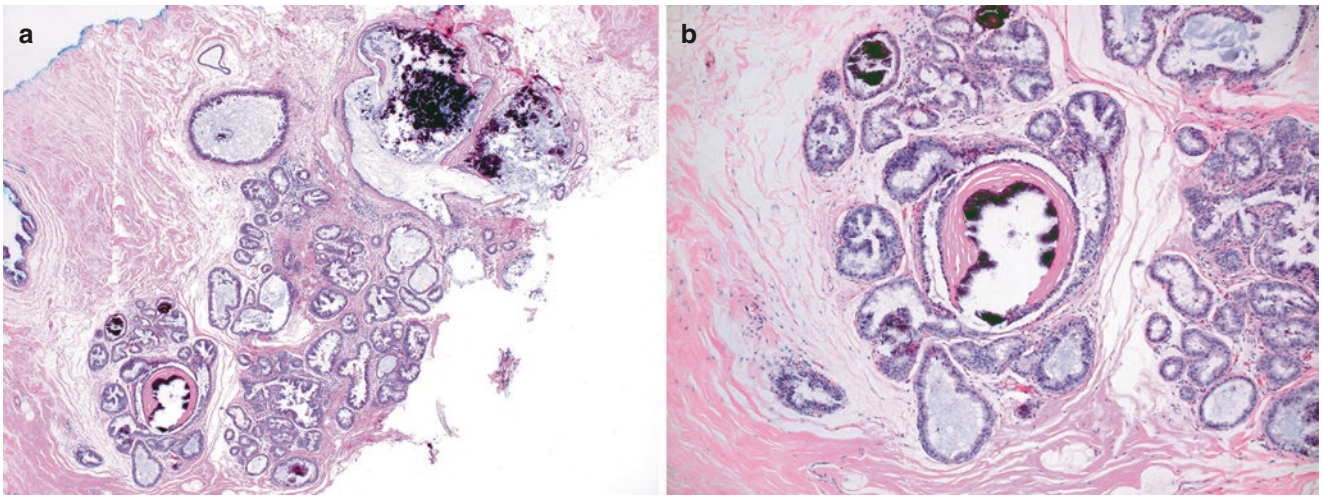

Fig. 5.25 Unusual lesion with hybrid features of MLL and columnar cell change (**a**, **b**)

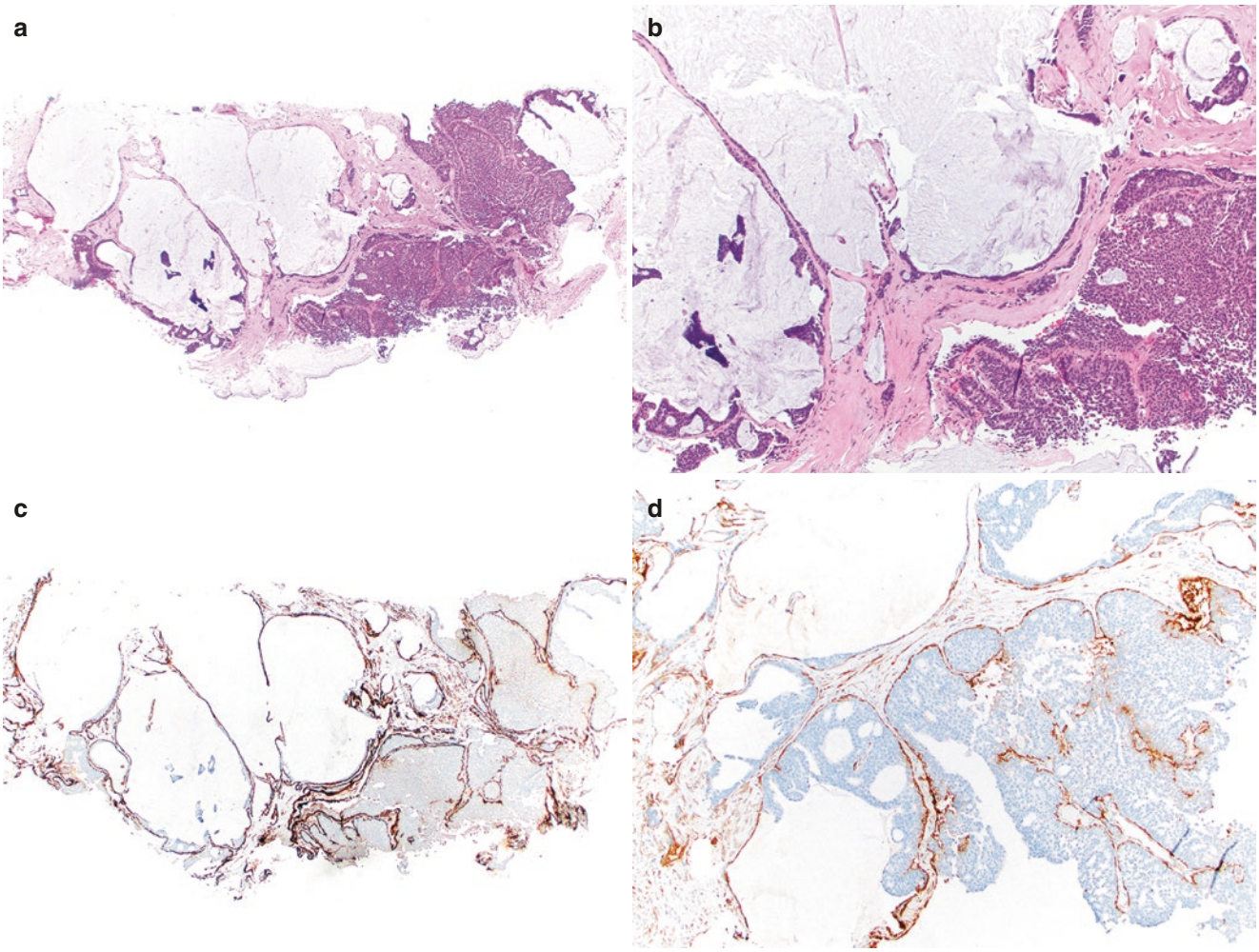

Fig. 5.26 Ductal carcinoma in situ with extracellular mucin production (**a**–**d**). The DCIS is associated with several ducts with marked dilation by mucinous contents and few free-floating atypical epithelial clusters. The residual epithelial lining at the perimeter of the mucin noted on H&E (**a**, **b**) and the underlying myoepithelial layer confirmed on immunohistochemical stain for SMM (**c**–**d**) are reassuring that the free-floating clusters do not represent mucinous carcinoma

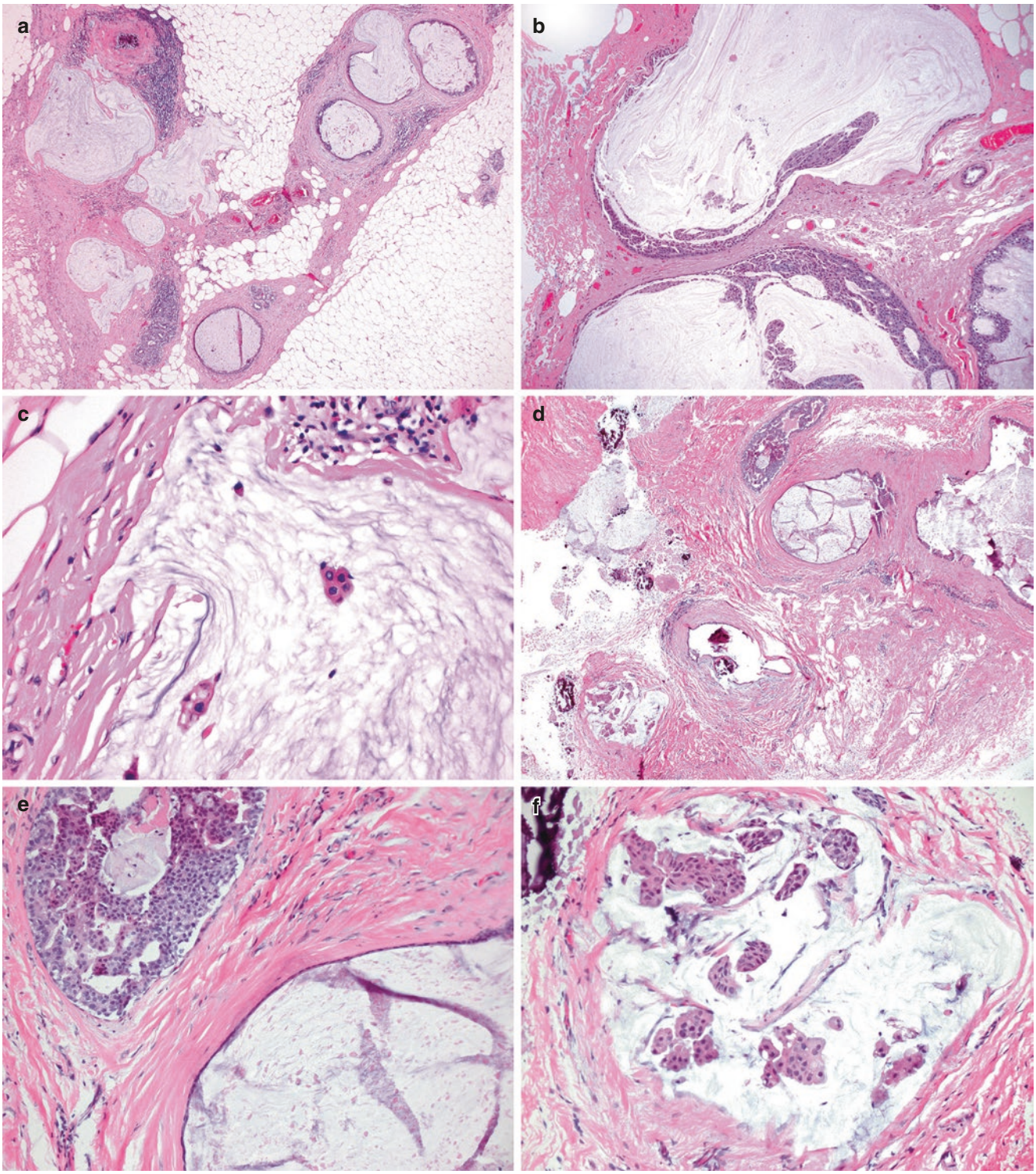

Fig. 5.27 Mucocele-like lesions associated with DCIS and invasive carcinoma (**a**–**f**). One case shows DCIS lifting off of the duct wall and rare clusters of atypical cells floating in mucin (**a**–**c**), indefinite for microinvasion (**c**). Another case contains DCIS adjacent to multiple clusters of atypical cells in extravasated mucin (**d**–**f**), consistent with a small focus of invasive mucinous carcinoma (**f**)

[152] characterized patterns of transition from intraductal to invasive carcinoma in 130 cases of mucinous carcinoma. Interestingly, one pattern of transition, which was exclusive to cases of type A mucinous carcinoma (dominant mucin component), involved overdistention and rupture of ducts with DCIS by luminal mucin. Extravasated mucin contained

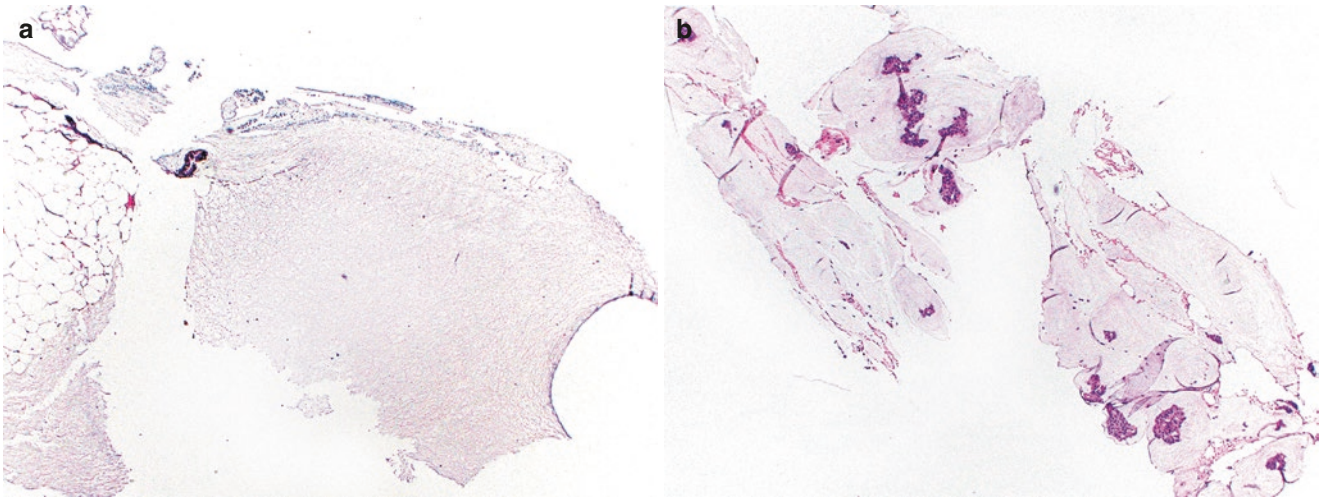

Fig. 5.28 Mucin with free-floating epithelial clusters in biopsy samples (**a**, **b**). A single banal cluster in mucin likely represents a benign lesion (**a**), while several atypical clusters in mucin are worrisome for mucinous carcinoma and should prompt consideration of excision

floating carcinoma cells in predominantly papillary clusters. Foci of residual DCIS and residual benign ducts with mucinous contents were located at the periphery of the invasive mucinous carcinoma. This study provided evidence in support of the theory that malignant MLLs serve as a precursor of mucinous carcinoma of the breast, more specifically those with type A morphology.

Clinical Management and Prognosis

Early series of MLLs consisting of excisional biopsies and mastectomies demonstrated that these lesions encompass a morphologic spectrum from benign to atypical to malignant. With the advent of CNBs, it was assumed that all MLLs should be excised in order to avoid issues related to inadequate sampling of a heterogeneous lesion, and this became the prevailing practice. At that time, there was little data to support or refute this recommendation. Since then, many studies have been limited by small numbers, insufficient radiologic-pathologic correlation, and varying definitions of what constitutes an upgrade (ADH versus DCIS), leading to widely variable upgrade rates ranging from 0% to 43% in the literature [98, 141, 142, 145, 147, 153–160]. Reflecting this, conflicting opinions exist regarding the management of MLLs diagnosed on CNB.

Several studies have shown that mucinous lesions can be reliably diagnosed on CNB. In these studies, the upgrade rates are acceptable, if an upgrade is strictly defined as malignancy (DCIS or invasive carcinoma) on excision. Renshaw [141] reviewed 22 cases of mucinous lesions diagnosed on CNB, ranging from benign MLLs to mucinous carcinomas, and found no changes in diagnosis from benign to malignant or vice versa for the 15 cases that were excised. Similarly, Wang et al. [142] evaluated benign and malignant mucinous lesions in 32 CNBs and corresponding excisions and found that all of the benign MLLs were benign on excision as well. Some authors have shown that important differences in upgrade rates exist for benign MLLs with and without atypia. Carkaci et al. [145] identified 44 cases of MLL diagnosed on CNB or fine needle aspiration, albeit only 16 of which were surgically excised. Three (19%) of 16 cases were upgraded to malignancy on excision. None of the cases of MLL without atypia were found to be malignant. However, all three cases of MLL with atypia on biopsy were upgraded to DCIS. Similarly, Sutton et al. [161] found an overall upgrade rate of 13% in their series of 38 excised MLLs. All 22 MLLs without atypia were found to be benign on excision, while five (31%) of the MLLs with atypia were upgraded to DCIS.

Other recent studies have shown that MLLs without atypia have a small risk of upgrade to malignancy, although this risk is still much lower than observed for atypical MLLs. For example, Towne et al. [162] found that 2 of 25 (8%) MLLs without atypia diagnosed on CNB were upgraded to DCIS on excision, while Zhang et al. [163] noted the same in 1 of 19 cases (5%). Rakha et al. [164] reviewed their own data as well as the literature to date. Two (4%) of 54 cases of MLL without atypia on CNB demonstrated DCIS on the subsequent excision specimen, concordant with an upgrade rate of 4% (4 of 106) for benign MLLs in the literature. A review of previous studies revealed that the frequency of malignancy is much higher at 21% (7 of 33) if there is atypia in the CNB. Overall, an analysis of the literature reveals that surgical excision of all MLLs involved by ADH or DCIS is clearly recommended. In contrast, it may be appropriate to consider more conservative management of benign MLLs without atypia in the setting of no radiologic mass lesion and close follow-up.

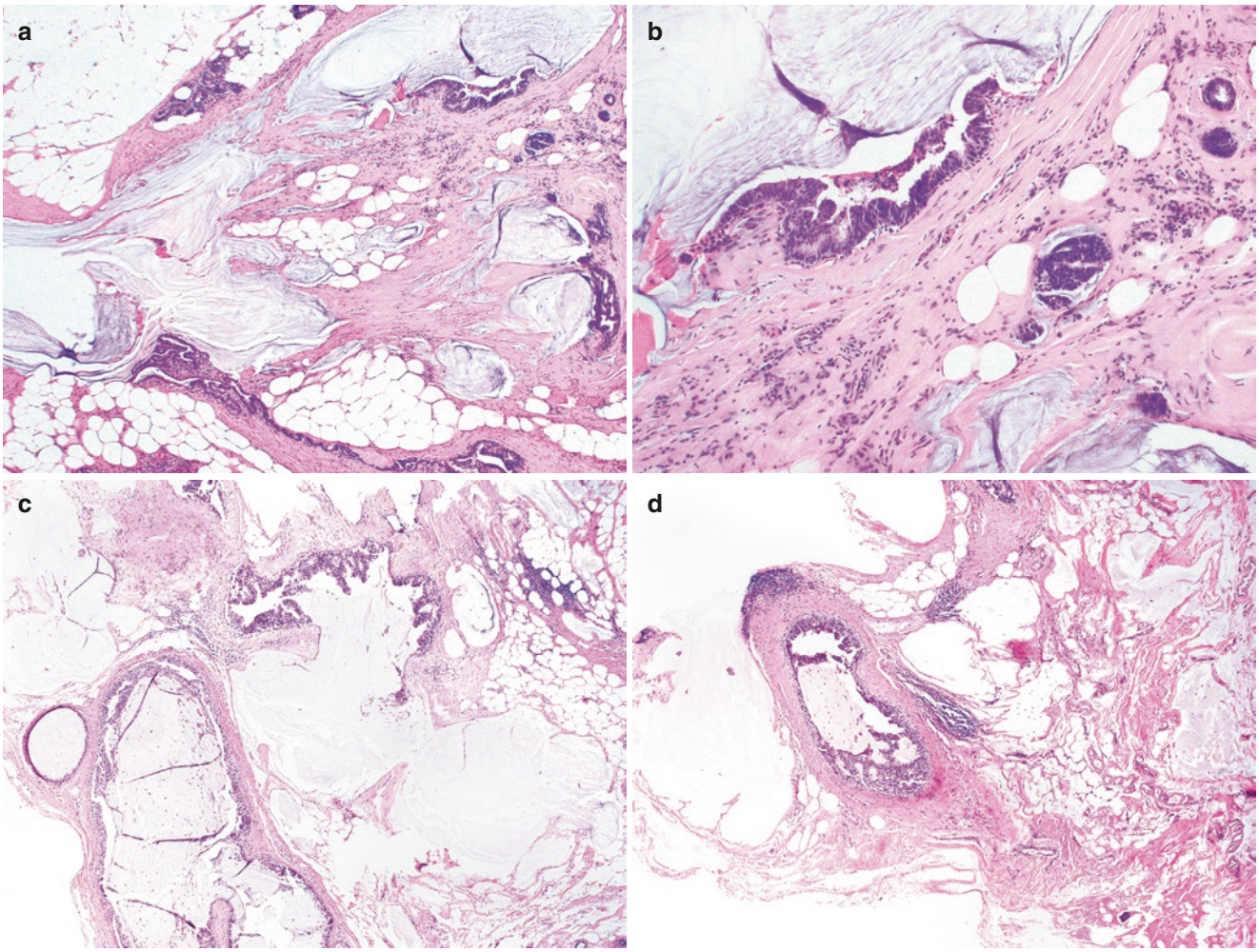

Fig. 5.29 Epithelial clusters of uncertain significance in the setting of atypical (**a**, **b**) or malignant (**c**, **d**) MLLs with lesional distortion by abundant mucin and surrounding stromal response. The small clusters in sclerotic stroma cannot be definitively diagnosed as microinvasion (**a**, **b**) nor can the rare, minute clusters floating in mucin be diagnosed as mucinous carcinoma (**c**, **d**). A diagnosis of mucinous carcinoma can be more confidently made with there are several atypical epithelial clusters within a pool of extravasated mucin separate from nearby DCIS and this pool shows more complex fibrovascular septation

Some authors advocate for the excision of all MLLs regardless of the presence of atypia. Much of this perspective results from few studies showing that ADH is found on the excision of some benign MLLs without atypia. In a small series by Carder et al. [154], 2 (33%) of 6 cases of benign MLL contained ADH in the excision. Again, 3 (75%) of 4 cases of MLL with ADH were upgraded to malignancy (two DCIS and one mucinous carcinoma). More recently, Jaffer et al. [159] evaluated 45 cases of benign MLL on CNBs and identified ADH in seven cases (16%) and DCIS is one case (2%) on excision. Both sets of authors argued that finding ADH would inform the patient and the clinician of an overall increased risk of breast cancer, providing an opportunity for more frequent screening and endocrine prophylaxis in certain patients. However, a diagnosis of ADH may or may not be treated in such a manner, and considering it as a true upgrade overestimates the risk associated with benign MLLs. It appears reasonable to recommend excision for MLLs, even those without atypia, in the setting of a radiologic mass to exclude the possibility of undersampling. However, in small lesions up to 1.0 cm that might be entirely sampled on core biopsy, clinical and radiologic follow-up without excision may be appropriate as long as there is no atypia and radiologic-pathologic correlation does not reveal discordant findings.

Recurrences of MLL are rare but have been noted in the literature. Fisher and Millis [165] reported a case of a mucocele-like tumor with atypia excised from a 31-year-old woman. One year later, three masses with histologic features of pure mucinous carcinoma with associated papillary intraductal carcinoma recurred at the same site. In a long-term follow-up study of 13 MLLs (5 with ADH, 3 with low grade

DCIS) diagnosed on excisional biopsy, Ohi et al. [166] found that one MLL with ADH recurred as an MLL with DCIS at 37 months after excision. Additionally, Hamele-Bena et al. [139] identified two patients with local recurrences in their series of 53 MLLs. One patient developed an MLL with coexistent LCIS 2 years after an excisional biopsy of an MLL with UDH. Another patient, who initially presented with an MLL with focal invasion and underwent excision of the lesion, subsequently developed an ipsilateral MLL with focal invasion 5 years later. The patient also had a contralateral MLL with DCIS. In this series, one of the largest ones, the length of follow-up for the entire group ranged from less than 1 to 15.3 years, with a mean follow-up of 3.7 years. All patients were alive and well without evidence of disease at the time of the report.

In summary, adenosis, radial scars, MGA, and MLLs constitute lesions that may sometimes be confused with invasive carcinoma, especially when they are only partially represented on CNB. Familiarity with these lesions, a high degree of suspicion, and judicious use of immunohistochemical studies will help the pathologist resolve most potential diagnostic dilemmas.

References

1. Foote FW, Stewart FW. Comparative studies of cancerous versus noncancerous breasts. Ann Surg. 1945;121(1):6–53.
2. Urban JA, Adair FE. Sclerosing adenosis. Cancer. 1949;2(4):625–34.
3. Heller EL, Fleming JC. Fibrosing adenomatosis of the breast. Am J Clin Pathol. 1950;20(2):141–6.
4. Visscher DW, et al. Sclerosing adenosis and risk of breast cancer. Breast Cancer Res Treat. 2014;144(1):205–12.
5. Taskin F, et al. Sclerosing adenosis of the breast: radiologic appearance and efficiency of core needle biopsy. Diagn Interv Radiol. 2011;17(4):311–6.
6. Gill HK, Ioffe OB, Berg WA. When is a diagnosis of sclerosing adenosis acceptable at core biopsy? Radiology. 2003;228(1):50–7.
7. Gunhan-Bilgen I, et al. Sclerosing adenosis: mammographic and ultrasonographic findings with clinical and histopathological correlation. Eur J Radiol. 2002;44(3):232–8.
8. Nielsen NS, Nielsen BB. Mammographic features of sclerosing adenosis presenting as a tumour. Clin Radiol. 1986;37(4):371–3.
9. DiPiro PJ, et al. Mammographic and sonographic appearances of nodular adenosis. AJR Am J Roentgenol. 2000;175(1):31–4.
10. Chen YL, et al. Sclerosing adenosis: ultrasonographic and mammographic findings and correlation with histopathology. Mol Clin Oncol. 2017;6(2):157–62.
11. Taylor HB, Norris HJ. Epithelial invasion of nerves in benign diseases of the breast. Cancer. 1967;20(12):2245–9.
12. Davies JD. Neural invasion in benign mammary dysplasia. J Pathol. 1973;109(3):225–31.
13. Gobbi H, et al. Atypical ductal hyperplasia and ductal carcinoma in situ of the breast associated with perineural invasion. Hum Pathol. 2001;32(8):785–90.
14. Eusebi V, Azzopardi JG. Vascular infiltration in benign breast disease. J Pathol. 1976;118(1):9–16.
15. Chan JK, Ng WF. Sclerosing adenosis cancerized by intraductal carcinoma. Pathology. 1987;19(4):425–8.
16. Fechner RE. Lobular carcinoma in situ in sclerosing adenosis. A potential source of confusion with invasive carcinoma. Am J Surg Pathol. 1981;5(3):233–9.
17. Fechner RE. Carcinoma in situ involving sclerosing adenosis. Histopathology. 1996;28(6):570.
18. Oberman HA, Markey BA. Noninvasive carcinoma of the breast presenting in adenosis. Mod Pathol. 1991;4(1):31–5.
19. Moritani S, et al. Topographical, morphological and immunohistochemical characteristics of carcinoma in situ of the breast involving sclerosing adenosis. Two distinct topographical patterns and histological types of carcinoma in situ. Histopathology. 2011;58(6):835–46.
20. Flotte TJ, Bell DA, Greco MA. Tubular carcinoma and sclerosing adenosis: the use of basal lamina as a differential feature. Am J Surg Pathol. 1980;4(1):75–7.
21. Ekblom P, et al. Basement membrane and apocrine epithelial antigens in differential diagnosis between tubular carcinoma and sclerosing adenosis of the breast. J Clin Pathol. 1984;37(4):357–63.
22. Jao W, Recant W, Swerdlow MA. Comparative ultrastructure of tubular carcinoma and sclerosing adenosis of the breast. Cancer. 1976;38(1):180–6.
23. Harrison BT, et al. Quality assurance in breast pathology: lessons learned from a review of amended reports. Arch Pathol Lab Med. 2017;141(2):260–6.
24. Cui X, Wei S. Carcinoma in situ involving sclerosing adenosis: seeking the salient histological characteristics to prevent overdiagnosis. Ann Clin Lab Sci. 2017;47(5):529–34.
25. Dewar R, et al. Best practices in diagnostic immunohistochemistry: myoepithelial markers in breast pathology. Arch Pathol Lab Med. 2011;135(4):422–9.
26. Werling RW, et al. Immunohistochemical distinction of invasive from noninvasive breast lesions: a comparative study of p63 versus calponin and smooth muscle myosin heavy chain. Am J Surg Pathol. 2003;27(1):82–90.
27. Shoker BS, et al. Abnormal regulation of the oestrogen receptor in benign breast lesions. J Clin Pathol. 2000;53(10):778–83.
28. Franquet T, et al. Spiculated lesions of the breast: mammographic-pathologic correlation. Radiographics. 1993;13(4):841–52.
29. Bianchi S, et al. Radial scar without associated atypical epithelial proliferation on image-guided 14-gauge needle core biopsy: analysis of 49 cases from a single-centre and review of the literature. Breast. 2012;21(2):159–64.
30. Jensen RA, et al. Invasive breast cancer risk in women with sclerosing adenosis. Cancer. 1989;64(10):1977–83.
31. London SJ, et al. A prospective study of benign breast disease and the risk of breast cancer. JAMA. 1992;267(7):941–4.
32. Dupont WD, Page DL. Risk factors for breast cancer in women with proliferative breast disease. N Engl J Med. 1985;312(3):146–51.
33. Calhoun BC, Booth CN. Atypical apocrine adenosis diagnosed on breast core biopsy: implications for management. Hum Pathol. 2014;45(10):2130–5.
34. Fuehrer N, et al. Atypical apocrine adenosis of the breast: long-term follow-up in 37 patients. Arch Pathol Lab Med. 2012;136(2):179–82.
35. Seidman JD, Ashton M, Lefkowitz M. Atypical apocrine adenosis of the breast: a clinicopathologic study of 37 patients with 8.7-year follow-up. Cancer. 1996;77(12):2529–37.
36. Tavassoli FA, Norris HJ. Intraductal apocrine carcinoma: a clinicopathologic study of 37 cases. Mod Pathol. 1994;7(8):813–8.
37. O'Malley FP, Bane A. An update on apocrine lesions of the breast. Histopathology. 2008;52(1):3–10.
38. O'Malley FP, Bane AL. The spectrum of apocrine lesions of the breast. Adv Anat Pathol. 2004;11(1):1–9.

39. Bianchi S, et al. Reproducibility of histological diagnoses and diagnostic accuracy of non palpable breast lesions. Pathol Res Pract. 1994;190(1):69–76.
40. Selim AG, Wells CA. Immunohistochemical localisation of androgen receptor in apocrine metaplasia and apocrine adenosis of the breast: relation to oestrogen and progesterone receptors. J Clin Pathol. 1999;52(11):838–41.
41. Selim AG, El-Ayat G, Wells CA. Expression of c-erbB2, p53, Bcl-2, Bax, c-myc and Ki-67 in apocrine metaplasia and apocrine change within sclerosing adenosis of the breast. Virchows Arch. 2002;441(5):449–55.
42. Selim AG, El-Ayat G, Wells CA. c-erbB2 oncoprotein expression, gene amplification, and chromosome 17 aneusomy in apocrine adenosis of the breast. J Pathol. 2000;191(2):138–42.
43. Wells CA, et al. Apocrine adenosis: a precursor of aggressive breast cancer? J Clin Pathol. 1995;48(8):737–42.
44. Chang Sen LQ, Berg WA, Carter GJ. Upgrade rate and imaging features of atypical apocrine lesions. Breast J. 2017;23(5):569–78.
45. Hou Y, et al. Surgical follow-up results for apocrine adenosis and atypical apocrine adenosis diagnosed on breast core biopsy. Ann Diagn Pathol. 2016;24:4–6.
46. Carter DJ, Rosen PP. Atypical apocrine metaplasia in sclerosing lesions of the breast: a study of 51 patients. Mod Pathol. 1991;4(1):1–5.
47. Semb CB. Pathologico-anatomical and clinical investigations of fibroadenomatosis cystica mammae: and its relation to other pathological conditions in the mamma, especially cancer. Acta Chirurgica Scandinavica. 1928;64:1–484.
48. Fenoglio C, Lattes R. Sclerosing papillary proliferations in the female breast. A benign lesion often mistaken for carcinoma. Cancer. 1974;33(3):691–700.
49. Tremblay G, Buell RH, Seemayer TA. Elastosis in benign sclerosing ductal proliferation of the female breast. Am J Surg Pathol. 1977;1(2):155–66.
50. Fisher ER, et al. A nonencapsulated sclerosing lesion of the breast. Am J Clin Pathol. 1979;71(3):240–6.
51. Azzopardi JG, Ahmed A, Millis RR. Problems in breast pathology. In: Major problems in pathology. Philadelphia: W.B. Saunders Company; 1979. p. 466.
52. Rickert RR, Kalisher L, Hutter RV. Indurative mastopathy: a benign sclerosing lesion of breast with elastosis which may simulate carcinoma. Cancer. 1981;47(3):561–71.
53. Hamperl H. [Radial scars (scarring) and obliterating mastopathy (author's transl)]. Virchows Arch A Pathol Anat Histol. 1975;369(1):55–68.
54. Page DL, Anderson TJ. Diagnostic histopathology of the breast. Edinburgh: Churchill Livingstone; 1987.
55. Schnitt SJ, Collins LC. Biopsy interpretation of the breast, Biopsy interpretation series. 2nd ed. Philadelphia, PA: Lippincott Williams & Wilkins; 2009.
56. Sahin A, Collins LC. Radial scar/complex sclerosing lesion. In: WHO Classification of Tumours Editorial Board, editor. Breast tumours. Lyon: International Agency for Research on Cancer; 2019. p. 30–31.
57. Linell F, Ljungberg O. Breast carcinoma. Progression of tubular carcinoma and a new classification. Acta Pathol Microbiol Scand A. 1980;88(1):59–60.
58. Burnett SJ, et al. Benign biopsies in the prevalent round of breast screening: a review of 137 cases. Clin Radiol. 1995;50(4):254–8.
59. Cawson JN, et al. Fourteen-gauge needle core biopsy of mammographically evident radial scars: is excision necessary? Cancer. 2003;97(2):345–51.
60. Berg JC, et al. Breast cancer risk in women with radial scars in benign breast biopsies. Breast Cancer Res Treat. 2008;108(2):167–74.
61. Jacobs TW, et al. Radial scars in benign breast-biopsy specimens and the risk of breast cancer. N Engl J Med. 1999;340(6):430–6.
62. Sanders ME, et al. Interdependence of radial scar and proliferative disease with respect to invasive breast carcinoma risk in patients with benign breast biopsies. Cancer. 2006;106(7):1453–61.
63. Tabar L, Dean PB. Teaching atlas of mammography. Stuttgart: Georg Thieme Verlag; 1985.
64. Mitnick JS, et al. Differentiation of radial scar from scirrhous carcinoma of the breast: mammographic-pathologic correlation. Radiology. 1989;173(3):697–700.
65. Hassell P, et al. Radial sclerosing lesions of the breast: mammographic and pathologic correlation. Can Assoc Radiol J. 1999;50(6):370–5.
66. Boute V, et al. Are the criteria of Tabar and Dean still relevant to radial scar? Eur J Radiol. 2006;60(2):243–9.
67. Mitnick JS, Harris MN, Roses DF. Mammographic detection of carcinoma of the breast in patients with augmentation prostheses. Surg Gynecol Obstet. 1989;168(1):30–2.
68. Denley H, et al. Metaplastic carcinoma of the breast arising within complex sclerosing lesion: a report of five cases. Histopathology. 2000;36(3):203–9.
69. Gobbi H, et al. Metaplastic spindle cell breast tumors arising within papillomas, complex sclerosing lesions, and nipple adenomas. Mod Pathol. 2003;16(9):893–901.
70. Wilsher MJ. Adenosquamous proliferation of the breast and low grade adenosquamous carcinoma: a common precursor of an uncommon cancer? Pathology. 2014;46(5):402–10.
71. Wilsher MJ, Owens TW, Allcock RJ. Next generation sequencing of the nidus of early (adenosquamous proliferation rich) radial sclerosing lesions of the breast reveals evidence for a neoplastic precursor lesion. J Pathol Clin Res. 2017;3(2):115–22.
72. Eberle CA, et al. Infiltrating epitheliosis of the breast: characterization of histological features, immunophenotype and genomic profile. Histopathology. 2016;68(7):1030–9.
73. Hilson JB, Schnitt SJ, Collins LC. Phenotypic alterations in myoepithelial cells associated with benign sclerosing lesions of the breast. Am J Surg Pathol. 2010;34(6):896–900.
74. Kawaguchi K, Shin SJ. Immunohistochemical staining characteristics of low-grade adenosquamous carcinoma of the breast. Am J Surg Pathol. 2012;36(7):1009–20.
75. Oh EY, Collins LC. Keratin expression patterns in stromal cells of benign sclerosing lesions of the breast: a potential diagnostic pitfall. Arch Pathol Lab Med. 2015;139(9):1143–8.
76. Elston CW, Ellis IO. The breast. Edinburgh: Churchill Livingstone; 1998.
77. Anderson TJ, Battersby S. Radial scars of benign and malignant breasts: comparative features and significance. J Pathol. 1985;147(1):23–32.
78. Jacobs TW, et al. Radial scars of the breast and breast carcinomas have similar alterations in expression of factors involved in vascular stroma formation. Hum Pathol. 2002;33(1):29–38.
79. Iqbal M, et al. Molecular and genetic abnormalities in radial scar. Hum Pathol. 2002;33(7):715–22.
80. Wolters KL, et al. Frequent PIK3CA mutations in radial scars. Diagn Mol Pathol. 2013;22(4):210–4.
81. Bataillon G, et al. High rate of PIK3CA mutations but no TP53 mutations in low-grade adenosquamous carcinoma of the breast. Histopathology. 2018;73(2):273–83.
82. Ang D, et al. Novel method for PIK3CA mutation analysis: locked nucleic acid—PCR sequencing. J Mol Diagn. 2013;15(3):312–8.
83. Troxell ML, et al. High prevalence of PIK3CA/AKT pathway mutations in papillary neoplasms of the breast. Mod Pathol. 2010;23(1):27–37.
84. Troxell ML, et al. Phosphatidylinositol-3-kinase pathway mutations are common in breast columnar cell lesions. Mod Pathol. 2012;25(7):930–7.

85. Dahlstrom JE, et al. Diagnostic accuracy of stereotactic core biopsy in a mammographic breast cancer screening programme. Histopathology. 1996;28(5):421–7.
86. Dershaw DD, et al. Nondiagnostic stereotaxic core breast biopsy: results of rebiopsy. Radiology. 1996;198(2):323–5.
87. Lee AH, et al. Excision biopsy findings of patients with breast needle core biopsies reported as suspicious of malignancy (B4) or lesion of uncertain malignant potential (B3). Histopathology. 2003;42(4):331–6.
88. Lee CH, et al. Cost-effectiveness of stereotactic core needle biopsy: analysis by means of mammographic findings. Radiology. 1997;202(3):849–54.
89. Meyer JE, et al. Large-needle core biopsy: nonmalignant breast abnormalities evaluated with surgical excision or repeat core biopsy. Radiology. 1998;206(3):717–20.
90. Jackman RJ, et al. Stereotactic, automated, large-core needle biopsy of nonpalpable breast lesions: false-negative and histologic underestimation rates after long-term follow-up. Radiology. 1999;210(3):799–805.
91. Kirwan SE, et al. Multiple 14G stereotactic core biopsies in the diagnosis of mammographically detected stellate lesions of the breast. Clin Radiol. 2000;55(10):763–6.
92. Philpotts LE, et al. Uncommon high-risk lesions of the breast diagnosed at stereotactic core-needle biopsy: clinical importance. Radiology. 2000;216(3):831–7.
93. Brenner RJ, et al. Percutaneous core needle biopsy of radial scars of the breast: when is excision necessary? AJR Am J Roentgenol. 2002;179(5):1179–84.
94. Brodie C, O'Doherty A, Quinn C. Fourteen-gauge needle core biopsy of mammographically evident radial scars: is excision necessary? Cancer. 2004;100(3):652–3; author reply 653–4.
95. Becker L, et al. Management of radial scars found at percutaneous breast biopsy. Can Assoc Radiol J. 2006;57(2):72–8.
96. Lopez-Medina A, et al. Radial scars diagnosed at stereotactic core-needle biopsy: surgical biopsy findings. Eur Radiol. 2006;16(8):1803–10.
97. Dillon MF, et al. Predictive value of breast lesions of "uncertain malignant potential" and "suspicious for malignancy" determined by needle core biopsy. Ann Surg Oncol. 2007;14(2):704–11.
98. El-Sayed ME, et al. Predictive value of needle core biopsy diagnoses of lesions of uncertain malignant potential (B3) in abnormalities detected by mammographic screening. Histopathology. 2008;53(6):650–7.
99. Lieske B, et al. Screen-detected breast lesions with an indeterminate (B3) core needle biopsy should be excised. Eur J Surg Oncol. 2008;34(12):1293–8.
100. Hayes BD, O'Doherty A, Quinn CM. Correlation of needle core biopsy with excision histology in screen-detected B3 lesions: the Merrion breast screening unit experience. J Clin Pathol. 2009;62(12):1136–40.
101. Linda A, et al. Radial scars without atypia diagnosed at imaging-guided needle biopsy: how often is associated malignancy found at subsequent surgical excision, and do mammography and sonography predict which lesions are malignant? AJR Am J Roentgenol. 2010;194(4):1146–51.
102. Rakha EA, et al. Outcome of breast lesions diagnosed as lesion of uncertain malignant potential (B3) or suspicious of malignancy (B4) on needle core biopsy, including detailed review of epithelial atypia. Histopathology. 2011;58(4):626–32.
103. Rakha EA, et al. Screen-detected malignant breast lesions diagnosed following benign (B2) or normal (B1) needle core biopsy diagnoses. Eur J Cancer. 2010;46(10):1835–40.
104. Rajan S, Wason AM, Carder PJ. Conservative management of screen-detected radial scars: role of mammotome excision. J Clin Pathol. 2011;64(1):65–8.
105. Rakha EA, et al. Characterization and outcome of breast needle core biopsy diagnoses of lesions of uncertain malignant potential (B3) in abnormalities detected by mammographic screening. Int J Cancer. 2011;129(6):1417–24.
106. Resetkova E, et al. Management of radial sclerosing lesions of the breast diagnosed using percutaneous vacuum-assisted core needle biopsy: recommendations for excision based on seven years' of experience at a single institution. Breast Cancer Res Treat. 2011;127(2):335–43.
107. Sloane JP, Mayers MM. Carcinoma and atypical hyperplasia in radial scars and complex sclerosing lesions: importance of lesion size and patient age. Histopathology. 1993;23(3):225–31.
108. Matrai C, et al. Advocating nonsurgical management of patients with small, incidental radial scars at the time of needle core biopsy: a study of 77 cases. Arch Pathol Lab Med. 2015;139:1137–42.
109. Lee KA, et al. Risk of malignancy when microscopic radial scars and microscopic papillomas are found at percutaneous biopsy. AJR Am J Roentgenol. 2012;198(2):W141–5.
110. Park VY, et al. Mammographically occult asymptomatic radial scars/complex sclerosing lesions at ultrasonography-guided core needle biopsy: follow-up can be recommended. Ultrasound Med Biol. 2016;42(10):2367–71.
111. Farshid G, Buckley E. Meta-analysis of upgrade rates in 3163 radial scars excised after needle core biopsy diagnosis. Breast Cancer Res Treat. 2019;174(1):165–77.
112. McDivitt RW, Stewart FW, Berg JW, Universities Associated for Research and Education in Pathology. Tumors of the breast. In: Armed Forces Institute of Pathology (US), editor. Atlas of tumor pathology, second series, fascicle 2. Washington, DC: Armed Forces Institute of Pathology; 1968.
113. Clement PB, Azzopardi JG. Microglandular adenosis of the breast—a lesion simulating tubular carcinoma. Histopathology. 1983;7(2):169–80.
114. Rosen PP. Microglandular adenosis. A benign lesion simulating invasive mammary carcinoma. Am J Surg Pathol. 1983;7(2):137–44.
115. Tavassoli FA, Norris HJ. Microglandular adenosis of the breast. A clinicopathologic study of 11 cases with ultrastructural observations. Am J Surg Pathol. 1983;7(8):731–7.
116. Khalifeh IM, et al. Clinical, histopathologic, and immunohistochemical features of microglandular adenosis and transition into in situ and invasive carcinoma. Am J Surg Pathol. 2008;32(4):544–52.
117. Geyer FC, et al. Microglandular adenosis or microglandular adenoma? A molecular genetic analysis of a case associated with atypia and invasive carcinoma. Histopathology. 2009;55(6):732–43.
118. Geyer FC, et al. Molecular evidence in support of the neoplastic and precursor nature of microglandular adenosis. Histopathology. 2012;60(6B):E115–30.
119. Shin SJ, et al. Molecular evidence for progression of microglandular adenosis (MGA) to invasive carcinoma. Am J Surg Pathol. 2009;33(4):496–504.
120. Rosen PP. Rosen's breast pathology. 3rd ed. Philadelphia, PA: Lippincott Williams & Wilkins; 2008. p. 1136.
121. Sabate JM, et al. Microglandular adenosis of the breast in a BRCA1 mutation carrier: radiological features. Eur Radiol. 2002;12(6):1479–82.
122. Brogi E. Adenosis and microglandular adenosis. In: Brogi E, Hoda SA, Koerner FC, Rosen PP, editors. Rosen's breast pathology. Philadelphia, PA: Lippincott Williams & Wilkins; 2014.
123. Tavassoli FA, Bratthauer GL. Immunohistochemical profile and differential diagnosis of microglandular adenosis. Mod Pathol. 1993;6(3):318–22.

124. Rosenblum MK, Purrazzella R, Rosen PP. Is microglandular adenosis a precancerous disease? A study of carcinoma arising therein. Am J Surg Pathol. 1986;10(4):237–45.
125. Koenig C, et al. Carcinoma arising in microglandular adenosis: an immunohistochemical analysis of 20 intraepithelial and invasive neoplasms. Int J Surg Pathol. 2000;8(4):303–15.
126. James BA, Cranor ML, Rosen PP. Carcinoma of the breast arising in microglandular adenosis. Am J Clin Pathol. 1993;100(5):507–13.
127. Resetkova E, Flanders DJ, Rosen PP. Ten-year follow-up of mammary carcinoma arising in microglandular adenosis treated with breast conservation. Arch Pathol Lab Med. 2003;127(1):77–80.
128. Shui R, Yang W. Invasive breast carcinoma arising in microglandular adenosis: a case report and review of the literature. Breast J. 2009;15(6):653–6.
129. Lee YH, et al. Young-aged woman with invasive ductal carcinoma arising in atypical microglandular adenosis: a case report. Pathol Int. 2010;60(10):685–9.
130. Acs G, et al. Microglandular adenosis with transition into adenoid cystic carcinoma of the breast. Am J Surg Pathol. 2003;27(8):1052–60.
131. Rosen PP. So-called acinic cell carcinoma of the breast arises from microgladular adenosis and is not a distinct entity. Mod Pathol. 2017;30(10):1504.
132. Wen YH, Weigelt B, Reis-Filho JS. Microglandular adenosis: a non-obligate precursor of triple-negative breast cancer? Histol Histopathol. 2013;28(9):1099–108.
133. Geyer FC, et al. Genetic analysis of microglandular adenosis and acinic cell carcinomas of the breast provides evidence for the existence of a low-grade triple-negative breast neoplasia family. Mod Pathol. 2017;30(1):69–84.
134. Foschini MP, Eusebi V. Microglandular adenosis of the breast: a deceptive and still mysterious benign lesion. Hum Pathol. 2018;82:1–9.
135. Eusebi V, et al. Microglandular adenosis, apocrine adenosis, and tubular carcinoma of the breast. An immunohistochemical comparison. Am J Surg Pathol. 1993;17(2):99–109.
136. Guerini-Rocco E, et al. Microglandular adenosis associated with triple-negative breast cancer is a neoplastic lesion of triple-negative phenotype harbouring TP53 somatic mutations. J Pathol. 2016;238(5):677–88.
137. Radner M, et al. Chromosome 2q gain and epigenetic silencing of GATA3 in microglandular adenosis of the breast. J Pathol Clin Res. 2021;7(3):220–32.
138. Rosen PP. Mucocele-like tumors of the breast. Am J Surg Pathol. 1986;10(7):464–9.
139. Hamele-Bena D, Cranor ML, Rosen PP. Mammary mucocele-like lesions. Benign and malignant. Am J Surg Pathol. 1996;20(9):1081–5.
140. Weaver MG, Abdul-Karim FW, Al-Kaisi N. Mucinous lesions of the breast. A pathological continuum. Pathol Res Pract. 1993;189(8):873–6.
141. Renshaw AA. Can mucinous lesions of the breast be reliably diagnosed by core needle biopsy? Am J Clin Pathol. 2002;118(1):82–4.
142. Wang J, et al. Can core biopsy reliably diagnose mucinous lesions of the breast? Am J Clin Pathol. 2007;127(1):124–7.
143. Park YJ, Kim EK. A pure mucocele-like lesion diagnosed on ultrasonography-guided core-needle biopsy: is imaging follow-up sufficient? Ultrasonography. 2014; https://doi.org/10.14366/usg.14036.
144. Kim JY, et al. Benign and malignant mucocele-like tumors of the breast: mammographic and sonographic appearances. AJR Am J Roentgenol. 2005;185(5):1310–6.
145. Carkaci S, et al. Do all mucocele-like lesions of the breast require surgery? Clin Imaging. 2011;35(2):94–101.
146. Cheng L, Lee WY, Chang TW. Benign mucocele-like lesion of the breast: how to differentiate from mucinous carcinoma before surgery. Cytopathology. 2004;15(2):104–8.
147. Glazebrook K, Reynolds C. Original report. Mucocele-like tumors of the breast: mammographic and sonographic appearances. AJR Am J Roentgenol. 2003;180(4):949–54.
148. Chopra S, et al. Pure mucinous breast cancer-mammographic and ultrasound findings. Clin Radiol. 1996;51(6):421–4.
149. Coyne JD. Columnar cell hyperplasia with intraluminal crystalloids and features of a mucocoele-like lesion. Histopathology. 2004;44(4):401–3.
150. Fadare O, Mariappan MR. Mucocele-like tumor and columnar cell hyperplasia of the breast occurring in a morphologic continuum. J Med Case Rep. 2008;2:138.
151. Tan PH, Tse GM, Bay BH. Mucinous breast lesions: diagnostic challenges. J Clin Pathol. 2008;61(1):11–9.
152. Kryvenko ON, et al. Precursor lesions of mucinous carcinoma of the breast: analysis of 130 cases. Am J Surg Pathol. 2013;37(7):1076–84.
153. Deschryver K, Radford DM, Schuh ME. Pathology of large-caliber stereotactic biopsies in nonpalpable breast lesions. Semin Diagn Pathol. 1999;16(3):224–34.
154. Carder PJ, Murphy CE, Liston JC. Surgical excision is warranted following a core biopsy diagnosis of mucocoele-like lesion of the breast. Histopathology. 2004;45(2):148–54.
155. Ramsaroop R, et al. Mucocele-like lesions of the breast: an audit of 2 years at BreastScreen Auckland (New Zealand). Breast J. 2005;11(5):321–5.
156. Begum SM, et al. Mucin extravasation in breast core biopsies–clinical significance and outcome correlation. Histopathology. 2009;55(5):609–17.
157. Ouldamer L, et al. [Mucocele-like lesions of the breast: management after diagnosis on ultrasound guided core biopsy or stereotactic vacuum-assisted biopsy]. Gynecol Obstet Fertil. 2010;38(7–8):455–9.
158. Flegg KM, et al. Surgical outcomes of borderline breast lesions detected by needle biopsy in a breast screening program. World J Surg Oncol. 2010;8:78.
159. Jaffer S, Bleiweiss IJ, Nagi CS. Benign mucocele-like lesions of the breast: revisited. Mod Pathol. 2011;24(5):683–7.
160. Weigel S, et al. Minimal invasive biopsy results of "uncertain malignant potential" in digital mammography screening: high prevalence but also high predictive value for malignancy. Rofo. 2011;183(8):743–8.
161. Sutton B, et al. Mucocele-like lesions diagnosed on breast core biopsy: assessment of upgrade rate and need for surgical excision. Am J Clin Pathol. 2012;138(6):783–8.
162. Towne WS, Michaels AY, Ginter PS. Mucocele-like lesion of the breast diagnosed on core biopsy: histologic and clinical analysis of 78 cases with focus on features associated with upgrade. Arch Pathol Lab Med. 2021; https://doi.org/10.5858/arpa.2020-0497-OA.
163. Zhang G, et al. Mucocele-like lesions diagnosed on breast core biopsy: low risk of upgrade and subsequent carcinoma. Breast J. 2018;24(3):314–8.
164. Rakha EA, et al. Outcome of pure mucocele-like lesions diagnosed on breast core biopsy. Histopathology. 2013;62(6):894–8.
165. Fisher CJ, Millis RR. A mucocoele-like tumour of the breast associated with both atypical ductal hyperplasia and mucoid carcinoma. Histopathology. 1992;21(1):69–71.
166. Ohi Y, et al. Mucocele-like lesions of the breast: a long-term follow-up study. Diagn Pathol. 2011;6:29.

Papillary and Epithelial–Myoepithelial Tumors

6

Paula S. Ginter and Timothy M. D'Alfonso

Papillary Lesions

Overview

Papillary lesions comprise a clinically and histologically diverse group of epithelial proliferations composed of supportive fibrovascular cores lined by variable amounts of epithelial and myoepithelial cells. Both benign and malignant papillary lesions may develop in any component of the duct-lobular system, but they are disproportionately more frequent in lactiferous and subareolar central ducts.

Because of their high degree of cellularity or accompanying periductal stromal changes, benign papillary lesions can mimic malignancy, especially in limited samples that do not provide much context of lesional extent or size. On the other hand, papillary carcinomas are often bland in appearance, with most characterized by subtle cytological features of malignancy that may be confused with benign processes. For these reasons, papillary lesions present a common and sometimes difficult diagnostic problem in core needle biopsies.

When evaluating papillary lesions in any type of sample, pathologists should bear in mind that benign papillary lesions are characterized by the presence of myoepithelial cells which can be demonstrated with immunohistochemical stains [1]. Papillary carcinomas, however, either lack myoepithelial cells or show attenuation of myoepithelial staining. Second, most papillary breast carcinomas are diagnosed in women older than 60 years, whereas papilloma is generally a lesion encountered in pre- and perimenopausal age groups. Accordingly, one should have a higher index of suspicion when evaluating a papillary lesion from an older patient. Adenomyoepithelial tumors are multinodular papillary lesions in which the myoepithelial component is particularly prominent.

The following discussion will encompass the spectrum of benign (papilloma), atypical (papilloma with atypical ductal hyperplasia), and malignant (papillary carcinoma) papillary lesions in the breast. Ductal carcinoma in situ (DCIS) which can show a variety of architectural patterns including papillary typically involves multiple ducts and is discussed within the broader context of DCIS in Chap. 9.

Intraductal Papilloma

Overview and Clinical Presentation

Papillomas can be solitary or multiple. Solitary papillomas typically arise in subareolar large ducts and affect patients in their 40–60s who most commonly are biopsied for benign breast disease. Rarely, papillomas may also develop in children and adolescents. These tumors are especially prone to cause nipple discharge, which is unilateral, and either clear or bloody in appearance. Although most papillomas are not palpable, some patients may present with a subareolar nodule, particularly in those that are greater than 2 cm in size. Smaller papillomas may be detected on screening imaging, or as incidental histologic findings in biopsy or excision specimens. In contrast, multiple papillomas arise within peripheral terminal duct-lobular units and affected patients are usually younger than those having solitary, centrally located papillomas. Patients with multiple papillomas have a tendency to have synchronous, recurrent, or bilateral proliferative breast lesions. Despite these clinical differences, the histologic appearance and pathologic workup in problematic cases remain the same for pathologists.

P. S. Ginter
Department of Pathology and Laboratory Medicine, Weill Cornell Medicine, New York, NY, USA
e-mail: psg9003@med.cornell.edu

T. M. D'Alfonso (✉)
Department of Pathology, Memorial Sloan Kettering Cancer Center, New York, NY, USA
e-mail: dalfonst@mskcc.org

© The Author(s), under exclusive license to Springer Nature Switzerland AG 2022
S. J. Shin et al. (eds.), *A Comprehensive Guide to Core Needle Biopsies of the Breast*,
https://doi.org/10.1007/978-3-031-05532-4_6

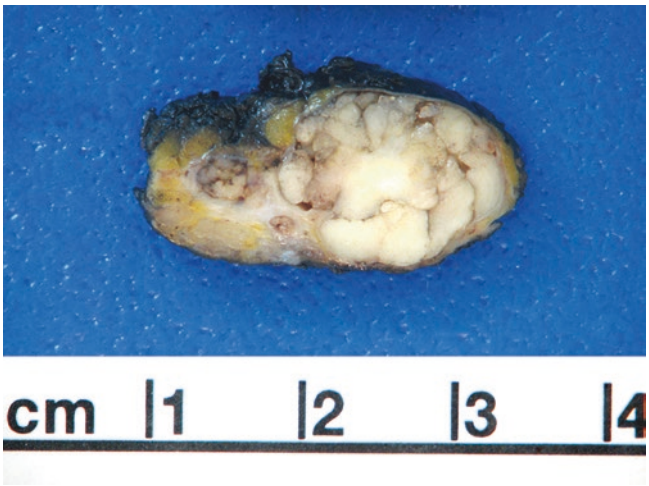

Fig. 6.1 Gross appearance of intraductal papilloma. An excisional biopsy specimen shows a dilated duct with an intraductal papillary mass

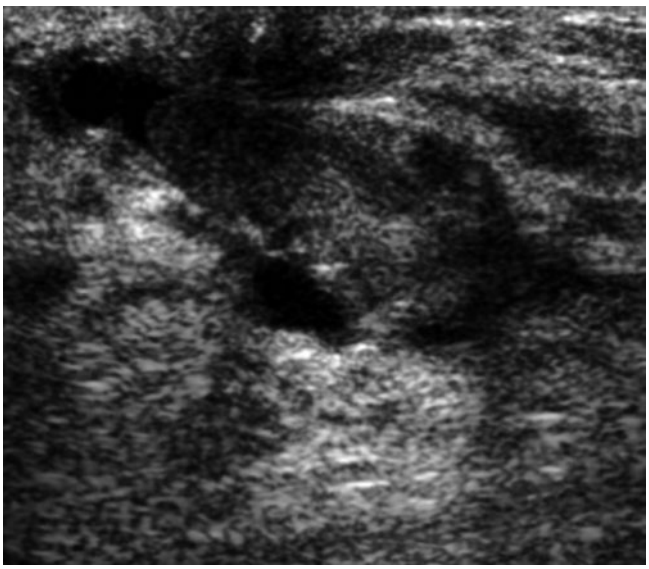

Fig. 6.2 Ultrasound appearance of intraductal papilloma. A solid mass within a dilated duct is seen

Gross and Radiographic Features

Grossly, a papilloma may appear as a polypoid nodule within a dilated duct and may show papillary excrescences (Fig. 6.1). Associated hemorrhage may be present. In cases that have undergone prior biopsy, a papilloma can grossly appear as an ill-defined mass. On mammography, papilloma may appear as a circumscribed mass within a cystically dilated duct. Calcifications may be evident, which correspond to stromal mineralization or calcifications associated with glandular tissue. In many cases, papillomas are not apparent on mammography due to their small size [2, 3]. In a series of 22 patients with nipple discharge reported by Orel et al., five patients with negative mammograms had intraductal papillomas on excisional biopsy that ranged in size from 0.4 to 0.7 cm [4]. Many papillomas are associated with dilated ducts, which may be the only abnormality seen on imaging [2, 5]. Ultrasound shows a well-defined hypoechoic nodule with or without ductal dilatation (Fig. 6.2) [5].

Microscopic Features

Intraductal papilloma is characterized by an arborizing proliferation of fibrovascular cores lined by an inner layer of myoepithelial cells and outer layer of ductal epithelial cells. The papilloma is typically seen arising within a dilated or fibrotic duct (Fig. 6.3). The histologic appearance of papilloma can be quite heterogeneous and show variable degrees of epithelial proliferation, coexisting fibrocystic changes, inflammation, and stromal sclerosis.

As with other papillary lesions in core biopsy samples, papillomas may appear as detached tissue fragments that have been separated from their surrounding duct (Fig. 6.4). At low magnification, the dense cell population may impart a more "solid" than arborescent architecture and may lack obvious branching papillae (Fig. 6.5). Fibrovascular cores can be slender or broad and are lined by cuboidal to columnar epithelial cells that are oriented perpendicular to the basement membrane (Fig. 6.6). The epithelial cells lack significant cytologic atypia. Mitoses should be absent in all but an occasional case where they may be rare. Myoepithelial cells may be flattened and inconspicuous or cuboidal, round, and prominent (Fig. 6.7). Clear cell change can be seen in myoepithelial cells. In some cases, papillomas show adenomyoepitheliomatous features, in which the myoepithelial populations are prominent and distinct from the epithelium with more abundant cytoplasm (Fig. 6.8). The evenly disposed architecture of myoepithelium in these cases is of use in distinguishing them from cases of atypical lobular hyperplasia or lobular carcinoma in situ (lobular neoplasia) involving a papilloma (see below).

Intraductal papilloma may be accompanied by or contain virtually all manifestations of non-proliferative and proliferative fibrocystic change. "Secondary" proliferative lesions are present in over one half of patients with solitary papillomas, and generally provide reassurance that a particular lesion is completely benign. Common findings include foci of adenosis which expands the interior of these lesions (Fig. 6.9). Florid usual ductal hyperplasia of the epithelial lining of papillomas often grows within and distends the potential space between the papilloma and the duct from which it is arising (Fig. 6.10). In some cases it is sufficiently florid to obscure the underlying papillary lesion or worse, mimic solid papillary carcinoma (discussed below).

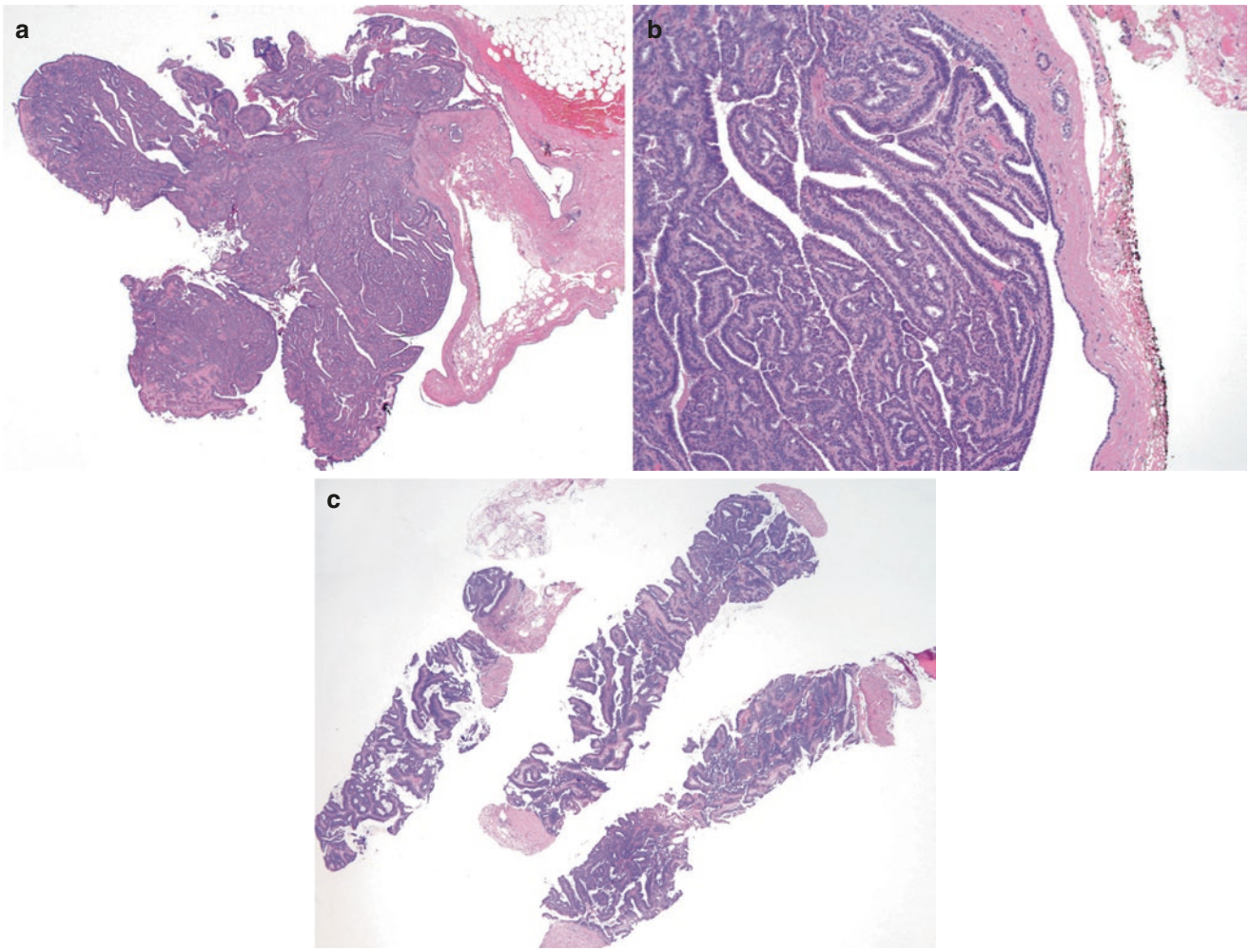

Fig. 6.3 Intraductal papilloma in a core biopsy. (**a**–**c**) Two examples of papilloma showing papillary proliferations arising within dilated and fibrotic ducts

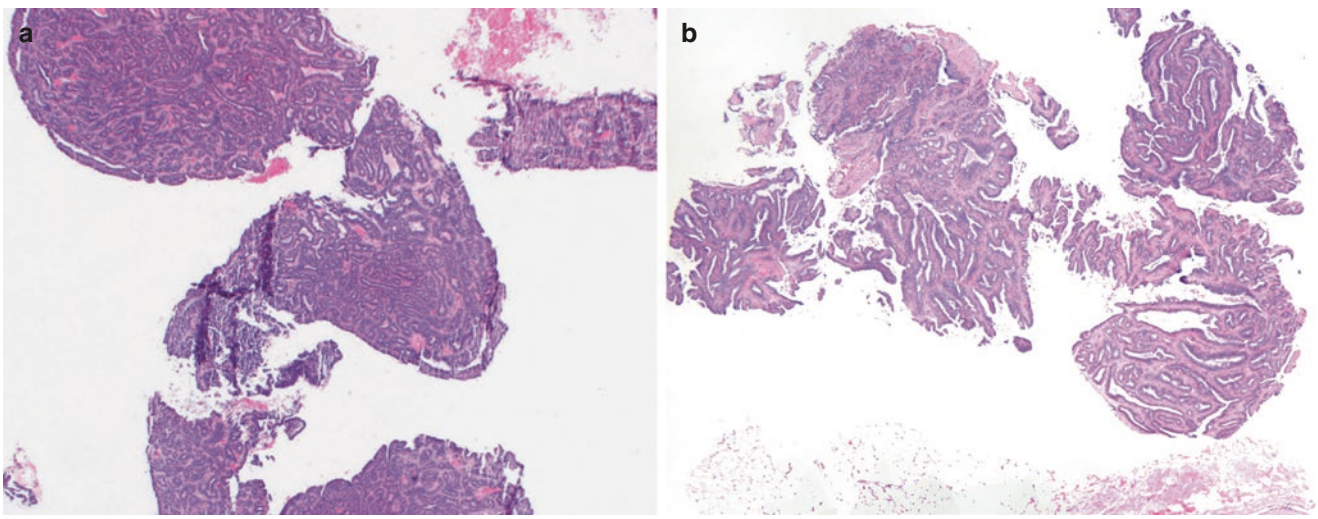

Fig. 6.4 Intraductal papilloma in core biopsy. (**a**, **b**) Papillomas appear fragmented in these core biopsies and are separated from the involved duct

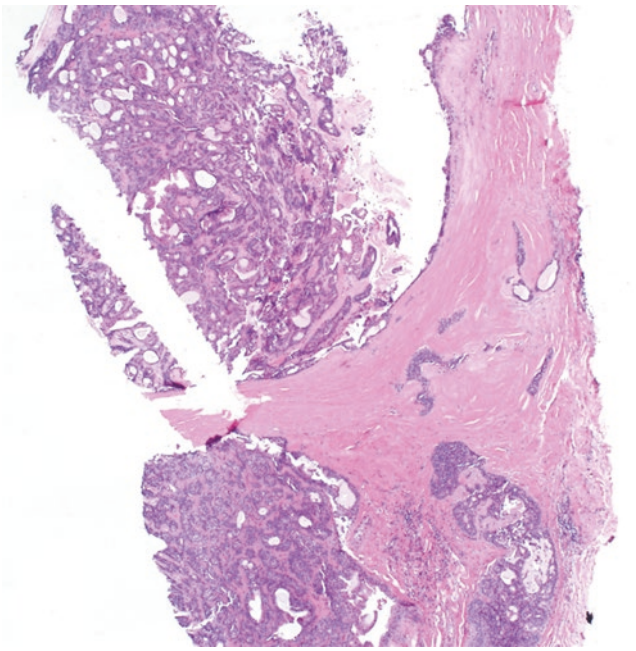

Fig. 6.5 Intraductal papilloma in core biopsy. The intraductal proliferation shows solid architecture and lacks obvious branching papillae in this case

Apocrine metaplasia is present in up to one-third of papillomas (Fig. 6.11); this is often characterized by variable nuclear enlargement which may be misconstrued as true apocrine atypia. This finding can be particularly problematic in core biopsy samples, and if there is an expansile focus of apocrine cells demonstrating a threefold increase in nuclear size (i.e., relative of "normal" apocrine cells) and other concerning features such as mitoses or single cell necrosis, excisional biopsy of the lesion should be recommended to exclude apocrine DCIS.

Papillomas can undergo acute or organizing infarction, which may be the result of a previous needling by FNA [6]. This can be diffuse or focal within the papilloma. If recent, infarction is characterized by a well-demarcated area of hypereosinophilic coagulative necrosis (Fig. 6.12). Squamous metaplasia is often present in such cases, but can also occur independent of infarction and generally considered a finding associated with papillomas (benignity) (Fig. 6.13).

The term "sclerosing papilloma" is used for papillomas with periductal sclerosis associated with fibroblastic proliferation, altered extracellular matrix, and "entrapped" ductules (Fig. 6.14). These lesions show some overlapping

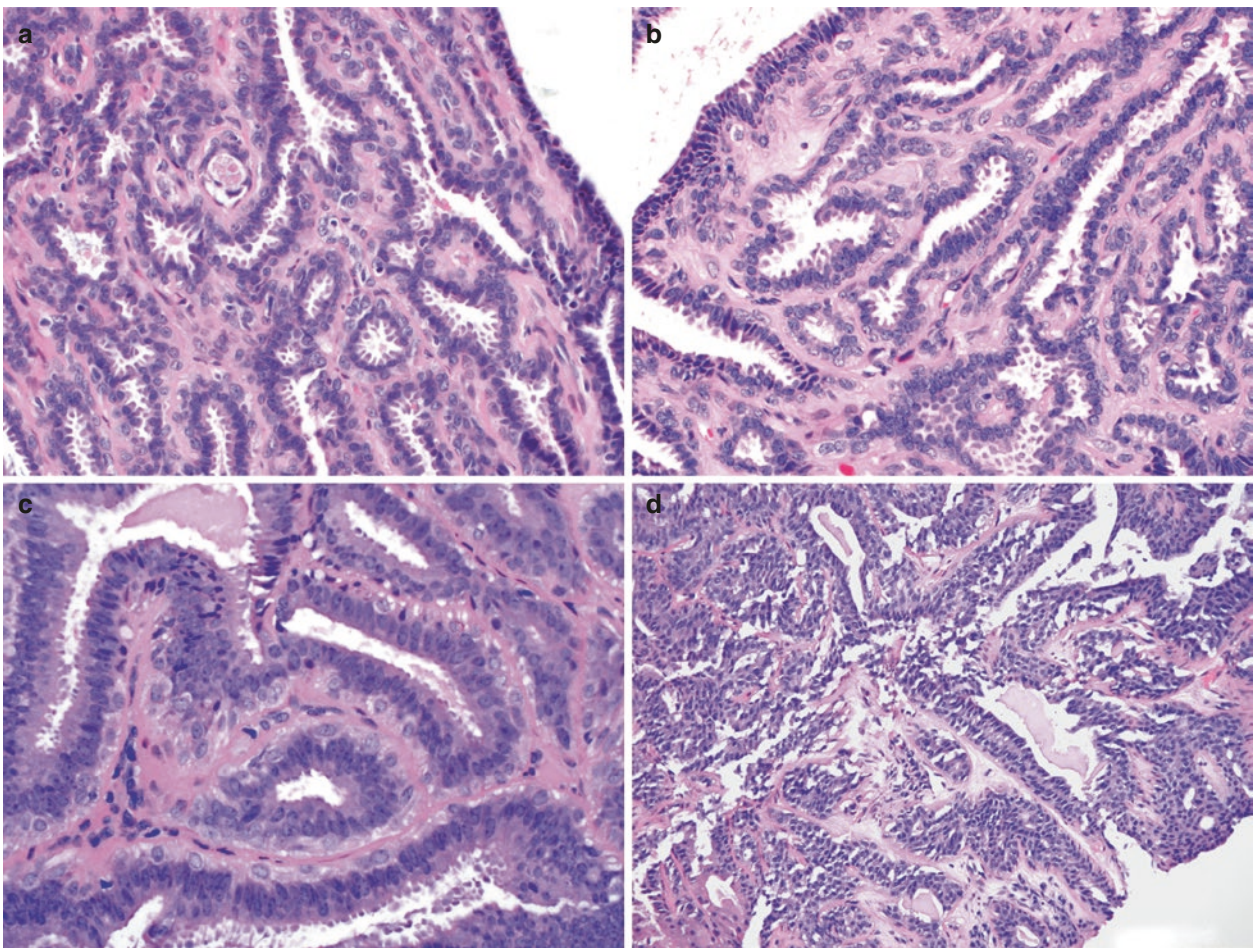

Fig. 6.6 Intraductal papilloma. (**a**–**d**) Intraductal papilloma is characterized by fibrovascular cores lined by cuboidal to columnar epithelium oriented perpendicular to the basement membrane. Cells lack significant cytologic atypia

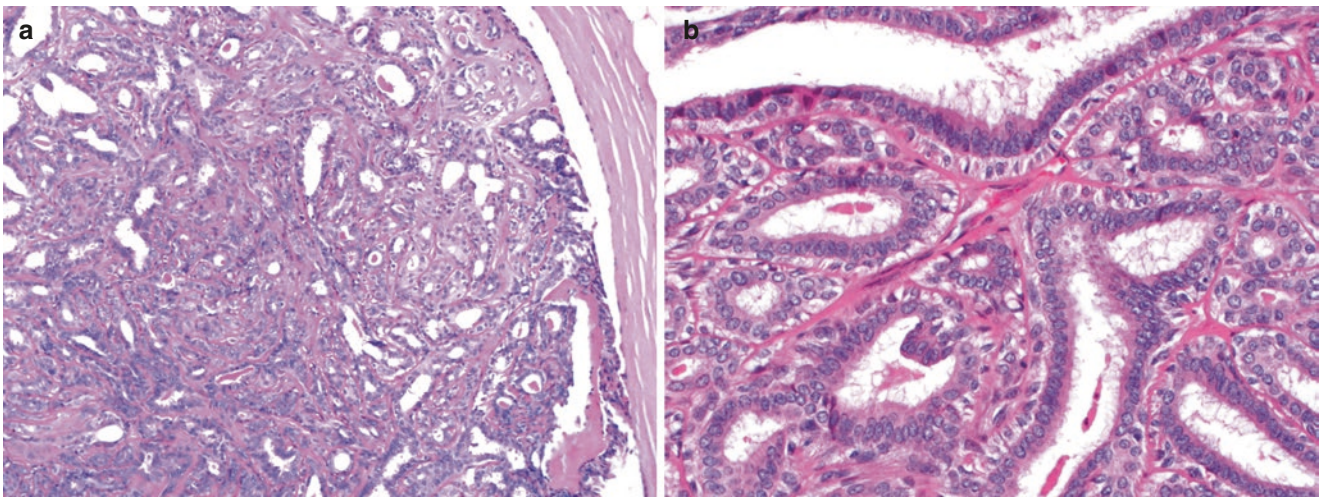

Fig. 6.7 Myoepithelial cells in intraductal papilloma. (**a**, **b**) Myoepithelial cells are cuboidal with clear cytoplasm and are prominent in these examples

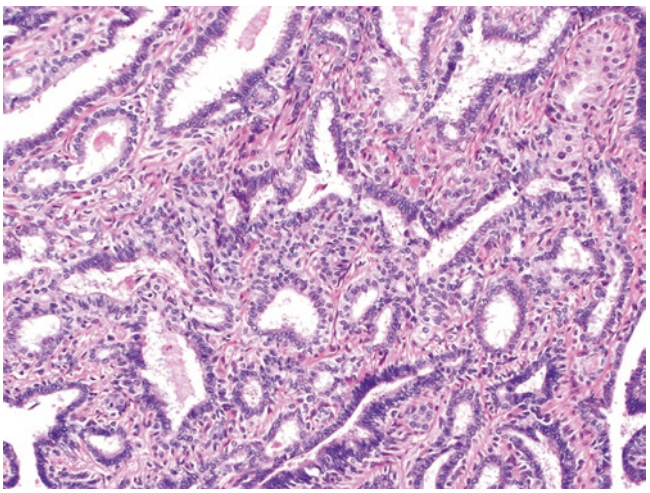

Fig. 6.8 Papilloma with myoepithelial cell hyperplasia. Myoepithelial cells are prominent and show small foci of hyperplasia within papillae

features with radial scars/complex sclerosing lesions, and in some instances the distinction may not be possible in core needle biopsy material (Fig. 6.15). A descriptive term of the histologic findings such as "radial sclerosing papillary lesion" may be necessary with deferral of diagnosis to be rendered at the time of excisional biopsy.

A characteristic but particularly difficult pattern of sclerosis seen in papillomas is characterized by tortuous or band-like small ducts alternating with an admixture of cellular and hyalinized stroma which can pose as a diagnostic pitfall for invasive carcinoma. Owing to their resemblance to a desmoplastic host response seen with infiltrative small glands of invasive carcinoma, these may be confused with malignancy, particularly in a limited core needle biopsy sample (Fig. 6.16). As a general rule of thumb, worrisome sclerosing lesions should be interpreted with great caution particularly if there is unequivocal evidence of a papilloma in the specimen. In the vast majority of these instances, the areas concerning for invasive carcinoma represent sclerosis adjacent to a papilloma which only becomes evident at the time of excisional biopsy. Sclerotic areas with benign entrapped glands generally affect the periphery of a papilloma and the directional pattern of the glands is parallel to the papilloma's contour (Fig. 6.17). True invasion in association with papillary lesions exhibits different morphologic traits which will be discussed below. However, it should be fully acknowledged that the distinction can be exceedingly difficult in core biopsy samples, and in general erring on the side of caution is strongly recommended in this setting.

Papilloma with atypical ductal hyperplasia (ADH) (*atypical papilloma*) [7–9] is characterized by growth of a monotonous cell population within a papilloma with cytologic and/or architectural atypia that would ordinarily qualify for a diagnosis of atypical ductal hyperplasia outside of a papilloma (Figs. 6.18 and 6.19). The World Health Organization (WHO) recommends diagnosing papilloma with ADH when the atypical focus is less than 3 mm in size and papilloma with DCIS when the atypical focus is ≥3 mm [10]. These criteria imply that the bulk of the lesion should comprise recognizable benign papilloma. However, since size-threshold criteria are problematic in fragmented core biopsy samples, caution is recommended to avoid overdiagnosis of malignancy in these cases. In contrast to atypical papilloma, DCIS associated with a papilloma often involves multiple adjacent ducts which may be helpful in establishing a diagnosis of DCIS in a core biopsy sample, if adjacent ducts are fortuitously sampled (Fig. 6.20).

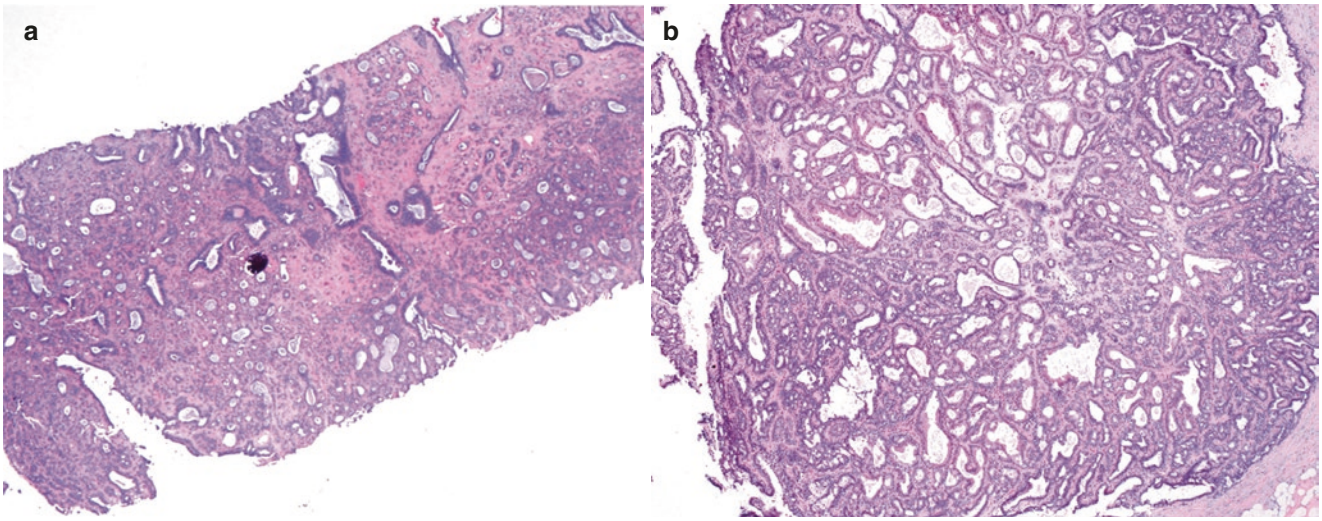

Fig. 6.9 Examples of intraductal papilloma involved by sclerosing adenosis. (**a**) Core biopsy that shows a papillary proliferation that is expanded by sclerosing adenosis involving the lesion. (**b**) Intraductal papilloma with sclerosing adenosis in an excisional biopsy

Atypical lobular hyperplasia (ALH)/lobular carcinoma in situ (LCIS) can arise within or adjacent to papillomas. When ALH/LCIS involves a papilloma, its presence can be subtle and difficult to recognize, requiring a high index of suspicion for initial detection, owing to focal or patchy pagetoid growth within papillomas (Fig. 6.21). ALH/LCIS cells have a tendency to arrange themselves individually or in small clusters within the interior of the papilloma, and may thereby resemble prominent myoepithelium, owing to their relatively clear cytoplasm. Diagnosis is facilitated by recognition of monotonous, round, centrally placed nuclei and asymmetric distribution of lobular cells within the papilloma. E-cadherin immunostaining is useful in confirming lobular neoplasia, although sometimes difficult to interpret due to frequent admixture with other proliferative (E-cadherin positive) elements common in papillomas.

Differential Diagnosis and Immunohistochemical Features

Most ordinary papillomas can be diagnosed without the use of immunostains, even when focally present in core needle biopsy samples. In difficult cases, staining for myoepithelial cells, which may be inconspicuous, provides reassurance that the lesion is benign. Useful stains for demonstrating myoepithelium include calponin, muscle-specific actin, smooth muscle myosin heavy chain (SMM), and p63 (Fig. 6.22). Cytokeratin 5/6 is expressed in myoepithelial cells but may also be seen in ductal hyperplasia and ALH/LCIS.

In most papillomas, myoepithelial cells form a continuous single layer around the outside of all luminal type or hyperplastic epithelium. In some papillomas, myoepithelial hyperplasia may be seen as small nodular foci. In situations of discerning entrapped glands in sclerosis from invasion, attempts to identify myoepithelial cells in the former can be wrought with its own pitfalls. The myoepithelium investing entrapped benign glands can be attenuated and employment of myoepithelial immunostains may reveal attenuated or even focally absent staining falsely suggesting invasion (Fig. 6.23). All myoepithelial markers are not "created equal" as some are less specific. Smooth muscle actin and CD10, for example, show cross-reactivity with adjacent stromal myofibroblasts. Conversely, despite ease of interpretation due to its nuclear distribution, p63 tends to be less sensitive for myoepithelial cells in papillary lesions and can show false-negative staining more often than others in certain diagnostic situations such as this. As such, if this investigation by immunohistochemistry is to be pursued, a panel of myoepithelial stains (p63, SMM, calponin) should be used provided there is enough diagnostic tissue available for study.

Estrogen receptor (ER) typically shows a variable staining pattern in usual ductal hyperplasia within a papilloma, similar to hyperplasia outside of a papilloma, whereas ADH and DCIS will typically show diffuse ER positivity. This can be diagnostically useful. One caveat, however, is that some benign papillomas may show diffuse ER staining (Fig. 6.24), and therefore malignancy should not be inferred solely by the presence of diffuse or intense immunoreactivity for ER in this setting.

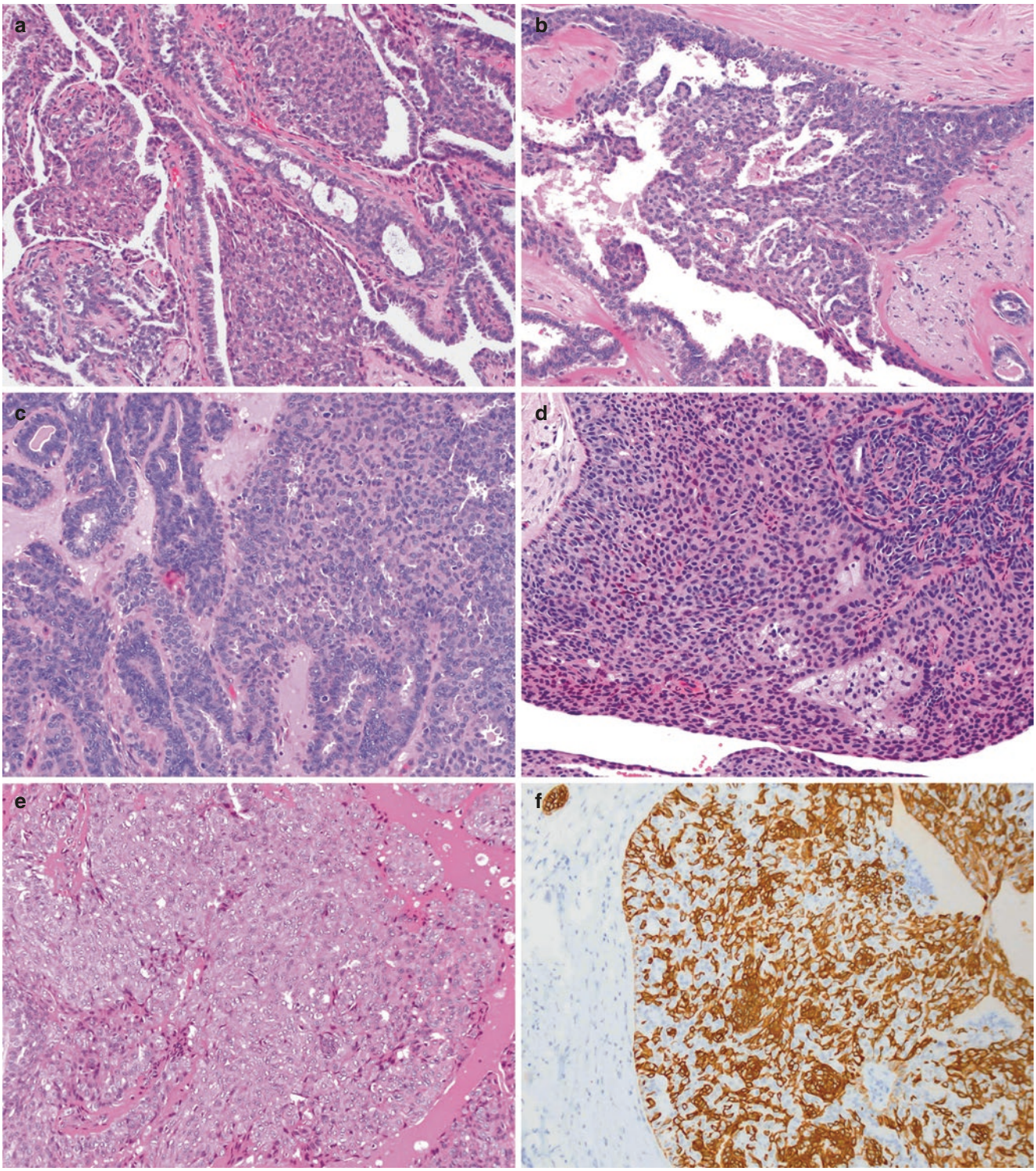

Fig. 6.10 Intraductal papillomas with florid usual ductal hyperplasia. (**a**–**e**) Florid ductal hyperplasia arises from the walls of ducts and shows a streaming growth pattern of polymorphic cells, similar to florid ductal hyperplasia seen outside of papillomas. (**f**) A CK5/6 immunostain shows a mosaic pattern of staining in florid ductal hyperplasia

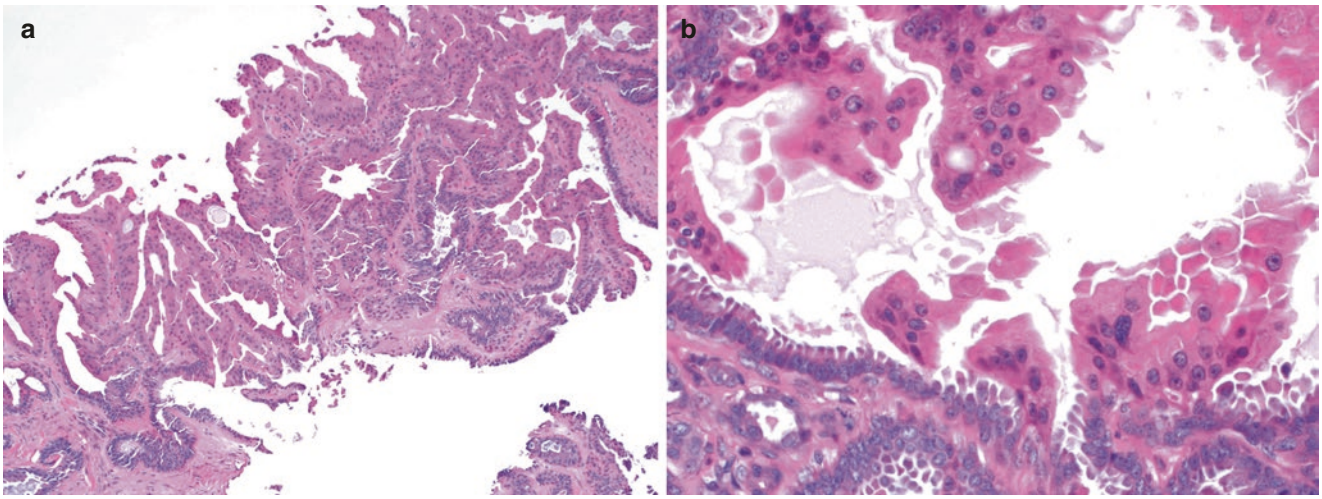

Fig. 6.11 Apocrine metaplasia in papilloma. (**a**) Core biopsy of papilloma with apocrine metaplasia. (**b**) Rare cells show apocrine-type atypia, characterized by enlarged nuclei

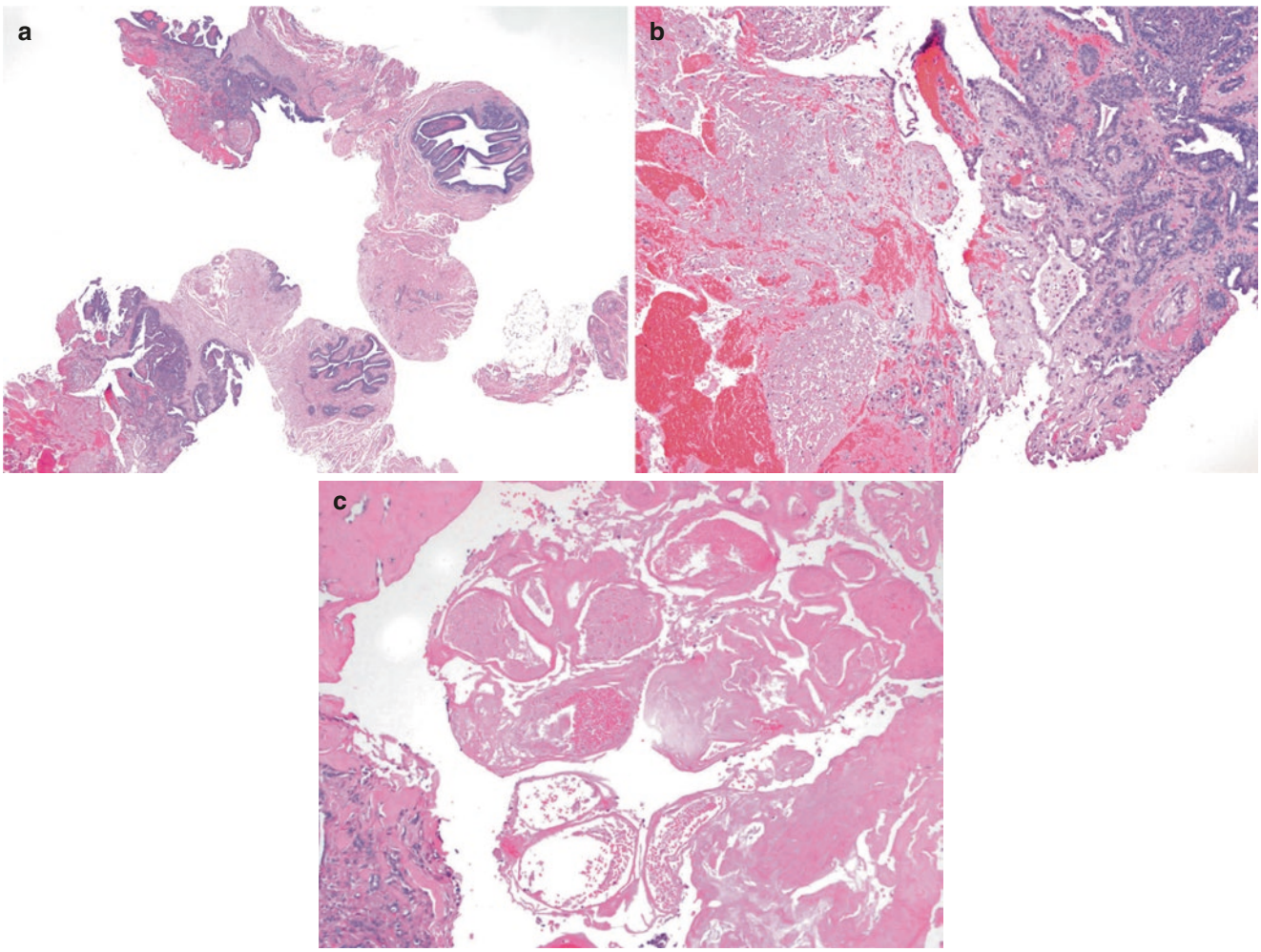

Fig. 6.12 Infarction in papilloma. (**a**) Low-power view of a core biopsy showing a papilloma that has undergone infarction (infarcted portions of papilloma on *left side* of image). (**b**, **c**) Infarcted areas of papilloma are eosinophilic and retain the underlying papillary growth pattern of the lesion

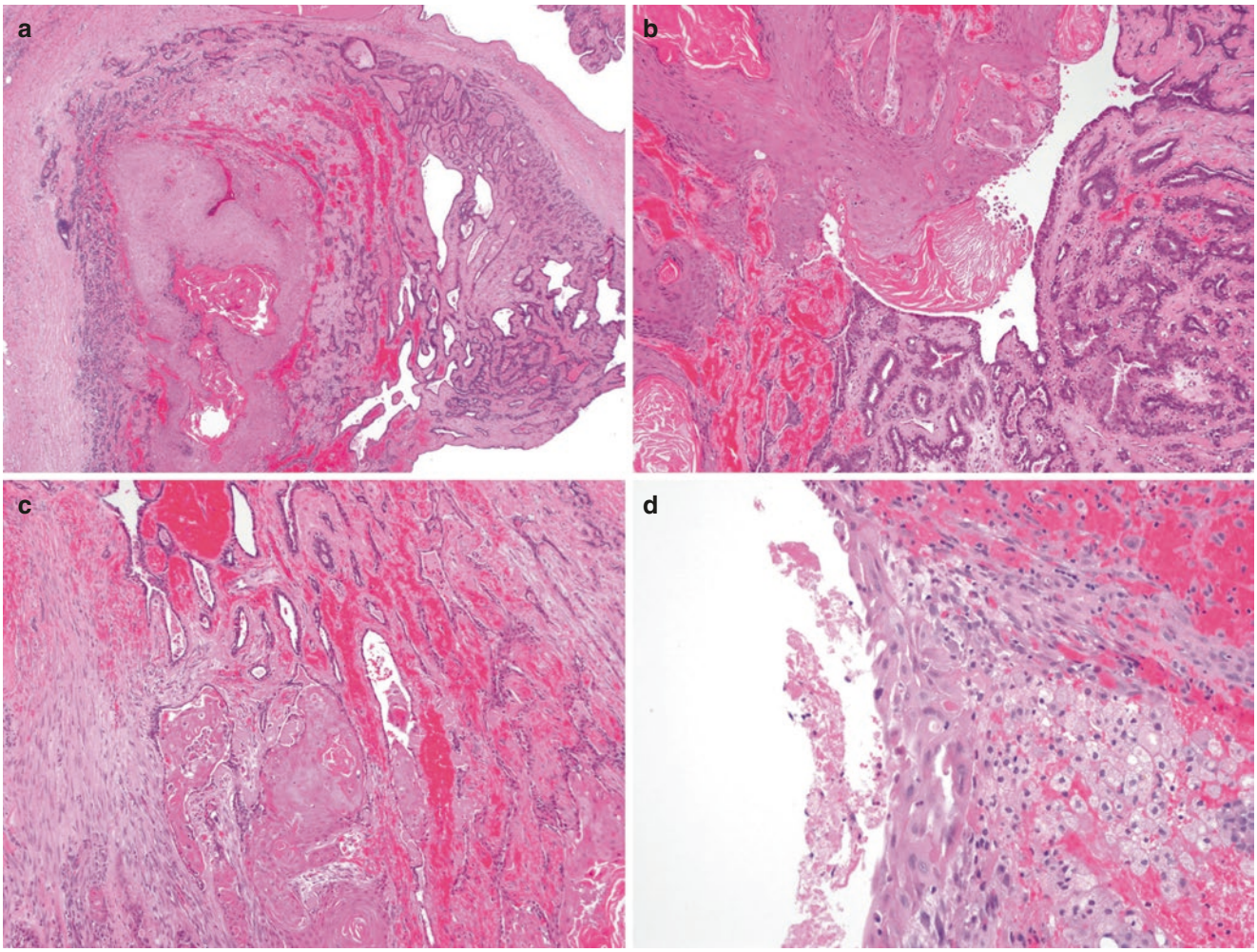

Fig. 6.13 Squamous metaplasia in papilloma. (**a**–**c**) Squamous metaplasia occurs within the stroma of papillae and within glandular lumina. (**d**) Squamous metaplasia in areas of inflammation and hemorrhage at the edge of a papilloma

Molecular Features of Intraductal Papilloma

Molecular analyses of intraductal papilloma have shown that papillomas are clonal neoplasms that show frequent (over 2/3 cases) alterations in the PIK3CA/AKT/mTOR signaling pathway [11–14]. Some studies have reported a greater frequency of *PIK3CA* mutations in papillomas with florid ductal hyperplasia [12, 15]. One study reported clonal-relatedness between a subset of papillomas and associated carcinomas (invasive and DCIS), with atypical papillomas more frequently clonally related to coexisting carcinoma than papillomas without atypia [14].

Management of Papilloma in Core Needle Biopsy

Surgical excision has been the traditional management for all papillomas diagnosed in core needle biopsies. The rationale behind excising these lesions is that there is a possibility that carcinoma arising within or in close association with the papilloma has gone unsampled. There has been a wide range of reported pathologic upgrade rates for papillomas diagnosed on core biopsy [16–22]. As with other studies of its kind, these have included small numbers of cases, have had variable inclusion criteria, and suffered possible selection bias as to which patients underwent excision.

More recent data support observation, rather than routine excision, of benign papillomas when there is radiologic-pathologic concordance. Studies employing strict-pathologic correlation and histologic review have shown upgrade rates on excision to DCIS or invasive carcinoma to be less than 5% [23–28]. One multi-institutional prospective analysis with radiologic-pathologic concordance reported an upgrade rate of less than 2% for asymptomatic benign papillomas diagnosed in core needle biopsies [26]. These recent data suggest that routine excision of papillomas is not indicated, and thus many centers have moved towards not recommending surgery for patients diagnosed with papilloma.

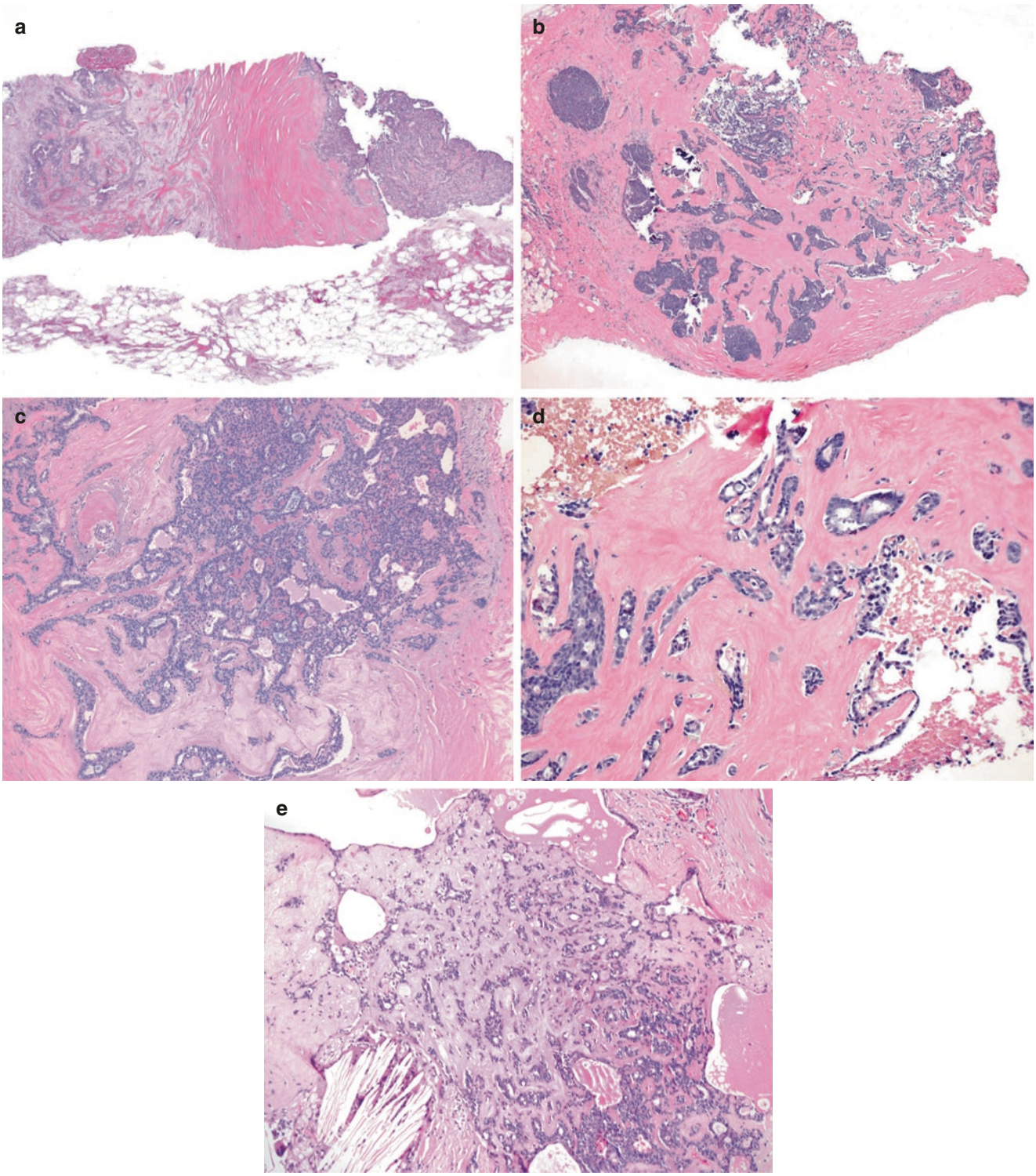

Fig. 6.14 Sclerosing papilloma. (**a**–**e**) Sclerosing papilloma is characterized by entrapped glands in dense sclerosis that have an infiltrative appearance

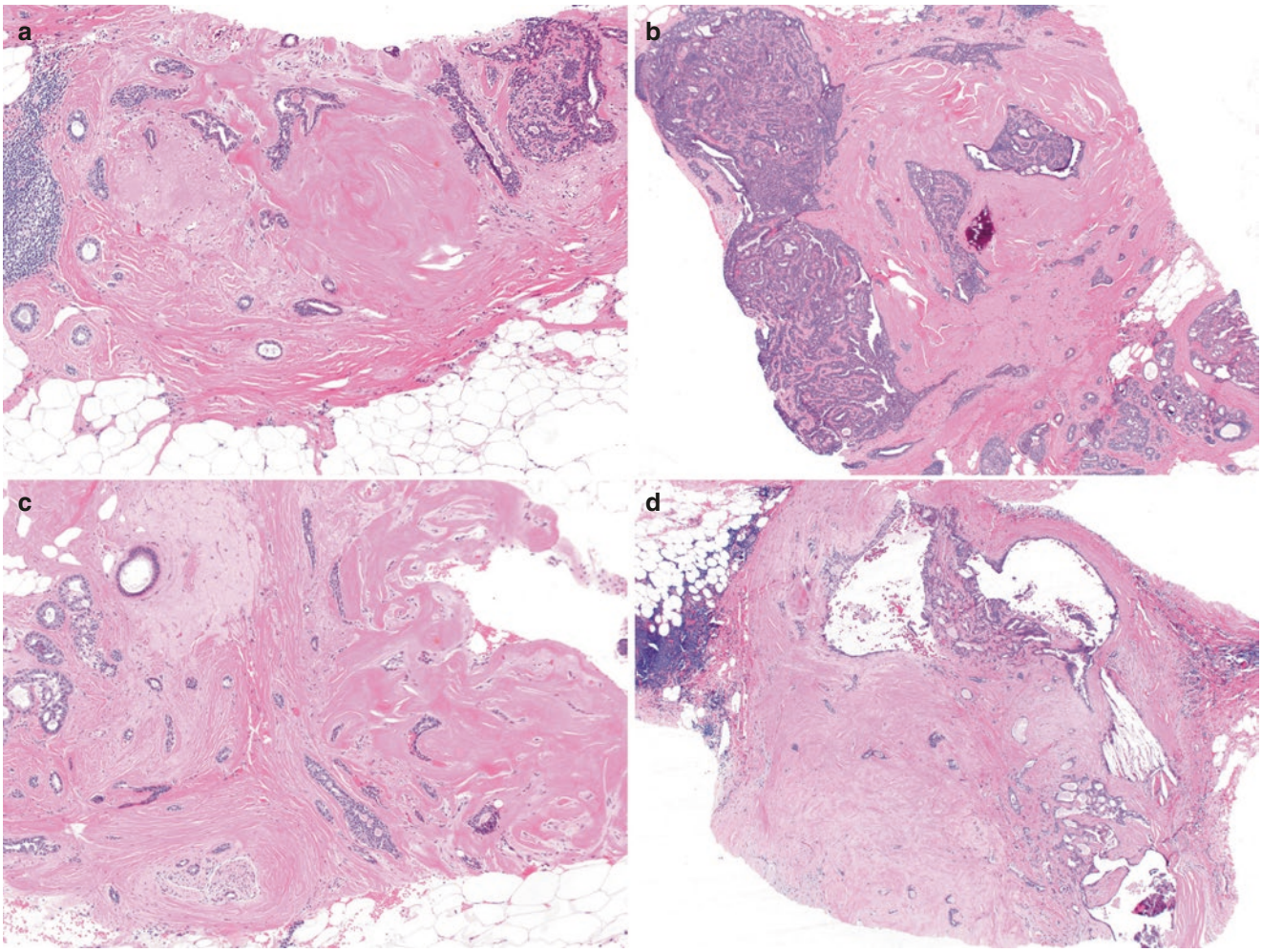

Fig. 6.15 Lesions classified as "radial sclerosing papillary lesions" in core needle biopsies. (**a**–**d**) These lesions are densely sclerotic with variable degrees of papillary proliferation while also having features of radial scar, such as stromal elastosis and angulated and distorted glands. Some lesions undergo calcification of the stroma, as seen in (**b**)

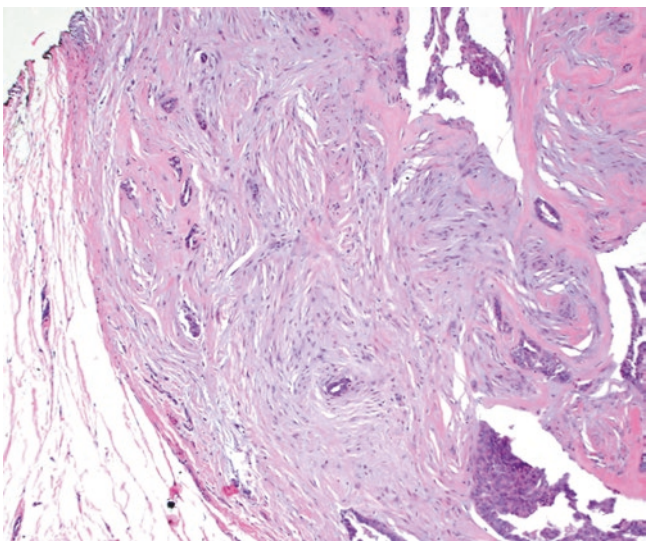

Fig. 6.16 Papilloma with small ducts embedded in cellular stroma. The cellular stroma in this sclerosing papilloma has a blue myxoid appearance, which can mimic stromal desmoplasia in some cases

Currently, papillomas with ADH or DCIS require excision. Surgical excision of non-atypical papillomas is considered for symptomatic papillomas and for patients at high-risk for breast cancer development.

Prognosis

Intraductal papilloma is not considered to represent a direct precursor lesion to invasive breast carcinoma. It connotes a lifetime breast cancer risk about twice that of the general population, which is similar to other non-atypical proliferative fibrocystic changes. Atypical papilloma conveys breast cancer risk similar to atypical ductal hyperplasia (relative risk of 4–5) [7, 9].

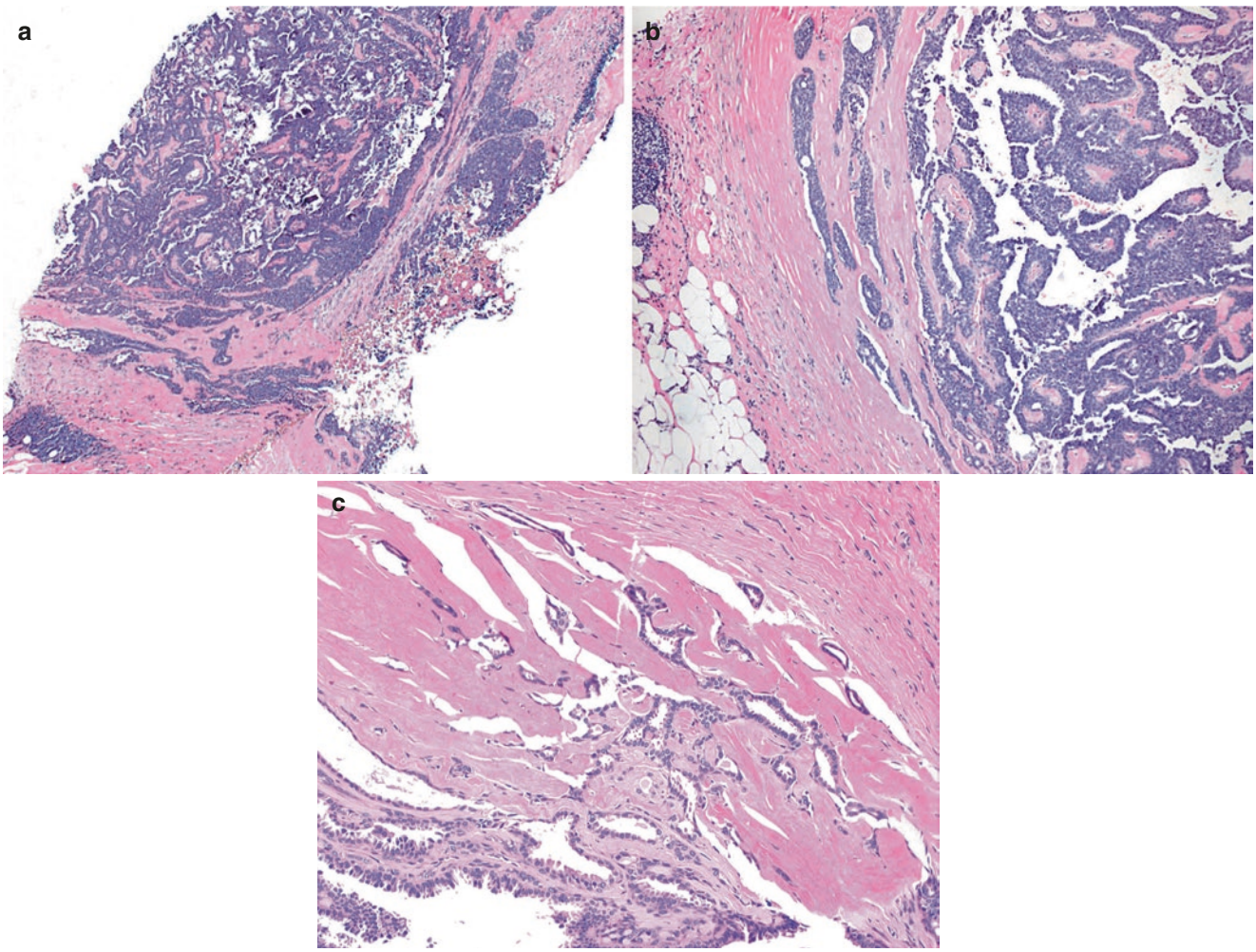

Fig. 6.17 Entrapped glands in papilloma. (**a**–**c**) Entrapped glands present in sclerotic stroma are oriented parallel to the papilloma's contour and are not associated with a desmoplastic stromal reaction

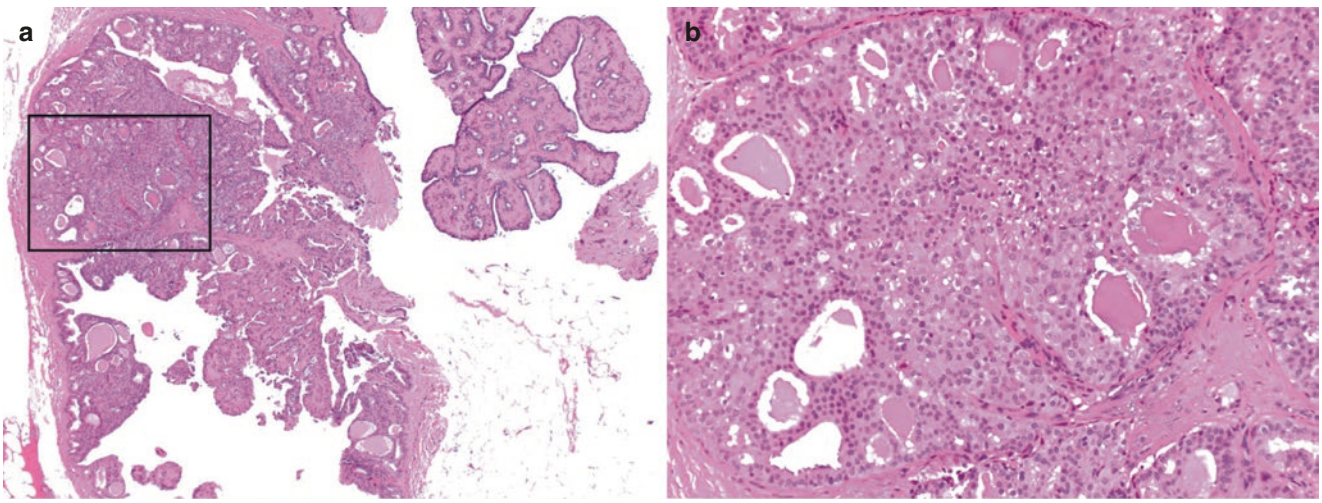

Fig. 6.18 Papilloma with ADH. (**a**) Core biopsy shows an intraductal papilloma with a focus of atypical cribriform ductal hyperplasia (*box*). (**b**) Higher power view of area in *box* from (**a**) shows punched-out cribriform spaces, characteristic of atypical ductal hyperplasia. (**c**–**f**) Two examples of atypical ductal hyperplasia occurring at the edge of intraductal papillomas

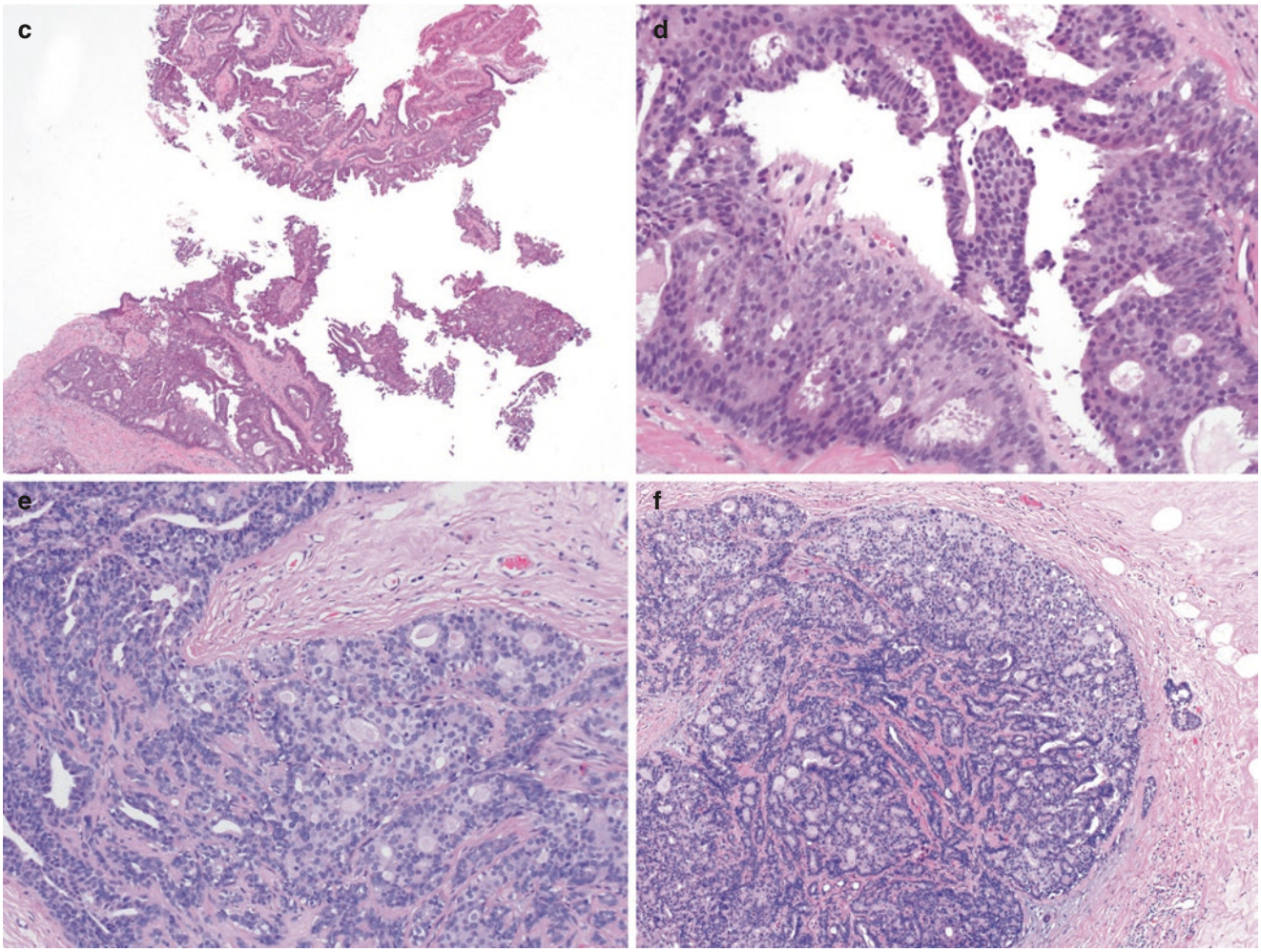

Fig. 6.18 (continued)

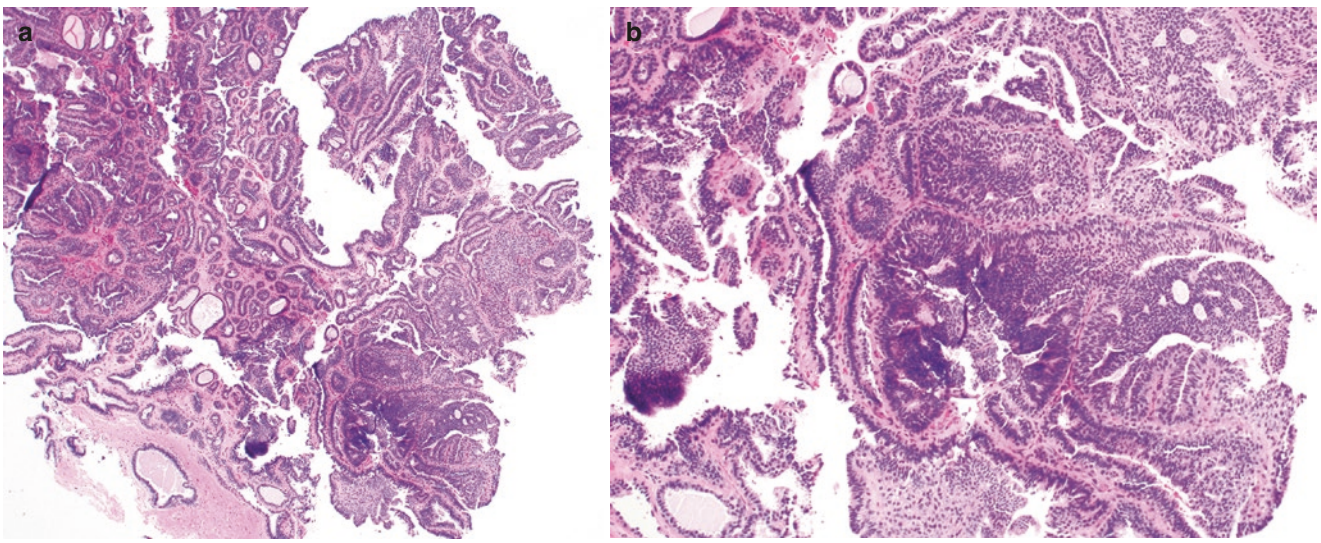

Fig. 6.19 Papilloma with ADH. (**a**) Core biopsy shows an intraductal papilloma with a focus of solid and cribriform growth (right of image). (**b**) Higher power examination of this focus shows monotonous cells growing in a solid and cribriform pattern. The remaining papilloma (left of images) appears benign

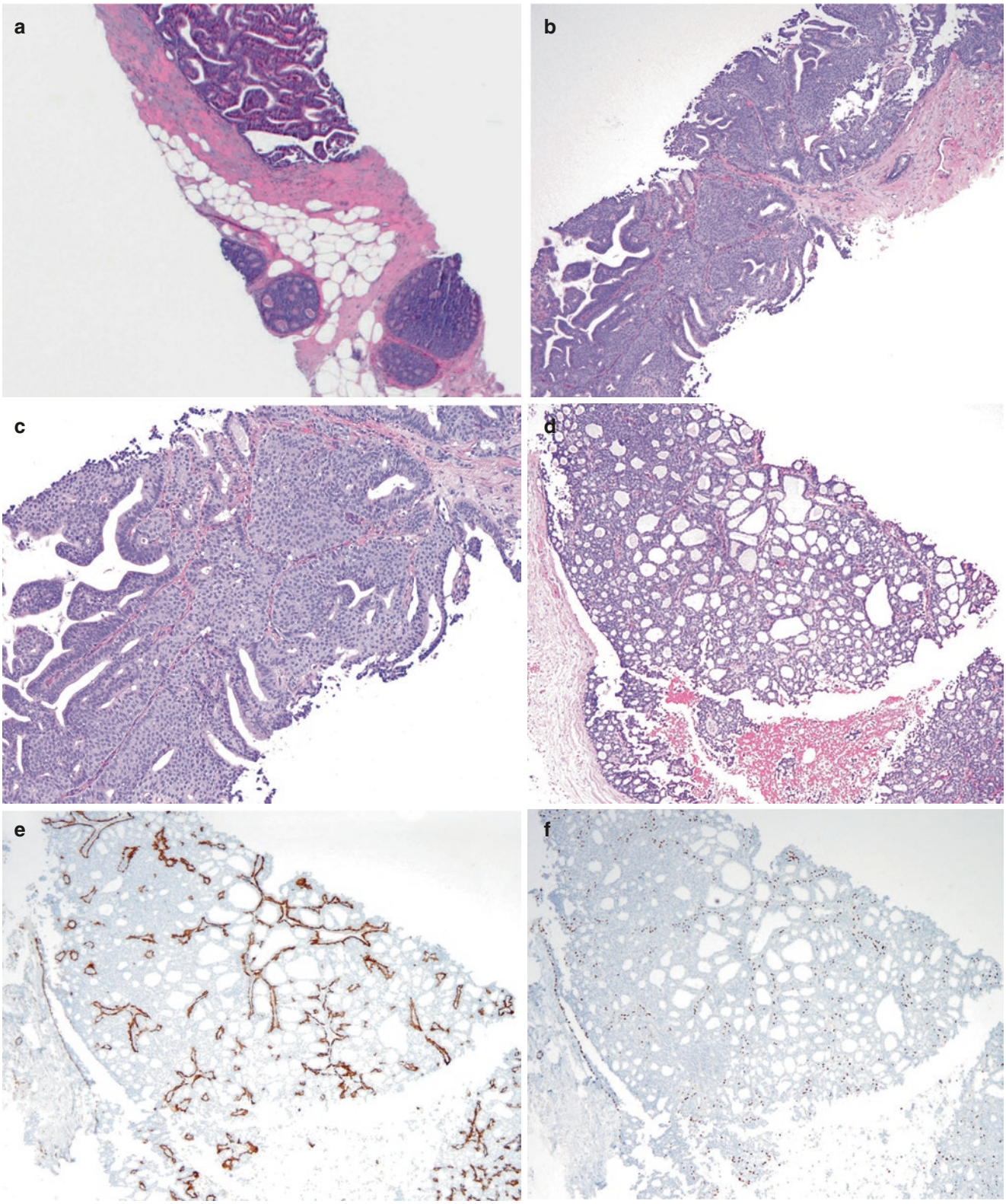

Fig. 6.20 Ductal carcinoma in situ (DCIS) involving papilloma. (**a**) A helpful clue to the diagnosis of DCIS withing a papilloma is conventional cribriform, micropapillary, or solid DCIS growing in adjacent ducts. (**b**, **c**) Solid type DCIS involving a papilloma in a core biopsy. (**d**) DCIS with cribriform features involving a papilloma. Variable myoepithelial staining with (**e**) calponin and (**f**) p63 is seen with some foci showing complete lack of staining

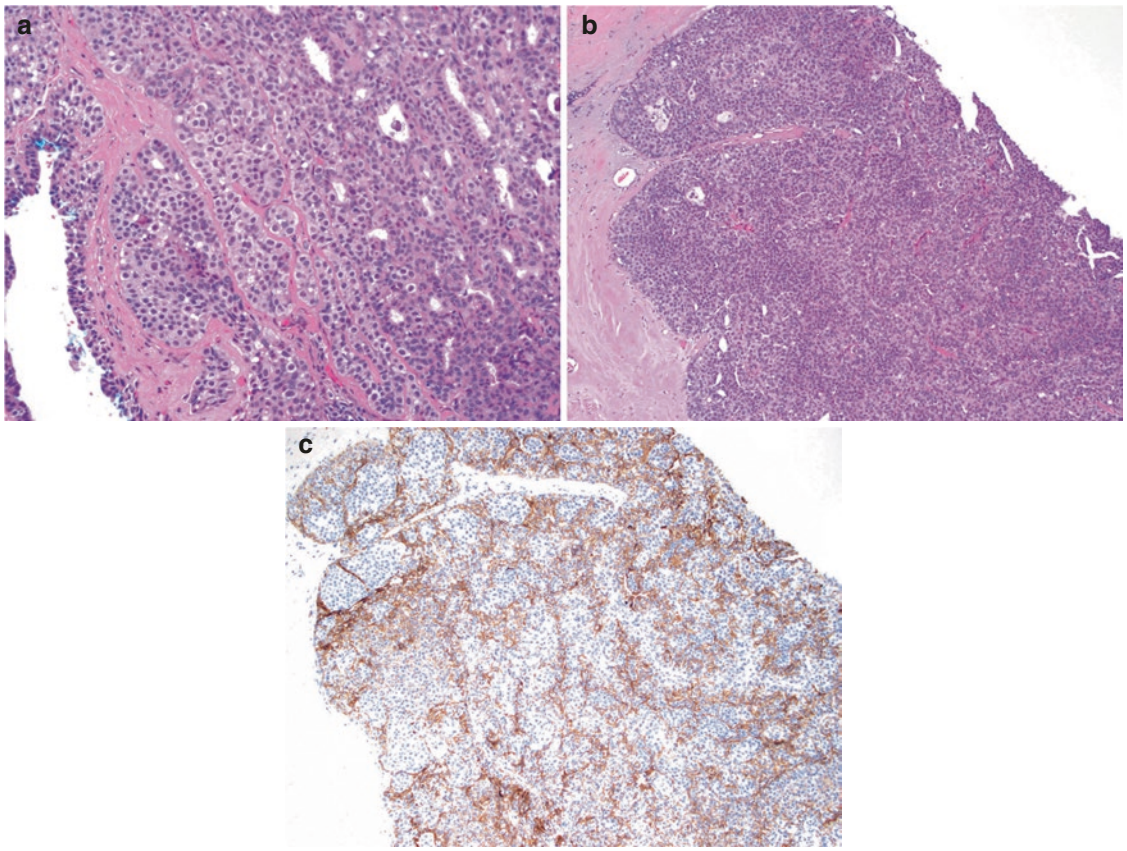

Fig. 6.21 Lobular carcinoma in situ (LCIS) involving papilloma. (**a**, **b**) Classic type LCIS shows pagetoid growth within the glands of the papilloma. (**c**) An E-cadherin immunostain highlights residual ductal epithelium in the papilloma, while LCIS cells are negative

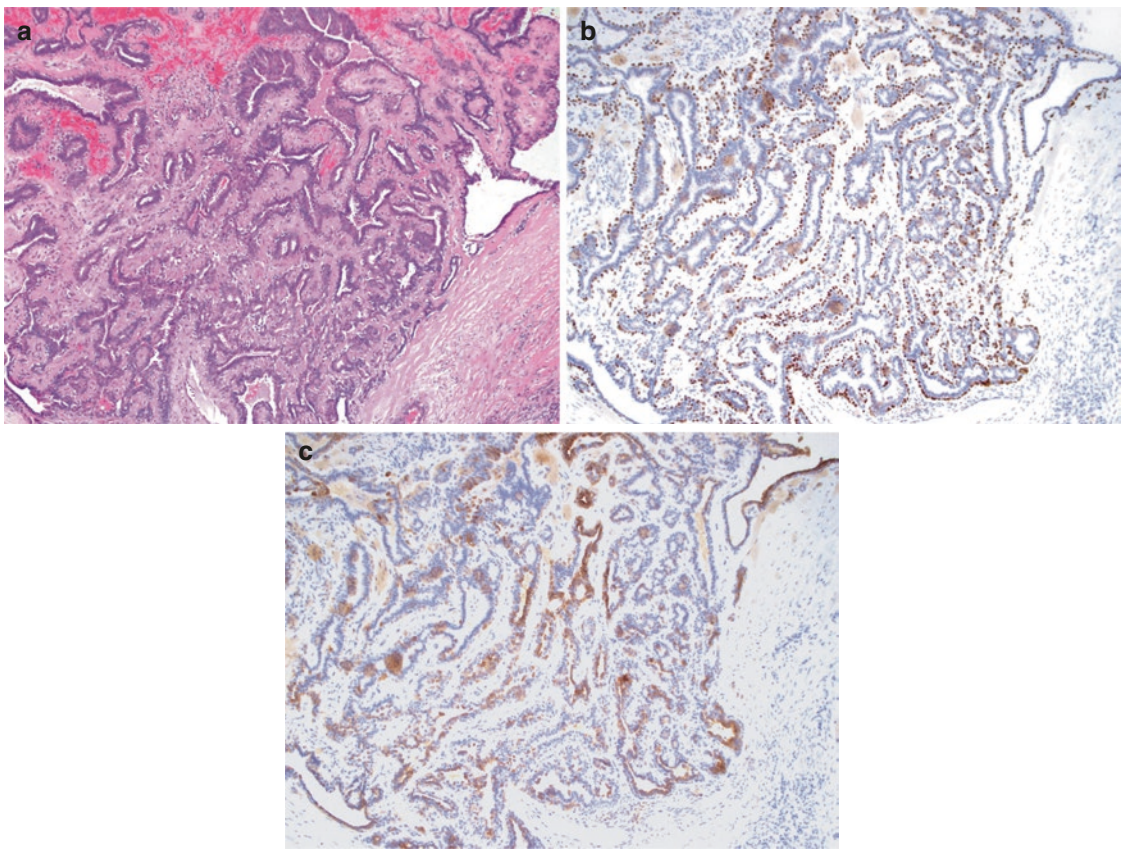

Fig. 6.22 Myoepithelial staining in papilloma. (**a**) Papilloma shows positive staining of myoepithelial cells with (**b**) p63 and (**c**) CK5/6

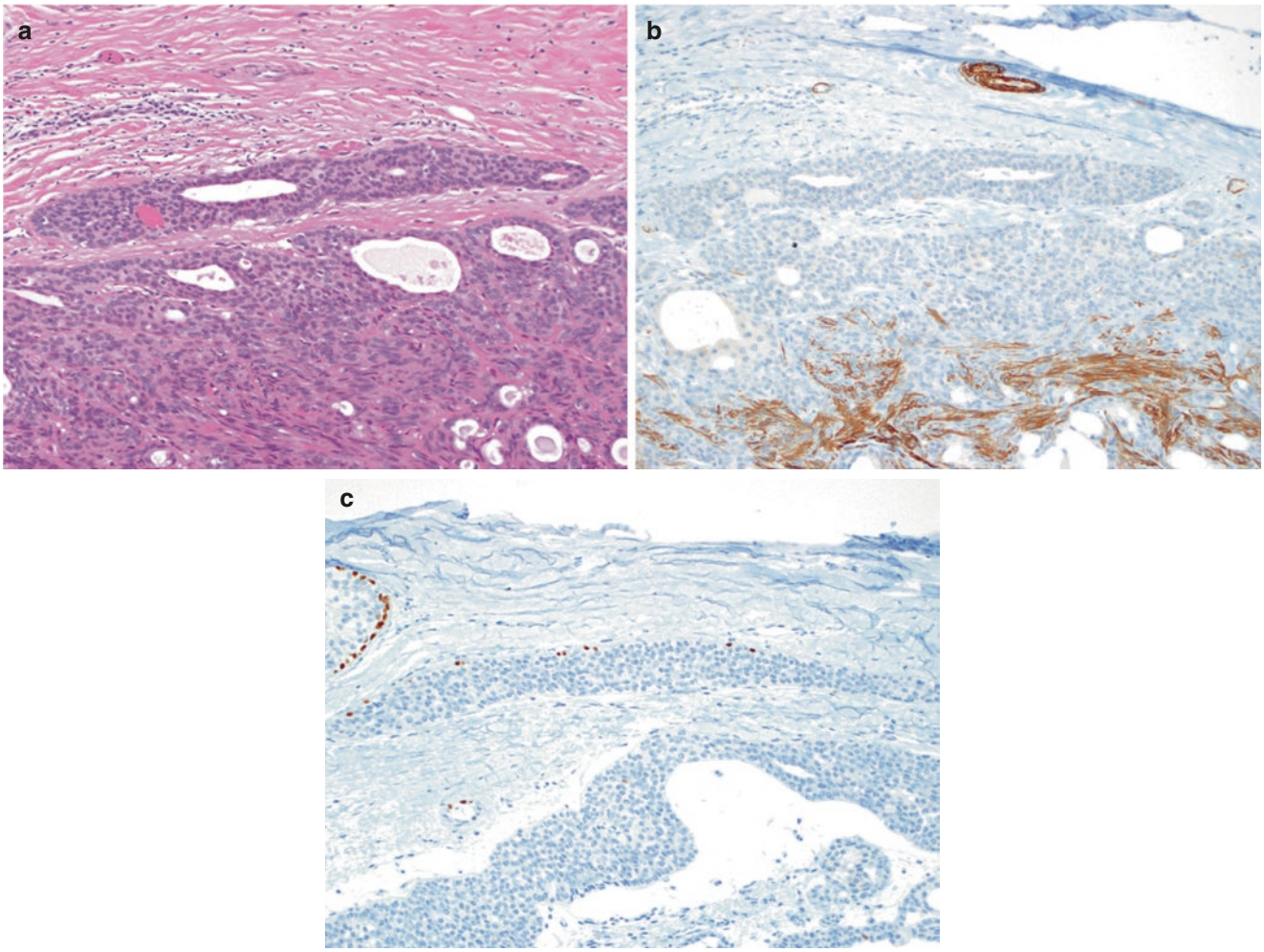

Fig. 6.23 Attenuated myoepithelial staining in glands at periphery of papilloma, (**a**) A gland at the edge of an intraductal papilloma shows (**b**) no staining with smooth muscle myosin heavy chain, while (**c**) discontinuous p63 staining is seen in the same gland

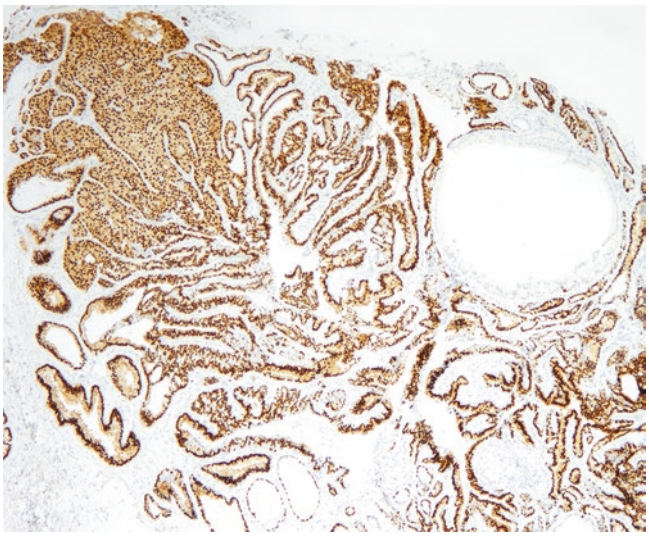

Fig. 6.24 Estrogen receptor (ER) expression in papilloma. ER expression is strong and diffuse not only in DCIS (*top left* of image) but also in areas of the benign papilloma uninvolved by DCIS

Papillary Carcinoma

Overview

The term "papillary carcinoma" is a generic designation for carcinomas that exhibit growth along fibrovascular cores and show diminished or complete lack of myoepithelial cells. Papillary carcinomas can be in situ or invasive processes. The WHO recognizes four specific types of papillary carcinoma: papillary DCIS, encapsulated papillary carcinoma (EPC), solid papillary carcinoma (SPC), and invasive papillary carcinoma [10]. These differ mainly in their morphologic features and distribution of myoepithelial cells. All types of papillary carcinoma tend to occur in postmenopausal women. Use of the term "papillary carcinoma" generally implies indolent clinical behavior to clinicians. Invasive carcinomas associated with papillary carcinoma or invasive types of papillary carcinoma are generally managed similar to other grade and stage-matched non-papillary invasive carcinomas.

The main considerations for evaluating papillary carcinomas in core biopsies are (1) distinguishing papillary carcinomas from benign papillomas and (2) determining whether there is associated invasive carcinoma with a papillary carcinoma. As many core biopsies containing papillary carcinoma are fragmented, it is often impossible to determine whether true stromal invasive carcinoma is present. A diagnosis of "fragments of papillary carcinoma" is usually sufficient for a core biopsy, provided clinicians understand that in such cases assessment of the presence or absence of invasive carcinoma should be made in the excision specimen. Specifying the histologic type of papillary carcinoma (e.g., papillary DCIS vs. EPC) in a core biopsy is often not possible and not necessary as these are managed in a similar fashion.

Gross and Radiographic Features

Most papillary carcinomas appear suspicious on imaging and are generally larger than papillomas. They often present as a circumscribed mass on imaging and may be cystic. Some cases present with unilateral nipple discharge. Papillary DCIS, which is often present with other types of DCIS may present as mammographic calcifications. Papillary carcinoma shows a variable gross appearance and may be solid and circumscribed or may appear as a cystic mass with grossly identifiable papillary structures.

Microscopic Features

There are certain histologic features that distinguish papilloma from various types of papillary carcinoma and recognition of these features aid in their distinction in a core biopsy sample. Papillary carcinomas tend to be loosely cohesive and fragmented with delicate fibrovascular cores (Figs. 6.25 and 6.26), while papillomas typically have cohesive growth with broader fibrovascular cores.

Papillary carcinoma cells are less crowded, busy, and overlapped than the cell populations of papilloma. Papillary carcinomas are characterized by evenly spaced monotonous cells—which may be cuboidal or columnar in shape (Fig. 6.27). Nuclei are small to medium sized and lack pleomorphism, although they are noticeably hyperchromatic (Fig. 6.28). Some cases of papillary carcinoma have a dimorphic appearance due to the so-called globoid cells which are neoplastic epithelial cells that can mimic myoepithelial cells (Fig. 6.29). Presence of mitotic figures is significant; they are present consistently in malignant papillary lesions yet uncommon in papillomas with rare exception. Individual cell necrosis is another finding that may be seen, which is rare in benign papillary lesions. Although the term papillary carcinoma implies arborescent architecture, many have variable admixtures of (secondary) cribriform growth, particularly near the edges of involved spaces (Fig. 6.30).

Excluding invasion may become problematic when evaluating periductal clusters of tumor cells in small biopsies; despite lack of myoepithelium, most experts would consider tumor cells within the fibrous wall surrounding papillary carcinoma to represent "pinched-off" or entrapped epithelium rather than true invasion (Fig. 6.31). Invasive carcinoma arising in association with papillary carcinoma (in situ) occurs as invasive carcinoma, no special type (NST), growing in an irregular configuration that is typically growing perpendicular to the orientation of the involved duct (Fig. 6.32). Areas of true invasion are often <1.0 cm and thus less conspicuous in imaging than the cystic component of some tumors; hence, they may not be represented in core needle biopsy material.

Subtypes of Papillary Carcinoma: Specific Key Features

Papillary DCIS

Papillary DCIS refers to a type of DCIS in which carcinoma cells line fibrovascular cores that lack myoepithelium [10]. This growth pattern of DCIS is usually present in association with other types of DCIS including cribriform, micropapillary, and solid types. Papillary DCIS lacks an underlying benign papillary lesion, which distinguishes papillary DCIS from papilloma with DCIS. The latter shows benign areas of papilloma that contain myoepithelial cells in fibrovascular cores. Myoepithelial cells in papillary DCIS tend to be absent in fibrovascular cores but are present at periphery of the lesion. In some cases, myoepithelial cells are markedly diminished or absent at the periphery of papillary DCIS, and this should not be interpreted as invasive carcinoma. As with other types of papillary carcinoma (in situ) the presence of rounded contours without irregular growth into stroma supports an in situ designation. Papillary DCIS is staged as in situ carcinoma (Tis) according the American Joint Committee on Cancer (AJCC) [29].

Encapsulated Papillary Carcinoma

Encapsulated papillary carcinoma (EPC), previously referred to as "intracystic papillary carcinoma," or "encysted papillary carcinoma" is a type of papillary carcinoma that lacks myoepithelial cells along fibrovascular cores as well as at the periphery of the tumor. EPC characteristically grows within a cystic space lined by fibrous tissue with inflammatory changes (Figs. 6.33 and 6.34). Multinodular growth with multiple cystic spaces may be seen. Cells of EPC usually show low or intermediate nuclear grade and are present along delicate fibrovascular cores. Solid and/or cribriform growth is often present. Myoepithelial cells are not apparent on H&E or by immunohistochemistry along the fibrovascu-

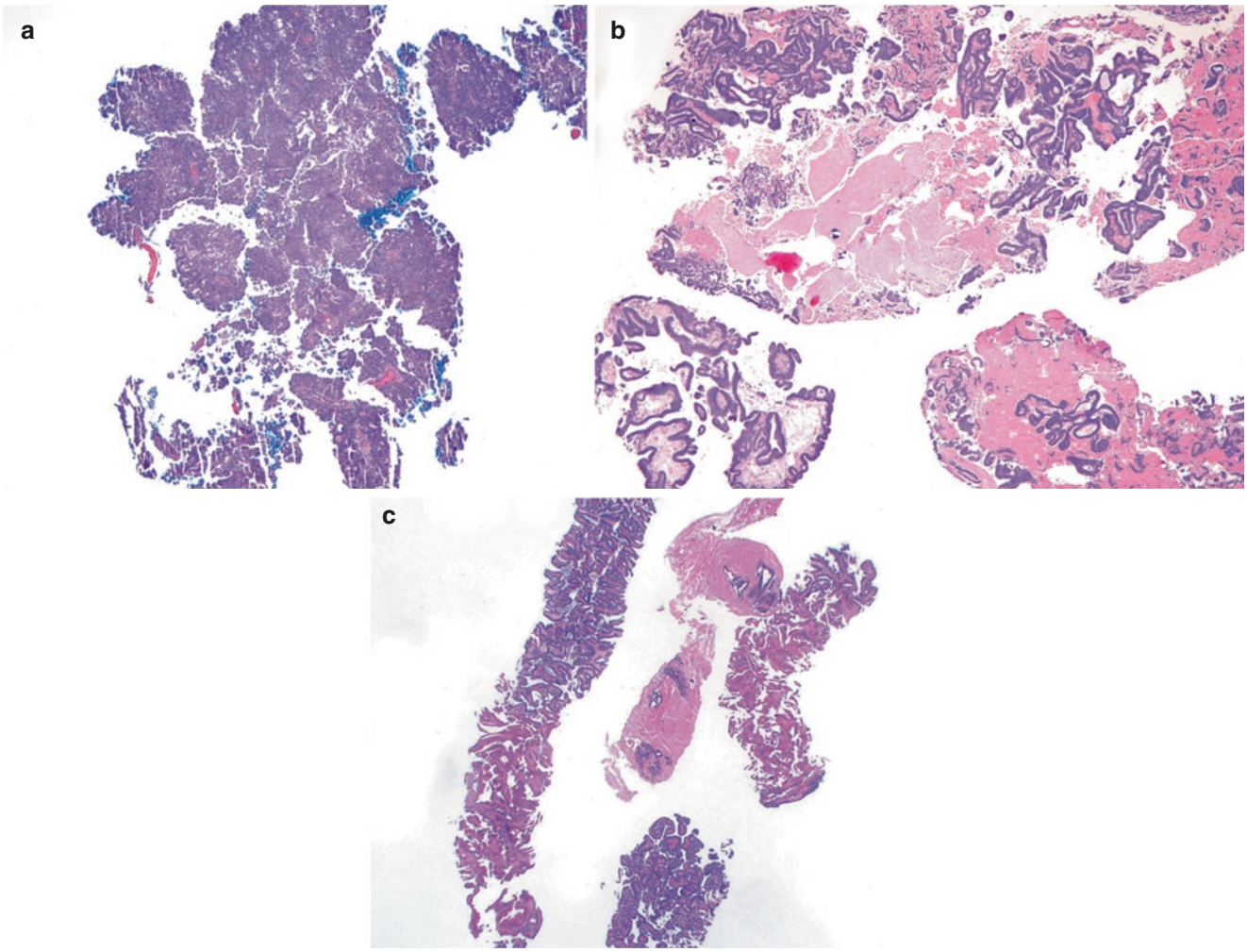

Fig. 6.25 Needle core biopsies of papillary carcinoma compared with papilloma. (**a**, **b**) Papillary carcinomas appear fragmented and basophilic on low-power examination, while (**c**) papilloma is more cohesive and eosinophilic in appearance

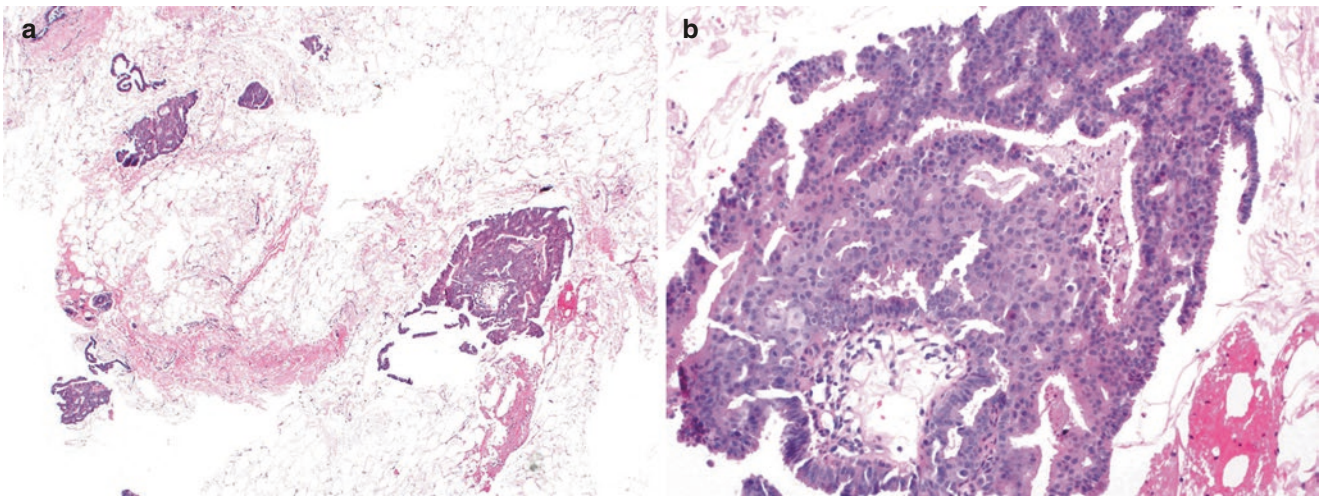

Fig. 6.26 Fragments of papillary carcinoma in a core biopsy. (**a**) Low-power view of the core biopsy shows displaced fragments of epithelium. (**b**) Higher power magnification shows an atypical papillary proliferation with necrosis that is diagnostic for papillary carcinoma. Assessment of invasion cannot be performed in these instances

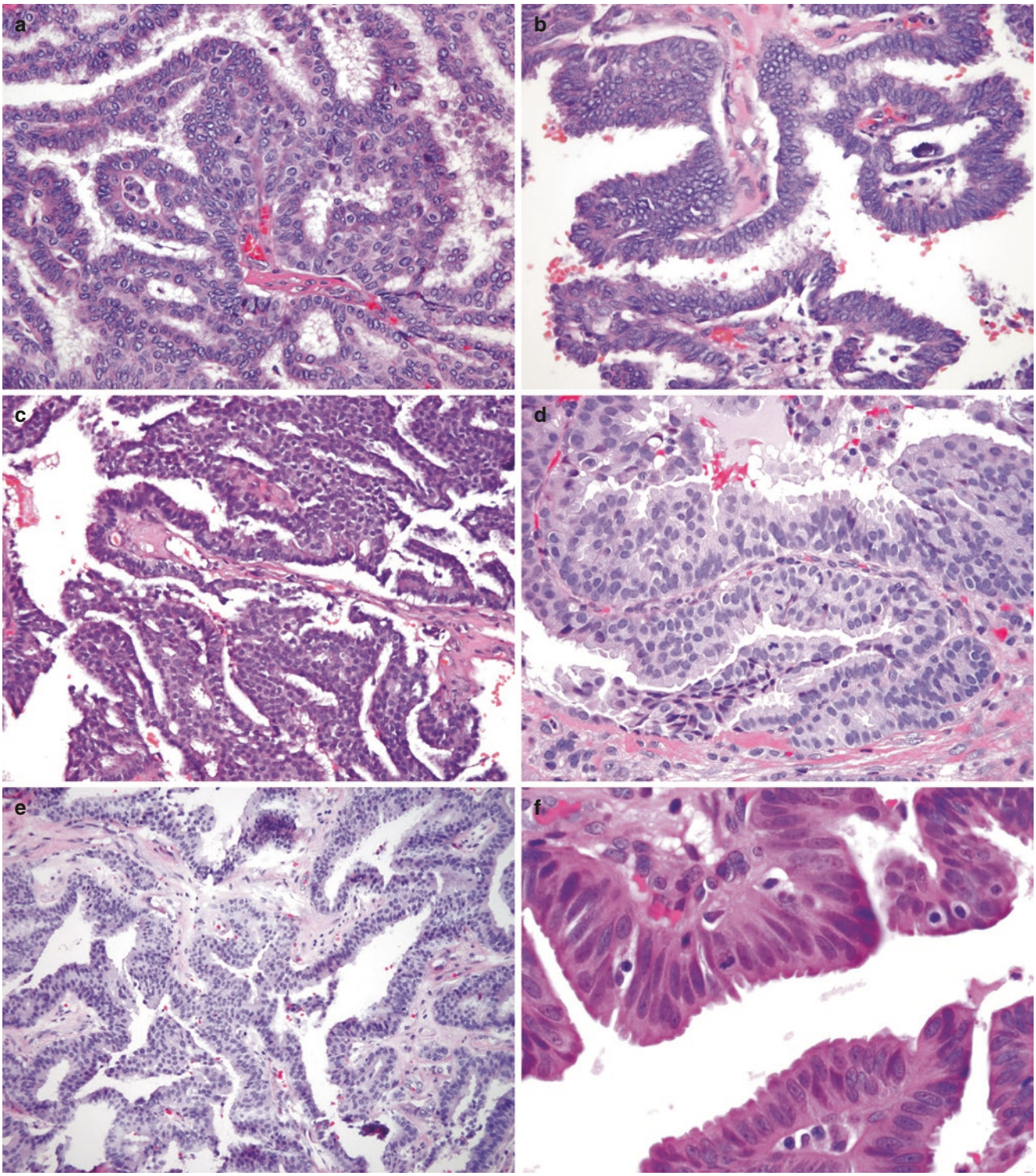

Fig. 6.27 Papillary carcinoma. (**a**–**f**) Papillary carcinoma is characterized by evenly spaced monotonous cells that are typically present on slender fibrovascular cores as seen in these examples. Mitotic figures can be easily identified in (**a**, **d**, and **f**)

lar cores or at the periphery of the tumor (Fig. 6.35). A subset (less than 10%) of EPCs show high-grade cytologic features with pleomorphic nuclei and exhibit more solid growth [30, 31]. In contrast to low-intermediate grade EPCs which are ER-positive and HER2-negative, high-grade tumors frequently show a triple-negative phenotype [30].

EPC is currently regarded by the WHO as a low-grade form of invasive carcinoma with a pushing border [10],

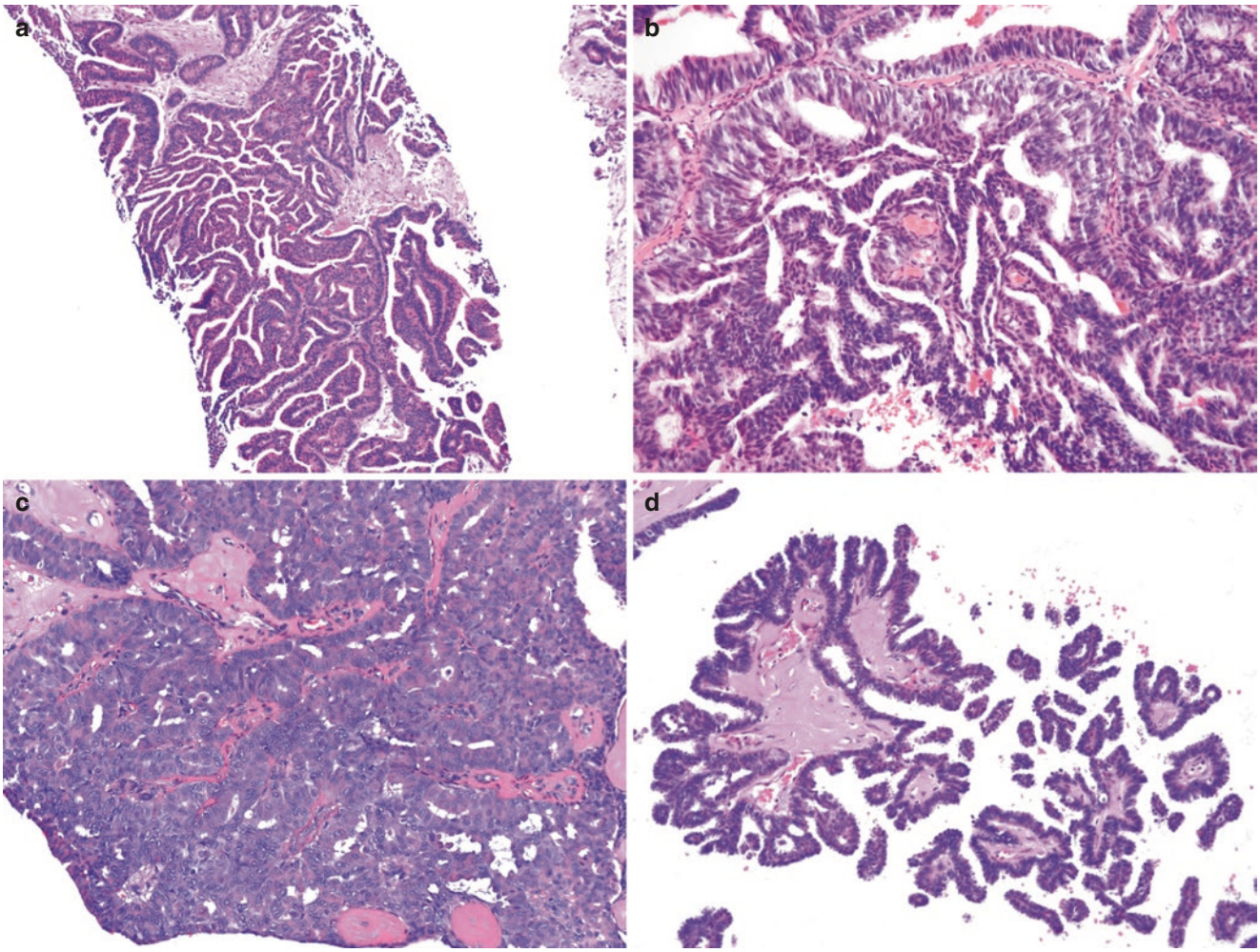

Fig. 6.28 Papillary carcinoma. (**a**–**d**) Examples of papillary carcinomas in core biopsies. These examples appear hyperchromatic on lower power examination due to the high nuclear-to-cytoplasmic ratio of cells

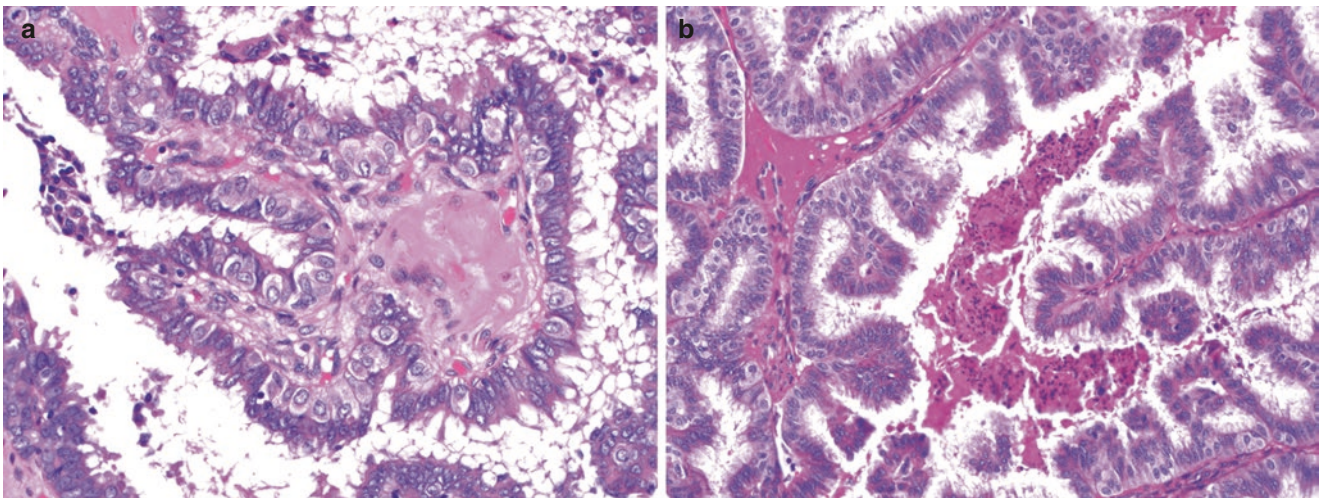

Fig. 6.29 Papillary carcinoma with dimorphic cellular proliferation due to the so-called globoid cells. (**a**, **b**) A second population of ductal neoplastic cells with abundant clear cytoplasm can mimic myoepithelial cells in papillary carcinoma

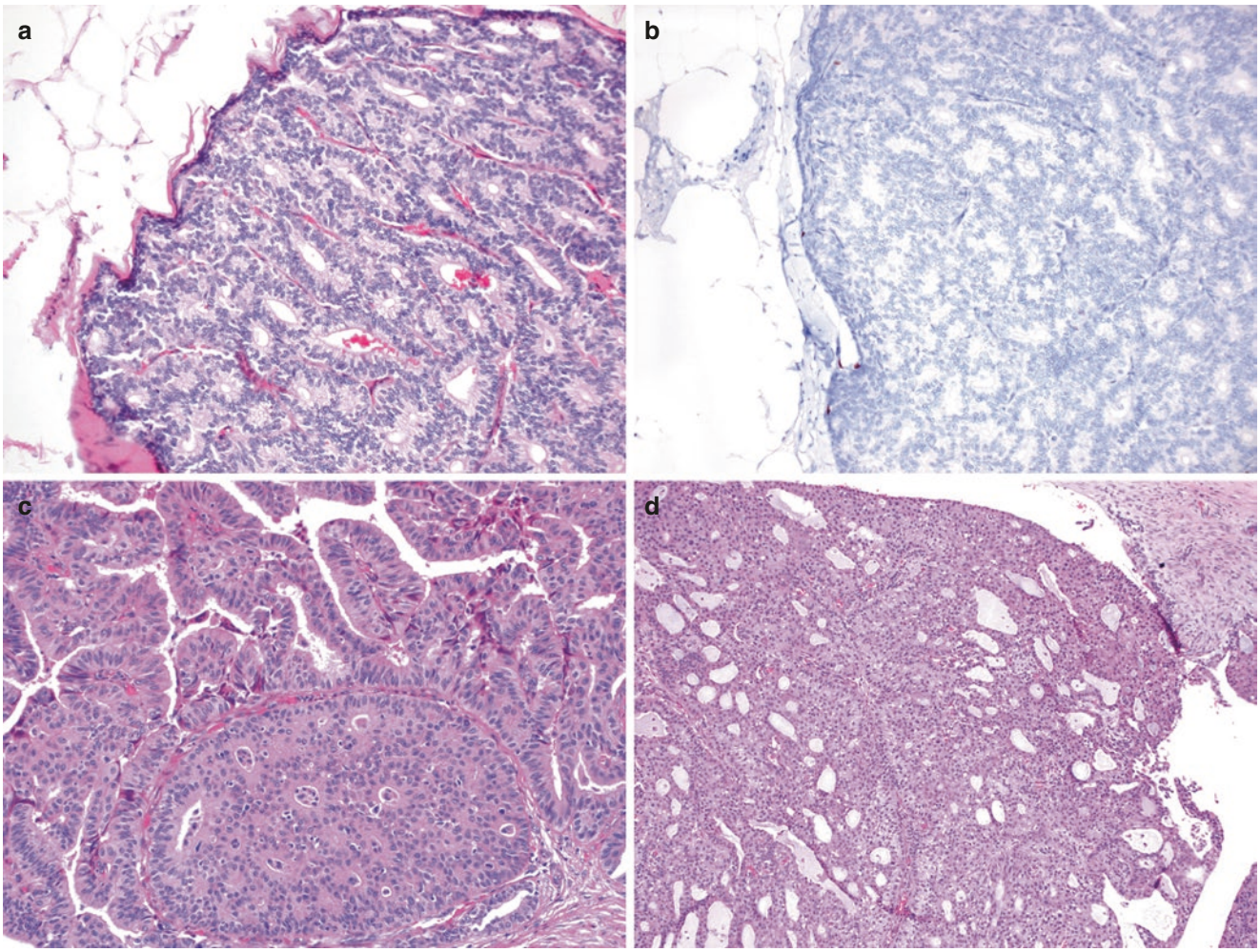

Fig. 6.30 Papillary DCIS (**a**) Secondary cribriform growth can be seen at the edge of papillary carcinomas. (**b**) A p63 highlights rare cells at the periphery of the duct, while no staining is seen in the inner papillary and cribriform components. (**c**) Focus of cribriform growth in papillary carcinoma and in (**d**) solid papillary carcinoma with mucinous features

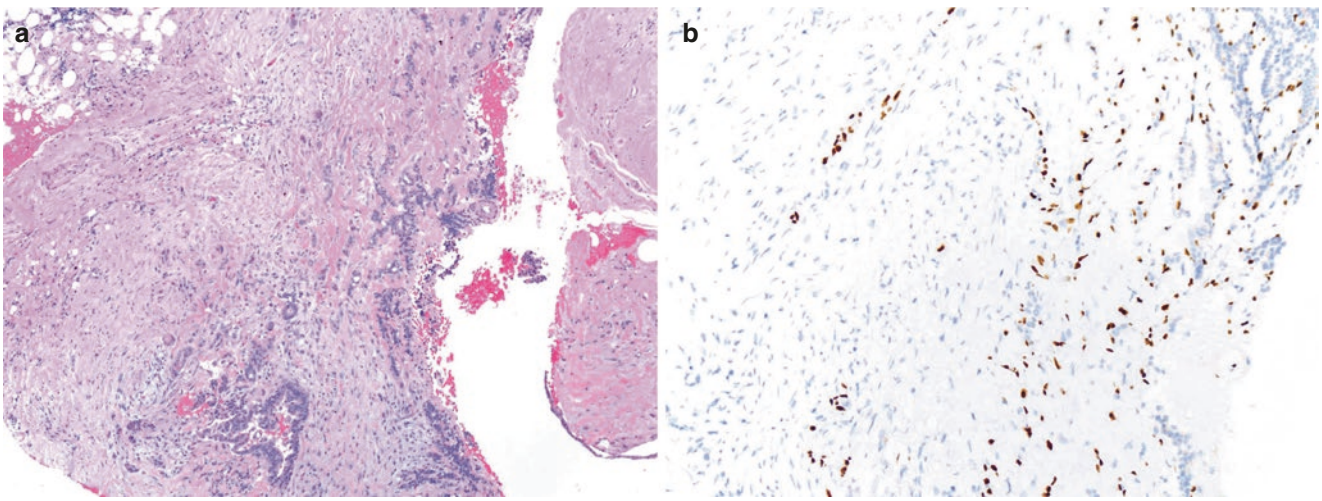

Fig. 6.31 Papillary carcinoma—pseudoinvasive glands. (**a**, **b**) Low- and high-power views of entrapped glands in reactive stroma surrounding papillary carcinoma (in situ). (**c**) Another focus of entrapped glands in this case is (**d**) highlighted by p63

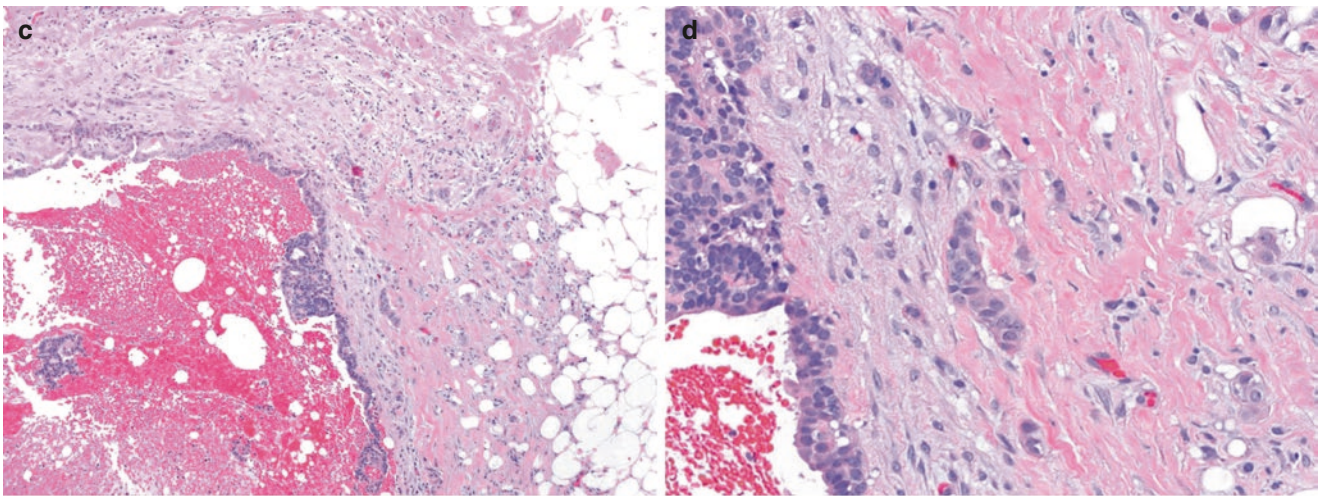

Fig. 6.31 (continued)

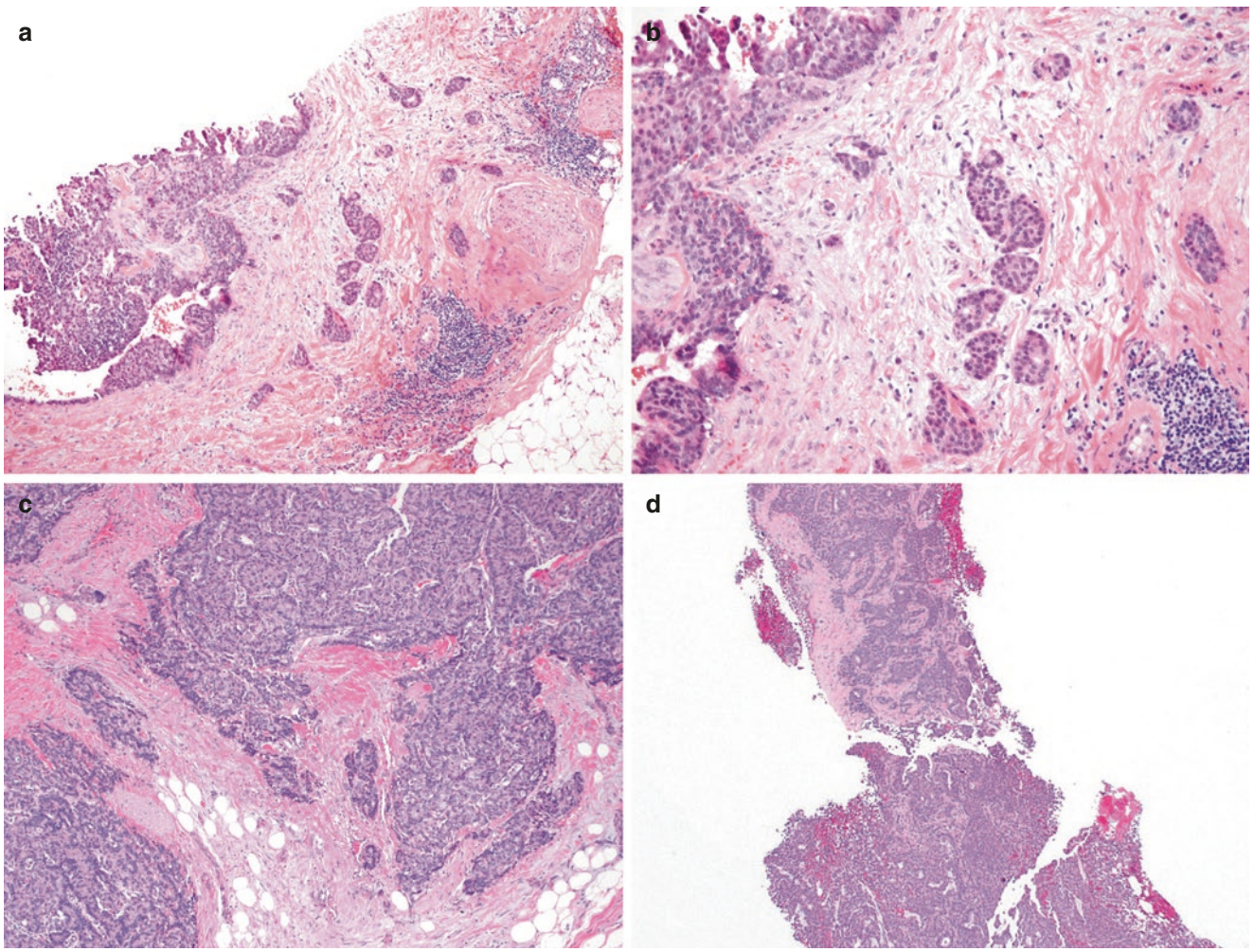

Fig. 6.32 Papillary carcinoma with invasion. (**a–c**) Invasive carcinoma arising from papillary carcinoma grows perpendicular to the papillary carcinoma's contour. (**d**) Core biopsy with invasive carcinoma (*top*) arising from papillary carcinoma (bottom)

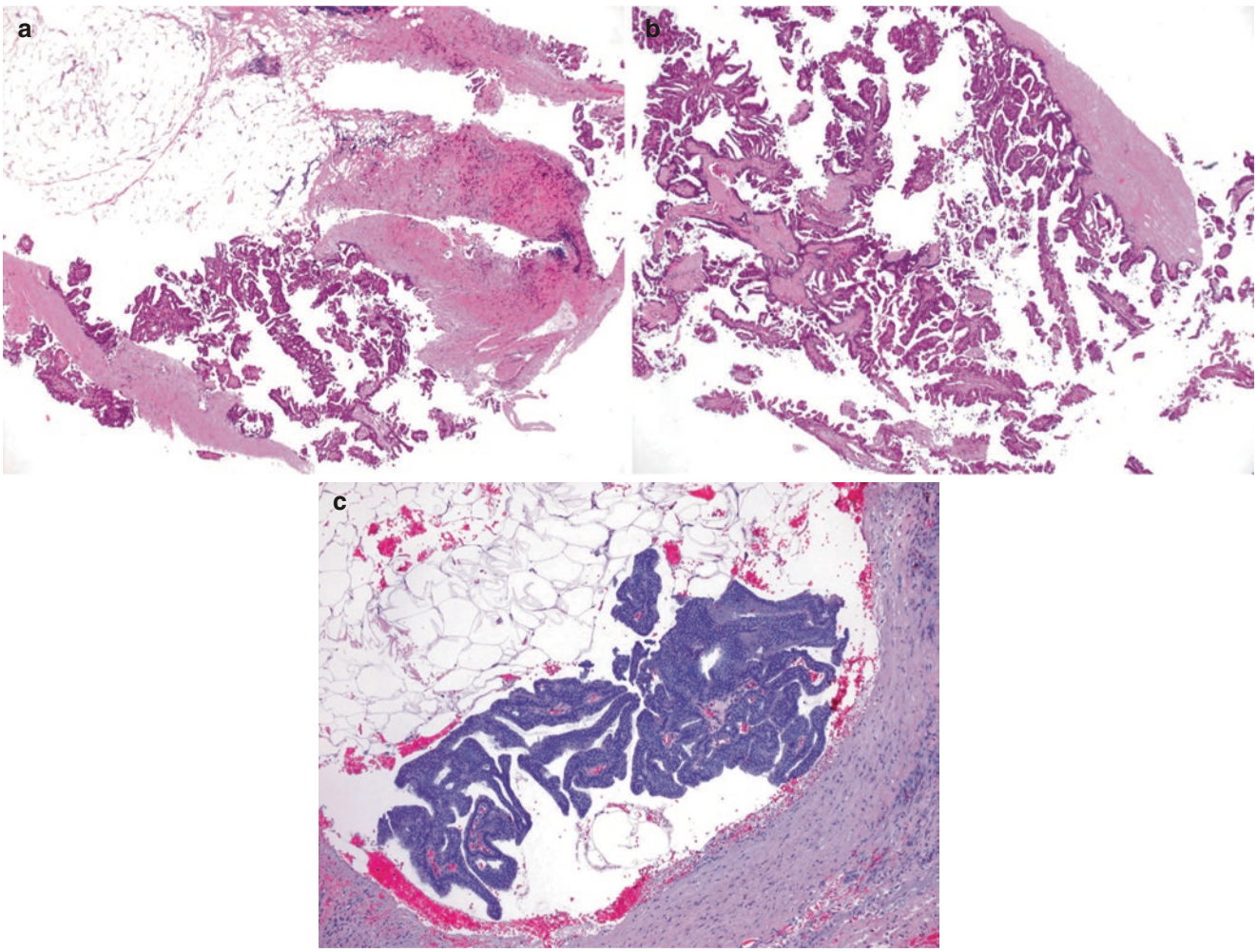

Fig. 6.33 Encapsulated papillary carcinoma in core needle biopsy. (**a**–**c**) Papillary carcinoma appears loosely attached or detached from the thick fibrous walls of the tumor

although this has been a matter of debate. This notion is based on the lack of myoepithelial cells in the tumor as well as reports of axillary and distant metastases in patients with EPC [10, 32]. Due to its excellent prognosis, similar to that of conventional DCIS, EPC is staged as in situ (Tis) according to the AJCC [29]. Invasive carcinoma associated with EPC is staged according to the largest contiguous focus of invasive carcinoma. It is recommended that high-grade triple-negative carcinomas with a encapsulated papillary growth pattern be regarded and treated as a triple-negative invasive carcinoma [10, 30].

Solid Papillary Carcinoma

Solid papillary carcinoma (SPC) is a clinically and genomically distinct form of ER-positive breast cancer in that it is characterized by its tendency to present in older postmenopausal women and show frequent neuroendocrine differentiation [10]. SPC is a well-circumscribed or multinodular mass that can be appreciated on imaging and gross examination (Fig. 6.36).

SPC is so named for its tendency to grow as solid intraductal proliferations of cells that have a "streaming" architecture (Fig. 6.37) with inconspicuous fibrovascular cores. The low magnification growth pattern of SPC bears considerable resemblance to florid examples of usual ductal hyperplasia (UDH) (Fig. 6.38). However, unlike most UDH, solid papillary carcinoma typically presents in a "tumor-like" manner, with masses of cells distending several adjacent, crowded duct-like spaces, all of which are embedded within bland collagenous stroma, thereby forming a nodular mass. Involved ducts in these nodules have a distorted "geographic" shape and sometimes appear sufficiently close so as to "fit together."

Despite the resemblance to UDH there are a number of high magnification features that help in the identification of SPC. These features include a tendency for the cells to be

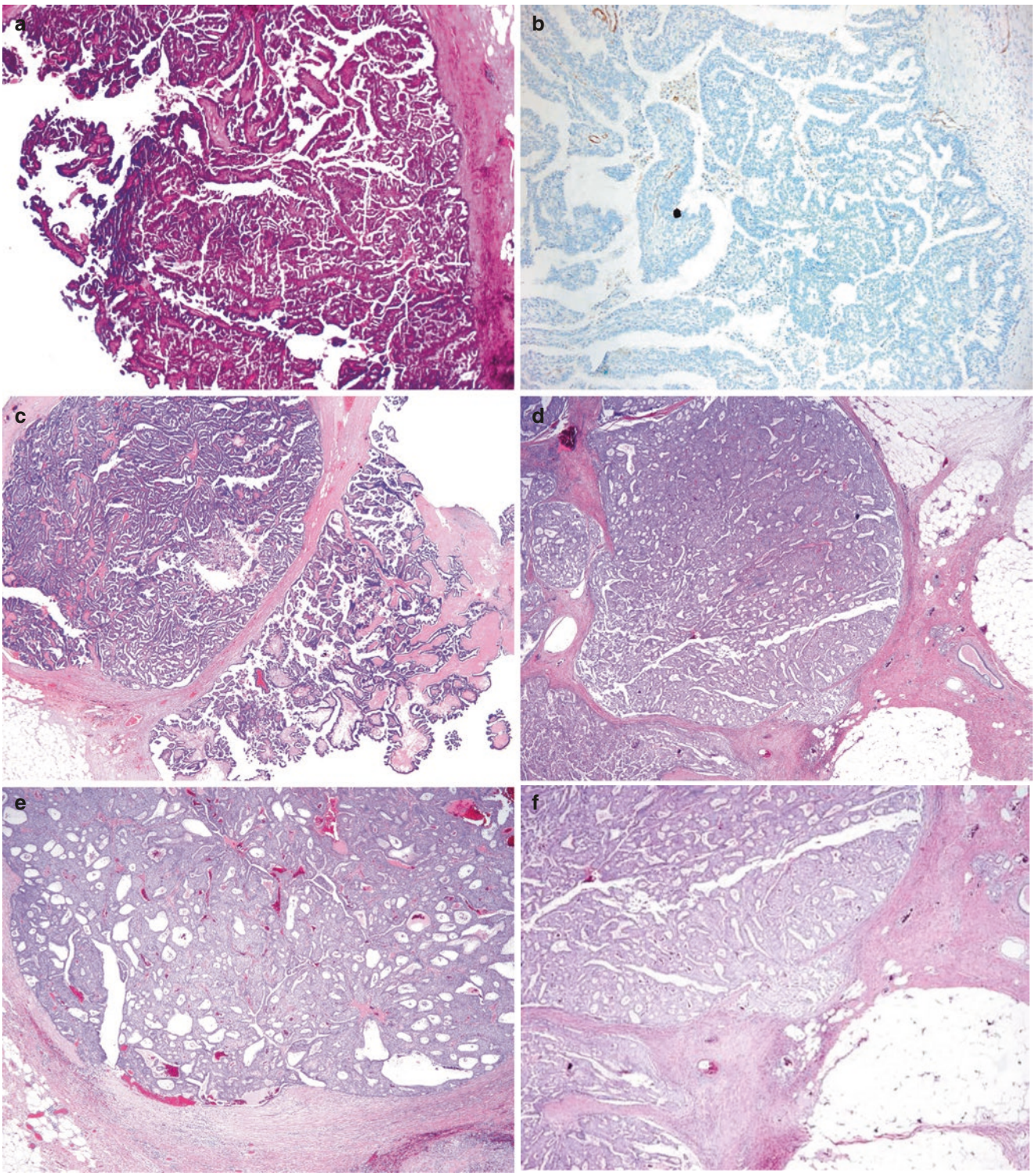

Fig. 6.34 Encapsulated papillary carcinoma. (**a**) Papillary carcinoma is present within a fibrous cyst wall. (**b**) No staining is seen with smooth muscle myosin heavy chain. (**c**) Encapsulated papillary carcinoma in a core biopsy. (**d**, **e**) Example of encapsulated papillary carcinoma. Pseudoinvasion of carcinoma is seen in (**f**)

less overlapping, show greater monotony, and demonstrate more hyperchromasia than those of UDH (Fig. 6.39). A subset of SPCs display mucinous differentiation, which may be present as intracytoplasmic mucin vacuoles or extracellular mucin (Fig. 6.40). Some cases of invasive SPC exhibit abundant extracellular mucin in which solid papillary glands are floating in pools of mucin, similar to mucinous carcinoma. Neuroendocrine differentiation is frequently observed,

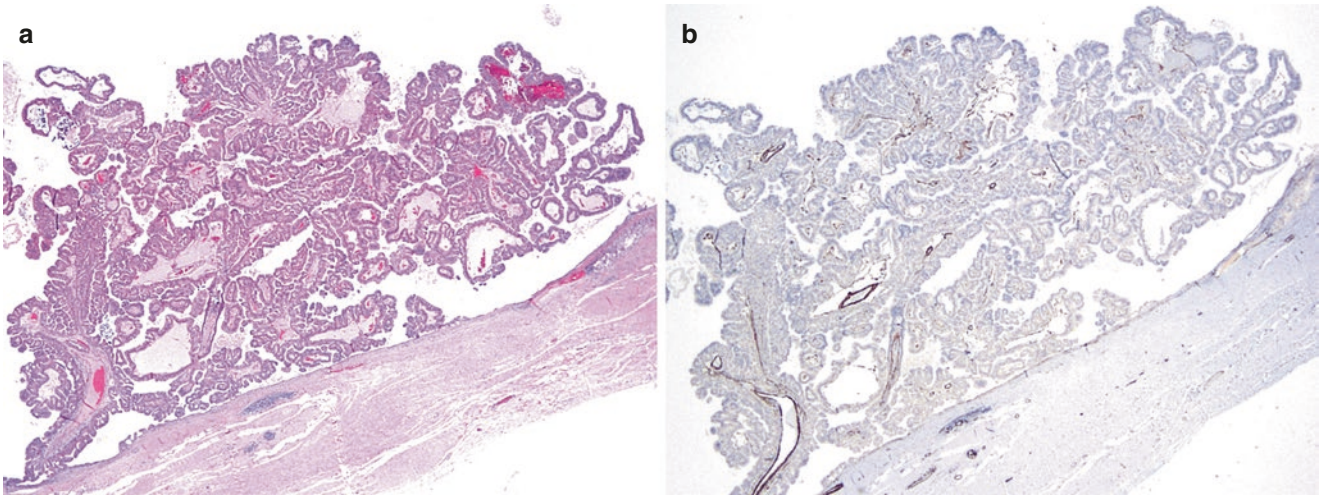

Fig. 6.35 Encapsulated papillary carcinoma—myoepithelial staining. (**a**) Encapsulated papillary carcinoma showing (**b**) negative staining within the papillary carcinoma and cyst wall with smooth muscle myosin heavy chain

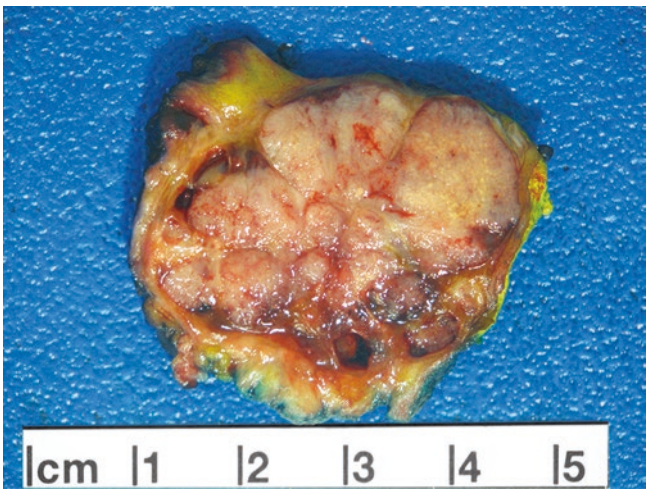

Fig. 6.36 Solid papillary carcinoma—gross appearance. Solid papillary carcinoma shows a multinodular brown-to-red mass in this lumpectomy specimen

including cases with mucinous differentiation. SPCs with neuroendocrine differentiation often show eosinophilic granular cytoplasm forming a "perinuclear hof" (Fig. 6.41). Neuroendocrine differentiation can be confirmed with immunostains including synaptophysin, chromogranin, CD56, and insulinoma-associated protein 1 (INSM1); however, currently there is no clinical significance for demonstrating neuroendocrine differentiation in these tumors.

Invasive carcinoma arising within SPC or "invasive solid papillary carcinoma" shows solid nests of cells infiltrating fibrous tissue or adipose tissue (Fig. 6.42). A stromal desmoplastic reaction is typically absent with this type of invasion and the epithelium sometimes appears "pushed" into surrounding stroma, similar to what is seen with artifactual displacement of tissue. SPC with rounded contours that lack irregular growth should be regarded as in situ solid papillary carcinomas, even in the absence of myoepithelial expression or in cases with attenuated myoepithelial staining (Fig. 6.43).

SPCs are generally associated with a favorable outcome, and lymph node metastases are infrequent (<5% of cases) [10, 33]. The vast majority of SPCs show strong expression of ER (±PR) and are negative for HER2 overexpression. Invasive solid papillary carcinoma or invasive carcinoma, NST associated with solid papillary carcinoma is graded and staged like conventional types of invasive carcinoma.

Invasive Papillary Carcinoma

Invasive papillary carcinoma is an exceedingly rare type of invasive carcinoma in which virtually the entire tumor is composed of papillary glandular structures with infiltrative growth and completely devoid of myoepithelial cells [10]. Invasive papillary carcinoma is distinguished from other types of papillary carcinoma with invasion in that the latter most often show non-papillary growth. When an invasive tumor shows entirely papillary growth in a core biopsy, metastasis from another site should be excluded. Lung carcinomas (TTF-1+/napsin-A+) and gynecologic serous tumors (PAX8+/WT1+) can be distinguished from invasive papillary carcinomas using immunohistochemistry.

Due to the rarity of invasive papillary carcinoma, there are virtually no outcome data related to these tumors. Invasive papillary carcinomas are graded according to the Nottingham system and staged according to AJCC system [29].

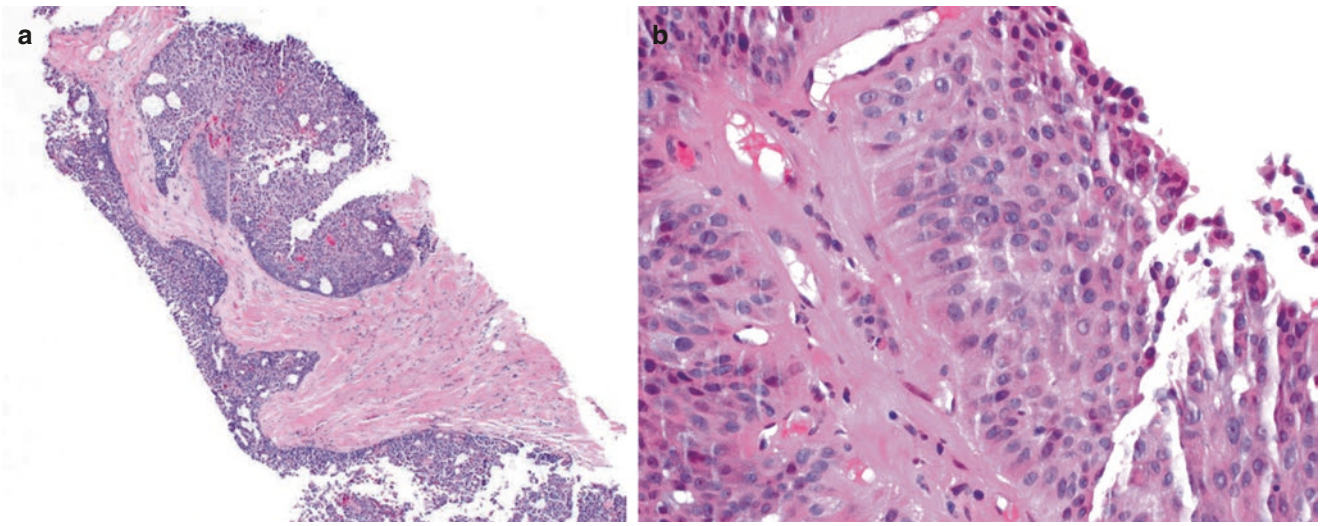

Fig. 6.37 Solid papillary carcinoma in core needle biopsy samples. (**a**) Solid papillary carcinoma shows a solid proliferation of cells expanding ducts on low-power view. (**b**) Cells are monotonous with eosinophilic cytoplasm

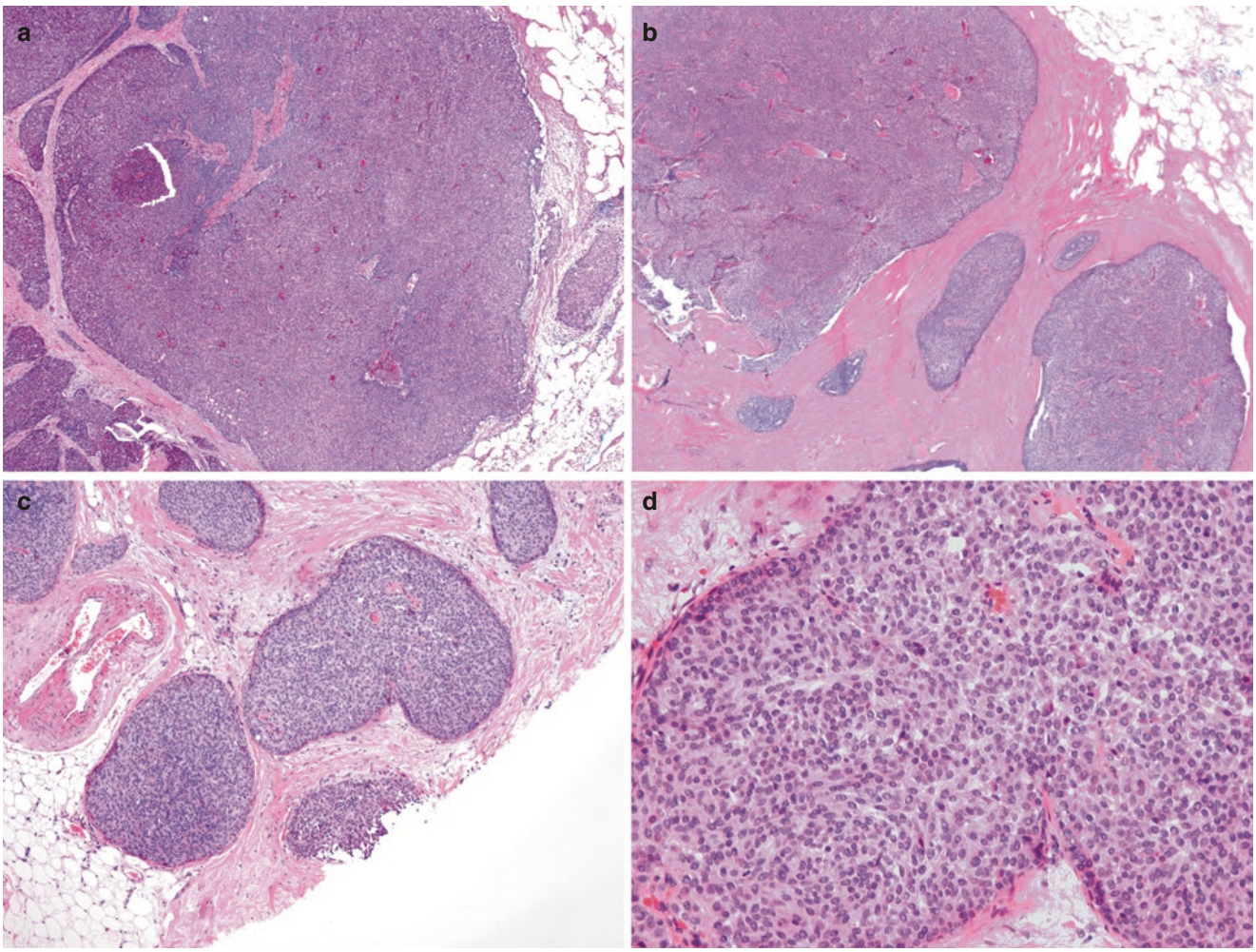

Fig. 6.38 Solid papillary carcinoma. (**a**–**e**) Solid papillary carcinoma is characterized by large expanded ducts and has a similar appearance to florid ductal hyperplasia on low-power examination. (**f**) High-power view shows a uniform population of cells growing in a streaming pattern. Fibrovascular cores are evident within the ducts

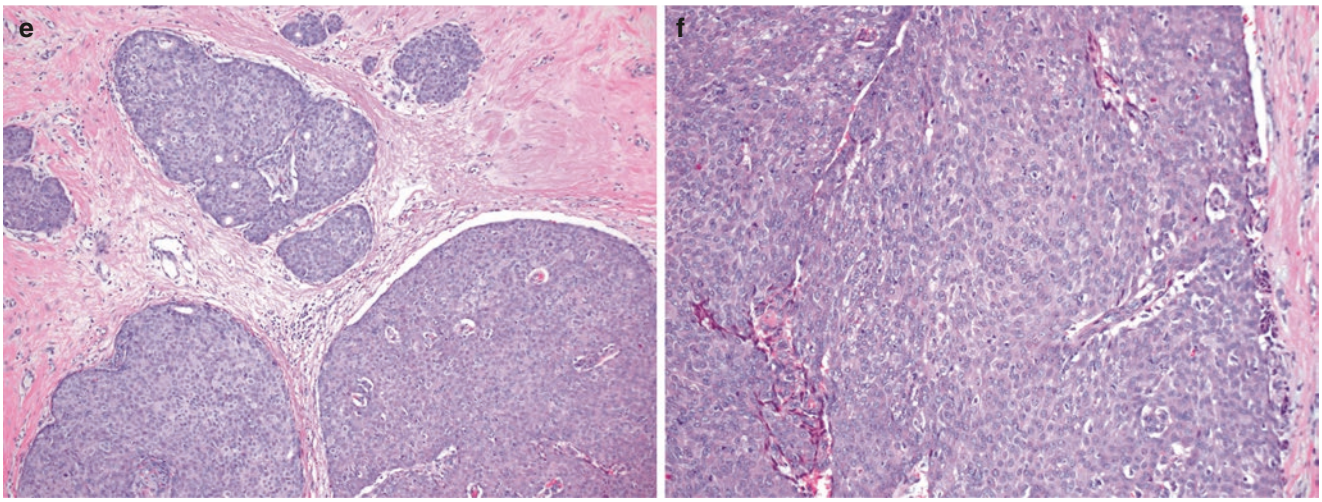

Fig. 6.38 (continued)

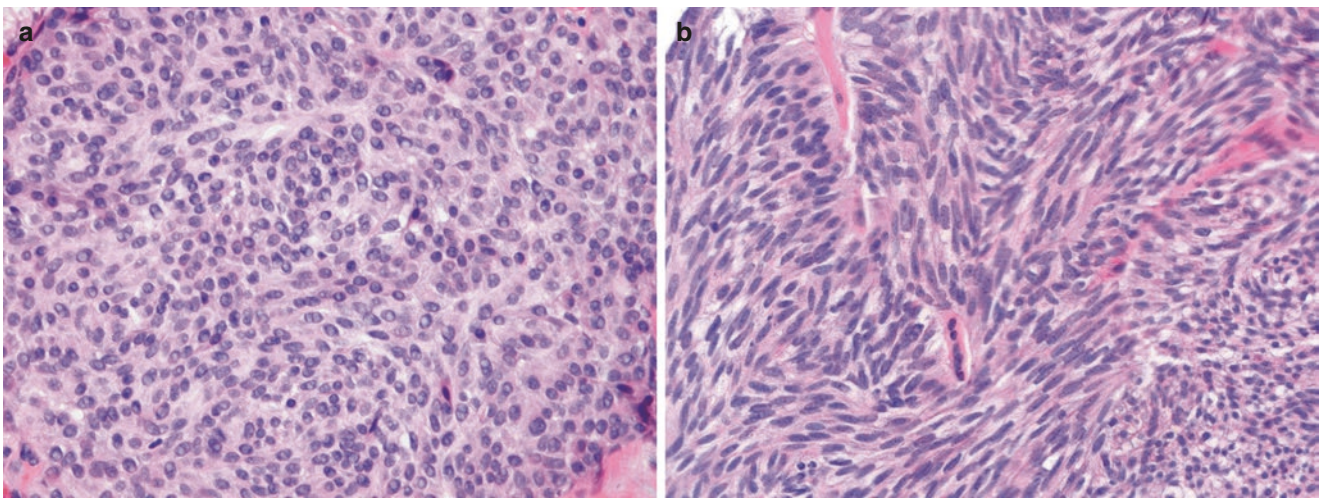

Fig. 6.39 Solid papillary carcinoma–cytologic features. (**a**) Cells are monomorphic with low-grade atypia and grow in a streaming fashion. (**b**) Spindle cell growth in solid papillary carcinoma

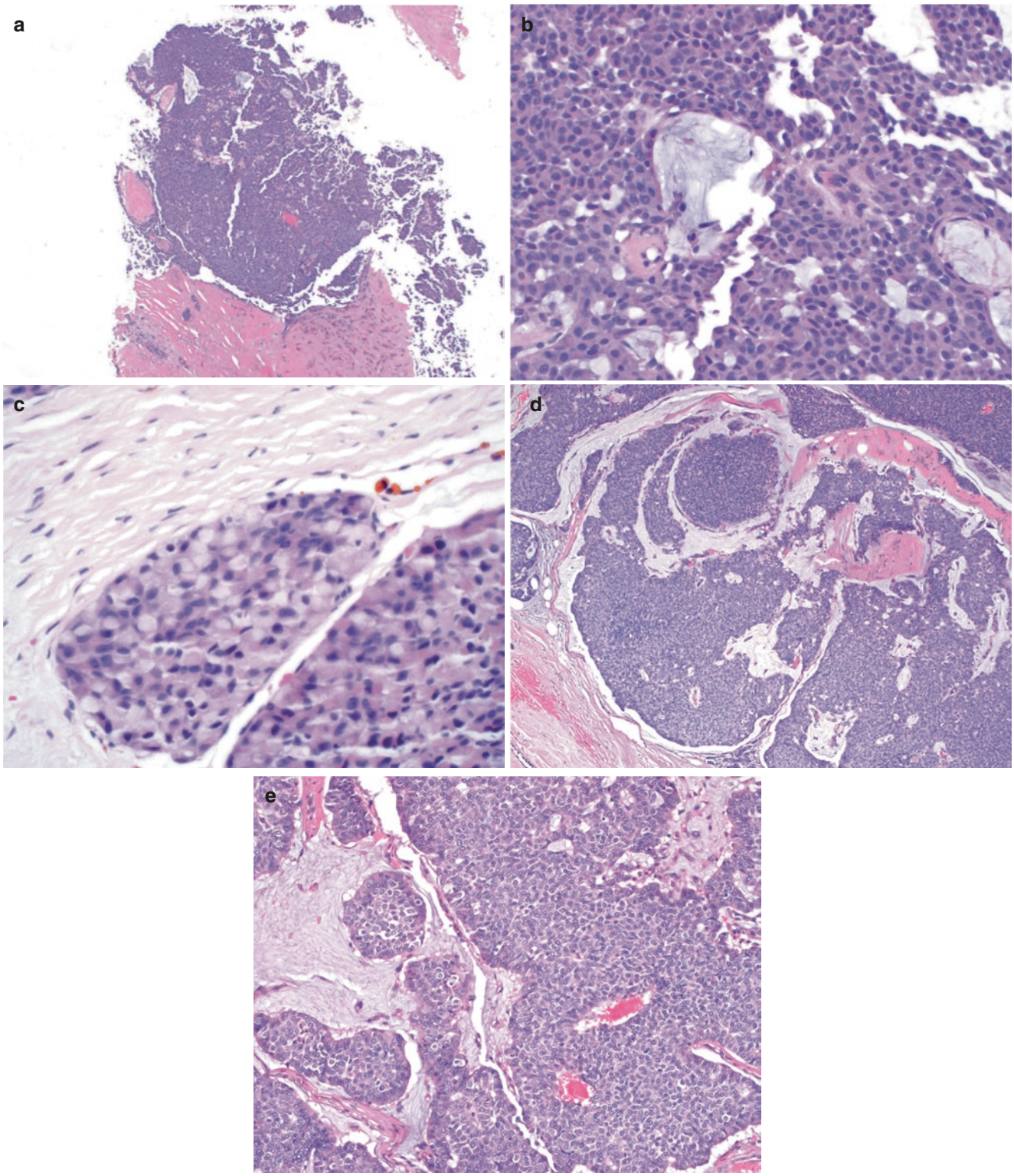

Fig. 6.40 Mucin-producing solid papillary carcinoma. (**a**, **b**) Low- and high-power views of solid papillary carcinoma (in situ) with mucinous features. (**c**) Intracellular mucin in solid papillary carcinoma. (**d**, **e**) Invasive solid papillary carcinoma growing in extracellular pools of mucin

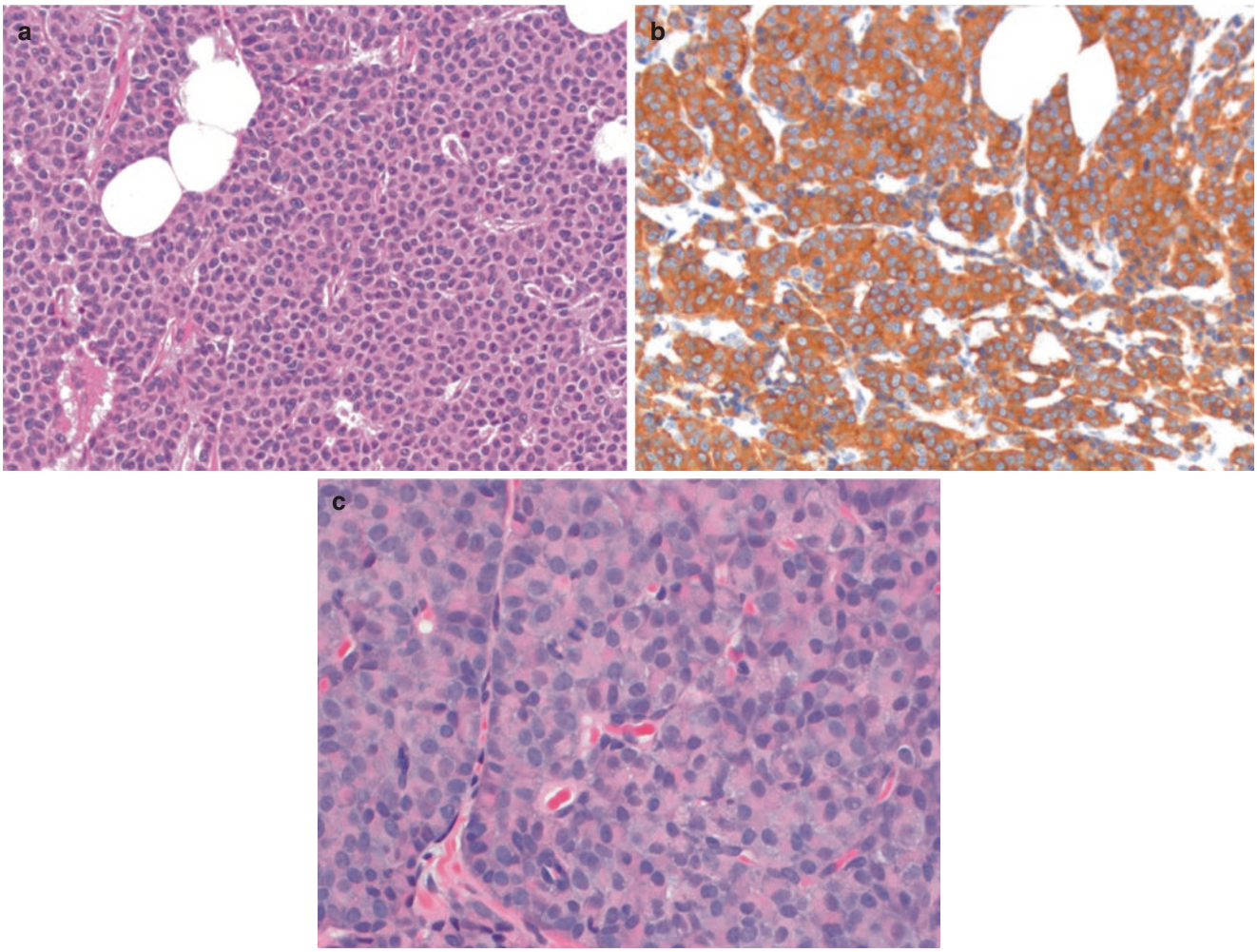

Fig. 6.41 Neuroendocrine differentiation in solid papillary carcinoma. (**a**) Solid papillary carcinoma with a pink appearance from low-power examination. (**b**) Diffuse reactivity with synaptophysin is seen. (**c**) Cells show a perinuclear eosinophilic hof

Molecular Features of Papillary Carcinoma

Papillary carcinomas have been shown to have relatively simple genomic profiles with copy number profiles (including 16q losses, 1q gains, and 16p gains) and *PIK3CA* mutation rates similar to grade and ER-matched invasive carcinomas, NST [34, 35]. Solid papillary carcinomas have been shown to have greater expression of genes associated with neuroendocrine differentiation including *RET*, *ASCL1,* and *DOK7*, compared with EPCs [35]. One study examining the genomics of EPC reported recurrent alterations in genes related to chromatin remodeling, including *KMT2A* and *CREBBP* [36]. In the same study, invasive carcinomas associated with EPC were found to have similar copy number profiles as the EPCs, but with greater enrichment in pathways related to invasion [36].

Other Considerations with Core Needle Biopsy

Papillary lesions, whether benign or malignant, are particularly friable and tend to fragment during the core biopsy procedure. Consequently, the phenomenon of "epithelial displacement," which occurs to variable degrees in both benign and malignant papillary lesions, can be seen in the subsequent excisional biopsy material of these cases. The displaced epithelial cells or cell clusters can mimic invasive carcinoma which can be diagnostically problematic if accompanying findings favoring displacement such as squamous metaplastic changes and retraction artifact of these cells/cell clusters embedded in the needle biopsy tract are not clearly seen (Fig. 6.44). Further discussion of epithelial displacement after core biopsy procedures can be found in Chap. 1.

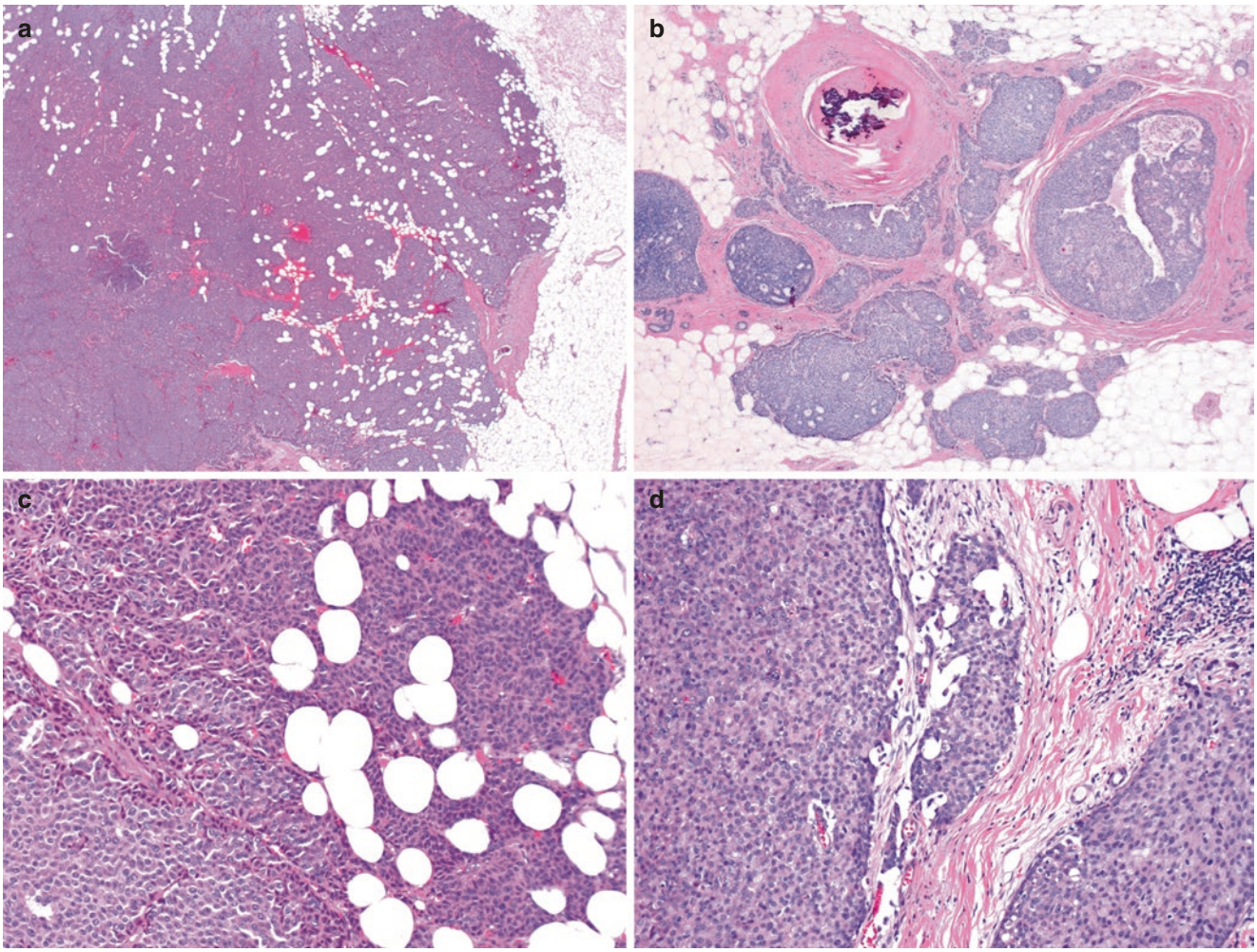

Fig. 6.42 Solid papillary carcinoma with invasion. (**a**) Invasive solid papillary carcinoma characterized by infiltrative growth into adipose tissue. (**b**) Invasive carcinoma arising from solid papillary carcinoma in situ shows multiple infiltrative nests of cells. (**c**) Invasive carcinoma growing in fat without stromal reaction. (**d**) Focal invasive carcinoma arising from in situ solid papillary carcinoma

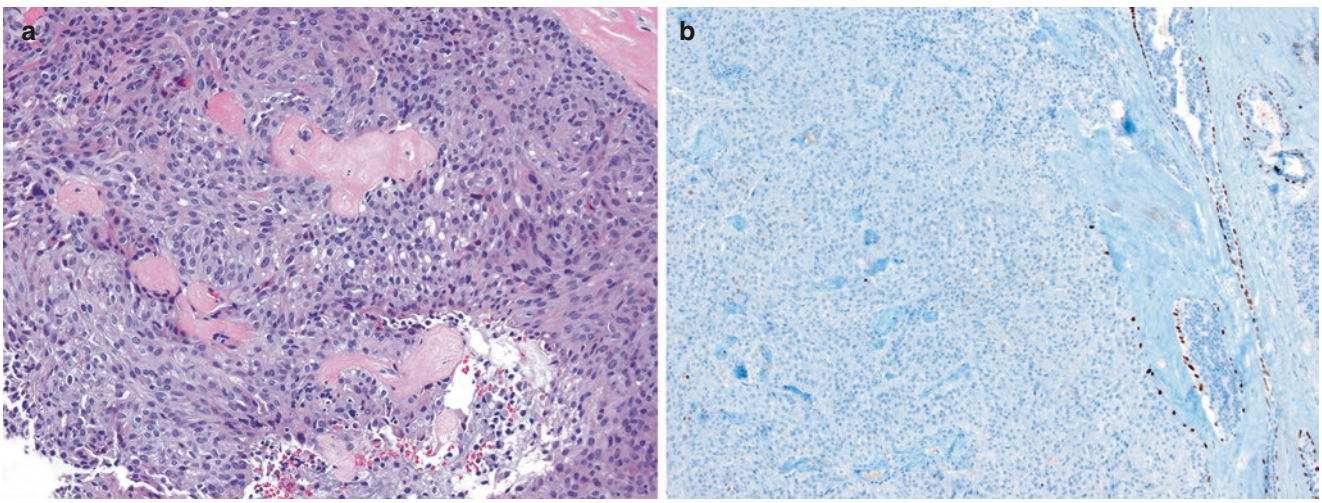

Fig. 6.43 Myoepithelial cell staining in solid papillary carcinoma. (**a**) Solid papillary carcinoma with streaming growth. (**b**) p63 shows focal reactivity at the perimeter of the tumor while adjacent benign glands show continuous positivity

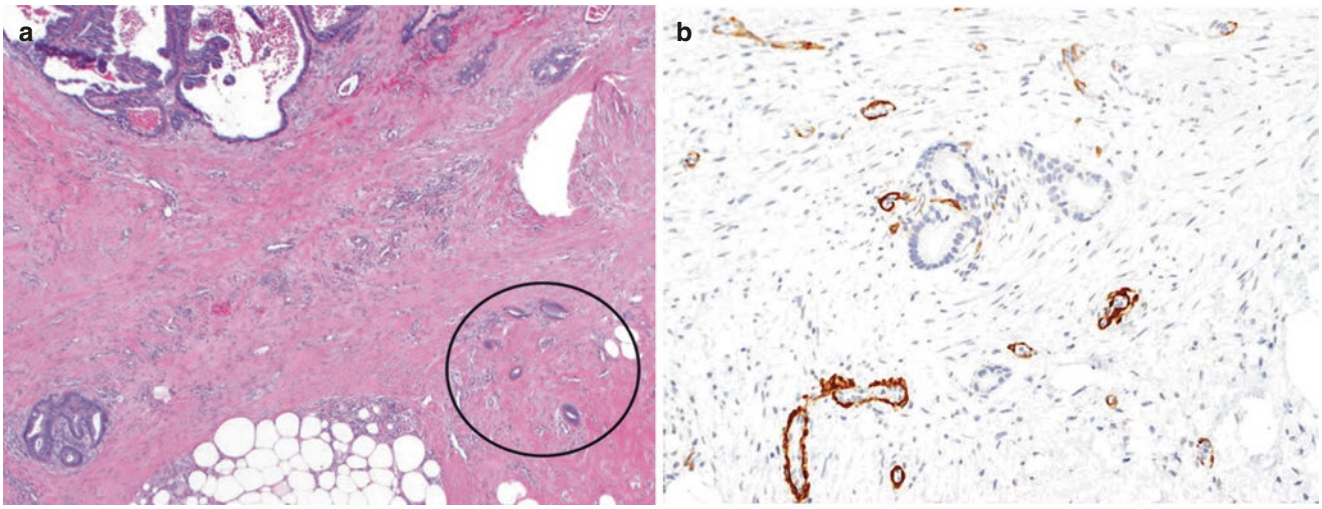

Fig. 6.44 Epithelial displacement following core biopsy of a papillary carcinoma. (**a**) Excisional biopsy shows displaced glands (*circle*) within a biopsy tract associated with in situ papillary carcinoma (*top* of image). (**b**) Displaced glands are negative for smooth muscle myosin heavy chain which should not be mistaken for invasion

Epithelial–Myoepithelial Tumors

Mammary epithelial–myoepithelial tumors are biphasic neoplasms that consist of both epithelial and myoepithelial components. Pleomorphic adenoma (PA) and adenomyoepithelioma (AME) are benign whereas malignant adenomyoepithelioma (AME-M) and adenoid cystic carcinoma are malignant. We will discuss the first three entities in this chapter. Adenoid cystic carcinoma will be discussed in Chap. 12 which is dedicated to rare and salivary gland-type tumors.

Pleomorphic Adenoma

Overview

Pleomorphic adenoma (PA) is a rare, benign neoplasm composed of epithelial and myoepithelial components. These elements which demonstrate variable cytologic and architectural features are embedded in a chondromyxoid stroma. The first description of mammary PA was in 1906 by Lec'ene [37], with additional reports of at least 85 cases since that time [38–41]. The common retro or peri-areolar location of PA has led some to suggest that it arises from large lactiferous ducts; however, rarely PAs have been described in other quadrants of the breast [42–44]. While PAs have been typically described in adult women (range: 19–89 years, mean: 60 years) [45, 46], reports of male PA have been documented [47].

Gross and Radiographic Features

Grossly, PAs are typically well-circumscribed, solid nodules with glistening cut surfaces [48–50]. Generally, they are typically less than 3 cm in size; however, long-standing tumors may grow to be much larger (up to 17 cm) [38–41]. PAs typically present as solitary, palpable, central masses; however, cases presenting with nipple discharge have been described [42, 51]. PAs are circumscribed, lobulated masses and only rarely associated with calcifications [50, 52]. Lesions with irregular infiltrative edges have also been reported [53]. On ultrasound, PAs are round to ovoid hypoechoic lesions with well-circumscribed margins [49, 54] or lobulated masses with irregular margins [48, 55]. In some circumstances, PAs can present as a cystic lesion when they demonstrate intraductal growth [56].

Microscopic Features and Differential Diagnosis

Akin to its salivary gland counterpart, mammary PA is characterized by a mixture of epithelial cells surrounded by an outer layer of bland, spindle or stellate myoepithelial cells embedded within a myxoid, chondroid, or osteoid stroma (Fig. 6.45) [38, 47, 56, 57]. The cellularity of PAs ranges from sparse to high. The epithelial component may be arranged as tubular structures, islands, cords, or sheets. The epithelial cells are characterized by pink cytoplasm with small, oval nuclei. Apocrine metaplasia may be seen [39, 58]. Mitoses are infrequent. PAs are frequently circumscribed with a thin but sometimes incomplete pseudocapsule [43, 50, 59]. PAs may be seen arising within a lactiferous duct and may be associated with papillomatous areas [56, 60].

The differential diagnosis for mammary PA include mucinous carcinoma, matrix-producing metaplastic carcinoma (i.e., metaplastic carcinoma with heterologous mesenchymal differentiation), fibroepithelial tumors (i.e., fibroadenoma or phyllodes tumor), adenoid cystic carcinoma, adenomyoepi-

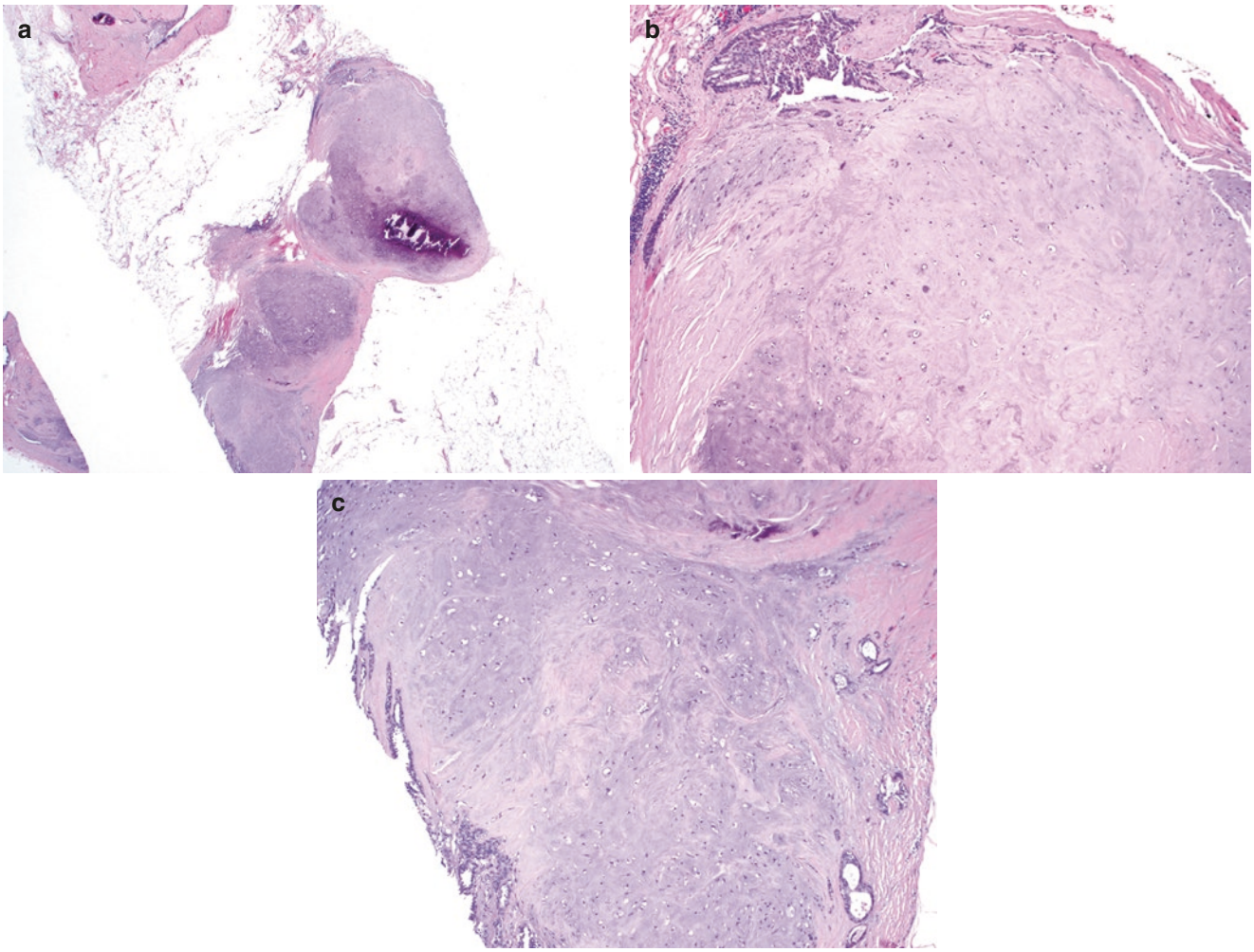

Fig. 6.45 Pleomorphic adenoma in core biopsy: (**a**) Pleomorphic adenoma shows a prominent chondroid stroma with intermixed glandular elements on low-power view. (**b**) Glandular element demonstrates benign epithelial proliferation at the periphery of the lesion and the cells within the chondroid stroma are small and bland. (**c**) The epithelial are arranged as tubular structures and nests. The investing myoepithelial component is inconspicuous

thelial tumors, and chondroid syringoma (i.e., cutaneous mixed tumor).

In some cases differentiating mucinous carcinoma from mammary PA can be problematic due the abundant mucoid stroma and bland cytologic features of the invasive carcinoma cells. Alcian blue and hyaluronidase may be used to distinguish this differential diagnosis since the extracellular mucin of mucinous carcinoma will stain positively with Alcian blue (at pH 1.0 and 2.5) which is resistant to hyaluronidase pretreatment. In contrast, hyaluronidase treatment results in loss of Alcian blue (at pH 1.0 and 2.5) positivity in PAs [60]. Immunostains for myoepithelial cells can be performed which would be present in PAs, and completely absent in mucinous carcinoma. Finally, strong and diffuse estrogen receptor positivity would favor mucinous carcinoma over PA.

Compared to mammary PA, matrix-producing metaplastic carcinoma demonstrates a significant degree of nuclear atypia, inconspicuous mitoses, and high proliferation index [54]. Furthermore, metaplastic carcinoma may show foci of necrosis. While metaplastic carcinomas can retain a myoepithelial phenotype, the well-organized biphasic pattern of myoepithelial cells surrounding the ductal structures in a PA should assist in differentiating these two entities (Fig. 6.46) [61].

While more frequently problematic in the cytologic differential diagnosis of PA, fibroepithelial tumors may also be considered in the differential diagnosis of a core biopsy specimen. Compared to mammary PA, fibroepithelial tumors (especially phyllodes or fibroadenomas with intracalicular growth) demonstrate compressed epithelial structures. Furthermore, benign fibroepithelial tumors, even those with

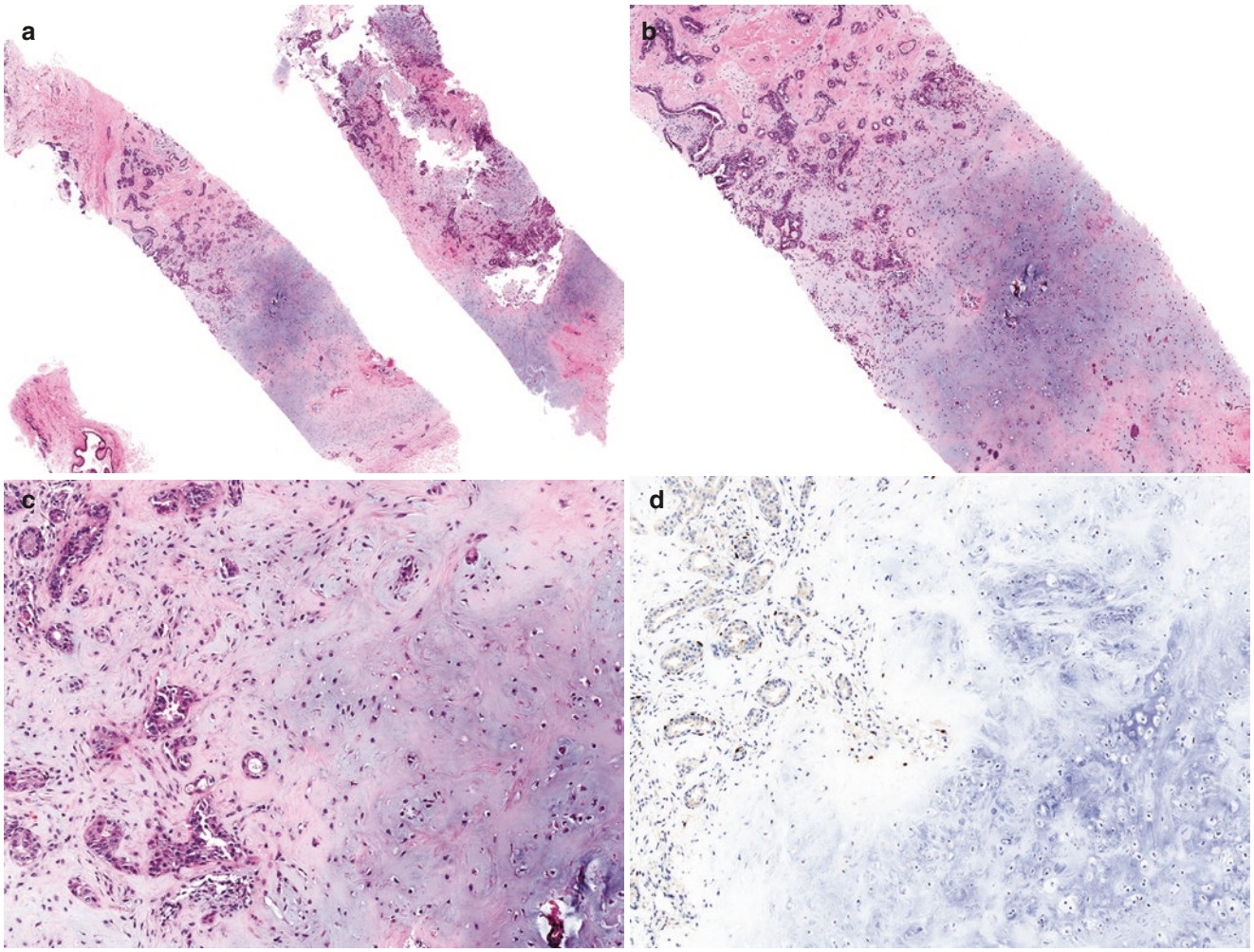

Fig. 6.46 Pleomorphic adenoma in core biopsy: (**a**, **b**) Pleomorphic adenoma shows a bland glandular proliferation embedded in chondromyxoid stroma with well-circumscribed borders on low power. (**c**) The glandular component and the cells embedded in the chondromyxoid stroma demonstrate low-grade cytomorphology. Mitoses are absent. (**d**) The investing myoepithelial component is highlighted by a p63 immunostain. (*Courtesy of Yunn-Yi Chen, MD PhD*)

myxoid stroma, generally lack chondroid or osseous components. In malignant fibroepithelial tumors, the degree of atypia within the stromal component that would be expected, including those with osseous or chondroid differentiation would be beyond that expected in PA.

Both mammary adenoid cystic carcinoma (AdCC) and PA are biphasic neoplasms that consist of both epithelial and myoepithelial components. Compared to AdCC, in which the glandular or cribriform structures may contain a myxoid acidic secretion, in PA, the biphasic elements are surrounded by an abundant myxoid stroma with or without chondroid or osteoid metaplasia. Furthermore, PA should have well-circumscribed borders whereas AdCC demonstrates infiltrative growth.

Differentiating adenomyoepithelioma (AME) from mammary PA may be quite difficult. While both are biphasic and well-demarcated lesions, AME is characterized by a prominent and often multilayered myoepithelial cells surrounding epithelial glands. While AME may occasionally demonstrate chondromyxoid stroma, the absence in most cases can be used to exclude PA. Finally, AME may demonstrate nuclear atypia and mitoses which are absent in PA.

Chondroid syringoma is morphologically indistinguishable from mammary PA. While the trunk is not a common location for this benign skin neoplasm, it may arise in the axilla and mimic a mammary neoplasm. The key in differentiating these entities is recognizing that a chondroid syringoma arises in the dermis or subcutis and not surrounded by mammary glandular tissue (which may be challenging in the core biopsy setting). Chondroid syringoma may also be classified as eccrine or apocrine, due to the morphological appearance of the tumor cells [52].

Immunohistochemistry

The biphasic nature of PA can be highlighted with the use of immunohistochemical stains. The epithelial component is positive for low molecular weight and pan-cytokeratins, epithelial membrane antigen (EMA), and carcinoembryonic antigen [39, 43, 50, 54]. The stromal and periglandular myoepithelial component is positive for CD10, p63, calponin, SMA, and high molecular weight cytokeratin (i.e., CK14, CK-K903) [49, 54]. Focal positivity for keratins (i.e., CAM 5.2 and AE1:AE3) and EMA may be noted in the myoepithelial cells [50]. S100 protein can have a variable expression, but found to be more intense in myoepithelial cells. Estrogen receptor and progesterone receptor positivity is variable [50, 54, 59, 62]. Rare studies have demonstrated immunoreactivity for HMGI-C and HMGI(Y) proteins in the nuclei of the spindle and myoepithelial cells, supporting a similar histogenesis compared to salivary gland PAs [39].

Molecular Features

Studies have demonstrated salivary gland PAs harbor chromosomal translocations, most often in the long arms of chromosomes 8 (8q12) and 12 (12q15), and in the short arm of chromosome 6 (6p21), corresponding to genes pleomorphic adenoma gene 1 (PLAG1), high mobility group protein gene HMGA2 (HMGI-C), and HMGIY, respectively [63–65]. The genetic/chromosomal alterations of mammary PA have yet to be evaluated and is therefore of limited diagnostic utility in this setting [63].

Management in Core Needle Biopsy

Generally, surgical excision is recommended for the management of PAs diagnosed in core needle biopsies. This is in part a reflection of difficulties in establishing a definitive diagnosis based on the morphologic and immunophenotypic overlap with other biphasic breast lesions (i.e., adenomyoepithelial tumors). Due to the rarity of mammary PAs, there are no published studies reporting "upgrade rates" for lesions diagnosed in core needle biopsy and referred for excision.

Prognosis

In general, PAs are indolent; however, local recurrences may occur if the lesion is incompletely excised [38, 42, 66]. Furthermore, there are reports of malignant PA (i.e., carcinoma ex PA) [61].

Adenomyoepithelioma

Overview

Adenomyoepithelioma (AME) is a rare mass-forming biphasic neoplasm. First described by Hamperl in 1970 [67], AME is characterized by epithelial lined tubular gland-like elements in close association with a conspicuous intervening myoepithelial cells. The alternating even placement of these distinct cell types results in a characteristic highly cellular mass with a microscopically organoid character. AMEs are characterized by a considerable range of histological appearances, depending on the differentiation and cytology of the constituent populations. While most AMEs follow a benign clinical course, distant metastases from benign appearing lesions have been reported. As such, AMEs may be regarded as neoplasms with low malignant potential [10]. While AMEs typically present as a palpable breast mass, however more widespread use of breast cancer screening programs have increased the detection of asymptomatic lesions [68]. AMEs have predominantly been described in female patients >50 years of age. Rare reports of AME in men exist [69, 70]. Any case that has undergone a recent change in size or character should be suspected of harboring carcinoma (to be discussed later in this chapter).

Gross and Radiographic Features

Grossly, these are circumscribed, homogeneous, bossellated, or multilobulated masses, typically 1.0–2.5 cm in diameter, but can reach up to 10 cm (Fig. 6.47) [71]. Cystic areas may be appreciated in some instances [72, 73].

On mammography, AMEs are usually round or lobulated dense masses with partially indistinct but mostly circumscribed margins that lack calcifications [74, 75]. By ultrasound, AMEs may be irregular to oval, solid or solid-cystic masses with well-to-poorly circumscribed margins and posterior or combined acoustic enhancement [74, 75]. Unless complicated by malignancy, size and imaging features should be stable over time. The radiographic differential diagnosis is generally fibroadenoma or duct adenoma.

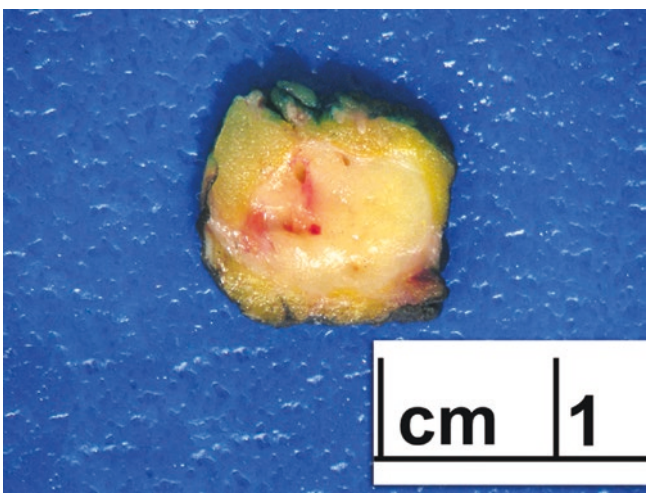

Fig. 6.47 Gross appearance of adenomyoepithelioma. An excisional biopsy specimen shows a well-circumscribed, homogeneous, pale yellow mass

Microscopic Features and Differential Diagnosis

Scanning magnification examination of AME reveals a cellular mass having a distinctly multilobulated appearance; however, this characteristic feature may be more subtle in limited core biopsy material (Fig. 6.48). AMEs frequently demonstrate a mixture of papillary, spindle, tubular, or lobulated architecture and that which predominates will determine the differential diagnosis. In most instances, the main differential to consider is the papilloma as they share many histologic features. For instance, AME consistently have a

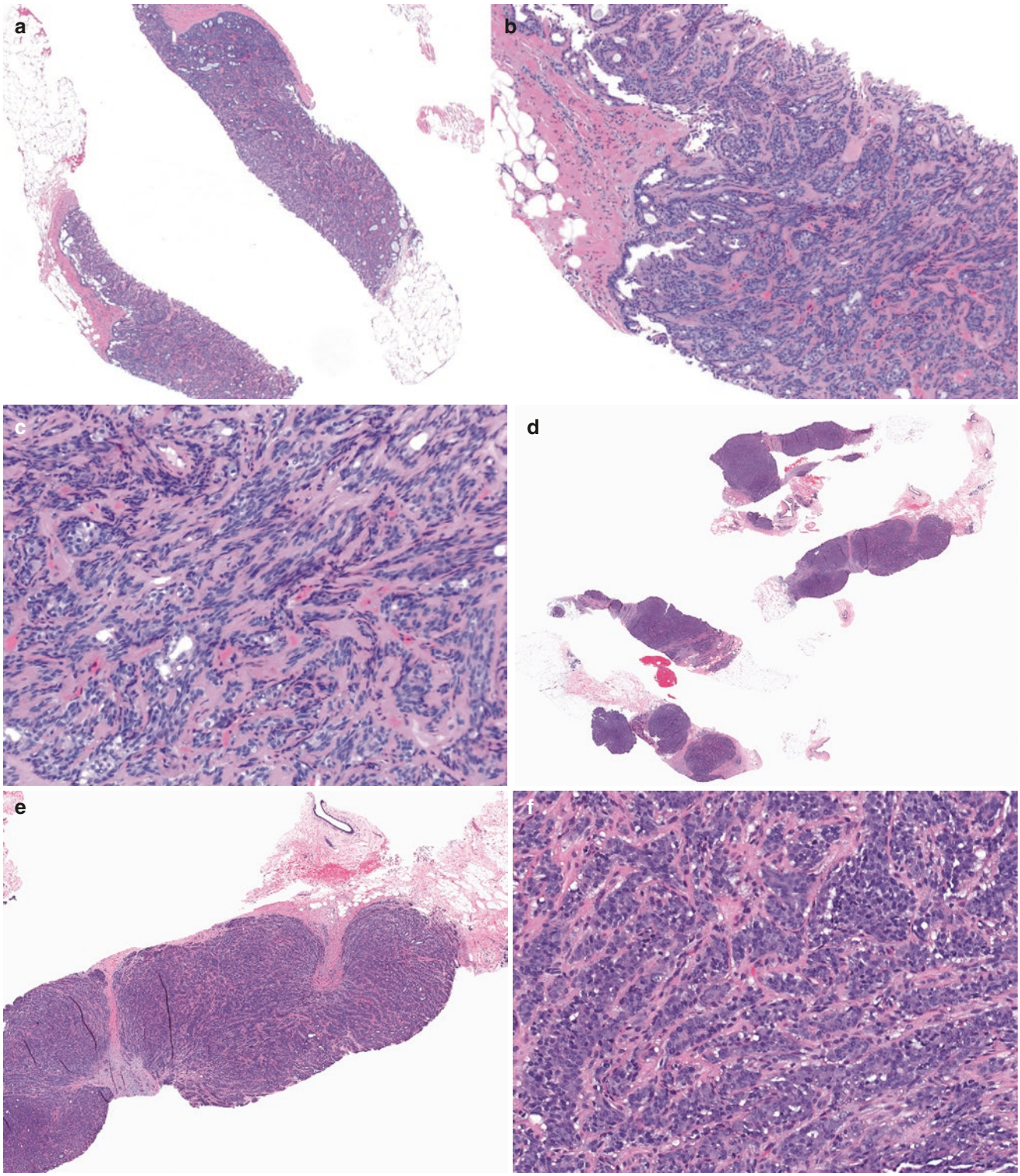

Fig. 6.48 Adenomyoepithelioma in core biopsy. (**a**) Low-power view shows a circumscribed nodular lesion in the core biopsy. (**b**) Papillary cores are evident. (**c**) Spindle cells and glands are present. Fibrovascular cores in the lesion can be seen. (**d**–**f**) Second case with prominent multinodular architecture and adenosis-like growth

non-infiltrative, pushing interface with surrounding tissue. The glandular component in most cases forms small monotonous acini of uniform diameter which can easily be mistaken for adenosis expanding the interior of a papilloma. In some cases, the epithelium is disposed in trabecular formations which can be a distinguishing feature as this is not appreciated in papillomas. If there is evidence of predominant intraluminal growth, the lesion should be classified as a papilloma. Epithelial populations alternate in a predictable, nonrandom manner with myoepithelial cells within variable amounts of hyaline collagenous matrix (Fig. 6.49). It is characteristic for the myoepithelial component to predominate; they often appear to outnumber epithelial populations or, focally, to form small nodules. This finding although charac-

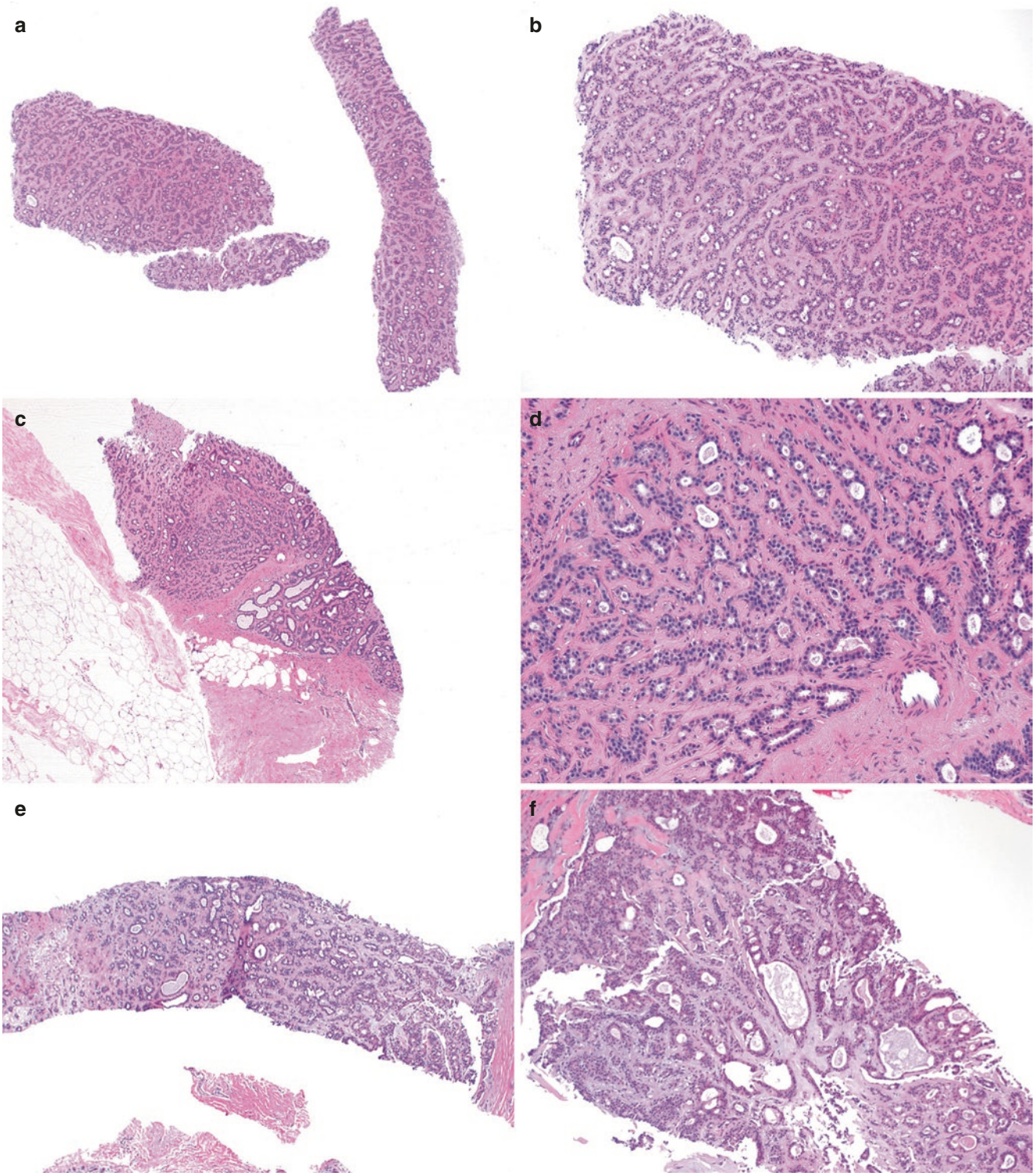

Fig. 6.49 Adenomyoepitheliomas with prominent glandular components. (**a**–**d**) Core biopsy shows a proliferation of small glands in a dense hyalinized stroma. (**e**, **f**) Second case with adenosis-like growth

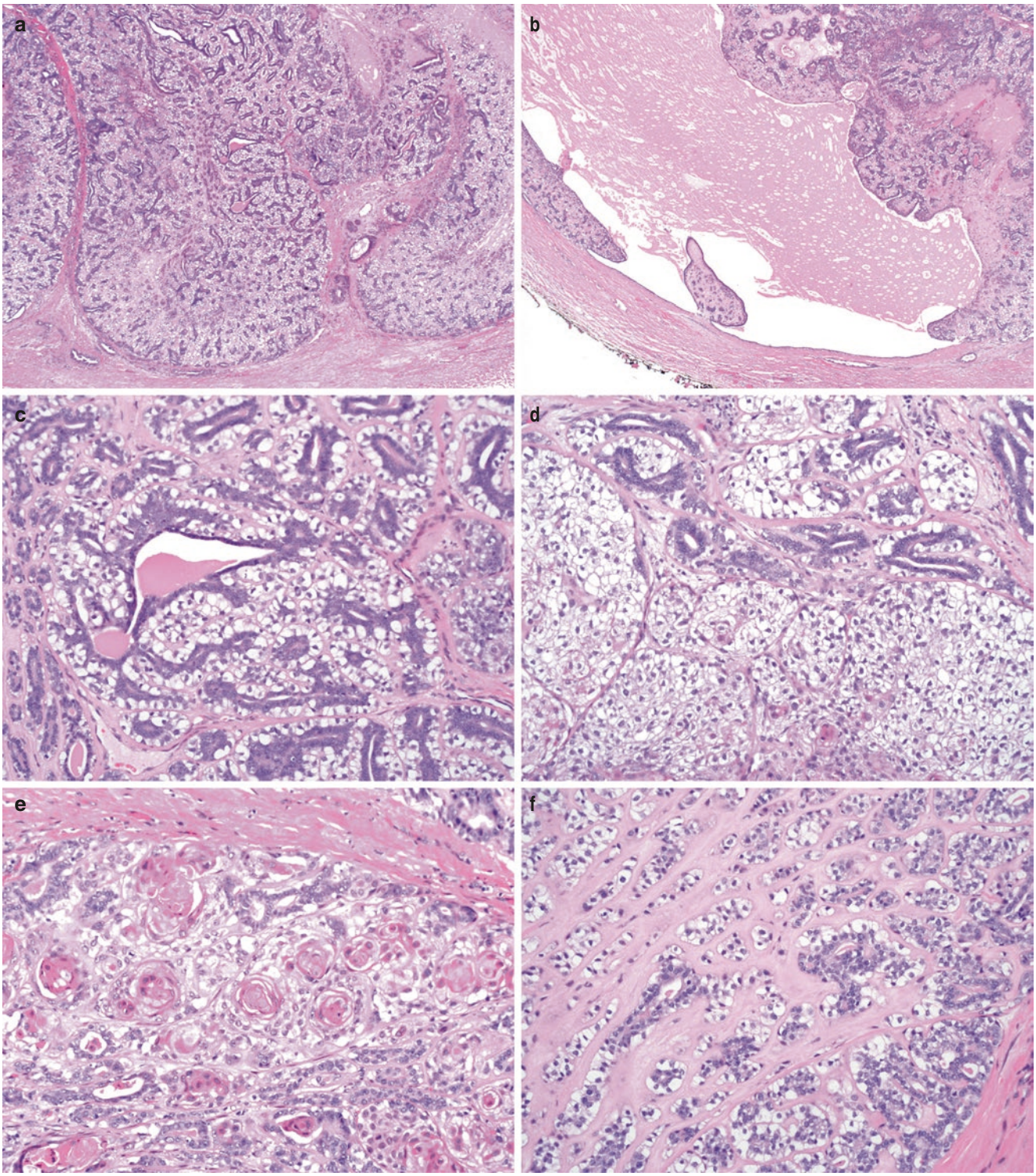

Fig. 6.50 Adenomyoepithelioma. (**a**) Multinodular growth in AME. (**b**) Cystic component in the tumor. (**c**, **d**) Clear cell change in myoepithelial cell cytoplasm. (**e**) Squamous metaplasia. (**f**) Eosinophilic matrix in the stroma

teristic for AME can also be seen focally in a subset of papillomas as discussed previously. Epithelial and myoepithelial nuclei are generally plump and usually have open chromatin (Fig. 6.50). The cytological features of the myoepithelial population may be mononuclear and undistinguished in character, although it is nearly always more obvious in adenomyoepithelioma than in papilloma. In many cases the myoepithelium declares itself with (glycogen-rich) clear cytoplasm. Mitoses may be present, but they should be inconspicuous at most.

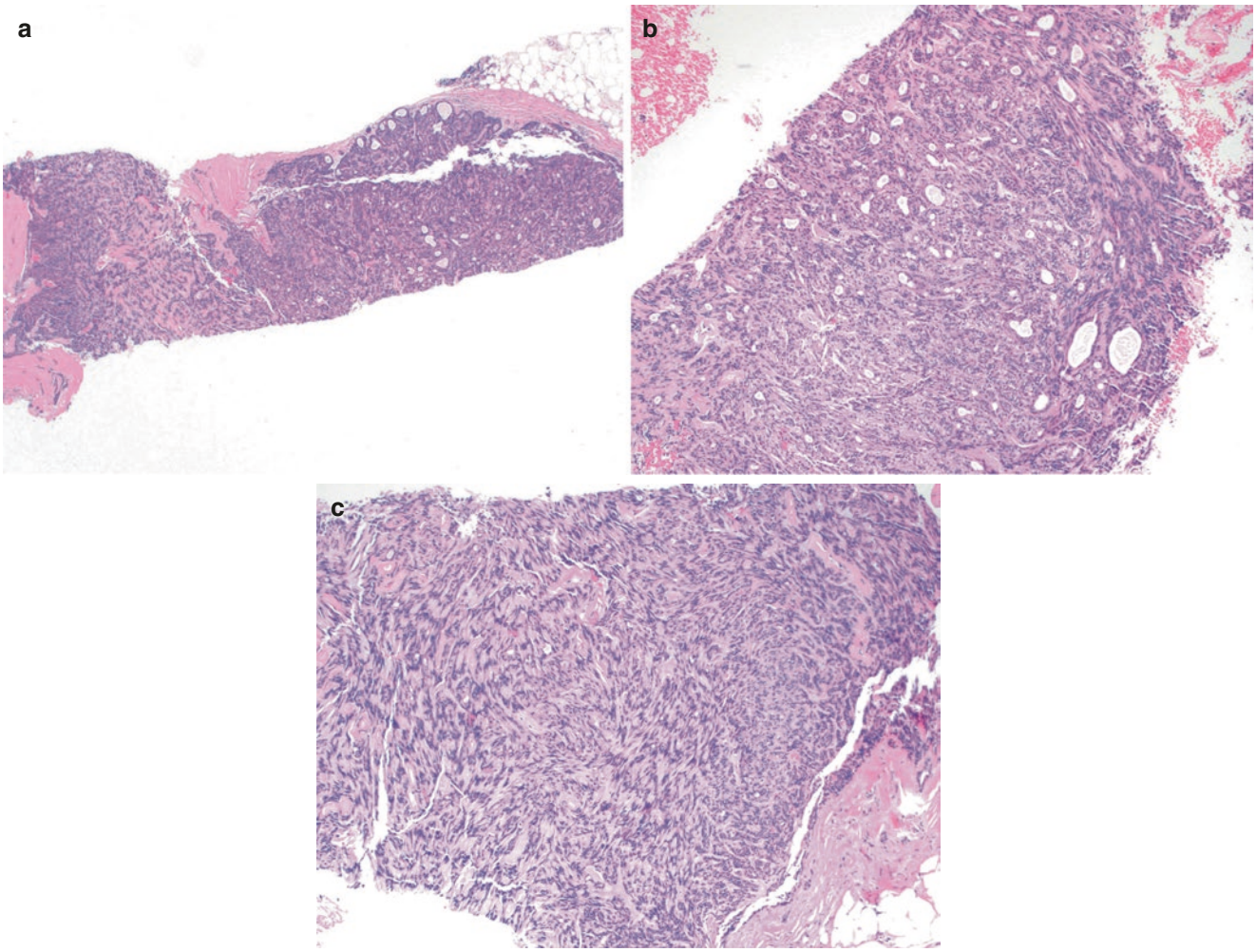

Fig. 6.51 Adenomyoepithelioma—spindle cell morphology. (**a–c**) AME with myoid differentiation in a core biopsy is composed mainly of spindle cells with rare open glands in the tumor

Some AME may assume a predominantly spindled appearance which can be particularly problematic in core needle biopsy samples (Fig. 6.51). If diffuse and the only areas sampled, the differential diagnosis entertained at that time is that of a spindle cell lesion, not a biphasic tumor. A concerted effort to identify any glandular/tubular formation within lesional tissue should be made which will alert the pathologist to consider AME in the differential diagnosis. Correlation with imaging findings may be of further assistance in these cases. On occasion, AME can show additional histologic features focally such as squamous or sebaceous differentiation, chondroid metaplasia, or collagenous spherulosis.

In AME with tubular architecture, small ductal structures are surrounded by conspicuous myoepithelial cells in a uniform arrangement, while those with lobulated architecture display nest of predominantly myoepithelial cells surrounded by dense hyalinized and sclerotic collagenous material. When either of these two patterns predominate, other entities in the differential diagnosis include adenosis, adenoid cystic carcinoma, and pleomorphic adenoma. Nodule-forming variants of adenosis may simulate adenomyoepithelioma with prominent tubular architecture but tend to lack the distinctive biphasic character of the latter (Fig. 6.52). Adenoid cystic carcinoma may also present as populations of mixed benign appearing glands with myoepithelial-like cells. However, the basal cell population in adenoid cystic carcinoma is less obviously myoepithelial in character. Further, adenoid cystic carcinoma should exhibit areas of infiltrative growth or "cylinders" of basophilic basal lamina material (Fig. 6.53). As previously mentioned, distinguishing AME from pleomorphic adenoma may be challenging, particularly in cases with lobulated architecture, where the hyalinized and sclerotic collagenous material may appear myoid or chondroid in nature.

Some cases are characterized by myoepithelial cell atypia, with focal or diffuse nuclear enlargement and pleomorphism. The significance of this finding is not clear but serves to reinforce the known phenomenon of malignancy arising is adenomyoepithelioma as most carcinomas arising in AME show "atypical" myoepithelial populations (see below).

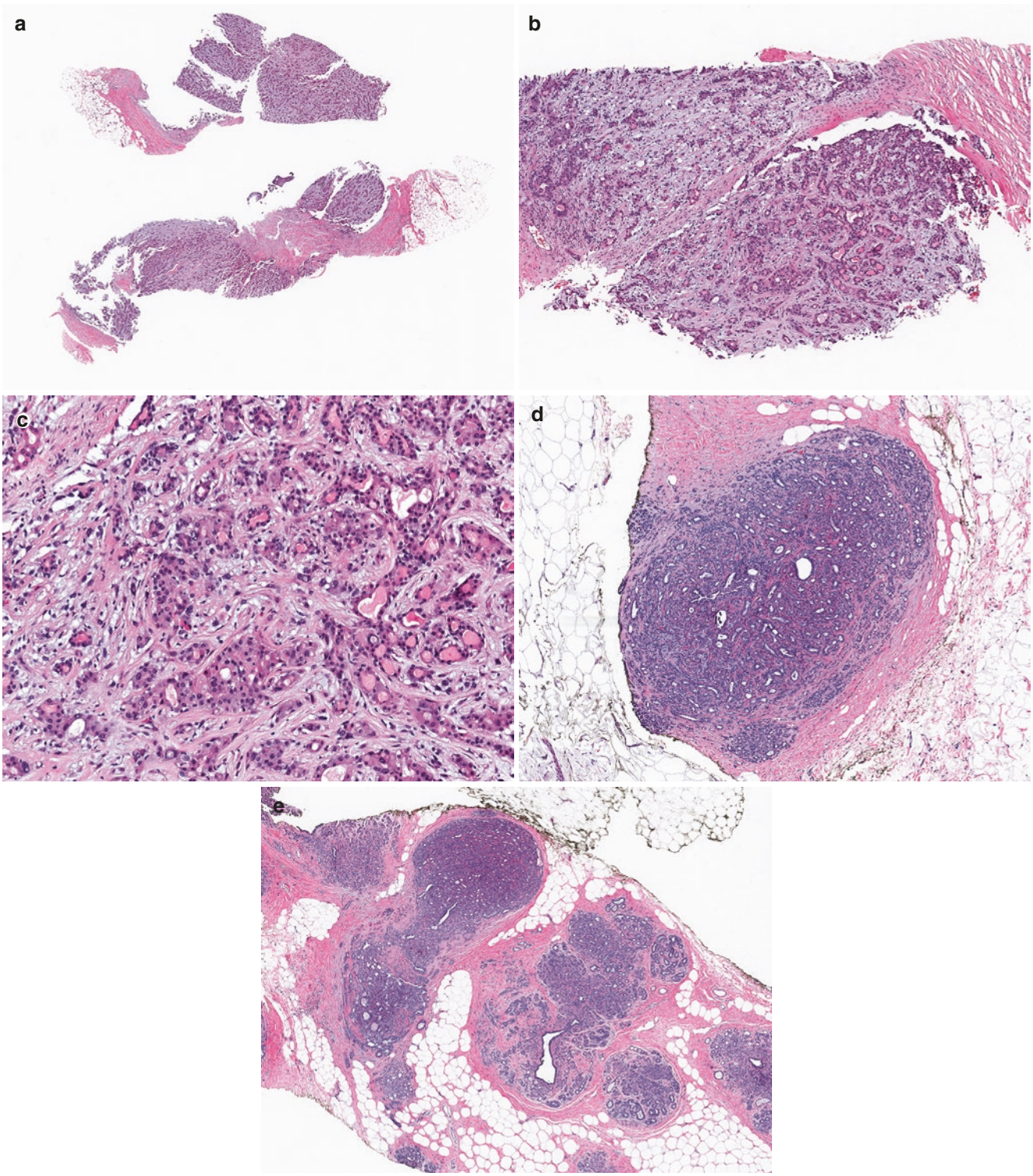

Fig. 6.52 Adenomyoepithelioma with adenosis pattern compared to nodular adenosis. (**a**, **b**) Core biopsy shows a circumscribed but nodular adenomyoepithelioma. (**c**) The tumor is composed of a biphasic proliferation of glands with eosinophilic epithelial cells with luminal secretions surrounded by a proliferation of clear to spindled myoepithelial cells. (**d**) Nodule of sclerosing adenosis with adenomyoepitheliomatous features due to prominent myoepithelial cells. (**e**) The surrounding breast tissue demonstrates additional foci of sclerosing adenosis that lacks biphasic characteristics

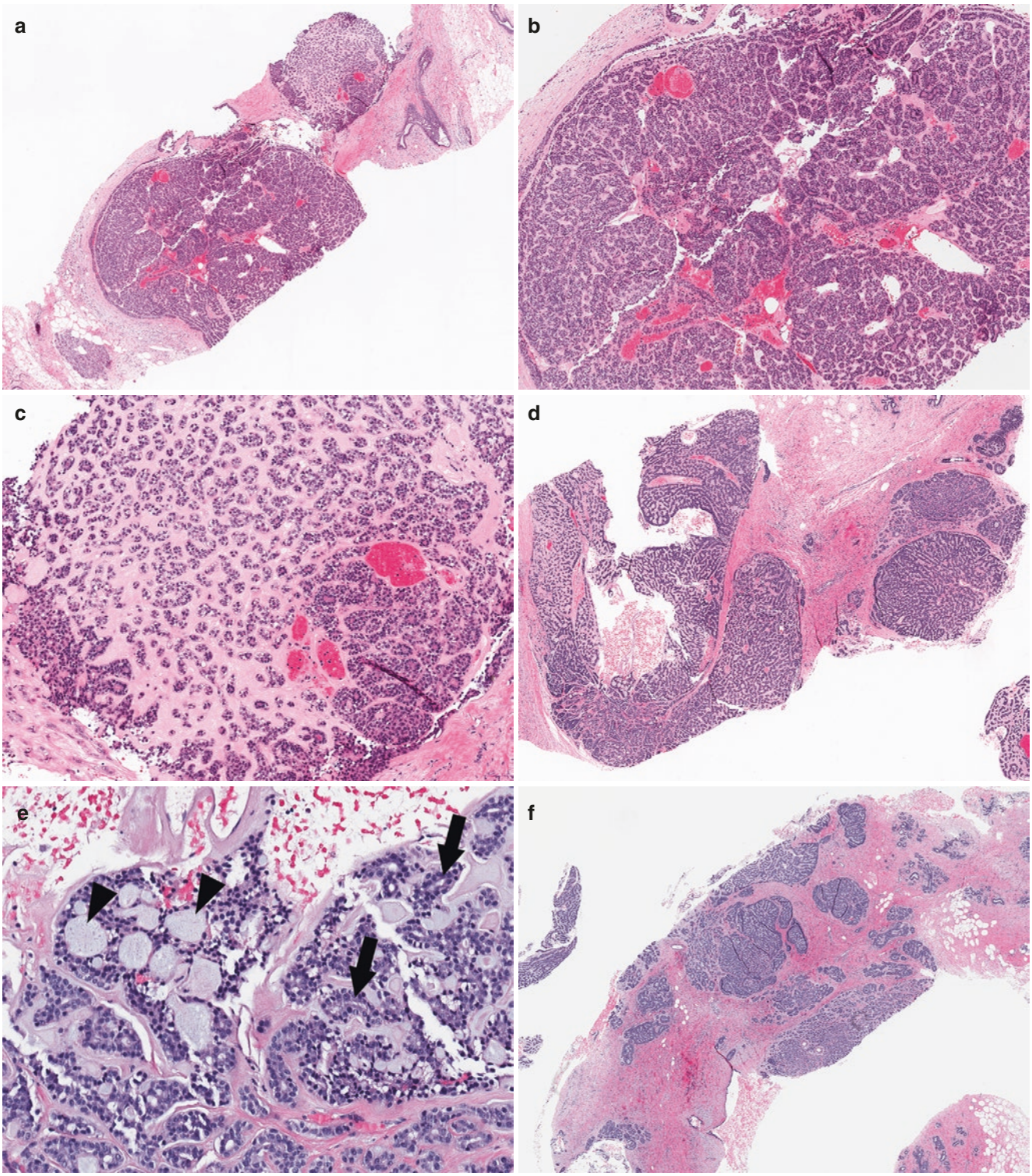

Fig. 6.53 Adenomyoepithelioma compared to adenoid cystic carcinoma. (**a**–**d**) Core biopsy shows a nodular but circumscribed adenomyoepithelioma. (**b**) The tumor is composed of densely packed glands that lack cribriform architecture. (**c**) In a portion of the tumor, the small glands are embedded in a dense hyalinized stroma. (**d**) Core biopsy shows an adenoid cystic carcinoma with multinodular and predominately circumscribed growth on low power. (**e**) At higher magnification, epithelial elements form true lumina (arrows) and basaloid myoepithelial-like cells form pseudolumina with cribriform architecture filled with myxoid stroma (arrowheads). (**f**) Additional core biopsies demonstrated nest and glands with infiltrative growth

Immunohistochemistry

In most cases, the diagnosis can be rendered on morphologic features alone; however, in the core biopsy setting, pathologists who do not commonly encounter these tumors may not have an initial high index of suspicion at the onset. Confirming the myoepithelial component of AME can be helpful and immunostains S-100 protein, SMM, and p63 can be utilized (Fig. 6.54). In general, there has been no published study spe-

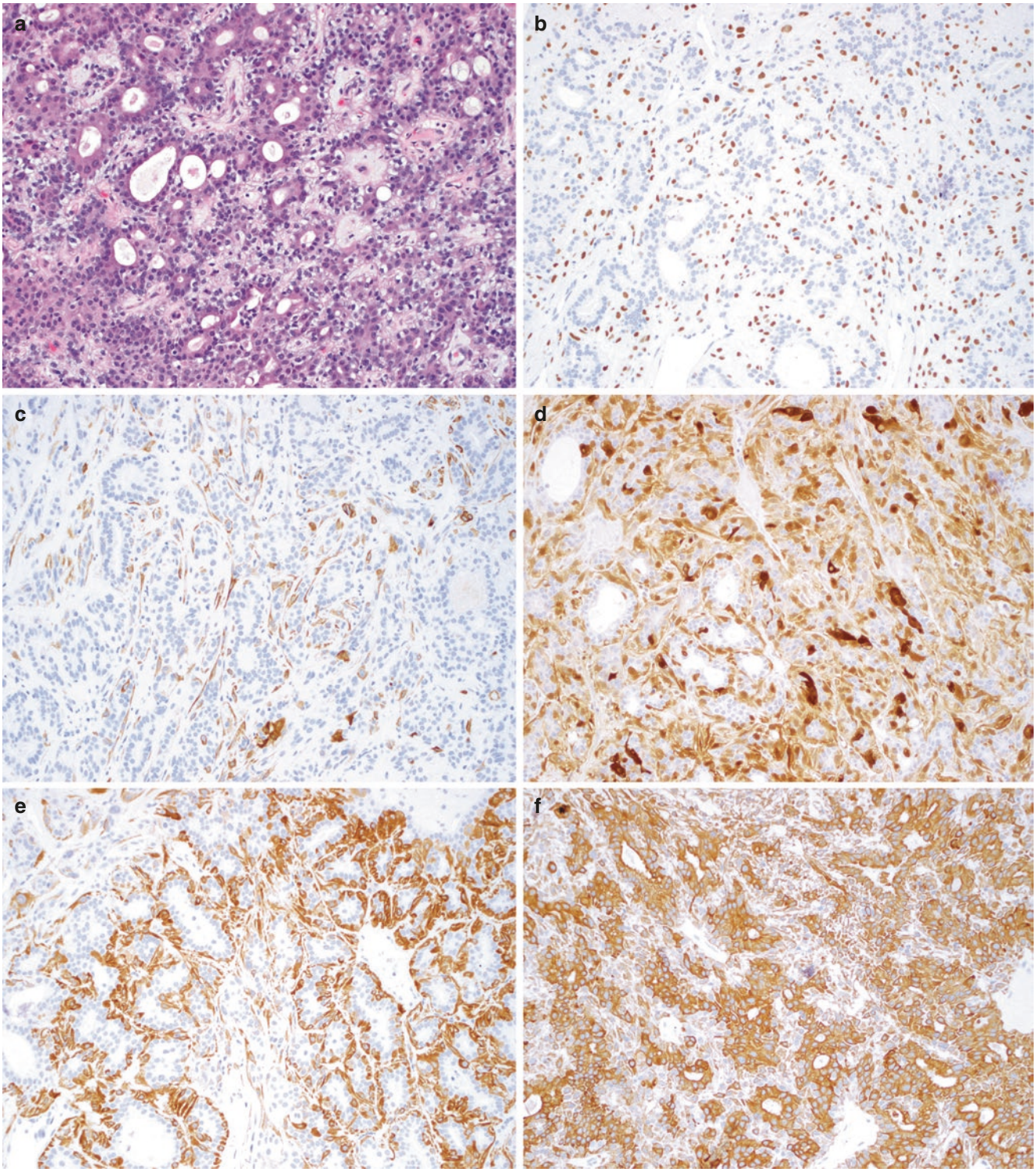

Fig. 6.54 Immunohistochemical staining in adenomyoepithelioma. (**a**) Adenomyoepithelioma with biphasic appearance. (**b**) p63 highlights myoepithelial cells. (**c**) CK14 shows variable staining of myoepithelial cells, while (**d**) S-100 protein shows a more diffuse pattern of staining of myoepithelial cells in this case. (**e**) Smooth muscle myosin heavy chain shows myoepithelial staining while (**f**) CK7 highlights luminal ductal cells in the lesion

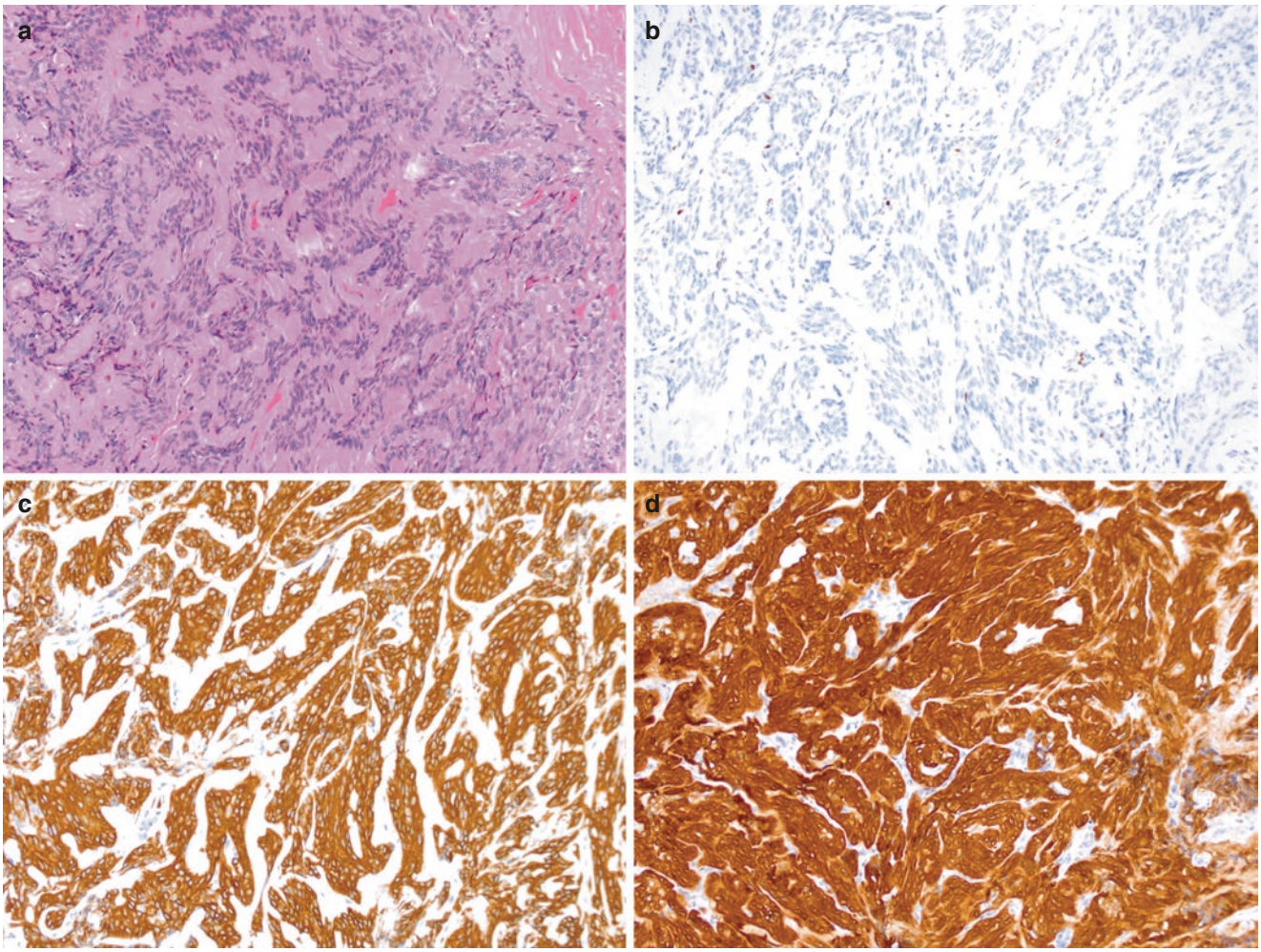

Fig. 6.55 Myoepithelial staining in adenomyoepithelioma. (**a**) Adenomyoepithelioma shows spindle cell features. Glandular elements are inconspicuous at best in this core sample. (**b**) p63 shows scattered single cell positivity which is unexpected in an AME. However, strong and diffuse staining is observed with other myoepithelial markers (**c**) CK5 and (**d**) S-100 protein

cifically characterizing AME by immunohistochemistry. One study in abstract form [76] reported the observation that rarely spindle cell areas of AME lack immunoreactivity for routinely utilized myoepithelial markers (p63) particularly in small samples where morphologically diagnostic areas may be inaccessible. Representing a possible diagnosis pitfall, it was reported that the myoepithelial nature of these areas could be better confirmed using S-100 protein or CK14 (Fig. 6.55).

Molecular Features

Microsatellite instability and reciprocal translocations of chromosomes 8 and 16 have been demonstrated in AMEs [77–79]. Studies have shown that estrogen receptor (ER)-positive adenomyoepithelial tumors frequently harbor PIK3CA and AKT1 activating mutations and ER-negative tumors frequently harbor HRAS mutations [79]. However, there is one report of a co-occurring HRAS and PIK3CA mutation in an ER-positive adenomyoepithelial tumor [80]. PIK3CA and AKT1 mutations appear to be mutually exclusive and co-occurring AKT1 and GNAS mutations may be seen [79–81].

Management in Core Needle Biopsy

Surgical excision should be considered when core biopsies show AME, especially for cases with worrisome or changing imaging findings, in order to rule out carcinoma arising in AME (see below). To date there are no published studies reporting "upgrade rates" or AME diagnosed in core needle biopsy and referred for excision. Myoepithelial cell atypia, frequent mitoses, and necrosis (even focal) are clues to the presence of coexisting malignancy.

Malignancy in Adenomyoepithelioma (Adenomyoepithelioma with Carcinoma)

Malignant adenomyoepithelioma (AME-M) is characterized by the presence of malignancy (either arising from the epithelial or myoepithelial components) within an AME, whereas the terminology "epithelial–myoepithelial carcinoma" is preferred when both the epithelial and myoepithelial compartments are malignant [10]. Carcinomas developing

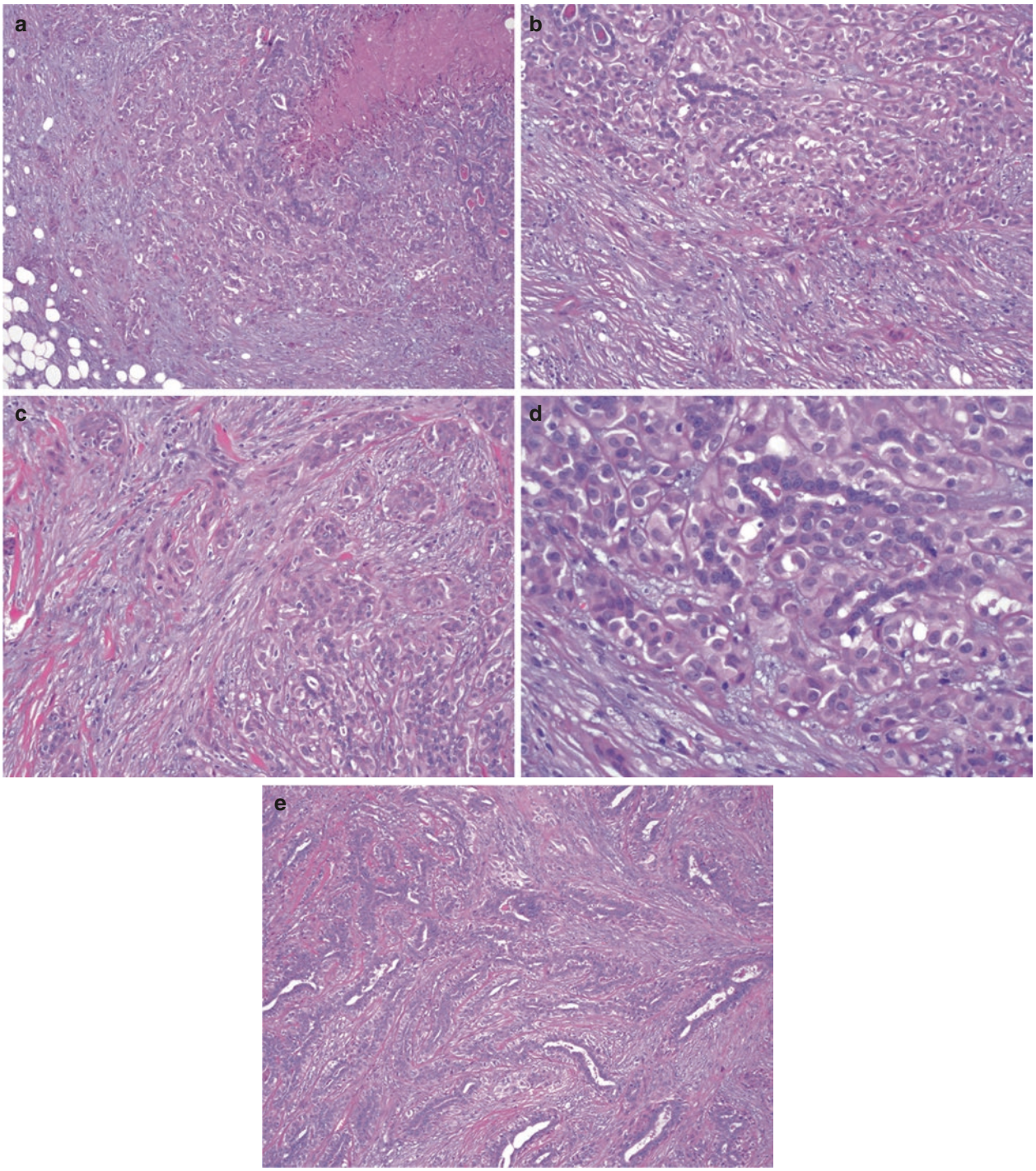

Fig. 6.56 Malignant adenomyoepithelioma. (**a**–**e**) Invasive carcinoma infiltrates the desmoplastic stroma. Tumoral necrosis is evident (**a**). The tumor is mitotically active and shows epithelioid and spindle cell features. Residual benign adenomyoepithelioma is present (**e**)

or arising in AME are well described, but the frequency of malignant transformation is unknown.

Malignant adenomyoepitheliomas are characterized by a large spectrum of histological patterns. When malignant change occurs within the epithelial component, it can be of no special type or special types (including invasive lobular carcinoma) [82, 83]. Furthermore, metaplastic differentiation is not infrequently encountered in AME-M [82, 84, 85]. In some cases, the carcinoma component is confined to the AME and the treatment of these patients should be similar to those diagnosed with DCIS. The presence of an invasive component can be confirmed when the neoplastic component grows beyond the confines of the AME and infiltrates the surrounding stroma with a desmoplastic reaction (Fig. 6.56). The treatment regimen is the same as those for conventional invasive breast carcinoma. In cases where myoepithelial component undergoes malignant transformation, the tumor will more closely resemble myoepithelial carci-

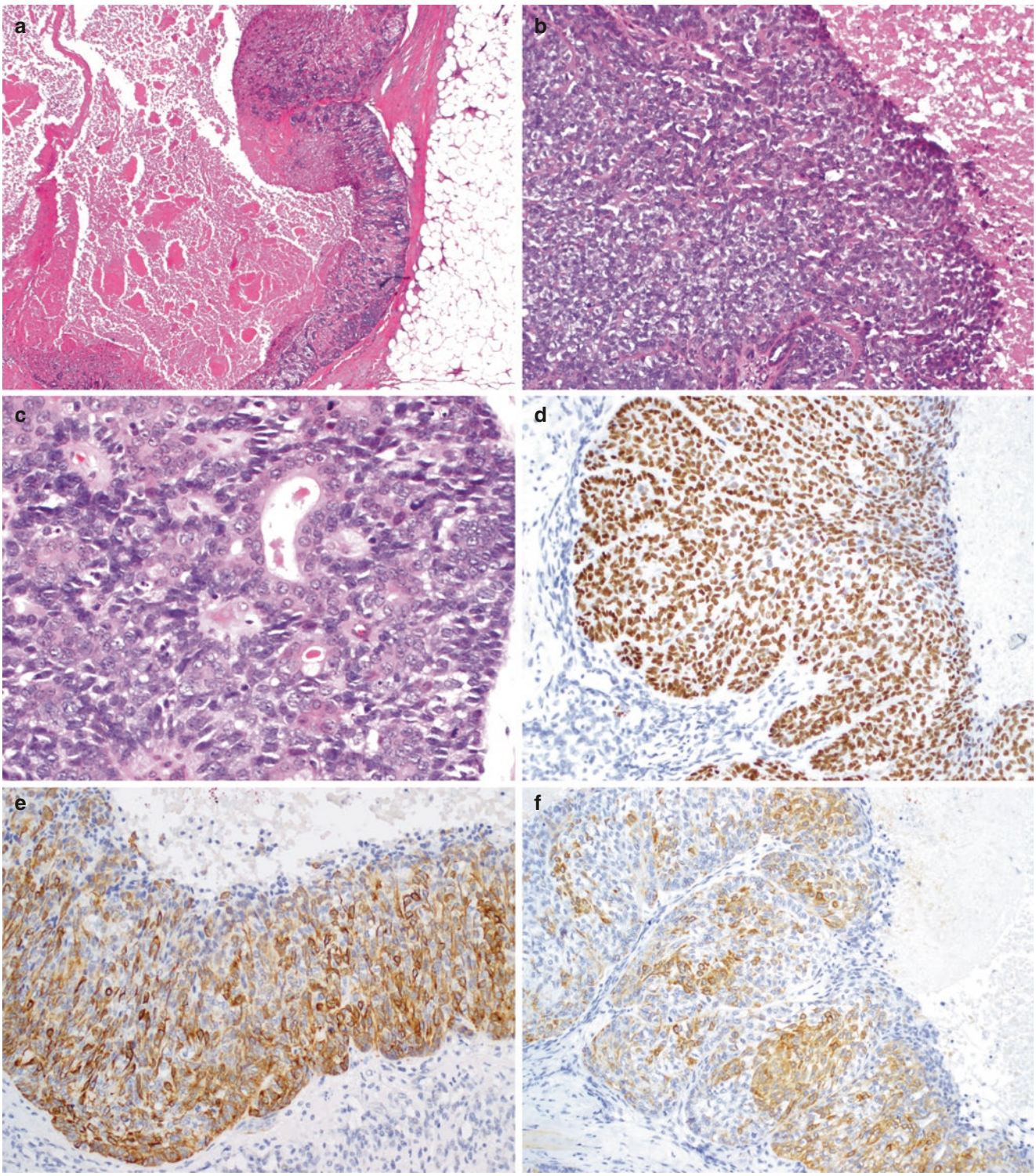

Fig. 6.57 Malignant adenomyoepithelioma. (**a**) The tumor is multinodular with abundant necrosis; however, the fundamental adenomyoepithelial structure is retained. (**b**, **c**) Cells show high-grade nuclear cytology and are mitotically active. Tumor cells are of myoepithelial differentiation by immunohistochemical stains (**d**) p63, (**e**) CK14, (**f**) CK5

noma with infiltrating nests of clear or spindled cells that demonstrate myoepithelial immunophenotyping (Fig. 6.57). The primary differential diagnosis in cases with a neoplastic myoepithelial component will be a pure malignant myoepithelioma, which can be excluded by identifying an underlying benign adenomyoepitheliomatous component. In cases

where both components undergo malignant transformation, the lesion will mimic poorly differentiated epithelial–myoepithelial carcinoma of salivary gland [78, 86].

Some carcinomas arising in AME have been characterized by aggressive or metastatic behavior and the prognosis is predominantly determined by the histologic type of malignancy arising within the AME-M [77, 87].

Importantly, the presence of cytologic atypia, increased mitoses, and/or necrosis of an adenomyoepithelial tumor identified on core biopsy ought to be considered suspicious for concurrent malignancy. In such cases, these findings should be clearly reported, as to ensure excision for complete pathologic examination.

References

1. Hill CB, Yeh IT. Myoepithelial cell staining patterns of papillary breast lesions: from intraductal papillomas to invasive papillary carcinomas. Am J Clin Pathol. 2005;123(1):36–44.
2. Francis A, England D, Rowlands D, Bradley S. Breast papilloma: mammogram, ultrasound and MRI appearances. Breast. 2002;11(5):394–7.
3. Carty NJ, Mudan SS, Ravichandran D, Royle GT, Taylor I. Prospective study of outcome in women presenting with nipple discharge. Ann R Coll Surg Engl. 1994;76(6):387–9.
4. Orel SG, Dougherty CS, Reynolds C, Czerniecki BJ, Siegelman ES, Schnall MD. MR imaging in patients with nipple discharge: initial experience. Radiology. 2000;216(1):248–54.
5. Han BK, Choe YH, Ko YH, Yang JH, Nam SJ. Benign papillary lesions of the breast: sonographic-pathologic correlation. J Ultrasound Med. 1999;18(3):217–23.
6. Flint A, Oberman HA. Infarction and squamous metaplasia of intraductal papilloma: a benign breast lesion that may simulate carcinoma. Hum Pathol. 1984;15(8):764–7.
7. Lewis JT, Hartmann LC, Vierkant RA, Maloney SD, Shane Pankratz V, Allers TM, et al. An analysis of breast cancer risk in women with single, multiple, and atypical papilloma. Am J Surg Pathol. 2006;30(6):665–72.
8. MacGrogan G, Tavassoli FA. Central atypical papillomas of the breast: a clinicopathological study of 119 cases. Virchows Arch. 2003;443(5):609–17.
9. Page DL, Salhany KE, Jensen RA, Dupont WD. Subsequent breast carcinoma risk after biopsy with atypia in a breast papilloma. Cancer. 1996;78(2):258–66.
10. WHO Classification of Tumors. Breast tumours. 5th ed. Lyon: IARC; 2019.
11. Lininger RA, Park WS, Man YG, Pham T, MacGrogan G, Zhuang Z, et al. LOH at 16p13 is a novel chromosomal alteration detected in benign and malignant microdissected papillary neoplasms of the breast. Hum Pathol. 1998;29(10):1113–8.
12. Troxell ML, Levine J, Beadling C, Warrick A, Dunlap J, Presnell A, et al. High prevalence of PIK3CA/AKT pathway mutations in papillary neoplasms of the breast. Mod Pathol. 2010;23(1):27–37.
13. Jahn SW, Kashofer K, Thuringer A, Abete L, Winter E, Eidenhammer S, et al. Mutation profiling of usual ductal hyperplasia of the breast reveals activating mutations predominantly at different levels of the PI3K/AKT/mTOR pathway. Am J Pathol. 2016;186(1):15–23.
14. Kader T, Elder K, Zethoven M, Semple T, Hill P, Goode DL, et al. The genetic architecture of breast papillary lesions as a predictor of progression to carcinoma. NPJ Breast Cancer. 2020;6:9.
15. Mishima C, Kagara N, Ikeda JI, Morii E, Miyake T, Tanei T, et al. Mutational analysis of AKT1 and PIK3CA in intraductal papillomas of the breast with special reference to cellular components. Am J Pathol. 2018;188(5):1106–12.
16. Jakate K, De Brot M, Goldberg F, Muradali D, O'Malley FP, Mulligan AM. Papillary lesions of the breast: impact of breast pathology subspecialization on core biopsy and excision diagnoses. Am J Surg Pathol. 2012;36(4):544–51.
17. Renshaw AA, Derhagopian RP, Tizol-Blanco DM, Gould EW. Papillomas and atypical papillomas in breast core needle biopsy specimens: risk of carcinoma in subsequent excision. Am J Clin Pathol. 2004;122(2):217–21.
18. Swapp RE, Glazebrook KN, Jones KN, Brandts HM, Reynolds C, Visscher DW, et al. Management of benign intraductal solitary papilloma diagnosed on core needle biopsy. Ann Surg Oncol. 2013;20(6):1900–5.
19. Rizzo M, Linebarger J, Lowe MC, Pan L, Gabram SG, Vasquez L, et al. Management of papillary breast lesions diagnosed on core-needle biopsy: clinical pathologic and radiologic analysis of 276 cases with surgical follow-up. J Am Coll Surg. 2012;214(3):280–7.
20. Jaffer S, Nagi C, Bleiweiss IJ. Excision is indicated for intraductal papilloma of the breast diagnosed on core needle biopsy. Cancer. 2009;115(13):2837–43.
21. Tseng HS, Chen YL, Chen ST, Wu YC, Kuo SJ, Chen LS, et al. The management of papillary lesion of the breast by core needle biopsy. Eur J Surg Oncol. 2009;35(1):21–4.
22. Collins LC, Schnitt SJ. Papillary lesions of the breast: selected diagnostic and management issues. Histopathology. 2008;52(1):20–9.
23. Pareja F, Corben AD, Brennan SB, Murray MP, Bowser ZL, Jakate K, et al. Breast intraductal papillomas without atypia in radiologic-pathologic concordant core-needle biopsies: rate of upgrade to carcinoma at excision. Cancer. 2016;122(18):2819–27.
24. Lee SJ, Wahab RA, Sobel LD, Zhang B, Brown AL, Lewis K, et al. Analysis of 612 benign papillomas diagnosed at core biopsy: rate of upgrade to malignancy, factors associated with upgrade, and a proposal for selective surgical excision. AJR Am J Roentgenol. 2021;217:1299–311.
25. Kim SY, Kim EK, Lee HS, Kim MJ, Yoon JH, Koo JS, et al. Asymptomatic benign papilloma without atypia diagnosed at ultrasonography-guided 14-gauge core needle biopsy: which subgroup can be managed by observation? Ann Surg Oncol. 2016;23(6):1860–6.
26. Nakhlis F, Baker GM, Pilewskie M, Gelman R, Calvillo KZ, Ludwig K, et al. The incidence of adjacent synchronous invasive carcinoma and/or ductal carcinoma in situ in patients with intraductal papilloma without atypia on core biopsy: results from a prospective multi-institutional registry (TBCRC 034). Ann Surg Oncol. 2021;28(5):2573–8.
27. Limberg J, Kucher W, Fasano G, Hoda S, Michaels A, Marti JL. Intraductal papilloma of the breast: prevalence of malignancy and natural history under active surveillance. Ann Surg Oncol. 2021;28:6032–40.
28. Grimm LJ, Bookhout CE, Bentley RC, Jordan SG, Lawton TJ. Concordant, non-atypical breast papillomas do not require surgical excision: a 10-year multi-institution study and review of the literature. Clin Imaging. 2018;51:180–5.
29. Amin MB, American Joint Committee on Cancer, American Cancer Society. AJCC cancer staging manual. American Joint Committee on Cancer, Springer: Chicago IL; 2017.
30. Rakha EA, Varga Z, Elsheik S, Ellis IO. High-grade encapsulated papillary carcinoma of the breast: an under-recognized entity. Histopathology. 2015;66(5):740–6.
31. Esposito NN, Dabbs DJ, Bhargava R. Are encapsulated papillary carcinomas of the breast in situ or invasive? A basement membrane study of 27 cases. Am J Clin Pathol. 2009;131(2):228–42.

32. Rakha EA, Gandhi N, Climent F, van Deurzen CH, Haider SA, Dunk L, et al. Encapsulated papillary carcinoma of the breast: an invasive tumor with excellent prognosis. Am J Surg Pathol. 2011;35(8):1093–103.
33. Tan BY, Thike AA, Ellis IO, Tan PH. Clinicopathologic characteristics of solid papillary carcinoma of the breast. Am J Surg Pathol. 2016;40(10):1334–42.
34. Duprez R, Wilkerson PM, Lacroix-Triki M, Lambros MB, MacKay A, A'Hern R, et al. Immunophenotypic and genomic characterization of papillary carcinomas of the breast. J Pathol. 2012;226(3):427–41.
35. Piscuoglio S, Ng CK, Martelotto LG, Eberle CA, Cowell CF, Natrajan R, et al. Integrative genomic and transcriptomic characterization of papillary carcinomas of the breast. Mol Oncol. 2014;8(8):1588–602.
36. Schwartz CJ, Boroujeni AM, Khodadadi-Jamayran A, Heguy A, Snuderl M, Jour G, et al. Molecular analysis of encapsulated papillary carcinoma of the breast with and without invasion. Hum Pathol. 2021;111:67–74.
37. Lec'ene AL. Observation d'un cas de tumeur "mixte" du sein. Rev Chir. 1906;33:434–8.
38. John BJ, Griffiths C, Ebbs SR. Pleomorphic adenoma of the breast should be excised with a cuff of normal tissue. Breast J. 2007;13(4):418–20.
39. Sato K, Ueda Y, Shimasaki M, Ozaki M, Nitta N, Chada K, et al. Pleomorphic adenoma (benign mixed tumor) of the breast: a case report and review of the literature. Pathol Res Pract. 2005;201(4):333–9.
40. Takahashi K. Diagnosis of an extremely rare pleomorphic adenoma of the breast with core needle biopsy: A case report. Ann Med Surg (Lond). 2018;36:242–5.
41. Teh J, Dessauvagie B, Kessell M, Dissanayake D, Wylie EJ. An atypically located pleomorphic adenoma: radiological and pathological correlation. J Med Imaging Radiat Oncol. 2022;66:105–6.
42. Diaz NM, McDivitt RW, Wick MR. Pleomorphic adenoma of the breast: a clinicopathologic and immunohistochemical study of 10 cases. Hum Pathol. 1991;22(12):1206–14.
43. Foschini MP, Morandi L, Asioli S, Giove G, Corradini AG, Eusebi V. The morphological spectrum of salivary gland type tumours of the breast. Pathology. 2017;49(2):215–27.
44. Moran CA, Suster S, Carter D. Benign mixed tumors (pleomorphic adenomas) of the breast. Am J Surg Pathol. 1990;14(10):913–21.
45. Kanter MH, Sedeghi M. Pleomorphic adenoma of the breast: cytology of fine-needle aspiration and its differential diagnosis. Diagn Cytopathol. 1993;9(5):555–8.
46. Narita T, Matsuda K. Pleomorphic adenoma of the breast: case report and review of the literature. Pathol Int. 1995;45(6):441–7.
47. Cuadros CL, Ryan SS, Miller RE. Benign mixed tumor (pleomorphic adenoma) of the breast: ultrastructural study and review of the literature. J Surg Oncol. 1987;36(1):58–63.
48. De Dominicis E, Perrone G, Verzi A, Bianchi A, Altomare V, Zobel BB, et al. Pleomorphic adenoma of the breast. Breast J. 2005;11(6):513–4.
49. Ginter PS, Scognamiglio T, Tauchi-Nishi P, Antonio LB, Hoda SA. Pleomorphic adenoma of breast: a radiological and pathological study of a common tumor in an uncommon location. Case Rep Pathol. 2015;2015:172750.
50. Iyengar P, Cody HS 3rd, Brogi E. Pleomorphic adenoma of the breast: case report and review of the literature. Diagn Cytopathol. 2005;33(6):416–20.
51. Khamechian T, Alizargar J, Mazoochi T. Reporting a rare case of pleomorphic adenoma of the breast. Case Rep Med. 2014;2014:387183.
52. Kelten C, Boyaci C, Trabulus DC, Sirin S. Benign mixed tumour of the breast and breast skin, two cases with diagnostic difficulties. BMJ Case Rep. 2015;2015 https://doi.org/10.1136/bcr-2015-210906.
53. Fiks T. Pleomorphic adenoma (benign "mixed" tumor) of the human female breast. Case report. Pol J Pathol. 1999;50(4):297–9.
54. Di Bonito M, Cantile M, Cerrone M, Liguori G, Botti G. Synchronous pleomorphic adenoma and invasive ductal carcinoma in distinct breasts. Breast J. 2015;21(4):428–30.
55. Mizukami Y, Takayama T, Takemura A, Ichikawa K, Onoguchi M, Miyati T, et al. Pleomorphic adenoma of the breast. Radiat Med. 2008;26(7):442–5.
56. Arslan A, Guldogan N, Kapucuoglu N, Esen G, Kara H, Uras C. A rare case of pleomorphic adenoma of the breast: ultrasonography and pathology findings. Breast J. 2018;24(6):1069–70.
57. Rakha EA, Aleskandarany MA, Samaka RM, Hodi Z, Lee AH, Ellis IO. Pleomorphic adenoma-like tumour of the breast. Histopathology. 2016;68(3):405–10.
58. Sakuma T, Mori M, Kokubo C, Deguchi K, Matsuo K, Tagami K. Cytology of breast pleomorphic adenoma associated with extensive apocrine metaplasia. Diagn Cytopathol. 2018;46(1):56–8.
59. Molland JG, Morgan GJ, Walker DM, Lin BP. Pleomorphic adenoma of the parotid and breast in a male patient. Pathology. 2005;37(3):263–5.
60. Reid-Nicholson M, Bleiweiss I, Pace B, Azueta V, Jaffer S. Pleomorphic adenoma of the breast. A case report and distinction from mucinous carcinoma. Arch Pathol Lab Med. 2003;127(4):474–7.
61. Hayes MM, Lesack D, Girardet C, Del Vecchio M, Eusebi V. Carcinoma ex-pleomorphic adenoma of the breast. Report of three cases suggesting a relationship to metaplastic carcinoma of matrix-producing type. Virchows Arch. 2005;446(2):142–9.
62. Chen KT. Pleomorphic adenoma of the breast. Am J Clin Pathol. 1990;93(6):792–4.
63. Pia-Foschini M, Reis-Filho JS, Eusebi V, Lakhani SR. Salivary gland-like tumours of the breast: surgical and molecular pathology. J Clin Pathol. 2003;56(7):497–506.
64. Geurts JM, Schoenmakers EF, Roijer E, Stenman G, Van de Ven WJ. Expression of reciprocal hybrid transcripts of HMGIC and FHIT in a pleomorphic adenoma of the parotid gland. Cancer Res. 1997;57(1):13–7.
65. Rohen C, Rogalla P, Meyer-Bolte K, Bartnitzke S, Chilla R, Bullerdiek J. Pleomorphic adenomas of the salivary glands: absence of HMGIY rearrangements. Cancer Genet Cytogenet. 1999;111(2):178–81.
66. Soreide JA, Anda O, Eriksen L, Holter J, Kjellevold KH. Pleomorphic adenoma of the human breast with local recurrence. Cancer. 1988;61(5):997–1001.
67. Hamperl H. The myothelia (myoepithelial cells). Normal state; regressive changes; hyperplasia; tumors. Curr Top Pathol. 1970;53:161–220.
68. Lee JH, Kim SH, Kang BJ, Lee AW, Song BJ. Ultrasonographic features of benign adenomyoepithelioma of the breast. Korean J Radiol. 2010;11(5):522–7.
69. Berna JD, Arcas I, Ballester A, Bas A. Adenomyoepithelioma of the breast in a male. AJR Am J Roentgenol. 1997;169(3):917–8.
70. Tamura G, Monma N, Suzuki Y, Satodate R, Abe H. Adenomyoepithelioma (myoepithelioma) of the breast in a male. Hum Pathol. 1993;24(6):678–81.
71. Foschini MP, Eusebi V. Carcinomas of the breast showing myoepithelial cell differentiation. A review of the literature. Virchows Arch. 1998;432(4):303–10.
72. Rosen PP. Adenomyoepithelioma of the breast. Hum Pathol. 1987;18(12):1232–7.
73. Tavassoli FA. Myoepithelial lesions of the breast. Myoepitheliosis, adenomyoepithelioma, and myoepithelial carcinoma. Am J Surg Pathol. 1991;15(6):554–68.
74. Hayes MM. Adenomyoepithelioma of the breast: a review stressing its propensity for malignant transformation. J Clin Pathol. 2011;64(6):477–84.

75. Moritz AW, Wiedenhoefer JF, Profit AP, Jagirdar J. Breast adenomyoepithelioma and adenomyoepithelioma with carcinoma (malignant adenomyoepithelioma) with associated breast malignancies: a case series emphasizing histologic, radiologic, and clinical correlation. Breast. 2016;29:132–9.
76. Yang W, Wells J, Nguyen M, Shin SJ. Immunohistochemical characterization of adenomyoepithelial tumors of the breast (Abstract); 2014.
77. Ericson-Lindquist K, Johansson A, Leveen P, Elmberger G, Jonsson G, Staaf J, et al. Targeted sequencing may facilitate differential diagnostics of pulmonary tumours: a case series. Diagn Pathol. 2017;12(1):31.
78. Baum JE, Sung KJ, Tran H, Song W, Ginter PS. Mammary epithelial-myoepithelial carcinoma: report of a case with HRAS and PIK3CA mutations by next-generation sequencing. Int J Surg Pathol. 2019;27(4):441–5.
79. Geyer FC, Li A, Papanastasiou AD, Smith A, Selenica P, Burke KA, et al. Recurrent hotspot mutations in HRAS Q61 and PI3K-AKT pathway genes as drivers of breast adenomyoepitheliomas. Nat Commun. 2018;9(1):1816.
80. Ginter PS, McIntire PJ, Kurtis B, Mirabelli S, Motanagh S, Hoda S, et al. Adenomyoepithelial tumors of the breast: molecular underpinnings of a rare entity. Mod Pathol. 2020;33(9):1764–72.
81. Lubin D, Toorens E, Zhang PJ, Jaffer S, Baraban E, Bleiweiss IJ, et al. Adenomyoepitheliomas of the breast frequently harbor recurrent hotspot mutations in PIK3-AKT pathway-related genes and a subset show genetic similarity to salivary gland epithelial-myoepithelial carcinoma. Am J Surg Pathol. 2019;43(7):1005–13.
82. Xu J, Tang X, Iida Y, Fuchinoue F, Kusumi T, Yagihashi N, et al. Adenomyoepithelioma with carcinoma of the breast: a report of two cases and a review of the literature. Pathol Res Pract. 2016;212(2):130–4.
83. Honda Y, Iyama K. Malignant adenomyoepithelioma of the breast combined with invasive lobular carcinoma. Pathol Int. 2009;59(3):179–84.
84. Oka K, Sando N, Moriya T, Yatabe Y. Malignant adenomyoepithelioma of the breast with matrix production may be compatible with one variant form of matrix-producing carcinoma: a case report. Pathol Res Pract. 2007;203(8):599–604.
85. Foschini MP, Pizzicannella G, Peterse JL, Eusebi V. Adenomyoepithelioma of the breast associated with low-grade adenosquamous and sarcomatoid carcinomas. Virchows Arch. 1995;427(3):243–50.
86. Ahmed AA, Heller DS. Malignant adenomyoepithelioma of the breast with malignant proliferation of epithelial and myoepithelial elements: a case report and review of the literature. Arch Pathol Lab Med. 2000;124(4):632–6.
87. Jones C, Tooze R, Lakhani SR. Malignant adenomyoepithelioma of the breast metastasizing to the liver. Virchows Arch. 2003;442(5):504–6.

Fibroepithelial Lesions

7

Gregor Krings and Yunn-Yi Chen

Mammary Hamartoma

Overview and Clinical Presentation

Hamartomas are abnormal dysgenetic benign growths of cells and tissue types normally present at that particular site. In the breast, the term hamartoma was introduced by Arrigoni et al. in 1971 and refers to radiologically evident or palpable nodules composed of variable admixtures of fibrous, epithelial, and adipose elements, although chondroid, osseous, and smooth muscle components can be present as well. One or more tissue types may predominate [1–14]. Hamartomas include lesions previously referred to as adenolipomas, lipofibroadenomas, fibroadenolipomas, chondrolipomas, and myoid hamartomas.

The incidence of mammary hamartomas is difficult to determine with accuracy, and reported estimates range from 0.1% to 0.7% in some studies to as high as 4.8% of all benign breast tumors in others [3, 8, 10, 11, 13]. Mammary hamartomas may present at essentially all adult ages, including before and after menopause, and have rarely been identified in adolescence [8, 10, 11, 14, 15]. The mean age at diagnosis ranged from 38 to 50 years in several studies [10, 12–14, 16]. Women are primarily affected, but rare myoid hamartomas have been reported in men [17].

Mammary hamartoma may present as a painless, mobile, and soft-to-firm palpable mass, as breast asymmetry, or may be identified incidentally on imaging [4, 8, 10, 12–15]. The clinical impression is often that of a fibroadenoma (FA) [13]. Hamartomas are almost always solitary, but multiple synchronous or metachronous lesions may rarely be seen [10, 13–15]. In one study, 12% of cases had coexistent FAs [14]. An exceedingly rare case of bilateral myoid hamartoma has been reported [18]. Studies have shown a wide size range (from <1 to 24 cm), with a mean of 3.9 cm in larger series [4, 6, 8, 10, 12–15]. A slightly increased incidence in the left compared to the right breast has been reported by some [11, 13, 14, 19, 20]. In a study by Wahner-Roedler et al., 67% of hamartomas were in the left breast, and 39% were in the upper outer quadrant [14]. Rare cases of hamartomas arising in ectopic mammary tissue of the inguinal region or axilla have been described [21, 22].

Gross and Radiologic Features

The typical mammographic appearance of mammary hamartoma is of a round to ovoid nodule of variable density with well-circumscribed margins and a thin peripheral radiopaque pseudocapsule [8, 13, 14, 23, 24]. The degree of lesional heterogeneity depends on the relative amounts of fibroglandular and adipose tissue, with predominantly fibrous lesions mimicking FA and predominantly fatty lesions mimicking lipoma or fat necrosis [23, 24]. Lobulated densities can be seen within the encapsulated fat, described as “slice of salami” [23–25]. The presence of normal breast components within a well-circumscribed mass has been described as a “breast within a breast” sign [26]. A peripheral radiolucent halo may be seen [3, 8, 13, 23]. Lesional margins may in some instances be irregular, indistinct, or obscured [14]. Small non-suspicious calcifications may be noted in some cases [14]. The most common sonographic finding is of a compressible well-encapsulated solid, hypoechoic mass with heterogeneous echogenicity and irregular hyperechoic bands or nodules between hypoechoic areas [13, 23, 27, 28]. The adjacent breast tissue is usually displaced mammographically and sonographically [13]. In a study by Sevim et al., ~15% of lesions revealed a partially irregular border by ultrasound [12]. In another series, 5 of 24 hamartomas were not visible on ultrasound [14]. By magnetic resonance imaging (MRI), hamartomas are well-encapsulated ovoid nodules

G. Krings (✉) · Y.-Y. Chen
Department of Pathology, University of California San Francisco, San Francisco, CA, USA
e-mail: gregor.krings@ucsf.edu; yunn-yi.chen@ucsf.edu

© The Author(s), under exclusive license to Springer Nature Switzerland AG 2022

S. J. Shin et al. (eds.), *A Comprehensive Guide to Core Needle Biopsies of the Breast*,
https://doi.org/10.1007/978-3-031-05532-4_7

with dark, smooth, and thin rims and internal heterogenicity, which show heterogeneous gadolinium enhancement [13].

On gross examination, mammary hamartomas are typically surgically enucleated, well-circumscribed, soft-to-firm solid masses and may be lentiform or disc-like [3, 6, 8, 15, 29]. Sharp separation from adjacent breast tissue is often obvious [10]. The nature of the cut surface varies depending on the relative amount and distribution of fibroglandular versus adipose tissue, with fibrous areas being white-tan, firm, and rubbery with a smooth, glistening surface, compared to soft pale yellow fatty areas [3, 6, 8, 15, 29]. The lesions may mimic FA, lipoma, or even normal breast tissue. One of nine hamartomas presenting in adolescent girls studied by Chang et al. was noted to have thin, slit-like spaces, but cleft-like spaces were not seen [15]. Small cysts may be noted.

Microscopic Features

The histologic features of hamartomas are variable, and earlier studies attempted to subclassify these lesions into different subgroups. McGuire and Cohn offered a classification system based on "fibrous," "fatty," and "fibrofatty" categories, whereas Jones et al. proposed four groups, namely "encapsulated fibrocystic changes," "FA with fibrous stroma," "FA-like," and "circumscribed adenolipoma" [30, 31]. However, these categories are not clinically relevant and are not recommended.

As a group, hamartomas are well-circumscribed, lobulated, and comprised of some combination of normal breast ducts and lobules with interlobular fibrosis and adipose tissue in variable proportions. They can range from predominantly fibrous and/or hyalinized to mostly fatty with scant fibroepithelial elements (Figs. 7.1 and 7.2). A characteristic feature in many cases is an impression of architectural disorganization. The borders are well-demarcated from the adjacent tissue, often with a compressed fibrous pseudocapsule. It has been suggested that the presence of fibrosis between and within individual lobules which obliterates the usual specialized intralobular mammary stroma is a characteristic feature of most hamartomas [3, 4, 6, 8, 13]. However, this feature is not unique to hamartomas and can be seen in other lesions, such as sclerosing lobular hyperplasia [13]. Stromal cellularity varies from paucicellular to mildly cellular. Benign stromal giant cells have been reported very rarely [3]. Pseudoangiomatous stromal hyperplasia (PASH) is not infrequent and may also involve adjacent breast tissue (Figs. 7.1 and 7.2) [4, 6, 8, 10, 13]. Focal stromal ossification may rarely be seen [13]. Adipose tissue is present to variable degree in most cases [3, 6, 8, 13, 30], although Chang et al. noted no fat in 5 of 9 hamartomas presenting in adolescent girls, with the remainder showing only minimal fat [15]. The epithelium is usually comprised of otherwise unremarkable breast ducts and lobules, which are often disorganized (Fig. 7.1). Lobules may be atrophic or poorly formed. Usual ductal hyperplasia may be seen [4, 8, 13]. Small cysts are not uncommon (up to 32% of cases in one study), and apocrine metaplasia or adenosis may be seen (Figs. 7.1 and 7.2) [4, 8, 10, 13, 15]. In rare cases, the epithelium may be involved by atypical hyperplasia, in situ carcinoma, or invasive carcinoma [13, 32–41].

Adenolipomas are composed predominantly of circumscribed lobulated adipose tissue with structurally normal but typically disorganized breast ducts and lobules (Fig. 7.3) [42]. As in other hamartomas, a thin peripheral fibrous pseudocapsule is present. The epithelium may form small cysts but is not usually hyperplastic. Adipose tissue is almost always mature, but rare adenolipomas with brown fat (*adenohibernomas*) have been described [43–45].

Myoid hamartomas are often considered to be a rare hamartoma variant [5, 7, 46, 47]. These lesions are characterized by variable amounts of smooth muscle bundles or fascicles admixed with adipose tissue, fibrous stroma, and epithelium (Fig. 7.4) [5, 48, 49]. The smooth muscle cells have eosinophilic cytoplasm with elongated cigar-shaped nuclei, but atypia should be absent [49]. Garfein et al. described the presence of occasional epithelioid cells within myoid hamartomas, which may mimic invasive lobular carcinoma [50]. A rare case of lobular neoplasia arising in myoid hamartoma has been reported [51].

Most *chondrolipomas* are composed of well-circumscribed lobulated fibroadipose tissue containing islands of benign hyaline cartilage, although a few cases of chondrolipomas with associated mammary ducts and lobules have been reported [2, 52–56]. Although generally considered hamartoma variants, these rare lesions do not strictly fulfill the definition of the term, given that cartilage is not a normal component of the breast.

Immunohistochemistry

Immunohistochemistry plays no role in the diagnosis of mammary hamartomas. Herbert et al. studied 24 hamartomas and found immunopositivity for estrogen and progesterone receptors in both epithelial and stromal cells in all cases, whereas other studies described hormone receptor positivity in epithelial cells only [4, 8, 10]. The stromal cells diffusely express vimentin, CD34 and Bcl-2, as do myofibroblasts in areas of PASH [4, 7]. Smooth muscle cells of myoid hamartomas express smooth muscle actin (SMA), desmin, and calponin, whereas these markers often highlight only scattered stromal cells in hamartomas without morphologically obvious myoid differentiation [4, 7, 8].

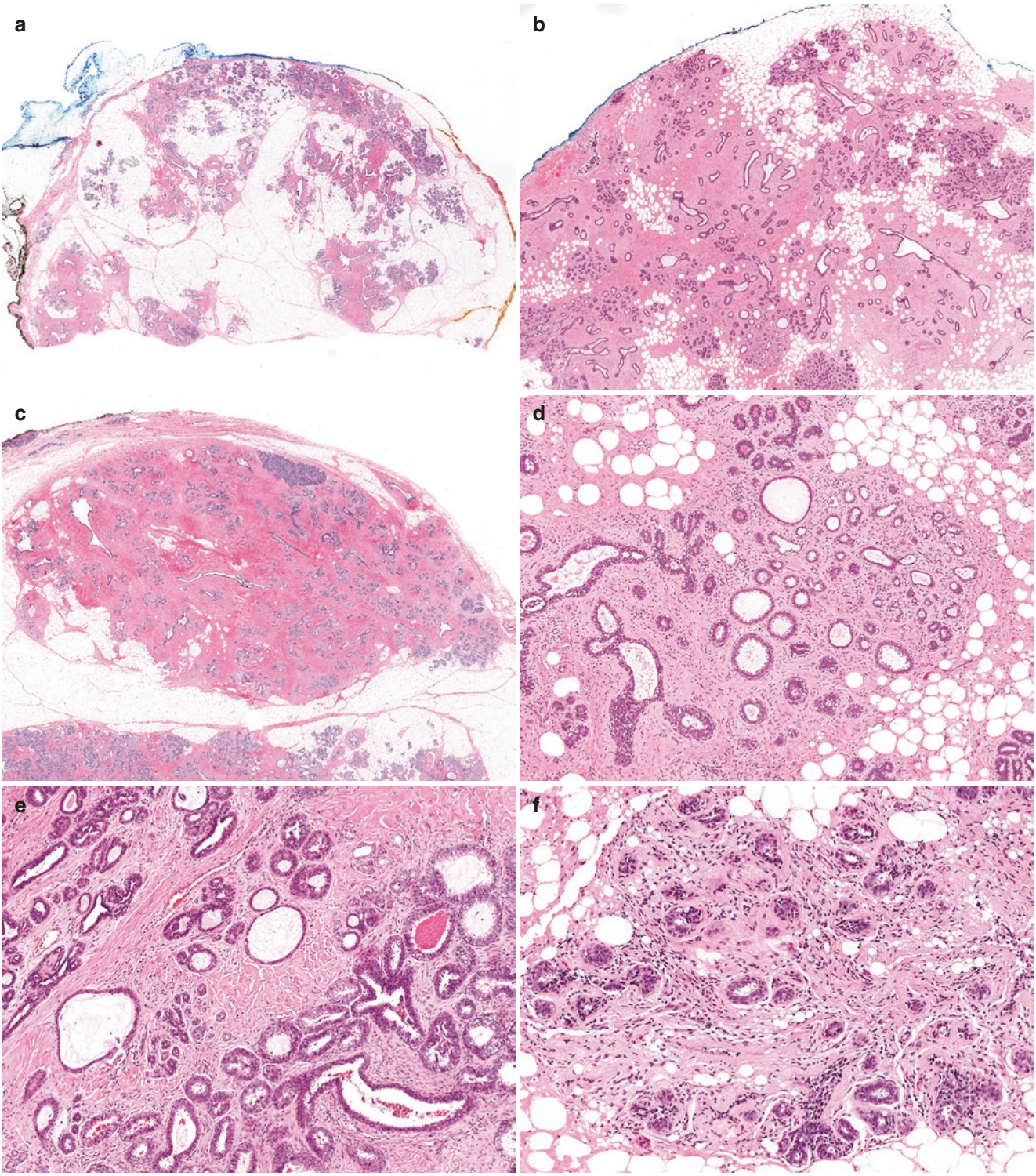

Fig. 7.1 Mammary hamartomas. (**a**–**c**) Mammary hamartomas are well circumscribed and well demarcated from the adjacent tissue, often with a delicate fibrous pseudocapsule. The lesions are composed of variable combinations of mammary epithelium, stroma, and adipose tissue, which overall may appear disorganized. (**d**) Lobular fibrosis is frequent and characteristically involves intralobular and interlobular stroma. (**e**) PASH and small cysts are common. (**f**) Lobules may appear atrophic

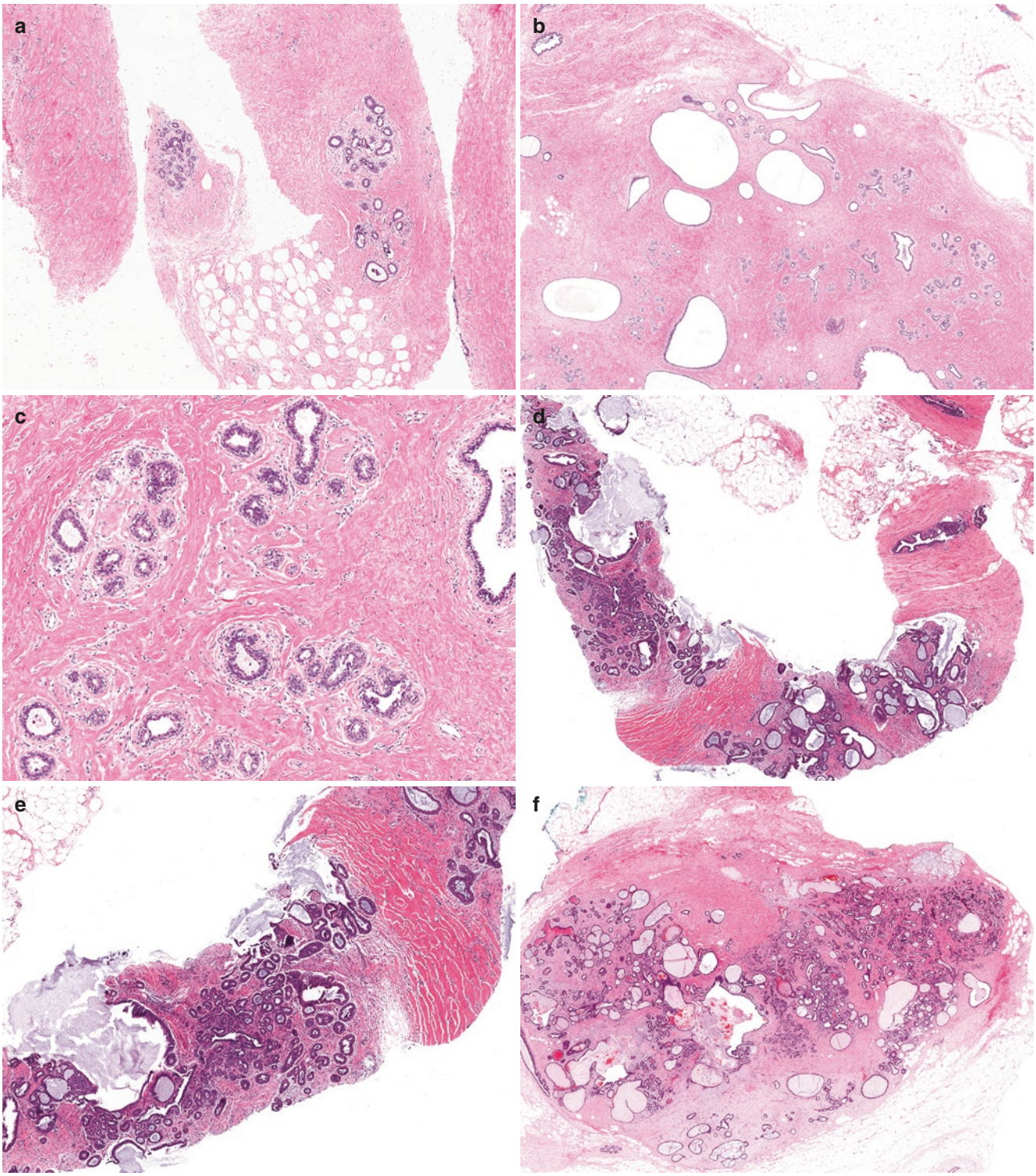

Fig. 7.2 Mammary hamartomas. (**a**) Sampling by core biopsy may mimic normal breast tissue, in this case showing PASH and fibrosis encasing adipose tissue. (**b**, **c**) Excision revealed a fibrous hamartoma with PASH, cysts, and apocrine metaplasia. (**d**, **e**) Core biopsy of another case demonstrated a benign fibroglandular proliferation with cysts, extruded luminal mucin, and PASH. (**f**) Excision specimen of the same case in (**d**) and (**e**). (**g**, **h**) Core biopsy of another case, revealing ducts and lobules intimately admixed with fibrosis and a prominent adipose component, with overall disorganized appearance. (**i**) Excision revealed a hamartoma with similar features

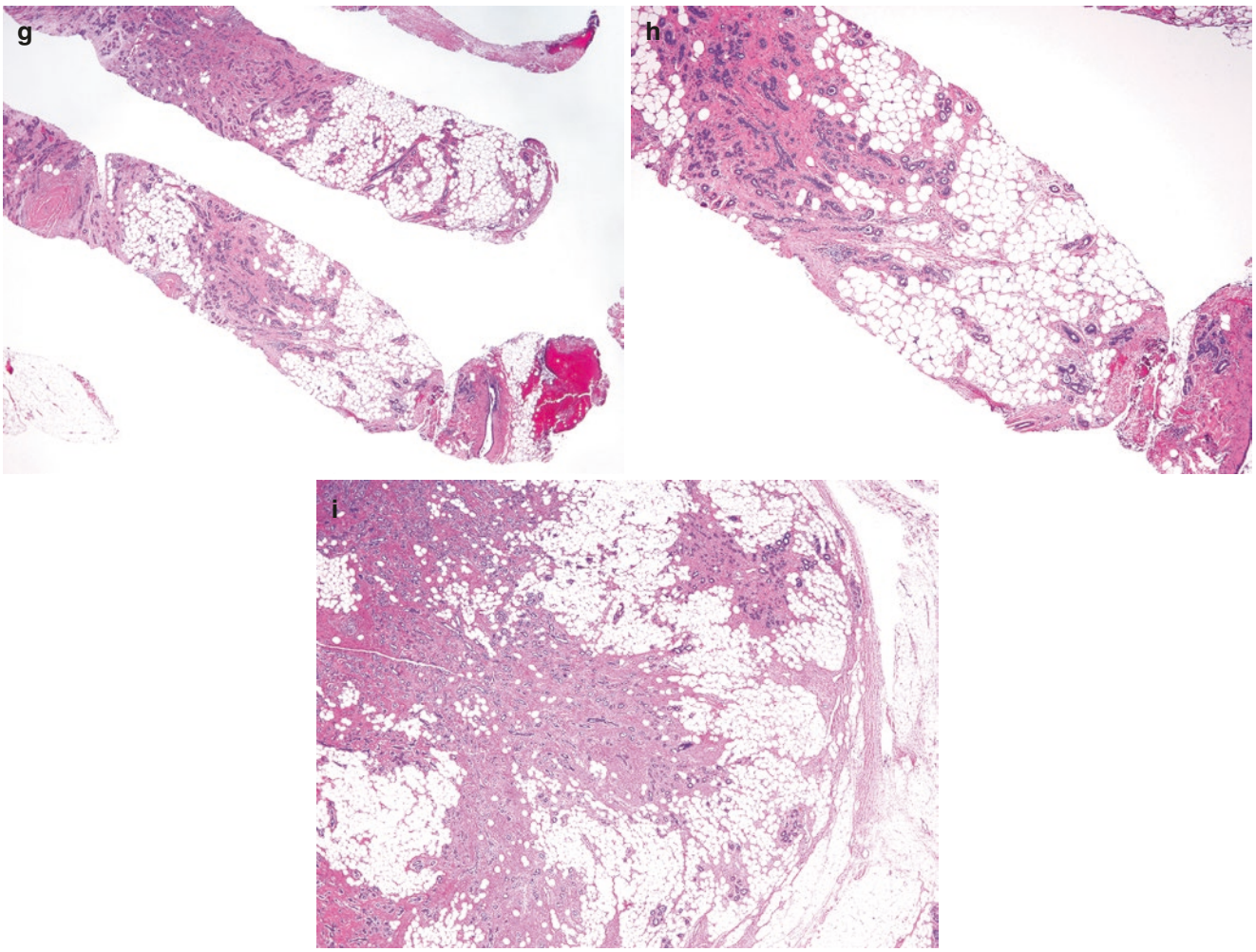

Fig. 7.2 (continued)

Differential Diagnosis

Because hamartomas are comprised of disorganized but histologically "normal" breast elements, diagnosis is often not possible based on histologic features alone on core-needle biopsy (CNB) and requires careful radiologic–pathologic and clinical correlation [13, 57–59]. The differential diagnosis may include normal breast tissue or benign fibroglandular changes (Figs. 7.2 and 7.3). The diagnosis is more straightforward in an excision specimen showing a mass lesion with pseudocapsule and the characteristic features of hamartoma.

Hamartomas may mimic FAs both clinically and radiologically, and distinction from FA variants or fibroadenomatous change may be challenging on CNB or even excision specimens. Fortunately, this distinction has no clinical relevance. Recognition of intracanalicular growth favors FA, whereas the presence of lobules can raise consideration of hamartoma. Adipose tissue within a fibroepithelial lesion on CNB can raise consideration of hamartoma versus FA with lipomatous metaplasia, phyllodes tumor (PT), or periductal stromal tumor. Recognized intracanalicular growth favors FA or PT. Significant stromal hypercellularity, stromal atypia, or mitoses would be concerning for PT or periductal stromal tumor. Distinction of hamartomas with PASH from nodular PASH or PASH involving FA may not be possible on CNB.

Diabetic mastopathy can have areas of dense fibrosis similar to what is seen in hamartomas, and both hamartomas and myoid hamartomas may demonstrate epithelioid myofibroblasts [50]. However, hamartomas lack the characteristic periepithelial and perivascular inflammation of diabetic mastopathy. The epithelioid myofibroblasts may also simulate invasive lobular carcinoma, and immunohistochemistry for pancytokeratin may be useful in this context.

Pathogenesis and Risk Factors

The pathogenesis of mammary hamartomas is largely unknown. Classification of myoid hamartomas as hamartomas is disputed by some, as smooth muscle may not be con-

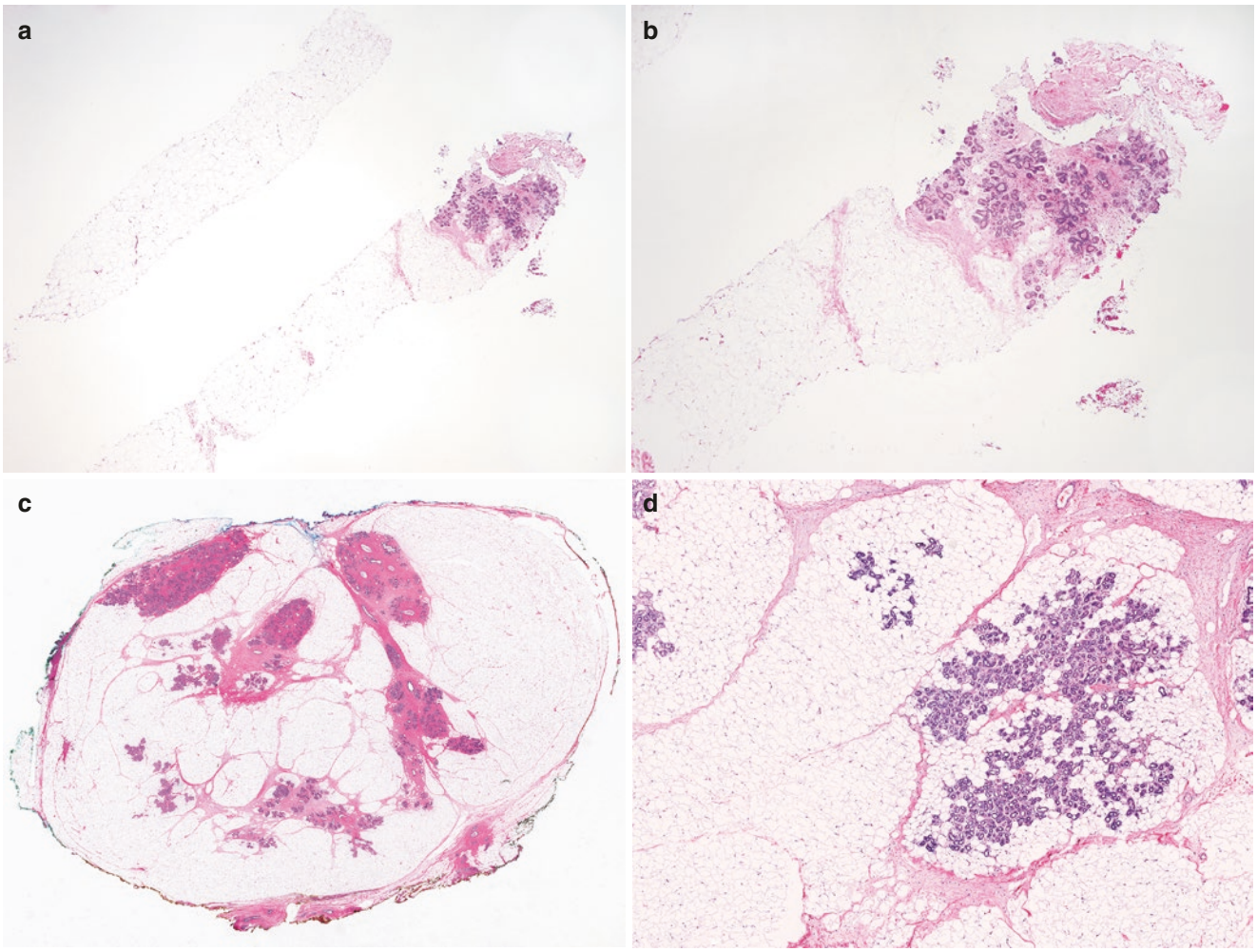

Fig. 7.3 Adenolipoma. (**a**, **b**) Core biopsy with abundant adipose tissue and adjacent lobules, which alone is not specific to make a diagnosis. (**c**, **d**) On excision, adenolipoma is well circumscribed and comprised of lobulated adipose tissue with associated disorganized ducts and lobules

sidered a normal constituent of breast tissue. Some consider myoid hamartomas to represent adenosis tumors with leiomyomatous myoid metaplasia of myoepithelial cells [46], whereas others have argued that the smooth muscle cells derive from metaplastic stromal cells, blood vessel walls, or a common stromal progenitor cell capable of divergent differentiation [5, 7, 47, 57, 60, 61].

Panagopoulos et al. identified rearrangement of high mobility group AT-hook 2 (*HMGA2*) in a myoid hamartoma [62]. Rohen et al. described an aberration at chromosome 12q in an adenolipoma from a 58-year-old woman, and Dietrich et al. described the presence of t(12;16) in one and del(1)(p22) in another adenolipoma [63, 64]. A 6p21 alteration involving the region encoding the *HMGA1* chromatin remodeling protein has also been described in a hamartoma with dense hyalinized connective tissue and prominent PASH [65]. Notably, 12q13-15 (encompassing *HMGA2*) or *HMGA1* alterations have been described in various benign mesenchymal tumors, such as lipomas, uterine leiomyomas, pulmonary hamartomas, pleomorphic adenomas, and breast fibroadenomas, suggesting a common role for these loci in these lesions [66–72].

Mammary hamartomas have been described in patients with Cowden syndrome, an autosomal dominant disorder characterized by mutations in the phosphatase and tensin homolog (*PTEN*) gene, which predisposes to the development of multiple benign and malignant lesions in the breast, skin, thyroid, and endometrium, among others [73–75]. Hamartomas developing in this context may be multiple or bilateral [75, 76]. In a retrospective study of breast lesions identified in 19 women with Cowden Syndrome, 17 (89%) had features suggestive of mammary hamartoma, with 84% and 47% of patients having multiple and bilateral lesions, respectively [75]. However, most mammary hamartomas are not associated with Cowden syndrome, and it is unknown if sporadic lesions harbor *PTEN* alterations.

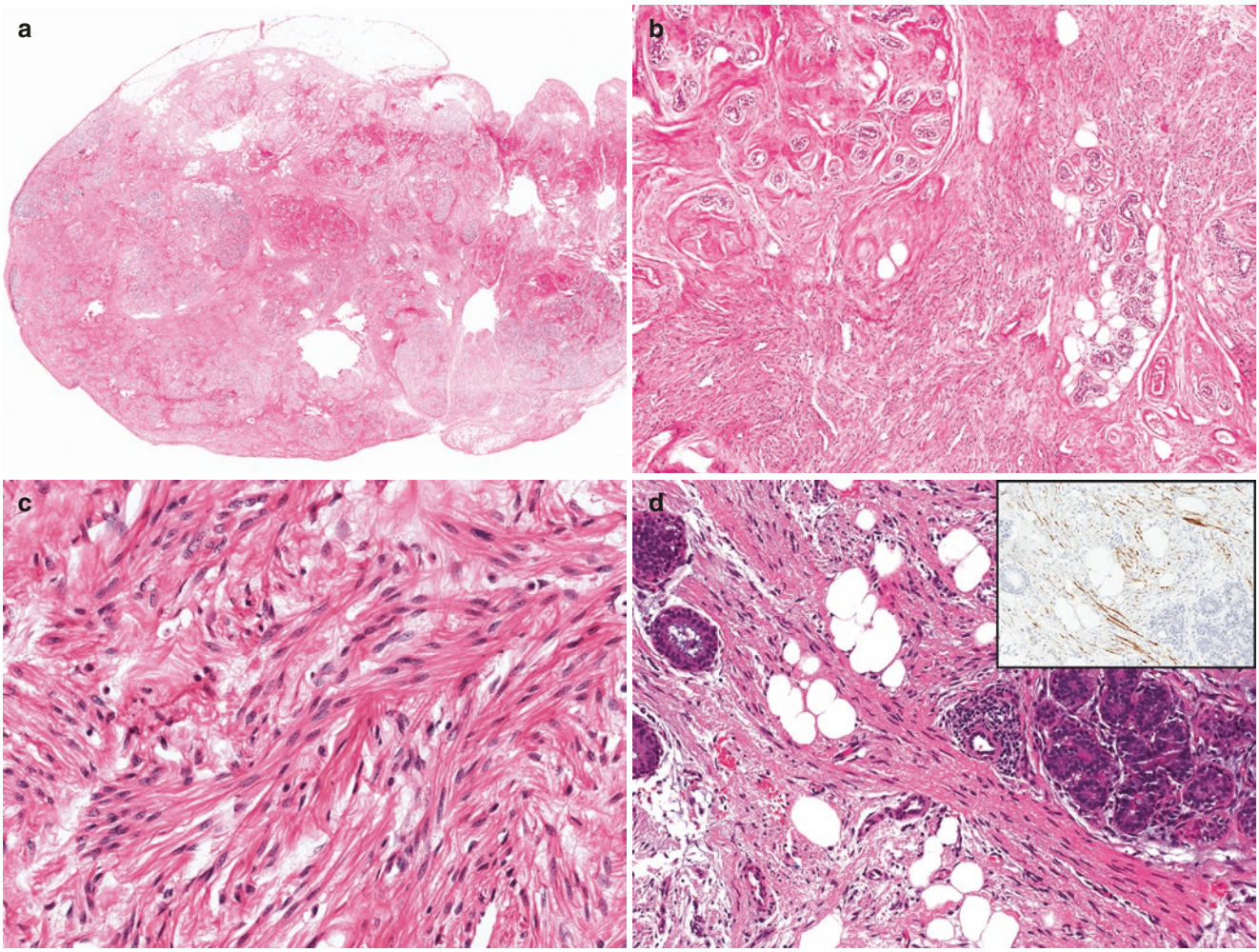

Fig. 7.4 Myoid hamartoma. Myoid hamartomas are rare hamartoma variants with smooth muscle differentiation. (**a**) This lesion shows features typical of hamartoma on low power. (**b**) Closer examination reveals intersecting cellular fascicles of spindled cells adjacent to the sclerotic lobules. Note the admixed fat. (**c**) The spindled cells have eosinophilic cytoplasm and bland elongated cigar-shaped nuclei, indicative of myoid differentiation. (**d**) Smooth muscle bundle in a myoid hamartoma on core biopsy and highlighted by desmin stain (inset)

Prognosis and Clinical Management

Hamartomas are benign and can be surgically enucleated [77] without risk of recurrence. Reports of rare recurrences have been associated with positive margins in the original excision and likely represent incomplete excision [6, 13, 15, 78].

Fibroadenoma

Overview and Clinical Presentation

FAs are the most common fibroepithelial tumors and the most common benign tumors of the breast. The incidence varies with age and is highest in women less than 30 years old [79]. FAs are the most common breast tumors in adolescents and young women. The true incidence is difficult to define, ranging from 9% to 23% in autopsy series and from 7% to 13% in specialty clinics in this age group [80, 81]. In one study, FAs accounted for 91% of all solid breast masses with confirmed tissue diagnosis in girls younger than 19 years of age [82]. FAs can also present in older age groups. In a large multicenter community-based screening population (Breast Cancer Surveillance Consortium), the overall incidence of FAs in women over 40 years old was 18.5%, with a peak incidence of ~24% at ages 40–49 decreasing to <15% in older age groups [83]. In another study, 20% of benign and 12% of all breast masses in postmenopausal women were FAs, with an overall incidence of 10% of biopsies in this population [84].

FAs usually present as a solitary palpable, mobile, firm, and painless mass, but non-palpable lesions may also be detected by mammography as a mass or calcifications [85–

88]. Infarcted tumors, as can occur during pregnancy or lactation, may be painful [89, 90]. Many FAs are small (often <3 cm), but large tumors up to 20 cm may be encountered, especially in adolescents with juvenile FAs, which may grow rapidly in size and/or cause marked breast distortion, raising clinical concern for PT [79, 91, 92]. FAs exceeding 5 cm in size have been called "giant fibroadenomas" and usually occur as single or multiple lesions in adolescent girls after puberty [93–97]. FAs may affect any region within the breast, although the upper outer quadrant is most common. When present in the axilla, FAs can clinically mimic lymphadenopathy. The left breast is involved slightly more often than the right [79]. Some women (13–16%) may develop multiple or, less commonly, bilateral (synchronous or metachronous) FAs, which is more often associated with a family history or other predisposing conditions, such as cyclosporine use [98–106]. FAs may also develop in ectopic mammary-like tissue in the chest wall and vulva [107–111].

Gross and Radiologic Features

On mammography, FAs typically present as round or oval, smooth masses with increased density, which may or may not be associated with coarse calcifications [112]. Alternatively, only coarse calcifications may be seen. An increasing number of non-palpable FAs are being detected by screening mammography [85–88]. It is not always possible to distinguish FAs from other lesions, including benign cysts, PTs, or invasive carcinoma by mammography [112, 113]. Characteristic ultrasound features of FA include a well-circumscribed round or oval homogeneous and hypoechoic mass with variable acoustic enhancement, which may have lobulations and a smooth, echogenic capsule [114–116]. In some cases, irregular borders, lesional heterogeneity, or posterior shadowing may simulate carcinoma [116]. Myxoid FAs may be more likely to simulate invasive mucinous carcinoma on ultrasound due to overlapping features [117]. Kim et al. reported enhanced posterior acoustic shadowing in juvenile FAs compared to conventional FAs [115], and Sanchez et al. reported an increased incidence of internal linear hyperechoic septae in juvenile FAs compared to conventional FAs [82]. Juvenile FAs have also been shown to demonstrate more vascularity by color Doppler than conventional FAs [82, 118]. MRI usually reveals a smooth lobulated mass showing low- or high-signal intensity on T2-weighted images [119]. Radiologic differentiation of FA from PT is often not reliable [119, 120].

The gross appearance of FA is of a well-circumscribed ovoid mass with a smooth, bosselated outer surface. The lesions are often less than 3 cm but show a wide size range, reaching sizes up to 20 cm in some cases [79, 96, 97, 121]. The cut surface is usually tan-gray or white, rubbery, and bulging, in some cases with appreciable lobulations and/or very small slit-like spaces. Variations exist depending on the nature of the stroma. Sclerotic/hyalinized FAs are firmer and white with or without associated calcifications, whereas myxoid FAs are soft and gelatinous or mucoid. Tubular adenomas tend to be more tan-brown and slightly softer than conventional FAs.

Microscopic Features

FAs are well-circumscribed but non-encapsulated, nodular or mass-like biphasic stromal and epithelium proliferations. Two distinct growth patterns may be seen: (1) *intracanalicular*, in which the stromal proliferation compresses ducts into distorted and elongated curvilinear structures with slit-like lumens or clefts (Fig. 7.5a–e), and (2) *pericanalicular*, in which the stroma proliferates circumferentially around ducts without epithelial compression and with open lumens (Figs. 7.5f–i). Both patterns may be seen in a given FA (Figs. 7.5j). The growth pattern has no known clinical significance. A pericanalicular pattern is often seen in FAs of children and young women in their second or third decade, including juvenile FAs. In the vast majority of cases, the tumor borders are sharply demarcated from adjacent breast tissue. A poorly defined lesion with histologic features of FA that lacks clearly demarcated borders and blends with surrounding breast parenchyma has been described as *fibroadenomatous* or *fibroadenomatoid* change (Fig. 7.6).

The stromal cellularity of conventional FAs is low (Fig. 7.5). The epithelial and stromal elements are generally evenly distributed throughout. Tumors with increased stromal cellularity may be encountered, especially in younger women (Fig. 7.7). These *cellular fibroadenomas* are defined by focal or diffuse mildly increased stromal cellularity, although evaluation of the degree of stromal cellularity is subjective, and a diagnostic threshold is lacking. Cellular FAs may show overlapping histological features with PTs in CNBs and excisions, especially in lesions with a prominent intracanalicular pattern. The absence of stromal-epithelial heterogeneity in cellular FAs is a useful discriminator in this context (Fig. 7.7d, e), especially in the absence of well-developed features of PTs. Subepithelial stromal accentuation is not seen in FAs, although this can be a subjective feature to evaluate, and some fibroadenomas have compressed intralobular stroma in subepithelial zones that can mimic subepithelial stromal accentuation.

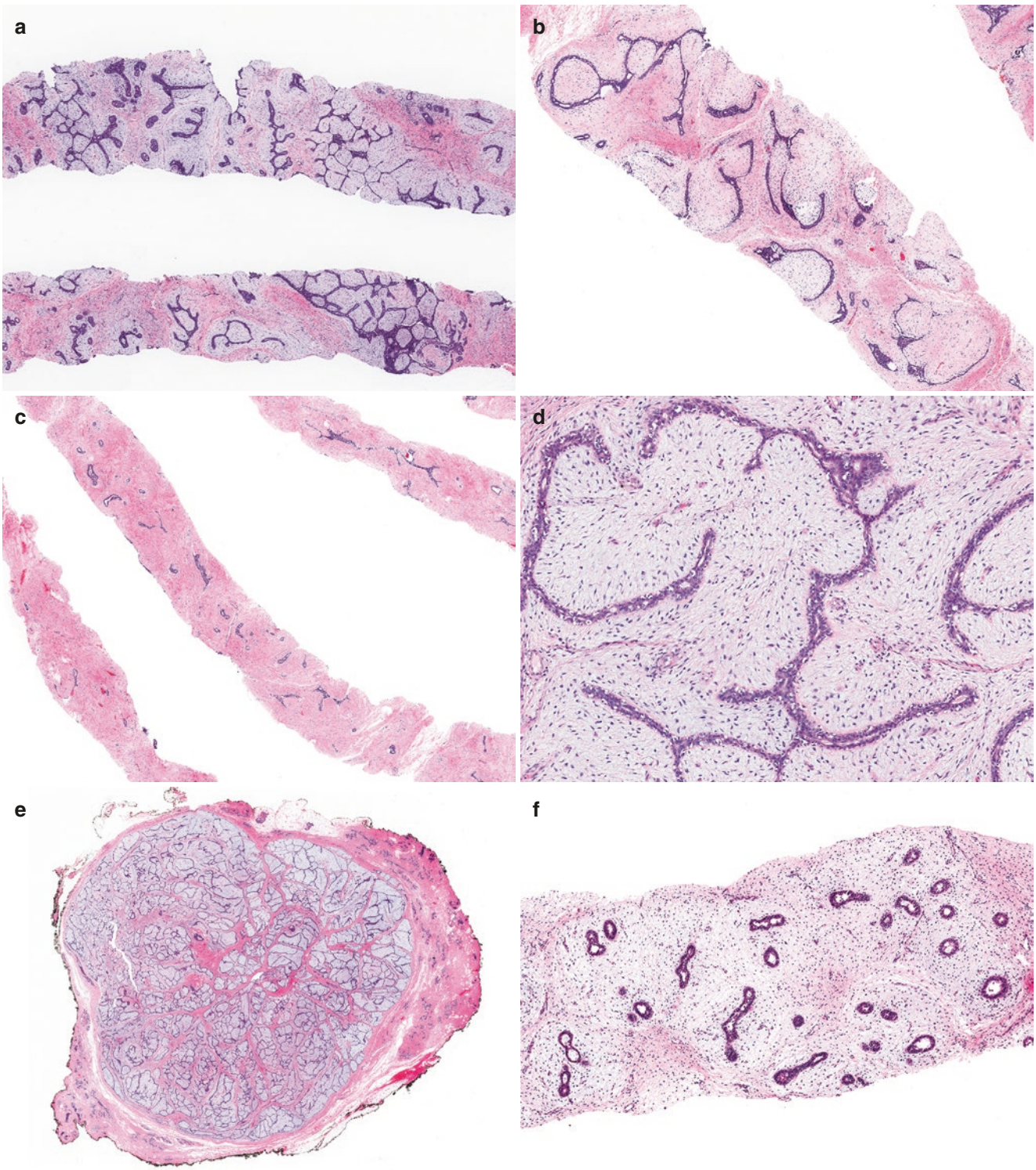

Fig. 7.5 Fibroadenomas and growth patterns. (**a**–**e**) Intracanalicular, (**f**–**i**) Pericanalicular, (**j**) Mixed intracanalicular (left), and pericanalicular (central and right)

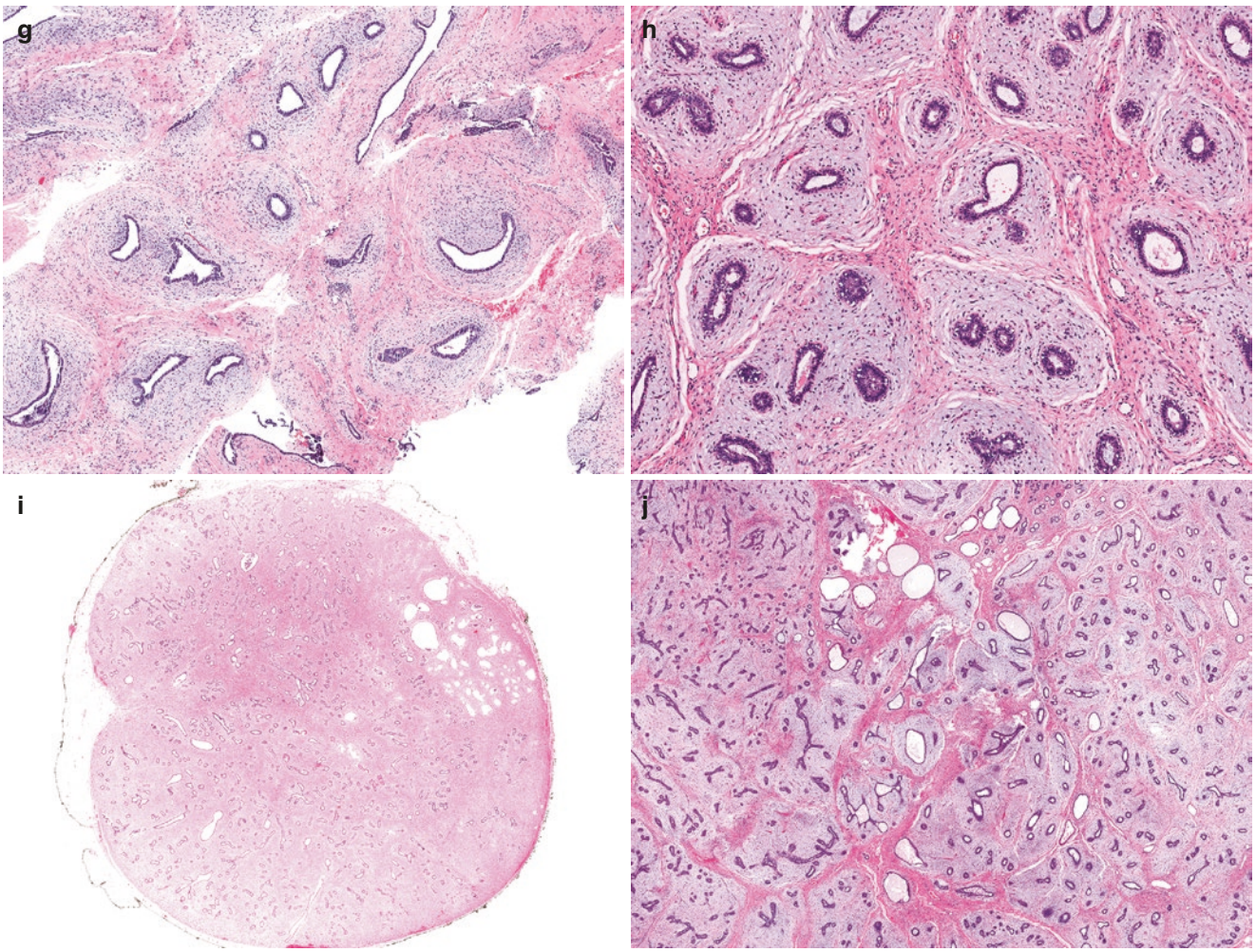

Fig. 7.5 (continued)

The stroma of FAs is usually composed of bland spindle cells with oval nuclei and variable amounts of collagen (Fig. 7.8a). Some lesions have myxoid stroma, and if comprising the entire lesion, are designated *myxoid FAs* (Fig. 7.8b). Myxoid FAs are commonly multicentric or bilateral in patients with Carney complex but are more often solitary if sporadic [122]. In addition to myxoid FAs, myxoid stromal changes were also noted to involve single or small groups of lobules and interlobular stroma in patients with Carney complex [122]. Some FAs are hypocellular with prominent sclerosis and hyalinization of the stroma that may calcify, and may present as coarse calcifications on mammography (Fig. 7.8c). These *hyalinized FAs* are common in older women and may be long-standing static or regressing tumors. Although most FAs show consistent stromal composition and appearance throughout, lesions with differing stromal composition may be encountered (Fig. 7.8d, e). PASH was identified in ~4% of FAs in one series [123]. Rare FAs may show benign stromal heterologous elements. Lipomatous metaplasia is seen most commonly, but myoid and cartilaginous metaplasia have also been described (Fig. 7.9). Rare ossification has been reported, predominantly in hyalinized FAs [124, 125].

Stromal mitotic activity is generally absent in conventional FAs, but cellular and juvenile FAs may have increased mitotic activity, especially in younger patients. The degree of mitotic activity overlaps with benign PTs, and an upper limit for mitotic activity within FAs in adults has not been established. Up to 2 mitotic figures/10 high-power fields (HPF) has been suggested to be acceptable in the proper histologic and clinicopathologic context [126–128]. The presence of mitotic activity in fibroepithelial tumors presenting in older women should prompt careful evaluation for the alternate diagnosis of PT. Excision should be considered for fibroepithelial tumors with mitoses in CNBs to exclude PT.

Benign multinucleated stromal giant cells may be encountered in fibroepithelial tumors, including FAs, although this is relatively rare (Fig. 7.8f, g) [129–137]. These cells have vari-

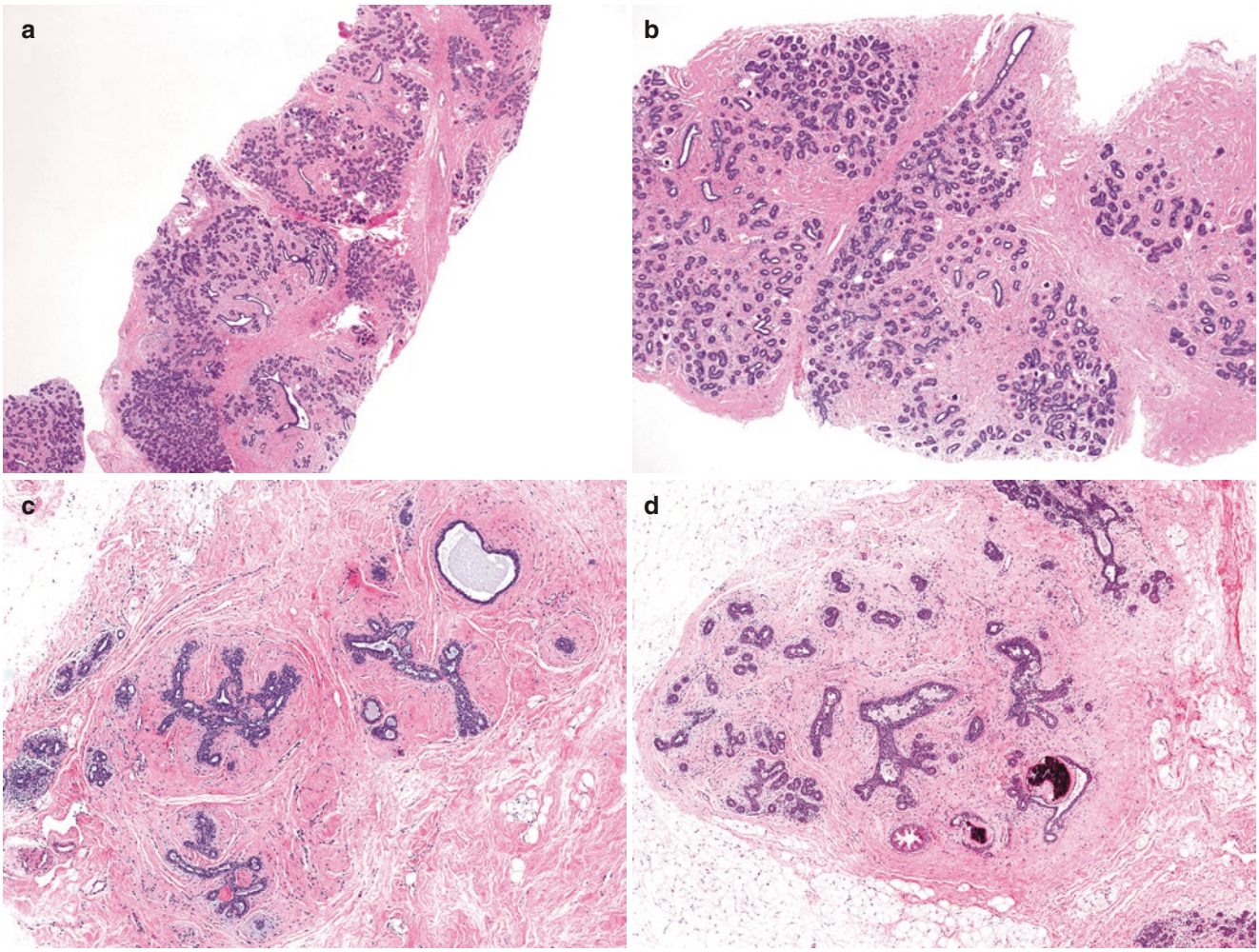

Fig. 7.6 Sclerosing lobular hyperplasia and fibroadenomatous change. (**a**, **b**) Sclerosing lobular hyperplasia can present as a mass lesion clinically resembling fibroadenoma but is composed of multiple enlarged lobules with increased ductules and intact architecture, associated with collagenized intralobular and often interlobular stroma. (**c**, **d**) Vaguely defined nodular areas with fibroadenomatous architecture and indistinct borders that merge with the surrounding tissue can be classified as fibroadenomatous change. Large calcifications associated with the lesion in (**d**) prompted the biopsy

able amounts of eosinophilic cytoplasm and enlarged, hyperchromatic nuclei, which may be pleomorphic. A floret pattern with multiple nuclei may be seen [46, 131, 135]. The chromatin is fine and smudgy with degenerative features, and nucleoli are either absent or inconspicuous. Nuclear inclusions may be seen. Cell size is variable but may be enlarged in some cases [131]. The giant cells often cluster without significantly increasing the degree of stromal cellularity. Mitotic activity is usually absent, but some studies have reported occasional mitoses [131, 137]. Although the cytologic features may be striking, these cells are of no known clinical significance. Benignity is supported by degenerative nuclear features similar to those found in benign giant cells of other organs (nasal polyps, bladder, gynecologic organs, anus), lack of evidence of recurrence in reported lesions, and lack of correlation with fibroadenoma versus phyllodes histology [129, 131, 135, 138]. The presence of multinucleated stromal giant cells in a fibroepithelial tumor with features of FA should not be used as evidence for PT.

Usual ductal hyperplasia, often with micropapillary or fenestrated architecture, can be seen in the epithelial component of FAs (Fig. 7.10c). In one series, usual ductal hyperplasia was found in ~44% of FAs [123]. Apocrine or uncommonly squamous metaplasia may be seen [123]. Atypical epithelial proliferations are uncommon and include atypical ductal or lobular hyperplasia and ductal or lobular carcinoma in situ (Fig. 7.10d–h) [123, 139–146]. The reported incidence of carcinoma involving FA ranges from 0.01% to 0.3% in screened populations, with the vast predominance being in situ carcinomas [139, 142, 144]. The

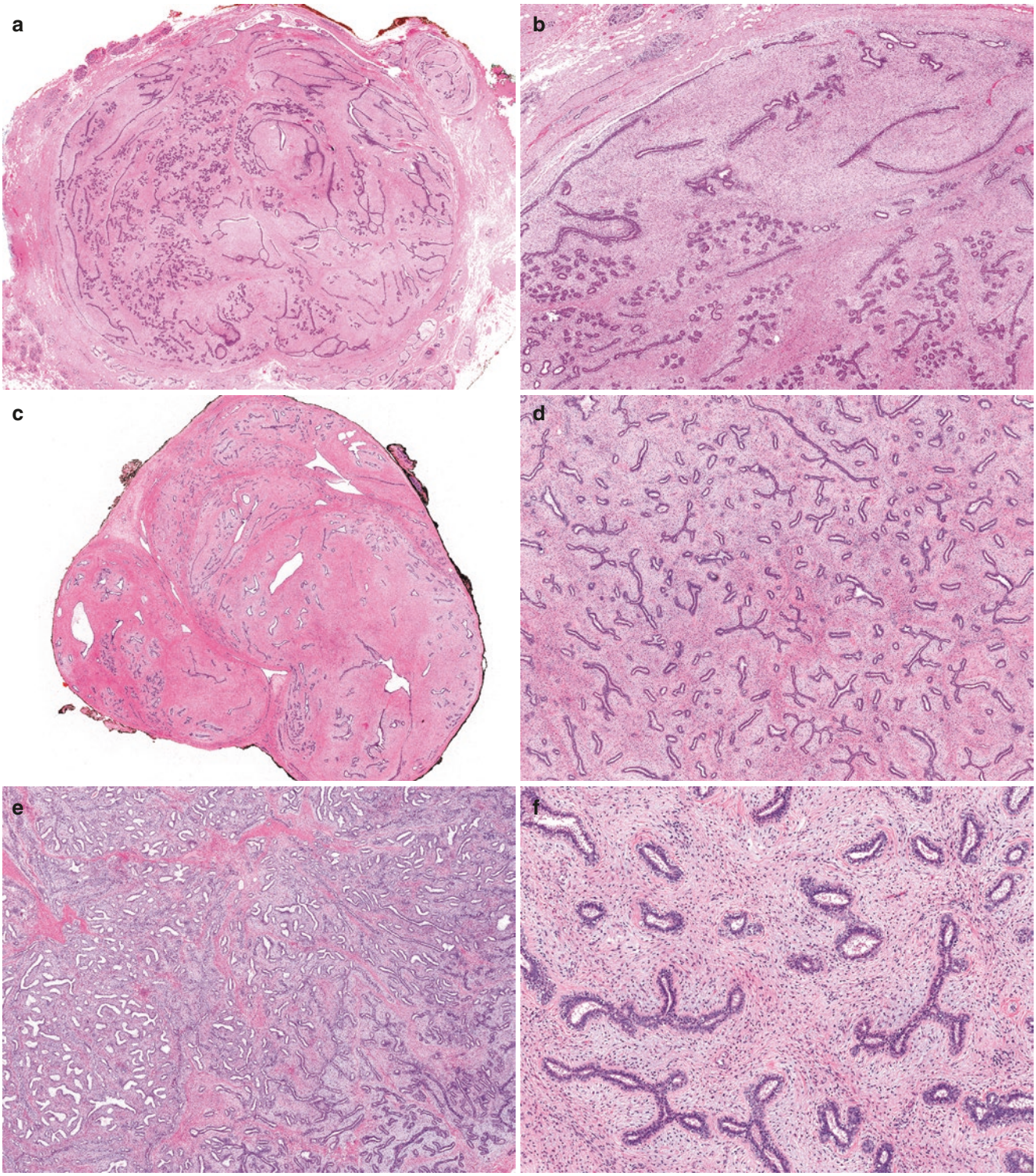

Fig. 7.7 Cellular fibroadenoma. (**a**–**c**) Cellular fibroadenomas are well circumscribed, with mildly increased stromal cellularity and evenly distributed epithelial and stromal components. (**d**, **e**) The even distribution of epithelium and stroma imparts a uniform appearance throughout the lesion. (**f**–**h**) Stromal cellularity is mildly increased, but there is no stromal cell atypia. (**i**) Stromal cellularity of conventional fibroadenoma, in contrast

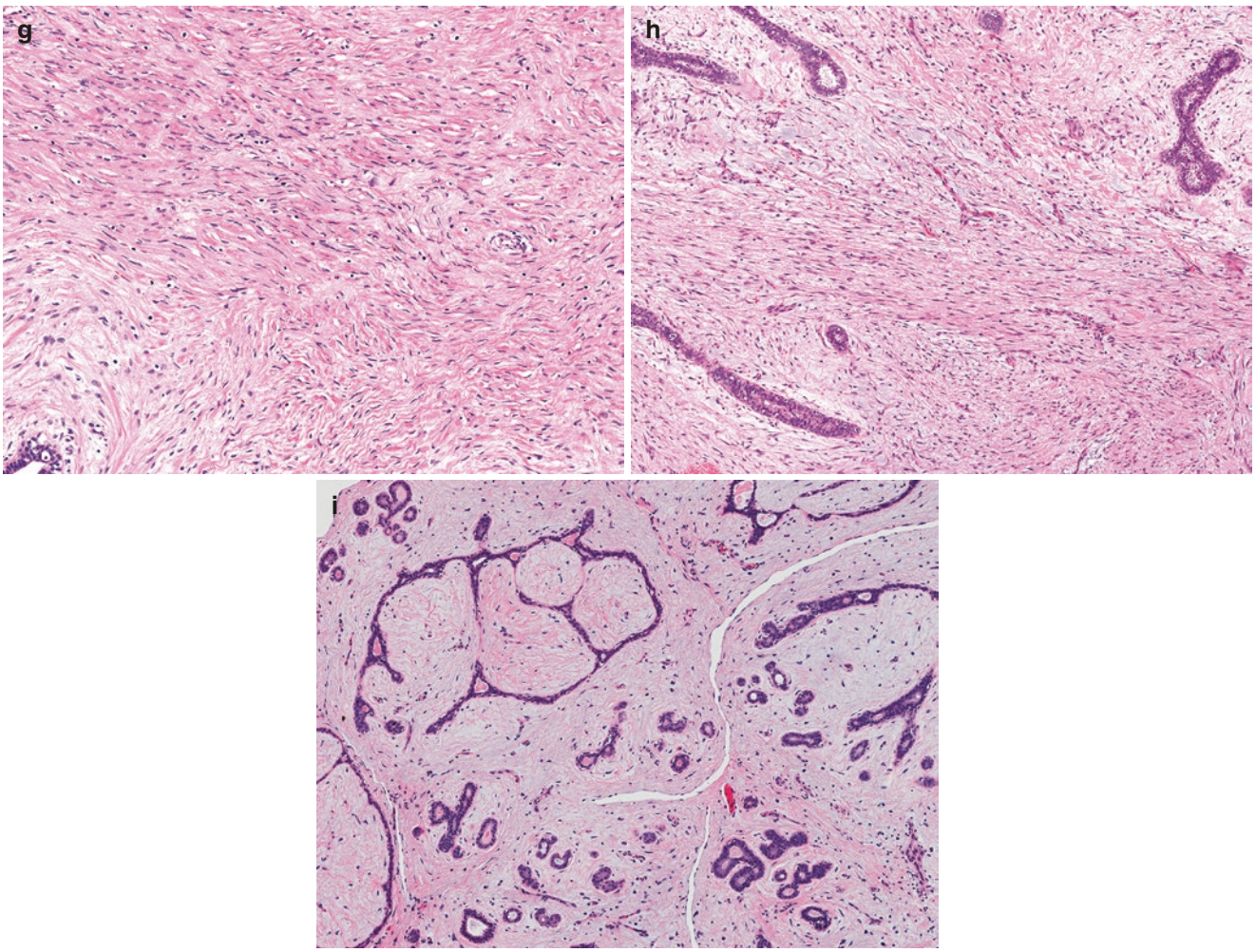

Fig. 7.7 (continued)

mean age of patients with associated carcinoma is 42–52 years, approximately 15–20 years older than patients presenting with FAs lacking carcinoma [123, 142, 145]. Whereas some studies reported a predominance of lobular carcinoma in situ, others have shown approximately equal incidence of ductal and lobular carcinoma in situ [123, 142, 145]. In situ carcinoma may also involve ducts adjacent to FAs with carcinoma [123, 142]. Atypical hyperplasia is less common, and flat epithelial atypia may also be seen [123]. Tangential sectioning of elongated non-atypical ducts may sometimes give a false impression of cribriforming (Fig. 7.10i).

FAs arising in children often have features that may otherwise be concerning for PT, such as increased stromal cellularity (mild to moderate) and focal stromal frond formation (Fig. 7.11), but these were not found to correlate with recurrence [147]. Stromal mitotic activity may also be increased beyond what is accepted for FA in adults (up to 7/10 HPF reported) [148]. These features should not necessarily point to a diagnosis of PT in this population in the absence of other diagnostic features.

Complex FAs are defined by the presence of sclerosing adenosis, papillary apocrine metaplasia, cysts greater than 3 mm in size, or epithelial calcifications (Fig. 7.12) [123, 149, 150]. In a large study, the presence of cysts was the single most common histologic feature of these lesions (~29%), with two or more of the features present in ~35% of cases [149]. Another series demonstrated sclerosing adenosis as the most common complex feature (~57%) [150]. Complex FAs occur in older patients (mean age of 35–47 years) and tend to be smaller than FAs without complex features, averaging approximately one-half the size (1.3 ± 0.57 cm) of conventional fibroadenomas (2.55 ± 1.44 cm) in one study [123, 150]. Proliferative epithelium has been noted to occur more often adjacent to complex versus non-complex FAs [149].

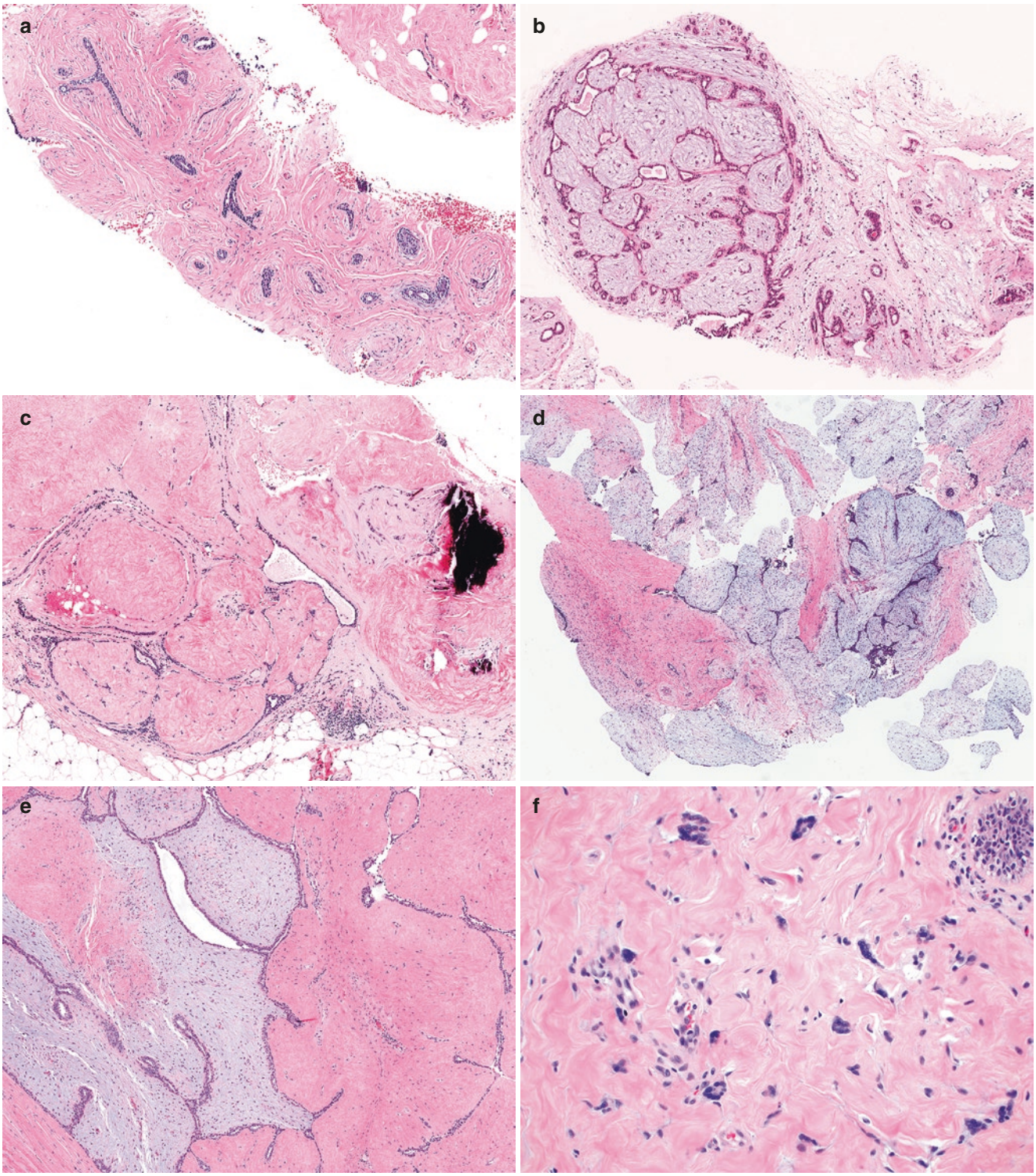

Fig. 7.8 Fibroadenoma stroma. (**a**) Fibroadenomas most commonly have a normocellular fibrous stroma. (**b**) Myxoid fibroadenoma. (**c**) Hyalinized fibroadenoma. The stroma of these tumors may calcify and present as coarse calcifications on mammography, leading to core biopsy. (**d**, **e**) Some fibroadenomas show mixed stromal features, fibrous and myxoid in this case. (**f**, **g**) Benign multinucleated giant cells with dark, degenerative chromatin, some arranged in florets (**f**). (**h**) Infarcted fibroadenoma in a pregnant woman

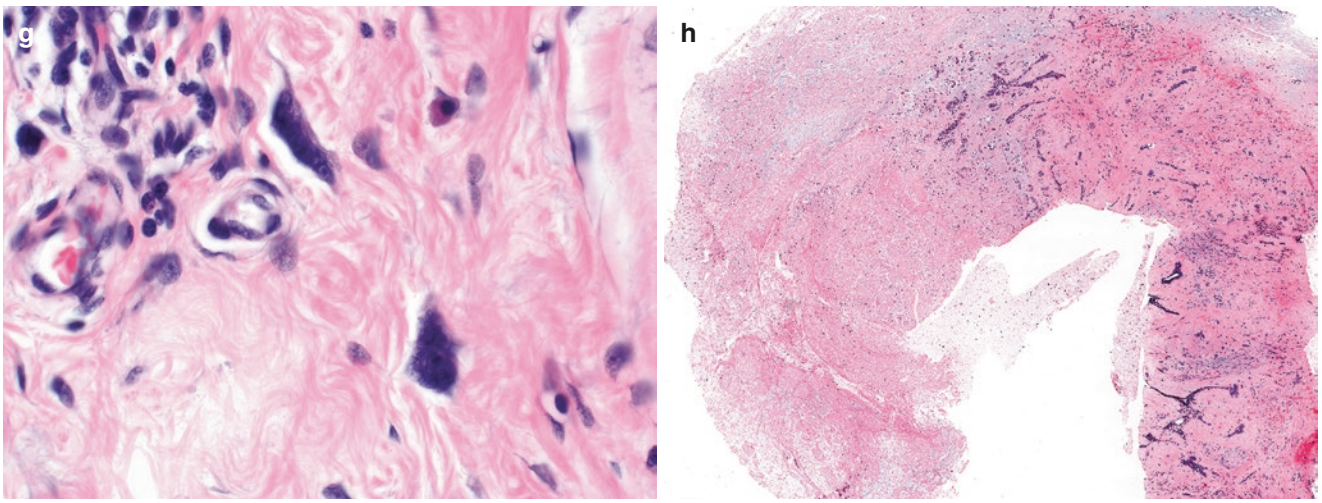

Fig. 7.8 (continued)

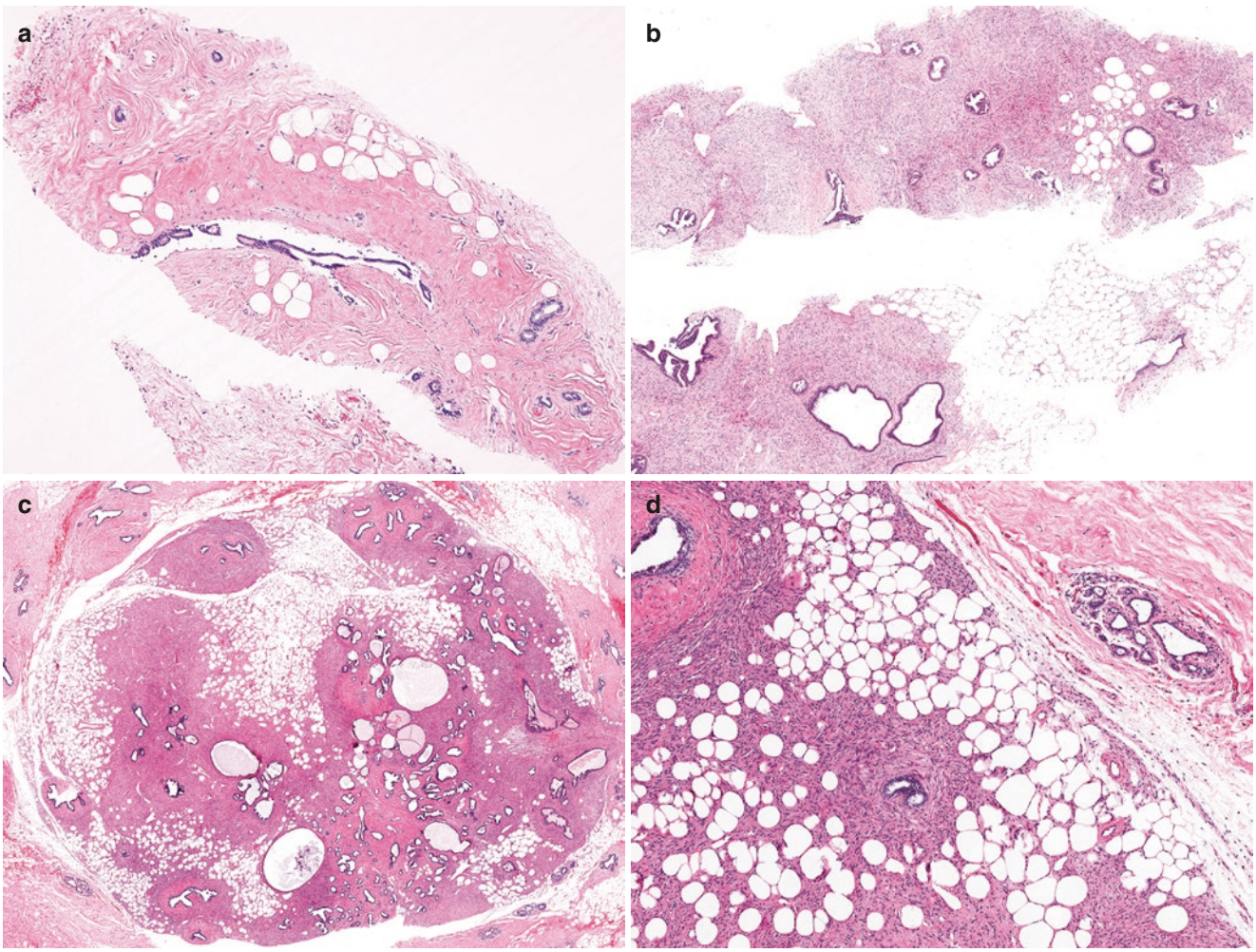

Fig. 7.9 Benign mesenchymal metaplasia in fibroadenoma. (**a**) Core biopsy of fibroadenoma with lipomatous metaplasia. (**b**–**d**) Cellular fibroadenoma with lipomatous metaplasia. The presence of fat in a cellular fibroepithelial lesion on core biopsy (**b**) raises suspicion for infiltrative growth of phyllodes tumor. On excision (**c**, **d**), mature fat is confined within the rounded lesional borders, giving the impression of being an inherent part of the lesion. (**e**, **f**) Core biopsy of fibroadenoma with myoid metaplasia. (**g**, **h**) Fibroadenoma with myoid metaplasia. Myoid bundles are highlighted by desmin immunostain (**h**)

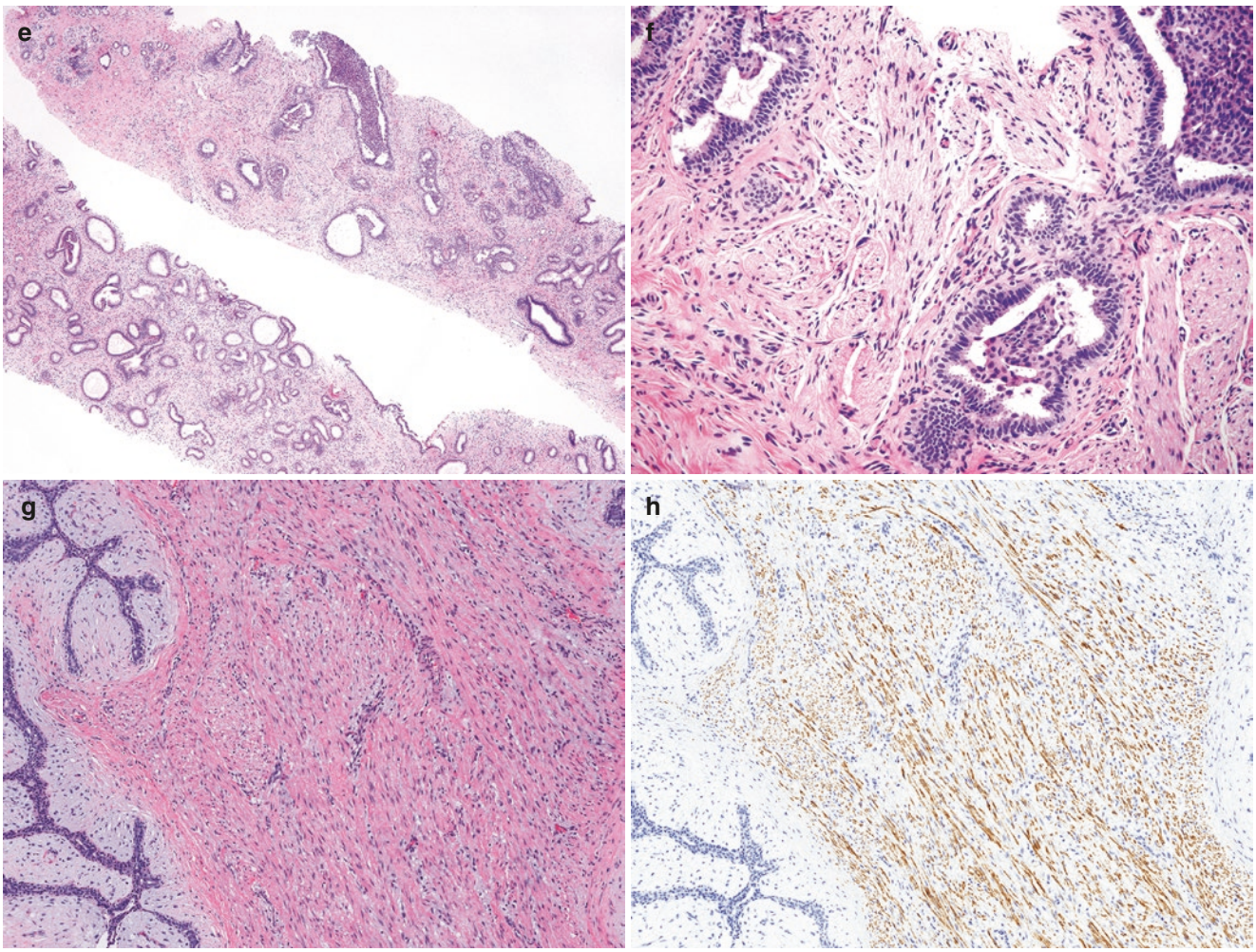

Fig. 7.9 (continued)

Juvenile FAs are more common in adolescents and women younger than 20 years of age, but the prevalence is bimodal, with a second peak in women >40 years old. Conventional FAs are more common than juvenile FAs even in adolescents and younger women [91, 151, 152]. Juvenile FAs demonstrate a mild to moderate increase in stromal cellularity and a pericanalicular or mixed growth pattern, typically with usual ductal hyperplasia. Hyperplasia is often micropapillary and in such cases has been referred to as "gynecomastoid hyperplasia," based on the resemblance to epithelial hyperplasia in gynecomastia. Stromal cellularity is evenly distributed throughout the lesion, although mild intralesional heterogeneity may occasionally be seen (Fig. 7.13). There is no stromal cytologic atypia. Mitotic activity may be present, especially in adolescents and younger women.

Tubular adenomas are characterized by an adenosis-like proliferation of closely packed rounded ductules with small lumina and little intervening stroma. These lesions are considered FA variants in which the epithelial proliferation has overtaken the stroma and is the dominant component. The ductules often have luminal eosinophilic secretions. Associated lymphocytic inflammation may be present in some cases (Fig. 7.14). During pregnancy or lactation, the epithelium of FAs or tubular adenomas may show focal or diffuse lactational/secretory changes, characterized by bubbly vacuolated cytoplasm, mildly increased nuclear size and hyperchromasia and/or nuclear hobnailing, as well as variable ductular dilatation (Fig. 7.10a, b). In contrast, so-called lactational adenomas (nodular lactational hyperplasia) are likely coalescent lactational lobules.

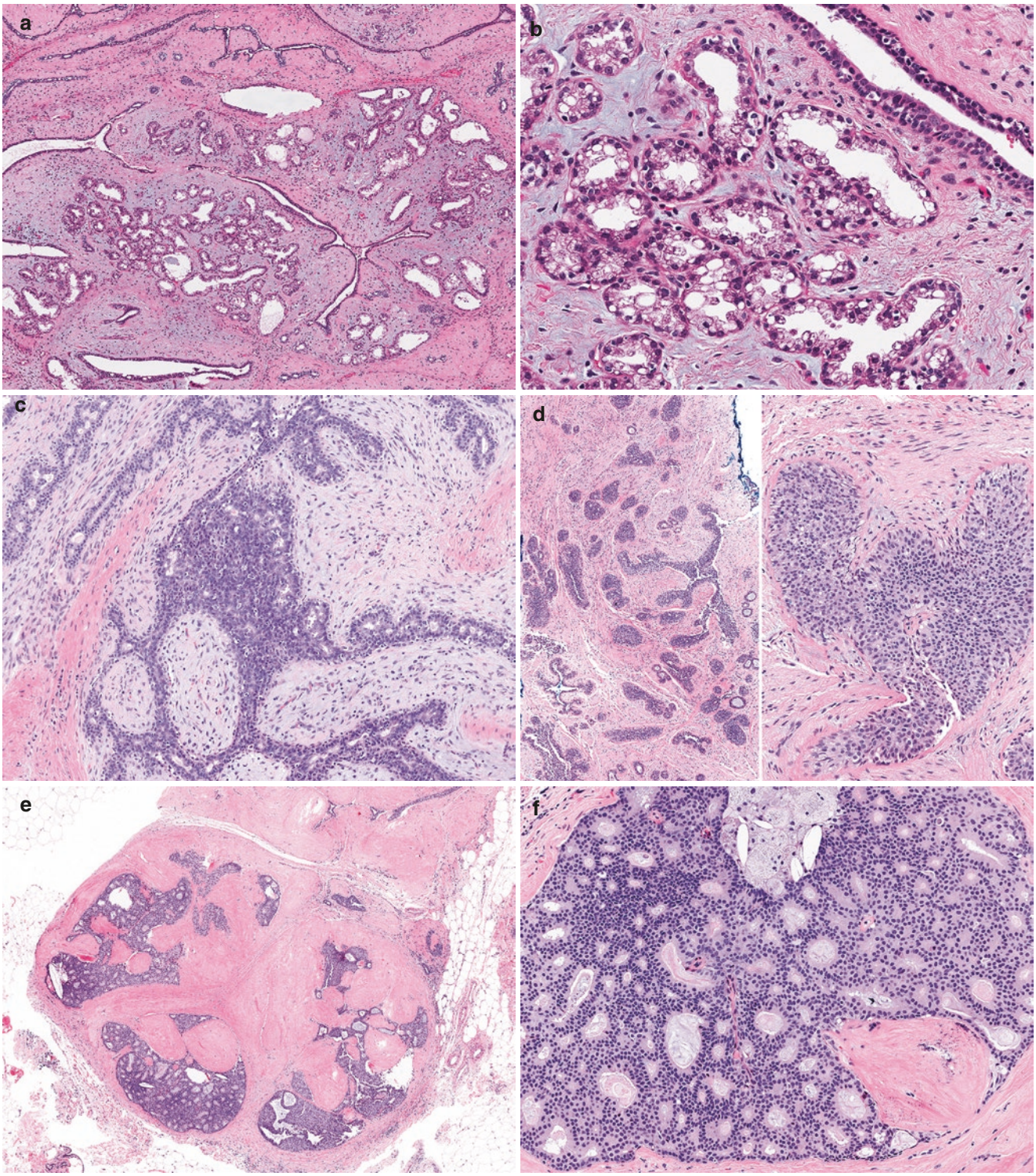

Fig. 7.10 Epithelial metaplasia, hyperplasia, and neoplasia in fibroadenoma. (**a**, **b**) Lactational or pregnancy-like changes. (**c**) Usual ductal hyperplasia. (**d**) Atypical ductal hyperplasia. (**e**, **f**) Ductal carcinoma in situ. (**g**) Atypical lobular hyperplasia, with negative E-cadherin immunostain in (**h**). (**i**) Tangential sectioning of the elongated ducts of fibroepithelial tumors should not be misinterpreted as atypical ductal hyperplasia

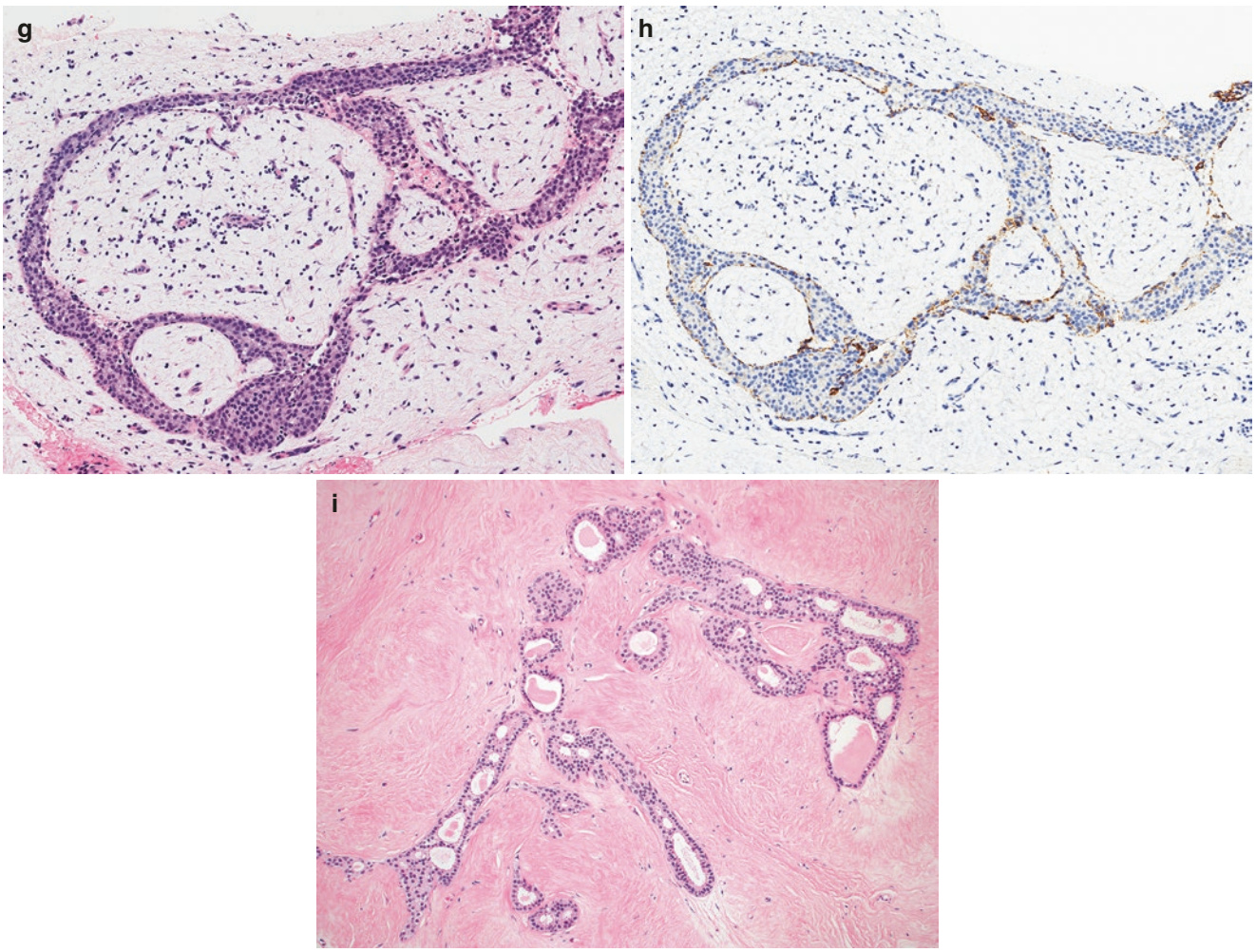

Fig. 7.10 (continued)

FAs can infarct in some instances, usually during pregnancy, lactation, or following fine-needle aspiration procedures (Fig. 7.8h). Rare cases of apparently spontaneous infarction have also been reported [89, 90, 153–156]. The presence of necrosis should therefore not necessarily preclude the diagnosis, although appropriate caution is warranted.

Immunohistochemistry

The stromal cells of FAs have an immunophenotype typical of mammary stroma, including CD34 and SMA positivity [157–159], and can express Bcl-2 and aberrant nuclear β-catenin [160–162]. Stromal cells in FAs express estrogen receptor (ER)β but not ERα, and this has been correlated with stromal cellularity and young age [163]. The luminal epithelium usually expresses ERα. Progesterone receptor (PR) may be expressed in the epithelium or stroma [164–167]. Immunohistochemistry plays no role in the distinction of FAs from PTs.

Differential Diagnosis

The diagnosis of conventional FA is often straight forward when typical features are present on CNB or excision. The presence of focal stromal fronds in some FAs can raise consideration of PT, but these are focal and less cellular than those of PTs, without subepithelial stromal accentuation (Fig. 7.15). On CNB, the false negative rate (with respect to PTs) has been estimated to be <1% despite the heterogeneous nature of some PTs [168, 169]. The triple approach of interpreting the pathology results in the context of clinical and radiologic input is suggested to avoid underdiagnosis of PT on CNB. In some cases, prominent hyperplastic epithe-

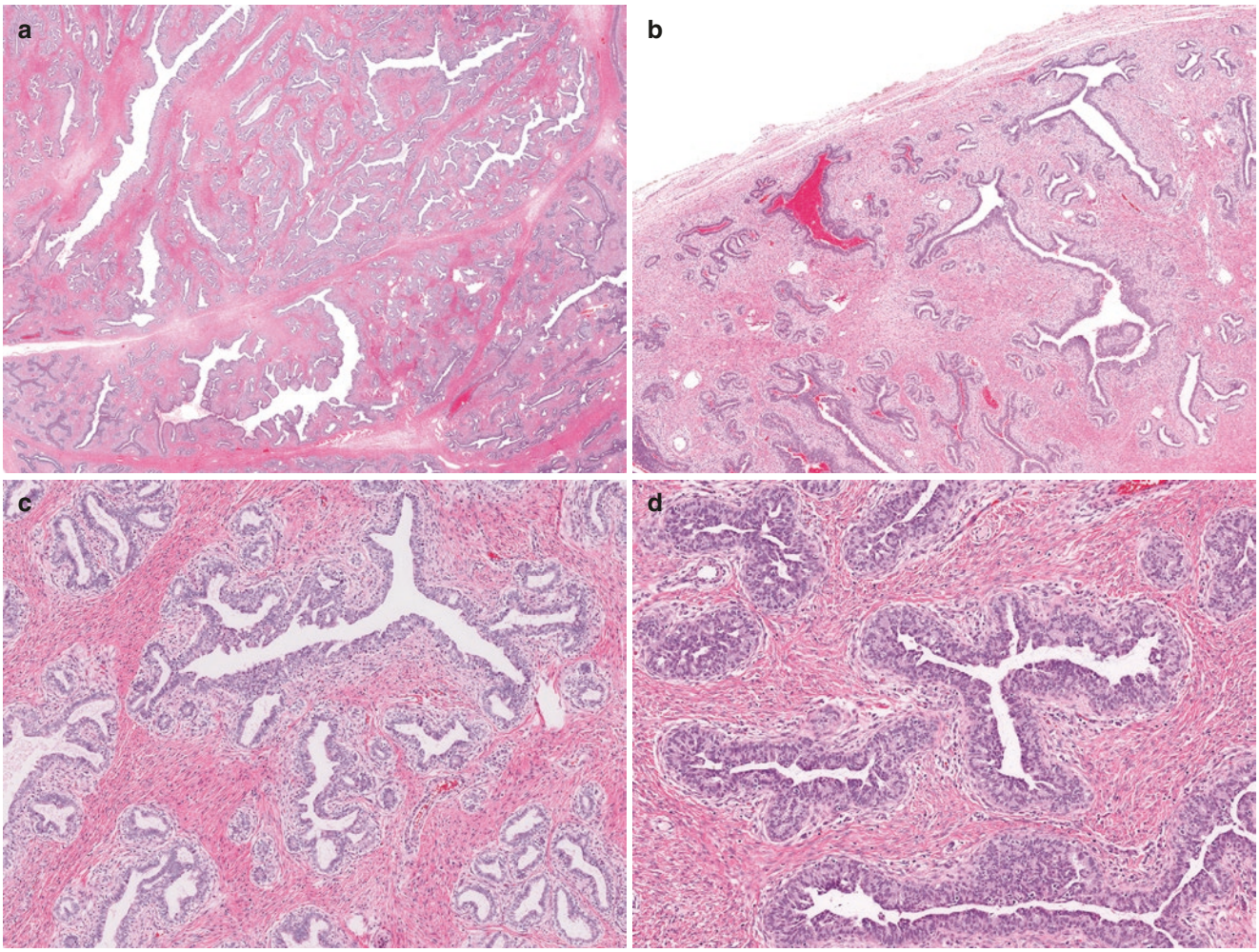

Fig. 7.11 Benign fibroepithelial tumor in 12-month-old girl. Fibroepithelial tumors in children may sometimes have (**a**) focal frond formation, (**b**–**d**) increased stromal cellularity, and elevated mitotic rate (up to 7 per 10 HPF in this case). (**c**, **d**) Micropapillary hyperplasia and pericanalicular growth are typical of juvenile fibroadenoma. Targeted DNA sequencing of this case using a panel that includes genes commonly mutated in fibroepithelial tumors did not reveal any genetic alterations

lium or well-developed PASH may distract from the presence of an underlying FA on CNB. Sclerosing adenosis, cysts, and/or apocrine change within a complex FA may mimic a radial sclerosing lesion on CNB, and vice versa (Fig. 7.12). FAs with lipomatous metaplasia may mimic hamartomas on CNB. Hamartomas tend to have more epithelial-stromal disorganization with intact lobules and lack well-developed intracanalicular or periductal growth patterns. Myxoid FAs can mimic mucinous carcinoma at low power on limited biopsy material. Immunohistochemistry for myoepithelial cells associated with ducts in myxoid FAs may be useful in these cases. Uncommonly, PTs (borderline or malignant) can show paradoxically hypocellular myxoid-appearing stroma, which can be deceptive as the stromal mitoses are only appreciated on higher magnification.

Sclerosing lobular hyperplasia (*fibroadenomatoid mastopathy*) refers to a mass lesion clinically mimicking FA but microscopically showing multiple enlarged lobules with intact architecture and increased numbers of ductules, characteristically associated with collagenized intralobular and sometimes interlobular stroma (Fig. 7.6a, b). Sclerosing lobular hyperplasia is often found adjacent to fibroadenomas and phyllodes tumors [170]. The differential diagnosis of tubular adenomas includes other mass-forming lesions with adenosis, including nodular adenosis, sclerosing intraductal papilloma or ductal adenoma, and sclerosing lobular hyperplasia. The packed ductules of tubular adenomas are round to oval, compared to more irregularly jagged contours in ductal adenoma, and the stroma of tubular adenomas is not hyalinized or sclerotic.

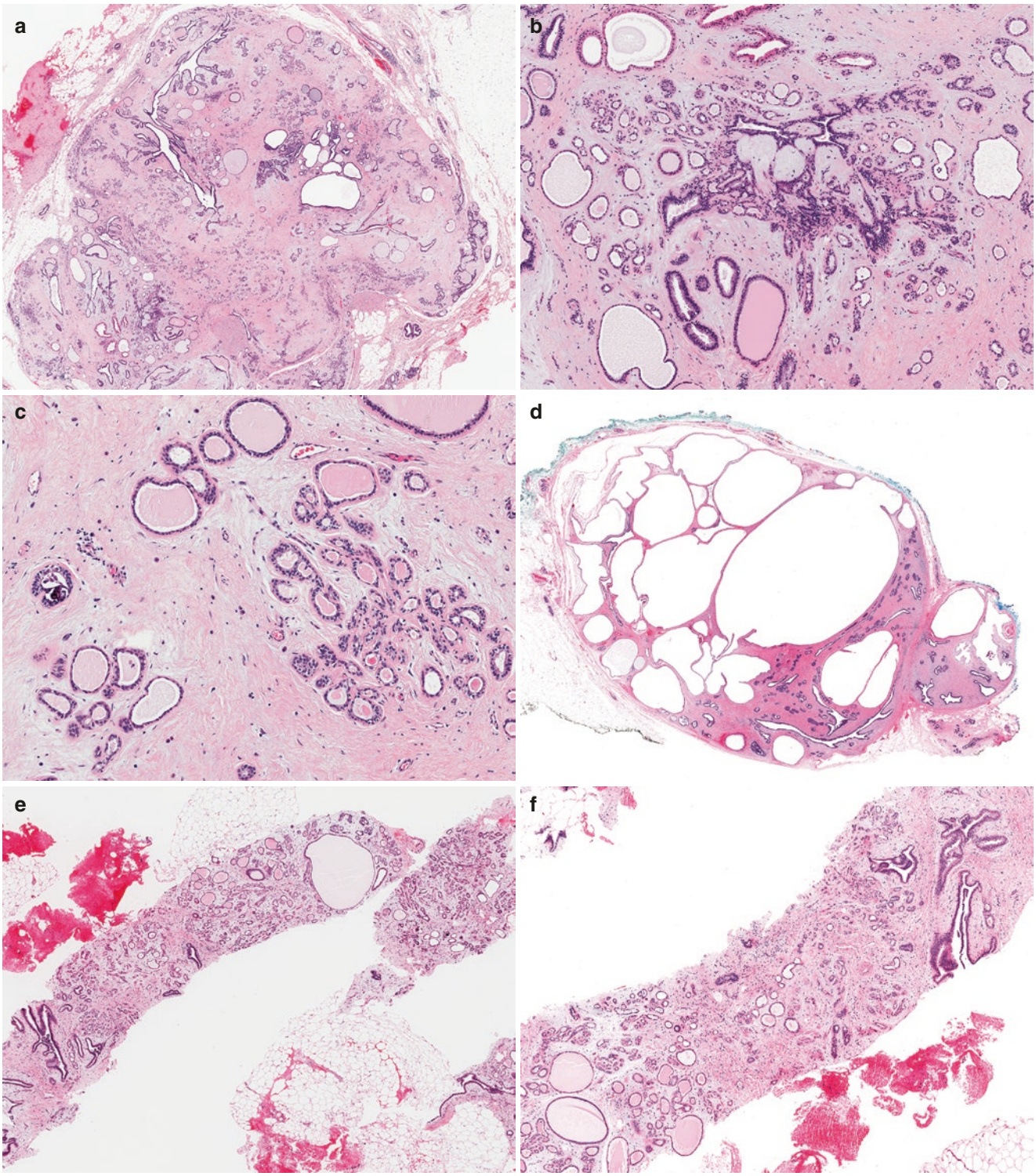

Fig. 7.12 Complex fibroadenoma. (**a**–**c**) Complex fibroadenoma with sclerosing adenosis, apocrine metaplasia, and epithelial calcifications. (**d**) Complex fibroadenoma with numerous large cysts. (**e**–**g**) This complex fibroadenoma was diagnosed as a complex sclerosing lesion on core biopsy. The presence of sclerosing adenosis, stromal fibrosis and variable duct dilatation can mimic a sclerosing lesion. (**g**) Focal elongated ducts with proliferative stroma point towards a fibroepithelial tumor

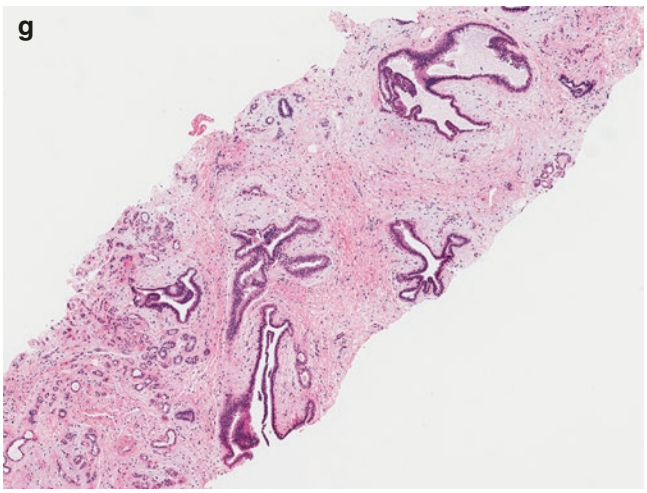

Fig. 7.12 (continued)

The most challenging differential diagnosis of cellular FA and juvenile FA is with benign PT. The distinction may be difficult in excision specimens and even more problematic in CNBs, where borderline PT could also be considered in the differential. The dilemma is due to overlapping and subjective histopathologic features (degree of stromal atypia, cellularity, and mitoses), limited sampling, and heterogeneity of PTs. For this reason, fibroepithelial tumors with increased stromal cellularity but lacking definitive features of PT, such as marked cellularity, obvious stromal overgrowth, well-developed cellular stromal fronds, obvious periductal stromal condensation, or at least moderate stromal cytologic atypia, are often diagnosed descriptively on CNB, for example, as *fibroepithelial neoplasm with cellular stroma*. More definitive characterization can be performed on the subsequent excision specimen (see sections "Phyllodes Tumors" and "Differential Diagnosis" for additional discussion).

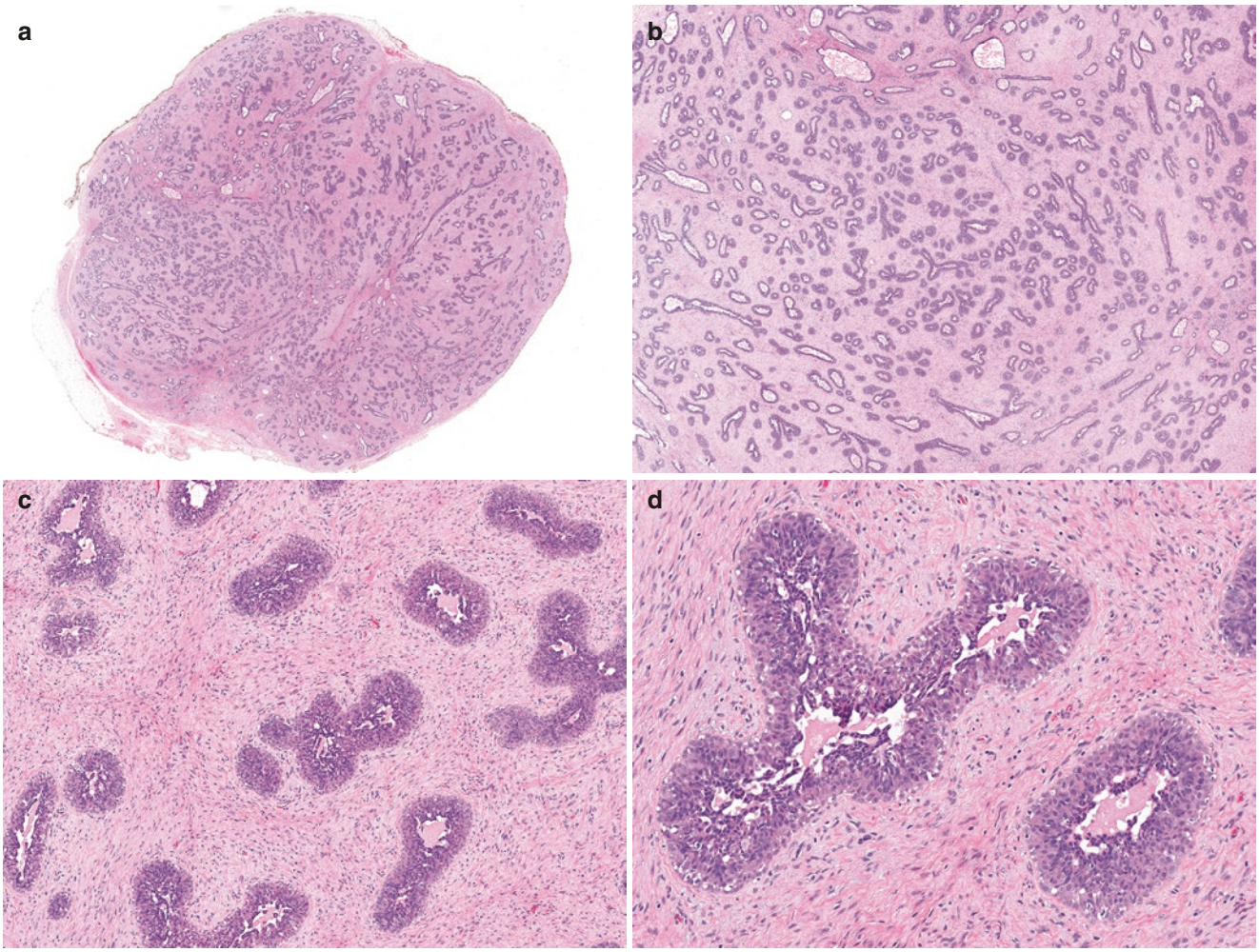

Fig. 7.13 Juvenile fibroadenoma. (**a**, **b**) and (**e**, **f**) These tumors characteristically have a pericanalicular growth pattern with relatively homogenous distribution of epithelial and stromal elements. (**c**, **d**, and **g**) The stroma is mildly hypercellular, and epithelium is proliferative, with a "gynecomastoid" (micropapillary) pattern of usual ductal hyperplasia. (**g**) Mitotic figures may be present. (**h**–**j**) Core biopsy of a juvenile fibroadenoma with similar features

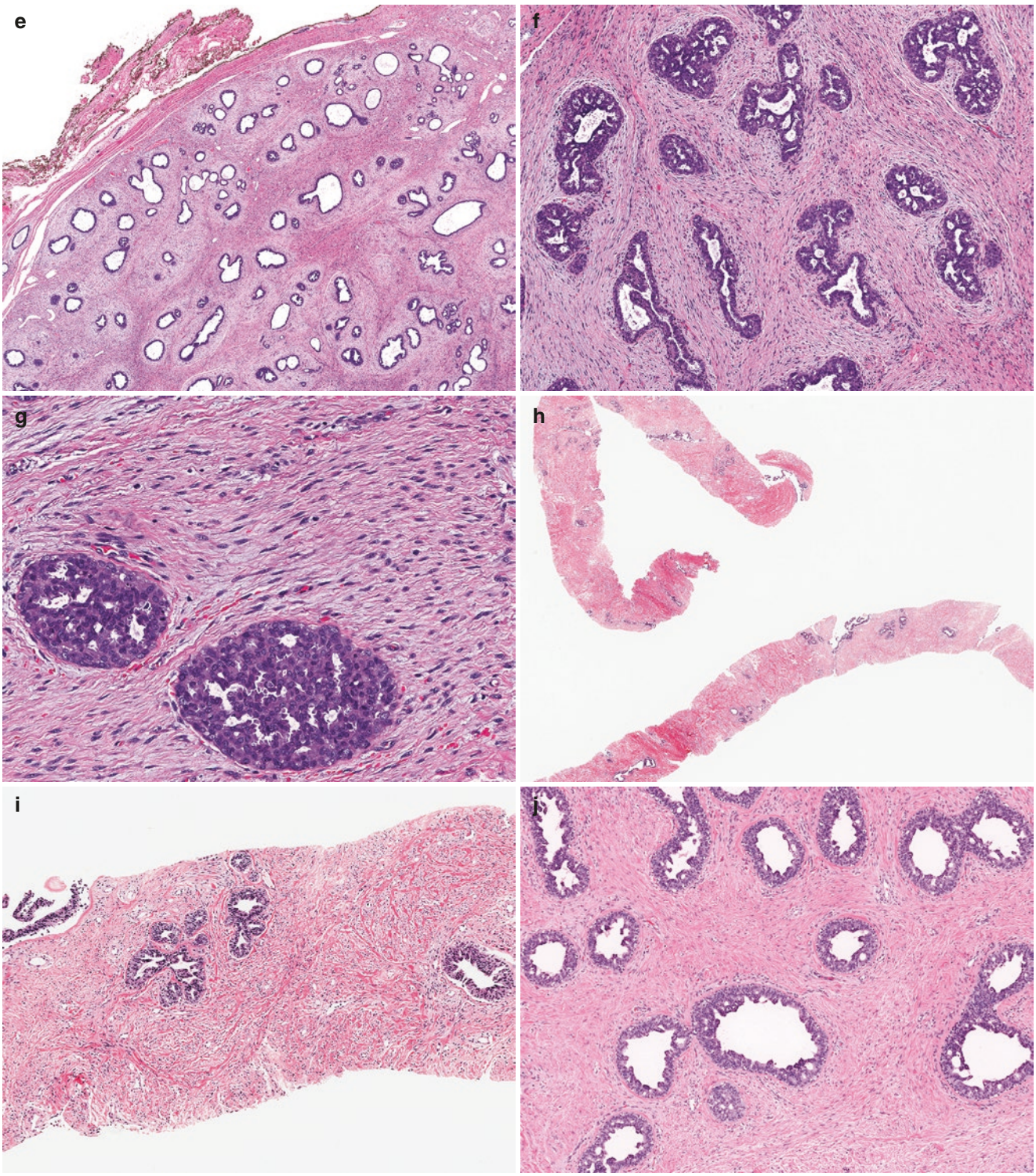

Fig. 7.13 (continued)

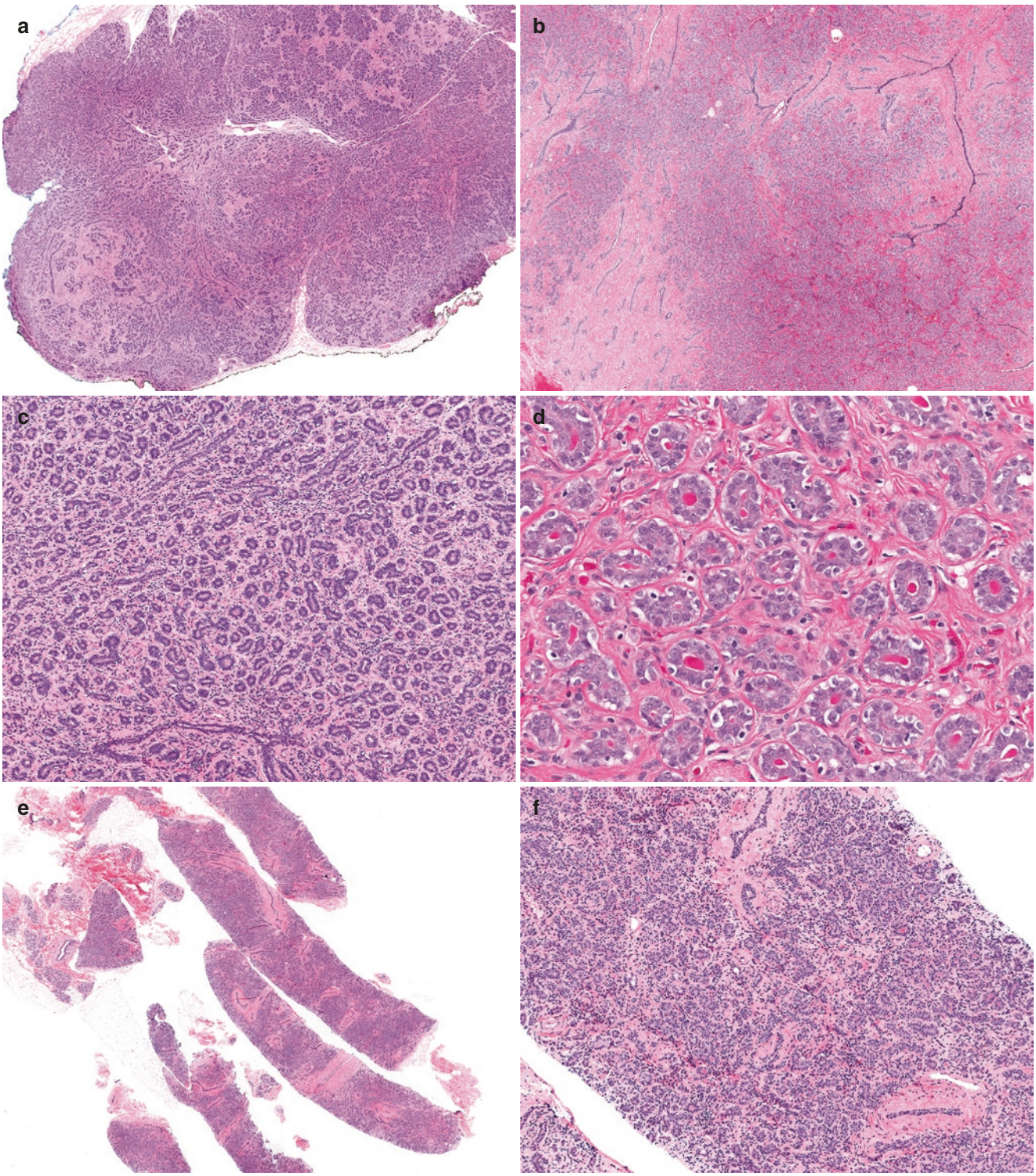

Fig. 7.14 Tubular adenoma. Tubular adenomas are fibroadenoma variants with prominent epithelial proliferation. (**a**, **b**) Features of the underlying fibroadenoma architecture are often identified. (**c**, **d**) Higher power reveals closely apposed ductules with rounded contours and luminal eosinophilic secretions. Scattered lymphocytic inflammation may be seen. (**e**, **f**) and (**g**, **h**) Core biopsies of tubular adenomas

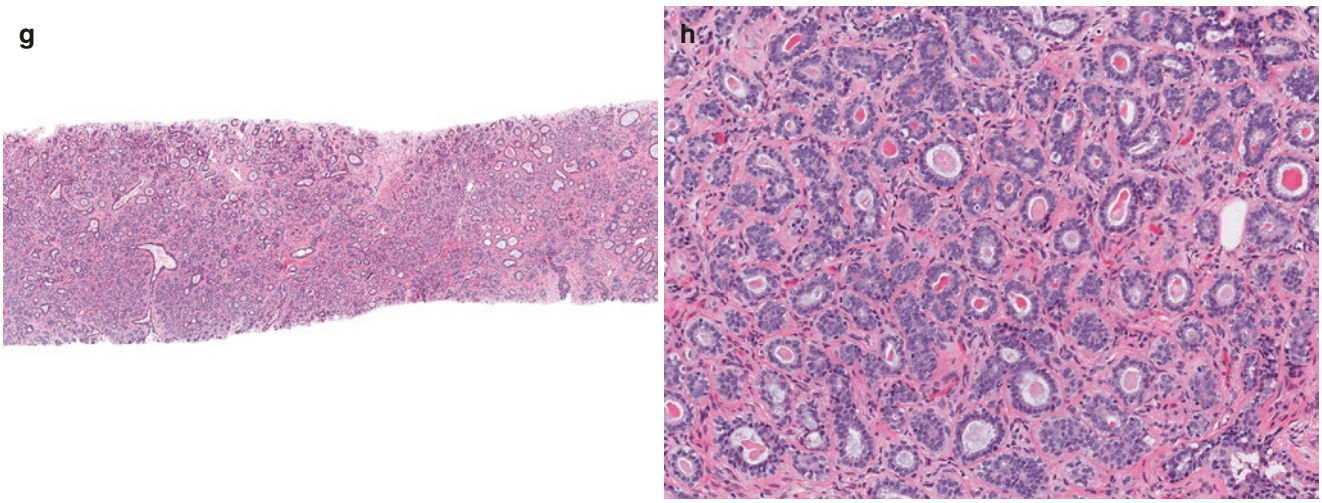

Fig. 7.14 (continued)

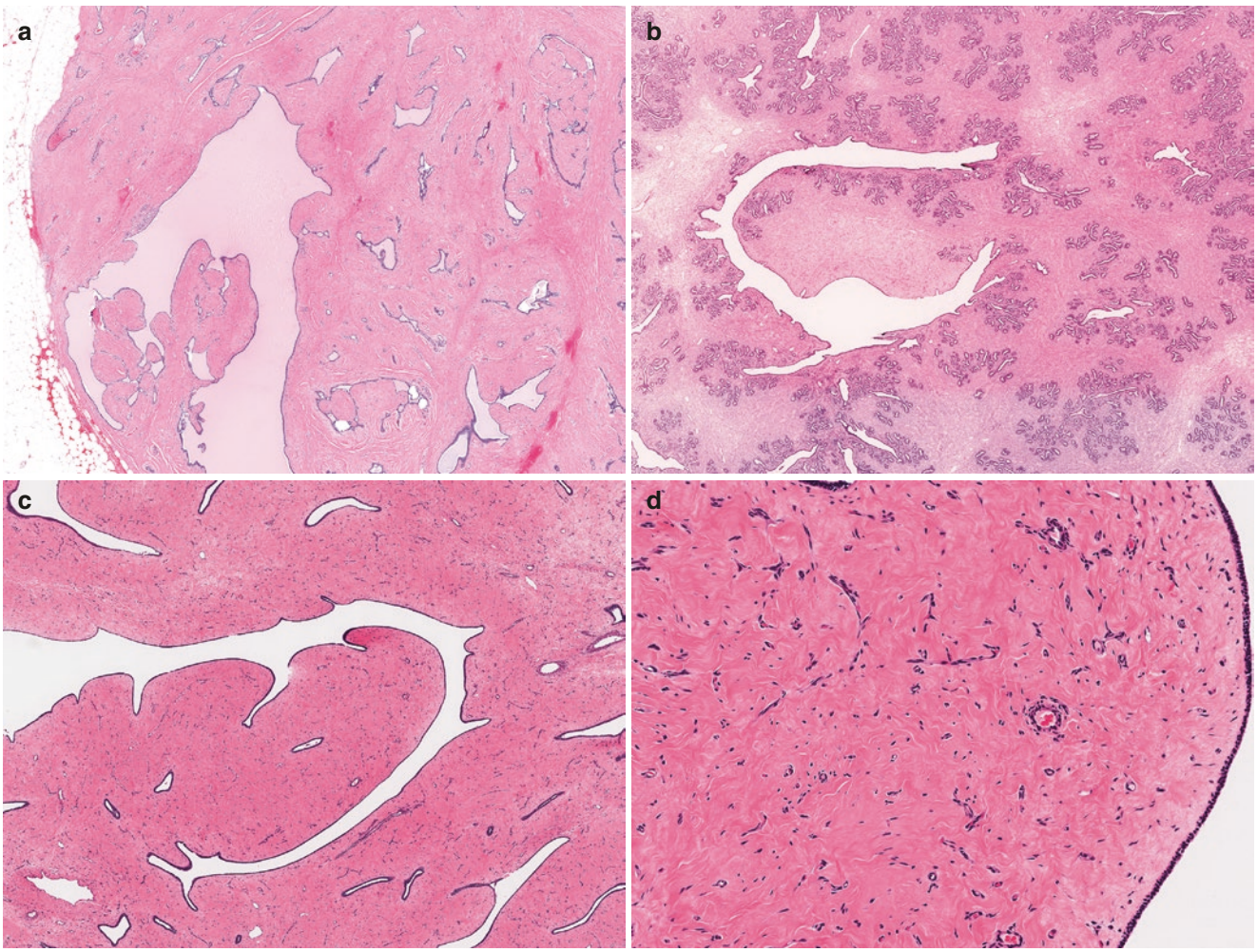

Fig. 7.15 Fibroadenomas with focal frond formation. (**a**) Conventional and (**b**) juvenile fibroadenoma with focal fronds. Fronds in fibroadenomas are typically focal and (**c**, **d**) hypocellular. Their presence should not preclude the diagnosis in the absence of other features of phyllodes tumor

Pathogenesis and Risk Factors

A role for hormonal influence in FA development and growth is suggested by the increased prevalence of FAs in young premenopausal women, regression or hyalinization with age, and increased risk associated with prior estrogen replacement therapy in postmenopausal women [79, 171, 172]. Women with FAs have also been shown to have elevated plasma estradiol levels compared to a control group and harbor single nucleotide polymorphisms (SNPs) in enzymes involved in estrogen metabolism [173]. The expression of ERβ in stromal cells of FA and the association with younger age and increased stromal cellularity can be interpreted as further support of hormonal influence in tumor development [163]. Additionally, the functional interaction of the Mediator complex, of which subunit 12 (*MED12*) is recurrently mutated in the majority of FAs, with ER signaling is consistent with this hypothesis [174–176] (see section "Molecular Pathology"). Studies analyzing associations of oral contraceptive use with risk of FA development are conflicting, with several but not all studies reporting decreased risk with oral contraceptive use [177–182]. Treatment with the selective ER modulator tamoxifen has been associated with decreased proliferative activity of FA stroma [183]. FAs are rare in men and have been associated with hormonal imbalance, such as gynecomastia, exogenous hormone use including estrogen supplementation in male-to-female transexuals, hormone-modulating agents for treatment of prostatic adenocarcinoma, or other drugs such as spironolactone [184–187]. The occurrence of FAs in men in the absence of such risk factors is extremely rare.

Organ transplant patients immunosuppressed with cyclosporine have an increased risk of developing FAs, which tend to be multiple and bilateral. Cyclosporine-associated FAs have been reported following renal, paired renal-pancreas, and liver transplantation, with intervals between transplantation and presentation of a breast mass ranging from 8 months to 13 years [98, 99, 101–104, 188, 189]. The average intervals were reported to be 3.5–4.8 years in larger cohorts [99, 103, 190]. Regression has been reported in some cyclosporine-associated FAs after cessation of cyclosporine treatment and replacement with tacrolimus, whereas others remained stable or decreased in size [191].

Myxoid FAs are associated with Carney complex, an autosomal dominant syndrome also associated with myxomas, spotty pigmentation, endocrine hyperactivity, and melanotic schwannomas [122, 192]. These lesions are often multicentric or bilateral [122]. However, the vast majority of myxoid FAs are sporadic.

Molecular Pathology

Early studies of FAs used cytogenetic analysis or comparative genomic hybridization (CGH) to identify karyotypic abnormalities in up to 44% of FAs. Recurrent chromosome level changes were not consistently identified [193, 194]. Additional studies using polymerase chain reaction (PCR)-based or CGH-based approaches found no evidence of monoclonality in either the epithelial or stromal components of most FAs, although some groups identified monoclonal stroma in FAs with either increased stromal cellularity, "phyllloid-like stromal expansion," or "a phyllodes component" [195–199]. SNP arrays and microsatellite analysis demonstrated only rare loss of heterozygosity (LOH) [200, 201].

More recent DNA sequencing studies have elucidated the genetics of FAs in greater detail and confirm their neoplastic nature. A landmark study by Lim et al. identified recurrent somatic mutations in exon 2 of *MED12* in the majority of FAs by whole exome and targeted sequencing [175]. *MED12* mutations were subsequently identified across the spectrum of fibroepithelial tumors, including 21–86% of FAs, with most aberrations being missense mutations in codon 44 [202–212]. *MED12* mutations were more common in intracanalicular FAs than other growth patterns [206, 208]. Notably, the spectrum of *MED12* mutations identified in FAs and PTs (within exon 2 and especially codon 44) is similar to that of uterine leiomyomas, another benign tumor associated with hormonal dysregulation [175, 213–216]. *MED12* exon 2 mutations were also identified in complex fibroadenomas [204, 217], juvenile FAs [204, 218], tubular adenomas [204], and FAs arising in children and adolescents [218, 219], but have not been identified in myxoid FAs [220]. Some studies have reported lower rates of *MED12* mutations in juvenile versus conventional FAs, which is consistent with the higher incidence of these mutations in tumors with intracanalicular growth [206, 218]. *MED12* mutations were restricted to the stromal component in cases where stroma and epithelium were microdissected and analyzed separately, and mutation status correlated with stromal but not epithelial mRNA and protein expression [175, 206, 217, 221].

MED12, located on the X chromosome, encodes a subunit of the multiprotein transcriptional regulator Mediator complex, which is involved in transcription regulation. MED12, MED13, Cyclin C, and CDK8 or CDK9 comprise a kinase module that interacts with the core Mediator complex to modulate transcriptional activity. MED12 activates the kinase activity of CDK8 through direct interaction of its first 100 amino acids (exons 1 and 2) with Cyclin C. The exon 2 mutations identified in fibroepithelial tumors disrupt this interaction, resulting in global gene expression changes,

which may include ER, Wnt, and TGFβ signaling pathways [176]. With regards to ER signaling, MED12 is known to interact with ERα and ERβ [174], and *MED12* mutations in FAs were found to correlate with dysregulated ER signaling by gene expression profiling [175]. However, the precise roles of *MED12* in the development of fibroepithelial tumors remain to be elucidated.

Other genes are recurrently mutated in FAs at much lower frequencies than *MED12*. Using a customized 16 gene panel of genes implicated in pathogenesis and progression of fibroepithelial tumors, the most frequently mutated genes in a large international cohort were *MED12* (45%), the histone methyl transferase and tumor suppressor *KMT2D* (15%), and the nuclear hormone receptor *RARA* (9%), with less frequent mutations in *FLNA* (6%), *TERT* (6%), *SETD2* (4%), *NF1* (4%), *PIK3CA* (3%), and *BCOR* (3%) [205]. *TERT* encodes the catalytic subunit of telomerase transcriptase, and hotspot mutations in *TERT* promoter have been identified in PTs at high frequency [202, 205, 207, 210, 212, 222, 223]. Some studies have identified *TERT* promoter mutations in a small number of FAs, while others have not [202, 205, 207, 210, 212, 223]. No *TERT* promoter mutations were identified in two series of FAs arising in children and adolescents [218, 219], consistent with the benign nature of these tumors, which can sometimes harbor histologic features otherwise raising consideration for PT [147, 148]. Cellular fibroadenomas have been found to have more frequent *PIK3CA* (9% vs 2%) and *MAP3K1* (4% vs 1%) mutations than conventional FAs [207]. There were no significant differences between FAs that recurred, FAs with subsequent ipsilateral recurrence or contralateral occurrence, and FAs without subsequent events, although the few events in this series limit the analysis.

Prognosis and Clinical Management

Risk of Development of Subsequent Carcinoma

The overall relative risk (RR) of developing subsequent carcinoma of the breast appears to be slightly increased (1.5–2.6) in women with a history of FA and is similar to the risk of other benign proliferative breast diseases [149, 224–228]. However, Dupont et al. reported no increased risk of carcinoma in patients with a history of excised FA without complex features in the absence of a family history of breast cancer [149]. Histologic features of FAs and adjacent non-fibroadenomatous tissue affected the RR estimates. Patients with complex FAs or with benign proliferative disease in adjacent breast tissue demonstrated overall RR of developing subsequent carcinoma of 3.1 and 3.47, respectively, and the risk remained elevated for more than 20 years following diagnosis. However, the increased RR associated with complex FAs was 3.72 in the presence of a family history of breast cancer but decreased to 2.6 in women without a family history, which was not significantly different from women with non-complex FAs without a family history (RR 2.06) [149]. More recently, Nassar et al. also described a slightly elevated subsequent breast cancer risk for women with complex FAs (RR 2.27 versus 1.49 for simple FA), but this was ascribed to other concomitant histologic features (proliferative breast disease and incomplete involution). When stratified by these additional factors, complex FA did not result in increased breast cancer risk [229]. In the study by Dupont et al., the RR associated with FAs showing atypical hyperplasia in the adjacent breast was 7.29, which is higher than the accepted RR (4.1–4.5) of atypical hyperplasia in the absence of FA [149, 230]. McDivitt et al. also reported an increased RR of 6.29 in patients with both FA and atypical hyperplasia, although the location of the atypical proliferation within and/or adjacent to the FA was not described [228]. When atypical ductal or lobular hyperplasia is confined to FAs without involvement of adjacent tissue, the risk for developing subsequent carcinoma is not increased relative to that of the FA alone [231].

Clinical Management and Outcomes

In the absence of cellular stroma, mitotic activity, or other atypical features, a diagnosis of FA can usually be made confidently on CNB, especially in conjunction with the triple approach of correlating pathology, radiology, and clinical features. False negativity rates (i.e., incorrect biopsy diagnosis of FA with subsequent diagnosis of PT on excision) have been estimated to be <1%) [169].

Surgical versus non-surgical treatment of conventional FAs diagnosed on CNB depends on patient preference and risk factors. In the absence of epithelial atypia, radiologic–pathologic discordance, or concerning clinical behavior such as rapid growth, observation with conservative clinical follow-up is a reasonable option, and this approach is recommended by the American Society of Breast Surgeons [126, 232, 233]. Fibroepithelial tumors with cellular stroma on CNB are often excised to exclude PT.

For women undergoing surgical excision, solitary FAs can be enucleated, and most FAs do not recur after complete excision. In a survey-based study of adolescents and young adults, fibroadenomas developed at or near the original surgical site in 12% of respondents [234]. Non-surgical therapeutic options include percutaneous vacuum-assisted image-guided biopsy (Mammotome) and cryoablation [235–245]. In one study, the recurrence rate following vacuum-assisted biopsy was 33%, with only lesions >2 cm showing clinical recurrence [236]. In a study by Kaufman et al. with 2.6 years average follow-up, 84% of FAs in women aged 13–66 years were non-palpable following cryoablation, with lesions ≤2 cm showing a better response compared to lesions >2 cm. Ultrasound revealed a median 99% reduction in FA

volume with treatment, and smaller lesions resorbed faster than larger lesions [239]. Rare residual palpable FAs have been excised following cryoablation due to patient preference, and these were reported to show necrotic debris without viable lesional tissue or "shrunken hyaline matrix with preserved collagenous architecture" [237, 240, 246].

Studies directly addressing management of complex FAs diagnosed on CNB are scarce. In a study of 20 complex FAs initially diagnosed on CNB, one was reclassified as benign PT on excision, and another with atypical lobular hyperplasia on biopsy was upgraded to invasive lobular carcinoma on excision [150]. Complex FAs are generally managed using the same principles as conventional FA.

Patients with juvenile FAs are not considered to be at increased risk for subsequent development of PTs or carcinoma [91, 151]. Although objective data are limited, most patients with juvenile FAs undergo excision, given the often large and rapidly growing size of these lesions in adolescents and the inability to definitively exclude PT on CNB [247, 248]. Excision should aim to preserve as much breast tissue as possible in adolescent girls in order to allow for proper breast development [91, 247, 249, 250]. Normal breast development can be seen after surgery, even in cases with only limited residual breast tissue remaining after excision [91]. In a study of juvenile FAs in adolescent girls, none of the solitary lesions recurred after local excision with or without a rim of normal adjacent tissue after a mean follow-up period of 3.8 years, whereas all six girls with multiple lesions developed additional lesions within 18 months following initial excision [91].

Excision is generally recommended for FAs with atypical ductal hyperplasia diagnosed on CNB. FAs with associated carcinoma should be managed similar to breast carcinoma in the usual setting [251].

Phyllodes Tumor

Overview and Clinical Presentation

PTs are biphasic epithelial and stromal neoplasms characterized by stromal hypercellularity and often characteristic exaggerated leaf-like intracanalicular architecture, with recurrence and/or metastatic potential, the likelihood of which varies along a spectrum from benign to malignant [252]. Johannes Mueller initially named these lesions *cystosarcoma phyllodes* in 1838 to reflect their fleshy, leaf-like, and sometimes cystic appearance [253]. However, this term is no longer used, as most PTs are benign, without sarcomatous features or aggressive behavior.

PTs are rare, reported to represent between 0.3% and 1% of all primary breast tumors and 2.5% of fibroepithelial tumors in women of European descent [252]. Because incidence studies are from tertiary care centers, the true incidence is likely to be lower [126]. The relative frequencies of benign, borderline, and malignant PTs are ~60–75%, 15–26%, and 8–20% [252, 254–257]. The average age at presentation is 40–50 years in most studies, which is 10–20 years older than that of FA [252, 257–264]. A Surveillance Epidemiology and End Results (SEER) study reported a mean age of 50 years for malignant PTs [262]. Although PTs are overall not common in women under 30 years old and are rare before menarche, they may present in essentially any age group, including children [147, 148, 265–269]. Most but not all PTs in children are benign [147, 148, 266–271].

PTs are more common in Asian and Latina white women, and these tumors may present at an earlier age [16, 252, 259]. In a study of Asian women of multiple ethnic backgrounds, the overall incidence of PT was 3.8%, and the average age of presentation was 25–30 years, with up to one-third of patients presenting in adolescence [16]. Latina white women born in Mexico, Central or South America have a three- to fourfold increased risk of developing malignant PTs compared to Latina white women born in the United States [259]. Asian women may also be at increased risk of recurrence [254].

PTs are rare in men, in whom they have been associated with gynecomastia, suggesting a role for hormonal imbalance in development [184, 272–277]. Consistent with a hormonal role in development, PTs have been reported during pregnancy or following in vitro fertilization in women [278–281].

PT often presents as a rapidly growing new mass or as rapid growth of a previously stable lesion [263, 264, 282, 283]. Gordon et al. suggested that PTs have a faster detectable growth rate as measured by ultrasound than FAs [284]. The average tumor size is 4–5 cm, but smaller tumors are detected due to screening mammography [254, 257, 258, 260, 263, 273, 285–288], and giant tumors >30 cm have been reported [289–291]. In a large study of 605 PTs, sizes ranged from 0.3 to 25 cm, with an average of 5.2 cm [257]. Malignant tumors can be larger than benign tumors, but there is broad overlap [254, 258, 288, 292]. In a study of 335 PTs, average tumor sizes were 4.3, 8.1, and 9.2 cm for benign, borderline, and malignant PTs, respectively, but ranged from 2 cm or less to more than 20 cm across all tumor grades [288]. Large tumors may cause skin discoloration, thinning, dilated subcutaneous veins, or ulceration [263, 264, 282, 287]. In one study, skin ulceration was found in 3 of 335 cases (all tumors ≥16.5 cm), two of which were malignant and one of which was borderline [288]. Tumors may invade the chest wall [263, 264, 293]. Bloody nipple discharge can occur from spontaneous infarction [294]. The vast majority of PTs are unilateral and clinically unifocal [254, 257, 258, 260, 263, 273, 285–287, 293], although satellite nodules may be iden-

tified on pathologic examination. Rare bilateral tumors have been reported [258, 263, 286, 288]. The left and right breasts are involved with approximately equal frequency [257, 263, 273, 295, 296]. The most common single site appears to be the upper outer quadrant, but larger tumors more often span multiple quadrants [263, 296]. Although axillary lymphadenopathy is relatively common at presentation (up to 20% of patients), lymph node metastases are very rare [264, 273, 285, 297–300]. In a SEER study of 1035 PTs, one-quarter of patients had some type of lymphadenectomy and 9% had at least ten lymph nodes removed, but nodal metastases were identified in only nine patients [299]. Rare cases of hypoglycemia associated with PTs have been described [301–304].

Gross and Radiologic Features

Mammography of PT usually reveals a rounded non-spiculated mass with smooth or lobulated borders and homogenous density [295, 305, 306]. A peripheral halo can be seen in some cases, due to compression of adjacent breast parenchyma [295, 305, 306]. A minority of tumors demonstrates areas of border irregularity, and tumors with loss of margin definition can mimic carcinomas radiologically [305, 306]. Calcifications are rarely identified and can be present in benign or malignant tumors, including tumors with necrosis or osseous differentiation [295]. Internal fat density has also been described in tumors with fatty metaplasia or liposarcoma-like differentiation [295]. By ultrasound, PTs similarly present as well-rounded oval or lobulated masses [305, 307]. Cysts and internal echoes with a heterogeneous pattern are often present [295, 305, 307]. Typical MRI findings of PTs include a round or lobulated mass with well-defined margins and heterogeneous internal structure with internal septations. Reliable distinction of PT from FA or among PT grades is not always possible by mammography, ultrasound, or MRI [120, 295, 305, 307–311]. In one MRI study, up to one-third of PTs (and 23% of FAs) showed contrast enhancement features suspicious for invasive carcinoma [120]. Admietz et al. studied PTs and FAs by real-time elastography and found that PTs often demonstrate an elastic center with a peripheral inelastic rim, which was present in only 5% of FAs [312].

PTs vary in gross appearance, due to tissue heterogeneity within and between tumors. Most tumors are well-circumscribed on gross examination and are often surgically enucleated without definitive preoperative diagnosis [252, 288]. Even tumors with microscopic tissue infiltration are usually macroscopically circumscribed. Smaller satellite nodules may be present at the periphery. The cut surface is usually tan-pink or gray and bulging and may be firm, mucoid, and/or fleshy. A characteristic finding is the presence of a whorled surface with curvilinear clefts and/or cystic spaces. However, smaller lesions may appear more homogenous [252]. Norris and Taylor noted gelatinous or translucent areas in 56% and cystic areas in 33% of tumors in their series [263]. Malignant PTs with extensive stromal overgrowth can appear solid, firm, and fibrous. Adipose metaplasia or liposarcoma-like elements are soft and yellow. Tumors with chondroid or osseous elements may be gritty or show frank cartilage or bone formation. Grossly evident necrosis or hemorrhage can be seen, especially in larger tumors, but is not common [263, 288]. Overlying skin may be ulcerated.

Microscopic Features

Histological Features

PTs are fibroepithelial neoplasms with stromal proliferation resulting in increased stromal cellularity. Classically, these tumors demonstrate an exaggerated intracanalicular growth pattern, with leaf-like stromal fronds surfaced by epithelium that protrude into dilated clefts or cyst-like spaces (Fig. 7.16 and 7.17). Well-developed stromal fronds are bulbous and may have smaller invaginating clefts or notches along their convexity. The stromal proliferation is often more pronounced in the area immediately subjacent to the epithelium, which has been referred to as periepithelial or subepithelial condensation or accentuation [252]. Mitotic activity may be increased in the subepithelial zone (Fig. 7.18). The combination of increased stromal cellularity and leaf-like architecture with or without subepithelial stromal accentuation can be used to distinguish PTs from FAs in classic cases. However, stromal fronds may be focal or absent in some PTs. Some tumors instead have elongated branching, clefted ducts, sometimes with a staghorn-like appearance, embedded within the cellular stroma (Fig. 7.19) [252, 313]. Stromal mitotic activity and atypia are variable and are important parameters for tumor grading. Marked stromal proliferation may give rise to stromal overgrowth, defined as the disproportionate proliferation of stroma with lack of epithelium in at least one low-power microscopic field, i.e., at 40× (4× lens with 10× ocular) magnification [252, 314]. Stromal overgrowth is typical of malignant tumors and may be focally present in some borderline tumors but is not a feature of benign tumors [252, 314, 315]. Although stromal hypercellularity is one of the key features of PTs, cellularity is not infrequently heterogeneous, as is the relative distribution of stroma and epithelium. Stromal het-

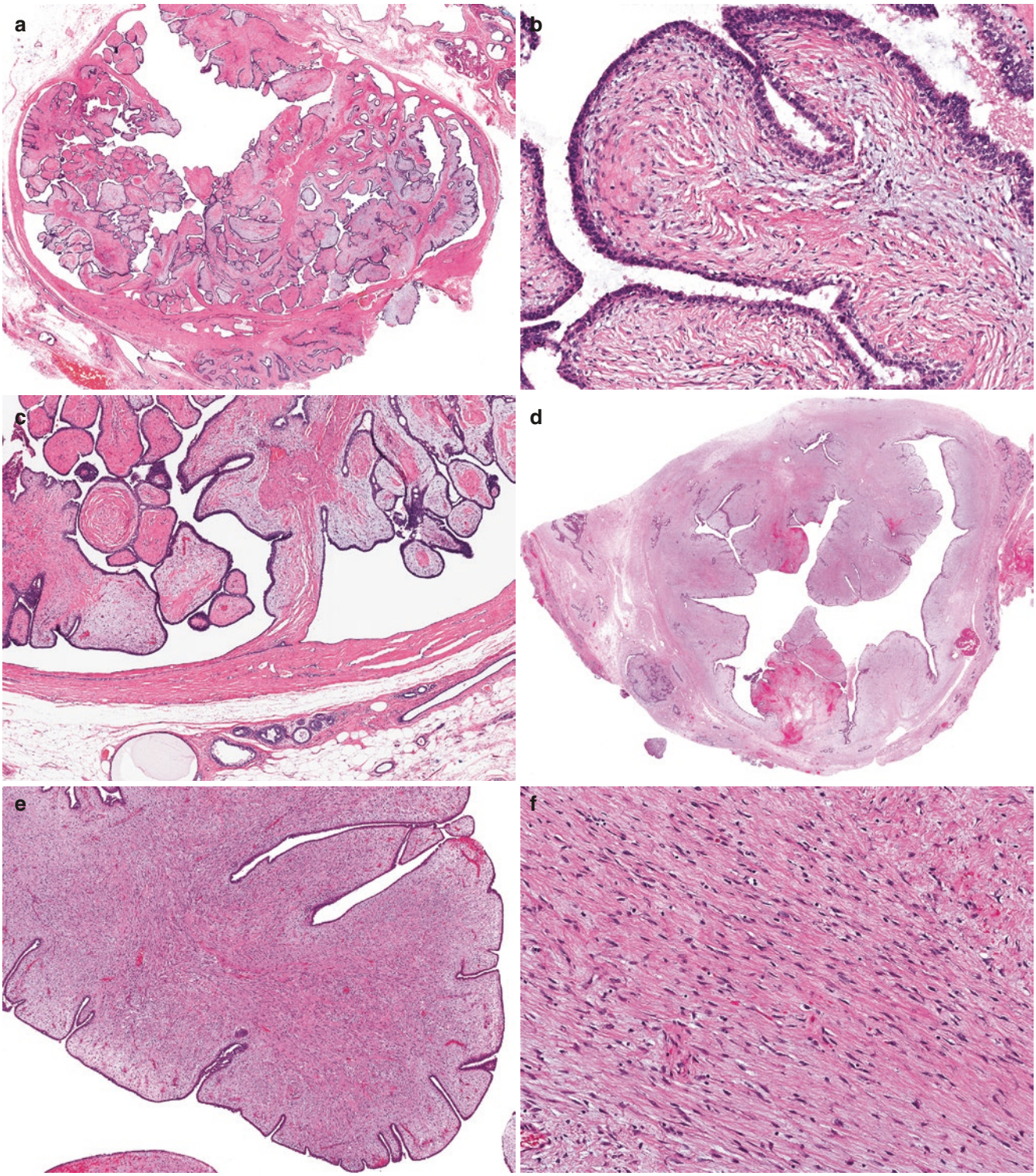

Fig. 7.16 Benign phyllodes tumor. (**a**–**c**) Benign phyllodes tumor showing circumscribed, pushing borders and well-developed leaf-like architecture, with epithelium-lined stromal fronds protruding into enlarged cystic spaces. (**d**–**f**) Another benign phyllodes tumor with similar features. (**b**, **e**, and **f**) Stroma is mildly hypercellular, with closely spaced and occasionally touching nuclei but infrequent nuclear overlap. There is no stromal overgrowth. Mitotic activity is low (0–4 mitotic figures/10 HPF)

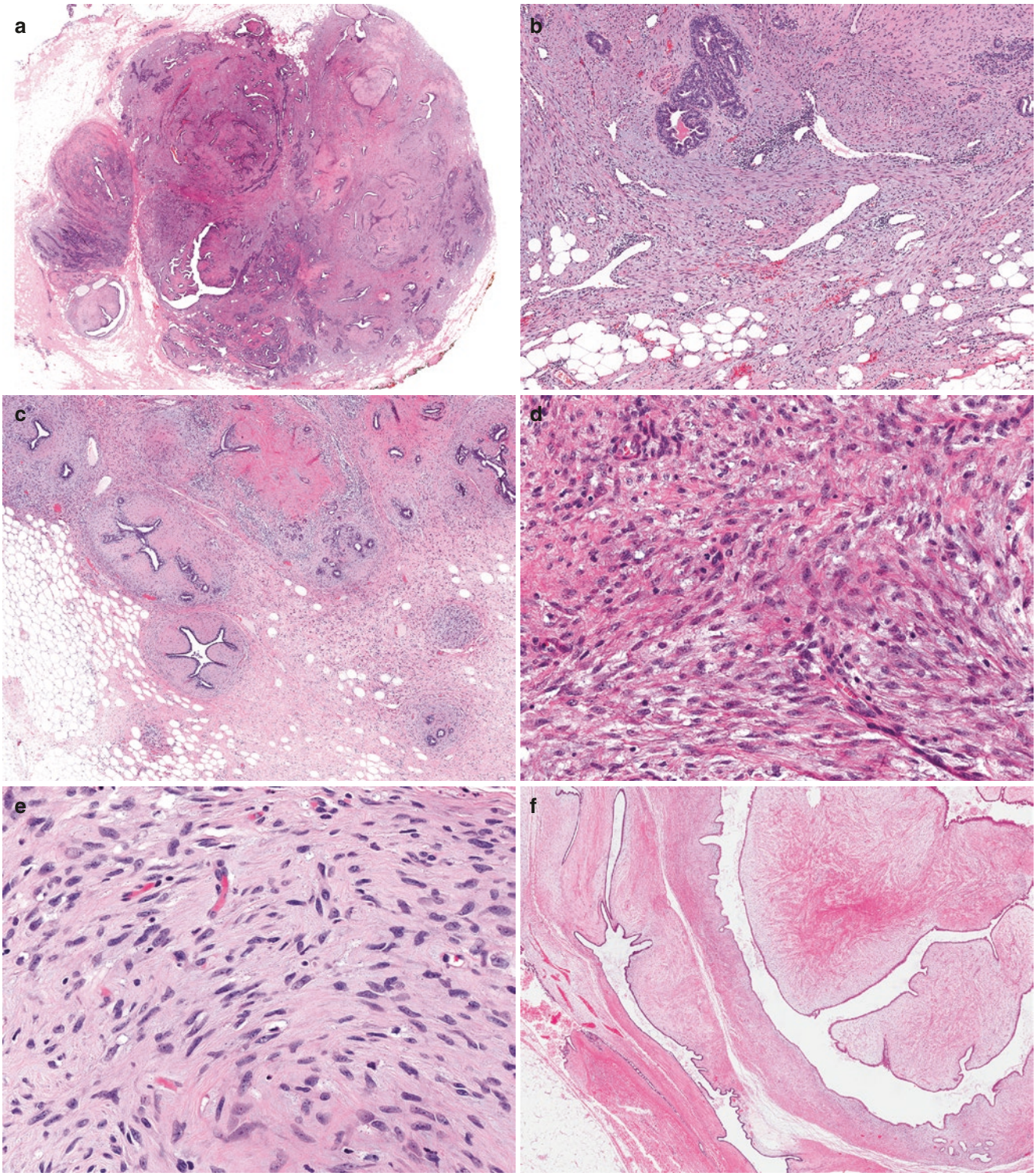

Fig. 7.17 Borderline phyllodes tumor. Borderline phyllodes tumors have features that are intermediate between benign and malignant tumors or demonstrate some but not all of the features of malignancy. (**a**–**c**) The tumors often have at least focally infiltrative tumor borders, with extension into the adjacent parenchyma. (**d**) Moderately hypercellular stroma can be seen, but cellularity can be heterogeneous. Mitotic activity is intermediate (5–9 per 10 HPF). (**e**) Moderate stromal cell atypia. (**f**–**h**) This borderline tumor had a circumscribed pushing border, well-developed leaf-like growth and mostly mild stromal hypercellularity. (**g**) However, a focal area of marked hypercellularity with (**h**) increased mitotic activity and moderate to severe cytologic atypia was present

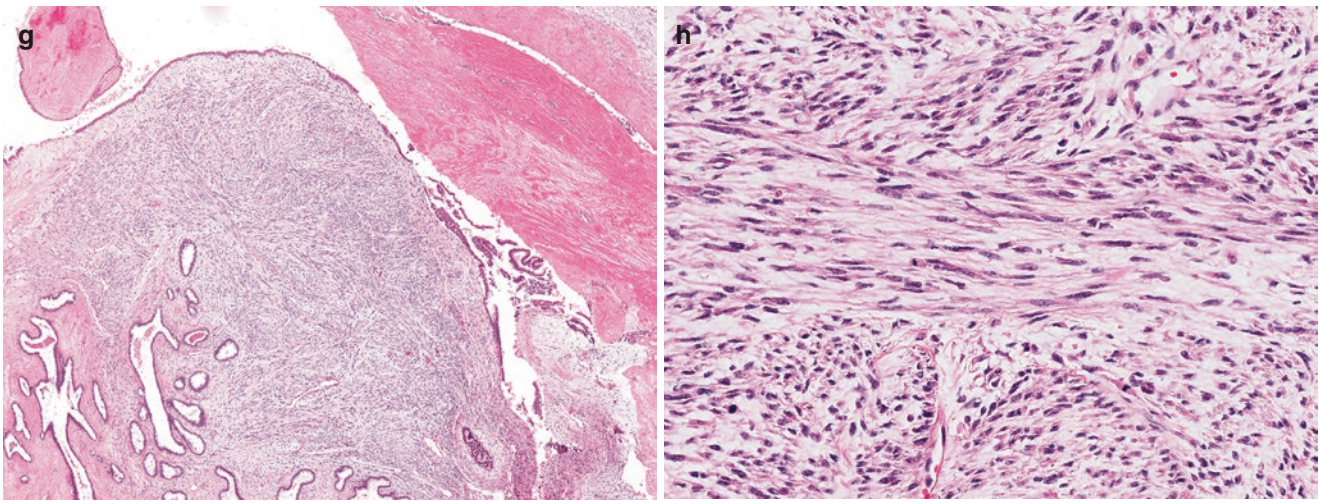

Fig. 7.17 (continued)

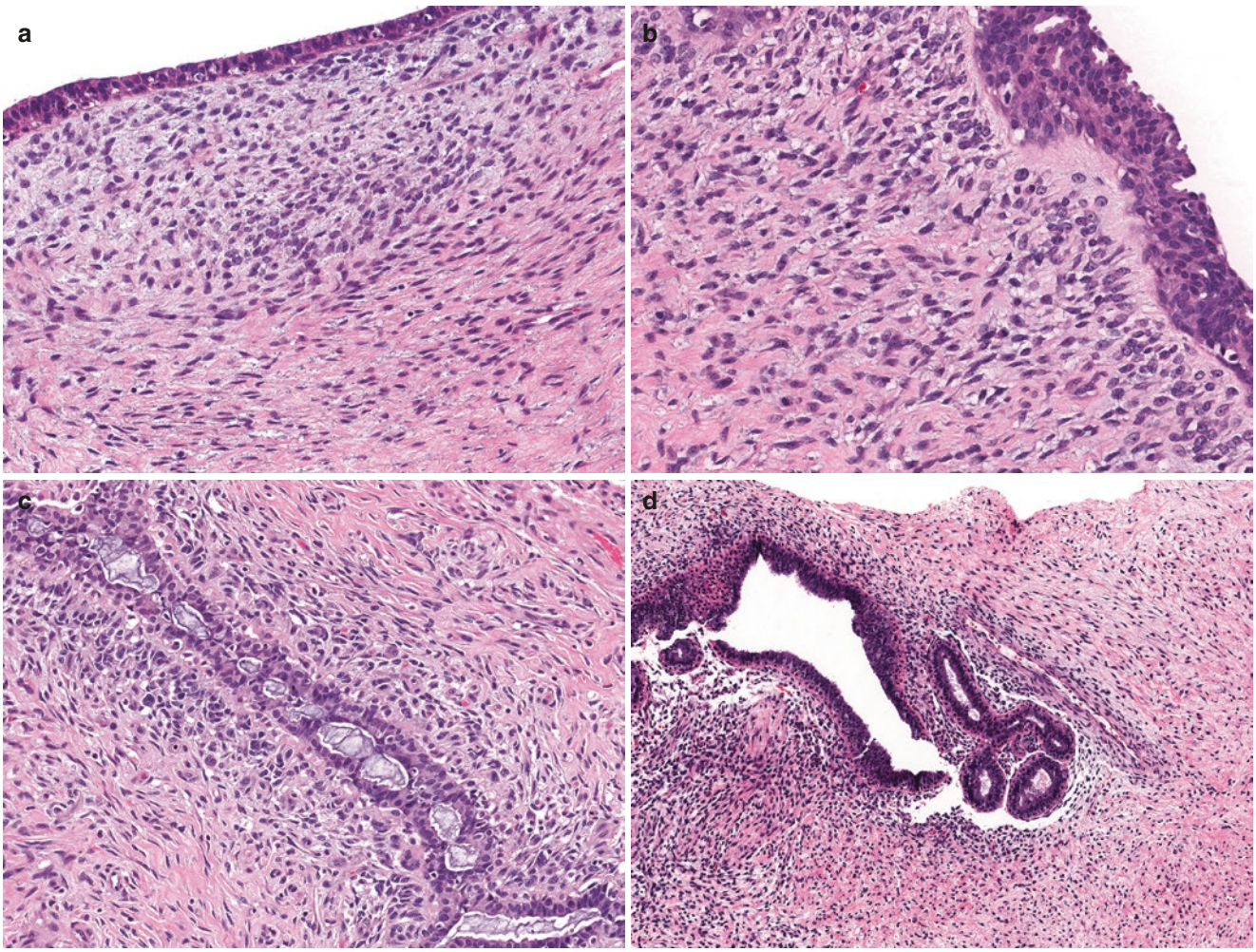

Fig. 7.18 Subepithelial stromal condensation of accentuation. (**a**–**d**) Increased density of the stromal proliferation in subepithelial zones is a useful feature in the diagnosis of phyllodes tumor. Mitotic activity is often increased in these areas

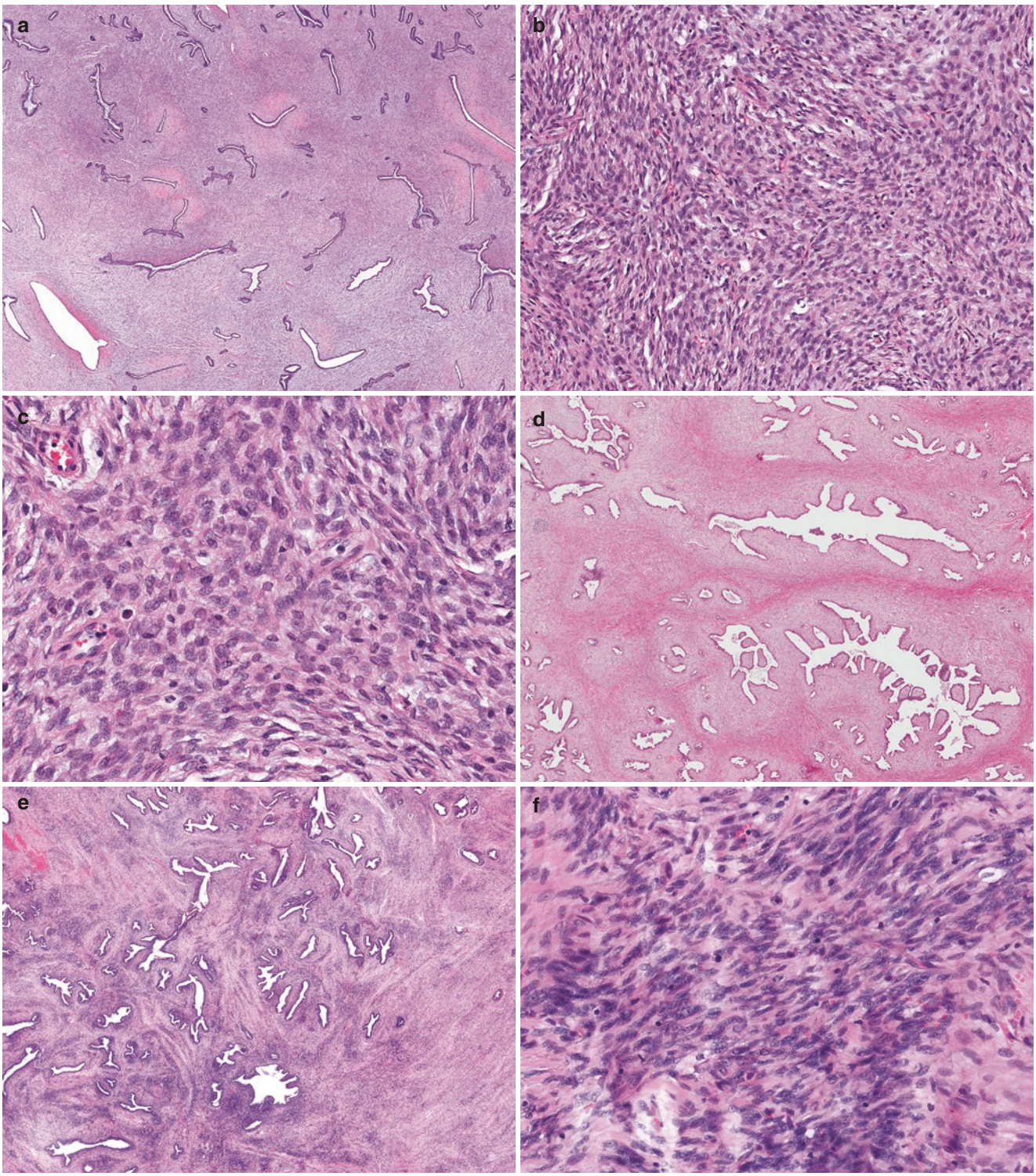

Fig. 7.19 Phyllodes tumors without leaf-like growth pattern. (**a**) This phyllodes tumor lacks leaf-like growth and shows relatively evenly distributed epithelial and stromal components. (**b**, **c**) However, stromal cellularity is moderate to marked, with sheets of closely packed and frequently overlapping nuclei, which is in excess of what is seen in cellular fibroadenomas. Mitotic activity was 4 per 10 HPF. (**d**, **e**) Other phyllodes tumors without well-developed stromal fronds, instead showing ducts with staghorn-like appearance embedded in cellular stroma. (**f**) Higher power magnification of the tumor in (**e**), with markedly cellular stroma and mitotic figures

erogeneity includes the presence of FA-like areas in some PTs (Figs. 7.20 and 7.21), and may infrequently lead to underdiagnosis in CNB or fine-needle aspiration biopsies if diagnostic cellular areas are not sampled (see section "Differential Diagnosis"). The stroma can vary from myxoid to hyalinized to more fibrous. Most (~87%) PTs in one large series showed myxoid degeneration [288]. PASH (Fig. 7.22) was described in ~73% of cases in one study, being more common in benign (~76%) compared to borderline (18%) or malignant (~6%) tumors [288]. In a core biopsy, the presence of PASH in a fibroepithelial tumor can raise consideration of PT over a cellular FA, and together with other features, would raise enough suspicion to advocate excisional biopsy for the patient. Multinucleated stromal giant cells may be present [135, 137]. One group reported the presence of stromal giant cells in ~9% of PTs, with increasing numbers correlated with increasing grade [288]. Benign stromal giant cells are typically focal and distinct, with degenerative-type atypia compared to background stromal cells, but distinction from neoplastic tumor cells can sometimes be problematic. In such cases, irregular nuclear borders, lack of degenerative-type chromatin, vesicular chromatin, prominent nucleoli, and especially mitotic figures favor neoplastic atypia (Fig. 7.22). Benign metaplastic stromal changes may be seen but are rare, with one series reporting an incidence of 0.3% each for benign adipose metaplasia and benign chondromyxoid metaplasia (Fig. 7.22) [288]. Heterologous differentiation is most commonly liposarcoma-like, although the presence of lipo-

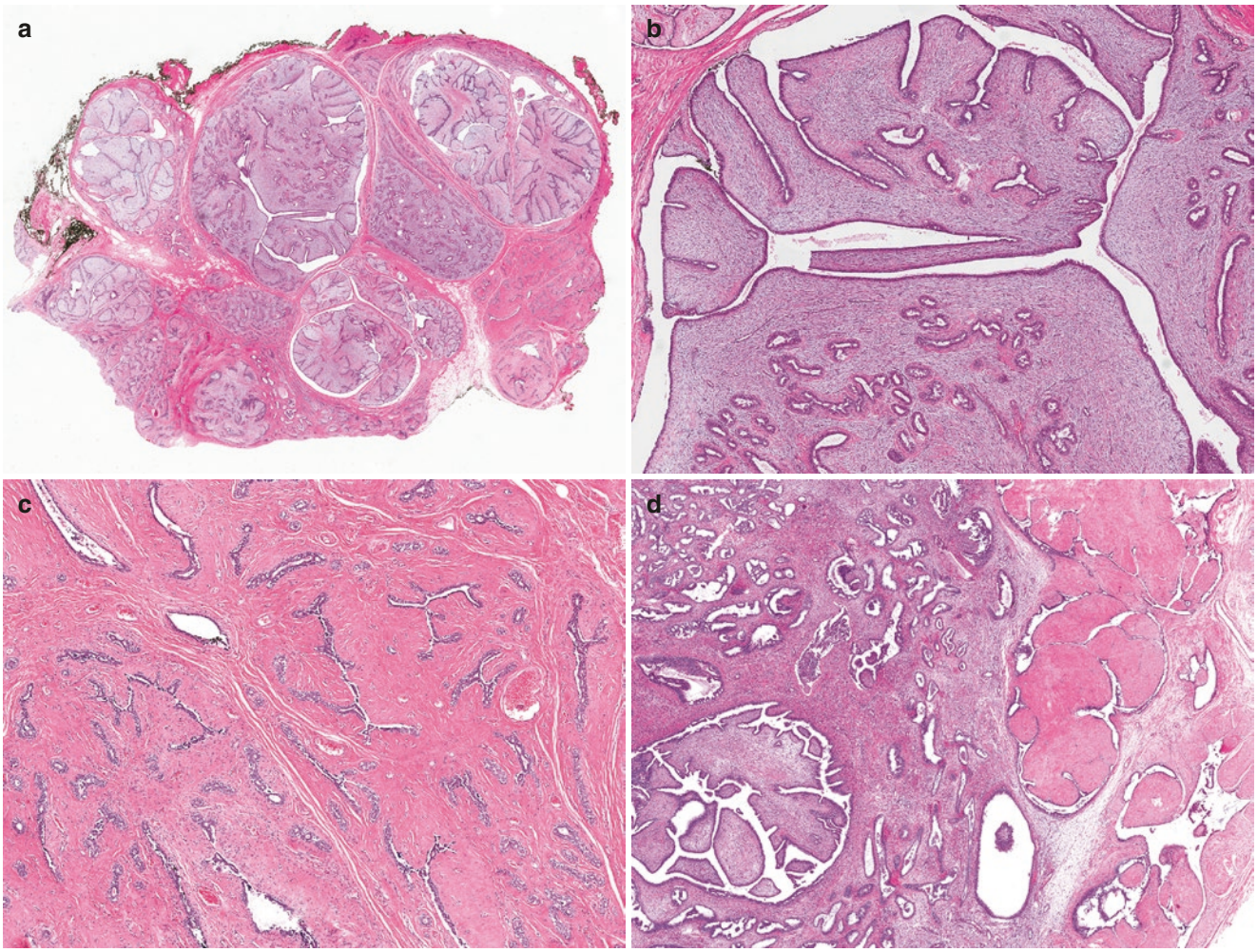

Fig. 7.20 Stromal heterogeneity in phyllodes tumors. (**a**–**c**) Benign phyllodes tumor with stromal heterogeneity, characterized by (**b**) areas of leaf-like growth and hypercellular stroma, and other areas of (**c**) hypocellular, hyalinized stroma indistinguishable from intracanalicular pattern fibroadenoma (lower right in (**a**)). (**d**) Another heterogeneous phyllodes tumor with fibroadenoma-like area (right) adjacent to hypercellular phyllodal area (left)

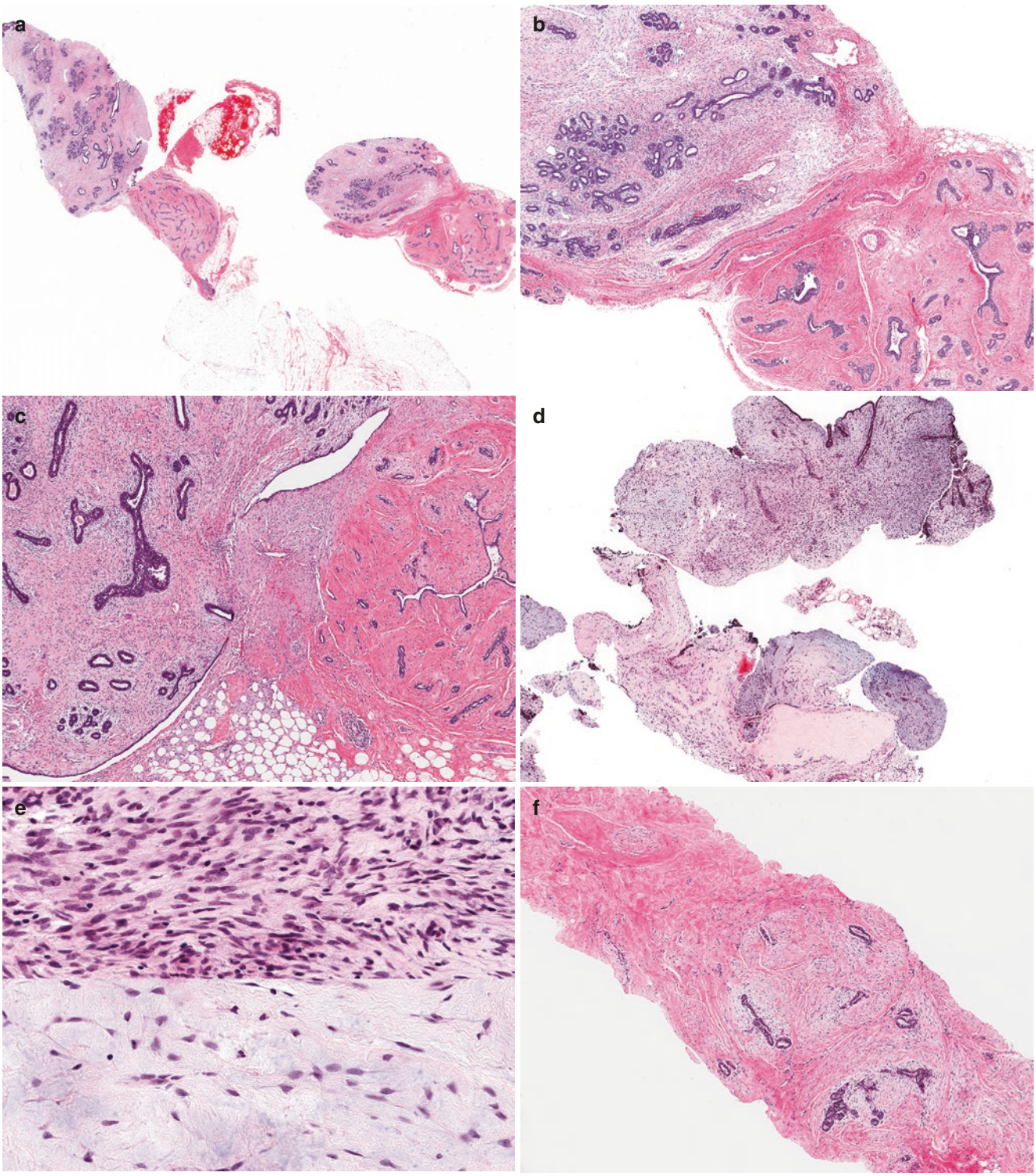

Fig. 7.21 Core-needle biopsy can sometimes reveal the stromal heterogeneity of phyllodes tumors. (**a**, **b**) Hyalinized hypocellular fibroadenoma-like foci adjacent to areas of stromal hypercellularity on core biopsy. (**c**) Excision revealed a phyllodes tumor with similar features. (**d**, **e**) Another core biopsy of phyllodes tumor showing stromal heterogeneity between core fragments. (**f**) Core biopsy of a mass presenting in a 36-year-old woman with mildly cellular fibroadenomatous change. (**g–i**) Excision revealed a borderline phyllodes tumor with marked stromal heterogeneity, including (**h**) hypercellular areas with stromal fronds and (**i**) areas reminiscent of fibroadenoma. (**j**, **k**) Core biopsy of a 3.8 cm lobulated mass in a 59-year-old woman showing a spindle cell neoplasm with moderate stromal cellularity and no epithelial component. (**l–n**) Excision revealed a heterogeneous borderline phyllodes tumor, with (**m**) hypercellular and infiltrative stromal overgrowth adjacent to (**n**) fibroadenoma-like areas at the periphery. The biopsy did not sample the areas of fibroepithelial growth

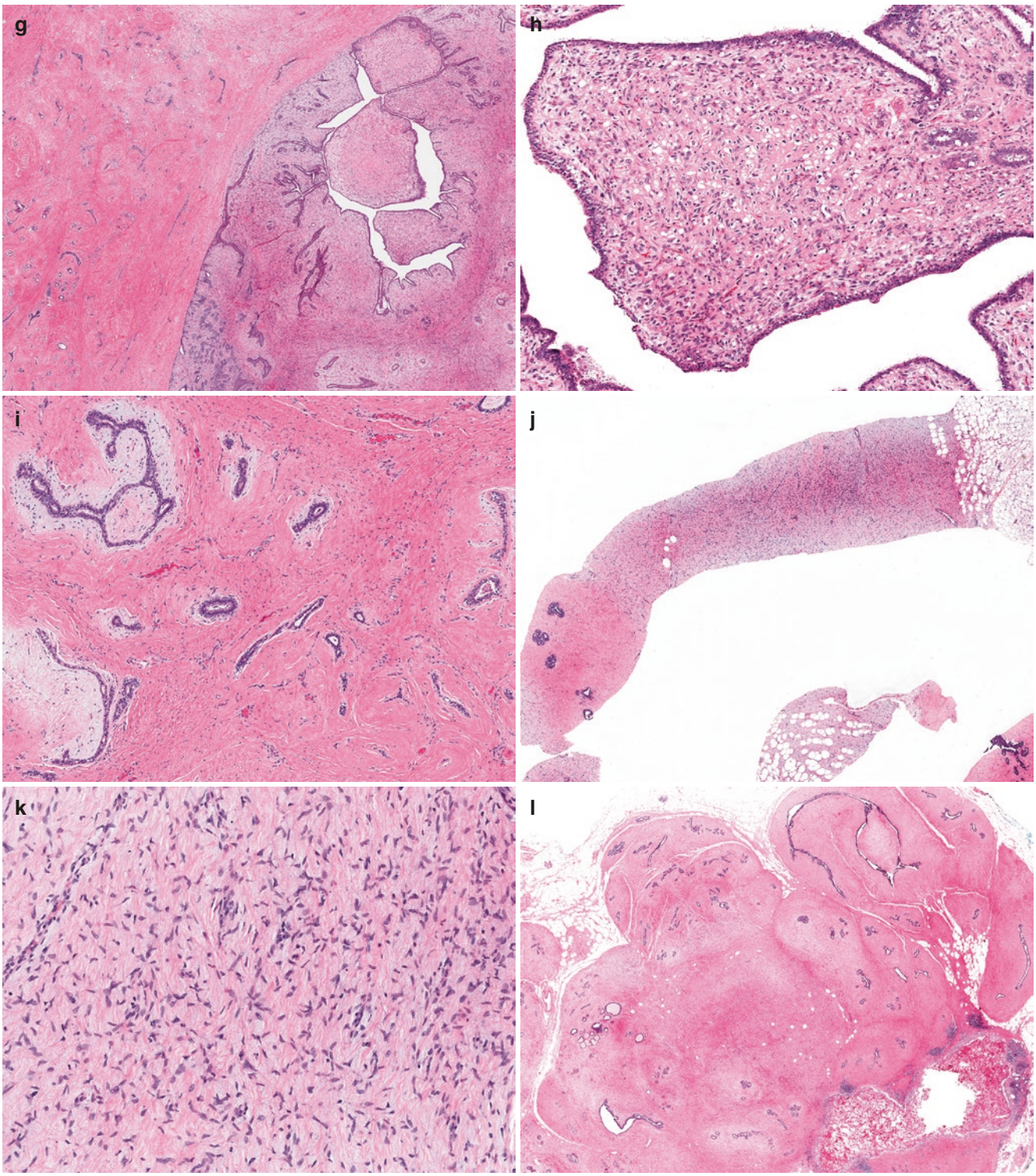

Fig. 7.21 (continued)

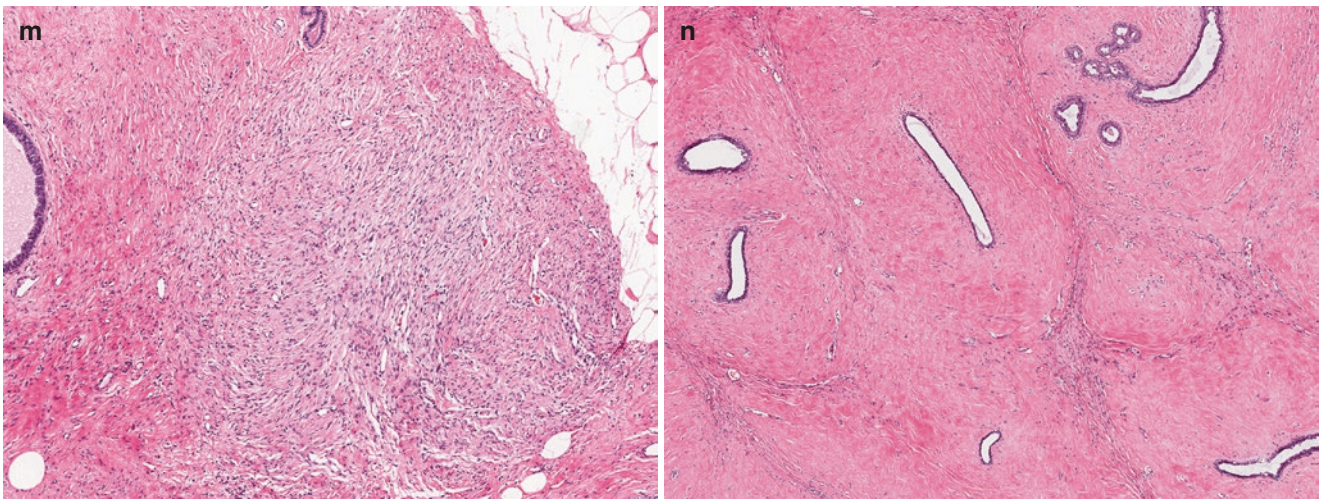

Fig. 7.21 (continued)

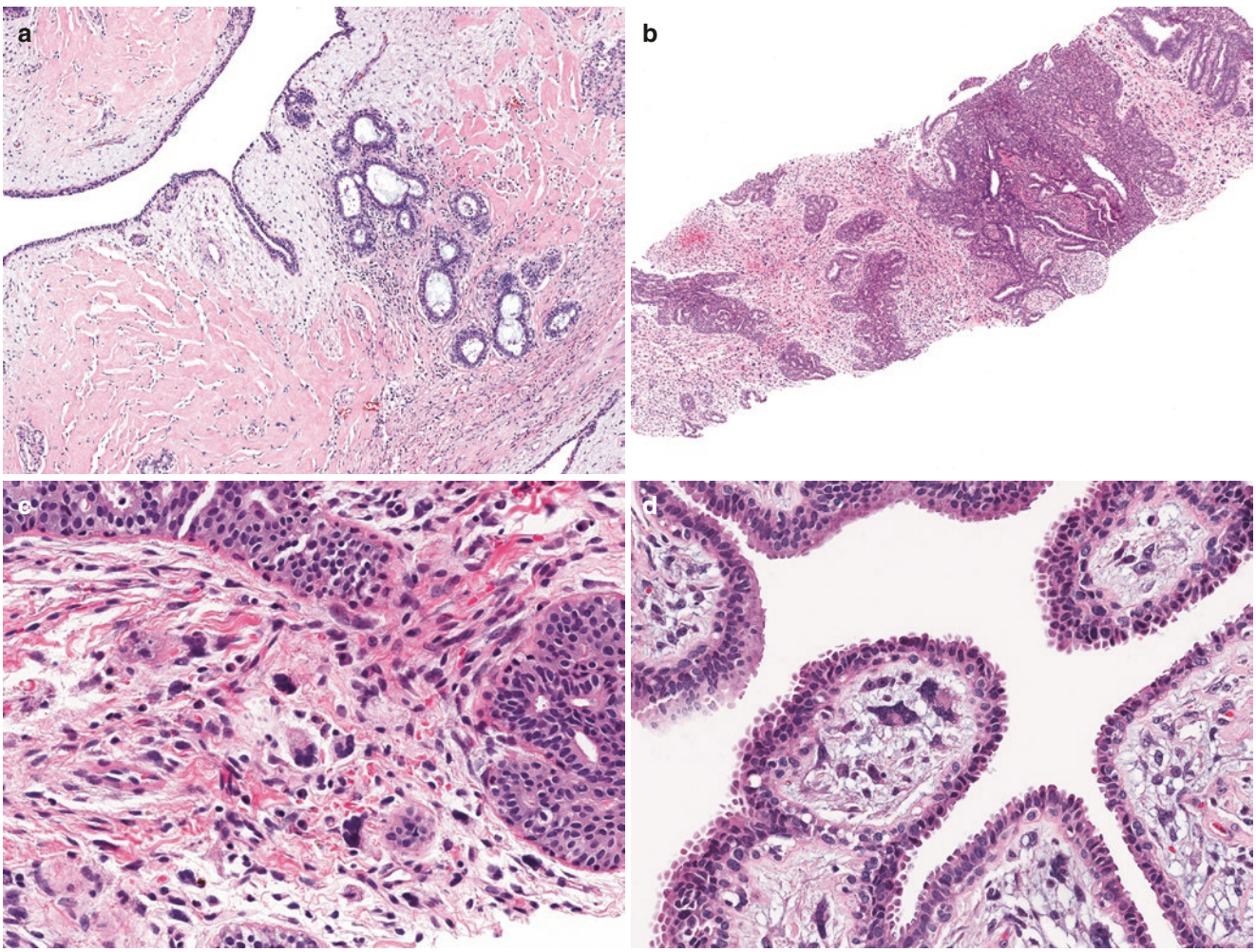

Fig. 7.22 Stromal changes in phyllodes tumor. (**a**) Pseudoangiomatous stromal hyperplasia. (**b**, **c**) Benign multinucleated stromal giant cells in a phyllodes tumor with usual ductal hyperplasia on core biopsy. Note the degenerative-like chromatin of the multinucleated cells and floret cells. (**d**–**g**) In contrast, neoplastic stromal giant cells of phyllodes tumor, with marked atypia and (**e**) mitotic activity. (**g**) Diffuse p53 positivity of the atypical multinucleated cells and background spindled cells in this case (same as (**g**)). (**h**–**j**) Myoid metaplasia, characterized by interlacing bundles of slender spindled cells with eosinophilic cytoplasm and elongated bland nuclei, which were positive for smooth muscle markers (desmin in (**j**)). (**k**, **l**) Lipomatous metaplasia in phyllodes tumor

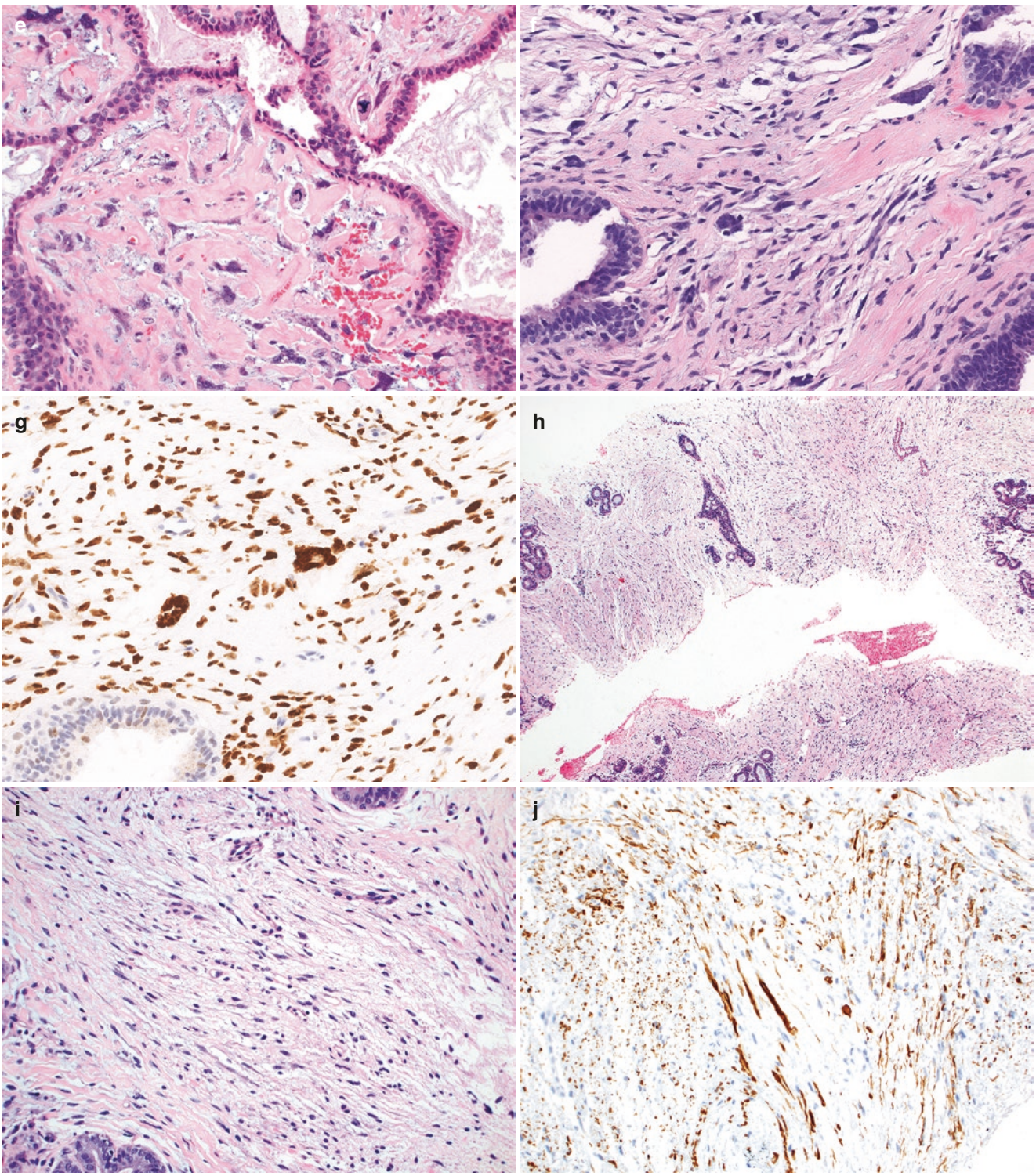

Fig. 7.22 (continued)

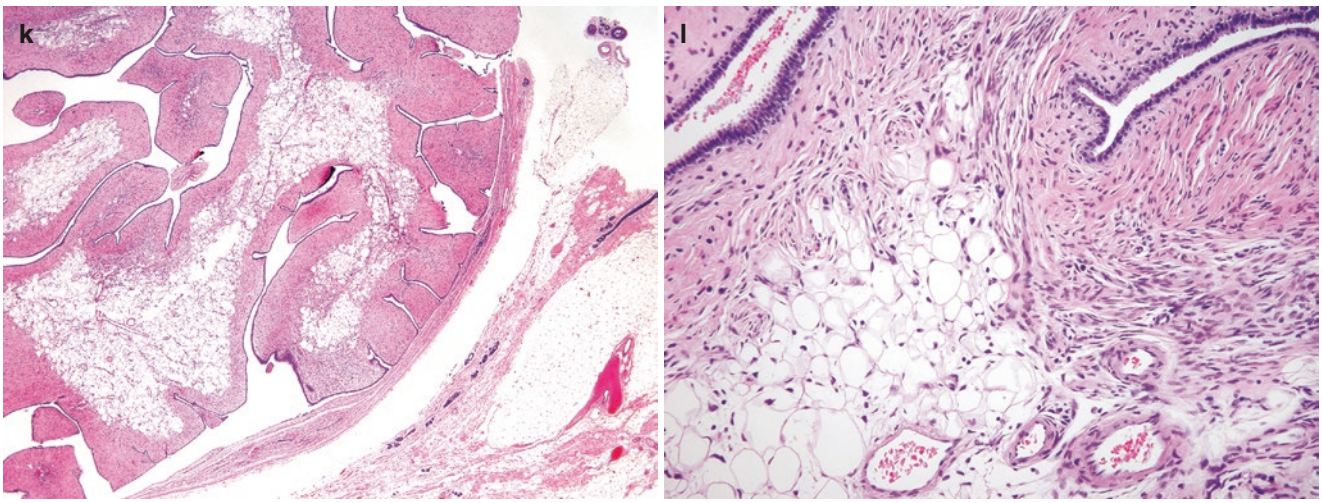

Fig. 7.22 (continued)

sarcoma within a PT is no longer considered a diagnostic feature of malignancy in the World Health Organization (WHO) classification of breast tumors [252]. Less common malignant heterologous elements, which are by themselves diagnostic of malignancy, include chondrosarcoma, osteosarcoma, and rhabdomyosarcoma (Fig. 7.23) [252, 257]. Mamoon et al. described an exceedingly unusual case of angiosarcoma arising in a recurrent PT [316].

The epithelium consists of bilayered luminal epithelium and myoepithelium. Usual ductal hyperplasia is not uncommon, with approximately 37%, 28%, and 9% of tumors showing mild, moderate, and florid hyperplasia in one study (Fig. 7.24e, f) [288]. Apocrine or squamous metaplasia may be present, the latter of which may line ducts or form squamous cysts (Fig. 7.24a–d) [254, 263, 288, 317]. Calcifications are rare and can be seen in association with epithelium or stroma. Atypical ductal or lobular hyperplasia is rare in PTs, and in situ or invasive ductal or lobular carcinoma is even less common (Fig. 7.24g–n) [318–323]. In a large study by Tan et al., only one malignant PT (0.03% of tumors in this series) showed ductal carcinoma in situ (DCIS), five cases (1.5%) showed atypical ductal hyperplasia, and 1 case (0.03%) each showed atypical lobular hyperplasia and lobular carcinoma in situ (LCIS) [288]. PTs of all grades may infarct, but tumor necrosis is far less common and mostly present in malignant tumors (Fig. 7.25) [288]. The ipsilateral or contralateral breast parenchyma may contain FAs or fibroadenomatous change, and some studies have correlated the presence of synchronous ipsilateral FAs or fibroadenomatous change with tumor recurrence [258, 288, 324–327]. Adjacent satellite PT nodules may also be seen.

Periductal stromal tumors are characterized by concentric stromal proliferations around dilated, non-compressed ducts, with adjacent proliferative nodules coalescing to form a larger mass (Fig. 7.26a–d). Because periductal stroma tumors may recur as PTs, and areas resembling periductal stromal tumor can be seen in some PTs, they are considered PT variants and are classified as a PT subtype in the WHO classification of breast tumors [252, 328]. The term p*eriductal stromal sarcoma* was originally used to describe tumors with moderate stromal cell atypia, at least three mitotic figures per 10 HPF, and infiltrative growth, whereas *periductal stromal hyperplasia* was non-infiltrative with less cytologic atypia and mitotic activity (Fig. 7.26e, f) [328]. Defined as such, 1 of 20 sarcomas recurred locally (and 1 distally), as did 1 of 7 hyperplasias. The term *sarcoma* is discouraged in lieu of *tumor* to more accurately reflect the variable but often non-malignant behavior. Associated ducts may show usual ductal hyperplasia, and associated PASH has been described in the adjacent tissue [328, 329].

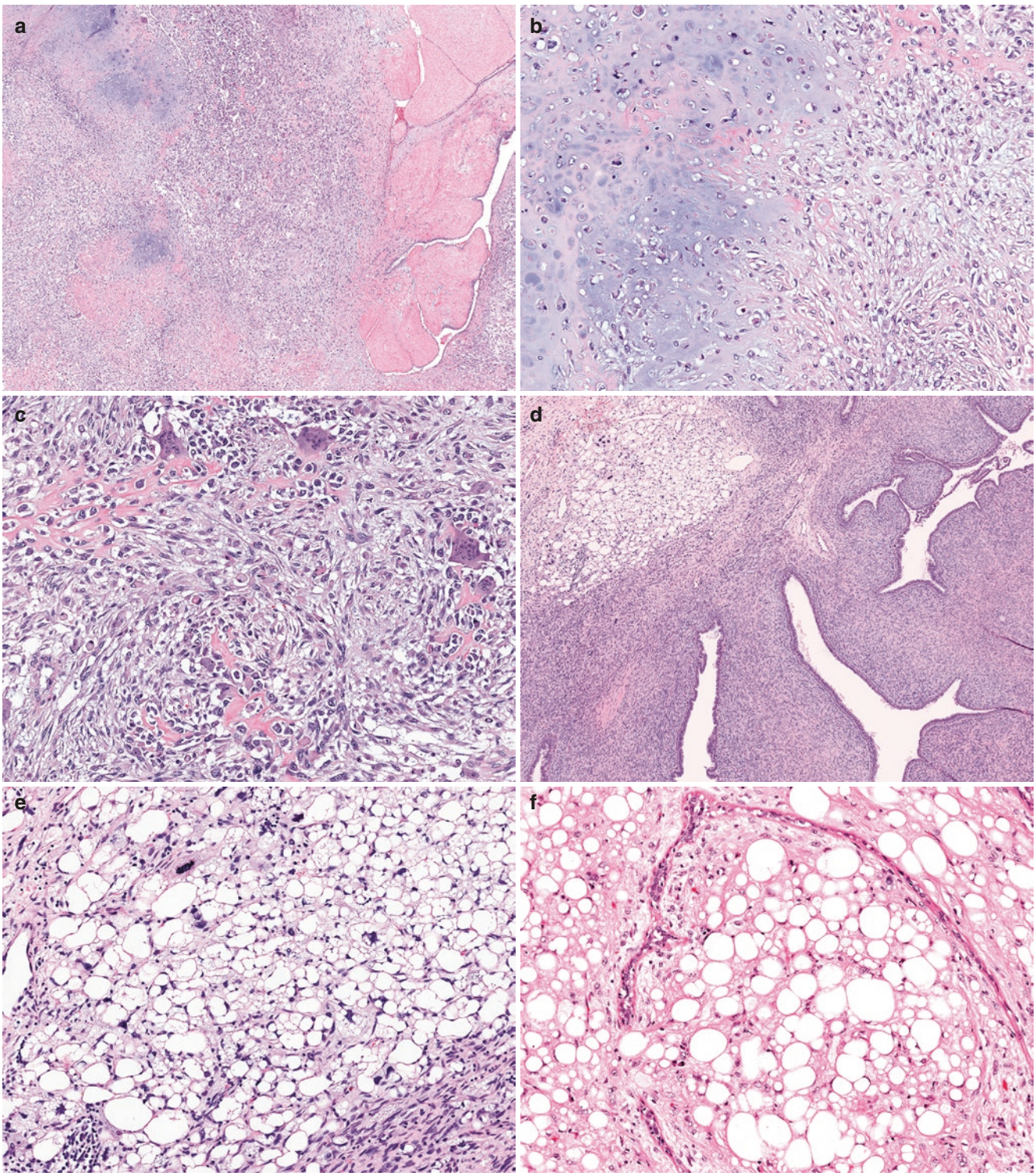

Fig. 7.23 Malignant heterologous differentiation in phyllodes tumor. (**a**–**c**) Phyllodes tumor with osteosarcomatous and chondrosarcomatous stromal overgrowth. (**b**) Chondrosarcomatous differentiation with neoplastic cells in lacunae within cartilaginous stroma. (**c**) Osteosarcomatous differentiation with osteoid production and osteoclast-like giant cells. (**d**–**f**) Liposarcoma-like differentiation with atypical adipocytes and lipoblasts. Previously considered to be diagnostic of malignancy, the presence of liposarcoma-like elements within a PT is no longer considered to be diagnostic of malignancy according to the WHO classification of breast tumors. (**g**) Leiomyosarcomatous differentiation, (**h**) supported by diffuse desmin expression

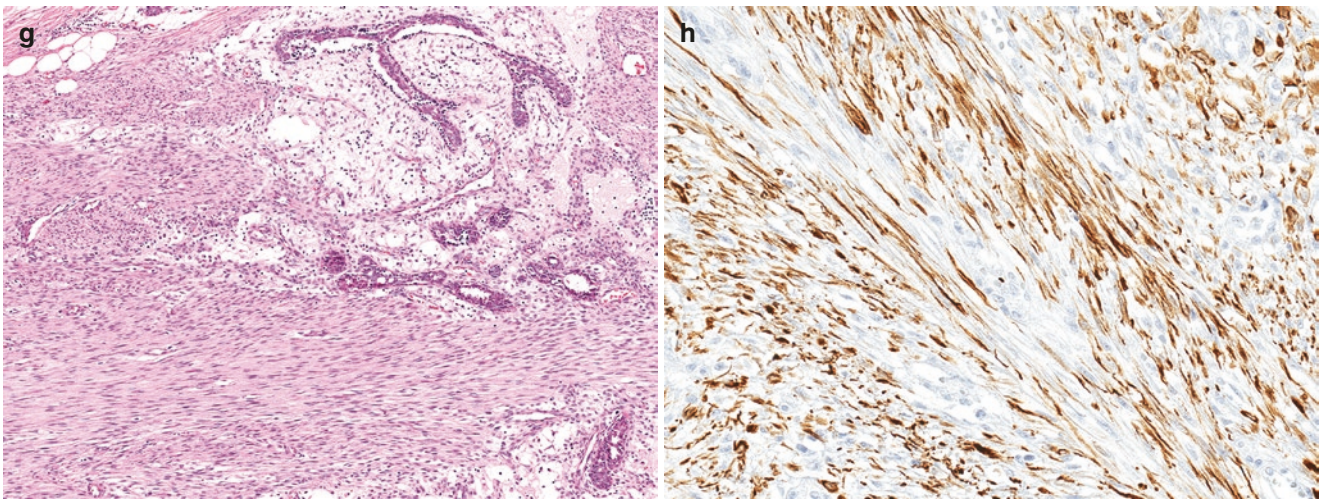

Fig. 7.23 (continued)

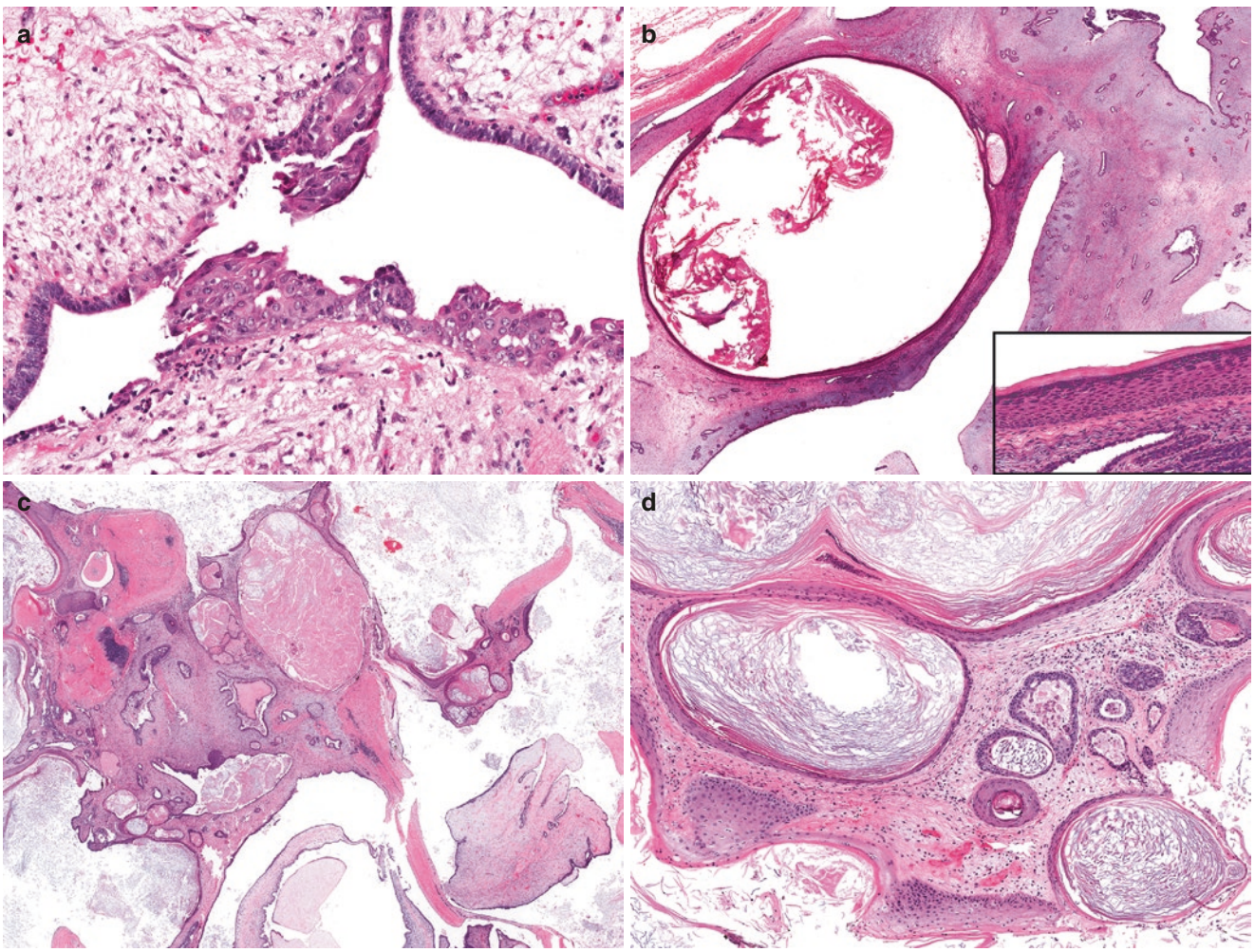

Fig. 7.24 Epithelial metaplasia, hyperplasia, and neoplasia in phyllodes tumor. (**a**–**d**) Squamous metaplasia is rare but more common in phyllodes tumors than fibroadenomas. Squamous metaplasia may be seen in (**a**) epithelium lining the stromal fronds, or (**b**–**d**) as cysts. (**e**, **f**) Usual ductal hyperplasia. (**g**–**i**) Atypical ductal hyperplasia. (**j**, **k**) Ductal carcinoma in situ, intermediate nuclear grade. (**l**, **m**) Lobular carcinoma in situ. (**n**–**p**) Invasive ductal carcinoma in a malignant phyllodes tumor with extensive stromal overgrowth, confirmed by negative myoepithelial cell staining (p63 shown in (**p**))

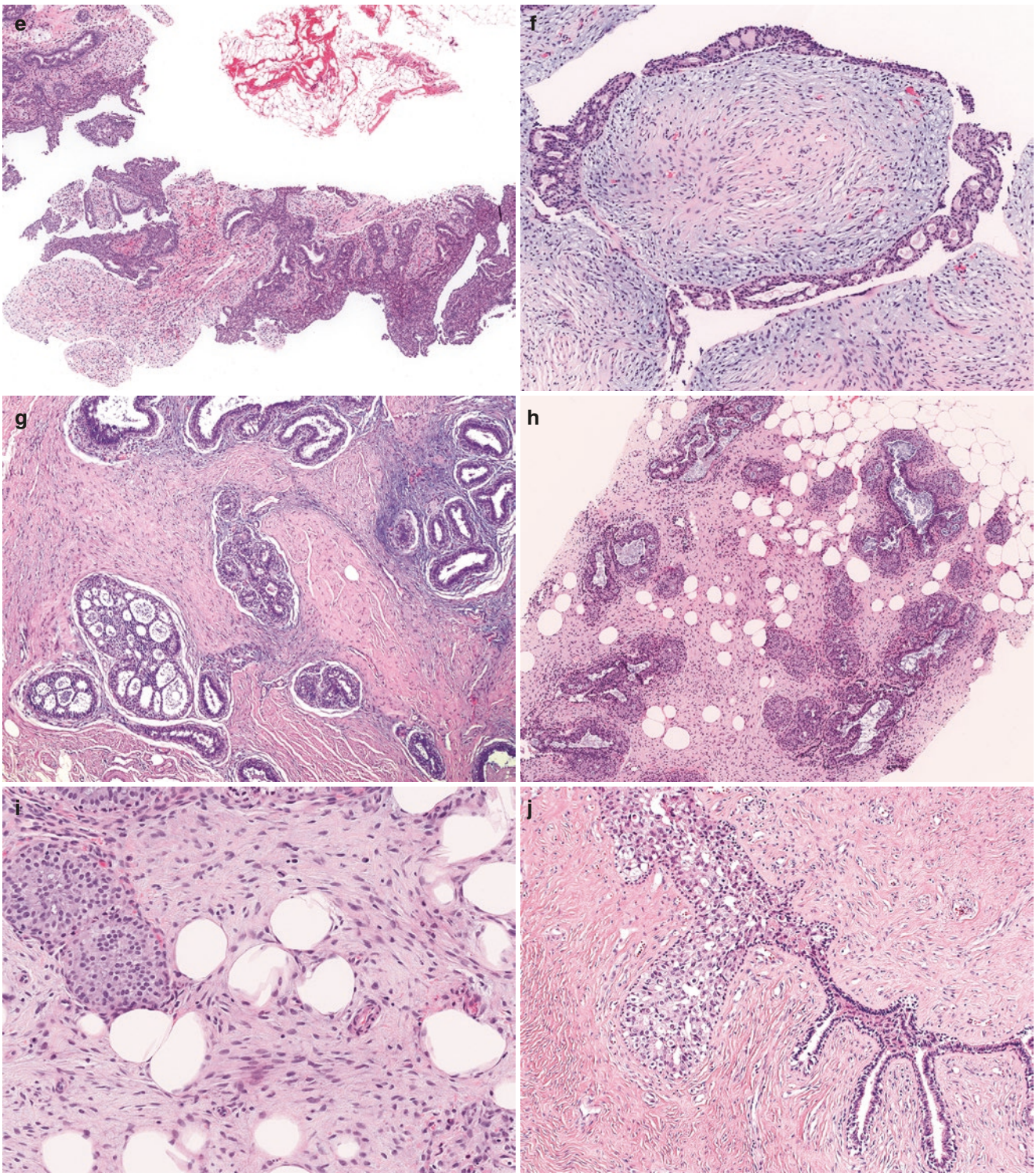

Fig. 7.24 (continued)

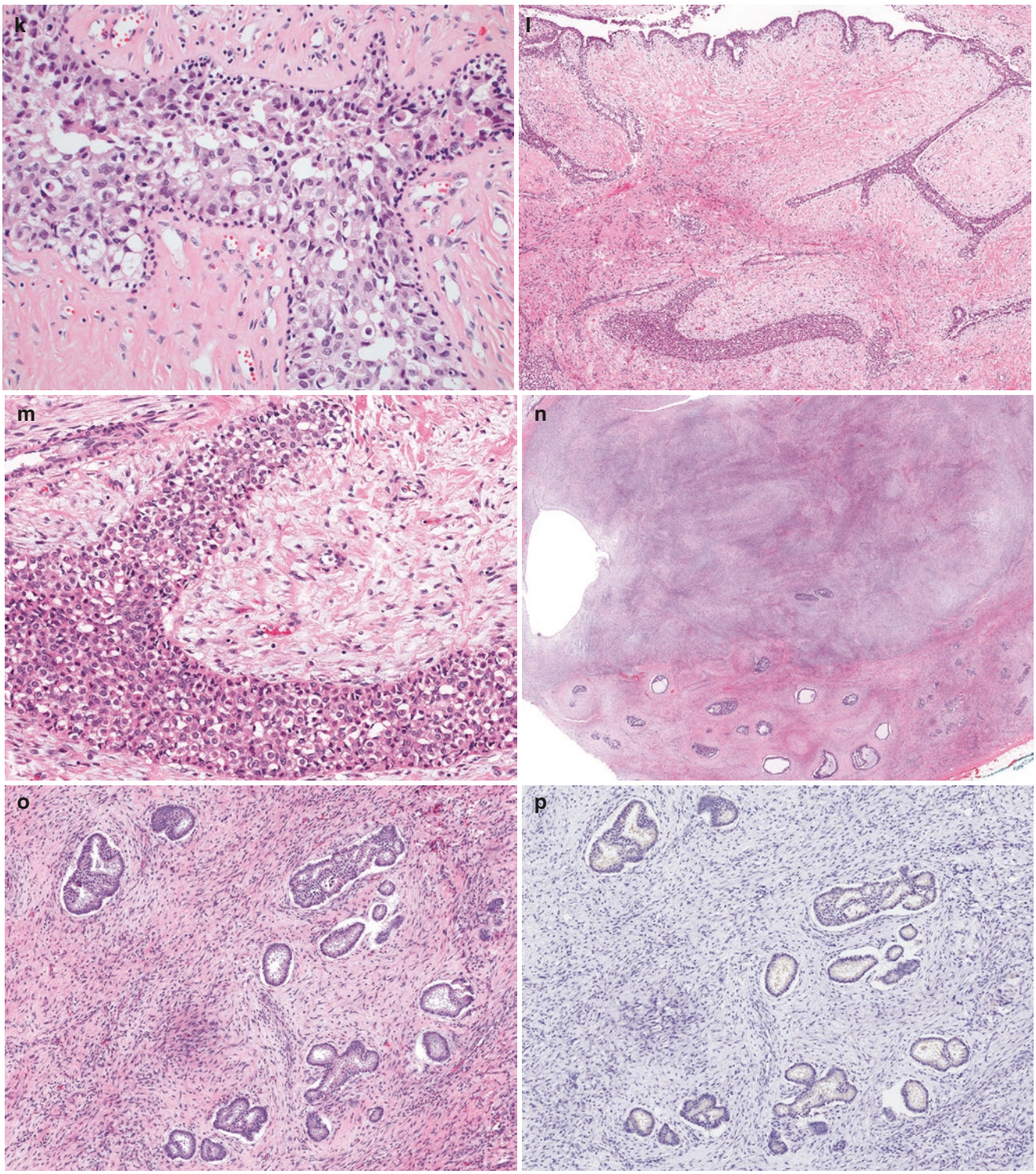

Fig. 7.24 (continued)

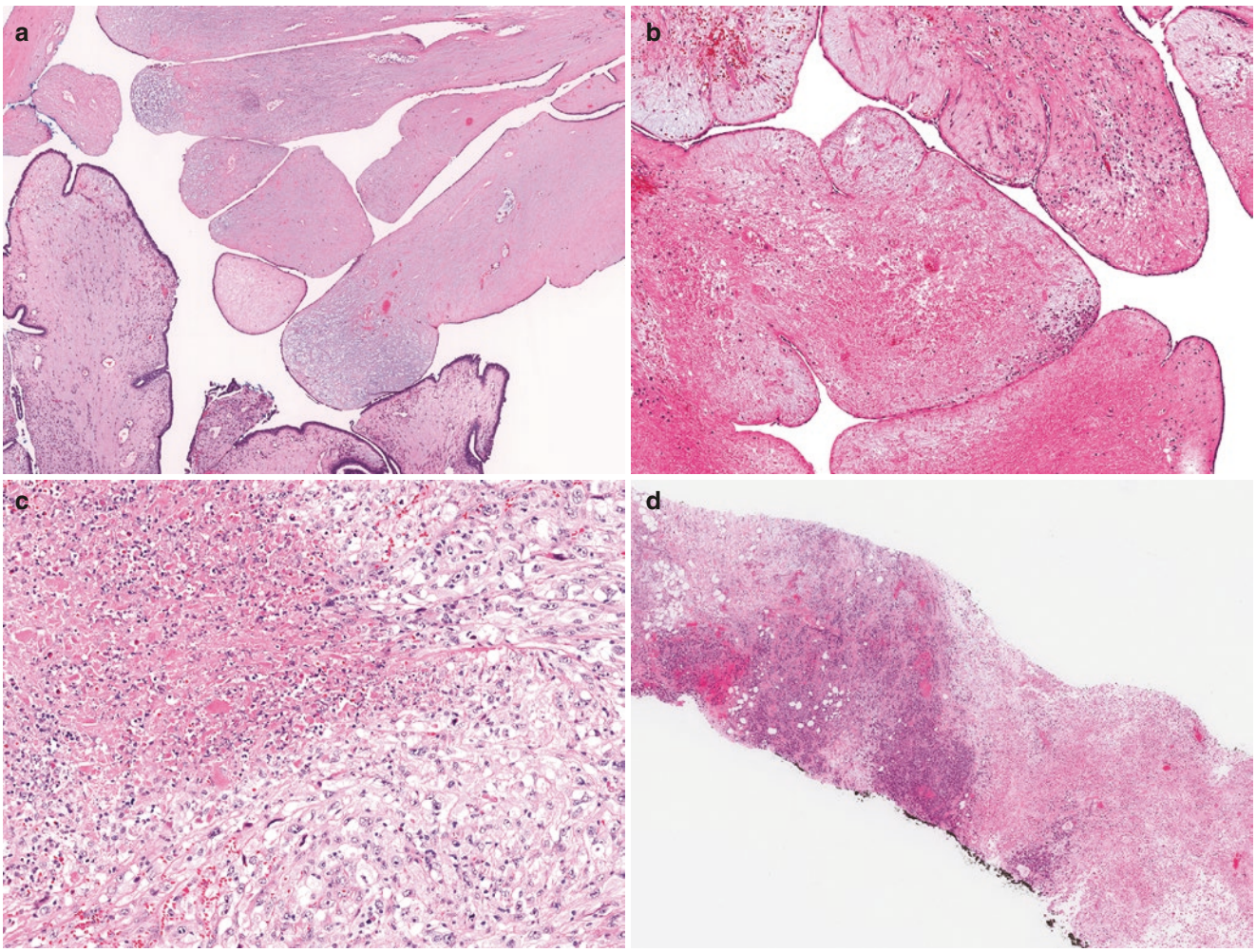

Fig. 7.25 Infarction and tumor necrosis of phyllodes tumor. (**a**, **b**) Infarction of stromal fronds. (**c**, **d**) Tumor necrosis

Phyllodes Tumor Grading

Numerous studies have attempted to identify clinicopathologic factors that may be useful to stratify PTs for risk of local recurrence and metastasis. Histologic features have included tumor border, stromal cellularity, mitotic activity, stromal cell atypia, stromal overgrowth, tumor necrosis, and the presence of malignant heterologous elements [258, 261, 263, 293, 314]. The WHO grading system classifies tumors as benign, borderline, or malignant based on the degree of stromal hypercellularity, stromal cell atypia, and stromal mitotic activity, as well as presence or absence of stromal overgrowth, infiltrative tumor borders, and/or malignant heterologous elements (Table 7.1) [252]. Histologic grading of PTs overall correlates with risk of recurrence or metastasis, but can be problematic due to the inherent subjectivity of the grading criteria and diagnostic thresholds used, with lower predictive power for determining individual tumor behavior [252, 257, 330].

Benign PTs are well-circumscribed, mildly hypercellular tumors with no to mild stromal cell atypia, low mitotic activity (0–4 mitotic figures/10 HPF) and pushing borders (Fig. 7.16). Stromal overgrowth and tumor necrosis are

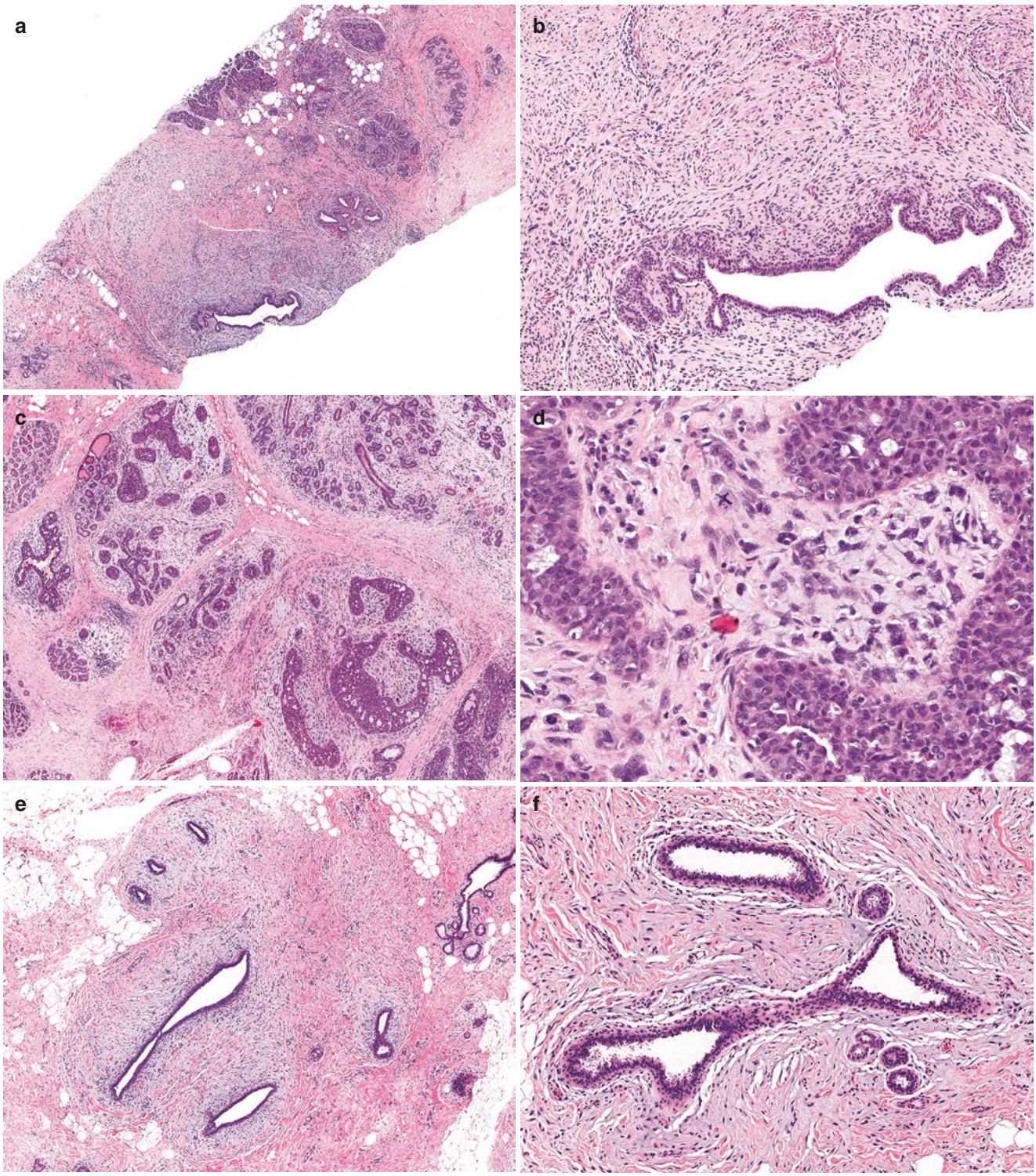

Fig. 7.26 Periductal stromal tumor and periductal stromal hyperplasia. (**a**, **b**) Core biopsy of periductal stromal tumor, with periductal proliferation of atypical spindled cells with infiltrative growth. (**c**, **d**) Excision of periductal stromal tumor showing (**c**) periductal growth pattern evident at low power and (**d**) marked stromal cell atypia with mitotic activity, including atypical mitotic figure. (**e**, **f**) Periductal stromal hyperplasia with bland spindle cells lacking nuclear atypia and mitotic activity

Table 7.1 Phyllodes tumor grading, WHO criteria

	Benign	Borderline	Malignant
Stromal hypercellularity	Mild, non-uniform or diffuse	Moderate, non-uniform or diffuse	Marked, usually diffuse
Stromal mitotic activity	0–4/10 HPF (<2.5/mm^2)	5–9/10 HPF (2.5 to <5/mm^2)	≥10/10 HPF (≥5/mm^2)
Stromal cell atypia	Mild or none	Mild or moderate	Marked
Stromal overgrowth	Absent	May be focal	Usually present, may be diffuse
Tumor borders	Circumscribed	Circumscribed or focally infiltrative	Infiltrative
Malignant heterologous differentiation	Absent	Absent	Present[a]

[a] Malignant heterologous differentiation, aside from liposarcoma-like differentiation, defines malignancy even in the absence of the other features. Liposarcoma-like differentiation alone is not considered malignant in PT

absent [252, 288]. Mature mesenchymal metaplasia may be seen very rarely and is often lipomatous when present [331]. Benign PTs are more likely to demonstrate PASH, multinucleated stromal giant cells, and epithelial hyperplasia than higher grade tumors [288].

On the other end of the spectrum, malignant PTs are characterized by areas of marked stromal cellularity, marked stromal cell atypia, and high mitotic activity (≥10 mitotic figures/10 HPF). The tumor border is at least focally infiltrative. Tumor infiltration may be obvious as tongues of infiltrating cellular stroma or may be more subtle, with wrapping and entrapment of adjacent fat. Stromal overgrowth is usually present and may be diffuse (Fig. 7.27). In fact, malignant PTs can mimic metaplastic spindle cell carcinoma or sarcoma due to the lack of or scant amount of epithelium, especially in CNBs (Figs. 7.28 and 7.29). Extensive sampling may be required (Fig. 7.30, 7.31, and 7.32). All five histologic features (marked cellularity, marked pleomorphism, ≥10 mitoses/10 HPF, permeative borders, and stromal overgrowth) should be present for a diagnosis of malignancy in the absence of malignant heterologous elements (Table 7.1) [252, 313]. Aside from liposarcoma-like differentiation, malignant heterologous stromal elements, such as chondrosarcoma, osteosarcoma, and rhabdomyosarcoma, define malignancy even in the absence of the other histologic features. A combination of heterologous components may be present (Fig. 7.23) [252, 257, 332–335]. Although liposarcomatous differentiation was previously considered to be diagnostic of malignancy in PT, these tumors are thought to have low metastatic risk, and liposarcoma-like differentiation in a PT alone is no longer considered a feature of malignancy [252, 336]. Consistent with this, despite the histologic similarity, PTs with liposarcoma-like elements lack *MDM2* or *CDK4* amplifications characteristic of extramammary well-differentiated liposarcomas [222, 337, 338]. Furthermore, the liposarcoma-like components of microdissected tumors were found to have less chromosomal aberrations than the non-heterologous component of the same tumors [222]. Accordingly, grading of PT with liposarcoma-like elements should be based on the other histologic parameters, akin to PTs without heterologous differentiation. For cases that do not meet criteria for malignancy using these features, it has been suggested to use the term "lipoblast-like areas" rather than liposarcoma to avoid confusion [339]. PTs with pleomorphic liposarcoma component may have worse outcomes [336].

Borderline PTs have intermediate histologic features between benign and malignant tumors (Table 7.1), and PTs with some but not all of the features of malignancy are classified as borderline (Fig. 7.17). Accordingly, these tumors have a varied morphologic appearance with a spectrum of stromal cellularity, atypia, and mitotic activity, but typically show mild or moderate stromal cellularity and/or mild to moderate stromal cell atypia with 5–9 mitotic figures/10 HPF. The tumor borders are often well-defined and pushing but may be focally infiltrative. Areas of stromal overgrowth can be seen but is not diffuse. Benign and borderline tumors may show significant heterogeneity [252].

In general, PTs should not be graded on CNB material. Choi et al. directly compared 129 PTs diagnosed and graded on excision specimens with the diagnosis and grade obtained in the preceding CNBs. Of 90 benign PTs, ~74% were correctly diagnosed and graded as benign PT in the CNB, with the remainder incorrectly diagnosed as FAs. Among 30 borderline and 9 malignant PTs, only ~27% and ~45% were correctly graded in the preceding CNB, respectively. All discordant diagnoses were underestimated on CNB in this study [292]. Another study found some correlation of stromal cellularity, pleomorphism, and mitotic activity between CNBs and excisions of PTs, with correlation coefficients of 0.6, 0.65, and 0.67, respectively. The degree of certainty increased with increasing tumor grade [340]. Discrepancies between grade on CNB versus excision are due to sampling,

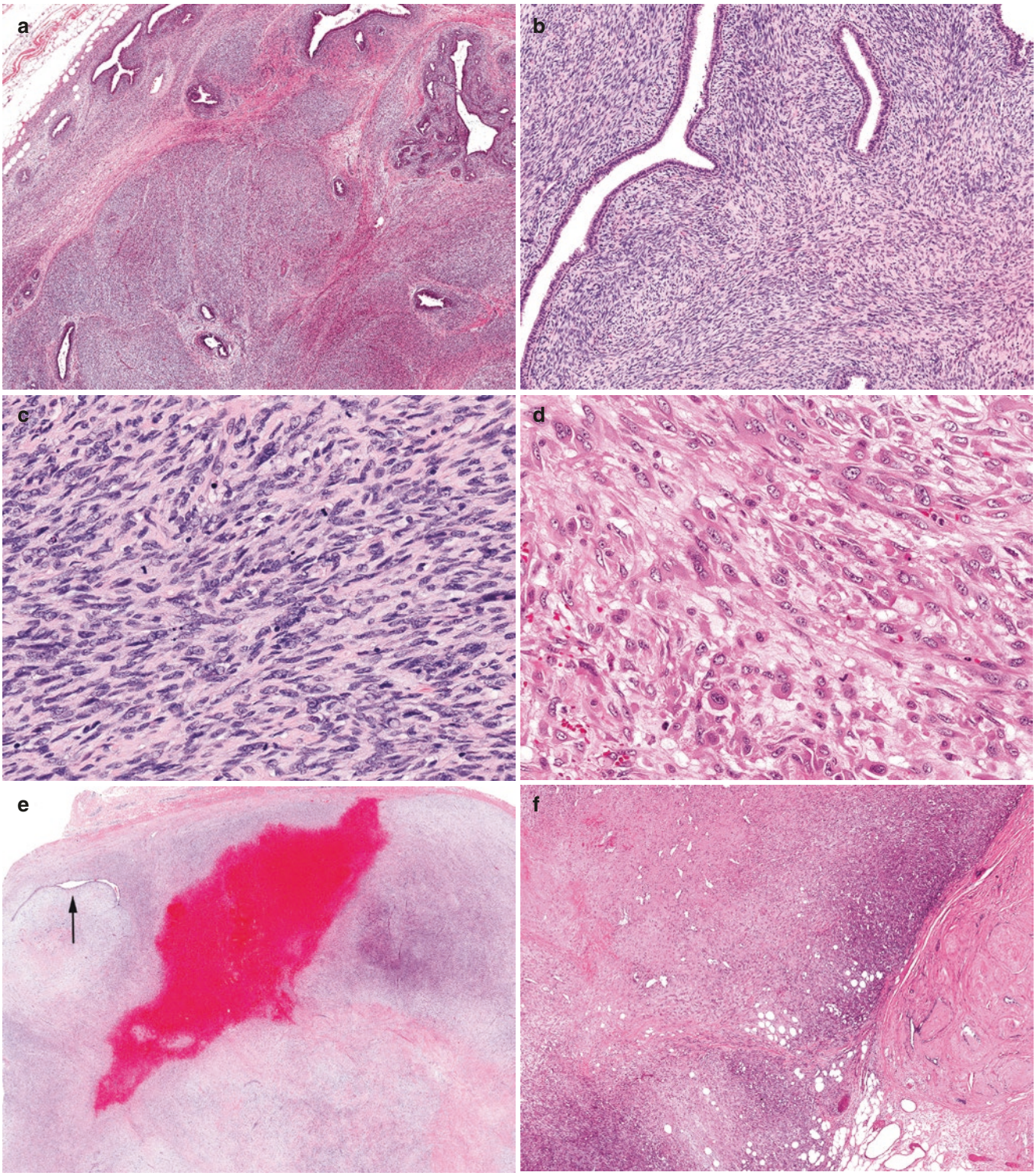

Fig. 7.27 Malignant phyllodes tumor. Malignant phyllodes tumors are defined by the presence of all five of the following features: (**a**–**d**) marked stromal hypercellularity, (**c**) high mitotic activity (≥10/10 HPF), (**c**, **d**) severe cytologic atypia, (**e**, **f**) stromal overgrowth, which may be diffuse, and (**g**, **h**) infiltrative borders. Extensive sampling may be necessary to identify the epithelial component, which may be a rare embedded elongated duct (**e**, arrow) or residual fibroadenoma-like area (right side of (**f**)). (**g**) Infiltrative borders may appear as obvious tongues of tumor cells frankly invading the adjacent parenchyma or (**h**) may be more subtle, with tumor stromal cells encroaching and encasing adjacent adipocytes

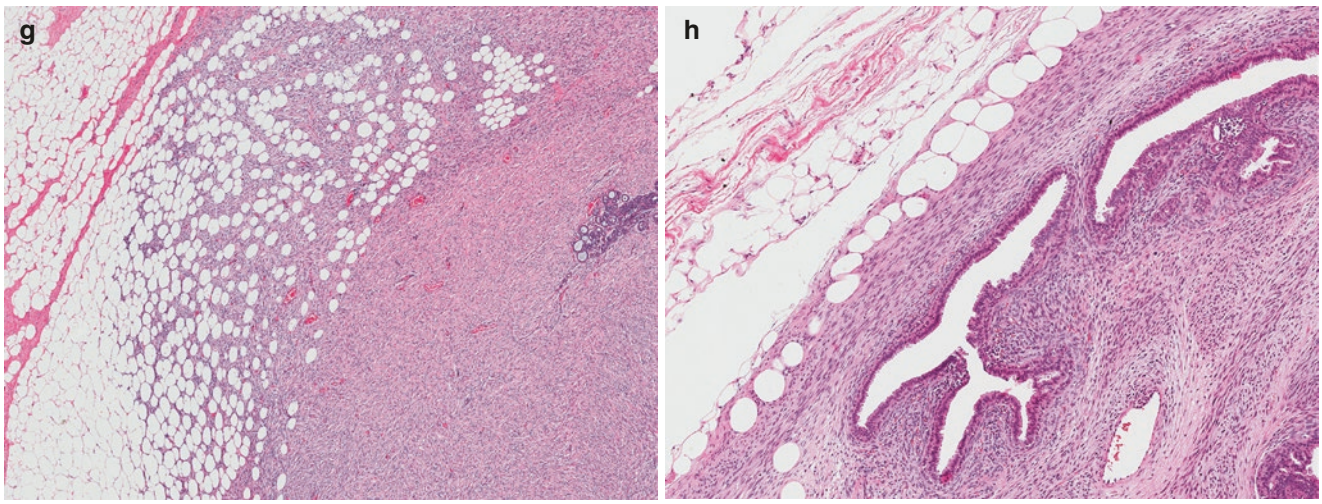

Fig. 7.27 (continued)

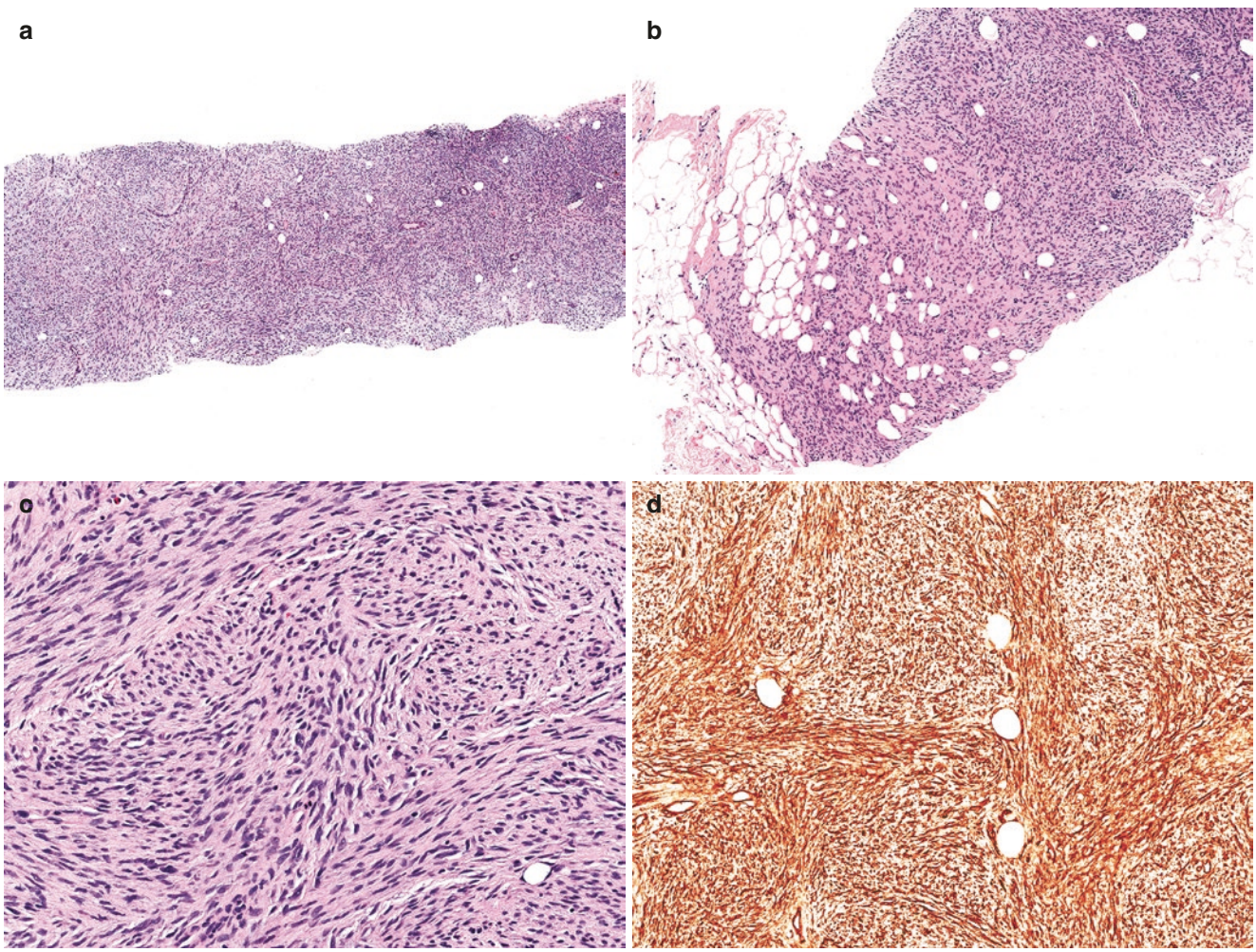

Fig. 7.28 Malignant phyllodes tumor with diffuse stromal overgrowth. (**a**, **b**) Core biopsy with cellular spindle cell neoplasm with infiltrative borders and entrapped fat. No epithelial component is present. (**c**) Higher power magnification highlighting intersecting atypical spindled cells with numerous mitotic figures. Immunohistochemistry showed (**d**) diffuse positive CD34 and (**e**) diffuse nuclear β-catenin expression, compatible with phyllodes tumor. (**f**) Excision revealed malignant phyllodes tumor with marked stromal overgrowth

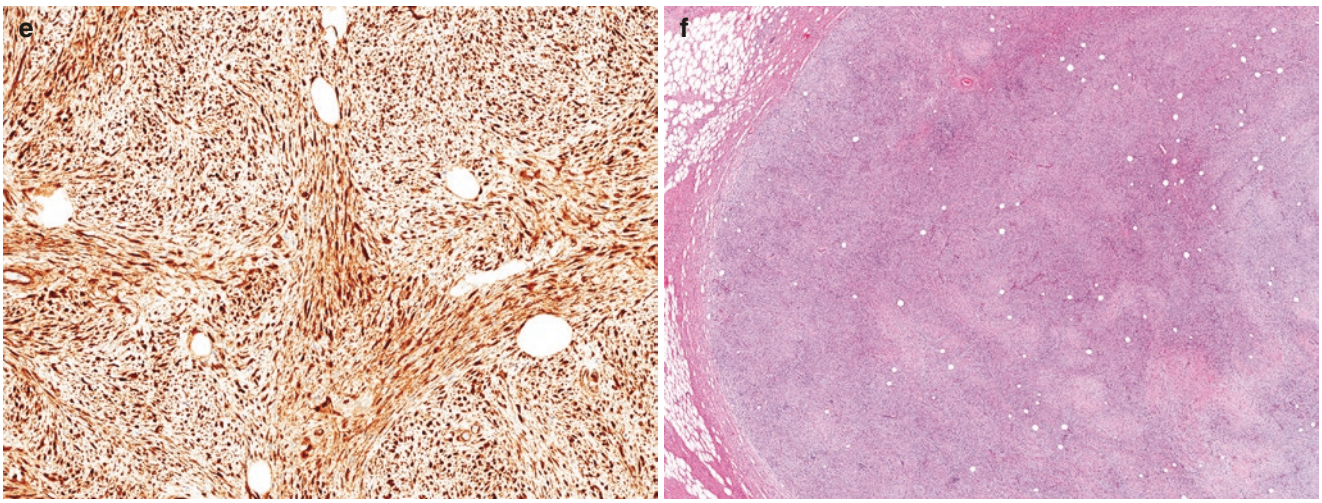

Fig. 7.28 (continued)

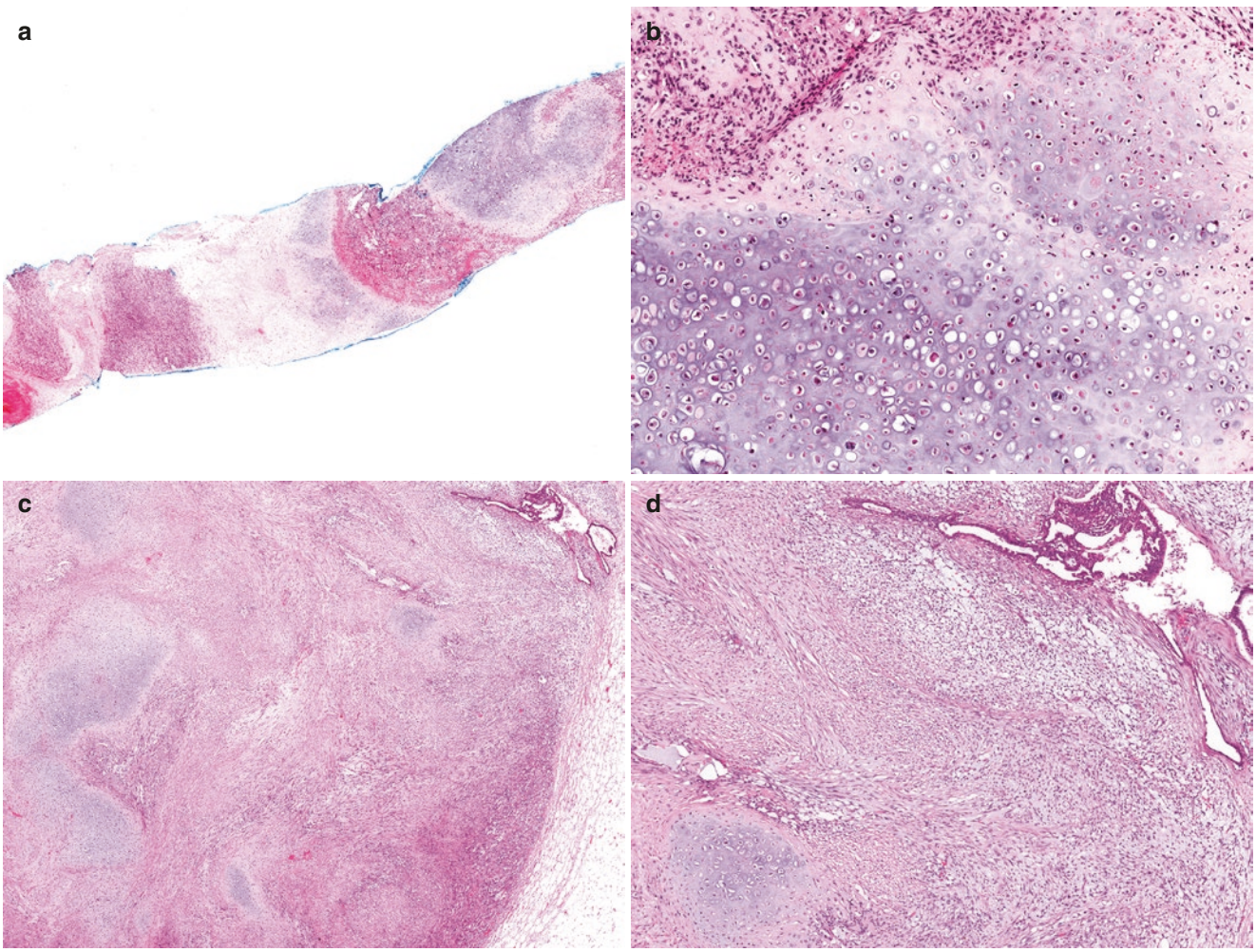

Fig. 7.29 Malignant phyllodes tumor with extensive chondrosarcomatous stromal overgrowth. (**a**, **b**) Core biopsy of large palpable breast mass in a 43-year-old woman showing a malignant spindle cell neoplasm with chondroid differentiation. (**c**, **d**) Mastectomy revealed a malignant tumor with extensive chondroid differentiation and only a rare long curvilinear duct. Targeted DNA sequencing revealed a *MED12* G44D mutation, consistent with malignant phyllodes tumor with chondrosarcomatous differentiation

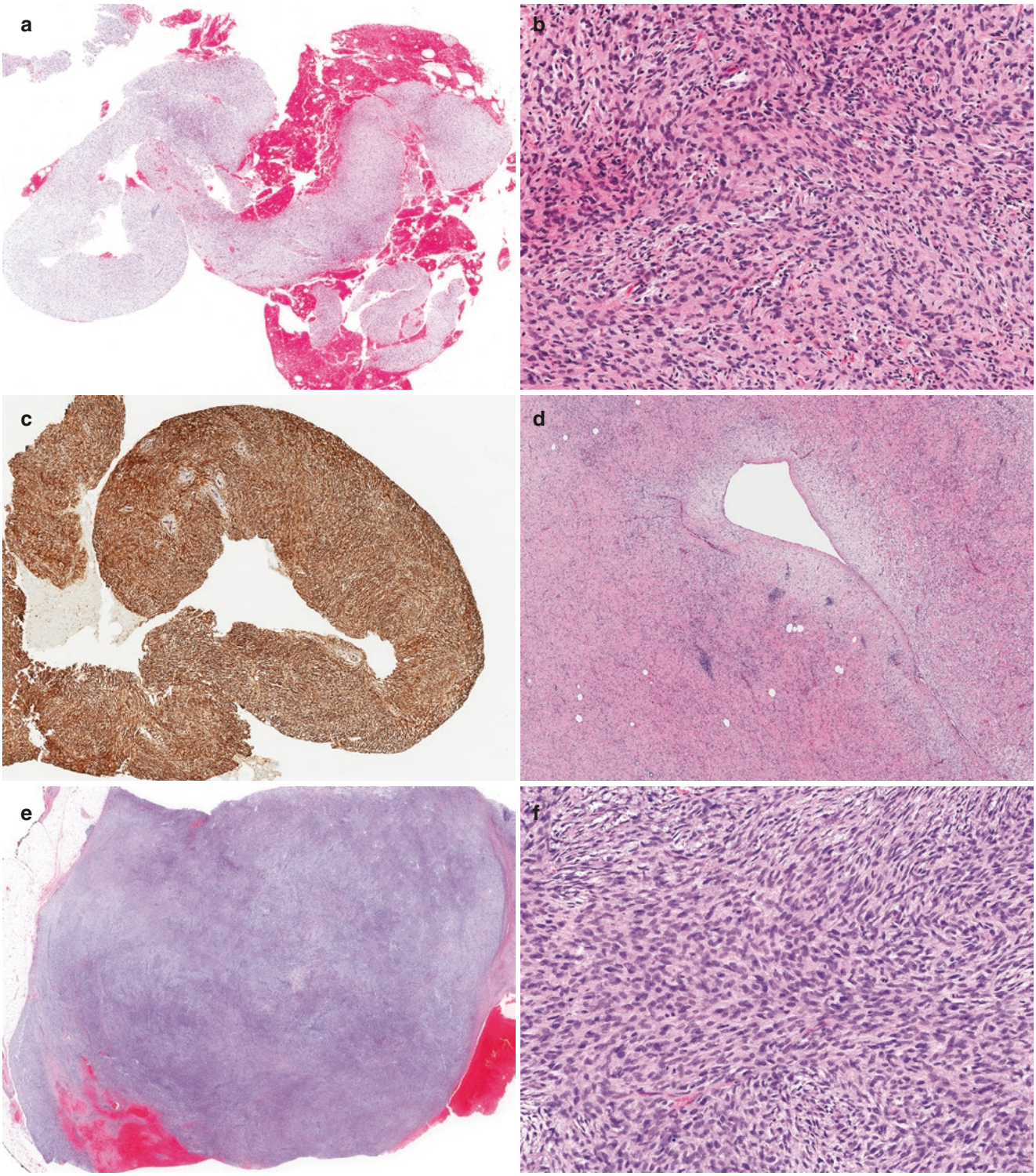

Fig. 7.30 Malignant phyllodes tumor with extensive stromal overgrowth. (**a**, **b**) Core biopsy demonstrating a cellular spindle cell neoplasm without associated epithelium. (**c**) The tumor cells diffusely express CD34, excluding metaplastic carcinoma and supporting phyllodes tumor. Multiple cytokeratins and p63 were negative. (**d**) Excision revealed a malignant phyllodes tumor with prominent stromal overgrowth and only a rare elongated lesional duct. (**e**–**f**) Another malignant phyllodes tumor with diffuse stromal overgrowth. (**g**) Extensive sampling revealed only one small focus of identifiable fibroepithelial growth

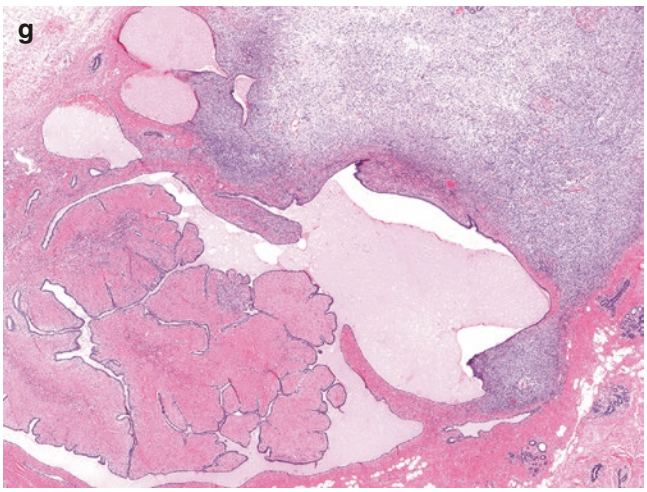

Fig. 7.30 (continued)

PT heterogeneity, and inability to evaluate the tumor borders, not to mention the difficulty discerning cellular FA from PT on CNB.

Recurrent and Metastatic Phyllodes Tumors

Local PT recurrences are most commonly of the same grade as the initial tumor [257, 258, 287]. In a large study, locally recurrent PTs were of the same grade as the initial tumor in 63% of 73 cases. Of 48 initially benign recurrent tumors, 21 (44%) recurred as higher grade, with most (81%) of these being borderline. Four (8.3%) of 48 benign tumors and 2 (12.5%) of 16 borderline tumors recurred as malignant tumors. Four (25%) borderline tumors but no malignant tumors recurred as benign lesions [257].

Metastatic PTs are essentially always comprised only of the stromal component, which demonstrates malignant spindle cell morphology in the vast majority of cases

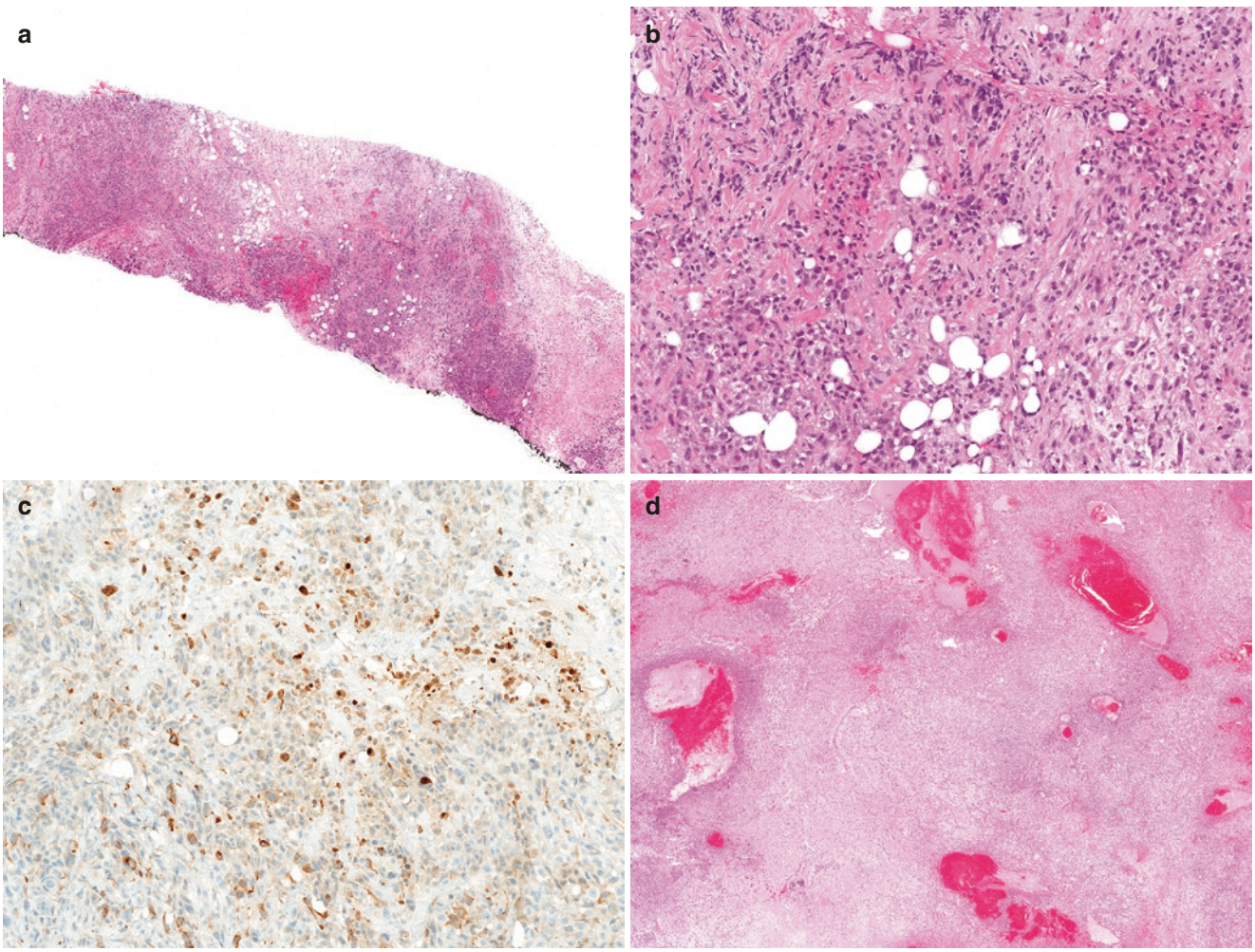

Fig. 7.31 Expression of cytokeratin and p63 in malignant phyllodes tumor with extensive osteosarcomatous and chondrosarcomatous stromal overgrowth. (**a**–**c**) Core biopsy of an enlarged, hard, and deformed breast with skin edema revealing a poorly differentiated malignant neoplasm with necrosis. (**b**) The tumor cells are variably epithelioid to spindled with marked pleomorphism. (**c**) Cytokeratin immunostain was positive in scattered tumor cells. (**d**–**i**) Mastectomy showed an 18 cm malignant phyllodes with (**e**) extensive osseous differentiation, characterized by osteoid matrix deposition and osteoclast-like multinucleated giant cells, and focal chondroid differentiation. (**f**, **g**) Foci of epithelium associated with intracanalicular stromal growth were identified upon extensive sampling, including (**g**) areas with infarcted stromal fronds, which solidified the diagnosis of malignant phyllodes tumor. The tumor cells showed (**h**) focal cytokeratin and (**i**) patchy p63 expression by immunohistochemistry

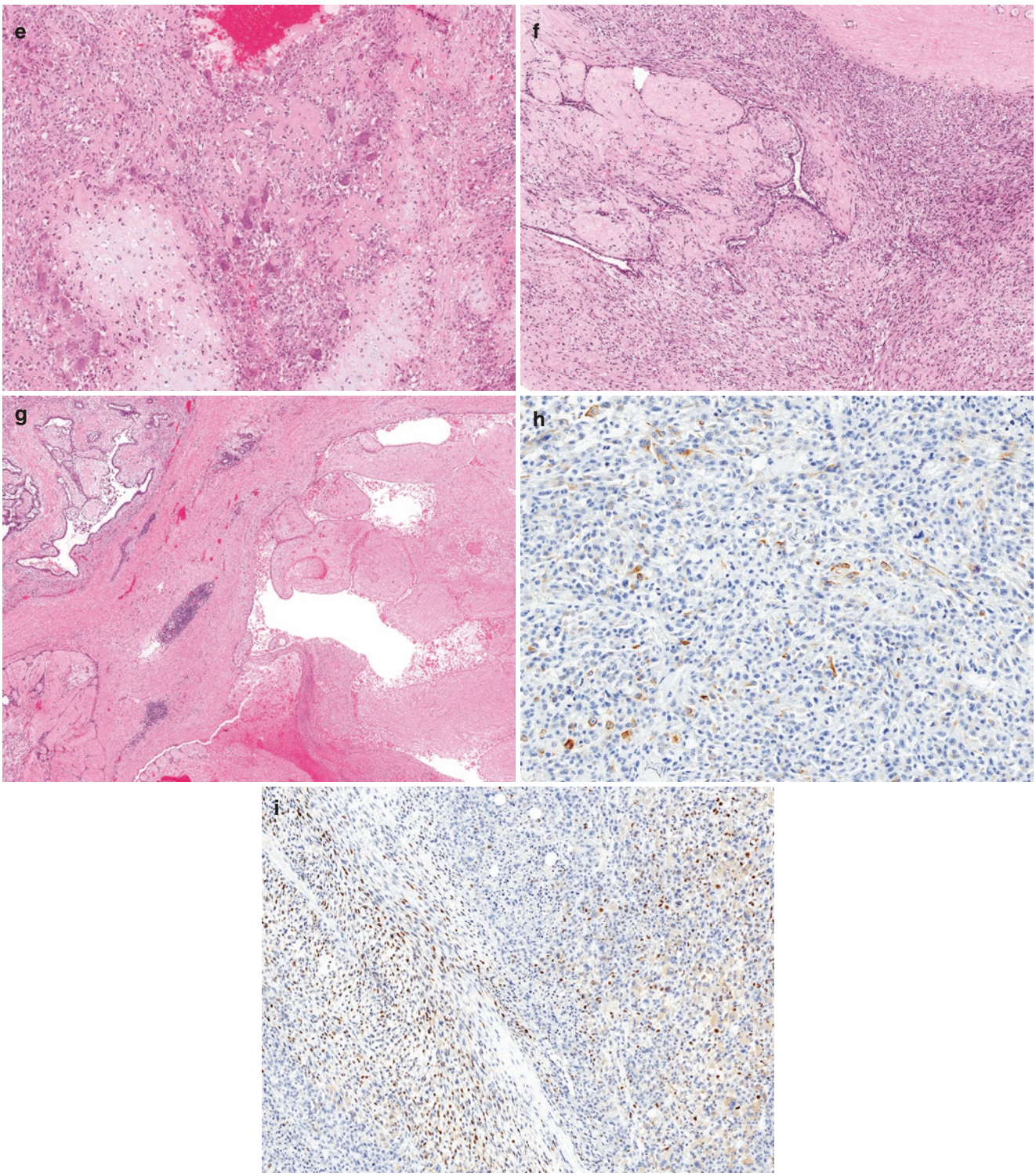

Fig. 7.31 (continued)

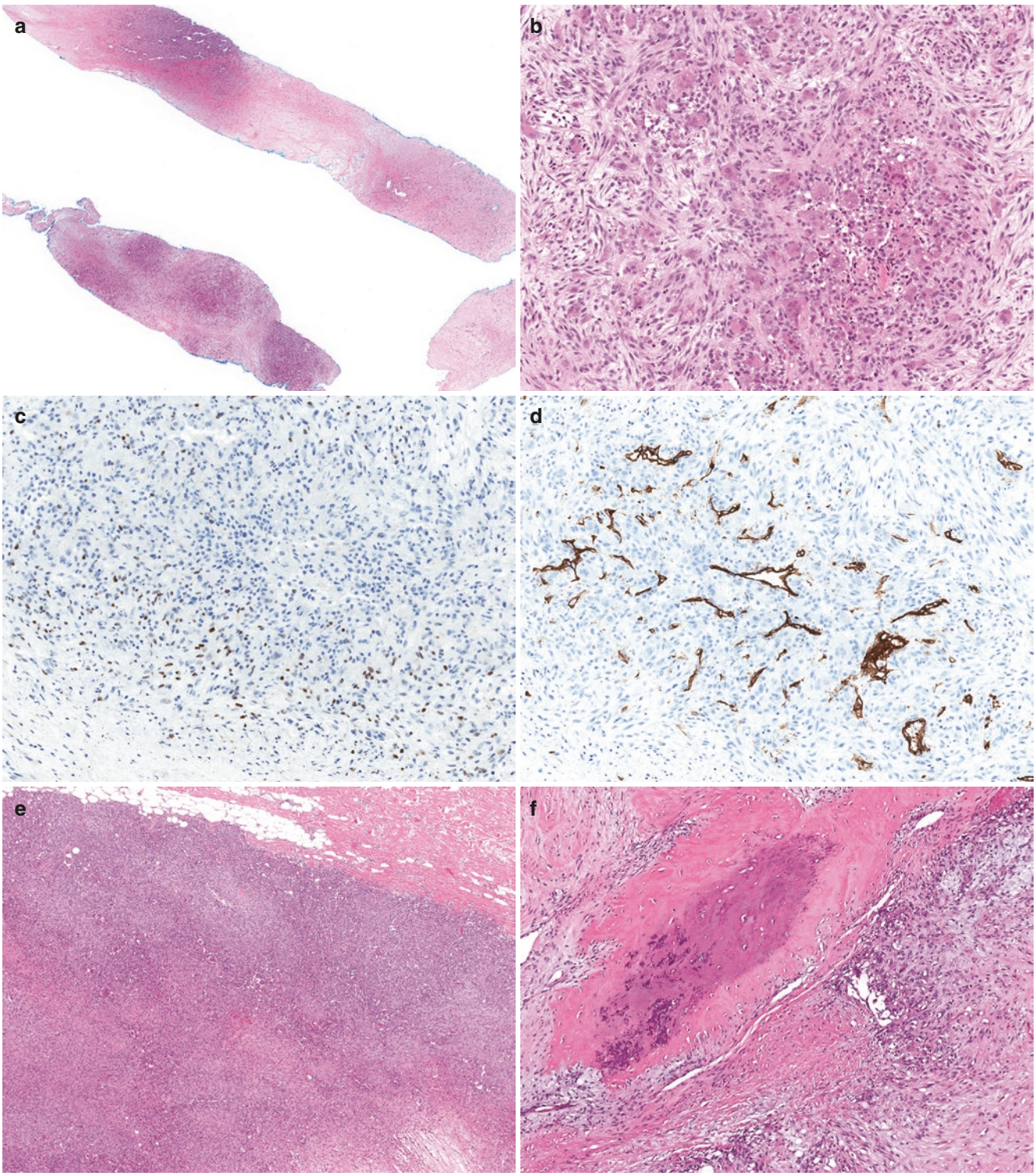

Fig. 7.32 Malignant phyllodes tumors with diffuse stromal overgrowth and p63 expression. (**a**–**d**) Core biopsy revealing malignant spindle cell neoplasm (**b**) with numerous multinucleated giant cells and no epithelial component. The tumor cells express (**c**) p63 and are (**d**) negative for CD34 and cytokeratins (not shown). (**e**–**g**) Mastectomy revealed a malignant phyllodes tumor with osteosarcomatous differentiation. (**g**) A rare fibroadenoma-like focus was identified after extensive tumor sampling. (**h**) Positive p63 immunostain. Targeted DNA sequencing revealed *MED12* G44D and *TERT* promoter mutations, confirming the diagnosis of malignant phyllodes tumor

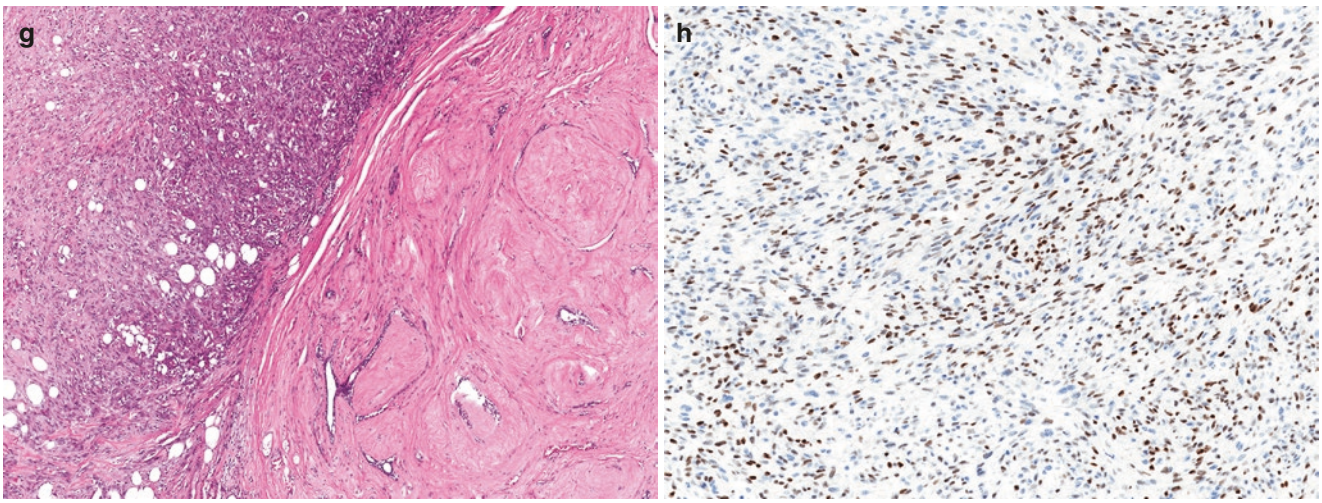

Fig. 7.32 (continued)

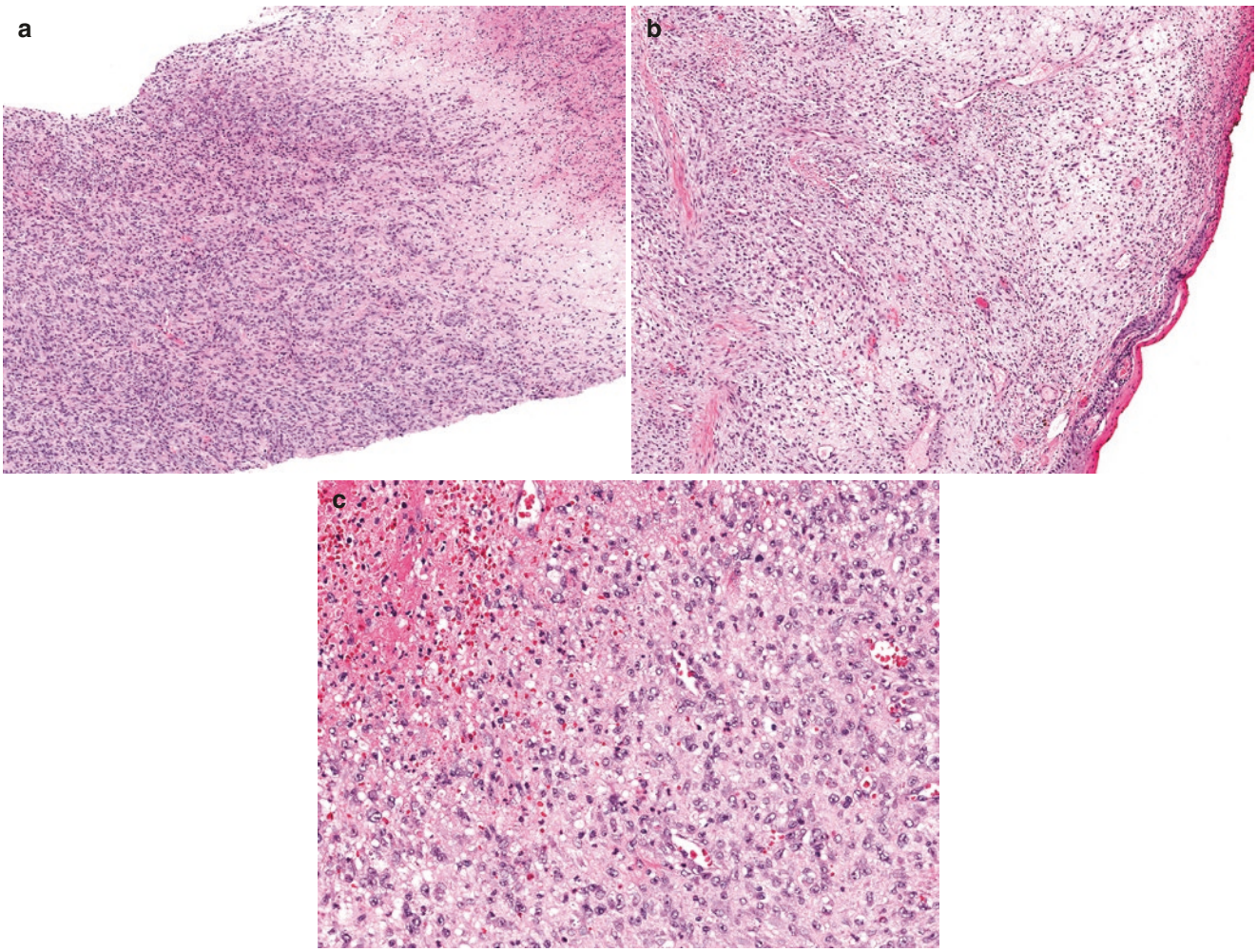

Fig. 7.33 Metastatic phyllodes tumor. (**a**) Metastatic malignant phyllodes tumor to the lung, with tumor necrosis. (**b**, **c**) Metastatic malignant phyllodes tumor to the vulva, (**b**) with skin ulceration and (**c**) tumor necrosis. Metastatic phyllodes tumors are comprised of the stromal component only

(Fig. 7.33). Heterologous sarcomatous elements present in the primary tumor may or may not be present in the metastasis [317, 332]. On the other hand, the metastatic tumor may very rarely demonstrate heterologous differentiation not seen in the primary tumor [341]. Only one unusual immunohistochemically confirmed case of PT with both epithelial and stromal metastasis to the lung has been reported [342].

Immunohistochemistry

Whereas the stromal cells of most FAs diffusely express CD34, such staining is less predictable in PTs and can be negative or variably positive (Fig. 7.28) [157, 159, 160, 343–345]. Stromal CD34 positivity decreases with increasing PT grade [160, 344–348]. One large study showed CD34 positivity in ~73% of 109 PTs, which decreased from ~79% of benign tumors to ~67% and ~44% of borderline and malignant tumors, respectively [345]. In a study of 57 CNBs designed to identify features that could predict PT on excision, all three CNBs that lacked CD34 staining were PTs on excision (two borderline and one malignant), whereas diffuse staining was seen in FAs and other PTs [349]. Stromal actin expression has been positively correlated with grade [344]. Sapino et al. observed stromal cell co-expression of ERβ, SMA, and calponin but no expression of ERα. In contrast to FAs, ERβ expression in PTs increased with age [163]. Stromal cells in PTs of all grades may express nuclear β-catenin (Fig. 7.28) [161, 162, 347, 350]. In a study of 119 PTs, Sawyer et al. observed stromal nuclear β-catenin staining in 86 (72%) tumors, with 7 of 8 malignant tumors showing absent or weak staining [350]. Others have also shown lower numbers of malignant PTs with staining [351]. *CTNNB1* mutations have not been identified [161, 210, 211, 222, 350, 352].

Earlier studies reported absence of stromal cytokeratin staining in PTs, suggesting utility in the differential diagnosis with spindle cell metaplastic carcinoma [343, 353, 354]. More recent studies have shown cytokeratin staining in PTs. In a study by Chia et al., MNF116 was positive in ~12%, 34βE12 in 22%, CK7 in ~28%, CK14 in ~2%, AE1/3 in ~8%, and CAM5.2 in ~2% of PTs. Stromal MNF116, 34βE12, and CAM5.2 positivity increased with tumor grade, and MNF116 also increased with cellularity, necrosis, and cystic change [345]. Staining in all positive cases was focal in this study, ranging from 1 to 5% of tumor cells [345]. Cimino-Mathews et al. described focal cytokeratin (AE1/3, 34βE12, or CK8/18) positivity in 1–5% of stromal cells in 3 (21%) of 14 malignant PTs but no FAs, benign or borderline PTs [346]. Earlier studies also reported lack of p63 staining in PTs [355–357]. More recent analysis revealed p63 positivity in stromal cells of 8 (57%) of 14 malignant PTs, but no staining in FAs, benign or borderline PTs [346]. Staining in most (63%) p63-positive malignant PTs was focal (1–5% of tumor cells), with none showing staining in >30% of cells. The ΔN p63 isoform p40 was expressed in 14% of malignant PTs but no benign or borderline PTs or FAs. Bansal et al. also described focal p63 and cytokeratin cocktail staining in 2 of 10 malignant PT but not in benign or borderline PT [358]. Differences in cytokeratin and p63 expression in PTs between earlier and more recent studies may be attributed to preferential staining of these markers in malignant PTs, few of which were included in earlier studies [346]. The findings have special relevance to CNB diagnosis, as positive staining for cytokeratins, p63, or p40 in spindle cell lesions cannot be used to exclude PT (Figs. 7.31, 7.32, and 7.34).

Many studies have evaluated the correlation of immunohistochemical markers with PT grade, histologic features used for grading, and/or recurrence or metastasis. These have included p53 [359–370], TERT [371], CD117 [344, 348, 368, 372–375], CD10 [165, 376], EGFR [377, 378], PDGF and PDGFRβ [379], VEGF [347, 380], and Ki-67 [359, 367, 381–385]. None were shown to independently predict recurrence or metastasis. In a study by Cimino-Mathews et al., 29% of malignant PTs showed diffuse strong p16 expression with RB loss, and 21% of malignant tumors showed the reverse immunophenotype of p16 loss with diffuse strong RB expression (Fig. 7.33). No FAs, benign or borderline PTs had this immunophenotype, suggesting that this pathway may contribute to PT progression in a subset of tumors [381].

The epithelial cells of PTs usually express ER and PR, and an inverse correlation with malignancy has been reported [386].

In a study designed to identify features of cellular fibroepithelial tumors that predict PT on subsequent excision, Jacobs et al. found significantly higher median stromal Ki-67 staining in biopsies of PTs (7.2%, range 0–18%) than cellular FAs (1.6%, range 0.4–4.4%), even among lesions of moderate stromal cellularity [127]. However, there was significant overlap, with CNBs from 3 of 9 PTs showing proliferative indices <4.4% [127]. Jara-Lazaro et al. reported that CNBs with stromal Ki-67 indices ≥5% were PTs on excision in 84% of cases, whereas all FAs showed no or <5% staining [349]. In practice, the significant degree of overlap in Ki-67 staining among fibroepithelial tumors precludes reliable diagnostic utility in most cases [127, 383].

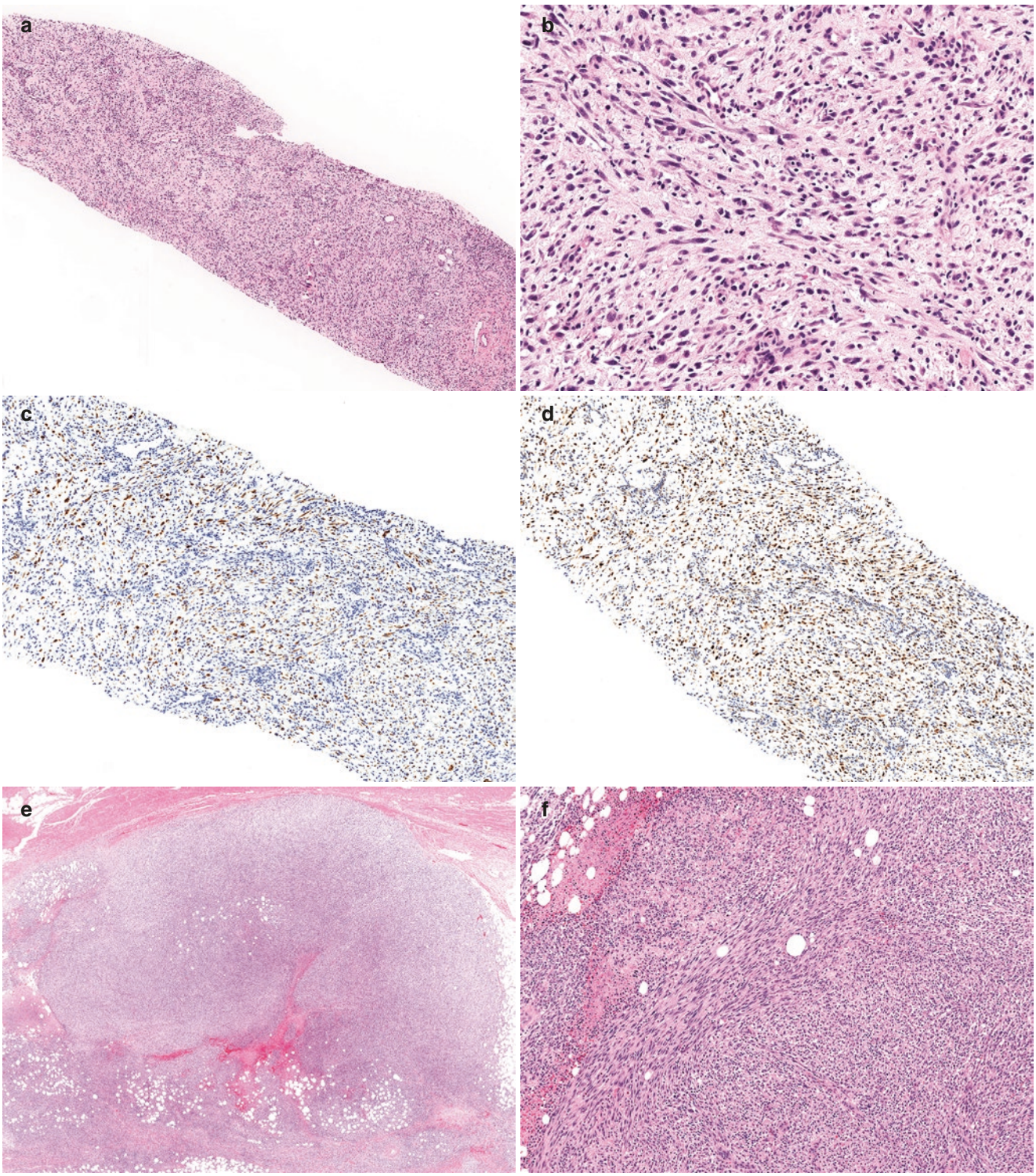

Fig. 7.34 Expression of cytokeratin and p63 in malignant phyllodes tumor with stromal overgrowth. (**a**–**d**) Core biopsy revealing malignant spindle cell neoplasm, with patchy immunohistochemical staining for (**c**) cytokeratin and (**d**) p63. (**e**, **f**) Excision revealed malignant phyllodes tumor with diffuse stromal overgrowth. Targeted DNA sequencing revealed mutations in *MED12* exon 2 and *TERT* promoter, among other aberrations, confirming the diagnosis

Table 7.2 Benign phyllodes tumor versus cellular fibroadenoma

	Benign phyllodes tumor	Cellular fibroadenoma
Leaf-like growth pattern	Present, typically well developed	Absent or focal
Subepithelial stromal condensation	May be present	Absent
Stromal heterogeneity	May be present	Usually absent
Stromal cell atypia	Mild	None[a]
Stromal hypercellularity	Mild	Mild
Stromal mitoses	0–4/10 HPF (<2.5/mm^2)	Few[b]
Pseudoangiomatous stromal hyperplasia	May be present	Rarely present
Squamous metaplasia	May be present	Virtually absent
TERT promoter mutation	Present in subset	Usually absent

[a] Multinucleated stromal giant cells in PT or FA should not be mistaken for atypia

[b] Typically ≤2/10 HPF, but may be more numerous in children and adolescents

Differential Diagnosis

The differential diagnosis of a cellular fibroepithelial tumor with mild to moderate stromal cellularity, no to minimal stromal cell atypia, and absent or low mitotic activity usually rests between benign PT and cellular FA (Table 7.2). The distinction of benign PT from cellular FA is often not problematic in an excision specimen if the lesion has well-developed frond-like architecture of PT and subepithelial stromal accentuation. However, not all PTs have well-developed stromal fronds, with the epithelium of some tumors arranged as elongated branching, clefted ducts, sometimes with a staghorn-like appearance (Fig. 7.19) [252, 313]. Lack of stromal fronds should therefore not necessarily exclude the diagnosis in the presence of other concerning features, such as increased stromal cellularity, mitotic activity, stromal atypia, stromal overgrowth, and/or infiltrative growth. On the other hand, focal stromal fronds may be seen in some FAs. These are generally focal and less cellular without subepithelial stromal accentuation (Fig. 7.15). Retracted stromal projections of some intracanalicular FAs can mimic stromal fronds, but these have the appearance of fitting together with one another like a jigsaw puzzle, as opposed to PT fronds that protrude more irregularly into gaping cystic spaces [127]. Assessment of stromal cellularity is subjective, and the lower threshold of PT cellularity overlaps with cellular FA. Significant and diffuse nuclear overlap or areas of sheet-like stromal growth are not features of cellular FA. Stromal cellularity and epithelial distribution is often heterogeneous in PTs, compared to the more uniform appearance of cellular FAs and juvenile FAs. This feature is more helpful when evaluating excision specimens than CNBs [126]. Although FAs are typically well-circumscribed, lesions otherwise indistinguishable from typical FAs may occasionally show irregular borders, which has also been documented in pediatric FAs [147]. In some cases, distinguishing cellular FAs from benign PTs may simply not be possible. In such cases, a diagnosis of *benign cellular fibroepithelial neoplasm* can be rendered, with an explanation of the features present, the difficulty in precise categorization, and the possible risk of local recurrence with essentially no risk for metastasis [126]. The diagnostic dilemma was highlighted in a study by Lawton et al., in which 21 fibroepithelial tumors that were difficult to classify as cellular FAs or PTs were independently reviewed by ten breast pathologists. Complete agreement among pathologists was seen in only two (9.5%) cases, and diagnoses ranged from FA to borderline PT in 43% of cases [387]. *TERT* promoter mutations are highly enriched in PTs compared to FAs (including cellular FAs) and may be useful to favor PT in challenging cases [205, 207, 210].

The distinction between cellular FA and PT is particularly problematic in CNBs (Figs. 7.35, 7.36, and 7.37). Patient age and tumor size are not useful in this context [127, 128, 340, 388]. Numerous studies have examined histopathologic features in CNBs of PTs compared to FAs [127, 128, 169, 340, 349, 388–391]. Many have identified stromal cellularity and/or mitotic activity to be useful in CNBs, with other features overall being less helpful (Fig. 7.35) [127, 128, 169, 340, 349, 391]. Jacobs et al. evaluated histopathologic features present in CNB diagnosed as fibroepithelial lesions with cellular stroma that could predict a diagnosis of PT versus FA on subsequent excision [127]. Only stromal cellularity (marked versus mild) and mitotic activity were found to be useful, with all markedly cellular lesions being PTs and all mildly cellular lesions being FAs. Mild cellularity was defined as twice the cellularity of normal perilobular stroma, and marked cellularity was defined as stromal cells in close contiguity "resulting in areas of confluence with many stromal cell nuclei appearing to touch." Although PTs of moderate cellularity showed higher mitotic counts (1–6 mitoses/10 HPF) than cellular FAs (1–2 mitoses/10 HPF), broad overlap was seen. Similarly, median Ki-67 indices were higher for these PT (7.2%, range 0–18%) than cellular FAs (1.6%, range 0–4.4%), but overlap prevented practical use as a single diagnostic feature. The authors suggested a diagnostic algorithm in which markedly cellular lesions or moderately cellular lesions with stromal mitotic activity or elevated proliferative indices are most likely to be PTs, whereas mildly cellular lesions, especially if lacking mitoses or elevated proliferative fractions, are more likely to be FAs [127]. Lee et al. found that increased stromal cellularity compared to typical FA in at least 50% of the biopsy material, stromal expansion with a 10× micro-

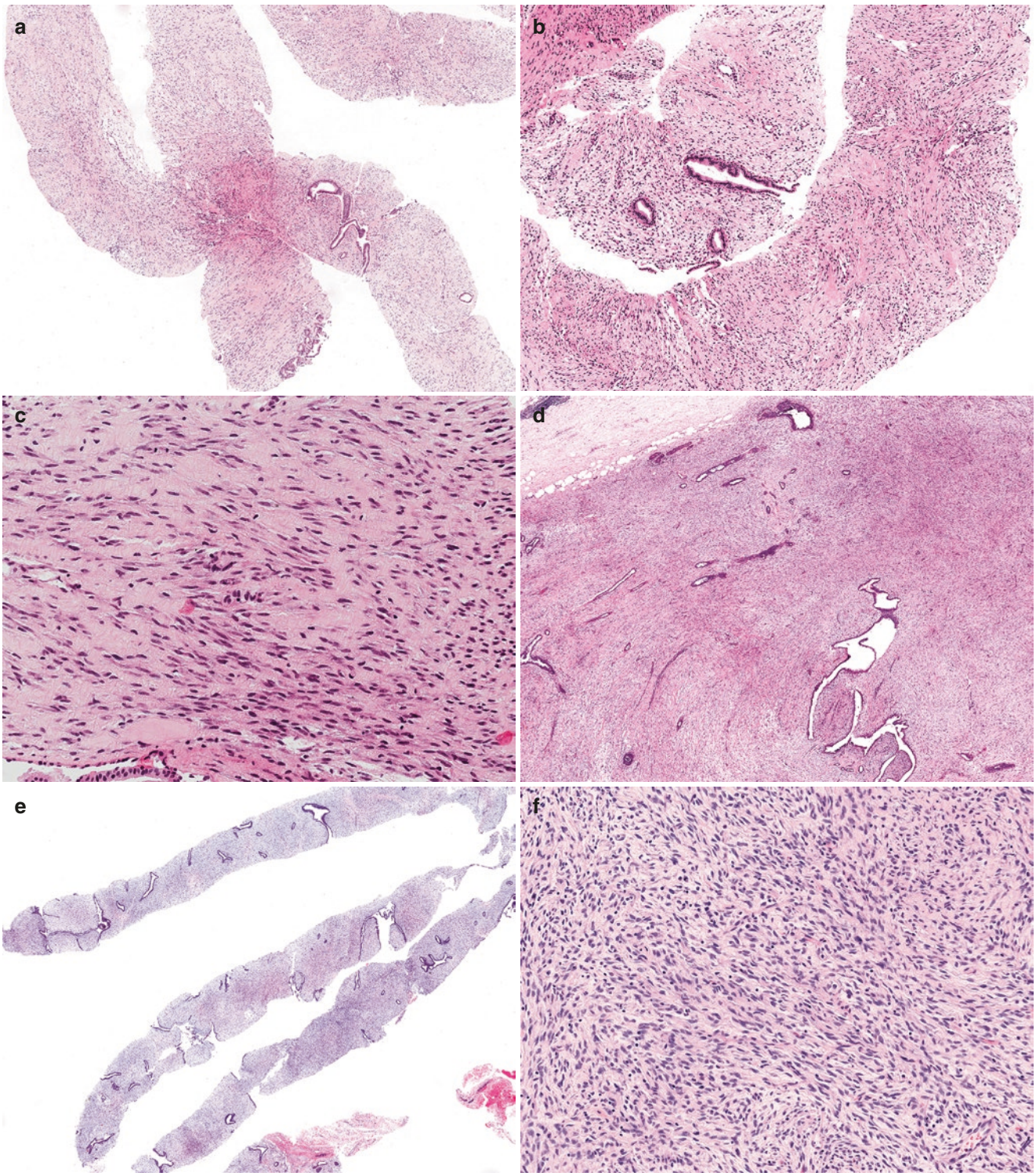

Fig. 7.35 Stromal cellularity and mitotic activity can be useful in the evaluation of fibroepithelial tumors with cellular stroma on core biopsy. (**a**–**c**) Core biopsy of cellular fibroepithelial tumor showing an excess of stroma relative to epithelium, with (**b**) moderate stromal hypercellularity and (**c**) scattered mitotic figures (three identified). (**d**) Excision revealed a borderline phyllodes tumor. (**e**–**g**) Fibroepithelial tumor with intracanalicular growth, hypercellular stroma, and numerous mitotic figures (3 in this HPF). The degree of stromal hypercellularity and mitotic activity favor phyllodes tumor. (**h**–**j**) Core biopsy of another cellular fibroepithelial tumor with exaggerated intracanalicular growth and moderate stromal hypercellularity. (**h**) Fragmentation of the biopsy is also noted. (**j**) Excision revealed a phyllodes tumor

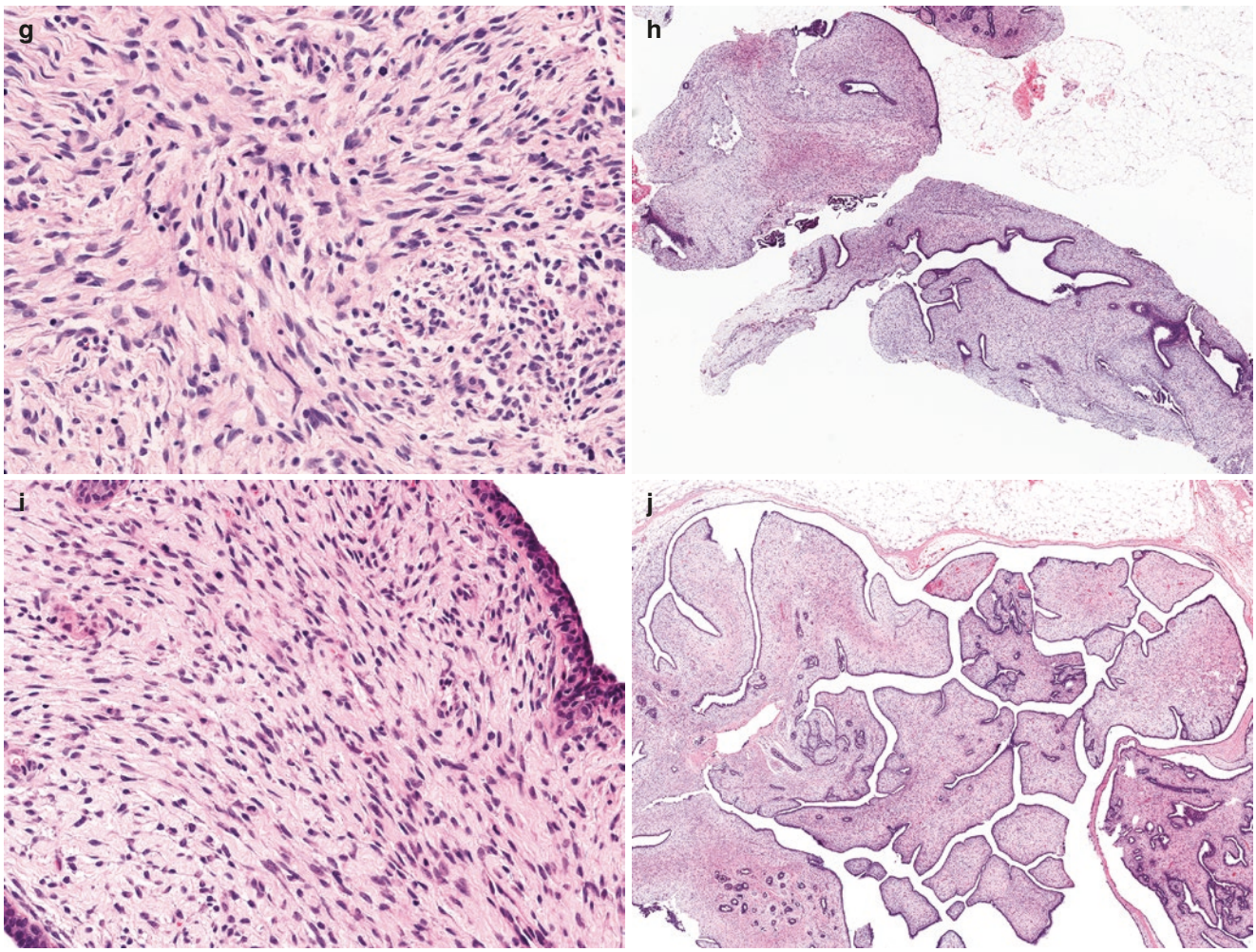

Fig. 7.35 (continued)

scope objective, tissue fragmentation and adipose tissue within lesional stroma were all significantly more common in CNBs from PTs compared to FAs (Figs. 7.35, 7.36, and 7.37) [169]. Tissue fragmentation likely reflects leaf-like growth, which is not always appreciated in CNBs. However, FAs with prominent intracanalicular growth may also fragment and form pseudofrond-like foci in CNBs, and this feature should be interpreted with caution (Fig. 7.37). A subsequent study applied these four features to CNBs of fibroepithelial tumors diagnosed as either PT or cellular FA on excision. This allowed for correct categorization in 19 of 21 PT and 70 of 91 FAs but predicted "unnecessary" excision of 31% of FAs [392]. Jara-Lazaro et al. studied fibroepithelial tumors in which PT could not be excluded on CNB and found that either marked stromal cellularity, marked nuclear atypia, stromal overgrowth (4× objective), ≥2 mitotic figures/10 HPF, or ill-defined lesional borders exclusively predicted PT on excision. Moderate stromal cellularity (20 of 27 PTs), moderate nuclear atypia (14 of 16 PTs) and PASH (19 of 23 PTs) were significantly more common in PTs. Of lesions with mild stromal cellularity, 42% were PTs on excision, whereas most lesions with moderate (74%) and all lesions with marked cellularity were PTs. Stromal mitoses of 0–1/10 HPF were present in similar numbers of PTs (42%) and FAs (58%), but all cases with 2 or more mitotic figures in 10 HPF were PTs. Eighty-four percent of lesions with Ki-67 index ≥5% and all lesions with topoisomerase labeling ≥5% were PTs on excision [349]. Yasir et al. used a combinatorial approach and concluded that the presence of any three or more of a number of different histologic features is useful in prediction of PT on CNB. These included mitotic activity, stromal expansion (10× objective), stromal fragmentation, adipose tissue infiltration or fat entrapment, stromal heterogeneity, stromal

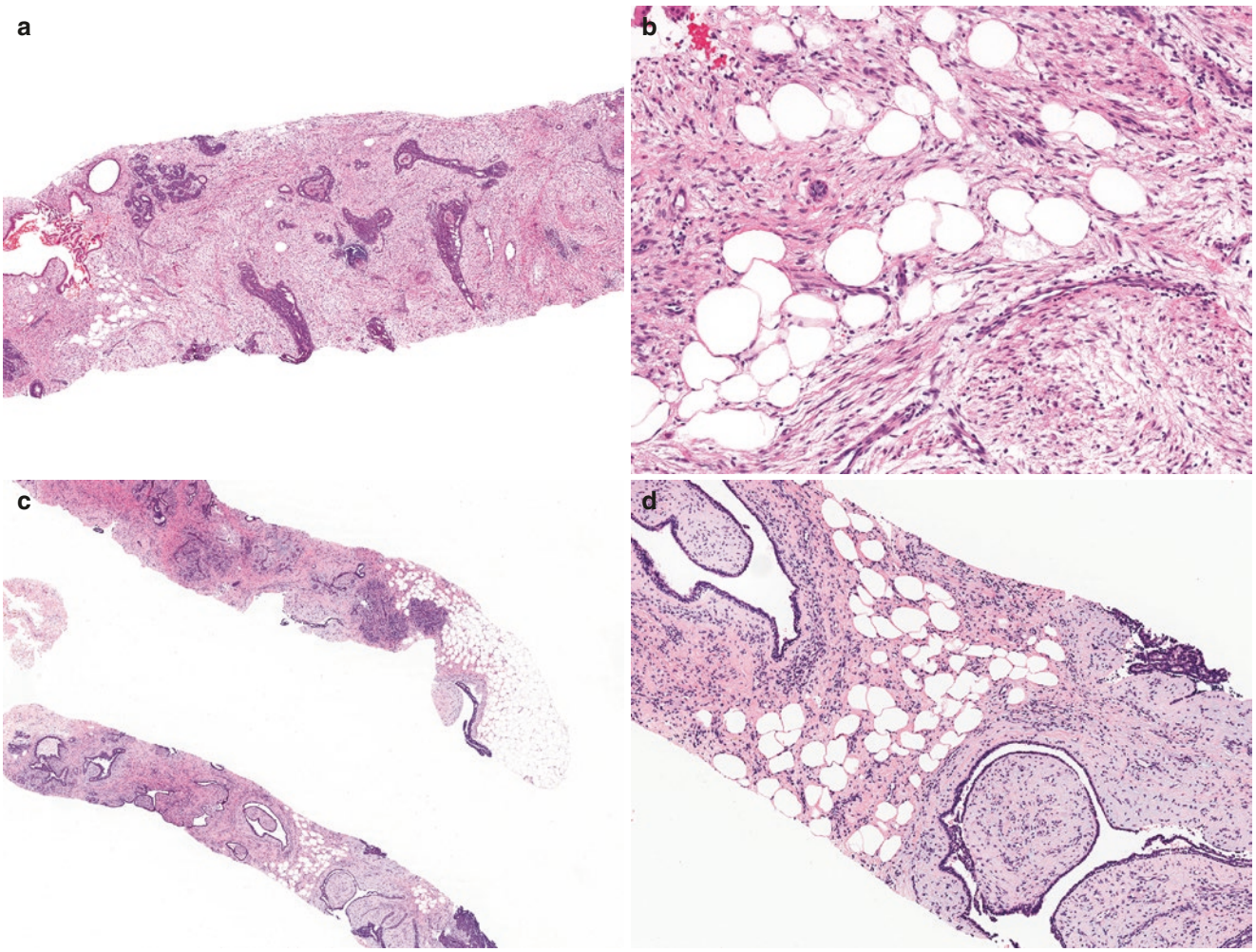

Fig. 7.36 Cellular fibroepithelial tumors with associated fat on core biopsy. (**a**, **b**) Core biopsy of moderately cellular fibroepithelial tumor infiltrating fat. (**c**, **d**) Core biopsy of another cellular fibroepithelial tumor with intralesional fat. The presence of fat within a cellular fibroepithelial tumor on core biopsy raises consideration for infiltrative growth of phyllodes tumor. Excision of both lesions revealed phyllodes tumor

condensation, and stromal cell pleomorphism. More features were seen on average in PTs (3.9) versus FAs (1.4). No lesions with 0–1 features were PTs, whereas 70%, 87.5%, and 100% of lesions with 3, 4, or 5 features were PTs, respectively. In particular, the combination of stromal heterogeneity, subepithelial condensation, and stromal pleomorphism were considered most useful. The sensitivity for detection of PT was 85.2% for the detection of 3 or more histologic features and 74.1% for the detection of three or more mitotic figures [128]. Differences between these studies are likely due to the sample populations, inherent heterogeneity of PTs, and the subjectivity and thresholds of evaluated histologic parameters between observers, which limits practical application. No feature(s) have been found to reliably predict PT versus FA in all cases. A CNB diagnosis of *fibroepithelial neoplasm with cellular stroma* is prudent in equivocal cases, with recommendation for excision.

On occasion, a spindle cell proliferation with associated benign epithelium can raise the differential of fascicular PASH versus cellular fibroepithelial tumor on CNB of a breast mass. The presence of fat within the lesion can especially raise concern for an infiltrative fibroepithelial tumor. The possibility of PASH within a fibroepithelial tumor may also be considered. Careful evaluation for fibroepithelial architecture (elongated and compressed ducts, subepithelial stromal growth) or other areas with classic PASH can point to the correct diagnosis.

The differential diagnosis of malignant PT primarily includes metaplastic carcinoma, primary and metastatic sarcoma, and melanoma (Table 7.3). If biphasic intracanalicu-

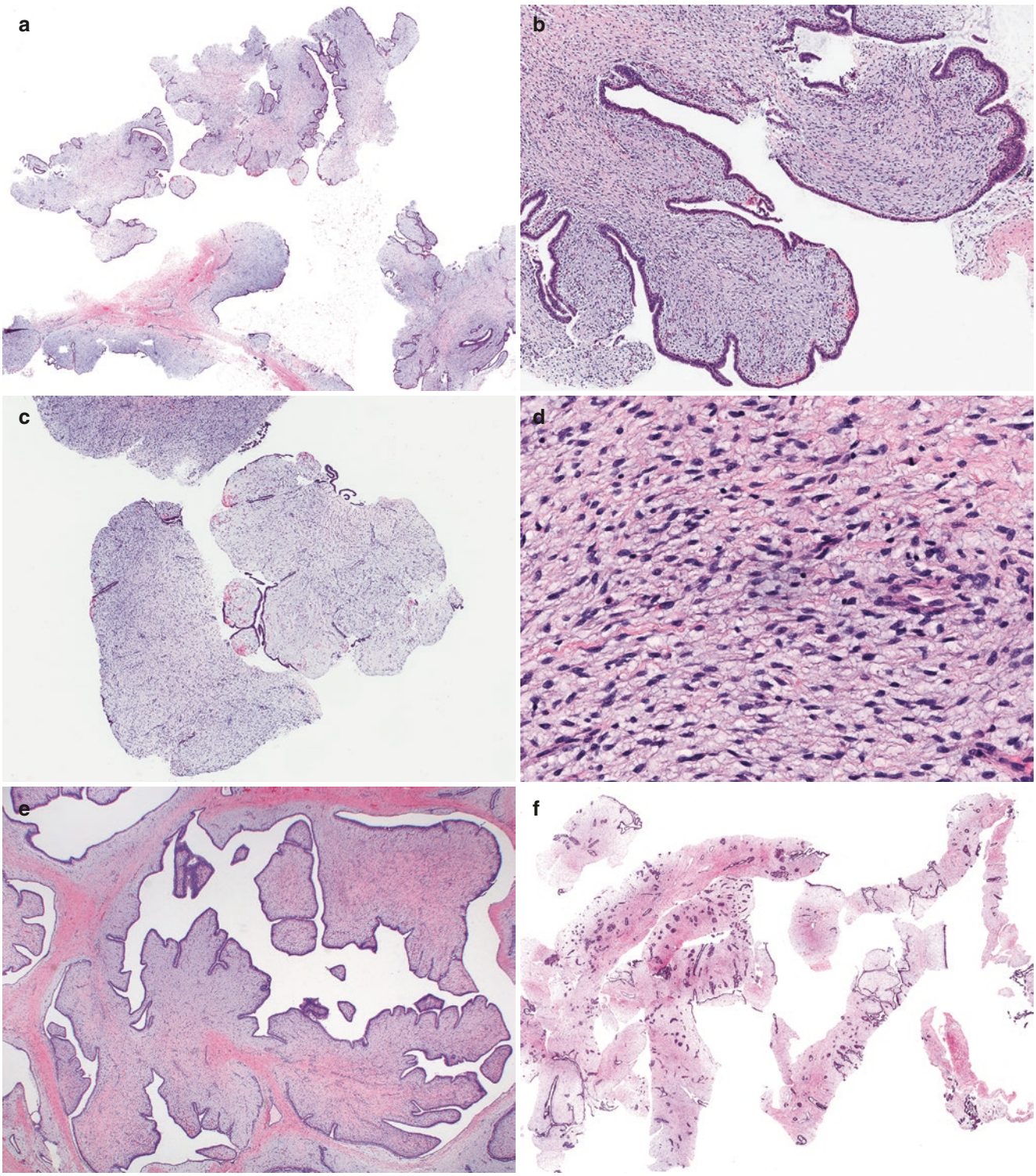

Fig. 7.37 Tissue fragmentation can be seen in core biopsies of phyllodes tumors but is not specific. (**a**–**d**) Cellular fibroepithelial tumor with fragmented bulbous stromal fronds, moderate stromal cellularity, and mitotic activity. (**e**) Excision revealed a borderline phyllodes tumor with well-developed leaf-like architecture. (**f**–**h**) Core biopsy of another cellular fibroepithelial tumor with prominent intracanalicular growth and hint of frond formation without significant tissue fragmentation. (**i**) Excision revealed a benign phyllodes tumor. (**j**, **k**) Core biopsy of a markedly fragmented fibroepithelial tumor with epithelial sloughing and suggestion of stromal fronds. (**l**) Excision revealed fibroadenoma

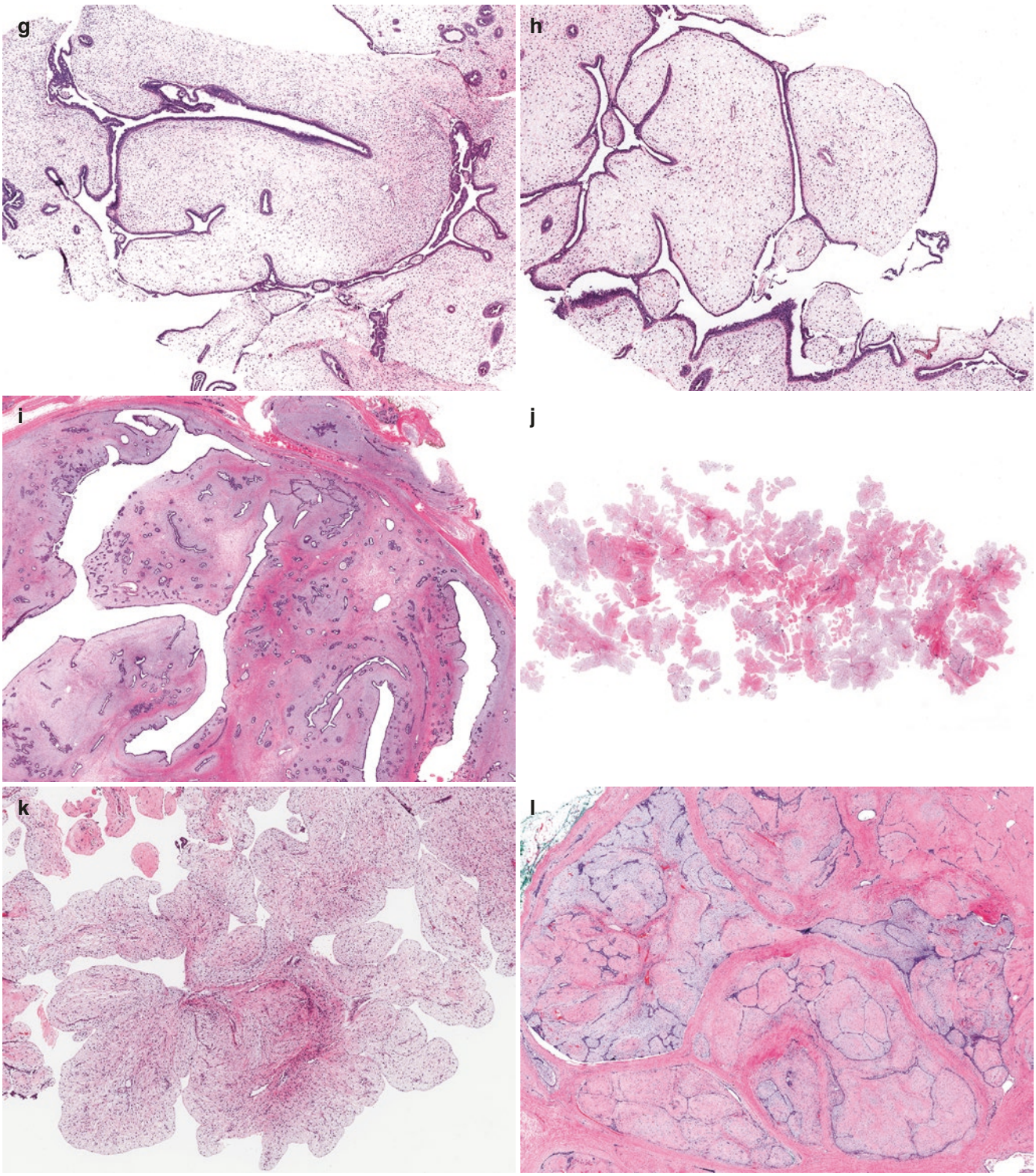

Fig. 7.37 (continued)

Table 7.3 Differential diagnosis of malignant spindle cell neoplasms of the breast

	Malignant phyllodes tumor	Metaplastic spindle cell carcinoma	Sarcoma (primary or metastatic)
Leaf-like growth pattern	Often present[a]	Absent	Absent
Heterologous differentiation	May be present	May be present	Tumor lineage-dependent
Conventional invasive carcinoma component	Absent (exceedingly rare)	May be present (may be squamous)	Absent
Ductal carcinoma in situ	Absent[b]	May be present	Absent
Cytokeratins[c]	Negative or focal	Positive, may be focal	Negative or focal
p63	Negative or focal	Positive, may be focal	Negative or focal
CD34	Positive or negative[d]	Negative	Positive or negative
MED12 mutation	Present in subset	Negative	Negative[e]

[a] May be focal or absent, especially with extensive stromal overgrowth and on core biopsy
[b] May very rarely be involved by ductal carcinoma in situ
[c] Panel of high- and low-molecular-weight cytokeratins is recommended
[d] Positivity decreases with increasing phyllodes tumor grade; often negative in malignant tumors
[e] Leiomyosarcomas may have *MED12* mutations

lar growth is recognized, the diagnosis of PT is straightforward (Fig. 7.27a, b). Atypical or frankly malignant epithelium (invasive or in situ) favors metaplastic carcinoma and is much less common in PTs and absent in sarcomas. Tumors consisting only of malignant spindle cells without an epithelial component are most problematic. In the breast, metaplastic carcinoma is more common than malignant PT (and sarcoma) and should be excluded in such cases. Extensive sampling of an excision specimen may be required to identify the epithelial component of PT, which may be very focal (Figs. 7.30, 7.31, and 7.32). Malignant heterologous elements can be seen in PTs, metaplastic carcinomas, and sarcomas and is not a useful differentiating factor (Fig. 7.29), with the exception of liposarcoma-like areas that would favor PT and essentially exclude metaplastic carcinoma.

The distinction between malignant PT with stromal overgrowth, metaplastic carcinoma, and sarcoma can be especially difficult in CNBs showing a malignant spindle cell neoplasm (Figs. 7.28, 7.29, 7.30, 7.31, 7.32, 7.34 and 7.38). The distinction has clinical implications, as patients with metaplastic carcinoma may undergo axillary sentinel node sampling at time of surgery, and neoadjuvant chemotherapy may be considered. Immunohistochemistry can sometimes be useful if pitfalls are avoided. Metaplastic carcinomas express cytokeratins, especially high-molecular-weight keratins 34βE12, CK5/6, CK14, and AE1/3, although the type and extent of cytokeratin staining varies between tumors and can be focal [346, 353, 357, 393–395]. However, PTs may also show focal (1–5%) cytokeratin positivity, including MNF116, 34βE12, CK7, CK8/18 CK14, AE1/3, and CAM5.2 (Figs. 7.31 and 7.34). MNF116, 34βE12, and CAM5.2 positivity increases with PT grade, and was only seen in malignant PT in one study [345, 346]. Metaplastic spindle cell carcinomas often express p63 [346, 356, 357, 396], but this marker can also be expressed in malignant PTs (57% in one study), as well as reactive stromal proliferations (Figs. 7.31, 7.32, and 7.34) [346, 397]. In one tissue microarray (TMA) study, 57% of malignant PTs were p63 positive (weak or moderate to strong intensity), with focal staining (1–5% of cells) in most (63%) of these cases and <30% of cells staining in all cases. In contrast, 62% of spindle cell carcinomas were p63 positive, which was of moderate to strong intensity in 20–100% of cells [346]. Accordingly, strong diffuse p63 and/or cytokeratin staining favor metaplastic carcinoma, but negative or focal staining is not informative. It has been suggested that p40 expression may be more specific (86% vs. 43%) but less sensitive (46% vs. 62%) than p63 for metaplastic carcinoma versus malignant PT [346]. CD34 is negative in metaplastic carcinomas and may be positive in PTs, but expression decreases with PT grade, such that many malignant PTs (43% in one study) are negative [160, 398]. Positive CD34 staining essentially excludes metaplastic carcinoma, whereas negative staining is not informative (Figs. 7.28, 7.30 and 7.32). In a TMA study, 7 of 13 metaplastic carcinomas (2 of 6 with spindled morphology) expressed GATA3, including 4 cases with at least 25% of cells staining positively, compared to only 1 of 14 malignant PTs, which showed weak staining in 6–25% of cells [29]. Another study observed GATA3 expression in most metaplastic carcinomas but in none of 33 (including 8 malignant) PTs [399]. The neural crest transcription factor SOX10 was found to be expressed in 66% of metaplastic carcinomas versus no PTs, including 14 malignant tumors [400].

In challenging cases, targeted genetic analysis can be useful in distinguishing malignant PT from metaplastic carcinoma (Figs. 7.29, 7.32 and 7.34). *MED12* mutations are the most frequent mutations in PTs with discriminatory potential in this context, having been identified in up to ~40% of malignant PTs across studies but not in metaplastic carcinomas [205, 210, 211, 222, 352, 401–409].

Sarcomas may be morphologically indistinguishable from malignant PTs with complete stromal overgrowth.

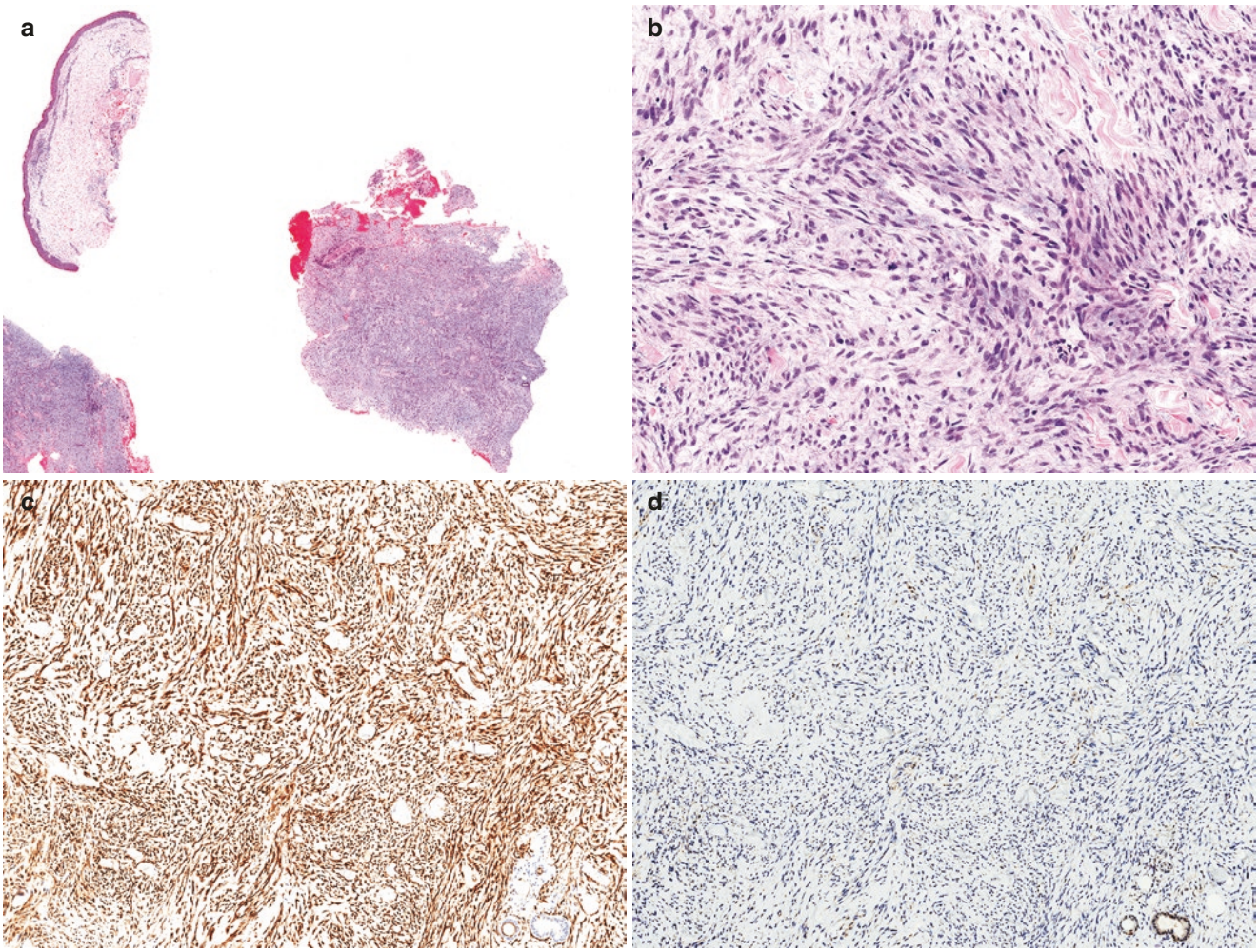

Fig. 7.38 Recurrent malignant phyllodes tumor, skin punch biopsy. (**a**, **b**) Skin punch biopsy of a markedly asymmetric breast showing a malignant spindle cell neoplasm with myxoid-like stroma infiltrating the deep dermis. Excision revealed recurrent malignant phyllodes tumor with extensive stromal overgrowth. (**c**) The tumor showed strong diffuse expression of p16 and (**d**) loss of RB expression, a non-specific immunophenotype that has been described in a subset of malignant but not benign or borderline phyllodes tumors. Multiple cytokeratins, p63, CD34, GATA3, SOX10, ER, SMA, and desmin were negative (not shown)

Exclusion of metastatic sarcoma is facilitated by clinical history. Primary breast sarcomas have identical features as in extramammary sites but, aside from angiosarcomas, are exceedingly rare in the breast and a diagnosis of exclusion. In one study, 5 of 6 tumors diagnosed as primary breast sarcomas were found to have genetic features of PTs (*MED12*, *TERT*, *FLNA*, and/or *BCOR* mutations), suggesting that these tumors have similar origins [410]. Clinicopathologic features and outcomes have been shown to be similar between PTs and primary breast sarcomas [411].

In the absence of a recognized biphasic component on CNB, the differential diagnosis also includes other spindle cell tumors. Although most fibromatoses express nuclear β-catenin, this marker is not specific in this context, being positive in some PTs and metaplastic carcinomas [350, 412]. Fibromatosis is CD34 negative. Melanomas and nerve sheath tumors are often SOX10 and S100 protein positive, and melanomas may express other melanocytic markers. Myofibroblastomas do not typically entrap epithelial elements, facilitating distinction from PTs with evidence of biphasic growth. Myofibroblastomas and PTs can be CD34 and SMA positive, but myofibroblastomas often express ER, PR, and AR, and may be more diffusely desmin positive, in contrast to PTs. Genetic analysis can also be helpful to distinguish PTs from other spindle cell lesions. Identification of a *MED12* exon 2 mutation favors a fibroepithelial tumor [413], and other aberrations can point to the alternate diagnosis (i.e., *CTNNB1* or *APC* mutations in fibromatosis, gene fusions specific to sarcoma types).

Pathogenesis, Molecular Pathology, and Risk Factors

PTs derive from specialized intralobular stroma. Early clonality studies showed that the stroma is monoclonal [197–199, 201, 414], with a monoclonal epithelial component identified in some tumors [197, 415]. Epithelial-stromal interactions have been suggested to play a role in PT pathogenesis. Consistent with this, stromal cellularity and mitotic activity is increased in subepithelial zones [416]. Wnt/β-catenin signaling has been implicated. Sawyer et al. found stromal β-catenin nuclear staining without *CTNNB1* mutations in PTs, with a direct correlation between epithelial Wnt ligand Wnt5a and stromal nuclear β-catenin expression in benign but not malignant PTs. Thus, epithelial-derived Wnt signaling may contribute to tumor development via stromal β-catenin activation, with stromal proliferation becoming independent of the epithelium during tumor progression [350, 416]. Additional evidence supportive of epithelial-stromal interaction in PT pathogenesis can be inferred from correlations between epithelial marker expression (ER, PR, E-cadherin) and stromal histologic features or grade [386, 417].

MED12 exon 2 mutations identical to those identified in FAs have been identified in stromal cells of PTs, and other genes (*RARA*, *SETD2*, *KMT2D*, *FLNA*, among others) are also recurrently mutated in both tumors [205, 208–211, 222, 401, 418], supporting a shared pathogenesis. Using a targeted sequencing panel of 16 genes implicated in fibroepithelial tumor pathogenesis, PTs were more likely to harbor multiple mutations compared to FAs, including when comparing only benign PTs to FAs [205]. Some PTs likely arise from FAs, although this remains controversial. Observational support for this hypothesis derives from the similar morphology and genetic profiles of both tumors, the relatively high frequency of FAs in patients with PTs, and the identification of FA-like areas in some PTs [258, 324]. More direct genetic evidence was first provided by Noguchi et al., who found evidence of stromal monoclonality with alteration of the same *AR* allele in three FAs that subsequently recurred as PTs [199]. More recently, studies of synchronous and metachronous ipsilateral fibroepithelial tumors revealed identical *MED12* mutations in paired FAs and PTs (including benign and malignant tumors), indicative of clonal relatedness [211, 419]. Furthermore, PTs with FA-like areas were found to be genetically distinct from PTs without FA-like areas [420]. In this context, the increased frequency of mutations in *RARA*, *TERT*, *FLNA*, and *SETD2* in PTs compared to FAs may additionally implicate these genes in progression to PT [205, 211, 212, 419]. Nonetheless, the high prevalence of FAs and relative rarity of PTs suggests that an event causing progression of FA to PT would be exceptionally rare [339].

Genetic features associated with grade progression among PTs have been characterized. *TERT* alterations, including promoter mutations, correlate with tumor grade and are among postulated drivers of tumor progression [205, 210, 222]. *TERT* alterations have been associated with increased *TERT* mRNA and TERT protein expression in stromal cells of PT [210, 371]. In the largest studies, *TERT* alterations were identified in 18–32% benign, 57–61% borderline, and 46–68% malignant tumors [205, 210, 212, 371]. *TERT* promoter mutations have only rarely been identified in FAs [205, 212]. Increased telomerase activity stemming from *TERT* aberrations may help overcome replicative senescence and allow for accumulation of additional aberrations during tumor progression [210, 339]. Mutations in *FLNA*, *TP53*, and *RB1* have also been found to correlate with increasing grade, and *PTEN* aberrations were enriched (11%) in malignant tumors [205], whereas *MED12* mutations appear to correlate negatively with grade, being less frequent in malignant PTs [205, 210]. Some studies identified *TP53*, *RB1*, *NF1*, *PIK3CA*, and *EGFR* aberrations exclusively in borderline or malignant tumors [210, 211, 401]. A pathogenic role for the tumor suppressor *TP53* is further supported by the finding that women with Li-Fraumeni syndrome harboring germline *TP53* mutations are susceptible to PT development [421]. Liu et al. identified genetic aberrations in tyrosine kinase (*FGFR1*/*EGFR*) and PI-3 kinase signaling pathways in 8 of 10 malignant phyllodes tumors, including activating *FGFR1*, *PIK3CA*, and *BRAF* mutations [222]. Activating hotspot mutations in *AKT1*, *NRAS*, *ERBB2*, and *ERBB3*, as well as *KIAA1549-BRAF* and *FGFR3-TACC3* gene fusions, have also been found in low frequency in malignant PTs [210, 352, 422]. Several of these aberrations are potentially targetable and could suggest therapeutic options for these aggressive tumors. Higher grade PTs also have increased karyotypic complexity with increased chromosomal copy number changes relative to lower grade tumors [201, 415, 423–427]. Recurrent 1q gain and 13q loss have been associated with borderline/malignant grade [426–431]. Gains of 7p and 8q, losses of 10 and 13q, losses in 9p21.3 (*CDKN2A/B*), and amplifications, including *EGFR*, are potential markers of malignant tumors [425].

There is evidence for *MED12*-dependent and *MED12*-independent pathways in PT development. In a study of 16 borderline and malignant PTs, Pareja et al. compared the genetic profiles of 7 PTs with FA-like areas and 9 PTs without FA-like areas and found *MED12* mutations to be significantly more frequent in the group with FA-like areas (71%) compared to the group without FA-like areas (11%), which had more frequent aberrations in *EGFR*, *TP53*, and *RB1*. The authors speculate that some borderline and malignant PTs may develop from *MED12*-mutated FAs, whereas others arise de novo via accumulation of genetic aberrations in

other cancer drivers [420]. Consistent with the concept of multiple pathogenic pathways, others have found more frequent aberrations in *TERT*, *RARA*, *SETD2*, *EGFR*, *ERBB4*, *MAP3K1*, and *IGF1R* in *MED12*-mutated tumors compared to *MED12*-wild-type tumors, which instead more often harbored *TP53* and *PIK3CA* mutations [205]. In this context, it is interesting that patients with malignant PT and a history of ipsilateral FA had a significantly longer survival than those without FA history [432], and *MED12*-mutated PTs had a lower recurrence rate than *MED12*-wild-type tumors [433].

Genetic analysis has uncovered intratumoral genetic heterogeneity in PTs, which at least in some cases, correlates with morphologic heterogeneity. Regions of increased stromal cellularity and atypia have been found to have increased mutational burden [434] and more chromosomal copy number changes and pathogenic mutations [222], compared to regions of less cellularity and atypia within the same tumors. Liu et al. additionally described more chromosomal aberrations in non-heterologous areas compared with liposarcomatous foci in microdissected PTs [222]. Histologically similar regions within PTs have also been shown to display differences in chromosomal copy number alterations, and acquired chromosomal aberrations in recurrent versus primary tumors were independent of histologic progression. These findings may provide an explanation for the imperfect correlation between histologic grading and tumor behavior and progression [330, 424].

Prognosis and Clinical Management

Local Recurrence

Most PTs are benign, and only a minority of tumors recur locally following excision [252]. In a large series of 605 PTs, the overall recurrence rate was ~13%, with the majority (91%) being local [257]. Most local recurrences occur within 2–3 years of diagnosis, although intervals greater than 20 years have been reported [252, 257, 258, 260, 263, 285, 287, 288, 293, 314]. In one study, 65% of patients experienced a single tumor recurrence, with 2, 3, and 6 recurrences occurring in ~29%, 5%, and ~1%, respectively [257]. Most local PT recurrences are of the same grade as the original tumor, although some may be higher grade [257, 287, 435]. In one study, the overall rate of progression of initially benign or borderline tumors to a higher grade recurrence was 31.5%. Twenty-one of 48 (~44%) initially benign tumors and 2 of 16 (~13%) initially borderline tumors recurred as higher grade, with ~9% (6 of 64) benign or borderline tumors recurring as malignant [257].

Recurrence risk has been correlated with tumor grade. A recent meta-analysis of 54 studies with a total of 9234 patients identified a local recurrence risk of 6–9%, 11–16%, and 14–21% for benign, borderline, and malignant PTs, respectively [436]. Features that have been correlated with increased recurrence risk include stromal mitotic activity, stromal cellularity, stromal pleomorphism, stromal overgrowth, myxoid stroma, tumor necrosis, infiltrative borders, and younger age [257, 258, 285, 288, 436–438]. Tan et al. developed a nomogram based on stromal cell atypia, mitotic activity, stromal overgrowth, and surgical margins (*AMOS* criteria) that could predict recurrence-free survival more accurately than an aggregate sum of predictive histologic factors. Although the nomogram does not distinguish between local recurrence and metastasis, the vast majority of events in this study were local [257]. The nomogram has been validated in other patient populations [20, 324, 439]. Positive surgical margin status has also been implicated as a strong predictive factor for local recurrence in numerous other studies [34, 255, 258, 260, 261, 286, 292, 438–441]. However, a recent meta-analysis identified a correlation between positive margin status and local recurrence for malignant PTs only, with a tendency for increased recurrence in benign and borderline tumors [436]. Furthermore, several recent studies have suggested that benign PTs have low recurrence risk that may be independent of margin status [287, 435, 436, 442–447].

Metastases and Survival

Axillary metastases of PTs are rare, and distant metastases are also uncommon, estimated to occur in ~2% of cases overall [252, 435, 448]. Essentially only malignant PTs metastasize, often after local recurrence [252, 257, 258, 288, 293, 300, 438]. Metastases usually occur within 5 years of diagnosis [252, 258, 263, 285, 287, 293, 449]. The most common sites of metastatic spread are lung and pleura, with less common sites including vertebrae, bones, gastrointestinal tract, and liver, among others [34, 257, 263, 314, 438, 449]. Metastases are essentially always comprised only of the stromal component. Predictors of metastasis include older age (>50 years) and indicators of tumor biology, such as stromal overgrowth, diffuse and marked stromal atypia, necrosis, infiltrative border, high mitotic count, size (>9 cm), and heterologous differentiation [258, 260, 314, 449–452]. In a large series of 605 PTs, 2% of women died of PT [257]. Deaths typically occur with malignant PT preceded by metastasis [288, 293, 314]. Local recurrence with chest wall invasion may also rarely be fatal [293]. Reinfuss et al. reported a median survival of 4 months for patients with metastatic disease, and in another study it was 17 months [438, 453].

Treatment

The primary treatment for PTs is surgical excision. Breast conserving surgery is typically preferred if feasible.

Mastectomy has been performed if breast conserving surgery is not possible due to large tumor size and/or high tumor to breast ratio or for recurring disease [34, 262, 285, 438, 441, 448, 454–457]. The likelihood of PT when CNB reveals a fibroepithelial tumor with cellular stroma is relatively high. In one study directly evaluating outcomes of patients with cellular fibroepithelial lesions initially diagnosed in CNBs, 41% of patients were found to have PT on excision [127]. In another study in which PT could not be excluded on CNB, 63% of patients had PT on excision [349]. In this context and due to the uncertainty and challenges in differentiating cellular FA from PT, surgical excision is often warranted for cellular fibroepithelial lesions identified on CNB [126]. Whereas FAs are routinely enucleated, PTs have typically been excised with the goal of achieving negative margins [34, 438, 448]. However, recent studies suggest that benign PTs have low recurrence risk that may be independent of margin status and may not require wide excision [255, 287, 435, 436, 442–447]. Guidelines from the National Comprehensive Cancer Network (NCCN), 2021 recommend excisional biopsy with complete mass removal but without the goal of obtaining negative margins, followed by observation, for indeterminate fibroepithelial tumors or benign PTs identified on CNB. Fibroepithelial tumors with features concerning for borderline or malignant PT on CNB should be excised to negative margins [458]. Fibroepithelial tumors involved by atypical hyperplasia or carcinoma are excised and managed according to guidelines for these lesions [458].

Adequate margin width for PT excision is controversial, and the adequate distance to negative margins has not been prospectively evaluated. A rim of at least 1 cm of uninvolved tissue has often been cited based on retrospective analyses [34, 258, 297, 438, 458]. However, this margin width is not consistently obtained in practice, and it is unlikely to be necessary for all PTs [435]. Recent studies and meta-analyses have failed to identify significant correlations between negative margin width and local recurrence [435, 437, 459–463]. This is particularly relevant in benign PTs, for which emerging data suggest that wider excision is unlikely to have significant impact on local recurrence [255, 287, 435, 436, 442–447]. The minimum width of a negative margin in borderline and malignant PTs remains uncertain, but several studies have suggested that 1 cm margins may not be necessary [437, 459, 462, 464, 465]. An expert consensus review has suggested that tumor on ink or <1 mm away be considered positive for PTs [313]. On the other hand, the NCCN currently recommends a 1 cm margin for borderline and malignant PTs, while noting that narrower margins are not an absolute indication for mastectomy [458].

Given the very low incidence of axillary nodal metastasis in PTs, axillary sentinel lymph node biopsy or dissection is not routinely indicated in the absence of concurrent invasive carcinoma or confirmed nodal metastasis [34, 435, 448, 458].

There are no randomized controlled prospective data to support the use of adjuvant radiation therapy for PT, and its routine use has not been established. However, patients with borderline and especially malignant tumors may be offered radiation treatment [262, 285, 297, 339, 455, 456, 466]. In a study using Surveillance, Epidemiology, and End Results Program (SEER) data from 1983 to 2013, 11% and 16% of patients with malignant PTs undergoing breast conserving surgery or mastectomy, respectively, were treated with adjuvant radiation [467]. Some studies have reported a decrease in local recurrences with use of adjuvant radiotherapy, but without an effect on survival [297, 467–472]. The NCCN guidelines suggest that radiation could be considered if recurrence could create significant morbidity, such as chest wall recurrence following mastectomy [458]. There is no proven benefit for chemotherapy in the treatment of PTs, which may be considered on a case-by-case basis in malignant tumors [339, 448, 473].

References

1. Arrigoni MG, Dockerty MB, Judd ES. The identification and treatment of mammary hamartoma. Surg Gynecol Obstet. 1971;133(4):577–82.
2. Banev SG, Filipovski VA. Chondrolipoma of the breast—case report and a review of literature. Breast. 2006;15(3):425–6.
3. Charpin C, Mathoulin MP, Andrac L, Barberis J, Boulat J, Sarradour B, et al. Reappraisal of breast hamartomas. A morphological study of 41 cases. Pathol Res Pract. 1994;190(4):362–71.
4. Chiacchio R, Panico L, D'Antonio A, Delrio P, Bifano D, Avallone M, et al. Mammary hamartomas: an immunohistochemical study of ten cases. Pathol Res Pract. 1999;195(4):231–6.
5. Davies JD, Riddell RH. Muscular hamartomas of the breast. J Pathol. 1973;111(3):209–11.
6. Daya D, Trus T, D'Souza TJ, Minuk T, Yemen B. Hamartoma of the breast, an underrecognized breast lesion. A clinicopathologic and radiographic study of 25 cases. Am J Clin Pathol. 1995;103(6):685–9.
7. Di Tommaso L, Pasquinelli G, Damiani S. Smooth muscle cell differentiation in mammary stromo-epithelial lesions with evidence of a dual origin: stromal myofibroblasts and myoepithelial cells. Histopathology. 2003;42(5):448–56.
8. Fisher CJ, Hanby AM, Robinson L, Millis RR. Mammary hamartoma—a review of 35 cases. Histopathology. 1992;20(2):99–106.
9. Hayashi H, Ito T, Matsushita K, Kitamura H, Kanisawa M. Mammary hamartoma: immunohistochemical study of two adenolipomas and one variant with cartilage, smooth muscle and myoepithelial proliferation. Pathol Int. 1996;46(1):60–5.
10. Herbert M, Sandbank J, Liokumovich P, Yanai O, Pappo I, Karni T, et al. Breast hamartomas: clinicopathological and immunohistochemical studies of 24 cases. Histopathology. 2002;41(1):30–4.
11. Linell F, Ostberg G, Soderstrom J, Andersson I, Hildell J, Ljungqvist U. Breast hamartomas. An important entity in mammary pathology. Virchows Arch A Pathol Anat Histol. 1979;383(3):253–64.

12. Sevim Y, Kocaay AF, Eker T, Celasin H, Karabork A, Erden E, et al. Breast hamartoma: a clinicopathologic analysis of 27 cases and a literature review. Clinics (Sao Paulo). 2014;69(8):515–23.
13. Tse GM, Law BK, Ma TK, Chan AB, Pang LM, Chu WC, et al. Hamartoma of the breast: a clinicopathological review. J Clin Pathol. 2002;55(12):951–4.
14. Wahner-Roedler DL, Sebo TJ, Gisvold JJ. Hamartomas of the breast: clinical, radiologic, and pathologic manifestations. Breast J. 2001;7(2):101–5.
15. Chang HL, Lerwill MF, Goldstein AM. Breast hamartomas in adolescent females. Breast J. 2009;15(5):515–20.
16. Chua CL, Thomas A, Ng BK. Cystosarcoma phyllodes—Asian variations. Aust N Z J Surg. 1988;58(4):301–5.
17. Ravakhah K, Javadi N, Simms R. Hamartoma of the breast in a man: first case report. Breast J. 2001;7(4):266–8.
18. Nangia A, Patiri K, Pujani M, Sehgal S. Bilateral myoid hamartoma of breast: an exceptionally rare lesion. Breast Dis. 2013;34(2):77–80.
19. Aggelatou R, Mouselimi M, Panou A. The role of mammography in the diagnostic approach of breast hamartomas. Eur J Gynaecol Oncol. 1998;19(4):399–400.
20. Chng TW, Lee JY, Lee CS, Li H, Tan MH, Tan PH. Validation of the Singapore nomogram for outcome prediction in breast phyllodes tumours: an Australian cohort. J Clin Pathol. 2016;69(12):1124–6.
21. Desai A, Ramesar K, Allan S, Marr A, Howlett DC. Breast hamartoma arising in axillary ectopic breast tissue. Breast J. 2010;16(4):433–4.
22. Dworak O, Reck T, Greskotter KR, Kockerling F. Hamartoma of an ectopic breast arising in the inguinal region. Histopathology. 1994;24(2):169–71.
23. Farrokh D, Hashemi J, Ansaripour E. Breast hamartoma: mammographic findings. Iran J Radiol. 2011;8(4):258–60.
24. Helvie MA, Adler DD, Rebner M, Oberman HA. Breast hamartomas: variable mammographic appearance. Radiology. 1989;170(2):417–21.
25. Berna JD, Nieves FJ, Romero T, Arcas I. A multimodality approach to the diagnosis of breast hamartomas with atypical mammographic appearance. Breast J. 2001;7(1):2–7.
26. Paraskevopoulos JA, Hosking SW, Stephenson T. Breast within a breast: a review of breast hamartomas. Br J Clin Pract. 1990;44(1):30–2.
27. Black J, Metcalf C, Wylie EJ. Ultrasonography of breast hamartomas. Australas Radiol. 1996;40(4):412–5.
28. Park SY, Oh KK, Kim EK, Son EJ, Chung WH. Sonographic findings of breast hamartoma: emphasis on compressibility. Yonsei Med J. 2003;44(5):847–54.
29. Cimino-Mathews A, Subhawong AP, Illei PB, Sharma R, Halushka MK, Vang R, et al. GATA3 expression in breast carcinoma: utility in triple-negative, sarcomatoid, and metastatic carcinomas. Hum Pathol. 2013;44(7):1341–9.
30. Jones MW, Norris HJ, Wargotz ES. Hamartomas of the breast. Surg Gynecol Obstet. 1991;173(1):54–6.
31. McGuire LI, Cohn D. Hamartoma of the breast. Aust N Z J Surg. 1991;61(9):713–6.
32. Anani PA, Hessler C. Breast hamartoma with invasive ductal carcinoma. Report of two cases and review of the literature. Pathol Res Pract. 1996;192(12):1187–94.
33. Baron M, Ladonne JM, Gravier A, Picquenot JM, Berry M. Invasive lobular carcinoma in a breast hamartoma. Breast J. 2003;9(3):246–8.
34. Chen WH, Cheng SP, Tzen CY, Yang TL, Jeng KS, Liu CL, et al. Surgical treatment of phyllodes tumors of the breast: retrospective review of 172 cases. J Surg Oncol. 2005;91(3):185–94.
35. Choi N, Ko ES. Invasive ductal carcinoma in a mammary hamartoma: case report and review of the literature. Korean J Radiol. 2010;11(6):687–91.
36. Coyne J, Hobbs FM, Boggis C, Harland R. Lobular carcinoma in a mammary hamartoma. J Clin Pathol. 1992;45(10):936–7.
37. Harigopal M, Mudrovich SA, Hoda SA, Rosen PP. Secondary tumors in mammary adenolipomas: a report of 2 unusual cases. Arch Pathol Lab Med. 2003;127(3):e151–4.
38. Kuroda N, Sugimoto T, Numoto S, Enzan H. Microinvasive lobular carcinoma associated with intraductal spread arising in a mammary hamartoma. J Clin Pathol. 2002;55(1):76–7.
39. Mester J, Simmons RM, Vazquez MF, Rosenblatt R. In situ and infiltrating ductal carcinoma arising in a breast hamartoma. AJR Am J Roentgenol. 2000;175(1):64–6.
40. Ruiz-Tovar J, Reguero-Callejas ME, Alaez AB, Ramiro C, Rojo R, Collado MV, et al. Infiltrating ductal carcinoma and ductal carcinoma in situ associated with mammary hamartoma. Breast J. 2006;12(4):368–70.
41. Tse GM, Law BK, Pang LM, Cheung HS. Ductal carcinoma in situ arising in mammary hamartoma. J Clin Pathol. 2002;55(7):541–2.
42. Yasuda S, Kubota M, Noto T, Mukai M, Tokuda Y, Hanaue H, et al. Two cases of adenolipoma of the breast. Tokai J Exp Clin Med. 1992;17(3–4):139–44.
43. Damiani S, Panarelli M. Mammary adenohibernoma. Histopathology. 1996;28(6):554–5.
44. Garijo MF, Torio B, Val-Bernal JF. Mammary hamartoma with brown adipose tissue. Gen Diagn Pathol. 1997;143(4):243–6.
45. Kapucuoglu N, Percinel S, Angelone A. Adenohibernoma of the breast. Virchows Arch. 2008;452(3):351–2.
46. Brogi E. Fibroepithelial neoplasms. In: Hoda S, Brogi E, Koerner FC, Rosen PR, editors. Rosen's breast pathology. 4th ed. Philedelphia: Wolters Kluwer; 2014. p. 1379.
47. Oberman HA. Hamartomas and hamartoma variants of the breast. Semin Diagn Pathol. 1989;6(2):135–45.
48. Bayar S, Dusunceli E, Heper AO, Guner R, Genc V, Demirkazik A. Myoid hamartoma of the breast: a very rare entity. Breast J. 2010;16(1):86–8.
49. Stafyla V, Kotsifopoulos N, Grigoriadis K, Bakoyiannis CN, Peros G, Sakorafas GH. Myoid hamartoma of the breast: a case report and review of the literature. Breast J. 2007;13(1):85–7.
50. Garfein CF, Aulicino MR, Leytin A, Drossman S, Hermann G, Bleiweiss IJ. Epithelioid cells in myoid hamartoma of the breast: a potential diagnostic pitfall for core biopsies. Arch Pathol Lab Med. 1996;120(7):676–80.
51. Mathers ME, Shrimankar J. Lobular neoplasia within a myoid hamartoma of the breast. Breast J. 2004;10(1):58–9.
52. Fushimi H, Kotoh K, Nishihara K, Fujinaka H, Takao T. Chondrolipoma of the breast: a case report with cytological and histological examination. Histopathology. 1999;35(5):478–9.
53. Kaplan L, Walts AE. Benign chondrolipomatous tumor of the human female breast. Arch Pathol Lab Med. 1977;101(3):149–51.
54. Lugo M, Reyes JM, Putong PB. Benign chondrolipomatous tumors of the breast. Arch Pathol Lab Med. 1982;106(13):691–2.
55. Marsh WL Jr, Lucas JG, Olsen J. Chondrolipoma of the breast. Arch Pathol Lab Med. 1989;113(4):369–71.
56. Perez MT, Alexis JB. Chondrolipoma of the breast presenting as calcifications in a routine mammogram. Histopathology. 1999;35(2):189–91.
57. Eusebi V, Cunsolo A, Fedeli F, Severi B, Scarani P. Benign smooth muscle cell metaplasia in breast. Tumori. 1980;66(5):643–53.
58. Gogas J, Markopoulos C, Gogas H, Skandalakis P, Kontzoglou K, Stavridou A. Hamartomas of the breast. Am Surg. 1994;60(6):447–50.

59. Herbert M, Schvimer M, Zehavi S, Mendlovic S, Karni T, Pappo I, et al. Breast hamartoma: fine-needle aspiration cytologic finding. Cancer. 2003;99(4):255–8.
60. Azzopardi JGAA, Millis RR. Problems in breast pathology. London: W.B. Saunders; 1979.
61. Magro G, Bisceglia M, Michal M, Eusebi V. Spindle cell lipoma-like tumor, solitary fibrous tumor and myofibroblastoma of the breast: a clinico-pathological analysis of 13 cases in favor of a unifying histogenetic concept. Virchows Arch. 2002;440(3):249–60.
62. Panagopoulos I, Gorunova L, Andersen HK, Pedersen TD, Lomo J, Lund-Iversen M, et al. Genetic characterization of myoid hamartoma of the breast. Cancer Genomics Proteomics. 2019;16(6):563–8.
63. Dietrich CU, Pandis N, Andersen JA, Heim S. Chromosome abnormalities in adenolipomas of the breast: karyotypic evidence that the mesenchymal component constitutes the neoplastic parenchyma. Cancer Genet Cytogenet. 1994;72(2):146–50.
64. Rohen C, Caselitz J, Stern C, Wanschura S, Schoenmakers EF, Van de Ven WJ, et al. A hamartoma of the breast with an aberration of 12q mapped to the MAR region by fluorescence in situ hybridization. Cancer Genet Cytogenet. 1995;84(1):82–4.
65. Dal Cin P, Wanschura S, Christiaens MR, Van den Berghe I, Moerman P, Polito P, et al. Hamartoma of the breast with involvement of 6p21 and rearrangement of HMGIY. Genes Chromosomes Cancer. 1997;20(1):90–2.
66. Dumollard JM, Ranchere-Vince D, Burel F, Coindre JM, Tallini G, Ligon AH, et al. [Spindle cell lipoma and 13q deletion: diagnostic utility of cytogenetic analysis]. Ann Pathol. 2001;21(4):303–10.
67. Kazmierczak B, Meyer-Bolte K, Tran KH, Wockel W, Breightman I, Rosigkeit J, et al. A high frequency of tumors with rearrangements of genes of the HMGI(Y) family in a series of 191 pulmonary chondroid hamartomas. Genes Chromosomes Cancer. 1999;26(2):125–33.
68. Sornberger KS, Weremowicz S, Williams AJ, Quade BJ, Ligon AH, Pedeutour F, et al. Expression of HMGIY in three uterine leiomyomata with complex rearrangements of chromosome 6. Cancer Genet Cytogenet. 1999;114(1):9–16.
69. Tallini G, Vanni R, Manfioletti G, Kazmierczak B, Faa G, Pauwels P, et al. HMGI-C and HMGI(Y) immunoreactivity correlates with cytogenetic abnormalities in lipomas, pulmonary chondroid hamartomas, endometrial polyps, and uterine leiomyomas and is compatible with rearrangement of the HMGI-C and HMGI(Y) genes. Lab Investig. 2000;80(3):359–69.
70. Wang X, Zamolyi RQ, Zhang H, Pannain VL, Medeiros F, Erickson-Johnson M, et al. Fusion of HMGA1 to the LPP/TPRG1 intergenic region in a lipoma identified by mapping paraffin-embedded tissues. Cancer Genet Cytogenet. 2010;196(1):64–7.
71. Williams AJ, Powell WL, Collins T, Morton CC. HMGI(Y) expression in human uterine leiomyomata. Involvement of another high-mobility group architectural factor in a benign neoplasm. Am J Pathol. 1997;150(3):911–8.
72. Xiao S, Lux ML, Reeves R, Hudson TJ, Fletcher JA. HMGI(Y) activation by chromosome 6p21 rearrangements in multilineage mesenchymal cells from pulmonary hamartoma. Am J Pathol. 1997;150(3):901–10.
73. Liaw D, Marsh DJ, Li J, Dahia PL, Wang SI, Zheng Z, et al. Germline mutations of the PTEN gene in Cowden disease, an inherited breast and thyroid cancer syndrome. Nat Genet. 1997;16(1):64–7.
74. Pilarski R. Risk perception among women at risk for hereditary breast and ovarian cancer. J Genet Couns. 2009;18(4):303–12.
75. Schrager CA, Schneider D, Gruener AC, Tsou HC, Peacocke M. Clinical and pathological features of breast disease in Cowden's syndrome: an underrecognized syndrome with an increased risk of breast cancer. Hum Pathol. 1998;29(1):47–53.
76. Gomez Garcia EB, Lobbes MB, van de Vijver K, Keymeulen K, van der Ent F, Yntema HG, et al. Occult breast cancer due to multiple calcified hamartomas in a patient with Cowden syndrome. Case Rep Radiol. 2012;2012:638725.
77. Tse G, Koo JS, Thicke AA. Hamartoma. In: The WHO Classification of Tumours Editorial Board, editor. WHO classification of tumours breast tumours. 5th ed. Lyon: International Agency for Research on Cancer; 2019. p. 166–7.
78. Yu L, Yang W, Xu X, Gu Y, Wang C, Lu H, et al. Myoid harmatoma of the breast: clinicopathologic analysis of a rare tumor indicating occasional recurrence potential. Breast J. 2011;17(3):322–4.
79. Foster ME, Garrahan N, Williams S. Fibroadenoma of the breast: a clinical and pathological study. J R Coll Surg Edinb. 1988;33(1):16–9.
80. Goehring C, Morabia A. Epidemiology of benign breast disease, with special attention to histologic types. Epidemiol Rev. 1997;19(2):310–27.
81. Santen RJ, Mansel R. Benign breast disorders. N Engl J Med. 2005;353(3):275–85.
82. Sanchez R, Ladino-Torres MF, Bernat JA, Joe A, DiPietro MA. Breast fibroadenomas in the pediatric population: common and uncommon sonographic findings. Pediatr Radiol. 2010;40(10):1681–9.
83. Weaver DL, Rosenberg RD, Barlow WE, Ichikawa L, Carney PA, Kerlikowske K, et al. Pathologic findings from the Breast Cancer Surveillance Consortium: population-based outcomes in women undergoing biopsy after screening mammography. Cancer. 2006;106(4):732–42.
84. Hunter TB, Roberts CC, Hunt KR, Fajardo LL. Occurrence of fibroadenomas in postmenopausal women referred for breast biopsy. J Am Geriatr Soc. 1996;44(1):61–4.
85. Dahlstrom JE, Jain S, Sutton T, Sutton S. Diagnostic accuracy of stereotactic core biopsy in a mammographic breast cancer screening programme. Histopathology. 1996;28(5):421–7.
86. Hermann G, Janus C, Schwartz IS, Krivisky B, Bier S, Rabinowitz JG. Nonpalpable breast lesions: accuracy of prebiopsy mammographic diagnosis. Radiology. 1987;165(2):323–6.
87. Thicke AABE, Harada O, Oyama T, Tse G. Fibroadenoma. In: The WHO Classification of Tumours Editorial Board, editor. WHO classification of tumours breast tumours. 5th ed. Lyon: International Agency for Research on Cancer; 2019. p. 168–71.
88. Varas X, Leborgne F, Leborgne JH. Nonpalpable, probably benign lesions: role of follow-up mammography. Radiology. 1992;184(2):409–14.
89. Ichihara S, Matsuyama T, Kubo K, Tamura Z, Aoyama H. Infarction of breast fibroadenoma in a postmenopausal woman. Pathol Int. 1994;44(5):398–400.
90. Skenderi F, Krakonja F, Vranic S. Infarcted fibroadenoma of the breast: report of two new cases with review of the literature. Diagn Pathol. 2013;8:38.
91. Pike AM, Oberman HA. Juvenile (cellular) adenofibromas. A clinicopathologic study. Am J Surg Pathol. 1985;9(10):730–6.
92. Song BS, Kim EK, Seol H, Seo JH, Lee JA, Kim DH, et al. Giant juvenile fibroadenoma of the breast: a case report and brief literature review. Ann Pediatr Endocrinol Metab. 2014;19(1):45–8.
93. Alagaratnam TT, Ng WF, Leung EY. Giant fibroadenomas of the breast in an oriental community. J R Coll Surg Edinb. 1995;40(3):161–2.
94. Farrow JH, Ashikari H. Breast lesions in young girls. Surg Clin North Am. 1969;49(2):261–9.
95. McCague A, Davis JV. Giant fibroadenoma in a 22 year old patient: case report and literature review. Breast Dis. 2010;31(1):49–52.

96. Noguchi S, Aihara T, Motomura K, Inaji H, Imaoka S, Koyama H, et al. Demonstration of polyclonal origin of giant fibroadenoma of the breast. Virchows Arch. 1995;427(3):343–7.
97. Oberman HA. Breast lesions in the adolescent female. Pathol Annu. 1979;14(Pt 1):175–201.
98. Alkhunaizi AM, Ismail A, Yousif BM. Breast fibroadenomas in renal transplant recipients. Transplant Proc. 2004;36(6):1839–40.
99. Baildam AD, Higgins RM, Hurley E, Furlong A, Walls J, Venning MC, et al. Cyclosporin A and multiple fibroadenomas of the breast. Br J Surg. 1996;83(12):1755–7.
100. Dent DM, Cant PJ. Fibroadenoma. World J Surg. 1989;13(6):706–10.
101. Kanaan N, Goffin E. Multiple bilateral fibroadenomas of the breasts requiring mastectomy in a renal transplant patient. Clin Nephrol. 2004;61(2):151–4.
102. Seo YL, Choi CS, Yoon DY, Yun EJ, Lee YJ, Park SJ, et al. Benign breast diseases associated with cyclosporine therapy in renal transplant recipients. Transplant Proc. 2005;37(10):4315–9.
103. Son EJ, Oh KK, Kim EK, Cho N, Lee JD, Kim SH, et al. Characteristic imaging features of breast fibroadenomas in women given cyclosporin A after renal transplantation. J Clin Ultrasound. 2004;32(2):69–77.
104. Weinstein SP, Orel SG, Collazzo L, Conant EF, Lawton TJ, Czerniecki B. Cyclosporin A-induced fibroadenomas of the breast: report of five cases. Radiology. 2001;220(2):465–8.
105. Williamson ME, Lyons K, Hughes LE. Multiple fibroadenomas of the breast: a problem of uncertain incidence and management. Ann R Coll Surg Engl. 1993;75(3):161–3.
106. Haagensen C. Diseases of the breast. Philadelphia: W.B. Saunders; 1971.
107. Atwal GS, O'Connor SR, Clamp M, Elston CW. Fibroadenoma occurring in supernumerary breast tissue. Histopathology. 2007;50(4):513–4.
108. Baisre A, Heller DS, Lee J, Zheng P. Fibroadenoma of the vulva. A report of two cases. J Reprod Med. 2002;47(11):949–51.
109. Fisher JH. Fibroadenoma of supernumerary mammary gland tissue in vulva. Am J Obstet Gynecol. 1947;53(2):335–7.
110. Kazakov DV, Spagnolo DV, Stewart CJ, Thompson J, Agaimy A, Magro G, et al. Fibroadenoma and phyllodes tumors of anogenital mammary-like glands: a series of 13 neoplasms in 12 cases, including mammary-type juvenile fibroadenoma, fibroadenoma with lactation changes, and neurofibromatosis-associated pseudoangiomatous stromal hyperplasia with multinucleated giant cells. Am J Surg Pathol. 2010;34(1):95–103.
111. Sington JD, Manek S, Hollowood K. Fibroadenoma of the mammary-like glands of the vulva. Histopathology. 2002;41(6):563–5.
112. Yilmaz E, Sal S, Lebe B. Differentiation of phyllodes tumors versus fibroadenomas. Acta Radiol. 2002;43(1):34–9.
113. Sickles EA. Breast masses: mammographic evaluation. Radiology. 1989;173(2):297–303.
114. Jackson VP, Rothschild PA, Kreipke DL, Mail JT, Holden RW. The spectrum of sonographic findings of fibroadenoma of the breast. Investig Radiol. 1986;21(1):34–40.
115. Kim SJ, Park YM, Jung SJ, Lee KH, Kim OH, Ryu JH, et al. Sonographic appearances of juvenile fibroadenoma of the breast. J Ultrasound Med. 2014;33(11):1879–84.
116. Skaane P, Engedal K. Analysis of sonographic features in the differentiation of fibroadenoma and invasive ductal carcinoma. AJR Am J Roentgenol. 1998;170(1):109–14.
117. Yamaguchi R, Tanaka M, Mizushima Y, Hirai Y, Yamaguchi M, Kaneko Y, et al. Myxomatous fibroadenoma of the breast: correlation with clinicopathologic and radiologic features. Hum Pathol. 2011;42(3):419–23.
118. Strano S, Gombos EC, Friedland O, Mozes M. Color Doppler imaging of fibroadenomas of the breast with histopathologic correlation. J Clin Ultrasound. 2004;32(7):317–22.
119. Kuhl CK. MRI of breast tumors. Eur Radiol. 2000;10(1):46–58.
120. Wurdinger S, Herzog AB, Fischer DR, Marx C, Raabe G, Schneider A, et al. Differentiation of phyllodes breast tumors from fibroadenomas on MRI. AJR Am J Roentgenol. 2005;185(5):1317–21.
121. Greenberg R, Skornick Y, Kaplan O. Management of breast fibroadenomas. J Gen Intern Med. 1998;13(9):640–5.
122. Carney JA, Toorkey BC. Myxoid fibroadenoma and allied conditions (myxomatosis) of the breast. A heritable disorder with special associations including cardiac and cutaneous myxomas. Am J Surg Pathol. 1991;15(8):713–21.
123. Kuijper A, Mommers EC, van der Wall E, van Diest PJ. Histopathology of fibroadenoma of the breast. Am J Clin Pathol. 2001;115(5):736–42.
124. Murali R, French JR, Sharma R, Bilous AM. Metaplastic ossification in mammary fibroadenoma. Breast J. 2006;12(3):276–7.
125. Nishida Y, Kohno N, Furuya Y, Nakatani T, Kaneko S, Sashikata T, et al. Mammary fibroadenoma showing osseous metaplasia: a case report. Gan No Rinsho. 1989;35(12):1461–5.
126. Jacobs TW. Update on fibroepithelial lesions of the breast. Surg Pathol Clin. 2009;2(2):301–17.
127. Jacobs TW, Chen YY, Guinee DG Jr, Holden JA, Cha I, Bauermeister DE, et al. Fibroepithelial lesions with cellular stroma on breast core needle biopsy: are there predictors of outcome on surgical excision? Am J Clin Pathol. 2005;124(3):342–54.
128. Yasir S, Gamez R, Jenkins S, Visscher DW, Nassar A. Significant histologic features differentiating cellular fibroadenoma from phyllodes tumor on core needle biopsy specimens. Am J Clin Pathol. 2014;142(3):362–9.
129. Berean K, Tron VA, Churg A, Clement PB. Mammary fibroadenoma with multinucleated stromal giant cells. Am J Surg Pathol. 1986;10(11):823–7.
130. Heneghan HM, Martin ST, Casey M, Tobbia I, Benani F, Barry KM. A diagnostic dilemma in breast pathology—benign fibroadenoma with multinucleated stromal giant cells. Diagn Pathol. 2008;3:33.
131. Huo L, Gilcrease MZ. Fibroepithelial lesions of the breast with pleomorphic stromal giant cells: a clinicopathologic study of 4 cases and review of the literature. Ann Diagn Pathol. 2009;13(4):226–32.
132. Kar R, Mohanty SK, Dey P. Fine-needle aspiration cytology of bilateral mammary fibroadenoma with multinucleated stromal giant cells. Diagn Cytopathol. 2005;32(4):247–8.
133. Nielsen BB, Ladefoged C. Fibroadenoma of the female breast with multinucleated giant cells. Pathol Res Pract. 1985;180(6):721–6.
134. Pitt MA, Knox WF, Haboubi NY. Multinucleated stromal giant cells of the colonic lamina propria in ulcerative colitis. J Clin Pathol. 1993;46(9):874–5.
135. Powell CM, Cranor ML, Rosen PP. Multinucleated stromal giant cells in mammary fibroepithelial neoplasms. A study of 11 patients. Arch Pathol Lab Med. 1994;118(9):912–6.
136. Ryska A, Reynolds C, Keeney GL. Benign tumors of the breast with multinucleated stromal giant cells. Immunohistochemical analysis of six cases and review of the literature. Virchows Arch. 2001;439(6):768–75.
137. Tse GM, Law BK, Chan KF, Mas TK. Multinucleated stromal giant cells in mammary phyllodes tumours. Pathology. 2001;33(2):153–6.
138. Rosen PP. Multinucleated mammary stromal giant cells: a benign lesion that simulates invasive carcinoma. Cancer. 1979;44(4):1305–8.

139. Buzanowski-Konakry K, Harrison EG Jr, Payne WS. Lobular carcinoma arising in fibroadenoma of the breast. Cancer. 1975;35(2):450–6.
140. Chintamani, Khandelwal R, Tandon M, Yashwant K, Kulshreshtha P, Aeron T, et al. Carcinoma developing in a fibroadenoma in a woman with a family history of breast cancer: a case report and review of literature. Cases J. 2009;2:9348.
141. Deschenes L, Jacob S, Fabia J, Christen A. Beware of breast fibroadenomas in middle-aged women. Can J Surg. 1985;28(4):372–4.
142. Diaz NM, Palmer JO, McDivitt RW. Carcinoma arising within fibroadenomas of the breast. A clinicopathologic study of 105 patients. Am J Clin Pathol. 1991;95(5):614–22.
143. McDivitt RW, Farrow JH, Stewart FW. Breast carcinoma arising in solitary fibroadenomas. Surg Gynecol Obstet. 1967;125(3):572–6.
144. Ozzello L, Gump FE. The management of patients with carcinomas in fibroadenomatous tumors of the breast. Surg Gynecol Obstet. 1985;160(2):99–104.
145. Pick PW, Iossifides IA. Occurrence of breast carcinoma within a fibroadenoma. A review. Arch Pathol Lab Med. 1984;108(7):590–4.
146. Stafyla V, Kotsifopoulos N, Grigoriades K, Kassaras G, Sakorafas GH. Lobular carcinoma in situ of the breast within a fibroadenoma. A case report. Gynecol Oncol. 2004;94(2):572–4.
147. Tay TK, Chang KT, Thike AA, Tan PH. Paediatric fibroepithelial lesions revisited: pathological insights. J Clin Pathol. 2015;68(8):633–41.
148. Ross DS, Giri DD, Akram MM, Catalano JP, Olcese C, Van Zee KJ, et al. Fibroepithelial lesions in the breast of adolescent females: a clinicopathological study of 54 cases. Breast J. 2017;23(2):182–92.
149. Dupont WD, Page DL, Parl FF, Vnencak-Jones CL, Plummer WD Jr, Rados MS, et al. Long-term risk of breast cancer in women with fibroadenoma. N Engl J Med. 1994;331(1):10–5.
150. Sklair-Levy M, Sella T, Alweiss T, Craciun I, Libson E, Mally B. Incidence and management of complex fibroadenomas. AJR Am J Roentgenol. 2008;190(1):214–8.
151. Fekete P, Petrek J, Majmudar B, Someren A, Sandberg W. Fibroadenomas with stromal cellularity. A clinicopathologic study of 21 patients. Arch Pathol Lab Med. 1987;111(5):427–32.
152. Mies C, Rosen PP. Juvenile fibroadenoma with atypical epithelial hyperplasia. Am J Surg Pathol. 1987;11(3):184–90.
153. Deshpande KM, Deshpande AH, Raut WK, Lele VR, Bobhate SK. Diagnostic difficulties in spontaneous infarction of a fibroadenoma in an adolescent: case report. Diagn Cytopathol. 2002;26(1):26–8.
154. Oh YJ, Choi SH, Chung SY, Yang I, Woo JY, Lee MJ. Spontaneously infarcted fibroadenoma mimicking breast cancer. J Ultrasound Med. 2009;28(10):1421–3.
155. Pinto RG, Couto F, Mandreker S. Infarction after fine needle aspiration. A report of four cases. Acta Cytol. 1996;40(4):739–41.
156. Vargas MP, Merino MJ. Infarcted myxoid fibroadenoma following fine-needle aspiration. Arch Pathol Lab Med. 1996;120(11):1069–71.
157. Chauhan H, Abraham A, Phillips JR, Pringle JH, Walker RA, Jones JL. There is more than one kind of myofibroblast: analysis of CD34 expression in benign, in situ, and invasive breast lesions. J Clin Pathol. 2003;56(4):271–6.
158. Ohtani H, Sasano N. Stromal cells of the fibroadenoma of the human breast. An immunohistochemical and ultrastructural study. Virchows Arch A Pathol Anat Histopathol. 1984;404(1):7–16.
159. Silverman JS, Tamsen A. Mammary fibroadenoma and some phyllodes tumour stroma are composed of CD34+ fibroblasts and factor XIIIa+ dendrophages. Histopathology. 1996;29(5):411–9.
160. Moore T, Lee AH. Expression of CD34 and bcl-2 in phyllodes tumours, fibroadenomas and spindle cell lesions of the breast. Histopathology. 2001;38(1):62–7.
161. Sawyer EJ, Hanby AM, Poulsom R, Jeffery R, Gillett CE, Ellis IO, et al. Beta-catenin abnormalities and associated insulin-like growth factor overexpression are important in phyllodes tumours and fibroadenomas of the breast. J Pathol. 2003;200(5):627–32.
162. Zhang L, Yang C, Pfeifer JD, Caprioli RM, Judd AM, Patterson NH, et al. Histopathologic, immunophenotypic, and proteomics characteristics of low-grade phyllodes tumor and fibroadenoma: more similarities than differences. NPJ Breast Cancer. 2020;6:27.
163. Sapino A, Bosco M, Cassoni P, Castellano I, Arisio R, Cserni G, et al. Estrogen receptor-beta is expressed in stromal cells of fibroadenoma and phyllodes tumors of the breast. Mod Pathol. 2006;19(4):599–606.
164. Branchini G, Schneider L, Cericatto R, Capp E, Brum IS. Progesterone receptors A and B and estrogen receptor alpha expression in normal breast tissue and fibroadenomas. Endocrine. 2009;35(3):459–66.
165. Mechtersheimer G, Kruger KH, Born IA, Moller P. Antigenic profile of mammary fibroadenoma and cystosarcoma phyllodes. A study using antibodies to estrogen- and progesterone receptors and to a panel of cell surface molecules. Pathol Res Pract. 1990;186(4):427–38.
166. Rao BR, Meyer JS, Fry CG. Most cystosarcoma phyllodes and fibroadenomas have progesterone receptor but lack estrogen receptor: stromal localization of progesterone receptor. Cancer. 1981;47(8):2016–21.
167. Umekita Y, Yoshida H. Immunohistochemical study of hormone receptor and hormone-regulated protein expression in phyllodes tumour: comparison with fibroadenoma. Virchows Arch. 1998;433(4):311–4.
168. Jacobs TWCY-Y, Guinee DG, Eby PR, Thike AA, Vohra P, Tan PH. Phyllodes tumor (PT) subsequent to a diagnosis of fibroadenoma (FA) on breast core needle biopsy (CNB): frequency and characteristics. Mod Pathol. 2014;27:34–90.
169. Lee AH, Hodi Z, Ellis IO, Elston CW. Histological features useful in the distinction of phyllodes tumour and fibroadenoma on needle core biopsy of the breast. Histopathology. 2007;51(3):336–44.
170. Kovi J, Chu HB, Leffall LD Jr. Sclerosing lobular hyperplasia manifesting as a palpable mass of the breast in young black women. Hum Pathol. 1984;15(4):336–40.
171. Dixon JM. Cystic disease and fibroadenoma of the breast: natural history and relation to breast cancer risk. Br Med Bull. 1991;47(2):258–71.
172. Trapido EJ, Brinton LA, Schairer C, Hoover R. Estrogen replacement therapy and benign breast disease. J Natl Cancer Inst. 1984;73(5):1101–5.
173. Hefler LA, Tempfer CB, Grimm C, Lebrecht A, Ulbrich E, Heinze G, et al. Estrogen-metabolizing gene polymorphisms in the assessment of breast carcinoma risk and fibroadenoma risk in Caucasian women. Cancer. 2004;101(2):264–9.
174. Kang YK, Guermah M, Yuan CX, Roeder RG. The TRAP/Mediator coactivator complex interacts directly with estrogen receptors alpha and beta through the TRAP220 subunit and directly enhances estrogen receptor function in vitro. Proc Natl Acad Sci U S A. 2002;99(5):2642–7.
175. Lim WK, Ong CK, Tan J, Thike AA, Ng CC, Rajasegaran V, et al. Exome sequencing identifies highly recurrent MED12 somatic mutations in breast fibroadenoma. Nat Genet. 2014;46(8):877–80.
176. Zhang S, O'Regan R, Xu W. The emerging role of mediator complex subunit 12 in tumorigenesis and response to chemotherapeutics. Cancer. 2020;126(5):939–48.

177. Canny PF, Berkowitz GS, Kelsey JL, LiVolsi VA. Fibroadenoma and the use of exogenous hormones. A case-control study. Am J Epidemiol. 1988;127(3):454–61.
178. Kelsey JL, Fischer DB, Holford TR, LiVoisi VA, Mostow ED, Goldenberg IS, et al. Exogenous estrogens and other factors in the epidemiology of breast cancer. J Natl Cancer Inst. 1981;67(2):327–33.
179. Ory H, Cole P, MacMahon B, Hoover R. Oral contraceptives and reduced risk of benign breast diseases. N Engl J Med. 1976;294(8):419–22.
180. Ravnihar B, Seigel DG, Lindtner J. An epidemiologic study of breast cancer and benign breast neoplasias in relation to the oral contraceptive and estrogen use. Eur J Cancer. 1979;15(4):395–405.
181. Vessey MP, Doll R, Sutton PM. Oral contraceptives and breast neoplasia: a retrospective study. Br Med J. 1972;3(5829):719–24.
182. Yu H, Rohan TE, Cook MG, Howe GR, Miller AB. Risk factors for fibroadenoma: a case-control study in Australia. Am J Epidemiol. 1992;135(3):247–58.
183. Bernardes JR Jr, Seixas MT, Lima GR, Marinho LC, Gebrim LH. The effect of tamoxifen on PCNA expression in fibroadenomas. Breast J. 2003;9(4):302–6.
184. Ansah-Boateng Y, Tavassoli FA. Fibroadenoma and cystosarcoma phyllodes of the male breast. Mod Pathol. 1992;5(2):114–6.
185. Gupta P, Foshee S, Garcia-Morales F, Gray T. Fibroadenoma in male breast: case report and literature review. Breast Dis. 2011;33(1):45–8.
186. Kanhai RC, Hage JJ, Bloemena E, van Diest PJ, Karim RB. Mammary fibroadenoma in a male-to-female transsexual. Histopathology. 1999;35(2):183–5.
187. Lemmo G, Garcea N, Corsello S, Tarquini E, Palladino T, Ardito G, et al. Breast fibroadenoma in a male-to-female transsexual patient after hormonal treatment. Eur J Surg Suppl. 2003;588:69–71.
188. Darwish A, Nasr AO, El Hassan LA, Fahal AH. Cyclosporine-A therapy-induced multiple bilateral breast and accessory axillary breast fibroadenomas: a case report. J Med Case Rep. 2010;4:267.
189. Yarak S, Floriano M, Decico JE, Konishi CT, Michalany NS, Enokihara MY, et al. First report of a fibro-adenoma in axillary mammary tissue of a renal transplant patient taking cyclosporin. Int J Dermatol. 2007;46(4):407–9.
190. Sangthawan P, Fox J, Atkins RC, Kerr PG. Increased incidence of benign breast disease in female renal transplant patients receiving cyclosporin. ANZ J Surg. 2002;72(3):222–5.
191. Iaria G, Pisani F, De Luca L, Sforza D, Manuelli M, Perrone L, et al. Prospective study of switch from cyclosporine to tacrolimus for fibroadenomas of the breast in kidney transplantation. Transplant Proc. 2010;42(4):1169–70.
192. Stratakis CA, Carney JA, Lin JP, Papanicolaou DA, Karl M, Kastner DL, et al. Carney complex, a familial multiple neoplasia and lentiginosis syndrome. Analysis of 11 kindreds and linkage to the short arm of chromosome 2. J Clin Invest. 1996;97(3):699–705.
193. Calabrese G, Di Virgilio C, Cianchetti E, Guanciali Franchi P, Stuppia L, Parruti G, et al. Chromosome abnormalities in breast fibroadenomas. Genes Chromosomes Cancer. 1991;3(3):202–4.
194. Stephenson CF, Davis RI, Moore GE, Sandberg AA. Cytogenetic and fluorescence in situ hybridization analysis of breast fibroadenomas. Cancer Genet Cytogenet. 1992;63(1):32–6.
195. Kasami M, Vnencak-Jones CL, Manning S, Dupont WD, Jensen RA, Page DL. Monoclonality in fibroadenomas with complex histology and phyllodal features. Breast Cancer Res Treat. 1998;50(2):185–91.
196. Kobayashi S, Iwase H, Kuzushima T, Iwata H, Toyama T, Hara Y, et al. Consecutively occurring multiple fibroadenomas of the breast distinguished from phyllodes tumors by clonality analysis of stromal tissue. Breast Cancer. 1999;6(3):201–6.
197. Kuijper A, Buerger H, Simon R, Schaefer KL, Croonen A, Boecker W, et al. Analysis of the progression of fibroepithelial tumours of the breast by PCR-based clonality assay. J Pathol. 2002;197(5):575–81.
198. Noguchi S, Motomura K, Inaji H, Imaoka S, Koyama H. Clonal analysis of fibroadenoma and phyllodes tumor of the breast. Cancer Res. 1993;53(17):4071–4.
199. Noguchi S, Yokouchi H, Aihara T, Motomura K, Inaji H, Imaoka S, et al. Progression of fibroadenoma to phyllodes tumor demonstrated by clonal analysis. Cancer. 1995;76(10):1779–85.
200. McCulloch RK, Sellner LN, Papadimitrou JM, Turbett GR. The incidence of microsatellite instability and loss of heterozygosity in fibroadenoma of the breast. Breast Cancer Res Treat. 1998;49(2):165–9.
201. Wang ZC, Buraimoh A, Iglehart JD, Richardson AL. Genome-wide analysis for loss of heterozygosity in primary and recurrent phyllodes tumor and fibroadenoma of breast using single nucleotide polymorphism arrays. Breast Cancer Res Treat. 2006;97(3):301–9.
202. Garcia-Dios DA, Levi D, Shah V, Gillett C, Simpson MA, Hanby A, et al. MED12, TERT promoter and RBM15 mutations in primary and recurrent phyllodes tumours. Br J Cancer. 2018;118(2):277–84.
203. Lae M, Gardrat S, Rondeau S, Richardot C, Caly M, Chemlali W, et al. MED12 mutations in breast phyllodes tumors: evidence of temporal tumoral heterogeneity and identification of associated critical signaling pathways. Oncotarget. 2016;7(51):84428–38.
204. Lien HC, Huang CS, Yang YW, Jeng YM. Mutational analysis of MED12 exon 2 in a spectrum of fibroepithelial tumours of the breast: implications for pathogenesis and histogenesis. Histopathology. 2016;68(3):433–41.
205. Md Nasir ND, Ng CCY, Rajasegaran V, Wong SF, Liu W, Ng GXP, et al. Genomic characterisation of breast fibroepithelial lesions in an international cohort. J Pathol. 2019;249(4):447–60.
206. Mishima C, Kagara N, Tanei T, Naoi Y, Shimoda M, Shimomura A, et al. Mutational analysis of MED12 in fibroadenomas and phyllodes tumors of the breast by means of targeted next-generation sequencing. Breast Cancer Res Treat. 2015;152(2):305–12.
207. Ng CCY, Md Nasir ND, Loke BN, Tay TKY, Thike AA, Rajasegaran V, et al. Genetic differences between benign phyllodes tumors and fibroadenomas revealed through targeted next generation sequencing. Mod Pathol. 2021;34:1320–32.
208. Pfarr N, Kriegsmann M, Sinn P, Klauschen F, Endris V, Herpel E, et al. Distribution of MED12 mutations in fibroadenomas and phyllodes tumors of the breast—implications for tumor biology and pathological diagnosis. Genes Chromosomes Cancer. 2015;54(7):444–52.
209. Piscuoglio S, Murray M, Fusco N, Marchio C, Loo FL, Martelotto LG, et al. MED12 somatic mutations in fibroadenomas and phyllodes tumours of the breast. Histopathology. 2015;67(5):719–29.
210. Piscuoglio S, Ng CK, Murray M, Burke KA, Edelweiss M, Geyer FC, et al. Massively parallel sequencing of phyllodes tumours of the breast reveals actionable mutations, and TERT promoter hotspot mutations and TERT gene amplification as likely drivers of progression. J Pathol. 2016;238(4):508–18.
211. Tan J, Ong CK, Lim WK, Ng CC, Thike AA, Ng LM, et al. Genomic landscapes of breast fibroepithelial tumors. Nat Genet. 2015;47(11):1341–5.
212. Yoshida M, Ogawa R, Yoshida H, Maeshima A, Kanai Y, Kinoshita T, et al. TERT promoter mutations are frequent and show association with MED12 mutations in phyllodes tumors of the breast. Br J Cancer. 2015;113(8):1244–8.

213. Je EM, Kim MR, Min KO, Yoo NJ, Lee SH. Mutational analysis of MED12 exon 2 in uterine leiomyoma and other common tumors. Int J Cancer. 2012;131(6):E1044–7.
214. Makinen N, Mehine M, Tolvanen J, Kaasinen E, Li Y, Lehtonen HJ, et al. MED12, the mediator complex subunit 12 gene, is mutated at high frequency in uterine leiomyomas. Science. 2011;334(6053):252–5.
215. McGuire MM, Yatsenko A, Hoffner L, Jones M, Surti U, Rajkovic A. Whole exome sequencing in a random sample of North American women with leiomyomas identifies MED12 mutations in majority of uterine leiomyomas. PLoS One. 2012;7(3):e33251.
216. Perot G, Croce S, Ribeiro A, Lagarde P, Velasco V, Neuville A, et al. MED12 alterations in both human benign and malignant uterine soft tissue tumors. PLoS One. 2012;7(6):e40015.
217. da Silva EM, Beca F, Sebastiao APM, Murray MP, Silveira C, Da Cruz PA, et al. Stromal MED12 exon 2 mutations in complex fibroadenomas of the breast. J Clin Pathol. 2020; https://doi.org/10.1136/jclinpath-2020-207062.
218. Tay TKY, Guan P, Loke BN, Nasir NDM, Rajasegaran V, Thike AA, et al. Molecular insights into paediatric breast fibroepithelial tumours. Histopathology. 2018;73(5):809–18.
219. Pareja F, Da Cruz PA, Murray MP, Hoang T, Gularte-Merida R, Brown D, et al. Recurrent MED12 exon 2 mutations in benign breast fibroepithelial lesions in adolescents and young adults. J Clin Pathol. 2019;72(3):258–62.
220. Lozada JR, Burke KA, Maguire A, Pareja F, Lim RS, Kim J, et al. Myxoid fibroadenomas differ from conventional fibroadenomas: a hypothesis-generating study. Histopathology. 2017;71(4):626–34.
221. Tan WJ, Chan JY, Thike AA, Lim JC, Md Nasir ND, Tan JS, et al. MED12 protein expression in breast fibroepithelial lesions: correlation with mutation status and oestrogen receptor expression. J Clin Pathol. 2016;69(10):858–65.
222. Liu SY, Joseph NM, Ravindranathan A, Stohr BA, Greenland NY, Vohra P, et al. Genomic profiling of malignant phyllodes tumors reveals aberrations in FGFR1 and PI-3 kinase/RAS signaling pathways and provides insights into intratumoral heterogeneity. Mod Pathol. 2016;29(9):1012–27.
223. Sim Y, Ng GXP, Ng CCY, Rajasegaran V, Wong SF, Liu W, et al. A novel genomic panel as an adjunctive diagnostic tool for the characterization and profiling of breast Fibroepithelial lesions. BMC Med Genet. 2019;12(1):142.
224. Carter CL, Corle DK, Micozzi MS, Schatzkin A, Taylor PR. A prospective study of the development of breast cancer in 16,692 women with benign breast disease. Am J Epidemiol. 1988;128(3):467–77.
225. El-Wakeel H, Umpleby HC. Systematic review of fibroadenoma as a risk factor for breast cancer. Breast. 2003;12(5):302–7.
226. Krieger N, Hiatt RA. Risk of breast cancer after benign breast diseases. Variation by histologic type, degree of atypia, age at biopsy, and length of follow-up. Am J Epidemiol. 1992;135(6):619–31.
227. Levi F, Randimbison L, Te VC, La Vecchia C. Incidence of breast cancer in women with fibroadenoma. Int J Cancer. 1994;57(5):681–3.
228. McDivitt RW, Stevens JA, Lee NC, Wingo PA, Rubin GL, Gersell D. Histologic types of benign breast disease and the risk for breast cancer. The Cancer and Steroid Hormone Study Group. Cancer. 1992;69(6):1408–14.
229. Nassar A, Visscher DW, Degnim AC, Frank RD, Vierkant RA, Frost M, et al. Complex fibroadenoma and breast cancer risk: a Mayo Clinic Benign Breast Disease Cohort Study. Breast Cancer Res Treat. 2015;153(2):397–405.
230. Dupont WD, Page DL. Risk factors for breast cancer in women with proliferative breast disease. N Engl J Med. 1985;312(3):146–51.
231. Carter BA, Page DL, Schuyler P, Parl FF, Simpson JF, Jensen RA, et al. No elevation in long-term breast carcinoma risk for women with fibroadenomas that contain atypical hyperplasia. Cancer. 2001;92(1):30–6.
232. Management of fibroadenomas of the breast. American Society of Breast Surgeons; 2008 [updated 29 Apr 2008]. Available from: https://www.breastsurgeons.org/docs/statements/Management-of-Fibroadenomas.pdf.
233. Cant PJ, Madden MV, Coleman MG, Dent DM. Non-operative management of breast masses diagnosed as fibroadenoma. Br J Surg. 1995;82(6):792–4.
234. Javed A, Jenkins SM, Labow B, Boughey JC, Lemaine V, Neal L, et al. Intermediate and long-term outcomes of fibroadenoma excision in adolescent and young adult patients. Breast J. 2019;25(1):91–5.
235. Fine RE, Israel PZ, Walker LC, Corgan KR, Greenwald LV, Berenson JE, et al. A prospective study of the removal rate of imaged breast lesions by an 11-gauge vacuum-assisted biopsy probe system. Am J Surg. 2001;182(4):335–40.
236. Grady I, Gorsuch H, Wilburn-Bailey S. Long-term outcome of benign fibroadenomas treated by ultrasound-guided percutaneous excision. Breast J. 2008;14(3):275–8.
237. Kaufman CS, Bachman B, Littrup PJ, Freeman-Gibb LA, White M, Carolin K, et al. Cryoablation treatment of benign breast lesions with 12-month follow-up. Am J Surg. 2004;188(4):340–8.
238. Kaufman CS, Bachman B, Littrup PJ, White M, Carolin KA, Freman-Gibb L, et al. Office-based ultrasound-guided cryoablation of breast fibroadenomas. Am J Surg. 2002;184(5):394–400.
239. Kaufman CS, Littrup PJ, Freeman-Gibb LA, Smith JS, Francescatti D, Simmons R, et al. Office-based cryoablation of breast fibroadenomas with long-term follow-up. Breast J. 2005;11(5):344–50.
240. Littrup PJ, Freeman-Gibb L, Andea A, White M, Amerikia KC, Bouwman D, et al. Cryotherapy for breast fibroadenomas. Radiology. 2005;234(1):63–72.
241. Nurko J, Mabry CD, Whitworth P, Jarowenko D, Oetting L, Potruch T, et al. Interim results from the FibroAdenoma Cryoablation Treatment Registry. Am J Surg. 2005;190(4):647–51; discussion 51–2.
242. Park HL, Kim LS. The current role of vacuum assisted breast biopsy system in breast disease. J Breast Cancer. 2011;14(1):1–7.
243. Polom K, Murawa D, Nowaczyk P, Adamczyk B, Giles E, Fertsch S, et al. Vacuum-assisted core-needle biopsy as a diagnostic and therapeutic method in lesions radiologically suspicious of breast fibroadenoma. Rep Pract Oncol Radiother. 2010;16(1):32–5.
244. Povoski SP. The utilization of an ultrasound-guided 8-gauge vacuum-assisted breast biopsy system as an innovative approach to accomplishing complete eradication of multiple bilateral breast fibroadenomas. World J Surg Oncol. 2007;5:124.
245. Sperber F, Blank A, Metser U, Flusser G, Klausner JM, Lev-Chelouche D. Diagnosis and treatment of breast fibroadenomas by ultrasound-guided vacuum-assisted biopsy. Arch Surg. 2003;138(7):796–800.
246. Kaufman CS, Littrup PJ, Freman-Gibb LA, Francescatti D, Stocks LH, Smith JS, et al. Office-based cryoablation of breast fibroadenomas: 12-month followup. J Am Coll Surg. 2004;198(6):914–23.
247. Matz D, Kerivan L, Reintgen M, Akman K, Lozicki A, Causey T, et al. Breast preservation in women with giant juvenile fibroadenoma. Clin Breast Cancer. 2013;13(3):219–22.
248. Simmons RM, Cance WG, Iacicca MV. A giant juvenile fibroadenoma in a 12-year-old girl: a case for breast conservation. Breast J. 2000;6(6):418–20.
249. Kuusk U. Multiple giant fibroadenomas in an adolescent female breast. Can J Surg. 1988;31(2):133–4.
250. Nikumbh DB, Desai SR, Madan PS, Patil NJ, Wader JV. Bilateral giant juvenile fibroadenomas of breasts:a case report. Pathol Res Int. 2011;2011:482046.
251. Wu YT, Chen ST, Chen CJ, Kuo YL, Tseng LM, Chen DR, et al. Breast cancer arising within fibroadenoma: collective analysis of

case reports in the literature and hints on treatment policy. World J Surg Oncol. 2014;12:335.
252. Tse GKJ, Thike AA. Phyllodes tumour. In: The WHO Classification of Tumours Editorial Board, editor. WHO classification of tumours breast tumours. 5th ed. Lyon: International Agency for Research in Cancer; 2019. p. 172–6.
253. Fiks A. Cystosarcoma phyllodes of the mammary gland—Muller's tumor. For the 180th birthday of Johannes Muller. Virchows Arch A Pathol Anat Histol. 1981;392(1):1–6.
254. Karim RZ, Gerega SK, Yang YH, Spillane A, Carmalt H, Scolyer RA, et al. Phyllodes tumours of the breast: a clinicopathological analysis of 65 cases from a single institution. Breast. 2009;18(3):165–70.
255. Kim S, Kim JY, Kim DH, Jung WH, Koo JS. Analysis of phyllodes tumor recurrence according to the histologic grade. Breast Cancer Res Treat. 2013;141(3):353–63.
256. Pimiento JM, Gadgil PV, Santillan AA, Lee MC, Esposito NN, Kiluk JV, et al. Phyllodes tumors: race-related differences. J Am Coll Surg. 2011;213(4):537–42.
257. Tan PH, Thike AA, Tan WJ, Thu MM, Busmanis I, Li H, et al. Predicting clinical behaviour of breast phyllodes tumours: a nomogram based on histological criteria and surgical margins. J Clin Pathol. 2012;65(1):69–76.
258. Barrio AV, Clark BD, Goldberg JI, Hoque LW, Bernik SF, Flynn LW, et al. Clinicopathologic features and long-term outcomes of 293 phyllodes tumors of the breast. Ann Surg Oncol. 2007;14(10):2961–70.
259. Bernstein L, Deapen D, Ross RK. The descriptive epidemiology of malignant cystosarcoma phyllodes tumors of the breast. Cancer. 1993;71(10):3020–4.
260. Cohn-Cedermark G, Rutqvist LE, Rosendahl I, Silfversward C. Prognostic factors in cystosarcoma phyllodes. A clinicopathologic study of 77 patients. Cancer. 1991;68(9):2017–22.
261. Hart WR, Bauer RC, Oberman HA. Cystosarcoma phyllodes. A clinicopathologic study of twenty-six hypercellular periductal stromal tumors of the breast. Am J Clin Pathol. 1978;70(2):211–6.
262. Macdonald OK, Lee CM, Tward JD, Chappel CD, Gaffney DK. Malignant phyllodes tumor of the female breast: association of primary therapy with cause-specific survival from the Surveillance, Epidemiology, and End Results (SEER) program. Cancer. 2006;107(9):2127–33.
263. Norris HJ, Taylor HB. Relationship of histologic features to behavior of cystosarcoma phyllodes. Analysis of ninety-four cases. Cancer. 1967;20(12):2090–9.
264. Reinfuss M, Mitus J, Smolak K, Stelmach A. Malignant phyllodes tumours of the breast. A clinical and pathological analysis of 55 cases. Eur J Cancer. 1993;29A(9):1252–6.
265. Amerson JR. Cystosarcoma phyllodes in adolescent females. A report of seven patients. Ann Surg. 1970;171(6):849–56.
266. Andersson A, Bergdahl L. Cystosarcoma phyllodes in young women. Arch Surg. 1978;113(6):742–4.
267. Briggs RM, Walters M, Rosenthal D. Cystosarcoma phylloides in adolescent female patients. Am J Surg. 1983;146(6):712–4.
268. Rajan PB, Cranor ML, Rosen PP. Cystosarcoma phyllodes in adolescent girls and young women: a study of 45 patients. Am J Surg Pathol. 1998;22(1):64–9.
269. Sorelli PG, Thomas D, Moore A, Khan M, Hoque H. Malignant phyllodes tumor in an 11-year-old premenarchal girl. J Pediatr Surg. 2010;45(2):e17–20.
270. Hoover HC, Trestioreanu A, Ketcham AS. Metastatic cystosarcoma phylloides in an adolescent girl: an unusually malignant tumor. Ann Surg. 1975;181(3):279–82.
271. Selamzade M, Gidener C, Koyuncuoglu M, Mevsim A. Borderline phylloides tumor in an 11-year-old girl. Pediatr Surg Int. 1999;15(5–6):427–8.
272. Kahan Z, Toszegi AM, Szarvas F, Gaizer G, Baradnay G, Ormos J. Recurrent phyllodes tumor in a man. Pathol Res Pract. 1997;193(9):653–8.
273. Keelan PA, Myers JL, Wold LE, Katzmann JA, Gibney DJ. Phyllodes tumor: clinicopathologic review of 60 patients and flow cytometric analysis in 30 patients. Hum Pathol. 1992;23(9):1048–54.
274. Konstantakos AK, Graham DJ. Cystosarcoma phyllodes tumors in men. Am Surg. 2003;69(9):808–11.
275. Nielsen VT, Andreasen C. Phyllodes tumour of the male breast. Histopathology. 1987;11(7):761–2.
276. Pantoja E, Llobet RE, Lopez E. Gigantic cystosarcoma phyllodes in a man with gynecomastia. Arch Surg. 1976;111(5):611.
277. Reingold IM, Ascher GS. Cystosarcoma phyllodes in a man with gynecomastia. Am J Clin Pathol. 1970;53(6):852–6.
278. Blaker KM, Sahoo S, Schweichler MR, Chagpar AB. Malignant phylloides tumor in pregnancy. Am Surg. 2010;76(3):302–5.
279. Pacchiarotti A, Selman H, Gentile V, Pacchiarotti A, Milazzo GN, Lanzilotti G, et al. First case of transformation for breast fibroadenoma to high-grade malignant phyllodes tumor in an in vitro fertilization patient: misdiagnosis of recurrence, treatment and review of the literature. Eur Rev Med Pharmacol Sci. 2013;17(18):2495–8.
280. Sharma JB, Wadhwa L, Malhotra M, Arora R, Singh S. A case of huge enlargement of cystosarcoma phylloides of breast in pregnancy. Eur J Obstet Gynecol Reprod Biol. 2004;115(2):237–9.
281. Way JC, Culham BA. Phyllodes tumour in pregnancy: a case report. Can J Surg. 1998;41(5):407–9.
282. Browder W, McQuitty JT Jr, McDonald JC. Malignant cystosarcoma phylloides. Treatment and prognosis. Am J Surg. 1978;136(2):239–41.
283. Dyer NH, Bridger JE, Taylor RS. Cystosarcoma phylloides. Br J Surg. 1966;53(5):450–5.
284. Gordon PB, Gagnon FA, Lanzkowsky L. Solid breast masses diagnosed as fibroadenoma at fine-needle aspiration biopsy: acceptable rates of growth at long-term follow-up. Radiology. 2003;229(1):233–8.
285. Asoglu O, Ugurlu MM, Blanchard K, Grant CS, Reynolds C, Cha SS, et al. Risk factors for recurrence and death after primary surgical treatment of malignant phyllodes tumors. Ann Surg Oncol. 2004;11(11):1011–7.
286. Moffat CJ, Pinder SE, Dixon AR, Elston CW, Blamey RW, Ellis IO. Phyllodes tumours of the breast: a clinicopathological review of thirty-two cases. Histopathology. 1995;27(3):205–18.
287. Tan EY, Tan PH, Yong WS, Wong HB, Ho GH, Yeo AW, et al. Recurrent phyllodes tumours of the breast: pathological features and clinical implications. ANZ J Surg. 2006;76(6):476–80.
288. Tan PH, Jayabaskar T, Chuah KL, Lee HY, Tan Y, Hilmy M, et al. Phyllodes tumors of the breast: the role of pathologic parameters. Am J Clin Pathol. 2005;123(4):529–40.
289. Chung J, Son EJ, Kim JA, Kim EK, Kwak JY, Jeong J. Giant phyllodes tumors of the breast: imaging findings with clinicopathological correlation in 14 cases. Clin Imaging. 2011;35(2):102–7.
290. Krishnamoorthy R, Savasere T, Prabhuswamy VK, Babu R, Shivaswamy S. Giant malignant phyllodes tumour of breast. Case Rep Oncol Med. 2014;2014:956856.
291. Liang MI, Ramaswamy B, Patterson CC, McKelvey MT, Gordillo G, Nuovo GJ, et al. Giant breast tumors: surgical management of phyllodes tumors, potential for reconstructive surgery and a review of literature. World J Surg Oncol. 2008;6:117.
292. Choi J, Koo JS. Comparative study of histological features between core needle biopsy and surgical excision in phyllodes tumor. Pathol Int. 2012;62(2):120–6.
293. Pietruszka M, Barnes L. Cystosarcoma phyllodes: a clinicopathologic analysis of 42 cases. Cancer. 1978;41(5):1974–83.

294. Tagaya N, Kodaira H, Kogure H, Shimizu K. A case of phyllodes tumor with bloody nipple discharge in juvenile patient. Breast Cancer. 1999;6(3):207–10.
295. Liberman L, Bonaccio E, Hamele-Bena D, Abramson AF, Cohen MA, Dershaw DD. Benign and malignant phyllodes tumors: mammographic and sonographic findings. Radiology. 1996;198(1):121–4.
296. Stebbing JF, Nash AG. Diagnosis and management of phyllodes tumour of the breast: experience of 33 cases at a specialist centre. Ann R Coll Surg Engl. 1995;77(3):181–4.
297. Belkacemi Y, Bousquet G, Marsiglia H, Ray-Coquard I, Magne N, Malard Y, et al. Phyllodes tumor of the breast. Int J Radiat Oncol Biol Phys. 2008;70(2):492–500.
298. Geisler DP, Boyle MJ, Malnar KF, McGee JM, Nolen MC, Fortner SM, et al. Phyllodes tumors of the breast: a review of 32 cases. Am Surg. 2000;66(4):360–6.
299. Gullett NP, Rizzo M, Johnstone PA. National surgical patterns of care for primary surgery and axillary staging of phyllodes tumors. Breast J. 2009;15(1):41–4.
300. Kapiris I, Nasiri N, A'Hern R, Healy V, Gui GP. Outcome and predictive factors of local recurrence and distant metastases following primary surgical treatment of high-grade malignant phyllodes tumours of the breast. Eur J Surg Oncol. 2001;27(8):723–30.
301. Aguiar Bujanda D, Rivero Vera JC, Cabrera Suarez MA, Aguiar Morales J, Christol R, Bohn Sarmiento U, et al. Hypoglycemic coma secondary to big insulin-like growth factor II secretion by a giant phyllodes tumor of the breast. Breast J. 2007;13(2):189–91.
302. Hikichi M, Kiriyama Y, Hayashi T, Ushimado K, Kobayashi N, Urano M, et al. A hypoglycemia-inducing giant borderline phyllodes tumor secreting high-molecular-weight insulin-like growth factor II: immunohistochemistry and a western blot analysis. Intern Med. 2018;57(2):237–41.
303. Hino N, Nakagawa Y, Ikushima Y, Yoshida M, Tsuyuguchi M. A case of a giant phyllodes tumor of the breast with hypoglycemia caused by high-molecular-weight insulin-like growth factor II. Breast Cancer. 2010;17(2):142–5.
304. Kataoka T, Haruta R, Goto T, Sugino K, Asahara T, Dohi K, et al. Malignant phyllodes tumor of the breast with hypoglycemia: report of a case. Jpn J Clin Oncol. 1998;28(4):276–80.
305. Buchberger W, Strasser K, Heim K, Muller E, Schrocksnadel H. Phylloides tumor: findings on mammography, sonography, and aspiration cytology in 10 cases. AJR Am J Roentgenol. 1991;157(4):715–9.
306. Page JE, Williams JE. The radiological features of phylloides tumour of the breast with clinico-pathological correlation. Clin Radiol. 1991;44(1):8–12.
307. Chao TC, Lo YF, Chen SC, Chen MF. Sonographic features of phyllodes tumors of the breast. Ultrasound Obstet Gynecol. 2002;20(1):64–71.
308. Farria DM, Gorczyca DP, Barsky SH, Sinha S, Bassett LW. Benign phyllodes tumor of the breast: MR imaging features. AJR Am J Roentgenol. 1996;167(1):187–9.
309. McCarthy E, Kavanagh J, O'Donoghue Y, McCormack E, D'Arcy C, O'Keeffe SA. Phyllodes tumours of the breast: radiological presentation, management and follow-up. Br J Radiol. 2014;87(1044):20140239.
310. Wiratkapun C, Piyapan P, Lertsithichai P, Larbcharoensub N. Fibroadenoma versus phyllodes tumor: distinguishing factors in patients diagnosed with fibroepithelial lesions after a core needle biopsy. Diagn Interv Radiol. 2014;20(1):27–33.
311. Yabuuchi H, Soeda H, Matsuo Y, Okafuji T, Eguchi T, Sakai S, et al. Phyllodes tumor of the breast: correlation between MR findings and histologic grade. Radiology. 2006;241(3):702–9.
312. Adamietz BR, Kahmann L, Fasching PA, Schulz-Wendtland R, Uder M, Beckmann MW, et al. Differentiation between phyllodes tumor and fibroadenoma using real-time elastography. Ultraschall Med. 2011;32(Suppl 2):E75–9.
313. Tan BY, Acs G, Apple SK, Badve S, Bleiweiss IJ, Brogi E, et al. Phyllodes tumours of the breast: a consensus review. Histopathology. 2016;68(1):5–21.
314. Ward RM, Evans HL. Cystosarcoma phyllodes. A clinicopathologic study of 26 cases. Cancer. 1986;58(10):2282–9.
315. Oberman HA. Cystosarcoma phyllodes; a clinicopathologic study of hypercellular periductal stromal neoplasms of breast. Cancer. 1965;18:697–710.
316. Mamoon N, Mushtaq S, Hassan U, Rashid R, Khadim MT, Sarfraz T, et al. Angiosarcoma arising in recurrent phyllodes tumour. Histopathology. 2009;54(7):913–6.
317. Grimes MM. Cystosarcoma phyllodes of the breast: histologic features, flow cytometric analysis, and clinical correlations. Mod Pathol. 1992;5(3):232–9.
318. Abdul Aziz M, Sullivan F, Kerin MJ, Callagy G. Malignant phyllodes tumour with liposarcomatous differentiation, invasive tubular carcinoma, and ductal and lobular carcinoma in situ: case report and review of the literature. Pathol Res Int. 2010;2010:501274.
319. Kodama T, Kameyama K, Mukai M, Sugiura H, Ikeda T, Okada Y. Invasive lobular carcinoma arising in phyllodes tumor of the breast. Virchows Arch. 2003;442(6):614–6.
320. Parfitt JR, Armstrong C, O'Malley F, Ross J, Tuck AB. In-situ and invasive carcinoma within a phyllodes tumor associated with lymph node metastases. World J Surg Oncol. 2004;2:46.
321. Ramdass MJ, Dindyal S. Phyllodes breast tumour showing invasive squamous-cell carcinoma with invasive ductal, clear-cell, secretory, and squamous components. Lancet Oncol. 2006;7(10):880.
322. Sugie T, Takeuchi E, Kunishima F, Yotsumoto F, Kono Y. A case of ductal carcinoma with squamous differentiation in malignant phyllodes tumor. Breast Cancer. 2007;14(3):327–32.
323. Yasumura T, Matsui S, Hamajima T, Nagashima K, Yamagishi H, Aikawa I, et al. Infiltrating ductal carcinoma developing within cystosarcoma phyllodes—a case report. Jpn J Surg. 1988;18(3):326–9.
324. Chng TW, Gudi M, Lim SH, Li H, Tan PH. Validation of the Singapore nomogram for outcome prediction in breast phyllodes tumours in a large patient cohort. J Clin Pathol. 2018;71(2):125–8.
325. Kario K, Maeda S, Mizuno Y, Makino Y, Tankawa H, Kitazawa S. Phyllodes tumor of the breast: a clinicopathologic study of 34 cases. J Surg Oncol. 1990;45(1):46–51.
326. Rowell MD, Perry RR, Hsiu JG, Barranco SC. Phyllodes tumors. Am J Surg. 1993;165(3):376–9.
327. Treves N, Sunderland DA. Cystosarcoma phyllodes of the breast: a malignant and a benign tumor; a clinicopathological study of seventy-seven cases. Cancer. 1951;4(6):1286–332.
328. Burga AM, Tavassoli FA. Periductal stromal tumor: a rare lesion with low-grade sarcomatous behavior. Am J Surg Pathol. 2003;27(3):343–8.
329. Coyne JD. Periductal stromal hyperplasia. Histopathology. 2007;50(6):814–5.
330. Karim RZ, O'Toole SA, Scolyer RA, Cooper CL, Chan B, Selinger C, et al. Recent insights into the molecular pathogenesis of mammary phyllodes tumours. J Clin Pathol. 2013;66(6):496–505.
331. Powell CM, Rosen PP. Adipose differentiation in cystosarcoma phyllodes. A study of 14 cases. Am J Surg Pathol. 1994;18(7):720–7.
332. Barnes L, Pietruszka M. Rhabdomyosarcoma arising within a cystosarcoma phyllodes. Case report and review of the literature. Am J Surg Pathol. 1978;2(4):423–9.

333. Silver SA, Tavassoli FA. Osteosarcomatous differentiation in phyllodes tumors. Am J Surg Pathol. 1999;23(7):815–21.
334. Tomas D, Bujas T, Stajduhar E, Kirac P, Mijic A, Kruslin B. Malignant phyllodes tumor with associated osteosarcomatous, chondrosarcomatous, and liposarcomatous overgrowth. APMIS. 2007;115(4):367–70.
335. Vera-Sempere F, Garcia-Martinez A. Malignant phyllodes tumor of the breast with predominant chondrosarcomatous differentiation. Pathol Res Pract. 2003;199(12):841–5.
336. Bacchi CE, Wludarski SC, Lamovec J, Ben Dor D, Ober E, Salviato T, et al. Lipophyllodes of the breast. A reappraisal of fat-rich tumors of the breast based on 22 cases integrated by immunohistochemical study, molecular pathology insights, and clinical follow-up. Ann Diagn Pathol. 2016;21:1–6.
337. Inyang A, Thomas DG, Jorns J. Heterologous liposarcomatous differentiation in malignant phyllodes tumor is histologically similar but immunohistochemically and molecularly distinct from well-differentiated liposarcoma of soft tissue. Breast J. 2016;22(3):282–6.
338. Lyle PL, Bridge JA, Simpson JF, Cates JM, Sanders ME. Liposarcomatous differentiation in malignant phyllodes tumours is unassociated with MDM2 or CDK4 amplification. Histopathology. 2016;68(7):1040–5.
339. Tan PH. Fibroepithelial lesions revisited: implications for diagnosis and management. Mod Pathol. 2021;34(Suppl 1):15–37.
340. Tsang AK, Chan SK, Lam CC, Lui PC, Chau HH, Tan PH, et al. Phyllodes tumours of the breast—differentiating features in core needle biopsy. Histopathology. 2011;59(4):600–8.
341. Graadt van Roggen JF, Zonderland HM, Welvaart K, Peterse JL, Hogendoorn PC. Local recurrence of a phyllodes tumour of the breast presenting with widespread differentiation to a telangiectatic osteosarcoma. J Clin Pathol. 1998;51(9):706–8.
342. Kracht J, Sapino A, Bussolati G. Malignant phyllodes tumor of breast with lung metastases mimicking the primary. Am J Surg Pathol. 1998;22(10):1284–90.
343. Aranda FI, Laforga JB, Lopez JI. Phyllodes tumor of the breast. An immunohistochemical study of 28 cases with special attention to the role of myofibroblasts. Pathol Res Pract. 1994;190(5):474–81.
344. Chen CM, Chen CJ, Chang CL, Shyu JS, Hsieh HF, Harn HJ. CD34, CD117, and actin expression in phyllodes tumor of the breast. J Surg Res. 2000;94(2):84–91.
345. Chia Y, Thike AA, Cheok PY, Yong-Zheng Chong L, Man-Kit Tse G, Tan PH. Stromal keratin expression in phyllodes tumours of the breast: a comparison with other spindle cell breast lesions. J Clin Pathol. 2012;65(4):339–47.
346. Cimino-Mathews A, Sharma R, Illei PB, Vang R, Argani P. A subset of malignant phyllodes tumors express p63 and p40: a diagnostic pitfall in breast core needle biopsies. Am J Surg Pathol. 2014;38(12):1689–96.
347. Ho SK, Thike AA, Cheok PY, Tse GM, Tan PH. Phyllodes tumours of the breast: the role of CD34, vascular endothelial growth factor and beta-catenin in histological grading and clinical outcome. Histopathology. 2013;63(3):393–406.
348. Noronha Y, Raza A, Hutchins B, Chase D, Garberoglio C, Chu P, et al. CD34, CD117, and Ki-67 expression in phyllodes tumor of the breast: an immunohistochemical study of 33 cases. Int J Surg Pathol. 2011;19(2):152–8.
349. Jara-Lazaro AR, Akhilesh M, Thike AA, Lui PC, Tse GM, Tan PH. Predictors of phyllodes tumours on core biopsy specimens of fibroepithelial neoplasms. Histopathology. 2010;57(2):220–32.
350. Sawyer EJ, Hanby AM, Rowan AJ, Gillett CE, Thomas RE, Poulsom R, et al. The Wnt pathway, epithelial-stromal interactions, and malignant progression in phyllodes tumours. J Pathol. 2002;196(4):437–44.
351. Tsang JY, Mendoza P, Lam CC, Yu AM, Putti TC, Karim RZ, et al. Involvement of alpha- and beta-catenins and E-cadherin in the development of mammary phyllodes tumours. Histopathology. 2012;61(4):667–74.
352. Nozad S, Sheehan CE, Gay LM, Elvin JA, Vergilio JA, Suh J, et al. Comprehensive genomic profiling of malignant phyllodes tumors of the breast. Breast Cancer Res Treat. 2017;162(3):597–602.
353. Dunne B, Lee AH, Pinder SE, Bell JA, Ellis IO. An immunohistochemical study of metaplastic spindle cell carcinoma, phyllodes tumor and fibromatosis of the breast. Hum Pathol. 2003;34(10):1009–15.
354. Santini D, Bazzocchi F, Paladini G, Gelli MC, Ricci M, Mazzoleni G, et al. Intermediate-sized filament proteins (keratin, vimentin, desmin) in metaplastic carcinomas, carcinosarcomas and stromal sarcomas of the breast. Int J Biol Markers. 1987;2(2):83–6.
355. Barbareschi M, Pecciarini L, Cangi MG, Macri E, Rizzo A, Viale G, et al. p63, a p53 homologue, is a selective nuclear marker of myoepithelial cells of the human breast. Am J Surg Pathol. 2001;25(8):1054–60.
356. Koker MM, Kleer CG. p63 expression in breast cancer: a highly sensitive and specific marker of metaplastic carcinoma. Am J Surg Pathol. 2004;28(11):1506–12.
357. Leibl S, Gogg-Kammerer M, Sommersacher A, Denk H, Moinfar F. Metaplastic breast carcinomas: are they of myoepithelial differentiation?: immunohistochemical profile of the sarcomatoid subtype using novel myoepithelial markers. Am J Surg Pathol. 2005;29(3):347–53.
358. Bansal M, Chen J, Wang X. Focal anomalous expression of cytokeratin and p63 in malignant phyllodes tumor: a comparison with spindle cell metaplastic carcinoma. Appl Immunohistochem Mol Morphol. 2018;26(3):198–201.
359. Erhan Y, Zekioglu O, Ersoy O, Tugan D, Aydede H, Sakarya A, et al. p53 and Ki-67 expression as prognostic factors in cystosarcoma phyllodes. Breast J. 2002;8(1):38–44.
360. Feakins RM, Mulcahy HE, Nickols CD, Wells CA. p53 expression in phyllodes tumours is associated with histological features of malignancy but does not predict outcome. Histopathology. 1999;35(2):162–9.
361. Gatalica Z, Finkelstein S, Lucio E, Tawfik O, Palazzo J, Hightower B, et al. p53 protein expression and gene mutation in phyllodes tumors of the breast. Pathol Res Pract. 2001;197(3):183–7.
362. Kleer CG, Giordano TJ, Braun T, Oberman HA. Pathologic, immunohistochemical, and molecular features of benign and malignant phyllodes tumors of the breast. Mod Pathol. 2001;14(3):185–90.
363. Korcheva VB, Levine J, Beadling C, Warrick A, Countryman G, Olson NR, et al. Immunohistochemical and molecular markers in breast phyllodes tumors. Appl Immunohistochem Mol Morphol. 2011;19(2):119–25.
364. Kuijper A, de Vos RA, Lagendijk JH, van der Wall E, van Diest PJ. Progressive deregulation of the cell cycle with higher tumor grade in the stroma of breast phyllodes tumors. Am J Clin Pathol. 2005;123(5):690–8.
365. Millar EK, Beretov J, Marr P, Sarris M, Clarke RA, Kearsley JH, et al. Malignant phyllodes tumours of the breast display increased stromal p53 protein expression. Histopathology. 1999;34(6):491–6.
366. Niezabitowski A, Lackowska B, Rys J, Kruczak A, Kowalska T, Mitus J, et al. Prognostic evaluation of proliferative activity and DNA content in the phyllodes tumor of the breast: immunohistochemical and flow cytometric study of 118 cases. Breast Cancer Res Treat. 2001;65(1):77–85.
367. Shpitz B, Bomstein Y, Sternberg A, Klein E, Tiomkin V, Kaufman A, et al. Immunoreactivity of p53, Ki-67, and c-erbB-2 in phyllodes tumors of the breast in correlation with clinical and morphologic features. J Surg Oncol. 2002;79(2):86–92.

368. Tan PH, Jayabaskar T, Yip G, Tan Y, Hilmy M, Selvarajan S, et al. p53 and c-kit (CD117) protein expression as prognostic indicators in breast phyllodes tumors: a tissue microarray study. Mod Pathol. 2005;18(12):1527–34.
369. Tse GM, Lui PC, Scolyer RA, Putti TC, Kung FY, Law BK, et al. Tumour angiogenesis and p53 protein expression in mammary phyllodes tumors. Mod Pathol. 2003;16(10):1007–13.
370. Tse GM, Putti TC, Kung FY, Scolyer RA, Law BK, Lau TS, et al. Increased p53 protein expression in malignant mammary phyllodes tumors. Mod Pathol. 2002;15(7):734–40.
371. Tsang JYS, Hui YK, Lee MA, Lacambra M, Ni YB, Cheung SY, et al. Association of clinicopathological features and prognosis of TERT alterations in phyllodes tumor of breast. Sci Rep. 2018;8(1):3881.
372. Liu J, Liu X, Feng X, Liu J, Lv S, Zhang W, et al. C-kit overexpression correlates with KIT gene copy numbers increases in phyllodes tumors of the breast. Breast Cancer Res Treat. 2015;149(2):395–401.
373. Sawyer EJ, Poulsom R, Hunt FT, Jeffery R, Elia G, Ellis IO, et al. Malignant phyllodes tumours show stromal overexpression of c-myc and c-kit. J Pathol. 2003;200(1):59–64.
374. Tan WJ, Thike AA, Tan SY, Tse GM, Tan MH, Bay BH, et al. CD117 expression in breast phyllodes tumors correlates with adverse pathologic parameters and reduced survival. Mod Pathol. 2015;28(3):352–8.
375. Tse GM, Putti TC, Lui PC, Lo AW, Scolyer RA, Law BK, et al. Increased c-kit (CD117) expression in malignant mammary phyllodes tumors. Mod Pathol. 2004;17(7):827–31.
376. Tse GM, Tsang AK, Putti TC, Scolyer RA, Lui PC, Law BK, et al. Stromal CD10 expression in mammary fibroadenomas and phyllodes tumours. J Clin Pathol. 2005;58(2):185–9.
377. Kersting C, Kuijper A, Schmidt H, Packeisen J, Liedtke C, Tidow N, et al. Amplifications of the epidermal growth factor receptor gene (egfr) are common in phyllodes tumors of the breast and are associated with tumor progression. Lab Investig. 2006;86(1):54–61.
378. Tse GM, Lui PC, Vong JS, Lau KM, Putti TC, Karim R, et al. Increased epidermal growth factor receptor (EGFR) expression in malignant mammary phyllodes tumors. Breast Cancer Res Treat. 2009;114(3):441–8.
379. Feakins RM, Wells CA, Young KA, Sheaff MT. Platelet-derived growth factor expression in phyllodes tumors and fibroadenomas of the breast. Hum Pathol. 2000;31(10):1214–22.
380. Tse GM, Lui PC, Lee CS, Kung FY, Scolyer RA, Law BK, et al. Stromal expression of vascular endothelial growth factor correlates with tumor grade and microvessel density in mammary phyllodes tumors: a multicenter study of 185 cases. Hum Pathol. 2004;35(9):1053–7.
381. Cimino-Mathews A, Hicks JL, Sharma R, Vang R, Illei PB, De Marzo A, et al. A subset of malignant phyllodes tumors harbors alterations in the Rb/p16 pathway. Hum Pathol. 2013;44(11):2494–500.
382. Kang Y, Kim JH, Lee TH, Kim TS, Jung WH, Chung HC, et al. Expression of anaphase-promoting complex7 in fibroadenomas and phyllodes tumors of breast. Hum Pathol. 2009;40(1):98–107.
383. Kocova L, Skalova A, Fakan F, Rousarova M. Phyllodes tumour of the breast: immunohistochemical study of 37 tumours using MIB1 antibody. Pathol Res Pract. 1998;194(2):97–104.
384. Ridgway PF, Jacklin RK, Ziprin P, Harbin L, Peck DH, Darzi AW, et al. Perioperative diagnosis of cystosarcoma phyllodes of the breast may be enhanced by MIB-1 index. J Surg Res. 2004;122(1):83–8.
385. Umekita Y, Yoshida H. Immunohistochemical study of MIB1 expression in phyllodes tumor and fibroadenoma. Pathol Int. 1999;49(9):807–10.
386. Tse GM, Lee CS, Kung FY, Scolyer RA, Law BK, Lau TS, et al. Hormonal receptors expression in epithelial cells of mammary phyllodes tumors correlates with pathologic grade of the tumor: a multicenter study of 143 cases. Am J Clin Pathol. 2002;118(4):522–6.
387. Lawton TJ, Acs G, Argani P, Farshid G, Gilcrease M, Goldstein N, et al. Interobserver variability by pathologists in the distinction between cellular fibroadenomas and phyllodes tumors. Int J Surg Pathol. 2014;22(8):695–8.
388. Resetkova E, Khazai L, Albarracin CT, Arribas E. Clinical and radiologic data and core needle biopsy findings should dictate management of cellular fibroepithelial tumors of the breast. Breast J. 2010;16(6):573–80.
389. Gould DJ, Salmans JA, Lassinger BK, Contreras A, Gutierrez C, Bonefas E, et al. Factors associated with phyllodes tumor of the breast after core needle biopsy identifies fibroepithelial neoplasm. J Surg Res. 2012;178(1):299–303.
390. Komenaka IK, El-Tamer M, Pile-Spellman E, Hibshoosh H. Core needle biopsy as a diagnostic tool to differentiate phyllodes tumor from fibroadenoma. Arch Surg. 2003;138(9):987–90.
391. Yohe S, Yeh IT. "Missed" diagnoses of phyllodes tumor on breast biopsy: pathologic clues to its recognition. Int J Surg Pathol. 2008;16(2):137–42.
392. Morgan JM, Douglas-Jones AG, Gupta SK. Analysis of histological features in needle core biopsy of breast useful in preoperative distinction between fibroadenoma and phyllodes tumour. Histopathology. 2010;56(4):489–500.
393. Adem C, Reynolds C, Adlakha H, Roche PC, Nascimento AG. Wide spectrum screening keratin as a marker of metaplastic spindle cell carcinoma of the breast: an immunohistochemical study of 24 patients. Histopathology. 2002;40(6):556–62.
394. Carter MR, Hornick JL, Lester S, Fletcher CD. Spindle cell (sarcomatoid) carcinoma of the breast: a clinicopathologic and immunohistochemical analysis of 29 cases. Am J Surg Pathol. 2006;30(3):300–9.
395. Rakha EA, Coimbra ND, Hodi Z, Juneinah E, Ellis IO, Lee AH. Immunoprofile of metaplastic carcinomas of the breast. Histopathology. 2017;70(6):975–85.
396. Tse GM, Tan PH, Chaiwun B, Putti TC, Lui PC, Tsang AK, et al. p63 is useful in the diagnosis of mammary metaplastic carcinomas. Pathology. 2006;38(1):16–20.
397. Bishop JA, Montgomery EA, Westra WH. Use of p40 and p63 immunohistochemistry and human papillomavirus testing as ancillary tools for the recognition of head and neck sarcomatoid carcinoma and its distinction from benign and malignant mesenchymal processes. Am J Surg Pathol. 2014;38(2):257–64.
398. Lee AH. Recent developments in the histological diagnosis of spindle cell carcinoma, fibromatosis and phyllodes tumour of the breast. Histopathology. 2008;52(1):45–57.
399. Jin C, Hacking S, Sajjan S, Kamanda S, Bhuiya T, Nasim M. GATA binding protein 3 (GATA3) as a marker for metaplastic spindle cell carcinoma of the breast. Pathol Res Pract. 2021;221:153413.
400. Cimino-Mathews A, Subhawong AP, Elwood H, Warzecha HN, Sharma R, Park BH, et al. Neural crest transcription factor Sox10 is preferentially expressed in triple-negative and metaplastic breast carcinomas. Hum Pathol. 2013;44(6):959–65.
401. Cani AK, Hovelson DH, McDaniel AS, Sadis S, Haller MJ, Yadati V, et al. Next-gen sequencing exposes frequent MED12 mutations and actionable therapeutic targets in phyllodes tumors. Mol Cancer Res. 2015;13(4):613–9.
402. Dieci MV, Smutna V, Scott V, Yin G, Xu R, Vielh P, et al. Whole exome sequencing of rare aggressive breast cancer histologies. Breast Cancer Res Treat. 2016;156(1):21–32.

403. Gatalica Z, Vranic S, Ghazalpour A, Xiu J, Ocal IT, McGill J, et al. Multiplatform molecular profiling identifies potentially targetable biomarkers in malignant phyllodes tumors of the breast. Oncotarget. 2016;7(2):1707–16.
404. Kim JY, Yu JH, Nam SJ, Kim SW, Lee SK, Park WY, et al. Genetic and clinical characteristics of phyllodes tumors of the breast. Transl Oncol. 2018;11(1):18–23.
405. Koh VCY, Ng CCY, Bay BH, Teh BT, Tan PH. The utility of a targeted gene mutation panel in refining the diagnosis of breast phyllodes tumours. Pathology. 2019;51(5):531–4.
406. Krings G, Chen YY. Genomic profiling of metaplastic breast carcinomas reveals genetic heterogeneity and relationship to ductal carcinoma. Mod Pathol. 2018;31(11):1661–74.
407. McCart Reed AE, Kalaw E, Nones K, Bettington M, Lim M, Bennett J, et al. Phenotypic and molecular dissection of metaplastic breast cancer and the prognostic implications. J Pathol. 2019;247(2):214–27.
408. Ng CKY, Piscuoglio S, Geyer FC, Burke KA, Pareja F, Eberle CA, et al. The landscape of somatic genetic alterations in metaplastic breast carcinomas. Clin Cancer Res. 2017;23(14):3859–70.
409. Yeong J, Thike AA, Young Ng CC, Md Nasir ND, Loh K, Teh BT, et al. A genetic mutation panel for differentiating malignant phyllodes tumour from metaplastic breast carcinoma. Pathology. 2017;49(7):786–9.
410. Lim SZ, Ng CCY, Rajasegaran V, Guan P, Selvarajan S, Thike AA, et al. Genomic profile of breast sarcomas: a comparison with malignant phyllodes tumours. Breast Cancer Res Treat. 2019;174(2):365–73.
411. Wang F, Jia Y, Tong Z. Comparison of the clinical and prognostic features of primary breast sarcomas and malignant phyllodes tumor. Jpn J Clin Oncol. 2015;45(2):146–52.
412. Lacroix-Triki M, Geyer FC, Lambros MB, Savage K, Ellis IO, Lee AH, et al. Beta-catenin/Wnt signalling pathway in fibromatosis, metaplastic carcinomas and phyllodes tumours of the breast. Mod Pathol. 2010;23(11):1438–48.
413. Lien HC, Huang CS, Yang YW, Jeng YM. MED12 exon 2 mutation as a highly sensitive and specific marker in distinguishing phyllodes tumours from other spindle neoplasms of the breast. APMIS. 2016;124(5):356–64.
414. Noguchi S, Aihara T, Koyama H, Motomura K, Inaji H, Imaoka S. Clonal analysis of benign and malignant human breast tumors by means of polymerase chain reaction. Cancer Lett. 1995;90(1):57–63.
415. Dietrich CU, Pandis N, Rizou H, Petersson C, Bardi G, Qvist H, et al. Cytogenetic findings in phyllodes tumors of the breast: karyotypic complexity differentiates between malignant and benign tumors. Hum Pathol. 1997;28(12):1379–82.
416. Sawhney N, Garrahan N, Douglas-Jones AG, Williams ED. Epithelial—stromal interactions in tumors. A morphologic study of fibroepithelial tumors of the breast. Cancer. 1992;70(8):2115–20.
417. Tsang JY, Mendoza P, Putti TC, Karim RZ, Scolyer RA, Lee CS, et al. E-cadherin expression in the epithelial components of mammary phyllodes tumors. Hum Pathol. 2012;43(12):2117–23.
418. Yoshida M, Sekine S, Ogawa R, Yoshida H, Maeshima A, Kanai Y, et al. Frequent MED12 mutations in phyllodes tumours of the breast. Br J Cancer. 2015;112(10):1703–8.
419. Piscuoglio S, Geyer FC, Burke KA, Murray MP, Ng CK, Mota A, et al. Massively parallel sequencing analysis of synchronous fibroepithelial lesions supports the concept of progression from fibroadenoma to phyllodes tumor. NPJ Breast Cancer. 2016;2:16035.
420. Pareja F, Geyer FC, Kumar R, Selenica P, Piscuoglio S, Ng CKY, et al. Phyllodes tumors with and without fibroadenoma-like areas display distinct genomic features and may evolve through distinct pathways. NPJ Breast Cancer. 2017;3:40.
421. Birch JM, Alston RD, McNally RJ, Evans DG, Kelsey AM, Harris M, et al. Relative frequency and morphology of cancers in carriers of germline TP53 mutations. Oncogene. 2001;20(34):4621–8.
422. Jardim DL, Conley A, Subbiah V. Comprehensive characterization of malignant phyllodes tumor by whole genomic and proteomic analysis: biological implications for targeted therapy opportunities. Orphanet J Rare Dis. 2013;8:112.
423. Dietrich CU, Pandis N, Bardi G, Teixeira MR, Soukhikh T, Petersson C, et al. Karyotypic changes in phyllodes tumors of the breast. Cancer Genet Cytogenet. 1994;78(2):200–6.
424. Jones AM, Mitter R, Springall R, Graham T, Winter E, Gillett C, et al. A comprehensive genetic profile of phyllodes tumours of the breast detects important mutations, intra-tumoral genetic heterogeneity and new genetic changes on recurrence. J Pathol. 2008;214(5):533–44.
425. Lae M, La Rosa P, Mandel J, Reyal F, Hupe P, Terrier P, et al. Whole-genome profiling helps to classify phyllodes tumours of the breast. J Clin Pathol. 2016;69(12):1081–7.
426. Lae M, Vincent-Salomon A, Savignoni A, Huon I, Freneaux P, Sigal-Zafrani B, et al. Phyllodes tumors of the breast segregate in two groups according to genetic criteria. Mod Pathol. 2007;20(4):435–44.
427. Lv S, Niu Y, Wei L, Liu Q, Wang X, Chen Y. Chromosomal aberrations and genetic relations in benign, borderline and malignant phyllodes tumors of the breast: a comparative genomic hybridization study. Breast Cancer Res Treat. 2008;112(3):411–8.
428. Ang MK, Ooi AS, Thike AA, Tan P, Zhang Z, Dykema K, et al. Molecular classification of breast phyllodes tumors: validation of the histologic grading scheme and insights into malignant progression. Breast Cancer Res Treat. 2011;129(2):319–29.
429. Jee KJ, Gong G, Ahn SH, Park JM, Knuutila S. Gain in 1q is a common abnormality in phyllodes tumours of the breast. Anal Cell Pathol. 2003;25(2):89–93.
430. Lu YJ, Birdsall S, Osin P, Gusterson B, Shipley J. Phyllodes tumors of the breast analyzed by comparative genomic hybridization and association of increased 1q copy number with stromal overgrowth and recurrence. Genes Chromosomes Cancer. 1997;20(3):275–81.
431. Tan WJ, Lai JC, Thike AA, Lim JC, Tan SY, Koh VC, et al. Novel genetic aberrations in breast phyllodes tumours: comparison between prognostically distinct groups. Breast Cancer Res Treat. 2014;145(3):635–45.
432. Abe M, Miyata S, Nishimura S, Iijima K, Makita M, Akiyama F, et al. Malignant transformation of breast fibroadenoma to malignant phyllodes tumor: long-term outcome of 36 malignant phyllodes tumors. Breast Cancer. 2011;18(4):268–72.
433. Ng CC, Tan J, Ong CK, Lim WK, Rajasegaran V, Nasir ND, et al. MED12 is frequently mutated in breast phyllodes tumours: a study of 112 cases. J Clin Pathol. 2015;68(9):685–91.
434. Tan BY, Md Nasir ND, Chang HY, Ng CCY, Guan P, Nagarajan S, et al. Morphologic and genetic heterogeneity in breast fibroepithelial lesions-a comprehensive mapping study. Mod Pathol. 2020;33(9):1732–45.
435. Rosenberger LH, Thomas SM, Nimbkar SN, Hieken TJ, Ludwig KK, Jacobs LK, et al. Contemporary multi-institutional cohort of 550 cases of phyllodes tumors (2007-2017) demonstrates a need for more individualized margin guidelines. J Clin Oncol. 2021;39(3):178–89.
436. Lu Y, Chen Y, Zhu L, Cartwright P, Song E, Jacobs L, et al. Local recurrence of benign, borderline, and malignant phyllodes tumors of the breast: a systematic review and meta-analysis. Ann Surg Oncol. 2019;26(5):1263–75.
437. Onkendi EO, Jimenez RE, Spears GM, Harmsen WS, Ballman KV, Hieken TJ. Surgical treatment of borderline and malignant phyllodes tumors: the effect of the extent of resection and

tumor characteristics on patient outcome. Ann Surg Oncol. 2014;21(10):3304–9.
438. Reinfuss M, Mitus J, Duda K, Stelmach A, Rys J, Smolak K. The treatment and prognosis of patients with phyllodes tumor of the breast: an analysis of 170 cases. Cancer. 1996;77(5):910–6.
439. Nishimura R, Tan PH, Thike AA, Tan MH, Taira N, Li HH, et al. Utility of the Singapore nomogram for predicting recurrence-free survival in Japanese women with breast phyllodes tumours. J Clin Pathol. 2014;67(8):748–50.
440. Barth RJ Jr. Histologic features predict local recurrence after breast conserving therapy of phyllodes tumors. Breast Cancer Res Treat. 1999;57(3):291–5.
441. Ben Hassouna J, Damak T, Gamoudi A, Chargui R, Khomsi F, Mahjoub S, et al. Phyllodes tumors of the breast: a case series of 106 patients. Am J Surg. 2006;192(2):141–7.
442. Borhani-Khomani K, Talman ML, Kroman N, Tvedskov TF. Risk of local recurrence of benign and borderline phyllodes tumors: a danish population-based retrospective study. Ann Surg Oncol. 2016;23(5):1543–8.
443. Cowan ML, Argani P, Cimino-Mathews A. Benign and low-grade fibroepithelial neoplasms of the breast have low recurrence rate after positive surgical margins. Mod Pathol. 2016;29(3):259–65.
444. Genco IS, Purohit V, Hackman K, Ferreira L, Tugertimur B, Hajiyeva S. Benign and borderline phyllodes tumors of the breast: clinicopathologic analysis of 205 cases with emphasis on the surgical margin status and local recurrence rate. Ann Diagn Pathol. 2021;51:151708.
445. Moo TA, Alabdulkareem H, Tam A, Fontanet C, Lu Y, Landers A, et al. Association between recurrence and re-excision for close and positive margins versus observation in patients with benign phyllodes tumors. Ann Surg Oncol. 2017;24(10):3088–92.
446. Moutte A, Chopin N, Faure C, Beurrier F, Ho Quoc C, Guinaudeau F, et al. Surgical management of benign and borderline phyllodes tumors of the breast. Breast J. 2016;22(5):547–52.
447. Noordman PCW, Kliioueva NM, Weimann MN, Borgstein PJ, Vrouenraets BC. Phyllodes tumors of the breast: a retrospective analysis of 57 cases. Breast Cancer Res Treat. 2020;181(2):361–7.
448. Guillot E, Couturaud B, Reyal F, Curnier A, Ravinet J, Lae M, et al. Management of phyllodes breast tumors. Breast J. 2011;17(2):129–37.
449. Hawkins RE, Schofield JB, Fisher C, Wiltshaw E, McKinna JA. The clinical and histologic criteria that predict metastases from cystosarcoma phyllodes. Cancer. 1992;69(1):141–7.
450. Koh VCY, Thike AA, Nasir NDM, Yip GWC, Bay BH, Tan PH. Size and heterologous elements predict metastases in malignant phyllodes tumours of the breast. Virchows Arch. 2018;472(4):615–21.
451. Li J, Tsang JY, Chen C, Chan SK, Cheung SY, Wu C, et al. Predicting outcome in mammary phyllodes tumors: relevance of clinicopathological features. Ann Surg Oncol. 2019;26(9):2747–58.
452. Slodkowska E, Nofech-Mozes S, Xu B, Parra-Herran C, Lu FI, Raphael S, et al. Fibroepithelial lesions of the breast: a comprehensive morphological and outcome analysis of a large series. Mod Pathol. 2018;31(7):1073–84.
453. de Roos WK, Kaye P, Dent DM. Factors leading to local recurrence or death after surgical resection of phyllodes tumours of the breast. Br J Surg. 1999;86(3):396–9.
454. Cheng SP, Chang YC, Liu TP, Lee JJ, Tzen CY, Liu CL. Phyllodes tumor of the breast: the challenge persists. World J Surg. 2006;30(8):1414–21.
455. Mitus J, Reinfuss M, Mitus JW, Jakubowicz J, Blecharz P, Wysocki WM, et al. Malignant phyllodes tumor of the breast: treatment and prognosis. Breast J. 2014;20(6):639–44.
456. Pezner RD, Schultheiss TE, Paz IB. Malignant phyllodes tumor of the breast: local control rates with surgery alone. Int J Radiat Oncol Biol Phys. 2008;71(3):710–3.
457. Telli ML, Horst KC, Guardino AE, Dirbas FM, Carlson RW. Phyllodes tumors of the breast: natural history, diagnosis, and treatment. J Natl Compr Cancer Netw. 2007;5(3):324–30.
458. NCCN. NCCN clinical practice guidelines in oncology. Version 4.2021. Phyllodes tumor 2021 [updated 28 Apr 2021]. Available from: https://www.nccn.org/professionals/physician_gls/pdf/breast.pdf.
459. Jang JH, Choi MY, Lee SK, Kim S, Kim J, Lee J, et al. Clinicopathologic risk factors for the local recurrence of phyllodes tumors of the breast. Ann Surg Oncol. 2012;19(8):2612–7.
460. Lin CC, Chang HW, Lin CY, Chiu CF, Yeh SP. The clinical features and prognosis of phyllodes tumors: a single institution experience in Taiwan. Int J Clin Oncol. 2013;18(4):614–20.
461. Shaaban M, Barthelmes L. Benign phyllodes tumours of the breast: (Over) treatment of margins—a literature review. Eur J Surg Oncol. 2017;43(7):1186–90.
462. Thind A, Patel B, Thind K, Isherwood J, Phillips B, Dhaliwal K, et al. Surgical margins for borderline and malignant phyllodes tumours. Ann R Coll Surg Engl. 2020;102(3):165–73.
463. Yom CK, Han W, Kim SW, Park SY, Park IA, Noh DY. Reappraisal of conventional risk stratification for local recurrence based on clinical outcomes in 285 resected phyllodes tumors of the breast. Ann Surg Oncol. 2015;22(9):2912–8.
464. Mitus JW, Blecharz P, Jakubowicz J, Reinfuss M, Walasek T, Wysocki W. Phyllodes tumors of the breast. The treatment results for 340 patients from a single cancer centre. Breast. 2019;43:85–90.
465. Spanheimer PM, Murray MP, Zabor EC, Stempel M, Morrow M, Van Zee KJ, et al. Long-term outcomes after surgical treatment of malignant/borderline phyllodes tumors of the breast. Ann Surg Oncol. 2019;26(7):2136–43.
466. Barth RJ Jr, Wells WA, Mitchell SE, Cole BF. A prospective, multi-institutional study of adjuvant radiotherapy after resection of malignant phyllodes tumors. Ann Surg Oncol. 2009;16(8):2288–94.
467. Kim YJ, Kim K. Radiation therapy for malignant phyllodes tumor of the breast: An analysis of SEER data. Breast. 2017;32:26–32.
468. Boutrus RR, Khair S, Abdelazim Y, Nasr S, Ibraheem MH, Farahat A, et al. Phyllodes tumors of the breast: adjuvant radiation therapy revisited. Breast. 2021;58:1–5.
469. Chao X, Chen K, Zeng J, Bi Z, Guo M, Chen Y, et al. Adjuvant radiotherapy and chemotherapy for patients with breast phyllodes tumors: a systematic review and meta-analysis. BMC Cancer. 2019;19(1):372.
470. Gnerlich JL, Williams RT, Yao K, Jaskowiak N, Kulkarni SA. Utilization of radiotherapy for malignant phyllodes tumors: analysis of the National Cancer Data Base, 1998-2009. Ann Surg Oncol. 2014;21(4):1222–30.
471. Zeng S, Zhang X, Yang D, Wang X, Ren G. Effects of adjuvant radiotherapy on borderline and malignant phyllodes tumors: a systematic review and meta-analysis. Mol Clin Oncol. 2015;3(3):663–71.
472. Zhao W, Tian Q, Zhao A, Wang B, Yang J, Wang L, et al. The role of adjuvant radiotherapy in patients with malignant phyllodes tumor of the breast: a propensity-score matching analysis. Breast Cancer. 2021;28(1):110–8.
473. Khosravi-Shahi P. Management of non metastatic phyllodes tumors of the breast: review of the literature. Surg Oncol. 2011;20(4):e143–8.

Columnar Cell Lesions and Flat Epithelial Atypia

8

Beth T. Harrison, Timothy M. D'Alfonso, and Stuart J. Schnitt

Overview

Columnar cell lesions (CCLs) of the breast belong to a family of lesions characterized by columnar alteration of the luminal epithelium of the terminal duct lobular units (TDLUs), encompassing a spectrum from benign to atypical and neoplastic. Pathologists have long recognized such lesions and described them under various names in the literature. In the past, benign lesions had been termed "columnar alteration of lobules" [1], "columnar alteration with prominent apical snouts and secretions" [2], "enlarged lobular units with columnar alteration" [3], and "blunt duct adenosis" [4], whereas atypical forms had been referred to as "pretubular hyperplasia" [5], "atypical cystic lobules" [6], "atypical cystic duct" [7], "small ectatic ducts lined by atypical ductal cells with apocrine snouts" [8], "ductal intraepithelial neoplasia of the flat monomorphic type" [9], and "clinging carcinoma (monomorphic type)" [10], among others. In the most recent edition of the World Health Organization Classification of Breast Tumours [11], CCLs are categorized as (1) columnar cell change (CCC) and columnar cell hyperplasia (CCH) and (2) flat epithelial atypia (FEA).

CCLs are commonly encountered by pathologists in core needle biopsies (CNBs), especially those performed for mammographic microcalcifications. Of particular interest in current practice is the diagnosis of FEA on CNB due to controversies regarding its optimal classification and management. FEA, which consists of cells with low-grade monomorphic cytologic atypia, is analogous to the lesions originally described by Professor John Azzopardi in his classical monograph from 1979, *Problems in Breast Pathology* [10], as "clinging carcinoma (monomorphic type)" and considered a type of low-grade ductal carcinoma in situ (DCIS). Although it is now understood that FEA does not confer the same risk of breast cancer as DCIS [12] and should not be classified as such, FEA often co-exists with atypical ductal hyperplasia (ADH) and low-grade DCIS [13], shares similar genetic alterations [14], and thus likely represents the earliest morphologically identifiable neoplastic alteration among CCLs.

Due to concerns of finding a worse lesion at surgical excision and upgrade rates reported to be as high as 40% in some studies [15, 16], FEA diagnosed on CNB has traditionally been managed with surgical excision at many institutions. However, in recent years, accumulating evidence suggests that the risk of contemporaneous and subsequent breast cancer may not be as high as once thought, and a more conservative approach may be prudent in at least some patients.

Clinical and Radiographic Features

CCLs are common microscopic lesions in breast tissue from patients spanning a wide range of ages. These lesions tend to present at a slightly younger age than ADH or DCIS, with a mean patient age ranging from the mid-40s to early 50s [17]. CCLs, which frequently display intraluminal calcifications histologically, represent the fifth most common pathological finding associated with mammographic calcifications, behind fibrocystic change, fibroadenoma, DCIS, and sclerosing adenosis [18]. CCLs have been noted in over 40% of consecutive needle localization excisional biopsies for microcalcifications, directly associated with the microcalcifications in three-quarters of those cases [2].

B. T. Harrison (✉) · S. J. Schnitt
Department of Pathology, Brigham and Women's Hospital and Harvard Medical School, Boston, MA, USA
e-mail: bharrison3@bwh.harvard.edu; sschnitt@bwh.harvard.edu

T. M. D'Alfonso
Department of Pathology, Memorial Sloan Kettering Cancer Center, New York, NY, USA
e-mail: dalfonst@mskcc.org

© The Author(s), under exclusive license to Springer Nature Switzerland AG 2022
S. J. Shin et al. (eds.), *A Comprehensive Guide to Core Needle Biopsies of the Breast*,
https://doi.org/10.1007/978-3-031-05532-4_8

In this modern era of screening mammography, CCLs are frequently present in stereotactic CNBs for mammographic microcalcifications and are detected in approximately 40% of these specimens [19]. FEA, in particular, is present in 1–10% of CNBs [15, 20]. The targeted microcalcifications have a clustered distribution and their morphology has been described as amorphous and indistinct, fine pleomorphic, or round, but not linear and branching [19, 21, 22]. The radiologic risk is most often categorized as Breast Imaging-Reporting and Data System (BI-RADS) category 4, suspicious for malignancy, or as BI-RADS category 3, probably benign [19, 23]. CCLs have also been detected in ultrasound-guided CNBs for complex or simple cystic lesions and solid masses, with predominantly regular or indistinct contours, as well as in MRI-guided biopsies for non-mass enhancement [21, 24]. However, CCLs may not always represent the correlate for a mass lesion and careful radiologic-pathologic correlation is necessary to ensure that the benign finding is concordant. There is no difference in imaging findings between cases with atypia (FEA) and without atypia (CCC and CCH) [9, 23, 25, 26].

Microscopic Features

Columnar cell lesions are found in TDLUs with variably enlarged and dilated acini with rounded or irregular contours. *Columnar cell change* is characterized by one to two layers of cuboidal-to-columnar epithelium, whereas *columnar cell hyperplasia* demonstrates cellular stratification of greater thickness. The columnar epithelial cells contain ovoid or elongated nuclei with evenly dispersed chromatin and inconspicuous nucleoli. The nuclei are basally located and oriented perpendicular to the basement membrane (Fig. 8.1). In CCH, the proliferating columnar cells are crowded, with overlapping nuclei, and they form small mounds, tufts or short micropapil-

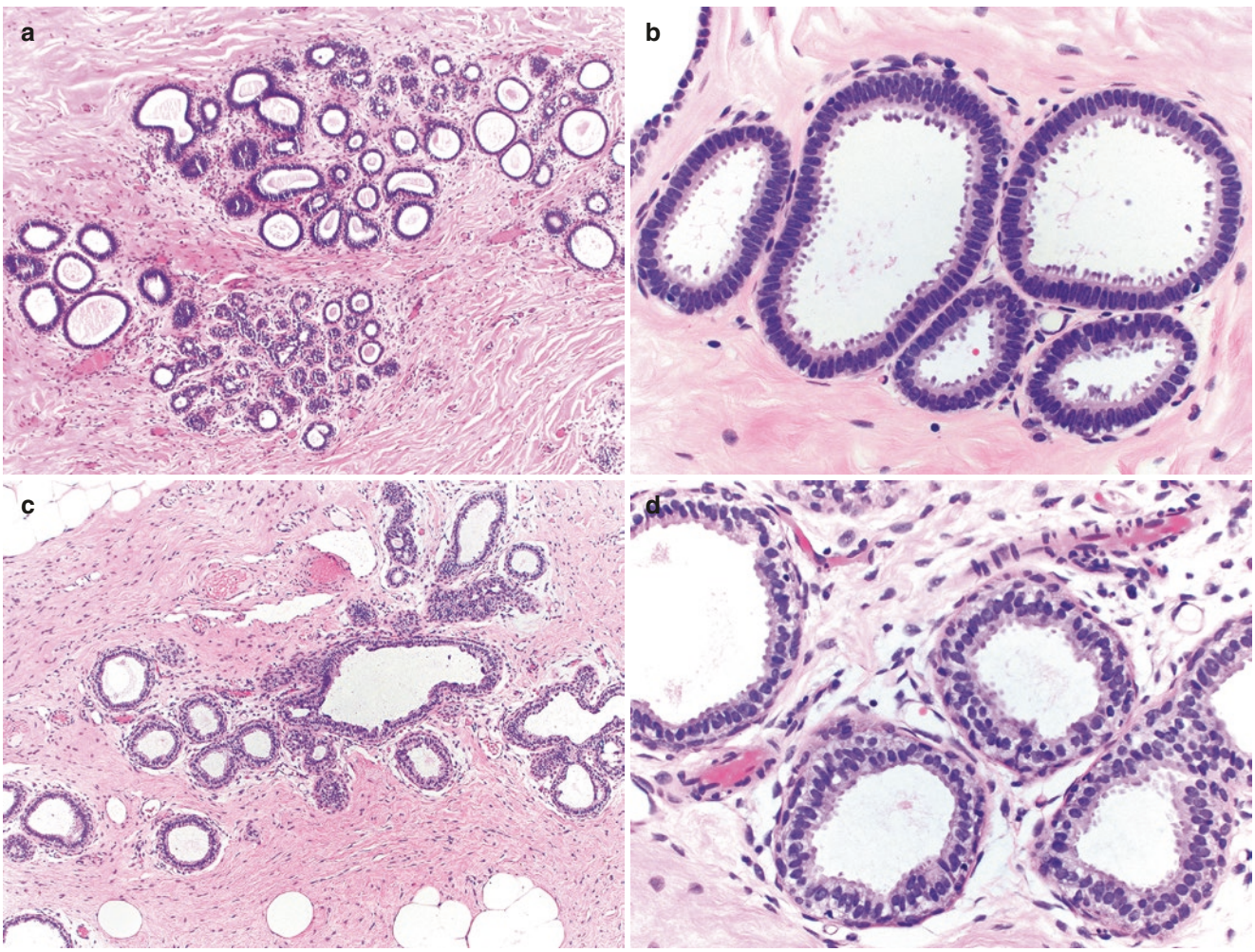

Fig. 8.1 Columnar cell change. (**a**–**d**) Terminal duct lobular units display variably dilated acini. (**b**, **d**) The acini are lined by 1–2 layers of columnar epithelial cells oriented perpendicular to the basement membrane. The cells have basally oriented, oval-to-elongated nuclei with finely dispersed chromatin and inconspicuous nucleoli

lations that give the luminal border an undulating contour (Figs. 8.2 and 8.3). Apical snouts or blebs are often present at the luminal border of the cells, and may be exaggerated, imparting a hobnail appearance (Fig. 8.4). Mitotic figures are absent to rare. The lesions are commonly associated with flocculent intraluminal secretions and basophilic calcifications of the calcium phosphate type (Figs. 8.5 and 8.6).

Flat epithelial atypia (FEA) is defined as a lesion in which lobular acini are lined by one to several layers of mildly atypical cuboidal-to-columnar cells with the features of low-grade DCIS [11], although a maximum thickness of 5 layers has been proposed by some authors [27]. At scanning magnification, FEA may be suspected in the presence of a TDLU with dilated acini with a distinctively round contour and thickened, band-like epithelium with a flat luminal border, which contrasts with the more irregular acinar contours often seen with CCC and CCH (Figs. 8.7 and 8.8). In the most readily recognized form of FEA, the lining epithelium is composed of 3–4 layers of evenly spaced, monomorphic cells with an increased nuclear-to-cytoplasmic ratio and loss of polarity. The cells have small, round nuclei with finely dispersed chromatin and variably prominent nucleoli. FEA also includes more subtle lesions consisting of 1–2 layers of columnar cells with oval-to-elongated nuclei, which maintain orientation perpendicular to the basement membrane, resembling CCC. However, in contrast to CCC, the cells display cytologic atypia in the form of an increased nuclear-to-cytoplasmic ratio, mild-to-moderate nuclear pleomorphism, marginated or clumped chromatin, and distinct nucleoli (Fig. 8.9). The appearance of these cells may be similar to the cells of tubular carcinoma (TC), or rarely colonic adenomas. Like other CCLs, FEA frequently exhibits prominent apical snouts, intraluminal secretions, and calcifications. Lymphocytic infiltrates are sometimes present in the intralobular stroma of TDLUs involved by FEA but are not typically seen in association with CCC and CCH. Mitotic figures may be present. As its name implies, FEA should have a flat growth pattern; while occasional cellular tufts or mounds are allowable, the presence of well-developed arcades, bridges, and micropapillary formations should preclude the diagnosis (Fig. 8.10).

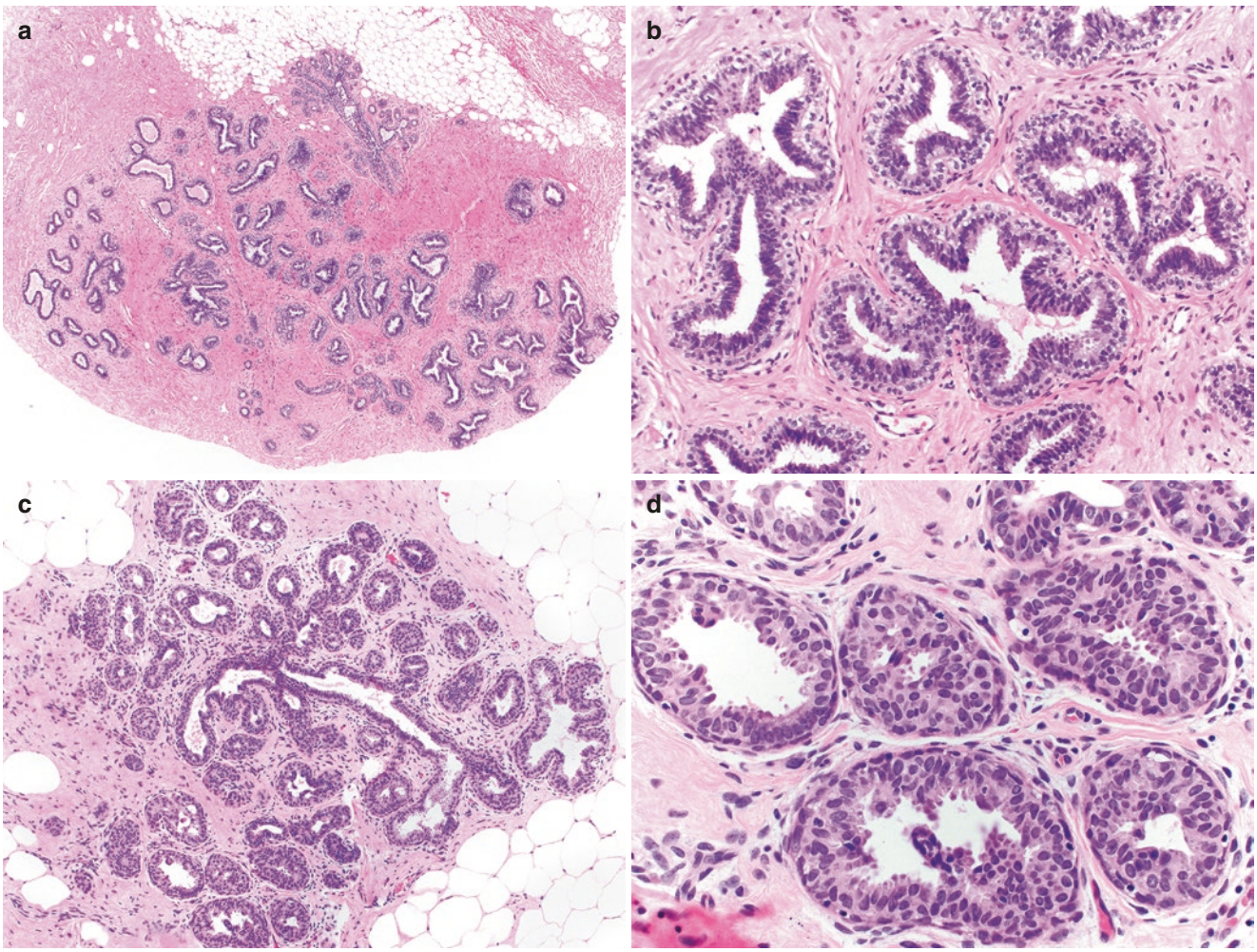

Fig. 8.2 Columnar cell hyperplasia. (**a**–**d**) Terminal duct lobular units have dilated acini with irregular contours. (**b**, **d**) The epithelial lining shows cellular stratification and tufting, which imparts an undulating luminal border

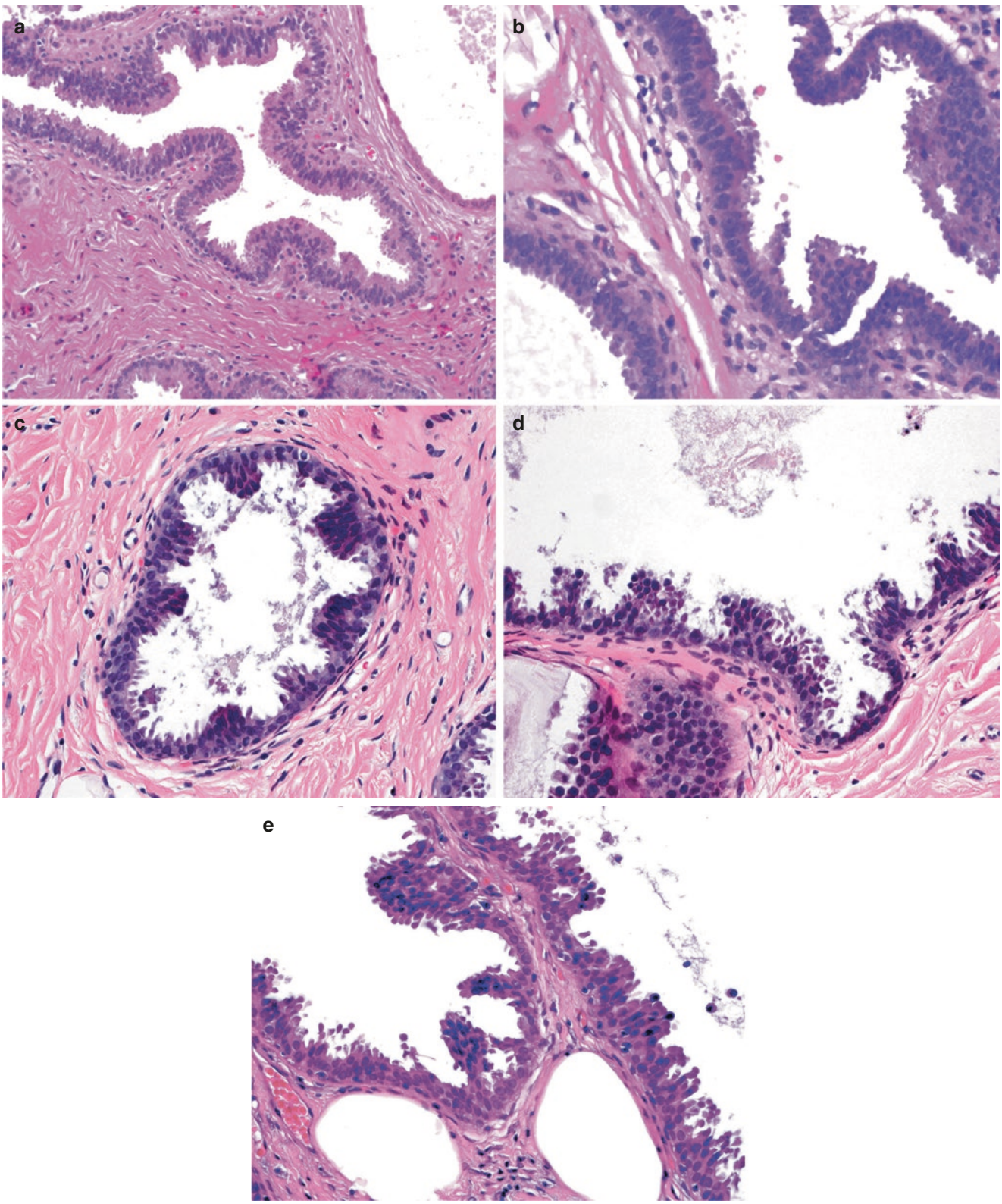

Fig. 8.3 Columnar cell hyperplasia. (**a**, **b**) Glands show columnar epithelium with stratification and retained polarization. Glands are more irregular in shape compared with columnar cell change. (**c**–**e**) Columnar cell hyperplasia may show micropapillary hyperplastic tufts without complex or rigid growth

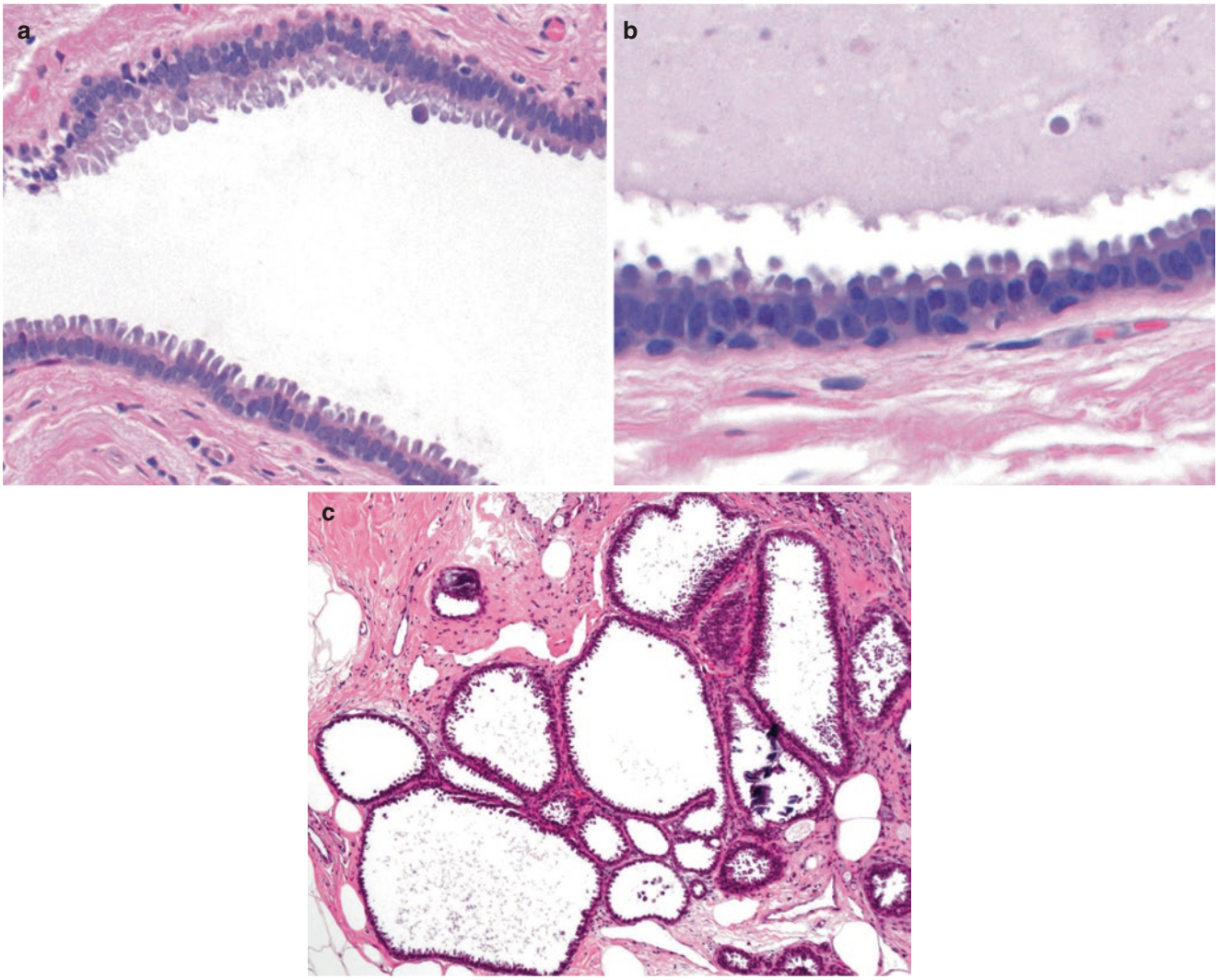

Fig. 8.4 Apical cytoplasmic snouts are characteristic of columnar cell lesions. (**a**, **b**) Columnar cell change with apical snouts. (**c**) Cytoplasmic snouts can be seen from low power in this case of columnar cell change and hyperplasia

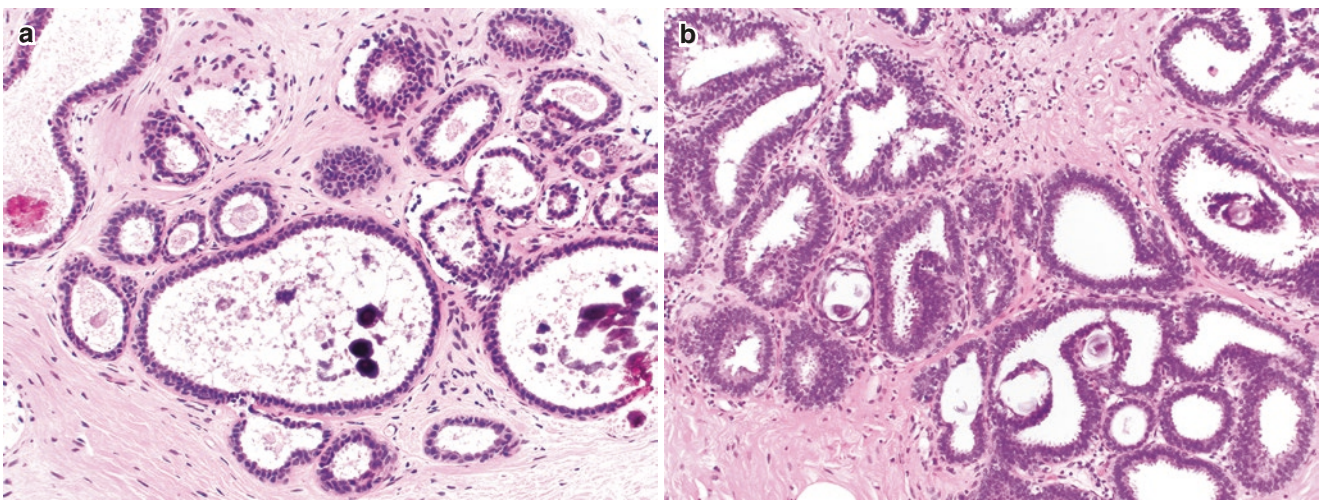

Fig. 8.5 Columnar cell lesions with associated calcifications. (**a**) Columnar cell change and (**b**) columnar cell hyperplasia commonly harbor intraluminal calcifications that correlate with the targeted mammographic calcifications

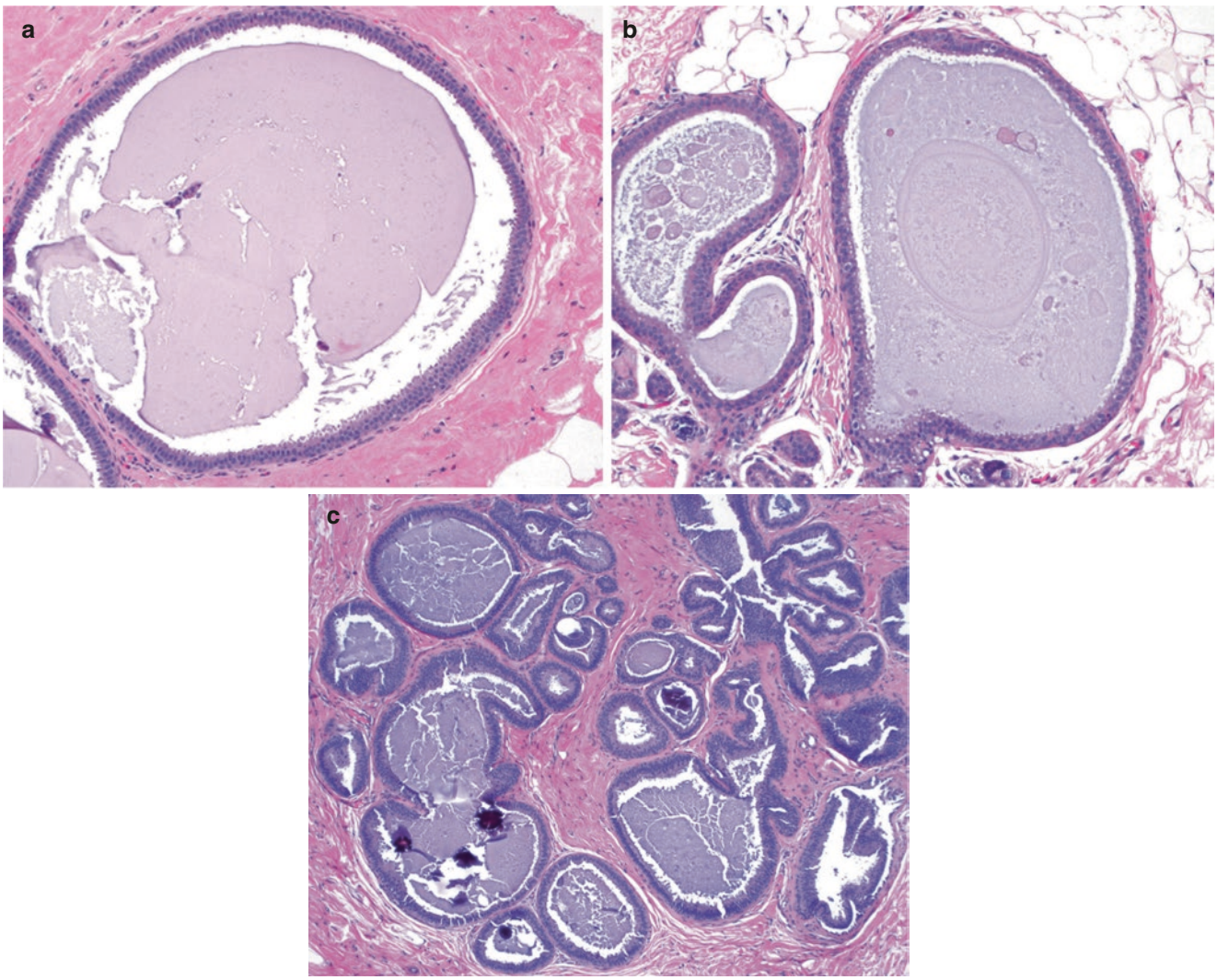

Fig. 8.6 Columnar cell change with secretions. (**a**–**c**) The thin secretion in columnar cell change varies from pink to dark blue in color

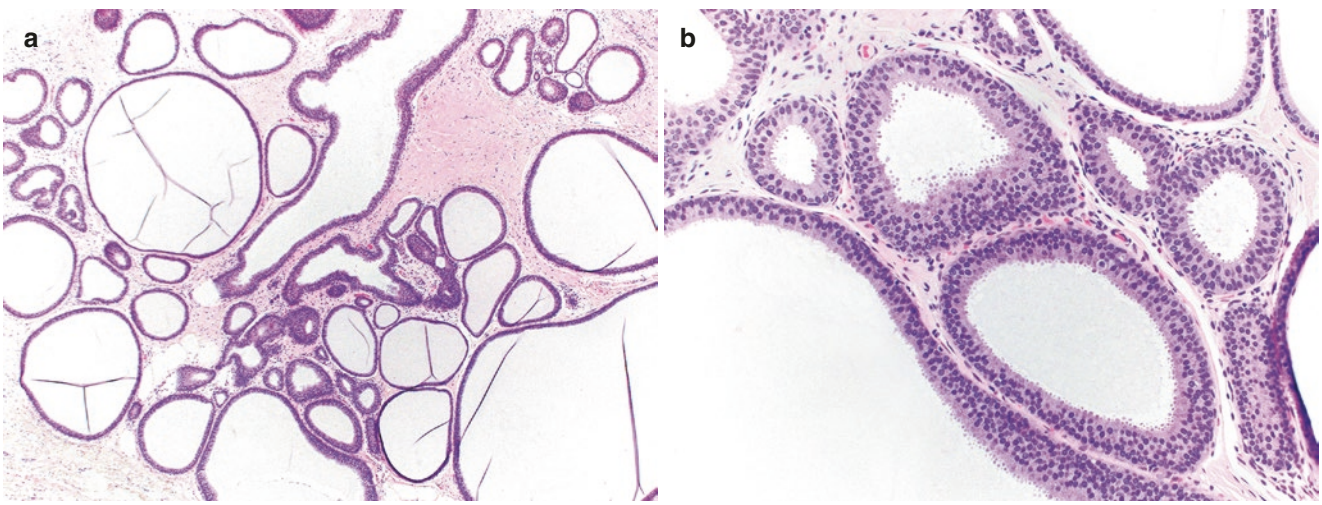

Fig. 8.7 Flat epithelial atypia. (**a**–**d**) Terminal duct lobular units involved by FEA are characterized by dilated acini with a round contour. The dilated acini (**e**) and terminal ducts (**f**) are often lined by 2–5 layers of evenly spaced, monomorphic cells with round nuclei. The nuclei may fine chromatin and inconspicuous nucleoli (**e**) or open chromatin with small, distinct nucleoli (**d**)

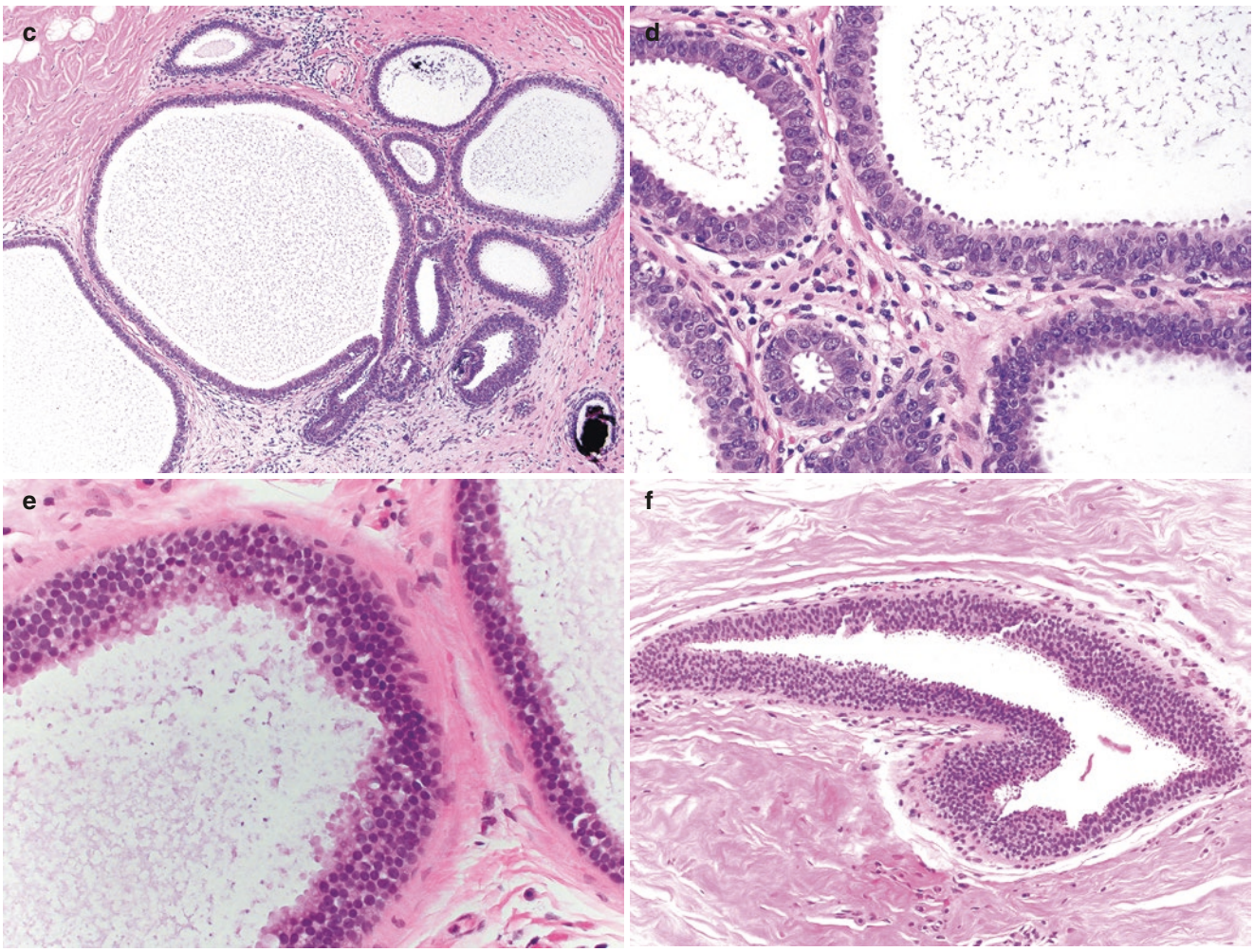

Fig. 8.7 (continued)

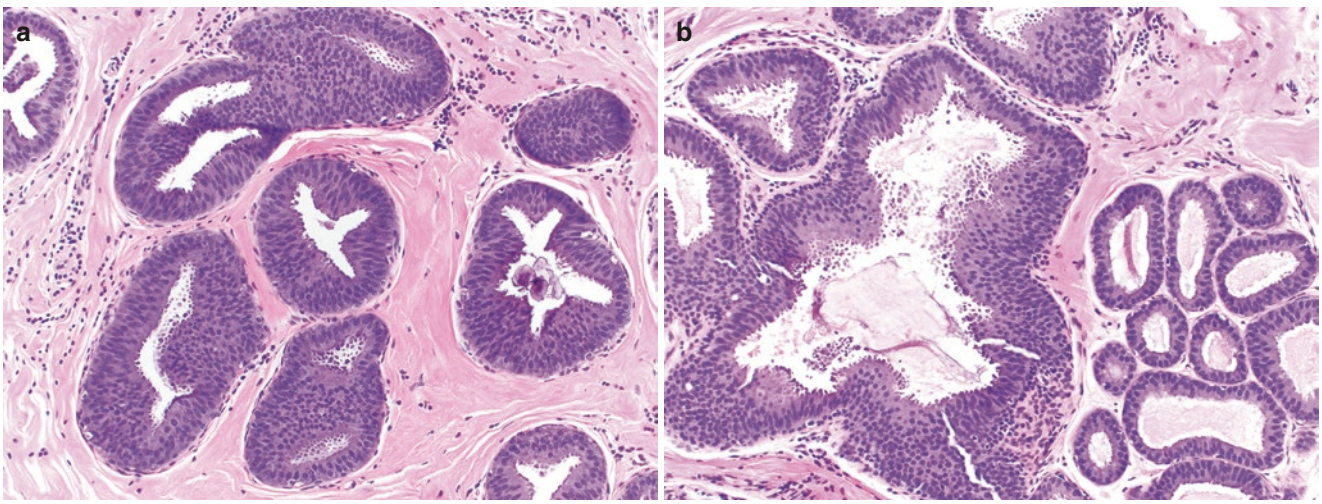

Fig. 8.8 Flat epithelial atypia with prominent cellular stratification. (**a**, **b**) Occasional examples of FEA have more than the 5 layers of cells. Although this lesion demonstrates low-grade cytologic atypia, the cellular tufting and the resultant irregular acinar contour and luminal border may resemble columnar cell hyperplasia. In the absence of rigid micropapillae and bridges, this lesion falls short of atypical ductal hyperplasia

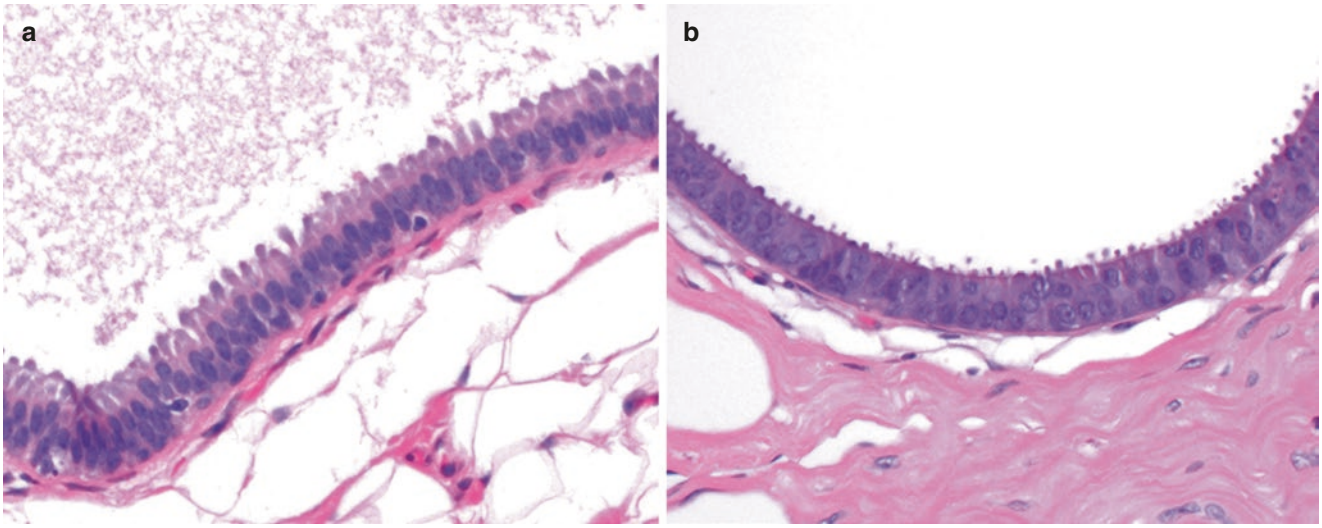

Fig. 8.9 Flat epithelial atypia compared with columnar cell change. (**a**) Columnar cell change shows uniform columnar cells arranged in an orderly configuration perpendicular to the basement membrane. (**b**) Cells of FEA, in comparison, are round to cuboidal and show low-grade cytologic atypia with prominent nucleoli. There is a loss of cellular polarity in FEA

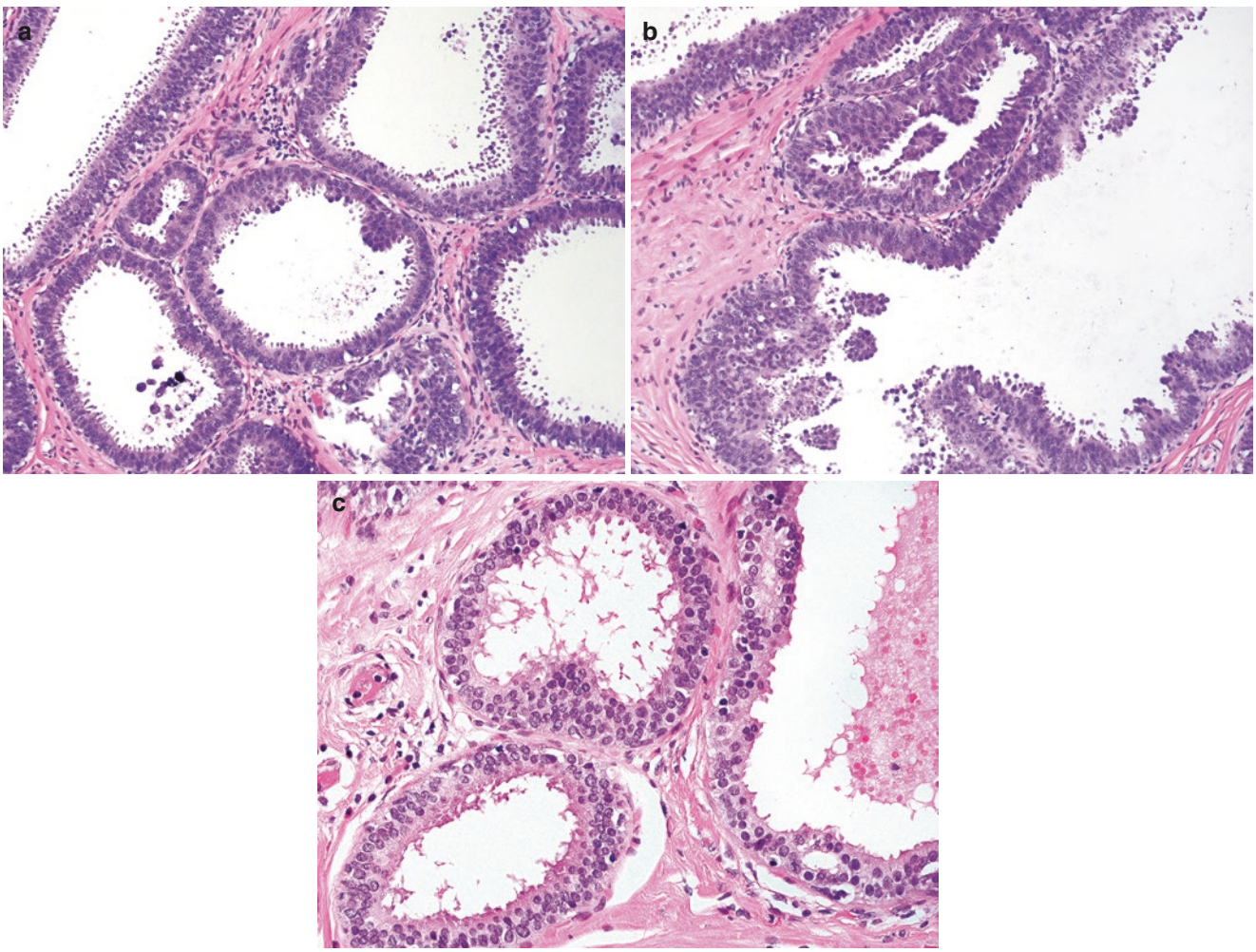

Fig. 8.10 Flat epithelial atypia with focal architectural atypia is challenging on core biopsy. A diagnosis of FEA is allowable in the presence of small cellular mounds (**a**), while a diagnosis of focal atypical ductal hyperplasia arising in a background of FEA should be made in the presence of well-developed micropapillae or arcades (**b**, **c**)

CCC, CCH, and FEA are often found in breast parenchyma that harbors other benign changes, such as cysts and proliferative epithelial lesions. More importantly, as will be further discussed below, CCLs are strongly associated with other lesions in the low-grade breast neoplasia pathway, including lobular neoplasia (LN), ADH, low-grade DCIS, tubular carcinoma (TC), and invasive lobular carcinoma (ILC) [13, 28] (Figs. 8.11, 8.12 and 8.13). In DCIS cases, the presence of concurrent FEA is significantly associated with DCIS of low nuclear grade, micropapillary and cribriform architectural patterns and absence of comedo necrosis [29].

A *mucinous variant of columnar cell lesions* (Fig. 8.14) has been described, with mucin production noted in approximately 5% of cases of CCLs with and without atypia and 15% of cases of ADH arising in CCLs [30]. Coyne [31] and Fadare and Mariappan [32] have also reported cases of CCH in morphologic continuum with mucocele-like lesions (MLLs). One lesion consisted of mucin-producing CCH associated with large basophilic calcifications, intraluminal crystalloids, and extravasated mucin, while the other lesion comprised benign mucinous cysts with an attenuated lining that transitioned to CCH. It is well established that mucocele-like lesions arise in the setting of various pathologic processes—CCC, CCH, FEA, and ADH among them—and those with atypia are referred to as *mucocele-like lesions with atypia*.

Blunt duct adenosis, although offered as a term synonymous with non-atypical columnar cell lesions [11], is considered by some authors to represent a distinct entity—a form of terminal duct hyperplasia with abortive lobule formation. Blunt duct adenosis has been described as a lobule-like aggregate of branching and tubular ducts with columnar luminal epithelium surrounded by a prominent myoepithelial cell layer and expanded, cellular intralobular stroma [33, 34]. It is usually associated with benign lesions, not precursor lesions, and it does not harbor 16q loss like other

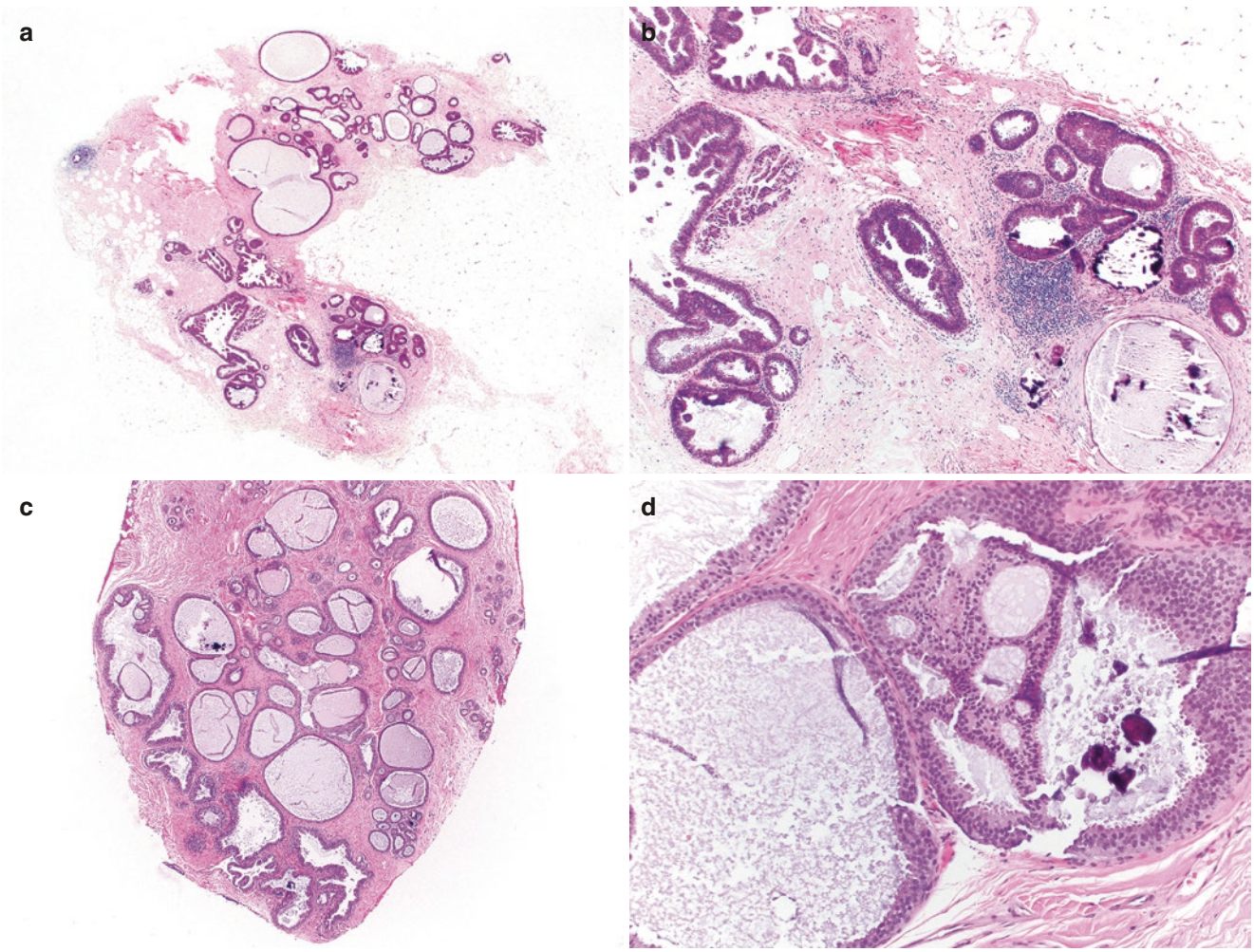

Fig. 8.11 Flat epithelial atypia associated with atypical ductal hyperplasia on core biopsy. (**a**, **c**) On low power, there are cystically dilated acini with intraluminal secretions and calcifications. (**b**, **d**) On higher power, architectural atypia in the form of micropapillary (**b**) and focal cribriform (**d**) proliferations can be appreciated, consistent with the diagnosis of atypical ductal hyperplasia

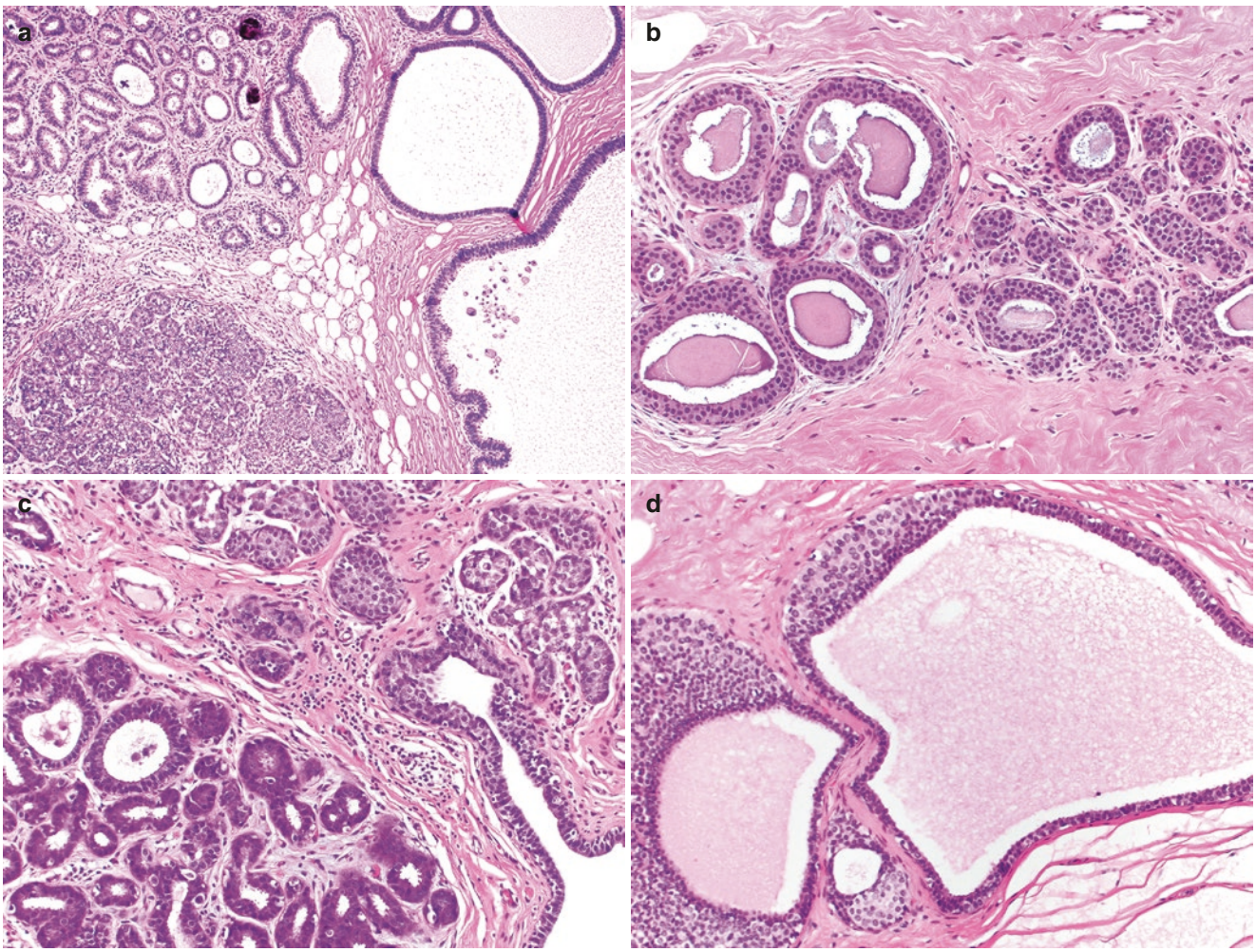

Fig. 8.12 Flat epithelial atypia associated with atypical lobular hyperplasia. The lobular neoplasia is present as poorly cohesive cells with low-grade cytologic atypia, which may fill the lobular acini (**a**, **b**), spread in a pagetoid fashion along terminal ducts (**c**), and even be seen in the same acinus as FEA (**d**). This finding may be subtle (**b**) and should be carefully excluded. Lobular neoplasia diagnosed on core biopsy is considered incidental and may not change management

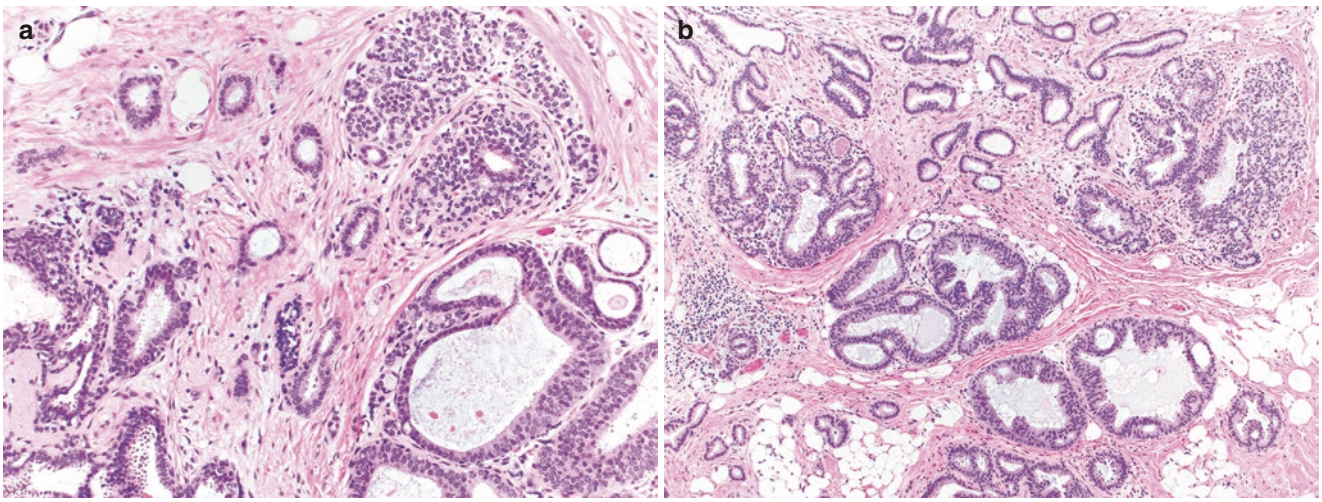

Fig. 8.13 Flat epithelial atypia belongs to the low-grade breast neoplasia family. This case includes the "Rosen triad" of FEA, lobular neoplasia and tubular carcinoma (**a**) as well as atypical ductal hyperplasia (**b**)

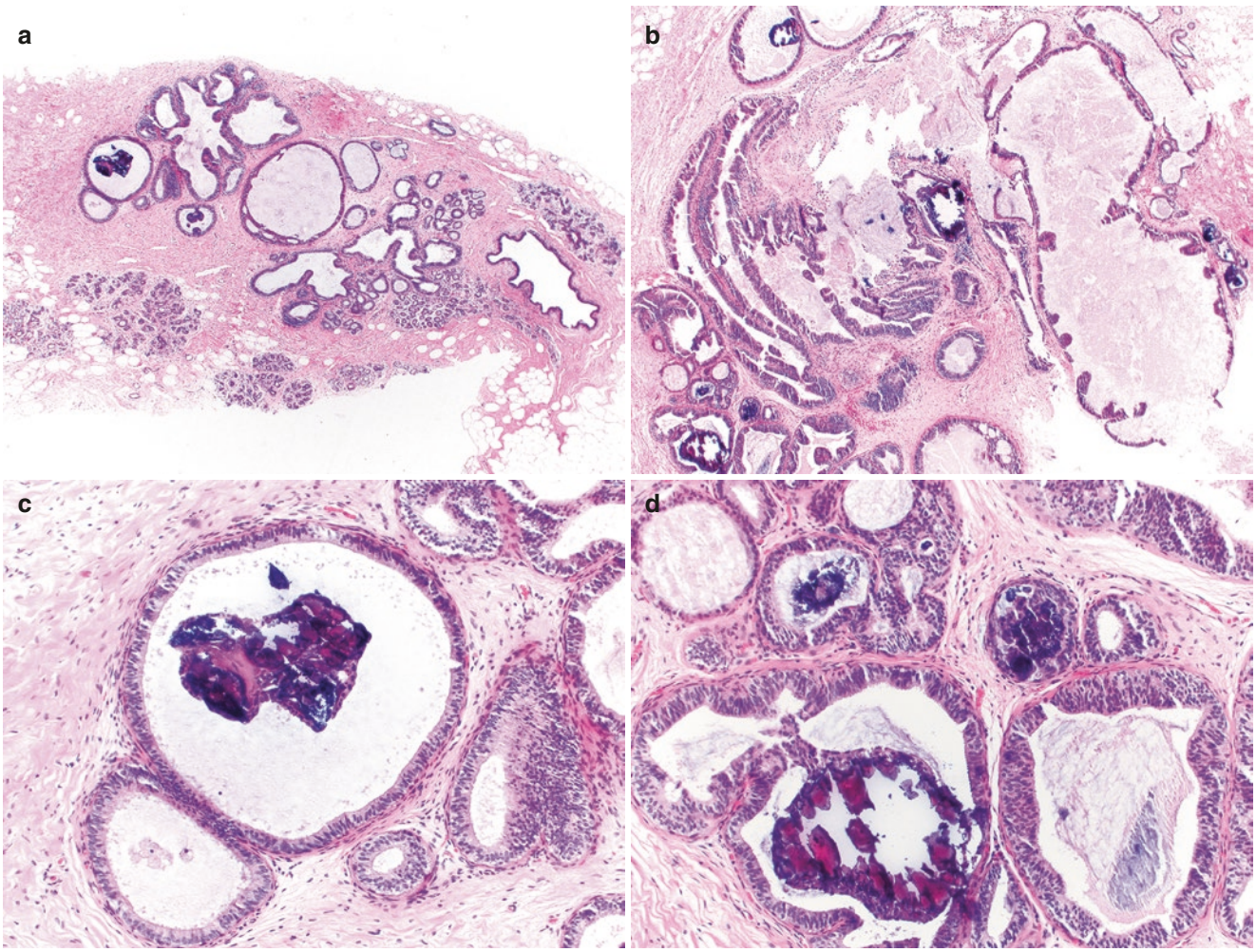

Fig. 8.14 Mucinous variant of columnar cell lesion on core biopsy. (**a**, **b**) The lesion consists of a mucocele-like lesion with focal atypia (**a**) and extravasated mucin (**b**) arising in a background of columnar cell change (**c**) and flat epithelial atypia (**d**). Note the characteristically coarse calcifications associated with the mucin

members of the low-grade breast neoplasia family [35]. Given this, it has been argued that this is best considered a benign polyclonal lesion distinct from CCLs [34]. However, we do not use the term blunt duct adenosis in our pathology reports.

Differential Diagnosis

In the approach to the diagnosis of CCLs on CNB, it is most important to appreciate the histologic features that distinguish FEA from non-atypical CCLs and other benign lesions, as the diagnosis of FEA should prompt careful exclusion of other higher risk lesions, such as ADH or lobular neoplasia, and may lead to a difference in management at some institutions. Several benign lesions may be considered in the differential diagnosis of FEA, as well as CCLs without atypia, and are likewise encountered in biopsies for microcalcifications. The following discussion emphasizes the distinction of FEA from other lesions as it is of greater clinical significance.

At low magnification, FEA may be completely overlooked, and examples may be misinterpreted as benign *microcysts*. Both of these lesions are composed of small round cysts, which are associated with intraluminal secretions and calcifications, and both are frequently found in a background of CCC. However, on closer inspection, microcysts are lined by an attenuated and banal epithelium, whereas FEA is distinguished by cellular stratification, monomorphism, and other features of low-grade atypia (Fig. 8.15a–c). Conversely, benign metaplastic and hyperplastic changes may be overdiagnosed as FEA. *Apocrine metaplasia* displays apocrine snouts, although not as exaggerated as the snouts of FEA, and its distinctive nuclear features—round-to-oval nuclei with vesicular chromatin and prominent nucleoli—may be misinterpreted as atypical. In

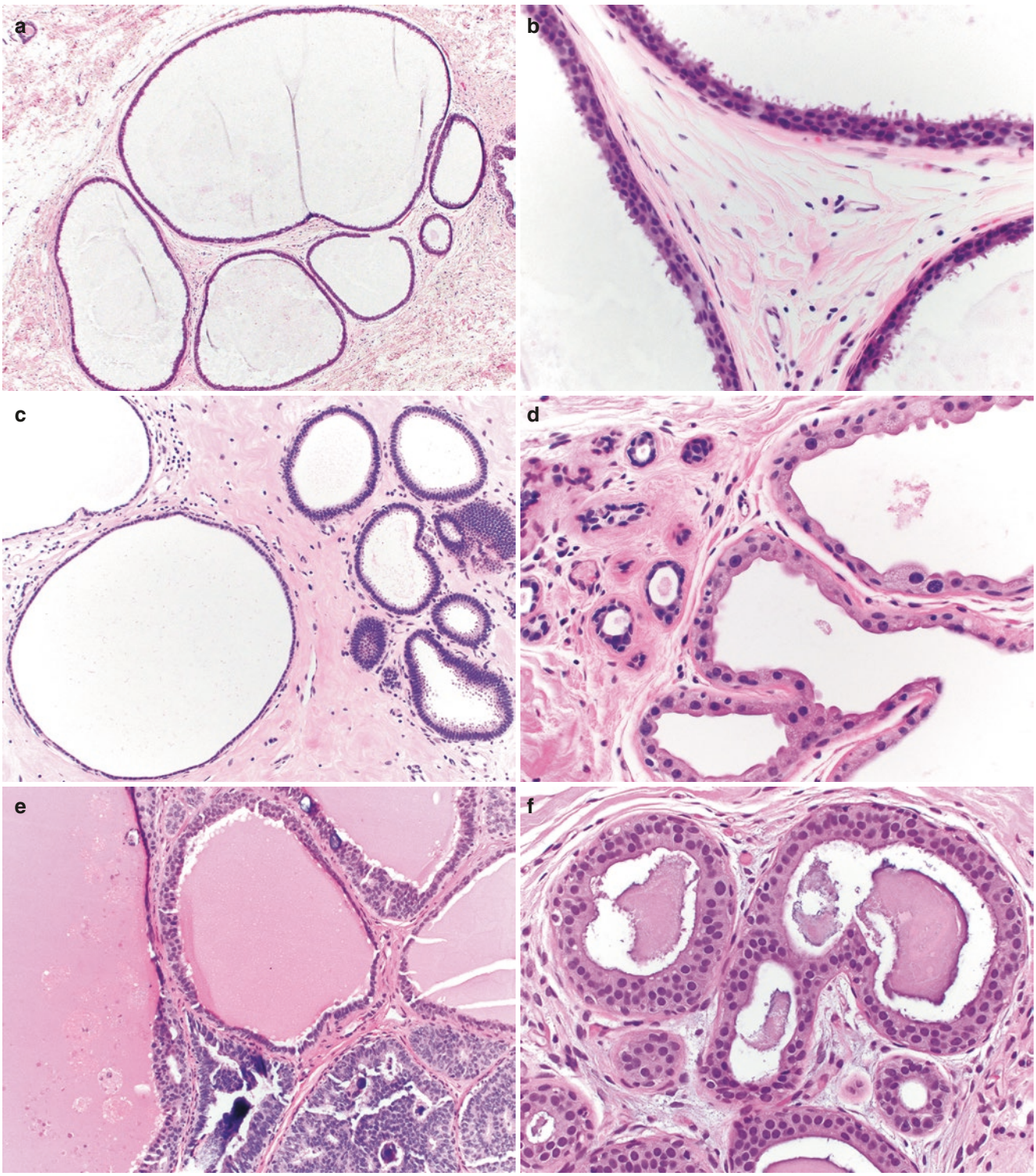

Fig. 8.15 Differential diagnosis of flat epithelial atypia. On low power, cystic FEA (**a**, **b**) may resemble microcysts (**c**) or apocrine cysts (**d**); however, on higher power, the cyst has a multilayered epithelial lining with cellular monomorphism and loss of polarity diagnostic of FEA. Like FEA, microcysts often arise in the setting of columnar cell change (**c**). Apocrine change is characterized by larger cells with abundant granular eosinophilic cytoplasm and larger oval nuclei with prominent nucleoli. Cystic hypersecretory lesions with atypia may raise consideration for FEA (with associated ADH or DCIS) but they are distinguished by colloid-like dense eosinophilic secretions (**e**) rather than the flocculent basophilic to eosinophilic secretions of FEA (**f**)

contrast to FEA, apocrine metaplasia has larger cells with more abundant eosinophilic cytoplasm, greater variation in nuclear size, and larger nucleoli, and it tends to be associated with optically clear, refractile calcium oxalate crystals (Fig. 8.15d). *Pregnancy-like (pseudolactational) hyperplasia* (PLH) and *cystic hypersecretory hyperplasia* (CHH) may also be confused with FEA due to cytologic alterations. PLH is characterized by swollen glandular cells with abundant pale vacuolated cytoplasm, small darkly stained nuclei, and apical cytoplasmic blebs. The cytoplasmic blebs, when compared to those in FEA, are enlarged and contain vacuolated cytoplasm as well as nuclei that are extruded into the lumen. CHH, which often co-exists with PLH, is composed of dilated cysts lined by flat-to-cuboidal epithelium, but these cysts are characteristically filled with colloid-like eosinophilic secretions [36] (Fig. 8.15e, f). Apocrine and hypersecretory lesions may display cytologic atypia and neoplastic transformation, but such lesions are characterized by significant nuclear pleomorphism and likely represent biologic processes distinct from low-grade neoplasia.

One of the more challenging aspects of the diagnosis of FEA is distinguishing it from CCC and CCH, as these lesions frequently coexist in the same breast, the same TDLU, or even the same space, and the features of atypia may be subtle. The diagnostic criteria for each of these lesions are detailed above and summarized in Table 8.1. Interobserver and intraobserver reproducibility has been addressed in multiple studies, which have shown fair to excellent reproducibility [37–40]. O'Malley et al. [40] demonstrated that the diagnosis of FEA and its distinction from CCLs without atypia is highly reproducible when pathologists are provided with a tutorial consisting of written criteria and representative digital images. Overall agreement among eight pathologists with a particular interest in breast pathology in the evaluation of images from 30 cases was 91.8% (95% CI, 84.0–96.9%), while the multi-rater kappa value was 0.83 (95% CI, 0.67–0.94), which is within the "excellent agreement" range. This suggests that observer agreement can be facilitated by standardized histologic criteria and sufficient training. Despite this, it should be acknowledged that the level of agreement found in this study may not be attainable under routine practice conditions or in the general practice setting.

Underscoring this point, results from the Breast Pathology (B-Path) study [41], a large investigation examining the under- and over-interpretation of breast biopsy specimens by U.S. pathologists, revealed wide variation in the diagnosis of FEA. This study included 115 pathologists representing diverse practice settings and levels of experience, but all with at least 1 year of experience interpreting breast specimens. Participants were provided with 60-case test sets composed of benign entities (30%), ADH (30%), DCIS (30%), and invasive carcinoma (10%). The diagnosis of FEA was assessed in the test set, 6 reference FEA cases, and 72 reference benign cases without FEA [including normal breast tissue, CCC, CCH, usual ductal hyperplasia (UDH), and ALH]. Pathologists rendered a diagnosis of FEA in 0–35% of the cases. Agreement with the FEA diagnosis for the 6 reference FEA cases ranged from 17% to 52%. Six of the non-FEA benign cases were considered to have FEA by 20% or more of the pathologists. The findings from this study suggest substantial variability exists among pathologists with respect to

Table 8.1 Diagnostic criteria for columnar cell lesions of the breast

	Columnar cell change	Columnar cell hyperplasia	Flat epithelial atypia
Features of involved TDLUs	Variably dilated acini	Variably dilated acini	Variably dilated acini
	Irregular acinar contours	Irregular acinar contours	Rounded acinar contours
			Darkly stained, thickened, band-like appearance of epithelium on low power
Epithelial lining	Single layer	Multilayering, with tufts and mounds	Single or multiple cell layers
			Often flat luminal border, but tufts and mounds allowable
			No well-formed arcades, bridges, or micropapillae
Cytology	Columnar cells with nuclei oriented perpendicular to basement membrane	Columnar cells with nuclei oriented perpendicular to basement membrane; nuclei may appear crowded and overlap	Rounded cells with loss of polarization with respect to basement membrane
	Ovoid or elongated nuclei	Ovoid or elongated nuclei	Rounded, monomorphic nuclei
	Nucleoli absent or inconspicuous	Nucleoli absent or inconspicuous	Variably prominent nucleoli
	Apical snouts	Apical snouts, may be exaggerated	Apical snouts, may be exaggerated
Luminal contents	Secretions	Secretions, may be prominent	Secretions, may be prominent
	Microcalcifications	Calcifications, occasionally psammomatous	Calcifications, occasionally psammomatous

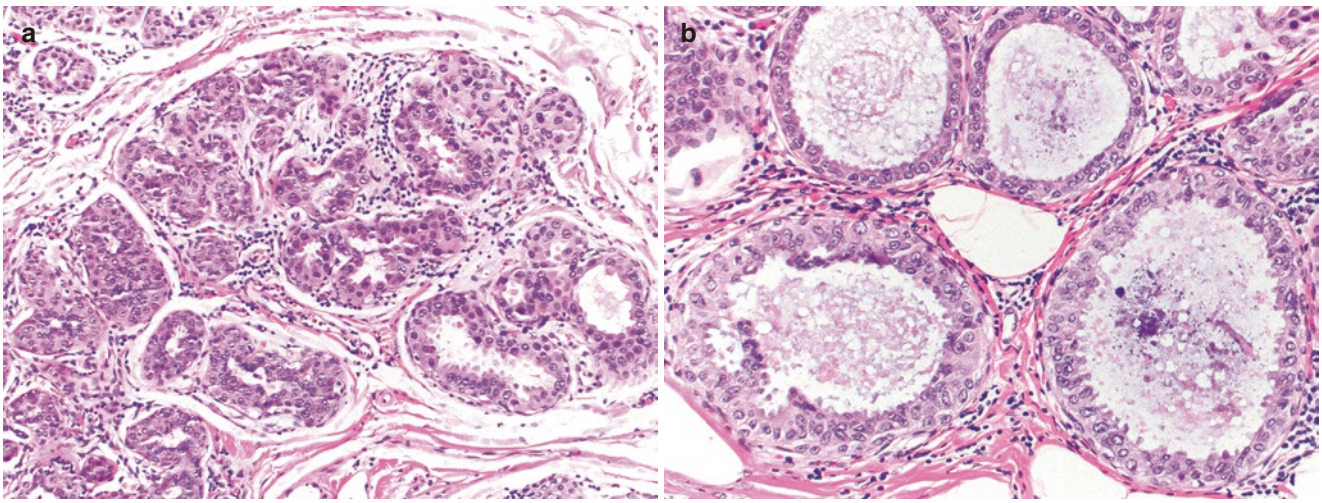

Fig. 8.16 Flat epithelial atypia with greater nuclear atypia than typically seen in this lesion. (**a**, **b**) These lesions show variation in nuclear size and shape, vesicular chromatin, and conspicuous nucleoli. The findings fall short of the high-grade nuclear atypia required for a diagnosis of DCIS with a clinging growth pattern

the diagnostic threshold and application of diagnostic criteria for FEA.

It can be argued that the ability to reproducibly distinguish FEA from non-atypical CCLs and other benign lesions on CNB is becoming less critical as accumulating evidence suggests that FEA may be managed more conservatively. On the other hand, at the other end of the spectrum, it is prudent to make every effort to exclude the possibility of coexistent ADH and DCIS, as these are high-risk lesions for which surgical excision is the standard of care. For cases in which FEA is identified on a CNB performed for mammographic microcalcifications, we recommend careful correlation with the specimen radiograph if available. If the microcalcifications visualized on the specimen radiograph appear more prominent or more numerous than the calcifications present in the tissue, additional levels should be performed. The same is true for any biopsy in which FEA exhibits focal architectural irregularity. Again, FEA may have occasional cellular tufts or mounds, whereas ADH should be diagnosed in the presence of well-developed arcades, bridges, and well-developed micropapillary formations. It has been shown that FEA evolves to ADH at the same site at an average of 3–4 tissue levels in 17% of cases [42].

Flat lesions with high-grade cytologic atypia should be classified as DCIS of the clinging type [43]. While this is undisputed, it remains uncertain how best to handle flat lesions in which there is greater nuclear atypia than typical for FEA, but still insufficient for diagnosis of high-grade DCIS; in other words, flat lesions composed of cells with intermediate-grade nuclear atypia (Fig. 8.16). Little is known about the molecular biology and natural history of these lesions. Although formal guidance is lacking, anecdotally, it has been our experience that many expert breast pathologists would not categorize this type of flat lesion as a form of intermediate-grade DCIS, and we agree. When such lesions are encountered on CNB, our approach is to note that the atypia exceeds that typically seen in FEA and to recommend surgical excision for final classification.

Immunohistochemical Features

The immunohistochemical profile is largely the same for all CCLs, including CCC, CCH, and FEA. All CCLs are characterized by strong and diffuse immunoreactivity for estrogen and progesterone receptors (ER and PR) and bcl-2 (an anti-apoptotic proto-oncogene). The epithelial cells in all of these lesions express luminal cytokeratins using antibodies to CK7, CK8, CK18, and CK19, but are negative for basal/high molecular weight (HMW) cytokeratins using antibodies to CK5, CK5/6, CK14, and CK17. Thus, the absence of basal/HMW cytokeratin expression cannot be used to distinguish FEA from non-atypical CCL as it is used to distinguish ADH from usual ductal hyperplasia. CCLs are also HER2 and p53 negative (wildtype-pattern heterogeneous staining). Cyclin D1 staining is increased compared to background. The MIB-1 proliferation index is also increased in CCH and FEA, but is low [44, 45].

Although immunohistochemistry is of little utility in the diagnosis of CCLs, these lesions are commonly noted on ER stains performed for other purposes, with the strong, diffuse staining of the cells comprising these lesions contrasting with the variable staining in normal breast epithelium, microcysts, and other benign non-proliferative and proliferative changes, and the absence of staining in apocrine metaplasia (Fig. 8.17). The immunophenotype of CCLs is similar to that

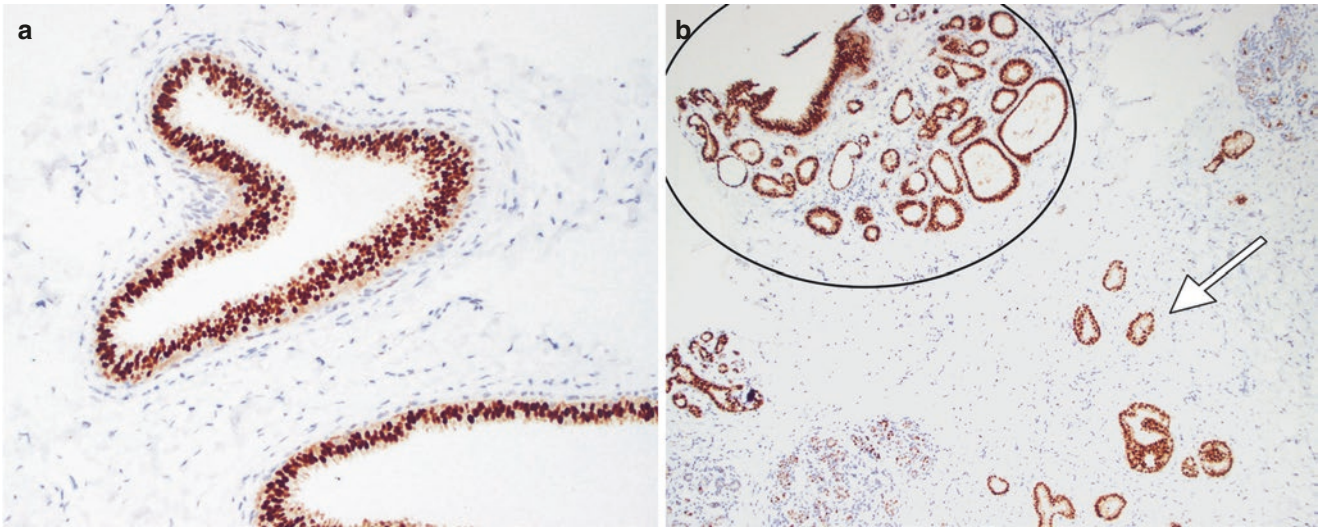

Fig. 8.17 Estrogen receptor expression in columnar cell lesions. (**a**) Flat epithelial atypia shows strong and diffuse reactivity with ER. (**b**) Strong ER expression in columnar cell change (circle) and adjacent tubular carcinoma (arrow), and weaker variable expression in benign lobules (bottom left and top right of image)

of other entities in the low-grade breast neoplasia pathway, and therefore it should be emphasized that these markers neither differentiate CCLs from one another nor from ADH and low-grade DCIS.

Pathogenesis

Convincing morphologic, immunohistochemical, and molecular genetic evidence suggests that CCLs represent the earliest non-obligate precursors in the low-grade breast neoplasia pathway, which includes invasive carcinomas and precursor lesions characterized by low nuclear grade, ER positivity, lack of expression of HER2 and basal markers, relatively few genomic alterations, and highly recurrent 16q loss [46–48]. Origins of this concept date back several decades ago when Professor Azzopardi, in his description of clinging carcinoma of the monomorphic type, observed that the cells of this lesion analogous to FEA were quite similar to the neoplastic cells of low-grade DCIS with a solid, cribriform, or micropapillary architectural pattern, and thus he considered it a form of DCIS [10]. Although it is now understood that FEA is not associated with sufficient breast cancer risk to be classified as DCIS, Professor Azzopardi's recognition of the link between FEA and low-grade DCIS was quite prescient.

Several studies from the mid-1990s to mid-2000s demonstrated that FEA—and synonymous lesions reported under other names—is strongly associated with the synchronous presence of low-grade DCIS, tubular carcinoma (TC), and lobular neoplasia (LN). In particular, the coexistence of CCLs, lobular carcinoma in situ (LCIS), and TC has been referred to as the "Rosen triad" as a tribute by Brandt and colleagues [49] to Dr. Paul Peter Rosen, who made the first categorical description in 1999 [28]. In their corresponding study of the Rosen triad, the same authors reported that all cases of TC were associated with CCLs, half of which also had associated LCIS. "Atypical CCH" was the predominant type of CCL seen with TCs [49]. Leibl et al. [50] suggested that FEA may be present in almost 90% of LN cases, whereas Collins et al. [29] showed that FEA is associated with low-grade DCIS with micropapillary and cribriform architectural patterns as well as the presence of ADH, LN, and other CCLs.

Expanding on this, Abdel-Fatah et al. [13, 45] provided additional evidence of the association of CCLs and other precursor lesions with low-grade breast carcinomas and proposed the concept of the low-grade breast neoplasia family. Back-to-back studies by this group revealed the significant coexistence of CCLs, LN, and ADH/low-grade DCIS with low-grade invasive carcinomas of tubular (TC), tubulolobular (TLC), classic lobular (ILC), and ductal/no special type (IDC) subtypes. CCLs, ADH/low-grade DCIS, and LN were detected in 78%, 71%, and 51% of low-grade breast carcinomas, respectively. CCLs co-localized with LN in 60% of ILCs and with ADH/DCIS in 85% of TCs. FEA was the most common of the CCLs, observed in 84% of TCs, 86% of TLCs, and 54% of ILCs [13]. Furthermore, the putative precursor lesions of this family—including CCC, CCH, FEA, ADH/low-grade DCIS, and LN—shared a similar immunophenotype. ER-α and bcl-2 were strongly and diffusely positive in the epithelial cells of these lesions, while cyclin D1 showed a stepwise increase in the percentage of positive cells from normal to CCC to CCH/FEA to ADH/DCIS to invasive carcinoma. The MIB-1 proliferation index was sig-

nificantly elevated in CCH, FEA, ADH/DCIS, and LN (>5%) as compared with normal TDLUs (1%). Low-grade breast carcinomas displayed a similar profile [45].

Molecular studies published during that time period and since then have reinforced the concept of a low-grade neoplasia family and elucidated the molecular genetic mechanisms underpinning the stepwise progression from precursor to invasive carcinoma in this pathway. Moinfar et al. [14], in an early loss of heterozygosity (LOH) study, were the first authors to demonstrate that ductal intraepithelial neoplasia (DIN)—flat type (monomorphic variant)/FEA harbors genetic changes and is clonally related to DCIS and IDC, and therefore likely represents one of the earliest neoplastic alterations in the breast. Simpson et al. [44], utilizing high-resolution comparative genomic hybridization (CGH), investigated the molecular genetic profiles of CCLs more broadly. All categories of CCLs, including CCC, CCH, and FEA, exhibited a variety of chromosomal alterations. Recurrent copy number alterations included loss of 16q, 17p, and X and gains of 15q, 16p, and 19. The low numbers of chromosomal alterations overall, the more frequent genomic losses relative to gains, and the recurrent loss of 16q observed in CCLs were consistent with the known genetic hallmarks of low-grade DCIS and low-grade invasive breast carcinomas [46–48]. Other studies have confirmed that FEA is clonally related to coexistent low-grade DCIS and TC [51] and have highlighted genetic transitions between FEA and ADH/DCIS [52], further supporting a direct precursor role for FEA.

Recently, *PIK3CA*-activating point mutations have been noted in a significant fraction of cases of CCC, FEA, ADH, DCIS, and invasive carcinoma. However, the presence of discordant genotypes between CCC and concurrent carcinoma, as well as the presence of mutations in UDH, indicates that these mutations may play a role in epithelial proliferation rather than neoplastic transformation [53, 54].

Taken together, the body of evidence supports a model of stepwise progression in the low-grade breast neoplasia pathway from CCLs to ADH/low-grade DCIS to low-grade invasive breast carcinomas. While the initial genetic alterations arise in a subset of CCLs without atypia, FEA represents the earliest morphologically identifiable precursor lesion of this pathway.

Management in Core Needle Biopsy

The clinical management of CCLs diagnosed on CNB is highly dependent on the presence or absence of atypia. CCC and CCH are considered benign entities that do not require surgical excision in the setting of radiologic-pathologic concordance, whereas it is controversial whether FEA must be excised when it is diagnosed as the most advanced lesion on biopsy. Given that FEA is cytologically atypical, and often found in breast tissue that harbors other low-grade precursor lesions and breast carcinomas, surgical excision has been the standard of care at many U.S. institutions in the years since this entity was defined in the 2003 WHO classification system. More recently, as accumulating evidence suggests that the risk of contemporaneous and subsequent breast cancer may be less than once thought, and as current practice trends favor de-escalation in the surgical management of breast disease, the management of FEA has been evolving to a more conservative approach.

Numerous retrospective, single institution studies have been published on the likelihood of finding malignancy (DCIS and invasive carcinoma), as well as high-risk lesions (ADH, ALH and LCIS), on surgical excision following a diagnosis of FEA on CNB, with reported upgrade rates widely varying [15, 16]. Recent meta-analyses have rigorously evaluated the literature on this topic. Rudin et al. [16] analyzed 32 studies published from 2003 to 2015 and found rates of upgrade of FEA to cancer ranging from 0% to 42%, with an overall pooled estimate of 11%. When the review was restricted to 16 higher quality studies that included only FEA cases diagnosed in 2003 or later (after the WHO definition was formalized), the pooled estimate dropped to 7.5%, with a rate of upgrade to invasive cancer of 3%. Wahab et al. [15] performed a similar analysis of 42 studies of pure FEA published from 2004 to 2020, which revealed pooled upgrade rates of 5% for breast cancer (1% for invasive carcinoma and 2% for DCIS). One notable trend in the published literature is that the upgrade rates have changed over time, with lower upgrade rates observed with later publication dates. In the last 5 years, several of the largest studies have reported no upgrades to invasive cancer at surgical excision [20, 55–57] (Table 8.2). Rates of co-occurrence of high-risk lesions (ADH, ALH, LCIS) on excision have ranged from 0% to 60%, with pooled estimates of 17.9% for ADH only and 27.1% for any high-risk lesion [16].

The extent of removal of the targeted mammographic microcalcifications is an important factor influencing the upgrade rate. Wahab et al. [15] noted that removal of at least 90% of the targeted microcalcifications at CNB, which was reported for 312 cases of FEA in 11 studies, is associated with a pooled upgrade rate of 0% (Table 8.3). For example, in a recent series of 40 cases of FEA diagnosed on CNB from 2012 to 2018, Grabenstetter et al. [26] found two invasive carcinomas on excision, yielding an upgrade rate of 5%. Microcalcifications represented the targeted radiologic lesion in the vast majority of cases, with residual microcalcifications identified on post-biopsy imaging in half, including the two upgraded ones. The upgraded cases were associated with microcalcifications spanning over 1.5 cm. Complete removal of the microcalcifications by CNB was achieved with smaller mammographic lesions (<1.0 cm), and no can-

Table 8.2 Select contemporary studies of upgrade of pure FEA to breast cancer

Study	Excisions, no.	Inv Ca, no. (%)	DCIS, no. (%)	Cancer total, no. (%)
Calhoun et al. (2015)	73	2 (2.7%)	3 (4.1%)	5 (6.8%)
Dialani et al. (2015)	35	0 (0%)	1 (2.9%)	1 (2.9%)
Acott et al. (2016)	48	0 (0%)	1 (2.1%)	1 (2.1%)
Mooney et al. (2016)	55	3 (5.5%)	3 (5.5%)	6 (10.9%)
Berry et al. (2016)	27	0 (0%)	3 (11.1%)	3 (11.1%)
Lamb et al. (2017)	208	0 (0%)	5 (2.4%)	5 (2.4%)
Ouidamer et al. (2018)	70	2 (2.9%)	3 (4.3%)	5 (7.1%)
McCroskey et al. (2018)	43	0 (0%)	0 (0%)	0 (0%)
Chan et al. (2018)	120	0 (0%)	1 (0.8%)	1 (0.8%)
Carrillo et al. (2019)	52	0 (0%)	2 (3.8%)	2 (3.8%)
Hugar et al. (2019)	94	0 (0%)	0 (0%)	0 (0%)
Srour et al. (2019)	34	1 (2.9%)	0 (0%)	1 (2.9%)
Grabenstetter et al. (2020)	34	2 (5.9%)	0 (0%)	2 (5.9%)
Liu et al. (2020)	89	0 (0%)	0 (0%)	0 (0%)
	982	10 (1.0%)	22 (2.2%)	32 (3.3%)

Table 8.3 Overall upgrade of FEA to breast cancer when at least 90% of microcalcifications removed at core needle biopsy

Study	Cases, no.	Breast cancer, no. (%)
Piubello et al. (2009)	14	0 (0%)
Solorzano et al. (2011)	8	1 (12.5%)
Lavoue et al. (2011)	18	1 (5.6%)
Bianchi et al. (2012)	42	2 (4.8%)
Villa et al. (2013)	85	0 (0%)
Ceunargt et al. (2013)	38	2 (5.3%)
Calhoun et al. (2015)	14	0 (0%)
Dialani et al. (2015)	23	0 (0%)
Acott et al. (2016)	19	0 (0%)
Hugar et al. (2019)	42	0 (0%)
Grabenstetter et al. (2020)	18	0 (0%)
	321	6 (1.9%)

cers were identified in this setting. Several other studies have similarly shown no upgrade to breast cancer when all microcalcifications are removed [20, 23, 25, 58–60]. It is worth noting that all studies with complete or near complete removal of the targeted calcifications employed 12-gauge or larger bore needles, which facilitates more generous sampling of the tissue. Other predictors of underestimation of malignancy have included the presence of a genetic predisposition to breast cancer [55], a targeted radiologic lesion other than microcalcifications [61], larger radiologic lesions (e.g., extent >1.0 cm) [62], more extensive FEA [62, 63], and concomitant high-risk lesions [60, 61].

At present, the management of FEA diagnosed on CNB is institution-dependent, although routine surgical excision is commonplace. An argument can be made for this approach given that the BI-RADS guidelines [64] recommend surgical excision for lesions with an upgrade rate of >2% and the overall upgrade to cancer is 5–7% in the literature to date [15, 16]. Surgical excision also facilitates the identification of co-occurring high-risk lesions (ADH, ALH, LCIS) in a nontrivial fraction of cases, which informs risk assessment and screening and risk reduction strategies, although whether this alone justifies surgery is debatable. On the other hand, it must be acknowledged that published upgrade rates have fallen in recent years, and the likelihood of finding cancer is exceedingly low when post-biopsy mammogram confirms that all microcalcifications have been removed. Thus, optimal management may be individualized based on correlation with imaging studies and a conservative approach with surveillance rather than surgery may be advocated in at least selected cases.

The current National Comprehensive Cancer Center (NCCN) guidelines suggest that FEA is a lesion that may not require surgical excision, although the details identifying patients suitable for observation are not specified [65]. The International Consensus Conference on lesions of uncertain malignant potential in the breast (B3 lesions) recommends therapeutic excision of the lesion seen on imaging by vacuum-assisted biopsy and no longer by open surgery, with follow-up surveillance imaging for 5 years [66, 67].

Prognosis

It has been consistently demonstrated in the literature that CCLs, including FEA, are associated with a very low risk of subsequent breast cancer. Boulos et al. [68] reported that CCLs were associated with only a mild increase in overall cancer risk (relative risk, 1.47) in the Nashville Breast Cohort, on the order of that associated with proliferative lesions without atypia, and there was no significant difference in the risk among the three categories of CCLs (e.g., CCC, CCH, and FEA). Similarly, using an established nested case-control study of benign breast disease within the Nurses' Health Study, Aroner et al. [69] found that women with CCLs had an increased risk of breast cancer compared to those without CCLs (odds ratio, 1.44), although this was no longer significant after adjustment for the presence of proliferative breast disease. Similarly, in a study by Said et al. [12] comparing the risk of breast cancer in women with benign breast disease in the Mayo Cohort to an external reference population, FEA did not convey independent risk of

breast cancer beyond that of proliferative disease without atypia (PDWA), as women with FEA and PDWA and those with PDWA alone both displayed approximately twofold elevated risk.

Most retrospective studies with long-term follow-up have shown very few instances of breast cancer following a diagnosis of FEA. While Martel et al. [9] reported that 14.3% of patients with flat DIN 1 (FEA) developed invasive carcinoma after 8 years of follow-up, there were no cases of invasive carcinoma or DCIS among 25 patients with clinging carcinoma of the monomorphic type (FEA) after an average follow-up period of 19.2 years in an analysis by Eusebi et al. [70], as well as no local recurrences after a median of 5.4 years among 59 patients who had the same diagnosis in a randomized clinical trial conducted by the European Organization for Research and Treatment of Cancer [71]. de Mascarel et al. [72] reported that none of the 84 patients who had FEA as an isolated lesion on excision progressed to a worse lesion in 10 years of follow-up. Furthermore, in studies of FEA managed with observation only, Ouldamer et al. [62] reported two ipsilateral breast cancers (intermediate-grade DCIS and IDC) in 50 patients followed for a mean follow-up of 4.7 years, whereas Uzoaru et al. [73] found no cancer during a median follow-up of 5 years.

Thus, the evidence suggests that patients diagnosed with FEA have a low risk of breast cancer and they can be potentially spared not only surgery but also the increased surveillance and risk reducing therapies offered to those with high-risk lesions such as ADH, ALH, and LCIS.

References

1. Page DL, Anderson TJ. Diagnostic histopathology of the breast. Edinburgh: Churchill Livingstone; 1987.
2. Fraser JL, Raza S, Chorny K, Connolly JL, Schnitt SJ. Columnar alteration with prominent apical snouts and secretions: a spectrum of changes frequently present in breast biopsies performed for microcalcifications. Am J Surg Pathol. 1998;22(12):1521–7.
3. McLaren BK, Gobbi H, Schuyler PA, Olson SJ, Parl FF, Dupont WD, et al. Immunohistochemical expression of estrogen receptor in enlarged lobular units with columnar alteration in benign breast biopsies: a nested case-control study. Am J Surg Pathol. 2005;29(1):105–8.
4. Ellis IO, Pinder SE, Bobrow L, et al. NHS publication no. 58. Pathology reporting of breast disease. Sheffield: NHS; 2005.
5. Rosen PP. Ductal hyperplasia. In: Rosen PP, editor. Rosen's breast pathology. Philadelphia, PA: Lippincott Williams & Wilkins; 2009. p. 230–63.
6. Oyama T, Maluf H, Koerner F. Atypical cystic lobules: an early stage in the formation of low-grade ductal carcinoma in situ. Virchows Arch. 1999;435(4):413–21.
7. Kusama R, Fujimori M, Matsuyama I, Fu L, Ishii K, Hama Y, et al. Clinicopathological characteristics of atypical cystic duct (ACD) of the breast: assessment of ACD as a precancerous lesion. Pathol Int. 2000;50(10):793–800.
8. Goldstein NS, O'Malley BA. Cancerization of small ectatic ducts of the breast by ductal carcinoma in situ cells with apocrine snouts: a lesion associated with tubular carcinoma. Am J Clin Pathol. 1997;107(5):561–6.
9. Martel M, Barron-Rodriguez P, Tolgay Ocal I, Dotto J, Tavassoli FA. Flat DIN 1 (flat epithelial atypia) on core needle biopsy: 63 cases identified retrospectively among 1,751 core biopsies performed over an 8-year period (1992-1999). Virchows Arch. 2007;451(5):883–91.
10. Azzopardi JG, Ahmed A, Millis RR. Problems in breast pathology. Major Probl Pathol. 1979;11:i–xvi, 1–466.
11. Schnitt SJ, Morris EA, Vincent-Salomon A. Columnar cell lesions, including flat epithelial atypia. In: Board WCoTE, editor. Breast tumours. 5th ed. Lyon: International Agency for Research on Cancer; 2019. p. 15–7.
12. Said SM, Visscher DW, Nassar A, Frank RD, Vierkant RA, Frost MH, et al. Flat epithelial atypia and risk of breast cancer: a Mayo cohort study. Cancer. 2015;121(10):1548–55.
13. Abdel-Fatah TM, Powe DG, Hodi Z, Lee AH, Reis-Filho JS, Ellis IO. High frequency of coexistence of columnar cell lesions, lobular neoplasia, and low grade ductal carcinoma in situ with invasive tubular carcinoma and invasive lobular carcinoma. Am J Surg Pathol. 2007;31(3):417–26.
14. Moinfar F, Man YG, Bratthauer GL, Ratschek M, Tavassoli FA. Genetic abnormalities in mammary ductal intraepithelial neoplasia-flat type ("clinging ductal carcinoma in situ"): a simulator of normal mammary epithelium. Cancer. 2000;88(9):2072–81.
15. Wahab RA, Lee SJ, Mulligan ME, Zhang B, Mahoney MC. Upgrade rate of pure flat epithelial atypia diagnosed at Core needle biopsy: a systematic review and meta-analysis. Radiol Imaging Cancer. 2021;3(1):e200116.
16. Rudin AV, Hoskin TL, Fahy A, Farrell AM, Nassar A, Ghosh K, et al. Flat epithelial atypia on core biopsy and upgrade to cancer: a systematic review and meta-analysis. Ann Surg Oncol. 2017;24(12):3549–58.
17. Jara-Lazaro AR, Tse GM, Tan PH. Columnar cell lesions of the breast: an update and significance on core biopsy. Pathology. 2009;41(1):18–27.
18. Dabbs DJ, Carter G, Fudge M, Peng Y, Swalsky P, Finkelstein S. Molecular alterations in columnar cell lesions of the breast. Mod Pathol. 2006;19(3):344–9.
19. Senetta R, Campanino PP, Mariscotti G, Garberoglio S, Daniele L, Pennecchi F, et al. Columnar cell lesions associated with breast calcifications on vacuum-assisted core biopsies: clinical, radiographic, and histological correlations. Mod Pathol. 2009;22(6):762–9.
20. Hugar SB, Bhargava R, Dabbs DJ, Davis KM, Zuley M, Clark BZ. Isolated flat epithelial atypia on core biopsy specimens is associated with a low risk of upgrade at excision. Am J Clin Pathol. 2019;151(5):511–5.
21. Elif A, Burcu S, Nazan C, Sumru CZ, Kemal AN. Columnar cell lesions of the breast: radiological features and histological correlation. Med Ultrason. 2015;17(2):147–54.
22. Kim MJ, Kim EK, Oh KK, Park BW, Kim H. Columnar cell lesions of the breast: mammographic and US features. Eur J Radiol. 2006;60(2):264–9.
23. Calhoun BC, Sobel A, White RL, Gromet M, Flippo T, Sarantou T, et al. Management of flat epithelial atypia on breast core biopsy may be individualized based on correlation with imaging studies. Mod Pathol. 2015;28(5):670–6.
24. Kim SJ, Kim WG. Sonographic features of flat epithelial atypia manifesting as a non-mass-like lesion: a case report. Am J Case Rep. 2019;20:340–4.
25. Dialani V, Venkataraman S, Frieling G, Schnitt SJ, Mehta TS. Does isolated flat epithelial atypia on vacuum-assisted breast core biopsy require surgical excision? Breast J. 2014;20(6):606–14.
26. Grabenstetter A, Brennan S, Salagean ED, Morrow M, Brogi E. Flat epithelial atypia in breast core needle biopsies with radiologic-

pathologic concordance: is excision necessary? Am J Surg Pathol. 2020;44(2):182–90.
27. Lerwill MF. Flat epithelial atypia of the breast. Arch Pathol Lab Med. 2008;132(4):615–21.
28. Rosen PP. Columnar cell hyperplasia is associated with lobular carcinoma in situ and tubular carcinoma. Am J Surg Pathol. 1999;23(12):1561.
29. Collins LC, Achacoso NA, Nekhlyudov L, Fletcher SW, Haque R, Quesenberry CP Jr, et al. Clinical and pathologic features of ductal carcinoma in situ associated with the presence of flat epithelial atypia: an analysis of 543 patients. Mod Pathol. 2007;20(11):1149–55.
30. Verschuur-Maes AH, Van Diest PJ. The mucinous variant of columnar cell lesions. Histopathology. 2011;58(6):847–53.
31. Coyne JD. Columnar cell hyperplasia with intraluminal crystalloids and features of a mucocoele-like lesion. Histopathology. 2004;44(4):401–3.
32. Fadare O, Mariappan MR. Mucocele-like tumor and columnar cell hyperplasia of the breast occurring in a morphologic continuum. J Med Case Rep. 2008;2:138.
33. Brogi E. Adenosis and microglandular adenosis. In: Hoda SA, Brogi E, Koerner FC, et al., editors. Rosen's breast pathology. 4th ed. Philadelphia, PA: Lippincott Williams & Wilkins; 2014. p. 183–212.
34. de Boer M, van Diest PJ. Blunt duct adenosis: a separate entity from columnar cell lesions? J Clin Pathol. 2021; https://doi.org/10.1136/jclinpath-2020-207359.
35. de Boer M, Verschuur-Maes AHJ, Buerger H, Moelans CB, Steenkamer M, Savola S, et al. Role of columnar cell lesions in breast carcinogenesis: analysis of chromosome 16 copy number changes by multiplex ligation-dependent probe amplification. Mod Pathol. 2018;31(12):1816–33.
36. Shin SJ, Rosen PP. Pregnancy-like (pseudolactational) hyperplasia: a primary diagnosis in mammographically detected lesions of the breast and its relationship to cystic hypersecretory hyperplasia. Am J Surg Pathol. 2000;24(12):1670–4.
37. Gomes DS, Porto SS, Balabram D, Gobbi H. Inter-observer variability between general pathologists and a specialist in breast pathology in the diagnosis of lobular neoplasia, columnar cell lesions, atypical ductal hyperplasia and ductal carcinoma in situ of the breast. Diagn Pathol. 2014;9:121.
38. Tan PH, Ho BC, Selvarajan S, Yap WM, Hanby A. Pathological diagnosis of columnar cell lesions of the breast: are there issues of reproducibility? J Clin Pathol. 2005;58(7):705–9.
39. Darvishian F, Singh B, Simsir A, Ye W, Cangiarella JF. Atypia on breast core needle biopsies: reproducibility and significance. Ann Clin Lab Sci. 2009;39(3):270–6.
40. O'Malley FP, Mohsin SK, Badve S, Bose S, Collins LC, Ennis M, et al. Interobserver reproducibility in the diagnosis of flat epithelial atypia of the breast. Mod Pathol. 2006;19(2):172–9.
41. Samples LS, Rendi MH, Frederick PD, Allison KH, Nelson HD, Morgan TR, et al. Surgical implications and variability in the use of the flat epithelial atypia diagnosis on breast biopsy specimens. Breast. 2017;34:34–43.
42. Chivukula M, Bhargava R, Tseng G, Dabbs DJ. Clinicopathologic implications of "flat epithelial atypia" in core needle biopsy specimens of the breast. Am J Clin Pathol. 2009;131(6):802–8.
43. Azzopardi JGAA, Millis RR. Problems in breast pathology, vol. 466. London: W.B. Saunders Company; 1979.
44. Simpson PT, Gale T, Reis-Filho JS, Jones C, Parry S, Sloane JP, et al. Columnar cell lesions of the breast: the missing link in breast cancer progression? A morphological and molecular analysis. Am J Surg Pathol. 2005;29(6):734–46.
45. Abdel-Fatah TM, Powe DG, Hodi Z, Reis-Filho JS, Lee AH, Ellis IO. Morphologic and molecular evolutionary pathways of low nuclear grade invasive breast cancers and their putative precursor lesions: further evidence to support the concept of low nuclear grade breast neoplasia family. Am J Surg Pathol. 2008;32(4):513–23.
46. Simpson PT, Reis-Filho JS, Gale T, Lakhani SR. Molecular evolution of breast cancer. J Pathol. 2005;205(2):248–54.
47. Roylance R, Gorman P, Harris W, Liebmann R, Barnes D, Hanby A, et al. Comparative genomic hybridization of breast tumors stratified by histological grade reveals new insights into the biological progression of breast cancer. Cancer Res. 1999;59(7):1433–6.
48. Bombonati A, Sgroi DC. The molecular pathology of breast cancer progression. J Pathol. 2011;223(2):307–17.
49. Brandt SM, Young GQ, Hoda SA. The "Rosen Triad": tubular carcinoma, lobular carcinoma in situ, and columnar cell lesions. Adv Anat Pathol. 2008;15(3):140–6.
50. Leibl S, Regitnig P, Moinfar F. Flat epithelial atypia (DIN 1a, atypical columnar change): an underdiagnosed entity very frequently coexisting with lobular neoplasia. Histopathology. 2007;50(7):859–65.
51. Aulmann S, Elsawaf Z, Penzel R, Schirmacher P, Sinn HP. Invasive tubular carcinoma of the breast frequently is clonally related to flat epithelial atypia and low-grade ductal carcinoma in situ. Am J Surg Pathol. 2009;33(11):1646–53.
52. Aulmann S, Braun L, Mietzsch F, Longerich T, Penzel R, Schirmacher P, et al. Transitions between flat epithelial atypia and low-grade ductal carcinoma in situ of the breast. Am J Surg Pathol. 2012;36(8):1247–52.
53. Ang DC, Warrick AL, Shilling A, Beadling C, Corless CL, Troxell ML. Frequent phosphatidylinositol-3-kinase mutations in proliferative breast lesions. Mod Pathol. 2014;27(5):740–50.
54. Troxell ML, Brunner AL, Neff T, Warrick A, Beadling C, Montgomery K, et al. Phosphatidylinositol-3-kinase pathway mutations are common in breast columnar cell lesions. Mod Pathol. 2012;25(7):930–7.
55. Lamb LR, Bahl M, Gadd MA, Lehman CD. Flat epithelial atypia: upgrade rates and risk-stratification approach to support informed decision making. J Am Coll Surg. 2017;225(6):696–701.
56. Chan PMY, Chotai N, Lai ES, Sin PY, Chen J, Lu SQ, et al. Majority of flat epithelial atypia diagnosed on biopsy do not require surgical excision. Breast. 2018;37:13–7.
57. Liu C, Dingee CK, Warburton R, Pao JS, Kuusk U, Bazzarelli A, et al. Pure flat epithelial atypia identified on core needle biopsy does not require excision. Eur J Surg Oncol. 2020;46(2):235–9.
58. Piubello Q, Parisi A, Eccher A, Barbazeni G, Franchini Z, Iannucci A. Flat epithelial atypia on core needle biopsy: which is the right management? Am J Surg Pathol. 2009;33(7):1078–84.
59. Villa A, Chiesa F, Massa T, Friedman D, Canavese G, Baccini P, et al. Flat epithelial atypia: comparison between 9-gauge and 11-gauge devices. Clin Breast Cancer. 2013;13(6):450–4.
60. Acott AA, Mancino AT. Flat epithelial atypia on core needle biopsy, must we surgically excise? Am J Surg. 2016;212(6):1211–3.
61. Yu CC, Ueng SH, Cheung YC, Shen SC, Kuo WL, Tsai HP, et al. Predictors of underestimation of malignancy after image-guided core needle biopsy diagnosis of flat epithelial atypia or atypical ductal hyperplasia. Breast J. 2015;21(3):224–32.
62. Ouldamer L, Poisson E, Arbion F, Bonneau C, Vilde A, Body G, et al. All pure flat atypical atypia lesions of the breast diagnosed using percutaneous vacuum-assisted breast biopsy do not need surgical excision. Breast. 2018;40:4–9.
63. Berry JS, Trappey AF, Vreeland TJ, Pattyn AR, Clifton GT, Berry EA, et al. Analysis of clinical and pathologic factors of pure, flat epithelial atypia on core needle biopsy to aid in the decision of excision or observation. J Cancer. 2016;7(1):1–6.
64. D'Orsi CJ, Sickles EA, Mendelson EB, Morris EA. ACR BI-RADS Atlas: breast imaging reporting and data system. Reston, VA: American College of Radiology; 2013.
65. Bevers TB, Helvie M, Bonaccio E, Calhoun KE, Daly MB, Farrar WB, et al. Breast cancer screening and diagnosis, version 3.2018,

NCCN clinical practice guidelines in oncology. J Natl Compr Cancer Netw. 2018;16(11):1362–89.
66. Rageth CJ, O'Flynn EAM, Pinker K, Kubik-Huch RA, Mundinger A, Decker T, et al. Second international consensus conference on lesions of uncertain malignant potential in the breast (B3 lesions). Breast Cancer Res Treat. 2019;174(2):279–96.
67. Rageth CJ, O'Flynn EA, Comstock C, Kurtz C, Kubik R, Madjar H, et al. First international consensus conference on lesions of uncertain malignant potential in the breast (B3 lesions). Breast Cancer Res Treat. 2016;159(2):203–13.
68. Boulos FI, Dupont WD, Simpson JF, Schuyler PA, Sanders ME, Freudenthal ME, et al. Histologic associations and long-term cancer risk in columnar cell lesions of the breast: a retrospective cohort and a nested case-control study. Cancer. 2008;113(9):2415–21.
69. Aroner SA, Collins LC, Schnitt SJ, Connolly JL, Colditz GA, Tamimi RM. Columnar cell lesions and subsequent breast cancer risk: a nested case-control study. Breast Cancer Res. 2010;12(4):R61.
70. Eusebi V, Foschini MP, Cook MG, Berrino F, Azzopardi JG. Long-term follow-up of in situ carcinoma of the breast with special emphasis on clinging carcinoma. Semin Diagn Pathol. 1989;6(2):165–73.
71. Bijker N, Peterse JL, Duchateau L, Julien JP, Fentiman IS, Duval C, et al. Risk factors for recurrence and metastasis after breast-conserving therapy for ductal carcinoma-in-situ: analysis of European Organization for Research and Treatment of Cancer Trial 10853. J Clin Oncol. 2001;19(8):2263–71.
72. de Mascarel I, MacGrogan G, Mathoulin-Pelissier S, Vincent-Salomon A, Soubeyran I, Picot V, et al. Epithelial atypia in biopsies performed for microcalcifications. Practical considerations about 2,833 serially sectioned surgical biopsies with a long follow-up. Virchows Arch. 2007;451(1):1–10.
73. Uzoaru I, Morgan BR, Liu ZG, Bellafiore FJ, Gaudier FS, Lo JV, et al. Flat epithelial atypia with and without atypical ductal hyperplasia: to re-excise or not. Results of a 5-year prospective study. Virchows Arch. 2012;461(4):419–23.

Intraductal Proliferations (DCIS, ADH, and UDH)

9

Kimberly H. Allison and Kristin C. Jensen

Introduction

Intraductal epithelial proliferations of the breast can present a diagnostic challenge to pathologists because of subtle differences in the diagnostic features and biologic characteristics of these proliferations. These lesions include ductal carcinoma in situ (DCIS), atypical ductal hyperplasia (ADH), and usual ductal hyperplasia. Each of these diagnostic categories carries a different risk of development of invasive carcinoma and has different treatment strategies. While diagnostic agreement rates on the diagnosis of high-grade ductal carcinoma are excellent, low-grade intraductal proliferations have notoriously low diagnostic agreement rates because these lesions present with a spectrum of very similar histologic findings [1, 2]. Reproducible evaluation of these lesions on core needle biopsy requires using current diagnostic criteria but also often must take into account clinical context. Figure 9.1 shows an overview of the main diagnostic categories and their characteristics.

The diagnosis of intraductal proliferative lesions on core biopsy requires evaluation of the cytologic and architectural features present as well as the extent of the process. Figure 9.2 shows an overview of the steps in this evaluative process. If the cytology is intermediate to high grade, a diagnosis of high-grade DCIS and its mimics should be considered, regardless of the extent or architecture. However, for lesions with low or borderline intermediate grade cytology, evaluation of the architecture of the proliferation is the next step in establishing the most accurate diagnosis. Are there architectural structures being formed that are associated with low-grade neoplasia, such as cribriform structures with polarized spaces, club-shaped micropapillae, or rigid bridges of uniform thickness? Or is the architecture more typical of a polyclonal process like usual ductal hyperplasia with swirling, overlapping cells, and non-polarized slit-like spaces?

The architectural and cytologic features are not always straightforward. Solid or spindled proliferations can be diagnostically challenging, but additional immunohistochemical studies can often help clarify the nature of the process and will be discussed. Lesions with a papillary architecture can also present a particular challenge in this diagnostic spectrum but will be discussed separately in Chap. 6.

When a diagnosis of low-grade DCIS versus ADH is being considered based on the cytologic and architectural features present, evaluation of the extent of the lesion becomes important when deciding which diagnostic category to assign. Both the uniformity of the process and the size of the lesion enter into the evaluation of extent. Are the spaces partially or completely involved by the atypical proliferation (is the process uniform or non-uniform)? Is the lesion larger than 2 mm, the size threshold used by Tavassoli and Norris to diagnose low-grade DCIS (when cytologic and architectural criteria are met) [3]? When in doubt, particularly on core needle biopsies where the entire extent of the lesion is still unclear, assigning a borderline diagnosis such as "ADH bordering on low-grade DCIS" or "ADH suspicious for low-grade DCIS" may be the most appropriate diagnosis to render to avoid overdiagnosis and overtreatment.

This chapter will begin with a discussion of DCIS and then follow with ADH and usual ductal hyperplasia.

K. H. Allison (✉)
Department of Pathology, Stanford University School of Medicine, Stanford, CA, USA
e-mail: allisonk@stanford.edu

K. C. Jensen
Department of Pathology, Stanford University School of Medicine, Stanford, CA, USA

Pathology and Laboratory Medicine Service, Veteran Affairs Palo Alto Health Care System, Palo Alto, CA, USA
e-mail: kjensen1@stanford.edu

© The Author(s), under exclusive license to Springer Nature Switzerland AG 2022
S. J. Shin et al. (eds.), *A Comprehensive Guide to Core Needle Biopsies of the Breast*,
https://doi.org/10.1007/978-3-031-05532-4_9

High Grade DCIS	Low-Intermediate Grade DCIS	ADH	UDH
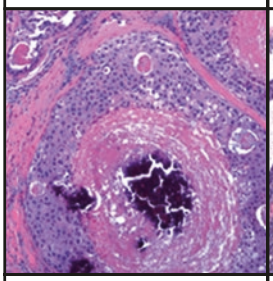	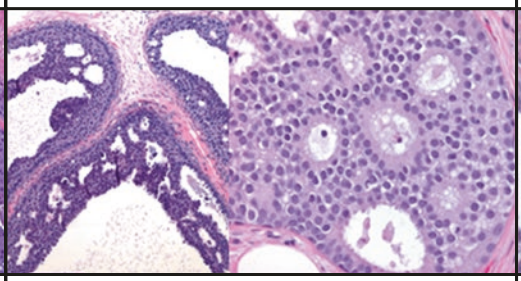	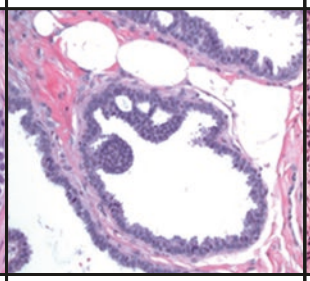	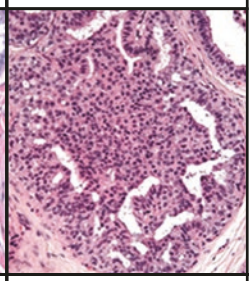
• More frequently ER negative/Low ER expression • Detection: Mass or screening mammography • Frequent HER2 amplification, p53 mutations • Risk of invasion: Typically within a decade	• Typically uniformly ER positive • Detection: Typically screening mammography • Frequent 16q and 1q abnormalities • Risk of invasion: Extends over decades	• Uniformly ER positive • Detection: Typically screening mammography • Treated as a risk lesion but most lesions are clonal • Diagnostic agreement an issue	• Variable ER expression • Not considered a precursor lesion

Fig. 9.1 Spectrum of intraductal proliferative lesions

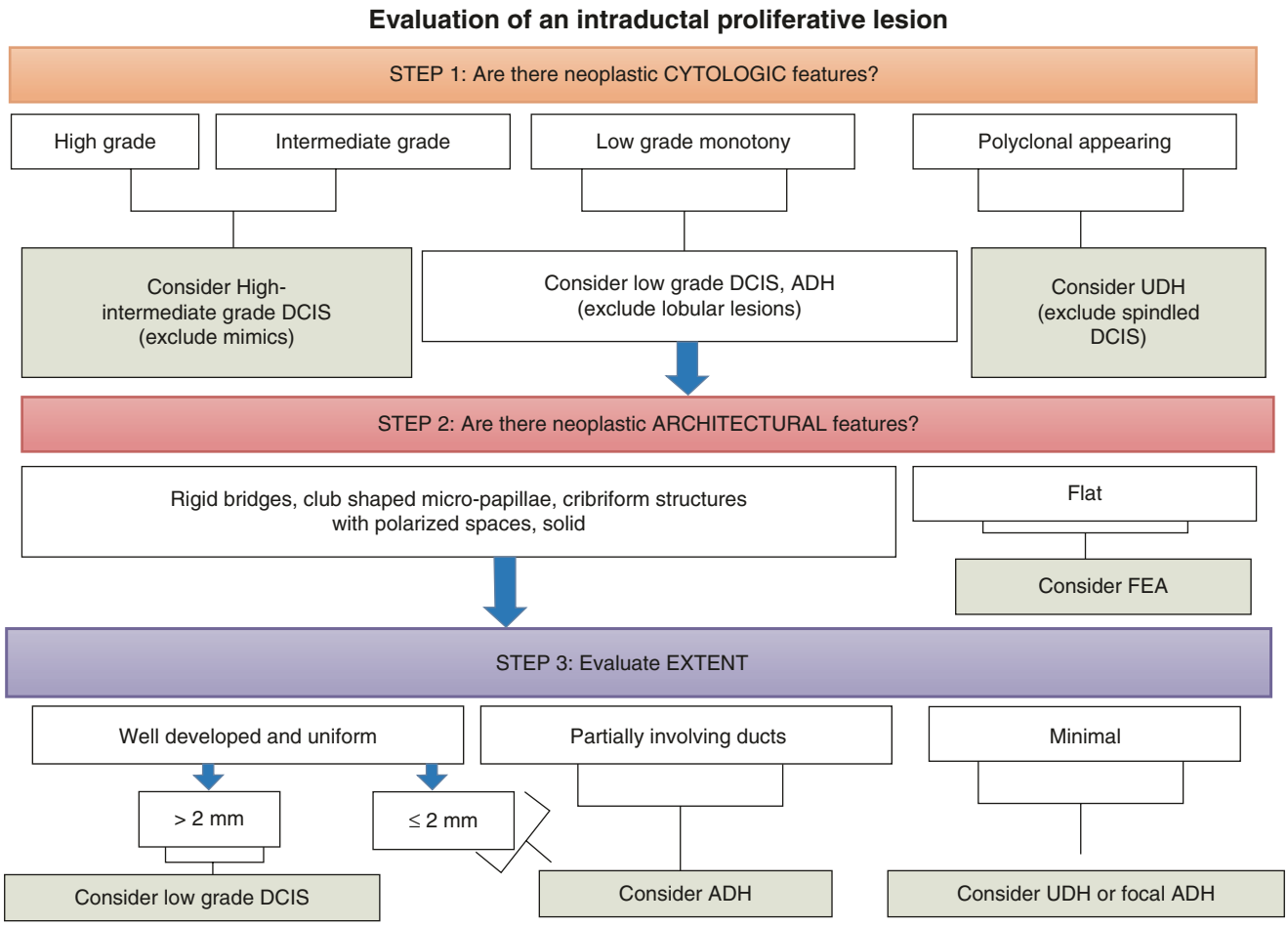

Fig. 9.2 Algorithm for diagnosing intraductal proliferative lesions

Ductal Carcinoma In Situ

Overview

DCIS is a non-obligate precursor to invasive breast cancer. In contrast to atypical lesions, which carry a bilateral risk of developing invasive cancer, DCIS is classically treated as an ipsilateral precursor to invasion with complete surgical removal for local control purposes. Natural history studies on DCIS detected in the pre-screening era indicate that when left completely untreated, it can evolve into invasive carcinoma in the same area in the majority of patients. However, high-grade DCIS has a more immediate risk of invasion within 5 years, while low-grade DCIS has a much longer time-course to invasion that extends over many decades [4–8]. These differences imply a spectrum of biology and behavior for lesions classified as DCIS. In fact, DCIS is a heterogeneous group of noninvasive neoplastic lesions with different clinical presentations, risks, and potential management strategies.

The incidence of ductal carcinoma in situ (DCIS) and its frequency on breast biopsy has increased dramatically in the era of mammographic screening [9–11]. In 1975, 5.8 US women per 100,000 were diagnosed with DCIS, while in 2012, this rate had climbed to 32.5 women per 100,000 [12]. This increase has largely been due to detection of smaller, low-grade, non-comedo DCIS with the incidence of high-grade DCIS remaining relatively stable [13, 14]. In population-based studies, 5–6% of breast core biopsies contain DCIS as the clinically most significant diagnosis, but the proportion of breast biopsies with DCIS increases with age and will also depend on practice characteristics and patient demographics [9].

Gross and Radiologic Features

In general, 80–85% of DCIS is detected by mammography with the remainder presenting as a mass and some in high-risk patients as MRI findings [15, 16]. Less commonly, DCIS can be present initially as bloody nipple discharge, Paget's disease of the nipple or as an incidental finding in breast tissue removed for other reasons. If core biopsies were performed for calcifications, radiographs of the cores are typically performed by radiology to confirm the presence of calcifications in the samples. The presence of calcifications in these films should be correlated with the presence of calcifications microscopically. If the targeted calcifications are not identified on histology, additional levels or radiography of the tissue blocks should be performed.

With any case of DCIS, the gross examination and tissue sampling procedures will be key to determining if there is also invasive carcinoma present. The College of American Pathologists recommends serial sequential sampling of the entire area of interest to exclude invasion, evaluate margins, and determine an accurate extent of disease [17]. This is especially true in cases of high-grade DCIS, where the presence of occult invasive carcinoma is higher. Creating a "map" of where tissue is submitted from is also crucial to determining an accurate size of both the DCIS and any occult-invasive carcinomas identified.

High-Grade DCIS Spectrum

While most high-grade DCIS is detected as calcifications on screening mammography, in contrast to low-grade DCIS, it can also frequently present as a mass or architectural distortion [18]. Less commonly, it presents as Paget's disease of the nipple or nipple discharge. On screening mammography, high-grade DCIS appears most commonly as abundant, linear, pleomorphic, or course heterogeneous calcifications, while granular segmental calcifications are more frequently associated with low-grade DCIS. Calcifications in high-grade DCIS are often associated with necrosis histologically.

MRI has become a useful imaging adjunct to mammography in high-risk patients and has a higher sensitivity for detection and evaluation of DCIS extent [19]. On MRI, high-grade DCIS presents as non-mass enhancement, a finding that can also be present in benign disease. MRI is particularly sensitive for high-grade DCIS with studies showing sensitivities of up to 98% on MRI versus only 56% on mammography [20]. The extent of DCIS on MRI is also often larger than the extent noted on mammography, but it can also be occult on MRI and only apparent as calcifications on mammography [21]. The largest lesion size on any imaging modality should be used to determine the extent of gross tissue sampling so that the true extent of disease present microscopically can be accurately measured.

Grossly, high-grade DCIS frequently has a gritty texture due to the comedo-necrosis and associated calcifications present. Comedo-necrosis can be grossly apparent as punctate secretions. However, these gross findings will be difficult to appreciate on a non-surgical, core needle biopsy specimen.

Low-Grade DCIS Spectrum

Low-intermediate grade DCIS is largely a screen-detected lesion. Granular segmental calcifications are the finding that prompts biopsy, with only rare cases presenting as a mass, architectural distortion, or nipple discharge. Paget's disease of the nipple is not associated with low-grade DCIS but may be intermediate-high grade DCIS.

While the span of the calcifications on screening mammography is used to estimate extent, these calcifications do not always correlate with the microscopic extent. Calcifications can also be present in adjacent risk lesions, columnar cell change, and fibro-proliferative changes, resulting in an overestimate of the extent of DCIS. DCIS can also extend far beyond the area of calcifications. Therefore, it is essential to closely correlate the imaging, gross and macroscopic findings when estimating size/extent of DCIS. On a core biopsy, reporting the presence of calcifications and if they are in the DCIS or surrounding changes can be helpful in guiding preoperative surgical treatment options.

Microscopic Features

High-Grade DCIS Spectrum

High-grade DCIS is characterized by its high nuclear grade, with pleomorphic nuclei. Mitotic figures are frequently seen, including atypical mitotic figures. Unlike low-grade DCIS, there is no requirement for a specific architectural pattern or extent and the diagnosis is made when there is an intraductal proliferation with high-grade cytology (see section "Differential Diagnosis" below).

High-grade DCIS can take on a variety of histologic growth patterns, many of which are also common in low-intermediate grade DCIS. The classic, "comedo-DCIS" is most characteristic of high-grade DCIS (Fig. 9.3a–c). It is typically solid in growth pattern with central areas of comedo-necrosis. The stroma around high-grade DCIS is often desmoplastic, with increased cellularity and prominent lymphocytic inflammation. Sometimes, the involved ducts become quite sclerotic and there are only small amounts of residual high-grade epithelium. On a core biopsy sample, if sclerotic ducts with associated lymphocytic inflammation are seen, additional levels can reveal diagnostic areas with more high-grade epithelium.

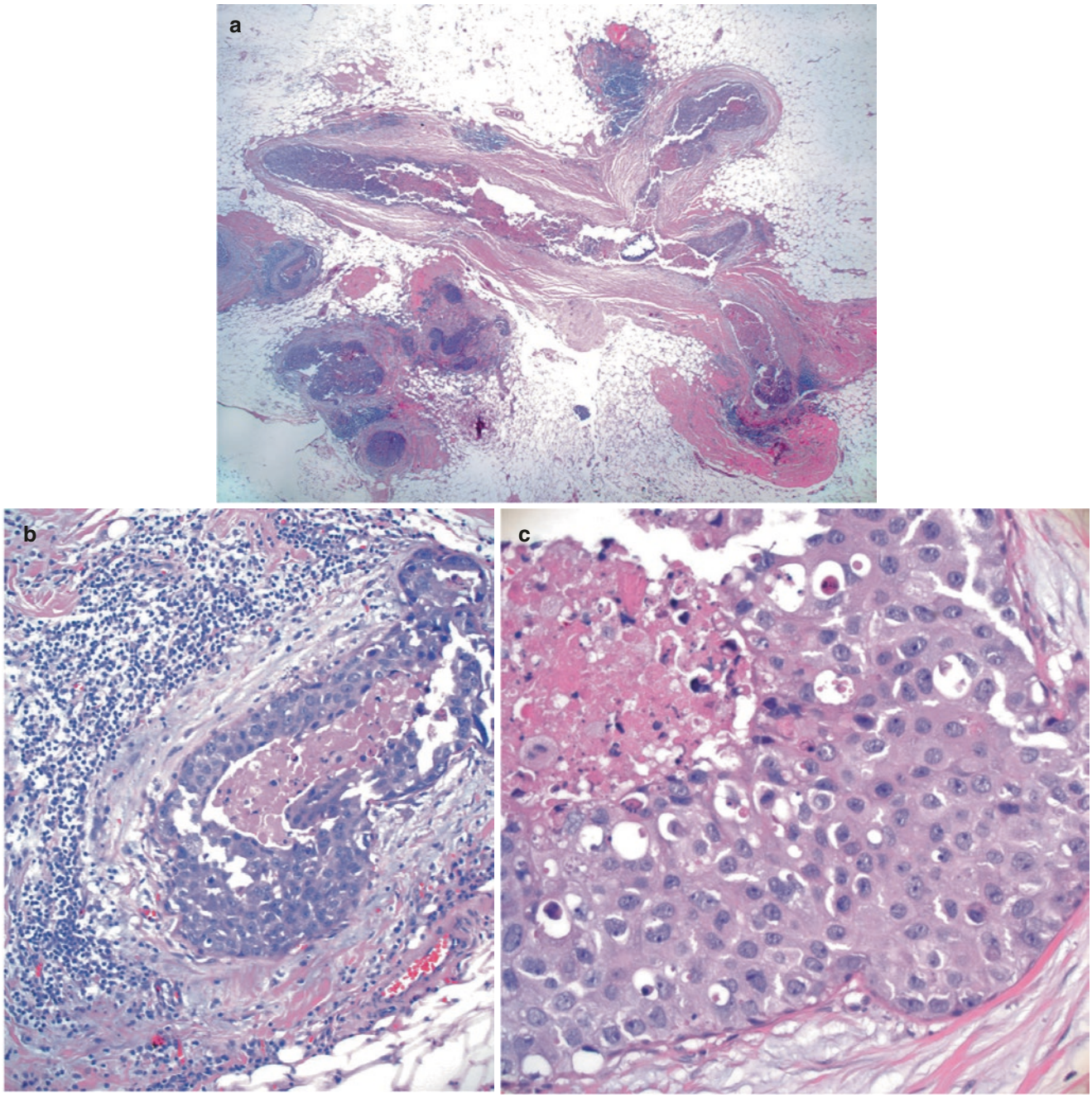

Fig. 9.3 High-grade DCIS, comedo-type with sclerosis around the ducts (**a**), and inflammation (**b**). The nuclear grade is high and there is central comedo-necrosis (**c**)

High-grade DCIS can extend from the ducts into the lobules, a process referred to as "cancerization of the lobules" (Fig. 9.4a–d). When there is a background of sclerosing adenosis involved by DCIS, the process can mimic invasion (Fig. 9.5a–d). Usually on H&E there are low-power, pattern-based clues that the process is more consistent with the nodular, "windswept" pattern of sclerosing adenosis involved by DCIS than the more infiltrative and diffuse pattern of invasive carcinoma. However, some cases are very challenging to distinguish from invasion. Examination of the patterns of sclerosing adenosis, atrophy, and fibro-proliferative changes in the background can be helpful for comparison. On higher power, close inspection often confirms the presence of basement membrane surrounding these areas. Myoepithelial cell stains can be very useful in this setting to confirm that the process is in situ (see section "Differential Diagnosis" below).

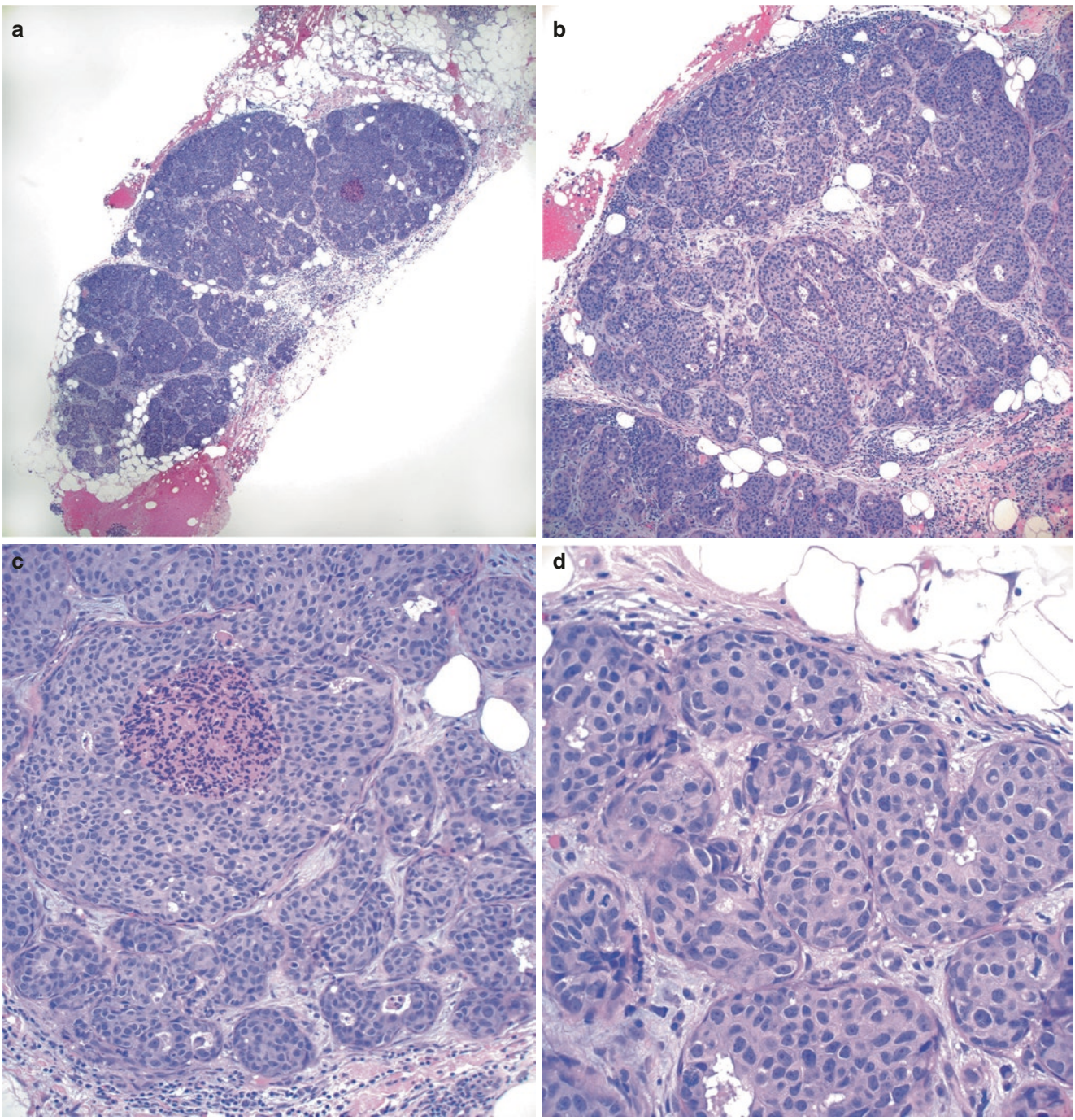

Fig. 9.4 High-grade DCIS with cancerization of lobules. On low power (**a**) and medium power (**b**) it is apparent this core biopsy has a population of hyperchromatic cells filling the terminal duct-lobular units. On higher power (**c**, **d**), the high grade cytology in areas of central necrosis are apparent (**c**)

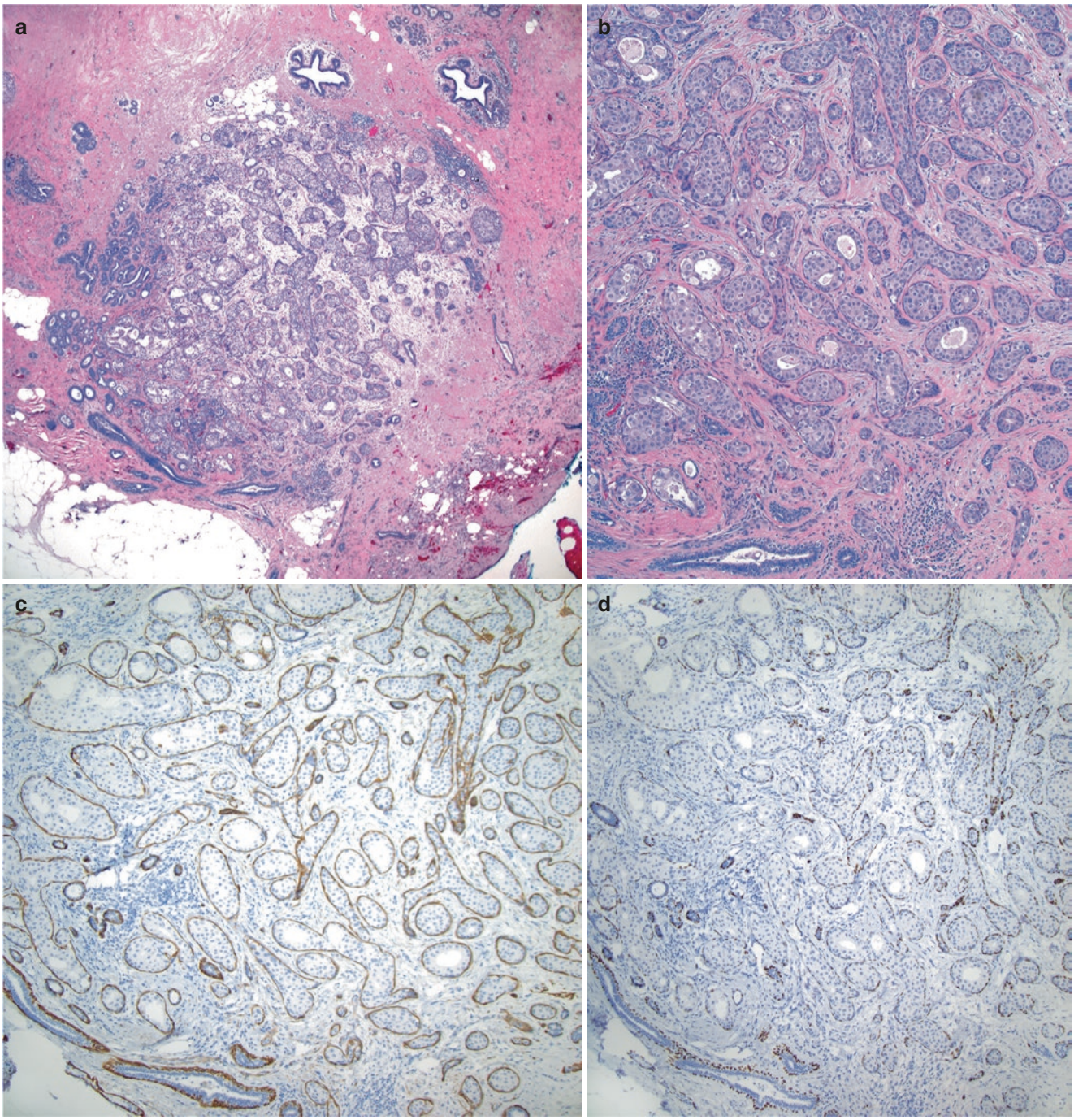

Fig. 9.5 High-grade DCIS involving sclerosing adenosis. On low power (**a**) the underlying architecture of sclerosing adenosis is more apparent than on higher power (**b**). Calponin (**c**) and p63 (**d**) stains outline the myoepithelial layer, ruling out an invasive process

Cribriform growth patterns are also common in high-grade DCIS, frequently with at least focal, single cell necrosis (Fig. 9.6). In contrast to low-grade DCIS, the spaces formed by the cribriform pattern in high-grade DCIS are not necessarily "punched out" or polarized. Micropapillary growth patterns can occur in high-grade DCIS (Fig. 9.7a, b) but are more common in low-intermediate grade DCIS.

Clinging carcinoma is a pattern specific to high-grade DCIS where a single or few cell-thick layers of pleomorphic cells (Fig. 9.8). The ducts are frequently dilated and filled with comedo-type necrosis. The high-grade cytologic atypia

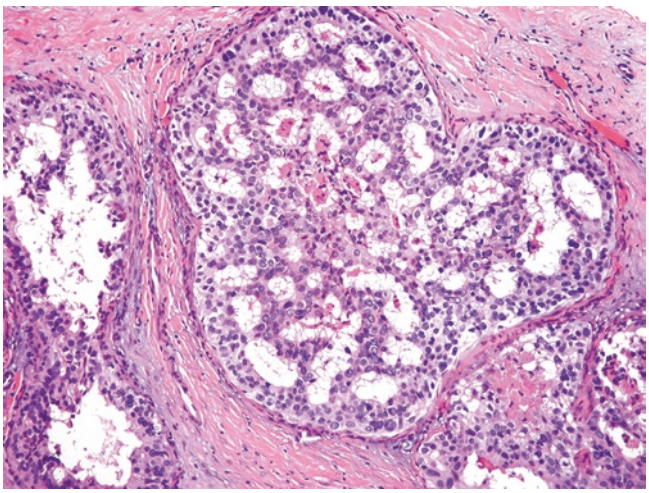

Fig. 9.6 Cribriform pattern high-grade DCIS

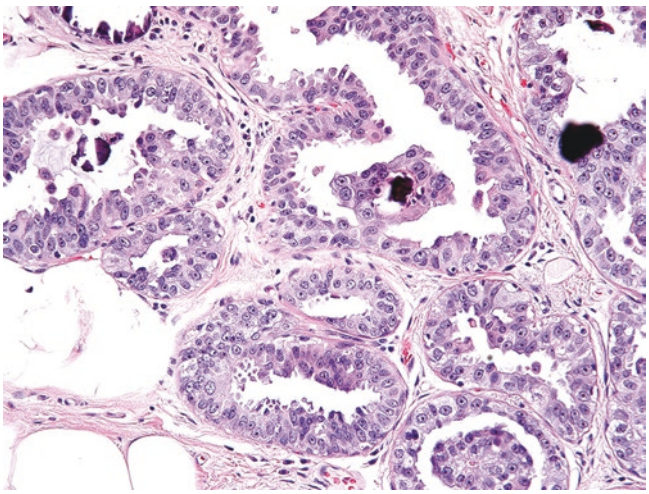

Fig. 9.8 Clinging carcinoma has a flat growth pattern but high-grade nuclei. Many cases also have central comedo-necrosis (not shown)

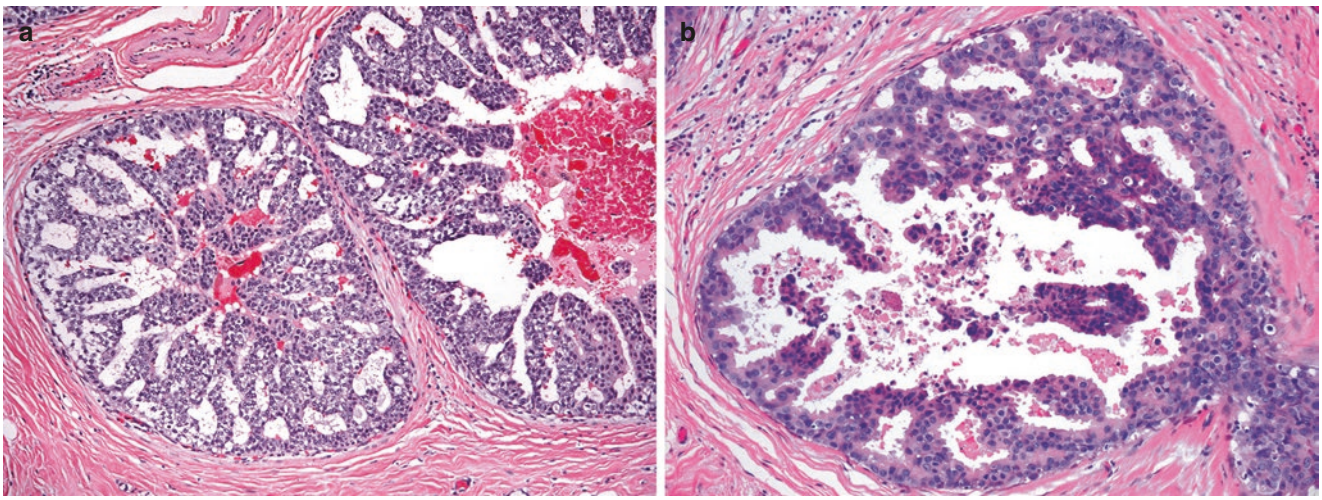

Fig. 9.7 High-grade micropapillary DCIS. (**a**) Extensive micropapillary projections are present with high-grade nuclei. (**b**) Single cell necrosis is present

is key to diagnosing this pattern. Care should be taken to exclude mimics such as atypical cystic hypersecretory or atypical pregnancy-like (pseudolactational) changes (see section "Differential Diagnosis").

High-grade DCIS frequently has apocrine cytologic features, with obviously high-grade nuclei and abundant eosinophilic, sometimes granular cytoplasm (Fig. 9.9). High-grade DCIS can have other less common types of cytologic differentiation including clear cell change (Fig. 9.10) and mucinous differentiation (although this is more common in low-grade DCIS). Rarely, small cell forms of high-grade DCIS are recognized. These specific histologic types have not been consistently shown to have outcomes different from other high-grade DCIS.

Cystic hypersecretory DCIS (also frequently called "cystic hypersecretory carcinoma") is a form of DCIS that is characterized by the dense eosinophilic, colloid-like secretions present in cystically dilated ducts/lobules (Fig. 9.11a–d). These lesions need to be distinguished from forms of cystic hypersecretory hyperplasia with or without atypia. An in-depth discussion of cystic hypersecretory carcinoma is discussed in Chap. 13.

Low-Grade DCIS Spectrum

The diagnosis of low-grade DCIS requires adherence to strict criteria that includes evaluation of the cytology, architecture, and extent. The nuclei of low-grade DCIS are small, very round, and have homogenous chromatin (Fig. 9.12a, b).

The cell borders are well defined and evenly spaced. Mitotic figures are rare but may be present and the monotony present is typically uniform. When the nuclear grade is intermediate, architectural and the extent criteria are not used.

The architectural features of low-grade DCIS include several characteristic patterns, many of which can be present in the same case. Cribriform spaces tend to be crisp and "punched out" appearing, but not always uniformly. The formation of polarized neo-lumens with the nuclei oriented away from the spaces is a reliable feature associated with low-grade neoplasia in this setting (Fig. 9.13a–d). Solid patterns of low-grade DCIS fill the involved ducts and lobules involved and can have only subtle polarized micro-acini present within it (Fig. 9.14a–d). Rarely, necrosis is present in association with this form of low-grade DCIS.

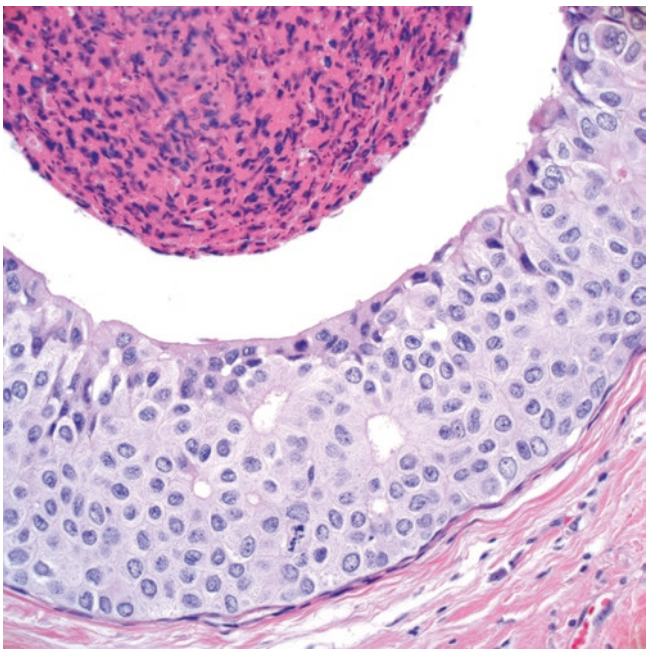

Fig. 9.9 High-grade DCIS with apocrine features (abundant eosinophilic cytoplasm) and comedo-necrosis

Low-intermediate grade micropapillary structures are club-shaped and maintain their uniform nuclei throughout the processes (Fig. 9.15a–d). The micropapillae can vary in length and development from club-shapes to elongate projections and rigid arcades. When extensive, the micropapillary projections can become maze-like in complexity. In contrast to micropapillary ADH, these micropapillae need to more completely involve the lesional ducts for a diagnosis of low-grade micropapillary DCIS (see below section on "Micropapillary ADH"). This pattern of DCIS tends to be more extensive and multifocal, is more often pure in pattern, and can be more challenging to excise to negative margins. In other instances, low-grade micropapillary DCIS arising intermittently in a background of micropapillary ADH can be seen. These cases are particularly difficult as the full spectrum of micropapillary proliferation is present and multifocal in distribution. Quantifying the extent of DCIS in these instances is particularly problematic. Despite similarities in nomenclature, micropapillary DCIS is *not* more frequently associated with micropapillary invasive carcinoma.

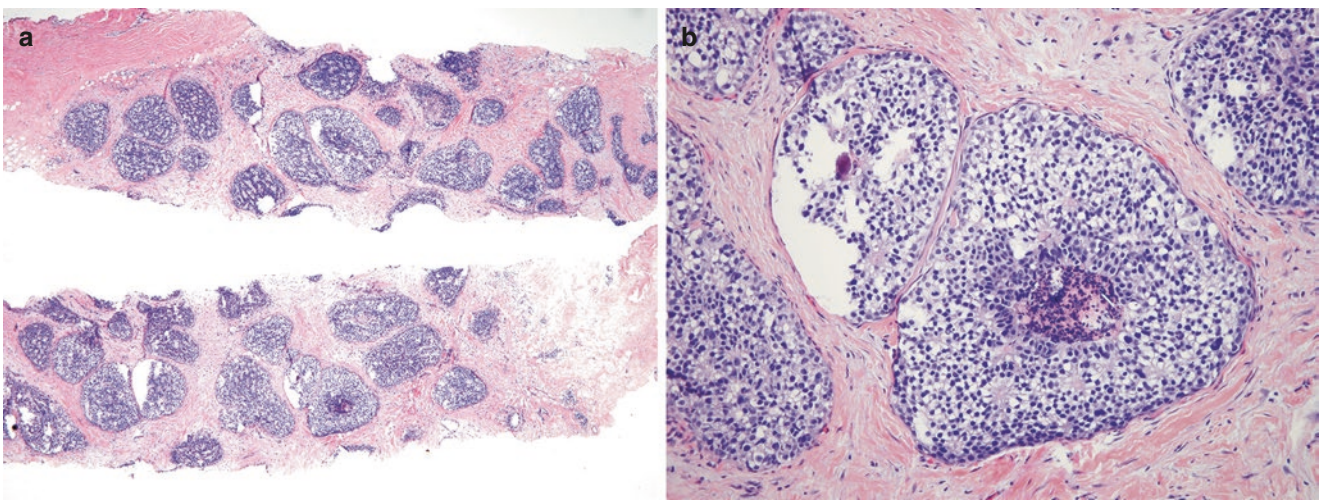

Fig. 9.10 Clear cell change in high-grade DCIS on core biopsy. (**a**) 1× magnification and (**b**) 10× magnification

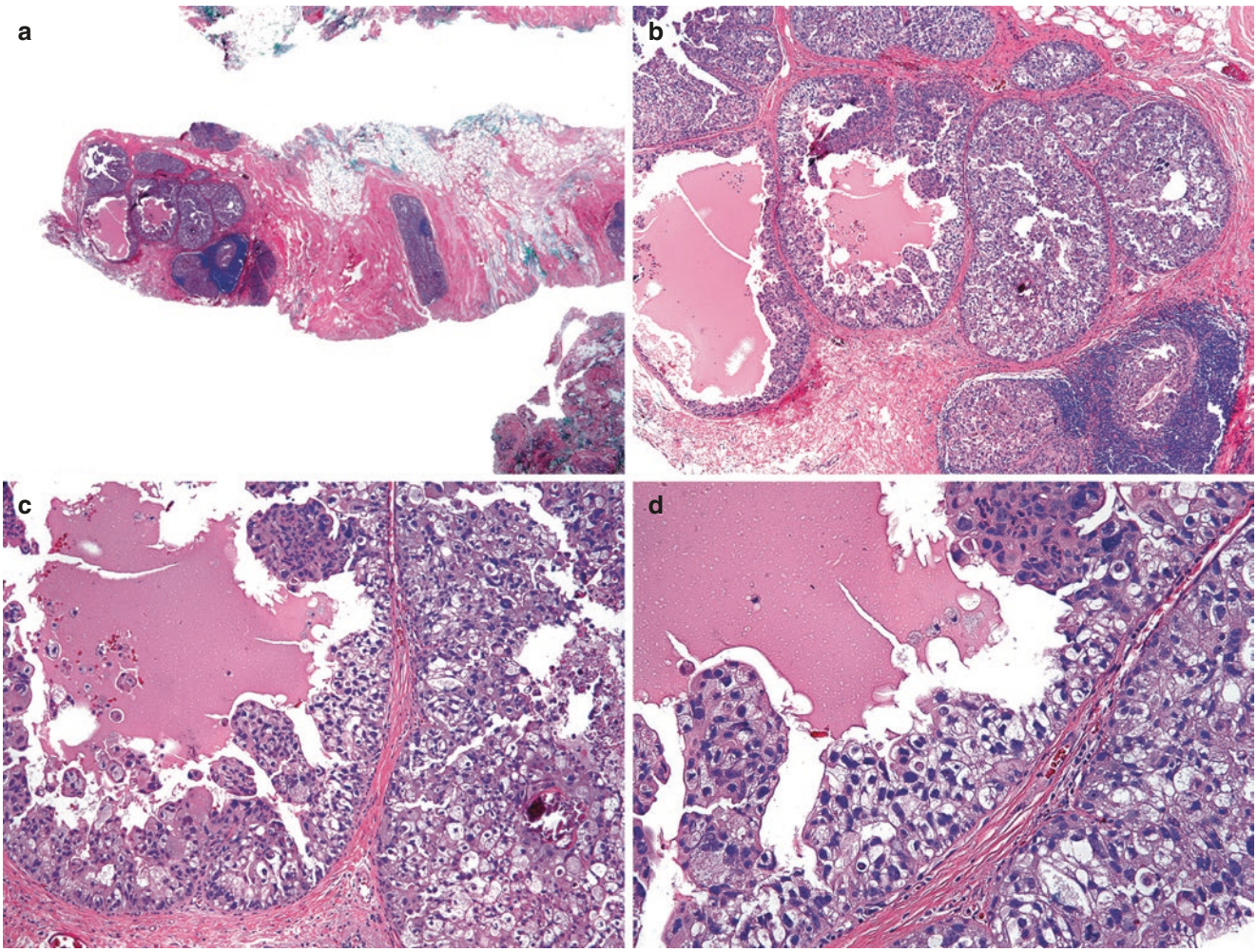

Fig. 9.11 Cystic hypersecretory DCIS on core biopsy at low-power magnification (**a**), intermediate (**b**) and high-power magnifications (**c**, **d**). Note the dense colloid-like secretion that has scalloped borders and is characteristic of hypersecretory lesions. The nuclei in this example are hyperchromatic, pleomorphic, and irregular

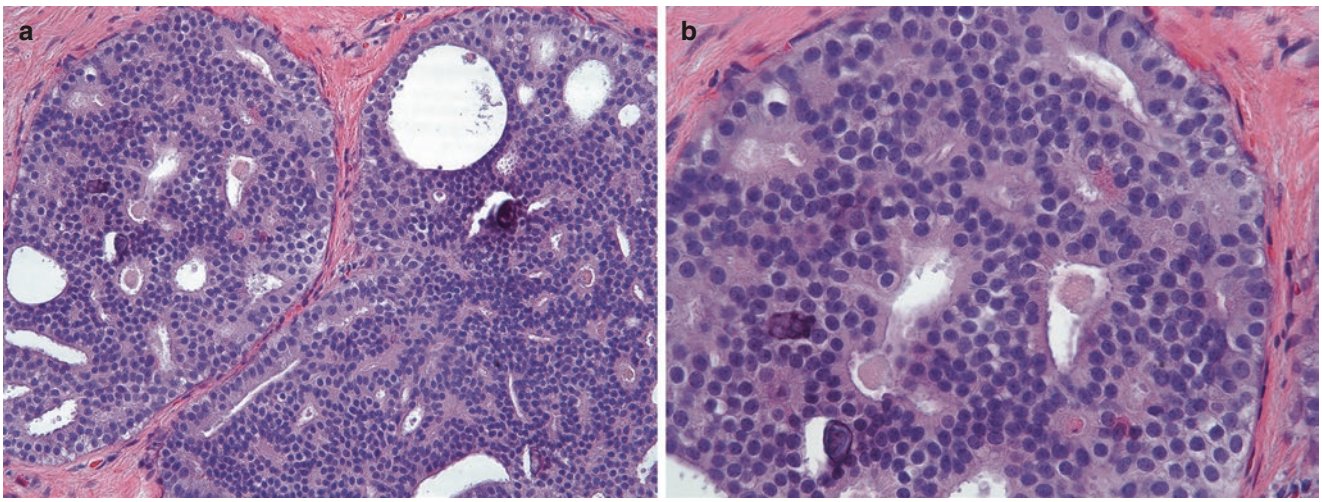

Fig. 9.12 Low-grade DCIS has cells with rounded, monotonous nuclei evenly distributed throughout the proliferation. (**a**) 20× magnification and (**b**) 40× magnification

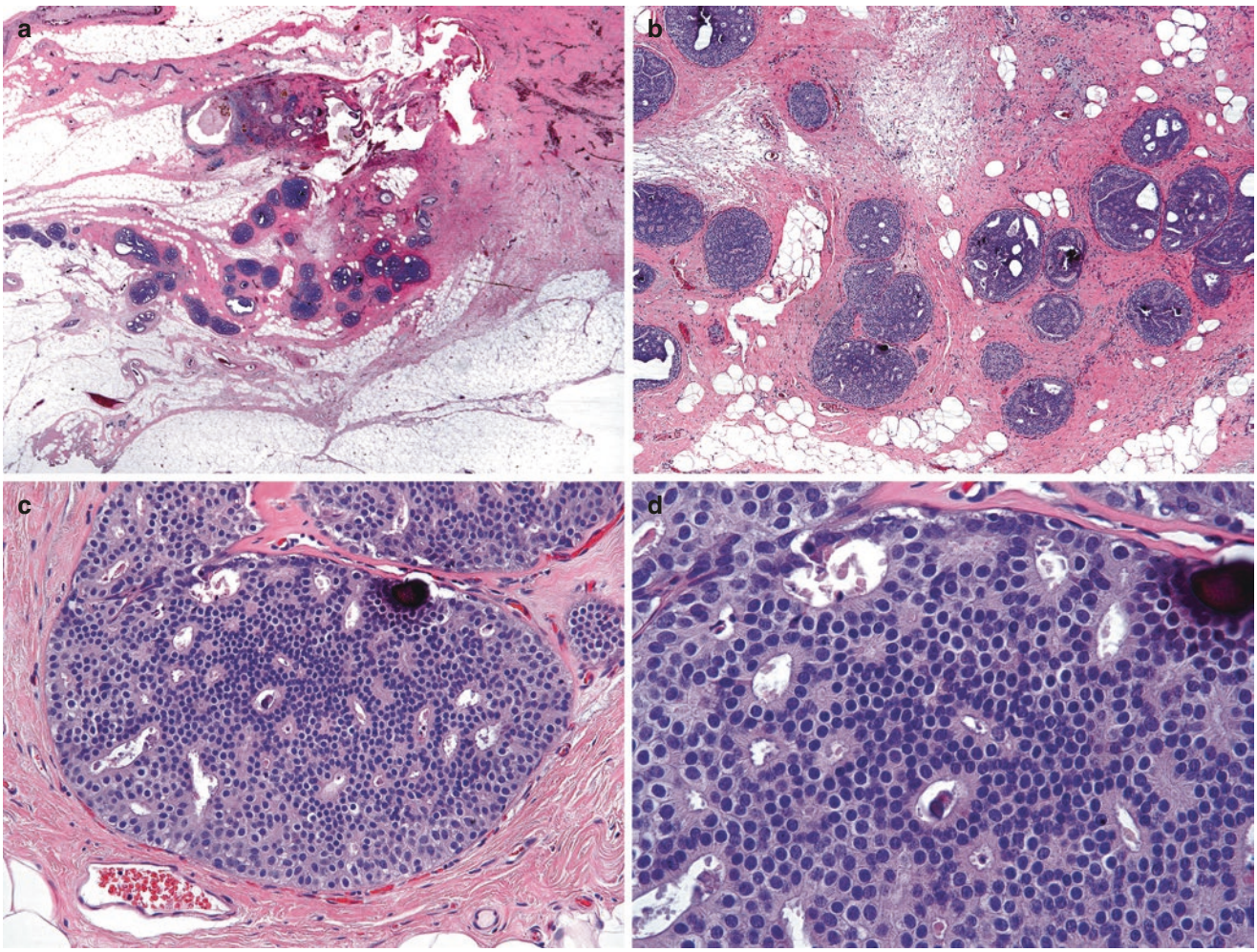

Fig. 9.13 (**a–d**) Core needle biopsy of a low-grade intraductal proliferation with cytologic monotony and cribriform architecture that is uniformly involving an area larger than 2 mm. These findings meet the criteria for a diagnosis of low-grade DCIS on core needle biopsy. The targeted calcifications are present within the low-grade DCIS. Note the polarized lumens being formed despite not all spaces being perfectly "punched out"

Low-grade DCIS is often present within a spectrum of low-grade neoplasia that includes ADH, flat epithelial atypia (FEA), and sometimes lobular lesions (Fig. 9.16a–d). On a core needle biopsy, description of this combination of findings and which lesions contain the targeted calcifications can be helpful to surgeons when planning surgical excision options. On excisional specimens, it can be challenging to differentiate between areas that qualify as low-grade DCIS versus lesions that are background ADH, etc. when evaluating size/extent and margin status of low-grade DCIS. Terminology such as "spectrum of low-grade in situ neoplasia, including low-grade DCIS, ADH, and FEA" can be helpful to describe these cases and their diagnostic challenges to clinicians. Pathologists must both use diagnostic criteria and their clinical judgment on such cases as these are more susceptible to higher interobserver variability.

The low-grade spectrum of DCIS also includes a papillary growth pattern which is characterized by monotonous tall columnar to rounded epithelial cells lining papillary structures containing fibrovascular cores (Fig. 9.17a, b). Myoepithelial cells are typically lacking within these fibrovascular cores but are maintained in the surrounding basal layer of the duct. This growth pattern of DCIS can be seen as a pure form but is also frequently admixed with micropapillary and cribriform patterns (Fig. 9.18a, b). When present, papillary DCIS can have a nodular growth pattern and be identified as multiple nodular areas on imaging. Low-grade DCIS can also involve benign papillary lesions or form dominant nodules ("encysted" or "encapsulated" papillary carcinomas). The spectrum of these more frequently solitary lesions are discussed in Chap. 6. On a core needle biopsy, for lesions that is predominantly papillary with a differential that

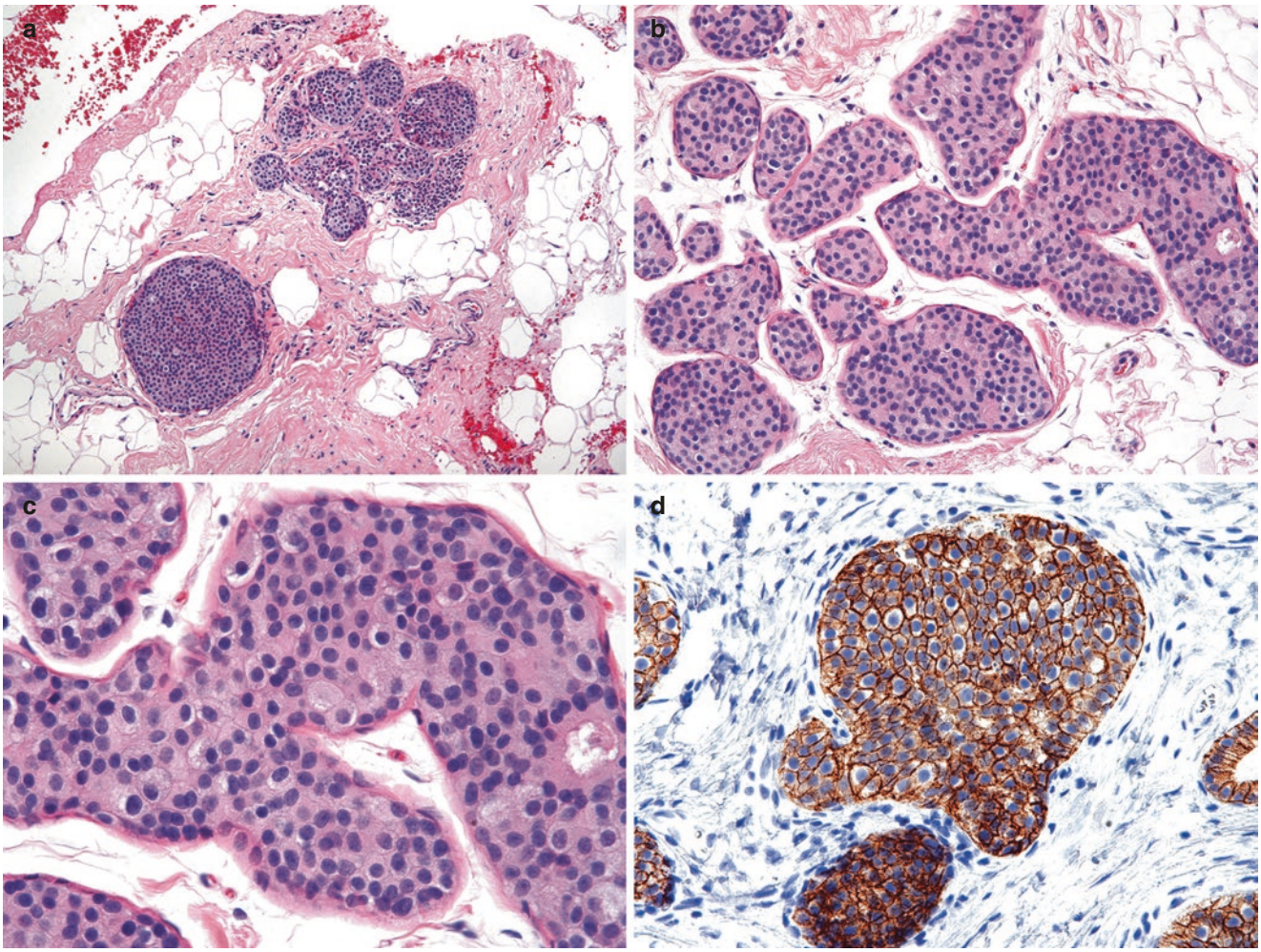

Fig. 9.14 (**a**–**d**) Examples of solid pattern, monotonous proliferations that raise the differential diagnosis of a low-grade DCIS versus lobular carcinoma in situ. Extension of the process into lobules can make this differential particularly challenging. Subtle clues to ductal differentiation include more crisp cell membranes and formation of subtle microacinar spaces (note a microacinar polarized space in the far left of image **c**). E-cadherin staining shows a membranous pattern in a ductal process, as in this case (**d**)

includes papillary DCIS, encysted papillary carcinoma, or ADH/DCIS involving a papilloma, a diagnosis of "atypical papillary lesion" can be most appropriate to defer evaluation of the entire lesion to an excisional specimen.

Low-grade apocrine DCIS is an uncommon DCIS variant characterized by abundant eosinophilic cytoplasm and bland but enlarged nuclei with prominent nucleoli. Because these cytologic features are similar to apocrine metaplasia and apocrine atypia, emphasis on the architectural growth patterns seen in other forms of DCIS is emphasized for a diagnosis. Most often, low-grade apocrine DCIS has a solid or cribriform growth pattern (Fig. 9.19). Caution should be used when evaluating micropapillary structures since benign apocrine metaplasia frequently forms club-shaped papillae. In addition, for lesions that only involve sclerosing adenosis without additional diagnostic areas, a diagnosis of atypical apocrine adenosis should be strongly considered.

Low-intermediate grade DCIS can take on a spindled growth pattern that mimics florid usual ductal hyperplasia. The cells contain nuclei that are elongated and hyperchromatic rather than rounded and are present in streaming patterns with solid growth (Fig. 9.20 a, b). The more intermediate-grade nuclear features are critical to the recognition of this form of DCIS. See the section "Differential Diagnosis" below which includes a discussion of features and immunohistochemical techniques used to distinguish between these two entities.

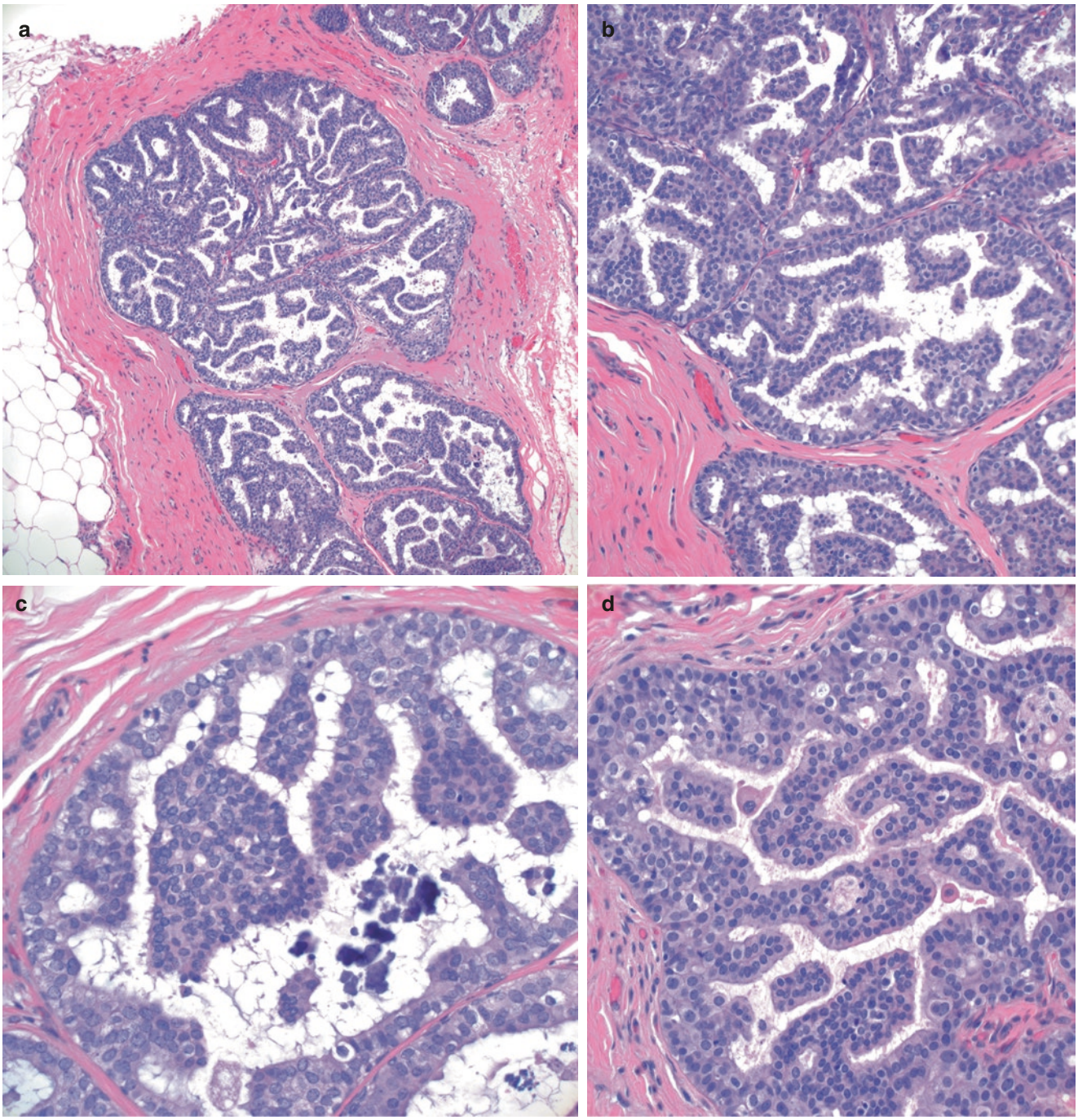

Fig. 9.15 (**a**–**d**) Micropapillary low-grade DCIS

Differential Diagnosis

High-Grade DCIS Spectrum

Invasion Versus High-Grade DCIS

When high-grade DCIS is extensive, it can be very challenging to rule out or differentiate from invasion due to the density of DCIS and the commonly present surrounding inflammation and sclerosis (Fig. 9.21a, b). However, because invasion in the setting of extensive high-grade DCIS is frequently also of high grade and HER2 positive, ruling out invasion is a critical job of the pathologist examining such a case [22] (Fig. 9.22a, b). A sentinel lymph node may be performed if invasion of any size is identified. According to the NCCN breast cancer treatment guidelines, treatment with chemotherapy (plus HER2 targeted therapy when HER2+) is

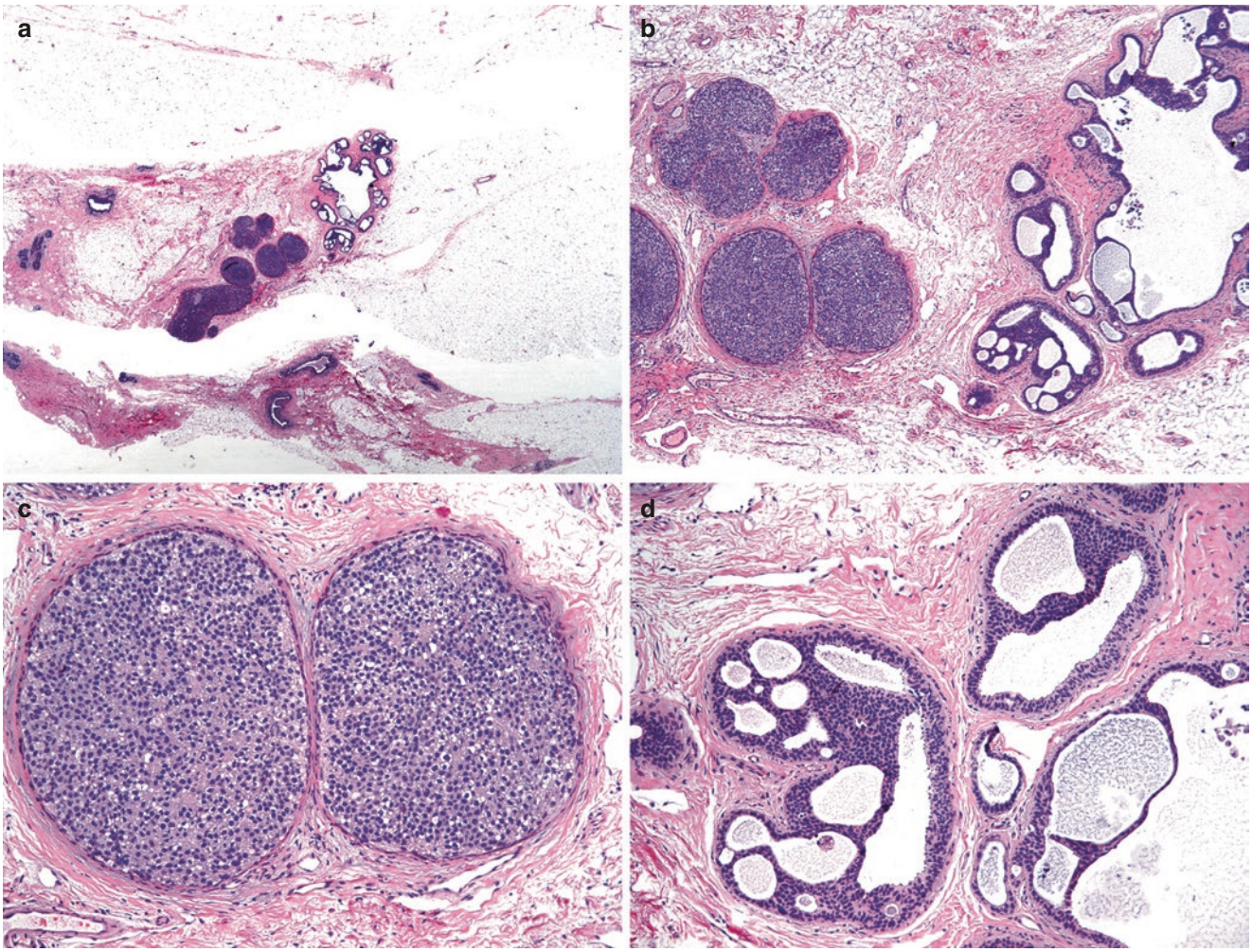

Fig. 9.16 Core needle biopsy with both low-intermediate grade DCIS and atypical ductal hyperplasia. (**a**, **b**) On low-power images, the DCIS is on the left-hand side and is distinguished by its complete involvement of multiple ducts by a solid pattern proliferation of cells with intermediate grade cytology (**c**) Higher power image of DCIS. (**d**) The ADH is on the right-hand side of the low-power images seen here in higher magnification.. In contrast to the DCIS in this case, it has a lower nuclear grade and only early architectural forms that are incompletely involving the ducts in this area

standard for hormone receptor-negative or HER2-positive invasion greater than 0.5 cm [23]. Oncologists may also consider these therapies when there are multiple smaller foci of invasion, but the evidence of benefit in this group is more limited.

Microinvasive foci of carcinoma (<1 mm) and larger foci can be masked in the lymphocytic background surrounding high-grade DCIS. Close examination of areas with more dense inflammation for single cells and clusters is recommended. A pan-cytokeratin stain, in addition to myoepithelial stains, can also be very useful to highlight the pattern of single cells and clusters of epithelial cells that lack myoepithelial cells (Fig. 9.21c–f). Some labs use combination stains that include two to three of these markers. Because these small foci can appear and disappear on immunostained levels and recuts, all additional material should be closely examined for invasion. In the context of a core needle biopsy with possible invasion, caution should be used if there is not 100% certainty about smaller foci of invasion. In this setting it can be appropriate to diagnose "DCIS with foci suspicious for microinvasion" and defer final classification of the process to the subsequent surgical specimen.

Solid, nested forms of high-grade invasive carcinoma can mimic DCIS (Fig. 9.23a–d). Because these foci are often larger than microinvasion, they are even more critical to diagnose and distinguish from clusters of DCIS. Clues to the diagnosis of invasion in these cases are the presence of a more complex, "puzzle-piece" pattern of growth than might be expected by diffuse involvement of ducts and lobules by DCIS. The edges of these nests are often more irregular than

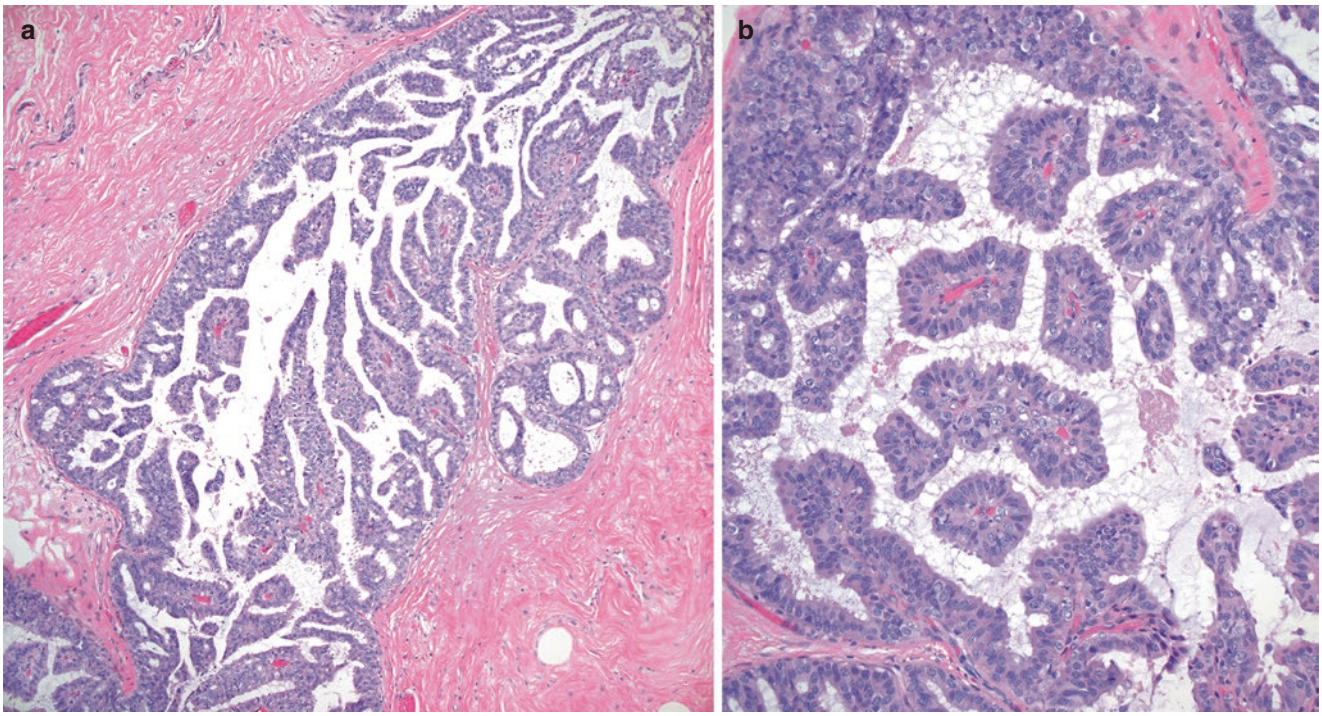

Fig. 9.17 (**a**, **b**) Papillary pattern DCIS contains papillary cores lined by low-grade cells with monotonous tall columnar to rounded nuclei. Despite its similarity to a benign papilloma, a myoepithelial layer is not apparent within the majority of the fibrovascular cores on H&E or on myoepithelial cell stains (not shown here)

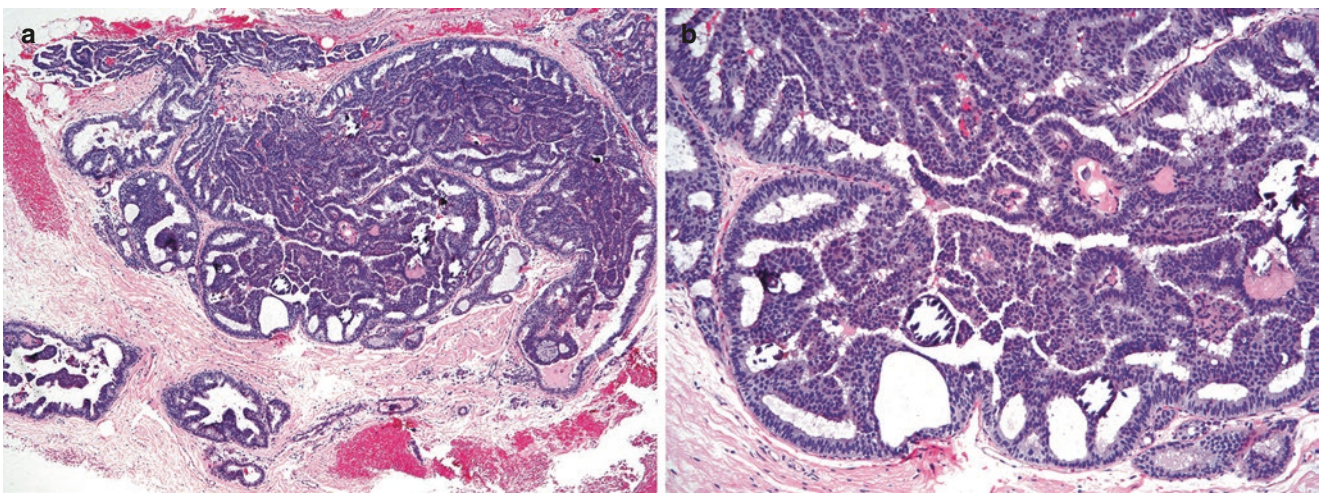

Fig. 9.18 (**a**, **b**) Low-intermediate grade DCIS with mixed papillary and micropapillary patterns

the rounded contours of DCIS. Myoepithelial stains will help in this differential. For cytoplasmic myoepithelial stains such as smooth muscle myosin heavy chain (SMM) and calponin, care should be taken not to interpret surrounding stromal positivity as a myoepithelial cell layer (Fig. 9.24a–d). The myoepithelial staining should be present within the outermost layer of the malignant cells in DCIS. This layer may be discontinuous and very attenuated in DCIS. Using a nuclear myoepithelial stain such as p63 in conjunction with a cytoplasmic one can help exclude "false positive" stromal staining. Some cases are very challenging and if there is uncertainty even after additional stains, consultation should be considered or this uncertainty should be clearly expressed in the report.

Pleomorphic LCIS

Pleomorphic lobular carcinoma (PLCIS) can also closely mimic high-grade DCIS. PLCIS will have high-grade nuclei and can also have central comedo-necrosis (Fig. 9.25a–d). Subtle areas of cellular discohesion or admixed areas of classical low-grade lobular carcinoma in situ (LCIS) or atypical lobular hyperplasia can be clues that raise this differential diagnosis. An E-cadherin stain can be used to determine the immunophenotype of the cells, with loss of expression being characteristic of PLCIS. This distinction can make big treatment differences since there is currently debate about whether PLCIS requires excision to negative margins, radiation, or hormonal therapy.

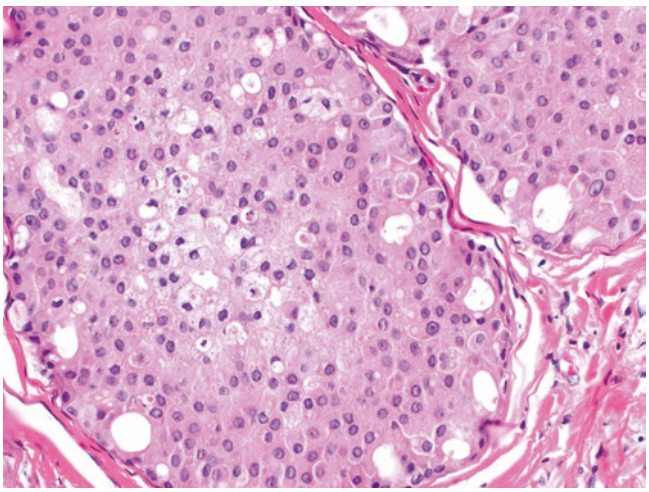

Fig. 9.19 Low-intermediate grade DCIS with apocrine differentiation

Atypical Cystic Hypersecretory or Atypical Pregnancy-Like (Pseudolactational) Changes

Another less common mimic of high-grade DCIS is atypical cystic hypersecretory or pregnancy-like (pseudolactational) change. This differential often arises when considering the diagnosis of "clinging carcinoma" or isolated lobular involvement by high-grade DCIS. Pregnancy-like (pseudolactational) change is characterized by its focal or patchy lobular distribution and vacuolated, bubbly cytoplasm. It can accumulate calcifications and be a reason for core biopsy [24]. These calcifications are often laminated or layered. Cystic hypersecretory change is characterized by the presence of dense eosinophilic secretion that appears similar to thyroid colloid. The secretion frequently has scalloped edges. Pregnancy-like (pseudolactational) change and cystic hypersecretory change can be present together. On a core biopsy, when there is only a focal lobule-based cytologically atypical process, caution should be used if there are features of pregnancy-like (pseudolactational) change or cystic hypersecretory change (Fig. 9.26a, b). This change is similar to the Arias-Stella reaction in the endometrium and can be present focally, in isolation and not associated with lactation. Cystic hypersecretory lesions and pregnancy-like lesions including their malignant counterparts are each discussed in Chaps. 13 and 21, respectively.

Posttreatment Changes

Radiation therapy can result in scattered cytologically atypical cells being present within ducts and lobules (Fig. 9.27). However, in contrast to high-grade DCIS, these changes are typically present as scattered enlarged cells with hyperchro-

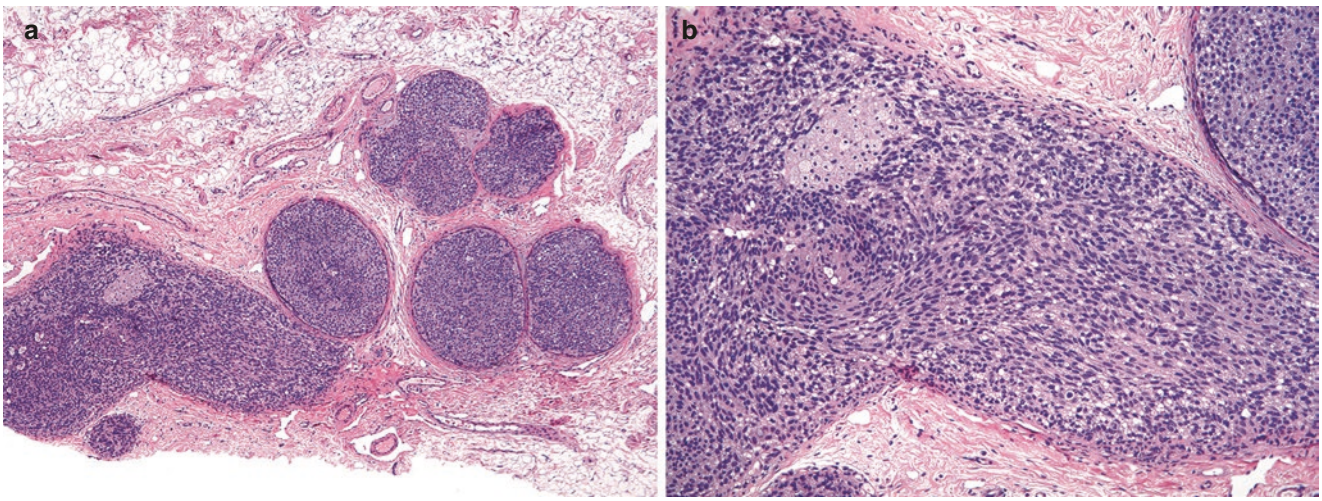

Fig. 9.20 (**a**, **b**) Spindled pattern low-intermediate grade DCIS

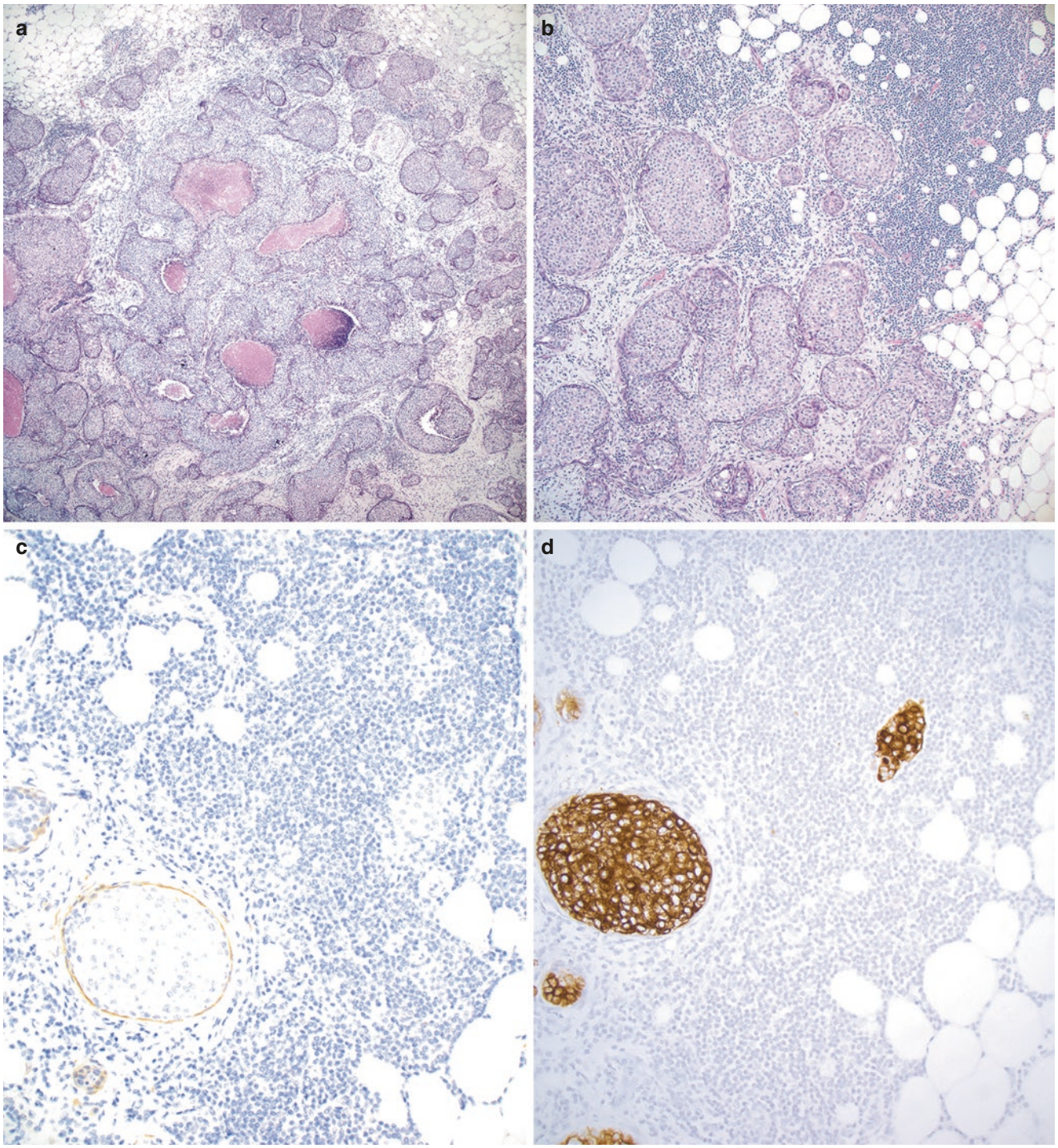

Fig. 9.21 (**a**) Low-power image of a case with extensive high-grade DCIS. The density of the DCIS with cancerization of lobules, surrounding sclerosis, and areas of inflammation can mask small foci of invasion. (**b**) Careful examination of areas with inflammation or irregular borders should be undertaken. There is a small focus of microinvasion present that is not easily visualized on H&E (**b**) or calponin immunostain (**c**), but is highlighted well on a pan-cytokeratin statin (**d**). Often more than one focus of microinvasion is present. Another focus of microinvasion is pictured in images (**e**) (calponin stain) and (**f**) (cytokeratin stain)

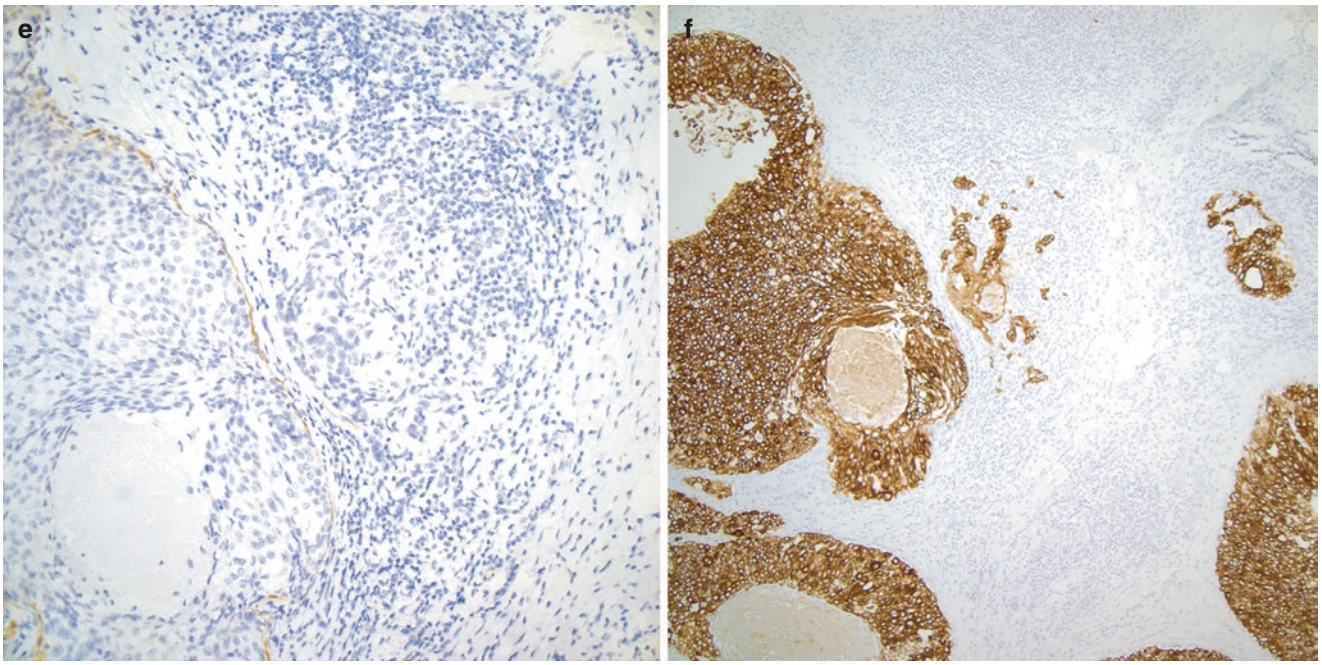

Fig. 9.21 (continued)

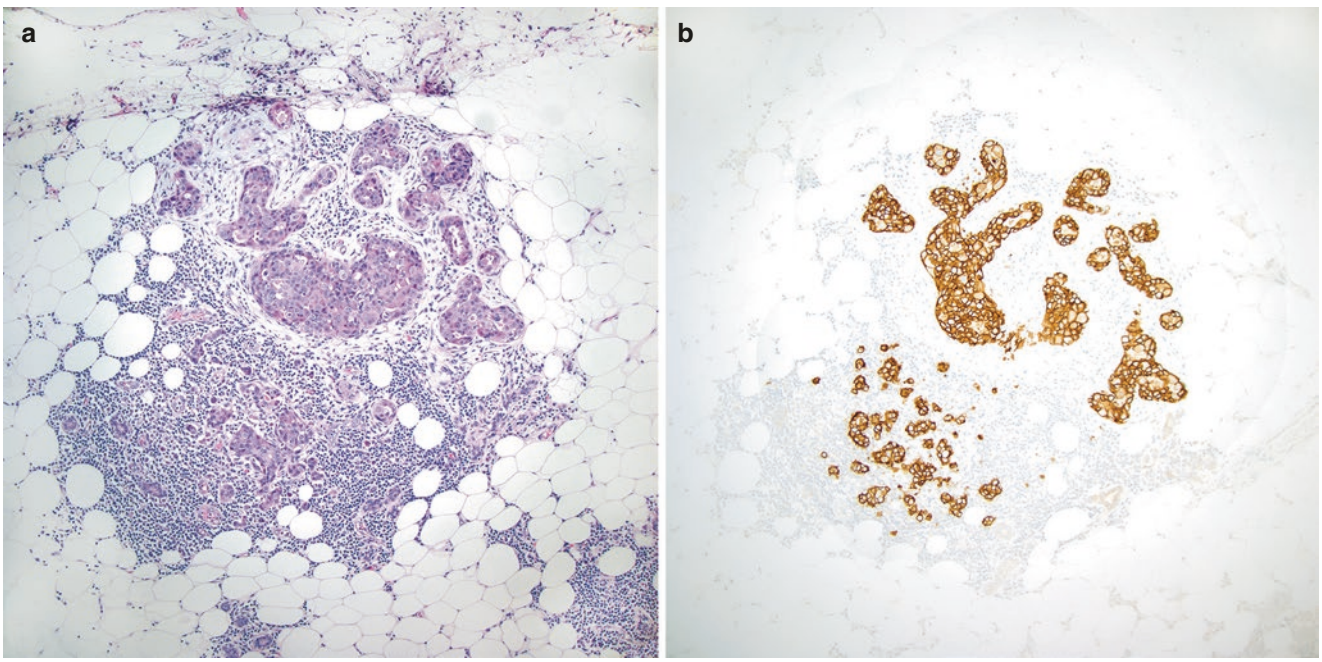

Fig. 9.22 Extensive high-grade DCIS is frequently associated with HER2-positive invasive disease. In this case, the scattered invasive tumor cells present in the inflammation adjacent to the DCIS (**a**) are positive for HER2 overexpression as well as the DCIS (**b**)

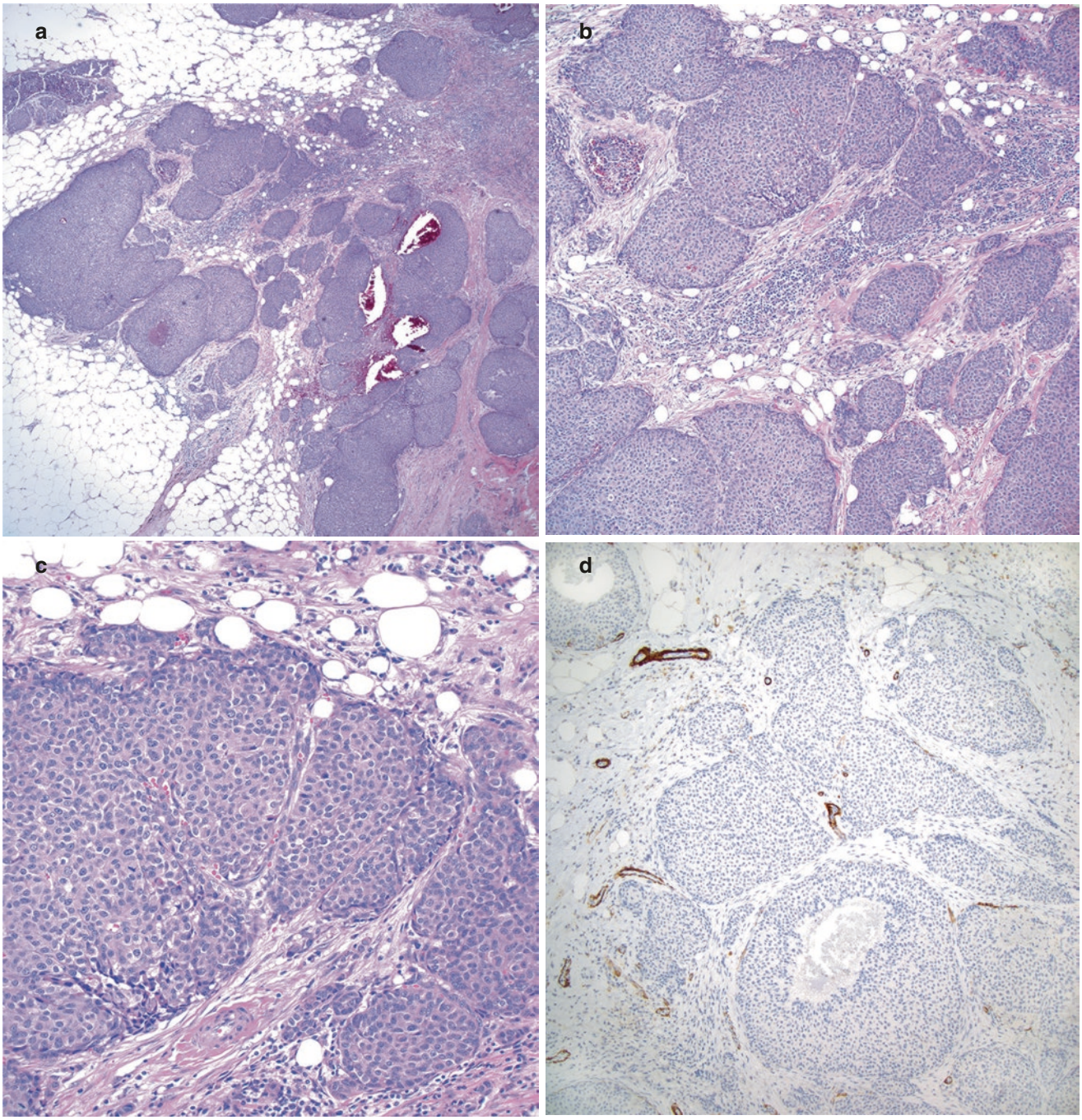

Fig. 9.23 The differential diagnosis between DCIS and solid, nested forms of invasive carcinoma can be a challenge. A diagnosis of invasive carcinoma should be considered even when the nests of carcinoma have rounded contours (similar to DCIS) when these areas appear to "fit" together like puzzle pieces in more complex patterns than that typically seen in DCIS (**a**). Some nests of carcinoma may have more irregular borders (**b**) or wrap around normal structures like adipocytes (**c**) or normal ducts. A negative result using myoepithelial cell markers will confirm the invasive nature of the process (**d**)

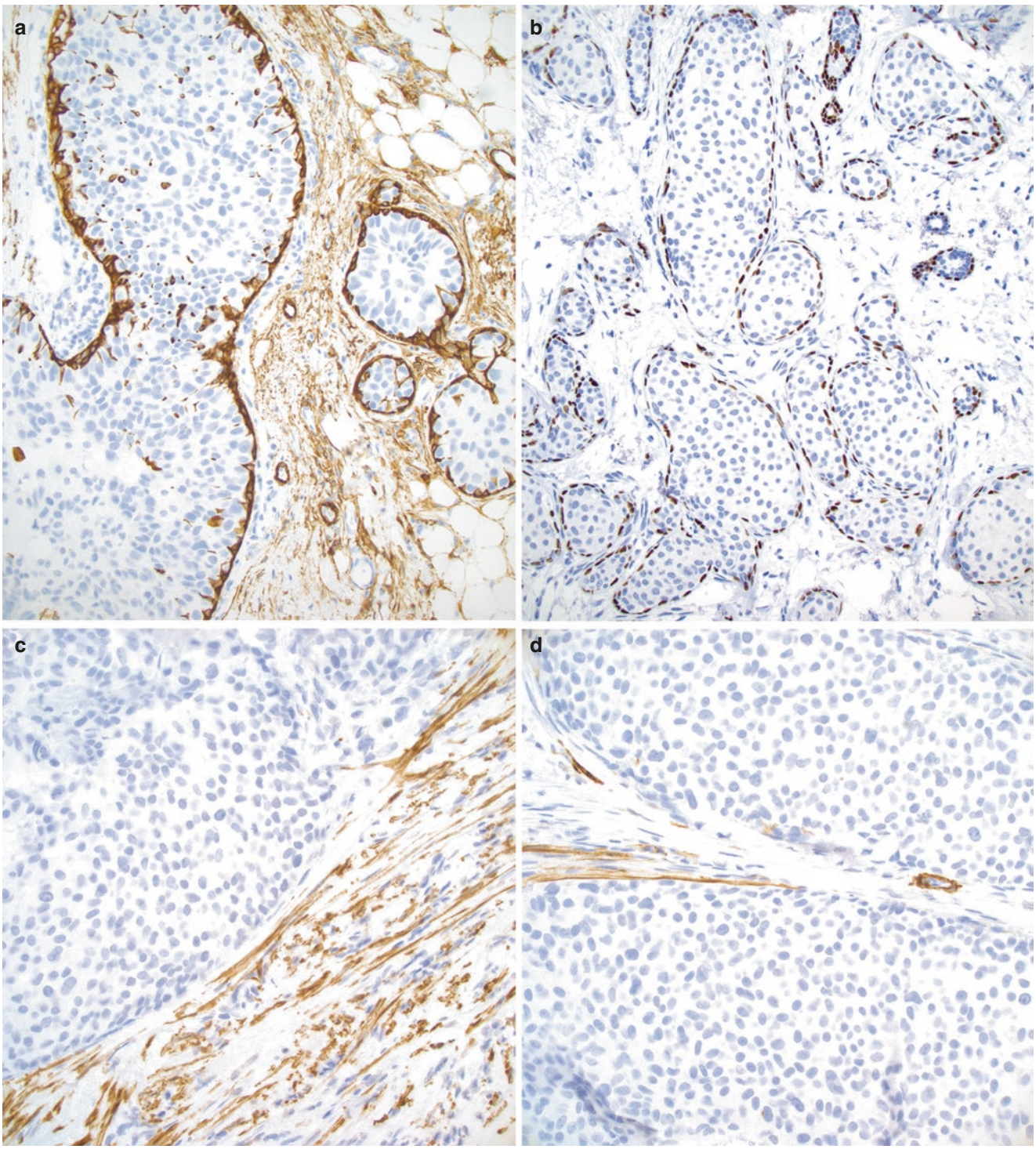

Fig. 9.24 A cytoplasmic myoepithelial stain such as smooth muscle myosin (SMM) should stain the cytoplasm of the basal myoepithelial cell layer in DCIS but may also stain surrounding stromal cells or small vessel walls (**a**). Note that the cells with cytoplasmic staining for SMM are located above the basement membrane and contain malignant appearing nuclei, in contrast to the stromal cells staining in the surrounding tissue. A nuclear myoepithelial cell marker such as p63 (**b**) can be helpful in conjunction since it should not stain the surrounding stromal cells. (**c**, **d**) show rounded nests of invasive carcinoma that lack a myoepithelial cell layer but on SMM stain there is stromal staining that is below the basement membrane that does not contain cells with malignant nuclei, and therefore should not be interpreted as a myoepithelial cell layer. (**d**) Also shows SMM staining of a small vessel

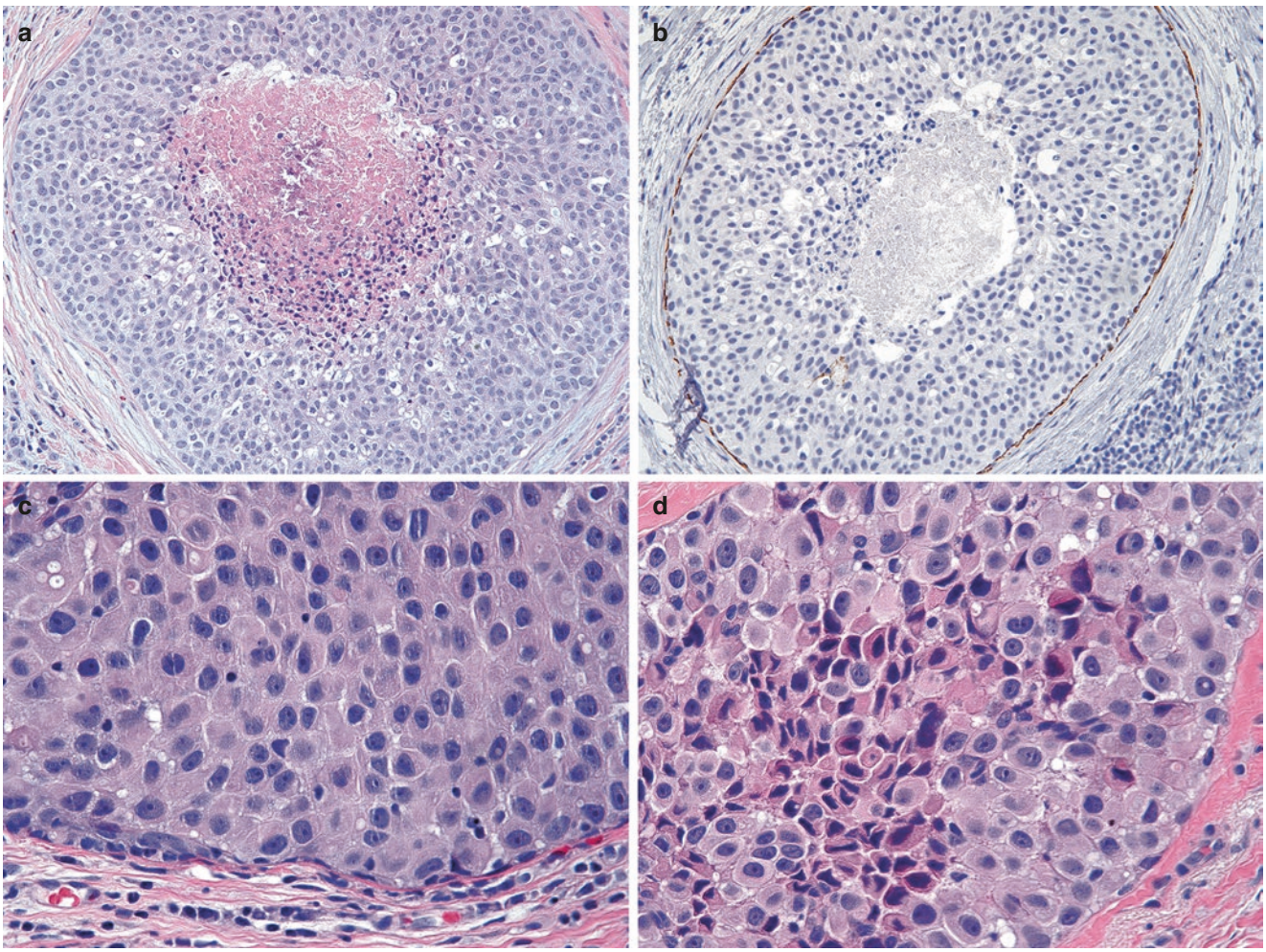

Fig. 9.25 Pleomorphic lobular carcinoma in situ (PLCIS) has high nuclear grade and can have central comedo-necrosis very similar to comedo-type DCIS (**a**). However, PLCIS will have loss of E-cadherin (**b**), in contrast to DCIS which should retain its E-cadherin expression. Subtle clues on H&E to a lobular process include intracytoplasmic lumens, less distinct cell borders, and rounding up of cells with discohesion (**c**, **d**, 40× magnification)

matic nuclei rather than a proliferation of atypical cells as is typically seen in high-grade DCIS. In the post-chemotherapy setting, residual "treated" DCIS can also present as atrophic sclerotic ducts lined by residual atypical epithelium. These ducts are often filled with histiocytes and debris as well. Knowing the clinical history is key to recognizing this as treated DCIS.

Low-Grade DCIS Spectrum

Limited Extent Low-Grade DCIS Versus ADH

Limited extent low-grade DCIS (2–3 mm) has many overlapping features with ADH, and determining the most appropriate of these diagnoses to use on a core biopsy sampling can be challenging. When either the cytologic or architectural features are considered borderline to qualify for a diagnosis of low-grade DCIS, a diagnosis of ADH is most appropriate. When there is clear cytologic monotony and there are early architectural forms characteristic of low-grade DCIS but not completely involving ducts or limited in development, again a diagnosis of ADH on core biopsy is more appropriate. Although originally developed in the excisional biopsy setting, the >2 mm threshold for a diagnosis of low-grade DCIS (when ducts are uniformly involved by a monotonous process with well-developed architecture) can serve as another useful threshold in the core biopsy setting. When close to this size threshold, a conservative approach should be used in the core biopsy setting. Diagnoses that reflect the borderline nature of the lesion should be utilized such as "ADH bordering on low-grade DCIS," "At least ADH, suspicious for low-

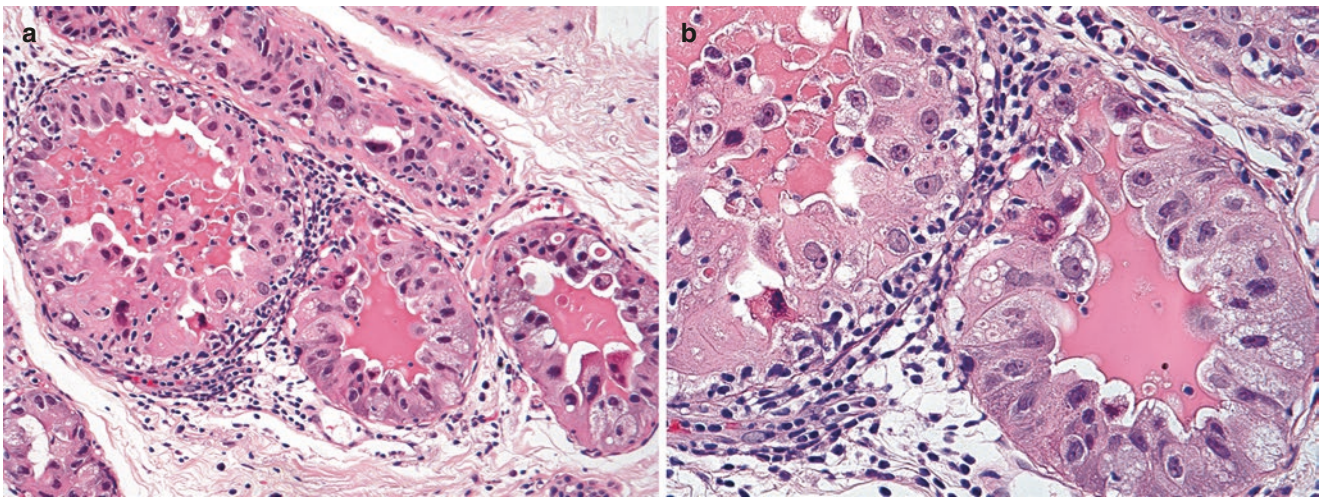

Fig. 9.26 Atypical cystic hypersecretory change (**a**: at 20× magnification, and **b**: at 40× magnification) can mimic high-grade DCIS involving a lobule. The dense thyroglobulin-like secretion with scalloped edges, which is characteristic of hypersecretory processes, should not be mistaken for necrosis. The cytoplasm in these images is bubbly and contains small granular secretions, suggesting a lactation-related phenotype. Although the nuclear atypia is marked, with prominent nucleoli and occasional multinucleated cells, if these changes are isolated to a few lobules in a core needle biopsy, a diagnosis of "severely atypical intraductal proliferation with hypersecretory features" should warrant excision to further clarify the extent and nature of the process. Cystic hypersecretory DCIS should be considered if there is more extensive proliferation involving ducts (see Fig. 9.11)

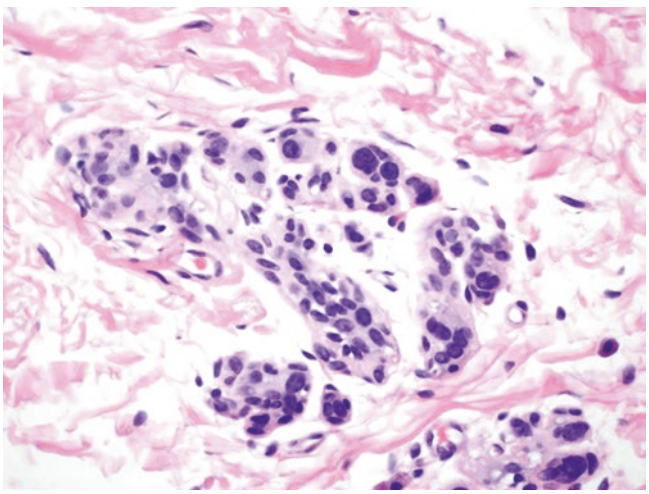

Fig. 9.27 Postradiation atypia can be seen in patients who were previously treated for breast cancer or other intrathoracic malignancies. In contrast to DCIS, the atypia is present as scattered hyperchromatic cells without significant proliferation

grade DCIS," and "Severely atypical intraductal proliferation." An example of a borderline lesion on core biopsy is shown in Fig. 9.28a–d. A definitive diagnosis of low-grade DCIS on core biopsy should be reserved for those cases where, if there are subsequently no additional findings on surgical excision, the pathologist can be confident that the extent of the lesion on core biopsy is enough to make treatment decisions that may include radiation.

Solid Patterns

Monotonous solid proliferations based on the terminal-duct/lobular unit can raise the differential diagnosis of low-grade DCIS versus LCIS (Fig. 9.14). The formation of subtle micro-acini can sometimes be evident and is supportive of ductal differentiation. The cell borders of low-grade DCIS also tend to be more crisp, while discohesion and indistinct cell borders are more suggestive of LCIS. However, often E-cadherin staining can be used to resolve this differential with loss of expression characteristic of lobular lesions. Occasionally, E-cadherin (or p120) staining has a mixed pattern of partial loss. In these cases, correlation with the histologic features (such as the presence of atypical lobular hyperplasia, pagetoid growth in a lobular pattern) may help favor one process over the other. It should be recognized that classification of a case as "in situ carcinoma with mixed ductal and lobular features" will result in treatment as DCIS by most clinicians, and in cases that are thought to be fundamentally lobular (i.e., pleomorphic LCIS), this term should not be used.

Cribriform Patterns

Cribriform DCIS can be mimicked by collagenous spherulosis, especially when there is concurrent LCIS present in the lesion (Fig. 9.29). Collagenous spherulosis is characterized by the formation of "punched out" spaces that are filled with basement membrane material and lined by myoepithelial cells. On H&E the basement membrane material is often evi-

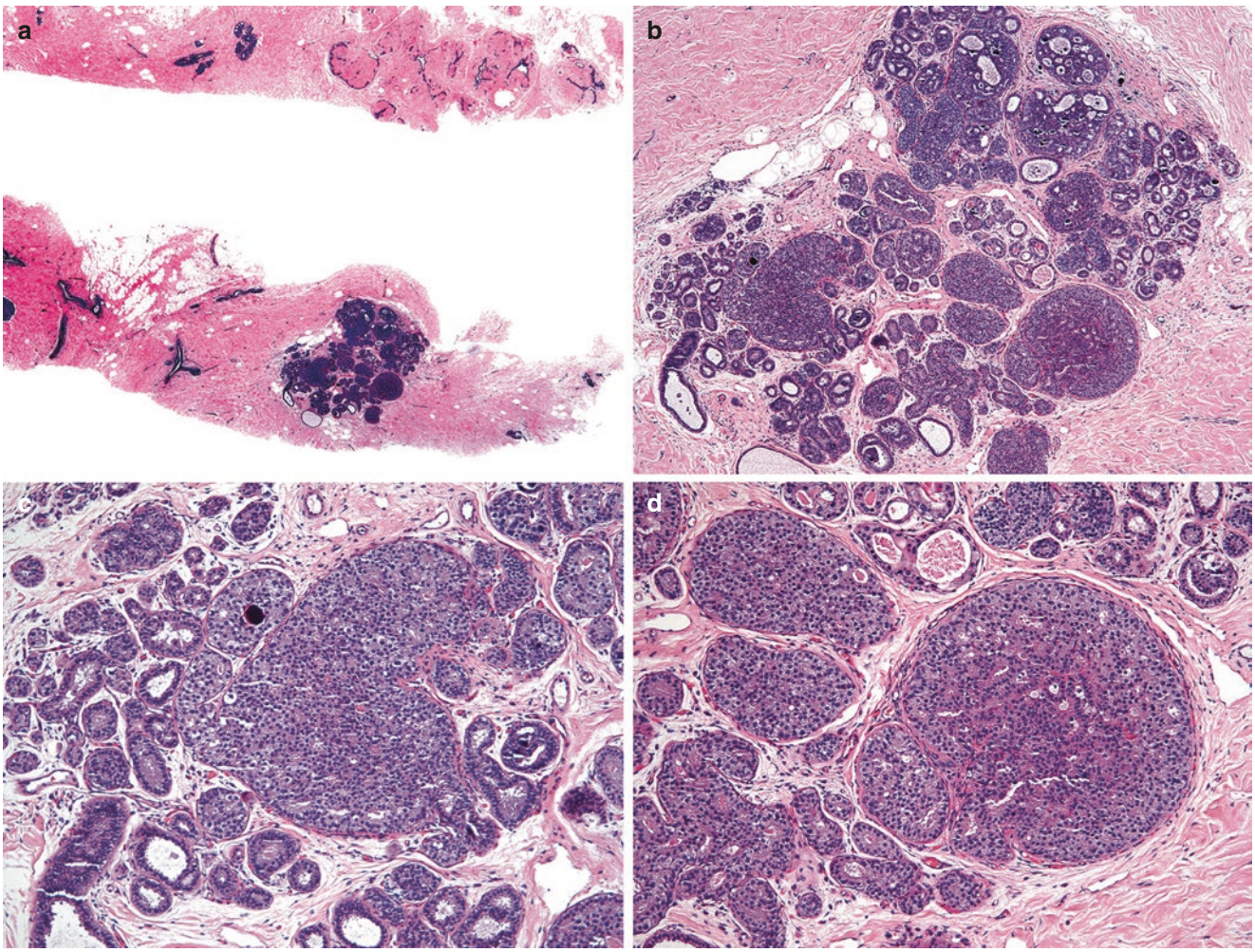

Fig. 9.28 (**a–d**) A core biopsy with an intraductal proliferation showing low-grade cytologic monotony and cribriform architecture. The proliferation developed in several ducts but not completely uniform throughout the lesion and measures <2 mm. When changes straddle between those of low-grade DCIS and ADH are present on a core biopsy, a diagnosis of "atypical ductal hyperplasia bordering on low-grade DCIS" (or similar terminology) should be considered. These borderline lesions will have high diagnostic disagreement, so consideration should also be given to a second pathologist review

dent but sometimes it degenerates and is only present as myxoid change or thin fibrils detached from the spaces. When there is the cytologic monotony of LCIS present in the background of these cribriform-like spaces, the appearance of low-grade DCIS can be quite striking. Because collagenous spherulosis is composed of a proliferation of both luminal epithelial and myoepithelial cell types, myoepithelial cell stains can aid in this diagnosis. In collagenous spherulosis, the myoepithelial cells should line the spaces formed, a pattern of staining not seen in DCIS. E-cadherin staining can also be helpful in cases to identify concurrent involvement by LCIS.

Invasive mimics of cribriform low-grade DCIS include adenoid cystic carcinoma and cribriform carcinoma. It is important to recognize the patterns of myoepithelial staining in adenoid cystic carcinoma, which has both luminal and basal/myoepithelial phenotypes admixed throughout the process, rather than only around the rim as in DCIS.

Spindled Patterns

Spindled forms of DCIS are challenging to diagnose due to their similarity to florid forms of UDH (Fig. 9.30a–d). When other more recognizable architectural patterns of DCIS are present, this can be helpful because it raises the differential of DCIS with a spindled pattern component. Spindled DCIS tends to have a more evenly distributed cellularity in involved ducts than compact forms of UDH, and should have more hyperchromatic, irregular, and enlarged nuclei. However, some cases are very difficult to differentiate without the help of immunohistochemistry. A CK5/6 stain is particularly use-

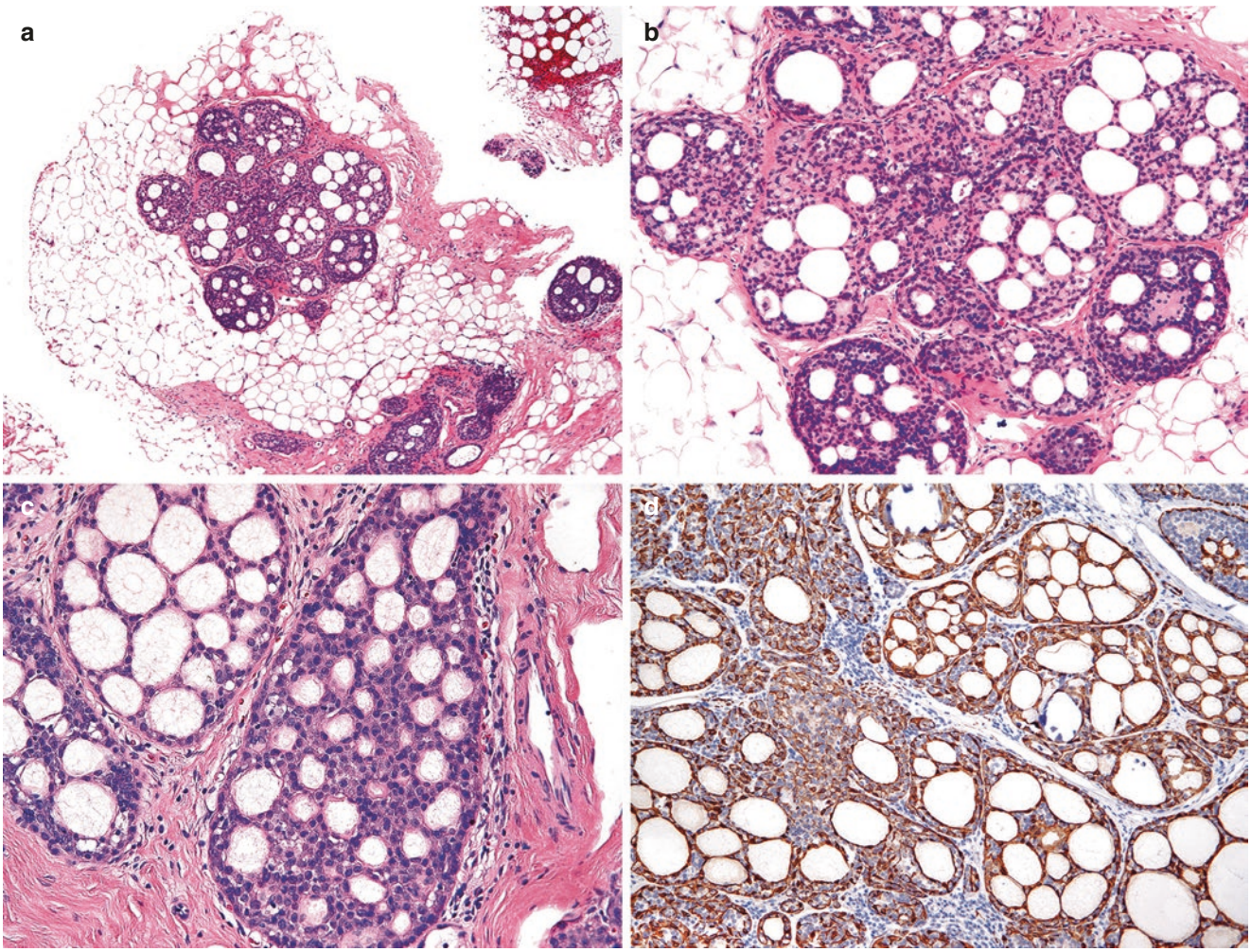

Fig. 9.29 (**a**–**d**) Collagenous spherulosis involved by LCIS mimicking low-grade cribriform DCIS. Collagenous spherulosis forms "punched out" crisp spaces within an intraductal proliferation. These spaces are lined or filled with basement membrane material that can be seen as a subtle "cuticle" surrounding the spaces or extending across the center of the space. Myoepithelial stains will highlight the mixed population of myoepithelial cells present that line these spaces. The monotony seen in this case is due to involvement of the process by LCIS (an E-cadherin stain—not shown—was negative in this cell population)

ful when the differential diagnosis includes intermediate-grade DCIS versus UDH. DCIS will be negative in the epithelial proliferation (while maintaining staining in the surrounding myoepithelial cell layer) while UDH will have a mixed or "mosaic" staining pattern. Including an ER stain can also be helpful since the cells of low-intermediate grade DCIS should be fairly uniformly and strongly positive, while the pattern of ER expression in UDH is more patchy and irregular.

Papillary Patterns

Papillary forms of DCIS can mimic benign papillomas especially when the lining epithelium is a single layer. The epithelium lining of papillary DCIS will appear darker at low power than a benign papilloma. This is due to the increased nuclear hyperchromasia and nuclear stratification present in papillary DCIS. Benign papillomas also have thicker fibrovascular cores than the thin ones that characterize papillary DCIS. High-power inspection of papillary DCIS will not identify obvious myoepithelial cells, as should be seen in a benign papilloma. When there is doubt, myoepithelial stains can be performed to differentiate, with myoepithelial layer present around the fibrovascular cores of benign papilloma but not the cores of papillary DCIS. Care should be taken not to interpret the staining of small vessels compressed around the edges of the fibrovascular cores as staining of a myoepithelial cell layer. Nuclear p63 staining should also be present in the myoepithelial cells. When in doubt, or if the differential includes other papillary lesions (such as encysted papillary carcinoma or papilloma involved by ADH or DCIS), a

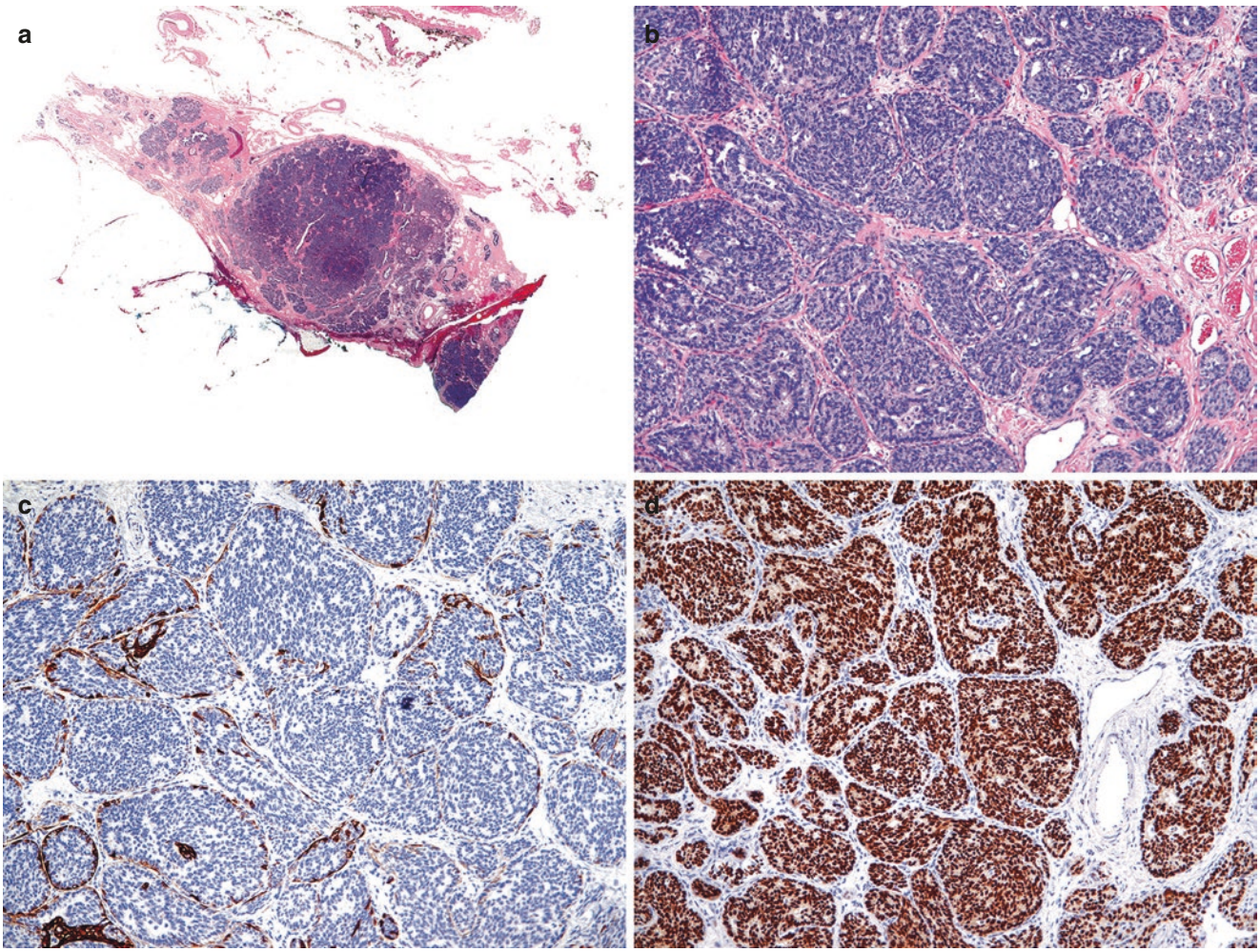

Fig. 9.30 (**a**, **b**) Spindled forms of DCIS can raise the differential of a florid usual ductal hyperplasia. When in doubt, additional immunohistochemistry can be helpful in this differential. Low-intermediate grade spindled DCIS should be negative for CK5/6 staining (**c**) and uniformly positive for ER expression (**d**). This is contrast to the "mosaic" CK5/6 staining pattern seen in UDH and more variable ER expression (see Fig. 9.41)

diagnosis of "atypical papillary lesion" can be appropriate on a core needle biopsy sample. Papillary lesions are discussed in more detail in Chap. 6.

Immunohistochemistry

Estrogen receptor staining is the only clinically relevant stain currently used in DCIS. Although high-grade DCIS is less likely to be ER positive than low-intermediate grade DCIS, an estimated 57% of comedo-DCIS is ER positive [25]. Patients with ER-positive DCIS can be offered Tamoxifen (or other hormonal-targeted therapies), to reduce the risk of recurrence in any residual breast tissue [26]. The threshold for ER positivity is 1% of cells with weak intensity staining, similar to criteria for invasive carcinoma [27]. A low-grade DCIS should be ER positive, and if it is not, this is considered a discordant result (Fig. 9.31). Both a re-evaluation of the histology as well as evaluation of possible testing error or a pre-analytical issue should be considered.

When a concurrent invasive carcinoma is hormone receptor negative and there is ER expression noted in the associated DCIS, both results should be reported since hormone-based treatment may be offered on the basis of the ER expression of the DCIS [26]. If a core biopsy sample contains only very limited ER-negative DCIS (or another factor limits the evaluation of ER expression), consideration for repeat testing on DCIS present in the subsequent surgical specimen is recommended if clinically relevant. Although progesterone receptor (PR) is frequently performed with ER on DCIS cases, there is not currently evidence that PR expression is clinically relevant in DCIS.

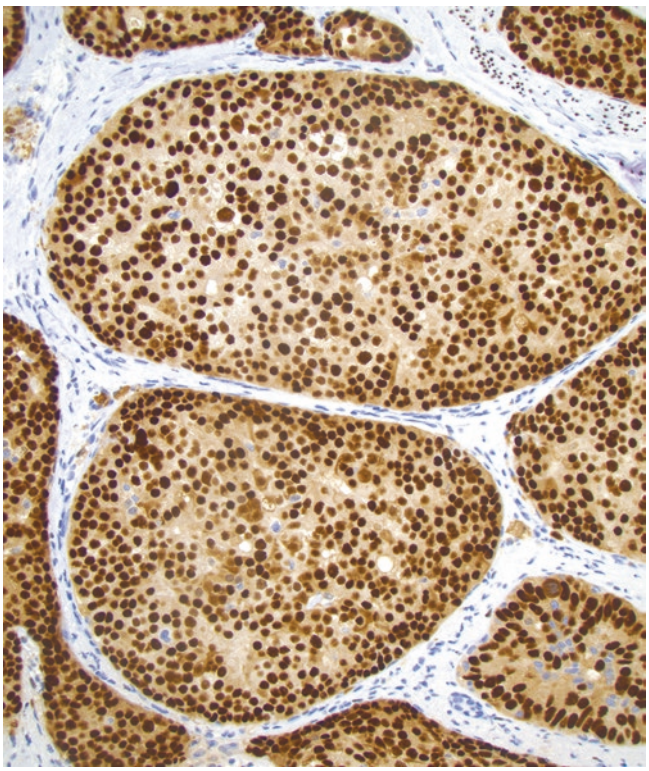

Fig. 9.31 Low-grade DCIS is typically uniformly and strongly ER positive

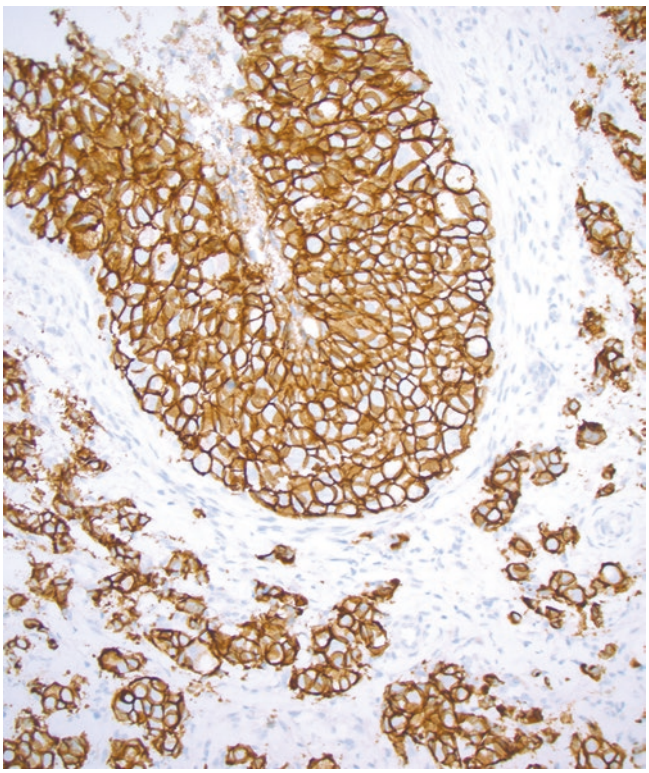

Fig. 9.32 High-grade invasive HER2-positive cancers are frequently associated with concurrent HER2-positive DCIS

HER2 staining is not standard in DCIS since there is currently no role for HER2 targeted therapies for pre-invasive disease. However, as mentioned earlier, high-grade DCIS is frequently HER2 positive with 60–100% HER2 positivity in high-grade, comedo-type DCIS [28, 29]. Twelve percent of ER-positive DCIS is estimated to be HER2 positive as well [30]. The vast majority of Paget's disease of the nipple is HER2 positive, ER negative, and high grade [31]. Extensive HER2-positive high-grade DCIS is more likely to harbor small foci of invasion, which has important implications for more extensive tissue sampling to identify any and possibly larger foci of invasive cancers [32] (Fig. 9.32).

Some argue that using IHC surrogates for molecular subtyping, including hormone receptors, HER2 and Ki-67, can help stratify DCIS patients by risk of upgrade [33]. High-grade DCIS is more often p53 positive and has higher proliferative rates on Ki-67 staining than low-grade DCIS.

CK5/6 staining is most often used to differentiate low-intermediate grade DCIS or ADH (CK5/6 negative) from UDH (mosaic pattern CK5/6 staining) and is less often useful in the diagnosis of high-grade DCIS. However, if used, it is important to recognize that some high-grade DCIS, especially the basal-like subtype, will be CK5/6 positive [34]. However, less than 10% of DCIS is estimated to be basal-like with the vast majority of invasive basal-like breast cancers not found to be associated with DCIS [35].

See the section "Differential Diagnosis" above for the utility of myoepithelial or E-cadherin staining in specific settings.

Pathogenesis

Just as it has become clear that there are distinct subtypes of invasive breast cancer with different molecular/phenotypic profiles and outcomes, there is also evidence that DCIS can be grouped into similar categories with differing pathogenesis [33, 36].

Estrogen receptor-positive DCIS is frequently low-intermediate grade and is associated with luminal-type invasive breast cancers that are most often low-intermediate grade and ER positive. It is considered a part of the "low-grade neoplasia family" which includes FEA, ADH, ALH, LCIS, low-grade DCIS, and low-grade invasive carcinomas [37, 38]. Low-grade DCIS contains recurrent losses of 16q and 17p as well as gains of 1q that are characteristic of this low-grade neoplasia family [39–41].

In contrast, hormone receptor negative (to low ER expressing) DCIS is typically high grade and is associated with the HER2 enriched and occasionally basal subtypes of high-grade invasive cancers [36]. When compared to the low-grade neoplasia family, high-grade DCIS more fre-

quently has HER2 amplification, basal marker expression, aneuploidy, and complex karyotypes [42, 43]. Of note, <30% of high-grade lesions have deletions of 16q, which is strongly associated with the low-grade pathway [36, 38, 44]. This finding suggests that most high-grade lesions have a different pathogenesis and do not evolve from low-grade ones. However, this pathway can occur in the minority of cases and the process of progression to invasion is complex [45].

Outcomes

The standards for treatment of DCIS are evolving as more is understood about its biology and outcomes. The most standard therapy is either partial mastectomy followed by whole-breast irradiation or a total mastectomy. Hormone targeting therapies are also commonly used to reduce recurrence rates in either breast in patients with hormone receptor-positive DCIS. However, as more is understood about the risks of the increasingly common low-grade DCIS spectrum, there is interest in more minimally treating this group by omitting radiation, performing partial breast irradiation, or even employing active surveillance protocols [46]. Although differences in local recurrence rates are apparent when radiation is added after lumpectomy for DCIS, there is not clear evidence of differences in overall survival using radiation [47–49]. Because benefits to overall mortality in treating this group of screen-detected low-grade cancers are currently unclear, there has been some recent concern that these lesions are overdetected or "overdiagnosed" and "overtreated" [50, 51].

There are many factors that have been associated with an increased risk of recurrence for DCIS, including margin status, age, and size, but one of the most powerful predictors appears to be nuclear grade. In one study with a median follow-up of 8.5 years, there was a 6.8% risk of recurrence of DCIS, 73% of which were in patients with high-grade DCIS [52]. After local therapy for DCIS, nuclear grade has been shown to be a predictive factor for ipsilateral breast cancer recurrence in a randomized clinical trial and meta-analysis [53–55].

The Van Nuys prognostic index, which combines size, margin width, nuclear grade, necrosis, and age, is used to calculate a score that predicts recurrence in conservatively treated DCIS [56, 57]. There is now at least one commercially available reverse transcriptase PCR-based assay that aims to determine which cases of DCIS are more likely to locally recur and respond to radiation therapy; however, its role in clinical practice is still unclear [58].

Given the currently evolving clinical management strategies for DCIS, a detailed, accurate pathologic diagnosis is and will continue to be key to individualizing treatment. Diagnostic agreement is estimated to be approximately 85% for breast biopsy samples containing DCIS (in a test set setting), with the majority of disagreements occurring in the low-grade end of the spectrum [1]. There is also a growing interest in developing biomarkers and clinical tests on DCIS tissue that can predict behavior and help determine treatment benefit [58, 59].

Atypical Ductal Hyperplasia

Overview

Atypical ductal hyperplasia (ADH) on core needle biopsy accounts for only 3–15% of breast biopsy diagnoses, but is a frequent topic in breast disease discussions because of the challenges presented by both their diagnosis and clinical management [60, 61]. ADH is a borderline lesion that has significant overlap of its diagnostic and molecular features with low-grade DCIS and UDH. Because ADH exists within this spectrum of changes and has no biologically distinct characteristics, its diagnosis is frequently problematic.

Diagnostic agreement rates for biopsies with ADH are quite low (40–60%), especially when compared to the much higher agreement for DCIS, invasive carcinoma, and benign breast lesions [1, 62]. Because the differences in diagnosis are frequently related to subtle differences of professional opinion and diagnostic thresholds, simply knowing the diagnostic criteria may not be enough to ensure a reproducible diagnosis of ADH [2]. These cases should be shown to colleagues or consultants such that a reproducible diagnostic consensus can be reached in these challenging lesions, particularly in the lesions that are considered to be borderline with either low-grade DCIS or UDH.

ADH is considered a bilateral "risk lesion" because it has been associated with 3–5× increased risk of developing invasive carcinoma in either breast [63, 64]. From a clinical perspective, when a lesion increases the risk of developing invasive cancer in either breast, it is managed as a generalized "risk lesion" rather than as a localized lesion that can be surgically excised. However, because of its association with low-grade DCIS and invasive cancers, when identified on core needle biopsy, an excision is typically performed to rule out unsampled carcinoma.

Patients with ADH as the clinically most significant lesion on a core biopsy are told that they have an increased risk of developing an invasive breast cancer, a risk which spans and slowly increases over several decades, and some are offered risk hormonal agents such as Tamoxifen to non-surgically reduce this risk [65]. Occasionally, a patient with ADH with or without other high-risk features may choose to reduce their future cancer risk surgically with bilateral mastectomies, although this is considered by most to be overtreatment. As such, although ADH is considered "benign," it is a

diagnosis that can have a significant clinical impact for any given patient and its diagnosis should be made with caution and with as much certainty as possible.

Gross and Radiologic Features

Similar to low-grade DCIS, ADH is most frequently diagnosed on core needle biopsy when calcifications are identified on screening mammogram. ADH does not present as a mass, unless it is involving a mass-forming lesion such as a papillary lesion or fibroadenoma. There are no radiologic features that help distinguish ADH and other risk lesions from calcifications present in low-grade DCIS or invasive carcinoma. Excisional biopsy is performed after identification of ADH as the clinically most significant lesion on a core biopsy to exclude the possibility of adjacent non-sampled DCIS or invasive carcinoma.

Microscopic Features

ADH is broadly described as a lesion that has "some but not all of the features of low-grade DCIS." The cytologic features of ADH are those of low-grade DCIS, with monotonous cells containing rounded nuclei with even chromatin (Fig. 9.33). Intermediate-to-high grade nuclear features are not considered to be in the spectrum of ADH. The cell border are well defined and the nucleo are evenly spaced, which are classic features of low-grade neoplasia.

The architectural features typical of ADH are earlier/less well developed than in low-grade DCIS, such as rigid bridges or bars of uniform thickness or "roman" arches and arcades. Partial involvement of a duct with more developed cribriform architecture or micropapillary structures also can be a feature (Fig. 9.34a–d). Solid patterns of ADH can be present if focal and occasionally have subtle polarized lumens present. The involved spaces may also contain admixed cell populations with features more suggestive of UDH, FEA, or non-proliferative epithelium. Two examples of core needle biopsies with ADH are shown in Figs. 9.35a–d and 9.36a–d.

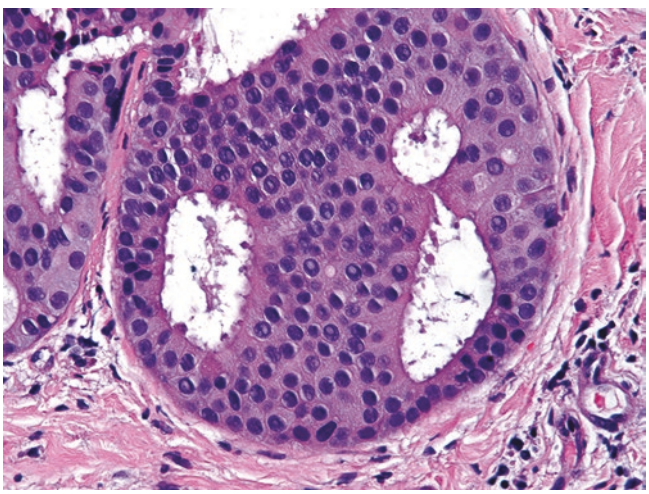

Fig. 9.33 Cytologic monotony with rounded and evenly spaced nuclei is present in a focus of atypical ductal hyperplasia. Similar nuclear monotony is present in low-grade DCIS

When the cytologic and architectural features of low-grade DCIS are present, many authors agree that smaller lesions with these findings should still be classified as ADH. There are different extent and size thresholds suggested by different authors. Page et al. proposed a system where these proliferations, if confined to no more than two duct spaces, could be classified as ADH instead of low-grade DCIS [66]. However, some authors argue that this low threshold would result in overtreatment of very limited extent low-grade DCIS that may not have significantly different outcomes from ADH. Tavassoli and Norris proposed that 2 mm (in size) be the threshold below which lesions with low-grade DCIS characteristics could be classified as ADH [3]. However, since both of these systems were developed in excisional biopsies, their use in core needle biopsies where the entire lesion may not be visualized should be done with caution. The WHO Working Group recommends a conservative approach when a core needle biopsy contains ADH versus limited extent low-grade DCIS, favoring classification as ADH or "at least ADH" with various qualifiers until the entire lesion can be evaluated on surgical excision [67].

Differential Diagnosis

ADH Borderline with Low-Grade DCIS

As mentioned above, this diagnostic differential is very challenging since there are no additional stains or molecular markers to aid in the distinction of ADH from limited extent low-grade DCIS. This differential most frequently arises when the cytology is clearly monotonous but the architecture is not uniformly well developed or the size of a lesion with uniform well-developed architecture is small (<2 mm). In general, if the lesion borders between ADH and low-grade DCIS, a diagnosis of ADH should be made on core needle biopsy. Figure 9.28a–d shows an example of a case with features that border on low-grade DCIS. Cytologic monotony is present and some early neoplastic architecture is evident. Two of the involved ducts have more complete involvement by the process. However, given the lack of uniformity of the architectural changes throughout the lesion, on a core needle biopsy this lesion should be classified as "ADH borderline with low-grade DCIS, with associated calcifications" and include a comment such as the following: "There is an atypical intraductal proliferation with features that border on a diagnosis of low-grade DCIS. However, given the limited

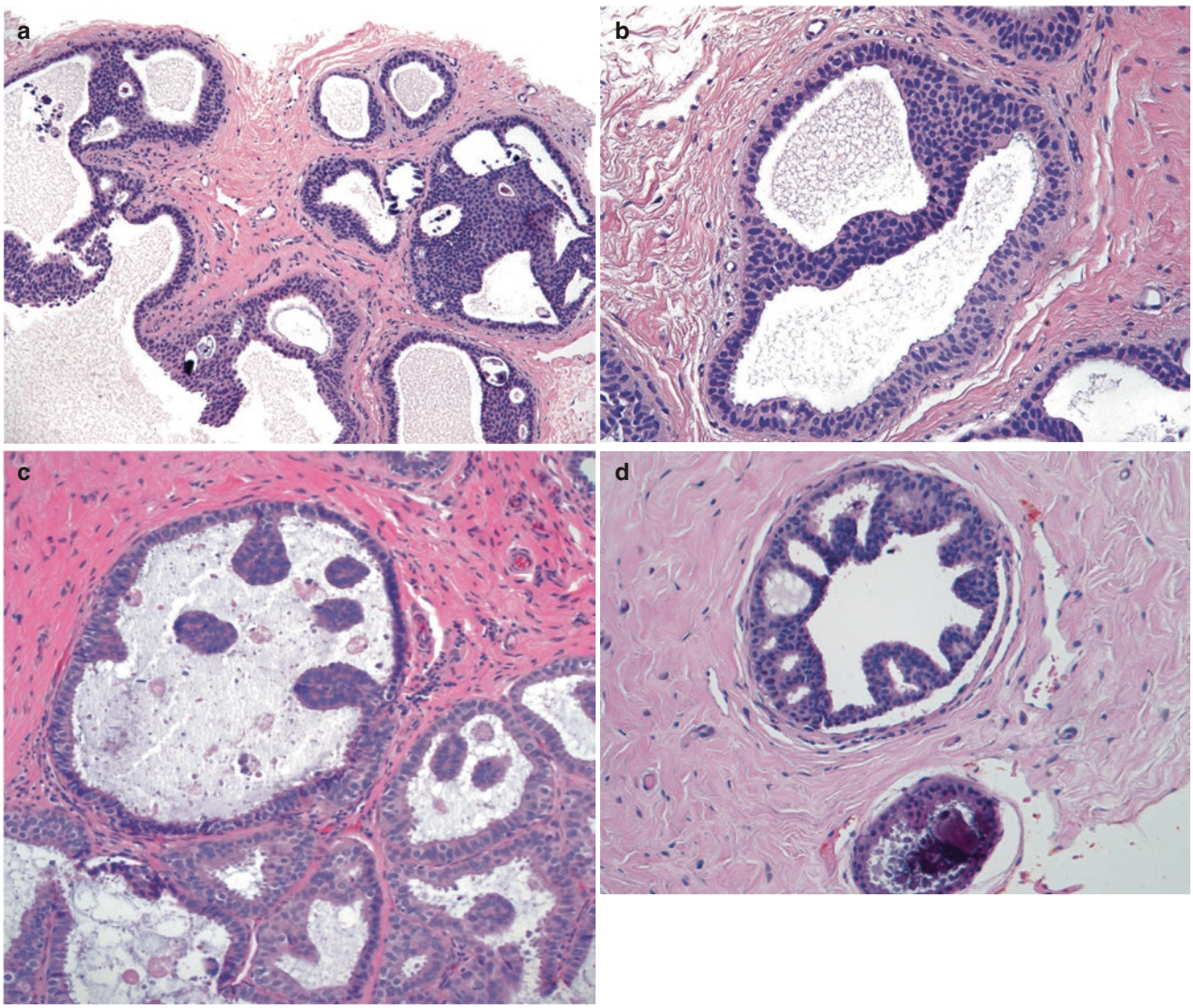

Fig. 9.34 (**a**, **b**) Architectural characteristics of ADH include the formation of rigid bridges or bars across duct spaces and early cribriform structures. (**c**) Micropapillary forms of ADH will have only a few early micropapillary structures present. (**d**) Roman bridges or arches can also be present. These early neoplastic structures do not uniformly fill the duct spaces or are limited in extent compared to low-grade DCIS

extent present in this core biopsy sampling, we would classify the findings as ADH and recommend correlation and final classification of the process on the anticipated excisional specimen." It is our policy to have a second pathologist review of all diagnoses of ADH on core biopsy (as the clinically most significant lesion), which would also be noted in the comment.

ADH Versus UDH

The other end of the spectrum of ADH includes the differential with non-atypical proliferative lesions such as UDH. UDH is characterized by a more polyclonal appearance, in contrast to the monotony seen in ADH. Sometimes cases have borderline cytologic features that can raise this differential. Evaluation of the architecture can offer clues to help resolve this differential. The spaces formed in ADH are frequently polarized, with the nuclei oriented away from the lumen of the space. This is in contrast to UDH, where the peripherally located spaces are non-polarized with nuclei immediately abutting the slit-like spaces that are formed. Bars and bridges formed in ADH should be rigid and contain cells without significant nuclear overlap. In contrast, UDH can form cellular bridges but they should be tapered and contain overlapping nuclei. When there are micropapillary structures being formed, ADH is favored when they are club-shaped and contain regularly spaced monotonous

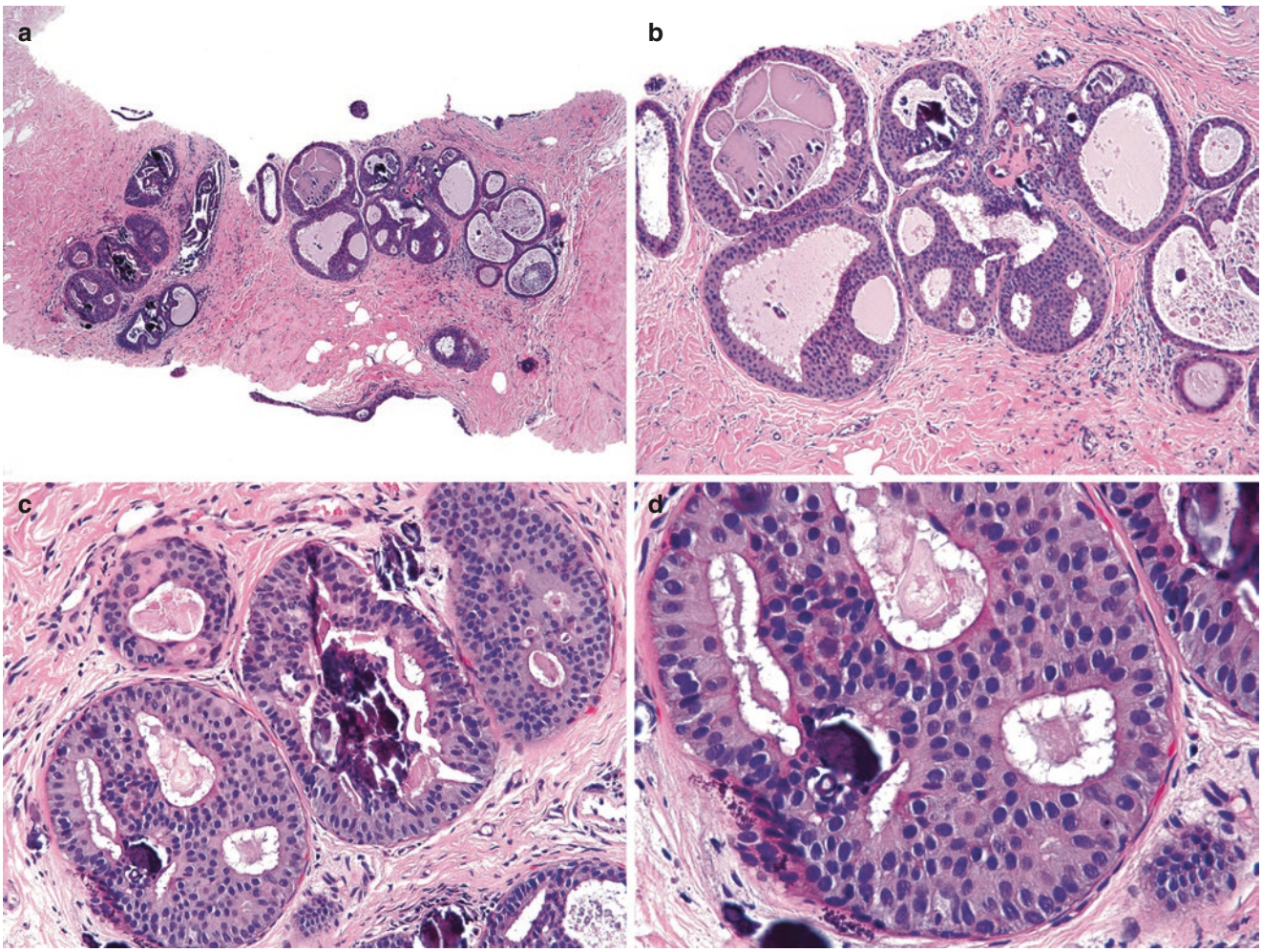

Fig. 9.35 (**a**–**d**) This core needle biopsy contains an intraductal proliferation with low-grade cytologic monotony and early, partially developed architectural changes. The architecture is not well developed or uniform enough for a diagnosis of low-grade DCIS. These findings on core needle biopsy are most consistent with atypical ductal hyperplasia. The targeted calcifications are present within the ADH

nuclei. UDH can form tufted or gynecomastoid hyperplastic structures that mimic micropapillae but they contain overlapping nuclei that are smaller at the ends of these structures and are non-uniform. Figure 9.37a–f shows side-by-side comparisons of these features in ADH versus UDH.

CK5/6 and ER staining, or ADH-5 (see below) can be helpful in cases when features are borderline. The cell population of ADH will stain similar to low-grade DCIS with loss of CK5/6 expression and uniform, strong ER staining within the proliferation. In contrast, UDH will have a mixed "mosaic" pattern of staining and variable ER expression.

When in doubt about the diagnosis of UDH versus ADH on a core biopsy, a review by a second pathologist can be helpful, but in general the low-grade diagnosis should be favored. A comment can be included that the diagnosis of ADH was considered but that the changes were insufficient for this diagnosis in this sample.

Minimal Extent ADH Versus FEA or Non-atypical Columnar Cell Change/Benign

ADH is frequently seen admixed with FEA and non-atypical columnar cell change. The targeted calcifications can be present throughout all of these lesions. When columnar cell change becomes monotonous with more rounded nuclei and there are early architectural formations, the diagnosis of minimal extent ADH should be considered (Fig. 9.38 a, b). When FEA is seen on a core biopsy sampling as the highest order diagnosis, because it is still unclear if excisional biopsy should follow, additional levels should be considered to identify any areas that are diagnostic of ADH. These areas are often minimal, early architectural formations such as a few rigid bridges or micropapillations within ducts lined by FEA. CK5/6 and ER stains are not useful in columnar cell lesions versus ADH since they can have very similar staining patterns.

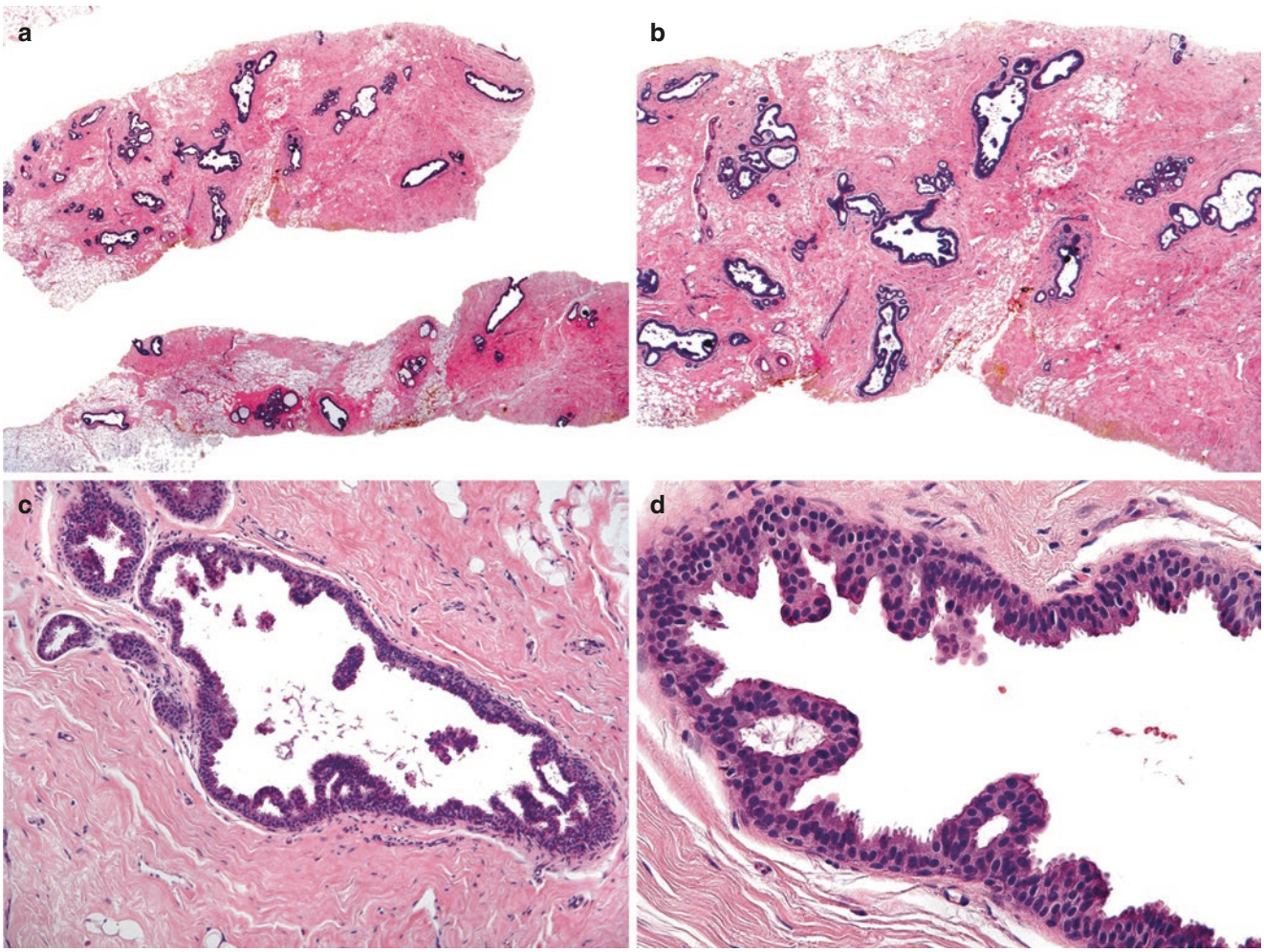

Fig. 9.36 (**a**–**d**) This core needle biopsy contains scattered ducts involved by a cytologically monotonous process that is forming early bridges and arches in portions of these ducts. Despite multiple ducts being involved, the development of the architectural forms is not considered sufficient for a diagnosis of low-grade DCIS (no definite club-shaped micropapillae, etc.). These findings are most consistent with a diagnosis of atypical ductal hyperplasia on core biopsy

In cases such as these, it can be helpful to clinicians to describe the truly minimal extent of the ADH present in the core biopsy sampling, since these very focal, not-suspicious lesions are less likely to upgrade on excision and it may not be mandatory to perform excisional biopsies in all such patients [68, 69].

Immunohistochemistry

There is no clinically indicated reason to apply ER staining to ADH. In contrast to DCIS, which has a spectrum of ER expression in lesions of different nuclear grade, ADH should be uniformly ER positive. Although the majority of women with ADH only do not receive hormone-targeted therapies for risk reduction, this therapy has been shown to reduce their long-term risk of invasive cancer.

As mentioned in the section "Differential Diagnosis," staining for basal cytokeratins CK5/6 can aid in the differential between UDH and ADH. There are additional antibody cocktail stains, such as the ADH-5 stain, which contains a combination of low and high molecular weight cytokeratins including CK5, 7, 14, 18, and p63. Some studies suggest that interobserver reproducibility can be improved when these stains are performed routinely [70].

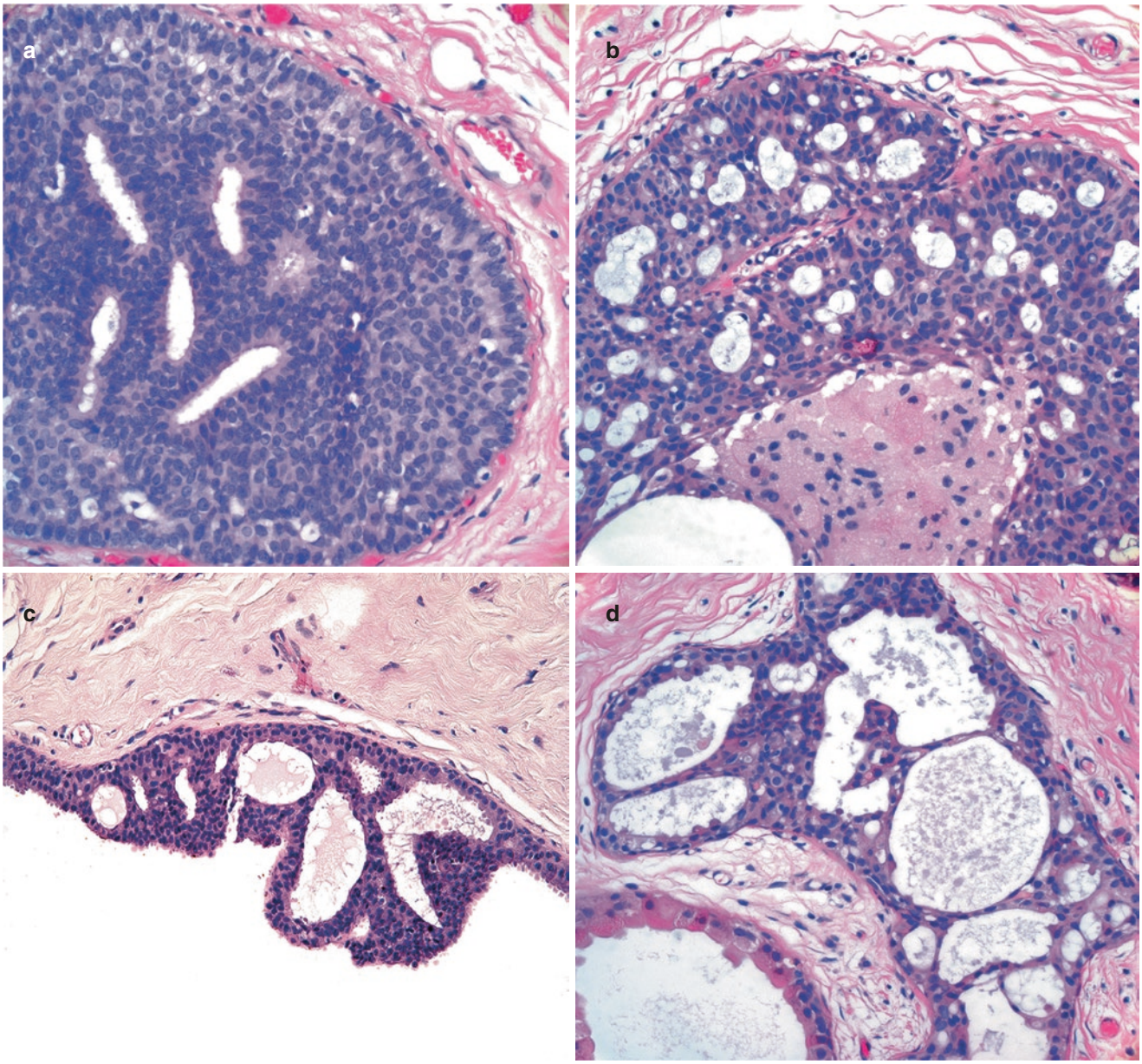

Fig. 9.37 (**a**) ADH with cytologic monotony and formation of early lumens that are slit-like but are polarized. (**b**) UDH can have more rounded spaces but they are not polarized and the cell population has a jumbled, polyclonal appearance. (**c**) ADH forming rigid arches that contain monotonous cells that have minimal overlap. (**d**) UDH with tapered, thin bridges containing cells with compressed nuclei. (**e**) ADH with partial involvement of a duct by elongated micropapillae containing monotonous cells with uniform nuclei. (**f**) UDH/columnar cell hyperplasia with formation of small micropapillae that contain jumbled nuclei which are smaller in size than those in the surrounding duct

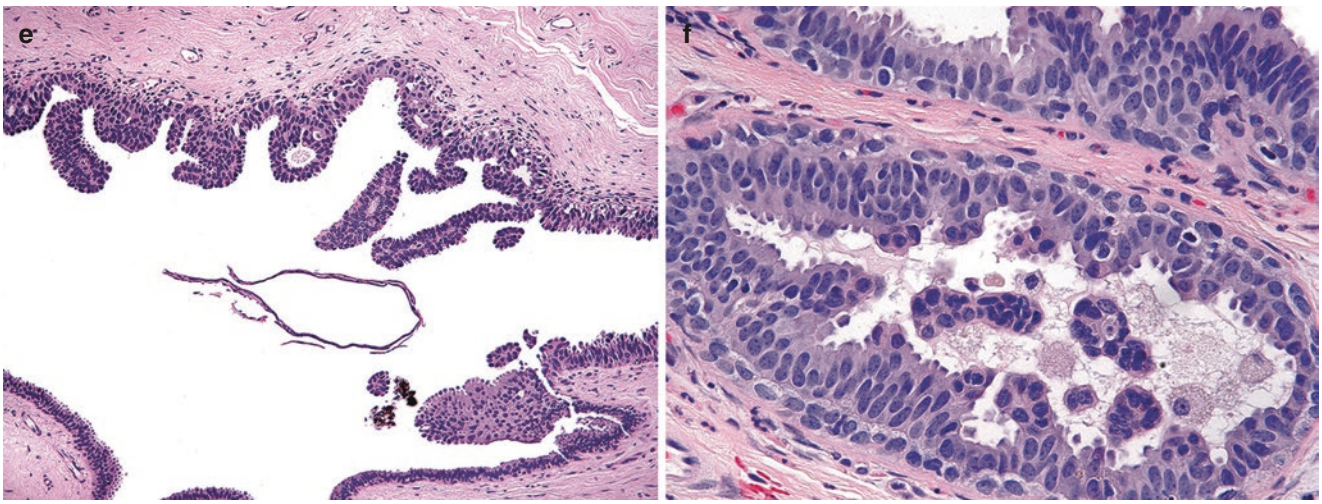

Fig. 9.37 (continued)

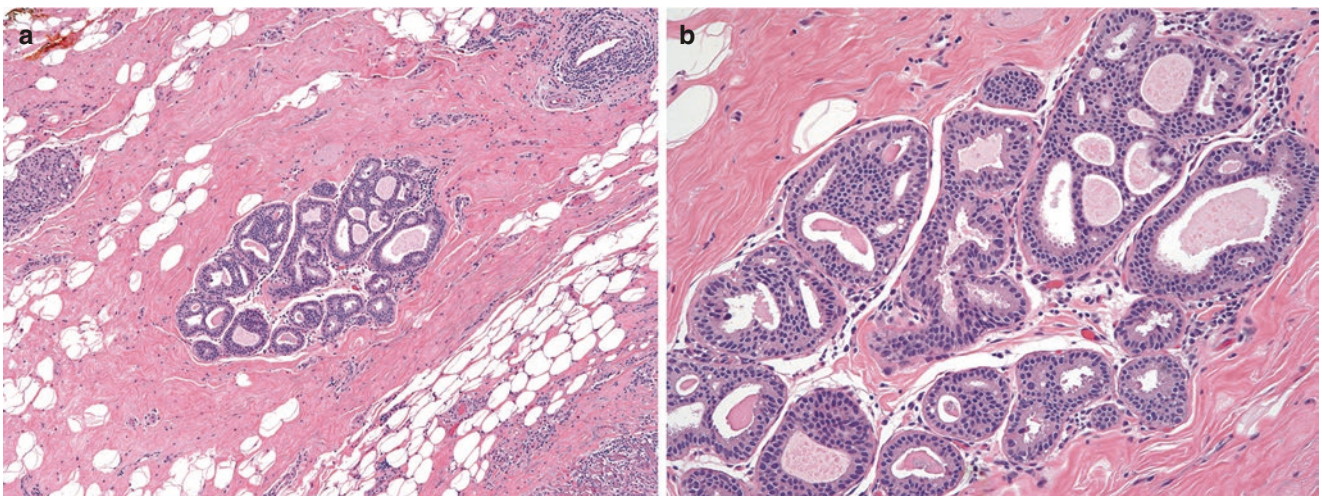

Fig. 9.38 (**a**, **b**) A core biopsy with a single focus <1 mm of an intraductal proliferation with enough cytologic monotony and early architectural changes to consider a diagnosis of minimal ADH

Pathogenesis

It is crucial to understand that there are differences between what a lesion is considered from a biologic standpoint and how it is managed clinically. Risk lesions such as ADH were initially defined and classified based on results of long-term follow-up after excisional biopsy without the benefit of molecular data. If the increased risk of developing invasive cancer over time was bilateral, it was considered a risk lesion, and if it was unilateral, it was considered a precursor lesion. Today, we know much more about the biology of these lesions and understand that some risk lesions, such as ADH, can be neoplastic and non-obligate precursors to invasion. Studies of loss of heterozygosity (LOH) in low-grade DCIS and ADH have shown similar genetic lesions, providing evidence that these are clonal processes and both therefore fulfill the basic concept of neoplasia [71]. The bilateral risk associated with risk lesions is likely a result of a tendency for the lesion to be distributed in a patchy, scattered, and bilateral pattern as can occur with ADH.

The current model of the pathogenesis of breast cancer places many of the high-risk lesions, including ADH, in the low-grade pathway to "luminal"/estrogen receptor-positive invasive disease [37]. ADH is thought to be a very early neoplastic step in the pathway to low-intermediate grade DCIS and estrogen receptor-positive, low-grade invasive ductal

carcinomas [36]. Allelic imbalances are seen with similar frequencies in ADH and low-grade DCIS and there are similar recurrent regions with LOH including loci on 1q, 16q, and 17p [40, 71, 72].

Outcomes

The identification of ADH as the clinically most significant lesion on a core needle biopsy will prompt most practices to offer a trip to the operating room for an excisional biopsy to rule out unsampled DCIS or invasive carcinoma. This is due to the upgrade rates for ADH on core biopsy, which range widely by study but in general are between 10% and 20% [60, 73–97].

Multiple studies have looked at ways to identify subgroups of ADH on core biopsy that are not at risk of upgrade and can avoid surgical excision. Lower upgrade rates can be achieved if cases are segregated by "low-risk features" such as complete removal of the targeted calcifications by core biopsy, very focal ADH without cytologic suspicion for an intermediate grade process, and no family or personal history of breast cancer. But even using these risk stratification strategies, it is challenging to find a reproducible set of criteria that will give a risk of upgrade that is <3%.

However, in the few available prospective studies that have used criteria to avoid excision in some patients with ADH on core biopsy, there have been minimal events although follow-up was limited [98]. This suggests that upgrade rates may not be the best measure of outcome. The majority of these lesions will not invade and if they do it will be a favorable biology-invasive disease over many years. In fact, some studies looking at SEER data on excised versus not excised low-grade DCIS suggest that there is no overall survival benefit for surgical excision [46]. Because of this, most authorities agree that performing bilateral mastectomies would be overtreatment for ADH even though their risk for developing invasive disease is bilateral (although more recent studies suggest there is an increased ipsilateral risk) [99]. Some authorities argue that the increased risk of cancer should be managed medically with hormonal therapies [65]. However, most opt for high-risk screening protocols in these patients as the only risk prevention intervention.

Usual Ductal Hyperplasia

Overview

UDH is a benign proliferative lesion that can range from mild to florid. On a core needle biopsy, its presence can distract from other areas and raise concern for atypical processes. It carries a mildly increased risk of future development of breast cancer, estimated to be 1.5–2.0× [100].

Gross and Radiologic Features

UDH has no distinguishing gross or radiologic features. It can be found as an incidental background finding in core biopsies, or can be associated with the imaging abnormality of interest. Dense breasts more often have proliferative changes such as UDH on biopsy. UDH is most commonly identified in core biopsies performed for calcifications on mammography (often incidentally but sometimes also associated with calcifications) but can also be seen in biopsies for MRI enhancement or associated with mass lesions. Because UDH can involve lesions like radial scars, it can also present as an architectural distortion. Biopsies performed for a mass that contain UDH frequently contain papillary lesions, sclerosing adenosis, or fibroadenomas that explain the presence of a mass on imaging.

Microscopic Features

UDH is characterized by a polyclonal proliferation of cells that have indistinct cell borders, creating a "syncytial" appearance that is often streaming or windswept in appearance. The nuclei have bland chromatin patterns and vary in shape and size, consistent with a polyclonal process. When spaces are formed within the proliferation, they are typically peripherally located within the duct and slit-like, without polarization of cells around these spaces (Fig. 9.39a–d). The compact form of hyperplasia has very dense collections of nuclei in the center of the duct, often with a spindled appearance. Micropapillary hyperplasia is characterized by tufts of columnar-type epithelium forming "pinched" or pyramid-shaped structures with smaller, crowded nuclei present toward the lumen aspect than the basal aspect (see Fig. 9.37f).

UDH that is more florid often contains collections of histiocytes and can rarely be so florid that there are areas of necrosis present (Fig. 9.40a–d). There are no well-defined criteria to distinguish florid from moderate to mild UDH. Florid UDH involving a papillary lesion, sclerosing lesions, or radial scar can complicate diagnosis. Myoepithelial stains in conjunction with CK5/6 staining can help clarify these processes as UDH involving these lesions. Mitotic figures can be present in usual ductal hyperplasia, but atypical mitotic figures should warrant consideration of DCIS.

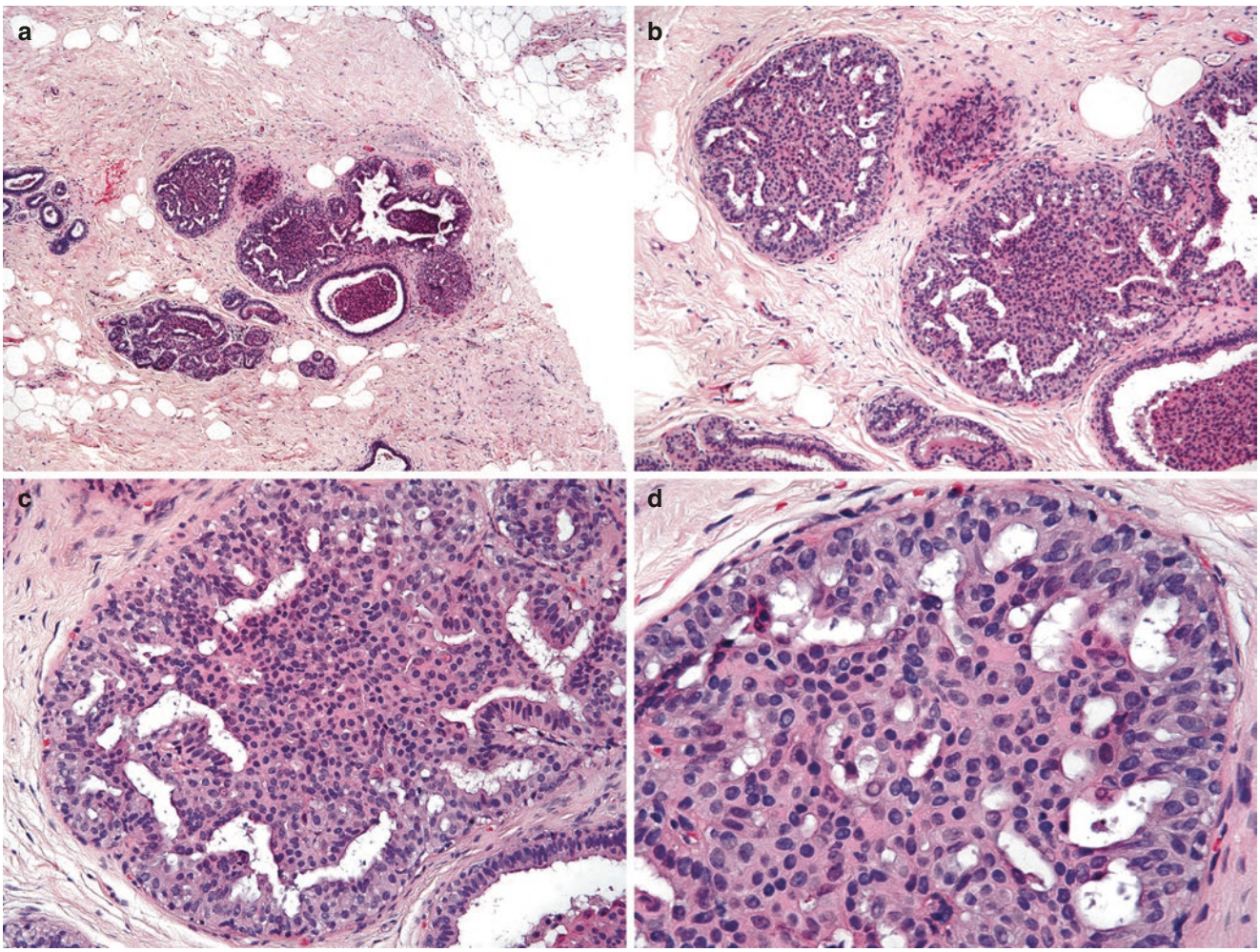

Fig. 9.39 (**a**–**d**) A core biopsy with an intraductal proliferation without cytologic monotony (cells are non-uniform, overlapping and of different sizes and shapes) and peripheral split-like spaces that are non-polarized. These features are diagnostic of usual ductal hyperplasia

Differential Diagnosis

The differential diagnosis of UDH has been discussed in sections on DCIS and ADH. Florid UDH with a compact pattern can mimic spindled DCIS (see section on "Differential Diagnosis" of spindled DCIS versus UDH above). UDH and ADH can also be in the differential diagnosis of cases containing proliferations with features that overlap between these diagnoses (see section on "Differential Diagnosis" of ADH versus UDH above).

Immunohistochemistry

There are no clinically relevant antibody stains to perform when a diagnosis of UDH is rendered. As discussed in the section "Differential Diagnosis," CK5/6 staining patterns in UDH are mixed or "mosaic" since UDH contains cells with both luminal and basal-type cytokeratins admixed (Fig. 9.41a, b). Estrogen receptor expression also tends to be similar but inverse in pattern, with the luminal-type epithelial cells staining more often than the admixed basal-type cells (Fig. 9.41c, d).

Pathogenesis

UDH is a benign, proliferative intraductal process. The frequency of LOH in cases of usual hyperplasia is low and typically at random sites, suggesting that in contrast to ADH and DCIS, it is non-neoplastic [71, 101]. Therefore, while it is difficult to find genetic distinctions between low-grade DCIS and ADH, the border between ADH and UDH is better defined from the standpoint of molecular alterations [102].

The formation of UDH and other proliferative lesions may be related to hormonally regulated changes, since it is more frequently found in younger patients with dense breasts and during the menstrual cycle. There is some debate about whether UDH is a step in the pathway to ADH and low-grade

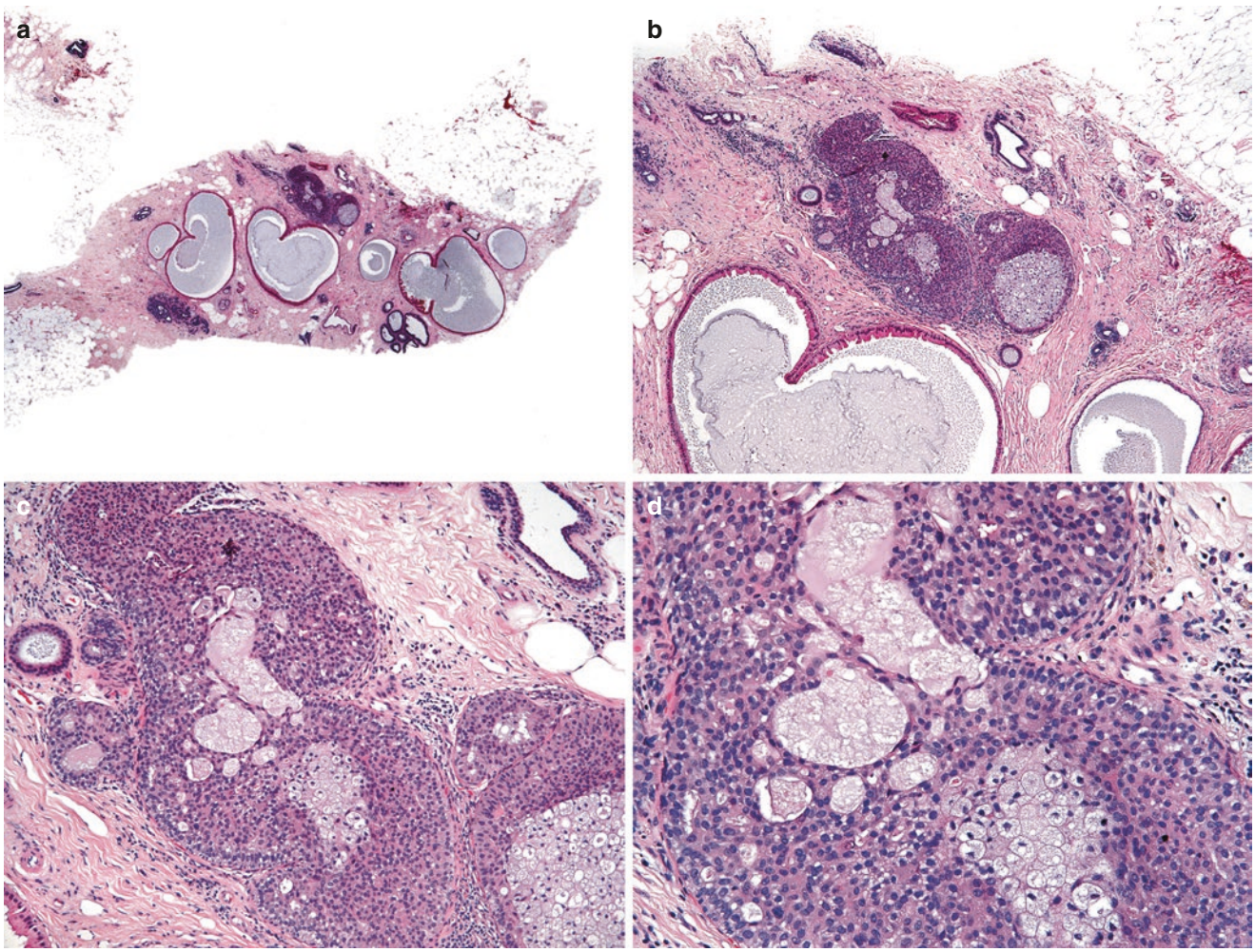

Fig. 9.40 (**a**–**d**) This core biopsy contains cysts as well as an intraductal proliferation that is filling some duct spaces. This proliferation contains polyclonal appearing cells with overlapping nuclei. There are collections of histiocytes and acellular secretions in the center of the proliferation. These features are most consistent with a diagnosis of usual ductal hyperplasia on core biopsy. If a diagnosis of forms of ADH or DCIS are being considered, a CK5/6 and ER stain can be helpful

carcinomas since UDH that shows higher levels of estrogen expression, higher Ki-67 proliferative rates, and is more frequently associated with patients who developed breast cancers [103–106].

Outcomes

UDH is not considered a lesion with a significant risk of upgrade to DCIS or invasive carcinoma on excision, so in general a diagnosis of UDH on a core biopsy has minimal impact. It can be important to describe the degree of the proliferative changes present on core biopsies with non-atypical proliferations like UDH such that appropriate radiologic–pathologic correlation can occur.

Although women with florid UDH are slightly more likely to develop invasive breast cancer in either breast and more frequently have other associated proliferative lesions of the breast, there are currently no medical management implications from this diagnosis.

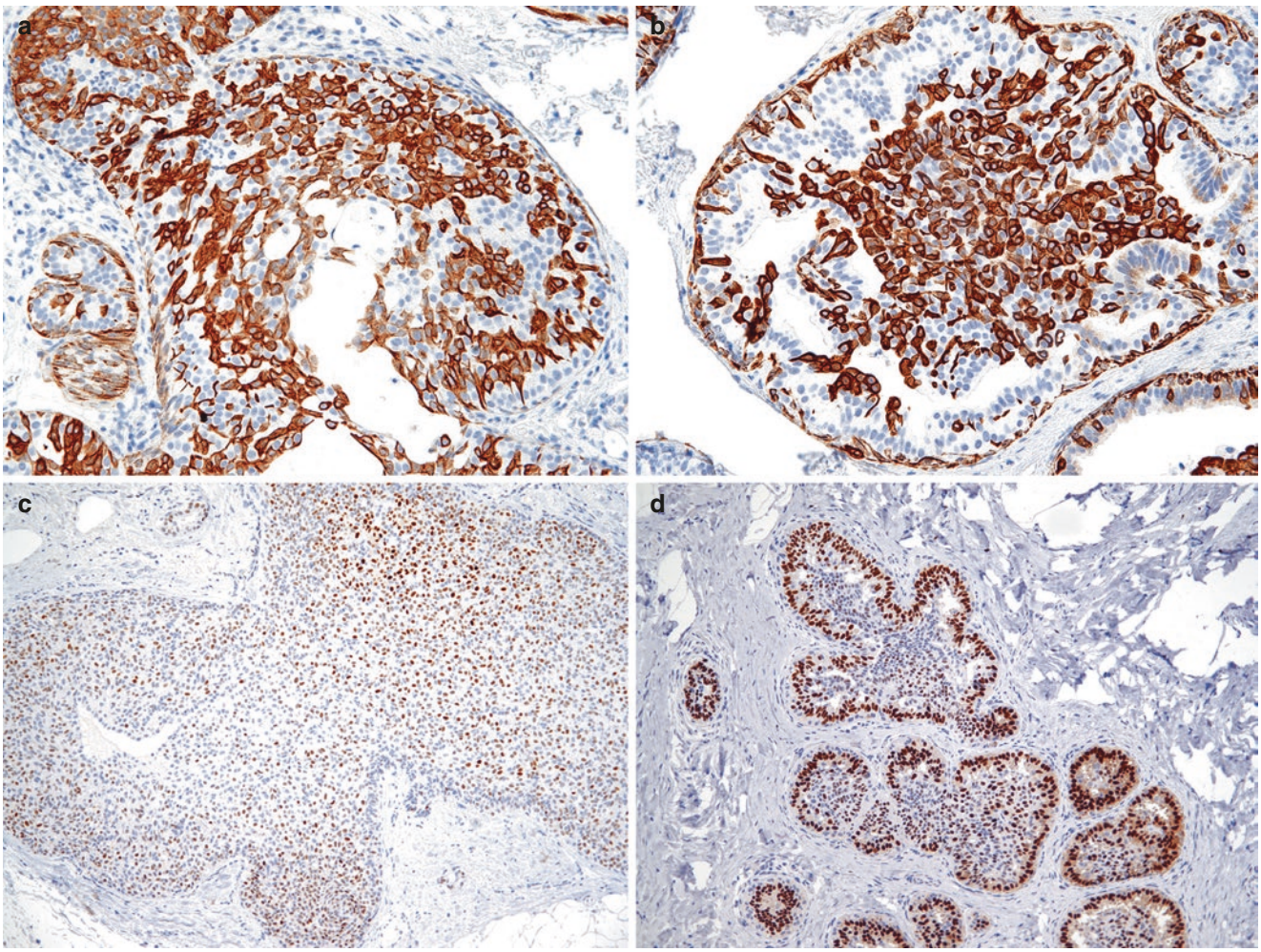

Fig. 9.41 (**a**, **b**) CK5/6 "mosaic" staining pattern seen in usual ductal hyperplasia (in contrast to the absent staining seen in low-grade DCIS/ADH). (**c**, **d**) Variable patterns of ER expression are seen in UDH (in contrast to the uniform strong expression expected throughout low-grade DCIS or ADH)

References

1. Elmore JG, Longton GM, Carney PA, et al. Diagnostic concordance among pathologists interpreting breast biopsy specimens. JAMA. 2015;313(11):1122–32.
2. Allison KH, Reisch LM, Carney PA, et al. Understanding diagnostic variability in breast pathology: lessons learned from an expert consensus review panel. Histopathology. 2014;65(2):240–51.
3. Tavassoli FA, Norris HJ. A comparison of the results of long-term follow-up for atypical intraductal hyperplasia and intraductal hyperplasia of the breast. Cancer. 1990;65(3):518–29.
4. Betsill WL Jr, Rosen PP, Lieberman PH, Robbins GF. Intraductal carcinoma. Long-term follow-up after treatment by biopsy alone. JAMA. 1978;239(18):1863–7.
5. Collins LC, Tamimi RM, Baer HJ, Connolly JL, Colditz GA, Schnitt SJ. Outcome of patients with ductal carcinoma in situ untreated after diagnostic biopsy: results from the Nurses' Health Study. Cancer. 2005;103(9):1778–84.
6. Page DL, Dupont WD, Rogers LW, Jensen RA, Schuyler PA. Continued local recurrence of carcinoma 15-25 years after a diagnosis of low grade ductal carcinoma in situ of the breast treated only by biopsy. Cancer. 1995;76(7):1197–200.
7. Sanders ME, Schuyler PA, Dupont WD, Page DL. The natural history of low-grade ductal carcinoma in situ of the breast in women treated by biopsy only revealed over 30 years of long-term follow-up. Cancer. 2005;103(12):2481–4.
8. Page DL, Dupont WD, Rogers LW, Landenberger M. Intraductal carcinoma of the breast: follow-up after biopsy only. Cancer. 1982;49(4):751–8.
9. Allison KH, Abraham LA, Weaver DL, et al. Trends in breast biopsy pathology diagnoses among women undergoing mammography in the United States: a report from the Breast Cancer Surveillance Consortium. Cancer. 2015;121(9):1369–78.
10. Kerlikowske K. Epidemiology of ductal carcinoma in situ. J Natl Cancer Inst Monogr. 2010;2010(41):139–41.
11. Sorum R, Hofvind S, Skaane P, Haldorsen T. Trends in incidence of ductal carcinoma in situ: the effect of a population-based screening programme. Breast. 2010;19(6):499–505.
12. Sacchini V, Fortunato L, Cody Iii HS, Van Zee KJ, Cutuli B, Bonanni B. Breast ductal carcinoma in situ. Int J Surg Oncol. 2012;2012:753267.
13. Virnig BA, Tuttle TM, Shamliyan T, Kane RL. Ductal carcinoma in situ of the breast: a systematic review of incidence, treatment, and outcomes. J Natl Cancer Inst. 2010;102(3):170–8.

14. Hofvind S, Sorum R, Thoresen S. Incidence and tumor characteristics of breast cancer diagnosed before and after implementation of a population-based screening-program. Acta Oncol. 2008;47(2):225–31.
15. Ernster VL, Ballard-Barbash R, Barlow WE, et al. Detection of ductal carcinoma in situ in women undergoing screening mammography. J Natl Cancer Inst. 2002;94(20):1546–54.
16. Evans DG, Kesavan N, Lim Y, et al. MRI breast screening in high-risk women: cancer detection and survival analysis. Breast Cancer Res Treat. 2014;145(3):663–72.
17. Lester SC, Bose S, Chen YY, et al. Protocol for the examination of specimens from patients with ductal carcinoma in situ of the breast. Arch Pathol Lab Med. 2009;133(1):15–25.
18. Stomper PC, Margolin FR. Ductal carcinoma in situ: the mammographer's perspective. AJR Am J Roentgenol. 1994;162(3):585–91.
19. Lehman CD. Magnetic resonance imaging in the evaluation of ductal carcinoma in situ. J Natl Cancer Inst Monogr. 2010;2010(41):150–1.
20. Kuhl CK, Schrading S, Bieling HB, et al. MRI for diagnosis of pure ductal carcinoma in situ: a prospective observational study. Lancet. 2007;370(9586):485–92.
21. Riedl CC, Luft N, Bernhart C, et al. Triple-modality screening trial for familial breast cancer underlines the importance of magnetic resonance imaging and questions the role of mammography and ultrasound regardless of patient mutation status, age, and breast density. J Clin Oncol. 2015;33(10):1128–35.
22. Borgquist S, Zhou W, Jirstrom K, et al. The prognostic role of HER2 expression in ductal breast carcinoma in situ (DCIS); a population-based cohort study. BMC Cancer. 2015;15:468.
23. Gradishar WJ, Anderson BO, Balassanian R, et al. Breast cancer version 2.2015. J Natl Compr Cancer Netw. 2015;13(4):448–75.
24. Shin SJ, Rosen PP. Pregnancy-like (pseudolactational) hyperplasia: a primary diagnosis in mammographically detected lesions of the breast and its relationship to cystic hypersecretory hyperplasia. Am J Surg Pathol. 2000;24(12):1670–4.
25. Bur ME, Zimarowski MJ, Schnitt SJ, Baker S, Lew R. Estrogen receptor immunohistochemistry in carcinoma in situ of the breast. Cancer. 1992;69(5):1174–81.
26. Allred DC, Anderson SJ, Paik S, et al. Adjuvant tamoxifen reduces subsequent breast cancer in women with estrogen receptor-positive ductal carcinoma in situ: a study based on NSABP protocol B-24. J Clin Oncol. 2012;30(12):1268–73.
27. Hammond ME, Hayes DF, Dowsett M, et al. American Society of Clinical Oncology/College Of American Pathologists guideline recommendations for immunohistochemical testing of estrogen and progesterone receptors in breast cancer. J Clin Oncol. 2010;28(16):2784–95.
28. Ho GH, Calvano JE, Bisogna M, et al. In microdissected ductal carcinoma in situ, HER-2/neu amplification, but not p53 mutation, is associated with high nuclear grade and comedo histology. Cancer. 2000;89(11):2153–60.
29. van de Vijver MJ, Peterse JL, Mooi WJ, et al. Neu-protein overexpression in breast cancer. Association with comedo-type ductal carcinoma in situ and limited prognostic value in stage II breast cancer. N Engl J Med. 1988;319(19):1239–45.
30. Collins LC, Schnitt SJ. HER2 protein overexpression in estrogen receptor-positive ductal carcinoma in situ of the breast: frequency and implications for tamoxifen therapy. Mod Pathol. 2005;18(5):615–20.
31. Sek P, Zawrocki A, Biernat W, Piekarski JH. HER2 molecular subtype is a dominant subtype of mammary Paget's cells. An immunohistochemical study. Histopathology. 2010;57(4):564–71.
32. Tot T. Early (<10 mm) HER2-positive invasive breast carcinomas are associated with extensive diffuse high-grade DCIS: implications for preoperative mapping, extent of surgical intervention, and disease-free survival. Ann Surg Oncol. 2015;22(8):2532–9.
33. Williams KE, Barnes NL, Cramer A, et al. Molecular phenotypes of DCIS predict overall and invasive recurrence. Ann Oncol. 2015;26(5):1019–25.
34. Bryan BB, Schnitt SJ, Collins LC. Ductal carcinoma in situ with basal-like phenotype: a possible precursor to invasive basal-like breast cancer. Mod Pathol. 2006;19(5):617–21.
35. Dabbs DJ, Chivukula M, Carter G, Bhargava R. Basal phenotype of ductal carcinoma in situ: recognition and immunohistologic profile. Mod Pathol. 2006;19(11):1506–11.
36. Lopez-Garcia MA, Geyer FC, Lacroix-Triki M, Marchio C, Reis-Filho JS. Breast cancer precursors revisited: molecular features and progression pathways. Histopathology. 2010;57(2):171–92.
37. Abdel-Fatah TM, Powe DG, Hodi Z, Reis-Filho JS, Lee AH, Ellis IO. Morphologic and molecular evolutionary pathways of low nuclear grade invasive breast cancers and their putative precursor lesions: further evidence to support the concept of low nuclear grade breast neoplasia family. Am J Surg Pathol. 2008;32(4):513–23.
38. Abdel-Fatah TM, Powe DG, Hodi Z, Lee AH, Reis-Filho JS, Ellis IO. High frequency of coexistence of columnar cell lesions, lobular neoplasia, and low grade ductal carcinoma in situ with invasive tubular carcinoma and invasive lobular carcinoma. Am J Surg Pathol. 2007;31(3):417–26.
39. Stratton MR, Collins N, Lakhani SR, Sloane JP. Loss of heterozygosity in ductal carcinoma in situ of the breast. J Pathol. 1995;175(2):195–201.
40. Buerger H, Otterbach F, Simon R, et al. Comparative genomic hybridization of ductal carcinoma in situ of the breast-evidence of multiple genetic pathways. J Pathol. 1999;187(4):396–402.
41. Gao Y, Niu Y, Wang X, Wei L, Lu S. Genetic changes at specific stages of breast cancer progression detected by comparative genomic hybridization. J Mol Med (Berl). 2009;87(2):145–52.
42. Reis-Filho JS, Simpson PT, Gale T, Lakhani SR. The molecular genetics of breast cancer: the contribution of comparative genomic hybridization. Pathol Res Pract. 2005;201(11):713–25.
43. Simpson PT, Reis-Filho JS, Gale T, Lakhani SR. Molecular evolution of breast cancer. J Pathol. 2005;205(2):248–54.
44. Natrajan R, Lambros MB, Geyer FC, et al. Loss of 16q in high grade breast cancer is associated with estrogen receptor status: evidence for progression in tumors with a luminal phenotype? Genes Chromosomes Cancer. 2009;48(4):351–65.
45. Hernandez L, Wilkerson PM, Lambros MB, et al. Genomic and mutational profiling of ductal carcinomas in situ and matched adjacent invasive breast cancers reveals intra-tumour genetic heterogeneity and clonal selection. J Pathol. 2012;227(1):42–52.
46. Sagara Y, Mallory MA, Wong S, et al. Survival benefit of breast surgery for low-grade ductal carcinoma in situ: a population-based cohort study. JAMA Surg. 2015;150(8):739–45.
47. EORTC Breast Cancer Cooperative Group, EORTC Radiotherapy Group, Bijker N, et al. Breast-conserving treatment with or without radiotherapy in ductal carcinoma-in-situ: ten-year results of European Organisation for Research and Treatment of Cancer randomized phase III trial 10853—a study by the EORTC Breast Cancer Cooperative Group and EORTC Radiotherapy Group. J Clin Oncol. 2006;24(21):3381–7.
48. Fisher ER, Dignam J, Tan-Chiu E, et al. Pathologic findings from the National Surgical Adjuvant Breast Project (NSABP) eight-year update of protocol B-17: intraductal carcinoma. Cancer. 1999;86(3):429–38.
49. Hughes LL, Wang M, Page DL, et al. Local excision alone without irradiation for ductal carcinoma in situ of the breast: a trial of the Eastern Cooperative Oncology Group. J Clin Oncol. 2009;27(32):5319–24.
50. Welch HG, Black WC. Overdiagnosis in cancer. J Natl Cancer Inst. 2010;102(9):605–13.

51. Esserman LJ, Thompson IM, Reid B, et al. Addressing overdiagnosis and overtreatment in cancer: a prescription for change. Lancet Oncol. 2014;15(6):e234–42.
52. Sue GR, Chagpar AB. Predictors of recurrence in patients diagnosed with ductal carcinoma in situ. Am Surg. 2015;81(1):48–51.
53. Benson JR, Wishart GC. Predictors of recurrence for ductal carcinoma in situ after breast-conserving surgery. Lancet Oncol. 2013;14(9):e348–57.
54. Wapnir IL, Dignam JJ, Fisher B, et al. Long-term outcomes of invasive ipsilateral breast tumor recurrences after lumpectomy in NSABP B-17 and B-24 randomized clinical trials for DCIS. J Natl Cancer Inst. 2011;103(6):478–88.
55. Wang SY, Shamliyan T, Virnig BA, Kane R. Tumor characteristics as predictors of local recurrence after treatment of ductal carcinoma in situ: a meta-analysis. Breast Cancer Res Treat. 2011;127(1):1–14.
56. Di Saverio S, Catena F, Santini D, et al. 259 patients with DCIS of the breast applying USC/Van Nuys prognostic index: a retrospective review with long term follow up. Breast Cancer Res Treat. 2008;109(3):405–16.
57. Silverstein MJ, Lagios MD, Craig PH, et al. A prognostic index for ductal carcinoma in situ of the breast. Cancer. 1996;77(11):2267–74.
58. Solin LJ, Gray R, Baehner FL, et al. A multigene expression assay to predict local recurrence risk for ductal carcinoma in situ of the breast. J Natl Cancer Inst. 2013;105(10):701–10.
59. Wood WC, Alvarado M, Buchholz DJ, et al. The current clinical value of the DCIS Score. Oncology (Williston Park). 2014;28(Suppl 2):C2, 1–8, C3.
60. Jackman RJ, Birdwell RL, Ikeda DM. Atypical ductal hyperplasia: can some lesions be defined as probably benign after stereotactic 11-gauge vacuum-assisted biopsy, eliminating the recommendation for surgical excision? Radiology. 2002;224(2):548–54.
61. Maganini RO, Klem DA, Huston BJ, Bruner ES, Jacobs HK. Upgrade rate of core biopsy-determined atypical ductal hyperplasia by open excisional biopsy. Am J Surg. 2001;182(4):355–8.
62. Schnitt SJ, Connolly JL, Tavassoli FA, et al. Interobserver reproducibility in the diagnosis of ductal proliferative breast lesions using standardized criteria. Am J Surg Pathol. 1992;16(12):1133–43.
63. Fitzgibbons PL, Henson DE, Hutter RV. Benign breast changes and the risk for subsequent breast cancer: an update of the 1985 consensus statement. Cancer Committee of the College of American Pathologists. Arch Pathol Lab Med. 1998;122(12):1053–5.
64. Dupont WD, Page DL. Risk factors for breast cancer in women with proliferative breast disease. N Engl J Med. 1985;312(3):146–51.
65. Hartmann LC, Degnim AC, Santen RJ, Dupont WD, Ghosh K. Atypical hyperplasia of the breast—risk assessment and management options. N Engl J Med. 2015;372(1):78–89.
66. Page DL, Dupont WD, Rogers LW, Rados MS. Atypical hyperplastic lesions of the female breast. A long-term follow-up study. Cancer. 1985;55(11):2698–708.
67. Simpson J, Schnitt S, Visscher D, van der Vijver MJ, Ellis I. Atypical ductal hyperplasia. In: Lakhani S, Ellis IO, Schnitt SJ, Tan PH, van der Vijver MJ, editors. WHO classification of tumours of the breast. Lyon: IARC Press; 2012. p. 88–9.
68. Allison KH, Eby PR, Kohr J, DeMartini WB, Lehman CD. Atypical ductal hyperplasia on vacuum-assisted breast biopsy: suspicion for ductal carcinoma in situ can stratify patients at high risk for upgrade. Hum Pathol. 2011;42(1):41–50.
69. Eby PR, Ochsner JE, DeMartini WB, Allison KH, Peacock S, Lehman CD. Frequency and upgrade rates of atypical ductal hyperplasia diagnosed at stereotactic vacuum-assisted breast biopsy: 9-versus 11-gauge. AJR Am J Roentgenol. 2009;192(1):229–34.
70. Jain RK, Mehta R, Dimitrov R, et al. Atypical ductal hyperplasia: interobserver and intraobserver variability. Mod Pathol. 2011;24(7):917–23.
71. Lakhani SR, Collins N, Stratton MR, Sloane JP. Atypical ductal hyperplasia of the breast: clonal proliferation with loss of heterozygosity on chromosomes 16q and 17p. J Clin Pathol. 1995;48(7):611–5.
72. Larson PS, de las Morenas A, Cerda SR, Bennett SR, Cupples LA, Rosenberg CL. Quantitative analysis of allele imbalance supports atypical ductal hyperplasia lesions as direct breast cancer precursors. J Pathol. 2006;209(3):307–16.
73. Fuhrman GM, Cederbom GJ, Bolton JS, et al. Image-guided core-needle breast biopsy is an accurate technique to evaluate patients with nonpalpable imaging abnormalities. Ann Surg. 1998;227(6):932–9.
74. Jackman RJ, Nowels KW, Rodriguez-Soto J, Marzoni FA Jr, Finkelstein SI, Shepard MJ. Stereotactic, automated, large-core needle biopsy of nonpalpable breast lesions: false-negative and histologic underestimation rates after long-term follow-up. Radiology. 1999;210(3):799–805.
75. Jackman RJ, Nowels KW, Shepard MJ, Finkelstein SI, Marzoni FA Jr. Stereotaxic large-core needle biopsy of 450 nonpalpable breast lesions with surgical correlation in lesions with cancer or atypical hyperplasia. Radiology. 1994;193(1):91–5.
76. Berg WA, Krebs TL, Campassi C, Magder LS, Sun CC. Evaluation of 14- and 11-gauge directional, vacuum-assisted biopsy probes and 14-gauge biopsy guns in a breast parenchymal model. Radiology. 1997;205(1):203–8.
77. Brown TA, Wall JW, Christensen ED, et al. Atypical hyperplasia in the era of stereotactic core needle biopsy. J Surg Oncol. 1998;67(3):168–73.
78. Burak WE Jr, Owens KE, Tighe MB, et al. Vacuum-assisted stereotactic breast biopsy: histologic underestimation of malignant lesions. Arch Surg. 2000;135(6):700–3.
79. Burbank F. Stereotactic breast biopsy of atypical ductal hyperplasia and ductal carcinoma in situ lesions: improved accuracy with directional, vacuum-assisted biopsy. Radiology. 1997;202(3):843–7.
80. Cangiarella J, Waisman J, Symmans WF, et al. Mammotome core biopsy for mammary microcalcification: analysis of 160 biopsies from 142 women with surgical and radiologic followup. Cancer. 2001;91(1):173–7.
81. Darling ML, Smith DN, Lester SC, et al. Atypical ductal hyperplasia and ductal carcinoma in situ as revealed by large-core needle breast biopsy: results of surgical excision. AJR Am J Roentgenol. 2000;175(5):1341–6.
82. Doren E, Hulvat M, Norton J, et al. Predicting cancer on excision of atypical ductal hyperplasia. Am J Surg. 2008;195(3):358–61; discussion 61–2.
83. Elston CW, Sloane JP, Amendoeira I, et al. Causes of inconsistency in diagnosing and classifying intraductal proliferations of the breast. European Commission Working Group on Breast Screening Pathology. Eur J Cancer. 2000;36(14):1769–72.
84. Gadzala DE, Cederbom GJ, Bolton JS, et al. Appropriate management of atypical ductal hyperplasia diagnosed by stereotactic core needle breast biopsy. Ann Surg Oncol. 1997;4(4):283–6.
85. Houssami N, Ciatto S, Ellis I, Ambrogetti D. Underestimation of malignancy of breast core-needle biopsy: concepts and precise overall and category-specific estimates. Cancer. 2007;109(3):487–95.
86. Jacobs TW, Connolly JL, Schnitt SJ. Nonmalignant lesions in breast core needle biopsies: to excise or not to excise? Am J Surg Pathol. 2002;26(9):1095–110.

87. Liberman L, Cohen MA, Dershaw DD, Abramson AF, Hann LE, Rosen PP. Atypical ductal hyperplasia diagnosed at stereotaxic core biopsy of breast lesions: an indication for surgical biopsy. AJR Am J Roentgenol. 1995;164(5):1111–3.
88. Liberman L, Dershaw DD, Glassman JR, et al. Analysis of cancers not diagnosed at stereotactic core breast biopsy. Radiology. 1997;203(1):151–7.
89. Liberman L, Kaplan JB, Morris EA, Abramson AF, Menell JH, Dershaw DD. To excise or to sample the mammographic target: what is the goal of stereotactic 11-gauge vacuum-assisted breast biopsy? AJR Am J Roentgenol. 2002;179(3):679–83.
90. Lin PH, Clyde JC, Bates DM, Garcia JM, Matsumoto GH, Girvin GW. Accuracy of stereotactic core-needle breast biopsy in atypical ductal hyperplasia. Am J Surg. 1998;175(5):380–2.
91. Lourenco AP, Mainiero MB, Lazarus E, Giri D, Schepps B. Stereotactic breast biopsy: comparison of histologic underestimation rates with 11- and 9-gauge vacuum-assisted breast biopsy. AJR Am J Roentgenol. 2007;189(5):W275–9.
92. Meyer JE, Smith DN, Lester SC, et al. Large-core needle biopsy of nonpalpable breast lesions. JAMA. 1999;281(17):1638–41.
93. Moore MM, Hargett CW 3rd, Hanks JB, et al. Association of breast cancer with the finding of atypical ductal hyperplasia at core breast biopsy. Ann Surg. 1997;225(6):726–31; discussion 31–3.
94. Nguyen M, McCombs MM, Ghandehari S, et al. An update on core needle biopsy for radiologically detected breast lesions. Cancer. 1996;78(11):2340–5.
95. Philpotts LE, Lee CH, Horvath LJ, Lange RC, Carter D, Tocino I. Underestimation of breast cancer with II-gauge vacuum suction biopsy. AJR Am J Roentgenol. 2000;175(4):1047–50.
96. Renshaw AA, Cartagena N, Schenkman RH, Derhagopian RP, Gould EW. Atypical ductal hyperplasia in breast core needle biopsies. Correlation of size of the lesion, complete removal of the lesion, and the incidence of carcinoma in follow-up biopsies. Am J Clin Pathol. 2001;116(1):92–6.
97. Tocino I, Garcia BM, Carter D. Surgical biopsy findings in patients with atypical hyperplasia diagnosed by stereotaxic core needle biopsy. Ann Surg Oncol. 1996;3(5):483–8.
98. Caplain A, Drouet Y, Peyron M, et al. Management of patients diagnosed with atypical ductal hyperplasia by vacuum-assisted core biopsy: a prospective assessment of the guidelines used at our institution. Am J Surg. 2014;208(2):260–7.
99. Hartmann LC, Radisky DC, Frost MH, et al. Understanding the premalignant potential of atypical hyperplasia through its natural history: a longitudinal cohort study. Cancer Prev Res (Phila). 2014;7(2):211–7.
100. Page DL, Dupont WD. Benign breast disease: indicators of increased breast cancer risk. Cancer Detect Prev. 1992;16(2):93–7.
101. Reis-Filho JS, Lakhani SR. The diagnosis and management of pre-invasive breast disease: genetic alterations in pre-invasive lesions. Breast Cancer Res. 2003;5(6):313–9.
102. Ellis IO, Pinder SE, Lee AH, Elston CW. A critical appraisal of existing classification systems of epithelial hyperplasia and in situ neoplasia of the breast with proposals for future methods of categorization: where are we going? Semin Diagn Pathol. 1999;16(3):202–8.
103. Shaaban AM, Sloane JP, West CR, Foster CS. Breast cancer risk in usual ductal hyperplasia is defined by estrogen receptor-alpha and Ki-67 expression. Am J Pathol. 2002;160(2):597–604.
104. Boecker W, Buerger H, Schmitz K, et al. Ductal epithelial proliferations of the breast: a biological continuum? Comparative genomic hybridization and high-molecular-weight cytokeratin expression patterns. J Pathol. 2001;195(4):415–21.
105. Shoker BS, Jarvis C, Clarke RB, et al. Estrogen receptor-positive proliferating cells in the normal and precancerous breast. Am J Pathol. 1999;155(6):1811–5.
106. Shekhar MP, Nangia-Makker P, Wolman SR, Tait L, Heppner GH, Visscher DW. Direct action of estrogen on sequence of progression of human preneoplastic breast disease. Am J Pathol. 1998;152(5):1129–32.

10 Invasive Breast Carcinoma of No Special Type, Microinvasive Carcinoma, Tubular Carcinoma, and Cribriform Carcinoma

Helena Hwang, Karan Saluja, and Sunati Sahoo

Invasive Breast Carcinoma of No Special Type

Overview

Invasive breast carcinoma of no special type (IBC-NST) is the most common invasive breast carcinoma (IBC). It is a diagnosis of exclusion and considered a "wastebasket" category for tumors that cannot be classified as a special type. In 2012, the World Health Organization (WHO) recommended a change in terminology from invasive ductal carcinoma not otherwise specified (IDC-NOS) to IBC-NST [1]. Invasive breast carcinoma NST comprises 70–80% of all IBC based on Surveillance Epidemiology and End Results (SEER) data and several published series [1–4]. A few studies have reported a lower incidence rate of 47–53%, as these authors segregated tumors showing mixed morphology (invasive carcinoma, NST admixed with some special type IBC) from tumors showing only IBC-NST [5, 6]. In the United States, the median age at diagnosis is 63 with the majority of cases occurring in women in their 50s and 60s [7]. Men in general are at low risk of developing breast cancer, with IBC-NST being the most common type.

Gross and Radiologic Features

Clinically, invasive breast carcinoma NST most commonly presents as a palpable mass. Pain as well as nipple retraction or inversion, skin retraction, or nipple discharge may be present. Rarely, primary breast carcinoma can present in the axilla without any abnormality detected in the breast.

On imaging, breast carcinomas usually present as a mass with some variability in presentation. Broberg et al. described five different groups for invasive carcinomas based on mammographic findings: Group A—presence of spiculated mass with or without calcifications, Group B—increased attenuation or structural variation in the parenchyma such as density or architectural distortion with or without calcifications, Group C—presence of clusters of heterogeneous calcifications without an evident mass, Group D—circumscribed lesions with or without calcifications, and Group E—tumors with no visible abnormality on mammogram [8]. The majority of histologically confirmed IBC are stellate masses without calcifications; some tumors may present as stellate or circumscribed masses with calcifications or as calcifications only (Figs. 10.1 and 10.2). The sensitivity of mammography alone in detecting invasive cancer is highly variable, ranging from 45% to 90%, and depends on a number of factors including age, size of the tumor, breast density, presence of an implant, and prior surgical procedures [9]. One study reported the detection rate to be 50% for tumors less than 10 mm and 88% for tumors greater than 10 mm in diameter [10].

Ultrasonography is not routinely used for screening as it is time consuming and has low sensitivity for calcifications [11, 12]. The sensitivity of ultrasound for mass-forming breast carcinoma is 80–90% [9]. Ultrasound as an adjunct to mammography increases the sensitivity of breast cancer detection in older women and in patients with increased breast density. Ultrasound alone is the recommended first-line breast imaging modality only in young high-risk women (<40 years). Additionally, ultrasound is used routinely to evaluate any suspicious mass found on mammography and to evaluate the axillary lymph nodes.

On ultrasonography, invasive carcinoma commonly presents as an irregular hypoechoic mass with ill-defined margins, sometimes accompanied by spiculation, posterior

H. Hwang · S. Sahoo (✉)
Department of Pathology, UT Southwestern Medical Center, Dallas, TX, USA
e-mail: helena.hwang@utsouthwestern.edu; sunati.sahoo@utsouthwestern.edu

K. Saluja
Department of Pathology, UT Health Science Center at Houston, Houston, TX, USA
e-mail: karan.saluja@uth.tmc.edu

© The Author(s), under exclusive license to Springer Nature Switzerland AG 2022
S. J. Shin et al. (eds.), *A Comprehensive Guide to Core Needle Biopsies of the Breast*,
https://doi.org/10.1007/978-3-031-05532-4_10

shadowing, or microlobulation [13] (Fig. 10.3). Other findings that are worrisome for malignancy include "taller than wide" mass as compared to "wider than tall" nodules that tend to be benign. Tall nodules suggest neoplastic growth across the normal tissue plane as the patient is scanned in a supine position [14], whereas benign lesions, such as fibroadenomas, grow along the normal tissue plane resulting in a wide mass [15].

Magnetic resonance imaging (MRI) has been shown to be highly sensitive, but mammography and ultrasound are still the principal imaging modalities to detect breast cancer. Recommendations for annual MRI screening along with mammography are limited to women with a high lifetime risk of breast cancer (20–25% or greater). These include carriers of *BRCA1* or *BRCA2* gene mutations, first-degree relatives with *BRCA1* or *BRCA2* gene mutations, patients who had radiation therapy to the chest between the ages of 10 and 30, and patients with either Li-Fraumeni or Cowden syndrome or who have first-degree relatives with these syndromes [16].

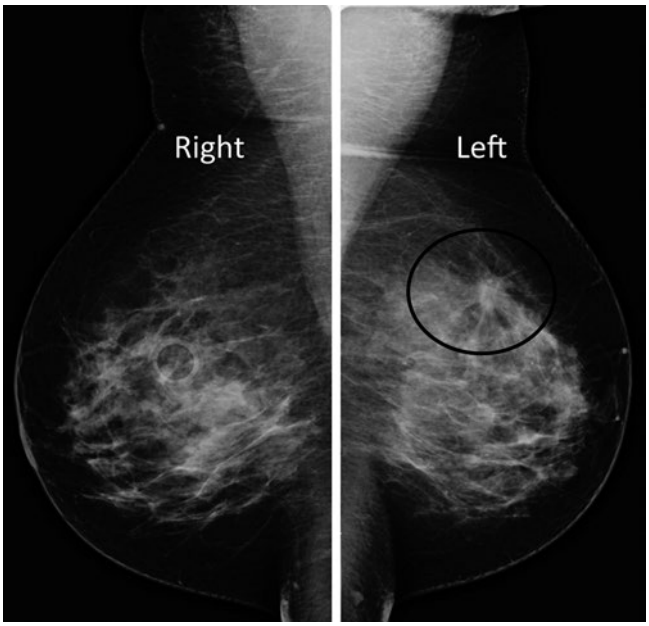

Fig. 10.1 Invasive breast carcinoma NST. Mammography demonstrates a 1.8 cm spiculated mass with associated architectural distortion in the middle depth of the left breast. (Courtesy of Stephen Seiler. Used with permission)

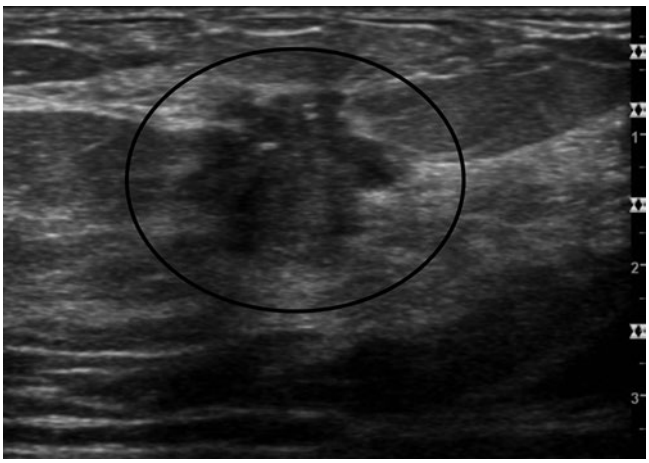

Fig. 10.3 Invasive breast carcinoma NST. Ultrasound shows an irregular hypoechoic mass with indistinct and angular margins (*circled*). (Courtesy of Stephen Seiler. Used with permission)

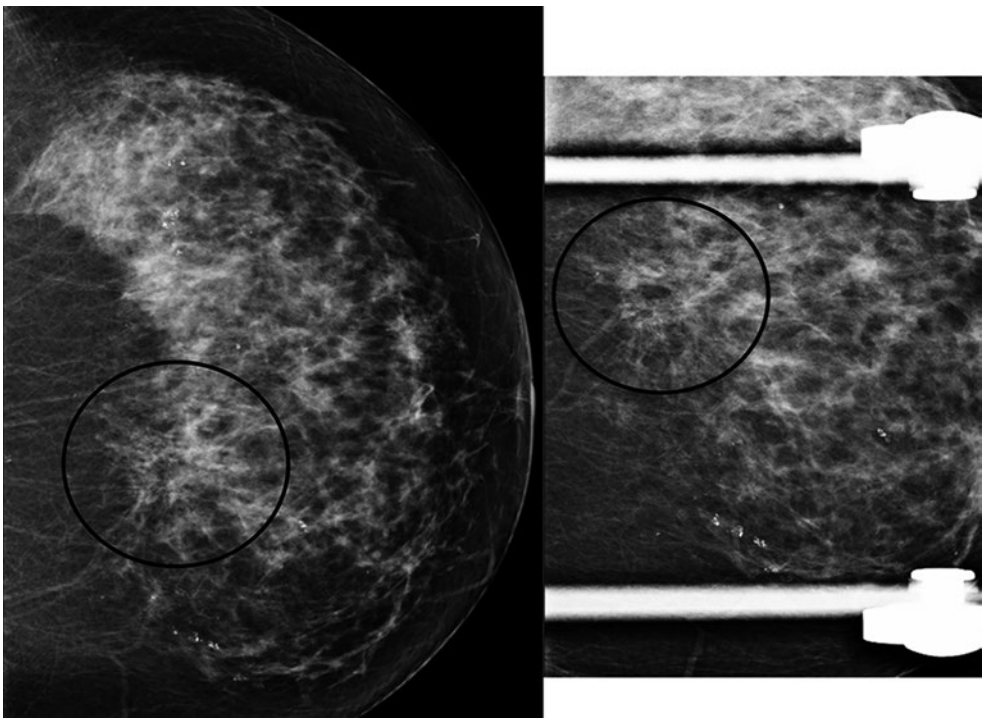

Fig. 10.2 Invasive breast carcinoma NST. Mammography demonstrates subtle architectural distortion in the middle to posterior depth of the medial left breast. This distortion persists on subsequent spot compression imaging (*circled*). (Courtesy of Stephen Seiler. Used with permission)

MRI is also commonly used to determine the extent of disease and detect additional tumors in newly diagnosed breast cancer patients. The tumor size obtained from MRI corresponds more closely to pathologic tumor size than measurements by mammography, ultrasound, or clinical assessment [9]. MRI has also proven to be the most accurate method for assessing treatment response and measuring residual tumor in patients who undergo neoadjuvant chemotherapy [17]. Although MRI is highly sensitive, the specificity for detecting carcinoma is low [18, 19]. Some of the benign lesions that can present as an enhancing lesion on MRI include inflammatory lesions and benign lesions such as fibroadenoma, sclerosing adenosis, intraductal papilloma, and apocrine metaplasia [18, 19].

On MRI, image morphology and contrast enhancement kinetics are used to determine how suspicious a lesion is. Lesions that are irregular and enhance rapidly on injection of the MR contrast agent Gadolinium, sometimes with ring enhancement, tend to be malignant, due to increased vascularity in malignant lesions. In contrast, benign lesions generally show slow and less avid enhancement. Lesions that show rapid contrast enhancement followed by rapid washout are highly predictive of malignancy (Fig. 10.4). Similarly, lesions that do not show any enhancement have a high negative predictive value for a malignant process. Schnall et al. reported a negative predictive value of 94% for invasive carcinoma and 88% for any malignant process. Of the non-enhancing lesions, 16% turned out to be ductal carcinoma in situ (DCIS) and 3% were invasive carcinoma on final pathologic assessment [20].

Digital breast tomosynthesis (DBT) is a newer imaging technology that is essentially "three-dimensional" mammography. While the benefits of DBT are currently being actively studied, it appears to increase the cancer detection rate and reduce recall rates. Tomosynthesis is particularly useful in assessing asymmetries and architectural distortions as it allows better assessment of the shape and margins of masses [21].

Grossly, IBC-NST appears as a white-tan to yellow-tan, firm-to-hard, stellate mass (Fig. 10.5). Close inspection may reveal white fibrous streaks extending into the surrounding fibroadipose tissue. A chalky-white appearance within the tumor is indicative of either necrosis or calcifications. About one-third of tumors can have somewhat circumscribed borders with a soft fleshy texture, although this feature is mostly seen with special types of mammary carcinoma such as mucinous, solid papillary, and basal-like triple-negative breast carcinoma (Fig. 10.6). Most IDCs induce fibroblastic stromal reaction (desmoplasia) and hence was described as scirrhous carcinoma in the past [22]. The consistency of an IDC depends primarily on the amount of desmoplastic or fibroblastic stroma present in the tumor.

Invasive breast carcinoma is most often identified in the upper outer quadrant (40–50%) irrespective of laterality,

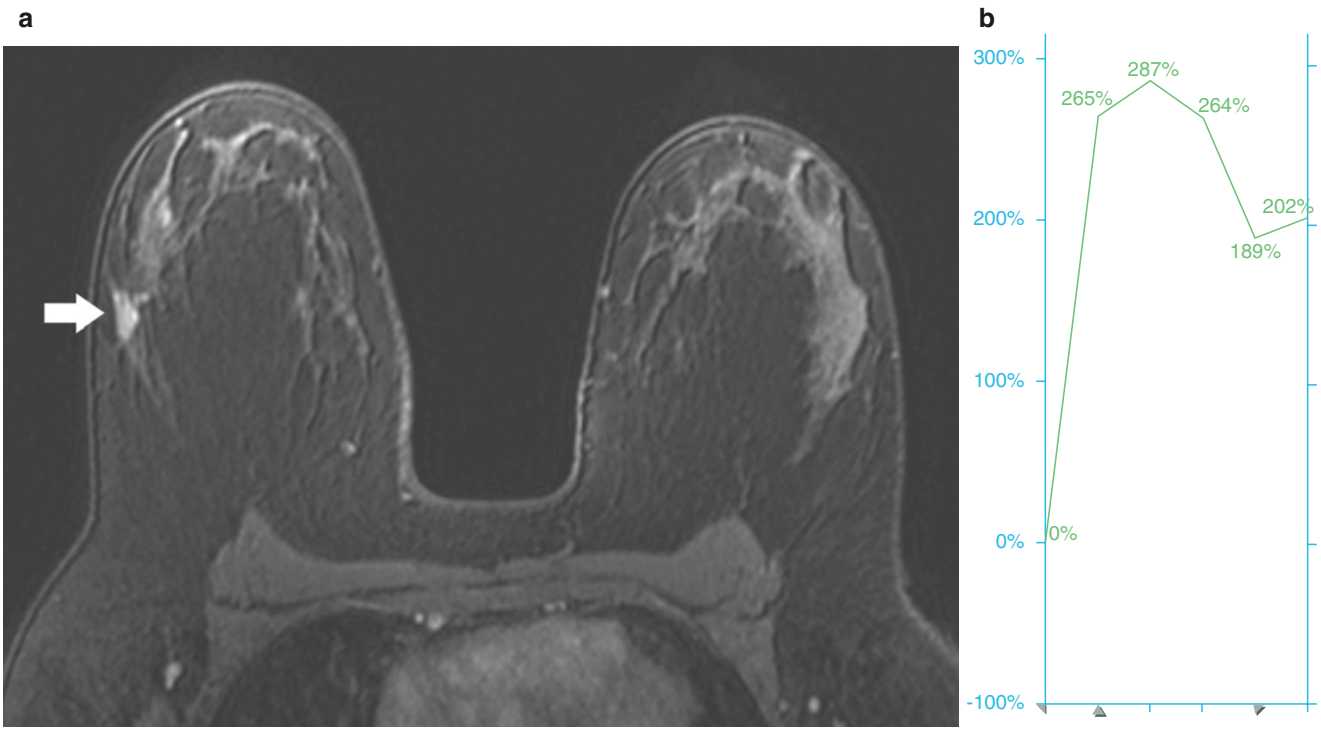

Fig. 10.4 Invasive breast carcinoma NST. MRI was performed for high-risk screening in this patient with a known *BRCA2* mutation. (**a**) An irregular heterogeneously enhancing mass is seen in the lateral right breast (*arrow*). (**b**) Time–intensity curve (kinetics) shows a rapid uptake and rapid wash out, a pattern typically seen with malignancy. (Courtesy of Stephen Seiler. Used with permission)

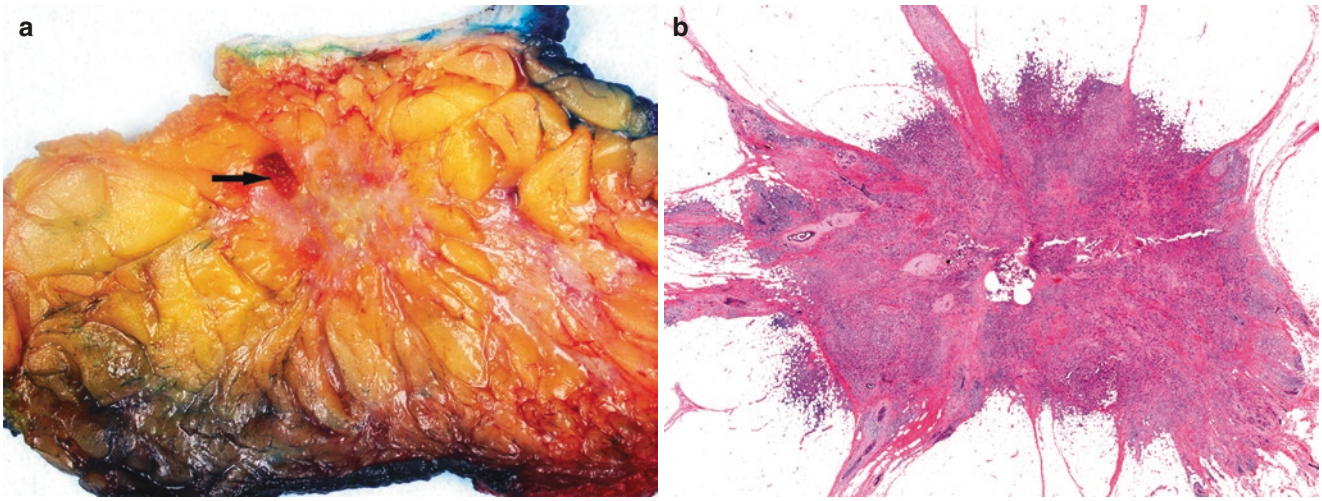

Fig. 10.5 Invasive breast carcinoma NST. (**a**) Gross appearance of a stellate mass with infiltrating margin and pink gelatinous material (hydrogel) indicative of the prior core biopsy site (*arrow*). (**b**) Scanning view depicts the stellate appearance of the tumor on histology

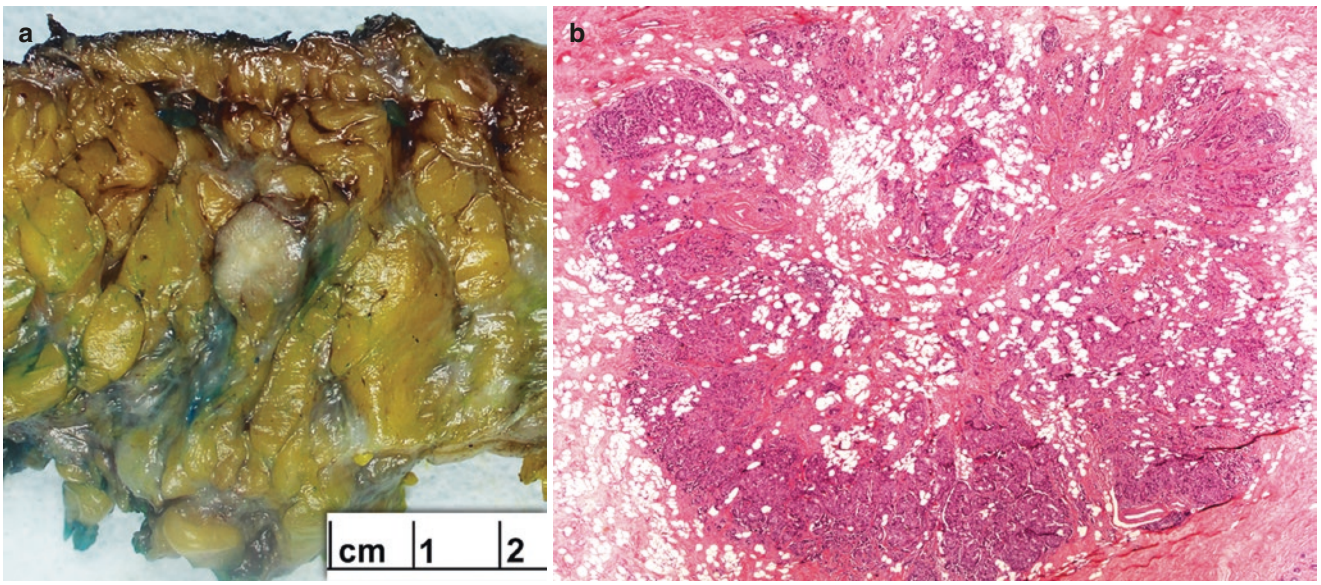

Fig. 10.6 Invasive breast carcinoma NST. A 7 mm IBC with relatively circumscribed borders, (**a**) gross appearance and (**b**) scanning view shows relatively well-delineated border on histology

followed by central breast, upper inner, lower outer and lower inner quadrants. The frequency corresponds with the amount of breast parenchyma present in the respective quadrants [2].

Microscopic Features

WHO defines pure IBC-NST as tumors showing less than 10% of a special subtype such as invasive lobular carcinoma (ILC). When a tumor shows a component of a special type such as tubular or lobular carcinoma, WHO recommends that the term "mixed IBC-NST and special subtype carcinoma" be used with the percentage of the special subtype given [1].

The morphology of IBC-NST is highly heterogeneous. The majority of tumors show a highly infiltrative border appreciated on scanning power, recapitulating the stellate appearance seen grossly (Fig. 10.7). The tumor may grow as cords, trabeculae, diffuse sheets, or a mixture of these patterns in addition to showing gland or tubule formation (Figs. 10.8, 10.9, and 10.10). Occasionally, tumors may exhibit single cell infiltration or a targetoid configuration entrapping benign ducts or lobules that resemble ILC at low-power examination but lacks the dyscohesion of lobular carcinoma (Fig. 10.11). Arps et al. termed IDC with prominent single cell infiltration as IDC with lobular features and reported that these tumors showed more aggressive behavior than ILC and IDC that did not show lobular features [23] (Fig. 10.12). Rarely, small foci of squamous or sebaceous

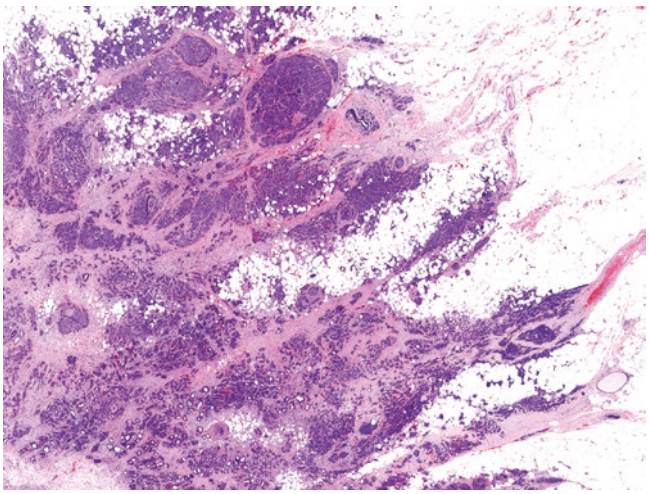

Fig. 10.7 Invasive breast carcinoma NST. Low power depicts the stellate appearance of the tumor due to infiltration of the fibrous bands by tumor cells with associated desmoplasia

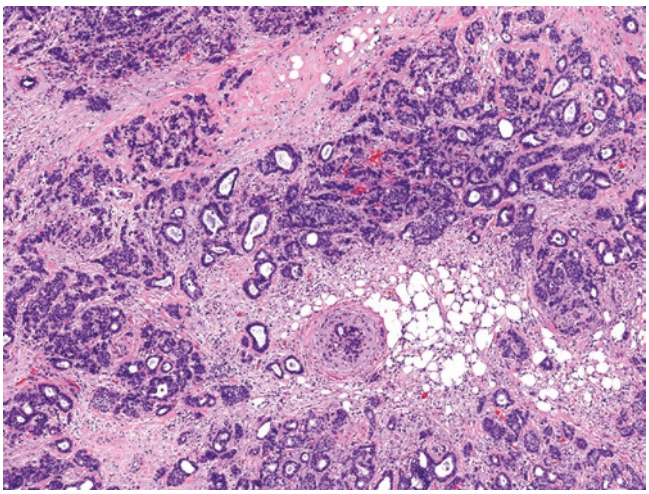

Fig. 10.8 Invasive breast carcinoma NST. Low power of the tumor displays varying architectural patterns comprising glands and solid nests

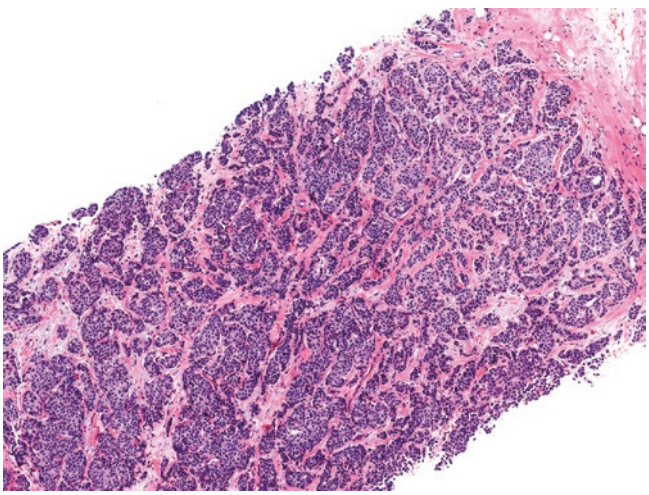

Fig. 10.9 Invasive breast carcinoma NST, with prominent nesting pattern and well-delineated border

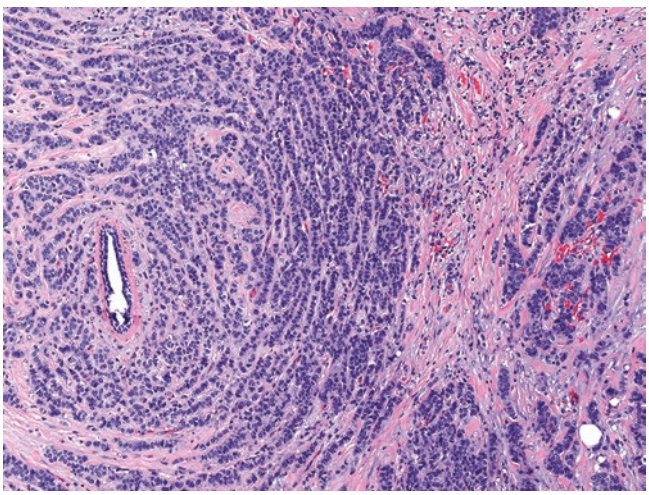

Fig. 10.11 Invasive breast carcinoma NST, with targetoid growth pattern around a benign duct (*left*)

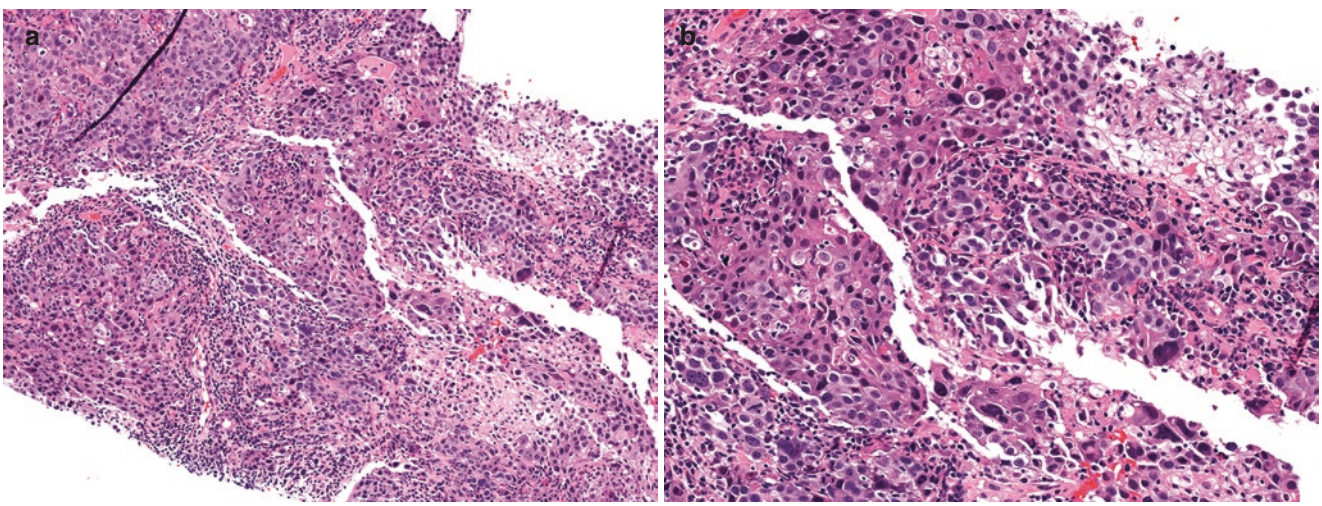

Fig. 10.10 Invasive breast carcinoma NST, poorly differentiated with highly pleomorphic tumor cells, (**a**) low-power and (**b**) high-power magnifications

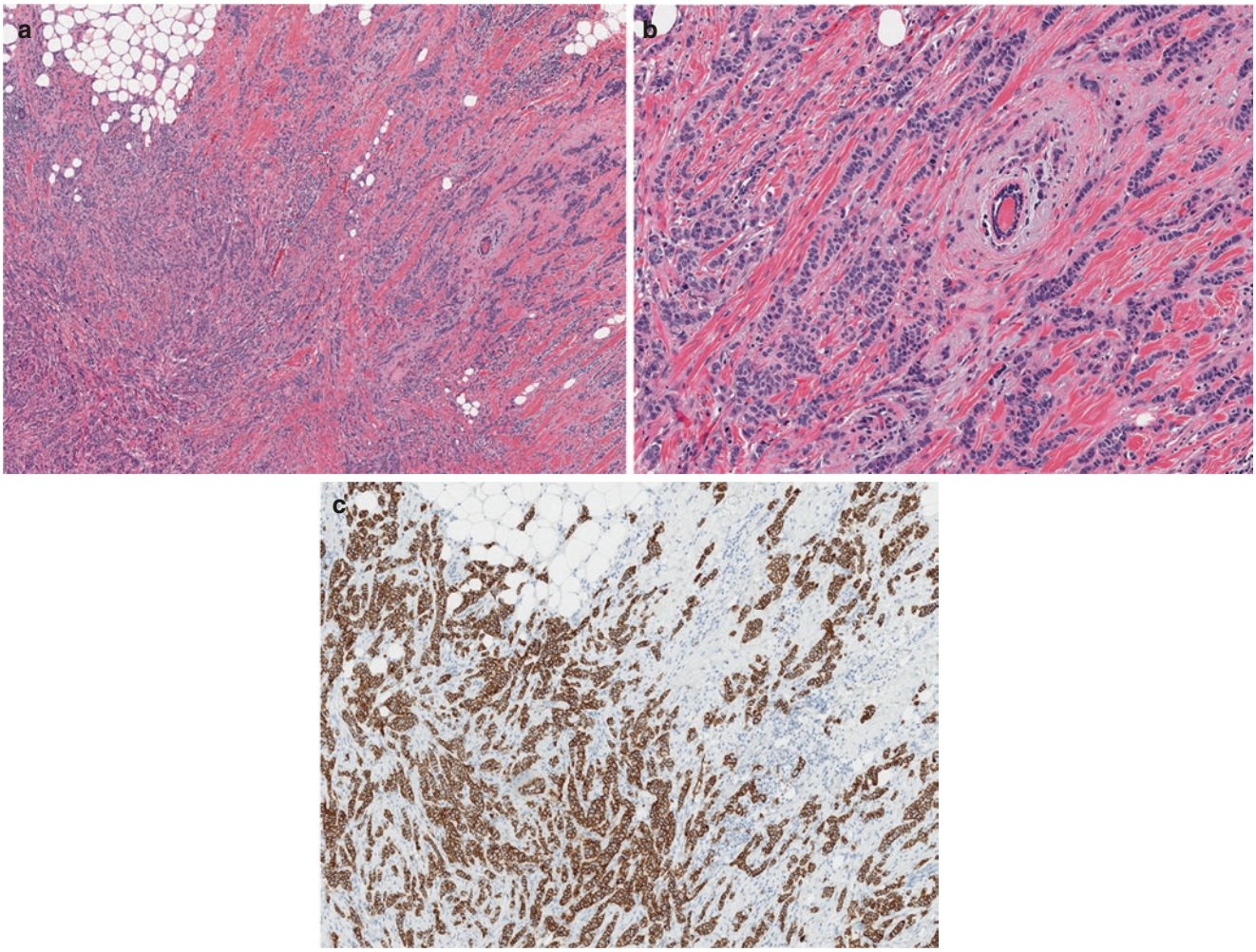

Fig. 10.12 Invasive breast carcinoma with lobular features. (**a**) Low-power view shows diffuse infiltration by single cells and thin cords of tumor, (**b**) high-power view shows invasive carcinoma cells with minimal nuclear pleomorphism, and (**c**) E-cadherin shows positive membrane staining in the tumor

differentiation can be seen, particularly in high-grade IBC NST (Figs. 10.13 and 10.14).

The stroma of IBC NST can be highly variable, ranging from pauci-cellular and edematous to showing marked desmoplasia, dense sclerosis, or hyalinization. It can also appear to be highly cellular due to an admixed lymphoplasmacytic infiltrate (Fig. 10.15). Some tumors may show a large central area of sclerosis (Fig. 10.16). Necrosis may be present, either as single cell necrosis/apoptosis or focal to extensive.

Histologic Grading

Histologic grading in IBC has been shown to be a reliable prognostic indicator, even though it can be subjective [24–27]. The Nottingham grading system, a modification of the original Scarff-Bloom-Richardson grading system, is used for histologic grading of breast carcinomas [25, 28, 29]. The Nottingham grade along with lymph node status and tumor size is collectively required for calculation of the Nottingham Prognostic Index (NPI) [30]. The higher the NPI score, the worse the prognosis. Patients are stratified into good, moderate, or poor prognostic groups using the NPI score [31].

Histologic grading requires assessment of three components of tumor morphology, each of which is given a score from 1 to 3. The final grade is calculated by adding the three scores. The three components are tubule/acinar/glandular formation, nuclear atypia/pleomorphism, and mitotic rate. Glandular formation is generally assessed at low-power examination and a score is given based on the percentage of tubule formation. A score of 1 is given when more than 75% of the tumor shows tubule formation, a score of 2 is for 10–75% tubule formation, and a score of 3 is for less than 10% gland formation. Tumor clusters with reverse polarization of tumor cells as seen in micropapillary carcinoma, solid tumor clusters floating in mucin pools as seen in mucinous carcinoma, and solid tumor nodules with a pushing border as seen in some invasive (solid) papillary carcinomas are by default scored as 3. Pure cribriform architecture is scored as 1.

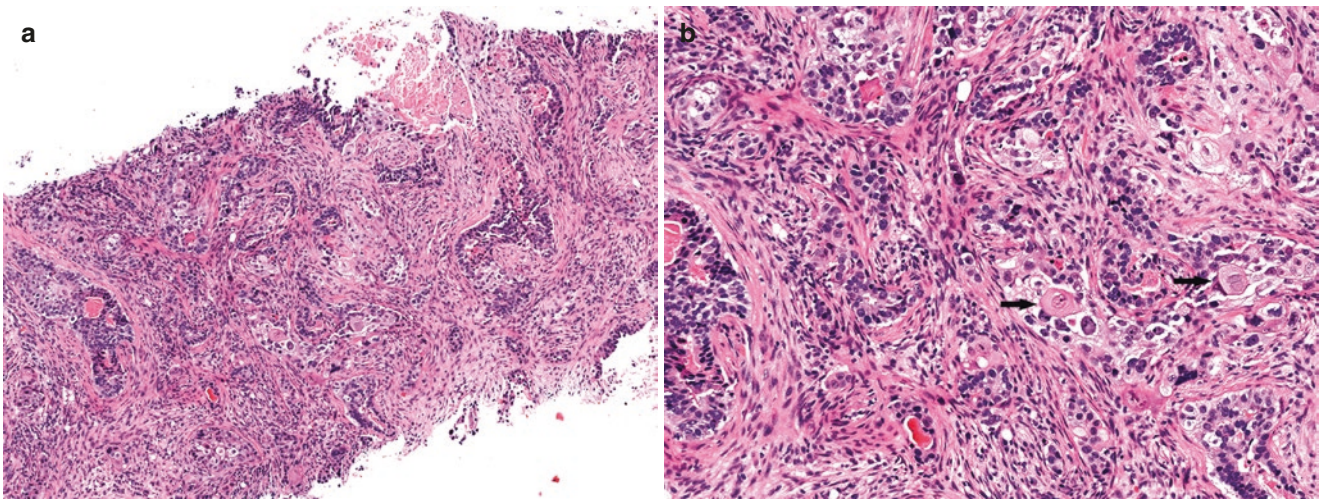

Fig. 10.13 Invasive breast carcinoma NST, poorly differentiated with focal squamous differentiation (*arrow*), (**a**) low-power and (**b**) high-power magnifications

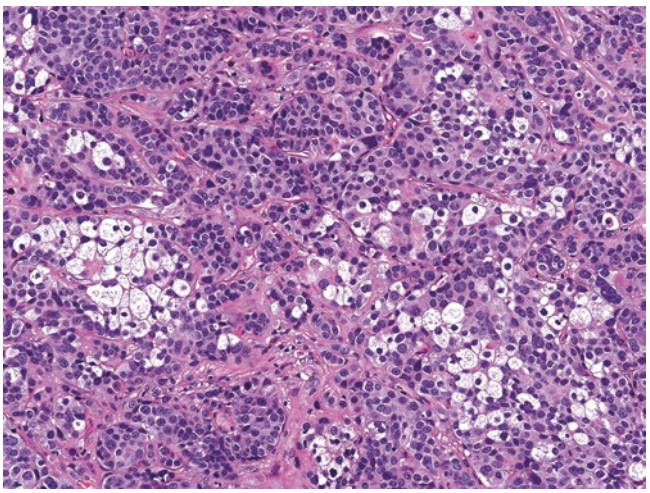

Fig. 10.14 Invasive breast carcinoma NST, moderately differentiated with focal sebaceous differentiation

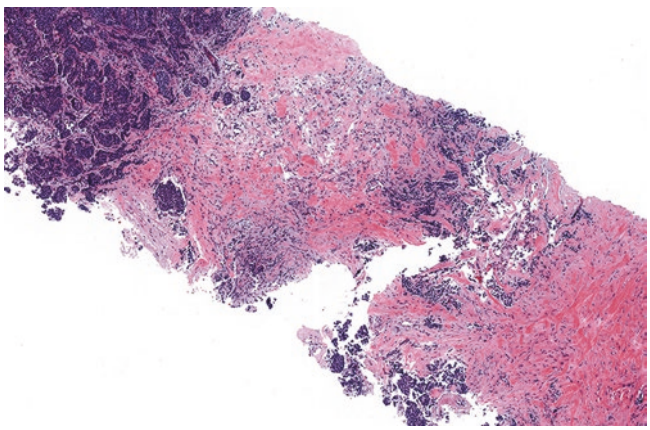

Fig. 10.16 Invasive breast carcinoma NST. Low power displays an IBC with a central zone of sclerosis

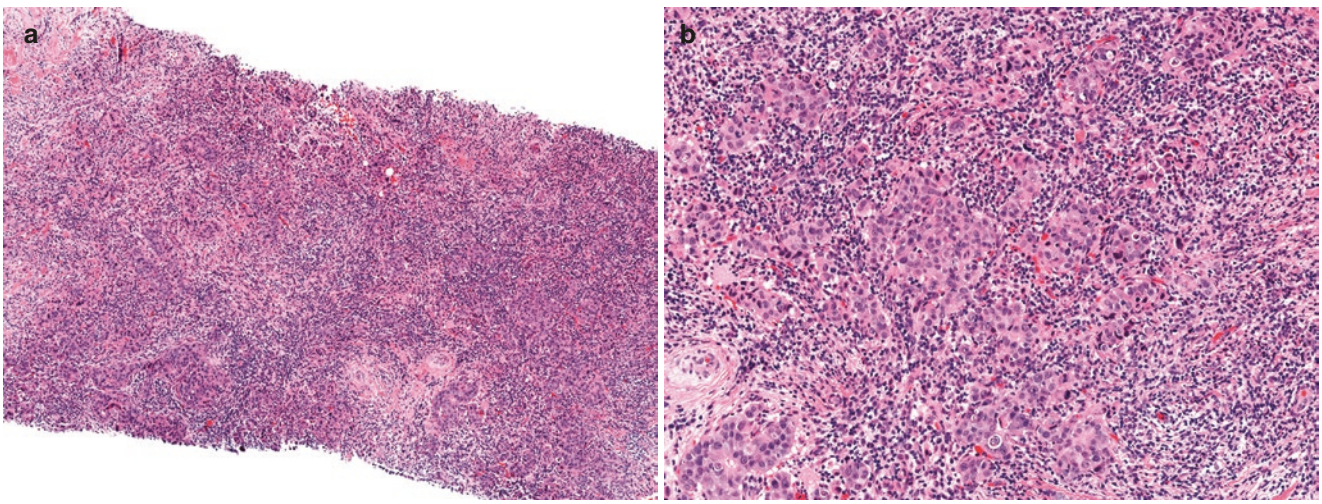

Fig. 10.15 Invasive breast carcinoma NST, high grade with prominent inflammatory cell infiltration, (**a**) low-power and (**b**) high-power magnifications

Nuclear pleomorphism refers to an amalgamation of variation in tumor nuclear size, chromatin characteristics, and the presence of nucleoli. Of the three components used for grading, nuclear grade is the most subjective. For nuclear size estimation, comparison with the adjacent or entrapped benign breast ductal epithelial cells should be used. If there are no benign breast epithelial cells nearby, stromal lymphocytes can be used as a reference. Tumors with small and regular nuclei with evenly dispersed chromatin and indistinct nucleoli, similar or slightly larger (up to 1.5 times) than the size of the adjacent normal breast epithelial cells is given a score of 1. Tumors with moderate variation in nuclear shape and size (1.5–2 times) than normal epithelial cells, occasional bigger nuclei among most tumor cells, uneven distribution of chromatin, vesicular nuclei with chromatin dispersed more peripherally towards the nuclear membrane and small visible nucleoli are given a score of 2. A score of 3 is reserved for tumors with marked nuclear size variation, frequent bizarre nuclei, nuclei with a predominant vesicular chromatin pattern and prominent to macro nucleoli. Some high-grade tumors with markedly enlarged nuclei with frequent mitoses may not show variation in nuclear size but should be scored as 3.

Strict criteria for the mitotic count should be adhered to, as the mitotic index is a reflection of the proliferative potential of the tumor and perhaps the most important semiquantitative component of the histologic grading system with prognostic implications. The current recommendation is to count mitotic figures on routine H&E stain. Immunohistochemistry/immunohistochemical (IHC) stains such as anti-phosphohistone H3 (pHH3) can highlight mitotic figures but at present is not recommended to assess mitotic count [32]. Only unequivocal mitotic figures should be counted. Care should be taken to distinguish apoptotic cells (characterized by dense pink eosinophilic cytoplasm and dark pyknotic nuclei often noted in higher grade tumors) and intratumoral lymphocytes from mitoses. The count should be performed at high-power field (400×), and the total number of mitoses per ten adjacent high-power fields should be used to estimate the mitotic score. In an excisional specimen, the area with the most mitotic activity should be counted; this generally corresponds to the leading edge or the periphery of the tumor. One should avoid counting mitosis in the center of the tumor, which often has sclerosis or low cellularity. The same rule also applies in core needle biopsy (CNB) samples, although it is highly dependent on sampling, i.e., the area and amount of tumor sampled. Additionally, crush artifact resulting from the biopsy procedure may impact mitosis count and nuclear grading in CNB samples (Fig. 10.17).

The size of a high-power field is variable and may differ up to sixfold from one microscope to another (Table 10.1).

Other factors that may affect mitotic count are the type of fixative and fixation time. Start et al. found that a delay in tissue fixation for up to 6 h reduced the number of visible mitoses by a mean of 53% without any effect on nuclear pleomorphism or tubule formation [33]. Robbins et al. reported that tissues fixed in B5 fixative rather than in buffered formalin/formaldehyde tend to show increased nuclear pleomorphism/size and higher mitotic count, though that difference was not statistically significant [34]. Therefore, the current recommendation is to use 10% neutral phosphate-buffered formalin at pH 7.0 with an optimal formalin-to-tissue ratio of 10:1. The tissue should be fixed in formalin as soon as possible. It is recommended that the time interval between tissue removed from the patient to its placement in formalin (cold ischemia time) be less than 1 h [35]. This is easily achievable in core needle biopsy (CNB) samples. However, for excision specimens, one needs to be mindful of ischemia time as inking and sectioning takes time. Minimizing the tissue ischemia time to less than 1 h is also important for biomarker studies.

Once the three components have been assessed, the scores are added to determine the histologic grade (Table 10.1). Tumors with a score of 3–5 are well differentiated (grade 1), score 6–7 are moderately differentiated (grade 2), and score 8–9 are poorly differentiated (grade 3) (Figs. 10.18, 10.19, and 10.20). The concordance rate for histologic grade between CNB and excision is reported to be 59–91% [36–39], with the majority of cases (30–40%) upgraded on excision by one level [40]. An upgrade rate of two levels, i.e., from grade 1 to grade 3, is very rare (0–2%) [41–43]. The discordance in tumor grade is mainly due to underestimation of mitotic count, followed by nuclear pleomorphism and tubule formation [41, 43]. One study reported better correlation between anti-pHH3 and MIB-1 staining with that of mitotic figures obtained from excision specimens than on CNBs [44]. The underestimation of mitotic activity in CNBs can be problematic, particularly when the difference in scoring results in an upgrade of the overall histologic grade on excision. Clinicians find this seemingly discordant histologic grade reported between the CNB and the subsequent excision specimen disconcerting and confusing. Hence, if such a scenario is foreseen, it is suggested that the histologic grade in the CNB be reported as "well to moderately differentiated (Grade 1–2)" so that both "options" are available to the pathologist who will be reporting the final histologic grade on the excision specimen. Alternatively, a statement such as "Final histologic grade should be based on the excision specimen" could be included in the comment of the pathology report.

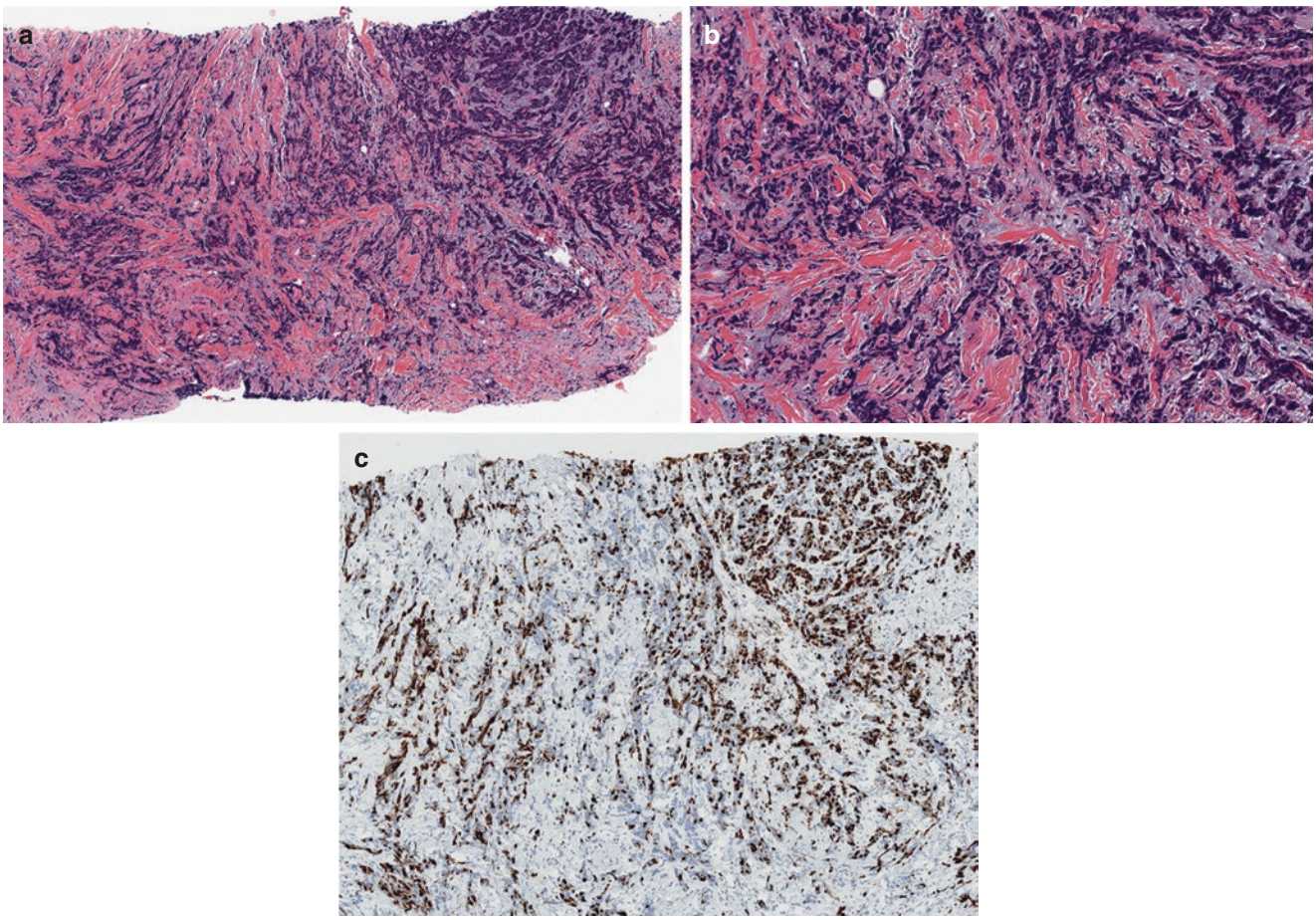

Fig. 10.17 Invasive breast carcinoma NST, with marked crush artifact that interferes with histologic grading, specifically nuclear pleomorphism and mitotic count, (**a**) low-power and (**b**) high-power magnifications, (**c**) Ki-67 stain shows high proliferation rate

Table 10.1 Nottingham scoring system to evaluate histologic grade for invasive breast carcinoma

	Score		
Parameters	1	2	3
Tubule/gland formation			
	>75%	10–75%	<10%
Nuclear pleomorphism/size			
	Small/regular nuclei with evenly dispersed chromatin and indistinct nucleoli; size 1.5× normal breast epithelial nuclei	Moderate variation in nuclear shape with uneven distribution of chromatin, vesicular nuclei, and occasional small visible nucleoli; size 1.5–2× normal breast epithelial nuclei	Marked nuclear size variation, frequently bizarre nuclei with a predominant vesicular chromatin pattern and prominent to macro nucleoli; size >2–2.5× normal breast epithelial nuclei
Mitotic count[a]			
Field diameter (mm)			
0.4	≤4	5–9	≥10
0.45	≤5	6–11	≥12
0.5	≤7	8–14	≥15
0.55	≤8	9–17	≥18
0.6	≤10	11–20	≥21
0.65	≤12	13–24	≥25

Reproduced from Elston, C.W. and Ellis, I.O. (1991), Pathological prognostic factors in breast cancer. I. The value of histological grade in breast cancer: experience from a large study with long-term follow-up. Histopathology, 19: 403–410. https://doi.org/10.1111/j.1365-2559.1991.tb00229.x, with permission of John Wiley and Sons

Final grade (addition of scores of each component): Grade 1: total score, 3–5. Grade 2: total score, 6 and 7. Grade 3: total score, 8 and 9. Based on Elston and Ellis modification of the original Scarff-Bloom-Richardson grading system [27]

[a] Mitotic count varies according to the field diameter and field area at high-power magnification (400×)

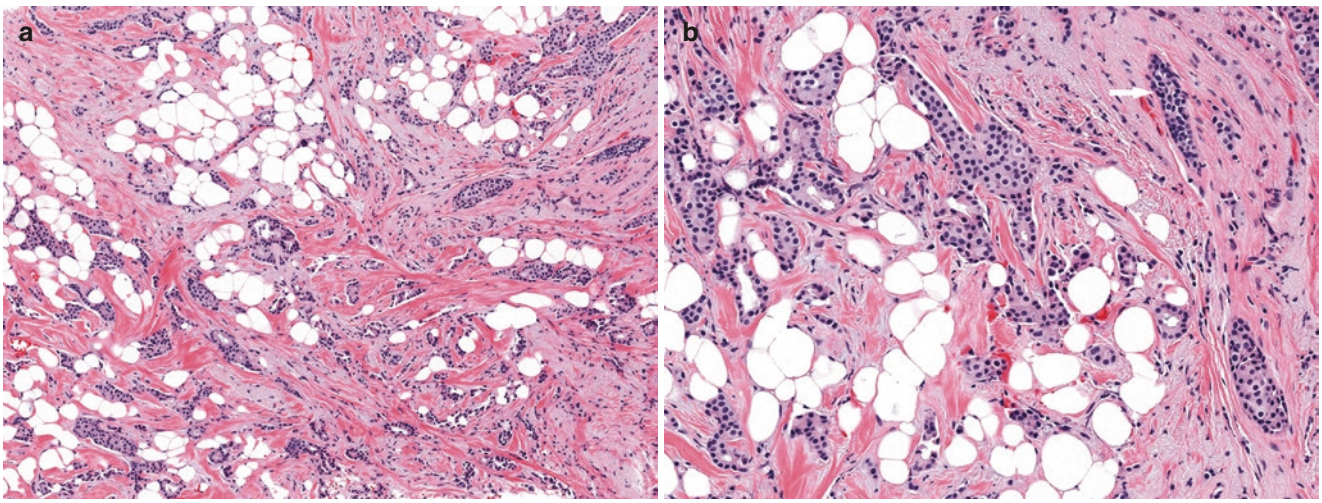

Fig. 10.18 Invasive breast carcinoma NST, grade 1, (**a**) low-power and (**b**) high-power magnifications (arrow indicates normal duct for comparison)

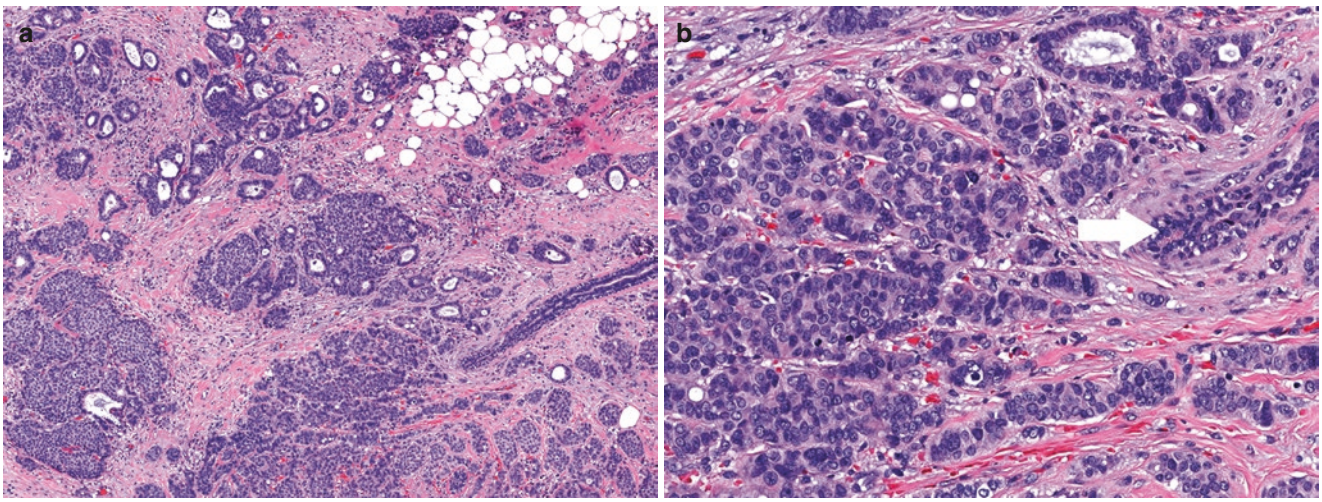

Fig. 10.19 Invasive breast carcinoma NST, grade 2, (**a**) low-power and (**b**) high-power magnifications (arrow indicates normal duct for comparison)

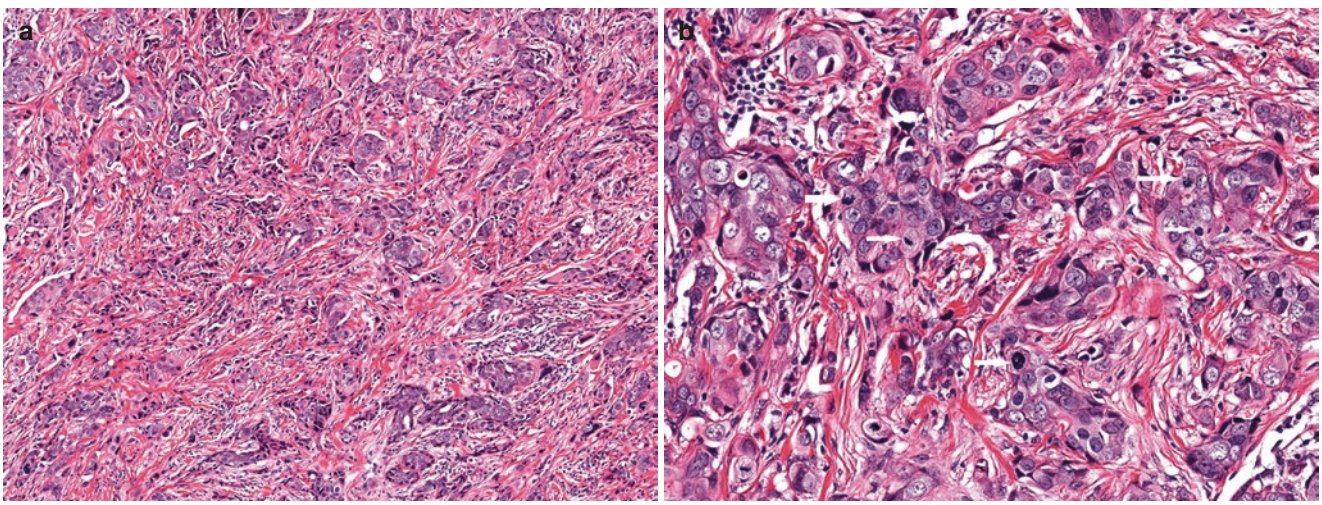

Fig. 10.20 Invasive breast carcinoma NST, grade 3, (**a**) low-power and (**b**) high-power magnifications (arrows indicating mitosis)

Reporting Core Needle Biopsy

A correct pathologic diagnosis of invasive carcinoma in a CNB is paramount as it not only guides further treatment but also provides important information for prognostic and predictive factors. In patients who undergo neoadjuvant therapy and have complete pathologic response, the CNB will be the only available tumor tissue for diagnosis and biomarker studies. As sampling is limited on a CNB, utmost vigilance should be taken not to overdiagnose invasive carcinoma. Several studies have reported high concordance rates ranging from 91% to 100% between CNB and the subsequent excision for a malignant diagnosis [45–47]. The sensitivity and specificity of diagnosing invasive carcinoma in CNB ranges from 85 to 100% and 96 to 100%, respectively [48–50].

Once the diagnosis of malignancy is established, every effort should be made to report tumor type, histologic grade, tumor size, the presence or absence of coexistent in situ carcinoma, lymphovascular invasion, the presence and extent of necrosis and tumor infiltrating lymphocytes (TILs). If coexistent DCIS is identified, its extent, architectural type, and nuclear grade should be reported. Recording the number of cores containing tumor and the largest linear extent of the tumor in core biopsies becomes important in certain instances: small tumors can be entirely removed with no residual tumor left in the excision specimen, the size of the tumor on the CNB can be larger than in the excision, and to ensure that there is more than minimal invasive component (at least more than 2 mm and ideally 5 mm of tumor tissue) available to perform and assess tumor biomarkers. The latter is extremely important in cases where neoadjuvant chemotherapy is planned. Routinely performing ER, PR, and HER2 on CNB samples rather than the excision is preferred as there is less variation in cold ischemia time and duration of fixation; the hormone receptor (HR) and HER2 status also dictate possible pre-surgical systemic therapy.

Differential Diagnosis

The differential diagnosis of IBC-NST includes both malignant and benign lesions. The main invasive carcinoma in the differential is ILC, particularly ILC variants, e.g., pleomorphic type, as they can show similar architecture and high-grade morphology (discussed in Chap. 15) (Fig. 10.21). Distinction between IBC NST and ILC is recommended because their clinical behavior and outcome are different [51, 52].

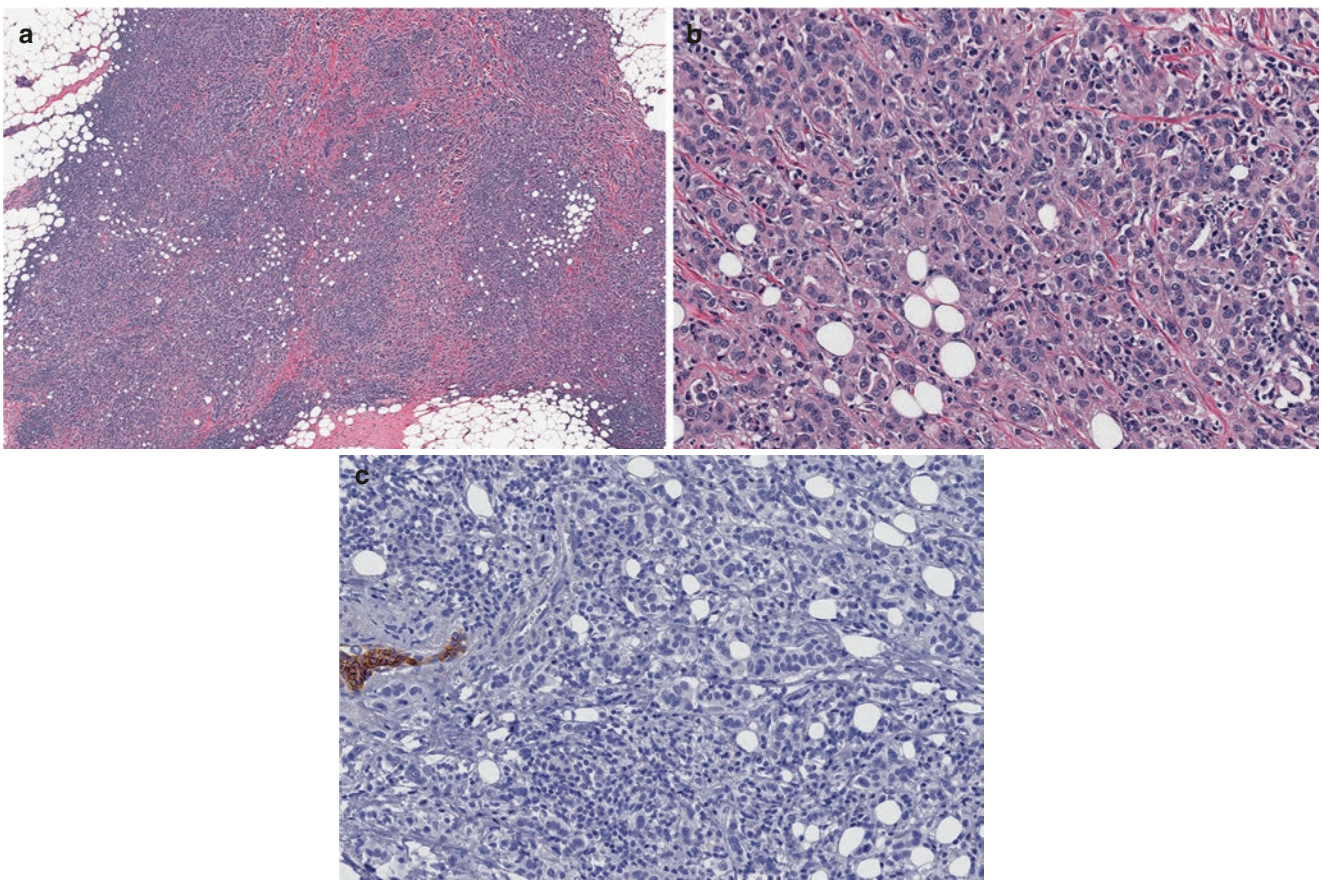

Fig. 10.21 Invasive lobular carcinoma mimicking ductal carcinoma, (**a**) low-power view shows a diffuse infiltration of tumor cells admixed with inflammatory infiltrate, (**b**) high-power view shows highly pleomorphic tumor cells growing in a trabecular pattern, and (**c**) E-cadherin shows negative staining in the tumor cells but positive staining of a normal duct on the left

Benign and in situ lesions that may mimic IBC-NST include nipple adenoma, sclerosing adenosis alone or secondarily involved by DCIS/lobular carcinoma in situ (LCIS), radial scar with epithelial hyperplasia, and complex sclerosing lesions involved by epithelial hyperplasia, DCIS or LCIS (Figs. 10.22, 10.23, 10.24, 10.25, and 10.26). Histological

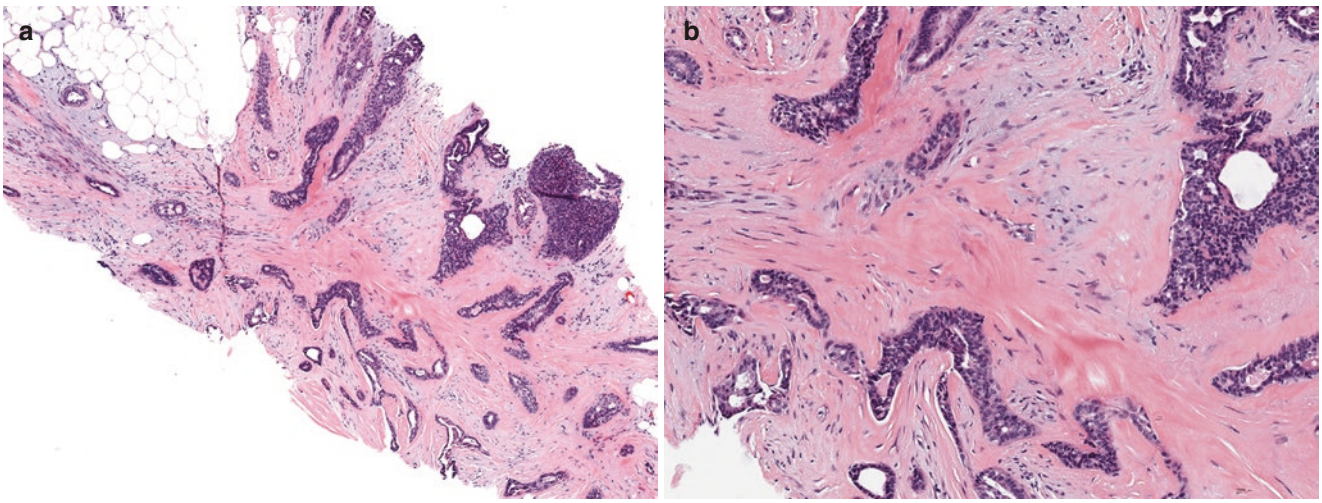

Fig. 10.22 Radial scar mimicking IBC-NST and DCIS. (**a**) Low-power and (**b**) high-power magnifications

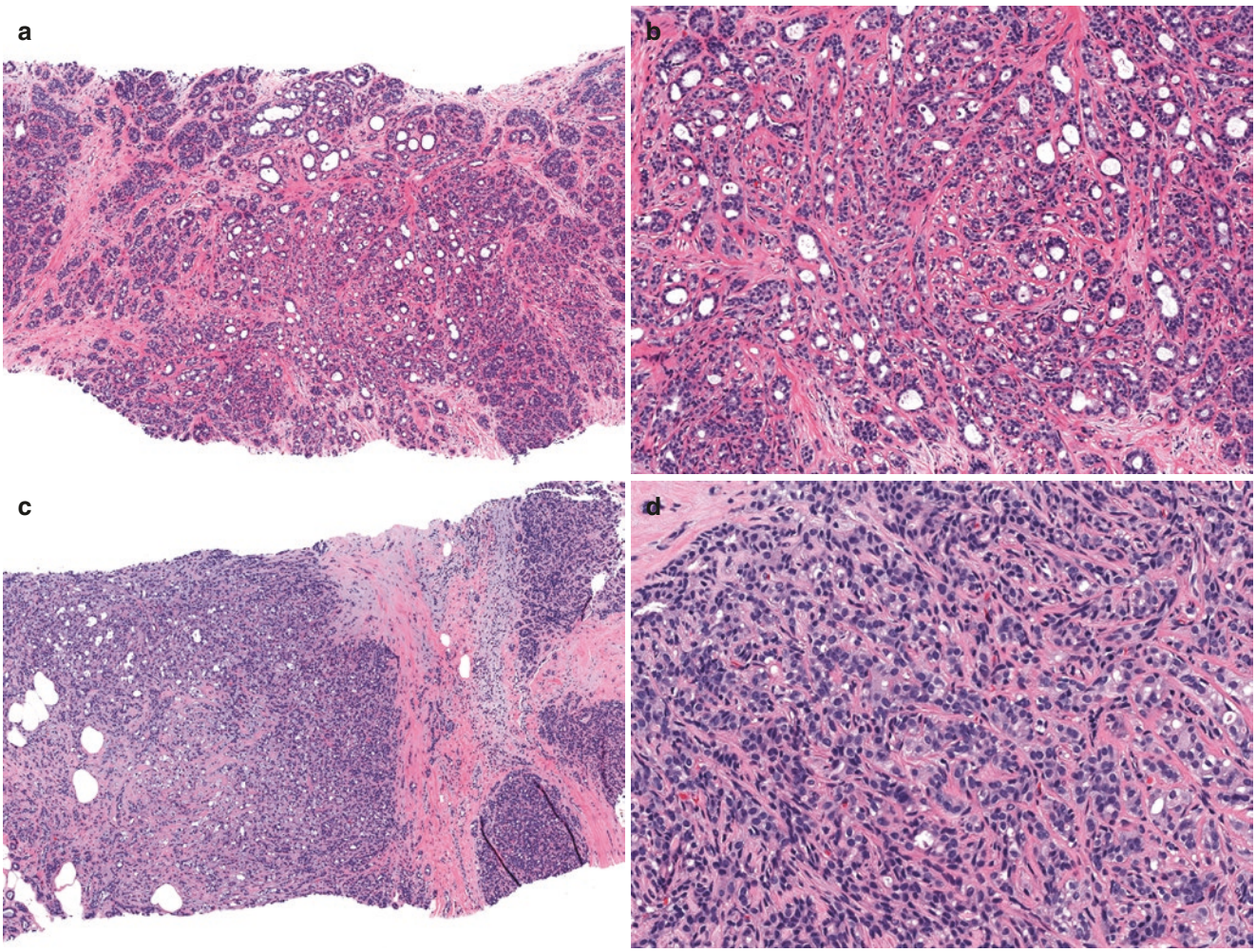

Fig. 10.23 Extensive mass-forming sclerosing adenosis. Example 1 (**a**, **b**). The distorted lobules and sclerosis mimic invasive carcinoma. Example 2 (**c**, **d**). The distorted lobules and areas of stromal sclerosis can easily be mistaken for invasive carcinoma

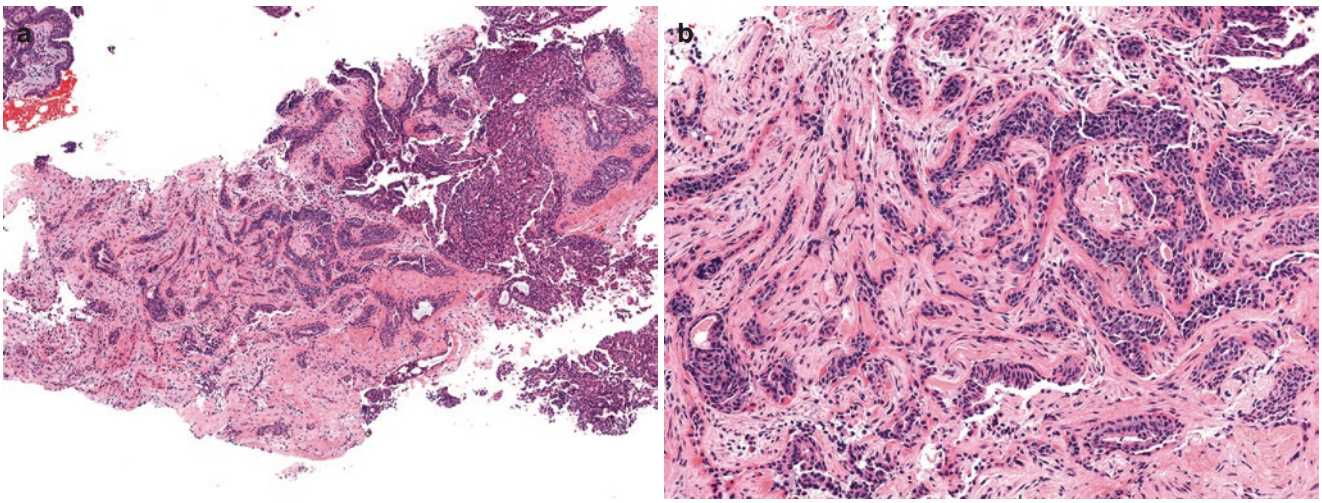

Fig. 10.24 Sclerosing papilloma. (**a**) Entrapped glands and sclerosis in an intraductal papilloma can be mistaken for invasive breast carcinoma NST. (**b**) High-power magnification reveals smooth outline of the entrapped glands by pink basement membrane

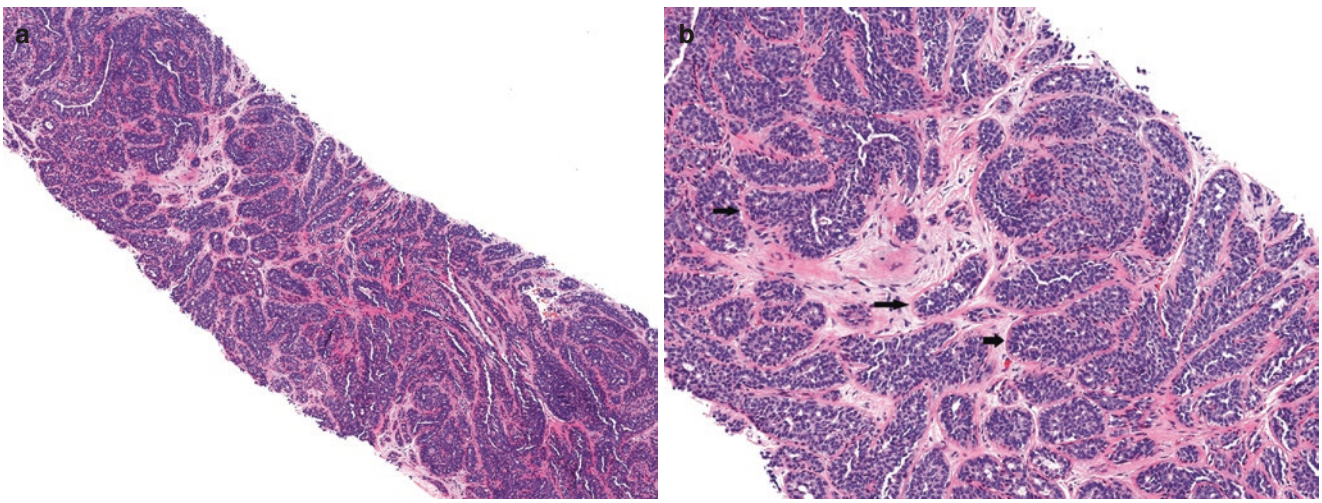

Fig. 10.25 Complex sclerosing lesion with epithelial hyperplasia. (**a**) Epithelial hyperplasia in the benign entrapped glands in a fibrotic stroma mimics invasive carcinoma. (**b**) High-power view shows benign epithelial cells and pink basement membrane (*arrows*)

features that can help to identify a lesion as benign include circumscribed or lobular configuration at low-power examination and most importantly identification of myoepithelial cells beneath the hyperplastic epithelium and the smooth outline of the distorted epithelial cells conferred by an intact basement membrane. Immunostains for myoepithelial cells such as smooth muscle myosin heavy chain (SMM), p63, or calponin can be extremely helpful in these cases. In cases where the nature of the lesion remains equivocal and the diagnosis cannot be made with confidence, it is preferable to request a repeat CNB or state that final classification will be performed after the evaluation of the excision specimen, rather than commit to a questionable diagnosis.

The majority of IBC-NST exhibits infiltrative margins but at times may show a circumscribed border with a pushing front. When necrosis is present in the center of large expansile solid nests of tumor cells that are high grade, it can resemble comedo-type DCIS. These high histologic grade circumscribed lesions are commonly "triple-negative" breast carcinoma or "IBC with medullary pattern" (Fig. 10.27). Careful assessment of the intervening stroma that usually reveals desmoplasia should prompt one to consider the diagnosis of invasive carcinoma, which can be further confirmed by myoepithelial stains. When low-to-intermediate grade IBC-NST with circumscribed/pushing edge is encountered, solid papillary carcinoma should be included in the differen-

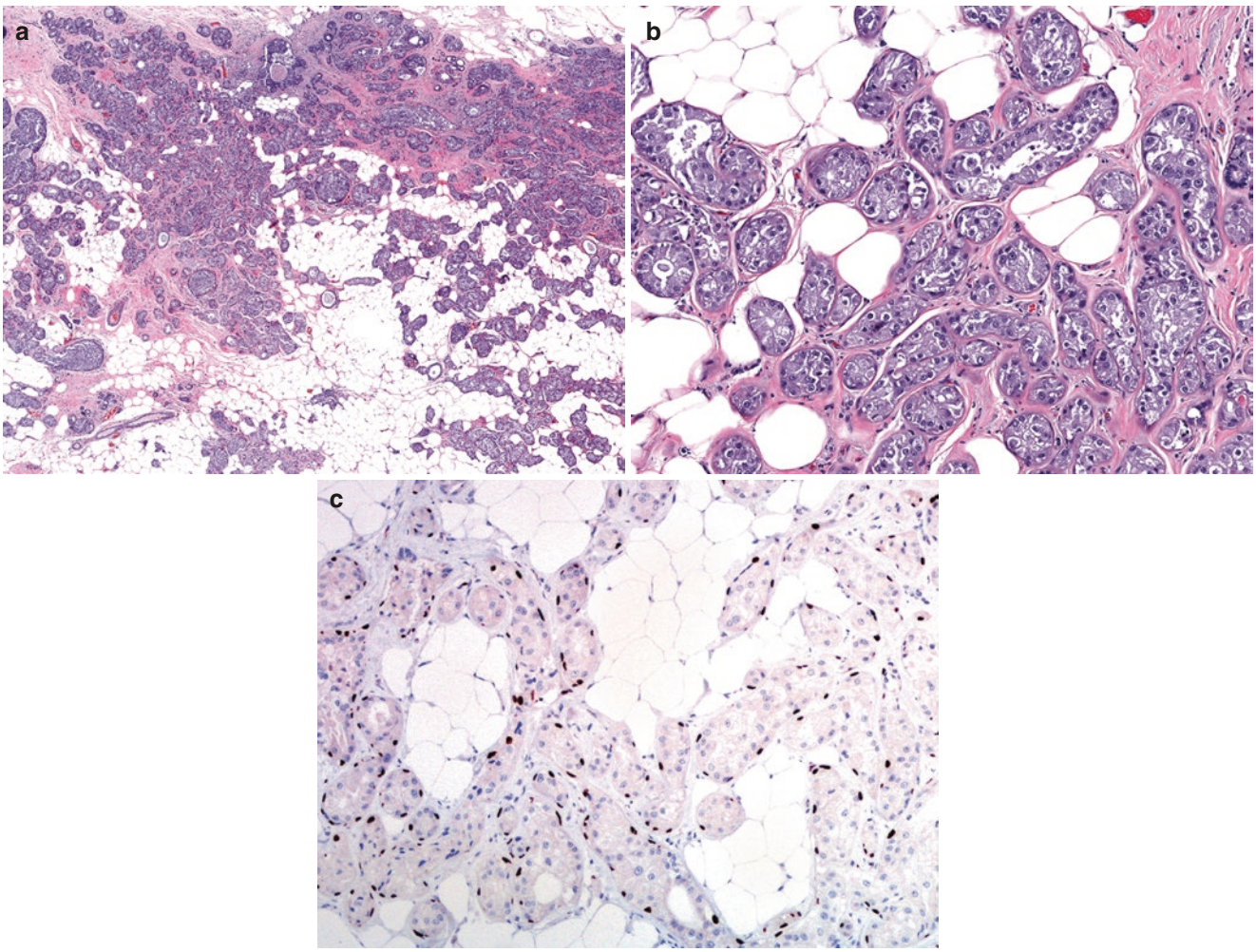

Fig. 10.26 DCIS involving sclerosing adenosis mimics invasive carcinoma. (**a**) Low-power and (**b**) high-power magnifications. (**c**) p63 stain shows intact myoepithelial cells around glands

tial diagnosis, especially in older women who tend to have these tumors. Occasionally, low-grade IBC-NST may show prominent large nests of tumor cells embedded in fibrotic stroma resembling DCIS (Fig. 10.28).

Lymphomas of the breast, whether primary or secondary, are rare. High-grade lymphoma can mimic high-grade IBC-NST with an inflammatory infiltrate [53, 54]. The most common primary breast lymphoma in most series is diffuse large B cell lymphoma (DLBCL), with frequency ranging from 49% to 64% [55, 56]. The next most common lymphomas encountered are extranodal marginal zone lymphoma of mucosa-associated lymphoid tissue (MALT) type (19–23%) and follicular lymphomas (14–19%) [55, 56]. Lymphoma usually presents as a mass lesion in the breast. High-grade lymphoma should be suspected when the lesion is diffuse, grows as sheets, and shows intimate mixture of neoplastic cells and other chronic inflammatory cells (Fig. 10.29).

Lastly, IBC-NST must be differentiated from metastases to the breast from extramammary sites. Although uncommon, metastases to the breast accounts for up to 3% of all breast masses [57]. Fortunately, most patients who present with metastases to the breast already have an earlier diagnosis of the primary tumor. The tumors that metastasize to the breast include melanoma and carcinomas from ovary, lung, thyroid, kidney, and liver [58–60]. Breast involvement by metastatic carcinoma may be a sign of rapid widespread dissemination with a survival rate of only 10.9 months [61]. Certain features that may be indicative of metastasis are absence of microcalcifications, lack of spiculations on imaging, or lack of skin involvement clinically, but none of these

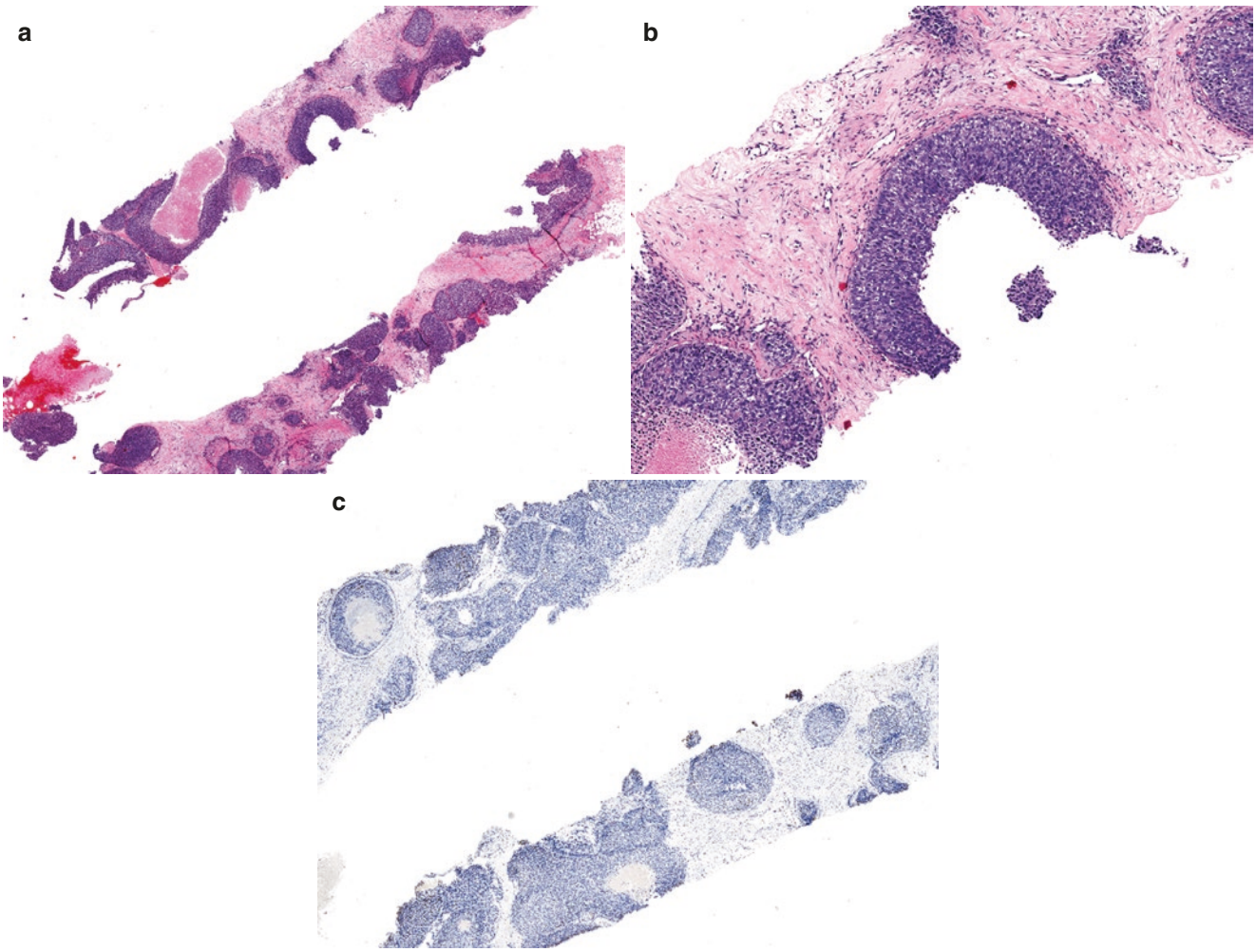

Fig. 10.27 Invasive breast carcinoma NST masquerading as DCIS. (**a**) A 2 cm mass that shows large solid nests of tumor with round borders and central necrosis resembling DCIS. (**b**) High-power view shows altered desmoplastic stroma between the nests distinct from normal breast stroma. (**c**) Immunostain for p63 shows lack of myoepithelial cells in the entire lesion

features are specific for metastatic disease. In a CNB, metastatic tumor to breast should be suspected when a malignant tumor with unusual morphology is encountered or when a tumor believed to be breast primary shows an unusual staining pattern with prognostic markers (Figs. 10.30 and 10.31). The presence of in situ carcinoma favors tumor of breast origin, although incidental DCIS can be present adjacent to metastatic tumor. In some cases, metastatic tumors may not display any of the above features. What is crucial in these cases is having a detailed clinical history. On the rare occasion when metastasis to the breast is the first manifestation of the tumor, a detailed discussion with clinicians is required to determine the primary site. A panel of immunostains may help determine the primary site, keeping in mind that no stain is pathognomonic for a site of origin. TTF1, for example, can be positive in breast carcinomas [62] and focal expression of WT1 in IBC with mucinous differentiation has been reported [63].

Immunohistochemistry

Invasive breast carcinomas tend to be CK7 positive and CK20 negative, consistent with most tumors found above the diaphragm. Immunostains that can help identify breast as the site of origin include ER, GATA3, GCDFP-15, and mammaglobin. ER is expressed in approximately 80% of IBC [64]. Strong, diffuse ER expression may be sufficient to ren-

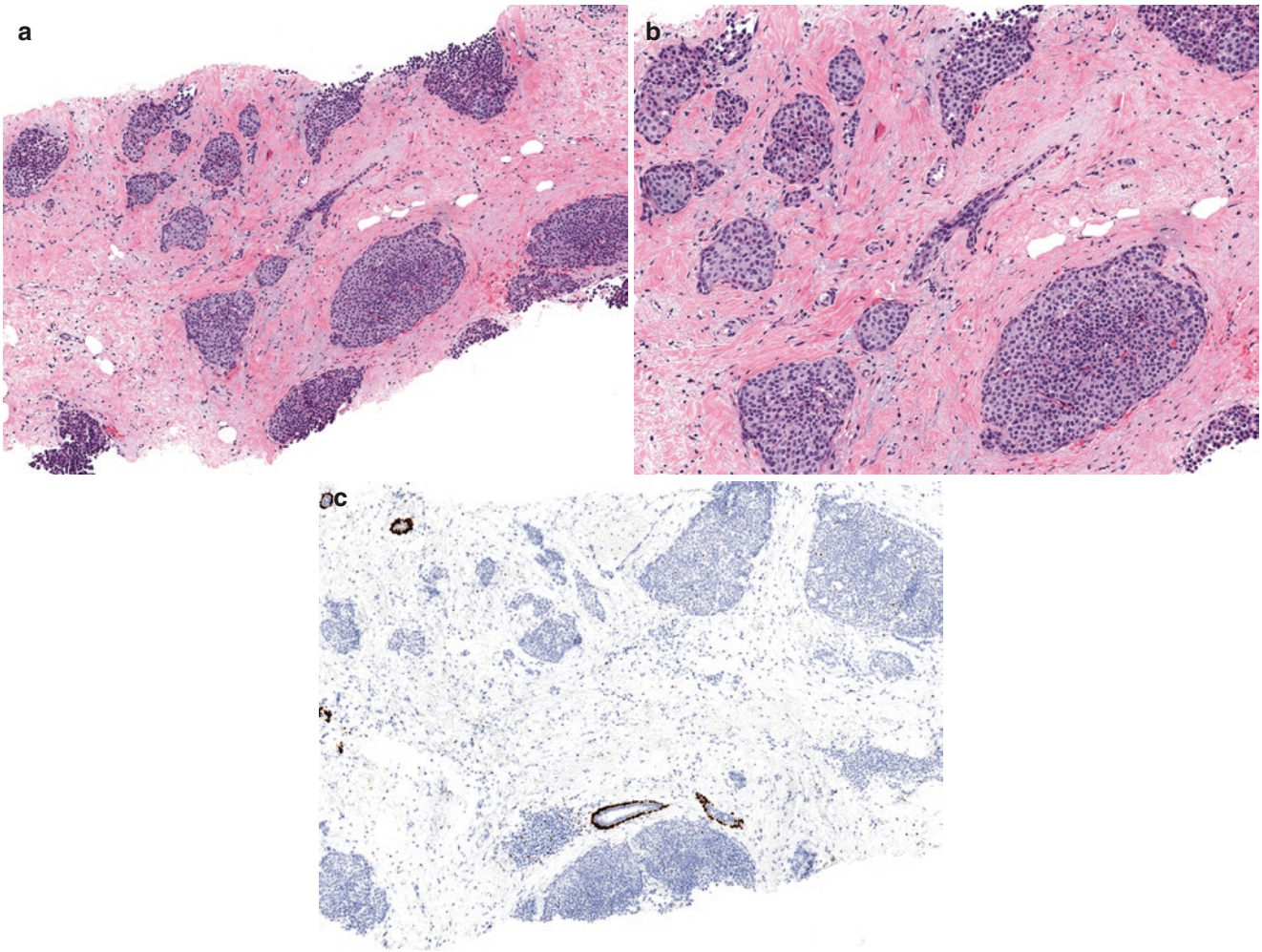

Fig. 10.28 Invasive breast carcinoma NST, moderately differentiated mimicking DCIS. (**a**) Low-power view shows solid nests of low nuclear grade cells with round to oval borders, (**b**) high-power view, and (**c**) SMM immunostain shows absence of staining around the nests confirming the tumor's invasive nature

der a diagnosis of metastatic breast carcinoma in the appropriate clinical setting. ER however is not specific and can be expressed in skin adnexal, salivary gland, and gynecologic tumors. Mammaglobin and GCDFP-15 are highly specific (both have >90% specificity) but have low sensitivity for IBC (mammaglobin 50%, GCDFP-15 20–50%) [65–68]. Staining for both markers also tends to be patchy. Similar to ER, other tumors that are likely to express both these markers are skin adnexal, salivary gland, and gynecologic tumors [66, 69]. GCDFP-15 is a marker of apocrine differentiation and accordingly is more sensitive in cases of apocrine carcinoma (75%) or IBC with apocrine differentiation (55%) compared to carcinoma without apocrine differentiation (23%) [70].

GATA3, a member of a zinc finger transcription factor family, is expressed in 70–90% of breast carcinomas [71, 72]. Of greater utility however, GATA3 is expressed in up to 70% of triple-negative breast carcinomas (TNBC) [73]. GATA3 is also expressed in a majority of skin adnexal, skin squamous cell, and urothelial carcinomas [72].

While well-differentiated metastatic IBC will usually express ER and GATA3, TNBC may not show expression of these markers which can make diagnosing metastatic TNBC challenging in some cases. One stain that may help in such a setting is SOX10. SOX10 is an immunostain that is primarily associated with nerve sheath tumors and melanoma but has also been shown to be expressed in up to 70% of TNBC [74].

Pathogenesis

Seminal papers by Wellings and colleagues demonstrated that both ductal and lobular neoplasia arise from the terminal

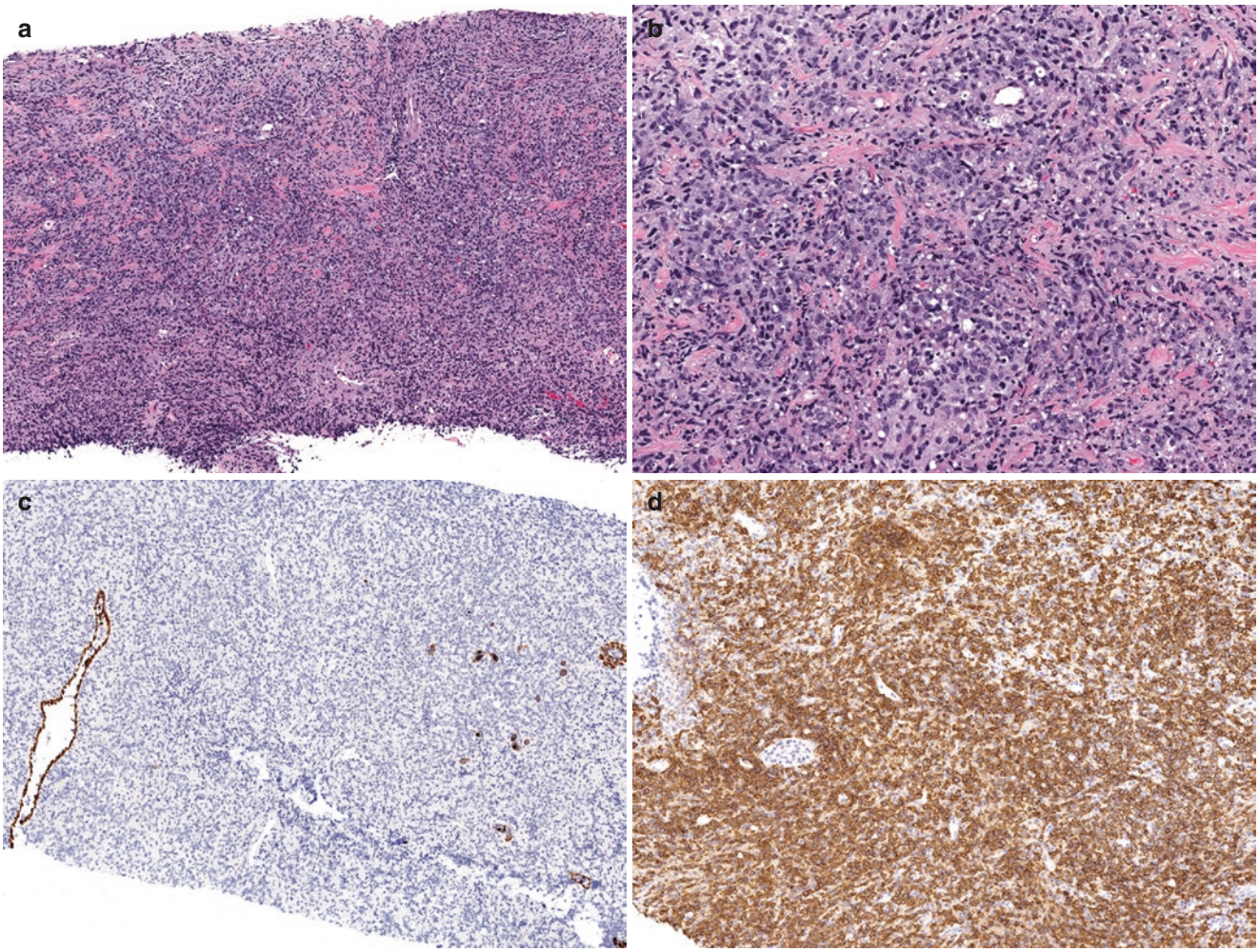

Fig. 10.29 Primary lymphoma of breast. (**a**) Core needle biopsy reveals a diffuse infiltrate with aggregates of neoplastic cells mimicking IBC-NST with inflammatory infiltrates. (**b**) High-power view shows larger neoplastic cells intimately admixed with inflammatory cells. (**c**) Cytokeratin stain shows complete lack of staining in neoplastic cells while (**d**) immunostain for CD20 is diffusely positive

duct lobular unit (TDLU) [75, 76], in contrast to the conventional thought at that time that lobular tumors arise from lobules and ductal tumors arise from ducts. Just as lobular neoplasia (atypical lobular hyperplasia and LCIS) is a non-obligate precursor to ILC [77–79], flat epithelial atypia (FEA), atypical ductal hyperplasia (ADH), and DCIS are considered non-obligate precursors to IBC-NST [75, 76, 80, 81]. Contrary to the historical belief that a tumor progresses from a precursor lesion to low-grade invasive carcinoma to high-grade invasive carcinoma, genetic and gene expression studies have supported two different pathways: a low-grade pathway and a high-grade pathway.

High-grade DCIS and poorly differentiated IBC share common genetic alterations whereas low-grade lesions, such as ADH, low-grade DCIS, and well-differentiated invasive carcinoma, exhibit similar genomic changes, providing little support for a transition from a low-grade carcinoma to a high-grade carcinoma. Comparative genomic hybridization (CGH) studies have revealed that the low-grade evolutionary pathway is characterized by frequent loss of chromosome 16q, gain of chromosome 1q, and infrequent amplification of 17q12 [82–84]. Similarly, various loss-of-heterozygosity (LOH) and CGH-based studies have demonstrated similar genetic alterations (16q loss and 1q gain) in FEA and ADH [82, 85, 86]. On the other hand, loss of chromosome 16q is infrequent in high-grade lesions further supporting segregation of low- and high-grade lesions [83, 84]. Furthermore, high-grade carcinomas (both in situ and invasive) demonstrate complex karyotypes such as loss of 8p, 11q, 13q, and 14q, gains of 1q, 5p, 8q, and 17q, and amplification of 17q12 and 11q13 [84, 87]. However, some studies have suggested, albeit in a small subset of tumors,

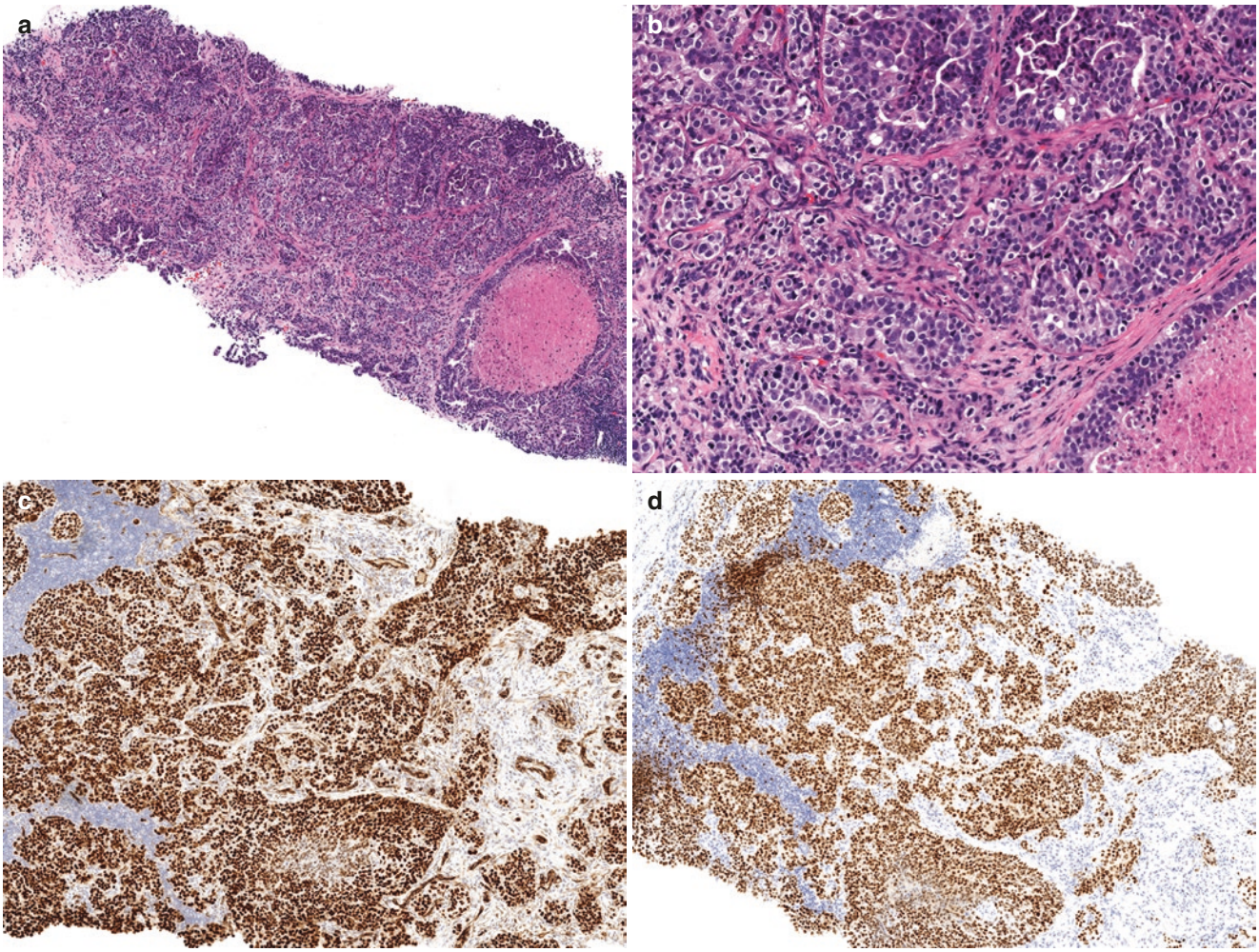

Fig. 10.30 Serous carcinoma of the ovary metastatic to breast. (**a**) Low-power magnification shows a high-grade invasive tumor with areas of necrosis mimicking in situ carcinoma, (**b**) high-power magnification, (**c**) WT1 and (**d**) PAX8 show diffuse nuclear staining in tumor cells confirming its Mullerian origin

that there might be a pathway leading from low-grade to high-grade as they demonstrated loss of 16q in high-grade lesions [88, 89]. Natrajan et al. noted 16q loss is more frequent in high-grade luminal subtype carcinomas compared to other high-grade carcinomas such as HER2 only or basal-like phenotypes [88].

Invasive breast carcinoma NST is a heterogenous disease, varying in histologic grades, HR/HER2 biomarker status, gene expression profiles, and genetic alterations. By gene expression profiling, IBCs-NST encompass all five intrinsic molecular subtypes: luminal A, luminal B, HER2-enriched, basal-like, and normal breast-like. Luminal A tumors (overall corresponding to low-grade, ER/PR-positive, HER2-negative IBC-NST with low Ki-67 proliferation rate) are enriched in *PIK3CA* mutations (~50%), whereas basal-like tumors (in general as high-grade ER/PR/HER2 triple-negative IBC-NST) have a high prevalence of *TP53* mutations (~85–90%). Studies from patients with genetic tumor syndromes have identified multiple genes that when altered are associated with an increased susceptibility to breast cancer. These breast cancer-predisposing genes include *BRCA1*, *BRCA2*, *PTEN* (Cowden syndrome), *TP53* (Li-Fraumeni syndrome), *ATM*, *PALB2*, and *CHEK2*, among others. Many of these genes are involved in DNA repair. Breast cancers occurring in these genetic tumor syndromes are mostly IBC-NST; however, tumors with mutations in select genes, either germline or somatically acquired, tend to show specific pathologic features. For example, most IBC with germline and/or somatic *BRCA1* mutations appear well-demarcated, have prominent lymphoplasmacytic infiltrate and are high grade with high mitotic activity. Breast cancers from Li-Fraumeni patients are most likely to be grade 3 IBC-NST

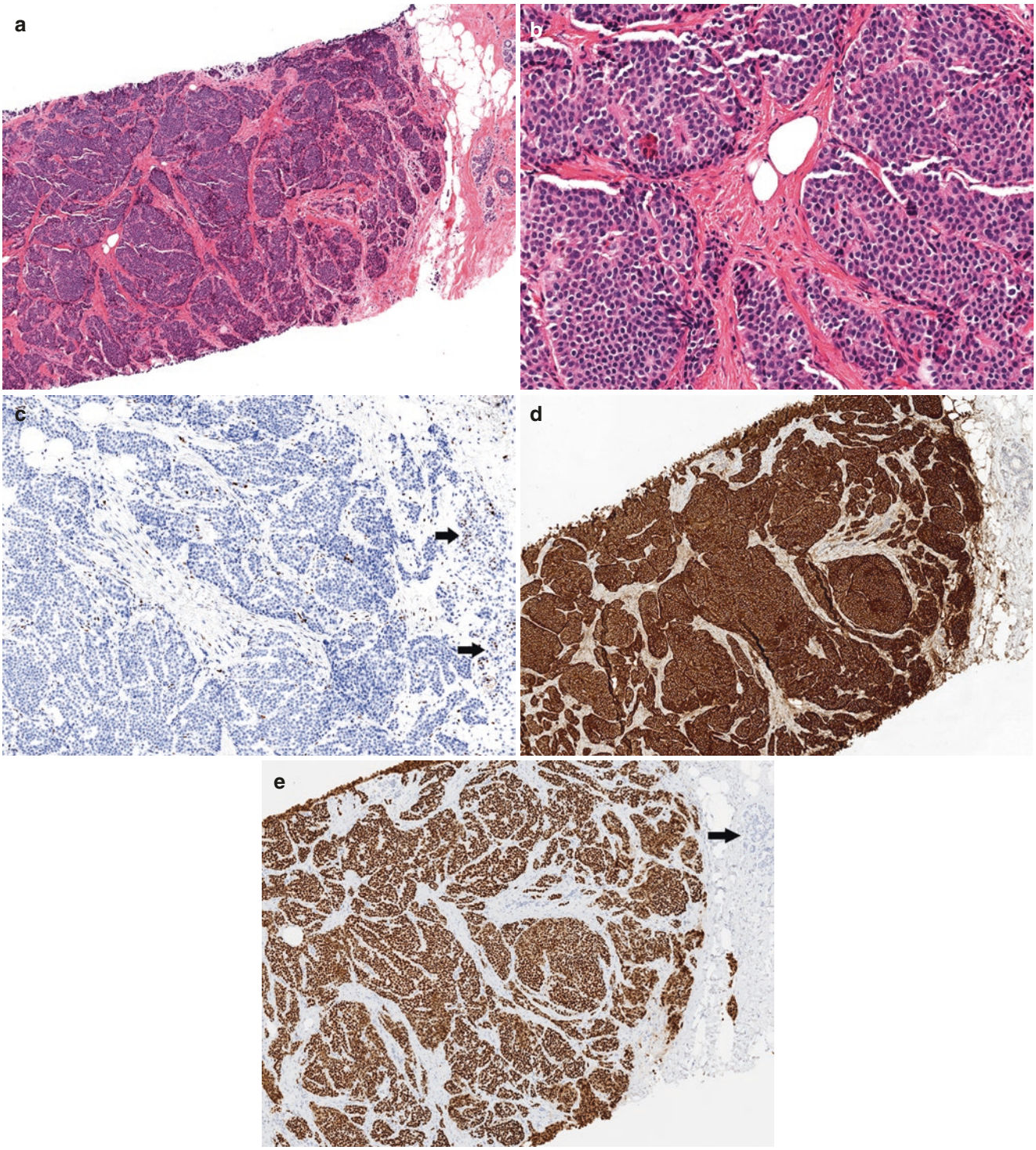

Fig. 10.31 Neuroendocrine tumor of ileum metastatic to breast. (**a**) Low-power view shows infiltrative growth pattern mimicking moderately differentiated IBC-NST. (**b**) High-power view shows prominent nesting and fine powdery chromatin of tumor cells. (**c**) Negative hormone receptor (ER/PR) staining (estrogen receptor stain shows compressed normal lobules with focal positive staining (*arrows*)) prompted further IHC investigation. (**d**) Chromogranin and (**e**) CDX2 show diffuse staining in tumor cells and no staining in normal lobule (*arrow*) (all breast-specific markers were negative, not shown)

with frequent HER2 overexpression/amplification (~60%), while apocrine differentiation is common in breast cancers from patients with germline *PTEN* mutations. Please refer to Chap. 23 for comprehensive discussion in molecular profiling of breast cancer.

Prognosis

The prognosis of IBC-NST depends on a number of factors. These include age, tumor size, histologic grade, lymph node status, hormone receptor (HR) status, and HER2 status. HR and HER2 status are also significant predictive factors for endocrine and anti-HER2 therapy, respectively (Fig. 10.32). Tumor infiltrating lymphocytes have recently been found to be a prognostic factor in TNBC and HER2-positive breast cancer [90]. Other factors that have been studied but found to be of uncertain significance include the presence of angioinvasion, perineural invasion, tumor necrosis, and DCIS (and its extent), among others [90]. Prognostic and predictive factors, including panel-based gene expression signatures (such as OncotypeDx®, MammaPrint®, Prosigna® and EndoPredict®), are further discussed in Chaps. 22 and 23.

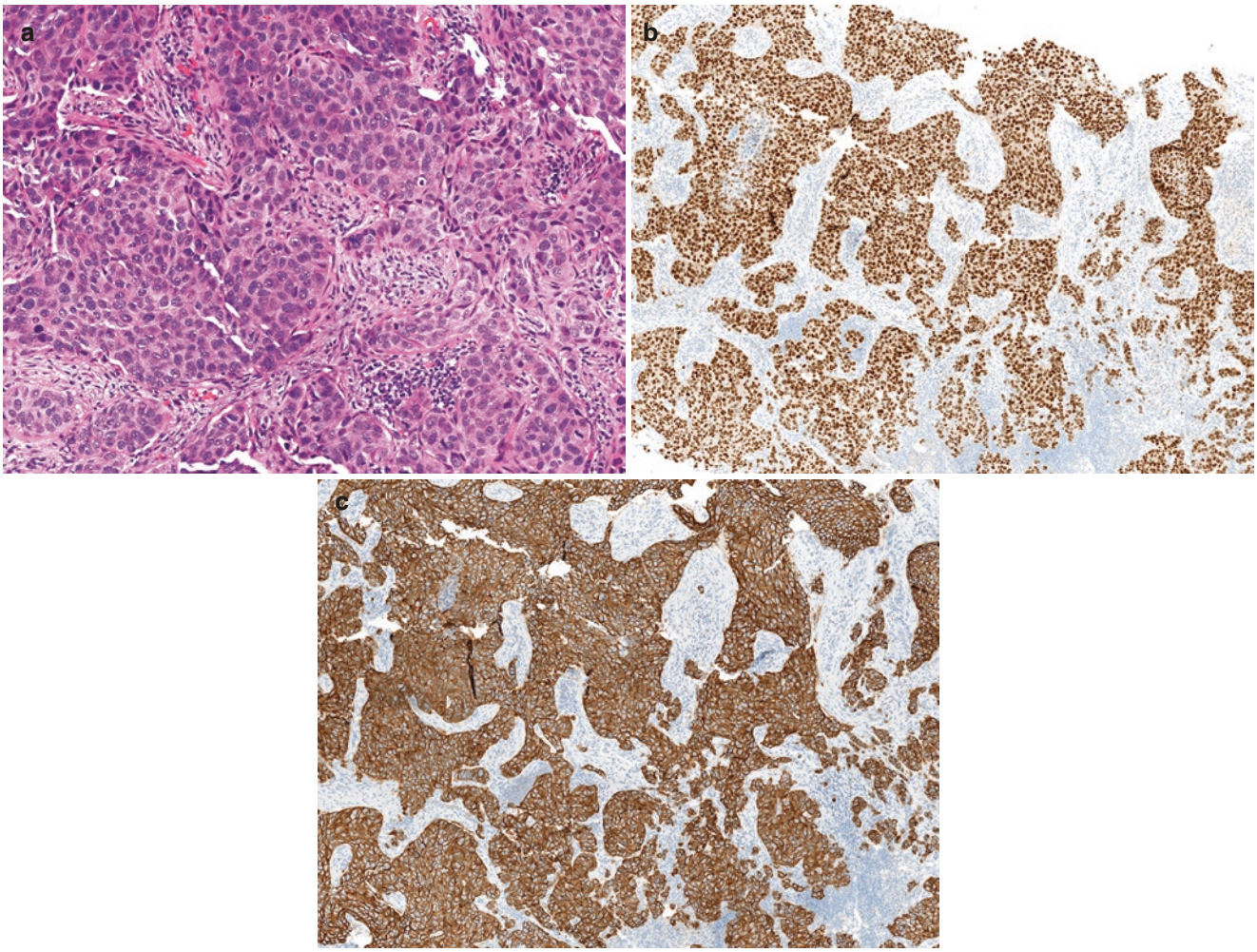

Fig. 10.32 Invasive breast carcinoma NST. (**a**) Low-power magnification, (**b**) diffuse strong nuclear staining with estrogen receptor, and (**c**) strong complete membranous staining with HER2

Microinvasive Breast Carcinoma

Overview

Microinvasive carcinoma (MIC) of the breast is defined as invasive carcinoma not exceeding 1 mm in greatest dimension [91]. MIC is uncommon and accounts for 0.68–2.4% of all IBCs [92–94]. It is usually associated with carcinoma in situ (CIS) and has been found in 9.5–13% of all DCIS cases [95, 96].

Microinvasion has been defined in various ways in the past. Some of the initial studies describing lymph node involvement in patients with MIC defined it as DCIS with stromal invasion without defining the size of invasion [97, 98]. Other definitions used previously include "DCIS with focal stromal invasion in less than or equal to 10% of the surface of histological section examined" [99], "more than single collection of cells outside the lobular unit or immediate periductal area" [100], "maximal extent of invasion…not more than 2 mm or comprising <10% of the tumor with 90% of DCIS" [101], "a single focus of invasive carcinoma ≤2 mm or up to three foci of invasion each not more than 1 mm in greatest dimension" [102], and "infiltration of neoplastic cells beyond the specialized lobular or intralobular stroma" [103]. In 1982, Lagios et al. defined microinvasion as invasive carcinoma less than 1 mm [104]. In 1996, the *American Joint Committee on Cancer* (AJCC) formally recognized MIC as invasive carcinoma measuring 1 mm or less, the definition of which has remained unchanged in subsequent editions of the *Cancer Staging Manual* [91].

Gross and Radiologic Features

MIC is a microscopic finding and does not have any specific clinical, radiological, or gross correlate that would distinguish it from "pure" DCIS of similar size and grade. However, certain radiologic features have been identified that are predictive of microinvasion or small invasive carcinoma. Large size DCIS (>5 cm), cases where the main mammographic feature is a mass, distortion, or asymmetry versus calcifications, and correspondingly patients who had ultrasound-guided CNB rather than a stereotactic CNB have been found to be associated with an upgrade to MIC when only DCIS was diagnosed on CNB [105–107]. Vieira et al. reviewed the ultrasound findings of 11 of 21 patients with MIC and found 10 manifested as a solid hypoechoic mass, supporting the association of microinvasion with mass-forming DCIS [105].

Microscopic Features

MIC is typically identified in association with high-grade DCIS (Fig. 10.33). It is unusual in the setting of low-grade DCIS (Fig. 10.34). Besides high-grade DCIS, MIC may be seen with LCIS, either classic or pleomorphic types [108] (Figs. 10.35 and 10.36). Histologic clues for microinvasion include high-grade DCIS, presence of periductal chronic inflammation, stromal edema, and stromal desmoplasia around DCIS (Fig. 10.37). The presence of excessive microcalcifications or comedonecrosis in high-grade DCIS is also associated with greater chance of finding MIC [95, 102, 109], but none of the above features are specific for microinvasion as they are often present in DCIS cases without invasion. If one is unable to follow the smooth outline around the branching ducts, lobules or other benign sclerosing lesions replaced by DCIS, MIC should be strongly suspected. The cells in microinvasive foci are cytologically identical to the adjacent in situ component and usually appear as single cells or small angulated clusters, often within the stroma immediately adjacent to the in situ component. Due to the limited amount of invasive tumor, assigning a combined histologic grade is not feasible. Therefore, it is recommended to specify only the nuclear grade for MIC or, if reasonable, the degree of differentiation based on tubular formation and nuclear grade. The presence of stromal retraction around the neoplastic nests, a finding often noted in frankly invasive carcinoma, is another helpful clue in the diagnosis of MIC (Figs. 10.38 and 10.39). Invasive foci may be multifocal in MIC and therefore a thorough sampling and search for additional (possibly larger) foci should be conducted when a single focus of MIC is identified in cases with extensive DCIS [109]. While the size of individual foci of MIC should not be added together to yield a single cumulative size of tumor, there are otherwise no standard guidelines dictating the minimum distance between foci to designate one as an individual focus.

Conversely, one should be careful not to overdiagnose MIC, a common pitfall highlighted by one retrospective review. This study found only 19.3% cases with an initial

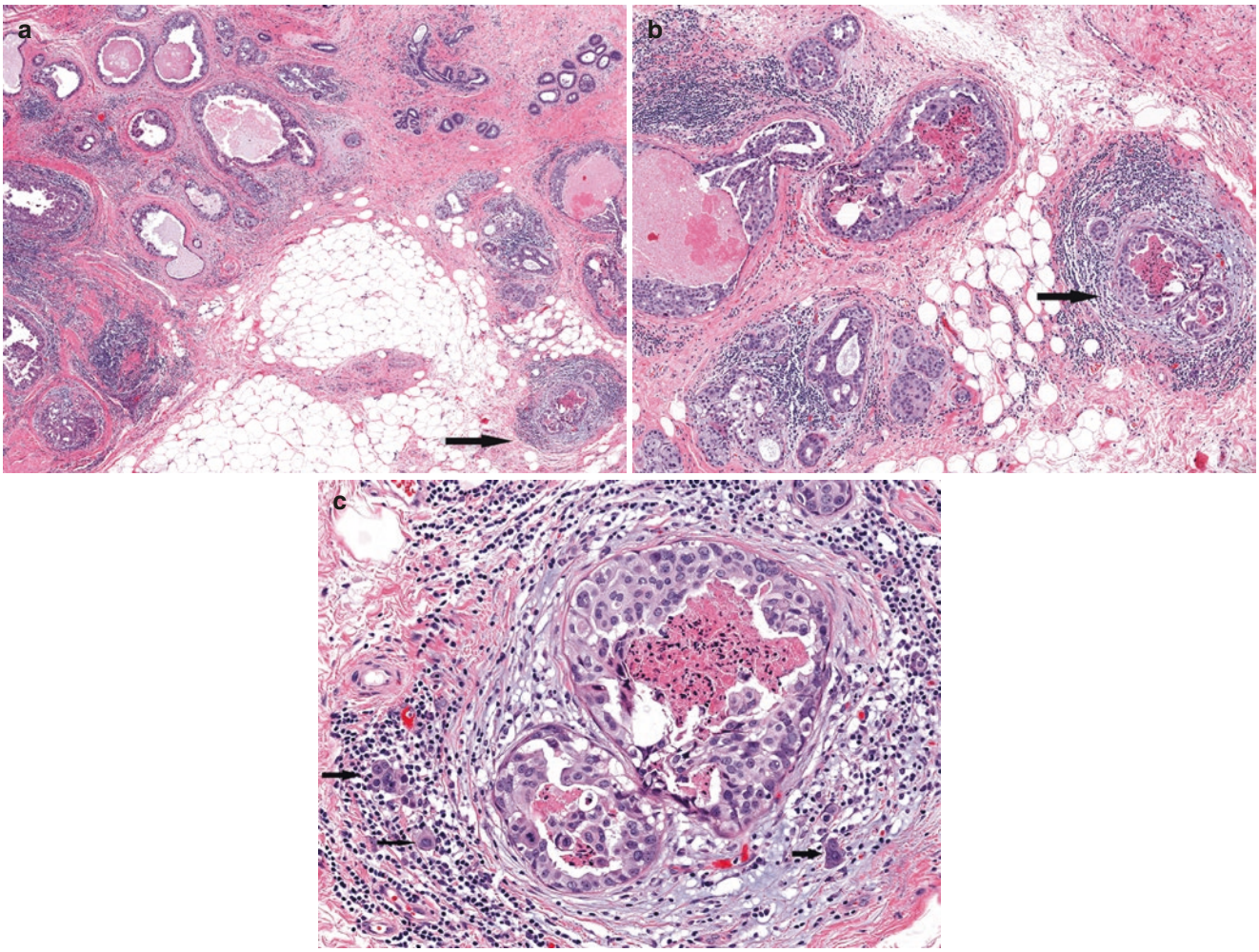

Fig. 10.33 High-grade DCIS with microinvasion. (**a**) Low-power view shows multiple ducts involved by high-grade DCIS with central necrosis and periductal fibrosis. (**b**) Medium power view reveals a focus of DCIS with prominent periductal fibrosis and inflammation (*arrow*). (**c**) Few single cells and small clusters of neoplastic cells in the intralobular stroma around DCIS are seen (*arrows*)

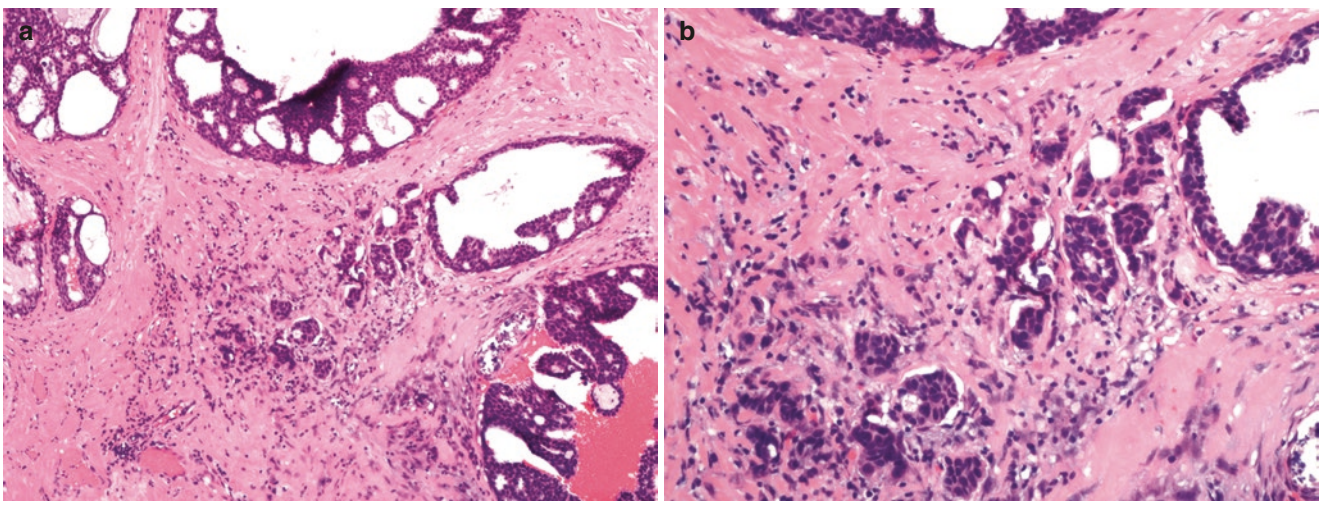

Fig. 10.34 Low-grade DCIS with microinvasion, (**a**) low-power and (**b**) high-power magnifications

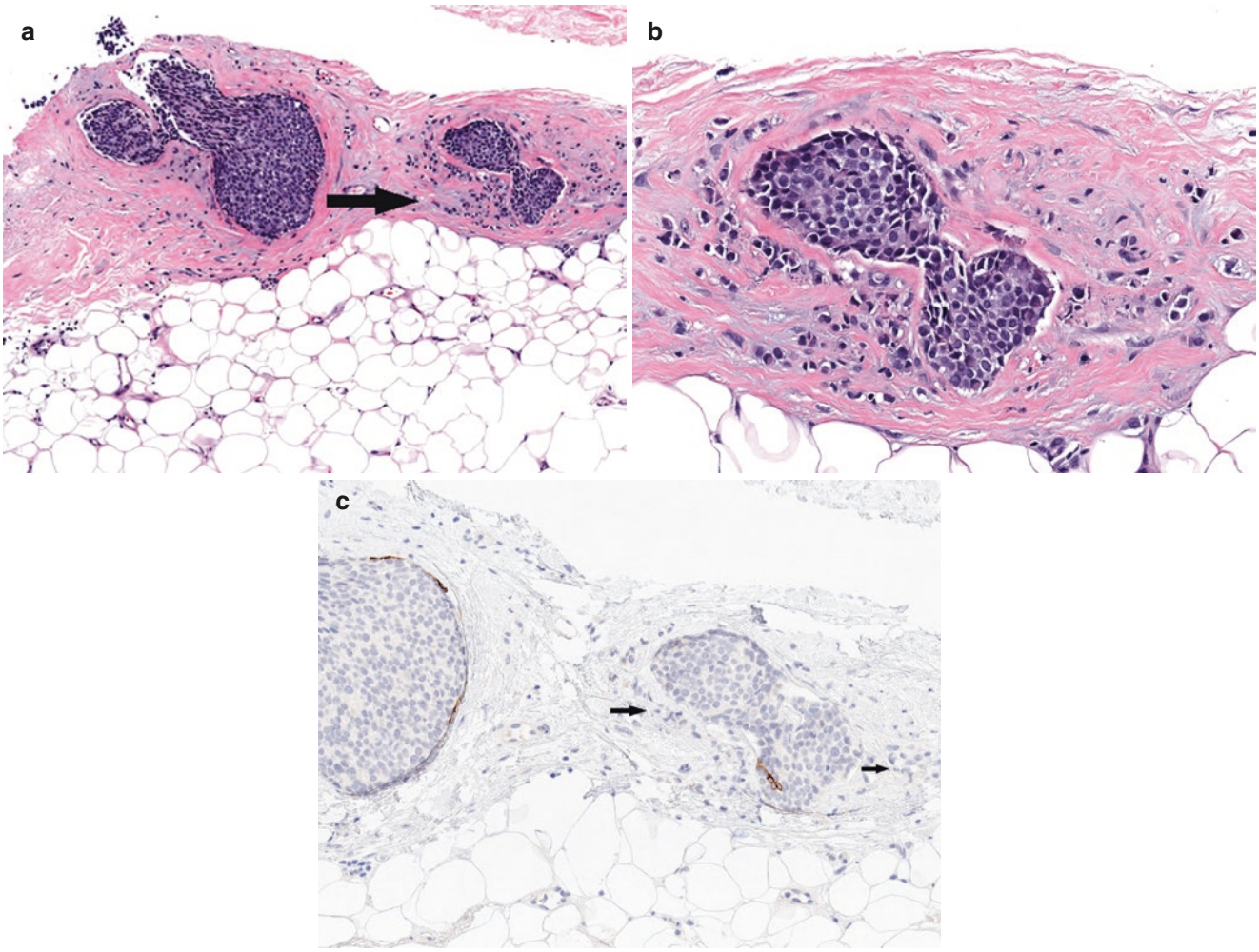

Fig. 10.35 Microinvasive lobular carcinoma associated with classic LCIS. (**a**) Low-power view shows microinvasive lobular carcinoma (*arrow*). (**b**) High-power view highlights linear infiltration by single tumor cells scattered around LCIS. (**c**) E-cadherin immunostain shows lack of staining in both in situ and invasive components (*arrow*) while focal weak positivity is retained in myoepithelium investing LCIS

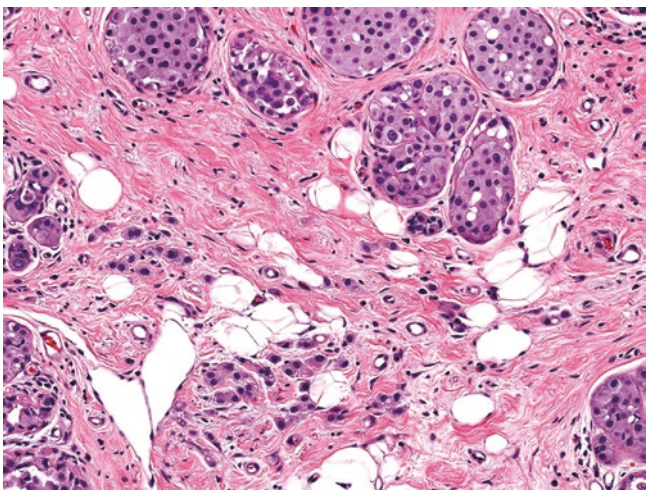

Fig. 10.36 Microinvasive lobular carcinoma (*center left*) associated with pleomorphic LCIS

diagnosis of MIC or suspicious for microinvasion were truly MIC [110]. Diagnosing MIC on CNB is of particular importance because of the implications for further management (discussed in the section "Prognosis").

Differential Diagnosis

Lesions that can mimic MIC or small invasive carcinoma in a CNB include lobular involvement by DCIS (cancerization of lobules), branching or budding ducts of DCIS distorted by fibrosclerosis, and sclerosing lesions including adenosis or radial scar involved by DCIS (Figs. 10.40, 10.41, 10.42, 10.43, and 10.44). This can be particularly challenging in a CNB where the underlying lesion, e.g., sclerosing adenosis, may not be present or apparent due to limited material. MIC should be cautiously diagnosed in limited samples unless it

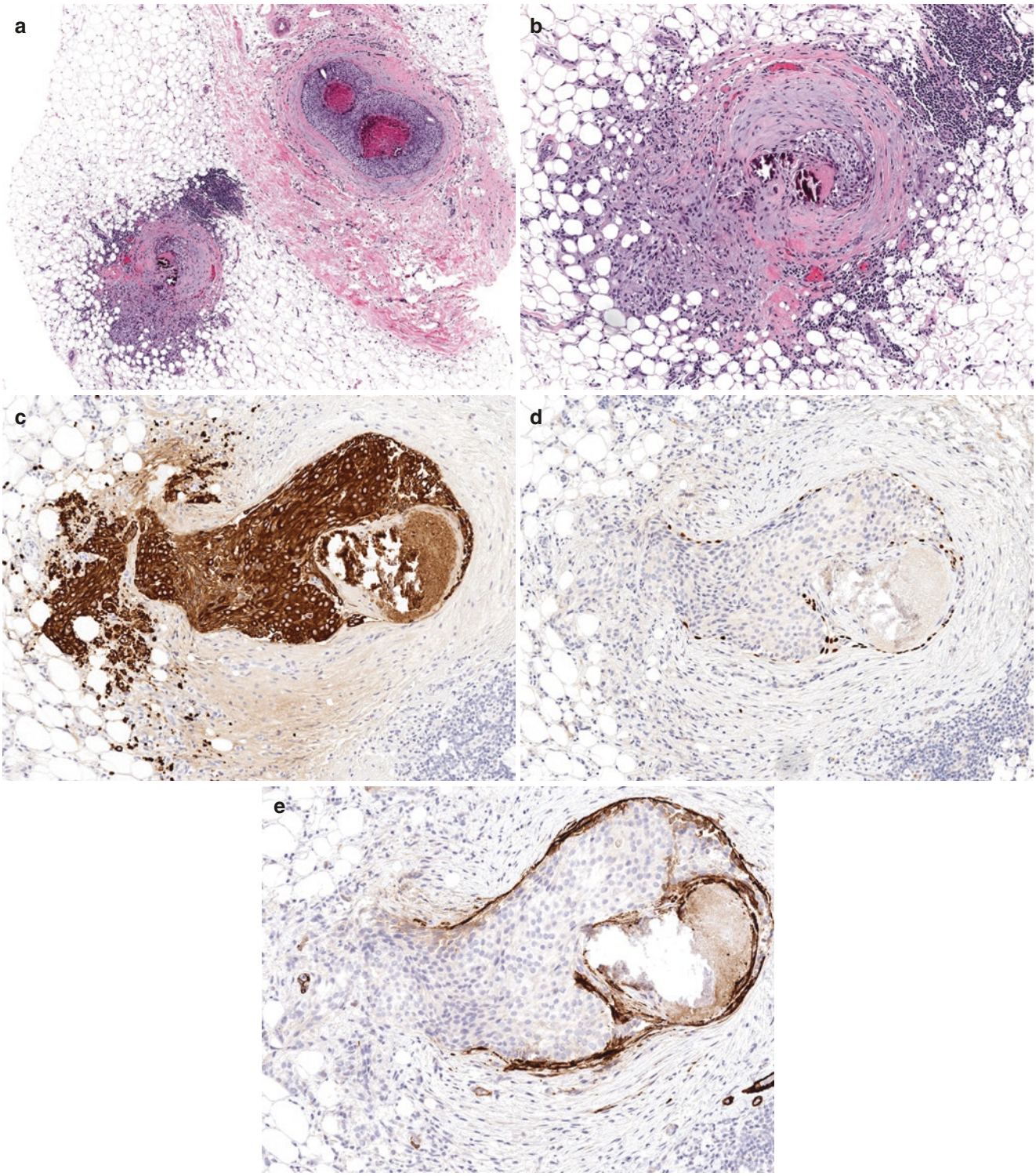

Fig. 10.37 DCIS with microinvasion. (**a**) Low-power view shows DCIS associated with marked periductal fibrosis and inflammation extending into the fat (*lower left*). (**b**) Higher power view shows the duct with disrupted wall but the presence of microinvasive carcinoma is difficult to discern. (**c**) Cytokeratin stain highlights the single cells dispersed in the fibrotic and inflammatory stroma. (**d**) Immunostain for p63 shows myoepithelial cells surrounding portion of the DCIS but absent in microinvasive carcinoma. (**e**) SMM shows similar pattern with loss of myoepithelial cells in the microinvasive focus

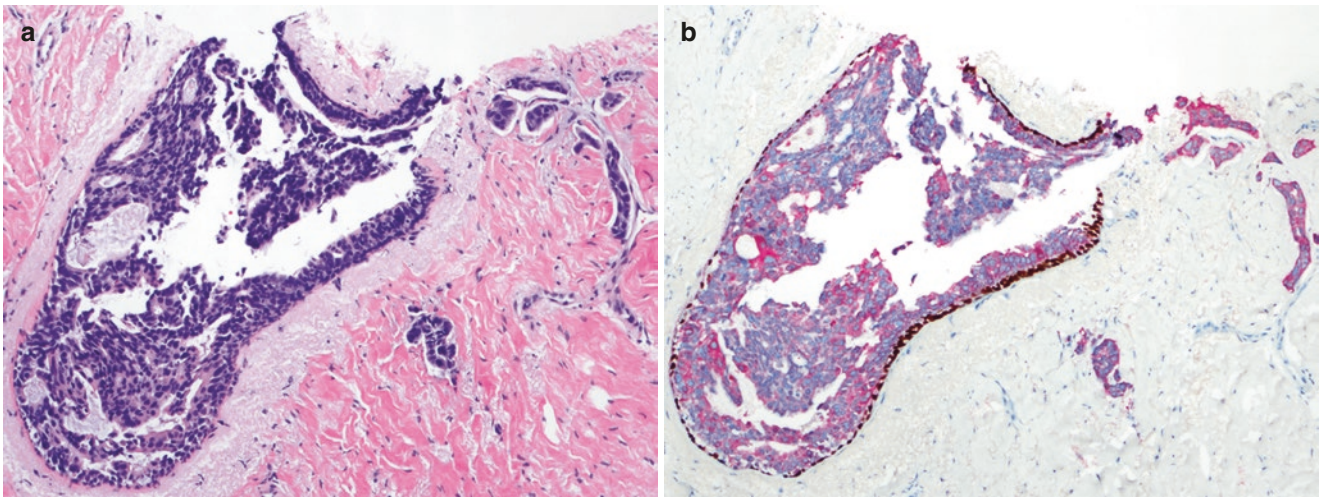

Fig. 10.38 Microinvasive carcinoma in a core needle biopsy adjacent to DCIS. (**a**) H&E section demonstrates stromal retraction around the invasive tumor nests. (**b**) Double IHC stain for p63 (brown chromogen) and cytokeratin (red chromogen) shows complete lack of myoepithelial staining around MIC

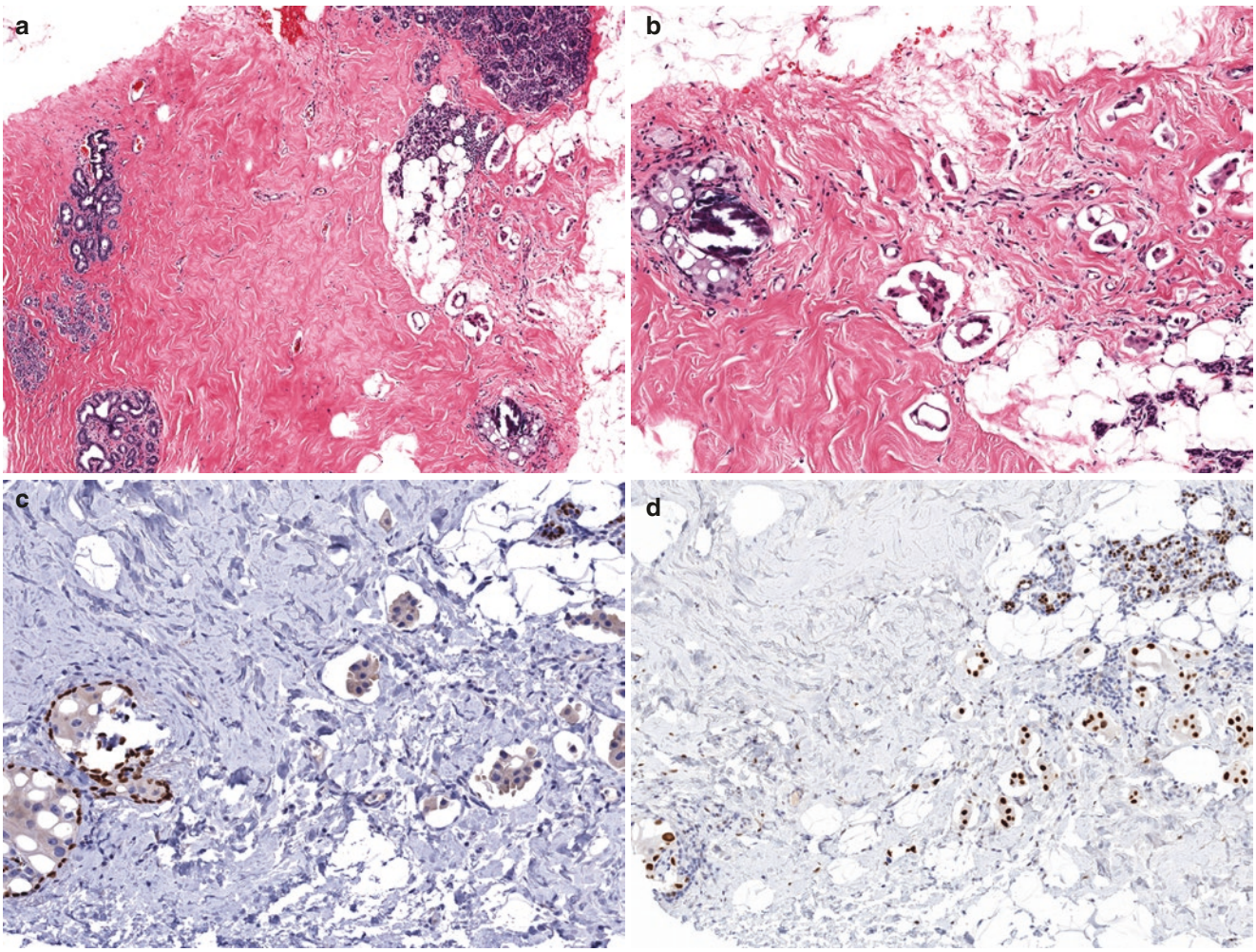

Fig. 10.39 Microinvasive carcinoma with marked retraction artifact. (**a**) Core needle biopsy with microinvasion and a small focus of DCIS with associated calcification. (**b**) High-power view highlights stromal retraction around the invasive tumor nests. (**c**) Immunostain for p63 shows lack of myoepithelial cells in microinvasive focus (*right*) while DCIS retains positivity (*left*). (**d**) Microinvasive carcinoma as well as DCIS are positive for estrogen receptor immunostain

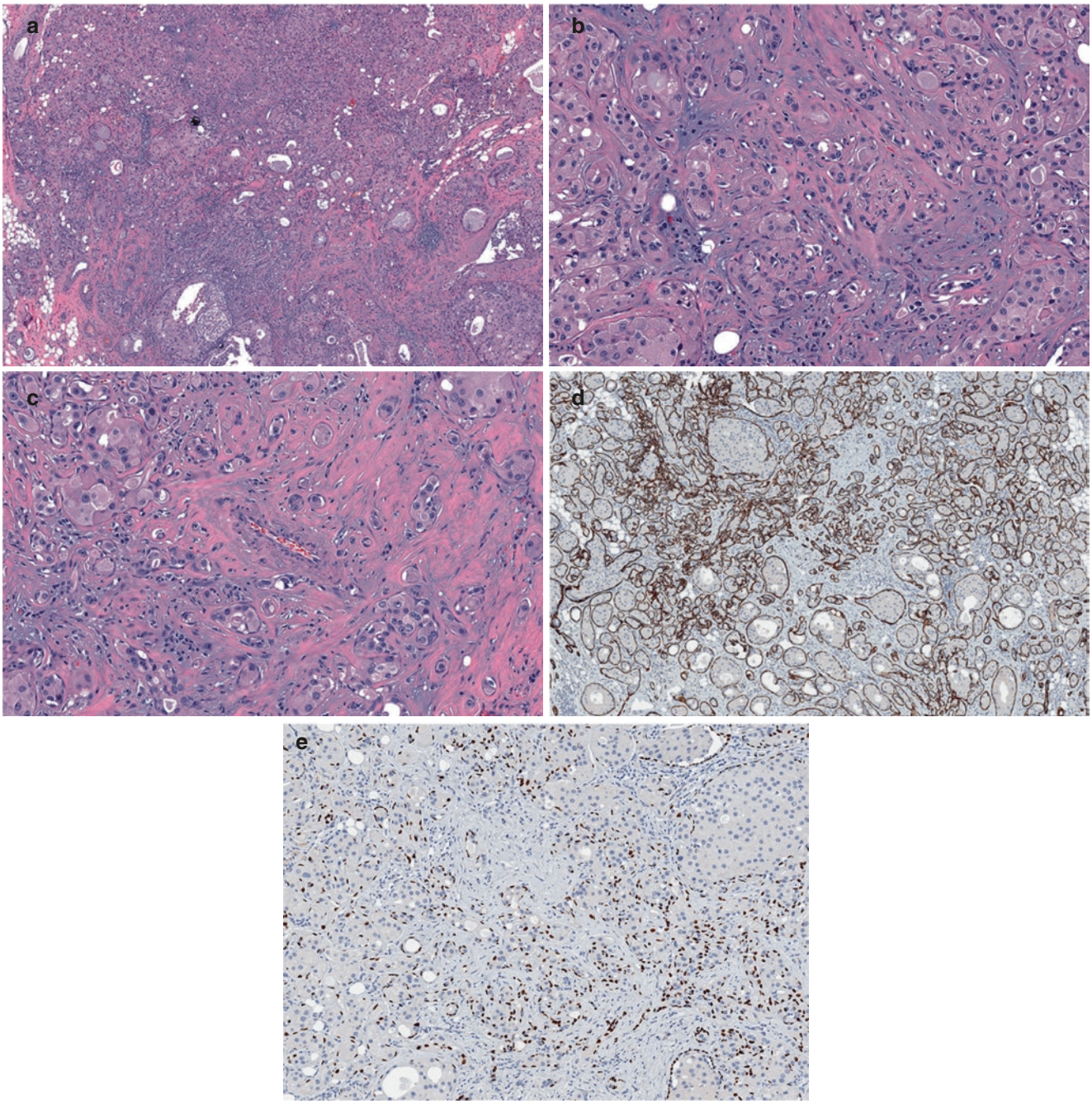

Fig. 10.40 Mass-forming DCIS. (**a**) Low-power and (**b**, **c**) high-power magnifications of different areas of the tumor consisting of sclerosis and entrapped cancerized lobules mimicking invasive carcinoma. (**d**) Immunostains for SMM and (**e**) p63 highlight intact myoepithelial cells throughout the lesion including sclerosing areas

is unequivocal. If the suspected microinvasive focus is depleted on myoepithelial immunostains or the immunostains are inconclusive, a diagnosis of "DCIS, suspicious for microinvasion" with an explanatory note is recommended.

One pitfall unique to excision specimens is the artifactual displacement of epithelial cells into the stroma, introduced at the time of a CNB or fine-needle aspiration. These embedded epithelial clusters can mimic MIC, particularly if the displaced cells are neoplastic (Fig. 10.45). Displaced epithelium can occur after a CNB for DCIS where neoplastic cells are easily dislodged [111, 112]. Microscopic clues including associated reparative fibrosis, fat necrosis, recent hemor-

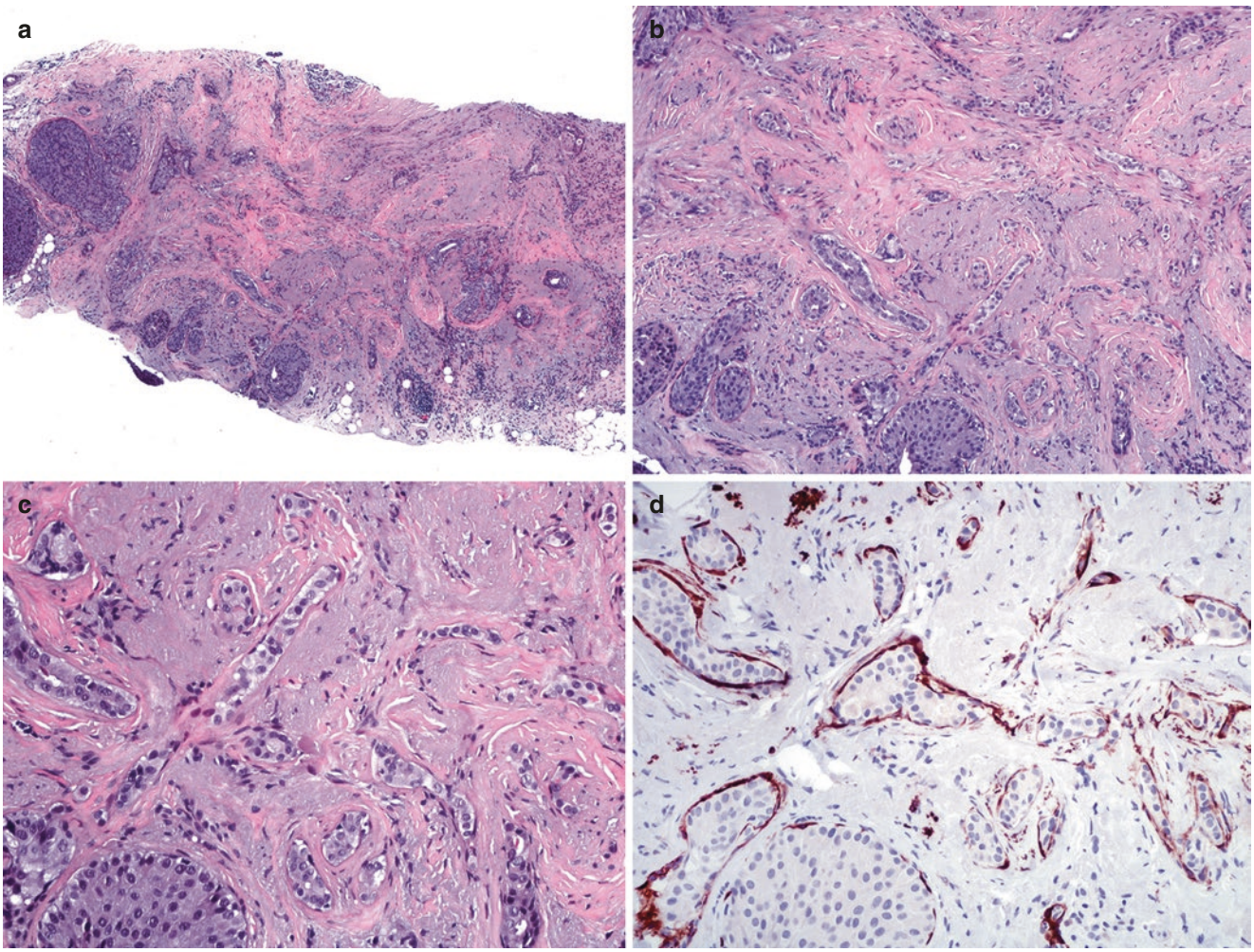

Fig. 10.41 Radial scar involved by DCIS. (**a**) Low-power view of CNB containing a sclerosing lesion, (**b**) center of the radial scar with elastosis and entrapped ducts and lobules involved by neoplastic cells. (**c**) Medium power view shows elongated entrapped neoplastic ductules. (**d**) SMM immunostain shows intact myoepithelial cells around entrapped ductules

rhage, or hemosiderin-laden macrophages in a previous core biopsy tract should make the pathologist to consider a diagnosis of epithelial displacement rather than invasive carcinoma [112]. Immunohistochemical stains for myoepithelial cells are only helpful in rare cases of displaced non-high-grade DCIS or benign entity where myoepithelium is still retained in the epithelial clusters. The absence of myoepithelium evidenced by negative staining, however, does not exclude the possibility of displaced epithelium.

Immunohistochemistry

As with any IBC, the most useful immunostains to confirm a diagnosis of MIC are those for myoepithelial cells. In addition, cytokeratin can be helpful, particularly in cases of DCIS with marked lymphocytic infiltrate, as it highlights single cells and small epithelial clusters of MIC (Fig. 10.37). Ideally, MIC is easier to confirm if double IHC staining for myoepithelial cells and cytokeratin is available (Fig. 10.38). Immunostains for basement membrane such as collagen type IV and laminin are not necessary and further can be difficult to interpret.

Due to the small size of MIC, residual MIC may not be present on subsequent stains for ER/PR/HER2 analysis. In many cases, however, the adjacent DCIS shows identical expression of these markers, and some may use this as a surrogate [113]. Cases of high-grade DCIS with MIC are often ER/PR negative and HER2 positive (Fig. 10.46).

The limited amount of invasive tumor available for IHC assessment underscores the importance of anticipating the stains needed and proceeding accordingly. When MIC is sus-

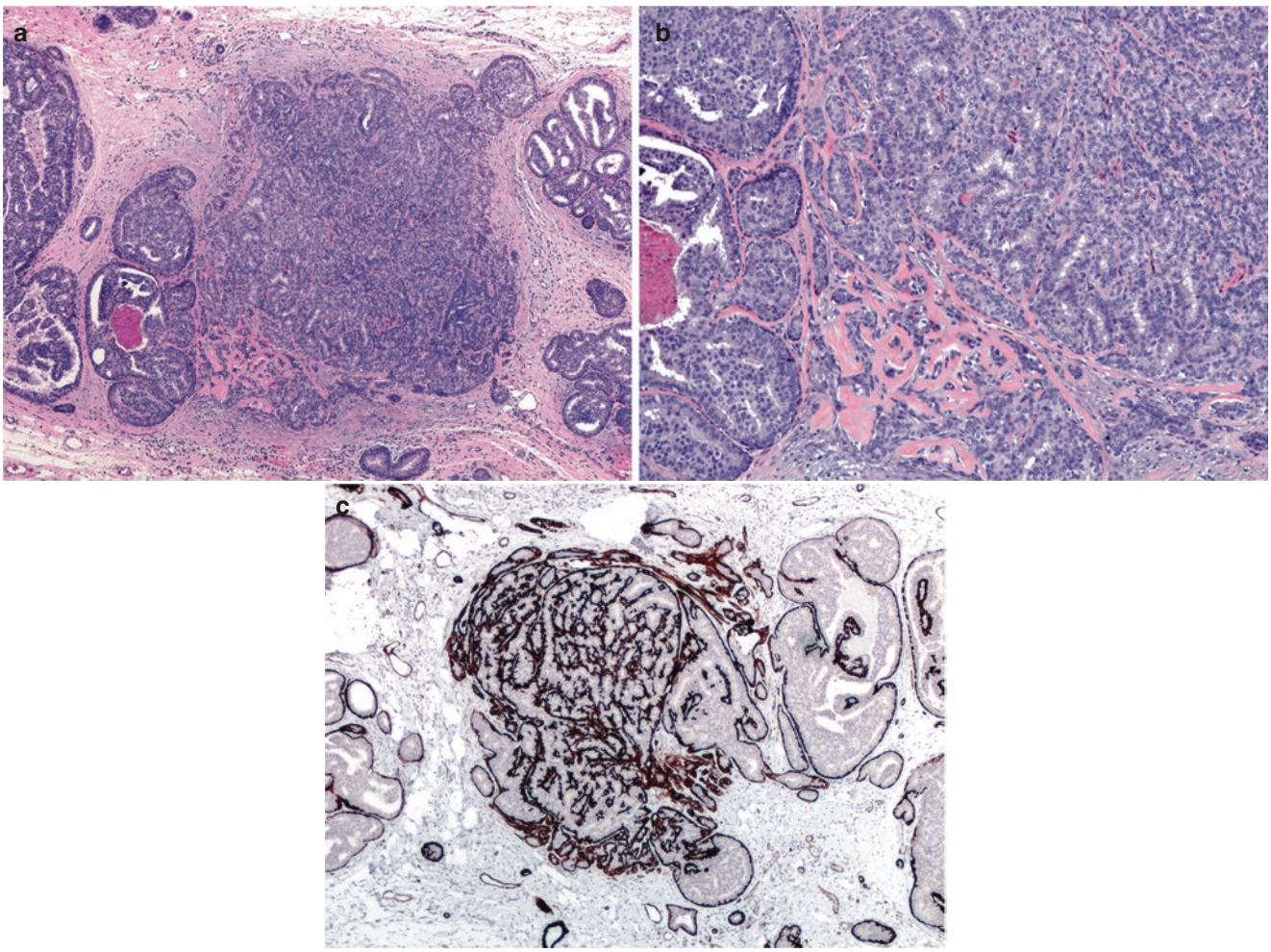

Fig. 10.42 Low-grade DCIS involving sclerosing adenosis. (**a**) Low-power and (**b**) high-power magnifications. (**c**) SMM immunostain shows intact myoepithelium

pected in a background of DCIS, performing at least two myoepithelial stains, a cytokeratin stain, ER, PR, and preparing at least three unstained slides for possible subsequent HER2 immunostain and HER2 FISH, with instructions that they all be cut from the paraffin block in one sitting is recommended. Implementing a breast MIC stain protocol may be prudent.

Prognosis

Few studies have addressed the upgrade of DCIS diagnosed on CNB to microinvasive or frankly invasive carcinoma. In one study, 13 of 93 patients (14%) with DCIS diagnosed on CNB also had microinvasion and another 31 (33%) had invasive carcinoma on excision [107]. Another study of 192 patients diagnosed as DCIS on vacuum-assisted CNB reported 10% and 29% upgrade to microinvasion and invasive carcinoma, respectively [114]. In the United Kingdom, 3% of DCIS cases diagnosed on CNB were upgraded to microinvasion and 18% to invasive carcinoma [115].

The incidence of sentinel lymph node metastasis in MIC is less than 5%. One meta-analysis that included 968 patients from 24 studies reported 3.2% macrometastasis (95% confidence interval (CI) 2.1–4.6%), 4% micrometastasis (95% CI 2.7–5.5%), and 2.9% isolated tumor cells (95% CI 1.6–4.6%) in MIC [116]. In addition, patients with MIC have a 0.95% risk of metastasis to non-sentinel lymph nodes as reported in one study [116]. Several studies have reported excellent prognosis in MIC irrespective of lymph node involvement [117, 118]. Disease-free survival and overall survival for patients with MIC closely resembles that of pure DCIS of equivalent size and grade [119]. The risk of distant metastasis is extremely low, ranging from 0% to 2% with a median follow-up of 4–9 years [117, 118, 120]. Another study however found the prognosis of microinvasive carcinoma to

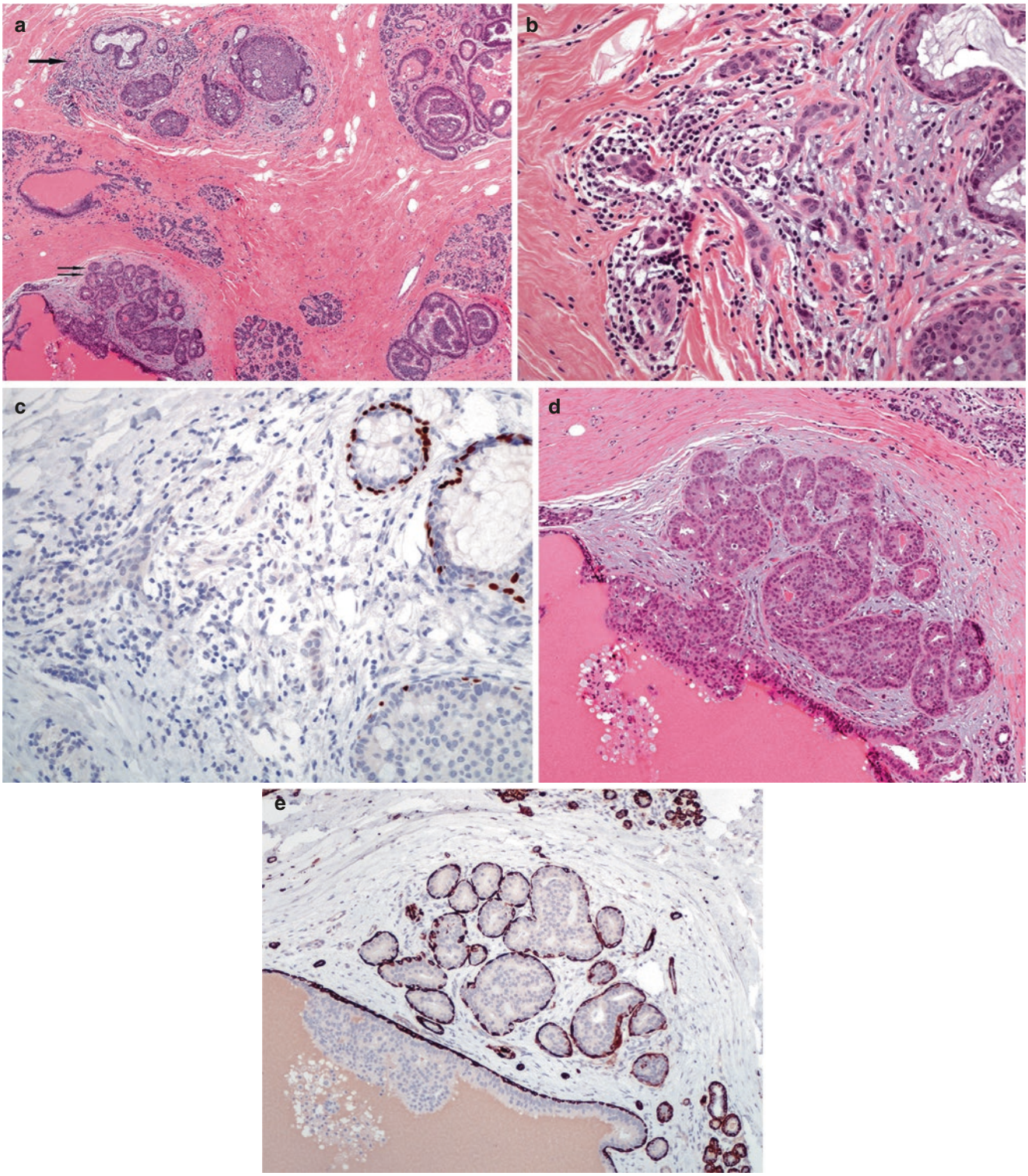

Fig. 10.43 Low-grade DCIS. Microinvasion vs cancerized lobules. (**a**) Low-power view shows microinvasion (*single arrow*) and cancerized lobules (*two arrows*). (**b**) High-power view of microinvasion. (**c**) p63 stain shows lack of staining in microinvasive carcinoma. (**d**) High-power view of cancerized lobules. (**e**) SMM immunostain shows intact myoepithelial cells around cancerized lobules

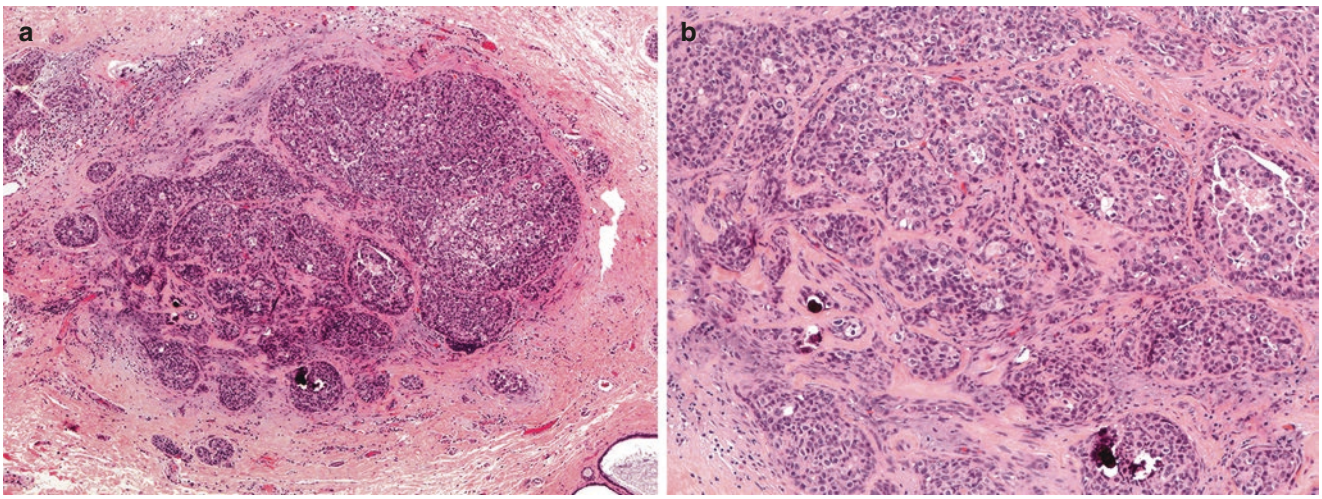

Fig. 10.44 High-grade DCIS with sclerosis. (**a**) Low-power view, (**b**) high-power view reveals the smooth outline of pink basement membrane around the distorted lobules which can be helpful if present

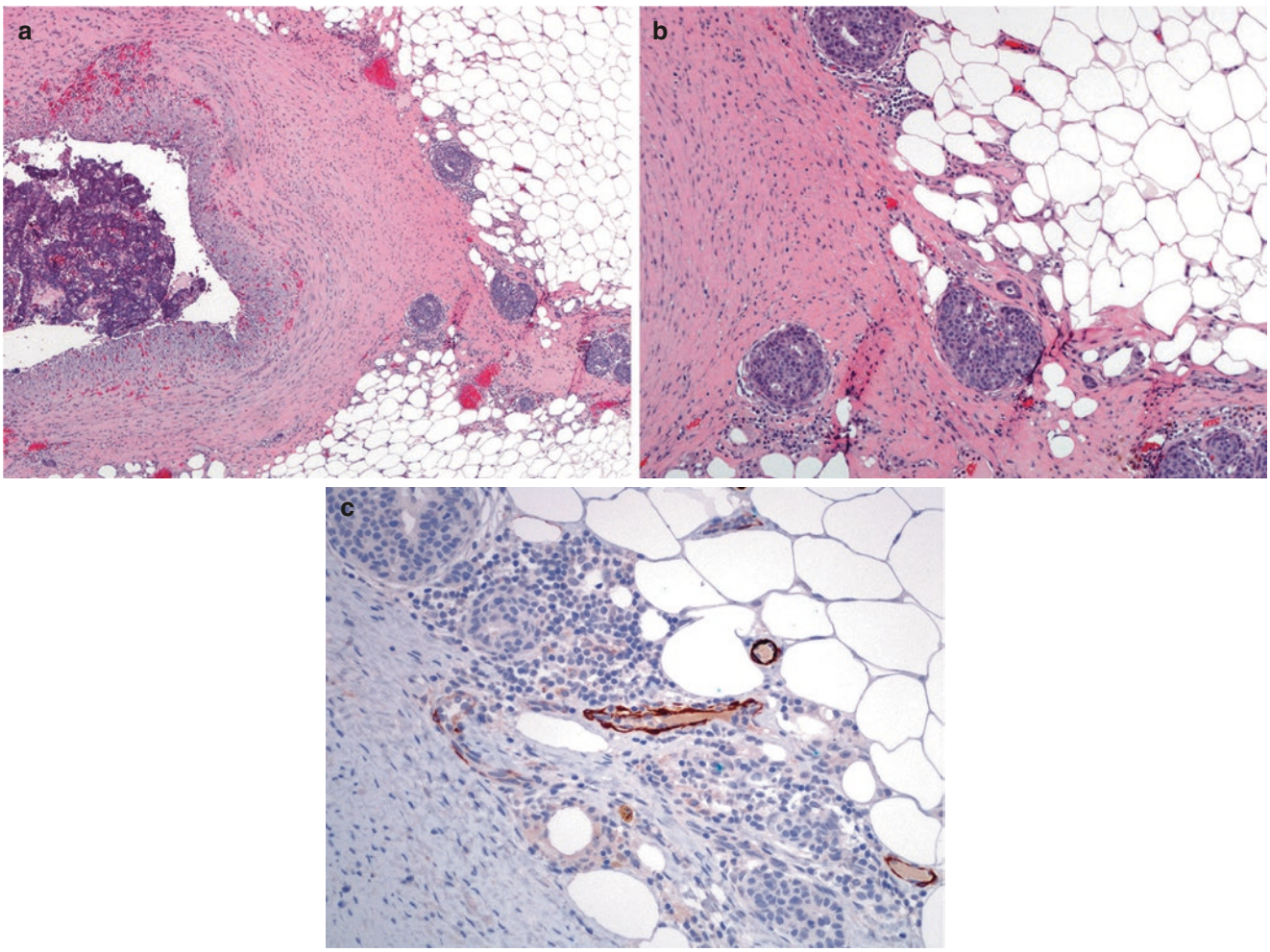

Fig. 10.45 Displaced neoplastic cells from a prior core biopsy of an encapsulated papillary carcinoma. (**a**) Low-power magnification shows the encapsulated papillary carcinoma and the needle tract with displaced neoplastic cells embedded in scar tissue. (**b**) High-power magnification reveals nests of neoplastic cells with associated fat necrosis. (**c**) Immunostain for SMM demonstrates lack of myoepithelial cells around the displaced nests

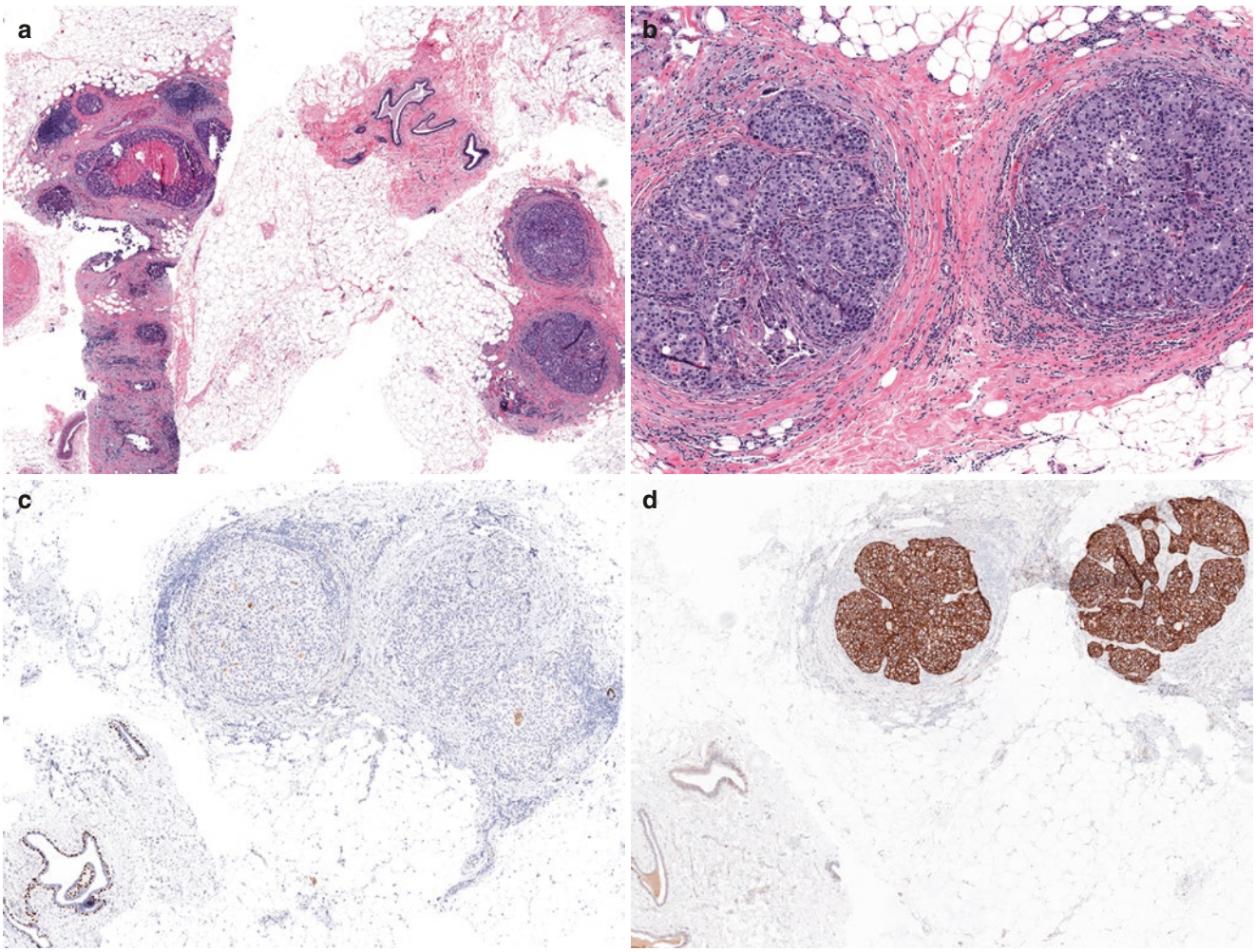

Fig. 10.46 Microinvasive carcinoma masquerading as DCIS. (**a**) Low-power view, (**b**) high-power view shows round contour in the invasive foci that can be misconstrued as in situ carcinoma. (**c**) Immunostain for SMM shows complete lack of staining in those foci. (**d**) HER2 stain shows strong positive membranous staining (3+) in MIC (both DCIS and MIC were negative for ER and PR, not shown)

resemble invasive carcinomas less than 1 cm in size while a SEER analysis found an increased mortality rate for microinvasive carcinoma versus DCIS [121, 122].

Whether sentinel lymph node biopsy (SLNB) is performed in patients diagnosed with pure DCIS or DCIS with microinvasion depends not only on whether the patient is undergoing breast-conserving surgery or total mastectomy but also on the clinical presentation and imaging findings. The 2014 *American Society of Clinical Oncology* (ASCO) guidelines recommend that SLNB be performed in cases of DCIS or DCIS with microinvasion diagnosed on CNB if mastectomy is planned as it obviates the need for subsequent axillary dissection if invasive carcinoma is found [120]. In patients undergoing breast-conserving surgery, this issue is more controversial. Some support routine SLNB because there is a 10–20% chance of an upgrade from DCIS with or without microinvasion to frank invasive carcinoma, especially when DCIS is large (≥5 cm), DCIS presents as a mass lesion by imaging and/or on physical examination, or high-grade DCIS is associated with comedonecrosis [123, 124].

Tubular Carcinoma

Overview

Tubular carcinoma is a well-differentiated invasive carcinoma with distinct morphologic features and an excellent prognosis. It is rare, often reported to comprise less than 2% of all IBC [125–128]. Most women are diagnosed in their late 50s or early 60s [127, 129–131]. SEER data shows that the majority of tubular carcinomas occur in non-Hispanic white women (90%), followed by African-American (3.6%), Asian/Pacific Islanders (3.5%), Hispanic white (2.3%), and American Indian/Alaska Native (0.5%) women [132]. Tubular carcinoma is also rare in men [133]. Tubular carci-

noma can be multifocal with one study finding 10 of 103 patients with pure tubular carcinomas having multiple foci ranging from 2 to 5 in number [134].

Gross and Radiologic Features

On mammogram, tubular carcinoma appears as a round, oval or lobulated, dense mass with irregular or spiculated margins, occasionally accompanied by microcalcifications [135, 136] (Fig. 10.47). Imaging findings are nonspecific and can overlap with patterns seen in sclerosing adenosis, radial scar, or IBC-NST [137, 138] (Fig. 10.48). Widespread mammographic screening has led to an increased incidence of tubular carcinomas as it detects non-palpable tumors (1 cm or less in size); small, incidental tumors are also found in biopsies performed for unrelated reasons [139–141]. Ultrasonography has been reported to be more helpful than mammography in detecting smaller-sized lesions [142] (Fig. 10.49).

Tubular carcinomas that are grossly identifiable are indistinguishable from other IBC-NST, appearing as tan-white to gray, ill-defined, firm to hard, stellate lesions. The stellate appearance is due to extensive elastosis and desmoplasia that often accompanies this tumor. The majority of tubular carcinomas are 1 cm or less, but larger tumors have been described [129, 131, 143]. The largest tubular carcinoma reported in the literature is 12 cm [144]. Larger tumors however are more likely to be mixed type with an IBC-NST component, rather than pure tubular carcinomas.

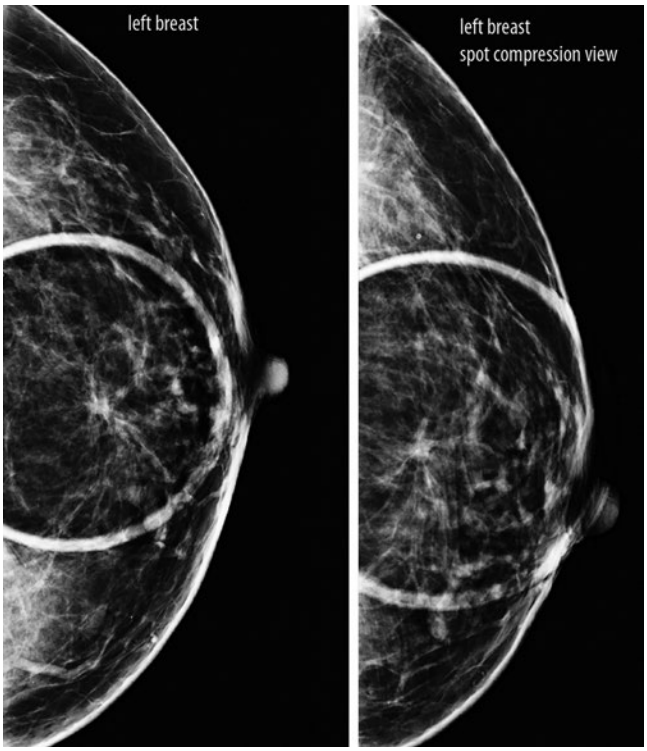

Fig. 10.47 Tubular carcinoma. Mammographic appearance of a 7 mm irregular mass with spiculated margins and associated architectural distortion seen at the 12 o'clock region that persists on spot compression view

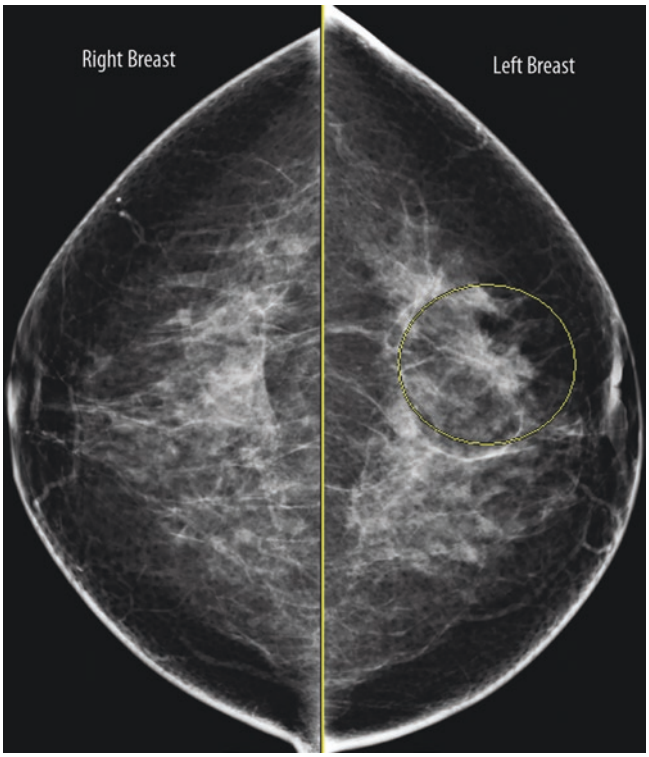

Fig. 10.48 Radial scar. Mammographic appearance of a 2.5 cm focal asymmetry (*circled*) that was interpreted as BIRADS 5, suspicious for invasive carcinoma

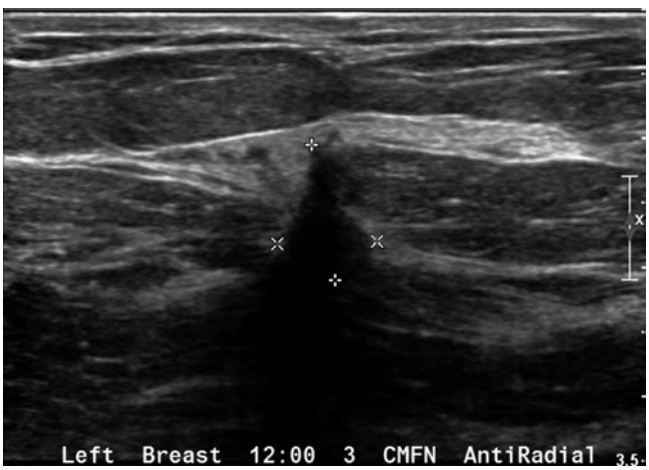

Fig. 10.49 Tubular carcinoma. Ultrasound of the tumor in Fig. 10.47 shows an oval hypoechoic mass

Microscopic Features

Tubular carcinoma is characterized by glands or tubules with open lumens lined by a single layer of neoplastic epithelium. In the majority of cases, the lesion is easily recognizable at low power because of the pale blue tincture of the stroma that appears different from the surrounding normal breast. The tubules are arranged in a haphazard manner, often embedded within a dense sclerotic and elastotic stroma, imparting a stellate appearance to the tumor (Figs. 10.50, 10.51, 10.52, 10.53, and 10.54). The tubules are round to oval, often angulated, lined by monotonous cuboidal to low columnar cells with eosinophilic to amphophilic cytoplasm and apical snouts (Fig. 10.55). Myoepithelial cells are absent around these tubules. The nuclei lining the tubules are low-grade, basally oriented, with evenly dispersed chromatin and inconspicuous nucleoli. Mitoses are rare. Microcalcifications are often identified in tubular carcinomas, either in the stroma, with associated benign lesions (discussed later), in associated DCIS, or in the neoplastic tubules. Lymphovascular invasion is extremely rare and necrosis is virtually non-existent.

In the past, the proportion of tubules required to classify a tumor as tubular carcinoma ranged from 75% to 100% [127,

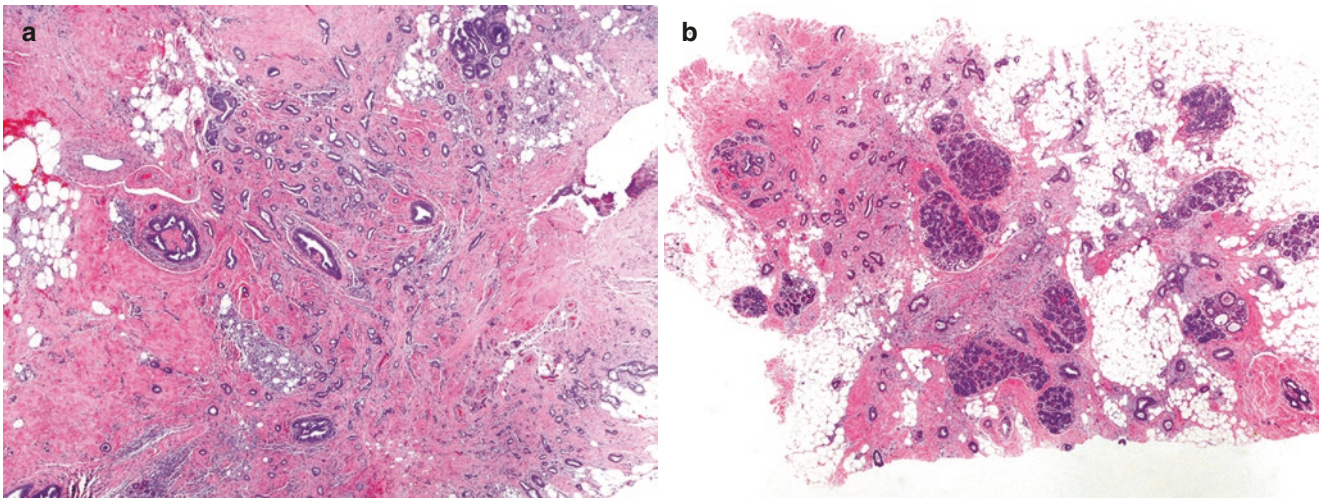

Fig. 10.50 Tubular carcinoma. (**a**) The haphazard arrangement of the tubules in a dense stroma contributes to the stellate appearance of the tumor. (**b**) Low-power view of a tubular carcinoma with pale appearing stroma

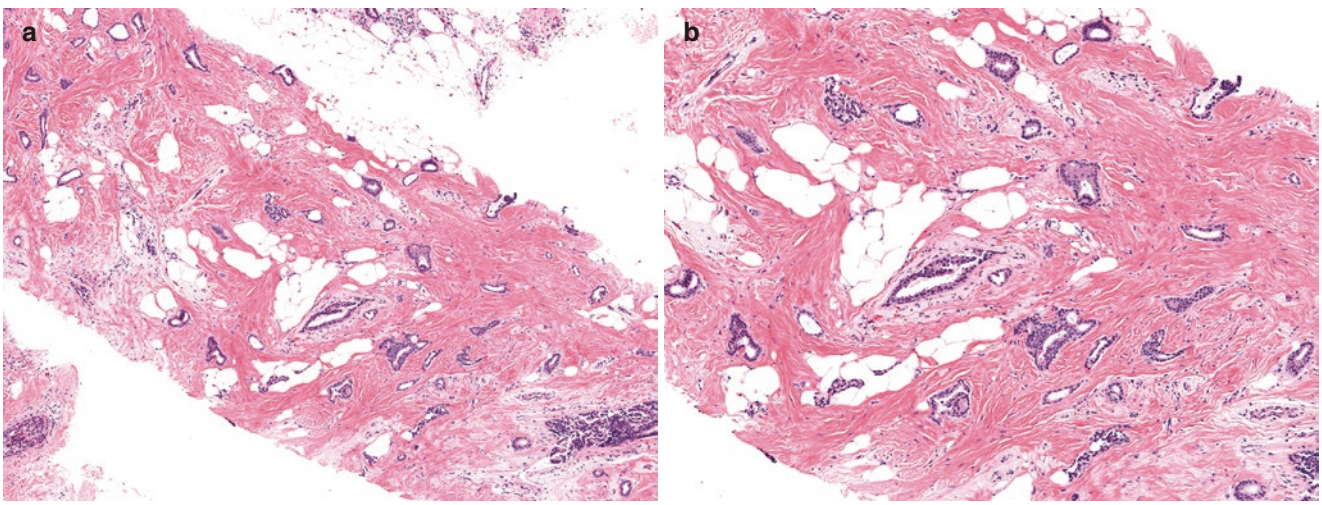

Fig. 10.51 Tubular carcinoma. (**a**) Low-power view shows the haphazard arrangement of tubules in dense stroma with focal elastosis. (**b**) High-power view shows angulated glands

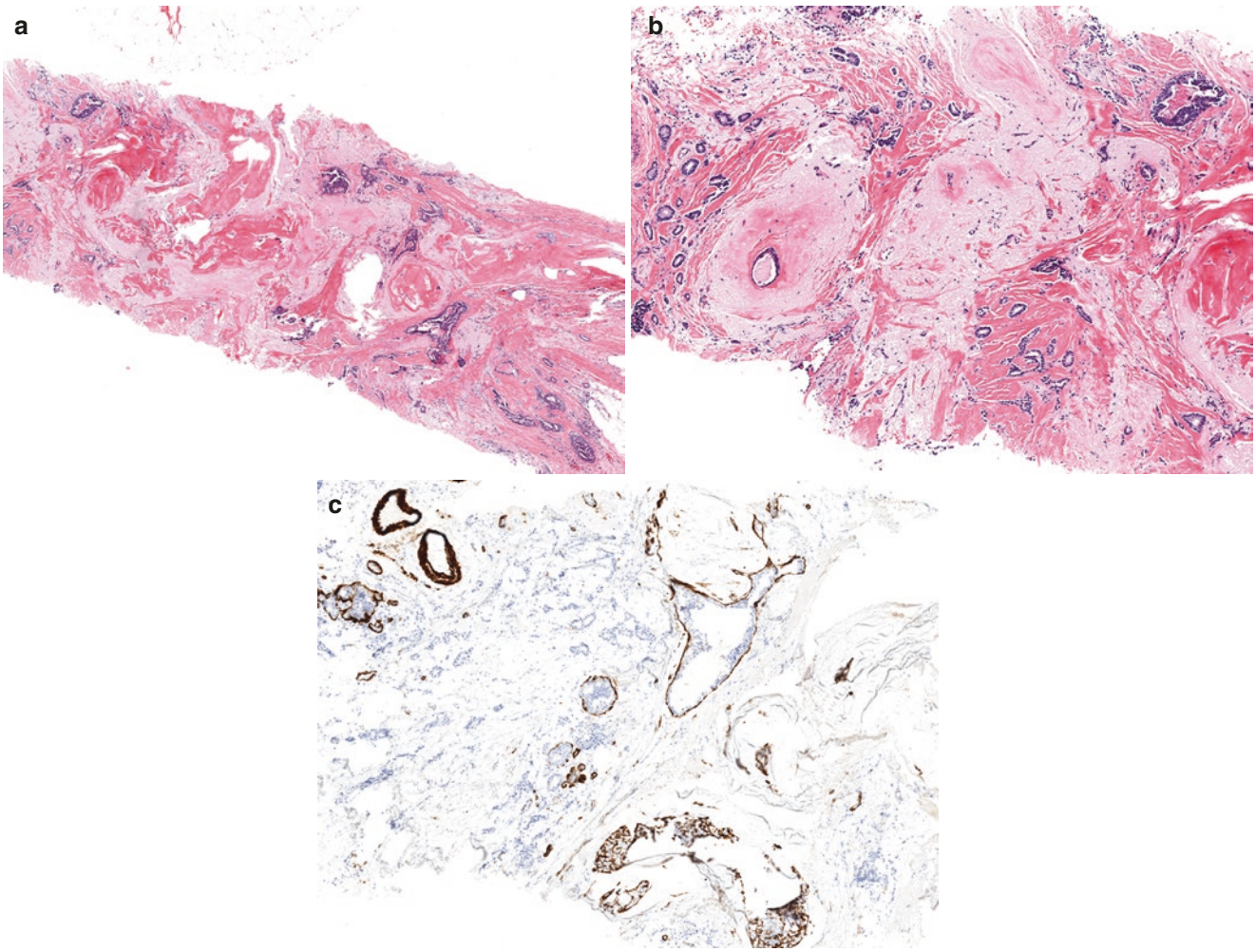

Fig. 10.52 Tubular carcinoma resembling a radial scar. (**a**) Low-power magnification shows extensive elastosis associated with neoplastic glands. (**b**) High-power magnification shows aggregates of angulated glands embedded in the stroma and a rare focus of DCIS (*upper right*). (**c**) SMM immunostain shows lack of myoepithelial staining around invasive neoplastic glands

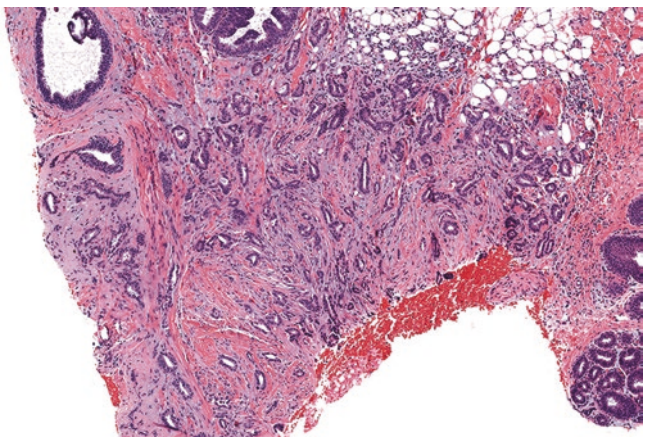

Fig. 10.53 Tubular carcinoma. Numerous angulated glands are embedded in a desmoplastic stroma with coexisting columnar cell lesion (*upper left* and *lower right*)

129, 134, 143]. Pure tubular carcinoma is currently defined as a tumor showing at least 90% tubule formation [145]. Inherently, tubular carcinoma is Nottingham histologic grade 1. In CNB samples, this assessment may not be possible in every case since only portions of the tumor are available for study. Therefore, it is recommended that such cases be reported as "well-differentiated invasive breast carcinoma with (prominent) tubular features" with a comment stating that final classification will be performed on the excisional specimen.

Tubular carcinomas are not uncommonly associated with columnar cell lesions, including FEA, and other low-grade lesions such as ADH, ALH, low-grade DCIS, and classic LCIS. The coexistence of tubular carcinomas, lobular neoplasia, and columnar cell lesions with or without atypia has been described as a "triad" or "Rosen triad" [146–148] (Fig. 10.56). Tubular carcinomas are more frequently associ-

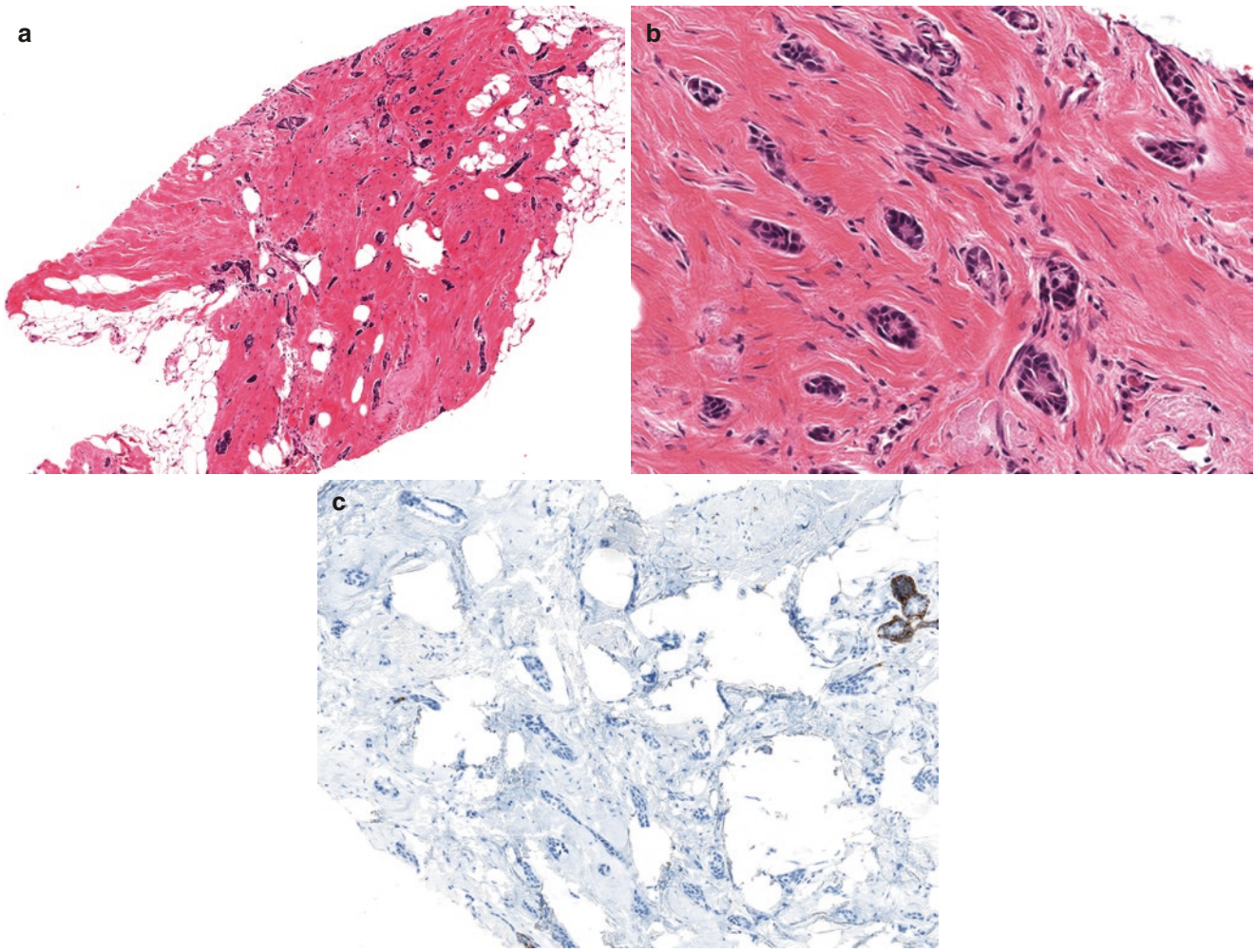

Fig. 10.54 Tubular carcinoma. (**a**) Angulated bland appearing glands of a tubular carcinoma in dense stroma mimics a benign process such as radial scar. (**b**) High-power view shows the low-grade tubular glands, some are compressed. (**c**) SMM immunostain is negative around the neoplastic tubules

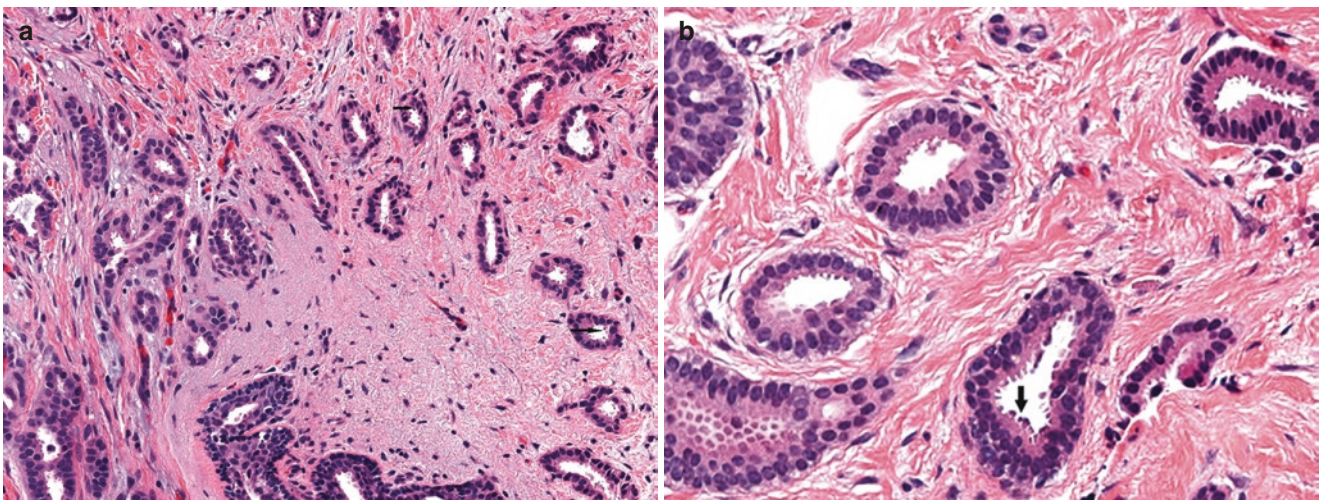

Fig. 10.55 Tubular carcinoma. (**a**) The neoplastic tubules are angular and have open lumens lined by a monolayer of low-grade neoplastic cells. (**b**) High-power view highlights the apical snouts (arrow)

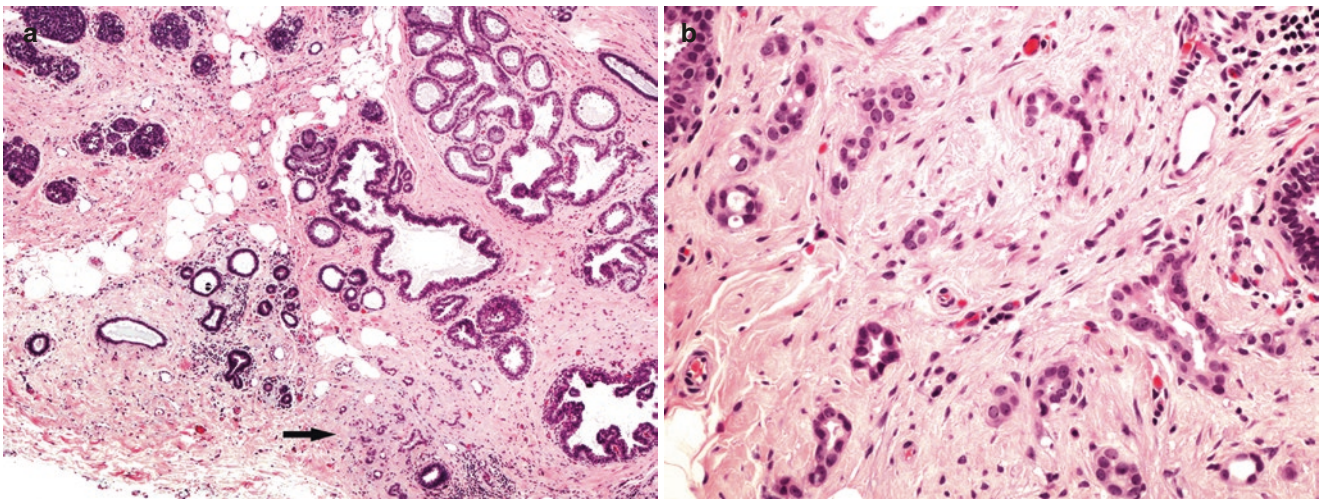

Fig. 10.56 Rosen triad. (**a**) Scanning view of an incidental tubular carcinoma (*arrow*) present in association with lobular neoplasia (*upper left*) and columnar cell lesion. (**b**) High-power magnification shows tubular carcinoma between the ductules with columnar cell change

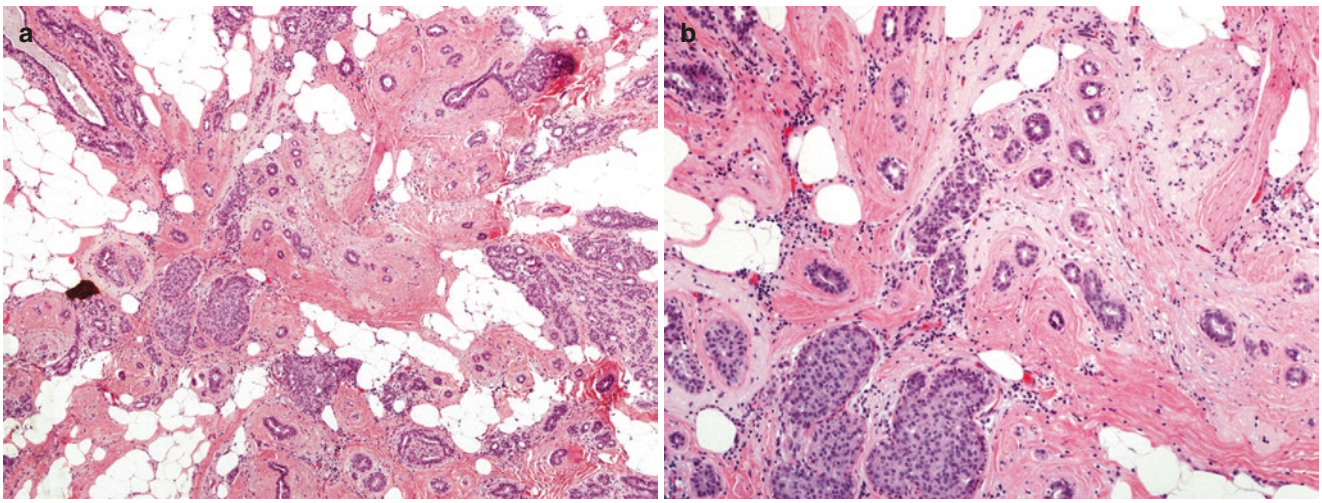

Fig. 10.57 Radial scar. (**a**) Scanning view of radial scar demonstrates a central dense nidus with entrapped glands from which the dilated ducts and ducts with epithelial proliferation radiate. (**b**) High-power magnification of the nidus

ated with columnar cell lesions (93% to almost 100%) than with lobular neoplasia (50%) or usual ductal hyperplasia (18%) [130, 148, 149]. The presence of one or more of these coexisting lesions in CNBs should prompt careful examination by the pathologist to exclude an occult tubular carcinoma.

Differential Diagnosis

The presence of small round to oval glands with bland neoplastic cells makes the diagnosis of tubular carcinoma challenging, especially in a CBN. Because of limited tissue sampling, various benign entities with similar morphologic appearance such as complex sclerosing lesions/radial scar, sclerosing adenosis, tubular adenosis, microglandular adenosis, and syringomatous tumor of the nipple-areolar region may mimic tubular carcinoma.

Complex Sclerosing Lesions/Radial Scar

Large radial scars can mimic invasive carcinoma on imaging studies and on gross examination. In excisional specimens, complex sclerosing lesions/radial scar is easier to recognize as the sclerotic or hyalinized nidus and the dilated and proliferative ducts that radiate from the nidus are seen together (Fig. 10.57). The center or nidus of a radial scar is composed

of dense stroma that often exhibits elastosis and contains entrapped benign glands that are often angulated, closely mimicking tubular carcinoma. Consequently, when the center of a radial scar is sampled in a core biopsy, it can lead to misdiagnosis (Fig. 10.58). Staining for myoepithelial markers generally resolves the dilemma in most cases, as radial scars will show positive staining for myoepithelial cells in the entrapped glands. It is worth noting that in larger or highly sclerotic radial scars, staining for myoepithelium may be absent in a few centrally located tubules but should be intact in the majority of the entrapped glands/tubules. Rarely, tubular carcinoma may involve a preexisting radial scar. One should be careful not to use this rare occurrence to overdiagnose tubular carcinoma when encountering a radial scar (Fig. 10.57).

Tubular Adenosis and Sclerosing Adenosis

The compressed, elongated, and angulated glands embedded in dense sclerotic stroma encountered in sclerosing adenosis may be mistaken for tubular carcinoma, particularly in CNBs. Examination at low-power magnification is extremely helpful as sclerosing adenosis is lobulocentric compared to the infiltrative appearance of tubular carcinoma. At higher magnification, sclerosing adenosis consists of proliferation of compact, swirled glands and tubules, which are compressed and distorted due to dense stromal proliferation, especially in the center of a lobule. At the periphery, glands are usually round and open with scant luminal secretions (Fig. 10.59). Recognizing spindled myoepithelial cells around the tubules may help to avoid misinterpretation. In challenging cases, immunostains for myoepithelial cells such as p63 or SMM can help. Smooth muscle actin (SMA) should be avoided, as it can stain adjacent stromal myofibroblasts in tubular carcinoma, leading to misinterpretation of tubular carcinoma as adenosis. Tubular adenosis is an uncommon benign non-lobulocentric lesion with an infiltrative appearance that may mimic tubular carcinoma. Depending on the plane of section, the glands may appear round or elongated (Fig. 10.60). However, myoepithelial cells and the basement membranes are intact and can be well demonstrated by appropriate IHC stains.

Microglandular Adenosis

Microglandular adenosis is a rare benign lesion composed of small, round, open glands lined by a single layer of epithelial cells without accompanying myoepithelial cells. Certain histological clues can aid in distinguishing between the two lesions. Microglandular adenosis is a diffuse lesion

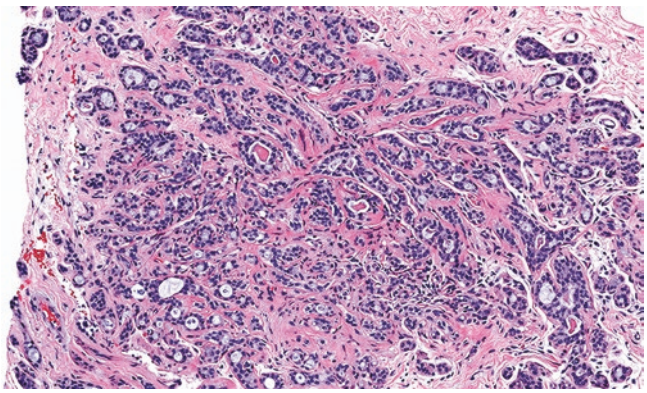

Fig. 10.59 Sclerosing adenosis superficially resembles well-differentiated invasive ductal carcinoma

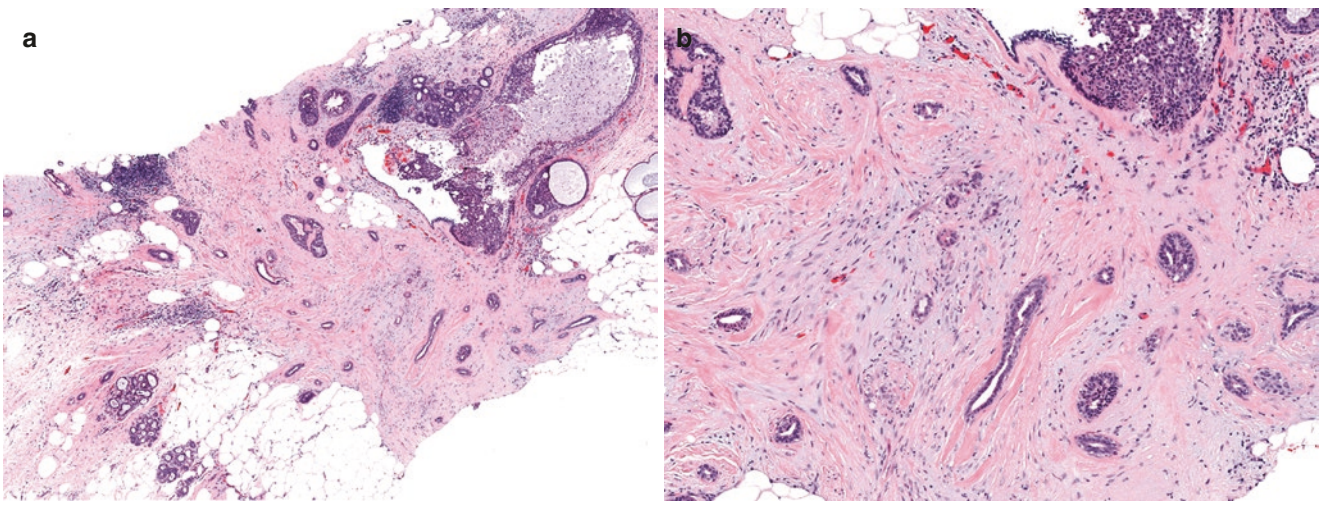

Fig. 10.58 Radial scar. (**a**) The center of a radial scar sampled in a CNB demonstrates sclerotic and elastotic stroma associated with entrapped angulated tubules and (**b**) high-power magnification shows compressed elongated and angulated tubular glands

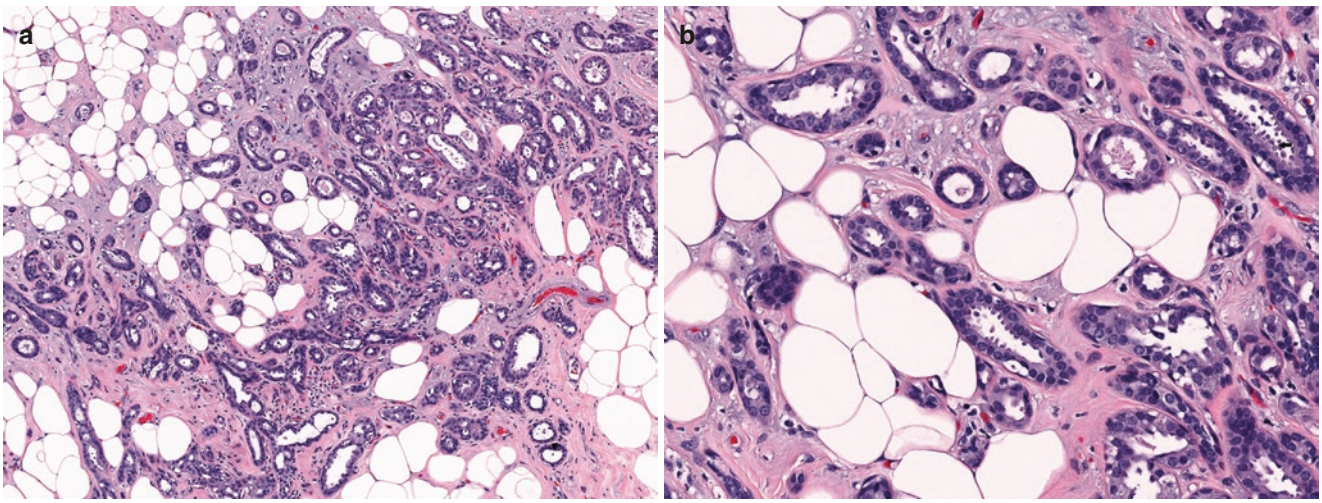

Fig. 10.60 Tubular adenosis. (**a**) Low-power view shows elongated tubular glands embedded in fibromyxoid stroma and (**b**) high-power view shows tubular glands with columnar cell change with apical snouts, myoepithelial cells, and distinct basement membrane around each tubule

with glands infiltrating haphazardly into the fibrous stroma and adipose tissue, whereas tubular carcinoma is more often localized. The neoplastic epithelium of tubular carcinoma has mild nuclear atypia and pleomorphism with apical snouts and tends to have amphophilic or basophilic secretions rather than the dense eosinophilic secretions seen in the round glands of microglandular adenosis [150]. Additionally, the stroma in tubular carcinoma is dense and elastotic whereas in microglandular adenosis the stroma is unaltered. Immunostains can be used to differentiate between these two entities, although myoepithelial stains are unhelpful as both lesions lack myoepithelial cells. The most useful stains are ER and S100 protein as tubular carcinoma is S100 protein negative and ER positive whereas microglandular adenosis shows the opposite pattern of staining. The basement membrane is intact in microglandular adenosis and can be highlighted by either reticulin, periodic acid–Schiff (PAS), or immunostain for collagen type IV or laminin (Fig. 10.61).

Syringomatous Tumor of the Nipple-Areolar Region

Syringomatous tumor is a locally infiltrative, recurring, and non-metastasizing lesion that almost always occurs in the nipple-areolar region (Fig. 10.62). In contrast, tubular carcinoma rarely occurs in the nipple-areolar region. The presence of squamous differentiation or squamous cysts, a characteristic trait of syringomatous tumor, is not seen in tubular carcinoma.

Other carcinomas that should be distinguished from tubular carcinoma are well-differentiated IBC with tubule formation, low-grade adenosquamous carcinoma, and tubulolobular carcinoma.

Well-Differentiated IBC with Tubule Formation

This tumor exhibits greater architectural complexity of its glands including branching or nesting (Fig. 10.63) or higher nuclear grade (Fig. 10.64) than tubular carcinoma.

Low-Grade Adenosquamous Carcinoma

Low-grade adenosquamous carcinoma is a rare type of metaplastic carcinoma with glandular and squamous differentiation typically distributed in a cellular or collagenized stroma. As its name states, it shows low-grade features including well-formed comma-shaped pointed glands, lined by two layers of cells that have low nuclear grade and low mitotic activity as seen in tubular carcinoma or syringomatous tumor. The key to diagnosis is appreciation of squamoid nests and the cellular stroma, particularly around neoplastic glands. Overt keratinization is not a feature. On CNB, the glandular component may predominate and be confused with tubular carcinoma. Immunostains can help, as low-grade adenosquamous carcinomas are HR negative and this lack of expression should make one question a diagnosis of tubular carcinoma. Additionally, immunostain for p63 in low-grade adenosquamous carcinoma shows intact staining around most tubules and positive staining of the squamoid nests and spindle cells (Fig. 10.65).

Tubulolobular Carcinoma

Morphologically tubulolobular carcinomas are low-grade invasive carcinomas that show an admixture of well-formed tubules and single cells arranged in cords as seen in lobular carcinoma in 75% of the tumor [151]. They tend to be HR positive and HER2 negative and are associated with a good prognosis [149, 151–154]. Most but not all examples express membranous E-cadherin, membranous p120 catenin, and

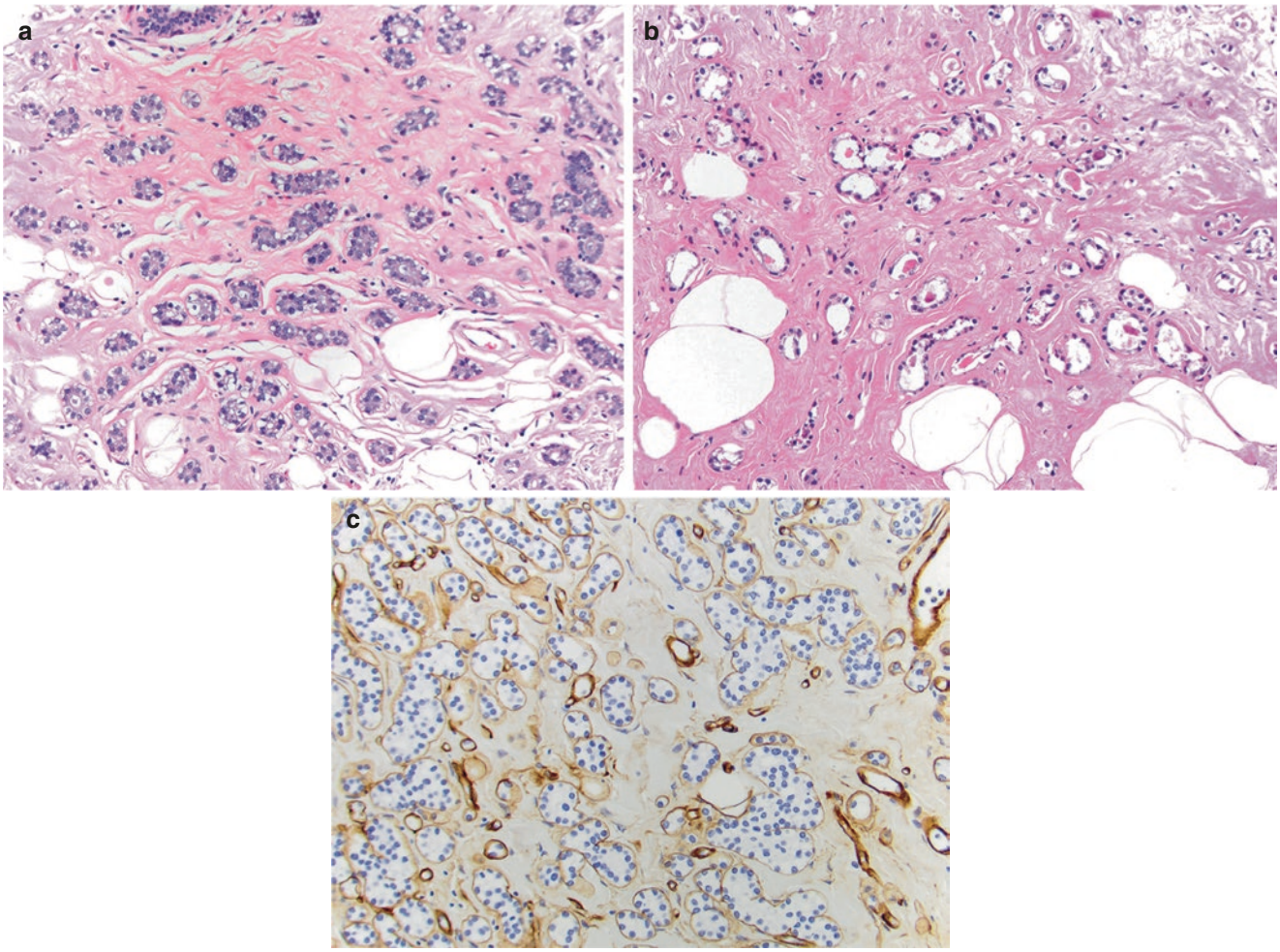

Fig. 10.61 Microglandular adenosis. (**a**, **b**) Small round open glands lined by a single layer of epithelial cells and containing bright eosinophilic secretions are distributed in the breast parenchyma without stromal alteration. (**c**) Collagen type IV immunostain demonstrates intact basement membrane while myoepithelial markers are negative (not shown)

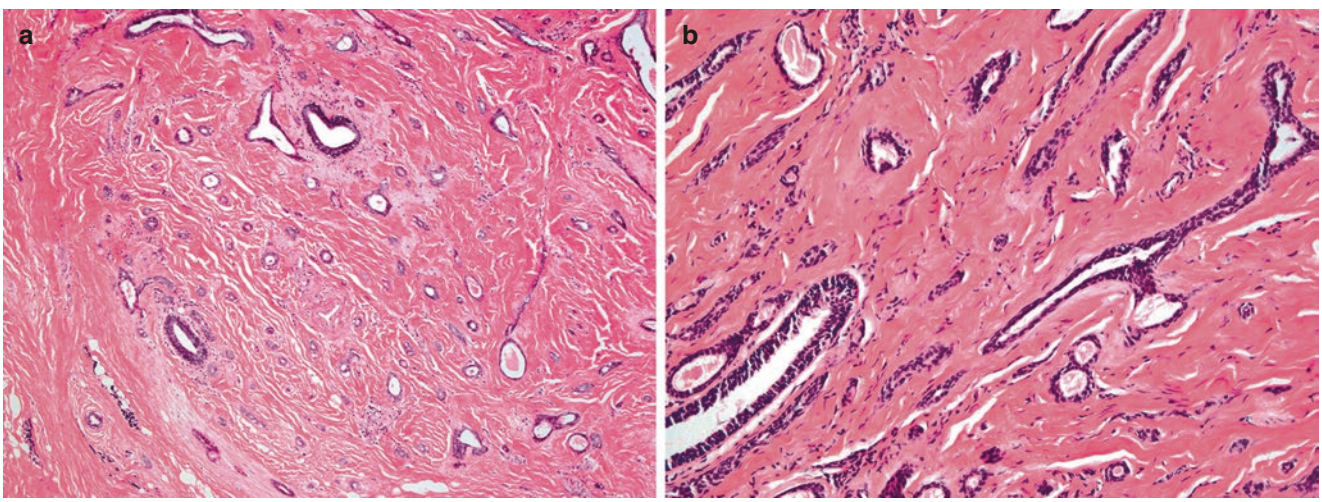

Fig. 10.62 Syringomatous tumor of the nipple. (**a**) Low-power view shows infiltration of the nipple stroma by tubules with pointed ends. (**b**) High-power view shows squamoid cysts characteristic of this entity

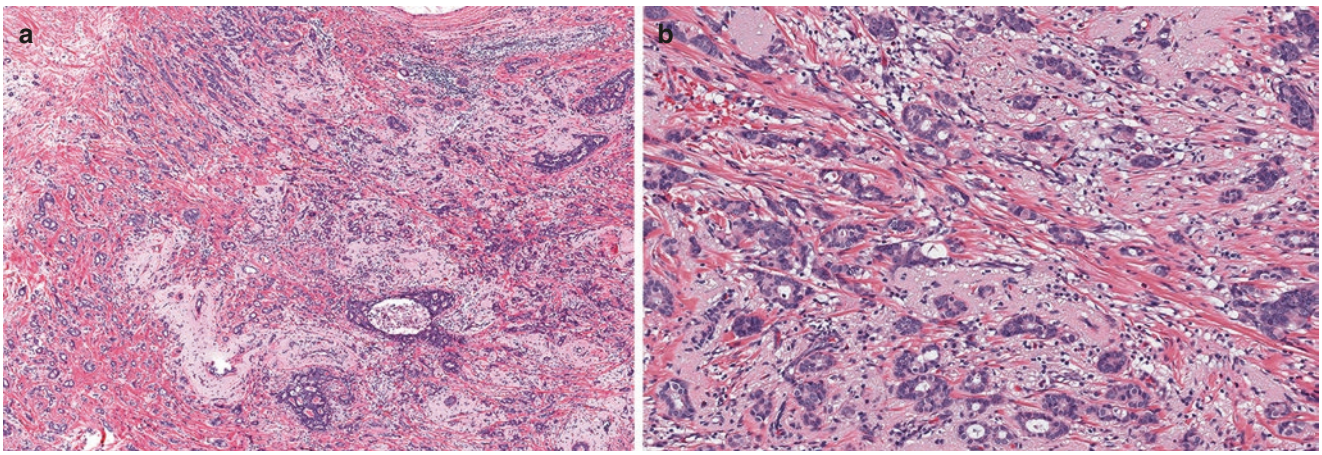

Fig. 10.63 A well-differentiated invasive breast carcinoma NST with predominant tubule formation. (**a**) Low-power and (**b**) high-power magnifications

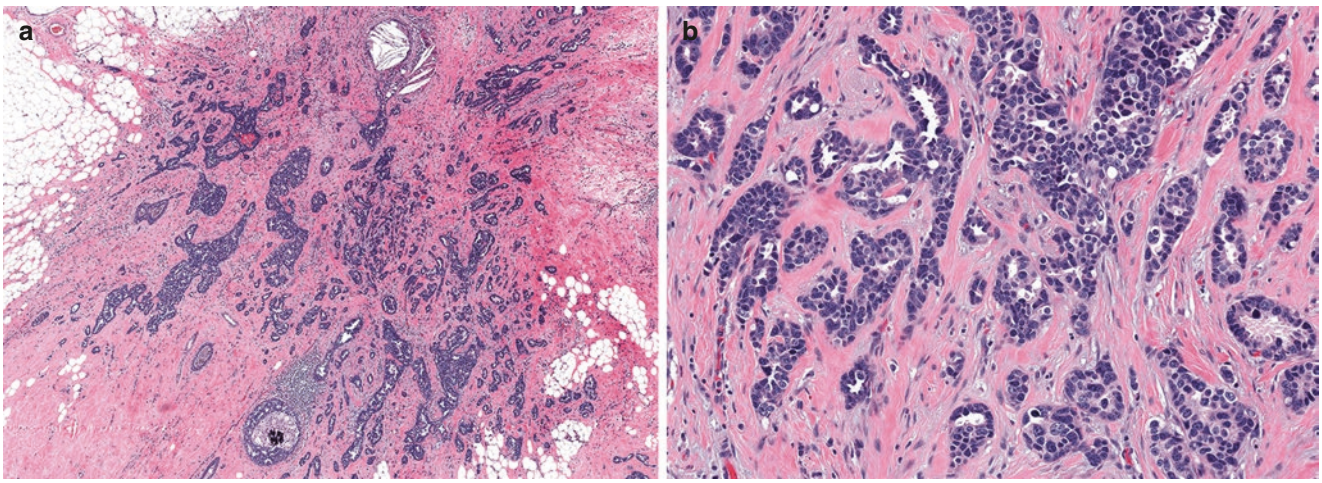

Fig. 10.64 A moderately differentiated invasive breast carcinoma NST. (**a**) Low-power view shows predominant tubule formation with minor component of solid nests of cells but (**b**) high-power view reveals tubular glands with high nuclear grade and focal intraluminal necrosis

beta-catenin staining and accordingly are grouped with ductal rather than lobular carcinomas [151, 152, 155]. Many are seen in association with lobular neoplasia, however, which most likely reflects their origins in the low-grade pathway (discussed previously). This diagnosis may not be highly reproducible as ILC can show some degree of tubule formation (Please see additional discussion of invasive carcinomas with mixed ductal/tubular and lobular morphology in Chap. 15).

Immunohistochemistry

Tubular carcinomas are invariably HR positive and HER2 negative (Fig. 10.66). ER has been reported to be positive in almost all cases, whereas 71–92% of cases have been reported to be PR positive [128–130, 156]. Rare cases of tubular carcinoma have been reported to be HER2 positive [128, 156]. If a tubular carcinoma is ER negative and/or HER2 positive, the diagnosis should be questioned and the case reviewed. The well-differentiated nature of tubular carcinoma is also reflected by a low (<10%) Ki-67 proliferation index and wild-type pattern of p53 expression [157–159].

Pathogenesis

Molecular and genetic studies have found tubular carcinoma to be distinct at the genomic level with a low level of chromosomal alterations compared to IBC-NST in general. However, tubular carcinoma and low-grade breast carcinoma appear more similar to each other than to high-grade carcinomas as both tumors show a higher frequency of 16q loss and 1q gain and lower frequency of 17p loss [160]. By gene expression profiling, the vast majority of tubular carcinomas are classified as luminal A molecular subtype,

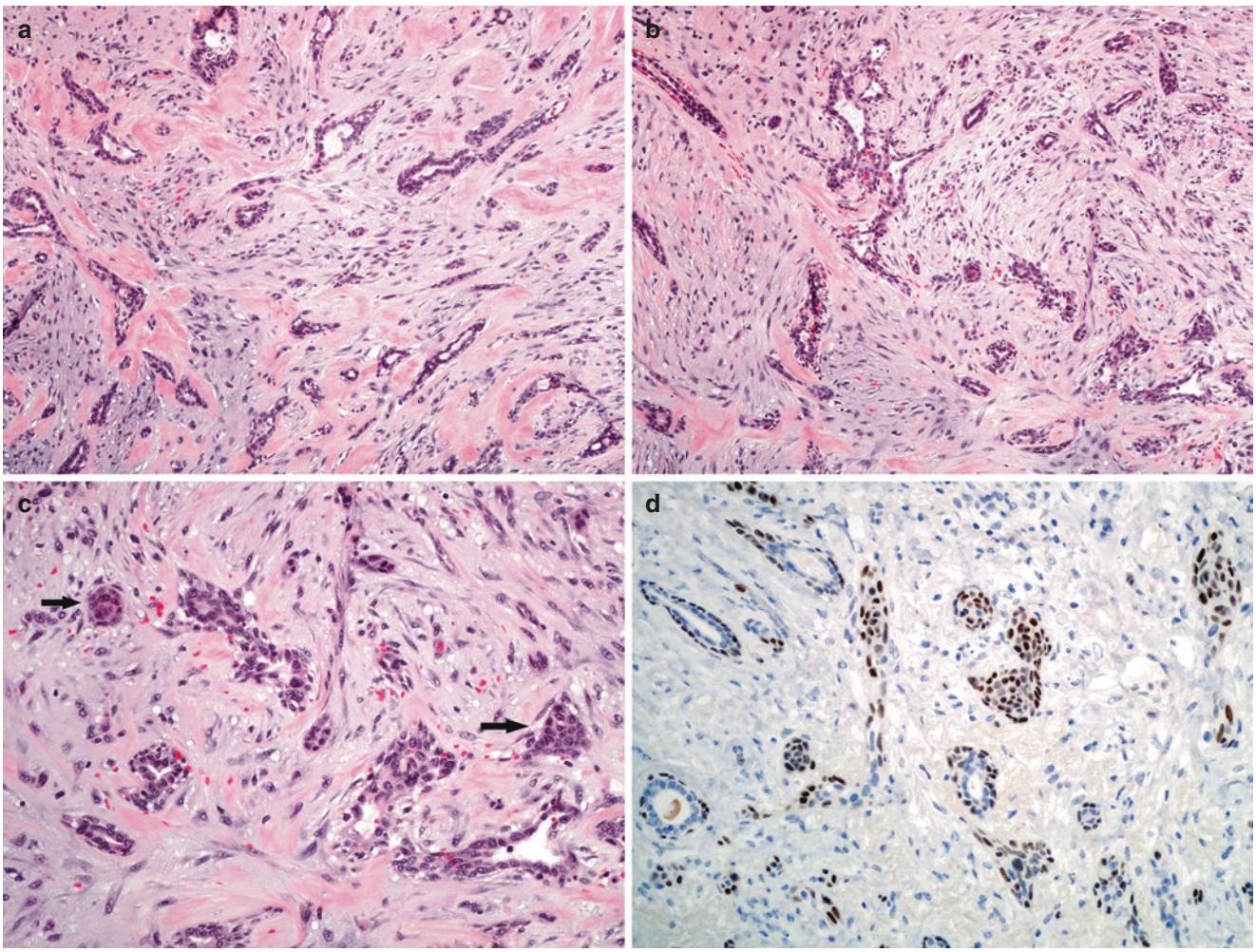

Fig. 10.65 Low-grade adenosquamous carcinoma. (**a**) Open angulated glands embedded in a fibrous cellular stroma showing focal hyalinization. (**b**) Different areas of the tumor show tubular glands and small nests of cells surrounded by cellular stroma. (**c**) High-power view shows squamoid nests with dense eosinophilic cytoplasm (*arrow*). (**d**) Immunostain for p63 reveals nuclear staining in the peripheral cells of the tubules and the squamoid nests. Spindle cells are also positive with CAM5.2 and focally with p63 (not shown)

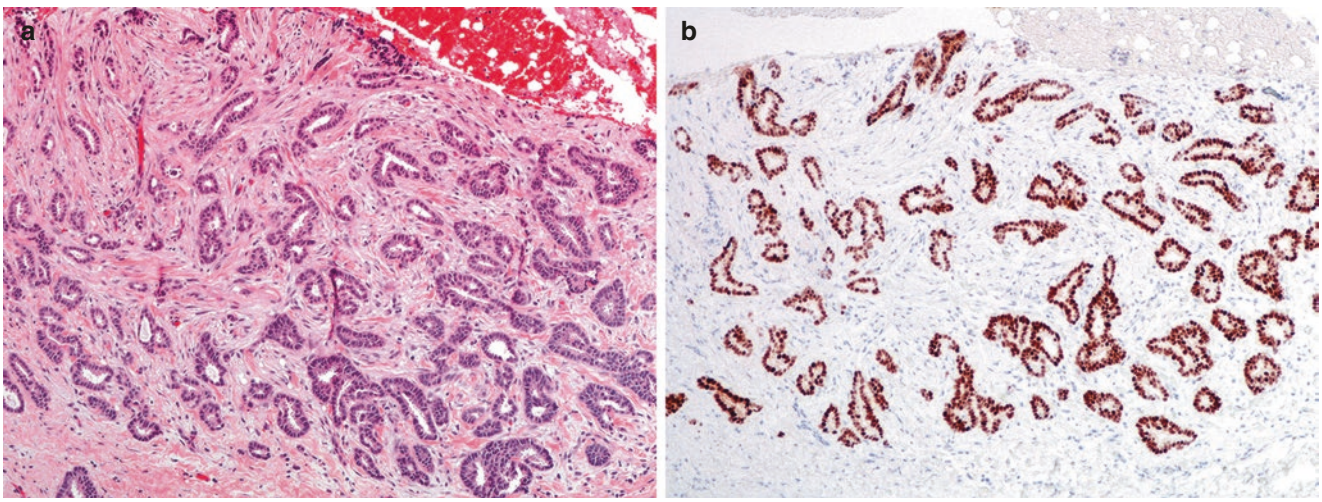

Fig. 10.66 Tubular carcinoma. (**a**) H&E stain and (**b**) strong diffuse nuclear staining for estrogen receptor

similar to low-grade IDC-NST. However, some differences between tubular carcinoma and low-grade IDC-NST have been elucidated by comparative transcriptomic analysis, with upregulation of the ER-driven signaling pathways (ESR1, CREBBP1, and NCOR1 signals) noted in tubular carcinoma [158].

Prognosis

Tubular carcinoma is known for its excellent prognosis. It has a low propensity for lymph node metastases (incidence 2–11%) [129, 130, 134, 143, 161, 162], a low rate of local recurrence (4–7%) [127, 129–131] and distant metastasis, and a high overall survival rate [130, 143, 156, 161]. The 5-year disease-free survival rate is generally more than 90% [129, 156, 161, 163] and the 10-year overall survival rate is comparable to that of the age-matched general population [131, 156, 163]. Due to its excellent prognosis, it is critical to differentiate tubular carcinoma from well-differentiated IBC NST. As mentioned previously, on a core biopsy, depending on the size of the tumor, it may be more appropriate to diagnose the tumor as "IBC with tubular features" and defer the final classification to the excision specimen.

The mainstay of treatment for tubular carcinoma is surgical excision. Due to the extremely favorable prognosis of tubular carcinomas, the impact of endocrine and radiation therapy have been questioned. Current NCCN guidelines state endocrine therapy should be considered but is not clearly recommended for tubular carcinomas less than 3 cm in size and/or in node-negative cases. In patients with macrometastasis in one or more axillary lymph nodes, endocrine therapy is recommended with the option of adjuvant chemotherapy [164]. Neoadjuvant chemotherapy is largely not considered in the treatment of tubular carcinoma [162]. Radiation therapy was found to be a favorable prognostic factor for overall survival in tubular carcinoma patients in a National Cancer Database study [165] while a SEER database study found that radiotherapy improved survival outcomes in patients aged <50 years [166].

While sentinel lymph node biopsy (SLNB) is a fairly standard indication in invasive carcinomas, some studies have questioned its routine use in tubular carcinomas. Few retrospective studies have reported a higher rate of lymph node involvement, mostly because of varying criteria used for this diagnosis [127, 130, 143, 162, 167]. Studies that examined lymph node involvement in "pure" tubular carcinoma, defined as >90% tubule formation with low-grade histology, found 4.6–6.2% cases with lymph node metastasis, including cases with isolated tumor cells [134, 167, 168]. A study by Lea et al. reported 13 patients with lymph node involvement (7 macrometastasis, 5 micrometastasis, and 1 with isolated tumor cells) in their series of 146 "pure" tubular carcinomas (defined as tumors with ≥90% tubule formation). However, in their series, three patients had grade 2 histology and six patients were not graded. Therefore nine cases did not fulfill the criteria for pure tubular histology. In addition, 28 patients in their study did not undergo any axillary lymph node sampling [169]. In a large multi-institutional study by Dejode and colleagues of 234 patients with pure tubular carcinoma, 6 patients (2.5%) had macrometastasis, 15 (6.4%) micrometastasis, and 2 (0.8%) isolated tumor cells. They also reported an overall low rate of non-sentinel lymph node involvement, found only in 3 (1.2%) patients, all of whom had macrometastasis in their sentinel lymph nodes. None of the patients with micrometastasis or isolated tumor cells had metastasis in non-sentinel lymph node on completion of axillary dissection [170].

Fedko and colleagues reported 5 (5.4%) cases with lymph node metastasis and 2 with isolated tumor cells in a study of 105 patients with tubular carcinoma. In their study, the tumor ranged from 0.9 to 1.5 cm in node-positive patients. Despite two node-positive patients with tumors less than 1 cm in size, the authors proposed forgoing axillary staging in patients with tumors measuring less than 1.8 cm [134]. Additionally in the study by Dejode et al., after multivariate analysis, the only parameter significantly linked to lymph node involvement was pathologic tumor size of greater than 10 mm ($p = 0.007$). Of the 122 patients with a pathologic tumor size less than 10 mm, none had macrometastasis, 4 had micrometastasis, and 1 had isolated tumor cells to the sentinel lymph node. They suggested that SLNB could be omitted in patients with tumors less than 10 mm in size, and further postulated that even those patients with metastasis in the sentinel lymph node might not require completion of axillary lymph node dissection [170].

Interestingly, the rate of lymph node involvement in pure tubular carcinoma is comparable to the accepted overall false-negative rate of 5–9.8% reported for sentinel lymph node metastases [171–173]. Long-term data from the prospective National Surgical Adjuvant Breast and Bowel Project (NSABP) B04 trial reported no difference in disease-free survival, relapse-free survival, distant disease-free survival, or overall survival in clinically node-negative women who were randomized to receive radical mastectomy, total mastectomy without axillary dissection but with postoperative radiation, or total mastectomy plus axillary dissection, if their nodes became clinically positive on follow-up [174]. Additionally, univariate analysis using data from the NSABP B06 trial revealed that when comparing node-negative patients ($n = 1090$) to node-positive patients ($n = 651$), those with tumors of favorable histology (including 120 with tubular carcinoma) experienced a significantly greater overall survival at 10 years compared to those without. On multivariate analysis, favorable histology proved to be an independent predictor of survival in node-negative patients [175].

Invasive Cribriform Carcinoma

Overview

Invasive cribriform carcinoma (ICC) is an uncommon morphologic variant of invasive carcinoma comprising less than 1% of all IBC [176, 177]. Page et al. first characterized this entity in 1983 as a well-differentiated carcinoma that often has a tubular component and is associated with a favorable prognosis [176]. The median age is 61 with a wide age range reported (7–91 years) [176, 178–181]. Multifocality has been found in 13.7–20% of cases [176, 180].

Gross and Radiologic Features

The imaging findings of most ICC are similar to other IBC-NST. ICC appears as an irregular high-density spiculated mass with or without associated calcifications on mammogram [179, 181]. One study reported four of eight cases to be mammographically occult [179]. Common features of ICC on ultrasound are irregular shape, hypoechogenicity, and no posterior acoustic shadow [179, 181, 182]. On MRI, most ICC present as an irregularly shaped enhancing mass.

Grossly, ICC appears similar to other mass-forming IBC-NST. The average tumor size ranges from 1.7 to 3.1 cm [176, 178–180].

Microscopic Features

ICC shows a sieve-like pattern or fenestrated appearance in which individual glands are angular or irregular (Fig. 10.67). The cribriform nests may have a round or irregular contour (Fig. 10.68). The neoplastic glands infiltrate between ducts and lobules of normal breast without disturbing their architecture (Fig. 10.69). The lumens may contain bluish mucinous secretions with or without associated microcalcifications [183] (Fig. 10.70). The tumor cells are small with eosinophilic to amphophilic cytoplasm, low-to-intermediate nuclear grade, finely dispersed chromatin, indistinct nucleoli, and infrequent mitoses (Fig. 10.71). The stroma usually shows a desmoplastic response, sometimes associated with inflammatory infiltrates or osteoclastic-like giant cells [160, 184] (Fig. 10.72). It is not uncommon to find neoplastic tubules intermixed with cribriform nests as well as prominent apical snouts in the cribriform nests. In the majority of cases, associated DCIS is seen, usually of cribriform type. ICCs are histologic grade-1 tumors.

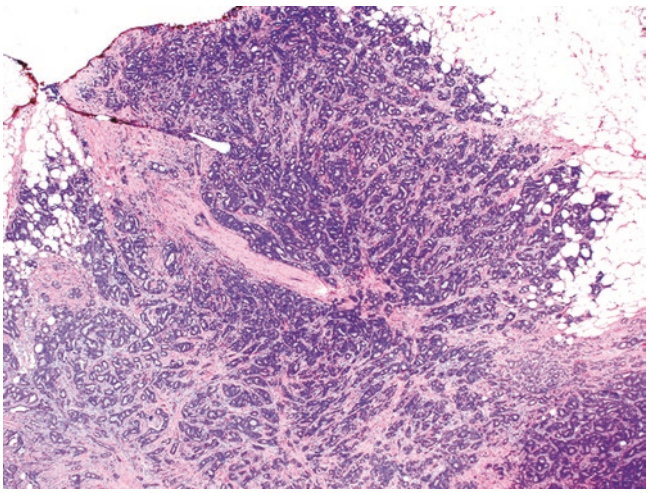

Fig. 10.67 Invasive cribriform carcinoma with sieve-like pattern apparent on scanning view

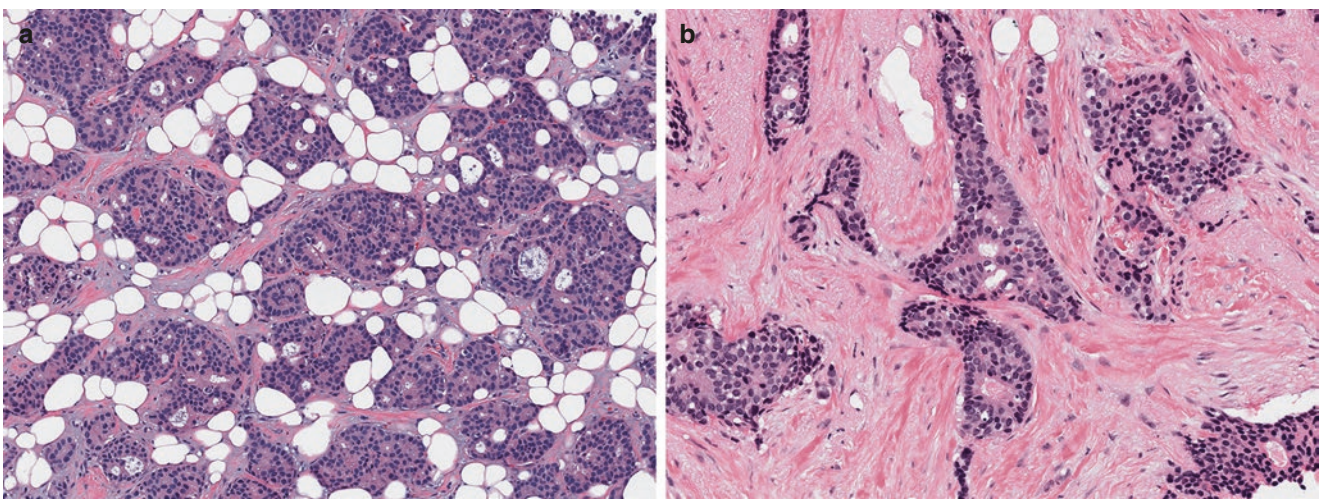

Fig. 10.68 Invasive cribriform carcinoma. (**a**) Individual tumor nests with round-to-oval contour and (**b**) a different case showing tumor nests with irregular and angulated contour

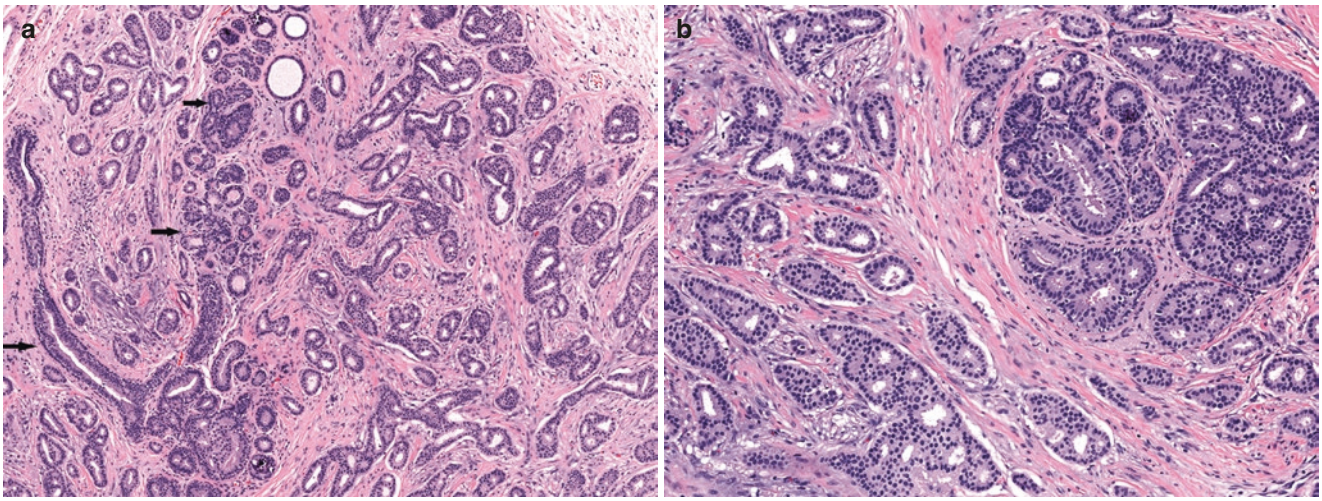

Fig. 10.69 Invasive cribriform carcinoma infiltrates between the normal glandular breast elements (*arrow*), (**a**) low power and (**b**) high power

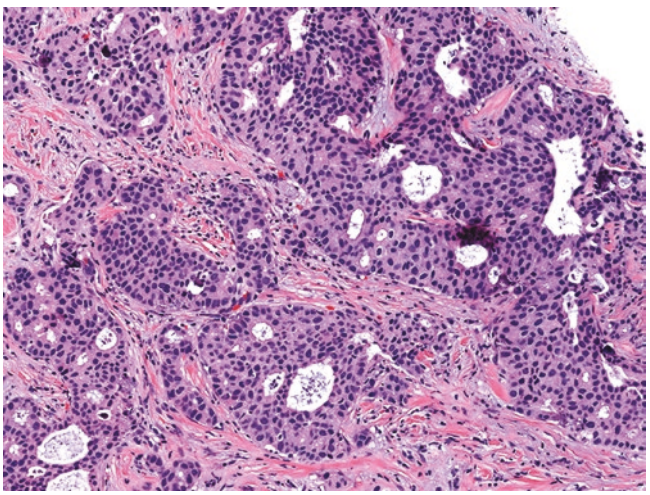

Fig. 10.70 Invasive cribriform carcinoma with basophilic luminal secretions and associated microcalcifications which can superficially resemble adenoid cystic carcinoma

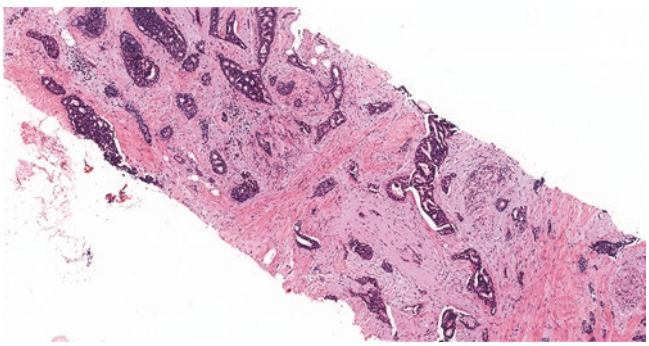

Fig. 10.72 Invasive cribriform carcinoma associated with a marked desmoplastic stromal reaction

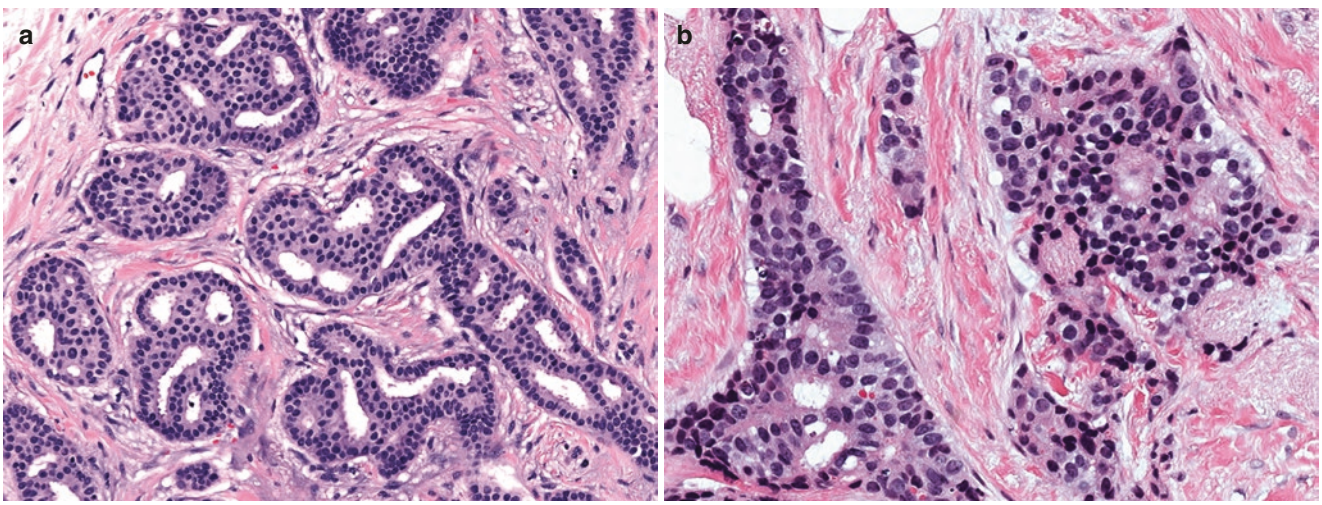

Fig. 10.71 Invasive cribriform carcinoma lined by monotonous low-grade cells with apical snouts and uniform nuclei with fine chromatin (**a**, **b**)

WHO defines pure ICC as tumors showing greater than 90% cribriform architecture. Page et al. originally classified ICC as "classical" or "mixed." Classical ICC was defined as tumors showing at least a 50% cribriform component with the remaining component showing a tubular pattern (Fig. 10.73). Mixed ICC was defined as tumors with at least a 50% cribriform component with any admixed component being non-tubular [176]. ICC should be distinguished from IBC-NST that shows a cribriform pattern but has aggressive characteristics such as high-grade nuclei, increased mitotic activity, or necrosis (Fig. 10.74). These should not be identified as ICC as they are not associated with the favorable prognosis of these tumors.

Differential Diagnosis

The most common differential diagnosis of ICC is cribriform DCIS. Other rare entities such as adenoid cystic carcinoma (AdCC), invasive mammary carcinoma with osteoclast-like giant cells, and collagenous spherulosis may superficially resemble ICC.

Cribriform DCIS

ICC and cribriform DCIS can be mistaken for one another, particularly in a CNB. Cribriform DCIS is often found within ICC, and they must be distinguished from one another in order to obtain an accurate measurement of the invasive

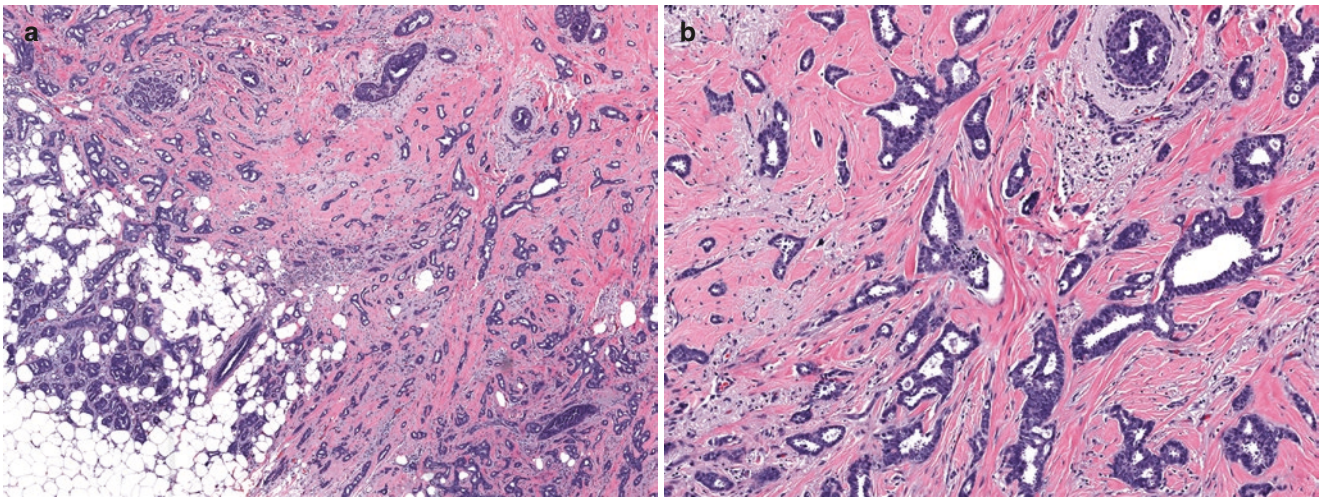

Fig. 10.73 Invasive cribriform carcinoma admixed with tubular carcinoma (**a**) low power and (**b**) high power

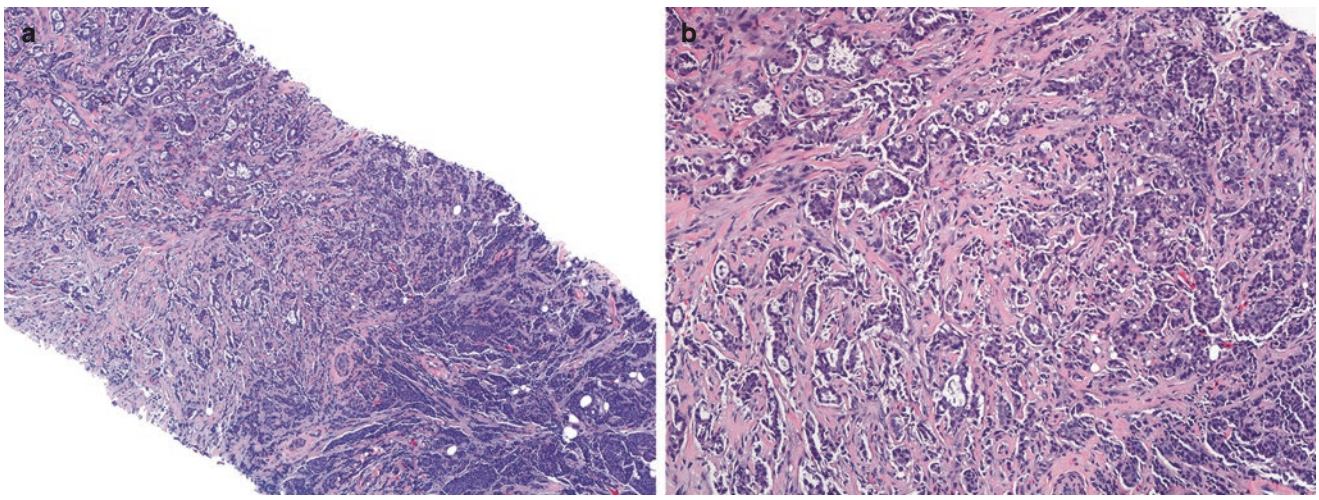

Fig. 10.74 Invasive breast carcinoma NST shows invasive cribriform growth pattern (**a**, **b**)

component for appropriate tumor staging. Cribriform DCIS has smooth round contours as opposed to the angular or irregular contours seen in ICC (Fig. 10.75). Also, cribriform DCIS does not distort the normal breast architecture or induce a desmoplastic reaction. In difficult cases, particularly in core biopsies, immunostains for myoepithelial cells can be invaluable in differentiating the two components (Fig. 10.76).

Adenoid Cystic Carcinoma (AdCC)

Low-grade AdCC can exhibit cribriform architecture resembling ICC (Fig. 10.77). The dual epithelial–myoepithelial cell population and intraluminal basement membrane material present in AdCC are distinguishing features, although ICC can also show intraluminal secre-

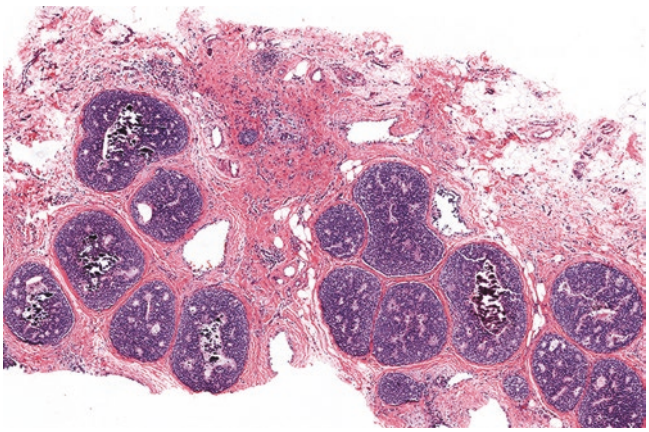

Fig. 10.75 Cribriform DCIS with round contour and normal breast stroma between the nests

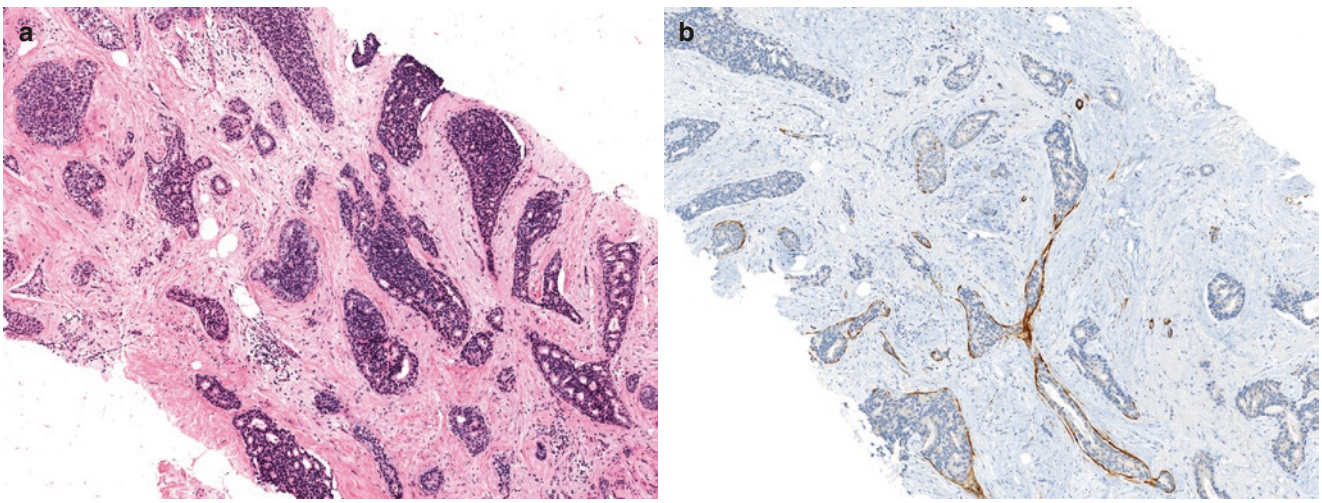

Fig. 10.76 An invasive cribriform carcinoma consisting of cribriform nests with round and irregular contours making it difficult to assess the extent of in situ versus invasive carcinoma, (**a**) H&E stain and (**b**) p63 helps to delineate the in situ and invasive components

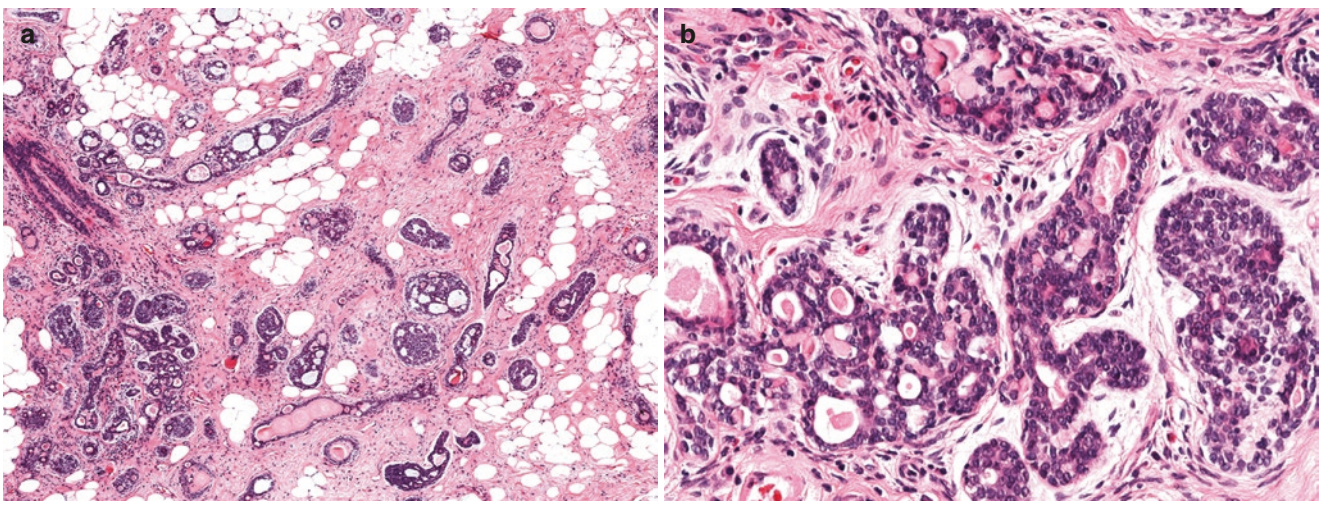

Fig. 10.77 Low-grade adenoid cystic carcinoma of the breast. (**a**) Low power and (**b**) high power shows accumulated basement membrane material (*left*) and the presence of intercalated ducts (*right*)

tions resembling the basement membrane material of AdCC. Immunostains are key as AdCC and ICC show different patterns of expression. One of the most useful stains is ER as AdCC is typically ER negative, whereas ICC expresses ER diffusely in virtually all cases. In addition, AdCC shows p63 expression by its neoplastic myoepithelial component and membranous and cytoplasmic CD117 (c-KIT) staining by its epithelial component while ICC is negative for myoepithelial markers [185] (see Chap. 12 for further discussion of AdCC).

Collagenous Spherulosis

Collagenous spherulosis can be associated with calcifications and hence be the target of CNB (Fig. 10.78). The hallmark of collagenous spherulosis is the presence of amorphous, acellular, dense eosinophilic spherules composed of basement membrane material analogous to the spherules seen in AdCC. Degenerative changes in the spherules may result in empty spaces or a basophilic appearance that can be mistaken for secretions (Fig. 10.79). The ductal cells have a smooth, round appearance with bland cytology. Myoepithelial cells typically surround the spherules and are also present at the periphery of the ductules. Myoepithelial markers such as p63 and SMM demonstrate different patterns of staining in AdCC and collagenous spherulosis, helping to distinguish between the two.

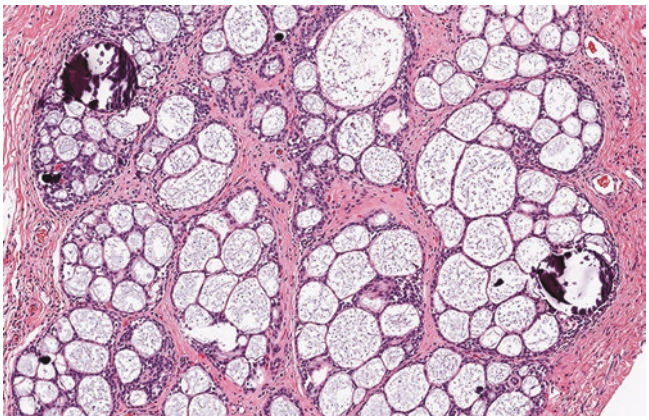

Fig. 10.78 Collagenous spherulosis with associated calcifications. Note the bluish appearing degenerated basement membrane material within the glandular lumens

Invasive Mammary Carcinoma with Osteoclast-Like Giant Cells

This is a rare type of IBC in which the invasive component may exhibit well, moderate-to-poor differentiation with associated cribriform growth pattern or less commonly non-cribriform patterns such as lobular, mucinous, papillary, squamous, or apocrine carcinomas (Fig. 10.80). Distinctive features of this entity include the grossly red–brown appearance of the tumor which microscopically represents numerous red blood cells and hemosiderin-laden macrophages in tumoral stroma, as well as the juxtaposition of numerous osteoclast-like giant cells of histiocytic origin and neoplastic glands. These tumors should be classified and graded according to the morphologic pattern and differentiation.

Immunohistochemistry

ICC is usually HR positive and HER2 negative (Fig. 10.81). Almost all cases are ER positive, and 70–90% are PR positive [178, 180, 181]. The proliferation rate is usually low (<14%) [180].

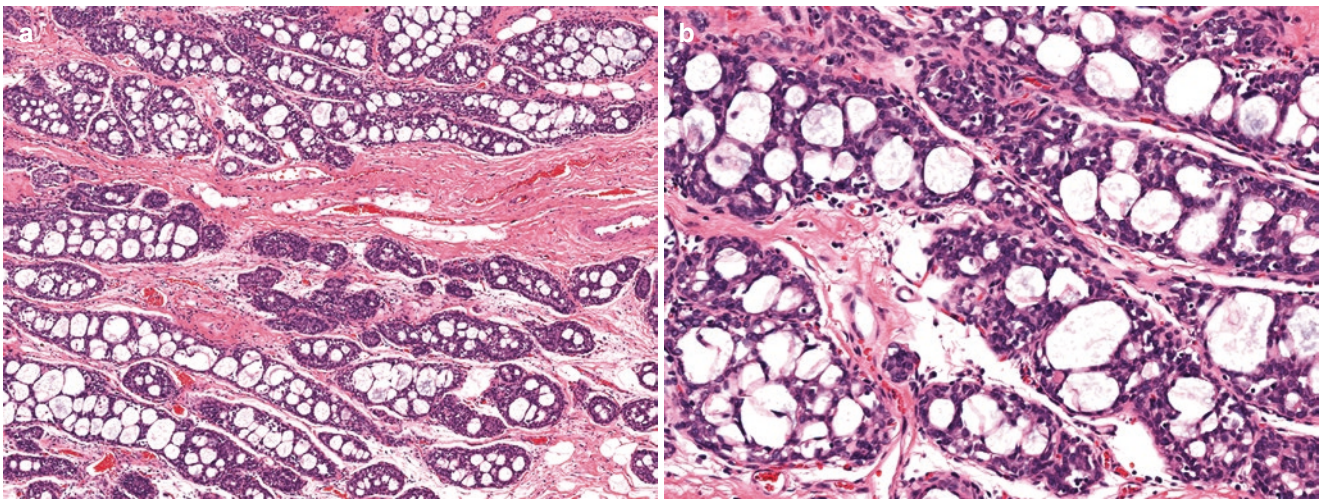

Fig. 10.79 Extensive collagenous spherulosis involved by LCIS. (**a**) Low-power view shows a sieve-like appearance resembling a cribriform growth pattern. (**b**) High-power view shows bluish basement membrane material

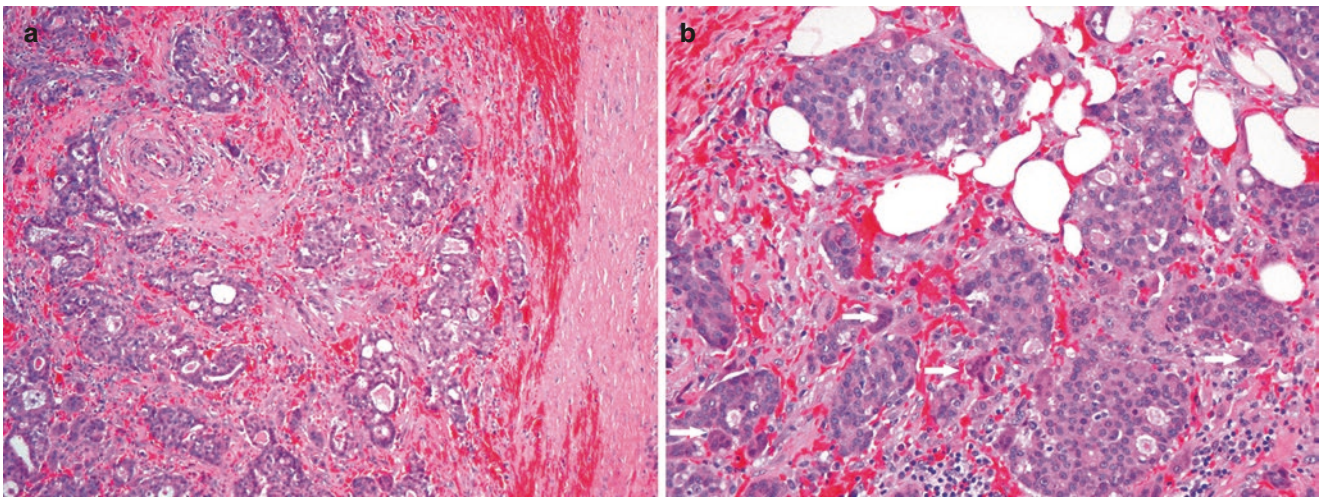

Fig. 10.80 Invasive mammary carcinoma with numerous red blood cells and osteoclast-like giant cells (*arrow*): (**a**) low power and (**b**) high power

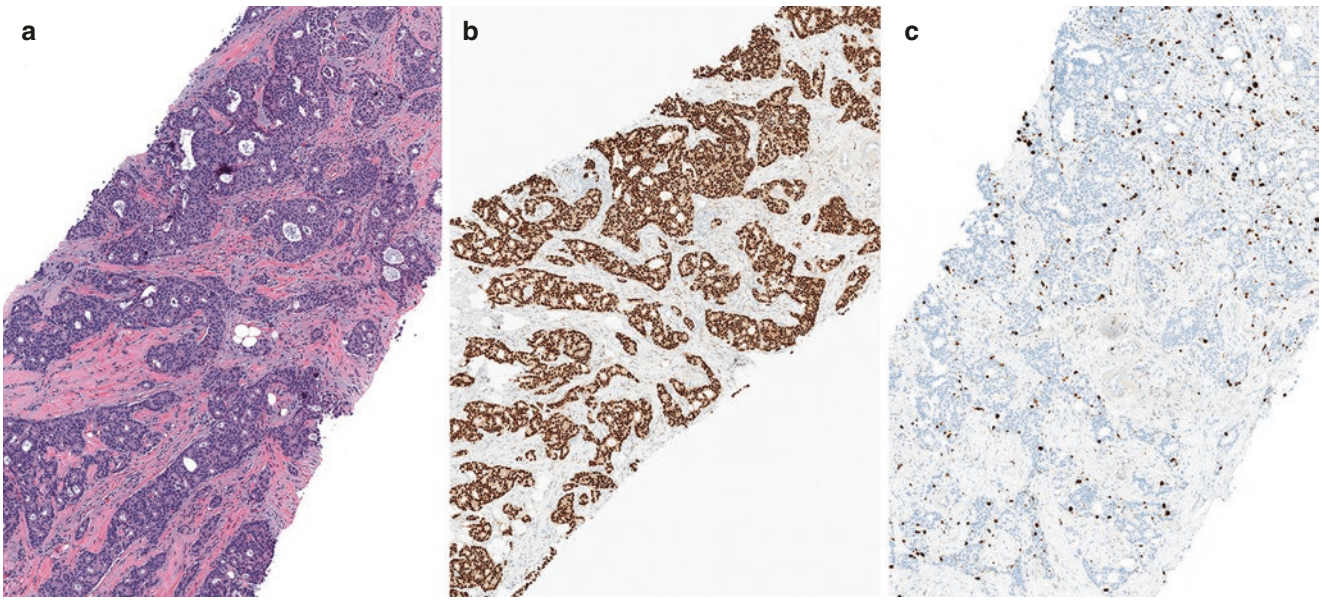

Fig. 10.81 Invasive cribriform carcinoma, (**a**) H&E stain, (**b**) strong and diffuse ER staining, and (**c**) Ki-67 shows low (<10%) proliferation index in tumor cells

Prognosis

Invasive cribriform carcinoma is associated with an excellent prognosis. The largest case series include the study by Page et al. where 51 cases were divided into classical and mixed types as defined above and Venable et al. with 62 cases of "pure" ICC, where essentially the entire tumor exhibited a cribriform pattern, and "mixed" ICC, where tumors displayed cribriform architecture mixed with tubular, papillary, ductal, or lobular patterns [176, 178].

With an average follow-up of 14.5 years, only one patient with classical ICC in Page's study died, but from contralateral breast squamous cell carcinoma [176]. Venable et al. found a 100% 5-year survival rate in those with tumors with ≥50% cribriform pattern [178]. A more recent SEER study found a 90% 5-year survival rate for ICC [177]. Axillary lymph node metastasis in ICC has been reported to range from 14% to 25% [176–178, 180, 181]. ICC is less likely to involve more than three lymph nodes compared to tumors with a smaller (<50%) cribriform component [178]. Interestingly, nodal metastasis from pure ICC maintains a cribriform pattern, whereas metastasis from mixed tumors are more likely to exhibit a non-cribriform component [176, 178]. One case of distant metastasis with ICC has been reported in a patient with untreated tumor for 13 years that eventually ulcerated through the skin. This patient was still alive 7 years after presenting with metastatic disease, demonstrating the indolent nature of this tumor [186].

References

1. Rakha EAAK, Bu H, Ellis IO, Foschini MP, Horii R, Masuda S, Penault-Llorca F, Schnitt SJ, Tsuda H, Vincent-Salomon A, Yang WT. WHO classification of tumours: breast tumours. 5th ed. Lyon: World Health Organization; 2019.
2. Anderson WF, Pfeiffer RM, Dores GM, Sherman ME. Comparison of age distribution patterns for different histopathologic types of breast carcinoma. Cancer Epidemiol Biomark Prev. 2006;15(10):1899–905.
3. Fisher CJ, Egan MK, Smith P, Wicks K, Millis RR, Fentiman IS. Histopathology of breast cancer in relation to age. Br J Cancer. 1997;75(4):593–6.
4. Li CI, Anderson BO, Daling JR, Moe RE. Trends in incidence rates of invasive lobular and ductal breast carcinoma. JAMA. 2003;289(11):1421–4.
5. Ellis IO, Galea M, Broughton N, Locker A, Blamey RW, Elston CW. Pathological prognostic factors in breast cancer. II. Histological type. Relationship with survival in a large study with long-term follow-up. Histopathology. 1992;20(6):479–89.
6. Fisher ER, Gregorio RM, Fisher B, Redmond C, Vellios F, Sommers SC. The pathology of invasive breast cancer. A syllabus derived from findings of the National Surgical Adjuvant Breast Project (protocol no. 4). Cancer. 1975;36(1):1–85.
7. Allred DC, Carlson RW, Berry DA, Burstein HJ, Edge SB, Goldstein LJ, et al. NCCN task force report: estrogen receptor and progesterone receptor testing in breast cancer by immunohistochemistry. J Natl Compr Cancer Network. 2009;7(Suppl 6):S1–21; quiz S2–3.
8. Broberg A, Glas U, Gustafsson SA, Hellstrom L, Somell A. Relationship between mammographic pattern and estrogen receptor content in breast cancer. Breast Cancer Res Treat. 1983;3(2):201–7.
9. Berg WA, Gutierrez L, NessAiver MS, Carter WB, Bhargavan M, Lewis RS, et al. Diagnostic accuracy of mammography, clinical examination, US, and MR imaging in preoperative assessment of breast cancer. Radiology. 2004;233(3):830–49.
10. Moss HA, Britton PD, Flower CD, Freeman AH, Lomas DJ, Warren RM. How reliable is modern breast imaging in differentiating benign from malignant breast lesions in the symptomatic population? Clin Radiol. 1999;54(10):676–82.
11. Sickies EA. Sonographic detectability of breast calcification. Proc SPIE. 1983;419:51–2.
12. Lambie RW, Hodgden D, Herman EM, Kopperman M. Sonomammographic manifestations of mammographically detectable breast microcalcifications. J Ultrasound Med. 1983;2(11):509–14.
13. Stavros AT, Thickman D, Rapp CL, Dennis MA, Parker SH, Sisney GA. Solid breast nodules: use of sonography to distinguish between benign and malignant lesions. Radiology. 1995;196(1):123–34.
14. Fornage BD, Sneige N, Faroux MJ, Andry E. Sonographic appearance and ultrasound-guided fine-needle aspiration biopsy of breast carcinomas smaller than 1 cm3. J Ultrasound Med. 1990;9(10):559–68.
15. Fornage BD, Lorigan JG, Andry E. Fibroadenoma of the breast: sonographic appearance. Radiology. 1989;172(3):671–5.
16. Saslow D, Boetes C, Burke W, Harms S, Leach MO, Lehman CD, et al. American Cancer Society guidelines for breast screening with MRI as an adjunct to mammography. CA Cancer J Clin. 2007;57(2):75–89.
17. Yeh E, Slanetz P, Kopans DB, Rafferty E, Georgian-Smith D, Moy L, et al. Prospective comparison of mammography, sonography, and MRI in patients undergoing neoadjuvant chemotherapy for palpable breast cancer. AJR Am J Roentgenol. 2005;184(3):868–77.
18. Jabbar SB, Lynch B, Seiler S, Hwang H, Sahoo S. Pathologic findings of breast lesions detected on magnetic resonance imaging. Arch Pathol Lab Med. 2017;141(11):1513–22.
19. Choudhery S, Lynch B, Sahoo S, Seiler SJ. Features of non-mass enhancing lesions detected on 1.5 T breast MRI: a radiologic and pathologic analysis. Breast Dis. 2015;35(1):13–7.
20. Schnall MD, Blume J, Bluemke DA, DeAngelis GA, DeBruhl N, Harms S, et al. Diagnostic architectural and dynamic features at breast MR imaging: multicenter study. Radiology. 2006;238(1):42–53.
21. Mandoul C, Verheyden C, Millet I, Orliac C, Pages E, Thomassin I, et al. Breast tomosynthesis: what do we know and where do we stand? Diagn Interv Imaging. 2019;100(10):537–51.
22. van Bogaert LJ, Maldague P. Scirrhous carcinoma of the female breast. Invest Cell Pathol. 1980;3(4):377–82.
23. Arps DP, Healy P, Zhao L, Kleer CG, Pang JC. Invasive ductal carcinoma with lobular features: a comparison study to invasive ductal and invasive lobular carcinomas of the breast. Breast Cancer Res Treat. 2013;138(3):719–26.
24. Galea MH, Blamey RW, Elston CE, Ellis IO. The Nottingham Prognostic Index in primary breast cancer. Breast Cancer Res Treat. 1992;22(3):207–19.
25. Elston CW, Ellis IO. Pathological prognostic factors in breast cancer. I. The value of histological grade in breast cancer: experience from a large study with long-term follow-up. Histopathology. 2002;41(3A):154–61.
26. Elston CW, Ellis IO. Pathological prognostic factors in breast cancer. I. The value of histological grade in breast cancer: experience from a large study with long-term follow-up. Histopathology. 2002;41(3A):151–2; discussion 2–3.
27. Elston CW, Ellis IO. Pathological prognostic factors in breast cancer. I. The value of histological grade in breast cancer: experience from a large study with long-term follow-up. Histopathology. 1991;19(5):403–10.
28. Bloom HJ, Richardson WW. Histological grading and prognosis in breast cancer; a study of 1409 cases of which 359 have been followed for 15 years. Br J Cancer. 1957;11(3):359–77.
29. Patey DH, Scarff RW. The position of histology in the prognosis of carcinoma of the breast. Lancet. 1928;1:801–4.
30. Haybittle JL, Blamey RW, Elston CW, Johnson J, Doyle PJ, Campbell FC, et al. A prognostic index in primary breast cancer. Br J Cancer. 1982;45(3):361–6.
31. Blamey RW, Ellis IO, Pinder SE, Lee AH, Macmillan RD, Morgan DA, et al. Survival of invasive breast cancer according to the Nottingham Prognostic Index in cases diagnosed in 1990-1999. Eur J Cancer. 2007;43(10):1548–55.
32. Cui X, Harada S, Shen D, Siegal GP, Wei S. The utility of phosphohistone H3 in breast cancer grading. Appl Immunohistochem Mol Morphol. 2015;23:689–95.
33. Start RD, Flynn MS, Cross SS, Rogers K, Smith JH. Is the grading of breast carcinomas affected by a delay in fixation? Virchows Arch A Pathol Anat Histopathol. 1991;419(6):475–7.
34. Robbins P, Pinder S, de Klerk N, Dawkins H, Harvey J, Sterrett G, et al. Histological grading of breast carcinomas: a study of interobserver agreement. Hum Pathol. 1995;26(8):873–9.
35. Yildiz-Aktas IZ, Dabbs DJ, Bhargava R. The effect of cold ischemic time on the immunohistochemical evaluation of estrogen receptor, progesterone receptor, and HER2 expression in invasive breast carcinoma. Mod Pathol. 2012;25(8):1098–105.
36. Usami S, Moriya T, Amari M, Suzuki A, Ishida T, Sasano H, et al. Reliability of prognostic factors in breast carcinoma determined by core needle biopsy. Jpn J Clin Oncol. 2007;37(4):250–5.
37. Shannon J, Douglas-Jones AG, Dallimore NS. Conversion to core biopsy in preoperative diagnosis of breast lesions: is it justified by results? J Clin Pathol. 2001;54(10):762–5.

38. McIntosh SA, Panchalingam L, Payne S, Miller ID, Sarkar TK, Hutcheon AW, et al. Freehand core biopsy in breast cancer: an accurate predictor of tumour grade following neoadjuvant chemotherapy? Breast. 2002;11(6):496–500.
39. Andrade VP, Gobbi H. Accuracy of typing and grading invasive mammary carcinomas on core needle biopsy compared with the excisional specimen. Virchows Arch. 2004;445(6):597–602.
40. Monticciolo DL. Histologic grading at breast core needle biopsy: comparison with results from the excised breast specimen. Breast J. 2005;11(1):9–14.
41. Rakha EA, Ellis IO. An overview of assessment of prognostic and predictive factors in breast cancer needle core biopsy specimens. J Clin Pathol. 2007;60(12):1300–6.
42. Denley H, Pinder SE, Elston CW, Lee AH, Ellis IO. Preoperative assessment of prognostic factors in breast cancer. J Clin Pathol. 2001;54(1):20–4.
43. Daveau C, Baulies S, Lalloum M, Bollet M, Sigal-Zafrani B, Sastre X, et al. Histological grade concordance between diagnostic core biopsy and corresponding surgical specimen in HR-positive/HER2-negative breast carcinoma. Br J Cancer. 2014;110(9):2195–200.
44. Kwok TC, Rakha EA, Lee AH, Grainge M, Green AR, Ellis IO, et al. Histological grading of breast cancer on needle core biopsy: the role of immunohistochemical assessment of proliferation. Histopathology. 2010;57(2):212–9.
45. Verkooijen HM, Peeters PH, Buskens E, Koot VC, Borel Rinkes IH, Mali WP, et al. Diagnostic accuracy of large-core needle biopsy for nonpalpable breast disease: a meta-analysis. Br J Cancer. 2000;82(5):1017–21.
46. Verkooijen HM, Core Biopsy After Radiological Localisation Study G. Diagnostic accuracy of stereotactic large-core needle biopsy for nonpalpable breast disease: results of a multicenter prospective study with 95% surgical confirmation. Int J Cancer. 2002;99(6):853–9.
47. Dillon MF, Hill AD, Quinn CM, O'Doherty A, McDermott EW, O'Higgins N. The accuracy of ultrasound, stereotactic, and clinical core biopsies in the diagnosis of breast cancer, with an analysis of false-negative cases. Ann Surg. 2005;242(5):701–7.
48. Ibrahim AE, Bateman AC, Theaker JM, Low JL, Addis B, Tidbury P, et al. The role and histological classification of needle core biopsy in comparison with fine needle aspiration cytology in the preoperative assessment of impalpable breast lesions. J Clin Pathol. 2001;54(2):121–5.
49. Brenner RJ, Fajardo L, Fisher PR, Dershaw DD, Evans WP, Bassett L, et al. Percutaneous core biopsy of the breast: effect of operator experience and number of samples on diagnostic accuracy. AJR Am J Roentgenol. 1996;166(2):341–6.
50. Bassett L, Winchester DP, Caplan RB, Dershaw DD, Dowlatshahi K, Evans WP 3rd, et al. Stereotactic core-needle biopsy of the breast: a report of the Joint Task Force of the American College of Radiology, American College of Surgeons, and College of American Pathologists. CA Cancer J Clin. 1997;47(3):171–90.
51. Rakha EA, Gill MS, El-Sayed ME, Khan MM, Hodi Z, Blamey RW, et al. The biological and clinical characteristics of breast carcinoma with mixed ductal and lobular morphology. Breast Cancer Res Treat. 2009;114(2):243–50.
52. Rakha EA, El-Sayed ME, Powe DG, Green AR, Habashy H, Grainge MJ, et al. Invasive lobular carcinoma of the breast: response to hormonal therapy and outcomes. Eur J Cancer. 2008;44(1):73–83.
53. Wiseman C, Liao KT. Primary lymphoma of the breast. Cancer. 1972;29(6):1705–12.
54. Telesinghe PU, Anthony PP. Primary lymphoma of the breast. Histopathology. 1985;9(3):297–307.
55. Talwalkar SS, Miranda RN, Valbuena JR, Routbort MJ, Martin AW, Medeiros LJ. Lymphomas involving the breast: a study of 106 cases comparing localized and disseminated neoplasms. Am J Surg Pathol. 2008;32(9):1299–309.
56. Ganjoo K, Advani R, Mariappan MR, McMillan A, Horning S. Non-Hodgkin lymphoma of the breast. Cancer. 2007;110(1):25–30.
57. Sauer T. Fine-needle aspiration cytology of extra mammary metastatic lesions in the breast: a retrospective study of 36 cases diagnosed during 18 years. Cytojournal. 2010;7:10.
58. Vaughan A, Dietz JR, Moley JF, Debenedetti MK, Aft RL, Gillanders WE, et al. Metastatic disease to the breast: the Washington University experience. World J Surg Oncol. 2007;5:74.
59. Saluja K, Thakral B, Bit-Ivan E, Kaufman M, Liu L. Fine-needle aspiration of metastatic renal cell carcinoma to a male breast: a rare initial presentation. Cytojournal. 2014;11:8.
60. Nasit JG, Shah B, Shah M. Metastatic hepatocellular carcinoma presenting as gynecomastia in male: a diagnostic dilema in fine needle aspiration cytology. Cytojournal. 2012;9:21.
61. Vassalli L, Ferrari VD, Simoncini E, Rangoni G, Montini E, Marpicati P, et al. Solitary breast metastases from a renal cell carcinoma. Breast Cancer Res Treat. 2001;68(1):29–31.
62. Robens J, Goldstein L, Gown AM, Schnitt SJ. Thyroid transcription factor-1 expression in breast carcinomas. Am J Surg Pathol. 2010;34(12):1881–5.
63. Domfeh AB, Carley AL, Striebel JM, Karabakhtsian RG, Florea AV, McManus K, et al. WT1 immunoreactivity in breast carcinoma: selective expression in pure and mixed mucinous subtypes. Mod Pathol. 2008;21(10):1217–23.
64. Howlader N, Altekruse SF, Li CI, Chen VW, Clarke CA, Ries LA, et al. US incidence of breast cancer subtypes defined by joint hormone receptor and HER2 status. J Natl Cancer Inst. 2014;106(5):dju055.
65. Wick MR, Lillemoe TJ, Copland GT, Swanson PE, Manivel JC, Kiang DT. Gross cystic disease fluid protein-15 as a marker for breast cancer: immunohistochemical analysis of 690 human neoplasms and comparison with alpha-lactalbumin. Hum Pathol. 1989;20(3):281–7.
66. Bhargava R, Beriwal S, Dabbs DJ. Mammaglobin vs GCDFP-15: an immunohistologic validation survey for sensitivity and specificity. Am J Clin Pathol. 2007;127(1):103–13.
67. Han JH, Kang Y, Shin HC, Kim HS, Kang YM, Kim YB, et al. Mammaglobin expression in lymph nodes is an important marker of metastatic breast carcinoma. Arch Pathol Lab Med. 2003;127(10):1330–4.
68. Lewis GH, Subhawong AP, Nassar H, Vang R, Illei PB, Park BH, et al. Relationship between molecular subtype of invasive breast carcinoma and expression of gross cystic disease fluid protein 15 and mammaglobin. Am J Clin Pathol. 2011;135(4):587–91.
69. Dennis JL, Hvidsten TR, Wit EC, Komorowski J, Bell AK, Downie I, et al. Markers of adenocarcinoma characteristic of the site of origin: development of a diagnostic algorithm. Clin Cancer Res. 2005;11(10):3766–72.
70. Mazoujian G, Bodian C, Haagensen DE Jr, Haagensen CD. Expression of GCDFP-15 in breast carcinomas. Relationship to pathologic and clinical factors. Cancer. 1989;63(11):2156–61.
71. Yang M, Nonaka D. A study of immunohistochemical differential expression in pulmonary and mammary carcinomas. Mod Pathol. 2010;23(5):654–61.
72. Miettinen M, McCue PA, Sarlomo-Rikala M, Rys J, Czapiewski P, Wazny K, et al. GATA3: a multispecific but potentially useful marker in surgical pathology: a systematic analysis of 2500 epithelial and nonepithelial tumors. Am J Surg Pathol. 2014;38(1):13–22.
73. Cimino-Mathews A, Subhawong AP, Illei PB, Sharma R, Halushka MK, Vang R, et al. GATA3 expression in breast carcinoma: utility in triple-negative, sarcomatoid, and metastatic carcinomas. Hum Pathol. 2013;44(7):1341–9.

74. Cimino-Mathews A, Subhawong AP, Elwood H, Warzecha HN, Sharma R, Park BH, et al. Neural crest transcription factor Sox10 is preferentially expressed in triple-negative and metaplastic breast carcinomas. Hum Pathol. 2013;44(6):959–65.
75. Wellings SR, Jensen HM, Marcum RG. An atlas of subgross pathology of the human breast with special reference to possible precancerous lesions. J Natl Cancer Inst. 1975;55(2):231–73.
76. Wellings SR, Jensen HM. On the origin and progression of ductal carcinoma in the human breast. J Natl Cancer Inst. 1973;50(5):1111–8.
77. Marshall LM, Hunter DJ, Connolly JL, Schnitt SJ, Byrne C, London SJ, et al. Risk of breast cancer associated with atypical hyperplasia of lobular and ductal types. Cancer Epidemiol Biomark Prev. 1997;6(5):297–301.
78. Lakhani SR, Audretsch W, Cleton-Jensen AM, Cutuli B, Ellis I, Eusebi V, et al. The management of lobular carcinoma in situ (LCIS). Is LCIS the same as ductal carcinoma in situ (DCIS)? Eur J Cancer. 2006;42(14):2205–11.
79. Hanby AM, Hughes TA. In situ and invasive lobular neoplasia of the breast. Histopathology. 2008;52(1):58–66.
80. Oyama T, Iijima K, Takei H, Horiguchi J, Iino Y, Nakajima T, et al. Atypical cystic lobule of the breast: an early stage of low-grade ductal carcinoma in-situ. Breast Cancer. 2000;7(4):326–31.
81. Lerwill MF. Flat epithelial atypia of the breast. Arch Pathol Lab Med. 2008;132(4):615–21.
82. Simpson PT, Reis-Filho JS, Gale T, Lakhani SR. Molecular evolution of breast cancer. J Pathol. 2005;205(2):248–54.
83. Roylance R, Gorman P, Harris W, Liebmann R, Barnes D, Hanby A, et al. Comparative genomic hybridization of breast tumors stratified by histological grade reveals new insights into the biological progression of breast cancer. Cancer Res. 1999;59(7):1433–6.
84. Buerger H, Otterbach F, Simon R, Poremba C, Diallo R, Decker T, et al. Comparative genomic hybridization of ductal carcinoma in situ of the breast-evidence of multiple genetic pathways. J Pathol. 1999;187(4):396–402.
85. O'Connell P, Pekkel V, Fuqua SA, Osborne CK, Clark GM, Allred DC. Analysis of loss of heterozygosity in 399 premalignant breast lesions at 15 genetic loci. J Natl Cancer Inst. 1998;90(9):697–703.
86. Moinfar F, Man YG, Bratthauer GL, Ratschek M, Tavassoli FA. Genetic abnormalities in mammary ductal intraepithelial neoplasia-flat type ("clinging ductal carcinoma in situ"): a simulator of normal mammary epithelium. Cancer. 2000;88(9):2072–81.
87. Tirkkonen M, Tanner M, Karhu R, Kallioniemi A, Isola J, Kallioniemi OP. Molecular cytogenetics of primary breast cancer by CGH. Genes Chromosomes Cancer. 1998;21(3):177–84.
88. Natrajan R, Lambros MB, Geyer FC, Marchio C, Tan DS, Vatcheva R, et al. Loss of 16q in high grade breast cancer is associated with estrogen receptor status: evidence for progression in tumors with a luminal phenotype? Genes Chromosomes Cancer. 2009;48(4):351–65.
89. Allred DC, Wu Y, Mao S, Nagtegaal ID, Lee S, Perou CM, et al. Ductal carcinoma in situ and the emergence of diversity during breast cancer evolution. Clin Cancer Res. 2008;14(2):370–8.
90. Denkert C, von Minckwitz G, Darb-Esfahani S, Lederer B, Heppner BI, Weber KE, et al. Tumour-infiltrating lymphocytes and prognosis in different subtypes of breast cancer: a pooled analysis of 3771 patients treated with neoadjuvant therapy. Lancet Oncol. 2018;19(1):40–50.
91. Amin M, Gress DM, Meyer Vega LR, Edge SB, Greene FL, Byrd DR, Brookland RK, Washington MK, Compton CC. AJCC cancer staging manual. 8th ed. Chicago, IL: Springer; 2017.
92. Veronesi P, Rodriguez-Fernandez J, Intra M. Controversies in the use of sentinel nodes: microinvasion, post surgery and after preoperative systemic treatment. Breast. 2007;16(Suppl 2):S67–70.
93. Hanna MG, Jaffer S, Bleiweiss IJ, Nayak A. Re-evaluating the role of sentinel lymph node biopsy in microinvasive breast carcinoma. Mod Pathol. 2014;27(11):1489–98.
94. Hoda SA, Chiu A, Prasad ML, Giri D, Hoda RS. Are microinvasion and micrometastasis in breast cancer mountains or molehills? Am J Surg. 2000;180(4):305–8.
95. Silverstein MJ, Waisman JR, Gamagami P, Gierson ED, Colburn WJ, Rosser RJ, et al. Intraductal carcinoma of the breast (208 cases). Clinical factors influencing treatment choice. Cancer. 1990;66(1):102–8.
96. Klauber-DeMore N, Tan LK, Liberman L, Kaptain S, Fey J, Borgen P, et al. Sentinel lymph node biopsy: is it indicated in patients with high-risk ductal carcinoma-in-situ and ductal carcinoma-in-situ with microinvasion? Ann Surg Oncol. 2000;7(9):636–42.
97. Schuh ME, Nemoto T, Penetrante RB, Rosner D, Dao TL. Intraductal carcinoma. Analysis of presentation, pathologic findings, and outcome of disease. Arch Surg. 1986;121(11):1303–7.
98. Kinne DW, Petrek JA, Osborne MP, Fracchia AA, DePalo AA, Rosen PP. Breast carcinoma in situ. Arch Surg. 1989;124(1):33–6.
99. Patchefsky AS, Schwartz GF, Finkelstein SD, Prestipino A, Sohn SE, Singer JS, et al. Heterogeneity of intraductal carcinoma of the breast. Cancer. 1989;63(4):731–41.
100. Page DL, Anderson TJ. Diagnostic histopathology of the breast. Edinburgh: Churchill Livingstone; 1987.
101. Solin LJ, Fowble BL, Yeh IT, Kowalyshyn MJ, Schultz DJ, Weiss MC, et al. Microinvasive ductal carcinoma of the breast treated with breast-conserving surgery and definitive irradiation. Int J Radiat Oncol Biol Phys. 1992;23(5):961–8.
102. Silver SA, Tavassoli FA. Mammary ductal carcinoma in situ with microinvasion. Cancer. 1998;82(12):2382–90.
103. National Coordinating Group for Breast Cancer Screening Pathology. Pathology reporting in breast cancer screening. Sheffield: NHSBSP Publications; 1995.
104. Lagios MD, Westdahl PR, Margolin FR, Rose MR. Duct carcinoma in situ. Relationship of extent of noninvasive disease to the frequency of occult invasion, multicentricity, lymph node metastases, and short-term treatment failures. Cancer. 1982;50(7):1309–14.
105. Vieira CC, Mercado CL, Cangiarella JF, Moy L, Toth HK, Guth AA. Microinvasive ductal carcinoma in situ: clinical presentation, imaging features, pathologic findings, and outcome. Eur J Radiol. 2010;73(1):102–7.
106. Sim YT, Litherland J, Lindsay E, Hendry P, Brauer K, Dobson H, et al. Upgrade of ductal carcinoma in situ on core biopsies to invasive disease at final surgery: a retrospective review across the Scottish Breast Screening Programme. Clin Radiol. 2015;70(5):502–6.
107. Dillon MF, McDermott EW, Quinn CM, O'Doherty A, O'Higgins N, Hill AD. Predictors of invasive disease in breast cancer when core biopsy demonstrates DCIS only. J Surg Oncol. 2006;93(7):559–63.
108. Nemoto T, Castillo N, Tsukada Y, Koul A, Eckhert KH Jr, Bauer RL. Lobular carcinoma in situ with microinvasion. J Surg Oncol. 1998;67(1):41–6.
109. Yang M, Moriya T, Oguma M, De La Cruz C, Endoh M, Ishida T, et al. Microinvasive ductal carcinoma (T1mic) of the breast. The clinicopathological profile and immunohistochemical features of 28 cases. Pathol Int. 2003;53(7):422–8.
110. Prasad ML, Osborne MP, Giri DD, Hoda SA. Microinvasive carcinoma (T1mic) of the breast: clinicopathologic profile of 21 cases. Am J Surg Pathol. 2000;24(3):422–8.
111. Diaz NM, Cox CE, Ebert M, Clark JD, Vrcel V, Stowell N, et al. Benign mechanical transport of breast epithelial cells to sentinel lymph nodes. Am J Surg Pathol. 2004;28(12):1641–5.
112. Carter BA, Jensen RA, Simpson JF, Page DL. Benign transport of breast epithelium into axillary lymph nodes after biopsy. Am J Clin Pathol. 2000;113(2):259–65.

113. Schnitt SJ, Collins LC. Microinvasive carcioma. In: Schnitt SJCLC, editor. Biopsy interpretation of the breast. Philadelphia, PA: Lippincott Williams & Wilkins; 2009. p. 236–48.
114. Tunon-de-Lara C, Chauvet MP, Baranzelli MC, Baron M, Piquenot J, Le-Bouedec G, et al. The role of sentinel lymph node biopsy and factors associated with invasion in extensive DCIS of the breast treated by mastectomy: the Cinnamome prospective multicenter study. Ann Surg Oncol. 2015;22(12):3853–60.
115. NHS Breast Screening Programme, Association of Breast Surgery. An audit of screen detected breast cancers for the year of screening April 2012 to March 2013. London: NHS Breast Screening Programme; 2014.
116. Gojon H, Fawunmi D, Valachis A. Sentinel lymph node biopsy in patients with microinvasive breast cancer: a systematic review and meta-analysis. Eur J Surg Oncol. 2014;40(1):5–11.
117. Parikh RR, Haffty BG, Lannin D, Moran MS. Ductal carcinoma in situ with microinvasion: prognostic implications, long-term outcomes, and role of axillary evaluation. Int J Radiat Oncol Biol Phys. 2012;82(1):7–13.
118. Murphy CD, Jones JL, Javid SH, Michaelson JS, Nolan ME, Lipsitz SR, et al. Do sentinel node micrometastases predict recurrence risk in ductal carcinoma in situ and ductal carcinoma in situ with microinvasion? Am J Surg. 2008;196(4):566–8.
119. Shatat L, Gloyeske N, Madan R, O'Neil M, Tawfik O, Fan F. Microinvasive breast carcinoma carries an excellent prognosis regardless of the tumor characteristics. Hum Pathol. 2013;44(12):2684–9.
120. Lyman GH, Temin S, Edge SB, Newman LA, Turner RR, Weaver DL, et al. Sentinel lymph node biopsy for patients with early-stage breast cancer: American Society of Clinical Oncology clinical practice guideline update. J Clin Oncol. 2014;32(13):1365–83.
121. Sopik V, Sun P, Narod SA. Impact of microinvasion on breast cancer mortality in women with ductal carcinoma in situ. Breast Cancer Res Treat. 2018;167(3):787–95.
122. Wang W, Zhu W, Du F, Luo Y, Xu B. The demographic features, clinicopathological characteristics and cancer-specific outcomes for patients with microinvasive breast cancer: a SEER database analysis. Sci Rep. 2017;7:42045.
123. van la Parra RF, Ernst MF, Barneveld PC, Broekman JM, Rutten MJ, Bosscha K. The value of sentinel lymph node biopsy in ductal carcinoma in situ (DCIS) and DCIS with microinvasion of the breast. Eur J Surg Oncol. 2008;34(6):631–5.
124. Dominguez FJ, Golshan M, Black DM, Hughes KS, Gadd MA, Christian R, et al. Sentinel node biopsy is important in mastectomy for ductal carcinoma in situ. Ann Surg Oncol. 2008;15(1):268–73.
125. Cooper HS, Patchefsky AS, Krall RA. Tubular carcinoma of the breast. Cancer. 1978;42(5):2334–42.
126. Carstens PH. Tubular carcinoma of the breast. A study of frequency. Am J Clin Pathol. 1978;70(2):204–10.
127. Kader HA, Jackson J, Mates D, Andersen S, Hayes M, Olivotto IA. Tubular carcinoma of the breast: a population-based study of nodal metastases at presentation and of patterns of relapse. Breast J. 2001;7(1):8–13.
128. Romano AM, Wages N, Smolkin M, Fortune K, Atkins K, Dillon PM. Tubular carcinoma of the breast: institutional and SEER database analysis supporting a unique classification. Breast Dis. 2015;35:103–11.
129. Sullivan T, Raad RA, Goldberg S, Assaad SI, Gadd M, Smith BL, et al. Tubular carcinoma of the breast: a retrospective analysis and review of the literature. Breast Cancer Res Treat. 2005;93(3):199–205.
130. Rakha EA, Lee AH, Evans AJ, Menon S, Assad NY, Hodi Z, et al. Tubular carcinoma of the breast: further evidence to support its excellent prognosis. J Clin Oncol. 2010;28(1):99–104.
131. Cabral AH, Recine M, Paramo JC, McPhee MM, Poppiti R, Mesko TW. Tubular carcinoma of the breast: an institutional experience and review of the literature. Breast J. 2003;9(4):298–301.
132. Li CI. Risk of mortality by histologic type of breast cancer in the United States. Hormones & Cancer. 2010;1(3):156–65.
133. Visfeldt J, Scheike O. Male breast cancer. I. Histologic typing and grading of 187 Danish cases. Cancer. 1973;32(4):985–90.
134. Fedko MG, Scow JS, Shah SS, Reynolds C, Degnim AC, Jakub JW, et al. Pure tubular carcinoma and axillary nodal metastases. Ann Surg Oncol. 2010;17(Suppl 3):338–42.
135. Sheppard DG, Whitman GJ, Huynh PT, Sahin AA, Fornage BD, Stelling CB. Tubular carcinoma of the breast: mammographic and sonographic features. AJR Am J Roentgenol. 2000;174(1):253–7.
136. Elson BC, Helvie MA, Frank TS, Wilson TE, Adler DD. Tubular carcinoma of the breast: mode of presentation, mammographic appearance, and frequency of nodal metastases. AJR Am J Roentgenol. 1993;161(6):1173–6.
137. Vega A, Garijo F. Radial scar and tubular carcinoma. Mammographic and sonographic findings. Acta Radiol. 1993;34(1):43–7.
138. Shin HJ, Kim HH, Kim SM, Kim DB, Lee YR, Kim MJ, et al. Pure and mixed tubular carcinoma of the breast: mammographic and sonographic differential features. Korean J Radiol. 2007;8(2):103–10.
139. Tweedie E, Tonkin K, Kerkvliet N, Doig GS, Sparrow RK, O'Malley FP. Biologic characteristics of breast cancer detected by mammography and by palpation in a screening program: a pilot study. Clin Invest Med. 1997;20(5):300–7.
140. Rajakariar R, Walker RA. Pathological and biological features of mammographically detected invasive breast carcinomas. Br J Cancer. 1995;71(1):150–4.
141. Anderson TJ, Lamb J, Alexander F, Lutz W, Chetty U, Forrest AP, et al. Comparative pathology of prevalent and incident cancers detected by breast screening. Edinburgh Breast Screening Project. Lancet. 1986;1(8480):519–23.
142. Mitnick JS, Gianutsos R, Pollack AH, Susman M, Baskin BL, Ko WD, et al. Tubular carcinoma of the breast: sensitivity of diagnostic techniques and correlation with histopathology. AJR Am J Roentgenol. 1999;172(2):319–23.
143. McDivitt RW, Boyce W, Gersell D. Tubular carcinoma of the breast. Clinical and pathological observations concerning 135 cases. Am J Surg Pathol. 1982;6(5):401–11.
144. Andersen JA, Carter D, Linell F. A symposium on sclerosing duct lesions of the breast. Pathol Annu. 1986;21(Pt 2):145–79.
145. van Deurzen CH, McMillan DC, Purdie CA. WHO classifications of tumours: breast tumours. 5th ed. Lyon: World Health Organization; 2019.
146. Sahoo S, Recant WM. Triad of columnar cell alteration, lobular carcinoma in situ, and tubular carcinoma of the breast. Breast J. 2005;11(2):140–2.
147. Rosen PP. Columnar cell hyperplasia is associated with lobular carcinoma in situ and tubular carcinoma. Am J Surg Pathol. 1999;23(12):1561.
148. Brandt SM, Young GQ, Hoda SA. The "Rosen Triad": tubular carcinoma, lobular carcinoma in situ, and columnar cell lesions. Adv Anat Pathol. 2008;15(3):140–6.
149. Abdel-Fatah TM, Powe DG, Hodi Z, Lee AH, Reis-Filho JS, Ellis IO. High frequency of coexistence of columnar cell lesions, lobular neoplasia, and low grade ductal carcinoma in situ with invasive tubular carcinoma and invasive lobular carcinoma. Am J Surg Pathol. 2007;31(3):417–26.
150. Clement PB, Azzopardi JG, Microglandular adenosis of the breast—a lesion simulating tubular carcinoma. Histopathology. 1983;7(2):169–80.
151. Wheeler DT, Tai LH, Bratthauer GL, Waldner DL, Tavassoli FA. Tubulolobular carcinoma of the breast: an analysis of 27 cases of a tumor with a hybrid morphology and immunoprofile. Am J Surg Pathol. 2004;28(12):1587–93.
152. Esposito NN, Chivukula M, Dabbs DJ. The ductal phenotypic expression of the E-cadherin/catenin complex in tubulolobular

carcinoma of the breast: an immunohistochemical and clinicopathologic study. Mod Pathol. 2007;20(1):130–8.
153. Green I, McCormick B, Cranor M, Rosen PP. A comparative study of pure tubular and tubulolobular carcinoma of the breast. Am J Surg Pathol. 1997;21(6):653–7.
154. Pereira H, Pinder SE, Sibbering DM, Galea MH, Elston CW, Blamey RW, et al. Pathological prognostic factors in breast cancer. IV: should you be a typer or a grader? A comparative study of two histological prognostic features in operable breast carcinoma. Histopathology. 1995;27(3):219–26.
155. Kuroda H, Tamaru J, Takeuchi I, Ohnisi K, Sakamoto G, Adachi A, et al. Expression of E-cadherin, alpha-catenin, and beta-catenin in tubulolobular carcinoma of the breast. Virchows Arch. 2006;448(4):500–5.
156. Diab SG, Clark GM, Osborne CK, Libby A, Allred DC, Elledge RM. Tumor characteristics and clinical outcome of tubular and mucinous breast carcinomas. J Clin Oncol. 1999;17(5):1442–8.
157. Alvarenga CA, Paravidino PI, Alvarenga M, Gomes M, Dufloth R, Zeferino LC, et al. Reappraisal of immunohistochemical profiling of special histological types of breast carcinomas: a study of 121 cases of eight different subtypes. J Clin Pathol. 2012;65(12):1066–71.
158. Lopez-Garcia MA, Geyer FC, Natrajan R, Kreike B, Mackay A, Grigoriadis A, et al. Transcriptomic analysis of tubular carcinomas of the breast reveals similarities and differences with molecular subtype-matched ductal and lobular carcinomas. J Pathol. 2010;222(1):64–75.
159. Rosen PP, Lesser ML, Arroyo CD, Cranor M, Borgen P, Norton L. p53 in node-negative breast carcinoma: an immunohistochemical study of epidemiologic risk factors, histologic features, and prognosis. J Clin Oncol. 1995;13(4):821–30.
160. Waldman FM, Hwang ES, Etzell J, Eng C, DeVries S, Bennington J, et al. Genomic alterations in tubular breast carcinomas. Hum Pathol. 2001;32(2):222–6.
161. Livi L, Paiar F, Meldolesi E, Talamonti C, Simontacchi G, Detti B, et al. Tubular carcinoma of the breast: outcome and loco-regional recurrence in 307 patients. Eur J Surg Oncol. 2005;31(1):9–12.
162. Javid SH, Smith BL, Mayer E, Bellon J, Murphy CD, Lipsitz S, et al. Tubular carcinoma of the breast: results of a large contemporary series. Am J Surg. 2009;197(5):674–7.
163. Min Y, Bae SY, Lee HC, Lee JH, Kim M, Kim J, et al. Tubular carcinoma of the breast: clinicopathologic features and survival outcome compared with ductal carcinoma in situ. J Breast Cancer. 2013;16(4):404–9.
164. National Comprehensive Cancer Network. Clinical practice guidelines in oncology—breast cancer. Version 4.2021; 2021. www.nccn.org
165. Stauber J, Chevli N, Haque W, Messer JA, Farach AM, Schwartz MR, et al. Prognostic impact of radiation therapy in tubular carcinoma of the breast. Radiother Oncol. 2021;159:202–8.
166. Chen JX, Zhang WW, Dong Y, Sun JY, He ZY, Wu SG. The effects of postoperative radiotherapy on survival outcomes in patients under 65 with estrogen receptor positive tubular breast carcinoma. Radiat Oncol. 2018;13(1):226.
167. Deos PH, Norris HJ. Well-differentiated (tubular) carcinoma of the breast. A clinicopathologic study of 145 pure and mixed cases. Am J Clin Pathol. 1982;78(1):1–7.
168. Papadatos G, Rangan AM, Psarianos T, Ung O, Taylor R, Boyages J. Probability of axillary node involvement in patients with tubular carcinoma of the breast. Br J Surg. 2001;88(6):860–4.
169. Lea V, Gluch L, Kennedy CW, Carmalt H, Gillett D. Tubular carcinoma of the breast: axillary involvement and prognostic factors. ANZ J Surg. 2014; https://doi.org/10.1111/ans.12791.
170. Dejode M, Sagan C, Campion L, Houvenaeghel G, Giard S, Rodier JF, et al. Pure tubular carcinoma of the breast and sentinel lymph node biopsy: a retrospective multi-institutional study of 234 cases. Eur J Surg Oncol. 2013;39(3):248–54.
171. Veronesi U, Viale G, Paganelli G, Zurrida S, Luini A, Galimberti V, et al. Sentinel lymph node biopsy in breast cancer: ten-year results of a randomized controlled study. Ann Surg. 2010;251(4):595–600.
172. Krag DN, Anderson SJ, Julian TB, Brown AM, Harlow SP, Ashikaga T, et al. Technical outcomes of sentinel-lymph-node resection and conventional axillary-lymph-node dissection in patients with clinically node-negative breast cancer: results from the NSABP B-32 randomised phase III trial. Lancet Oncol. 2007;8(10):881–8.
173. Goyal A, Newcombe RG, Chhabra A, Mansel RE, Group AT. Factors affecting failed localisation and false-negative rates of sentinel node biopsy in breast cancer—results of the ALMANAC validation phase. Breast Cancer Res Treat. 2006;99(2):203–8.
174. Fisher B, Jeong JH, Anderson S, Bryant J, Fisher ER, Wolmark N. Twenty-five-year follow-up of a randomized trial comparing radical mastectomy, total mastectomy, and total mastectomy followed by irradiation. N Engl J Med. 2002;347(8):567–75.
175. Fisher ER, Anderson S, Redmond C, Fisher B. Pathologic findings from the National Surgical Adjuvant Breast Project protocol B-06. 10-year pathologic and clinical prognostic discriminants. Cancer. 1993;71(8):2507–14.
176. Page DL, Dixon JM, Anderson TJ, Lee D, Stewart HJ. Invasive cribriform carcinoma of the breast. Histopathology. 1983;7(4):525–36.
177. Liu J, Zheng X, Han Z, Lin S, Han H, Xu C. Clinical characteristics and overall survival prognostic nomogram for invasive cribriform carcinoma of breast: a SEER population-based analysis. BMC Cancer. 2021;21(1):168.
178. Venable JG, Schwartz AM, Silverberg SG. Infiltrating cribriform carcinoma of the breast: a distinctive clinicopathologic entity. Hum Pathol. 1990;21(3):333–8.
179. Stutz JA, Evans AJ, Pinder S, Ellis IO, Yeoman LJ, Wilson AR, et al. The radiological appearances of invasive cribriform carcinoma of the breast. Nottingham Breast Team. Clin Radiol. 1994;49(10):693–5.
180. Zhang W, Zhang T, Lin Z, Zhang X, Liu F, Wang Y, et al. Invasive cribriform carcinoma in a Chinese population: comparison with low-grade invasive ductal carcinoma-not otherwise specified. Int J Clin Exp Pathol. 2013;6(3):445–57.
181. Lee YJ, Choi BB, Suh KS. Invasive cribriform carcinoma of the breast: mammographic, sonographic, MRI, and 18 F-FDG PET-CT features. Acta Radiol. 2014; https://doi.org/10.1177/0284185114538425.
182. Lim HS, Jeong SJ, Lee JS, Park MH, Yoon JH, Kim JW, et al. Sonographic findings of invasive cribriform carcinoma of the breast. J Ultrasound Med. 2011;30(5):701–5.
183. Wells CA, Ferguson DJ. Ultrastructural and immunocytochemical study of a case of invasive cribriform breast carcinoma. J Clin Pathol. 1988;41(1):17–20.
184. Saout L, Leduc M, Suy-Beng PT, Meignie P. [A new case of cribriform breast carcinoma associated with histiocytic giant cell reaction]. Arch Anat Cytol Pathol. 1985;33(1):58–61.
185. Rabban JT, Swain RS, Zaloudek CJ, Chase DR, Chen YY. Immunophenotypic overlap between adenoid cystic carcinoma and collagenous spherulosis of the breast: potential diagnostic pitfalls using myoepithelial markers. Mod Pathol. 2006;19(10):1351–7.
186. Zhang W, Lin Z, Zhang T, Liu F, Niu Y. A pure invasive cribriform carcinoma of the breast with bone metastasis if untreated for thirteen years: a case report and literature review. World J Surg Oncol. 2012;10:251.

Triple-Negative/Basal-Like Breast Carcinomas

11

Yaileen D. Guzmán-Arocho, Benjamin C. Calhoun, and Laura C. Collins

Overview

"Triple-negative" breast cancers (TNBCs) are defined by the absence of estrogen receptor (ER) and progesterone receptor (PR) protein expression by immunohistochemistry (IHC) and the absence of human epidermal growth factor 2 (HER2) protein overexpression or gene amplification on IHC and in situ hybridization studies, respectively. TNBC represents approximately 15–20% of all breast carcinomas [1, 2]. This group of breast cancers has a similar clinicopathologic profile to tumors categorized as basal-like carcinomas (BLC) through gene expression profiling studies performed in the early 2000s [3, 4]. Patients with BLC/TNBC are more likely to be of younger age or premenopausal; and women of African American or West African ancestry or who are *BRCA1* or *BRCA2* mutation carriers have a greater likelihood of developing TNBC [1, 5–7]. For these reasons, the current National Comprehensive Cancer Network Guidelines recommend referral of all patients with TNBC for genetic counseling and consideration for genetic testing [8].

BLC/TNBCs are associated with more aggressive tumor characteristics, more frequent relapse and metastasis, and decreased overall survival [9]. Patients with BLC/TNBC are more likely to have pulmonary, visceral, and central nervous system metastases than lymph node metastases compared to those with luminal and HER2-enriched subtypes, particularly within the first 5 years after diagnosis [10–12]. In what is known as the "triple-negative paradox," BLC/TNBCs show increased rates of complete pathologic response to chemotherapy but have lower disease-free and overall survival compared with the other breast cancer subtypes [13–16] suggesting heterogeneity within the group of BLC/TNBC.

At the time of writing, the use of multigene signatures for tumor classification is not current clinical practice (at least not for ER-negative tumors); thus, the term TNBC will be used in this chapter, unless particular reference is being made to tumors classified through molecular studies. In the years since the molecular subtype of BLC was first described, studies have demonstrated that BLC represents a group of tumors with diverse histology. In addition to invasive breast carcinomas of no special type (NST), BLC includes metaplastic carcinoma, carcinoma with medullary features, adenoid cystic carcinoma, and apocrine carcinoma [17]. More recently, tumors with the triple-negative phenotype have been shown to have an ever-expanding spectrum of gene expression profiles [18–21]. This chapter is dedicated to the discussion of TNBC NST; the special types of BLC/TNBC are discussed in Chap. 12.

Gross and Radiologic Features

On gross examination, TNBCs are often round or macrolobulated and well circumscribed. Sectioning reveals tan or white cut surfaces that may show areas of central fibrosis or necrosis.

TNBCs are less likely to be detected by screening mammography and are more likely to present as interval tumors compared to other breast cancer subtypes [12]. Additionally, the radiologic features of TNBCs differ from most image-detected breast cancers [22]; the most common mammographic finding is a density or mass that in many cases lacks the irregular shape, spiculated margins, and suspicious calcifications associated with other breast cancers [23–25]. Despite the often larger size at diagnosis compared to other tumor types [26], up to 18% of TNBCs can be occult on initial mammogram [23–25]. On ultrasound, TNBCs typically present as a mass with well-circumscribed borders and pos-

Y. D. Guzmán-Arocho · L. C. Collins (✉)
Department of Pathology, Beth Israel Deaconess Medical Center and Harvard Medical School, Boston, MA, USA
e-mail: yguzman@bidmc.harvard.edu; lcollins@bidmc.harvard.edu

B. C. Calhoun
Department of Pathology and Laboratory Medicine, University of North Carolina at Chapel Hill, Chapel Hill, NC, USA
e-mail: ben.calhoun@unchealth.unc.edu

© The Author(s), under exclusive license to Springer Nature Switzerland AG 2022
S. J. Shin et al. (eds.), *A Comprehensive Guide to Core Needle Biopsies of the Breast*,
https://doi.org/10.1007/978-3-031-05532-4_11

terior acoustic enhancement [23, 25, 27]. In this setting, posterior acoustic enhancement may indicate an internal fluid component corresponding to tumor necrosis [22].

Magnetic resonance imaging is used to screen populations at high risk for the development of breast cancer, including *BRCA* mutation carriers [28], and it may be the most sensitive imaging modality for TNBC, with tumors often showing a unifocal mass lesion with smooth margins, regular shape (round, oval, or lobulated), and peripheral (rim) pattern of enhancement [25, 29–32]. A high intratumoral signal on T2-weighted images is frequently seen in TNBC which has been shown to correlate with tumor necrosis [32]. The presumptive precursor lesion, triple-negative ductal carcinoma in situ (DCIS) also shows distinct imaging features [33]. When compared to other types of DCIS, triple-negative DCIS is infrequently associated with mammographically suspicious calcifications and more often manifests as a mass, architectural distortion, or asymmetric density [33–35]. Additionally, DCIS is less likely to be identified in association with TNBC when compared to other subtypes of breast cancer [34, 36].

Microscopic Features

As mentioned above, TNBCs are histologically diverse, but a large majority of TNBCs are invasive ductal carcinomas that have a solid growth pattern with absent tubule formation, large pleomorphic nuclei, and a very brisk mitotic rate (i.e., a high combined histologic grade). Furthermore, TNBCs are often associated with a limited or absent in situ component, zones of geographic necrosis, prominent lymphocytic infiltrates, central fibrotic foci or "acellular zones," and circumscribed or pushing (non-infiltrative) borders [4, 37–40]. Foci of metaplastic differentiation, such as squamous metaplasia, may also be present [4] (Figs. 11.1, 11.2,

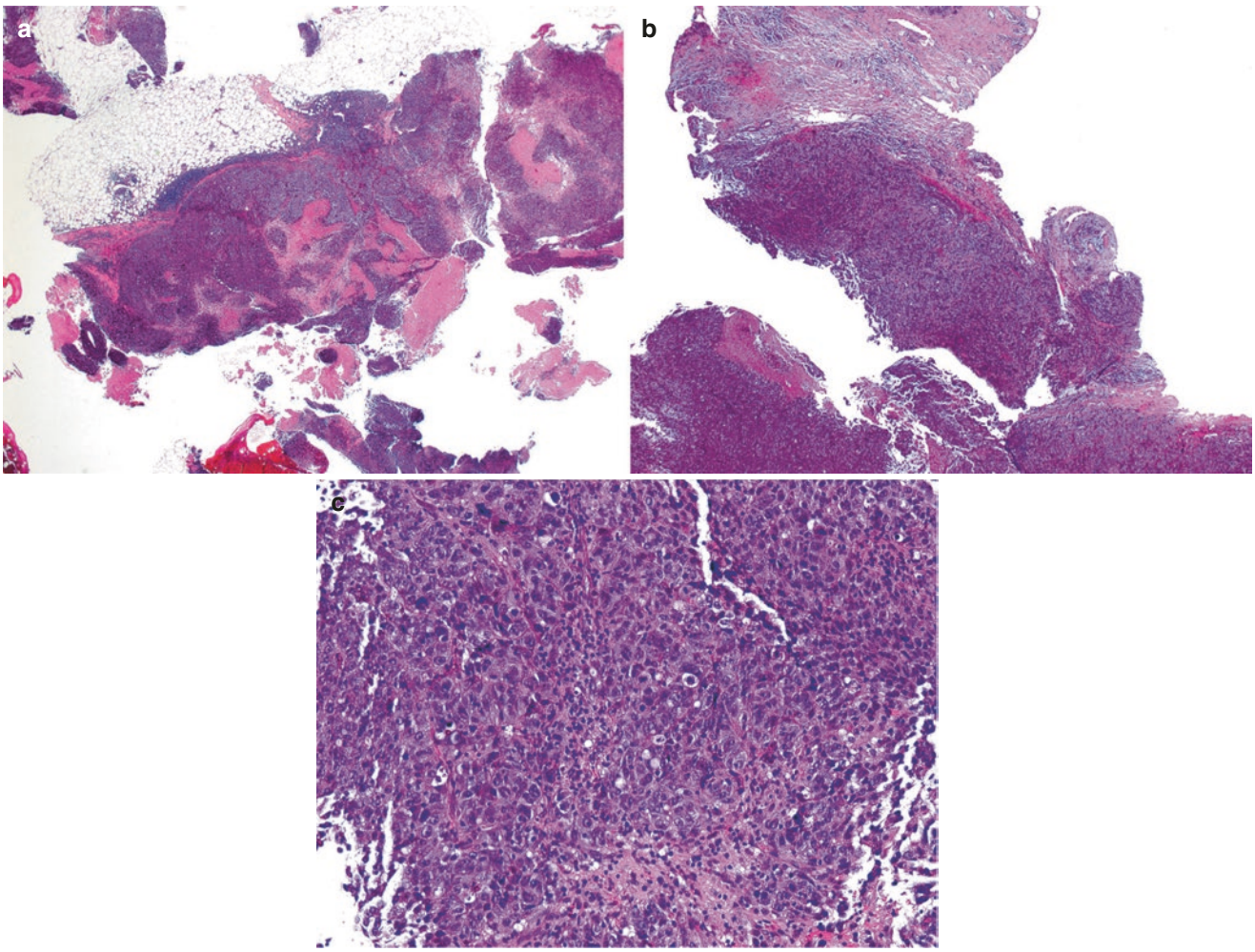

Fig. 11.1 Invasive ductal carcinoma. This low-power image illustrates many of the characteristic features of TNBCs. There is a circumscribed or pushing margin at the tumor-breast parenchyma interface. The tumor cells are arranged in solid sheets, with no tubule formation and little intervening stroma. Large areas of necrosis are present and there is a prominent lymphocytic infiltrate (**a**). On intermediate-power view, the circumscribed margin is better appreciated (**b**). On high-power view, the tumor cells have high-grade nuclei; the mitotic rate is brisk and there are admixed lymphocytes (**c**)

11.3, 11.4, 11.5, 11.6, 11.7, 11.8, 11.9, 11.10, 11.11, 11.12, 11.13, 11.14, 11.15, and 11.16) (Table 11.1). In addition to being negative for ER, PR, and HER2, these tumors fre-

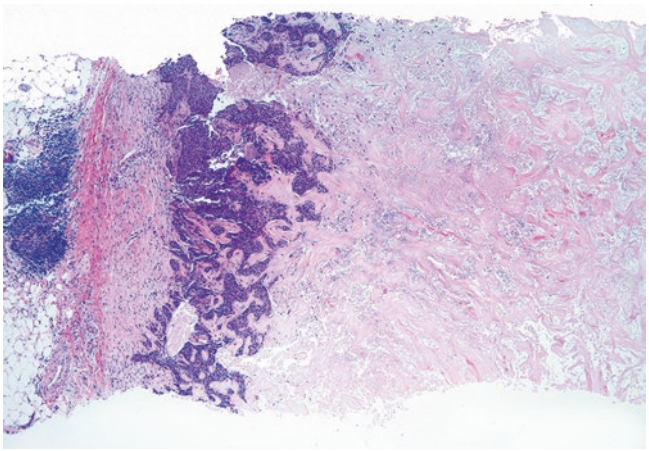

Fig. 11.2 Invasive ductal carcinoma with a circumscribed tumor margin (at *left*), solid tumor growth pattern, and a large zone of fibrosis (at *right*)

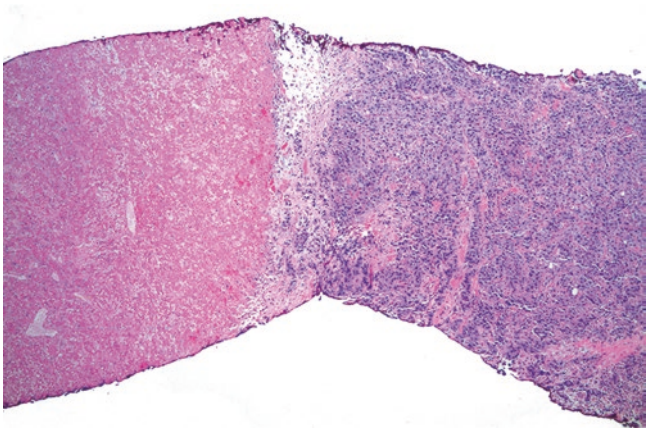

Fig. 11.3 Invasive ductal carcinoma with tumor cells arranged in solid sheets and a large zone of necrosis (at *left*)

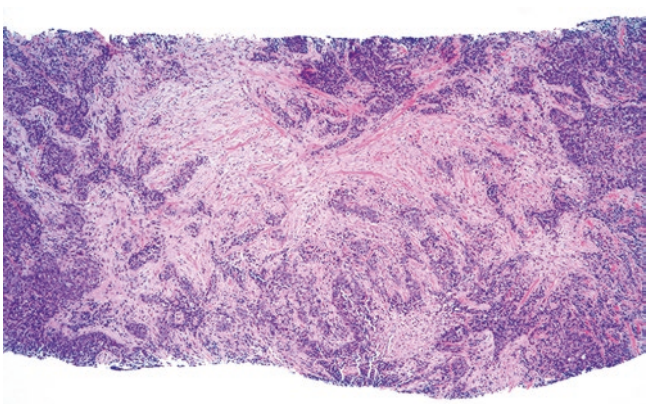

Fig. 11.4 Invasive ductal carcinoma. Note the absence of any tubule formation by the tumor cells

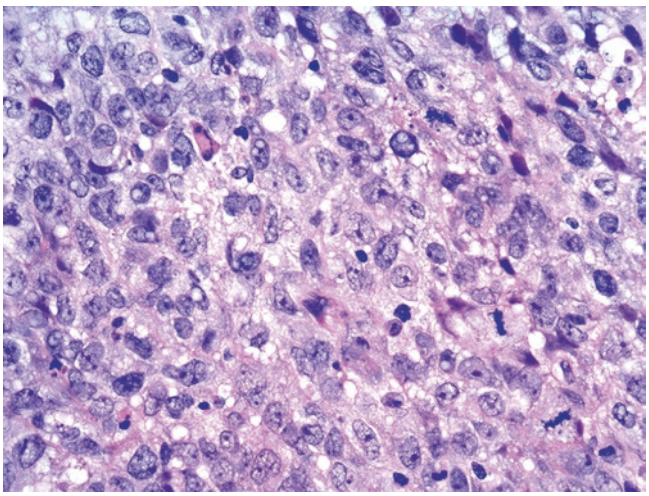

Fig. 11.5 Invasive ductal carcinoma. High-power image demonstrating the nuclear pleomorphism and brisk mitotic rate

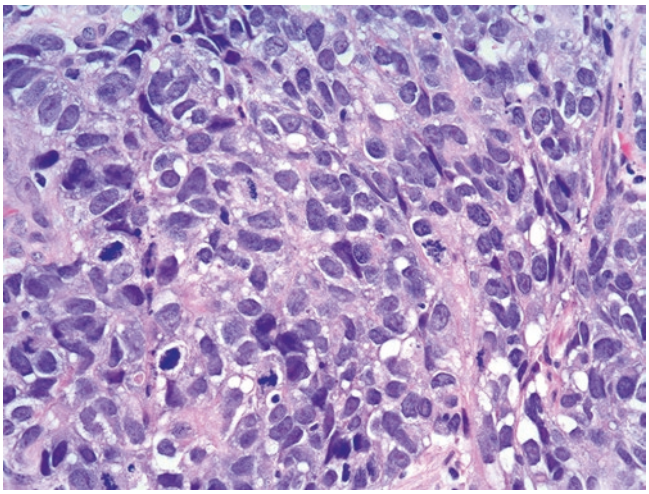

Fig. 11.6 Invasive ductal carcinoma. Another example illustrating the nuclear pleomorphism and brisk mitotic rate so characteristic of these tumors

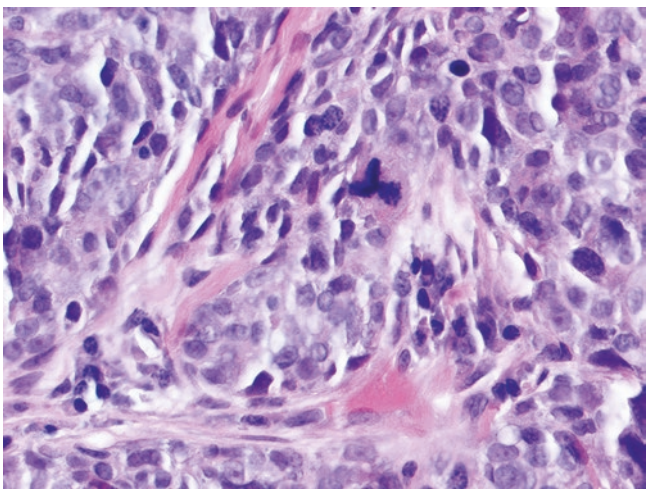

Fig. 11.7 Invasive ductal carcinoma. High-power image depicting an atypical mitotic figure

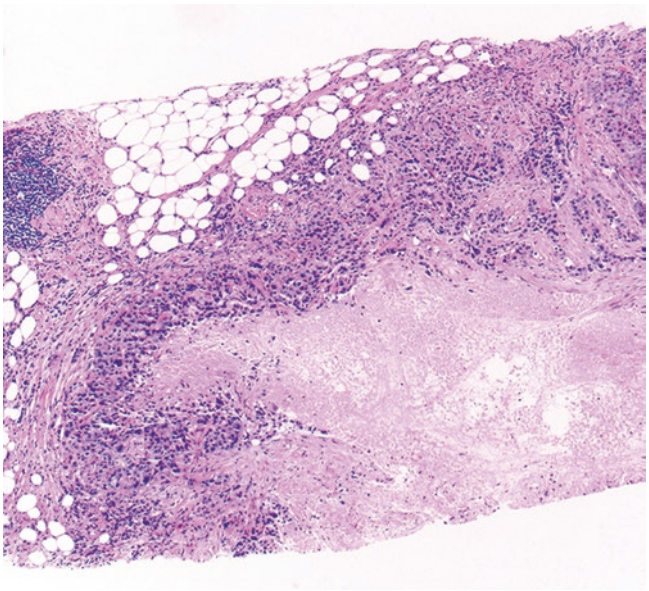

Fig. 11.8 Invasive ductal carcinoma. Intermediate-power image illustrating the circumscribed tumor margin and a large zone of necrosis. Once again note the absence of any tubule formation by the tumor cells

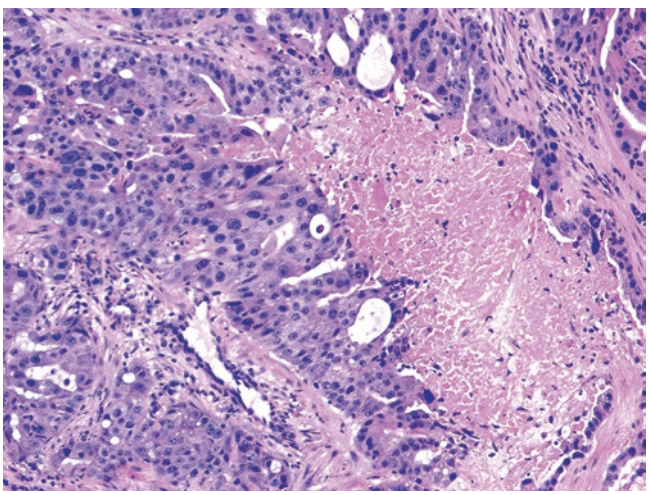

Fig. 11.9 Invasive ductal carcinoma. Higher power image illustrating the high-grade nuclear morphology and an area of necrosis

quently show expression of high-molecular-weight keratins such as cytokeratin 5/6 and 14, epidermal growth factor receptor, and p53 [3, 4, 41] (Fig. 11.17).

While the aforementioned histologic features are strongly suggestive of a TNBC, in most instances, hormone receptor and HER2 studies are performed and reported after the diagnosis is rendered, and the pathologist is not aware of whether a tumor is triple-negative when evaluating the core biopsy specimen. Furthermore, the limited material provided by the core needle biopsy (CNB) procedure may not sample some

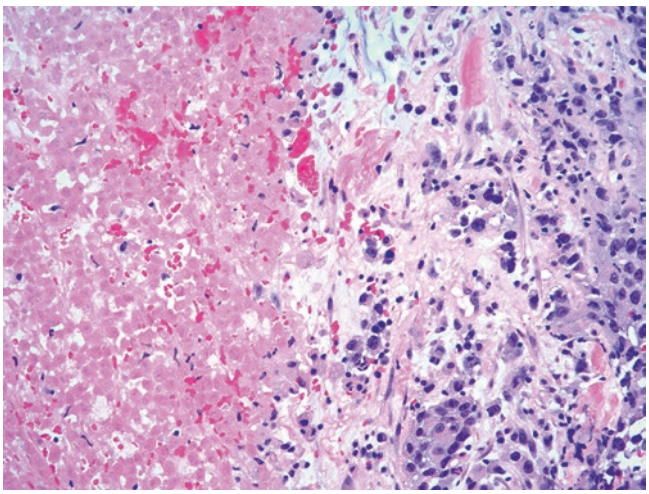

Fig. 11.10 Invasive ductal carcinoma. Another example illustrating the high-grade nuclear morphology and an area of necrosis

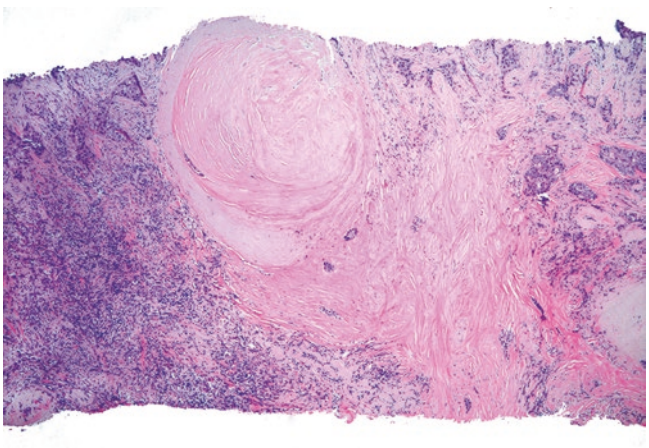

Fig. 11.11 Invasive ductal carcinoma. Low-power image illustrating a central fibrotic area with adjacent tumor cells

of the more characteristic areas of TNBC, such as the central zone of fibrosis or necrosis, or the circumscribed tumor border, particularly if the tumor is large.

Although consensus on a panel of surrogate IHC markers that could be used to define the BLC phenotype has been proposed [42–44], the addition of other markers such as high-molecular-weight keratins, epidermal growth factor receptor, and/or androgen receptor (AR) is not routine practice today [45]. Classifying tumors as TNBC NST, providing the histologic grade, and using the standard prognostic and predictive biomarkers, ER, PR, and HER2, provides the necessary information for appropriate clinical management. As discussed below, it is important to ensure the tumor is of breast origin whenever there are clinical or pathologic features to suggest otherwise.

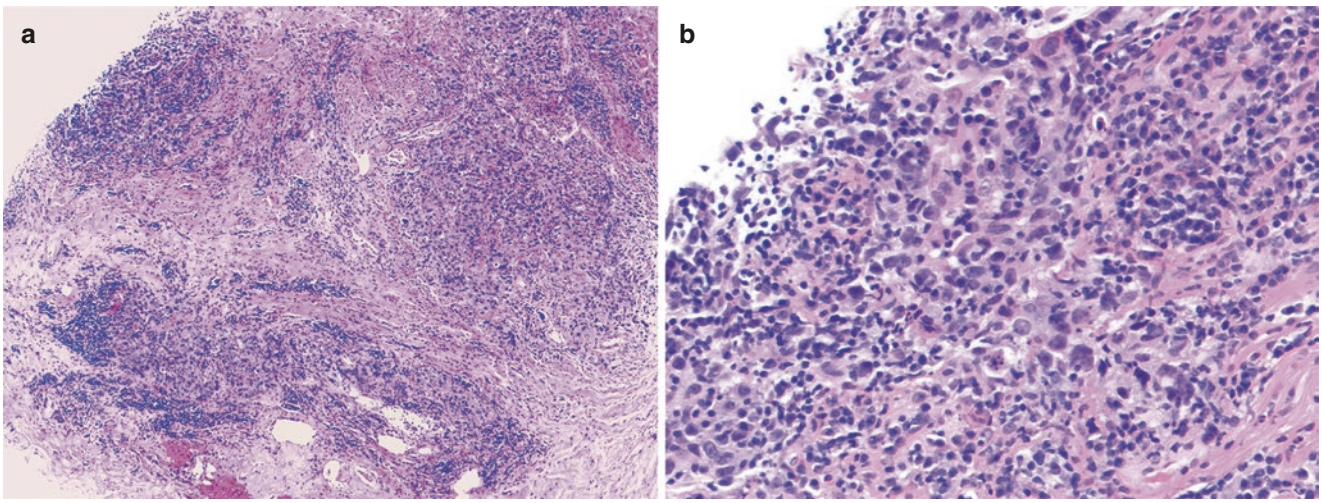

Fig. 11.12 Invasive ductal carcinoma with a prominent lymphoid infiltrate. On low-power magnification, some of the tumor cell nests are obscured by the dense lymphoid infiltrate (**a**). Even on higher power view, malignant epithelial cells can be difficult to appreciate among the lymphoid cells (**b**)

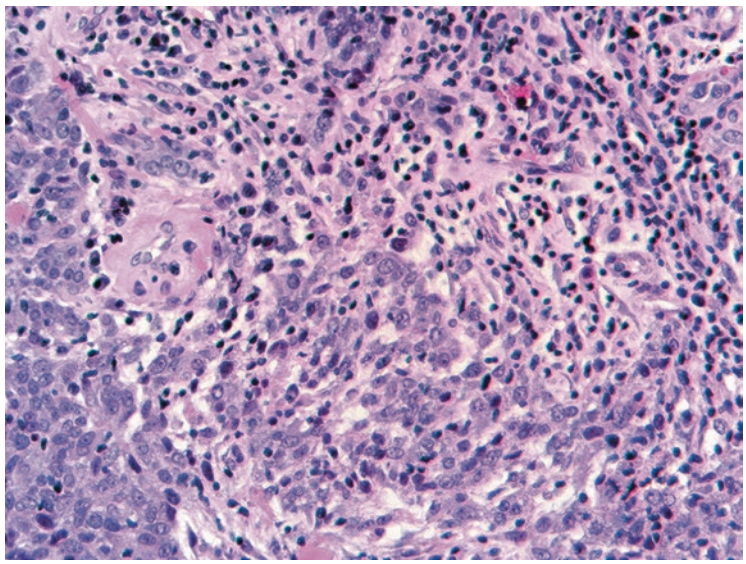

Fig. 11.13 Invasive ductal carcinoma with admixed lymphocytes. A prominent stromal lymphocytic infiltrate is one of the characteristic features of TNBCs

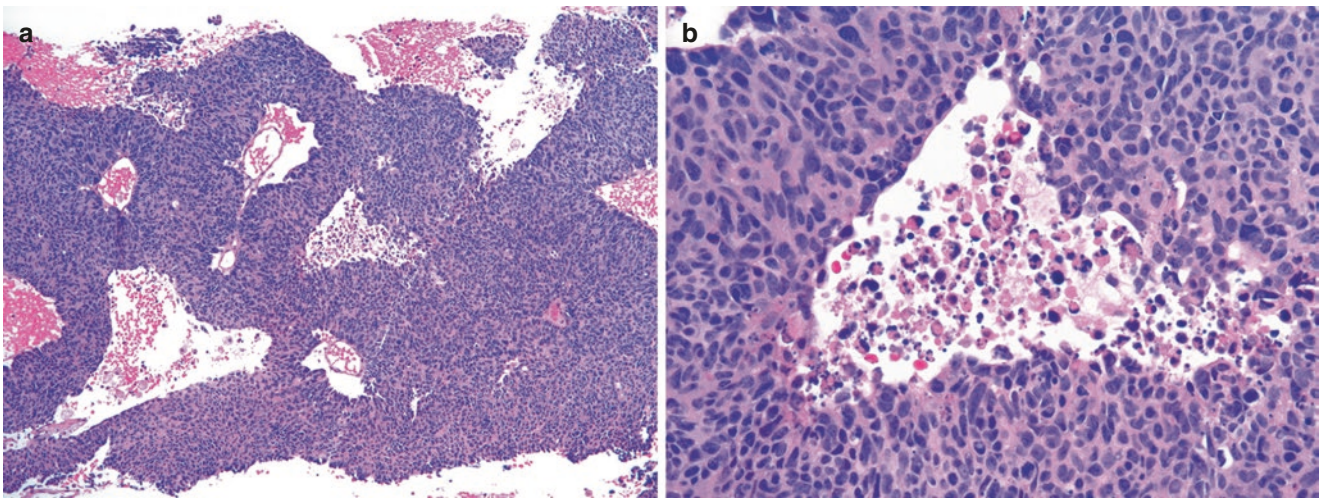

Fig. 11.14 Invasive ductal carcinoma. This lower power image depicts the solid growth pattern characteristic of TNBCs; there is little if any intervening stroma (**a**). On higher power view, the high-grade nuclear morphology can be appreciated as well as an area of necrosis (**b**)

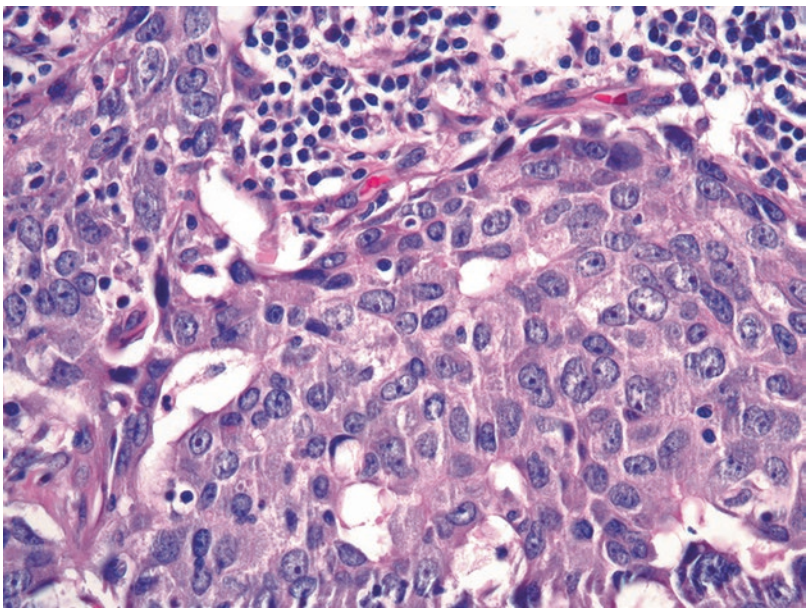

Fig. 11.15 Invasive ductal carcinoma. High-power image depicting solid sheets of tumor cells, with high-grade nuclei, and an associated lymphocytic infiltrate

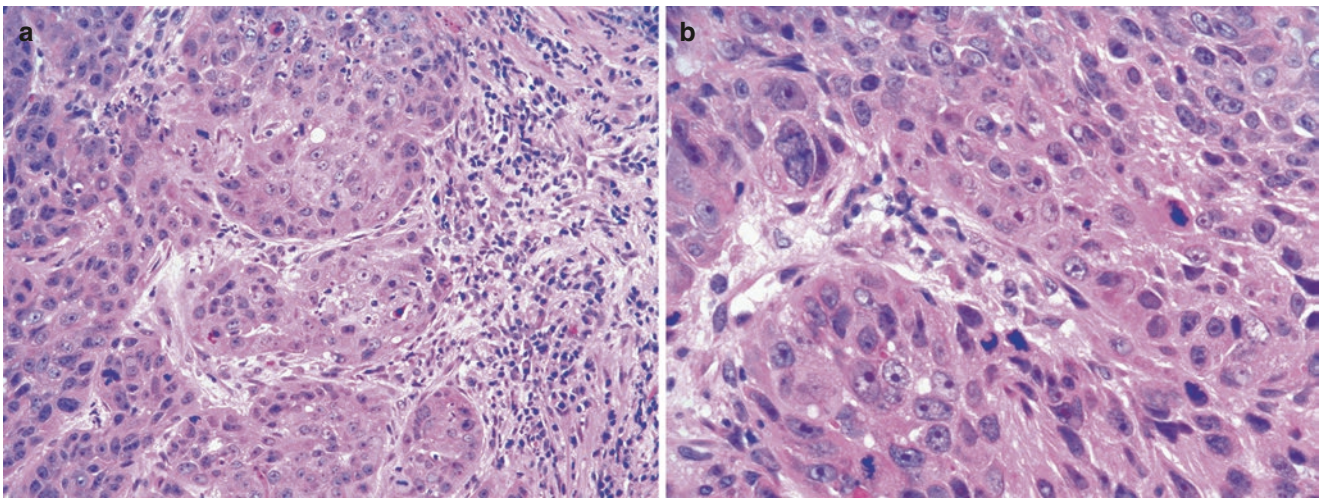

Fig. 11.16 Invasive ductal carcinoma with squamoid features. A characteristic of TNBCs is a propensity for metaplastic differentiation. In this case, the tumor cells have taken on a squamous appearance with relatively abundant, dense eosinophilic cytoplasm. Note also the associated lymphoid infiltrate (**a**). Higher power magnification better illustrates the nuclear pleomorphism and brisk mitotic rate (**b**)

Table 11.1 Key features of triple-negative breast carcinomas, no special type

• Solid growth pattern
• High nuclear grade
• Brisk mitotic rate
• Prominent stromal lymphocytic infiltrate
• Zones of necrosis or fibrosis
• Circumscribed tumor margin
• Metaplastic features
• Minimal/absent ductal carcinoma in situ

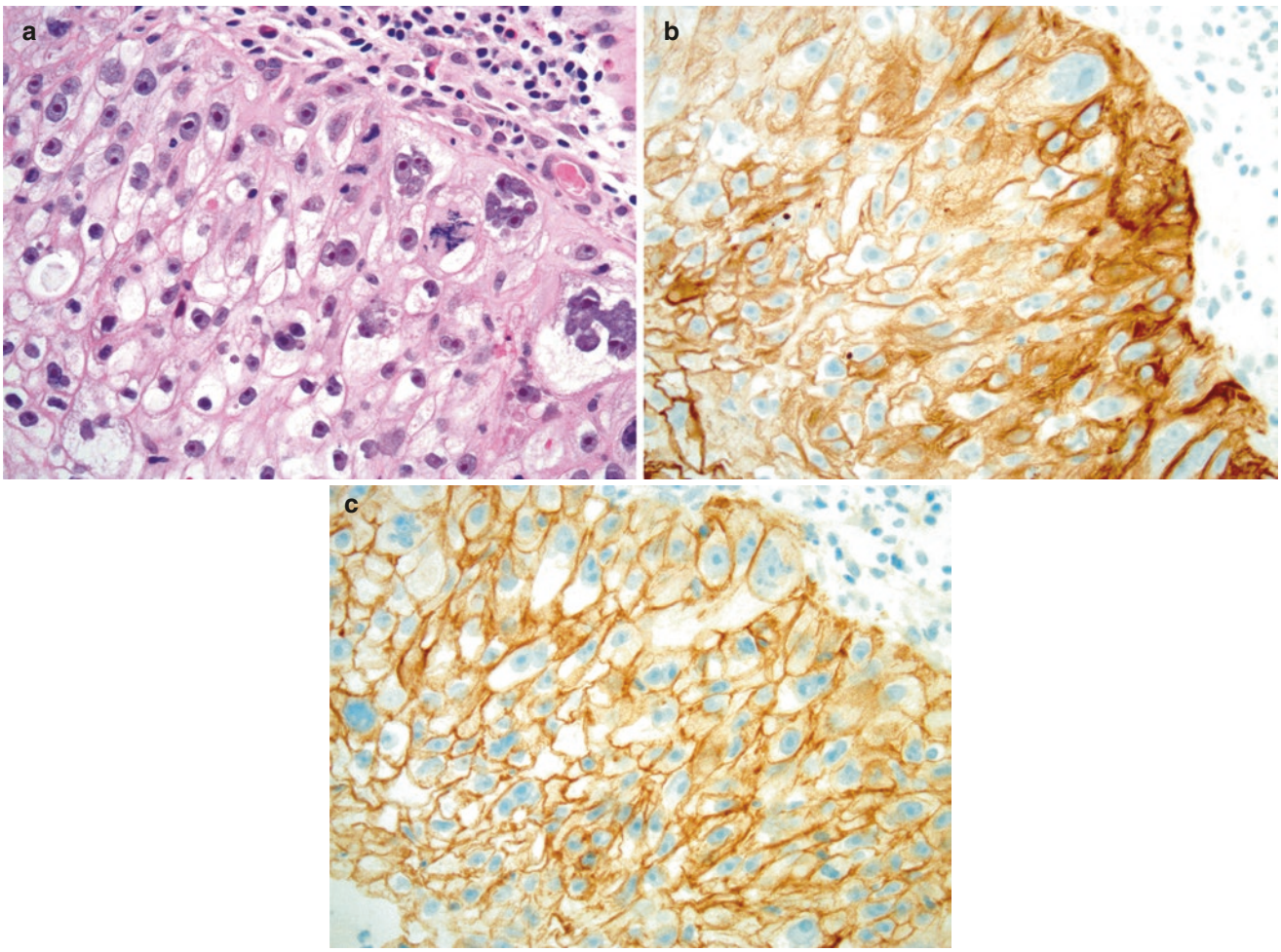

Fig. 11.17 Invasive ductal carcinoma. (**a**) H&E stain; (**b**) cytokeratin 5/6 immunostain; (**c**) epidermal growth factor receptor immunostain. This high-power image illustrates a high-grade TNBC with cytoplasmic clearing, multinucleation, and an atypical mitotic figure (**a**). Expression of high-molecular-weight keratins is a characteristic of triple-negative/basal-like carcinomas. In this image strong, diffuse cytoplasmic and membranous staining is present (**b**). A similar membranous pattern of staining is seen with epidermal growth factor receptor (**c**). In some studies, any staining with these antibodies is considered sufficient to characterize a tumor as "basal-like"

Differential Diagnosis

Given the limited sampling associated with the CNB procedure, the high-grade nature of the tumor, the frequent absence of an in situ component, and the triple-negative immunophenotype, a number of differential diagnoses merit consideration. Furthermore, in an era when neoadjuvant chemotherapy is increasingly the initial treatment option for patients with high-grade, hormone receptor negative cancers, it is critical that a triple-negative tumor diagnosed on CNB is consistent with primary breast carcinoma. Tumors that mimic TNBC include metastatic high-grade malignancies from another primary site, such as malignant melanoma (Fig. 11.18), colorectal carcinoma or renal cell carcinoma, as well as non-epithelial tumors primary to the breast, such as epithelioid angiosarcoma (Fig. 11.19), and high-grade large cell lymphomas (Fig. 11.20), either primary or secondary (Table 11.2). Clinical and radiographic information [e.g., multiple bilateral breast masses, history of another malignancy, violaceous or erythematous skin lesion(s), history of radiation therapy to the breast, serological tumor markers] can be invaluable. It is also important to ascertain whether the biopsy is from the breast itself or the skin or subcutaneous tissue of the breast, as this, too, may influence interpretation. As mentioned above, many TNBCs lack an in situ component, but in a CNB specimen the absence of DCIS in and of itself does not necessarily warrant evaluation for metastatic tumor. For certain special types of TNBCs that harbor specific molecular alterations, IHC can be a helpful surrogate marker for classification; examples include MYB (strong diffuse nuclear labeling) for adenoid cystic carcinoma [46], pan-TRK for secretory carcinoma [47], and IDH2 for tall cell carcinoma with reversed polarity [48] (see Chap. 12).

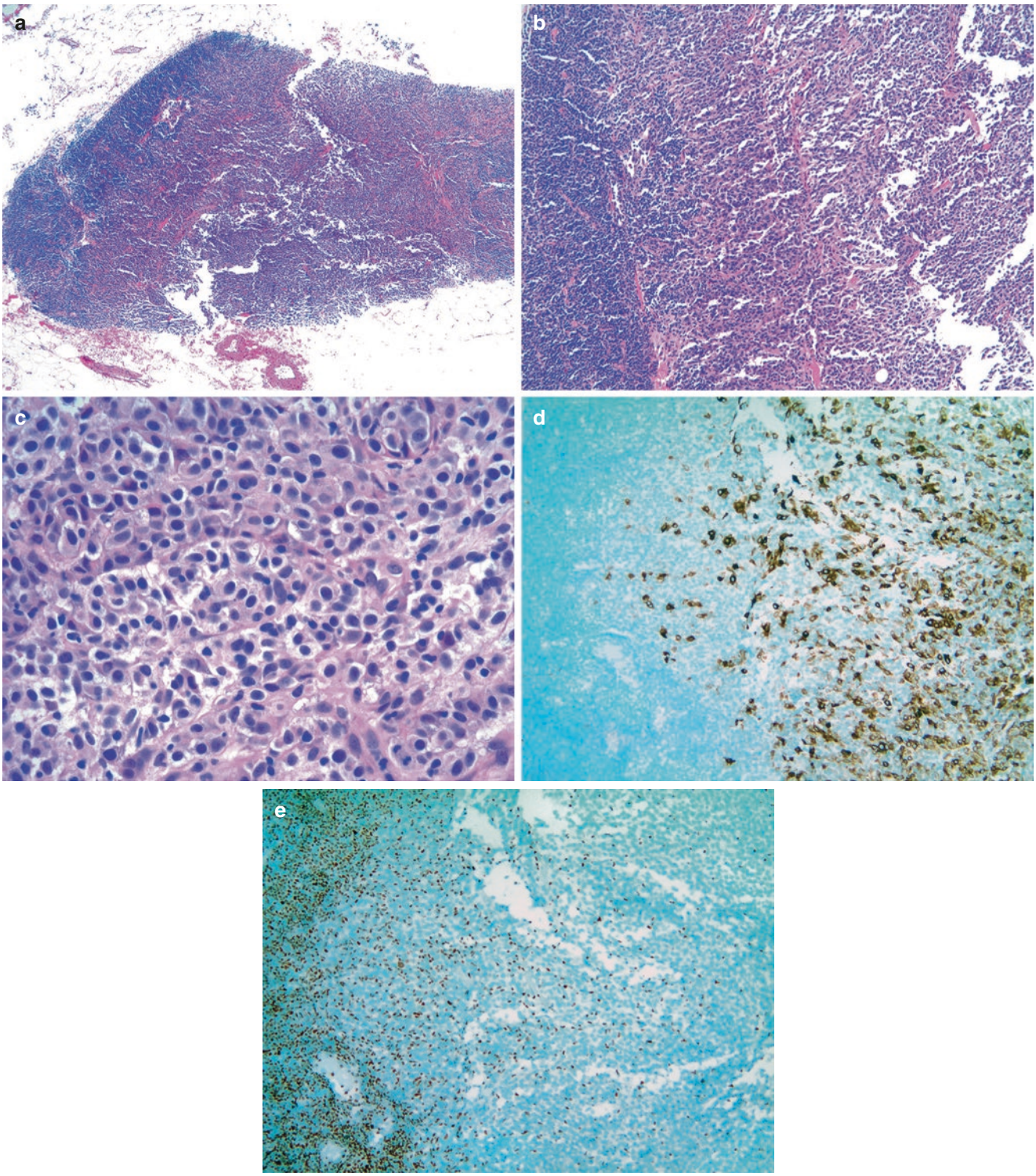

Fig. 11.18 Metastatic malignant melanoma. High-grade malignant tumors in the breast, with a triple-negative immunophenotype, represent a major potential pitfall for misdiagnosis on CNB. In this low-power image, the tumor cells are arranged in solid sheets; the tumor appears to have a circumscribed margin and there is a prominent associated lymphoid infiltrate (**a**). At intermediate-power view, the interface between the tumor cells and lymphocytes is better appreciated. There is little intervening stroma (**b**). At high-power view, the tumor cells have relatively abundant cytoplasm, round to oval nuclei that are slightly eccentrically placed in the cell. Mitotic activity is present (lower right of field) (**c**). Many of the aforementioned features are in keeping with a diagnosis of TNBC. Distinguishing features are subtle, but in this case, may include the relative lack of nuclear pleomorphism. An immunostain for HMB-45 helps confirm the diagnosis of metastatic melanoma. (**d**) Note that an S100 protein immunostain in isolation is not sufficient to confirm or exclude melanoma as a substantial number of breast carcinomas express S100 protein. A GATA3 immunostain is negative; the lymphocytes serve as an internal control (**e**)

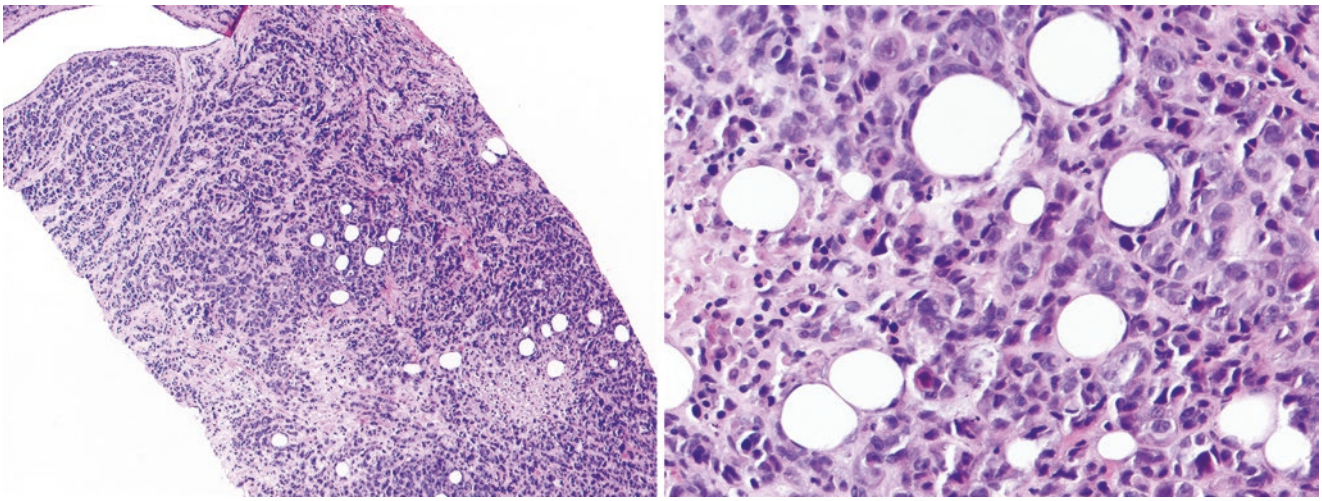

Fig. 11.19 Epithelioid angiosarcoma. This image demonstrates high-grade, malignant epithelioid cells growing in solid sheets with areas of tumor necrosis; the tumor had a triple-negative immunophenotype. This type of tumor is another example of a potential pitfall in the diagnosis of TNBCs. Critical to reaching the correct diagnosis is accurate clinical information (including history of radiation therapy and description of any skin changes) and use of supportive immunostains (see text)

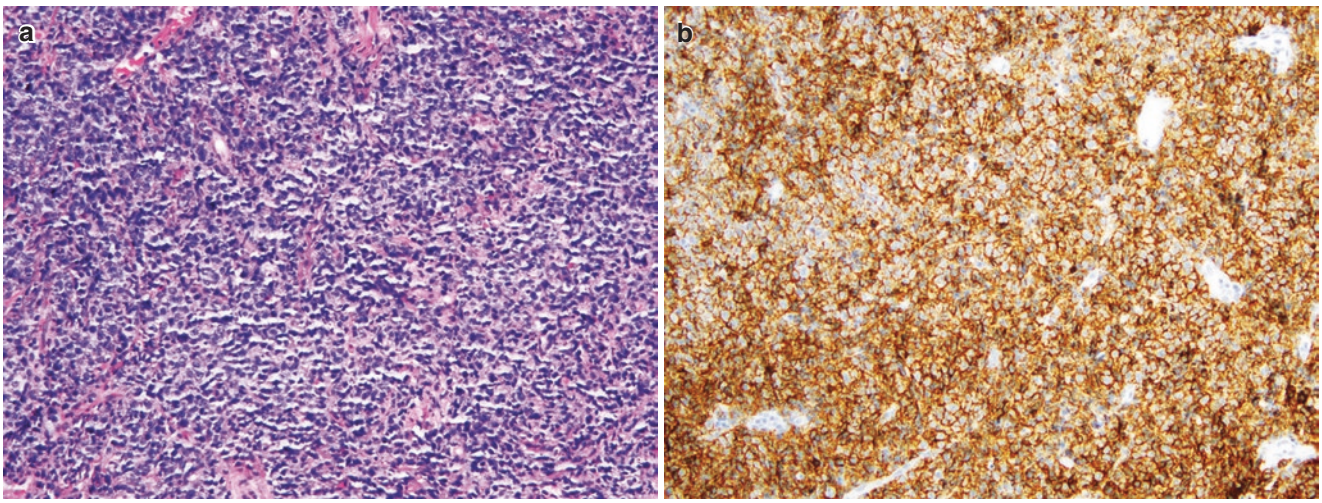

Fig. 11.20 Diffuse large B cell lymphoma. (**a**) H&E stain demonstrating diffuse sheets of large cells with reasonably abundant cytoplasm and an admixed lymphocytic infiltrate. (**b**) CD20 immunostain shows strong reactivity for the tumor cells. Further workup confirmed the tumor to be DLBCL

Table 11.2 Differential diagnostic considerations for triple-negative breast carcinomas

• Metastatic carcinomas (e.g., colon, renal cell)
• Epithelioid angiosarcoma
• Metastatic melanoma
• High-grade lymphoma

In addition to the aforementioned features, whenever the morphology is not typical of that of a breast primary, metastasis should be considered. In this scenario, IHC using a panel of antibodies such as differential cytokeratins (i.e., CK7, CK20) and markers of pulmonary (TTF1, Napsin A), gastrointestinal (CDX2), or Müllerian origin (PAX8, WT-1) may be helpful. Many breast cancers, especially those arising in association with microglandular adenosis (MGA) [49, 50], are positive for S100 protein; therefore, evaluation for metastatic melanoma should include additional markers such as HMB45, MART-1 (Melan A), or microphthalmia transcription factor (Fig. 11.18). In this setting of a high-grade tumor with a differential diagnosis of TNBC versus other, markers of mammary origin such as gross cystic disease fluid protein-15 (aka BRST-2) and mammaglobin are helpful when positive, but many high-grade breast carcinomas may not be immunoreactive for either antigen or may be only focally positive which can be a problem especially in a CNB specimen. GATA3 is another marker that can be helpful in identification of tumors

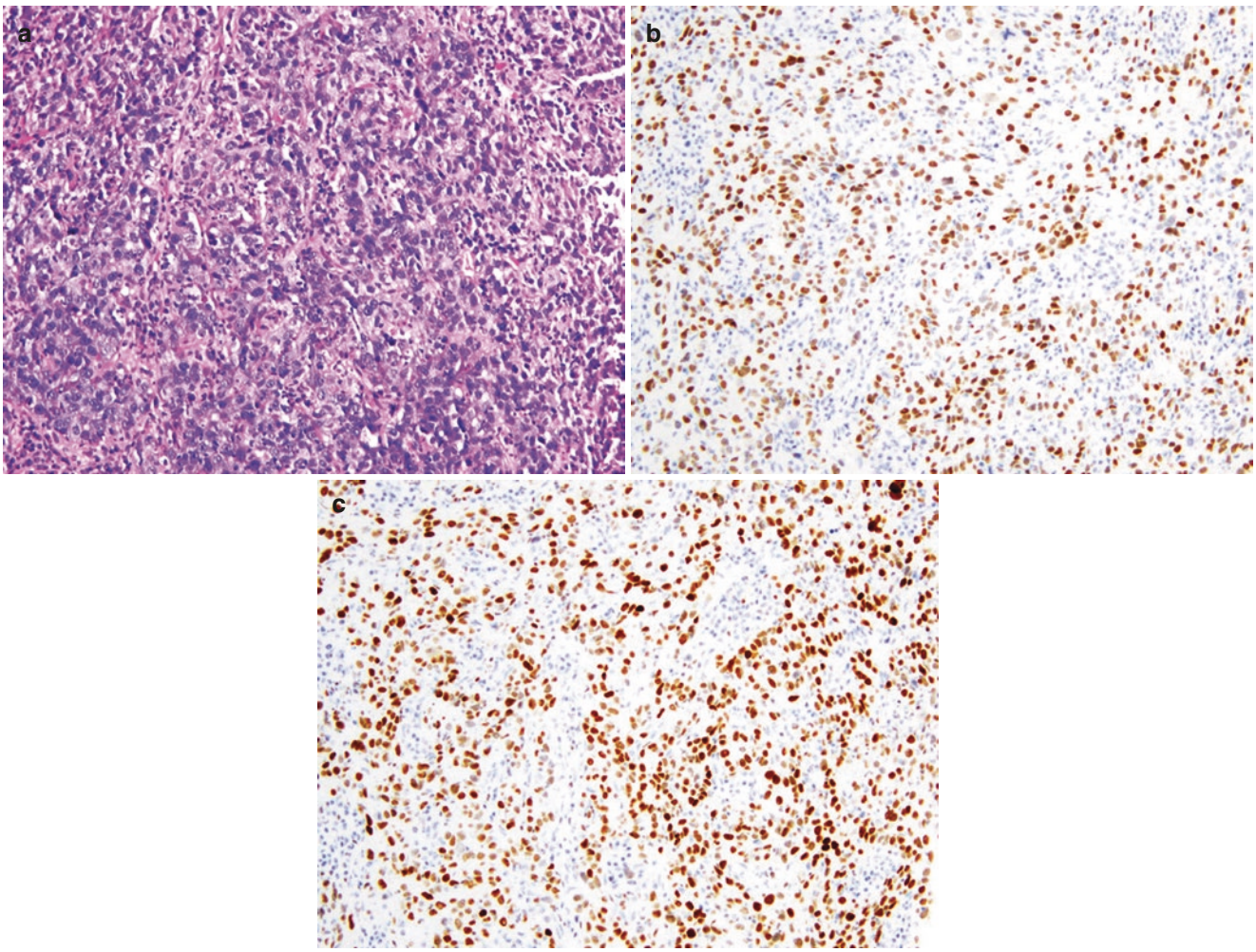

Fig. 11.21 Invasive ductal carcinoma. (**a**) H&E stain shows sheets of large pleomorphic cells. (**b**) GATA3 and (**c**) SOX10 immunostains are strongly positive supporting the diagnosis of breast origin in this triple-negative tumor of the breast

of breast origin (Fig. 11.21); however, while there is a high level of GATA3 expression in ER-positive breast carcinoma, expression in ER-negative tumors is lower, with only 40–60% of TNBC reported to express this marker [51–55]. It is important to note that GATA3 is not specific for tumors of breast origin; it labels urothelial carcinoma, squamous cell carcinoma, pancreatic adenocarcinoma, and malignant mesothelioma, among others [52, 56–58]. SOX10 (Fig. 11.21), a marker of neural crest origin, may also be positive in TNBC and trichorhinophalangeal syndrome type 1 (TRPS1) is a marker recently described to be highly expressed in TNBC. [59–65]. As with S100 protein, a pan-keratin should be evaluated in conjunction with SOX10, as it will label metastatic malignant melanoma, which is often a differential diagnostic consideration in this setting [66, 67].

Markers of vascular differentiation, such as Factor VIII, CD31, and ERG, will be important when epithelioid angiosarcoma is in the differential diagnosis [68, 69]. MYC expression by IHC and/or gene amplification by fluorescence in situ hybridization supports a diagnosis of angiosarcoma, particularly secondary angiosarcoma [70–74]. Some epithelioid angiosarcomas will show aberrant keratin expression, a potential diagnostic pitfall that could be compounded by the limited material available on hematoxylin and eosin (H&E) evaluation of core needle biopsies [75, 76].

Evaluation for involvement by lymphoma or leukemia (discussed in more detail in Chap. 20) should be performed if clinical and pathologic features raise this differential diagnostic consideration. Diffuse large B cell lymphoma (DLBCL) is the most common primary lymphoma of the breast [77, 78] and the histologic appearance of this tumor could be mistaken for a high-grade TNBC (Fig. 11.20). DLBCL is positive for the B cell markers CD20, CD79a, and PAX5 and negative for epithelial keratins [77]. Anaplastic large cell lymphoma is less common than DLBCL but has been reported in association with breast implants [79]. Most cases are positive for CD30 with variable immunoreactivity for T cell markers [80–82].

While not immediately relevant to the differential diagnoses under consideration in this chapter, it should be noted that HER2 overexpression and amplification can occur in non-mammary tumors [83]. Furthermore, the combination of ER positivity, particularly if the SP1 antibody clone is used, and TTF1 positivity may be seen in both lung and breast carcinomas [84–86]. All of this serves to emphasize the importance of a complete clinical history in the accurate interpretation of high-grade tumors on CNB specimens of the breast.

Pathogenesis: Histopathology and Biology

DCIS with triple-negative and basal-like phenotypes, the presumptive precursor for TNBC, occurs at a frequency of between 5% and 8% [87–96]. Patients with triple-negative and basal-like DCIS may be at increased risk of recurrence and have a worse prognosis compared with other subtypes of DCIS [95–97].

Although rare, invasive carcinomas may arise in association with MGA, which is another lesion with a triple-negative phenotype. The co-localization of MGA with some TNBCs, and the demonstration of shared genetic alterations, such as *TP53* mutations, in paired tumors suggests that MGA and/or atypical MGA may be a non-obligate precursor for the development of special types of TNBC [98–102]. Invasive tumors arising in the setting of MGA may be invasive ductal carcinoma NST with clear cell (Fig. 11.22) or basaloid morphology, metaplastic and matrix-producing carcinomas, adenoid cystic carcinoma, or acinic cell carcinoma [99] (see Chaps. 5 and 12).

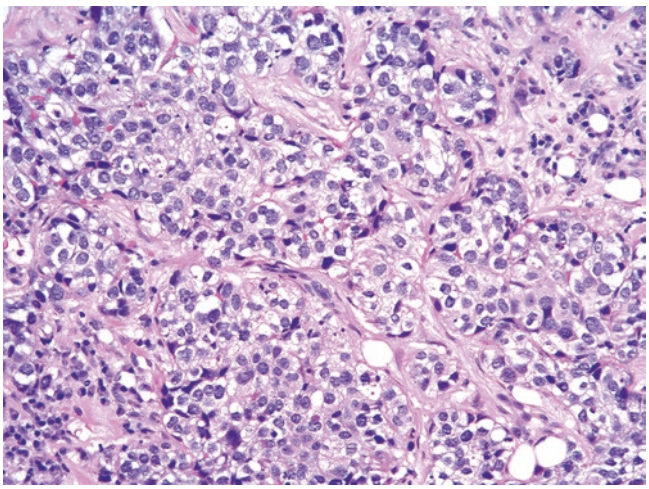

Fig. 11.22 Invasive ductal carcinoma with clear cell features. This high-grade, TNBC has clear cytoplasm. Carcinomas arising in association with microglandular adenosis (MGA) have a triple-negative immunophenotype and may have clear cell change. Evaluation for foci of MGA or atypical MGA is indicated, as this may represent the precursor lesion for these tumors (see text)

Mutations in genes involved in DNA repair such as *BRCA1* and *BRCA2* are known to play a role in the development of hereditary breast cancer [103–106]. DNA repair gene expression patterns have also been correlated with molecular subtypes of breast cancer and clinical outcomes [107]. Patients with mutations in *BRCA1* are predisposed to develop BLC/TNBCs with many of the gross and microscopic features described above [108–111]. Approximately 20% of BLC/TNBCs harbor mutations in *BRCA1* or *BRCA2* [112, 113]. Sporadic TNBCs also show related genetic and phenotypic features that have been referred to as "BRCAness" [114]. The inherited or sporadic alterations in DNA repair genes may make some types of TNBCs more sensitive to poly(ADP-ribose) polymerase (PARP) inhibitors and platinum-based chemotherapy in the adjuvant or neoadjuvant settings, as discussed in more detail below [115].

Prognosis and Review of the Core Needle Biopsy Literature and Its Significance to Clinical Management

The overall approach to the multidisciplinary treatment of TNBC is similar to other types of breast cancer with the notable exception that patients with TNBC will not benefit from endocrine therapy or HER2-targeted therapy [116]. It remains critical for pathologists to adhere to the current American Society of Clinical Oncology (ASCO)/College of American Pathologists (CAP) criteria for the interpretation of HER2 and hormone receptor testing so that TNBC is identified in a consistent and reproducible manner [116–120]. One issue with regard to ER reporting in TNBC is the demonstration that some tumors with low ER positivity are more similar morphologically and molecularly in gene expression profiling studies to BLC than to luminal (ER-positive) cancers [121–123]. The current recommendation by ASCO/CAP is to score tumor cell nuclear staining of ≥1% as positive, with the additional requirement that when only 1–10% of the tumor cell nuclei stain with ER, the result should be reported as low positive [122, 124–126]. Limited data suggest that low positive ER, HER2-negative tumors have higher pathological complete response (pCR) rates and show survival outcomes more similar to TNBCs than ER-positive carcinomas [127]. Whether these tumors truly behave and respond as ER-positive carcinomas or TNBCs remains to be determined, and whether these tumors should be considered for treatment and clinical trials for patients with TNBC is debatable; though it is noteworthy that several trials have relaxed eligibility requirements to include patients with low ER-positive, HER2-negative carcinomas. Given the lack of

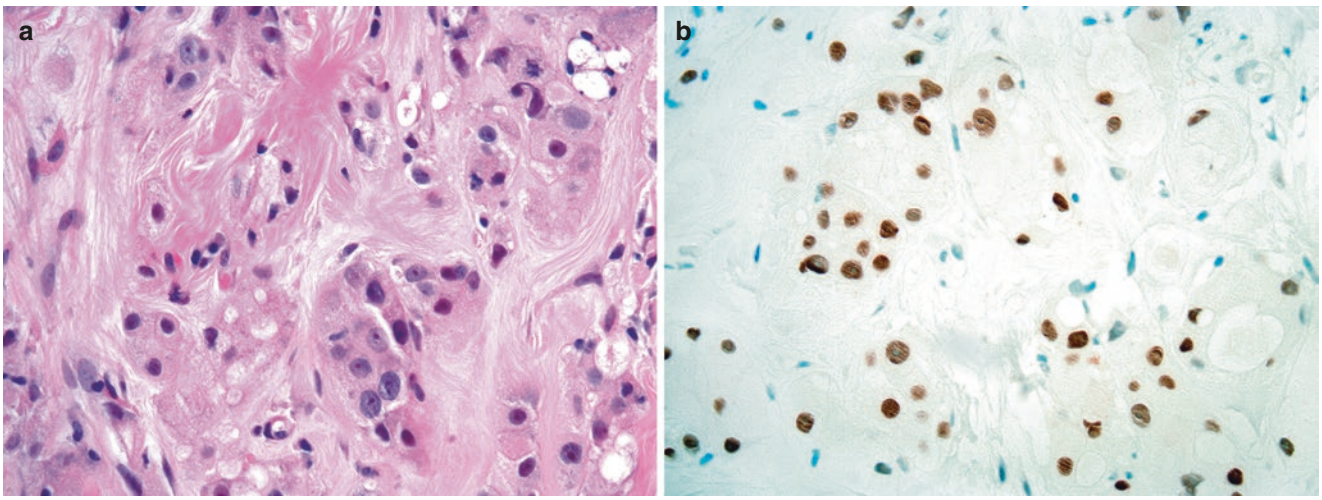

Fig. 11.23 Invasive ductal carcinoma, (**a**) H&E stain and (**b**) AR immunostain. In this TNBC the tumor cells show the characteristic high nuclear grade; some features suggestive of apocrine differentiation may be appreciated (**a**). An immunostain for AR was strongly positive (**b**). While the majority of AR-positive breast carcinomas are also ER positive, a substantial minority of TNBCs have been shown to express AR representing a possible therapeutic target

targetable therapies in TNBC, regimens of cytotoxic chemotherapy (i.e., doxorubicin, cyclophosphamide, paclitaxel, docetaxel, methotrexate, fluorouracil, and epirubicin) remain the current preoperative and/or adjuvant systemic therapy in patients with TNBC [128].

Insights from molecular profiling of TNBC and the treatment of *BRCA* mutation carriers show the potential for more tailored therapy in the future. After a core biopsy diagnosis of TNBC is rendered, pathologists may be called upon to perform and interpret additional IHC or molecular studies to identify TNBC that will be most likely to respond to a particular type of therapy. For example, the expression of AR in a subset of TNBC (Fig. 11.23), presumably corresponding to the described luminal AR molecular subtype [21], provides a potential target for directed therapy [129]. Expression of AR has been described in 10–50% of TNBC [130–137]. The prognosis is controversial among this group of tumors, with studies showing a lower rate of pCR after neoadjuvant chemotherapy [138, 139]. Three phase II clinical trials investigating the use of the AR-targeted therapies, bicalutamide, abiraterone acetate, and enzalutamide, have shown clinical benefit for some patients with AR-positive TNBC [140–142]. The immunohistochemical analysis of AR expression in studies of TNBC has been evaluated using different clones and thresholds for positive staining, which is problematic for clinical application. Recent studies have used a cutoff of >0% (any staining in tumor cells) [26], ≥1% (essentially applying the ASCO/CAP criteria developed for ER and PR) [143–146], >10% [140, 147], or a composite of the staining intensity and percentage of positive tumor cells [148].

Tumor-infiltrating lymphocytes (TILs) have been shown to be a positive prognostic factor in TNBC, with increased TILs linked to increased pCR rates [149, 150]. Despite the poor prognosis associated with TNBC, pCR is associated with improved outcomes [151, 152]. A standardized methodology has been proposed by the International TILs Working Group 2014 [153] and the International Immuno-Oncology Biomarker Working Group on Breast Cancer [154], with proven acceptable reproducibility [155–157], although reporting of TILs in breast cancer has not yet been routinely implemented in clinical settings [158]. A newer predictive maker in TNBC is programmed death-ligand 1 (PD-L1); two PD-L1 inhibitors, atezolizumab (in combination with paclitaxel protein-bound chemotherapy) [159] and pembrolizumab [160, 161], are approved by the United States Food and Drug Administration (FDA) for use in the setting of advanced or metastatic TNBC with PD-L1 positive immune cells demonstrated by IHC. At the time writing, Ventana PD-L1 (SP142) for atezolizumab and pharmDx PD-L1 (22C3) for pembrolizumab are the only PD-L1 companion diagnostic IHC tests with FDA approval for breast cancer [161]. New data, however, have prompted withdrawal of atezolizumab for this indication [162].

The potential sensitivity of TNBC to DNA-damaging agents suggests that platinum-based chemotherapy may be more effective in this rather than other subtypes of breast cancer. Studies of cisplatin in germline *BRCA* mutation carriers have shown a high rate of response and pCR [163, 164] but the response rate in sporadic TNBC may not be as high [165, 166]. Reports from two randomized phase II neoadjuvant trials in TNBC, Gepar Sixto and CALBG 4063, indicated that the addition of carboplatin increased pCR rates and overall survival; however, the rate of breast conservation was not improved [167–169]. Phase III clinical trials among

BRCA mutation carriers have shown clinical benefit from PARP inhibitors. Currently, two PARP inhibitors, Talazoparib [161, 170] and Olaparib [161, 171], have FDA approval for treatment of advanced breast cancer in this population. The mature survival data and correlative marker studies from these and other trials should provide more insight into the benefit of platinum-based therapy, PARP inhibitors, and anti-angiogenic therapy in TNBC [172, 173].

Conclusions

TNBC represents approximately 15–20% of all breast cancers. The correct identification and classification of these high-grade carcinomas on CNB is critical to patient management. With the increasing utilization of neoadjuvant chemotherapy as a treatment option, performance of biomarker studies for ER, PR, and HER2 on the CNB specimen has become routine. When there is only limited sampling of a high-grade, triple-negative malignancy located in the breast, careful consideration of whether the tumor is a primary carcinoma is warranted in every case.

References

1. Boyle P. Triple-negative breast cancer: epidemiological considerations and recommendations. Ann Oncol. 2012;23(Suppl 6):vi7–12.
2. Foulkes WD, Smith IE, Reis-Filho JS. Triple-negative breast cancer. N Engl J Med. 2010;363(20):1938–48.
3. Nielsen TO, Hsu FD, Jensen K, Cheang M, Karaca G, Hu Z, et al. Immunohistochemical and clinical characterization of the basal-like subtype of invasive breast carcinoma. Clin Cancer Res. 2004;10(16):5367–74.
4. Livasy CA, Karaca G, Nanda R, Tretiakova MS, Olopade OI, Moore DT, et al. Phenotypic evaluation of the basal-like subtype of invasive breast carcinoma. Mod Pathol. 2006;19(2):264–71.
5. Carey LA, Perou CM, Livasy CA, Dressler LG, Cowan D, Conway K, et al. Race, breast cancer subtypes, and survival in the Carolina Breast Cancer Study. JAMA. 2006;295(21):2492–502.
6. Collins LC, Martyniak A, Kandel MJ, Stadler ZK, Masciari S, Miron A, et al. Basal cytokeratin and epidermal growth factor receptor expression are not predictive of BRCA1 mutation status in women with triple-negative breast cancers. Am J Surg Pathol. 2009;33(7):1093–7.
7. Greenup R, Buchanan A, Lorizio W, Rhoads K, Chan S, Leedom T, et al. Prevalence of BRCA mutations among women with triple-negative breast cancer (TNBC) in a genetic counseling cohort. Ann Surg Oncol. 2013;20(10):3254–8.
8. Daly M, Pal T, Berry M, Buys S, Dickson P, Domcheck S, et al. Genetic/familial high-risk assessment: breast, ovarian, and pancreatic. National Comprehensive Cancer Network. 2022. https://www.nccn.org/.
9. Dent R, Trudeau M, Pritchard KI, Hanna WM, Kahn HK, Sawka CA, et al. Triple-negative breast cancer: clinical features and patterns of recurrence. Clin Cancer Res. 2007;13(15 Pt 1):4429–34.
10. Dent R, Hanna WM, Trudeau M, Rawlinson E, Sun P, Narod SA. Pattern of metastatic spread in triple-negative breast cancer. Breast Cancer Res Treat. 2009;115(2):423–8.
11. Lin NU, Claus E, Sohl J, Razzak AR, Arnaout A, Winer EP. Sites of distant recurrence and clinical outcomes in patients with metastatic triple-negative breast cancer: high incidence of central nervous system metastases. Cancer. 2008;113(10):2638–45.
12. Lin NU, Vanderplas A, Hughes ME, Theriault RL, Edge SB, Wong YN, et al. Clinicopathologic features, patterns of recurrence, and survival among women with triple-negative breast cancer in the National Comprehensive Cancer Network. Cancer. 2012;118(22):5463–72.
13. Carey LA, Dees EC, Sawyer L, Gatti L, Moore DT, Collichio F, et al. The triple negative paradox: primary tumor chemosensitivity of breast cancer subtypes. Clin Cancer Res. 2007;13(8):2329–34.
14. von Minckwitz G, Untch M, Blohmer JU, Costa SD, Eidtmann H, Fasching PA, et al. Definition and impact of pathologic complete response on prognosis after neoadjuvant chemotherapy in various intrinsic breast cancer subtypes. J Clin Oncol. 2012;30(15):1796–804.
15. Cortazar P, Zhang L, Untch M, Mehta K, Costantino JP, Wolmark N, et al. Pathological complete response and long-term clinical benefit in breast cancer: the CTNeoBC pooled analysis. Lancet. 2014;384(9938):164–72.
16. Bhargava R, Beriwal S, Dabbs DJ, Ozbek U, Soran A, Johnson RR, et al. Immunohistochemical surrogate markers of breast cancer molecular classes predicts response to neoadjuvant chemotherapy: a single institutional experience with 359 cases. Cancer. 2010;116(6):1431–9.
17. Weigelt B, Horlings HM, Kreike B, Hayes MM, Hauptmann M, Wessels LF, et al. Refinement of breast cancer classification by molecular characterization of histological special types. J Pathol. 2008;216(2):141–50.
18. Yin L, Duan JJ, Bian XW, Yu SC. Triple-negative breast cancer molecular subtyping and treatment progress. Breast Cancer Res. 2020;22(1):61.
19. Garrido-Castro AC, Lin NU, Polyak K. Insights into molecular classifications of triple-negative breast cancer: improving patient selection for treatment. Cancer Discov. 2019;9(2):176–98.
20. Prat A, Adamo B, Cheang MC, Anders CK, Carey LA, Perou CM. Molecular characterization of basal-like and non-basal-like triple-negative breast cancer. Oncologist. 2013;18(2):123–33.
21. Lehmann BD, Bauer JA, Chen X, Sanders ME, Chakravarthy AB, Shyr Y, et al. Identification of human triple-negative breast cancer subtypes and preclinical models for selection of targeted therapies. J Clin Invest. 2011;121(7):2750–67.
22. Dogan BE, Turnbull LW. Imaging of triple-negative breast cancer. Ann Oncol. 2012;23(Suppl 6):vi23–9.
23. Kim MY, Choi N. Mammographic and ultrasonographic features of triple-negative breast cancer: a comparison with other breast cancer subtypes. Acta Radiol. 2013;54(8):889–94.
24. Wang Y, Ikeda DM, Narasimhan B, Longacre TA, Bleicher RJ, Pal S, et al. Estrogen receptor-negative invasive breast cancer: imaging features of tumors with and without human epidermal growth factor receptor type 2 overexpression. Radiology. 2008;246(2):367–75.
25. Dogan BE, Gonzalez-Angulo AM, Gilcrease M, Dryden MJ, Yang WT. Multimodality imaging of triple receptor-negative tumors with mammography, ultrasound, and MRI. AJR Am J Roentgenol. 2010;194(4):1160–6.
26. Rakha EA, El-Sayed ME, Green AR, Lee AH, Robertson JF, Ellis IO. Prognostic markers in triple-negative breast cancer. Cancer. 2007;109(1):25–32.

27. Kojima Y, Tsunoda H. Mammography and ultrasound features of triple-negative breast cancer. Breast Cancer. 2011;18(3):146–51.
28. Lehman CD, Smith RA. The role of MRI in breast cancer screening. J Natl Compr Cancer Netw. 2009;7(10):1109–15.
29. Costantini M, Belli P, Distefano D, Bufi E, Matteo MD, Rinaldi P, et al. Magnetic resonance imaging features in triple-negative breast cancer: comparison with luminal and HER2-overexpressing tumors. Clin Breast Cancer. 2012;12(5):331–9.
30. Navarro Vilar L, Alandete Germán SP, Medina García R, Blanc García E, Camarasa Lillo N, Vilar SJ. MR imaging findings in molecular subtypes of breast cancer according to BIRADS system. Breast J. 2017;23(4):421–8.
31. Sung JS, Jochelson MS, Brennan S, Joo S, Wen YH, Moskowitz C, et al. MR imaging features of triple-negative breast cancers. Breast J. 2013;19(6):643–9.
32. Uematsu T, Kasami M, Yuen S. Triple-negative breast cancer: correlation between MR imaging and pathologic findings. Radiology. 2009;250(3):638–47.
33. Kojima Y, Tsunoda H, Honda S, Kikuchi M, Kawauchi N, Yoshida A, et al. Radiographic features for triple negative ductal carcinoma in situ of the breast. Breast Cancer. 2011;18(3):213–20.
34. Bae MS, Moon WK, Chang JM, Cho N, Park SY, Won JK, et al. Mammographic features of calcifications in DCIS: correlation with oestrogen receptor and human epidermal growth factor receptor 2 status. Eur Radiol. 2013;23(8):2072–8.
35. Kim MY, Kim HS, Choi N, Yang JH, Yoo YB, Park KS. Screening mammography-detected ductal carcinoma in situ: mammographic features based on breast cancer subtypes. Clin Imaging. 2015;39(6):983–6.
36. Yang WT, Dryden M, Broglio K, Gilcrease M, Dawood S, Dempsey PJ, et al. Mammographic features of triple receptor-negative primary breast cancers in young premenopausal women. Breast Cancer Res Treat. 2008;111(3):405–10.
37. Fulford LG, Easton DF, Reis-Filho JS, Sofronis A, Gillett CE, Lakhani SR, et al. Specific morphological features predictive for the basal phenotype in grade 3 invasive ductal carcinoma of breast. Histopathology. 2006;49(1):22–34.
38. Putti TC, El-Rehim DM, Rakha EA, Paish CE, Lee AH, Pinder SE, et al. Estrogen receptor-negative breast carcinomas: a review of morphology and immunophenotypical analysis. Mod Pathol. 2005;18(1):26–35.
39. Tsuda H, Takarabe T, Hasegawa F, Fukutomi T, Hirohashi S. Large, central acellular zones indicating myoepithelial tumor differentiation in high-grade invasive ductal carcinomas as markers of predisposition to lung and brain metastases. Am J Surg Pathol. 2000;24(2):197–202.
40. Tsuda H, Takarabe T, Hasegawa T, Murata T, Hirohashi S. Myoepithelial differentiation in high-grade invasive ductal carcinomas with large central acellular zones. Hum Pathol. 1999;30(10):1134–9.
41. Tan DS, Marchió C, Jones RL, Savage K, Smith IE, Dowsett M, et al. Triple negative breast cancer: molecular profiling and prognostic impact in adjuvant anthracycline-treated patients. Breast Cancer Res Treat. 2008;111(1):27–44.
42. Cheang MC, Voduc D, Bajdik C, Leung S, McKinney S, Chia SK, et al. Basal-like breast cancer defined by five biomarkers has superior prognostic value than triple-negative phenotype. Clin Cancer Res. 2008;14(5):1368–76.
43. Blows FM, Driver KE, Schmidt MK, Broeks A, van Leeuwen FE, Wesseling J, et al. Subtyping of breast cancer by immunohistochemistry to investigate a relationship between subtype and short and long term survival: a collaborative analysis of data for 10,159 cases from 12 studies. PLoS Med. 2010;7(5):e1000279.
44. Gazinska P, Grigoriadis A, Brown JP, Millis RR, Mera A, Gillett CE, et al. Comparison of basal-like triple-negative breast cancer defined by morphology, immunohistochemistry and transcriptional profiles. Mod Pathol. 2013;26(7):955–66.
45. Goldhirsch A, Winer EP, Coates AS, Gelber RD, Piccart-Gebhart M, Thürlimann B, et al. Personalizing the treatment of women with early breast cancer: highlights of the St Gallen International Expert Consensus on the primary therapy of early breast cancer 2013. Ann Oncol. 2013;24(9):2206–23.
46. Poling JS, Yonescu R, Subhawong AP, Sharma R, Argani P, Ning Y, et al. MYB labeling by immunohistochemistry is more sensitive and specific for breast adenoid cystic carcinoma than MYB labeling by FISH. Am J Surg Pathol. 2017;41(7):973–9.
47. Harrison BT, Fowler E, Krings G, Chen YY, Bean GR, Vincent-Salomon A, et al. Pan-TRK immunohistochemistry: a useful diagnostic adjunct for secretory carcinoma of the breast. Am J Surg Pathol. 2019;43(12):1693–700.
48. Pareja F, da Silva EM, Frosina D, Geyer FC, Lozada JR, Basili T, et al. Immunohistochemical analysis of IDH2 R172 hotspot mutations in breast papillary neoplasms: applications in the diagnosis of tall cell carcinoma with reverse polarity. Mod Pathol. 2020;33(6):1056–64.
49. James BA, Cranor ML, Rosen PP. Carcinoma of the breast arising in microglandular adenosis. Am J Clin Pathol. 1993;100(5):507–13.
50. Koenig C, Dadmanesh F, Bratthauer GL, Tavassoli FA. Carcinoma arising in microglandular Adenosis: an immunohistochemical analysis of 20 intraepithelial and invasive neoplasms. Int J Surg Pathol. 2000;8(4):303–15.
51. Krings G, Nystrom M, Mehdi I, Vohra P, Chen YY. Diagnostic utility and sensitivities of GATA3 antibodies in triple-negative breast cancer. Hum Pathol. 2014;45(11):2225–32.
52. Miettinen M, McCue PA, Sarlomo-Rikala M, Rys J, Czapiewski P, Wazny K, et al. GATA3: a multispecific but potentially useful marker in surgical pathology: a systematic analysis of 2500 epithelial and nonepithelial tumors. Am J Surg Pathol. 2014;38(1):13–22.
53. Yang M, Nonaka D. A study of immunohistochemical differential expression in pulmonary and mammary carcinomas. Mod Pathol. 2010;23(5):654–61.
54. Liu H, Shi J, Prichard JW, Gong Y, Lin F. Immunohistochemical evaluation of GATA-3 expression in ER-negative breast carcinomas. Am J Clin Pathol. 2014;141(5):648–55.
55. Clark BZ, Beriwal S, Dabbs DJ, Bhargava R. Semiquantitative GATA-3 immunoreactivity in breast, bladder, gynecologic tract, and other cytokeratin 7-positive carcinomas. Am J Clin Pathol. 2014;142(1):64–71.
56. Asch-Kendrick R, Cimino-Mathews A. The role of GATA3 in breast carcinomas: a review. Hum Pathol. 2016;48:37–47.
57. Liu H, Shi J, Wilkerson ML, Lin F. Immunohistochemical evaluation of GATA3 expression in tumors and normal tissues: a useful immunomarker for breast and urothelial carcinomas. Am J Clin Pathol. 2012;138(1):57–64.
58. Agostini-Vulaj D, Bratton LE, Dunne RF, Cates JMM, Zhou Z, Findeis-Hosey JJ, et al. Incidence and significance of GATA3 positivity in pancreatic ductal adenocarcinoma and cholangiocarcinoma. Appl Immunohistochem Mol Morphol. 2020;28(6):460–3.
59. Cimino-Mathews A, Subhawong AP, Elwood H, Warzecha HN, Sharma R, Park BH, et al. Neural crest transcription factor Sox10 is preferentially expressed in triple-negative and metaplastic breast carcinomas. Hum Pathol. 2013;44(6):959–65.
60. Qazi MS, McGregor SM. Combined use of SOX10 and GATA3 in mammary carcinoma. Pathol Res Pract. 2020;216(2):152801.
61. Jamidi SK, Hu J, Aphivatanasiri C, Tsang JY, Poon IK, Li JJ, et al. Sry-related high-mobility-group/HMG box 10 (SOX10) as a sen-

sitive marker for triple-negative breast cancer. Histopathology. 2020;77(6):936–48.
62. Nelson ER, Sharma R, Argani P, Cimino-Mathews A. Utility of Sox10 labeling in metastatic breast carcinomas. Hum Pathol. 2017;67:205–10.
63. Tozbikian GH, Zynger DL. A combination of GATA3 and SOX10 is useful for the diagnosis of metastatic triple-negative breast cancer. Hum Pathol. 2019;85:221–7.
64. Miettinen M, McCue PA, Sarlomo-Rikala M, Biernat W, Czapiewski P, Kopczynski J, et al. Sox10—a marker for not only schwannian and melanocytic neoplasms but also myoepithelial cell tumors of soft tissue: a systematic analysis of 5134 tumors. Am J Surg Pathol. 2015;39(6):826–35.
65. Yoon EC, Wang G, Parkinson B, Huo L, Peng Y, Wang J, et al. TRPS1, GATA3, and SOX10 expression in triple-negative breast carcinoma. Hum Pathol. 2022;125:97–107. https://doi.org/10.1016/j.humpath.2022.04.006. Epub 2022 Apr 9.
66. Szumera-Ciećkiewicz A, Bosisio F, Teterycz P, Antoranz A, Delogu F, Koljenović S, et al. SOX10 is as specific as S100 protein in detecting metastases of melanoma in lymph nodes and is recommended for sentinel lymph node assessment. Eur J Cancer. 2020;137:175–82.
67. Miettinen M, Fernandez M, Franssila K, Gatalica Z, Lasota J, Sarlomo-Rikala M. Microphthalmia transcription factor in the immunohistochemical diagnosis of metastatic melanoma: comparison with four other melanoma markers. Am J Surg Pathol. 2001;25(2):205–11.
68. Miettinen M, Lindenmayer AE, Chaubal A. Endothelial cell markers CD31, CD34, and BNH9 antibody to H- and Y-antigens—evaluation of their specificity and sensitivity in the diagnosis of vascular tumors and comparison with von Willebrand factor. Mod Pathol. 1994;7(1):82–90.
69. Miettinen M, Wang ZF, Paetau A, Tan SH, Dobi A, Srivastava S, et al. ERG transcription factor as an immunohistochemical marker for vascular endothelial tumors and prostatic carcinoma. Am J Surg Pathol. 2011;35(3):432–41.
70. Udager AM, Ishikawa MK, Lucas DR, McHugh JB, Patel RM. MYC immunohistochemistry in angiosarcoma and atypical vascular lesions: practical considerations based on a single institutional experience. Pathology. 2016;48(7):697–704.
71. Cornejo KM, Deng A, Wu H, Cosar EF, Khan A, St Cyr M, et al. The utility of MYC and FLT4 in the diagnosis and treatment of postradiation atypical vascular lesion and angiosarcoma of the breast. Hum Pathol. 2015;46(6):868–75.
72. Fernandez AP, Sun Y, Tubbs RR, Goldblum JR, Billings SD. FISH for MYC amplification and anti-MYC immunohistochemistry: useful diagnostic tools in the assessment of secondary angiosarcoma and atypical vascular proliferations. J Cutan Pathol. 2012;39(2):234–42.
73. Guo T, Zhang L, Chang NE, Singer S, Maki RG, Antonescu CR. Consistent MYC and FLT4 gene amplification in radiation-induced angiosarcoma but not in other radiation-associated atypical vascular lesions. Genes Chromosomes Cancer. 2011;50(1):25–33.
74. Ginter PS, Mosquera JM, MacDonald TY, D'Alfonso TM, Rubin MA, Shin SJ. Diagnostic utility of MYC amplification and anti-MYC immunohistochemistry in atypical vascular lesions, primary or radiation-induced mammary angiosarcomas, and primary angiosarcomas of other sites. Hum Pathol. 2014;45(4):709–16.
75. Fletcher CD, Beham A, Bekir S, Clarke AM, Marley NJ. Epithelioid angiosarcoma of deep soft tissue: a distinctive tumor readily mistaken for an epithelial neoplasm. Am J Surg Pathol. 1991;15(10):915–24.
76. Meis-Kindblom JM, Kindblom LG. Angiosarcoma of soft tissue: a study of 80 cases. Am J Surg Pathol. 1998;22(6):683–97.
77. Talwalkar SS, Miranda RN, Valbuena JR, Routbort MJ, Martin AW, Medeiros LJ. Lymphomas involving the breast: a study of 106 cases comparing localized and disseminated neoplasms. Am J Surg Pathol. 2008;32(9):1299–309.
78. Domchek SM, Hecht JL, Fleming MD, Pinkus GS, Canellos GP. Lymphomas of the breast: primary and secondary involvement. Cancer. 2002;94(1):6–13.
79. Thompson PA, Prince HM. Breast implant-associated anaplastic large cell lymphoma: a systematic review of the literature and mini-meta analysis. Curr Hematol Malig Rep. 2013;8(3):196–210.
80. Aladily TN, Medeiros LJ, Amin MB, Haideri N, Ye D, Azevedo SJ, et al. Anaplastic large cell lymphoma associated with breast implants: a report of 13 cases. Am J Surg Pathol. 2012;36(7):1000–8.
81. Li S, Lee AK. Silicone implant and primary breast ALK1-negative anaplastic large cell lymphoma, fact or fiction? Int J Clin Exp Pathol. 2009;3(1):117–27.
82. Taylor CR, Siddiqi IN, Brody GS. Anaplastic large cell lymphoma occurring in association with breast implants: review of pathologic and immunohistochemical features in 103 cases. Appl Immunohistochem Mol Morphol. 2013;21(1):13–20.
83. Tapia C, Glatz K, Novotny H, Lugli A, Horcic M, Seemayer CA, et al. Close association between HER-2 amplification and overexpression in human tumors of non-breast origin. Mod Pathol. 2007;20(2):192–8.
84. Robens J, Goldstein L, Gown AM, Schnitt SJ. Thyroid transcription factor-1 expression in breast carcinomas. Am J Surg Pathol. 2010;34(12):1881–5.
85. Gomez-Fernandez C, Mejias A, Walker G, Nadji M. Immunohistochemical expression of estrogen receptor in adenocarcinomas of the lung: the antibody factor. Appl Immunohistochem Mol Morphol. 2010;18(2):137–41.
86. Wei S, Said-Al-Naief N, Hameed O. Estrogen and progesterone receptor expression is not always specific for mammary and gynecologic carcinomas: a tissue microarray and pooled literature review study. Appl Immunohistochem Mol Morphol. 2009;17(5):393–402.
87. Kurbel S. In search of triple-negative DCIS: tumor-type dependent model of breast cancer progression from DCIS to the invasive cancer. Tumour Biol. 2013;34(1):1–7.
88. Beetch M, Harandi-Zadeh S, Yang T, Boycott C, Chen Y, Stefanska B, et al. DNA methylation landscape of triple-negative ductal carcinoma in situ (DCIS) progressing to the invasive stage in canine breast cancer. Sci Rep. 2020;10(1):2415.
89. Livasy CA, Perou CM, Karaca G, Cowan DW, Maia D, Jackson S, et al. Identification of a basal-like subtype of breast ductal carcinoma in situ. Hum Pathol. 2007;38(2):197–204.
90. Dabbs DJ, Chivukula M, Carter G, Bhargava R. Basal phenotype of ductal carcinoma in situ: recognition and immunohistologic profile. Mod Pathol. 2006;19(11):1506–11.
91. Bryan BB, Schnitt SJ, Collins LC. Ductal carcinoma in situ with basal-like phenotype: a possible precursor to invasive basal-like breast cancer. Mod Pathol. 2006;19(5):617–21.
92. Thike AA, Iqbal J, Cheok PY, Tse GM, Tan PH. Ductal carcinoma in situ associated with triple negative invasive breast cancer: evidence for a precursor-product relationship. J Clin Pathol. 2013;66(8):665–70.
93. Tamimi RM, Baer HJ, Marotti J, Galan M, Galaburda L, Fu Y, et al. Comparison of molecular phenotypes of ductal carcinoma in situ and invasive breast cancer. Breast Cancer Res. 2008;10(4):R67.
94. Clark SE, Warwick J, Carpenter R, Bowen RL, Duffy SW, Jones JL. Molecular subtyping of DCIS: heterogeneity of breast cancer reflected in pre-invasive disease. Br J Cancer. 2011;104(1):120–7.
95. Zhou W, Jirström K, Johansson C, Amini RM, Blomqvist C, Agbaje O, et al. Long-term survival of women with basal-like

ductal carcinoma in situ of the breast: a population-based cohort study. BMC Cancer. 2010;10:653.
96. Zhou W, Jirström K, Amini RM, Fjällskog ML, Sollie T, Lindman H, et al. Molecular subtypes in ductal carcinoma in situ of the breast and their relation to prognosis: a population-based cohort study. BMC Cancer. 2013;13:512.
97. Liu Y, Shou K, Li J, Wu Q, Hu Y, Wang J, et al. Ductal carcinoma in situ of the breast: perspectives on tumor subtype and treatment. Biomed Res Int. 2020;2020:7251431.
98. Guerini-Rocco E, Piscuoglio S, Ng CK, Geyer FC, De Filippo MR, Eberle CA, et al. Microglandular adenosis associated with triple-negative breast cancer is a neoplastic lesion of triple-negative phenotype harbouring TP53 somatic mutations. J Pathol. 2016;238(5):677–88.
99. Wen YH, Weigelt B, Reis-Filho JS. Microglandular adenosis: a non-obligate precursor of triple-negative breast cancer? Histol Histopathol. 2013;28(9):1099–108.
100. Geyer FC, Lacroix-Triki M, Colombo PE, Patani N, Gauthier A, Natrajan R, et al. Molecular evidence in support of the neoplastic and precursor nature of microglandular adenosis. Histopathology. 2012;60(6B):E115–30.
101. Geyer FC, Kushner YB, Lambros MB, Natrajan R, Mackay A, Tamber N, et al. Microglandular adenosis or microglandular adenoma? A molecular genetic analysis of a case associated with atypia and invasive carcinoma. Histopathology. 2009;55(6):732–43.
102. Shin SJ, Simpson PT, Da Silva L, Jayanthan J, Reid L, Lakhani SR, et al. Molecular evidence for progression of microglandular adenosis (MGA) to invasive carcinoma. Am J Surg Pathol. 2009;33(4):496–504.
103. Miki Y, Swensen J, Shattuck-Eidens D, Futreal PA, Harshman K, Tavtigian S, et al. A strong candidate for the breast and ovarian cancer susceptibility gene BRCA1. Science. 1994;266(5182):66–71.
104. Wooster R, Neuhausen SL, Mangion J, Quirk Y, Ford D, Collins N, et al. Localization of a breast cancer susceptibility gene, BRCA2, to chromosome 13q12-13. Science. 1994;265(5181):2088–90.
105. Wooster R, Bignell G, Lancaster J, Swift S, Seal S, Mangion J, et al. Identification of the breast cancer susceptibility gene BRCA2. Nature. 1995;378(6559):789–92.
106. Hall JM, Lee MK, Newman B, Morrow JE, Anderson LA, Huey B, et al. Linkage of early-onset familial breast cancer to chromosome 17q21. Science. 1990;250(4988):1684–9.
107. Santarpia L, Iwamoto T, Di Leo A, Hayashi N, Bottai G, Stampfer M, et al. DNA repair gene patterns as prognostic and predictive factors in molecular breast cancer subtypes. Oncologist. 2013;18(10):1063–73.
108. Armes JE, Egan AJ, Southey MC, Dite GS, McCredie MR, Giles GG, et al. The histologic phenotypes of breast carcinoma occurring before age 40 years in women with and without BRCA1 or BRCA2 germline mutations: a population-based study. Cancer. 1998;83(11):2335–45.
109. Foulkes WD, Stefansson IM, Chappuis PO, Bégin LR, Goffin JR, Wong N, et al. Germline BRCA1 mutations and a basal epithelial phenotype in breast cancer. J Natl Cancer Inst. 2003;95(19):1482–5.
110. Honrado E, Osorio A, Palacios J, Benitez J. Pathology and gene expression of hereditary breast tumors associated with BRCA1, BRCA2 and CHEK2 gene mutations. Oncogene. 2006;25(43):5837–45.
111. Lakhani SR, Jacquemier J, Sloane JP, Gusterson BA, Anderson TJ, van de Vijver MJ, et al. Multifactorial analysis of differences between sporadic breast cancers and cancers involving BRCA1 and BRCA2 mutations. J Natl Cancer Inst. 1998;90(15):1138–45.
112. Gonzalez-Angulo AM, Timms KM, Liu S, Chen H, Litton JK, Potter J, et al. Incidence and outcome of BRCA mutations in unselected patients with triple receptor-negative breast cancer. Clin Cancer Res. 2011;17(5):1082–9.
113. Network CGA. Comprehensive molecular portraits of human breast tumours. Nature. 2012;490(7418):61–70.
114. Turner N, Tutt A, Ashworth A. Hallmarks of 'BRCAness' in sporadic cancers. Nat Rev Cancer. 2004;4(10):814–9.
115. von Minckwitz G, Martin M. Neoadjuvant treatments for triple-negative breast cancer (TNBC). Ann Oncol. 2012;23(Suppl 6):vi35–9.
116. Anders CK, Zagar TM, Carey LA. The management of early-stage and metastatic triple-negative breast cancer: a review. Hematol Oncol Clin North Am. 2013;27(4):737–49, viii.
117. Wolff AC, Hammond MEH, Allison KH, Harvey BE, Mangu PB, Bartlett JMS, et al. Human epidermal growth factor receptor 2 testing in breast cancer: American Society of Clinical Oncology/College of American Pathologists clinical practice guideline focused update. Arch Pathol Lab Med. 2018;142(11):1364–82.
118. Wolff AC, Hammond MEH, Allison KH, Harvey BE, Mangu PB, Bartlett JMS, et al. Human epidermal growth factor receptor 2 testing in breast cancer: American Society of Clinical Oncology/College of American Pathologists clinical practice guideline focused update. J Clin Oncol. 2018;36(20):2105–22.
119. Penault-Llorca F, Viale G. Pathological and molecular diagnosis of triple-negative breast cancer: a clinical perspective. Ann Oncol. 2012;23(Suppl 6):vi19–22.
120. Cheang MC, Martin M, Nielsen TO, Prat A, Rodriguez-Lescure A, Ruiz A. Quantitative hormone receptors, triple-negative breast cancer (TNBC), and molecular pes: a collaborative effort of the BIG-NCI NABCG. In: Proceedings of the American Society of Clinical Oncology, 1–5 Jun 2012, Chicago, p. a1008.
121. Poon IK, Tsang JY, Li J, Chan SK, Shea KH, Tse GM. The significance of highlighting the oestrogen receptor low category in breast cancer. Br J Cancer. 2020;123(8):1223–7.
122. Iwamoto T, Booser D, Valero V, Murray JL, Koenig K, Esteva FJ, et al. Estrogen receptor (ER) mRNA and ER-related gene expression in breast cancers that are 1% to 10% ER-positive by immunohistochemistry. J Clin Oncol. 2012;30(7):729–34.
123. Gloyeske NC, Dabbs DJ, Bhargava R. Low ER+ breast cancer: is this a distinct group? Am J Clin Pathol. 2014;141(5):697–701.
124. Allison KH, Hammond MEH, Dowsett M, McKernin SE, Carey LA, Fitzgibbons PL, et al. Estrogen and progesterone receptor testing in breast cancer: ASCO/CAP guideline update. J Clin Oncol. 2020;38(12):1346–66.
125. Allison KH, Hammond MEH, Dowsett M, McKernin SE, Carey LA, Fitzgibbons PL, et al. Estrogen and progesterone receptor testing in breast cancer: American Society of Clinical Oncology/College of American Pathologists guideline update. Arch Pathol Lab Med. 2020;144(5):545–63.
126. Cheang MC, Treaba DO, Speers CH, Olivotto IA, Bajdik CD, Chia SK, et al. Immunohistochemical detection using the new rabbit monoclonal antibody SP1 of estrogen receptor in breast cancer is superior to mouse monoclonal antibody 1D5 in predicting survival. J Clin Oncol. 2006;24(36):5637–44.
127. Fujii T, Kogawa T, Dong W, Sahin AA, Moulder S, Litton JK, et al. Revisiting the definition of estrogen receptor positivity in HER2-negative primary breast cancer. Ann Oncol. 2017;28(10):2420–8.
128. Gradishar WJ, Moran MS, Abraham J, Aft R, Agnese D, Allison KH, et al. Breast cancer (Version 2.2021).
129. Shah PD, Gucalp A, Traina TA. The role of the androgen receptor in triple-negative breast cancer. Womens Health (Lond). 2013;9(4):351–60.
130. Niemeier LA, Dabbs DJ, Beriwal S, Striebel JM, Bhargava R. Androgen receptor in breast cancer: expression in estrogen

receptor-positive tumors and in estrogen receptor-negative tumors with apocrine differentiation. Mod Pathol. 2010;23(2):205–12.
131. Park S, Koo J, Park HS, Kim JH, Choi SY, Lee JH, et al. Expression of androgen receptors in primary breast cancer. Ann Oncol. 2010;21(3):488–92.
132. Micello D, Marando A, Sahnane N, Riva C, Capella C, Sessa F. Androgen receptor is frequently expressed in HER2-positive, ER/PR-negative breast cancers. Virchows Arch. 2010;457(4):467–76.
133. Ogawa Y, Hai E, Matsumoto K, Ikeda K, Tokunaga S, Nagahara H, et al. Androgen receptor expression in breast cancer: relationship with clinicopathological factors and biomarkers. Int J Clin Oncol. 2008;13(5):431–5.
134. Vellaisamy G, Tirumalae R, Inchara YK. Expression of androgen receptor in primary breast carcinoma and its relation with clinicopathologic features, estrogen, progesterone, and her-2 receptor status. J Cancer Res Ther. 2019;15(5):989–93.
135. He J, Peng R, Yuan Z, Wang S, Peng J, Lin G, et al. Prognostic value of androgen receptor expression in operable triple-negative breast cancer: a retrospective analysis based on a tissue microarray. Med Oncol. 2012;29(2):406–10.
136. Yu Q, Niu Y, Liu N, Zhang JZ, Liu TJ, Zhang RJ, et al. Expression of androgen receptor in breast cancer and its significance as a prognostic factor. Ann Oncol. 2011;22(6):1288–94.
137. Gucalp A, Traina TA. Targeting the androgen receptor in triple-negative breast cancer. Curr Probl Cancer. 2016;40(2–4):141–50.
138. Gerratana L, Basile D, Buono G, De Placido S, Giuliano M, Minichillo S, et al. Androgen receptor in triple negative breast cancer: a potential target for the targetless subtype. Cancer Treat Rev. 2018;68:102–10.
139. Masuda H, Baggerly KA, Wang Y, Zhang Y, Gonzalez-Angulo AM, Meric-Bernstam F, et al. Differential response to neoadjuvant chemotherapy among 7 triple-negative breast cancer molecular subtypes. Clin Cancer Res. 2013;19(19):5533–40.
140. Gucalp A, Tolaney S, Isakoff SJ, Ingle JN, Liu MC, Carey LA, et al. Phase II trial of bicalutamide in patients with androgen receptor-positive, estrogen receptor-negative metastatic breast cancer. Clin Cancer Res. 2013;19(19):5505–12.
141. Bonnefoi H, Grellety T, Tredan O, Saghatchian M, Dalenc F, Mailliez A, et al. A phase II trial of abiraterone acetate plus prednisone in patients with triple-negative androgen receptor positive locally advanced or metastatic breast cancer (UCBG 12-1). Ann Oncol. 2016;27(5):812–8.
142. Traina TA, Miller K, Yardley DA, Eakle J, Schwartzberg LS, O'Shaughnessy J, et al. Enzalutamide for the treatment of androgen receptor-expressing triple-negative breast cancer. J Clin Oncol. 2018;36(9):884–90.
143. Kensler KH, Poole EM, Heng YJ, Collins LC, Glass B, Beck AH, et al. Androgen receptor expression and breast cancer survival: results from the nurses' health studies. J Natl Cancer Inst. 2019;111(7):700–8.
144. Dieci MV, Tsvetkova V, Griguolo G, Miglietta F, Mantiero M, Tasca G, et al. Androgen receptor expression and association with distant disease-free survival in triple negative breast cancer: analysis of 263 patients treated with standard therapy for stage I-III disease. Front Oncol. 2019;9:452.
145. Collins LC, Cole KS, Marotti JD, Hu R, Schnitt SJ, Tamimi RM. Androgen receptor expression in breast cancer in relation to molecular phenotype: results from the Nurses' Health Study. Mod Pathol. 2011;24(7):924–31.
146. Hu R, Dawood S, Holmes MD, Collins LC, Schnitt SJ, Cole K, et al. Androgen receptor expression and breast cancer survival in postmenopausal women. Clin Cancer Res. 2011;17(7):1867–74.
147. McGhan LJ, McCullough AE, Protheroe CA, Dueck AC, Lee JJ, Nunez-Nateras R, et al. Androgen receptor-positive triple negative breast cancer: a unique breast cancer subtype. Ann Surg Oncol. 2014;21(2):361–7.
148. Loibl S, Müller BM, von Minckwitz G, Schwabe M, Roller M, Darb-Esfahani S, et al. Androgen receptor expression in primary breast cancer and its predictive and prognostic value in patients treated with neoadjuvant chemotherapy. Breast Cancer Res Treat. 2011;130(2):477–87.
149. Denkert C, von Minckwitz G, Darb-Esfahani S, Lederer B, Heppner BI, Weber KE, et al. Tumour-infiltrating lymphocytes and prognosis in different subtypes of breast cancer: a pooled analysis of 3771 patients treated with neoadjuvant therapy. Lancet Oncol. 2018;19(1):40–50.
150. Gao ZH, Li CX, Liu M, Jiang JY. Predictive and prognostic role of tumour-infiltrating lymphocytes in breast cancer patients with different molecular subtypes: a meta-analysis. BMC Cancer. 2020;20(1):1150.
151. Biswas T, Efird JT, Prasad S, Jindal C, Walker PR. The survival benefit of neoadjuvant chemotherapy and pCR among patients with advanced stage triple negative breast cancer. Oncotarget. 2017;8(68):112712–9.
152. Liedtke C, Mazouni C, Hess KR, André F, Tordai A, Mejia JA, et al. Response to neoadjuvant therapy and long-term survival in patients with triple-negative breast cancer. J Clin Oncol. 2008;26(8):1275–81.
153. Salgado R, Denkert C, Demaria S, Sirtaine N, Klauschen F, Pruneri G, et al. The evaluation of tumor-infiltrating lymphocytes (TILs) in breast cancer: recommendations by an International TILs Working Group 2014. Ann Oncol. 2015;26(2):259–71.
154. Dieci MV, Radosevic-Robin N, Fineberg S, van den Eynden G, Ternes N, Penault-Llorca F, et al. Update on tumor-infiltrating lymphocytes (TILs) in breast cancer, including recommendations to assess TILs in residual disease after neoadjuvant therapy and in carcinoma in situ: a report of the International Immuno-Oncology Biomarker Working Group on Breast Cancer. Semin Cancer Biol. 2018;52(Pt 2):16–25.
155. Tramm T, Di Caterino T, Jylling AB, Lelkaitis G, Lænkholm AV, Ragó P, et al. Standardized assessment of tumor-infiltrating lymphocytes in breast cancer: an evaluation of inter-observer agreement between pathologists. Acta Oncol. 2018;57(1):90–4.
156. Swisher SK, Wu Y, Castaneda CA, Lyons GR, Yang F, Tapia C, et al. Interobserver agreement between pathologists assessing tumor-infiltrating lymphocytes (TILs) in breast cancer using methodology proposed by the International TILs Working Group. Ann Surg Oncol. 2016;23(7):2242–8.
157. Kojima YA, Wang X, Sun H, Compton F, Covinsky M, Zhang S. Reproducible evaluation of tumor-infiltrating lymphocytes (TILs) using the recommendations of International TILs Working Group 2014. Ann Diagn Pathol. 2018;35:77–9.
158. Balic M, Thomssen C, Würstlein R, Gnant M, Harbeck N. St. Gallen/Vienna 2019: a brief summary of the consensus discussion on the optimal primary breast cancer treatment. Breast Care (Basel). 2019;14(2):103–10.
159. Narayan P, Wahby S, Gao JJ, Amiri-Kordestani L, Ibrahim A, Bloomquist E, et al. FDA approval summary: atezolizumab plus paclitaxel protein-bound for the treatment of patients with advanced or metastatic TNBC whose tumors express PD-L1. Clin Cancer Res. 2020;26(10):2284–9.
160. Cortes J, Cescon DW, Rugo HS, Nowecki Z, Im SA, Yusof MM, et al. Pembrolizumab plus chemotherapy versus placebo plus chemotherapy for previously untreated locally recurrent inoperable or metastatic triple-negative breast cancer (KEYNOTE-355): a randomised, placebo-controlled, double-blind, phase 3 clinical trial. Lancet. 2020;396(10265):1817–28.
161. Administration USFaD. List of cleared or approved companion diagnostic devices (in vitro and imaging tools).
162. Miles D, Gligorov J, André F, Cameron D, Schneeweiss A, Barrios C, et al. Primary results from IMpassion131, a double-blind, placebo-controlled, randomised phase III trial of

first-line paclitaxel with or without atezolizumab for unresectable locally advanced/metastatic triple-negative breast cancer. Ann Oncol. 2021;32(8):994–1004. https://doi.org/10.1016/j.annonc.2021.05.801. Epub 2021 Jul 1.
163. Byrski T, Huzarski T, Dent R, Gronwald J, Zuziak D, Cybulski C, et al. Response to neoadjuvant therapy with cisplatin in BRCA1-positive breast cancer patients. Breast Cancer Res Treat. 2009;115(2):359–63.
164. Byrski T, Huzarski T, Dent R, Marczyk E, Jasiowka M, Gronwald J, et al. Pathologic complete response to neoadjuvant cisplatin in BRCA1-positive breast cancer patients. Breast Cancer Res Treat. 2014;147(2):401–5.
165. Hahnen E, Lederer B, Hauke J, Loibl S, Kröber S, Schneeweiss A, et al. Germline mutation status, pathological complete response, and disease-free survival in triple-negative breast cancer: secondary analysis of the GeparSixto randomized clinical trial. JAMA Oncol. 2017;3(10):1378–85.
166. Silver DP, Richardson AL, Eklund AC, Wang ZC, Szallasi Z, Li Q, et al. Efficacy of neoadjuvant cisplatin in triple-negative breast cancer. J Clin Oncol. 2010;28(7):1145–53.
167. Loibl S, Weber KE, Timms KM, Elkin EP, Hahnen E, Fasching PA, et al. Survival analysis of carboplatin added to an anthracycline/taxane-based neoadjuvant chemotherapy and HRD score as predictor of response-final results from GeparSixto. Ann Oncol. 2018;29(12):2341–7.
168. von Minckwitz G, Schneeweiss A, Loibl S, Salat C, Denkert C, Rezai M, et al. Neoadjuvant carboplatin in patients with triple-negative and HER2-positive early breast cancer (GeparSixto; GBG 66): a randomised phase 2 trial. Lancet Oncol. 2014;15(7):747–56.
169. Sikov WM, Berry DA, Perou CM, Singh B, Cirrincione CT, Tolaney SM, et al. Impact of the addition of carboplatin and/or bevacizumab to neoadjuvant once-per-week paclitaxel followed by dose-dense doxorubicin and cyclophosphamide on pathologic complete response rates in stage II to III triple-negative breast cancer: CALGB 40603 (Alliance). J Clin Oncol. 2015;33(1):13–21.
170. Litton JK, Rugo HS, Ettl J, Hurvitz SA, Gonçalves A, Lee KH, et al. Talazoparib in patients with advanced breast cancer and a germline BRCA mutation. N Engl J Med. 2018;379(8):753–63.
171. Robson M, Im SA, Senkus E, Xu B, Domchek SM, Masuda N, et al. Olaparib for metastatic breast cancer in patients with a germline BRCA mutation. N Engl J Med. 2017;377(6):523–33.
172. O'Shaughnessy J, Schwartzberg L, Danso MA, Miller KD, Rugo HS, Neubauer M, et al. Phase III study of iniparib plus gemcitabine and carboplatin versus gemcitabine and carboplatin in patients with metastatic triple-negative breast cancer. J Clin Oncol. 2014;32(34):3840–7.
173. Tutt A, Balmana J, Robson M, Garber J, Kaufman B, Geyer C, et al. 331TiP—Olympia, neo-olympia and olympiad: randomized phase III trials of olaparib in patients (Pts) with breast cancer (Bc) and a germline Brca1/2 mutation (Gbrcam). Ann Oncol. 2014;25(Suppl 4):iv109.

Less Common Triple-Negative Breast Cancers

12

Poonam Vohra, Yunn-Yi Chen, and Gregor Krings

Adenoid Cystic Carcinoma

Overview and Clinical Presentation

Adenoid cystic carcinoma (AdCC) of the breast is a rare and histologically distinct triple-negative and basal-like cancer, which accounts for <0.1% of all breast carcinomas. Previously termed cylindroma, AdCC of the breast was first described by Geschickter [1]. Classic AdCC follow an indolent clinical course and generally has an excellent prognosis [2–4]. The incidence of mammary AdCC has remained stable over the last 30 years without a notable rise following widespread use of mammography since the 1980s. It occurs more frequently in the sixth or early seventh decade and is extremely unusual in younger and premenopausal women [2]. The incidence ratio for black women is 39% lower than for white women. Although far more common in women, AdCC has also been described in men [5, 6]. The tumor typically presents as a palpable mass that is occasionally tender to palpation. A few reported cases have been detected incidentally on routine screening mammograms of asymptomatic patients. AdCC is often located in the central or subareolar region [7]. Despite this central location, nipple discharge is rarely present. AdCC is only rarely fixed to the overlying skin, nipple, or pectoral muscles [7]. The right and left breasts are equally affected, and there is no predilection for AdCC to develop bilaterally [8].

Gross and Radiologic Features

On gross examination, AdCC is usually circumscribed and nodular, ranging from 0.5 to 12 cm in size, with an average of 3 cm. Microcysts (pink, tan, or gray) may occasionally be noted grossly [9].

On mammography, AdCC can appear either as a well-defined lobulated or ill-defined mass or occasionally as an asymmetric density with microcalcifications [7, 10]. Rare tumors may present as a spiculated lesion. In one case, MRI revealed an unusual pattern of early enhancement (but no washout) extending from the periphery to the center gradually [10]. These tumors exhibit minimal vascularity on color Doppler imaging and on positron emission tomography (PET) scan [11, 12]. AdCC usually does not show the typical appearance of invasive ductal carcinoma (IDC) on either mammogram or ultrasonography due to its well-defined nature with less surrounding architectural disruption and fibrosis. Accordingly, a "negative" finding or a benign-looking breast lesion on imaging cannot completely exclude the possibility of AdCC. On the other hand, the presence of a painful breast lesion without obvious inflammatory signs can lead to diagnostic suspicion [12].

Microscopic Features

AdCC demonstrates distinct histologic features analogous to its counterpart in the salivary glands, lung, and skin. Based on architectural and cytologic features, three subtypes have been recognized by the most recent World Health Organization (WHO) classification of breast tumors: classic AdCC, solid basaloid AdCC (SB-AdCC) and AdCC with high-grade transformation [13]. Classic AdCC constitutes the vast majority of breast AdCC. These tumors are composed of a dual population of luminal epithelial cells and abluminal myoepithelial/basaloid cells, arranged in varied architectural patterns including cribriform, tubular, reticular, solid, and mixed (Figs. 12.1, 12.2, 12.3, 12.4, 12.5, and 12.6). The most frequent cribriform variant is characterized by a sieve-like growth pattern, in which sheets of epithelial cells are punctuated by round or oval gland-like spaces

P. Vohra · Y.-Y. Chen · G. Krings (✉)
Department of Pathology, University of California San Francisco (UCSF), San Francisco, CA, USA
e-mail: Poonam.vohra@ucsf.edu; yunn-yi.chen@ucsf.edu; gregor.krings@ucsf.edu

© The Author(s), under exclusive license to Springer Nature Switzerland AG 2022

S. J. Shin et al. (eds.), *A Comprehensive Guide to Core Needle Biopsies of the Breast*,
https://doi.org/10.1007/978-3-031-05532-4_12

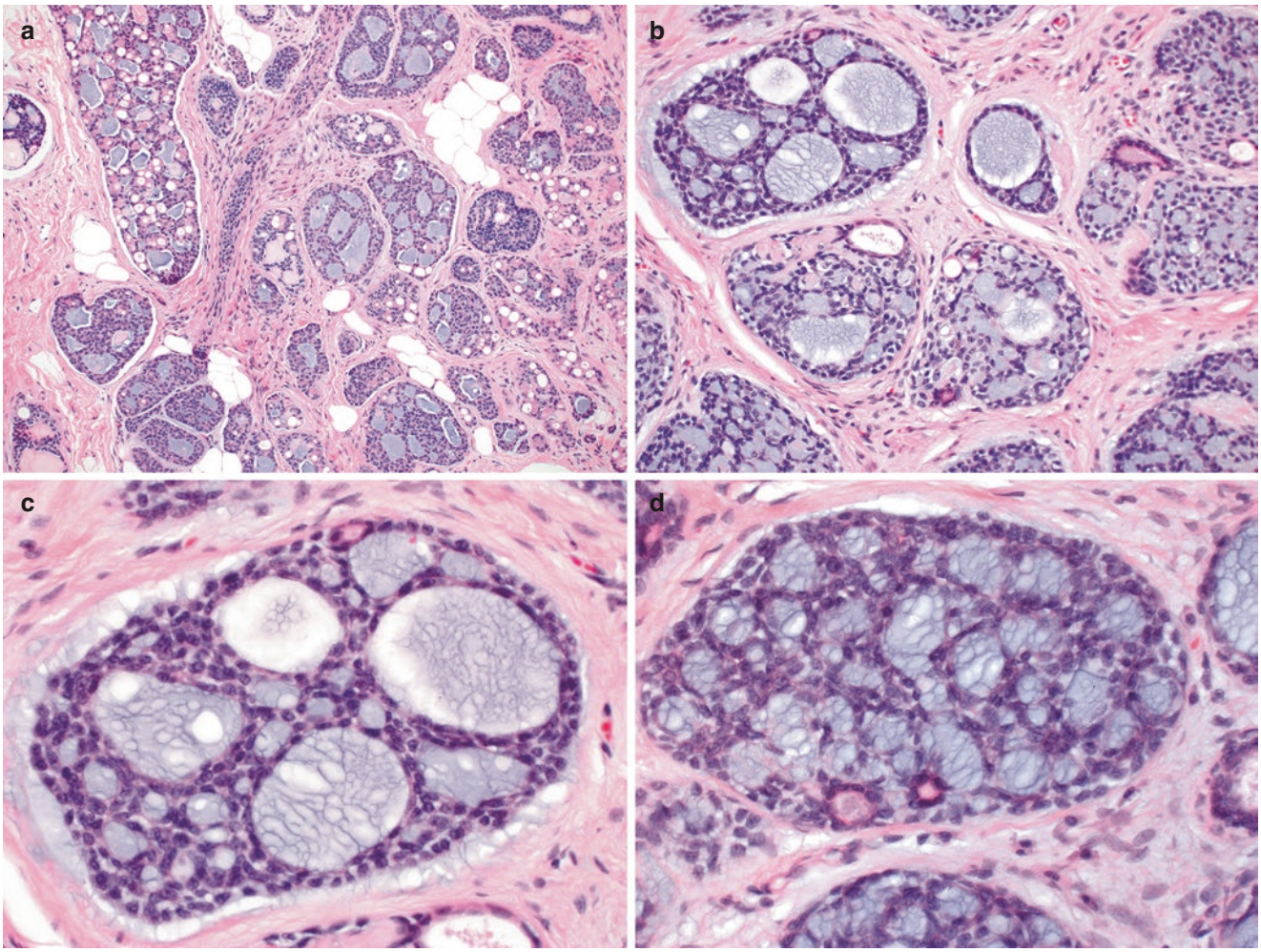

Fig. 12.1 Core needle biopsy of adenoid cystic carcinoma, cribriform growth pattern. (**a**–**d**) CNB reveals nests of tumor cells with a characteristic sieve-like (cribriform) growth pattern, in which clusters of neoplastic epithelial and myoepithelial cells are punctuated by round to oval spaces containing myxoid basement membrane material

(Fig. 12.1a–d). The dominant myoepithelial/basaloid cells have scant eosinophilic to clear cytoplasm and angulated to oval, hyperchromatic monomorphic nuclei, whereas the luminal epithelial cells are slightly larger, with modest amounts of eosinophilic cytoplasm and rounded nuclei (Fig. 12.2a–c). Mitotic activity is generally low. Two types of lumens are identified: "pseudolumens," comprising the characteristic cribriform spaces lined by myoepithelial cells, and true glandular lumens, lined by luminal epithelial cells (Fig. 12.4a–e). The pseudolumens contain basement membrane material, which may appear as Alcian blue-positive loose myxoid substance or PASD-positive eosinophilic hyalinized spherules. Immunostains for type IV collagen and laminin highlight the basement membrane components within the pseudolumens [14] (Fig. 12.4f, g). The true glandular lumens may show PAS-positive eosinophilic secretions.

AdCC may also assume a reticular architecture, in which the neoplastic cells are arranged in interconnected thin strands associated with myxoid or hyaline basement membrane material (Fig. 12.5a–d). Interspersed ductules may be appreciated on careful inspection. AdCC with tubular growth pattern comprises ductules or tubules lined by luminal epithelial cells and surrounding abluminal myoepithelial cells. The tubular pattern is often admixed with areas of cribriform growth (Fig. 12.6a–f).

First described by Shin and Rosen in 2002 [15], the rare SB-AdCC subtype is characterized by infiltrating irregular solid nests or islands of basaloid tumor cells within a hyalinized, myxoid, or desmoplastic stroma (Fig. 12.7a–d). Compared to classic AdCC, the tumor cells in the solid-basaloid subtype are larger, with hyperchromatic nuclei, moderate to marked atypia, and increased mitotic activity [15] (Fig. 12.8a, b). Foci of necrosis may be present, and

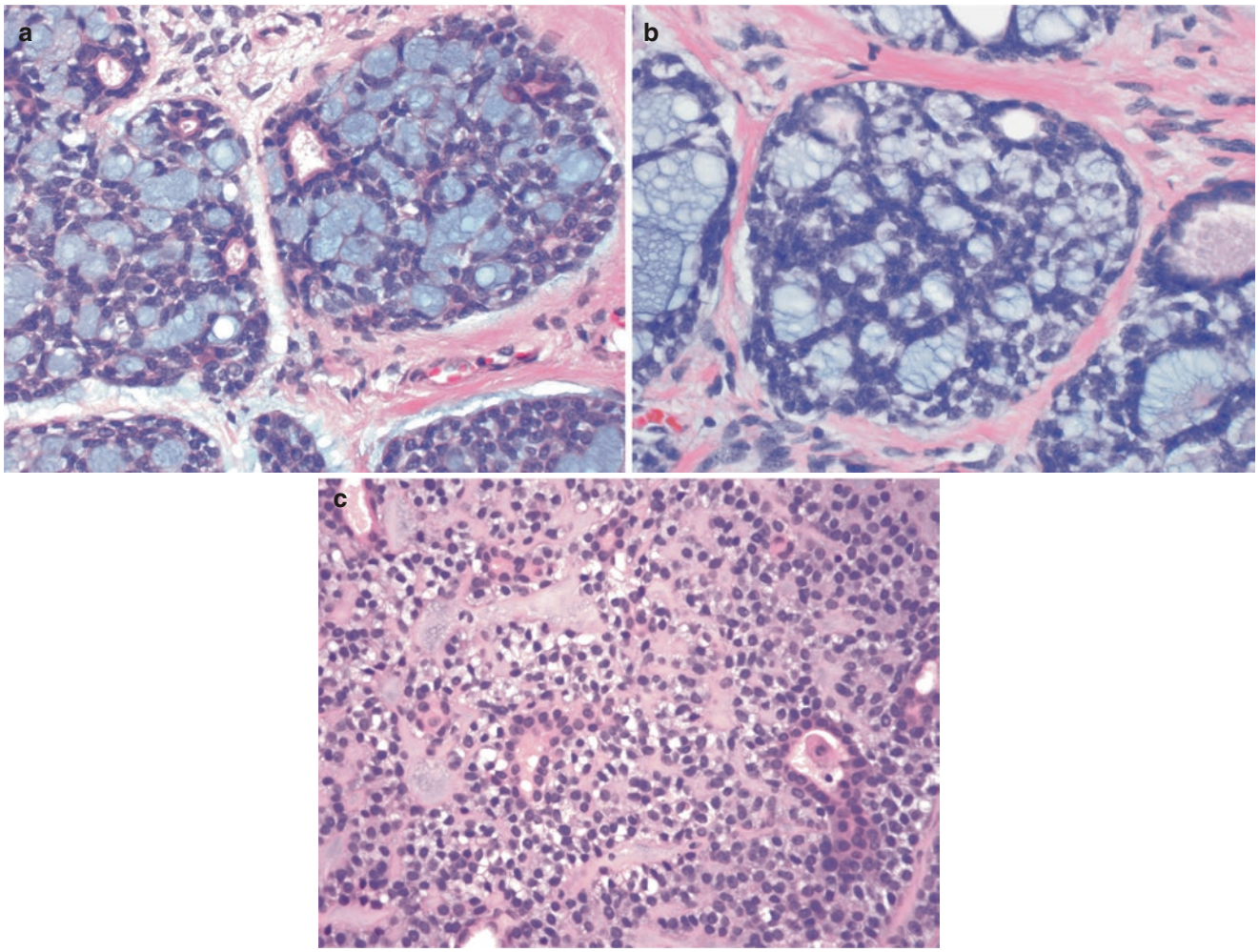

Fig. 12.2 Adenoid cystic carcinoma with dual population of tumor cells. (**a**, **b**) The myoepithelial/basaloid cells in these examples demonstrate scant cytoplasm and enlarged nuclei with irregular borders and open chromatin, whereas the luminal epithelial cells display more distinct eosinophilic cytoplasm and slightly smaller nuclei. (**c**) The myoepithelial cells of this case show scant pale to clear vacuolated cytoplasm and oval hyperchromatic nuclei. The luminal epithelial cells are larger, with more eosinophilic cytoplasm and rounded nuclei. Note the lumen formation by both populations of tumor cells in these examples

perineural invasion and lymphovascular invasion are frequent findings. Whereas a dual population of ductal and myoepithelial cells is considered to be the cardinal feature for diagnosis of AdCC, this phenotype is not conspicuous in the solid basaloid subtype, with the tumor showing basaloid cells, apparent loss of the biphasic cellular components, and decrease or loss of myoepithelial marker expression [15–18]. Immunostaining is often required to highlight any focal, subtle second cell population and true glandular lumens in SB-AdCC (Fig. 12.9a–f). The identification of so-called intercalated ducts, which appear eosinophilic in the background of dark basaloid cells, is helpful in recognizing this variant (Fig. 12.9). It has been suggested that the basaloid tumor cells probably represent poorly differentiated or undifferentiated primitive precursor cells capable of differentiating into myoepithelial-like or luminal-type cells [15, 16].

AdCC with high-grade transformation has been well documented in the salivary gland but is vanishingly rare in the breast. This subtype is characterized by either classic or SB-AdCC associated and merged with a high-grade carcinoma, which has been reported to include high-grade triple-negative breast cancer (TNBC) of no special type [19, 20] and small cell neuroendocrine carcinoma [21]. A rare metaplastic carcinoma with an associated AdCC component has been described [22].

In rare cases, the epithelial cells of AdCC can demonstrate squamous or sebaceous differentiation [2]. AdCC has been observed in association with microglandular adenosis,

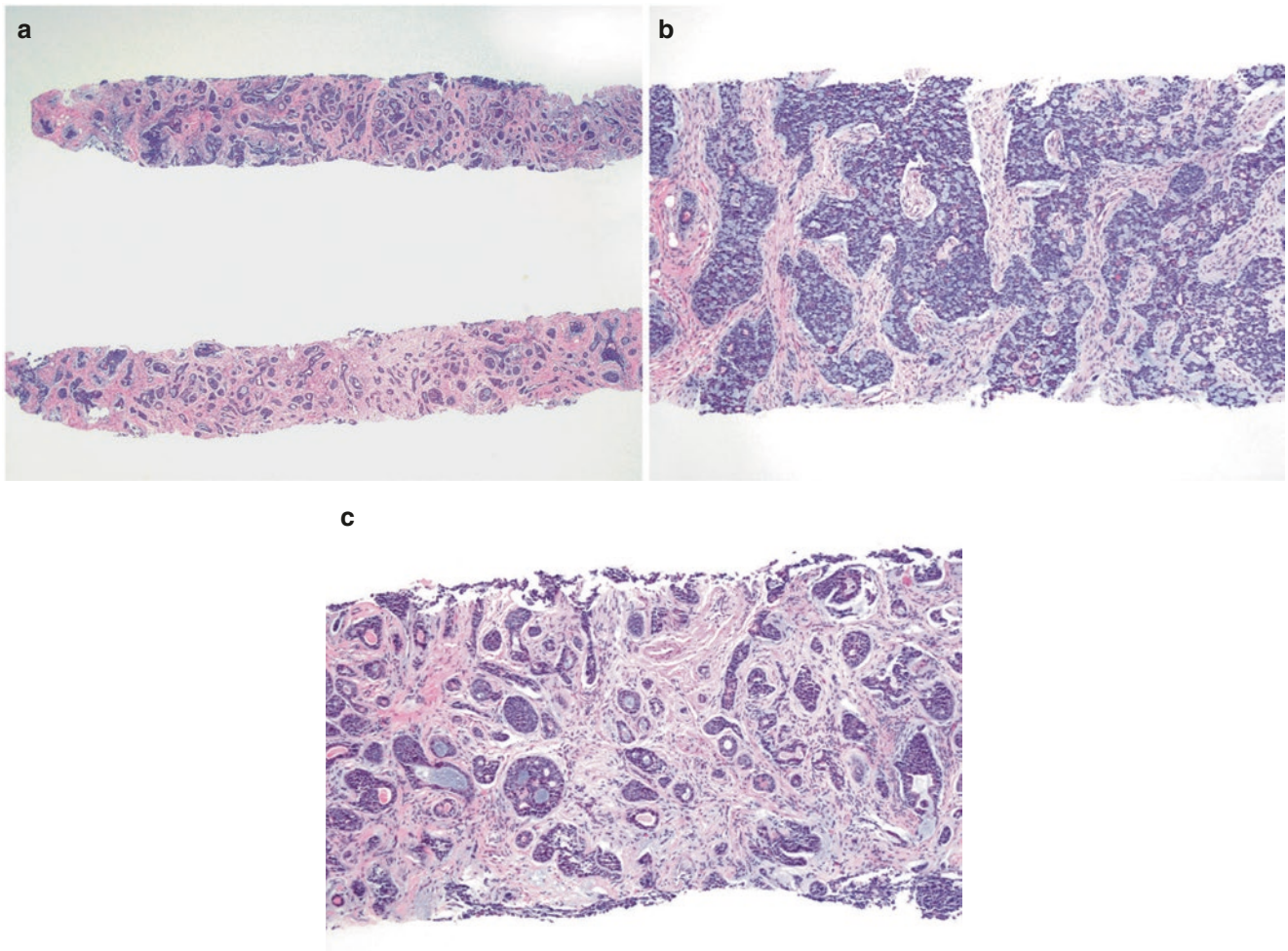

Fig. 12.3 Core needle biopsy of adenoid cystic carcinoma, mixed growth patterns. (**a**) This AdCC demonstrates varied growth patterns, (**b**) including some areas with irregular infiltrating trabeculae, (**c**) and other areas showing nested and glandular growth with focal cribriforming

tubular adenosis, papilloma, adenomyoepithelioma, and low-grade adenosquamous carcinoma [3, 23–25], suggesting a close relationship between breast lesions displaying biphasic epithelial–myoepithelial differentiation (Fig. 12.10). An in situ lesion with adenoid cystic features has been described [15, 23]. However, the distinction between in situ and invasive AdCC may be challenging.

Similar to its counterpart in the salivary gland but to a much lower frequency, AdCC of the breast can demonstrate perineural invasion [26, 27], which may be associated with the clinical finding of a painful breast mass (Fig. 12.11). Lymphatic tumor emboli are extremely uncommon in classic AdCC. As mentioned above, perineural invasion and lymphovascular invasion are more frequently observed in SB-AdCC. Despite being well circumscribed on imaging and gross evaluation, the tumor borders are usually at least focally infiltrative microscopically. In fact, scant tubular or cribriform glands may be noted at some distance (>1 cm away) from the grossly identified mass, sometimes in the form of perineural invasion. This feature may partly contribute to the local recurrence observed in some patients with AdCC after breast-conserving surgery.

Ro et al. suggested that AdCC can be stratified into three grades based on the proportion of solid growth within the tumor: grade I—no solid component; grade II—<30% solid component; and grade III—>30% solid component. Grade II and III tumors tended to be larger and were more likely to recur and rarely metastasize [3, 28]. However, the prognostic significance of this histologic grading scheme has not been confirmed by other studies [16, 29]. The current (eighth edition) American Joint Commission on Cancer staging manual recommends that the modified Scarf-Bloom-Richardson (SBR) grading system be applied for all breast cancer subtypes, including AdCC. Using the SBR grading system, most classic AdCC are grade 2, whereas SB-AdCC can be either grade 2 or 3 [18, 30]. Given the unclear significance of histo-

logic grading and the overall excellent prognosis of AdCC, except for the solid basaloid subtype, we generally do not grade these tumors on core needle biopsies (CNB).

Immunohistochemistry

The two different cell types of classic AdCC can be readily distinguished by immunohistochemistry. The myoepithelial cells are typically positive for high-molecular-weight cytokeratins (HMWCK; CK5/6, CK14, CK17) and a subset of myoepithelial cell markers (p63, smooth muscle actin [SMA], S100 protein), but are usually negative for other myoepithelial markers, which can include calponin, smooth muscle myosin (SMM), and CD10 (Figs. 12.12b–f, 12.13b, and 12.14c, d). This suggests an incomplete or aberrant myoepithelial phenotype. Which myoepithelial cell markers are positive or negative in a given tumor is not predictable. The luminal epithelial cells show positivity for CK7, CK8/18, CD117 (c-kit), epithelial membrane antigen (EMA), and car-

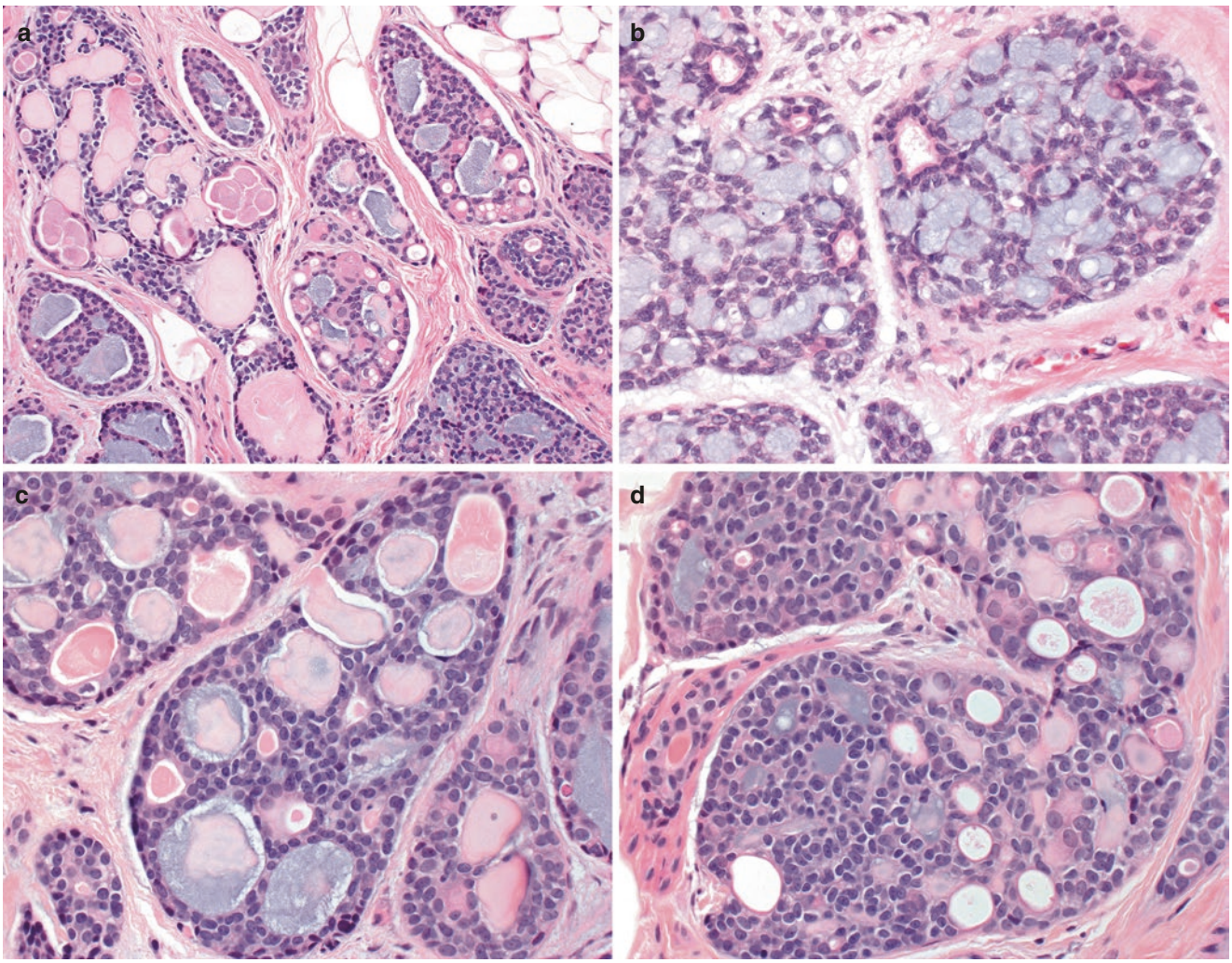

Fig. 12.4 True lumens and pseudolumens of adenoid cystic carcinoma. (**a**–**e**) Pseudolumens are lined by myoepithelial cells and often contain basement membrane material, which may appear as either loose myxoid substance or eosinophilic hyalinized spherules. In contrast, true glandular lumens are lined by luminal epithelial cells and may be empty or show intraluminal eosinophilic secretions. Immunostains for laminin (**f**) and (**g**) collagen type IV highlight the basement membrane material within pseudolumens

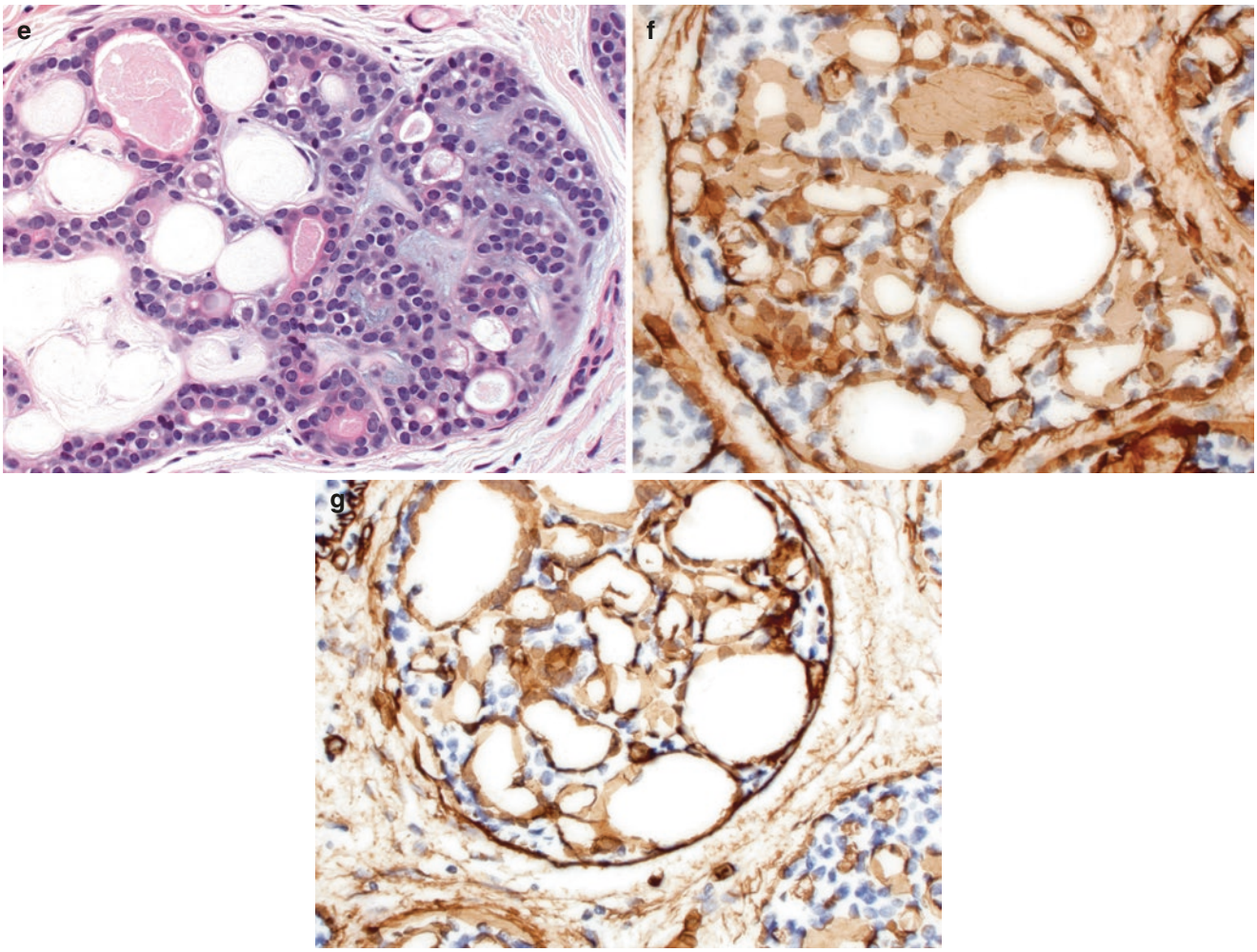

Fig. 12.4 (continued)

cinoembryonic antigen (CEA) [31] (Figs. 12.9c, 12.12f, 12.13c, and 12.14e). The basaloid cells in the SB-AdCC are often diffusely CK7 positive, and p63 may be negative or only focally positive, sometimes at the periphery of the tumor nests [15, 18, 30] (Figs. 12.9f and 12.15c). Therefore, negative or minimal staining for myoepithelial markers in a tumor with basaloid features does not exclude the diagnosis of SB-AdCC [15]. The MYB transcription factor is expressed predominantly in the myoepithelial cells of classic AdCC and is often positive in the basaloid cells of SB-AdCC [18, 32] (Figs. 12.14f and 12.15e). MYB expression is typically diffuse and strong in SB-AdCC on CNB, whereas only peripheral tumoral staining may be seen in some excised tumors, which may be due to short protein half-life and incomplete formalin fixation [18, 33]. SOX10 is expressed by both epithelial and myoepithelial cells [34] (Fig. 12.15d).

Expression of CD117, a tyrosine kinase receptor, is identified in virtually all AdCC. CD117 reactivity is usually limited to the ductular epithelial cells but may exhibit a more diffuse pattern in some cases, especially in SB-AdCC [18, 22] (Figs. 12.8c, 12.13c, and 12.14e). Although CD117 expression is helpful in the diagnosis of AdCC, this marker is not specific for this tumor type. Despite a high level of protein expression, recurrent *KIT* gene aberrations have not been identified [31].

AdCC are usually negative for estrogen receptor (ER) and progesterone receptor (PR) and consistently lack HER2 protein overexpression and gene amplification [35]. However, a small subset of AdCC may be ER/PR positive [15, 29, 35]. A novel 36 kDa isoform of ER (ER-α36) has been detected in AdCC [36]. Androgen receptor (AR) is usually negative [37, 38].

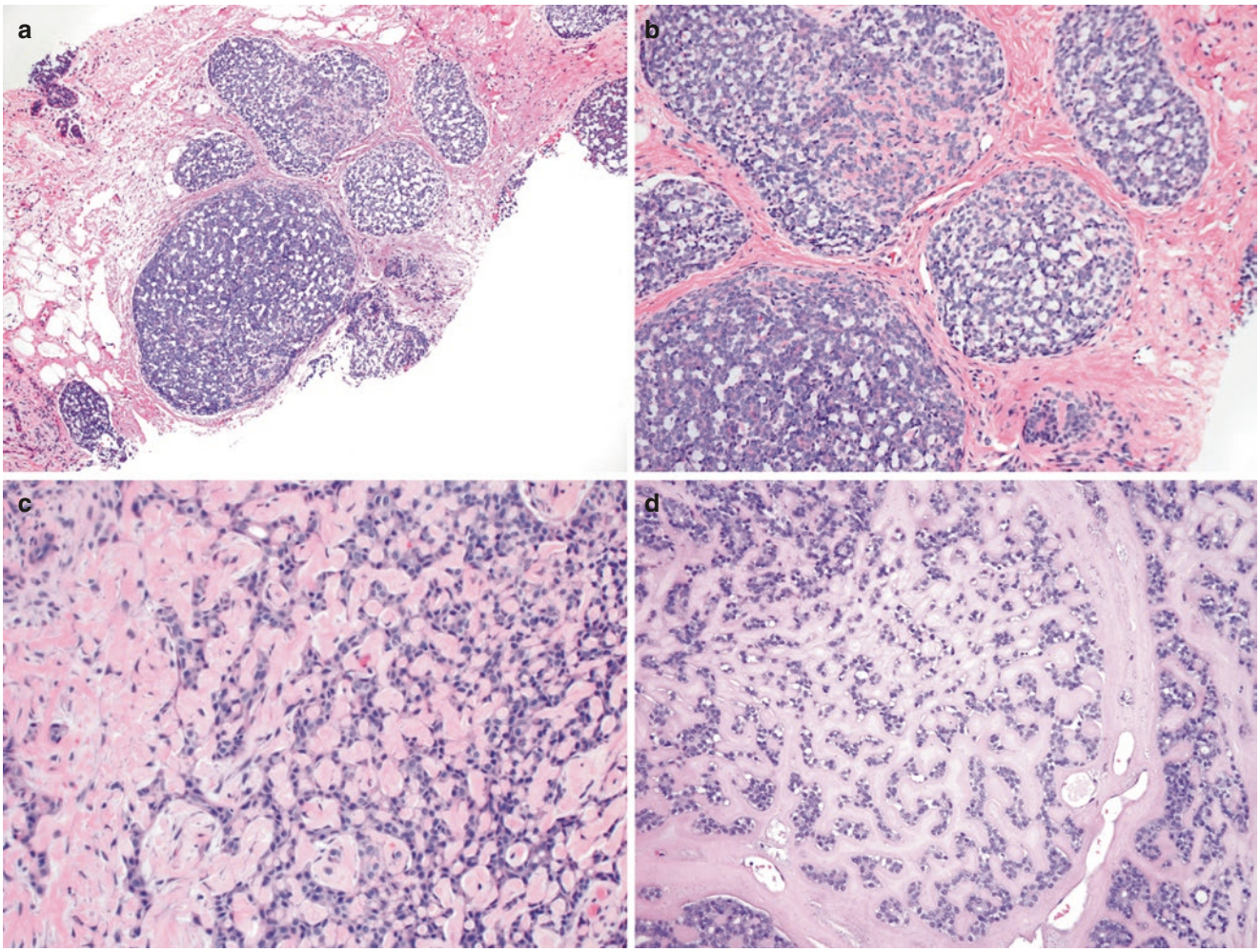

Fig. 12.5 Core needle biopsy of adenoid cystic carcinoma, reticular growth pattern. (**a**–**d**) The reticular growth pattern is characterized by neoplastic cells arranged as interconnected thin strands with associated myxoid or hyaline matrix. The matrix material may compress the glands

Although other TNBC generally have high proliferative activity, several studies have reported a low Ki-67 proliferation rate in classic AdCC (average ~5 to 10%) [18, 39, 40]. The SB-AdCC subtype, in agreement with increased mitotic count compared to classic AdCC, has a significantly higher Ki-67 proliferation index (average ~30%) [17, 18] (Fig. 12.15f).

Differential Diagnosis

The differential diagnosis of AdCC depends largely on the growth pattern. Cribriform pattern AdCC can mimic and be confused with invasive cribriform carcinoma, cribriform ductal carcinoma in situ (DCIS), and collagenous spherulosis, especially in small tissue samples obtained by CNB (Fig. 12.16a–f). The cribriform glands of invasive cribriform carcinoma are usually angulated, lined by a single population of luminal-type epithelial cells, and present within desmoplastic stroma. Luminal contents may contain calcifications and mucin. In contrast, cribriform AdCC demonstrates a dual cell population, with pseudolumens filled with basement membrane material. Immunophenotypically, invasive cribriform carcinoma is negative for myoepithelial markers and positive for ER and PR, whereas AdCC expresses at least some myoepithelial markers and is usually hormone receptor (HR) negative. Cribriform DCIS reveals a lobulocentric arrangement, with a single population of luminal-type epithelial cells comprising the proliferative component. Although myoepithelial cells are present in cribriform DCIS, they are limited to the periphery of the ducts and are not admixed with the epithelial cells as in AdCC. In

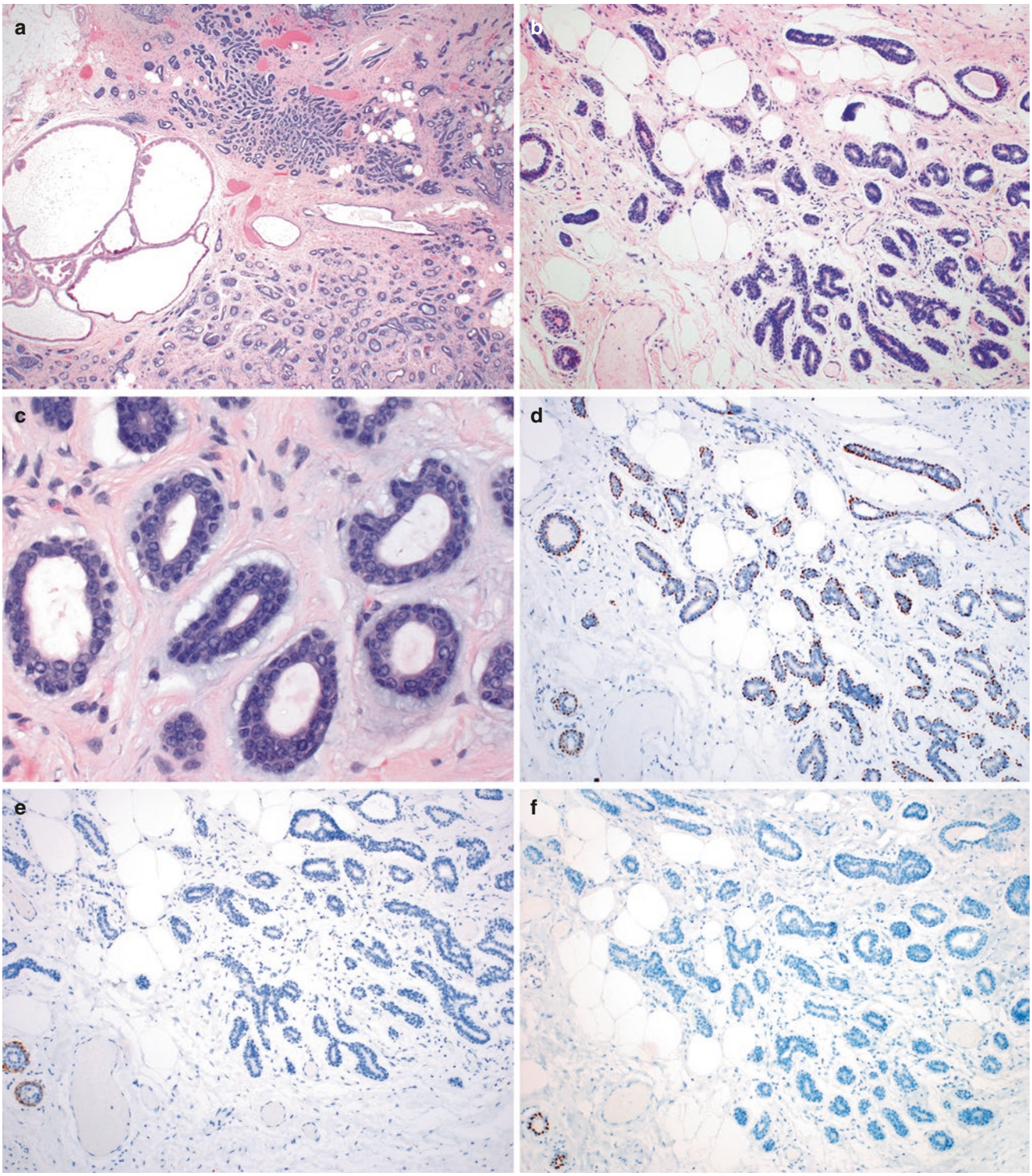

Fig. 12.6 Adenoid cystic carcinoma, tubular growth pattern. (**a**) The tubular growth pattern of AdCC demonstrates distinctly infiltrative ductules, (**b**, **c**) which on higher power are noted to be composed of luminal epithelial and abluminal myoepithelial cells. (**d**) The tubular glands show positive immunohistochemical staining for p63, which can be mistaken for a benign glandular proliferation such as a sclerosing lesion. Note the presence of two benign ducts in the lower left corner. Immunostains for other myoepithelial markers such as calponin (**e**) and SMM, and ER (**f**) are helpful in such cases, as calponin and SMM are usually negative in the neoplastic myoepithelial cells of AdCC but positive in myoepithelial cells associated with benign glandular lesions, while ER is negative in AdCC but patchy positive in benign glands

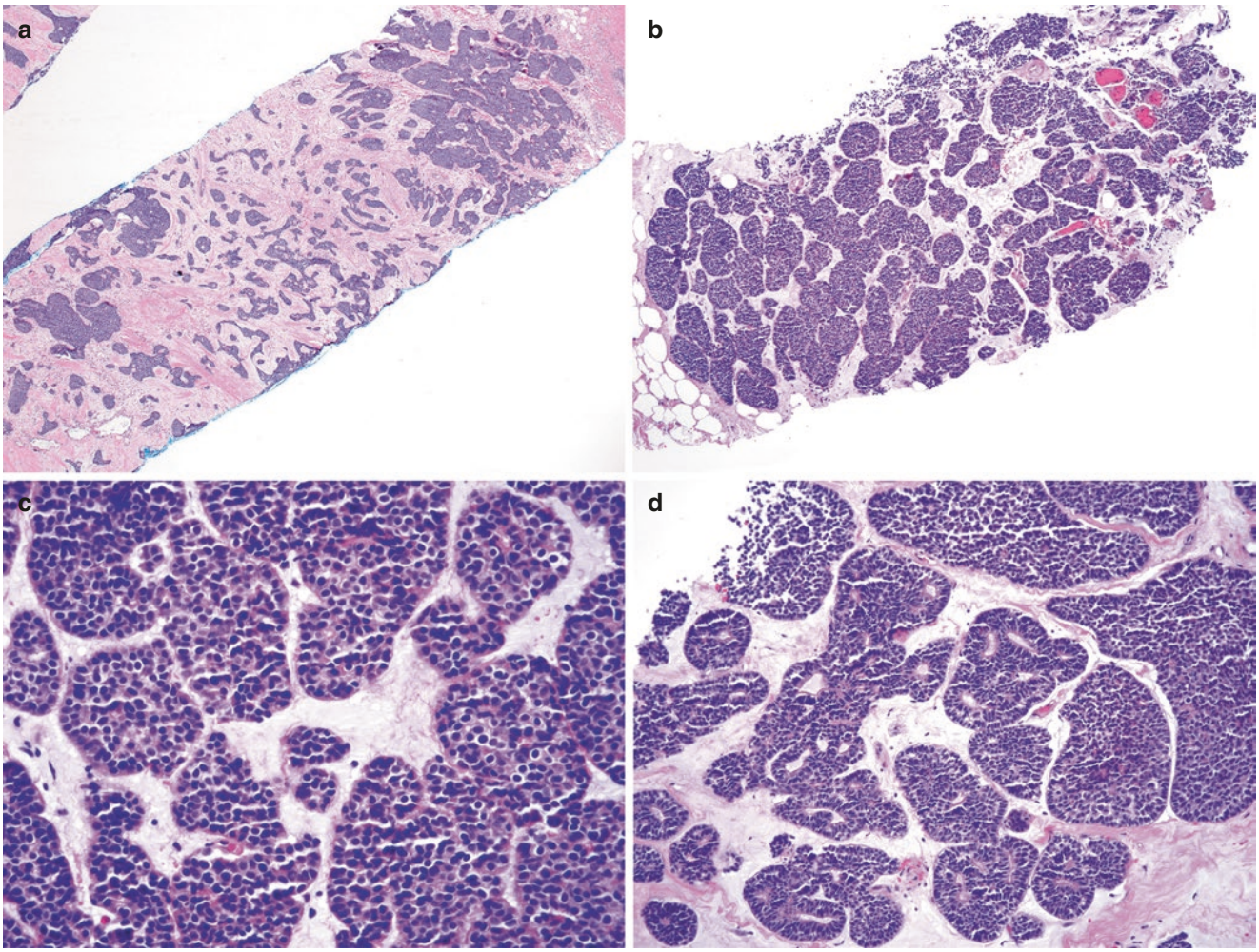

Fig. 12.7 Core needle biopsy of adenoid cystic carcinoma, solid-basaloid subtype. (**a**, **b**) Lower power view shows infiltrating irregular trabeculae and "geographic" solid nests in a hyalinized stroma. (**b**, **c**) Medium- and high-power views demonstrate solid nests of tumor cells with basaloid features. (**d**) Note the admixture of solid nests and focal cribriform growth in some areas

addition, cribriform DCIS is typically ER positive. CD117 immunoreactivity can be a helpful diagnostic adjunct in differentiating AdCC from invasive cribriform carcinoma and cribriform DCIS. The latter two cribriform lesions generally do not express CD117, as opposed to positive CD117 staining in most AdCC. However, it is important to note that lack of CD117 staining in a CNB does not necessarily exclude the cribriform pattern of AdCC, because CD117-positive ductular cells may be sparsely present. The distinction of AdCC from collagenous spherulosis may be challenging due to the biphasic nature of the epithelial–myoepithelial proliferation, the presence of true glandular and pseudolumens, and the accumulation of myxoid material and eosinophilic spherules shared by both lesions. However, collagenous spherulosis is a benign entity confined to preexisting ducts, lobules, or proliferative lesions and is not infiltrative. Furthermore, although both lesions demonstrate p63- and SMA-positive myoepithelial cells surrounding pseudolumens, the myoepithelial cells of AdCC often lack expression of SMM and calponin, whereas these markers are positive in the true myoepithelial cells of collagenous spherulosis (Fig. 12.16a–f). Figure 12.17 depicts a flow chart that is helpful in evaluating cribriform proliferations of the breast, and the characteristic immunoprofiles of these lesions are summarized in Table 12.1.

The tubular component of AdCC should be distinguished from tubular carcinoma, microglandular adenosis (MGA) and radial sclerosing lesion. Attention to the cellular components (single cell type versus biphasic epithelial-myoepithelial populations) and luminal contents (presence of basement membrane material) in conjunction with a selective panel of immunohistochemical markers are helpful to make the distinction, which are summarized in Table 12.2.

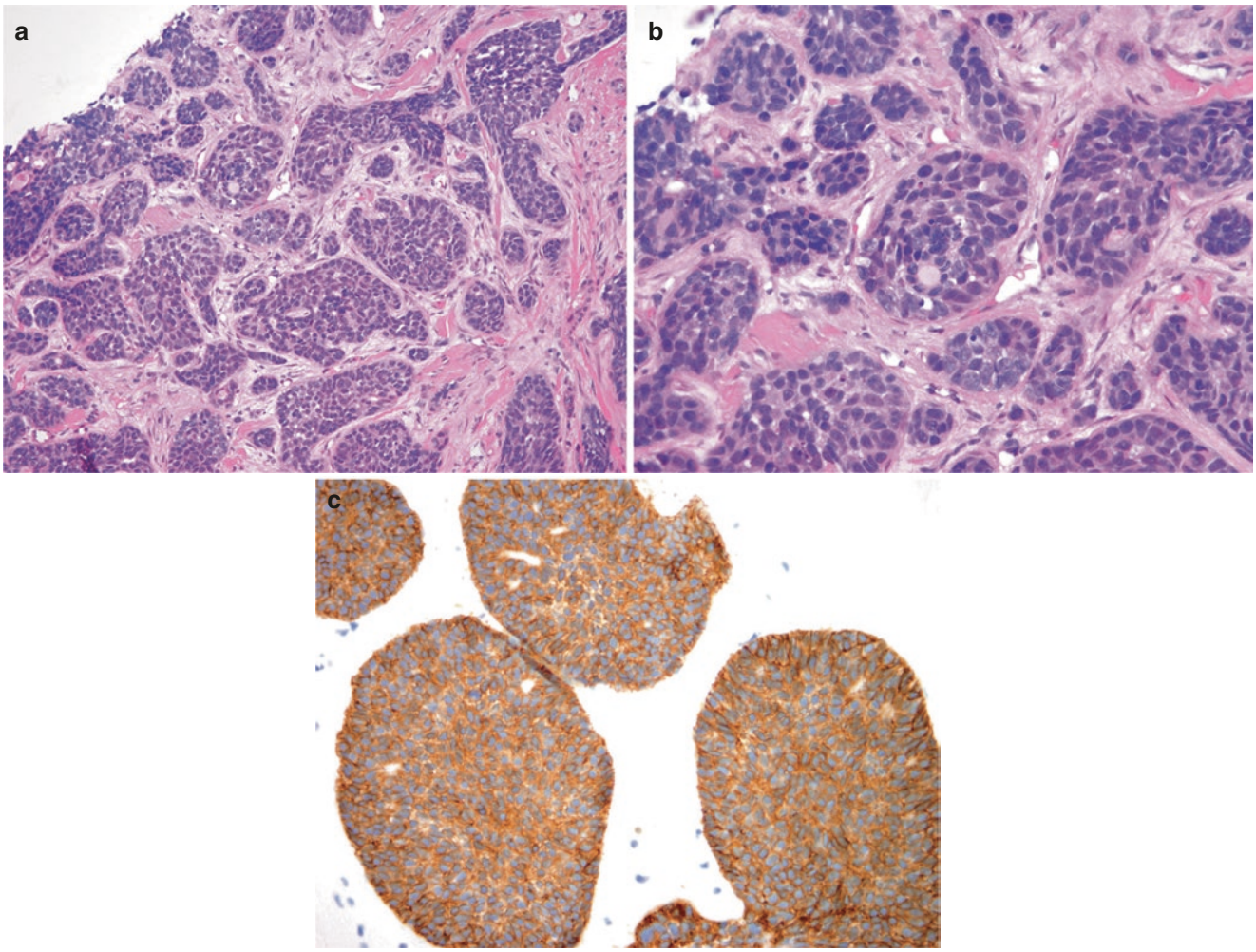

Fig. 12.8 Core needle biopsy of adenoid cystic carcinoma, solid-basaloid subtype. (**a**) High magnification reveals medium to large basaloid cells with scant cytoplasm, round to oval hyperchromatic nuclei, and inconspicuous nucleoli. The stroma is slightly desmoplastic in this case. (**b**) Note nuclear atypia is severe. (**c**) Diffuse positive immunostaining of the tumor cells for CD117

The main differential diagnosis for SB-AdCC includes high-grade IDC (especially tumors with basal-like features), small cell carcinoma (primary and metastatic), solid papillary carcinoma, Merkel cell carcinoma, lymphoma, and cylindroma of the breast. High-grade IDC with basal-like features often demonstrate large necrotic or fibrotic foci, pushing borders, and/or a prominent lymphoplasmacytic infiltrate. Small cell carcinoma is distinguished from SB-AdCC by prominent nuclear molding, necrosis with frequent apoptotic bodies, and significantly higher mitotic activity and Ki-67 proliferative index. In contrast to SB-AdCC, neuroendocrine markers may be positive in small cell carcinoma and Merkel cell carcinoma, the latter of which typically also expresses CK20 and neurofilament. Identification of intercalated ducts in SB-AdCC may be useful. In most cases, immunostains will be required to help establish the correct diagnosis. Table 12.3 summarizes the immunohistochemical markers useful in the workup of lesions with solid and "basaloid" features.

Cylindroma of the breast (dermal analog tumor) is a rare benign tumor with eccrine phenotype that can be confused with SB-AdCC, especially in CNB, as both tumors have nodular and trabecular patterns, basaloid cells with admixed duct structures, and hyaline globules of basement membrane material. However, infiltrative growth, cytologic atypia, mitotic activity, and lack of continuous, thickened basement membrane around tumor cell nests in SB-AdCC can help to differentiate the two. In addition, AdCC may be associated with mucin production, a feature not observed in cylindroma [41, 42].

Pathogenesis and Risk Factors

Although the origin of AdCC of the breast has been debated, it is generally accepted that this tumor is likely derived from undifferentiated cells that have the capacity to differentiate toward ductal and myoepithelial lineages [15, 16, 43].

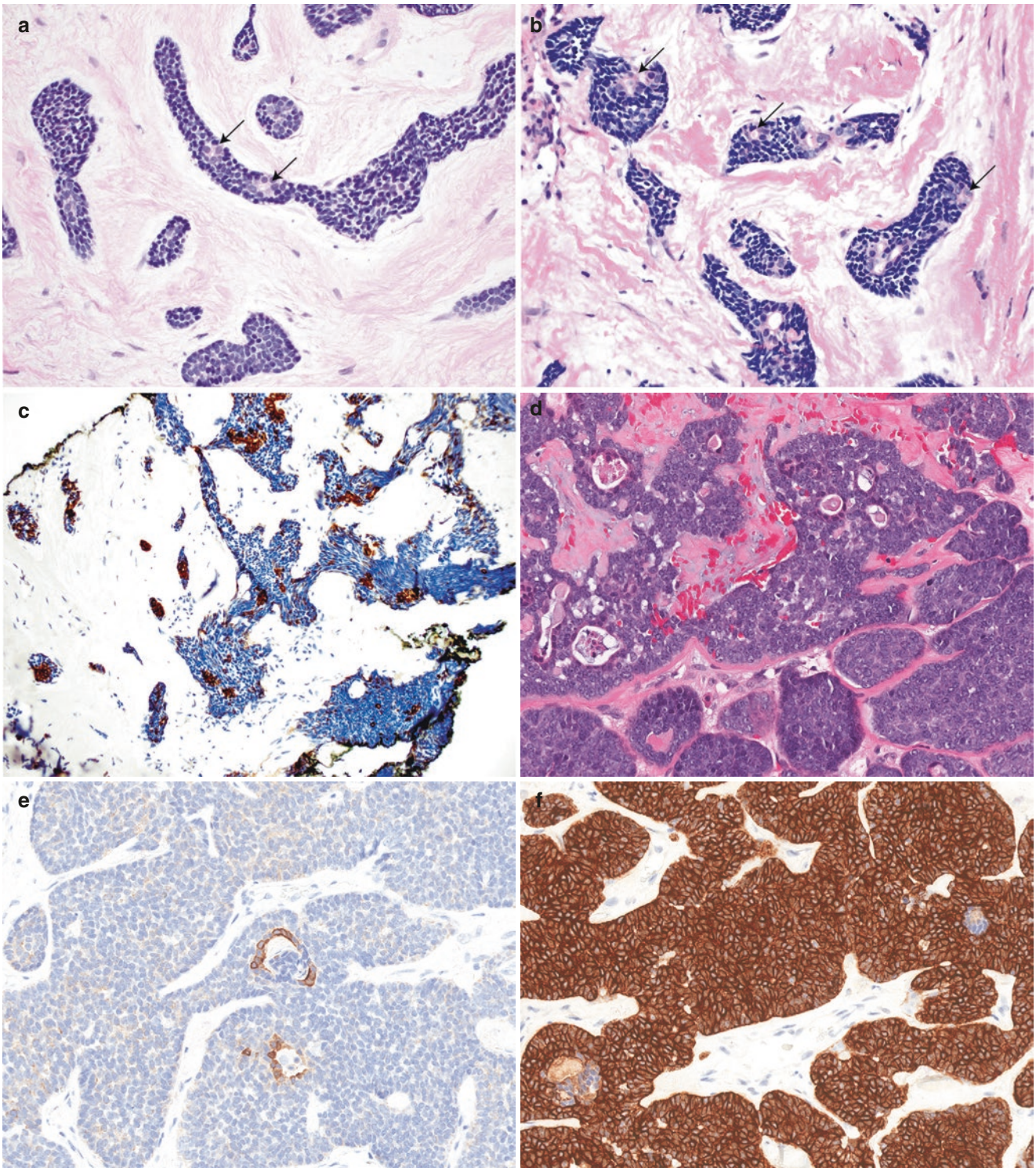

Fig. 12.9 Solid-basaloid subtype of adenoid cystic carcinoma, intercalated ducts. (**a**, **b**) Note slightly eosinophilic intercalated ducts subtly embedded within nests of dark basaloid cells. (**c**) CK7 highlights the glandular component and is negative in the basaloid cells. (**d**–**f**) Another example of SB-AdCC showing dispersed intercalated ducts within solid nests (**d**). The glandular component in this SB-AdCC is positive for CK5/6 (**e**) but negative for CK7 (**f**), while the basaloid cells are diffusely positive for CK7. These two examples illustrate that cytokeratin expression pattern is variable between different cases of SB-AdCC, likely reflecting the poorly differentiated state of the neoplastic cells

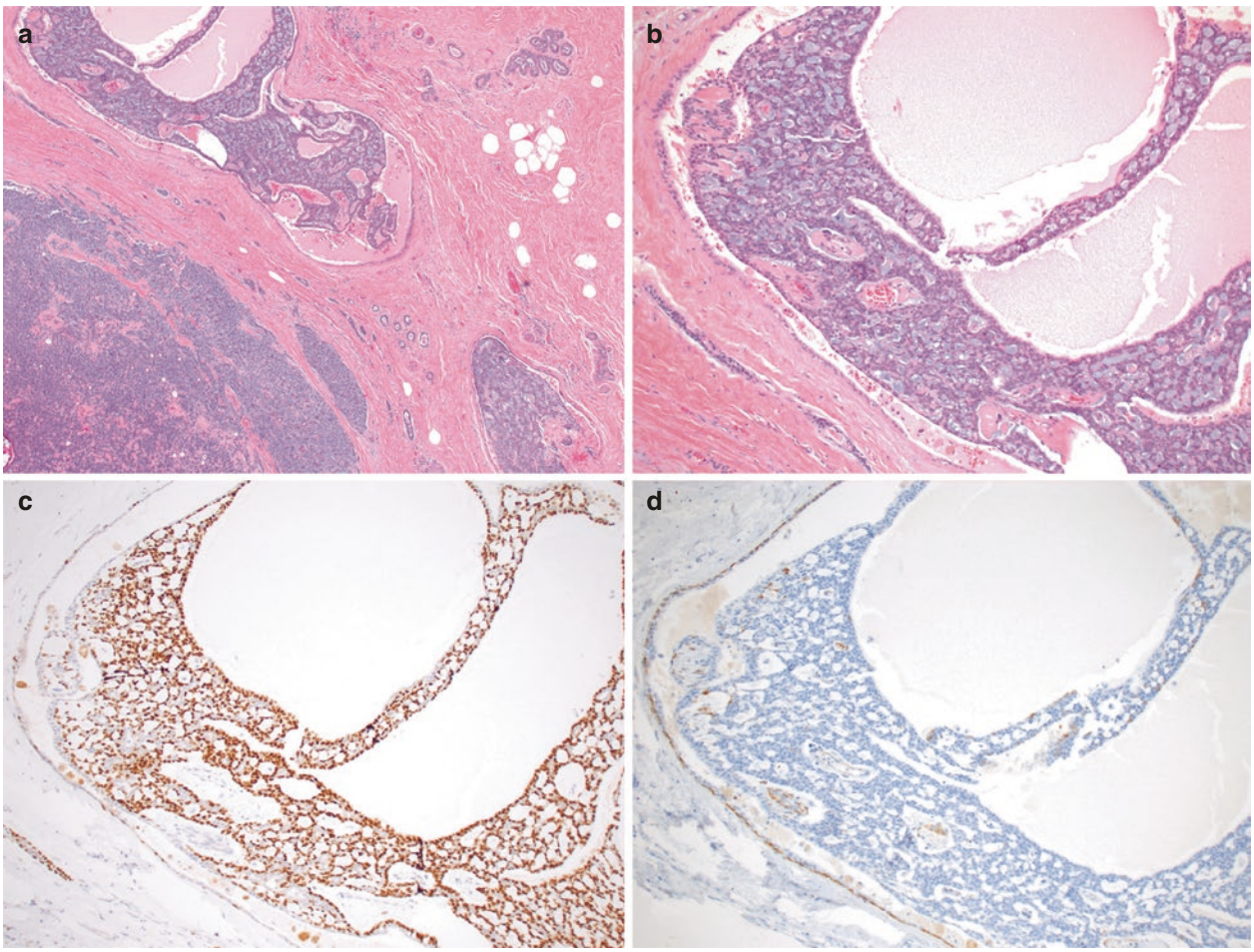

Fig. 12.10 Adenoid cystic carcinoma arising in association with intraductal papilloma. (**a**) This invasive AdCC (*lower left*) is arising in association with intraductal papillomas (*upper right*). (**b**) Higher power magnification demonstrates the typical biphasic epithelial and myoepithelial tumor cells of adenoid cystic carcinoma involving an underlying papilloma. Note the presence of residual papillary fibrovascular cores. (**c**) An immunohistochemical stain for p63 shows positive staining of the tumor cells and benign myoepithelial cells lining the periphery of the involved duct. (**d**) In contrast, an immunohistochemical stain for SMM is characteristically negative in the tumor cells but also highlights the benign myoepithelial cells of the involved duct

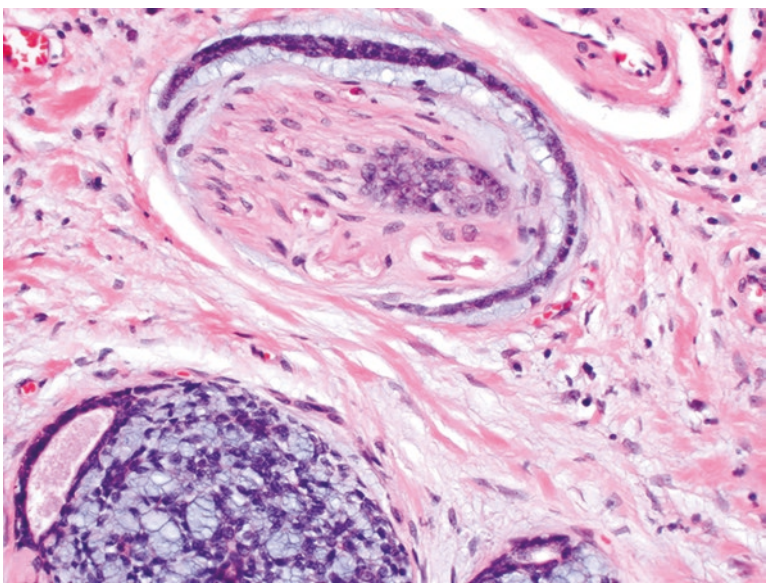

Fig. 12.11 Adenoid cystic carcinoma with perineural invasion. Similar to its counterpart in the salivary gland, albeit less frequently, AdCC of the breast can demonstrate perineural invasion and may be associated with clinical findings of a painful breast mass

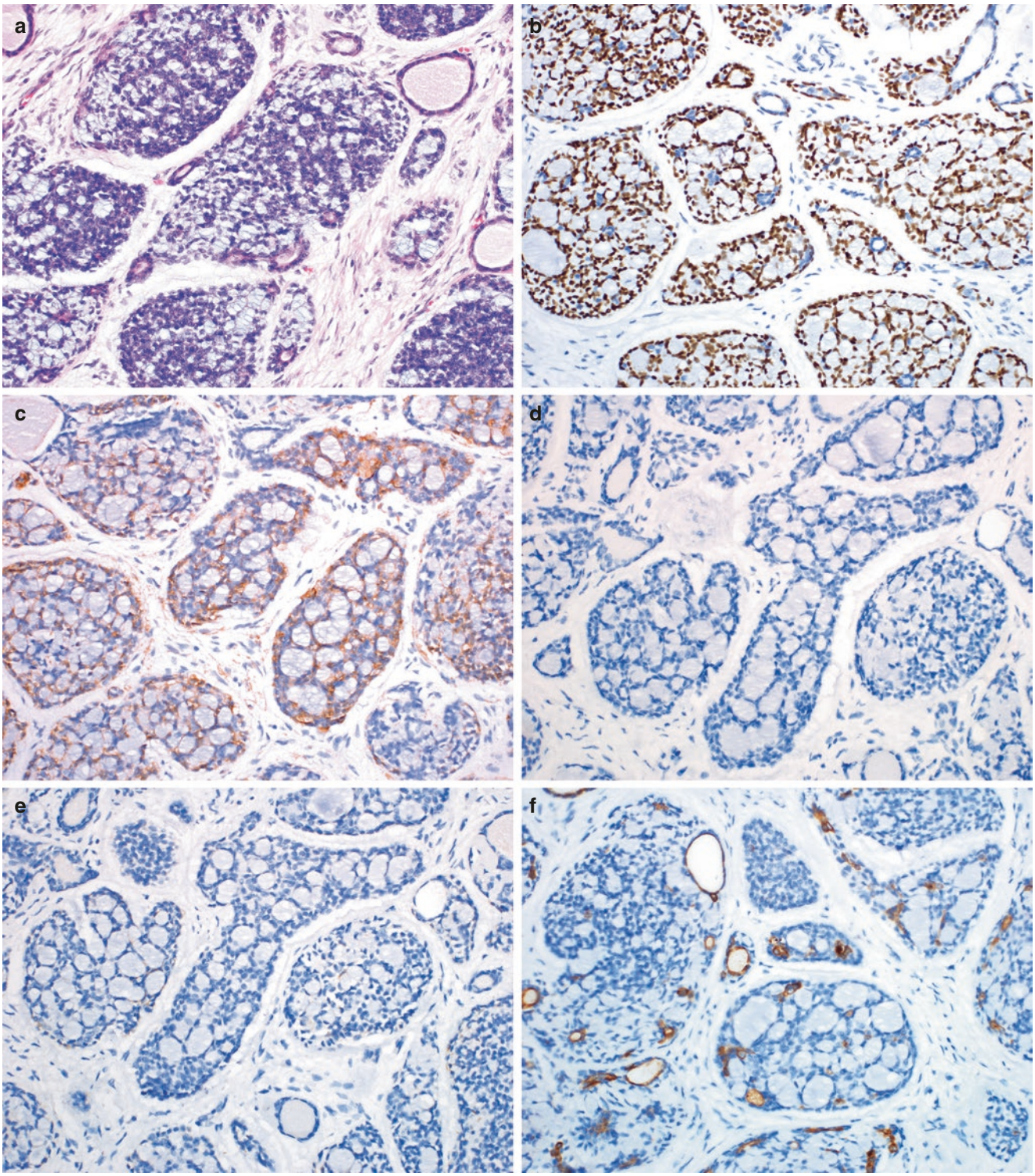

Fig. 12.12 Immunohistochemistry highlights the dual neoplastic cell populations in adenoid cystic carcinoma. (**a**) The neoplastic myoepithelial cells are immunopositive for (**b**) p63 and (**c**) SMA but are negative for (**d**) SMM and (**e**) calponin. In contrast, the neoplastic epithelial cells are decorated by (**f**) CK7

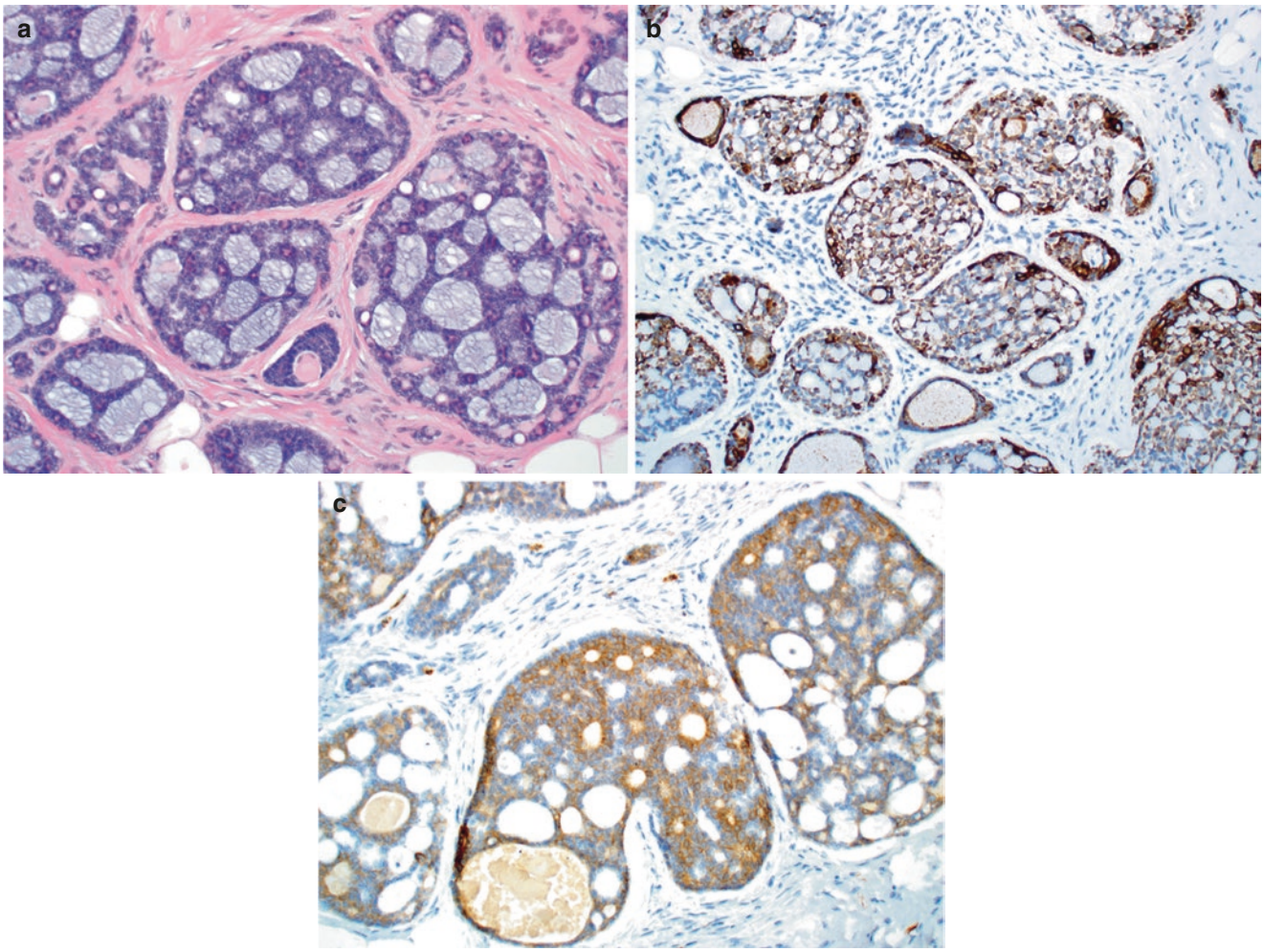

Fig. 12.13 Immunohistochemistry reveals a basal-like phenotype in AdCC. (**a**) This cribriform AdCC shows easily identified dual tumor cell populations. (**b**) The basaloid cells are typically immunoreactive for high-molecular-weight cytokeratins, such as CK5/6. (**c**) The basal marker CD117 is positive in most AdCC, often preferentially staining the luminal epithelial cells, as seen in this example

Similar to its counterpart at other anatomic sites, most classic AdCC of the breast harbor a t(6:9)(q22–23:p23–24) chromosomal translocation, which results in an expressed *MYB-NFIB* fusion gene [30, 44–46]. The fusion is thought to upregulate *MYB* RNA and MYB protein by removing microRNA binding sites in the *MYB* 3′ untranslated region or by super enhancer translocation [44]. The prevalence of *MYB-NFIB* is reported to be 33–100% in AdCC of the breast [39, 44, 47]. Alternate genetic drivers in AdCC lacking the *MYB-NFIB* fusion gene include *MYB* amplification, deletion of downstream sequences harboring presumed *MYB* regulatory element(s), and rearrangements involving *MYBL1*, which encodes A-MYB, a protein sharing extensive homology with c-MYB (encoded by *MYB*) [48]. In contrast to TNBC of no special type, classic AdCC have simple genomes, a low exonic mutation burden, and absence of *PIK3CA* and *TP53* mutations. Similar to salivary gland AdCC, classic breast AdCC harbor mutations in chromatin remodeling, cell adhesion, and canonical signaling pathway genes [45]. *MYB-NFIB* fusions are much less common (~13–19%) in SB-AdCC than classic AdCC [18, 30]. In contrast to classic AdCC and TNBC of no special type, SB-AdCC frequently harbor inactivating mutations in *CREBBP* and activating mutations in *NOTCH1* or *NOTCH2* [18]. SB-AdCC were also found to have less genomic instability and less frequent *TP53* mutations than TNBC of no special type [18]. The majority of AdCC (classic and SB-AdCC) express high levels of MYB protein, suggestive of a convergent phenotype in which activation of *MYB* and *MYBL1* and downstream targets can be driven by various mechanisms. Genetic analysis of AdCC with high-grade transformation is limited, but two tumors with transformation to high-grade TNBC were found

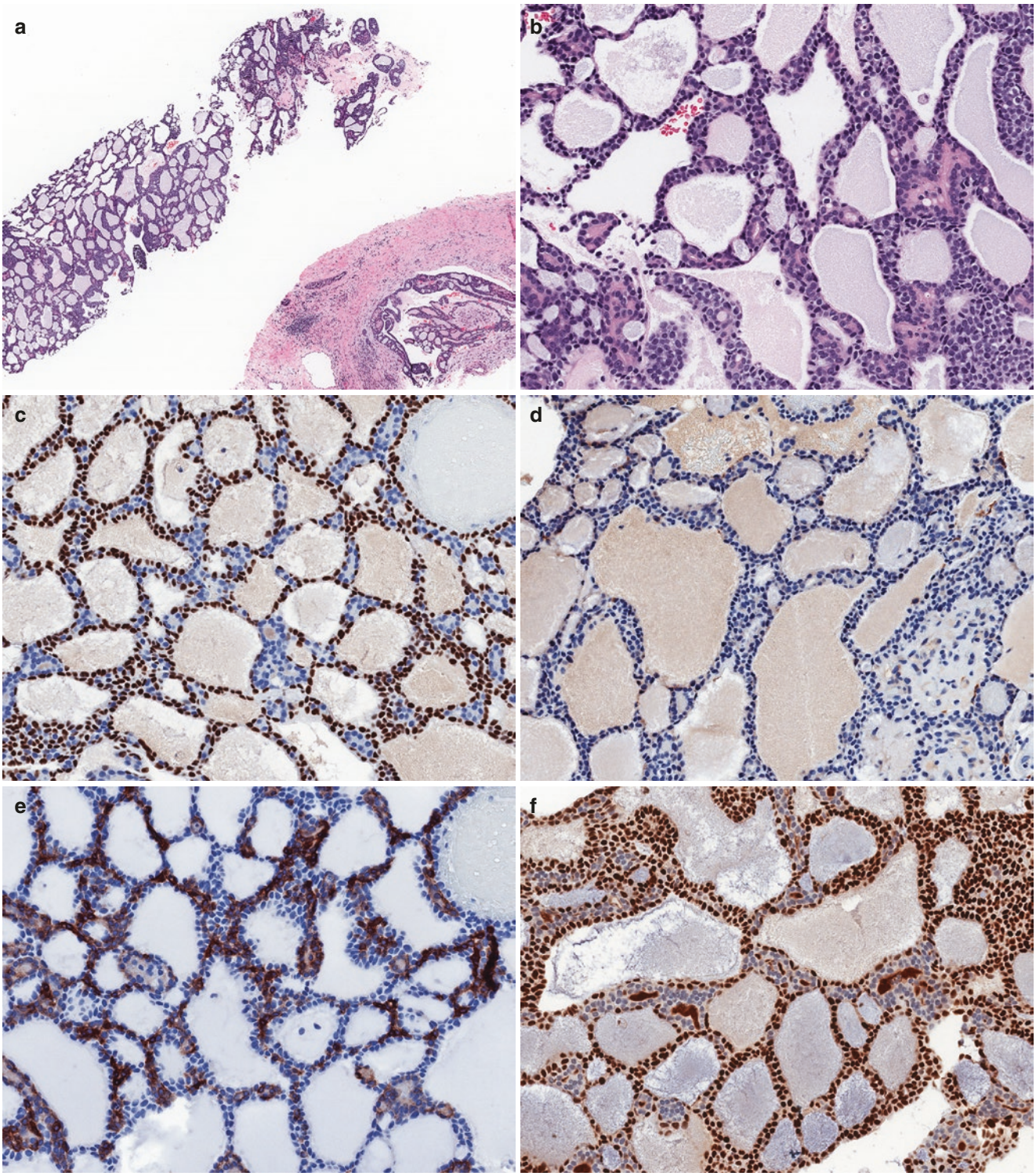

Fig. 12.14 Core needle biopsy of adenoid cystic carcinoma. (**a**) Low-power magnification shows an epithelial neoplasm arranged in cribriform growth pattern. (**b**) High magnification demonstrates dual neoplastic populations comprising basaloid cells surrounding larger lumens and slightly eosinophilic epithelial cells forming smaller lumens. Note the presence of lightly basophilic myxoid substance in the larger lumens. The basaloid cells are positive for p63 (**c**) and negative for calponin (**d**), while CD117 stain decorates the epithelial cells (**e**). The neoplastic cells show strong nuclear expression of MYB (**f**), predominantly in the basaloid cells. The morphologic features and immunophenotype support the diagnosis of AdCC, classic subtype

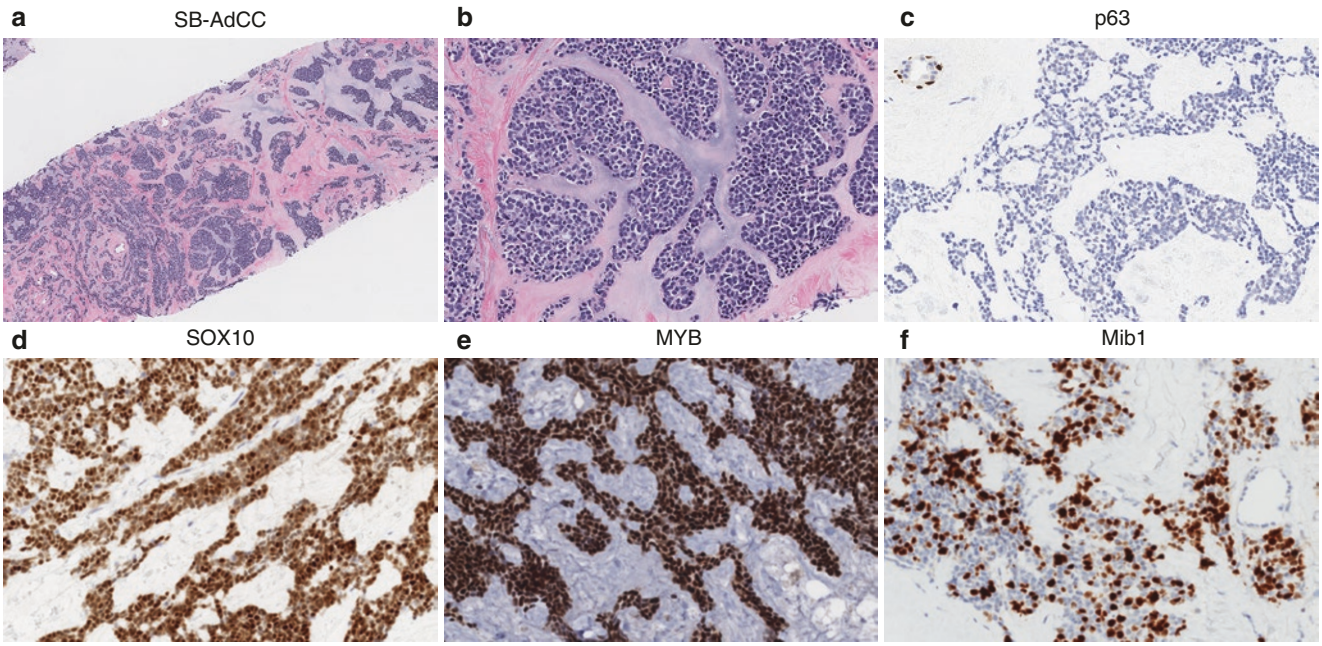

Fig. 12.15 Core needle biopsy of adenoid cystic carcinoma, solid-basaloid subtype. (**a**) Low-power view reveals an epithelial neoplasm infiltrating as irregular solid nests in a hyalinized and focally myxoid stroma. (**b**) High-power view demonstrates basaloid cells with high nuclear-to-cytoplasmic ratio and moderate to marked nuclear atypia. The neoplastic cells lack expression of myoepithelial markers p63 (**c**) and SMM (not shown) and are strongly positive for SOX10 (**d**) and MYB (**e**). The morphologic features and immunophenotype support the diagnosis of SB-AdCC. Note SB-AdCC has a higher Ki-67 proliferation index (**f**) than what is observed in classic AdCC

to harbor *MYB-NFIB* fusions in both the AdCC and high-grade TNBC components, with additional clonal aberrations in high-grade TNBC [20].

Because AdCC characteristically show MYB activation, MYB testing can be useful as a robust ancillary test in the workup of challenging cases where AdCC is included in the differential diagnosis. This includes (1) fluorescence in situ hybridization (FISH) using *MYB* break-apart probe, *MYB-NFIB* fusion probe, or *MYBL1* break-apart probe [30, 48] (Fig. 12.18a); (2) Next-generation sequencing, (3) detection of MYB protein overexpression by immunohistochemistry (Figs. 12.14f, 12.15e, and 12.18b) [18, 32, 48]; and (4) *MYB* RNA in situ hybridization (ISH) [49, 50]. FISH is very specific but least sensitive. Immunohistochemistry (with a positive result defined as strong staining in ≥50% tumor cells) is sensitive and readily available in many laboratories, but less specific. Immunohistochemistry is overall likely to be more useful in CNB than excision specimens due to poor staining in central areas of some excised tumors, which is likely related to fixation [18, 48]. In the salivary gland, *MYB* RNA ISH has been shown to provide superior sensitivity for the diagnosis of AdCC compared with *MYB* FISH and superior specificity compared with MYB immunohistochemistry [49].

AdCC displays a triple-negative and basal-like phenotype and clusters with basal-like breast cancers by gene expression profiling [37, 43, 51]. However, in contrast to other triple-negative tumors such as metaplastic carcinomas, AdCC forms a separate subgroup within the basal-like group by hierarchical clustering [37]. These findings further support the distinction of AdCC as a specific subtype of basal-like cancer. Some AdCC may belong to the claudin-low molecular subgroup, which is characterized by stem cell-like features and low expression of claudins, E-cadherin, and proliferation genes [31]. A characteristic CD44+/CD24—stem cell marker immunophenotype, which has been associated in some studies with tumor initiation, progression and survival and resistance to therapy, has been observed in AdCC [31, 52].

Prognosis and Clinical Management

Recognition of AdCC as a distinct subtype of TNBC is of clinical relevance due to the indolent behavior and excellent prognosis of classic AdCC [3, 4, 28]. Classic AdCC presents mostly as a localized disease (pathologic stage T1 or T2) with a low incidence of lymph node (0–5%) or dis-

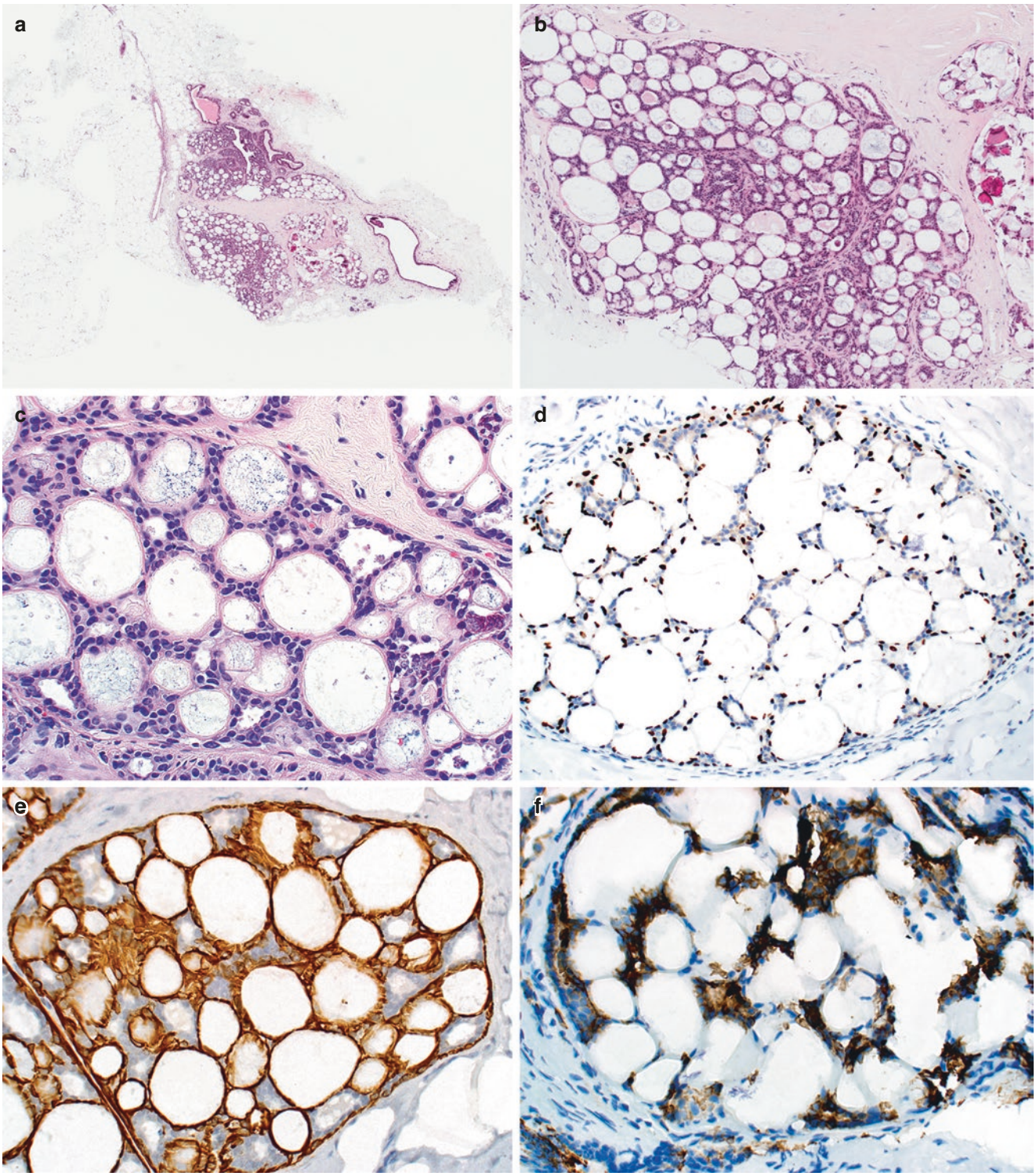

Fig. 12.16 Collagenous spherulosis (CS). (**a**, **b**) Core needle biopsy of CS, showing cribriform glands with associated calcifications. (**c**) The cribriform pattern with dual epithelial and myoepithelial cell populations and the presence of basement membrane material within pseudolumens can mimic the cribriform pattern of AdCC. Note the eosinophilic cuticles lining pseudolumens of CS, which are not a feature of AdCC. Immunohistochemical stains for (**d**) p63 and (**e**) SMM highlight the myoepithelial cells of CS, whereas neoplastic myoepithelial cells of AdCC are often negative for SMM. (**f**) The luminal epithelial cells of CS are immunoreactive for CAM5.2

tant (<3%) metastasis at the time of diagnosis [2, 51]. The most common sites of distant metastases are the lung and bone [2, 27, 53], in contrast to other TNBC, which frequently affect the brain and lung. At variance with TNBC of no special type, which usually recurs within the first 3 years after diagnosis, AdCC can recur both locally and with metastatic disease many years after the initial presentation. However, even with local recurrence or distant metastases, these patients have a prolonged and indolent clinical course, with a 10-year survival of 90–100% [38, 53, 54]. Death from AdCC of the breast is extremely unusual [55]. The development of a second malignancy following the diagnosis of AdCC has been documented, and all patients should continue to be followed for this risk [2, 53, 56].

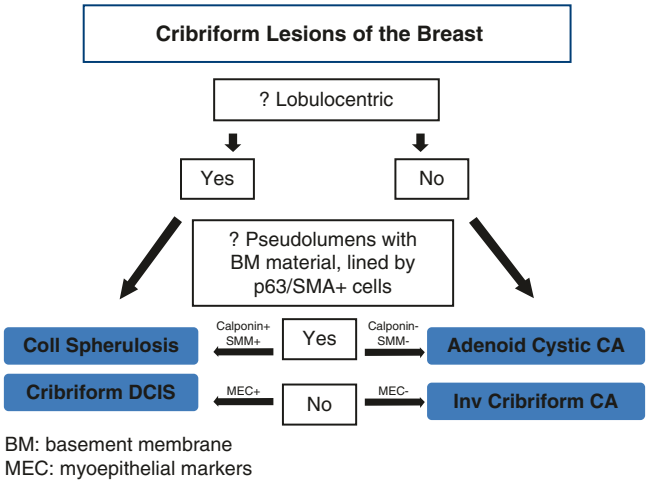

Fig. 12.17 Flow chart for cribriform proliferations of the breast

Limited data in the literature provide either no evidence or conflicting results on the prognostic value of histologic or nuclear grading and proliferative activity [16, 28, 29]. However, SB-AdCC appears to be associated with a more aggressive clinical course, with increased risk of axillary lymph node involvement and distant metastasis [17, 18, 30, 31]. Even with metastasis, patients with SB-AdCC may survive for an extended period, suggesting that this subtype is not as aggressive as high-grade TNBC of no special type.

Table 12.1 Immunophenotype of cribriform breast lesions

Immunostain	AdCC	Invasive cribriform carcinoma	Cribriform DCIS	Collagenous spherulosis
p63 and SMA	Myoepithelial cells +	–	Periphery of duct +	Myoepithelial cells within and at periphery of duct +
Calponin and SMM	Usually –	–	Periphery of duct +	Myoepithelial cells within and at periphery of duct +
Low-molecular-weight keratins (CK7, CAM5.2)	Epithelial cells +	Diffusely +	Diffusely +	Epithelial cells +
CD117	+, Usually in epithelial cells	–	–	– To patchy + in epithelial cells
Estrogen receptor (ER)	Usually –	Diffusely +	Diffusely +	Epithelial cells patchy +

Table 12.2 Morphologic features and immunohistochemical markers helpful in the distinction of tubular variant adenoid cystic carcinoma from histologic mimics

Histopathologic features	AdCC (tubular variant)	Tubular carcinoma	Microglandular adenosis	Radial sclerosing lesion
Cell types	Epithelial and myoepithelial	Epithelial	Epithelial	Epithelial and myoepithelial
Luminal contents	True lumens: Mucin or eosinophilic secretions Pseudo lumens: Myxoid or hyalinized basement membrane material	+/– Calcifications	PASD-positive colloid-like eosinophilic secretions	+/– Calcifications
Immunohistochemistry for myoepithelial markers (p63, SMM, calponin, SMA)	Positive for p63 and SMA; often negative (or variable staining) for calponin and SMM	Negative for all myoepithelial markers	Negative for all myoepithelial markers	Positive for all myoepithelial markers (attenuation in some cases)
Estrogen receptor	Negative	Diffusely and strongly positive	Negative	Positive, patchy staining with variable intensity
Other immunohistochemical markers	Diffusely and strongly positive for MYB (predominantly in myoepithelial cells)		Strongly positive for S100 protein; negative for MYB	

Table 12.3 Immunohistochemical markers useful in the distinction of solid basaloid AdCC from histologic mimics

	Pankeratin	CK 7	CK 20	p63	TTF-1	NSE	SYN	CHROMO	LCA
SB-AdCC	+	+[a]	–	–/+[b]	–	–	–	–	–
Small cell carcinoma (primary)	+[c]	+	–	–	–/+	+	+/–	+/–	–
Small cell carcinoma (secondary from lung)	+[c]	–	–	–	+	+	+/–	+/–	–
Merkel cell carcinoma of the skin	+[c]	–	+	–	–	+	+/–	+/–	–
Lymphoma	–	–	–	–	–	–	–	–	+

[a] Positive in basaloid cells
[b] Often negative or only focally positive
[c] May be patchy and weak, with perinuclear dot-like pattern

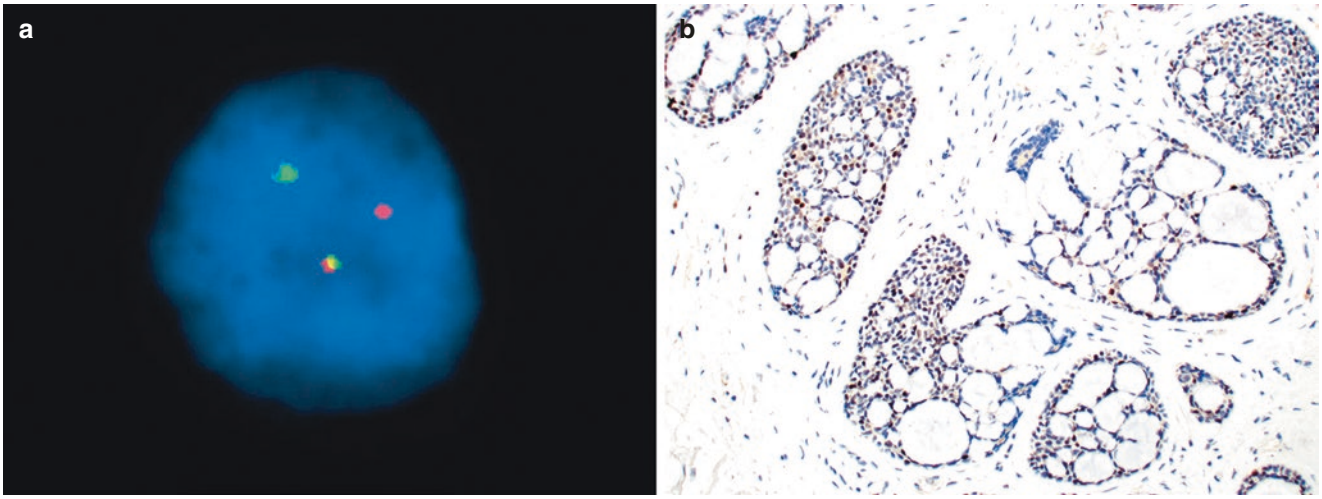

Fig. 12.18 *MYB-NFIB* translocation and MYB protein overexpression in adenoid cystic carcinoma. (**a**) Fluorescence in situ hybridization demonstrates evidence of *MYB* rearrangement (*MYB* break-apart probe). (**b**) The *MYB-NFIB* fusion results in MYB overexpression, which is highlighted by MYB immunostaining in this example of AdCC

Due to the rarity of AdCC in the breast, there is no consensus on the optimal management of patients with these tumors [33]. Current treatment generally includes complete surgical resection with or without axillary sentinel lymph node sampling or adjuvant radiotherapy [29]. In one study, a high rate (42%) of positive surgical margins was observed after breast-conserving surgery [57]. Reported recurrence rates ranged from 6 to 37% after local excision only [26, 29, 53, 56]. A large study from the California Cancer Registry reported a significant benefit for adjuvant radiotherapy on overall survival and disease-specific survival in patients with AdCC [58], and some suggest that postoperative radiation should be considered for all patients after lumpectomy irrespective of margin status, given the high rate of positive margins after breast-conserving surgery [55, 59]. Most patients are not eligible for hormonal therapy due to negative hormonal receptor status. For most patients with classic AdCC, chemotherapy is likely not indicated [60]. More frequent axillary and distant metastases in SB-AdCC may suggest a role for chemotherapy in patients with this rare subtype, and most reported SB-AdCC cases in the literature have received chemotherapy. Given their frequency in SB-AdCC, activating *NOTCH* mutations could be a potential future therapeutic target [61].

Tall Cell Carcinoma with Reversed Polarity

Overview and Clinical Presentation

Tall cell carcinoma with reversed polarity (TCCRP) is a rare triple-negative invasive breast carcinoma with characteristic histologic and molecular features, an indolent clinical course, and favorable prognosis [62–66]. TCCRP was first described by Eusebi et al. [62] in 2003 as "breast tumor resembling tall cell variant of papillary thyroid carcinoma" because of its morphological resemblance to papillary thyroid carcinoma (PTC), with less than 100 cases reported in the literature since [62, 64–78]. This tumor has also been referred to as "solid papillary carcinoma with reverse polarity" [63] and "solid papillary carcinoma resembling the tall cell variant of papillary thyroid carcinoma" [62–64, 66,

79]. The fifth edition of the WHO classification of breast tumors has included TCCRP as a distinct type of invasive breast carcinoma [80].

TCCRP primarily affect patients in the sixth decade (range of 39–89 years, median age 64), with all reported cases having been in women [63–78, 81, 82]. TCCRP usually presents as a palpable and well-defined nodule that is occasionally tender to palpation [71], or less frequently as a screen-detected non-palpable lesion with associated microcalcifications [64, 68, 70–73, 75, 77, 78].

Gross and Radiologic Features

On gross evaluation, TCCRP usually appears as a well-circumscribed, firm, white to gray mass ranging in size from 0.6 to 8.5 cm, with an average of 2.6 cm [62, 66–69, 72, 75, 77, 78]. The cut surface is generally solid and grayish-white to tan in color [77]. A brownish, translucent, multinodular cut surface resembling hyperplastic thyroid tissue may occasionally be observed [67].

TCCRP is often interpreted as benign on mammography or ultrasound examination due to its circumscribed margins. On mammography, these tumors present either as a mass or pleomorphic calcifications [68, 77]. On ultrasound, they can appear either as a round, mildly hypoechoic mass with microlobulated margins without acoustic shadowing [68, 70] or a well-circumscribed, hypoechoic mass with mixed posterior shadowing and enhancement and increased vascularity [77].

Microscopic Features

TCCRP has distinct morphology with cytoarchitectural features analogous to the tall cell variant of PTC. At low power, most tumors have overall pushing margins (Fig. 12.19a); however, focal infiltrative growth into fat and entrapment of benign glands can usually be appreciated on closer evaluation, which may help suggest an invasive process, especially in a CNB specimen [63, 64, 78] (Figs. 12.19b and 12.20). The tumor is composed of multiple circumscribed nests and nodules of epithelial cells haphazardly distributed in stroma. In some cases, the cellular nests are arranged in a jigsaw pattern (Fig. 12.20). Many of the nodules are solid and contain thin papillae with delicate fibrovascular cores, creating a solid papillary pattern, whereas others are partly cystic with more conspicuous papillae, imparting a papillary appearance [62, 63, 65, 66] (Fig. 12.21a, c). Aggregates of foamy histiocytes are frequently present within the fibrovascular cores (Fig. 12.21b). Foci of cystically dilated glands or follicle-like structures containing eosinophilic amorphous colloid-like material with a scalloped periphery, reminiscent of a thyroid follicular pattern, can be seen in some tumors [64, 66] (Fig. 12.21d). The tumoral stroma is usually collagenous with little to no desmoplasia. Networks of small capillary-like vessels are present in a delicate garland-like fashion encircling the tumor nests [64, 83].

Cytologically, the tumor cells in TCCRP are cuboidal to tall columnar, usually with abundant granular eosinophilic cytoplasm (Fig. 12.22). Occasionally, the cytoplasm can be less granular but strongly eosinophilic [64]. The characteris-

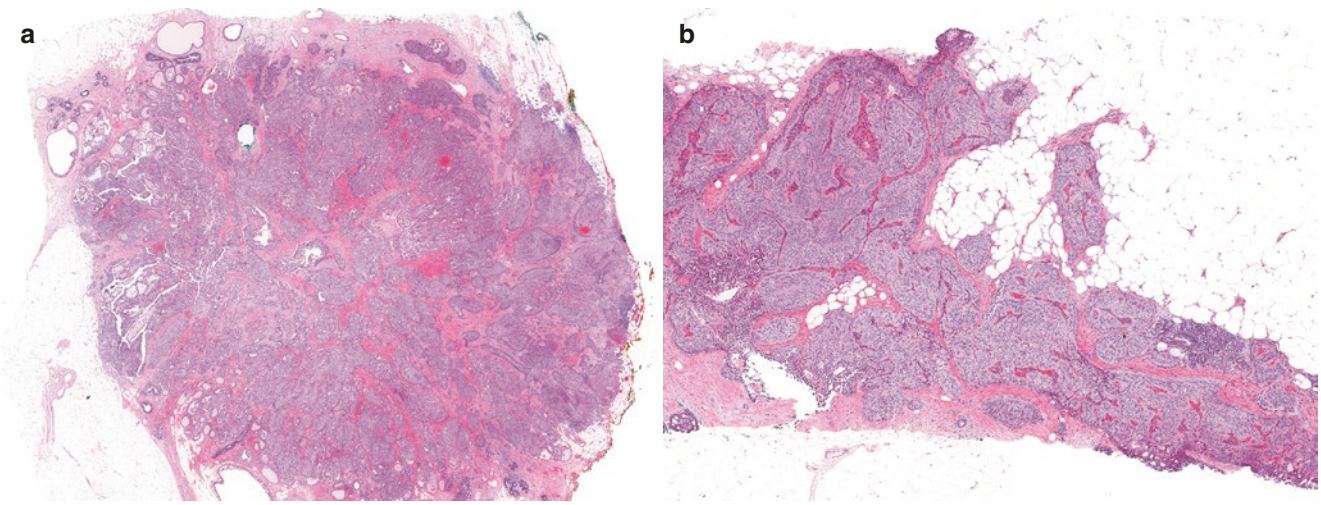

Fig. 12.19 Tall cell carcinoma with reversed polarity, tumor border. (**a**) Whole mount view of an excision for TCCRP demonstrates an overall circumscribed tumor with pushing margins that is often observed in this neoplasm. Note that the tumor is composed of multiple nodules and nests in the background of fibrotic stroma. (**b**) A CNB of TCCRP shows relatively circumscribed tumor-stroma interface, but with infiltration of tumor nests into fat

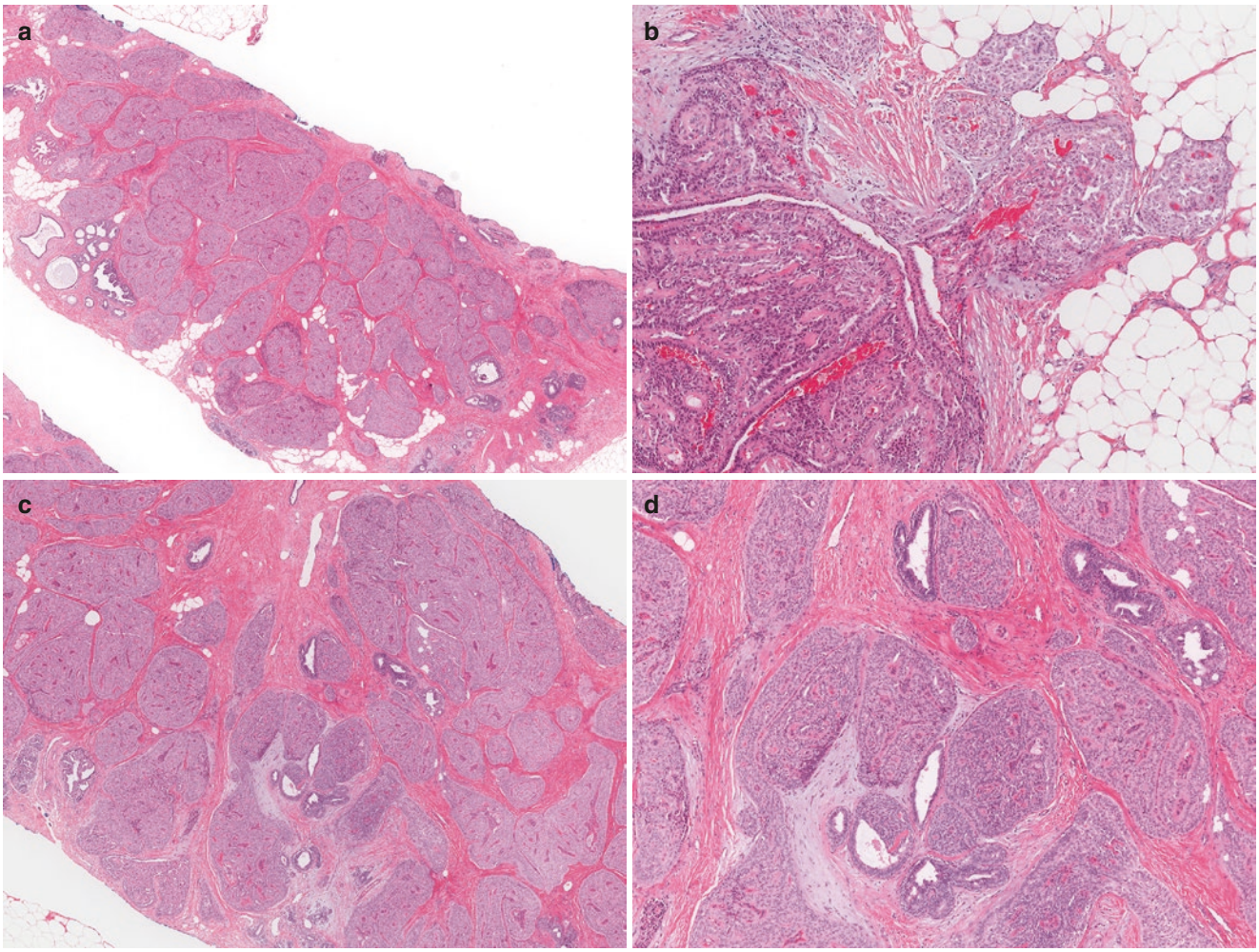

Fig. 12.20 Core needle biopsy of tall cell carcinoma with reversed polarity. (**a**) This example of TCCRP shows multiple solid circumscribed nodules haphazardly distributed throughout the breast stroma imparting a jigsaw pattern. (**b**) The presence of focal tumor nests in the fat raises the possibility of an invasive process in a CNB. (**c**) Low magnification demonstrates circumscribed solid papillary nodules growing around and between normal ducts, suggesting an invasive lesion. (**d**) Higher magnification further highlights normal ducts between tumor nodules. The stroma of TCCRP is typically collagenous and fibrotic, but may rarely show focal desmoplasia (lower central field)

tic cytoplasm has been shown to reflect the presence of abundant mitochondria using an anti-mitochondrial antibody [62, 66]. The neoplastic cells have round to oval, low- to intermediate-grade nuclei that often exhibit optical clearing, nuclear grooves, stratification, and cytoplasmic pseudoinclusions [62–65, 72, 78], similar to the nuclei of PTC (Fig. 12.22c). The most distinguishing cytologic feature is reverse polarization, with the nuclei localized to the apical or adluminal, rather than at the basal, pole of the columnar tumor cells [62–65, 72, 77] (Fig. 12.22d–f). Psammoma bodies [77] or granular calcifications may be identified within the colloid-like material or associated with the proliferative epithelium [62, 64, 66, 68, 77]. Mitotic activity is generally low, and there is no necrosis, or vascular or perineural invasion. Areas of mucinous differentiation or apocrine metaplasia may rarely be present [77]. Using the Nottingham grading system, most tumors are histological grade 1, receiving 2 points for nuclear grade, 1 point for mitotic activity, and 2 points for glandular differentiation.

An in situ component has been described in some cases of TCCRP [66]. The distinction between in situ and invasive cancer can be challenging in tumors that are composed of well-circumscribed round nodules, but myoepithelial markers such as p63 and SMM are helpful [63, 64]. Foci of flat epithelial atypia (FEA) have been observed at the periphery of the tumor in a few cases [64].

Immunohistochemistry

TCCRP typically shows strong and diffuse cytoplasmic expression for low-molecular-weight keratins (LMWCK,

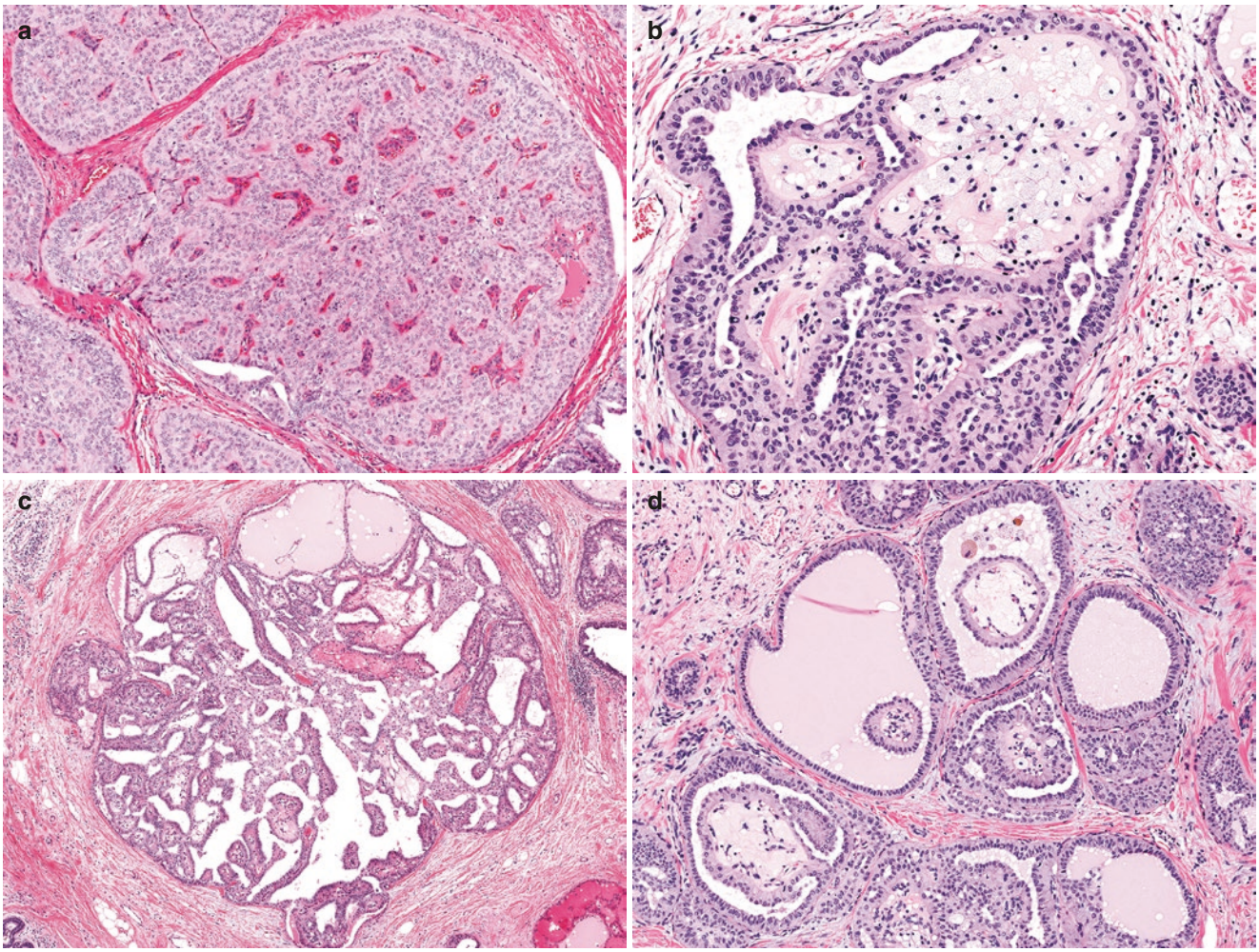

Fig. 12.21 Tall cell carcinoma with reversed polarity, architectural patterns. Tumor cells in TCCRP can be arranged in various growth patterns. (**a**) A major pattern is characterized by solid nodules containing thin papillae with delicate fibrovascular cores, imparting a solid papillary appearance. (**b**) The fibrovascular cores of tumor nodules often contain aggregates of foamy histiocytes. (**c**) Some tumor nodules are partly cystic with more conspicuous papillae, creating a frankly papillary appearance. (**d**) A follicular pattern features cystically dilated glands containing eosinophilic colloid-like material with a scalloped periphery, resembling thyroid follicles

e.g., CK7, CK19) and HMWCK (e.g., CK5/6, CK14 and CK34bE12) [62, 64, 66, 76] (Fig. 12.23). The tumor cells are also immunoreactive for calretinin (diffuse or focal), S100 protein, mitochondrial antigen (accentuated at the basal pole), CEA, and BCL-2 [64, 65, 69, 71]. Despite the morphologic resemblance to PTC, TTF-1, thyroglobulin, and HBME 1 are negative [70, 76, 77]. Breast origin is confirmed by variable staining for GATA3, mammaglobin, and GCDFP-15 (Fig. 12.23f, g), which are positive in ~60% of cases [64, 71, 75, 76].

E-cadherin stain shows strong lateral membrane expression with absent apical or basal expression, whereas MUC1 and EMA highlight localization of the nucleus to the apical aspect of the tumor cells (Fig. 12.23h), supporting the morphologic impression of reverse polarity [63]. No myoepithelial cells are identified along the fibrovascular cores or at the periphery of the papillary, solid, or follicular structures with immunohistochemical stains for p63, calponin, SMM, and CD10 [64, 65, 69, 71, 78] (Fig. 12.23b, c). The lack of a peripheral myoepithelial layer, together with the haphazard distribution of the tumor nodules and infiltrative growth, supports TCCRP as an invasive process.

TCRRPs are usually negative for ER and PR and consistently lack HER2 protein overexpression and gene amplification (Fig. 12.23i). However, a small subset of TCCRP may show weak and focal ER and PR expression in 1–10% of tumor cells [63, 66, 69, 77]. Most cases have either absent or low AR expression, arguing against apocrine differentiation [64, 82]. The Ki-67 proliferation index is low (Fig. 12.23j), ranging from 1 to 5% in most tumors [64, 65, 69, 71]. The rich capillary network around tumor nests can be highlighted by vascular markers, such as CD31, ERG, or CD34.

Antibodies against IDH2 R172 mutant proteins have been shown to be highly sensitive (>90%) and specific (100%) for

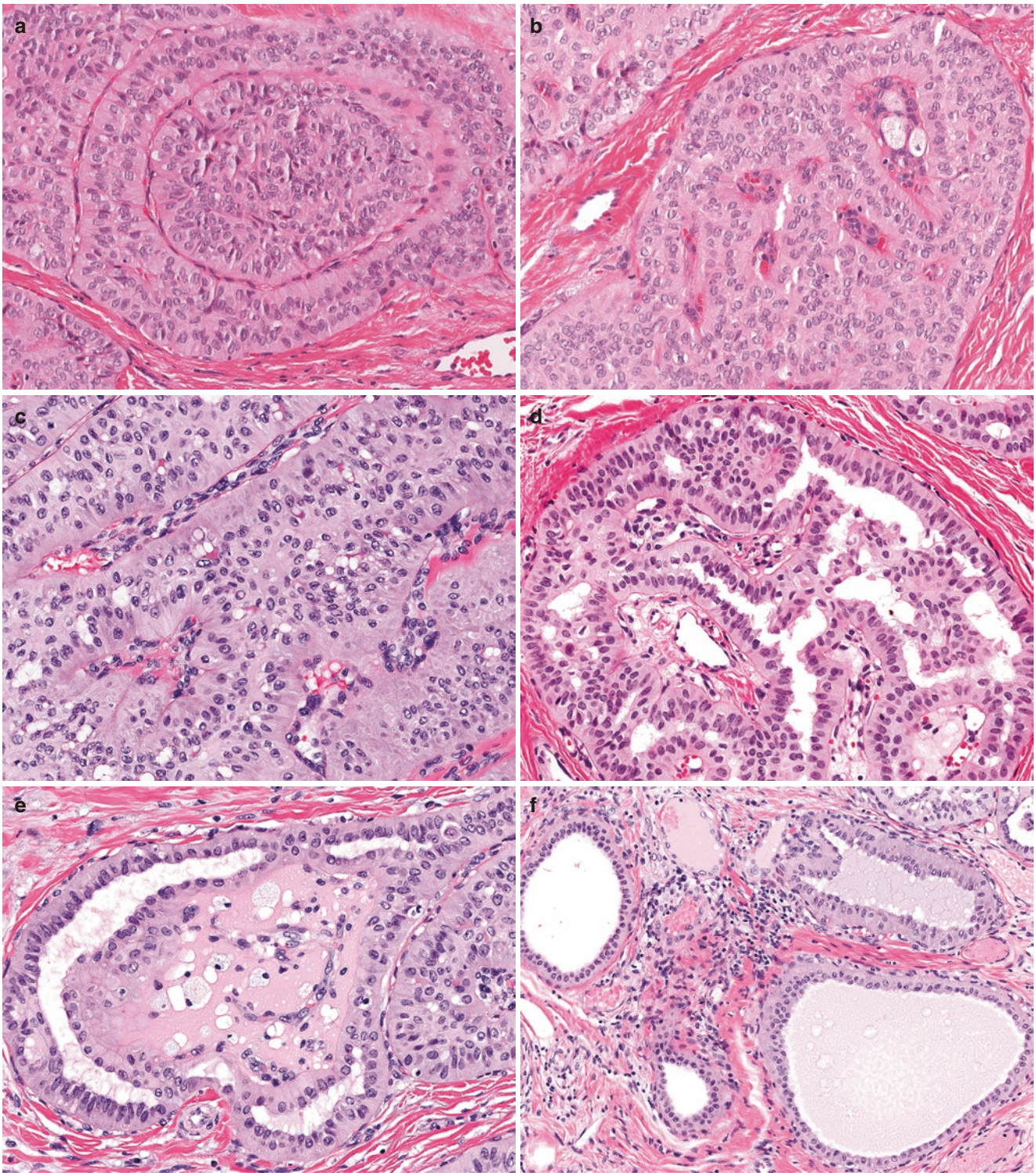

Fig. 12.22 Tall cell carcinoma with reversed polarity, cytologic features. (**a**, **b**) The tumor cells are tall columnar with abundant eosinophilic cytoplasm and low- to intermediate-grade nuclei. (**c**) The nuclei are crowded and overlapping and exhibit nuclear grooves with scattered cytoplasmic pseudoinclusions, features mimicking thyroid papillary carcinoma. (**d**–**f**) These images highlight the characteristic reverse polarization of TCCRP in which the nuclei are localized in the apical rather than at the basal poles of the neoplastic columnar cells

the detection of the *IDH2* R172 hotspot mutations in TCCRP, including in CNB [75, 82]. Using an antibody directed at IDH2 R172S, all tumors with either *R172S* or *R172T* mutations were found to be immunoreactive, showing diffuse and strong staining with a cytoplasmic granular pattern (Fig. 12.24). The single tumor in this study with *IDH2* R172I

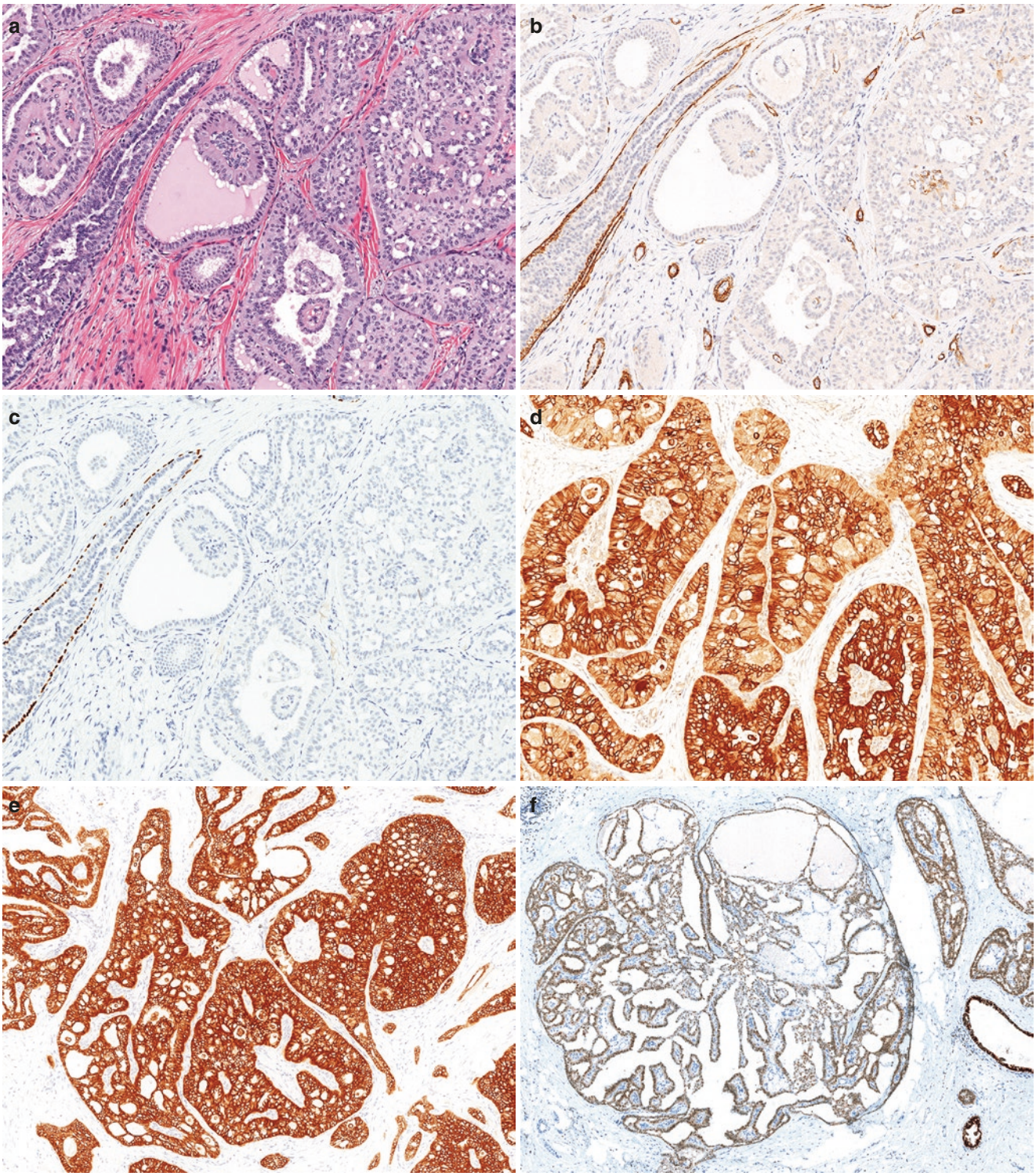

Fig. 12.23 Tall cell carcinoma with reversed polarity, immunophenotype. (**a**–**c**) Although the tumor nests are circumscribed with a rounded contour on H&E section (**a**), they lack an investing myoepithelial layer as shown by the SMM (**b**) and p63 (**c**) immunostains, supporting the invasive nature of TCCRP. Note the absence of myoepithelial cells both at the periphery of the tumor nodules and along all the fibrovascular cores, while the entrapped benign ducts are positive for SMM and p63. The neoplastic cells demonstrate diffuse and strong expression of both HMWCK CK5/6 (**d**) and LMWCK CAM5.2 (**e**). Breast markers GATA3 (**f**) and mammaglobin (**g**) are variably positive in the tumor cells. (**h**) An EMA immunostain decorates the apical side of the columnar cells where the nuclei are situated, confirming the reversed polarity of TCCRP. (**i**) The majority of these tumors are negative for ER (note positive staining in the entrapped normal ducts), PR (not shown), and HER2 (not shown). (**j**) The Ki-67 proliferation index is low

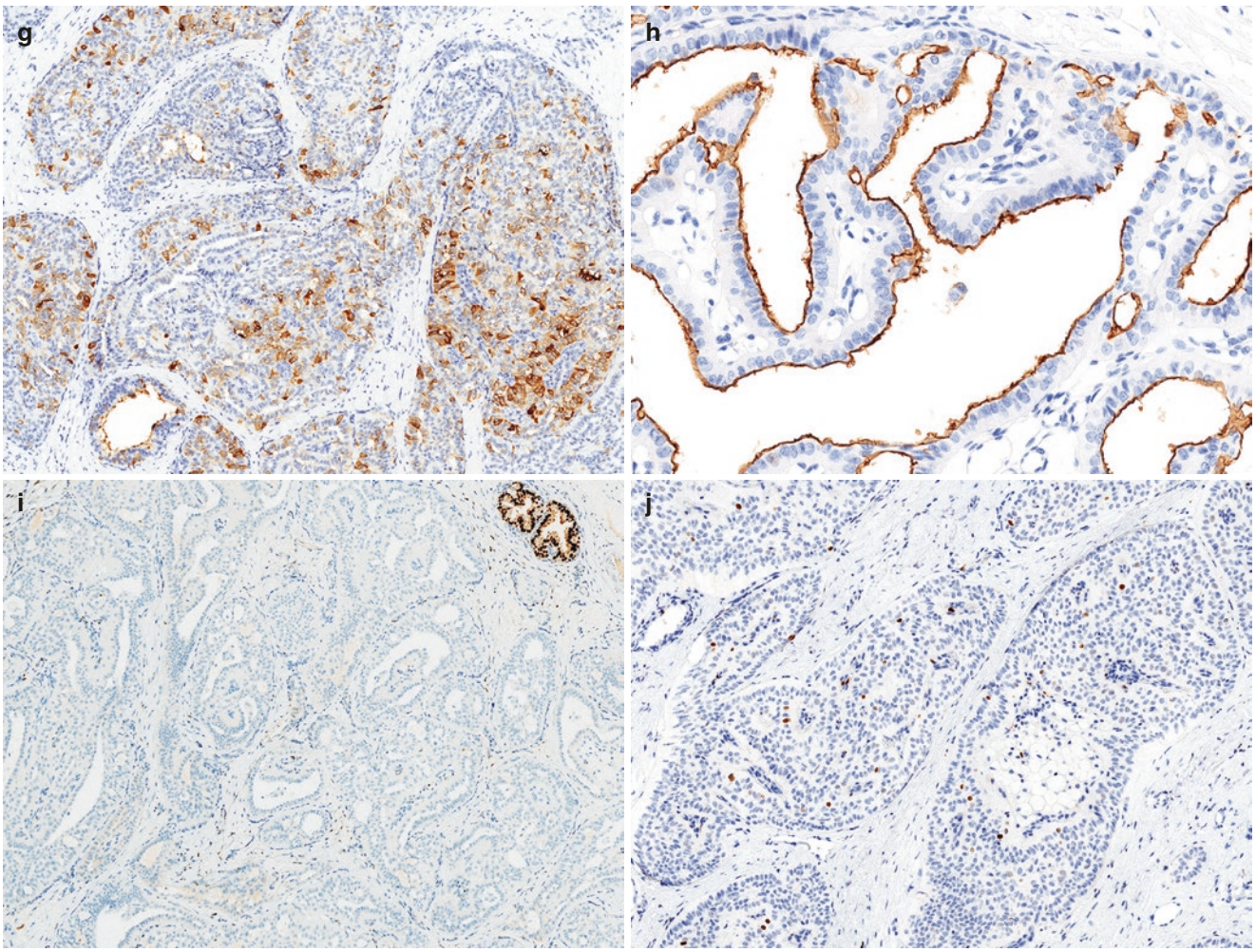

Fig. 12.23 (continued)

mutation was negative [82]. In another study, an antibody recognizing IDH2 epitopes R172A/C/D/E/G/L/Q/S/Y (MsMab-1) showed strong and diffuse immunopositivity in 6 of 7 TCCRP with *IDH2* mutations (R172G and R172S), with another tumor harboring an R172T mutation showing weak staining [75]. Other papillary neoplasms and all conventional TNBC tested in these studies were negative, with the exception of weak staining (H-score ≤ 40) in 3 non-TCCRP papillary lesions with MsMab-1 [75, 82]. Immunohistochemistry with IDH2 R172 mutation-specific antibodies can therefore be useful as a surrogate for genetic analysis or to triage tumors for sequencing of the *IDH2* R172 hotspot locus [75, 82], with the caveat that TCCRP with some less common *IDH2* R172 mutations may be negative with one or the other antibody, and tumors lacking *IDH2* mutations will be missed [63]. Accordingly, the diagnosis of TCCRP should not be excluded in cases displaying the unique histopathologic features of this entity if IDH2 R172 immunohistochemistry is negative.

Differential Diagnosis

Other papillary lesions of the breast: Due to its rarity, papillary architecture and unusual immunoprofile, TCCRP may be confused with other more common benign or malignant papillary neoplasms of the breast, especially in limited CNB material. These lesions include intraductal papilloma with usual ductal hyperplasia, solid papillary carcinoma (SPC), papillary pattern DCIS, and encapsulated papillary carcinoma (EPC) (Table 12.4). The cytologic features, including nuclear grooves and pseudoinclusions, and strong CK5/6 expression in TCCRP could mimic intraductal papilloma with usual ductal hyperplasia. However, TCCRP lacks myoepithelial cells along the fibrovascular papillae or around the papillary nodules and is typically ER negative, whereas papilloma has intact myoepithelial cell layers and is ER positive in a heterogeneous pattern. Like TCCRP, SPC is composed of circumscribed nodules with solid papillary architecture and an absence of myoepithelial cells along the fibrovascular cores.

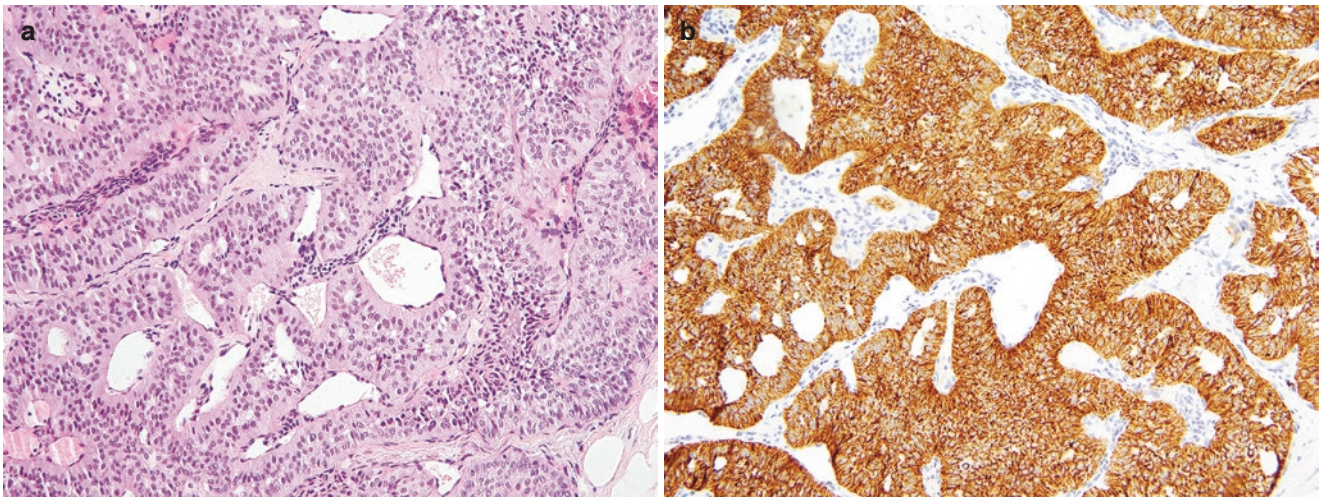

Fig. 12.24 Tall cell carcinoma with reversed polarity, detection of mutant IDH2 by mutant-specific antibody. TCCRP harbors recurrent *IDH2* mutations at R172. (**a**, **b**) Immunohistochemistry using an antibody to IDH2 R172 mutant protein demonstrates diffuse and strong staining with cytoplasmic granular pattern in the tumor cells, helpful in confirming the diagnosis of TCCRP (*Courtesy of Dr. Fresia Pareja*, Department of Pathology, Memorial Sloan Kettering Cancer Center with permission)

Table 12.4 Immunohistochemical markers helpful in the differential diagnosis of TCCRP and papillary mimics

	Tall cell carcinoma with reverse polarity	Papilloma with usual ductal hyperplasia	Solid papillary carcinoma (in situ and invasive)	Papillary pattern DCIS and encapsulated papillary carcinoma
CK5/6	Positive, diffuse	Positive, mosaic pattern	Negative	Negative
ER	Negative or focal weak	Positive, heterogeneous	Positive, diffuse	Positive, diffuse
Myoepithelial cell markers (p63, SMM, calponin)	Negative along papillae and around nodules	Positive along papillae and around ducts	Negative along papillae; Positive or negative around nodules	Negative along papillae; Positive around DCIS, negative around EPC
IDH2 R172	Positive	Negative	Negative	Negative

The helpful distinguishing morphologic features include tall columnar cells with apically located nuclei in TCCRP versus polygonal cells with evenly spaced round to oval nuclei, often accompanied by areas of spindled or plasmacytoid cytology, in SPC. Immunophenotypically, TCCRP is diffusely CK5/6 positive and ER negative, while SPC has the opposite staining pattern. Furthermore, SPC often expresses the neuroendocrine markers synaptophysin and chromogranin, which are consistently negative in TCCRP. The finding of circumscribed papillary ducts lacking myoepithelial cells in TCCRP could also raise the consideration of papillary pattern DCIS or EPC. Immunohistochemical analysis with CK5/6 and ER is again helpful in the distinction, as in the distinction from SPC. Furthermore, most TCCRP display strong and diffuse immunolabeling with an IDH2 R172-specific antibody, in contrast to the other papillary neoplasms in the differential. Careful evaluation of cytoarchitectural features supplemented by judicious use of immunohistochemical markers can therefore help establish the correct diagnosis, even in a CNB specimen (Table 12.4).

Metastatic papillary thyroid carcinoma: Because of the striking morphologic similarities between PTC and TCCRP and because ~5% of metastases to the breast are of thyroid origin [84], metastatic thyroid carcinoma is often considered in the differential diagnosis for TCCRP. Immunohistochemistry with tissue-specific markers is helpful in this context. TCCRP lacks expression of thyroid-specific markers, including TTF-1, thyroglobulin, and PAX8 [62, 66, 67, 75, 77], and instead shows positive, albeit patchy, staining for breast markers GATA3, mammaglobin, and GCDFP-15.

Infiltrating epitheliosis (IE): Another lesion that shares morphologic features and immunophenotype with TCCRP is infiltrating epitheliosis (IE), an exceedingly rare complex sclerosing lesion with overt CK5/6-positive epithelial proliferation [85], weak/patchy to absent ER expression, and attenuated to absent myoepithelial cell layers around the proliferating cells, similar to TCCRP. Moreover, *PIK3CA* or *PIK3R1* mutations have been reported in IE, and are also seen in TCCRP [86]. It has been suggested that there is a continuum between IE and TCCRP and that these papillary lesions represent a spectrum, with IE at the sclerosis-rich/epithelium-poor end and TCCRP at the epithelium-rich/stroma-poor end of the spectrum [65].

Pathogenesis and Risk Factors

TCCRP characteristically harbors recurrent *IDH2* hotspot mutations (often R172S or R172T), which have been reported in >80% of cases [63, 65, 71–73, 75, 78]. *IDH2* mutations appear to be pathognomonic for TCCRP in the context of breast neoplasms [63] but have also been identified in gliomas [87], myeloid leukemias [88], sinonasal undifferentiated carcinomas [89], chondrosarcomas [90], and cholangiocarcinomas [91]. *IDH2* encodes the mitochondrial enzyme isocitrate dehydrogenase 2. The precise mechanisms by which *IDH2* mutations function in cancer remain unknown. However, *IDH2* mutations lead to gain-of-function enzymatic activity that allows for NADPH-dependent reduction of α-ketoglutarate (αKG) to 2-hydroxyglutarate, which in turn inhibits αKG-dependent dioxygenases, including TET2, and alters genome-wide histone and DNA methylation, cell differentiation and survival, and extracellular matrix maturation [65, 75, 92–94]. In TCCRP, *IDH2* mutations often co-exist with genetic alterations in phosphatidylinositol-3 kinase (PI-3 K) signaling pathway genes, including activating *PIK3CA* and *PIK3R1* mutations [63, 65, 72, 75, 78]. Whereas PI-3 K pathway gene mutations are common in breast cancer, *IDH2* hotspot mutations are extremely rare or non-existent in other breast tumors, and their identification can be used as a confirmatory molecular finding for TCCRP [72, 95–97]. Functional studies have shown that forced expression of *IDH2* R172S and *PIK3CA* H1047R together result in a reverse polarization phenotype resembling that of TCCRP [63]. Truncating *TET2* mutations have been identified in a subset of TCCRP lacking the *IDH2* mutations [63, 65, 72, 75, 78]. Given that mutant IDH2 is thought to function through inhibition of TET2, TCCRP may be an example of a convergent phenotype stemming from *IDH2* or *TET2* mutations functioning in the same pathway [63, 87]. TCCRP has thus joined a growing list of breast tumors with unique genotypic-phenotypic correlation (Table 12.5) [72].

Table 12.5 Breast tumors with genotype-phenotype correlation

Tumor	Genetic Alterations
Lobular carcinoma in situ and invasive lobular carcinoma	*CDH1* mutation
Adenoid cystic carcinoma	*MYB-NFIB* fusion *MYBL1-NFIB* fusion *MYB* amplification
Secretory carcinoma	*ETV6-NTRK3* fusion
Mucoepidermoid carcinoma	*CRTC1-MAML2* fusion
Pleomorphic adenoma	*PLAG1* arrangement *HMGA2-WIF1* fusion
Fibroepithelial tumor (fibroadenoma and phyllodes tumor)	*MED12* exon 2 mutation
Tall cell carcinoma with reversed polarity	*IDH2* R172 mutation

BRAF mutations and *RET/PTC* rearrangements, which are frequently found in PTC and are thought to be responsible for the specific nuclear features in PTC, are consistently absent in TCCRP [77].

RNA sequencing of 9 TCCRP revealed expression profiles of either luminal A or basal intrinsic molecular subtypes [75].

Prognosis and Clinical Management

Limited available follow-up data on a small number of cases suggests that the majority of TCCRP follow an indolent clinical course with excellent prognosis despite the triple-negative or weakly ER-positive biomarker profile [62–71, 73, 75, 77]. TCCRP presents mostly as localized disease with a low incidence of lymph node metastasis at the time of diagnosis (reported in only 4 patients, including one intramammary node) [64, 66, 69, 76]. The single patient with intramammary lymph node metastases was alive and free of local or distant recurrence 10 years after diagnosis. Only one case with distant metastasis (to bone) has been reported [69]. However, it is not clear if this tumor was truly TCCRP, as it was ER positive and associated with DCIS with comedonecrosis, and with lymphovascular invasion.

Due to the rarity of TCCRP, there are no guidelines or consensus on the management of patients with these tumors. Current treatment generally includes surgical excision with lumpectomy or mastectomy [63–65]. Local recurrence has been reported, and complete excision with adequate margin is considered optimal. The role of radiation or systemic therapy is unclear. *IDH2* mutations may serve as a future target for therapeutic intervention in metastatic lesions.

Mucoepidermoid Carcinoma

Overview and Clinical Presentation

Mucoepidermoid carcinoma (MEC) of the breast is a triple-negative salivary gland-like tumor that shares distinctive histopathologic features, immunophenotype, and genetic alterations with its counterpart arising in other anatomic sites [98–100]. Whereas MEC is the most common salivary gland malignancy, it is an exceedingly rare diagnosis and less frequent than other salivary gland-like neoplasms in the breast, such as AdCC, secretory carcinoma, and adenomyoepithelioma. The estimated incidence has been cited as 0.2–0.3% of all breast cancers [101, 102], although it appears to be even less common in practice. Since the first description by Patchefsky et al. [103] in 1979, less than 50 cases of breast MEC have been reported in the English literature, mostly as single case reports [100, 102, 104].

All reported MEC cases are in adult women, ranging in age from 27 to 86 years (mean age 56 years) [104]. Patients usually present with a palpable lump that is often well-circumscribed but occasionally ill-defined on physical examination and may be tender to palpation [99, 103, 104]. Nipple discharge may be present when the tumor arises in the retroareolar region [99]. Some cases have been detected by screening mammography [100, 105, 106].

Gross and Radiologic Features

Most MEC are well circumscribed, gray to white, and firm with a solid or solid cystic cut surface. Cysts are often filled with mucoid material. Tumor size ranges from 0.5 to 11 cm (median 2.5 cm).

Radiographically, some MEC are considered to be benign. On mammography, MEC often presents as a round nodule and less frequently as an ill-defined mass. Ultrasonography demonstrates a hypoechoic or mixed hyperechoic and hypoechoic mass with smooth or irregular contours that may show posterior shadowing [100, 104, 105, 107, 108]. Some cases appear as a complex cystic and solid nodule [104, 109, 110]. An enhancing mass is observed on MRI [107, 108].

Microscopic Features

At scanning magnification, most MEC appear as a solid or partly cystic nodular lesion with pushing margins (Fig. 12.25). Some tumors are surrounded by a fibrous pseudocapsule [99, 108]. Stellate or irregular margins may be seen, usually in high-grade tumors. A dense lymphoplasmacytic infiltrate is frequently observed at the tumor periphery, which in the salivary gland has been termed tumor-associated lymphoid proliferation (TALP) (Fig. 12.25). MEC comprises a mixed population of mucinous (mucin-secreting) cells, epidermoid/squamoid cells, and intermediate cells in varying proportions and arranged in overall circumscribed macrocystic, microcystic/glandular, and solid patterns (Figs. 12.26, 12.27, and 12.28). Prominent extracellular basophilic and/or eosinophilic secretions often fill the cystic and glandular spaces.

Mucinous cells are usually located at the luminal/central aspects of the cysts, glands, and nests (Figs. 12.27a and 12.28c, g). These cells may be tall columnar or goblet shaped with obvious cytoplasmic mucin, or more subtle, requiring special stains, such as PASD, mucicarmine, or Alcian blue to highlight the mucin (Fig. 12.27b). Intermediate cells, which are most concentrated at the periphery of cysts and nodules, are small with relatively high nuclear-to-cytoplasmic ratio and oval hyperchromatic nuclei (Figs. 12.27a and 12.28g). Epidermoid cells are polygonal with well-defined cell borders and abundant eosinophilic cytoplasm (Figs. 12.27a and 12.28c, g). Focal intercellular bridges may be observed in rare cases, but true keratinization, such as squamous pearls or individual cell keratinization, should be absent. In addition to the most common three cell types as described above, salivary gland MEC may also have cells with prominent cytoplasmic clearing (clear cell changes), oncocytic cells, spindle cells, and rarely ciliated cells and cells with sebaceous differentiation. Clear cell changes are also observed in breast MEC and can be quite prominent in some tumors (Fig. 12.27c). An in situ component may be present and displays similar features, including the three characteristic cell types, mucinous/eosinophilic secretions, and periductal lymphoplasmacytic infiltrates [99, 108, 111] (Fig. 12.29).

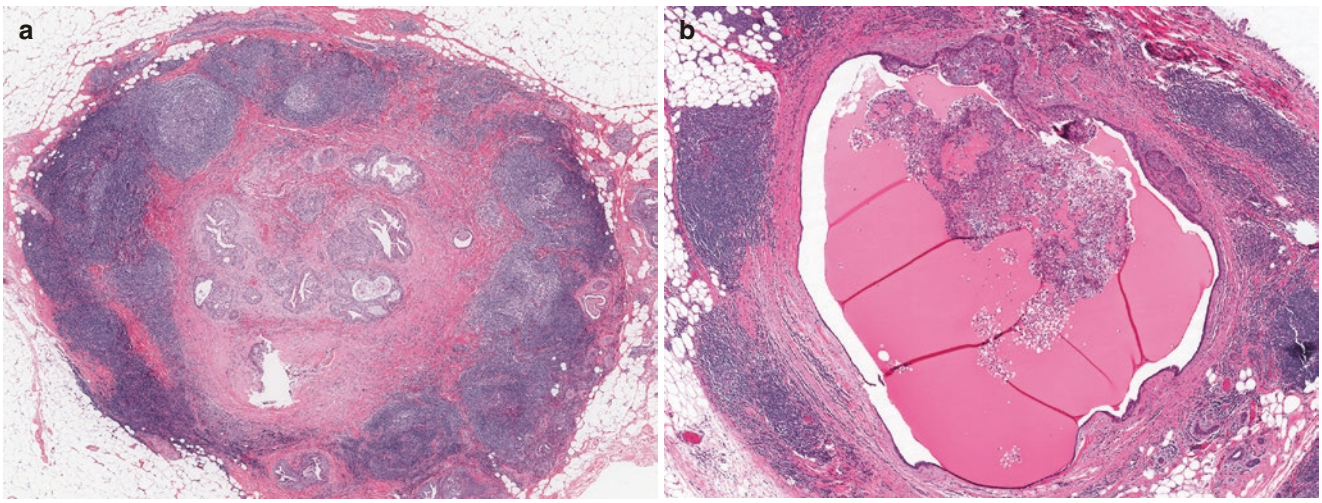

Fig. 12.25 Mucoepidermoid carcinoma, tumor border. (**a**, **b**) At scanning magnification, these two examples of MEC appear circumscribed with pushing margins. Note the prominent lymphoplasmacytic infiltrate at the periphery of the tumor, including lymphoid aggregates with germinal center formation. The tumor can be solid (**a**), cystic (**b**), or solid and cystic

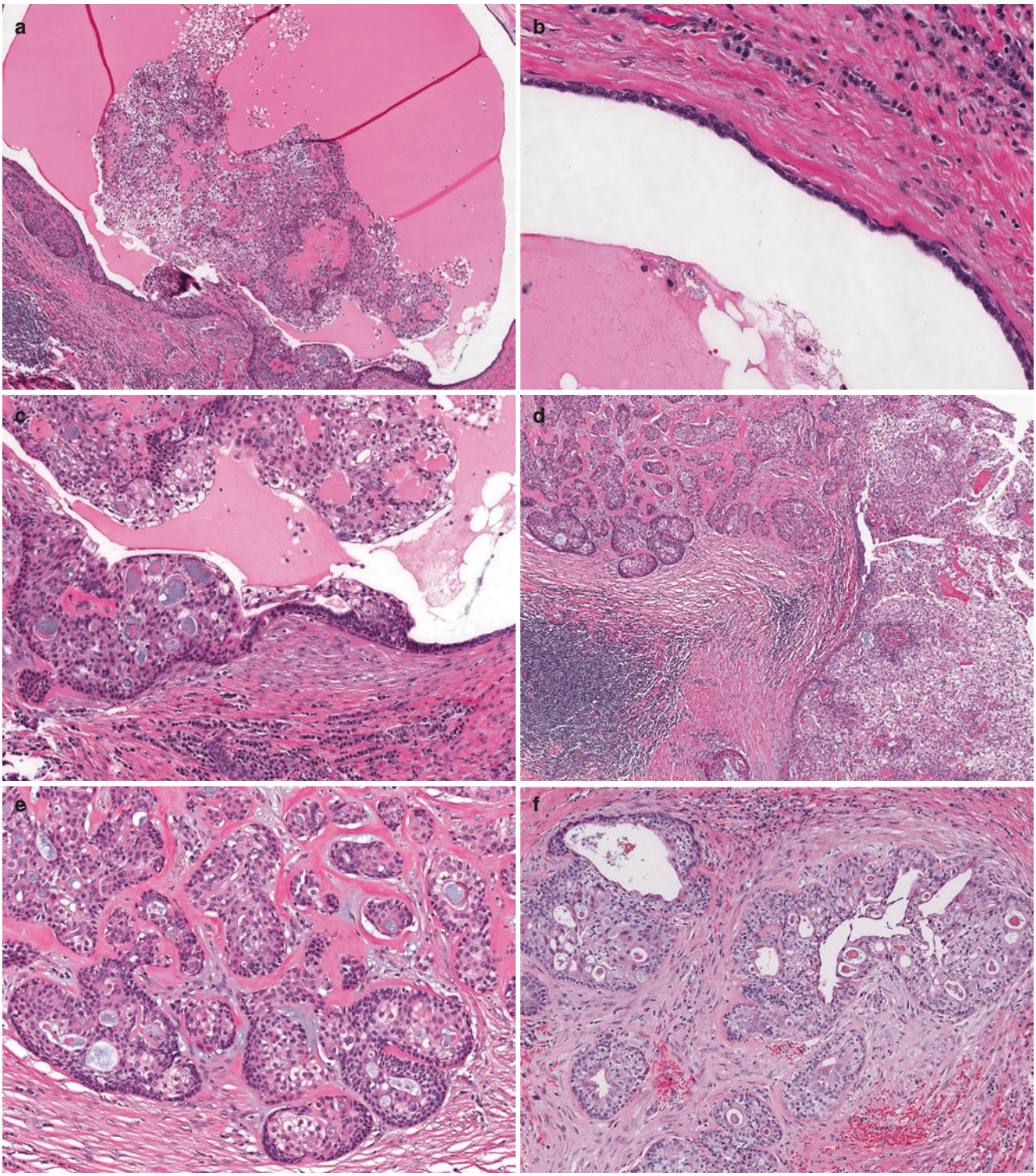

Fig. 12.26 Mucoepidermoid carcinoma, architectural pattern. The tumor cells in MEC can be arranged in macrocystic structures (**a**–**c**), solid nests (**d**, **e**) or microcystic/fenestrated glandular pattern (**e**, **f**), usually with varying proportion in a given lesion. In the macrocystic pattern, the tumor cells can grow as a mural papillary nodule (**a**); while the majority of the cyst wall can be lined by one to a few layers of neoplastic epithelial cells (**b**, **c**). In the solid growth pattern, the nests can be large (**d**, right) or small (**d**, left, and **e**). The small solid nests may be admixed with microcystic elements (**e**). Note the presence of prominent secretions within the macrocytic spaces and glandular lumens, which can be eosinophilic or basophilic. The stroma associated with the tumor nests/glands can be hyalinized/fibrotic (**e**) or desmoplastic (**f**)

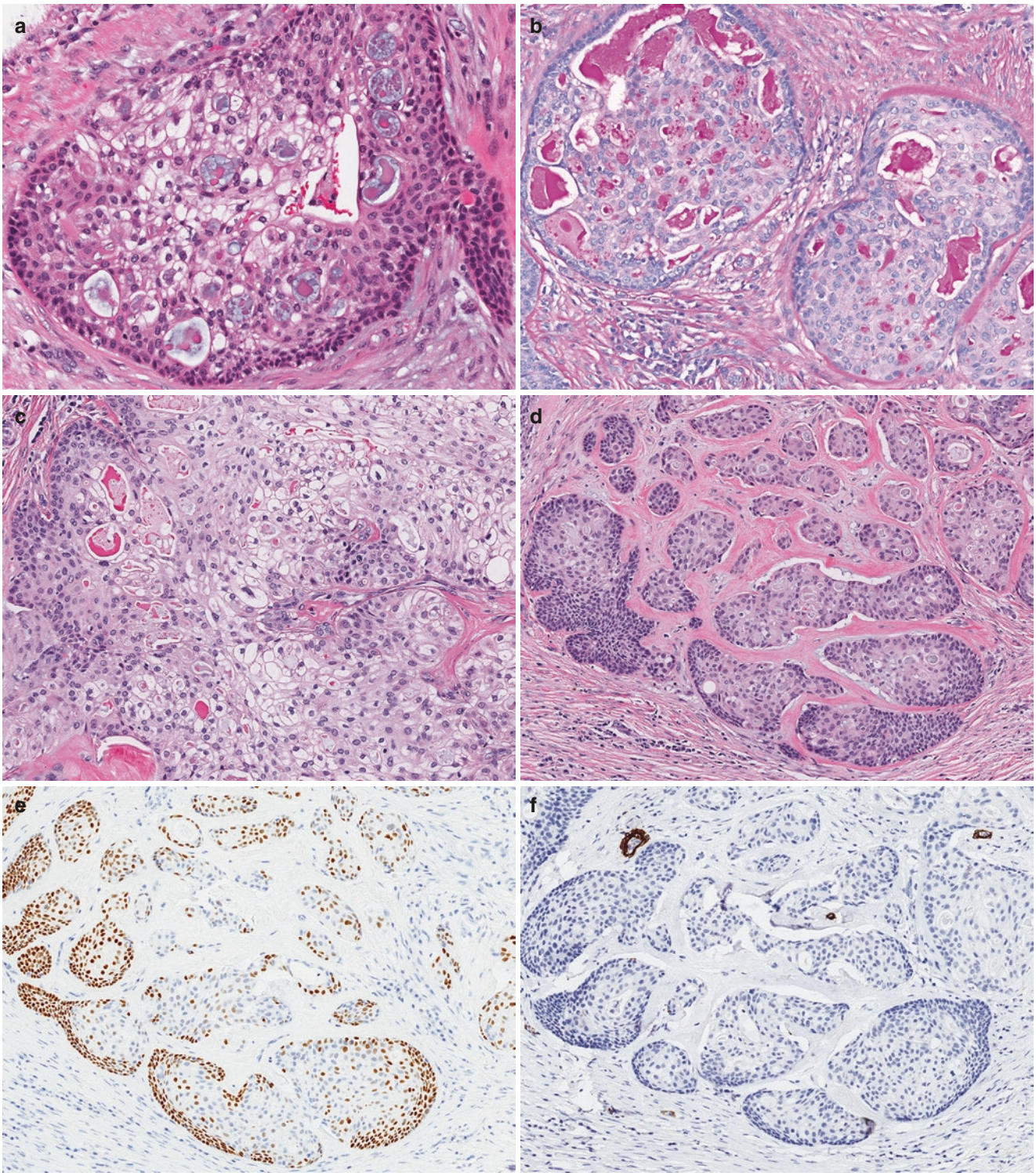

Fig. 12.27 Mucoepidermoid carcinoma, cytologic features. (**a**) MEC is composed of a mixed population of intermediate cells (which are most concentrated at the periphery of the tumor cysts/glands/nests), epidermoid/squamoid cells (which have distinct cell borders and abundant eosinophilic cytoplasm), and mucin-secreting cells (which are preferentially localized at the luminal/central aspects of tumor cysts/glands/nests). (**b**) A PASD stain highlights the intracytoplasmic mucin in the mucin-secreting cells as well as the mucinous secretion within the glandular lumens. (**c**) Clear cell changes may be observed in the neoplastic cells and are prominent in this example. (**d**) The various tumor cell types and their spatial arrangement create a distinct appearance to the tumor nests with darker cells at the periphery and paler cells toward the center. The intermediate cells (and to various extent, the epidermoid cells) are positive for p63 immunostain (**e**), which may be mistaken as being myoepithelial cells. However, the tumor nests and glands are negative for other myoepithelial markers, including SMM (**f**), calponin and SMA (not shown)

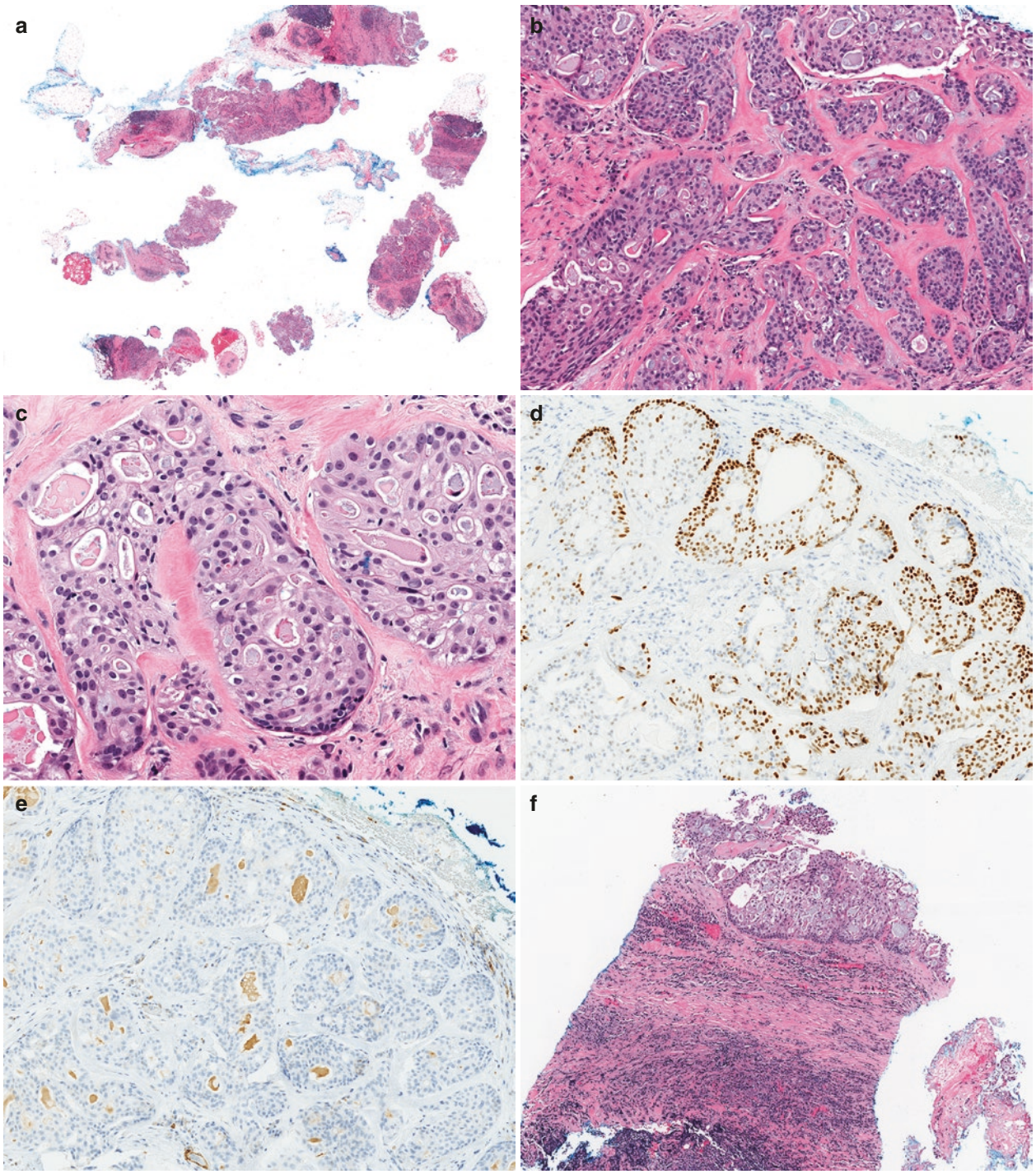

Fig. 12.28 Mucoepidermoid carcinoma, features in core needle biopsy specimen. The characteristic architectural and cytologic features of MEC can be appreciated in this CNB specimen targeted for a breast mass (**a**). (**b**) Some core fragments contain microcystic glands and small solid nests in a fibrotic/hyalinized stroma. (**c**) High magnification reveals a mixed cell population and eosinophilic/basophilic secretions within glandular lumens (**c**). The microcystic glands and solid nests have peripheral p63-positive cells (**d**) and are negative for SMM immunostain (**e**). (**f–i**) One core fragment appears to sample part of a cyst wall that is lined by multiple layers of epithelial cells. Note the prominent lymphoplasmacytic infiltrate in the cyst wall (**f**), and the mixed intermediate cells (dark cells with high nuclear-to-cytoplasmic ratio at the periphery of the cyst), epidermoid cells, and mucin-secreting cells (**g**). Also noted is the basophilic to eosinophilic secretory material within the glandular spaces. Similar to the microcystic elements and solid nests, the macrocystic structure is positive for p63 immunostain with a predominant peripheral staining pattern (**h**) and negative for SMM (**i**). (**j–l**) Another core fragment samples a part of a cyst that is lined by only one to two flat layers of bland epithelial cells, which could easily be misinterpreted as a benign simple cyst. Again, note the presence of a dense lymphoplasmacytic infiltrate in the cyst wall. Also note the presence of subtle mucin secretion in the thin cyst lining (upper part of the cyst in **j**), which would not be expected in simple cyst. The cyst is lined by p63-positive cells (**k**), but is completely negative for SMM (**l**), which along with other features (dense lymphoplasmacytic infiltrate and mucin secretion) should alert the pathologist to question the impression of a benign simple cyst

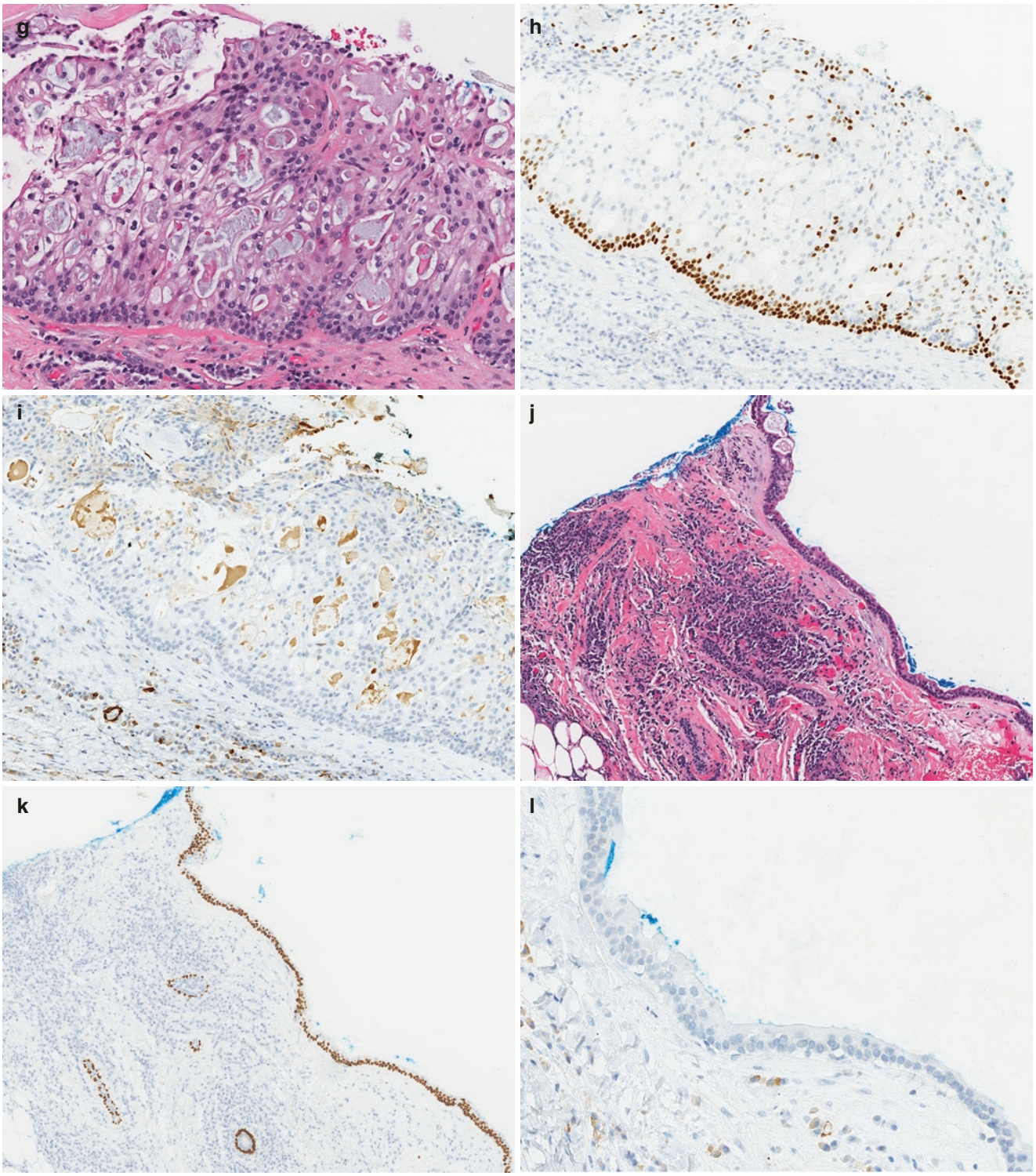

Fig. 12.28 (continued)

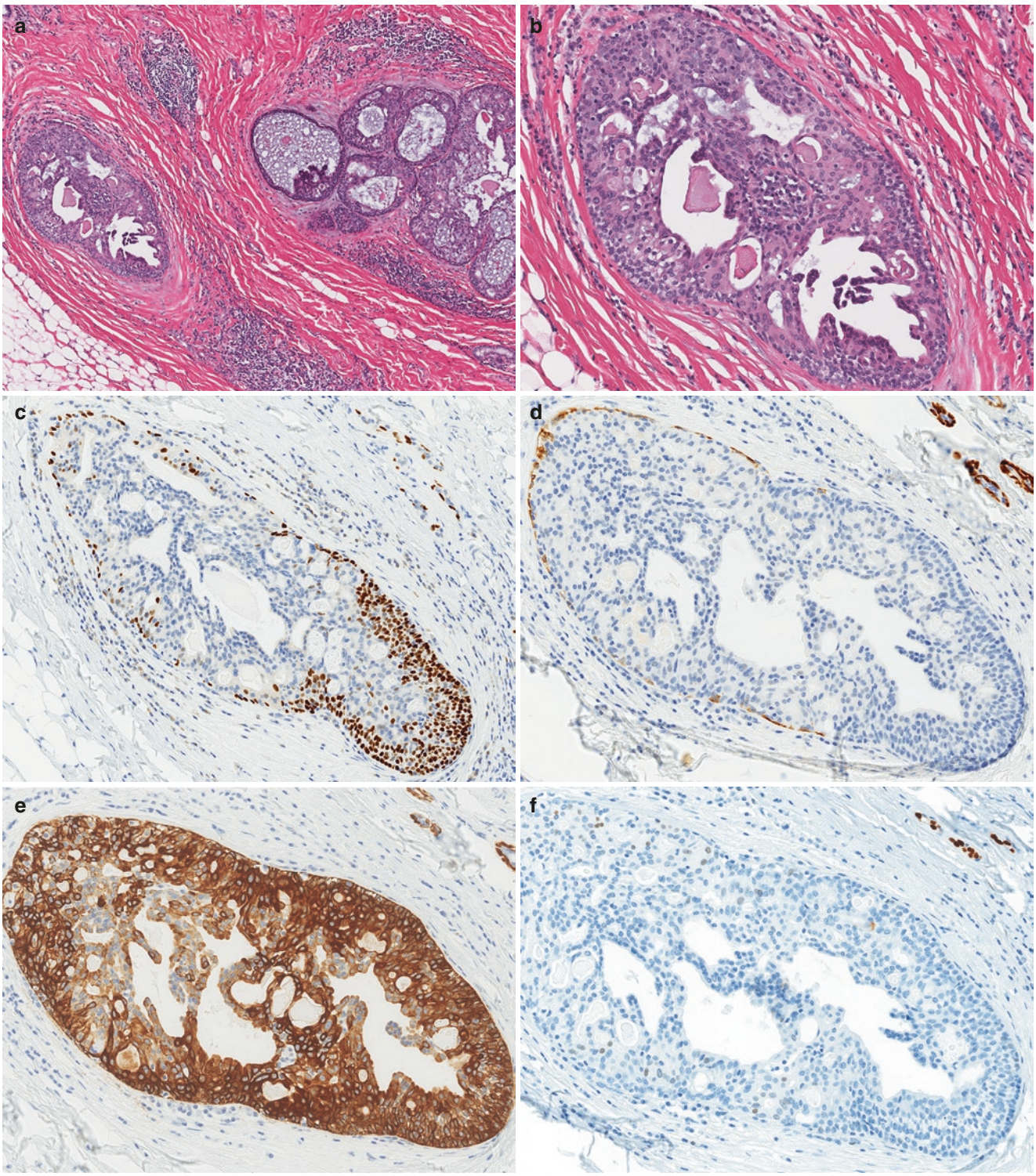

Fig. 12.29 Mucoepidermoid carcinoma, in situ component. (**a–f**) An in situ component of MEC may be present in some cases and exhibit similar features as those observed in the invasive component, including the associated lymphoplasmacytic infiltrate (**a**) and the mixed population of neoplastic cells and luminal secretions (**b**). The mixed (hence appearing to be heterogeneous) epithelial types with squamoid features and irregular fenestrations could mimic usual ductal hyperplasia. Strong expression for CK5/6 (**e**) further complicates the issue. However, the neoplastic cells in the MEC (both in situ and invasive forms) are completely negative to minimally positive for ER (in the range 1–2%) (**f**), which helps to distinguish the lesion from usual ductal hyperplasia. The in situ component of MEC is invested by a myoepithelial layer, highlighted by p63 (**c**) and calponin (**d**) immunostains

Accurate grading of breast MEC is important in providing prognostic information. In the salivary gland, the most commonly used grading systems for MEC are The Brandwein and Armed Forces Institute of Pathology (AFIP) methods, which are three-tiered and point-based systems incorporating various adverse histologic features (Table 12.6). For breast MEC, the AFIP system and the modified Scarff-Bloom-Richardson (SBR) system appear to be largely interchangeable and yield similar prognostic data [99]. With the AFIP grading scheme, ~55% of breast MEC are low grade, <10% are intermediate grade, and ~40% are high grade [100, 104, 112].

Cystic architecture with abundant mucinous cells predominates in low-grade MEC, and the tumor cells have bland round to oval nuclei and infrequent mitoses (0–3/10 HPF). High-grade MEC are usually arranged in solid nests with scant mucinous cells, greater nuclear atypia, and increased mitotic activity. Infiltration of tumor nests into surrounding breast tissue may be present. Necrosis, lymphovascular invasion, and perineural invasion are typically only identified in high-grade tumors. Accurate diagnosis of high-grade MEC can be challenging based on morphologic grounds alone. High-grade MEC of the salivary gland has been well documented in the literature to include a heterogeneous group of different entities upon re-review by expert pathologists. FISH is a useful ancillary test to help identify MEC in the breast (see section "Pathogenesis" and "Differential Diagnosis").

Table 12.6 AFIP and Brandwein semiquantitative methods for assessing histological grade in salivary gland MEC

	AFIP method	Brandwein method
Intracystic component	2 (<20%)	2 (<25%)
Border/invasive front	NA	2 (small nests and islands)
Nuclear anaplasia/ pleomorphism	4	2
Mitosis	3 (≥4/10 HPF)	3 (≥5/10 HPF)
Perineural invasion	2	3
Necrosis	3	3
Lymphovascular invasion	NA	3
Bony invasion	NA	3
	Total score	Total score
Low grade	0–4	0
Intermediate grade	5–6	2–3
High grade	7–14	4+

Adapted from Cipriani et al. [113]

Immunohistochemistry

MEC is overall positive for LMWCK (CK7, CAM5.2), HMWCK (CK5/6, CK14), and p63 [99, 100] (Figs. 12.27e, 12.28d, h, k, 12.30, and 12.31b). Expression of these markers is correlated with cell type, and immunohistochemistry is helpful in highlighting the various cell populations and their distribution in the tumor nests and cysts. Intermediate cells are typically positive for p63 and HMWCK and negative for LMWCK; epidermoid cells usually react with both LMWCK and HMWCK, with variable staining for p63; and mucinous cells preferentially express LMWCK. This differential staining pattern with LMWCK-positive cells concentrated in the central/luminal part of the tumor nests and HMWCK-positive cells predominantly located in the outer layers of the nests creates a "zoning phenomenon" (Fig. 12.30), that is shared by salivary gland and breast MEC and is helpful in

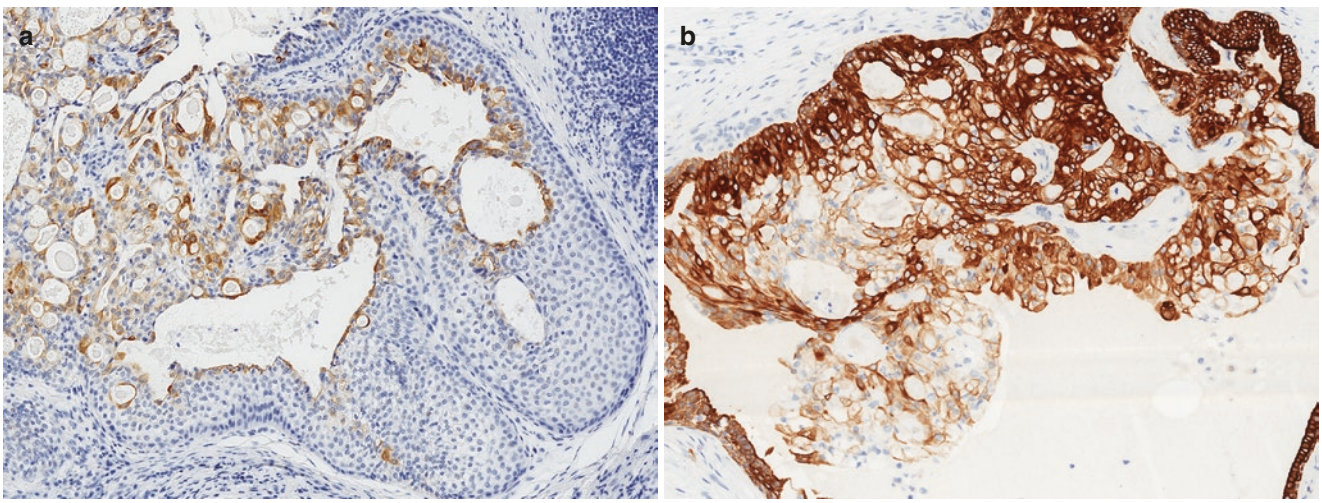

Fig. 12.30 Mucoepidermoid carcinoma, zoning phenomenon with cytokeratin immunostains. (**a**, **b**) The various cell types in MEC tend to exhibit different expression for cytokeratins, in which LMWCK such as CAM5.2 shows preferential staining of the mucin-secreting cells (**a**) whereas HMWCK such as CK14 decorates predominantly the intermediate and epidermoid cells (**b**), creating a distinctive "zoning" phenomenon that is helpful for the diagnosis of MEC

establishing the diagnosis [99]. Expression of p63 by intermediate cells at the periphery of tumor nests and cysts may be misinterpreted as myoepithelial differentiation; however, the tumor cells are negative for other myoepithelial cell markers, including SMM, calponin, and SMA [99] (Figs. 12.27f and 12.28e, i, l). On the other hand, the in situ component has a peripheral myoepithelial layer that can be highlighted with SMM, calponin, SMA stains, in addition to p63 (Fig. 12.29d).

All reported breast MEC have been ER and PR negative or rarely weakly positive and are consistently HER2 negative (Fig. 12.31c). Therefore, MEC falls into the group of basal-like triple-negative breast cancers by immunophenotype.

There is limited information about expression of other markers in MEC. Based on analyses of two breast MEC, these tumors were also patchy or diffusely positive for MUC4, GATA3, and mammaglobin and negative for GCDFP-15 [100] (Fig. 12.31d).

Differential Diagnosis

The characteristic histological features and immunophenotype of MEC are distinctive in the breast. However, pathologists may not necessarily consider this very rare subtype of breast cancer, and MEC can be confused with various benign and malignant lesions when assessing limited CNB material, depending on the architectural pattern and dominant cell type sampled.

Simple cysts: CNB which samples only a portion of a macrocyst lined by one to a few layers of intermediate cells with or without epidermoid cells could easily be misinterpreted as a simple cyst with or without squamous metaplasia (Figs. 12.26b and 12.28j). Features that would be unusual for simple cyst include the presence of mucinous cells (which can be very subtle), a prominent lymphoplasmacytic infiltrate in the cyst wall, and lack of myoepithelial cells at the cyst periphery by SMM and calponin immunohistochemistry

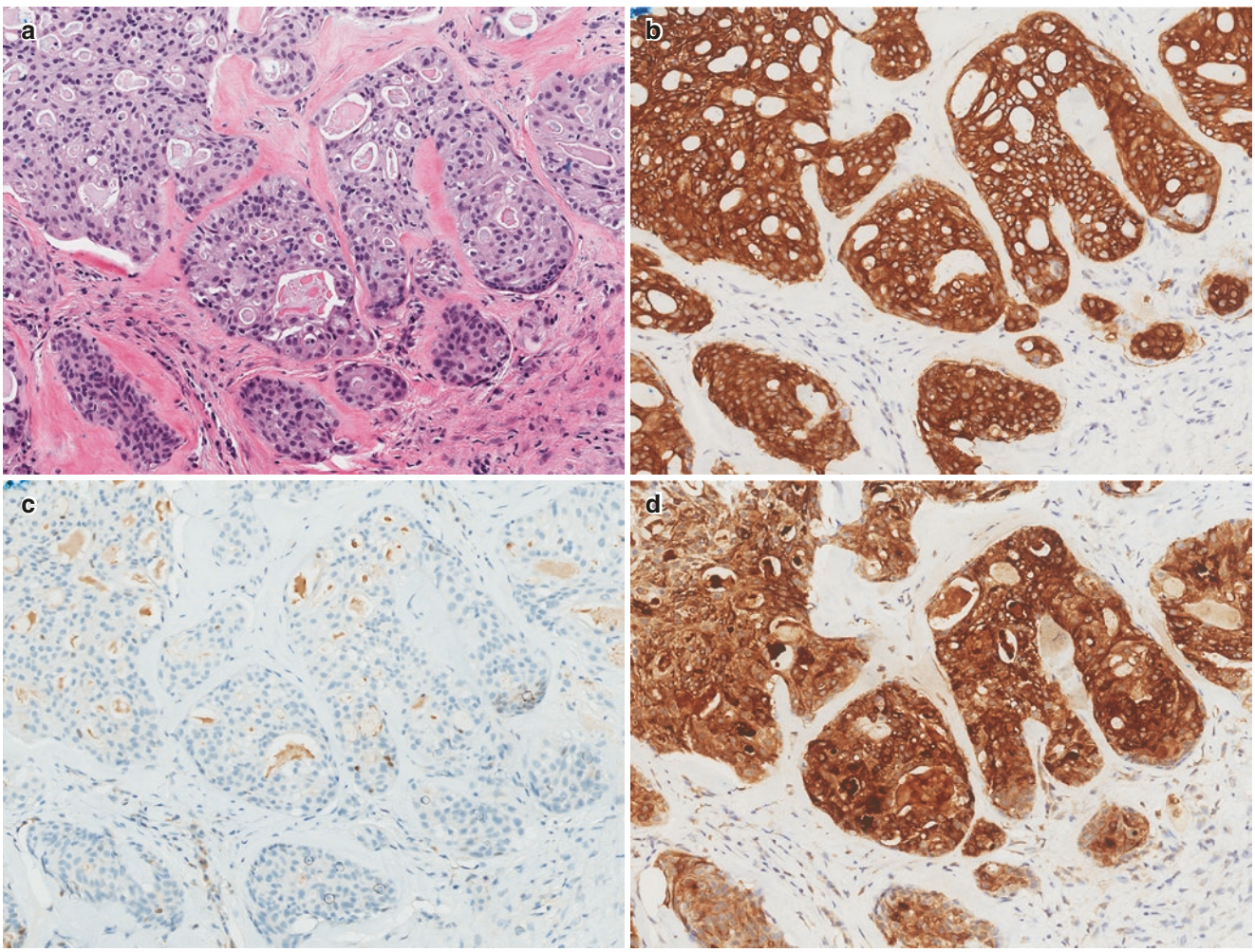

Fig. 12.31 Mucoepidermoid carcinoma, additional immunostaining profile. (**a–d**) The neoplastic cells in MEC are positive for CK5/6 (**b**) and negative for ER (**c**), PR (not shown), and HER2 (now shown), thus exhibiting a basal-like and triple-negative immunophenotype. MEC typically shows strong expression of mammaglobin (**d**)

(Fig. 12.28j–l). In these situations, radiologic-pathologic correlation is important to determine the presence of discordant findings and the need for re-biopsy to pursue a conclusive diagnosis.

Usual ductal hyperplasia: The bland cytology, different cell types (heterogeneous cell population), and often irregular microcystic spaces of MEC, especially in the DCIS component, may mimic usual ductal hyperplasia (Fig. 12.29a, b). Clues to the correct diagnosis include recognizing tumor cells with epidermoid, mucinous, and intermediate features, the presence of mucin, and the associated periductal lymphoplasmacytic infiltrate. CK5/6 and ER immunohistochemistry is helpful in making the distinction, with positive CK5/6 (in zonal pattern) and negative ER expression in MEC, and positive CK5/6 (in mosaic pattern) and heterogeneous ER expression in usual ductal hyperplasia (Fig. 12.29).

Ductal carcinoma in situ: Epidermoid cells with well-defined cell borders and microcystic architecture in MEC can also raise consideration of cribriform pattern DCIS of no special type. Helpful features for the correct diagnosis are the heterogeneous cell population, as well as the CK5/6-positive, ER-negative, and p63-positive phenotype in MEC, compared to the uniform cell population with negative CK5/6 and p63 and strongly ER-positive expression pattern in DCIS.

Papillary lesions: MEC with macrocystic structures containing mural cellular nodules can resemble either intraductal papilloma with usual ductal hyperplasia and squamous metaplasia or papillary carcinoma, including EPC (Fig. 12.26a). As in the discussion for usual ductal hyperplasia and DCIS above, appreciation of the various cell types and characteristic immunophenotype can help to arrive at the correct diagnosis.

Secretory carcinoma: Low-grade MEC can be mistaken for secretory carcinoma, another rare salivary gland-type carcinoma. Both tumors can have a prominent cystic component, abundant PASD-positive secretory material, and cytologically bland cells that may have eosinophilic, clear, or vacuolated cytoplasm (Fig. 12.32). In addition, both tumors express MUC4, GATA3, and mammaglobin [100, 114]. However, in contrast to the strong S100 protein-positive and p63-negative profile of secretory carcinoma, MEC is consistently positive for p63 and is negative or only focally positive

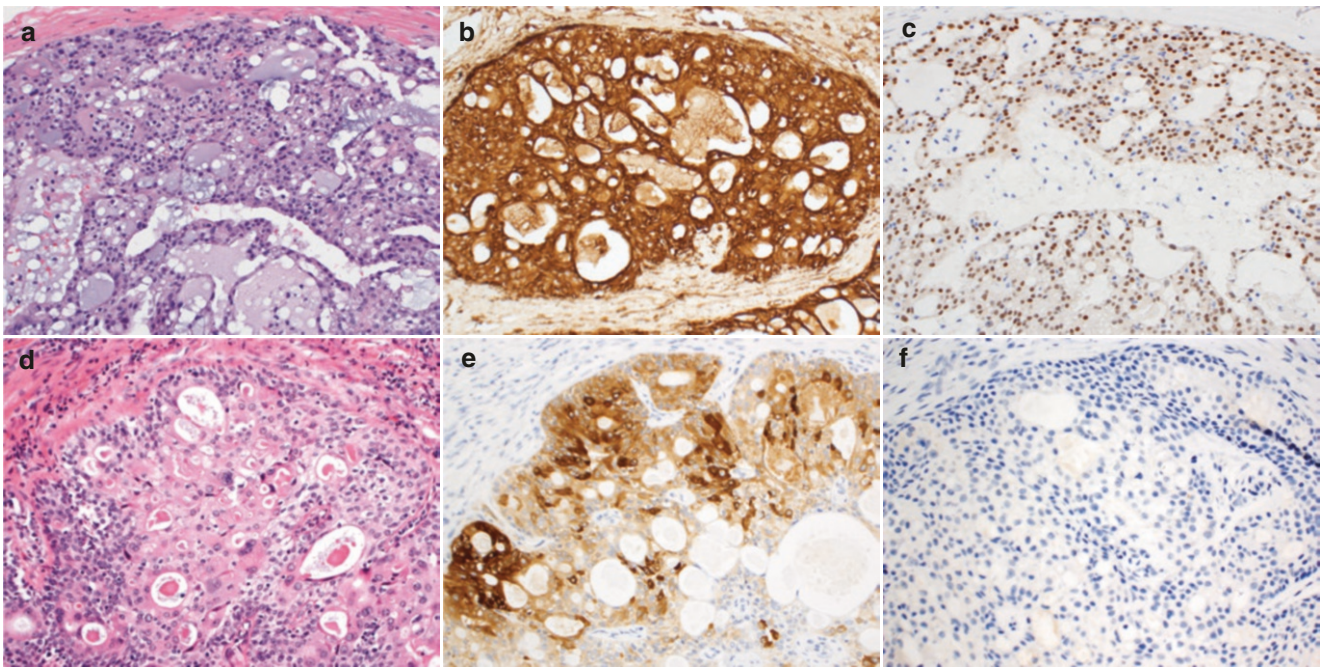

Fig. 12.32 Mucoepidermoid carcinoma versus secretory carcinoma. Secretory carcinoma (**a–c**) and MEC (**d–f**) are both salivary gland-like carcinomas with a triple-negative biomarker profile, share similar morphologic features with a microcystic pattern, bland cytology and prominent secretions (**a**, **d**) and strong mammaglobin expression (**b**, **e**), and may be confused with each other. However, each tumor type is characterized by a distinct chromosomal translocation, with *ETV6-NTRK3* fusion gene in secretory carcinoma and *CRTC1-MAML2* fusion gene in MEC. The diagnosis can therefore be supported by immunohistochemistry with a pan-TRK antibody, which shows nuclear staining in secretory carcinoma (**c**) and is negative in MEC (**f**)

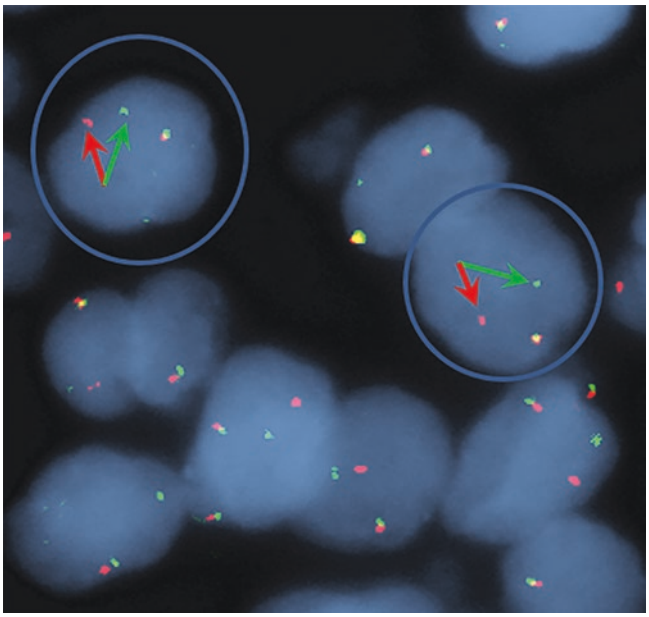

Fig. 12.33 *CRTC1-MAML2* translocation in mucoepidermoid carcinoma. The hallmark chromosomal translocation in MEC, *CRTC1-MAML2*, can be detected using a break-apart fluorescence in situ hybridization (FISH) probe to *MAML2* gene. Note the split-apart green and orange signals of the altered *MAML2* allele and the fused yellow signal from the normal *MAML2* allele. This FISH result is from the case shown in Fig. 12.28. (*Courtesy of Dr. Joaquin Garcia*, Department of Laboratory Medicine and Pathology, Mayo Clinic with permission)

for S100 protein. Furthermore, the tumors each harbor pathognomonic chromosomal translocations and resultant fusion genes (*CRTC1-MAML2* in MEC and *ETV6-NTRK3* in secretory carcinoma), allowing for distinction by FISH using *MAML2* and *ETV6* break-apart probes or sequencing technologies (Fig. 12.33). Immunostaining with a pan-TRK antibody can also be useful, with the majority of secretory carcinomas showing positive nuclear expression, while MEC are negative [115, 116] (Fig. 12.33c, f).

Metaplastic carcinoma: The epidermoid cells and immunophenotype (positive CK5/6 and p63, triple negative) of MEC may raise consideration of metaplastic squamous cell carcinoma. This distinction has significant management implications as diagnosis of metaplastic carcinoma in a CNB may lead to treatment with neoadjuvant chemotherapy. MEC is composed of circumscribed nodules and cysts with mixed cell types including mucinous cells, whereas metaplastic squamous cell carcinoma infiltrates as irregular nests lacking mucinous cells. The presence of true keratinization is not observed in MEC and favors metaplastic squamous cell carcinoma. Low-grade adenosquamous carcinoma may also enter into the differential diagnosis, but this tumor has a different growth pattern consisting of small glands with varying degree of squamous differentiation and lacks mucinous cells (see section "Metaplastic Carcinoma").

Breast tumors with clear cell cytology: MEC with prominent clear cell features and positive p63 expression may be confused with adenomyoepithelioma exhibiting clear cell change of the neoplastic myoepithelial cells. MEC lacks myoepithelial differentiation and is negative for myoepithelial markers SMM, calponin, and SMA. MEC with clear cell features must also be differentiated from invasive breast carcinomas with glycogen-rich clear cell carcinoma pattern and lipid-rich carcinoma pattern. Both of these latter tumors lack mucinous cells and are usually negative for CK5/6 and p63.

Metastatic renal cell carcinoma: Metastatic renal cell carcinoma is also a potential consideration in the differential diagnosis of MEC with prominent clear cell changes. Correlation with history and radiologic findings together with immunohistochemistry is helpful in establishing the diagnosis. Tissue-specific markers (mammaglobin, GATA3, and PAX8) and cytokeratins (CK7 and CK5/6) are differentially expressed in these tumors, with MEC being positive for mammaglobin, GATA3, CK7, and CK5/6, whereas clear cell renal cell carcinoma expresses PAX8 and is negative for CK7 and CK5/6.

Hidradenoma arising in the breast: Hidradenoma (HA) is a skin adnexal tumor that shares overlapping morphological features and immunophenotype with MEC (see Chap. 25). In addition, the signature *MAML2* rearrangement of MEC has also been identified in HA, predominantly as a *CRTC1-MAML2* translocation and rarely as a *CRTC3-MAML2* translocation [117, 118]. These findings raise the question as to whether HA is a distinct cutaneous adnexal neoplasm that shares histopathologic and genetic characteristics with MEC, or whether it represents a cutaneous counterpart of MEC. HA in the breast usually arises in the nipple and subareolar region, although it may also be located in the deeper parenchyma. Differentiating HA of the breast skin from low-grade MEC is diagnostically challenging, if not impossible, in a CNB [119–121]. An infiltrative growth pattern or irregular borders favor MEC, while the presence of ductal or tubular structures lined by SOX10-positive basophilic cuboidal cells is suggestive of HA [122]. Complete excision to evaluate the entire lesion is required for a definitive diagnosis.

Finally, although metastatic MEC from the salivary gland or other anatomic locations could be considered in the differential diagnosis, this is very unlikely. Salivary gland tumors rarely metastasize to the breast, and low-grade MEC does not carry a risk for distant metastasis. Nevertheless, clinical history is helpful in excluding metastasis. A DCIS component, if present, supports MEC of the breast.

Pathogenesis

MEC arising in salivary gland and other sites are characterized by recurrent chromosomal translocations involving the *MAML2* gene, most commonly t(11;19), which results in *CRTC1-MAML2* fusion, and less frequently t(11;15), which results in *CRTC3-MAML2* fusion [123–125]. *MAML2* gene rearrangements and *CRTC1-MAML2* fusions have also been identified in breast MEC by FISH, reverse transcription polymerase chain reaction (RT-PCR), and RNA sequencing [100, 105, 111, 112]. *MAML2* rearrangements are thus considered the hallmark genetic alteration of MEC regardless of anatomic location. Detection of *MAML2* rearrangement using a commercially available *MAML2* break-apart FISH probe (Fig. 12.33) or detection of *CRTC1-MAML2* fusion by RT-PCR or sequencing technologies can be performed on formalin-fixed paraffin-embedded tissue to confirm the diagnosis of this rare breast cancer subtype, especially in challenging CNB specimens.

CRTC1 (*C*REB *R*egulated *T*ranscriptional *C*oactivator) controls the expression of specific CREB-activated genes, and *MAML2* gene is a member of the mastermind-like family that augments Notch signaling. The *CRTC1-MAML2* fusion gene has been shown to activate Notch signaling and has transforming activity in cell lines, with silencing of the fusion inhibiting tumor growth [126]. Expression of *CRTC1-MAML2* in a transgenic mouse model causes formation of salivary gland tumors that resemble histological and molecular characteristics of human MEC [127]. Together, in vitro and in vivo studies support *CRCT1-MAML2* fusion as the major oncogenic driver in MEC.

In addition to *CRTC1-MAML2* fusions, breast MEC have been found to have simple genomes with no copy number alterations and a very low exonic mutational burden, similar to other fusion gene-driven special breast cancer subtypes (e.g., AdCC and secretory carcinoma) and distinct from high-grade TNBC of no special type [100].

Prognosis and Clinical Management

The prognosis of breast MEC is correlated with histologic grade and clinical stage. High-grade tumors portend aggressive behavior with frequent metastasis to axillary lymph nodes and distant organs. Approximately 30% of high-grade MEC in the literature developed distant metastasis and eventually led to death. In contrast, only rare axillary metastasis and no distant spread have been documented for low- and intermediate-grade MEC, and none of the patients died of disease [104, 105, 122]. Low-grade MEC of the breast can be considered to have indolent biological behavior and favorable clinical outcome, similar to other salivary gland-like carcinomas in the breast, such as AdCC and secretory carcinoma.

Given the rarity of MEC in the breast, there is limited data to guide treatment. Complete excision with clear margins has been proposed as the standard surgical approach. Most patients are not eligible for hormonal therapy due to the triple-negative status of these tumors. Radiation has been offered to some patients in case reports. Chemotherapy is not likely to be recommended for node-negative low-grade tumors [104, 105].

Secretory Carcinoma

Overview

Secretory carcinoma is a rare salivary gland-type breast carcinoma characterized by distinct morphologic and immunophenotypic features and underpinned by a hallmark t(12;15)(p13;q25) chromosomal translocation and resultant *ETV6-NTRK3* gene fusion. These tumors account for <0.05% of invasive breast carcinomas [128, 129]. Secretory carcinoma was initially described in children by McDivitt and Stewart and was called "juvenile breast carcinoma" [130] and remains the most common breast cancer of childhood. However, these tumors have subsequently been found to occur predominantly in adults [130–139], and the term juvenile breast carcinoma is not recommended. Unlike other salivary gland-type carcinomas of the breast, secretory carcinoma was first recognized in the breast, with analog tumors that harbor the same *ETV6-NTRK3* fusion (previously termed mammary analog secretory carcinomas [MASC]) subsequently described at other anatomic sites including salivary gland [140–143], sinonasal mucosa [144], skin [145–147], lung [148], vulva [149], and thyroid gland [150–152]. The number of salivary gland secretory carcinomas reported in the literature has now surpassed that of its breast counterpart.

Secretory carcinomas of the breast occur predominantly in women but may also be seen in men [128, 132, 133, 153, 154]. Most of these tumors present in the fourth to seventh decade (range 3–87 years), with a mean patient age of 53 [130–139, 154, 155]. The most common presentation is of a slow-growing, firm, painless, well-circumscribed, mobile breast mass, occasionally with nipple discharge. In women, secretory carcinomas most frequently arise in the upper outer quadrant or near the nipple, but any region of the breast can be involved, including ectopic breast tissue [130–133, 155,

156]. In children or men, the tumors commonly arise in the subareolar region [130, 132, 133].

Gross and Radiologic Features

Gross examination generally reveals a well-circumscribed mass with grayish-white or yellowish-tan, firm cut surfaces. Mean tumor size is approximately 1–2 cm, but a wide range in sizes has been reported (up to 16 cm) [128, 130–135, 137, 138, 157].

On ultrasound, secretory carcinoma presents as a well-circumscribed, round to oval, macrolobulated, isoechoic to hypoechoic, mass mimicking fibroadenoma [158–160] or sometimes as a hypoechoic, irregularly shaped, spiculated mass with heterogeneous internal echoes [161, 162]. Mammographic findings are variable and nonspecific, including a discrete nodular density with irregular margins [158, 159, 162, 163], heterogeneously dense pattern with no evidence of a mass [160], or as an isodensity mass with an obscured margin [161].

Microscopic Features

Secretory carcinomas are composed of polygonal tumor cells with moderate amounts of eosinophilic vacuolated or granular cytoplasm and rounded to oval nuclei, which infiltrate in various growth patterns, including microcystic/honeycomb, papillary, tubular, and solid (Fig. 12.34). Most tumors have mixed growth patterns. The microcystic spaces and tubular lumens are filled with prominent eosinophilic or amphophilic bubbly secretions. Intracellular secretory vacuoles and extracellular secretions stain positively for PASD, mucicarmine, and Alcian blue. The tumor nuclei are usually small to medium in size and rounded to oval with open, vesicular chromatin and small nucleoli (mild to moderate nuclear pleomorphism). Mitotic activity is generally low. Accordingly, the vast majority of secretory carcinomas are histological grade 1 or 2 by modified Scarff-Bloom-Richardson grading. High-grade tumors have been reported but are exceptionally rare [134]. The tumor stroma is often sclerotic. An in situ component may be present, usually with similar secretory features, low- or intermediate-grade nuclei, and cribriform and solid patterns [133, 135, 137, 154]. Distinction of in situ carcinoma from invasive carcinoma with microcystic architecture and rounded contours may be challenging by H&E alone and can be assisted with immunohistochemical stains for myoepithelial markers (Fig. 12.35). Pure secretory carcinoma in situ is exceedingly rare [164].

Immunohistochemistry

The tumor cells typically express S100 protein, CEA (polyclonal), mammaglobin, SOX10, and MUC4, usually in a strong and diffuse staining pattern (Fig. 12.36a–e). GATA3, CK8/18, CD117, and vimentin may also be positive. GCDFP-15 is usually negative or only focally positive (Fig. 12.36f). Most secretory carcinomas show a basal immunophenotype with expression of cytokeratins 5/6, 14, and 17 and EGFR, although positivity may be focal (Fig. 12.37) [132–134, 137, 139]. Secretory carcinomas are often triple negative for ER, PR, and HER2, although weak ER/PR expression is not uncommon [133, 134, 137]. The Ki-67 proliferation index is often <20% but variable across tumors [132, 134, 135].

Most secretory carcinomas show nuclear staining using a pan-TRK antibody [116, 165, 166] (Fig. 12.38). In one study, diffuse (>50% of cells) and/or at least focally strong nuclear staining was found to be sensitive (~83%) and specific (100%) for the diagnosis of breast secretory carcinoma [116]. Cytoplasmic staining is not specific in this context.

Differential Diagnosis

The architectural pattern (microcystic/fenestrated, papillary, tubular, or solid), cytologic features (ample eosinophilic, clear, or vacuolated cytoplasm), and prominent secretory material in secretory carcinoma can mimic several benign and malignant lesions of the breast, especially in a limited CNB sample.

Lactational or lactational-like change: Secretory carcinoma bears superficial resemblance to lactational (or lactational-like) change, as both lesions feature prominent eosinophilic secretions and epithelial cells with vacuolated cytoplasm (Fig. 12.39a, b). However, lactational change is a lobulocentric process and lacks microcystic, papillary, or solid architecture, whereas secretory carcinoma has infiltrative growth with various architectural patterns. In challenging cases with limited material, immunohistochemical stains with myoepithelial markers and pan-TRK antibody can help with the differential diagnosis [116]. The glands of lactational change have intact myoepithelial layers and lack nuclear pan-TRK expression.

Cystic hypersecretory lesions: Secretory carcinoma may also be confused with cystic hypersecretory lesions (including cystic hypersecretory hyperplasia and cystic hypersecretory carcinoma), as these lesions all have densely eosinophilic (thyroid colloid-like) secretions that may retract from the luminal epithelium (Fig. 12.39c, d). However, the tinctorial

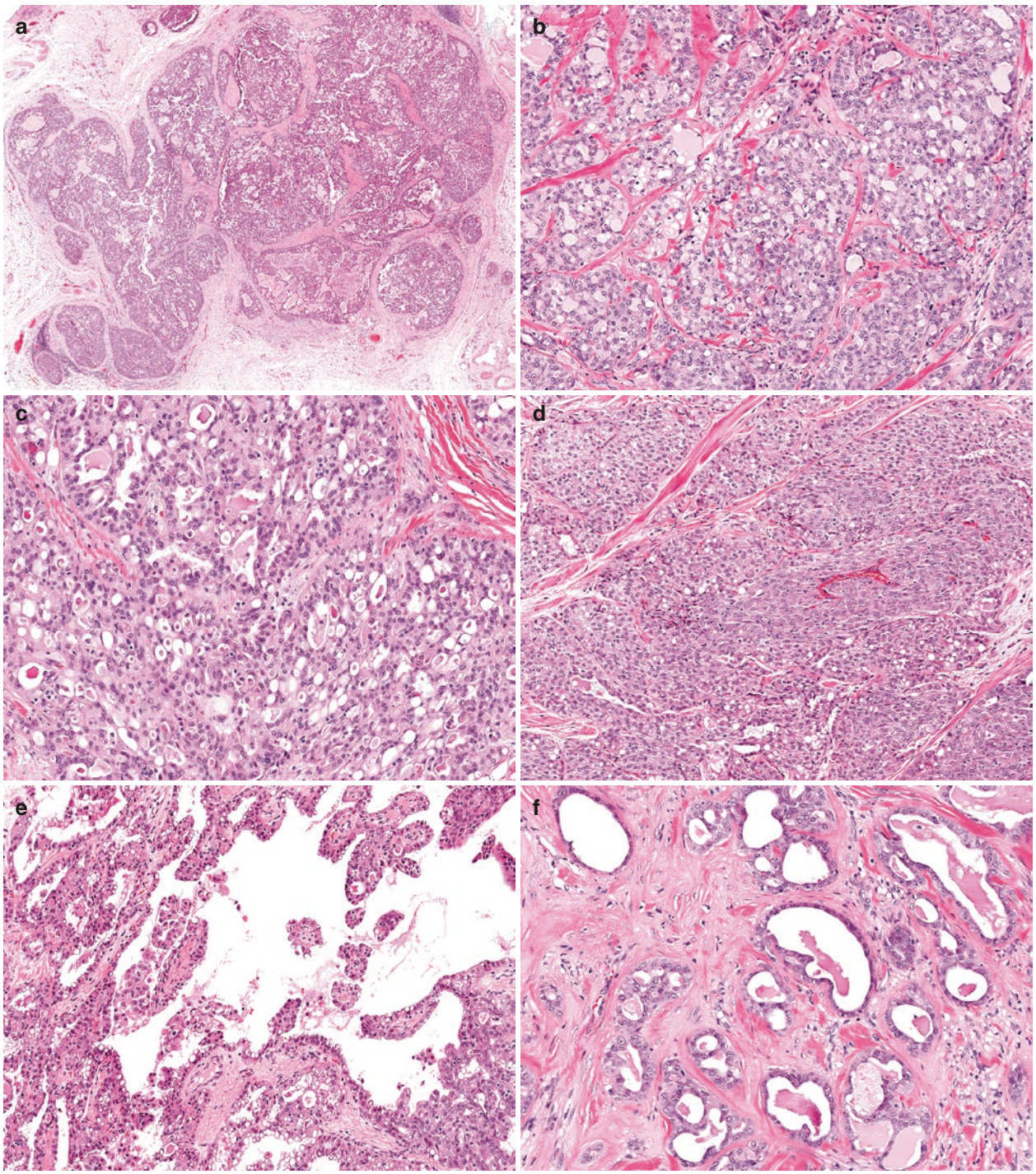

Fig. 12.34 Secretory carcinoma, histologic features. (**a**) Low magnification demonstrates tumor cells arranged in glandular structures and nests of variable size and shape within a fibrotic/sclerotic stroma. The tumor cells are organized in various architectural patterns, including microcystic/fenestrated/honeycomb pattern (**b**, **c**), solid nests (**d**), papillary structures (**e**), and tubular/follicular pattern (**f**). The microcystic pattern is usually the predominant architectural component. However, these patterns are often admixed in various proportions in an individual tumor. Note that the glandular spaces contain prominent secretions, which may be densely eosinophilic (thyroid colloid-like), amphophilic, or basophilic (mucin-like) and often have a bubbling appearance. (**g**, **h**) Cytologically, the tumor cells have moderate to abundant eosinophilic to vacuolated cytoplasm and low- to intermediate-grade nuclei that are usually oval in shape with small nucleoli. Note the vacuolated/bubbly cytoplasm in (**h**). (**i**) In rare examples, scattered tumor cells may have apocrine features, with coarse eosinophilic granules that can be highlighted by GCDFP-15 immunohistochemical stain (*not shown*). (**j**) This tumor shows higher grade nuclear features than is typical, with enlarged nuclei, vesicular chromatin, and prominent nucleoli. Rare tumors with high-grade nuclei, increased mitotic activity and necrosis have been reported and are associated with more aggressive behavior. (**k**, **l**) In this core needle biopsy, the characteristic microcystic glandular pattern with prominent secretions and cytologically bland tumor cells can be appreciated to suggest the diagnosis, which can be confirmed with appropriate immunohistochemical stains and *ETV6* FISH

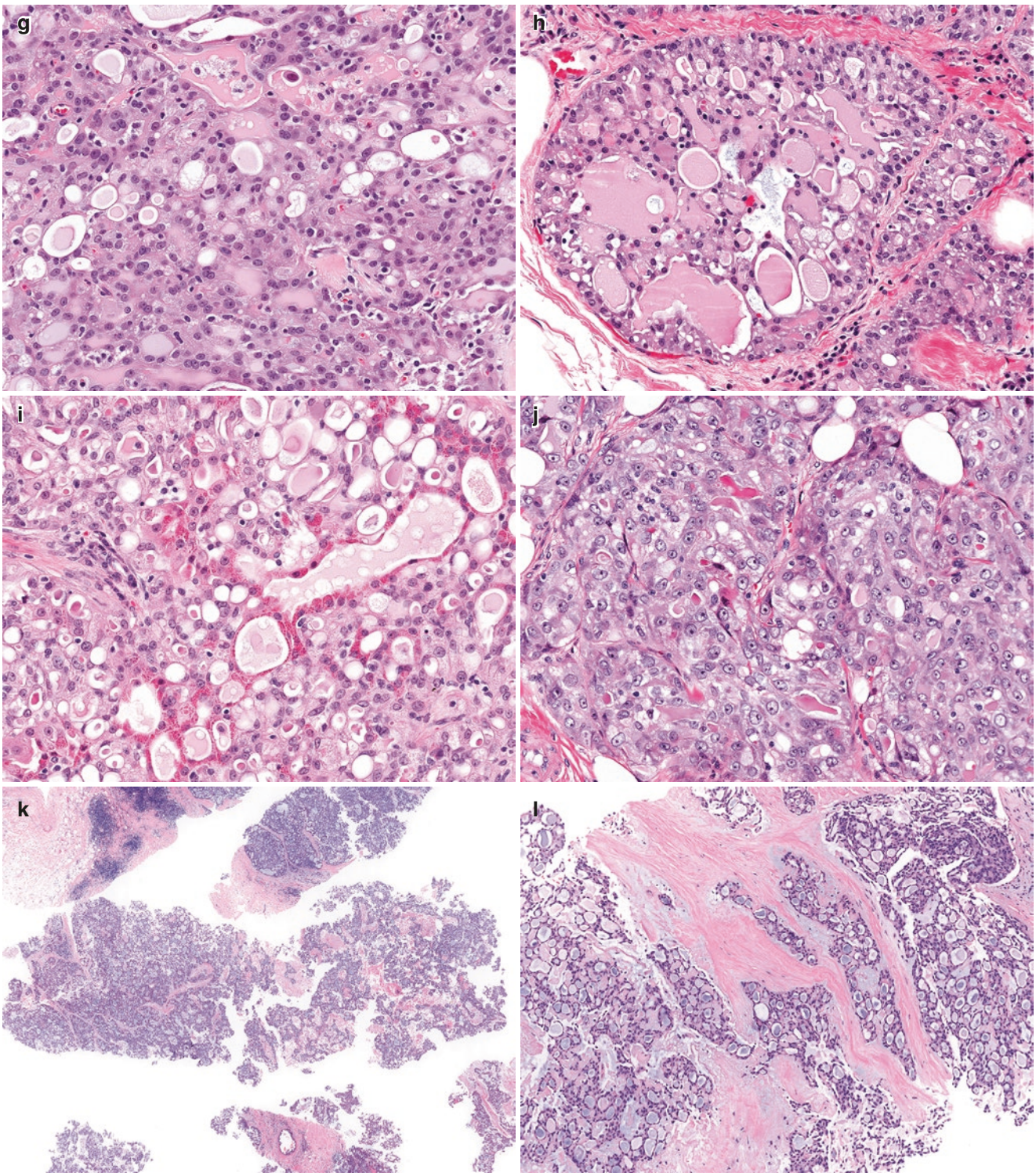

Fig. 12.34 (continued)

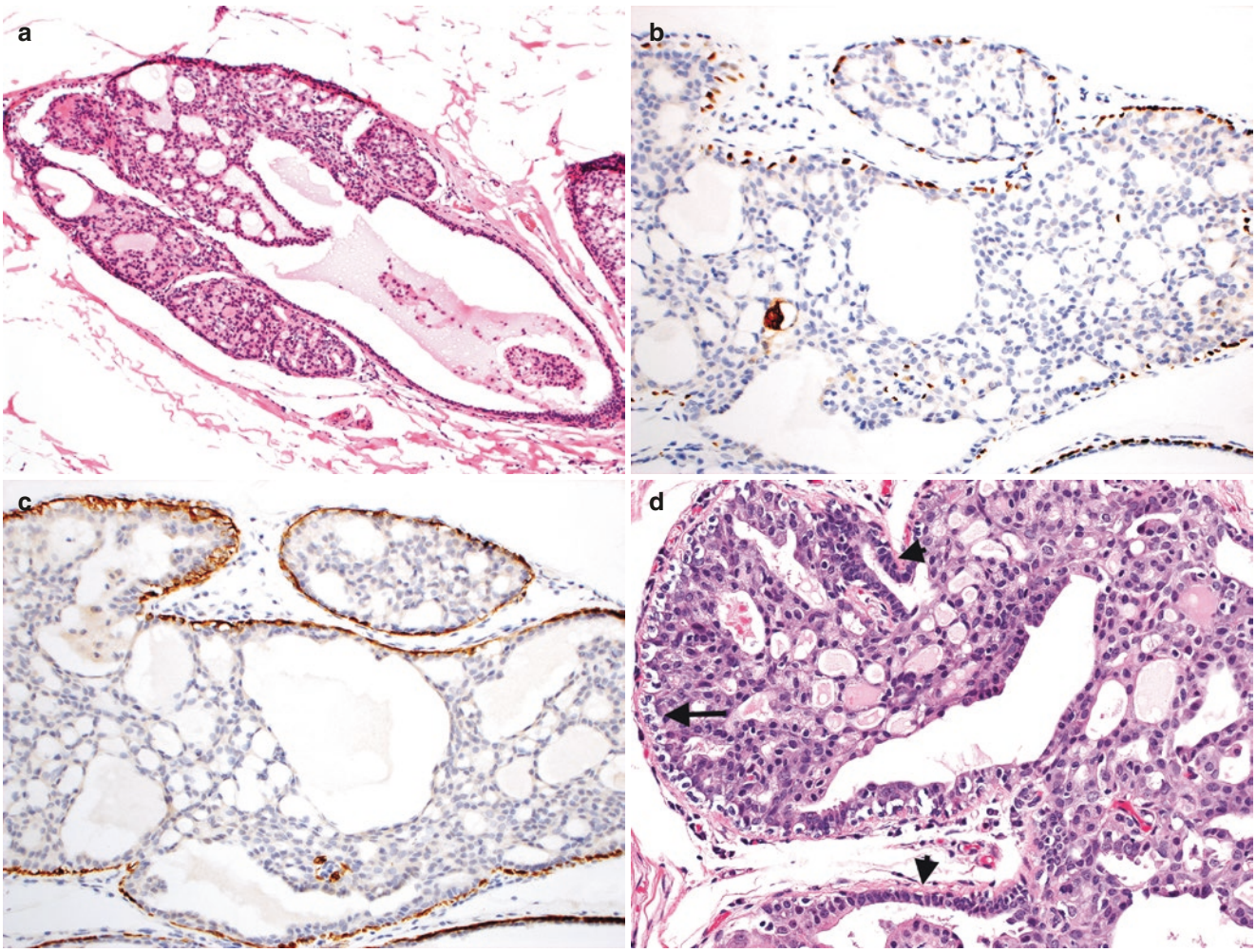

Fig. 12.35 Secretory carcinoma, in situ component. (**a–c**) An in situ component may be present in some cases and typically demonstrates a cribriform/fenestrated pattern, prominent eosinophilic secretions in the glandular spaces, and low- to intermediate-grade nuclei, as appreciated on the H&E stain (**a**) in this example. Immunohistochemical stains for myoepithelial markers p63 (**b**) and SMM (**c**) highlight the peripheral myoepithelial layer and support an in situ lesion. (**d**) Another example of secretory carcinoma in situ. Note the layer of myoepithelial cells with clear cytoplasm at the periphery of the duct (*arrows*) and residual normal luminal epithelium (*arrowheads*)

quality of the secretions is different: the secretions in cystic hypersecretory lesions often show parallel linear cracks (but not always), while secretions in secretory carcinoma have an overall bubbling appearance without parallel linear cracks. Cystic hypersecretory lesions are not infiltrative and lack expression of nuclear pan-TRK and basal markers (CK5/6 and EGFR). Most cystic hypersecretory lesions are ER positive (see also Chap. 13).

Usual ductal hyperplasia: In a limited CNB sample, the microcystic/fenestrated pattern, bland cytologic features, and patchy CK5/6 expression of secretory carcinoma may mimic usual ductal hyperplasia (Fig. 12.39e). The prominent luminal secretions and negative (or minimal) ER expression are clues to reconsider the diagnosis.

Low-grade mucoepidermoid carcinoma: A major differential diagnostic consideration for secretory carcinoma is low-grade MEC. These two salivary gland-type carcinomas share overlapping architectural patterns, PASD-positive secretions, bland cytologic features, and a similar immunophenotype, which includes positive mammaglobin, MUC4, and CK5/6 and triple-negative biomarker status (see also section "Mucoepidermoid Carcinoma" in this chapter and Fig. 12.32). Distinction of the two can be facilitated by FISH using *MAML2* and *ETV6* break-apart probes to identify the hallmark rearrangements of each (Figs. 12.33 and 12.38a), and/or pan-TRK immunohistochemistry (Fig. 12.32).

Acinic cell carcinoma: Secretory carcinoma may be confused with acinic cell carcinoma when the latter has follicular and/or solid architecture, luminal secretions, and clear cytoplasm with less conspicuous cytoplasmic granules. Furthermore, both tumor types are strongly S100 positive. However, the large PASD-positive cytoplasmic zymogen-like granules typical of acinic cell carcinoma are absent in

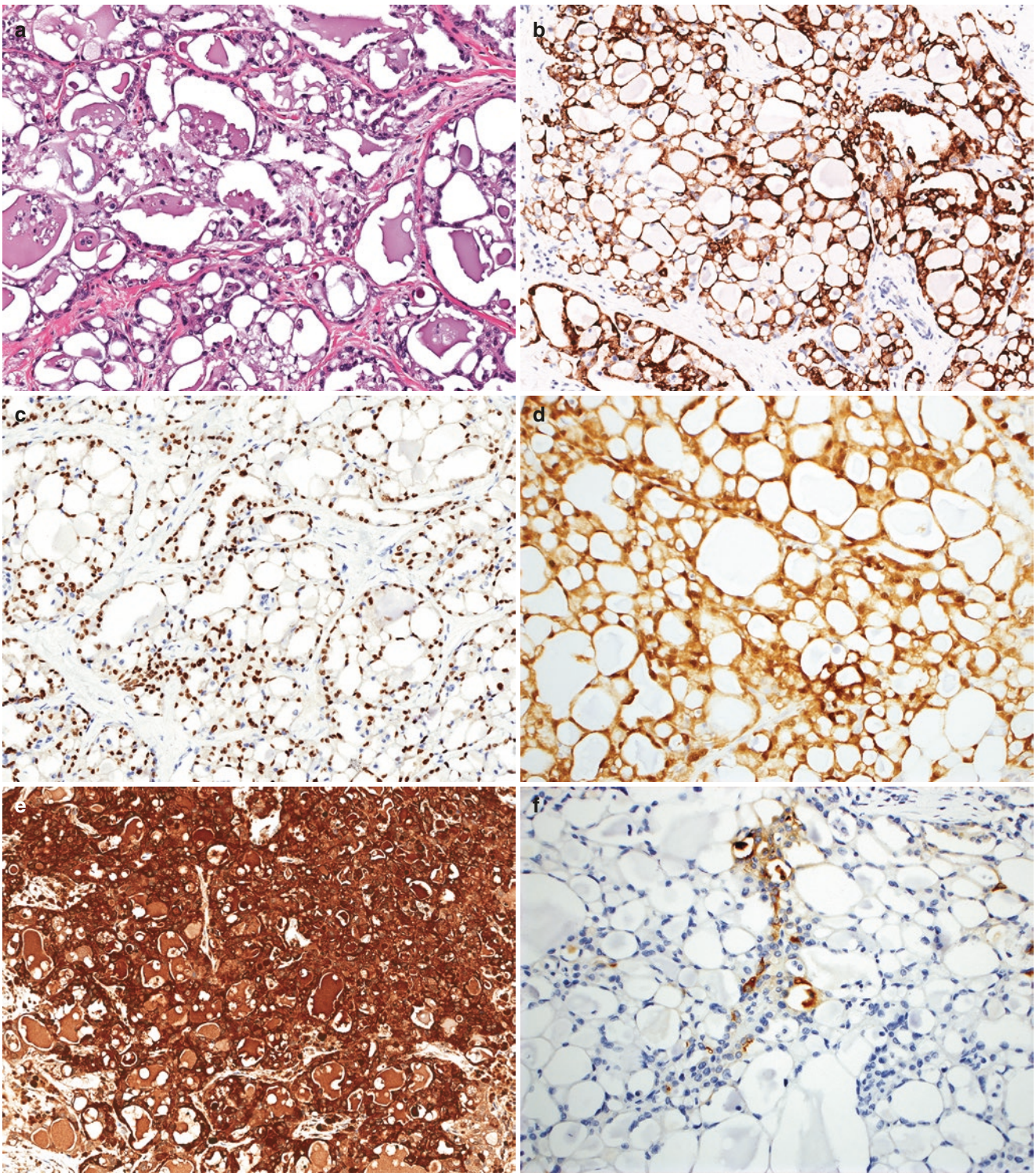

Fig. 12.36 Secretory carcinoma, immunohistochemical profile. Although not specific, secretory carcinoma (**a**) shows a characteristic immunostaining pattern that is helpful in establishing the diagnosis. This includes typically diffuse and strong immunoreactivity to MUC4 (**b**), SOX10 (**c**), S100 protein (**d**), and mammaglobin (**e**). Most tumors are either negative or only focally positive for GCDFP-15 (**f**). However, rare examples with strong GCDFP-15 expression have been noted

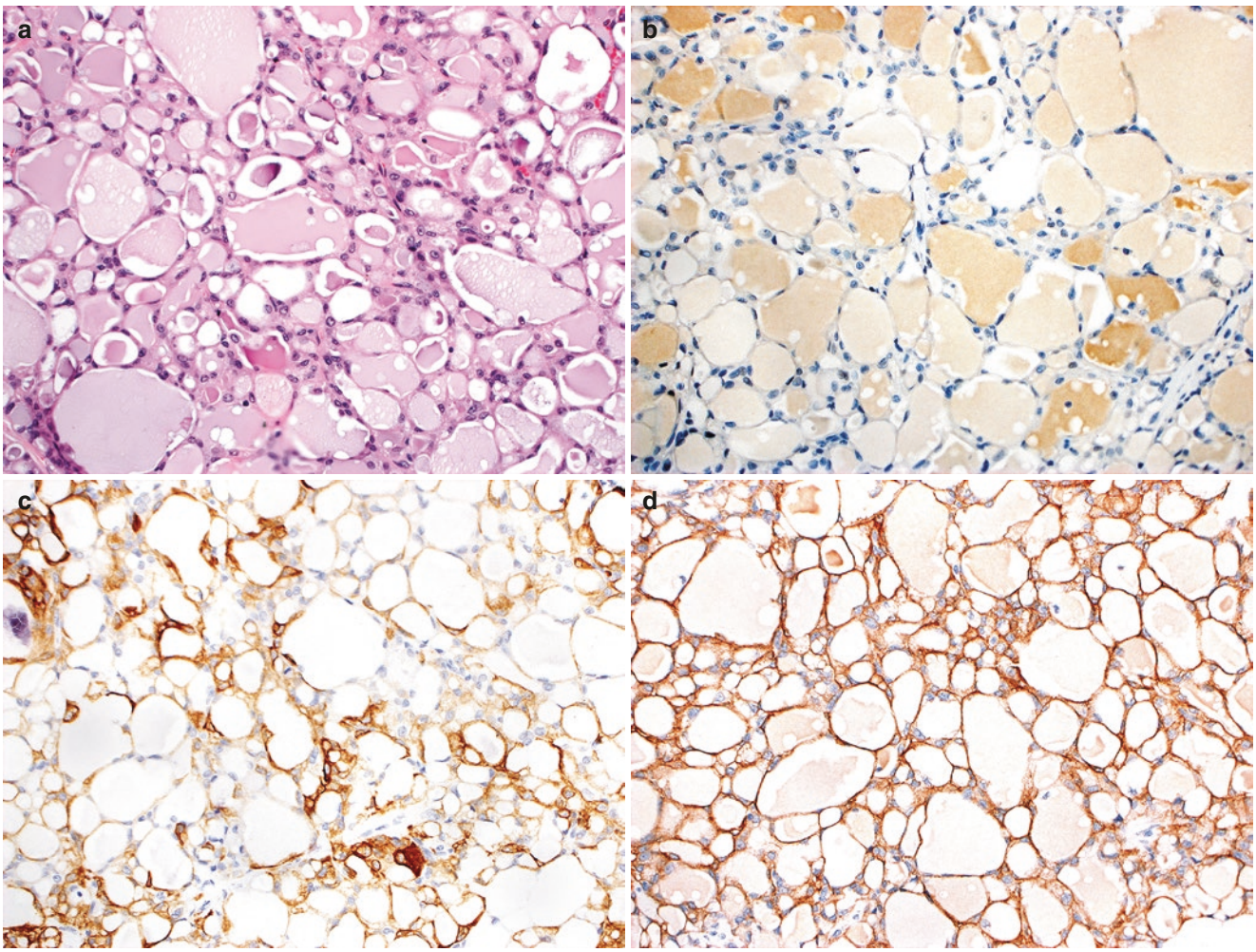

Fig. 12.37 Secretory carcinoma, basal-like immunophenotype. (**a**, **b**) Most secretory carcinomas are negative for ER (**b**), PR (*not shown*) and HER2 (*not shown*). These tumors usually express basal markers, such as CK5/6 (**c**) and EGFR (**d**), although expression may be focal

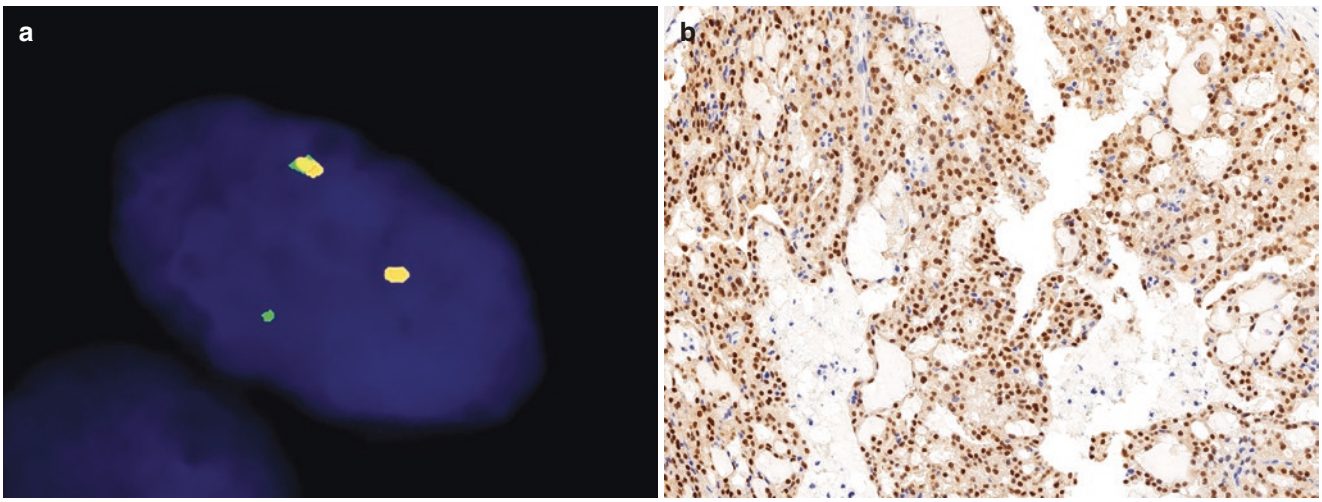

Fig. 12.38 *ETV6-NTRK3* and pan-TRK immunohistochemistry in secretory carcinoma. (**a**) *ETV6* rearrangement can be demonstrated by fluorescence in situ hybridization using an *ETV6* break-apart probe. Note the separate green and orange signals from the rearranged *ETV6* allele and the single fused yellow signal from the other intact *ETV6* allele. The *ETV6-NTRK3* fusion can be directly detected using *ETV6* and *NTRK3* convergence probes (*not shown*) or next-generation sequencing methods. (**b**) Overexpression of the chimeric ETV6-NTRK3 protein can be detected using a pan-TRK antibody, which shows diffuse and/or at least focally strong nuclear staining

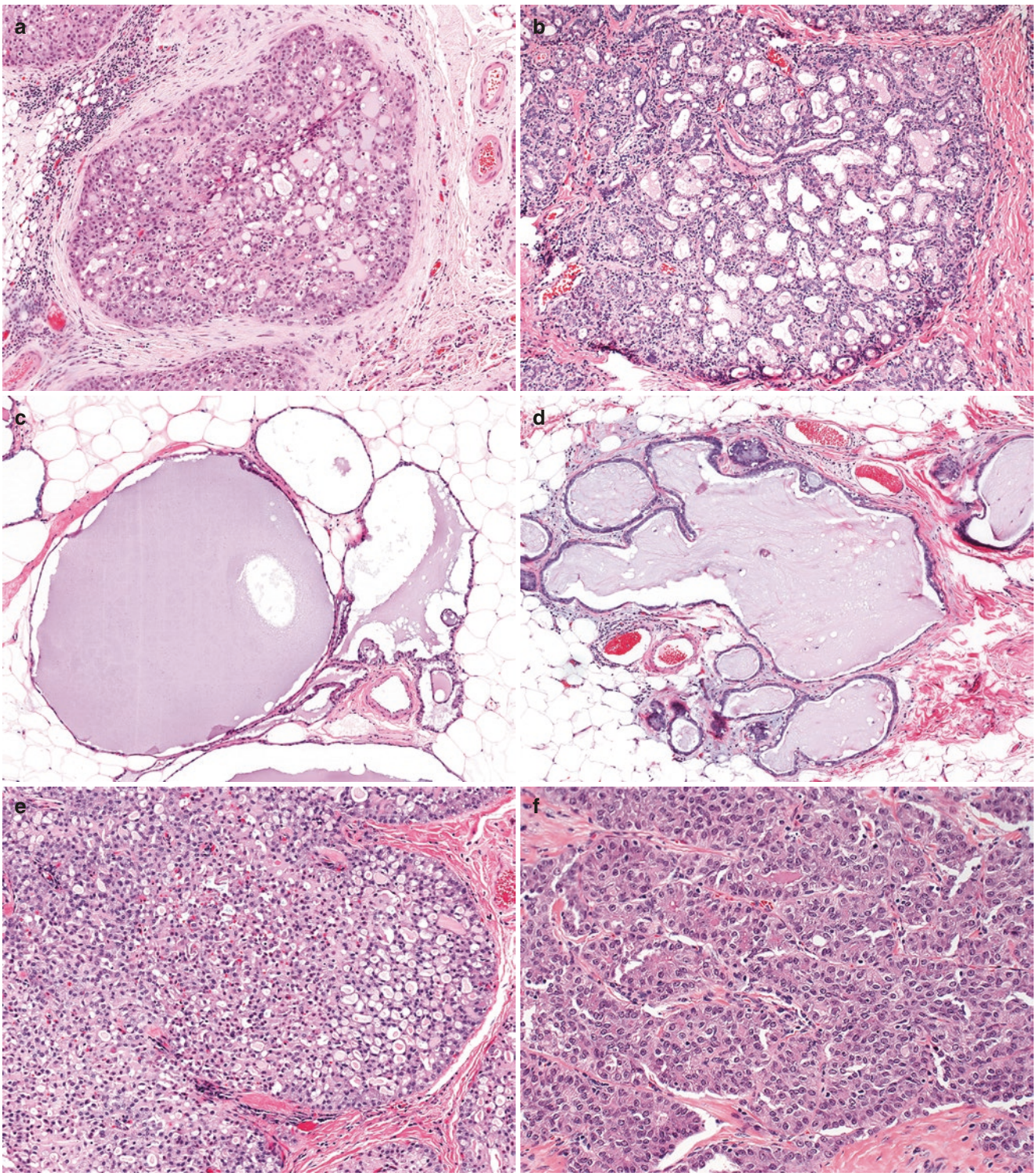

Fig. 12.39 Secretory carcinoma, morphologic mimics. Secretory carcinoma can mimic a number of benign and malignant breast lesions. At low power, the prominent secretions and vacuolated cytoplasm in secretory carcinoma (**a**) can resemble lactational change (**b**). Secretory carcinoma (**c**), especially the follicular pattern, can mimic atypical cystic hypersecretory hyperplasia (**d**). Sometimes, secretory carcinoma with fenestrated pattern and bland cytology (**e**) can be misconstrued as usual ductal hyperplasia. Secretory carcinoma with solid nested growth pattern and eosinophilic cytoplasm (**f**) may be confused with apocrine carcinoma (**g**). (**h**) The dense eosinophilic secretions in this secretory carcinoma impart a thyroid colloid-like appearance, which could suggest metastatic follicular thyroid carcinoma. The triple-negative biomarker profile may further complicate the issue. Strong mammaglobin expression that is typical of secretory carcinoma would help exclude a metastatic carcinoma

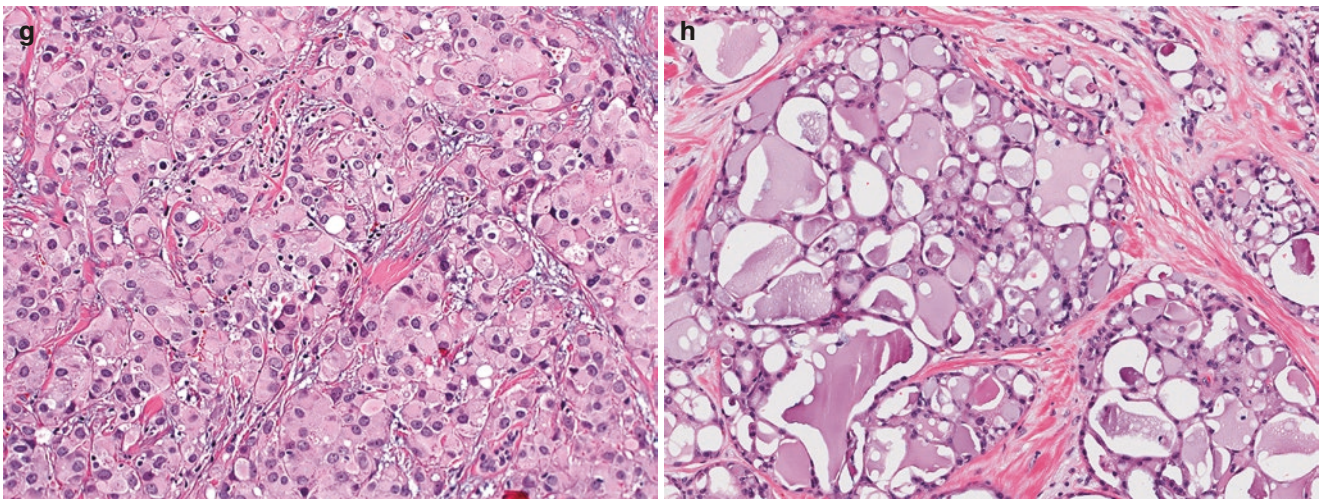

Fig. 12.39 (continued)

secretory carcinoma. Acinic cell carcinoma lacks *ETV6-NTRK3* and is negative for nuclear pan-TRK expression (see also sections "Carcinoma with Apocrine Differentiation" and "Differential Diagnosis" in this chapter).

Carcinoma with apocrine differentiation: Secretory carcinoma can mimic carcinoma with apocrine differentiation, especially when growing in tubular and solid patterns (Figs. 12.34i and 12.39f, g). Carcinoma with apocrine differentiation lacks the typical luminal secretions of secretory carcinoma and the apocrine cells have round nuclei with prominent nucleoli. Immunohistochemically, carcinoma with apocrine differentiation typically shows diffuse and strong expression of GCDFP-15 and AR, and is negative for mammaglobin, S100 protein, and pan-TRK antibody.

Tall cell carcinoma with reversed polarity: TCCRP is another potential consideration in the differential diagnosis of secretory carcinoma, as both tumor types can have papillary and follicular components, eosinophilic colloid-like secretions, and epithelial cells with abundant eosinophilic cytoplasm and low- to intermediate-grade nuclei. Both tumors also share a triple-negative and CK5/6-positive, basal-like immunoprofile. However, TCCRP exhibits distinguishing cytological features, including reverse polarization, nuclear grooves, and cytoplasmic pseudoinclusions. In contrast to secretory carcinoma, TCCRP shows variable and less mammaglobin expression and is negative or only focally positive for S100 protein. Recurrent *IDH2* hotspot mutations of TCCRP can be detected by IDH2 R172 mutant-specific immunohistochemical stain (see also section "Tall Cell Carcinoma with Reversed Polarity" in this chapter).

Pathogenesis

Secretory carcinoma canonically harbors a t(12;15)(p13;q25) chromosomal translocation that results in an *ETV6-NTRK3* fusion gene, which has been identified in both in situ and invasive carcinoma components, consistent with an early oncogenic event [133, 137, 154, 167]. The rearrangement joins the N-terminal dimerization domain of *ETV6* with the C-terminal tyrosine kinase domain of *NTRK3* to produce a ligand-independent, constitutively activated chimeric tyrosine kinase that signals through RAS-mitogen activated protein kinase (MAPK) and PI-3 K pathways and can transform cells of multiple lineages [133, 167–173]. *ETV6-NTRK3* has also been described in secretory carcinomas arising in other anatomic sites [133, 141, 146, 151]. Together, the shared morphologic, immunophenotypic, and genetic features of secretory carcinomas are consistent with a common pathogenesis for these tumors, regardless of anatomic site. Secretory carcinomas with *ETV6* rearrangements lacking *ETV6-NTRK3* fusions have been described in the salivary gland, with identified fusions in these tumors including *ETV6-RET*, *ETV6-MAML3*, and *ETV6-MET* [174–181]. However, such alternate fusions have not been identified in secretory carcinomas of the breast.

Consistent with *ETV6-NTRK3* as the main oncogenic driver of secretory carcinomas, targeted DNA sequencing of primary breast and salivary gland secretory carcinomas did not identify additional driver mutations in these tumors, which were additionally found to have a low exonic mutational burden and quiet genomes with no to few chromo-

somal copy number changes and no focal amplifications or deletions [133]. Accordingly, secretory carcinomas of the breast are genetically distinct from invasive breast carcinomas of no special type (IBC-NST), including common basal-like carcinomas. Instead, akin to other fusion gene-driven salivary gland-like breast carcinomas (AdCC, MEC), secretory carcinomas appear to be genetically more similar to their counterparts at other anatomic sites [45, 100, 133]. A recent study found additional aberrations in distant metastases of two aggressive secretory carcinomas, including amplification of the 16p13.3 locus (containing *PDPK1*), a hotspot *TERT* promotor mutation, and loss of 9p21.3 locus (*CDKN2A, CDKN2B*) [154].

In addition to secretory carcinomas, *ETV6-NTRK3* fusions have been described in a variety of other tumor types, including infantile fibrosarcoma [182], cellular mesoblastic nephroma [183], glioma [165], acute myeloid leukemia [184], ALK-negative inflammatory myofibroblastic tumor [185], Spitz-tumor [186], and radiation-induced thyroid carcinoma [152]. However, *ETV6-NTRK3* appears to be specific for secretory carcinoma in the context of breast cancer and has not been identified in other breast carcinomas [187]. Detection of the hallmark translocation or gene fusion by FISH or next-generation sequencing analysis, respectively, can be used to confirm the diagnosis. *ETV6* break-apart (likely most often used) (Fig. 12.38a), *NTRK3* break-apart, and *ETV6-NTRK3* convergence probes (most specific) are commercially available. In addition, immunohistochemistry using a pan-TRK antibody has been shown to be a highly specific (100%) and slightly less sensitive (~83%) marker for secretory carcinoma in the breast (Fig. 12.38b). In addition to its diagnostic utility, demonstration of the *ETV6-NTRK3* fusion has additional clinical value, as *ETV6-NTRK3* fusions may be targeted for treatment (see sections "Prognosis and Clinical Management").

Prognosis and Clinical Management

Secretory carcinomas generally have an indolent clinical course with favorable outcome, especially in children and young adults and even in the context of axillary nodal metastasis [128, 130, 131, 137]. Five- and ten-year survival rates are 87% and 77%, respectively, and 5- and 10-year cause-specific survival rates are 94% and 91%, respectively [128]. Axillary metastases have been reported in ~20–35% of patients overall [128, 131–134, 154]. Recurrences and distant metastases are uncommon, and deaths are rare [131, 134, 153, 154, 157]. However, some tumors, often in older adult patients, may be more aggressive [154, 157].

The primary treatment is surgical excision to negative margins with sentinel lymph node sampling [128, 162, 188]. In children, preservation of breast tissue is attempted if possible to ensure normal breast development [188]. The efficacy of adjuvant radiation is uncertain, but radiotherapy has been reported to be increasingly used in adults [128]. Similarly, the role of chemotherapy is unknown, although reports suggest poor responses in patients with metastatic tumors [189]. Small molecule inhibitors (larotrectinib, entrectinib) targeting NTRK3 and other NTRK family members show promising efficacy in patients with TRK fusion cancers [190–192], including breast secretory carcinoma [193].

Carcinoma with Apocrine Differentiation

Overview and Clinical Presentation

Carcinoma with apocrine differentiation is defined as invasive carcinoma with cytologic features of apocrine cells in more than 90% of the tumor cell population [194]. However, recognition of what constitutes apocrine cytology can be subjective, especially at the lower end of the morphologic spectrum, and variable apocrine cytologic features can also be seen in other subtypes of breast carcinomas, including IDC (of no special type), lobular, micropapillary, mucinous, and papillary carcinomas. Furthermore, carcinomas with apocrine morphology can vary in terms of ER and HER2 status and exhibit heterogeneous intrinsic gene expression patterns [37, 195]. Gene expression signatures associated with these tumors (molecular apocrine, luminal androgen receptor [LAR]) lack ER and are enriched for AR expression and hormonally regulated pathways, but do not exclusively correlate with apocrine histology [196, 197]. It is therefore not surprising that different series in the literature have reported variable clinical outcomes for invasive carcinomas with apocrine features. A combination of apocrine cytomorphology and immunophenotype (ER and PR negative, AR positive) has been used to refine the classification. As such, these tumors, which may be triple negative or HER2 positive, have also been referred to as pure apocrine carcinomas, and comprise a subset of the carcinomas identified as LAR or molecular apocrine by gene expression [196–198]. Invasive carcinomas with apocrine morphologic features but lacking the above immunophenotype have been referred to as apocrine-like car-

cinomas [194, 199, 200]. For the purpose of discussion in this chapter, apocrine carcinoma is used synonymously with carcinoma with apocrine differentiation and defined by cytologic features. The term pure apocrine carcinoma is adopted when the tumor is known to also demonstrate an ER- and PR-negative and AR-positive immunophenotype.

Using strict diagnostic criteria, apocrine carcinoma is rare and comprises <1% of all breast cancers [201–203]. The clinical presentation is similar to IBC-NST. Patients may be asymptomatic or present with a hard, palpable, irregular breast lump with or without skin or nipple retraction. Presentation with bloody nipple discharge is uncommon [194]. Apocrine carcinoma is usually unilateral but can be multifocal/multicentric, and rare cases of bilateral tumors considered to be independent primaries have been reported [204]. Overall, patients tend to be postmenopausal and older than patients presenting with IBC-NST [205–214].

Gross and Radiologic Features

Imaging and gross pathologic findings are not distinctive from IBC-NST. Triple-negative apocrine carcinomas (TNAC) have been reported to be smaller than IBC-NST [208, 210, 212, 213, 215].

Microscopic Features

Microscopically, apocrine carcinomas demonstrate architectural growth patterns similar to those of IBC-NST but differ in their cytologic appearance [216] (Fig. 12.40). These tumors are characteristically composed of large cells with abundant cytoplasm, round and/or pleomorphic vesicular nuclei and prominent nucleoli, occasionally associated with apical cytoplasmic "snouts" projecting into the glandular

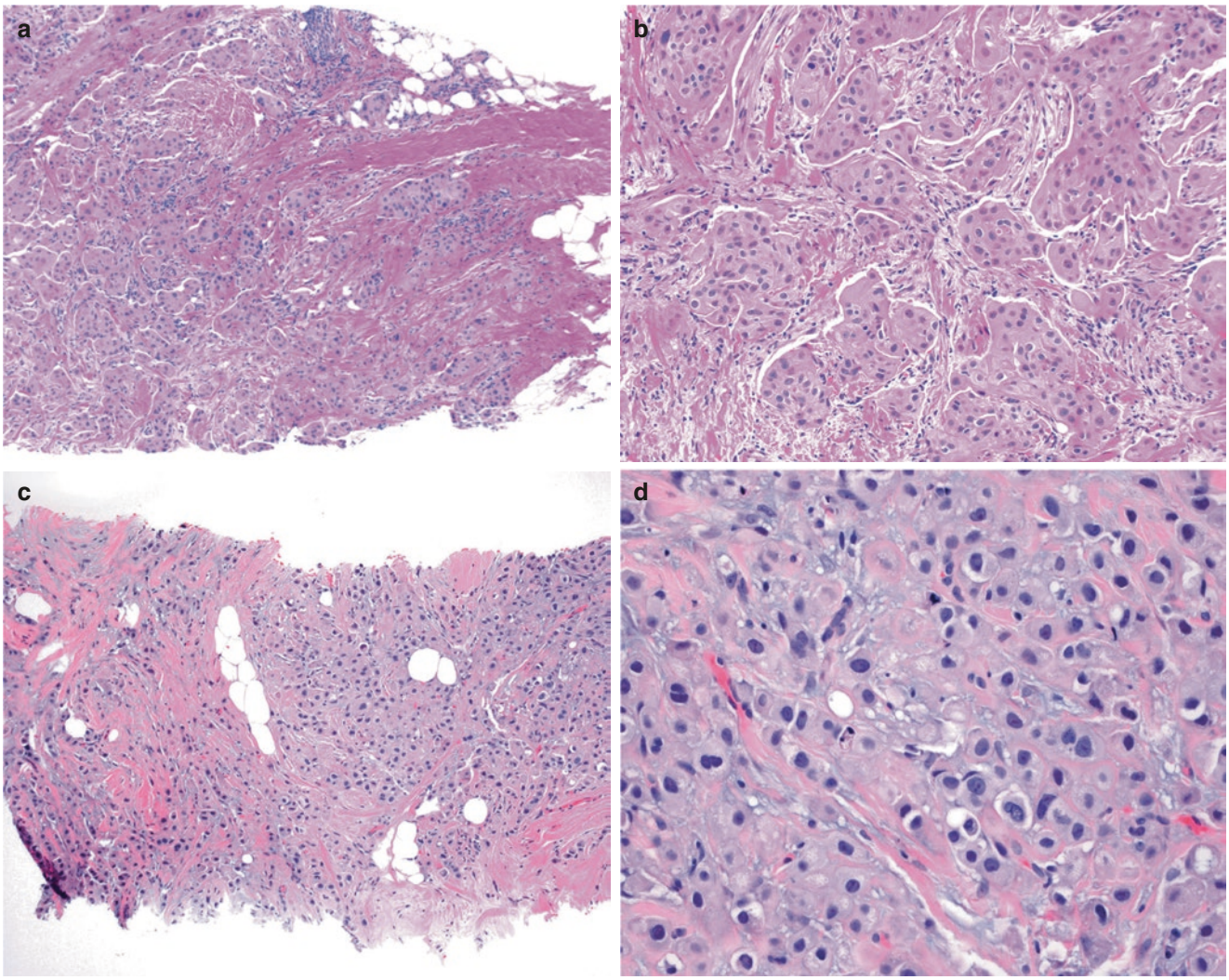

Fig. 12.40 Core needle biopsy showing growth patterns of invasive apocrine carcinoma. (**a**–**d**) Most apocrine carcinomas invade as irregular nests and small tumor clusters. (**e**–**g**) In some cases, glandular differentiation is present, which rarely exceeds 75%. (**h**) Note the apical cytoplasmic snouts projecting into the glandular lumens of this case

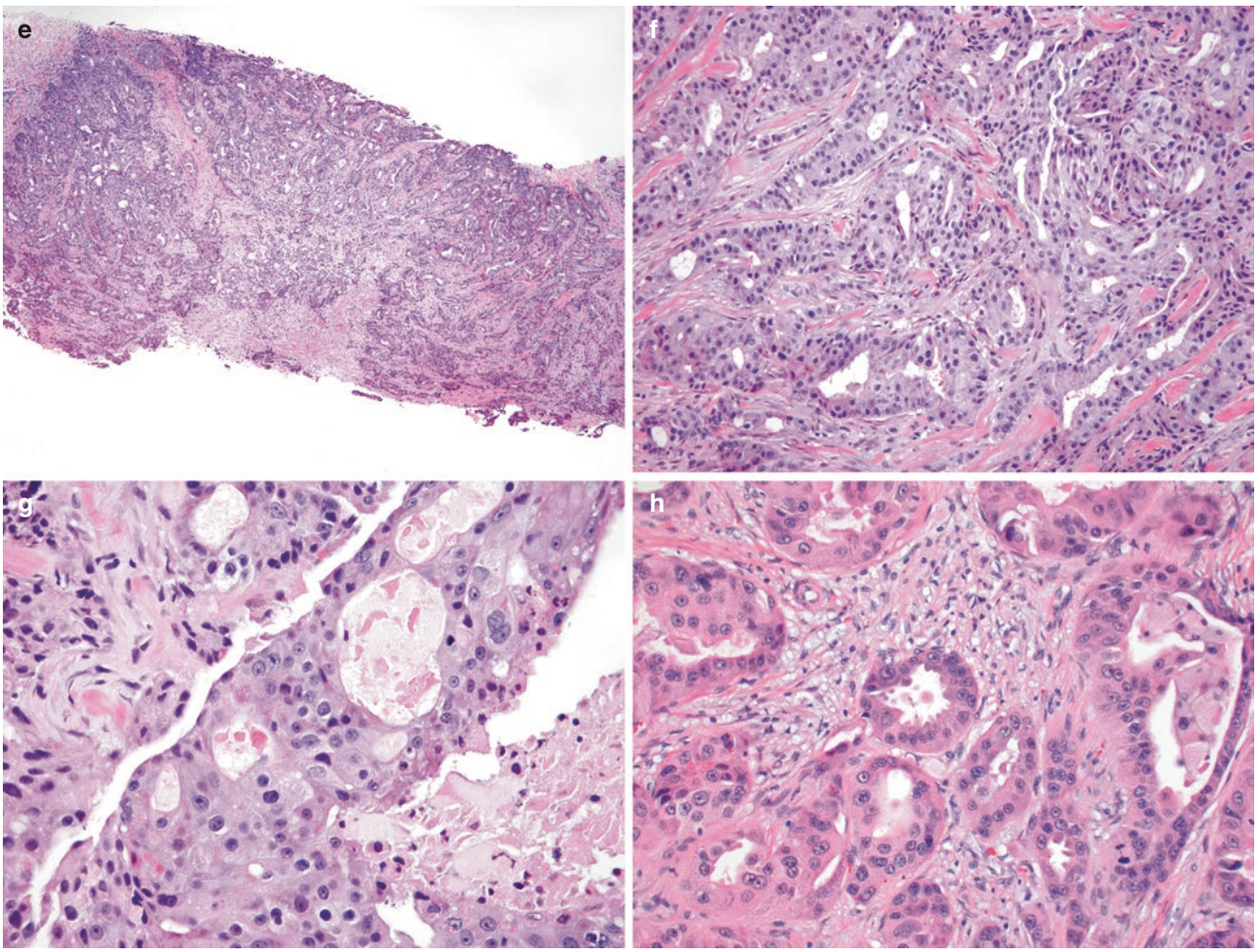

Fig. 12.40 (continued)

lumen (Figs. 12.40h and 12.41). The nuclear chromatin is irregular and often condensed along the periphery of the nuclear membrane. The cell borders are typically sharply defined (Fig. 12.41b) but may be indistinct in some cases (Fig. 12.42h, i). The abundant cytoplasm is eosinophilic, granular, and diastase-resistant periodic-acid-Schiff (PAS) positive (type A cells), vacuolated clear or foamy (type B cells), or a combination of both (Figs. 12.41 and 12.43). Intracytoplasmic lipid, as well as intracytoplasmic and intraluminal mucin, has also been observed (Fig. 12.41b). The majority of these tumors exhibit moderate nuclear pleomorphism, and tubule formation is rarely greater than 75% (Fig. 12.40e–g). Mitotic activity is often moderate or high. Most apocrine carcinomas are graded as modified SBR grade 2 or 3 [217]. TNAC tends to be of lower histological grade (predominantly grade 2) than other TNBC [203, 208, 212, 215]. The in situ component, when present, usually also demonstrates apocrine features, often with intermediate to high nuclear grade with or without comedo necrosis [202] (Fig. 12.44).

Pleomorphic invasive lobular carcinoma may also show apocrine differentiation (Fig. 12.45), and an apocrine variant of pleomorphic lobular carcinoma in situ has been characterized [218–221]. Histiocytoid carcinomas are rare, mostly lobular, invasive carcinomas that may show apocrine features. The neoplastic cells have indistinct borders, abundant foamy or eosinophilic cytoplasm, and regular to slightly pleomorphic nuclei, resembling histiocytes [222]. However, none of these tumors are classified as apocrine carcinomas (see also Chap. 14—Atypical Lobular Hyperplasia and Lobular Carcinoma in Situ and Chap. 15—Invasive Lobular Carcinoma).

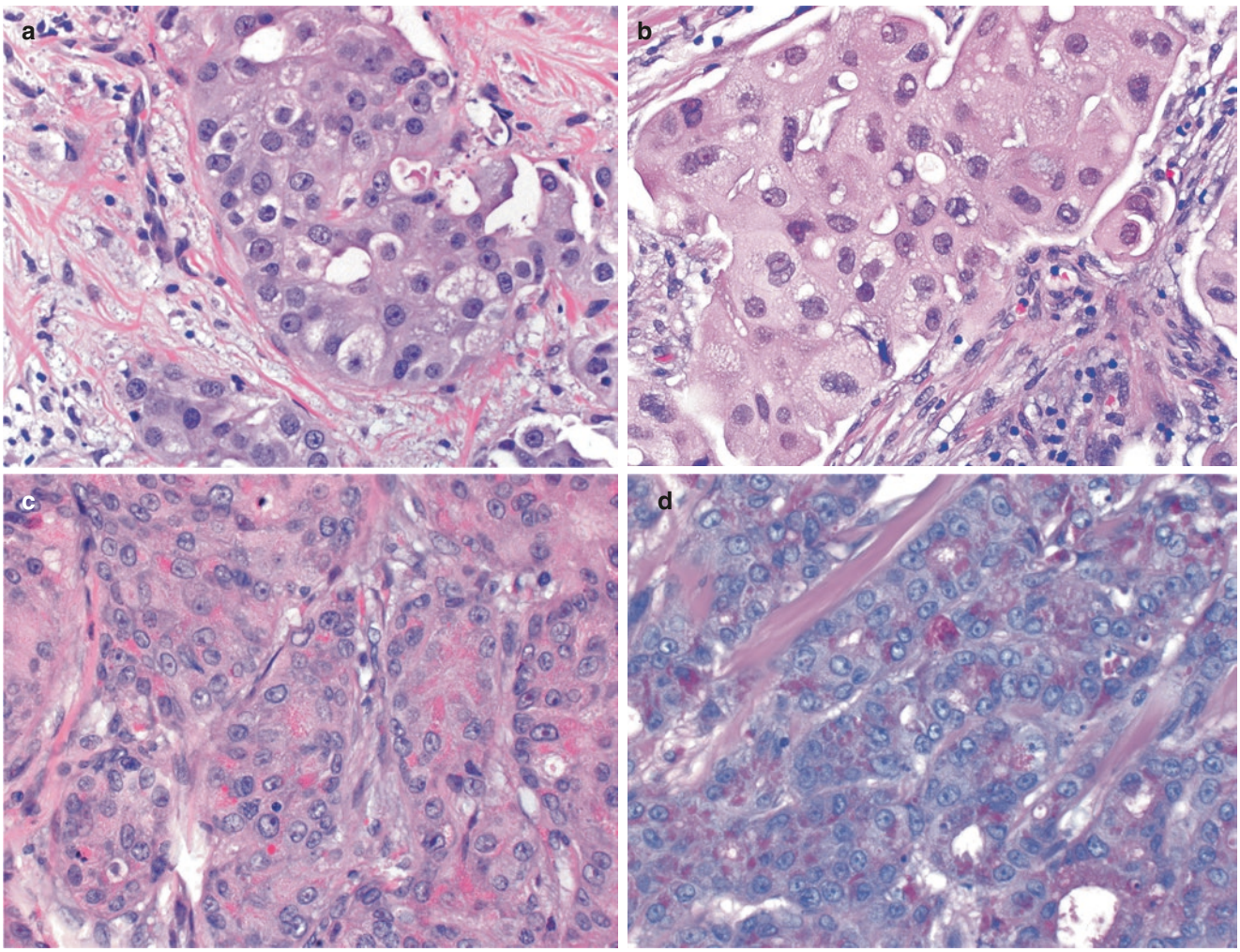

Fig. 12.41 Cytologic features of invasive apocrine carcinoma, granular variant (type A). (**a**) The tumor cells are large with sharply defined borders, abundant eosinophilic granular cytoplasm, and rounded pleomorphic nuclei with vesicular chromatin and prominent nucleoli. (**b**) Rare cases may demonstrate intracytoplasmic mucin. (**c**, **d**) This example shows prominent, coarse, and brightly eosinophilic cytoplasmic granules, which are highlighted by diastase-resistant PAS stain

Immunohistochemistry

ER, PR, AR, and HER2 Biomarkers

The majority of apocrine carcinomas are negative for ER and PR and demonstrate strong AR expression (Fig. 12.46) [199, 223]. Pure apocrine carcinomas are by definition ER negative, PR negative, and AR positive (at least 10% of cells has been suggested) [199]. The ERα isoform ER-α36 was found to be frequently overexpressed in pure apocrine carcinoma [36]. AR expression is much less common in ER-negative carcinomas compared to ER-positive/luminal carcinomas but is not entirely unique to apocrine carcinomas among ER-negative tumors [197, 224, 225]. In contrast to pure apocrine carcinomas, only ~58% of molecular apocrine tumors were found to express AR by immunohistochemistry in one study, despite high AR mRNA expression [197]. AR expression has been associated with HER2 overexpression and/or *ERBB2* amplification [199, 226]. HER2 overexpression and *ERBB2* amplification have been observed in up to 57% of pure apocrine carcinomas [199], which is significantly higher than the incidence of HER2 overexpression in IDC-NST. The remaining pure apocrine carcinomas are triple negative (TNAC) [199, 203]. HER2 overexpression has been inversely correlated with EGFR expression in apocrine carcinomas, with the vast majority of TNAC overexpressing EGFR [199].

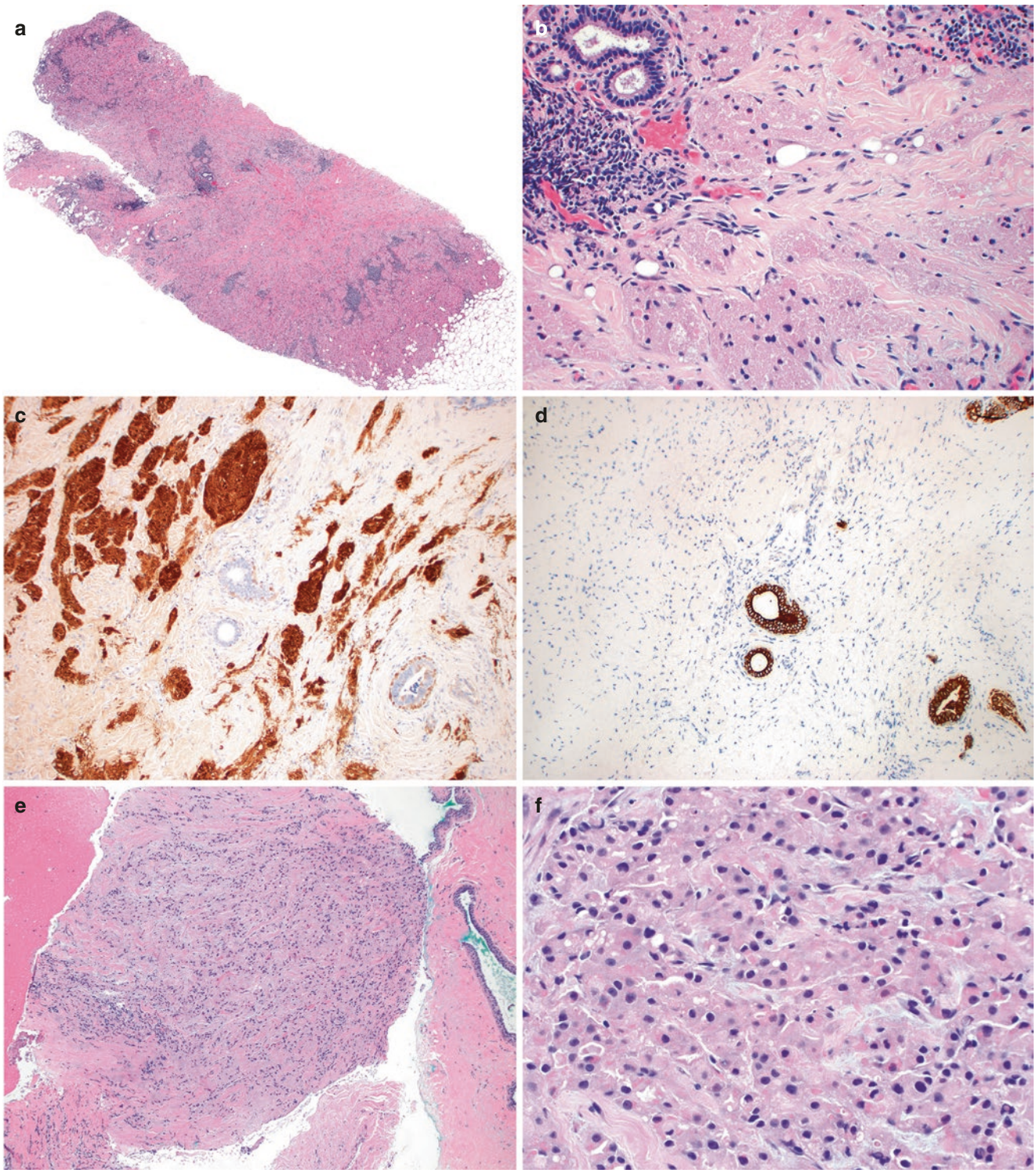

Fig. 12.42 Granular cell tumor may mimic invasive apocrine carcinoma. (**a**, **b**) Granular cell tumor shows infiltrating clusters of epithelioid cells with abundant granular eosinophilic cytoplasm, which may mimic apocrine carcinoma (**e**, **f**). Note the small, bland nuclei of granular cell tumor, in contrast to the larger, more atypical nuclei of apocrine carcinoma. Granular cell tumors (**c**) show strong and diffuse positivity for S100 protein, (**d**) but are negative for keratin, (**g**) in contrast to apocrine carcinomas. (**h**–**k**) The invasive component of this apocrine carcinoma (**h**, **i**) shows infiltrative tumor cell clusters with indistinct cell borders and abundant granular eosinophilic cytoplasm in a dense sclerotic stroma, mimicking granular cell tumor. (**j**) In this case, an associated in situ component shows well-developed apocrine features and is useful to help establish the correct diagnosis. (**k**) An immunostain for ER is negative in invasive apocrine carcinoma (and granular cell tumor)

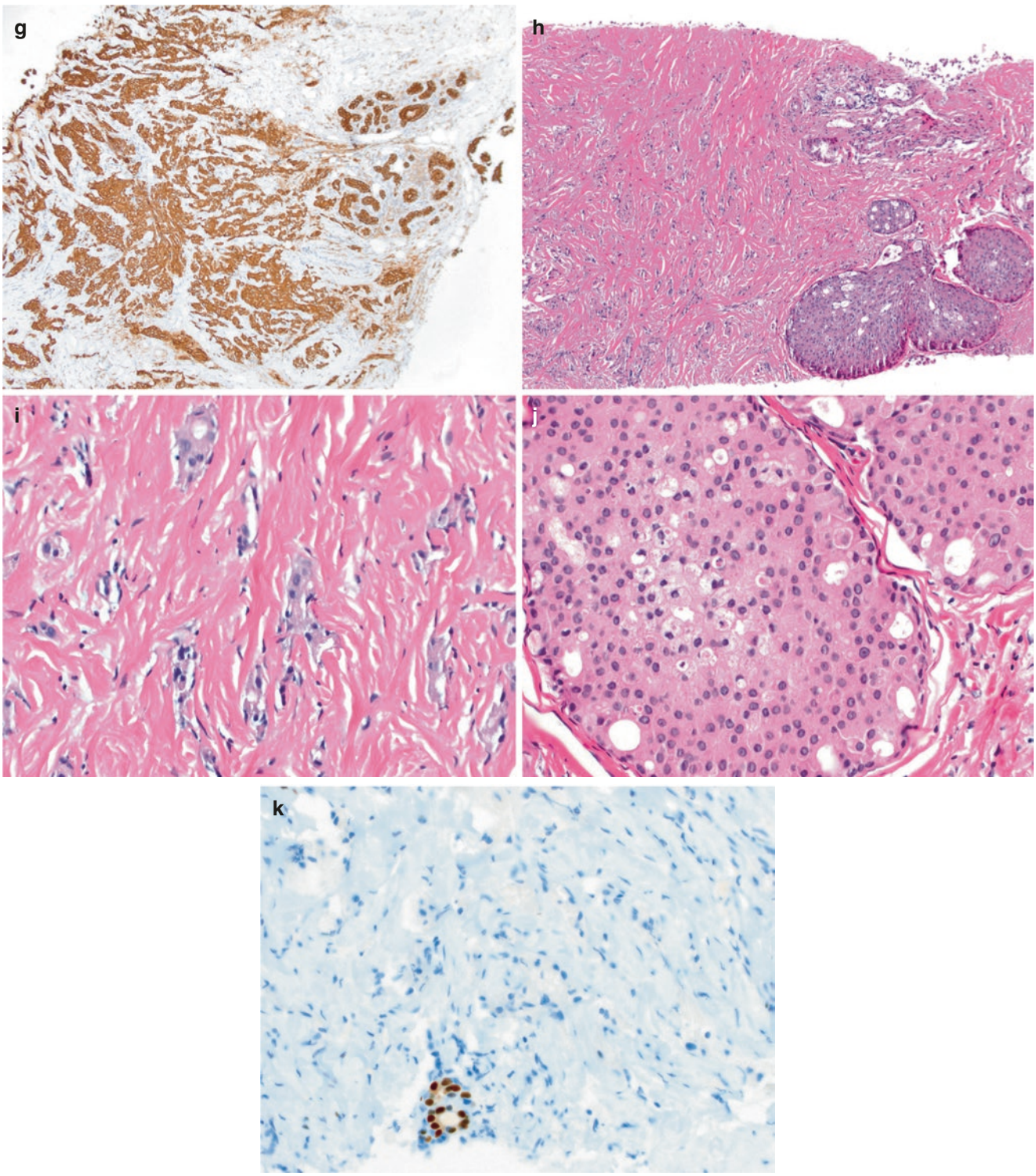

Fig. 12.42 (continued)

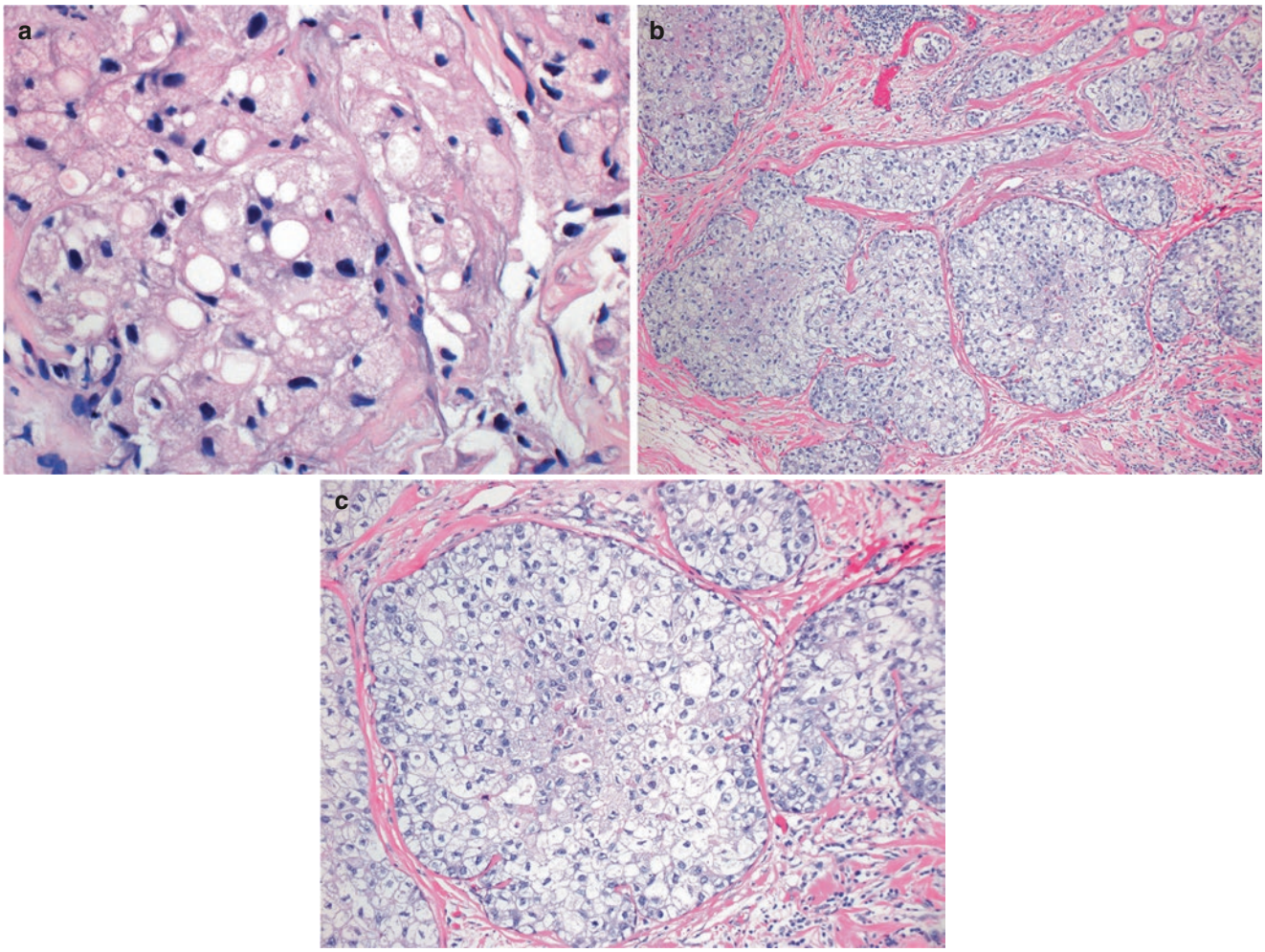

Fig. 12.43 Cytologic features of invasive apocrine carcinoma, foamy variant (type B). The tumor cells of this variant have abundant (**a**) foamy to (**b**, **c**) vacuolated clear cytoplasm

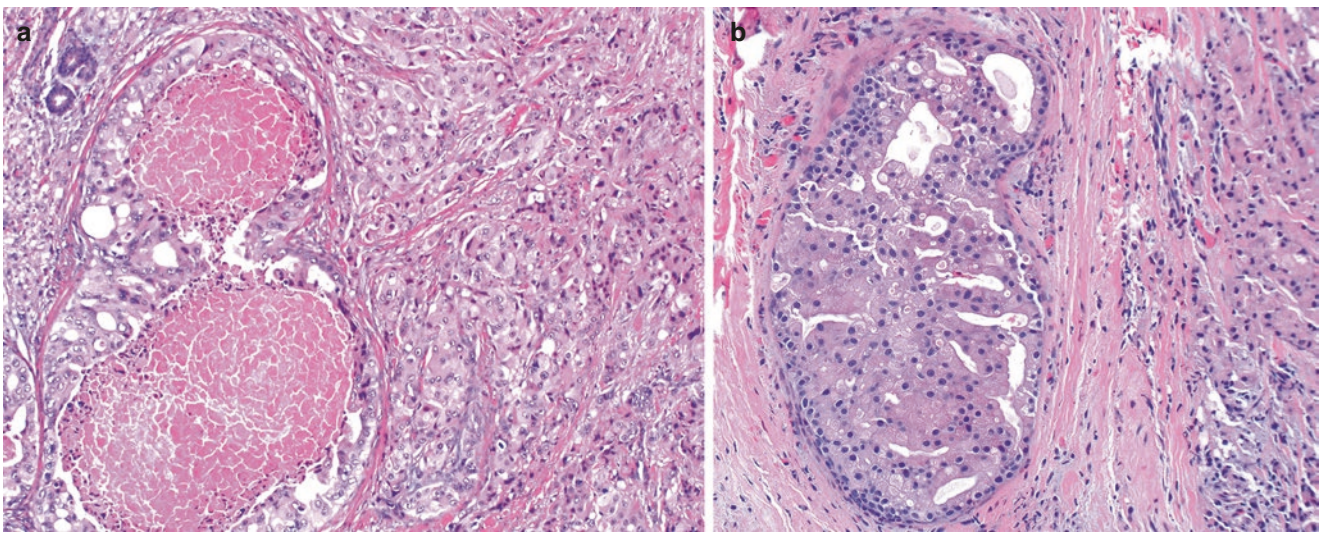

Fig. 12.44 Apocrine ductal carcinoma in situ. (**a**, **b**) The in situ component associated with invasive apocrine carcinoma often displays similar apocrine cytologic features

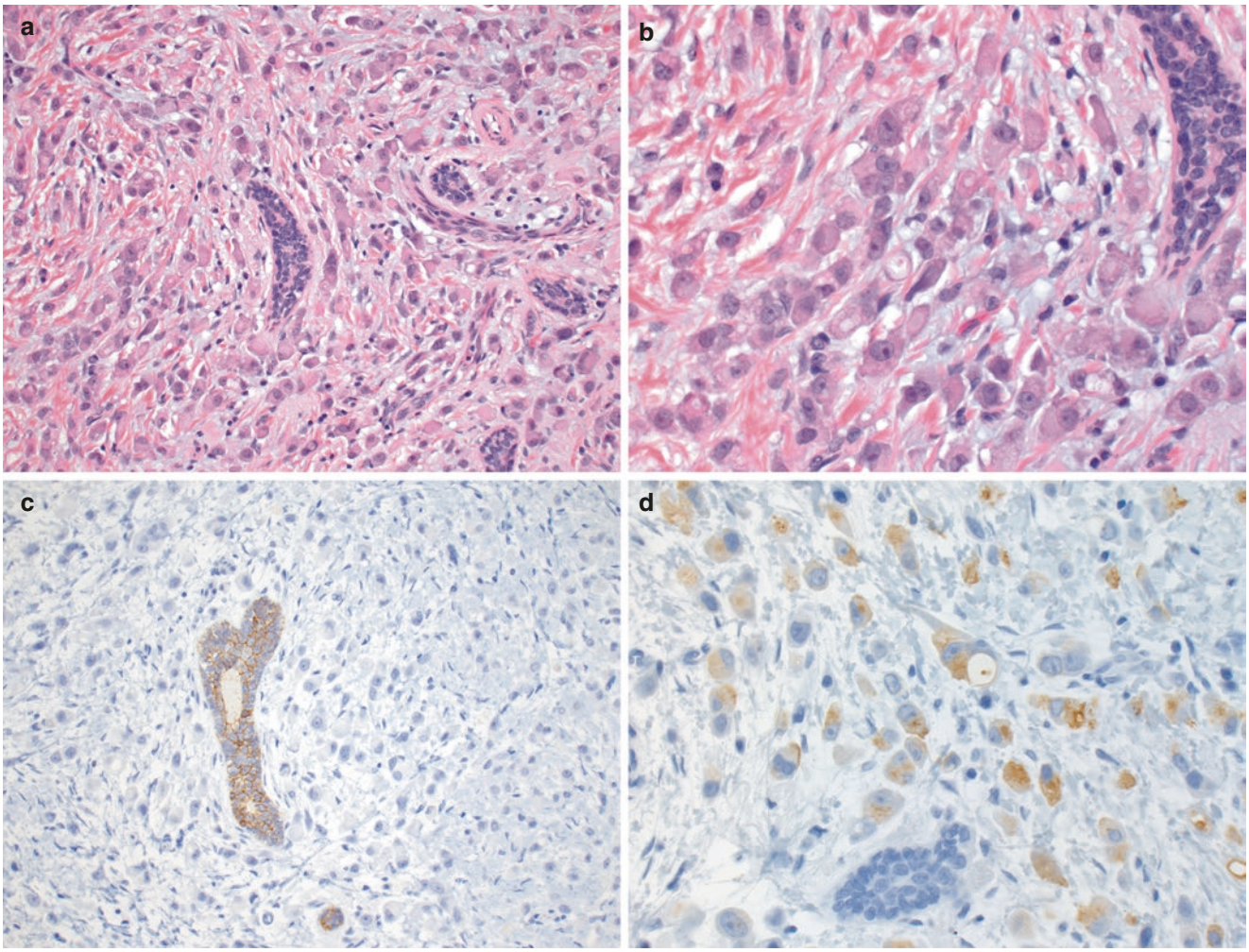

Fig. 12.45 Invasive pleomorphic lobular carcinoma with apocrine features. (**a**) These tumors are characterized by discohesive tumor cells with vacuolated cytoplasm infiltrating as single cells and small cell groups, with permeative and targetoid growth patterns. (**b**) In contrast to classic invasive lobular carcinoma, the tumor cells are large and demonstrate abundant eosinophilic granular cytoplasm with pleomorphic nuclei and prominent nucleoli, indicative of apocrine differentiation. (**c**) Negative or aberrant E-cadherin immunostaining supports the lobular phenotype. (**d**) Similar to invasive apocrine carcinomas, in general, these tumors express GCDFP-15

Markers of Apocrine Differentiation

GCDFP-15 is an AR-regulated protein that is often regarded as a functional marker of apocrine differentiation in benign and malignant cells (Fig. 12.46a, b) [227]. GCDFP-15 has been found to strongly correlate with AR expression and with carcinomas showing a surrogate molecular apocrine immunophenotype (ER-, PR-, AR+), and was associated with but not specific for apocrine morphology in the latter group [197, 228]. Pure apocrine carcinomas were positive for GCDFP-15 in ~71% of cases in one study [228]. However, GCDFP-15 has also been positively correlated with HR and HER2 expression and is not limited to apocrine carcinomas [197, 228–230]. With respect to HR-negative carcinomas, one study observed GCDFP-15 expression in molecular apocrine tumors but not in basal-like carcinomas of the control group. However, the vast majority (93%) of molecular apocrine carcinomas in this study lacked apocrine morphologic features [197]. Decreased GCDFP-15 expression has been demonstrated in lymph node-positive apocrine carcinomas and in advanced disease [229, 231], which also limits its use as a reliable marker for the apocrine phenotype.

Celis et al. defined a specific apocrine protein signature analogous to that of apocrine sweat glands, which included markers consistently expressed in apocrine cells (such as AR, CD24, 15-PDGH [prostaglandin dehydrogenase], ACSMS1 [acyl-CoA synthetase medium-chain family number 1]), as well as markers which are typically not expressed [232]. 5α-Reductase, an enzyme that converts testosterone to dihydrotestosterone, was expressed in approximately 60% of apocrine carcinomas and correlated with adverse prognostic parameters [230]. Other markers reported to be specific for apocrine differentiation include gamma-glutaminyl transfer-

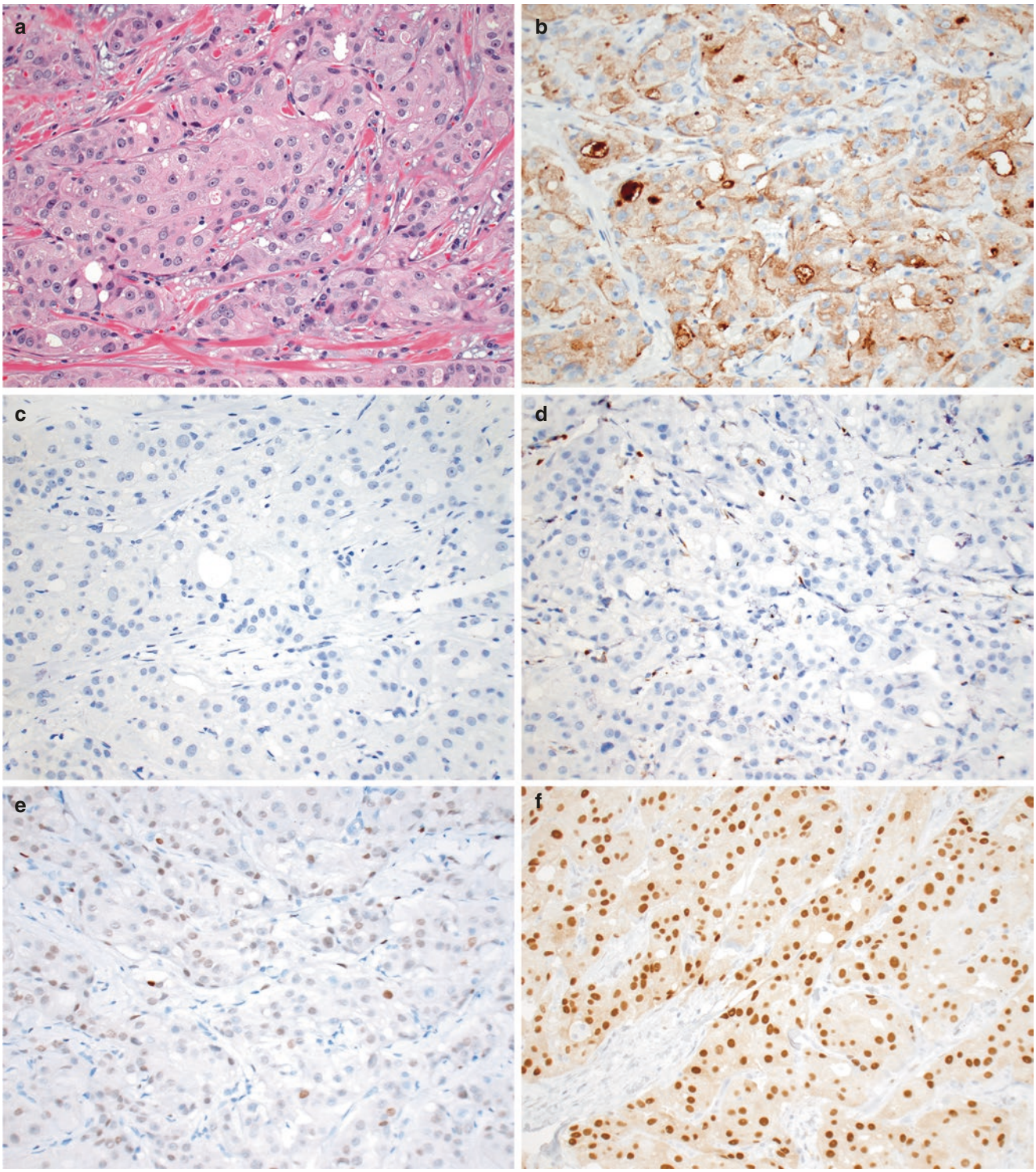

Fig. 12.46 Immunophenotype of invasive apocrine carcinoma. (**a**) Invasive apocrine carcinoma is characterized by strong immunoreactivity to (**b**) GCDFP-15, whereas (**c**) mammaglobin, another commonly utilized breast-specific marker, is typically negative. (**d**) BCL2 is typically negative in these tumors. (**e**, **f**) This invasive apocrine carcinoma shows characteristic immunopositivity for (**e**) GATA3 and (**f**) AR. ER and PR were negative (*not shown*)

ase 1 (GGT-1), tumor-associated glycoprotein-72, HMGCS2, and FAB7 [233–235]. However, none of these markers are currently used for routine clinical application.

Other Immunohistochemical Markers

Apocrine carcinoma cells are immunoreactive for epithelial markers, including EMA and LMWCK (e.g., CK7, CK8, CK18, CK19) [37, 236]. In one study, CK20 reactivity was detected in 50% (4/8) of apocrine carcinomas, while none of the non-apocrine breast carcinomas were CK20 positive [236]. The immunohistochemical profile (expression of luminal CKs, negative for basal cytokeratins CK5/6 and CK14) is consistent with gene expression studies indicating that apocrine carcinomas are generally not basal-like by molecular profiling [37, 196, 198]. CEA positivity has also been observed in apocrine carcinomas [237]. Apocrine cells, both benign and malignant, are usually negative or only focally positive for the breast marker mammaglobin (Fig. 12.46c). In contrast, GATA3, a sensitive marker for breast carcinomas including TNBC, is usually positive in apocrine carcinomas [114, 238, 239] (Fig. 12.46e) and has also been correlated with AR expression in TNBC [240]. Apocrine carcinomas are typically negative for neuroendocrine markers, such as synaptophysin, chromogranin A, and CD56 [37]. TNAC tend to have a lower Ki-67 proliferation index compared to non-apocrine TNBC [208, 210, 212].

Differential Diagnosis

The most common morphologic mimic of invasive apocrine carcinoma is sclerosing adenosis involved by atypical apocrine cells (atypical apocrine adenosis) or apocrine DCIS (Fig. 12.47). Appreciation of the lobulocentric growth of the

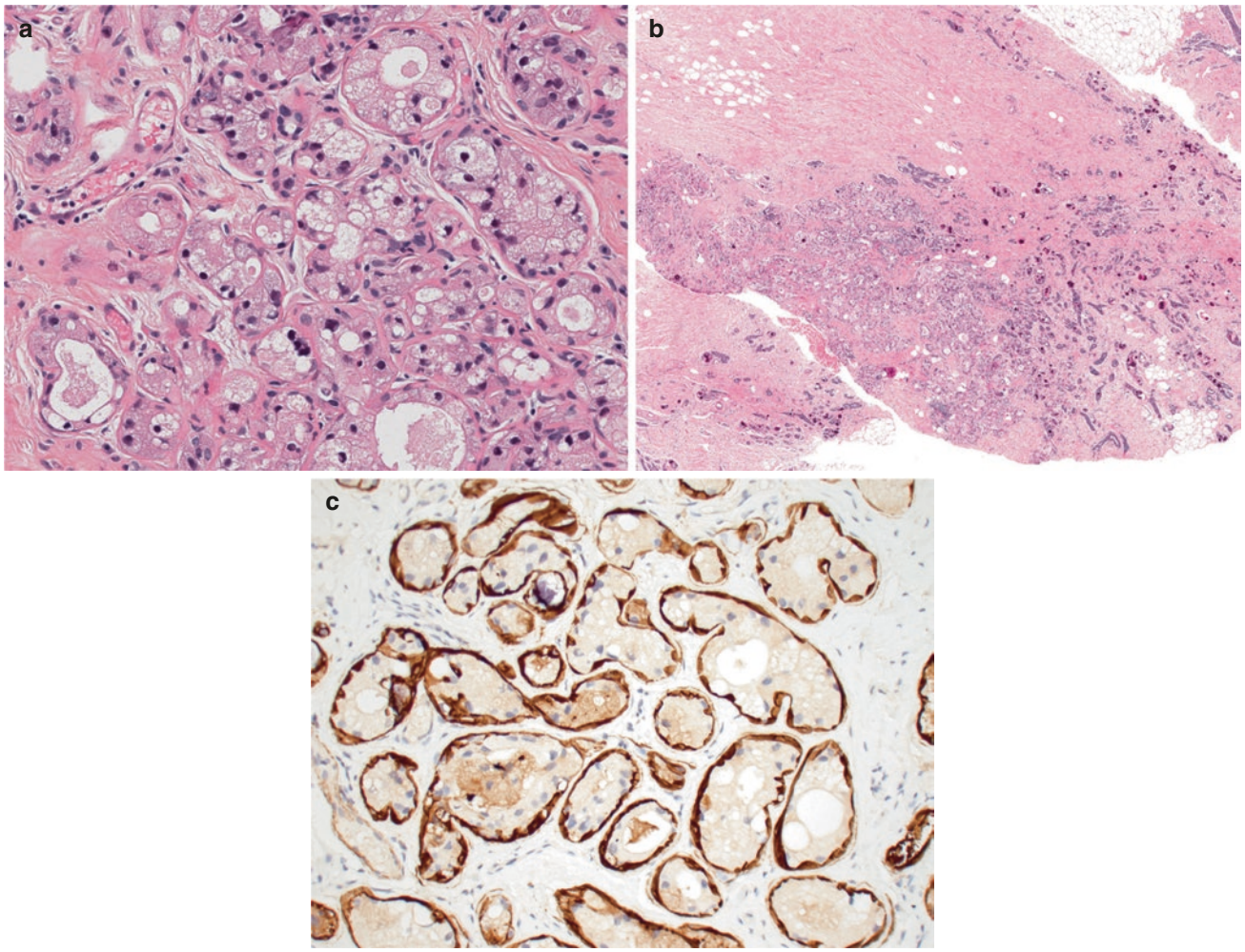

Fig. 12.47 Atypical apocrine adenosis may mimic invasive apocrine carcinoma. (**a**) The nuclei of apocrine cells in atypical apocrine adenosis are enlarged (at least three times the size of normal apocrine cells) and often hyperchromatic. Mitotic figures may be present (*not shown*). The ductules appear crowded and haphazardly arranged on high magnification, which, in combination with the cytologic features, may mimic invasive carcinoma with apocrine differentiation. (**b**) Lower magnification is helpful to appreciate the lobulocentric nature of the lesion, although this may not be well visualized in scant core biopsy specimens. (**c**) Immunohistochemistry for myoepithelial cell markers (SMM in this case) may be helpful to exclude invasive carcinoma and establish the correct diagnosis. Note that myoepithelial cell staining may be attenuated in some apocrine lesions (*not shown here*)

latter lesions on low-power magnification is helpful in making the distinction but may not be apparent in limited core biopsy material. Immunostains can help to highlight the myoepithelial cells of sclerosing lesions in challenging cases. In this context, it should be remembered that myoepithelial cells may be attenuated in non-invasive apocrine and sclerosing lesions [241, 242].

A variety of benign and malignant lesions characterized by large epithelioid cells with abundant eosinophilic or pale vacuolated cytoplasm may be confused with apocrine carcinoma, especially in a limited core biopsy specimen.

Granular cell tumor can rarely arise in the breast and may be misinterpreted as apocrine carcinoma. Contrary to apocrine carcinoma, cells of granular cell tumors have small nuclei with absent to indistinct nucleoli and no to only rare mitotic figures. Cytokeratin immunohistochemistry will stain tumor cells of apocrine carcinoma but is negative in granular cell tumors. Conversely, S100 protein is diffusely and intensely positive in granular cell tumor but is negative or shows only focal weak reactivity in apocrine carcinoma (Fig. 12.42).

An inflammatory process with accumulation of foamy histiocytes may sometimes simulate apocrine carcinoma. However, the histiocytes in such cases have bland cytologic features, in contrast to the atypical nuclei of apocrine carcinomas. Immunohistochemical stains for cytokeratin and histiocytic markers such as CD68 and CD163 can be used to establish the correct diagnosis in cases that are equivocal on H&E (Fig. 12.48a–d).

In addition to apocrine carcinoma, invasive breast carcinoma with oncocytic pattern, acinic cell carcinoma, and neuroendocrine tumors are characterized by eosinophilic

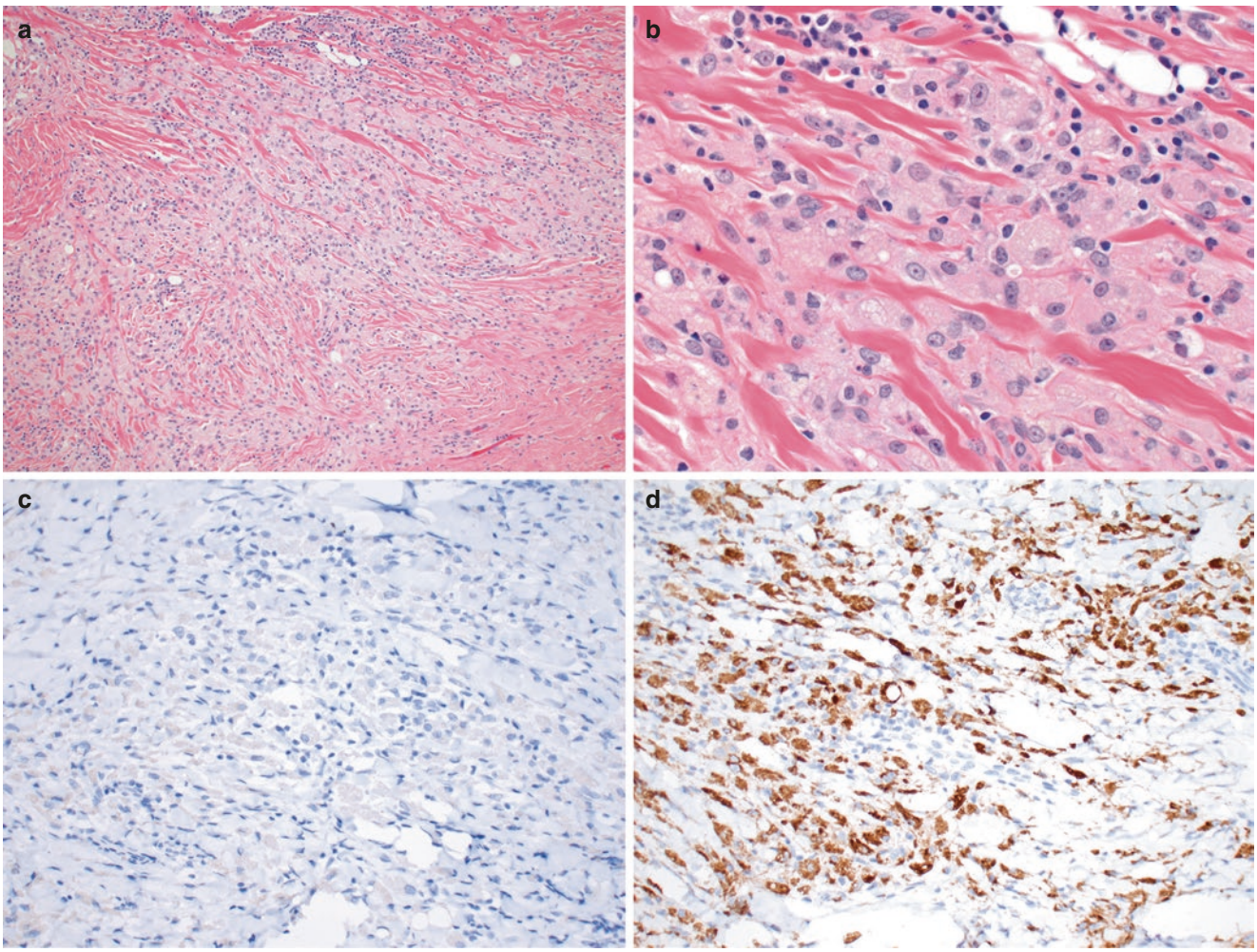

Fig. 12.48 Histiocytic infiltrates may be mistaken for invasive apocrine carcinoma. (**a**, **b**) The cytologic features and nested growth pattern of prominent histiocytic reactions may sometimes mimic invasive apocrine carcinoma, especially in limited core biopsy material. (**d**) CD68 and other histiocytic markers, such as CD163, are positive in such cases, whereas (**c**) keratin is negative

granular cytoplasm. Oncocytic carcinoma was first described by Damiani et al. and characterized by Ragazzi et al. as an invasive carcinoma composed of at least 70% oncocytic cells displaying strong immunoreactivity for anti-mitochondrial antibody [243, 244]. These tumors usually demonstrate a solid growth pattern with pushing margins. The oncocytic cells have well-defined borders and abundant granular eosinophilic cytoplasm, which is due to diffuse accumulation of mitochondria, similar to oncocytes at other anatomic sites. The nuclei range from low grade to pleomorphic. Although apocrine cells and oncocytes share similar morphological features, recognition of a few differences can be helpful to distinguish these tumors. Immunophenotypically, anti-mitochondrial antibody is positive in a diffuse strong granular pattern in invasive breast carcinoma with oncocytic pattern but is negative or focal in apocrine carcinoma. Furthermore, invasive breast carcinoma with oncocytic pattern is often ER positive (~80% of cases) and GCDFP-15 negative (~70%), whereas pure apocrine carcinoma exhibits the reverse immunophenotype [243, 244]. Although considered a rare pattern of invasive breast carcinoma, one study using anti-mitochondrial antibody found that ~20% of 76 consecutive invasive carcinomas were rich in mitochondria [243]. Oncocytic carcinomas or mitochondrion-rich carcinomas of the breast appear to be molecularly heterogeneous, with most classified as luminal or HER2 subtype [245]. A subset of tumors was found to have chromosomal gains of 11q13.1-q13.2 and 19p13, similar to oncocytic tumors of the kidney and thyroid [245]. The clinical features and prognosis of invasive breast carcinoma with oncocytic pattern appear to be similar to other IDC-NST when matched for grade and stage [243, 246, 247].

Acinic cell carcinoma, first described by Roncaroli et al. in 1996 [248], is an exceedingly rare subtype of breast cancer, which displays serous acinar differentiation and is morphologically similar to its salivary gland counterpart. These tumors may present as a palpable mass and show infiltrative growth grossly [249, 250]. The tumor cells exhibit solid, microglandular, or microcystic architectural patterns and have moderate to abundant, amphophilic to eosinophilic granular cytoplasm and round to oval nuclei. The granules are often large, coarse, and bright red in color, resembling those seen in intestinal Paneth cells (Figs. 12.49 and 12.51). Clear cells with hypernephroid appearance may be observed. The cytoplasm stains with PAS after diastase digestion and may also be focally positive for GCDFP-15, similar to apocrine carcinoma. However, most of the tumor cells are immunoreactive to amylase, alpha-1 antichymotrypsin, lysozyme, S100 protein, and EMA, which confirms the diagnosis (Figs. 12.50 and 12.51). Acinic cell carcinomas are consistently negative for ER, PR, AR, and HER2 [250–252] (Fig. 12.51h). Guerini-Rocco et al. revealed complex genomic patterns of gains and losses in acinic cell carcinoma, similar to other types of high-grade TNBC. Most tumors were also noted to harbor *TP53* mutation [253]. A close relationship has been reported between microglandular adenosis and acinic cell carcinoma [254, 255]. Despite being triple negative, acinic cell carcinomas of the breast have an indolent clinical behavior [250]. A subset of acinic cell carcinomas are found in association with high-grade TNBC of NST (Fig. 12.52), and one study demonstrated shared identical mutations in both components, suggesting that some acinic cell carcinomas might constitute the substrate for the development of a more aggressive form of triple-negative carcinomas [253].

Table 12.7 summarizes the distinguishing features of primary breast carcinomas with granular cytoplasm.

The differential diagnosis of apocrine carcinoma with clear cell features primarily includes metastatic renal cell carcinoma (RCC) of clear cell type, as well as adenomyoepithelioma (Fig. 12.43). Clinical history is critical in suspecting the diagnosis of metastatic RCC. In contrast to apocrine carcinoma, clear cell RCC shows negative immunoreactivity for CK7 and CK20 and is typically positive for PAX2, PAX8, and RCC markers. Lastly, exceedingly rare invasive breast carcinomas with sebaceous, lipid-rich, or glycogen-rich patterns are included in the differential diagnosis (see Chap. 10).

Fig. 12.49 Acinic cell carcinoma of the breast. (**a**–**c**) Core needle biopsy of an acinic cell carcinoma showing infiltrative microglandular growth of tumor cells with eosinophilic granular cytoplasm and bland rounded nuclei. (**d**–**f**) Subsequent excision revealed predominantly microglandular and focal solid growth. Note the abundance of distinctive coarse eosinophilic cytoplasmic granules resembling zymogen granules of intestinal Paneth cells (**f**). (*Courtesy of Dr. Jose Jessurun*, Department of Pathology and Laboratory Medicine, Weill Cornell Medicine with permission)

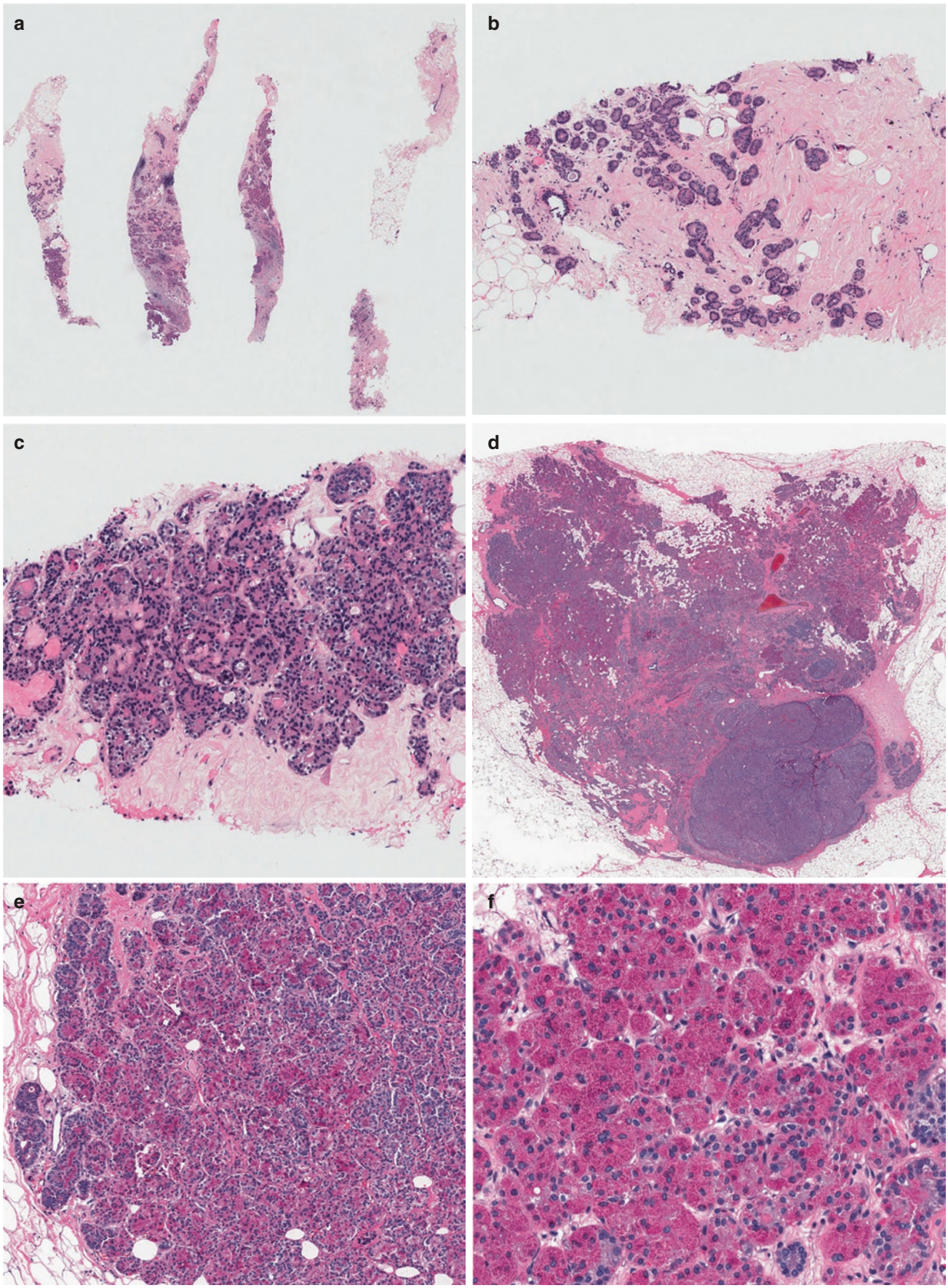
a
b
c
d
e
f

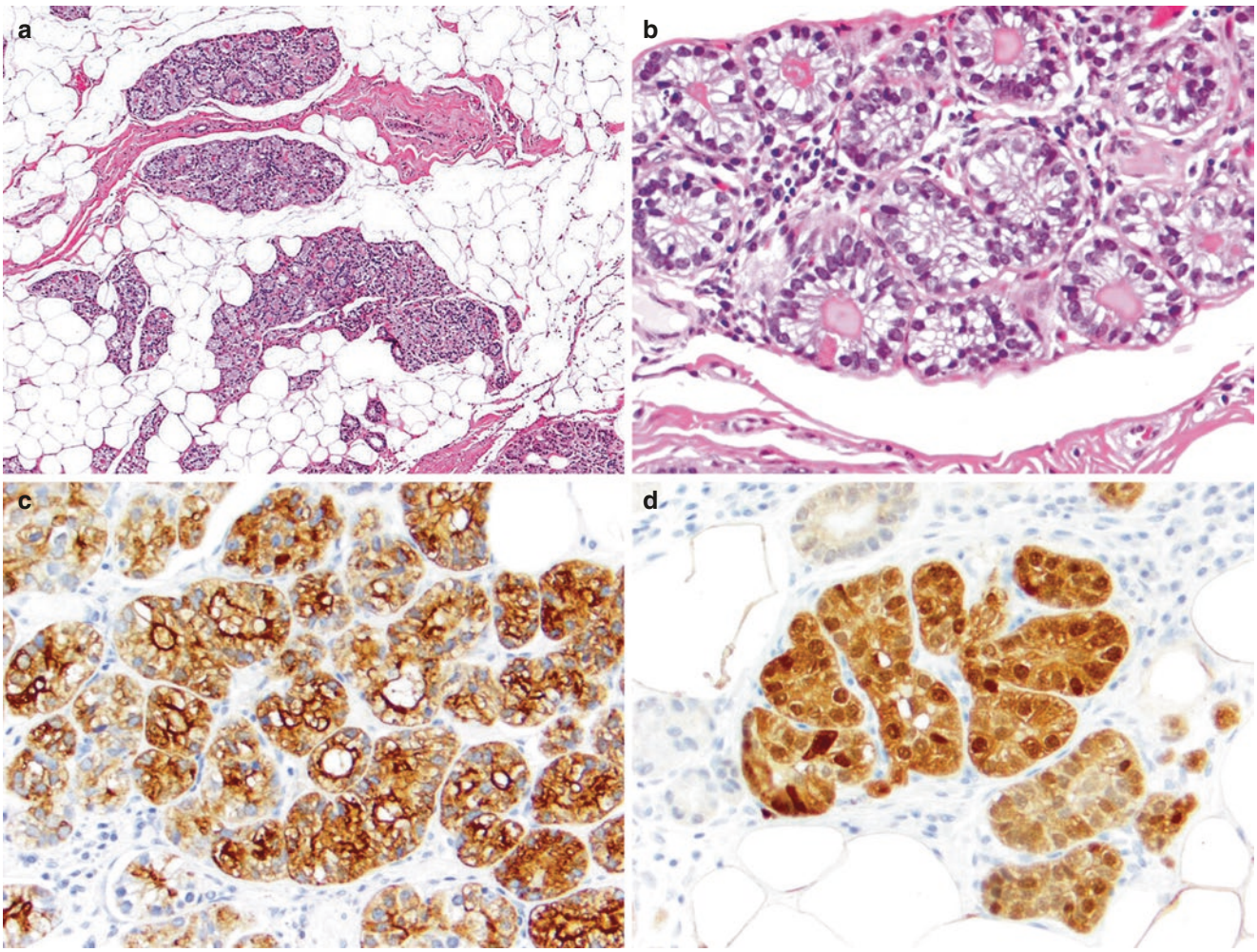

Fig. 12.50 Acinic cell carcinoma of the breast. (**a**, **b**) This example of acinic cell carcinoma demonstrates columnar tumor cells with clear cytoplasm and orderly polarized rounded nuclei arranged in an acinar pattern. Note the presence of large eosinophilic granules in the apical cytoplasm in some tumor cells. The tumor cells are strongly immunoreactive for (**c**) lysozyme and (**d**) S100 protein. (*Courtesy of Dr. Laura C. Collins*, Department of Pathology, Beth Israel Deaconess Medical Center with permission)

Pathogenesis and Risk Factors

The origin and pathogenesis of carcinomas with apocrine differentiation is poorly understood. Using comparative genomic hybridization, one study found evidence of clonality in benign cysts with papillary apocrine hyperplasia, and some of these benign lesions showed chromosomal copy number alterations also identified in apocrine DCIS and invasive apocrine carcinomas (including 2q and 13q gains; 1p, 16q, and 17q losses). These findings suggest that a subset of benign apocrine proliferations may be non-obligate precursors to carcinomas with apocrine differentiation [256]. Given how common apocrine metaplasia and hyperplasia is, such an event would be predicted to be exceedingly rare.

Patients with Cowden disease have germline *PTEN* mutations and an increased risk of breast cancer. Banneau et al. reported that the gene expression profiles of breast carcinomas in patients with Cowden disease at least partially overlap with the molecular apocrine signature, and many of these tumors show apocrine morphologic and immunophenotypic (AR+, ER-, PR-, HER2+/−) features [234]. Benign breast lesions in patients with Cowden disease also frequently show apocrine differentiation [257, 258]. Together, the observations suggest a possible link between germline *PTEN* mutation and apocrine phenotype. However, most apocrine carcinomas are unrelated to Cowden disease.

Gene expression profiling studies have defined a molecular apocrine signature based on ER-negative breast carcinomas that express high levels of AR, as well as genes typically expressed in ER-positive/luminal tumors. Up to one-half of these tumors are HER2 positive, with the remainder being triple negative. Many but not all of the

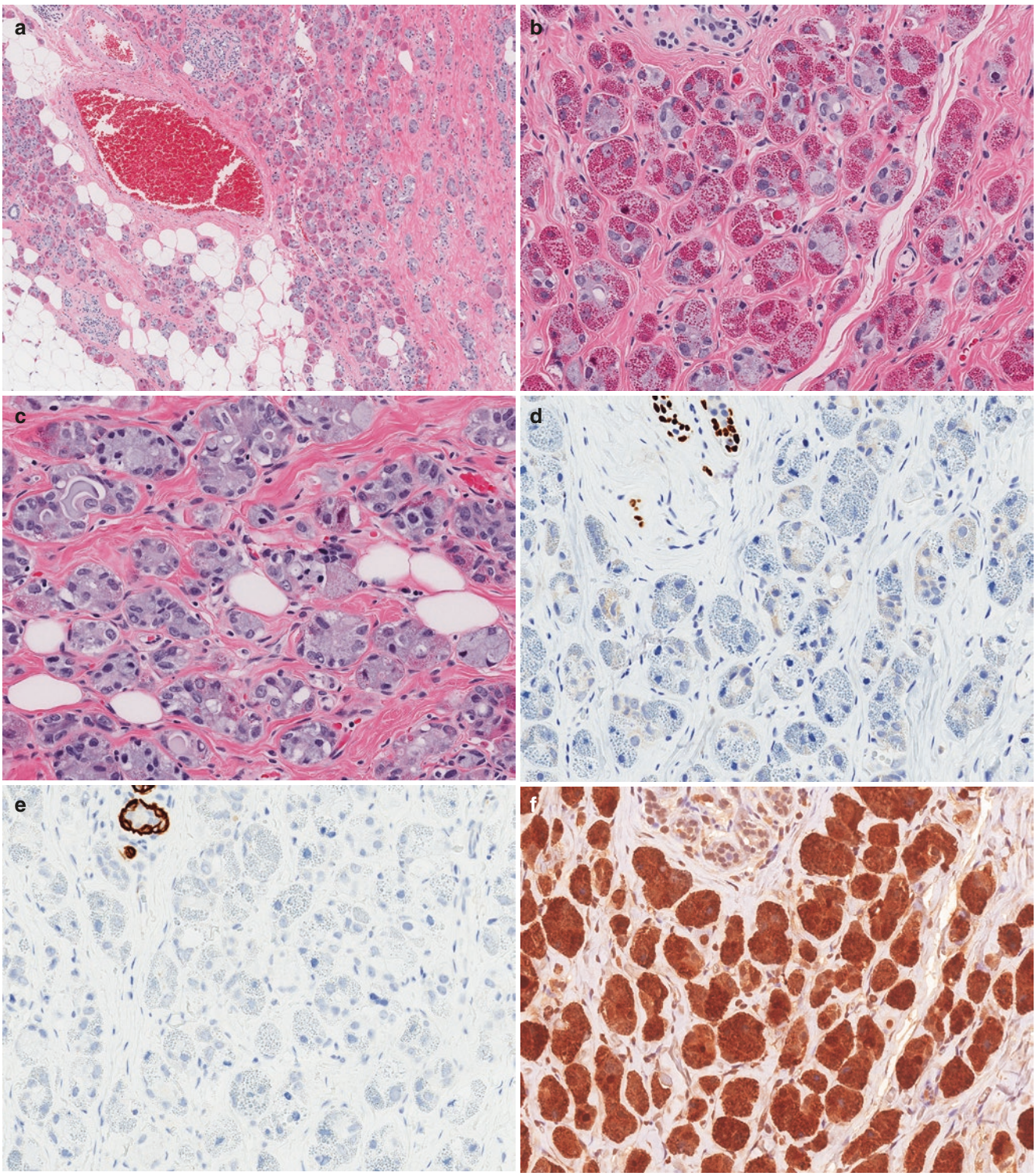

Fig. 12.51 Acinic cell carcinoma of the breast. (**a**–**c**) Another example of acinic cell carcinoma showing infiltrating small glands in fibrofatty stroma without desmoplastic reaction. The tumor cells forming the microglands have abundant amphophilic cytoplasm, many of which containing large, coarse, and bright eosinophilic granules (**b**, **c**). The small glands lack a myoepithelial layer, as seen with p63 (**d**) and SMM (**e**) immunostains. The neoplastic cells are strongly positive for lysozyme (**f**) and S100 protein (**g**). Acinic cell carcinoma is typically negative for ER (**h**), PR (not shown) and HER2 (not shown)

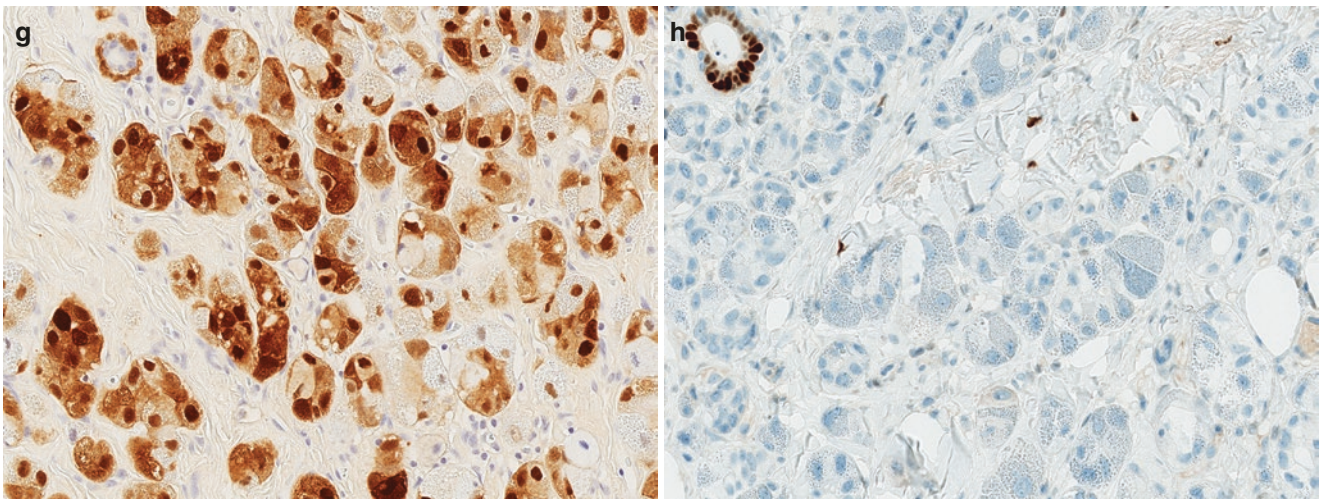

Fig. 12.51 (continued)

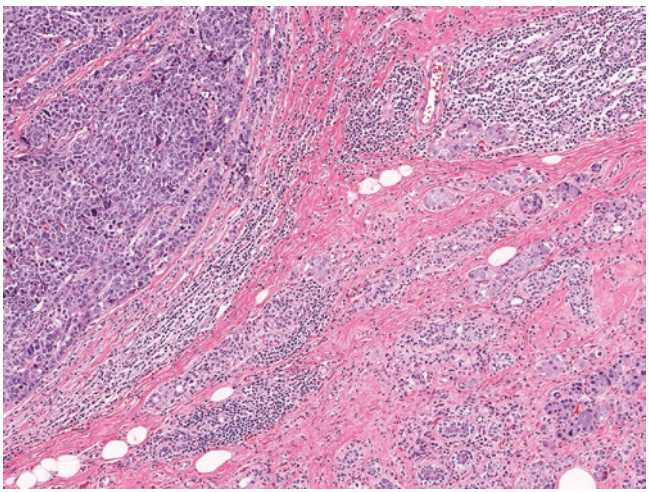

Fig. 12.52 Acinic cell carcinoma (right lower field) with adjacent high-grade, triple-negative IBC-NST (left upper field)

tumors in the combined studies showed morphologic features of apocrine differentiation [198, 259]. Pleomorphic invasive lobular carcinomas with apocrine differentiation have also been found to cluster with the molecular apocrine group [37]. However, in a study that classified molecular apocrine carcinomas based on expression of a targeted subset of genes from the signature, only 7% of tumors had apocrine morphology [197]. Accordingly, apocrine carcinoma shows overlap with but does not always correlate with the molecular apocrine expression signature. Lehmann et al. described an LAR gene expression signature in ~10% of TNBC, which was characterized by increased expression of AR and AR-regulated genes, as well as other features typical of ER-positive luminal carcinomas. This group likely includes the subset of HER2-negative molecular apocrine tumors [196].

Apocrine carcinomas frequently harbor mutations in PI-3K pathway genes, most often *PIK3CA*, as well as *PTEN, PIK3R1,* and *AKT1* [195, 208, 215]. In a study of 18 TNAC, the most frequently mutated genes were *PIK3CA* (~72%), *PTEN* (~33%), and *TP53* (~28%). *TP53* mutations are less common compared to other TNBC [208, 215]. Additional alterations include RAS/RAF/MEK pathway genes, growth factor receptors, and cell cycle genes [208]. A single TNAC with a potentially actionable novel *FGFR2-TACC2* fusion has been reported [208]. Genomic instability of TNAC is low, in contrast to other TNBC [208, 215].

Prognosis and Clinical Management

Data on the prognosis of patients with apocrine carcinoma have been contradictory, which is likely due to retrospective series with relatively low numbers of patients and the lack of uniform defining criteria (morphology alone, versus morphology with ER and/or AR and/or HER2 status, versus molecular subtype without histology). Some studies have reported similar [209, 231, 260–263] or worse [203, 214] outcomes of apocrine carcinomas compared to IDC-NST. These studies have generally included ER-positive or HER2-positive apocrine carcinomas in the analyses, which are likely to drive tumor behavior, treatment, and prognosis. In a SEER study, poor outcomes of patients with apocrine carcinomas compared to IDC-NST improved after correction for demographic and clinicopathologic (grade, stage, ER, PR, HER2, nodal status) factors [214]. A number of studies have observed better outcomes of TNAC compared to other TNBC [207, 210, 211, 264, 265]. This would be consistent with the smaller size, lower grade, and lower Ki-67 indices often associated with TNAC [203, 208, 210–213, 215, 265]. Rates of lymphovascular invasion and lymph node metastasis may be similar

Table 12.7 Distinguishing pathologic features of breast carcinomas with granular cytoplasm

	Apocrine carcinoma	Acinic cell carcinoma	Invasive carcinoma with oncocytic pattern	Neuroendocrine tumor
Growth pattern	Variable (nests, glands, micropapillary, papillary, single cells)	Microglandular, solid, microcystic	Solid growth with pushing margin	Nests (organoid), solid papillary
Cytologic features	Large cells; well-defined cell border; abundant eosinophilic granular to foamy or clear cytoplasm; apical cytoplasmic snouts may be present if glandular	Monotonous cuboidal/columnar to polygonal cells; moderate to abundant, amphophilic to eosinophilic granular or clear cytoplasm	Large round cells; well-defined cell border; abundant eosinophilic granular cytoplasm	Polygonal, plasmacytoid or spindled cells; moderate eosinophilic granular cytoplasm
Nuclear features	Round to pleomorphic; prominent nucleoli	Round to oval	Centrally located; low grade to pleomorphic; prominent nucleoli	Low to intermediate grade
Granules	Electron-dense secretory granules; coarse eosinophilic granules	Zymogen granules; coarse bright red granules	Mitochondria; fine eosinophilic granules	Neurosecretory granules; fine eosinophilic granules
Defining IHC[a] profile	ER−, PR−, AR+	Amylase+, lysozyme+, alpha-1 antichymotrypsin+	Mitochondrial antibody strong staining in ≥70% tumor cells	Synaptophysin+, chromogranin+
Additional IHC profile	GCDFP-15+, BCL2−	ER−, PR−, HER2−, S100+, EMA+	ER+ (~80%), GCDFP-15− (~70%)	ER+, HER2−

[a]Abbreviations: *IHC* immunohistochemical

in TNAC compared to other TNBC [207]. Worse outcomes have been reported in LAR tumors compared to other TNBC and in molecular apocrine carcinomas compared to other molecular subtypes, but these groups defined by either gene expression or immunohistochemistry do not correlate perfectly with apocrine carcinoma [196, 265, 266].

Treatment for apocrine carcinoma is often similar to IBC-NST. The role of adjuvant chemotherapy is limited by paucity of data. Population-based studies have shown that patients with TNAC overall receive chemotherapy at a lower rate than other TNBC, yet outcomes were more favorable [207, 211, 265]. There is little data on the response of apocrine carcinomas to neoadjuvant chemotherapy. Lower rates of pathologic complete response have been observed in apocrine carcinomas, although outcomes remained favorable [262]. Pathologic complete response rates were reported to be variable for LAR tumors [267, 268] and similar to basal-like TNBC for molecular apocrine tumors [266], but apocrine morphology was not considered in these analyses. Apocrine carcinomas with HER2 overexpression are eligible for anti-HER2 targeted therapies.

Given the high frequency of AR expression in apocrine carcinomas or molecularly defined groups (molecular apocrine or LAR tumors), androgen blockade may offer a therapeutic approach for these tumors [269, 270]. The high frequency of PI-3K/mTOR pathway mutations suggests that targeted inhibitors of this pathway may also be therapeutic candidates [271]. Preclinical models have suggested that AR-positive/LAR TNBC are sensitive to CDK4/6 inhibition [272, 273]. A number of clinical trials are examining the utility of PI-3 K and CDK4/6 inhibitors in combination with anti-androgens in TNBC [274].

Metaplastic Carcinoma

Overview and Clinical Presentation

Metaplastic breast carcinomas constitute a heterogeneous group of predominantly triple-negative invasive breast cancers characterized by differentiation of the neoplastic epithelium into squamous and/or mesenchymal-like elements, including spindle cell, chondroid, or osseous components and rarely others [275]. These tumors are uncommon, representing 0.2–1% of all breast carcinomas [275–278]. Differences in the definition of metaplastic carcinoma likely account for the reported variability in prevalence. In general, metaplastic components should comprise >10% of the tumor cells for a diagnosis of metaplastic carcinoma, although some authors have used different cutoffs including <10% or ≥20% [279–281]. IDC-NST may also occasionally show focal metaplastic components.

Various terminologies have been applied in the literature to categorize the different morphologic features that can be seen in metaplastic carcinomas. These tumors have been described as being monophasic, with only one metaplastic component present, or biphasic, with more than one component present. Biphasic tumors may have only metaplastic components or include metaplastic and adenocarcinoma components. Some metaplastic carcinomas are purely epithelial (squamous cell carcinoma, adenosquamous carcinoma) or purely sarcomatoid (spindle cell carcinoma), whereas others are biphasic epithelial and sarcomatoid. The WHO classification uses a practical descriptive system of metaplastic carcinoma patterns based on the histologic type of metaplastic components present: low-grade adenosqua-

mous carcinoma (LGASC), fibromatosis-like metaplastic carcinoma (FLMBC), squamous cell carcinoma (SCC), spindle cell carcinoma, metaplastic carcinoma with heterologous mesenchymal differentiation (MCMD), and mixed metaplastic carcinoma [275]. When a metaplastic carcinoma is composed of multiple different components, it is recommended to report each component and its estimated percentage [275]. LGASC and FLMBC are considered low-grade metaplastic carcinomas and tend to have a favorable prognosis, despite the triple-negative phenotype. The other groups generally have more aggressive behavior and worse outcomes, although retrospective analyses suggest differences in outcomes between some groups [275, 279, 282]. An international study of 364 metaplastic carcinomas from centers in Europe and Asia showed the following frequency distribution: 32% spindle cell carcinoma, 29% matrix-producing carcinoma (mesenchymal differentiation), 21% SCC, 13% mixed squamous and spindle cell carcinoma, and 5% FLMBC [279]. Another study of 347 tumors in the Asia-Pacific Metaplastic Breast Cancer (AP-MBC) consortium found mixed (72%), pure squamous (16%), and pure spindle cell (8%) metaplastic carcinomas to comprise ~96% of cases [282].

The clinical features and patient age distribution of metaplastic carcinomas are overall similar to those of ER-negative IBC-NST, although patients with metaplastic carcinoma tend to present at a higher stage [276, 283]. Most patients (85% in one study) present with a palpable lump [284]. A lower incidence of lymph node involvement has been found compared to IDC-NST [13, 277, 278, 285–287].

Gross and Radiologic Features

Some metaplastic carcinomas display imaging features more often associated with benign lesions, such as round or oval masses with circumscribed margins [288]. However, in a recent series of 71 metaplastic carcinomas, >90% showed imaging features concerning for malignancy, most commonly being an ill-defined mass. Fifteen percent of the tumors in this study were classified as interval cancers [284]. Calcifications are uncommon but may be associated with DCIS or tumors with osseous differentiation [284, 288, 289].

Metaplastic breast carcinomas are often larger than IBC-NST, with a reported mean size of 3.9 cm, ranging from 2 to >10 cm [275, 278, 283, 287]. The gross features are overall not different from those of IBC-NST, with some cases appearing relatively circumscribed and others having irregular, ill-defined borders. Cystic change may be seen, especially in squamous cell carcinomas [290]. Tumors with heterologous cartilaginous differentiation may appear gelatinous, and those with osseous differentiation are hard and gritty. Additional features relevant to specific subtypes are discussed in the appropriate sections below.

Low-Grade Adenosquamous Carcinoma

First described by Rosen and Ernsberger in 1987, LGASC is a distinct and uncommon type of metaplastic carcinoma with low-grade features [291]. In contrast to most other metaplastic carcinomas (except FLMBC), LGASC generally have an indolent clinical course, although they can be locally aggressive [292, 293]. The diagnosis can be especially challenging in CNB due to tissue fragmentation, inconsistent sampling of lesional tissue, and variable staining with epithelial and myoepithelial markers [291, 294]. Familiarity with the morphologic features and unique immunophenotype is thus important for diagnosis [292].

These tumors are overall smaller than other types of metaplastic carcinoma, with a median size of 2–2.8 cm (ranging from 0.5 to 8.6 cm). Grossly, LGASC has a stellate configuration with irregular borders and a firm to hard yellow cut surface [291].

Microscopic Features

Microscopically, LGASC are composed of infiltrating small glands intermixed with solid nests of squamous cells in a spindle cell background (Fig. 12.53a). The growth pattern is occasionally centrifugal and can resemble a radial scar on low magnification. The glands are usually small, elongated, and compressed, forming slender extensions suggestive of syringomatous differentiation [291, 293]. The glands are lined by biphasic luminal epithelial cells and myoepithelial cells, with variable degrees of squamous differentiation of the luminal epithelial cells (Fig. 12.53b–e). The glandular lumens may contain eosinophilic amorphous material with a condensed, inspissated appearance. The squamous nests are of various sizes and shapes, including thin strands and single cells. Squamous pearls or squamous cysts may also be present (Fig. 12.53f). Both the glandular and squamous cells exhibit low-grade cytology, low mitotic activity, and a lack of necrosis, which correlates with the indolent clinical course [291–293]. The stroma of LGASC is typically composed of cellular spindle cells but may be fibrotic and paucicellular. The stromal cells are often arranged in a concentric fashion around the epithelial elements, from which they appear to emanate. A prominent lymphocytic response is often observed at the periphery of the tumor, sometimes in a "cannon ball" pattern. Osteocartilaginous metaplasia may rarely be seen in the stroma [293]. LGASC are highly infiltrative, with the small tumor glands and squamous nests insinuating between and into normal undistorted lobules (Fig. 12.54c).

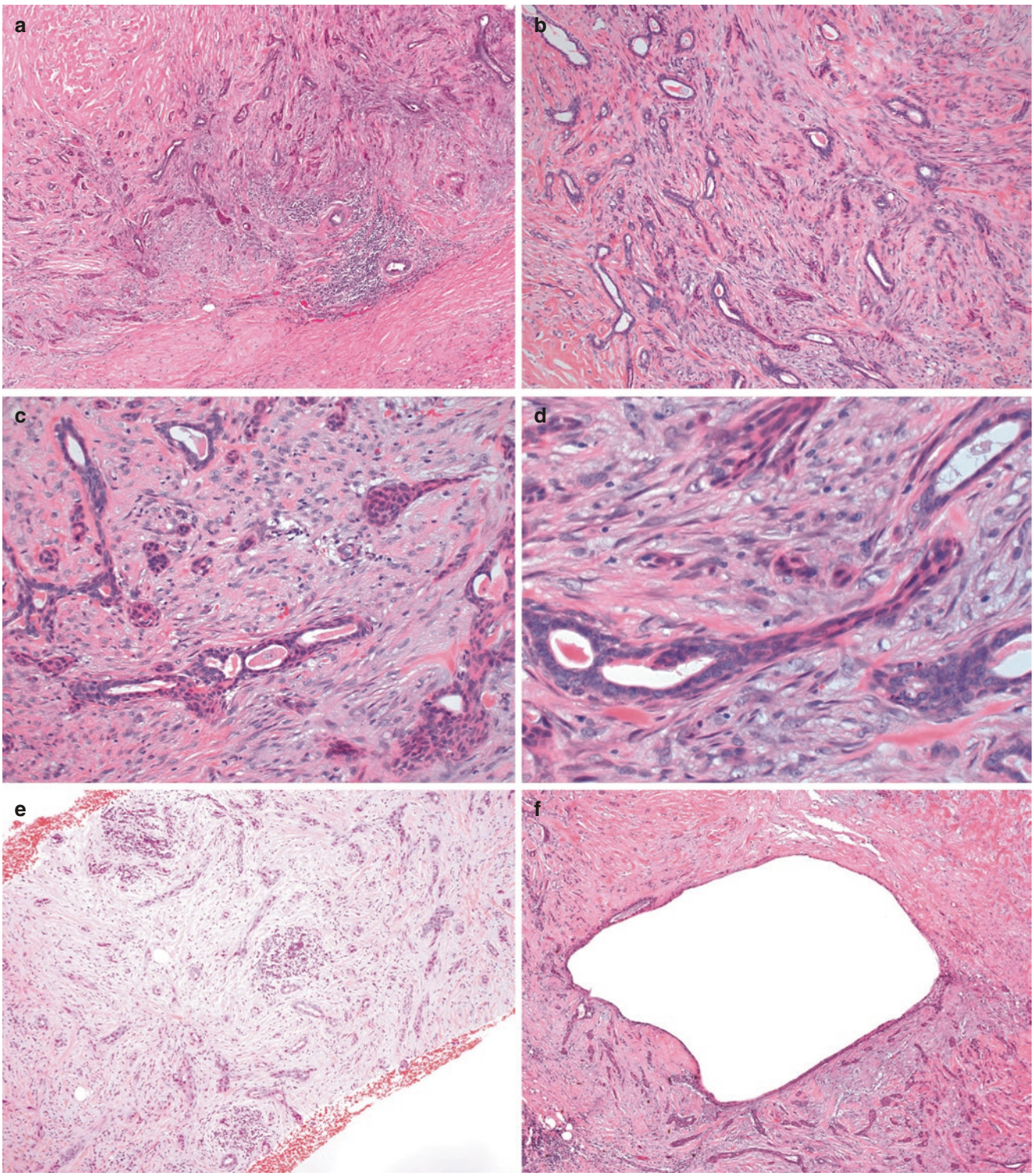

Fig. 12.53 Low-grade adenosquamous carcinoma. (**a**) LGASC showing infiltrating small glands and nests of squamous cells within a desmoplastic to focally fibrotic stroma. Note the lymphoid aggregates, which are usually present at the periphery of the tumor. (**b–d**) Higher power views highlighting the infiltrative glands, which are typically elongated and/or compressed and show variable squamous differentiation. Note some of the cell nests with tear-drop extensions, suggestive of syringomatous differentiation. (**e**) These features can be appreciated on core biopsy. (**f**) Squamous cysts may be seen in some cases

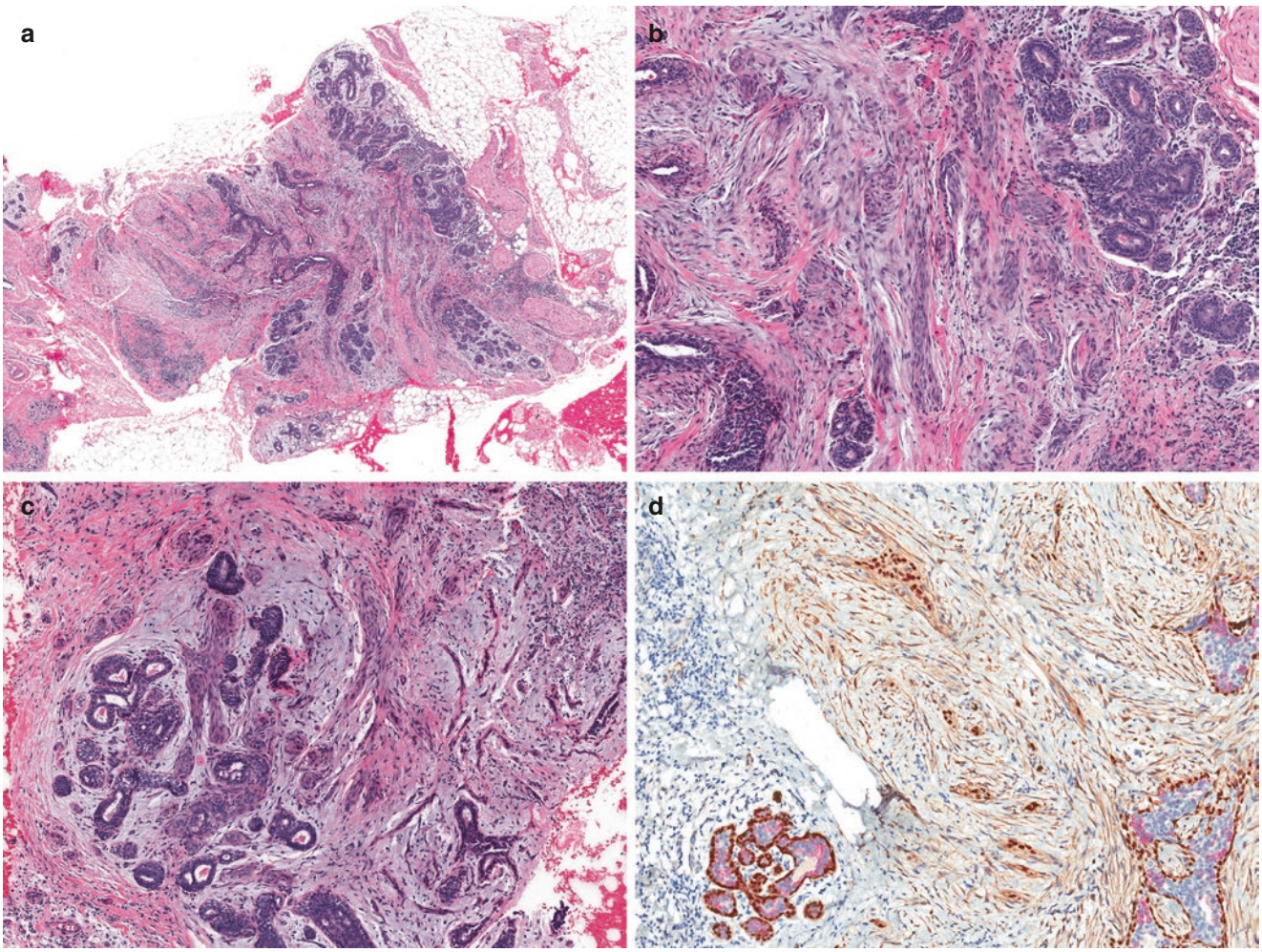

Fig. 12.54 Low-grade adenosquamous carcinoma mimicking sclerosing lesion. (**a**) The low-power architecture of this LGASC is suggestive of a sclerosing lesion. (**b**) On medium power, slender compressed glands are present within a cellular stroma, which is accentuated around the tumor nests. Note the lymphocytic infiltrates at the tumor periphery (right side of images **a** and **b**). (**c**) The neoplastic glands show squamous differentiation and infiltrate between and within the benign lobules. (**d**) Immunohistochemical triple stain (p63 and calponin in brown chromogen and CAM5.2 in red) shows that the tumor cell nests are positive for p63 and negative for both calponin and CAM5.2

Rare cases may demonstrate coexisting DCIS or IDC-NST or show transition to higher grade metaplastic components [292, 295, 296].

LGASC may arise in association with a central sclerosing proliferative lesion, such as radial scar, sclerosing adenosis, or sclerosing papilloma [292, 293, 297]. Association with adenomyoepithelioma has also been reported [298]. In these settings, the small glands and squamous nests of LGASC surround and intermingle with the background distorted ducts and can be easily overlooked and misinterpreted as part of the entrapped epithelial structures characteristic of these sclerosing lesions. However, the stroma of LGASC is desmoplastic rather than fibroelastotic, and the morphologic features of the epithelium, including squamous cell nests, should alert the pathologist to the possibility of LGASC mimicking a benign sclerosing lesion (Fig. 12.54a–d).

Immunohistochemistry

Immunophenotypically, LGASC demonstrate an unusual "consistently variable" staining pattern with myoepithelial markers. In a study of a large series of LGASC, myoepithelial markers (p63, SMM, calponin, SMA, CD10) were found to exhibit a spectrum of complete, discontinuous, or absent staining around the epithelial nests within the same tumor in over one-third of the cases, with 11% of tumors demonstrating complete circumferential staining (Fig. 12.55f, g) [294]. No tumor showed complete absence of staining by any of the myoepithelial markers. Glandular luminal staining for p63 was observed in approximately 75% of LGASC, further supporting squamous differentiation of these glandular structures. In addition, a distinctive lamellar (concentric) staining pattern of stromal cells surrounding glands was noted with

SMM and/or calponin in more than half of the lesions, which can complicate interpretation of true myoepithelial staining (Fig. 12.55e). Another feature is the core staining pattern observed with various cytokeratins, in which the luminally located epithelial cells of neoplastic glands stained stronger than the adjacent basal cells within the same glands (Fig. 12.55d). These unique inconsistent staining patterns with epithelial and myoepithelial markers may be diagnostically valuable in problematic cases to support the suspicion of LGASC (Fig. 12.55a–g). LGASC are triple negative for ER, PR, and HER2 (Fig. 12.55h) and show consistent expression of basal cytokeratins (CK5/6, CK14, CK17) [295, 296, 299–302], indicative of a basal-like immunophenotype. EGFR is variably expressed [295, 299, 302].

Differential Diagnosis

The differential diagnosis of LGASC includes benign fibrosclerosing lesions (sclerosing adenosis, radial scar/complex sclerosing lesion), reactive squamous metaplasia, tubular carcinoma, and syringomatous adenoma of the nipple [292, 294]. Fibrosclerosing lesions usually do not demonstrate squamous differentiation, and the associated stroma is typically fibroelastotic and hypocellular. These lesions also lack infiltrative growth of glands between and into normal lobules, and the glands are often surrounded by a complete myoepithelial layer (Fig. 12.54a–d). However, rare squamous metaplasia may be observed in fibrosclerosing lesions, and decreased or focal lack of myoepithelial marker expression can be seen [241]. Early cellular sclerosing lesions can

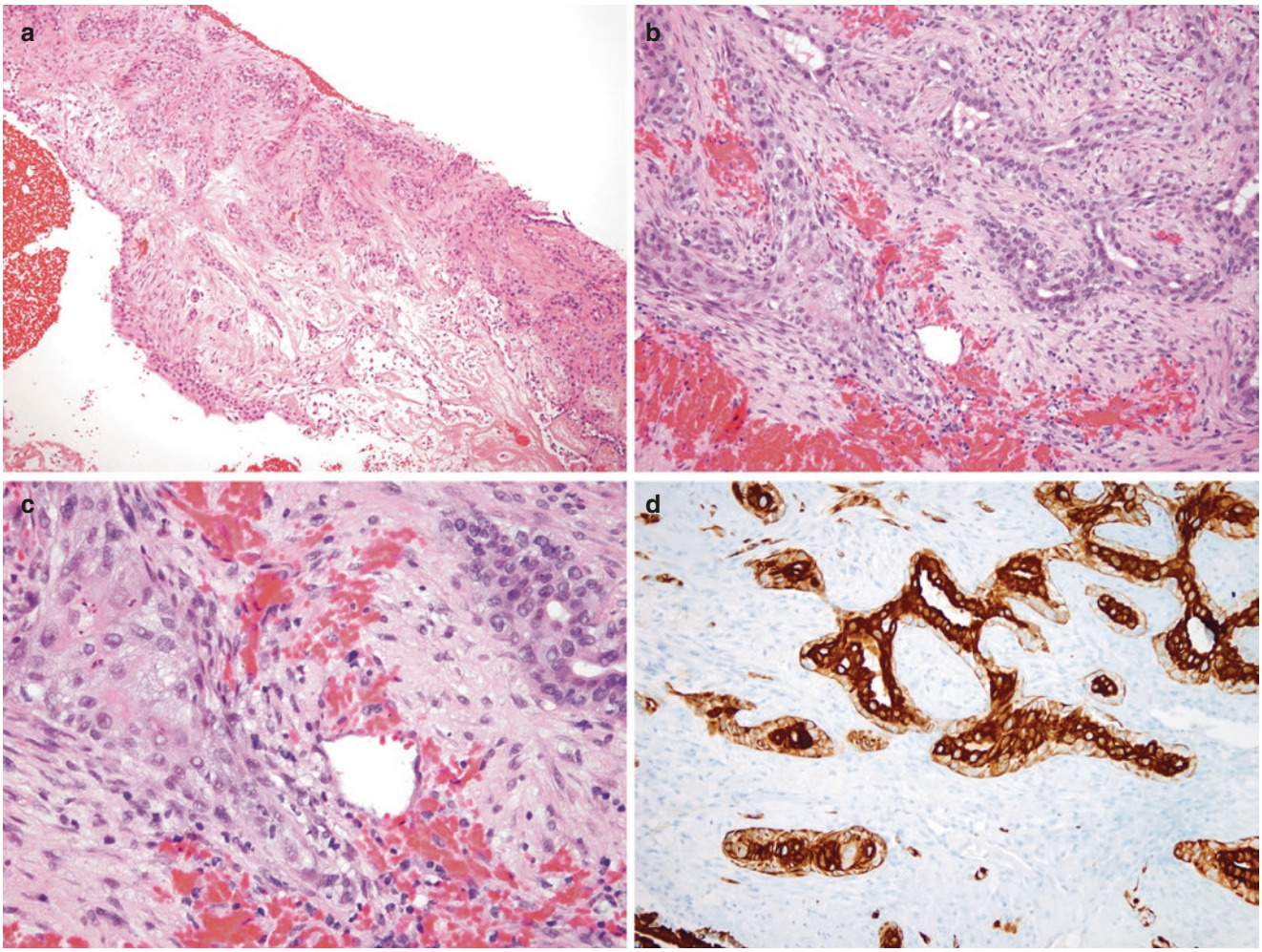

Fig. 12.55 Core needle biopsy of low-grade adenosquamous carcinoma. (**a–c**) This CNB shows nests and glands of tumor cells with squamous features embedded within a cellular spindle cell stroma. (**d**) Immunohistochemical staining for CK7 demonstrates characteristic "core staining" pattern, with stronger staining of luminal epithelial cells than surrounding basally located cells. (**e**) SMM immunostain highlights stromal cell cuffing around lesional cells giving characteristic "lamellar" staining pattern. (**f**, **g**) p63 and calponin immunostains show the consistently variable staining pattern, with a spectrum of complete, discontinuous, and absent staining pattern around the tumor nests within the same lesion. (**h**) The tumor cells lack ER expression

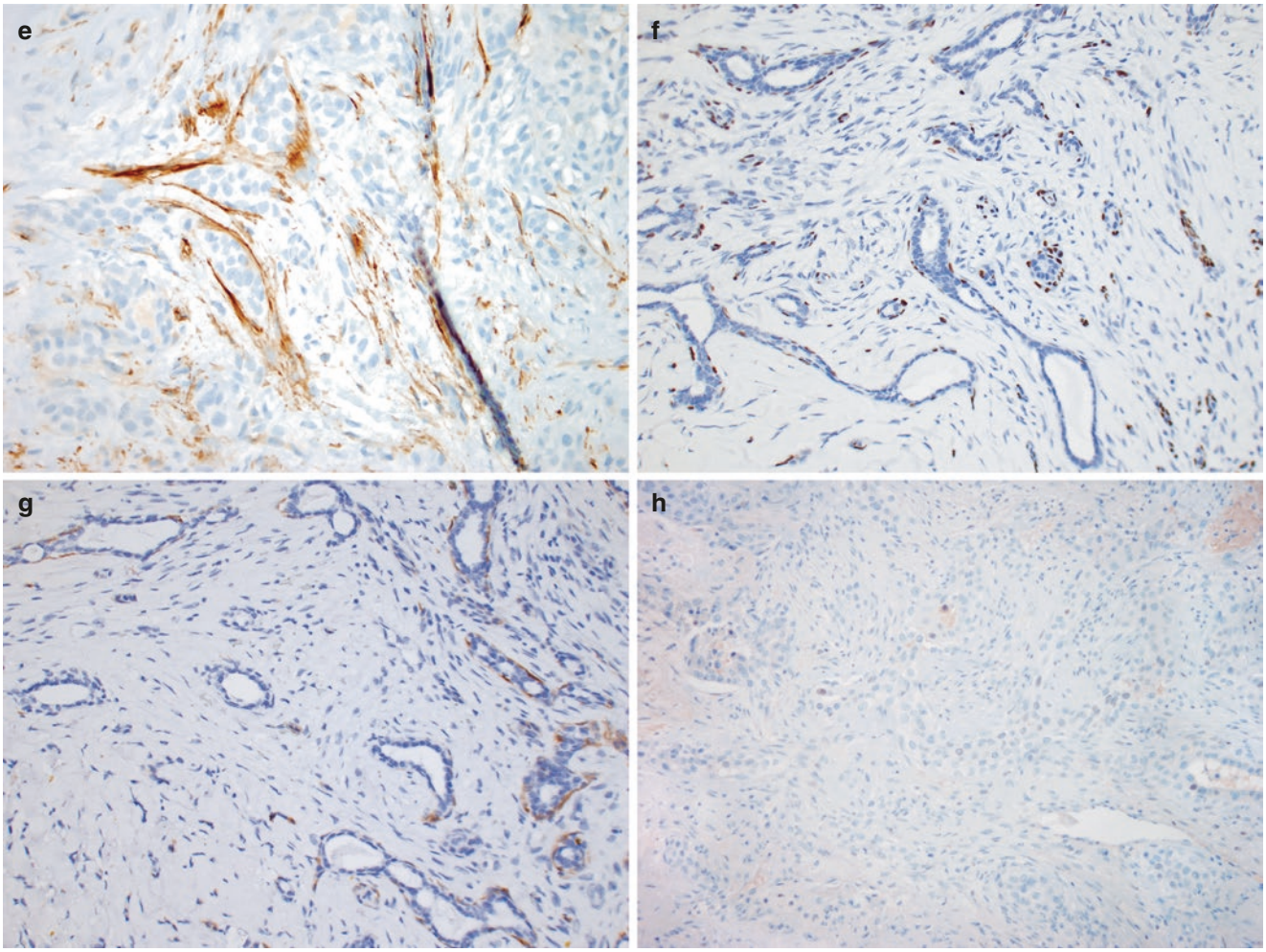

Fig. 12.55 (continued)

harbor adenosquamous-like areas in the central nidus, raising consideration for LGASC [303]. Therefore, the distinction between LGASC and benign fibrosclerosing lesions may be difficult even with immunohistochemical stains in a core biopsy specimen. In such challenging cases, a descriptive diagnosis of "atypical sclerosing lesion" with a comment to recommend excision can be considered.

Tubular carcinomas feature angulated glands in a cellular desmoplastic stroma, which may be confused with LGASC. However, tubular carcinomas do not show squamous differentiation. Furthermore, LGASCs demonstrate inconsistent staining patterns with myoepithelial markers, whereas the neoplastic glands of tubular carcinomas lack myoepithelial staining altogether. Lastly, tubular carcinomas are strongly positive for ER, in sharp contrast to the negative ER immunophenotype of LGASC.

The most difficult differential diagnosis of LGASC is with syringomatous tumor of the nipple, as both lesions share identical or nearly identical morphologic and immunohistochemical features, and both have a propensity for local recurrence [275, 292, 301]. Tumor location is also not a strong discriminating feature, as both can occur in the retroareolar region [294]. Syringomatous tumor of the nipple may exhibit a similar inconsistent staining pattern with myoepithelial markers as is typical of LGASC, although the "lamellar" myoepithelial and core "cytokeratin" staining patterns are not likely to be seen in the former [294].

LGASC should be distinguished from high-grade adenosquamous carcinoma (SCC mixed with IBC-NST), due to the often-aggressive behavior of the latter.

Fibromatosis-Like Metaplastic Carcinoma

FLMBC was first described by Gobbi et al. in 1999 as a low-grade variant of metaplastic carcinoma that mimics fibromatosis [304]. Compared to other metaplastic carcinomas, these tumors are associated with unique clinical behavior

characterized by low malignant potential, a high incidence of local recurrence, and very rare distant metastases. FLMBC has shown predilection for older women and the left breast [305].

Grossly, FLMBC appears as a hard mass with homogenous gritty, gray white cut surfaces, ranging in size from 1 to 7 cm. Some lesions are circumscribed, whereas others have irregular borders or may even be cystic in appearance [305].

Microscopic Features

Histologically, FLMBC exhibit an infiltrative, fibromatosis-like growth pattern [304, 306]. The tumors comprise bland spindle cells arranged as interlacing fascicles and embedded in a collagenized stroma, comprising at least 95% of the total tumor area [307] (Figs. 12.56, 12.57, 12.58a–c, and 12.59a–c). Tumor cell nuclei are slender with tapered edges and finely distributed chromatin [275]. Nuclear atypia is absent or mild. Scattered foci of more plump and polygonal (epithelioid) cells with rounded nuclei, eosinophilic cytoplasm, and foci of glandular or squamous elements may be seen but should comprise <5% of the lesion [304, 306] (Figs. 12.57b, 12.59c, and 12.60). Not infrequently, the epithelioid cells are arranged in a perivascular pattern (Fig. 12.59b) [297, 304]. Mitotic activity is absent to low (<2/10 HPF). The majority of tumors have a mild chronic inflammatory infiltrate admixed with the neoplastic spindle cells [306] (Fig. 12.58a–c). It should be noted that these tumors demonstrate significant intertumoral and even intratumoral variation in the degree of cellularity and amount of stromal collagen. Tumors with extensive collagenous stroma and scant spindle cells

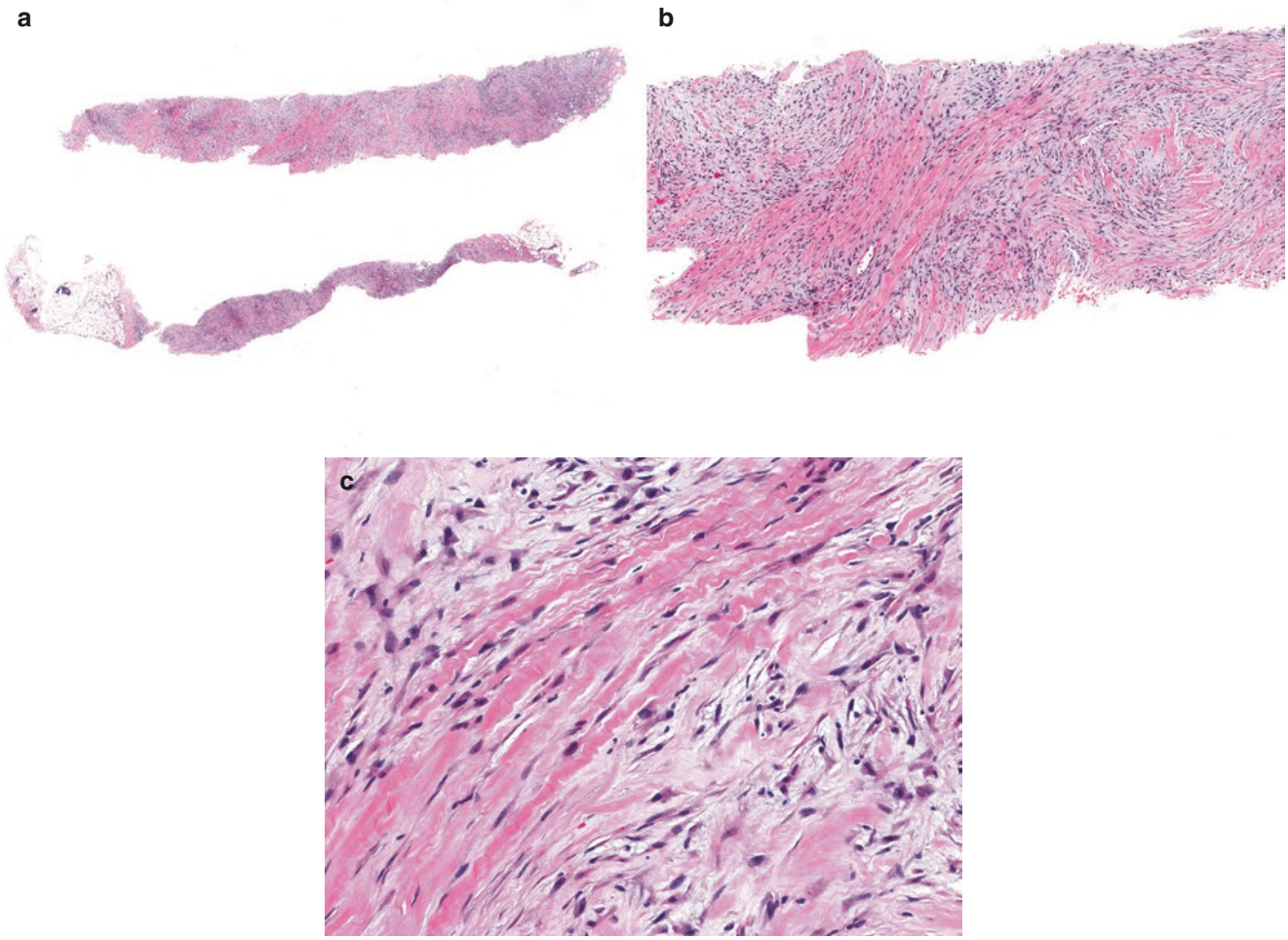

Fig. 12.56 Fibromatosis-like metaplastic carcinoma. (**a**, **b**) Core needle biopsy demonstrates spindled tumor cells arranged in long fascicles mimicking fibromatosis. (**c**) On higher magnification, the spindled cells demonstrate pale eosinophilic cytoplasm and bland, slender nuclei with tapered edges, and finely distributed chromatin. Note the abundant stromal collagen in the background

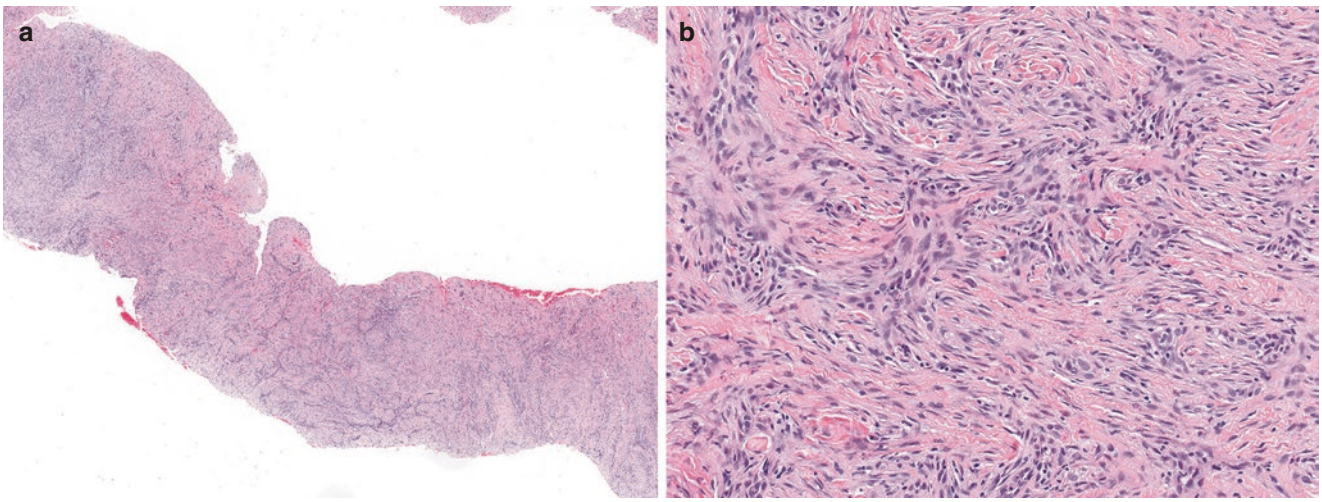

Fig. 12.57 Fibromatosis-like metaplastic carcinoma (FLMBC). (**a**, **b**) FLMBC showing higher cellularity and foci of epithelioid tumor cells with more rounded nuclei. Nuclear features are bland, and mitotic activity is low

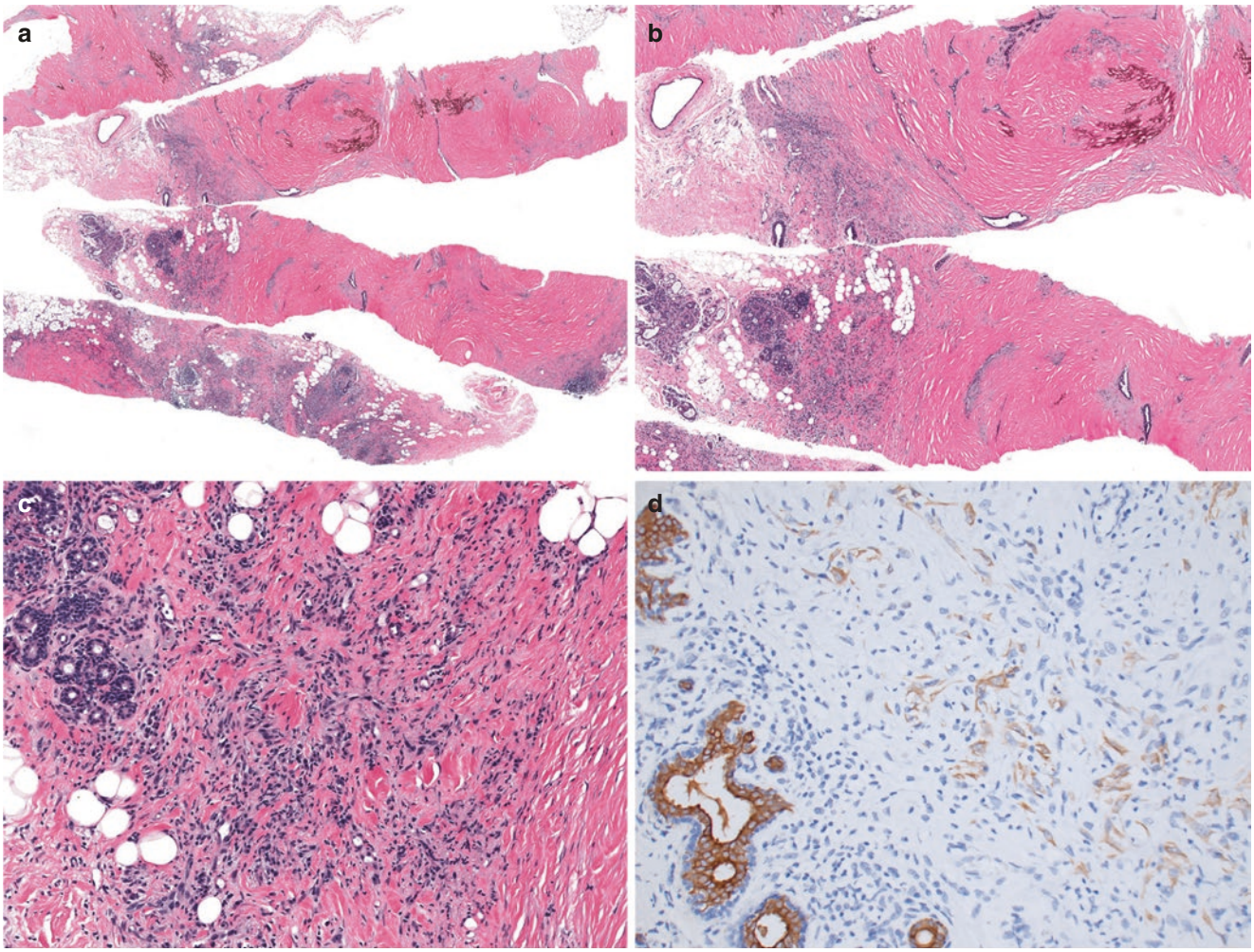

Fig. 12.58 Fibromatosis-like metaplastic carcinoma (FLMBC). (**a**, **b**) This FLMBC shows extensive sclerotic and hypocellular stroma involving multiple core fragments, with peripheral inflammatory foci noted on low power. This case could easily be mistaken for a fibroinflammatory process. (**c**) Higher magnification reveals the subtle presence of atypical spindle cells in association with the inflammatory lymphohistiocytic infiltrates. Immunostains for (**d**) keratin AE1/AE3 and (**e**) p63 highlight the infiltrative growth of the atypical spindle cells and confirm the diagnosis

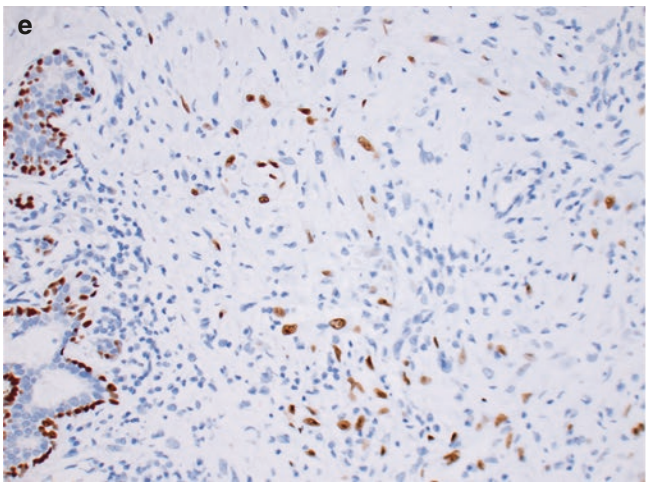

Fig. 12.58 (continued)

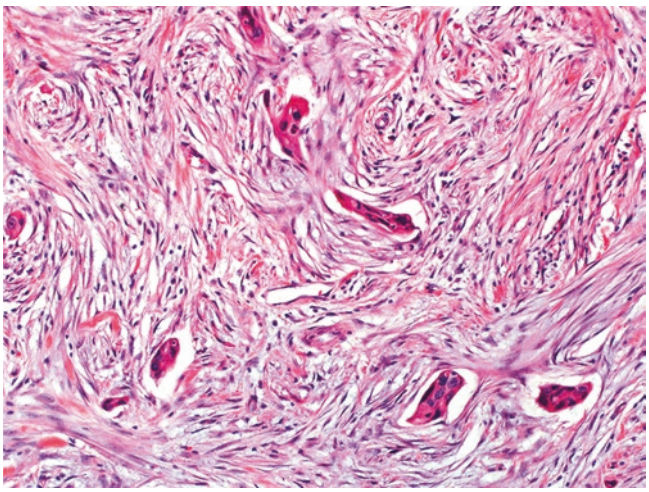

Fig. 12.60 Fibromatosis-like metaplastic carcinoma (FLMBC) with squamous tumor cells. Small clusters of squamous cells are embedded within the spindle cell proliferation of this FLMBC. These squamous cells should comprise <5% of the tumor

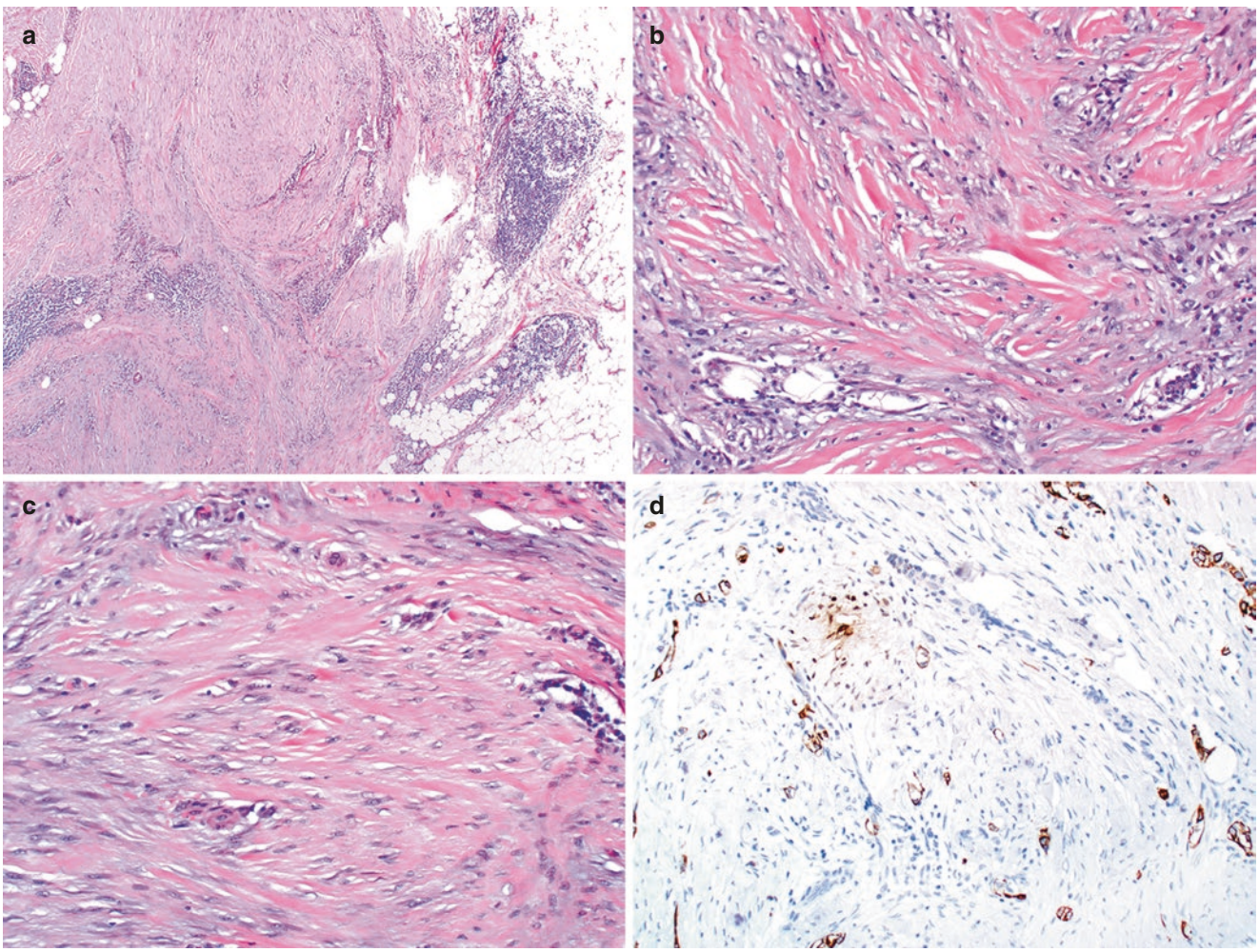

Fig. 12.59 Fibromatosis-like metaplastic carcinoma (FLMBC) mimicking scar tissue. (**a**) This FLMBC demonstrates low-power features suggestive of scar tissue. (**b**) High-power examination reveals abundant dense collagen with associated bland spindle cells and a mild inflammatory infiltrate. (**c**) Rare single and small clusters of epithelioid cells with squamoid features are identified after thorough searching. (**d**) HMWCK (34βE12) immunostain highlights the neoplastic cells

have been mistaken as a scar or fibroinflammatory process (Figs. 12.58 and 12.59).

Immunohistochemistry

FLMBC are consistently p63 and cytokeratin positive, which is useful to establish the diagnosis (Figs. 12.58d, e and 12.59d) [282, 302, 304, 308]. However, the immunoreactivity may be focal and sometimes largely restricted to areas with epithelioid cells. The spindle cells express vimentin and may be EMA or SMA positive [302]. Like other types of metaplastic carcinoma, FLMBC are triple negative for ER, PR, and HER2 [302, 306] (see additional discussion in section "Spindle Cell Carcinoma" and Table 12.8 for immunohistochemical markers useful in the diagnosis of metaplastic carcinoma).

Differential Diagnosis

FLMBC should always be considered in a breast core biopsy of a bland spindle cell proliferation. The differential diagnosis of FLMBC encompasses various bland spindle cell lesions, including scar, fibromatosis, nodular fasciitis, myofibroblastoma, and inflammatory myofibroblastic tumor. These lesions can be all distinguished from FLMBC by lack of epithelioid clusters and cytokeratin and p63 expression [304]. CD34 shows strong positivity in myofibroblastoma but is negative in metaplastic carcinoma. Of note, aberrant nuclear staining for beta-catenin is characteristic of fibromatosis but can also be observed in some metaplastic carcinomas and phyllodes tumors [309]. FLMBC should be distinguished from metaplastic spindle cell carcinoma, which is not associated with the same indolent clinical behavior as FLMBC. Spindle cell carcinomas are higher grade tumors with moderate or marked nuclear pleomorphism and higher mitotic activity.

Table 12.8 Useful immunohistochemical markers in the diagnostic workup of spindle cell metaplastic carcinoma

Markers	Utility and interpretation
CK (MNF116, AE1/3, 34βE12, CAM5.2, CK5/6, CK14, CK19)	Positive in metaplastic carcinoma, especially AE1/3 and MNF116 (~80%) and basal keratins (34βE12, CK5/6, CK14, CK19) (~70%); luminal keratins (CK7, CK8/18, CK19) less frequently positive (~30–60%) May be positive in phyllodes tumors[a]
p63	Positive in metaplastic carcinoma, especially FLMBC, but also other types May be positive in phyllodes tumors[a], as well as benign and malignant mesenchymal tumors
CD34	Positive in fibroadenoma, phyllodes tumor, PASH, myofibroblastoma, angiosarcoma and dermatofibrosarcoma protuberans Negative in metaplastic carcinoma, fibromatosis, and nodular fasciitis
β-Catenin	Aberrant nuclear expression in fibromatosis, but not specific (also in some phyllodes tumors and metaplastic carcinomas)
SOX10	Sensitive marker for melanoma and nerve-sheath-derived tumors May be positive in metaplastic carcinoma
Other markers	Based on morphologic features and history: S100 protein, SOX10, HMB-45 (melanoma); SMA, desmin, myogenin (muscle tumor); RB loss (myofibroblastoma); ERG, CD31, MYC (vascular tumor), etc.

[a]CK and p63 reactivity, when detected in phyllodes tumors, is often focal

Spindle Cell Carcinoma

Microscopic Features

Spindle cell carcinomas are composed of atypical elongated to plump spindled cells arranged in cellular fascicular, herringbone, fasciitis-like, vaguely storiform, or patternless growth patterns (Fig. 12.61a–d). The spindle cells can entrap native ducts and lobules or obliterate the normal breast architecture. Microcystic or pseudovascular spaces may occasionally be seen and can mimic angiosarcoma. Nuclear pleomorphism is typically moderate or marked. The mitotic rate is variable, and markedly atypical mitotic figures are common in higher grade tumors [310]. The tumor cells may be focally more epithelioid or squamous, which can be a clue to the diagnosis. A chronic inflammatory infiltrate is often present, and scattered multinucleated osteoclast-like giant cells may be seen (Figs. 12.62, 12.63a, b, and 12.64a–d). Focal myxoid change or stromal hyalinization may be seen. Small foci of chondroid or osseous differentiation may also be present but should be focal. Most spindle cell carcinomas have infiltrative borders, but some may show a rounded pushing edge. DCIS may occasionally be seen in association with the invasive spindle cell component, which supports the epithelial nature of the tumor and can facilitate the diagnosis [311] (Fig. 12.65).

Immunohistochemistry

Immunohistochemistry is essential to demonstrate epithelial differentiation of the spindle cells in spindle cell carcinoma, especially in cases lacking associated DCIS. A panel of epithelial markers is recommended and should include broad spectrum keratins (MNF116, AE1/AE3), high-molecular-weight keratins (34βE12, CK5/6, CK14), and p63 [312] (Figs. 12.61e, f, 12.63c, d, and 12.64e). In general, the spindle cells are more likely to express high-molecular-weight keratins, whereas luminal keratins (CAM5.2, CK7, CK19) are more often negative [302, 313]. It should be emphasized that no single keratin is consistently positive in metaplastic

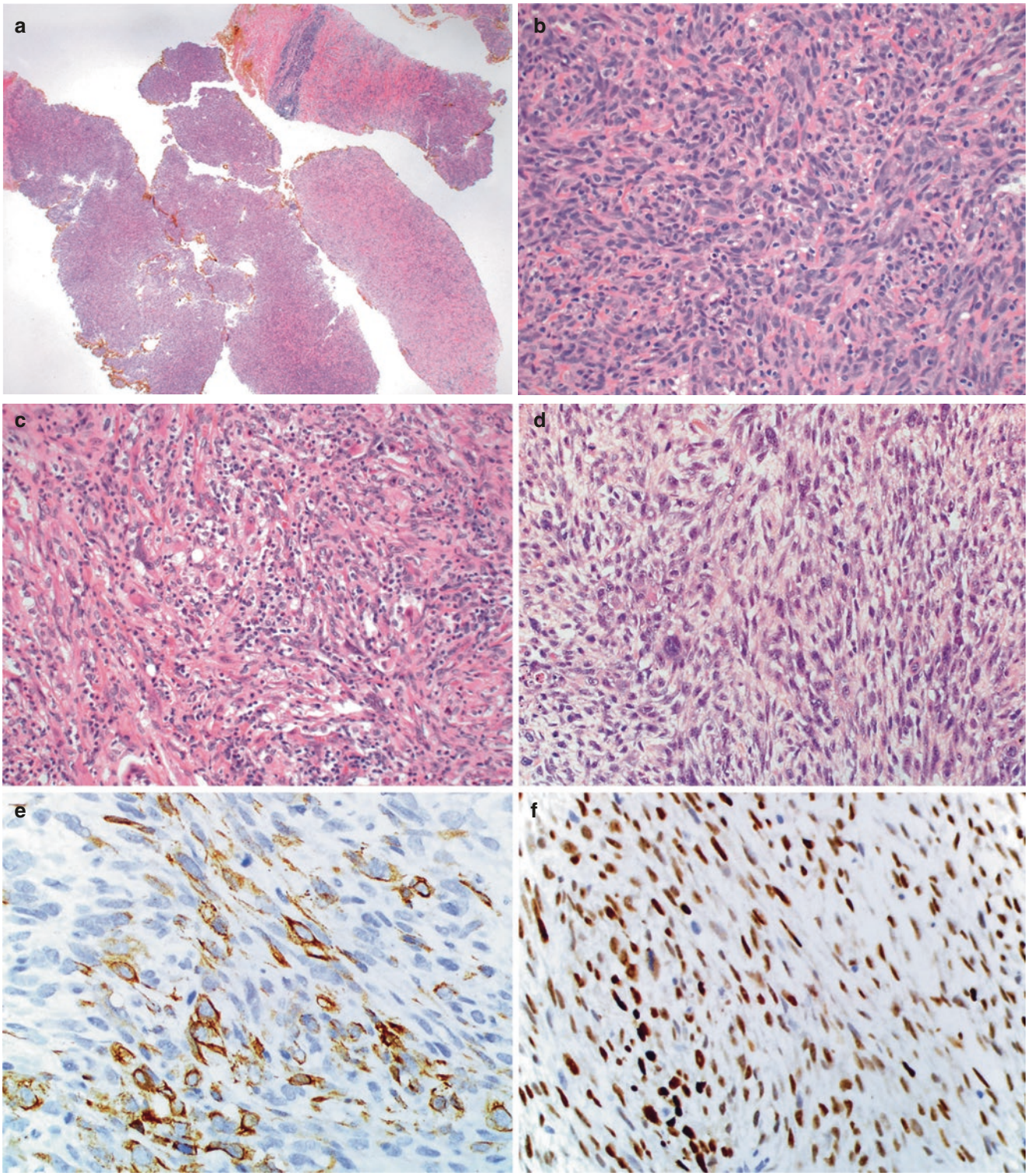

Fig. 12.61 Spindle cell carcinoma. (**a**, **b**) Core needle biopsy of this breast mass reveals a hypercellular spindle cell neoplasm with a storiform growth pattern, moderate nuclear atypia, and scattered mitotic figures. (**c**, **d**) Other examples showing a more sarcomatoid appearance, featuring fascicles of spindled tumor cells with severe cytologic atypia. (**e**, **f**) Immunostains for keratins (in this case, MNF116) and p63 are helpful to confirm the epithelial nature of the spindle cells

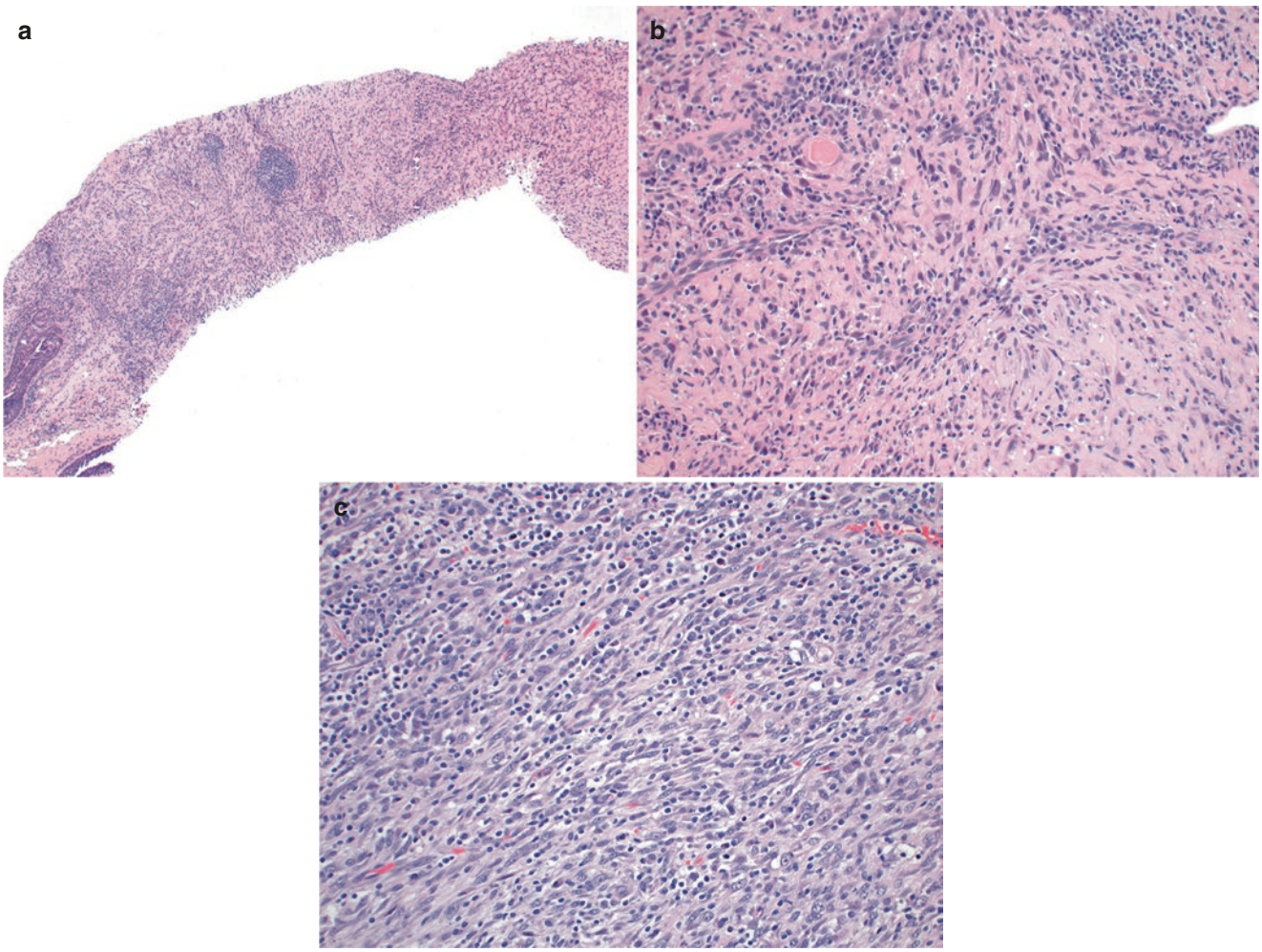

Fig. 12.62 Spindle cell carcinoma with prominent lymphoplasmacytic inflammation. (**a–c**) These two cases of spindle cell carcinoma show prominent associated lymphoplasmacytic infiltrates associated with the tumor cells

carcinoma. In addition, keratin positivity may be very focal [314]. Therefore, negative keratin staining in a core biopsy specimen does not exclude the diagnosis of metaplastic carcinoma. Immunohistochemical testing of multiple blocks of a surgical excision specimen may be required to reveal keratin reactivity in some cases. P63 is a sensitive marker for metaplastic carcinoma but is not specific and can be expressed in a variety of benign and malignant mesenchymal lesions, notably including malignant phyllodes tumors, which are often high in the differential diagnosis, especially in a core biopsy [315–318] (see section "Differential Diagnosis"). In addition to p63, other markers expressed by myoepithelial cells, such as SOX10, SMA, S100 protein, CD10, and maspin, can also be positive in spindle cell (and other) metaplastic carcinomas, supporting the notion that some of these tumors have myoepithelial-like differentiation and are on a spectrum with myoepithelial carcinoma [302, 319].

Metaplastic carcinomas may exhibit aberrant nuclear staining for beta-catenin, a feature traditionally regarded as characteristic of fibromatosis [309]. GATA3 may also be positive in metaplastic carcinomas (~20–50%), including spindle cell carcinomas, with most positive cases showing weak staining [319–321]. A recent immunohistochemical study found overexpression of TRPS1, a GATA transcription factor and regulator of mammary epithelial cell growth and differentiation, in 86% of metaplastic carcinomas, including spindle cell carcinoma, SCC, and MCMD. Additional studies will be required to validate these results and their diagnostic utility [321]. CD34, a marker expressed in several mesenchymal tumors of the breast including phyllodes tumors, is typically negative in spindle cell carcinoma. Table 12.8 summarizes useful immunohistochemical markers that can be used in the diagnostic workup of spindle cell carcinoma.

Like other metaplastic carcinomas, spindle cell carcinomas are triple negative for ER, PR, and HER2. EGFR overexpression is frequent, with EGFR gene amplification described in a subset of cases [322, 323].

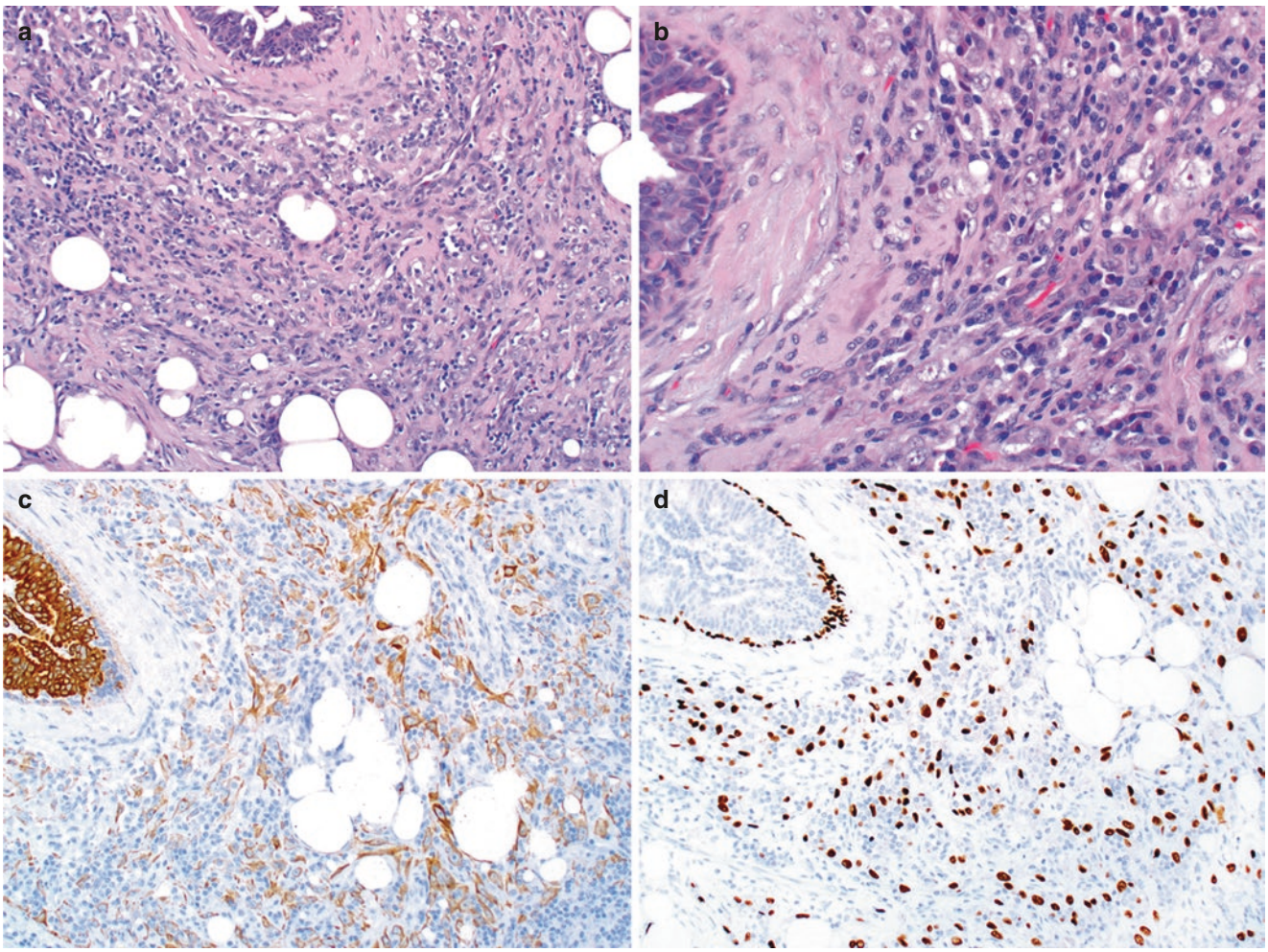

Fig. 12.63 Spindle cell carcinoma mimicking mastitis. (**a**) In this example, marked inflammatory infiltrates obscure the underlying neoplastic spindle cells and impart an appearance of mastitis on lower power evaluation. (**b**) Higher power magnification reveals the atypical spindle and epithelioid cells dispersed within the inflammation. (**c**, **d**) Broad spectrum cytokeratin antibody MNF116 and p63 demonstrate positive staining in the tumor cells, respectively. Note the lace-like pattern of the numerous tumor cells highlighted by MNF116

Differential Diagnosis

Despite a long list of differential diagnoses, metaplastic carcinoma is by far the most common spindle cell lesion of the breast (~45%), followed by phyllodes tumor, fibromatosis, and myofibroblastoma (each ~10%) [324]. Primary or metastatic sarcomas, including angiosarcoma, must also be included in the differential, but these tumors are rare in the breast. Accordingly, metaplastic carcinoma with a spindle cell component should always be considered when encountering a spindle cell proliferation arising in the breast. Identification of associated DCIS or small squamous foci helps support the epithelial nature of the tumor to facilitate the diagnosis. Therefore, adequate tumor sampling with careful evaluation for DCIS or epithelioid/squamous foci is critical in an excision specimen. However, DCIS may be scant or absent and not sampled by core biopsy. A panel of immunohistochemical markers is often required to demonstrate the epithelial nature of the spindle cells and establish the correct diagnosis (Table 12.8).

Distinction of spindle cell metaplastic carcinoma from malignant phyllodes tumor with stromal overgrowth is often problematic, especially in core biopsies. Like metaplastic carcinomas, the stromal cells of malignant phyllodes tumors can be p63 or keratin positive, although staining in phyllodes tumors is usually focal [317, 318] (Fig. 12.66). The ΔN p63 isoform p40 was suggested in one study to be more specific but less sensitive than p63 for the diagnosis of spindle cell carcinoma, although this requires further validation [317]. Focal expression of keratin, p63, and/or p40 in a spindle cell neoplasm of the breast therefore does not exclude phyllodes tumor, especially in a core biopsy specimen. CD34 may be helpful in this setting, as a subset of malig-

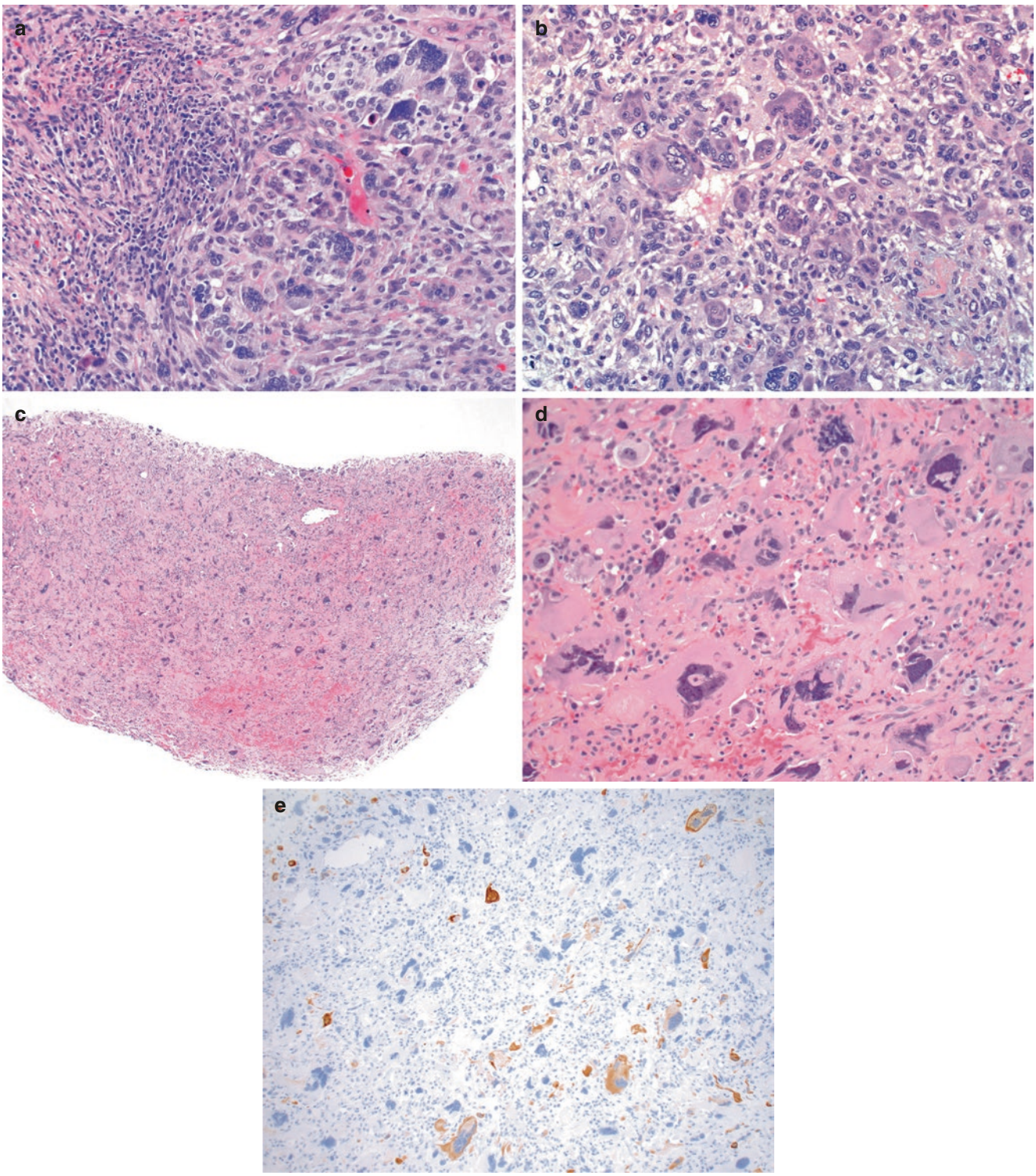

Fig. 12.64 Spindle cell carcinoma with giant cells. (**a, b**) Spindle cell carcinoma with osteoclastic-like giant cells. The tumor-associated giant cells demonstrate abundant eosinophilic cytoplasm and multiple small bland oval clustered nuclei, typical of osteoclastic-like giant cells. These cells are benign and are considered to belong to the histiocytic lineage. (**c–e**) In contrast, this spindle cell carcinoma is composed of markedly pleomorphic neoplastic epithelial cells, supported by positive keratin immunostain

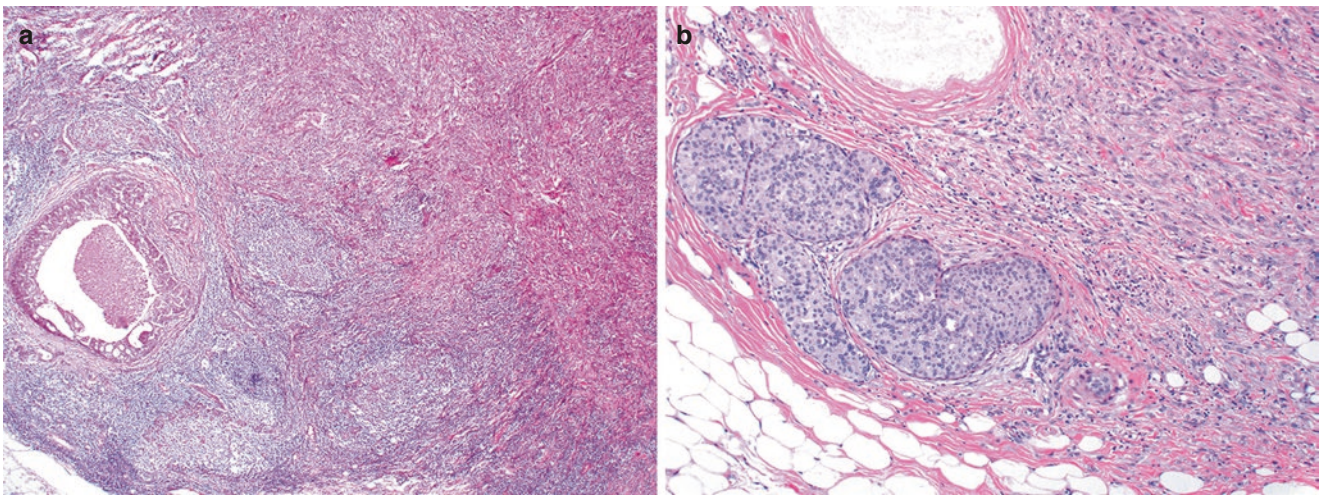

Fig. 12.65 Conventional ductal carcinoma in situ (DCIS) associated with spindle cell carcinoma. (**a**, **b**) The presence of DCIS associated with a spindle cell neoplasm helps support a diagnosis of metaplastic carcinoma, even if immunohistochemical stains for keratin are negative

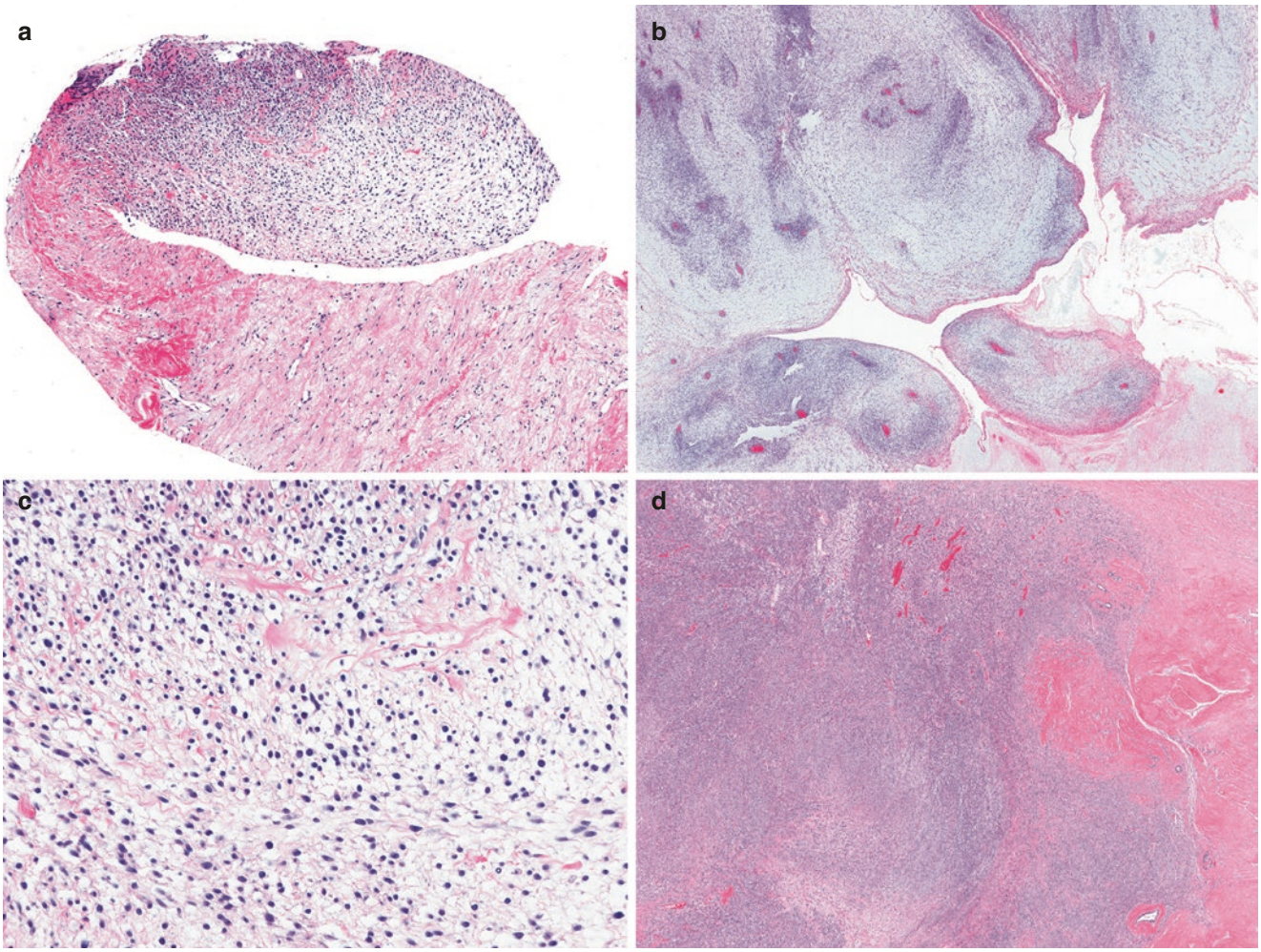

Fig. 12.66 Cytokeratin expression in a spindle cell neoplasm of the breast does not exclude phyllodes tumor. (**a**, **c**) This CNB demonstrates a spindle cell neoplasm with epithelioid features, including areas of cytoplasmic clearing and rounded hyperchromatic nuclei, but no glandular or ductal component. (**e**) An immunostain for pancytokeratin is positive in <5% of the spindle cells. (**b**, **d**) Excision revealed a malignant phyllodes tumor (**b**) with hypercellular areas of characteristic leaf-like growth, as well as (**d**) abundant stromal overgrowth. Note the presence of a residual hyalinized fibroepithelial area at the right of the image. (**f**) Immunohistochemistry also revealed focal (<5%) cytokeratin positivity of the phyllodes tumor stromal cells in the excision specimen

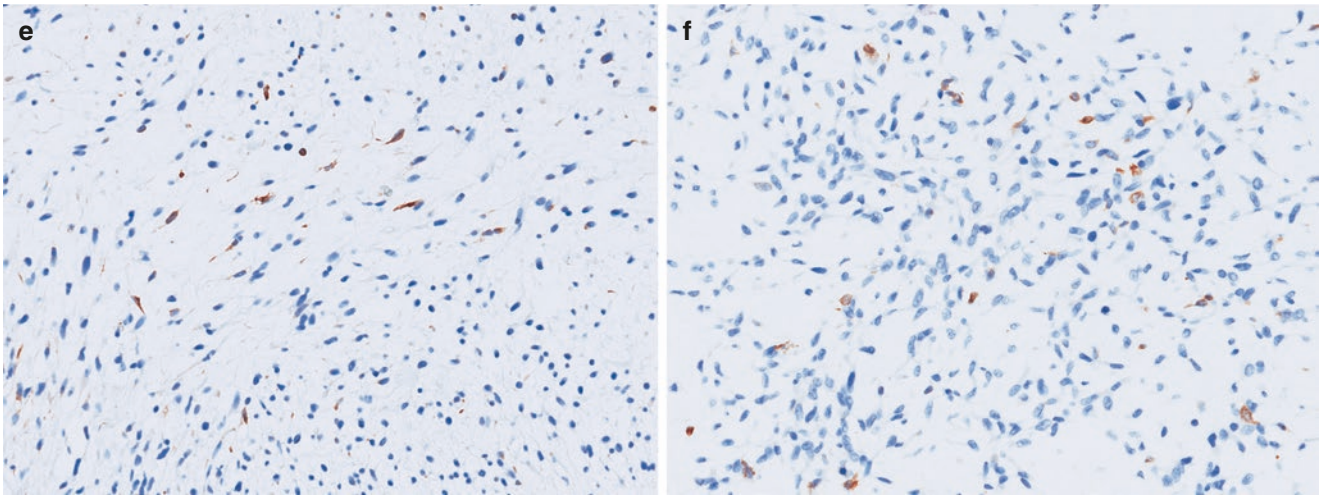

Fig. 12.66 (continued)

nant phyllodes tumors express this marker, which is negative in spindle cell carcinoma [313, 325]. Strong and diffuse keratin and p63 staining favors spindle cell carcinoma. Conversely, negative staining p63 and keratin staining in a core biopsy does not exclude metaplastic carcinoma, as expression can be focal (see also Chap. 7, sections "Phyllodes Tumor—Immunohistochemistry" and "Differential Diagnosis"). In the absence of histologic or immunophenotypic evidence for epithelial differentiation, it may not be possible to differentiate metaplastic carcinoma from phyllodes tumor or sarcoma on core biopsy. In such cases, a descriptive diagnosis such as "atypical spindle cell proliferation" or "spindle cell neoplasm" should be rendered, with recommendation for surgical excision. Indeed, unless epithelial differentiation is obvious and/or keratin immunopositivity is diffuse, a spindle cell neoplasm in the breast should be excised for definitive classification. In challenging cases, targeted sequencing could be useful in distinguishing metaplastic carcinoma from malignant PT. Specifically, the identification of a hotspot *MED12* mutation would confirm a fibroepithelial tumor and essentially exclude metaplastic carcinoma [282, 311, 326–332].

Squamous Cell Carcinoma

Primary squamous cell carcinoma (SCC) of the breast is a rare type of metaplastic carcinoma, accounting for <0.1% of all breast tumors [333, 334]. Pure SCC is almost entirely (>90%) composed of squamous cell carcinoma [335], but SCC may also be mixed with other types of metaplastic carcinoma, most commonly with a spindle cell pattern, or with IBC-NST, the latter of which is classified as high-grade adenosquamous carcinoma. Primary cutaneous or metastatic SCC must be excluded prior to making a diagnosis of metaplastic SCC.

The etiology of metaplastic SCC is not known. It has been hypothesized that these tumors can arise from squamous metaplasia associated with either benign breast lesions or ductal carcinoma [336–339]. Rare SCC have been identified in association with inflammatory lesions, such as abscesses, chronic cysts, chronic mastitis, or implant capsules, suggesting that chronic inflammation may be a contributing factor to tumor development in some cases [337, 338, 340–343].

Microscopic Features

SCC of the breast can present with various histomorphologic patterns of the invasive squamous cells, including keratinizing, non-keratinizing, cystic, papillary, clear cell, and acantholytic [344]. In most cases, the squamous cells are keratinized with eosinophilic glassy cytoplasm, intercellular bridges, and keratin debris accompanied by necrosis, desmoplastic stromal reaction, and prominent inflammation (Figs. 12.67a–c and 12.68). Cystic degeneration is common, with portions of the tumor composed of squamous lined cysts with variable nuclear pleomorphism [345] (Fig. 12.69). Acantholytic change in SCC is characterized by the presence of vascular like channels and pseudoglandular structures that can mimic angiosarcoma [344, 346]. The following pathological criteria are required to establish a diagnosis of metaplastic SCC of the breast: (1) the tumor is not derived from the overlying skin or nipple; (2) the infiltrative component is predominantly (>90%) of squamous type; (3) no other invasive neoplastic elements (ductal, mesenchymal, or other) are present in significant

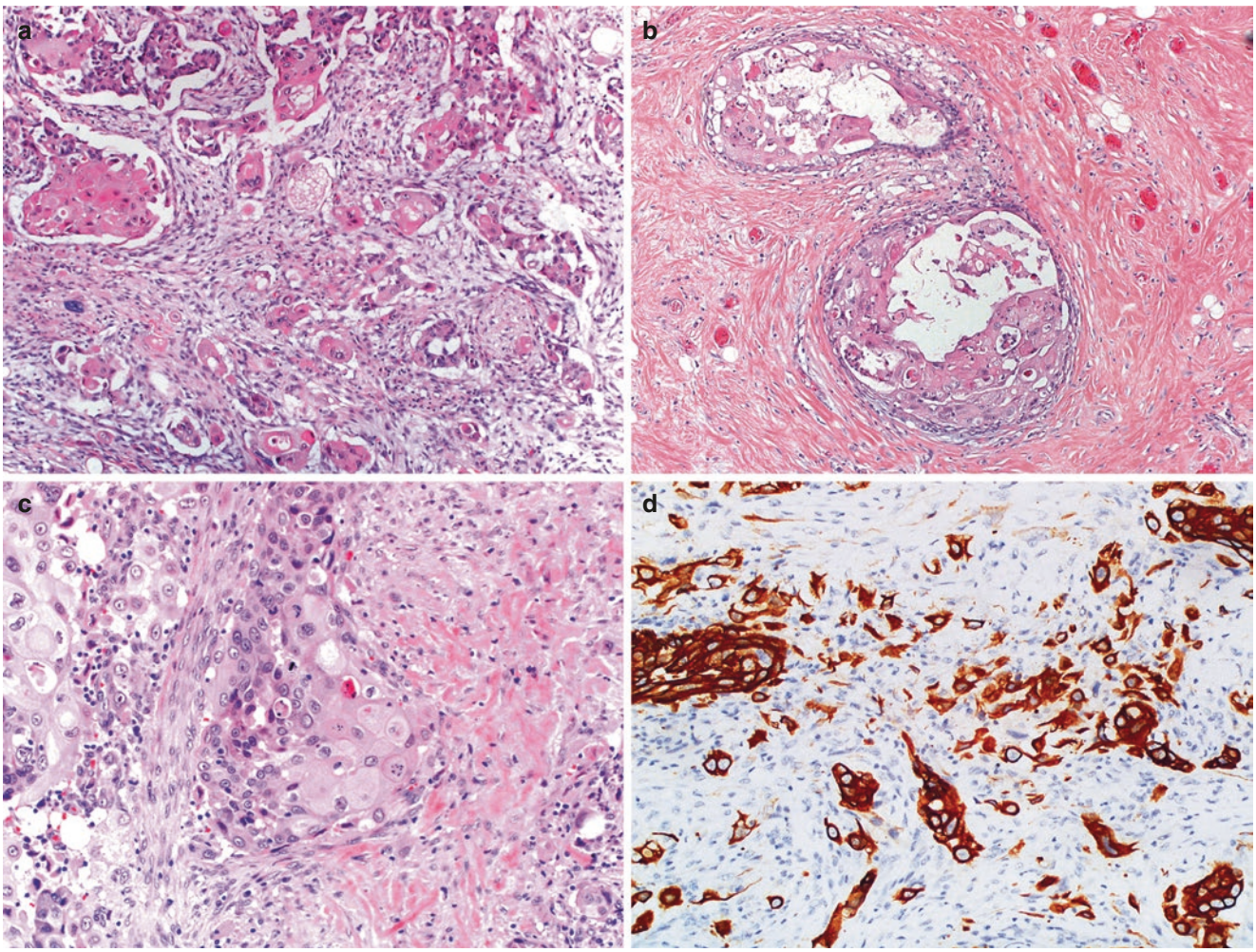

Fig. 12.67 Metaplastic squamous cell carcinoma. (**a**) This metaplastic carcinoma demonstrates infiltrating nests of squamous carcinoma cells with well-developed cytoplasmic keratinization. (**b**) Associated carcinoma in situ in this case also shows prominent squamous differentiation. (**c**) Another case of metaplastic SCC showing clusters of pleomorphic squamous cells, characterized by well-defined cell borders and glassy eosinophilic cytoplasm indicative of keratinization. (**d**) An immunostain for CK5/6 shows strong and diffuse positivity in the tumor cells

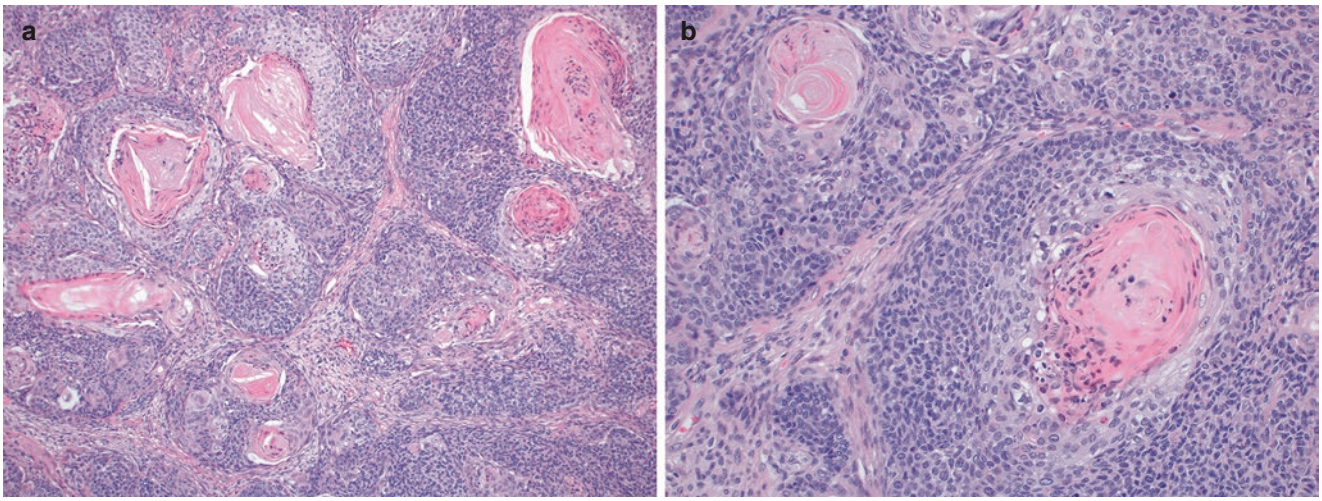

Fig. 12.68 Metaplastic squamous cell carcinoma. (**a**, **b**) Another example of metaplastic SCC showing keratin pearl formation. Note the presence of intercellular bridges in the malignant squamous cells surrounding the keratin pearls on high magnification

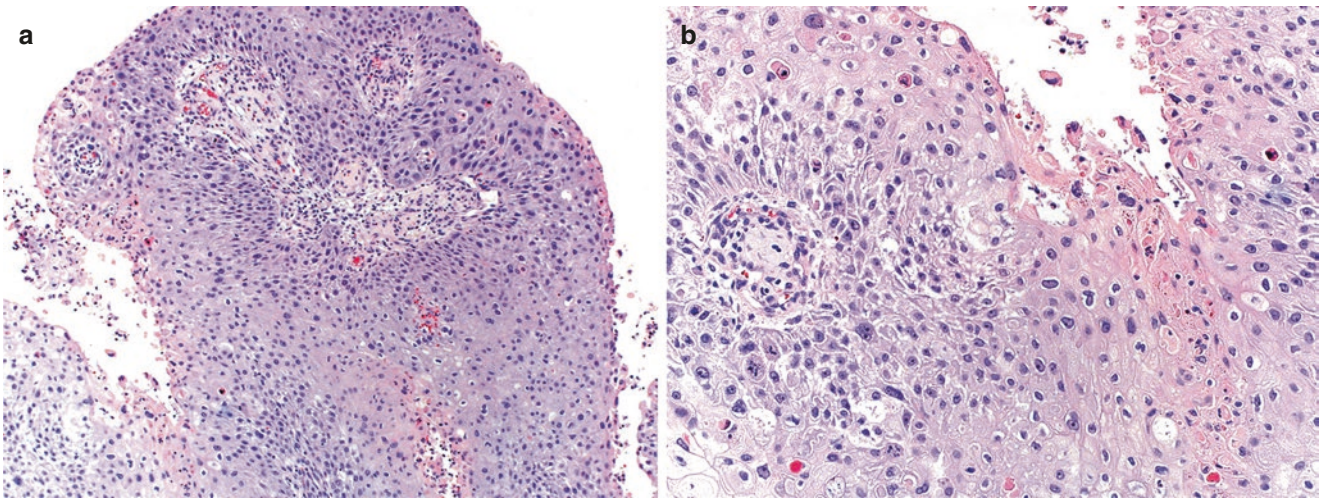

Fig. 12.69 Metaplastic squamous cell carcinoma with cystic degeneration. (**a**) CNB of this metaplastic SCC demonstrates foci of cystic degeneration, which may mimic sampling of an epidermal inclusion cyst. (**b**) Higher magnification illustrates distinct cytologic atypia, mitotic figures, and apoptotic cells

amounts (<10% total) after thorough sampling; and (4) metastatic SCC from another primary site has been excluded [337, 344].

Immunohistochemistry

The diagnosis of SCC is established primarily based on the cytologic features of squamous differentiation and not by immunohistochemical staining, although the latter can help support the diagnosis. SCC express basal keratins (CK5/6, CK14), p63, and p40 (Fig. 12.67d). These tumors are usually triple negative for ER, PR, and HER2, although, like other metaplastic carcinoma types, some SCC may be ER or HER2 positive [302, 311, 335, 347]. EGFR is frequently expressed [302, 335].

Differential Diagnosis

High-grade invasive ductal carcinomas, particularly those with abundant eosinophilic cytoplasm, may exhibit cytologic features suggestive of SCC. Strict morphologic criteria should be adopted when assessing a carcinoma for squamous differentiation. These include well-developed intercellular bridges, unequivocal keratinized cells, or squamous pearls. Necrotic and degenerating cells can mimic keratinized cells, as both may have hyperchromatic pyknotic nuclei and dense eosinophilic cytoplasm. The presence of perinuclear halos can help favor keratinized cells. Immunohistochemistry may not be helpful, because reactivity to CK5/6, p63, and p40 is not specific for SCC but is also noted in basal-like triple-negative IDC-NST.

Diagnosis of metaplastic SCC requires exclusion of cutaneous or metastatic SCC. In the absence of associated DCIS or overlying skin with dysplasia, this distinction can usually not be made based on histologic review of a core biopsy specimen alone and requires correlation with clinical history and tumor location (deep versus superficial).

Mucoepidermoid carcinoma (MEC) of the breast may also be mistaken for SCC. In contrast to SCC, MEC is composed of a mixture of intermediate, epidermoid, and mucinous cells (Figs. 12.28 and 12.70a–c). Focal squamous differentiation may be observed in the epidermoid cells. However, true keratinization with formation of squamous pearls excludes the diagnosis of MEC and favors SCC. Immunohistochemistry of MEC demonstrates a "zoning phenomenon," in which high-molecular-weight keratin (such as CK14) highlights the intermediate and epidermoid cells at the periphery of the tumor nests and cysts, and low-molecular-weight keratin (such as CAM5.2) decorates mucinous cells in the central regions of the nests [348] (Fig. 12.30). This unique staining pattern is not seen in SCC. Immunohistochemical stain p63 shows differential expression in the various components of MEC, with consistent expression in the intermediate cells, variable reactivity in epidermoid cells, and lack of expression in the mucinous areas (Figs. 12.28 and 12.70d). Intra- and extracellular mucin is PASD and mucicarmine positive, which can also be helpful in the differential diagnosis with SCC, which is PASD and mucicarmine negative (Figs. 12.27b and 12.70e). In contrast to SCC, MEC harbors *MAML2* rearrangement [100, 105, 111, 112] (see also section "Mucoepidermoid Carcinoma" in this chapter).

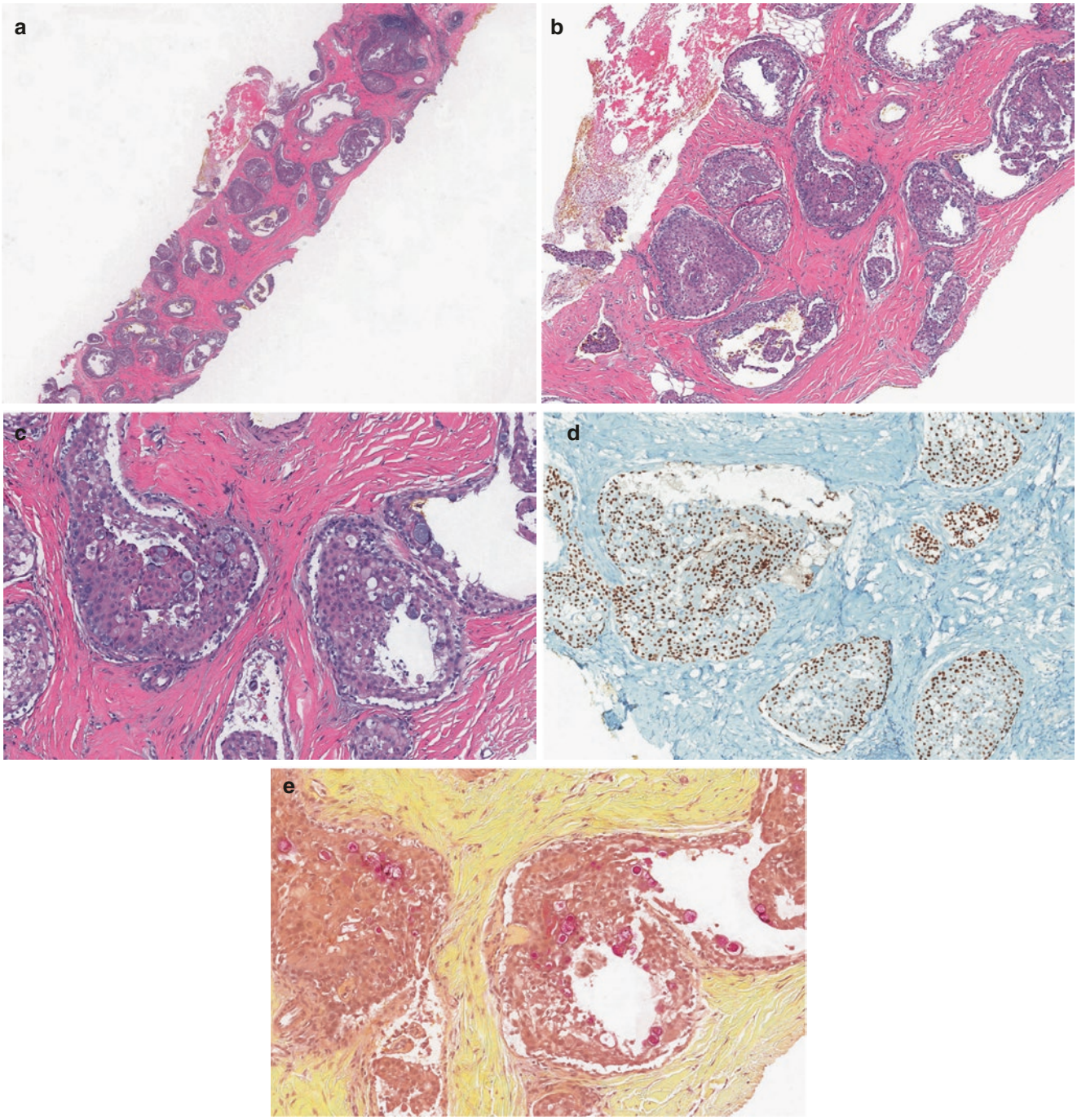

Fig. 12.70 Mucoepidermoid carcinoma of the breast, core needle biopsy. (**a**, **b**) This MEC shows a predominantly nested growth pattern with admixed microcystic spaces. (**c**) Higher magnification reveals the presence of epidermoid, intermediate, and mucinous tumor cells, which is diagnostic. (**d**) Immunohistochemistry for p63 is positive in the intermediate and epidermoid cells, whereas the mucinous cells are p63 negative. (**e**) In contrast, mucicarmine stain highlights the mucinous cells

Metaplastic Carcinoma with Heterologous Mesenchymal Differentiation

Microscopic Features

MCMD are invasive carcinomas composed of heterologous mesenchymal-like elements often admixed with carcinomatous areas. The mesenchymal-like component is often chondroid (Figs. 12.71, 12.72, 12.73, and 12.74), osseous (Fig. 12.75), or less frequently rhabdomyoid (Fig. 12.76), and the carcinomatous component is typically akin to moderately or poorly differentiated IDC-NST or squamous. The mesenchymal component may appear differentiated or frankly malignant, resembling chondrosarcoma and osteosarcoma of soft tissue [280]. Wargotz and Norris originally described a group of "matrix-producing carcinomas," which are characterized by direct transition from ductal carcinoma to areas with cartilaginous or osseous matrix deposition, without an intervening spindle cell component [349] (Figs. 12.71 and 12.74). Matrix-producing carcinomas with chondroid differentiation tend to have circumscribed borders and large areas of central necrosis, with viable tumor cells concentrated near the peripheral rim of the tumor (Fig. 12.71). The stromal matrix, which can range from chondroid to chondromyxoid, is composed of acid mucopolysaccharides that stain metachromatically with Alcian blue and aldehyde fuchsin and are resistant to hyaluronidase and diastase digestion. A conventional adenocarcinoma component is often present to variable extent, but in some cases extensive sampling may be required to identify these areas, which help to differentiate these tumors from soft tissue chondrosarcoma or osteosarcoma. Associated DCIS is identified in a subset of cases, and when present, can be of NST or rarely show lumi-

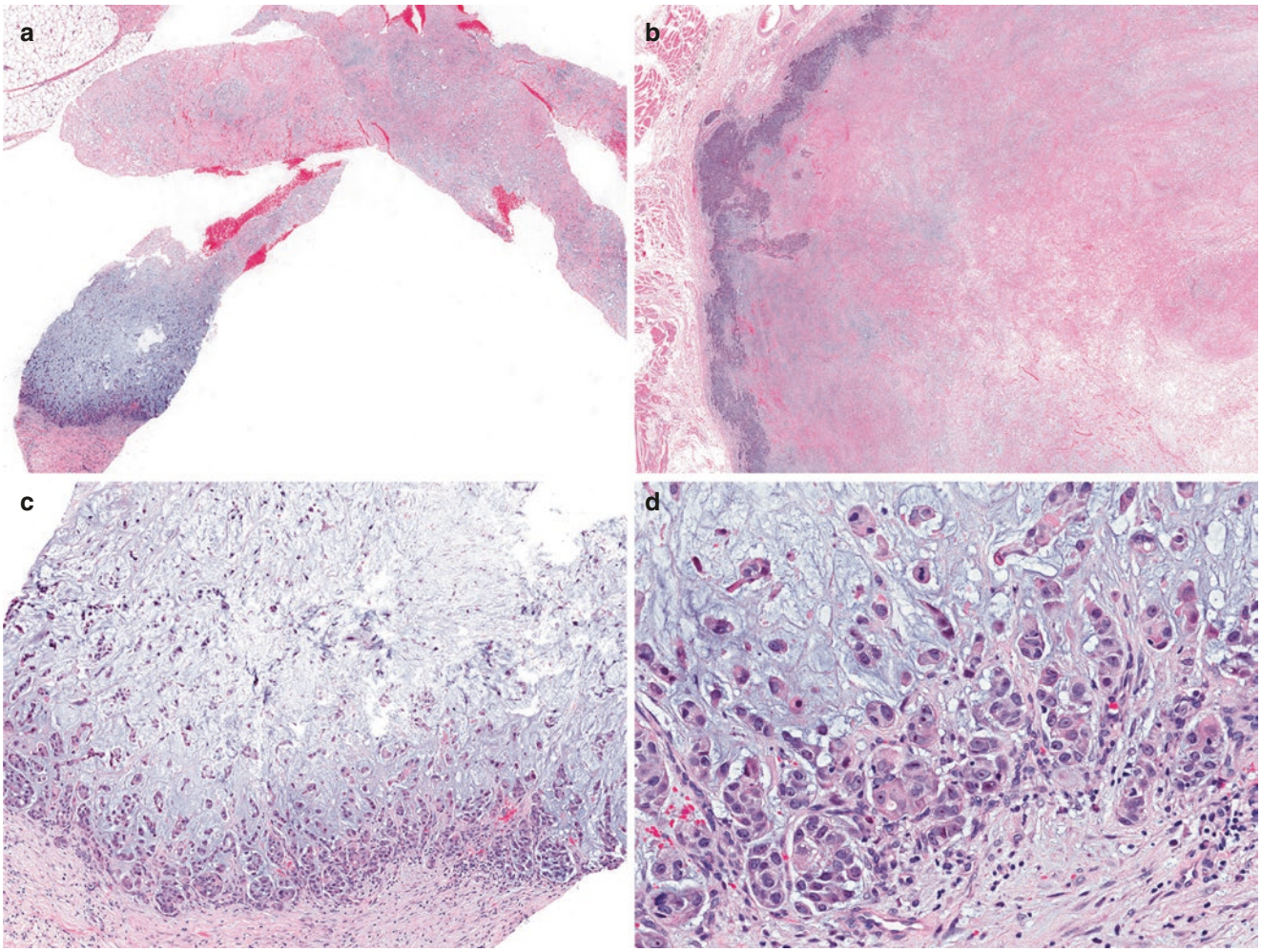

Fig. 12.71 Metaplastic carcinoma with heterologous mesenchymal (chondroid) differentiation, matrix-producing carcinoma. (**a**, **c**) On CNB, the chondroid matrix of this metaplastic carcinoma is obvious at low magnification, with increased cellularity noted at the tumor periphery and other areas being hypocellular and necrotic. (**b**) On excision, these tumors are often relatively well circumscribed at low power, with large areas of central necrosis and the bulk of tumor cellularity concentrated at the tumor periphery. (**d**) High-power evaluation reveals moderate cytologic atypia and scattered mitotic figures

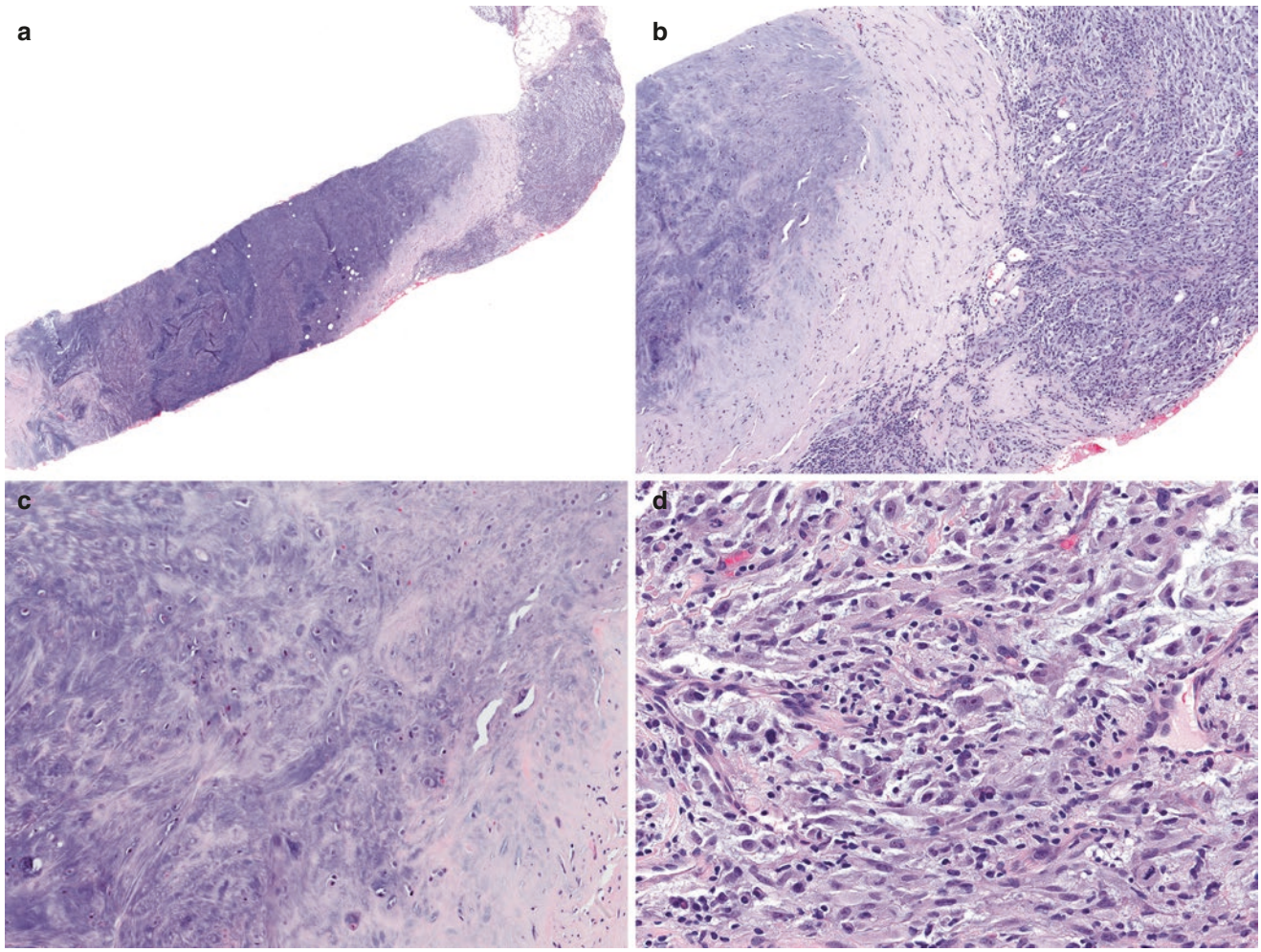

Fig. 12.72 Metaplastic carcinoma with heterologous mesenchymal (chondroid) differentiation. (**a**, **b**) On CNB, an area of hypocellular chondroid matrix is appreciated adjacent to a focal hypercellular spindle cell area. (**c**) The chondroid area is distinctly hypocellular with well-formed lacunae but no significant cytologic atypia. (**d**) In contrast, higher magnification of the hypercellular focus reveals malignant spindle cells with moderate nuclear atypia and prominent mitotic activity within myxoid stroma. Focal spindle cells are allowable in a tumor that otherwise meets criteria for matrix-producing carcinoma

nal matrix secretion (Fig. 12.77). Metaplastic carcinomas with chondroid differentiation can arise in association with microglandular adenosis [25, 350–352].

Immunohistochemistry

As for other metaplastic carcinomas, immunohistochemistry is essential to demonstrate epithelial differentiation of MCMD, especially in cases lacking a histologically recognizable invasive carcinomatous/ductal component or associated DCIS. A panel of epithelial markers including broad spectrum keratins (MNF116, AE1/AE3), high-molecular-weight keratins (34βE12, CK5/6, CK14), luminal keratins (CAM5.2, CK7), and p63 is suggested, as it is not possible to predict which marker(s) will be positive and staining may be focal. Keratin and p63 may be positive in epithelial and/or spindle cell components. MCMD may also express myoepithelial markers in addition to p63, such as SMA, CD10, SOX10, and S100 protein [302, 319] (Figs. 12.75d, e and 12.78). Like other metaplastic carcinomas, these tumors are usually triple negative for ER, PR, and HER2. EGFR can be positive in a subset [302].

Differential Diagnosis

MCMD should be distinguished from other lesions that have chondroid or osseous matrix. On the malignant end of the spectrum, this includes malignant phyllodes tumor with heterologous differentiation and primary or metastatic sarcoma (chondrosarcoma or osteosarcoma). In the absence of a

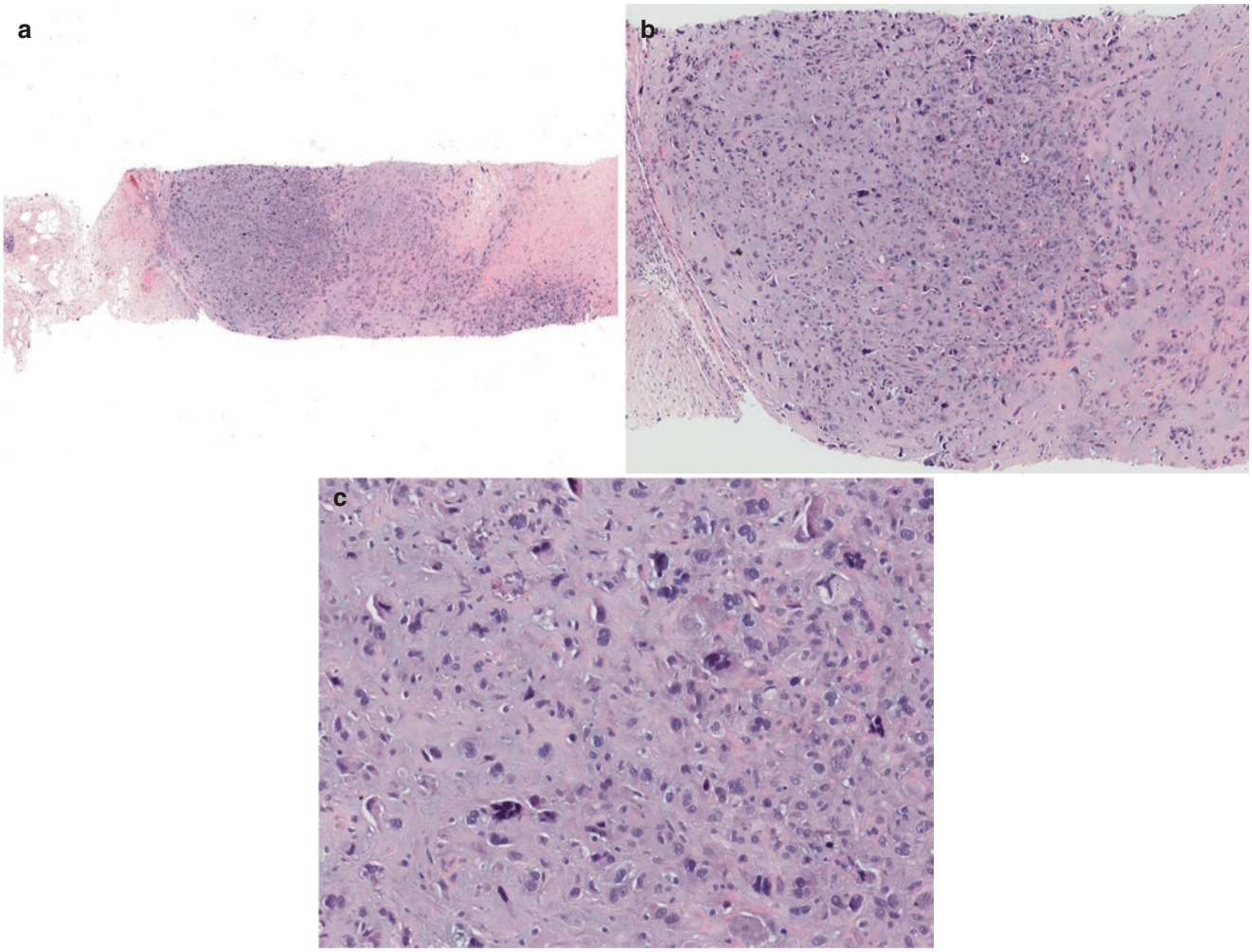

Fig. 12.73 Metaplastic carcinoma with heterologous mesenchymal (chondroid) differentiation. (**a–c**) On CNB, metaplastic carcinoma with chondroid differentiation and high-grade cytologic features may be indistinguishable from primary or metastatic soft tissue chondrosarcoma. Keratin immunopositivity or the presence of a diagnostic epithelial component can make this distinction (not shown)

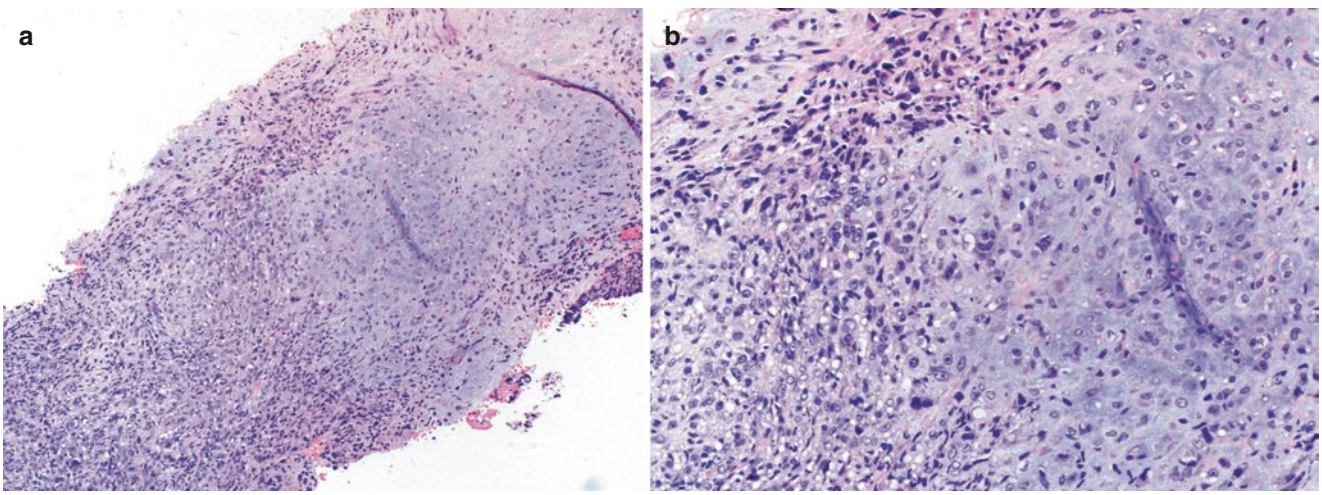

Fig. 12.74 Metaplastic carcinoma with heterologous mesenchymal (chondroid) differentiation. (**a**, **b**) Another example of chondroid matrix-producing carcinoma with prominent cytological atypia on core needle biopsy

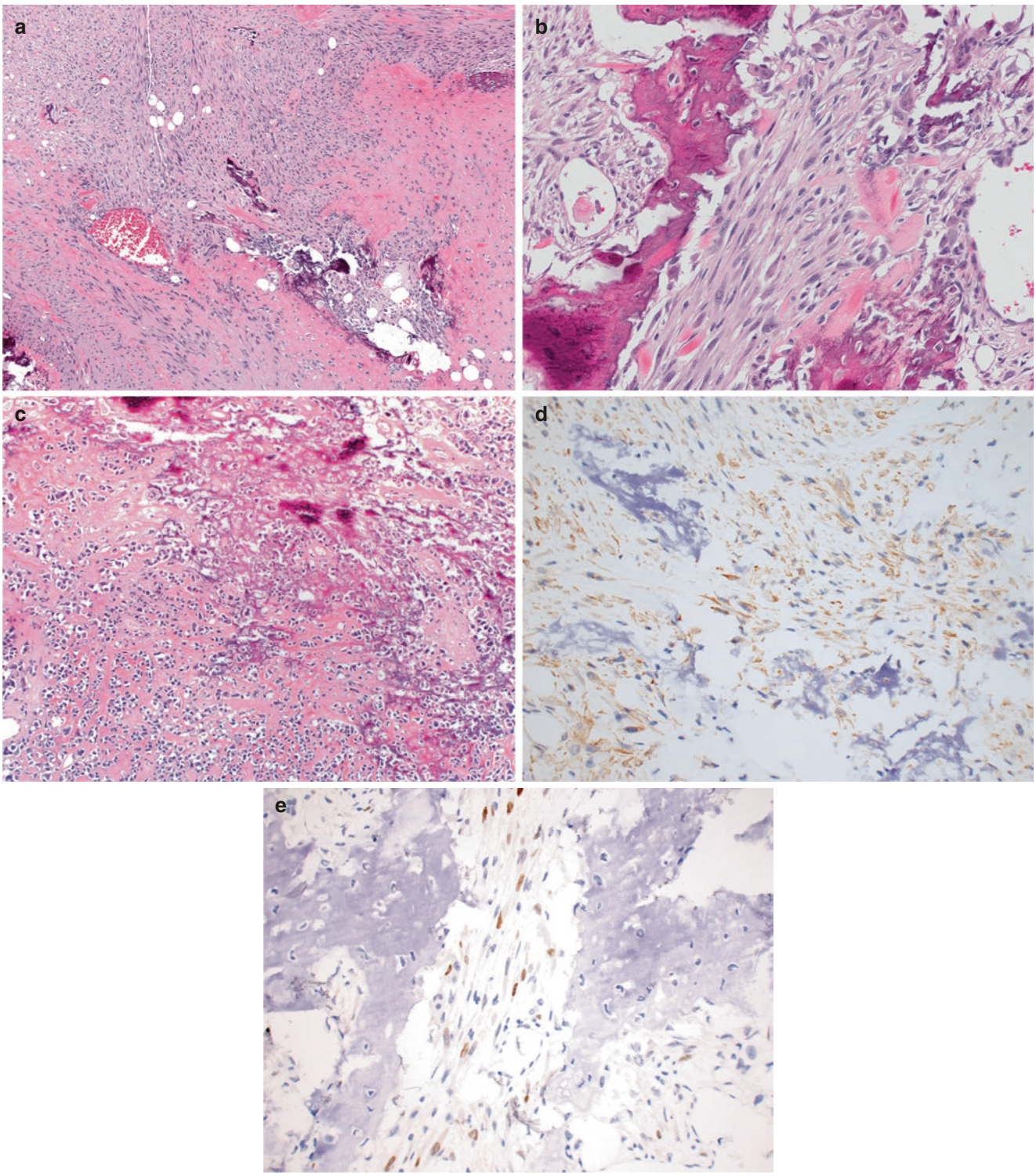

Fig. 12.75 Metaplastic carcinoma with heterologous mesenchymal (osseous) differentiation. (**a**, **b**) This metaplastic carcinoma shows areas of malignant spindle cells admixed with areas of osteoid and bone formation. (**c**) Another example of metaplastic carcinoma with osseous differentiation. Positive immunohistochemistry for (**d**) keratins (in this case CK14) and/or (**e**) p63 is useful in such cases to support the epithelial nature of the malignant tumor cells

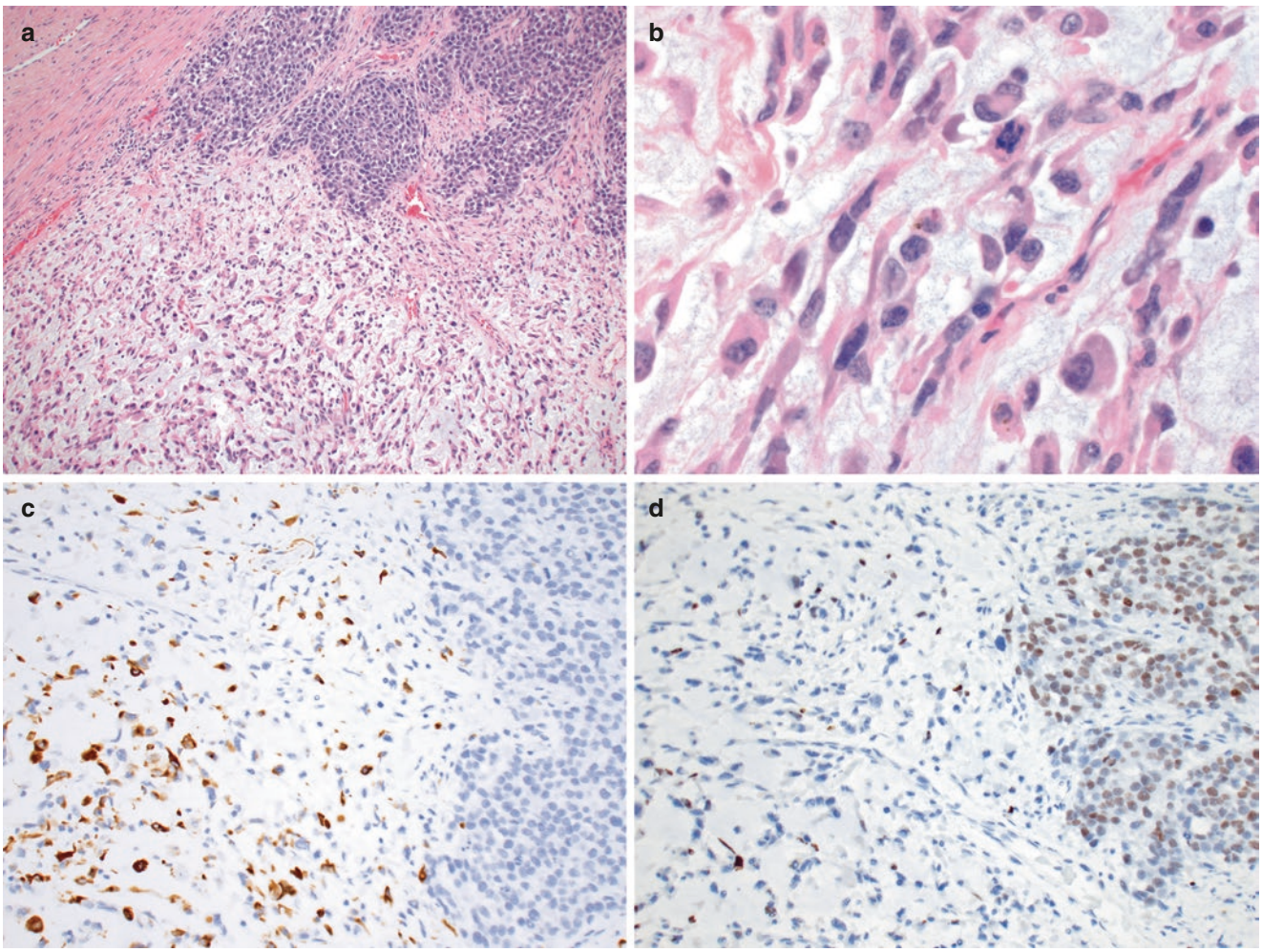

Fig. 12.76 Metaplastic carcinoma with rhabdomyoid differentiation. (**a**) This metaplastic carcinoma shows an abrupt transition between areas of cohesive epithelioid carcinoma cells (upper right) and discohesive spindled tumor cells. (**b**) Higher magnification reveals pleomorphic spindled tumor cells with rhabdoid features, including prominent eosinophilic cytoplasm and eccentrically located nuclei. (**c**) Immunohistochemistry for desmin is positive in the spindled tumor cells, further supporting the muscle phenotype. The spindle cells are also positive for myogenin (not shown). (**d**) In contrast, immunohistochemistry for p63 is diffusely positive in the epithelioid cells but only decorates rare spindled tumor cells

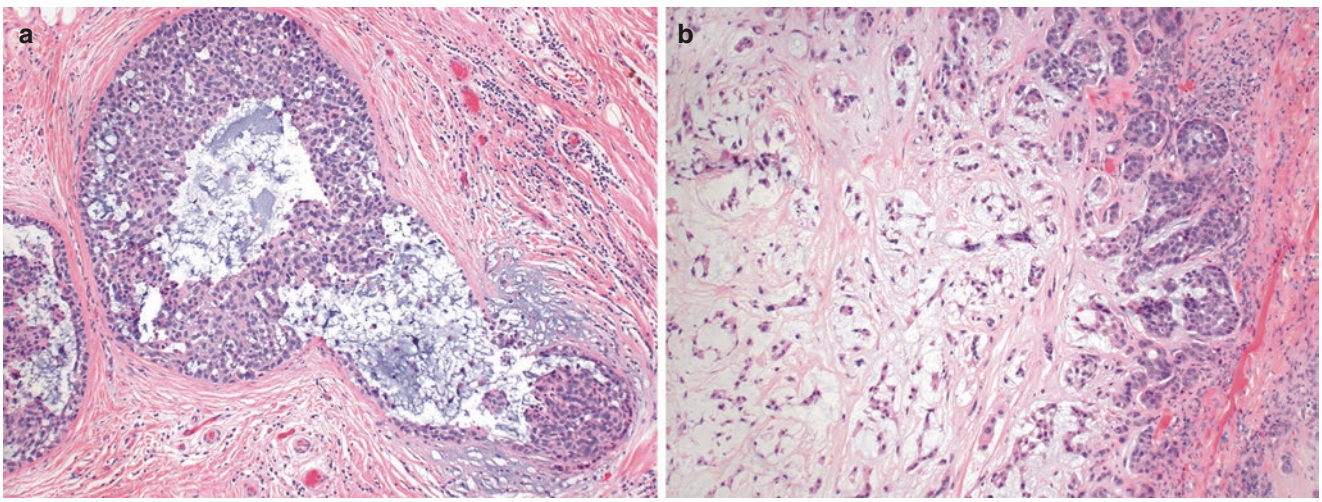

Fig. 12.77 Ductal carcinoma in situ with chondromyxoid features. (**a**) The in situ component of this carcinoma shows chondromyxoid features similar to that of (**b**) the associated matrix-producing carcinoma

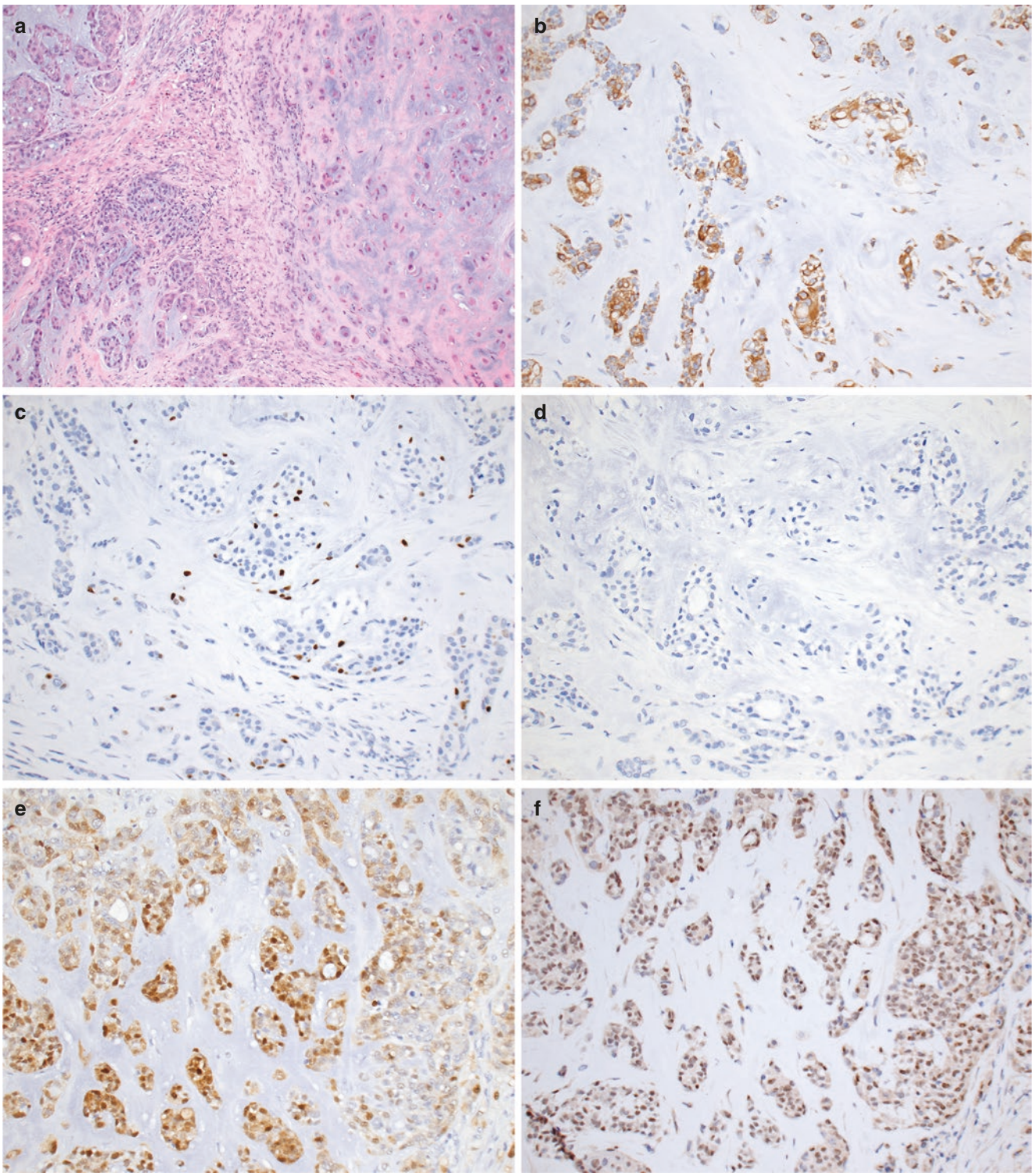

Fig. 12.78 Immunohistochemistry of metaplastic carcinoma with heterologous chondroid differentiation. (**a**) Immunohistochemistry of this metaplastic carcinoma shows positive staining of the chondroid matrix-associated tumor cells for (**b**) keratin AE1/AE3 and (**c**) patchy staining for p63, whereas (**d**) low-molecular-weight keratin CAM5.2 is negative. Metaplastic carcinoma, especially those with chondroid differentiation, often demonstrate expression of (**e**) S100 protein and (**f**) SOX10

conventional invasive carcinoma component or DCIS, the distinction from malignant phyllodes tumor rests on the identification of an associated benign epithelial component with intracanalicular architecture or embedded elongated and compressed ducts in phyllodes tumor, which may be absent in a core biopsy. A panel of immunohistochemical stains for keratins, p63, and CD34 may be useful, with the caveat that some phyllodes tumors can express keratins and p63 and may be CD34 negative (see sections "Spindle Cell Carcinoma" and "Differential Diagnosis," and Chap. 7, section "Phyllodes Tumor—Immunohistochemistry" and "Differential Diagnosis") [313, 317, 318, 325]. Chondrosarcoma or osteosarcoma, either primary or metastatic to the breast, is exceedingly rare and is a diagnosis of exclusion which can only be made after extensive tumor sampling and thorough immunohistochemical workup to exclude epithelial differentiation, as well as review of the clinical history.

MCMD with loose chondromyxoid matrix may also be confused with mucinous carcinoma in small biopsy specimens. Mucinous carcinomas do not show large areas of zonal necrosis, and the neoplastic cells usually exhibit less cytologic atypia and are more evenly distributed throughout the mucin. In addition, mucinous carcinomas are strongly positive for ER and luminal cytokeratins, whereas metaplastic carcinoma is ER negative.

Benign entities with chondromyxoid matrix are in the differential diagnosis on limited core biopsy material, including sclerosing papilloma with chondroid metaplasia and pleomorphic adenoma (Figs. 12.79 and 12.80a, b). In comparison to metaplastic carcinomas, pleomorphic adenomas lack necrosis and consist of biphasic epithelial and myoepithelial cells with bland cytology and no to rare mitotic figures (Fig. 12.80a–d).

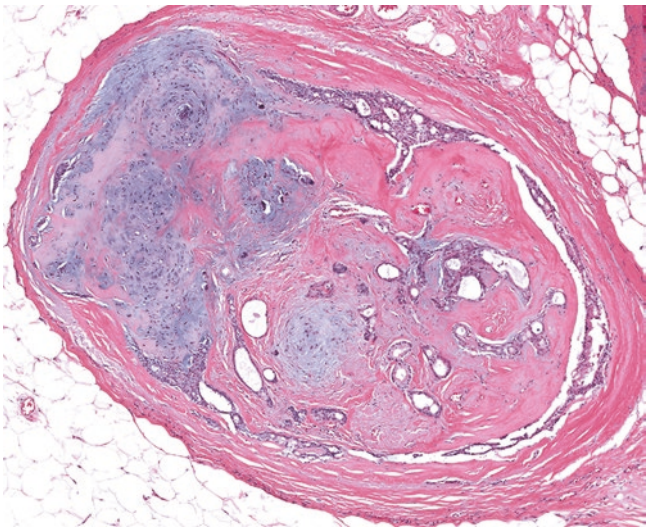

Fig. 12.79 Sclerosing papilloma with chondroid stroma. Chondroid metaplasia involving a sclerosed papilloma may raise the differential diagnosis of metaplastic carcinoma with chondroid differentiation. This may be especially challenging on core needle biopsy. The presence of associated sclerosed benign epithelial elements, lack of cytologic atypia, hypocellularity, and overall circumscription can be useful to make the distinction

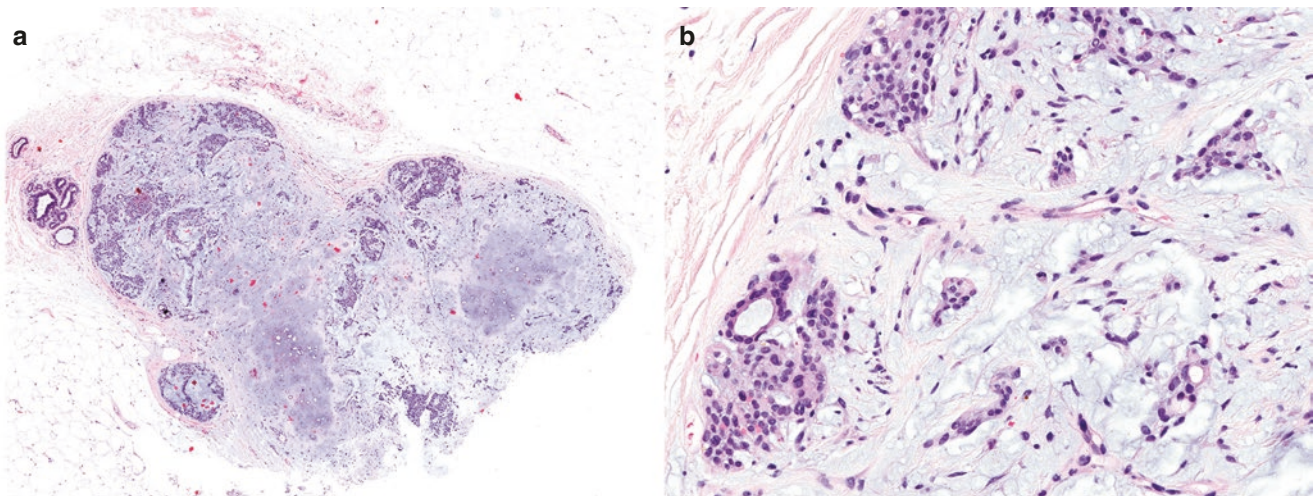

Fig. 12.80 Metaplastic carcinoma with heterologous chondroid differentiation versus pleomorphic adenoma. The distinction of these lesions can be challenging, especially on limited core needle biopsy material. (**a**) Low-power view of pleomorphic adenoma shows a well-circumscribed lobulated nodule composed of chondromyxoid matrix with associated cellular proliferation and without areas of necrosis. Note the benign breast lobule in the upper left corner. (**b**) High-power magnification reveals the characteristic biphasic tubule-forming epithelial and admixed myoepithelial proliferation, each with bland cytology and lack of mitotic activity. (**c**) In contrast, metaplastic carcinoma with heterologous chondroid differentiation displays central necrosis (right) with subtle infiltrative growth (left) into fat. (**d**) On high power, the cells are more atypical with larger hyperchromatic nuclei and scattered mitoses

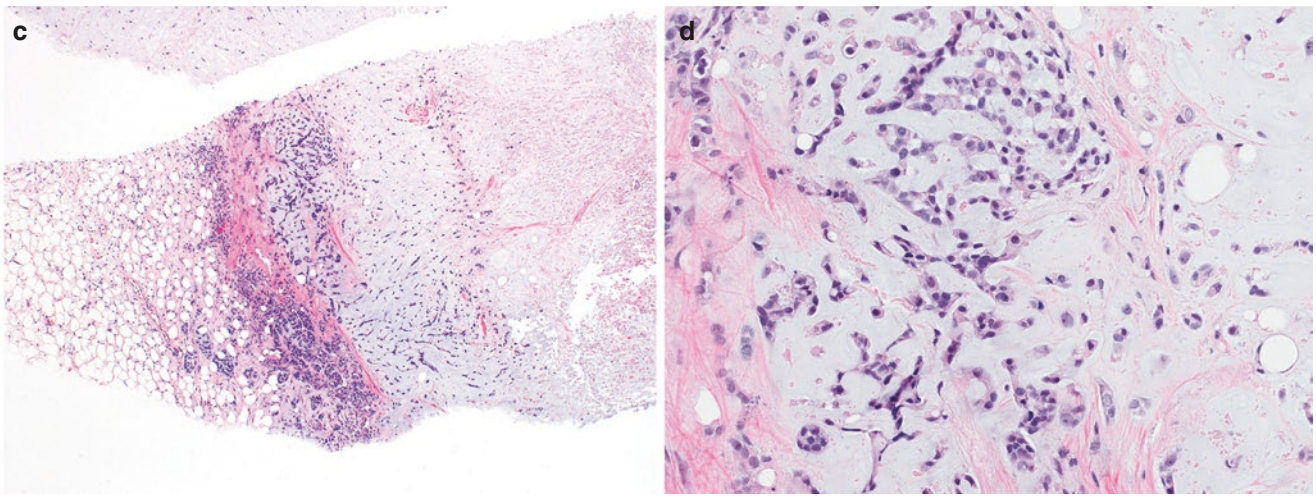

Fig. 12.80 (continued)

Mixed Metaplastic Carcinomas

A significant proportion of metaplastic carcinomas harbor a mixture of different metaplastic elements or metaplastic elements with conventional carcinoma (Fig. 12.81). These cases are classified as mixed metaplastic carcinoma. Each of the various components present should be recorded in the pathology report [275].

Pathogenesis and Risk Factors

The cell of origin of metaplastic carcinomas is unknown. It has been postulated that this heterogeneous group of tumors may develop from dedifferentiation events later during carcinogenesis, rather than malignant transformation of a particular cancer stem cell [353]. Regardless, genetic studies have confirmed a shared monoclonal origin of the various heterologous and conventional carcinomatous components, as well as associated DCIS [311, 354–358]. Metaplastic carcinomas show stem cell-like features, with enrichment for markers of tumor-initiating cells (ALDH1, $CD44^{+}/CD42^{-/low}$) and characteristics of epithelial-mesenchymal transition (EMT), such as increased expression of vimentin and E-cadherin repressors (ZEB1, SLUG, TWIST) and decreased cell-cell adhesion proteins, including E-cadherin and claudins [359–361]. Consistent with this, these tumors generally cluster with the basal-like and claudin-low intrinsic gene expression subgroups, the latter of which is enriched for EMT and cancer stem cell-like features [360–364]. The stem cell-like and EMT features of metaplastic carcinomas may explain their relative chemoresistance [365]. Transcriptomic heterogeneity between morphological types has been described, with spindle cell carcinomas being claudin-low, and SCC and metaplastic carcinomas with chondroid differentiation being enriched for basal-like profiles. Using the TNBC gene expression classifier, metaplastic carcinomas with chondroid differentiation were all mesenchymal-like, whereas other types showed variable or unstable phenotypes [366].

Genetic studies have begun to elucidate the mutational landscape of metaplastic carcinomas. As a group (excluding LGASC and FLMBC), these tumors are enriched for mutations in *TP53*, PI-3 K pathway (*PIK3CA*, *PIK3R1*, *PTEN*), MAPK pathway (*KRAS*, *HRAS*, *NF1*), and Wnt pathway (*FAT1*, *CCN6*) genes, as well as *TERT* promoter. Chromatin remodeling genes are also frequently mutated (*ARID1A*, *KMT2C*, *KMT2D*) [282, 311, 331, 363, 367–370]. Metaplastic carcinomas and associated DCIS share identical sets of mutations, including in PI-3 K (*PIK3CA*, *PIK3R1*, *AKT1*, *PTEN*) and MAPK (*KRAS*, *HRAS*) pathway genes, highlighting an early role for these pathways in tumor development [311]. Overall, mutations in PI-3 K (*PIK3CA*, *PIK3R1*, *PTEN*) and MAPK (*NF1*, *HRAS*, *KRAS*) pathway genes are significantly more frequent in metaplastic carcinomas compared to other TNBC [311, 331]. However, differences in the mutational repertoire have been identified in morphologic types. Metaplastic carcinomas with chondroid differentiation (matrix-producing carcinomas) lack *PIK3CA* mutations, which are enriched in carcinomas with spindle cell and/or squamous differentiation [311, 331]. Similarly, *TERT* promoter mutations were found to be enriched in spindle cell carcinomas, SCC, and mixed metaplastic carcinomas with spindle and squamous differentiation, but absent in matrix-producing carcinomas [311]. *TP53* mutations appear to be less common in spindle cell carcinomas compared to

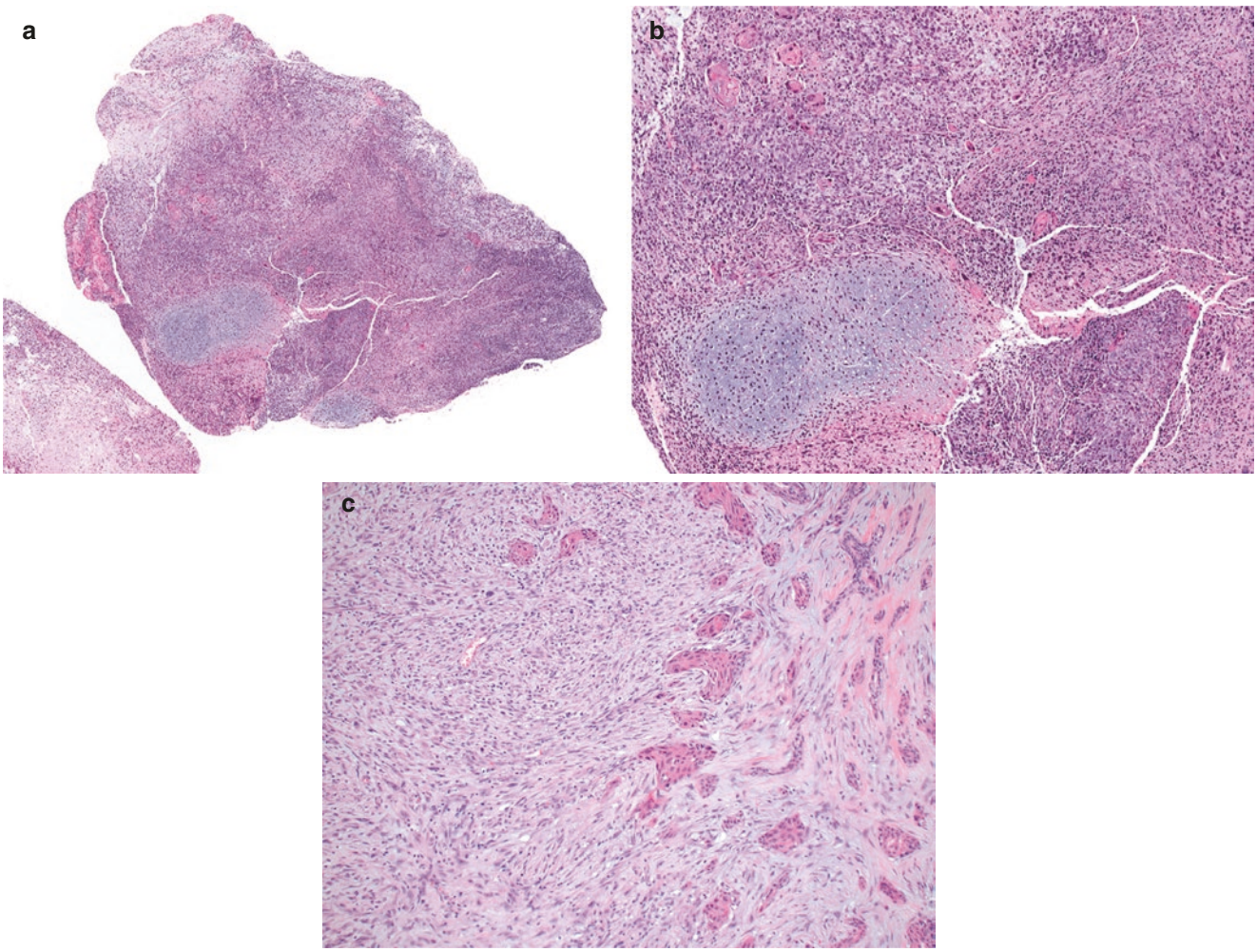

Fig. 12.81 Mixed metaplastic carcinoma with chondroid, squamous and spindle cell differentiation. (**a–c**) This metaplastic carcinoma shows mixed differentiation, with admixed chondroid and squamous differentiation and adjacent spindle cell areas

the other groups [311, 371]. Aside from LGASC and FLMBC, metaplastic carcinomas have complex genomes, including a subset with chromosomal alterations characteristically associated with *BRCA1/2* inactivation (BRCAness) [311, 331, 360, 366].

Case reports of metaplastic carcinoma arising in patients with neurofibromatosis suggest a possible, albeit rare, association [372–374]. Loss of heterozygosity at the variant germline *NF1* allele was described in one case arising in a 41-year-old woman [372].

The molecular features of low-grade metaplastic carcinomas (LGASC and FLMBC) have been characterized in less detail than high-grade metaplastic carcinomas. LGASC are basal-like carcinomas by surrogate immunohistochemical profiling (triple negative, CK5/6/14/17 positive, EGFR positive) [295, 299]. These tumors frequently have hotspot *PIK3CA* mutations and lack *TP53* mutations [295]. Chromosomal copy number analysis revealed a simple genome with few gains and losses in one tumor and a firestorm pattern with EGFR amplification in another [299]. Case reports describe rare LGASC arising in a patient with germline *BRCA1* mutation [375] and in another with germline *BRIP1* mutation [376], although genetic analysis of the tumors was not performed. It has been postulated that LGASC arise from adenosquamous proliferations associated with radial sclerosing lesions, which could explain the histologic association of these entities. Like LGASC, adenosquamous proliferations have been found to be clonal with *PIK3CA* mutations [303].

FLMBC are basal-like carcinomas with a claudin-low phenotype by immunohistochemistry, exhibiting low expression of adhesion molecules, a tumor-initiating cell phenotype (CD44+/CD24-), and features of EMT (vimentin expression with lack of E-cadherin) [307]. A limited number of tumors have been analyzed genetically. *PIK3CA* and *TERT* promoter hotspot mutations were each identified in three of four tumors analyzed by targeted DNA sequencing, akin to metaplastic spindle cell carcinomas [377]. Chromosomal copy number analysis of three tumors identified very few alterations, with

9p21.3 loss (including *CDKN2A*, which encodes p16) identified in two of the cases [378].

Prognosis and Clinical Management

With the exception of LGASC and FLMBC, metaplastic carcinomas are aggressive tumors with 3-year, 5-year, and 10-year survival rates of approximately 77%, 62%, and 53%, respectively [276, 277, 379, 380]. Outcome analyses have been overall limited by retrospective study design with selection bias, population-based or local studies without central pathology review, and lack of matching for stage in some cases. Nonetheless, patient outcomes are generally considered to be worse for metaplastic carcinoma than for other TNBC, with increased local recurrence risk and shorter disease-free and overall survival in the former, despite low rates of nodal involvement [279, 283, 310, 381–383]. On the other hand, metaplastic carcinomas tend to present with higher stage than IDC-NST [276, 278, 283, 379], and a large multi-institutional study found similar outcomes to IDC-NST matched for age, grade, ER, and HER2 status if analysis was limited to early stage (pT1/pT2) tumors [279]. Others have found similar results [384–386]. Distant metastases are common, even in the absence of nodal metastasis [278, 283, 381, 383, 387], with brain and lung being frequent sites.

Regarding conventional breast cancer prognostic factors in metaplastic carcinoma, inferior outcomes have been associated with older patient age [276, 278, 382, 388], nodal involvement, [278, 279, 383, 387, 388], lymphovascular invasion [279], and large tumor size [278, 282, 379, 389, 390]. Others have found no prognostic association with tumor size [279]. In a population-based study using SEER data, there were no differences in 5-year survival between hormone receptor positive and negative metaplastic carcinoma [277]. HER2-positive metaplastic carcinomas may have more favorable outcomes than triple-negative metaplastic carcinomas [276].

Intriguingly, there are data to suggest that different morphologic types of metaplastic carcinoma may have different outcomes. Mixed metaplastic carcinomas have been associated with worse outcomes compared to other morphologic types in several studies [279, 282, 388, 389]. In a large international consortium study of metaplastic carcinomas (AP-MBC), mixed metaplastic carcinomas and spindle cell carcinomas had worse 10-year breast cancer-specific survival (BCSS) than SCC. Moreover, mixed metaplastic carcinomas with more than three morphological components had worse outcomes than those with only two or three components [282]. Accordingly, the number and percentage of morphologic components in a metaplastic carcinoma should be reported by the pathologist [275]. In another international study, Rakha et al. observed longest BCSS for patients with matrix-producing carcinomas, and shortest BCSS for those with spindle cell carcinomas or mixed spindle and squamous cell carcinomas. These associations were maintained even after exclusion of locally advanced tumors [279]. In contrast to these studies, others have found no significant associations between morphologic type and outcome [383, 388]. EGFR overexpression and lack of keratin expression (CK AE1/3) have been correlated with poor outcomes [282]. The prognostic significance of histologic grade is uncertain [275, 279, 282].

There are no specific NCCN guidelines for the treatment of metaplastic carcinoma, and these tumors are in general treated like other IBC-NST/TNBC [391]. Chemotherapy is routinely offered, although metaplastic carcinomas appear to have poor responses [262, 275, 278, 333, 335, 379, 383, 385, 386, 388, 389, 392–396]. Response rates to neoadjuvant chemotherapy are low, with complete pathologic responses of 0–17% across studies [262, 335, 379, 383, 386, 388, 389, 396]. There is evidence to suggest that matrix-producing carcinomas may achieve better responses to neoadjuvant chemotherapy than other types [388, 396]. Radiation therapy may provide survival benefit for patients undergoing breast-conserving surgery and for high-risk patients with large (>5 cm) tumors or extensive nodal disease [277, 278, 380, 390, 395, 397, 398].

Given the high rate of PI-3K pathway aberrations in metaplastic carcinomas, these patients are potential candidates for *PIK3CA* or mTOR inhibitors. In a study of 52 women with advanced metaplastic carcinoma, a 21% objective response rate was reported for a regimen consisting of the mTOR inhibitors temsirolimus or everolimus in combination with doxorubicin and bevacizumab. *PIK3CA* mutations were significantly associated with improved objective response rate (31 versus 0%) but not clinical benefit rate [399]. Patients with metaplastic carcinoma treated with this regimen had better long-term outcomes compared to patients with TNBC treated with the same regimen [399]. Given the high rate of homologous recombination repair deficiency signatures in metaplastic carcinomas [400], one could postulate that these patients may benefit from PARP inhibitor therapy [397].

Variable PD-L1 tumor cell and immune cell expression has been reported in metaplastic carcinomas, with staining being more frequent than in other TNBC [367, 401–404]. In one study, positive PD-L1 expression was observed in 95% of metaplastic carcinomas using the FDA-approved SP142 antibody and scoring criteria used in the Impassion130 trial (≥1% immune cell staining), which is significantly higher than the positivity of TNBC in the trial (41%) [404, 405]. These findings suggest that most advanced metaplastic carcinomas are potentially eligible for anti-PD-L1 therapy. Indeed, case reports have described durable responses to Pembrolizumab (anti-PD-1)/nab-paclitaxel and durvalumab (anti-PD-L1)/paclitaxel in metaplastic spindle cell carci-

noma and metaplastic carcinoma with squamous elements, respectively [406, 407].

FLMBC and LGASC are low-grade metaplastic carcinoma subtypes that are recognized to have more indolent clinical behavior with overall favorable prognosis [293, 297]. The incidence of nodal or distant metastasis is extremely low. However, both FLMBC and LGASC exhibit potentially locally aggressive behavior with high risk of recurrence. Accordingly, these tumors are generally treated by excision to clear margins. The role of chemotherapy is undetermined. The NCCN guidelines note that limited data support local excision only for these tumors, with consideration of systemic or targeted therapy only in node-positive disease [391].

Invasive Breast Carcinoma with Medullary Pattern

Overview and Clinical Presentation

Medullary carcinoma of the breast (MC) was previously described as a rare subtype of breast cancer with distinct morphology and favorable prognosis, despite its high-grade histopathologic features and often triple-negative immunophenotype. However, classification was notoriously complicated by poor interobserver and intraobserver diagnostic reproducibility [408–414]. MC and related tumors have undergone multiple rounds of reclassification over the years. In the first formal definition of MC in 1945, Moore and Foote described a unique tumor with well-circumscribed borders, poorly differentiated cells, and a prominent lymphoid infiltrate [415]. Based on strict diagnostic criteria initially proposed by Ridolfi et al. that correlated with favorable outcomes, the first three editions of the WHO classification included MC as a breast cancer subtype with circumscribed borders, syncytial architecture, pleomorphic nuclei, and a prominent lymphoplasmacytic inflammatory infiltrate [408]. In recognition of the poor reproducibility of the diagnosis and challenges in consistent reporting, the fourth edition introduced the category of "carcinomas with medullary features" to include MC, atypical medullary carcinomas (AMC), and a subset of IDC-NST [416]. However, aside from poor diagnostic reproducibility, these tumors as a group were found to show broad histopathologic overlap with basal-like carcinomas and carcinomas arising in *BRCA1* carriers. In addition, it has been recognized that the favorable prognosis of MC and other invasive carcinomas not meeting strict MC criteria is likely explained by the presence of large numbers of tumor infiltrating lymphocytes (TILs), which is associated with better outcomes in TNBC [275, 417–421]. This recognition has reduced the necessity of diagnostically differentiating these tumors. Accordingly, invasive carcinomas with medullary features are considered in the fifth edition to represent one end of the histopathologic spectrum of TIL-rich IBC-NST and classified as a morphologic pattern, rather than a separate subtype [422]. A descriptive modifier indicating the medullary pattern or basal-like features should be included with the diagnosis.

Invasive carcinomas meeting the previous criteria for MC are rare and account for <1% of invasive breast cancers. A higher prevalence can be expected if other invasive carcinomas with medullary pattern are included (up to 7% in some studies) [423–427]. The average age at presentation typically ranges from 45 to 54 years across various series, although patients tend to be relatively younger compared to those with other invasive breast carcinomas, with one study showing higher numbers of patients with MC in the 35 years or younger group [409, 412, 415, 426, 428–431]. These tumors are rare in men [424].

The clinical presentation is similar to other IBC-NST, with most tumors presenting as a palpable mass. Average size of tumors previously classified as MC ranged from 2 to 3.2 cm [409, 411, 424, 431, 432]. Ipsilateral lymphadenopathy is not uncommon and is reactive in many cases [433].

Gross and Radiologic Features

Grossly, invasive carcinomas with medullary pattern are well-circumscribed, soft to moderately firm tumors, and may show a characteristic shiny, pearly white appearance that bulges above the cut surfaces [434]. Foci of hemorrhage or necrosis may be present, the latter of which may cause cystic degeneration. Prominent cystic degeneration is seen usually in larger tumors [221]. Some tumors may be poorly circumscribed, due to irregular extension of the inflammatory infiltrate beyond the margins of tumor [408].

On mammography, invasive carcinomas with medullary pattern are well circumscribed round, oval, or lobulated with smooth borders and without calcifications. Ultrasound shows a well-circumscribed hypoechoic mass. Given their circumscription, these tumors may be mistaken radiographically for fibroadenomas [435]. On MRI, invasive carcinomas with medullary pattern are also round or lobular with well-circumscribed smooth margins. Peripheral rim enhancement with or without enhancing internal septations is often noted [436, 437].

Microscopic Features

Histologic features of invasive carcinoma with medullary pattern include circumscribed tumor borders, syncytial growth, high Nottingham/SBR grade, and a prominent lymphoplasmacytic inflammatory infiltrate, features which overlap with basal-like carcinomas and carcinomas associated with *BRCA1* mutations.

Although the WHO no longer classifies tumors as MC, AMC, or invasive carcinomas with medullary features, the previously used diagnostic criteria for these tumors are included here for reference and context. Ridolfi et al. defined MC as an invasive carcinoma with a well-circumscribed rounded tumor border without infiltration into adjacent tissue, >75% syncytial growth, associated moderate to marked diffuse lymphocytic infiltrate, intermediate or high nuclear grade, absence of glandular features, and lack of an intraductal component (Figs. 12.82, 12.83, 12.84, and 12.85). AMC referred to tumors with at least 75% syncytial growth but lacking one or two of the other features, and non-medullary carcinomas lacked at least 75% syncytial growth or three or more medullary features [408]. Using the Ridolfi classification, studies showed 10-year MC survival rates of 84–95%, compared to 53–80% for AMC and 51–70% for non-medullary carcinomas [408, 424, 438]. Tumors classified as AMC only due to the presence of an intraductal component had outcomes similar to MC [408]. Wargotz and Silverberg used similar criteria but allowed for intraductal carcinoma, focal marginal infiltration, or a sparse lymphocytic infiltrate and observed similarly favorable outcome for MC [409]. Pedersen et al. proposed a simplified classification system that defined MC as having syncytial growth, diffuse stromal lymphocytic inflammation, <25% necrosis, and lack of tubular growth [428]. This was further simplified by Marginean et al., who required only 30% anastomosing growth and prominent inflammation, which also correlated well with survival outcomes [439]. Overall, the Ridolfi criteria were most commonly applied and correlated well with outcomes but are the strictest with the worst interobserver reproducibility [411]. It is now recognized that invasive car-

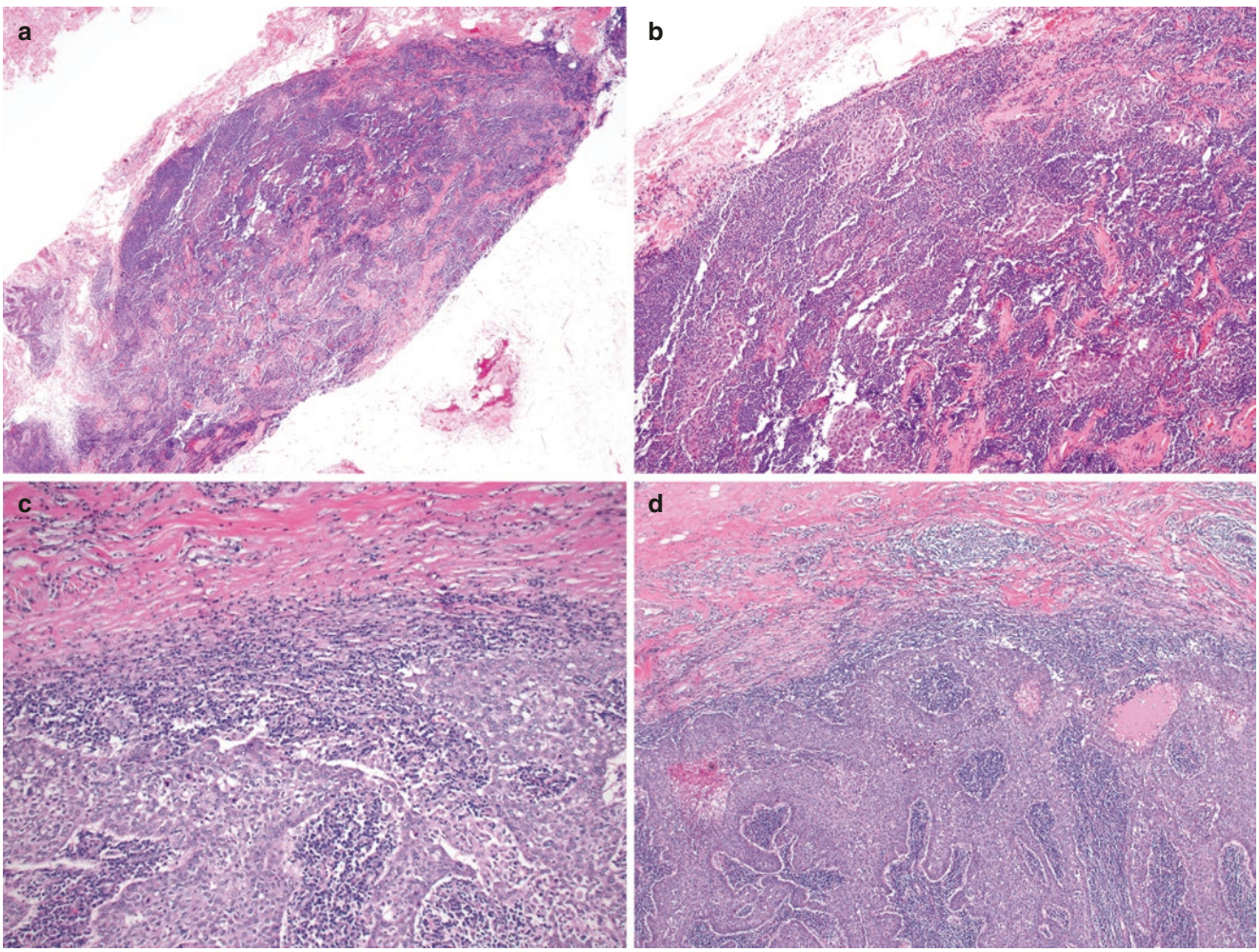

Fig. 12.82 Invasive breast carcinoma with medullary pattern, with well-circumscribed borders. (**a**, **b**) Core needle biopsy of this invasive breast carcinoma with medullary pattern reveals a rounded circumscribed border, without infiltration of tumor syncytium into adjacent fat. (**c**, **d**) Another example of invasive breast carcinoma with medullary pattern with well-circumscribed borders and a pushing-type of invasion. Note that the associated lymphoplasmacytic infiltrate is present throughout the tumor and at the periphery, where it may infiltrate the adjacent tissue

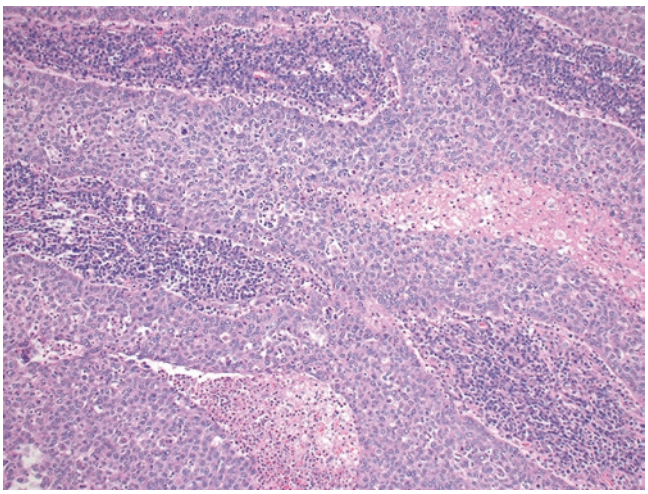

Fig. 12.83 Syncytial growth pattern of invasive breast carcinoma with medullary pattern. Syncytial growth is characterized by interanastomosing sheets of pleomorphic tumor cells with ill-defined cell membranes and borders. The typical lymphoplasmacytic infiltrate with scant collagenous stroma is present between areas of tumor syncytium. Note the presence of tumor necrosis in this case

cinomas with a medullary pattern exist along a morphologic continuum, with outcomes likely explained by their association with TILs, and discrete separation is no longer suggested.

Syncytial growth of invasive breast carcinomas with medullary pattern is characterized by broad interanastomosing sheets of tumor cells with indistinct cell borders (Figs. 12.83 and 12.84). The features may sometimes impart a squamoid appearance. Well-circumscribed tumors have rounded peripheral contours with a pushing-type convex border and lack of tumor infiltration into adjacent tissue. The inflammatory infiltrate is lymphoplasmacytic and often diffuse (Fig. 12.82). TILs can be quantitated in these tumors if clinically indicated, using the international consensus scoring recommendations [440]. A practical guide to TILs evaluation can be accessed online: https://www.tilsinbreastcancer.org. Lymphoid follicles with germinal center formation may be present. The inflammatory infiltrate may percolate among adjacent ducts and lobules at the tumor edge (Fig. 12.82d). Benign lobules distant from the tumor may show a similar

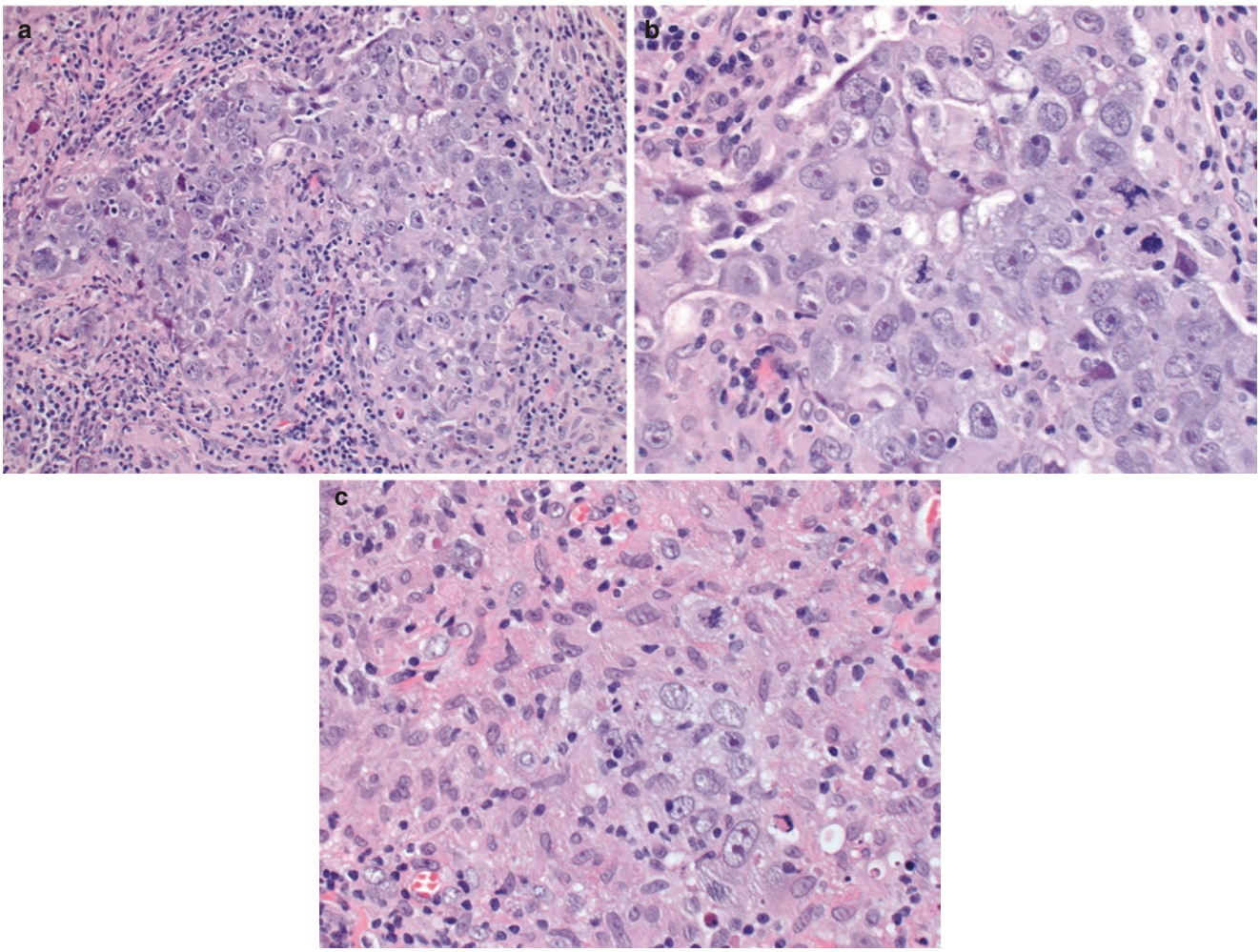

Fig. 12.84 Cytologic features of invasive breast carcinoma with medullary pattern. (**a**–**c**) The tumor cells are markedly pleomorphic, with grade 3 nuclei that have vesicular chromatin and prominent nucleoli. Mitotic activity is robust. Note also the syncytial appearance of the tumor cells and associated lymphoplasmacytic inflammatory infiltrate

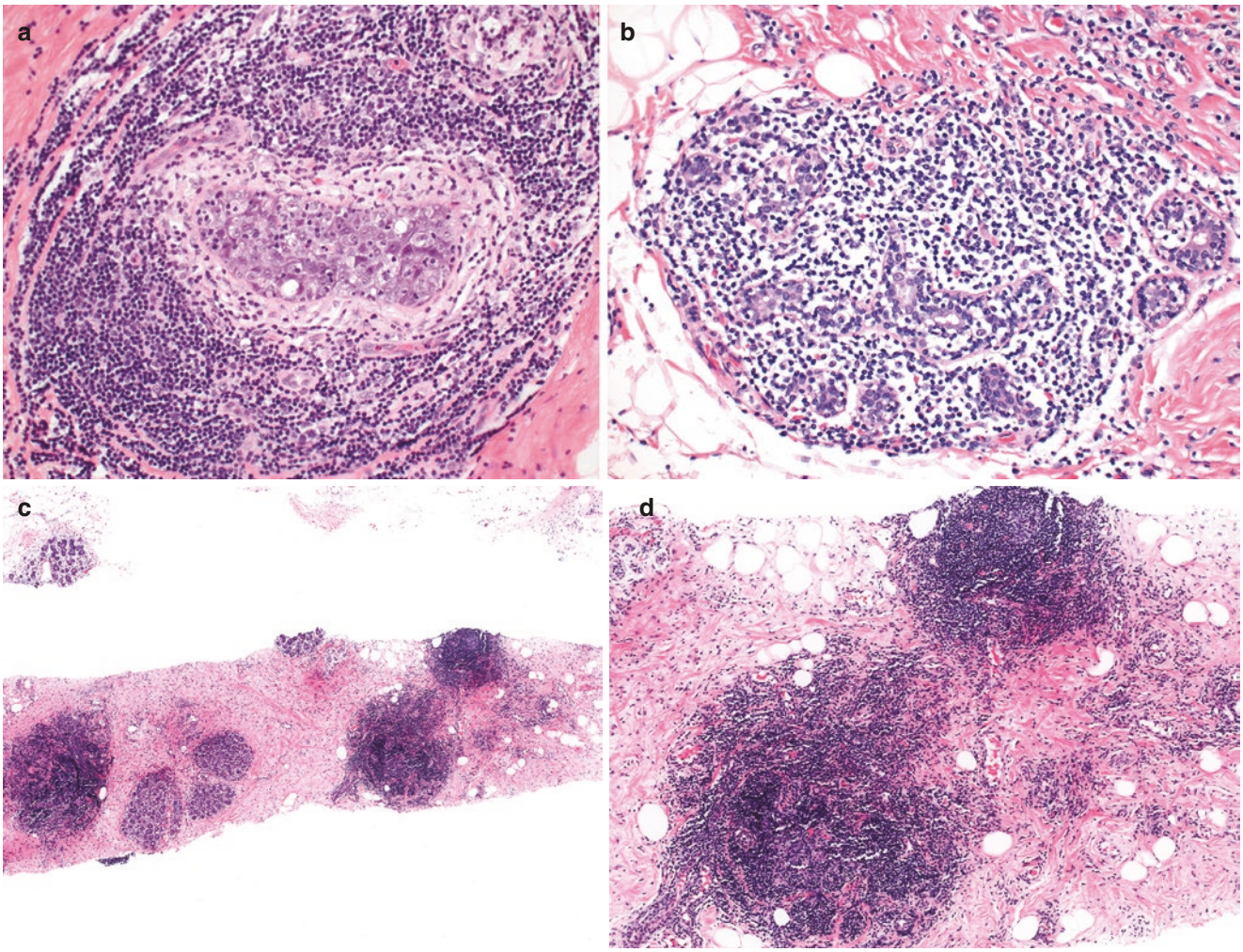

Fig. 12.85 Perilobular inflammatory infiltrates of invasive breast carcinoma with medullary pattern. (**a**) Intraductal carcinoma associated with invasive breast carcinoma with medullary pattern is characteristically high grade, in this example with a solid growth pattern. Note the associated perilobular lymphoplasmacytic infiltrate, which is typical. (**b**) Benign lobules may also demonstrate a similar prominent lymphoplasmacytic infiltrate, which may be seen at some distance from the carcinoma. (**c**, **d**) This CNB targeted for a breast mass demonstrates benign breast tissue with prominent lymphoplasmacytic infiltrates associated with some lobules and no carcinoma. The findings in the CNB were interpreted as lymphocytic mastitis. Excision revealed invasive breast carcinoma with medullary pattern (*not shown*). This case illustrates prominent perilobular lymphoplasmacytic infiltrate that is often observed in benign tissue adjacent to these tumors and also highlights the importance of radiological-pathological correlation in evaluating a breast CNB specimen

infiltrate (Fig. 12.85b–d). The tumor cells are enlarged and pleomorphic, with abundant cytoplasm and grade 2 or 3 nuclei with coarse or vesicular chromatin and often one or several prominent nucleoli (Fig. 12.84). Atypical giant cells with bizarre nuclei may be present. Focal squamous differentiation can be seen [408, 441]. Frequent mitotic figures, including abnormal forms, are common, as are pyknotic nuclei and smudged cells [434]. Areas of necrosis can lead to cystic degeneration. An intraductal component is not uncommon, usually with identical cytologic features and solid or comedo pattern, with or without lobular extension. A lymphoplasmacytic infiltrate is also often present surrounding the in situ carcinoma (Fig. 12.85a).

Immunohistochemistry

Invasive breast carcinomas with medullary pattern are usually triple (ER, PR, HER2) negative, although some tumors can be ER and PR positive [413, 417, 442–446]. HER2 overexpression is uncommon [417, 442, 443, 447–449]. These tumors express LMWCK (CK8/18 and CK7), with variable expression of HMWCK (such as CK5/6, CK14, and CK17) and other basal markers (EGFR, p-cadherin) [411, 417, 442, 443, 447, 450, 451]. In one series, a basal-like immunophenotype (triple negative with expression of either CK5/6 or EGFR) was demonstrated in ~63% of invasive carcinomas with medullary features compared to ~19% of matched IBC-

NST [442]. SMA, S100 protein, and p53 may be positive [417, 418, 442, 443, 452, 453], with p53 overexpression generally being due to *TP53* mutation [418, 443]. Ki-67 is usually >50% (~50–90%) [417, 442].

The lymphoplasmacytic infiltrate is predominantly composed of CD3+, CD8+, TIA-1+, and granzyme B+ lymphocytes [454–456].

Invasive breast carcinomas with medullary pattern may be positive for the immune checkpoint protein PD-L1 using either SP142 or 22C3 companion assays [457].

Differential Diagnosis

With the understanding that invasive breast carcinomas with medullary pattern belong to a morphologic continuum and that clinical behavior and outcomes are likely linked to TILs in these tumors, there is less necessity to categorically differentiate these tumors. Instead, the medullary pattern should be used as a descriptor for IBC-NST.

Some authors have described lymphoepithelioma-like carcinoma (LEC) of the breast, which is morphologically similar to LEC arising at other sites and tends to lack circumscribed borders and syncytial growth [458]. In contrast to extramammary LEC, LEC is generally negative for Epstein–Barr virus (EBV) by immunohistochemistry, in situ hybridization, and polymerase chain reaction [459]. LEC is not recognized as a breast cancer subtype in the WHO classification, and it is unclear if these tumors represent morphologic variants along the spectrum of invasive breast carcinomas with medullary pattern.

Due to the prominence of the lymphoplasmacytic infiltrate in some invasive breast carcinomas with medullary pattern, the differential diagnosis may include lymphoma, especially in scant CNB material. Immunohistochemical stains for cytokeratin can be helpful in these cases (Fig. 12.86).

Invasive breast carcinomas with medullary pattern can mimic metastatic carcinoma within a lymph node, especially in tumors presenting as an axillary mass, and this can be particularly problematic in CNB or fine needle aspiration. The presence of germinal centers is not helpful, as these may be seen in invasive breast carcinomas with medullary pattern. Identification of a lymph node capsule and/or subcapsular sinus is useful if present (Fig. 12.87).

The differential diagnosis may also include a variety of reactive processes, including diabetic mastopathy, granulomatous mastitis, and mammary Rosai–Dorfman disease (RDD), all of which can be associated with a prominent lymphoplasmacytic inflammatory infiltrate. Attention to cytomorphologic features helps to distinguish the histiocytes of granulomatous mastitis and RDD from high-grade carcinoma cells, although limited sampling in CNB material may be problematic. Cytokeratin immunohistochemistry is helpful in challenging cases. The histiocytes of granulomatous mastitis and RDD are positive for histiocytic markers, including CD68 and CD163. Immunohistochemistry for S100 protein is less useful, as RDD histiocytes and invasive carcinoma cells may both be positive [417].

Pathogenesis and Risk Factors

Invasive breast carcinomas with medullary pattern share many features with *BRCA1*-associated breast cancers, including younger age at presentation, high-grade histopathologic features with high mitotic activity, prominent lymphoplasmacytic infiltration, pushing borders, triple negative or basal phenotype, and frequent *TP53* mutations. Indeed, a high proportion of germline *BRCA1*-associated breast carcinomas demonstrate medullary-like features [460–466]. Conversely, carcinomas with medullary-like features harbor higher rates of *BRCA1* mutations than other IBC-NST, and often show *BRCA1* promoter hypermethylation [462, 467]. These tumors are also genomically unstable with high large-scale state transition (LST) status, indicative of a BRCAness phenotype due to deficient DNA repair [443]. *TP53* mutations are common [443].

The vast majority of tumors previously classified as MC are basal-like by gene expression profiling and surrogate immunohistochemistry [37, 442, 443, 468]. Using the original 6-group TNBC classification developed by Lehmann et al. (TNBCtype), most of these tumors belonged to the immunomodulatory (IM) group, which is enriched for gene ontologies in immune cell processes [196, 469]. Immune signaling genes in the IM subgroup overlap with a previously identified gene expression signature for MC, which includes genes related to the immune response, antigen processing and apoptosis [468]. Using a refined 4-group TNBC molecular classification, the tumors belong to the basal-like 1 (BL1) group, which is enriched for cell cycle and DNA damage response genes [196]. Teschendorff et al. similarly found that invasive carcinomas previously classified as MC clustered with a prognostically favorable ER-negative group enriched for genes in cell cycle and immune response genes [470]. Together, gene expression studies and association of these tumors with *BRCA1* aberrations and a BRCAness phenotype highlight the importance of immune regulation and DNA repair deregulation in pathogenesis.

Prognosis and Clinical Management

Despite the basal-like and triple-negative phenotype, the prognosis of MC has been historically favorable, with most studies finding improved 5- and 10-year survival rates compared to non-medullary invasive carcinomas, although out-

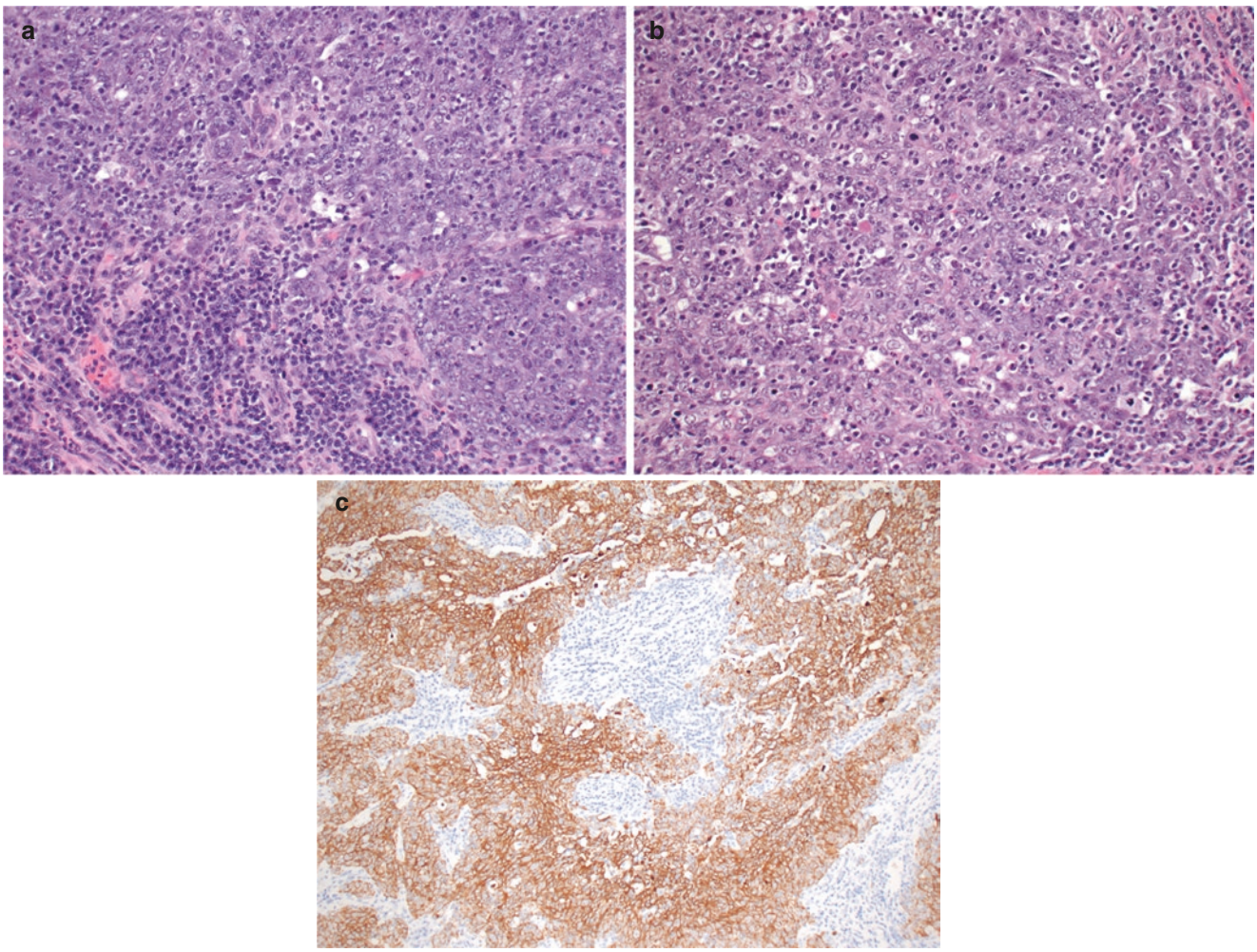

Fig. 12.86 Lymphoplasmacytic infiltrate of invasive breast carcinoma with medullary pattern may mask carcinoma cells. (**a**, **b**) In some cases, the inflammatory infiltrate may be very pronounced and mask the associated carcinoma cells, raising consideration for lymphoma. (**c**) Keratin immunostain is helpful in such cases to highlight the epithelial nature of the malignant cells. Note the interanastomosing sheets of syncytial epithelial cells

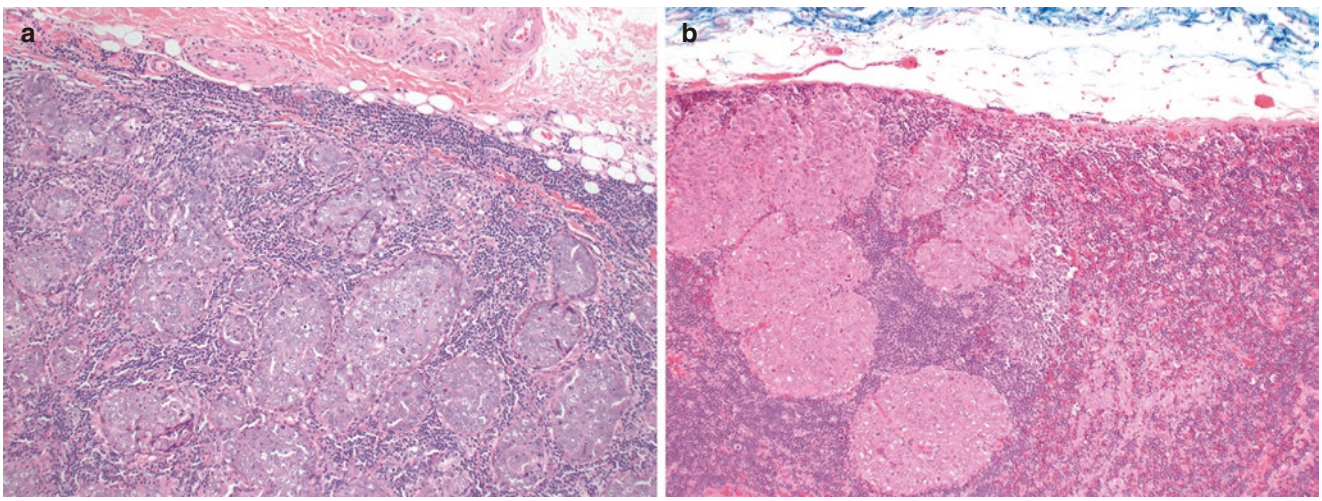

Fig. 12.87 Invasive breast carcinoma with medullary pattern may mimic metastatic carcinoma in a lymph node. (**a**) The prominent lymphoplasmacytic infiltrate and well-circumscribed tumor border of invasive breast carcinoma with medullary pattern may mimic metastatic carcinoma in a lymph node. The lack of a capsule and/or subcapsular sinus may be helpful in such cases. (**b**) In contrast, this lymph node with metastatic carcinoma demonstrates a distinct albeit compressed capsule

comes were generally dependent on strict and poorly reproducible diagnostic criteria. Most studies also observed decreased rates of axillary lymph node metastasis in patients with MC, and these patients had excellent long-term prognosis. Survival of patients with AMC were found to be intermediate between MC and non-medullary carcinomas, similar to non-medullary carcinomas, or similar to MC, depending on the study [408–412, 425, 431, 471, 472].

More recently, the prognostic impact of TILs has been discovered in high-grade carcinomas with and without medullary histologic features. High numbers of TILs are associated with improved response to neoadjuvant chemotherapy and longer disease-free survival in TNBC [419, 420, 472]. Moreover, survival in MC was not found to be significantly different from grade 3 IDC with prominent inflammation, but survival in both was significantly better than grade 3 IDC without prominent lymphocytic inflammation. There were no survival differences between MC and AMC in this study [472]. In another study, superior outcomes observed in invasive carcinomas with medullary features compared to other TNBC were lost once TILs were included in multivariate analysis [473]. Consistent with these findings, a gene expression signature for MC that is enriched for immune response genes was able to identify a prognostically favorable subgroup of basal-like carcinomas [474]. The data together suggest that the favorable outcomes ascribed to invasive breast carcinomas with medullary pattern are related to the prominent lymphoplasmacytic infiltrates in these tumors.

Rates of local tumor recurrence following breast conservation therapy are similar for patients with tumors previously classified as MC and IDC-NST [431, 475, 476]. Treatment of invasive breast carcinomas with medullary features is generally similar to other IBC-NST. Given the prominence of TILs in these tumors, immune checkpoint inhibitor therapy with PD-L1 (atezolizumab) or PD-1 (pembrolizumab) inhibitors can be an option for eligible patients [457].

References

1. Geschickter CF. Diseases of the breast: diagnosis, pathology, treatment. 2nd ed. Philadelphia, PA: JB Lippincott; 1945.
2. Arpino G, Clark GM, Mohsin S, Bardou VJ, Elledge RM. Adenoid cystic carcinoma of the breast: molecular markers, treatment, and clinical outcome. Cancer. 2002;94(8):2119–27.
3. Da Silva L, Buck L, Simpson PT, Reid L, McCallum N, Madigan BJ, et al. Molecular and morphological analysis of adenoid cystic carcinoma of the breast with synchronous tubular adenosis. Virchows Arch. 2009;454(1):107–14.
4. Miyai K, Schwartz MR, Divatia MK, Anton RC, Park YW, Ayala AG, et al. Adenoid cystic carcinoma of breast: recent advances. World J Clin Cases. 2014;2(12):732–41.
5. Ferlito A, Di Bonito L. Adenoid cystic carcinoma of the male breast: report of a case. Am Surg. 1974;40(1):72–6.
6. Hjorth S, Magnusson PH, Blomquist P. Adenoid cystic carcinoma of the breast. Report of a case in a male and review of the literature. Acta Chir Scand. 1977;143(3):155–8.
7. Santamaria G, Velasco M, Zanon G, Farrus B, Molina R, Sole M, et al. Adenoid cystic carcinoma of the breast: mammographic appearance and pathologic correlation. AJR Am J Roentgenol. 1998;171(6):1679–83.
8. Rosen PP. Adenoid cystic carcinoma of the breast. A morphologically heterogeneous neoplasm. Pathol Annu. 1989;24(Pt 2):237–54.
9. Tavassoli FA, Norris HJ. Mammary adenoid cystic carcinoma with sebaceous differentiation. A morphologic study of the cell types. Arch Pathol Lab Med. 1986;110(11):1045–53.
10. Tsuboi N, Ogawa Y, Inomata T, Nishioka A, Yoshida D, Yoshida S, et al. Dynamic MR appearance of adenoid cystic carcinoma of the breast in a 67-year-old female. Radiat Med. 1998;16(3):225–8.
11. Glazebrook KN, Reynolds C, Smith RL, Gimenez EI, Boughey JC. Adenoid cystic carcinoma of the breast. AJR Am J Roentgenol. 2010;194(5):1391–6.
12. Sheen-Chen SM, Eng HL, Chen WJ, Cheng YF, Ko SF. Adenoid cystic carcinoma of the breast: truly uncommon or easily overlooked? Anticancer Res. 2005;25(1B):455–8.
13. Foschini MPGF, Hayes MM, Marchio C, Nishimura R. Adenoid cystic carcinoma. In: WHO Classification of Tumours. Editorial Board, editors. WHO Classification of Breast Tumours. 5th ed. Lyon: International Agency for Research on Cancer (IARC); 2019. p. 142–5.
14. Kasami M, Olson SJ, Simpson JF, Page DL. Maintenance of polarity and a dual cell population in adenoid cystic carcinoma of the breast: an immunohistochemical study. Histopathology. 1998;32(3):232–8.
15. Shin SJ, Rosen PP. Solid variant of mammary adenoid cystic carcinoma with basaloid features: a study of nine cases. Am J Surg Pathol. 2002;26(4):413–20.
16. Lamovec J, Us-Krasovec M, Zidar A, Kljun A. Adenoid cystic carcinoma of the breast: a histologic, cytologic, and immunohistochemical study. Semin Diagn Pathol. 1989;6(2):153–64.
17. Foschini MP, Rizzo A, De Leo A, Laurino L, Sironi M, Rucco V. Solid variant of adenoid cystic carcinoma of the breast: a case series with proposal of a new grading system. Int J Surg Pathol. 2016;24(2):97–102.
18. Masse J, Truntzer C, Boidot R, Khalifa E, Perot G, Velasco V, et al. Solid-type adenoid cystic carcinoma of the breast, a distinct molecular entity enriched in NOTCH and CREBBP mutations. Mod Pathol. 2020;33(6):1041–55.
19. Righi A, Lenzi M, Morandi L, Flamminio F, De Biase D, Farnedi A, et al. Adenoid cystic carcinoma of the breast associated with invasive duct carcinoma: a case report. Int J Surg Pathol. 2011;19(2):230–4.
20. Fusco N, Geyer FC, De Filippo MR, Martelotto LG, Ng CK, Piscuoglio S, et al. Genetic events in the progression of adenoid cystic carcinoma of the breast to high-grade triple-negative breast cancer. Mod Pathol. 2016;29(11):1292–305.
21. Cabibi D, Cipolla C, Maria Florena A, Fricano S, Barresi E, Vieni S, et al. Solid variant of mammary "adenoid cystic carcinoma with basaloid features" merging with "small cell carcinoma". Pathol Res Pract. 2005;201(10):705–11.
22. Noske A, Schwabe M, Pahl S, Fallenberg E, Richter-Ehrenstein C, Dietel M, et al. Report of a metaplastic carcinoma of the breast with multi-directional differentiation: an adenoid cystic carcinoma, a spindle cell carcinoma and melanoma. Virchows Arch. 2008;452(5):575–9.
23. Acs G, Simpson JF, Bleiweiss IJ, Hugh J, Reynolds C, Olson S, et al. Microglandular adenosis with transition into adenoid cystic carcinoma of the breast. Am J Surg Pathol. 2003;27(8):1052–60.

24. James BA, Cranor ML, Rosen PP. Carcinoma of the breast arising in microglandular adenosis. Am J Clin Pathol. 1993;100(5):507–13.
25. Khalifeh IM, Albarracin C, Diaz LK, Symmans FW, Edgerton ME, Hwang RF, et al. Clinical, histopathologic, and immunohistochemical features of microglandular adenosis and transition into in situ and invasive carcinoma. Am J Surg Pathol. 2008;32(4):544–52.
26. McClenathan JH, de la Roza G. Adenoid cystic breast cancer. Am J Surg. 2002;183(6):646–9.
27. Peters GN, Wolff M. Adenoid cystic carcinoma of the breast. Report of 11 new cases: review of the literature and discussion of biological behavior. Cancer. 1983;52(4):680–6.
28. Ro JY, Silva EG, Gallager HS. Adenoid cystic carcinoma of the breast. Hum Pathol. 1987;18(12):1276–81.
29. Kleer CG, Oberman HA. Adenoid cystic carcinoma of the breast: value of histologic grading and proliferative activity. Am J Surg Pathol. 1998;22(5):569–75.
30. D'Alfonso TM, Mosquera JM, MacDonald TY, Padilla J, Liu YF, Rubin MA, et al. MYB-NFIB gene fusion in adenoid cystic carcinoma of the breast with special focus paid to the solid variant with basaloid features. Hum Pathol. 2014;45(11):2270–80.
31. Vranic S, Bender R, Palazzo J, Gatalica Z. A review of adenoid cystic carcinoma of the breast with emphasis on its molecular and genetic characteristics. Hum Pathol. 2013;44(3):301–9.
32. Poling JS, Yonescu R, Subhawong AP, Sharma R, Argani P, Ning Y, et al. MYB labeling by immunohistochemistry is more sensitive and specific for breast adenoid cystic carcinoma than MYB labeling by FISH. Am J Surg Pathol. 2017;41(7):973–9.
33. Kim M, Lee DW, Im J, Suh KJ, Keam B, Moon HG, et al. Adenoid cystic carcinoma of the breast: a case series of six patients and literature review. Cancer Res Treat. 2014;46(1):93–7.
34. Yang C, Zhang L, Sanati S. SOX10 is a sensitive marker for breast and salivary gland adenoid cystic carcinoma: immunohistochemical characterization of adenoid cystic carcinomas. Breast Cancer (Auckl). 2019;13:1178223419842185.
35. Trendell-Smith NJ, Peston D, Shousha S. Adenoid cystic carcinoma of the breast: a tumour commonly devoid of oestrogen receptors and related proteins. Histopathology. 1999;35(3):241–8.
36. Vranic S, Gatalica Z, Deng H, Frkovic-Grazio S, Lee LM, Gurjeva O, et al. ER-alpha36, a novel isoform of ER-alpha66, is commonly over-expressed in apocrine and adenoid cystic carcinomas of the breast. J Clin Pathol. 2011;64(1):54–7.
37. Weigelt B, Horlings HM, Kreike B, Hayes MM, Hauptmann M, Wessels LF, et al. Refinement of breast cancer classification by molecular characterization of histological special types. J Pathol. 2008;216(2):141–50.
38. Vranic S, Frkovic-Grazio S, Lamovec J, Serdarevic F, Gurjeva O, Palazzo J, et al. Adenoid cystic carcinomas of the breast have low Topo IIalpha expression but frequently overexpress EGFR protein without EGFR gene amplification. Hum Pathol. 2010;41(11):1617–23.
39. Wetterskog D, Lopez-Garcia MA, Lambros MB, A'Hern R, Geyer FC, Milanezi F, et al. Adenoid cystic carcinomas constitute a genomically distinct subgroup of triple-negative and basal-like breast cancers. J Pathol. 2012;226(1):84–96.
40. Pastolero G, Hanna W, Zbieranowski I, Kahn HJ. Proliferative activity and p53 expression in adenoid cystic carcinoma of the breast. Mod Pathol. 1996;9(3):215–9.
41. Albores-Saavedra J, Heard SC, McLaren B, Kamino H, Witkiewicz AK. Cylindroma (dermal analog tumor) of the breast: a comparison with cylindroma of the skin and adenoid cystic carcinoma of the breast. Am J Clin Pathol. 2005;123(6):866–73.
42. Mahmoud A, Hill DH, O'Sullivan MJ, Bennett MW. Cylindroma of the breast: a case report and review of the literature. Diagn Pathol. 2009;4:30.
43. Azoulay S, Lae M, Freneaux P, Merle S, Al Ghuzlan A, Chnecker C, et al. KIT is highly expressed in adenoid cystic carcinoma of the breast, a basal-like carcinoma associated with a favorable outcome. Mod Pathol. 2005;18(12):1623–31.
44. Persson M, Andren Y, Mark J, Horlings HM, Persson F, Stenman G. Recurrent fusion of MYB and NFIB transcription factor genes in carcinomas of the breast and head and neck. Proc Natl Acad Sci U S A. 2009;106(44):18740–4.
45. Martelotto LG, De Filippo MR, Ng CK, Natrajan R, Fuhrmann L, Cyrta J, et al. Genomic landscape of adenoid cystic carcinoma of the breast. J Pathol. 2015;237(2):179–89.
46. Drier Y, Cotton MJ, Williamson KE, Gillespie SM, Ryan RJ, Kluk MJ, et al. An oncogenic MYB feedback loop drives alternate cell fates in adenoid cystic carcinoma. Nat Genet. 2016;48(3):265–72.
47. Hudson JB, Collins BT. MYB gene abnormalities t(6;9) in adenoid cystic carcinoma fine-needle aspiration biopsy using fluorescence in situ hybridization. Arch Pathol Lab Med. 2014;138(3):403–9.
48. Kim J, Geyer FC, Martelotto LG, Ng CK, Lim RS, Selenica P, et al. MYBL1 rearrangements and MYB amplification in breast adenoid cystic carcinomas lacking the MYB-NFIB fusion gene. J Pathol. 2018;244(2):143–50.
49. Rooper LM, Lombardo KA, Oliai BR, Ha PK, Bishop JA. MYB RNA in situ hybridization facilitates sensitive and specific diagnosis of adenoid cystic carcinoma regardless of translocation status. Am J Surg Pathol. 2021;45(4):488–97.
50. Butcher MRL, Argani P, White M, Cimino-Mathews A. MYB RNA in situ hybridization is a useful tool to distinguish breast adenoid cystic carcinoma from other triple negative breast carcinomas (abstract). US Can Acad Pathol (USCAP). 2021;101:87.
51. Mastropasqua MG, Maiorano E, Pruneri G, Orvieto E, Mazzarol G, Vento AR, et al. Immunoreactivity for c-kit and p63 as an adjunct in the diagnosis of adenoid cystic carcinoma of the breast. Mod Pathol. 2005;18(10):1277–82.
52. Idowu MO, Kmieciak M, Dumur C, Burton RS, Grimes MM, Powers CN, et al. CD44(+)/CD24(-/low) cancer stem/progenitor cells are more abundant in triple-negative invasive breast carcinoma phenotype and are associated with poor outcome. Hum Pathol. 2012;43(3):364–73.
53. Millar BA, Kerba M, Youngson B, Lockwood GA, Liu FF. The potential role of breast conservation surgery and adjuvant breast radiation for adenoid cystic carcinoma of the breast. Breast Cancer Res Treat. 2004;87(3):225–32.
54. Vranic S, Bilalovic N, Lee LM, Kruslin B, Lilleberg SL, Gatalica Z. PIK3CA and PTEN mutations in adenoid cystic carcinoma of the breast metastatic to kidney. Hum Pathol. 2007;38(9):1425–31.
55. Page DL. Adenoid cystic carcinoma of breast, a special histopathologic type with excellent prognosis. Breast Cancer Res Treat. 2005;93(3):189–90.
56. Sumpio BE, Jennings TA, Merino MJ, Sullivan PD. Adenoid cystic carcinoma of the breast. Data from the Connecticut Tumor Registry and a review of the literature. Ann Surg. 1987;205(3):295–301.
57. Hodgson NC, Lytwyn A, Bacopulos S, Elavathil L. Adenoid cystic breast carcinoma: high rates of margin positivity after breast conserving surgery. Am J Clin Oncol. 2010;33(1):28–31.
58. Coates JM, Martinez SR, Bold RJ, Chen SL. Adjuvant radiation therapy is associated with improved survival for adenoid cystic carcinoma of the breast. J Surg Oncol. 2010;102(4):342–7.
59. Khanfir K, Kallel A, Villette S, Belkacemi Y, Vautravers C, Nguyen T, et al. Management of adenoid cystic carcinoma of the breast: a Rare Cancer Network study. Int J Radiat Oncol Biol Phys. 2012;82(5):2118–24.
60. Goldhirsch A, Wood WC, Coates AS, Gelber RD, Thurlimann B, Senn HJ, et al. Strategies for subtypes--dealing with the diversity of breast cancer: highlights of the St. Gallen International Expert

Consensus on the Primary Therapy of Early Breast Cancer 2011. Ann Oncol. 2011;22(8):1736–47.
61. Moore G, Annett S, McClements L, Robson T. Top notch targeting strategies in cancer: a detailed overview of recent insights and current perspectives. Cells. 2020;9(6):1503.
62. Eusebi V, Damiani S, Ellis IO, Azzopardi JG, Rosai J. Breast tumor resembling the tall cell variant of papillary thyroid carcinoma: report of 5 cases. Am J Surg Pathol. 2003;27(8):1114–8.
63. Chiang S, Weigelt B, Wen HC, Pareja F, Raghavendra A, Martelotto LG, et al. IDH2 mutations define a unique subtype of breast cancer with altered nuclear polarity. Cancer Res. 2016;76(24):7118–29.
64. Foschini MP, Asioli S, Foreid S, Cserni G, Ellis IO, Eusebi V, et al. Solid papillary breast carcinomas resembling the tall cell variant of papillary thyroid neoplasms: a unique invasive tumor with indolent behavior. Am J Surg Pathol. 2017;41(7):887–95.
65. Bhargava R, Florea AV, Pelmus M, Jones MW, Bonaventura M, Wald A, et al. Breast tumor resembling tall cell variant of papillary thyroid carcinoma: a solid papillary neoplasm with characteristic immunohistochemical profile and few recurrent mutations. Am J Clin Pathol. 2017;147(4):399–410.
66. Tosi AL, Ragazzi M, Asioli S, Del Vecchio M, Cavalieri M, Eusebi LH, et al. Breast tumor resembling the tall cell variant of papillary thyroid carcinoma: report of 4 cases with evidence of malignant potential. Int J Surg Pathol. 2007;15(1):14–9.
67. Colella R, Guerriero A, Giansanti M, Sidoni A, Bellezza G. An additional case of breast tumor resembling the tall cell variant of papillary thyroid carcinoma. Int J Surg Pathol. 2015;23(3):217–20.
68. Chang SY, Fleiszer DM, Mesurolle B, El Khoury M, Omeroglu A. Breast tumor resembling the tall cell variant of papillary thyroid carcinoma. Breast J. 2009;15(5):531–5.
69. Cameselle-Teijeiro J, Abdulkader I, Barreiro-Morandeira F, Ruiz-Ponte C, Reyes-Santias R, Chavez E, et al. Breast tumor resembling the tall cell variant of papillary thyroid carcinoma: a case report. Int J Surg Pathol. 2006;14(1):79–84.
70. Pitino A, Squillaci S, Spairani C, Rassu PC, Cosimi MF. Tall cell variant of papillary breast carcinoma: an additional case with review of the literature. Pathologica. 2017;109(3):162–7.
71. Jassim M, Premalata CS, Okaly G, Srinivas C. Tall cell carcinoma with reverse polarity of breast: report of a case with unique morphologic and molecular features. Turk Patoloji Derg. 2021;37(2):183–8.
72. Lozada JR, Basili T, Pareja F, Alemar B, Paula ADC, Gularte-Merida R, et al. Solid papillary breast carcinomas resembling the tall cell variant of papillary thyroid neoplasms (solid papillary carcinomas with reverse polarity) harbour recurrent mutations affecting IDH2 and PIK3CA: a validation cohort. Histopathology. 2018;73(2):339–44.
73. Haefliger S, Muenst S, Went P, Bihl M, Dellas S, Weber WP, et al. Tall cell carcinoma of the breast with reversed polarity (TCCRP) with mutations in the IDH2 and PIK3CA genes: a case report. Mol Biol Rep. 2020;47(6):4917–21.
74. Gai L, Done SJ, Cook D, Denic N, Erivwo P, Voisey K, et al. Breast tumour resembling tall cell variant of papillary thyroid carcinoma: case presentation (in a patient with Lynch syndrome). J Clin Pathol. 2018;71(11):1031–2.
75. Alsadoun N, MacGrogan G, Truntzer C, Lacroix-Triki M, Bedgedjian I, Koeb MH, et al. Solid papillary carcinoma with reverse polarity of the breast harbors specific morphologic, immunohistochemical and molecular profile in comparison with other benign or malignant papillary lesions of the breast: a comparative study of 9 additional cases. Mod Pathol. 2018;31(9):1367–80.
76. Toss MS, Billingham K, Egbuniwe IU, Moreno F, Abass A, Rakha EA. Breast tumours resembling the tall cell variant of thyroid papillary carcinoma: are they part of the papillary carcinoma spectrum or a distinct entity? Pathobiology. 2019;86(2-3):83–91.
77. Masood S, Davis C, Kubik MJ. Changing the term "breast tumor resembling the tall cell variant of papillary thyroid carcinoma" to "tall cell variant of papillary breast carcinoma". Adv Anat Pathol. 2012;19(2):108–10.
78. Zhong E, Scognamiglio T, D'Alfonso T, Song W, Tran H, Baek I, et al. Breast tumor resembling the tall cell variant of papillary thyroid carcinoma: molecular characterization by next-generation sequencing and histopathological comparison with tall cell papillary carcinoma of thyroid. Int J Surg Pathol. 2019;27(2):134–41.
79. Hameed O, Perry A, Banerjee R, Zhu X, Pfeifer JD. Papillary carcinoma of the breast lacks evidence of RET rearrangements despite morphological similarities to papillary thyroid carcinoma. Mod Pathol. 2009;22(9):1236–42.
80. Yang WTBH, Foschini MP, Schnitt SJ. Tall cell carcinoma with reversed polarity. In: WHO Classification of Tumours. Editorial Board, editors. WHO Classification of Breast Tumours. 5th ed. Lyon: International Agency for Research on Cancer (IARC); 2019. p. 153–4.
81. Ding LM, Hu HX, Wang YJ, Ji D, Ni LY, Sun ZH, et al. Tall cell variant of papillary breast carcinoma: report of a case. Zhonghua Bing Li Xue Za Zhi. 2019;48(10):815–7.
82. Pareja F, da Silva EM, Frosina D, Geyer FC, Lozada JR, Basili T, et al. Immunohistochemical analysis of IDH2 R172 hotspot mutations in breast papillary neoplasms: applications in the diagnosis of tall cell carcinoma with reverse polarity. Mod Pathol. 2020;33(6):1056–64.
83. Agoumi M, Giambattista J, Hayes MM. Practical considerations in breast papillary lesions: a review of the literature. Arch Pathol Lab Med. 2016;140(8):770–90.
84. Fiche M, Cassagnau E, Aillet G, Bailly J, Chupin M, Classe JM, et al. Breast metastasis from a "tall cell variant" of papillary thyroid carcinoma. Ann Pathol. 1998;18(2):130–2.
85. Eusebi V, Millis RR. Epitheliosis, infiltrating epitheliosis, and radial scar. Semin Diagn Pathol. 2010;27(1):5–12.
86. Eberle CA, Piscuoglio S, Rakha EA, Ng CK, Geyer FC, Edelweiss M, et al. Infiltrating epitheliosis of the breast: characterization of histological features, immunophenotype and genomic profile. Histopathology. 2016;68(7):1030–9.
87. Yan H, Parsons DW, Jin G, McLendon R, Rasheed BA, Yuan W, et al. IDH1 and IDH2 mutations in gliomas. N Engl J Med. 2009;360(8):765–73.
88. Green A, Beer P. Somatic mutations of IDH1 and IDH2 in the leukemic transformation of myeloproliferative neoplasms. N Engl J Med. 2010;362(4):369–70.
89. Dogan S, Chute DJ, Xu B, Ptashkin RN, Chandramohan R, Casanova-Murphy J, et al. Frequent IDH2 R172 mutations in undifferentiated and poorly-differentiated sinonasal carcinomas. J Pathol. 2017;242(4):400–8.
90. Amary MF, Bacsi K, Maggiani F, Damato S, Halai D, Berisha F, et al. IDH1 and IDH2 mutations are frequent events in central chondrosarcoma and central and periosteal chondromas but not in other mesenchymal tumours. J Pathol. 2011;224(3):334–43.
91. Borger DR, Tanabe KK, Fan KC, Lopez HU, Fantin VR, Straley KS, et al. Frequent mutation of isocitrate dehydrogenase (IDH)1 and IDH2 in cholangiocarcinoma identified through broad-based tumor genotyping. Oncologist. 2012;17(1):72–9.
92. Yang H, Ye D, Guan KL, Xiong Y. IDH1 and IDH2 mutations in tumorigenesis: mechanistic insights and clinical perspectives. Clin Cancer Res. 2012;18(20):5562–71.
93. Lu C, Ward PS, Kapoor GS, Rohle D, Turcan S, Abdel-Wahab O, et al. IDH mutation impairs histone demethylation and results in a block to cell differentiation. Nature. 2012;483(7390):474–8.
94. Xu W, Yang H, Liu Y, Yang Y, Wang P, Kim SH, et al. Oncometabolite 2-hydroxyglutarate is a competitive inhibitor

of alpha-ketoglutarate-dependent dioxygenases. Cancer Cell. 2011;19(1):17–30.
95. Ciriello G, Gatza ML, Beck AH, Wilkerson MD, Rhie SK, Pastore A, et al. Comprehensive molecular portraits of invasive lobular breast cancer. Cell. 2015;163(2):506–19.
96. Pereira B, Chin SF, Rueda OM, Vollan HK, Provenzano E, Bardwell HA, et al. The somatic mutation profiles of 2,433 breast cancers refines their genomic and transcriptomic landscapes. Nat Commun. 2016;7:11479.
97. The Cancer Genome Atlas N. Comprehensive molecular portraits of human breast tumours. Nature. 2012;490(7418):61–70.
98. Foschini MPGF, Marchio C, Nishimura R. Mucoepidermoid carcinoma. In: WHO Classification of Tumours. Editorial Board, editors. WHO Classification of Breast Tumours. 5th ed. Lyon: International Agency for Reseasrch on Cancer (IARC); 2019. p. 149–50.
99. Di Tommaso L, Foschini MP, Ragazzini T, Magrini E, Fornelli A, Ellis IO, et al. Mucoepidermoid carcinoma of the breast. Virchows Arch. 2004;444(1):13–9.
100. Bean GR, Krings G, Otis CN, Solomon DA, Garcia JJ, van Zante A, et al. CRTC1-MAML2 fusion in mucoepidermoid carcinoma of the breast. Histopathology. 2019;74(3):463–73.
101. Fisher ER, Palekar AS, Gregorio RM, Paulson JD. Mucoepidermoid and squamous cell carcinomas of breast with reference to squamous metaplasia and giant cell tumors. Am J Surg Pathol. 1983;7(1):15–27.
102. Cheng M, Geng C, Tang T, Song Z. Mucoepidermoid carcinoma of the breast: four case reports and review of the literature. Medicine (Baltimore). 2017;96(51):e9385.
103. Patchefsky AS, Frauenhoffer CM, Krall RA, Cooper HS. Low-grade mucoepidermoid carcinoma of the breast. Arch Pathol Lab Med. 1979;103(4):196–8.
104. Ye RP, Liao YH, Xia T, Kuang R, Long HA, Xiao XL. Breast mucoepidermoid carcinoma: a case report and review of literature. Int J Clin Exp Pathol. 2020;13(12):3192–9.
105. Yan M, Gilmore H, Harbhajanka A. Mucoepidermoid carcinoma of the breast with MAML2 rearrangement: a case report and literature review. Int J Surg Pathol. 2020;28(7):787–92.
106. Hornychova H, Ryska A, Betlach J, Bohac R, Cizek T, Tomsova M, et al. Mucoepidermoid carcinoma of the breast. Neoplasma. 2007;54(2):168–72.
107. Fujino M, Mori D, Akashi M, Yamamoto H, Aibe H, Matake K, et al. Mucoepidermoid carcinoma of the breast found during treatment of lymphoma. Case Rep Oncol. 2016;9(3):806–14.
108. Horii R, Akiyama F, Ikenaga M, Iwase T, Sakamoto G. Muco-epidermoid carcinoma of the breast. Pathol Int. 2006;56(9):549–53.
109. Sherwell-Cabello S, Maffuz-Aziz A, Rios-Luna NP, Pozo-Romero M, Lopez-Jimenez PV, Rodriguez-Cuevas S. Primary mucoepidermoid carcinoma of the breast. Breast J. 2017;23(6):753–5.
110. Basbug M, Akbulut S, Arikanoglu Z, Sogutcu N, Firat U, Kucukoner M. Mucoepidermoid carcinoma in a breast affected by burn scars: comprehensive literature review and case report. Breast Care (Basel). 2011;6(4):293–7.
111. Camelo-Piragua SI, Habib C, Kanumuri P, Lago CE, Mason HS, Otis CN. Mucoepidermoid carcinoma of the breast shares cytogenetic abnormality with mucoepidermoid carcinoma of the salivary gland: a case report with molecular analysis and review of the literature. Hum Pathol. 2009;40(6):887–92.
112. Pareja F, Da Cruz PA, Gularte-Merida R, Vahdatinia M, Li A, Geyer FC, et al. Pleomorphic adenomas and mucoepidermoid carcinomas of the breast are underpinned by fusion genes. NPJ Breast Cancer. 2020;6:20.
113. Cipriani NA, Lusardi JJ, McElherne J, Pearson AT, Olivas AD, Fitzpatrick C, et al. Mucoepidermoid carcinoma: a comparison of histologic grading systems and relationship to MAML2 rearrangement and prognosis. Am J Surg Pathol. 2019;43(7):885–97.
114. Krings G, Nystrom M, Mehdi I, Vohra P, Chen YY. Diagnostic utility and sensitivities of GATA3 antibodies in triple-negative breast cancer. Hum Pathol. 2014;45(11):2225–32.
115. Hung YP, Jo VY, Hornick JL. Immunohistochemistry with a pan-TRK antibody distinguishes secretory carcinoma of the salivary gland from acinic cell carcinoma. Histopathology. 2019;75(1):54–62.
116. Harrison BT, Fowler E, Krings G, Chen YY, Bean GR, Vincent-Salomon A, et al. Pan-TRK immunohistochemistry: a useful diagnostic adjunct for secretory carcinoma of the Breast. Am J Surg Pathol. 2019;43(12):1693–700.
117. Kyrpychova L, Kacerovska D, Vanecek T, Grossmann P, Michal M, Kerl K, et al. Cutaneous hidradenoma: a study of 21 neoplasms revealing neither correlation between the cellular composition and CRTC1-MAML2 fusions nor presence of CRTC3-MAML2 fusions. Ann Diagn Pathol. 2016;23:8–13.
118. Kuma Y, Yamada Y, Yamamoto H, Kohashi K, Ito T, Furue M, et al. A novel fusion gene CRTC3-MAML2 in hidradenoma: histopathological significance. Hum Pathol. 2017;70:55–61.
119. Kazakov DV, Vanecek T, Belousova IE, Mukensnabl P, Kollertova D, Michal M. Skin-type hidradenoma of the breast parenchyma with t(11;19) translocation: hidradenoma of the breast. Am J Dermatopathol. 2007;29(5):457–61.
120. Hsieh MS, Lien HC, Hua SF, Kuo WH, Lee YH. Clear cell hidradenoma of the breast with MAML2 gene rearrangement. Pathology. 2017;49(1):84–7.
121. Memon RA, Prieto Granada CN, Wei S. Clear cell papillary neoplasm of the breast with MAML2 gene rearrangement: clear cell hidradenoma or low-grade mucoepidermoid carcinoma? Pathol Res Pract. 2020;216(10):153140.
122. Yan M, Gilmore H, Harbhajanka A. Low-grade mucoepidermoid carcinoma versus nodular hidradenoma: potential diagnostic challenge in breast pathology. Int J Surg Pathol. 2021;29(3):346–7.
123. Fehr A, Roser K, Heidorn K, Hallas C, Loning T, Bullerdiek J. A new type of MAML2 fusion in mucoepidermoid carcinoma. Genes Chromosomes Cancer. 2008;47(3):203–6.
124. Lennerz JK, Perry A, Dehner LP, Pfeifer JD, Lind AC. CRTC1 rearrangements in the absence of t(11;19) in primary cutaneous mucoepidermoid carcinoma. Br J Dermatol. 2009;161(4):925–9.
125. Tonon G, Modi S, Wu L, Kubo A, Coxon AB, Komiya T, et al. t(11;19)(q21;p13) translocation in mucoepidermoid carcinoma creates a novel fusion product that disrupts a Notch signaling pathway. Nat Genet. 2003;33(2):208–13.
126. Komiya T, Park Y, Modi S, Coxon AB, Oh H, Kaye FJ. Sustained expression of Mect1-Maml2 is essential for tumor cell growth in salivary gland cancers carrying the t(11;19) translocation. Oncogene. 2006;25(45):6128–32.
127. Chen Z, Ni W, Li JL, Lin S, Zhou X, Sun Y, et al. The CRTC1-MAML2 fusion is the major oncogenic driver in mucoepidermoid carcinoma. JCI Insight. 2021;6(7):e139497.
128. Horowitz DP, Sharma CS, Connolly E, Gidea-Addeo D, Deutsch I. Secretory carcinoma of the breast: results from the survival, epidemiology and end results database. Breast. 2012;21(3):350–3.
129. Botta G, Fessia L, Ghiringhello B. Juvenile milk protein secreting carcinoma. Virchows Arch A Pathol Anat Histol. 1982;395(2):145–52.
130. McDivitt RW, Stewart FW. Breast carcinoma in children. JAMA. 1966;195(5):388–90.
131. Tavassoli FA, Norris HJ. Secretory carcinoma of the breast. Cancer. 1980;45(9):2404–13.
132. Li D, Xiao X, Yang W, Shui R, Tu X, Lu H, et al. Secretory breast carcinoma: a clinicopathological and immunophenotypic

study of 15 cases with a review of the literature. Mod Pathol. 2012;25(4):567–75.
133. Krings G, Joseph NM, Bean GR, Solomon D, Onodera C, Talevich E, et al. Genomic profiling of breast secretory carcinomas reveals distinct genetics from other breast cancers and similarity to mammary analog secretory carcinomas. Mod Pathol. 2017;30(8):1086–99.
134. Del Castillo M, Chibon F, Arnould L, Croce S, Ribeiro A, Perot G, et al. Secretory breast carcinoma: a histopathologic and genomic spectrum characterized by a joint specific ETV6-NTRK3 gene fusion. Am J Surg Pathol. 2015;39(11):1458–67.
135. Diallo R, Schaefer KL, Bankfalvi A, Decker T, Ruhnke M, Wülfing P, et al. Secretory carcinoma of the breast: a distinct variant of invasive ductal carcinoma assessed by comparative genomic hybridization and immunohistochemistry. Hum Pathol. 2003;34(12):1299–305.
136. Din NU, Idrees R, Fatima S, Kayani N. Secretory carcinoma of breast: clinicopathologic study of 8 cases. Ann Diagn Pathol. 2013;17(1):54–7.
137. Laé M, Fréneaux P, Sastre-Garau X, Chouchane O, Sigal-Zafrani B, Vincent-Salomon A. Secretory breast carcinomas with ETV6-NTRK3 fusion gene belong to the basal-like carcinoma spectrum. Mod Pathol. 2009;22(2):291–8.
138. Oberman HA. Secretory carcinoma of the breast in adults. Am J Surg Pathol. 1980;4(5):465–70.
139. Rosen PP, Cranor ML. Secretory carcinoma of the breast. Arch Pathol Lab Med. 1991;115(2):141–4.
140. Bishop JA. Unmasking MASC: bringing to light the unique morphologic, immunohistochemical and genetic features of the newly recognized mammary analogue secretory carcinoma of salivary glands. Head Neck Pathol. 2013;7(1):35–9.
141. Skálová A, Vanecek T, Sima R, Laco J, Weinreb I, Perez-Ordonez B, et al. Mammary analogue secretory carcinoma of salivary glands, containing the ETV6-NTRK3 fusion gene: a hitherto undescribed salivary gland tumor entity. Am J Surg Pathol. 2010;34(5):599–608.
142. Connor A, Perez-Ordoñez B, Shago M, Skálová A, Weinreb I. Mammary analog secretory carcinoma of salivary gland origin with the ETV6 gene rearrangement by FISH: expanded morphologic and immunohistochemical spectrum of a recently described entity. Am J Surg Pathol. 2012;36(1):27–34.
143. Majewska H, Skálová A, Stodulski D, Klimková A, Steiner P, Stankiewicz C, et al. Mammary analogue secretory carcinoma of salivary glands: a new entity associated with ETV6 gene rearrangement. Virchows Arch. 2015;466(3):245–54.
144. Wu B, Loh TKS, Vanecek T, Michal M, Petersson F. (Mammary Analogue) Secretory carcinoma of the nasal cavity: report of a rare case with p63 and DOG1 expression and uncommon exon 4-exon 14 ETV6-NTRK3 fusion diagnosed with next generation sequencing. Head Neck Pathol. 2020;14(2):542–9.
145. Amin SM, Beattie A, Ling X, Jennings LJ, Guitart J. Primary cutaneous mammary analog secretory carcinoma with ETV6-NTRK3 translocation. Am J Dermatopathol. 2016; 38(11):842–5.
146. Bishop JA, Taube JM, Su A, Binder SW, Kazakov DV, Michal M, et al. Secretory carcinoma of the skin harboring ETV6 gene fusions: a cutaneous analogue to secretory carcinomas of the breast and salivary glands. Am J Surg Pathol. 2017;41(1):62–6.
147. Chang MD, Arthur AK, García JJ, Sukov WR, Shon W. ETV6 rearrangement in a case of mammary analogue secretory carcinoma of the skin. J Cutan Pathol. 2016;43(11):1045–9.
148. Huang T, McHugh JB, Berry GJ, Myers JL. Primary mammary analogue secretory carcinoma of the lung: a case report. Hum Pathol. 2018;74:109–13.
149. Nguyen JK, Bridge JA, Joshi C, McKenney JK. Primary mammary analog secretory carcinoma (MASC) of the vulva with ETV6-NTRK3 fusion: a case report. Int J Gynecol Pathol. 2019;38(3):283–7.
150. Dettloff J, Seethala RR, Stevens TM, Brandwein-Gensler M, Centeno BA, Otto K, et al. Mammary analog secretory carcinoma (MASC) involving the thyroid gland: a report of the first 3 cases. Head Neck Pathol. 2017;11(2):124–30.
151. Dogan S, Wang L, Ptashkin RN, Dawson RR, Shah JP, Sherman EJ, et al. Mammary analog secretory carcinoma of the thyroid gland: a primary thyroid adenocarcinoma harboring ETV6-NTRK3 fusion. Mod Pathol. 2016;29(9):985–95.
152. Leeman-Neill RJ, Kelly LM, Liu P, Brenner AV, Little MP, Bogdanova TI, et al. ETV6-NTRK3 is a common chromosomal rearrangement in radiation-associated thyroid cancer. Cancer. 2014;120(6):799–807.
153. Arce C, Cortes-Padilla D, Huntsman DG, Miller MA, Dueñnas-Gonzalez A, Alvarado A, et al. Secretory carcinoma of the breast containing the ETV6-NTRK3 fusion gene in a male: case report and review of the literature. World J Surg Oncol. 2005;3:35.
154. Hoda RS, Brogi E, Pareja F, Nanjangud G, Murray MP, Weigelt B, et al. Secretory carcinoma of the breast: clinicopathologic profile of 14 cases emphasising distant metastatic potential. Histopathology. 2019;75(2):213–24.
155. Krings GCY, Sorensen PHB, Yang WT. Secretory carcinoma. In: WHO Classification of Tumours. Editorial Board, editors. WHO Classification of Breast Tumours. 5th ed. Lyon: International Agency for Research on Cancer (IARC); 2019. p. 146–8.
156. Shin SJ, Sheikh FS, Allenby PA, Rosen PP. Invasive secretory (juvenile) carcinoma arising in ectopic breast tissue of the axilla. Arch Pathol Lab Med. 2001;125(10):1372–4.
157. Krausz T, Jenkins D, Grontoft O, Pollock DJ, Azzopardi JG. Secretory carcinoma of the breast in adults: emphasis on late recurrence and metastasis. Histopathology. 1989;14(1):25–36.
158. Siegel JR, Karcnik TJ, Hertz MB, Gelmann H, Baker SR. Secretory carcinoma of the breast. Breast J. 1999;5(3):204–7.
159. Mun SH, Ko EY, Han BK, Shin JH, Kim SJ, Cho EY. Secretory carcinoma of the breast: sonographic features. J Ultrasound Med. 2008;27(6):947–54.
160. Paeng MH, Choi HY, Sung SH, Moon BI, Shim SS. Secretory carcinoma of the breast. J Clin Ultrasound. 2003;31(8):425–9.
161. Wu IK, Lai YC, Chiou HJ, Hsu CY. Secretory carcinoma of the breast: a case report and literature review. J Med Ultrasound. 2021;29(1):57–9.
162. Lee SG, Jung SP, Lee HY, Kim S, Kim HY, Kim I, et al. Secretory breast carcinoma: a report of three cases and a review of the literature. Oncol Lett. 2014;8(2):683–6.
163. Montalvo N, Posso V, Redrobán L. Secretory carcinoma in a 79-year-old woman: an exceptionally rare type of breast carcinoma. Rare Tumors. 2016;8(4):6650.
164. Yang Y, Wang Z, Pan G, Li S, Wu Y, Liu L. Pure secretory carcinoma in situ: a case report and literature review. Diagn Pathol. 2019;14(1):95.
165. Gatalica Z, Xiu J, Swensen J, Vranic S. Molecular characterization of cancers with NTRK gene fusions. Mod Pathol. 2019;32(1):147–53.
166. Hechtman JF, Benayed R, Hyman DM, Drilon A, Zehir A, Frosina D, et al. Pan-Trk Immunohistochemistry Is an Efficient and Reliable Screen for the Detection of NTRK Fusions. Am J Surg Pathol. 2017;41(11):1547–51.
167. Tognon C, Knezevich SR, Huntsman D, Roskelley CD, Melnyk N, Mathers JA, et al. Expression of the ETV6-NTRK3 gene fusion as a primary event in human secretory breast carcinoma. Cancer Cell. 2002;2(5):367–76.
168. Tognon C, Garnett M, Kenward E, Kay R, Morrison K, Sorensen PH. The chimeric protein tyrosine kinase ETV6-NTRK3 requires both Ras-Erk1/2 and PI3-kinase-Akt signaling for fibroblast transformation. Cancer Res. 2001;61(24):8909–16.

169. Lannon CL, Sorensen PH. ETV6-NTRK3: a chimeric protein tyrosine kinase with transformation activity in multiple cell lineages. Semin Cancer Biol. 2005;15(3):215–23.
170. Jin W, Yun C, Hobbie A, Martin MJ, Sorensen PH, Kim SJ. Cellular transformation and activation of the phosphoinositide-3-kinase-Akt cascade by the ETV6-NTRK3 chimeric tyrosine kinase requires c-Src. Cancer Res. 2007;67(7):3192–200.
171. Wai DH, Knezevich SR, Lucas T, Jansen B, Kay RJ, Sorensen PH. The ETV6-NTRK3 gene fusion encodes a chimeric protein tyrosine kinase that transforms NIH3T3 cells. Oncogene. 2000;19(7):906–15.
172. Cetinbas N, Huang-Hobbs H, Tognon C, Leprivier G, An J, McKinney S, et al. Mutation of the salt bridge-forming residues in the ETV6-SAM domain interface blocks ETV6-NTRK3-induced cellular transformation. J Biol Chem. 2013;288(39):27940–50.
173. Tognon CE, Mackereth CD, Somasiri AM, McIntosh LP, Sorensen PH. Mutations in the SAM domain of the ETV6-NTRK3 chimeric tyrosine kinase block polymerization and transformation activity. Mol Cell Biol. 2004;24(11):4636–50.
174. Skálová A, Vanecek T, Simpson RH, Laco J, Majewska H, Baneckova M, et al. Mammary analogue secretory carcinoma of salivary glands: molecular analysis of 25 ETV6 gene rearranged tumors with lack of detection of classical ETV6-NTRK3 fusion transcript by standard RT-PCR: report of 4 cases harboring ETV6-X gene fusion. Am J Surg Pathol. 2016;40(1):3–13.
175. Ito Y, Ishibashi K, Masaki A, Fujii K, Fujiyoshi Y, Hattori H, et al. Mammary analogue secretory carcinoma of salivary glands: a clinicopathologic and molecular study including 2 cases harboring ETV6-X fusion. Am J Surg Pathol. 2015;39(5):602–10.
176. Skálová A, Stenman G, Simpson RHW, Hellquist H, Slouka D, Svoboda T, et al. The role of molecular testing in the differential diagnosis of salivary gland carcinomas. Am J Surg Pathol. 2018;42(2):e11–27.
177. Skalova A, Vanecek T, Martinek P, Weinreb I, Stevens TM, Simpson RHW, et al. Molecular profiling of mammary analog secretory carcinoma revealed a subset of tumors harboring a novel ETV6-RET translocation: report of 10 cases. Am J Surg Pathol. 2018;42(2):234–46.
178. Rooper LM, Karantanos T, Ning Y, Bishop JA, Gordon SW, Kang H. Salivary secretory carcinoma with a novel ETV6-MET fusion: expanding the molecular spectrum of a recently described entity. Am J Surg Pathol. 2018;42(8):1121–6.
179. Guilmette J, Dias-Santagata D, Nosé V, Lennerz JK, Sadow PM. Novel gene fusions in secretory carcinoma of the salivary glands: enlarging the ETV6 family. Hum Pathol. 2019;83:50–8.
180. Black M, Liu CZ, Onozato M, Iafrate AJ, Darvishian F, Jour G, et al. Concurrent identification of novel EGFR-SEPT14 fusion and ETV6-RET fusion in secretory carcinoma of the salivary gland. Head Neck Pathol. 2020;14(3):817–21.
181. Salgado CM, Alaggio R, Reyes-Múgica M, Zin A, de Vito R. Clinicopathologic and Molecular Characterization of Four Cases of Pediatric Salivary Secretory Carcinoma (SSC), One with ETV6-RET Fusion. Head Neck Pathol. 2021;15(3):796–802.
182. Knezevich SR, McFadden DE, Tao W, Lim JF, Sorensen PH. A novel ETV6-NTRK3 gene fusion in congenital fibrosarcoma. Nat Genet. 1998;18(2):184–7.
183. Knezevich SR, Garnett MJ, Pysher TJ, Beckwith JB, Grundy PE, Sorensen PH. ETV6-NTRK3 gene fusions and trisomy 11 establish a histogenetic link between mesoblastic nephroma and congenital fibrosarcoma. Cancer Res. 1998;58(22):5046–8.
184. De Braekeleer E, Douet-Guilbert N, Morel F, Le Bris MJ, Basinko A, De Braekeleer M. ETV6 fusion genes in hematological malignancies: a review. Leuk Res. 2012;36(8):945–61.
185. Alassiri AH, Ali RH, Shen Y, Lum A, Strahlendorf C, Deyell R, et al. ETV6-NTRK3 is expressed in a subset of ALK-negative inflammatory myofibroblastic tumors. Am J Surg Pathol. 2016;40(8):1051–61.
186. Yeh I, Tee MK, Botton T, Shain AH, Sparatta AJ, Gagnon A, et al. NTRK3 kinase fusions in Spitz tumours. J Pathol. 2016;240(3):282–90.
187. Makretsov N, He M, Hayes M, Chia S, Horsman DE, Sorensen PH, et al. A fluorescence in situ hybridization study of ETV6-NTRK3 fusion gene in secretory breast carcinoma. Genes Chromosomes Cancer. 2004;40(2):152–7.
188. Costa NM, Rodrigues H, Pereira H, Pardal F, Matos E. Secretory breast carcinoma--case report and review of the medical literature. Breast. 2004;13(4):353–5.
189. Herz H, Cooke B, Goldstein D. Metastatic secretory breast cancer. Non-responsiveness to chemotherapy: case report and review of the literature. Ann Oncol. 2000;11(10):1343–7.
190. Drilon A, Li G, Dogan S, Gounder M, Shen R, Arcila M, et al. What hides behind the MASC: clinical response and acquired resistance to entrectinib after ETV6-NTRK3 identification in a mammary analogue secretory carcinoma (MASC). Ann Oncol. 2016;27(5):920–6.
191. Drilon A, Laetsch TW, Kummar S, DuBois SG, Lassen UN, Demetri GD, et al. Efficacy of larotrectinib in TRK fusion-positive cancers in adults and children. N Engl J Med. 2018;378(8):731–9.
192. Kheder ES, Hong DS. Emerging targeted therapy for tumors with NTRK fusion proteins. Clin Cancer Res. 2018;24(23):5807–14.
193. Shukla N, Roberts SS, Baki MO, Mushtaq Q, Goss PE, Park BH, et al. Successful targeted therapy of refractory pediatric ETV6-NTRK3 fusion-positive secretory breast carcinoma. JCO Precis Oncol. 2017;2017:PO.17.00034.
194. Provenzano EGZ, Vranic S. Carcinoma with apocrine differentiation. In: WHO Classification of Tumours. Editorial Board, editors. WHO Classification of Breast Tumours. 5th ed. Lyon: International Agency for Research on Cancer (IARC); 2019. p. 131–3.
195. Vranic S, Marchio C, Castellano I, Botta C, Scalzo MS, Bender RP, et al. Immunohistochemical and molecular profiling of histologically defined apocrine carcinomas of the breast. Hum Pathol. 2015;46(9):1350–9.
196. Lehmann BD, Bauer JA, Chen X, Sanders ME, Chakravarthy AB, Shyr Y, et al. Identification of human triple-negative breast cancer subtypes and preclinical models for selection of targeted therapies. J Clin Invest. 2011;121(7):2750–67.
197. Lehmann-Che J, Hamy AS, Porcher R, Barritault M, Bouhidel F, Habuellelah H, et al. Molecular apocrine breast cancers are aggressive estrogen receptor negative tumors overexpressing either HER2 or GCDFP15. Breast Cancer Res. 2013;15(3):R37.
198. Farmer P, Bonnefoi H, Becette V, Tubiana-Hulin M, Fumoleau P, Larsimont D, et al. Identification of molecular apocrine breast tumours by microarray analysis. Oncogene. 2005;24(29):4660–71.
199. Vranic S, Tawfik O, Palazzo J, Bilalovic N, Eyzaguirre E, Lee LM, et al. EGFR and HER-2/neu expression in invasive apocrine carcinoma of the breast. Mod Pathol. 2010;23(5):644–53.
200. D'Arcy C, Quinn CM. Apocrine lesions of the breast: part 2 of a two-part review. Invasive apocrine carcinoma, the molecular apocrine signature and utility of immunohistochemistry in the diagnosis of apocrine lesions of the breast. J Clin Pathol. 2019;72(1):7–11.
201. Yamazaki M, Nagata Y, Monji S, Shigematsu Y, Baba T, Shimokawa H, et al. Apocrine carcinoma of the breast. J UOEH. 2011;33(4):293–301.
202. Vranic S, Schmitt F, Sapino A, Costa JL, Reddy S, Castro M, et al. Apocrine carcinoma of the breast: a comprehensive review. Histol Histopathol. 2013;28(11):1393–409.
203. Dellapasqua S, Maisonneuve P, Viale G, Pruneri G, Mazzarol G, Ghisini R, et al. Immunohistochemically defined subtypes

and outcome of apocrine breast cancer. Clin Breast Cancer. 2013;13(2):95–102.
204. Schmitt FC, Soares R, Seruca R. Bilateral apocrine carcinoma of the breast. Molecular and immunocytochemical evidence for two independent primary tumours. Virchows Arch. 1998;433(6):505–9.
205. Mossler JA, Barton TK, Brinkhous AD, McCarty KS, Moylan JA, McCarty KS Jr. Apocrine differentiation in human mammary carcinoma. Cancer. 1980;46(11):2463–71.
206. Gerhard R, Costa JL, Schmitt F. Benign and malignant apocrine lesions of the breast. Expert Rev Anticancer Ther. 2012;12(2):215–21.
207. Arciero CA, Diehl AH 3rd, Liu Y, Sun Q, Gillespie T, Li X, et al. Triple-negative apocrine carcinoma: a rare pathologic subtype with a better prognosis than other triple-negative breast cancers. J Surg Oncol. 2020;122(6):1232–9.
208. Sun X, Zuo K, Yao Q, Zhou S, Shui R, Xu X, et al. Invasive apocrine carcinoma of the breast: clinicopathologic features and comprehensive genomic profiling of 18 pure triple-negative apocrine carcinomas. Mod Pathol. 2020;33(12):2473–82.
209. Imamovic D, Bilalovic N, Skenderi F, Beslagic V, Ceric T, Hasanbegovic B, et al. A clinicopathologic study of invasive apocrine carcinoma of the breast: a single-center experience. Breast J. 2018;24(6):1105–8.
210. Meattini I, Pezzulla D, Saieva C, Bernini M, Orzalesi L, Sanchez LJ, et al. Triple negative apocrine carcinomas as a distinct subtype of triple negative breast cancer: a case-control study. Clin Breast Cancer. 2018;18(5):e773–e80.
211. Montagna E, Cancello G, Pagan E, Bagnardi V, Munzone E, Dellapasqua S, et al. Prognosis of selected triple negative apocrine breast cancer patients who did not receive adjuvant chemotherapy. Breast. 2020;53:138–42.
212. Mills AM, Gottlieb CE, Wendroth SM, Brenin CM, Atkins KA. Pure apocrine carcinomas represent a clinicopathologically distinct androgen receptor-positive subset of triple-negative breast cancers. Am J Surg Pathol. 2016;40(8):1109–16.
213. Zhao S, Ma D, Xiao Y, Jiang YZ, Shao ZM. Clinicopathologic features and prognoses of different histologic types of triple-negative breast cancer: a large population-based analysis. Eur J Surg Oncol. 2018;44(4):420–8.
214. Zhang N, Zhang H, Chen T, Yang Q. Dose invasive apocrine adenocarcinoma has worse prognosis than invasive ductal carcinoma of breast: evidence from SEER database. Oncotarget. 2017;8(15):24579–92.
215. Weisman PS, Ng CK, Brogi E, Eisenberg RE, Won HH, Piscuoglio S, et al. Genetic alterations of triple negative breast cancer by targeted next-generation sequencing and correlation with tumor morphology. Mod Pathol. 2016;29(5):476–88.
216. Ogiya A, Horii R, Osako T, Ito Y, Iwase T, Eishi Y, et al. Apocrine metaplasia of breast cancer: clinicopathological features and predicting response. Breast Cancer. 2010;17(4):290–7.
217. Durham JR, Fechner RE. The histologic spectrum of apocrine lesions of the breast. Am J Clin Pathol. 2000;113(suppl_1):S3–18.
218. Shamir ER, Chen YY, Krings G. Genetic analysis of pleomorphic and florid lobular carcinoma in situ variants: frequent ERBB2/ERBB3 alterations and clonal relationship to classic lobular carcinoma in situ and invasive lobular carcinoma. Mod Pathol. 2020;33(6):1078–91.
219. Chen YY, Hwang ES, Roy R, DeVries S, Anderson J, Wa C, et al. Genetic and phenotypic characteristics of pleomorphic lobular carcinoma in situ of the breast. Am J Surg Pathol. 2009;33(11):1683–94.
220. Zhong E, Solomon JP, Cheng E, Baum J, Song W, Hoda SA. Apocrine variant of pleomorphic lobular carcinoma in situ: further clinical, histopathologic, immunohistochemical, and molecular characterization of an emerging entity. Am J Surg Pathol. 2020;44(8):1092–103.
221. Hoda SA, Brogi E, Koerner FC, Rosen PP. Rosen's breast pathology. Philadelphia, PA: Lippincott Williams and Williams; 2014.
222. Hood CI, Font RL, Zimmerman LE. Metastatic mammary carcinoma in the eyelid with histiocytoid appearance. Cancer. 1973;31(4):793–800.
223. Astvatsaturyan K, Yue Y, Walts AE, Bose S. Androgen receptor positive triple negative breast cancer: clinicopathologic, prognostic, and predictive features. PLoS One. 2018;13(6):e0197827.
224. Collins LC, Cole KS, Marotti JD, Hu R, Schnitt SJ, Tamimi RM. Androgen receptor expression in breast cancer in relation to molecular phenotype: results from the Nurses' Health Study. Mod Pathol. 2011;24(7):924–31.
225. Niemeier LA, Dabbs DJ, Beriwal S, Striebel JM, Bhargava R. Androgen receptor in breast cancer: expression in estrogen receptor-positive tumors and in estrogen receptor-negative tumors with apocrine differentiation. Mod Pathol. 2010;23(2):205–12.
226. Daemen A, Manning G. HER2 is not a cancer subtype but rather a pan-cancer event and is highly enriched in AR-driven breast tumors. Breast Cancer Res. 2018;20(1):8.
227. Loos S, Schulz KD, Hackenberg R. Regulation of GCDFP-15 expression in human mammary cancer cells. Int J Mol Med. 1999;4(2):135–40.
228. Darb-Esfahani S, von Minckwitz G, Denkert C, Ataseven B, Hogel B, Mehta K, et al. Gross cystic disease fluid protein 15 (GCDFP-15) expression in breast cancer subtypes. BMC Cancer. 2014;14:546.
229. Honma N, Takubo K, Akiyama F, Sawabe M, Arai T, Younes M, et al. Expression of GCDFP-15 and AR decreases in larger or node-positive apocrine carcinomas of the breast. Histopathology. 2005;47(2):195–201.
230. Kasashima S, Kawashima A, Ozaki S, Nakanuma Y. Expression of 5alpha-reductase in apocrine carcinoma of the breast and its correlation with clinicopathological aggressiveness. Histopathology. 2012;60(6B):E51–7.
231. Tanaka K, Imoto S, Wada N, Sakemura N, Hasebe K. Invasive apocrine carcinoma of the breast: clinicopathologic features of 57 patients. Breast J. 2008;14(2):164–8.
232. Celis JE, Cabezon T, Moreira JM, Gromov P, Gromova I, Timmermans-Wielenga V, et al. Molecular characterization of apocrine carcinoma of the breast: validation of an apocrine protein signature in a well-defined cohort. Mol Oncol. 2009;3(3):220–37.
233. Honma N, Takubo K, Arai T, Younes M, Kasumi F, Akiyama F, et al. Comparative study of monoclonal antibody B72.3 and gross cystic disease fluid protein-15 as markers of apocrine carcinoma of the breast. APMIS. 2006;114(10):712–9.
234. Banneau G, Guedj M, MacGrogan G, de Mascarel I, Velasco V, Schiappa R, et al. Molecular apocrine differentiation is a common feature of breast cancer in patients with germline PTEN mutations. Breast Cancer Res. 2010;12(4):R63.
235. Gromov P, Espinoza JA, Talman ML, Honma N, Kroman N, Timmermans Wielenga V, et al. FABP7 and HMGCS2 are novel protein markers for apocrine differentiation categorizing apocrine carcinoma of the breast. PLoS One. 2014;9(11):e112024.
236. Shao MM, Chan SK, Yu AM, Lam CC, Tsang JY, Lui PC, et al. Keratin expression in breast cancers. Virchows Arch. 2012;461(3):313–22.
237. Shousha S, Bull TB, Southall PJ, Mazoujian G. Apocrine carcinoma of the breast containing foam cells. An electron microscopic and immunohistological study. Histopathology. 1987;11(6):611–20.

238. Deftereos G, Sanguino Ramirez AM, Silverman JF, Krishnamurti U. GATA3 immunohistochemistry expression in histologic subtypes of primary breast carcinoma and metastatic breast carcinoma cytology. Am J Surg Pathol. 2015;39(9):1282–9.
239. Wendroth SM, Mentrikoski MJ, Wick MR. GATA3 expression in morphologic subtypes of breast carcinoma: a comparison with gross cystic disease fluid protein 15 and mammaglobin. Ann Diagn Pathol. 2015;19(1):6–9.
240. Kim S, Moon BI, Lim W, Park S, Cho MS, Sung SH. Expression patterns of GATA3 and the androgen receptor are strongly correlated in patients with triple-negative breast cancer. Hum Pathol. 2016;55:190–5.
241. Hilson JB, Schnitt SJ, Collins LC. Phenotypic alterations in myoepithelial cells associated with benign sclerosing lesions of the breast. Am J Surg Pathol. 2010;34(6):896–900.
242. Tramm T, Kim JY, Tavassoli FA. Diminished number or complete loss of myoepithelial cells associated with metaplastic and neoplastic apocrine lesions of the breast. Am J Surg Pathol. 2011;35(2):202–11.
243. Ragazzi M, de Biase D, Betts CM, Farnedi A, Ramadan SS, Tallini G, et al. Oncocytic carcinoma of the breast: frequency, morphology and follow-up. Hum Pathol. 2011;42(2):166–75.
244. Damiani S, Eusebi V, Losi L, D'Adda T, Rosai J. Oncocytic carcinoma (malignant oncocytoma) of the breast. Am J Surg Pathol. 1998;22(2):221–30.
245. Geyer FC, de Biase D, Lambros MB, Ragazzi M, Lopez-Garcia MA, Natrajan R, et al. Genomic profiling of mitochondrion-rich breast carcinoma: chromosomal changes may be relevant for mitochondria accumulation and tumour biology. Breast Cancer Res Treat. 2012;132(1):15–28.
246. Pia-Foschini M, Reis-Filho JS, Eusebi V, Lakhani SR. Salivary gland-like tumours of the breast: surgical and molecular pathology. J Clin Pathol. 2003;56(7):497–506.
247. Costa MJ, Silverberg SG. Oncocytic carcinoma of the male breast. Arch Pathol Lab Med. 1989;113(12):1396–9.
248. Roncaroli F, Lamovec J, Zidar A, Eusebi V. Acinic cell-like carcinoma of the breast. Virchows Arch. 1996;429(1):69–74.
249. Foschini MPGF, Marchio C, Nishimura R. Acinic cell carcinoma. In: WHO Classification of Tumours. Editorial Board, editors. WHO Classification of Breast Tumours. 5th ed. Lyon: International Agency for Research on Cancer (IARC); 2019. p. 139–41.
250. Limite G, Di Micco R, Esposito E, Sollazzo V, Cervotti M, Pettinato G, et al. Acinic cell carcinoma of the breast: review of the literature. Int J Surg. 2014;12(Suppl 1):S35–9.
251. Foschini MP, Eusebi V. Carcinomas of the breast showing myoepithelial cell differentiation. A review of the literature. Virchows Arch. 1998;432(4):303–10.
252. Peintinger F, Leibl S, Reitsamer R, Moinfar F. Primary acinic cell carcinoma of the breast: a case report with long-term follow-up and review of the literature. Histopathology. 2004;45(6):645–8.
253. Guerini-Rocco E, Hodi Z, Piscuoglio S, Ng CK, Rakha EA, Schultheis AM, et al. The repertoire of somatic genetic alterations of acinic cell carcinomas of the breast: an exploratory, hypothesis-generating study. J Pathol. 2015;237(2):166–78.
254. Kahn R, Holtveg H, Nissen F, Holck S. Are acinic cell carcinoma and microglandular carcinoma of the breast related lesions? Histopathology. 2003;42(2):195–6.
255. Geyer FC, Lacroix-Triki M, Colombo PE, Patani N, Gauthier A, Natrajan R, et al. Molecular evidence in support of the neoplastic and precursor nature of microglandular adenosis. Histopathology. 2012;60(6B):E115–30.
256. Jones C, Damiani S, Wells D, Chaggar R, Lakhani SR, Eusebi V. Molecular cytogenetic comparison of apocrine hyperplasia and apocrine carcinoma of the breast. Am J Pathol. 2001;158(1):207–14.
257. Schrager CA, Schneider D, Gruener AC, Tsou HC, Peacocke M. Clinical and pathological features of breast disease in Cowden's syndrome: an underrecognized syndrome with an increased risk of breast cancer. Hum Pathol. 1998;29(1):47–53.
258. Schrager CA, Schneider D, Gruener AC, Tsou HC, Peacocke M. Similarities of cutaneous and breast pathology in Cowden's syndrome. Exp Dermatol. 1998;7(6):380–90.
259. Doane AS, Danso M, Lal P, Donaton M, Zhang L, Hudis C, et al. An estrogen receptor-negative breast cancer subset characterized by a hormonally regulated transcriptional program and response to androgen. Oncogene. 2006;25(28):3994–4008.
260. d'Amore ES, Terrier-Lacombe MJ, Travagli JP, Friedman S, Contesso G. Invasive apocrine carcinoma of the breast: a long term follow-up study of 34 cases. Breast Cancer Res Treat. 1988;12(1):37–44.
261. Abati AD, Kimmel M, Rosen PP. Apocrine mammary carcinoma. A clinicopathologic study of 72 cases. Am J Clin Pathol. 1990;94(4):371–7.
262. Nagao T, Kinoshita T, Hojo T, Tsuda H, Tamura K, Fujiwara Y. The differences in the histological types of breast cancer and the response to neoadjuvant chemotherapy: the relationship between the outcome and the clinicopathological characteristics. Breast. 2012;21(3):289–95.
263. Cha YJ, Jung WH, Koo JS. The clinicopathologic features of molecular apocrine breast cancer. Korean J Pathol. 2012;46(2):169–76.
264. Liao HY, Zhang WW, Sun JY, Li FY, He ZY, Wu SG. The clinicopathological features and survival outcomes of different histological subtypes in triple-negative breast cancer. J Cancer. 2018;9(2):296–303.
265. Wu W, Wu M, Peng G, Shi D, Zhang J. Prognosis in triple-negative apocrine carcinomas of the breast: a population-based study. Cancer Med. 2019;8(18):7523–31.
266. Bonnefoi H, MacGrogan G, Poncet C, Iggo R, Pommeret F, Grellety T, et al. Molecular apocrine tumours in EORTC 10994/BIG 1-00 phase III study: pathological response after neoadjuvant chemotherapy and clinical outcomes. Br J Cancer. 2019;120(9):913–21.
267. Masuda H, Baggerly KA, Wang Y, Zhang Y, Gonzalez-Angulo AM, Meric-Bernstam F, et al. Differential response to neoadjuvant chemotherapy among 7 triple-negative breast cancer molecular subtypes. Clin Cancer Res. 2013;19(19):5533–40.
268. Lehmann BD, Jovanovic B, Chen X, Estrada MV, Johnson KN, Shyr Y, et al. Refinement of triple-negative breast cancer molecular subtypes: implications for neoadjuvant chemotherapy selection. PLoS One. 2016;11(6):e0157368.
269. Grellety T, Callens C, Richard E, Briaux A, Velasco V, Pulido M, et al. Enhancing abiraterone acetate efficacy in androgen receptor-positive triple-negative breast cancer: Chk1 as a potential target. Clin Cancer Res. 2019;25(2):856–67.
270. Gucalp A, Traina TA. Androgen receptor-positive, triple-negative breast cancer. Cancer. 2017;123(10):1686–8.
271. Pascual J, Turner NC. Targeting the PI3-kinase pathway in triple-negative breast cancer. Ann Oncol. 2019;30(7):1051–60.
272. Asghar US, Barr AR, Cutts R, Beaney M, Babina I, Sampath D, et al. Single-cell dynamics determines response to CDK4/6 inhibition in triple-negative breast cancer. Clin Cancer Res. 2017;23(18):5561–72.
273. Christenson JL, O'Neill KI, Williams MM, Spoelstra NS, Jones KL, Trahan GD, et al. Activity of combined androgen receptor antagonism and cell cycle inhibition in androgen receptor positive triple negative breast cancer. Mol Cancer Ther. 2021;20(6):1062–71.
274. Marra A, Trapani D, Viale G, Criscitiello C, Curigliano G. Practical classification of triple-negative breast cancer: intra-

tumoral heterogeneity, mechanisms of drug resistance, and novel therapies. NPJ Breast Cancer. 2020;6:54.
275. Reis-Filho JSGH, McCart Read AE, Rakha EA, Shin SJ, Sotiriou C, Vincent-Salomon A. Metaplastic carcinoma. In: WHO Classification of Tumours. Editorial Board, editors. WHO Classification of Breast Tumours. 5th ed. Lyon: International Agency for Research on Cancer (IARC); 2019. p. 134–8.
276. Schroeder MC, Rastogi P, Geyer CE Jr, Miller LD, Thomas A. Early and locally advanced metaplastic breast cancer: presentation and survival by receptor status in surveillance, epidemiology, and end results (SEER) 2010-2014. Oncologist. 2018;23(4):481–8.
277. Paul Wright G, Davis AT, Koehler TJ, Melnik MK, Chung MH. Hormone receptor status does not affect prognosis in metaplastic breast cancer: a population-based analysis with comparison to infiltrating ductal and lobular carcinomas. Ann Surg Oncol. 2014;21(11):3497–503.
278. Nelson RA, Guye ML, Luu T, Lai LL. Survival outcomes of metaplastic breast cancer patients: results from a US population-based analysis. Ann Surg Oncol. 2015;22(1):24–31.
279. Rakha EA, Tan PH, Varga Z, Tse GM, Shaaban AM, Climent F, et al. Prognostic factors in metaplastic carcinoma of the breast: a multi-institutional study. Br J Cancer. 2015; 112(2):283–9.
280. Downs-Kelly E, Nayeemuddin KM, Albarracin C, Wu Y, Hunt KK, Gilcrease MZ. Matrix-producing carcinoma of the breast: an aggressive subtype of metaplastic carcinoma. Am J Surg Pathol. 2009;33(4):534–41.
281. Gwin K, Wheeler DT, Bossuyt V, Tavassoli FA. Breast carcinoma with chondroid differentiation: a clinicopathologic study of 21 triple negative (ER-, PR-, Her2/neu-) cases. Int J Surg Pathol. 2010;18(1):27–35.
282. McCart Reed AE, Kalaw E, Nones K, Bettington M, Lim M, Bennett J, et al. Phenotypic and molecular dissection of metaplastic breast cancer and the prognostic implications. J Pathol. 2019;247(2):214–27.
283. El Zein D, Hughes M, Kumar S, Peng X, Oyasiji T, Jabbour H, et al. Metaplastic carcinoma of the breast is more aggressive than triple-negative breast cancer: a study from a single institution and review of literature. Clin Breast Cancer. 2017;17(5):382–91.
284. Langlands F, Cornford E, Rakha E, Dall B, Gutteridge E, Dodwell D, et al. Imaging overview of metaplastic carcinomas of the breast: a large study of 71 cases. Br J Radiol. 2016;89(1064):20140644.
285. Oberman HA. Metaplastic carcinoma of the breast. A clinicopathologic study of 29 patients. Am J Surg Pathol. 1987;11(12):918–29.
286. Tse GM, Tan PH, Putti TC, Lui PC, Chaiwun B, Law BK. Metaplastic carcinoma of the breast: a clinicopathological review. J Clin Pathol. 2006;59(10):1079–83.
287. Pezzi CM, Patel-Parekh L, Cole K, Franko J, Klimberg VS, Bland K. Characteristics and treatment of metaplastic breast cancer: analysis of 892 cases from the National Cancer Data Base. Ann Surg Oncol. 2007;14(1):166–73.
288. Yang WT, Hennessy B, Broglio K, Mills C, Sneige N, Davis WG, et al. Imaging differences in metaplastic and invasive ductal carcinomas of the breast. AJR Am J Roentgenol. 2007;189(6):1288–93.
289. Kashyap R, Vellathussery Chakkalakkoombil S, Ch Toi P, Satheesan D. Metaplastic breast carcinoma with osseous differentiation presenting as calcified breast mass-Radio-pathological correlation. Breast J. 2020;26(9):1825–7.
290. Cardoso F, Leal C, Meira A, Azevedo R, Mauricio MJ, Leal da Silva JM, et al. Squamous cell carcinoma of the breast. Breast. 2000;9(6):315–9.
291. Rosen PP, Ernsberger D. Low-grade adenosquamous carcinoma. A variant of metaplastic mammary carcinoma. Am J Surg Pathol. 1987;11(5):351–8.
292. Soo K, Tan PH. Low-grade adenosquamous carcinoma of the breast. J Clin Pathol. 2013;66(6):506–11.
293. Van Hoeven KH, Drudis T, Cranor ML, Erlandson RA, Rosen PP. Low-grade adenosquamous carcinoma of the breast. A clinicopathologic study of 32 cases with ultrastructural analysis. Am J Surg Pathol. 1993;17(3):248–58.
294. Kawaguchi K, Shin SJ. Immunohistochemical staining characteristics of low-grade adenosquamous carcinoma of the breast. Am J Surg Pathol. 2012;36(7):1009–20.
295. Bataillon G, Fuhrmann L, Girard E, Menet E, Lae M, Capovilla M, et al. High rate of PIK3CA mutations but no TP53 mutations in low-grade adenosquamous carcinoma of the breast. Histopathology. 2018;73(2):273–83.
296. Denley H, Pinder SE, Tan PH, Sim CS, Brown R, Barker T, et al. Metaplastic carcinoma of the breast arising within complex sclerosing lesion: a report of five cases. Histopathology. 2000;36(3):203–9.
297. Gobbi H, Simpson JF, Jensen RA, Olson SJ, Page DL. Metaplastic spindle cell breast tumors arising within papillomas, complex sclerosing lesions, and nipple adenomas. Mod Pathol. 2003;16(9):893–901.
298. Foschini MP, Pizzicannella G, Peterse JL, Eusebi V. Adenomyoepithelioma of the breast associated with low-grade adenosquamous and sarcomatoid carcinomas. Virchows Arch. 1995;427(3):243–50.
299. Geyer FC, Lambros MB, Natrajan R, Mehta R, Mackay A, Savage K, et al. Genomic and immunohistochemical analysis of adenosquamous carcinoma of the breast. Mod Pathol. 2010;23(7):951–60.
300. Tan QT, Chuwa EW, Chew SH, Lim-Tan SK, Lim SH. Low-grade adenosquamous carcinoma of the breast: a diagnostic and clinical challenge. Int J Surg. 2015;19:22–6.
301. Boecker W, Stenman G, Loening T, Andersson MK, Sinn HP, Barth P, et al. Differentiation and histogenesis of syringomatous tumour of the nipple and low-grade adenosquamous carcinoma: evidence for a common origin. Histopathology. 2014;65(1):9–23.
302. Rakha EA, Coimbra ND, Hodi Z, Juneinah E, Ellis IO, Lee AH. Immunoprofile of metaplastic carcinomas of the breast. Histopathology. 2017;70(6):975–85.
303. Wilsher MJ, Owens TW, Allcock RJ. Next generation sequencing of the nidus of early (adenosquamous proliferation rich) radial sclerosing lesions of the breast reveals evidence for a neoplastic precursor lesion. J Pathol Clin Res. 2017;3(2):115–22.
304. Gobbi H, Simpson JF, Borowsky A, Jensen RA, Page DL. Metaplastic breast tumors with a dominant fibromatosis-like phenotype have a high risk of local recurrence. Cancer. 1999;85(10):2170–82.
305. Nonnis R, Paliogiannis P, Giangrande D, Marras V, Trignano M. Low-grade fibromatosis-like spindle cell metaplastic carcinoma of the breast: a case report and literature review. Clin Breast Cancer. 2012;12(2):147–50.
306. Sneige N, Yaziji H, Mandavilli SR, Perez ER, Ordonez NG, Gown AM, et al. Low-grade (fibromatosis-like) spindle cell carcinoma of the breast. Am J Surg Pathol. 2001;25(8):1009–16.
307. Rito M, Schmitt F, Pinto AE, Andre S. Fibromatosis-like metaplastic carcinoma of the breast has a claudin-low immunohistochemical phenotype. Virchows Arch. 2014;465(2):185–91.
308. Koker MM, Kleer CG. p63 expression in breast cancer: a highly sensitive and specific marker of metaplastic carcinoma. Am J Surg Pathol. 2004;28(11):1506–12.
309. Lacroix-Triki M, Geyer FC, Lambros MB, Savage K, Ellis IO, Lee AH, et al. beta-catenin/Wnt signalling pathway in fibromato-

sis, metaplastic carcinomas and phyllodes tumours of the breast. Mod Pathol. 2010;23(11):1438–48.
310. Carter MR, Hornick JL, Lester S, Fletcher CD. Spindle cell (sarcomatoid) carcinoma of the breast: a clinicopathologic and immunohistochemical analysis of 29 cases. Am J Surg Pathol. 2006;30(3):300–9.
311. Krings G, Chen YY. Genomic profiling of metaplastic breast carcinomas reveals genetic heterogeneity and relationship to ductal carcinoma. Mod Pathol. 2018;31(11):1661–74.
312. Dunne B, Lee AH, Pinder SE, Bell JA, Ellis IO. An immunohistochemical study of metaplastic spindle cell carcinoma, phyllodes tumor and fibromatosis of the breast. Hum Pathol. 2003;34(10):1009–15.
313. Lee AH. Recent developments in the histological diagnosis of spindle cell carcinoma, fibromatosis and phyllodes tumour of the breast. Histopathology. 2008;52(1):45–57.
314. Rakha EA, Quinn CM, Foschini MP, Munoz Martin M, Dabbs DJ, Lakhani S, et al. Metaplastic carcinomas of the breast without evidence of epithelial differentiation: a diagnostic approach for management. Histopathology. 2021;78(5):759–71.
315. Jo VY, Fletcher CD. p63 immunohistochemical staining is limited in soft tissue tumors. Am J Clin Pathol. 2011;136(5):762–6.
316. Bishop JA, Montgomery EA, Westra WH. Use of p40 and p63 immunohistochemistry and human papillomavirus testing as ancillary tools for the recognition of head and neck sarcomatoid carcinoma and its distinction from benign and malignant mesenchymal processes. Am J Surg Pathol. 2014;38(2):257–64.
317. Cimino-Mathews A, Sharma R, Illei PB, Vang R, Argani P. A subset of malignant phyllodes tumors express p63 and p40: a diagnostic pitfall in breast core needle biopsies. Am J Surg Pathol. 2014;38(12):1689–96.
318. Bansal M, Chen J, Wang X. Focal anomalous expression of cytokeratin and p63 in malignant phyllodes tumor: a comparison with spindle cell metaplastic carcinoma. Appl Immunohistochem Mol Morphol. 2018;26(3):198–201.
319. Cimino-Mathews A, Subhawong AP, Elwood H, Warzecha HN, Sharma R, Park BH, et al. Neural crest transcription factor Sox10 is preferentially expressed in triple-negative and metaplastic breast carcinomas. Hum Pathol. 2013;44(6):959–65.
320. Jin C, Hacking S, Sajjan S, Kamanda S, Bhuiya T, Nasim M. GATA binding protein 3 (GATA3) as a marker for metaplastic spindle cell carcinoma of the breast. Pathol Res Pract. 2021;221:153413.
321. Ai D, Yao J, Yang F, Huo L, Chen H, Lu W, et al. TRPS1: a highly sensitive and specific marker for breast carcinoma, especially for triple-negative breast cancer. Mod Pathol. 2021;34(4):710–9.
322. Leibl S, Moinfar F. Metaplastic breast carcinomas are negative for Her-2 but frequently express EGFR (Her-1): potential relevance to adjuvant treatment with EGFR tyrosine kinase inhibitors? J Clin Pathol. 2005;58(7):700–4.
323. Reis-Filho JS, Milanezi F, Carvalho S, Simpson PT, Steele D, Savage K, et al. Metaplastic breast carcinomas exhibit EGFR, but not HER2, gene amplification and overexpression: immunohistochemical and chromogenic in situ hybridization analysis. Breast Cancer Res. 2005;7(6):R1028–35.
324. Varma S, Shin SJ. An algorithmic approach to spindle cell lesions of the breast. Adv Anat Pathol. 2013;20(2):95–109.
325. Moore T, Lee AH. Expression of CD34 and bcl-2 in phyllodes tumours, fibroadenomas and spindle cell lesions of the breast. Histopathology. 2001;38(1):62–7.
326. Md Nasir ND, Ng CCY, Rajasegaran V, Wong SF, Liu W, Ng GXP, et al. Genomic characterisation of breast fibroepithelial lesions in an international cohort. J Pathol. 2019;249(4):447–60.
327. Piscuoglio S, Ng CK, Murray M, Burke KA, Edelweiss M, Geyer FC, et al. Massively parallel sequencing of phyllodes tumours of the breast reveals actionable mutations, and TERT promoter hotspot mutations and TERT gene amplification as likely drivers of progression. J Pathol. 2016;238(4):508–18.
328. Tan J, Ong CK, Lim WK, Ng CC, Thike AA, Ng LM, et al. Genomic landscapes of breast fibroepithelial tumors. Nat Genet. 2015;47(11):1341–5.
329. Liu SY, Joseph NM, Ravindranathan A, Stohr BA, Greenland NY, Vohra P, et al. Genomic profiling of malignant phyllodes tumors reveals aberrations in FGFR1 and PI-3 kinase/RAS signaling pathways and provides insights into intratumoral heterogeneity. Mod Pathol. 2016;29(9):1012–27.
330. Nozad S, Sheehan CE, Gay LM, Elvin JA, Vergilio JA, Suh J, et al. Comprehensive genomic profiling of malignant phyllodes tumors of the breast. Breast Cancer Res Treat. 2017;162(3):597–602.
331. Ng CKY, Piscuoglio S, Geyer FC, Burke KA, Pareja F, Eberle CA, et al. The landscape of somatic genetic alterations in metaplastic breast carcinomas. Clin Cancer Res. 2017;23(14):3859–70.
332. Yeong J, Thike AA, Young Ng CC, Md Nasir ND, Loh K, Teh BT, et al. A genetic mutation panel for differentiating malignant phyllodes tumour from metaplastic breast carcinoma. Pathology. 2017;49(7):786–9.
333. Menes T, Schachter J, Morgenstern S, Fenig E, Lurie H, Gutman H. Primary squamous cell carcinoma (SqCC) of the breast. Am J Clin Oncol. 2003;26(6):571–3.
334. Grabowski J, Saltzstein SL, Sadler G, Blair S. Squamous cell carcinoma of the breast: a review of 177 cases. Am Surg. 2009;75(10):914–7.
335. Hennessy BT, Krishnamurthy S, Giordano S, Buchholz TA, Kau SW, Duan Z, et al. Squamous cell carcinoma of the breast. J Clin Oncol. 2005;23(31):7827–35.
336. Stevenson JT, Graham DJ, Khiyami A, Mansour EG. Squamous cell carcinoma of the breast: a clinical approach. Ann Surg Oncol. 1996;3(4):367–74.
337. Behranwala KA, Nasiri N, Abdullah N, Trott PA, Gui GP. Squamous cell carcinoma of the breast: clinico-pathologic implications and outcome. Eur J Surg Oncol. 2003;29(4):386–9.
338. Olsen DL, Keeney GL, Chen B, Visscher DW, Carter JM. Breast implant capsule-associated squamous cell carcinoma: a report of 2 cases. Hum Pathol. 2017;67:94–100.
339. Huws AM, Semkin L, Moalla A, Udayasankar S, Holt SDH, Sharaiha YM. Primary squamous cell carcinoma of the breast in association with Zuska's disease. Breast Cancer. 2018;25(3):365–9.
340. Tan YM, Yeo A, Chia KH, Wong CY. Breast abscess as the initial presentation of squamous cell carcinoma of the breast. Eur J Surg Oncol. 2002;28(1):91–3.
341. Gupta C, Malani AK, Weigand RT, Rangineni G. Pure primary squamous cell carcinoma of the breast: a rare presentation and clinicopathologic comparison with usual ductal carcinoma of the breast. Pathol Res Pract. 2006;202(6):465–9.
342. Wrightson WR, Edwards MJ, McMasters KM. Primary squamous cell carcinoma of the breast presenting as a breast abscess. Am Surg. 1999;65(12):1153–5.
343. Goldberg MT, Llaneras J, Willson TD, Boyd JB, Venegas RJ, Dauphine C, et al. Squamous cell carcinoma arising in breast implant capsules. Ann Plast Surg. 2021;86(3):268–72.
344. Nayak A, Wu Y, Gilcrease MZ. Primary squamous cell carcinoma of the breast: predictors of locoregional recurrence and overall survival. Am J Surg Pathol. 2013;37(6):867–73.
345. Wargotz ES, Norris HJ. Metaplastic carcinomas of the breast. IV. Squamous cell carcinoma of ductal origin. Cancer. 1990;65(2):272–6.
346. Eusebi V, Lamovec J, Cattani MG, Fedeli F, Millis RR. Acantholytic variant of squamous-cell carcinoma of the breast. Am J Surg Pathol. 1986;10(12):855–61.

347. Lei T, Pu T, Wei B, Fan Y, Yang L, Shen M, et al. Clinicopathologic characteristics of HER2-positive metaplastic squamous cell carcinoma of the breast. J Clin Pathol. 2022;75(1):18–23.
348. Foschini MP, Marucci G, Eusebi V. Low-grade mucoepidermoid carcinoma of salivary glands: characteristic immunohistochemical profile and evidence of striated duct differentiation. Virchows Arch. 2002;440(5):536–42.
349. Wargotz ES, Norris HJ. Metaplastic carcinomas of the breast. I. Matrix-producing carcinoma. Hum Pathol. 1989;20(7):628–35.
350. Rosenblum MK, Purrazzella R, Rosen PP. Is microglandular adenosis a precancerous disease? A study of carcinoma arising therein. Am J Surg Pathol. 1986;10(4):237–45.
351. Kim GE, Kim NI, Lee JS, Park MH. Metaplastic carcinoma with chondroid differentiation arising in microglandular adenosis. J Pathol Transl Med. 2017;51(4):418–21.
352. Schwartz CJ, Dolgalev I, Yoon E, Osman I, Heguy A, Vega-Saenz de Miera EC, et al. Microglandular adenosis is an advanced precursor breast lesion with evidence of molecular progression to matrix-producing metaplastic carcinoma. Hum Pathol. 2019;85:65–71.
353. van Deurzen CH, Lee AH, Gill MS, Menke-Pluijmers MB, Jager A, Ellis IO, et al. Metaplastic breast carcinoma: tumour histogenesis or dedifferentiation? J Pathol. 2011;224(4):434–7.
354. Teixeira MR, Qvist H, Bohler PJ, Pandis N, Heim S. Cytogenetic analysis shows that carcinosarcomas of the breast are of monoclonal origin. Genes Chromosomes Cancer. 1998;22(2):145–51.
355. Geyer FC, Weigelt B, Natrajan R, Lambros MB, de Biase D, Vatcheva R, et al. Molecular analysis reveals a genetic basis for the phenotypic diversity of metaplastic breast carcinomas. J Pathol. 2010;220(5):562–73.
356. Lien HC, Lin CW, Mao TL, Kuo SH, Hsiao CH, Huang CS. p53 overexpression and mutation in metaplastic carcinoma of the breast: genetic evidence for a monoclonal origin of both the carcinomatous and the heterogeneous sarcomatous components. J Pathol. 2004;204(2):131–9.
357. Avigdor BE, Beierl K, Gocke CD, Zabransky DJ, Cravero K, Kyker-Snowman K, et al. Whole-exome sequencing of metaplastic breast carcinoma indicates monoclonality with associated ductal carcinoma component. Clin Cancer Res. 2017;23(16):4875–84.
358. Zhuang Z, Lininger RA, Man YG, Albuquerque A, Merino MJ, Tavassoli FA. Identical clonality of both components of mammary carcinosarcoma with differential loss of heterozygosity. Mod Pathol. 1997;10(4):354–62.
359. Zhang Y, Toy KA, Kleer CG. Metaplastic breast carcinomas are enriched in markers of tumor-initiating cells and epithelial to mesenchymal transition. Mod Pathol. 2012;25(2):178–84.
360. Hennessy BT, Gonzalez-Angulo AM, Stemke-Hale K, Gilcrease MZ, Krishnamurthy S, Lee JS, et al. Characterization of a naturally occurring breast cancer subset enriched in epithelial-to-mesenchymal transition and stem cell characteristics. Cancer Res. 2009;69(10):4116–24.
361. Gerhard R, Ricardo S, Albergaria A, Gomes M, Silva AR, Logullo AF, et al. Immunohistochemical features of claudin-low intrinsic subtype in metaplastic breast carcinomas. Breast. 2012;21(3):354–60.
362. Weigelt B, Ng CK, Shen R, Popova T, Schizas M, Natrajan R, et al. Corrigendum: metastatic breast carcinomas display genomic and transcriptomic heterogeneity. Mod Pathol. 2015;28(4):607.
363. Piscuoglio S, Ng CKY, Geyer FC, Burke KA, Cowell CF, Martelotto LG, et al. Genomic and transcriptomic heterogeneity in metaplastic carcinomas of the breast. NPJ Breast Cancer. 2017;3:48.
364. Prat A, Parker JS, Karginova O, Fan C, Livasy C, Herschkowitz JI, et al. Phenotypic and molecular characterization of the claudin-low intrinsic subtype of breast cancer. Breast Cancer Res. 2010;12(5):R68.
365. May CD, Sphyris N, Evans KW, Werden SJ, Guo W, Mani SA. Epithelial-mesenchymal transition and cancer stem cells: a dangerously dynamic duo in breast cancer progression. Breast Cancer Res. 2011;13(1):202.
366. Weigelt B, Ng CK, Shen R, Popova T, Schizas M, Natrajan R, et al. Metaplastic breast carcinomas display genomic and transcriptomic heterogeneity [corrected]. Mod Pathol. 2015;28(3):340–51.
367. Joneja U, Vranic S, Swensen J, Feldman R, Chen W, Kimbrough J, et al. Comprehensive profiling of metaplastic breast carcinomas reveals frequent overexpression of programmed death-ligand 1. J Clin Pathol. 2017;70(3):255–9.
368. Edenfield J, Schammel C, Collins J, Schammel D, Edenfield WJ. Metaplastic breast cancer: molecular typing and identification of potential targeted therapies at a single institution. Clin Breast Cancer. 2017;17(1):e1–e10.
369. Pareja F, Ferrando L, Lee SSK, Beca F, Selenica P, Brown DN, et al. The genomic landscape of metastatic histologic special types of invasive breast cancer. NPJ Breast Cancer. 2020;6:53.
370. Hayes MJ, Thomas D, Emmons A, Giordano TJ, Kleer CG. Genetic changes of Wnt pathway genes are common events in metaplastic carcinomas of the breast. Clin Cancer Res. 2008;14(13):4038–44.
371. Ross JS, Badve S, Wang K, Sheehan CE, Boguniewicz AB, Otto GA, et al. Genomic profiling of advanced-stage, metaplastic breast carcinoma by next-generation sequencing reveals frequent, targetable genomic abnormalities and potential new treatment options. Arch Pathol Lab Med. 2015;139(5):642–9.
372. Suarez-Kelly LP, Akagi K, Reeser JW, Samorodnitsky E, Reeder M, Smith A, et al. Metaplastic breast cancer in a patient with neurofibromatosis type 1 and somatic loss of heterozygosity. Cold Spring Harb Mol Case Stud. 2018;4(2):a002352.
373. Lee HS, Jung EJ, Kim JY, Song EJ, Jeong CY, Ju YT, et al. Metaplastic spindle cell carcinoma of the breast in a patient with neurofibromatosis type 1. Breast J. 2018;24(3):391–4.
374. Natsiopoulos I, Chatzichristou A, Stratis I, Skordalaki A, Makrantonakis N. Metaplastic breast carcinoma in a patient with Von Recklinghausen's disease. Clin Breast Cancer. 2007;7(7):573–5.
375. Noel JC, Buxant F, Engohan-Aloghe C. Low-grade adenosquamous carcinoma of the breast--A case report with a BRCA1 germline mutation. Pathol Res Pract. 2010;206(7):511–3.
376. Nam G, Strenger R, Cutitar M, Wang Y. Low-grade adenosquamous carcinoma of the breast: a case with pathogenic germline mutation in the BRIP1 gene. Case Reports. 2020;22:200444.
377. Zhong S, Zhou S, Li A, Lv H, Li M, Tang S, et al. High frequency of PIK3CA and TERT promoter mutations in fibromatosis-like spindle cell carcinomas. J Clin Pathol. 2022;75(7):477–82.
378. Takano EA, Hunter SM, Campbell IG, Fox SB. Low-grade fibromatosis-like spindle cell carcinomas of the breast are molecularly exiguous. J Clin Pathol. 2015;68(5):362–7.
379. Hennessy BT, Giordano S, Broglio K, Duan Z, Trent J, Buchholz TA, et al. Biphasic metaplastic sarcomatoid carcinoma of the breast. Ann Oncol. 2006;17(4):605–13.
380. Tseng WH, Martinez SR. Metaplastic breast cancer: to radiate or not to radiate? Ann Surg Oncol. 2011;18(1):94–103.
381. Jung SY, Kim HY, Nam BH, Min SY, Lee SJ, Park C, et al. Worse prognosis of metaplastic breast cancer patients than other patients with triple-negative breast cancer. Breast Cancer Res Treat. 2010;120(3):627–37.
382. Lester TR, Hunt KK, Nayeemuddin KM, Bassett RL Jr, Gonzalez-Angulo AM, Feig BW, et al. Metaplastic sarcomatoid carcinoma of the breast appears more aggressive than other triple receptor-negative breast cancers. Breast Cancer Res Treat. 2012;131(1):41–8.
383. Zhang Y, Lv F, Yang Y, Qian X, Lang R, Fan Y, et al. Clinicopathological features and prognosis of metaplastic breast

carcinoma: experience of a major chinese cancer center. PLoS One. 2015;10(6):e0131409.
384. Beatty JD, Atwood M, Tickman R, Reiner M. Metaplastic breast cancer: clinical significance. Am J Surg. 2006;191(5): 657–64.
385. Bae SY, Lee SK, Koo MY, Hur SM, Choi MY, Cho DH, et al. The prognoses of metaplastic breast cancer patients compared to those of triple-negative breast cancer patients. Breast Cancer Res Treat. 2011;126(2):471–8.
386. Corso G, Frassoni S, Girardi A, De Camilli E, Montagna E, Intra M, et al. Metaplastic breast cancer: prognostic and therapeutic considerations. J Surg Oncol. 2021;123(1):61–70.
387. Lee H, Jung SY, Ro JY, Kwon Y, Sohn JH, Park IH, et al. Metaplastic breast cancer: clinicopathological features and its prognosis. J Clin Pathol. 2012;65(5):441–6.
388. Han M, Salamat A, Zhu L, Zhang H, Clark BZ, Dabbs DJ, et al. Metaplastic breast carcinoma: a clinical-pathologic study of 97 cases with subset analysis of response to neoadjuvant chemotherapy. Mod Pathol. 2019;32(6):807–16.
389. Cimino-Mathews A, Verma S, Figueroa-Magalhaes MC, Jeter SC, Zhang Z, Argani P, et al. A clinicopathologic analysis of 45 patients with metaplastic breast carcinoma. Am J Clin Pathol. 2016;145(3):365–72.
390. Takala S, Heikkilä P, Nevanlinna H, Blomqvist C, Mattson J. Metaplastic carcinoma of the breast: prognosis and response to systemic treatment in metastatic disease. Breast J. 2019;25(3):418–24.
391. Gradishar WJ, Moran MS, Abraham J, Aft R, Agnese D, Allison KH, et al. NCCN guidelines(R) insights: breast cancer, version 4.2021. J Natl Compr Canc Netw. 2021;19(5):484–93.
392. Honda M, Saji S, Horiguchi S, Suzuki E, Aruga T, Horiguchi K, et al. Clinicopathological analysis of ten patients with metaplastic squamous cell carcinoma of the breast. Surg Today. 2011;41(3):328–32.
393. Liu J, Yu Y, Sun JY, He SS, Wang X, Yin J, et al. Clinicopathologic characteristics and prognosis of primary squamous cell carcinoma of the breast. Breast Cancer Res Treat. 2015;149(1):133–40.
394. Lan T, Lu Y, Zheng R, Shao X, Luo H, He J, et al. The Role of adjuvant chemotherapy in metaplastic breast carcinoma: a competing risk analysis of the SEER database. Front Oncol. 2021;11:572230.
395. He X, Ji J, Dong R, Liu H, Dai X, Wang C, et al. Prognosis in different subtypes of metaplastic breast cancer: a population-based analysis. Breast Cancer Res Treat. 2019;173(2):329–41.
396. Wong W, Brogi E, Reis-Filho JS, Plitas G, Robson M, Norton L, et al. Poor response to neoadjuvant chemotherapy in metaplastic breast carcinoma. NPJ Breast Cancer. 2021;7(1):96.
397. Tray N, Taff J, Adams S. Therapeutic landscape of metaplastic breast cancer. Cancer Treat Rev. 2019;79:101888.
398. Haque W, Verma V, Naik N, Butler EB, Teh BS. Metaplastic breast cancer: practice patterns, outcomes, and the role of radiotherapy. Ann Surg Oncol. 2018;25(4):928–36.
399. Basho RK, Gilcrease M, Murthy RK, Helgason T, Karp DD, Meric-Bernstam F, et al. Targeting the PI3K/AKT/mTOR pathway for the treatment of mesenchymal triple-negative breast cancer: evidence from a phase 1 trial of mTOR inhibition in combination with liposomal doxorubicin and bevacizumab. JAMA Oncol. 2017;3(4):509–15.
400. Moukarzel LA, Ferrando L, Da Cruz PA, Brown DN, Geyer FC, Pareja F, et al. The genetic landscape of metaplastic breast cancers and uterine carcinosarcomas. Mol Oncol. 2021;15(4):1024–39.
401. Lien HC, Lee YH, Chen IC, Lin CH, Chen TW, Lu YT, et al. Tumor-infiltrating lymphocyte abundance and programmed death-ligand 1 expression in metaplastic breast carcinoma: implications for distinct immune microenvironments in different metaplastic components. Virchows Arch. 2021;478(4):669–78.
402. Morgan E, Suresh A, Ganju A, Stover DG, Wesolowski R, Sardesai S, et al. Assessment of outcomes and novel immune biomarkers in metaplastic breast cancer: a single institution retrospective study. World J Surg Oncol. 2020;18(1):11.
403. Chao X, Liu L, Sun P, Yang X, Li M, Luo R, et al. Immune parameters associated with survival in metaplastic breast cancer. Breast Cancer Res. 2020;22(1):92.
404. Grabenstetter A, Jungbluth AA, Frosina D, Hoda R, Dos Anjos CH, Patil S, et al. PD-L1 expression in metaplastic breast carcinoma using the PD-L1 SP142 assay and concordance among PD-L1 immunohistochemical assays. Am J Surg Pathol. 2021;45(9):1274–81.
405. Schmid P, Adams S, Rugo HS, Schneeweiss A, Barrios CH, Iwata H, et al. Atezolizumab and Nab-paclitaxel in advanced triple-negative breast cancer. N Engl J Med. 2018;379(22): 2108–21.
406. Adams S. Dramatic response of metaplastic breast cancer to chemo-immunotherapy. NPJ Breast Cancer. 2017;3:8.
407. Al Sayed AD, Elshenawy MA, Tulbah A, Al-Tweigeri T, Ghebeh H. Complete response of chemo-refractory metastatic metaplastic breast cancer to paclitaxel-immunotherapy combination. Am J Case Rep. 2019;20:1630–5.
408. Ridolfi RL, Rosen PP, Port A, Kinne D, Mike V. Medullary carcinoma of the breast: a clinicopathologic study with 10 year follow-up. Cancer. 1977;40(4):1365–85.
409. Wargotz ES, Silverberg SG. Medullary carcinoma of the breast: a clinicopathologic study with appraisal of current diagnostic criteria. Hum Pathol. 1988;19(11):1340–6.
410. Pedersen L, Zedeler K, Holck S, Schiodt T, Mouridsen HT. Medullary carcinoma of the breast, proposal for a new simplified histopathological definition. Based on prognostic observations and observations on inter- and intraobserver variability of 11 histopathological characteristics in 131 breast carcinomas with medullary features. Br J Cancer. 1991;63(4):591–5.
411. Jensen ML, Kiaer H, Andersen J, Jensen V, Melsen F. Prognostic comparison of three classifications for medullary carcinomas of the breast. Histopathology. 1997;30(6):523–32.
412. Pedersen L, Zedeler K, Holck S, Schiodt T, Mouridsen HT. Medullary carcinoma of the breast. Prevalence and prognostic importance of classical risk factors in breast cancer. Eur J Cancer. 1995;31A(13-14):2289–95.
413. Pedersen L, Holck S, Schiodt T, Zedeler K, Mouridsen HT. Inter- and intraobserver variability in the histopathological diagnosis of medullary carcinoma of the breast, and its prognostic implications. Breast Cancer Res Treat. 1989;14(1):91–9.
414. Gaffey MJ, Mills SE, Frierson HF Jr, Zarbo RJ, Boyd JC, Simpson JF, et al. Medullary carcinoma of the breast: interobserver variability in histopathologic diagnosis. Mod Pathol. 1995;8(1):31–8.
415. Moore OS Jr, Foote FW Jr. The relatively favorable prognosis of medullary carcinoma of the breast. Cancer. 1949;2(4):635–42.
416. Jacquemier JR-FJ, Lakhani SR, Rakha E. Carcinoma with medullary features. In: WHO Classification of Tumours. Editorial Board, editors. WHO Classification of Breast Tumours. 4th ed. Lyon: International Agency for Research on Cancer (IARC); 2012.
417. Jacquemier J, Padovani L, Rabayrol L, Lakhani SR, Penault-Llorca F, Denoux Y, et al. Typical medullary breast carcinomas have a basal/myoepithelial phenotype. J Pathol. 2005;207(3):260–8.
418. de Cremoux P, Salomon AV, Liva S, Dendale R, Bouchind'homme B, Martin E, et al. p53 mutation as a genetic trait of typical medullary breast carcinoma. J Natl Cancer Inst. 1999;91(7):641–3.
419. Denkert C, von Minckwitz G, Darb-Esfahani S, Lederer B, Heppner BI, Weber KE, et al. Tumour-infiltrating lymphocytes and prognosis in different subtypes of breast cancer: a pooled analysis of 3771 patients treated with neoadjuvant therapy. Lancet Oncol. 2018;19(1):40–50.

420. Loi S, Drubay D, Adams S, Pruneri G, Francis PA, Lacroix-Triki M, et al. Tumor-infiltrating lymphocytes and prognosis: a pooled individual patient analysis of early-stage triple-negative breast cancers. J Clin Oncol. 2019;37(7):559–69.
421. Loi S, Michiels S, Salgado R, Sirtaine N, Jose V, Fumagalli D, et al. Tumor infiltrating lymphocytes are prognostic in triple negative breast cancer and predictive for trastuzumab benefit in early breast cancer: results from the FinHER trial. Ann Oncol. 2014;25(8):1544–50.
422. Rakha EAAK, Bu H, Ellis IO, Foschini MP, Horii R, Masuda S, Penault-Llorca F, Schnitt SJ, Tsuda H, Vincent-Salomon A, Yang WT. Invasive breast carcinoma of no special type. In: WHO Classification of Tumours. Editorial Board, editors. WHO Classification of Breast Tumours. 5th ed. Lyon: International Agency for Research on Cancer (IARC); 2019. p. 104.
423. Fisher ER, Gregorio RM, Fisher B, Redmond C, Vellios F, Sommers SC. The pathology of invasive breast cancer. A syllabus derived from findings of the National Surgical Adjuvant Breast Project (protocol no. 4). Cancer. 1975;36(1):1–85.
424. Rapin V, Contesso G, Mouriesse H, Bertin F, Lacombe MJ, Piekarski JD, et al. Medullary breast carcinoma. A reevaluation of 95 cases of breast cancer with inflammatory stroma. Cancer. 1988;61(12):2503–10.
425. Huober J, Gelber S, Goldhirsch A, Coates AS, Viale G, Ohlschlegel C, et al. Prognosis of medullary breast cancer: analysis of 13 International Breast Cancer Study Group (IBCSG) trials. Ann Oncol. 2012;23(11):2843–51.
426. Richardson WW. Medullary carcinoma of the breast; a distinctive tumour type with a relatively good prognosis following radical mastectomy. Br J Cancer. 1956;10(3):415–23.
427. Bloom HJ, Richardson WW, Field JR. Host resistance and survival in carcinoma of breast: a study of 104 cases of medullary carcinoma in a series of 1,411 cases of breast cancer followed for 20 years. Br Med J. 1970;3(5716):181–8.
428. Pedersen L, Holck S, Schiodt T, Zedeler K, Mouridsen HT. Medullary carcinoma of the breast, prognostic importance of characteristic histopathological features evaluated in a multivariate Cox analysis. Eur J Cancer. 1994;30A(12):1792–7.
429. Maier WP, Rosemond GP, Goldman LI, Kaplan GF, Tyson RR. A ten year study of medullary carcinoma of the breast. Surg Gynecol Obstet. 1977;144(5):695–8.
430. Li CI, Uribe DJ, Daling JR. Clinical characteristics of different histologic types of breast cancer. Br J Cancer. 2005;93(9):1046–52.
431. Vu-Nishino H, Tavassoli FA, Ahrens WA, Haffty BG. Clinicopathologic features and long-term outcome of patients with medullary breast carcinoma managed with breast-conserving therapy (BCT). Int J Radiat Oncol Biol Phys. 2005;62(4):1040–7.
432. Rubens JR, Lewandrowski KB, Kopans DB, Koerner FC, Hall DA, McCarthy KA. Medullary carcinoma of the breast. Overdiagnosis of a prognostically favorable neoplasm. Arch Surg. 1990;125(5):601–4.
433. Neuman ML, Homer MJ. Association of medullary carcinoma with reactive axillary adenopathy. AJR Am J Roentgenol. 1996;167(1):185–6.
434. Kleer CG. Carcinoma of the breast with medullary-like features: diagnostic challenges and relationship with BRCA1 and EZH2 functions. Arch Pathol Lab Med. 2009;133(11):1822–5.
435. Meyer JE, Amin E, Lindfors KK, Lipman JC, Stomper PC, Genest D. Medullary carcinoma of the breast: mammographic and US appearance. Radiology. 1989;170(1 Pt 1):79–82.
436. Jeong SJ, Lim HS, Lee JS, Park MH, Yoon JH, Park JG, et al. Medullary carcinoma of the breast: MRI findings. AJR Am J Roentgenol. 2012;198(5):W482–7.
437. Yoo JL, Woo OH, Kim YK, Cho KR, Yong HS, Seo BK, et al. Can MR Imaging contribute in characterizing well-circumscribed breast carcinomas? Radiographics. 2010;30(6):1689–702.
438. Reinfuss M, Stelmach A, Mitus J, Rys J, Duda K. Typical medullary carcinoma of the breast: a clinical and pathological analysis of 52 cases. J Surg Oncol. 1995;60(2):89–94.
439. Marginean F, Rakha EA, Ho BC, Ellis IO, Lee AH. Histological features of medullary carcinoma and prognosis in triple-negative basal-like carcinomas of the breast. Mod Pathol. 2010;23(10):1357–63.
440. Salgado R, Denkert C, Demaria S, Sirtaine N, Klauschen F, Pruneri G, et al. The evaluation of tumor-infiltrating lymphocytes (TILs) in breast cancer: recommendations by an International TILs Working Group 2014. Ann Oncol. 2015;26(2):259–71.
441. Rosen PP, Lesser ML, Kinne DW. Breast carcinoma at the extremes of age: a comparison of patients younger than 35 years and older than 75 years. J Surg Oncol. 1985;28(2):90–6.
442. Rodriguez-Pinilla SM, Rodriguez-Gil Y, Moreno-Bueno G, Sarrio D, Martin-Guijarro Mdel C, Hernandez L, et al. Sporadic invasive breast carcinomas with medullary features display a basal-like phenotype: an immunohistochemical and gene amplification study. Am J Surg Pathol. 2007;31(4):501–8.
443. Vincent-Salomon A, Gruel N, Lucchesi C, MacGrogan G, Dendale R, Sigal-Zafrani B, et al. Identification of typical medullary breast carcinoma as a genomic sub-group of basal-like carcinomas, a heterogeneous new molecular entity. Breast Cancer Res. 2007;9(2):R24.
444. Chu Z, Lin H, Liang X, Huang R, Zhan Q, Jiang J, et al. Clinicopathologic characteristics of typical medullary breast carcinoma: a retrospective study of 117 cases. PLoS One. 2014;9(11):e111493.
445. Reiner A, Reiner G, Spona J, Schemper M, Holzner JH. Histopathologic characterization of human breast cancer in correlation with estrogen receptor status. A comparison of immunocytochemical and biochemical analysis. Cancer. 1988;61(6):1149–54.
446. Stierer M, Rosen H, Weber R, Hanak H, Spona J, Tuchler H. Immunohistochemical and biochemical measurement of estrogen and progesterone receptors in primary breast cancer. Correlation of histopathology and prognostic factors. Ann Surg. 1993;218(1):13–21.
447. Flucke U, Flucke MT, Hoy L, Breuer E, Goebbels R, Rhiem K, et al. Distinguishing medullary carcinoma of the breast from high-grade hormone receptor-negative invasive ductal carcinoma: an immunohistochemical approach. Histopathology. 2010;56(7):852–9.
448. Soomro S, Shousha S, Taylor P, Shepard HM, Feldmann M. c-erbB-2 expression in different histological types of invasive breast carcinoma. J Clin Pathol. 1991;44(3):211–4.
449. Somerville JE, Clarke LA, Biggart JD. c-erbB-2 overexpression and histological type of in situ and invasive breast carcinoma. J Clin Pathol. 1992;45(1):16–20.
450. Tot T. The cytokeratin profile of medullary carcinoma of the breast. Histopathology. 2000;37(2):175–81.
451. Larsimont D, Lespagnard L, Degeyter M, Heimann R. Medullary carcinoma of the breast: a tumour lacking keratin 19. Histopathology. 1994;24(6):549–52.
452. Kajiwara M, Toyoshima S, Yao T, Tanaka M, Tsuneyoshi M. Apoptosis and cell proliferation in medullary carcinoma of the breast: a comparative study between medullary and non-medullary carcinoma using the TUNEL method and immunohistochemistry. J Surg Oncol. 1999;70(4):209–16.
453. Domagala W, Harezga B, Szadowska A, Markiewski M, Weber K, Osborn M. Nuclear p53 protein accumulates preferentially in medullary and high-grade ductal but rarely in lobular breast carcinomas. Am J Pathol. 1993;142(3):669–74.
454. Guo X, Fan Y, Lang R, Gu F, Chen L, Cui L, et al. Tumor infiltrating lymphocytes differ in invasive micropapillary carcinoma and medullary carcinoma of breast. Mod Pathol. 2008;21(9):1101–7.

455. Kuroda H, Tamaru J, Sakamoto G, Ohnisi K, Itoyama S. Immunophenotype of lymphocytic infiltration in medullary carcinoma of the breast. Virchows Arch. 2005;446(1):10–4.
456. Yakirevich E, Izhak OB, Rennert G, Kovacs ZG, Resnick MB. Cytotoxic phenotype of tumor infiltrating lymphocytes in medullary carcinoma of the breast. Mod Pathol. 1999;12(11):1050–6.
457. Carter JM, Polley MC, Leon-Ferre RA, Sinnwell J, Thompson KJ, Wang X, et al. Characteristics and spatially-defined immune (micro)landscapes of early-stage PD-L1-positive triple-negative breast cancer. Clin Cancer Res. 2021;27(20):5628–37.
458. Dadmanesh F, Peterse JL, Sapino A, Fonelli A, Eusebi V. Lymphoepithelioma-like carcinoma of the breast: lack of evidence of Epstein-Barr virus infection. Histopathology. 2001;38(1):54–61.
459. Lespagnard L, Cochaux P, Larsimont D, Degeyter M, Velu T, Heimann R. Absence of Epstein-Barr virus in medullary carcinoma of the breast as demonstrated by immunophenotyping, in situ hybridization and polymerase chain reaction. Am J Clin Pathol. 1995;103(4):449–52.
460. Lakhani SR, Gusterson BA, Jacquemier J, Sloane JP, Anderson TJ, van de Vijver MJ, et al. The pathology of familial breast cancer: histological features of cancers in families not attributable to mutations in BRCA1 or BRCA2. Clin Cancer Res. 2000;6(3):782–9.
461. Shousha S. Medullary carcinoma of the breast and BRCA1 mutation. Histopathology. 2000;37(2):182–5.
462. Eisinger F, Jacquemier J, Charpin C, Stoppa-Lyonnet D, Bressac-de Paillerets B, Peyrat JP, et al. Mutations at BRCA1: the medullary breast carcinoma revisited. Cancer Res. 1998;58(8):1588–92.
463. Marcus JN, Watson P, Page DL, Narod SA, Lenoir GM, Tonin P, et al. Hereditary breast cancer: pathobiology, prognosis, and BRCA1 and BRCA2 gene linkage. Cancer. 1996;77(4):697–709.
464. Marcus JN, Watson P, Page DL, Narod SA, Tonin P, Lenoir GM, et al. BRCA2 hereditary breast cancer pathophenotype. Breast Cancer Res Treat. 1997;44(3):275–7.
465. Lakhani SR, Jacquemier J, Sloane JP, Gusterson BA, Anderson TJ, van de Vijver MJ, et al. Multifactorial analysis of differences between sporadic breast cancers and cancers involving BRCA1 and BRCA2 mutations. J Natl Cancer Inst. 1998;90(15):1138–45.
466. Breast Cancer Linkage Consortium. Pathology of familial breast cancer: differences between breast cancers in carriers of BRCA1 or BRCA2 mutations and sporadic cases. Lancet. 1997;349(9064):1505–10.
467. Esteller M, Silva JM, Dominguez G, Bonilla F, Matias-Guiu X, Lerma E, et al. Promoter hypermethylation and BRCA1 inactivation in sporadic breast and ovarian tumors. J Natl Cancer Inst. 2000;92(7):564–9.
468. Bertucci F, Finetti P, Cervera N, Charafe-Jauffret E, Mamessier E, Adelaide J, et al. Gene expression profiling shows medullary breast cancer is a subgroup of basal breast cancers. Cancer Res. 2006;66(9):4636–44.
469. Romero P, Benhamo V, Deniziaut G, Fuhrmann L, Berger F, Manie E, et al. Medullary breast carcinoma, a triple-negative breast cancer associated with BCLG overexpression. Am J Pathol. 2018;188(10):2378–91.
470. Teschendorff AE, Miremadi A, Pinder SE, Ellis IO, Caldas C. An immune response gene expression module identifies a good prognosis subtype in estrogen receptor negative breast cancer. Genome Biol. 2007;8(8):R157.
471. Fisher ER, Kenny JP, Sass R, Dimitrov NV, Siderits RH, Fisher B. Medullary cancer of the breast revisited. Breast Cancer Res Treat. 1990;16(3):215–29.
472. Rakha EA, Aleskandarany M, El-Sayed ME, Blamey RW, Elston CW, Ellis IO, et al. The prognostic significance of inflammation and medullary histological type in invasive carcinoma of the breast. Eur J Cancer. 2009;45(10):1780–7.
473. Leon-Ferre RA, Polley MY, Liu H, Gilbert JA, Cafourek V, Hillman DW, et al. Impact of histopathology, tumor-infiltrating lymphocytes, and adjuvant chemotherapy on prognosis of triple-negative breast cancer. Breast Cancer Res Treat. 2018;167(1):89–99.
474. Sabatier R, Finetti P, Cervera N, Lambaudie E, Esterni B, Mamessier E, et al. A gene expression signature identifies two prognostic subgroups of basal breast cancer. Breast Cancer Res Treat. 2011;126(2):407–20.
475. Weiss MC, Fowble BL, Solin LJ, Yeh IT, Schultz DJ. Outcome of conservative therapy for invasive breast cancer by histologic subtype. Int J Radiat Oncol Biol Phys. 1992;23(5):941–7.
476. Kurtz JM, Amalric R, Brandone H, Ayme Y, Jacquemier J, Pietra JC, et al. Local recurrence after breast-conserving surgery and radiotherapy. Frequency, time course, and prognosis. Cancer. 1989;63(10):1912–7.

13

Special Histologic Types and Special Morphologic Patterns of Invasive Ductal Carcinoma of No Special Type: Mucinous, Micropapillary, Mucinous Cystadenocarcinoma, Neuroendocrine Neoplasm, Cystic Hypersecretory, Glycogen-Rich Clear Cell, Carcinoma with Osteoclast-Like Giant Cells

Yun Wu, Sandra J. Shin, and Aysegul A. Sahin

Mucinous Carcinoma

Overview

Mucinous carcinoma, also known as "colloid carcinoma," is a special histologic type of breast cancer, which accounts for approximately 2% of all breast cancers [1]. By definition, greater than 90% of tumor cells must be present within mucinous stroma. Many other types of breast carcinoma can show focal mucin production, and those tumors where <90% of the tumor is mucinous should be classified as "mixed tumors with a mucinous carcinoma component" or as "invasive carcinomas with focal mucinous features."

Pure mucinous carcinoma typically occurs in older patients [2, 3] with a median age at diagnosis of 71 years (mean: 68 years, range: 25–85 years) as compared to those with invasive ductal carcinoma of no special type (NST) (median and mean age: 61 years) [2, 3]. Approximately one-third of patients with mucinous carcinoma present with a palpable breast mass, while the remaining two-thirds are detected by screening mammography or sonography.

Pure mucinous carcinoma is associated with a favorable clinical outcome, as well as favorable pathologic features, including smaller tumor size, lower frequency of regional lymph node involvement, and high probability of hormone receptor positivity [2, 3].

Y. Wu (✉) · A. A. Sahin
Department of Pathology, The University of Texas MD Anderson Cancer Center, Houston, TX, USA
e-mail: yunwu@mdanderson.org; asahin@mdanderson.org

S. J. Shin
Department of Pathology and Laboratory Medicine, Albany Medical College, Albany, NY, USA
e-mail: shins1@amc.edu

Invasive mucinous micropapillary carcinoma is a variant that has distinct histomorphology and clinical behavior apart from pure invasive mucinous carcinoma. While it should still be classified fundamentally as a mucinous carcinoma, this variant is important to recognize as it has been found to be biologically more aggressive than pure mucinous carcinoma. Since it was first described in 2002, there have been increasing reports of this variant in the literature [4–12].

Invasive mucinous micropapillary carcinoma tends to occur in younger patients with a median age range of 44–55 years [4, 7–12]. These tumors typically show higher tumor grade and Ki-67 proliferation rate and more frequent human epidermal growth factor 2 (HER2) overexpression and are associated with higher incidences of lymphovascular invasion and axillary lymph node metastasis. Consequently, affected patients experience a more aggressive clinical course and adverse outcome as compared to those with conventional mucinous carcinomas [8–12].

Gross and Radiologic Features

Grossly, the tumors are typically lobulated and well circumscribed with soft gelatinous/glistening cut surfaces. More than 95% of tumors are less than 5 cm with a mean size of 1.5–2.0 cm [2, 3].

Mammography often shows a well-circumscribed lesion [13, 14], and by sonography, these lesions are hypoechoic or isoechoic [14]. Due to their innocuous appearing features by imaging, a significant number are misinterpreted as benign, resulting in delayed diagnosis [15].

© The Author(s), under exclusive license to Springer Nature Switzerland AG 2022

S. J. Shin et al. (eds.), *A Comprehensive Guide to Core Needle Biopsies of the Breast*,
https://doi.org/10.1007/978-3-031-05532-4_13

Microscopic Features

Microscopically, mucinous carcinoma is characterized by islands of tumor cells suspended in extracellular mucin pools. The tumor cells are arranged in nested, trabecular, tubular, papillary, or micropapillary configurations and exhibit low-to-intermediate nuclear grade. Delicate fibrous septa with vascular proliferation are identified within mucin pools.

As previously mentioned, pure mucinous carcinoma is defined as a tumor where >90% of the neoplastic cells are immersed in mucin pools, and consequently, such a diagnosis cannot be rendered in core needle biopsy (CNB) material since the tumor has only been representatively sampled. A diagnosis of "invasive mammary (or ductal) carcinoma with prominent mucinous features" with a note stating that final classification would be performed after the evaluation of the entire tumor in the forthcoming surgical excision specimen would be appropriate to state in the core biopsy report. When examining the excisional biopsy specimen, if the non-mucinous component is present in >10% of the tumor, the tumor should be classified as "mixed mucinous carcinoma."

Traditionally, mucinous carcinomas have been further categorized into two types: type A, hypocellular, and type B, hypercellular (Figs. 13.1 and 13.2) [1]. Type A tumors often have mucin content of 60–90%, with predominantly trabecu-

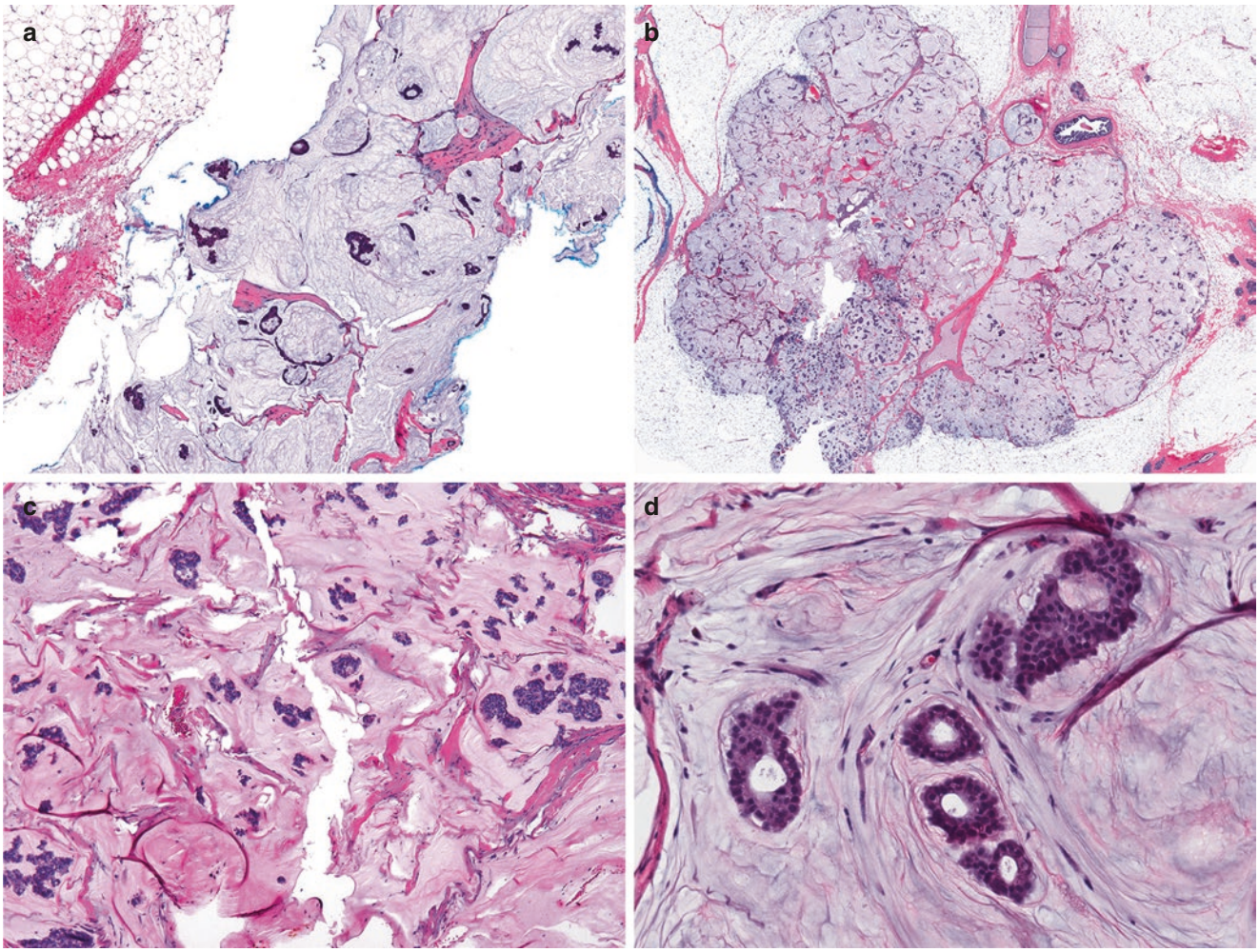

Fig. 13.1 Type A, hypocellular mucinous carcinoma. (**a**) CNB shows cords, glands, and small nests of tumor cells suspended in a pool of mucin. (**b**) Specimen from surgical resection demonstrates that >90% of the tumor cells are confined within a pool of mucin. (**c**) Medium-power view demonstrates that the mucin pool is supported by fibrous septa with vascular proliferation. (**d**) The neoplastic cells are uniform and low grade

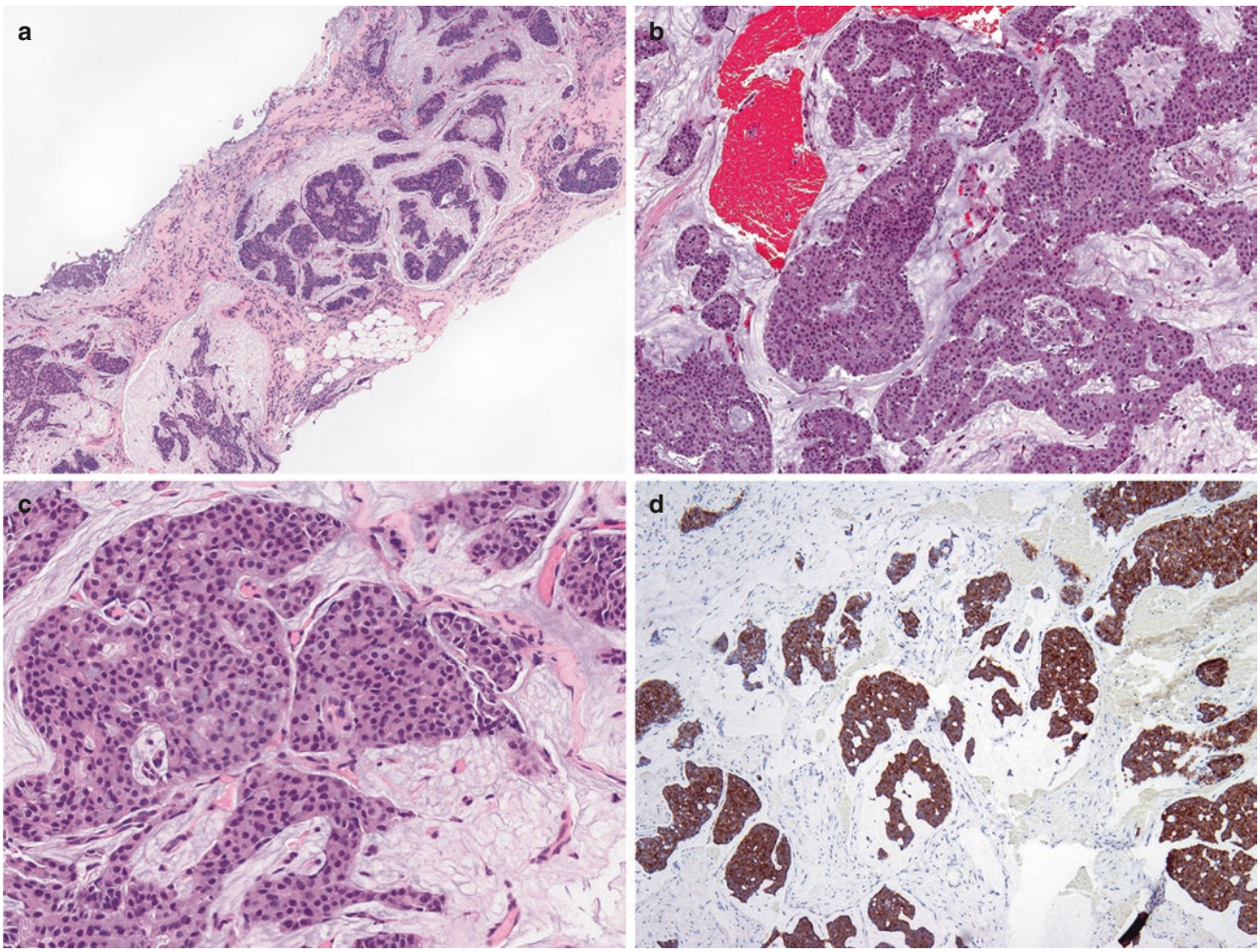

Fig. 13.2 Type B, hypercellular mucinous carcinoma. (**a**) CNB shows large nests and cores of tumor cells suspended in a mucin pool. (**b**) The tumor cells are uniform and low grade. (**c**) Another case of hypercellular mucinous carcinoma shows solid papillary configuration (**d**) with diffuse neuroendocrine differentiation, demonstrated by positive immunoreactivity for synaptophysin

lar and glandular cellular arrangement, while type B tumors often have mucin content <50%, and tumor cells often form nests or sheets. Type B tumors can sometimes show focal solid papillary architecture and may be associated with neuroendocrine differentiation (Fig. 13.2d). In routine practice, further classification as type A or type B mucinous carcinoma is not included in pathology reports. But a recent molecular study showed that these two types of tumor have distinct molecular profiles [16]. The clinicopathologic differences between these two types of tumor have not yet been investigated; additional studies are warranted.

Even in core biopsy samples, it is important to recognize whether the tumor may represent the invasive mucinous micropapillary carcinoma variant (Fig. 13.3). Like its conventional counterpart, >90% of the mucinous micropapillary carcinoma is mucinous, but tumor cells suspended in mucin pools additionally show a predominantly micropapillary configuration with pseudoacinar formation. The solid sheets, cribriform, trabecular, or ribbonlike arrangements that are frequently seen in conventional type are not formations seen in mucinous micropapillary carcinoma and, if identified, should exclude the possibility of this variant.

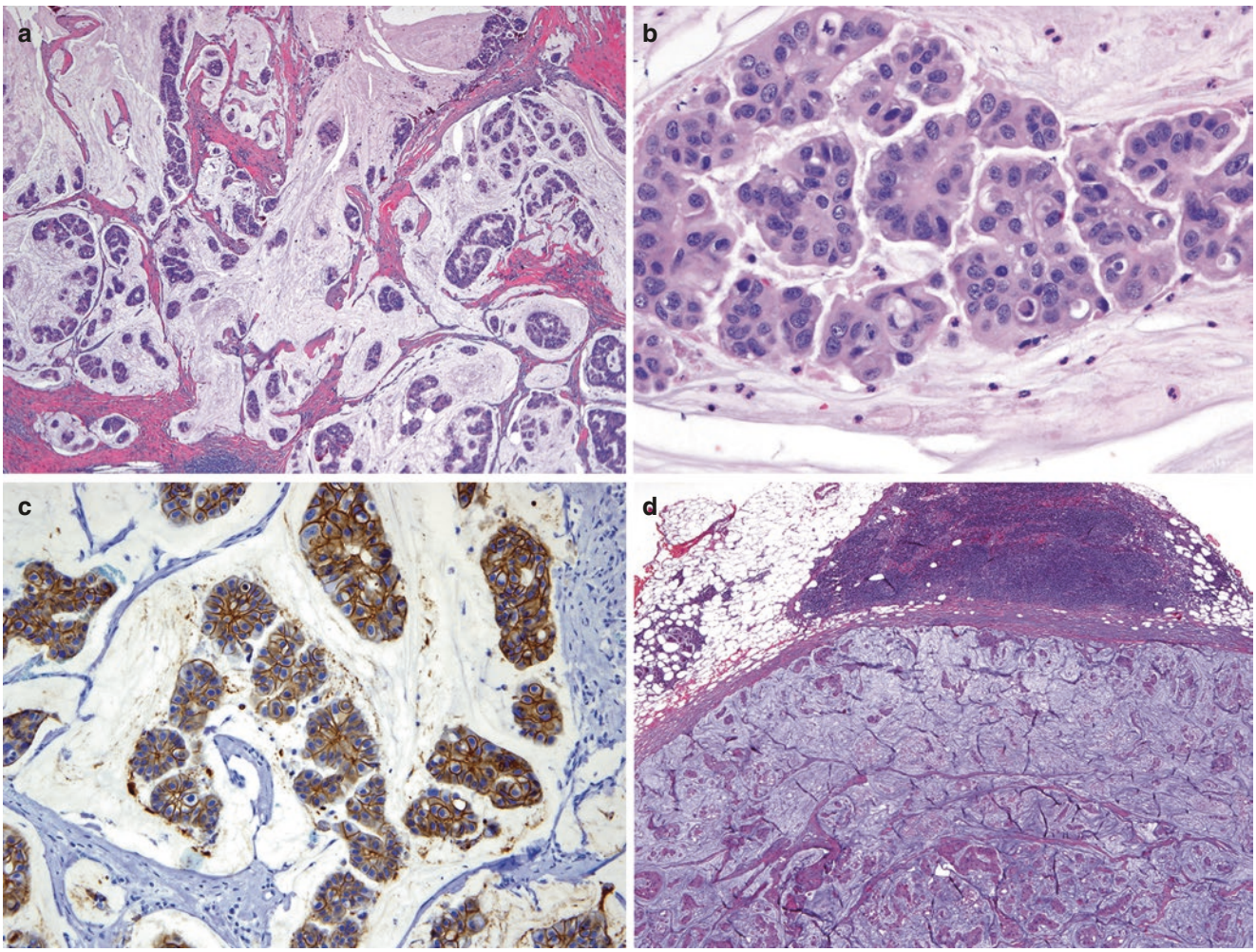

Fig. 13.3 Invasive mucinous micropapillary carcinoma. (**a**, **b**) The neoplastic cells in the mucin pool demonstrate micropapillary configuration, and the neoplastic cells are intermediate to high grade. (**c**) Twenty percent of mucinous micropapillary carcinomas are positive for HER2/neu overexpression as shown in this case. (**d**) Up to one-third of these cases have regional lymph node metastasis as shown in this case

Differential Diagnosis

The most important considerations in the differential diagnosis for mucinous carcinoma are other mucinous lesions of the breast and metastatic mucinous tumors from extramammary sites. Among the former group, mucocele-like lesion (MLL) is the most frequently encountered mucinous lesion in CNBs. MLLs are mucin-filled dilated ducts with or without concomitant rupture and mucin extravasation into the surrounding stroma. MLLs are usually small in size (0.1–0.6 cm) [17]. More than 90% of cases are the target of CNB due to their association with mammographically evident microcalcifications. The remainder of cases form a mass lesion that can be detected by sonogram [17]. Depending on the type of epithelial cells lining the dilated ducts, MLLs can be benign or contain atypical ductal hyperplasia (ADH) or ductal carcinoma in situ (DCIS). A recent study showed that more than half of MLLs are benign (57%), 33% are associated with ADH and the remaining 10% with DCIS [18].

Benign MLLs are comprised of dilated ducts lined by uniform cuboidal or columnar cells with or without concomitant extravasated acellular mucin. Occasionally, usual ductal hyperplasia may be present. A diagnostic pitfall is the occasional instance of benign epithelium detaching and shedding into luminal mucin, and thus mimicking invasive mucinous carcinoma (Fig. 13.4a). In these cases, it is important to see that the contour of the mucin pool is usually rounded and similarly shaped to the adjacent intact dilated ducts. Also, despite being detached from the duct wall, benign epithelium remains as strips with myoepithe-

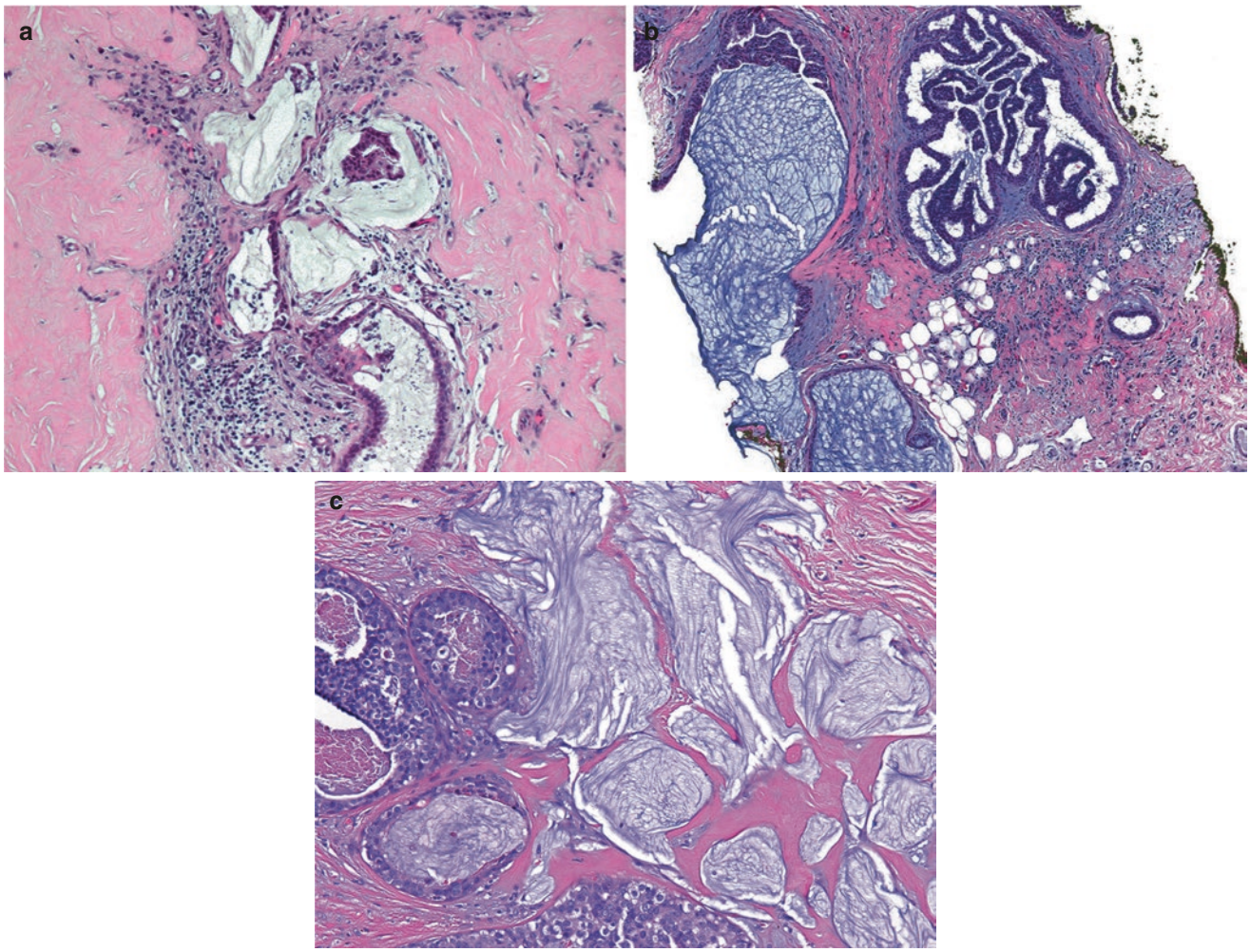

Fig. 13.4 Mucocele-like lesions. (**a**) A cluster of detached epithelial cells floated in the extravasated mucin, mimicking invasive mucinous carcinoma. However, the cell cluster contains mixed epithelial and myoepithelial cells (highlighted by myoepithelial staining, not shown). MLL may also be associated with (**b**) ADH and (**c**) DCIS. Both lesions have extravasated mucin into adjacent stroma. Deeper levels are warranted in these cases to rule out the presence of invasive carcinoma

lial cells as seen in normal duct-lining epithelium. In challenging cases, the presence of myoepithelial cells can be demonstrated using myoepithelial immunostains. In contrast, floating tumor cells of invasive mucinous carcinoma form clusters and lack myoepithelial cells. Additionally, vascular proliferations within the delicate septa of the mucin pools are usually prominent in mucinous carcinoma and not present in MLLs, as angiogenesis is the hallmark of cancer. When MLL is associated with ADH or DCIS, the epithelial lining contains monotonous cells with regular spacing and distinct cell borders, forming cribriform or micropapillary architecture (Fig. 13.4b, c).

Mucinous carcinomas of other organs, such as colorectum, lung, or gynecologic tract, metastatic to breast have been rarely encountered (Fig. 13.5). A good clinical history is helpful in the differentiation of metastatic mucinous carcinoma from primary mucinous carcinoma. Histologically, primary mucinous carcinoma of the breast has relatively low histologic grade. Immunohistochemical stains are positive for hormone receptors in most primary breast tumors as compared to metastatic mucinous carcinomas. Tissue-specific markers such as GATA3, TTF1, CDX2, and PAX8 are useful for identifying tumor origin. WT1 staining is not useful in the differential diagnosis, as it can be positive in mucinous carcinoma of the breast.

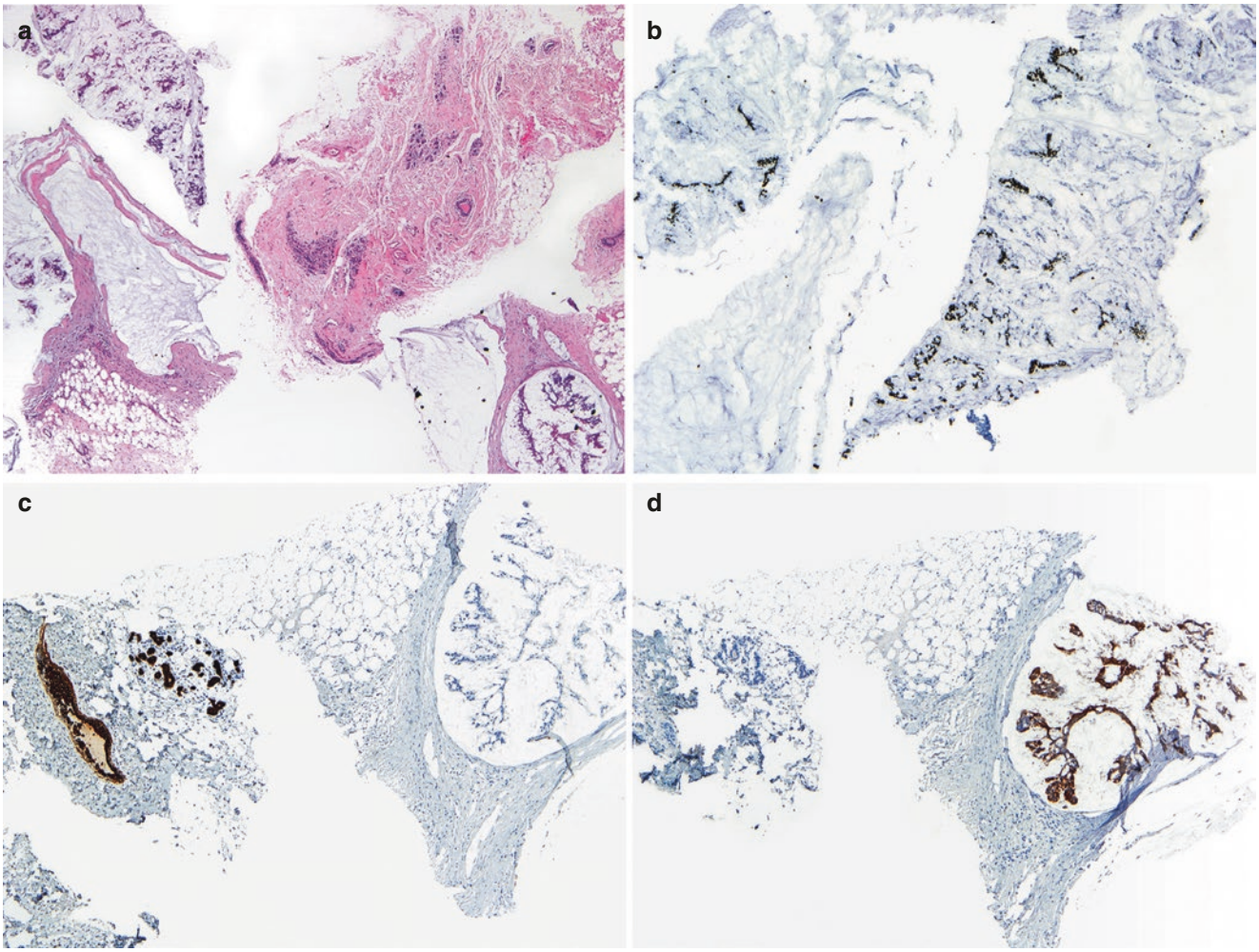

Fig. 13.5 Mucinous carcinoma from colorectal origin metastatic to the breast. (**a**) CNB demonstrates mixed mucinous carcinoma and normal breast tissue. The tumor cells are negative for hormone receptors, raising suspicion for metastatic carcinoma. Further workup demonstrates that the tumor cells are positive for (**b**) CDX2 and (**d**) CK20 and negative for (**c**) CK7; in contrast, the normal breast tissue is positive for CK7 and negative for CK20. The history of rectal mucinous carcinoma also supports the above diagnosis

Immunohistochemical Workup

More than 90% of mucinous carcinomas are estrogen receptor (ER) positive, and about 70–80% of them are progesterone receptor (PR) positive [2, 3]. HER2 overexpression or amplification is uncommon in conventional mucinous carcinoma but can be seen in 20–33% of mucinous micropapillary carcinoma [8, 9].

Pathogenesis

The pathogenesis of mucinous carcinoma is still under investigation. Available data show that mucinous carcinoma has a different molecular pathogenesis than invasive ductal carcinoma NST [16, 19]. A low level of genetic instability is identified in these tumors [16]. The gene profile of hypocellular mucinous carcinoma is different from that of the hypercellular type. The genetic profile of hypercellular mucinous carcinoma is similar to that of neuroendocrine carcinoma (NEC), which is consistent with the clinicopathologic finding that some hypercellular mucinous carcinomas show neuroendocrine differentiation [16].

Prognosis

Conventional pure mucinous carcinoma in general is associated with an excellent prognosis [2, 3]. The largest series with more than 11,000 patients showed disease-specific survival of 94% (5 years), 89% (10 years), 85% (15 years), and 81% (20 years) as compared to 82% (5 years), 72% (10 years), 66% (15 years), and 72% (20 years) in patients with invasive ductal carcinoma NST [3]. An earlier study

showed that the 5-year overall survival of patients with mucinous carcinoma was similar to that of the age-matched general population [2]; however, late distant recurrence may occur after 25 years [2]. While rates of regional nodal involvement are low (12–14%) [3, 20], nodal status is the most significant prognostic factor followed by age, tumor size, hormonal receptor status, and nuclear grade [3]. The prognostic significance of neuroendocrine differentiation in mucinous carcinoma remains unclear.

As mentioned previously, mucinous micropapillary carcinoma appears to be a distinct clinicopathologic entity with a more aggressive clinical course [8–12]. Early local recurrence has been reported in affected patients. A recent study with 10-year follow-up showed that patients with invasive mucinous micropapillary carcinoma experienced worse recurrence-free and overall survival than those with stage (II–III)-matched conventional mucinous carcinoma [10]. However, the prognosis of patients with invasive mucinous micropapillary carcinoma is still better than that of patients with invasive micropapillary carcinoma in all stage I–III-matched cases [10]. Therefore, it appears that the prognosis of patients with invasive mucinous micropapillary carcinoma is in between that of those with conventional mucinous carcinoma and invasive micropapillary carcinoma.

Invasive Micropapillary Carcinoma

Overview

Invasive micropapillary carcinoma was first described by Fisher et al. in 1980 [21] and further defined by Petersen [22] and Siriaunkgul and Tavassoli in 1993 [23]. Pure invasive micropapillary carcinoma accounts for <2% of all invasive breast carcinomas. However, about 7% of invasive ductal carcinomas of NST contain a focal micropapillary component [24]. Pure micropapillary carcinoma and mixed micropapillary carcinoma have higher frequencies of lymphovascular invasion and axillary nodal metastasis as compared to invasive mammary carcinoma NST [24].

About half of the patients with invasive micropapillary carcinoma present with a palpable mass. The age at diagnosis is similar to that of patients with invasive mammary carcinoma NST.

Gross and Radiologic Features

Invasive micropapillary carcinomas do not have specific gross or radiographic features. Similar to invasive carcinoma NST, it often presents as an irregular mass with white/tan firm cut surfaces on gross examination. Radiographically, both mammogram and ultrasound display imaging findings that are highly suspicious for malignancy [25, 26]. Mammogram often shows a high-density irregular mass with infiltrating margins and associated microcalcifications. Sonogram similarly shows an irregular hypoechoic mass.

Microscopic Features

Characteristically, the tumor cells are arranged in small nests or glands surrounded by clear stromal spaces. In contrast to true papillary structures, fibrovascular cores are absent within tumor cell nests (Figs. 13.6 and 13.7). The tumor cells have reverse polarity, with the apical aspect of cytoplasmic membrane facing the empty stromal space instead of the luminal space. This histologic feature can be confirmed by

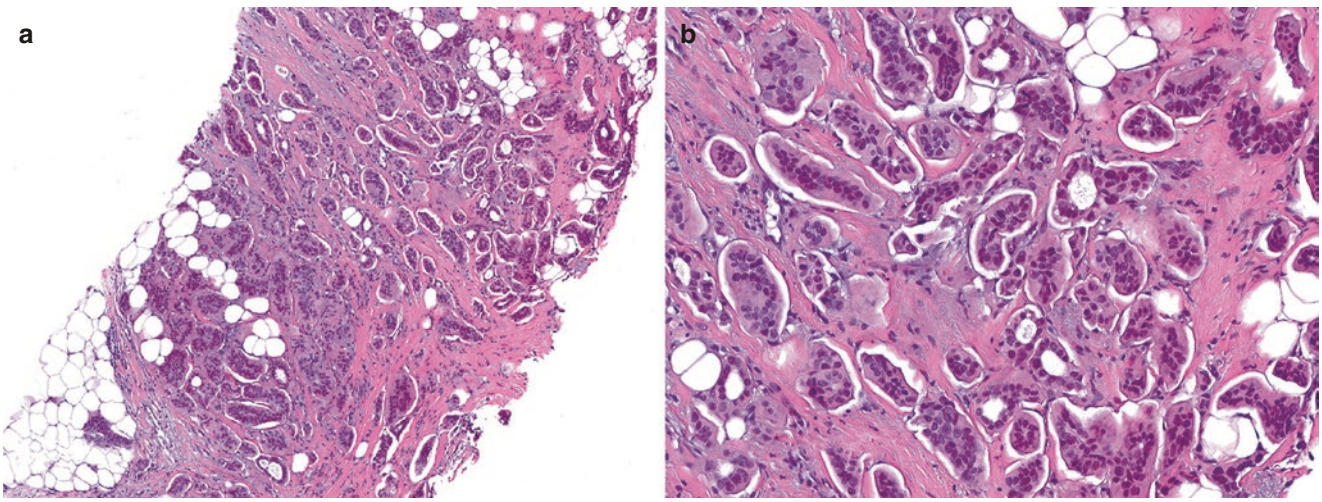

Fig. 13.6 Invasive micropapillary carcinoma. (**a**) CNB reveals small nests and glands of tumor cells with clear spaces around them. (**b**) The tumor cells are low grade in this case

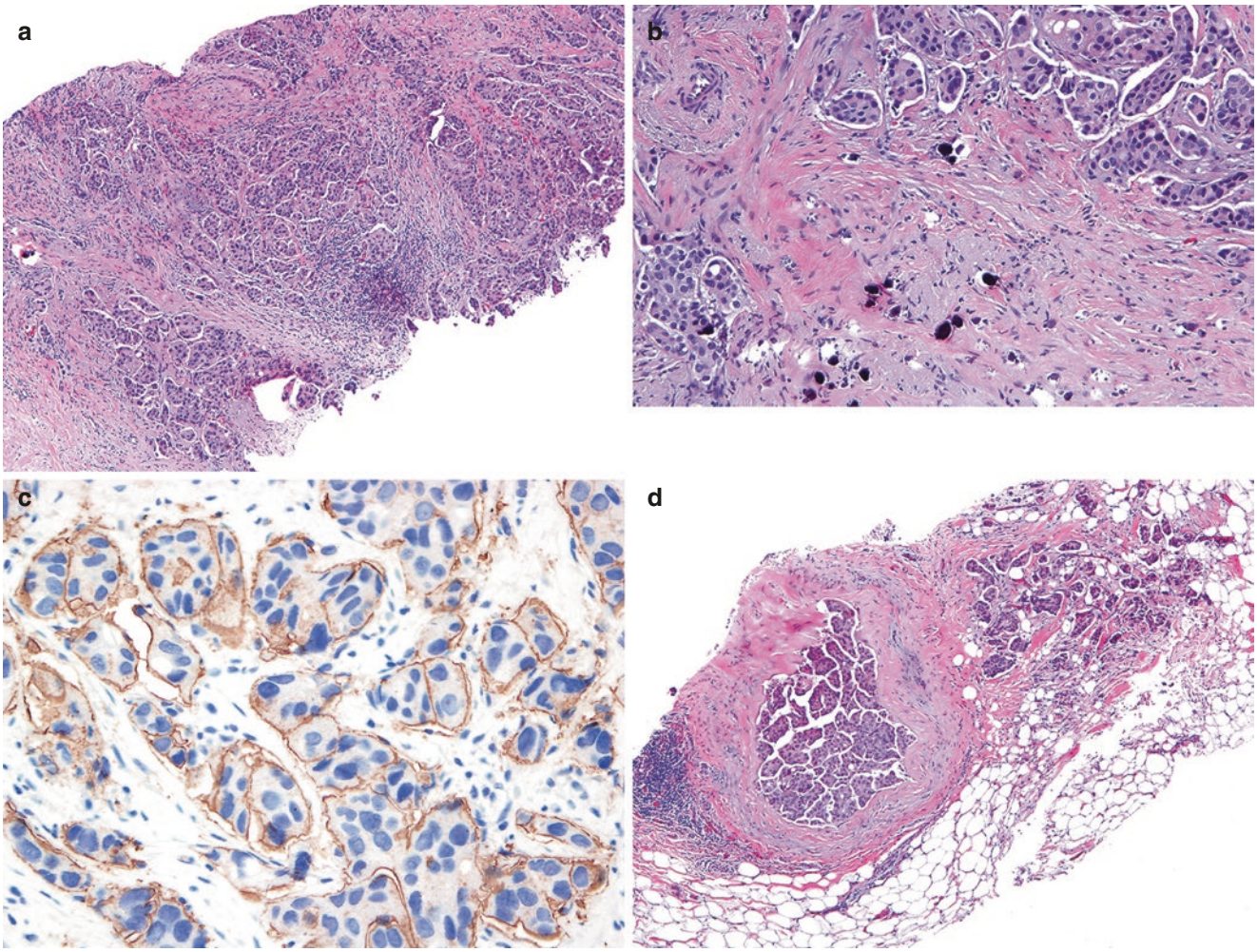

Fig. 13.7 Invasive micropapillary carcinoma with associated psammoma bodies. (**a**, **b**) CNB shows small nests of tumor cells with clear spaces around them. Psammoma bodies are readily identified in the tumor stroma. The tumor cells in this case are moderately differentiated. (**c**) Immunohistochemical staining of EMA highlights the outside cellular membranes of the tumor cell nests, indicating the "inside-out" reverse polarity of the tumor cells. (**d**) Vascular invasion is also identified in the adjacent tissue

MUC1 or epithelial membrane antigen (EMA) immunohistochemical staining (Fig. 13.7c) [27, 28]. The MUC1 and EMA staining highlight the cellular membrane facing the stromal surface in micropapillary carcinoma, while inner/luminal cell surfaces are highlighted in non-micropapillary carcinoma. Only a minority (7%) of invasive ductal carcinomas with no clear-cut micropapillary pattern show the staining pattern seen in micropapillary carcinoma [29]. Psammomatous calcifications are occasionally present (Fig. 13.7a). Invasive micropapillary carcinoma is often of low to intermediate grade, and overt nuclear pleomorphism is rare. Occasionally, invasive micropapillary carcinoma with apocrine features is seen.

The characteristic presence of a clear space around individual tumor cell nests can be difficult to distinguish from true lymphovascular invasion. However, true lymphovascular invasion is more easily identified in the peri-tumoral lymphovascular bundles (Fig. 13.7d).

Differential Diagnosis

Invasive micropapillary carcinoma needs to be distinguished from invasive carcinoma with retraction artifact. Tumor cells with retraction artifact lack the typical reverse polarity of the glands of invasive micropapillary carcinoma, and this can be confirmed by immunohistochemical staining with MUC1 or EMA.

Another important consideration is the possibility of metastatic carcinoma with micropapillary features from other organs, such as the gynecologic tract or lung. Serous carcinoma of the gynecologic tract is one of the most common

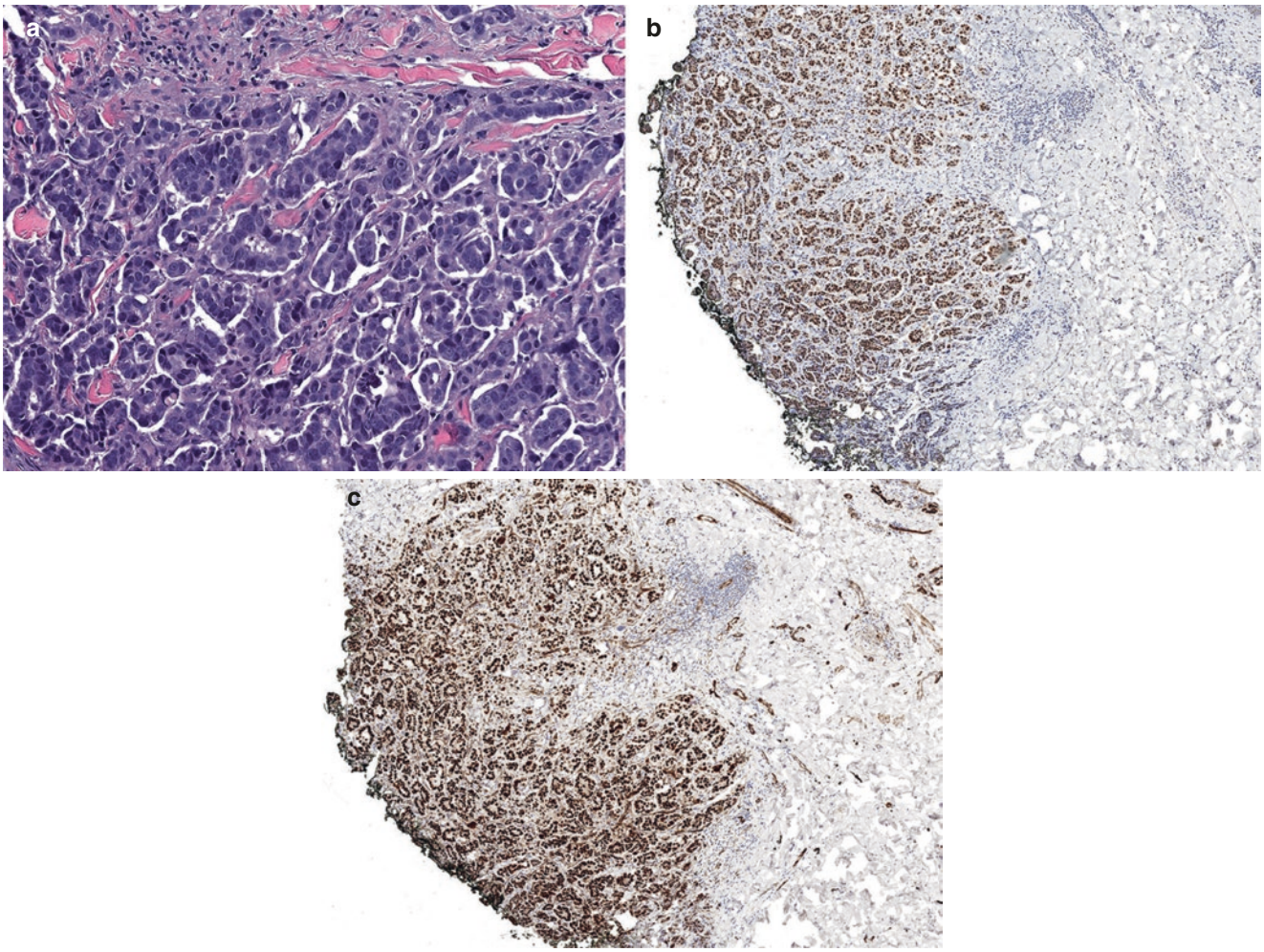

Fig. 13.8 Papillary serous carcinoma metastatic to the breast mimics primary invasive micropapillary carcinoma. (**a**) In this case, patient presented clinically as inflammatory breast cancer with diffuse erythematous skin change. CNB shows the tumor with micropapillary configuration within clear spaces. Prominent lymphovascular invasion is present. Due to prior history of serous carcinoma, immunohistochemical staining of tissue-specific markers was performed, and it revealed that the tumor cells were (**b**) PAX8 positive, (**c**) WT1 positive, and GATA3 negative (not shown), supporting the diagnosis metastatic serous carcinoma

carcinomas metastatic to the breast [30]. Metastatic micropapillary carcinomas from other organs are histologically similar or identical to mammary micropapillary carcinoma, and occasionally they can present clinically as inflammatory breast cancer with extensive dermal lymphatic invasion [31]. Tissue-specific immunohistochemical stains (e.g., TTF1, PAX8, GATA3) and clinical history can be helpful in excluding this possibility (Fig. 13.8).

Immunohistochemical Workup

Most invasive micropapillary carcinomas are ER positive (61–100%) and PR positive (46–83%) [24]. HER2 overexpression is variable and is present in approximately one-third of cases.

MUC-1 or EMA can be used to differentiate true invasive micropapillary carcinoma from retraction artifact, and tissue-specific markers such as GATA3 (breast), TTF1 (lung), PAX8, and WT1 (GYN tract) can be used to differentiate primary versus metastatic carcinoma.

Pathogenesis

The pathogenesis of micropapillary carcinoma is still under investigation. Recent studies show that compared to invasive carcinoma NST, invasive micropapillary carcinoma has a distinct molecular profile including recurrent amplification of the oncogenes *c-MYC*, *CCND1*, and *FGFR1* [32]. In addition, somatic mutations of genes involved in cellular polarity and shape have been identified in pure invasive micropapil-

lary carcinoma, which may contribute to the morphological features of these tumors [33].

Prognosis

Due to the high rate of lymphovascular invasion and regional nodal metastasis, patients with invasive micropapillary carcinoma often present with higher clinical and pathologic stages, and therefore have a relatively poor prognosis [34–36]. The reported 5-year overall survival rate ranges from 59 to 85% [36–38]. The 5-year disease-specific survival rate ranges from 70 to 92% [38, 39]. Nevertheless, when adjusted for stage, patients with micropapillary carcinoma experience similar overall survival as compared to those with invasive mammary carcinoma NST [37].

Similar prognostic factors have been identified in association with invasive micropapillary carcinoma as in invasive mammary carcinoma NST. Age less than 50 years at diagnosis, large tumor size (>2 cm), and negative hormonal receptor status are adverse prognostic factors [38]. Patients with four or more positive regional lymph nodes have a worse prognosis than node-negative patients. However, patients with 1–3 positive lymph nodes have similar disease-specific and overall survival as compared to node-negative patients [38]. It is unclear whether the survival benefits of contemporary chemoradiation therapy in breast cancer patients with low-volume regional nodal disease as seen in the ACOSOG Z0011 trial are also seen in this group of patients [40].

Mucinous Cystadenocarcinoma

Overview

Mucinous cystadenocarcinoma is an exceedingly rare form of breast carcinoma, which was first described in 1998 by Koenig and Tavassoli in their series of four patients [41]. Subsequently, there have been fewer than 30 cases reported in the literature, largely as case reports or small series. Patients are usually postmenopausal and slightly older than those women who develop invasive carcinoma NST [42, 43]. Most recently, the 2019 edition of the WHO Classification of Tumours added this as a special type of breast carcinoma [44].

Gross and Radiologic Features

The typical presentation is that of a solitary breast mass. Grossly, these tumors are described as well-delineated, occasionally lobulated, tumor masses ranging from 0.8 to 19 cm in size [41, 43]. The cut surface is gray-white or tan in color with a cystic and/or mucinous, gelatinous appearance [41, 42]. On mammogram, these tumors are of medium to high density, by ultrasound show mixed hypoechogenicity, or by magnetic resonance imaging show enhancement [45, 46].

Microscopic Features

Histologically, mucinous cystadenocarcinoma consists of closely approximated variably sized cystic spaces lined by neoplastic mucinous epithelial cells, which collectively demonstrate a pushing tumor border. The single layer of epithelium also forms tufts and branching papillae. These cells are cytologically bland with basally located nuclei and abundant intracellular mucin (Fig. 13.9). In some instances, the cells show increasing cytologic atypia and mucin depletion and may rarely demonstrate squamoid features [41, 42]. Luminal mucin has been found extravasated in the adjacent stroma in about one-third of reported cases, however, without floating neoplastic cells [45]. Coexisting invasive carcinomas of NST or mucinous type or with metaplastic features (squamoid, sarcomatous) have been reported [41, 45, 47]. Moreover, concurrent conventional DCIS with intermediate or high nuclear grade or with mucinous features has been reported [45, 47, 48].

Differential Diagnosis

Among other mammary entities, mucinous cystadenocarcinoma should be distinguished from other more common malignancies such as mucinous carcinoma, solid papillary carcinoma with invasion (mucinous carcinoma), and cystic hypersecretory carcinoma. Lobular carcinoma in situ with signet ring cell morphology is a lower priority consideration.

More importantly, exclusion of metastatic carcinoma from the pancreas, appendix, or ovary is paramount. The presence of in situ carcinoma is helpful in excluding metastasis in the differential diagnosis; however, a thorough clinical evaluation and imaging workup should be performed. Immunohistochemical workup is particularly helpful in this regard (see below).

Morphologically, invasive mucinous carcinoma consists of neoplastic epithelial cells floating in pools of extravasated mucin. An important distinction from mucinous cystadenoma is that neoplastic epithelial cells in mucinous carcinoma do not contain abundant intracytoplasmic mucin. A more obvious distinction is that mucinous carcinomas lack a multicystic appearance. In fact, mucinous cystadenocarcinoma is more likely to be mistaken for in situ carcinoma that can accompany invasive mucinous carcinoma exhibiting both intracytoplasmic and luminal, extracellular mucin, however, still lacking a multicystic appearance. Although mucinous cystadenocarcinoma and cystic hypersecretory

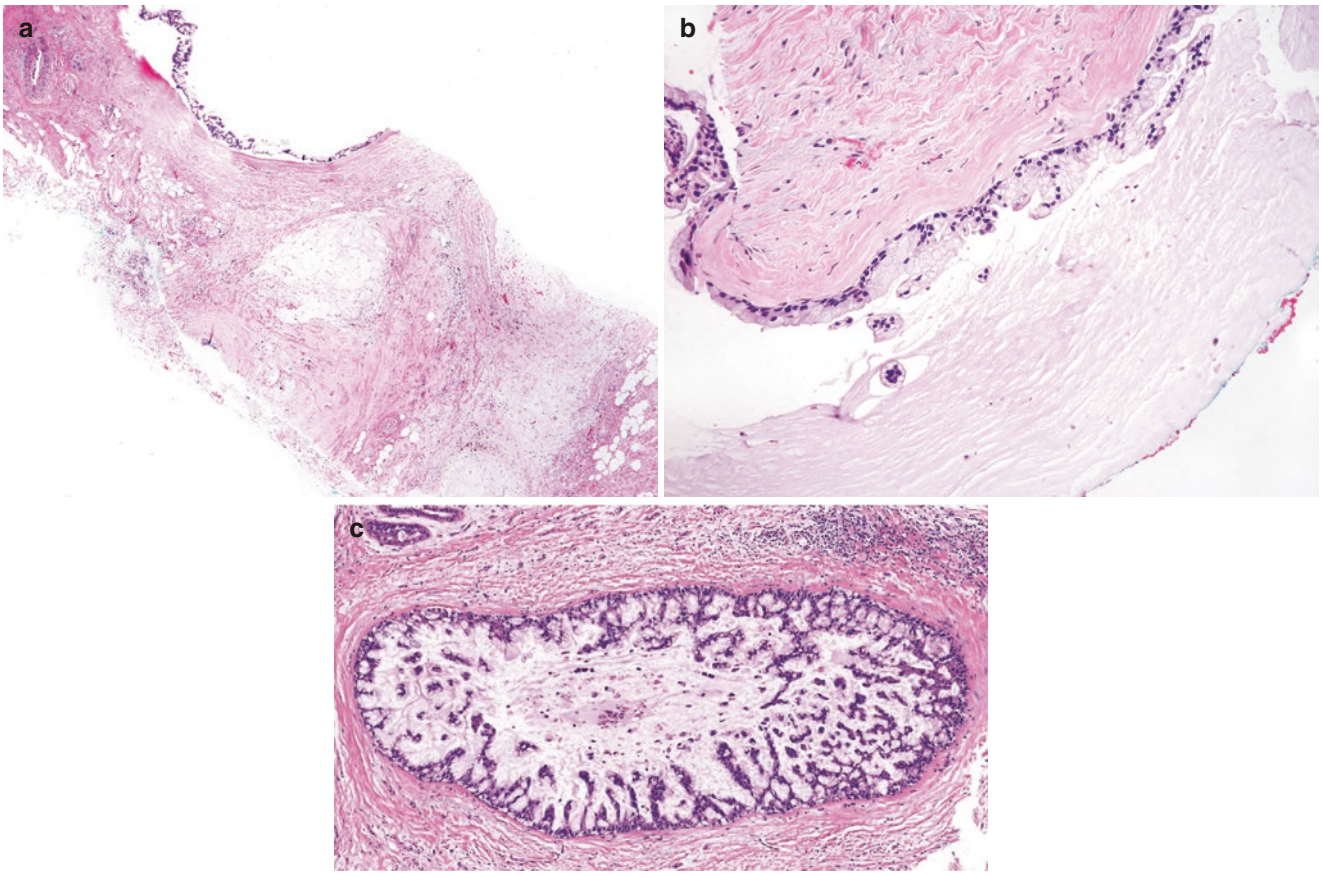

Fig. 13.9 Mucinous cystadenocarcinoma of the breast. (**a**) Low-power magnification of CNB showing a transected cystic space lined by neoplastic mucinous columnar epithelium. (**b**) Higher magnification highlighting neoplastic epithelium with abundant intracellular mucin and basally located nuclei, and abundant luminal mucin. (**c**) Another example of mucinous cystadenocarcinoma with prominent papillae, *courtesy of Dr. Chengqin Wang, Qingdao University Medical College,* with permission

carcinoma share a multicystic appearance at low magnification, the presence of eosinophilic colloid-like luminal secretions and absence of intracellular mucin in the latter are discerning features. Some examples of solid papillary carcinomas produce intracytoplasmic mucin, which can become extracellular and lead to evidence of invasion (mucinous carcinoma). Morphologically, these should be easily distinguishable from mucinous cystadenocarcinoma. See Chap. 6 regarding more information on solid papillary carcinoma with invasion. While there is similarity on the epithelial cellular level, lobular carcinoma in situ with signet ring cell features characteristically obscures the lumens of the terminal duct lobular units in which they occupy.

Immunohistochemical Workup

Mucinous cystadenocarcinomas are triple-negative (ER−/PR−/HER2−) breast carcinomas and typical of invasive carcinomas lack investment by myoepithelial cells as evidenced by absence of staining for myoepithelial markers [41, 45]. Rare HER2+ examples have been reported [49]. Interestingly, Ki-67 proliferation index is notably high in these tumors (20.5–90% in reported cases) despite its characteristically favorable prognosis [45, 49]. Like other breast carcinomas, mucinous cystadenocarcinomas show an immunoprofile of CK7+/CK20−/CDX2−, whereas metastatic mucinous adenocarcinomas from the ovary/pancreas or colon show different immunoprofiles of CK7+/CK20+/CDX2+ and CK7−/CK20+/CDX2+, respectively. It is important to note that markers considered to be breast specific (GATA3, GCDFP-15, mammaglobin) can be negative. In contrast to mucinous cystadenocarcinomas, invasive mucinous carcinomas are typically ER+/PR+ and exhibit a low Ki-67 proliferation index. More recently, investigators have found that these tumors exhibit a MUC5+/MUC2− immunoprofile, which appears to distinguish them from other mucinous-type carcinomas both primary and metastatic to the breast [43, 50]. More studies are needed to validate this potentially unique characteristic of mucinous cystadenocarcinoma.

Pathogenesis

The pathogenesis is currently uncertain, largely due to the inability to study this rare tumor in sufficient numbers. With that said, Nayak et al. surmised that due to the presence of "focal abrupt squamous differentiation" in several cases including their own, as well as other reports of sarcomatous transformation, mucinous cystadenocarcinomas are a result of metaplastic differentiation in the breast [45]. Chen W-Y et al. separately described a transition from conventional DCIS to "mucinous cystadenocarcinoma in situ," suggesting a process of metaplasia [47].

Prognosis

Patients experience a favorable prognosis, and recurrence is infrequent. Most reported patients are alive without evidence of disease; three cases have reportedly died of disease in 14 months to 9 years [48].

Neuroendocrine Neoplasm

Overview

Neuroendocrine neoplasm (NEN) of the breast is an evolving and controversial entity. Its prevalence is reported to be <1% of all breast carcinomas [51]. Nevertheless, the true prevalence is hard to assess as neuroendocrine markers are not routinely evaluated on breast cancers. It was first recognized in 1963 by Feyrter and Hartmann who reported two invasive breast cancers with carcinoid growth pattern [52]. Later, it was described by Cubilla and Woodruff as "carcinoid tumor of the breast" due to its morphological similarity to carcinoid tumors of other organs [53].

In the distant past, a modified silver (Grimelius) stain and electron microscopy were utilized to identify neurosecretory granules [54]. Currently, however, neuroendocrine differentiation is demonstrated by immunohistochemical staining for neuroendocrine-specific markers, such as synaptophysin and chromogranin.

Limited numbers of case reports and case series have been published in the literature using various cutoffs for neuroendocrine differentiation [55–74]. Mammary NEN was first officially adopted into the World Health Organization (WHO) Classification of Tumours in 2003 as "neuroendocrine carcinoma," a subtype of invasive mammary carcinoma bearing histologic features similar to NEN of the lung and gastrointestinal tract, with expression of neuroendocrine markers in >50% of the tumor cells [75].

In the 2012 edition of the WHO Classification of Tumours, the spectrum of mammary NEN was broadened into a category of "carcinoma with neuroendocrine features," which included well-differentiated neuroendocrine tumor, poorly differentiated neuroendocrine carcinoma, and invasive carcinoma with neuroendocrine differentiation [51]. The requirement for >50% tumor cells expressing neuroendocrine markers was not present in the 2012 WHO edition.

Most recently, the 2019 edition of the WHO Classification of Tumours lists "neuroendocrine neoplasm" as a separately defined entity with regard to invasive breast carcinoma NST [76]. This change is based on a recommendation from the expert panel of the International Agency for Research on Cancer that a uniform classification for neuroendocrine neoplasms should be applied to all organ systems, including breast [77]. As a result, the WHO currently defines breast NEN as tumors with >90% neuroendocrine histologic pattern and diffuse (>50%), uniform immunoreactivity for synaptophysin and/or chromogranin. NEN is further subclassified as well-differentiated neuroendocrine tumor (NET) or NEC based on diagnostic criteria similar to those used in the gastrointestinal tract and lung. Special entities including mucinous carcinoma with neuroendocrine differentiation and solid papillary carcinoma are no longer classified as NEN of the breast [76].

A large database study showed that the age of patients with mammary NEN ranged from 26 to 99 years (mean: 64 years), which is slightly older than patients with invasive carcinoma NST (mean: 61 years) [71]. More than 50% of patients presented with palpable masses; however, approximately 25% were asymptomatic and had tumors detected by screening mammography.

Gross and Radiologic Features

Most tumors are lobulated, with white-to-tan cut surfaces similar to invasive carcinoma NST. Some show red-to-brown and slightly soft cut surfaces due to high intratumoral vascularity. Tumor sizes range from <1 to 11 cm (median: 2.5 cm) [71]. Lobulated mass lesions are the most common radiographic findings by mammography and sonography [78].

Microscopic Features

Neuroendocrine neoplasm of the breast shows morphologic features similar to its counterparts in the lung or gastrointestinal tract. Well-differentiated NET often exhibits a nested histologic pattern, which can be dispersed or packed to form large tumor nodules, with sinusoid-like vasculature. The tumor cells can be round, ovoid, plasmacytoid, or spindled. The cytoplasm is typically eosinophilic, granular, or clear [79]. Examples are shown in Figs. 13.10, 13.11, and 13.12. Whereas well-differentiated NETs in the gastrointestinal tract are classified as grades 1, 2, or 3 based on mitotic rate

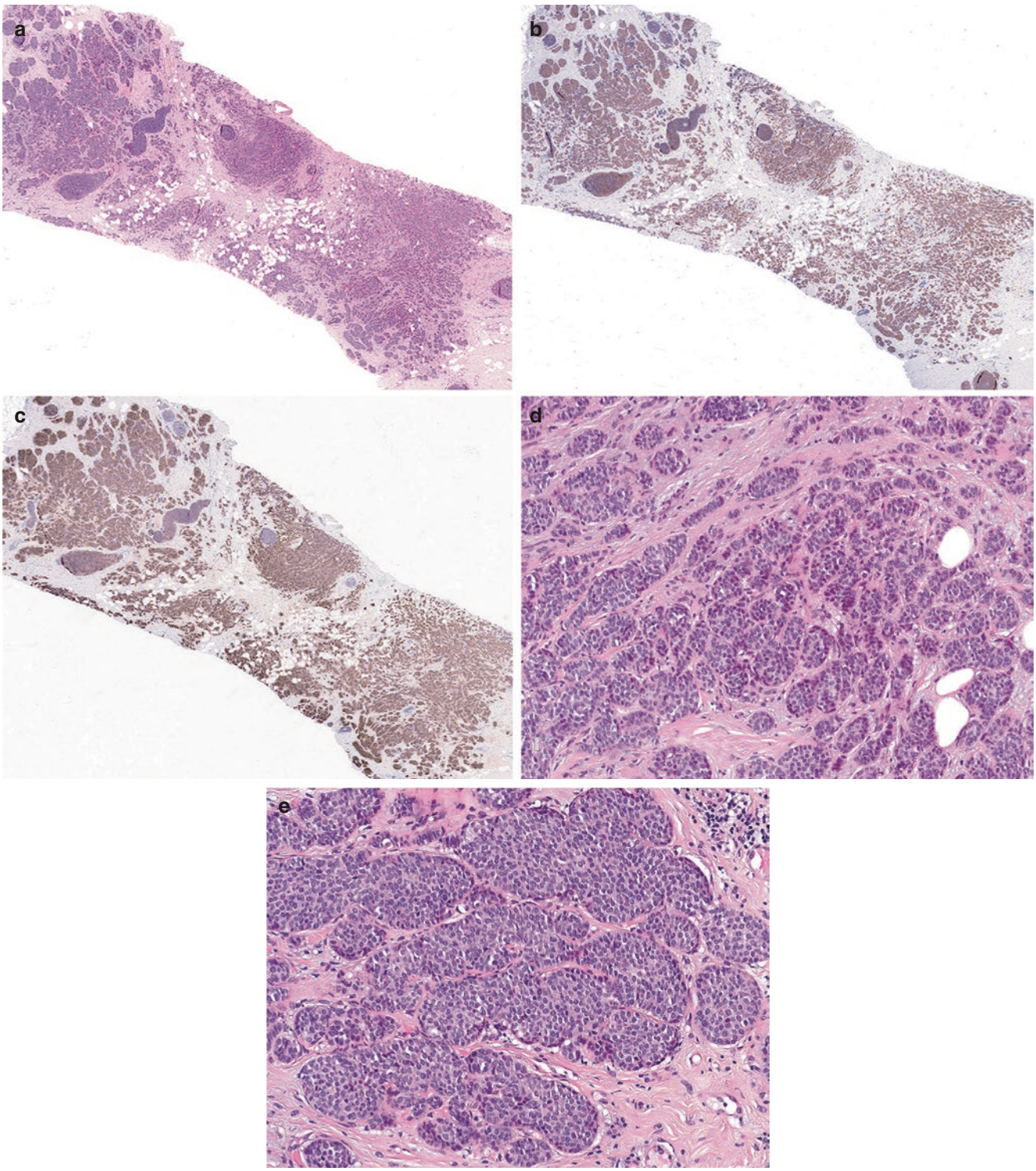

Fig. 13.10 Neuroendocrine tumor with a nested growth pattern. (**a**) Low-power view shows an invasive component with associated carcinoma in situ. Both invasive and in situ tumor cells are diffusely positive for (**b**) synaptophysin and (**c**) chromogranin. (**d**, **e**) Medium- and high-power views show that the tumor cells are uniformly low grade

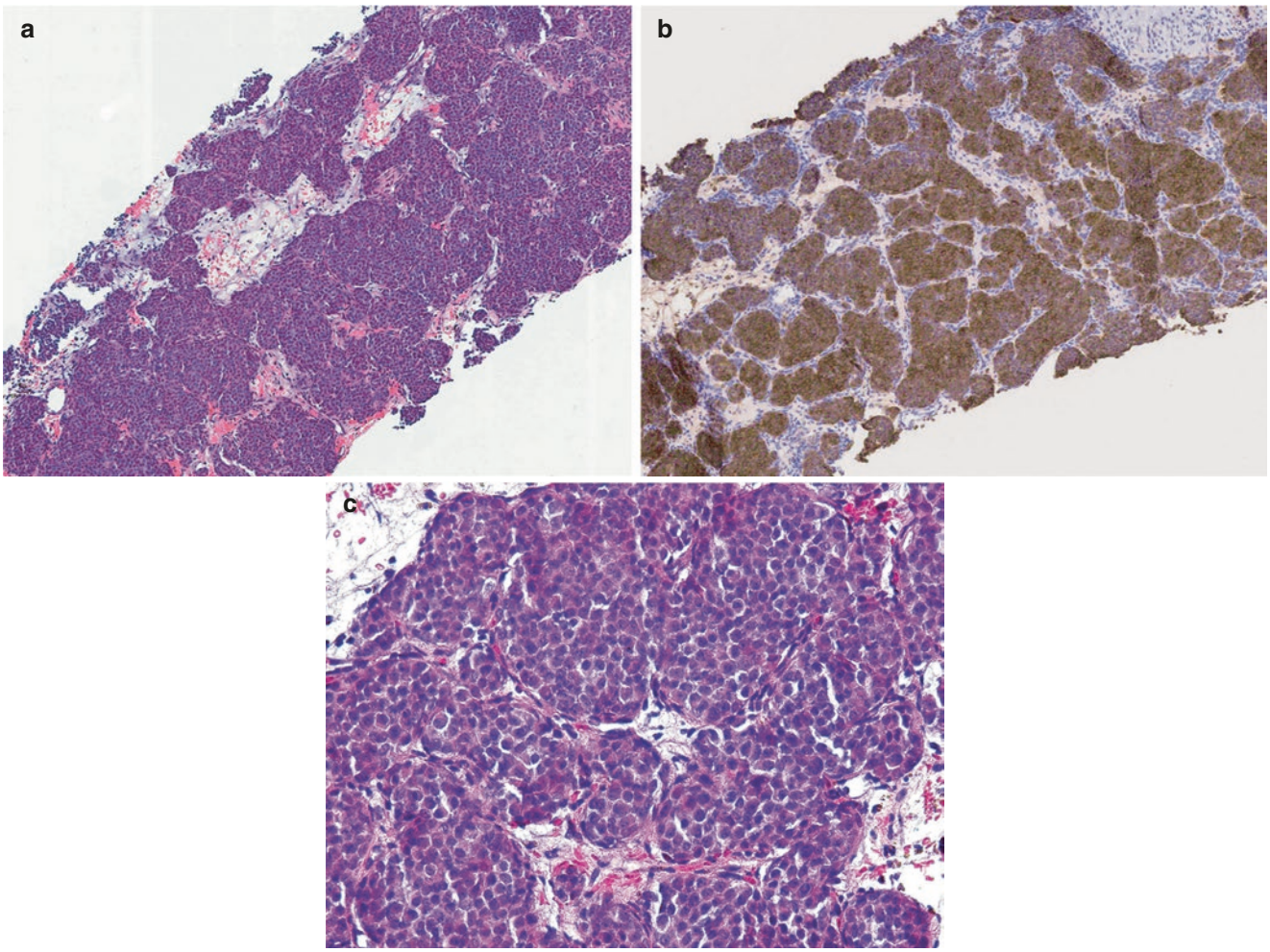

Fig. 13.11 Neuroendocrine tumor with an alveolar growth pattern. (**a**) Low-power view shows tumor cells arranged in organoid nests with intervening sinusoidal vasculature. (**b**) Tumor cells are diffusely positive for synaptophysin. (**c**) Medium-power view shows that the tumor cells are low to intermediate grade

and Ki-67 proliferation index, the WHO still recommends Nottingham histologic grading for breast neuroendocrine neoplasms. Nevertheless, both grading schemes are highly concordant as mitotic count constitutes one of the main parameters in both systems.

Poorly differentiated NECs are subdivided into large-cell neuroendocrine carcinoma and small-cell carcinoma. Small-cell carcinoma of the breast is histologically identical to its counterparts in other organs. It is composed of densely packed tumor cells with hyperchromatic nuclei, inconspicuous nucleoli, and scant cytoplasm. Nuclear molding, brisk mitoses, and tumor necrosis are frequent (Fig. 13.13). Most mammary small-cell carcinomas are associated with an in situ carcinoma. Half are associated with invasive ductal carcinoma NST or invasive lobular carcinoma [80].

Large-cell NEC is composed of nests of large tumor cells with abundant granular or clear cytoplasm, vesicular nuclei, and prominent nucleoli. Tumor nodules are often supported by fibrovascular septa with rich vasculature. Brisk mitotic activity and tumor necrosis are frequently present (Fig. 13.14). Differentiating large-cell NEC from grade 3 well-differentiated NET can sometimes be challenging. Compared to grade 3 NET, large-cell NEC shows significantly more cytologic atypia and lacks the classic architectural pattern of NET. Table 13.1 lists a few additional features that can help to differentiate the two.

Differential Diagnosis

The main differential diagnosis for primary mammary NEN is metastatic NEN from other organs to the breast. Due to their overlapping or identical histologic features, clinical history in conjunction with tissue-specific markers such as GATA3 (breast), TRPS1 (breast), TTF1 (lung), and CDX2 (gastrointestinal tract) is essential for correct diagnosis [82, 81]. The presence of DCIS supports mammary primary; however, it is important to bear in mind that metastatic NEN

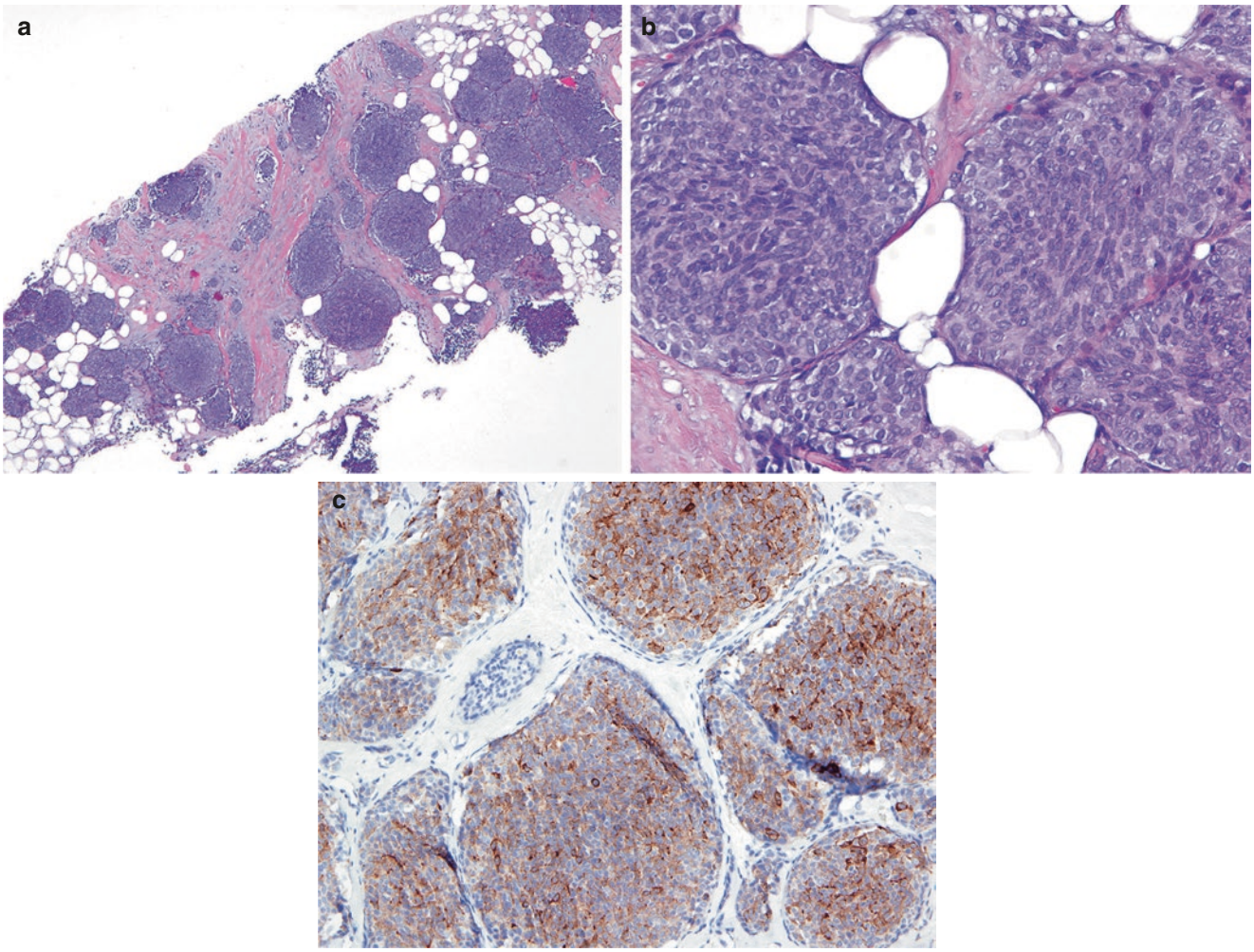

Fig. 13.12 Neuroendocrine tumor with prominent spindled cells. (**a**) The tumor cells are arranged in variably sized nests infiltrating fibroadipose tissue. (**b**, **c**) High-power views demonstrate that the tumor cells are predominantly spindled and are diffusely positive for synaptophysin

can morphologically mimic in situ carcinoma (Fig. 13.15). Histologically and immunohistochemically, primary mammary small-cell carcinoma is indistinguishable from metastatic small-cell carcinoma. Therefore, the presence of DCIS or an invasive carcinoma NST component and clinical history are key in distinguishing between the two.

Immunohistochemical Workup

By definition, >50% of the tumor cells should express neuroendocrine markers. Synaptophysin and chromogranin are considered to be the most specific markers for neuroendocrine differentiation [83]. Other markers such as neuron-specific enolase (NSE) and CD56 are sensitive, but not specific, for NEN [83]. INSM1, a potential novel neuroendocrine marker, is currently under investigation.

Most mammary NETs express estrogen receptor (77–95%) and progesterone receptor (40–70%) and are negative for HER2 overexpression or amplification. Breast NENs also express GATA3 and TRPS1, which can be used to differentiate primary mammary tumors from metastases. Of note, TTF1 is not helpful for differentiating primary mammary small-cell carcinoma from metastatic small-cell carcinoma as both mammary and non-mammary small-cell carcinomas can express TTF1.

Pathogenesis

The pathogenesis of mammary NEN is still under investigation. Unlike the lung and gastrointestinal tract, endogenous endocrine cells do not reside in normal breast tissue. One hypothesis is that mammary NENs are derived from argyrophilic cells of neural crest origin, which migrate to the breast. Recently, two studies showed the presence of isolated and hyperplastic benign-appearing neuroendocrine cells in breast parenchyma containing NEN, suggesting that neuroendo-

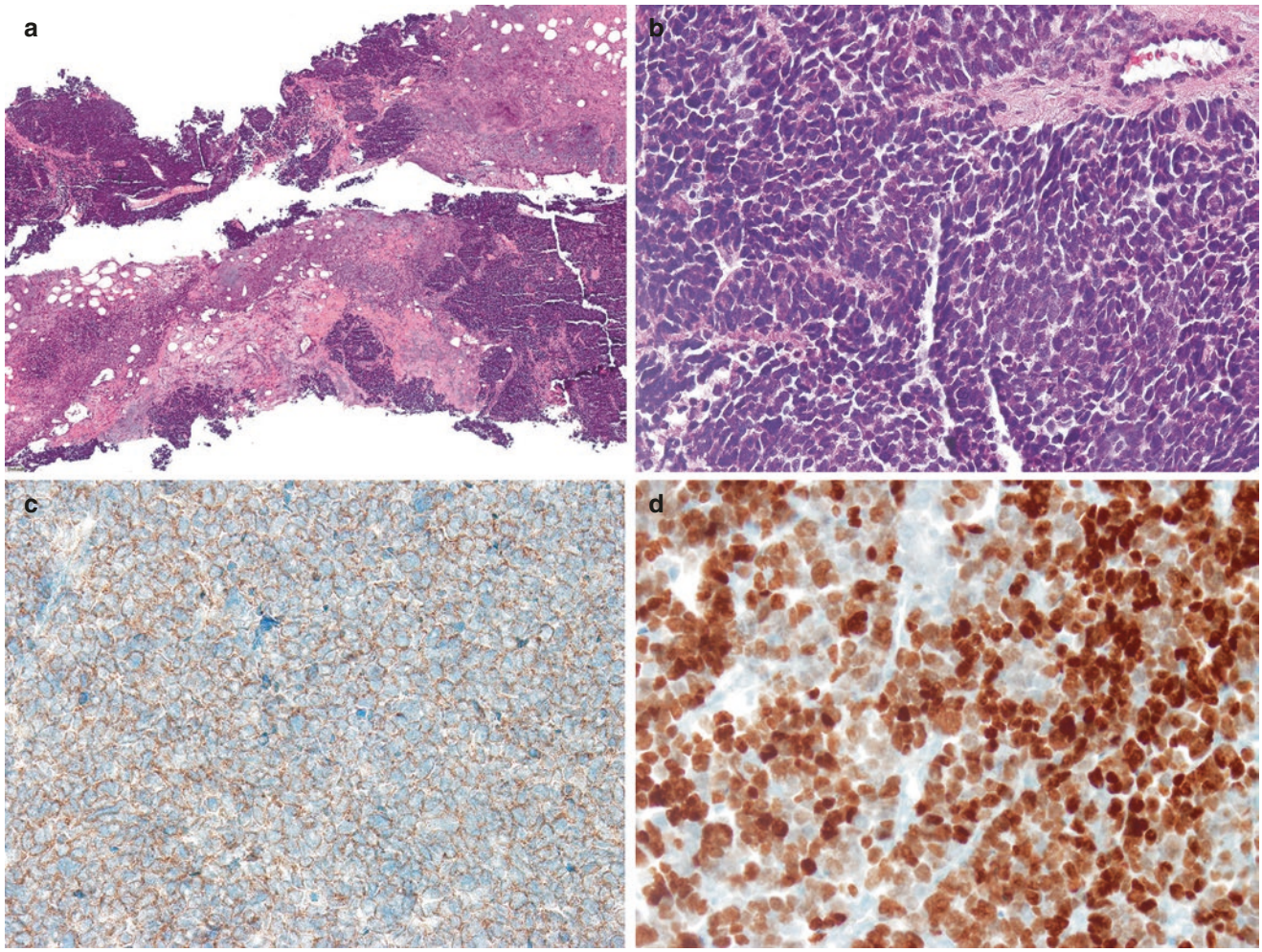

Fig. 13.13 Small-cell carcinoma. (**a**) CNB shows a friable tumor with a large area of necrosis. (**b**) Medium-power view shows densely packed tumor cells with scant cytoplasm, hyperchromatic nuclei, and absence of nucleoli. Nuclear molding is prominent. Mitoses are also readily identified. The tumor cells are diffusely positive for (**c**) synaptophysin and (**d**) TTF1

crine cell hyperplasia might be a precursor lesion to NEN in the breast [84, 85].

Another hypothesis is that mammary NEN originates from cancer stem cells with divergent luminal epithelial and neuroendocrine differentiation. A recent study showed that most mammary NENs fell into the luminal B molecular subtype of breast cancer [86]. Consistent with the wide morphological spectrum of NEN, limited cytogenetic studies have revealed various genetic changes with low-grade mammary NET sharing some cytogenetic abnormalities seen in low-grade NETs of the lung and gastrointestinal tract, while poorly differentiated mammary NECs demonstrate considerably more complex genetic abnormalities, suggesting that different molecular alterations underlie various types of NEN in the breast [87].

Next-generation sequencing (NGS) analysis has revealed the presence of mutations in *FGFR1*, *FGFR2*, *VEGFR2*, and *HRAS* genes, which are extremely rare in invasive mammary carcinoma NST. These findings suggest the potential for targeted therapy against specific tyrosine kinase receptors for breast NENs [88].

Prognosis

The clinical outcome varies and depends on the type of NEN. Poorly differentiated NEC, whether small or large cell, carries a very poor prognosis.

There are conflicting results concerning the clinical outcomes of the vast majority of mammary NEN, namely, the well-differentiated NETs [57, 60, 61, 63, 64, 66–75]. Some of these conflicting results are secondary to differing diagnostic criteria for neuroendocrine differentiation used in previous years. However, most of the recent large series studies indicate that mammary NET has a worse clinical outcome as compared with invasive carcinoma NST [68–70, 72–74, 89].

The most recent surveillance, epidemiology, and end result database study showed that both NET and NEC have

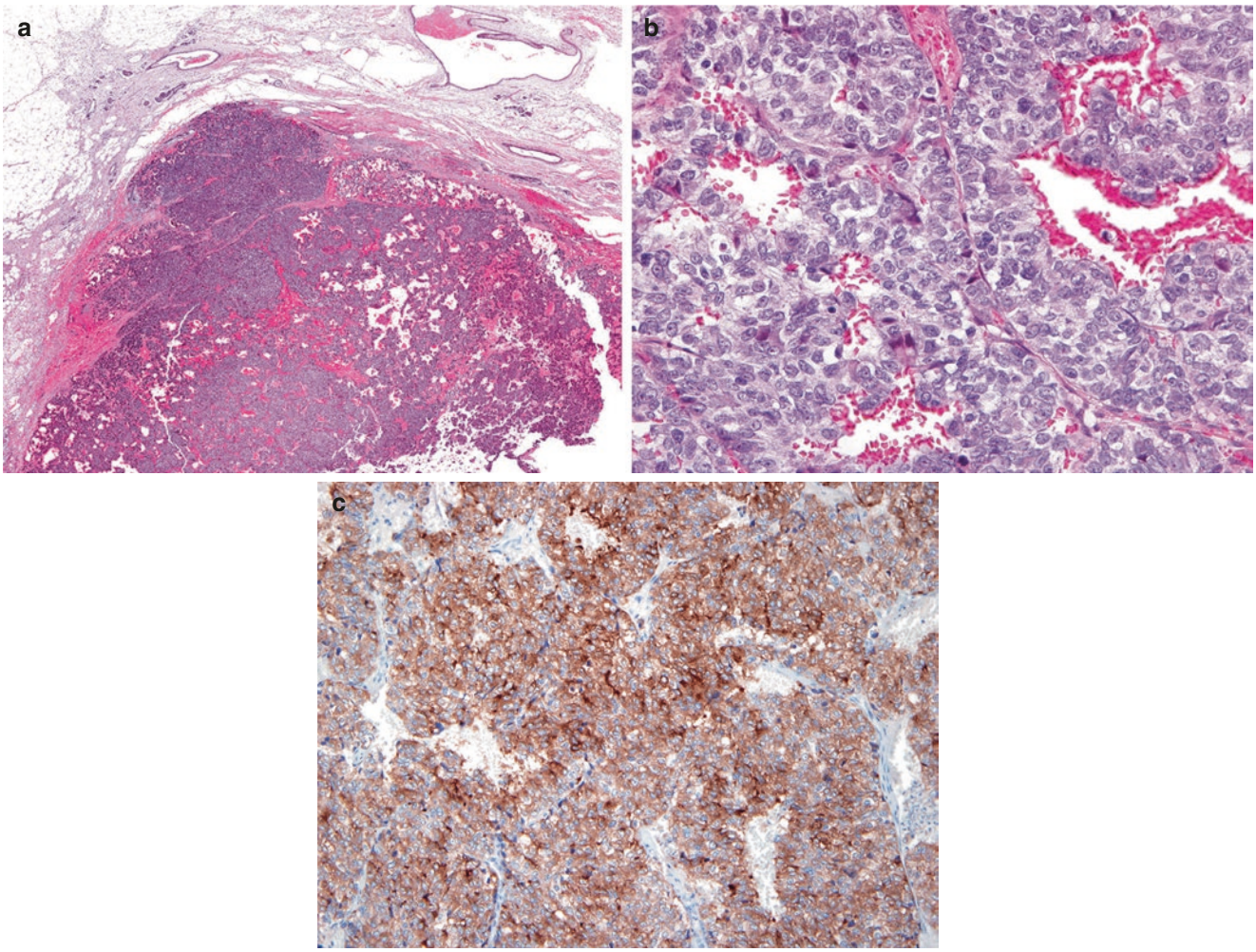

Fig. 13.14 Large-cell neuroendocrine carcinoma. (**a**) The tumor is relatively well circumscribed. (**b**) Tumor cells are large with clear to granular cytoplasm, vesicular nuclei, and prominent nucleoli and show brisk mitosis. Prominent vasculature is present. (**c**) Tumor cells are diffusely positive for synaptophysin

Table 13.1 Differentiating grade 3 neuroendocrine tumor from large-cell neuroendocrine carcinoma

	Mitoses (per 10 HPF)	Ki-67 index (%)	Loss of RB protein/ p53 mutation
Grade 3 NET	Often >20	>20, usually <55	–
Large-cell NEC	Usually >20	Usually >55	+

worse overall survival (OS) and disease-specific survival (DSS) than invasive ductal carcinoma NST [89]. The 5-year OS rates for NET, NEC, and invasive ductal carcinoma NST are 56%, 39%, and 83%, respectively. The 5-year DSS rates for NET, NEC, and invasive ductal carcinoma NST are 63%, 46%, and 89%, respectively. While NEN tends to present with more advanced disease (36% with regional nodal metastasis and 20% with systemic metastasis), even within the same stage or grade, NET and NEC have worse OS and DSS than corresponding stage or grade invasive ductal carcinoma NST [89]. Several case-control studies that matched clinical and pathologic parameters, including age, stage, hormone receptor status, and surgical procedure, further confirm the adverse outcome of patients with NEN compared to those with invasive carcinoma NST [67, 72, 74].

Of note, invasive carcinoma with neuroendocrine differentiation (<50% of the tumor cells expressing neuroendocrine markers) is no longer classified as NEN of the breast. It may constitute up to 30% of invasive breast cancer NST. Early studies indicated that invasive carcinoma with focal neuroendocrine differentiation does not differ prognostically from invasive carcinoma NST [60, 61].

Multivariate analyses show that positive regional nodal status, negative PR status, and lack of surgery are adverse independent prognostic factors for DSS [71] and that posi-

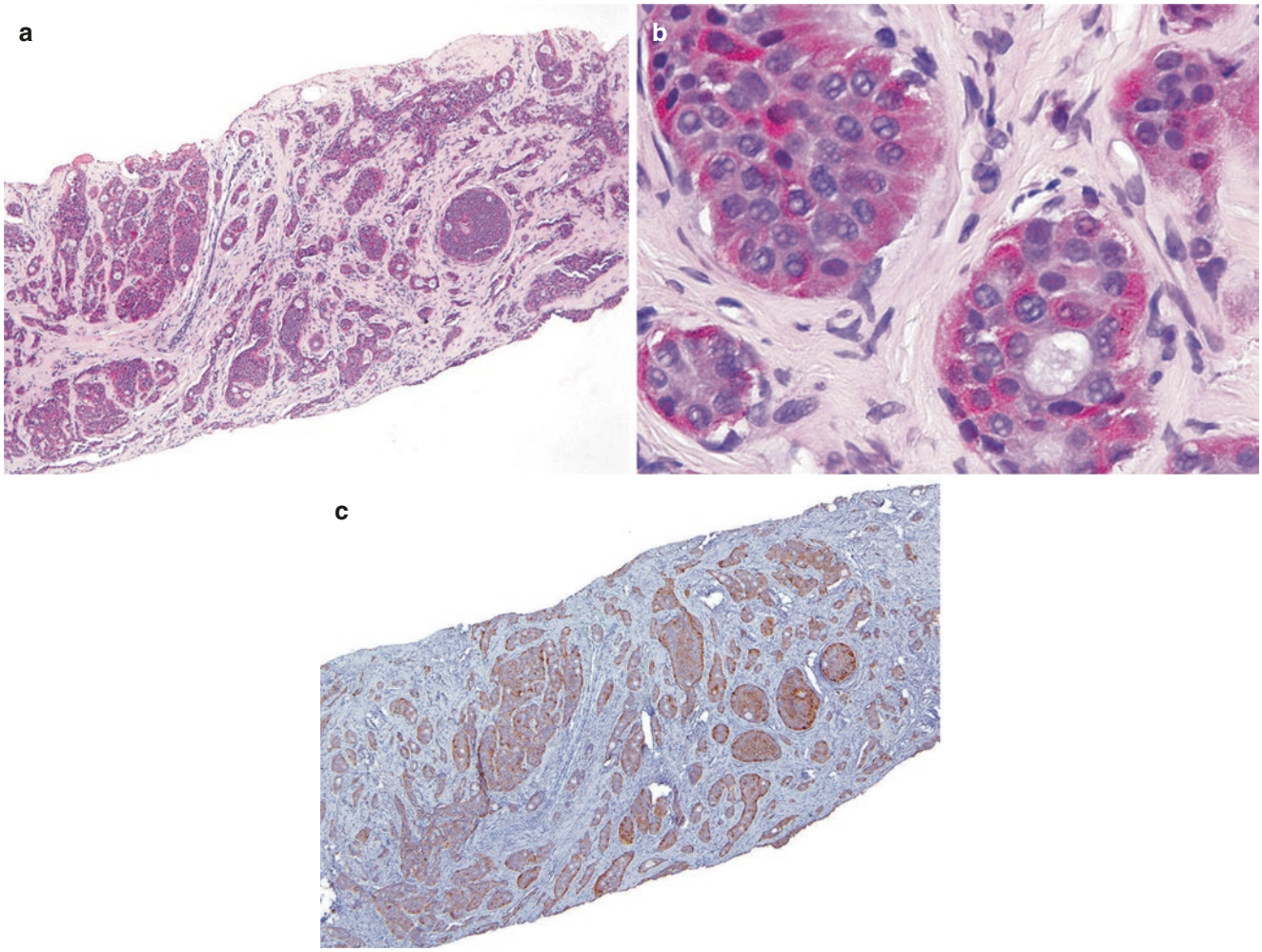

Fig. 13.15 Metastatic neuroendocrine tumor from ileum mimicking primary neuroendocrine tumor of the breast. (**a**) Low-power view of the CNB shows tumor cells arranged in solid nests, cords, and glands, mimicking invasive ductal carcinoma with DCIS. (**b**) High-power view demonstrates prominent eosinophilic neuroendocrine granules. (**c**) Neuroendocrine differentiation is confirmed by immunohistochemical staining with synaptophysin

tive regional nodal status, advanced age (>60 years), and high Ki-67 proliferation rate are independent adverse prognostic factors for OS in mammary NEN [71, 89, 90].

Cystic Hypersecretory Lesions Including Cystic Hypersecretory Carcinoma

Overview

Cystic hypersecretory lesions (CHLs) include cystic hypersecretory hyperplasia (CHH), CHH with atypia, and cystic hypersecretory (in situ) carcinoma (CHC), all of which share a common histologic characteristic of closely arranged cysts of varying sizes. CHLs come to medical attention due to their tendency to form a breast mass or cause nipple discharge and more recently present as a radiographic abnormality including mammographically detected calcifications [91]. The epithelial lining of these cysts varies from benign to atypical to carcinomatous, which in turn determines their classification as CHH, CHH with atypia, and CHC, respectively.

Cystic hypersecretory carcinoma is a distinct histologic type of in situ carcinoma that is associated with an indolent clinical course. Rarely, invasive carcinoma can arise in a CHL (invariably also containing areas of CHC), and a subset of these patients are also found to have metastatic involvement of axillary lymph nodes.

Gross and Radiologic Features

CHLs commonly form a grossly evident mass, which can attain a large size (up to 10 cm) but typically average about 5 cm in greatest diameter [91–100]. They are firm, and the cut surface is gray-brown with multiple cysts. The cysts vary in size and are filled with viscous gelatinous or mucoid material. Areas that are histologically found to be CHC versus CHH are indistinguishable by gross examination.

The mammographic appearance of mass-forming CHLs is varied and ranges from unremarkable to a focal asymmetry or a mass without calcifications [91, 98, 101, 102]. More recently, some examples have been identified mammographically by their association with calcifications [91]. By sonography, mass-forming CHLs have been described as an anechoic heterogeneous mass containing multiple small cysts and dilated ducts [97, 101, 103].

Microscopic Features and Differential Diagnosis

The fundamental structure of CHLs should be obvious on low-power magnification where a localized arrangement of closely approximated and rounded cysts filled with eosinophilic luminal secretions is appreciated (Figs. 13.16 and 13.17). Not uncommonly, scattered lymphoid infiltrates and histiocytes are seen in the adjacent stroma, likely secondary to the rupture of some lesional cysts (Fig. 13.18).

Luminal secretions in CHLs are a diagnostic requirement and typically abundant in CHH and CHH with atypia. In contrast, luminal secretions are notably diminished in CHC, which may serve as a helpful clue in some cases.

The appearance of luminal secretions can vary from case to case. Luminal secretions of CHLs are best known

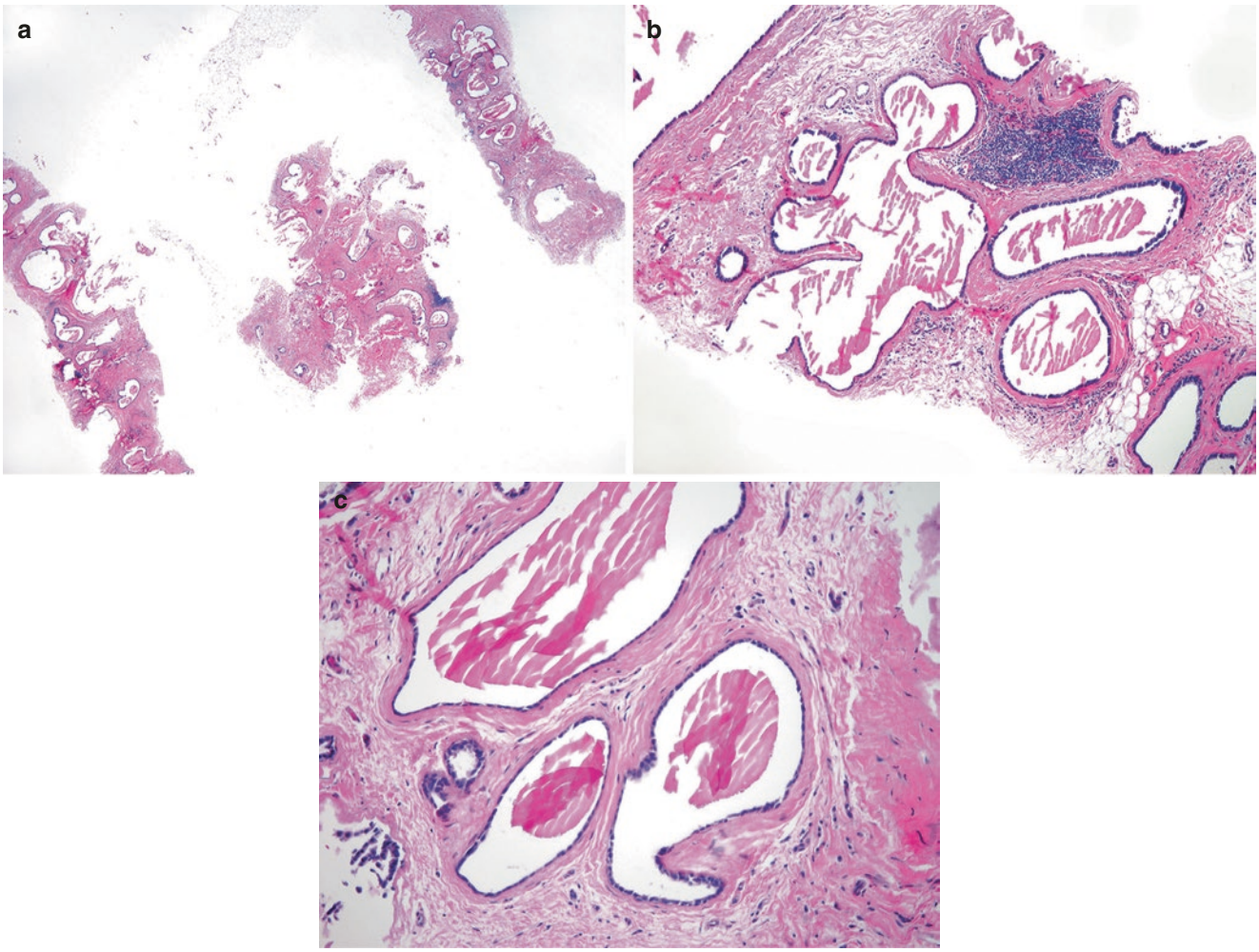

Fig. 13.16 Cystic hypersecretory hyperplasia. (**a**–**c**) CNB samples showing multiple closely approximated cysts with characteristic pink luminal secretions

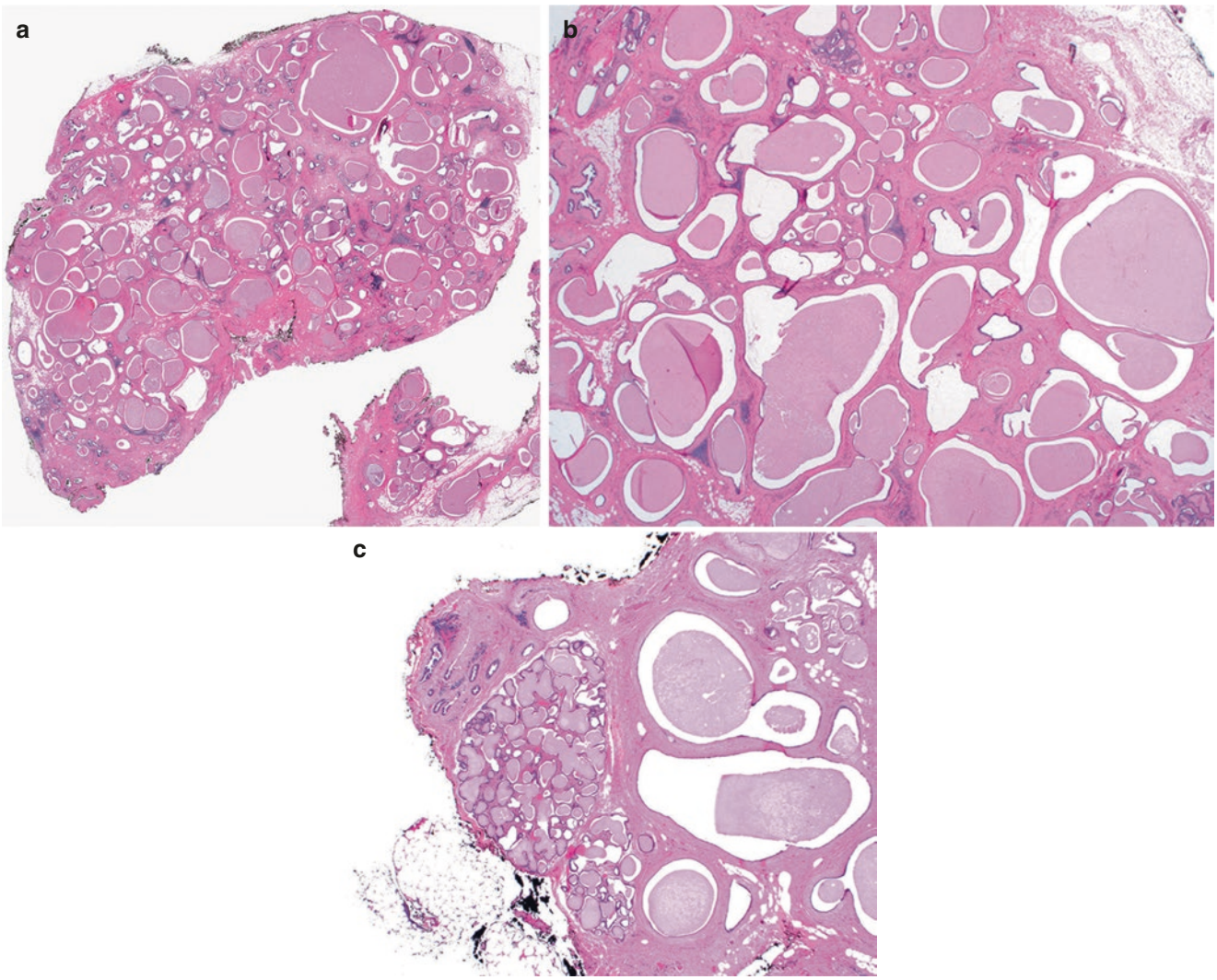

Fig. 13.17 Cystic hypersecretory hyperplasia. (**a**) Scanning view of an excisional biopsy performed for a breast mass showing a nodular mass of variably sized cysts. (**b**) Another example on medium-power view showing abundant opaque pink secretions in many of the cysts. (**c**) Cystic hypersecretory hyperplasia is seen here extending into a terminal duct lobular unit

to be dense and brightly eosinophilic, resemble thyroidal colloid, and also show prominent retraction with or without scalloped edges from the cyst wall (Fig. 13.19). Less commonly, secretions can assume a lighter shade of pink, appear less dense, and contain "pock" marks (Fig. 13.20). In other instances, the secretions can appear textured (Fig. 13.21). The presence of parallel cracks in the secretions reminiscent of venetian blinds is also a trait of CHLs, and in some instances, fragmented secretions can fall away from the lumen and dislodge into the surrounding breast parenchyma (Fig. 13.22). In addition, luminal histiocytes can be seen admixed with pink secretions in certain examples (Fig. 13.23).

CHH represents the benign end of the cystic hypersecretory proliferative spectrum and, in its simplest form, is characterized by cysts lined by a single layer of bland cuboidal or minimally columnar shaped epithelium. The epithelial lining can appear flattened and sometimes be extremely attenuated and difficult to evaluate histologically (Fig. 13.24).

The main entities to consider in the differential diagnosis are benign cysts as part of the spectrum of fibrocystic dis-

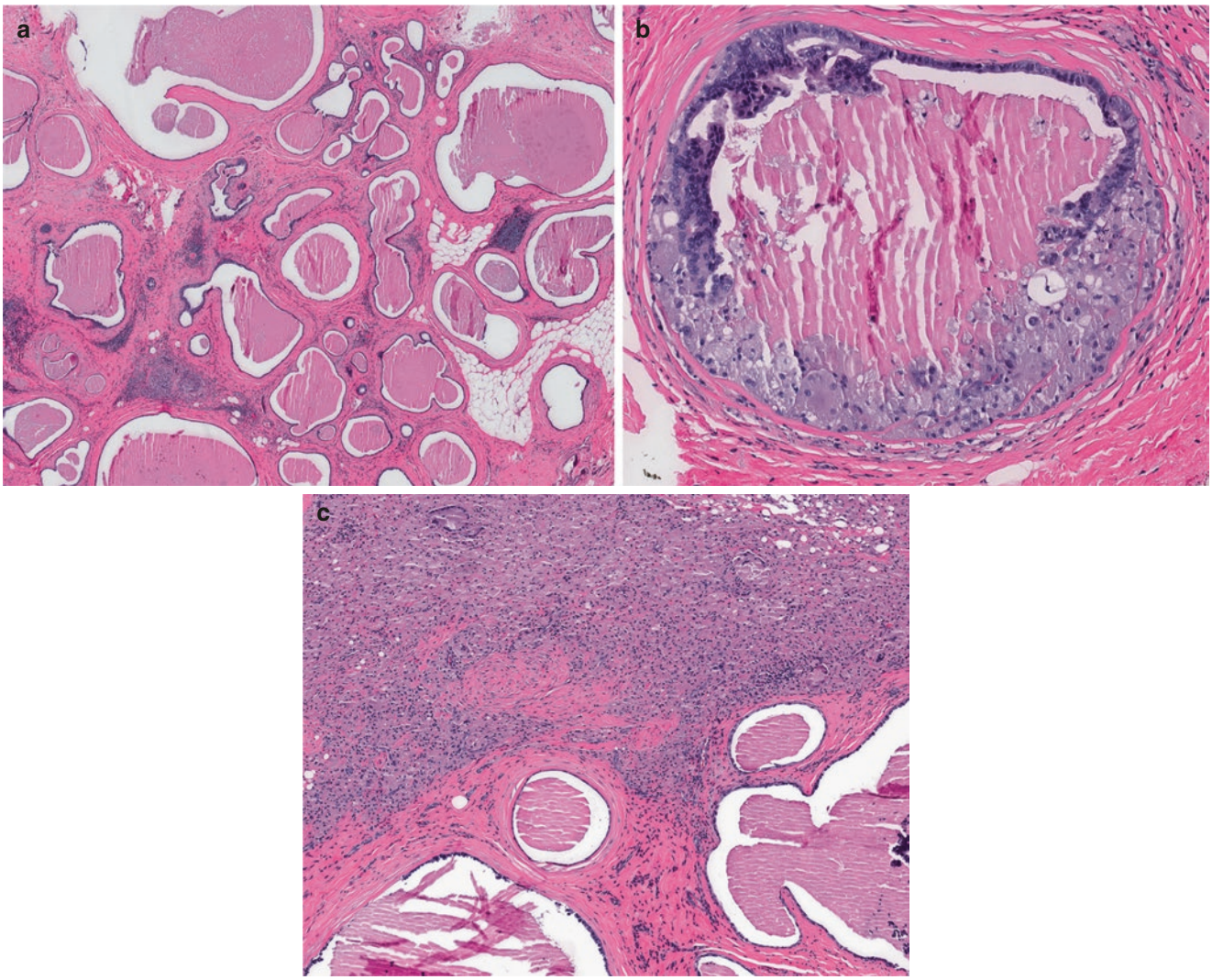

Fig. 13.18 Stromal changes seen in cystic hypersecretory lesions. (**a**) Low-power magnification shows scattered lymphoid aggregates and infiltrates between cysts. (**b**) Some cysts undergo rupture eliciting a histiocytic reaction in the stroma. (**c**) The stromal histiocytes are particularly abundant in this cystic hypersecretory lesion

ease, CHH with atypia, and CHC. Low-power scanning of multiple cysts lined by simple epithelium and containing pink luminal secretions can be easily mistaken for evidence of fibrocystic disease; however, the localized highly concentrated number of cysts should alert one to consider other entities. At this junction, juvenile papillomatosis could be considered as it is also characterized by a localized arrangement of cysts. However, unlike CHLs, juvenile papillomatosis will also contain proliferative elements such as ductal hyperplasia, apocrine metaplasia, and papillomas. Once the presence of these coexisting entities is excluded, the possibility of juvenile papillomatosis can be excluded. The more ominous pitfall is the failure to recognize CHH with atypia or CHC, which can manifest as a single layer of cytologically atypical or frankly carcinomatous epithelium, respectively, in lesional cysts (Fig. 13.25). This underscores the importance of high-magnification evaluation of all CHLs. It is also essential to know that the epithelial changes seen in one cyst can be markedly different from adjacent cysts, and not uncommonly, a spectrum of epithelial changes ranging

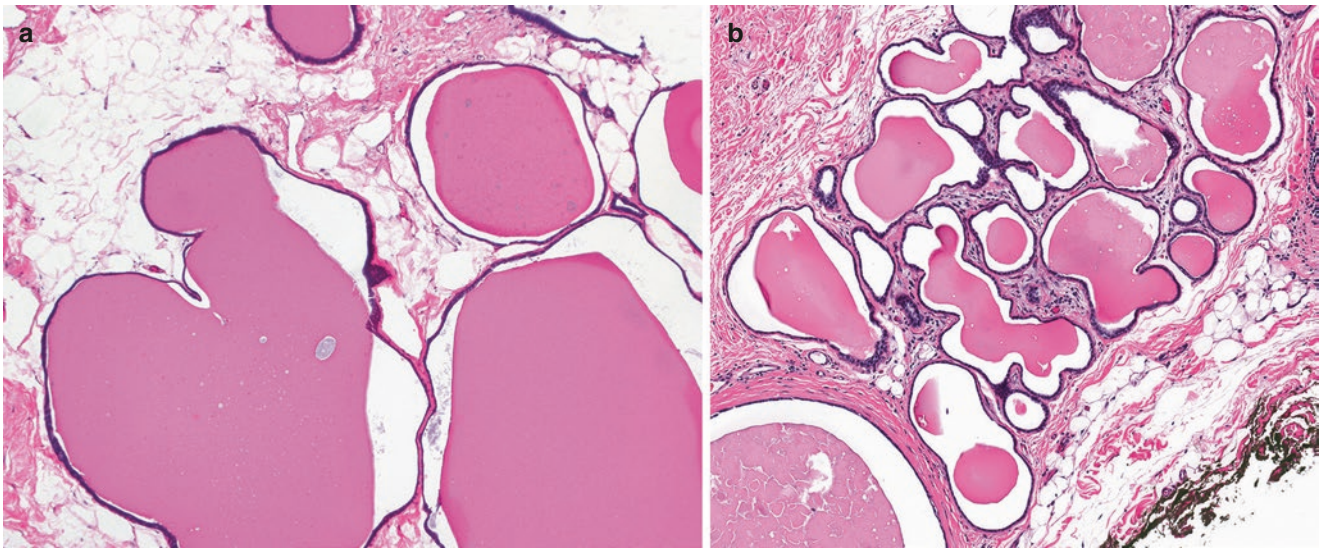

Fig. 13.19 Secretions in cystic hypersecretory lesions. (**a**) Luminal secretions in this entity are typically pink but sometimes can have a reddish hue. Characteristically, the pink secretions can be dense, thyroidal colloid-like, and glassy appearing with prominent retraction from the cyst wall. (**b**) Another example of dark pink, glassy secretions involving a lobule

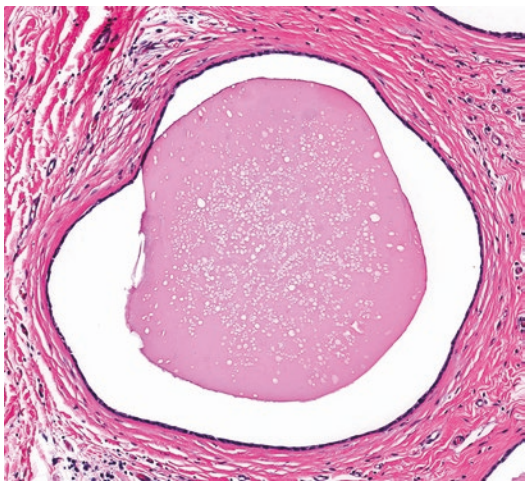

Fig. 13.20 Other characteristics of cystic hypersecretory secretions. This image shows typical "pock" marks seen in some secretions. Note the lighter shade of pink and greater translucency seen in this example containing pockmarks in contrast to the typical thyroidal colloid-like secretions seen in Fig. 13.19

from benign to carcinoma can be seen within a single cyst with or without morphologic transition (Figs. 13.26 and 13.27).

CHH can also be mildly proliferative where the epithelial cells are piled up but maintain cytologic and architectural benignity. The growth pattern is largely seen as abortive papillary tufts (Fig. 13.24c–e). It is necessary to scrutinize these proliferative examples of CHH on higher magnification to exclude the possibility of atypia in which case a diagnosis of CHH with atypia would be more appropriate. The diagnostic criteria used for conventional ADH are similarly applied to hyperplasia in this setting, and the degree of atypia would fall short of that necessary for a diagnosis of in situ carcinoma.

When the epithelial lining of a CHL is frankly malignant, then the diagnosis of cystic hypersecretory carcinoma is made. In the majority of cases, the in situ carcinoma demonstrates micropapillary (usual or flat/clinging) or papillary architecture with intermediate or high nuclear grade. Solid growth pattern can be seen in a minority of cases. Mitoses are readily identified. Some but not all examples contain luminal necrosis and/or calcifications [95]. Luminal secretions are diminished as previously mentioned. CHC can also involve neighboring terminal duct lobular units (Figs. 13.28, 13.29, 13.30, and 13.31).

CHC invariably arises in a clinically evident CHL, but CHC, itself, may not constitute the bulk of the lesion. CHC arising within a CHL is typically multifocal, making the assessment of tumor burden difficult. In one report, CHC comprised at most 50% of the gross tumor mass (CHL) while the remainder represented CHH or CHH with atypia [102]. Clearly communicating the distribution and extent of CHC in the pathology report will avoid having clinicians misconstrue gross tumor size as representing the extent of the in situ carcinoma in these cases. Concurrent conventional DCIS is not found. Associated Paget's disease has been reported in one case [102].

Invasive ductal carcinoma has been found in approximately 20% of reported CHC cases [96, 97, 103]. These examples are typically poorly and sometimes moderately differentiated without cystic hypersecretory features (Fig. 13.32).

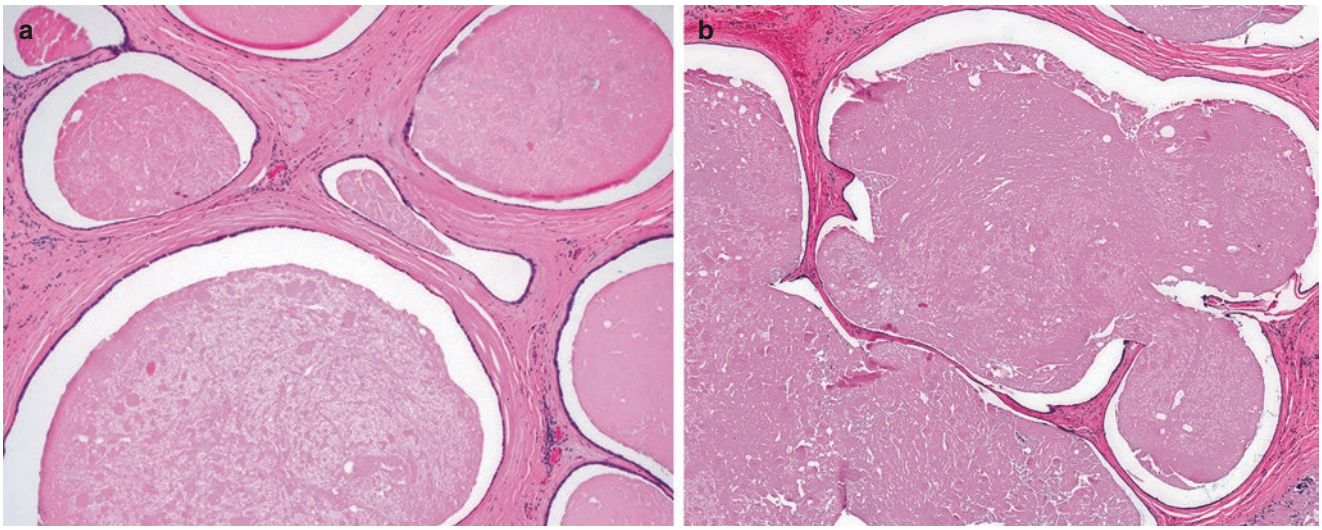

Fig. 13.21 Cystic hypersecretory secretions. (**a**, **b**) Occasionally, luminal secretions demonstrate a textured appearance that has a woven or fabric-like quality

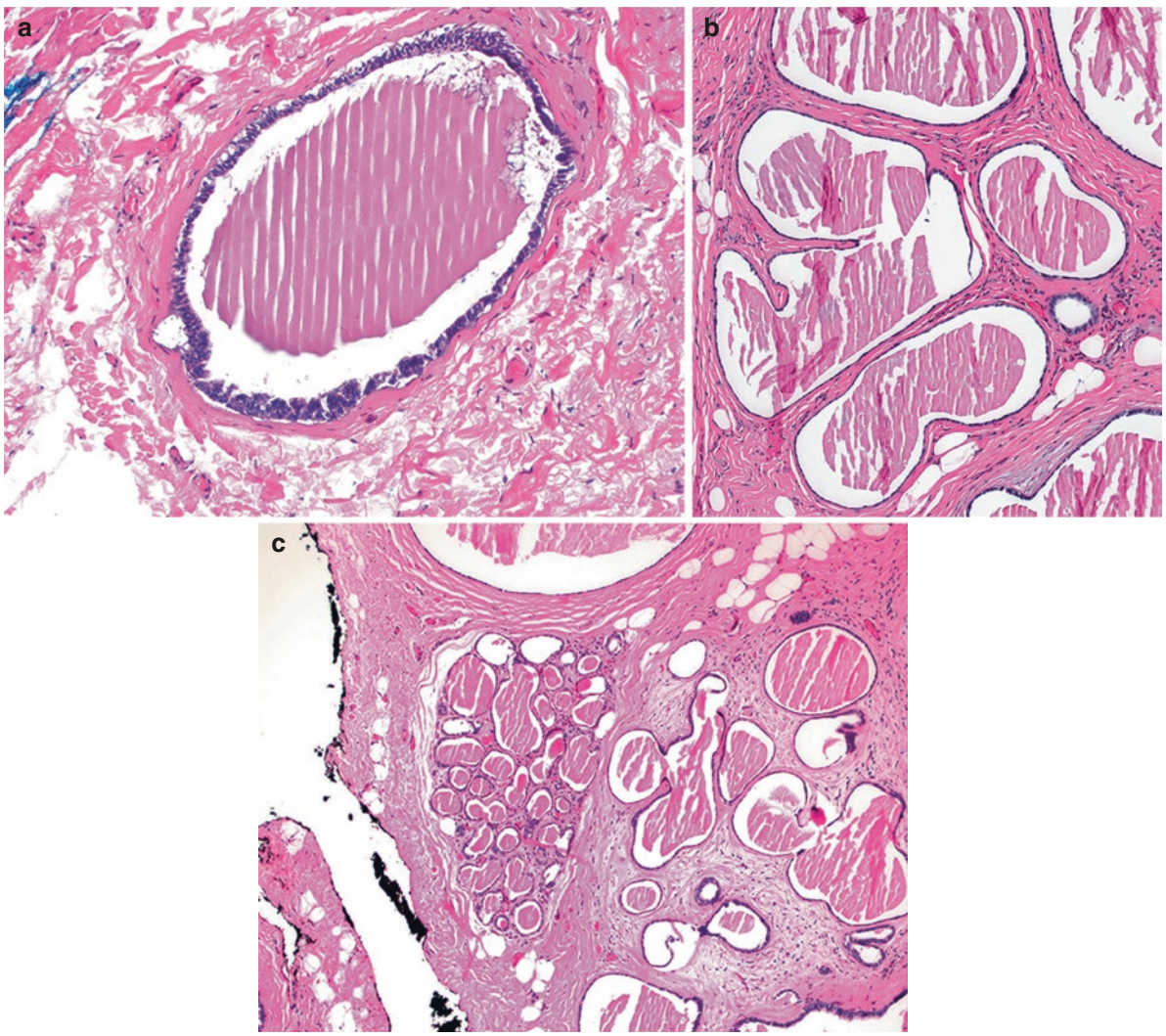

Fig. 13.22 Luminal secretions with a "venetian blind" appearance. (**a**, **b**) These parallel cracks throughout the span of the secretions can become dislodged in some areas. (**c**) This appearance can even be appreciated in a terminal duct lobular unit

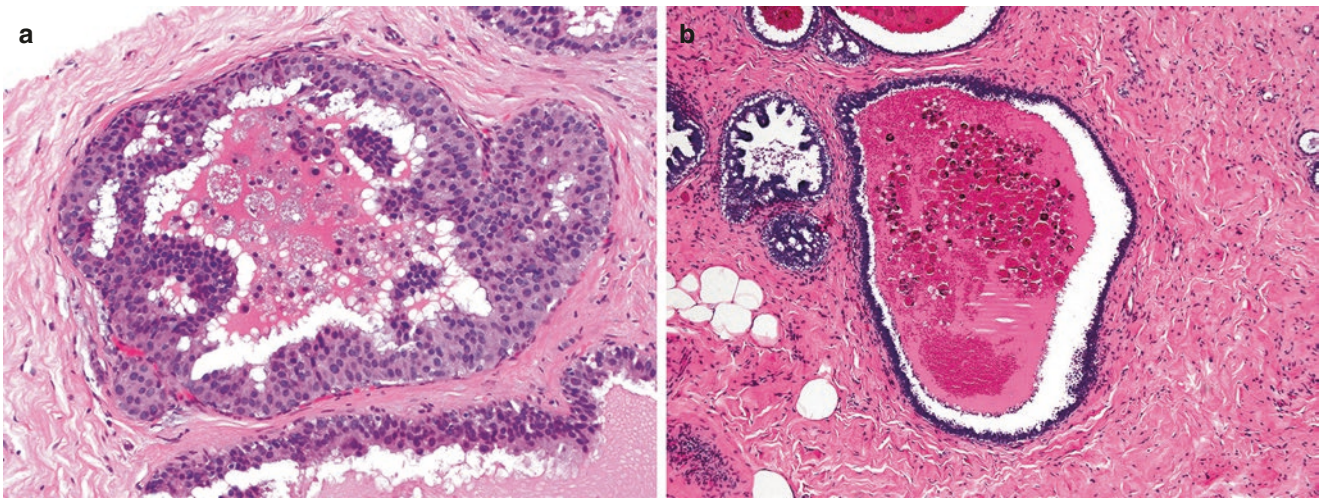

Fig. 13.23 Luminal histiocytes in cystic hypersecretory lesions. (**a**, **b**) Luminal histiocyte examples

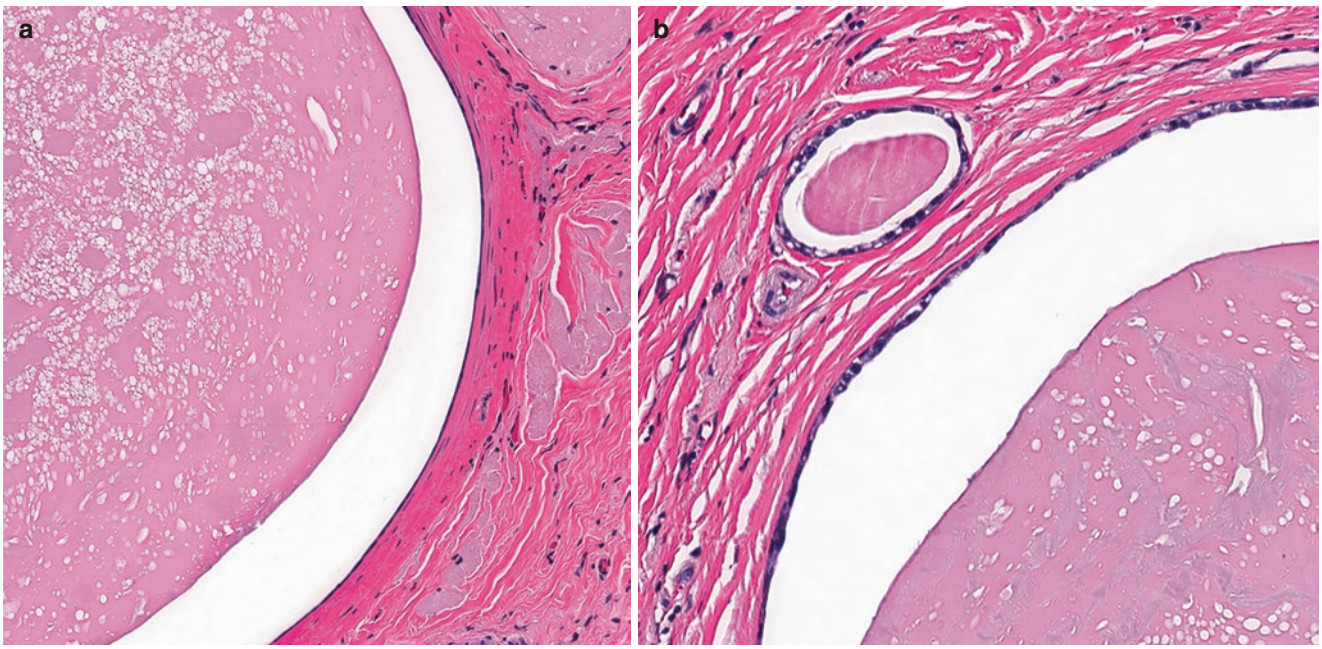

Fig. 13.24 Cystic hypersecretory hyperplasia. (**a**, **b**) The lining of cysts can be very inconspicuous consisting of a single layer of bland flattened cuboidal epithelium. (**c**, **d**) Another example of cystic hypersecretory hyperplasia which is mildly proliferative. (**e**) Cystic hypersecretory hyperplasia containing individual cysts that are non-proliferative and proliferative

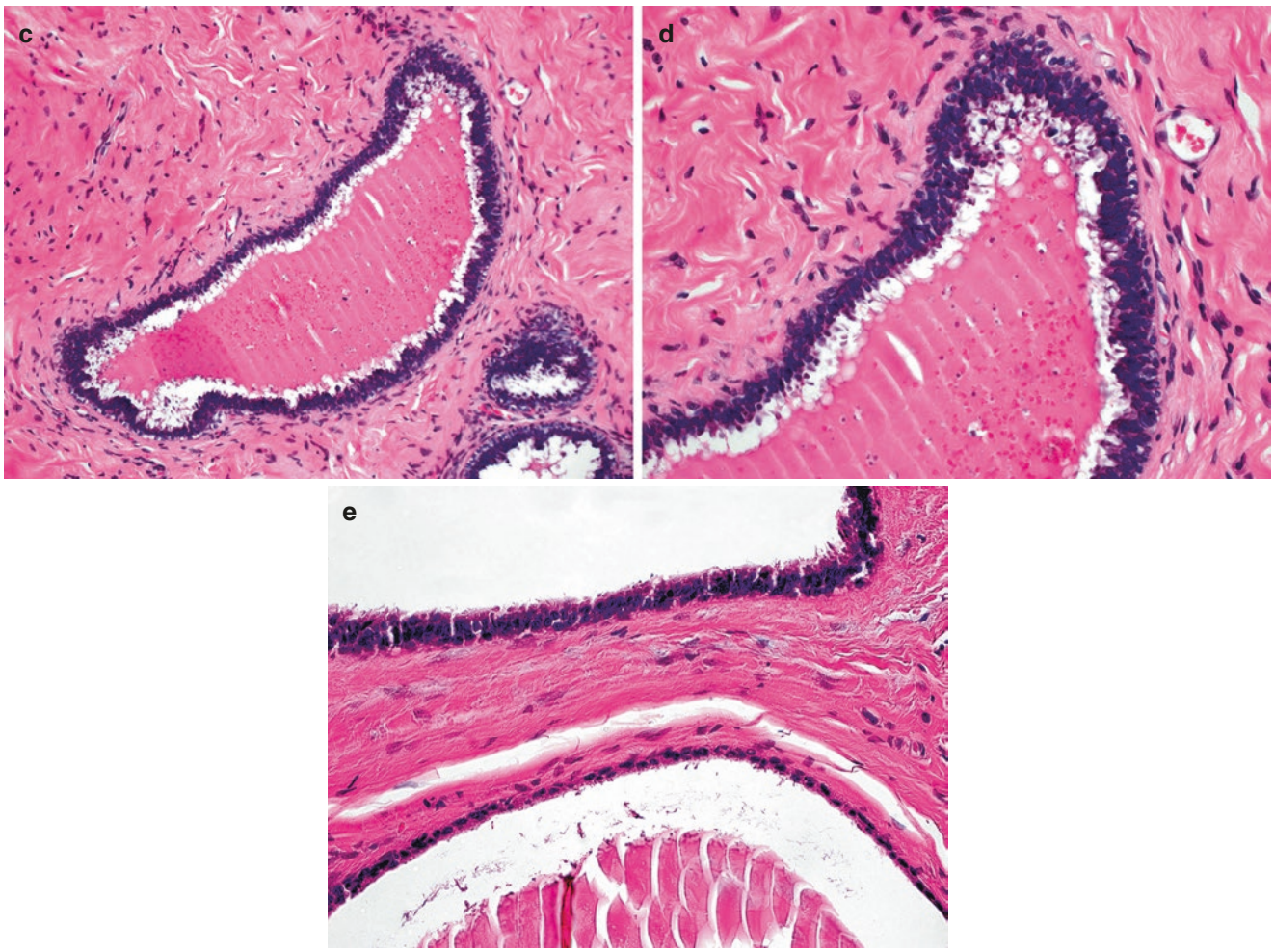

Fig. 13.24 (continued)

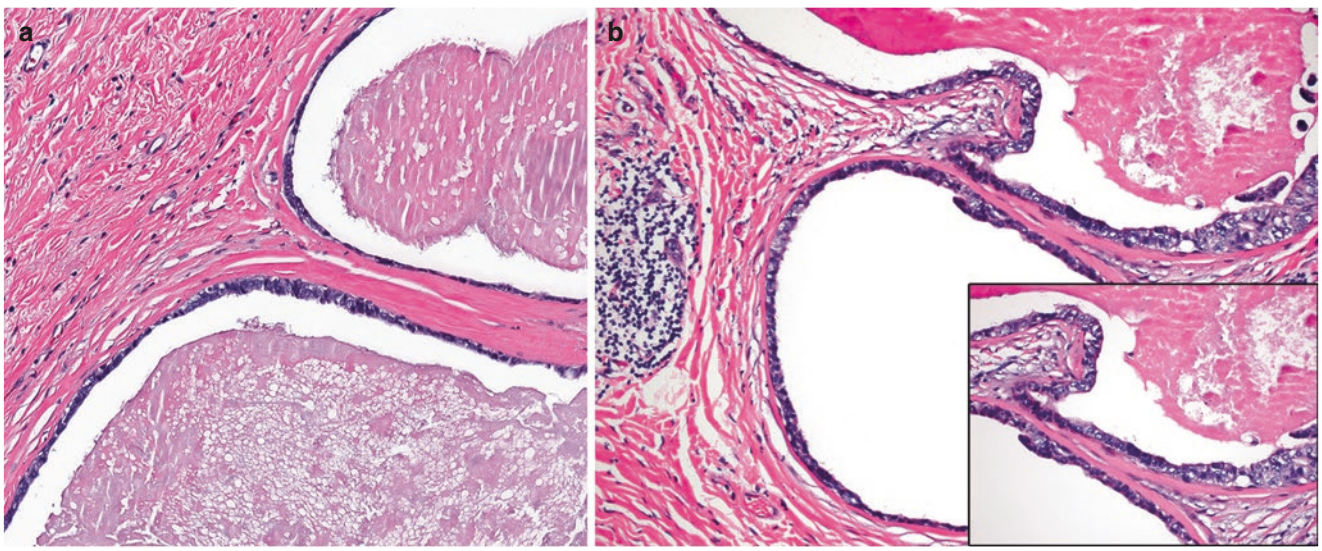

Fig. 13.25 Atypical cystic hypersecretory hyperplasia misconstrued as cystic hypersecretory hyperplasia. (**a**, **b**) Similar to columnar cell change with atypia (i.e., flat epithelial atypia), atypia in these lesions can be easily missed if scanning on low magnification. (**c**) In some cases, nuclear hyperchromasia can be detected at low magnification, which is helpful but still requires a high index of suspicion. (**d**) Malignant epithelium is confirmed on high-magnification examination in this case of minimally proliferative cystic hypersecretory in situ carcinoma

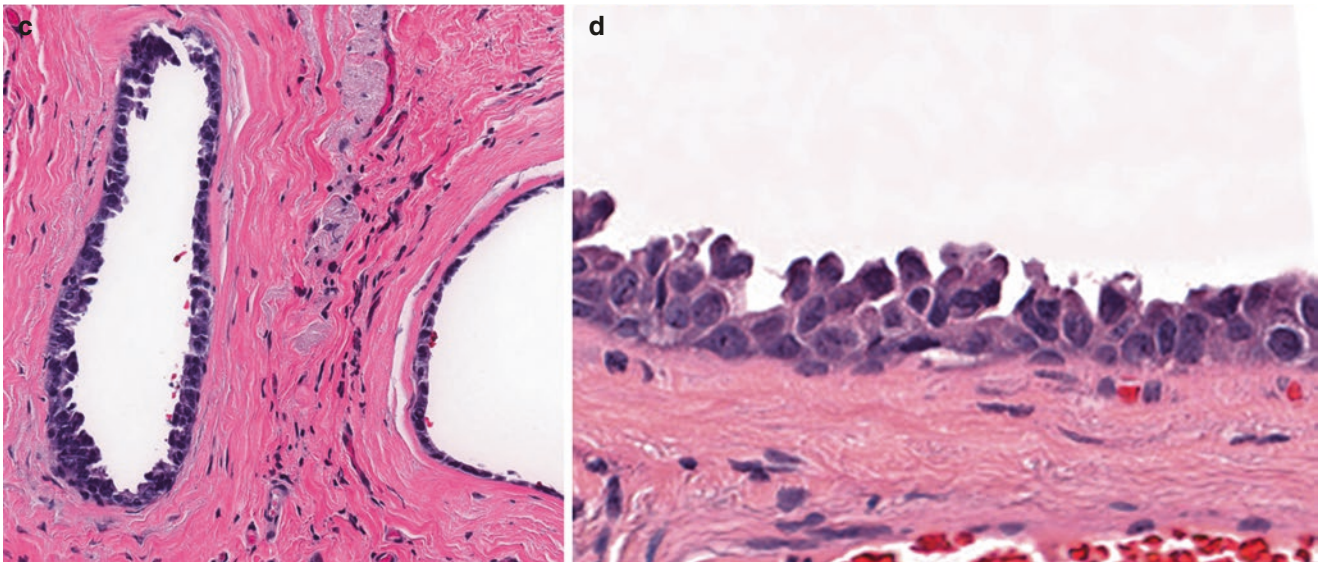

Fig. 13.25 (continued)

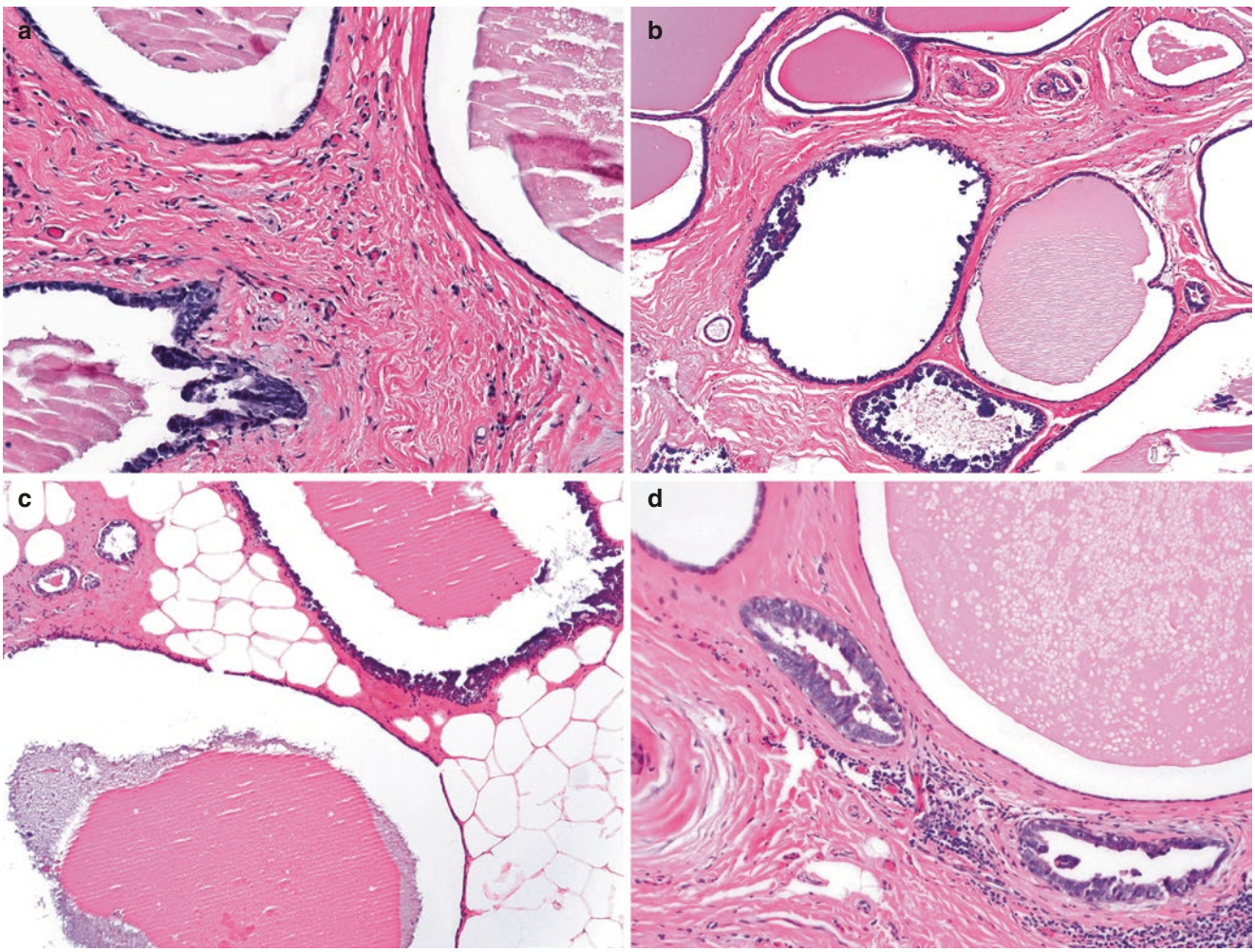

Fig. 13.26 Benign, atypical, and carcinomatous cystic hypersecretory lesions. (**a**–**d**) These are typically juxtaposed to one another

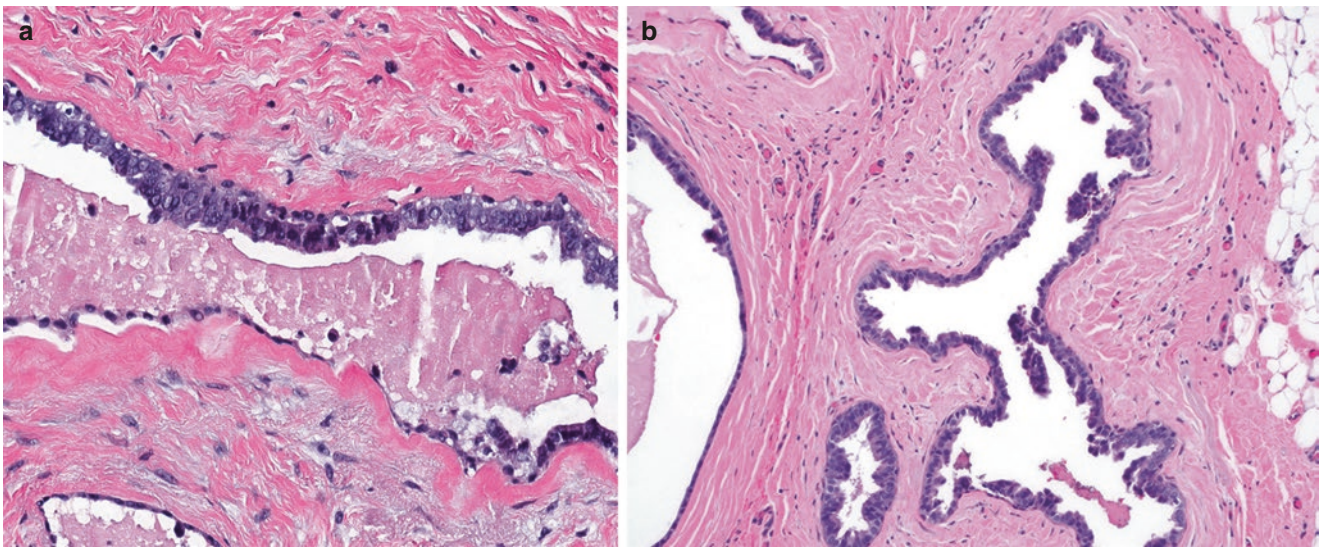

Fig. 13.27 Cystic hypersecretory lesions. (**a**) The epithelial lining of a single cyst can show cytologic transition from benign to carcinoma. (**b**) This phenomenon can be appreciated in the cyst on the left, while the one in the center is completely involved by atypical epithelium

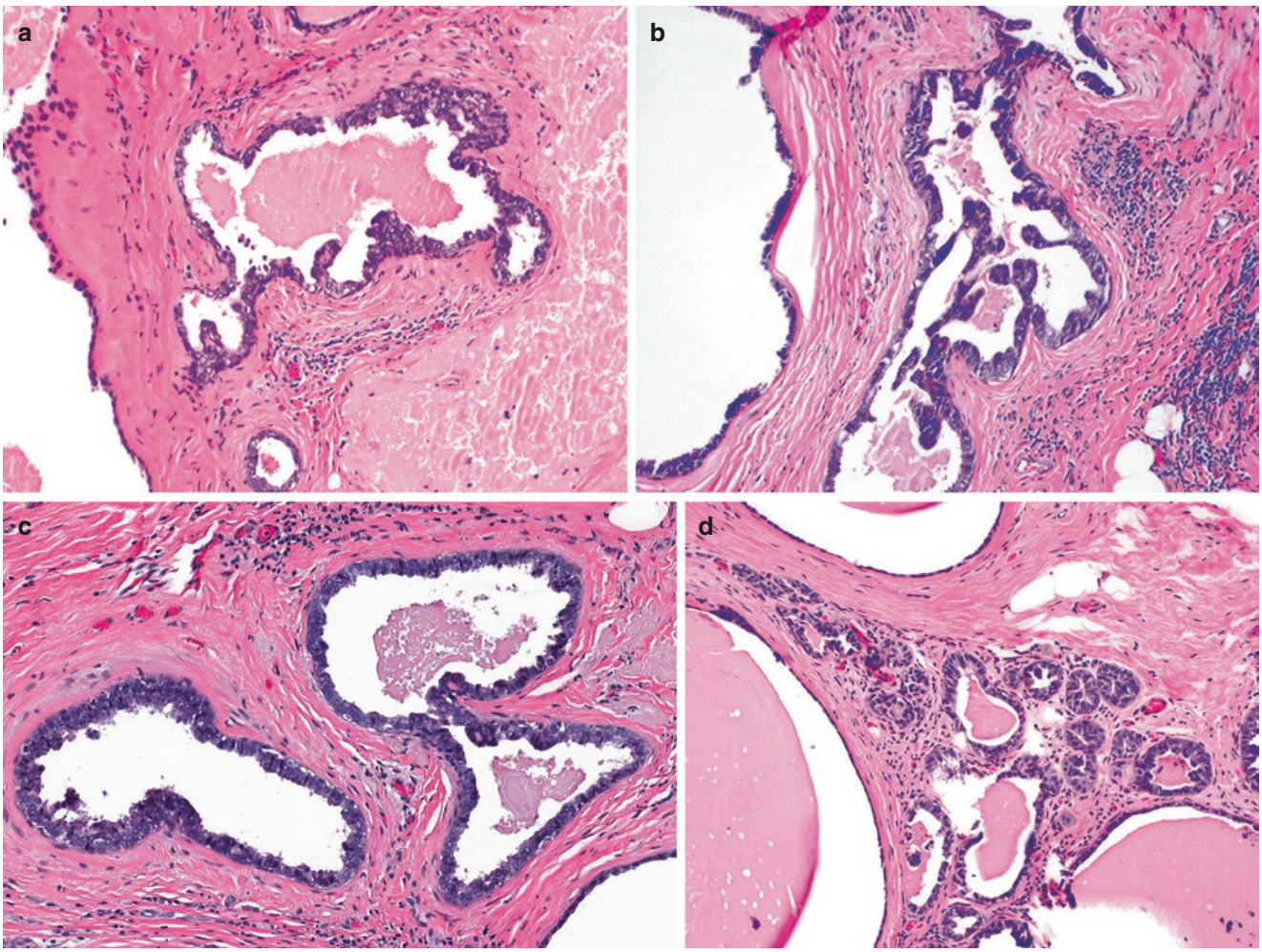

Fig. 13.28 Cystic hypersecretory carcinoma. (**a**–**c**) The most common architectural growth pattern in this type of in situ carcinoma is micropapillary. Both usual and flat (clinging) types can be seen. (**d**) CHC can involve lobules. (**e**) This focus of cystic hypersecretory carcinoma shows focal weak immunoreactivity for ER. Note in figures (**a**–**c**) that the luminal secretions are noticeably diminished in these malignant cases

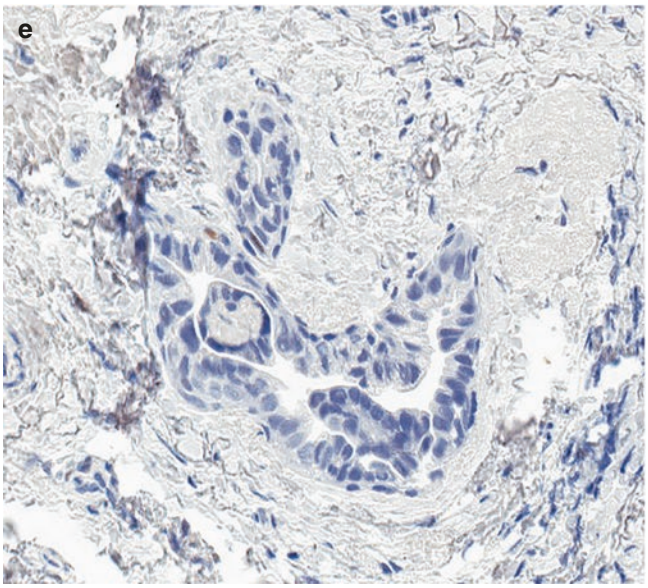

Fig. 13.28 (continued)

Rarely, metastatic disease has been reported in these patients, all of which manifested as axillary lymph node involvement with the exception of one case of bone metastasis [92].

Immunohistochemical Workup

Myoepithelium investing CHLs can be demonstrated using immunostains routinely used for this purpose [p63, smooth muscle myosin heavy chain (SMM), calponin]; however, rarely these stains can be negative similar to that seen in some papillary carcinomas [91, 104].

CHCs are typically negative for basal-like carcinoma markers such as epidermal growth factor receptor (EGFR), CK14, and CK5 [91]. These in situ carcinomas are variably positive for ER and PR, but the majority of studies have found CHC to be ER positive [91, 93, 96–98, 102, 103, 105–107]. One study also studied androgen receptor (AR) expression, which was

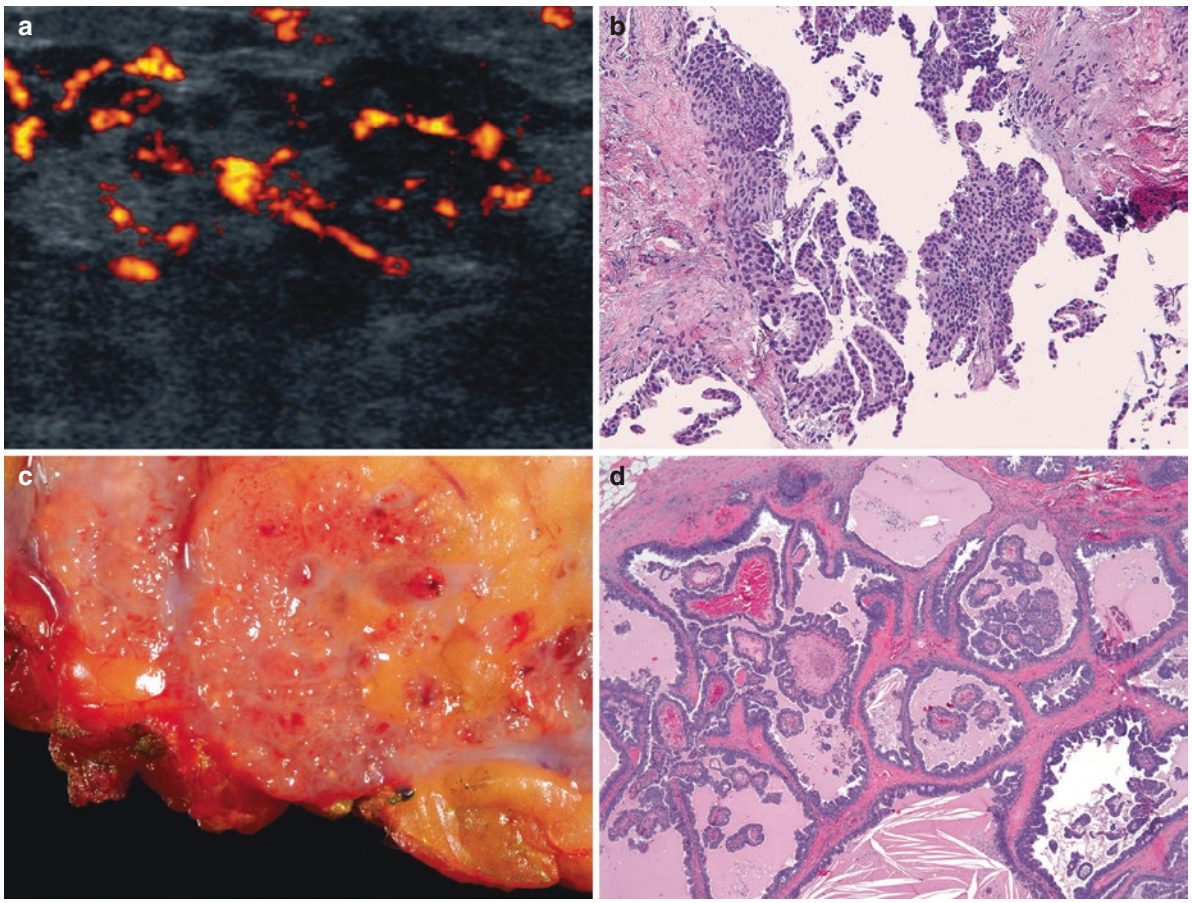

Fig. 13.29 Cystic hypersecretory carcinoma. (**a**) A large ill-defined lesion was examined under sonography, which showed numerous small anechoic cysts and dilated ducts, with substantially increased vascularity. Ultrasound-guided CNB was performed and yielded small tissue fragments. (**b**) Focal area showed collapsed ducts with focal micropapillary atypical proliferation. Due to discordant clinical, pathologic, and radiographic findings, segmental mastectomy was performed. (**c**) Fresh resection specimen shows numerous cysts and dilated ducts filled with viscous translucent material. (**d**) Histologic examination revealed many cysts and dilated ducts filled with dense and eosinophilic secretions and lined by carcinomatous epithelium with papillary and micropapillary growth patterns

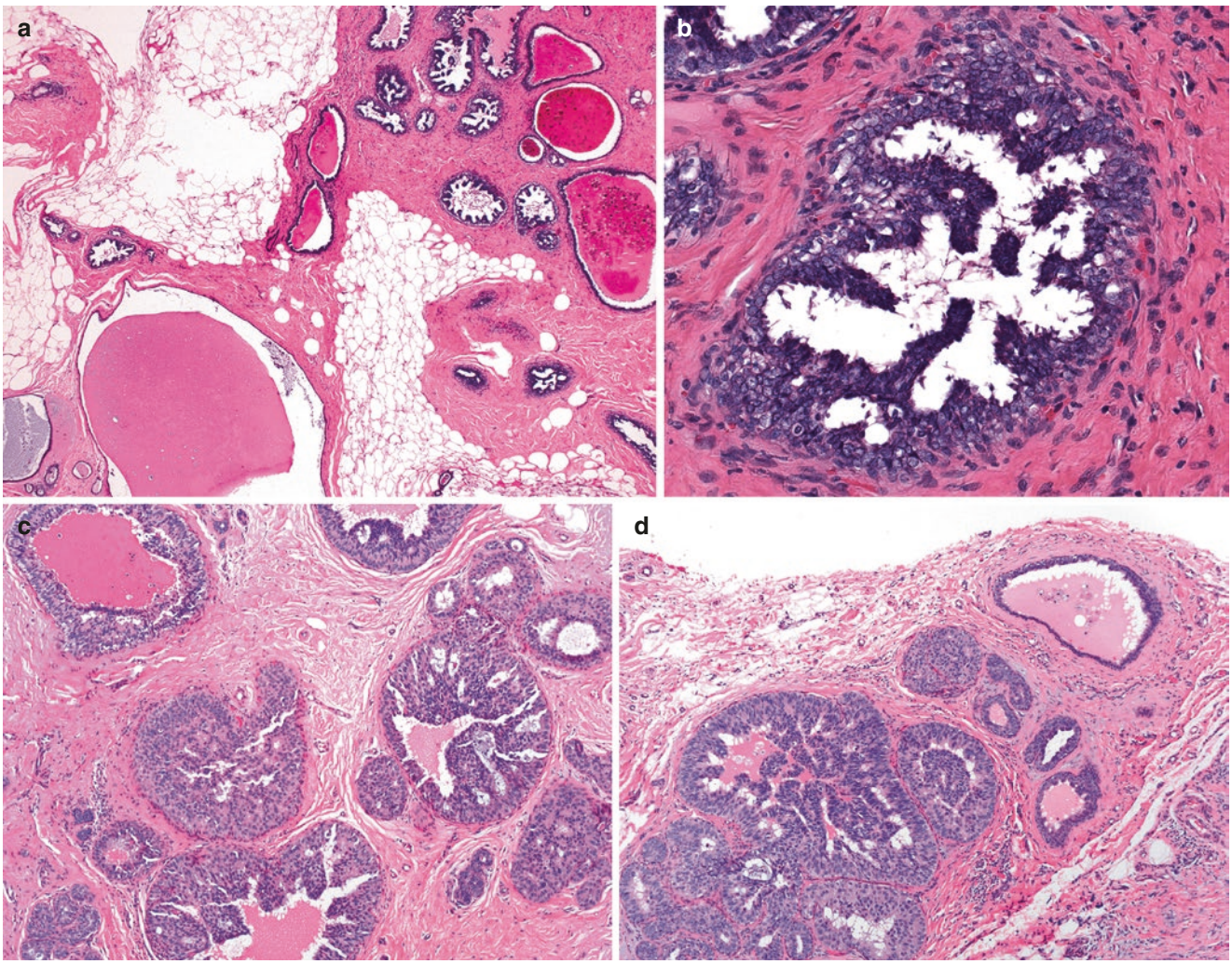

Fig. 13.30 Cystic hypersecretory carcinoma. (**a**) At low-power magnification, lesional cysts are lined by noticeably darker staining epithelium (flat or micropapillary) in contrast to cystic hypersecretory hyperplasia, which is also seen in the same field (*lower left*). (**b**) High-power view confirms the overtly malignant features of the micropapillary epithelial lining of cystic hypersecretory carcinoma. (**c**, **d**) A second example of CHC exhibiting more proliferative micropapillary growth pattern

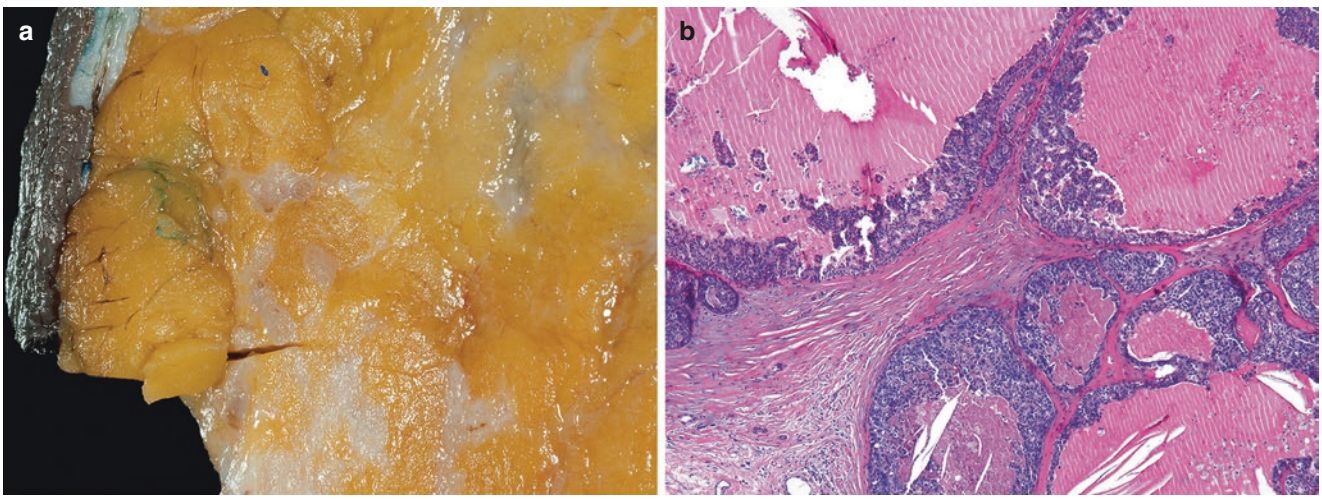

Fig. 13.31 Cystic hypersecretory carcinoma. (**a**) Another example of cystic hypersecretory carcinoma from a fixed gross specimen. Multiple cysts can be appreciated within fibrous areas. (**b**) Histologic examination shows dilated ducts and cysts filled with dense, eosinophilic secretions with cracks. Cystic hypersecretory carcinoma shows micropapillary and flat micropapillary (clinging) growth patterns

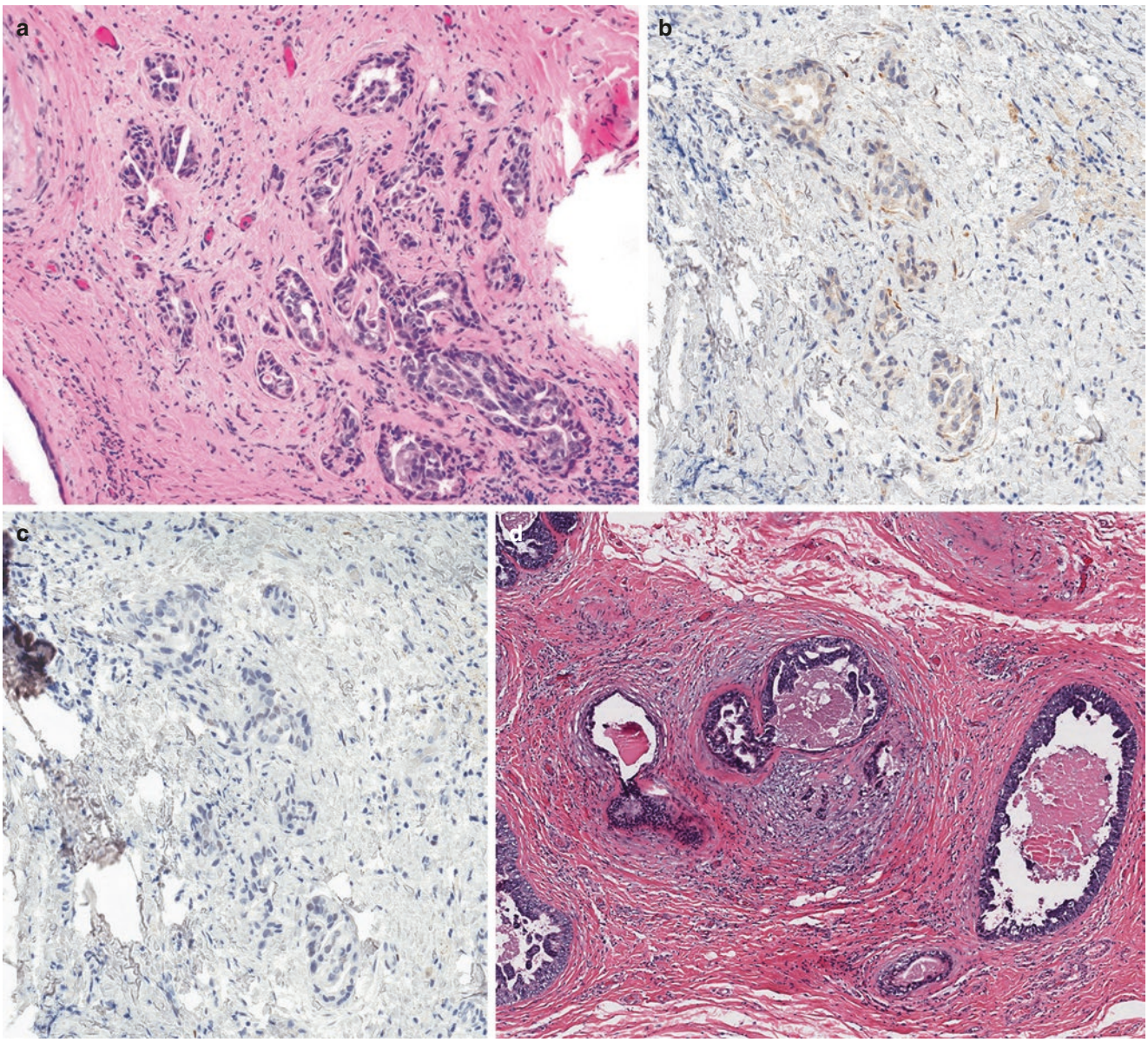

Fig. 13.32 Invasive ductal carcinoma arising in cystic hypersecretory carcinoma. (**a**) The invasive carcinoma is moderately differentiated and measured 3 mm in size. (**b**) Calponin immunostain demonstrates lack of myoepithelium in the invasive carcinoma. Neighboring blood vessels are positive (not shown). (**c**) The invasive carcinoma is focally and very weakly positive for ER. (**d**) Another example of invasive ductal carcinoma directly arising adjacent to cystic hypersecretory carcinoma. This focus is microinvasive in size and shows high nuclear grade. Note that cystic hypersecretory traits are not apparent in the invasive components of either example

also found to be variably positive [91]. The HER2 status of CHC has not been well studied but was not found to be overexpressed (3+ staining) in one study [91]. Invasive carcinoma arising in this setting shows similar biomarker expression as CHC, and when studied, similar immunoexpression has been observed in both in situ and invasive components [91].

Pathogenesis

The variable biomarker expression in CHC suggests that this entity is a heterogeneous preinvasive carcinoma much like that of conventional DCIS. This may in part explain why (most) examples are associated with an indolent clinical

course while a minor subset progress to invasive carcinoma and even metastasize. Much more investigation is needed to elucidate the biologic underpinnings of this special type of in situ carcinoma, which has been largely limited by the scarcity of this distinctive carcinoma.

Prognosis and Management in the Core Biopsy Setting

Patients diagnosed with CHH in excisional biopsies experience a benign course. Obtaining negative surgical margins is not indicated. However, in the CNB setting, cystic hypersecretory proliferations of any type should be further investigated by surgical excision due to the multifocal, scattered distribution by which CCH with atypia and CHC arise in CHLs and therefore can easily go unsampled at the time of initial biopsy.

In some instances, cystic hypersecretory changes can be seen in concert with pregnancy-like (pseudolactational) proliferations at the time of initial CNB [108], and moreover, in situ or invasive carcinoma (some cystic hypersecretory in type) has been found to arise in this morphologic background [109]. These two seemingly unrelated lesions can be found together (coexisting or histologically merging) in CNB samples targeted for calcifications associated with pregnancy-like change/hyperplasia, and not infrequently, atypia of one or both components is seen in the subsequent excisional biopsy [108] (Fig. 13.33). These observations have led to the recommendation of excisional biopsy in such instances even if both components are benign in the CNB sample [108].

If CHH with atypia is found in a CNB sample, excisional biopsy is recommended to further evaluate the area and to exclude a clinically more significant lesion (i.e., CHC, invasive carcinoma). However, it is not clear at this time how to clinically manage a patient with CHH with atypia as the highest order diagnosis (in an excisional biopsy).

Patients with CHC are treated similarly to those affected by conventional forms of in situ ductal carcinoma (surgery ± radiotherapy, hormonal therapy). The clinical course has been reported to be indolent with the most recent reported series showing no evidence of disease in four patients with long-term follow-up (mean: 5.5 years) including one who also harbored microinvasive disease.

Despite the nonaggressive course associated with CHC, the invasive carcinomas that arise in this setting are typically poorly or moderately differentiated. Cystic hypersecretory traits are not appreciated in invasive or metastatic counterparts of CHC [92]. So-called invasive cystic hypersecretory carcinomas described in the literature are in fact cases of CHLs from which only a portion of the tumor represents invasive carcinoma [91, 99, 109, 110]. It is imperative to clearly state in the pathology report the size of only the invasive carcinoma for proper staging as the gross tumor size of the CHL is invariably much larger.

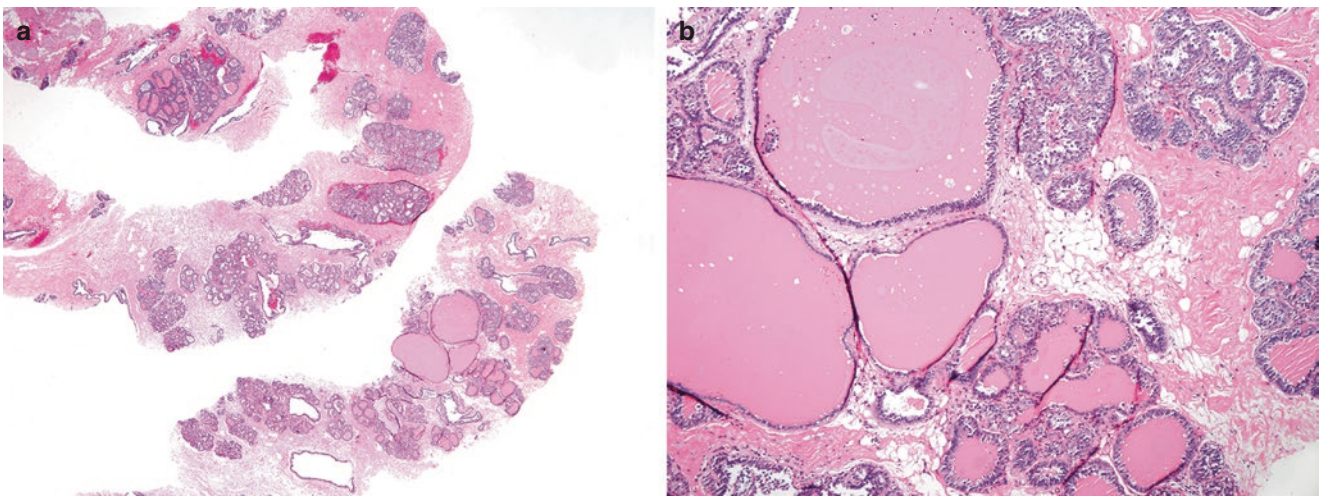

Fig. 13.33 Cystic hypersecretory hyperplasia merged with pregnancy-like hyperplasia. (**a**, **b**) CNB samples show ectatic lobular glands showing pregnancy-like hyperplasia, which in areas are merged with large cysts filled with eosinophilic secretions typical of cystic hypersecretory hyperplasia

Glycogen-Rich Clear-Cell Carcinoma

Overview

Glycogen-rich clear-cell carcinoma (GRCCC) is an uncommon breast carcinoma, which constitutes approximately 1–3% of breast carcinomas [111]. The first case was reported by Hull et al. in 1981 [112]. Since then, fewer than 100 cases have been reported in the literature [113–124]. The median age at presentation is 51 years (range, 31–81 years) [124]. The clinical presentation of patients with this tumor is no different from those with invasive carcinoma NST [111]. Most patients present with a breast mass, while others additionally experience nipple discharge. A rare case manifesting as inflammatory breast cancer has also been reported [124]. This tumor is now considered to be a special histologic pattern under the invasive breast carcinoma of no special type in the most current WHO classification [125].

Gross and Radiologic Features

No specific gross features are associated with GRCCC. The tumor size ranges from 1 to 8 cm, and most of them are 2–5 cm.

Radiographically, a high-density mass with intratumoral calcifications is the most common mammographic finding, while sonography often shows a hypoechoic mass with or without calcifications [124].

Microscopic Features

By definition, GRCCC is an invasive carcinoma where >90% of the tumor cells have abundant cytoplasm containing glycogen (Fig. 13.34). The tumor cells are usually intermediate to high nuclear grade. The tumor cells are arranged in cords, solid nests, or papillary configurations

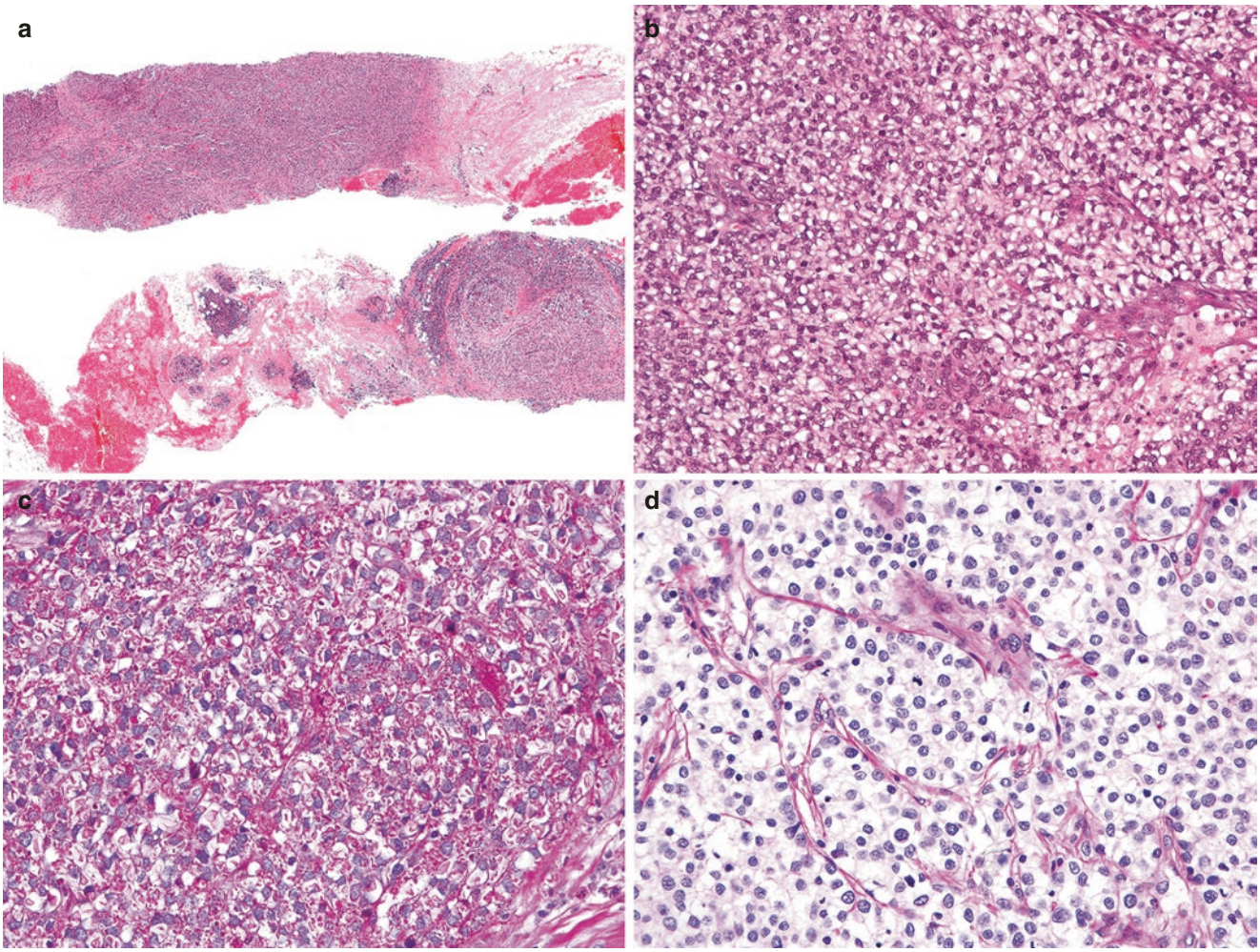

Fig. 13.34 Glycogen-rich carcinoma. (**a**) Low-power magnification of a biopsy core of glycogen-rich carcinoma. The tumor cells with clear cytoplasm and sharp cytoplasmic membrane form a well-circumscribed tumor nodule. (**b**) Cytoplasmic glycogens are highlighted by (**c**) PAS staining, and (**d**) digested by diastase

and, individually, are polygonal with sharp cytoplasmic borders. The cytoplasm is clear or granular, containing PAS-positive diastase-labile glycogen (Fig. 13.34c, d). Associated in situ carcinoma shows similar histologic features. Glycogen-rich clear-cell DCIS as a primary diagnosis has also been reported [126].

As CNB only representatively samples the tumor, the diagnosis of GRCCC cannot be rendered on this material as it requires microscopic examination of the entire tumor. The diagnosis of GRCCC can be suspected on CNB ("invasive carcinoma with glycogen-rich or clear-cell features") and confirmed on final resection specimen.

Differential Diagnosis

GRCCC is not a distinct clinicopathologic entity. But due to its peculiar histologic features, it should be differentiated from other carcinomas with clear-cell features, including lipid-rich carcinoma, myoepithelial carcinoma, primary NEC with clear-cell features, and metastatic clear-cell renal cell carcinoma.

Lipid-rich carcinoma also has clear and vacuolated cytoplasm in >90% of the tumor cells. However, the cytoplasm contains lipids instead of glycogen, which are positive for oil red O or Sudan Black.

Pure spindle cell myoepithelial carcinoma is histologically and immunophenotypically indistinguishable from spindle cell metaplastic carcinoma and is considered as a type of metaplastic carcinoma by most pathologists [127]. However, rare myoepithelial carcinomas are composed of epithelioid polygonal cells with clear cytoplasm, resembling clear-cell myoepithelial tumors of the salivary glands [128, 129], and should be differentiated from GRCCC. Myoepithelial carcinoma is negative for glycogen and positive for myoepithelial markers S100 protein and smooth muscle actin. Anecdotal glycogen-rich clear-cell myoepithelial carcinoma has been reported [130].

In some examples, NEC of the breast may have clear-cell cytoplasm and should be distinguished from GRCCC. With that said, a rare case of GRCCC with neuroendocrine differentiation has been reported, wherein, in addition to having the diagnostic features of GRCCC, the tumor cells were also found to be diffusely positive for neuroendocrine markers synaptophysin and chromogranin-A [131].

Metastatic clear-cell renal cell carcinoma is another entity which can be morphologically mistaken for GRCCC. The presence of rich vasculature, lack of in situ carcinoma, and previous clinical history can often lead to the correct diagnosis.

Immunohistochemical Workup

Special stains periodic acid–Schiff (PAS) and PAS-D (with diastase) are used to confirm the diagnosis of GRCCC as cytoplasmic glycogen stains positively for PAS but negatively for PAS-D. GRCCC has variable expression of hormonal receptors and has no specific immunophenotypic profile. A recent study reported that GRCCC showed a similar biomarker profile as invasive ductal carcinoma NST with 64% of them being ER positive, 60% being PR positive, and HER2 overexpression or amplification seen in 12% of the cases [124].

To differentiate GRCCC from other neoplasms with clear cytoplasm particularly clear-cell renal cell carcinoma, tissue-specific markers CD10, PAX8, and PAX2 (kidney) and GATA3 (breast) are helpful for the correct diagnosis.

Pathogenesis

The pathogenesis of GRCCC is unclear.

Prognosis

Conflicting data regarding the prognosis for GRCCC are reported in the literature. Some studies show a good prognosis [112, 113], while others show aggressive clinical course [124, 126, 130]. However, the prognosis of GRCCC is no different from invasive carcinoma NST when the tumors are matched by size, grade, and lymph node status [117, 124].

Invasive Mammary Carcinoma with Osteoclast-like Giant Cells

Overview

Invasive breast carcinoma with osteoclast-like multinucleated giant cells is a rare variant of primary breast carcinoma. Osteoclast-like multinucleated giant cells can occur in many different tumor types including carcinomas and sarcomas of various organs such as lung, liver, gallbladder, thyroid, pancreas, kidney, and urinary tract [132–137]. Factor et al. first described two cases of invasive mammary carcinoma with osteoclast-like giant cells in the English literature in 1977 [138], which was followed by a small series of eight cases reported by Angnantis and Rosen in 1979 [139]. Identification of osteoclast-like multinucleated giant in association with invasive breast carcinoma is described in less than 2% of breast cancer patients. Only about 250 cases have been published in the literature thus far [140–146]. Due to its distinctive

histologic appearance, this tumor type is recognized as invasive breast carcinoma NST with special morphological patterns by the most recent WHO classification [147]. Since osteoclast-like multinucleated giant cells can be associated with almost all histologic types of breast cancer, it is viewed as a histologic finding rather than a distinct histologic subtype.

Gross and Radiologic Features

Clinical features of breast cancer with osteoclast-like multinucleated giant cells are similar to those of invasive carcinoma NST. It can occur in a wide range of ages (range: 28–88 years) [142]. The tumor size ranges from 0.5 to 10 cm [139, 142]. The most described cases are reported to be round well-circumscribed masses with microcalcifications. A red-brown gross appearance usually due to hemorrhage and associated hemosiderin deposition is commonly described as a characteristic of this tumor.

Microscopic Features

The defining histologic feature is the presence of varying amounts of osteoclast-like multinucleated giant cells in the stroma of invasive carcinoma (Fig. 13.35). Osteoclast-like multinucleated giant cells have been reported in various histological types of invasive breast cancer, including invasive

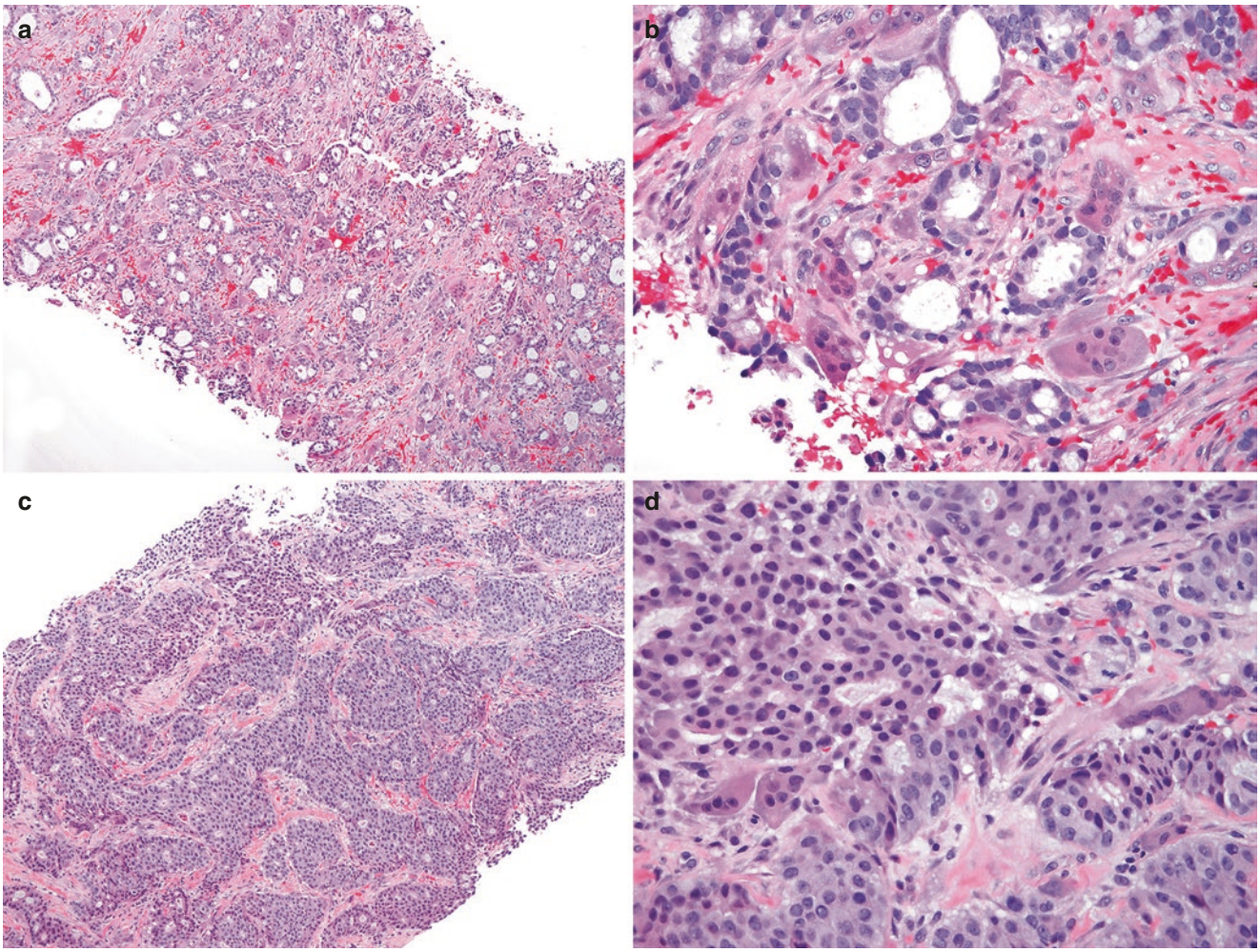

Fig. 13.35 Invasive ductal carcinoma with osteoclast-like giant cells. (**a**, **b**) CNB of a well-differentiated invasive ductal carcinoma shows associated multinucleated osteoclast-like giant cells. (**c**, **d**) Another example of moderately differentiated invasive ductal carcinoma with rare, scattered osteoclast-like giant cells

ductal carcinoma, invasive cribriform carcinoma, tubular carcinoma, mucinous carcinoma, papillary carcinoma, lobular carcinoma, and pleomorphic and metaplastic carcinoma [139, 143, 148, 149]. Osteoclast-like multinucleated giant cells have also been reported in association with both ductal and lobular carcinoma in situ [150]. The number of osteoclast-like multinucleated giant cells present in stroma may be quite variable from case to case and even in different areas of a tumor. Osteoclast-like multinucleated giant cells show bland cytologic features without atypia and most importantly without mitotic activity. Hemorrhage and hemosiderin deposition are common in the tumoral stroma.

Differential Diagnosis

The diagnosis of invasive carcinoma with osteoclast-like giant cells is straightforward when both multinucleated osteoclast-like giant cell and invasive carcinoma are readily identified. It can become diagnostically challenging when the carcinoma component is not readily identified, particularly in limited CNB material.

The differential diagnosis includes a benign reactive process with a giant cell component or malignant neoplasms of epithelial and/or mesenchymal origin. In a benign reactive process, atypical cells are not identified. However, when atypical cells, e.g., spindle cells or pleomorphic cells, are present together with osteoclast-like giant cells, the differential diagnosis includes pleomorphic carcinoma, metaplastic/sarcomatoid carcinoma with osteoclast-like giant cells, and sarcoma (Fig. 13.36). Definitive diagnosis can be deferred to the resection specimen in uncertain cases.

Immunohistochemical Workup

The associated multinucleated giant cells are of histiocytic origin, and they are CD68 positive and S100 protein negative. The carcinoma associated with osteoclast-like giant cells will be positive for cytokeratin and additionally may be associated with in situ carcinoma. In contrast, sarcomas will not be immunoreactive for cytokeratins and will lack an in situ carcinoma component.

Invasive carcinomas with osteoclast-like giant cells are frequently positive for hormonal receptors (ER and/or PR) and negative for HER2, although high-grade tumors including metaplastic carcinoma can be triple negative (ER−/PR−/HER−).

Pathogenesis

The mechanism for formation of osteoclast-like giant cells is still unknown. Immunohistochemical studies have confirmed histiocytic lineage of osteoclast-like multinucleated giant cells since they are positive for CD68 and negative for S100 protein. Secretion of specific cytokines, such as vascular endothelial growth factor and matrix metallopeptidase 12, has been described, and it has been hypothesized that the characteristic inflammatory and hypervascular stroma, which is commonly observed in breast carcinoma with osteoclast-like multinucleated giant cells, may be associated with the activation of these cytokines [151, 152].

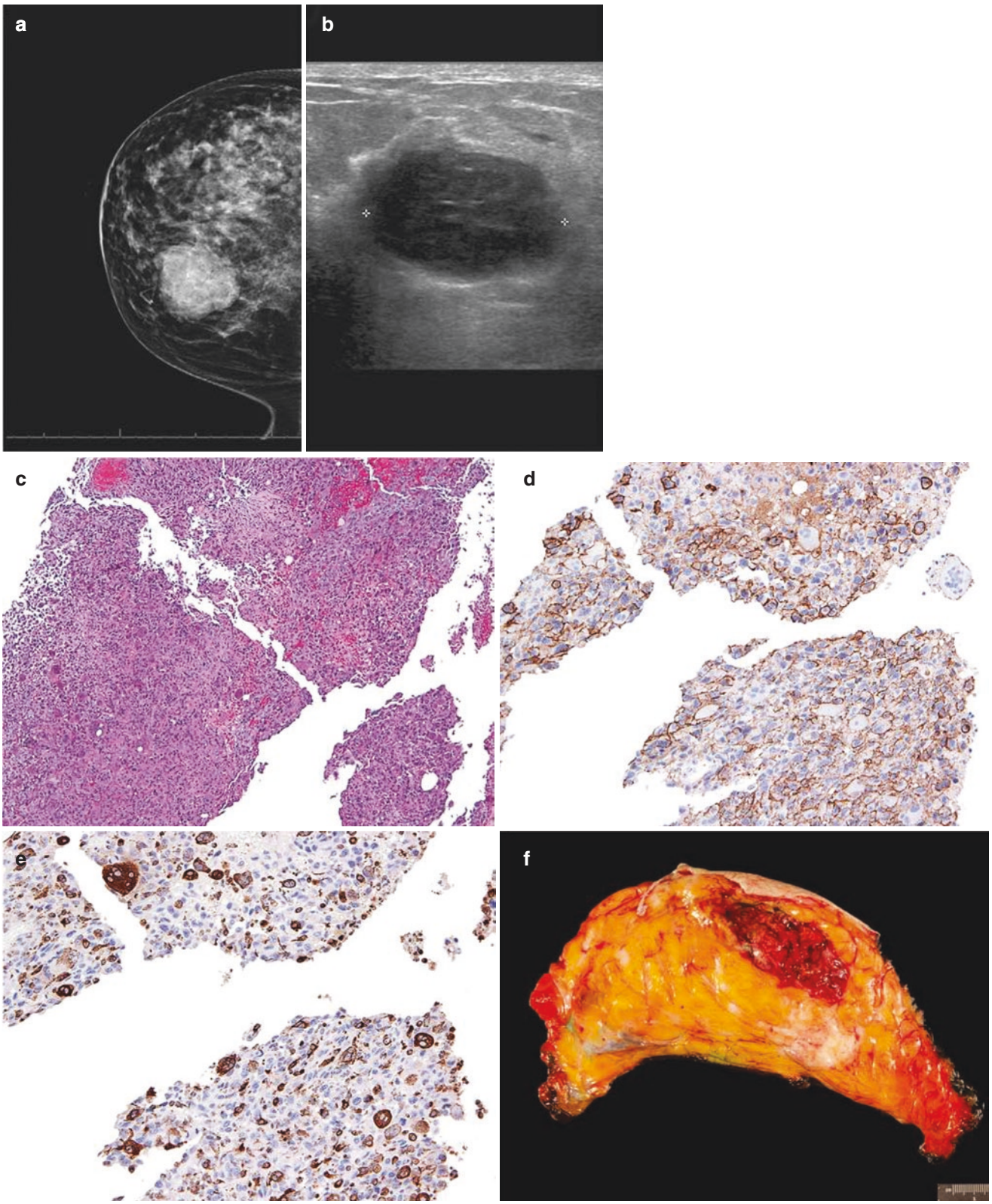

Fig. 13.36 Metaplastic/sarcomatoid carcinoma with osteoclast-like giant cells. (**a**) A 52-year-old women presented with a large palpable mass in her right breast. Diagnostic mammogram revealed a 4 cm lobulated, partially circumscribed, partially obscured mass, which was further confirmed by (**b**) sonogram. (**c**) Core needle biopsy was performed and showed a cellular high-grade neoplasm with mixed spindle, pleomorphic cells and osteoclast-like giant cells. The differential diagnosis includes metaplastic/sarcomatoid carcinoma versus sarcoma. (**d**, **e**) Further work-up showed the pleomorphic and spindle cells were positive for EMA (**d**) and multinuclear giant cells were positive for CD68 (**e**). Metaplastic/sarcomatoid carcinoma was favored. Patient underwent total mastectomy. (**f**) Gross evaluation revealed a well-demarcated large mass with brown hemorrhagic soft cut surface. (**g**, **h**) Histologic examination showed sheets of pleomorphic and spindle cells with admixed multinucleated giant cells; (**i**) focal area of high grade ductal carcinoma in situ was also present

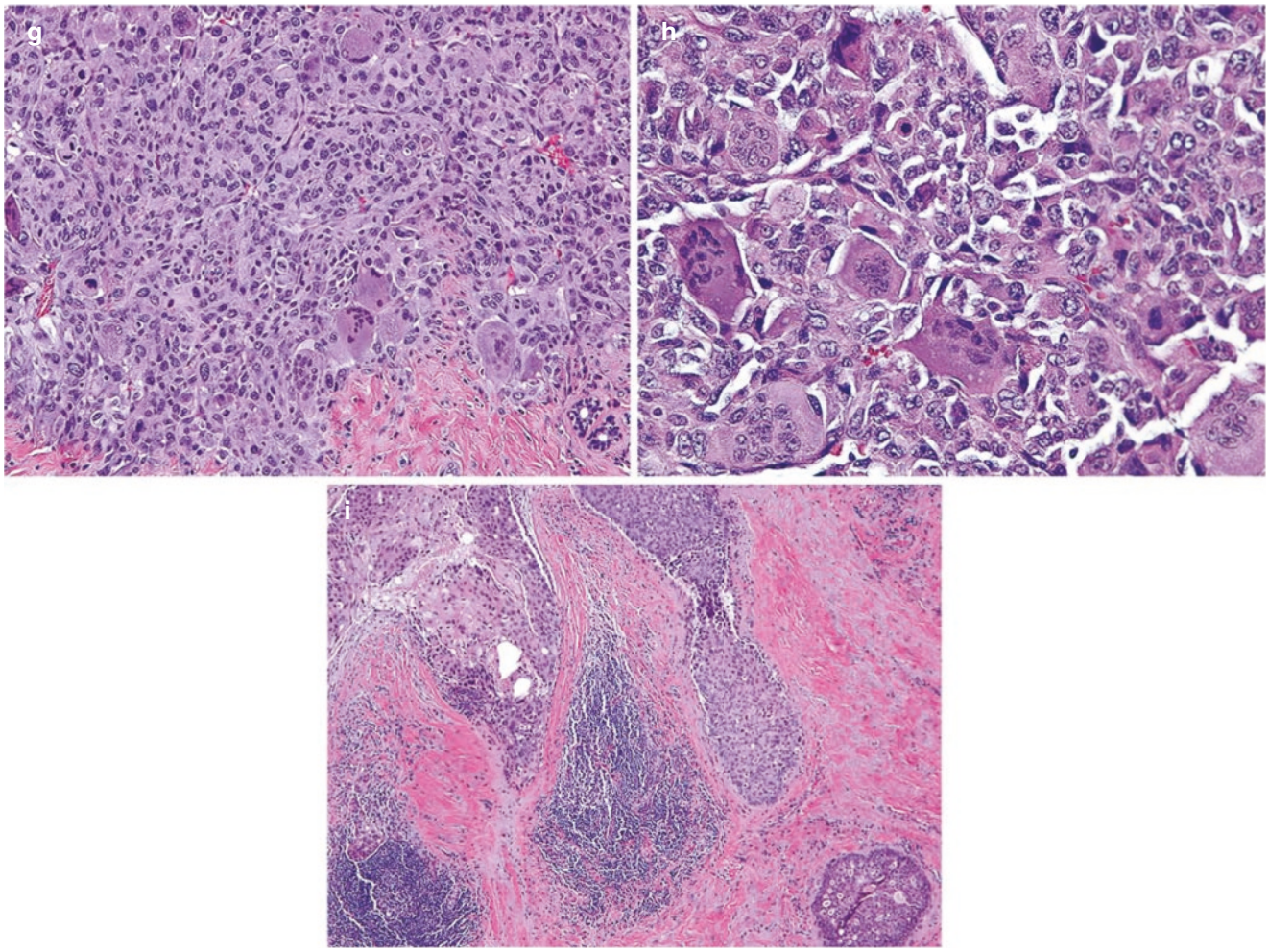

Fig. 13.36 (continued)

References

1. Wen HY, et al. Mucinous carcinoma. In: Allison KH, Brogi E, et al., editors. WHO classification of tumors of the breast. Lyon: IARC Press; 2019. p. 123–5.
2. Diab SG, Clark GM, et al. Tumor characteristics and clinical outcome of tubular and mucinous breast carcinomas. J Clin Oncol. 1999;17:1442–8.
3. Di Saverio S, et al. A retrospective review with long term follow up of 11,400 cases of pure mucinous breast carcinoma. Breast Cancer Res Treat. 2008;111(3):541–7.
4. Ng WK. Fine-needle aspiration cytology findings of an uncommon micropapillary variant of pure mucinous carcinoma of the breast: review of patients over an 8-year period. Cancer. 2002;96(5):280–8.
5. Madur B, et al. Cytologic findings in infiltrating micropapillary carcinoma and mucinous carcinomas with micropapillary pattern. Acta Cytol. 2007;51(1):25–32.
6. Shet T, Chinoy R. Presence of a micropapillary pattern in mucinous carcinomas of the breast and its impact on the clinical behavior. Breast J. 2008;14(5):412–20.
7. Bal A, et al. Prognostic significance of micropapillary pattern in pure mucinous carcinoma of the breast. Int J Surg Pathol. 2008;16(3):251–6.
8. Ranade A, et al. Clinicopathological evaluation of 100 cases of mucinous carcinoma of breast with emphasis on axillary staging and special reference to a micropapillary pattern. J Clin Pathol. 2010;63(12):1043–7.
9. Barbashina V, et al. Mucinous micropapillary carcinoma of the breast: an aggressive counterpart to conventional pure mucinous tumors. Hum Pathol. 2013;44:1577–85.
10. Liu F, et al. Invasive micropapillary mucinous carcinoma of the breast is associated with poor prognosis. Breast Cancer Res Treat. 2015;151(2):443–51.
11. Sun P, et al. Mucinous carcinoma with micropapillary features is morphologically, clinically and genetically distinct from pure mucinous carcinoma of breast. Mod Pathol. 2020;33(10):1945–60.
12. Pareja F, et al. Micropapillary variant of mucinous carcinoma of the breast shows genetic alterations intermediate between those of mucinous carcinoma and micropapillary carcinoma. Histopathology. 2019;75(1):139–45.
13. Matsuda M, et al. Mammographic and clinicopathological features of mucinous carcinoma of the breast. Breast Cancer. 2000;7(1):65–70.
14. Memis A, et al. Mucinous (colloid) breast cancer: mammographic and US features with histologic correlation. Eur J Radiol. 2000;35(1):39–43.
15. Dhillon R, et al. Screen-detected mucinous breast carcinoma: potential for delayed diagnosis. Clin Radiol. 2006;61(5):423–30.
16. Lacroix-Triki M, et al. Mucinous carcinoma of the breast is genomically distinct from invasive ductal carcinomas of no special type. J Pathol. 2010;222(3):282–98.

17. Jaffer S, et al. Benign mucocele-like lesions of the breast: revisited. Mod Pathol. 2011;24(5):683–7.
18. Begum SM, et al. Mucin extravasation in breast core biopsies—clinical significance and outcome correlation. Histopathology. 2009;55(5):609–17.
19. Fujii H, et al. Mucinous cancers have fewer genomic alterations than more common classes of breast cancer. Breast Cancer Res Treat. 2002;76(3):255–60.
20. Komenaka IK, et al. Pure mucinous carcinoma of the breast. Am J Surg. 2004;187(4):528–32.
21. Fisher ER, et al. Pathologic findings from the National Surgical Adjuvant Breast Project (protocol no. 4). VI. Invasive papillary cancer. Am J Clin Pathol. 1980;73(3):313–22.
22. Petersen JL. Breast carcinomas with an unexpected inside-out growth pattern: rotation of polarization associated with angioinvasion. Pathol Res Pract. 1993;189:A780.
23. Siriaunkgul S, Tavassoli FA. Invasive micropapillary carcinoma of the breast. Mod Pathol. 1993;6:660–2.
24. Marchio C, et al. Invasive micropapillary carcinoma. In: Allison KH, Brogi E, et al., editors. WHO classification of tumors of the breast. Lyon: IARC Press; 2019. p. 128–30.
25. Adrada B, et al. Invasive micropapillary carcinoma of the breast: mammographic, sonographic, and MRI features. AJR Am J Roentgenol. 2009;193(1):W58–63.
26. Alsharif S, et al. Mammographic, sonographic and MR imaging features of invasive micropapillary breast cancer. Eur J Radiol. 2014;83(8):1375–80.
27. Luna-Moré S, et al. Invasive micropapillary carcinoma of the breast. A new special type of invasive mammary carcinoma. Pathol Res Pract. 1994;190(7):668–74.
28. Nassar H, et al. Pathogenesis of invasive micropapillary carcinoma: role of MUC1 glycoprotein. Mod Pathol. 2004;17(9):1045–50.
29. Acs G, et al. Invasive ductal carcinomas of the breast showing partial reversed cell polarity are associated with lymphatic tumor spread and may represent part of a spectrum of invasive micropapillary carcinoma. Am J Surg Pathol. 2010;34(11):1637–46.
30. DeLair DF, et al. Non-mammary metastases to the breast and axilla: a study of 85 cases. Mod Pathol. 2013;26(3):343–9.
31. Khalifeh I, et al. Primary peritoneal serous carcinoma presenting as inflammatory breast cancer. Breast J. 2009;15(2):176–81.
32. Marchio C, et al. Genomic and immunophenotypical characterization of pure micropapillary carcinomas of the breast. J Pathol. 2008;215:398–410.
33. Gruel N, et al. Polarity gene alterations in pure invasive micropapillary carcinomas of the breast. Breast Cancer Res. 2014;16(3):R46.
34. Pettinato G, et al. Invasive micropapillary carcinoma of the breast: clinicopathologic study of 62 cases of a poorly recognized variant with highly aggressive behavior. Am J Clin Pathol. 2004;121:857–66.
35. Vingiani A, et al. The clinical relevance of micropapillary carcinoma of the breast: a case-control study. Histopathology. 2013;63:217–24.
36. Chen L, et al. Breast carcinoma with micropapillary features: clinicopathologic study and long-term follow-up of 100 cases. Int J Surg Pathol. 2008;16:155–63.
37. Yu JI, et al. Differences in prognostic factors and patterns of failure between invasive micropapillary carcinoma and invasive ductal carcinoma of the breast: matched case-control study. Breast. 2010;19:231–7.
38. Chen AC, et al. Prognostic markers for invasive micropapillary carcinoma of the breast: a population-based analysis. Br J Cancer. 2014;111(3):619–22.
39. Middleton LP, et al. Infiltrating micropapillary carcinoma of the breast. Mod Pathol. 1999;12:499–504.
40. Giuliano AE, et al. Axillary dissection vs no axillary dissection in women with invasive breast cancer and sentinel node metastasis: a randomized clinical trial. JAMA. 2011;305(6):569–75.
41. Koenig C, Tavassoli FA. Mucinous cystadenocarcinoma of the breast. Am J Surg Pathol. 1998;6:698–703.
42. Honma N, Sakamoto G, Ikenaga M, et al. Mucinous cystadenocarcinoma of the breast: a case report and review of the literature. Arch Pathol Lab Med. 2003;127:1031–3.
43. Jain E, Kumar A, Jain R, et al. Primary mucinous cystadenocarcinoma of the breast: a rare case report with review of the literature. Int J Surg Pathol. 2021; Feb 26 (Online ahead of print)
44. Wen HY, et al. Mucinous cystadenocarcinoma. In: Allison KH, Brogi E, et al., editors. WHO Classification of tumors of the Breast. Lyon: IARC Press; 2019. p. 126–7.
45. Nayak A, Bleiweiss IJ, Dumoff K, et al. Mucinous cystadenocarcinoma of the breast: report of 2 cases including one with long-term local recurrence. Int J Surg Pathol. 2018;26:749–57.
46. Li X, Peng J, Zhang Z, et al. Mammary mucinous cystadenocarcinoma. Breast J. 2012;18:282–3.
47. Chen W-Y, Chen C-S, Chen H-C, et al. Mucinous cystadenocarcinoma of the breast coexisting with infiltrating ductal carcinoma. Pathol Int. 2004;54:781–6.
48. Wang X, Li Y, Zhao P, et al. Primary mucinous cystadenocarcinoma of the breast: a clinicopathologic analysis of one case and review of the literature. Int J Clin Exp Pathol. 2020;13:2562–8.
49. Petersson F, Pang B, Thamboo TP, et al. Mucinous cystadenocarcinoma of the breast with amplification of the HER2-gene confirmed by FISH: the first case reported. Hum Pathol. 2009;41:910–3.
50. Kim SE, Park JH, Hong SW, et al. Primary mucinous cystadenocarcinoma of the breast: cytologic finding and expression of MUC5 are different from mucinous carcinoma. Korean J Pathol. 2012;46:611–6.
51. Bussolati G, Badve S. Carcinomas with neuroendocrine features. In: Lakhani S, Ellis IO, Schnitt SJ, Tan PH, van de Vijver MJ, editors. WHO classification of tumours of the breast. Lyon: IARC Press; 2012. p. 62–3.
52. Feyrter F, Hartmann G. On the carcinoid growth form of the carcinoma mammae, especially the carcinoma solidum (Gelatinosum) mammae. Frankf Z Pathol. 1963;73:24–39.
53. Cubilla AL, Woodruff JM. Primary carcinoid tumor of the breast. A report of eight patients. Am J Surg Pathol. 1977;1:283–92.
54. Azzopardi JG, et al. 'Carcinoid' tumours of the breast: the morphological spectrum of argyrophil carcinomas. Histopathology. 1982;6:549–69.
55. Fisher ER, Palekar AS. Solid and mucinous varieties of so-called mammary carcinoid tumors. Am J Clin Pathol. 1979;1979(72):909–16.
56. Papotti M, et al. Neuroendocrine differentiation in carcinomas of the breast: a study of 51 cases. Semin Diagn Pathol. 1989;6:174–88.
57. Rosen PP, Oberman HA. Invasive carcinoma. In: Rosen PP, Oberman HA, editors. Tumors of the mammary gland. Atlas of tumor pathology. Washington, DC: AFIP Press; 1993. p. 236–40.
58. Maluf HM, Koerner FC. Solid papillary carcinoma of the breast. A form of intraductal carcinoma with endocrine differentiation frequently associated with mucinous carcinoma. Am J Surg Pathol. 1995;19:1237–44.
59. Sapino A, et al. Expression of apocrine differentiation markers in neuroendocrine breast carcinomas of aged women. Mod Pathol. 2001;14:768–76.
60. Miremadi A, et al. Neuroendocrine differentiation and prognosis in breast adenocarcinoma. Histopathology. 2002;40:215–22.
61. Makretsov N, et al. Tissue microarray analysis of neuroendocrine differentiation and its prognostic significance in breast cancer. Hum Pathol. 2003;34:1001–8.
62. Zekioglu O, et al. Neuroendocrine differentiated carcinomas of the breast: a distinct entity. Breast. 2003;12:251–7.
63. van Krimpen C, et al. The prognostic influence of neuroendocrine differentiation in breast cancer: results of a long term follow-up study. Breast. 2004;13:329–33.

64. Lopez-Bonet E, et al. Solid neuroendocrine breast carcinomas: incidence, clinico-pathological features and immunohistochemical profiling. Oncol Rep. 2008;20:1369–74.
65. Rovera F, et al. Neuroendocrine carcinomas of the breast. Int J Surg. 2008;6(Suppl 1):S113–5.
66. Righi L, et al. Neuroendocrine differentiation in breast cancer: established facts and unsolved problems. Semin Diagn Pathol. 2010;27:69–76.
67. Wei B, et al. Invasive neuroendocrine carcinoma of the breast: a distinctive subtype of aggressive mammary carcinoma. Cancer. 2010;116:4463–73.
68. Zhang Y, et al. Invasive neuroendocrine carcinoma of the breast: a prognostic research of 107 Chinese patients. Neoplasma. 2013;60(2):215–22.
69. Angarita FA, et al. Locally-advanced primary neuroendocrine carcinoma of the breast: case report and review of the literature. World J Surg Oncol. 2013;11:128.
70. Rovera F, et al. Neuroendocrine breast cancer: retrospective analysis of 96 patients and review of literature. Int J Surg. 2013;11(Suppl 1):S79–83.
71. Wang J, et al. Invasive neuroendocrine carcinoma of the breast: a population-based study from the surveillance, epidemiology and end results (SEER) database. BMC Cancer. 2014;14:147.
72. Kwon SY, et al. Neuroendocrine differentiation correlates with hormone receptor expression and decreased survival in patients with invasive breast carcinoma. Histopathology. 2014;64(5):647–59.
73. Cloyd JM, et al. Impact of histological subtype on long-term outcomes of neuroendocrine carcinoma of the breast. Breast Cancer Res Treat. 2014;148(3):637–44.
74. Bogina G, et al. Neuroendocrine differentiation in breast carcinoma: clinicopathological features and outcome. Histopathology. 2016;68(3):422–32.
75. Ellis IO, et al. Invasive breast carcinoma. In: Tavassoli FA, Devilee P, editors. Pathology and genetics. Tumors of the breast and female genital organs. WHO series on classification of tumours. Lyon: IARC Press; 2003. p. 32–4.
76. Rakha EA, et al. Neuroendocrine neoplasms. In: Allison KH, Brogi E, et al., editors. WHO classification of tumors of the breast. Lyon: IARC Press; 2019. p. 155–61.
77. Rindi G, et, al. A common classification framework for neuroendocrine neoplasms: an International Agency for Research on Cancer (IARC) and World Health Organization (WHO) expert consensus proposal. Mod Pathol. 2018;31(12):1770–86.
78. Park YM, et al. Primary neuroendocrine carcinoma of the breast: clinical, imaging, and histologic features. Am J Roentgenol. 2014;203:W221–30.
79. Tang F, et al. Invasive mammary carcinoma with neuroendocrine differentiation: histological features and diagnostic challenges. Histopathology. 2011;59:106–15.
80. Shin SJ, et al. Small cell carcinoma of the breast: a clinicopathologic and immunohistochemical study of nine patients. Am J Surg Pathol. 2000;24(9):1231–8.
81. Perry KD, et al. Metastatic neuroendocrine tumour in the breast: a potential mimic of in-situ and invasive mammary carcinoma. Histopathology. 2011;59(4):619–30.
82. Ai D, et al. TRPS1: a highly sensitive and specific marker for breast carcinoma, especially for triple-negative breast cancer. Mod Pathol. 2021;34:710–9.
83. Dabbs DJ, Thompsom LD. Diagnostic immunohistochemistry: theranostic and genomic applications. 4th ed. Philadelphia, PA: Elsevier Sanders; 2014. p. 264.
84. Kawasaki T, et al. Neuroendocrine cells associated with neuroendocrine carcinoma of the breast: nature and significance. J Clin Pathol. 2012;65(8):699–703.
85. Miura K, et al. Double neuroendocrine ductal carcinomas in situ coexisting with a background of diffuse idiopathic neuroendocrine cell hyperplasia of breast: a case report and hypothesis of neuroendocrine tumor development. Pathol Int. 2012;62(5):331–4.
86. Wachter DL, et al. Expression of neuroendocrine markers in different molecular subtypes of breast carcinoma. Biomed Res Int. 2014;2014:408459.
87. Xiang D, et al. Molecular cytogenetic characterization of mammary neuroendocrine carcinoma. Hum Pathol. 2014;45:1951–6.
88. Ang D, et al. Novel mutations in neuroendocrine carcinoma of the breast: possible therapeutic targets. Appl Immunohistochem Mol Morphol. 2015;23(2):97–103.
89. Yang L, et al. Validation of prognostic significance of the proposed uniform classification framework in neuroendocrine neoplasms of the breast. Breast Cancer Res Treat. 2021;186:403–15.
90. Tian Z, et al. Prognostic significance of tumor grading and staging in mammary carcinomas with neuroendocrine differentiation. Hum Pathol. 2011;42(8):1169–77.
91. D'Alfonso TM, Ginter PS, Liu YF, Shin SJ. Cystic hypersecretory (in-situ) carcinoma of the breast: a clinicopathologic and immunohistochemical characterization of 10 cases with clinical follow-up. Am J Surg Pathol. 2014;38(1):45–53.
92. Rosen PP, Scott M. Cystic hypersecretory duct carcinoma of the breast. Am J Surg Pathol. 1984;8:31–41.
93. Colandrea JM, Shmookler BM, O'Dowd GJ, et al. Cystic hypersecretory duct carcinoma of the breast. Report of a case with fine-needle aspiration. Arch Pathol Lab Med. 1988;112:560–56.
94. Adams GD, Lacey S. Cystic hypersecretory breast carcinoma. An unusual breast cancer. Nebr Med J. 1990;75:104–8.
95. Kim MK, Kwon GY, Gong GY. Fine needle aspiration cytology of cystic hypersecretory carcinoma of the breast. Acta Cytol. 1997;41(3):892–6.
96. Herrmann ME, McClatchey KD, Siziopikou KP. Invasive cystic hypersecretory ductal carcinoma of breast: a case report and review of the literature. Arch Pathol Lab Med. 1999;123:1108–10.
97. Lee JS, Lee YJ. Invasive cystic hypersecretory carcinoma of the breast: a case report. J Korean Med Sci. 2004;19:149–51.
98. Skalova A, Ryska A, Kajo K, et al. Cystic hypersecretory carcinoma: rare and poorly recognized variant of intraductal carcinoma of the breast. Report of five cases. Histopathology. 2005;46:43–9.
99. Gupta P, Dhingra S, Musa O, et al. Invasive cystic hypersecretory carcinoma of the breast associated with papillary pattern: a rare and poorly recognised variant of ductal carcinoma of the breast. Ecancermedicalscience. 2014;8:477.
100. Singh K, Falkenberry S, Eklund B, et al. Cystic hypersecretory hyperplasia of breast. Int J Surg Pathol. 2018;26(5):432–3.
101. Song SW, Whang IY, Chang ED. Cystic hypersecretory ductal carcinoma of the breast: a rare cause of cystic breast mass. Jpn J Radiol. 2011;29:660–2.
102. Sahoo S, Gopal P, Roland L, et al. Cystic hypersecretory carcinoma of the breast with Paget disease of the nipple: a diagnostic challenge. Int J Surg Pathol. 2008;16:208–12.
103. Resetkova E, Padula A, Albarraccin CT, et al. Pathologic quiz case: a large, ill-defined cystic breast mass. Invasive cystic hypersecretory duct carcinoma. Arch Pathol Lab Med. 2005;129:e79–80.
104. Hill CB, Yeh IT. Myoepithelial cell staining patterns of papillary breast lesions: from intraductal papillomas to invasive papillary carcinomas. Am J Clin Pathol. 2005;123:36–44.
105. Park JM, Seo MR. Cystic hypersecretory duct carcinoma of the breast: report of two cases. Clin Radiol. 2002;57:312–5.
106. Shah AK, Banerjee SN, Sehonanda AS, et al. Cystic hypersecretory duct carcinoma of the breast. Breast J. 2000;6:269–72.
107. Cserni G, Viragh S. Immunohistochemical and ultrastructural analysis of a mammary cystic hypersecretory carcinoma. Pathol Oncol Res. 1997;3:287–92.
108. Shin SJ, Rosen PP. Pregnancy-like (pseudolactational) hyperplasia: a primary diagnosis in mammographically detected lesions of the breast and its relationship to cystic hypersecretory hyperplasia. Am J Surg Pathol. 2000;24:1670–4.
109. Shin SJ, Rosen PP. Carcinoma arising from preexisting pregnancy-like and cystic hypersecretory hyperplasia lesions of the breast:

a clinicopathologic study of 9 patients. Am J Surg Pathol. 2004;28:789–93.
110. Guerry P, Erlandson RA, Rosen PP. Cystic hypersecretory hyperplasia and cystic hypersecretory duct carcinoma of the breast. Pathology, therapy, and follow-up of 39 patients. Cancer. 1988;61:1611–20.
111. Eusebi, et al. Exceptionally rare types and variants. In: Lakhani S, Ellis IO, Schnitt SJ, Tan PH, van de Vijver MJ, editors. WHO classification of tumours of the breast. Lyon: IARC Press; 2012. p. 74–5.
112. Hull MT, et al. Glycogen-rich clear cell carcinoma of the breast: a light and electron microscopic study. Cancer. 1981;48(9):2003–9.
113. Benisch B, et al. Solid glycogen-rich clear cell carcinoma of the breast (a light and ultrastructural study). Am J Clin Pathol. 1983;79(2):243–5.
114. Ficher ER, et al. Glycogen-rich, clear cell breast cancer: with comments concerning other clear cell variants. Hum Pathol. 1985;16(11):1085–90.
115. Hull MT. Glycogen-rich clear cell carcinomas of the breast. A clinicopathologic and ultrastructural study. Am J Surg Pathol. 1986;10(8):553–9.
116. Toikkanen S, Joensuu H. Glycogen-rich clear-cell carcinoma of the breast: a clinicopathologic and flow cytometric study. Hum Pathol. 1991;22(1):81–3.
117. Hayes MM, et al. Glycogen-rich clear cell carcinoma of the breast. A clinicopathologic study of 21 cases. Am J Surg Pathol. 1995;19(8):904–11.
118. Gurbuz Y, Ozkara SK. Clear cell carcinoma of the breast with solid papillary pattern: a case report with immunohistochemical profile. J Clin Pathol. 2003;56(7):552–4.
119. Kuroda H, et al. Clinical and pathological features of glycogen-rich clear cell carcinoma of the breast. Breast Cancer. 2005;12(3):189–95.
120. Markopoulos C, et al. Glycogen-rich clear cell carcinoma of the breast. World J Surg Oncol. 2008;6:44.
121. Thondavadi SR, et al. A case report of glycogen-rich clear cell carcinoma of breast. Indian J Pathol Microbiol. 2010;53(2):374–5.
122. Martín-Martín B, et al. An unusual case of locally advanced glycogen-rich clear cell carcinoma of the breast. Case Rep Oncol. 2011;4(3):452–7.
123. Kim SE, et al. Immunophenotypes of glycogen rich clear cell carcinoma. Yonsei Med J. 2012;53(6):1142–6.
124. Ma X, et al. Clinicopathologic characteristics and prognosis of glycogen-rich clear cell carcinoma of the breast. Breast J. 2014;20(2):166–73.
125. Rakha EA, et al. Invasive breast carcinoma of no special type. In: Allison KH, Brogi E, et al., editors. WHO classification of tumors of the breast. Lyon: IARC Press; 2019. p. P108–9.
126. Salemis NS. Intraductal glycogen-rich clear cell carcinoma of the breast: a rare presentation and review of the literature. Breast Care (Basel). 2012;7(4):319–21.
127. Leibl S, et al. Metaplastic breast carcinomas: are they of myoepithelial differentiation?: immunohistochemical profile of the sarcomatoid subtype using novel myoepithelial markers. Am J Surg Pathol. 2005;29(3):347–53.
128. Cartagena N Jr, et al. Clear cell myoepithelial neoplasm of the breast. Hum Pathol. 1988;19(10):1239–43.
129. Mandal S, et al. Clear cell malignant myoepithelioma—breast presenting as a fungating mass. Breast J. 2007;13(6):618–20.
130. Son HJ, et al. Glycogen-rich clear cell mammary malignant myoepithelioma. Breast. 2004;13(6):506–9.
131. Di Tommaso L, et al. Glycogen-rich clear-cell breast carcinoma with neuroendocrine differentiation features. Pathologica. 2001;93(6):676–80.
132. Akatsu T, et al. Gallbladder carcinoma with osteoclast-like giant cells. J Gastroenterol. 2006;41:83–7.
133. Wada Y, et al. Adenocarcinoma of the liver with osteoclast-like giant cells. Pathol Int. 2013;63:476–8.
134. Temesgen WM, et al. Osteoclastic giant cell tumor of the pancreas. Int J Surg Case Rep. 2014;5(4):175–9.
135. Yamabe S, et al. Case of giant cell anaplastic ductal carcinoma of the pancreas. Nihon Shokakibyo Gakkai Zasshi. 2014;111(2):334–9.
136. McCash SI, et al. Undifferentiated carcinoma of the renal pelvis with osteoclast-like giant cells: a report of two cases. APMIS. 2010;118:407–12.
137. Singh M, et al. Osteoclastic giant cell rich carcinoma cervix: a rare entity. J Obstet Gynaecol. 2012;32(5):499–501.
138. Factor SM, et al. Carcinoma of the breast with multinucleated reactive stroma giant cells. Virchows Arch A Pathol Anat Histol. 1977;374:1–12.
139. Agnantis NT, Rosen PP. Mammary carcinoma with osteoclast-like giant cells. A study of eight cases with follow-up data. Am J Clin Pathol. 1979;72:383–9.
140. Zhou S, et al. Invasive breast carcinomas of no special type with osteoclast-like giant cells frequently have a luminal phenotype. Virchows Arch. 2014;464(6):681–8.
141. Holland R, van Haelst UJ. Mammary carcinoma with osteoclast-like giant cells. Additional observations on six cases. Cancer. 1984;53:1963–73.
142. Tavassoli FA, Norris HJ. Breast carcinoma with osteoclast like giant cells. Arch Pathol Lab Med. 1986;110:636–9.
143. Trojani M, et al. Osteoclastic type giant cell carcinoma of the breast. Ann Pathol. 1989;9:189–94.
144. Mukkamala A, et al. Breast carcinoma with osteoclastic giant cells. Breast J. 1999;5:149–50.
145. Yang YL, et al. Invasive ductal carcinoma with osteoclastic giant cells of breast: clinicopathologic characteristics. Breast J. 2013;19(3):329–30.
146. Niu Y, et al. Breast carcinoma with osteoclastic giant cells: case report and review of the literature. Int J Clin Exp Pathol. 2014;7(4):1788–91.
147. Rakha EA, et al. Invasive breast carcinoma of no special type. In: Allison KH, Brogi E, et al, eds. WHO classification of tumors of the breast. Lyon: IARC Press; 2019. p. 105–106.
148. Kurokawa K, et al. Pleomorphic carcinoma with osteoclastic giant cells of the breast: immunohistochemical differentiation between coexisting neoplastic and reactive giant cells. Pathol Int. 2009;59:91–7.
149. Wargotz ES, Norris HJ. Metaplastic carcinomas of the breast: V. metaplastic carcinoma with osteoclastic giant cells. Hum Pathol. 1990;21:1142–50.
150. Coyne JD. DCIS and LCIS with multinucleated giant cells-a report of 4 cases. Histopathology. 2007;50(5):669–71.
151. Shishido-Hara Y, et al. Two cases of breast carcinoma with osteoclastic giant cells: are the osteoclastic giant cells pro-tumoural differentiation of macrophages? Diagn Pathol. 2010;5:55.
152. Albawardi AS, et al. Mammary carcinoma with osteoclast-like giant cells: a case report. Int J Clin Exp Pathol. 2014;7:9038–43.

Atypical Lobular Hyperplasia and Lobular Carcinoma In Situ

14

Gregor Krings, Helena Hwang, and Yunn-Yi Chen

Overview

Atypical lobular hyperplasia (ALH) and lobular carcinoma in situ (LCIS) are noninvasive neoplastic proliferative lesions comprised of generally small, dyscohesive cells originating in the terminal duct lobular units (TDLUs), with or without pagetoid extension to terminal ducts [1, 2]. The loss of cell-to-cell cohesion is secondary to absence or dysfunction of E-cadherin. ALH and LCIS are distinguished from one another by the degree of involvement of the TDLUs, with ALH showing less involvement (Figs. 14.1 and 14.2). Both lesions are often grouped under the term lobular neoplasia (LN), which was first introduced by Haagensen et al. in 1978 [3]. Lesions consistent with LN were noted as early as 1850 in a book by John Birkett, who pictorialized "cecal terminations of glandular tissue" [4]. A few other LN references subsequently followed, most notably in 1919 by James Ewing, who in his book *Neoplastic Diseases* showed two photographs which resembled LCIS and pagetoid involvement of duct that were described as "atypical proliferation of

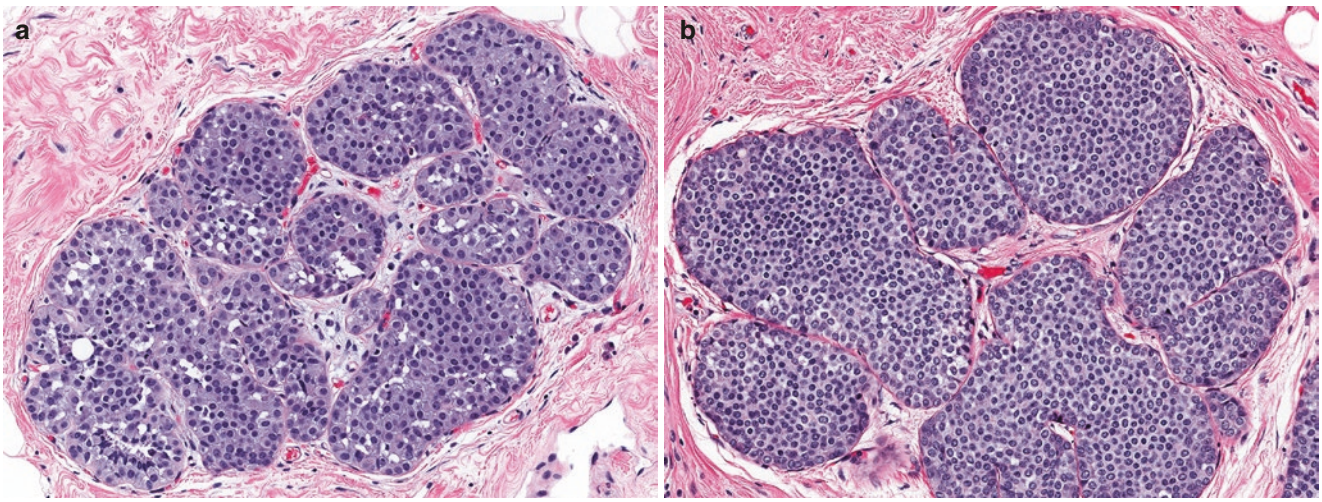

Fig. 14.1 Classic LCIS. (**a**, **b**) More than 50% of the acini in these TDLUs are filled and expanded by loosely cohesive monomorphic cells with pale cytoplasm, small uniform round nuclei, and inconspicuous nucleoli

G. Krings · Y.-Y. Chen (✉)
Department of Pathology, University of California San Francisco, San Francisco, CA, USA
e-mail: Gregor.krings@ucsf.edu; Yunn-yi.chen@ucsf.edu

H. Hwang
Department of Pathology, UT Southwestern Medical Center, Dallas, TX, USA
e-mail: Helena.hwang@utsouthwestern.edu

© The Author(s), under exclusive license to Springer Nature Switzerland AG 2022
S. J. Shin et al. (eds.), *A Comprehensive Guide to Core Needle Biopsies of the Breast*,
https://doi.org/10.1007/978-3-031-05532-4_14

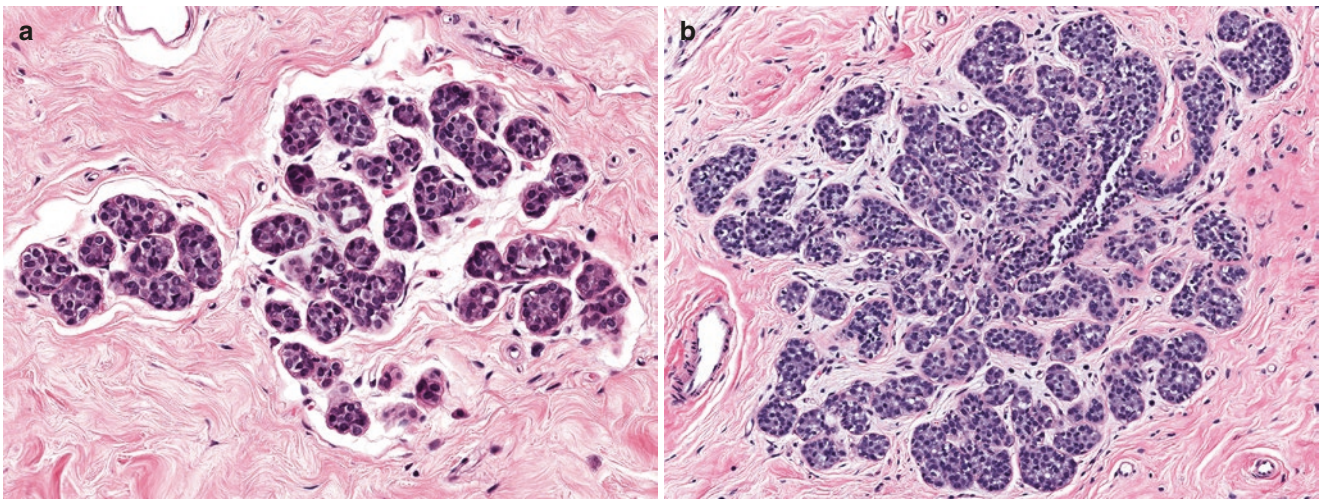

Fig. 14.2 ALH. (**a**, **b**) The acini in these TDLUs are filled and minimally expanded (with less than 50% of the acini with <8 cells in diameter) by small non-cohesive monomorphic cells with scant cytoplasm and small uniform nuclei

acinar cells" and "atypical proliferation of a segment of a duct" [5]. However, it was not until 1941 that Foote and Stewart first coined the term LCIS in their seminal paper [6]. Most of their detailed descriptions on the clinical and pathological features of LCIS have remained remarkably current more than 80 years later.

Our understanding of LCIS has evolved over the years. In the ensuing three decades after the work by Foote and Stewart, the prevailing opinion was that LCIS was a premalignant lesion and, analogous to DCIS, would progress to invasive carcinoma. Therefore, mastectomy was the recommended treatment for LCIS [6]. Subsequent long-term outcome data suggested that LCIS behaves more as a risk factor for future invasive carcinoma than a true malignant precursor condition [3, 7–9]. Therefore, Haagensen et al. introduced the term LN to convey the more indolent nature of this proliferative process and to avoid the carcinoma connotation and overtreatment [3]. Since the late 1990s, morphologic variants of LCIS have been recognized and defined [2, 10]. The last two decades have seen emerging evidence from molecular studies that reveal the clonal relationship between LCIS and invasive lobular carcinoma (ILC), including pleomorphic LCIS and florid LCIS, supporting the notion that LCIS can also be a direct but non-obligate precursor lesion to ILC. As our understanding of LN continues to evolve, so does the pathologic evaluation of preinvasive lobular lesions and management for patients with these lesions, especially in core biopsy specimens.

Nomenclature and Classification

ALH and LCIS are the recommended and most widely used terminologies for intraepithelial neoplastic lobular proliferations. However, there is merit in understanding other classification systems.

LCIS was so named because it was believed to originate from lobules, whereas DCIS was initially thought to arise from ducts until evidence emerged that DCIS also originates from the TDLU [11]. In 1978, Haagensen et al. proposed the term LN to reflect the indolent nature of LCIS, stating "the correct choice of a name for a disease is very important, not only because it identifies it, but also because it prejudices the choice of treatment" as "most surgeons amputate breasts when the lesion is classified as carcinoma" [3].

The origin of the term ALH is more difficult to pinpoint, but it appears to have been in the pathology lexicon for some time. Foote and Stewart preferred the term "lobular hyperplasia" for lesions they felt were an "early stage of LCIS" [12], while Wheeler et al. described ALH in 1974 as "cells not distending the terminal ducts, or not totally replacing all normal cells … of at least one terminal duct" [8]. It was not until 1985 that ALH was strictly defined by Page et al. [13]. Strictly speaking, the term ALH is a misnomer, however, as these lesions have been shown to be clonal and neoplastic [14–16].

Differentiating ALH from LCIS can be highly subjective with intra- and interobserver variability [17]. Some authors have therefore advocated diagnosing these lesions as LN, particularly in core biopsies [18, 19]. However, given the differences in long-term risk of invasive cancer development, as well as different upgrade rates to carcinoma on core biopsies (see section "Prognosis and Management"), it is clinically relevant to separate ALH from classic LCIS when possible.

Tavassoli created a three-tiered system for classification of LN, employing the term lobular intraepithelial neoplasia (LIN) [20]. LIN1 is a proliferation of neoplastic lobular cells that fill but do not distend acini, LIN2 fills and distends acini

with acinar outlines remaining distinct, and LIN3 includes lesions with massive acinar distension, necrosis, pleomorphic cells, or signet ring cells. It was suggested that LIN1 and LIN2 be combined in practice and simply diagnosed as LIN, whereas LIN3 should be further subclassified into four types: LIN—necrotic type, LIN—pleomorphic type, LIN—macroacinar type, and LIN—signet ring cell type [21].

LCIS lesions as originally described by Foote and Stewart and consisting of uniform small cells are considered classic LCIS. Haagensen further noted that larger lobular cells (type B cells) can be observed in classic LCIS in addition to the small cells (type A cells) [3]. Morphologic variants of LCIS that deviate from classic LCIS have been recognized, especially after the introduction of E-cadherin immunohistochemistry (IHC). Pleomorphic LCIS was first described by Frost et al. in 1996 as an in situ lesion associated with pleomorphic ILC and composed of "one or multiple distended lobules with enlarged and dyscohesive cells, irregularly shaped nuclei, and abundant eosinophilic cytoplasm" [22]. The term florid LCIS was coined by Shin and Rosen for LCIS lesions showing "marked expansion of the TDLUs by a solid proliferation of dyshesive nonpleomorphic cells with or without necrosis and/or calcifications" [23, 24]. Tavassoli proposed necrotic, pleomorphic, macroacinar, and signet ring cell types of LIN3 that should be distinguished from classic LIN [21]. Other terms that have been used by pathologists include "necrotic LCIS," "LCIS with necrosis," "non-classic LCIS," and "variant LCIS." These morphologic variants should be distinguished from classic LCIS, as they appear to have more worrisome histopathologic features, more advanced molecular alterations, and more aggressive biologic behavior with implications for clinical management. The current WHO classification recognizes two subtypes of LCIS in addition to classic LCIS: pleomorphic LCIS and florid LCIS. Use of the terms "non-classic LCIS" or "variant LCIS" is not recommended without further clarification, due to lack of sufficient specificity to guide patient management [2, 10].

The term mixed carcinoma in situ was previously used in the literature, mainly before the advent of E-cadherin immunostaining, to describe lesions equivocal for DCIS versus LCIS. Using IHC, Jacobs et al. and Maluf et al. were able to classify such previously diagnosed equivocal lesions as either DCIS or LCIS based on membranous expression of E-cadherin. In some cases, DCIS and LCIS were found to coexist within the same duct [25, 26], a phenomenon that Rosen had also described long before E-cadherin immunostaining was routinely used [27]. Koerner and Maluf later suggested that most of these lesions appeared to be pagetoid involvement of DCIS by LN [28]. DCIS and LCIS occurring adjacent to one another are more common than coexisting DCIS and LCIS within the same duct [28]. The terms "mixed carcinoma in situ" or "ductal lobular carcinoma in situ" should be avoided, as these designations are not clear and confusing for patient management. Immunostains for E-cadherin and other components of the E-cadherin-catenin complex should help classify equivocal in situ lesions on hematoxylin and eosin stain, including coexisting DCIS and LCIS within the same duct space (Fig. 14.3) (see sections "Immunohistochemistry" and "Differential Diagnosis").

In the core biopsy setting, pathologists are encouraged to categorize noninvasive lobular lesions using the terms and criteria recommended by the WHO classification [1, 2]. Whereas some practices may use LN to encompass ALH and LCIS, it is clinically relevant to separate ALH from classic LCIS whenever possible. The LIN classification system is not recommended, as this terminology is not widely accepted and is accordingly at risk for confusion by treating physi-

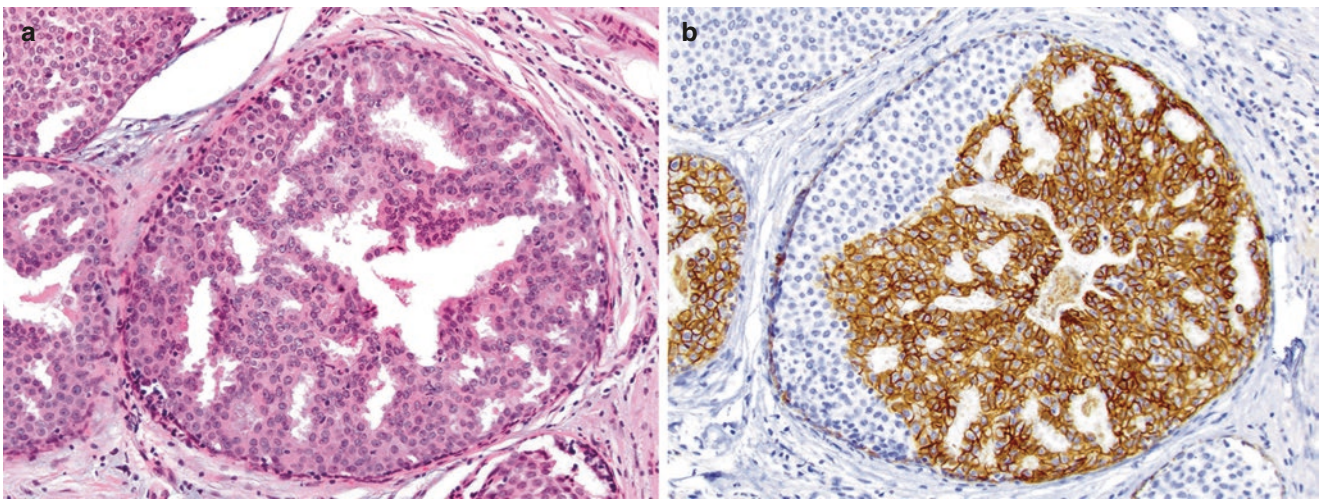

Fig. 14.3 Coexisting DCIS and classic LCIS in a duct. (**a**) H&E stain and (**b**) E-cadherin immunostain showing membranous staining in DCIS cells and loss of membranous staining in LCIS cells within the same duct

cians. It is most important to distinguish classic LCIS from pleomorphic and florid subtypes, as the latter two subtypes have distinct clinical and management implications when diagnosed on core biopsy.

Clinical Features

ALH and classic LCIS are often multicentric and bilateral [3, 20, 29–32]. In contrast, pleomorphic and florid LCIS have been noted to be unifocal and continuous in distribution, often colocalized with ILC in the background of multicentric classic LCIS [33, 34]. Classic LCIS is predominantly found in premenopausal women with a mean age of ~50 years, 10–15 years earlier than that for ILC [3, 29, 35, 36]. Pleomorphic LCIS and florid LCIS, on the other hand, are diagnosed primarily in postmenopausal women (mean age ~ 60 years) [24, 34, 37, 38].

ALH and classic LCIS are not clinically detectable and usually an incidental microscopic finding in breast biopsies performed for other indications [6]. As a result, the true incidence of these lesions in the general population is unknown. ALH and classic LCIS have been identified in ~0.5–1.2% and 0.5–3.6% of otherwise benign core biopsies, respectively, and 1.6–2.9% and 0.04–1.2% of reduction mammoplasty specimens, respectively [1, 2]. Population-based studies demonstrated a fourfold increase in the incidence of LCIS from the late 1970s to 1990s, with the largest increase occurring in women 50–79 years old. The increase was attributed to a rise in biopsies resulting from widespread mammographic screening, as well as the use of hormone replacement therapy for menopause; the rate has since plateaued [39, 40].

Contrary to classic LCIS and similar to DCIS, pleomorphic LCIS and florid LCIS usually present with abnormal imaging findings, most frequently suspicious calcifications, that lead to core biopsy [24, 34, 37, 41–46]. Pure pleomorphic LCIS (without associated invasive carcinoma or DCIS) on core biopsy can also rarely present as a palpable mass, including pleomorphic LCIS involving a sclerosing lesion [34, 47]. Pleomorphic LCIS and florid LCIS without associated DCIS or invasive carcinoma on core biopsy are uncommon, accounting for only 4.7% of 316 pure LN lesions in a large prospective study [48].

Gross and Radiologic Features

Foote and Stewart noted that "there is no way a clinical diagnosis of LCIS can be made … and there is no way LCIS can be recognized grossly," which remains essentially true to this day [6]. LCIS is typically not apparent on gross examination.

Radiologic Features in ALH and Classic LCIS

ALH and classic LCIS have been considered radiographically occult. One of the earliest studies on the utility of mammography in LN reported that calcifications in LCIS cases were usually present in benign tissue near LCIS but rarely in the lesion itself [49]. This often remains the case in classic LN, with the targeted calcifications correlating to lesions such as columnar cell change, sclerosing adenosis, collagenous spherulosis, and other entities. On the other hand, calcifications have also been increasingly recognized in association with classic LN, perhaps due to widespread screening (Fig. 14.4). In such cases, classic LCIS often manifests as clustered punctate or grouped amorphous calcifications [50–52]. Studies analyzing upgrade rates from core biopsy found that classic LN was the targeted lesion in 3–37% of cases biopsied for calcifications [53–57]. This

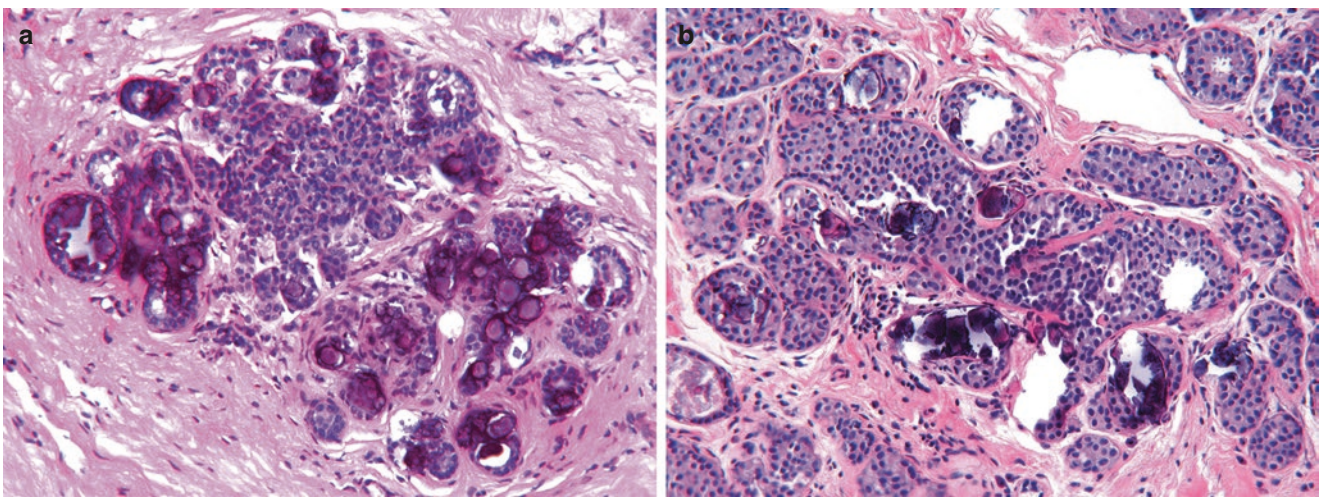

Fig. 14.4 Classic LN associated with calcifications. (**a**) ALH and (**b**) LCIS

should be distinguished from the occasional minute calcifications in LN that would not explain the calcifications targeted for biopsy.

Rarely, classic LCIS can present with ultrasound or MRI abnormalities that are targeted for biopsy. Scoggins et al. reported three cases of classic LCIS presenting as a shadowing, avascular, irregular, hypoechoic mass on ultrasound [52]. Rare cases of classic LCIS have been found to manifest as enhancing nodules or as heterogeneous non-mass-like enhancement with persistent enhancement kinetics on MRI [52, 58].

Radiologic Features in Pleomorphic and Florid LCIS

In contrast to classic LCIS, which is typically radiographically occult, almost all pleomorphic and florid LCIS present with imaging abnormalities. Mammographically, most of these lesions show suspicious pleomorphic or granular, coarse calcifications, similar to the patterns observed in DCIS (Fig. 14.5) [24, 34, 37, 41–47, 50, 59, 60]. Some cases may present with architectural distortion/density/mass with or without microcalcifications on mammogram [34, 37, 53, 61]. Pleomorphic and florid LCIS can occasionally present as a mass lesion or asymmetry on ultrasound [53, 60] or be detected by screening MRI as non-mass enhancement or mass [24, 34, 47].

Microscopic Features

The key feature of all LN is loss of cellular cohesion. ALH is distinguished from classic LCIS by the extent of acinar involvement within the TDLU. Pleomorphic LCIS and florid LCIS differ from classic LCIS with regard to the degree of nuclear atypia and lobular acinar expansion, respectively (Table 14.1).

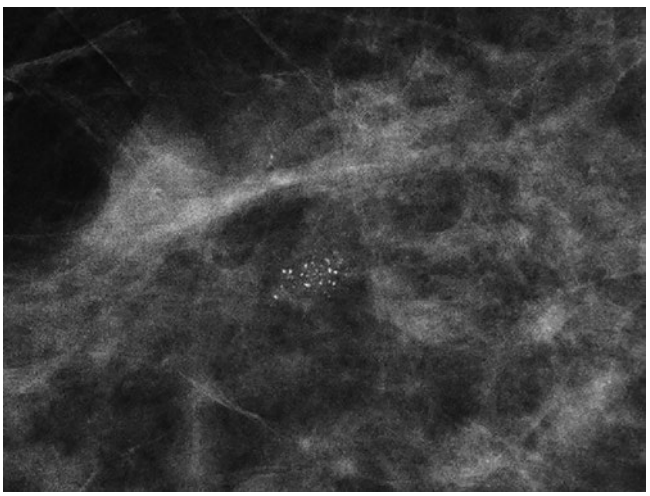

Fig. 14.5 A screening mammogram with clustered pleomorphic calcifications proven to be pleomorphic LCIS

Table 14.1 Histopathologic features of LCIS subtypes

	Classic LCIS	Pleomorphic LCIS	Florid LCIS
Loss of cellular cohesion	Present	Present	Present
Cytologic features	Type A, type B, or mixture of type A and B cells[a]	Marked nuclear pleomorphism akin to high-grade DCIS (~two- to three-fold size variation) and/or at least some nuclei ≥4× size of lymphocyte nucleus	Type A, type B, or mixture of type A and B cells; often type B cells
Architectural requirement	At least 50% of acini in TDLU distended[b]	None	(1) No or little intervening stroma between markedly expanded acini of TDLU and/or (2) expanded acinus/duct entirely fills one high-power field (~40–50 cells diameter)
Comedo necrosis (central confluent necrosis)	Absent[c]	May be present	May be present

Adapted from Shamir et al. [34]
[a] See text for definition of type A and type B cells
[b] See the text for criteria of distension
[c] Single-cell apoptosis and minute foci of necrosis may rarely be seen in classic LCIS

Atypical Lobular Hyperplasia and Classic LCIS

Both ALH and classic LCIS are comprised of solid proliferations of monomorphic dyshesive epithelial cells originating in the TDLU, with or without pagetoid involvement of ducts (Figs. 14.1 and 14.2). The epithelial cells are of two types: Type A cells are small with scant cytoplasm and uniform, round, hyperchromatic nuclei (1–1.5× the size of a lymphocyte nucleus) with inconspicuous nucleoli; type B cells have more abundant cytoplasm and slightly larger vesicular nuclei (about 2× the size of a lymphocyte nucleus) with more variability in nuclear size and shape and evident nucleoli (Fig. 14.6) [3, 45]. Type A and type B cells may be admixed in individual cases, even within a single space (Fig. 14.6). Distinction of type A and B cells is of no known clinical significance, but it is important not to confuse lesions containing type B cells with pleomorphic LCIS (see below). In all neoplastic lobular cells (ALH, LCIS, and ILC), intracytoplasmic lumina (also termed vacuoles) are often present and may appear clear or contain central

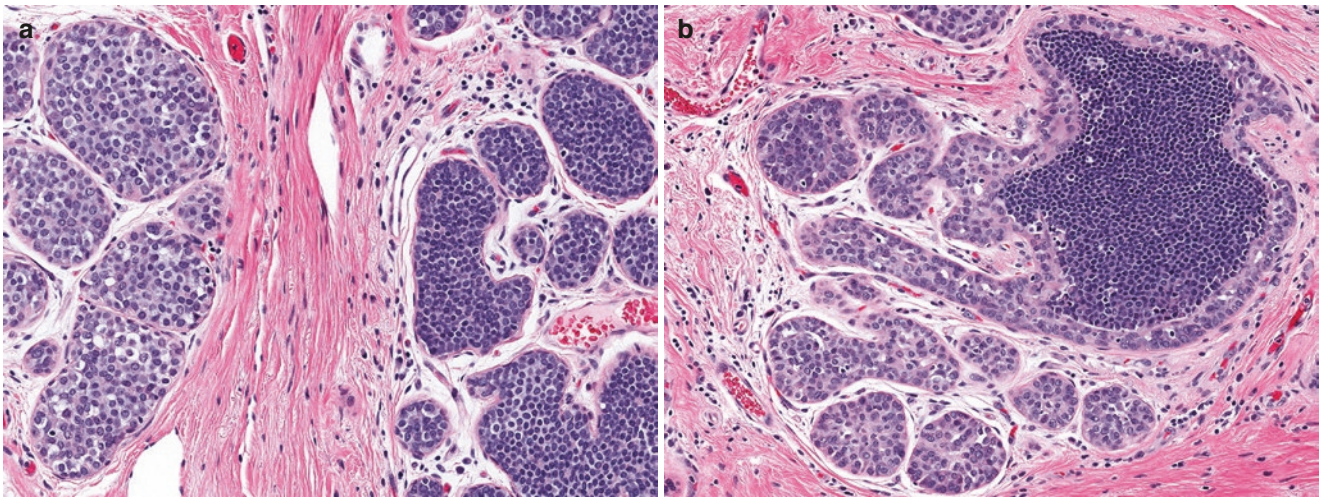

Fig. 14.6 Classic LCIS), type A and type B cells. (**a**) This classic LCIS case is composed of type A and B cells in adjacent TDLUs. Type A cells (LCIS in the right TDLU) are small with scant cytoplasm and uniform nuclei displaying fine chromatin and no visible nucleoli, whereas type B cells (LCIS in the left TDLU) have more cytoplasm and slightly larger vesicular nuclei with more variability in nuclear size and shape and evident nucleoli. (**b**) Type A and B cells are present within the same TDLU in this example

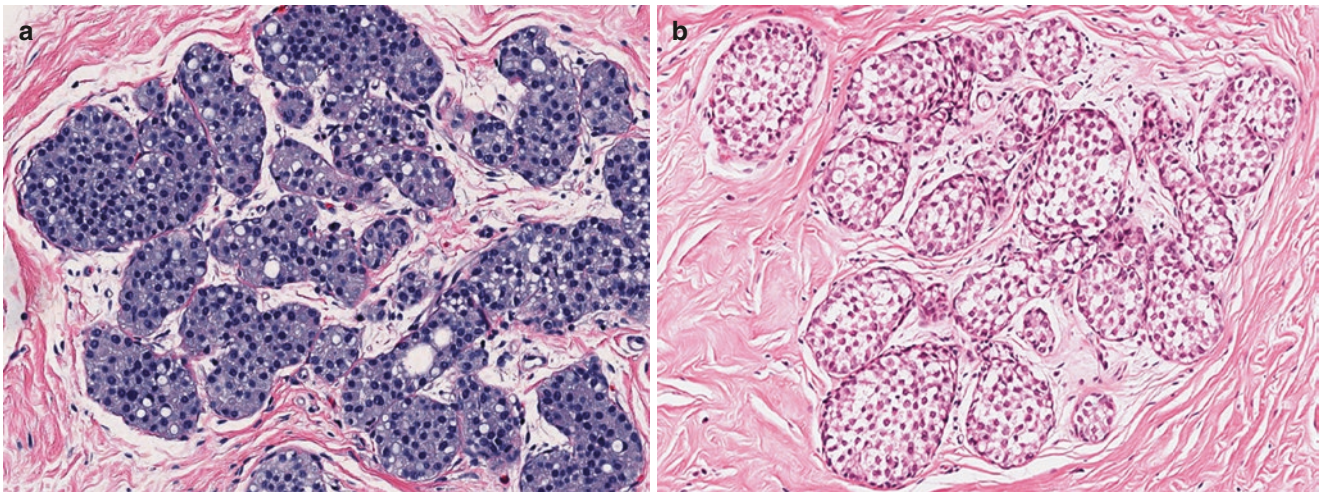

Fig. 14.7 Classic LCIS, intracytoplasmic lumina/vacuoles. (**a**) The presence of intracytoplasmic lumina is a characteristic cytologic feature of lobular lesions and is particularly prominent in this classic LCIS. (**b**) The neoplastic cells in this LCIS have pronounced clear intracytoplasmic lumina, imparting a bubbly appearance to the lesion

mucoid inclusions or eosinophilic globules (Fig. 14.7). These lumina can be large enough to indent the nuclei, imparting a signet ring cell appearance (Fig. 14.8). Glandular architecture is absent (unless LN involves another underlying lesion), and mitoses are rare. Classic LCIS may rarely exhibit single-cell apoptosis and even minute foci of necrosis, the presence of which does not exclude the diagnosis of classic LCIS in the context of other appropriate cytologic and architectural features. Microcalcifications are uncommon in ALH and classic LCIS; when present, they are usually related to underlying lesions that are secondarily colonized by LN, such as LN involving sclerosing adenosis or collagenous spherulosis.

According to the criteria proposed by Page et al. and adopted by the WHO classification, ALH and classic LCIS differ in the extent to which the TDLU is involved by the atypical lobular cell proliferation. In LCIS, more than half of the acini in a TDLU are filled and expanded or distended by the neoplastic cells. Lesser involvement is classified as ALH [62]. Given this descriptive and relatively subjective definition and the known interobserver variability in differentiating ALH from LCIS, the most recent WHO classification has suggested two approaches that have been proposed by some authorities and may serve as guideposts for what constitutes "filling and expansion" or "distension" of the acini. The first approach is based on estimating the number of cells in the

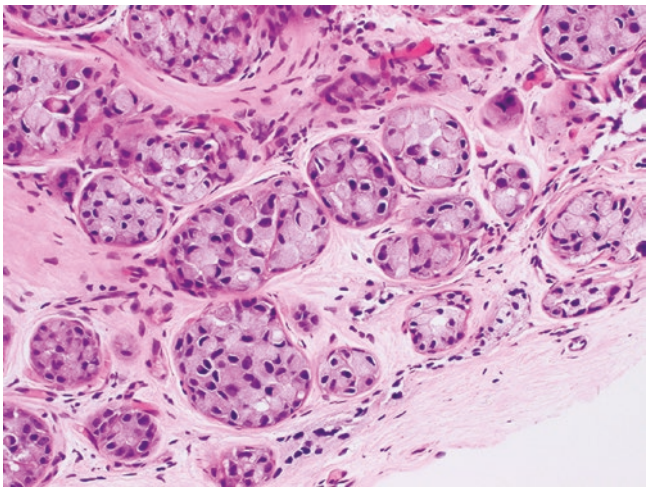

Fig. 14.8 Classic LCIS with signet ring cell features. The cytoplasm of the LCIS cells is filled with blue mucin displacing the nucleus to the periphery and creating a signet ring cell appearance

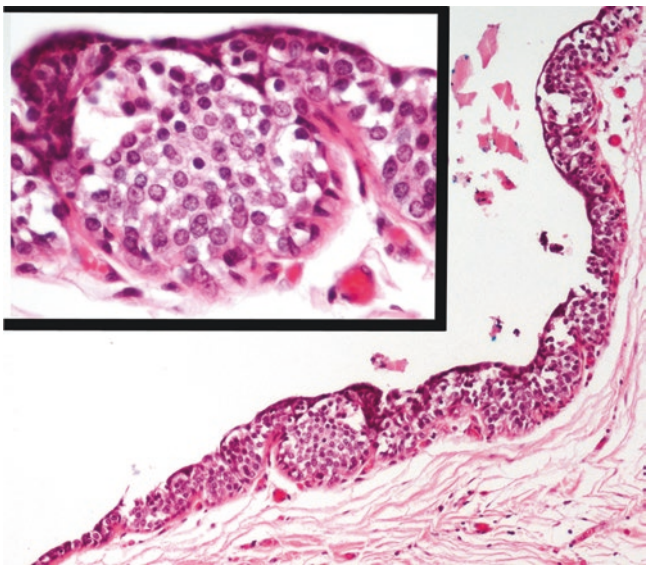

Fig. 14.9 Classic LCIS with pagetoid spread to a duct. The neoplastic lobular cells grow between the luminal epithelial cells and myoepithelial cells. Note the compression and attenuation of the overlying luminal epithelial cells by the loosely cohesive neoplastic cells with intracytoplasmic lumina (inset)

involved acini: if ≥8 lobular cells span the diameter of an acinus, it is considered expanded or distended [63, 64]. The second approach compares the caliber of the involved acini to that of acini in adjacent uninvolved lobules: if the involved acini are larger than the uninvolved acini, they are considered expanded or distended [21]. Although these criteria may be helpful for pathologists in their clinical practice, scientific evidence for these criteria to define expansion is lacking.

ALH and LCIS can show pagetoid growth in involved ducts, which is characterized by the neoplastic cells insinuating between the preexisting luminal epithelial cells and myoepithelial cells, resulting in compression and attenuation of the overlying luminal layer (Fig. 14.9). Cross sections of ducts with pagetoid LN often have a cloverleaf pattern (Fig. 14.10). Lobular neoplastic cells may also colonize various underlying lesions, such as sclerosing adenosis, radial scars, fibroadenomas, usual ductal hyperplasia, papillary lesions, and collagenous spherulosis. In these settings, the underlying lesions may mask the presence of LN or create a histologic pattern that can mimic invasive carcinoma or DCIS (see section "Differential Diagnosis").

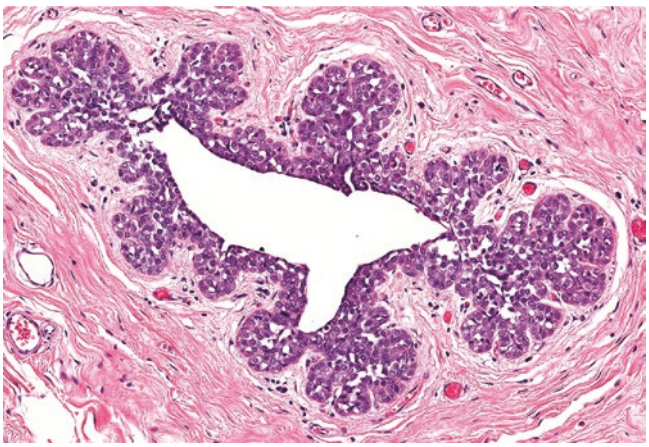

Fig. 14.10 Lobular neoplasia with cloverleaf appearance. The cross section of a duct with pagetoid involvement by LN often has a cloverleaf appearance, which is a helpful clue at low-power evaluation to suggest the presence of LN

Pleomorphic LCIS

Pleomorphic LCIS shares with classic LCIS the solid proliferation of dyshesive neoplastic cells within TDLUs but differs from classic LCIS with regard to the degree of nuclear atypia. Pleomorphic LCIS is defined by marked nuclear pleomorphism, with at least some nuclei being >4× the size of a lymphocyte nucleus, and/or nuclear pleomorphism equivalent to that seen in high-grade DCIS (Fig. 14.11) [2, 45]. Multinucleated cells are observed in approximately 25% of pleomorphic LCIS but are generally absent in classic LCIS. As such, when multinucleation is noted in LCIS, the possibility of pleomorphic LCIS should be considered (Fig. 14.11c) [65]. In contrast to classic LCIS, pleomorphic LCIS frequently demonstrates central confluent or comedo necrosis and is often associated with calcifications (Fig. 14.11d).

A subset of pleomorphic LCIS can exhibit apocrine cytologic features with abundant eosinophilic, granular cytoplasm and large rounded nuclei with prominent nucleoli. These lesions have been variously designated as apocrine pleomorphic LCIS, pleomorphic apocrine LCIS, or pleomorphic LCIS with apocrine features (Fig. 14.12) [37]. Similar to classic LCIS, signet ring cells but with pleomorphic high-

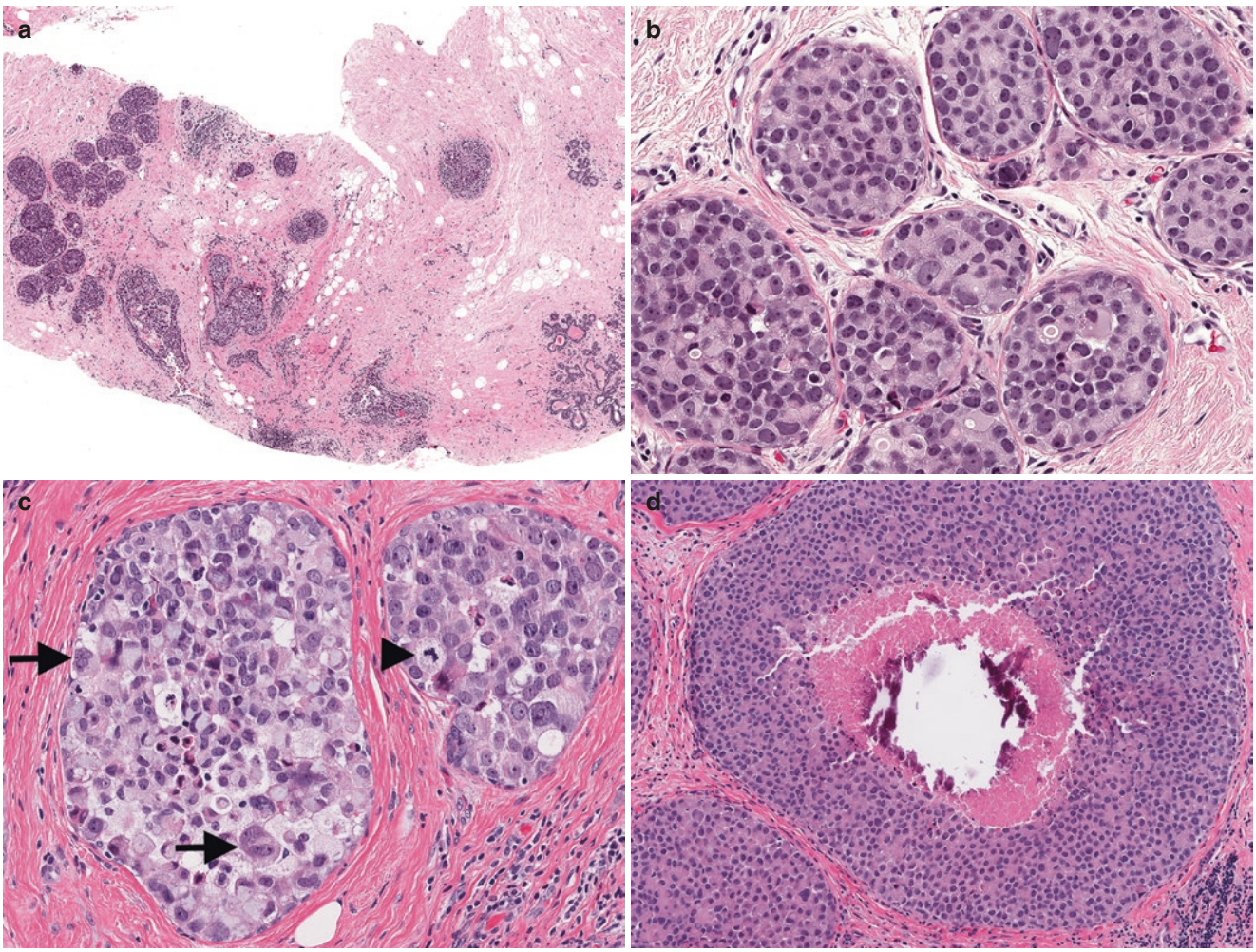

Fig. 14.11 Pleomorphic LCIS. (**a**, **b**) A core biopsy for calcifications demonstrates lobular acini filled and expanded by loosely cohesive cells with marked cytologic atypia, equivalent to high-grade DCIS. E-cadherin immunostain was negative in the neoplastic cells (not shown). (**c**) This pleomorphic LCIS features a dyscohesive proliferation of neoplastic cells with marked nuclear pleomorphism, including multinucleated cells (arrows). Also present are mitoses (arrowhead), apoptotic cells, and signet ring cells. (**d**) In some examples, pleomorphic LCIS demonstrates marked expansion of the terminal ducts with associated central confluent necrosis and calcifications

grade nuclei may be observed in pleomorphic LCIS and can be quite conspicuous in some cases (Fig. 14.13). Lobular acini involved by pleomorphic lobular cells are often substantially expanded, not infrequently to the degree observed in florid LCIS (Figs. 14.11d and 14.12b). On the other hand, the acini may also be only mildly distended or show no distension. Such lesions still qualify as pleomorphic LCIS, as the diagnosis is based on cytologic features, and there is no recognized category of pleomorphic ALH.

Florid LCIS

Florid LCIS is defined by its architectural features. In these lesions, the LCIS cells exhibit cytologic features of classic LCIS (type A, type B, or a mixture of type A and B cells; often type B cells), but there is marked distension of TDLUs or ducts, imparting a confluent mass-like appearance (Fig. 14.14). Florid LCIS should have at least one of the two architectural features: (1) little to no intervening stroma between markedly distended acini of involved TDLUs (Fig. 14.14) and/or (2) a minimum size cutoff of an expanded acinus or duct filling at least one high-power field (an area equivalent to ~40–50 cells in diameter) (Fig. 14.15) [24, 34, 66, 67]. Similar to pleomorphic LCIS, florid LCIS often develops central confluent necrosis and/or luminal calcifications (Figs. 14.14a and 14.15b).

In some cases, pleomorphic LCIS may also exhibit a florid growth pattern, and these lesions should be classified as pleomorphic LCIS (Figs. 14.11d and 14.12b) [10]. Other LCIS cases may have a florid growth pattern with a spectrum of cytologic atypia ranging from classic to pleomorphic, and a designation of mixed pleomorphic and florid LCIS can be applied [10]. Foci of classic LCIS are often present in tissue adjacent to either pleomorphic LCIS or florid LCIS. A diagnosis of "LCIS, mixed pleomorphic and classic types," or

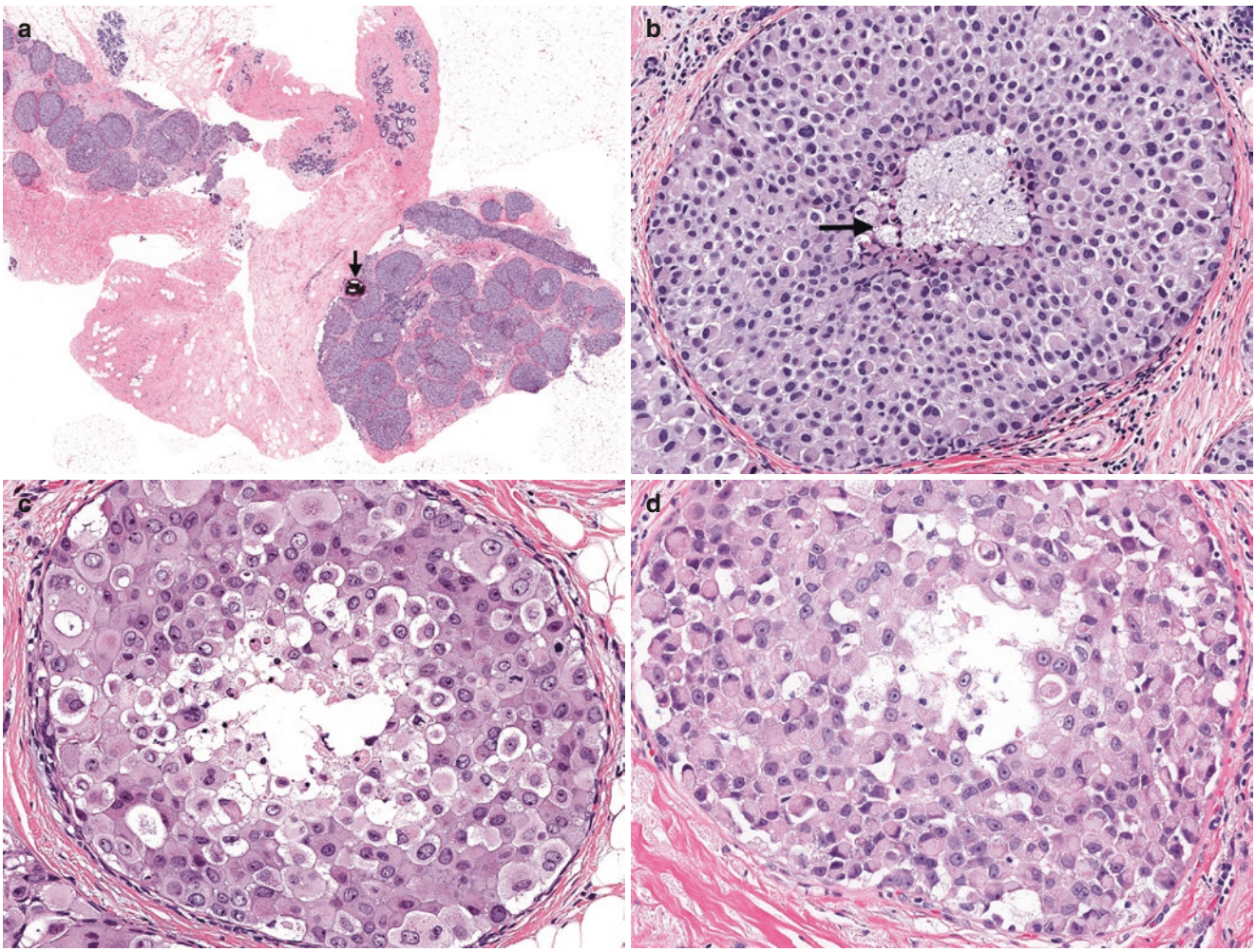

Fig. 14.12 Pleomorphic LCIS with apocrine features. (**a**, **b**) This core biopsy was performed for pleomorphic calcifications and demonstrates marked expansion of the TDLUs by loosely cohesive large cells with abundant eosinophilic granular cytoplasm and large round nuclei with prominent nucleoli. Note the associated calcifications (arrow in **a**) and small foci of necrosis (arrow in **b**). (**c**, **d**) Two more examples highlight apocrine cytologic features in pleomorphic LCIS. The neoplastic cells in all of these cases are negative for E-cadherin expression (now shown)

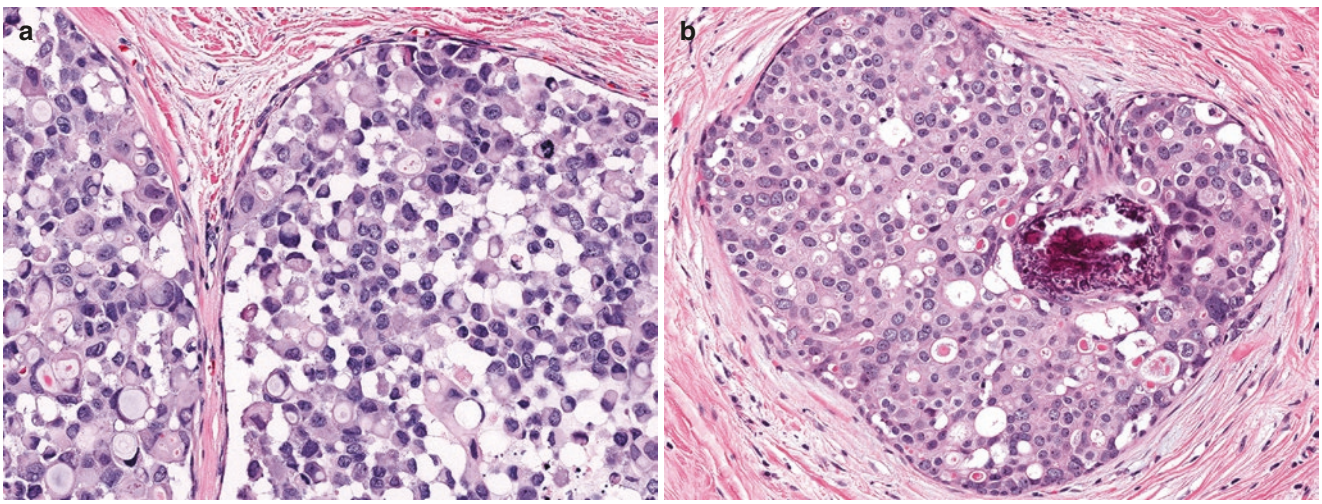

Fig. 14.13 Pleomorphic LCIS, cytologic features. (**a**) Prominent signet ring cell features are noted in this pleomorphic LCIS. (**b**) In another example of pleomorphic LCIS, the neoplastic cells have large intracytoplasmic lumina containing eosinophilic globules. The large intracytoplasmic lumina may mimic glandular structures, leading to misclassification of DCIS

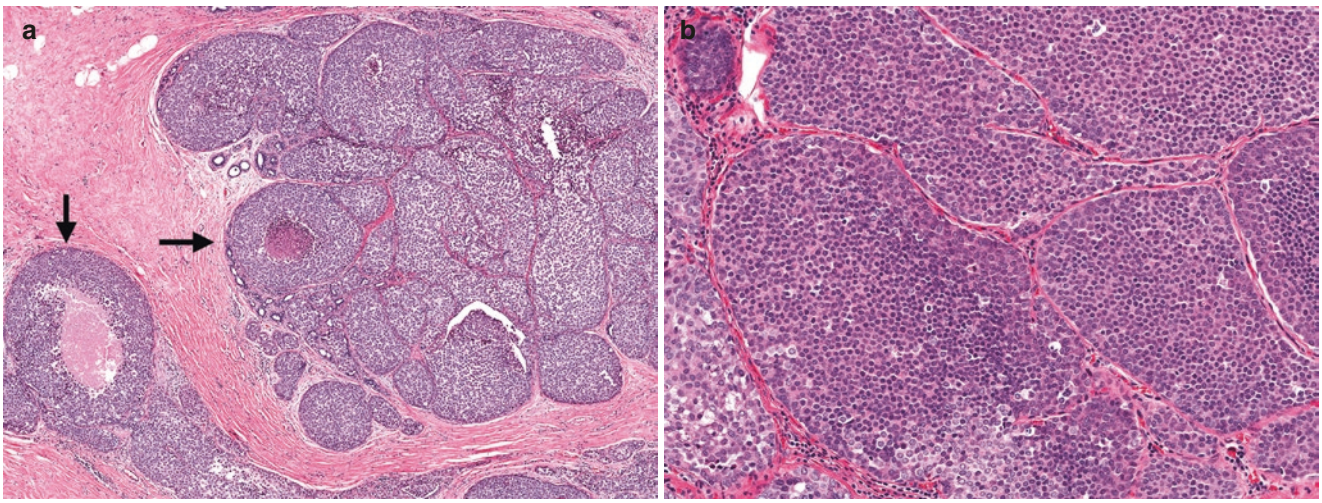

Fig. 14.14 Florid LCIS. (**a**) Florid LCIS shows marked distension of TDLUs or ducts, imparting a confluent mass-like appearance at low-power view. Note the presence of central confluent necrosis in some duct spaces (arrows). (**b**) Higher magnification reveals cytologic features akin to classic LCIS (non-pleomorphic). Note that there is little to no intervening stroma between the markedly distended acini and ducts

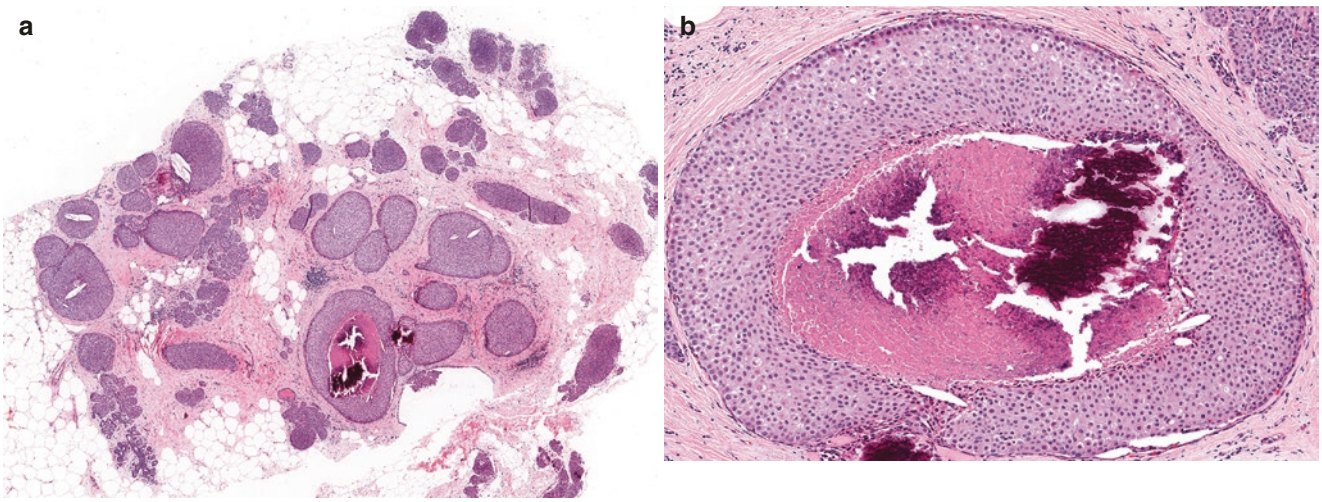

Fig. 14.15 Florid LCIS. (**a**) This MRI-guided core biopsy for focal clumped non-mass enhancement demonstrates solid pattern in situ carcinoma involving both ducts and lobules. (**b**) The duct is markedly expanded, occupying at least one high-power field (an area equivalent to >40–50 cells in diameter), and the neoplastic cells show similar cytologic features as the adjacent classic LCIS (right upper corner), the presence of which should raise the possibility of florid LCIS rather than solid-pattern DCIS. E-cadherin stain was negative in all in situ components (not shown), supporting florid LCIS and classic LCIS. Note the presence of comedo necrosis and calcifications in the florid LCIS

"LCIS, mixed florid and classic types," would be appropriate for these mixed lesions (Fig. 14.16). Occasionally, both classic and pleomorphic lobular cells can be present in the same TDLU or even the same acinus (Fig. 14.17). The finding of classic LCIS associated with solid pattern carcinoma in situ should raise the possibility of an LCIS subtype rather than solid DCIS (see sections "Differential Diagnosis" and "Distinguishing Between LCIS and DCIS").

Figure 14.18 summarizes and compares the histological features of ALH and the various LCIS subtypes.

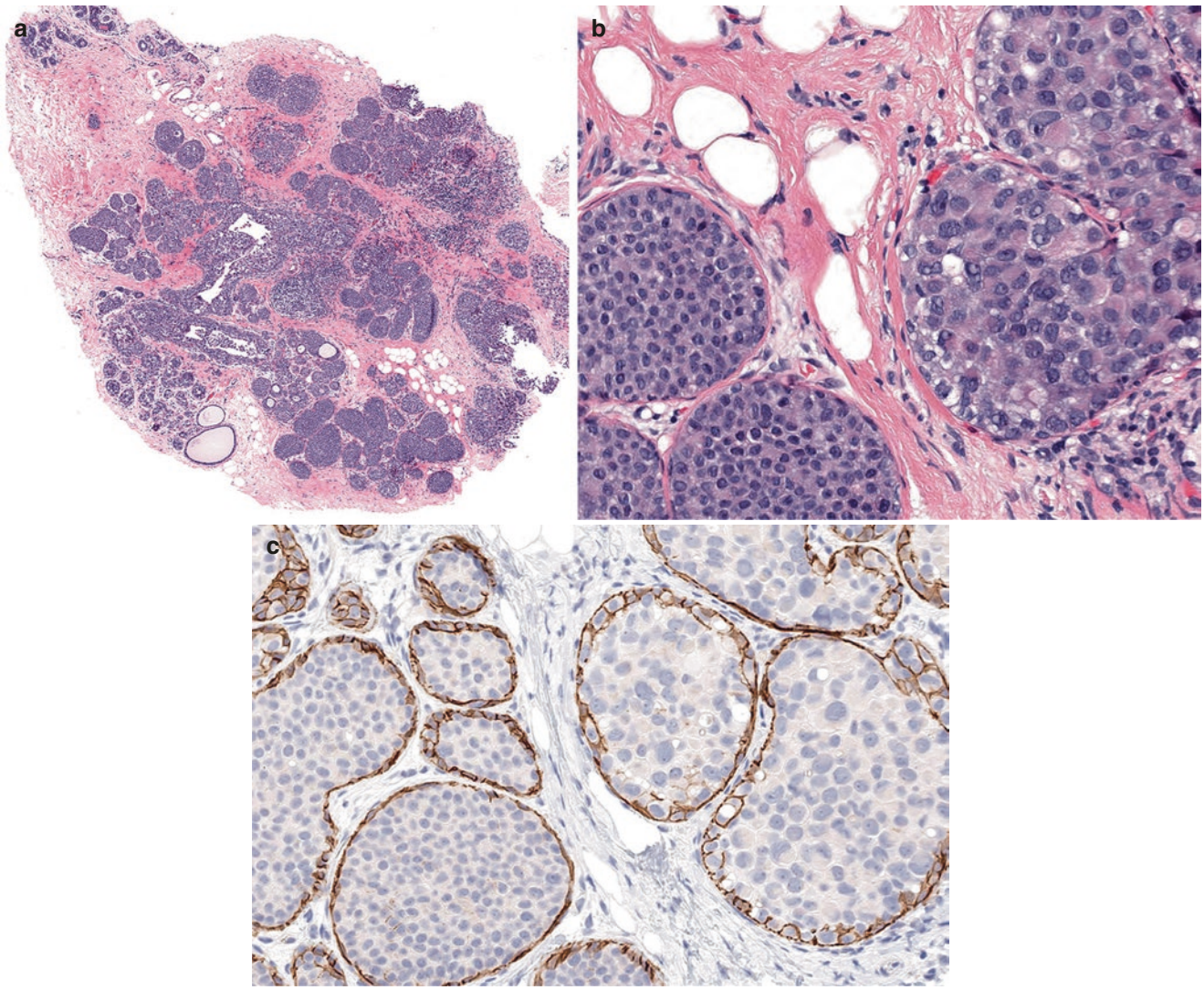

Fig. 14.16 Pleomorphic and classic LCIS in a same core biopsy. (**a**) Low magnification and (**b**) higher magnification show pleomorphic LCIS (right upper in **b**) and classic LCIS (left lower in **b**) in adjacent TDLUs, which is confirmed by (**c**) negative E-cadherin immunostain in both components

Immunohistochemistry

Classic LCIS typically exhibits strong estrogen receptor (ER) expression without human epidermal growth factor 2 (HER2) overexpression/*ERBB2* amplification and has a low Ki-67 proliferation index [68–72]. Florid LCIS has an overall similar biomarker profile but can infrequently demonstrate HER2 overexpression/*ERBB2* amplification and may have a higher Ki-67 index [24, 34]. Cyclin D1 overexpression has been described in florid LCIS, but *CCND1* amplification has also been observed in pleomorphic LCIS and rare classic LCIS [24, 34, 47, 73, 74]. Pleomorphic LCIS is more likely to be ER negative (especially lesions with apocrine features) or HER2 positive (up to ~30%) and has moderate-to-high Ki-67 proliferation index (Fig. 14.19) [34, 37, 45, 75]. Approximately 10–15% of pleomorphic

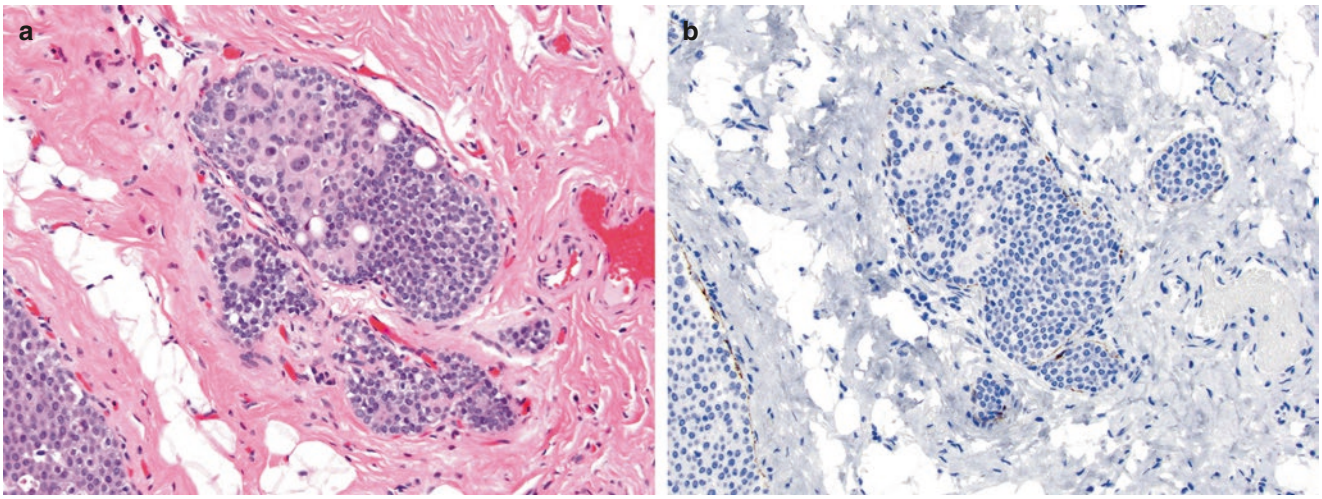

Fig. 14.17 LCIS, pleomorphic and classic cells found in same acinus. (**a**) Pleomorphic cells are in the upper left and classic type in the lower right aspects of the acinus. (**b**) Immunohistochemistry for E-cadherin is negative, supporting LCIS

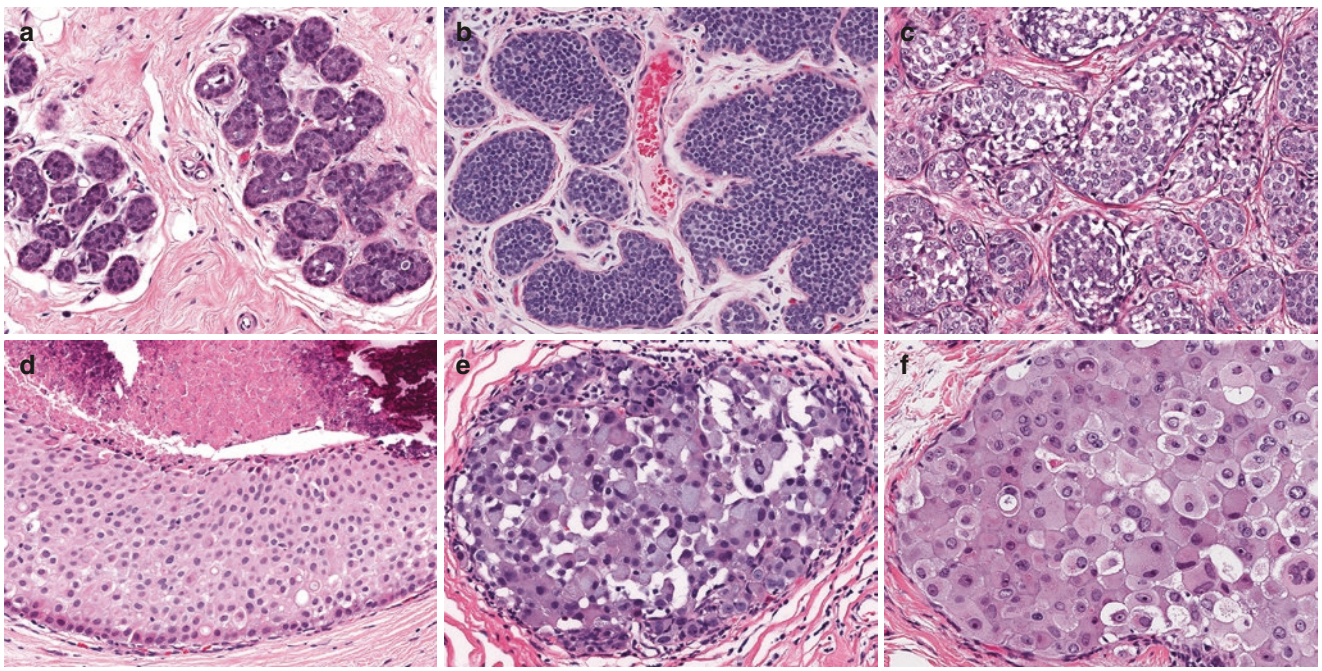

Fig. 14.18 Comparison of histologic features of ALH and the various LCIS subtypes, with all the images taken at the same magnification (40×). (**a**) ALH; (**b**) classic LCIS comprised of type A cells; (**c**) classic LCIS comprised of type B cells; (**d**) florid LCIS; (**e**) pleomorphic LCIS; and (**f**) apocrine pleomorphic LCIS

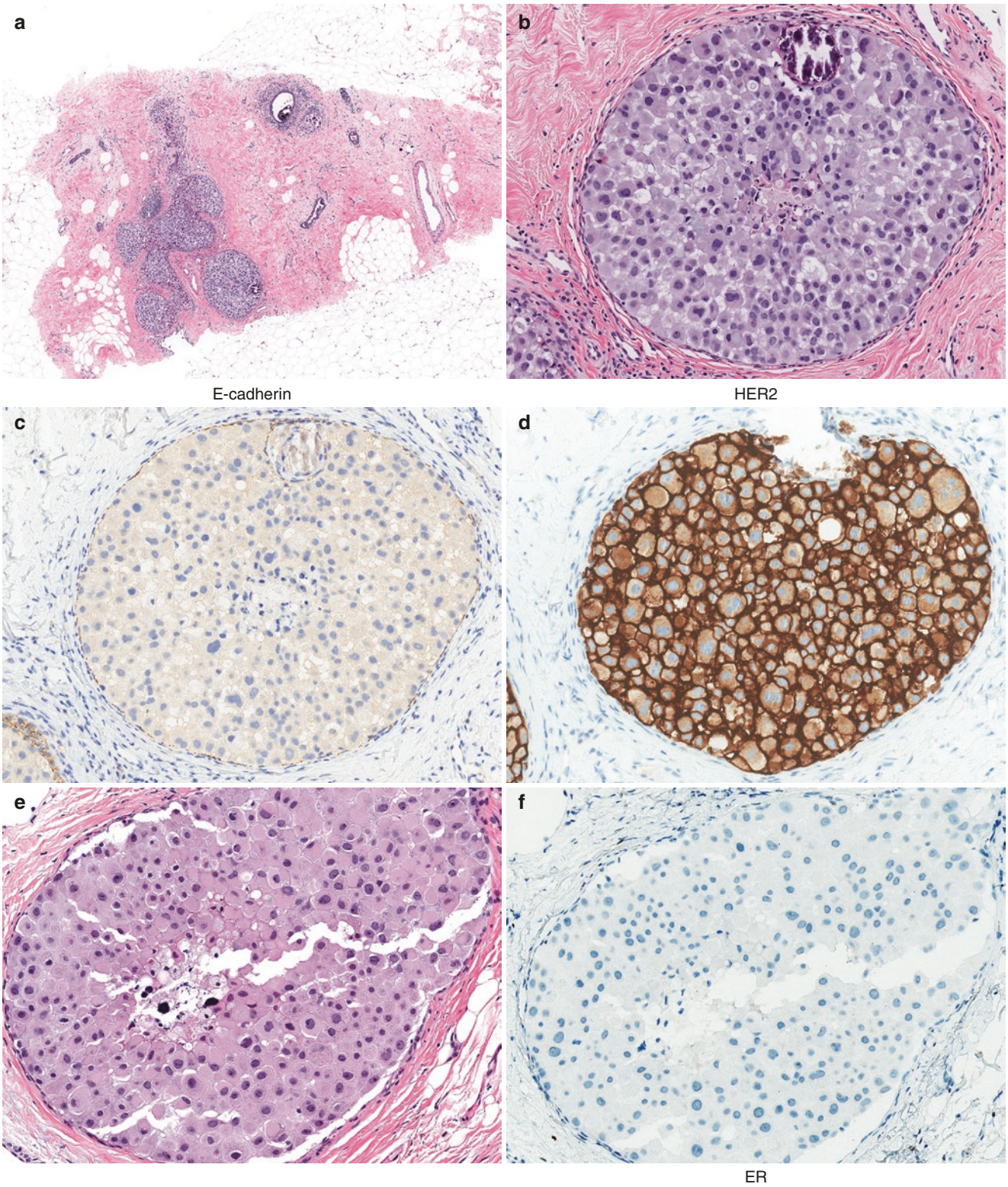

Fig. 14.19 Pleomorphic LCIS may be HER2 positive or ER negative. (**a–d**) HER2-positive pleomorphic LCIS. H&E stains at low (**a**) and high (**b**) magnification and E-cadherin (**c**) immunostain demonstrate an apocrine pleomorphic LCIS that exhibits HER2 overexpression by immunohistochemistry (**d**). (**e**) H&E stain shows another example of apocrine pleomorphic LCIS that is (**f**) negative for ER

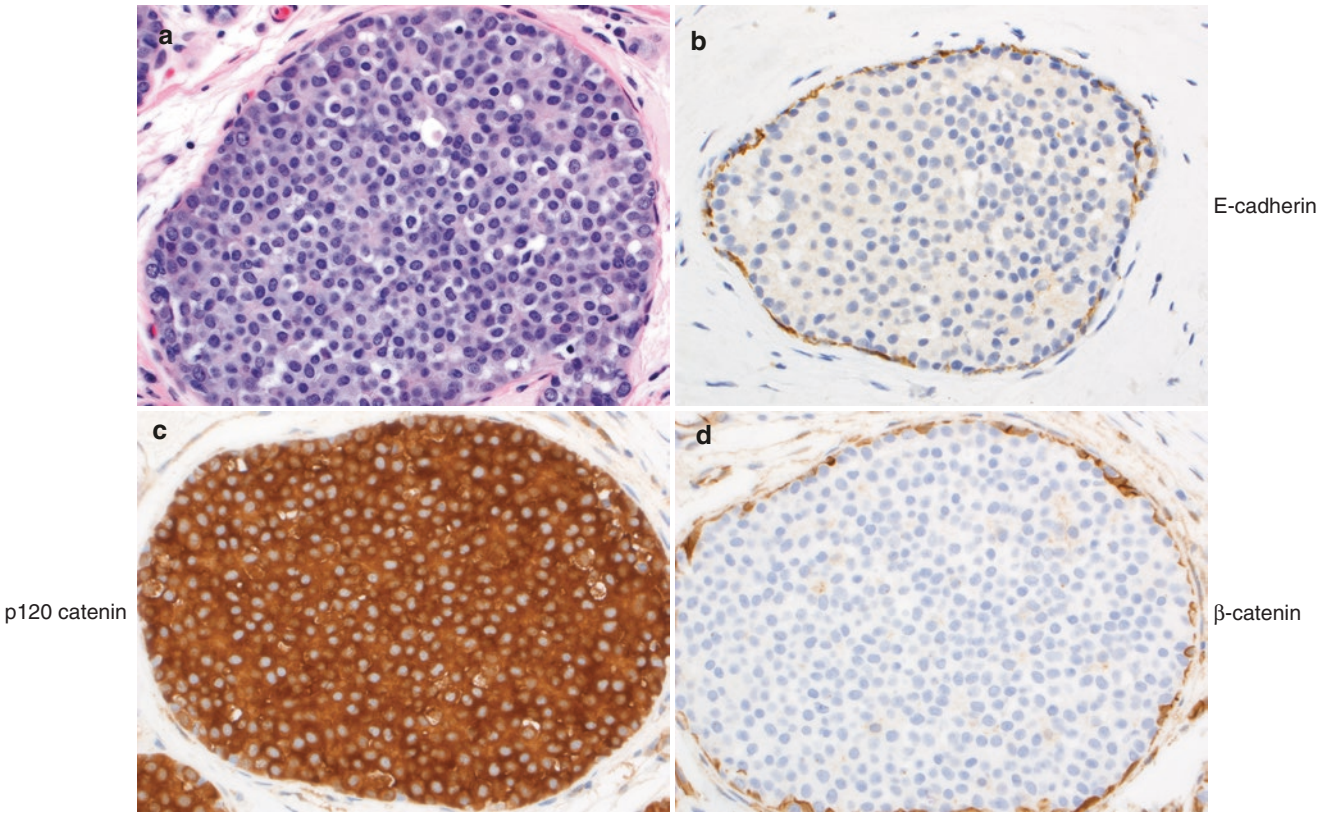

Fig. 14.20 LCIS, typical immunostaining pattern of the E-cadherin-catenin complex. (**a**) H&E stain of a classic LCIS. (**b**) E-cadherin immunostain demonstrates loss of membranous expression (note the positive staining from the surrounding myoepithelial cells). (**c**) p120 catenin immunostain reveals strong cytoplasmic staining pattern (in contrast to membranous staining pattern in ductal-type lesions). (**d**) The LCIS cells show loss of membranous expression of β-catenin (note the positive staining from the surrounding myoepithelial cells)

LCIS cases are triple negative [34, 44, 73]. All LCIS subtypes typically show a strong expression of androgen receptor (AR) [37, 75].

All neoplastic lobular cells (ALH, LCIS regardless of subtype, and ILC) are characterized by the absence or dysfunction of E-cadherin. E-cadherin is a calcium-dependent transmembrane protein that regulates epithelial cell adhesion and cell polarity via adherens junctions between cells and is linked to the actin cytoskeleton. E-cadherin is tethered to actin by binding alpha-, beta-, and gamma-catenins via its intracytoplasmic domain, and this complex is strengthened by p120 catenin. Immunohistochemical analysis of the components of the E-cadherin-catenin protein complex is a valuable adjunct to help evaluate these lesions in clinical practice. Lobular lesions exhibit loss of membranous E-cadherin and β-catenin expression, along with increased cytoplasmic (and lack of membranous) expression of p120 catenin (Fig. 14.20) [76, 77] (see also Chap. 15", section "Immunohistochemistry", and Table 15.2). Among these immunohistochemical markers, E-cadherin is most frequently used by pathologists. Although most LCIS lesions completely lack E-cadherin expression, aberrant staining can be observed in some cases, including attenuated membranous, incomplete membranous, diffuse cytoplasmic, or dot-like Golgi staining patterns (Fig. 14.21) [78–80]. It is important to recognize that staining variability can also arise from different E-cadherin antibody clones [80]. In some instances, suboptimal antibody optimization and validation can lead to false-positive staining in LN (Fig. 14.22) [81]. Comparison of staining quality and intensity of neighboring ducts and lobules (positive internal control) should be routinely performed when interpreting an E-cadherin stain. Caution should also be exercised to avoid misinterpretation of weak, discontinuous myoepithelial

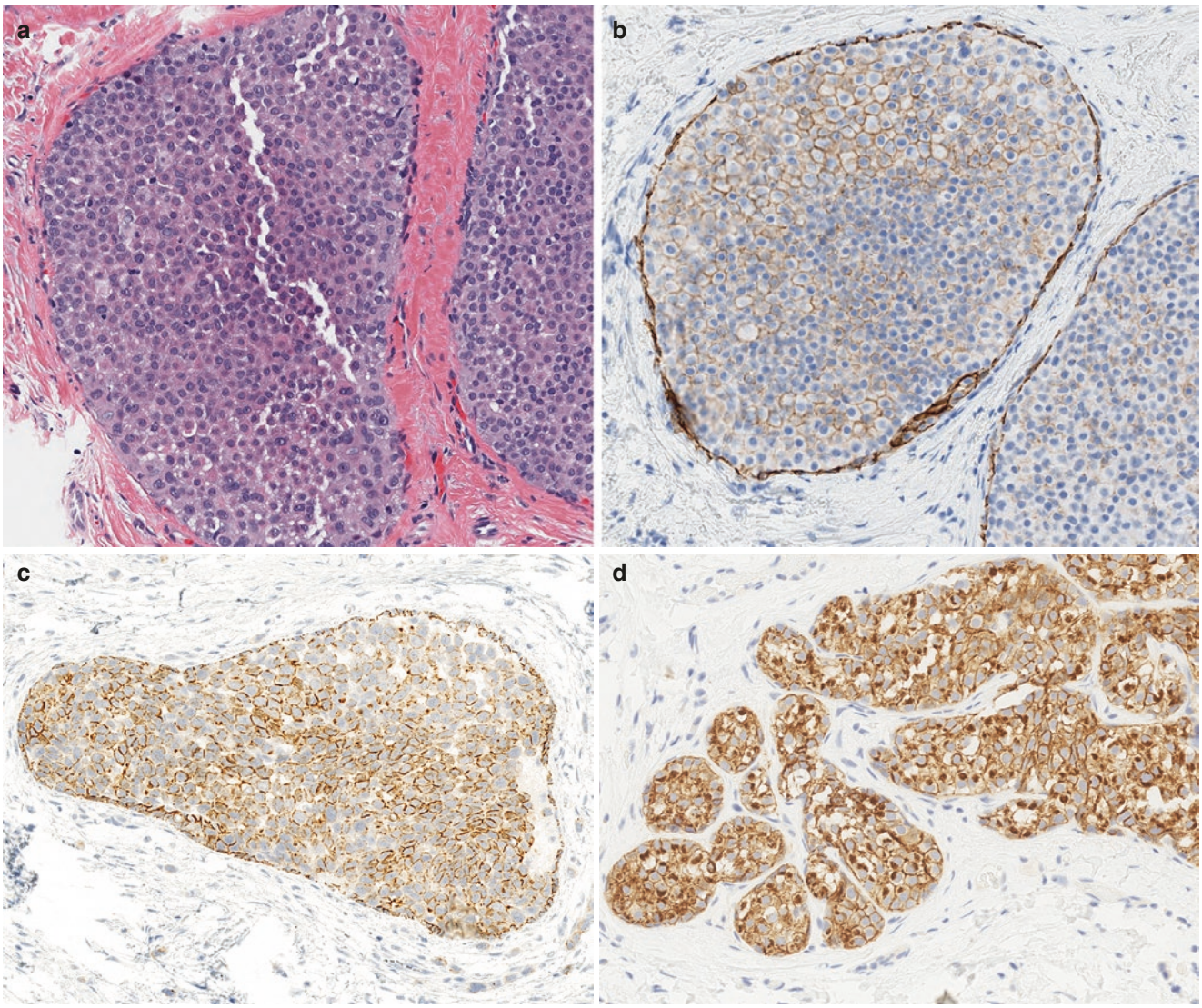

Fig. 14.21 LCIS with aberrant E-cadherin staining. (**a**, **b**) H&E stain (**a**) and corresponding E-cadherin immunostain (**b**) show a LCIS with weak complete to partial fragmented membranous staining that should not be interpreted as DCIS. Note relatively decreased staining intensity in LCIS compared to residual ductal and myoepithelial cells at the periphery. (**c**) This LCIS demonstrates aberrant E-cadherin expression with variable staining in the neoplastic cells, ranging from absent, partial/beaded membrane and circumferential membrane to perinuclear dot-like staining patterns. Staining heterogeneity for E-cadherin within the same lesion is a feature not infrequently observed in LCIS (and ILC) with aberrant E-cadherin expression. (**d**) Another example of aberrant E-cadherin expression in which the LCIS cells exhibit a prominent perinuclear dot-like staining pattern along with cytoplasmic and fragmented membranous staining

cell staining or staining of residual underlying epithelial cells as staining of LN cells (more likely to be encountered in ALH but can also be seen in LCIS).

In general, absolute reliance on E-cadherin IHC should be avoided. As with any other immunostain, interpretation of E-cadherin stain is best carried out in the context of the histologic features. In cases of equivocal E-cadherin expression, p120 catenin and/or β-catenin stains can be helpful to interrogate the functionality of the E-cadherin-catenin complex (Fig. 14.23) [82, 83]. However, interpretation of p120 catenin can be problematic in some cases, as distinguishing between cytoplasmic and membranous staining can be subjective and challenging, especially in cells with scant cytoplasm.

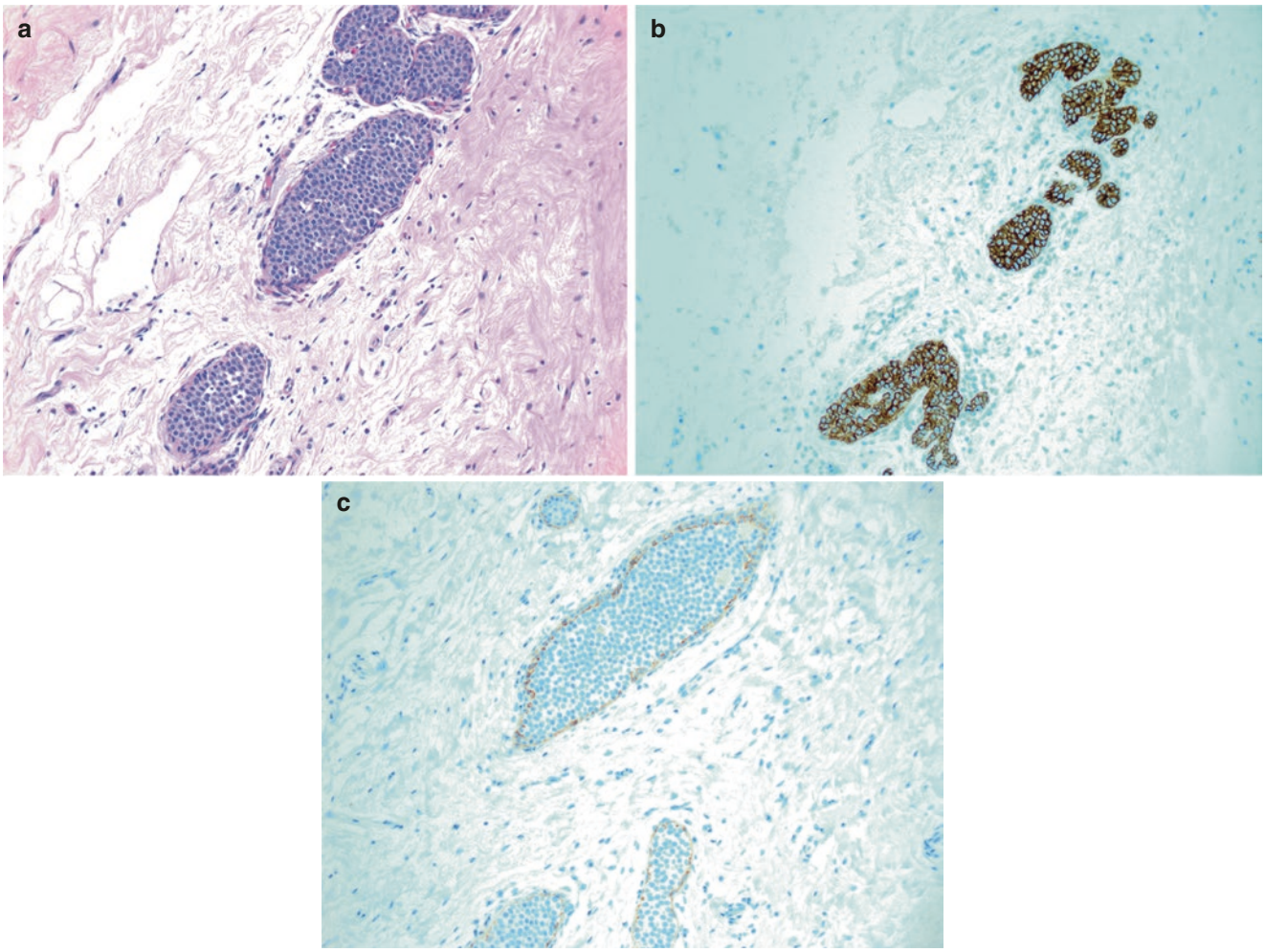

Fig. 14.22 Suboptimal E-cadherin staining protocol can lead to a false-positive result. (**a**) H&E stain of classic LCIS. (**b**) E-cadherin immunostain (from another facility) using suboptimal staining protocol leading to false-positive membranous staining of lobular cells. (**c**) Repeat E-cadherin immunostain revealing appropriate lack of staining in lobular cells

Differential Diagnosis

Distinction of ALH from Classic LCIS

A common dilemma in clinical practice is to distinguish the upper end of ALH from the lower end of classic LCIS using the criteria established by Page [13]. The distinction can be highly subjective, and some authors have therefore advocated for grouping these lesions together as LN, particularly in core biopsies [18, 19]. However, given the differences in long-term risk of invasive cancer development and different upgrade rates on subsequent excision (see section "Prognosis and Management"), it is helpful to separate ALH from classic LCIS when possible using one of the two semiquantitative approaches suggested by the WHO classification (see section "Microscopic Features") [1]. It should be noted that the distinction between ALH and classic LCIS is based on the extent of acinar distension within a given TDLU and not on the number of involved TDLUs. Cases with multiple TDLUs minimally involved by the lobular cells do not qualify as classic LCIS. In addition, both ALH and LCIS can demonstrate pagetoid extension to ducts, and the presence of this finding does not help the distinction.

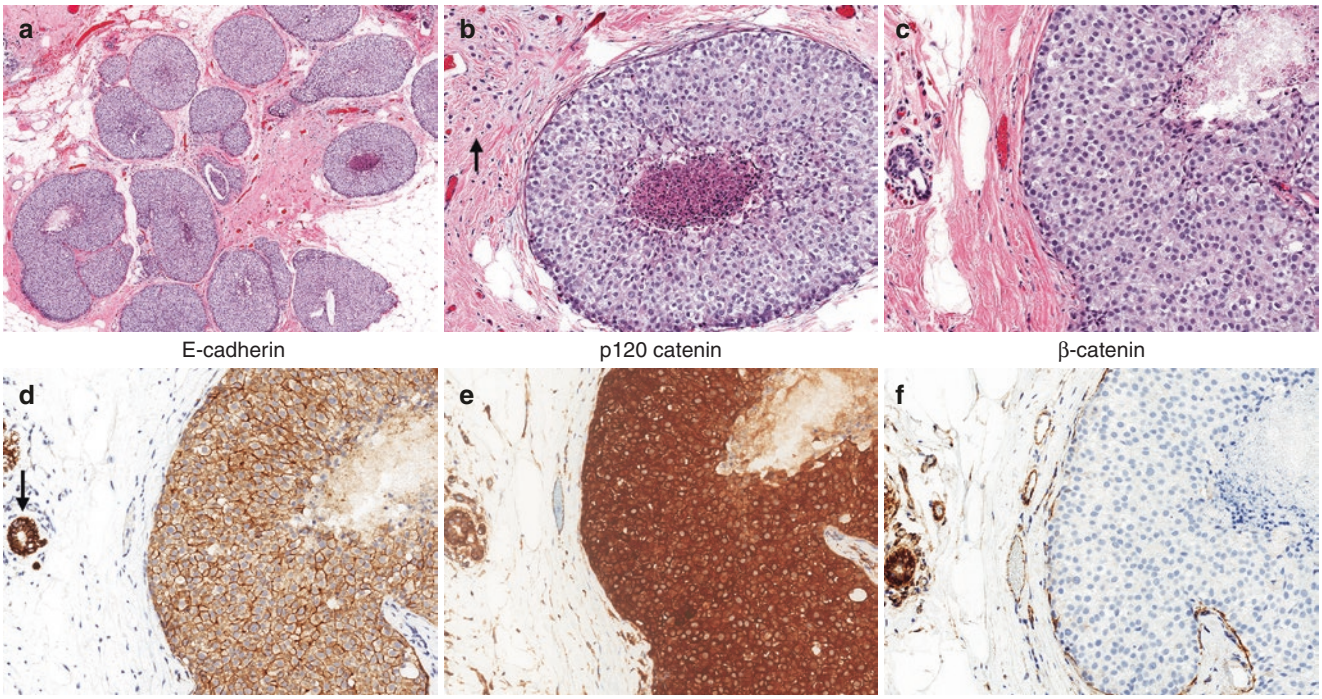

Fig. 14.23 Florid LCIS with aberrant E-cadherin staining. (**a**) H&E stain shows pure solid-pattern carcinoma in situ with comedo necrosis. (**b**) A microscopic focus of invasive lobular carcinoma (arrow) is noted adjacent to the in situ carcinoma. The findings of exclusively solid-pattern in situ component and associated invasive lobular carcinoma should alert the pathologist to the possibility of an LCIS subtype (florid LCIS in this case) rather than solid-pattern DCIS. (**c**) H&E stain showing carcinoma in situ (right) and an adjacent benign duct (left). (**d**) E-cadherin immunostain reveals complete membranous staining in the neoplastic cells. However, the staining intensity is slightly less intense than that observed in adjacent benign duct (arrow), suggesting the possibility of aberrant E-cadherin expression. (**e**) p120 catenin immunostain demonstrates strong cytoplasmic staining pattern. (**f**) β-catenin immunostain highlights loss of expression. This case shows how morphologic evaluation could suggest an LCIS subtype rather than DCIS and also illustrates how immunohistochemistry with other components of the E-cadherin-catenin complex is helpful in confirming aberrant E-cadherin expression and a dysfunctional E-cadherin-catenin complex to support the diagnosis of LCIS

Distinction of ALH from Benign Mimics

Another pitfall is the interpretation of benign changes as ALH and vice versa. Inadequate fixation of specimens can result in a dyshesive appearance of normal lobules and ductal lesions that can be mistaken for ALH (and classic LCIS), a problem encountered more often in excisional than core biopsy specimens. Prominent myoepithelial cells or myoepithelial hyperplasia, particularly cases with clear cytoplasm, can mimic ALH (Fig. 14.24). These acini and ductules typically have normal-appearing luminal epithelial cells, in contrast to the compressed/attenuated luminal epithelial cells often observed in ALH. Clear-cell change is an uncommon benign metaplastic change of cells in the lobules, which may be misinterpreted as ALH (Fig. 14.25) [84]. The epithelial cells in clear-cell change have abundant clear to finely granular cytoplasm and a small central nucleus and lack intracytoplasmic lumina typical of neoplastic lobular cells. Finally, one should not mistake intraepithelial histiocytes or lymphocytes as pagetoid spread by lobular cells (Fig. 14.26). E-cadherin may be of value in distinguishing between these benign mimics and ALH, but caution should be taken to avoid misinterpretation of weak, discontinuous myoepithelial cell staining as LN with loss of staining. Differential staining should be more straightforward if ruling out clear-cell change. Additional immunohistochemical stains, such as p63, keratin, or CD68, can also be useful to exclude hyperplastic myoepithelial cells and intraepithelial histiocytes mimicking pagetoid spread by lobular cells (Fig. 14.26).

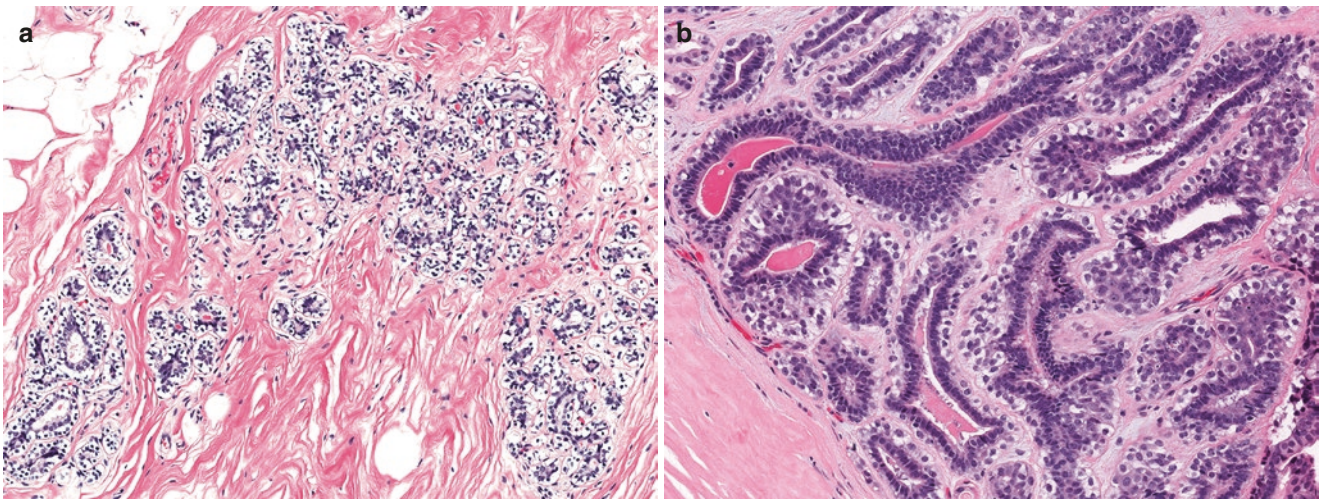

Fig. 14.24 Prominent myoepithelial cells can mimic ALH. (**a**) Acini showing prominent myoepithelial cells with clear cytoplasm. (**b**) Ductules lined by hyperplastic myoepithelial cells with clear cytoplasm. Both examples can simulate ALH. Note that the overlying luminal epithelial cells are normal appearing with cuboidal to columnar shape, in contrast to the compressed and attenuated luminal cells often observed in ALH

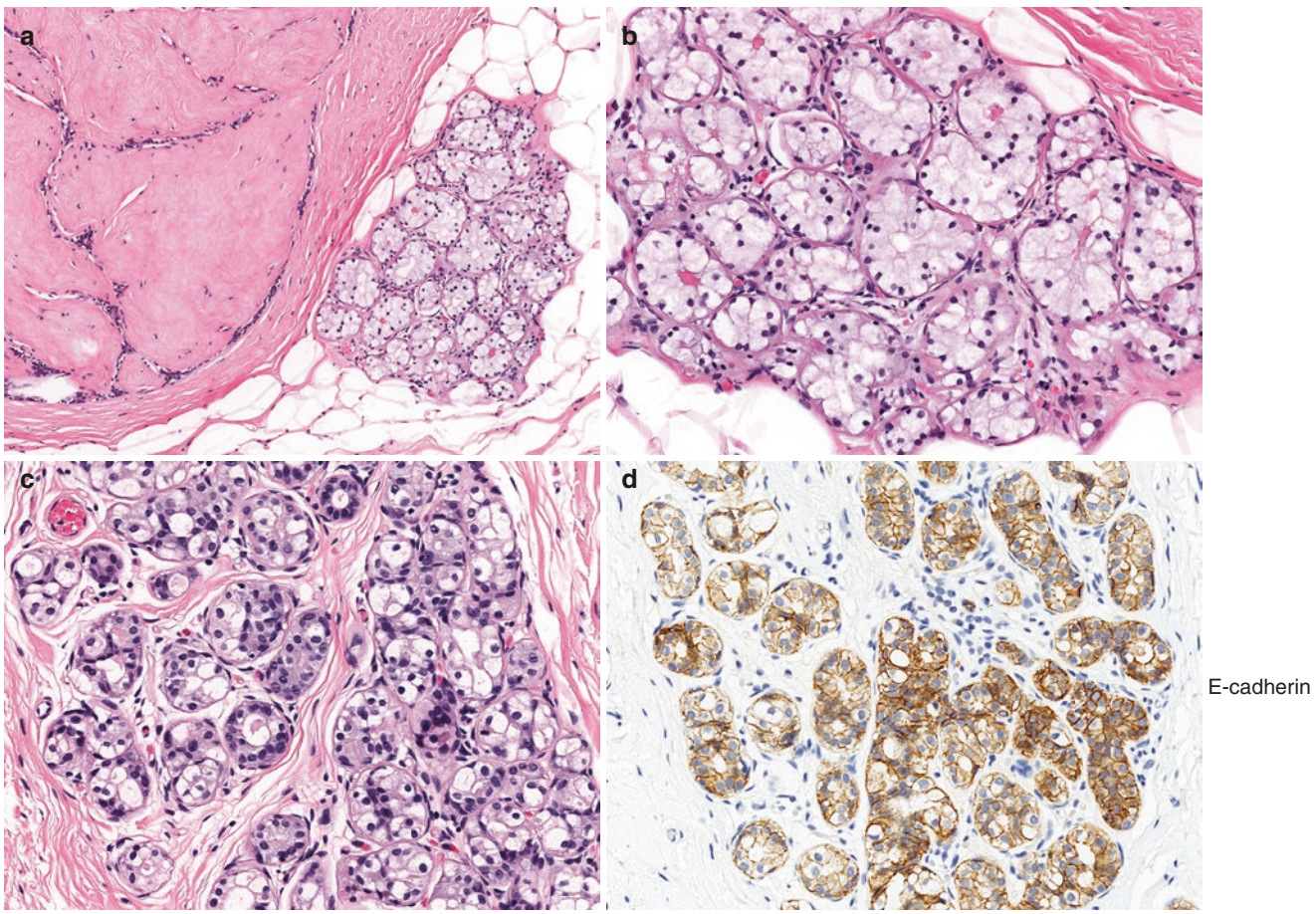

Fig. 14.25 Clear-cell change mimicking ALH. (**a**, **b**) Lobule with clear-cell change can be confused with ALH, especially at low magnification (**a**). The epithelial cells at high magnification (**b**) are characterized by abundant clear to finely granular cytoplasm and a small, generally centrally located nucleus. (**c**, **d**) Another example of clear-cell change. H&E stain (**c**) and E-cadherin immunostain (**d**) showing positive membranous staining

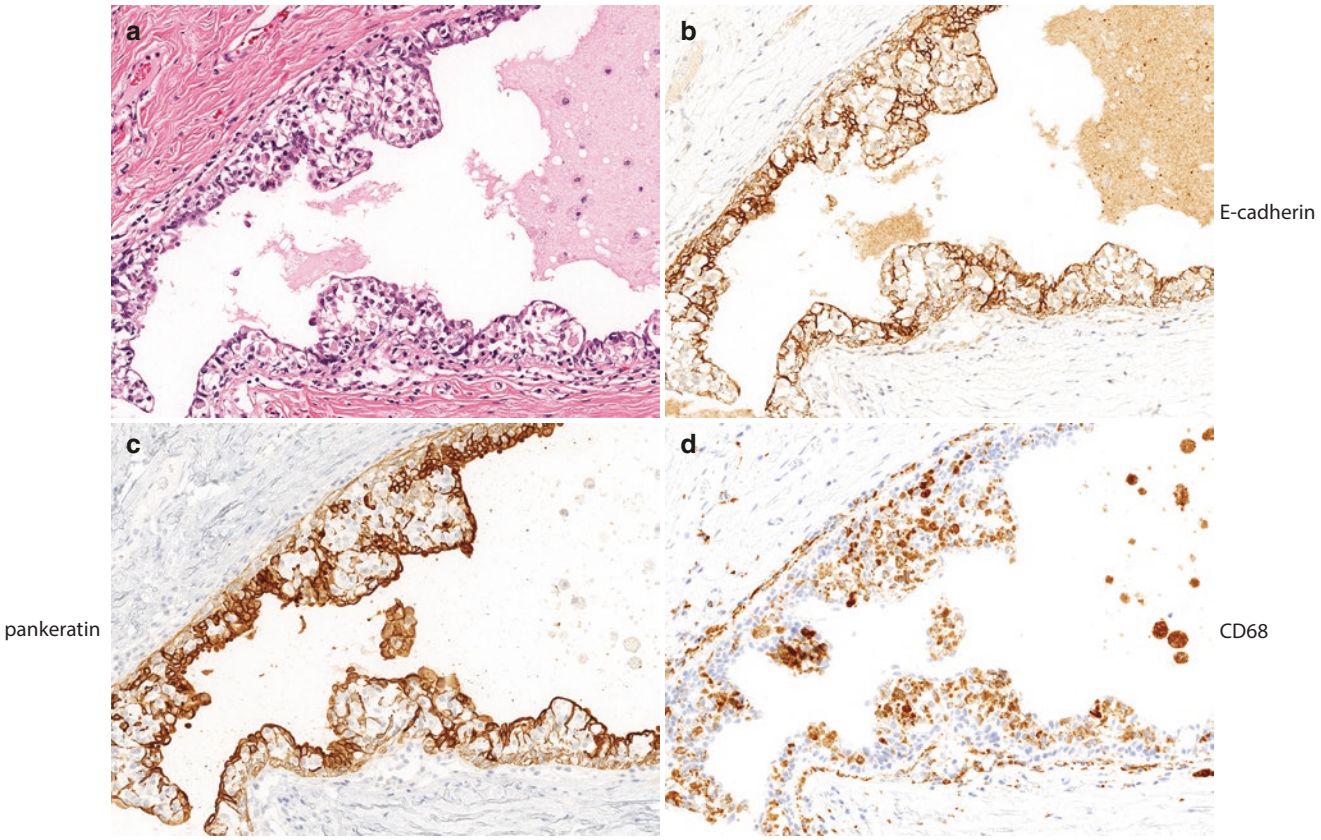

Fig. 14.26 Intraepithelial histiocytes simulate pagetoid spread of LN. (**a**) H&E stain of a duct with prominent intraepithelial histiocytes mimicking pagetoid spread of LN, including vacuolated cytoplasm of the histiocytes and compressed overlying luminal epithelial cells. (**b**) Negative E-cadherin expression could be further misleading. (**c**) Pancytokeratin and (**d**) CD68 immunostains help to highlight these cells as histiocytes and not epithelial cells

Another problem with ALH is missing the subtle lesion. In postmenopausal women, the extent to which the lobular cells fill and distend the TDLU tends to be less conspicuous than in younger patients. An atrophic lobule with ALH may not be distended, instead manifesting as a single layer of dyshesive cells that can be easily overlooked, especially at low power (Fig. 14.27). ALH involving atrophic lobules can be unequivocally diagnosed with E-cadherin IHC. One helpful clue to spot subtle ALH on low-power examination is to note the loss of acinar lumens in ALH compared to background normal TDLUs where the acinar lumens remain patent. An increase in the number of nuclei can also usually be appreciated.

Distinguishing Between LCIS and DCIS

The most important diagnostic decision for solid pattern carcinoma in situ is the distinction between solid pattern DCIS and LCIS, especially pleomorphic LCIS and florid LCIS. Classic LCIS and florid LCIS may be misclassified as low- or intermediate-grade DCIS, whereas pleomorphic LCIS can be easily mistaken for high-grade DCIS. Correct categorization has important clinical implications, as DCIS and LCIS are considered to be biologically distinct with differences in patient management (Table 14.2).

Differentiating solid pattern DCIS from LCIS, including pleomorphic and florid subtypes, can usually be established by careful evaluation of cytoarchitectural features, as summarized in Table 14.3. It should be emphasized that these histopathologic features are not entirely specific and show overlap between LCIS and DCIS. Loss of cell-to-cell cohesion is the key defining morphologic feature of LCIS. However, dyscohesion may not be apparent in some LCIS lesions, especially when the spaces are significantly expanded and tightly packed with the neoplastic cells, as in florid LCIS. Conversely, DCIS with necrosis/degeneration or suboptimal fixation may appear dyshesive. Intracytoplasmic lumina and signet ring cells are typically observed and may be quite prominent in LCIS, but these features are not specific for a lobular phenotype and may also be seen in DCIS, usually in mucin-producing DCIS. In a high-grade solid pattern in situ lesion, the presence of multinucleated cells favors pleomorphic LCIS, but multinucleation can also be observed in some examples of DCIS. DCIS and LCIS display preferential but overlapping distribution within the ductal-lobular

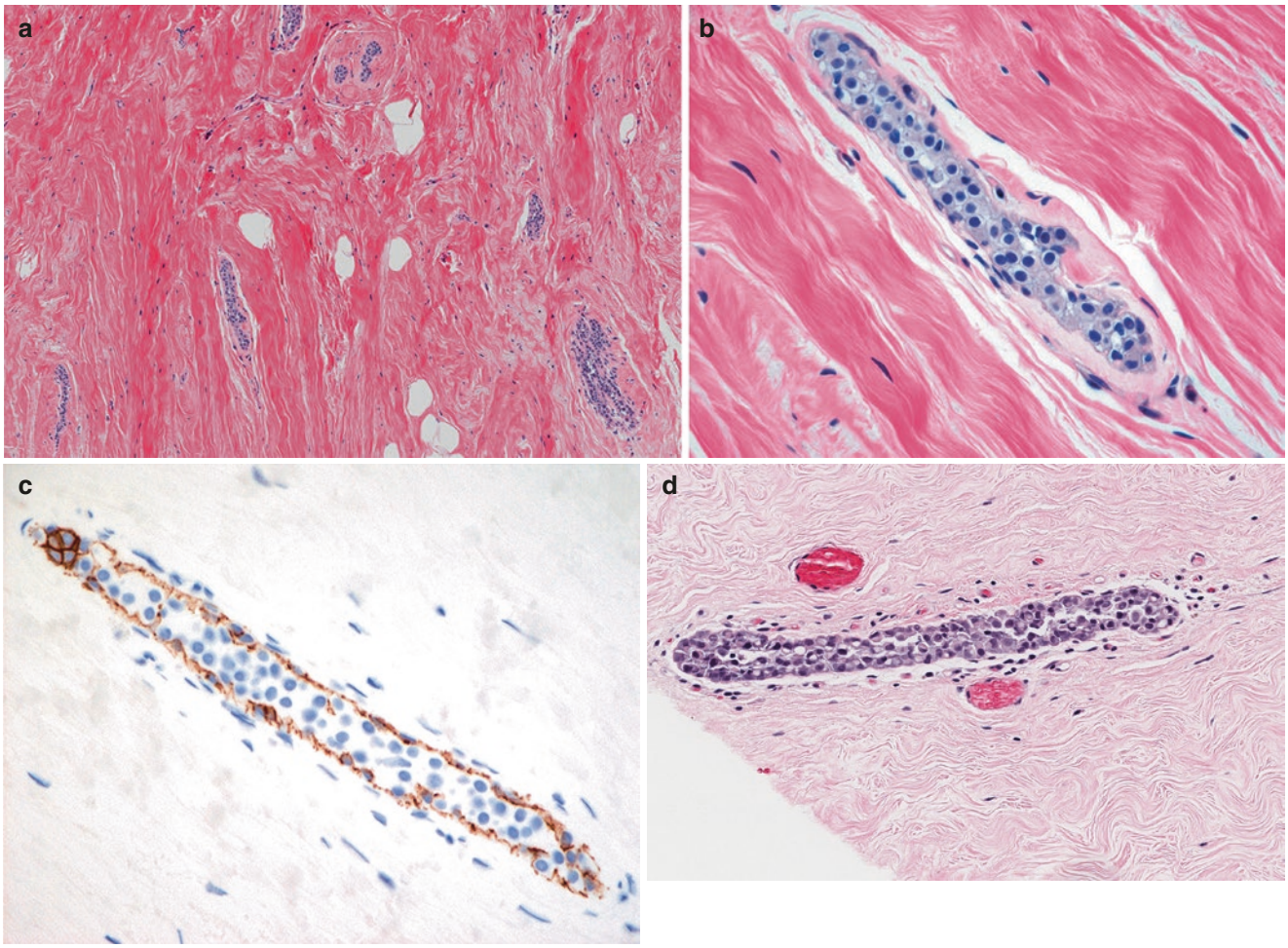

Fig. 14.27 ALH in lobular atrophy. (**a**) At low-power view, the atrophic lobules involved by ALH from this postmenopausal patient are not distended and may be overlooked. (**b**) High-power view demonstrates a single layer of subtly dyshesive epithelial cells, suggestive of ALH. (**c**) Immunohistochemistry highlights loss of E-cadherin expression, helping to establish the correct diagnosis. (**d**) Another example of ALH in an atrophic duct featuring non-cohesive, monomorphic epithelial cells with intracytoplasmic lumina

Table 14.2 Clinical distinction between LCIS subtypes and DCIS

	DCIS	Classic LCIS	Pleomorphic and florid LCIS
Current understanding of biology	Direct precursor of invasive cancer	Risk factor for future invasive cancer; may also be a non-obligate precursor	Likely a direct precursor of invasive lobular carcinoma
Future invasive cancer risk	8–10× risk; same site as DCIS; mostly as IDC	8–10× risk; bilateral; IDC > ILC	Lack of sufficient long-term follow-up data
Recommended treatment	Surgical excision, ± radiation therapy and hormonal therapy	Lifelong follow-up ± chemoprevention with hormonal therapy	Surgical excision, ± hormonal therapy; role of adjuvant radiation therapy unknown
Margins on excision	Margin status reported; excision to negative margins	Not evaluated	Recommended to report margin status; no consensus on negative surgical margins
If identified on core biopsy	Excision indicated	1. Excision if pathology discordant with imaging, limited sampling or other high-risk lesion also present 2. Observation with clinical/imaging follow-up ± chemoprevention if pathology concordant with imaging	Excision indicated

Table 14.3 Morphologic features useful in distinction between LCIS and DCIS

Morphologic features	Favor LCIS	Favor DCIS
Loss of cellular cohesion	+	
Prominent intracytoplasmic lumina and/or signet ring cell morphology	+	
Multinucleation	+[a]	
Pure solid pattern	+	
Lobular growth with pagetoid pattern in ducts	+	
Classic LCIS and/or ALH in adjacent breast	+	
Sharply defined cell membranes		+
Microacinar formation and polarization of cells around extracellular lumina and/or at the periphery of involved spaces		+

Adapted from [10]
[a] Multinucleation raises consideration of pleomorphic LCIS

system. Although LCIS characteristically involves lobules, DCIS can also extend into lobules (designated as cancerization of lobules by DCIS) (Fig. 14.28). Similarly, pagetoid ductal spread is not pathognomonic of LCIS and can be seen in DCIS (Figs. 14.29 and 14.30a). Furthermore, pagetoid growth of LCIS may occasionally impart a micropapillary/papillary appearance or may completely fill the ducts, features that can simulate DCIS (Fig. 14.30b). Formation of intraductal glandular structures with polarization of cells around the extracellular lumina is indicative of DCIS, and well-formed microacini are not expected in LCIS. However, LCIS involving other lesions, such as collagenous spherulosis or intraductal papillomas, can mimic neoplastic glandular structures of DCIS (see below). Although sharply defined cell membranes are characteristic of DCIS, LCIS may also

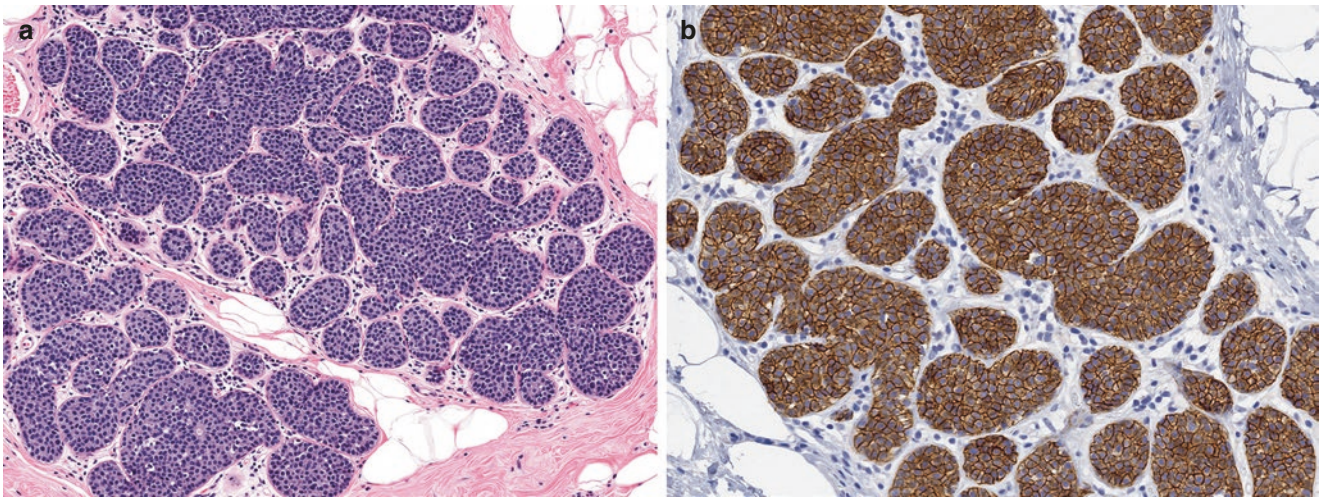

Fig. 14.28 Cancerization of lobules by DCIS can mimic LCIS. (**a**) Expansion of lobules by a monotonous population of low-grade epithelial cells. (**b**) The neoplastic cells exhibit strong membranous E-cadherin staining, supporting the diagnosis of DCIS

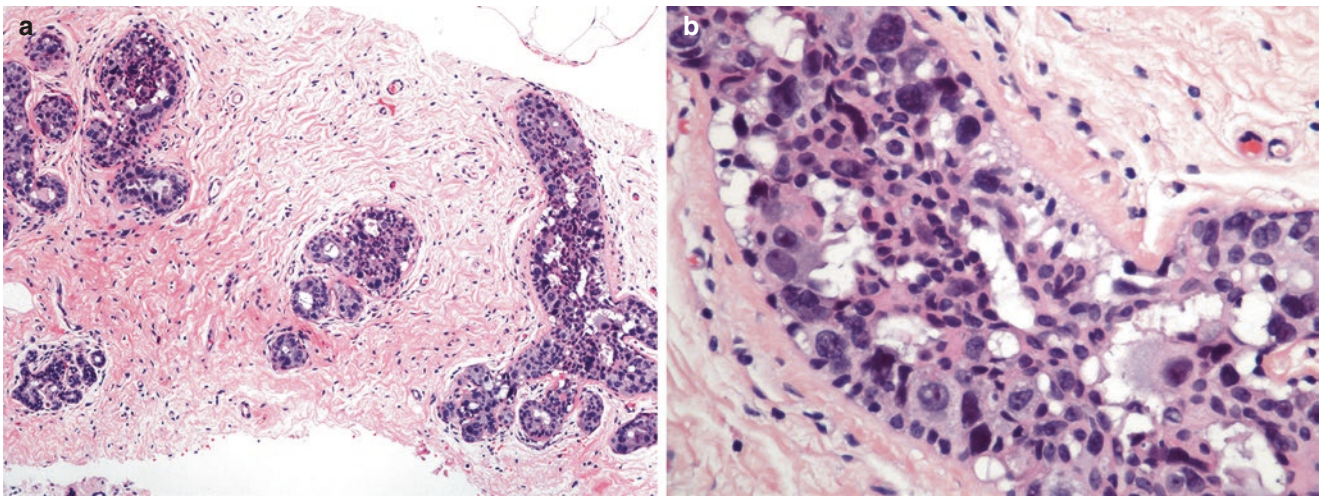

Fig. 14.29 Pleomorphic LCIS as pure pagetoid spread in ducts. (**a**) Low-magnification and (**b**) high-magnification views. This incidental finding was interpreted as DCIS in a core biopsy performed for calcifications identified in association with columnar cell change (not shown)

exhibit this feature, usually concurrent with apparent cohesive growth in significantly expanded spaces, thereby further confounding the diagnosis. The majority of DCIS lesions have mixed architectural patterns. When an in situ carcinoma is entirely solid in pattern, the possibility of (pleomorphic or florid) LCIS should be considered. Lastly, the vast majority of pleomorphic LCIS and florid LCIS are seen in association with classic LCIS and/or ALH. Although classic LCIS and ALH can be seen in association with DCIS, their presence should alert the pathologist to the possibility of an LCIS subtype. Similarly, the type of associated invasive carcinoma may be another helpful clue, as LCIS is usually found in association with ILC and DCIS with invasive ductal carcinoma (IDC). Of course, LCIS can also coexist with IDC, and DCIS with ILC. Similarly, LCIS and DCIS can involve the same lesion (Fig. 14.31) and even co-localize in the same duct space (Fig. 14.3). Given the overlapping morphological features of DCIS and LCIS (especially pleomorphic LCIS and florid LCIS), immunohistochemical stains for E-cadherin and other components of the E-cadherin-catenin complex can be useful for correct classification but should be interpreted in the context of the histologic features.

Distinguishing Classic LCIS from Pleomorphic/Florid LCIS

The distinction between classic LCIS and pleomorphic LCIS or florid LCIS can usually be made using the cytologic and architectural criteria outlined by the WHO classification.

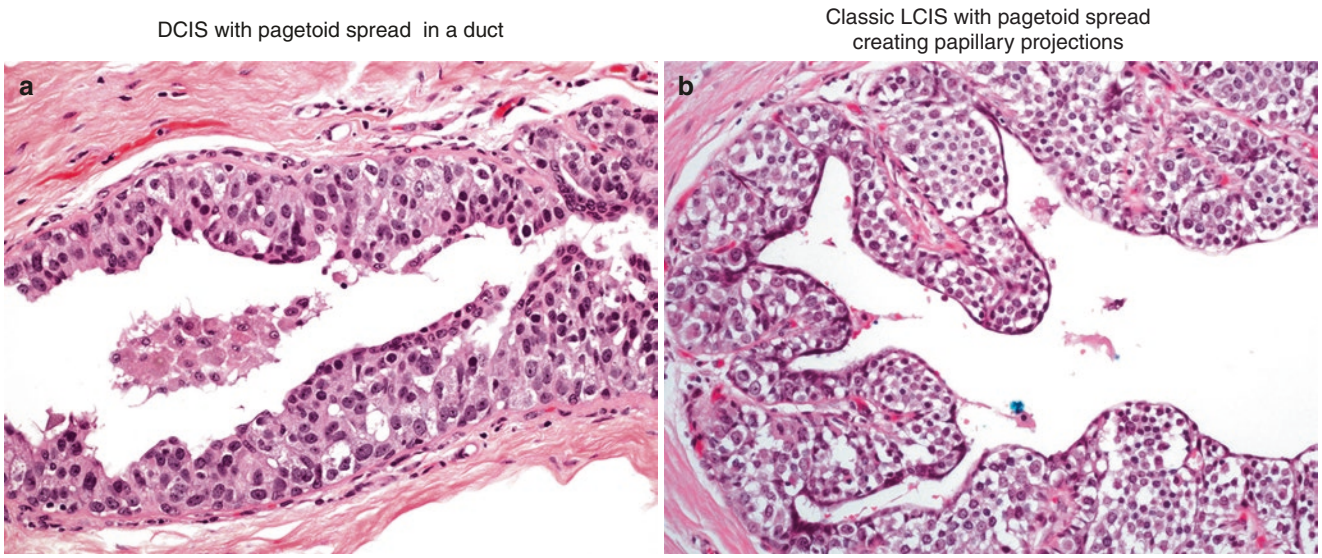

Fig. 14.30 Pagetoid growth pattern can be seen in both DCIS and LCIS. (**a**) DCIS with pagetoid growth pattern in a duct that could be misinterpreted as LCIS. (**b**) In this example, classic LCIS with pagetoid spread creates papillary projections, a feature that could mimic DCIS

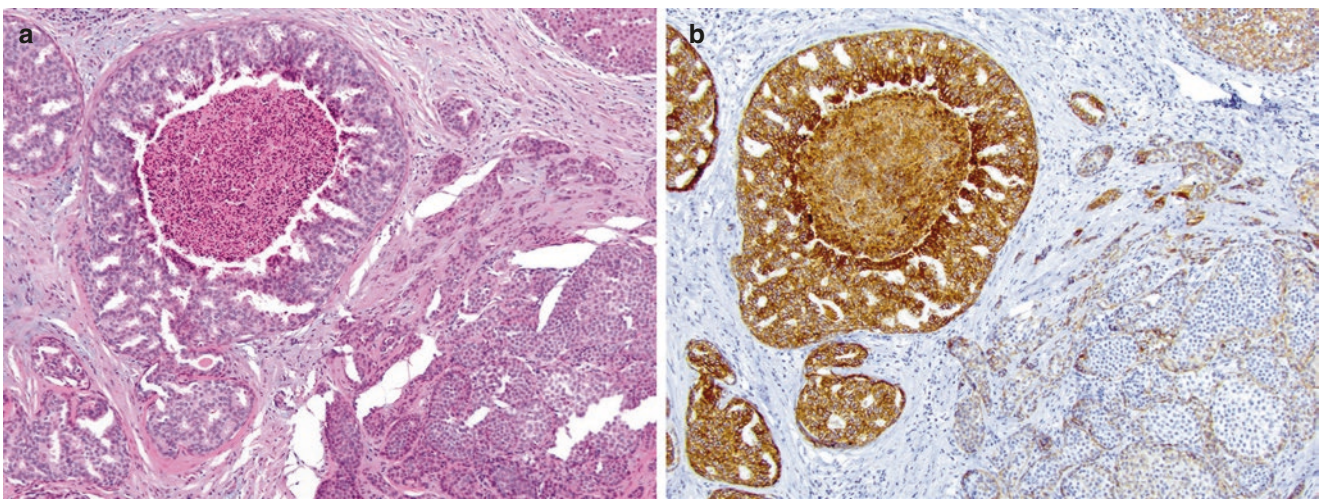

Fig. 14.31 DCIS and adjacent classic LCIS. (**a**) Micropapillary DCIS with comedo necrosis in the upper left and classic LCIS involving sclerosing adenosis in the lower right. (**b**) Immunostain for E-cadherin is positive in DCIS and negative in LCIS

However, some LCIS lesions may not fit neatly into any of the accepted categories due to borderline and overlapping features. Some cases have nuclear features that are borderline between classic LCIS and pleomorphic LCIS or architectural features that are borderline between classic LCIS and florid LCIS. A conservative approach is recommended for these borderline lesions, akin to recommendations for ductal proliferations advocated by Page and Rogers [10, 85]. Therefore, LCIS with nuclear atypia on the borderline between classic type B cells and pleomorphic LCIS should generally be classified as classic LCIS. Similarly, LCIS with type A or type B cells and acinar distension bordering between classic LCIS and florid LCIS should be designated as classic LCIS. It is important to note that extensive LCIS with involvement of numerous TDLUs but lacking marked acinar expansion should not be characterized as "florid," to avoid confusion with florid LCIS.

Diagnosis of Subtle Invasive Lobular Carcinoma Arising in Association with LCIS

ILC may be quite subtle and easily missed. In contrast to classic LCIS, which is not infrequently encountered in pure in situ form without associated invasive carcinoma, most (~59–87%) cases of pleomorphic LCIS and florid LCIS are ultimately associated with invasive carcinoma either on core biopsy or on surgical excision, with the majority (~84–100%) of these being ILC [33, 34, 86–88]. Therefore, the presence of these LCIS subtypes should prompt a careful search for subtle invasion in the adjacent tissue, which may manifest as a subtle increase in cellularity or could be masked by inflammatory cells (Figs. 14.32, 14.33, and 14.34). Immunohistochemical stains, such as cytokeratin or multiplex stains composed of low molecular keratin and myoepithelial markers, can be very helpful to highlight subtle invasive foci (Fig. 14.32).

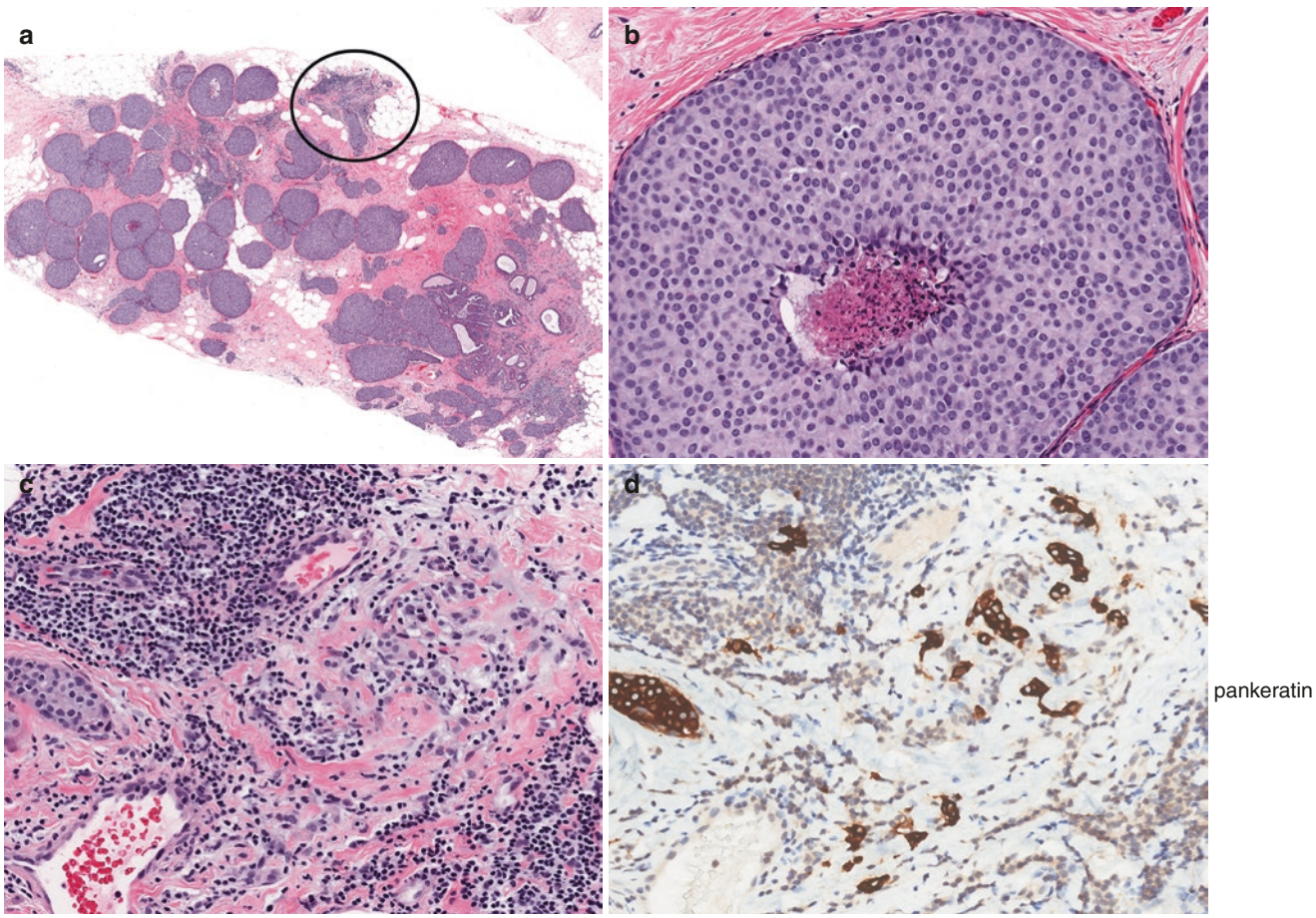

Fig. 14.32 Florid LCIS with subtle invasive lobular carcinoma masked by inflammatory infiltrate. (**a**, **b**) Core biopsy for non-mass enhancement shows florid LCIS with central confluent necrosis. Note a focus of dense lymphoid infiltrate in the stroma (circled area in **a**). (**c**) High-power evaluation from the circled area in (**a**) reveals subtle single and small clusters of cells admixed with the lymphoid infiltrate, suspicious for invasive carcinoma. (**d**) An immunostain for pancytokeratin confirms invasive lobular carcinoma

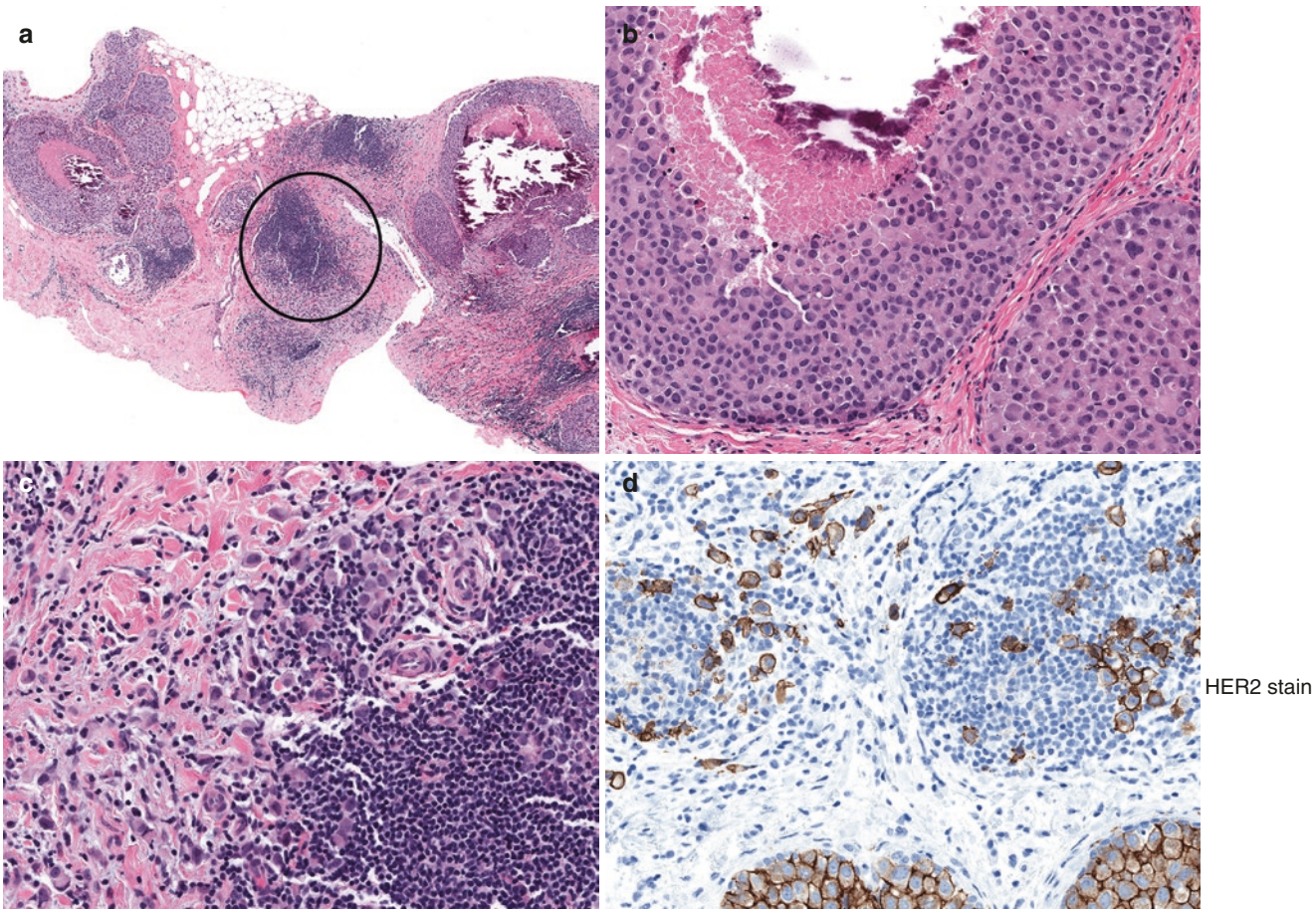

Fig. 14.33 Pleomorphic LCIS with subtle invasive lobular carcinoma masked by dense inflammatory infiltrate. (**a**, **b**) Core biopsy for pleomorphic calcifications shows pleomorphic LCIS with comedo necrosis and calcifications. Note a few foci of dense lymphoid infiltrate (one of which circled in (**a**)). (**c**) High-power examination from the circled area in (**a**) demonstrates subtle single epithelioid cells admixed with the lymphoid infiltrate, highly suspicious for invasive carcinoma. A keratin immunostain confirmed the diagnosis of invasion (not shown). (**d**) HER2 immunostain highlights HER2 overexpression in the invasive carcinoma and associated pleomorphic LCIS

Lobular Neoplasia (or LCIS) Involving Different Lesions

LN does not infrequently involve other lesions, such as fibroadenomas, sclerosing adenosis, radial scars, and papillomas, among others (Figs. 14.35, 14.36, 14.37, 14.38, and 14.39). It is important to be aware of this phenomenon in order not to overlook LN in an otherwise benign breast lesion or to avoid a misdiagnosis of invasive carcinoma or DCIS.

A well-recognized pitfall is LN involving collagenous spherulosis. Collagenous spherulosis is often associated with calcifications that can be targeted for core biopsy. LN involving collagenous spherulosis is most likely to be mistaken for cribriform pattern DCIS (Fig. 14.40). Collagenous spherulosis can be recognized by the basophilic myxoid material or hyalinized spherules of basement membrane material within the cribriform pseudolumina. Immunohistochemical stains for p63, calponin, or smooth muscle myosin heavy chain (SMM) can be used to highlight myoepithelial cells surrounding the pseudolumina, and E-cadherin will show absent membranous staining in the LN population (Fig. 14.40). Care should be taken not to misinterpret weak E-cadherin staining of admixed myoepithelial cells as evidence of retained E-cadherin expression and consequent misclassification as DCIS.

Another common pitfall is LN involving sclerosing adenosis and radial scar. The pseudo-infiltrative pattern of sclerosing adenosis involved by neoplastic cells can easily lead to an erroneous diagnosis of invasive carcinoma (Figs. 14.41, 14.42, 14.43, and 14.44). Although it is fairly simple to prove the diagnosis with immunohistochemical stains (myoepithelial markers to demonstrate lack of invasion and absence of E-cadherin in the neoplastic cells), the challenge lies in considering this possibility in the differential diagnosis. The underlying lesion may not be easily appreciated in limited core biopsy material. The presence of LN or sclerosing adenosis in their pure forms in the adjacent tissue is an

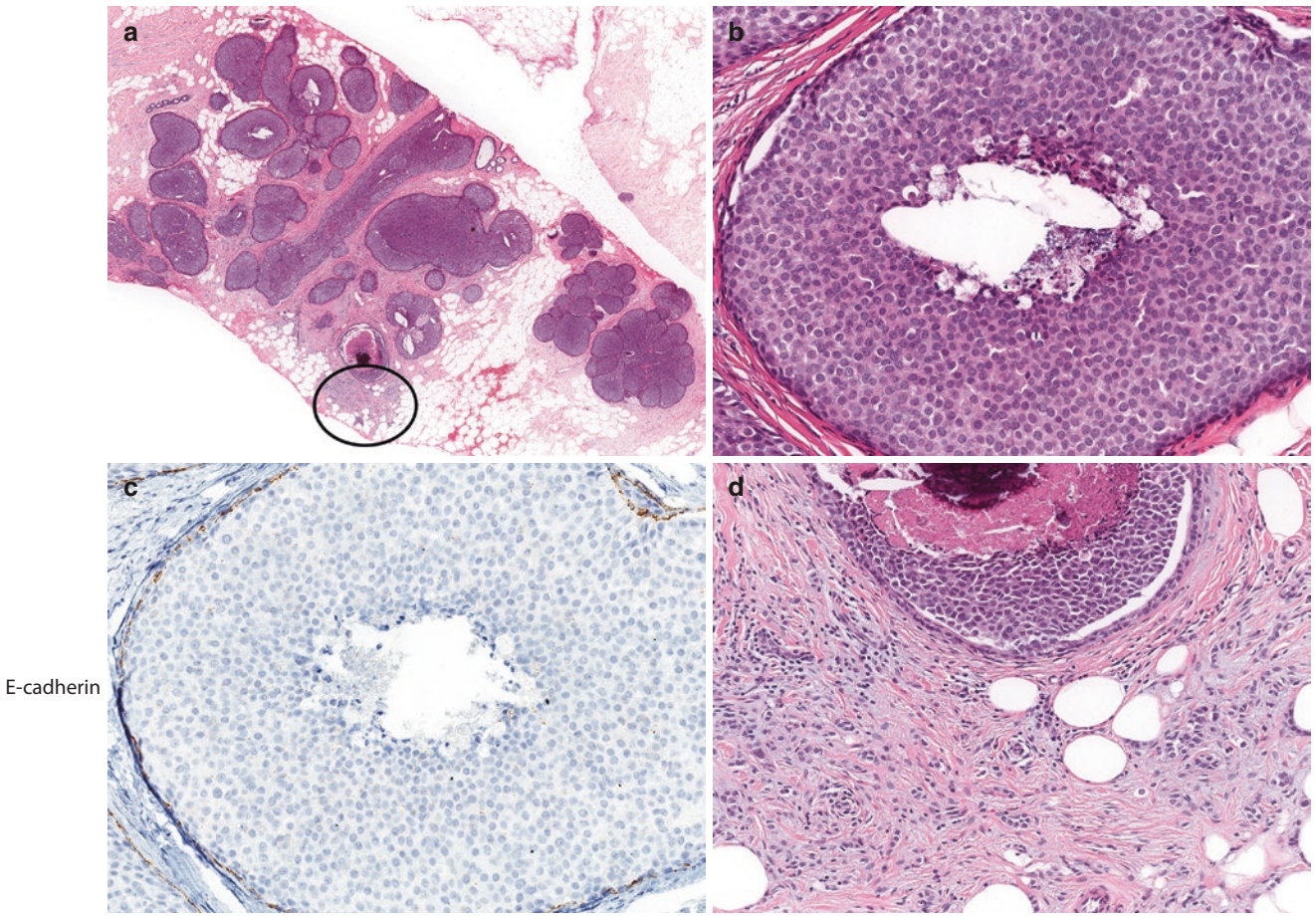

Fig. 14.34 Florid LCIS with subtle invasive lobular carcinoma. (**a, b**) H&E stains and (**c**) E-cadherin immunostain from a core biopsy show florid LCIS with confluent necrosis and calcifications. One small area appears to have a subtle increase in cellularity at low magnification (circled area in (**a**)). (**d**) High magnification from the circled area in (**a**) reveals the presence of invasive lobular carcinoma

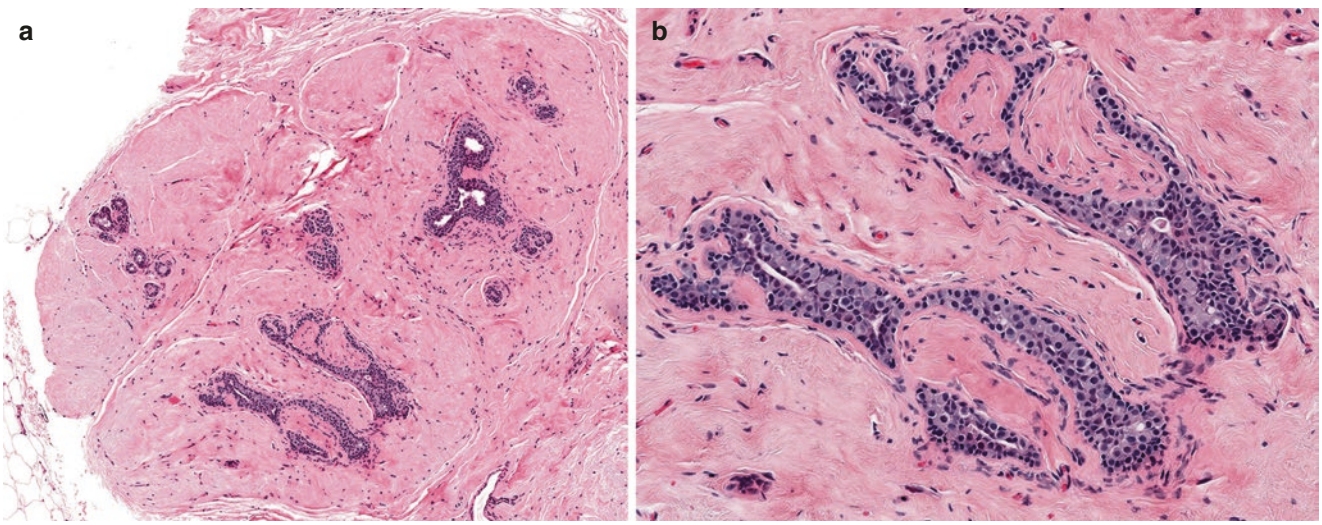

Fig. 14.35 Core biopsy performed for a mass shows incidental ALH involving a fibroadenoma. (**a**) Low magnification and (**b**) high magnification

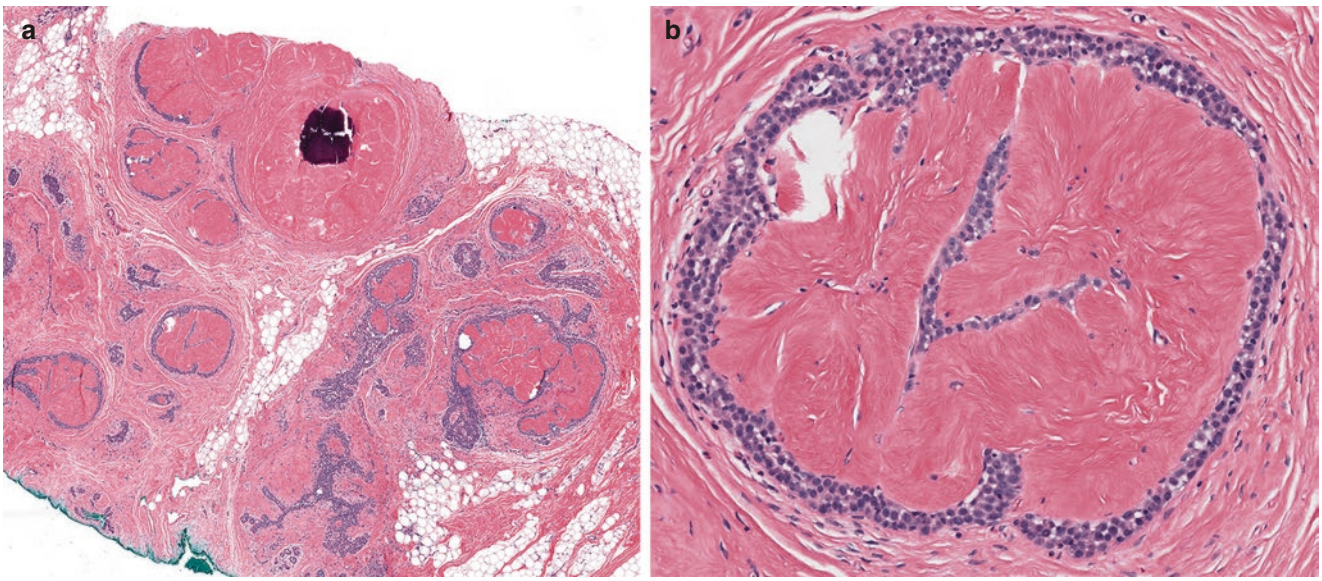

Fig. 14.36 Core biopsy performed for calcifications shows incidental ALH in fibroadenomatous change with calcifications. (**a**) Low magnification and (**b**) high magnification

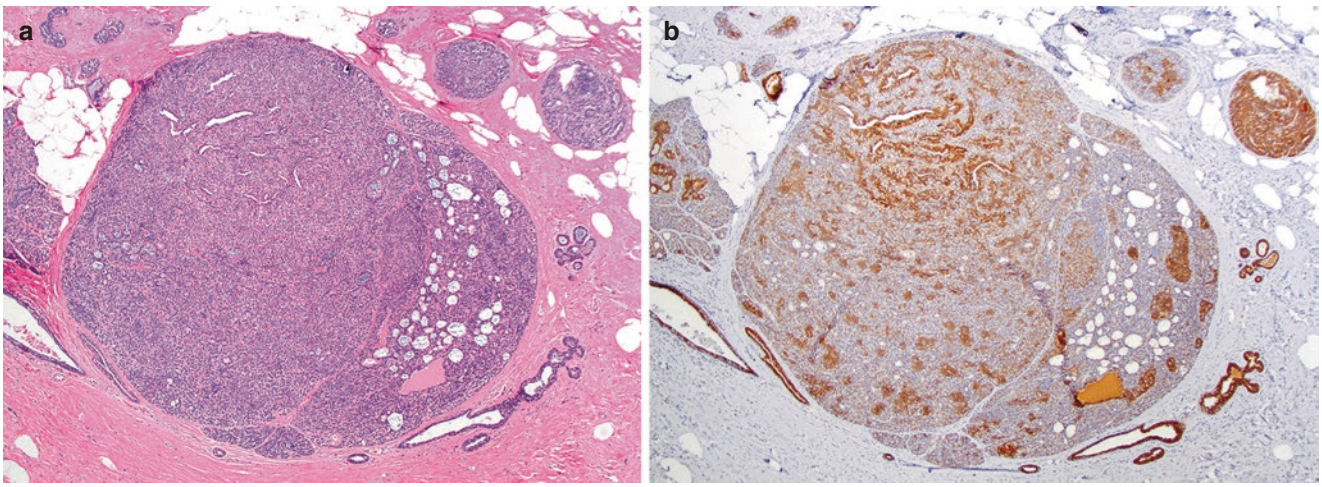

Fig. 14.37 Classic LCIS involving nodular adenosis. (**a**) H&E stain. (**b**) E-cadherin immunostain is negative in the LCIS cells

important clue to the diagnosis. Radial scars can themselves be mistaken for invasive carcinoma, and involvement by LN may further complicate the diagnosis.

Pathogenesis

Lobular lesions of the breast are defined by the absence or dysfunction of the E-cadherin protein, resulting in loss of cell-to-cell cohesion, and altered organization of the lobules and giving rise to the characteristic morphologic appearance of LN [89, 90]. E-cadherin is encoded by the *CDH1* gene localized on the long arm of chromosome 16 (16q22.1). E-cadherin alterations are an early event in LN, being present in ALH and persisting in LCIS (all subtypes) and ILC. Loss of E-cadherin expression is most commonly caused by *CDH1* mutations accompanied by loss of the wild-type allele at 16q [77, 91]. Most *CDH1* mutations are truncating, but missense mutations and in-frame deletions have been observed and may more likely account for aberrant E-cadherin expression [92]. E-cadherin may also be down-regulated by promoter hypermethylation or other types of transcriptional repression [93, 94]. Germline *CDH1* mutations may rarely be associated with the development of lobular breast cancers [95, 96].

All LCIS subtypes harbor recurrent chromosomal gain of 1q and loss of 16q, a pattern typical of the low-grade breast neoplasia pathway [14, 24, 37, 73, 74, 97, 98]. As expected,

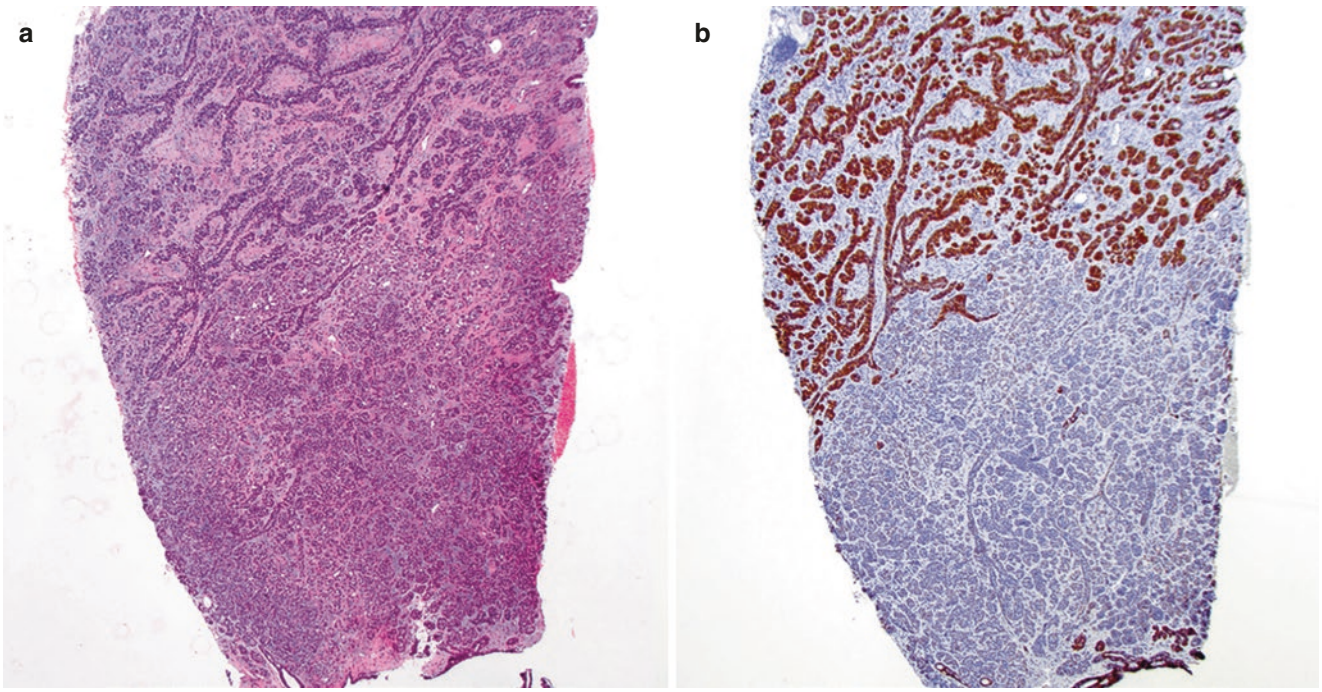

Fig. 14.38 Extensive classic LCIS involving a sclerosing papilloma, biopsied for a mass. (**a**) Low magnification shows the sclerosis in the upper half that is secondarily involved by LCIS in the lower half of the image. (**b**) Immunostain for E-cadherin highlights the preexisting ductal epithelium and shows lack of staining in LCIS

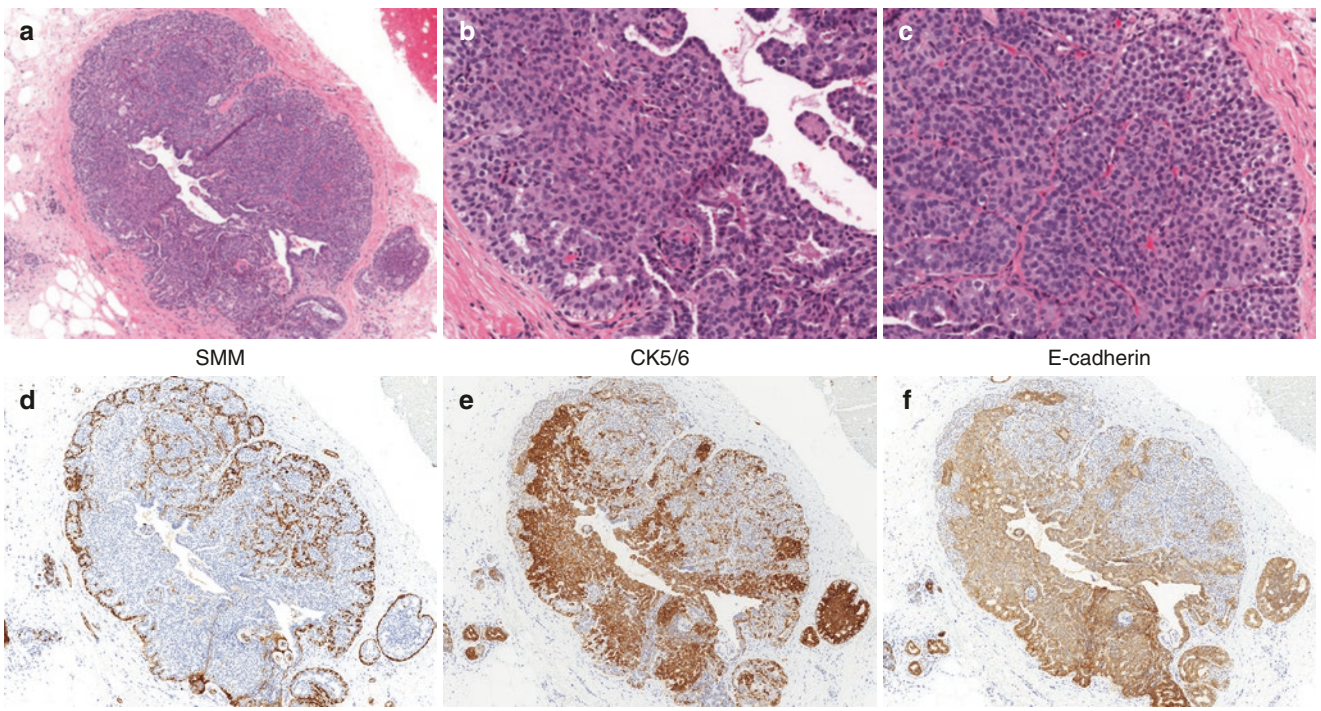

Fig. 14.39 Papilloma involved by both classic LCIS and usual ductal hyperplasia. (**a**) Low-power view shows a papilloma involved by epithelial proliferation. (**b**, **c**) Higher power views demonstrate features of usual ductal hyperplasia with heterogeneous overlapping nuclei in some areas (**b**) and atypical proliferation with monomorphic low-grade nuclei and intracytoplasmic lumina in other areas (**c**). (**d**) SMM immunostain highlights the myoepithelial cells lining the papillae. (**e**) CK5/6 immunostain confirms foci of usual ductal hyperplasia (positive staining) and atypical proliferation (negative staining). (**f**) The atypical proliferation is negative for E-cadherin, supporting LCIS

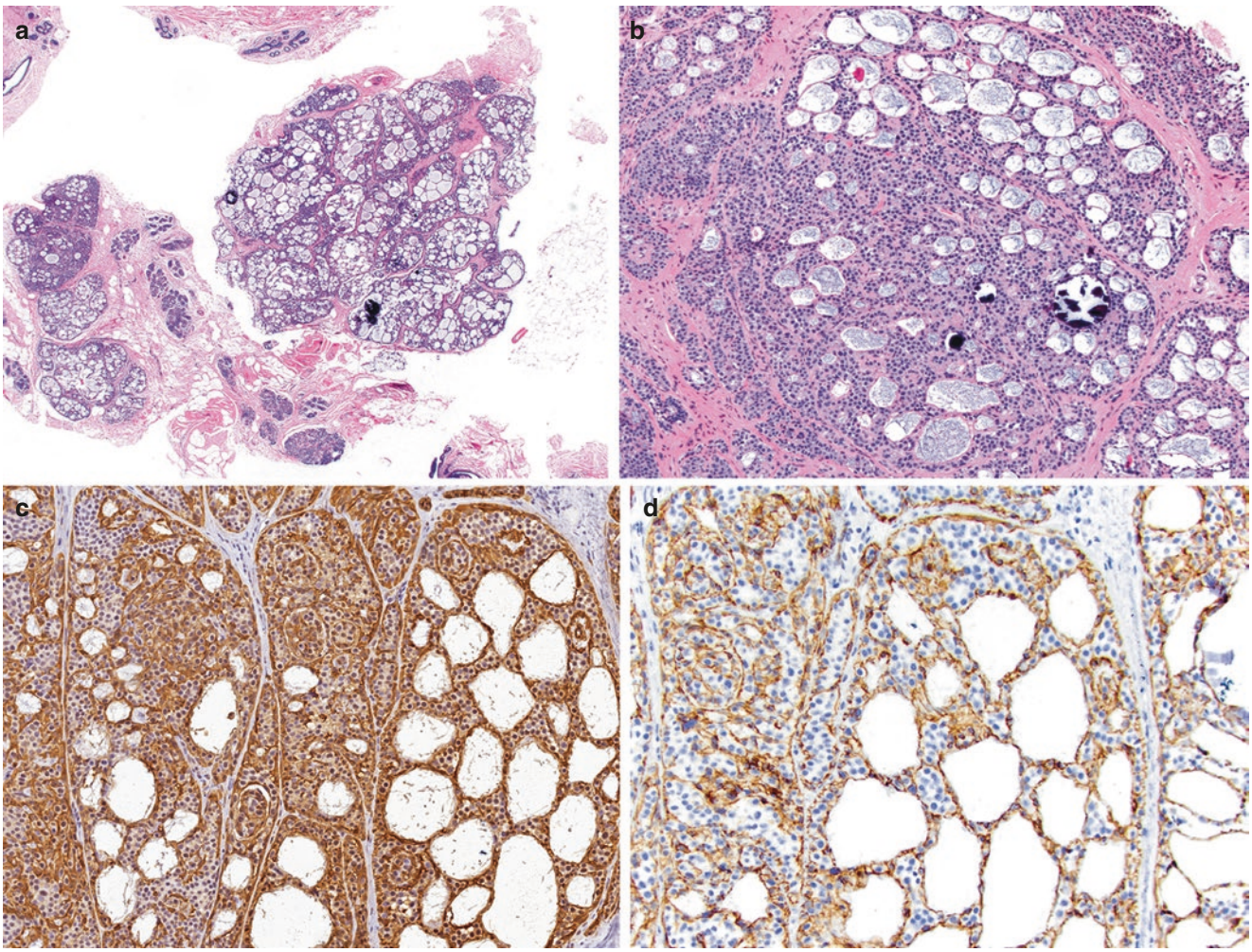

Fig. 14.40 Classic LCIS involving collagenous spherulosis. (**a**) Core biopsy performed for calcifications shows a confluent area with cribriform architecture due to collagenous spherulosis. (**b**) Higher magnification demonstrates a monotonous population of low-grade cells that can easily be mistaken for low-grade DCIS in the context of the cribriform architecture. Note the basophilic myxoid spherules within the cribriform pseudoglandular spaces. (**c**) Immunostain for calponin reveals myoepithelial cells around the spherules and at the periphery of the lesion. (**d**) E-cadherin immunostain is negative in the LCIS cells but highlights the residual ductal and myoepithelial cells

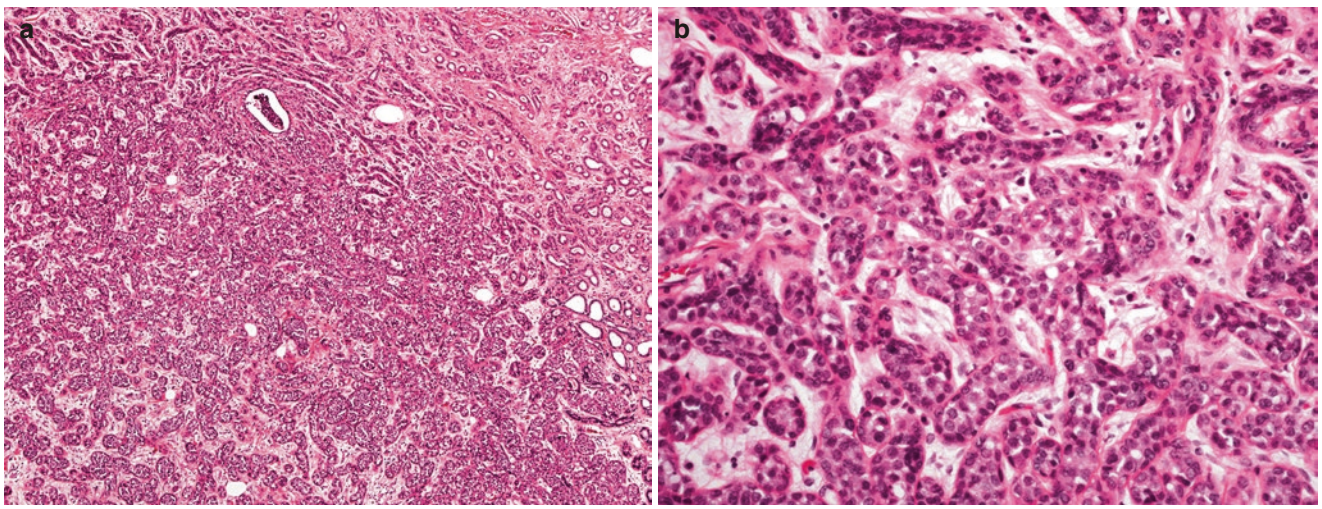

Fig. 14.41 Classic LCIS involving extensive sclerosing adenosis mimics invasive carcinoma. (**a**) The combination of pseudo-infiltrative growth pattern and monomorphic neoplastic cells can be misdiagnosed as invasive carcinoma. (**b**) Higher magnification reveals lobular neoplastic cells surrounded by intact basement membrane. Immunohistochemistry with myoepithelial markers is helpful to confirm the presence of myoepithelial cells and avoid a misdiagnosis of invasion

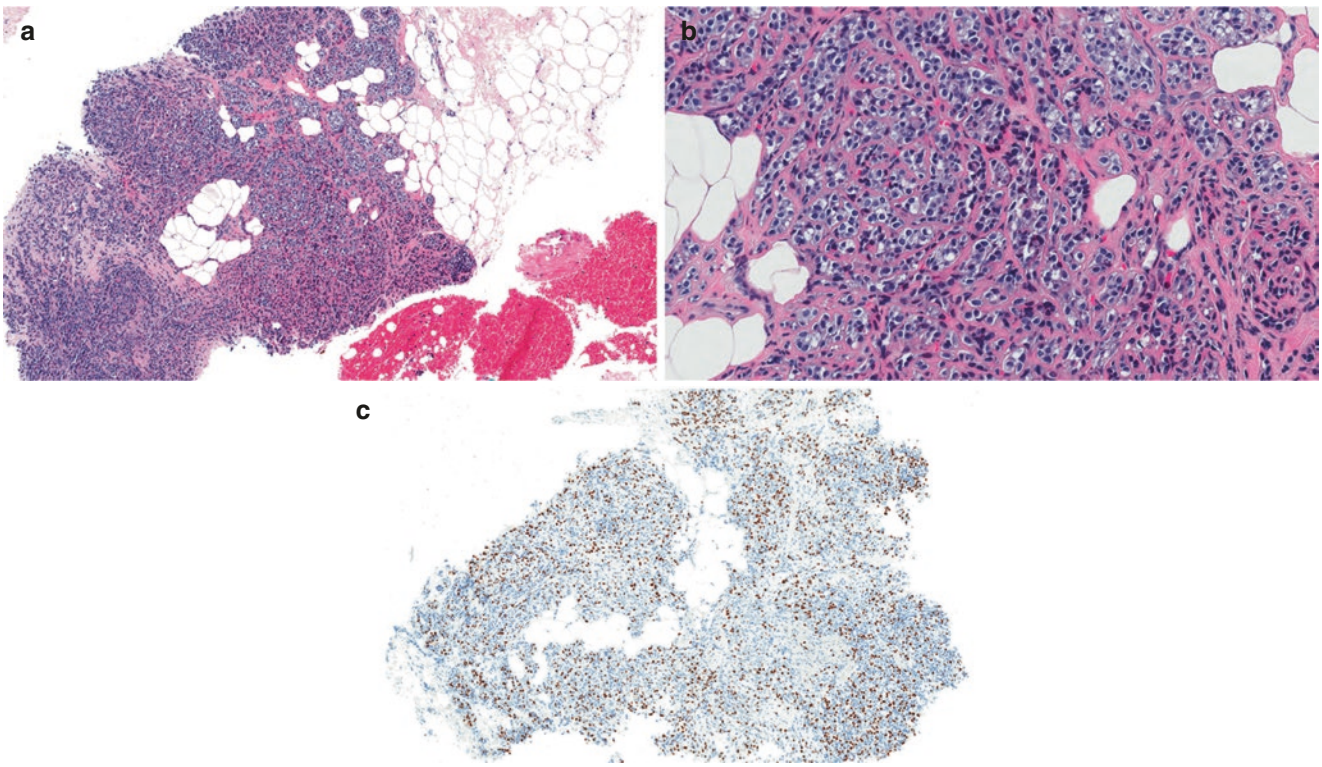

Fig. 14.42 Classic LN involving sclerosing adenosis in a core biopsy. (**a**, **b**) Low- and high-power views show infiltrative-appearing small epithelial nests, raising the possibility of an invasive carcinoma. (**c**) p63 immunostain shows intact myoepithelial cells

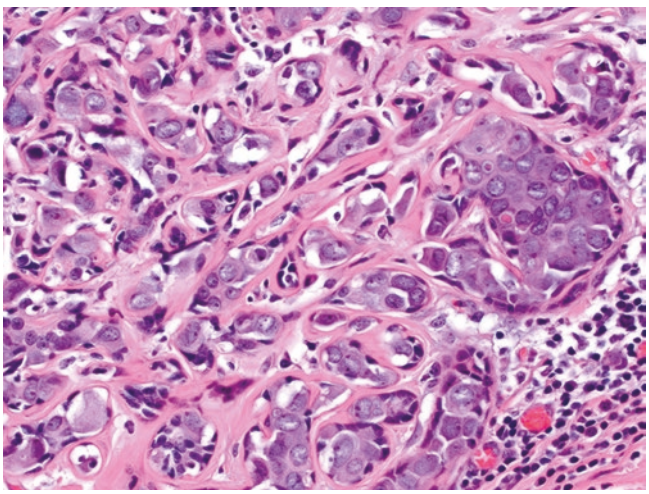

Fig. 14.43 Pleomorphic LCIS involving sclerosing adenosis and mimicking high-grade invasive ductal carcinoma

CDH1 mutations have been identified in the majority (~80–90%) of sequenced LCIS lesions of all subtypes [73, 74, 99–101]. Other frequently mutated genes that have been identified in all LCIS subtypes include *PIK3CA*, *CBFB*, *RUNX1*, *TBX3*, *FOXA1*, and *GATA3*, a genetic profile that is typical of luminal type breast cancers and especially ILC [73, 74, 99, 100, 102]. Analyses of synchronous ILC and classic LCIS pairs have found that most shared identical mutations, including *CDH1* and *PIK3CA*, among others [74, 100]. In one study, anatomically distinct foci of classic LCIS within the same breast quadrant were clonally related to one another in all cases, and foci from different quadrants were clonally related to one another in 67% of cases. Synchronous ILC and DCIS were found to be clonally related to at least one sequenced focus of classic LCIS in 77% and 56% of cases, respectively [99]. These findings provide evidence that LCIS is a clonal neoplastic lesion and that at least some classic LCIS is a non-obligate precursor to ILC.

Compared to classic LCIS, pleomorphic LCIS and florid LCIS are genomically more complex, with more copy number alterations (CNA) in addition to 1q gain and 16q loss [24, 37, 74]. Pleomorphic LCIS with apocrine features and florid LCIS were found to be genomically more complex than non-apocrine pleomorphic LCIS [24, 37]. In paired analysis, pleomorphic LCIS and florid LCIS were found to harbor identical shared pathogenic mutations (including *CDH1*, *PIK3CA*, and others) and CNA as synchronous classic LCIS, indicative of a common clonality between classic LCIS and these LCIS subtypes [74]. However, pleomorphic LCIS is a genetically more advanced lesion than classic LCIS, with most pleomorphic LCIS showing a higher mutational load, more CNA, and additional driver alterations [74]. These most notably include highly recurrent *ERBB2* and *ERBB3*

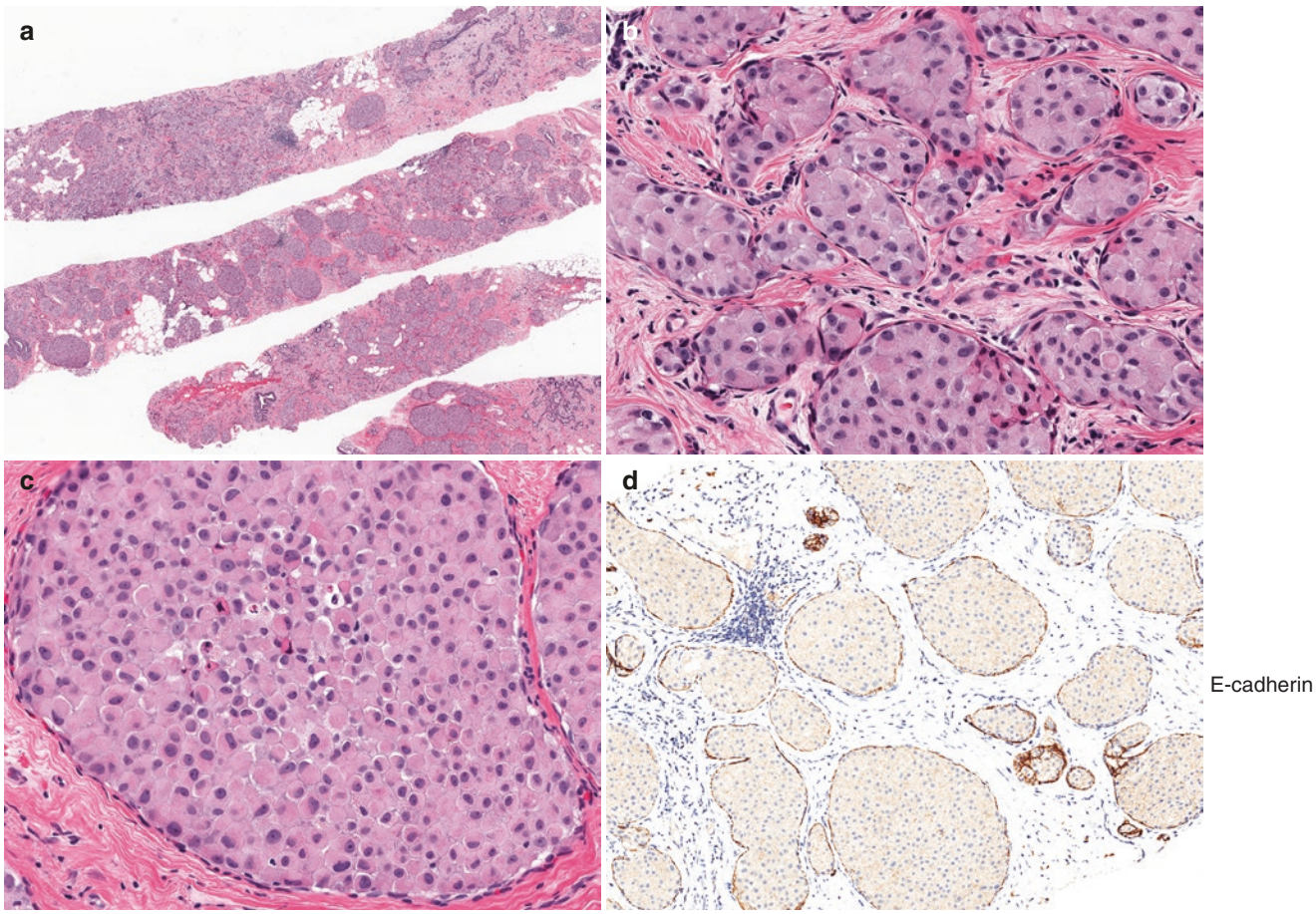

Fig. 14.44 Apocrine pleomorphic LCIS involving a sclerosing lesion presenting as a palpable mass. (**a**) Low-power view of the core biopsy shows confluent atypical epithelial nests, giving the impression of invasive carcinoma. (**b**, **c**) Higher power views demonstrate small and large solid nests comprised of apocrine cells with pleomorphic nuclei, suggesting invasive apocrine carcinoma associated with apocrine DCIS. However, the possible basement membrane around cell nests and focal loss of cell-to-cell cohesion could raise the possibility of an LCIS. (**d**) The neoplastic cells lack E-cadherin expression. Note the positive E-cadherin staining from the surrounding myoepithelial cells. Immunostains for E-cadherin and myoepithelial markers (not shown) support apocrine pleomorphic LCIS involving an underlying sclerosing lesion

aberrations (*ERBB2* mutations and/or amplifications and *ERBB3* mutations) and less commonly *TP53* mutations and *CCND1* amplifications, all of which, when present in pleomorphic LCIS, are typically shared with synchronous ILC [37, 73, 74]. Progression from pleomorphic LCIS to paired ILC has been associated with the accumulation of mutations in other cancer genes and additional CNA in a subset of cases [74]. In concert with the pleomorphic cytomorphologic features and more aggressive biomarker profile, the genetic data support the notion that, compared to clonally related classic LCIS, pleomorphic LCIS is a more advanced precursor lesion with frequent *ERBB2* and *ERBB3* alterations. Florid LCIS also harbors frequent *ERBB2* and *ERBB3* mutations [73, 74]. However, data on the genetic relationship of florid LCIS to paired classic LCIS and ILC are more limited. An analysis of three paired cases, each with clonally related classic LCIS, florid LCIS, and ILC, showed additional clonal or subclonal pathogenic mutations (*PIK3R1*, *FOXA1*, *KRAS*, *KMT2C*) in florid LCIS compared to classic LCIS in all three, but these were not shared with synchronous ILC. Synchronous ILC in one of these cases was genetically more similar to paired classic LCIS than florid LCIS [74].

ERBB2 and *ERBB3* encode the oncogenic epidermal growth factor receptors HER2 and HER3, respectively. Most *ERBB2* (missense, insertions) and *ERBB3* (missense) mutations in pleomorphic LCIS and florid LCIS are localized to the tyrosine kinase domain and predicted to be activating [73, 74, 103]. A high frequency of *ERBB2* mutations has also been described in pleomorphic or solid pattern ILC [92, 104] and relapsed ILC, and it is associated with worse outcomes in patients with ILC [105–107]. *ERBB2* and *ERBB3* alterations were found to be more common in pleomorphic LCIS and florid LCIS and in ILC associated with these LCIS subtypes than ILC from The Cancer Genome Atlas (TCGA) dataset. Similarly, *TP53* mutations were more common in ILC associated with pleomorphic LCIS than in the TCGA

ILC [74]. In sum, *ERRB2*, *ERRB3*, and *TP53* likely help drive the histologic and biologic progression of classic LCIS toward these LCIS subtypes and provide further evidence for their more aggressive potential.

Table 14.4 compares the clinical-pathologic and molecular features of classic LCIS, pleomorphic LCIS, and florid LCIS.

Prognosis and Management

When LCIS was first described, it was considered a premalignant condition and a precursor lesion to invasive carcinoma. Several decades later, the opposite conclusion was reached, as classic LCIS was found to be indolent and regarded as a risk factor for the development of future invasive carcinoma. Currently, histologic observations, clinical follow-up data, and genetic studies support LN being both a risk factor for and a non-obligate precursor to invasive carcinoma.

Lobular Neoplasia as a Risk Factor for Invasive Breast Carcinoma

Our current understanding of the prognosis and outcomes of patients with ALH and classic LCIS is derived from long-term follow-up studies (Tables 14.5 and 14.6). Long-term follow-up data of patients with pleomorphic LCIS and florid LCIS is very limited, and the natural history of these subtypes is currently less clear.

Table 14.4 Clinical-pathologic and molecular features between classic LCIS, pleomorphic LCIS, and florid LCIS

	Classic LCIS	Pleomorphic LCIS	Florid LCIS
Age	Premenopausal (mean ~ 50 years)	Postmenopausal (mean ~ 60 years)	Postmenopausal (mean ~ 60 years)
Clinical presentation	Incidental microscopic finding	Imaging detection (most often mammographic calcifications)	Imaging detection (most often mammographic calcifications)
Biomarkers	ER+, HER2−, low Ki-67 (favorable)	More often ER−, HER2+, TN or aberrant p53, more often high Ki-67	Usually ER+, HER2−/+, more often high Ki-67
Chromosomal copy number alterations	1q+/16q−; no or few other alterations	1q+/16q−; plus additional alterations	1q+/16q−; plus additional alterations
Genetics	*CDH1* mutation, luminal genetic profile, including frequent *PIK3CA* mutations	*CDH1* mutation, luminal genetic profile, including frequent *PIK3CA* mutations; plus additional alterations (*ERBB2, ERBB3, TP53, CCND1*)	*CDH1* mutation, luminal genetic profile, including frequent *PIK3CA* mutations; plus additional alterations (*ERBB2, ERBB3, CCND1*)
Adjacent invasive carcinoma	Low incidence (IDC or ILC)	High incidence (majority ILC)	High incidence (majority ILC)

Table 14.5 Long-term follow-up studies of patients with ALH

ALH studies	Data source	Time period of patient enrollment	Follow-up (years)	Total Pts	Developed IBC/DCIS	% ILC	Ipsilateral	Contralateral	RR
Page et al. [13]	Nashville breast studies	1950–1985	17	252[a]	50[b]	18%	68%	24%	4.2
									3.1
Page et al. [112]									–
McLaren et al. [125]									
Degnim et al. [122]	Mayo benign breast disease cohort	1967–2001	12.1	327	75[c]	17%	65%	32%	3.67
Hartmann et al. [110]									–
Marshall et al. [111]	Nurses' health Study[d]	1976–1996, 1989–1995[e]	9.1	–	–	–	61%	–	5.3[f]
Collins et al. [108]									5.49[f]

Pts patients, *IBC* invasive breast carcinoma, *DCIS* ductal carcinoma in situ, *ILC* invasive lobular carcinoma, *RR* relative risk
Total pts. only include patients with follow-up; %ILC = ILC/total cases of invasive carcinoma
[a] Includes 15 patients with concomitant atypical ductal hyperplasia
[b] Includes only IBC
[c] Includes IBC and DCIS
[d] 36 cases, 42 controls
[e] Nurses' Health Study I from 1976 to 1996 and Nurses' Health Study II from 1989 to 1995
[f] Odds ratio

Table 14.6 Long-term follow-up studies of LN

LCIS/LIN/LN studies	Type of LN	Source	Enrollment period	Follow-up in years	Total patients	Developed CA	% ILC	Ipsilateral	Contralateral	RR
Haagensen et al. [3]	LN	CPMC	1930–1972	14	210	36[a]	66%[b]	19[c]	19[c]	7.2
Rosen et al. [9]	LCIS	MSKCC	1940–1950	24	84	32[a]	42%[b]	18[c]	18[c]	9
Page et al. [114]	LCIS	Nashville breast studies	1950–1968	19	39	9[d]	70%	5	3	9
Bodian et al. [116]	LN	CPMC	1930–1982	18	236	62[e]	34%[b]	48%[f]	39%[f]	5.4
Fisher et al. [115]	LIN	NSABP	1985–1990	12	180	36[a]	82%[b]	26[c]	14[c]	–
Chuba et al. [120]	LCIS	SEER	1973–1988	–	4853	350[d]	23%	–	–	–
Li et al. [126]	LCIS	SEER	1988–2001	–	4490	282[d]	49%	7.3/1000[g]	5.2/1000[g]	–

LCIS lobular carcinoma in situ, *LIN* lobular intraepithelial neoplasia, *LN* lobular neoplasia, *CA* carcinoma, *IBC* invasive breast carcinoma, *DCIS* ductal carcinoma in in situ, *LCIS* lobular carcinoma in situ, *ILC* invasive lobular carcinoma, *CPMC* Columbia Presbyterian Medical Center, *MSKCC* Memorial Sloan Kettering Cancer Center, *NSABP* National Surgical Adjuvant Breast and Bowel Project, *SEER* Surveillance, Epidemiology, and End Results Program, and RR relative risk

Total patients only include patients with follow-up; %ILC = ILC/total cases of invasive carcinoma

[a] Includes IBC, DCIS, and LCIS

[b] Haagensen et al. (19 ILC ["small-cell carcinoma"] of 29 IBC); Rosen et al. (13 ILC of 31 IBC); Bodian et al. (45 carcinomas classified on their review, 35 were IBC with 12 ILC and 10 DCIS); Fisher et al. (19 total IBC but only 17 had histology reviewed with 14 ILC confirmed)

[c] Some patients developed more than one carcinoma

[d] Includes only IBC

[e] Includes IBC and DCIS

[f] Study only provided percentage of cases

[g] Person-years

For patients with ALH and LCIS, the relative risk for subsequent development of breast cancer is often cited to be 4–5× and 8–10× the risk in the general population, respectively [3, 7, 9, 13, 108–116]. The absolute risk of breast cancer associated with ALH is estimated to be about 1% per year and fairly constant over time, with a cumulative incidence of 30% at 25 years [117]. The absolute risk for classic LCIS is in the range of 1–2% per year, with a cumulative long-term rate of >20% at 20 years and a lifetime risk of 30–40% [36, 115, 118, 119]. The risk is bilateral, albeit with an ipsilateral predominance. The invasive carcinoma can be either lobular or ductal, but with an overrepresentation of ILC [120, 121].

Follow-up studies have also identified clinical and histologic features that could modify the relative risk. Younger patient age at diagnosis, lesser degree of age-related lobular involution, a positive family history, multiple foci of LN, and focal E-cadherin staining have been found to further increase the risk of breast cancer, whereas chemoprevention has proven to lower the risk [32, 36, 109, 111, 117, 122, 123]. A gene expression profiling study identified genes that may play a role in LCIS progression [124], but whether this signature will be of clinical value in predicting the risk of subsequent invasion remains to be determined.

LN as a Non-obligate Precursor of Invasive Breast Carcinoma

A role for classic LCIS as a precursor to ILC was initially suggested by histopathological observations: neoplastic cells in LCIS and ILC are cytologically similar; LCIS and ILC are seen synchronously, and LCIS is essentially always present in cases with microinvasive ILC [3–5, 127, 128]. The invasive carcinomas that develop after a diagnosis of LN are enriched for lobular type with an ipsilateral predominance [121, 125]. Patients with classic LN appear to have a propensity to develop invasive carcinomas with a good prognosis. Haagensen et al. observed that almost all of the carcinomas that developed were favorable types [3]. Similarly, 42% of invasive carcinomas that developed in the Nashville Breast Studies were special type, including ILC, tubulolobular carcinomas, and tubular carcinomas [125]. The well-documented association of LN with tubular carcinomas and columnar cell change/flat epithelial atypia has been referred to as "Rosen's triad" (Fig. 14.45) and is reflective of the shared clonality between these lesions, considered a part of the low-grade breast neoplasia pathway that also includes ILC and intraepithelial ductal neoplasia [129–132]. Together, observational studies suggest that classic LCIS can behave as both a risk factor and a non-obligate precursor for the development of invasive carcinoma.

Clinical observational studies also support a more immediate precursor role for pleomorphic and florid LCIS subtypes compared to classic LCIS. In contrast to classic LCIS, most (59–87%) pleomorphic LCIS and florid LCIS are associated with invasive carcinoma either on core needle biopsy or on subsequent excision, and the majority (84–100%) of these are ILC [33, 34, 86–88]. Brautthauer and Tavassoli

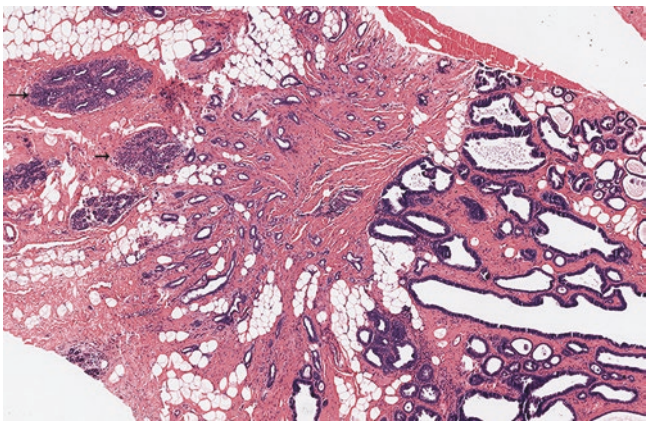

Fig. 14.45 Triad of lobular neoplasia (left, arrows), columnar cell lesion (flat epithelial atypia, right), and tubular carcinoma (center)

found that 23% of LIN3 lesions (some of which would meet the current criteria of florid or pleomorphic LCIS) versus 14% of LIN1 (equivalent to ALH) and 18% of LIN2 (equivalent to classic LCIS) lesions were associated with synchronous invasive carcinoma, suggestive of more aggressive behavior of LIN3. In this study, ILC comprised 86% of invasive carcinomas associated with LIN3, compared to 11% with LIN1 and 47% with LIN2 [133]. Shamir et al. observed that pleomorphic LCIS and florid LCIS were unifocal and co-localized with associated invasive lobular carcinoma in 20 of 20 spatially mapped cases, compared to synchronous classic LCIS in these specimens, which was more frequently multifocal with a wider distribution [34]. In this study, of invasive carcinomas associated with pleomorphic LCIS and florid LCIS, all grade 1 invasive carcinomas were associated with florid LCIS and all grade 3 carcinomas were associated with pleomorphic LCIS [34]. Pleomorphic LCIS is also typically associated with pleomorphic ILC, which usually has a more aggressive biomarker profile (ER negative, HER2 positive, or triple negative) and other clinicopathologic features (higher stage, higher grade, lymphovascular invasion) that contribute to less favorable outcomes [34, 134, 135] (see also Chap. 15).

Genetic studies more directly support a precursor role for classic LCIS, pleomorphic LCIS, and florid LCIS (see section "Pathogenesis" for additional discussion). Initial studies showed loss of heterozygosity and chromosomal copy gains and losses in ALH, which were also shared by associated LCIS and ILC in these cases [14–16]. Others have found that classic LCIS and synchronous ILC share identical mutations and CNA, reflective of a common clonality and indicating that classic LCIS is already a fairly advanced lesion capable of progressing to invasive carcinoma [74, 99, 100, 136–138]. Pleomorphic LCIS and florid LCIS (with or without synchronous ILC) share identical mutations and CNA with synchronous classic LCIS, but harbor additional genetic aberrations (especially *ERBB2* mutations/amplifications, *ERBB3* mutations, and *TP53* mutations) that are not usually observed in classic LCIS. The genetic profile of pleomorphic LCIS is largely shared with synchronous ILC, with some ILC accumulating additional pathogenic mutations [74]. Data regarding the genetic relationship of florid LCIS with classic LCIS and ILC are more limited, but also indicate a shared clonality between these lesions [74]. These findings indicate that pleomorphic LCIS and florid LCIS are clonally related to classic LCIS but are genetically more advanced, and at least pleomorphic LCIS is likely to be a direct precursor to ILC [73, 74, 139].

Management of ALH and Classic LCIS

Clinical management for LN differs significantly depending on the subtype of LCIS and whether the lesion is found on core biopsy or surgical excision.

The management of ALH and classic LCIS identified on core biopsy has been controversial, largely due to a wide range of reported upgrade rates to invasive carcinoma and DCIS on surgical excision (ranging from 0 to 60%). The retrospective nature of most studies introduces inherent selection bias, as some cases undergo observation and others excision. Other limitations in some of the studies include lack of radiologic-pathologic correlation, inclusion of cases with other risk lesions (atypical ductal hyperplasia) in the biopsy, variable definition of what constitutes an upgrade on excision, and lack of pathology review. The upgrade rates are generally higher when radiological-pathological correlation is not addressed or when classic LN represents the radiological target, and the rates are even higher in cases biopsied for mass lesions and in imaging-discordant cases. Most recent studies report much lower excisional upgrade rates of incidental classic LN (ALH alone, classic LCIS alone, or ALH plus classic LCIS) when concordant imaging-histologic correlation to a different target lesion was documented (Table 14.7). Among these, three prospective studies and one from an institution where classic LN cases were routinely excised (thereby avoiding potential bias in excising those lesions that are more likely to be upgraded) reveal very low upgrade rates in the range of 1–3.5% [48, 140–142]. A recent systematic review and meta-analysis of literature regarding imaging-concordant classic LN diagnosed on core biopsy found that the pooled risks for upgrade to any malignancy (invasive carcinoma and DCIS) were 3.1% for all classic LN, 2.5% for ALH, and 5.8% for classic LCIS, while the risks for upgrade to invasive carcinoma were 1.3% for all LN, 0.4% for ALH, and 3.5% for LCIS [143]. Although the overall upgrade rates are low, the data additionally support differentiating ALH from classic LCIS in pathology reports.

When ALH and classic LCIS are diagnosed on core biopsy, careful radiologic-pathologic correlation is required. According to the current National Comprehensive Cancer

Table 14.7 Select studies of upgrade rate for ALH/classic LCIS diagnosed on core biopsy with radiologic-pathologic correlation

Studies[a]	Year	# with excision[a]	# (%) with upgrade
ALH			
Subhawong et al. [151]	2010	56	0 (0)
Zhao et al. [152]	2012	163	5 (3%)
Shah-khan et al. [54]	2012	81	1 (1%)
Genco et al. [146]	2020	172	3 (2%)
Total		472	9 (2%)
Classic LCIS			
Subhawong et al. [151]	2010	12	4 (33%)
Zhao et al. [152]	2012	74	6 (8%)
Shah-khan et al. [54]	2012	20	1 (5%)
D'Alfonso et al. [53]	2013	53[b]	4 (7.5%)[c]
Genco et al. [146]	2020	115	8 (7%)
Pride et al. [148]	2021	81	11 (14%)[c]
Total		355	34 (10%)
ALH/classic LCIS			
Karabakhtsian et al. [57]	2007	77	8 (10%)
Hwang et al. [153]	2008	71[b]	1 (1%)
Nagi et al. [154]	2008	45	2 (4%)
Purdie et al. [155]	2010	45	8 (18%)
Rendi et al. [142][e]	2012	67	2 (3%)
Niell et al. [156]	2012	60	5 (8)
Atkins et al. [157]	2013	38	0 (0%)
Murray et al. [140][d]	2013	72	2 (3%)
Chaudhary et al. [158]	2013	87	3 (3%)
Nakhlis et al. [141][d]	2016	75	1 (1%)
Susnik et al. [48][d]	2016	228	8 (3.5%)
Schmidt et al. [150]	2018	107	5 (5%)
Total		972	45 (5%)

All studies are retrospective except where noted otherwise. All upgrades are DCIS and invasive carcinoma except where noted otherwise

[a] Includes only studies of classic lobular neoplasia with radiologic-pathologic correlation and pathology review. Number in total cases excluded those with discordant radiological-pathological findings

[b] Excluded cases of LCIS variants on core biopsy

[c] One upgrade was to pleomorphic LCIS as the most significant lesion

[d] Prospective study

[e] Retrospective study; however, all lobular neoplasia was excised at this institution

Network (NCCN) Guidelines and the American Society of Breast Surgeons (ASBS) Consensus Guidelines, if multidisciplinary review concludes that ALH or classic LCIS in an adequately sampled core biopsy is incidental with concordant imaging findings and that there are no other high-risk lesions which themselves would indicate excision (such as atypical ductal hyperplasia), routine excision is not required. These patients can be followed with clinical-radiological surveillance and counseled regarding risk reduction with chemoprevention. When ALH or classic LCIS diagnosed on core biopsy is discordant with the imaging findings, surgical excision is prudent [144, 145].

Several clinical-pathologic features of ALH and classic LCIS have been suggested as risk factors that might be associated with an increased upgrade rate on excision. These include a personal history of prior or concurrent breast cancer, extensive (>4 foci) LN on core biopsy, larger lesion size on imaging, imaging for high-risk indications (in contrast to routine mammographic screening), and detection by MRI-guided core biopsy [142, 146–148]. However, more studies are needed to determine whether any of these features could be of value in routine clinical management (i.e., recommending excision over surveillance).

Short-term follow-up studies of patients with classic LN on core biopsy who did not undergo excision have been reported. Shah-Khan et al. found that 4 of 65 patients developed ipsilateral cancer (mean 53 months) [54]. Two developed ILC and two DCIS, 7–78 months after biopsy. Only the case that developed cancer 7 months after core biopsy was in the same quadrant as the initial biopsy site, whereas the others were found in other quadrants. Four patients from the entire study group of 156 patients (those who did and did not undergo excision) developed contralateral invasive carcinoma, all IDC, 7–36 months after core biopsy. None of the 30 women who underwent chemoprevention developed subsequent invasive carcinoma or DCIS during the study period. Middleton et al. reported on 104 patients who did not undergo immediate surgical excision (median 3.4 years) [149]. Five patients developed DCIS or invasive carcinoma, all ipsilateral: two were diagnosed with DCIS and ILC at the initial core biopsy site at 66 months and 38 months, respectively, and three developed IDC or DCIS elsewhere in the breast at 17, 24, and 60 months. Schmidt et al. found that 2 of 54 (4%) patients developed invasive carcinoma during follow-up (mean 55 months). One was diagnosed with ILC at the initial core biopsy site 3 years later, and the other developed invasive carcinoma at a different location in the ipsilateral breast. Fourteen patients received antihormonal medication during the follow-up period. Neither of the two patients who subsequently developed carcinoma during observation were on endocrine therapy [150].

The clinical management of classic LCIS diagnosed in excision specimens is more straightforward with general consensus. There is no indication that excision of classic LCIS to negative margins is useful, and it is therefore not necessary to assess or report the margin status for classic LCIS, including classic LCIS found in association with florid LCIS, pleomorphic LCIS, and/or ILC.

Management of Pleomorphic LCIS and Florid LCIS

Pleomorphic LCIS and florid LCIS are rare and underrecognized lesions, and long-term follow-up studies are lacking. In addition, the diagnostic criteria and terminologies used to classify these lesions have been inconsistent in the literature. For these reasons, there are no clear guidelines for the appropriate clinical management of these LCIS subtypes, in particular with regard to optimal surgical treatment and adjuvant therapy.

Studies on the upgrade rates at excision for LCIS lesions that were variably termed pleomorphic LCIS, florid LCIS, non-classic LCIS, or variant LCIS have been retrospective and included relatively small numbers of patients. Nonetheless, these studies consistently report a high upgrade risk, ranging from 18 to 100% and averaging almost 40% across the pooled data (Table 14.8). Consistent with the elevated upgrade rate, more aggressive biomarker profile, and advanced genetic profile, the most recent WHO Classification of Tumours editorial board recommends surgical excision for pleomorphic LCIS and florid LCIS diagnosed on core biopsy [2].

The optimal treatment for patients with excised pleomorphic and florid LCIS is more problematic, including the need to achieve negative margins and the role of adjuvant radiation therapy [10, 159]. Overall, there are few studies, all retrospective in nature, with few adverse events, which limits the conclusions that can be drawn. Consistent with this, a survey of breast surgeons found no consensus for the management of surgical margins in cases of pleomorphic LCIS. Approximately one-quarter of respondents reported routine re-excision when pleomorphic LCIS is found at the surgical margin, whereas another quarter reported sometimes re-excising, and the remaining one-half reported never re-excising [159]. By pooling available series addressing post-lumpectomy recurrence rates for pure "non-classic" LCIS by final margin status, Hoffman et al. found that only 3/85 (3.5%) patients with negative margins developed recurrence, compared to 5/19 (26.3%) with <1 mm margin and 8/22 (36.4%) with a positive margin [47]. However, multi-institutional, prospective data will be required to more definitively assess the association between recurrence risk and margin status.

There is also lack of consensus agreement for adjuvant therapy after excision for pleomorphic LCIS and florid LCIS, with some patients receiving hormonal therapy alone, adjuvant radiation alone, both, or neither. Based on a lack of sufficient data, it is impossible to draw conclusions regarding the benefit of adjuvant radiation therapy for these LCIS subtypes [10]. The available data are also insufficient to demonstrate statistically significant benefit of hormonal therapy. However, based on chemoprevention trials for ALH and classic LCIS and the knowledge that almost all florid LCIS and most (>70%) pleomorphic LCIS are ER positive [24, 34, 37, 47, 73], and that the majority of florid LCIS and pleomorphic LCIS are associated with hormone receptor-positive classic LCIS [24, 34, 37], it seems prudent to consider that patients with pleomorphic and florid LCIS could benefit from hormonal therapy.

Studies addressing the local recurrence risk or development of invasive carcinoma after excision of pleomorphic LCIS are also limited in number and retrospective in nature, which precludes drawing definitive conclusions [41, 43–45, 60, 160]. Based on a pooled analysis of published series, Singh et al. reported that all recurrences following excision of pleomorphic or florid LCIS were ipsilateral and most were lobular phenotype, a pattern that is in contrast to classic LCIS [60].

Given the paucity of outcome data to provide guidance on the need for excision to clear margins and/or potential benefit of adjuvant radiation therapy for pleomorphic LCIS and florid LCIS, a pragmatic approach is to individualize the management of these patients based on multidisciplinary evaluation and overall risk assessment [10]. It is recommended that pathologists assess and report margin status for pleomorphic LCIS and florid LCIS in order to help inform management decisions [2].

Table 14.8 Upgrade rate at excision for LCIS subtypes diagnosed on core needle biopsy

Studies	Year	LCIS subtype	# with excisions	# (%) with upgrade
Georgian-Smith and Lawton [50]	2001	P-LCIS	5	2 (40%)
Lavoue et al. [161]	2007	P-LCIS	10	3 (33%)
Chivukula et al. [61]	2008	P-LCIS	12	3 (25%)
Hwang et al. [153]	2008	V-LCIS	6	3 (50%)
		P-LCIS	7	3 (43%)
Carder et al. 2010 [162]	2010	P-LCIS	8	2 (25%)
Sullivan et al. [46]	2010	V-LCIS	11	4 (36%)
		P-LCIS	17	3 (18%)
Niell et al. [156]	2012	P-LCIS	4	4 (100%)
Meroni et al. [163]	2014	P-LCIS	12	6 (50%)
Flanagan et al. [43]	2015	P-LCIS	21	11 (52%)
Susnik et al. [48]	2016	V-LCIS	15	4 (27%)
Guo et al. [38]	2018	P-LCIS	23	14 (60%)
Savage et al. [164]	2018	P-LCIS	15	4 (27%)
Massanat et al. [88]	2018	P-LCIS	22	8 (36.3%)
Shamir et al. [34]	2019	P-LCIS, F-LCIS	14	5 (36%)
Foschini et al. [87]	2019	P-LCIS, F-LCIS	70	31 (44%)
Nakhlis et al. [165]	2019	V-LCIS	76	27 (36%)
Singh et al. [60]	2020	P-LCIS, F-LCIS	24	6 (25%)
Total			372	143 (38%)

Adapted from Schnitt et al. [10]
P-LCIS pleomorphic lobular carcinoma in situ, *F-LCIS* florid lobular carcinoma in situ, *V-LCIS* variant lobular carcinoma in situ (including either a combination of pleomorphic and florid LCIS or cases in which the variants were not clearly defined according to current criteria)

References

1. Chen YYDT, King TA, Palacios J, Reis-Filho JS, Shin SJ, Simpson PT. Atypical lobular hyperplasia. In: WHO classification of Tumours editorial board, editors. WHO classification of breast Tumours. 5th ed. Lyon: International Agency for Research on Cancer (IARC); 2019. p. 68–70.

2. Chen YYDT, King TA, Palacios J, Shin SJ, Simpson PT. Lobular carcinoma in situ. In: WHO classification of Tumours editorial board, editors. WHO classification of breast Tumours. 5th ed. Lyon: International Agency for Research on Cancer (IARC); 2019. p. 71–4.
3. Haagensen CD, Lane N, Lattes R, Bodian C. Lobular neoplasia (so-called lobular carcinoma in situ) of the breast. Cancer. 1978;42(2):737–69.
4. Hajdu SI, Tang P. Lobular carcinoma in situ. Ann Clin Lab Sci. 2009;39(4):413–5.
5. Ewing J. Neoplastic diseases, a text-book on tumors. Philadelphia, PA: W.B. Saunders Company; 1919.
6. Foote FW, Stewart FW. Lobular carcinoma in situ: a rare form of mammary cancer. Am J Pathol. 1941;17(4):491–63.
7. Andersen JA. Lobular carcinoma in situ of the breast. An approach to rational treatment. Cancer. 1977;39(6):2597–602.
8. Wheeler JE, Enterline HT, Roseman JM, Tomasulo JP, McIlvaine CH, Fitts WT Jr, et al. Lobular carcinoma in situ of the breast. Long-term follow-up. Cancer. 1974;34(3):554–63.
9. Rosen PP, Kosloff C, Lieberman PH, Adair F, Braun DW Jr. Lobular carcinoma in situ of the breast. Detailed analysis of 99 patients with average follow-up of 24 years. Am J Surg Pathol. 1978;2(3):225–51.
10. Schnitt SJ, Brogi E, Chen YY, King TA, Lakhani SR. American registry of pathology expert opinions: the spectrum of lobular carcinoma in situ: diagnostic features and clinical implications. Ann Diagn Pathol. 2020;45:151481.
11. Wellings SR, Jensen HM. On the origin and progression of ductal carcinoma in the human breast. J Natl Cancer Inst. 1973;50(5):1111–8.
12. Foote FW, Stewart FW. Comparative studies of cancerous versus noncancerous breasts. Ann Surg. 1945;121(1):6–53.
13. Page DL, Dupont WD, Rogers LW, Rados MS. Atypical hyperplastic lesions of the female breast. A long-term follow-up study. Cancer. 1985;55(11):2698–708.
14. Lu YJ, Osin P, Lakhani SR, Di Palma S, Gusterson BA, Shipley JM. Comparative genomic hybridization analysis of lobular carcinoma in situ and atypical lobular hyperplasia and potential roles for gains and losses of genetic material in breast neoplasia. Cancer Res. 1998;58(20):4721–7.
15. Mastracci TL, Shadeo A, Colby SM, Tuck AB, O'Malley FP, Bull SB, et al. Genomic alterations in lobular neoplasia: a microarray comparative genomic hybridization signature for early neoplastic proliferation in the breast. Genes Chromosomes Cancer. 2006;45(11):1007–17.
16. Nayar R, Zhuang Z, Merino MJ, Silverberg SG. Loss of heterozygosity on chromosome 11q13 in lobular lesions of the breast using tissue microdissection and polymerase chain reaction. Hum Pathol. 1997;28(3):277–82.
17. Fitzgibbons PL. Atypical lobular hyperplasia of the breast: a study of pathologists' responses in the College of American Pathologists Performance Improvement Program in surgical pathology. Arch Pathol Lab Med. 2000;124(3):463–4.
18. O'Malley FP, Pinder SE, Mulligan AM. Breast pathology. Philadelphia, PA: Saunders; 2011.
19. Ellis IO. Pathology reporting of breast disease: a joint document incorporating the third edition of the NHS breast screening Programme's guidelines for pathology reporting in breast cancer screening and the second edition of the Royal College of pathologists' minimum dataset for breast cancer histopathology. Sheffield/London: NHS Cancer Screening Programmes, The Royal College of Pathologists; 2005.
20. Tavassoli F. Pathology of the breast. Norwalk, CT: Appleton & Lange; 1992.
21. Tavassoli FA, Eusebi V. Tumors of the mammary gland. Washington, DC: American Registry of Pathology, Armed Forces Institute of Pathology; 2009.
22. Frost AR, Tsangaris TN, Silverberg SG. Pleomorphic lobular carcinoma in situ. Pathol Case Rev. 1996;1:27–31.
23. Rosen PP. Rosen's breast pathology. 2nd ed. Philadelphia, PA: Lippincott Williams & Wilkins; 2001.
24. Shin SJ, Lal A, De Vries S, Suzuki J, Roy R, Hwang ES, et al. Florid lobular carcinoma in situ: molecular profiling and comparison to classic lobular carcinoma in situ and pleomorphic lobular carcinoma in situ. Hum Pathol. 2013;44(10):1998–2009.
25. Jacobs TW, Pliss N, Kouria G, Schnitt SJ. Carcinomas in situ of the breast with indeterminate features: role of E-cadherin staining in categorization. Am J Surg Pathol. 2001;25(2):229–36.
26. Maluf HM, Swanson PE, Koerner FC. Solid low-grade in situ carcinoma of the breast: role of associated lesions and E-cadherin in differential diagnosis. Am J Surg Pathol. 2001;25(2): 237–44.
27. Rosen PP. Coexistent lobular carcinoma in situ and intraductal carcinoma in a single lobular-duct unit. Am J Surg Pathol. 1980;4(3):241–6.
28. Koerner F, Maluf H. Uncommon morphologic patterns of lobular neoplasia. Ann Diagn Pathol. 1999;3(4):249–59.
29. Beute BJ, Kalisher L, Hutter RV. Lobular carcinoma in situ of the breast: clinical, pathologic, and mammographic features. AJR Am J Roentgenol. 1991;157(2):257–65.
30. Lambird PA, Shelley WM. The spatial distribution of lobular in situ mammary carcinoma. Implications for size and site of breast biopsy. JAMA. 1969;210(4):689–93.
31. Rosen PP, Senie R, Schottenfeld D, Ashikari R. Noninvasive breast carcinoma: frequency of unsuspected invasion and implications for treatment. Ann Surg. 1979;189(3):377–82.
32. Schnitt SJ, Morrow M. Lobular carcinoma in situ: current concepts and controversies. Semin Diagn Pathol. 1999;16(3): 209–23.
33. Bagaria SP, Shamonki J, Kinnaird M, Ray PS, Giuliano AE. The florid subtype of lobular carcinoma in situ: marker or precursor for invasive lobular carcinoma? Ann Surg Oncol. 2011;18(7):1845–51.
34. Shamir ER, Chen YY, Chu T, Pekmezci M, Rabban JT, Krings G. Pleomorphic and florid lobular carcinoma in situ variants of the breast: a clinicopathologic study of 85 cases with and without invasive carcinoma from a single academic center. Am J Surg Pathol. 2019;43(3):399–408.
35. Frykberg ER. Lobular carcinoma in situ of the breast. Breast J. 1999;5(5):296–303.
36. King TA, Pilewskie M, Muhsen S, Patil S, Mautner SK, Park A, et al. Lobular carcinoma in situ: a 29-year longitudinal experience evaluating clinicopathologic features and breast cancer risk. J Clin Oncol. 2015;33(33):3945–52.
37. Chen YY, Hwang ES, Roy R, DeVries S, Anderson J, Wa C, et al. Genetic and phenotypic characteristics of pleomorphic lobular carcinoma in situ of the breast. Am J Surg Pathol. 2009;33(11):1683–94.
38. Guo T, Wang Y, Shapiro N, Fineberg S. Pleomorphic lobular carcinoma in situ diagnosed by breast core biopsy: clinicopathologic features and correlation with subsequent excision. Clin Breast Cancer. 2018;18(4):e449–e54.
39. Eheman CR, Shaw KM, Ryerson AB, Miller JW, Ajani UA, White MC. The changing incidence of in situ and invasive ductal and lobular breast carcinomas: United States, 1999-2004. Cancer Epidemiol Biomark Prev. 2009;18(6):1763–9.
40. Li CI, Anderson BO, Daling JR, Moe RE. Changing incidence of lobular carcinoma in situ of the breast. Breast Cancer Res Treat. 2002;75(3):259–68.

41. De Brot M, Koslow Mautner S, Muhsen S, Andrade VP, Mamtani A, Murray M, et al. Pleomorphic lobular carcinoma in situ of the breast: a single institution experience with clinical follow-up and centralized pathology review. Breast Cancer Res Treat. 2017;165(2):411–20.
42. Fasola CE, Chen JJ, Jensen KC, Allison KH, Horst KC. Characteristics and clinical outcomes of pleomorphic lobular carcinoma in situ of the breast. Breast J. 2018;24(1):66–9.
43. Flanagan MR, Rendi MH, Calhoun KE, Anderson BO, Javid SH. Pleomorphic lobular carcinoma in situ: radiologic-pathologic features and clinical management. Ann Surg Oncol. 2015;22(13):4263–9.
44. Khoury T, Karabakhtsian RG, Mattson D, Yan L, Syriac S, Habib F, et al. Pleomorphic lobular carcinoma in situ of the breast: clinicopathological review of 47 cases. Histopathology. 2014;64(7):981–93.
45. Sneige N, Wang J, Baker BA, Krishnamurthy S, Middleton LP. Clinical, histopathologic, and biologic features of pleomorphic lobular (ductal-lobular) carcinoma in situ of the breast: a report of 24 cases. Mod Pathol. 2002;15(10):1044–50.
46. Sullivan ME, Khan SA, Sullu Y, Schiller C, Susnik B. Lobular carcinoma in situ variants in breast cores: potential for misdiagnosis, upgrade rates at surgical excision, and practical implications. Arch Pathol Lab Med. 2010;134(7):1024–8.
47. Hoffman DI, Zhang PJ, Tchou J. Breast-conserving surgery for pure non-classic lobular carcinoma in situ: a single institution's experience. Surg Oncol. 2019;28:190–4.
48. Susnik B, Day D, Abeln E, Bowman T, Krueger J, Swenson KK, et al. Surgical outcomes of lobular neoplasia diagnosed in core biopsy: prospective study of 316 cases. Clin Breast Cancer. 2016;16(6):507–13.
49. Hutter RV, Snyder RE, Lucas JC, Foote FW Jr, Farrow JH. Clinical and pathologic correlation with mammographic findings in lobular carcinoma in situ. Cancer. 1969;23(4):826–39.
50. Georgian-Smith D, Lawton TJ. Calcifications of lobular carcinoma in situ of the breast: radiologic-pathologic correlation. AJR Am J Roentgenol. 2001;176(5):1255–9.
51. Maxwell AJ, Clements K, Dodwell DJ, Evans AJ, Francis A, Hussain M, et al. The radiological features, diagnosis and management of screen-detected lobular neoplasia of the breast: findings from the Sloane project. Breast. 2016;27:109–15.
52. Scoggins M, Krishnamurthy S, Santiago L, Yang W. Lobular carcinoma in situ of the breast: clinical, radiological, and pathological correlation. Acad Radiol. 2013;20(4):463–70.
53. D'Alfonso TM, Wang K, Chiu YL, Shin SJ. Pathologic upgrade rates on subsequent excision when lobular carcinoma in situ is the primary diagnosis in the needle core biopsy with special attention to the radiographic target. Arch Pathol Lab Med. 2013;137(7):927–35.
54. Shah-Khan MG, Geiger XJ, Reynolds C, Jakub JW, Deperi ER, Glazebrook KN. Long-term follow-up of lobular neoplasia (atypical lobular hyperplasia/lobular carcinoma in situ) diagnosed on core needle biopsy. Ann Surg Oncol. 2012;19(10):3131–8.
55. Crisi GM, Mandavilli S, Cronin E, Ricci A Jr. Invasive mammary carcinoma after immediate and short-term follow-up for lobular neoplasia on core biopsy. Am J Surg Pathol. 2003;27(3):325–33.
56. Esserman LE, Lamea L, Tanev S, Poppiti R. Should the extent of lobular neoplasia on core biopsy influence the decision for excision? Breast J. 2007;13(1):55–61.
57. Karabakhtsian RG, Johnson R, Sumkin J, Dabbs DJ. The clinical significance of lobular neoplasia on breast core biopsy. Am J Surg Pathol. 2007;31(5):717–23.
58. Van Goethem M, Schelfout K, Kersschot E, Colpaert C, Verslegers I, Biltjes I, et al. Enhancing area surrounding breast carcinoma on MR mammography: comparison with pathological examination. Eur Radiol. 2004;14(8):1363–70.
59. Sapino A, Frigerio A, Peterse JL, Arisio R, Coluccia C, Bussolati G. Mammographically detected in situ lobular carcinomas of the breast. Virchows Arch. 2000;436(5):421–30.
60. Singh K, Sung CJ, Quddus MR. Descriptive study comparing outcomes of classic and nonclassic lobular carcinoma in situ (florid and pleomorphic) initially diagnosed on core needle biopsy. Breast J. 2020;26(12):2350–6.
61. Chivukula M, Haynik DM, Brufsky A, Carter G, Dabbs DJ. Pleomorphic lobular carcinoma in situ (PLCIS) on breast core needle biopsies: clinical significance and immunoprofile. Am J Surg Pathol. 2008;32(11):1721–6.
62. Page DL, Dupont WD, Rogers LW. Ductal involvement by cells of atypical lobular hyperplasia in the breast: a long-term follow-up study of cancer risk. Hum Pathol. 1988;19(2):201–7.
63. Simpson PT, Gale T, Fulford LG, Reis-Filho JS, Lakhani SR. The diagnosis and management of pre-invasive breast disease: pathology of atypical lobular hyperplasia and lobular carcinoma in situ. Breast Cancer Res. 2003;5(5):258–62.
64. Simpson J, Page D. Lobular neoplasia. In: Elston CW, Ellis IO, editors. The breast. Systematic pathology. 13. 3rd ed. London: Churchill Livingstone; 1998.
65. Blanco LZ, Thurow TA, Mahajan A, Susnik B, Helenowski I, Chmiel JS, et al. Multinucleation is an objective feature useful in the diagnosis of pleomorphic lobular carcinoma in situ. Am J Clin Pathol. 2015;144(5):722–6.
66. Alvarado-Cabrero I, Picon Coronel G, Valencia Cedillo R, Canedo N, Tavassoli FA. Florid lobular intraepithelial neoplasia with signet ring cells, central necrosis and calcifications: a clinicopathological and immunohistochemical analysis of ten cases associated with invasive lobular carcinoma. Arch Med Res. 2010;41(6):436–41.
67. Wen HY, Brogi E. Lobular carcinoma in situ. Surg Pathol Clin. 2018;11(1):123–45.
68. Albonico G, Querzoli P, Ferretti S, Rinaldi R, Nenci I. Biological profile of in situ breast cancer investigated by immunohistochemical technique. Cancer Detect Prev. 1998;22(4):313–8.
69. Bur ME, Zimarowski MJ, Schnitt SJ, Baker S, Lew R. Estrogen receptor immunohistochemistry in carcinoma in situ of the breast. Cancer. 1992;69(5):1174–81.
70. Pallis L, Wilking N, Cedermark B, Rutqvist LE, Skoog L. Receptors for estrogen and progesterone in breast carcinoma in situ. Anticancer Res. 1992;12(6B):2113–5.
71. Ramachandra S, Machin L, Ashley S, Monaghan P, Gusterson BA. Immunohistochemical distribution of c-erbB-2 in in situ breast carcinoma: a detailed morphological analysis. J Pathol. 1990;161(1):7–14.
72. Rudas M, Neumayer R, Gnant MF, Mittelbock M, Jakesz R, Reiner A. p53 protein expression, cell proliferation and steroid hormone receptors in ductal and lobular in situ carcinomas of the breast. Eur J Cancer. 1997;33(1):39–44.
73. Harrison BT, Nakhlis F, Dillon DA, Soong TR, Garcia EP, Schnitt SJ, et al. Genomic profiling of pleomorphic and florid lobular carcinoma in situ reveals highly recurrent ERBB2 and ERRB3 alterations. Mod Pathol. 2020;33(7):1287–97.
74. Shamir ER, Chen YY, Krings G. Genetic analysis of pleomorphic and florid lobular carcinoma in situ variants: frequent ERBB2/ERBB3 alterations and clonal relationship to classic lobular carcinoma in situ and invasive lobular carcinoma. Mod Pathol. 2020;33(6):1078–91.
75. Zhong E, Solomon JP, Cheng E, Baum J, Song W, Hoda SA. Apocrine variant of pleomorphic lobular carcinoma in situ: further clinical, histopathologic, immunohistochemical, and molecular characterization of an emerging entity. Am J Surg Pathol. 2020;44(8):1092–103.
76. Canas-Marques R, Schnitt SJ. E-cadherin immunohistochemistry in breast pathology: uses and pitfalls. Histopathology. 2016;68(1):57–69.

77. Dabbs DJ, Schnitt SJ, Geyer FC, Weigelt B, Baehner FL, Decker T, et al. Lobular neoplasia of the breast revisited with emphasis on the role of E-cadherin immunohistochemistry. Am J Surg Pathol. 2013;37(7):e1–11.
78. Da Silva L, Parry S, Reid L, Keith P, Waddell N, Kossai M, et al. Aberrant expression of E-cadherin in lobular carcinomas of the breast. Am J Surg Pathol. 2008;32(5):773–83.
79. Rakha EA, Patel A, Powe DG, Benhasouna A, Green AR, Lambros MB, et al. Clinical and biological significance of E-cadherin protein expression in invasive lobular carcinoma of the breast. Am J Surg Pathol. 2010;34(10):1472–9.
80. Choi YJ, Pinto MM, Hao L, Riba AK. Interobserver variability and aberrant E-cadherin immunostaining of lobular neoplasia and infiltrating lobular carcinoma. Mod Pathol. 2008;21(10):1224–37.
81. Wells JM, Pipa J, Shin SJ. Lobular neoplasia of the breast revisited with emphasis on the role of E-cadherin immunohistochemistry. Am J Surg Pathol. 2014;38(3):434–5.
82. Sarrio D, Perez-Mies B, Hardisson D, Moreno-Bueno G, Suarez A, Cano A, et al. Cytoplasmic localization of p120ctn and E-cadherin loss characterize lobular breast carcinoma from preinvasive to metastatic lesions. Oncogene. 2004;23(19):3272–83.
83. Shibata T, Kokubu A, Sekine S, Kanai Y, Hirohashi S. Cytoplasmic p120ctn regulates the invasive phenotypes of E-cadherin-deficient breast cancer. Am J Pathol. 2004;164(6):2269–78.
84. Vina M, Wells CA. Clear cell metaplasia of the breast: a lesion showing eccrine differentiation. Histopathology. 1989;15(1):85–92.
85. Page DL, Rogers LW. Combined histologic and cytologic criteria for the diagnosis of mammary atypical ductal hyperplasia. Hum Pathol. 1992;23(10):1095–7.
86. Fadare O, Dadmanesh F, Alvarado-Cabrero I, Snyder R, Stephen Mitchell J, Tot T, et al. Lobular intraepithelial neoplasia [lobular carcinoma in situ] with comedo-type necrosis: a clinicopathologic study of 18 cases. Am J Surg Pathol. 2006;30(11):1445–53.
87. Foschini MP, Miglio R, Fiore R, Baldovini C, Castellano I, Callagy G, et al. Pre-operative management of pleomorphic and florid lobular carcinoma in situ of the breast: report of a large multi-institutional series and review of the literature. Eur J Surg Oncol. 2019;45(12):2279–86.
88. Masannat YA, Husain E, Roylance R, Heys SD, Carder PJ, Ali H, et al. Pleomorphic LCIS what do we know? A UK multicenter audit of pleomorphic lobular carcinoma in situ. Breast. 2018;38:120–4.
89. Derksen PW, Braumuller TM, van der Burg E, Hornsveld M, Mesman E, Wesseling J, et al. Mammary-specific inactivation of E-cadherin and p53 impairs functional gland development and leads to pleomorphic invasive lobular carcinoma in mice. Dis Model Mech. 2011;4(3):347–58.
90. Derksen PW, Liu X, Saridin F, van der Gulden H, Zevenhoven J, Evers B, et al. Somatic inactivation of E-cadherin and p53 in mice leads to metastatic lobular mammary carcinoma through induction of anoikis resistance and angiogenesis. Cancer Cell. 2006;10(5):437–49.
91. McCart Reed AE, Kutasovic JR, Lakhani SR, Simpson PT. Invasive lobular carcinoma of the breast: morphology, biomarkers and 'omics. Breast Cancer Res. 2015;17:12.
92. Rosa-Rosa JM, Caniego-Casas T, Leskela S, Cristobal E, Gonzalez-Martinez S, Moreno-Moreno E, et al. High frequency of ERBB2 activating mutations in invasive lobular breast carcinoma with pleomorphic features. Cancers (Basel). 2019;11(1):74.
93. Ciriello G, Gatza ML, Beck AH, Wilkerson MD, Rhie SK, Pastore A, et al. Comprehensive molecular portraits of invasive lobular breast cancer. Cell. 2015;163(2):506–19.
94. Sarrio D, Moreno-Bueno G, Hardisson D, Sanchez-Estevez C, Guo M, Herman JG, et al. Epigenetic and genetic alterations of APC and CDH1 genes in lobular breast cancer: relationships with abnormal E-cadherin and catenin expression and microsatellite instability. Int J Cancer. 2003;106(2):208–15.
95. Corso G, Figueiredo J, La Vecchia C, Veronesi P, Pravettoni G, Macis D, et al. Hereditary lobular breast cancer with an emphasis on E-cadherin genetic defect. J Med Genet. 2018;55(7):431–41.
96. Corso G, Intra M, Trentin C, Veronesi P, Galimberti V. CDH1 germline mutations and hereditary lobular breast cancer. Familial Cancer. 2016;15(2):215–9.
97. Boldt V, Stacher E, Halbwedl I, Popper H, Hultschig C, Moinfar F, et al. Positioning of necrotic lobular intraepithelial neoplasias (LIN, grade 3) within the sequence of breast carcinoma progression. Genes Chromosomes Cancer. 2010;49(5):463–70.
98. Etzell JE, Devries S, Chew K, Florendo C, Molinaro A, Ljung BM, et al. Loss of chromosome 16q in lobular carcinoma in situ. Hum Pathol. 2001;32(3):292–6.
99. Lee JY, Schizas M, Geyer FC, Selenica P, Piscuoglio S, Sakr RA, et al. Lobular carcinomas in situ display intralesion genetic heterogeneity and clonal evolution in the progression to invasive lobular carcinoma. Clin Cancer Res. 2019;25(2):674–86.
100. Sakr RA, Schizas M, Carniello JV, Ng CK, Piscuoglio S, Giri D, et al. Targeted capture massively parallel sequencing analysis of LCIS and invasive lobular cancer: repertoire of somatic genetic alterations and clonal relationships. Mol Oncol. 2016;10(2):360–70.
101. Shah V, Nowinski S, Levi D, Shinomiya I, Kebaier Ep Chaabouni N, Gillett C, et al. PIK3CA mutations are common in lobular carcinoma in situ, but are not a biomarker of progression. Breast Cancer Res. 2017;19(1):7.
102. Desmedt C, Zoppoli G, Gundem G, Pruneri G, Larsimont D, Fornili M, et al. Genomic characterization of primary invasive lobular breast cancer. J Clin Oncol. 2016;34(16):1872–81.
103. Bose R, Kavuri SM, Searleman AC, Shen W, Shen D, Koboldt DC, et al. Activating HER2 mutations in HER2 gene amplification negative breast cancer. Cancer Discov. 2013;3(2):224–37.
104. Deniziaut G, Tille JC, Bidard FC, Vacher S, Schnitzler A, Chemlali W, et al. ERBB2 mutations associated with solid variant of high-grade invasive lobular breast carcinomas. Oncotarget. 2016;7(45):73337–46.
105. McCart Reed AE, Lal S, Kutasovic JR, Wockner L, Robertson A, de Luca XM, et al. LobSig is a multigene predictor of outcome in invasive lobular carcinoma. NPJ Breast Cancer. 2019;5:18.
106. Ping Z, Siegal GP, Harada S, Eltoum IE, Youssef M, Shen T, et al. ERBB2 mutation is associated with a worse prognosis in patients with CDH1 altered invasive lobular cancer of the breast. Oncotarget. 2016;7(49):80655–63.
107. Ross JS, Wang K, Sheehan CE, Boguniewicz AB, Otto G, Downing SR, et al. Relapsed classic E-cadherin (CDH1)-mutated invasive lobular breast cancer shows a high frequency of HER2 (ERBB2) gene mutations. Clin Cancer Res. 2013;19(10):2668–76.
108. Collins LC, Baer HJ, Tamimi RM, Connolly JL, Colditz GA, Schnitt SJ. Magnitude and laterality of breast cancer risk according to histologic type of atypical hyperplasia: results from the nurses' health study. Cancer. 2007;109(2):180–7.
109. Coopey SB, Mazzola E, Buckley JM, Sharko J, Belli AK, Kim EM, et al. The role of chemoprevention in modifying the risk of breast cancer in women with atypical breast lesions. Breast Cancer Res Treat. 2012;136(3):627–33.
110. Hartmann LC, Radisky DC, Frost MH, Santen RJ, Vierkant RA, Benetti LL, et al. Understanding the premalignant potential of atypical hyperplasia through its natural history: a longitudinal cohort study. Cancer Prev Res (Phila). 2014;7(2):211–7.
111. Marshall LM, Hunter DJ, Connolly JL, Schnitt SJ, Byrne C, London SJ, et al. Risk of breast cancer associated with atypical hyperplasia of lobular and ductal types. Cancer Epidemiol Biomark Prev. 1997;6(5):297–301.

112. Page DL, Schuyler PA, Dupont WD, Jensen RA, Plummer WD Jr, Simpson JF. Atypical lobular hyperplasia as a unilateral predictor of breast cancer risk: a retrospective cohort study. Lancet. 2003;361(9352):125–9.
113. Worsham MJ, Abrams J, Raju U, Kapke A, Lu M, Cheng J, et al. Breast cancer incidence in a cohort of women with benign breast disease from a multiethnic, primary health care population. Breast J. 2007;13(2):115–21.
114. Page DL, Kidd TE Jr, Dupont WD, Simpson JF, Rogers LW. Lobular neoplasia of the breast: higher risk for subsequent invasive cancer predicted by more extensive disease. Hum Pathol. 1991;22(12):1232–9.
115. Fisher ER, Land SR, Fisher B, Mamounas E, Gilarski L, Wolmark N. Pathologic findings from the National Surgical Adjuvant Breast and bowel project: twelve-year observations concerning lobular carcinoma in situ. Cancer. 2004;100(2):238–44.
116. Bodian CA, Perzin KH, Lattes R. Lobular neoplasia. Long term risk of breast cancer and relation to other factors. Cancer. 1996;78(5):1024–34.
117. Hartmann LC, Degnim AC, Santen RJ, Dupont WD, Ghosh K. Atypical hyperplasia of the breast—risk assessment and management options. N Engl J Med. 2015;372(1):78–89.
118. Fisher ER, Costantino J, Fisher B, Palekar AS, Paik SM, Suarez CM, et al. Pathologic findings from the National Surgical Adjuvant Breast Project (NSABP) protocol B-17. Five-year observations concerning lobular carcinoma in situ. Cancer. 1996;78(7):1403–16.
119. To T, Wall C, Baines CJ, Miller AB. Is carcinoma in situ a precursor lesion of invasive breast cancer? Int J Cancer. 2014;135(7):1646–52.
120. Chuba PJ, Hamre MR, Yap J, Severson RK, Lucas D, Shamsa F, et al. Bilateral risk for subsequent breast cancer after lobular carcinoma-in-situ: analysis of surveillance, epidemiology, and end results data. J Clin Oncol. 2005;23(24):5534–41.
121. Ansquer Y, Delaney S, Santulli P, Salomon L, Carbonne B, Salmon R. Risk of invasive breast cancer after lobular intraepithelial neoplasia: review of the literature. Eur J Surg Oncol. 2010;36(7):604–9.
122. Degnim AC, Visscher DW, Berman HK, Frost MH, Sellers TA, Vierkant RA, et al. Stratification of breast cancer risk in women with atypia: a Mayo cohort study. J Clin Oncol. 2007;25(19):2671–7.
123. Fisher B, Costantino JP, Wickerham DL, Redmond CK, Kavanah M, Cronin WM, et al. Tamoxifen for prevention of breast cancer: report of the National Surgical Adjuvant Breast and bowel project P-1 study. J Natl Cancer Inst. 1998;90(18):1371–88.
124. Andrade VP, Morrogh M, Qin LX, Olvera N, Giri D, Muhsen S, et al. Gene expression profiling of lobular carcinoma in situ reveals candidate precursor genes for invasion. Mol Oncol. 2015;9(4):772–82.
125. McLaren BK, Schuyler PA, Sanders ME, Jensen RA, Simpson JF, Dupont WD, et al. Excellent survival, cancer type, and Nottingham grade after atypical lobular hyperplasia on initial breast biopsy. Cancer. 2006;107(6):1227–33.
126. Li CI, Malone KE, Saltzman BS, Daling JR. Risk of invasive breast carcinoma among women diagnosed with ductal carcinoma in situ and lobular carcinoma in situ, 1988-2001. Cancer. 2006;106(10):2104–12.
127. Nemoto T, Castillo N, Tsukada Y, Koul A, Eckhert KH Jr, Bauer RL. Lobular carcinoma in situ with microinvasion. J Surg Oncol. 1998;67(1):41–6.
128. Ross DS, Hoda SA. Microinvasive (T1mic) lobular carcinoma of the breast: clinicopathologic profile of 16 cases. Am J Surg Pathol. 2011;35(5):750–6.
129. Abdel-Fatah TM, Powe DG, Hodi Z, Lee AH, Reis-Filho JS, Ellis IO. High frequency of coexistence of columnar cell lesions, lobular neoplasia, and low grade ductal carcinoma in situ with invasive tubular carcinoma and invasive lobular carcinoma. Am J Surg Pathol. 2007;31(3):417–26.
130. Abdel-Fatah TM, Powe DG, Hodi Z, Reis-Filho JS, Lee AH, Ellis IO. Morphologic and molecular evolutionary pathways of low nuclear grade invasive breast cancers and their putative precursor lesions: further evidence to support the concept of low nuclear grade breast neoplasia family. Am J Surg Pathol. 2008;32(4):513–23.
131. Rosen PP. Columnar cell hyperplasia is associated with lobular carcinoma in situ and tubular carcinoma. Am J Surg Pathol. 1999;23(12):1561.
132. Sahoo S, Recant WM. Triad of columnar cell alteration, lobular carcinoma in situ, and tubular carcinoma of the breast. Breast J. 2005;11(2):140–2.
133. Bratthauer GL, Tavassoli FA. Lobular intraepithelial neoplasia: previously unexplored aspects assessed in 775 cases and their clinical implications. Virchows Arch. 2002;440(2):134–8.
134. Mukhtar RA, Krings G, Chen YY, Mamounas ME, Fahrner-Scott K, Wong J, et al. Mitotic score and pleomorphic histology in invasive lobular carcinoma of the breast: impact on disease-free survival. Breast Cancer Res Treat. 2020;181(1):23–9.
135. Yang LP, Sun HF, Zhao Y, Chen MT, Zhang N, Jin W. Clinicopathological characteristics and survival outcomes in pleomorphic lobular breast carcinoma of the breast: a SEER population-based study. Cancer Med. 2017;6(12):2867–75.
136. Hwang ES, Nyante SJ, Yi Chen Y, Moore D, DeVries S, Korkola JE, et al. Clonality of lobular carcinoma in situ and synchronous invasive lobular carcinoma. Cancer. 2004;100(12):2562–72.
137. Andrade VP, Ostrovnaya I, Seshan VE, Morrogh M, Giri D, Olvera N, et al. Clonal relatedness between lobular carcinoma in situ and synchronous malignant lesions. Breast Cancer Res. 2012;14(4):R103.
138. Morandi L, Marucci G, Foschini MP, Cattani MG, Pession A, Riva C, et al. Genetic similarities and differences between lobular in situ neoplasia (LN) and invasive lobular carcinoma of the breast. Virchows Arch. 2006;449(1):14–23.
139. Reis-Filho JS, Simpson PT, Jones C, Steele D, Mackay A, Iravani M, et al. Pleomorphic lobular carcinoma of the breast: role of comprehensive molecular pathology in characterization of an entity. J Pathol. 2005;207(1):1–13.
140. Murray MP, Luedtke C, Liberman L, Nehhozina T, Akram M, Brogi E. Classic lobular carcinoma in situ and atypical lobular hyperplasia at percutaneous breast core biopsy: outcomes of prospective excision. Cancer. 2013;119(5):1073–9.
141. Nakhlis F, Gilmore L, Gelman R, Bedrosian I, Ludwig K, Hwang ES, et al. Incidence of adjacent synchronous invasive carcinoma and/or ductal carcinoma in-situ in patients with lobular neoplasia on core biopsy: results from a prospective multi-institutional registry (TBCRC 020). Ann Surg Oncol. 2016;23(3):722–8.
142. Rendi MH, Dintzis SM, Lehman CD, Calhoun KE, Allison KH. Lobular in-situ neoplasia on breast core needle biopsy: imaging indication and pathologic extent can identify which patients require excisional biopsy. Ann Surg Oncol. 2012;19(3):914–21.
143. Shehata MN, Rahbar H, Flanagan MR, Kilgore MR, Lee CI, Ryser MD, et al. Risk for upgrade to malignancy after breast core needle biopsy diagnosis of lobular neoplasia: a systematic review and meta-analysis. J Am Coll Radiol. 2020;17(10):1207–19.
144. American Society of Breast Surgeons. Consensus Guideline on Concordance Assessment of Image-Guided Breast Biopsies and Management of Borderline or High-Risk Lesions. https://www.breastsurgeons.org/resources/statements. Accessed 1 Aug 2021.
145. National Comprehensive Cancer Network Guidelines. Version 1. 2021. Breast Cancer Screening and Diagnosis. https://www.nccn.org. Accessed 1 Aug 2021.
146. Genco IS, Tugertimur B, Chang Q, Cassell L, Hajiyeva S. Outcomes of classic lobular neoplasia diagnosed on breast core

needle biopsy: a retrospective multi-center study. Virchows Arch. 2020;476(2):209–17.
147. Khoury T, Kumar PR, Li Z, Karabakhtsian RG, Sanati S, Chen X, et al. Lobular neoplasia detected in MRI-guided core biopsy carries a high risk for upgrade: a study of 63 cases from four different institutions. Mod Pathol. 2016;29(1):25–33.
148. Pride RM, Jimenez RE, Hoskin TL, Degnim AC, Hieken TJ. Upgrade at excisional biopsy after a core needle biopsy diagnosis of classic lobular carcinoma in situ. Surgery. 2021;169(3):644–8.
149. Middleton LP, Sneige N, Coyne R, Shen Y, Dong W, Dempsey P, et al. Most lobular carcinoma in situ and atypical lobular hyperplasia diagnosed on core needle biopsy can be managed clinically with radiologic follow-up in a multidisciplinary setting. Cancer Med. 2014;3(3):492–9.
150. Schmidt H, Arditi B, Wooster M, Weltz C, Margolies L, Bleiweiss I, et al. Observation versus excision of lobular neoplasia on core needle biopsy of the breast. Breast Cancer Res Treat. 2018;168(3):649–54.
151. Subhawong AP, Subhawong TK, Khouri N, Tsangaris T, Nassar H. Incidental minimal atypical lobular hyperplasia on core needle biopsy: correlation with findings on follow-up excision. Am J Surg Pathol. 2010;34(6):822–8.
152. Zhao C, Desouki MM, Florea A, Mohammed K, Li X, Dabbs D. Pathologic findings of follow-up surgical excision for lobular neoplasia on breast core biopsy performed for calcification. Am J Clin Pathol. 2012;138(1):72–8.
153. Hwang H, Barke LD, Mendelson EB, Susnik B. Atypical lobular hyperplasia and classic lobular carcinoma in situ in core biopsy specimens: routine excision is not necessary. Mod Pathol. 2008;21(10):1208–16.
154. Nagi CS, O'Donnell JE, Tismenetsky M, Bleiweiss IJ, Jaffer SM. Lobular neoplasia on core needle biopsy does not require excision. Cancer. 2008;112(10):2152–8.
155. Purdie CA, McLean D, Stormonth E, Macaskill EJ, McCullough JB, Edwards SL, et al. Management of in situ lobular neoplasia detected on needle core biopsy of breast. J Clin Pathol. 2010;63(11):987–93.
156. Niell B, Specht M, Gerade B, Rafferty E. Is excisional biopsy required after a breast core biopsy yields lobular neoplasia? AJR Am J Roentgenol. 2012;199(4):929–35.
157. Atkins KA, Cohen MA, Nicholson B, Rao S. Atypical lobular hyperplasia and lobular carcinoma in situ at core breast biopsy: use of careful radiologic-pathologic correlation to recommend excision or observation. Radiology. 2013;269(2):340–7.
158. Chaudhary S, Lawrence L, McGinty G, Kostroff K, Bhuiya T. Classic lobular neoplasia on core biopsy: a clinical and radiopathologic correlation study with follow-up excision biopsy. Mod Pathol. 2013;26(6):762–71.
159. Blair SL, Emerson DK, Kulkarni S, Hwang ES, Malcarne V, Ollila DW. Breast surgeon's survey: no consensus for surgical treatment of pleomorphic lobular carcinoma in situ. Breast J. 2013;19(1):116–8.
160. Downs-Kelly E, Bell D, Perkins GH, Sneige N, Middleton LP. Clinical implications of margin involvement by pleomorphic lobular carcinoma in situ. Arch Pathol Lab Med. 2011;135(6):737–43.
161. Lavoue V, Graesslin O, Classe JM, Fondrinier E, Angibeau H, Leveque J. Management of lobular neoplasia diagnosed by core needle biopsy: study of 52 biopsies with follow-up surgical excision. Breast. 2007;16(5):533–9.
162. Carder PJ, Shaaban A, Alizadeh Y, Kumarasuwamy V, Liston JC, Sharma N. Screen-detected pleomorphic lobular carcinoma in situ (PLCIS): risk of concurrent invasive malignancy following a core biopsy diagnosis. Histopathology. 2010;57(3):472–8.
163. Meroni S, Bozzini AC, Pruneri G, Moscovici OC, Maisonneuve P, Menna S, et al. Underestimation rate of lobular intraepithelial neoplasia in vacuum-assisted breast biopsy. Eur Radiol. 2014;24(7):1651–8.
164. Savage JL, Jeffries DO, Noroozian M, Sabel MS, Jorns JM, Helvie MA. Pleomorphic lobular carcinoma in situ: imaging features, upgrade rate, and clinical outcomes. AJR Am J Roentgenol. 2018;211(2):462–7.
165. Nakhlis F, Harrison BT, Giess CS, Lester SC, Hughes KS, Coopey SB, et al. Evaluating the rate of upgrade to invasive breast cancer and/or ductal carcinoma in situ following a core biopsy diagnosis of non-classic lobular carcinoma in situ. Ann Surg Oncol. 2019;26(1):55–61.

Invasive Lobular Carcinoma

15

Eliah R. Shamir, Helena Hwang, and Yunn-Yi Chen

Overview

Invasive lobular carcinoma (ILC) accounts for up to 15% of all invasive breast carcinomas and represents the second most common histological type after invasive ductal carcinoma (IDC) [1–3]. The first description of ILC is attributed to Cornil, who in 1865 noted a diffusely infiltrative tumor of small round cells [4]. Foote and Stewart coined the term lobular carcinoma in the 1940s in their seminal work describing the classical features of these tumors, including the characteristic loss of cellular cohesion and association with lobular carcinoma in situ (LCIS) [5, 6]. This lack of cellular cohesion has since been shown at the molecular level to reflect inactivation of the E-cadherin gene *CDH1*, a defining feature that distinguishes these tumors from IDC. Classic ILC is characterized by small round cells with cytologically bland nuclei infiltrating the stroma in a distinctive single-file pattern. In 1982, Dixon et al. described a pleomorphic variant of ILC that demonstrates the same classic growth pattern but shows high nuclear grade [7]. ILC can also show other architectural patterns such as solid growth, trabecular or alveolar nests, and tubule formation, and rare variants with distinct cytological features have been recognized. The advent of E-cadherin immunostaining has helped to better classify ILC, particularly the pleomorphic type. Classic ILC constitutes the majority of ILC and is typically hormone receptor (HR) positive and HER2 negative, with a low proliferation rate. Pleomorphic ILC, which comprises less than 15% of all ILC, has higher mitotic activity and is more likely to be triple negative or demonstrate HER2 overexpression and gene amplification [8–11]. Recent landmark studies have comprehensively defined the genomic features of ILC and highlighted its distinct biology, including enrichment of *ERBB2* and *ERBB3* alterations particularly in the pleomorphic variant and in metastatic disease [12]. Although ILC is considered to have a similar or more favorable prognosis to IDC early after diagnosis, several studies suggest worse long-term outcomes.

Incidence and Clinical Presentation

Numerous studies have reported that ILC comprises between 5 and 15% of all invasive breast carcinomas. Though many studies in the United States and internationally report a rate of 6.5–8.5% [3, 8, 13–20], those that have included ILC morphologic variants cite higher rates [21, 22]. A higher percentage of ILC is also reported when mixed invasive ductal and lobular carcinomas are included [3].

ILC occurs in slightly older women than invasive breast carcinoma, no special type (IBC-NST), with a median age of 57–65 years [13, 14, 19, 23, 24]. The etiology is likely multifactorial and due to a combination of lifestyle, hormonal/reproductive, and genetic factors. Factors that increase exposure to endogenous estrogens (e.g., early menarche, late menopause, and low parity) or exogenous hormones (e.g., oral contraceptives) increase breast cancer risk [25]. Among genetic risk factors, ILC is underrepresented in patients with germline mutations in *BRCA1* and *TP53.* In contrast, patients with rare germline *E-cadherin* mutations, which are also associated with hereditary diffuse gastric cancer, have a cumulative risk for developing ILC of about 42% by 80 years and present at a younger age (mean 46 years) [26].

ILC is more strongly associated with female hormonal exposure than IBC-NST, resulting in more variation in incidence over the past few decades [25]. From 1987 to 1999, the

E. R. Shamir · Y.-Y. Chen (✉)
Department of Pathology, University of California San Francisco, San Francisco, CA, USA
e-mail: Eliah.Shamir@ucsf.edu; Yunn-yi.chen@ucsf.edu

H. Hwang
Department of Pathology, UT Southwestern Medical Center, Dallas, TX, USA
e-mail: Helena.hwang@utsouthwestern.edu

© The Author(s), under exclusive license to Springer Nature Switzerland AG 2022
S. J. Shin et al. (eds.), *A Comprehensive Guide to Core Needle Biopsies of the Breast*,
https://doi.org/10.1007/978-3-031-05532-4_15

incidence of ILC significantly increased relative to that of IBC-NST [3, 27]. This shift has been attributed to the increased use of hormonal replacement therapy in menopausal women [3, 28, 29] as well as increased alcohol consumption [30]. Improved recognition and classification of ILC may have also played a role [19]. ILC incidence subsequently decreased relative to IBC-NST from 1999 to 2004 [31], which may be due to decreased use of hormonal therapy following publication of the Women's Health Initiative trial results [32] and increasing rates of mammography screening [33, 34].

Incidence varies across racial groups, with ILC comprising a greater percentage of invasive breast carcinomas in Caucasian women compared to African-American women (9.1% versus 5.5%) [13]. This parallels the finding that estrogen receptor (ER)-positive tumors are more common in Caucasian than African-American women [35]. ILC is also less common in Asian-American women, comprising 5.3% of all IBC (SEER data 2007–2011), and East Asian countries have reported rates as low as 2.3% [36, 37].

In addition to patient age, ILC shows several differences from IDC in clinical presentation. Tumors tend to be slightly larger in ILC and are more frequently Nottingham grade 1 and ER positive [14, 16, 17, 19, 38]. Some studies have reported a higher rate of multifocality [39], but other clinicopathologic and radiologic analyses have found no significant differences from IDC [19, 40]. There are also no clear differences in the rate of axillary lymph node metastasis. Some studies report similar rates in ILC and IDC [14, 16, 20, 41], whereas others have variably observed lower [23, 42] or higher [38] rates in ILC. Differences in prognosis are discussed later in the chapter.

As with LCIS, ILC has historically been associated with an increased incidence of contralateral carcinoma; however, there is conflicting data on this issue. Several older studies included LCIS in addition to invasive carcinoma and ductal carcinoma in situ (DCIS) in their bilaterality rates, making it difficult to assess ILC independent of LCIS [43, 44]. Kollias et al. found ILC to be a significant predictor of contralateral breast cancer (invasive breast carcinomas or DCIS) [45], and Arpino et al. found in a large retrospective series that bilaterality was almost twice as common in ILC as in IDC (20.9% versus 11.2%, respectively) [14]. In contrast, other studies found that after excluding LCIS, ILC showed a total incidence of bilateral breast cancer (synchronous or metachronous) of approximately 17%, which was not significantly different from that of IDC [46, 47]. In a large prospective series, Pestalozzi et al. reported similar rates of contralateral breast cancer at 20 years in ILC (8.1%) and IDC (5.7%) [16]. Several other studies have also found no statistically significant difference in bilaterality between ILC and IDC [19, 41, 48, 49].

Gross and Radiologic Features

ILC is less likely than IBC-NST to be clinically, radiographically, and grossly apparent and therefore tends to be larger in size at the time of diagnosis. Classic ILC typically presents as a poorly defined, palpable mass or is subclinical. When ILC does present clinically, the findings can be vague on physical examination, often described as a thickening rather than a discrete mass. Due to ILC's diffuse infiltrative growth pattern, it can be missed on fine needle aspiration and core needle biopsies due to low cellularity and the bland nature of the cells. In contrast, ILC histologic variants such as solid and alveolar patterns are more likely to manifest as a mass lesion.

ILC can be detected through various imaging modalities. Mammography has the lowest sensitivity, ranging from 57% to 89%, with false-negative rates up to 19% [40, 50–53]. ILC is often described as having low opacity on mammogram, similar to normal breast parenchyma [50, 54]. The most common mammographic findings are a spiculated or ill-defined mass, architectural distortion, or asymmetric density [50, 55] (Fig. 15.1). Microcalcifications are uncommon [54–56].

Ultrasound shows better sensitivity (78–98%) than mammography, particularly with high-frequency ultrasound transducers [51, 52, 55–59]. ILC most often presents sonographically as a hypoechoic mass with irregular or indistinct margins with or without posterior acoustic shadowing (Fig. 15.2) [55, 57]. Classic ILC is more likely to be associ-

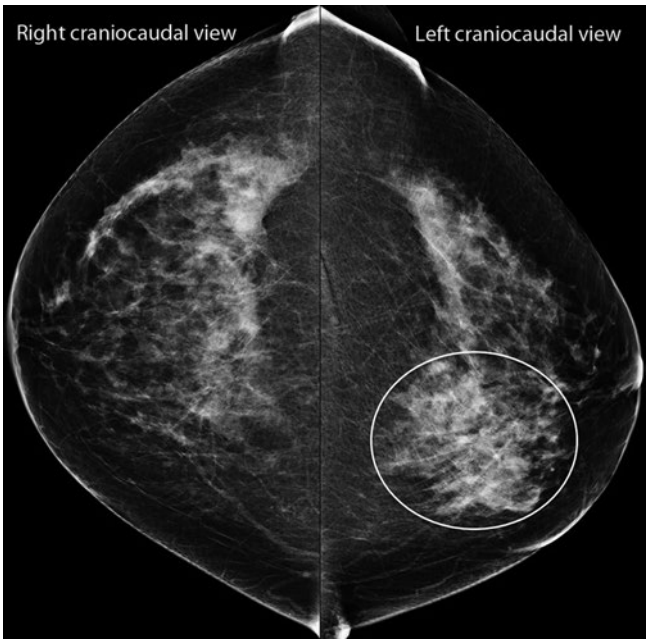

Fig. 15.1 ILC, classic type (mammography). This irregular left-breast mass (circled) showed indistinct margins and associated architectural distortion

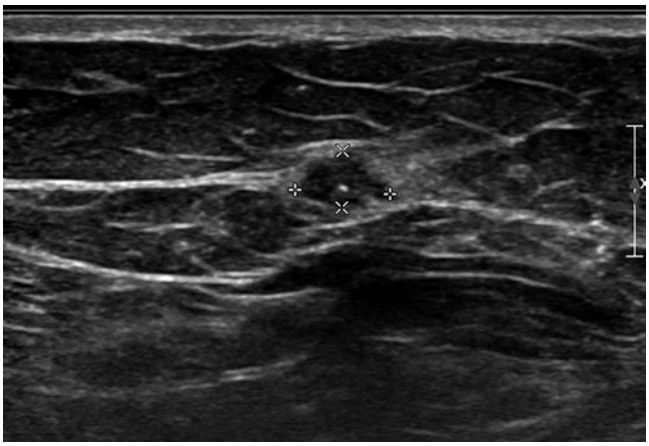

Fig. 15.2 ILC with variant histology (ultrasound). This carcinoma presented as a 10 mm hypoechoic mass with irregular margins

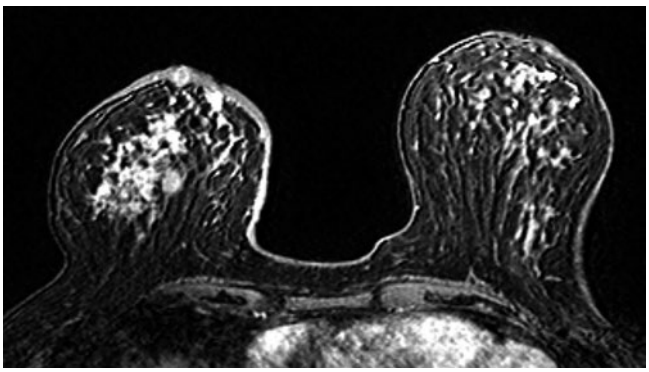

Fig. 15.3 ILC, classic type (MRI). ILC appears as a solitary enhancing mass in the central breast

ated with false-negative findings, whereas solid, alveolar, and signet ring cell growth patterns more often manifest as a lobulated or well-circumscribed mass [57]. Importantly, ultrasound significantly underestimates the size of ILC, more so than with other invasive breast carcinomas [60, 61].

MRI has the highest sensitivity for detecting ILC at 96–100%; however, MRI is not highly specific and can lead to false positives [58, 62]. ILC most often presents as a solitary enhancing mass or multiple small enhancing foci [63, 64] (Fig. 15.3). MRI provides the most accurate assessment of the extent of disease and multifocality, though it can overestimate tumor size [61, 62, 64–67]. MRI has shown a much higher correlation to pathologic size than mammogram or ultrasound [65, 67, 68]. Thus, in the setting of an ILC diagnosis on core needle biopsy, MRI is recommended as an important component of surgical planning [68, 69].

There is scant information on the radiographic manifestations of pleomorphic ILC. A small retrospective study comparing pleomorphic versus classic ILC found no differentiating features based on imaging findings [70]. However, a larger study observed that pleomorphic ILC was more likely to exhibit microcalcifications and skin or trabecular thickening on mammography and to show mixed echogenicity, parenchymal edema, and posterior acoustic enhancement on ultrasound [71]. Nevertheless, sizing of both classic and pleomorphic ILC was significantly underestimated on mammography and ultrasound [71].

The size of ILC is similarly challenging to define macroscopically and is often larger than gross findings. The diffuse growth pattern and lack of significant stromal change or desmoplasia in classic ILC can manifest as an irregular, ill-defined lesion or induration or thickening of the parenchyma that is difficult to discern from adjacent nonneoplastic breast tissue [72]. This issue is highlighted in a study where the gross measurement typically underestimated the microscopic size of ILC [73]. Thorough sampling of contiguous sections can reveal a greater extent of ILC than detected clinically or radiographically, providing a more accurate measurement of tumor size as well as revealing possible additional tumors not detected by imaging. In general, cases of ILC with a predominant alveolar or solid growth pattern are more likely to manifest as a discrete mass and correspondingly show less discrepancy between gross and microscopic size than those growing in a classic, single-file pattern.

Microscopic Features

Classic ILC

The hallmark of classic ILC is dyscohesive small cells that are individually dispersed or arranged in single-file linear cords with little to no stromal desmoplasia [6, 21] (Fig. 15.4a, b). A concentric or targetoid pattern of growth around normal ducts is another common feature (Fig. 15.4c). Peritumoral lymphovascular invasion is only detected in 7.5–13.5% of ILC, significantly less than the frequency seen with IBC-NST [42, 74]. Cytologically, the tumor cells show analogous features to those in atypical lobular hyperplasia or LCIS, which is present in the background breast in 63–99% of cases (Fig. 15.4d) [7, 75–77]. The tumor cells have round to notched ovoid nuclei of low to intermediate grade and a scant rim of cytoplasm. Although there is variation in nuclear size from tumor to tumor, a wide range of nuclear atypia within a tumor is uncommon. Mitotic activity is typically low. Due to its bland cytology, ILC can easily be mistaken for chronic inflammatory cells such as lymphocytes or plasma cells, particularly in a core biopsy or when present as a small focus (Fig. 15.4a).

At least some tumor cells in ILC demonstrate intracytoplasmic lumina, which are best appreciated in well-fixed specimens and can be a useful diagnostic feature (Fig. 15.5). In suboptimal fixed tissue, these lumina may appear as clear

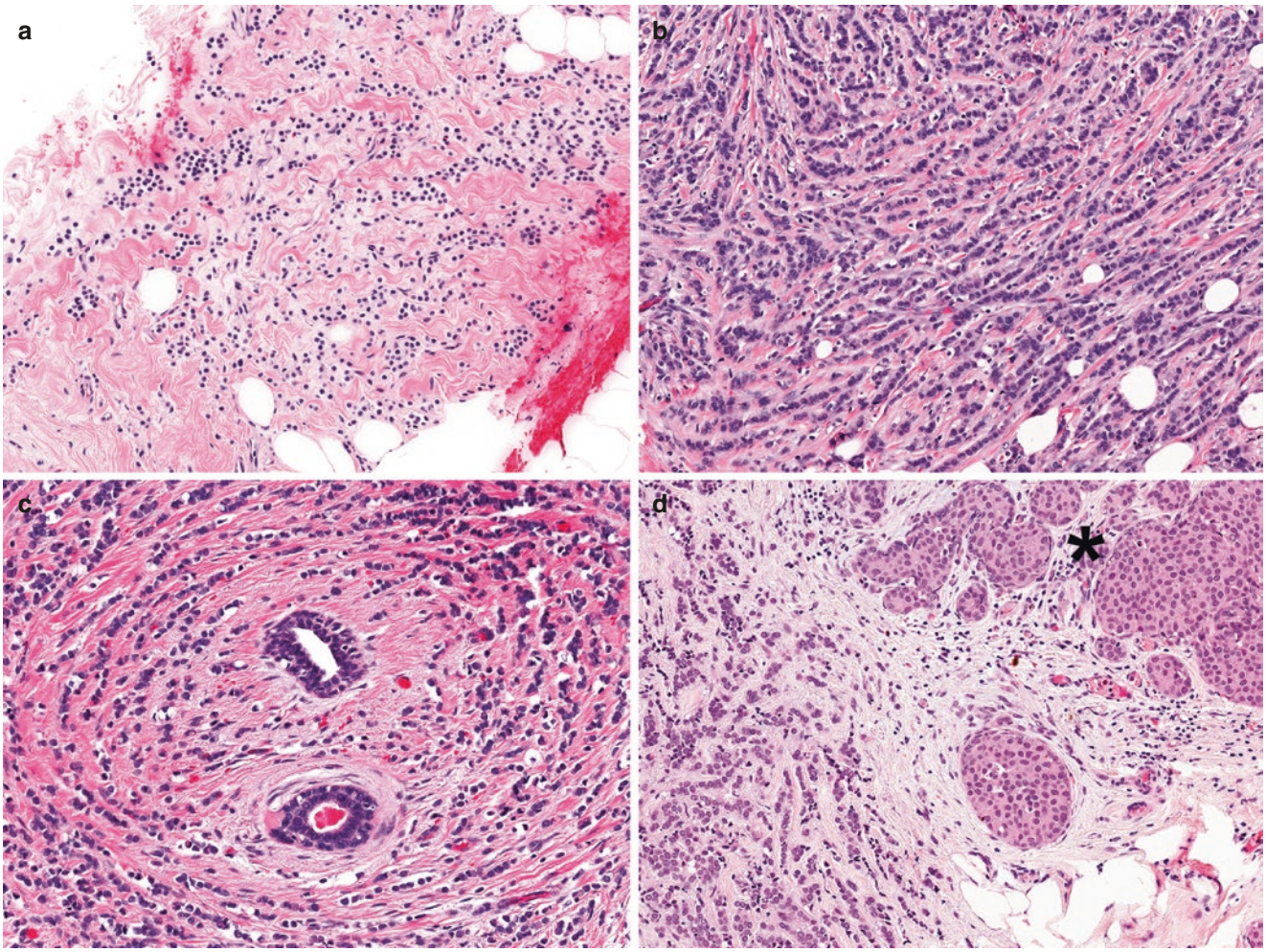

Fig. 15.4 ILC, classic type, architectural features. (**a, b**) Small, dyscohesive tumor cells are individually dispersed (**a**) or arranged in a linear, single-file pattern (**b**) with minimal to no stromal response. (**c**) The tumor cells often form a targetoid growth pattern around normal breast ducts. (**d**) Concurrent classic lobular carcinoma in situ (LCIS) (asterisk) is often present adjacent to ILC or in the background breast

vacuoles (Fig. 15.5a); however, positive immunoreactivity for epithelial membrane antigen (EMA) (Fig. 15.5d) confirms that these represent true lumens [78]. Better fixed specimens may demonstrate lumina containing either central mucoid inclusions (Fig. 15.5b) or eosinophilic globules (Fig. 15.5c). The latter can be quite prominent in some tumors. When large enough, the intracytoplasmic lumina can indent the nucleus and impart a signet ring cell appearance.

Morphologic Variants of ILC

Several morphologic variants of ILC have been described that deviate from classic ILC by either architectural or cytologic features, although there are no clear guidelines or absolute criteria as to their classification. These are currently best included in the diagnosis as special morphologic patterns, variants, or subtypes within the larger histologic type of ILC (e.g., "ILC, alveolar pattern"; "ILC, pleomorphic type").

Pleomorphic ILC (ILC, pleomorphic type) is the most well-recognized and -studied morphologic variant. Pleomorphic ILC typically retains the architectural pattern of classic ILC but is distinguished cytologically by marked nuclear atypia and pleomorphism equivalent to grade 3 (high-grade) nuclei [79] (Fig. 15.6). A subset of pleomorphic ILC shows apocrine features characterized by abundant granular eosinophilic cytoplasm and enlarged round, vesicular nuclei with prominent nucleoli [80] (Fig. 15.7). Mitotic activity is higher than that in classic ILC, and the stroma may show desmoplasia [81]. Associated pleomorphic LCIS is often present as well as classic LCIS, which can provide a clue to the diagnosis [82].

ILC with either classic or pleomorphic cytology can show nonclassical architectural features that still retain the charac-

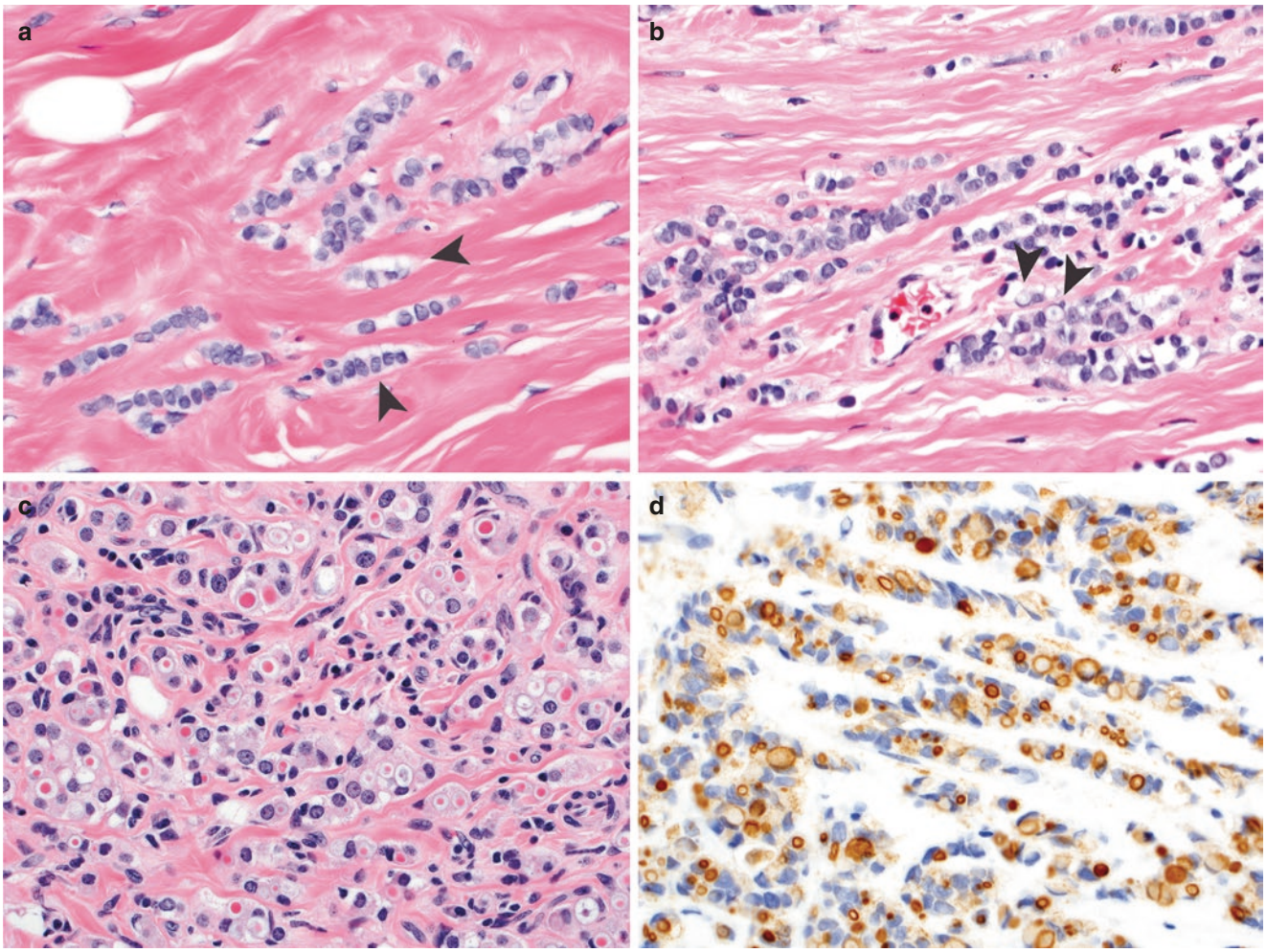

Fig. 15.5 ILC, classic type, cytologic features. (**a**) Tumor cells in ILC demonstrate occasional intracytoplasmic lumina that may appear clear or empty, imparting a bubbly appearance to the cells (arrowheads). (**b**, **c**) Lumina may also contain subtle mucoid material (**b**, arrowheads) or prominent dot-like eosinophilic globules (**c**). (**d**) Immunohistochemistry for epithelial membrane antigen (EMA) highlights intracytoplasmic lumina in ILC

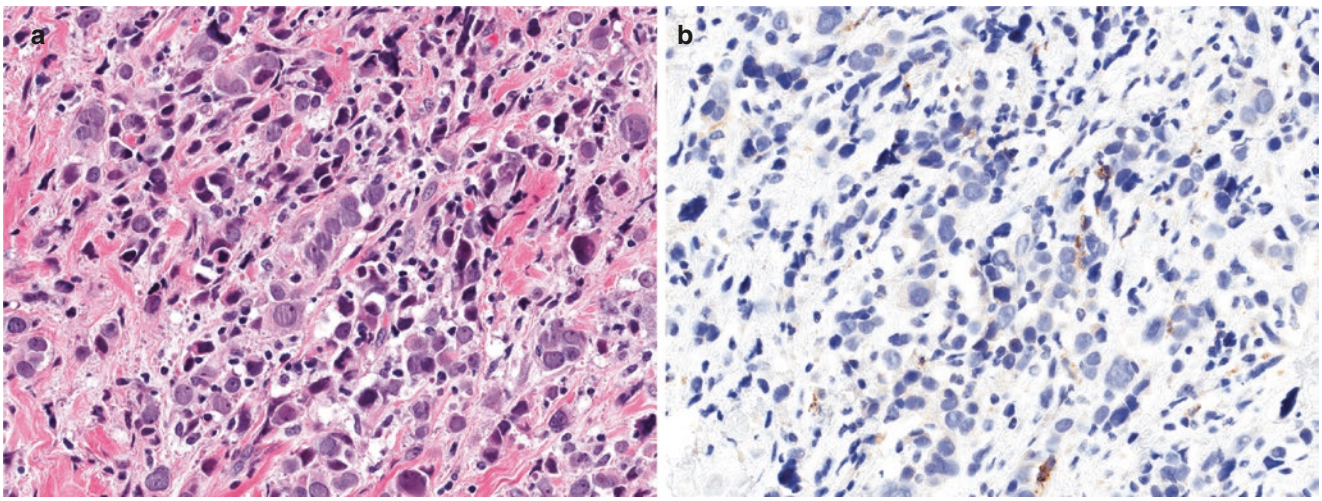

Fig. 15.6 ILC, pleomorphic type. (**a**) The tumor cells have marked nuclear atypia and pleomorphism with focal multinucleation. (**b**) Immunohistochemistry for E-cadherin is negative, supporting lobular differentiation

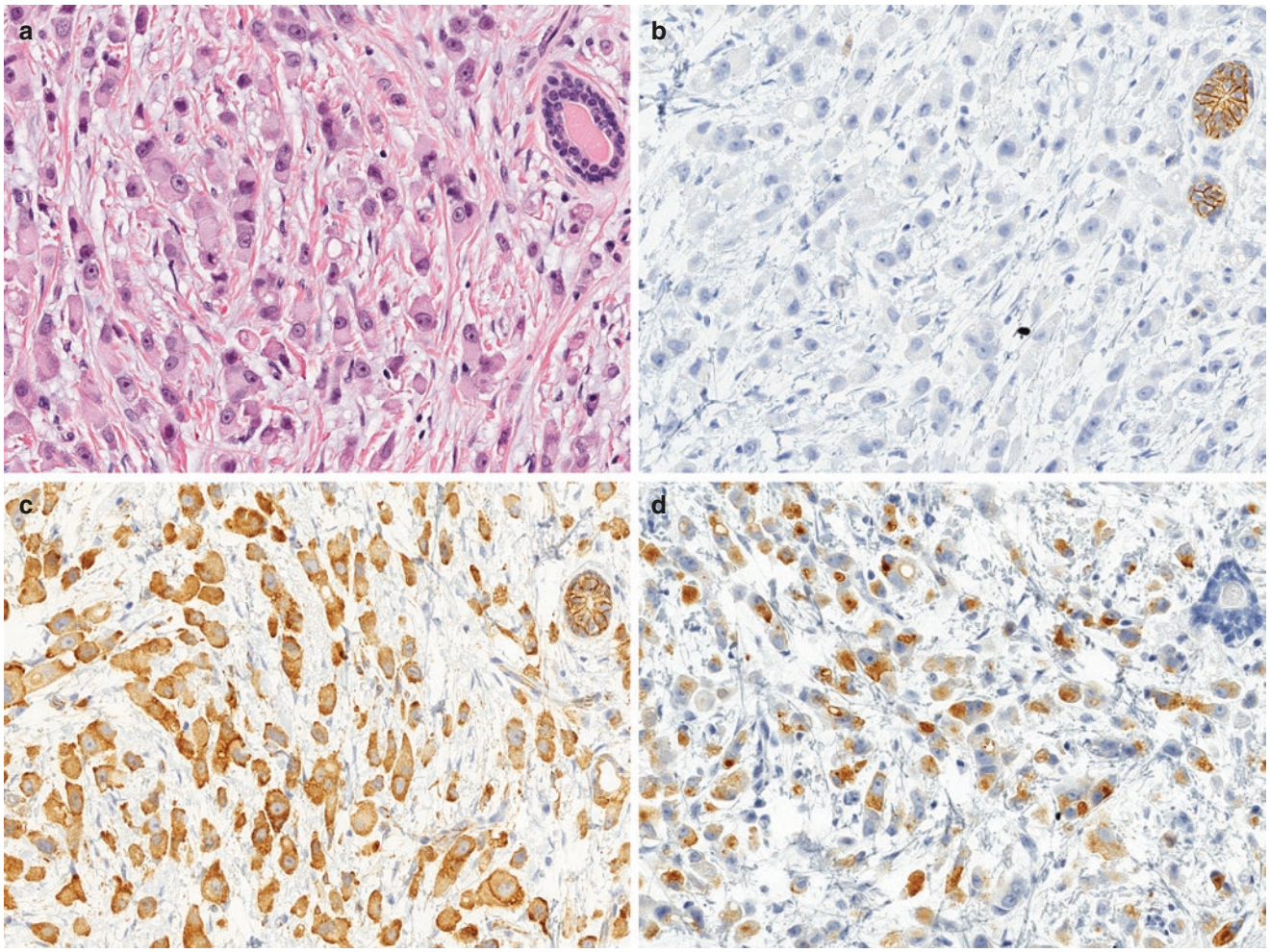

Fig. 15.7 ILC, pleomorphic type with apocrine features. (**a**) The tumor cells show apocrine features characterized by abundant granular eosinophilic cytoplasm and large nuclei with prominent nucleoli. (**b, c**) Immunohistochemistry shows absent membranous staining for E-cadherin in the tumor cells (**b**) and cytoplasmic localization of p120-catenin (**c**). (**d**) GCDFP-15 immunohistochemical staining is often diffusely positive

teristic lack of cell-cell cohesion. The solid pattern is composed of confluent sheets of dyscohesive cells with little to no intervening stroma and higher mitotic activity than classic type (Fig. 15.8) [83]. The alveolar pattern consists of loose globular aggregates of 20 or more cells separated by thin fibrovascular stroma [21] (Fig. 15.9). Finally, the trabecular pattern is characterized by thin-to-broad bands of cells 1–3 layers thick [21] (Fig. 15.10). These trabeculae can be short or long and may form an anastomosing pattern. Unlike other architectural patterns (e.g., alveolar) that still show prominent dyscohesion, trabeculae of ILC show variable loss of cell-cell cohesion and may be indistinguishable from those seen in IDC. These morphologic variants can thus easily be misdiagnosed as IDC, particularly on low-power evaluation, and require careful examination for subtle features of cellular dyscohesion on high power. In such cases, immunostaining for E-cadherin and p120-catenin is helpful to confirm lobular differentiation.

Other variants of ILC variably retain the classic diffuse infiltrative growth pattern but instead show distinct cytologic features. A rare histiocytoid variant consists of cytologically bland cells with low- to intermediate-grade nuclei and abundant foamy, finely vacuolated, amphophilic cytoplasm, resembling histiocytes [84, 85] (Fig. 15.11). Some have considered histiocytoid features to be within the spectrum of apocrine differentiation, and the two variants have often been used interchangeably in the literature. However, we define histiocytoid in keeping with the original description by Hood et al. as having grade 1 or 2 nuclei with uniform chromatin and inconspicuous nucleoli [85]. The cytomorphology can pose diagnostic pitfalls on limited core biopsy material or in recognizing metastases, which have been misinterpreted as

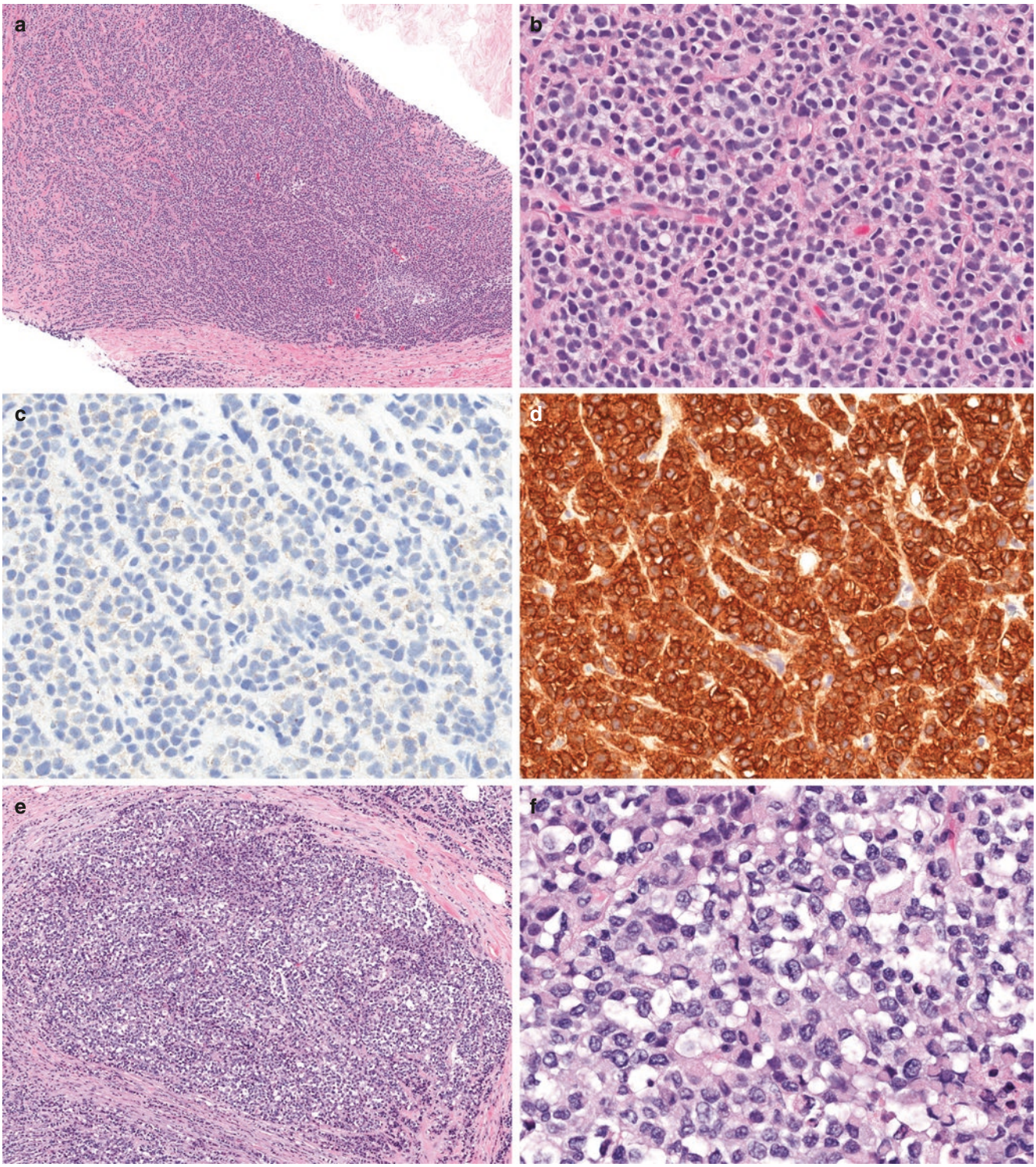

Fig. 15.8 ILC, solid pattern. (**a**) H&E stain of a core biopsy at low power shows an invasive carcinoma with sheetlike growth. (**b**) Higher power demonstrates dyscohesive tumor cells with intermediate-grade nuclei and focal clear intracytoplasmic lumina. (**c, d**) Immunohistochemistry shows lack of E-cadherin expression (**c**) and cytoplasmic p120-catenin (**d**). (**e, f**) A different example of solid-pattern growth in an ILC with pleomorphic nuclei and prominent intracytoplasmic lumina

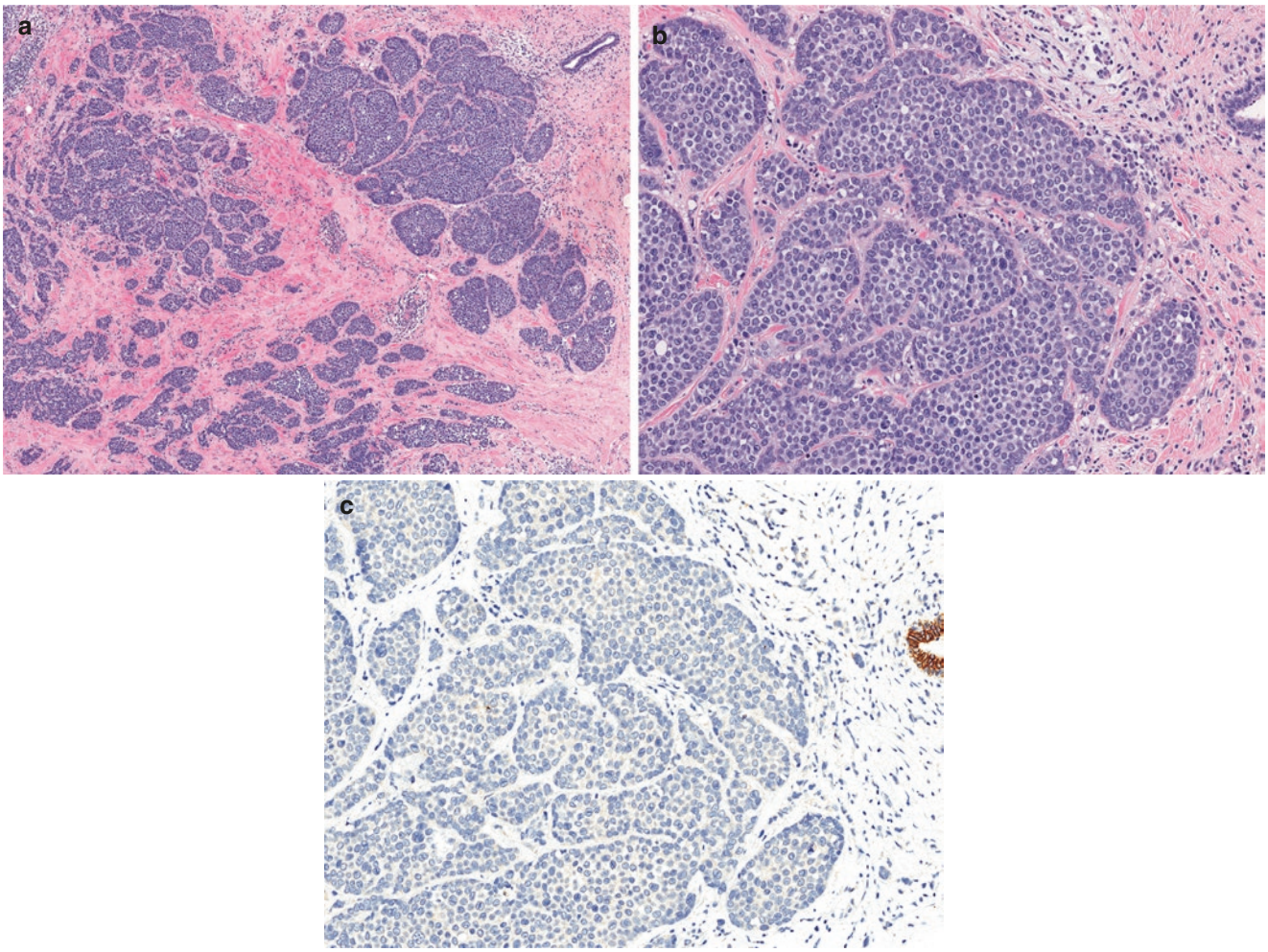

Fig. 15.9 ILC, alveolar pattern. (**a, b**) H&E stain at low and high power demonstrates tumor cells clustered in aggregates of >20 cells. (**c**) An E-cadherin immunostain is negative in tumor cells

benign sinus histiocytes in lymph nodes or xanthomatous lesions in the skin [84]. Tumor cells with more cytologic atypia, intracytoplasmic vacuoles, or more classic ILC morphology accompanied by immunohistochemistry (IHC) can help to confirm the correct diagnosis.

ILC with signet ring cell features describes a vague subtype composed of cells with abundant intracellular mucin pushing the nucleus to one side and an absence of extracellular mucin [86]. The nuclei may be low (Fig. 15.12a) or high grade (Fig. 15.12b). Notably, the quantity of these features is not well defined, and this subtype has not been associated with specific clinical or molecular features. Rather, the importance of recognizing signet ring cell morphology is to rule out metastatic signet ring cell carcinoma from the gastrointestinal (GI) tract, which is exceedingly rare. In addition, signet ring cell morphology is not specific to ILC and can be observed in IDC.

Signet ring cells are also found in a recently recognized rare morphologic variant, ILC with extracellular mucin (ILCEM). ILCEM demonstrates single cells, clusters, or linear arrays of tumor cells floating in pools of extracellular mucin [87–89] (Fig. 15.13). Extracellular mucin can also rarely be seen in nodal and distant metastases [89]. Limited data suggest that ILCEM more frequently displays nonclassical lobular features, including grade 3 nuclei, prominent signet ring cells, and solid-pattern growth [88, 89]. Pseudoglandular or pseudocribriform structures within extracellular mucin can mimic mucinous carcinoma. Importantly, these tumors always harbor a non-mucinous ILC component, which is a clue to the lobular phenotype [89].

Although tubule formation is generally considered to be a sign of a ductal phenotype, scattered abortive to sometimes well-formed tubules can be seen in ILC. The classification of tumors with mixed histology remains challenging as some

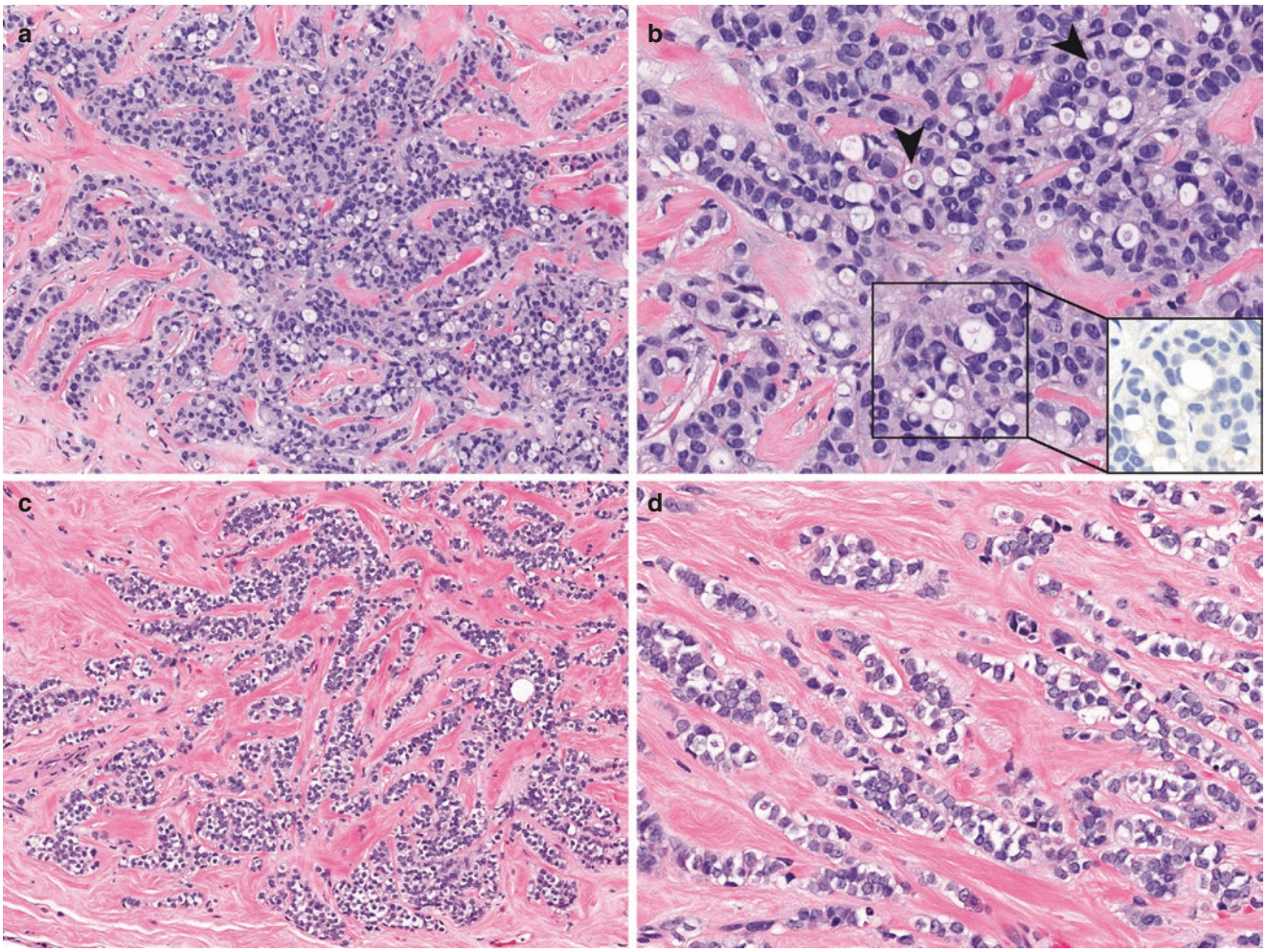

Fig. 15.10 ILC, trabecular pattern. (**a**) H&E stain at low power shows ILC arranged in irregularly anastomosing broad bands or trabeculae. The tumor cells display more cohesion than the single-file cords of classic ILC and may mimic IDC. (**b**) Higher power demonstrates prominent intracytoplasmic lumina with eosinophilic globules (arrowheads). The tumor cells lack E-cadherin expression (inset), confirming lobular differentiation. (**c, d**) A different example of an ILC with trabecular growth at low (**c**) and high (**d**) power. Note that the trabeculae are of different cell widths and variable lengths

retain E-cadherin immunoreactivity (Fig. 15.14) whereas others show complete loss (Fig. 15.15) (Table 15.1). Fisher et al. first described "tubulolobular carcinoma" (TLC) as a variant of ILC that displays an admixture of small, round-to-angulated tubules and single-file linear cords [90]. Others have since regarded TLC as a variant of ductal carcinoma with a lobular growth pattern. Three studies observed that almost all TLC were E-cadherin positive in both the invasive tubular and lobular components [91–93]. In addition, a majority of tumors expressed membranous α-catenin and β-catenin, supporting retention of the adherens junction [92, 93]. An in situ component was present in ~80% of cases and was ductal, lobular, or mixed (separate foci of ductal and lobular) [91, 93]. Interestingly, Christgen et al. recently described a series of E-cadherin-negative tumors with tubules of variable size and shape comprising ~20% of the tumor area (range 5–60%) [94]. These tumors, which they termed "ILC with tubular elements," showed focal E-cadherin to P-cadherin switching within the tubular component [94]. β-catenin was lost in dyscohesive tumor cells but retained in tubular elements, indicating focal rescue of adherens junction formation (Fig. 15.15b) [94]. Taken together, tumors with mixed histomorphology likely represent a heterogenous group that exist within the spectrum of lesions within the low-grade mammary neoplasia pathway [75]. Given the confusing terminology surrounding this topic, we propose using the term "tubulolobular pattern" as a modifier of IDC or ILC to reflect the underlying histologic type of the tumor (Table 15.1). Importantly, clinical management remains similar regardless of E-cadherin expression.

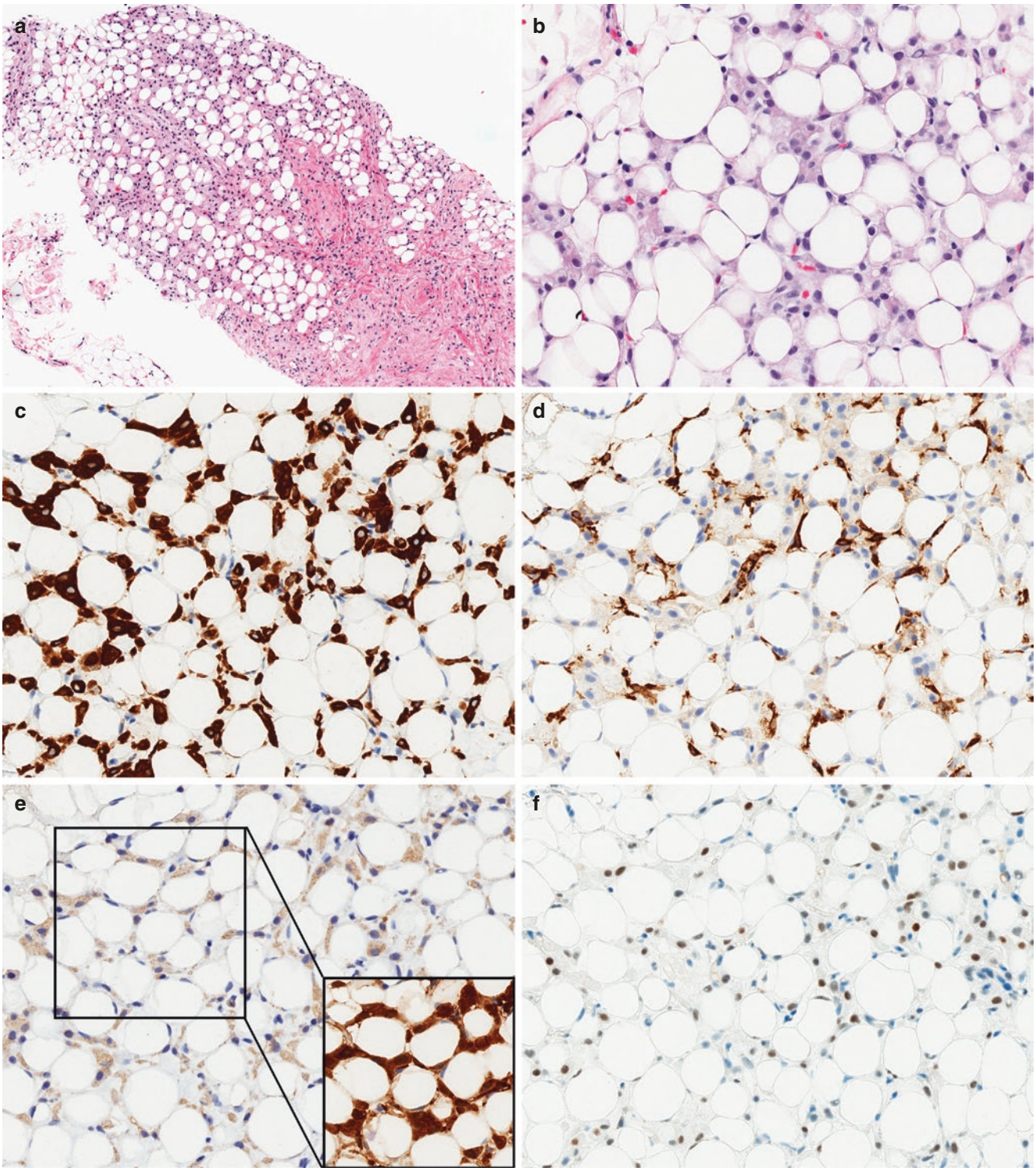

Fig. 15.11 ILC, histiocytoid variant. (**a**) H&E stain of a core biopsy at low power shows subtle infiltration of carcinoma within adipose tissue. (**b**) Higher power demonstrates tumor cells with abundant foamy cytoplasm. (**c, d**) Immunostains are positive for keratin (**c**) and negative for CD163 (**d**). (**e**) The tumor cells lack E-cadherin expression and show cytoplasmic p120-catenin (inset). (**f**) Testing for estrogen receptor (ER) shows a low level of expression (ER low positive)

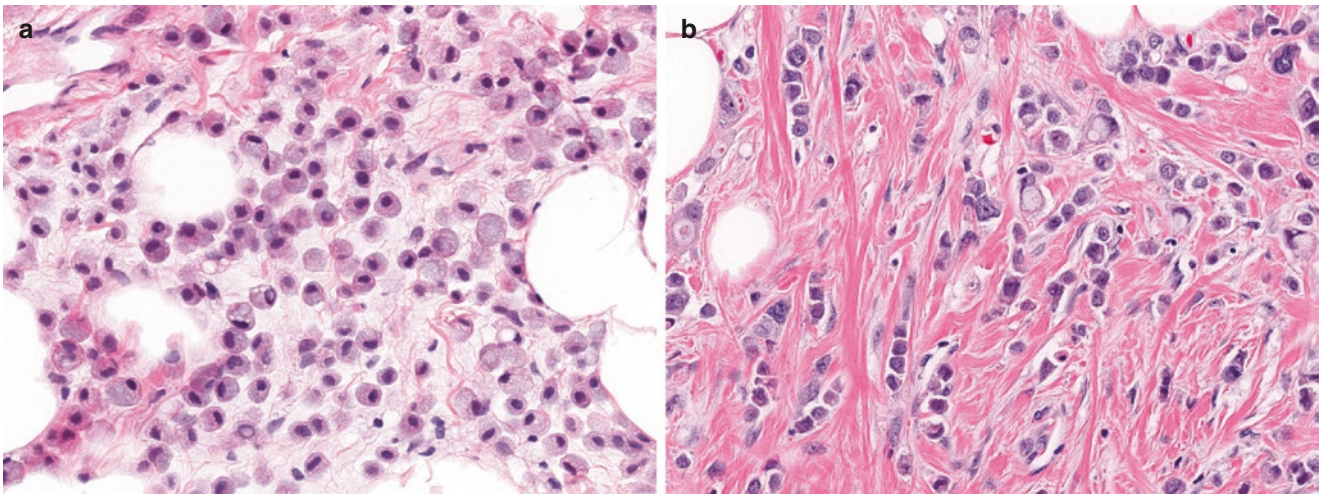

Fig. 15.12 ILC with signet ring cell features. (**a, b**) Signet ring cells can be seen in tumors with low (**a**) or high (**b**) nuclear grade

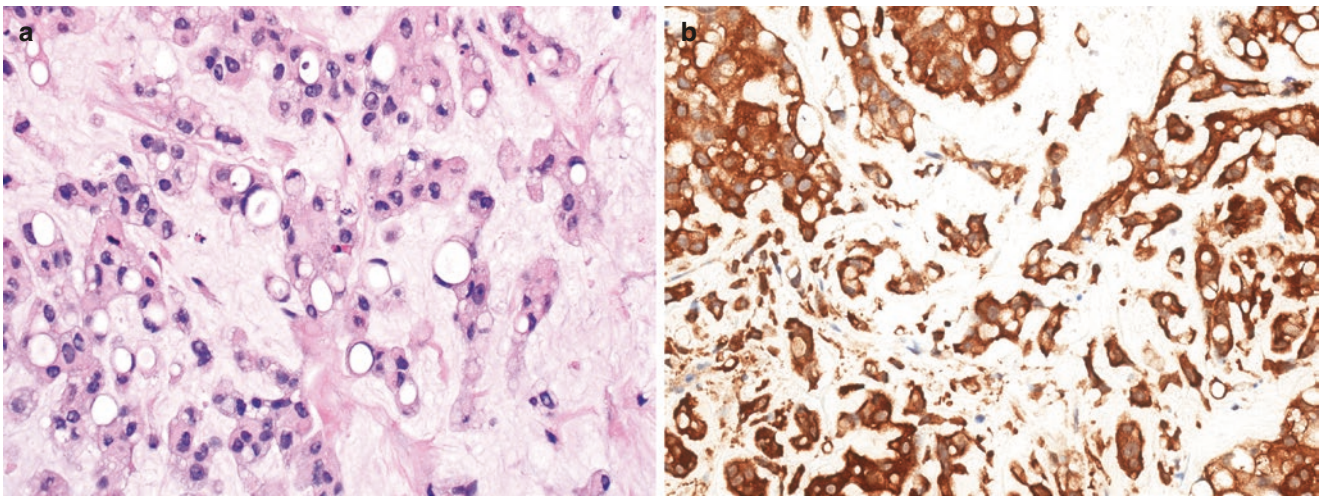

Fig. 15.13 ILC with extracellular mucin (ILCEM). (**a**) ILCEM is characterized by the presence of both extracellular mucin and single cells and/or clusters with intracellular mucin (i.e., signet ring cells). (**b**) Cytoplasmic expression of p120-catenin confirms lobular differentiation. (*Courtesy of Dr. Gregory Bean, Department of Pathology, Stanford University Medical Center*)

Finally, ILC of mixed type is composed of classic ILC with one or more variant patterns (e.g., "ILC, mixed classic, solid, and pleomorphic types"), without a specific quantitative requirement for the contribution of individual components. In a single-institution study, Raka et al. found that the vast majority of ILC (89%) is of classic type (55%) or mixed lobular subtypes (34%) [99]. Morphologic variants of ILC in their pure form are relatively rare.

Histologic Grading

ILC should be graded using the widely accepted modified Scarff–Bloom–Richardson (mSBR)/Nottingham grading system. Most (78–85%) ILC are grade 2 tumors, with a majority showing a moderate degree of nuclear pleomorphism (2 points) and low mitotic activity (1 point) [17, 100, 101]. Classic ILC are largely grade 2 or 1, while pleomorphic ILC can be grade 2 or 3. As mitotic activity tends to be low in classic ILC, the variation in overall grade is mainly due to nuclear grade (Fig. 15.16). ILC with variant architectural patterns tend to be of higher histologic grade. Rakha et al. found histologic grade to be prognostically significant, with grade 3 pleomorphic ILC having a worse prognosis than grade 2 pleomorphic ILC, suggesting that survival is associated with mitotic count, not with nuclear pleomorphism [102]. Therefore, the importance of recognizing nonclassical growth patterns and high nuclear grade in ILC is to not mis-

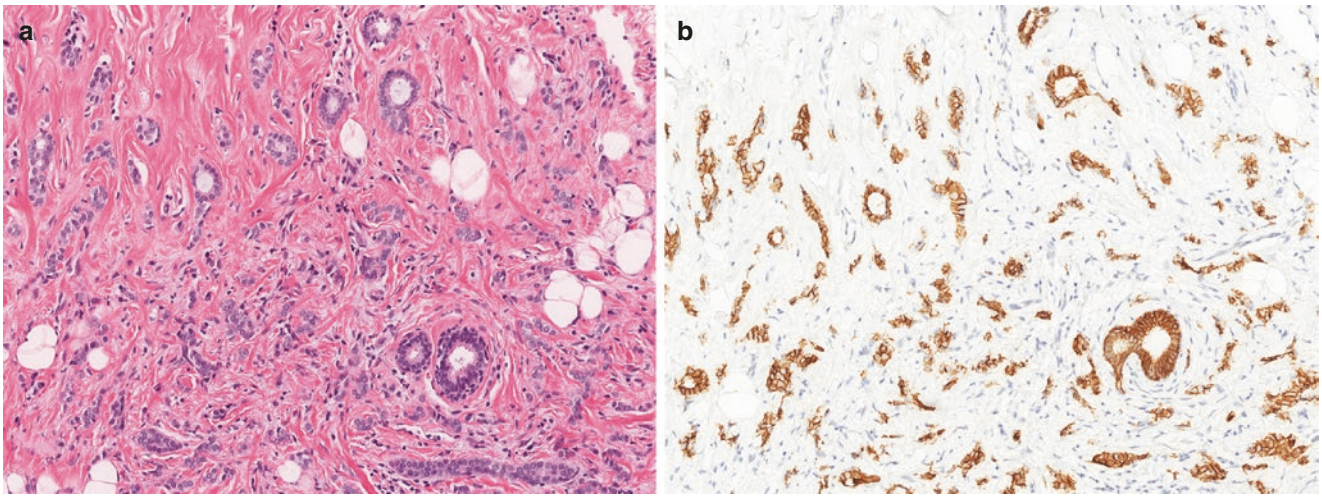

Fig. 15.14 IDC, tubulolobular pattern. (**a**) This tumor displays well-formed tubules admixed with single-file cords of cells. (**b**) An E-cadherin immunohistochemical stain is positive in both components

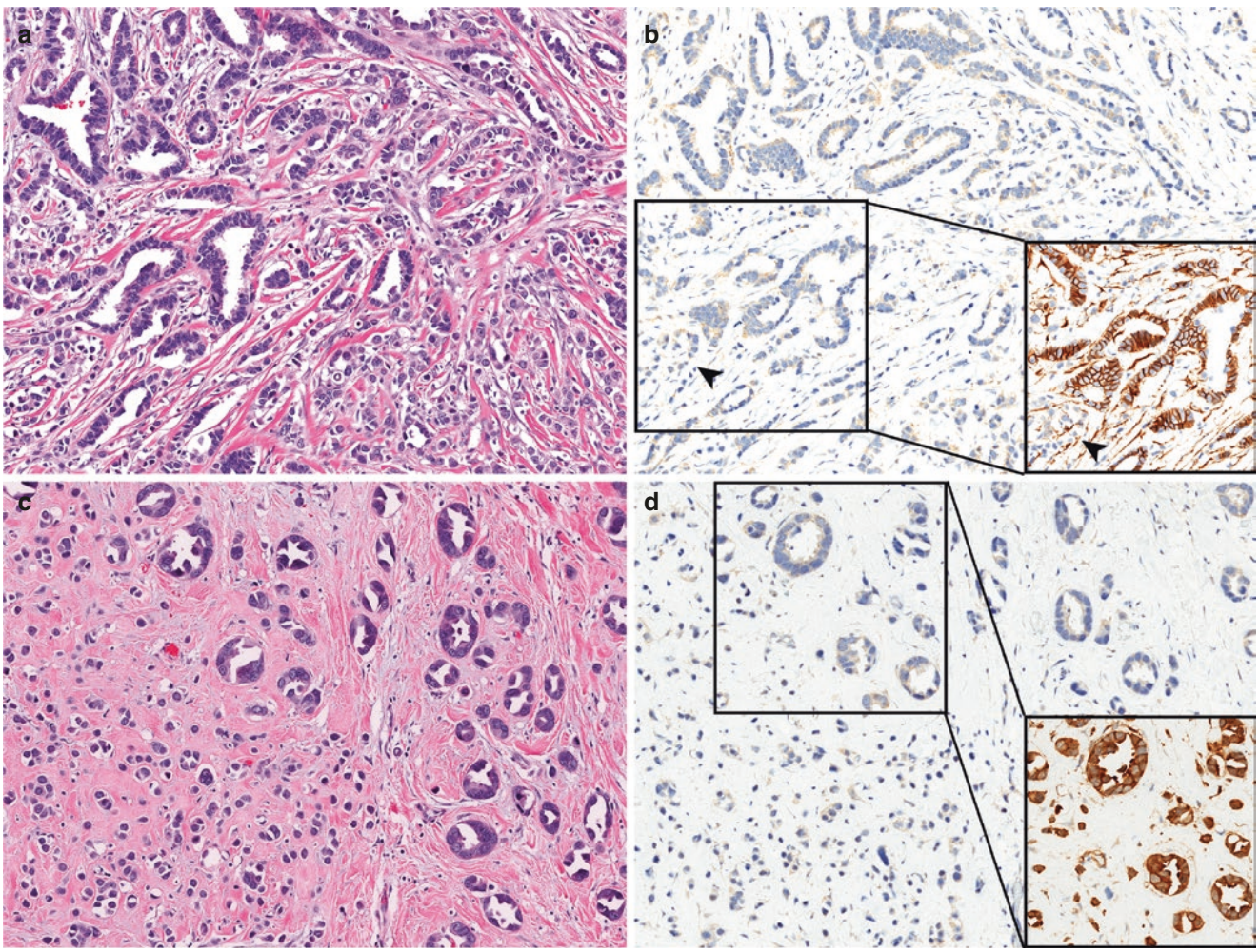

Fig. 15.15 ILC, tubulolobular pattern. (**a–d**) This tumor shows mixed (ductal and lobular) histology. The ductal component consists of both longitudinal, angulated tubules (**a**, top left) and small, round tubules with narrow lumens (**c**, top right). The admixed lobular component consists of single-file cords (**a**, bottom right) and individually dispersed cells (**c**, bottom left). Immunohistochemistry for E-cadherin is negative in both components (**b**, **d**). However, the tubules retain membrane-localized β-catenin, while the lobular component (arrowhead) is negative (**b**, inset). Expression of p120-catenin within the tubules is more ambiguous and may still appear cytoplasmic (**d**, inset). (**e, f**) This ILC with tubulolobular pattern was associated with both DCIS (asterisk) and LCIS (arrow), highlighted by E-cadherin immunostaining (**f**)

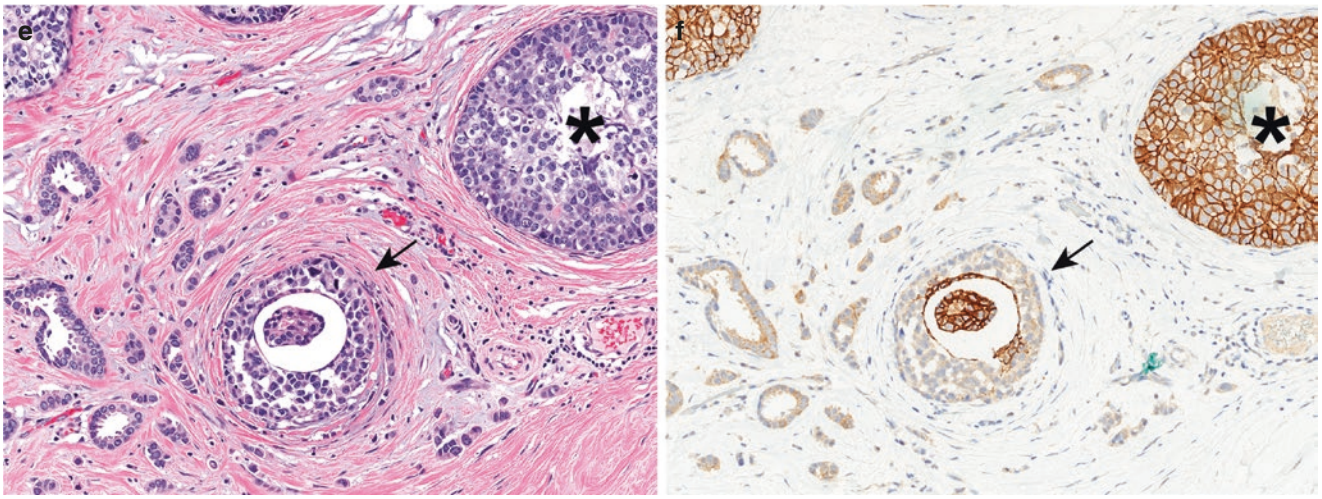

Fig. 15.15 (continued)

Table 15.1 Invasive breast carcinomas with mixed (lobular and ductal) histology

	Dyscohesive cells (Lobular component)	Tubules (Ductal component)	Alternative names	Comment	References
Mixed ductal and lobular carcinoma	E-cad aberrant > negative	E-cad positive		Components arise from a common ancestor (not a collision tumor); more often associated with DCIS than LCIS	[95, 96]
ILC, tubulolobular pattern	E-cad negative	E-cad negative (P-cad positive)	ILC with tubular elements; ILC with ductal features	Often associated with LCIS; original "tubulolobular carcinoma" described by Fisher et al.	[90, 94, 97]
IDC, tubulolobular pattern	E-cad positive	E-cad positive	Tubulolobular carcinoma; IDC with lobular features	Often associated with LCIS and/or DCIS	[91–93]
Invasive carcinoma with ductal and lobular features	Ambiguous	Ambiguous		Hybrid or indeterminate features by H&E and IHC do not permit definitive categorization	[98]

take these cases for IDC, as different growth patterns and pleomorphism do not appear to provide additional prognostic information not already conferred by histologic grading. In core biopsies, histologic grading of ILC should be performed and reported, although crush artifact may preclude definitive nuclear grading and proper evaluation of mitotic count in some cases.

Tumor Microenvironment

Studies of the tumor microenvironment have uncovered differences between ILC and IBC-NST. Levels of tumor-infiltrating lymphocytes (TILs) are significantly lower in ILC compared with ER+/HER2− IBC-NST. Nevertheless, about 15% of ILC show high numbers of TILs (defined as >5% [103] or >10% [104]), and these cases are associated with a younger age at diagnosis, lymph node metastasis, high proliferation rates, and ultimately worse prognosis [103, 104]. This finding contrasts with the typically favorable prognosis of high TIL levels in HER2+ and triple-negative IBC-NST. The presence of immune infiltration also seems to correlate with ILC morphologic variants, with the alveolar subtype being more often TIL negative and mixed pattern tumors mostly TIL enriched [103]. Further studies are needed to better understand the detailed immune composition within ILC, which may provide greater insight into the biological behavior of these tumors and the potential efficacy of immuno-oncology therapeutics.

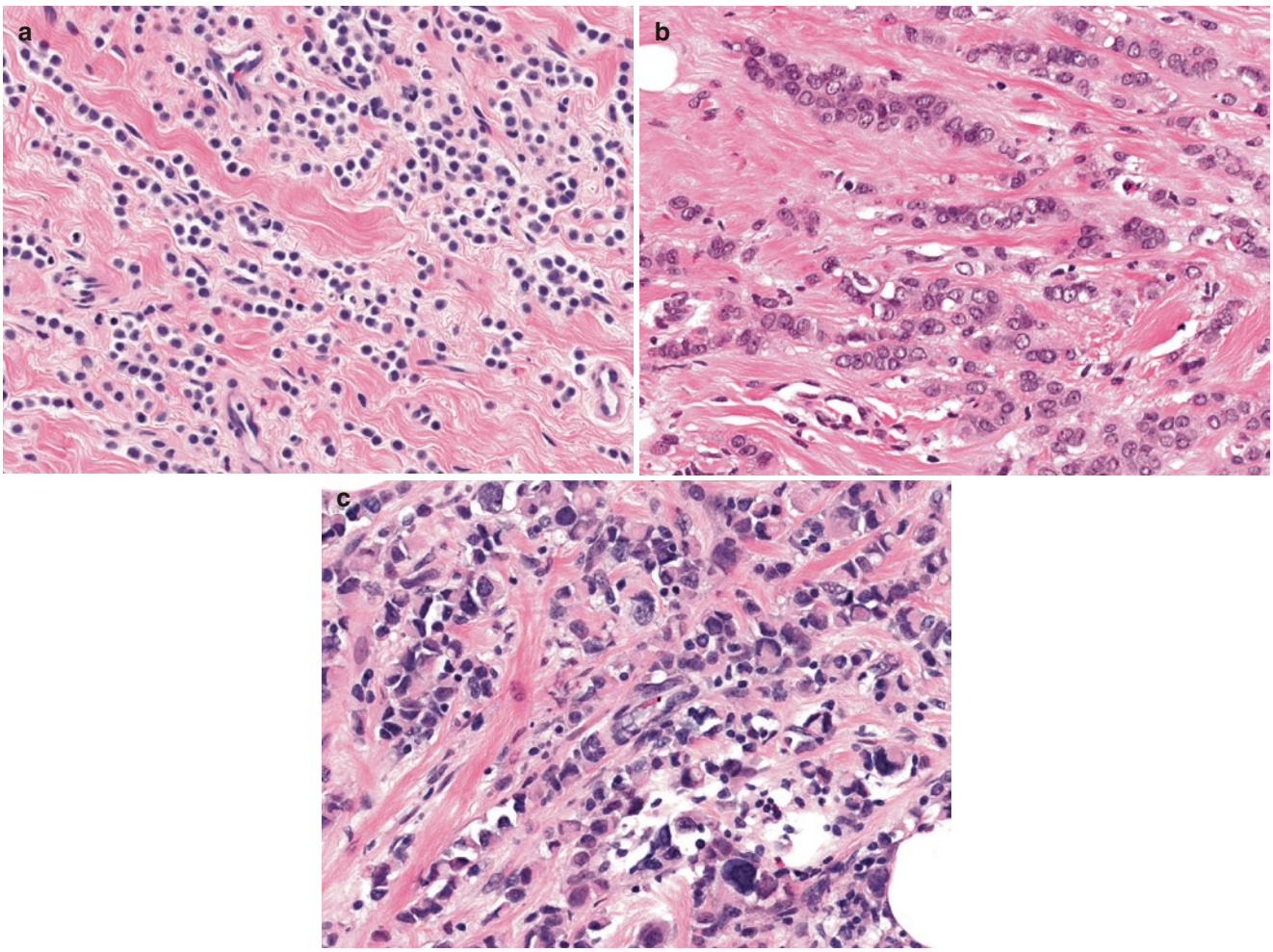

Fig. 15.16 ILC of nuclear grades 1 (**a**), 2 (**b**), and 3 (**c**) taken at the same magnification

Immunohistochemistry

Loss of E-cadherin was found to be a key feature of both ILC and lobular neoplasia in the late 1990s and represents the major molecular driver of dyscohesion seen in these tumors [105–107]. E-cadherin is the major transmembrane protein within epithelial cell adherens junctions, which facilitates calcium-dependent cell-cell adhesion via homotypic interactions, regulates the actin cytoskeleton, and mediates intracellular signaling [108]. Immunohistochemical staining for E-cadherin and other components of the cytoplasmic complex of adherens junctions has been increasingly used to help distinguish between ductal and lobular neoplasms (Table 15.2). The intracellular domain of E-cadherin interacts with a β-catenin–α-catenin complex to bind to the actin cytoskeleton and with p120-catenin to stabilize adherens junctions at the plasma membrane. Loss or disruption of E-cadherin typically results in concurrent absence of expression of β-catenin and α-catenin and upregulation and accumulation of p120-catenin in the cytoplasm [109]. The diffuse cytoplasmic staining pattern of p120-catenin is particularly useful to differentiate lobular from ductal lesions, which show membranous staining [110–112]. This stain is best used in conjunction with, but not in place of, E-cadherin, as distinguishing pure cytoplasmic from membranous staining can be challenging in tumor cells that have scant cytoplasm.

Table 15.2 Immunohistochemical workup to distinguish lobular and ductal neoplasms

	ILC and LCIS	Invasive ductal carcinoma and DCIS[a]
E-cadherin	Negative (or aberrant)	Membranous
p120 catenin	Cytoplasmic	Membranous
β-catenin	Negative (or aberrant)	Membranous

[a]This staining pattern is also seen in normal breast epithelium and benign duct lesions

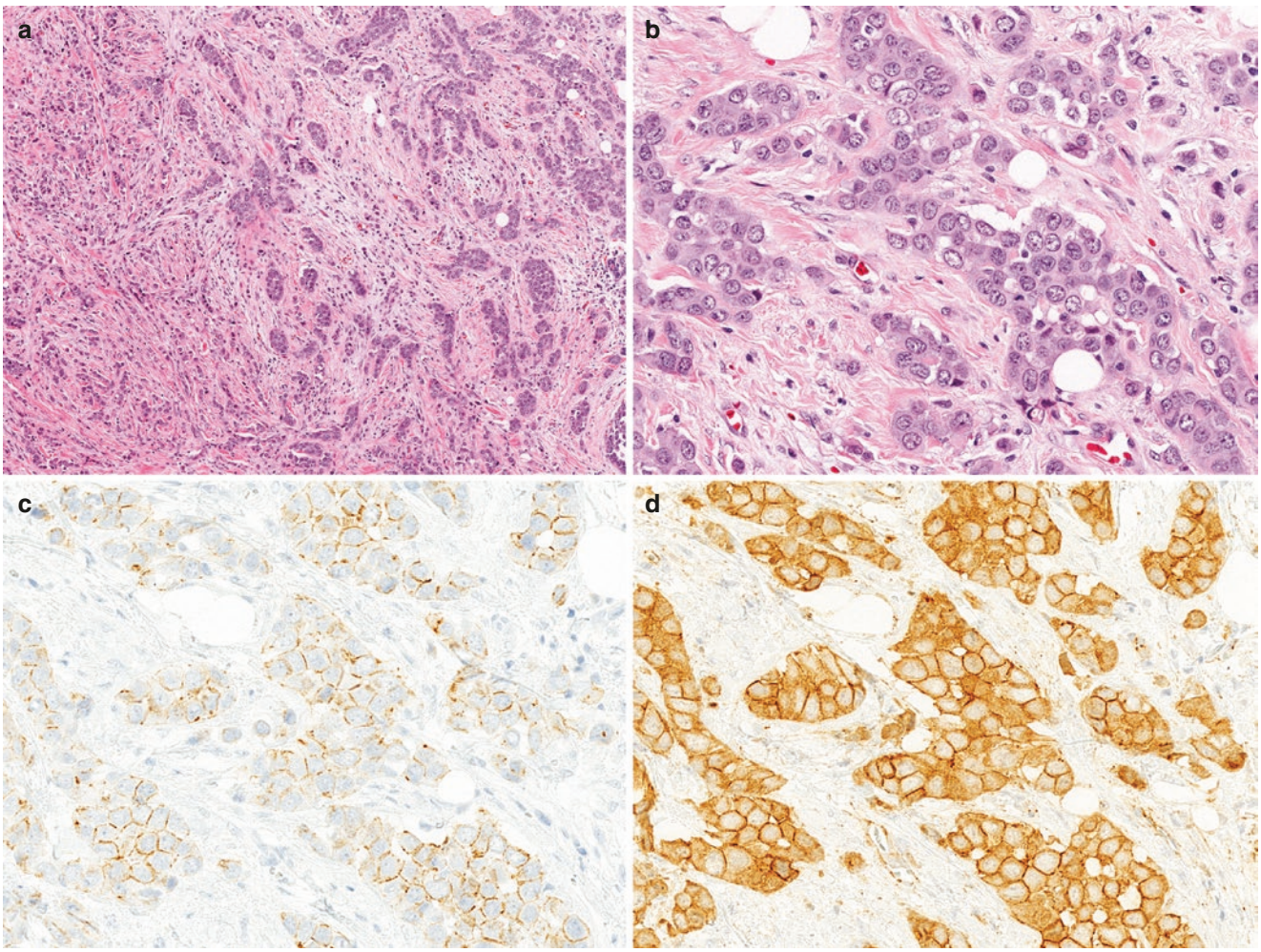

Fig. 15.17 ILC with aberrant (partial membranous) E-cadherin expression. (**a, b**) H&E stain at low and high power of ILC with classic and alveolar growth patterns. (**c**) The tumor cells showed variable incomplete membranous E-cadherin expression, leading to a misdiagnosis as IDC. (**d**) Immunohistochemistry for p120-catenin showed cytoplasmic expression, supporting lobular differentiation

Although most ILC completely lack E-cadherin expression, aberrant positivity can also be seen, including incomplete membrane (Fig. 15.17), diffuse cytoplasmic (Figs. 15.18 and 15.19), or dot-like Golgi (Fig. 15.20) staining patterns [105, 107, 113–115]. Genomic features commonly associated with ILC (16q loss, 1q gain, and 11q loss) have been demonstrated in cases with aberrant staining, suggesting that E-cadherin may be nonfunctional in these cases [116]. In addition, such cases have been shown to exhibit p120 cytoplasmic staining suggestive of a dysfunctional adherens junction [114, 117, 118]. Thus, "positive" E-cadherin staining should not be used to exclude a diagnosis of ILC. Moreover, it is important to recognize that variability in staining can arise from different E-cadherin antibody clones (Fig. 15.20) [114]. Suboptimal antibody optimization and validation that lead to overstaining can also alter the final interpretation and result in a misdiagnosis [119].

E-cadherin can rarely be negative in ductal neoplasms. Among non-lobular breast cancers, E-cadherin expression is reduced or lost in >40% of basal-like breast carcinomas [120]. Rare cases of IDC with predominantly well-formed glands have been found to lack E-cadherin immunoreactivity [121]. Rakha et al. found 7% of 1516 cases of IDC on a tissue microarray to be E-cadherin negative, with E-cadherin positivity defined as greater than or equal to 10% membranous staining [122]. However, in a follow-up study in which the authors stained full-face sections using two different E-cadherin antibodies, only three cases remained classified as E-cadherin negative, and all cases showed membranous staining for p120 and β-catenin, suggesting a functional adherens junction [118].

In everyday practice, fragmented, focal, or circumferential membranous staining that is relatively weaker in intensity to that observed in adjacent ductal epithelium (positive

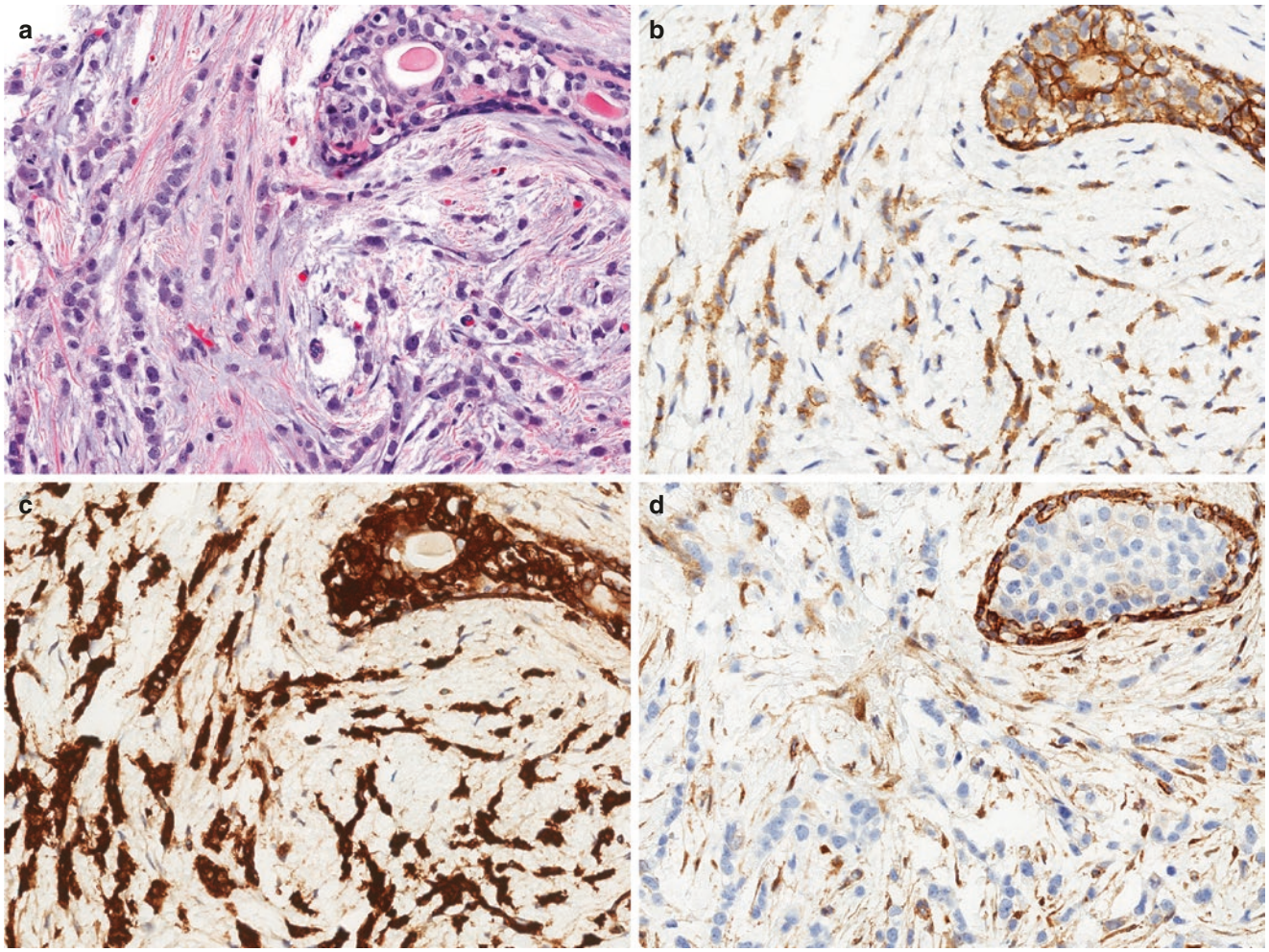

Fig. 15.18 ILC with aberrant (cytoplasmic) E-cadherin expression. (**a**) H&E stain of ILC with associated LCIS. (**b**) E-cadherin staining was difficult to interpret, with tumor cells showing variable cytoplasmic/granular (bottom right) to weak, incomplete membranous (bottom left) expression. (**c**) A p120-catenin immunostain showed predominantly strong cytoplasmic staining. (**d**) Immunohistochemistry for β-catenin was negative and helped to confirm a lobular phenotype

internal control) is diagnostically acceptable to confirm a lobular phenotype. About 15% of ILC show variable membranous expression of E-cadherin, often accompanied by perimembranous cytoplasmic expression, but a majority of these cases demonstrate impairment of the E-cadherin-catenin complex (e.g., via cytoplasmic p120 or aberrant localization of β and/or α-catenin) [114, 117]. Please also refer to Figs. 14.20, 14.21, 14.22, and 14.23 for the interpretation of E-cadherin immunostain and evaluation of ductal versus lobular lesions using immunohistochemistry/immunohistochemical (IHC) stains to the E-cadherin-catenin complex. Therefore, we reiterate the recommendations of Dabbs et al. that [1] E-cadherin staining should be avoided in cases with clear-cut classic lobular histology; [2] p120 and/or β-catenin IHC stains may be useful in equivocal cases with aberrant E-cadherin expression; and [3] a diagnosis of "invasive carcinoma with ductal and lobular features" is appropriate in some cases with equivocal histologic features and indeterminate findings by IHC (Table 15.1) [123].

Prognostic/Predictive Markers

Classic ILC is typically strongly and diffusely positive for ER, variably positive for PR, and negative for HER2, with a low Ki-67 proliferation index. ILC are more frequently ER positive (80–95%) than IBC-NST (70–80%) but express PR at about the same rate (60–70%) [14, 17, 19]. ILC is rarely HR negative, triple negative, or HER2 positive. Deviation from the usual immunoprofile is more likely to occur in pleomorphic or grade 3 ILC. Therefore, if classic ILC is not ER positive, one should question the diagnosis or consider a false-negative staining result (e.g., due to assay failure,

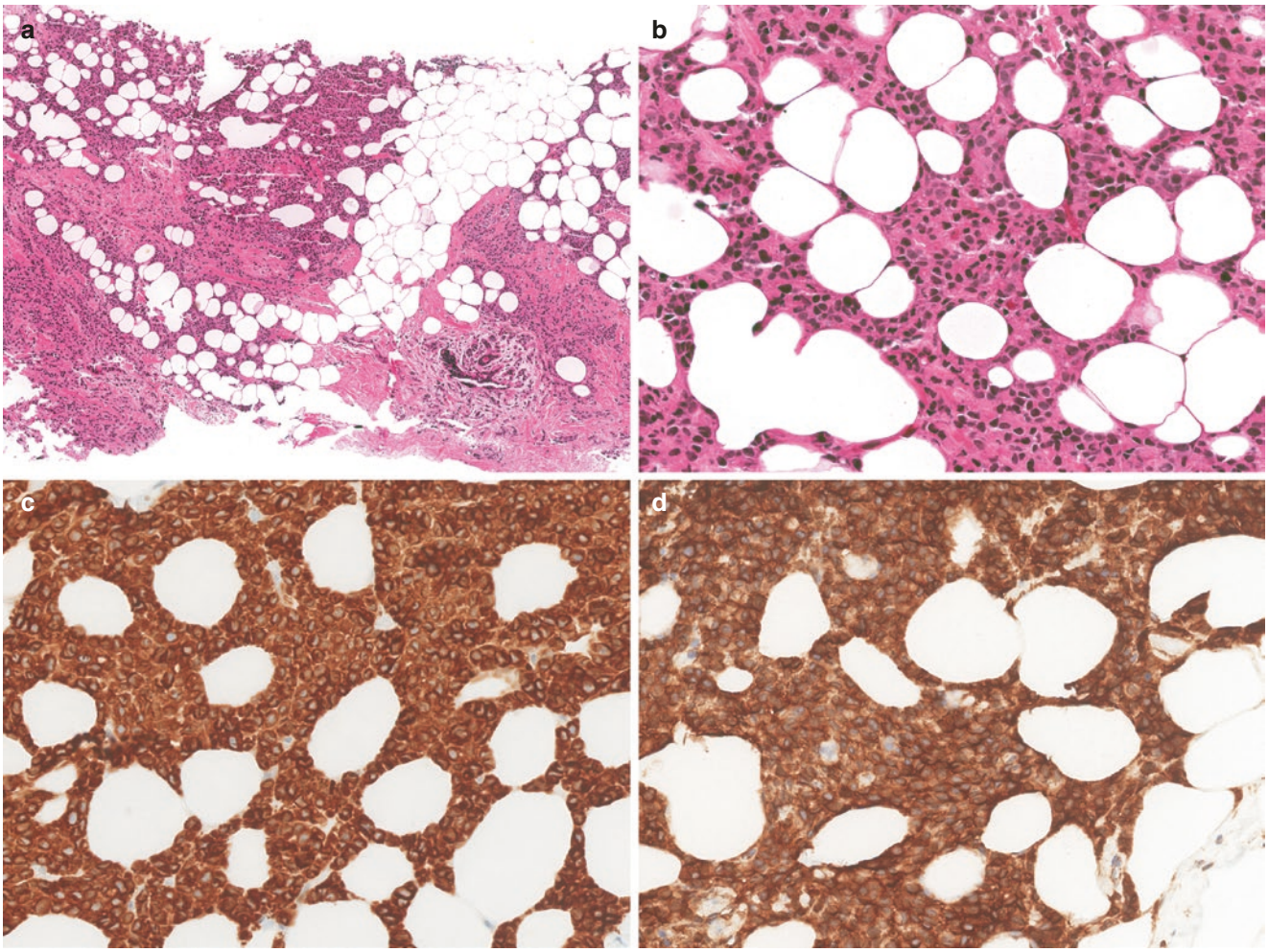

Fig. 15.19 ILC with aberrant (strong cytoplasmic) E-cadherin expression. (**a, b**) H&E stain of a core biopsy at low and high power demonstrates cytologically bland tumor cells infiltrating as single cells and linear arrays. (**c**) The tumor cells showed intense, predominantly cytoplasmic staining for E-cadherin, leading to a misdiagnosis as IDC. (**d**) Cytoplasmic localization of p120-catenin helped to appropriately classify the tumor as ILC

decalcification, or improper fixation). Similarly, if classic ILC appears HER2 positive by IHC, the results should be interpreted with caution and confirmed by fluorescence in situ hybridization (FISH) testing. However, rare instances of HER2-positive classic ILC have been reported. Yu et al. identified 12 cases of classic ILC with HER2 overexpression at their institution over a 3-year period and observed a significant association with histiocytoid morphology and absent PR expression [124].

Pleomorphic ILC is usually ER positive (77–96%) and PR positive (63–93%); however, this variant is more likely to be HR negative than classic ILC [8, 82, 102, 125–128]. A wide range (2–35%) of HER2 positivity has been reported in pleomorphic ILC (Fig. 15.21) compared to 0–2% for classic ILC [11, 102, 126–129]. The apocrine variant of pleomorphic ILC is more often ER negative and HER2 positive. Approximately 13–16% of pleomorphic ILC are triple negative [9, 10, 126]. The Ki-67 proliferation index is generally higher compared to classic ILC but significantly lower than that in poorly differentiated IDC [125]. Among other morphologic variants of ILC, ILCEM has been shown to be HER2 positive in 19% of reported cases [88].

Other Immunohistochemical Adjuncts

Due to the diffuse infiltrative growth pattern of ILC, cytokeratin immunostaining can serve as a useful ancillary test in several situations: [1] to detect inconspicuous lymph node metastases; [2] to evaluate margins in an excision specimen; [3] to identify scant residual tumor cells after neoadjuvant chemotherapy; and [4] to confirm epithelial origin in rare morphologic subtypes that mimic other cell types (e.g., histiocytoid variant).

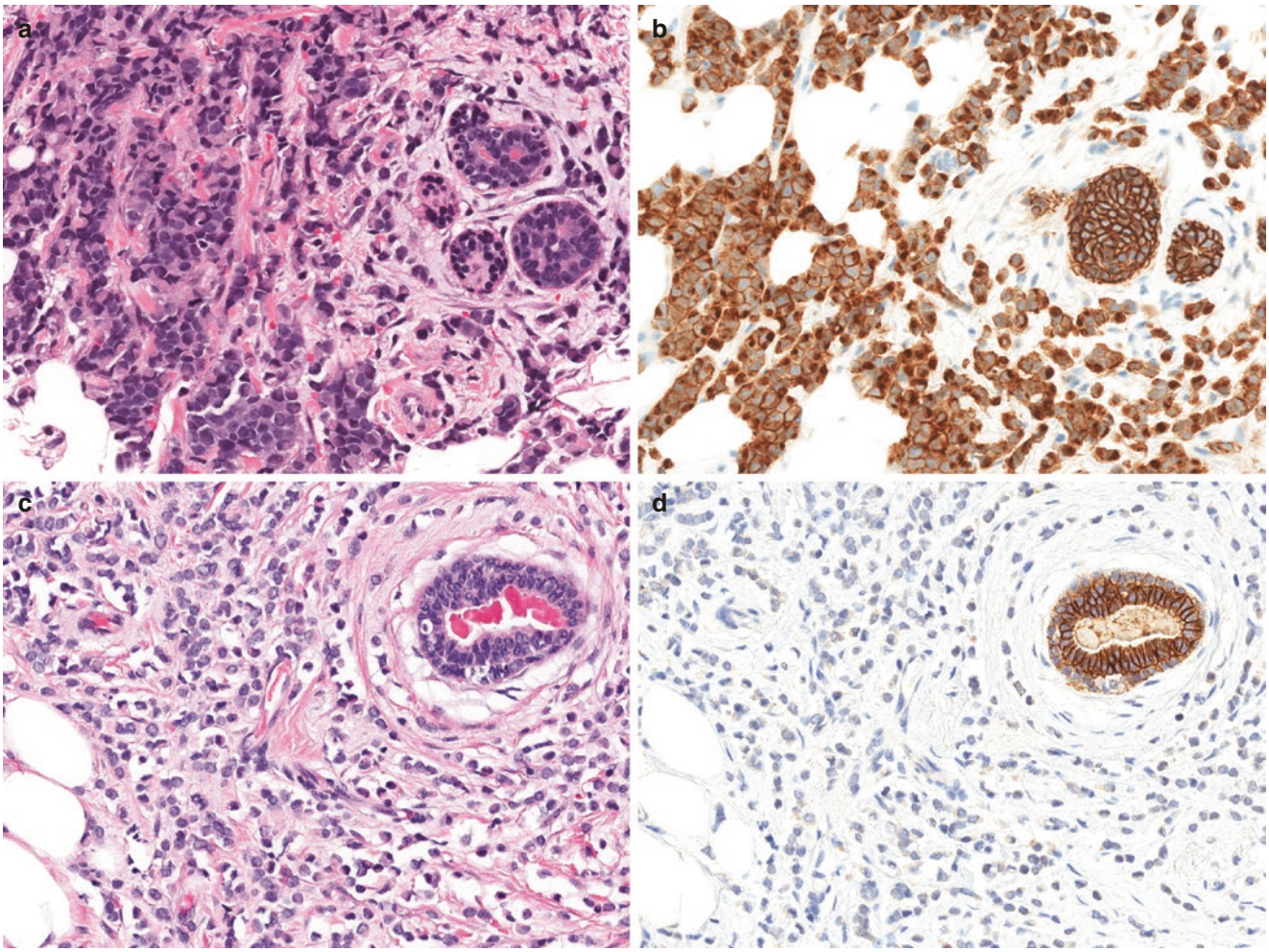

Fig. 15.20 ILC with aberrant (dot-like) E-cadherin expression. (**a, b**) On core biopsy, this invasive carcinoma demonstrated aberrant E-cadherin expression, including prominent large, cytoplasmic, dot-like (Golgi pattern) staining and weak/discontinuous membrane staining (**b**). (**c, d**) E-cadherin immunostaining on the excision specimen, performed in a different lab with a different clone/protocol, showed complete loss of expression (**d**)

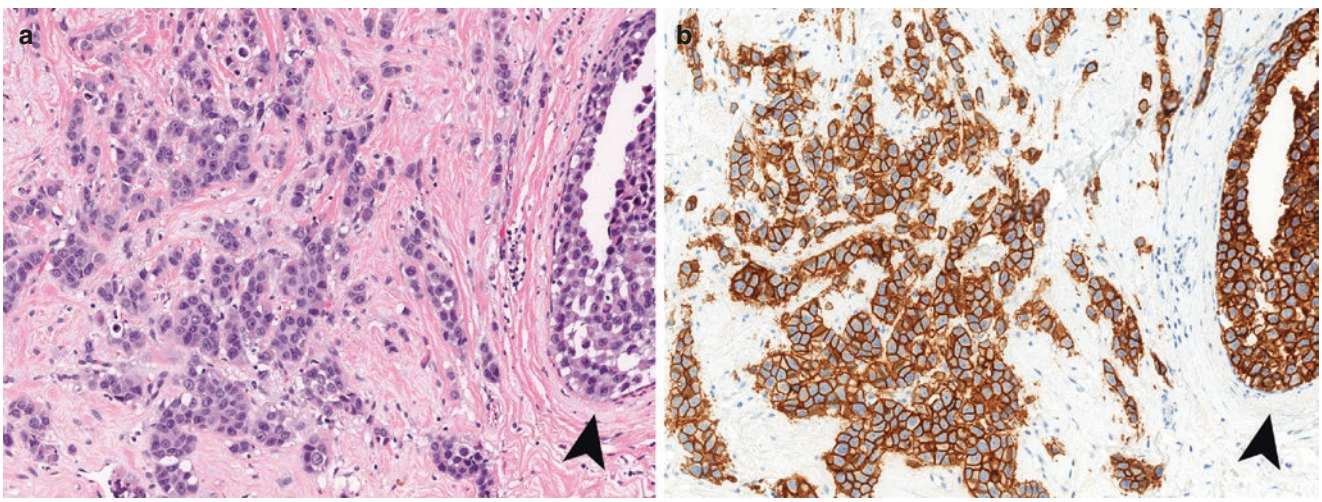

Fig. 15.21 ILC, pleomorphic type. (**a**) This ILC demonstrates pleomorphic nuclei and is associated with pleomorphic LCIS (arrowhead). (**b**) Both the invasive and in situ components show overexpression for HER2 (3+ staining)

ILC are typically negative for basal epithelial markers (CK5/6, CK14), myoepithelial markers, and p53. Additional immunohistochemical markers may be helpful to identify specific morphologic subtypes. For example, apocrine and histiocytoid variants of ILC typically show diffuse positivity (>50% of cell staining) for gross cystic disease fluid protein 15 (GCDFP-15) (Fig. 15.7) [80, 84]. ILCEM shows abnormal cytoplasmic localization of MUC1, which is normally membranous, as well as cytoplasmic expression of the intestinal mucins MUC2 and MUC6 [88].

Neuroendocrine differentiation can rarely be observed in ILC, as determined by immunohistochemical expression of neuroendocrine markers such as synaptophysin and chromogranin (Fig. 15.22) [130, 131]. However, neuroendocrine differentiation does not warrant designation as a distinct subtype in ILC and currently has no relevance for clinical outcomes or therapeutic management [97]. When a tumor with neuroendocrine differentiation is encountered in a core biopsy and no in situ component is identified, it is important to exclude metastasis, especially from the lung and GI tract.

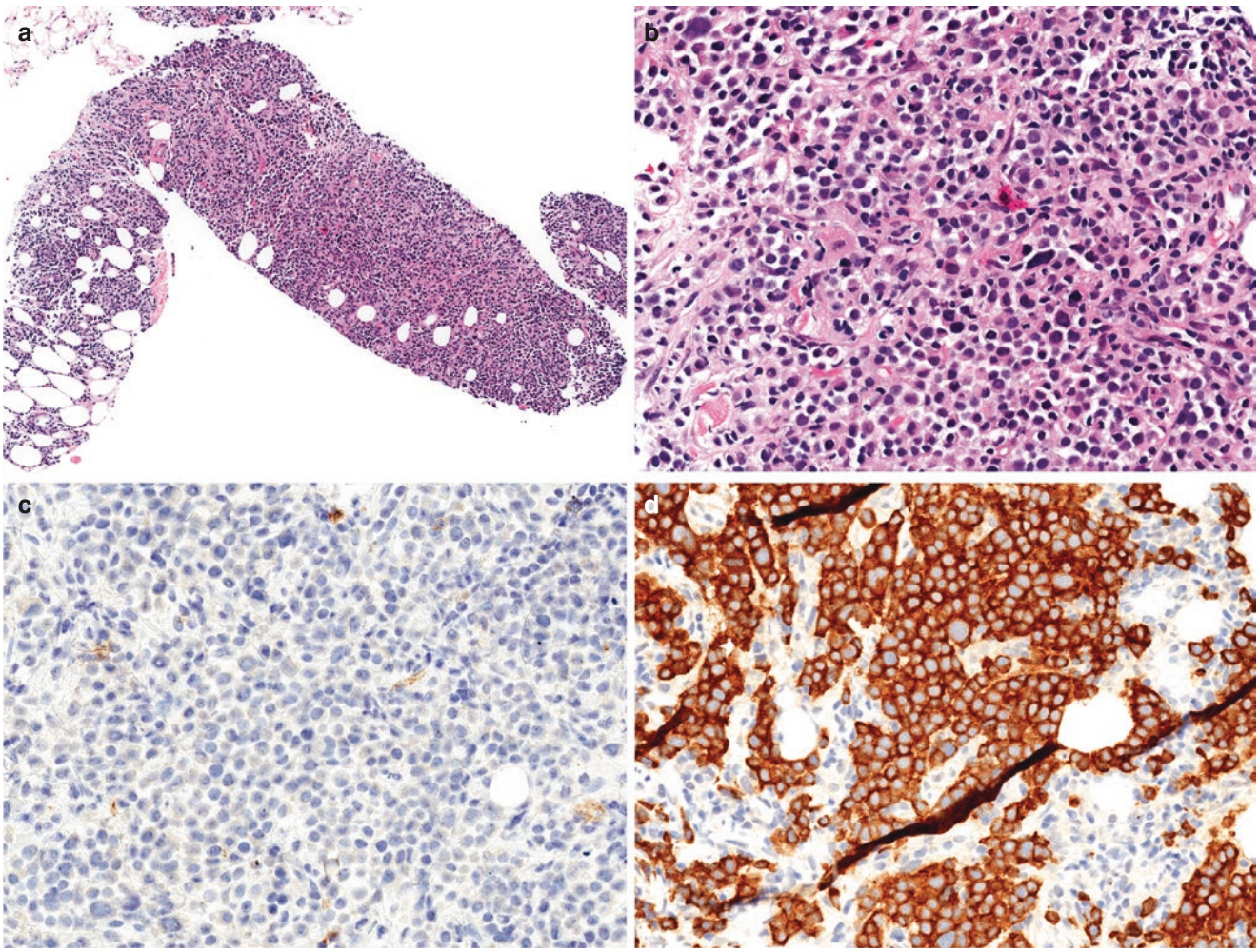

Fig. 15.22 ILC with pleomorphic features and neuroendocrine differentiation. (**a**) H&E stain of a core biopsy at low power shows a malignant neoplasm with sheetlike growth-infiltrating fibroadipose tissue. (**b**) Higher power demonstrates dyscohesive tumor cells with intermediate- to scattered high-grade nuclei and rare intracytoplasmic vacuoles. (**c, d**) The tumor cells lack E-cadherin expression (**c**) and are diffusely positive for synaptophysin (**d**). (**e, f**) Positive staining for GATA3 (**e**) and ER (**f**) and negative staining for TTF1 (**e**, inset) support breast origin

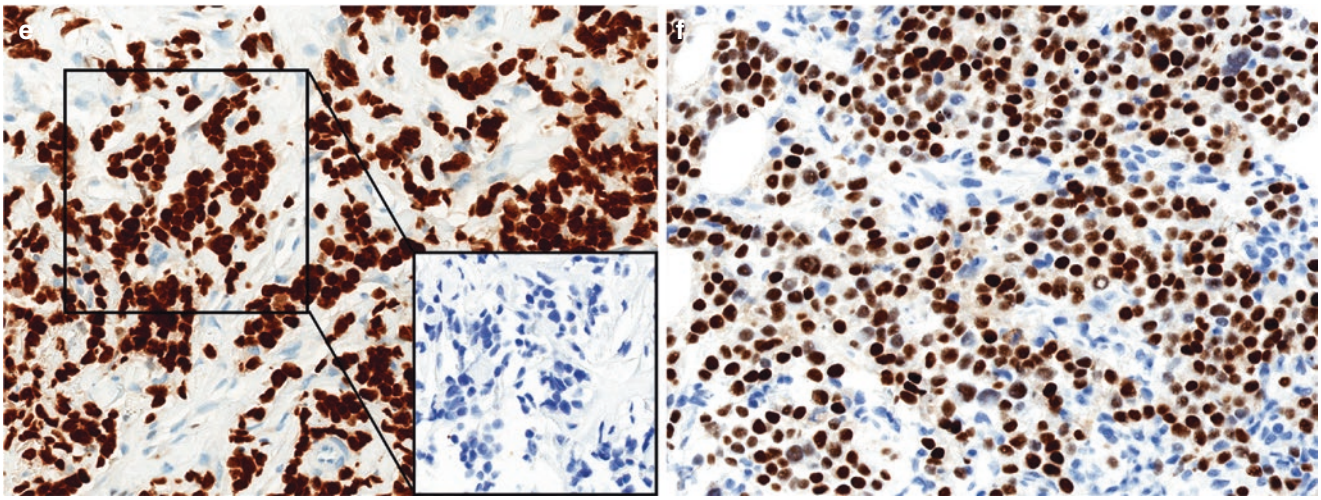

Fig. 15.22 (continued)

Differential Diagnosis

Invasive ductal versus lobular carcinoma: Not infrequently, grade 2 or 3 IDC will show cells in a single-file pattern or small solid nests that can mimic classic and alveolar growth patterns, respectively. IDC can also show signet ring cell differentiation. E-cadherin immunostaining should show membranous staining in the entire tumor, including areas with single-cell filing. A "pseudo" single-file growth pattern can also be seen when IDC infiltrates tissue that is particularly dense, such as sclerotic stroma or skin dermis (often in recurrent carcinoma or after neoadjuvant chemotherapy), leading to compressed, restricted growth (Fig. 15.23).

Pleomorphic ILC can also be mistaken for IDC, particularly the apocrine variant, which can mimic invasive apocrine carcinoma of ductal type. The presence of concurrent pleomorphic LCIS may be further misleading due to the high-grade cytology that mimics DCIS. Again, an E-cadherin stain can be helpful in these cases. In contrast, some poorly differentiated IDC can exhibit prominent dyscohesion, often due to under-fixation, and can be mistaken for ILC.

As discussed above, some invasive carcinomas show mixed lobular and ductal histology (Table 15.1). These tumors may represent mixed invasive ductal and lobular carcinoma; ILC, tubulolobular pattern; or IDC, tubulolobular pattern. In contrast to the latter two entities, mixed invasive ductal and lobular carcinomas demonstrate positive membranous E-cadherin expression within the ductal component of the tumor and aberrant or absent staining within the lobular component (Fig. 15.24). Whole-exome sequencing of these individual components has demonstrated that they arise from a common ancestor, with evidence for clonal progression from ductal to lobular histology [95]. Immunohistochemical evaluation for the integrity of the adherens junction (E-cadherin, p120 catenin, and β-catenin) can facilitate appropriate classification of such cases.

Solid or encapsulated papillary carcinoma: ILC can rarely present with architectural features that mimic solid papillary or encapsulated papillary carcinoma (Fig. 15.25). Such tumors demonstrate a well-defined, solid growth pattern containing fibrovascular cores with or without a peripheral fibrous capsule [132–134]. Subtle dyscohesion among the tumor cells as well as surrounding satellite foci of classic ILC can provide clues to the diagnosis. Absence of E-cadherin and myoepithelial markers is useful to confirm the lobular phenotype and invasive nature of the tumor, respectively.

Myofibroblastoma, epithelioid variant: Myofibroblastomas are rare benign spindle cell neoplasms arising from myofibroblasts that usually present as a mass lesion. In the epithelioid variant of myofibroblastoma, the tumor cells are rounded rather than spindled and form clusters or single-cell files, closely mimicking ILC (Fig. 15.26). Diffuse positivity for ER and PR and negative staining for E-cadherin in the neoplastic cells of myofibroblastoma further complicate the distinction. However, most myofibroblastomas present as a well-circumscribed mass in contrast to ILC, which usually presents as a spiculated mass or architectural distortion. Histologically, ILC shows an infiltrative growth pattern around normal ducts and lobules. Additional immunostains are particularly useful in a core biopsy in which the margins of the lesion cannot be assessed. Myofibroblastomas are positive for desmin and CD34 and negative for keratin.

Lymphoma and inflammatory infiltrates: Primary breast lymphomas are rare and usually present as mass lesions. When sampled in a core biopsy, low- or intermediate-grade lymphomas (e.g., small lymphocytic lymphoma, mantle cell

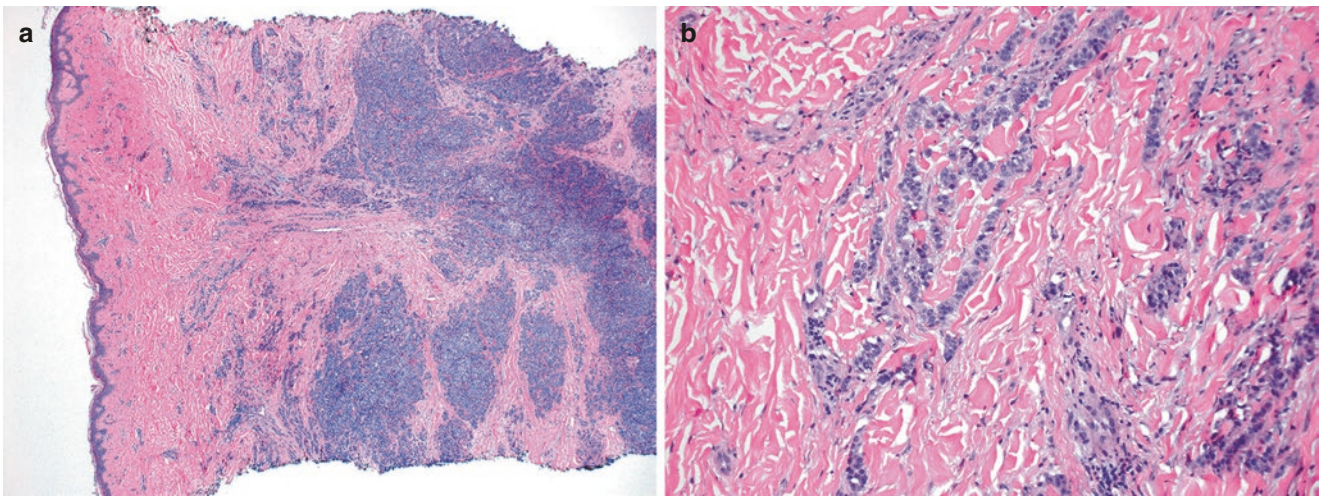

Fig. 15.23 IDC involving skin dermis. (**a**) H&E stain of a punch biopsy at low power shows a recurrent poorly differentiated IDC infiltrating the dermis. (**b**) Higher power shows focal single-file invasion reminiscent of ILC

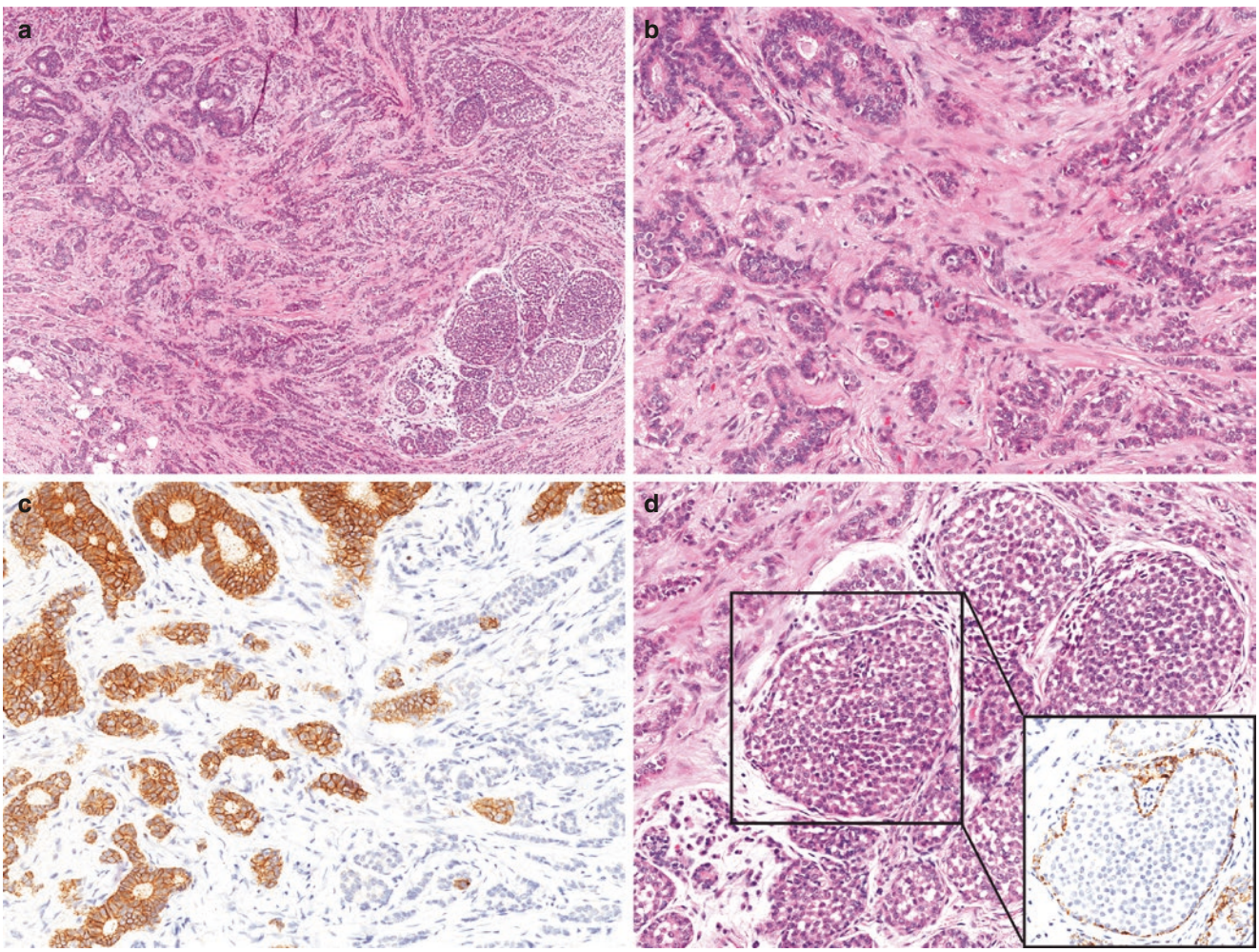

Fig. 15.24 Mixed ductal and lobular carcinoma. (**a**) This invasive carcinoma demonstrates mixed (predominantly lobular and focal ductal) histology and associated solid-pattern carcinoma in situ. (**b, c**) The ductal component (top left) consists of well-formed tubules and demonstrates positive membranous E-cadherin staining. The adjacent lobular component (bottom right) is composed of small nests and cords that lack E-cadherin expression. (**d**) The in situ carcinoma consists of small, monomorphic, dyscohesive cells that are negative for E-cadherin (inset), supporting LCIS

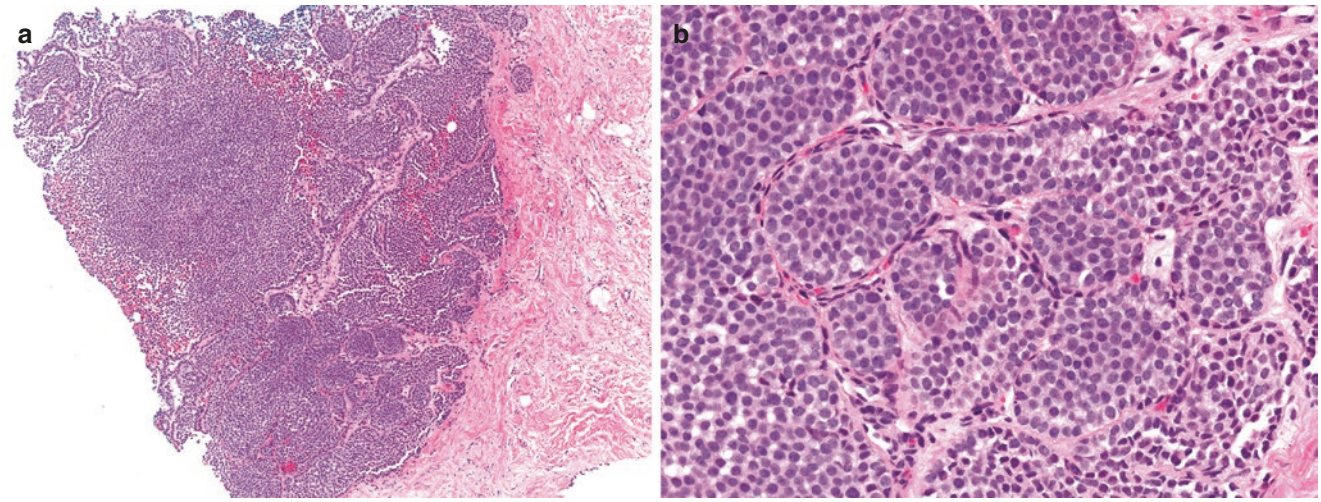

Fig. 15.25 ILC, solid pattern, mimicking solid papillary carcinoma. (**a**) H&E stain of a core biopsy at low power shows ILC arranged in a solid papillary pattern with peripheral budding into small tumor nests. (**b**) Higher power reveals monomorphic tumor cells with focal dyscohesive growth. E-cadherin staining was negative (not shown)

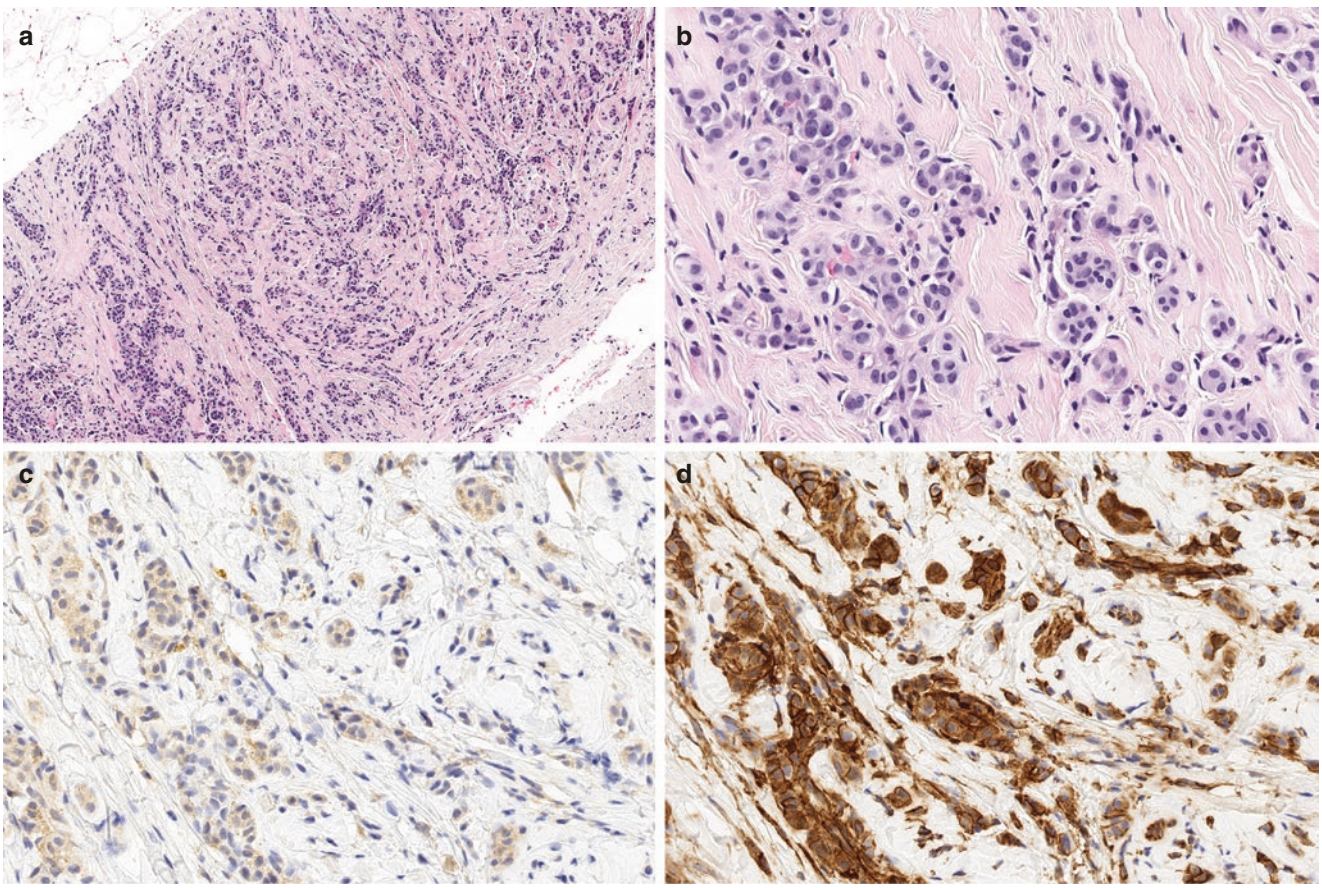

Fig. 15.26 Epithelioid myofibroblastoma. (**a**) H&E stain of a core biopsy at low power shows a haphazard, infiltrative-appearing proliferation of epithelioid cells. (**b**) The cells have bland round-to-oval nuclei and are variably arranged in small clusters or single cells. (**c, d**) The neoplastic cells show weak cytoplasmic staining for E-cadherin (**c**) and cytoplasmic and membranous expression of p120-catenin (**d**), leading to a false impression of ILC. (**e**) ER is diffusely positive. (**f–h**) Additional immunostains reveal that the neoplastic cells are negative for pankeratin (**f**) and patchy positive for CD34 (**g**) and desmin (**h**), supporting a diagnosis of epithelioid myofibroblastoma

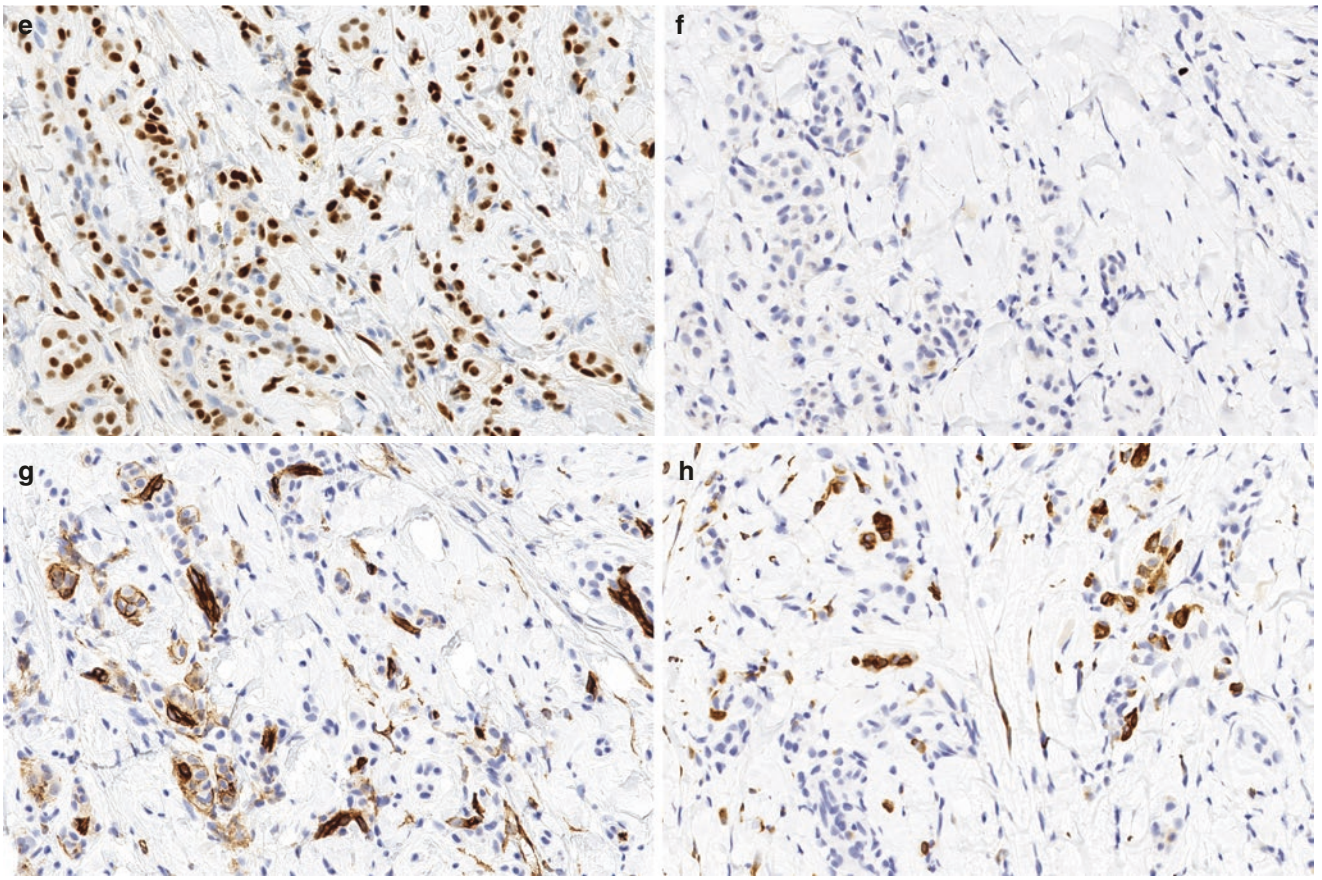

Fig. 15.26 (continued)

lymphoma) can be mistaken for ILC as both can grow as single cells, linear arrays, clusters, or solid sheets. Clues to the diagnosis of ILC include the presence of concurrent LCIS. Tumor cells in ILC also typically have more cytoplasm than in lymphoma and often demonstrate intracytoplasmic lumens (Figs. 15.5 and 15.8). IHC is helpful in challenging cases, as ILC is keratin positive and CD45 negative, whereas lymphoma shows the opposite staining pattern (Fig. 15.27). In the event one misdiagnoses a low-grade lymphoma as ILC on H&E stain, a negative ER immunostain should raise reconsideration of the diagnosis. This is particularly important in a core biopsy, as the management of these two neoplasms is markedly different.

ILC can also mimic other inflammatory processes. Extramedullary hematopoiesis can be seen in the breast, particularly following neoadjuvant chemotherapy, as a single-cell infiltrate of hematopoietic cells that closely resembles classic ILC at low power [135]. Myeloid differentiation can be confirmed through absent keratin immunoreactivity and positive staining for myeloperoxidase (Fig. 15.28). Similarly, infiltrates of lymphocytes or plasma cells can mimic ILC at low power. Finally, ILC with histiocytoid features is often ER weakly positive or negative and morphologically can be confused with histiocytes. Immunostains for keratin and CD68 will confirm the diagnosis (Fig. 15.11).

Granular cell tumor: This benign tumor of Schwann cell origin may show an infiltrative growth pattern as solid nests or cords of tumor cells with bland, vesicular nuclei and abundant coarsely granular, eosinophilic cytoplasm that can mimic ILC with histiocytoid or apocrine features. Granular cell tumors are keratin negative and positive for S-100 protein and CD68 (see Chap. 12).

Metastatic melanoma: Melanoma is one of the most common tumor types to metastasize to the breast and may present with an occult primary or a remote clinical history of melanoma. The tumor cells are dyscohesive and often grow in sheets or solid nests, imparting an appearance akin to solid- or alveolar-pattern ILC (Fig. 15.29). The diagnosis can be especially challenging on fine needle aspiration biopsy. Melanoma should be considered if the tumor cells are negative for hormone receptors and LCIS is absent. Other histologic features favoring melanoma include intranuclear inclusions, spindle cells, and melanin pigment, though this feature is rarely present [136]. Immunostains for melanoma

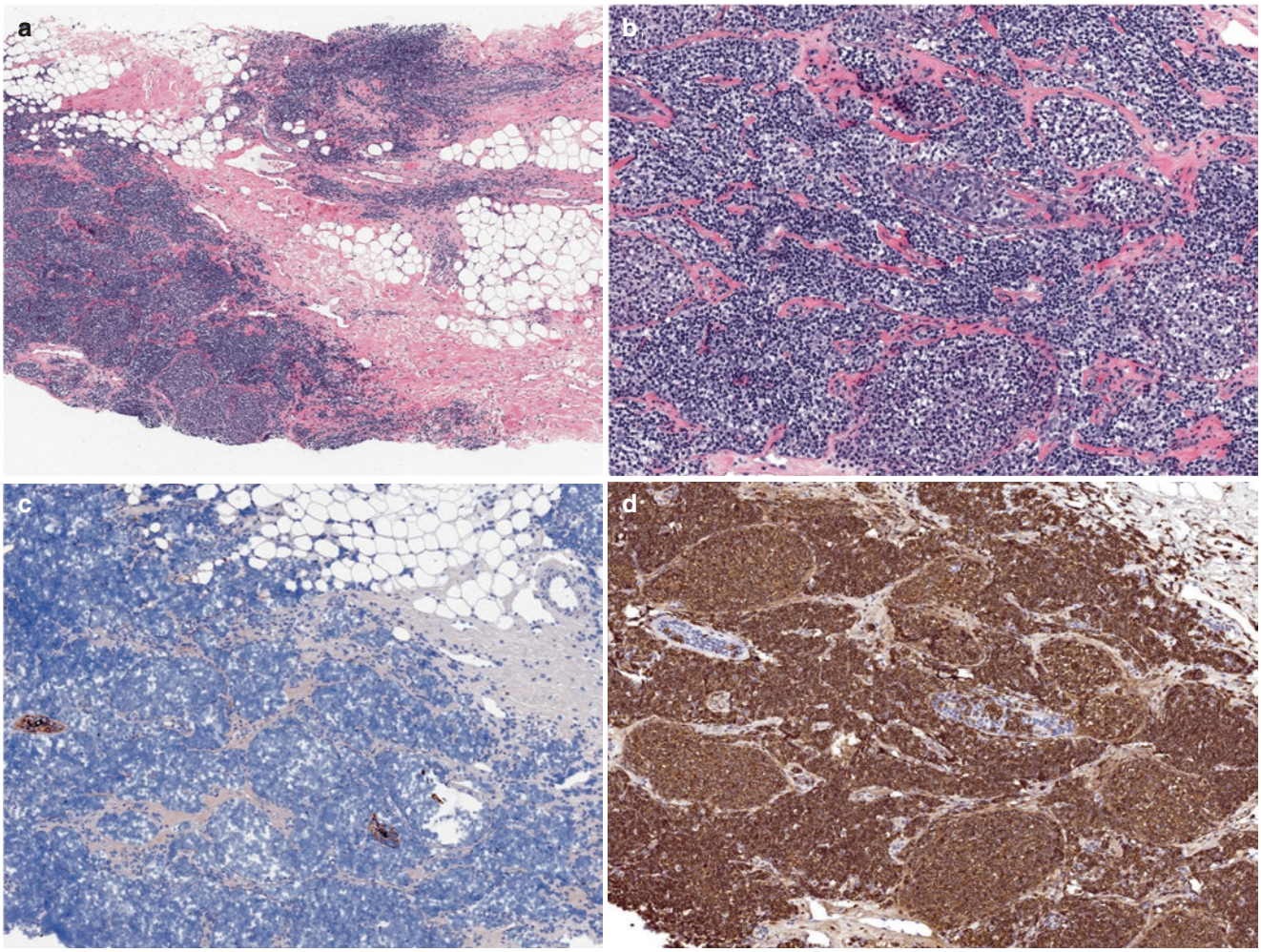

Fig. 15.27 Primary breast lymphoma. (**a, b**) H&E stain of a core biopsy at low and high power shows diffuse infiltration of breast tissue by small- to medium-sized, dyscohesive cells. (**c**) A keratin immunostain is negative in the tumor cells. (**d**) CD45 shows diffuse immunoreactivity

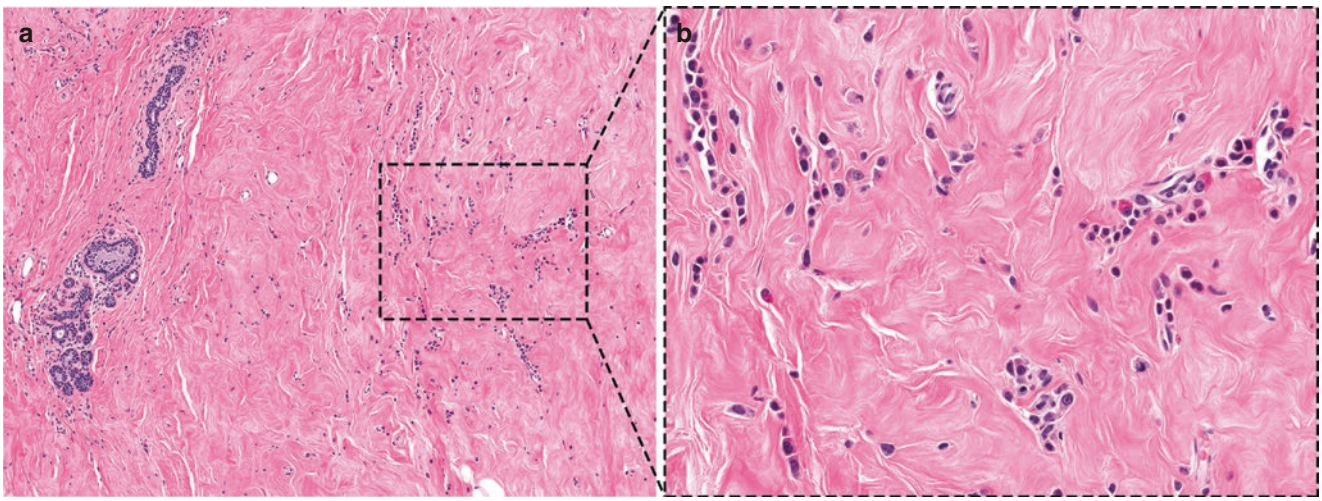

Fig. 15.28 Extramedullary hematopoiesis. (**a, b**) This breast excision specimen following neoadjuvant chemotherapy showed a small focus of epithelioid cells growing singly and in linear arrays, resembling ILC. (**c, d**) Immunohistochemical stains in this focus were negative for pan-keratin (**c**) and positive for myeloperoxidase (**d**)

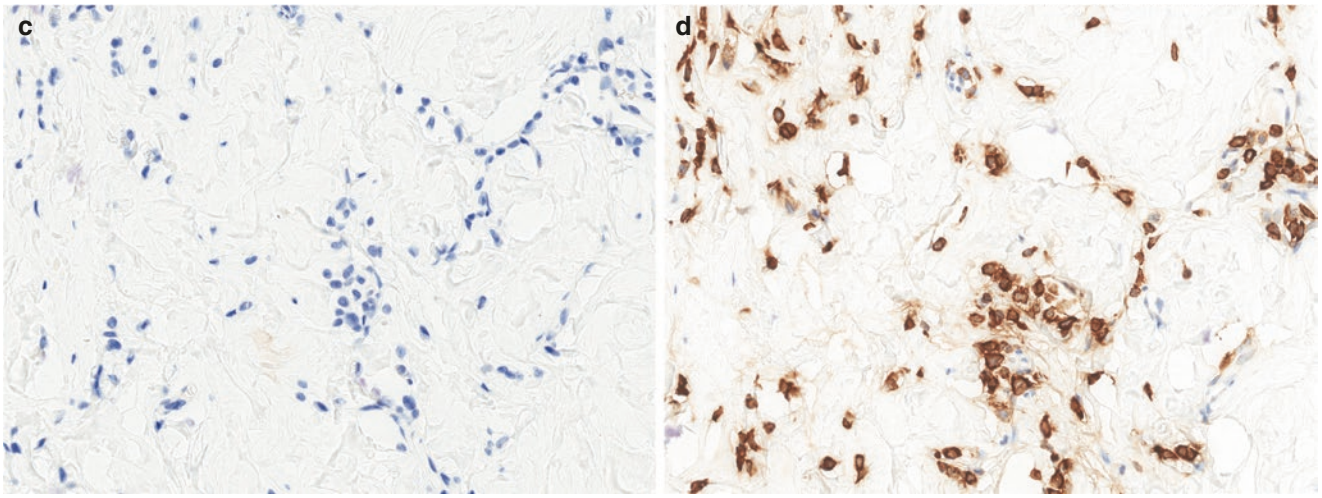

Fig. 15.28 (continued)

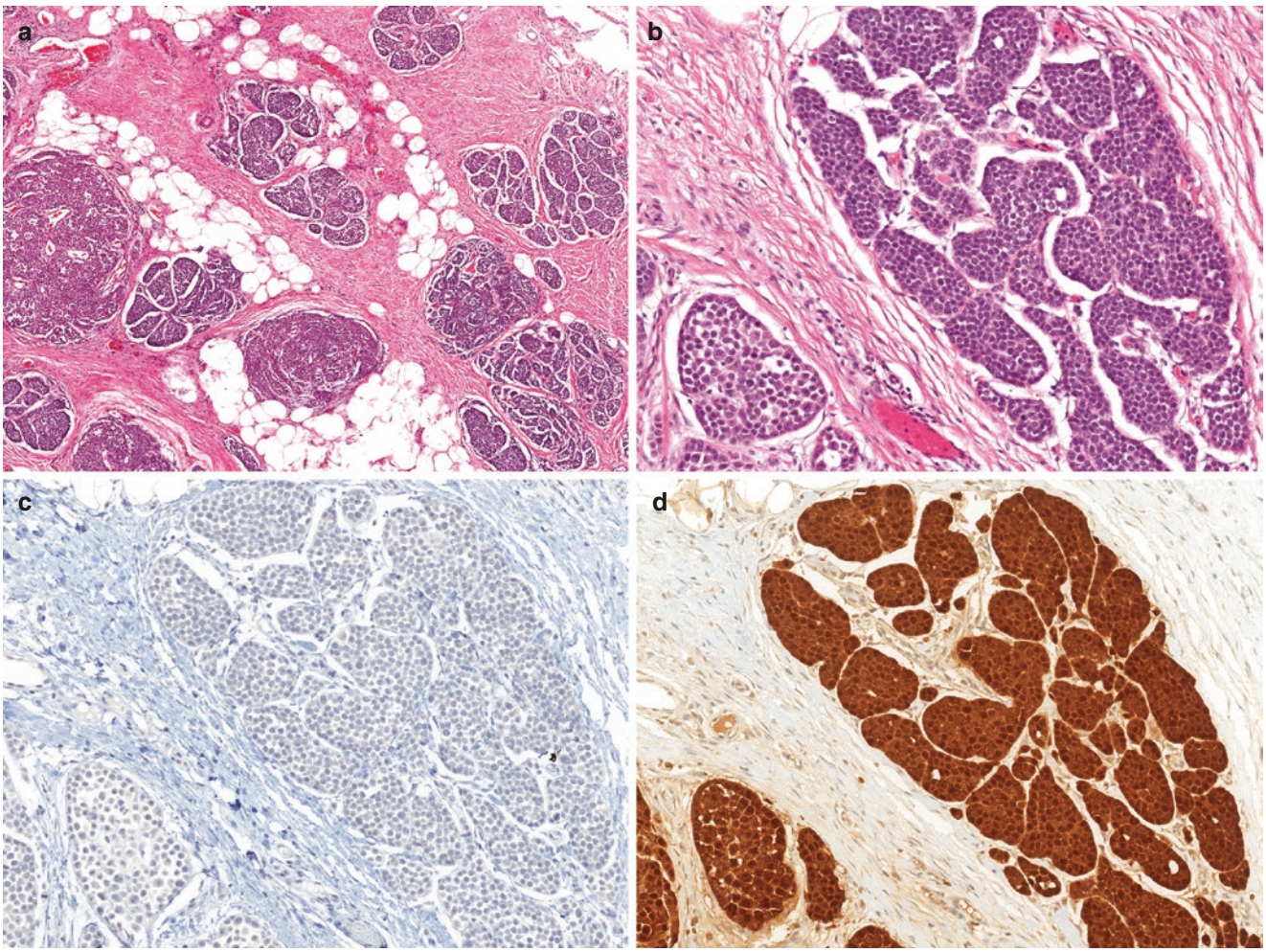

Fig. 15.29 Metastatic melanoma to the axilla. (**a**) H&E stain at low power shows a malignant neoplasm infiltrating fibroadipose tissue as solid nests of epithelioid cells arranged in a lobular pattern, mimicking the alveolar pattern of ILC. (**b**) Higher power reveals dyscohesive tumor cells with relatively uniform round, intermediate-grade nuclei. (**c–e**) Immunohistochemical stains are negative for pankeratin (**c**) and positive for the melanoma markers S100 protein (**d**) and HMB-45 (**e**). (**f**) Focally, the tumor cells showed more nuclear atypia with rare nuclear pseudoinclusions (yellow arrowhead)

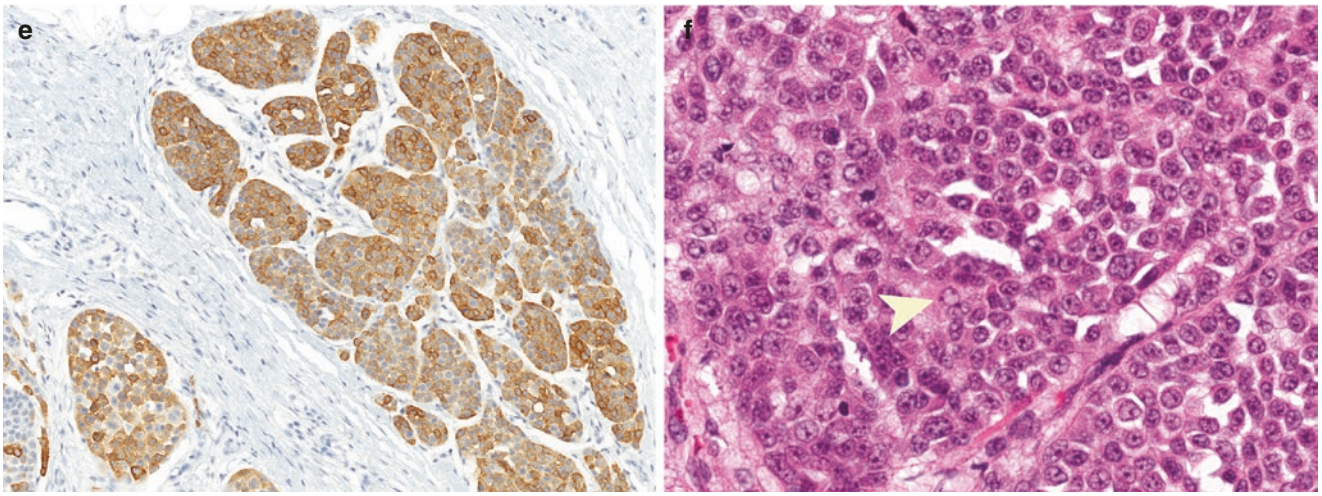

Fig. 15.29 (continued)

markers (Melan-A, HMB-45, and S100) can be used in conjunction with keratin and GATA3 to distinguish between these two entities.

Metastatic ILC versus other primaries: ILC with signet ring cell features appears identical to diffuse-type gastric adenocarcinoma, both of which are E-cadherin negative. Individuals with germline *CDH1* mutations are at increased risk for both types of carcinoma [137, 138]. ILC may metastasize to the stomach (Fig. 15.30), including in the setting of an occult primary; however, gastric adenocarcinomas rarely metastasize to the breast. In such cases, IHC is useful to determine the site of origin. ILC tends to be ER, GATA3, GCDFP-15, and mammaglobin positive, whereas gastric adenocarcinoma is usually negative [139–141]. In contrast, CDX-2 and CK20 are relatively sensitive and specific for gastrointestinal origin [141].

In the metastatic setting, GATA3 has the highest sensitivity for breast origin (100% of ILC compared to 92–96% of IDC) but is not entirely specific [142]. The sensitivity of mammaglobin and GCDFP-15 is based less on ductal versus lobular differentiation and more on grade, ER, and HER2 expression. Lewis et al. found that ER-positive/HER2-negative tumors expressed GCDFP-15 and mammaglobin more frequently than basal-like and triple-negative breast cancers (65% versus 5%, and 82% versus 25%, respectively) [143]. Since most classic ILC are low grade, ER positive, and HER2 negative, they are more likely to be positive for these markers than IBC-NST [144].

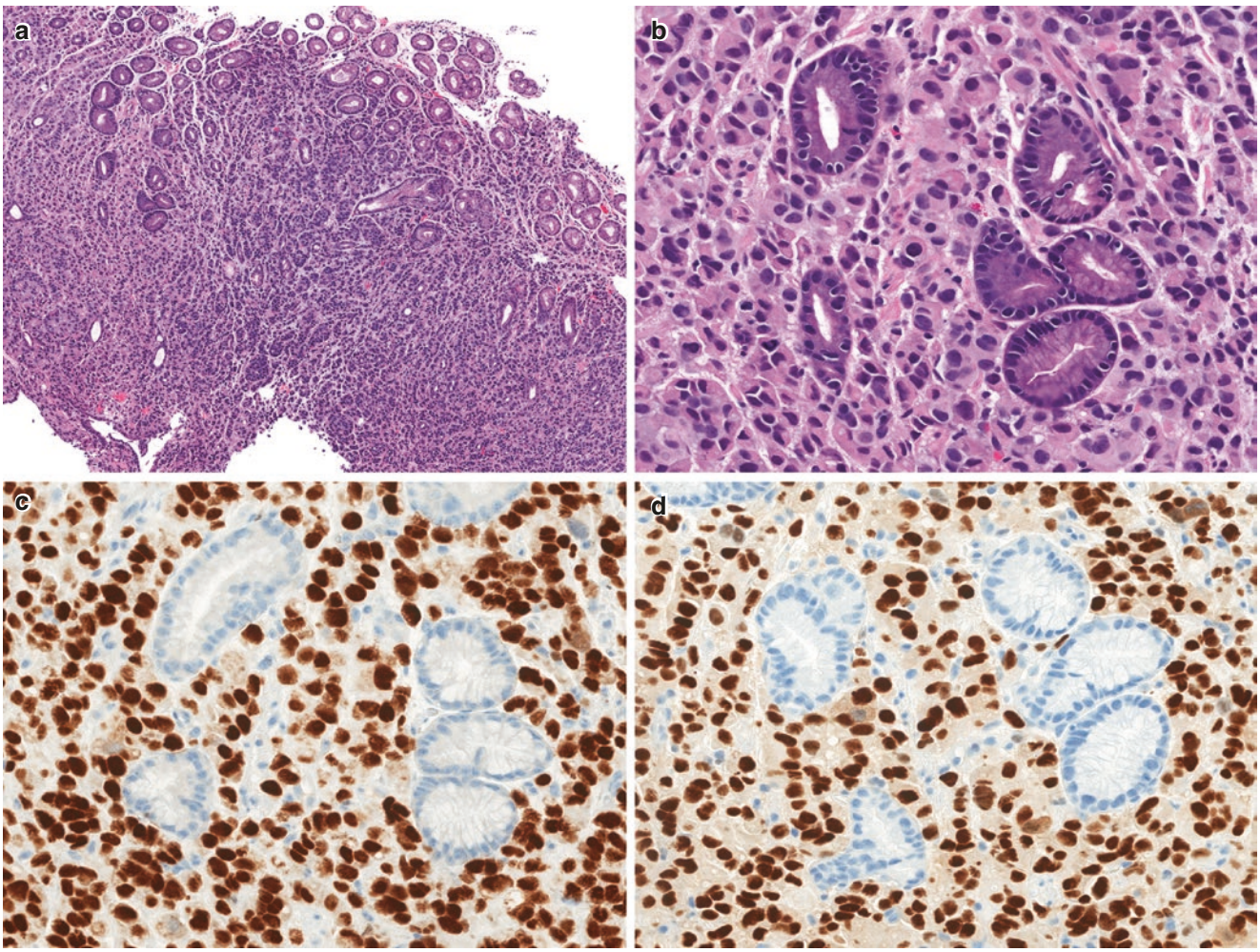

Fig. 15.30 Metastatic ILC to the stomach. (**a, b**) H&E stain of a gastric mucosal biopsy at low and high power demonstrates diffuse involvement by a carcinoma infiltrating as single cells and linear arrays. (**c, d**) The tumor cells are diffusely positive for GATA3 (**c**) and ER (**d**)

Pathogenesis

E-cadherin was originally discovered by Rolf Kemler et al. in 1977 [145] and is encoded by the *CDH1* gene. ILC is defined by dysfunction of the E-cadherin-catenin complex, the majority due to inactivating *CDH1* mutations combined with loss of heterozygosity of the wild-type allele at 16q22.1 [146]. Most *CDH1* mutations are truncating, but missense and splice-site mutations have been observed and may be more prone to result in aberrant E-cadherin expression [147]. Although *CDH1* mutation is pathognomonic for ILC, the wide range of reported mutation frequencies (43–82%) may be due to variability in sensitivity across sequencing platforms (whole genome, exome, targeted panel) combined with low tumor cellularity due to the diffuse infiltrative tumor growth pattern [148–151]. *E-cadherin* downregulation via promoter hypermethylation is also possible, though its role remains controversial [148, 152].

In addition to *CDH1*, over half of ILC show activation of the phosphatidylinositol 3-kinase (PI3K) pathway via activating mutations in *PIK3CA* (~40% of cases) or the downstream kinase *AKT1*, or via homozygous deletions or mutations in *PTEN* [148–150]. Mutations in these three genes are typically mutually exclusive. Compared to luminal A-matched IBC-NST, ILC harbor more frequent mutations in *CDH1*, *PTEN*, *TBX3*, and *FOXA1* and fewer mutations in *GATA3* [148]. Common copy number alterations include loss of 16q (~90% of cases), gain of 1q, and focal amplifications of 11q13 (*CCND1* locus), 8q24 (*MYC* locus), 8p11 (*FGFR1* locus), and 6q25 (*ESR1*) [150].

A number of studies have demonstrated that *ERBB2* mutations are more frequent in primary ILC compared to IBC-NST and are enriched in the setting of recurrence and metastasis [151, 153–156]. Pleomorphic LCIS and ILC also show a higher frequency of *ERBB2* and *ERBB3* alterations than classic LCIS and ILC [147, 150, 157]. These alterations

include both amplifications (*ERRB2*) and activating oncogenic mutations (*ERBB2* and *ERBB3*), predominantly within the tyrosine kinase domain of the respective genes. Notably, activating mutations in *ERBB2* enhance tyrosine kinase activity but do not result in overexpression of the mutant ERBB2 protein [158]. As most *ERBB2*-mutated tumors do not show concurrent amplification, these cases are not detected by routine HER2 IHC or FISH, raising consideration for whether a subset of ILC patients would benefit from *ERBB2* mutation testing [155]. Though associated with worse 10-year overall survival, *ERBB2/ERBB3* mutations may provide new actionable targets amenable to HER-targeted therapies [153].

Limited analysis has been performed on genomic features associated with specific histologic variants of ILC. The solid variant of ILC is enriched in *TP53, ERBB2*, and *ARID1A* mutations, *ARID1A* deletions, and *ESR1* copy number gains; the alveolar subtype is more likely to harbor *CCND1* and *PAK1* gains; and pleomorphic ILC frequently shows mutations in *TP53, ERBB2, and ERBB3* [147, 150, 157]. Nevertheless, most tumors with variant morphology show mixed growth patterns, including some areas with classic appearance. Further studies that separately sequence different growth patterns within the same tumor may improve our understanding of the biology of these subtypes and better inform their classification.

Molecular subtyping has served as another means of tumor classification. By gene expression profiling, most classic ILC are classified as luminal A [159, 160]. In contrast, pleomorphic ILC are more commonly HER2 positive or molecular apocrine subtype [160, 161]. Rare triple-negative ILC may further represent a distinct subtype of more aggressive tumors associated with elderly patients and the luminal androgen receptor (AR) subtype of triple-negative breast cancer described by Lehmann et al. [162]. These tumors express AR but not basal markers and show recurrent hotspot mutations (53.8% of cases) in *estrogen-related receptor alpha (ESRRA)*, an orphan nuclear receptor with structural homology to the estrogen receptor α/β [163]. Despite being HR negative, these tumors show estrogen signaling pathway activation, suggesting that they may be sensitive to traditional endocrine therapy [163].

The role of mutational drivers in therapeutic resistance represents an important emerging area of research to guide clinical management of ILC. *ESR1* alterations have been associated with disease recurrence, hormone therapy resistance, and metastasis in ILC, akin to IBC-NST [164, 165]. However, relative to IBC-NST, metastatic ILC show enrichment for activating *ERRB2* mutations and *NF1* loss-of-function mutations, both of which are mutually exclusive with *ESR1* mutations and may represent a biologically distinct mechanism for endocrine therapy resistance [151, 156, 166]. Finally, though >90% of ILC have low genomic complexity and low tumor mutation burden (<10 mutations/Mb), a small subset of tumors show mutational signatures associated with (a) somatic hypermutation via APOBEC mutagenesis; (b) complex structural rearrangements in clustered sets of chromosomes; or (c) homologous recombination DNA repair deficiency [167]. Higher mutation burden is associated with higher grade, ER-negative and triple-negative status, *TP53* and *ERBB2* mutations, and histologic subtype (highest in the solid variant) [167]. Taken together, elucidating the impact of specific genomic alterations or mutational signatures on prognosis and therapeutic response will be important for defining molecular parameters to guide clinical management.

Prognosis and Clinical Management

Classic ILC has multiple favorable prognostic features, including low grade, HR positivity, and a low proliferation index. However, these are offset by larger tumor size, more advanced stage at presentation (stage III/IV), and older patient age compared to IBC-NST [13, 14, 168–170]. The rate of axillary lymph node metastasis in classic ILC and IBC-NST is similar [19, 23, 72, 171]; however, ILC exhibit a distinct pattern of distant metastasis. Compared to IBC-NST, ILC is more likely to metastasize to the gastrointestinal tract, uterus, ovary, peritoneum, meninges, and skin and less likely to the lungs [14, 16, 19, 171–181]. Both ILC and IBC-NST commonly metastasize to bone, with several studies demonstrating a statistically significant higher rate of bone metastasis in ILC versus IBC-NST [172, 177, 179].

Studies comparing outcomes between ILC and IBC-NST have variably reported a similar [14, 19, 24, 41, 48, 49, 170, 182–185] or a better [23, 38, 76, 168, 186] prognosis for ILC, but some of this variation may be due to the follow-up period. Two large series with longer follow-up demonstrated that ILC has a similar or better prognosis than IBC-NST in the first 10 years after diagnosis; however, in the long term, outcomes are worse, with an increased risk of late recurrence, distant metastasis, and death [16, 17]. Late recurrence of ILC is consistent with recurrence patterns of ER-positive tumors. While ER-negative tumors are more likely to recur within 5 years, half of ER-positive tumors recur after 5 years [187, 188], and latency periods of up to 20–25 years have been reported [189]. Nevertheless, Rakha et al. found that the risk of late recurrence in ILC was independent of ER status [17]. Interestingly, a recent study of Mexican breast cancer patients found that 5-year overall survival in triple-negative and HER2-positive ILC is significantly worse compared to triple-negative and HER2-positive IBC-NST [190], suggesting that these subgroups within ILC carry distinct prognoses and warrant different clinical management.

Histologic grading using the mSBR/Nottingham method is an independent predictor of outcome in ILC [99, 100, 102, 191–193]. Separate analysis of the three components of grade has revealed that mitotic activity has the most prognostic significance for recurrence-free survival and overall survival [99, 102, 191]. Most ILC are grade 2, and grade 3 tumors are predominantly of variant morphology [100]. Limited data suggest that different histologic subtypes confer different prognoses, with more favorable outcomes in classic, tubulolobular, and alveolar subtypes and worse outcomes in pleomorphic and solid variants [42, 167, 186, 194, 195]. Pleomorphic ILC presents at a more advanced stage than classic ILC and exhibits more aggressive clinical behavior, which parallels its morphology and immunophenotype [8, 81, 128, 196]. However, other studies have found that after adjusting for clinicopathologic factors, there is no difference in disease-free survival between pleomorphic ILC and matched classic ILC controls [127], or between pleomorphic ILC and IDC [128, 197]. Indeed, Rakha et al. found that classification as the pleomorphic subtype does not provide any additional prognostic information beyond histologic grading [102]. Similarly, Mukhtar et al. demonstrated that only mitotic score, receptor subtype, and pathologic stage, not pleomorphic histology, are independent predictors of disease-free survival [10].

Despite clear biological differences in mutational landscape and metastatic patterns, ILC is largely still managed akin to IBC-NST. Based on the guidelines from the American Society of Clinical Oncology, hormonal therapy is used in the neoadjuvant and adjuvant setting for ER-positive tumors up to 10 years after surgery, as extended therapy has been shown to improve survival and decrease the risk of recurrence and contralateral breast cancer [198]. Recently, more attention has been paid to assessing the magnitude of benefit from different endocrine therapies in ILC versus IDC. A retrospective analysis of patients with early-stage IDC or classic ILC in the Breast International Group (BIG) 1–98 trial compared the relative effectiveness of 5 years of adjuvant monotherapy with the aromatase inhibitor letrozole versus tamoxifen [199]. Patients with ILC showed a significant reduction in disease-free survival with letrozole compared to tamoxifen, whereas a benefit in favor of letrozole was only seen in the luminal B-like subset of IDC [199]. Molecular studies in ILC cell lines and xenografts also demonstrate that ER regulates a different set of genes in ILC versus IDC [200]. While these findings need to be validated in larger prospective cohorts, they highlight the need for clinical research design that allows for more informed and tailored therapeutic decisions for ILC patients.

Classic ILC shows a poor response to chemotherapy and is more often treated with mastectomy than breast-conserving therapy [16, 201, 202]. The rate of pathologic complete response (pCR) following neoadjuvant chemotherapy is 0–11% in ILC compared to 9–25% in IBC-NST [116, 202–205]. However, this difference can be explained by differences in molecular characteristics (HR and HER2 status), rather than lobular histology [205]. Higher grade and/or HR-negative ILC are more likely to respond to chemotherapy, with a pCR rate of 17.8% versus 4.2% in HR-positive and low/intermediate-grade ILC [203]. Of note, pleomorphic ILC is often conflated with grade 3 ILC and thus treated with chemotherapy more commonly than classic ILC; however, mitotic count, not nuclear pleomorphism, is predictive of chemotherapy benefit and should drive treatment decisions [10].

The advent of genomic data on ILC has now allowed for correlation between specific genetic alterations, prognosis, and response to targeted therapy. The presence of *TP53* mutations and *ERBB2* alterations (mutations and amplifications) is associated with worse prognosis in ILC patients but offers opportunities for additional treatment [153, 167]. Patients with *ERBB2*-amplified ILC benefit from adjuvant trastuzumab [206], and there is increasing interest in using HER-targeted agents for tumors with activating *ERBB2/ERBB3* mutations. Clinical trials to determine the benefit of anti-HER2 therapy for *ERBB2*-mutated tumors are ongoing (e.g., SUMMIT trial and mutHER trial). Notably, the most frequently observed *ERBB2* hotspot mutation in ILC, p.L755S, confers resistance to the HER2 inhibitor lapatinib but is sensitive to the irreversible small-molecule inhibitor neratinib [158, 207]. *ERBB3* mutations are less well studied but are thought to promote ligand-independent oncogenic signaling that is amenable to blockade by anti-ERBB antibodies and small-molecule inhibitors [208]. Given that some ILC harbor multiple co-occurring *ERBB2/ERBB3* alterations [150, 157], it will also be important to evaluate the role of combination therapy using agents with different mechanisms of action.

The clinical utility and cost-effectiveness of existing commercially available prognostic and predictive assays for ILC remain an ongoing area of study. Most molecular diagnostic tests have been developed from ER-positive IBC-NST and do not account for tumor histology in their algorithms. The highly utilized 21-gene Oncotype DX assay calculates a recurrence score (RS) that estimates both the risk of distant recurrence and the likelihood of benefit from chemotherapy in HR-positive, HER2-negative, early-stage breast cancer [209, 210]. A recent multivariate analysis from SEER data demonstrated that the Oncotype DX RS is an independent prognostic factor in patients with ILC [211]. Nevertheless, several groups have demonstrated that the RS distribution in ILC differs significantly from that of IBC-NST [212–215], with only 7–8% of ILC patients falling into the high RS category (>25) that supports a definite recommendation for chemotherapy and predicts worse 5-year breast cancer-specific mortality [213, 214, 216]. In turn, one

study has suggested that PR status and tumor grade could be valuable parameters for cost-effective Oncotype DX testing in ILC: PR-negative disease and high grade are independent predictors of a high RS, whereas only 3% and 6% of PR-positive/grade 1 and 2 tumors, respectively, fall into the high-risk cohort [217]. Other genomic companion diagnostic tests such as MammaPrint [218, 219] and Prosigna/PAM50 [220] have recently been shown to have prognostic value for ILC patients, but their predictive value regarding decisions about chemotherapy remains unclear. Notably, a recently described 194-metagene signature developed specifically for ILC (termed "LobSig") outperformed other diagnostic tests, including Oncotype DX and Prosigna, in prognosticating ILC patient outcome at 10 years, particularly in stratifying grade 2 tumors [221]. Only 14% of the LobSig gene set included proliferation genes, and high-risk tumors were enriched in *ERBB2*, *ERBB3*, *TP53*, *AKT1*, and *ROS1* mutations, reflecting the distinct genomic landscape of these tumors [221]. Further development and validation of such signatures are warranted in prospective cohorts yet remain challenging due to the often long latency period between diagnosis and recurrence. Nevertheless, the increasing interest in diagnostic and therapeutic approaches tailored to the unique clinicopathologic and molecular features of ILC combined with rapidly emerging targeted therapies raises exciting opportunities to advance care for these patients.

References

1. Rakha EA, Ellis IO. Lobular breast carcinoma and its variants. Semin Diagn Pathol. 2010;27:49–61. https://doi.org/10.1053/j.semdp.2009.12.009.
2. Hanby AM, Hughes TA. In situ and invasive lobular neoplasia of the breast. Histopathology. 2008;52:58–66. https://doi.org/10.1111/j.1365-2559.2007.02891.x.
3. Li CI, Anderson BO, Daling JR, Moe RE. Trends in incidence rates of invasive lobular and ductal breast carcinoma. JAMA. 2003;289:1421–4.
4. Moore MM, et al. Association of infiltrating lobular carcinoma with positive surgical margins after breast-conservation therapy. Ann Surg. 2000;231:877–82.
5. Foote FW, Stewart FW. Lobular carcinoma in situ: a rare form of mammary cancer. Am J Pathol. 1941;17:491–496.3.
6. Foote FW Jr, Stewart FW. A histologic classification of carcinoma of the breast. Surgery. 1946;19:74–99.
7. Dixon JM, Anderson TJ, Page DL, Lee D, Duffy SW. Infiltrating lobular carcinoma of the breast. Histopathology. 1982;6:149–61.
8. Buchanan CL, et al. Is pleomorphic lobular carcinoma really a distinct clinical entity? J Surg Oncol. 2008;98:314–7. https://doi.org/10.1002/jso.21121.
9. Harbhajanka A, et al. Correlation of clinicopathologic parameters and immunohistochemical features of triple-negative invasive lobular carcinoma. Appl Immunohistochem Mol Morphol. 2014;22:e18–26. https://doi.org/10.1097/PAI.0b013e3182a5a02d.
10. Mukhtar RA, et al. Mitotic score and pleomorphic histology in invasive lobular carcinoma of the breast: impact on disease-free survival. Breast Cancer Res Treat. 2020;181:23–9. https://doi.org/10.1007/s10549-020-05606-5.
11. Lien HC, Chen YL, Juang YL, Jeng YM. Frequent alterations of HER2 through mutation, amplification, or overexpression in pleomorphic lobular carcinoma of the breast. Breast Cancer Res Treat. 2015; https://doi.org/10.1007/s10549-015-3336-0.
12. McCart Reed AE, Kalinowski L, Simpson PT, Lakhani SR. Invasive lobular carcinoma of the breast: the increasing importance of this special subtype. Breast Cancer Res. 2021;23:6. https://doi.org/10.1186/s13058-020-01384-6.
13. Li CI, Uribe DJ, Daling JR. Clinical characteristics of different histologic types of breast cancer. Br J Cancer. 2005;93:1046–52. https://doi.org/10.1038/sj.bjc.6602787.
14. Arpino G, Bardou VJ, Clark GM, Elledge RM. Infiltrating lobular carcinoma of the breast: tumor characteristics and clinical outcome. Breast Cancer Res. 2004;6:R149–56. https://doi.org/10.1186/bcr767.
15. Gonzalez-Angulo AM, et al. Biologic markers in axillary node-negative breast cancer: differential expression in invasive ductal carcinoma versus invasive lobular carcinoma. Clin Breast Cancer. 2006;7:396–400. https://doi.org/10.3816/CBC.2006.n.056.
16. Pestalozzi BC, et al. Distinct clinical and prognostic features of infiltrating lobular carcinoma of the breast: combined results of 15 International Breast Cancer Study Group clinical trials. J Clin Oncol. 2008;26:3006–14. https://doi.org/10.1200/jco.2007.14.9336.
17. Rakha EA, et al. Invasive lobular carcinoma of the breast: response to hormonal therapy and outcomes. Eur J Cancer. 2008;44:73–83. https://doi.org/10.1016/j.ejca.2007.10.009.
18. Rosen PP, et al. A comparative study of some pathologic features of mammary carcinoma in Tokyo, Japan and New York, USA. Cancer. 1977;39:429–34.
19. Sastre-Garau X, et al. Infiltrating lobular carcinoma of the breast. Clinicopathologic analysis of 975 cases with reference to data on conservative therapy and metastatic patterns. Cancer. 1996;77:113–20. https://doi.org/10.1002/(SICI)1097-0142(19960101)77:1<113::AID-CNCR19>3.0.CO;2-8.
20. Yeatman TJ, et al. Tumor biology of infiltrating lobular carcinoma. Implications for management. Ann Surg. 1995;222:549–59.; discussion 559-561.
21. Martinez V, Azzopardi JG. Invasive lobular carcinoma of the breast: incidence and variants. Histopathology. 1979;3:467–88.
22. Ellis IO, et al. Pathological prognostic factors in breast cancer. II. Histological type. Relationship with survival in a large study with long-term follow-up. Histopathology. 1992;20:479–89.
23. Toikkanen S, Pylkkanen L, Joensuu H. Invasive lobular carcinoma of the breast has better short- and long-term survival than invasive ductal carcinoma. Br J Cancer. 1997;76:1234–40.
24. Biglia N, et al. Clinical-pathologic features, long term-outcome and surgical treatment in a large series of patients with invasive lobular carcinoma (ILC) and invasive ductal carcinoma (IDC). Eur J Surg Oncol. 2013;39:455–60. https://doi.org/10.1016/j.ejso.2013.02.007.
25. Dossus L, Benusiglio PR. Lobular breast cancer: incidence and genetic and non-genetic risk factors. Breast Cancer Res. 2015;17:37. https://doi.org/10.1186/s13058-015-0546-7.
26. Corso G, Intra M, Trentin C, Veronesi P, Galimberti V. CDH1 germline mutations and hereditary lobular breast cancer. Familial Cancer. 2016;15:215–9. https://doi.org/10.1007/s10689-016-9869-5.
27. Li CI, et al. Changing incidence rate of invasive lobular breast carcinoma among older women. Cancer. 2000;88:2561–9.
28. Daling JR, et al. Relation of regimens of combined hormone replacement therapy to lobular, ductal, and other histologic types of breast carcinoma. Cancer. 2002;95:2455–64. https://doi.org/10.1002/cncr.10984.

29. Reeves GK, Beral V, Green J, Gathani T, Bull D. Hormonal therapy for menopause and breast-cancer risk by histological type: a cohort study and meta-analysis. Lancet Oncol. 2006;7:910–8. https://doi.org/10.1016/s1470-2045(06)70911-1.
30. Li CI, et al. Alcohol consumption and risk of postmenopausal breast cancer by subtype: the women's health initiative observational study. J Natl Cancer Inst. 2010;102:1422–31. https://doi.org/10.1093/jnci/djq316.
31. Eheman CR, et al. The changing incidence of in situ and invasive ductal and lobular breast carcinomas: United States, 1999-2004. Cancer Epidemiol Biomark Prev. 2009;18:1763–9. https://doi.org/10.1158/1055-9965.epi-08-1082.
32. Rossouw JE, et al. Risks and benefits of estrogen plus progestin in healthy postmenopausal women: principal results From the Women's Health Initiative randomized controlled trial. JAMA. 2002;288:321–33.
33. Jemal A, Ward E, Thun MJ. Recent trends in breast cancer incidence rates by age and tumor characteristics among U.S. women. Breast Cancer Res. 2007;9:R28. https://doi.org/10.1186/bcr1672.
34. Li CI, Daling JR. Changes in breast cancer incidence rates in the United States by histologic subtype and race/ethnicity, 1995 to 2004. Cancer Epidemiol Biomark Prev. 2007;16:2773–80. https://doi.org/10.1158/1055-9965.epi-07-0546.
35. Danforth DN Jr. Disparities in breast cancer outcomes between Caucasian and African American women: a model for describing the relationship of biological and nonbiological factors. Breast Cancer Res. 2013;15:208. https://doi.org/10.1186/bcr3429.
36. Fu L, Tsuchiya S, Matsuyama I, Ishii K. Clinicopathologic features and incidence of invasive lobular carcinoma in Japanese women. Pathol Int. 1998;48:348–54.
37. Lee JH, Park S, Park HS, Park BW. Clinicopathological features of infiltrating lobular carcinomas comparing with infiltrating ductal carcinomas: a case control study. World J Surg Oncol. 2010;8:34. https://doi.org/10.1186/1477-7819-8-34.
38. Wasif N, Maggard MA, Ko CY, Giuliano AE. Invasive lobular vs. ductal breast cancer: a stage-matched comparison of outcomes. Ann Surg Oncol. 2010;17:1862–9. https://doi.org/10.1245/s10434-010-0953-z.
39. Lynch SP, et al. Multifocality and multicentricity in breast cancer and survival outcomes. Ann Oncol. 2012;23:3063–9. https://doi.org/10.1093/annonc/mds136.
40. Le Gal M, et al. Mammographic features of 455 invasive lobular carcinomas. Radiology. 1992;185:705–8. https://doi.org/10.1148/radiology.185.3.1438749.
41. Fortunato L, et al. Lobular breast cancer: same survival and local control compared with ductal cancer, but should both be treated the same way? analysis of an institutional database over a 10-year period. Ann Surg Oncol. 2012;19:1107–14. https://doi.org/10.1245/s10434-011-1907-9.
42. Orvieto E, et al. Clinicopathologic characteristics of invasive lobular carcinoma of the breast: results of an analysis of 530 cases from a single institution. Cancer. 2008;113:1511–20. https://doi.org/10.1002/cncr.23811.
43. Ashikari R, Huvos AG, Urban JA, Robbins GF. Infiltrating lobular carcinoma of the breast. Cancer. 1973;31:110–6.
44. Fechner RE. Infiltrating lobular carcinoma without lobular carcinoma in situ. Cancer. 1972;29:1539–45. https://doi.org/10.1002/1097-0142(197206)29:6<1539::aid-cncr2820290618>3.0.co;2-p.
45. Kollias J, Ellis IO, Elston CW, Blamey RW. Clinical and histological predictors of contralateral breast cancer. Eur J Surg Oncol. 1999;25:584–9. https://doi.org/10.1053/ejso.1999.0711.
46. Baker RR, Kuhajda FP. The clinical management of a normal contralateral breast in patients with lobular breast cancer. Ann Surg. 1989;210:444–7.; discussion 447-448.
47. Yeatman TJ, et al. Bilaterality and recurrence rates for lobular breast cancer: considerations for treatment. Ann Surg Oncol. 1997;4:198–202.
48. Korhonen T, Huhtala H, Holli K. A comparison of the biological and clinical features of invasive lobular and ductal carcinomas of the breast. Breast Cancer Res Treat. 2004;85:23–9. https://doi.org/10.1023/B:BREA.0000021038.97593.8b.
49. Santiago RJ, Harris EE, Qin L, Hwang WT, Solin LJ. Similar long-term results of breast-conservation treatment for Stage I and II invasive lobular carcinoma compared with invasive ductal carcinoma of the breast: The University of Pennsylvania experience. Cancer. 2005;103:2447–54. https://doi.org/10.1002/cncr.21071.
50. Krecke KN, Gisvold JJ. Invasive lobular carcinoma of the breast: mammographic findings and extent of disease at diagnosis in 184 patients. AJR Am J Roentgenol. 1993;161:957–60. https://doi.org/10.2214/ajr.161.5.8273634.
51. Albayrak ZK, Onay HK, Karatag GY, Karatag O. Invasive lobular carcinoma of the breast: mammographic and sonographic evaluation. Diagn Interv Radiol. 2011;17:232–8. https://doi.org/10.4261/1305-3825.dir.598-06.3.
52. Boetes C, et al. Breast tumors: comparative accuracy of MR imaging relative to mammography and US for demonstrating extent. Radiology. 1995;197:743–7. https://doi.org/10.1148/radiology.197.3.7480749.
53. Hilleren DJ, Andersson IT, Lindholm K, Linnell FS. Invasive lobular carcinoma: mammographic findings in a 10-year experience. Radiology. 1991;178:149–54. https://doi.org/10.1148/radiology.178.1.1984294.
54. Mendelson EB, Harris KM, Doshi N, Tobon H. Infiltrating lobular carcinoma: mammographic patterns with pathologic correlation. AJR Am J Roentgenol. 1989;153:265–71. https://doi.org/10.2214/ajr.153.2.265.
55. Selinko VL, Middleton LP, Dempsey PJ. Role of sonography in diagnosing and staging invasive lobular carcinoma. J Clin Ultrasound. 2004;32:323–32. https://doi.org/10.1002/jcu.20052.
56. Watermann DO, Tempfer C, Hefler LA, Parat C, Stickeler E. Ultrasound morphology of invasive lobular breast cancer is different compared with other types of breast cancer. Ultrasound Med Biol. 2005;31:167–74. https://doi.org/10.1016/j.ultrasmedbio.2004.11.005.
57. Butler RS, et al. Sonographic evaluation of infiltrating lobular carcinoma. AJR Am J Roentgenol. 1999;172:325–30. https://doi.org/10.2214/ajr.172.2.9930776.
58. Berg WA, et al. Diagnostic accuracy of mammography, clinical examination, US, and MR imaging in preoperative assessment of breast cancer. Radiology. 2004;233:830–49. https://doi.org/10.1148/radiol.2333031484.
59. Rissanen T, Tikkakoski T, Autio AL, Apaja-Sarkkinen M. Ultrasonography of invasive lobular breast carcinoma. Acta Radiol. 1998;39:285–91. https://doi.org/10.1080/02841859809172196.
60. Pritt B, Ashikaga T, Oppenheimer RG, Weaver DL. Influence of breast cancer histology on the relationship between ultrasound and pathology tumor size measurements. Mod Pathol. 2004;17:905–10.
61. Gruber IV, et al. Measurement of tumour size with mammography, sonography and magnetic resonance imaging as compared to histological tumour size in primary breast cancer. BMC Cancer. 2013;13:328. https://doi.org/10.1186/1471-2407-13-328.
62. Boetes C, et al. The role of MRI in invasive lobular carcinoma. Breast Cancer Res Treat. 2004;86:31–7. https://doi.org/10.1023/B:BREA.0000032921.10481.dc.
63. Qayyum A, et al. MR imaging features of infiltrating lobular carcinoma of the breast. Am J Roentgenol. 2002;178:1227–32. https://doi.org/10.2214/ajr.178.5.1781227.

64. Schelfout K, et al. Preoperative breast MRI in patients with invasive lobular breast cancer. Eur Radiol. 2004;14:1209–16. https://doi.org/10.1007/s00330-004-2275-7.
65. Mann RM, et al. The value of MRI compared to mammography in the assessment of tumour extent in invasive lobular carcinoma of the breast. Eur J Surg Oncol. 2008;34:135–42. https://doi.org/10.1016/j.ejso.2007.04.020.
66. Munot K, et al. Role of magnetic resonance imaging in the diagnosis and single-stage surgical resection of invasive lobular carcinoma of the breast. Br J Surg. 2002;89:1296–301. https://doi.org/10.1046/j.1365-2168.2002.02208.x.
67. Rodenko GN, et al. MR imaging in the management before surgery of lobular carcinoma of the breast: correlation with pathology. AJR Am J Roentgenol. 1996;167:1415–9. https://doi.org/10.2214/ajr.167.6.8956569.
68. Caramella T, et al. Value of MRI in the surgical planning of invasive lobular breast carcinoma: a prospective and a retrospective study of 57 cases: comparison with physical examination, conventional imaging, and histology. Clin Imaging. 2007;31:155–61. https://doi.org/10.1016/j.clinimag.2007.01.001.
69. Mann RM, Kuhl CK, Kinkel K, Boetes C. Breast MRI: guidelines from the European Society of Breast Imaging. Eur Radiol. 2008;18:1307–18. https://doi.org/10.1007/s00330-008-0863-7.
70. Jung HN, Shin JH, Han BK, Ko EY, Cho EY. Are the imaging features of the pleomorphic variant of invasive lobular carcinoma different from classic ILC of the breast? Breast. 2013;22:324–9. https://doi.org/10.1016/j.breast.2012.07.016.
71. Yeap PM, Evans A, Purdie CA, Jordan LB, Vinnicombe SJ. A comparison of the imaging features of pleomorphic and classical invasive lobular carcinoma. Breast Cancer Res Treat. 2018;172:381–9. https://doi.org/10.1007/s10549-018-4914-8.
72. Silverstein MJ, et al. Infiltrating lobular carcinoma. Is it different from infiltrating duct carcinoma? Cancer. 1994;73:1673–7. https://doi.org/10.1002/1097-0142(19940315)73:6<1673::aid-cncr2820730620>3.0.co;2-b.
73. Moatamed NA, Apple SK. Extensive sampling changes T-staging of infiltrating lobular carcinoma of breast: a comparative study of gross versus microscopic tumor sizes. Breast J. 2006;12:511–7. https://doi.org/10.1111/j.1524-4741.2006.00338.x.
74. Fernandez B, et al. Lymph-node metastases in invasive lobular carcinoma are different from those in ductal carcinoma of the breast. J Clin Pathol. 2011;64:995–1000. https://doi.org/10.1136/jclinpath-2011-200151.
75. Abdel-Fatah TM, et al. High frequency of coexistence of columnar cell lesions, lobular neoplasia, and low grade ductal carcinoma in situ with invasive tubular carcinoma and invasive lobular carcinoma. Am J Surg Pathol. 2007;31:417–26. https://doi.org/10.1097/01.pas.0000213368.41251.b9.
76. DiCostanzo D, Rosen PP, Gareen I, Franklin S, Lesser M. Prognosis in infiltrating lobular carcinoma. An analysis of "classical" and variant tumors. Am J Surg Pathol. 1990;14:12–23.
77. Newman W. Lobular carcinoma of the female breast. Report of 73 cases. Ann Surg. 1966;164:305–14.
78. Quincey C, Raitt N, Bell J, Ellis IO. Intracytoplasmic lumina--a useful diagnostic feature of adenocarcinomas. Histopathology. 1991;19:83–7. https://doi.org/10.1111/j.1365-2559.1991.tb00898.x.
79. Page DL, Anderson TJ. Diagnostic histopathology of the breast. Edinburgh: Churchill Livingstone; 1987.
80. Eusebi V, Magalhaes F, Azzopardi JG. Pleomorphic lobular carcinoma of the breast: an aggressive tumor showing apocrine differentiation. Hum Pathol. 1992;23:655–62.
81. Weidner N, Semple JP. Pleomorphic variant of invasive lobular carcinoma of the breast. Hum Pathol. 1992;23:1167–71.
82. Middleton LP, et al. Pleomorphic lobular carcinoma: morphology, immunohistochemistry, and molecular analysis. Am J Surg Pathol. 2000;24:1650–6.
83. Fechner RE. Histologic variants of infiltrating lobular carcinoma of the breast. Hum Pathol. 1975;6:373–8.
84. Tan PH, Harada O, Thike AA, Tse GM. Histiocytoid breast carcinoma: an enigmatic lobular entity. J Clin Pathol. 2011;64:654–9. https://doi.org/10.1136/jcp.2011.088930.
85. Hood CI, Font RL, Zimmerman LE. Metastatic mammary carcinoma in the eyelid with histiocytoid appearance. Cancer. 1973;31:793–800. https://doi.org/10.1002/1097-0142(197304)31:4<793::aid-cncr2820310406>3.0.co;2-a.
86. Steinbrecher JS, Silverberg SG. Signet-ring cell carcinoma of the breast. The mucinous variant of infiltrating lobular carcinoma? Cancer. 1976;37:828–40. https://doi.org/10.1002/1097-0142(197602)37:2<828::aid-cncr2820370231>3.0.co;2-n.
87. Rosa M, Mohammadi A, Masood S. Lobular carcinoma of the breast with extracellular mucin: new variant of mucin-producing carcinomas? Pathol Int. 2009;59:405–9. https://doi.org/10.1111/j.1440-1827.2009.02385.x.
88. Singh K, DiazGomez B, Wang Y, Ou J, Hansen K. Invasive lobular carcinoma with extracellular mucin: not all mucinous mammary carcinomas are ductal! Int J Surg Pathol. 2019;27:55–8. https://doi.org/10.1177/1066896918788660.
89. Cserni G, et al. Invasive lobular carcinoma with extracellular mucin production-a novel pattern of lobular carcinomas of the breast. Clinico-pathological description of eight cases. Virchows Arch. 2017;471:3–12. https://doi.org/10.1007/s00428-017-2147-6.
90. Fisher ER, Gregorio RM, Redmond C, Fisher B. Tubulolobular invasive breast cancer: a variant of lobular invasive cancer. Hum Pathol. 1977;8:679–83.
91. Wheeler DT, Tai LH, Bratthauer GL, Waldner DL, Tavassoli FA. Tubulolobular carcinoma of the breast: an analysis of 27 cases of a tumor with a hybrid morphology and immunoprofile. Am J Surg Pathol. 2004;28:1587–93.
92. Esposito NN, Chivukula M, Dabbs DJ. The ductal phenotypic expression of the E-cadherin/catenin complex in tubulolobular carcinoma of the breast: an immunohistochemical and clinicopathologic study. Mod Pathol. 2007;20:130–8. https://doi.org/10.1038/modpathol.3800721.
93. Kuroda H, et al. Expression of E-cadherin, alpha-catenin, and beta-catenin in tubulolobular carcinoma of the breast. Virchows Arch. 2006;448:500–5. https://doi.org/10.1007/s00428-005-0096-y.
94. Christgen M, et al. E-cadherin to P-cadherin switching in lobular breast cancer with tubular elements. Mod Pathol. 2020;33:2483–98. https://doi.org/10.1038/s41379-020-0591-3.
95. McCart Reed AE, et al. Mixed ductal-lobular carcinomas: evidence for progression from ductal to lobular morphology. J Pathol. 2018;244:460–8. https://doi.org/10.1002/path.5040.
96. Qureshi HS, Linden MD, Divine G, Raju UB. E-cadherin status in breast cancer correlates with histologic type but does not correlate with established prognostic parameters. Am J Clin Pathol. 2006;125:377–85.
97. Shin SJ, Desmedt C, Kristiansen G, Ries-Filho JS, Sasano H. Invasive lobular carcinoma. In: WHO Classification of Tumours Editorial Board, editors. WHO Classification of Breast Tumours, 5th edition. Lyon, France: International Agency for Research on Cancer (IARC); 2019. p. 114–8.
98. Schnitt SJ, Brogi E, Chen YY, King TA, Lakhani SR. American registry of pathology expert opinions: the spectrum of lobular carcinoma in situ: diagnostic features and clinical implications. Ann Diagn Pathol. 2020;45:151481. https://doi.org/10.1016/j.anndiagpath.2020.151481.
99. Rakha EA, et al. Histologic grading is an independent prognostic factor in invasive lobular carcinoma of the breast. Breast Cancer Res Treat. 2008;111:121–7. https://doi.org/10.1007/s10549-007-9768-4.

100. Talman ML, Jensen MB, Rank F. Invasive lobular breast cancer. Prognostic significance of histological malignancy grading. Acta Oncol. 2007;46:803–9. https://doi.org/10.1080/02841860601137397.
101. Engstrom MJ, Opdahl S, Vatten LJ, Haugen OA, Bofin AM. Invasive lobular breast cancer: the prognostic impact of histopathological grade, E-cadherin and molecular subtypes. Histopathology. 2015;66:409–19. https://doi.org/10.1111/his.12572.
102. Rakha EA, et al. Pleomorphic lobular carcinoma of the breast: is it a prognostically significant pathological subtype independent of histological grade? Mod Pathol. 2013;26:496–501. https://doi.org/10.1038/modpathol.2012.197.
103. Tille JC, et al. Tumor-infiltrating lymphocytes are associated with poor prognosis in invasive lobular breast carcinoma. Mod Pathol. 2020;33:2198–207. https://doi.org/10.1038/s41379-020-0561-9.
104. Desmedt C, et al. Immune infiltration in invasive lobular breast cancer. J Natl Cancer Inst. 2018;110:768–76. https://doi.org/10.1093/jnci/djx268.
105. Gamallo C, et al. Correlation of E-cadherin expression with differentiation grade and histological type in breast carcinoma. Am J Pathol. 1993;142:987–93.
106. Moll R, Mitze M, Frixen UH, Birchmeier W. Differential loss of E-cadherin expression in infiltrating ductal and lobular breast carcinomas. Am J Pathol. 1993;143:1731–42.
107. Rasbridge SA, Gillett CE, Sampson SA, Walsh FS, Millis RR. Epithelial (E-) and placental (P-) cadherin cell adhesion molecule expression in breast carcinoma. J Pathol. 1993;169:245–50. https://doi.org/10.1002/path.1711690211.
108. Hartsock A, Nelson WJ. Adherens and tight junctions: structure, function and connections to the actin cytoskeleton. Biochim Biophys Acta. 2008;1778:660–9. https://doi.org/10.1016/j.bbamem.2007.07.012.
109. De Leeuw WJF, et al. Simultaneous loss of E-cadherin and catenins in invasive lobular breast cancer and lobular carcinoma in situ. J Pathol. 1997;183:404–11. https://doi.org/10.1002/(sici)1096-9896(199712)183:4<404::Aid-path1148>3.0.Co;2-9.
110. Sarrio D, et al. Cytoplasmic localization of p120ctn and E-cadherin loss characterize lobular breast carcinoma from preinvasive to metastatic lesions. Oncogene. 2004;23:3272–83. https://doi.org/10.1038/sj.onc.1207439.
111. Shibata T, Kokubu A, Sekine S, Kanai Y, Hirohashi S. Cytoplasmic p120ctn regulates the invasive phenotypes of E-cadherin-deficient breast cancer. Am J Pathol. 2004;164:2269–78. https://doi.org/10.1016/s0002-9440(10)63783-2.
112. Dabbs DJ, Bhargava R, Chivukula M. Lobular versus ductal breast neoplasms: the diagnostic utility of p120 catenin. Am J Surg Pathol. 2007;31:427–37. https://doi.org/10.1097/01.pas.0000213386.63160.3f.
113. Acs G, Lawton TJ, Rebbeck TR, LiVolsi VA, Zhang PJ. Differential expression of E-cadherin in lobular and ductal neoplasms of the breast and its biologic and diagnostic implications. Am J Clin Pathol. 2001;115:85–98. https://doi.org/10.1309/fdhx-l92r-batq-2ge0.
114. Choi YJ, Pinto MM, Hao L, Riba AK. Interobserver variability and aberrant E-cadherin immunostaining of lobular neoplasia and infiltrating lobular carcinoma. Mod Pathol. 2008;21:1224–37. https://doi.org/10.1038/modpathol.2008.106.
115. Da Silva L, et al. Aberrant expression of E-cadherin in lobular carcinomas of the breast. Am J Surg Pathol. 2008;32:773–83.
116. Cocquyt VF, et al. Different responses to preoperative chemotherapy for invasive lobular and invasive ductal breast carcinoma. Eur J Surg Oncol (EJSO). 2003;29:361–7. https://doi.org/10.1053/ejso.2002.1404.
117. Rakha EA, et al. Clinical and biological significance of E-cadherin protein expression in invasive lobular carcinoma of the breast. Am J Surg Pathol. 2010;34:1472–9. https://doi.org/10.1097/PAS.0b013e3181f01916.
118. Rakha EA, et al. Further evidence that E-cadherin is not a tumour suppressor gene in invasive ductal carcinoma of the breast: an immunohistochemical study. Histopathology. 2013;62:695–701. https://doi.org/10.1111/his.12066.
119. Wells JM, Pipa J, Shin SJ. Lobular neoplasia of the breast revisited with emphasis on the role of E-cadherin immunohistochemistry. Am J Surg Pathol. 2014;38:434–5. https://doi.org/10.1097/pas.0000000000000159.
120. Mahler-Araujo B, Savage K, Parry S, Reis-Filho JS. Reduction of E-cadherin expression is associated with non-lobular breast carcinomas of basal-like and triple negative phenotype. J Clin Pathol. 2008;61:615–20. https://doi.org/10.1136/jcp.2007.053991.
121. Harigopal M, et al. Aberrant E-cadherin staining patterns in invasive mammary carcinoma. World J Surg Oncol. 2005;3:73. https://doi.org/10.1186/1477-7819-3-73.
122. Rakha EA, Abd El Rehim D, Pinder SE, Lewis SA, Ellis IO. E-cadherin expression in invasive non-lobular carcinoma of the breast and its prognostic significance. Histopathology. 2005;46:685–93. https://doi.org/10.1111/j.1365-2559.2005.02156.x.
123. Dabbs DJ, et al. Lobular neoplasia of the breast revisited with emphasis on the role of E-cadherin immunohistochemistry. Am J Surg Pathol. 2013;37:e1–11. https://doi.org/10.1097/PAS.0b013e3182918a2b.
124. Yu J, Dabbs DJ, Shuai Y, Niemeier LA, Bhargava R. Classical-type invasive lobular carcinoma with HER2 overexpression: clinical, histologic, and hormone receptor characteristics. Am J Clin Pathol. 2011;136:88–97. https://doi.org/10.1309/ajcp7uriw0qettat.
125. Frolik D, Caduff R, Varga Z. Pleomorphic lobular carcinoma of the breast: its cell kinetics, expression of oncogenes and tumour suppressor genes compared with invasive ductal carcinomas and classical infiltrating lobular carcinomas. Histopathology. 2001;39:503–13.
126. Monhollen L, Morrison C, Ademuyiwa FO, Chandrasekhar R, Khoury T. Pleomorphic lobular carcinoma: a distinctive clinical and molecular breast cancer type. Histopathology. 2012;61:365–77. https://doi.org/10.1111/j.1365-2559.2012.04230.x.
127. Narendra S, Jenkins SM, Khoor A, Nassar A. Clinical outcome in pleomorphic lobular carcinoma: a case-control study with comparison to classic invasive lobular carcinoma. Ann Diagn Pathol. 2015; https://doi.org/10.1016/j.anndiagpath.2015.01.005.
128. Jung SP, et al. Invasive pleomorphic lobular carcinoma of the breast: clinicopathologic characteristics and prognosis compared with invasive ductal carcinoma. J Breast Cancer. 2012;15:313–9. https://doi.org/10.4048/jbc.2012.15.3.313.
129. Simpson PT, et al. Molecular profiling pleomorphic lobular carcinomas of the breast: evidence for a common molecular genetic pathway with classic lobular carcinomas. J Pathol. 2008;215:231–44. https://doi.org/10.1002/path.2358.
130. Marchio C, et al. The genetic landscape of breast carcinomas with neuroendocrine differentiation. J Pathol. 2017;241:405–19. https://doi.org/10.1002/path.4837.
131. Gradinaru SE, Bumbea H, Onisai MC, Stoicea M. Neuroendocrine differentiation in invasive lobular breast carcinoma. Acta Endocrinol (Buchar). 2017;13:246–8. https://doi.org/10.4183/aeb.2017.246.
132. Rakha EA, Abbas A, Sheeran R. Invasive lobular carcinoma mimicking papillary carcinoma: a report of three cases. Pathobiology. 2016;83:221–7. https://doi.org/10.1159/000442884.
133. Motanagh SA, Muller KE. Invasive lobular carcinoma with papillary features: a newly described variant that poses a difficult histologic differential diagnosis. Breast J. 2020;26:1231–3. https://doi.org/10.1111/tbj.13784.
134. Christgen M, et al. Subclonal analysis in a lobular breast cancer with classical and solid growth pattern mimicking a solid-

papillary carcinoma. J Pathol Clin Res. 2017;3:191–202. https://doi.org/10.1002/cjp2.76.
135. Wang J, Darvishian F. Extramedullary hematopoiesis in breast after neoadjuvant chemotherapy for breast carcinoma. Ann Clin Lab Sci. 2006;36:475–8.
136. Bacchi CE, et al. Metastatic melanoma presenting as an isolated breast tumor: a study of 20 cases with emphasis on several primary mimickers. Arch Pathol Lab Med. 2013;137:41–9. https://doi.org/10.5858/arpa.2011-0552-OA.
137. Schrader KA, et al. Hereditary diffuse gastric cancer: association with lobular breast cancer. Familial Cancer. 2008;7:73–82. https://doi.org/10.1007/s10689-007-9172-6.
138. Guilford P, et al. E-cadherin germline mutations in familial gastric cancer. Nature. 1998;392:402–5. https://doi.org/10.1038/32918.
139. O'Connell FP, Wang HH, Odze RD. Utility of immunohistochemistry in distinguishing primary adenocarcinomas from metastatic breast carcinomas in the gastrointestinal tract. Arch Pathol Lab Med. 2005;129:338–47. https://doi.org/10.1043/1543-2165(2005)129<338:uoiidp>2.0.co;2.
140. Wei S, Said-Al-Naief N, Hameed O. Estrogen and progesterone receptor expression is not always specific for mammary and gynecologic carcinomas: a tissue microarray and pooled literature review study. Appl Immunohistochem Mol Morphol. 2009;17:393–402. https://doi.org/10.1097/PAI.0b013e31819faa07.
141. Hui Y, et al. Differentiating breast carcinoma with signet ring features from gastrointestinal signet ring carcinoma: assessment of immunohistochemical markers. Hum Pathol. 2018;77:11–9. https://doi.org/10.1016/j.humpath.2018.01.002.
142. Miettinen M, et al. GATA3: a multispecific but potentially useful marker in surgical pathology: a systematic analysis of 2500 epithelial and nonepithelial tumors. Am J Surg Pathol. 2014;38:13–22. https://doi.org/10.1097/PAS.0b013e3182a0218f.
143. Lewis GH, et al. Relationship between molecular subtype of invasive breast carcinoma and expression of gross cystic disease fluid protein 15 and mammaglobin. Am J Clin Pathol. 2011;135:587–91. https://doi.org/10.1309/ajcpmfr6oa8ichnh.
144. Bhargava R, Beriwal S, Dabbs DJ. Mammaglobin vs GCDFP-15: an immunohistologic validation survey for sensitivity and specificity. Am J Clin Pathol. 2007;127:103–13. https://doi.org/10.1309/tdp92pqlde2hleet.
145. Kemler R, Babinet C, Eisen H, Jacob F. Surface antigen in early differentiation. Proc Natl Acad Sci U S A. 1977;74:4449–52.
146. Berx G, et al. EMBO J. 1995;14:6107–15.
147. Rosa-Rosa JM, et al. High frequency of ERBB2 activating mutations in invasive lobular breast carcinoma with pleomorphic features. Cancers (Basel). 2019;11:74. https://doi.org/10.3390/cancers11010074.
148. Ciriello G, et al. Comprehensive molecular portraits of invasive lobular breast cancer. Cell. 2015;163:506–19. https://doi.org/10.1016/j.cell.2015.09.033.
149. Michaut M, et al. Integration of genomic, transcriptomic and proteomic data identifies two biologically distinct subtypes of invasive lobular breast cancer. Sci Rep. 2016;6:18517. https://doi.org/10.1038/srep18517.
150. Desmedt C, et al. Genomic characterization of primary invasive lobular breast cancer. J Clin Oncol. 2016;34:1872–81. https://doi.org/10.1200/JCO.2015.64.0334.
151. Pareja F, et al. The genomic landscape of metastatic histologic special types of invasive breast cancer. NPJ Breast Cancer. 2020;6:53. https://doi.org/10.1038/s41523-020-00195-4.
152. Sarrio D, et al. Epigenetic and genetic alterations of APC and CDH1 genes in lobular breast cancer: relationships with abnormal E-cadherin and catenin expression and microsatellite instability. Int J Cancer. 2003;106:208–15. https://doi.org/10.1002/ijc.11197.
153. Kurozumi S, et al. Targetable ERBB2 mutation status is an independent marker of adverse prognosis in estrogen receptor positive, ERBB2 non-amplified primary lobular breast carcinoma: a retrospective in silico analysis of public datasets. Breast Cancer Res. 2020;22:85. https://doi.org/10.1186/s13058-020-01324-4.
154. Ross JS, et al. Relapsed classic E-cadherin (CDH1)-mutated invasive lobular breast cancer shows a high frequency of HER2 (ERBB2) gene mutations. Clin Cancer Res. 2013;19:2668–76. https://doi.org/10.1158/1078-0432.CCR-13-0295.
155. Ross JS, et al. Nonamplification ERBB2 genomic alterations in 5605 cases of recurrent and metastatic breast cancer: An emerging opportunity for anti-HER2 targeted therapies. Cancer. 2016;122:2654–62. https://doi.org/10.1002/cncr.30102.
156. Razavi P, et al. The genomic landscape of endocrine-resistant advanced breast cancers. Cancer Cell. 2018;34:427–438 e426. https://doi.org/10.1016/j.ccell.2018.08.008.
157. Shamir ER, Chen YY, Krings G. Genetic analysis of pleomorphic and florid lobular carcinoma in situ variants: frequent ERBB2/ERBB3 alterations and clonal relationship to classic lobular carcinoma in situ and invasive lobular carcinoma. Mod Pathol. 2020;33:1078–91. https://doi.org/10.1038/s41379-019-0449-8.
158. Bose R, et al. Activating HER2 mutations in HER2 gene amplification negative breast cancer. Cancer Discov. 2013;3:224–37. https://doi.org/10.1158/2159-8290.CD-12-0349.
159. Curtis C, et al. The genomic and transcriptomic architecture of 2,000 breast tumours reveals novel subgroups. Nature. 2012;486:346–52. https://doi.org/10.1038/nature10983.
160. Horlings HM, et al. Genomic profiling of histological special types of breast cancer. Breast Cancer Res Treat. 2013;142:257–69. https://doi.org/10.1007/s10549-013-2740-6.
161. Weigelt B, et al. Refinement of breast cancer classification by molecular characterization of histological special types. J Pathol. 2008;216:141–50. https://doi.org/10.1002/path.2407.
162. Lehmann BD, et al. Identification of human triple-negative breast cancer subtypes and preclinical models for selection of targeted therapies. J Clin Invest. 2011;121:2750–67. https://doi.org/10.1172/JCI45014.
163. Bergeron A, et al. Triple-negative breast lobular carcinoma: a luminal androgen receptor carcinoma with specific ESRRA mutations. Mod Pathol. 2021; https://doi.org/10.1038/s41379-021-00742-9.
164. Cao L, et al. Frequent amplifications of ESR1, ERBB2 and MDM4 in primary invasive lobular breast carcinoma. Cancer Lett. 2019;461:21–30. https://doi.org/10.1016/j.canlet.2019.06.011.
165. Basudan A, et al. Frequent ESR1 and CDK pathway copy-number alterations in metastatic breast cancer. Mol Cancer Res. 2019;17:457–68. https://doi.org/10.1158/1541-7786.MCR-18-0946.
166. Sokol ES, et al. Loss of function of NF1 is a mechanism of acquired resistance to endocrine therapy in lobular breast cancer. Ann Oncol. 2019;30:115–23. https://doi.org/10.1093/annonc/mdy497.
167. McCart Reed AE, et al. The genomic landscape of lobular breast cancer. Cancers (Basel). 2021;13:1950. https://doi.org/10.3390/cancers13081950.
168. Bharat A, Gao F, Margenthaler JA. Tumor characteristics and patient outcomes are similar between invasive lobular and mixed invasive ductal/lobular breast cancers but differ from pure invasive ductal breast cancers. Am J Surg. 2009;198:516–9. https://doi.org/10.1016/j.amjsurg.2009.06.005.
169. Lim ST, et al. A comparison of the clinical outcomes of patients with invasive lobular carcinoma and invasive ductal carcinoma of the breast according to molecular subtype in a Korean population. World J Surg Oncol. 2014;12:56. https://doi.org/10.1186/1477-7819-12-56.

170. Kwast AB, et al. Histological type is not an independent prognostic factor for the risk pattern of breast cancer recurrences. Breast Cancer Res Treat. 2012;135:271–80. https://doi.org/10.1007/s10549-012-2160-z.
171. Jain S, Fisher C, Smith P, Millis RR, Rubens RD. Patterns of metastatic breast cancer in relation to histological type. Eur J Cancer. 1993;29A:2155–7.
172. Dixon AR, Ellis IO, Elston CW, Blamey RW. A comparison of the clinical metastatic patterns of invasive lobular and ductal carcinomas of the breast. Br J Cancer. 1991;63:634–5.
173. Harris M, et al. A comparison of the metastatic pattern of infiltrating lobular carcinoma and infiltrating duct carcinoma of the breast. Br J Cancer. 1984;50:23–30.
174. Lamovec J, Bracko M. Metastatic pattern of infiltrating lobular carcinoma of the breast: an autopsy study. J Surg Oncol. 1991;48:28–33.
175. Taal BG, den Hartog Jager FC, Steinmetz R, Peterse H. The spectrum of gastrointestinal metastases of breast carcinoma: I. Stomach. Gastrointest Endosc. 1992;38:130–5.
176. Taal BG, den Hartog Jager FC, Steinmetz R, Peterse H. The spectrum of gastrointestinal metastases of breast carcinoma: II. The colon and rectum. Gastrointest Endosc. 1992;38:136–41.
177. Borst MJ, Ingold JA. Metastatic patterns of invasive lobular versus invasive ductal carcinoma of the breast. Surgery. 1993;114:637–41.; discussion 641-632.
178. Winston CB, et al. Metastatic lobular carcinoma of the breast: patterns of spread in the chest, abdomen, and pelvis on CT. AJR Am J Roentgenol. 2000;175:795–800. https://doi.org/10.2214/ajr.175.3.1750795.
179. Ferlicot S, et al. Wide metastatic spreading in infiltrating lobular carcinoma of the breast. Eur J Cancer. 2004;40:336–41.
180. Korhonen T, et al. The impact of lobular and ductal breast cancer histology on the metastatic behavior and long term survival of breast cancer patients. Breast. 2013;22:1119–24. https://doi.org/10.1016/j.breast.2013.06.001.
181. Inoue M, et al. Specific sites of metastases in invasive lobular carcinoma: a retrospective cohort study of metastatic breast cancer. Breast Cancer. 2017;24:667–72. https://doi.org/10.1007/s12282-017-0753-4.
182. Jayasinghe UW, Bilous AM, Boyages J. Is survival from infiltrating lobular carcinoma of the breast different from that of infiltrating ductal carcinoma? Breast J. 2007;13:479–85. https://doi.org/10.1111/j.1524-4741.2007.00468.x.
183. Moran MS, Yang Q, Haffty BG. The Yale University experience of early-stage invasive lobular carcinoma (ILC) and invasive ductal carcinoma (IDC) treated with breast conservation treatment (BCT): analysis of clinical-pathologic features, long-term outcomes, and molecular expression of COX-2, Bcl-2, and p53 as a function of histology. Breast J. 2009;15:571–8. https://doi.org/10.1111/j.1524-4741.2009.00833.x.
184. Peiro G, et al. The influence of infiltrating lobular carcinoma on the outcome of patients treated with breast-conserving surgery and radiation therapy. Breast Cancer Res Treat. 2000;59:49–54.
185. Viale G, et al. Lack of prognostic significance of "classic" lobular breast carcinoma: a matched, single institution series. Breast Cancer Res Treat. 2009;117:211–4. https://doi.org/10.1007/s10549-008-0112-4.
186. du Toit RS, et al. Invasive lobular carcinomas of the breast—the prognosis of histopathological subtypes. Br J Cancer. 1989;60:605–9.
187. Hess KR, Pusztai L, Buzdar AU, Hortobagyi GN. Estrogen receptors and distinct patterns of breast cancer relapse. Breast Cancer Res Treat. 2003;78:105–18.
188. Zhang XH, Giuliano M, Trivedi MV, Schiff R, Osborne CK. Metastasis dormancy in estrogen receptor-positive breast cancer. Clin Cancer Res. 2013;19:6389–97. https://doi.org/10.1158/1078-0432.ccr-13-0838.
189. Karrison TG, Ferguson DJ, Meier P. Dormancy of mammary carcinoma after mastectomy. J Natl Cancer Inst. 1999;91:80–5.
190. Flores-Diaz D, et al. Impact of invasive lobular carcinoma on long-term outcomes in Mexican breast cancer patients. Breast Cancer Res Treat. 2019;176:243–9. https://doi.org/10.1007/s10549-019-05234-8.
191. Bane AL, Tjan S, Parkes RK, Andrulis I, O'Malley FP. Invasive lobular carcinoma: to grade or not to grade. Mod Pathol. 2005;18:621–8. https://doi.org/10.1038/modpathol.3800273.
192. Mokbel K. Grading of infiltrating lobular carcinoma. Eur J Surg Oncol. 2001;27:609–10. https://doi.org/10.1053/ejso.2001.1126.
193. Pereira H, et al. Pathological prognostic factors in breast cancer. IV: Should you be a typer or a grader? A comparative study of two histological prognostic features in operable breast carcinoma. Histopathology. 1995;27:219–26.
194. Shousha S, Backhous CM, Alaghband-Zadeh J, Burn I. Alveolar variant of invasive lobular carcinoma of the breast. A tumor rich in estrogen receptors. Am J Clin Pathol. 1986;85:1–5. https://doi.org/10.1093/ajcp/85.1.1.
195. Iorfida M, et al. Invasive lobular breast cancer: subtypes and outcome. Breast Cancer Res Treat. 2012;133:713–23. https://doi.org/10.1007/s10549-012-2002-z.
196. Sahin S, Karatas F, Erdem GU, Hacioglu B, Altundag K. Invasive pleomorphic lobular histology is an adverse prognostic factor on survival in patients with breast cancer. Am Surg. 2017;83:359–64.
197. Yang LP, et al. Clinicopathological characteristics and survival outcomes in pleomorphic lobular breast carcinoma of the breast: a SEER population-based study. Cancer Med. 2017;6:2867–75. https://doi.org/10.1002/cam4.1244.
198. Burstein HJ, et al. Adjuvant endocrine therapy for women with hormone receptor-positive breast cancer: ASCO clinical practice guideline focused update. J Clin Oncol. 2019;37(5):423–38. https://doi.org/10.1200/JCO.18.01160. Epub 2018 Nov 19. PMID: 30452337.
199. Metzger Filho O, et al. Relative effectiveness of letrozole compared with tamoxifen for patients with lobular carcinoma in the BIG 1-98 trial. J Clin Oncol. 2015;33:2772–9. https://doi.org/10.1200/JCO.2015.60.8133.
200. Sikora MJ, et al. Invasive lobular carcinoma cell lines are characterized by unique estrogen-mediated gene expression patterns and altered tamoxifen response. Cancer Res. 2014;74:1463–74. https://doi.org/10.1158/0008-5472.CAN-13-2779.
201. Petrelli F, Barni S. Response to neoadjuvant chemotherapy in ductal compared to lobular carcinoma of the breast: a meta-analysis of published trials including 1,764 lobular breast cancer. Breast Cancer Res Treat. 2013;142:227–35. https://doi.org/10.1007/s10549-013-2751-3.
202. Cristofanilli M, et al. Invasive lobular carcinoma classic type: response to primary chemotherapy and survival outcomes. J Clin Oncol. 2005;23:41–8. https://doi.org/10.1200/jco.2005.03.111.
203. Loibl S, et al. Response and prognosis after neoadjuvant chemotherapy in 1,051 patients with infiltrating lobular breast carcinoma. Breast Cancer Res Treat. 2014;144:153–62. https://doi.org/10.1007/s10549-014-2861-6.
204. Tubiana-Hulin M, et al. Response to neoadjuvant chemotherapy in lobular and ductal breast carcinomas: a retrospective study on 860 patients from one institution. Ann Oncol. 2006;17:1228–33. https://doi.org/10.1093/annonc/mdl114.
205. Lips EH, et al. Lobular histology and response to neoadjuvant chemotherapy in invasive breast cancer. Breast Cancer Res Treat. 2012;136:35–43. https://doi.org/10.1007/s10549-012-2233-z.

206. Metzger-Filho O, et al. Magnitude of trastuzumab benefit in patients with HER2-positive, invasive lobular breast carcinoma: results from the HERA trial. J Clin Oncol. 2013;31:1954–60. https://doi.org/10.1200/JCO.2012.46.2440.
207. Kancha RK, et al. Differential sensitivity of ERBB2 kinase domain mutations towards lapatinib. PLoS One. 2011;6:e26760. https://doi.org/10.1371/journal.pone.0026760.
208. Jaiswal BS, et al. Oncogenic ERBB3 mutations in human cancers. Cancer Cell. 2013;23:603–17. https://doi.org/10.1016/j.ccr.2013.04.012.
209. Paik S, et al. A multigene assay to predict recurrence of tamoxifen-treated, node-negative breast cancer. N Engl J Med. 2004;351:2817–26. https://doi.org/10.1056/NEJMoa041588.
210. Paik S, et al. Gene expression and benefit of chemotherapy in women with node-negative, estrogen receptor-positive breast cancer. J Clin Oncol. 2006;24:3726–34. https://doi.org/10.1200/JCO.2005.04.7985.
211. Wang J, et al. The distribution and outcomes of the 21-gene recurrence score in T1-T2N0 estrogen receptor-positive breast cancer with different histologic subtypes. Front Genet. 2018;9:638. https://doi.org/10.3389/fgene.2018.00638.
212. Kelly CM, et al. Utility of oncotype DX risk estimates in clinically intermediate risk hormone receptor-positive, HER2-normal, grade II, lymph node-negative breast cancers. Cancer. 2010;116:5161–7. https://doi.org/10.1002/cncr.25269.
213. Baehner FL, Shak S, Miller DP, Petkov VI. SEER study of breast cancer specific mortality (BCSM) in patients with lobular tumors treated based on recurrence score results. J Clin Oncol. 2017;35:11568. https://doi.org/10.1200/JCO.2017.35.15_suppl.11568.
214. Felts JL, Zhu J, Han B, Smith SJ, Truica CI. An analysis of oncotype DX recurrence scores and clinicopathologic characteristics in invasive lobular breast cancer. Breast J. 2017;23:677–86. https://doi.org/10.1111/tbj.12751.
215. Siegelmann-Danieli N, et al. The impact of the oncotype DX recurrence score on treatment decisions and clinical outcomes in patients with early breast cancer: the Maccabi Healthcare Services experience with a unified testing policy. Ecancermedicalscience. 2013;7:380. https://doi.org/10.3332/ecancer.2013.380.
216. Christgen M, et al. Differential impact of prognostic parameters in hormone receptor-positive lobular breast cancer. Cancer. 2020;126:4847–58. https://doi.org/10.1002/cncr.33104.
217. Wu SG, et al. Progesterone receptor status and tumor grade predict the 21-gene recurrence score of invasive lobular breast cancer. Biomark Med. 2019;13:1005–12. https://doi.org/10.2217/bmm-2019-0209.
218. Beumer IJ, et al. Prognostic value of MammaPrint((R)) in invasive lobular breast cancer. Biomark Insights. 2016;11:139–46. https://doi.org/10.4137/BMI.S38435.
219. Metzger O, et al. Clinical utility of MammaPrint testing in invasive lobular carcinoma: results from the MINDACT phase III trial. Eur J Cancer. 2020;138:S5–6. https://doi.org/10.1016/S0959-8049(20)30542-6.
220. Laenkholm AV, et al. Population-based study of prosigna-PAM50 and outcome among postmenopausal women with estrogen receptor-positive and HER2-negative operable invasive lobular or ductal breast cancer. Clin Breast Cancer. 2020;20:e423–32. https://doi.org/10.1016/j.clbc.2020.01.013.
221. McCart Reed AE, et al. LobSig is a multigene predictor of outcome in invasive lobular carcinoma. NPJ Breast Cancer. 2019;5:18. https://doi.org/10.1038/s41523-019-0113-y.

Benign and Malignant Mesenchymal Tumors

16

Ashley Cimino-Mathews, Emily B. Ambinder, Pedram Argani, and Marissa J. White

Overview

Mesenchymal tumors of the breast demonstrate differentiation towards the non-epithelial components of the breast, including the vasculature, adipose tissue, smooth muscle, nerve sheath elements, and stromal myofibroblasts. Vascular lesions of the breast will be discussed in a separate chapter (Chap. 17). Mesenchymal tumors can be benign or malignant neoplasms and morphologically resemble their counterparts in other soft-tissue sites. The hamartomatous lesions are disorganized proliferations of the normal mesenchymal components admixed with the breast epithelial component.

Benign Adipose, Smooth Muscle, and Hamartomatous Lesions

Lipoma

Overview

Lipomas of the breast are typically unilateral, solitary, small, soft, and palpable masses that can occur in any age range and are reported to account for 4.6% of breast masses in adult females [1, 2]. Although most are small, "giant lipomas" defined as those measuring over 10 cm in size have been reported [3–5].

Gross and Radiologic Features

Grossly, lipomas are well-circumscribed oval or lobulated masses. Palpable lipomas are not always visible on imaging, with one series reporting only 3% of lipomas detectable on mammography and 21% detectable on ultrasound [1]. When visible on mammography, breast lipomas have distinct features and are radiolucent, with the same density as fat (Fig. 16.1). A thin fibrous capsule distinguishes these from the normal breast adipose tissue [1]. On ultrasound, breast lipomas are echogenic compared to normal fatty breast tissue and are typically oval or round with circumscribed margins and no blood flow. On ultrasound alone, the differential diagnosis includes other fat-containing benign lesions such as hematoma, angiolipoma, fat necrosis, hamartoma, and less commonly pseudoangiomatous stromal hyperplasia (PASH). On magnetic resonance imaging (MRI), breast lipomas have fat signal on all sequences and do not enhance.

Microscopic Features

Lipomas are composed of sheets of mature adipocytes characterized by cells with abundant clear cytoplasm and small, peripheral bland nuclei (Fig. 16.2). Lipomas are separated from the adjacent breast parenchyma by a thin fibrous capsule [1]. Morphologic variants of lipoma include angiolipoma (further discussed below), hibernoma (further discussed below), chondrolipoma, and spindle cell lipoma. Chondrolipomas contain associated lobules of mature cartilage [6–8] and are classified in some textbooks as a hamartoma variant [9]. Spindle cell lipomas contain a mixture of adipocytes, bland spindled cells, and associated wavy, ropy collagen bundles and are considered to be on the spectrum of mammary myofibroblastomas (further discussed below) [10–13].

A. Cimino-Mathews (✉) · P. Argani
Departments of Pathology and Oncology, The Johns Hopkins Hospital, Baltimore, MD, USA
e-mail: acimino@jhmi.edu; pargani@jhmi.edu

E. B. Ambinder
The Russell H. Morgan Department of Radiology and Radiologic Science, The Johns Hopkins Hospital, Baltimore, MD, USA
e-mail: emcinto8@jhmi.edu

M. J. White
Department of Pathology, The Johns Hopkins Hospital, Baltimore, MD, USA
e-mail: mwhite44@jhmi.edu

© The Author(s), under exclusive license to Springer Nature Switzerland AG 2022
S. J. Shin et al. (eds.), *A Comprehensive Guide to Core Needle Biopsies of the Breast*,
https://doi.org/10.1007/978-3-031-05532-4_16

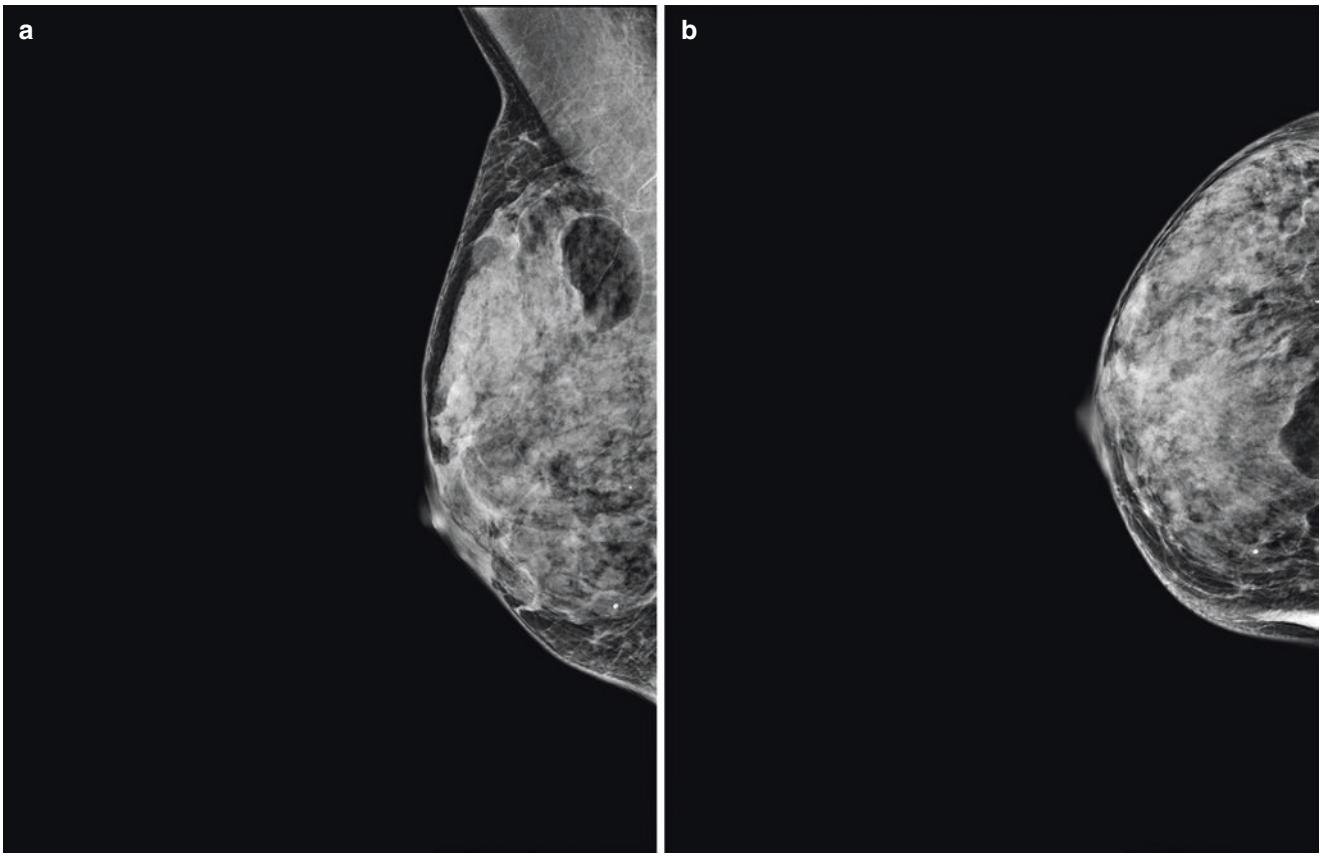

Fig. 16.1 Mammographic features of a breast lipoma. (**a**, **b**) Screening digital mammography in an asymptomatic female reveals a posterior right-breast mass at the 12:00 position, located just anterior to the pectoralis muscle. The mass is oval, circumscribed, and fat containing, consistent with a lipoma

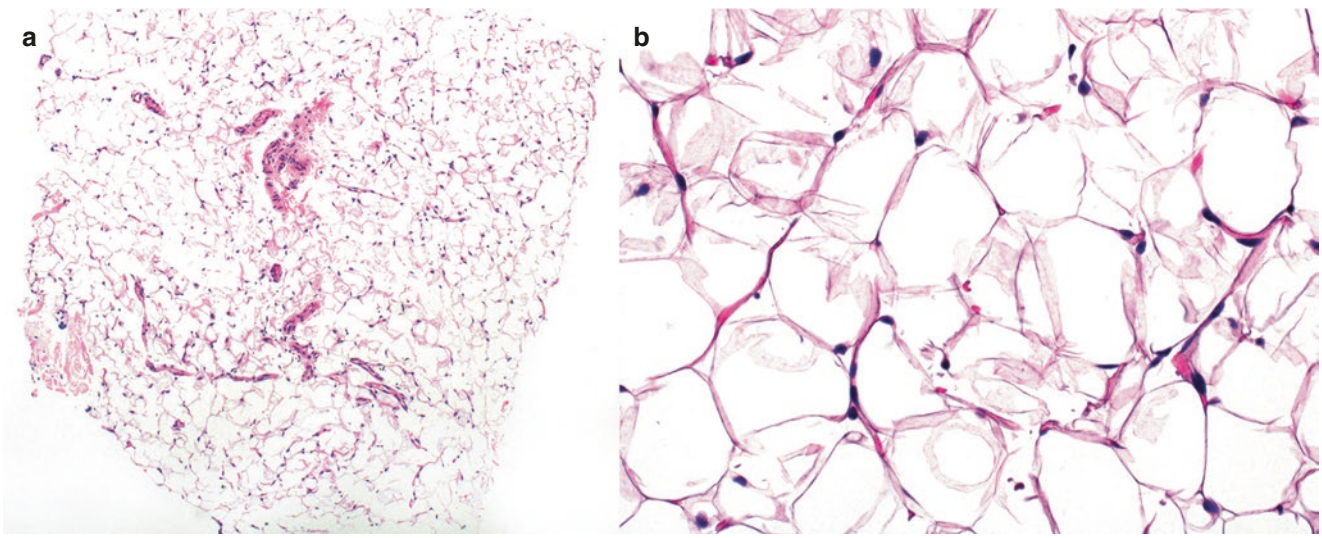

Fig. 16.2 Histologic features of a breast lipoma. (**a**, **b**) CNB of a soft palpable breast mass reveals mature adipocytes with abundant cytoplasm and small, peripheral bland nuclei. Unless there is a fibrous capsule separating the fatty lesion from the adjacent breast parenchyma, it may not be possible to definitively distinguish a fat lobule from a lipoma

Differential Diagnosis

The differential diagnosis of breast lipoma includes breast fat lobules, hamartoma, and rarely liposarcoma. Fat lobules lack a fibrous capsule, although its absence cannot be entirely confirmed on core needle biopsy (CNB) material. Hamartomas contain an admixture of other breast stromal and epithelial elements, including smooth muscle, stromal myofibroblasts, and breast lobules and ducts. Liposarcomas in the breast are rare [14–16], but even the well-differentiated liposarcomas will display nuclear atypia including hyperchromasia, nuclear enlargement, and lipoblasts, which distinguish them from benign lipomas.

Immunohistochemical Workup

In general, the diagnosis of a lipoma is made on the radiologic and histologic features alone. Adipocytes are immunoreactive for S100 protein. If the diagnosis of well-differentiated liposarcoma is being considered in the differential, immunohistochemistry (IHC) or fluorescence in situ hybridization for MDM2 amplification can be used to distinguish a well-differentiated liposarcoma from a lipoma [17, 18].

Pathogenesis

In general, benign lipomas lack specific genetic changes. However, spindle cell lipomas, like mammary myofibroblastomas, display alterations in chromosomes 13q and 16q [19].

Prognosis and Management

Lipomas are benign neoplasms and may be monitored expectantly or sufficiently treated with excisional biopsy.

Angiolipoma

Overview

Angiolipomas of the breast are lipoma variants that are typically small and subcutaneous and primarily affect adult females [2, 20, 21]. Unlike subcutaneous angiolipomas of other sites, breast angiolipomas are typically painless [20].

Gross and Radiologic Features

Like other lipomas, angiolipomas are grossly well circumscribed and thinly encapsulated. Similar to conventional lipomas, not all angiolipomas are visible on imaging. In one series, 57% of angiolipomas were detectable on mammogram and 71% were detectable on ultrasound [21]. When visible on mammography, angiolipomas are usually round or oval in shape with circumscribed margins (Fig. 16.3a). In contrast to lipomas, angiolipomas are often isodense to the breast parenchyma, which reflects the combination of adipose tissue and vascular proliferation that comprise these lesions. It is likely that the more vascular tumors are denser on mammography. The mammographic features are not diagnostic, and ultrasound is often performed to further evaluate these lesions. On ultrasound, angiolipomas are oval with some gentle lobulations and a thin echogenic pseudocapsule (Fig. 16.3b). Generally, these are hyperechoic relative to fat, but some display mixed echogenicity. Most angiolipomas have benign imaging characteristics; however, some display atypical features such as posterior acoustic shadowing. The differential diagnosis on the basis of imaging typically includes lipoma, fat necrosis, hamartoma, fibroadenoma, and PASH.

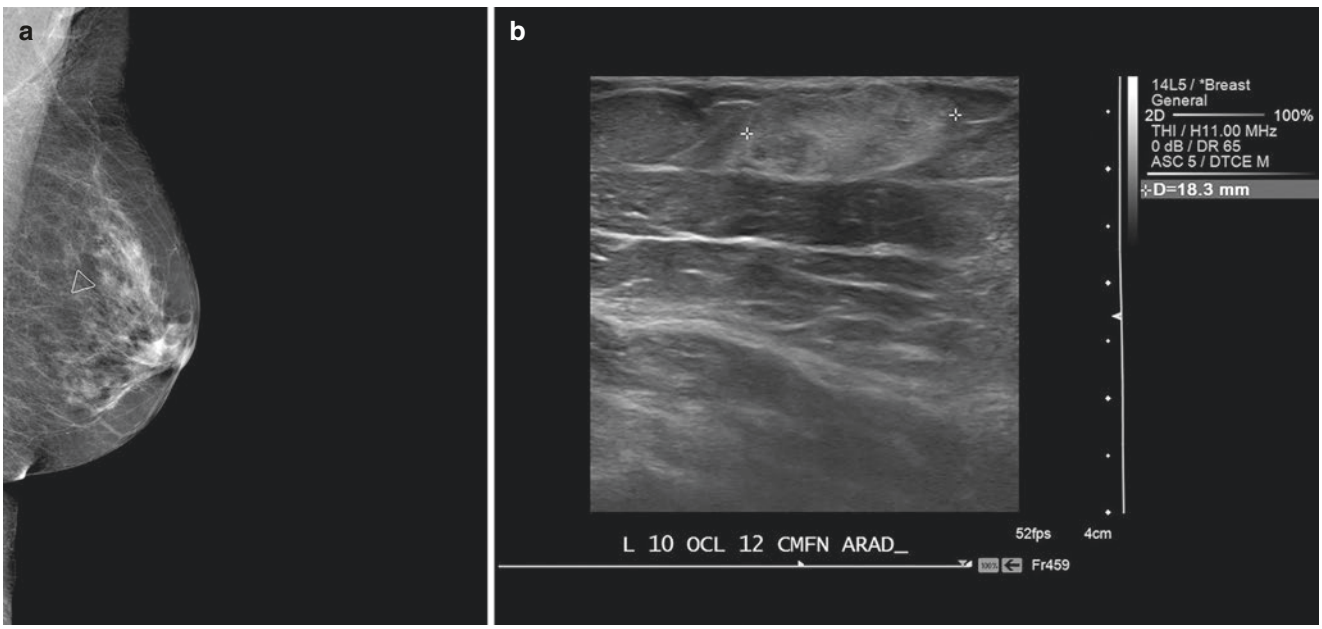

Fig. 16.3 Mammographic and ultrasound features of a breast angiolipoma. A 66-year-old female presents with a palpable left-breast mass. (**a**) No mass is seen on mammography (a *triangular* marker designates the site of the palpable mass). (**b**) Ultrasound shows an oval, parallel, and circumscribed mass with a heterogeneous echogenic and hypoechoic echopattern and no posterior sound change

Microscopic Features

Angiolipomas of any site are composed of mature adipose tissue with admixed capillary vasculature (Fig. 16.4a, b) that ranges from low to high vascularity. The endothelial cells are a single layer without appreciable atypia. The presence of fibrin thrombi within the vasculature spaces is a characteristic feature (Fig. 16.4c). Some lesions display scattered mast cells and interstitial myxoid change and fibrosis (Fig. 16.4d). Occasionally, extramedullary hematopoietic cells such as megakaryocytes can be seen in these lesions as well.

Differential Diagnosis

The differential diagnosis of angiolipoma of the breast includes vascular neoplasms (such as hemangioma or well-differentiated angiosarcoma) as well as other fatty tumors (such as lipoma). On CNB, a cellular angiolipoma is most likely to be confused for a vascular neoplasm, as the well-circumscribed and -encapsulated nature of an angiolipoma may not be well appreciated on the limited sampling of a CNB. If included as a vascular lesion, angiolipomas would comprise 52% of all vascular tumors of the breast in one single institution series [20]. Angiolipomas may show atypical features including nuclear hyperchromasia [22]. However, in contrast to angiolipomas, angiosarcomas should display an infiltrative pattern, mitotic activity, and greater nuclear atypia. The most difficult distinction in core biopsy samples, however, is discerning between an angiolipoma and a well-differentiated angiosarcoma involving adipose tissue (Fig. 16.5a–c). Nuclear atypia such as hyperchromasia and enlargement may be very subtle, and mitotic activity is characteristically very low and easily unappreciated in limited samplings (Fig. 16.5d). Clinical and radiologic correlation to ascertain the tumor size and location within the breast (superficial versus deep) is helpful. The presence of fibrin thrombi favors angiolipoma as they are not seen in well-differentiated angiosarcomas; however, not all angiofibro-

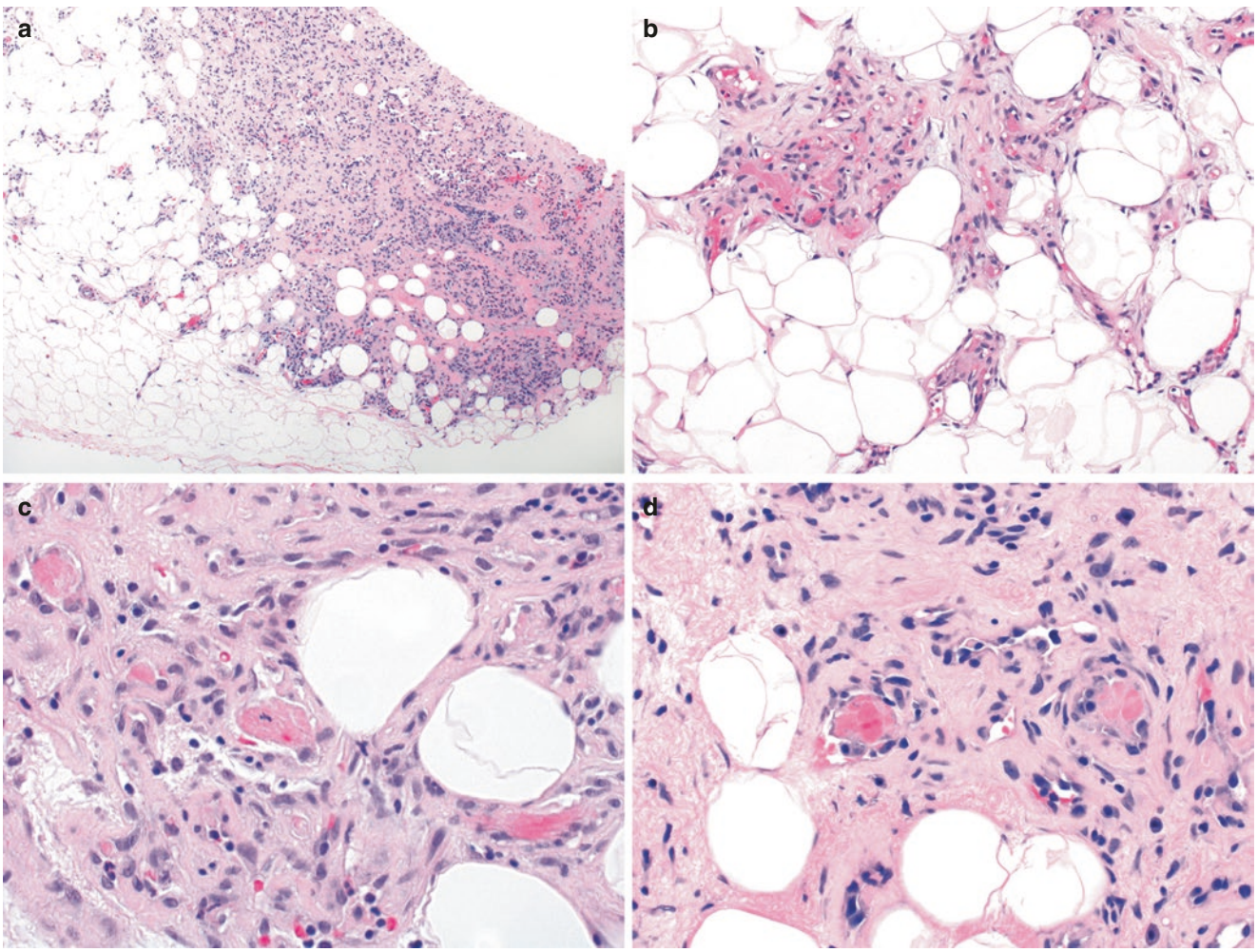

Fig. 16.4 Histologic features of a breast angiolipoma. (**a**, **b**) CNB of a palpable superficial breast mass shows a fairly well-demarcated lesion composed of mature adipose tissue with admixed benign capillaries of varying density. (**c**) The presence of fibrin thrombi within the vascular spaces is diagnostic. (**d**) Angiolipomas may display interstitial fibrosis and scattered mast cells

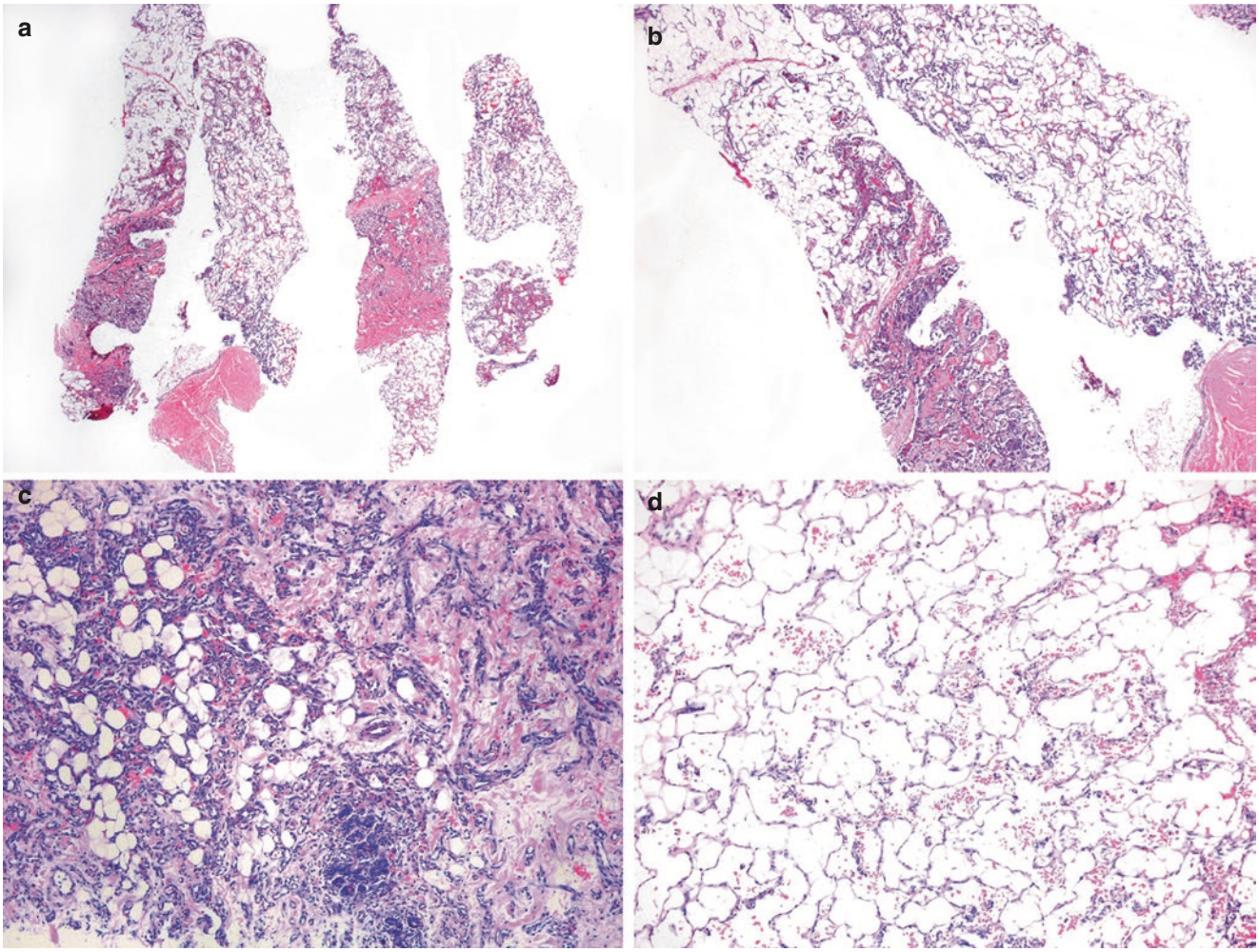

Fig. 16.5 Histologic features of a breast parenchymal well-differentiated angiosarcoma. (**a**, **b**) CNB of a deep parenchymal breast mass shows a variably cellular vascular lesion involving mature adipose tissue. (**c**) Areas of the lesion are composed of anastomosing vascular spaces lined by endothelial cells with subtle nuclear hyperchromasia and enlargement. (**d**) Other regions of the lesion display hypocellularity and minimal atypia, virtually indistinguishable from an angiolipoma; however, fibrin thrombi are absent

mas demonstrate fibrin thrombi in limited material. In such cases, excisional biopsy is recommended to finalize the diagnosis. By definition, hemangiomas should not have a lipomatous component and hence should appear more densely vascular than angiolipomas even in core biopsy samples. However, hemangiomas may undergo lipomatous metaplasia over time, resulting in intermingling of fat cells within the lesion.

Immunohistochemical Workup

IHC is not necessary in the diagnosis of angiolipoma. However, the endothelial cells label for vascular markers such as CD34. Ki-67 is helpful if cases where well-differentiated angiosarcoma needs to be excluded. In the absence of prior biopsy/trauma, angiolipomas and hemangiomas typically show a low Ki-67 index (<2%) (Fig. 16.6a, b), whereas differentiated angiosarcomas are highly proliferative (>50%) (Fig. 16.6c, d) [23]. The use of Ki-67 is most helpful at the opposite ends of the spectrum (straightforward hemangioma at one end, and angiosarcoma at the other) and is not recommended for assessing lesions in the middle (i.e., predominantly benign-appearing vascular lesion with some atypical features), particularly in core biopsy samples where only limited portions of the lesions are seen.

Pathogenesis

Angiolipomas do not harbor the genetic changes seen in other lipomas such as spindle cell lipomas [24]. A subset of soft-tissue angiolipomas demonstrate mutations in *PRKD2*,

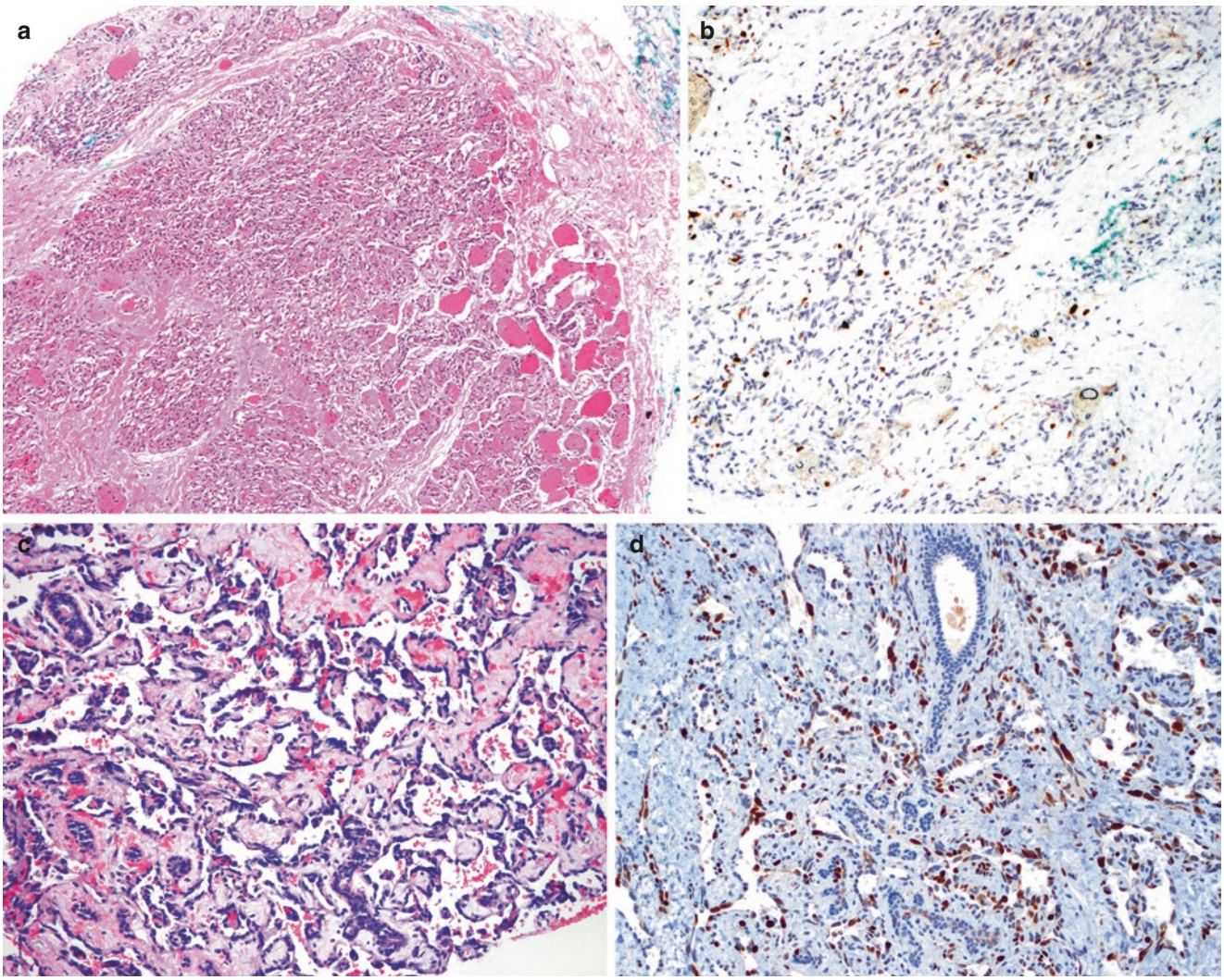

Fig. 16.6 Ki-67 immunoreactivity in vascular lesions. (**a**, **b**) Hemangioma showing low (<5%) Ki-67 index in comparison to (**c**, **d**) angiosarcoma, which shows a high Ki-67 index

whose protein kinase product PKD2 induces endothelial cell proliferation, suggesting that the adipocytes induce the vascular proliferation within the angiolipoma [25].

Prognosis and Management

Angiolipomas are benign neoplasms, and malignant transformation of an angiolipoma has not been reported. They do not require surgical excision if diagnosed unequivocally on CNB [20, 26]. If there is any suspicion that the biopsied lesion may represent angiosarcoma, particularly well-differentiated forms, due to the presence of one or more atypical features or lack of radiographic-pathologic correlation, it is prudent to recommend excisional biopsy for further evaluation. In the past, surgical excision was recommended for all vascular lesions detected on breast CNB; however, that is no longer necessary in cases with radiographic-pathologic concordance and lack of atypia [26, 27].

Hibernoma

Overview

Hibernomas are variant lipomas composed of brown fat. They may involve the axilla, breast axillary tail, breast, or chest wall and have been reported in the breasts of both adults and children [28].

Gross and Radiologic Features

Like classic lipomas, hibernomas are grossly well circumscribed and may have a thin fibrous capsule on cut surface. Hibernomas of the breast may be detected by palpation or by

screening mammography [29]. On mammography, hibernomas are typically denser than the surrounding mature adipose tissue. On ultrasound, these lesions are echogenic and have circumscribed margins [30]. On MRI, hibernomas have signal intensity of fat but will also show post-contrast enhancement [31]. The differential diagnosis includes lipoma, hamartoma, fat necrosis, capillary hemangioma, normal interlobular stromal fibrous tissue, and low-grade liposarcomas.

Microscopic Features

Hibernomas are composed of lobules of polygonal brown fat adipocytes (Fig. 16.7), which are characterized by eosinophilic, granular cytoplasm with multiple cytoplasmic vacuoles. The eosinophilic granularity of the cytoplasm is attributed to abundant mitochondria. As with classic lipomas, the nuclei are small, bland, and peripherally located.

Differential Diagnosis

The differential diagnosis of hibernoma includes other fatty tumors such as lipoma and liposarcoma, as well as residual brown fat, fat necrosis, granular cell tumor, and histiocytoid invasive lobular carcinoma (ILC). Classic lipomas do not contain the multiple granular vacuoles seen in hibernomas. Liposarcomas display nuclear atypia and lipoblasts. Residual brown fat would be seen primarily in children and does not form a distinct mass. Granular cell tumors have granular cytoplasm, but are not vacuolated and are immunoreactive for both S100 protein and CD68. Histiocytoid ILCs demonstrate an infiltrative growth pattern, display nuclear atypia, and are immunoreactive for cytokeratin (CK).

Immunohistochemical Workup

As with classic lipomas, the diagnosis of a hibernoma is made on the histologic features alone. Like other fatty tumors, hibernomas are immunoreactive for S100 protein and negative for CD68.

Pathogenesis

Hibernomas are reported throughout the body, both in areas that could theoretically contain residual physiologic brown fat (such as the axilla) and those that are not known to contain brown fat (such as the thigh) [28]. Thus, some hibernomas may arise from residual brown fat and some may arise from reprogramming of "white fat" (otherwise mature adipose tissue).

Prognosis and Management

Hibernomas are benign neoplasms and are not known to recur if surgically excised.

Leiomyoma

Overview

Leiomyomas of the breast are benign proliferations of smooth muscle that can occur in the subareolar region of males or females [32, 33], or deep ("intraparenchymal") within the breast parenchyma in females [34–36]. Most cases are detected by palpation, and some may be painful [36].

Gross and Radiologic Features

Grossly, leiomyomas are typically well circumscribed with a whorled, homogeneous cut surface. The leiomyomas of the

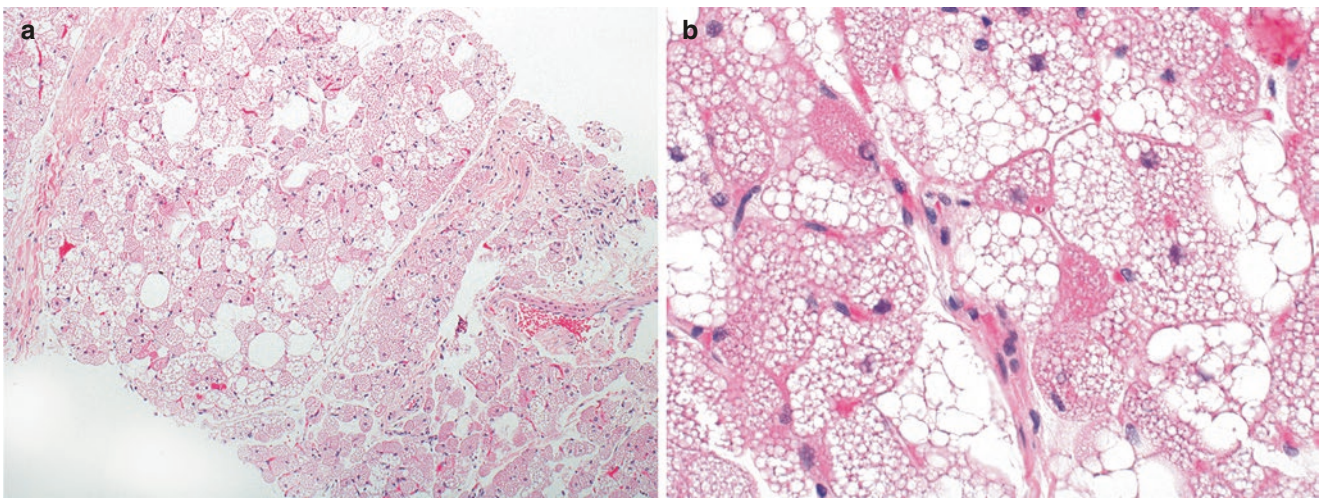

Fig. 16.7 Histologic features of an axillary hibernoma. (**a**, **b**) CNB of this axillary tail mass shows lobules of brown fat characterized by adipocytes with granular, eosinophilic cytoplasm containing multiple small vacuoles and bland nuclei

nipple are typically small [32], whereas the intraparenchymal leiomyomas have been reported to reach up to 14 cm [35]. The larger lesions may display hemorrhage. On mammography, intraparenchymal leiomyomas are homogenous, oval masses with distinct borders and no microcalcifications. On ultrasound, they are typically homogeneous and solid. The differential diagnosis includes fibroadenoma and hamartoma.

Microscopic Features

Leiomyomas of the breast, as in any soft-tissue site, are composed of fascicles of smooth muscle. The spindled cells are characterized by cigar-shaped, blunt-ended nuclei with minimal to no atypia and pale, eosinophilic cytoplasm (Fig. 16.8). The diagnosis of leiomyoma should be limited to those lesions that have pure smooth muscle differentiation and no admixed epithelial or fatty component.

Differential Diagnosis

The differential diagnosis of breast leiomyoma includes myoid hamartoma, myofibroblastoma (leiomyomatous variant), myoid metaplasia of breast myoepithelial cells, and leiomyosarcoma [37]. Breast hamartomas (discussed in detail below) contain an admixture of several tissue types of the breast parenchyma, including adipose tissue, stroma, and lobules. Myofibroblastomas (discussed in detail below) are proliferations of the stromal myofibroblasts and typically do not show the packeted, fascicular growth of leiomyomas except in the leiomyomatous variant. Unlike breast leiomyomas, these variant myofibroblastomas have a lipomatous component as is typical of other myofibroblastoma variants. However, this may not be fully evident in core biopsy samples, and as such, the distinction between these two entities may be impossible until the entire lesion is examined in an excisional biopsy specimen. Myoepithelial cells of the breast may display prominent myoid metaplasia or differentiation,

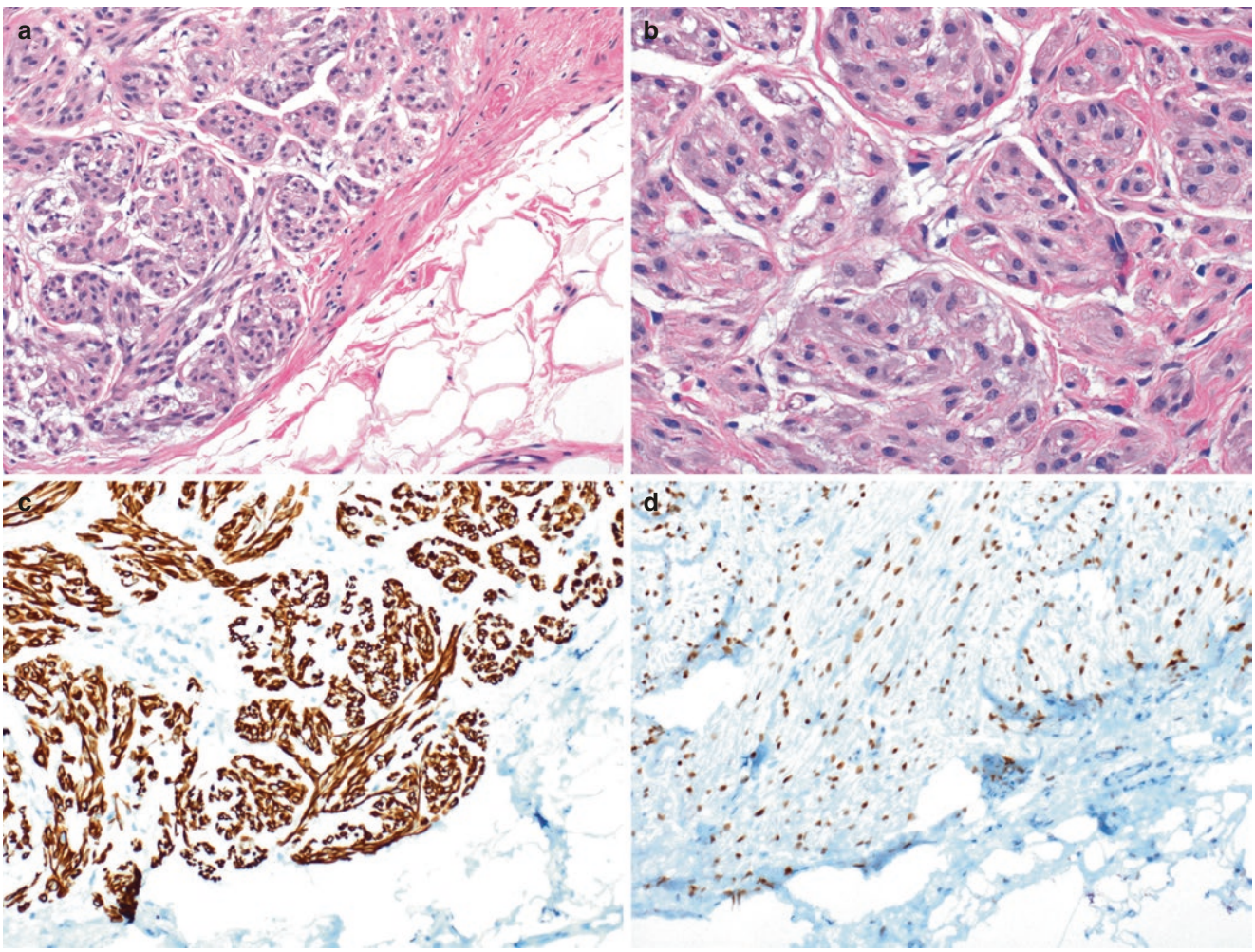

Fig. 16.8 Histologic features of an intraparenchymal leiomyoma. (**a**, **b**) CNB of a palpable, movable intraparenchymal breast mass reveals a well-circumscribed and thinly encapsulated solid mass composed of fascicles of spindled cells cut primarily on cross section. The cells have bland, hypochromatic nuclei and pale eosinophilic cytoplasm. The cells that are oriented longitudinally display cigar-shaped or blunt-ended nuclei. The cells are immunoreactive for (**c**) desmin and (**d**) ER

but they are intimately associated with benign breast lobules and ducts. Finally, leiomyosarcomas of the breast display atypical features including nuclear hyperchromasia, frequent mitoses, and necrosis (Fig. 16.9).

Immunohistochemical Workup

The histologic features of leiomyomas are characteristic of smooth muscle differentiation, and the lesional cells are immunoreactive for markers of smooth muscle differentiation such as desmin (Fig. 16.8c), smooth muscle actin (SMA), and calponin. Leiomyomas of the breast, like leiomyomas of the uterus and retroperitoneum in females, are also immunoreactive for estrogen receptor (ER) (Fig. 16.8d). Multifocal leiomyomas can raise the possibility of hereditary leiomyomatosis and renal cell carcinoma syndrome (HLRCC), which demonstrate loss of immunolabeling for fumarate hydratase [38, 39]. Although myofibroblastomas display immunolabeling for SMA, calponin, and ER like breast leiomyomas, they differ from leiomyomas in that they are also immunoreactive for BCL2, CD10, and CD34. It should be noted that leiomyomatous myofibroblastomas can be CD34 poor (or negative) [40], and therefore, results of this immunostain should not be heavily relied upon in CNB samples.

Pathogenesis

Leiomyomas of the subareolar region likely arise from the smooth muscle bundles of the nipple-areolar complex. The intraparenchymal leiomyomas may arise from blood vessel walls or from myoid metaplasia of the myoepithelial cells [35].

Prognosis and Management

The diagnosis of breast leiomyoma can be made on CNB if sufficient tissue is present in the sample to adequately reflect the entire lesion; however, in some cases, a diagnosis of myoid hamartoma or leiomyomatous myofibroblastoma cannot be entirely excluded, and examination of the entire lesion on simple excision may be necessary to make the distinction. Regardless, these lesions are benign and are adequately treated with conservative simple excision. Additionally, limited sampling of a large but bland smooth muscle lesion may also represent a well-differentiated leiomyosarcoma, so complete excision is advised.

Hamartoma

Overview

Hamartomas of any organ are defined as disorganized proliferations of a mixture of tissue types that are normally present in that organ. Hamartomas account for approximately 4.8% of benign breast tumors [41] and consist of varying degrees of fat, stroma, and epithelial components (lobules and terminal ducts) in an abnormal arrangement. Several variants have been described, including adenolipoma, chondrolipoma, and myoid hamartoma [9]. However, chondrolipoma is also considered a lipoma subtype [42].

Gross and Radiologic Features

Grossly, hamartomas are well-circumscribed lesions that are sharply delineated from the adjacent breast parenchyma. Depending upon the proportion of fat within the

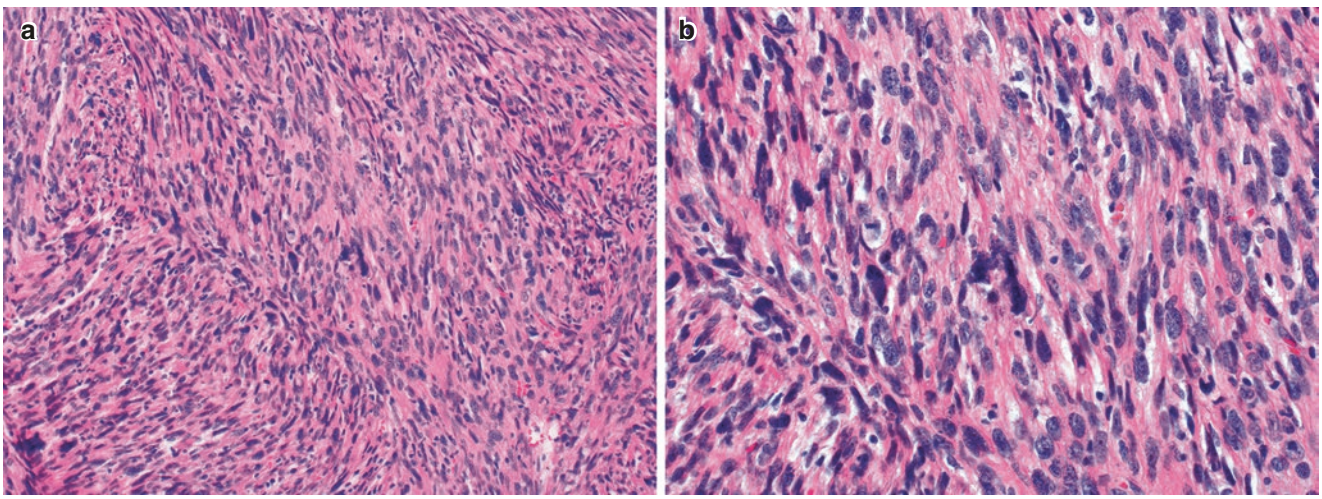

Fig. 16.9 Histologic features of a primary breast leiomyosarcoma. (**a**, **b**) CNB of a well-circumscribed breast mass reveals intersecting fascicles of spindled cells with blunt-ended, hyperchromatic nuclei, and scattered chronic inflammatory cells. The lesional cells are immunoreactive for SMA and desmin (not shown). The patient has no other known site of disease

lesion, a hamartoma may appear more or less fibrous or fatty on cut section. Hamartomas may be detected by palpation [43, 44] or on screening mammography [45]. On mammogram, hamartomas are typically circumscribed, round, or oval masses with mixed density due to having a combination of fat and fibroglandular tissue (Fig. 16.10). A pseudocapsule is sometimes seen as well. On ultrasound, these are well-circumscribed masses with variable echogenicity and no specific diagnostic findings [46]. The differential diagnosis includes fibroadenoma, but the presence of fat density within the mass favors a hamartomatous lesion.

Microscopic Features

Microscopically, mammary hamartomas are composed of varying degrees of mature adipose tissue, stromal fibrous tissue, and ducts and lobules (Fig. 16.11). Hamartomas classified as "adenolipomas" contain abundant mature adipose tissue and foci of benign breast lobules (Fig. 16.12). The stromal component may show very prominent myoid metaplasia ("myoid hamartoma") (Fig. 16.13a–c) [47], or changes of PASH [43, 44, 48]. "Chondrolipomas" consist of mature adipose tissue with foci of mature cartilage.

Differential Diagnosis

The differential diagnosis includes benign breast tissue and fibroadenoma. The features of a hamartoma on CNB may be entirely those of "benign breast tissue" with no obvious feature to suggest a mass lesion (Fig. 16.12a). Thus, it is imperative to correlate with the radiographic findings to know that a mass lesion is present, and the corresponding excisional specimen will confirm a well-circumscribed mass that is easily "shelled out" from the adjacent breast parenchyma (Fig. 16.12b). It may also not be possible to definitively distinguish between a hamartoma and a fibroadenoma on the limited sampling of a CNB.

Immunohistochemical Workup

The diagnosis of mammary hamartoma is made on the basis of the radiographic and histologic features; however, the stromal component will label as do the native benign myofibroblasts. In particular, myoid hamartomas will be immunoreactive for SMA, desmin, and ER (Fig. 16.13d–f).

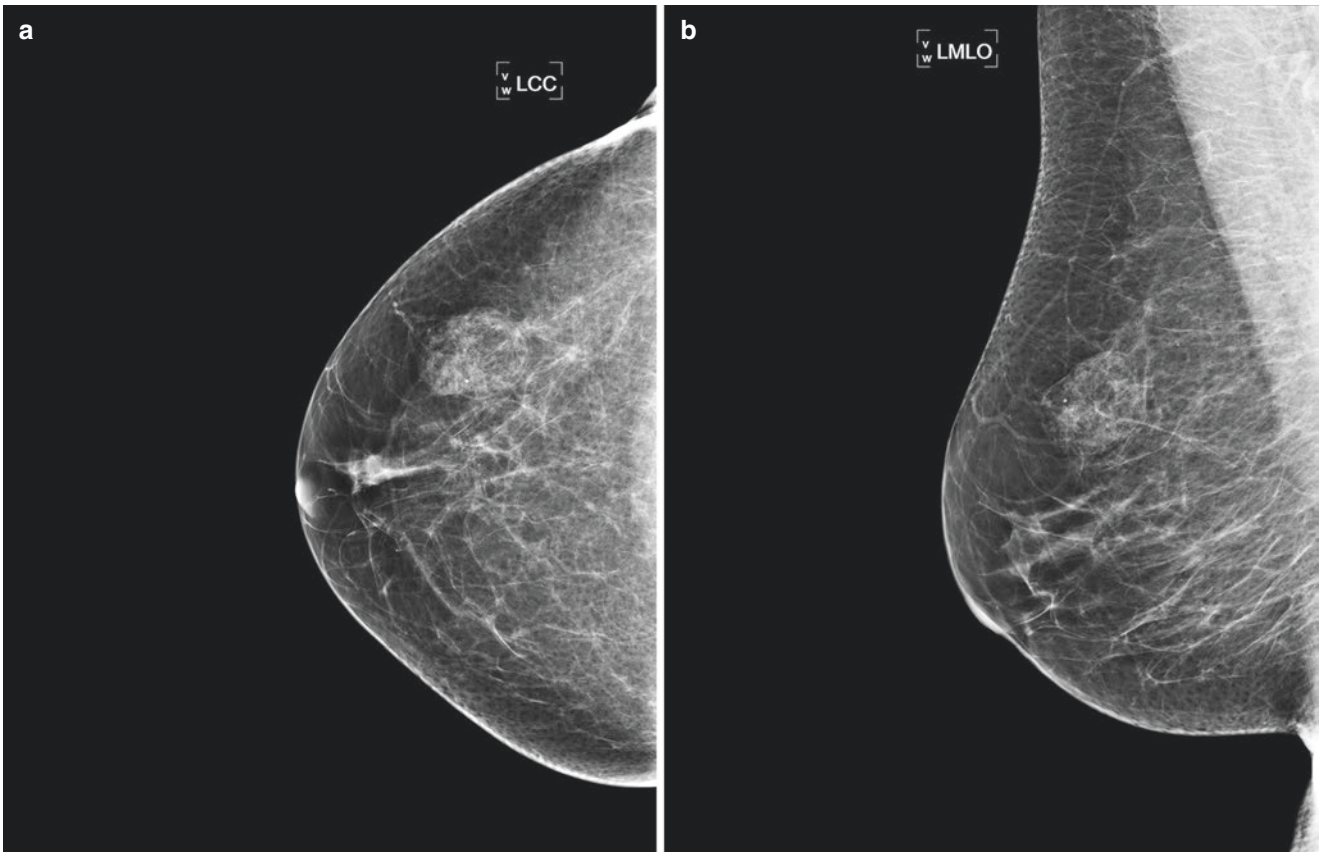

Fig. 16.10 Mammographic features of a mammary hamartoma. (**a**, **b**) Screening mammography in an asymptomatic patient reveals a mixed fat density mass with a thin capsule. The mixed fat density favors a hamartoma over a fibroadenoma

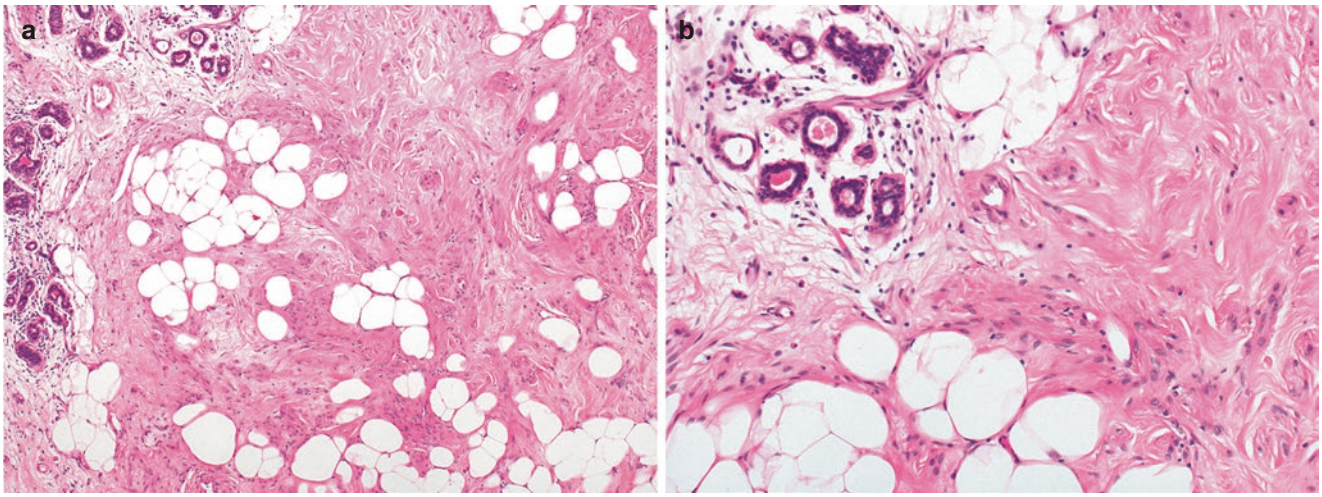

Fig. 16.11 Histologic features of a mammary hamartoma. (**a**, **b**) CNB of a well-circumscribed mass detected on screening mammography shows a haphazard admixture of mature adipose tissue, fibrous breast stroma with focal myoid differentiation, and benign breast lobules

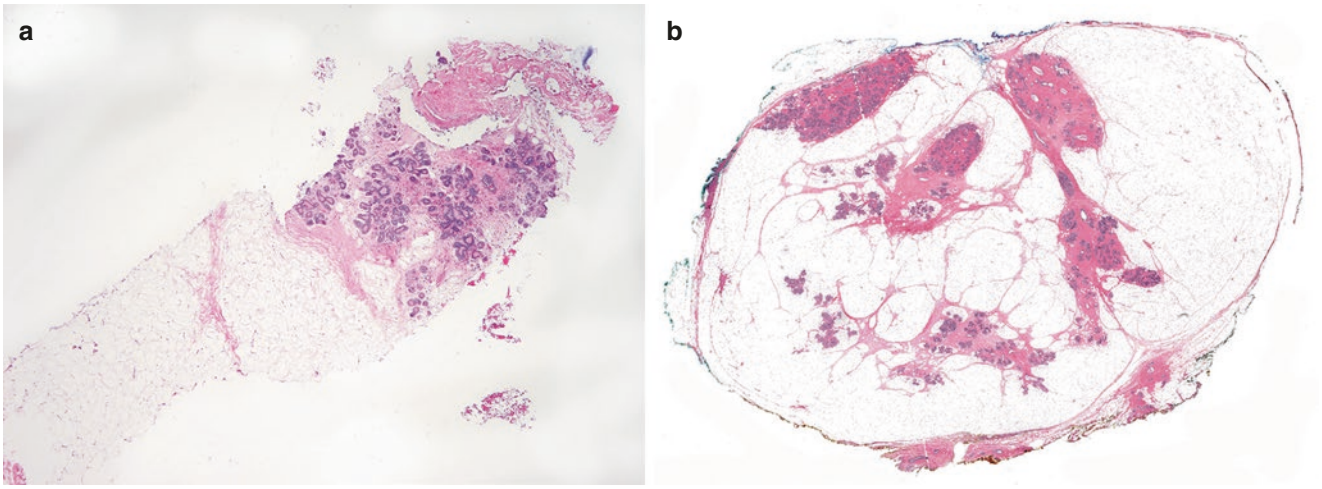

Fig. 16.12 Histologic features of an adenolipoma (mammary hamartoma) and correlation of the CNB with the excisional specimen. (**a**) CNB of the breast reveals mature fibroadipose tissue and benign breast lobules. A definitive diagnosis of an adenolipoma (breast hamartoma) may not be possible on CNB in this case without a clinical history of a palpable mass and a corresponding radiographic finding of a well-circumscribed and demarcated mass. (**b**) On excision, this mass is clearly well circumscribed and consistent with an adenolipoma (hamartoma)

Pathogenesis

The majority of breast hamartomas are sporadic, but they have been reported in association with Cowden syndrome [49], an autosomal dominant disorder due to *PTEN* gene loss that leads to a predisposition for multiple hamartomas, trichilemmomas, oral fibromas, and an increased risk of cancer including breast carcinoma [50, 51].

Prognosis and Management

Hamartomas are benign and are adequately managed with excisional biopsy.

Nodular Mucinosis

Overview

Mucinosis is an extremely rare breast lesion with no definite cellular origin that typically involves the nipple of young women [9].

Gross and Radiologic Features

Grossly, nodular mucinosis is firm and polypoid. On mammography, mucinosis presents as a circumscribed oval or round mass without calcifications [52]. On ultrasound,

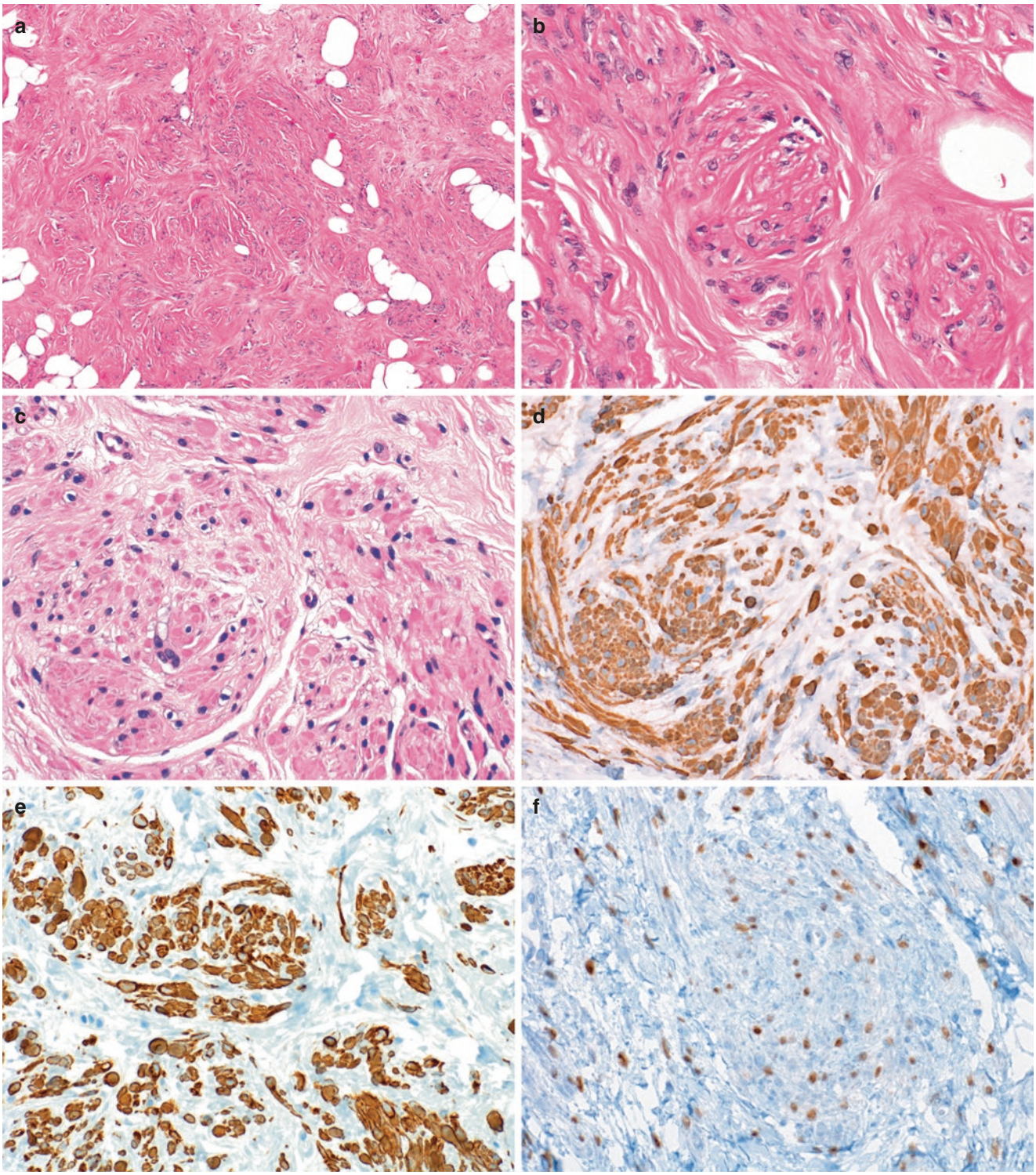

Fig. 16.13 Histologic and immunohistochemical features of a myoid mammary hamartoma. (**a**–**c**) CNB of a well-circumscribed mass reveals fascicles of smooth muscle cells and admixed fat. The presence of the fat differentiates this lesion from a pure leiomyoma. The myoid cells are immunoreactive for (**d**) SMA, (**e**) desmin, and (**f**) ER

mucinosis is circumscribed and homogeneously hypoechoic [52, 53].

Microscopic Features

Nodular mucinosis is composed of myxoid matrix material without any associated epithelial component. There are scattered spindled cells and may be associated histiocytes in the myxoid material.

Differential Diagnosis

The primary diagnostic pitfall in the differential diagnosis is a mucinous (colloid) carcinoma, which would have associated epithelial and glandular elements floating within the mucinous material. Other lesions with abundant myxoid stroma should be considered, such as myxoid fibroadenoma, myxoid nerve sheath tumor, and myxoma.

Immunohistochemical Workup

There is no specific immunohistochemical workup for nodular mucinosis; the spindled cells may be immunoreactive for SMA and are negative for CK [53]. The matrix material stains for Alcian blue and colloidal iron [53].

Pathogenesis

There is no known pathogenesis for this rare tumor. The SMA immunoreactivity in the spindled cells within the myxoid matrix raises the possibility that nodular mucinosis represents a variant of myofibroblastoma [53].

Prognosis and Management

Nodular mucinosis is benign but is best managed by excisional biopsy to exclude a mucinous (colloid) carcinoma.

Myofibroblast/Fibroblast-Derived Lesions

Myofibroblastoma

Overview

Myofibroblastomas are benign proliferations of the breast stromal myofibroblasts. Although originally described as a tumor primarily of the male breast [54], myofibroblastomas are increasingly recognized in adult females, likely attributable to increased diagnosis due to screening mammography [55].

Gross and Radiologic Features

Grossly, myofibroblastomas are typically firm, well-circumscribed, nonencapsulated masses that may rarely show myxoid or lipomatous areas [55, 56]. On mammography, myofibroblastomas are typically high-density oval circumscribed masses with or without associated calcifications [57]. On ultrasound, they are well circumscribed with heterogeneous echogenicity and variable posterior acoustic shadowing (Fig. 16.14). Rarely, these can be hypervascular on ultrasound [57].

Microscopic Features

Mammary myofibroblastomas can show a wide range of histologic features (Figs. 16.15, 16.16, 16.17, 16.18, 16.19, 16.20, 16.21, 16.22, 16.23, 16.24, and 16.25) [56, 58]. Classic myofibroblastomas are composed of spindled cells with pale amphophilic cytoplasm and bland, oval nuclei admixed with a prominent eosinophilic collagen matrix (Figs. 16.15 and 16.16). The lesional vessels may be hyalinized (Figs. 16.16 and 16.17). Benign breast lobules and

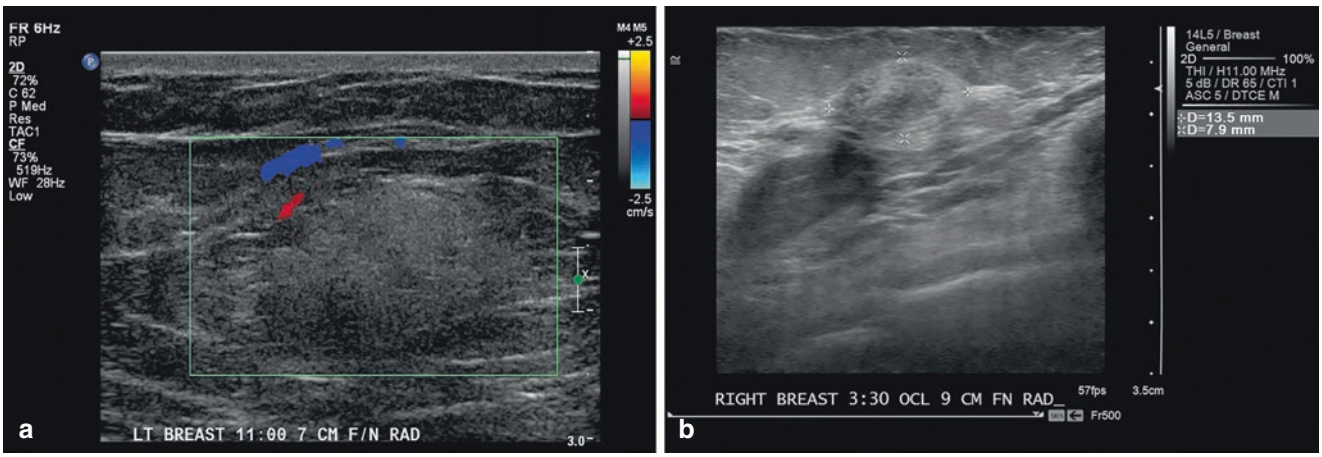

Fig. 16.14 Ultrasound features of mammary myofibroblastomas in a male and a female patient. Ultrasound findings in (**a**) a male and (**b**) a female patient with palpable breast lumps, each revealing an oval, parallel, and circumscribed mass with heterogeneous echo pattern, minimal vascularity, and no posterior acoustic shadowing

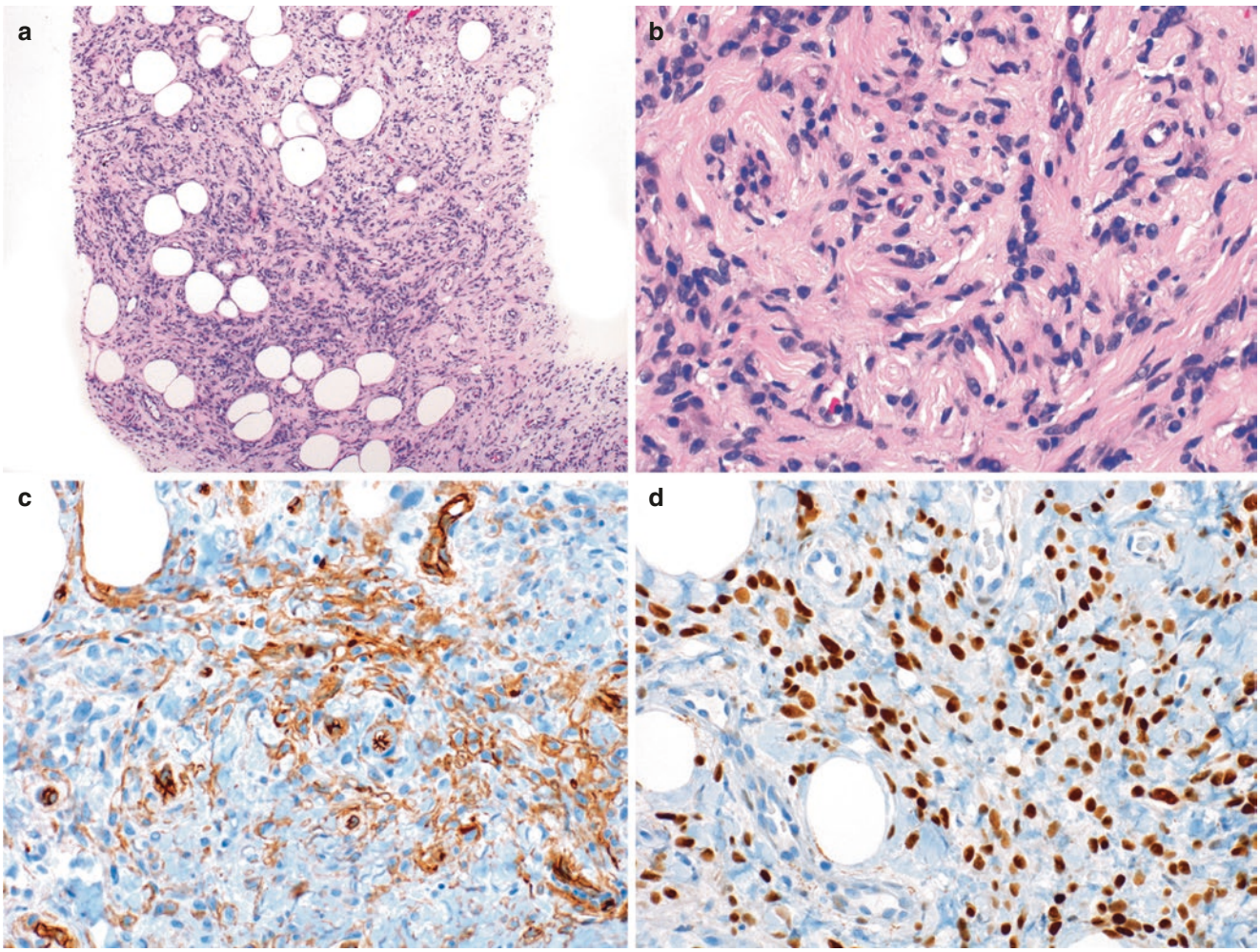

Fig. 16.15 Histologic features of a classic-type mammary myofibroblastoma. (**a**, **b**) CNB of a breast mass reveals a spindle cell neoplasm with admixed mature adipocytes. The lesional cells are oval to spindled with euchromatic nuclei and indistinct cell borders and are imbedded in a collagenous stroma. The cells are immunoreactive for (**c**) CD34 and (**d**) ER and are negative for CK (not shown)

terminal ducts are usually not present within the mass, although myofibroblastomas may rarely display an infiltrative growth pattern. Although classically arranged in nests or fascicles, the myofibroblasts may consist of single cells or cords of cells dissecting the associated collagen and mimicking ILC (Fig. 16.18a, b). Myofibroblastomas lack atypical features such as necrosis or atypical or frequent mitotic figures.

Variant morphologies and patterns include *cellular* myofibroblastomas (Figs. 16.17 and 16.19); *lipomatous* or fat-rich myofibroblastomas that resemble spindle cell lipomas (Fig. 16.20) [11, 12]; *epithelioid* myofibroblastomas with plump round cells (Fig. 16.21) [59]; myofibroblastomas with *chondroid metaplasia* (Fig. 16.22); myofibroblastomas with *myoid metaplasia* (leiomyomatous) (Fig. 16.23) [60]; *myxoid* myofibroblastomas with abundant myxoid stroma (Fig. 16.24) [13]; *deciduoid-like* myofibroblastomas [61]; *collagenized/fibrous* myofibroblastomas (Fig. 16.25) [56]; and *infiltrative* myofibroblastoma [56]. Rarely, myofibroblastomas may contain multinucleated floret-like cells similar to those seen in pleomorphic lipomas, as well as hemangiopericytoma-like areas [62]. Any one given lesion may also show a range of morphologic patterns.

Differential Diagnosis

The differential diagnosis of myofibroblastomas depends upon the morphologic pattern. In general, the differential diagnosis includes other spindle cell proliferations that involve the breast [37], including spindle cell metaplastic carcinoma, phyllodes tumor, rare mammary myofibrosarcoma [63–65], fibromatosis (discussed below), PASH (dis-

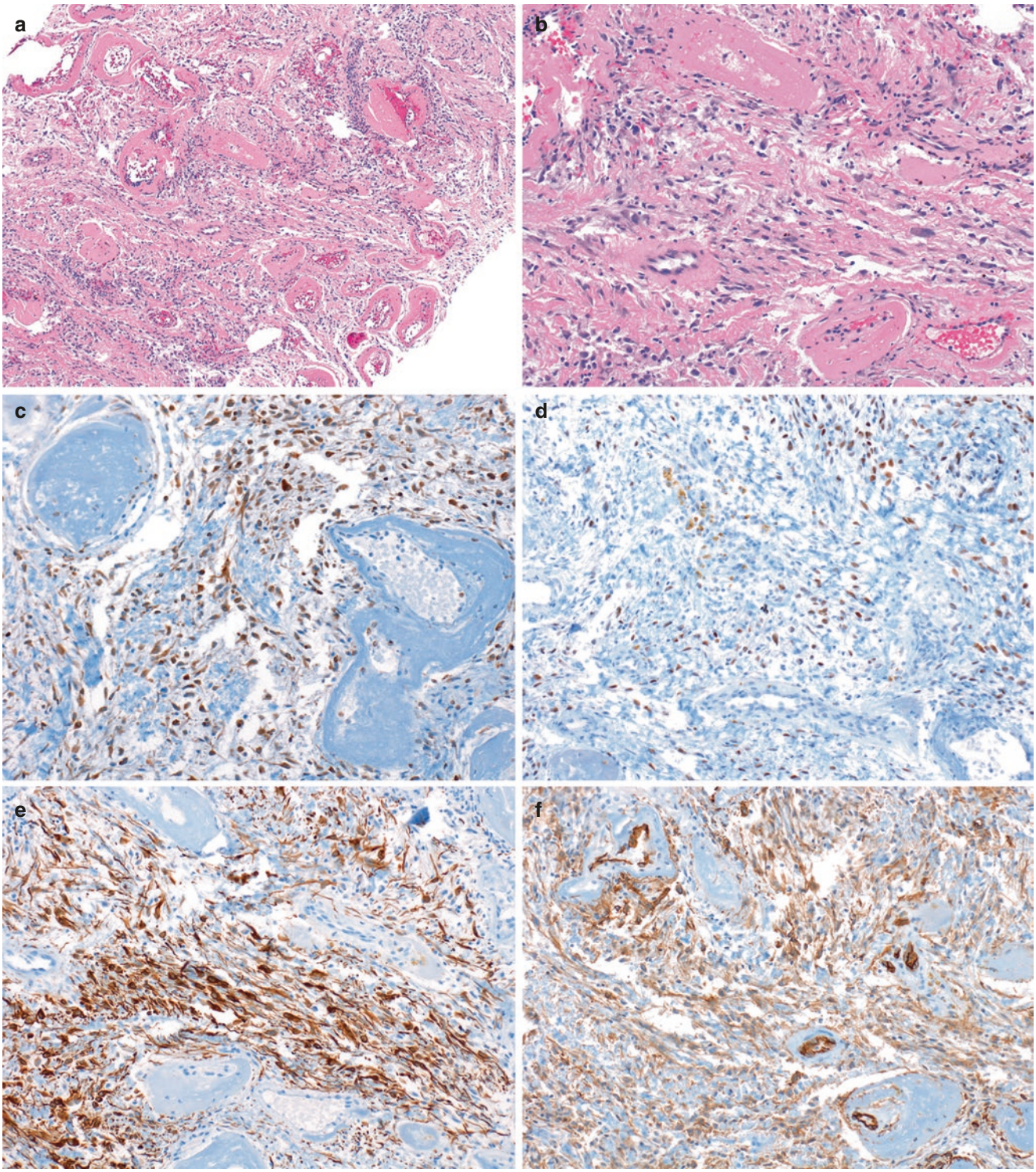

Fig. 16.16 Histologic features of a mammary myofibroblastoma with hyalinized vessels. (**a**, **b**) CNB of an incidentally discovered breast mass in a female shows a spindle cell neoplasm composed of small cells with oval to spindled nuclei, occasional intranuclear inclusions, and indistinct cell borders. The associated stroma comprises delicate eosinophilic, wavy collagen fibrils with scattered chronic inflammatory cells and vessels with hyalinization. The lesional cells are immunoreactive for (**c**) BCL2, (**d**) ER, (**e**) desmin, and (**f**) CD34

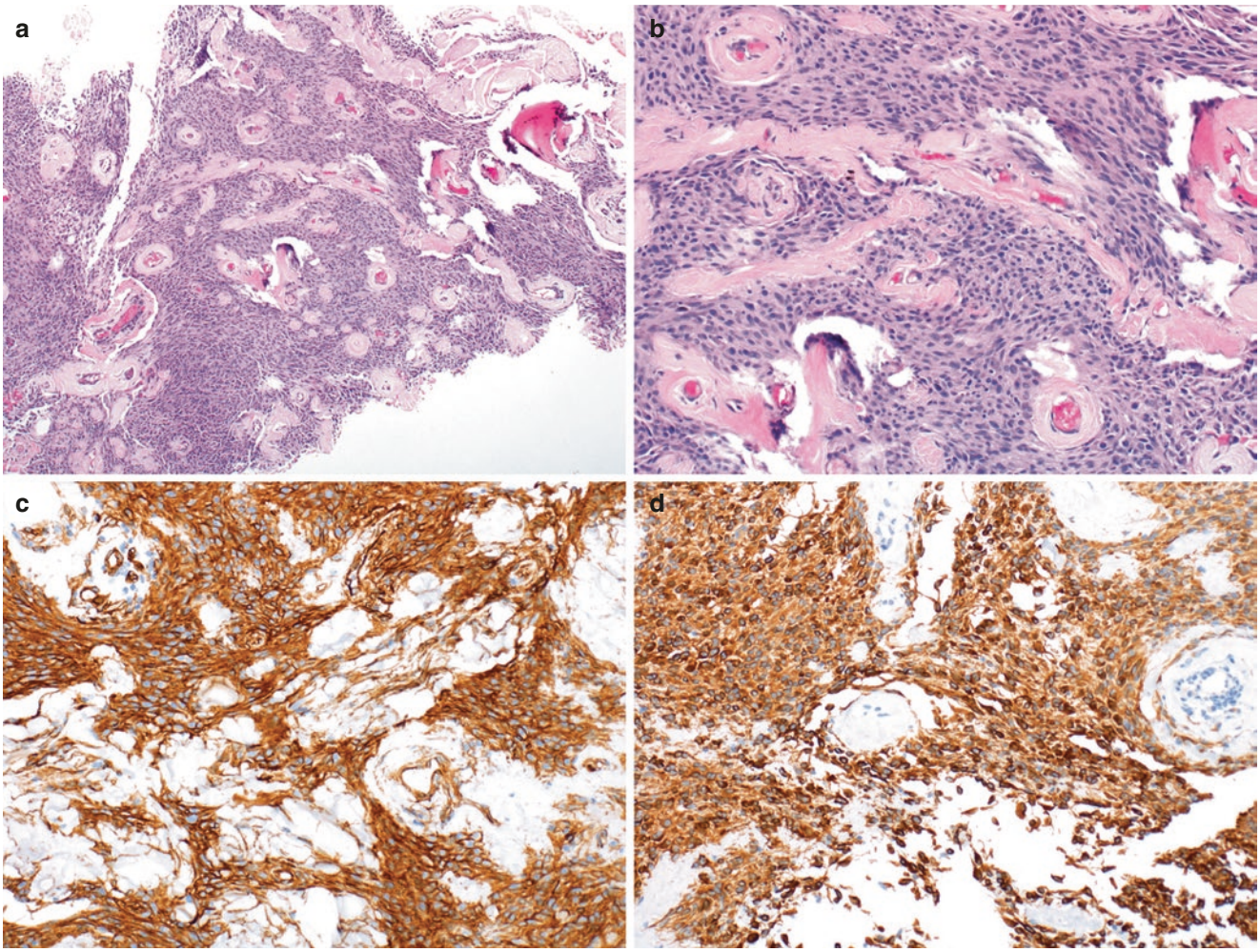

Fig. 16.17 Histologic features of a cellular mammary myofibroblastoma with prominent hyalinized vessels. (**a**, **b**) CNB reveals a cellular lesion composed of spindled to epithelioid cells with amphophilic cytoplasm and indistinct cell borders. There is no prominent collagen matrix here, but the small to medium-sized blood vessels display striking hyalinization. The morphologic features resemble a nerve sheath tumor; however, the lesional cells are immunoreactive for (**c**) CD34 and (**d**) desmin and are negative for S100 protein (not shown)

cussed below), and nodular fasciitis. Myofibrosarcomas display hypercellularity, nuclear atypia and pleomorphism, increased mitotic rate, and infiltrative growth. Epithelioid myofibroblastomas and myofibroblastomas with cord-like architecture mimic invasive carcinoma, particularly ILC. Cellular and palisading myofibroblastomas may resemble peripheral nerve sheath tumors such as schwannoma [66], and myxoid myofibroblastomas closely resemble neurofibromas; however, myofibroblastomas are negative for S100 protein. Myofibroblastomas with myoid metaplasia resemble leiomyomas.

Immunohistochemical Workup

Myofibroblastomas label by IHC as benign stromal myofibroblasts do; they are variably immunoreactive for SMA, desmin, CD34, BCL2, CD99, and hormone receptors including ER and androgen receptor (Figs. 16.15, 16.16, 16.17, 16.18, 16.22, 16.23, 16.24, and 16.25). However, rarely, myofibroblastomas can be CD34 negative [40]. Myofibroblastomas are negative for CKs and S100 protein. Loss of RB expression by IHC has been reported [58], reflecting the associated deletion of 13q14 containing the *RB1* locus. The ER immunoreactivity in myofibroblastomas

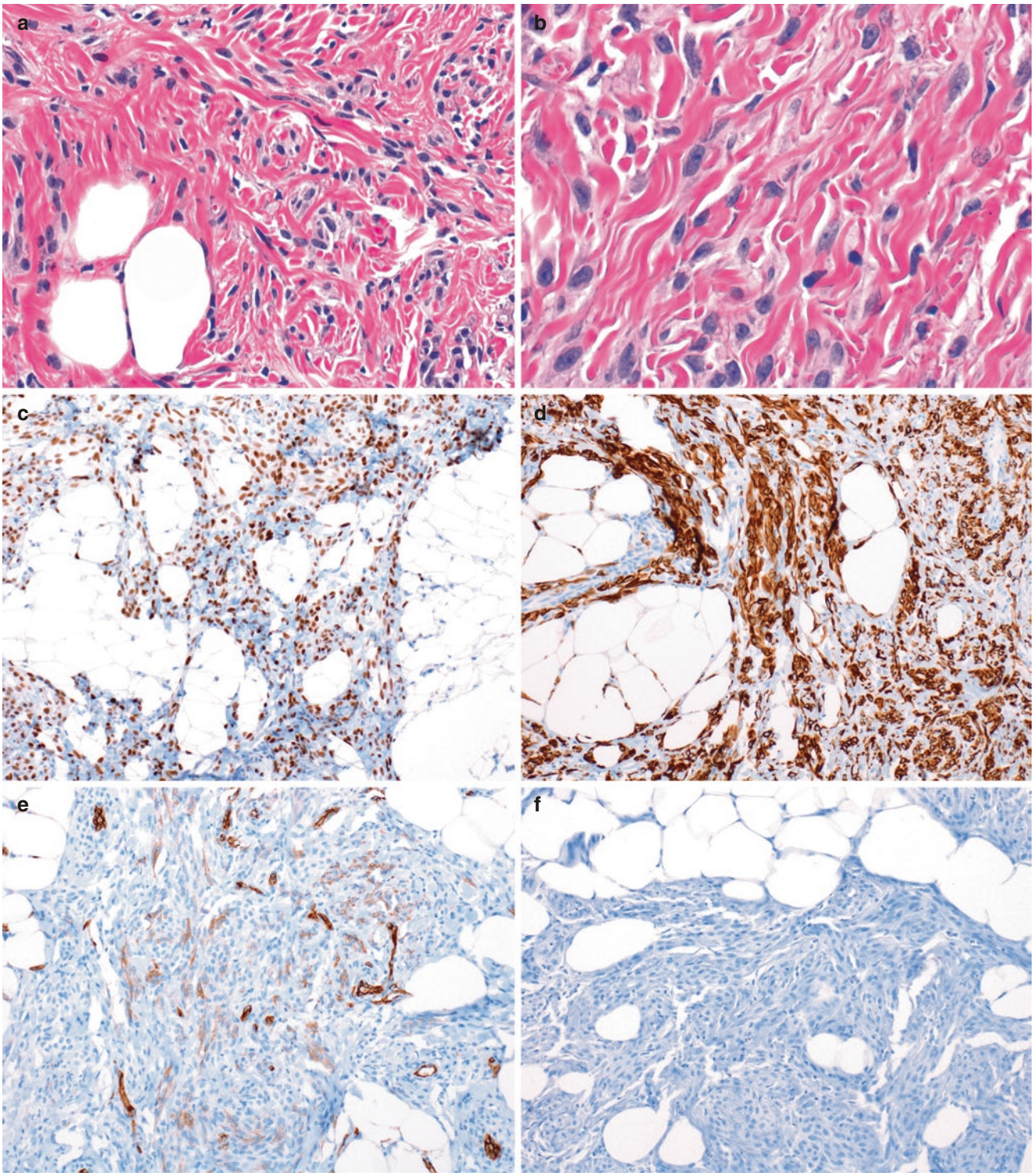

Fig. 16.18 Histologic features of a mammary myofibroblastoma mimicking invasive lobular carcinoma. (**a**, **b**) CNB of a breast mass reveals cords of oval to spindled cells with indistinct cell borders, amphophilic cytoplasm, oval irregular nuclei with punctate nucleoli, and associated bright eosinophilic collagen fibers. The lesional cells are immunoreactive for (**c**) ER, (**d**) desmin, and (**e**) CD34 and are negative for (**f**) CK AE1/AE3

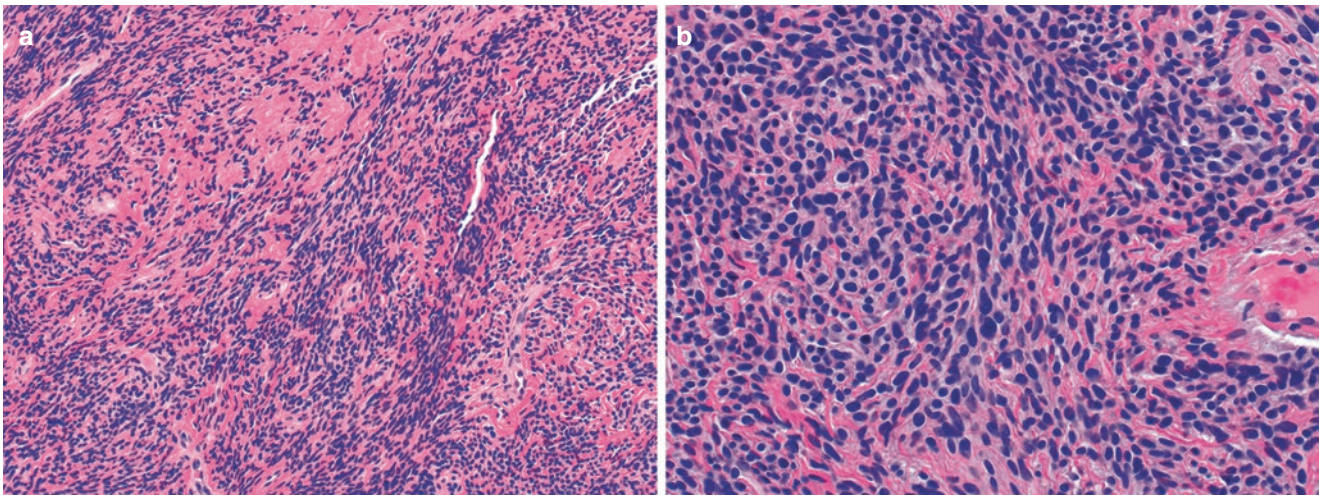

Fig. 16.19 Histologic features of a cellular myofibroblastoma. (**a**, **b**) Occasionally, myofibroblastomas may exhibit increased cellularity due to spindled to epithelioid cells with amphophilic cytoplasm tightly packed within an eosinophilic collagen matrix. These features may resemble a cellular or epithelioid schwannoma, but the cells are negative for S100 protein (not shown)

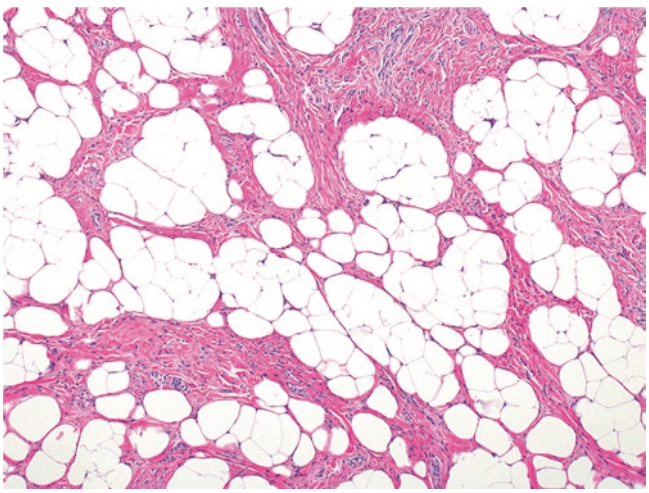

Fig. 16.20 Histologic features of a lipomatous mammary myofibroblastoma. CNB reveals a mass with admixed mature adipose tissue and bland spindled cells embedded in bands of brightly eosinophilic collagen. The morphology resembles a spindle cell lipoma

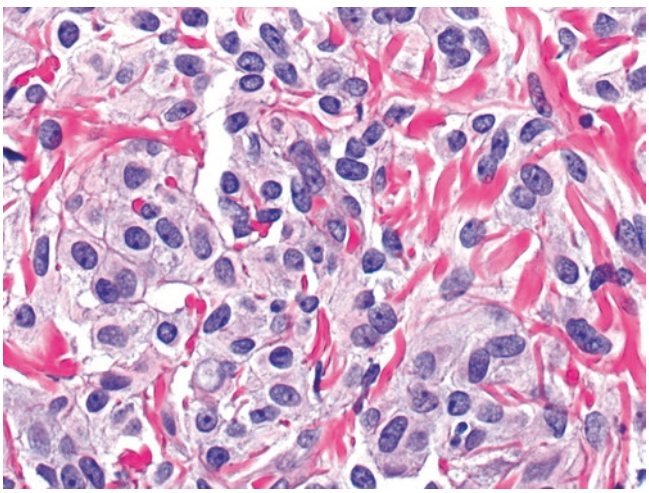

Fig. 16.21 Histologic features of an epithelioid mammary myofibroblastoma. Although myofibroblastomas are classically composed of spindled cells, epithelioid myofibroblastomas display plump, round cells with round to oval nuclei, punctate nucleoli, and occasional intranuclear vacuoles

is a potential diagnostic pitfall in the differential diagnosis of an invasive mammary carcinoma, and a CK immunostain should be included in the immunopanel for this differential.

Pathogenesis

Myofibroblastomas arise from the stromal myofibroblasts. They are considered on the spectrum of spindle cell lipomas and share similar genetic alterations, including chromosomal loss or rearrangements in 13q and 16q [19, 67].

Prognosis and Management

Myofibroblastomas are benign neoplasms, and conservative excision is generally recommended when myofibroblastomas are diagnosed on CNB [9]. Myofibroblastomas are not known to recur after excision.

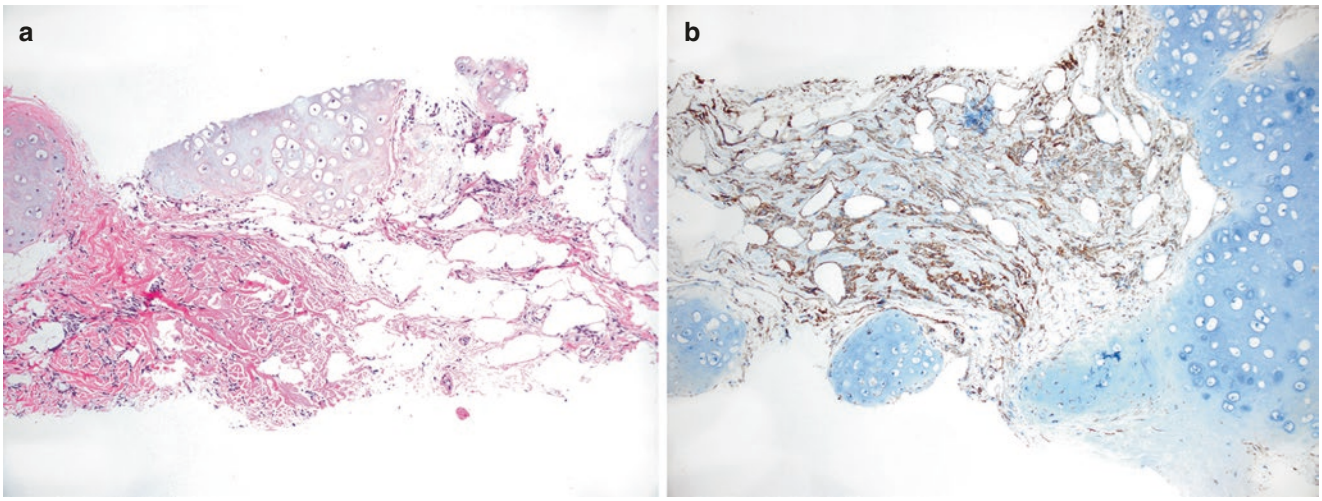

Fig. 16.22 Histologic features of a mammary myofibroblastoma with chondroid metaplasia. (**a**) CNB of this breast mass reveals bland spindled cells with associated bright eosinophilic collagen and mature cartilage. The spindled cells are immunoreactive for (**b**) CD34

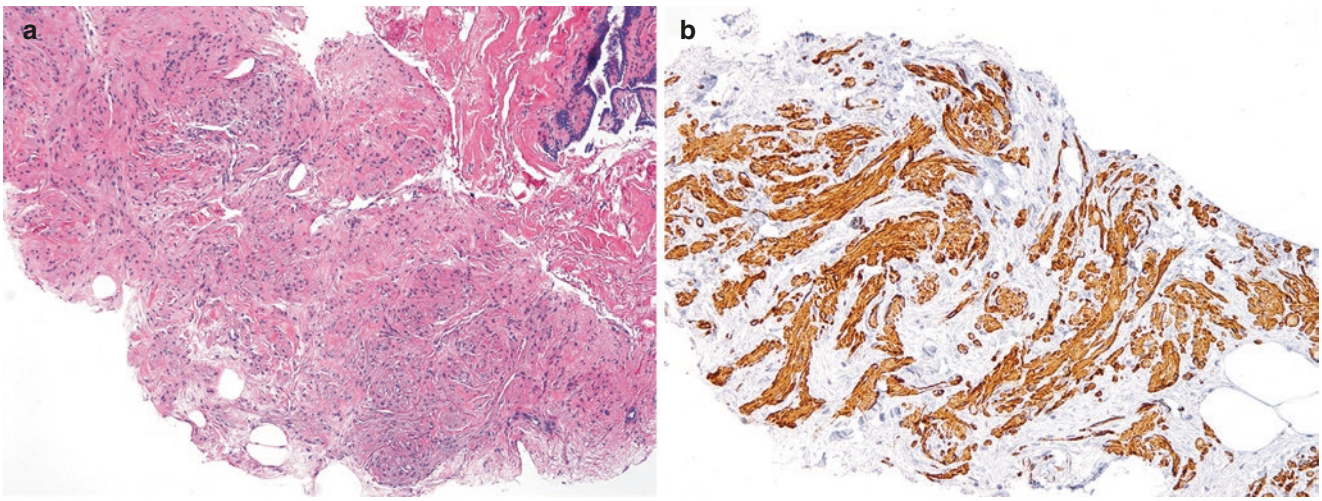

Fig. 16.23 Histologic features of a mammary myofibroblastoma with myoid metaplasia. (**a**) Regions of this leiomyomatous myofibroblastoma on CNB show fascicles of plump cells that in isolation resemble a leiomyoma. However, the presence of admixed adipocytes makes the diagnosis of leiomyoma less likely but rather raises the possibility of myoid hamartoma. Excisional biopsy would be needed to finalize the diagnosis. The cells are immunoreactive for (**b**) caldesmon as well as CD34 (not shown)

Pseudoangiomatous Stromal Hyperplasia

Overview

Pseudoangiomatous stromal hyperplasia (PASH) is a myofibroblastic stromal proliferation that is most often an incidental finding on a CNB or an excision performed for another benign or malignant process [68–70], and PASH is reportedly present in 23% of all routine breast biopsy specimens [71]. However, tumoral or nodular PASH can also form a discrete mass that mimics a fibroadenoma clinically and radiographically. PASH is felt to be hormonally driven. It most commonly affects premenopausal women [72] and is frequently associated with oral contraceptive use [73], but it has also been reported in males typically in association with gynecomastia [74]. PASH has also been rarely reported in pediatric patients [75].

Gross and Radiologic Features

Non-mass-forming PASH is an incidental microscopic finding with no gross correlate; however, non-mass-forming PASH can be detected on imaging. PASH is a concordant biopsy result for focal or clumped non-mass enhancement on MRI. This will typically have a segmental distribution and persistent enhancement [76].

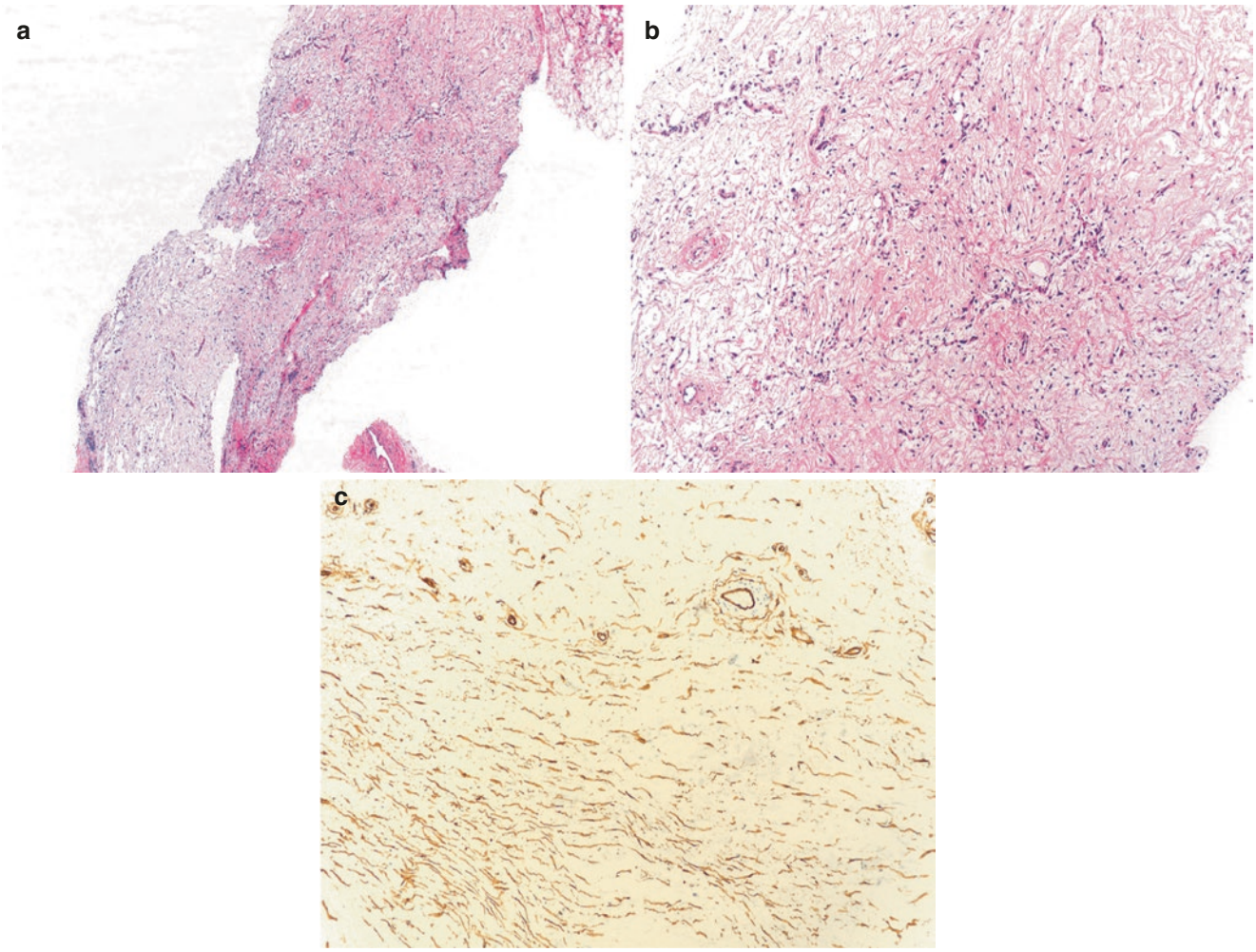

Fig. 16.24 Histologic features of a myxoid mammary myofibroblastoma. (**a**, **b**) CNB of a breast mass reveals a lesion with abundant loose myxoid stroma, delicate capillary vasculature, and bland spindled cells. The lesional cells are immunoreactive for (**c**) CD34 and ER (not shown) and are negative for S100 protein (not shown)

In contrast, nodular PASH is a grossly firm, fibrous lesion that is typically well circumscribed or lobulated. Mass-forming, nodular PASH can present as a palpable mass or be detected on screening mammography, which commonly shows a circumscribed mass without calcifications (Fig. 16.26a) [77]. However, the margins can rarely be irregular and spiculated [76]. On ultrasound, nodular PASH presents as a solid, circumscribed, and hypoechoic or heterogeneous mass with variable posterior acoustic shadowing (Fig. 16.26b, c and d) [77]. Larger lesions can have a lacelike pattern of reticulation with cystic changes. The most common differential diagnoses for mass-forming PASH are fibroadenoma, stromal fibrosis, and phyllodes tumor.

Microscopic Features

PASH is aptly named because it is a proliferation of myofibroblasts forming empty, "pseudoangiomatous" slit-like spaces that may be anastomosing and mimic vascular channels (Figs. 16.27, 16.28, and 16.29). The slit-like spaces are indeed lined by myofibroblasts and not endothelial cells. The slit-like spaces are admixed with benign ducts and lobules and are dispersed through a dense interlobular collagenous stroma and may also involve the intralobular stroma (Fig. 16.28). PASH is frequently accompanied by gynecomastia-like changes, including usual duct hyperplasia and periductular edema (Fig. 16.28) [73]. PASH may be isolated, widely dispersed, or infiltrative (Fig. 16.29).

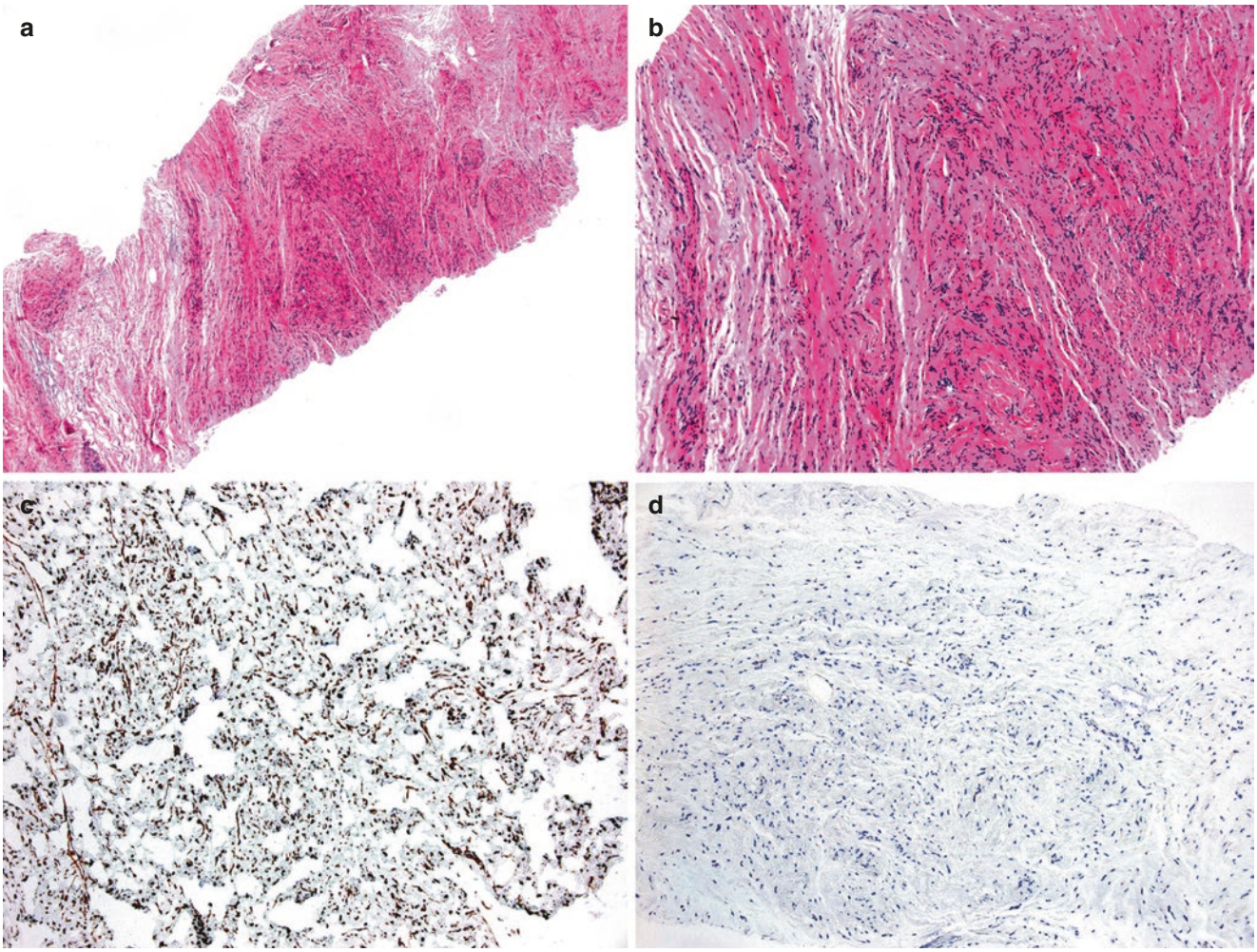

Fig. 16.25 Histologic features of a collagenized/fibrous mammary myofibroblastoma. (**a**, **b**) CNB of this breast mass reveals a variably cellular to hypocellular mass with prominent, dense, and fibrous collagen bundles with inconspicuous bland spindled cells that are immunoreactive for (**c**) CD34 and negative for (**d**) S100 protein

Occasionally, the myofibroblasts may form fascicular bundles and morphologically merge into the spectrum of myofibroblastoma.

Differential Diagnosis

The differential diagnosis for PASH includes vascular lesions, myofibroblastoma, and invasive carcinoma. The primary diagnostic pitfall for PASH is a vascular lesion such as angiosarcoma, in which the slit-like spaces are true endothelial-lined vascular spaces with atypia.

Immunohistochemical Workup

The myofibroblasts of PASH are immunoreactive for CD34 and SMA, as well as hormone receptors [69]. The PASH myofibroblasts are more often immunoreactive for PR than ER [68] and are negative for CKs and endothelial-specific markers.

Pathogenesis

The occurrence of PASH in premenopausal women, its association with gynecomastia in men, and the hormone receptor positivity imply a hormonal etiology [78].

Prognosis and Management

Incidentally discovered, non-mass-forming PASH on CNB does not require subsequent excision [69]. PASH is a benign proliferation, and there is no increased risk of subsequent breast carcinoma [79]. However, there are rare reports of malignancies associated with PASH. There is one reported case of a sarcoma arising in PASH [80], and there are reports of associated invasive [73] and ductal carcinoma in situ [72].

There are reports of nodular PASH recurring after excision [81], with one series reporting a 13–26% recurrence or progression rate [82]. Nevertheless, it is possible that rather than a recurrence, these subsequent lesions represent new

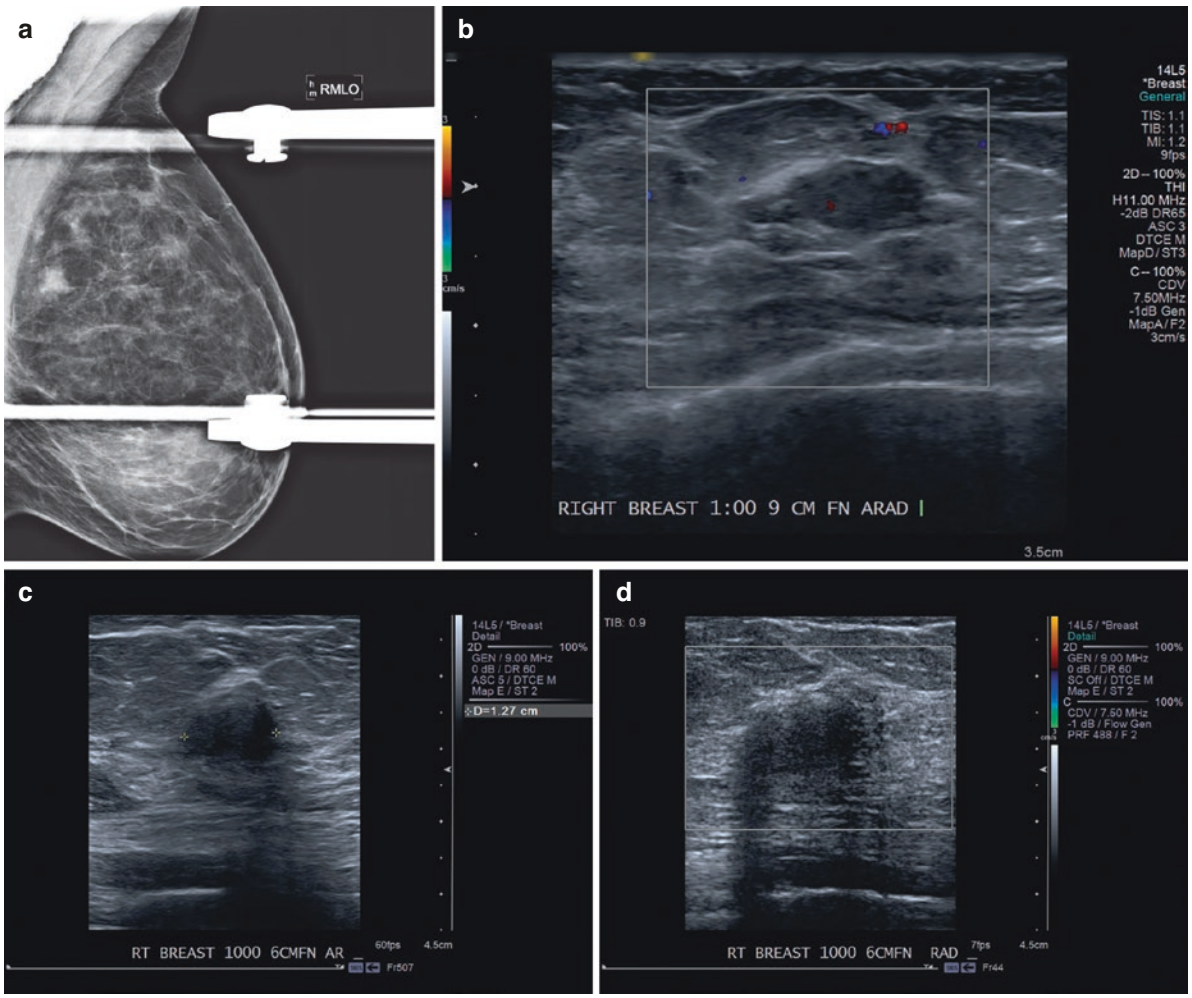

Fig. 16.26 Mammographic and ultrasound features of nodular PASH. (**a**) Screening mammography in a 44-year-old female detects a dense, round mass with indistinct margins and no calcifications in the upper inner, posterior right breast, which on ultrasound (**b**) is oval, parallel, and circumscribed with no posterior sound change and heterogeneous echogenicity. These findings favor a benign process. (**c**, **d**) In contrast, ultrasound images of an incidentally discovered mass in a 49-year-old female show an irregular mass with indistinct margins and posterior acoustic shadowing. These findings are radiographically suspicious for malignancy

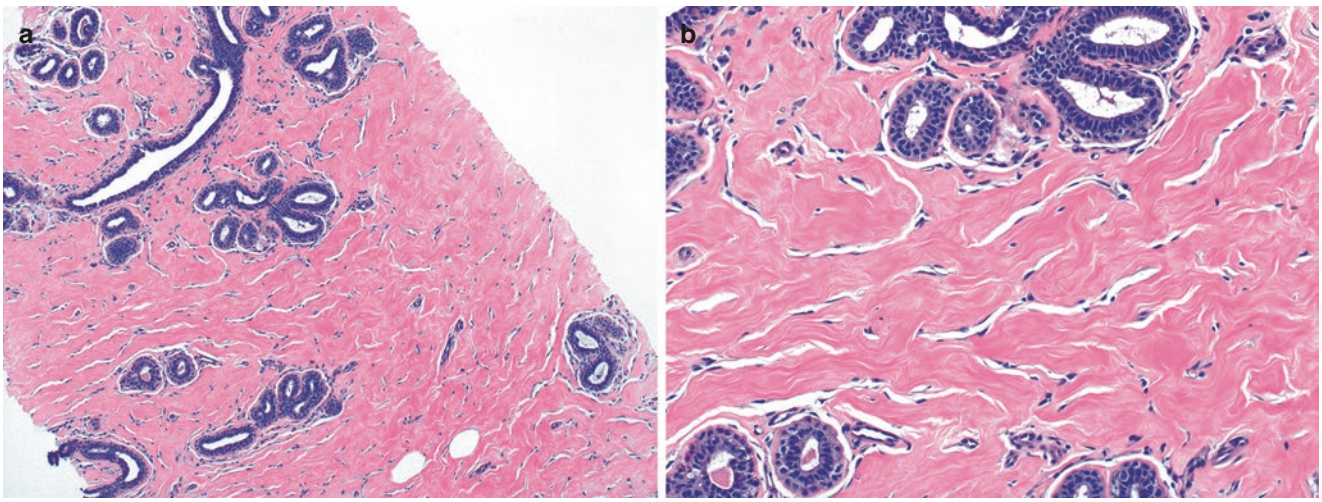

Fig. 16.27 Histologic features of pseudoangiomatous stromal hyperplasia (PASH). (**a**) CNB of a non-mass-like enhancement detected on MRI reveals a dense collagenized stroma with empty slit-like spaces permeating the interlobular stroma. (**b**) The slit-like spaces are lined by bland spindled cells with no atypia or mitotic figures

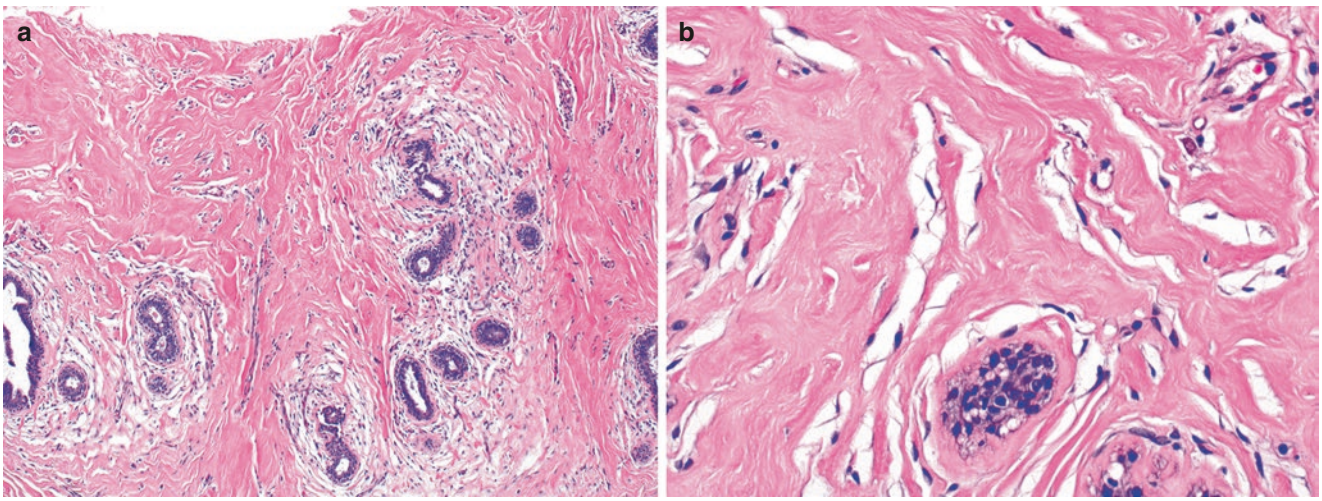

Fig. 16.28 Histologic features of PASH with associated gynecomastia-like changes. (**a**) CNB of a radiographically discovered mass in a female patient reveals dense fibrous stroma with slit-like spaces, usual ductal hyperplasia, and periductal stromal edema. (**b**) The slit-like spaces permeate the inter- and intralobular stroma

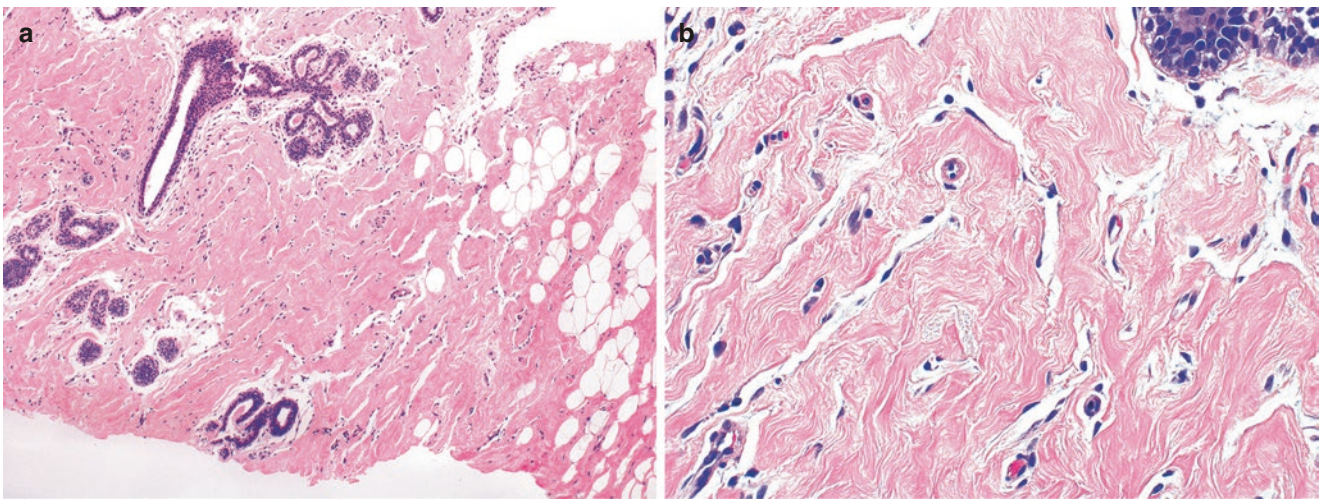

Fig. 16.29 Histologic features of PASH with an infiltrative growth pattern. (**a**, **b**) CNB reveals densely collagenized stroma with slit-like spaces that permeate the mature adipose tissue in an infiltrative growth pattern. The slit-like spaces are empty, focally anastomosing, and lined by bland spindled cells

PASH lesions, as the residual breast tissue is subject to the same hormonal influences that led to the initial occurrence of PASH in the first place. In addition, some lesions may regress spontaneously [68]. Furthermore, in one series, all cases of nodular PASH that were not excised remained radiographically stable, suggesting that clinical follow-up may be adequate in these patients [73]. These findings suggest that expectant, conservative management (i.e., clinicoradiographic follow-up rather than excision) may be appropriate for both incidentally discovered PASH and uncomplicated, nodular PASH diagnosed on CNB.

Fibromatosis

Overview

Fibromatosis (extra-abdominal desmoid tumor) can occur in the chest wall, axilla, superficial breast, or deep breast parenchyma and morphologically and immunophenotypically resembles deep fibromatoses elsewhere in the body. Although deep fibromatoses are associated with Gardner's syndrome, fibromatosis in the breast is most commonly non-syndromic and often seen in patients with a history of prior breast surgery or trauma [83, 84].

Gross and Radiologic Features

Breast fibromatosis commonly presents as a palpable breast mass that is clinically and radiographically suspicious for carcinoma [83, 85]. The lesions are grossly irregular, poorly circumscribed, and infiltrative. On mammography, breast fibromatoses can be round or irregular masses with indistinct or spiculated margins (Fig. 16.30a) and tethering of Cooper's ligaments, mimicking primary breast carcinoma [85, 86]. On ultrasound, they are irregular masses with thick echogenic rim, variable echogenicity, and variable posterior acoustic shadowing (Fig. 16.30b, c). On MRI, they are T2 bright with suspicious-pattern enhancement [86] (Fig. 16.31). MRI can be especially beneficial to show the full extent of disease including chest wall involvement, important in surgical planning.

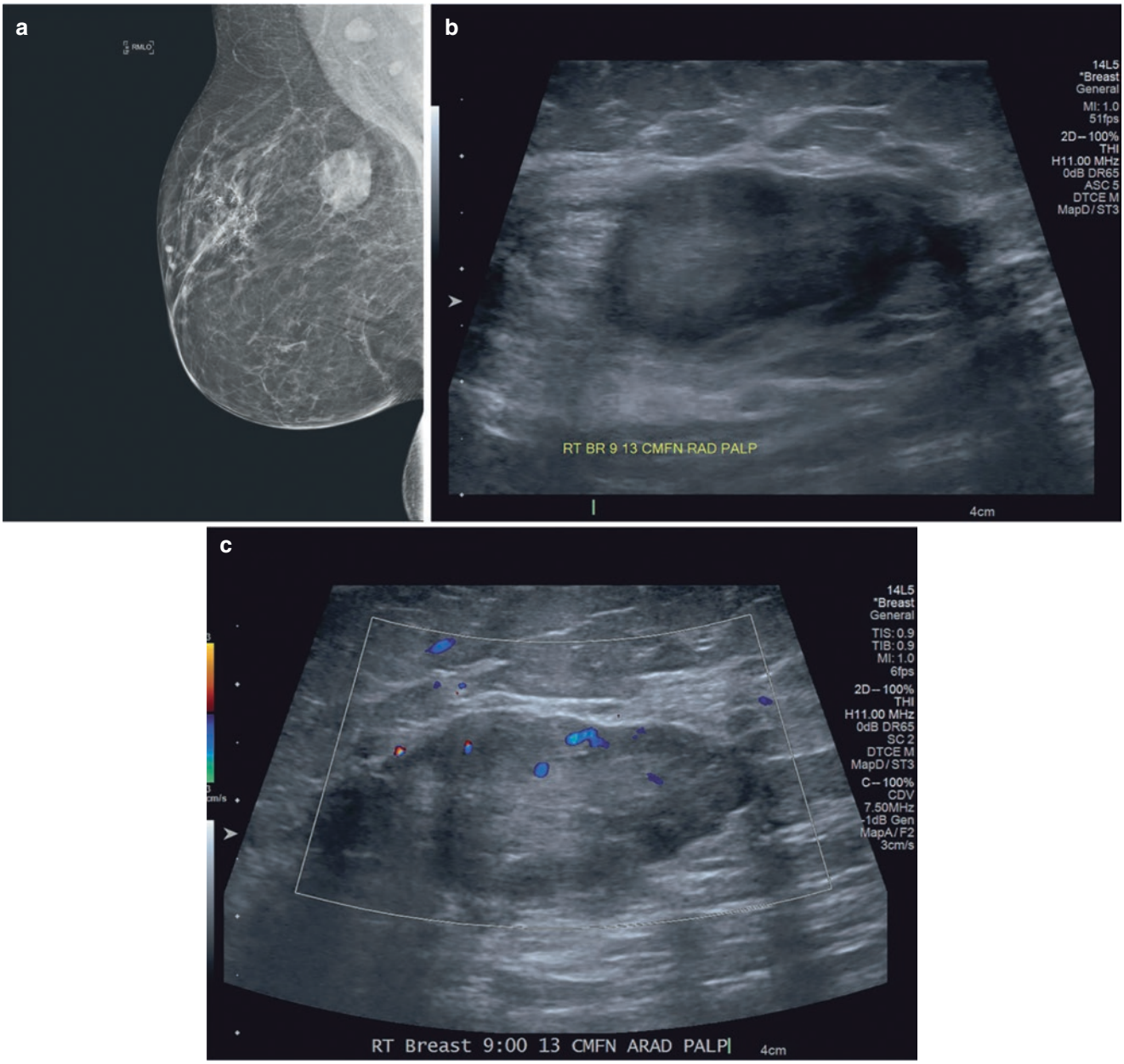

Fig. 16.30 Mammographic and ultrasound features of a fibromatosis in the breast. (**a**) Mammography of a palpable breast mass shows a high-density, round mass with partially circumscribed and partially obscured margins and no calcifications. (**b**, **c**) Corresponding ultrasounds show a vascular, oval, parallel, and circumscribed mass with heterogeneously hypo- and hyperechoic echo patterns and no posterior sound change

Fig. 16.31 Radiographic features of a fibromatosis associated with a breast implant. A 22-year-old female presents with breast asymmetry several years following placement of silicone breast implants for augmentation. Sagittal post-contrast subtracted MRI image shows a large, irregular, heterogeneously enhancing mass posterior to a retropectoral silicone implant. This mass involves the inferior breast and chest wall

Microscopic Features

Microscopically, fibromatoses of the breast and chest wall show identical morphologic features as those elsewhere in the body. The lesions are composed of fascicles of bland spindled cells with elongated nuclei that are hypochromatic in relation to the lesional blood vessels, such that the blood vessels appear to "stand out" at low power (Figs. 16.32 and 16.33). There is often a small space between the blood vessel and the adjacent spindled cells. The stroma can be variably collagenized and may display dense "keloidal" collagen (Fig. 16.33). The appearance of both "young" loose connective tissue and "older" densely fibrous collagenized tissue should be recognized as a characteristic of fibromatoses. The spindle cells may display occasional mitoses, but no atypical mitotic figures or significant nuclear atypia. Fibromatoses often have an infiltrative growth pattern, and peripheral lymphoid aggregates are commonly seen.

Differential Diagnosis

The differential diagnosis for fibromatosis in the breast includes other benign, malignant, and reactive spindle cell proliferations including spindle cell metaplastic carcinoma, phyllodes tumor, primary or metastatic sarcoma such as fibrosarcoma or leiomyosarcoma, myofibroblastoma variants (e.g., fibrous/collagenized), inflammatory myofibroblastic tumor, dermatofibroma, nodular fasciitis, and scar. The primary diagnostic pitfall for breast fibromatosis is fibromatosis-like metaplastic carcinoma of the breast [87, 88], which morphologically resembles fibromatosis with bland infiltrative spindled cells and a collagenized stroma.

Immunohistochemical Workup

Fibromatoses are immunoreactive for SMA and nuclear β-catenin (Figs. 16.32d and 16.33c) and negative for S100 protein, CD31, CD34, CKs, and EMA [89], as well as hormone receptors [90]. Cytoplasmic β-catenin labeling is nonspecific and not indicative of fibromatosis. Nuclear β-catenin is more specific; however, it can also be seen in benign fibroepithelial neoplasms [91]. Of note, however, more importantly nuclear β-catenin labeling has also been documented in 23% of metaplastic breast carcinomas [92], which is a potential diagnostic pitfall in the differential diagnosis of a breast fibromatosis. However, unlike fibromatoses, none of the metaplastic carcinomas studied harbored any evidence of mutation in the β-catenin encoding gene *CTNNB1* [92]. Breast metaplastic carcinomas and specifically fibromatosis-like metaplastic carcinomas of the breast are invariably immunoreactive for CK [87], particularly high-molecular-weight cytokeratin. Furthermore, β-catenin negatively does not exclude the diagnosis of a fibromatosis, as up to 18% of breast fibromatoses [93] and 44% of superficial fibromatoses [94] lack nuclear β-catenin reactivity. In summary, an immunopanel including β-catenin and CKs may be necessary to distinguish between fibromatosis and fibromatosis-like metaplastic carcinoma on CNB or excision. The combination of nuclear β-catenin immunoreactivity and CK negativity supports a diagnosis of fibromatosis.

Pathogenesis

Fibromatoses of the breast harbor somatic mutations in the APC/β-catenin signaling pathway, including mutations in the β-catenin encoding gene (*CTNNB1*), *APC* gene mutations, or allelic loss of 5q [93]. Fibromatoses of the breast have been reported in patients with a history of previous breast surgery [83], breast trauma [84], or breast implants (Fig. 16.31) [84]. The vast majority of cases in the breast are non-syndromic.

Prognosis and Management

Fibromatoses are benign yet can be locally aggressive, particularly if incompletely excised. Local recurrences are reported after surgical excision [95]; however, the relationship between margin status and recurrence rate is unclear [96]. Traditionally, treatment was complete excision to achieve negative margins. However, there is a trend towards a conservative, nonoperative "active surveillance" approach with consideration of tyrosine kinase inhibitors for extra-abdominal desmoid fibromatoses [97], including breast fibromatoses [98, 99].

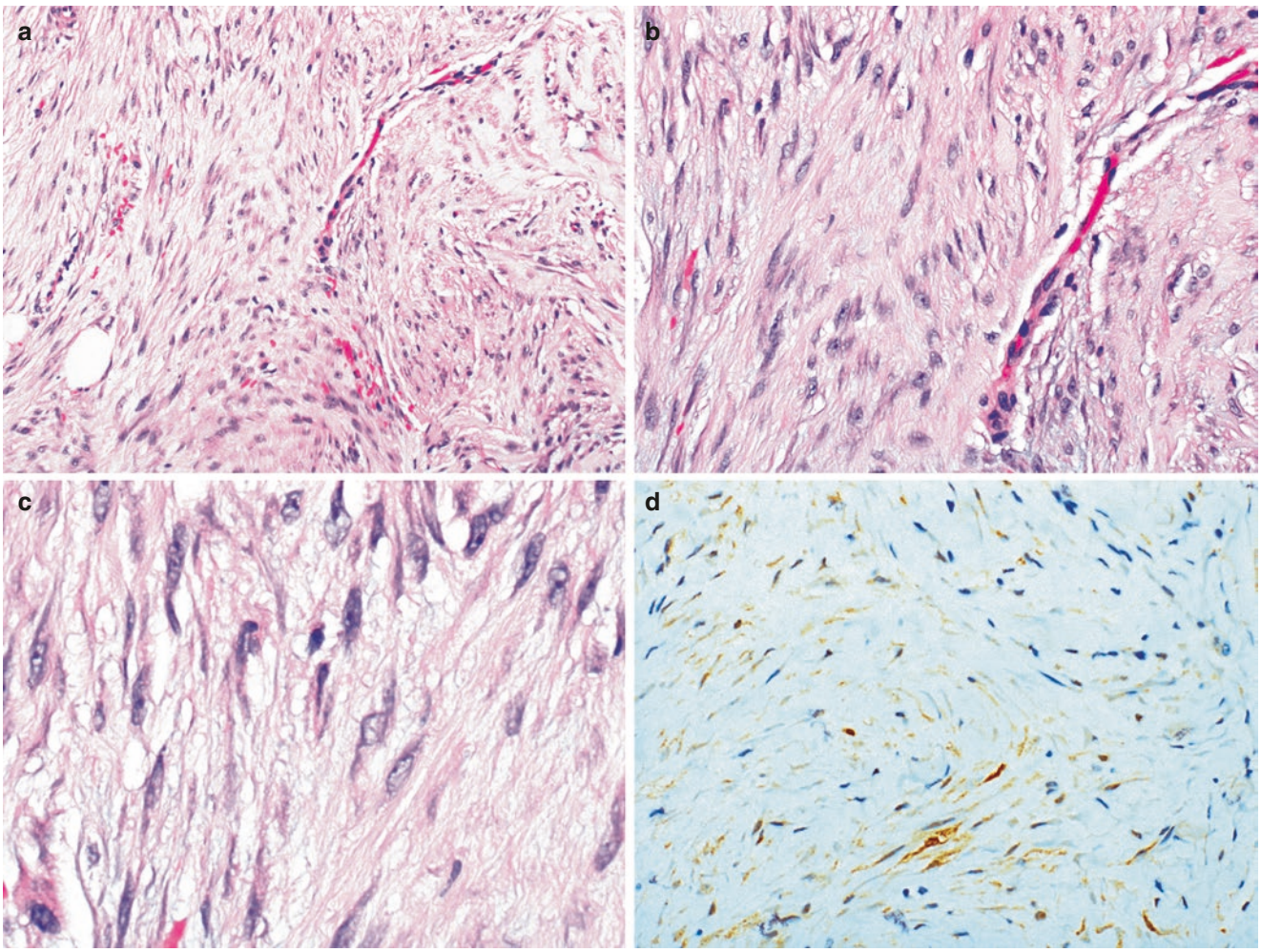

Fig. 16.32 Histologic features of a fibromatosis in the breast. (**a**–**c**) CNB of a palpable breast mass shows a spindle cell neoplasm composed of bland spindled cells that are hypochromatic in relation to the lesional capillaries, and there is a small space between the lesional cells and the blood vessels. The lesional cells are immunoreactive for (**d**) nuclear β-catenin, and they are negative for CK (not shown)

Dermatofibroma

Overview

Dermatofibroma (benign fibrous histiocytoma) is a superficial, cutaneous lesion that may be encountered on breast skin punch biopsy or CNB. Clinically, a dermatofibroma may mimic an accessory nipple [100, 101] or a cutaneous metastasis from breast carcinoma [102].

Gross and Radiologic Features

Clinically, dermatofibromas appear as tan or brown skin papules that characteristically display "dimpling" when compressed or squeezed. The appearance may resemble an accessory nipple both on clinical exam and on dermoscopy [100, 101]. Grossly, dermatofibromas are firm, well-circumscribed masses. Dermatofibromas are typically detected by palpation or clinical inspection and have no specific mammographic findings.

Microscopic Features

Microscopically, dermatofibromas are typically well-circumscribed, nonencapsulated spindle cell proliferations centered in the superficial dermis with a gap ("grenz zone") between the lesion and the overlying epidermis (Fig. 16.34a). The overlying epidermis may have flattened rete ridges with a pigmented basal layer, or alternatively display pseudoepitheliomatous hyperplasia. The spindled cells may be fibroblastic or histiocytoid and display a patternless pattern or whorled pattern (Fig. 16.34a–d). The dermis is collagenized with round nodules of collagen ("collagen balls") entrapped

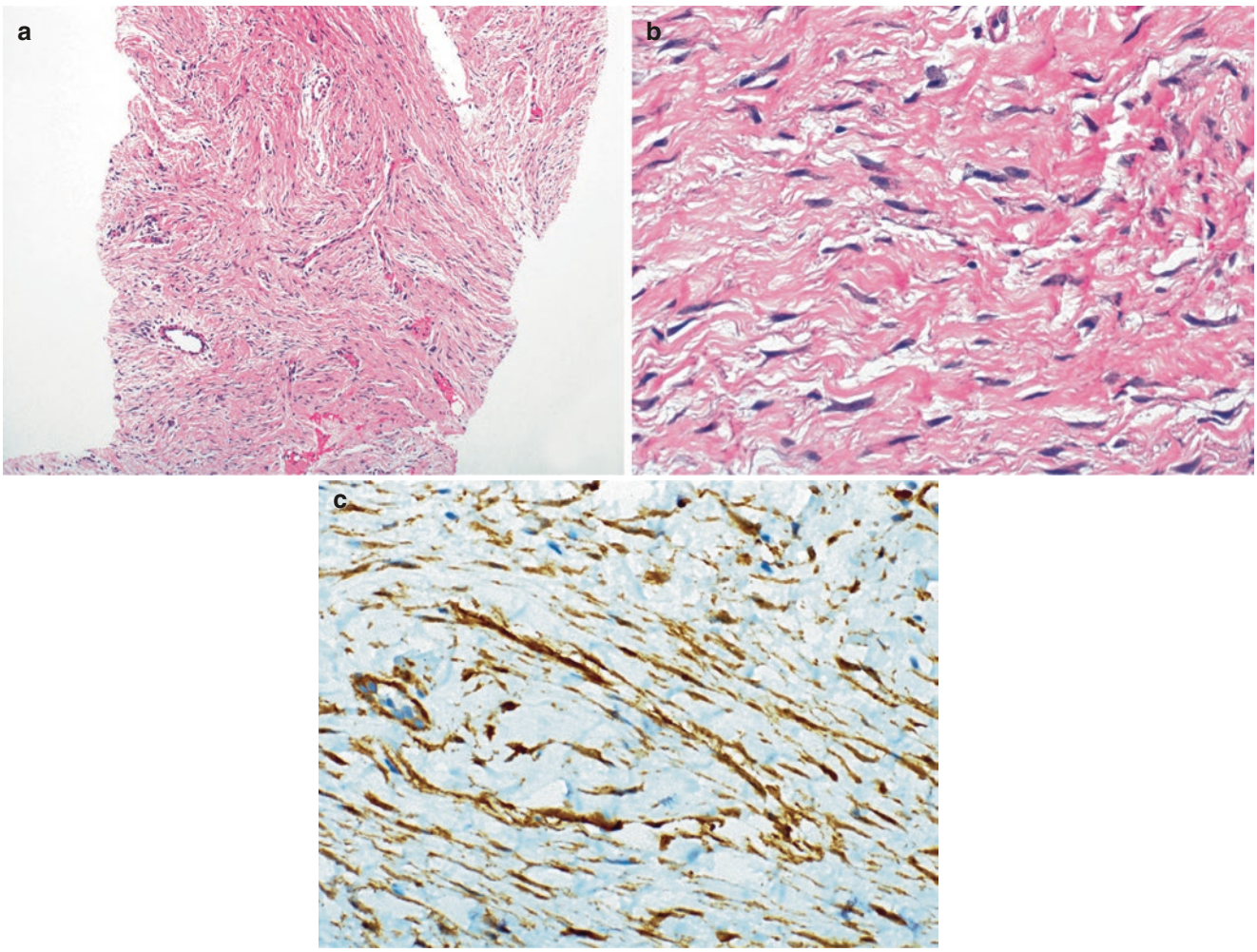

Fig. 16.33 Histologic features of a fibromatosis in the breast with associated keloidal collagen. (**a**, **b**) CNB of a breast mass shows an infiltrative spindle cell neoplasm composed of fascicles of bland spindled cells that are hypochromatic in relation to the lesional capillaries. The collagen is brightly eosinophilic, dense, and keloidal in areas. The lesional cells are immunoreactive for (**c**) nuclear β-catenin and negative for CK (not shown)

by the spindled cells at the periphery of the lesion (Fig. 16.34b). Dermatofibromas may display a range of morphologic variants, including sclerotic, hypocellular, osteoclastic, or myxoid.

Differential Diagnosis

The differential diagnosis of a dermatofibroma on breast punch biopsy or CNB includes other spindle cell proliferations of the skin and breast, including dermatofibrosarcoma protuberans (DFSP), atypical fibroxanthoma, spindle cell metaplastic carcinoma, myofibroblastoma, vascular neoplasms (such as angiosarcoma), neurofibroma, leiomyoma or leiomyosarcoma, scar, and metastasis to the breast skin. The superficial nature of the lesion, centered immediately below the epidermis, should raise the possibility of a cutaneous lesion. When dermatofibromas are especially collagenized or sclerotic, the single individual fibroblasts mimic chronic inflammatory cells or those of ILC.

Immunohistochemical Workup

Dermatofibromas have a variable immunoprofile depending upon the cellular composition of the lesion (i.e., more fibroblastic or histiocytic) [103]. In general, dermatofibromas are immunoreactive for factor XIIIa and variably positive for CD68. They are negative for CD34, BCL2, desmin, and CKs. In contrast, DFSP and myofibroblastoma are immunoreactive for CD34, and spindle cell metaplastic carcinomas are immunoreactive for CKs.

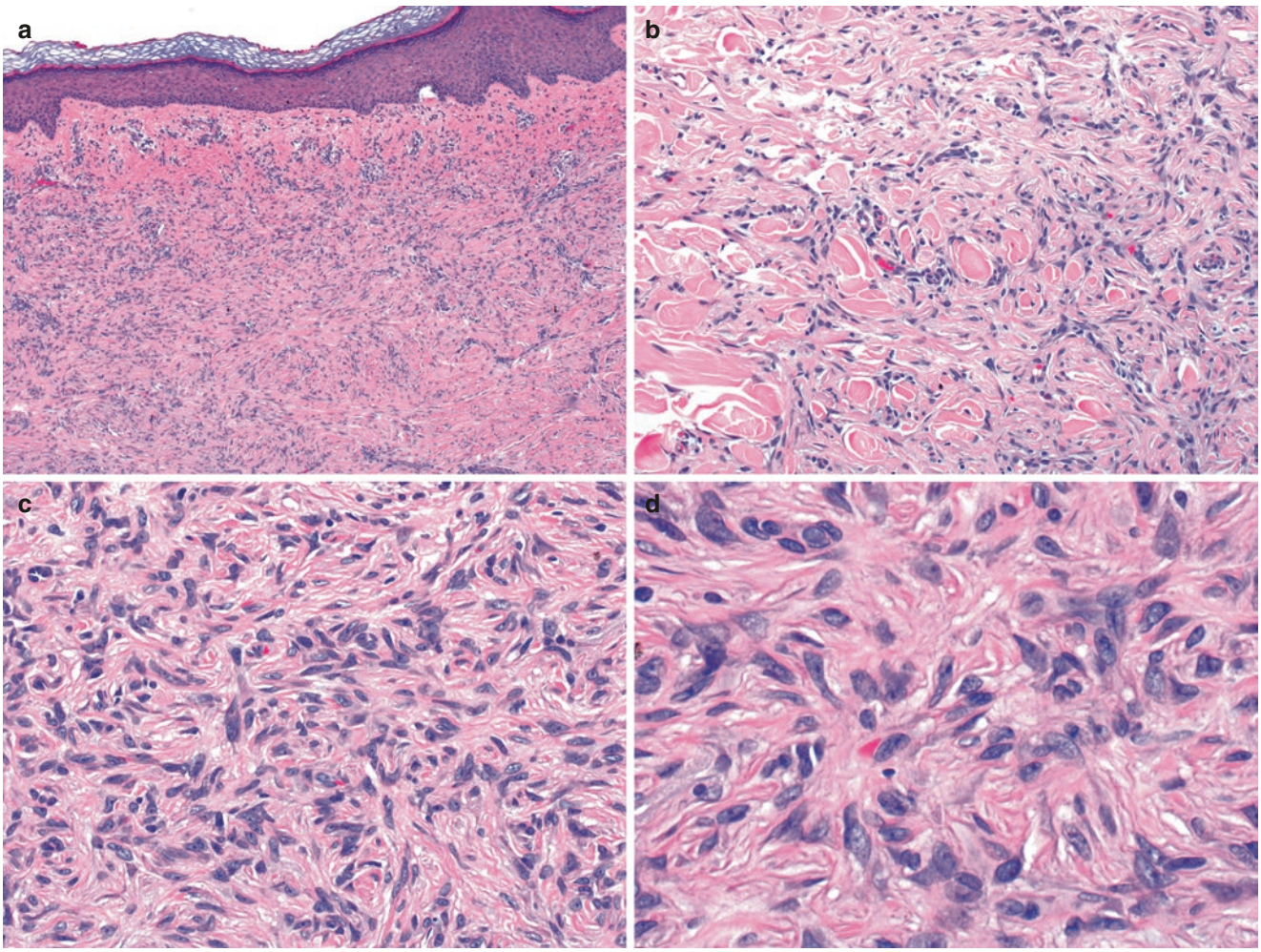

Fig. 16.34 Histologic features of a dermatofibroma in the breast skin. (**a**) Punch biopsy of a lesion in the breast skin reveals a spindle cell lesion centered in the superficial dermis with a collagenized gap (grenz zone) between the lesion and an overlying, flattened epidermis. (**b**) The periphery of the lesion shows rounded nodules of pink collagen ("collagen balls") entrapped by the lesional cells. (**c**, **d**) The lesional cells are spindled to epithelioid, with oval, bland nuclei, indistinct amphophilic cytoplasm, a vaguely storiform growth pattern, and admixed pink collagen fibers

Pathogenesis

Dermatofibromas in the breast skin are sporadic with no specific genetic changes.

Prognosis and Management

Dermatofibromas are benign neoplasms with very rare local recurrences. They are treated by local excision.

Neural Derived Tumors

Granular Cell Tumor

Overview

Granular cell tumors arise from the Schwann cells of peripheral nerves [104]. Although characteristically involving the head and neck region, granular cell tumors can occur throughout the body, and in fact up to 8.5% occur in the breast [105]. Granular cell tumors of the breast most often affect adult women but can also be seen in male [106] and pediatric [107] patients. Granular cell tumors typically grow in an infiltrative fashion and can mimic breast carcinoma clinically, radiographically, and histologically.

Gross and Radiologic Features

Grossly, granular cell tumors can be well circumscribed or infiltrative [108]. Most lesions present as a palpable mass, with approximately 25% detected incidentally on screening mammography [106]. The breast imaging findings are nonspecific but can be suspicious for malignancy [106, 109]. On mammography, granular cell tumors are most often noncalcified masses with spiculated margins (Fig. 16.35a, b)

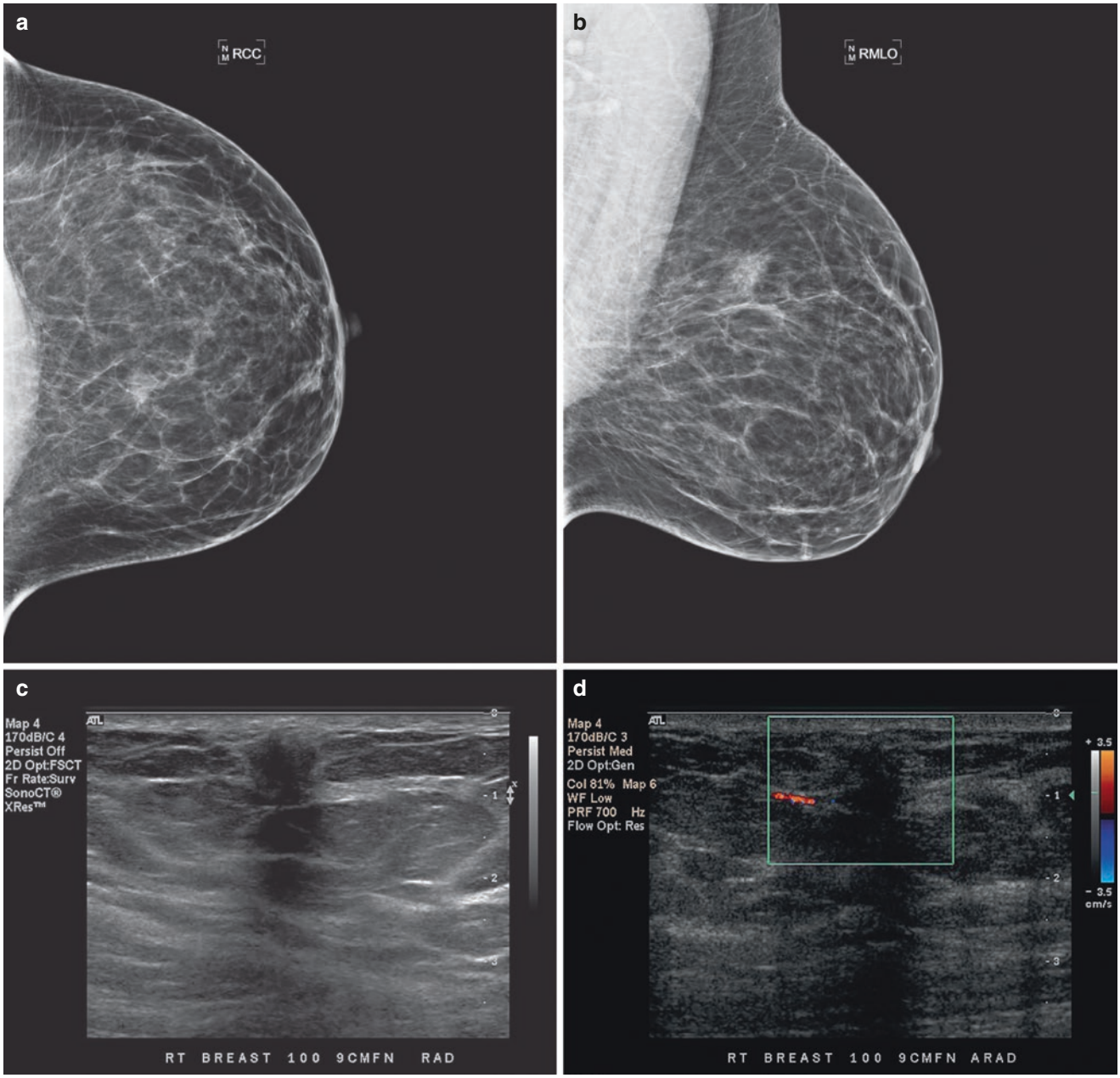

Fig. 16.35 Radiographic features of a granular cell tumor in the breast. (**a**, **b**) Screening mammography shows a dense irregular mass with indistinct margins and no associated calcifications located at 1:00 posteriorly in the right breast. (**c**, **d**) On ultrasound, the mass is minimally vascular, hypoechoic, and irregular with microlobulated margins, an echogenic rim, and posterior acoustic shadowing

due to the infiltrative growth pattern, yet circumscribed margins may also be seen. There may be associated skin thickening or retraction on imaging and clinical exam, mimicking a breast primary carcinoma. On ultrasound, granular cell tumors are usually hypoechoic and can have either posterior acoustic shadowing or posterior enhancement (Fig. 16.35c, d). On MRI, there is variable enhancement including rim and homogeneous enhancement [110]. The differential diagnosis is most significant for primary breast carcinoma; however, fibrosis and PASH can also have similar radiographic appearances.

Microscopic Features

Microscopically, benign granular cell tumors are typically characterized by nests of round to polygonal cells with euchromatic round nuclei, occasionally prominent nucleoli, and abundant eosinophilic, granular cytoplasm (Fig. 16.36a–c). The cells can be difficult to recognize at low magnification

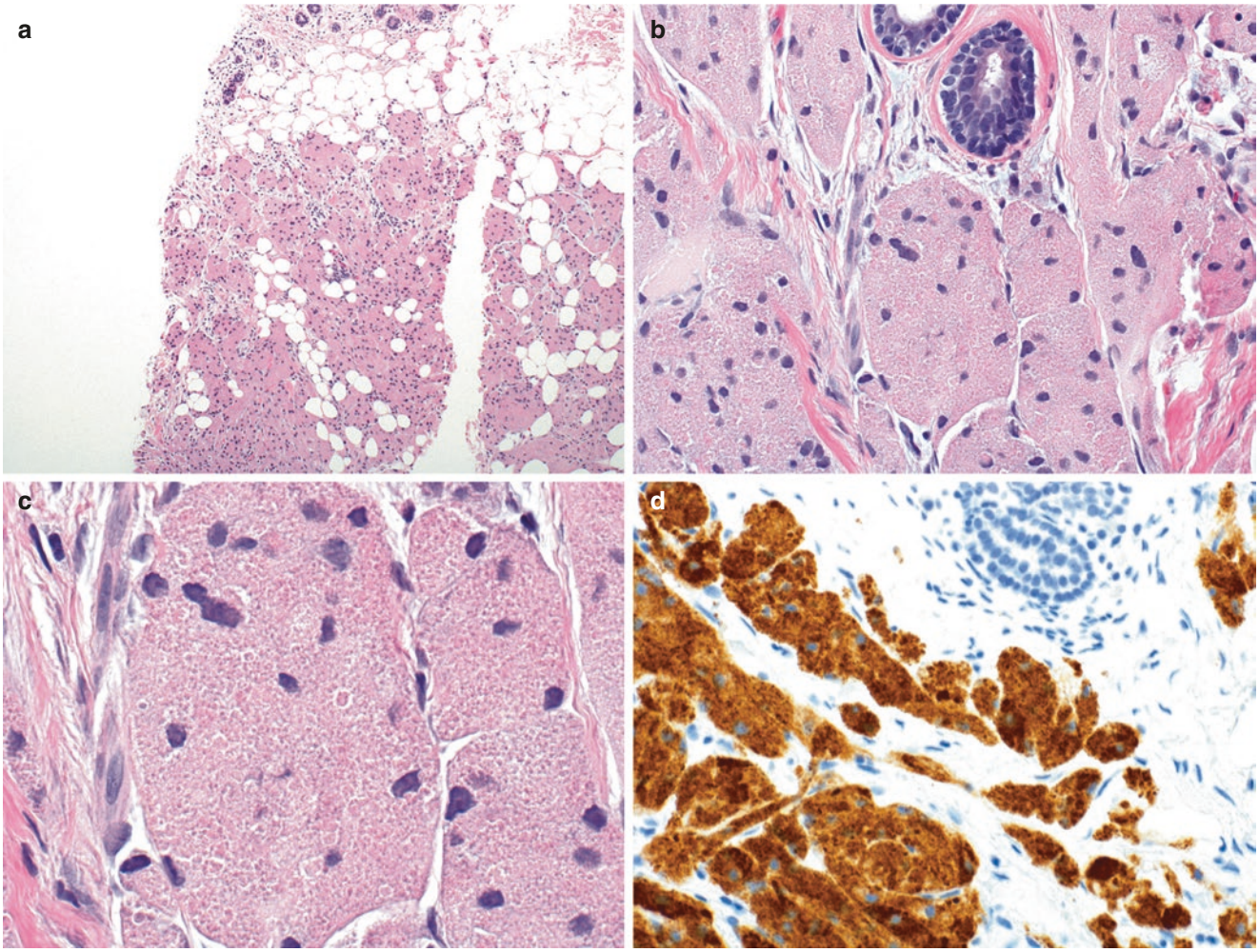

Fig. 16.36 Histologic and immunohistochemical features of a benign granular cell tumor in the breast. (**a**–**c**) CNB of a radiographically suspicious mass shows nests of round cells with indistinct cell borders, abundant eosinophilic and granular cytoplasm, euchromatic nuclei, and focally prominent nucleoli. The nests of cells infiltrate into the mature adipose tissue and around benign breast lobules. The cells are diffusely immunoreactive for (**d**) inhibin and negative for CK (not shown)

if arranged in cords and accompanied by a dense collagenous stroma (Fig. 16.37). When granular cell tumors occur beneath the skin or a mucosal surface, they incite a pseudoepitheliomatous hyperplasia response that can mimic in situ or invasive squamous carcinoma [105]. Mitoses can be seen in benign or malignant granular cell tumors (Fig. 16.38), but having three or more of the following features suggests malignancy, including the presence of necrosis, increased mitotic activity (>2 mitoses per 10 high-power fields), vesicular nuclei with markedly prominent nucleoli, and pleomorphism [111].

Differential Diagnosis

Granular cell tumors mimic primary invasive mammary carcinoma both clinically, due to the presence of a firm, spiculated mass, and histologically, due to the infiltrative nature of the cells and abundant eosinophilic cytoplasm (mimicking apocrine carcinoma). In particular, when granular cell tumors infiltrate as cords of cells (Fig. 16.37), they can morphologically resemble histiocytoid ILC. The differential diagnosis also includes histiocytic proliferations, such as xanthogranulomatous inflammation or fat necrosis.

Immunohistochemical Workup

Granular cell tumors are immunoreactive for inhibin (Fig. 16.36d), S100 protein, neuron-specific enolase (NSE), and CD68 [112, 113]. The cytoplasmic granules are periodic acid–Schiff (PAS) positive and diastase resistant. In contrast to invasive mammary carcinoma, granular cell tumors are negative for CK [113].

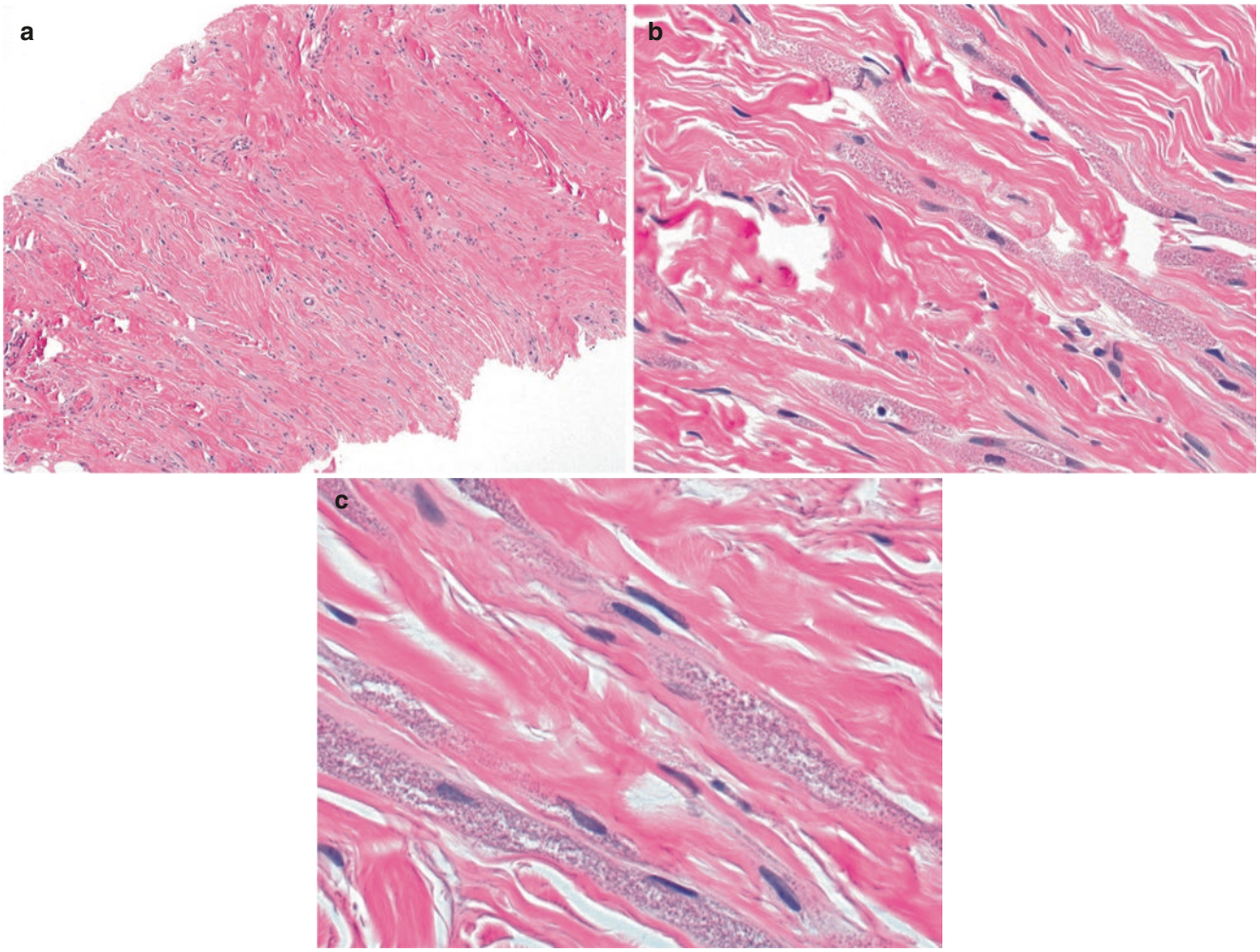

Fig. 16.37 Histologic features of a benign granular cell tumor mimicking invasive lobular carcinoma in the breast. (**a**–**c**) CNB of a radiographically suspicious mass reveals dense collagenized stroma with subtle infiltrating cords of cells with elongated, bland nuclei and eosinophilic, granular cytoplasm. The cells are immunoreactive for inhibin and CD68 (not shown) and negative for CK (not shown)

Pathogenesis

Granular cell tumors frequently display loss-of-function mutations in *ATP6AP1* or *ATP6AP2* genes [114], which results in abnormal endosome distribution and accumulation of intracytoplasmic vacuoles. Most granular cell tumors are sporadic but have been reported in association with a variety of rare syndromes. In addition, granular cell tumors in the breast have been reported in association with mastectomy scars in patients with primary breast carcinoma [115].

Prognosis and Management

The vast majority of granular cell tumors are benign and are adequately treated with local excision. However, approximately 2% of granular cell tumors are malignant (Fig. 16.38), including those in the breast [116], and data is limited on the optimal treatment of these rare tumors.

Neurofibroma

Overview

Neurofibromas are peripheral nerve sheath tumors that contain all the cellular components of the nerve sheath, including Schwann cells, perineurial cells, dendritic cells, axons, and fibroblasts [104]. Neurofibromas of the breast are rare and most commonly reported to involve the nipple-areolar complex in patients with neurofibromatosis type 1 [117].

Gross and Radiologic Features

Neurofibromas of the breast are typically detected as palpable superficial masses, but they may also be detected as incidental parenchymal breast masses on screening mammography [118]. Grossly, neurofibromas may be solitary or

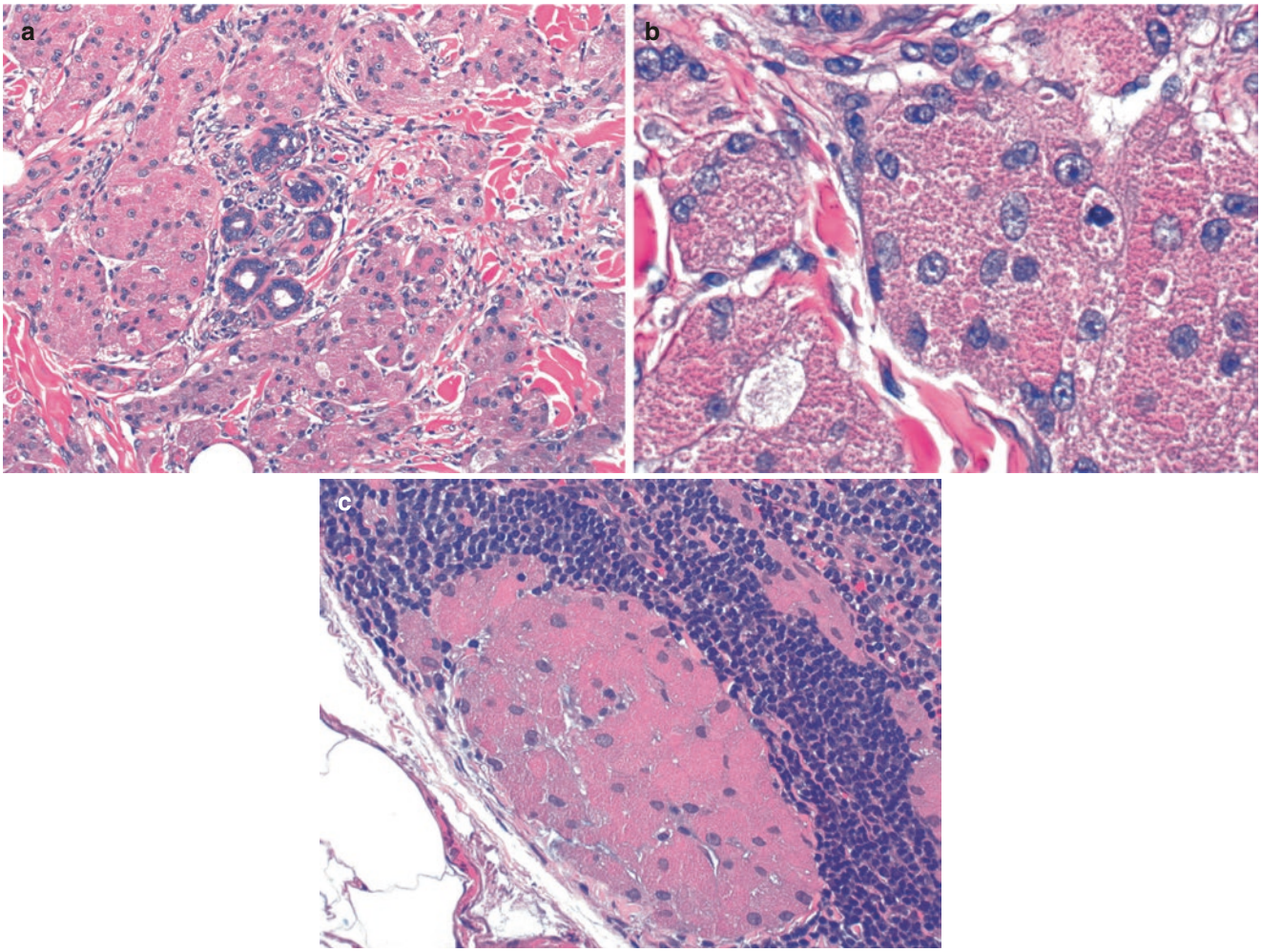

Fig. 16.38 Histologic features of a malignant granular cell tumor in the breast. (**a**, **b**) CNB of a radiographically suspicious, superficial breast mass reveals infiltrative nests of atypical cells with vesicular nuclei, prominent nucleoli, abundant mitotic figures, and eosinophilic granular cytoplasm. The cells infiltrate through the dermis and deep into the breast parenchyma, surrounding the benign breast lobules. (**c**) Metastatic granular cell tumor is present in one axillary lymph node

multinodular, and they may be well circumscribed or indistinct. On mammography, neurofibromas are most often round or oval masses with circumscribed margins [118]. On ultrasound, neurofibromas are typically round or oval, hypoechoic masses with posterior acoustic enhancement (Fig. 16.39) and can be mistaken for cysts.

Microscopic Features

Microscopically, neurofibromas are characterized by bland spindled cells with wavy nuclei in a loose, myxoid matrix with "shredded carrot-like" collagen fibrils and scattered mast cells (Fig. 16.40). Mitoses and atypia are rare. The lesion may form a distinct solitary mass (solitary neurofibroma), infiltrate around adnexal structures or breast epithelium (diffuse neurofibroma), or be multinodular (plexiform neurofibroma).

Differential Diagnosis

The differential diagnosis of neurofibroma includes other benign nerve sheath tumors such as schwannoma or less commonly malignant peripheral nerve sheath tumor, as well as myxoid myofibroblastoma. Schwannomas display regions of alternative hyper- and hypocellularity (Antoni A and B regions) and nuclear palisading (Verocay bodies) and are composed entirely of Schwann cells. Myofibroblastomas are composed of stromal myofibroblasts and label for CD34, SMA, BCL2, and ER.

Immunohistochemical Workup

The histologic features of neurofibroma are typically characteristic. Neurofibromas are typically focally immunoreactive for S100 protein (labeling the schwannian component of the neoplasm) and are negative for CK, SMA, and ER.

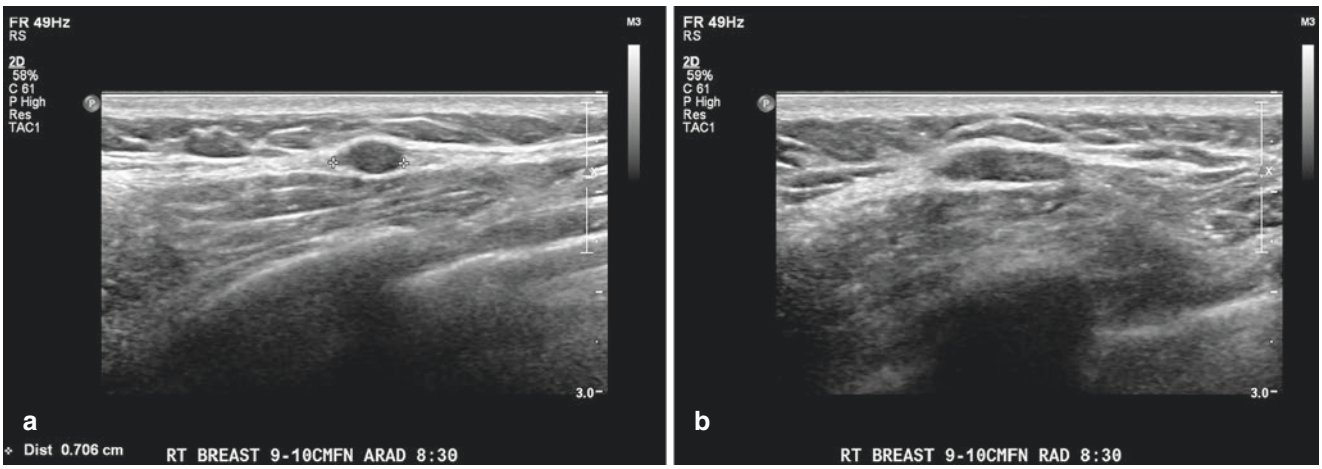

Fig. 16.39 Radiographic features of a neurofibroma in the breast. (**a**, **b**) A 43-year-old female presents with a palpable breast mass. Ultrasound evaluation reveals a parallel, circumscribed avascular and hypoechoic oval mass with no posterior sound change

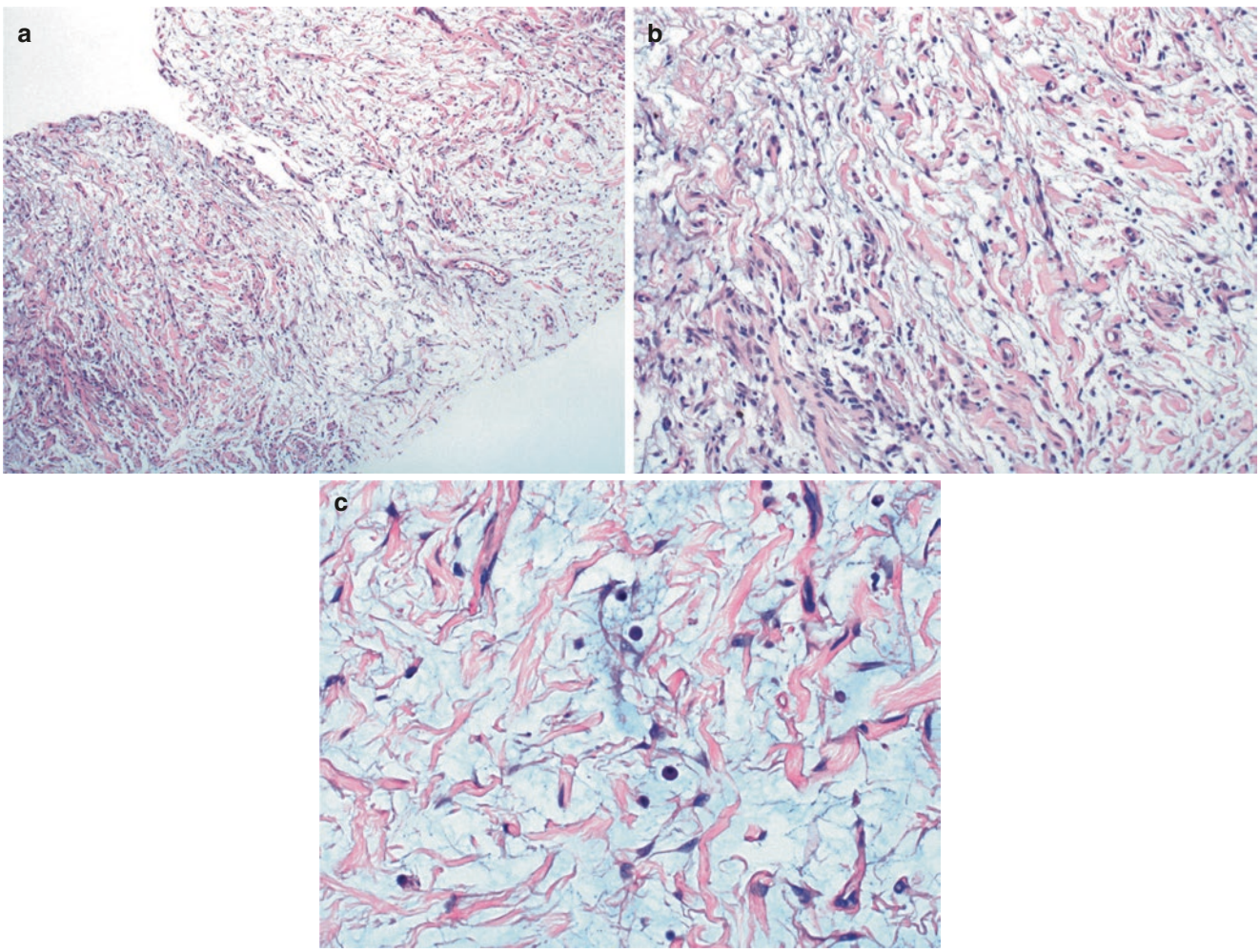

Fig. 16.40 Histologic features of a subareolar neurofibroma. (**a**–**c**) CNB of a superficial breast mass reveals bland spindled cells in a myxoid stroma with "shredded carrot" collagen, delicate capillary vasculature, and scattered mast cells. No breast epithelium is identified

Pathogenesis

Solitary neurofibromas of the breast are rare [118, 119], and most neurofibromas of the breast are associated with neurofibromatosis type 1 [117, 120].

Prognosis and Management

Neurofibromas of the breast are managed with local excision.

Schwannoma

Overview

Schwannomas are benign nerve sheath tumors that rarely involve the breast but have been reported in both female and male patients [121]. Like neurofibromas, schwannomas of the breast are typically superficial lesions [121], but they can rarely involve the deep breast parenchyma [122].

Gross and Radiologic Features

Most schwannomas of the breast present as palpable masses [121], but may be detected incidentally on imaging. Grossly, schwannomas are most often circumscribed but can be infiltrative or exophytic [123], mimicking primary breast carcinoma. On mammogram and ultrasound, schwannomas are typically round or oval, circumscribed masses without calcifications [122]. If cystic areas are present, the differential diagnosis includes a phyllodes tumor [121].

Microscopic Features

Schwannomas are composed of spindled cells characterized by long, wavy nuclei with bipolar tapering ends (Fig. 16.41) [104]. These cells are arranged in alternating cellular and hypocellular areas (Antoni A and Antoni B regions, respectively). The nuclei can palisade in parallel rows known as Verocay bodies (Fig. 16.41). Ancient schwannomas may display degenerative nuclear atypia. Schwannomas characteristically contain prominent, gaping, and hyalinized blood vessels.

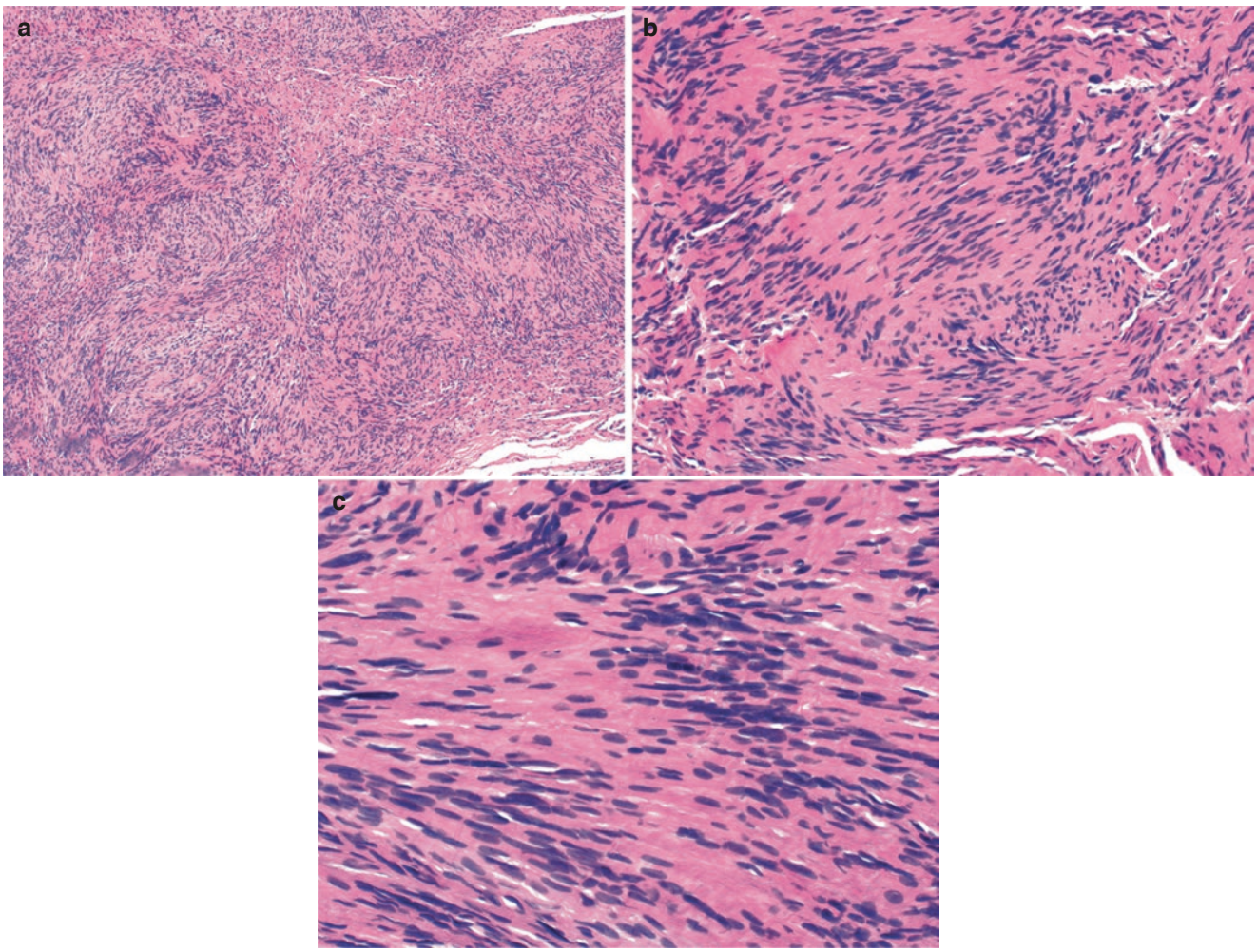

Fig. 16.41 Histologic features of a schwannoma in the breast. (**a**–**c**) CNB of a radiographically detected breast mass reveals a cellular neoplasm composed of spindled cells with wavy, tapering nuclei arranged in parallel ("Verocay bodies") with delicate pink schwannian stroma

Differential Diagnosis

The histologic differential diagnosis of schwannomas includes other peripheral nerve sheath tumors such as neurofibroma, as well as other spindle cell lesions of the breast such as myofibroblastoma, spindle cell metaplastic carcinoma, phyllodes tumor, fibromatosis, and leiomyoma. The distinctive morphology of Antoni A regions, Antoni B regions, and Verocay bodies is typically characteristic of a schwannoma.

Immunohistochemical Workup

Schwannomas are diffusely and strongly immunoreactive for S100 protein and SOX10. The majority of schwannomas are negative for CK; however, focal keratin labeling has been reported [124].

Pathogenesis

Most reported breast schwannomas are sporadic [121]; however, multiple nerve sheath tumors should raise the possibility of syndromes such as neurofibromatosis or schwannomatosis.

Prognosis and Management

Schwannomas are benign neoplasms and are adequately treated with excisional biopsy. Nonsurgical observation may be considered for patients with small, unchanging, and uncomplicated lesions [125].

Primary Breast Sarcomas

Overview

Primary sarcomas of the breast are extremely rare and account for less than 0.1% of all malignant breast neoplasms [126]. It is typically not possible to definitively diagnose primary breast sarcomas on CNB, as malignant spindle cell neoplasms of the breast may display marked lesional heterogeneity, and examination of the entire lesion after excision is often necessary to render a definitive diagnosis. The differential diagnostic entities of spindle cell metaplastic carcinoma and malignant phyllodes tumor are much more common than primary breast sarcomas and thus must be completely excluded.

Primary sarcomas of the breast include leiomyosarcoma [126–128], fibrosarcoma [14, 126, 129–131], liposarcoma [14, 15], malignant peripheral nerve sheath tumor [132, 133], osteosarcoma [14, 126, 134, 135], DFSP [14, 136–139], hemangiopericytoma [126], myofibrosarcoma [63–65, 130], malignant fibrous histiocytoma/pleomorphic undifferentiated sarcoma [14, 126, 129–131, 140], and angiosarcoma [14, 126, 130, 141–144]. Angiosarcoma will be discussed in a separate chapter devoted to vascular neoplasms (Chap. 17). A subset of primary breast sarcomas occur secondary to radiation for prior breast carcinoma [145–147].

Gross and Radiologic Features

Primary breast sarcomas typically present as palpable breast masses [126]. Grossly, primary breast sarcomas can be well circumscribed or infiltrative, and fibrous or lipomatous, depending upon their cellular composition. In general, the radiographic features of a primary breast sarcoma are nonspecific. On mammography, primary breast sarcomas are typically round or oval, dense masses without calcifications (Fig. 16.42a). On ultrasound, primary breast sarcomas are homogenously hypoechoic with no posterior sound change (Fig. 16.42b). On MRI, they often display rapid enhancement with suspicious washout kinetics [148]. The differen-

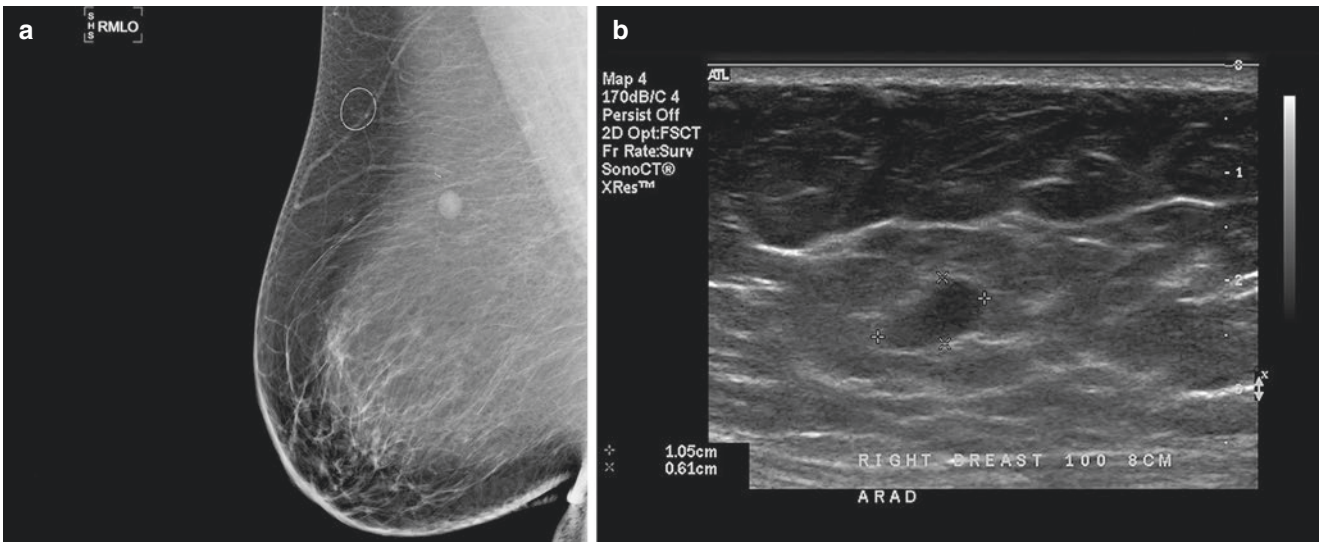

Fig. 16.42 Mammographic and ultrasound features of a primary breast sarcoma. (**a**) Screening mammography detects a new mass in a 45-year-old female. The mass is dense, round, and circumscribed within fat density tissue and has no associated calcifications. (**b**) On ultrasound, the mass is oval, parallel, hypoechoic, and avascular with circumscribed margins and no posterior sound change

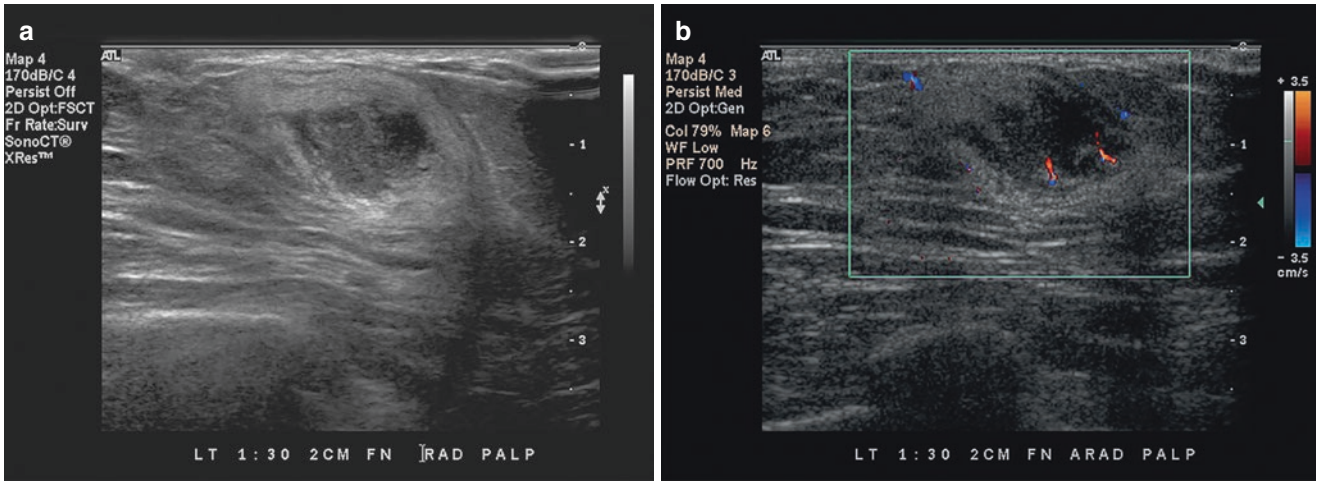

Fig. 16.43 Ultrasound features of a superficial dermatofibrosarcoma protuberans in the breast. (**a**, **b**) A 23-year-old female presents with a palpable, superficial breast mass. Ultrasound shows a vascular, oval mass with indistinct margins and heterogeneous echo pattern including an echogenic rim. The mass touches the deep dermis

tial diagnosis on the basis of imaging includes primary breast carcinoma, PASH, fibroadenoma, and metastatic lesions including metastatic sarcomas. Imaging is crucial in excluding the possibility of a primary chest wall or bony lesion extending into the breast, mimicking a primary breast neoplasm.

Among primary sarcomas occurring in the breast, DFSP may display unique imaging characteristics (Fig. 16.43), as they often arise in the deep dermis and not within the breast parenchyma. On mammography, DFSP is usually a dense, circumscribed, and superficial mass without calcifications [139, 149]. On ultrasound, these lesions are subcutaneous and have internal vascularity [138, 139, 149].

Postradiation sarcomas may not display any specific imaging findings, although some (particularly angiosarcomas) show mammographically apparent skin and trabecular thickening that is progressive and not in the region of previous surgical scar, which can be useful findings [147]. The differential diagnosis of skin and trabecular thickening on imaging includes infection, recurrent breast carcinoma with an inflammatory component, lymphangitic metastatic spread, and radiation-induced skin changes.

Microscopic Features

The morphologic features of primary breast sarcomas are identical to those of the sarcoma in other soft-tissue sites, and tumors should generally be graded using the criteria employed in other soft-tissue sites. Primary breast leiomyosarcoma displays intersecting fascicles of spindled cells with blunt-ended nuclei, perinuclear vacuoles, nuclear atypia including hyperchromasia, and an increased mitotic rate (Fig. 16.9). Primary breast fibrosarcoma displays infiltrative, atypical spindled cells arranged in a herringbone growth pattern (Fig. 16.44). Primary breast liposarcoma displays atypical adipocytes and scattered lipoblasts (Fig. 16.45). DFSP may present in either the superficial breast or deep within the breast parenchyma (Figs. 16.46 and 16.47). The lesional cells are short spindled cells arranged in a whorled, storiform pattern and are extensively infiltrative. High-grade pleomorphic sarcomas are undifferentiated neoplasms composed of markedly atypical, pleomorphic cells with nuclear hyperchromasia, prominent nucleoli, and abundant mitotic figures (Fig. 16.48). Primary breast osteosarcomas display pleomorphic spindled or oval cells with an associated chondroid or osseous matrix; they may be chondroblastic or osteoblastic [134]. Primary breast malignant peripheral nerve sheath tumors consist of cellular, hyperchromatic spindled cells that often condense beneath staghorn-like blood vessels. Postradiation sarcomas may display any morphologic pattern.

Differential Diagnosis

The differential diagnosis of a primary breast sarcoma includes spindle cell metaplastic breast carcinoma and malignant phyllodes tumor, both of which are far more common in the breast. The presence of an associated conventional invasive or in situ mammary carcinoma component or diffuse CK immunoreactivity would support a diagnosis of metaplastic carcinoma, while the presence of a leaflike epithelial component supports a diagnosis of a malignant phyllodes tumor. In addition, a metastatic sarcoma from another soft-tissue primary site to the breast must be excluded, such as a uterine leiomyosarcoma or deep-tissue liposarcoma, and in general clinical history is necessary as the morphologic

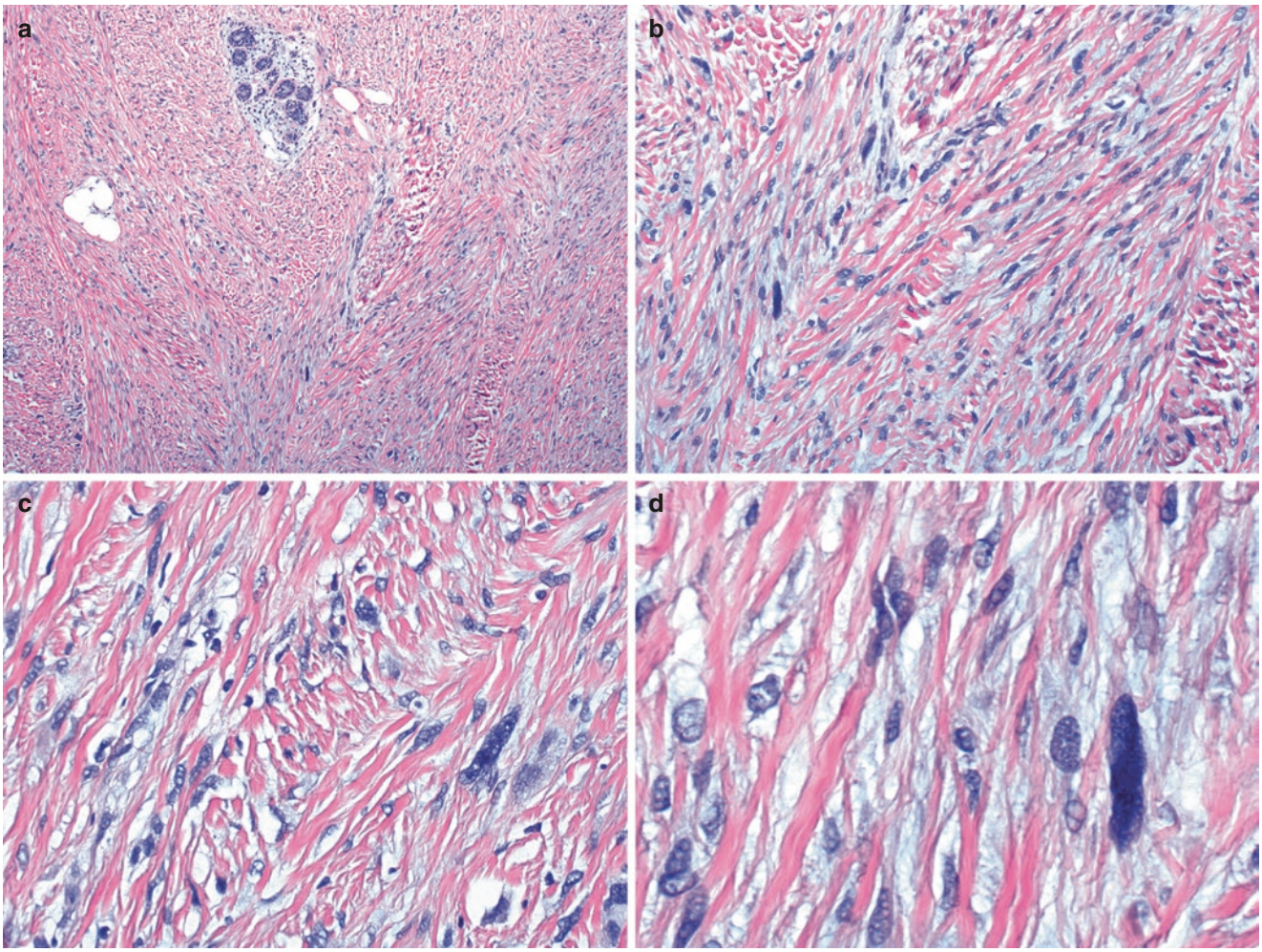

Fig. 16.44 Histologic features of a primary breast fibrosarcoma. (**a**–**d**) CNB of a palpable breast mass reveals an infiltrative spindle cell neoplasm with a herringbone growth pattern. The nuclei are oval to spindled with scattered pleomorphism including enlarged and hyperchromatic forms. The patient has no other known site of disease

features of the primary or metastatic lesion would be identical. However, the primary site may not be known at the time of breast biopsy [150]. The differential diagnosis of spindled to epithelioid malignant neoplasms in the breast also includes metastatic melanoma.

Both metaplastic carcinomas [151] and malignant phyllodes tumors [152] not only display malignant spindle cells but also frequently contain malignant heterologous elements such as osseous, chondroid, or liposarcomatous differentiation, which can be a potential diagnostic pitfall. On the limited material of a CNB, the diagnostic histologic features may not always be present to definitively exclude other entities in the differential diagnosis and to definitively diagnose a primary breast sarcoma. For instance, CNB of a breast mass may reveal a malignant spindle cell neoplasm (Fig. 16.49) composed of atypical spindled cells with hyperchromatic nuclei and abundant mitotic figures. Although this may represent a primary breast sarcoma, it is not possible to definitively exclude a metaplastic carcinoma or a malignant phyllodes tumor without examination of the complete lesion and employing a targeted immunopanel, as discussed below. The best diagnosis on CNB is "malignant spindle cell neoplasm," with recommendation of complete excision for final classification. This is important, as neoadjuvant chemotherapy may be considered for metaplastic carcinomas, whereas chemotherapy typically does not have a role for primary breast sarcomas or malignant phyllodes tumors.

Immunohistochemical Workup

IHC has a role in the workup of spindle cell neoplasms of the breast on CNB, but reaching the final diagnosis often requires examination of the excisional specimen. In general, leiomyosarcomas display smooth muscle differentiation and are

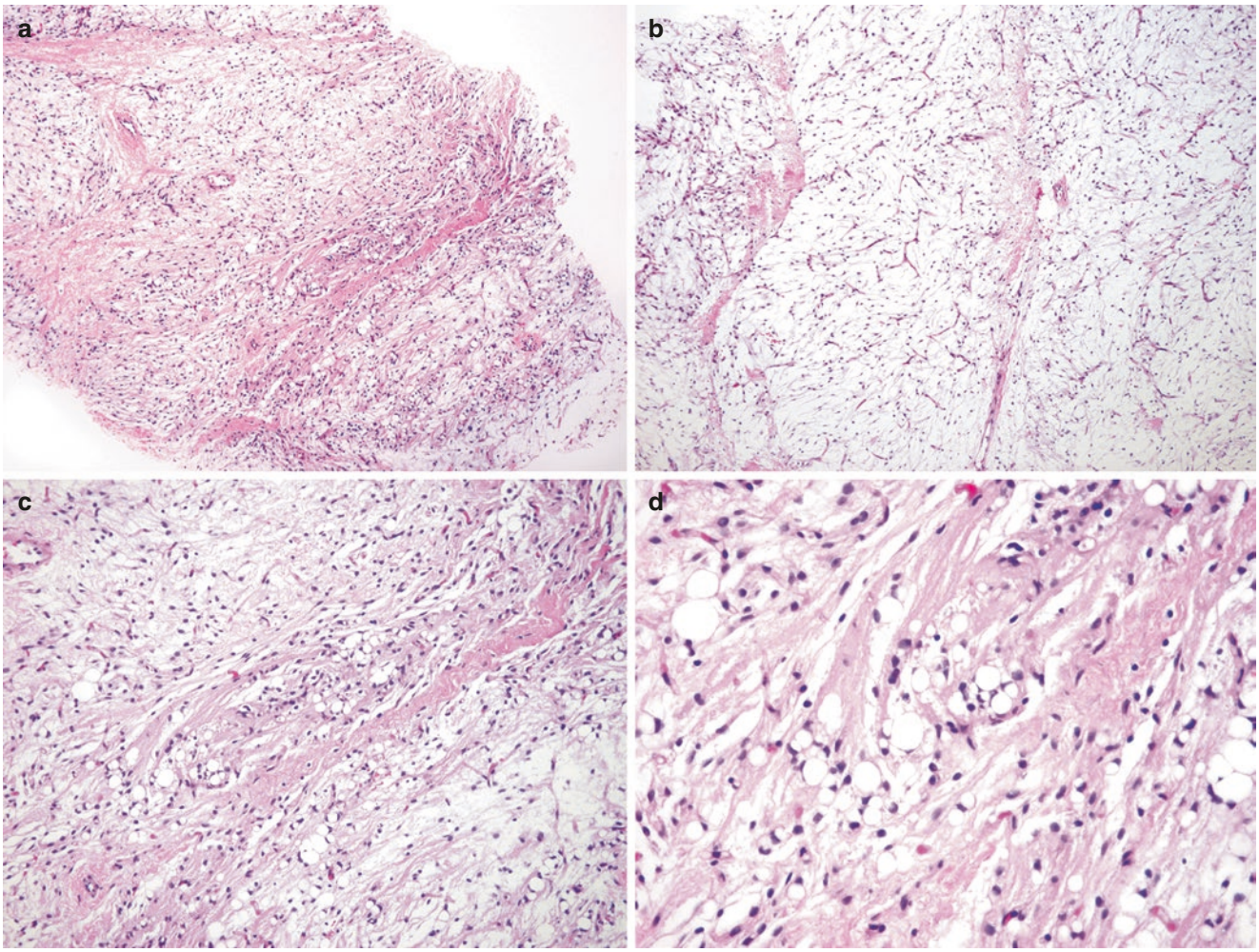

Fig. 16.45 Histologic features of a primary breast liposarcoma with myxoid features. (**a**–**d**) CNB of a palpable breast mass reveals an adipocyte-rich mass composed of spindled cells in a loose myxoid stroma with a delicate capillary vasculature network. Close examination reveals scattered lipoblasts. No benign breast parenchyma is identified. The patient has no other known site of disease

immunoreactive for SMA and desmin. Well-differentiated/dedifferentiated liposarcomas may display MDM2 immunoreactivity even on CNB [17]. Malignant peripheral nerve sheath tumors are focally immunoreactive for S100 protein. DFSP is immunoreactive for CD34, BCL2, and SMA (Figs. 16.46d and 16.47c).

In general, CK immunoreactivity is used to support a diagnosis of metaplastic carcinoma, while primary breast sarcomas are negative for CK. It may be necessary to employ several CK antibodies, as a metaplastic carcinoma may be negative by one or more given CK antibodies. However, negative CK immunoreactivity on the limited sampling of a CNB does not entirely exclude the possibility of a metaplastic carcinoma because of potential lesional heterogeneity, and the immunostains may need to be repeated on the excisional specimen.

Immunoreactivity for p63 is another marker that has traditionally been used to support epithelial differentiation in metaplastic carcinomas [89, 153, 154]; however, p63 labeling is increasingly recognized in both benign [155] and malignant [156] stromal neoplasms, as well as reactive stromal proliferations [155]. There are also notable exceptions to the use of CK immunoreactivity to support a diagnosis of carcinoma. While leiomyosarcomas are immunoreactive for desmin and SMA [127], they can also display CK and EMA immunoreactivity [157]. In addition, malignant phyllodes tumor can display immunoreactivity for both CK and p63 [158]. Thus, focal CK labeling alone on a CNB cannot be used to definitively diagnose a metaplastic carcinoma.

Pathogenesis

Primary breast sarcomas are rare, and the majority are sporadic. Postradiation sarcomas are a rare potential sequela of irradiation for primary breast carcinoma, and the incidence increases with time, with one series reporting an incidence of

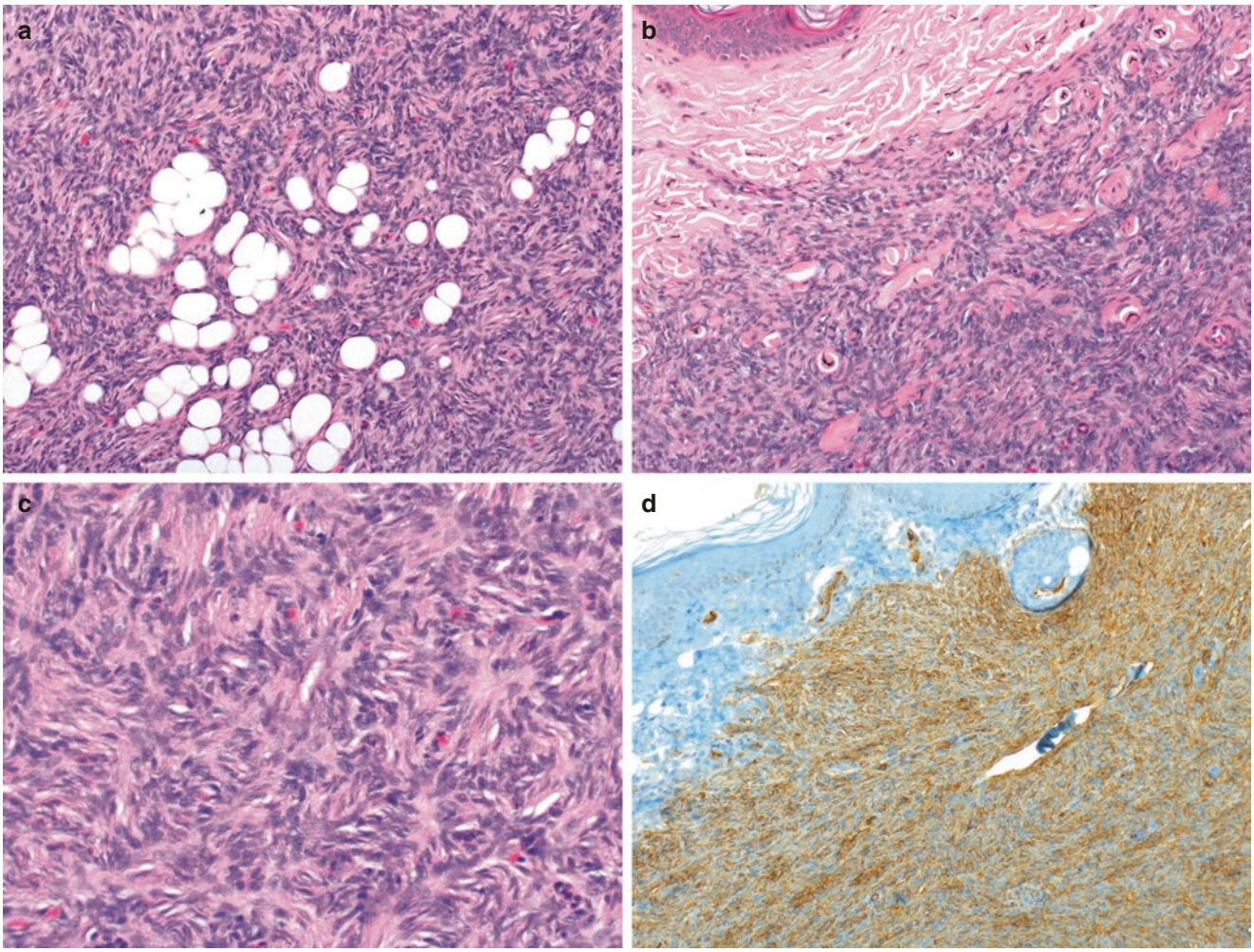

Fig. 16.46 Histologic features of superficial dermatofibrosarcoma protuberans in the breast. (**a**–**c**) Core biopsy of a superficial breast mass reveals a spindle cell neoplasm extending from the superficial dermis to the deep subcutaneous and mammary adipose tissue. The lesional cells are short spindled cells arranged in a storiform pattern with associated pink collagen. The lesional cells are immunoreactive for (**d**) CD34

0.07% at 5 years postradiation and 0.48% at 15 years [146]. Postradiation sarcomas most commonly occur in the breast but may also involve other areas of the radiation field including the axilla, chest wall, scapula, sternum, and supraclavicular region [146]. Angiosarcomas of the skin are the most common type of postradiation sarcoma; however, any sarcoma type can occur including pleomorphic undifferentiated sarcoma (Fig. 16.48), osteosarcoma, leiomyosarcoma, fibrosarcoma, and rhabdomyosarcoma [146].

Prognosis and Management

The overall prognosis for primary breast sarcoma is poor [14, 126, 130, 131, 159], with disease-free survival as low as 39% at 3 years [130]. The survival for postradiation sarcomas is similarly low, with one series reporting a 5-year survival of 36% [146]. The treatment for primary breast sarcomas is complete surgical excision with widely clear margins; there is no role for axillary lymph node staging [159]. Chemotherapy and radiation therapy may have a role in certain circumstances [148], but in general have not been shown to improve survival [14, 160]. Tumor size [126, 159] and margin status [130] are prognostic factors for overall survival. Complete surgical excision is imperative.

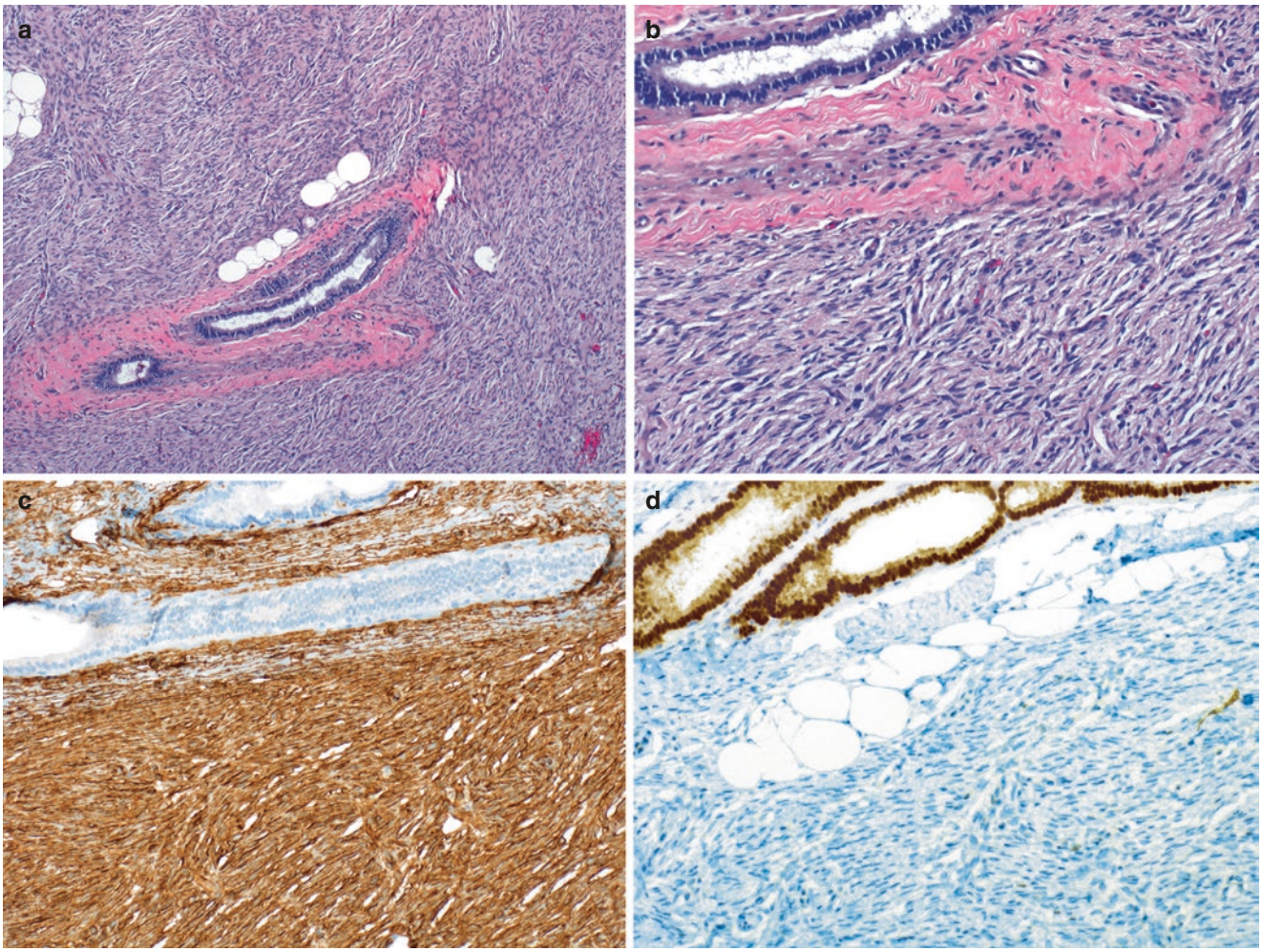

Fig. 16.47 Histologic features of a deep dermatofibrosarcoma protuberans in the breast. (**a**, **b**) CNB of a breast mass shows a spindle cell neoplasm that infiltrates throughout the breast adipose tissue and around benign ducts and lobules. The lesional cells are short spindled cells in a storiform pattern. The cells are immunoreactive for (**c**) CD34 and negative for (**d**) ER as well as CKs (not shown)

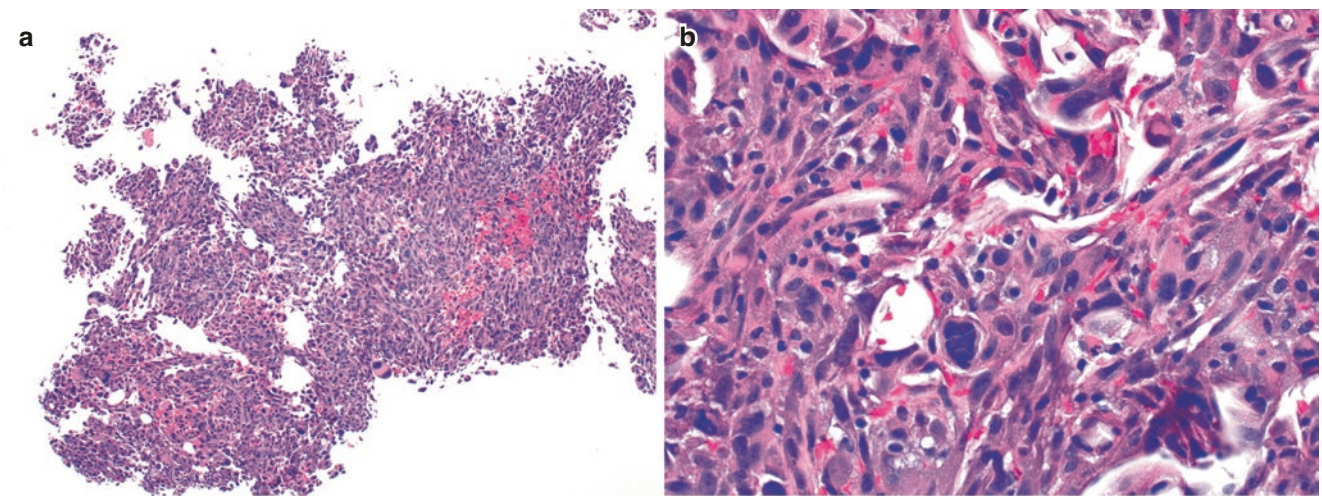

Fig. 16.48 Histologic features of a postradiation pleomorphic sarcoma in the breast. (**a**–**c**) CNB of a new breast mass shows a high-grade spindle cell neoplasm with marked nuclear pleomorphism, hyperchromasia, prominent nuclei, and abundant mitotic figures including atypical mitoses. The lesional cells are immunoreactive for vimentin and negative for SMA, desmin, myogenin, CD34, CD31, ERG, and CKs (not shown). (**d**) The background breast parenchyma shows radiation change

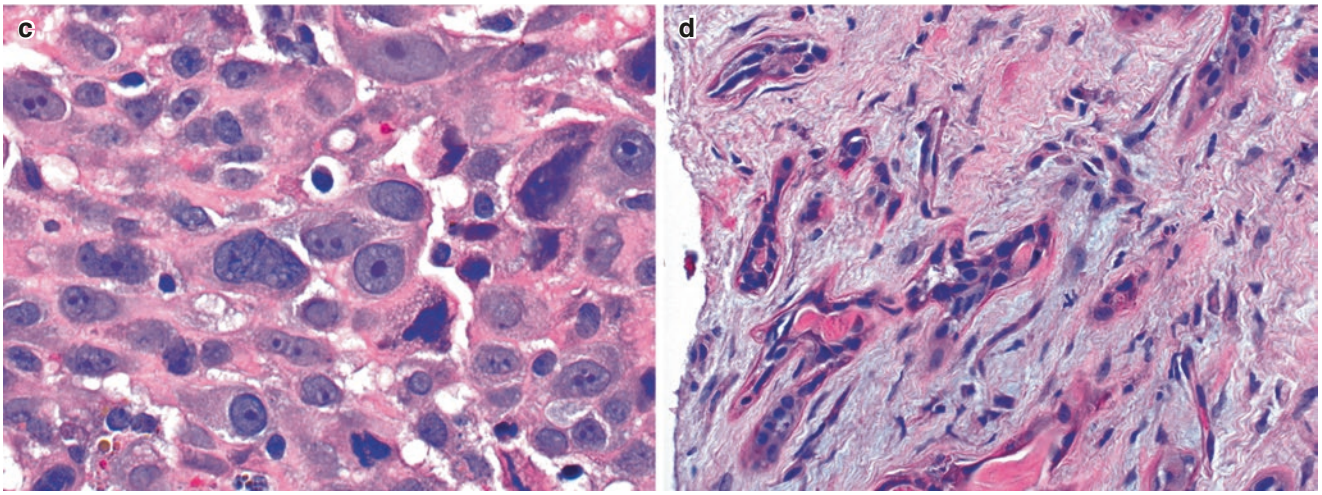

Fig. 16.48 (continued)

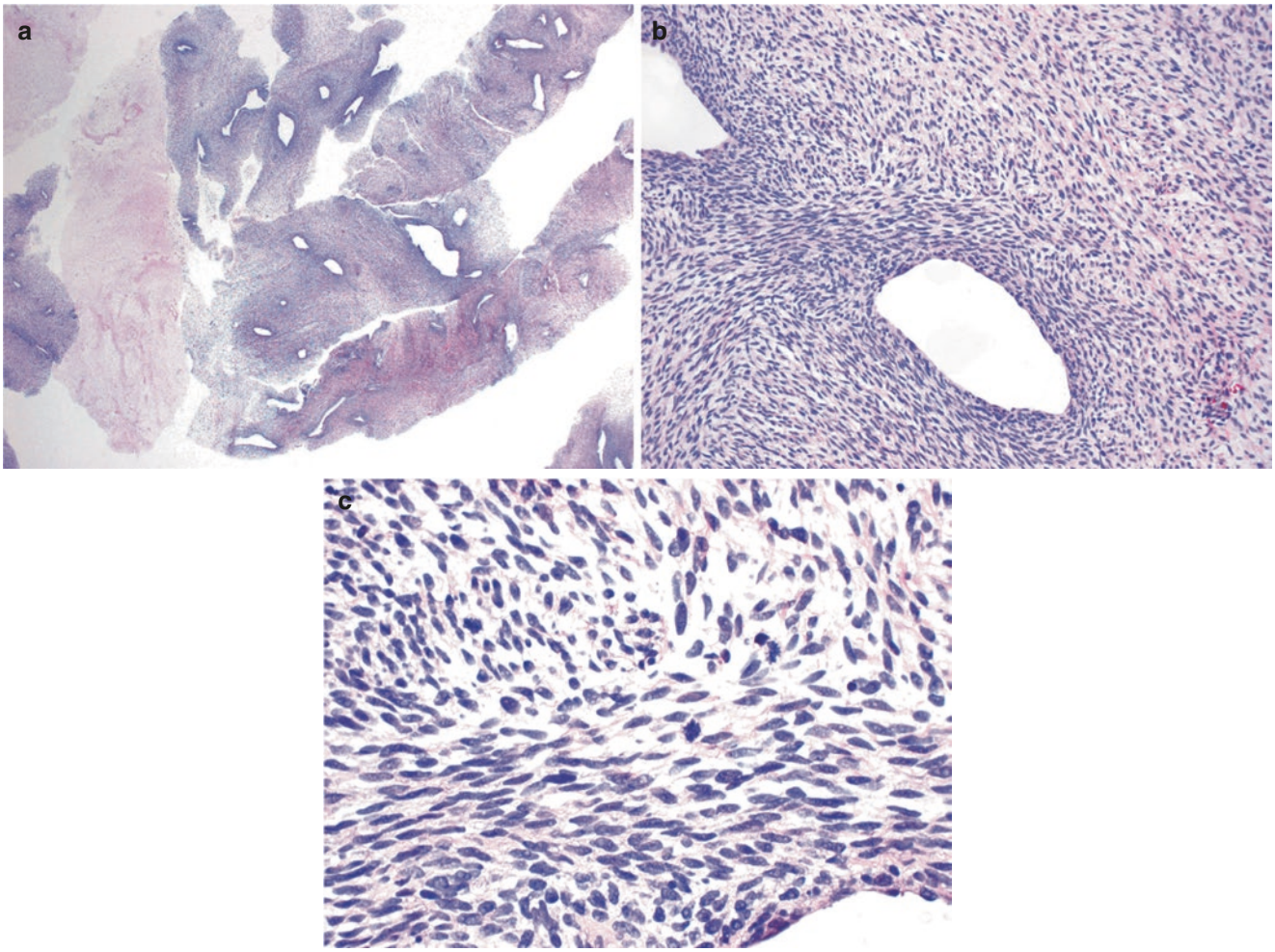

Fig. 16.49 Histologic features of a high-grade spindle cell neoplasm on CNB. (**a**–**c**) CNB of a large palpable breast mass reveals fascicles of atypical spindled cells with hyperchromatic nuclei and abundant mitotic figures. The best diagnosis on CNB is "malignant spindle cell neoplasm"

References

1. Lanng C, Eriksen BO, Hoffmann J. Lipoma of the breast: a diagnostic dilemma. Breast. 2004;13(5):408–11. Epub 2004/09/30
2. Rowe JJ, Cheah AL, Calhoun BC. Lipomatous tumors of the breast: a contemporary review. Semin Diagn Pathol. 2017;34(5):453–61. https://doi.org/10.1053/j.semdp.2017.05.008. Epub 2017 May 29
3. Li YF, Lv MH, Chen LF, Wu YF. Giant lipoma of the breast: a case report and review of the literature. Clin Breast Cancer. 2011;11(6):420–2. Epub 2011/07/07
4. Kirova YM, Feuilhade F, Le Bourgeois JP. Breast lipoma. Breast J. 2002;8(2):117–8. Epub 2002/03/19
5. Ramirez-Montano L, Vargas-Tellez E, Dajer-Fadel WL, Espinosa MS. Giant lipoma of the breast. Arch Plast Surg. 2013;40(3):244–6. Epub 2013/06/05
6. Marsh WL Jr, Lucas JG, Olsen J. Chondrolipoma of the breast. Arch Pathol Lab Med. 1989;113(4):369–71. Epub 1989/04/01
7. Banev SG, Filipovski VA. Chondrolipoma of the breast—case report and a review of literature. Breast. 2006;15(3):425–6. Epub 2005/09/01
8. Baric A, Jewell W, Chang CH, Damjanov I. Chondrolipoma of the breast. Breast J. 2005;11(3):212–3. Epub 2005/05/06
9. Lerwill MF, Koerner FC. Benign mesenchymal lesions. In: Hoda SA, Brogi E, Koerner FC, Rosen PP, editors. Rosen's Breast Pathology, 5th Ed. Philadelphia, PA: Lippincott Williams & Wilkins; 2021. p. 1125–1208.
10. Magro G, Bisceglia M, Michal M, Eusebi V. Spindle cell lipoma-like tumor, solitary fibrous tumor and myofibroblastoma of the breast: a clinico-pathological analysis of 13 cases in favor of a unifying histogenetic concept. Virchows Arch. 2002;440(3):249–60. Epub 2002/03/13
11. Magro G, Michal M, Vasquez E, Bisceglia M. Lipomatous myofibroblastoma: a potential diagnostic pitfall in the spectrum of the spindle cell lesions of the breast. Virchows Arch. 2000;437(5):540–4. Epub 2001/01/09
12. Magro G, Longo FR, Salvatorelli L, Vasquez E, Vecchio GM. Lipomatous myofibroblastoma of the breast: case report with diagnostic and histogenetic considerations. Pathologica. 2014;106(2):36–40. Epub 2014/10/09
13. Magro G. Mammary myofibroblastoma: an update with emphasis on the most diagnostically challenging variants. Histol Histopathol. 2016;31(1):1–23. Epub 2015 Sep 2
14. Blanchard DK, Reynolds CA, Grant CS, Donohue JH. Primary nonphylloides breast sarcomas. Am J Surg. 2003;186(4):359–61. Epub 2003/10/14
15. Austin RM, Dupree WB. Liposarcoma of the breast: a clinicopathologic study of 20 cases. Hum Pathol. 1986;17(9):906–13. Epub 1986/09/01
16. Briski LM, Jorns JM. Primary breast atypical lipomatous tumor/well-differentiated liposarcoma and dedifferentiated liposarcoma. Arch Pathol Lab Med. 2018;142(2):268–74. https://doi.org/10.5858/arpa.2016-0380-RSR2.
17. Weaver J, Rao P, Goldblum JR, Joyce MJ, Turner SL, Lazar AJ, et al. Can MDM2 analytical tests performed on core needle biopsy be relied upon to diagnose well-differentiated liposarcoma? Mod Pathol. 2010;23(10):1301–6. Epub 2010/05/25
18. Binh MB, Sastre-Garau X, Guillou L, de Pinieux G, Terrier P, Lagacé R, Aurias A, Hostein I, Coindre JM. MDM2 and CDK4 immunostainings are useful adjuncts in diagnosing well-differentiated and dedifferentiated liposarcoma subtypes: a comparative analysis of 559 soft tissue neoplasms with genetic data. Am J Surg Pathol. 2005;29(10):1340–7. https://doi.org/10.1097/01.pas.0000170343.09562.39. PMID: 16160477
19. Pauwels P, Sciot R, Croiset F, Rutten H, Van den Berghe H, Dal CP. Myofibroblastoma of the breast: genetic link with spindle cell lipoma. J Pathol. 2000;191(3):282–5. Epub 2000/07/06
20. Kryvenko ON, Chitale DA, VanEgmond EM, Gupta NS, Schultz D, Lee MW. Angiolipoma of the female breast: clinicomorphological correlation of 52 cases. Int J Surg Pathol. 2011;19(1):35–43. Epub 2010/11/23
21. Darling ML, Babagbemi TO, Smith DN, Brown FM, Lester SC, Meyer JE. Mammographic and sonographic features of angiolipoma of the breast. Breast J. 2000;6(3):166–70. Epub 2001/05/12
22. Hoda SA, Cranor ML, Rosen PP. Hemangiomas of the breast with atypical histological features. Further analysis of histological subtypes confirming their benign character. Am J Surg Pathol. 1992;16(6):553–60. Epub 1992/06/01
23. Shin SJ, Lesser M, Rosen PP. Hemangiomas and angiosarcomas of the breast: diagnostic utility of cell cycle markers with emphasis on Ki-67. Arch Pathol Lab Med. 2007;131(4):538–44. Epub 2007/04/12
24. Sciot R, Akerman M, Dal Cin P, De Wever I, Fletcher CD, Mandahl N, Mertens F, Mitelman F, Rosai J, Rydholm A, Tallini G, Van den Berghe H, Vanni R, Willen H. Cytogenetic analysis of subcutaneous angiolipoma: further evidence supporting its difference from ordinary pure lipomas: a report of the CHAMP study group. Am J Surg Pathol. 1997;21(4):441–4. https://doi.org/10.1097/00000478-199704000-00010. PMID: 9130991
25. Hofvander J, Arbajian E, Stenkula KG, Lindkvist-Petersson K, Larsson M, Nilsson J, Magnusson L, von Steyern FV, Rissler P, Hornick JL, Mertens F. Frequent low-level mutations of protein kinase D2 in angiolipoma. J Pathol. 2017;241(5):578–82. https://doi.org/10.1002/path.4865. Epub 2017 Feb 27
26. Sebastiano C, Gennaro L, Brogi E, Morris E, Bowser ZL, Antonescu CR, Pareja F, Brennan S, Murray MP. Benign vascular lesions of the breast diagnosed by core needle biopsy do not require excision. Histopathology. 2017;71(5):795–804. https://doi.org/10.1111/his.13291. Epub 2017 Sep 8. PMID: 28644513; PMCID: PMC5708168
27. Mantilla JG, Koenigsberg T, Reig B, Shapiro N, Villanueva-Siles E, Fineberg S. Core biopsy of vascular neoplasms of the breast: pathologic features, imaging, and clinical findings. Am J Surg Pathol. 2016;40(10):1424–34. https://doi.org/10.1097/PAS.0000000000000668. PMID: 27340752
28. Furlong MA, Fanburg-Smith JC, Miettinen M. The morphologic spectrum of hibernoma: a clinicopathologic study of 170 cases. Am J Surg Pathol. 2001;25(6):809–14. Epub 2001/06/08
29. Colville J, Feigin K, Tang L, Keating D, Cohen MA. Mammary hibernoma. Breast J. 2006;12(6):563–5. Epub 2007/01/24
30. Hardes J, Scheil-Bertram S, Hartwig E, Gebert C, Gosheger G, Schulte M. Sonographic findings of hibernoma. A report of two cases. J Clin Ultrasound. 2005;33:298–301.
31. Martini N, Londero V, Machin P, Travaini LL, Zuiani C, Bazzocchi M, Paganelli G. An unusual breast lesion: the ultrasonographic, mammographic, MRI and nuclear medicine findings of mammary hibernoma. Br J Radiol. 2010;83(985):e1–4. https://doi.org/10.1259/bjr/17929543. PMID: 20139247; PMCID: PMC3487266.
32. Ku J, Campbell C, Bennett I. Leiomyoma of the nipple. Breast J. 2006;12(4):377–80. Epub 2006/07/20
33. Nascimento AG, Karas M, Rosen PP, Caron AG. Leiomyoma of the nipple. Am J Surg Pathol. 1979;3(2):151–4. Epub 1979/04/01
34. Vecchio GM, Cavaliere A, Cartaginese F, Lucaccioni A, Lombardi T, Parenti R, et al. Intraparenchymal leiomyoma of the breast: report of a case with emphasis on needle core biopsy-based diagnosis. Pathologica. 2013;105(4):122–7. Epub 2014/01/29

35. Ende L, Mercado C, Axelrod D, Darvishian F, Levine P, Cangiarella J. Intraparenchymal leiomyoma of the breast: a case report and review of the literature. Ann Clin Lab Sci. 2007;37(3):268–73. Epub 2007/08/22
36. Minami S, Matsuo S, Azuma T, Uga T, Hayashi T, Eguchi S, et al. Parenchymal leiomyoma of the breast: a case report with special reference to magnetic resonance imaging findings and an update review of literature. Breast Cancer. 2011;18(3):231–6. Epub 2011/03/19
37. Krings G, McIntire P, Shin SJ. Myofibroblastic, fibroblastic and myoid lesions of the breast. Semin Diagn Pathol. 2017;34(5):427–37. https://doi.org/10.1053/j.semdp.2017.05.010. Epub 2017 May 28
38. Carter CS, Skala SL, Chinnaiyan AM, McHugh JB, Siddiqui J, Cao X, Dhanasekaran SM, Fullen DR, Lagstein A, Chan MP, Mehra R. Immunohistochemical characterization of fumarate hydratase (FH) and succinate dehydrogenase (SDH) in cutaneous leiomyomas for detection of familial cancer syndromes. Am J Surg Pathol. 2017;41(6):801–9. https://doi.org/10.1097/PAS.0000000000000840. PMID: 28288038; PMCID: PMC5423817
39. Buelow B, Cohen J, Nagymanyoki Z, Frizzell N, Joseph NM, McCalmont T, Garg K. Immunohistochemistry for 2-succinocysteine (2SC) and fumarate hydratase (FH) in cutaneous leiomyomas may aid in identification of patients With HLRCC (hereditary leiomyomatosis and renal cell carcinoma syndrome). Am J Surg Pathol. 2016;40(7):982–8. https://doi.org/10.1097/PAS.0000000000000626.
40. D'Alfonso TM, Subramaniyam S, Ginter PS, Mosquera JM, Croyle J, Liu YF, Rubin MA, Shin SJ. Characterization of CD34-deficient myofibroblastomas of the breast. Breast J. 2018;24(1):55–61. https://doi.org/10.1111/tbj.12835. Epub 2017 May 30
41. Charpin C, Mathoulin MP, Andrac L, Barberis J, Boulat J, Sarradour B, et al. Reappraisal of breast hamartomas. A morphological study of 41 cases. Pathol Res Pract. 1994;190(4):362–71. Epub 1994/04/01
42. Neilsen TO, CDM F, TKY T. Lipoma. In: WHO classification of Tumours editorial board. Breast tumours, WHO classification of tumours series, vol. 2. 5th ed. Lyon: International Agency for Research on Cancer; 2019. p. 221–2.
43. Herbert M, Sandbank J, Liokumovich P, Yanai O, Pappo I, Karni T, et al. Breast hamartomas: clinicopathological and immunohistochemical studies of 24 cases. Histopathology. 2002;41(1):30–4. Epub 2002/07/18
44. Tse GM, Law BK, Ma TK, Chan AB, Pang LM, Chu WC, et al. Hamartoma of the breast: a clinicopathological review. J Clin Pathol. 2002;55(12):951–4. Epub 2002/12/04
45. Wahner-Roedler DL, Sebo TJ, Gisvold JJ. Hamartomas of the breast: clinical, radiologic, and pathologic manifestations. Breast J. 2001;7(2):101–5. Epub 2001/05/01
46. Adrada B, Wu Y, Yang W. Hyperechoic lesions of the breast: radiologic-histopathologic correlation. AJR Am J Roentgenol. 2013;200(5):W518–30. https://doi.org/10.2214/AJR.12.9263.
47. Murugesan JR, Joglekar S, Valerio D, Bradley S, Clark D, Jibril JA. Myoid hamartoma of the breast: case report and review of the literature. Clin Breast Cancer. 2006;7(4):345–6. Epub 2006/11/10
48. Fisher CJ, Hanby AM, Robinson L, Millis RR. Mammary hamartoma—a review of 35 cases. Histopathology. 1992;20(2):99–106. Epub 1992/02/01
49. Schrager CA, Schneider D, Gruener AC, Tsou HC, Peacocke M. Clinical and pathological features of breast disease in Cowden's syndrome: an underrecognized syndrome with an increased risk of breast cancer. Hum Pathol. 1998;29(1):47–53. Epub 1998/01/28
50. Pilarski R. Cowden syndrome: a critical review of the clinical literature. J Genet Couns. 2009;18(1):13–27. Epub 2008/10/31
51. Molière S, Mathelin C. The Cowden Syndrome. N Engl J Med. 2020;382(15):e29. https://doi.org/10.1056/NEJMicm1910478. PMID: 32268030
52. Koide N, Akashi-Tanaka S, Fukutomi T, Nanasawa T, Hasegawa T. Nodular mucinosis of the breast: a case report with clinical and imaging findings. Breast Cancer. 2002;9(3):261–4. Epub 2002/08/20
53. Sanati S, Leonard M, Khamapirad T, Eltorky MA. Nodular mucinosis of the breast: a case report with pathologic, ultrasonographic, and clinical findings and review of the literature. Arch Pathol Lab Med. 2005;129(3):e58–61. Epub 2005/03/02
54. Wargotz ES, Weiss SW, Norris HJ. Myofibroblastoma of the breast. Sixteen cases of a distinctive benign mesenchymal tumor. Am J Surg Pathol. 1987;11(7):493–502. Epub 1987/07/01
55. McMenamin ME, DeSchryver K, Fletcher CD. Fibrous lesions of the breast: a review. Int J Surg Pathol. 2000;8(2):99–108. Epub 2001/08/09
56. Magro G. Mammary myofibroblastoma: a tumor with a wide morphologic spectrum. Arch Pathol Lab Med. 2008;132(11):1813–20. Epub 2008/11/04
57. Shanmugasiva VV, Ramli Hamid MT, Fadzli F, Shaleen Kaur KS, Abd Rahman N, Rahmat K. Myofibroblastoma of the breast. Malays J Pathol. 2018;40(3):349–53. PMID: 30580368
58. Howitt BE, Fletcher CD. Mammary-type Myofibroblastoma: clinicopathologic characterization in a series of 143 cases. Am J Surg Pathol. 2016;40(3):361–7. https://doi.org/10.1097/PAS.0000000000000540. PMID: 26523539
59. Magro G. Epithelioid-cell myofibroblastoma of the breast: expanding the morphologic spectrum. Am J Surg Pathol. 2009;33(7):1085–92. Epub 2009/04/25
60. D'Alfonso TM, Subramaniyam S, Ginter PS, Mosquera JM, MacDonald TY, Noorzad Z, Orta LY, Liu YF, Rubin MA, Shin SJ. Characterization of the leiomyomatous variant of myofibroblastoma: a rare subset distinct from other smooth muscle tumors of the breast. Hum Pathol. 2016;58:54–61. https://doi.org/10.1016/j.humpath.2016.07.018. Epub 2016 Aug 3. PMID: 27498061
61. Magro G, Gangemi P, Greco P. Deciduoid-like myofibroblastoma of the breast: a potential pitfall of malignancy. Histopathology. 2008;52(5):652–4. Epub 2008/03/29
62. Magro G, Fraggetta F, Torrisi A, Emmanuele C, Lanzafame S. Myofibroblastoma of the breast with hemangiopericytoma-like pattern and pleomorphic lipoma-like areas. Report of a case with diagnostic and histogenetic considerations. Pathol Res Pract. 1999;195(4):257–62. Epub 1999/05/25
63. Gocht A, Bosmuller HC, Bassler R, Tavassoli FA, Moinfar F, Katenkamp D, et al. Breast tumors with myofibroblastic differentiation: clinico-pathological observations in myofibroblastoma and myofibrosarcoma. Pathol Res Pract. 1999;195(1):1–10. Epub 1999/02/27
64. Stark M, Hoffmann A, Xiong Z. Mammary myofibrosarcoma: case report and literature review. Breast J. 2011;17(3):300–4. Epub 2011/05/07
65. Taccagni G, Rovere E, Masullo M, Christensen L, Eyden B. Myofibrosarcoma of the breast: review of the literature on myofibroblastic tumors and criteria for defining myofibroblastic differentiation. Am J Surg Pathol. 1997;21(4):489–96. Epub 1997/04/01
66. Magro G, Foschini MP, Eusebi V. Palisaded myofibroblastoma of the breast: a tumor closely mimicking schwannoma: report of 2 cases. Hum Pathol. 2013;44(9):1941–6. Epub 2013/04/12
67. Magro G, Righi A, Casorzo L, Antonietta T, Salvatorelli L, Kacerovska D, et al. Mammary and vaginal myofibroblastomas are genetically related lesions: fluorescence in situ hybridization analysis shows deletion of 13q14 region. Hum Pathol. 2012;43(11):1887–93. Epub 2012/05/12

68. Powell CM, Cranor ML, Rosen PP. Pseudoangiomatous stromal hyperplasia (PASH). A mammary stromal tumor with myofibroblastic differentiation. Am J Surg Pathol. 1995;19(3):270–7. Epub 1995/03/01
69. Virk RK, Khan A. Pseudoangiomatous stromal hyperplasia: an overview. Arch Pathol Lab Med. 2010;134(7):1070–4. Epub 2010/07/01
70. AbdullGaffar B. Pseudoangiomatous stromal hyperplasia of the breast. Arch Pathol Lab Med. 2009;133(8):1335–8. Epub 2009/08/06
71. Ibrahim RE, Sciotto CG, Weidner N. Pseudoangiomatous hyperplasia of mammary stroma. Some observations regarding its clinicopathologic spectrum. Cancer. 1989;63(6):1154–60. Epub 1989/03/15
72. Bowman E, Oprea G, Okoli J, Gundry K, Rizzo M, Gabram-Mendola S, et al. Pseudoangiomatous stromal hyperplasia (PASH) of the breast: a series of 24 patients. Breast J. 2012;18(3):242–7. Epub 2012/05/16
73. Ferreira M, Albarracin CT, Resetkova E. Pseudoangiomatous stromal hyperplasia tumor: a clinical, radiologic and pathologic study of 26 cases. Mod Pathol. 2008;21(2):201–7. Epub 2007/12/18
74. Badve S, Sloane JP. Pseudoangiomatous hyperplasia of male breast. Histopathology. 1995;26(5):463–6. Epub 1995/05/01
75. Shehata BM, Fishman I, Collings MH, Wang J, Poulik JM, Ricketts RR, et al. Pseudoangiomatous stromal hyperplasia of the breast in pediatric patients: an underrecognized entity. Pediatr Dev Pathol. 2009;12(6):450–4. Epub 2009/07/18
76. Jones KN, Glazebrook KN, Reynolds C. Pseudoangiomatous stromal hyperplasia: imaging findings with pathologic and clinical correlation. AJR Am J Roentgenol. 2010;195(4):1036–42. Epub 2010/09/23
77. Hargaden GC, Yeh ED, Georgian-Smith D, Moore RH, Rafferty EA, Halpern EF, et al. Analysis of the mammographic and sonographic features of pseudoangiomatous stromal hyperplasia. AJR Am J Roentgenol. 2008;191(2):359–63. Epub 2008/07/24
78. Anderson C, Ricci A Jr, Pedersen CA, Cartun RW. Immunocytochemical analysis of estrogen and progesterone receptors in benign stromal lesions of the breast. Evidence for hormonal etiology in pseudoangiomatous hyperplasia of mammary stroma. Am J Surg Pathol. 1991;15(2):145–9. Epub 1991/02/11
79. Degnim AC, Frost MH, Radisky DC, Anderson SS, Vierkant RA, Boughey JC, et al. Pseudoangiomatous stromal hyperplasia and breast cancer risk. Ann Surg Oncol. 2010;17(12):3269–77. Epub 2010/06/23
80. Nassar H, Elieff MP, Kronz JD, Argani P. Pseudoangiomatous stromal hyperplasia (PASH) of the breast with foci of morphologic malignancy: a case of PASH with malignant transformation? Int J Surg Pathol. 2010;18(6):564–9. Epub 2008/07/10
81. Vuitch MF, Rosen PP, Erlandson RA. Pseudoangiomatous hyperplasia of mammary stroma. Hum Pathol. 1986;17(2):185–91. Epub 1986/02/01
82. Gresik CM, Godellas C, Aranha GV, Rajan P, Shoup M. Pseudoangiomatous stromal hyperplasia of the breast: a contemporary approach to its clinical and radiologic features and ideal management. Surgery. 2010;148(4):752–7. discussion 7-8. Epub 2010/08/17
83. Neuman HB, Brogi E, Ebrahim A, Brennan MF, Van Zee KJ. Desmoid tumors (fibromatoses) of the breast: a 25-year experience. Ann Surg Oncol. 2008;15(1):274–80. Epub 2007/09/27
84. Rosen PP, Ernsberger D. Mammary fibromatosis. A benign spindle-cell tumor with significant risk for local recurrence. Cancer. 1989;63(7):1363–9. Epub 1989/04/01
85. Liu H, Zeng H, Zhang H, Wang H, Cheng Z, Hu Y, Wu Z. Breast fibromatosis: imaging and clinical findings. Breast J. 2020;26(11):2217–22. https://doi.org/10.1111/tbj.14008. Epub 2020 Aug 4
86. Erguvan-Dogan B, Dempsey PJ, Ayyar G, Gilcrease MZ. Primary desmoid tumor (extraabdominal fibromatosis) of the breast. AJR Am J Roentgenol. 2005;185(2):488–9. Epub 2005/07/23
87. Sneige N, Yaziji H, Mandavilli SR, Perez ER, Ordonez NG, Gown AM, et al. Low-grade (fibromatosis-like) spindle cell carcinoma of the breast. Am J Surg Pathol. 2001;25(8):1009–16. Epub 2001/07/28
88. Gobbi H, Simpson JF, Borowsky A, Jensen RA, Page DL. Metaplastic breast tumors with a dominant fibromatosis-like phenotype have a high risk of local recurrence. Cancer. 1999;85(10):2170–82. Epub 1999/05/18
89. Dunne B, Lee AH, Pinder SE, Bell JA, Ellis IO. An immunohistochemical study of metaplastic spindle cell carcinoma, phyllodes tumor and fibromatosis of the breast. Hum Pathol. 2003;34(10):1009–15. Epub 2003/11/11
90. Devouassoux-Shisheboran M, Schammel MD, Man YG, Tavassoli FA. Fibromatosis of the breast: age-correlated morphofunctional features of 33 cases. Arch Pathol Lab Med. 2000;124(2):276–80. Epub 2000/02/03
91. Sawyer EJ, Hanby AM, Rowan AJ, Gillett CE, Thomas RE, Poulsom R, et al. The Wnt pathway, epithelial-stromal interactions, and malignant progression in phyllodes tumours. J Pathol. 2002;196(4):437–44. Epub 2002/03/29
92. Lacroix-Triki M, Geyer FC, Lambros MB, Savage K, Ellis IO, Lee AH, et al. Beta-catenin/Wnt signalling pathway in fibromatosis, metaplastic carcinomas and phyllodes tumours of the breast. Mod Pathol. 2010;23(11):1438–48. Epub 2010/08/10
93. Abraham SC, Reynolds C, Lee JH, Montgomery EA, Baisden BL, Krasinskas AM, Wu TT. Fibromatosis of the breast and mutations involving the APC/beta-catenin pathway. Hum Pathol. 2002;33(1):39–46. https://doi.org/10.1053/hupa.2002.30196. Erratum in: Hum Pathol 2002;33(3):379. PMID: 11823972
94. Carlson JW, Fletcher CD. Immunohistochemistry for beta-catenin in the differential diagnosis of spindle cell lesions: analysis of a series and review of the literature. Histopathology. 2007;51(4):509–14. Epub 2007/08/23
95. Wargotz ES, Norris HJ, Austin RM, Enzinger FM. Fibromatosis of the breast. A clinical and pathological study of 28 cases. Am J Surg Pathol. 1987;11(1):38–45. Epub 1987/01/01
96. van de Rijn M, Brogi E, Charville GW, Liegl-Atzwanger B, Shin SJ. Desmoid fibromatosis. In: WHO Classification of Tumours Editorial Board. Breast tumours, WHO Classification of tumours series, vol. 2. 5th ed. Lyon: International Agency for Research on Cancer; 2019. p. 206–8.
97. Colombo C, Miceli R, Le Péchoux C, Palassini E, Honoré C, Stacchiotti S, Mir O, Casali PG, Dômont J, Fiore M, Le Cesne A, Gronchi A, Bonvalot S. Sporadic extra abdominal wall desmoid-type fibromatosis: surgical resection can be safely limited to a minority of patients. Eur J Cancer. 2015;51(2):186–92. https://doi.org/10.1016/j.ejca.2014.11.019. Epub 2014 Dec 11. PMID: 25500145
98. Kuba MG, Lester SC, Giess CS, Bertagnolli MM, Wieczorek TJ, Brock JE. Fibromatosis of the breast: diagnostic accuracy of core needle biopsy. Am J Clin Pathol. 2017;148(3):243–50. https://doi.org/10.1093/ajcp/aqx065.
99. Boland MR, Nugent T, Nolan J, O'Mahony J, O'Keeffe S, Gillham CC, Maguire A, Geraghty J, McCartan D, Evoy D, Prichard RS, McDermott EW, Alazawi D, Boyle TJ, Connolly EM. Fibromatosis of the breast: a 10-year multi-institutional experience and review of the literature. Breast Cancer. 2021;28(1):168–74. https://doi.org/10.1007/s12282-020-01145-5. Epub 2020 Aug 11. PMID: 32780320

100. Blum A, Roehm S. Accessory nipple looks like dermatofibroma in dermoscopy. Arch Dermatol. 2003;139(7):948–9. Epub 2003/07/23
101. Kiyohara T, Takahashi H, Kumakiri M. Supernumerary breast tissue with Toker cells clinically and dermoscopically mimicking atrophic dermatofibroma: the efficacy of estrogen receptor immunoreactivity. J Dermatol. 2012;39(10):873–5. Epub 2011/12/16
102. Hussein MR. Skin metastasis: a pathologist's perspective. J Cutan Pathol. 2010;37(9):e1–20. Epub 2009/11/20
103. Prieto VG, Reed JA, Shea CR. Immunohistochemistry of dermatofibromas and benign fibrous histiocytomas. J Cutan Pathol. 1995;22(4):336–41. Epub 1995/08/01
104. Charu V, Cimino-Mathews A. Peripheral nerve sheath tumors of the breast. Semin Diagn Pathol. 2017;34(5):420–6. https://doi.org/10.1053/j.semdp.2017.05.011. Epub 2017 May 27. PMID: 28647116
105. Lack EE, Worsham GF, Callihan MD, Crawford BE, Klappenbach S, Rowden G, et al. Granular cell tumor: a clinicopathologic study of 110 patients. J Surg Oncol. 1980;13(4):301–16. Epub 1980/01/01
106. Brown AC, Audisio RA, Regitnig P. Granular cell tumour of the breast. Surg Oncol. 2011;20(2):97–105. Epub 2010/01/16
107. De Simone N, Aggon A, Christy C. Granular cell tumor of the breast: clinical and pathologic characteristics of a rare case in a 14-year-old girl. J Clin Oncol. 2011;29(22):e656–7. Epub 2011/06/08
108. Adeniran A, Al-Ahmadie H, Mahoney MC, Robinson-Smith TM. Granular cell tumor of the breast: a series of 17 cases and review of the literature. Breast J. 2004;10(6):528–31. Epub 2004/12/01
109. Gibbons D, Leitch M, Coscia J, Lindberg G, Molberg K, Ashfaq R, et al. Fine needle aspiration cytology and histologic findings of granular cell tumor of the breast: review of 19 cases with clinical/radiologic correlation. Breast J. 2000;6(1):27–30. Epub 2001/05/12
110. Scaranelo AM, Bukhanov K, Crystal P, Mulligan AM, O'Malley FP. Granular cell tumour of the breast: MRI findings and review of the literature. Br J Radiol. 2007;80(960):970–4. Epub 2007/10/18
111. Fanburg-Smith JC, Meis-Kindblom JM, Fante R, Kindblom LG. Malignant granular cell tumor of soft tissue: diagnostic criteria and clinicopathologic correlation. Am J Surg Pathol. 1998;22(7):779–94. Epub 1998/07/21
112. Le BH, Boyer PJ, Lewis JE, Kapadia SB. Granular cell tumor: immunohistochemical assessment of inhibin-alpha, protein gene product 9.5, S100 protein, CD68, and Ki-67 proliferative index with clinical correlation. Arch Pathol Lab Med. 2004;128(7):771–5. Epub 2004/06/25
113. Montagnese MD, Roshong-Denk S, Zaher A, Mohamed I, Staren ED. Granular cell tumor of the breast. Am Surg. 2004;70(1):52–4. Epub 2004/02/18
114. Pareja F, Brandes AH, Basili T, Selenica P, Geyer FC, Fan D, Da Cruz PA, Kumar R, Brown DN, Gularte-Mérida R, Alemar B, Bi R, Lim RS, de Bruijn I, Fujisawa S, Gardner R, Feng E, Li A, da Silva EM, Lozada JR, Blecua P, Cohen-Gould L, Jungbluth AA, Rakha EA, Ellis IO, Edelweiss MIA, Palazzo J, Norton L, Hollmann T, Edelweiss M, Rubin BP, Weigelt B, Reis-Filho JS. Loss-of-function mutations in ATP6AP1 and ATP6AP2 in granular cell tumors. Nat Commun. 2018;9(1):3533. https://doi.org/10.1038/s41467-018-05886-y. PMID: 30166553; PMCID: PMC6117336
115. Rosso R, Scelsi M, Carnevali L. Granular cell traumatic neuroma: a lesion occurring in mastectomy scars. Arch Pathol Lab Med. 2000;124(5):709–11. Epub 2000/04/27
116. Akahane K, Kato K, Ogiso S, Sakaguchi K, Hashimoto M, Ishikawa A, et al. Malignant granular cell tumor of the breast: case report and literature review. Breast Cancer. 2015;22(3):317–23. Epub 2012/04/03
117. Bongiorno MR, Doukaki S, Arico M. Neurofibromatosis of the nipple-areolar area: a case series. J Med Case Rep. 2010;4:22. Epub 2010/03/09
118. Thompson SKS, Poppiti RJ, Collado-Mesa F, Rabinovich K. Solitary neurofibroma of the breast. Radiol Case Rep. 2012;7(4):1–3.
119. Jeyaretna DS, Oriolowo A, Smith ME, Watkins RM. Solitary neurofibroma in the male breast. World J Surg Oncol. 2007;5:23. Epub 2007/02/28
120. Murat A, Kansiz F, Kabakus N, Kazez A, Ozercan R. Neurofibroma of the breast in a boy with neurofibromatosis type 1. Clin Imaging. 2004;28(6):415–7. Epub 2004/11/09
121. Uchida N, Yokoo H, Kuwano H. Schwannoma of the breast: report of a case. Surg Today. 2005;35(3):238–42. Epub 2005/03/18
122. Bellezza G, Lombardi T, Panzarola P, Sidoni A, Cavaliere A, Giansanti M. Schwannoma of the breast: a case report and review of the literature. Tumori. 2007;93(3):308–11. Epub 2007/08/08
123. Lee EK, Kook SH, Kwag HJ, Park YL, Bae WG. Schwannoma of the breast showing massive exophytic growth: a case report. Breast. 2006;15(4):562–6. Epub 2006/07/18
124. Fanburg-Smith JC, Majidi M, Miettinen M. Keratin expression in schwannoma; a study of 115 retroperitoneal and 22 peripheral schwannomas. Mod Pathol. 2006;19(1):115–21. Epub 2005/12/17
125. Halteh P, Patel A, Eskreis-Winkler S, D'Alfonso TM. Schwannoma of the breast: a common tumor in an uncommon location. Breast J. 2018;24(2):206–7. https://doi.org/10.1111/tbj.12872. Epub 2017 Jul 14
126. Adem C, Reynolds C, Ingle JN, Nascimento AG. Primary breast sarcoma: clinicopathologic series from the Mayo Clinic and review of the literature. Br J Cancer. 2004;91(2):237–41. Epub 2004/06/10
127. Falconieri G, Della Libera D, Zanconati F, Bittesini L. Leiomyosarcoma of the female breast: report of two new cases and a review of the literature. Am J Clin Pathol. 1997;108(1):19–25. Epub 1997/07/01
128. Szekely E, Madaras L, Kulka J, Jaray B, Nagy L. Leiomyosarcoma of the female breast. Pathol Oncol Res. 2001;7(2):151–3. Epub 2001/07/18
129. Jones MW, Norris HJ, Wargotz ES, Weiss SW. Fibrosarcoma-malignant fibrous histiocytoma of the breast. A clinicopathological study of 32 cases. Am J Surg Pathol. 1992;16(7):667–74. Epub 1992/07/01
130. Pandey M, Mathew A, Abraham EK, Rajan B. Primary sarcoma of the breast. J Surg Oncol. 2004;87(3):121–5. Epub 2004/08/31
131. Terrier P, Terrier-Lacombe MJ, Mouriesse H, Friedman S, Spielmann M, Contesso G. Primary breast sarcoma: a review of 33 cases with immunohistochemistry and prognostic factors. Breast Cancer Res Treat. 1989;13(1):39–48. Epub 1989/01/01
132. Dhingra KK, Mandal S, Roy S, Khurana N. Malignant peripheral nerve sheath tumor of the breast: case report. World J Surg Oncol. 2007;5:142. Epub 2007/12/25
133. Medina-Franco H, Gamboa-Dominguez A, de La Medina AR. Malignant peripheral nerve sheath tumor of the breast. Breast J. 2003;9(4):332. Epub 2003/07/09
134. Bahrami A, Resetkova E, Ro JY, Ibanez JD, Ayala AG. Primary osteosarcoma of the breast: report of 2 cases. Arch Pathol Lab Med. 2007;131(5):792–5. Epub 2007/05/10
135. Silver SA, Tavassoli FA. Primary osteogenic sarcoma of the breast: a clinicopathologic analysis of 50 cases. Am J Surg Pathol. 1998;22(8):925–33. Epub 1998/08/26
136. Djilas-Ivanovic D, Prvulovic N, Bogdanovic-Stojanovic D, Vicko F, Sveljo O, Ivkovic-Kapicl T. Dermatofibrosarcoma protuberans of the breast: mammographic, ultrasound, MRI and MRS features. Arch Gynecol Obstet. 2009;280(5):827–30. Epub 2009/03/03

137. Kim MK, Chang ED, Kim JS, Whang IY. Dermatofibrosarcoma protuberans of the breast. Breast J. 2013;19(4):442–3. Epub 2013/06/01
138. Lin JY, Sheen-Chen SM, Hsu W, Huang CC, Ko SF, Eng HL. Dermatofibrosarcoma protuberans of the breast. Tumori. 2008;94(6):861–3. Epub 2009/03/10
139. Liu SZ, Ho TL, Hsu SM, Zhan HL, Chou CP. Imaging of dermatofibrosarcoma protuberans of breast. Breast J. 2010;16(5):541–3. Epub 2010/07/16
140. Hartel PH, Bratthauer G, Hartel JV, Fanburg-Smith JC. Primary malignant fibrous histiocytoma (myxofibrosarcoma/pleomorphic sarcoma not otherwise specified) of the breast: clinicopathologic study of 19 cases. Ann Diagn Pathol. 2011;15(6):407–13. Epub 2011/10/11
141. Nascimento AF, Raut CP, Fletcher CD. Primary angiosarcoma of the breast: clinicopathologic analysis of 49 cases, suggesting that grade is not prognostic. Am J Surg Pathol. 2008;32(12):1896–904. Epub 2008/09/25
142. Sher T, Hennessy BT, Valero V, Broglio K, Woodward WA, Trent J, et al. Primary angiosarcomas of the breast. Cancer. 2007;110(1):173–8. Epub 2007/06/02
143. Vorburger SA, Xing Y, Hunt KK, Lakin GE, Benjamin RS, Feig BW, et al. Angiosarcoma of the breast. Cancer. 2005;104(12):2682–8. Epub 2005/11/17
144. Wang XY, Jakowski J, Tawfik OW, Thomas PA, Fan F. Angiosarcoma of the breast: a clinicopathologic analysis of cases from the last 10 years. Ann Diagn Pathol. 2009;13(3):147–50. Epub 2009/05/13
145. Arbabi L, Warhol MJ. Pleomorphic liposarcoma following radiotherapy for breast carcinoma. Cancer. 1982;49(5):878–80. Epub 1982/03/01
146. Kirova YM, Vilcoq JR, Asselain B, Sastre-Garau X, Fourquet A. Radiation-induced sarcomas after radiotherapy for breast carcinoma: a large-scale single-institution review. Cancer. 2005;104(4):856–63. Epub 2005/06/28
147. Sheth GR, Cranmer LD, Smith BD, Grasso-Lebeau L, Lang JE. Radiation-induced sarcoma of the breast: a systematic review. Oncologist. 2012;17(3):405–18. Epub 2012/02/16
148. Al-Benna S, Poggemann K, Steinau HU, Steinstraesser L. Diagnosis and management of primary breast sarcoma. Breast Cancer Res Treat. 2010;122(3):619–26. Epub 2010/05/19
149. Ferreira ALS, Souza JA, Gibbons IL, Lellis RF, Oliveira VS, de Sousa Rosas CH, Guatelli CS, Bitencourt AGV. Clinical and imaging features of dermatofibrosarcoma protuberans in the breast. Breast J. 2021;27(1):92–4. https://doi.org/10.1111/tbj.14104. Epub 2020 Nov 27. PMID: 33246353
150. DeLair DF, Corben AD, Catalano JP, Vallejo CE, Brogi E, Tan LK. Non-mammary metastases to the breast and axilla: a study of 85 cases. Mod Pathol. 2013;26(3):343–9. Epub 2012/11/24
151. Tse GM, Tan PH, Putti TC, Lui PC, Chaiwun B, Law BK. Metaplastic carcinoma of the breast: a clinicopathological review. J Clin Pathol. 2006;59(10):1079–83. Epub 2006/02/10
152. Powell CM, Rosen PP. Adipose differentiation in cystosarcoma phyllodes. A study of 14 cases. Am J Surg Pathol. 1994;18(7):720–7. Epub 1994/07/01
153. Koker MM, Kleer CG. p63 expression in breast cancer: a highly sensitive and specific marker of metaplastic carcinoma. Am J Surg Pathol. 2004;28(11):1506–12. Epub 2004/10/19
154. Tse GM, Tan PH, Chaiwun B, Putti TC, Lui PC, Tsang AK, et al. p63 is useful in the diagnosis of mammary metaplastic carcinomas. Pathology. 2006;38(1):16–20. Epub 2006/02/18
155. Bishop JA, Montgomery EA, Westra WH. Use of p40 and p63 immunohistochemistry and human papillomavirus testing as ancillary tools for the recognition of head and neck sarcomatoid carcinoma and its distinction from benign and malignant mesenchymal processes. Am J Surg Pathol. 2014;38(2):257–64. Epub 2014/01/15
156. Jo VY, Fletcher CD. p63 immunohistochemical staining is limited in soft tissue tumors. Am J Clin Pathol. 2011;136(5):762–6. Epub 2011/10/28
157. Miettinen M. Immunoreactivity for cytokeratin and epithelial membrane antigen in leiomyosarcoma. Arch Pathol Lab Med. 1988;112(6):637–40. Epub 1988/06/01
158. Cimino-Mathews A, Sharma R, Illei PB, Vang R, Argani P. A subset of malignant phyllodes tumors express p63 and p40: a diagnostic pitfall in breast core needle biopsies. Am J Surg Pathol. 2014;38(12):1689–96. Epub 2014/07/22
159. Fields RC, Aft RL, Gillanders WE, Eberlein TJ, Margenthaler JA. Treatment and outcomes of patients with primary breast sarcoma. Am J Surg. 2008;196(4):559–61. Epub 2008/08/30
160. Lee JS, Yoon K, Onyshchenko M. Sarcoma of the breast: clinical characteristics and outcomes of 991 patients from the national cancer database. Sarcoma. 2021;21(2021):8828158. https://doi.org/10.1155/2021/8828158. PMID: 33542674; PMCID: PMC7843167

Vascular Lesions of the Breast

17

Melinda E. Sanders and Justin M. Cates

Benign Vascular Lesions

Overview

Benign vascular lesions of the breast may be encountered in the breast parenchyma or overlying dermis and subcutis. These lesions are typically incidental findings and rarely detected on routine screening imaging studies. Benign vascular lesions are seldom biopsied when there is strong clinical/radiographic evidence of the diagnosis. If biopsy is clinically indicated, an excisional procedure is preferred to reduce the risk of hemorrhage. Collectively, benign vascular lesions are well circumscribed and lack the cytologic atypia, endothelial hyperplasia, and anastomosing channels that characterize angiosarcoma. Morphologic variants recognized in the breast include perilobular, capillary, cavernous, and venous hemangioma; arteriovenous malformations and angiolipomas may occur in the breast rarely. There is no evidence to suggest that any of these types of hemangiomas develop into angiosarcomas over time. Other benign vascular lesions which may be rarely encountered in the breast include papillary endothelial hyperplasia and angiomatosis. The practical importance of recognizing these lesions is their distinction from angiosarcoma, which can be difficult on limited material such as in core needle biopsies (CNBs).

Clinical and Radiologic Features

Perilobular capillary hemangiomas are the most common vascular lesions of the breast and are observed in 1–12% of breast specimens [1]. They are almost always microscopic, incidental findings but may sometimes be detected clinically or by imaging. Capillary, cavernous, and venous hemangiomas appear as an oval or lobulated mass with well-circumscribed or microlobulated margins on mammogram and as an ill-defined, hyperechoic, or well-defined, hypoechoic mass on ultrasound. Most cases are superficial [2, 3]. By dynamic contrast-enhanced magnetic resonance imaging (MRI), hemangioma typically appears as a homogeneously enhancing mass with well-defined margins. The T1-weighted image shows intermediate signal, while in T2-weighted images the signal is intermediate to high [4, 5].

Angiomatosis occurs in young women and may be acquired or congenital [6, 7]. Clinically, angiomatosis presents as breast swelling or a large mass, in some cases measuring over 20 cm [6, 7], and is typically painless. Hyperpigmentation, discoloration, or papules of the overlying skin may be present [8]. Ultrasound examination shows large cystic spaces separated by septa with moderate blood flow [3]. MRI demonstrates a large septated mass, frequently with displacement and compression of the normal breast tissue. The cystic spaces are hypointense with respect to the glandular tissue on T1-weighted images and hyperintense compared to the glandular tissue on T2 images [3].

Microscopic Features

Perilobular hemangioma is a circumscribed proliferation of thin-walled capillaries lined by attenuated endothelial cells with small nuclei lacking atypia (Fig. 17.1a). Mitotic activity is absent. They may involve the intralobular or the extralobular stroma (Fig. 17.1b). Occasional lesions may be less circumscribed, raising concern for well-differentiated angiosarcoma on low-power examination; however, the endothelial cells lack atypia (Fig. 17.1c).

Capillary hemangiomas are characterized by a circumscribed proliferation of small vascular spaces with a lobular appearance, similar to lobular capillary hemangioma (pyogenic granuloma) from other anatomic sites (Fig. 17.2a, b). The endothelial cells lining these spaces are flat to slightly cuboidal without evidence of atypia (Fig. 17.2c). In *cavernous hemangiomas*, the vascular spaces are composed of larger vessels with dilated lumens and thin walls (Fig. 17.3a, b). The endothelial cells are flat and lack atypia (Fig. 17.3c). Stromal

M. E. Sanders (✉) · J. M. Cates
Department of Pathology, Microbiology and Immunology, Vanderbilt University Medical Center, Nashville, TN, USA
e-mail: melinda.sanders@vumc.org; justin.m.cates@vumc.org

© The Author(s), under exclusive license to Springer Nature Switzerland AG 2022
S. J. Shin et al. (eds.), *A Comprehensive Guide to Core Needle Biopsies of the Breast*,
https://doi.org/10.1007/978-3-031-05532-4_17

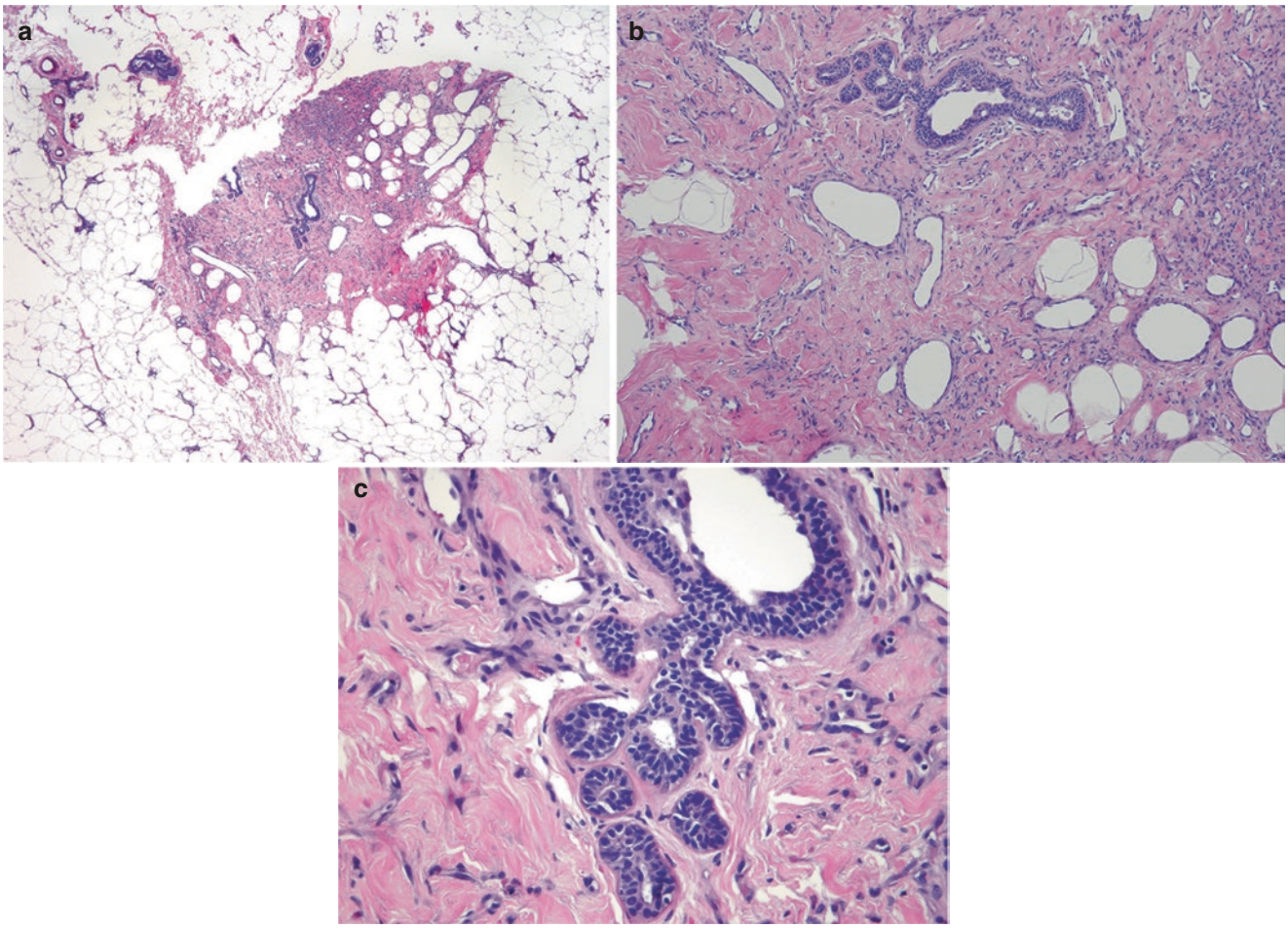

Fig. 17.1 (**a**) In this perilobular hemangioma, the proliferation of small capillaries has a slightly irregular contour but is circumscribed; (**b**) and both the interlobular and extralobular stroma are involved. (**c**) The capillaries proliferate around but do not distort the normal mammary structures

calcifications may be present. *Complex hemangiomas* contain a mixture of small vessels characteristic of the capillary type and dilated vessels typical of the cavernous type. *Venous hemangiomas* are uncommon and are characterized by large venous channels with variably thickened muscular walls lined by flat endothelial cells without atypia [9] (Fig. 17.4). Thrombosis, with or without secondary changes thereof (i.e., organizing thrombus, dystrophic calcifications, papillary endothelial hyperplasia [see below]), may occur in any of the hemangioma subtypes. Otherwise, benign hemangiomas showing focal endothelial cell atypia or anastomosing vascular channels have been termed "atypical hemangiomas" and may represent degenerative changes as are sometimes seen in other long-standing soft-tissue tumors [10].

Papillary endothelial hyperplasia represents exuberant organization and recanalization of a thrombus. Its appearance in the breast is identical to that seen in other sites [9, 11, 12]. Histologically, papillary endothelial hyperplasia is a relatively circumscribed intravascular proliferation of endothelial cells lining hyaline papillary stalks [13] (Fig. 17.5a). The endothelial cells are usually attenuated and lack necrosis or atypia (Fig. 17.5b). Ectatic vascular spaces frequently observed surrounding the papillary endothelial nodule are suggestive of origin from or association with a preexisting cavernous hemangioma [13]. An intravascular location can often be confirmed by an elastic stain. As papillae fuse, anastomosing vascular channels can develop and mimic angiosarcoma [13]. However, lesional circumscription, purely intravascular growth, and absence of significant cytologic atypia, necrosis, aberrant mitotic figures, or foci of solid growth usually make the distinction straightforward. Excisional biopsy is certainly an adequate treatment.

Angiomatosis is an uncommon lesion in which cystically dilated, anastomosing vascular spaces involve large areas of the breast without infiltration of breast parenchyma [7] (Fig. 17.6a). The vascular spaces are lined by flat endothelial cells without atypia or mitotic activity (Fig. 17.6b). The walls between the spaces contain wispy

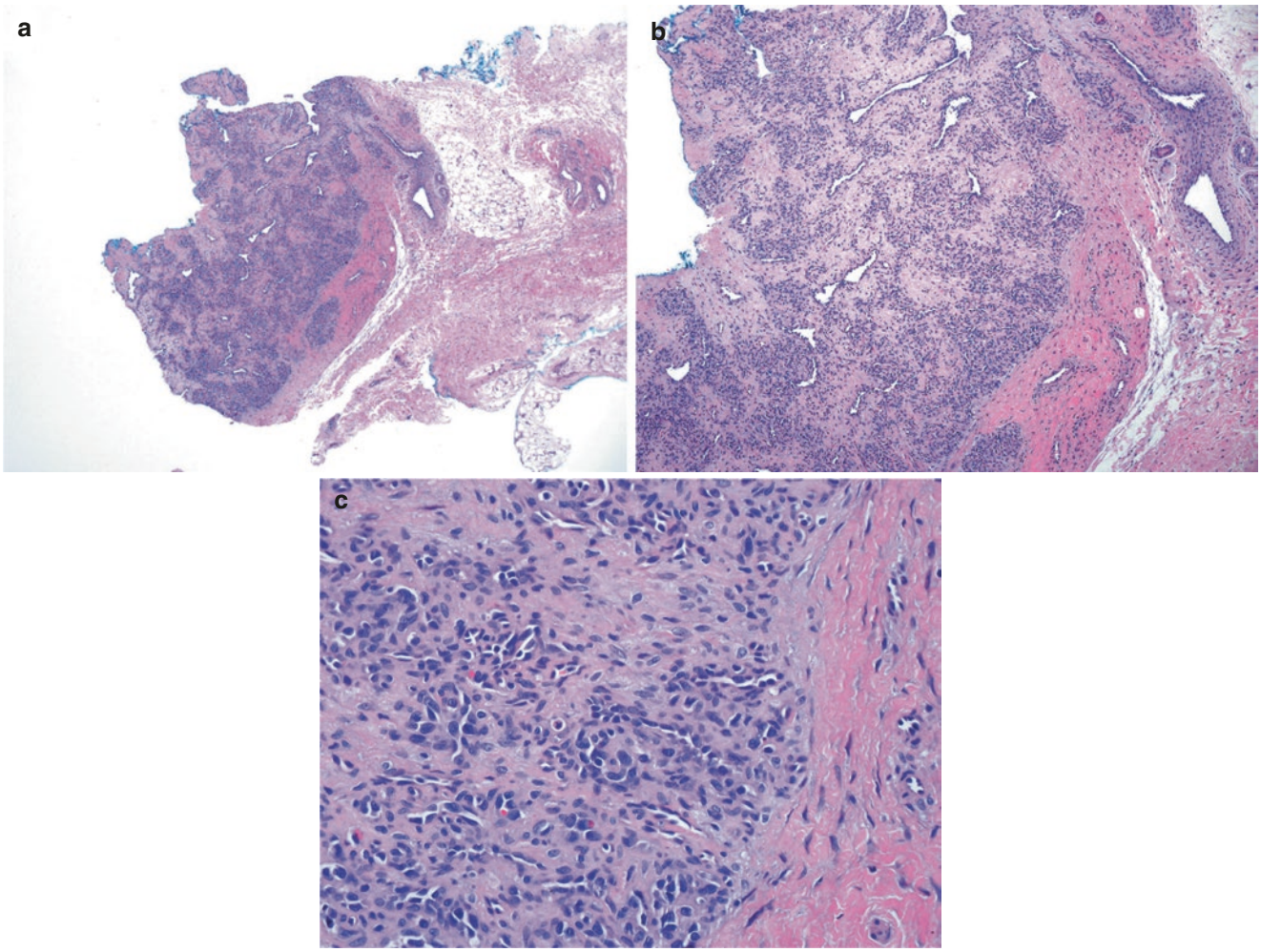

Fig. 17.2 (**a** and **b**) Capillary hemangioma consists of a circumscribed proliferation of small vessels with a lobulated appearance and mild associated inflammation. (**c**) The endothelial cells are cuboidal or flat without atypia

smooth muscle fibers, scattered mononuclear cells, or lymphoid aggregates (Fig. 17.6c). Distinction from low-grade angiosarcoma may be difficult, as angiomatosis can be large and less circumscribed than other benign vascular lesions. However, in contrast to angiosarcoma, the vascular proliferation entraps mammary ducts and lobules, instead of aggressively infiltrating them. In addition, angiomatosis lacks prominent nuclei and endothelial multilayering seen in angiosarcomas. Extensive sampling may be required to exclude malignancy [7].

Diffuse dermal angiomatosis is a reactive cutaneous capillary proliferation, which may involve the breast [14–20] and also mimic angiosarcoma. It is a distinct disorder in the spectrum of cutaneous reactive angiomatoses. The typical patient is a middle-aged woman with macromastia, obesity, and a history of tobacco use and/or vasculopathic disorders. Diffuse dermal angiomatosis typically presents with reticulated erythematous to purple patches on large pendulous breasts, which may ulcerate easily. The pathogenesis is thought to be related to tissue hypoxemia resulting from subclinical torsion, compression, and increased venous hydrostatic pressure due to macromastia, which is further aggravated by coexistent ischemic conditions such as hypertension or diabetes. Mammography demonstrates diffuse cutaneous and trabecular thickening, raising concern for inflammatory breast carcinoma [18]. Histologically, diffuse dermal angiomatosis consists of a diffuse proliferation of benign endothelial cells between the collagen bundles throughout the dermis (Fig. 17.7a). A diffuse proliferation of bland endothelial cells and pericytes insinuates between dermal collagen bundles, forming rudimentary capillary-like vessels (Fig. 17.7b–d). Reduction mammoplasty is a viable treatment option, which can be considered in patients who fail conservative therapy.

Angiolipomas are more often seen in the subcutis than in the breast parenchyma. As in other sites, they are often pain-

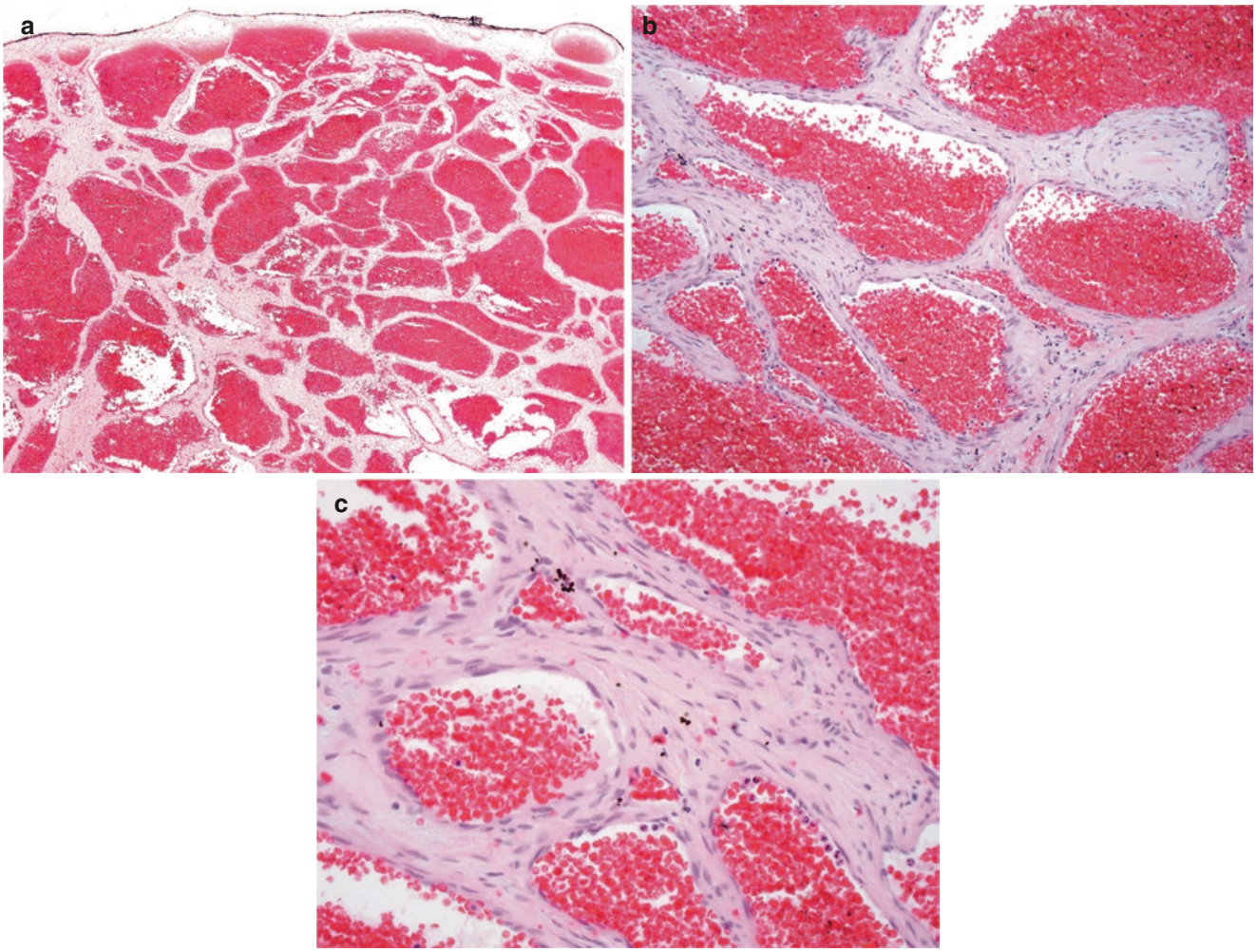

Fig. 17.3 (**a**) Cavernous hemangioma is composed of dilated vessels, larger than those of a capillary hemangioma. (**b**) The endothelial cells are flat and lack atypia. (**c**) High-power view of the flat endothelial cells. Note that the vascular walls are thick

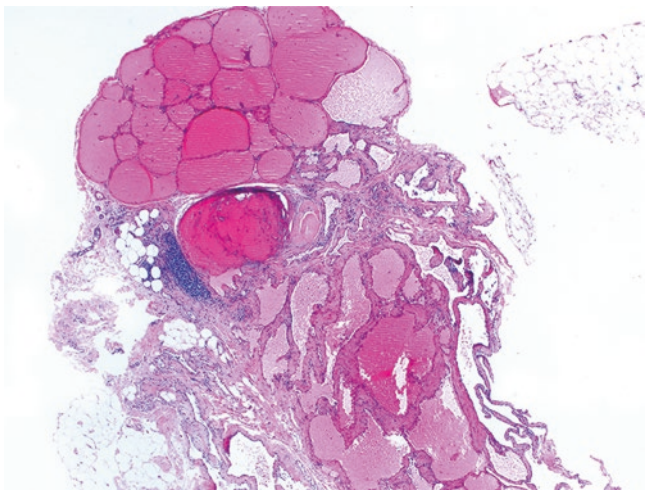

Fig. 17.4 Venous hemangioma is composed of large venous channels with variably thickened muscular walls lined by flat endothelial cells without atypia

ful and may be multiple. Angiolipomas are well-circumscribed lesions composed of an admixture of mature adipose tissue and benign capillary hemangioma components (Fig. 17.8a). The presence of intravascular hyaline microthrombi is characteristic (Fig. 17.8b). Angiolipomas lack the infiltrative pattern and atypia of angiosarcoma. These benign vascular lesions do not require excision.

Differential Diagnosis

The most important differential diagnosis for all the vascular lesions described above is angiosarcoma, which is characterized by poorly circumscribed borders, an infiltrative growth pattern, anastomosing vascular channels, nuclear atypia, and often endothelial multilayering. It is well recognized, however, that these features may not be fully developed or represented in a CNB specimen. When sampling is limited, diagnostic features of angiosarcoma may not be present. Conversely, benign vascular lesions may be confused with

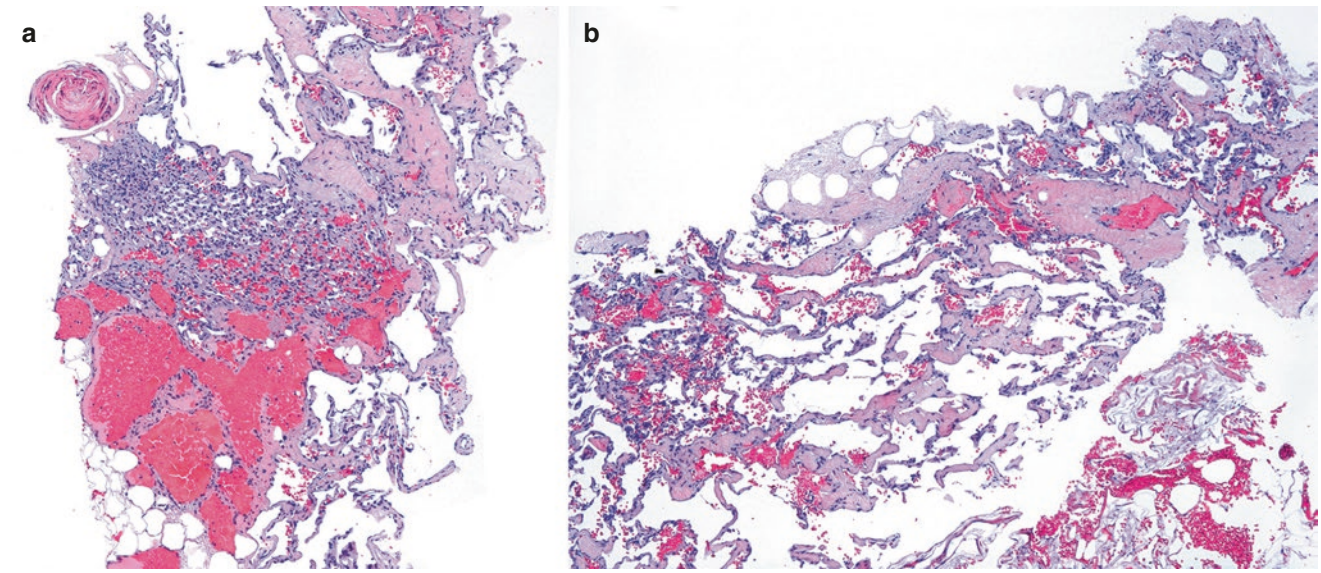

Fig. 17.5 (**a**) The low-power observation of circumscription is the key to recognition of papillary endothelial hyperplasia, which represents organization and recanalization of a thrombus. (**b**) A proliferation of endothelial cells lining hyaline papillary stalks is characteristic

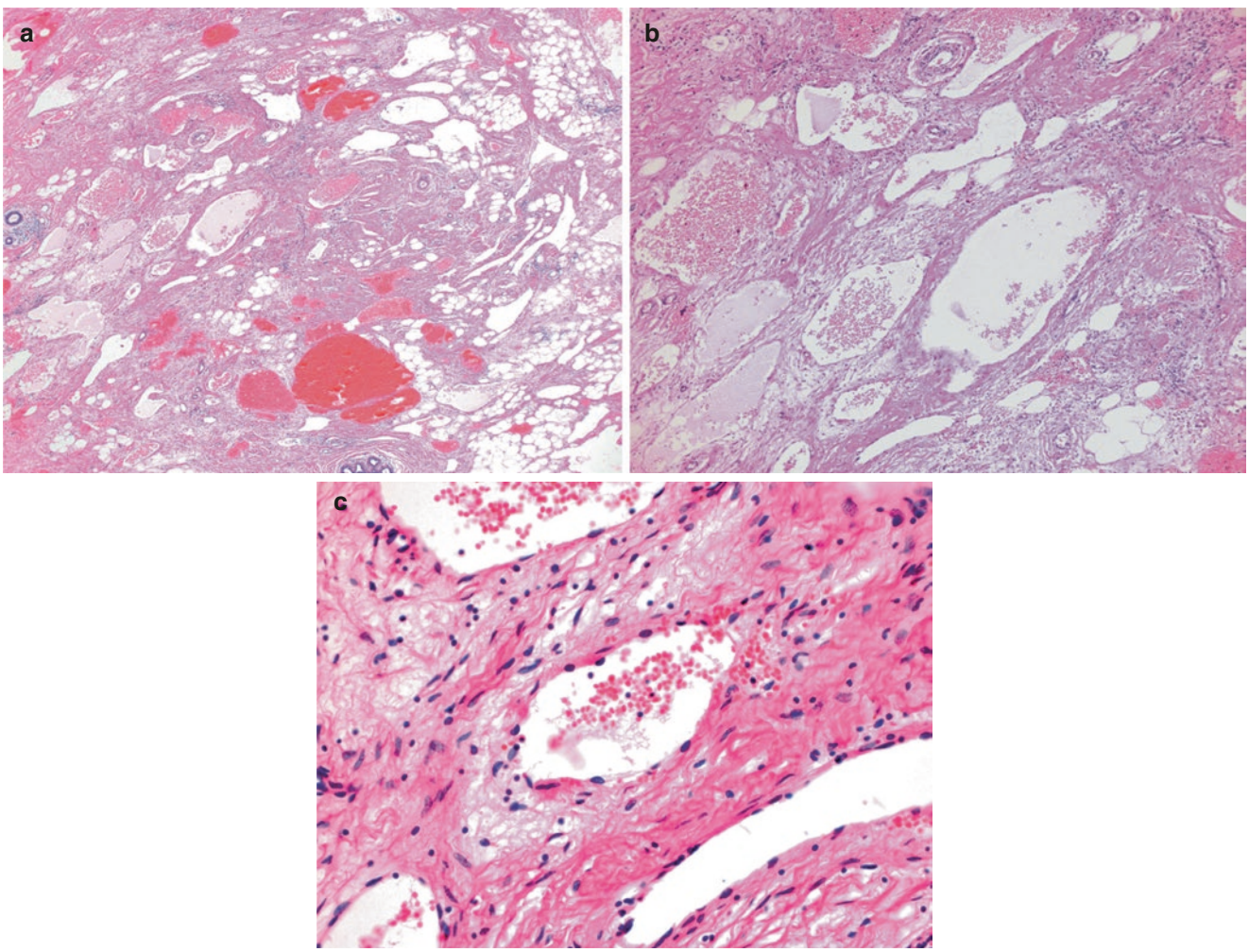

Fig. 17.6 (**a**) Angiomatosis is composed of cystically dilated, anastomosing vascular channels which frequently form a large mass. (**b**) The walls between the spaces contain wispy smooth muscle fibers, scattered mononuclear cells, and lymphoid aggregates. (**c**) The vascular spaces are lined by flat endothelial cells without atypia or mitotic activity

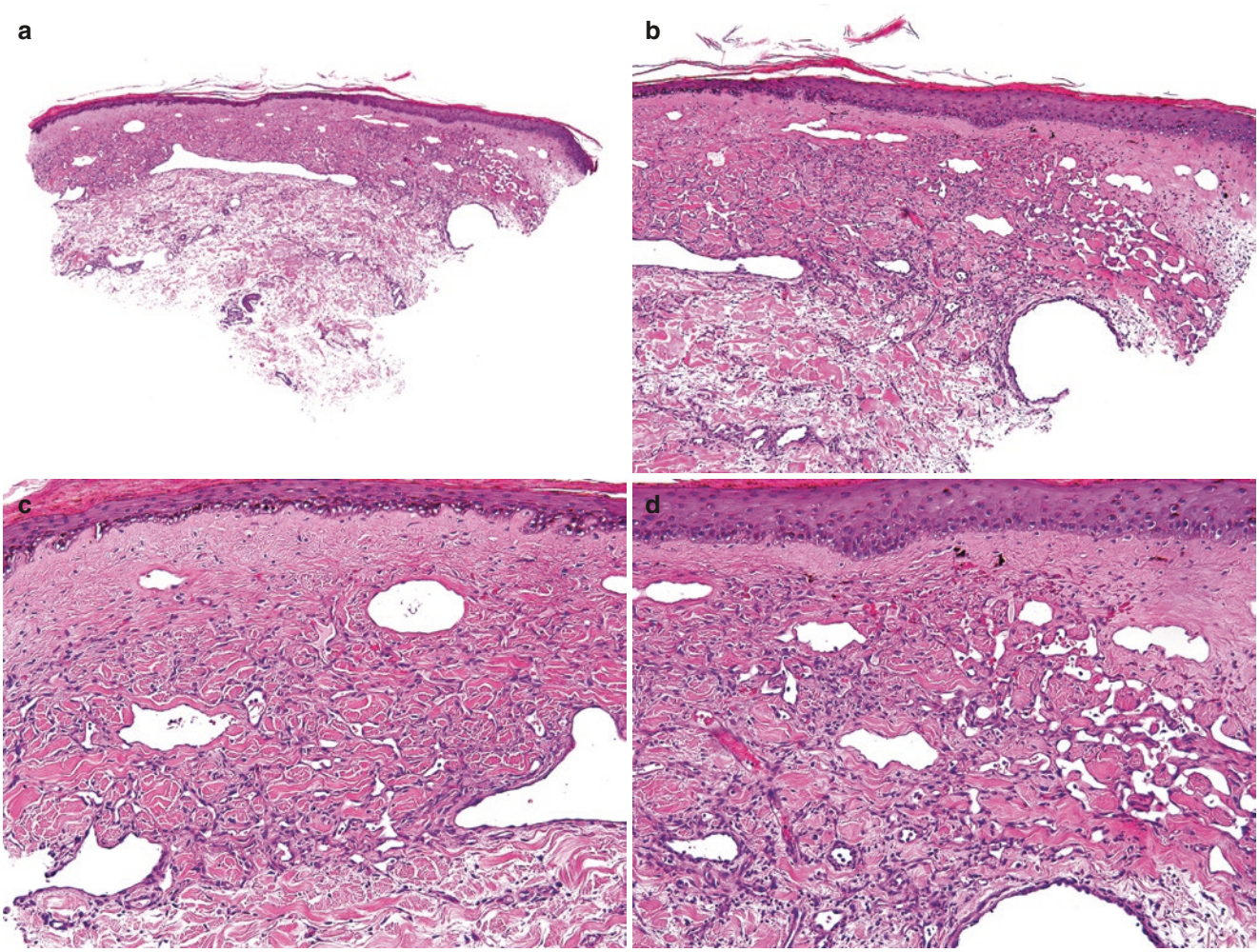

Fig. 17.7 (**a**) Diffuse dermal angiomatosis manifests a diffuse proliferation of benign endothelial cells between the collagen bundles, which is typically concentrated in the superficial half of the dermis. (**b**) The density and distribution of the vascular proliferation are highly variable mimicking angiosarcoma. (**c**) The diffuse proliferation of endothelial cells and pericytes, which insinuate between dermal collagen bundles, is bland. (**d**) The rudimentary capillary-like vessels lack hobnailing and atypia

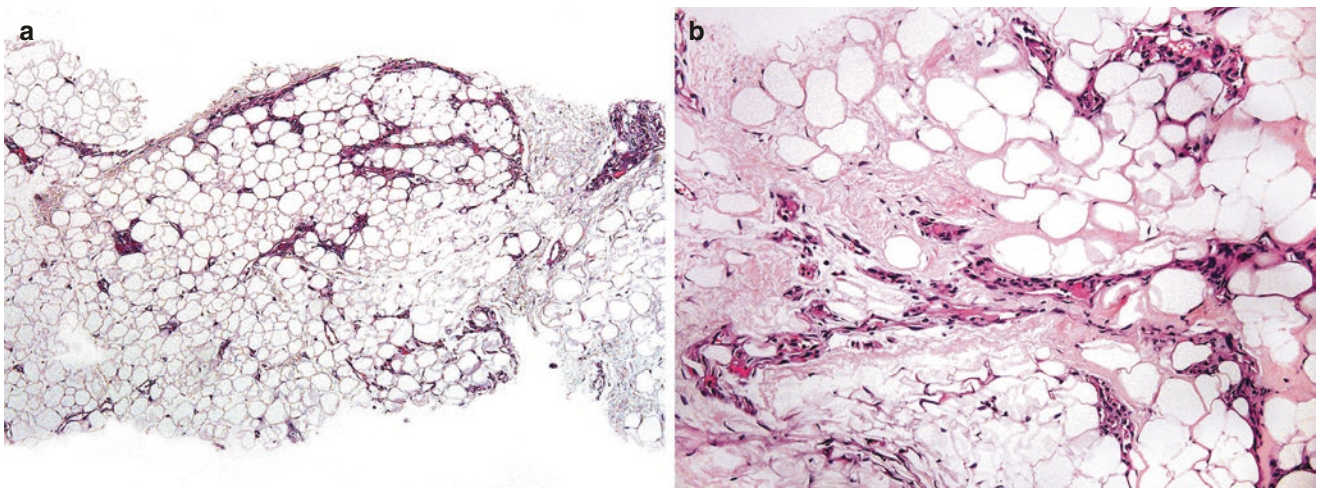

Fig. 17.8 (**a**) Angiolipomas consist of a circumscribed mass of adipose tissue admixed with a benign capillary hemangioma component. (**b**) Intravascular hyaline microthrombi are a characteristic finding

angiosarcoma on the basis of pseudoinfiltrative areas, apparent lack of circumscription, or presence of exuberant papillary endothelial hyperplasia with slight cytologic atypia (see above). Thus, in cases with overlapping or equivocal features, excision may be necessary to accurately characterize the lesion.

Immunohistochemical Workup

Benign vascular lesions demonstrate immunoreactivity for a variety of conventional vascular markers (ERG, CD31, CD34, FLI1, factor VIII-related antigen). However, routine use of these markers is unnecessary for the diagnosis of an obviously vasogenic lesion.

Treatment and Prognosis

In the majority of cases, benign vascular lesions do not require excision. When the diagnosis is made on CNB and the entire lesion cannot be fully visualized, excision may be recommended to fully characterize the lesion. In contrast, complete excision with negative margins or simple mastectomy is recommended for angiomatosis, since there is significant potential for local recurrence if the lesion is incompletely excised [6, 7, 21].

Angiosarcoma

Overview

Angiosarcoma arises in the breast more than in any other site [1]. Mammary angiosarcoma is also the most common type of breast sarcoma, representing approximately 8% of all breast sarcomas [22]. With an annual incidence rate of 1.2 per million women, angiosarcoma accounts for only 0.04% of all malignant neoplasms of the breast [23]. Most angiosarcomas of the breast are secondary to prior radiation therapy or less commonly chronic lymphedema [24–28]. Conversely, primary mammary angiosarcoma is a very rare disease that typically affects younger patients (<50 years of age). Both primary and secondary angiosarcomas show aggressive clinical behavior similar to angiosarcomas arising in other cutaneous or soft-tissue sites. They carry a propensity for local recurrence and a high risk for metastasis and tumor-related death. For this reason, all angiosarcomas are considered of high histologic grade [29–31].

Clinical and Radiologic Features

Patients with primary angiosarcoma range in age from 17 to 70 years (median 38 years) [32]. All reported cases of postradiation angiosarcoma have occurred in women over 50 years of age, which is on average 20 years older than women with primary mammary angiosarcoma [33]. Most cases occur 2.5–11.5 years (median 4.5 years) after radiation therapy [34–37]. This latency period is substantially shorter than for other radiation-associated malignancies in which the time between radiation therapy and malignancy is often more than 10 years. Although radiation-associated mammary angiosarcoma is uncommon, the incidence has increased significantly given the trend for more conservative surgical therapy for breast cancer combined with adjuvant radiation therapy [34, 36, 38, 39]. The estimated risk of either cutaneous or parenchymal disease following radiation therapy is approximately 0.3–0.4% [37, 40].

Whereas primary mammary angiosarcoma is typically a solitary, painless mass (usually >5 cm [1], range < 1.0 cm to >20 cm [41]) located deep in the mammary parenchyma [42], most postradiation angiosarcomas are multifocal and cutaneous (but may secondarily invade subjacent breast parenchyma) [34, 43–45]. If the lesion is located deep in the breast, there may be no external features to suggest angiosarcoma. More superficial tumors may show purple-blue discoloration of the skin due to hemorrhage and vascularity (Fig. 17.9). Mammography in primary angiosarcoma typically shows architectural distortion without microcalcifications or a large ill-defined density within the breast parenchyma [5, 46]. Radiation-associated cutaneous angiosarcoma presents as erythematous plaques, papules, or nodules within the field of radiation. MRI can be useful in defining the size in postradiation angiosarcoma [5].

Gross and Microscopic Features

Grossly, angiosarcomas are hemorrhagic masses. Areas of necrosis and cystic degeneration may be seen, especially in larger tumors [41]. The classic mammary angiosarcoma is characterized microscopically by complex, anastomosing vascular channels that infiltrate the dermis and/or underlying

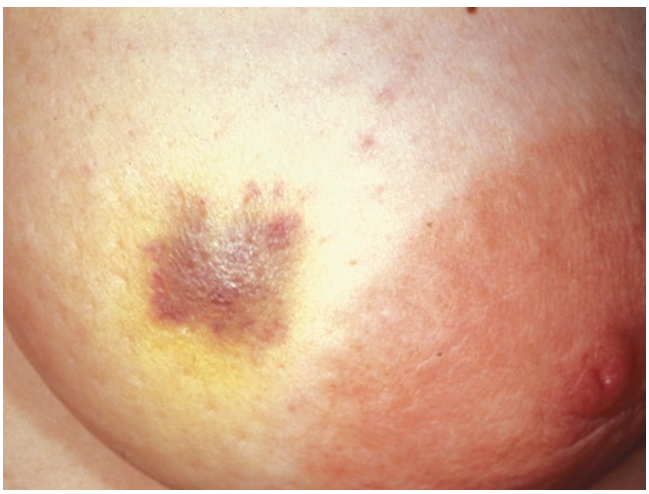

Fig. 17.9 Postradiation angiosarcoma lateral to the areola characterized by an irregular border and purple-blue discoloration of the skin due to its vascularity

breast parenchyma (Fig. 17.10). Angiosarcoma has a variety of histologic appearances ranging from well-differentiated, obviously vasoformative lesions to solid, poorly differentiated neoplasms requiring immunohistochemistry (IHC) for classification. In addition, the histologic features and degree of cellular differentiation can vary considerably within a given lesion. At the well-differentiated (low-grade) end of the spectrum, the vascular spaces are well defined and lined by cells with prominent nuclei that protrude into the vascular lumen (Figs. 17.11a, b). Endothelial tufting is minimal, and papillary formations are absent [32, 47]. Well-differentiated angiosarcoma may subtly permeate adipose tissue simulating angiolipoma (Fig. 17.12). Solid or spindle cell foci, blood lakes, mitoses, and necrosis are typically absent as well. Less differentiated variants [32, 47] (intermediate- and high-grade tumors) show prominent endothelial cell tufting, papillary formations (Fig. 17.13), or multilayered growth of obviously malignant, mitotically active endothelial cells (Fig. 17.14a, b). Focally, the papillary formations may mimic papillary endothelial hyperplasia, a potential diagnostic pitfall in a CNB where sampling may be limited (Figs. 17.15a, b). The anastomosing vascular channels of angiosarcoma commonly dissect around lobular units, a feature facilitating diagnosis on core biopsy (Fig. 17.16a, b). Solid or spindle cell foci, blood lakes (Fig. 17.17a, b), and necrosis (Fig. 17.18a, b) are usually present in poorly differentiated tumors, and some may show limited evidence of vascular differentiation (vasoformation). Occasionally poorly differentiated angiosarcomas have an epithelioid appearance resembling carcinoma (see below).

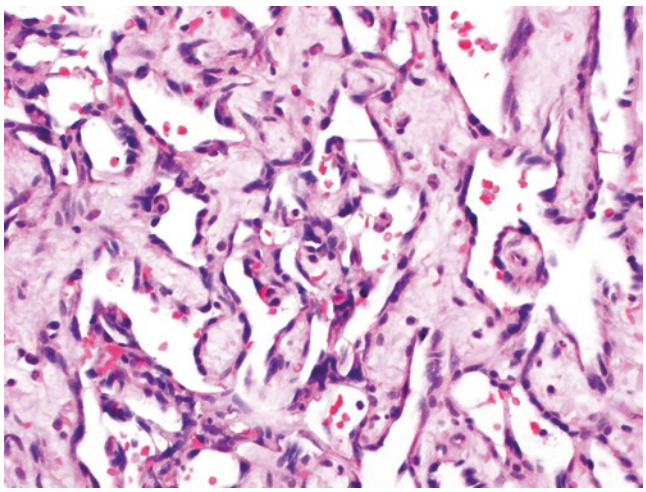

Fig. 17.10 Angiosarcomas are readily diagnosed when characteristic complex anastomosing vascular channels infiltrating the mammary parenchyma and/or dermis are present

For many years, considerable effort was extended in grading mammary angiosarcoma [32, 47], since early studies suggested a relationship between histologic grade and outcome [32, 47, 48]. However, a more recent study by Nascimento and coworkers with strict morphologic criteria indicated that angiosarcomas of the breast behave poorly regardless of grade, with 60% of patients developing distant metastases at a mean follow-up of 49 months [30].

Most cases of radiation-associated angiosarcoma are solid with an epithelioid morphology (see below), spindle cell morphology (Fig. 17.19a, b), or a mixture of the two patterns (Fig. 17.20). Occasionally, lesions with structural patterns typical of well- or moderately differentiated tumors are seen, but the malignant cells have marked nuclear hyperchromasia and conspicuous mitotic activity [1] (Fig. 17.21). Variable numbers of slit-like spaces containing intraluminal or extravasated erythrocytes or interstitial hemorrhage with the formation of blood lakes are often present in poorly differentiated lesions.

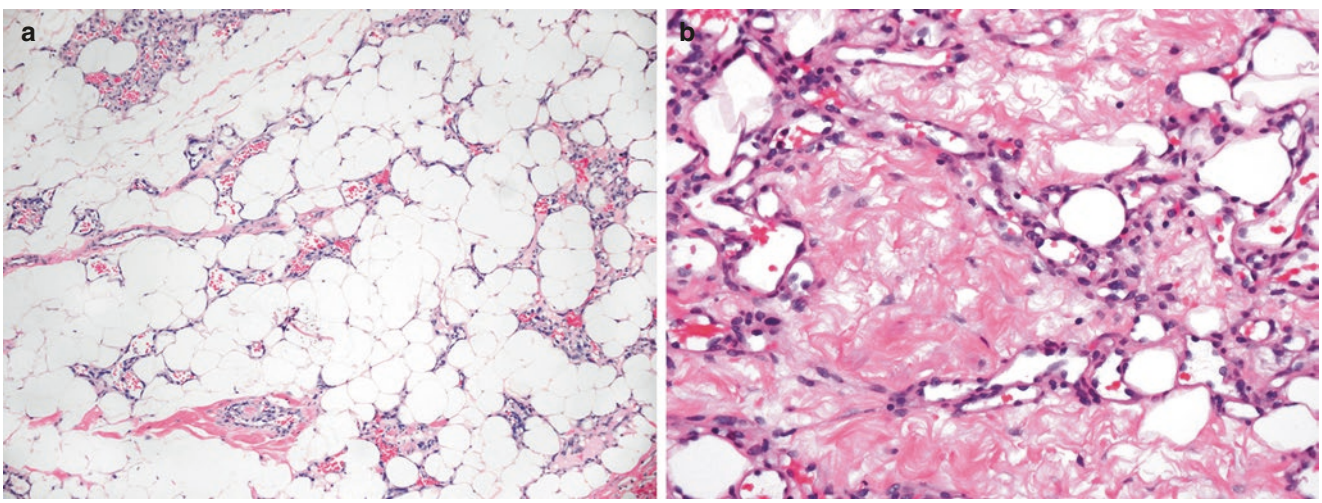

Fig. 17.11 (**a**) Well-differentiated angiosarcomas are composed of well-defined vascular spaces (**b**) lined by endothelial cells with prominent nuclei, which project into the vascular lumens

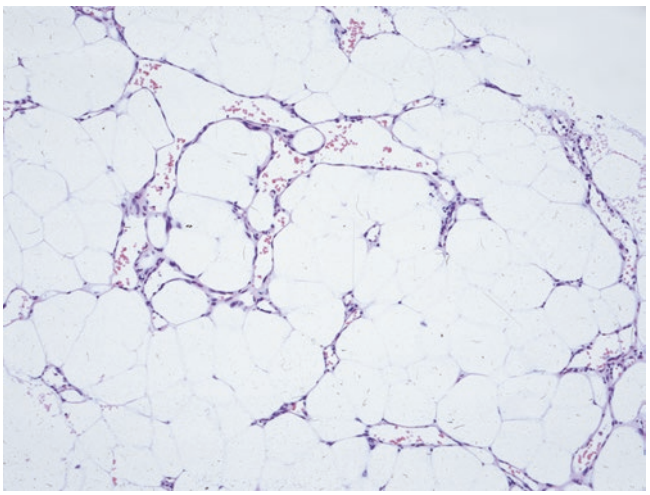

Fig. 17.12 This well-differentiated angiosarcoma subtly permeates adipose tissue simulating an angiolipoma

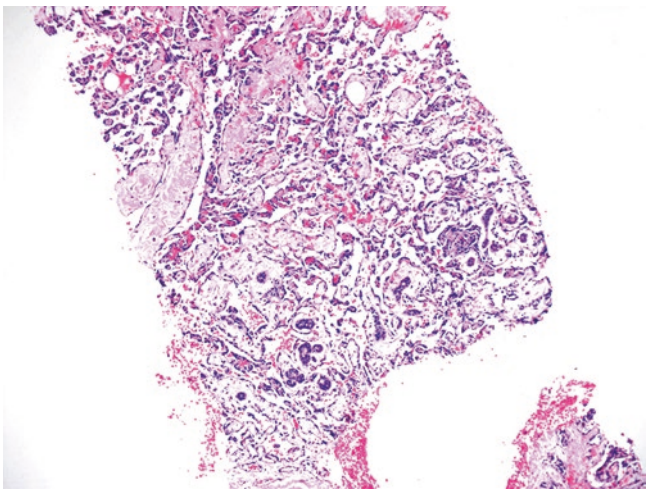

Fig. 17.13 Poorly differentiated angiosarcomas frequently contain papillary formations

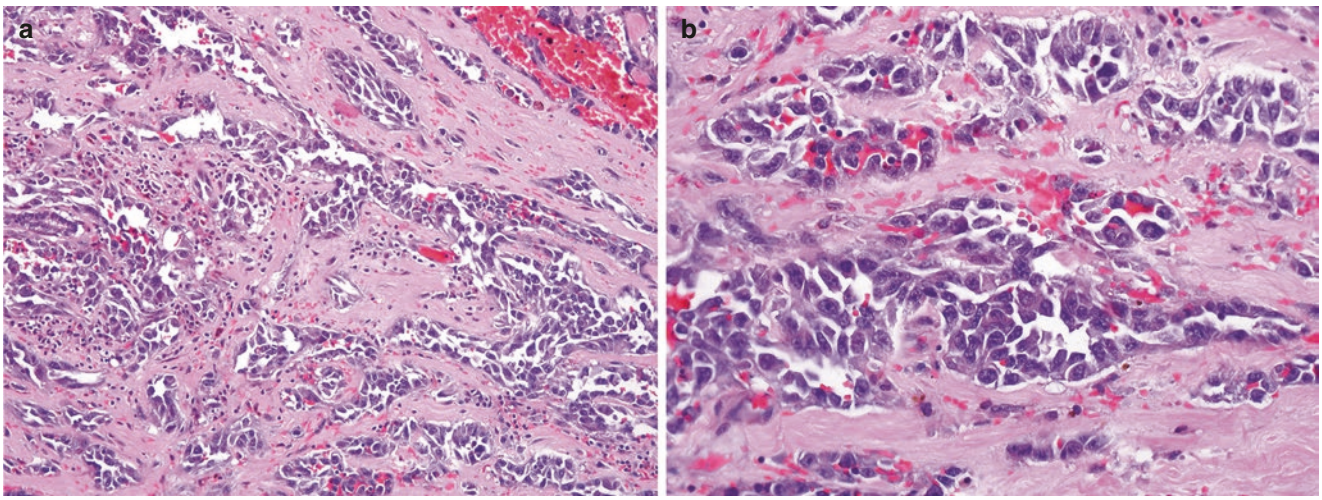

Fig. 17.14 (**a**) Poorly differentiated angiosarcomas frequently contain endothelial cell tufting and multilayered growth of (**b**) obviously malignant, mitotically active cells

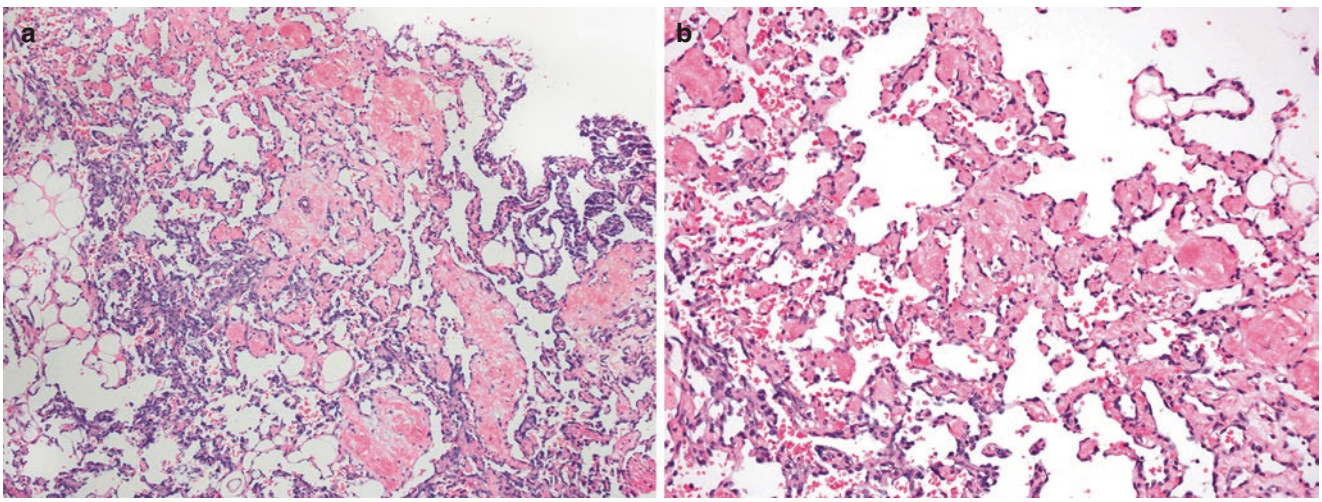

Fig. 17.15 (**a** and **b**) The papillary formations in angiosarcoma may mimic papillary endothelial hyperplasia, a potential diagnostic pitfall in a CNB

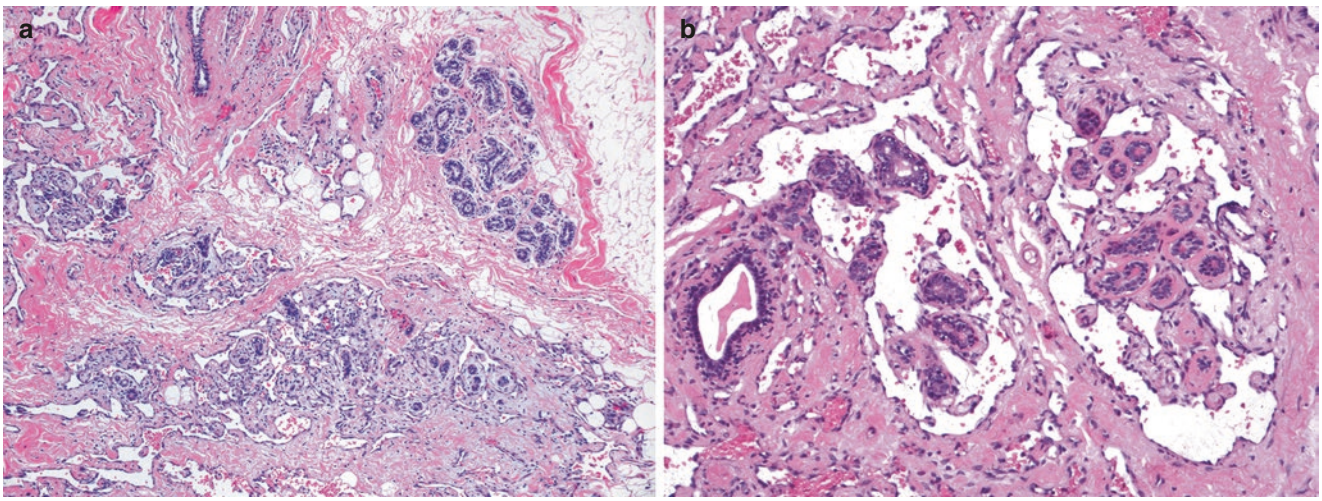

Fig. 17.16 (**a** and **b**) The anastomosing vascular channels of angiosarcoma in the breast commonly dissect around lobular units, a helpful feature in distinguishing angiosarcoma from perilobular capillary hemangioma in a limited sample

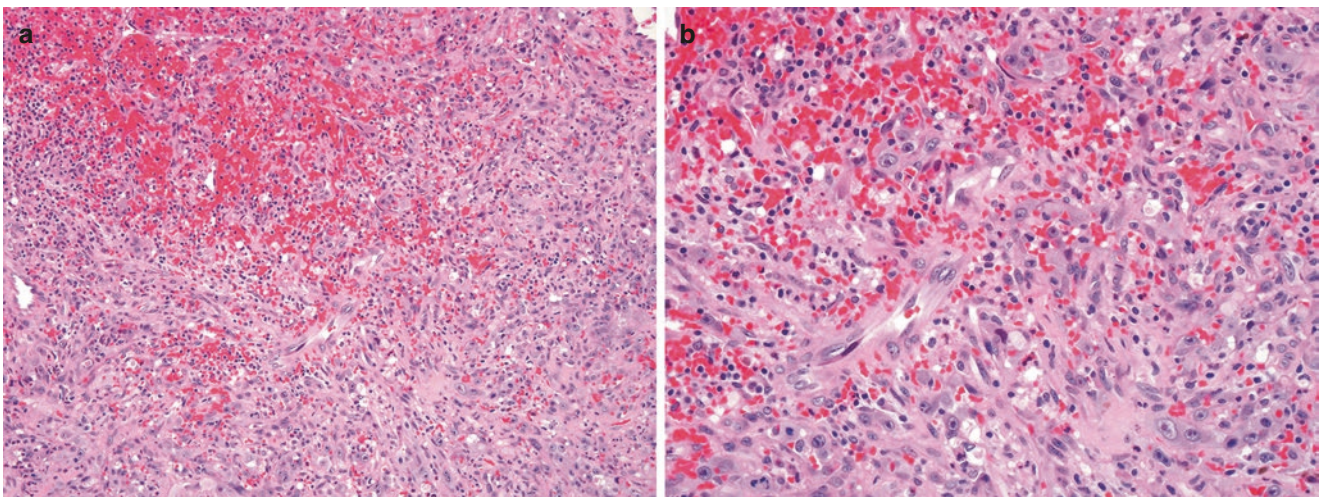

Fig. 17.17 (**a**) Poorly differentiated angiosarcomas frequently contain "blood lakes" characterized by (**b**) anaplastic tumor cells admixed with red blood cells without formation of defined vascular spaces

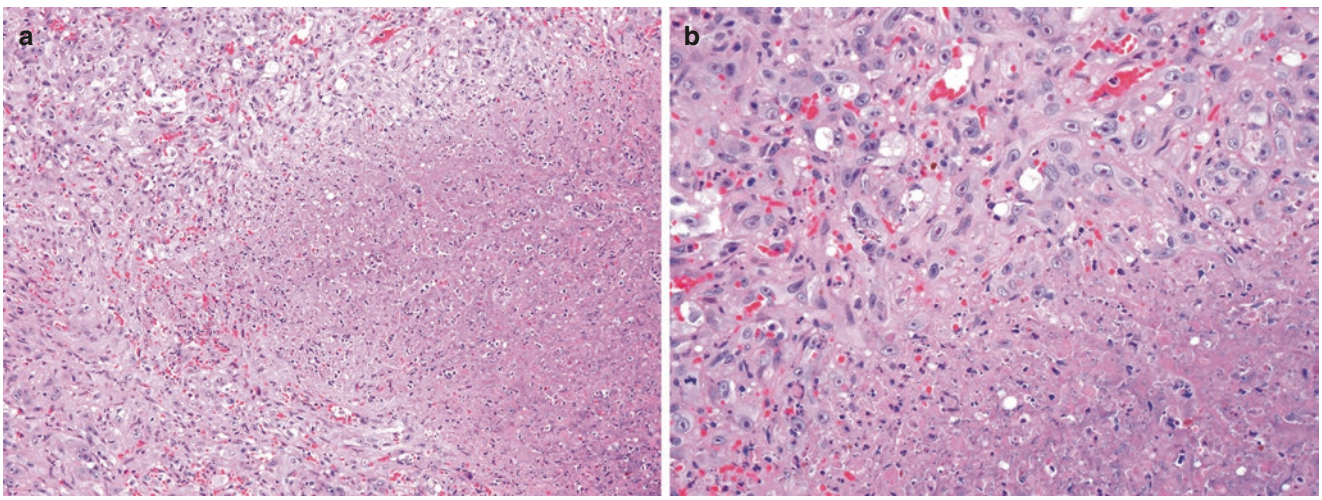

Fig. 17.18 (**a** and **b**) Geographic areas of necrosis are a frequent finding in poorly differentiated angiosarcomas

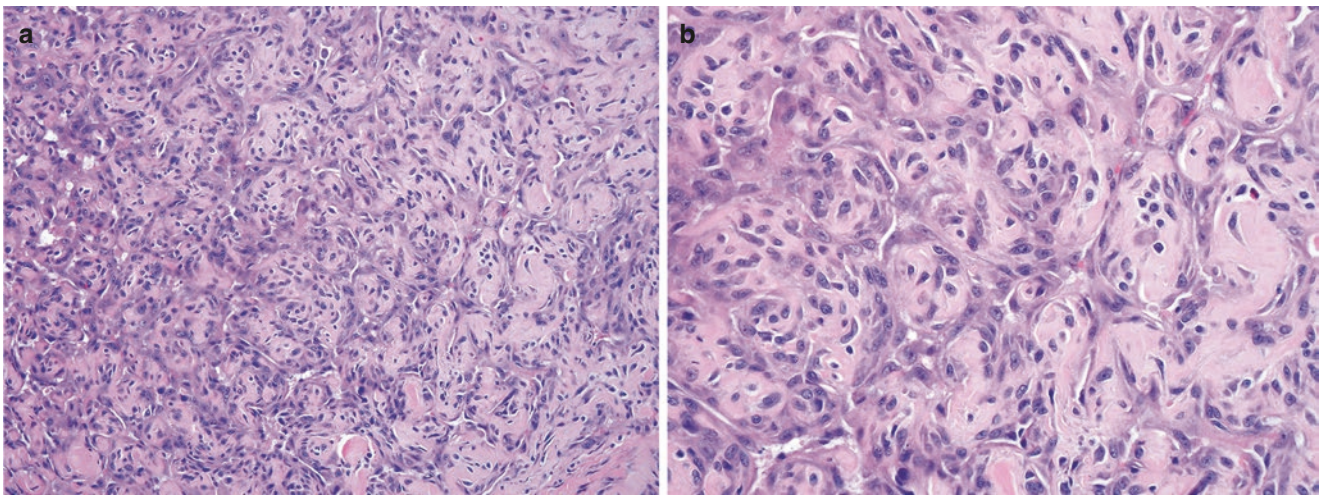

Fig. 17.19 (**a**) Angiosarcomas with spindle cell morphology typically have ovoid to elongated nuclei with prominent nucleoli. (**b**) Vasoformative spaces are poorly defined to absent

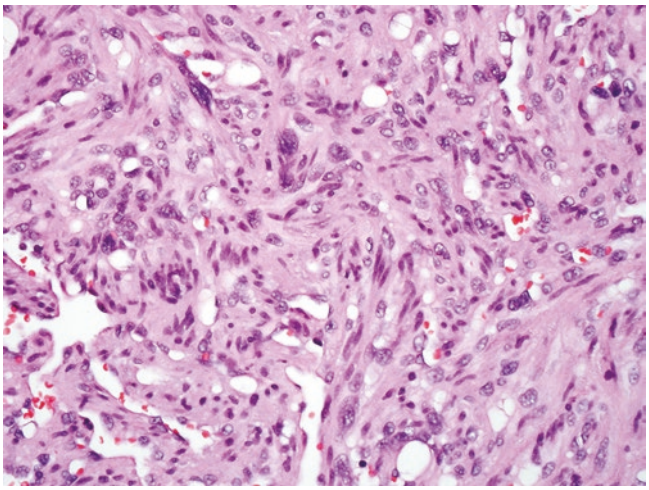

Fig. 17.20 Angiosarcoma with a mixed spindle cell and epithelioid morphology

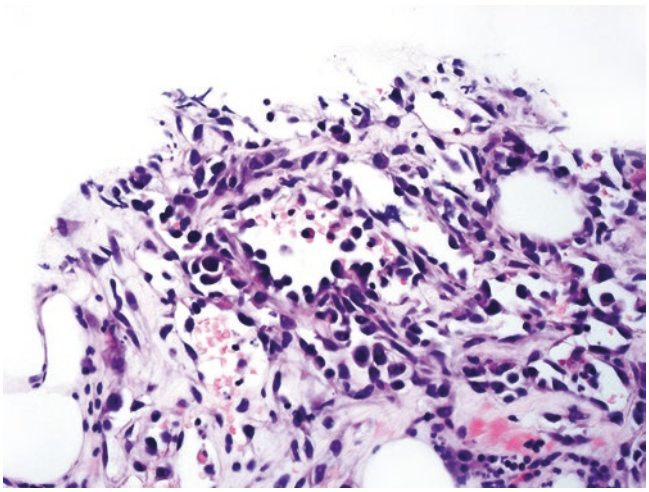

Fig. 17.21 Angiosarcoma with the typical vasoformative architecture of a well- to moderately differentiated tumor but lined by malignant endothelial cells with marked nuclear atypia

Epithelioid Angiosarcoma

Epithelioid angiosarcoma is a rare variant of angiosarcoma composed predominantly or exclusively of large "epithelioid" endothelial cells with ill-defined cell borders, abundant amphophilic to eosinophilic cytoplasm, and large vesicular nuclei (Fig. 17.22c). It has been reported to occur in diverse sites but uncommonly in the breast [1, 30, 49–53]. When arising at this site, epithelioid angiosarcoma is almost exclusively seen in patients with a history of radiation therapy [1, 30, 50–53]. Histologically, epithelioid angiosarcoma is a poorly circumscribed, infiltrative process which may extensively involve the deep dermis, mammary parenchyma, or both (Fig. 17.22a). When the lesion involves the mammary parenchyma, solid islands of tumor infiltrate around or obliterate acinar structures (Fig. 17.22b). Mitoses, including atypical forms, are abundant. Vascular spaces, blood lakes, or slit-like spaces containing extravasated erythrocytes are infrequently apparent. Therefore, IHC may be an important adjunct to reaching the correct diagnosis (see discussion below and Fig. 17.22d–f).

Differential Diagnosis

The differential diagnosis of well-differentiated angiosarcoma includes hemangioma, atypical vascular lesion, pseudoangiomatous stromal hyperplasia (PASH), and angiolipoma. In contrast to the infiltrating growth pattern, anastomosing vascular channels, and endothelial atypia seen in angiosarcoma, conventional hemangiomas and angiolipomas are well-circumscribed lesions that show no evidence of dissection through normal structures, anastomosing growth

patterns, or cytologic atypia. Atypical vascular lesions may show anastomosing vascular spaces, but nuclear atypia and endothelial multilayering are absent. Finally, PASH may resemble well-differentiated angiosarcoma at low power, but it is not a true vascular lesion; the cells lining the pseudovascular spaces are instead fibroblasts and/or myofibroblasts

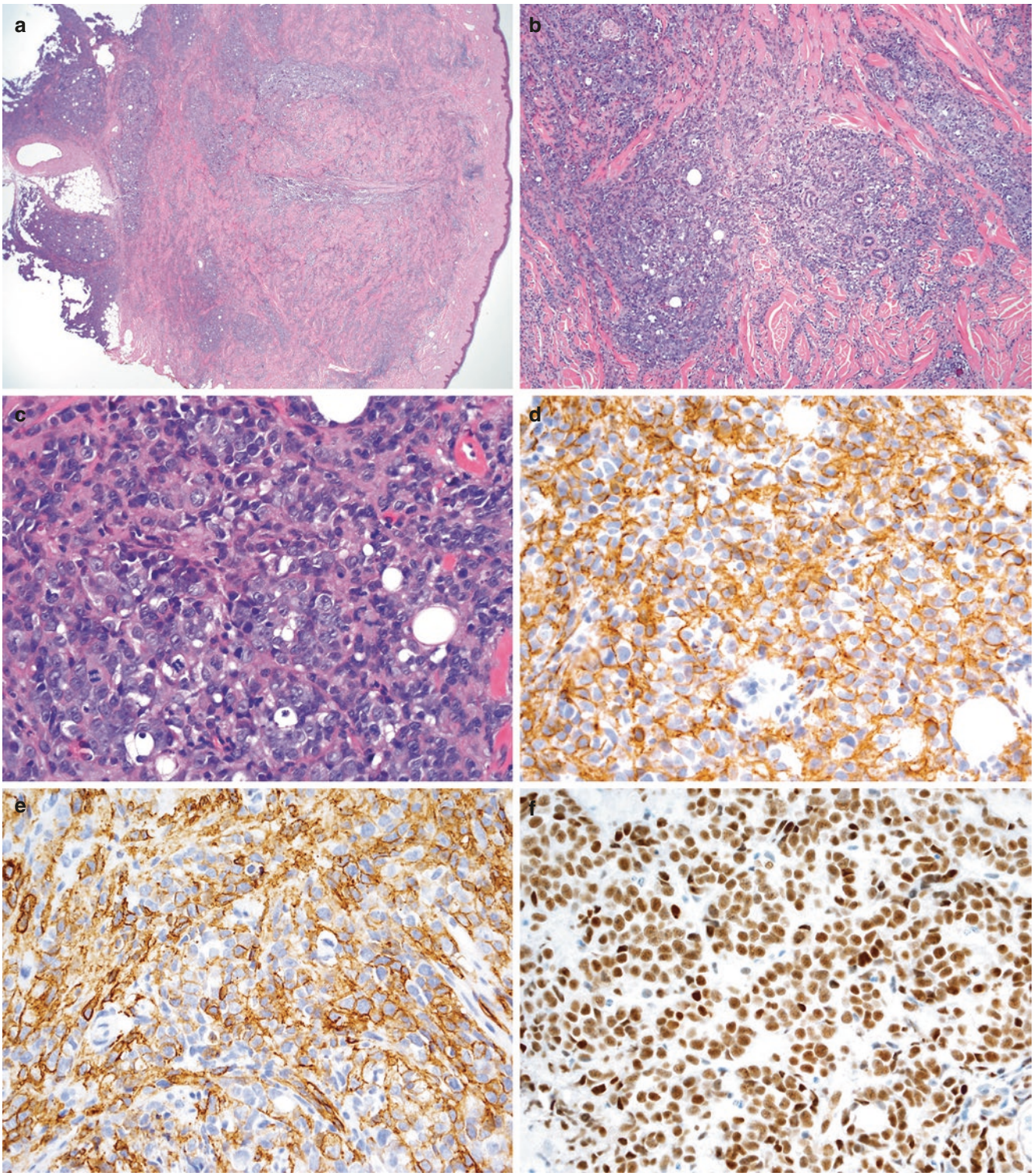

Fig. 17.22 (**a**) On low power, this postradiation epithelioid angiosarcoma extensively infiltrates the dermis, has a solid pattern and lacks vasoformative areas. (**b**) The epithelioid cells splay the dermal collagen. (**c**) At the deep aspect of the biopsy, the angiosarcoma cells infiltrate and obliterate much of the subjacent mammary parenchyma. The epithelioid angiosarcoma cells show diffuse, strong expression of multiple vascular markers including (**d**) CD31, (**e**) CD34, and (**f**) FLI1

that may express CD34 and SMA, but not endothelial markers.

The differential diagnosis of poorly differentiated angiosarcoma of the breast includes high-grade invasive mammary carcinoma of no special type, high-grade spindle cell metaplastic carcinoma, malignant melanoma, and epithelioid or other pleomorphic sarcomas. Distinction between epithelioid angiosarcoma and these other entities is greatly assisted by IHC (discussed below).

Immunohistochemistry and Molecular Alterations

Angiosarcoma typically demonstrates strong immunoreactivity for multiple vascular markers including CD31 [54–56], CD34 [55–57], factor VIII-related antigen [54–56], VEGFR-3 [56–58], D2–40 [59], FLI1 [60], and ERG [61], but use of IHC is only necessary for characterization of poorly differentiated tumors with limited or absent vasoformative areas. Since poorly differentiated angiosarcomas may demonstrate limited expression of endothelial cell markers, use of a battery of markers for endothelial differentiation in conjunction with other appropriate markers to resolve the differential diagnosis cannot be overemphasized.

CD31 and, more recently, ERG [61–64] (Fig. 17.23) are the gold standard for demonstrating endothelial differentiation in angiosarcoma. ERG is as sensitive and more specific for endothelial differentiation than CD31 [61]. Although CD31 and CD34 are both commonly used endothelial markers, CD31, while rather specific (it can be positive in intratumoral macrophages), is not particularly sensitive and is often lost or poorly expressed in angiosarcoma. In contrast, while CD34 is very sensitive (positive in >90% of vascular tumors), it is certainly not specific for endothelial cells, as it is expressed by many other mesenchymal cell types. ERG, a transcription factor that regulates angiogenesis, is a sensitive and relatively specific nuclear marker for endothelial cells (particularly clones directed at the N-terminus of the protein [65]). Thus far, the only other consistently ERG-positive tumor is prostatic adenocarcinoma [66]. A minority of Ewing sarcomas [67], epithelioid sarcomas [65, 68, 69], and acute myeloid leukemias [63] express ERG. These tumors show distinct clinical as well as morphologic and additional IHC profiles compared to angiosarcoma. A number of lymphatic-associated antibodies have also been recently developed (D2–40, Prox-1, and VEGFR-3) [56–58] and shown to be frequently expressed in angiosarcoma, suggesting that lymphatic or mixed lymphatic/blood vascular differentiation is common in malignant vascular tumors.

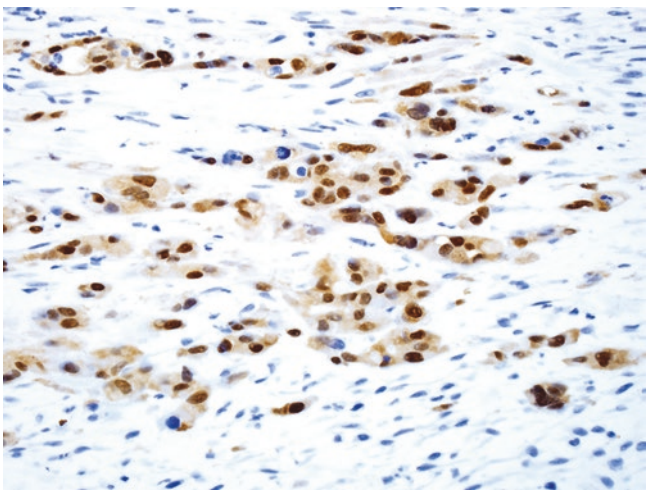

Fig. 17.23 IHC stain for ERG, currently the most sensitive and specific marker for demonstrating endothelial differentiation in angiosarcomas and benign vascular lesions

Cytokeratin (CK) and epithelial membrane antigen (EMA) immunoreactivity is not infrequent in angiosarcomas and may lead the pathologist toward an erroneous diagnosis of carcinoma. Weak to moderate or rarely strong expression of pankeratin (CAM5.2 and AE1/AE3) in a minority of tumor cells has been reported in 3–20% of non-epithelioid angiosarcomas [70, 71] and up to 50% of epithelioid angiosarcomas. EMA expression of similar distribution and intensity has been reported in 10–35% of non-epithelioid angiosarcomas and 25% of epithelioid angiosarcomas [70, 71]. Cautious interpretation of such expression in conjunction with the characteristic clinical and morphologic features of the tumor and expression of endothelial cell antigens will avoid this potential pitfall. High-grade invasive mammary carcinoma of no special type (ductal) is the most common differential diagnostic consideration for CK-expressing, high-grade angiosarcomas. However, carcinoma will usually show much stronger and more diffuse CK immunoreactivity and be negative for endothelial markers. Angiosarcomas composed of predominantly spindle cells may mimic a high-grade spindle cell metaplastic carcinoma. In angiosarcoma, the spindle cells form lobulated nests, whereas in metaplastic carcinoma the spindle cells form linear arrays with ill-defined, infiltrative borders.

The spindle cells of metaplastic carcinoma usually show moderate to strong expression of p63 [72] and its isoform p40 (ΔN p63), but the latter is less useful given its lower sensitivity [73, 74]. Spindle cell metaplastic carcinoma also shows patchy moderate to diffusely strong expression of high-molecular-weight CKs (CK5/6, CK34βE12) throughout the lesion and lacks expression of endothelial markers.

The proximal type of epithelioid sarcoma typically has a multinodular growth pattern and may occasionally show a pseudovascular appearance that can be mistaken for abortive attempts at vasoformation. Cytologically, the cells are large and epithelioid with marked cytologic atypia, vesicular nuclei, and prominent nucleoli. A significant proportion of epithelioid sarcomas also express endothelial markers, including N-terminal ERG, CD34 (up to 50%), FLI1, and

D2–40, further complicating distinction from angiosarcoma [63]. Although epithelioid sarcoma is typically strongly CK positive (75% of cases) [65], it should be recalled that malignant vascular tumors may aberrantly express CKs. However, in contrast to angiosarcoma, epithelioid sarcoma is negative for CD31 and often shows loss of nuclear INI1/SMARCB1 expression [75–77].

Melanoma metastatic to the breast frequently demonstrates epithelioid histology, thus falling within the differential diagnosis of epithelioid and poorly differentiated angiosarcoma. Most melanomas strongly express S-100 protein, SOX10, Melan-A, and HMB45, whereas angiosarcomas are negative for these markers; the importance of thorough clinical history cannot be overemphasized.

At the opposite end of the clinical spectrum, lower grade angiosarcomas arising in the postradiation setting must be distinguished from atypical vascular lesions. This distinction is important given the significant difference in clinical management and prognosis. However, their distinction can be exceptionally challenging and in some cases impossible to resolve with certainty on CNB material given their histomorphologic and immunophenotypic overlap. It is also important to note that angiosarcomas may contain peripheral atypical vascular lesion-like areas (Fig. 17.24a, b). The discovery that the c-*MYC* locus is amplified in over half of postradiation angiosarcomas [26, 78–81] and a variable fraction of non-radiation-associated angiosarcomas [26, 81–84], but not in atypical vascular lesions, now allows resolution of this differential diagnosis in most cases (Fig. 17.25a–f). IHC for c-MYC shows nearly 100% concordance with *c-MYC* fluorescence in situ hybridization (FISH) [24, 82, 85]. However, it should be noted that c-*MYC* amplification is not detected in all cases of radiation-associated angiosarcoma, especially when the lesion is well differentiated and unfortunately more likely confused with an atypical vascular lesion; therefore, lack of expression does not exclude angiosarcoma [26, 84–87].

The *FLT4* gene is co-amplified with c-*MYC* in 18–25% of secondary angiosarcomas, but not in primary angiosarcomas or atypical vascular lesions [78, 83], and is detectable by both FISH and immunohistochemistry. *FLT4* encodes the vascular endothelial growth factor receptor-3 (VEGFR3) [26, 88–91]. The high sensitivity and specificity of FLT4 immunohistochemistry are of therapeutic interest, since it may be a rapid screening tool to identify patients who would benefit from kinase inhibitor therapy. For example, pazopanib, a multikinase inhibitor with activity against VEGFR-1/2/3, was recently approved for soft-tissue sarcomas previously treated with chemotherapy [92, 93].

Genomic sequencing has identified activating mutations in *KDR* gene, which encodes vascular endothelial growth factor 2 in approximately 10% of mammary angiosarcomas, regardless of radiation exposure [94]. Mutations in *PTPRB* and *PLCG1* (genes related to angiogenesis) have also been described in some angiosarcomas [95]. While c-*MYC* amplification may be seen in tumors with *KDR* mutations, *FLT4* amplification appears to be mutually exclusive with *KDR* alterations [83]. Collectively, these findings suggest that therapeutic targeting of these angiogenic pathways may improve outcomes in these typically chemo- and radiation therapy-resistant tumors [86, 87].

Treatment and Prognosis

Total mastectomy is the treatment of choice for angiosarcoma as wide excision alone results in an unacceptable rate of local recurrence [96]. Axillary dissection is not necessary since metastases rarely involve these lymph nodes [96]. Occasionally, a small lesion (with respect to total breast volume, typically <2 cm) may be completely excised by lumpec-

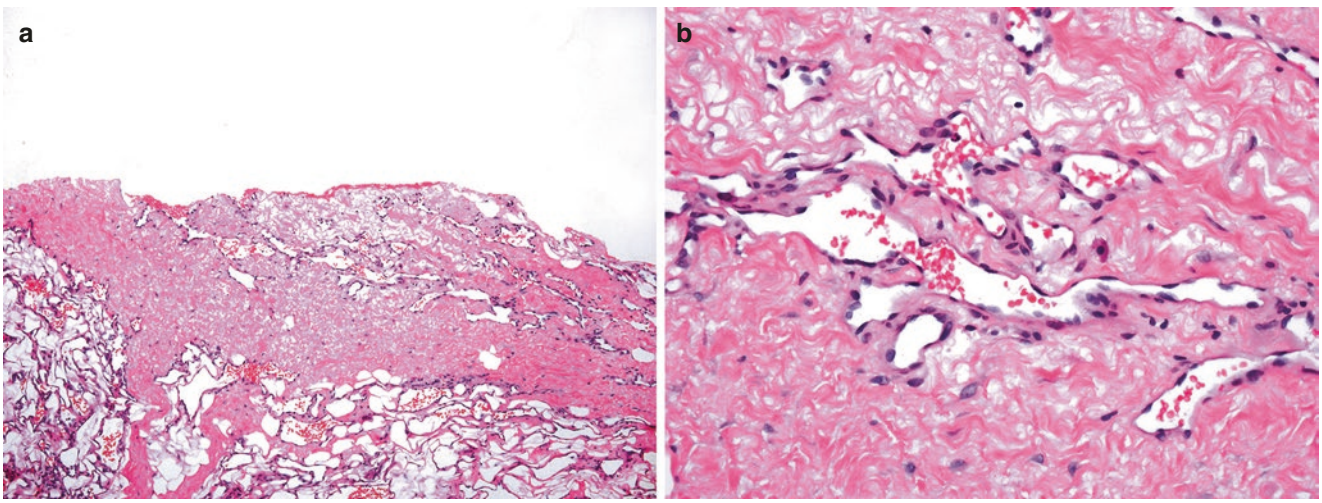

Fig. 17.24 (**a**) Low-grade angiosarcoma with complex anastomosing vascular channels centrally and peripheral atypical vascular lesion-like area at the edge of this CNB. (**b**) Plump, mildly atypical endothelial cells line these vascular spaces

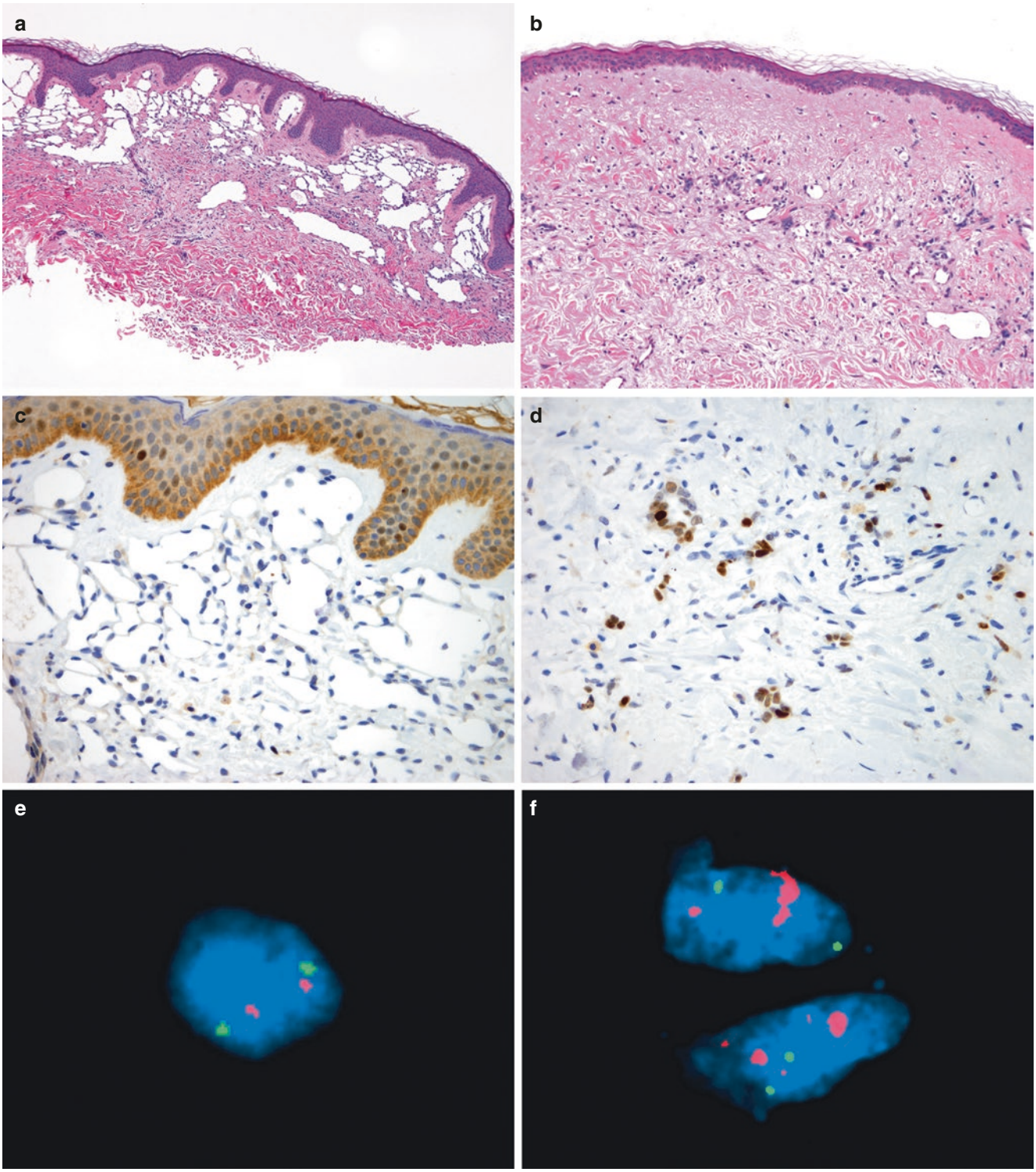

Fig. 17.25 Concurrent IHC for MYC and FISH for c-*MYC* performed on an atypical vascular lesion (**a**) and well-differentiated angiosarcoma (**b**), each arising in the breast skin following radiation therapy, demonstrates lack of overexpression (**c**) or amplification (**e**) in the atypical vascular lesion; however, the angiosarcoma demonstrates strong MYC expression by IHC (**d**) a benign endothelial cell with 2 copies of the *MYC* gene (red probe) and 2 copies of the chromosome 8 centromere (green probe) contrasts with (**f**) *MYC* amplification as detected by multiple gene copies (red signals) by FISH. (Images reproduced from Ginter PS, Mosquera JM, MacDonald TM, Rubin MA, Shin SJ. Diagnostic utility of MYC amplification and anti-MYC immunohistochemistry in atypical vascular lesions, primary or radiation-induced mammary angiosarcomas, and primary angiosarcomas of other sites. Human Pathology 2014;45(4):709–716, with permission of Elsevier)

tomy. Nearly all studies to date conclude that radiotherapy and chemotherapy are largely ineffective for both primary and post-radiotherapy angiosarcomas [31, 97, 98]; thus, the current interest in the employment of targeted agents to improve outcome is high (as discussed above). One recent study suggested that only patients with radiation-associated angiosarcoma derive benefit from chemotherapy [99], while another found chemotherapy benefit for patients with tumors >5 cm [100]. Immunotherapy may also be effective in some patients [101].

As with angiosarcoma of other anatomic sites, those arising in the breast (both primary and secondary to radiation therapy) are highly aggressive neoplasms with a poor prognosis. Indeed, most patients die shortly after diagnosis [102], and the median survival of patients with mammary angiosarcoma is only 1–2 years [33, 34]. Local recurrence is common, even after surgical resection with negative margins [39, 85, 103]. Metastases generally occur in the lungs, bone, liver, contralateral breast, and distant skin and soft tissues [85, 97]. Although older studies suggested a relationship between histologic grade and patient outcome for primary mammary angiosarcoma [32, 47], more recent data derived from the well-annotated cases reported by Nascimento and others failed to demonstrate an association between grade and outcome [30], analogous to angiosarcomas arising at other anatomic sites and those secondary to radiation therapy [34]. In Nascimento's series, 10 of 41 (24%) patients experienced local recurrence, 24 (59%) developed metastasis, and 18 (44%) died. Stratification of the tumors by histologic grade using Rosen's 3-tiered grading system showed no significant differences in relapse-free or overall survival [32, 47]. This result was subsequently replicated by Taffurelli et al. in a series of 112 patients [31].

Atypical Vascular Lesions

Overview

Atypical vascular lesions are most commonly seen in the skin of the breast following radiation therapy for breast cancer [24, 36, 38, 39, 44, 104]. They are thought to arise as a consequence of lymphatic obstruction after surgery and radiation, causing superficial dilatation of vascular channels [85, 105]. These lesions are not frankly malignant, and their potential to transform into angiosarcoma is low [106]. However, they are surrogate markers for exposure to radiation.

Clinical and Radiologic Features

The typical age at presentation is the sixth and seventh decades of life. Most patients present with a solitary, small, red, brown, or pink erythematous papule or plaque, but between 20% and 50% of patients have multiple synchronous or metachronous lesions [27, 38, 85, 86, 107]. Atypical vascular lesions are typically <5 mm, but some as large as 20 mm or more have been reported [27, 38]. Compared to postradiation angiosarcomas, atypical vascular lesions tend to occur in slightly younger patients and within a shorter time interval (average 3–4 years) following radiation exposure [85, 108].

Microscopic Features

On a well-oriented and adequate skin biopsy, atypical vascular lesions appear as a wedge-shaped aggregation of variably dilated, thin-walled vascular spaces lined by a single layer of cytologically bland endothelial cells limited to the dermis resembling lymphangioma (Fig. 17.26a). Rarely, the deep aspect of the reticular dermis or underlying subcutis may be involved [38, 85, 106, 108–110]. Small narrow vessels are also present and may show a focally anastomosing pattern with dissection through dermal collagen. Nuclear hobnailing and hyperchromasia are frequently observed (Fig. 17.26b, c). However, overt nuclear atypia, endothelial multilayering, and mitotic activity are not seen in atypical vascular lesions and if present should heighten the concern for well-differentiated angiosarcoma [109]. Thin projections of endothelium-covered stroma commonly project into the vascular spaces [86, 109]. Subtypes of atypical vascular lesion have been described based on the vascular lining cells: lymphatic type, vascular type, and those with mixed features [108]. The lymphatic type consists of empty, variably ectatic vessels resembling lymphangioma [109] (Fig. 17.27a–d). The vascular type is reminiscent of a capillary hemangioma and is composed of irregularly arranged, variably attenuated capillaries lined by hobnail endothelial cells [108, 110] that may demonstrate mild cytologic atypia [108] (Fig. 17.28a–d). There is no evidence that the subtypes differ in their very low rate of malignant progression [85, 86, 108]; thus, their distinction is only of academic interest.

On CNB, atypical vascular lesions can be difficult to differentiate from angiosarcoma. Features suggestive of atypical vascular lesion include small size, lack of overt endothelial atypia, and confinement to the dermis, without involvement of subcutaneous or breast parenchymal structures. Although the presence of anastomosing vascular spaces lined by plump

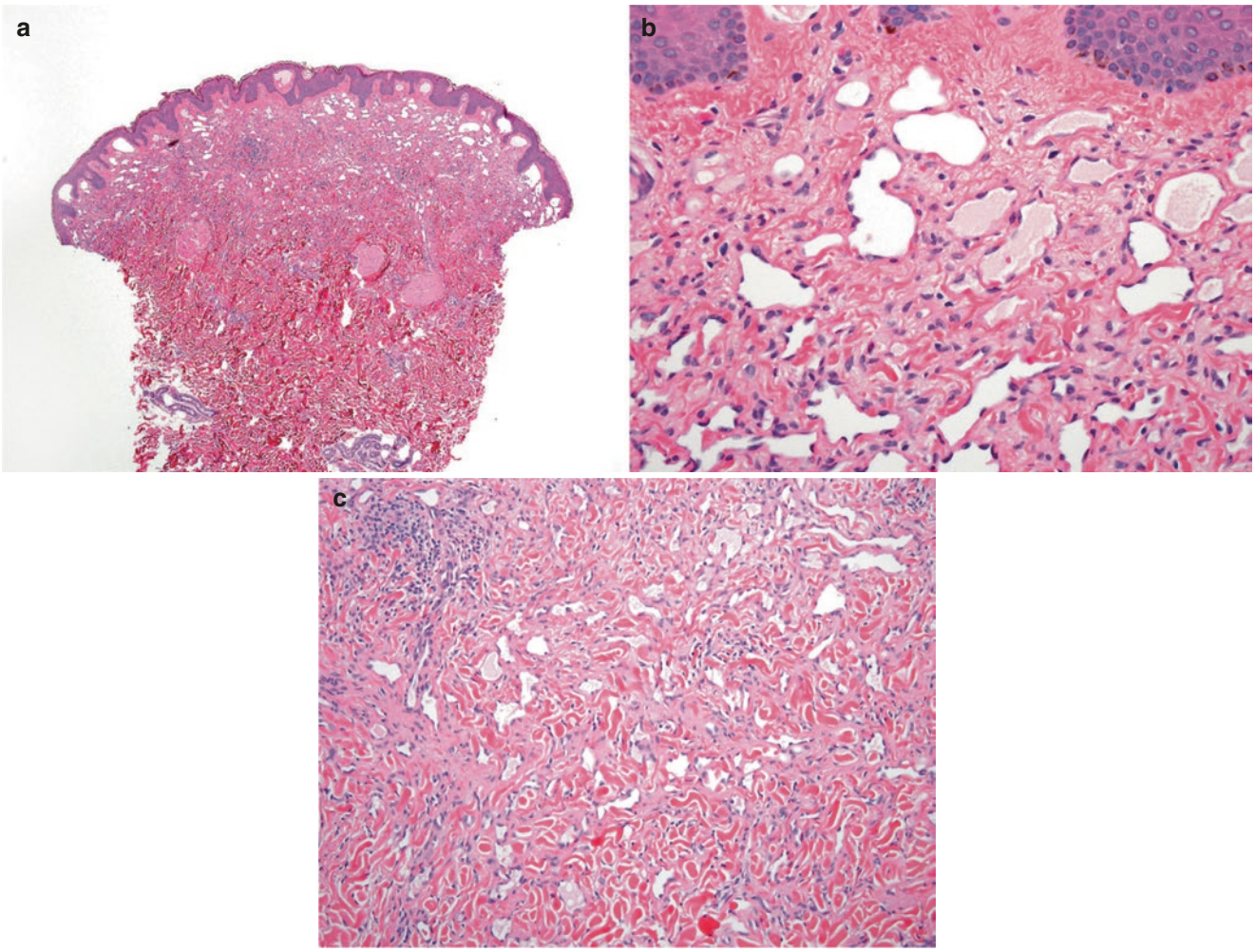

Fig. 17.26 (**a**) On low power, this atypical vascular lesion forms a broad wedge in the dermis. (**b**) The vascular spaces typically do not anastomose and lining endothelial cells show nuclear hobnailing and hyperchromasia. (**c**) The vascular spaces are haphazardly arranged and dissect the dermal collagen

endothelial cells is concerning, recognition of lesional circumscription and limited extent of the dissecting growth pattern will prevent overdiagnosis.

Differential Diagnosis

Distinction of atypical vascular lesions from angiosarcoma is critical to avoid excessive surgery and inappropriate prognostication as discussed in detail above in the differential diagnostic considerations for angiosarcoma. The histologic differential diagnosis also includes dermal vascular ectasia due to radiation and scar.

Immunohistochemistry

The endothelial cells of both the lymphatic and vascular types of atypical vascular lesion are positive for a variety of vascular markers including factor VIII-related antigen, ERG, CD31, CD34, and FLI1. The lymphatic type is also positive for D2–40 [108, 110]. Staining for smooth muscle myosin demonstrates the vessels of the vascular type with circumferential pericytes [108, 110]. Importantly, IHC for MYC has been shown to resolve the differential diagnosis of atypical vascular lesion and angiosarcoma with high specificity (Fig. 17.25 c, d) [24, 82, 85].

Treatment and Prognosis

The majority of these lesions pursue a benign clinical course, with only a few reported cases of progression to angiosarcoma [27, 34, 38, 40]. However, since these lesions are a surrogate marker for prior radiation exposure and may indicate a higher propensity to develop malignant vascular tumors, atypical vascular lesions diagnosed on CNB should be excised with the aim of obtaining negative margins. In addition, a small subset of these lesions may be upgraded to angiosarcoma on excision [108, 111].

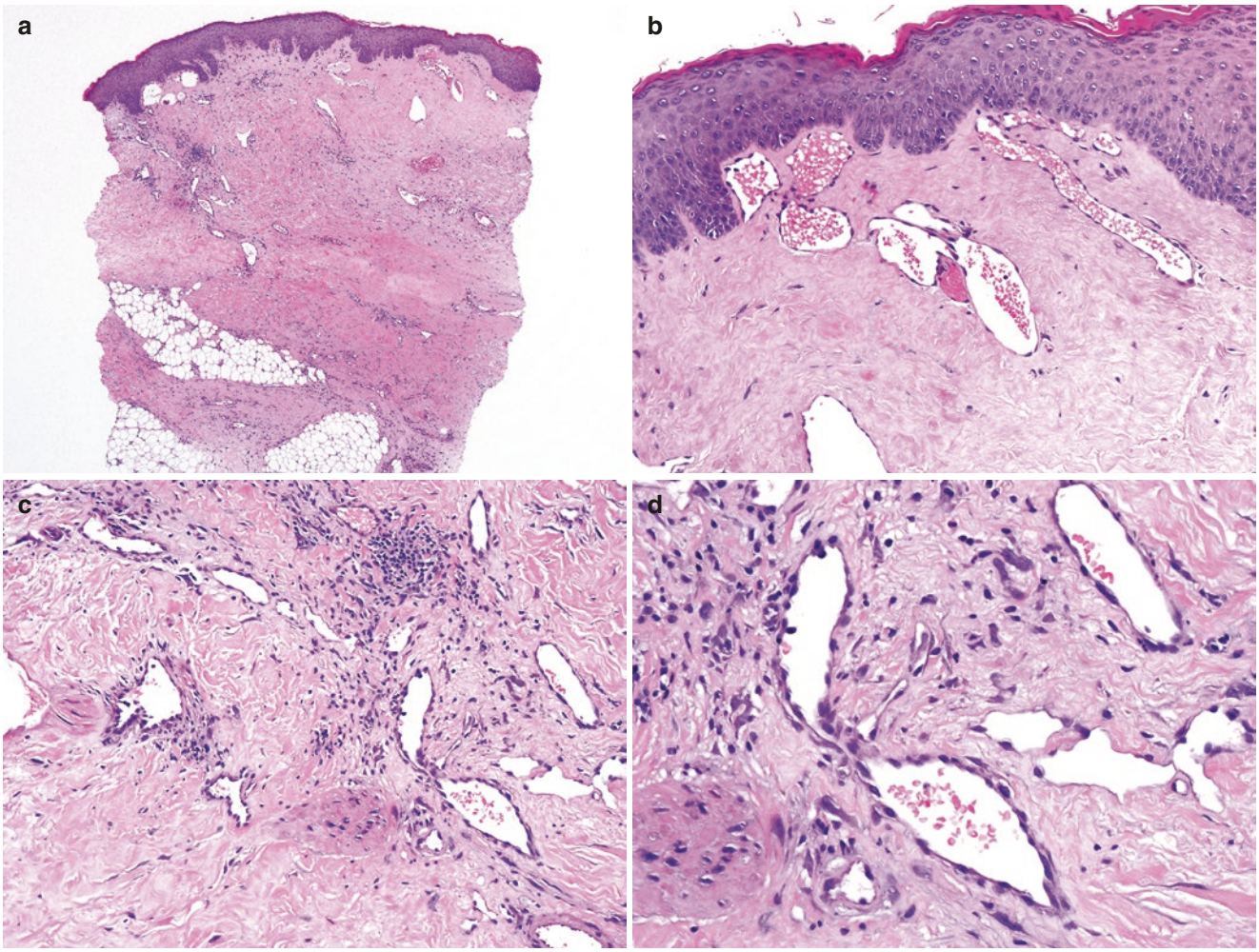

Fig. 17.27 Atypical vascular lesion, lymphatic type. (**a**) Low-power view shows empty, variably ectatic vessels in the dermis resembling lymphangioma. (**b**) The vessels may be dilated with enlarged endothelial cells or (**c**) focally anastomosing with dissection through dermal collagen and more prominent hobnail endothelial cells. (**d**) Prominent hobnail endothelial cells may be present but lack significant atypia

A series of ten radiation-induced intradermal vascular lesions with micropapillary tufts and architectural and/or cytologic atypia have been reported [106]. In contrast to angiosarcoma, the neoplasms were described as relatively well circumscribed and did not recur after complete excision. Although these authors concluded that atypical postradiation vascular lesions are characterized by a benign clinical course, others report that these types of lesions may have a higher incidence of local recurrence or malignant progression [38, 108]. In summary, it would appear that the risk of tumor progression is associated with atypical morphological features such as complex vascular architecture, involvement of deeper dermal and subcutaneous structures, and cytologic atypia [108]. Thus, excision with negative margins and close clinical follow-up for lesions lacking c-*MYC* amplification/overexpression remains warranted.

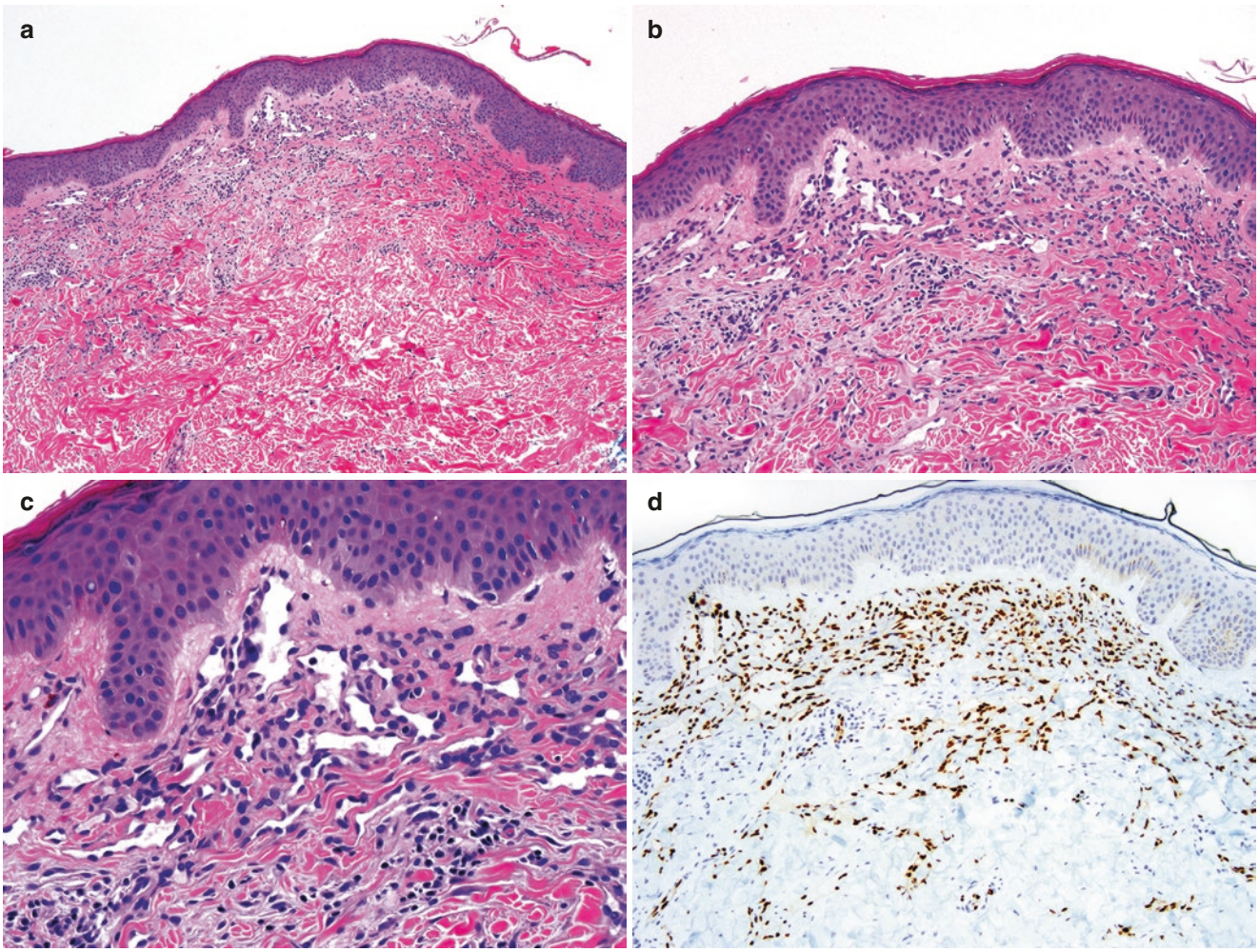

Fig. 17.28 Atypical vascular lesion, vascular type. (**a**) At low power, this vascular proliferation is confined to the superficial dermis and (**b**) is composed of irregularly arranged, variably attenuated capillaries lined by hobnail endothelial cells, reminiscent of a capillary hemangioma. (**c**) The hobnail endothelial cells are relatively uniform and demonstrate only mild cytologic atypia. (**d**) IHC for ERG highlights the lesional endothelial cells and clarifies the overall circumscription of the process. FISH studies for *c-MYC* amplification were negative

References

1. Rosen PP. Rosen's breast pathology. Philadelphia, PA: Lippincott-Raven; 1997.
2. Chung SY, Oh KK. Mammographic and sonographic findings of a breast subcutaneous hemangioma. J Ultrasound Med. 2002;21(5):585–8.
3. Ciurea A, et al. Diffuse angiomatosis of the breast--sonographic appearance. J Clin Ultrasound. 2014;42(8):498–501.
4. Ameen R, et al. Breast hemangioma: MR appearance with histopathological correlation. J Clin Imaging Sci. 2012;2:53.
5. Yang WT, et al. Mammary angiosarcomas: imaging findings in 24 patients. Radiology. 2007;242(3):725–34.
6. Morrow M, Berger D, Thelmo W. Diffuse cystic angiomatosis of the breast. Cancer. 1988;62(11):2392–6.
7. Rosen PP. Vascular tumors of the breast. III Angiomatosis. Am J Surg Pathol. 1985;9(9):652–8.
8. Ginter PS, McIntire PJ, Shin SJ. Vascular tumours of the breast: a comprehensive review with focus on diagnostic challenges encountered in the core biopsy setting. Pathology. 2017;49(2):197–214.
9. Rosen PP. Vascular tumors of the breast. V. Nonparenchymal hemangiomas of mammary subcutaneous tissues. Am J Surg Pathol. 1985;9(10):723–9.
10. Hoda SA, Cranor ML, Rosen PP. Hemangiomas of the breast with atypical histological features. Further analysis of histological subtypes confirming their benign character. Am J Surg Pathol. 1992;16(6):553–60.
11. Murao T, Nakai M, Hamada E. Intravascular papillary endothelial hyperplasia of the breast--report of a case with scanning electron microscopic observations. Gan No Rinsho. 1986;32(11):1471–4.

12. Romani J, et al. Masson's intravascular papillary endothelial hyperplasia mimicking Stewart-Treves syndrome: report of a case. Cutis. 1997;59(3):148–50.
13. Branton PA, Lininger R, Tavassoli FA. Papillary endothelial hyperplasia of the breast: the great impostor for angiosarcoma: a clinicopathologic review of 17 cases. Int J Surg Pathol. 2003;11(2):83–7.
14. Ferreli C, et al. Diffuse dermal angiomatosis of the breast: an emerging entity in the setting of cutaneous reactive angiomatoses. Clin Dermatol. 2021;39(2):271–7.
15. Frikha F, et al. Diffuse dermal angiomatosis of the breast with adjacent fat necrosis: a case report and review of the literature. Dermatol Online J. 2018;24(5)
16. Galambos J, et al. Diffuse dermal angiomatosis of the breast: a distinct entity in the spectrum of cutaneous reactive angiomatoses - clinicopathologic study of two cases and comprehensive review of the literature. Case Rep Dermatol. 2017;9(3):194–205.
17. Ho JD, Wolpowitz D, Phillips TJ. Breast nodularity and ulceration: diffuse dermal angiomatosis a corticosteroid responsive disease. Dermatol Online J. 2016;22(11)
18. Hui Y, et al. Diffuse dermal angiomatosis mimicking inflammatory breast carcinoma. Breast J. 2018;24(2):196–8.
19. Nguyen N, et al. Diffuse dermal angiomatosis of the breast. Proc (Bayl Univ Med Cent). 2020;33(2):273–5.
20. Strausburg MB, et al. Diffuse dermal angiomatosis of the breast with an apparent etiology of underlying calcified thrombosed artery with adjacent fat necrosis. Am J Dermatopathol. 2016;38(11):838–41.
21. Chung SY, Oh KK, Kim DJ. Mammographic and sonographic findings of a breast cystic lymphangioma. J Ultrasound Med. 2003;22(3):307–9.
22. May DS, Stroup NE. The incidence of angiosarcomas of the breast among women in the United States, 1973-1986. Plast Reconstr Surg. 1991;87:193–4.
23. Myerowitz RL, Pietruszka M, Barnes EL. Primary angiosarcoma of the breast. JAMA. 1978;239(5):403.
24. Fernandez AP, et al. FISH for MYC amplification and anti-MYC immunohistochemistry: useful diagnostic tools in the assessment of secondary angiosarcoma and atypical vascular proliferations. J Cutan Pathol. 2012;39(2):234–42.
25. Lagrange JL, et al. Sarcoma after radiation therapy: retrospective multiinstitutional study of 80 histologically confirmed cases. Radiation Therapist and Pathologist Groups of the Federation Nationale des Centres de Lutte Contre le Cancer. Radiology. 2000;216(1):197–205.
26. Manner J, et al. MYC high level gene amplification is a distinctive feature of angiosarcomas after irradiation or chronic lymphedema. Am J Pathol. 2010;176(1):34–9.
27. Weaver J, Billings SD. Postradiation cutaneous vascular tumors of the breast: a review. Semin Diagn Pathol. 2009;26(3):141–9.
28. Bonito FJP, et al. Radiation-induced angiosarcoma of the breast: A review. Breast J. 2020;26(3):458–63.
29. Fletcher CD, Unni K, Mertens F, editors. Vascular tumours in World Health Organization classification of tumours: pathology and genetics of tumours of soft tissue and bone. Lyon: IARC Press; 2002. p. 155–77.
30. Nascimento AF, Raut CP, Fletcher CD. Primary angiosarcoma of the breast: clinicopathologic analysis of 49 cases, suggesting that grade is not prognostic. Am J Surg Pathol. 2008;32(12):1896–904.
31. Taffurelli M, et al. Secondary breast angiosarcoma: a multicentre retrospective survey by the national Italian association of Breast Surgeons (ANISC). Breast. 2019;45:56–60.
32. Rosen PP, Kimmel M, Ernsberger D. Mammary angiosarcoma. The prognostic significance of tumor differentiation. Cancer. 1988;62(10):2145–51.
33. Vorburger SA, et al. Angiosarcoma of the breast. Cancer. 2005;104(12):2682–8.
34. Billings SD, et al. Cutaneous angiosarcoma following breast-conserving surgery and radiation: an analysis of 27 cases. Am J Surg Pathol. 2004;28(6):781–8.
35. Del Mastro L, et al. Angiosarcoma of the residual breast after conservative surgery and radiotherapy for primary carcinoma. Ann Oncol. 1994;5(2):163–5.
36. Strobbe LJ, et al. Angiosarcoma of the breast after conservation therapy for invasive cancer, the incidence and outcome. An unforeseen sequela. Breast Cancer Res Treat. 1998;47(2):101–9.
37. Wijnmaalen A, et al. Angiosarcoma of the breast following lumpectomy, axillary lymph node dissection, and radiotherapy for primary breast cancer: three case reports and a review of the literature. Int J Radiat Oncol Biol Phys. 1993;26(1):135–9.
38. Brenn T, Fletcher CD. Radiation-associated cutaneous atypical vascular lesions and angiosarcoma: clinicopathologic analysis of 42 cases. Am J Surg Pathol. 2005;29(8):983–96.
39. Monroe AT, Feigenberg SJ, Mendenhall NP. Angiosarcoma after breast-conserving therapy. Cancer. 2003;97(8):1832–40.
40. Slotman BJ, et al. Angiosarcoma of the breast following conserving treatment for breast cancer. Eur J Cancer. 1994;30A(3):416–7.
41. Baker GM, Schnitt SJ. Vascular lesions of the breast. Semin Diagn Pathol. 2017;34(5):410–9.
42. Steingaszner LC, Enzinger FM, Taylor HB. Hemangiosarcoma of the breast. Cancer. 1965;18:352–61.
43. Karlsson P, et al. Soft tissue sarcoma after treatment for breast cancer—a Swedish population-based study. Eur J Cancer. 1998;34(13):2068–75.
44. Yap J, et al. Sarcoma as a second malignancy after treatment for breast cancer. Int J Radiat Oncol Biol Phys. 2002;52(5):1231–7.
45. Tavassoli FA, Deville P. Angiosarcoma. In: World Health Organization classification of tumours: tumours of the breast and female genital organs. Lyon: IARC Press; 2003. p. 94–6.
46. Liberman L, et al. Angiosarcoma of the breast. Radiology. 1992;183(3):649–54.
47. Donnell RM, et al. Angiosarcoma and other vascular tumors of the breast. Am J Surg Pathol. 1981;5(7):629–42.
48. Merino MJ, Carter D, Berman M. Angiosarcoma of the breast. Am J Surg Pathol. 1983;7(1):53–60.
49. Carter E, Ulusarac O, Dyess DL. Axillary lymph node involvement in primary epithelioid angiosarcoma of the breast. Breast J. 2005;11(3):219–20.
50. Farina MC, et al. Epithelioid angiosarcoma of the breast involving the skin: a highly aggressive neoplasm readily mistaken for mammary carcinoma. J Cutan Pathol. 2003;30(2):152–6.
51. Macias-Martinez V, et al. Epithelioid angiosarcoma of the breast. Clinicopathological, immunohistochemical, and ultrastructural study of a case. Am J Surg Pathol. 1997;21(5):599–604.
52. Muzumder S, et al. Primary epithelioid angiosarcoma of the breast masquerading as carcinoma. Curr Oncol. 2010;17(1):64–9.
53. Wang ZS, et al. Primary epithelioid angiosarcoma of the male breast: report of a case. Surg Today. 2007;37(9):782–6.
54. Ohsawa M, et al. Use of immunohistochemical procedures in diagnosing angiosarcoma. Evaluation of 98 cases. Cancer. 1995;75(12):2867–74.
55. Poblet E, Gonzalez-Palacios F, Jimenez FJ. Different immunoreactivity of endothelial markers in well and poorly differentiated areas of angiosarcomas. Virchows Arch. 1996;428(4–5):217–21.
56. Yang XJ, et al. Angiosarcomas of the head and neck: a clinicoimmunohistochemical study of 8 consecutive patients. Int J Oral Maxillofac Surg. 2010;39(6):568–72.
57. Traweek ST, et al. The human hematopoietic progenitor cell antigen (CD34) in vascular neoplasia. Am J Clin Pathol. 1991;96(1):25–31.

58. Folpe AL, et al. Vascular endothelial growth factor receptor-3 (VEGFR-3): a marker of vascular tumors with presumed lymphatic differentiation, including Kaposi's sarcoma, kaposiform and Dabska-type hemangioendotheliomas, and a subset of angiosarcomas. Mod Pathol. 2000;13(2):180–5.
59. Cuda J, et al. Diagnostic utility of Fli-1 and D2-40 in distinguishing atypical fibroxanthoma from angiosarcoma. Am J Dermatopathol. 2013;35(3):316–8.
60. Folpe AL, et al. Expression of Fli-1, a nuclear transcription factor, distinguishes vascular neoplasms from potential mimics. Am J Surg Pathol. 2001;25(8):1061–6.
61. Sullivan HC, et al. The utility of ERG, CD31 and CD34 in the cytological diagnosis of angiosarcoma: an analysis of 25 cases. J Clin Pathol. 2015;68(1):44–50.
62. McKay KM, et al. Expression of ERG, an Ets family transcription factor, distinguishes cutaneous angiosarcoma from histological mimics. Histopathology. 2012;61(5):989–91.
63. Miettinen M, et al. ERG transcription factor as an immunohistochemical marker for vascular endothelial tumors and prostatic carcinoma. Am J Surg Pathol. 2011;35(3):432–41.
64. Minner S, et al. High level of Ets-related gene expression has high specificity for prostate cancer: a tissue microarray study of 11 483 cancers. Histopathology. 2012;61(3):445–53.
65. Stockman DL, et al. ERG and FLI1 protein expression in epithelioid sarcoma. Mod Pathol. 2014;27(4):496–501.
66. Liu H, et al. Immunohistochemical evaluation of ERG expression in various benign and malignant tissues. Ann Clin Lab Sci. 2013;43(1):3–9.
67. Wang WL, et al. Expression of ERG, an Ets family transcription factor, identifies ERG-rearranged Ewing sarcoma. Mod Pathol. 2012;25(10):1378–83.
68. Kohashi K, et al. ERG and SALL4 expressions in SMARCB1/INI1-deficient tumors: a useful tool for distinguishing epithelioid sarcoma from malignant rhabdoid tumor. Hum Pathol. 2015;46(2):225–30.
69. Miettinen M, et al. ERG expression in epithelioid sarcoma: a diagnostic pitfall. Am J Surg Pathol. 2013;37(10):1580–5.
70. Miettinen M, Franssila KO. Variable expression of keratins and nearly uniform lack of thyroid transcription factor 1 in thyroid anaplastic carcinoma. Hum Pathol. 2000;31(9):1139–45.
71. Rao P, et al. Angiosarcoma: a tissue microarray study with diagnostic implications. Am J Dermatopathol. 2013;35(4):432–7.
72. Tse GM, et al. p63 is useful in the diagnosis of mammary metaplastic carcinomas. Pathology. 2006;38(1):16–20.
73. D'Alfonso TM, et al. Expression of p40 and laminin 332 in metaplastic spindle cell carcinoma of the breast compared with other malignant spindle cell tumours. J Clin Pathol. 2015;68(7):516–21.
74. Kim SK, Jung WH, Koo JS. p40 (DeltaNp63) expression in breast disease and its correlation with p63 immunohistochemistry. Int J Clin Exp Pathol. 2014;7(3):1032–41.
75. Chbani L, et al. Epithelioid sarcoma: a clinicopathologic and immunohistochemical analysis of 106 cases from the French sarcoma group. Am J Clin Pathol. 2009;131(2):222–7.
76. Miettinen M, Wang ZF. Prox1 transcription factor as a marker for vascular tumors-evaluation of 314 vascular endothelial and 1086 nonvascular tumors. Am J Surg Pathol. 2012;36(3):351–9.
77. Modena P, et al. SMARCB1/INI1 tumor suppressor gene is frequently inactivated in epithelioid sarcomas. Cancer Res. 2005;65(10):4012–9.
78. Cornejo KM, et al. The utility of MYC and FLT4 in the diagnosis and treatment of postradiation atypical vascular lesion and angiosarcoma of the breast. Hum Pathol. 2015;46(6):868–75.
79. Ko JS, et al. Fully automated dual-color dual-hapten silver in situ hybridization staining for MYC amplification: a diagnostic tool for discriminating secondary angiosarcoma. J Cutan Pathol. 2014;41(3):286–92.
80. Mentzel T, et al. Postradiation cutaneous angiosarcoma after treatment of breast carcinoma is characterized by MYC amplification in contrast to atypical vascular lesions after radiotherapy and control cases: clinicopathological, immunohistochemical and molecular analysis of 66 cases. Mod Pathol. 2012;25(1):75–85.
81. Shon W, et al. MYC amplification and overexpression in primary cutaneous angiosarcoma: a fluorescence in-situ hybridization and immunohistochemical study. Mod Pathol. 2014;27(4):509–15.
82. Ginter PS, et al. Diagnostic utility of MYC amplification and anti-MYC immunohistochemistry in atypical vascular lesions, primary or radiation-induced mammary angiosarcomas, and primary angiosarcomas of other sites. Hum Pathol. 2014;45(4):709–16.
83. Guo T, et al. Consistent MYC and FLT4 gene amplification in radiation-induced angiosarcoma but not in other radiation-associated atypical vascular lesions. Genes Chromosomes Cancer. 2011;50(1):25–33.
84. Italiano A, et al. The miR-17-92 cluster and its target THBS1 are differentially expressed in angiosarcomas dependent on MYC amplification. Genes Chromosomes Cancer. 2012;51(6):569–78.
85. Fraga-Guedes C, et al. Angiosarcoma and atypical vascular lesions of the breast: diagnostic and prognostic role of MYC gene amplification and protein expression. Breast Cancer Res Treat. 2015;151(1):131–40.
86. Flucke U, Requena L, Mentzel T. Radiation-induced vascular lesions of the skin: an overview. Adv Anat Pathol. 2013;20(6):407–15.
87. Park MS, Ravi V, Araujo DM. Inhibiting the VEGF-VEGFR pathway in angiosarcoma, epithelioid hemangioendothelioma, and hemangiopericytoma/solitary fibrous tumor. Curr Opin Oncol. 2010;22(4):351–5.
88. Aprelikova O, et al. FLT4, a novel class III receptor tyrosine kinase in chromosome 5q33-qter. Cancer Res. 1992;52(3):746–8.
89. Galland F, et al. Chromosomal localization of FLT4, a novel receptor-type tyrosine kinase gene. Genomics. 1992;13(2):475–8.
90. Galland F, et al. The FLT4 gene encodes a transmembrane tyrosine kinase related to the vascular endothelial growth factor receptor. Oncogene. 1993;8(5):1233–40.
91. Partanen TA, Alitalo K, Miettinen M. Lack of lymphatic vascular specificity of vascular endothelial growth factor receptor 3 in 185 vascular tumors. Cancer. 1999;86(11):2406–12.
92. Ranieri G, et al. Pazopanib a tyrosine kinase inhibitor with strong anti-angiogenetic activity: a new treatment for metastatic soft tissue sarcoma. Crit Rev Oncol Hematol. 2014;89(2):322–9.
93. Schoffski P, et al. Soft tissue sarcoma: an update on systemic treatment options for patients with advanced disease. Oncol Res Treat. 2014;37(6):355–62.
94. Antonescu CR, et al. KDR activating mutations in human angiosarcomas are sensitive to specific kinase inhibitors. Cancer Res. 2009;69(18):7175–9.
95. Behjati S, et al. Recurrent PTPRB and PLCG1 mutations in angiosarcoma. Nat Genet. 2014;46(4):376–9.
96. Chen KT, Kirkegaard DD, Bocian JJ. Angiosarcoma of the breast. Cancer. 1980;46(2):368–71.
97. Tavassoli FA. Pathology of the Breast. 2nd ed. Stamford: Appleton-Lange; 1999.
98. Torres KE, et al. Long-term outcomes in patients with radiation-associated angiosarcomas of the breast following surgery and radiotherapy for breast cancer. Ann Surg Oncol. 2013;20(4):1267–74.
99. Gutkin PM, et al. Angiosarcoma of the breast: management and outcomes. Am J Clin Oncol. 2020;43(11):820–5.
100. McClelland S 3rd, et al. Extent of resection and role of adjuvant treatment in resected localized breast angiosarcoma. Breast Cancer Res Treat. 2019;175(2):409–18.
101. Ju T, et al. Skin angiography assisted mastectomy in secondary breast angiosarcoma: complete clinical response after neoadjuvant immunotherapy. Breast J. 2021;27(9):723–5.

102. Adem C, et al. Primary breast sarcoma: clinicopathologic series from the Mayo Clinic and review of the literature. Br J Cancer. 2004;91(2):237–41.
103. Seinen JM, et al. Radiation-associated angiosarcoma after breast cancer: high recurrence rate and poor survival despite surgical treatment with R0 resection. Ann Surg Oncol. 2012;19(8):2700–6.
104. Uchin JM, Billings SD. Radiotherapy-associated atypical vascular lesions of the breast. J Cutan Pathol. 2009;36(1):87–8.
105. Brodie C, Provenzano E. Vascular proliferations of the breast. Histopathology. 2008;52(1):30–44.
106. Gengler C, et al. Vascular proliferations of the skin after radiation therapy for breast cancer: clinicopathologic analysis of a series in favor of a benign process: a study from the French Sarcoma Group. Cancer. 2007;109(8):1584–98.
107. Brenn T, Fletcher CD. Postradiation vascular proliferations: an increasing problem. Histopathology. 2006;48(1):106–14.
108. Patton KT, Deyrup AT, Weiss SW. Atypical vascular lesions after surgery and radiation of the breast: a clinicopathologic study of 32 cases analyzing histologic heterogeneity and association with angiosarcoma. Am J Surg Pathol. 2008;32(6):943–50.
109. Fineberg S, Rosen PP. Cutaneous angiosarcoma and atypical vascular lesions of the skin and breast after radiation therapy for breast carcinoma. Am J Clin Pathol. 1994;102(6):757–63.
110. Requena L, et al. Benign vascular proliferations in irradiated skin. Am J Surg Pathol. 2002;26(3):328–37.
111. Mattoch IW, et al. Post-radiotherapy vascular proliferations in mammary skin: a clinicopathologic study of 11 cases. J Am Acad Dermatol. 2007;57(1):126–33.

Breast Tumors in Adolescents/Children and Males

18

Melinda E. Sanders

Children and Adolescents

Overview

Children are defined as being younger than 13 years, and adolescents are those between 13 and 19 years. Breast lesions in children and adolescents are rare [1] and differ from adult breast disease. First, breast disease in children and adolescents consists almost exclusively of benign lesions related to normal breast development and benign tumors [2–4]. Secondly, malignancies in children and adolescents are very rare [5]. Breast cancers in adolescents account for 0.1% of all breast cancers and less than 1% of all pediatric cancers [5, 10]. Thirdly, the developing mammary gland is highly sensitive to ionizing radiation and dense. Ultrasonography is thus the preferred imaging modality as it can identify lesions in dense breast tissue and avoid radiation exposure [5–8]. Thus, most pediatric breast lesions should be managed conservatively. Surgical treatment may affect developing breast buds in children and adolescents and should be recommended cautiously based on clinical and imaging features [5, 7, 8]. Although the vast majority of mass-forming lesions in these patients are benign, core needle biopsy (CNB) is a useful way to exclude malignancy in appropriately selected patients with a discrete mass. CNB should be considered in the rare event of abnormal imaging findings, such as non-circumscribed margins, complex solid and cystic components, posterior acoustic shadowing, size above 3 cm, or interval increase in mass size. CNB is highly accurate and avoids irreparable damage in pediatric patients [9]. A clinical history that includes a risk factor for malignancy, such as prior chest irradiation, known concurrent cancer not involving the breast, or family history of breast cancer, should prompt consideration of CNB even if the lesion has a benign appearance radiologically [9].

Developmental and Congenital Abnormalities

Knowledge of developmental abnormalities of the breast is important to avoid biopsy and surgery for these conditions, which may irreparably damage the developing breast. Premature thelarche is defined as the onset of breast development before 8 years of age, and delayed thelarche is defined as the onset after 13 years of age [5, 6, 8]. Early development of the breast may occur alone or accompanying precocious puberty. Idiopathic premature thelarche may occur in girls aged 1–3 years, which is not associated with precocious puberty and usually regresses. In such cases, hypoechoic subareolar breast buds can be identified by ultrasonography, and clinical follow-up is adequate [5, 6, 8]. When early breast development is associated with precocious puberty, the treating clinician should measure bone age and order appropriate studies to exclude an adrenal gland tumor [5, 6, 8].

An accessory nipple (polythelia) (Fig. 18.1) and an accessory breast (polymastia) are congenital anomalies associated with incomplete regression of the mammary ridge [5]. These anomalies can occur anywhere along the embryonic mammary ridge from the axilla to the groin, but most commonly occur in the axilla or inframammary fold [5]. An accessory nipple is found in 1–2% of the population and can be misdiagnosed clinically as a nevus [5–8]. Clinically, an accessory breast in the axilla usually manifests as periodic pain and protrusion into the axilla. Ultrasonography can confirm the presence of axillary fibroglandular tissue [5–8]. Hypoplasia and amastia (absence of breast tissue, nipple, and areola) are rare and may occur in association with Poland syndrome [11, 12]. Amazia, the presence of the nipple and areola but absence of underlying breast tissue, is most commonly attributable to iatrogenic resection of the breast buds or radiation therapy before adolescence [5, 8, 13].

M. E. Sanders (✉)
Department of Pathology, Microbiology and Immunology, Vanderbilt University Medical Center, Nashville, TN, USA
e-mail: melinda.sanders@vumc.org

© The Author(s), under exclusive license to Springer Nature Switzerland AG 2022
S. J. Shin et al. (eds.), *A Comprehensive Guide to Core Needle Biopsies of the Breast*,
https://doi.org/10.1007/978-3-031-05532-4_18

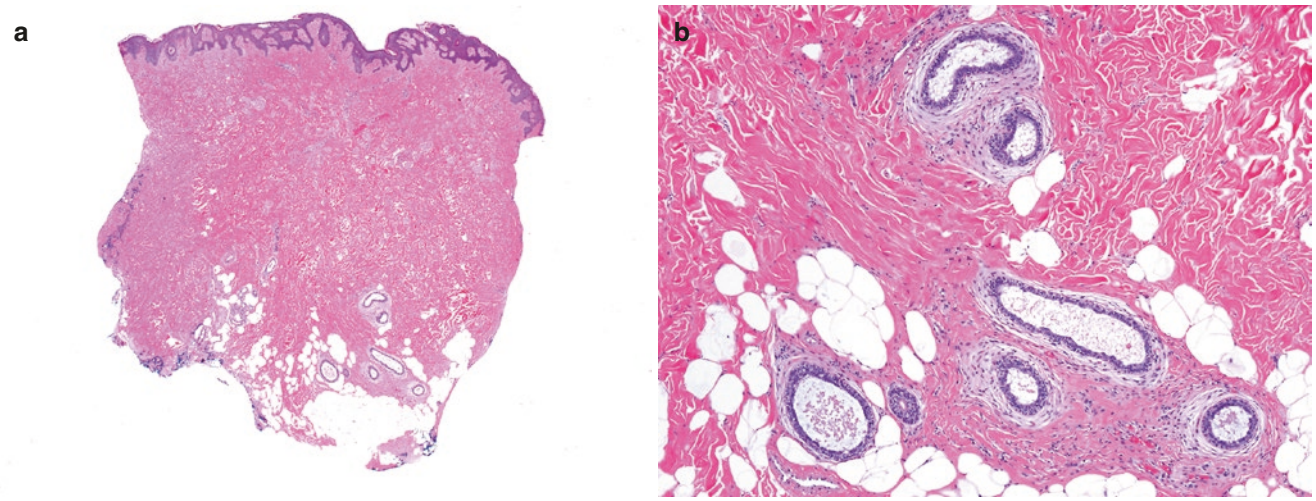

Fig. 18.1 (**a**) Supernumerary nipple from a 17-year-old female composed of mammary ducts at the junction of the dermis and subcutis. (**b**) The ducts have a prepubertal appearance

Nonneoplastic Lesions

Simple cysts are common in the adult female breast but can be found at any age. Cysts may arise from dilated acini or duct obstruction [14, 15]. A cyst in the adolescent breast presents as an asymptomatic mass adjacent to the nipple and is occasionally accompanied by inflammation or nipple discharge [5, 15, 16]. On ultrasonography, a cyst appears as a round or oval anechoic mass with posterior acoustic enhancement and lacks internal blood flow on a color Doppler study. Simple asymptomatic cysts with typical imaging features do not require further examination or intervention. However, cysts with atypical imaging features, such as internal echogenicity, fluid-fluid levels, internal septations, or a thick wall, may require aspiration to differentiate from galactocele, abscess, or complicated cyst [6, 8].

Duct ectasia rarely occurs in newborns and young children. Clinically, patients with duct ectasia present with bloody nipple discharge or a palpable mass in the breast. On ultrasound, multi-septate subareolar cyst-like masses or tubular anechoic structures are seen. The etiology of duct ectasia is unknown and is likely related to maternal hormones. Conservative treatment is indicated in newborns with these findings, including temporary cessation of breastfeeding and antibiotic administration [5, 6, 8].

Mastitis and abscess, common conditions in lactating women, can also occur in children with a bimodal distribution including infants (aged <2 months) and older children (aged 8–17 years) [17]. Mastitis is a clinical diagnosis based on signs and symptoms of infection, such as fever, erythema, and tenderness. The most common causative organisms in adolescence are Staphylococcus and pneumococci [5–8]. Treatment of mastitis with abscess includes antibiotic therapy and drainage with fine needle aspiration. A large abscess may require surgical incision and drainage with follow-up examination to confirm resolution [5–8, 16].

Galactocele is a retention cyst filled with milk caused by obstruction of a lactiferous duct. It is commonly seen in pregnant or lactating women but may also occur in infants and adolescents [18, 19]. Uncomplicated galactoceles with no atypical imaging features are self-limiting and do not need further evaluation or treatment. As with simple cysts, CNB is only indicated in patients with symptoms and those with atypical imaging features [5, 8].

Benign Masses

The overwhelming majority of benign masses presenting in female children and adolescents are fibroadenomas. Fibroadenomas form the largest group of lesions within the fibroepithelial lesion spectrum, a group of biphasic tumors consisting of fibroadenomas, phyllodes tumors, and hamartomas. The typical fibroadenoma and its variants as observed among adolescents will be reviewed. Pseudoangiomatous stromal hyperplasia (PASH) and the rarer entity, juvenile papillomatosis, which clinically present as a mass-mimicking fibroadenoma in this age group, will also be discussed.

Fibroadenoma

Fibroadenomas are the most common benign tumors in children and adolescents, accounting for 54–94% of breast lesions [5, 10, 17]. They are usually solitary; however, multiple and bilateral lesions have been reported [20, 21]. A diagnosis of Carney syndrome could be considered when multiple tumors with abundant myxoid stroma are present [22, 23]. Ultrasound findings typical of fibroadenoma are a round-to-oval hypoechoic mass with circumscribed margins,

oriented parallel to the skin [17]. Posterior acoustic enhancement is frequently seen, and altered blood flow can be observed on color Doppler ultrasound [8, 16]. Occasionally, fibroadenomas show atypical features on ultrasound, such as an angular border or posterior acoustic shadowing [6, 10], which warrant consideration of CNB.

Most fibroadenomas are slow growing, presenting as non-tender, firm, well-defined, mobile nodules. Grossly, ranging from 2 to 5 cm, fibroadenomas are well delineated from the surrounding breast tissue and demonstrate a lobulated, bulging white-gray cut surface with a few slit-like spaces. Some tumors contain myxoid areas. Histologically, fibroadenomas demonstrate two classic patterns, *pericanalicular* and *intracanalicular,* which are readily identified in CNB specimens. Most fibroadenomas contain a mixture of both patterns. The *pericanalicular* pattern develops from a circumferential stromal proliferation around open ductal structures (Fig. 18.2a). The *intracanalicular* pattern results from proliferation of stromal cells leading to collapsed slit-like ductal structures (Fig. 18.2b). Distinction of the two patterns is not clinically important; however, a prominent intracanalicular pattern can occasionally create a focally leaflike pattern which mimics a benign phyllodes tumor (Fig. 18.3a, b). *Cellular fibroadenomas* are defined by increased stromal cellularity, approximately twice that of the typical fibroadenoma [24], but limited mitotic activity (usually <3 per 10 HPF) and an absence of stromal atypia or overgrowth (Fig. 18.4a–c). A greater number of mitoses may even be permissible if accompanied by a similarly proliferative epithelial component also accompanied by evident mitotic activity. Furthermore, cellular fibroadenomas lack the cleft-like spaces and leafy projections characteristic of benign phyllodes tumors. Periductal stromal condensation, which is seen in many benign phyllodes tumors, is also absent. While most fibroadenomas are clearly delineated from the adjacent normal breast parenchyma, occasional lesions may have focally irregular margins [25]. Such foci are not of concern in the absence of other diagnostic fea-

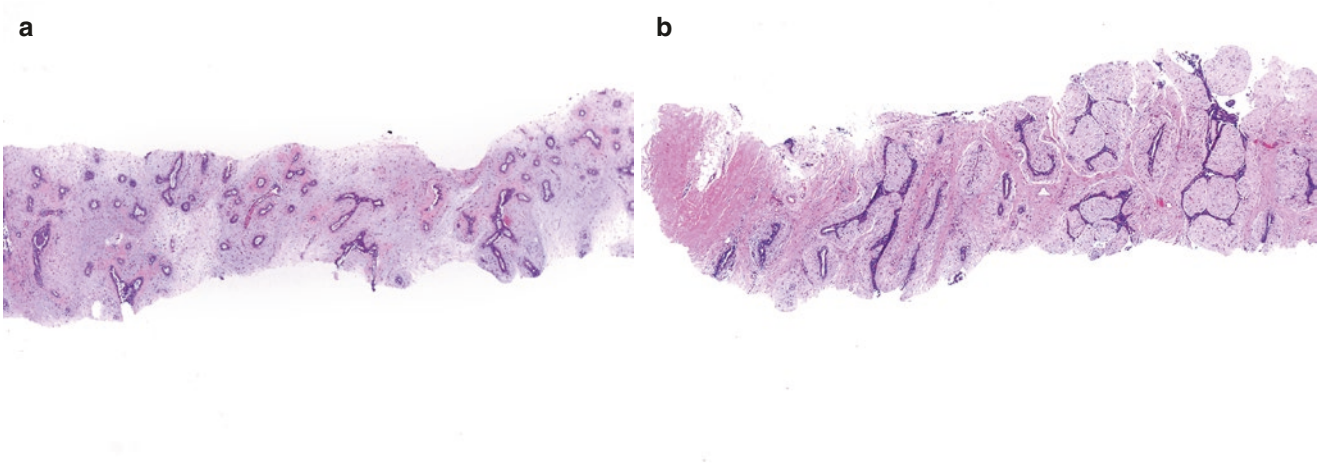

Fig. 18.2 (**a**) Fibroadenoma with a pericanalicular pattern characterized by circumferential stromal proliferation around open ductal structures. (**b**) The *intracanalicular* pattern results from proliferation of stromal cells leading to collapsed slit-like ductal structures

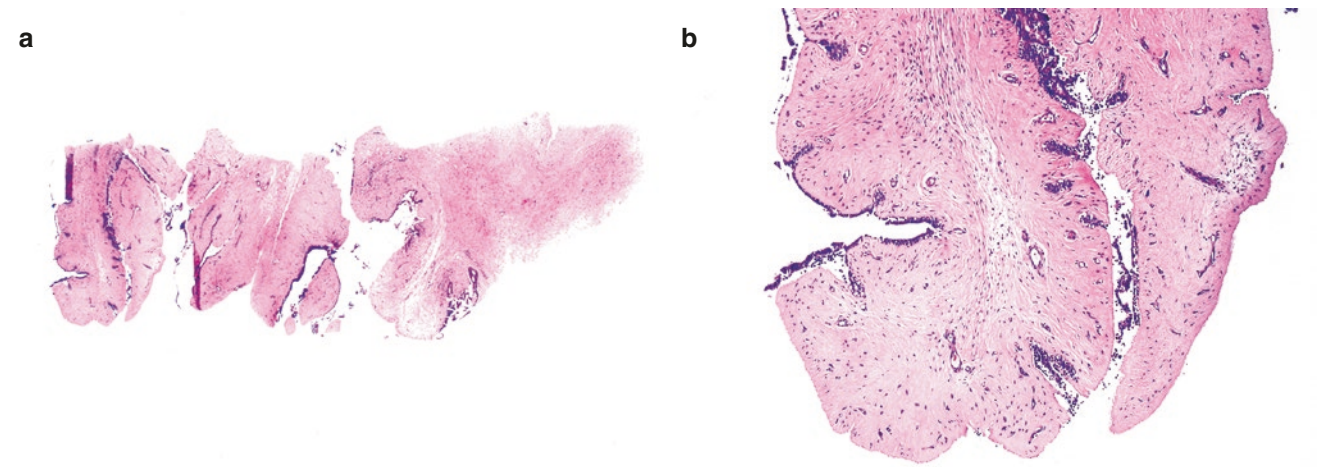

Fig. 18.3 Fibroadenoma with a prominent intracanalicular pattern with a focally leaflike pattern, which mimics a benign phyllodes tumor; however, the cellularity is very low, and atypia is lacking (**a, b**)

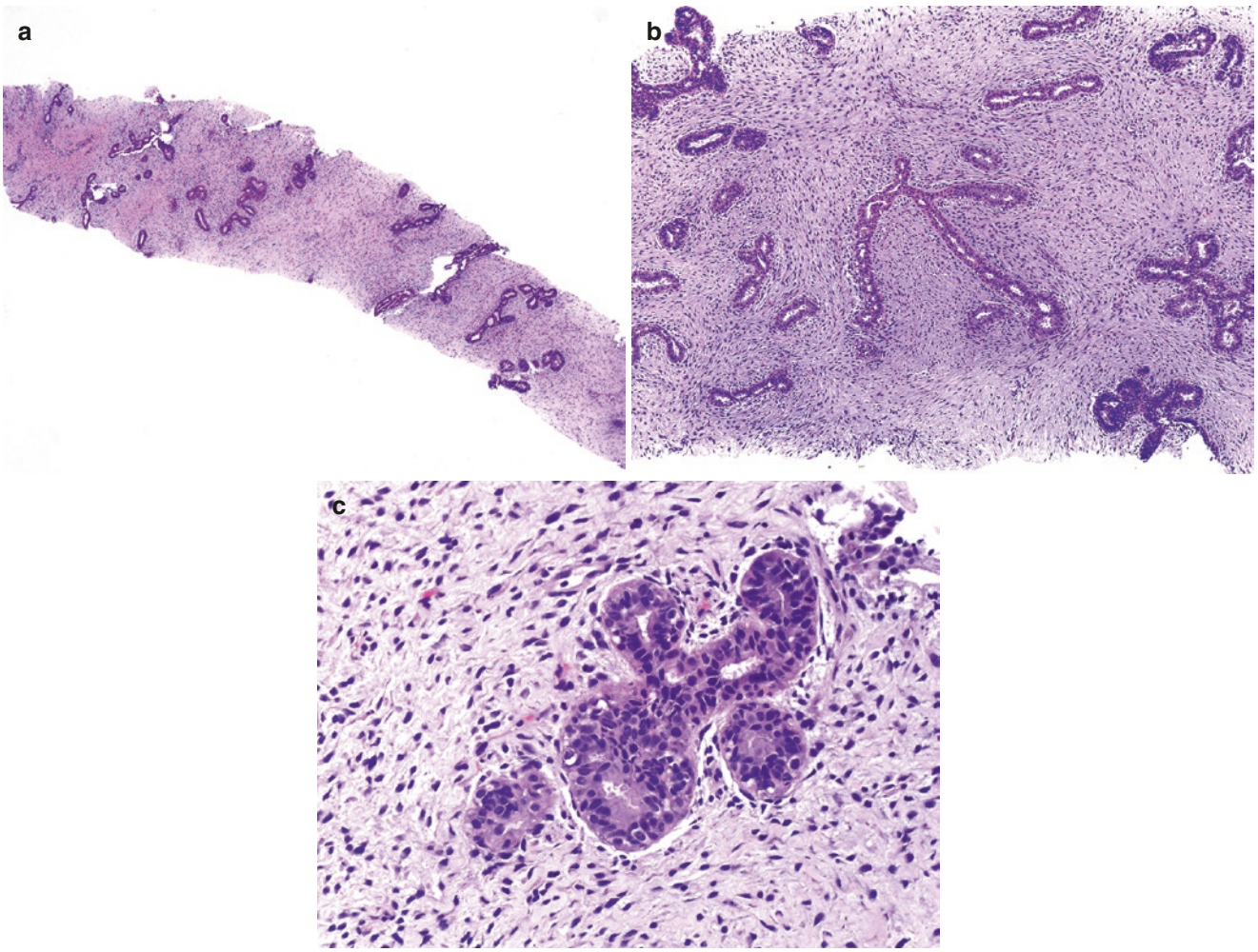

Fig. 18.4 (**a**) Increased stromal cellularity, approximately twice that of the typical fibroadenoma, is evident at low power in this cellular fibroadenoma from a 15-year-old female. (**b**) There is mild stromal expansion; however, the ratio of stroma to epithelium remains constant. (**c**) The stromal cells lack atypia, and a few mitoses are evident in the epithelial component

tures of phyllodes tumor. The clinical entity "*giant*" or "*juvenile*" fibroadenoma accounts for 7–8% of cases [5, 6, 8, 17] and is defined by a history of rapid growth [3, 5, 25] and sizes of 5–10 cm or more. These lesions are typically cellular and may show focal areas with branching, elongated clefts reminiscent of benign phyllodes tumor. The term "complex fibroadenoma" is used for fibroadenomas containing foci of sclerosing adenosis, apocrine change, or cysts larger than 3 mm. The lesion was originally recognized because it was associated with a slightly increased relative risk for later carcinoma development, while fibroadenomas without these features have no increase in relative risk [26, 27].

Regardless of the architectural pattern, the stroma of fibroadenomas may exhibit multinucleated giant cells, myxoid change (Fig. 18.5a–c), myofibroblastic stroma (Fig. 18.6a–c), pseudoangiomatous stromal hyperplasia (PASH), hyalinization with or without calcification, and rarely ossification. Lipomatous, smooth muscle, and osteochondroid metaplasia may rarely occur [25, 28]. The epithelial component often shows varying degrees of usual ductal hyperplasia, which is frequently mitotically active. Rare examples of atypical ductal hyperplasia (ADH) occurring in fibroadenomas in adolescents have been reported [29]. Although the significance of ADH in fibroadenomas has not been systematically studied in adolescents, limited follow-up studies of ADH in this age group have shown no risk implication [30, 31]. In addition, ADH when confined to a fibroadenoma in adult women has no prognostic significance [26, 27]. Extensive myoepithelial proliferation can also be seen, and care should be taken to avoid its misdiagnosis as ADH. Immunohistochemistry for smooth mus-

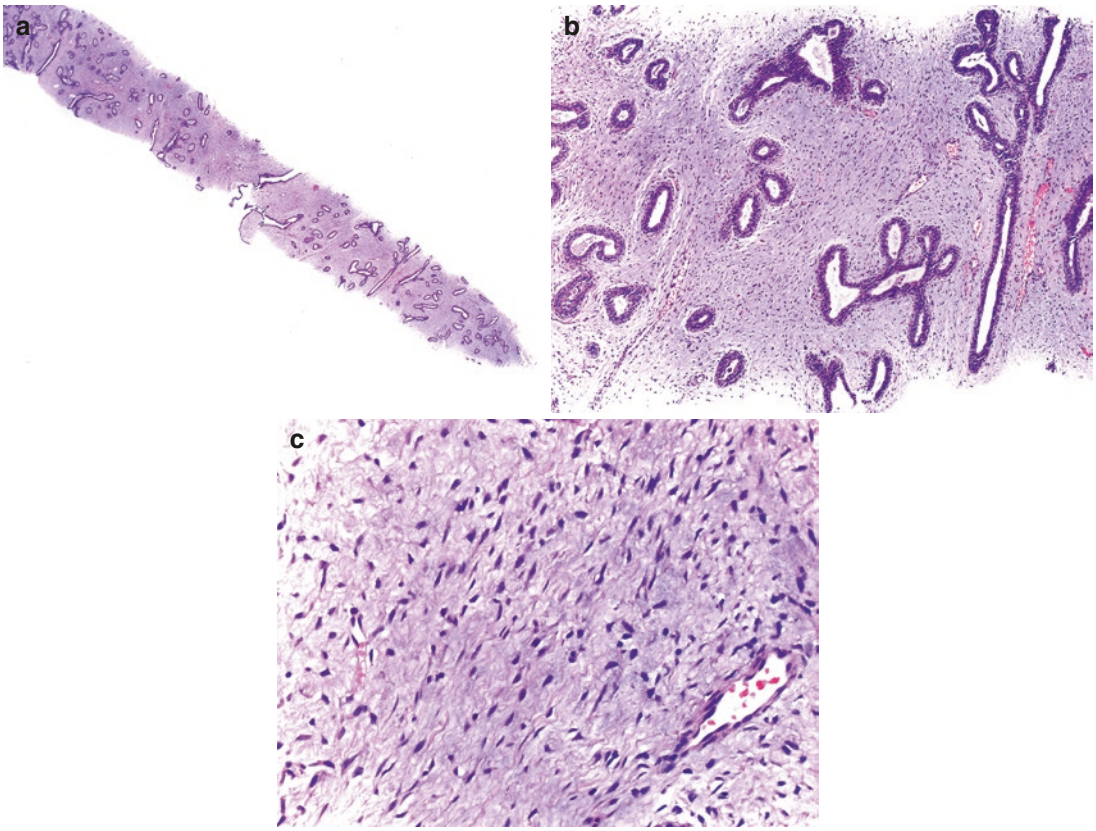

Fig. 18.5 (**a**) Fibroadenoma from a 17-year-old female with myxoid stroma. (**b**) The myxoid change is noted in the entirety of the stromal component, a finding of no known clinical significance. (**c**) The stromal cells display bland nonoverlapping nuclei and lack atypia

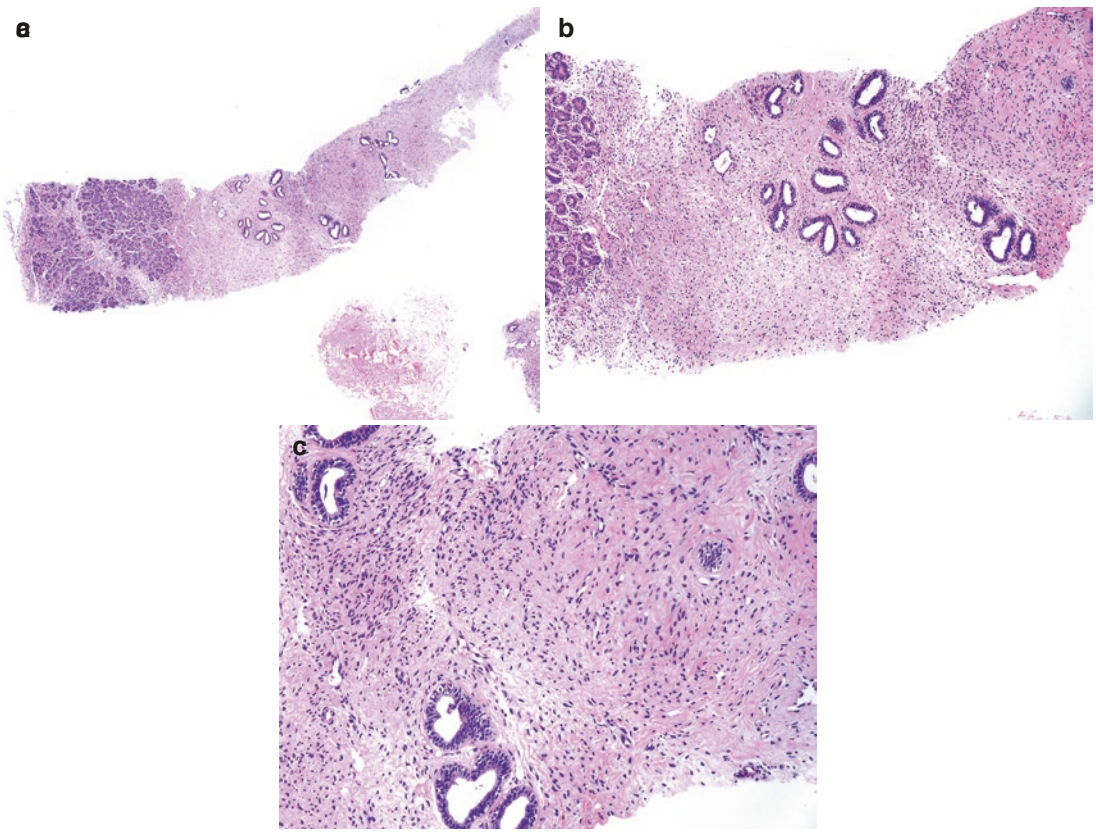

Fig. 18.6 (**a**) Fibroadenoma with myofibroblastic stroma from a 13-year-old female showing both tubular and pericanalicular patterns. (**b** and **c**) The bland myofibroblastic stromal cells are identical to those seen in a myofibroblastoma

cle actin (SMA) and p63 can be used to confirm the myoepithelial nature of these cells. DCIS is occasionally associated with fibroadenomas in adult women and is even less often seen in the adolescent population [32].

The terms "tubular adenoma" and "lactating adenoma" are best considered as variants of fibroadenoma since they behave in a benign fashion. Thus, the terms *tubular variant of fibroadenoma* and *nodular gestational hyperplasia*, respectively, are preferred. Both entities are clinically and macroscopically well circumscribed with a homogeneous white-tan cut surface in the tubular variant and a softer tan-yellow surface in nodular gestational hyperplasia. Histologically, the tubular variant displays abundant compact uniform acini, with the normal dual-cell population composed of an inner layer of cuboidal-to-columnar epithelial cells and an outer layer of myoepithelial cells with minimal intervening stroma (Fig. 18.7a–c). Nodular gestational hyperplasia occurs during pregnancy or the postpartum period. The clinically detectable mass demonstrates histologically a typical fibroadenoma with superimposed lactational change (Fig. 18.8a–c) or tubular variant architecture with superimposed secretory change characterized by luminal epithelial cells with large nuclei and abundant vacuolated cytoplasm (Fig. 18.9a–c). Of importance and particularly during pregnancy, nodular gestational hyperplasia may infarct and should not be taken as evidence of malignancy based solely on the presence of necrosis [33].

Pseudoangiomatous Stromal Hyperplasia (PASH)

PASH is a benign hormone-dependent myofibroblastic stromal proliferation that is reminiscent of a vascular lesion due to the formation of small slit-like spaces [34–36]. PASH can be seen in children, adolescents, and adults [37, 38]. Clinical and ultrasound findings are similar to those of fibroadenoma.

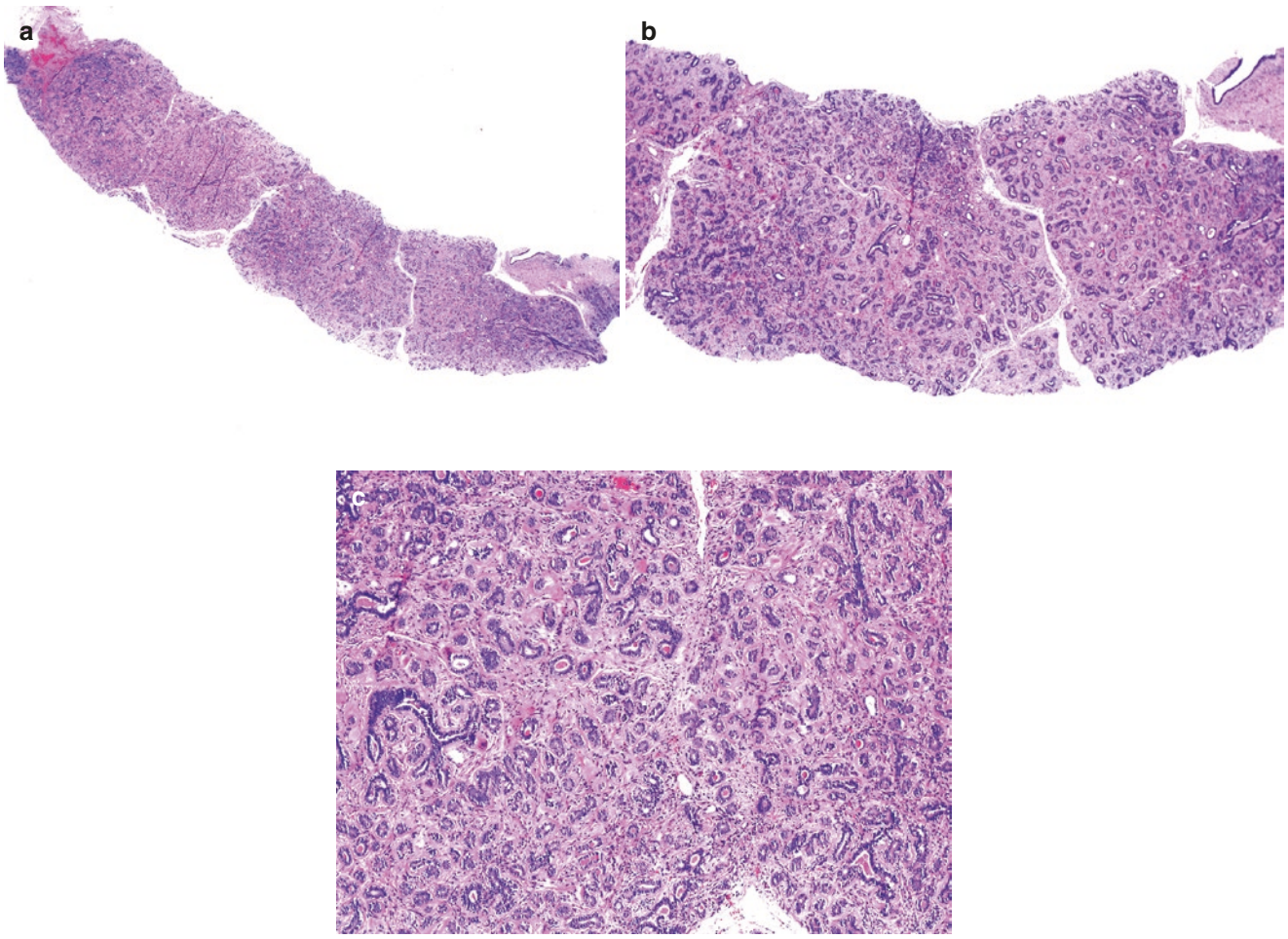

Fig. 18.7 (**a**) Fibroadenomas with a tubular pattern are densely cellular at low power and rarely encountered beyond adolescence. (**b**) The abundant, tightly compacted, uniform acini create a lesion resembling a massive lobular unit. (**c**) The acini are composed of an inner layer of cuboidal-to-columnar epithelial cells and an outer layer of myoepithelial cells with minimal intervening stroma

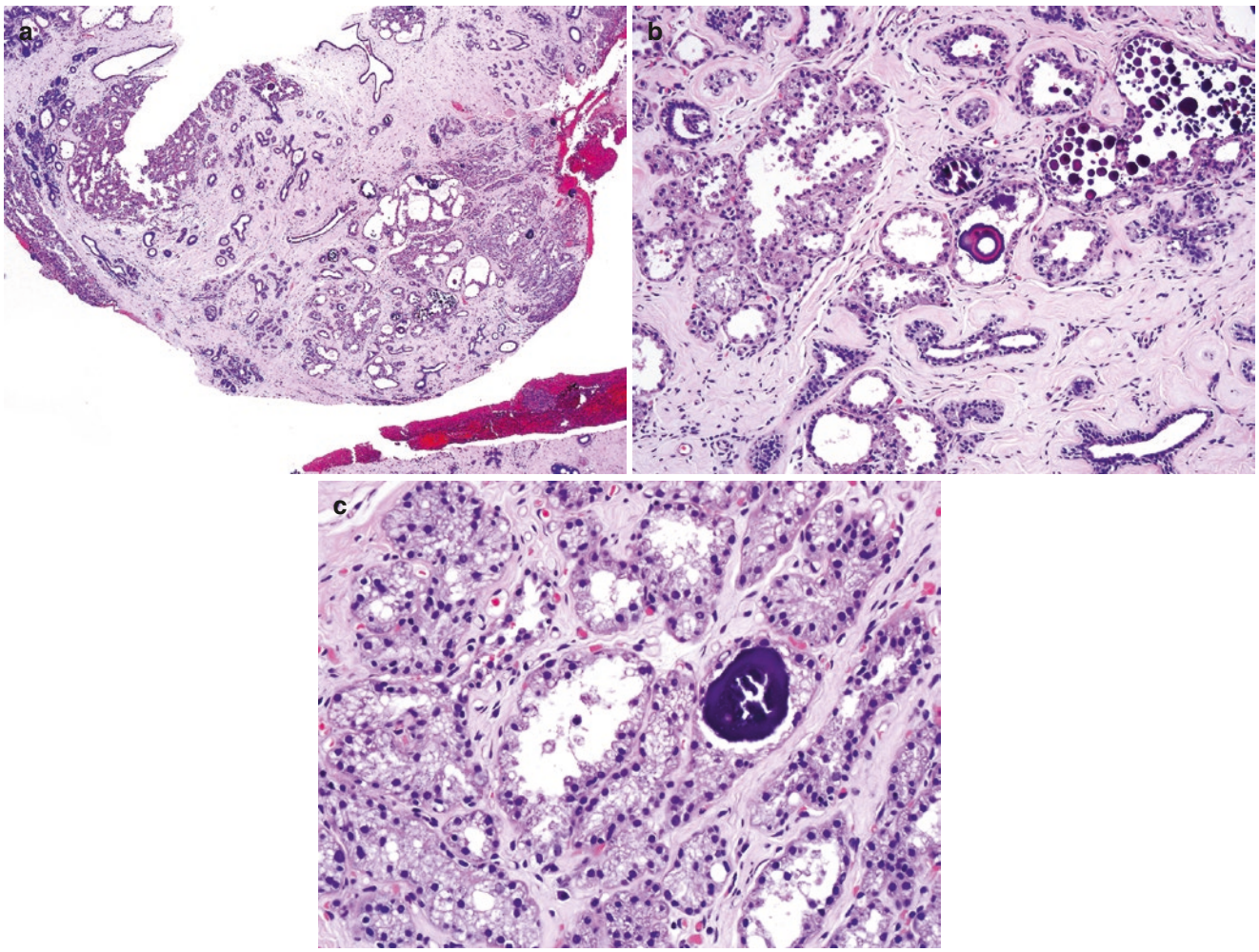

Fig. 18.8 (**a**) During an adolescent pregnancy, the epithelium of a pre-existing fibroadenoma may show lactational change and present as a palpable mass. (**b**) Milk of calcium-type calcifications may be evident. (**c**) Small round basal nuclei and abundant foamy cytoplasm are characteristics

Cases warranting diagnosis of PASH present as a mass, which is typically palpable. PASH is characterized by a proliferation of myofibroblasts, which form slit-shaped, pseudovascular spaces within a dense keloid-like stroma (Fig. 18.10a–c). These spaces do not contain red blood cells. The spindle-shaped myofibroblasts resemble endothelial cells but lack expression of specific endothelial (factor VIII, CD31, D2–40) and epithelial markers. The histologic features on H&E are usually defining, making immunohistochemistry unnecessary. However, the myofibroblastic origin of the cells can be confirmed by CD34 positivity in the absence of other specific endothelial markers [39]. These myofibroblasts also express desmin, SMA, calponin, and BCL-2 [39]. The hormonal basis of this process is evidenced by the expression of progesterone receptors by the myofibroblasts [40]. The hyalinized stroma is usually sharply demarcated from the surrounding breast or ill-defined, blending imperceptibly with the surrounding normal stroma. PASH does not exhibit mitotic activity, nuclear atypia, necrosis, or calcifications. Microscopic foci of PASH are often incidentally noted as a component of other lesions such as fibroadenoma but do not require specific comment. Excision is not required, although surgery may be indicated for large lesions causing a deformity.

Juvenile Papillomatosis

Occasionally, localized fibrocystic changes dominated by apocrine cysts, sclerosing micropapillomas, and usual ductal hyperplasia can present as a clinical mass in late adolescence, which is indistinguishable clinically from fibroadenoma (Fig. 18.11a–c). Ultrasound can facilitate the diagnosis

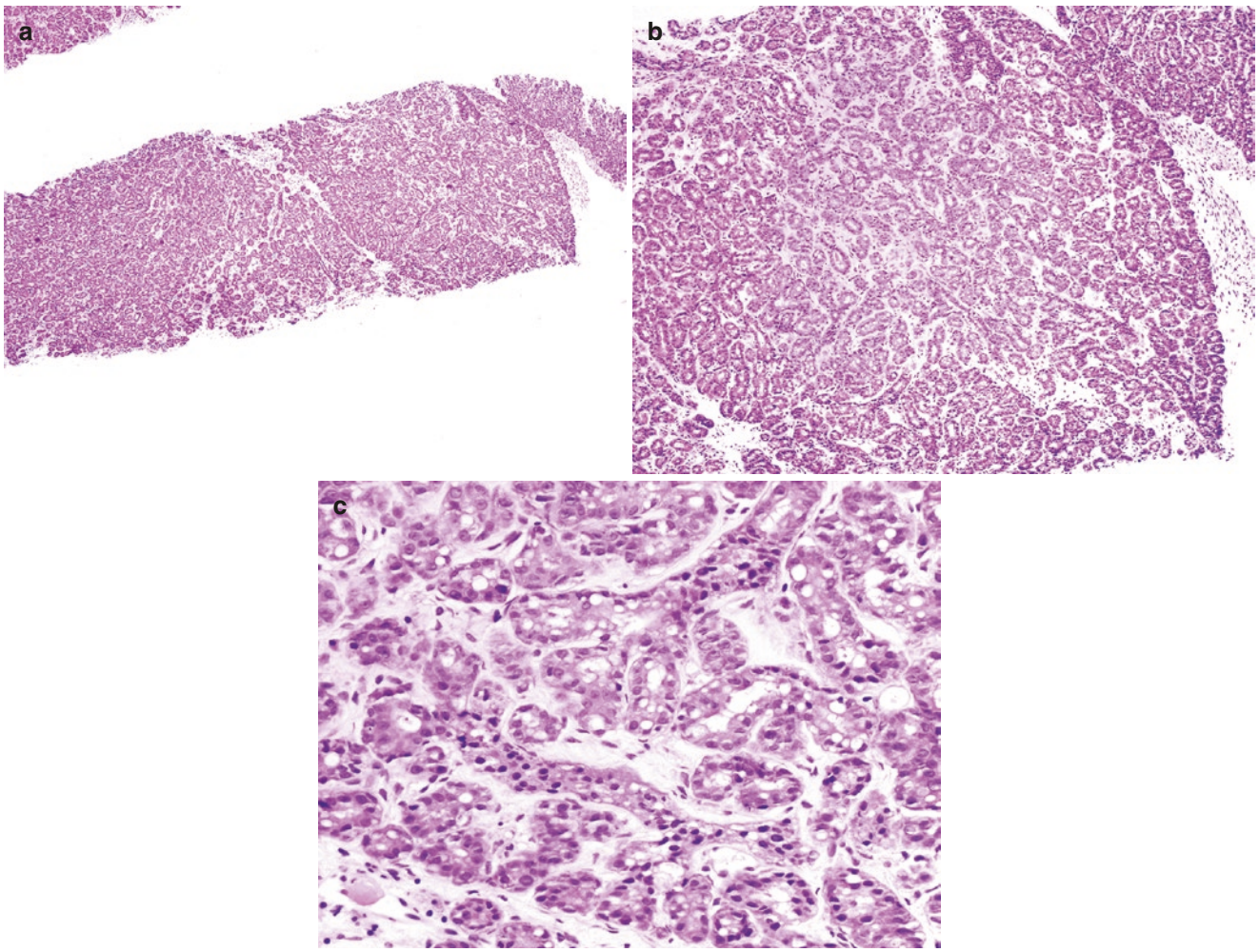

Fig. 18.9 (**a**) Tubular adenomas in adolescents may display diffuse lactational change during late pregnancy and during lactation. (**b**) At medium power, the cytoplasmic secretory material is evident within the epithelial cells comprising the tightly compacted acini. (**c**) Within individual acini, the nuclei are bland and inconspicuous while the cytoplasm is vacuolated and abundant

by revealing multiple small cysts with ill-defined margins within the mass. Historically, this presentation has been called juvenile papillomatosis [3, 41] or "Swiss cheese disease" [3, 41]. Despite theorization that this process may pose a risk for subsequent carcinoma [42, 43], no link has been established. Following the diagnostic excision, clinical follow-up is all that is required.

Carcinoma

Primary breast cancer is extremely rare in children and adolescents. The incidence of breast cancer is 1 in 1,000,000 in women younger than 20 years [5, 10]. Secretory carcinoma is the most common carcinoma to develop in these age groups; however, invasive mammary carcinomas of no special type (ductal) are also well documented in children and adolescents. All are considered to be extremely rare [1, 44–47]. Radiation therapy to the chest wall is a major risk factor. Furthermore, the risk of breast cancer has been reported to increase by 75-fold when a patient aged 10–16 years is treated with radiotherapy for Hodgkin's disease [6, 7]. Risk factors for breast cancer include gene mutations such as *BRCA1* or *BRCA2* [5, 6, 8].

The histologic features of invasive carcinomas and DCIS are identical to their adult counterparts and should be

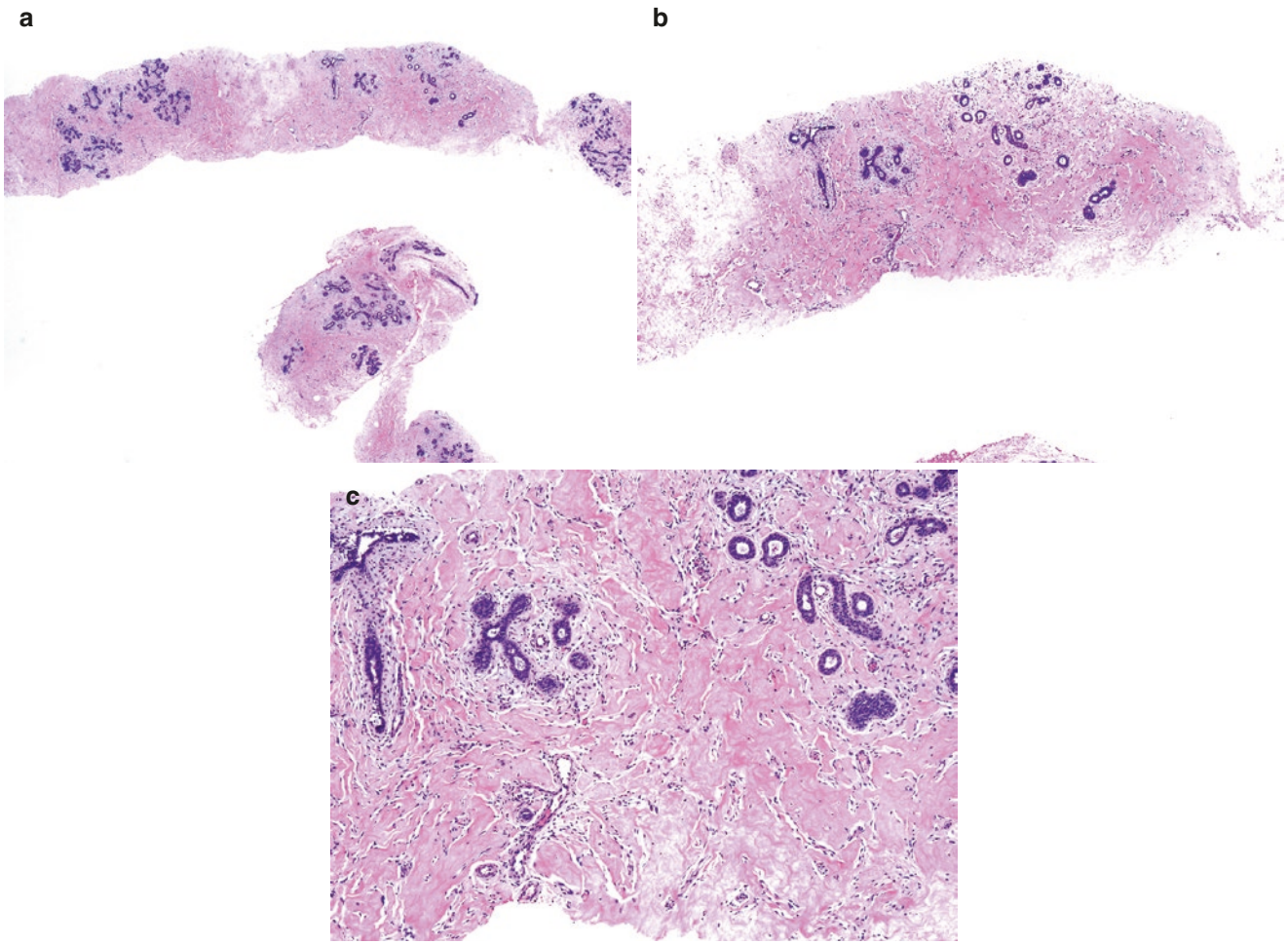

Fig. 18.10 (**a**) At low power, PASH is characterized by replacement of the interlobular stroma by dense fibrosis and associated epithelial atrophy yet with relative maintenance of the underlying terminal duct lobular unit architecture. (**b**) The fibrosis results from proliferation of myofibroblasts, which form slit-shaped, pseudovascular spaces within a dense keloid-like stroma. (**c**) The spindle-shaped myofibroblasts resemble endothelial cells but lack the expression of specific endothelial markers. In long-standing cases, the fibrosis may also replace the specialized connective tissue of the lobular units

graded, typed, and staged according to the Modified Nottingham Grading System and the American Joint Committee on Cancer guidelines, respectively [48]. Rare cases of DCIS in children present as a palpable mass or nodule and are low to intermediate grade with cribriform architecture (Fig. 18.12a–c). Reported cases of invasive carcinoma are of low and rarely intermediate combined histologic grade. The routine immunohistochemical hormone receptor studies and evaluation for HER2 overexpression/amplification performed on breast cancers in adult women should be performed on all pediatric invasive breast cancers as they similarly inform treatment strategy. Invasive carcinoma of no special type and DCIS in children or adolescents are presently managed the same as in adults. In females, breast conservation is the surgical procedure of choice for both invasive carcinoma and DCIS when anatomically feasible, while in males, total mastectomy is the usual definitive surgery. Sentinel lymph node biopsy (SLNB) is used to evaluate the axilla in adolescents with invasive carcinoma.

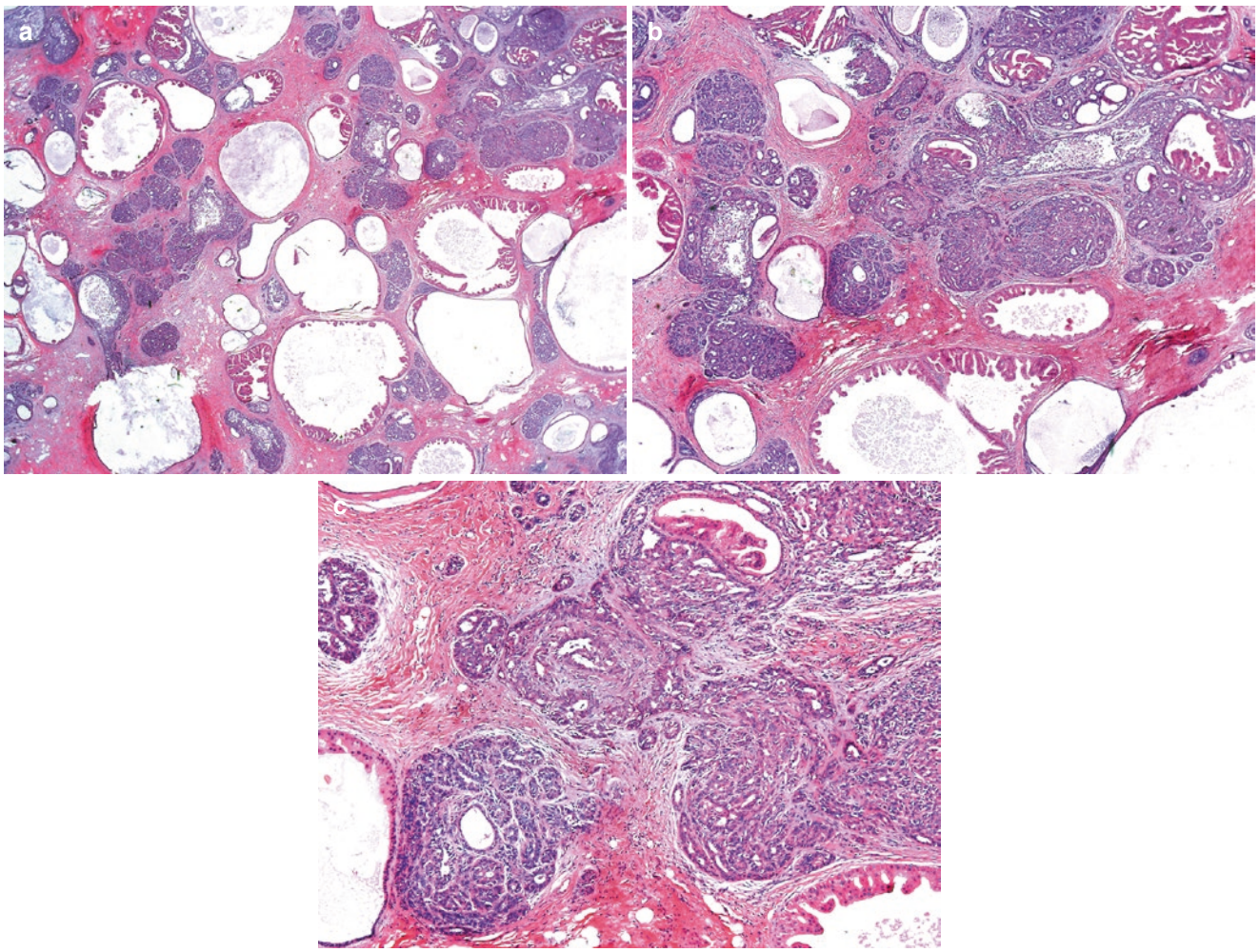

Fig. 18.11 (**a**) The numerous apocrine cysts and dense fibrocystic changes characteristic of juvenile papillomatosis are evident at low power. (**b**) Cysts with papillary apocrine change coalesce with micropapillomas, sclerosing adenosis, and usual ductal hyperplasia within a dense fibrous stroma to form a clinically evident mass. (**c**) Sclerosed micropapillomas and foci of sclerosing adenosis are abundant, while formal patterns of atypical hyperplasia are absent

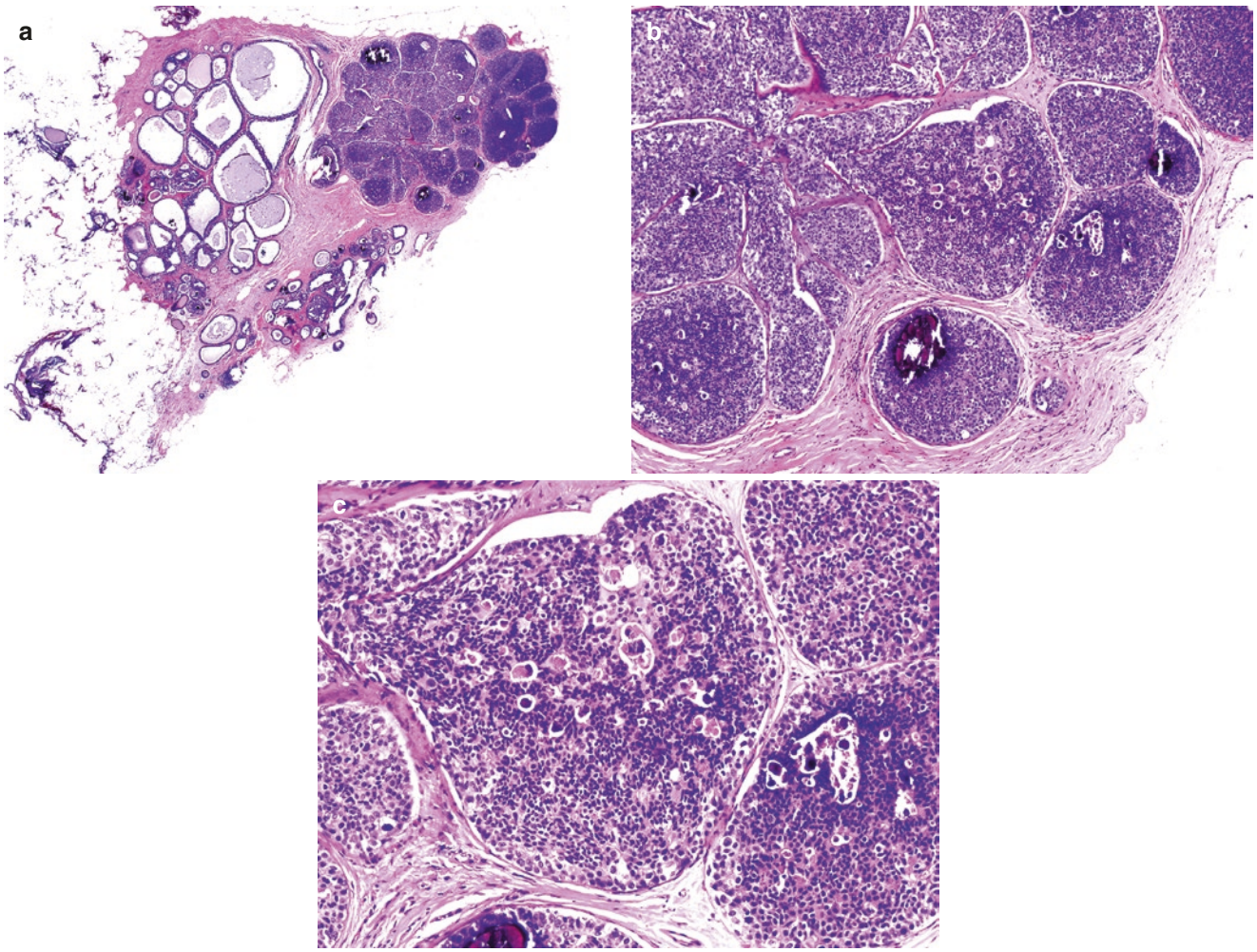

Fig. 18.12 (**a**) DCIS presenting as a palpable nodule in a 6-year-old girl. (**b**) Multiple distended epithelial spaces are replaced by intermediate-grade ductal carcinoma cells. (**c**) A subtle cribriform and rosette-like pattern is formed by the DCIS cells

Secretory Carcinoma

Overview

Secretory carcinoma is the most common carcinoma in children and occurs equally among males and females. Secretory carcinoma was originally termed juvenile carcinoma [49] because cases were identified in children; however, it is now recognized that less than half of all cases present in patients less than 20 years [50]. Secretory carcinoma usually presents as an asymptomatic firm subareolar mass in prepubertal males and females and is frequently associated with nipple discharge. They are firm, painless, well-circumscribed, mobile lesions which are distinct from the nipple.

Gross and Radiologic Features

Tumors range from 1.0 to 5.0 cm in diameter and have a gray-white firm cut surface, which may grossly mimic the appearance of fibroadenomas. Ultrasound is the initial imaging study, and mammography is reserved for selected cases in older adolescents [5]. In younger children, the high ratio of fibroglandular to fatty tissue makes mass detection difficult and exposes these children to radiation. Computed tomography is similarly avoided because of the risks of ionizing radiation in this population. Magnetic resonance imaging may be of value for children with masses involving deeper structures such as the chest wall [5]. Additionally, surgical intervention places immature breasts at risk for abnormal development. Given the extremely low prevalence of malignant breast tumors in the pediatric and adolescent populations, a conservative clinical, radiologic, and pathologic approach is recommended to avoid iatrogenic complications of overtreatment [31].

Microscopic Features

Microscopically, secretory carcinoma has a characteristic appearance consisting of one or several tumor islands and serpentine chords separated by prominent bands of densely

sclerotic collagen (Fig. 18.13a). The islands of tumor cells contain haphazardly arranged nuclei and numerous round-to-ovoid spaces containing abundant eosinophilic secretions, which impart an overall microcystic appearance (Fig. 18.13b, c). Although infrequently described in the literature, limited foci of in situ carcinoma may be present [51] (Fig. 18.13c). Most tumors are of low or occasionally intermediate Modified Nottingham grade. In some cases, the tumor islands are broad with solid areas (Fig. 18.14a). However, a pushing border, relative circumscription, and collagenous stroma are important clues to the diagnosis at low power. Some examples may be more cellular with moderately pleomorphic nuclei; however, the characteristic microcytic pattern assures the diagnosis in the pediatric/adolescent population (Fig. 18.14b). Solid, tubular, and papillary patterns have also been described [52, 53]. Individual tumor cells show mild-to-moderate cytologic atypia. The cytoplasm may be finely granular or clear as a result of vacuolization.

Immunohistochemistry and Molecular Characterization

Immunohistochemical stains which may facilitate confirmation of secretory carcinoma are epithelial membrane antigen (EMA) and S100 protein, which are strongly positive. These tumors are variably positive for basal markers with 80% demonstrating expression of CK5/6 and 40% EGFR expression [54]. In addition, secretory carcinomas are invariably negative for ER, PR, and HER2. The intra- and intercellular secretions are positive for Alcian blue and periodic acid-Schiff (diastase resistant) [55].

Secretory carcinoma has also been shown to have a recurrent translocation, t(12;15)(p12;q26.1), which was initially reported in congenital fibrosarcoma/mesoblastic nephroma

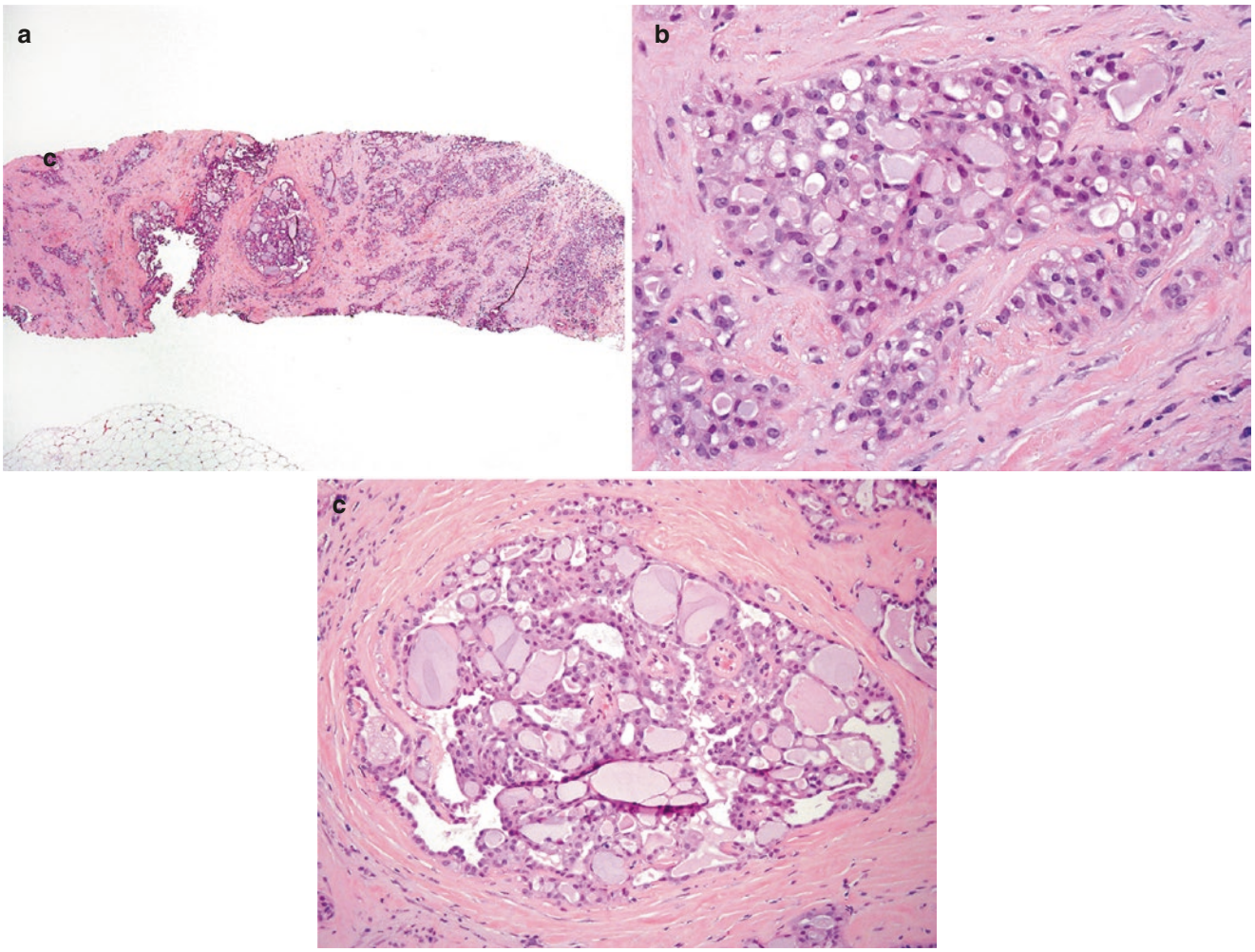

Fig. 18.13 (**a**) Secretory carcinoma is characterized by tumor islands and serpentine tumor chords separated by prominent bands of densely sclerotic collagen in this core needle biopsy from a 13-year-old girl. (**b**) The apocrine tumor cells form microcystic spaces containing abundant secretions. (**c**) Although infrequently described in the literature, limited foci of in situ carcinoma may be associated with the tumor

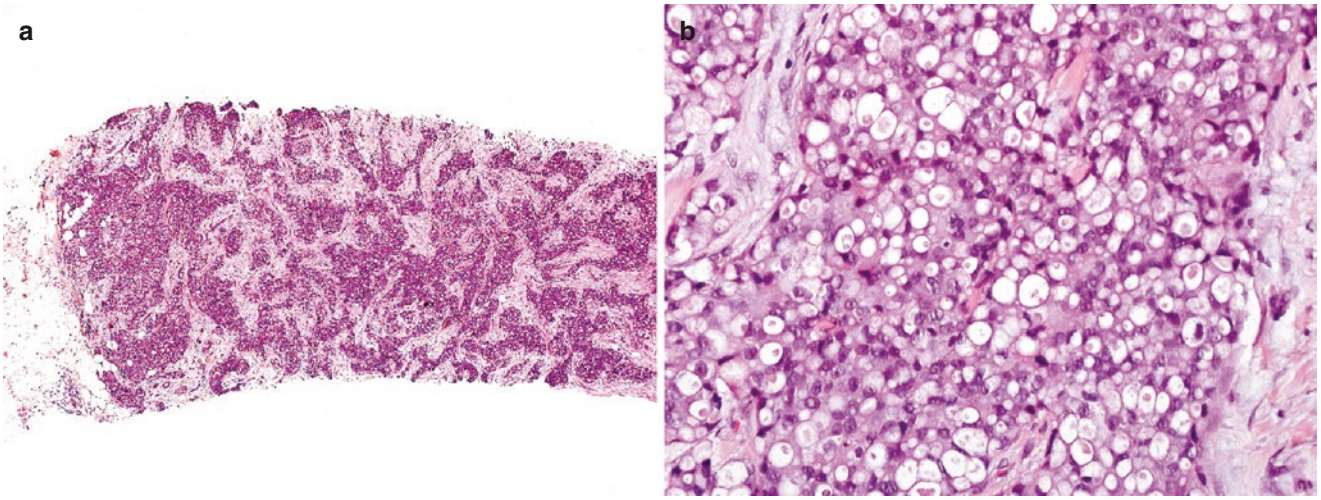

Fig. 18.14 (**a**) In this example of secretory carcinoma, the tumor islands are broad with solid areas. A pushing border, relative circumscription, and collagenous stroma are important clues to the diagnosis at low power. (**b**) This case is more cellular with moderately pleomorphic nuclei; however, the characteristic microcytic pattern assures the diagnosis

[56–60]. The resulting ETV6-NTRK3 fusion gene encodes a chimeric tyrosine kinase oncoprotein [61, 62]. Routine testing for the translocation is unnecessary in straightforward cases as there are no known treatments directed at the alteration.

As a rule of thumb, a diagnosis of breast carcinoma other than secretory carcinoma in young patients should call into question the possibility of a BRCA1/2 or p53 mutation; thus, genetic testing should be recommended for all pediatric patients [63–67].

Treatment and Prognosis

Secretory carcinoma is treated by surgical excision to negative margins and sentinel lymph node mapping [68]. Care to remove a limited amount of normal adjacent breast tissue is prudent to avoid deformity and abnormal breast development. In children, these tumors have indolent behavior and an excellent prognosis, even with axillary nodal involvement [3, 69–72]. Axillary metastasis to lymph nodes is found in 15–30% of cases when all ages are considered but is rare in children and adolescents [73–75]. Usually, a single node is involved which has no effect on the usually excellent prognosis in this age group [54]. Rare reports of late local recurrence have been recorded, and mortality due to metastatic secretory carcinoma is extremely rare [76]. Evidence of efficacy of postoperative radiation therapy and/or chemotherapy for secretory carcinoma is lacking, and thus it is not routinely used [77–79].

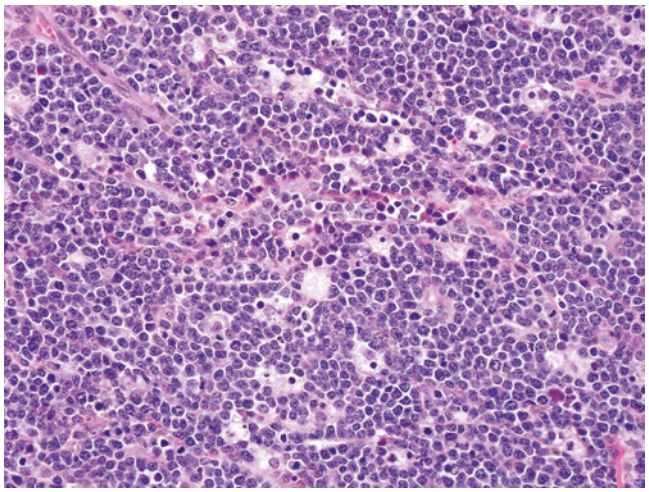

Fig. 18.15 Burkitt's lymphoma characterized by a "starry sky" pattern of immunoblasts and reactive histiocytes

Other Malignant Tumors

Although rare, other malignancies are seen in the breast of children and adolescents including tumors of hematologic or soft tissue origin and metastatic disease. Primary lymphoma of the breast is rare in children [80, 81]. Intermediate- and high-grade non-Hodgkin's B-cell lymphomas [82], especially Burkitt's lymphoma [83, 84] (Fig. 18.15), are the most common hematopoietic neoplasms with mammary

involvement in the pediatric and adolescent populations. Burkitt's lymphoma has a predilection for breast involvement of young pregnant or lactating women [85, 86]. Primary mammary Hodgkin's disease has also been reported [87] (Fig. 18.16a, b). Rarely, the breast may be the site of initial presentation of acute myelogenous leukemia but is more commonly seen in the setting of relapse (Fig. 18.17a, b).

A variety of pediatric malignancies may metastasize to the breast. Of these, alveolar rhabdomyosarcoma is the most common usually presenting as a rapidly growing mobile mass with no skin involvement [88]. Approximately 7% of all rhabdomyosarcomas are associated with breast metastases (Fig. 18.18a–c) at some point during the patient's course [89], which can manifest as a single tumor, multiple tumors in the same breast, or a bilateral disease. Strong expression of myogenin, MyoD1, and desmin and lack of expression of cytokeratin are characteristics of this small round blue cell tumor (Fig. 18.18d–f). Other reported metastases include neuroblastoma, medullary carcinoma of the thyroid, medulloblastoma, primitive neuroectodermal tumor-Ewing sarcoma, and malignant melanoma.

Primary soft-tissue sarcomas are extremely rare in the breast of children and adolescents [90–94]. Angiosarcoma [94, 95], fibrosarcoma, and rhabdomyosarcoma are among those reported.

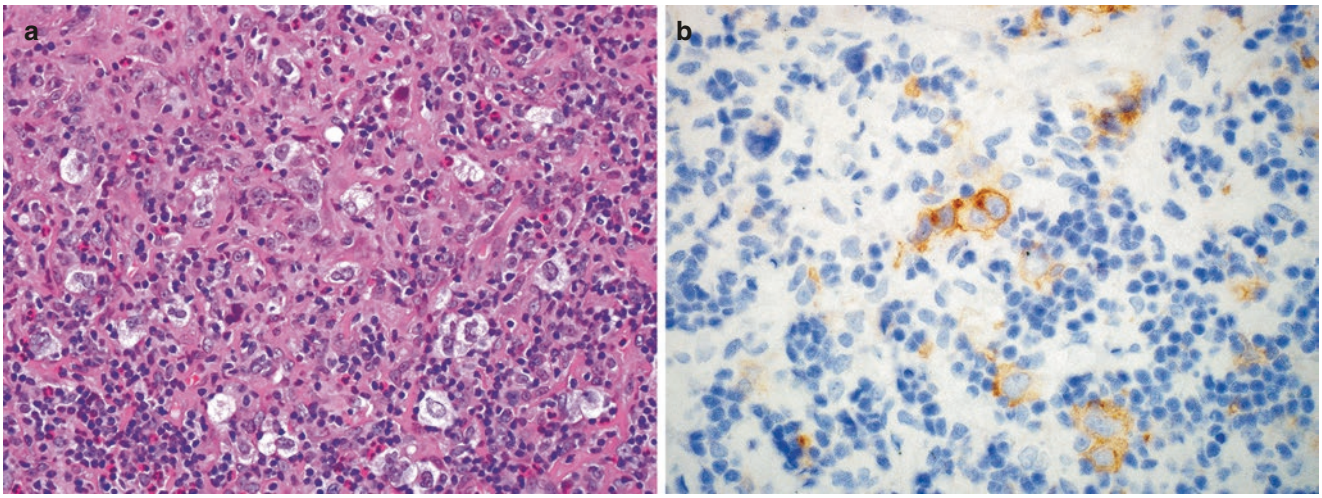

Fig. 18.16 (**a**) Example in an adolescent female characterized by classic Reed-Sternberg cells in a background of mononuclear and eosinophilic inflammation and sclerosis. (**b**) Immunohistochemistry for CD30 is a characteristic of Reed-Sternberg cells

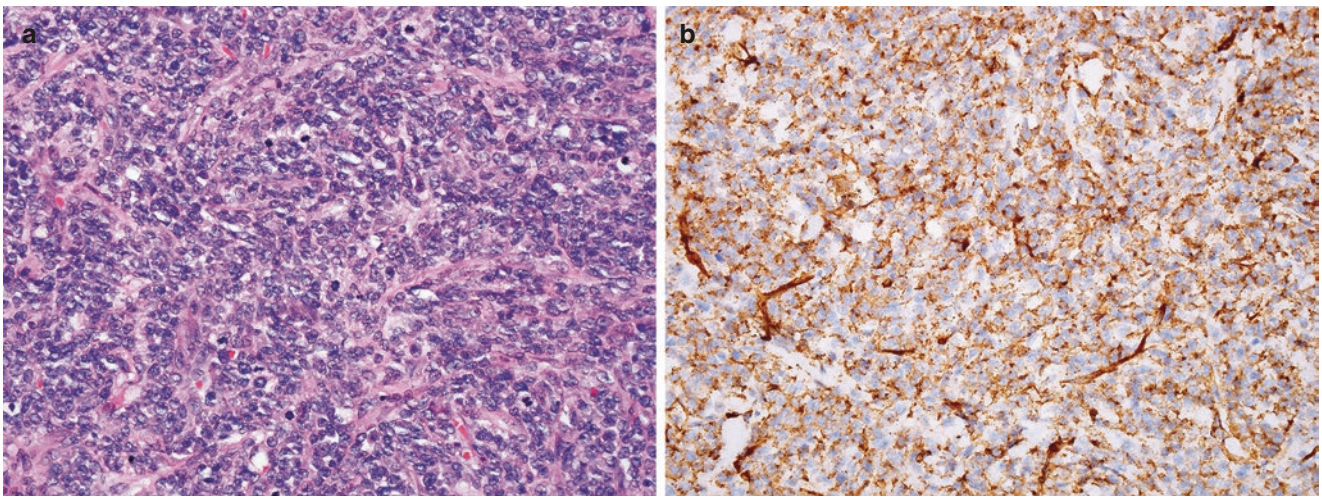

Fig. 18.17 (**a**) Patient with mammary involvement by acute myelogenous leukemia in relapse presenting as a granulocytic sarcoma. (**b**) Diffuse strong CD34 positivity is a characteristic of granulocytic sarcoma in this setting

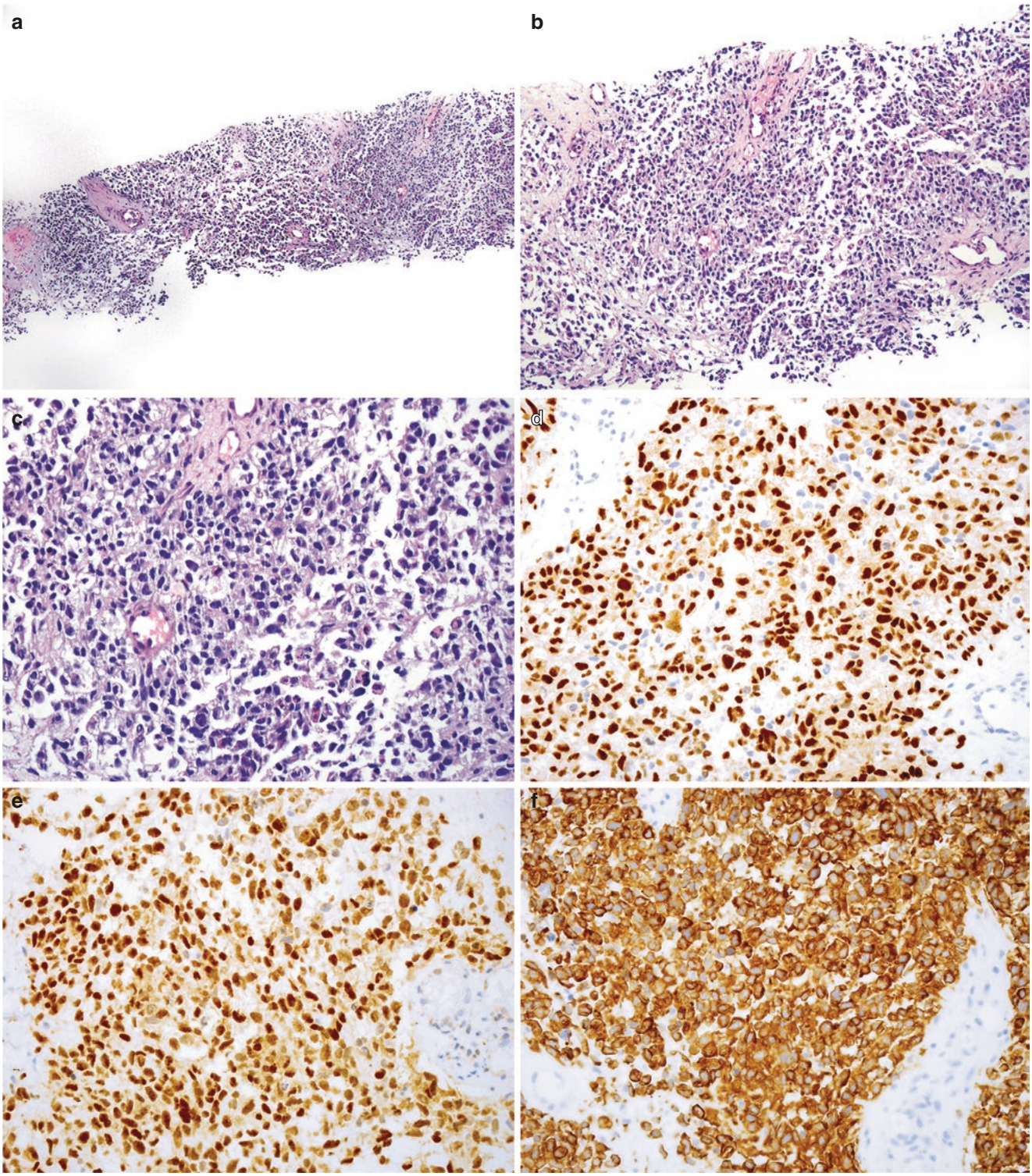

Fig. 18.18 (**a**) Metastatic alveolar rhabdomyosarcoma composed of poorly differentiated small round blue cells. (**b**) The neoplastic infiltrate has obliterated the normal mammary architecture. (**c**) The tumor cells are pleomorphic, hyperchromatic, and mitotically active. Strong positivity for (**d**) myogenin, (**e**) MyoD1, and (**f**) desmin is the classic immunohistochemical profile for alveolar rhabdomyosarcoma

Males Including Adolescents

Gynecomastia

Overview

Gynecomastia is the most common lesion of the male breast, caused by hormonal stimulation resulting in a proliferation of stromal and ductal components. Presenting as female-appearing breast development, gynecomastia is nonneoplastic and often reversible [96]. An excess, (either exogenous or endogenous) of estrogen is responsible for the changes. The three peaks in incidence are in neonates, adolescents, and elderly males. In most cases, the etiology is unknown, but may occasionally be related to endocrine disorders (congenital adrenal hyperplasia or Klinefelter's syndrome), drugs (digitalis, spironolactone, or antiandrogens used to treat prostate cancer), or topical agents (lavender and tea tree oils) [97]. Gynecomastia may be localized or generalized and can be unilateral or bilateral. Unilateral cases have a statistically nonsignificantly higher prevalence of pathology [98]. Gynecomastia alone is not a risk factor for subsequent carcinoma.

Gross and Radiologic Features

Mammographically, gynecomastia appears as a diffuse increase in fibroglandular density. Microcalcifications are occasionally identified. Ultrasound can also be used to rule out malignancy. In the absence of suspicious abnormality, routine imaging of gynecomastia is discouraged as the probability of finding cancer is negligible [99]. The gross appearance of breast tissue with gynecomastia is nonspecific, typically appearing as a gray-white fibrous tissue admixed with fat without an identifiable mass lesion.

Microscopic Features (Including ADH and DCIS Arising in Gynecomastia)

Gynecomastia has different stages of development, and the subsequent histologic findings change with the duration of the condition. In all stages, the number of ducts is increased. In the early and intermediate phases, the periductal stroma is cellular with an admixture of fibroblasts, myofibroblasts, lymphocytes, and plasma cells. Sometimes, the stroma is myxoid (Fig. 18.19). The luminal epithelium has a characteristic pattern of hyperplasia featuring tapered, pyknotic, and "pinched-appearing" tufts (Fig. 18.20b). These projections seem stuck to the luminal surface, which is often composed of several layers of epithelium, rather than attached to the basement membrane as in micropapillary ADH and DCIS. In the inactive fibrous phase, the ducts are lined by a single layer of atrophic luminal epithelial cells and there is progressive periductal fibrosis and stromal hyalinization. The stroma may show pseudoangiomatous stromal hyperplasia in any phase (Fig. 18.20).

The epithelial hyperplasia seen in gynecomastia may occasionally meet both cytologic and architectural features for ADH. Because the male breast is composed of ducts only, strict criteria for ADH cannot be applied but must be adapted to include an incompletely developed process partially occupying the involved spaces and limited in extent (Fig. 18.21). The atypical proliferation is characterized by uniform cells that have small round nuclei, pale cytoplasm, and even cell placement typically forming a cribriform, solid, or mixed pattern (Fig. 18.21c). Normal epithelial and myoepithelial cells lining a portion of each duct remain. Peripheral irregular, slit-like spaces heralding an admixture of the process with usual hyperplasia are characteristic. Given the rarity of this diagnosis, the subsequent breast cancer risk associated

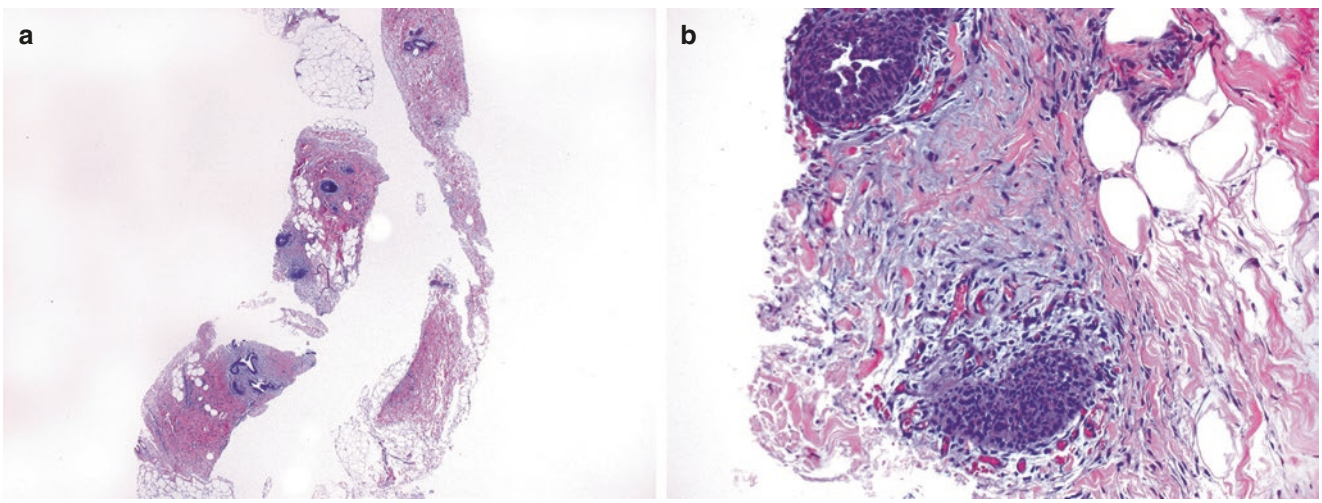

Fig. 18.19 (**a**) CNB performed to evaluate a distinct, tender 1.5 cm mass in a 54-year-old male with intermediate-phase gynecomastia revealed epithelial hyperplasia and periductal myxoid stroma. (**b**) The hyperplastic epithelium shows cellular variability, overlapping nuclei, and characteristic "pinched-appearing" tufts

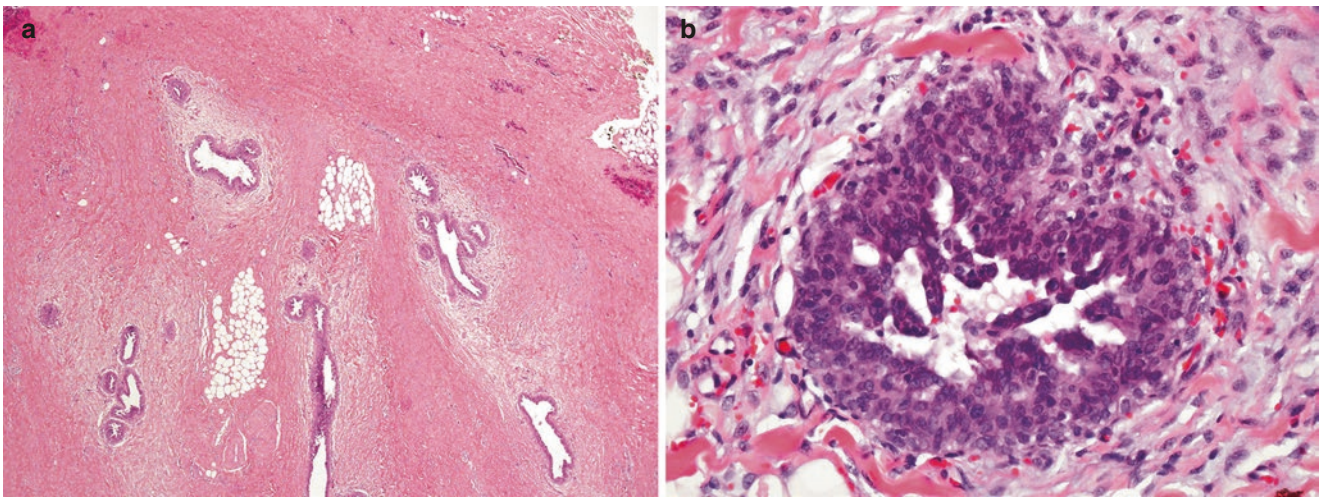

Fig. 18.20 (**a**) Florid-phase gynecomastia with increased number of ductal structures, florid hyperplasia, and extensive pseudoangiomatous stromal hyperplasia. (**b**) The variably hyperplastic ductal epithelium is characterized by tapered, pyknotic, and "pinched-appearing" tufts. These projections seem stuck to the luminal surface, which is often composed of several layers of epithelium, rather than attached to the basement membrane as in micropapillary ADH and DCIS. The surrounding stroma shows well-developed PASH

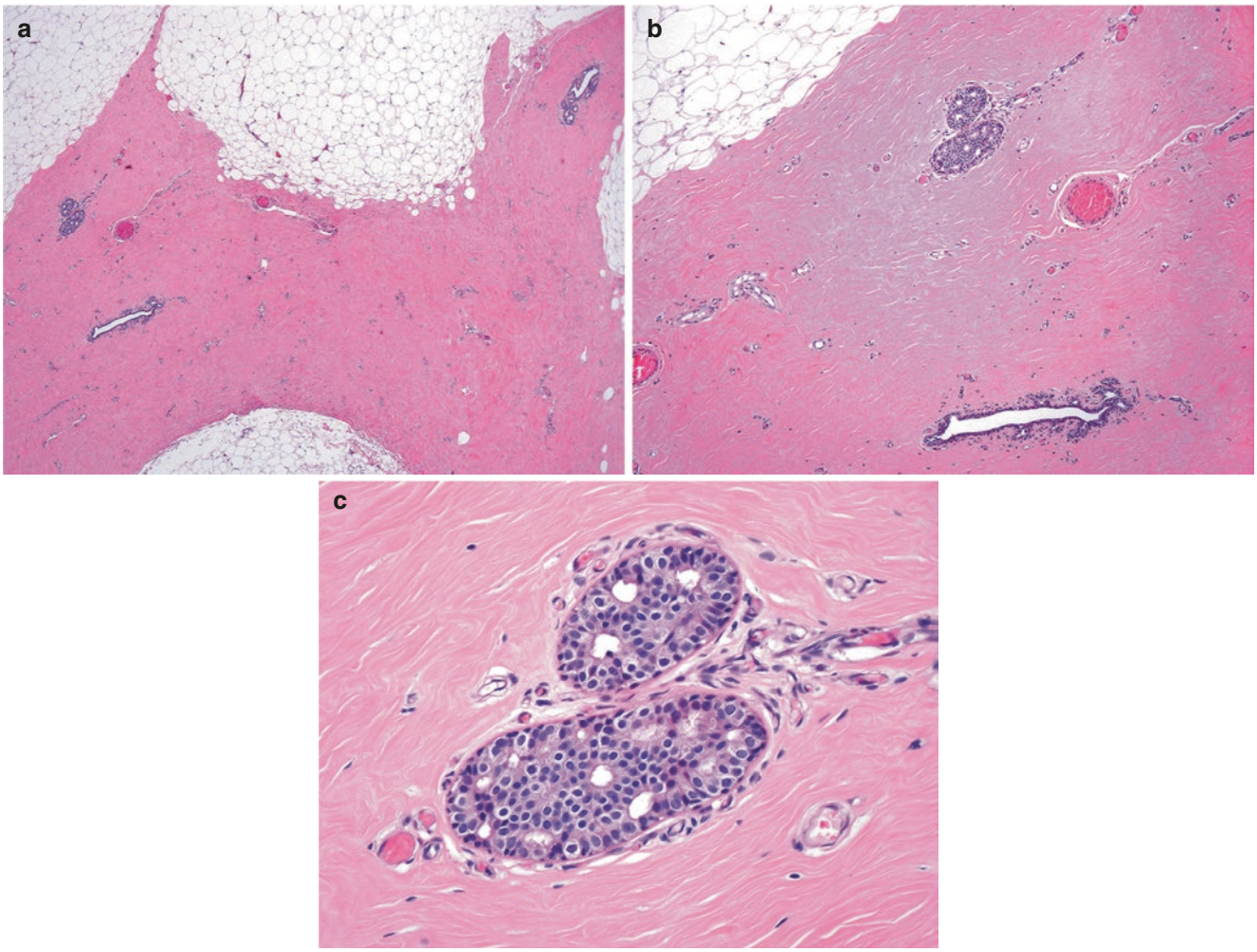

Fig. 18.21 (**a**) ADH in a 17-year-old obese adolescent with long-standing gynecomastia shows occasional ducts with hyperplastic epithelium and surrounding densely fibrotic stroma. (**b**) The process appears limited in extent but distinctive on low power. (**c**) On high power, the uniform cells that have small round nuclei, pale cytoplasm, and even cell placement typically form a cribriform pattern

with a diagnosis of ADH in the male breast is unknown. The threshold for diagnosing ADH in the setting of gynecomastia should be high as ADH is treated by mastectomy in males. Gynecomastia alone has not been shown to be a risk factor for subsequent carcinoma.

The extent of the atypical epithelial proliferation seen in gynecomastia may occasionally be extensive enough to warrant a diagnosis of DCIS. The diagnosis should be reserved for cases in which the atypical intraductal process is well developed and extensive (Fig. 18.22). These cases are almost exclusively low grade. In borderline cases, especially in a CNB, a diagnosis of well-developed ADH is preferable with a note in the report that the lesion will be best categorized at the time of mastectomy. DCIS has been reported in four adolescent males, all of whom had gynecomastia [100–103]. One of these cases was bilateral [102], occurring in a morbidly obese, pubertal 15-year-old. These adolescents presented with palpable nodules or were asymptomatic and had undergone surgery for psychosocial reasons [102]. All cases were low grade, showing a combination of cribriform, solid, and micropapillary patterns [100–103].

Immunohistochemistry

Immunohistochemistry is not useful in making the diagnosis of gynecomastia. Loss of CK5/6 expression in ADH or low-grade DCIS may facilitate confirmation of the H&E diagnosis but should not be the sole basis on which the diagnosis is made.

Treatment and Prognosis

Idiopathic adolescent gynecomastia does not require treatment, and most examples regress [97]. The subset of patients with persistence of the condition may seek surgical removal of the breast for psychosocial reasons. Older males who desire treatment are typically offered mastectomy. In male adolescents and older men, both ADH and DCIS are treated by complete mastectomy. SLNB is reserved for high-grade histology or coexistent invasive carcinoma.

Ductal Carcinoma In Situ (DCIS)

Overview

DCIS of the male breast is uncommon, representing approximately 7–10% of all male breast cancers [104]. DCIS in men occurs later than in women, with the peak in the sixth decade. DCIS of the male breast usually involves a solitary intraductal papilloma in a retroareolar or central location and is frequently palpable and accompanied by bloody nipple discharge [105].

Gross and Radiologic Features

On ultrasound, these papillary lesions appear as a complex cystic mass with hypoechoic areas representing fluid and a hyperechoic mass projecting from the wall [106]. DCIS may be associated with microcalcifications.

Microscopic Features

The most common presentation of DCIS in the male breast is DCIS involving or near-totally replacing a solitary intraductal papilloma (encapsulated, noninvasive papillary carcinoma). Features of encapsulated papillary carcinoma in the male breast are indistinguishable from those seen in the female breast. These lesions are most commonly of low or intermediate grade; however, any architectural pattern may be seen (Fig. 18.23), most commonly cribriform and solid. In

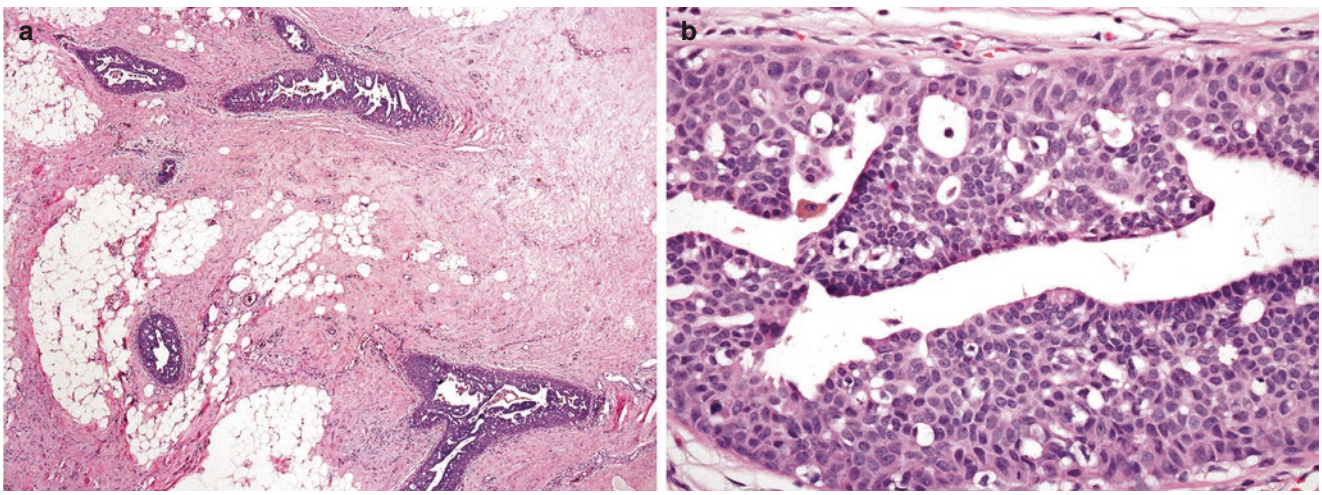

Fig. 18.22 (**a**) An extensive proliferation of atypical cells with intermediate-grade nuclei completely replaces the ducts in this example of DCIS in an adult male with a long-standing history of gynecomastia. Note the densely fibrotic surrounding stroma. (**b**) Higher power examination reveals moderate pleomorphism and evenly placed cells

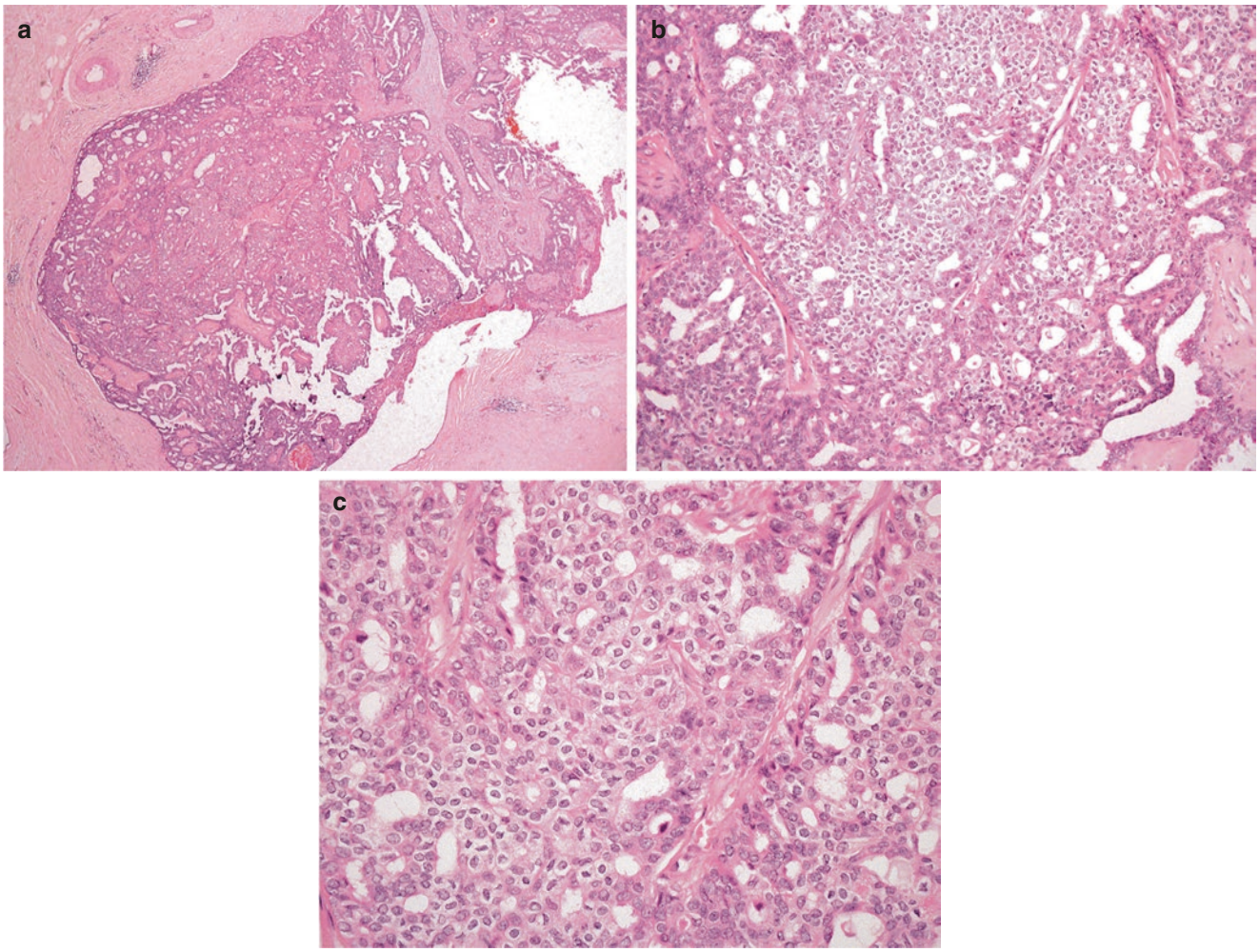

Fig. 18.23 (**a**) The papillary lesion is composed of a monotonous cell population, which near-totally replaces the normal papillary architecture. (**b**) The neoplastic population forms numerous cribriform spaces and solid areas diagnostic of low-grade DCIS. (**c**) The nonoverlapping tumor cells have discrete cell membranes and appear frozen in time

cases with a solid pattern, a densely fibrotic surrounding duct wall and fibrovascular cores are features critical to avoiding overdiagnosis of a solid-pattern invasive carcinoma (Fig. 18.24). DCIS in the absence of a papillary lesion is rare, and reported patients have long-standing gynecomastia (Fig. 18.22). High-grade DCIS is uncommon in the absence of an invasive carcinoma. Comedo necrosis is relatively uncommon. Paget's disease can present as a pigmented lesion and should be differentiated from melanoma.

Differential Diagnosis

The differential diagnosis for DCIS in adult males is an intraductal papilloma with florid hyperplasia or florid-phase gynecomastia. The florid hyperplasia in papillomas in men shows the same diagnostic features as in women: a proliferation characterized by cellular variability, uneven cell placement, and peripheral, slit-like secondary spaces. In contrast to the bulbous micropapillae of micropapillary DCIS, the hyperplastic epithelium in gynecomastia shows multiple tapering tufts projecting into the lumen (Fig. 18.20b). The tapered papillae appear tethered to the surface epithelium rather than anchored to the basement membrane. The epithelium shows irregular cell placement, cell swirling, and nuclear variability including larger nuclei near the basement membrane and small, pyknotic nuclei in the papillae. The surrounding stroma also shows stromal hyalinization with areas of pseudoangiomatous stromal hyperplasia (PASH).

Immunohistochemistry

All DCIS in men should be tested for ER and PR; the results inform treatment strategy as in women. Caution should be exercised in using immunohistochemistry to evaluate the presence of invasion. In the setting of DCIS involving an intraductal papilloma, a diagnosis of invasive carcinoma should be made when there is an unequivocal focus of invasion beyond the encysting fibrous tissue of the papilloma

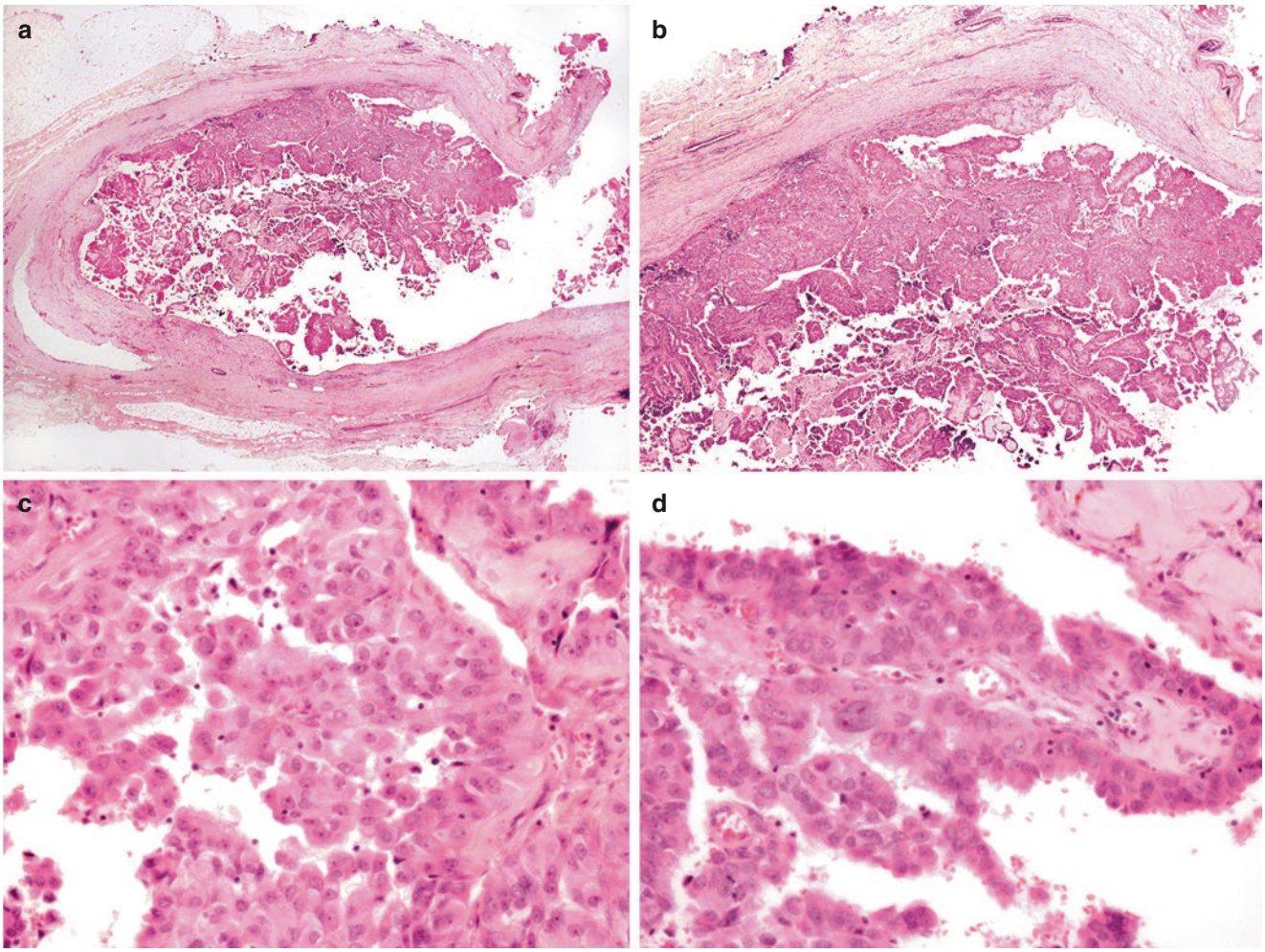

Fig. 18.24 (**a**) This high-grade DCIS involving an intraductal papilloma is surrounded by a dense fibrotic wall. (**b**) The encysting fibrous tissue delimits the friable papillary lesion from the surrounding mammary parenchyma. (**c**) The neoplastic cells have a dominantly solid pattern, which replaces the papillary architecture. (**d**) The residual fibrovascular cores are lined entirely by DCIS. Scattered mitotic figures are evident

similar to what is seen in the female breast. Absence of myoepithelial markers does not equate to the presence of invasion.

Treatment and Prognosis

Similar to the female breast, DCIS should be staged as pT0 per AJCC guidelines [48]. The preferred treatment for pure DCIS is mastectomy without axillary dissection. Similar to women, DCIS in the male breast has an excellent prognosis.

Invasive Carcinoma

Overview

In the United States, breast cancer is an uncommon malignancy in men, representing 0.5–1% of all breast cancers and less than 0.1% of all cancer deaths in men annually [107]. Men are 5–10 years older on average than women diagnosed with breast cancer. Incidence rates rise steadily with age with a unimodal distribution (single peak at around 75 years) [107]. This contrasts with the bimodal distribution of breast cancer in women (early onset and late). Approximately 2000 men are diagnosed with breast cancer annually, and the incidence appears to be slowly rising [108–112] by 1.1% annually [110, 113].

Similar genetic, hormonal, and environmental risk factors have been shown to play a role in both male and female breast cancer. Men with a first-degree relative with breast cancer have a 2.0X increased relative risk, which becomes more than 5X increased with the number of affected relatives with early onset of disease [114]. Studies indicate that up to 10% of all male breast cancers result from inherited germline mutations in well-known breast cancer susceptibility genes [115, 116]. Mutations in the BRCA2 gene are estimated to

account for 60–76% of male breast cancers occurring in high-risk breast cancer families, whereas BRCA1 mutation frequency ranges from 10% to 16% [117, 118]. Approximately 5–10% of men with BRCA2 mutations develop breast cancer (approximately 100-fold higher risk than in the general male population) [115, 116], and 4–14% of men with breast cancer in the United States or the UK are found to have deleterious BRCA2 mutations [119–121]. Male breast cancer has also been associated with alterations in PTEN [122], p53 [123], and CHEK2 [124]. p53 mutation rates in men are similar to those seen in women [123, 125].

Men with conditions associated with low levels of androgens are at higher risk of developing breast cancer, including hypogonadism from a variety of causes including Klinefelter's syndrome, orchitis, cryptorchidism, and testicular injury [126]. Other risk factors resulting in relative estrogen excess include exogenous estrogen or testosterone use [127], obesity [126, 128], finasteride therapy [129], and liver disease [130]. An association with prior chest wall radiation for treatment of gynecomastia and thymic enlargement has been reported [131]. The presence of gynecomastia has not been shown to increase risk [132].

Invasive carcinoma typically occurs in older men (median age 67 years) [133], which is slightly older than the average at diagnosis in women (61 years). Seventy-five to 95% of men present with a self-detected, painless subareolar mass that may involve the nipple, unlike the upper outer quadrant presentation that frequently characterizes breast cancer in women. Unlike gynecomastia, carcinoma tends to be located eccentrically in relation to the nipple. Clinically suspicious axillary lymph nodes are present in 40–55% of men at the time of diagnosis. Other common presenting symptoms include nipple discharge (10–51%), nipple ulceration (4–17%), nipple bleeding (2–9%), and local pain (4–20%) [132]. Rarely, male breast cancer presents with axillary adenopathy alone [134] or Paget's disease with ulceration of the nipple [135]. Paget's disease in men is nearly always associated with an underlying invasive cancer [136]. Less than 2% of male breast cancer is bilateral [137]. A recent review of 160 male breast cancer patients with distant metastases reported 10% of patients with metastasis at primary presentation and 25% at the time of recurrence [138]. The most common sites of distant metastasis were bone (14%), lung (13%), liver, and brain, similar to women.

Gross and Radiologic Features

The average tumor size at the time of diagnosis is 3.0 cm (range < 0.5–12 cm), and the gross appearance is similar to that seen in females. Mammographically invasive male breast cancers appear as a distinct, spiculated mass, eccentric to nipple. Calcifications are identified in a majority of cases. On ultrasound, the mass is hypoechoic, typically taller than wide, with indistinct or irregular margins. The presence of gynecomastia may obscure the presence of tumor, delaying diagnosis [139]. Ultrasound examination can also be used to aid in the differential diagnosis of benign cyst and, to a limited extent, fat necrosis.

Microscopic Features

Invasive carcinomas of the male breast are most commonly of no special type [140], similar to women, but are more likely to express ER and PR [141]. Male breast cancers should be graded, typed, and staged according to the Modified Nottingham Grading System and the American Joint Committee on Cancer guidelines, respectively [48]. The majority are intermediate and high combined histologic grade tumors (Figs. 18.25 and 18.26). Low combined histologic grade tumors are few. However, special types of invasive carcinoma, including secretory [142, 143] and mucinous carcinoma [144], have been described in men. Invasive lobular carcinoma and lobular carcinoma in situ are extremely rare, appearing only in case reports [145–147], with invasive lobular carcinoma representing far less than 1% of all male breast cancers compared to over 10% in females [133]. Extremely rare cases of inflammatory breast carcinoma have been reported in men [148]. As in women, invasive carcinoma in men is frequently associated with DCIS.

Studies of histologic correlates of the BRCA phenotypes found the majority of BRCA1-related male breast cancers to be hormone receptor-negative, HER2-negative, high-grade tumors with a high proliferative rate, a phenotype similar to that observed in women. On the other hand, BRCA2-associated male breast cancers display a characteristic phenotype not identified in women [149]. BRCA2-associated male breast cancers present with high tumor grade and lack progesterone receptor (PR) expression or HER2 [150] overexpression.

Differential Diagnosis

Clinically, the differential diagnosis for invasive carcinoma in men includes gynecomastia, lipoma, leiomyoma, myofibroblastoma, fat necrosis, epidermal inclusion cyst, skin adnexal lesions, and intraductal papillary and stromal lesions. A combination of radiologic findings and CNB histology usually confirm the diagnosis preoperatively.

Immunohistochemistry (Biomarkers)

The routine immunohistochemical hormone receptor studies and evaluation of HER2 overexpression/amplification using a combination of immunohistochemistry and fluorescence in situ hybridization (FISH) performed on breast cancers in women should be performed on all male breast cancers as they similarly inform treatment strategy. In general, male breast cancer resembles postmenopausal female breast cancer, and male breast cancer treatment follows the same approach as for postmenopausal female breast cancers.

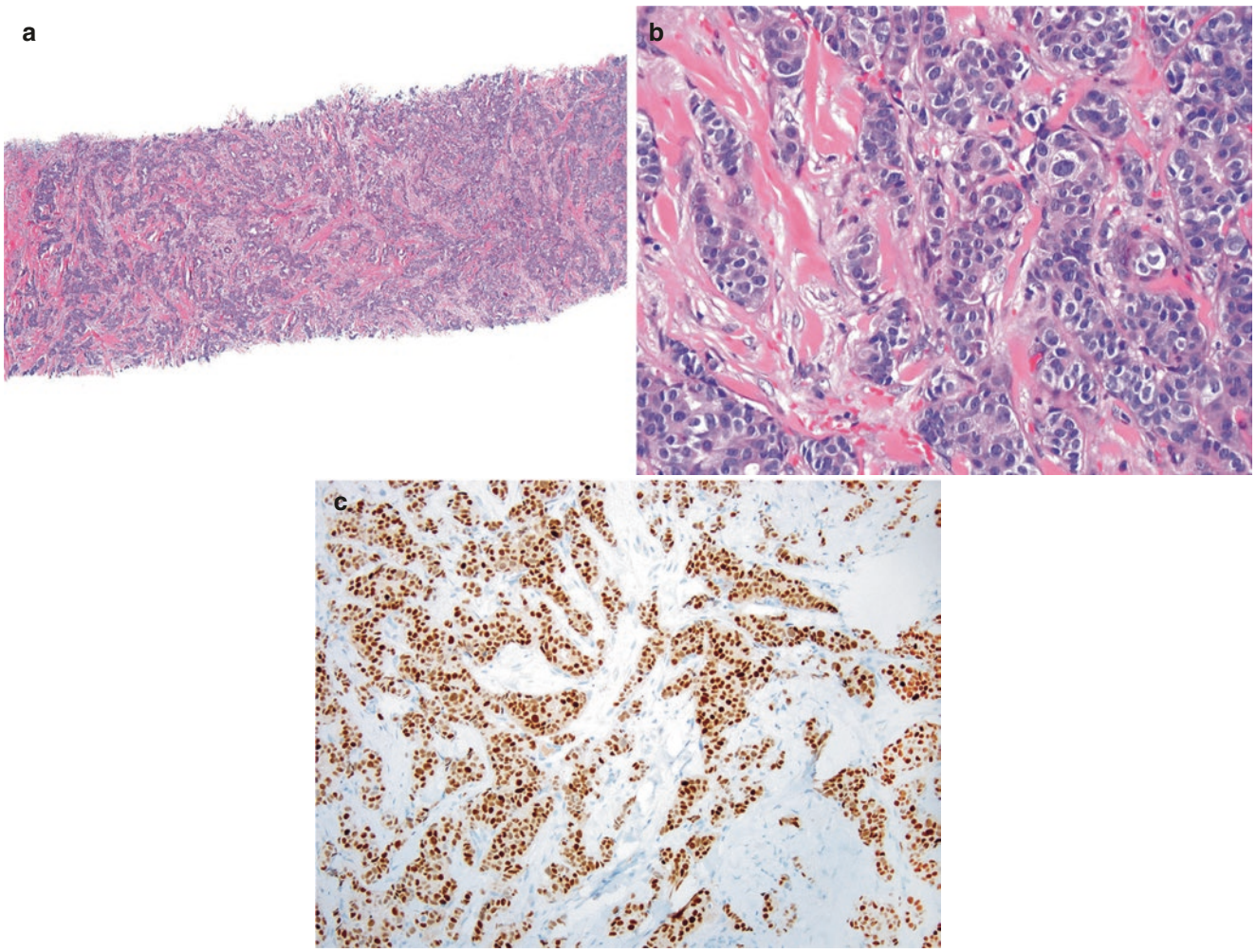

Fig. 18.25 (**a**) The infiltrative pattern of this mammary carcinoma in the breast of this adult male is histologically indistinguishable from similar lesions in the female breast. (**b**) Cords and nests of moderately pleomorphic tumor cells with occasional mitoses and lack of gland formation characterize this intermediate combined histologic grade carcinoma. (**c**) Strong expression for estrogen receptor is typical of male breast carcinomas irrespective of grade

Up to 80% of male breast cancers express ER and PR compared to 70% of female breast cancers [133, 151]. However, their expression does not appear to show the same strong association with grade and survival that are seen in female breast cancers [151].

Analysis of HER2 overexpression has been performed in male breast cancer, and rates of overexpression/amplification are similar [152–155] or lower (2–15%) [130] than those seen in female breast cancer. Although experience is limited, it appears that HER2 overexpression/amplification heralds the potential for an aggressive clinical course but also has an excellent response to trastuzumab in approximately half of the patients.

Neuroendocrine differentiation as evidenced by cytologic characteristics on H&E and by immunohistochemistry is not uncommon but is not found to have prognostic significance. Androgen receptor expression is extremely common in male breast cancers and has been reported in up to 90% of cases [156]. Androgen receptor expression correlates with survival in some but not all studies [155, 157].

Treatment and Prognosis

Compared with female tumors, male breast cancers are more likely to involve lymph nodes and invade the chest wall and are thus diagnosed at a more advanced stage and associated with a worse prognosis [158]. This is likely due to a combination of anatomic and socioeconomic factors. Due to the small volume of male breast tissue, rates of chest wall invasion and retroareolar infiltration are greater than those in women and may lead to more rapid access of tumor cells to

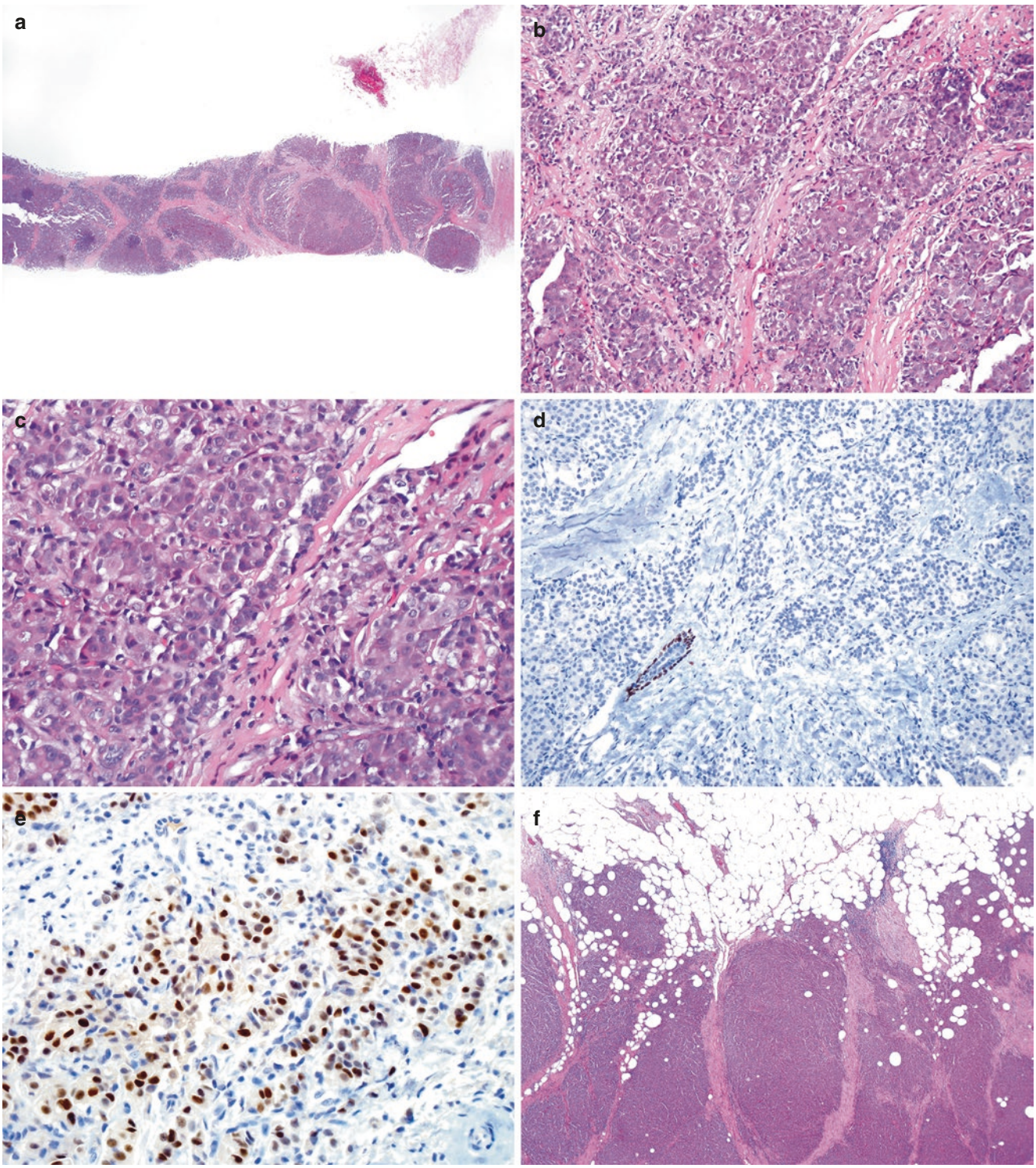

Fig. 18.26 (**a**) A high combined histologic grade invasive carcinoma in a male breast demonstrating a nodular pattern. (**b**) The tumor nests have subtly infiltrative borders. (**c**) On high power, pleomorphic tumor cells and mitotic activity are evident. (**d**) Loss of p63 expression supports the H&E interpretation of invasive carcinoma with residual staining of myoepithelial cells in a few benign ducts. (**e**) There is strong expression of estrogen receptor in tumor cells, a common feature of high-grade carcinomas in men. (**f**) The periphery of the lesion in the subsequent resection specimen showed numerous infiltrative nodules. (**g**) Tumor cells invade the surrounding adipose tissue

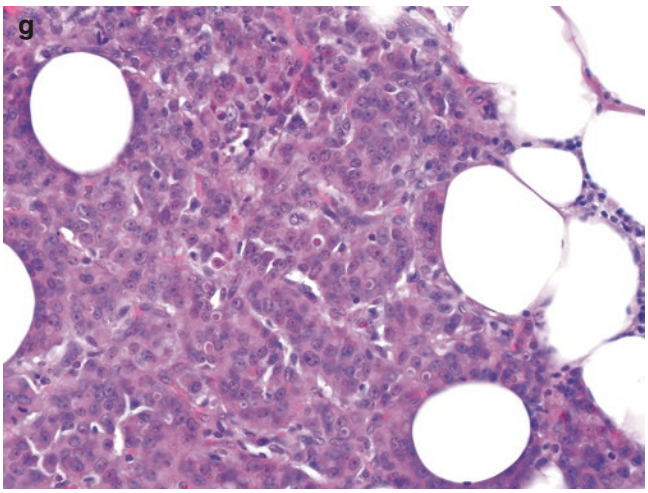

Fig. 18.26 (continued)

lymphatics. Poor awareness of the disease may also contribute by delaying diagnosis [159–162]. Lower socioeconomic status has also been suggested to be a poor prognostic indicator. However, the prognosis for male breast cancer, when adjusted for tumor size, histological grade, and lymph node status, is similar to that for female patients [138, 163–165].

Because of the rarity of male breast cancer, randomized clinical trials have not been carried out and treatment has not been standardized to the extent as it has been in women. However, given similarities in hormone receptor status, male breast cancers are treated like female breast cancers, with surgery followed by adjuvant hormone and/or chemotherapy and/or radiation as appropriate.

The surgical procedure of choice is a simple mastectomy as it remains the procedure with the lowest recurrence rates. In contrast to female breast cancer reconstruction aiming at volume replacement for an acceptable cosmetic outcome, male breast reconstruction focuses on primary skin closure [166]. This is frequently challenging as approximately 40% of male breast cancer patients present with stage III disease requiring extensive resection.

SNLB is the initial procedure for staging the axilla [167]. In the absence of clinically palpable lymph nodes, SNLB has been shown to be as effective in men as it is in women [168].

Adjuvant treatments for men are similar to those used for women. Since the overwhelming majority of male breast cancers are ER positive, tamoxifen is used as the standard therapy. Small retrospective studies show a benefit from endocrine therapy [169, 170]. High incidence of adverse effects including weight gain, sexual dysfunction, hot flashes, neurocognitive deficits, and thromboembolic events often limit the duration of tamoxifen therapy in older men [171, 172]. Surgical methods of hormonal therapy such as orchiectomy have also been used with some success [173]. The role of aromatase inhibitors in the treatment of male breast cancer is unclear, and anecdotal evidence suggests that they may not be as useful as in female breast cancer [174–176].

Optimal chemotherapy regimens for male breast cancer are not well defined due to the relative rarity of the disease. However, most patients are treated with combination chemotherapy based on the efficacy in women. Chemotherapy is typically reserved for stage II disease and beyond, intermediate- or high-grade tumors, and ER-negative tumors [177]. Trastuzumab plus chemotherapy is used for HER2-positive cancers as it appears to be similarly effective in men and women. Because more than 30% of male breast cancer patients are over 70 years of age, complications related to toxicity are high [178].

Mortality in male breast cancer has continued to improve over the past 30 years despite late-stage presentation [179]. Survival is significantly impacted by the presence of comorbidities in this relatively elderly patient population, with up to 40% of male breast cancer patients dying from unrelated causes [133].

Factors found to independently increase mortality include patient age greater than 65 years, large tumor size, high tumor grade, and involved lymph nodes [133]. The overall 5- and 10-year survival rates for male breast cancer are 63% and 42%, respectively [133]. Staging is particularly important, with 5-year survival for stage I disease at 78%, falling to 19% for stage IV. Men have a lower survival rate at each stage than women with equivalent disease. However, when the figures are adjusted to account for population variation in age, sex, and race, the survival rates become comparable.

Metastases to the Adult Male Breast

Breast metastasis from extra-mammary malignancy is rare. An incidence of 0.4–1.3% has been reported in literature regardless of gender. Metastases have been reported from cancers arising in a variety of primary sites including lung, prostate, bladder, and kidney, as well as malignant melanoma (Fig. 18.27).

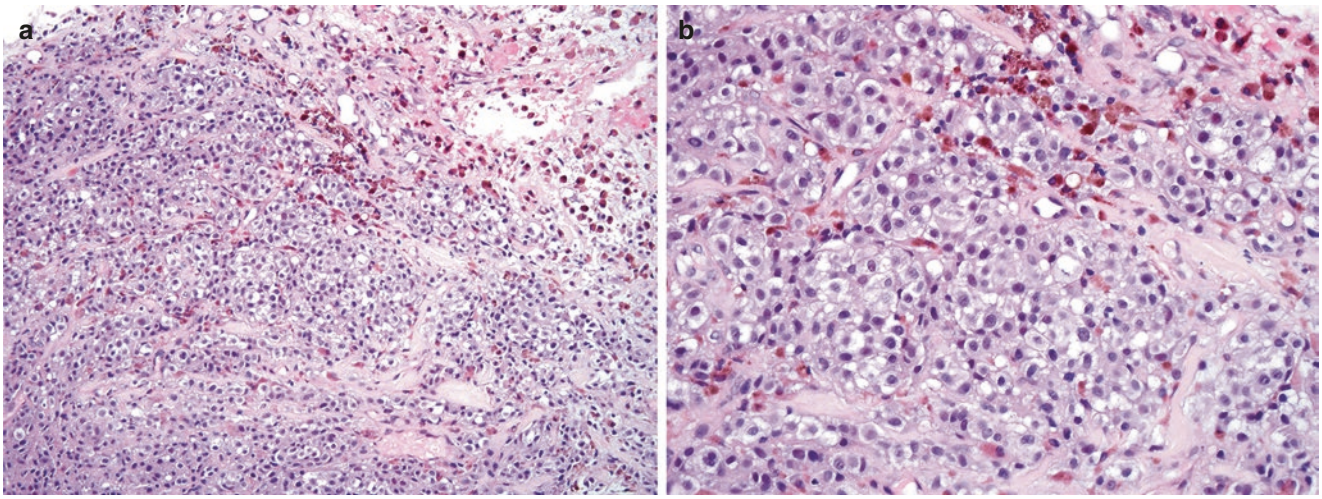

Fig. 18.27 (**a**) Metastatic melanoma involving the breast of a 57-year-old male characterized by epithelioid cells with abundant cytoplasm. (**b**) High-power examination shows moderately pleomorphic nuclei with prominent nucleoli and scattered adjacent melanophages

References

1. Ciftci AO, et al. Female breast masses during childhood: a 25-year review. Eur J Pediatr Surg. 1998;8(2):67–70.
2. Bower R, Bell MJ, Ternberg JL. Management of breast lesions in children and adolescents. J Pediatr Surg. 1976;11(3):337–46.
3. Dehner LP, Hill DA, Deschryver K. Pathology of the breast in children, adolescents, and young adults. Semin Diagn Pathol. 1999;16(3):235–47.
4. Goldstein DP, Miler V. Breast masses in adolescent females. Clin Pediatr (Phila). 1982;21(1):17–9.
5. Chung EM, et al. From the archives of the AFIP: breast masses in children and adolescents: radiologic-pathologic correlation. Radiographics. 2009;29(3):907–31.
6. Gao Y, et al. How to approach breast lesions in children and adolescents. Eur J Radiol. 2015;84(7):1350–64.
7. Kaneda HJ, et al. Pediatric and adolescent breast masses: a review of pathophysiology, imaging, diagnosis, and treatment. AJR Am J Roentgenol. 2013;200(2):W204–12.
8. Valeur NS, Rahbar H, Chapman T. Ultrasound of pediatric breast masses: what to do with lumps and bumps. Pediatr Radiol. 2015;45(11):1584–99. quiz 1581-3
9. Lee EJ, et al. Breast lesions in children and adolescents: diagnosis and management. Korean J Radiol. 2018;19(5):978–91.
10. Gutierrez JC, et al. Malignant breast cancer in children: a review of 75 patients. J Surg Res. 2008;147(2):182–8.
11. Baban A, et al. Poland syndrome with bilateral features: case description with review of the literature. Am J Med Genet A. 2009;149A(7):1597–602.
12. Urschel HC Jr. Poland syndrome. Semin Thorac Cardiovasc Surg. 2009;21(1):89–94.
13. Nso-Roca AP, Aguirre-Balsalobre FJ, Juste Ruiz M. Isolated unilateral amazia: an exceptional breast anomaly. J Pediatr Adolesc Gynecol. 2012;25(6):e147–8.
14. Weinstein SP, et al. Spectrum of US findings in pediatric and adolescent patients with palpable breast masses. Radiographics. 2000;20(6):1613–21.
15. Huneeus A, et al. Retroareolar cysts in the adolescent. J Pediatr Adolesc Gynecol. 2003;16(1):45–9.
16. Garcia CJ, et al. Breast US in children and adolescents. Radiographics. 2000;20(6):1605–12.
17. Sanchez R, et al. Breast fibroadenomas in the pediatric population: common and uncommon sonographic findings. Pediatr Radiol. 2010;40(10):1681–9.
18. Lau CT, Wong KK, Tam P. Galactocele in a male infant with transient hyperprolactinaemia: an extremely rare cause of breast enlargement in children. Case Rep Pediatr. 2016;2016:9487616.
19. Perez-Boscollo AC, et al. Galactocele: an unusual cause of breast enlargement in children. J Pediatr Surg. 2009;44(7):e1–3.
20. Lee KC, Chan JK, Ho LC. Histologic changes in the breast after fine-needle aspiration. Am J Surg Pathol. 1994;18(10):1039–47.
21. Moore RL, et al. Bilaterally symmetric juvenile fibroadenomas and tubular breast deformity in a prepubescent girl. J Pediatr Surg. 2007;42(6):1133–6.
22. Carney JA, Toorkey BC. Myxoid fibroadenoma and allied conditions (myxomatosis) of the breast. A heritable disorder with special associations including cardiac and cutaneous myxomas. Am J Surg Pathol. 1991;15(8):713–21.
23. Courcoutsakis NA, et al. Syndrome of spotty skin pigmentation, myxomas, endocrine overactivity, and schwannomas (Carney complex): breast imaging findings. Radiology. 1997;205(1):221–7.
24. Jacobs TW, et al. Fibroepithelial lesions with cellular stroma on breast core needle biopsy: are there predictors of outcome on surgical excision? Am J Clin Pathol. 2005;124(3):342–54.
25. Sanders M, Boulos F. The breast. In: Gilbert-Barness E, editor. Potter's pathology of the fetus, infant and child. Philadelphia, PA: Mosby Elsevier; 2007. p. 2093–114.
26. Dupont WD, et al. Long-term risk of breast cancer in women with fibroadenoma. N Engl J Med. 1994;331(1):10–5.
27. Carter BA, et al. No elevation in long-term breast carcinoma risk for women with fibroadenomas that contain atypical hyperplasia. Cancer. 2001;92(1):30–6.
28. Spagnolo DV, Shilkin KB. Breast neoplasms containing bone and cartilage. Virchows Arch A Pathol Anat Histopathol. 1983;400(3):287–95.
29. Mies C, Rosen PP. Juvenile fibroadenoma with atypical epithelial hyperplasia. Am J Surg Pathol. 1987;11(3):184–90.
30. Eliasen CA. Letter to the editor: atypical duct hyperplasia in young females. Am J Surg Pathol. 1992;16(9):1.
31. Eliasen CA, Cranor ML, Rosen PP. Atypical duct hyperplasia of the breast in young females. Am J Surg Pathol. 1992;16(3):246–51.
32. Tea MK, et al. Surgical breast lesions in adolescent females. Pediatr Surg Int. 2009;25(1):73–5.

33. Majmudar B, Rosales-Quintana S. Infarction of breast fibroadenomas during pregnancy. JAMA. 1975;231(9):963–4.
34. AbdullGaffar B. Pseudoangiomatous stromal hyperplasia of the breast. Arch Pathol Lab Med. 2009;133(8):1335–8.
35. Ferreira M, Albarracin CT, Resetkova E. Pseudoangiomatous stromal hyperplasia tumor: a clinical, radiologic and pathologic study of 26 cases. Mod Pathol. 2008;21(2):201–7.
36. Powell CM, Cranor ML, Rosen PP. Pseudoangiomatous stromal hyperplasia (PASH). A mammary stromal tumor with myofibroblastic differentiation. Am J Surg Pathol. 1995;19(3):270–7.
37. Baker M, et al. Pseudoangiomatous stromal hyperplasia of the breast in a 10-year-old girl. J Pediatr Surg. 2011;46(8):e27–31.
38. Shehata BM, et al. Pseudoangiomatous stromal hyperplasia of the breast in pediatric patients: an underrecognized entity. Pediatr Dev Pathol. 2009;12(6):450–4.
39. Sanders MP, Brooks JS, Palazzo JP. Mesenchymal lesions of the breast. In: Palazzo JP, editor. Difficult diagnoses in breast pathology. New York: Demos Medical; 2011. p. 172–95.
40. Virk RK, Khan A. Pseudoangiomatous stromal hyperplasia: an overview. Arch Pathol Lab Med. 2010;134(7):1070–4.
41. Rosen PP, et al. Juvenile papillomatosis (Swiss cheese disease) of the breast. Am J Surg Pathol. 1980;4(1):3–12.
42. Rosen PP, et al. Juvenile papillomatosis and breast carcinoma. Cancer. 1985;55(6):1345–52.
43. Bazzocchi F, et al. Juvenile papillomatosis (epitheliosis) of the breast. A clinical and pathologic study of 13 cases. Am J Clin Pathol. 1986;86(6):745–8.
44. Bauer BS, Jones KM, Talbot CW. Mammary masses in the adolescent female. Surg Gynecol Obstet. 1987;165(1):63–5.
45. Boothroyd A, Carty H. Breast masses in childhood and adolescence. A presentation of 17 cases and a review of the literature. Pediatr Radiol. 1994;24(2):81–4.
46. Jonides L, Rudy C, Walsh S. Breast masses in adolescent girls. J Pediatr Health Care. 1992;6(5 Pt 1):274. 287-8
47. Siegal A, Kaufman Z, Siegal G. Breast masses in adolescent females. J Surg Oncol. 1992;51(3):169–73.
48. Simpson JF. Breast. In: Edge S, et al., editors. AJCC cancer staging manual. New York: Springer-Verlag; 2010. p. 347–76.
49. Masse SR, Rioux A, Beauchesne C. Juvenile carcinoma of the breast. Hum Pathol. 1981;12(11):1044–6.
50. Horowitz DP, et al. Secretory carcinoma of the breast: results from the survival, epidemiology and end results database. Breast. 2012;21(3):350–3.
51. Lae M, et al. Secretory breast carcinomas with ETV6-NTRK3 fusion gene belong to the basal-like carcinoma spectrum. Mod Pathol. 2009;22(2):291–8.
52. Din NU, et al. Secretory carcinoma of breast: clinicopathologic study of 8 cases. Ann Diagn Pathol. 2013;17(1):54–7.
53. Osako T, et al. Secretory carcinoma of the breast and its histopathological mimics: value of markers for differential diagnosis. Histopathology. 2013;63(4):509–19.
54. Li D, et al. Secretory breast carcinoma: a clinicopathological and immunophenotypic study of 15 cases with a review of the literature. Mod Pathol. 2012;25(4):567–75.
55. Page DL, Anderson T. Diagnostic histopathology of the breast. Edinburgh: Churchill Livingstone; 1987.
56. Eguchi M, et al. Fusion of ETV6 to neurotrophin-3 receptor TRKC in acute myeloid leukemia with t(12;15)(p13;q25). Blood. 1999;93(4):1355–63.
57. Knezevich SR, et al. ETV6-NTRK3 gene fusions and trisomy 11 establish a histogenetic link between mesoblastic nephroma and congenital fibrosarcoma. Cancer Res. 1998;58(22):5046–8.
58. Knezevich SR, et al. A novel ETV6-NTRK3 gene fusion in congenital fibrosarcoma. Nat Genet. 1998;18(2):184–7.
59. Rubin BP, et al. Congenital mesoblastic nephroma t(12;15) is associated with ETV6-NTRK3 gene fusion: cytogenetic and molecular relationship to congenital (infantile) fibrosarcoma. Am J Pathol. 1998;153(5):1451–8.
60. Tognon C, et al. Expression of the ETV6-NTRK3 gene fusion as a primary event in human secretory breast carcinoma. Cancer Cell. 2002;2(5):367–76.
61. Liu Q, et al. Signal transduction and transforming properties of the TEL-TRKC fusions associated with t(12;15)(p13;q25) in congenital fibrosarcoma and acute myelogenous leukemia. EMBO J. 2000;19(8):1827–38.
62. Wai DH, et al. The ETV6-NTRK3 gene fusion encodes a chimeric protein tyrosine kinase that transforms NIH3T3 cells. Oncogene. 2000;19(7):906–15.
63. Claus EB, Risch N, Thompson WD. Autosomal dominant inheritance of early-onset breast cancer. Implications for risk prediction. Cancer. 1994;73(3):643–51.
64. Elger BS, Harding TW. Testing adolescents for a hereditary breast cancer gene (BRCA1): respecting their autonomy is in their best interest. Arch Pediatr Adolesc Med. 2000;154(2):113–9.
65. Malone KE, et al. BRCA1 mutations and breast cancer in the general population: analyses in women before age 35 years and in women before age 45 years with first-degree family history. JAMA. 1998;279(12):922–9.
66. Sidransky D, et al. Inherited p53 gene mutations in breast cancer. Cancer Res. 1992;52(10):2984–6.
67. Thompson WD. Genetic epidemiology of breast cancer. Cancer. 1994;74(1 Suppl):279–87.
68. Costa NM, et al. Secretory breast carcinoma--case report and review of the medical literature. Breast. 2004;13(4):353–5.
69. Farrow JH, Ashikari H. Breast lesions in young girls. Surg Clin North Am. 1969;49(2):261–9.
70. Oberman HA, Stephens PJ. Carcinoma of the breast in childhood. Cancer. 1972;30(2):470–4.
71. Tanimura A, Konaka K. Carcinoma of the breast in a 5 years old girl. Acta Pathol Jpn. 1980;30(1):157–60.
72. Tavassoli FA, Norris HJ. Secretory carcinoma of the breast. Cancer. 1980;45(9):2404–13.
73. Oberman HA. Secretory carcinoma of the breast in adults. Am J Surg Pathol. 1980;4(5):465–70.
74. Roth JA, Discafani C, O'Malley M. Secretory breast carcinoma in a man. Am J Surg Pathol. 1988;12(2):150–4.
75. Serour F, et al. Secretory breast cancer in childhood and adolescence: report of a case and review of the literature. Med Pediatr Oncol. 1992;20(4):341–4.
76. Kavalakat AJ, Covilakam RK, Culas TB. Secretory carcinoma of breast in a 17-year-old male. World J Surg Oncol. 2004;2:17.
77. Herz H, Cooke B, Goldstein D. Metastatic secretory breast cancer. Non-responsiveness to chemotherapy: case report and review of the literature. Ann Oncol. 2000;11(10):1343–7.
78. Serour F, et al. Penetration of aminoglycosides into human peritoneal tissue. Chemotherapy. 1990;36(4):251–3.
79. Szanto J, et al. Secretory breast cancer in a 7.5-year old boy. Breast. 2004;13(5):439–42.
80. Lin Y, Govindan R, Hess JL. Malignant hematopoietic breast tumors. Am J Clin Pathol. 1997;107(2):177–86.
81. Meis JM, Butler JJ, Osborne BM. Hodgkin's disease involving the breast and chest wall. Cancer. 1986;57(9):1859–65.
82. Lin P, et al. Precursor B-cell lymphoblastic lymphoma: a predominantly extranodal tumor with low propensity for leukemic involvement. Am J Surg Pathol. 2000;24(11):1480–90.
83. Fahmy JL, Wood BP, Miller JH. Bilateral breast involvement in a teenage girl with Burkitt lymphoma. Pediatr Radiol. 1995;25(1):56–7.
84. Hubner KF, Littlefield LG. Burkitt lymphoma in three American children. Clinical and cytogenetic observations. Am J Dis Child. 1975;129(10):1219–23.

85. Arber DA, et al. Non-Hodgkin's lymphoma involving the breast. Am J Surg Pathol. 1994;18(3):288–95.
86. Fadiora SO, et al. Generalised Burkitt's lymphoma involving both breasts--a case report. West Afr J Med. 2005;24(3):280–2.
87. Rogers DA, et al. Breast malignancy in children. J Pediatr Surg. 1994;29(1):48–51.
88. Binokay F, et al. Primary and metastatic rhabdomyosarcoma in the breast: report of two pediatric cases. Eur J Radiol. 2003;48(3):282–4.
89. Howarth CB, Caces JN, Pratt CB. Breast metastases in children with rhabdomyosarcoma. Cancer. 1980;46(11):2520–4.
90. Altomare DF, et al. Fatal breast rhabdomyosarcoma in a 15 year old primigravida. Eur J Gynaecol Oncol. 1990;11(2):149–51.
91. Gutman H, et al. Sarcoma of the breast: implications for extent of therapy. The M D Anderson experience. Surgery. 1994;116(3):505–9.
92. Herrera LJ, Lugo-Vicente H. Primary embryonal rhabdomyosarcoma of the breast in an adolescent female: a case report. J Pediatr Surg. 1998;33(10):1582–4.
93. Mazzocchi A, et al. Kasabach-Merritt syndrome associated to angiosarcoma of the breast. A case report and review of the literature. Tumori. 1993;79(2):137–40.
94. Rosen PP, Kimmel M, Ernsberger D. Mammary angiosarcoma. The prognostic significance of tumor differentiation. Cancer. 1988;62(10):2145–51.
95. Rainwater LM, et al. Angiosarcoma of the breast. Arch Surg. 1986;121(6):669–72.
96. Biro FM, et al. Hormonal studies and physical maturation in adolescent gynecomastia. J Pediatr. 1990;116(3):450–5.
97. Harman SM, et al. Longitudinal effects of aging on serum total and free testosterone levels in healthy men. Baltimore Longitudinal Study of Aging. J Clin Endocrinol Metab. 2001;86(2):724–31.
98. Lapid O, Jolink F, Meijer SL. Pathological findings in gynecomastia: analysis of 5113 breasts. Ann Plast Surg. 2015;74(2):163–6.
99. Lapid O, Siebenga P, Zonderland HM. Overuse of imaging the male breast-findings in 557 patients. Breast J. 2015;21(3):219–23.
100. Chang HL, et al. A 16-year-old male with gynecomastia and ductal carcinoma in situ. Pediatr Surg Int. 2008;24(11):1251–3.
101. Corroppolo M, et al. Ductal carcinoma in situ in a 15-year-old boy with gynaecomastia: a case report. Pediatr Surg Int. 2008;24(8):943–5.
102. Lemoine C, et al. Incidental finding of synchronous bilateral ductal carcinoma in situ associated with gynecomastia in a 15-year-old obese boy: case report and review of the literature. J Pediatr Surg. 2011;46(9):e17–20.
103. Wadie GM, et al. Ductal carcinoma in situ in a 16-year-old adolescent boy with gynecomastia: a case report. J Pediatr Surg. 2005;40(8):1349–53.
104. Anderson WF, Devesa SS. In situ male breast carcinoma in the Surveillance, Epidemiology, and End Results database of the National Cancer Institute. Cancer. 2005;104(8):1733–41.
105. Ruddy KJ, Winer EP. Male breast cancer: risk factors, biology, diagnosis, treatment, and survivorship. Ann Oncol. 2013;24(6):1434–43.
106. Yang WT, et al. Sonographic features of primary breast cancer in men. AJR Am J Roentgenol. 2001;176(2):413–6.
107. Anderson WF, et al. Comparison of age-specific incidence rate patterns for different histopathologic types of breast carcinoma. Cancer Epidemiol Biomark Prev. 2004;13(7):1128–35.
108. Contractor KB, et al. Male breast cancer: is the scenario changing. World J Surg Oncol. 2008;6:58.
109. Hodgson NC, et al. Male breast cancer: is the incidence increasing? Ann Surg Oncol. 2004;11(8):751–5.
110. Speirs V, Shaaban AM. The rising incidence of male breast cancer. Breast Cancer Res Treat. 2009;115(2):429–30.
111. Stang A, Thomssen C. Decline in breast cancer incidence in the United States: what about male breast cancer? Breast Cancer Res Treat. 2008;112(3):595–6.
112. White J, et al. Male breast carcinoma: increased awareness needed. Breast Cancer Res. 2011;13(5):219.
113. Jemal A, et al. Cancer statistics, 2010. CA Cancer J Clin. 2010;60(5):277–300.
114. Thompson D, Easton D. The genetic epidemiology of breast cancer genes. J Mammary Gland Biol Neoplasia. 2004;9(3):221–36.
115. Evans DG, et al. Risk of breast cancer in male BRCA2 carriers. J Med Genet. 2010;47(10):710–1.
116. Tai YC, et al. Breast cancer risk among male BRCA1 and BRCA2 mutation carriers. J Natl Cancer Inst. 2007;99(23):1811–4.
117. Ford D, et al. Genetic heterogeneity and penetrance analysis of the BRCA1 and BRCA2 genes in breast cancer families. The Breast Cancer Linkage Consortium. Am J Hum Genet. 1998;62(3):676–89.
118. Frank TS, et al. Clinical characteristics of individuals with germline mutations in BRCA1 and BRCA2: analysis of 10,000 individuals. J Clin Oncol. 2002;20(6):1480–90.
119. Basham VM, et al. BRCA1 and BRCA2 mutations in a population-based study of male breast cancer. Breast Cancer Res. 2002;4(1):R2.
120. Couch FJ, et al. BRCA2 germline mutations in male breast cancer cases and breast cancer families. Nat Genet. 1996;13(1):123–5.
121. Friedman LS, et al. Mutation analysis of BRCA1 and BRCA2 in a male breast cancer population. Am J Hum Genet. 1997;60(2):313–9.
122. Fackenthal JD, et al. Male breast cancer in Cowden syndrome patients with germline PTEN mutations. J Med Genet. 2001;38(3):159–64.
123. Anelli A, et al. Mutations of the p53 gene in male breast cancer. Cancer. 1995;75(9):2233–8.
124. Meijers-Heijboer H, et al. Low-penetrance susceptibility to breast cancer due to CHEK2(*)1100delC in noncarriers of BRCA1 or BRCA2 mutations. Nat Genet. 2002;31(1):55–9.
125. Dawson PJ, Schroer KR, Wolman SR. ras and p53 genes in male breast cancer. Mod Pathol. 1996;9(4):367–70.
126. Brinton LA, et al. Etiologic factors for male breast cancer in the U.S. Veterans Affairs medical care system database. Breast Cancer Res Treat. 2010;119(1):185–92.
127. Medras M, et al. Breast cancer and long-term hormonal treatment of male hypogonadism. Breast Cancer Res Treat. 2006;96(3):263–5.
128. Johnson KC, et al. Risk factors for male breast cancer in Canada, 1994-1998. Eur J Cancer Prev. 2002;11(3):253–63.
129. Lee SC, Ellis RJ. Male breast cancer during finasteride therapy. J Natl Cancer Inst. 2004;96(4):338–9.
130. Gomez-Raposo C, et al. Male breast cancer. Cancer Treat Rev. 2010;36(6):451–7.
131. Sasco AJ, Lowenfels AB, Pasker-de Jong P. Review article: epidemiology of male breast cancer. A meta-analysis of published case-control studies and discussion of selected aetiological factors. Int J Cancer. 1993;53(4):538–49.
132. Giordano SH, Buzdar AU, Hortobagyi GN. Breast cancer in men. Ann Intern Med. 2002;137(8):678–87.
133. Giordano SH, et al. Breast carcinoma in men: a population-based study. Cancer. 2004;101(1):51–7.
134. Agrawal A, Cheung KL, Robertson JF. Fulvestrant in advanced male breast cancer. Breast Cancer Res Treat. 2007;101(1):123.
135. Gu GL, et al. Axillary metastasis as the first manifestation of male breast cancer: a case report. Cases J. 2008;1(1):285.
136. Gennari R, et al. Male breast cancer: a special therapeutic problem. Anything new? (Review). Int J Oncol. 2004;24(3):663–70.
137. Buzdar AU. Breast cancer in men. Oncology (Williston Park). 2003;17(10):1361–4; discussion 1364, 1369–72

138. Foerster R, et al. Metastatic male breast cancer: a retrospective cohort analysis. Breast Care (Basel). 2014;9(4):267–71.
139. Doyle S, Steel J, Porter G. Imaging male breast cancer. Clin Radiol. 2011;66(11):1079–85.
140. Burga AM, et al. Invasive carcinomas of the male breast: a morphologic study of the distribution of histologic subtypes and metastatic patterns in 778 cases. Virchows Arch. 2006;449(5):507–12.
141. Pant K, Dutta U. Understanding and management of male breast cancer: a critical review. Med Oncol. 2008;25(3):294–8.
142. Arce C, et al. Secretory carcinoma of the breast containing the ETV6-NTRK3 fusion gene in a male: case report and review of the literature. World J Surg Oncol. 2005;3:35.
143. Gabal S, Talaat S. Secretory carcinoma of male breast: case report and review of the literature. Int J Breast Cancer. 2011;2011:704657.
144. Peschos D, et al. Mucinous breast carcinoma presenting as Paget's disease of the nipple in a man: a case report. Diagn Pathol. 2008;3:42.
145. Nance KV, Reddick RL. In situ and infiltrating lobular carcinoma of the male breast. Hum Pathol. 1989;20(12):1220–2.
146. Sanchez AG, Villanueva AG, Redondo C. Lobular carcinoma of the breast in a patient with Klinefelter's syndrome. A case with bilateral, synchronous, histologically different breast tumors. Cancer. 1986;57(6):1181–3.
147. Zahir MN, Minhas K, Shabbir-Moosajee M. Pleomorphic lobular carcinoma of the male breast with axillary lymph node involvement: a case report and review of literature. BMC Clin Pathol. 2014;14:16.
148. Spigel JJ, et al. Male inflammatory breast cancer. Clin Breast Cancer. 2001;2(2):153–5.
149. Mavaddat N, et al. Pathology of breast and ovarian cancers among BRCA1 and BRCA2 mutation carriers: results from the Consortium of Investigators of Modifiers of BRCA1/2 (CIMBA). Cancer Epidemiol Biomark Prev. 2012;21(1):134–47.
150. Ottini L, et al. Clinical and pathologic characteristics of BRCA-positive and BRCA-negative male breast cancer patients: results from a collaborative multicenter study in Italy. Breast Cancer Res Treat. 2012;134(1):411–8.
151. Nahleh ZA, et al. Male breast cancer in the veterans affairs population: a comparative analysis. Cancer. 2007;109(8):1471–7.
152. Bruce DM, et al. Male breast cancer: clinico-pathological features, immunocytochemical characteristics and prognosis. Eur J Surg Oncol. 1996;22(1):42–6.
153. Leach IH, Ellis IO, Elston CW. c-erb-B-2 expression in male breast carcinoma. J Clin Pathol. 1992;45(10):942.
154. Rudlowski C, et al. Her-2/neu gene amplification and protein expression in primary male breast cancer. Breast Cancer Res Treat. 2004;84(3):215–23.
155. Shaaban AM, et al. A comparative biomarker study of 514 matched cases of male and female breast cancer reveals gender-specific biological differences. Breast Cancer Res Treat. 2012;133(3):949–58.
156. Murphy CE, et al. Steroid hormone receptor expression in male breast cancer. Eur J Surg Oncol. 2006;32(1):44–7.
157. Kwiatkowska E, et al. BRCA2 mutations and androgen receptor expression as independent predictors of outcome of male breast cancer patients. Clin Cancer Res. 2003;9(12):4452–9.
158. Atalay C, Kanlioz M, Altinok M. Prognostic factors affecting survival in male breast cancer. J Exp Clin Cancer Res. 2003;22(1):29–33.
159. Ciatto S, et al. Male breast carcinoma: review of a multicenter series of 150 cases. Coordinating Center and Writing Committee of FONCAM (National Task Force for Breast Cancer), Italy. Tumori. 1990;76(6):555–8.
160. Gnerlich JL, et al. Poorer survival outcomes for male breast cancer compared with female breast cancer may be attributable to in-stage migration. Ann Surg Oncol. 2011;18(7):1837–44.
161. Thalib L, Hall P. Survival of male breast cancer patients: population-based cohort study. Cancer Sci. 2009;100(2):292–5.
162. Winchester DJ. Male breast carcinoma: a multiinstitutional challenge. Cancer. 1998;83(3):399–400.
163. Borgen PI, et al. Carcinoma of the male breast: analysis of prognosis compared with matched female patients. Ann Surg Oncol. 1997;4(5):385–8.
164. Temmim L, et al. Evaluation of prognostic factors in male breast cancer. Breast. 2001;10(2):166–75.
165. Willsher PC, et al. A comparison outcome of male breast cancer with female breast cancer. Am J Surg. 1997;173(3):185–8.
166. Donegan WL, Redlich PN. Breast cancer in men. Surg Clin North Am. 1996;76(2):343–63.
167. Wong SL, et al. Accuracy of sentinel lymph node biopsy for patients with T2 and T3 breast cancers. Am Surg. 2001;67(6):522–6. discussion 527-8
168. Flynn LW, et al. Sentinel lymph node biopsy is successful and accurate in male breast carcinoma. J Am Coll Surg. 2008;206(4):616–21.
169. Fogh S, et al. Use of tamoxifen with postsurgical irradiation may improve survival in estrogen and progesterone receptor-positive male breast cancer. Clin Breast Cancer. 2011;11(1):39–45.
170. Ribeiro G, Swindell R. Adjuvant tamoxifen for male breast cancer (MBC). Br J Cancer. 1992;65(2):252–4.
171. Cutuli B, et al. Breast-conserving therapy for ductal carcinoma in situ of the breast: the French Cancer Centers' experience. Int J Radiat Oncol Biol Phys. 2002;53(4):868–79.
172. Pemmaraju N, et al. Retrospective review of male breast cancer patients: analysis of tamoxifen-related side-effects. Ann Oncol. 2012;23(6):1471–4.
173. Volm MD. Male breast cancer. Curr Treat Options in Oncol. 2003;4(2):159–64.
174. Bradley KL, et al. Contemporary systemic therapy for male breast cancer. Clin Breast Cancer. 2014;14(1):31–9.
175. Maugeri-Sacca M, et al. Aromatase inhibitors for metastatic male breast cancer: molecular, endocrine, and clinical considerations. Breast Cancer Res Treat. 2014;147(2):227–35.
176. Zagouri F, et al. Aromatase inhibitors in male breast cancer: a pooled analysis. Breast Cancer Res Treat. 2015;151(1):141–7.
177. Patten DK, Sharifi LK, Fazel M. New approaches in the management of male breast cancer. Clin Breast Cancer. 2013;13(5):309–14.
178. Giordano SH, et al. Use and outcomes of adjuvant chemotherapy in older women with breast cancer. J Clin Oncol. 2006;24(18):2750–6.
179. Korde LA, et al. Multidisciplinary meeting on male breast cancer: summary and research recommendations. J Clin Oncol. 2010;28(12):2114–22.

Lesions of the Nipple

19

Nicole B. Johnson and Laura C. Collins

Overview

Lesions of the nipple are rarely, if ever, sampled by core needle biopsy (CNB); however, skin punch biopsies may be performed, and many of the same issues concerning small sample size and associated loss of overall architectural features remain relevant.

The normal structure of the nipple consists of mammary ducts, lactiferous sinuses, and lactiferous ducts. Histologically, the mammary ducts of the nipple-areolar complex have a serrated architecture on cross section and are lined by columnar epithelium. These ducts empty into lactiferous sinuses, which transition from columnar epithelium to squamous epithelium in the distal 1–2 mm just deep to the epidermis (Fig. 19.1). Prominent smooth muscle is present in the stroma, which is responsible for erection of the nipple and also aiding in expression of milk. The skin of the areola is pigmented, with many sebaceous glands in the dermis. The sebaceous glands may form large mounds or tubercles, known as Montgomery's tubercles, when associated with a lactiferous duct.

Lesions of the nipple are varied but typically present as either an erythematous rash, often with pruritus and an exudative crust, with or without associated tenderness, or as a palpable mass. Lesions involving the nipple can be divided into those that involve the ducts, which may be inflammatory or neoplastic: those that involve the smooth muscle of the nipple (i.e., leiomyoma), and those that involve the skin (i.e., Paget disease). Dermatologic conditions that may affect the nipple, such as eczema, psoriasis, dermatitis, and cutaneous malignancies, will not be discussed in this chapter. Entities specific to the nipple will be discussed with an emphasis on issues inherent to small biopsy samples.

N. B. Johnson
Presbyterian Pathology Group, Novant Health Presbyterian Medical Center, Charlotte, NC, USA

L. C. Collins (✉)
Department of Pathology, Beth Israel Deaconess Medical Center and Harvard Medical School, Boston, MA, USA
e-mail: lcollins@bidmc.harvard.edu

© The Author(s), under exclusive license to Springer Nature Switzerland AG 2022
S. J. Shin et al. (eds.), *A Comprehensive Guide to Core Needle Biopsies of the Breast*,
https://doi.org/10.1007/978-3-031-05532-4_19

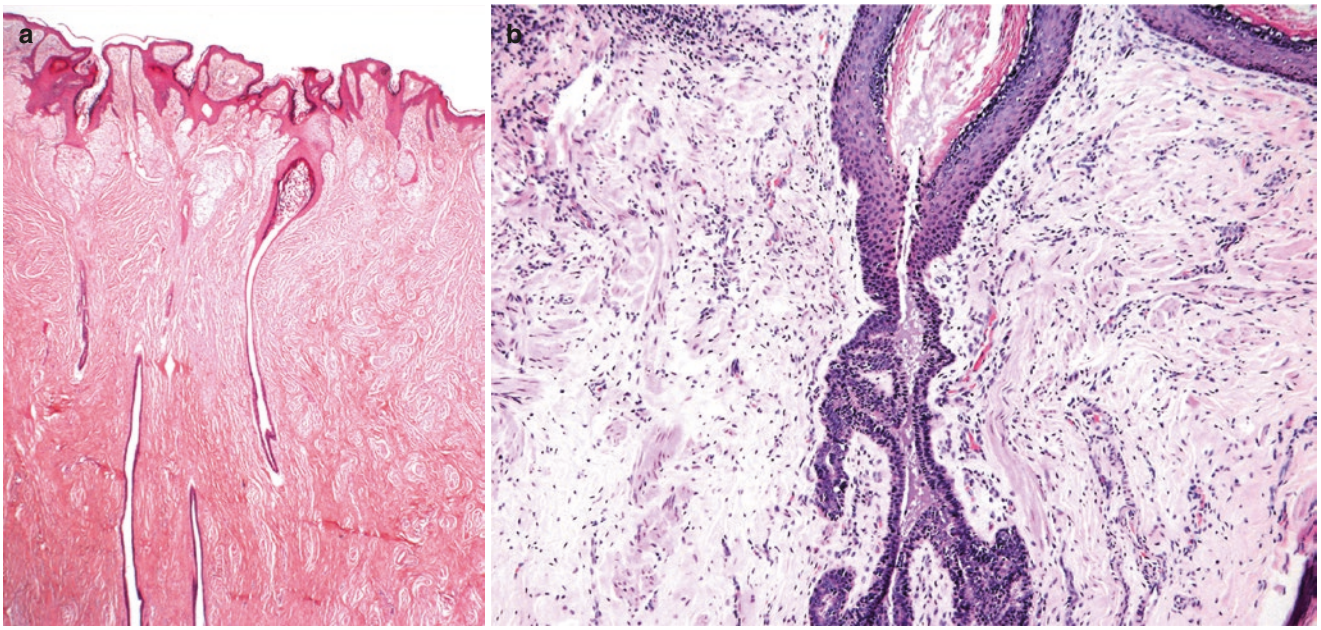

Fig. 19.1 (**a**) Normal nipple. This low-power image of the normal nipple consists of mammary ducts, a lactiferous sinus, and a lactiferous duct. Ducts empty into lactiferous sinuses, which transition from columnar epithelium to squamous epithelium in the distal 1–2 mm just deep to the epidermis. Smooth muscle is present in the stroma. Sebaceous glands may form large mounds or tubercles, known as Montgomery's tubercles, when associated with a lactiferous duct. (**b**) This high-power image of a nipple duct illustrates the normal transition of squamous epithelium at the surface (top of image) to glandular epithelium deeper in the duct (bottom of image)

Lesions of the Large Lactiferous Ducts

Squamous Metaplasia of Lactiferous Ducts

Squamous metaplasia of lactiferous ducts (SMOLD) is also known as Zuska disease, after one of the authors who first described five cases in 1951 [1]. The name SMOLD was first suggested by Crile and Chatty, and the role of the squamous epithelium in the disease was described at that time [2]. The median age at presentation is 47 years (range: 32–69 years) [3]. Patients are characteristically smokers who have suffered from recurrent episodes of periareolar abscesses or fistulas [3, 4]. SMOLD may be bilateral and can also affect men.

Gross and Radiologic Features

Patients present with tenderness, induration, and often a draining sinus at the periphery of the areola. With pressure, foul-smelling material may be expressed through the sinus or nipple. On mammography, a retroareolar asymmetry is the characteristic finding, typically medial in location. The ultrasound correlate is an ill-defined hypoechoic lesion with increased vascularity seen on color Doppler. Duct dilatation is usually present, and abscess or fistula formation may be seen [3].

Microscopic Features

By the time a biopsy is performed, there is usually a profound inflammatory reaction with microabscess formation. Identification of the involved duct with its squamous epithelial lining or of keratin fragments, which are sometimes within giant cells, may be difficult due to the obscuring inflammation (Figs. 19.2 and 19.3). Consideration of the diagnosis, especially in a smoker, is the key to recognizing this lesion histopathologically and, thereby, to directing appropriate patient management.

Differential Diagnosis

The differential diagnosis includes periductal mastitis, which has a similar inflammatory response in a retroareolar location but lacks keratinaceous debris and squamous-lined ducts. Granulomatous patterns of mastitis may be considered, but those patients are typically younger, nonsmokers with a recent history of pregnancy and lactation. Microscopically, the inflammatory picture includes granulomatous inflammation centered on the terminal duct lobular units, which differs from the picture described above for SMOLD. Other differential diagnostic considerations include a ruptured epidermal inclusion cyst, which is a squamous epithelial-lined cyst with keratinaceous debris and abundant inflammation, including foreign-body giant cells;

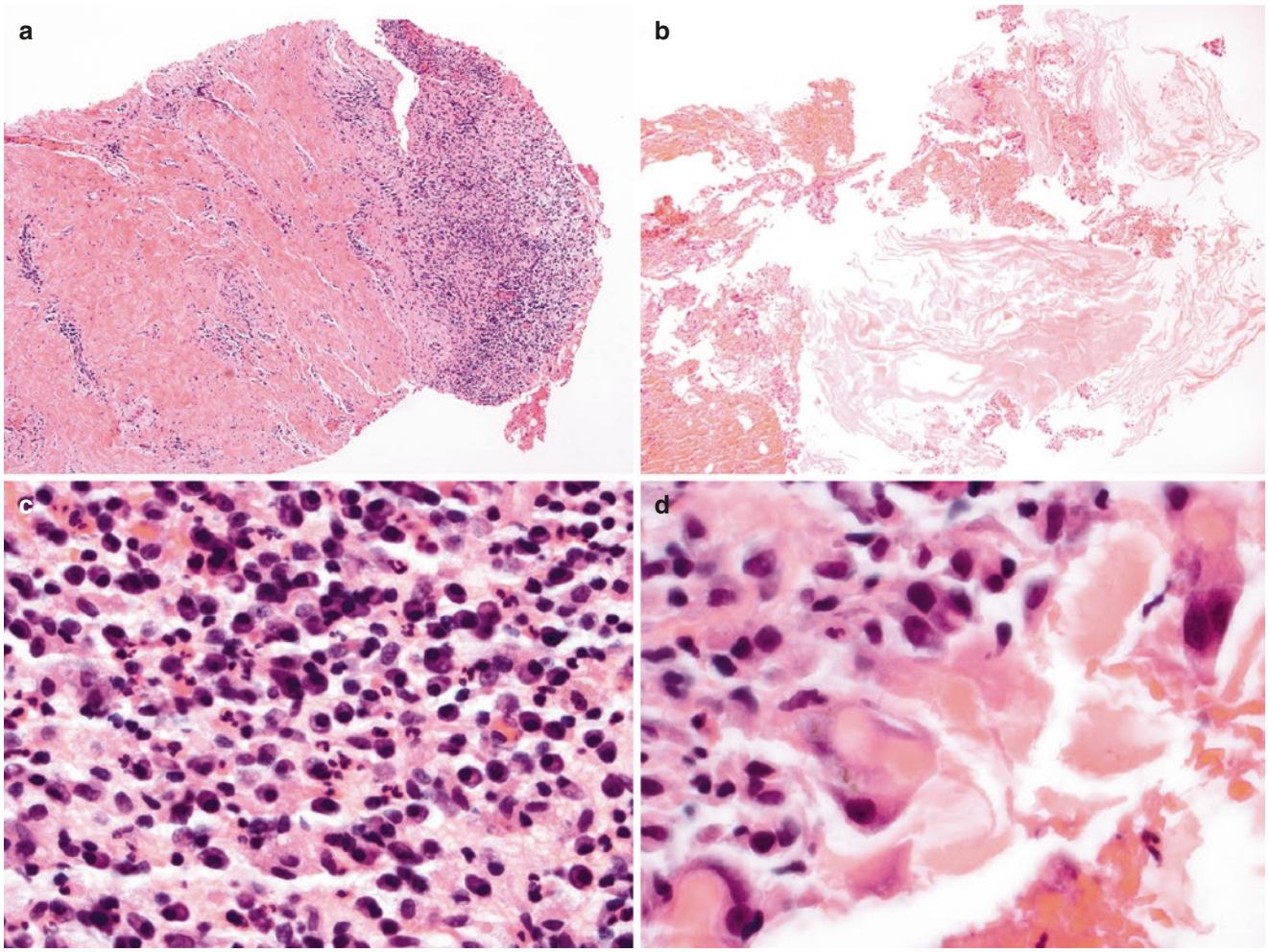

Fig. 19.2 Core needle biopsy of an inflammatory lesion with some features of SMOLD (**a**). It is unusual for all the features characteristic of SMOLD to be present in a single biopsy. The constellation of features present in this case: mixed inflammatory infiltrate (**b**), giant cells, and keratin fragments (**c**, and at higher power **d**) may be sufficient to suggest the diagnosis. It is important to evaluate any ducts present in the biopsy for metaplastic squamous epithelium, which may be a further clue to the diagnosis

and multiple periareolar fistulas with granulomatous inflammation as a cutaneous manifestation of Crohn disease [5]. However, in a ruptured epidermal inclusion cyst, typically there is only a single cystic structure that does not connect to the lactiferous ducts and no clinical correlate of a significant smoking history. Finally, cutaneous manifestations of Crohn disease lack the squamous epithelium of SMOLD.

Pathogenesis: Histopathology and Biology

As described above, the normal keratinizing epithelium of the nipple extends 1–2 mm into the lactiferous duct. SMOLD occurs when there is extension of the squamous epithelium more deeply into the lactiferous duct. Keratin accumulates within the duct causing obstruction, which leads to distention and subsequent infection with duct rupture, abscess, and possible fistula formation. SMOLD may involve one or multiple ducts.

Prognosis and Clinical Management

Recognition of the lesion histopathologically is critical to the eradication of the disease process. Patients often carry a diagnosis of "mastitis" and are managed conservatively with antibiotics and/or incision and drainage, which does not treat the underlying problem of keratin accumulation within the ducts. Effective treatment requires excision of the involved duct, often with a wedge resection of the nipple. Patients should also be counseled to discontinue smoking. Malignant transformation has not been described.

Mammary Duct Ectasia

Mammary duct ectasia is the constellation of periductal inflammation and fibrosis, with duct dilatation. It is more common in perimenopausal and postmenopausal women.

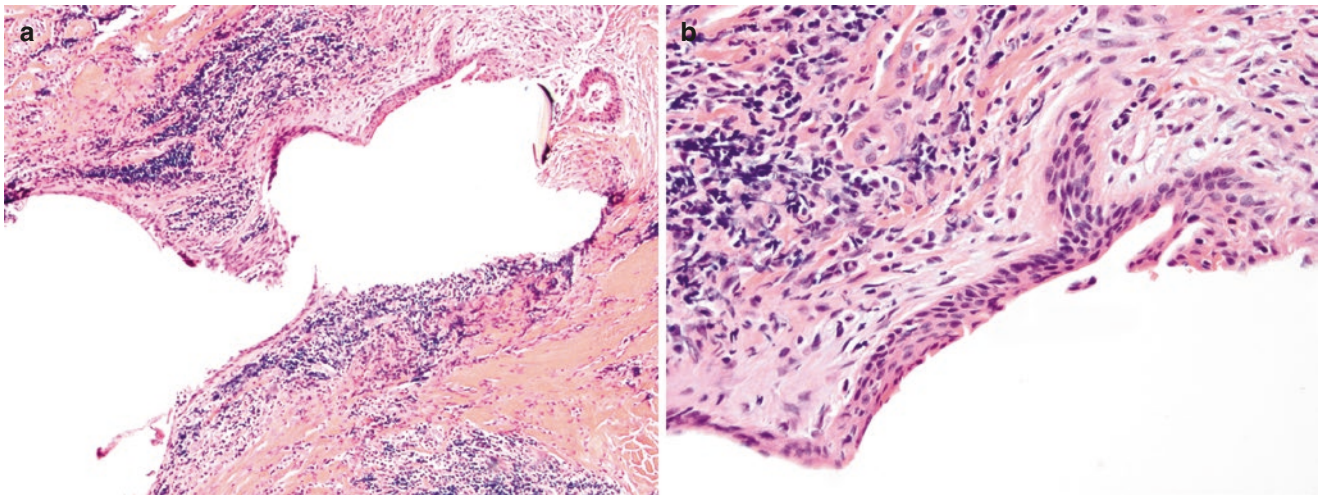

Fig. 19.3 Incisional biopsy of an inflammatory lesion deep to the nipple with features suggestive of SMOLD. (**a**) In this low-power image, chronic inflammation and a dilated duct with a squamous epithelial lining are present. (**b**) On higher power, the squamous epithelium of the duct and the adjacent chronic inflammatory cell infiltrate are better appreciated. While keratinaceous debris is not present in the biopsy material provided, the aforementioned features should raise this differential diagnostic consideration in the appropriate clinical setting

Gross and Radiologic Features

Patients with mammary duct ectasia typically present with pain and/or nipple discharge. There may be an associated mass or nipple retraction, raising concern for malignancy. On ultrasound, dilated ducts may be appreciated. A subtle feature described is hypoechoic layering around the dilated duct indicative of segmental duct ectasia [6]. Mammogram may demonstrate radiodense, serpiginous tubular structures that converge on the nipple-areolar complex; secretions and/or coarse calcifications may be appreciated within the duct [7]. The appearance of a ductal pattern of calcifications may raise suspicion for ductal carcinoma in situ (DCIS). On ultrasound examination, movement of particles in the secretions may be seen, suggesting the diagnosis of mammary duct ectasia [8].

Microscopic Features

The histopathologic features of mammary duct ectasia include dilated ducts with inspissated lipid-rich, luminal secretions and a prominent periductal chronic inflammatory cell infiltrate. Histiocytes are present both within the duct lumen and infiltrating the epithelium lining the duct (Fig. 19.4). Occasionally, periductal fibrosis is the more prominent component which may result in obliteration of the duct lumen. On CNB, the constellation of aforementioned features may be difficult to appreciate, due to sampling issues. It should be noted that the presence of dilated (or ectatic) ducts does not constitute mammary duct ectasia. The pathologic features together with the appropriate clinical signs and symptoms are required before rendering the diagnosis.

Differential Diagnosis

Due to the limitations of sampling by CNB, only part of the duct may be seen, leading to consideration of a cyst as the target lesion, or the inflammatory component may be sampled without the duct itself, suggesting "mastitis" or cyst with rupture as a possible diagnostic consideration. Correlation with the clinical and imaging findings is most helpful in reaching the correct diagnosis.

Pathogenesis: Histopathology and Biology

The pathogenesis of duct ectasia remains unclear. Some authors have suggested a relationship to smoking as a causative agent [4, 9, 10], though others have not found this association [11, 12]. It is hypothesized that periductal inflammation is the initial event with subsequent development of periductal fibrosis and ductal dilation. A second hypothesis argues that periductal mastitis and mammary duct ectasia are two different conditions and that it is periductal mastitis alone that is associated with a history of smoking [11, 12].

Prognosis and Clinical Management

Management is usually conservative, with surgery reserved for those patients for whom the condition is particularly debilitating.

Nipple Adenoma

Nipple adenoma, also known as florid papillomatosis or erosive adenomatosis (of the nipple), among other names, is a

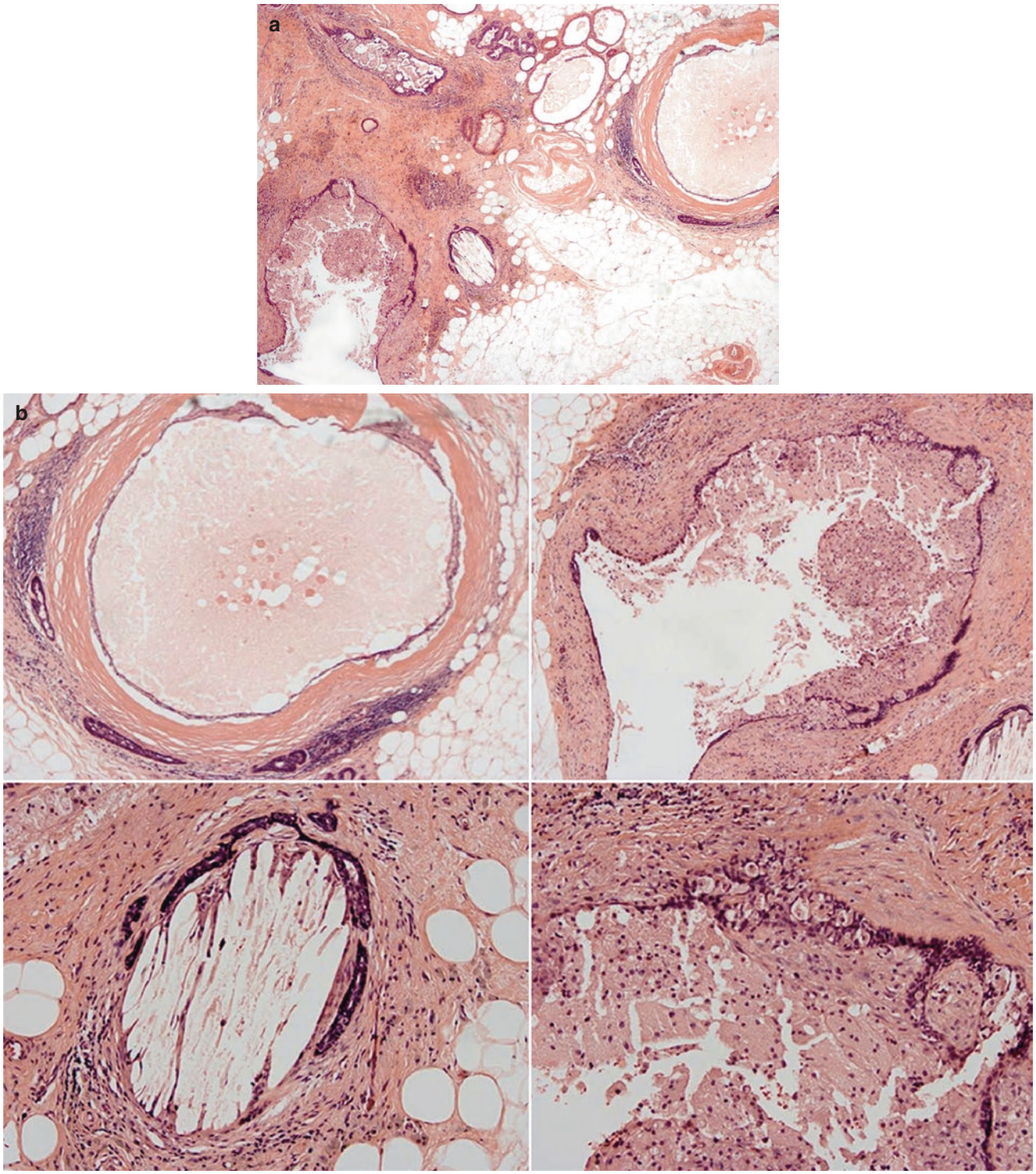

Fig. 19.4 Mammary duct ectasia. (**a**) At low power, this example of mammary duct ectasia demonstrates the dilated ducts with surrounding inflammatory cells, histocytes within the duct lumen, and some periductal fibrosis at the upper right corner. (**b**) This composite image shows the features of mammary duct ectasia at higher power: periductal fibrosis with lymphocytic infiltrate; histocytes within the duct lumen and within the ductal epithelium, which is better appreciated at higher power in the lower two images

benign proliferative lesion of the nipple typically occurring in the fourth decade [13].

Gross and Radiologic Features

Patients with nipple adenoma present with swelling, soreness, or itching of the nipple and on occasion a serous or serosanguinous nipple discharge. Nipple ulceration/erosion or a firm nodule may be apparent on clinical and gross examination. The clinical presentation mimics Paget disease. On imaging, nipple adenomas have been reported to be hyperdense with or without associated microcalcifications on mammography; hypoechoic with posterior enhancement on ultrasonography; and/or to present as a solid, enhancing mass on magnetic resonance imaging [14].

Microscopic Features

On microscopic examination, nipple adenomas have a relatively circumscribed growth pattern composed of benign glands, which may be simple tubular structures, or there may be expansion by florid usual ductal hyperplasia (UDH) (Figs. 19.5, 19.6, and 19.7). The epithelium may undergo squamous or apocrine metaplasia, and foci of necrosis may be seen in areas of UDH. The glands are arrayed in an adenosis-like pattern and are embedded in a fibrotic stroma. Focal papilloma formation may also be present. Distortion of glands by the fibrotic stroma may give the impression of an infiltrative growth pattern, particularly on a limited biopsy sample [13]. The glandular structures may extend to the skin surface, accounting for the erosion or ulceration seen clini-

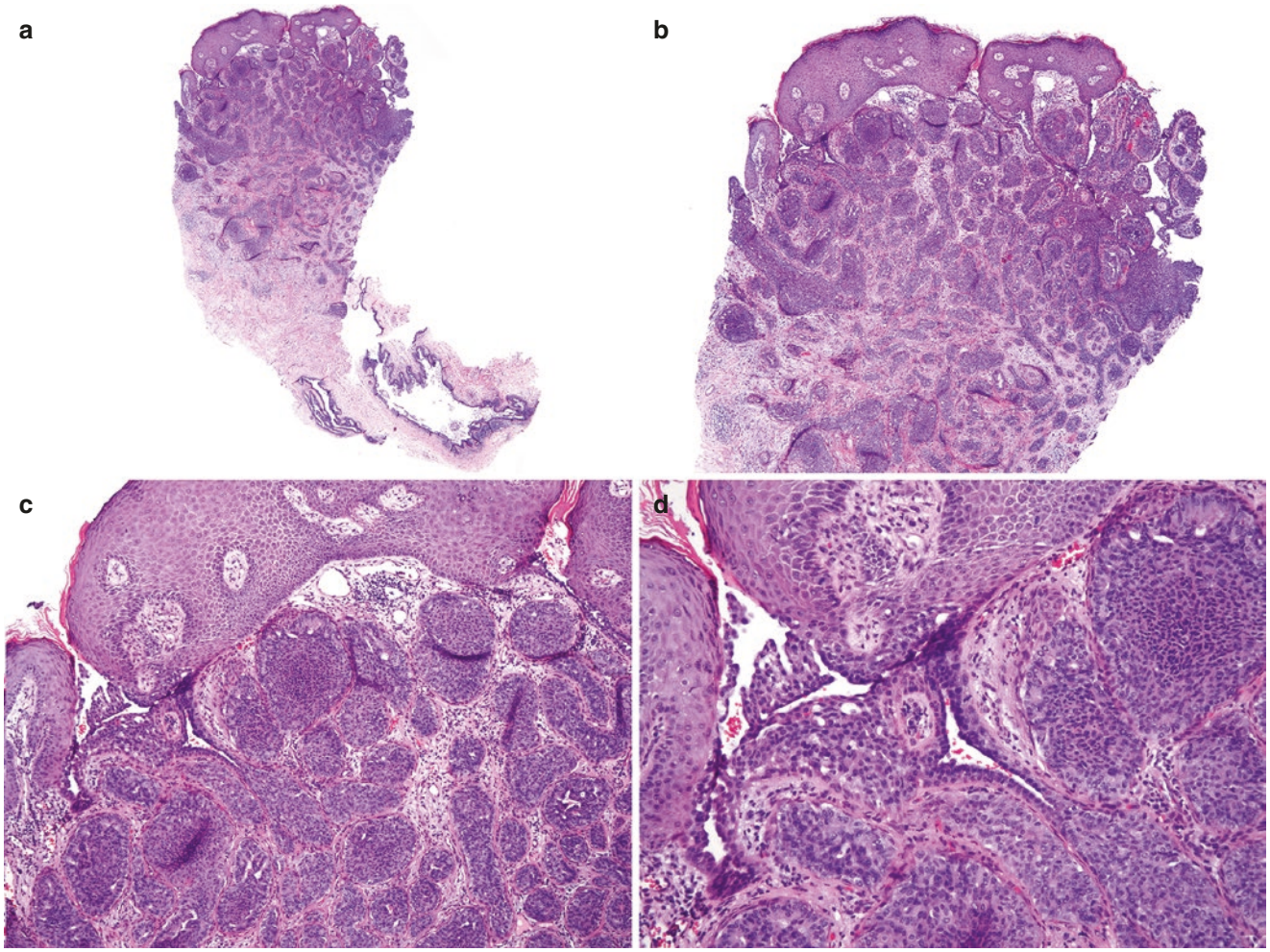

Fig. 19.5 Nipple adenoma. (**a**) At low-power view, this punch biopsy of the nipple demonstrates a proliferative lesion involving the superficial and deep dermis and extending toward the underlying breast parenchyma. (**b**) In this intermediate-power image, the complex architecture of the lesion is better appreciated, with crowded nests of cells with round-to-irregular borders. (**c**) The proliferation is present just beneath the epidermis of the nipple with focal extension of the glandular proliferation up into the epidermis. (**d**) At higher power view, a heterogeneous population of ductal epithelial cells which are streaming and overlapping, and which form peripheral slit-like spaces, can be appreciated; intranuclear inclusions are also present. Taken together, these features are diagnostic of florid UDH in a nipple adenoma

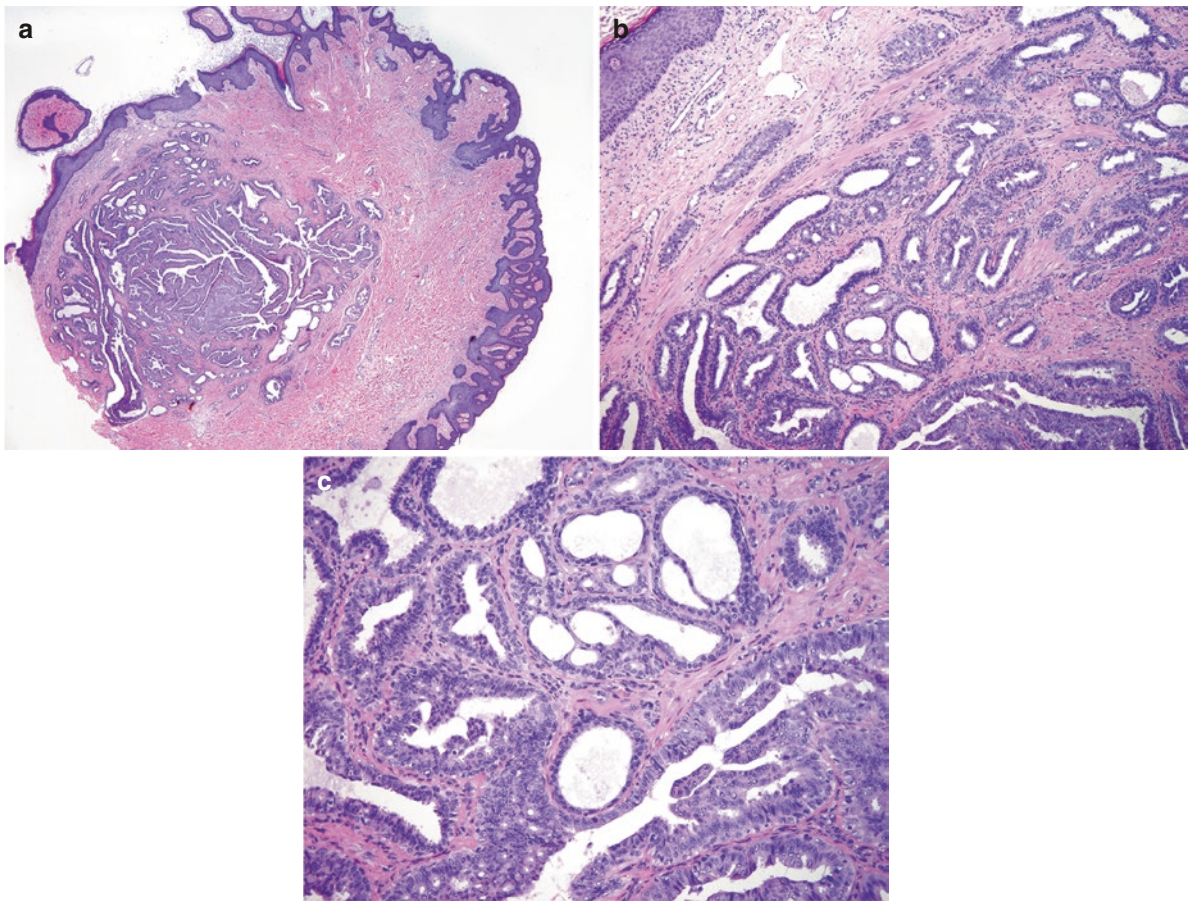

Fig. 19.6 Nipple adenoma. (**a**) This excisional biopsy specimen is of a nipple adenoma with a more papillary architecture, and with the characteristic well-rounded contour. (**b**) In contrast to the case in Fig. 19.5, the glandular structures in this example are more dilated and are lined by a columnar epithelial proliferation with areas of UDH. (**c**) On highest magnification, the histologic features of UDH can be appreciated: attenuated epithelial bridges and haphazardly placed epithelial cells with variable nuclear features; the spaces present are both rounded and slit-like but are preferentially placed at the periphery of the involved ducts

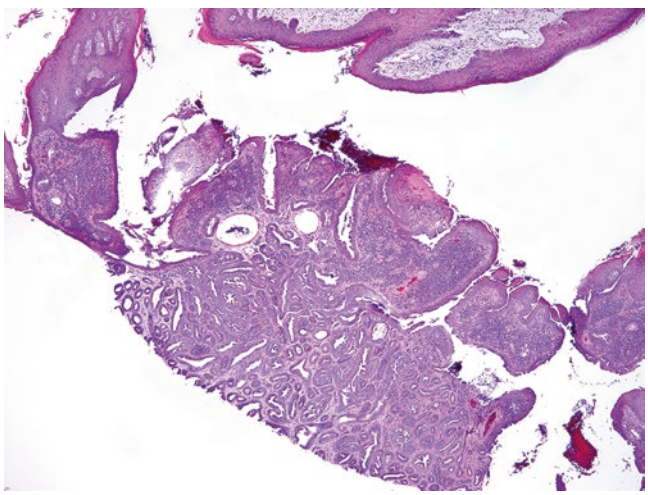

Fig. 19.7 Nipple adenoma. In this shave biopsy, the edge of the lesion is not captured making it difficult to appreciate the circumscribed nature of the proliferation. However, the variability of the epithelial proliferation and the slit-like spaces favor a benign process, even at this low power. Note also the extension of the glandular epithelium onto the surface of the nipple, a feature characteristic of nipple adenoma

cally (Fig. 19.8). Typically, these lesions are sampled either by a punch biopsy or by an excisional biopsy. Sampling by CNB is rare. The presence of nipple skin in the punch biopsy is important as it confirms the location of the lesion. If the biopsy is devoid of skin, then the lesion is likely arising beneath the nipple (subareolar region) and consequently excludes nipple adenoma from the differential diagnosis.

Differential Diagnosis

The differential diagnosis of nipple adenoma includes, primarily, tubular carcinoma and syringomatous adenoma (discussed below). The low-power impression of a more circumscribed, non-infiltrative lesion is helpful in distinguishing nipple adenoma from tubular carcinoma, if the edge of the lesion has been sampled. Tubular carcinoma lacks a myoepithelial cell layer, whereas myoepithelial cells are present in nipple adenoma and can be confirmed with immunohistochemical stains if the need arises.

Another potential problem is distinguishing florid UDH with associated necrosis (Fig. 19.9) from DCIS, which may

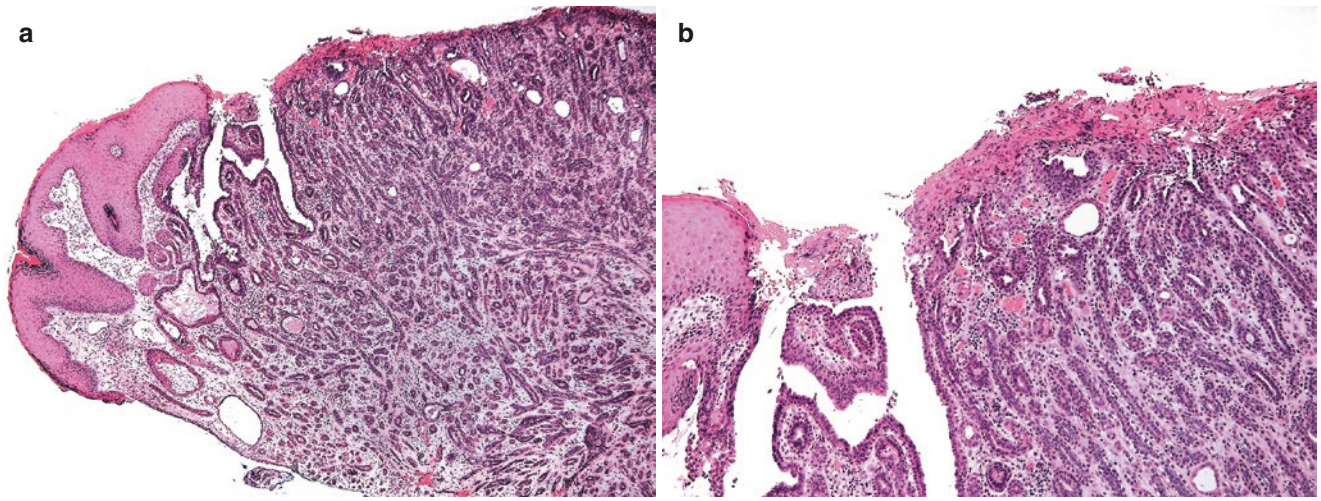

Fig. 19.8 Nipple adenoma with ulceration. (**a**) In this example of a nipple adenoma, the glandular epithelium has extended to the surface of the nipple resulting in extensive erosion and ulceration of the surface squamous epithelium. (**b**) This high-power image demonstrates ulceration of the squamous epithelium, illustrating why nipple adenoma is also known as erosive adenomatosis

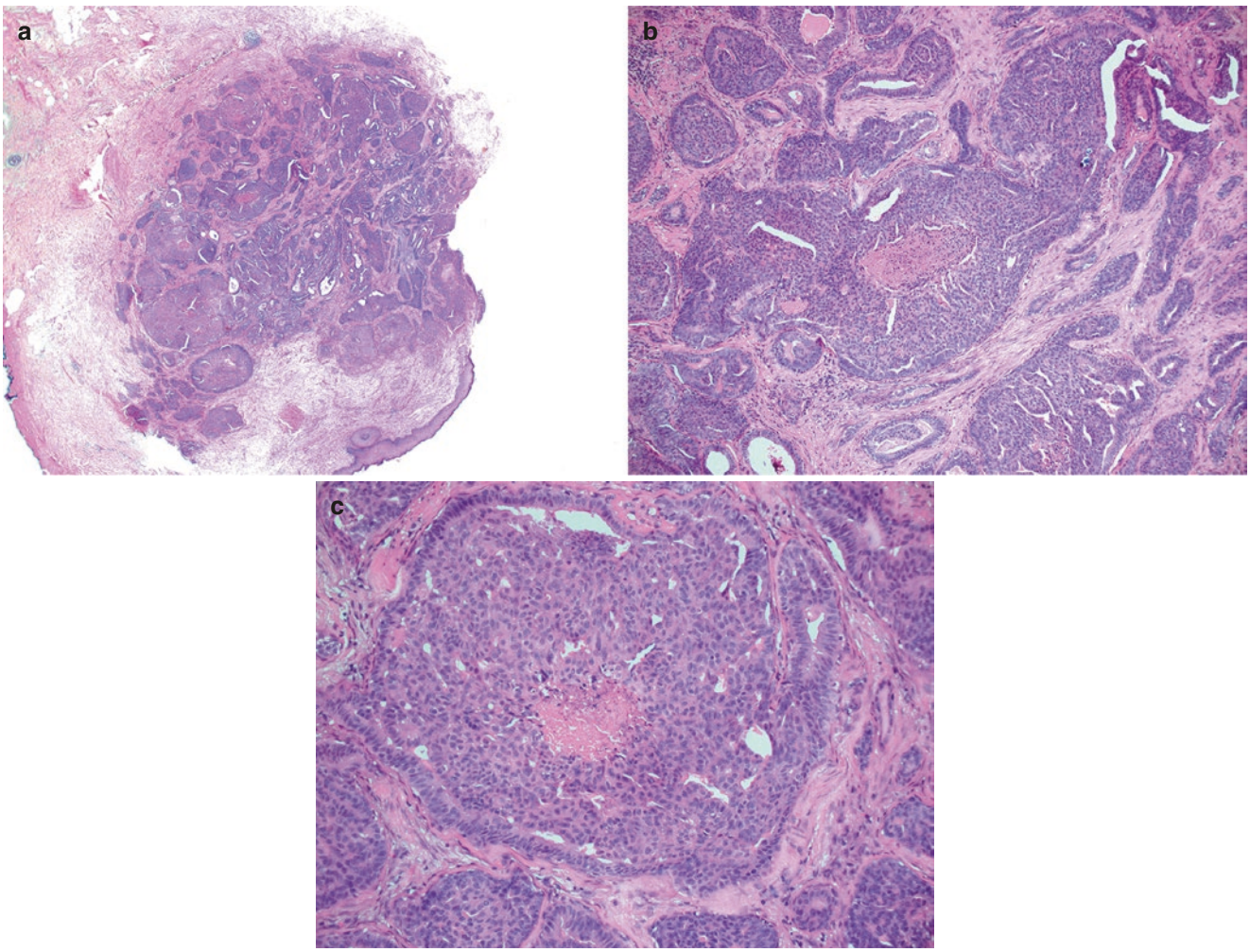

Fig. 19.9 Nipple adenoma with florid UDH and necrosis. (**a**) At low-power view, this excision demonstrates a lobulated, proliferative lesion involving the superficial and deep dermis of the nipple, with areas in the center of the field suggestive of necrosis. (**b**) In the intermediate- and (**c**) high-power images, the proliferation is seen to be composed of a heterogeneous population of overlapping ductal epithelial cells with slit-like spaces preferentially located at the periphery of the involved ducts. Central necrosis is also present. While the necrosis may raise concern for DCIS, the aforementioned features are characteristic of florid UDH

involve a nipple adenoma. The features of UDH involving a nipple adenoma are the same as elsewhere in the breast: a heterogeneous population of cells, with streaming and swirling of the nuclei; slit-like spaces preferentially located at the periphery of the duct; nuclear grooves; and intranuclear inclusions. In problematic cases, immunohistochemical stains for cytokeratin (CK) 5/6 and estrogen receptor (ER) are very helpful. In UDH, these stains are variably positive, staining some, but not all, of the cells; however, in low- and intermediate-grade DCIS, CK5/6 is negative, and ER is strongly and diffusely positive. As with any small biopsy, if there is uncertainty about the diagnosis, it is advisable to request further sampling before a definitive surgical procedure is performed. This is particularly important at this site, as mastectomy may be the next surgical procedure performed if a malignant diagnosis involving the nipple is rendered. Rare examples of invasive ductal carcinoma arising in association with nipple adenoma have been described [15].

Pathogenesis: Histopathology and Biology

The pathogenesis of nipple adenoma is unknown.

Prognosis and Clinical Management

Nipple adenoma is a benign lesion that is treated with excision. Recurrences are rare but have been reported [16].

Subareolar Sclerosing Duct Hyperplasia

Although not technically in the nipple, subareolar sclerosing duct hyperplasia (SSDH) is included in this chapter for the sake of completeness. This lesion occurs beneath the nipple-areolar complex, in the subareolar or central region. It is a benign proliferative lesion similar to nipple adenoma when involving the nipple and resembling radial scar when involving deeper breast tissue. Rosen first described 12 cases of this entity in 1987 [17]. Most patients present in the fourth or fifth decade (range 18–80 years [17–19]).

Gross and Radiologic Features

All reported cases presented with firm tumors beneath the nipple or areola without erosion or ulceration of the nipple. Patients may also present with bloody nipple discharge or rarely with nipple retraction [19]. The typical gross appearance described is of a firm mass, gray or brown in color with occasional yellow streaks, an indistinct border, and an average size of 1.2 cm (range 0.4–3.0 cm) [19]. The mammographic findings are not well documented.

Microscopic Features

Similar to radial scars, these lesions tend to have sclerosis centrally with hyperplastic ducts more prominent at the periphery. However, SSDH does not typically exhibit stromal elastosis. The lesion has both epithelial and stromal proliferation. In most cases, the lesion is composed of a few ducts expanded by UDH, resulting in rounded contours (Fig. 19.10). In some cases, there may be many small proliferative ducts at the periphery, resulting in an irregular border to the lesion. The hyperplastic proliferation often displays papillary architecture. SSDH may be associated with atypical ductal hyperplasia (ADH) or DCIS [17, 19]. Other reported coexisting lesions include low-grade adenosquamous carcinoma and lobular carcinoma in situ. Rare cases show apocrine metaplasia.

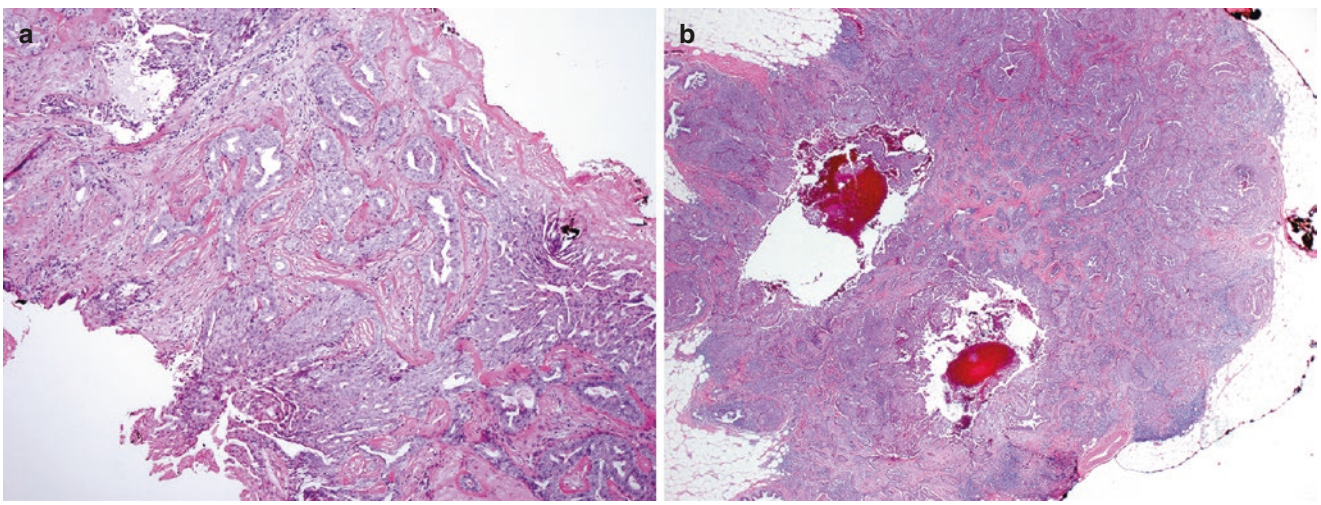

Fig. 19.10 Subareolar sclerosing ductal hyperplasia. (**a**) In this core biopsy of a subareolar lesion, the characteristic features of SSDH can be seen. Several ducts involved by florid UDH are embedded in a sclerotic stroma. Exact knowledge of the subareolar location within the breast is required in order to render this diagnosis. If there is doubt, a descriptive diagnosis is appropriate. (**b**) In the excision specimen from the same case, the circumscribed nature of the lesion is now appreciated, along with the extensive florid UDH and the central area of sclerosis, typical of the lesion

Differential Diagnosis

The differential diagnosis includes nipple adenoma and radial scar. As mentioned earlier, this differential diagnosis is sorted out based on the location in the breast. Nipple adenomas occur in the nipple, and radial scars occur deeper in the breast tissue. In contrast, SSDH occurs in the subareolar tissue. Only rarely has nipple tissue been reported to be included in the excisional specimens, and when explicitly reported, all lesions were entirely surrounded by breast parenchyma [17]. In addition, microscopic differences include more rounded contours in SSDH compared to the stellate architecture of radial scars. As noted above, SSDH does not display stromal elastosis, cystic or apocrine change, or squamous metaplasia.

Pathogenesis: Histopathology and Biology

The pathogenesis of SSDH is unknown.

Prognosis and Clinical Management

SSDH appears to behave in a similar manner to radial scars. Excisional biopsy is usually sufficient, although two of nine cases excised in the Rosen series developed recurrences and required re-excision. In the other reported series, no recurrences occurred, including those that were associated with carcinoma [18, 19].

Syringomatous Tumor

Syringomatous tumor (formerly adenoma) is a rare lesion of the nipple which may occur at any age, but the average age reported is 40 years. The name syringomatous adenoma was coined by Rosen in 1983 in a report in which he described five cases, noting the similarity of this lesion with syringoma of the eccrine duct [20]. Recently, the World Health Organization Expert Panel reporting in the Classification of Breast Tumours expressed a preference for use of the term syringomatous tumor [21].

Gross and Radiologic Features

Patients typically present with a subareolar mass, which may be associated with itching, pain, ulceration, nipple discharge, and/or nipple inversion. Radiologic findings are nonspecific, largely due to the difficulty of imaging in this location. On mammography, a subareolar mass, either circumscribed or spiculated and with or without associated microcalcifications, may be seen. Ultrasound findings reportedly vary from well-circumscribed to poorly defined hypoechoic lesions with posterior acoustic shadowing [22]. In practice, it is the clinical examination that is more important in this region. On gross examination, these tumors are usually ill-defined with a gray-white, firm cut surface. Reported tumor size ranges from 1.0 to 3.5 cm (median: 1.5 cm).

Microscopic Features

Syringomatous tumor is composed of small glands, tubules, nests, and cords of bland-appearing epithelial cells embedded in a fibrous stroma. Infiltration between ducts and into the smooth muscle of the nipple is often seen. Nests of squamous cells and squamous-lined cysts are also present, usually in the superficial aspect of the lesion (Figs. 19.11 and 19.12) [23]. These squamous cysts occasionally rupture, eliciting a chronic inflammatory response that may mask the glandular proliferation. Characteristically, many of the glands and tubules have a comma- or teardrop-shaped appearance with eosinophilic material in the lumina, comparable to that seen in syringomatous tumors of the skin [20]. Perineural invasion may be seen. The tubules are lined by two layers of epithelium, including an outer myoepithelial cell-like layer and a luminal layer [24]. The peripheral cell layer may stain for p63 and/or high-molecular-weight keratins (CK5/6, CK14), with variable expression of other myoepithelial cell markers [23]. The more glandular (luminal) elements stain with low-molecular-weight keratins such as CK8/18 [21].

Differential Diagnosis

On a CNB or a punch biopsy of the skin of the nipple, syringomatous tumor may be difficult to recognize. The infiltrative growth pattern can raise the differential diagnostic consideration of tubular carcinoma. Tubular carcinoma arising in the nipple is unusual. Morphologically, tubular carcinoma has open, angular, but not teardrop-shaped, glands with cytoplasmic snouts. The nuclei of tubular carcinoma are monomorphic and round. Frequently, there is associated ADH or low-grade DCIS, which is absent in syringomatous tumor. Finally, squamous metaplasia and squamous-lined cysts are not a feature of tubular carcinoma. Caution should be used when interpreting immunostains for myoepithelial cell markers as there may be an absence of staining around some of the nests in syringomatous tumor. Tubular carcinoma is strongly and diffusely positive for ER, which should enable distinction from syringomatous tumor, which shows only focal, weak staining, in the event that interpretation of myoepithelial markers is problematic.

Nipple adenoma is distinguished from syringomatous tumor by the more circumscribed nature of the lesion and the presence of florid UDH. Squamous metaplasia, if present in a nipple adenoma, would be focal as compared to syringomatous tumor where the squamous appearance is diffuse and fundamental to the lesion.

Low-grade adenosquamous carcinoma is a tumor with a similar histologic appearance to syringomatous tumor of the nipple, but occurs deeper in the breast parenchyma.

Pathogenesis: Histopathology and Biology

The pathogenesis of syringomatous tumor is incompletely understood. It has been suggested that syringomatous tumor

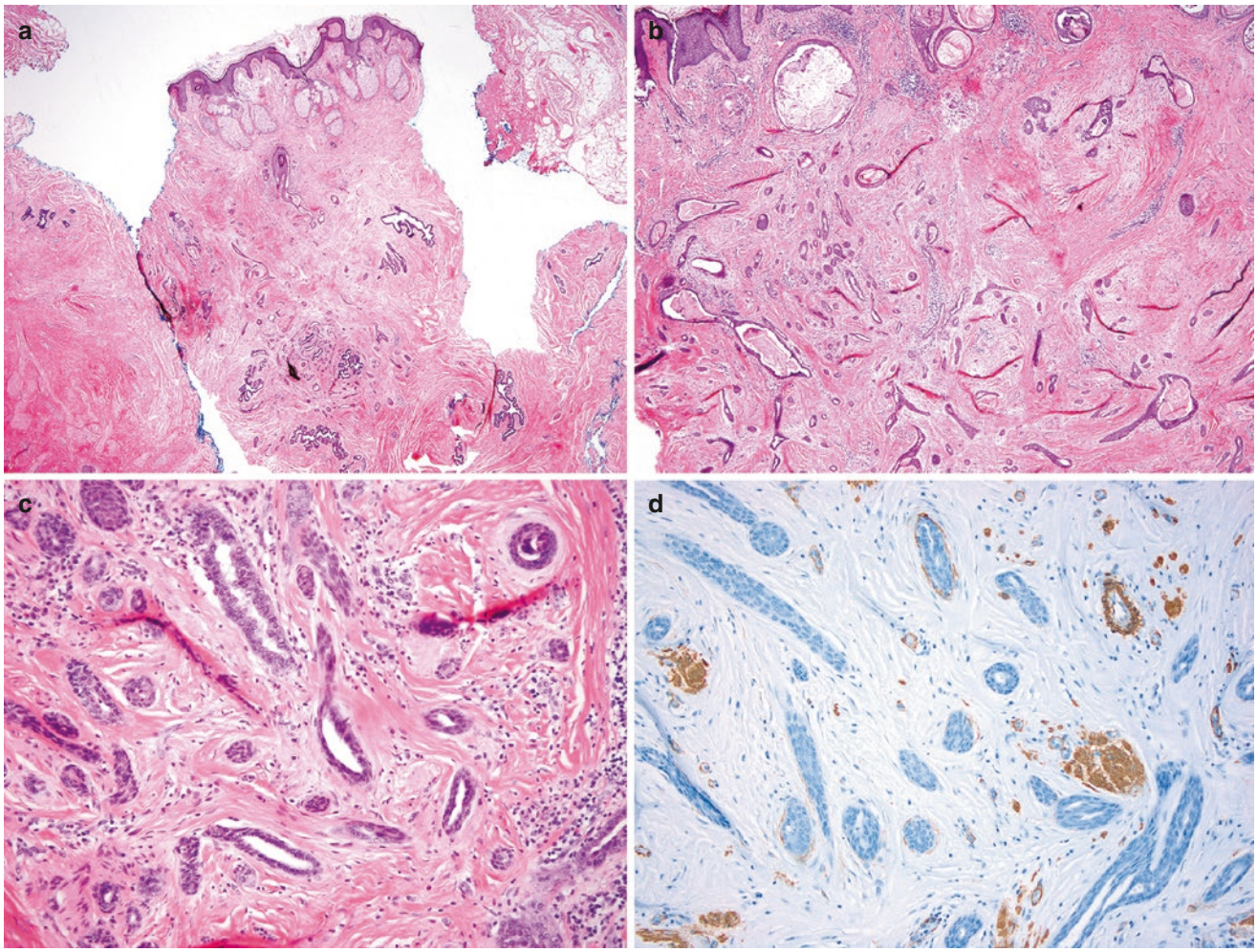

Fig. 19.11 Syringomatous tumor. (**a**) In this low-power image of several punch biopsies of a nipple lesion, the small glandular proliferation is subtle, though the presence of tubules, nests, and cords of epithelial cells infiltrating between the ducts of the nipple should prompt consideration of this diagnosis. (**b**) At intermediate power, the extent of the infiltration by the glands and cords of epithelial cells around the nipple ducts can be better appreciated. Several of the glands have eosinophilic material in the lumen. A squamous cyst is also present in this field. (**c**) At higher power view, the characteristic comma- or teardrop-shaped appearance of the glands with bland epithelial cells can be seen. (**d**) A smooth muscle actin immunostain demonstrates an absence of staining around the glandular elements and solid nests

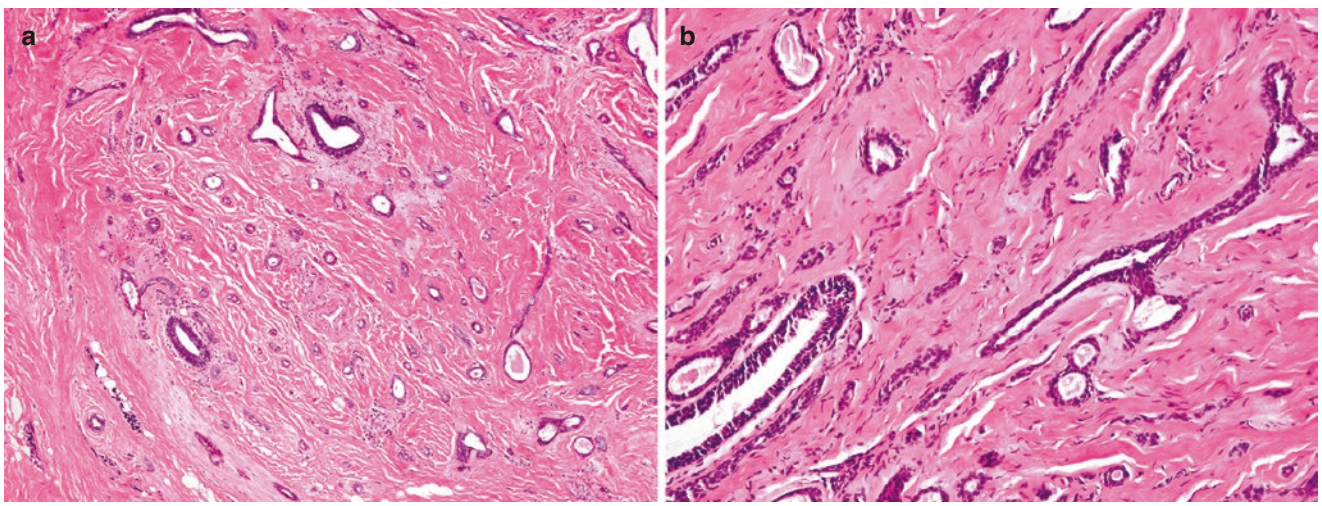

Fig. 19.12 Syringomatous tumor. In this punch biopsy of the nipple, small, somewhat teardrop-shaped glands can be seen infiltrating around normal nipple ducts, as is typical of this lesion; on (**a**) low and (**b**) higher power

has its origins in either the cutaneous appendages of the nipple-areolar complex [25] or the nipple duct epithelium [26]. Recent evidence suggests similarities in the cell of origin (p63+ and CK5/14+) for syringomatous tumor and low-grade adenosquamous carcinoma that may account for the morphologic and immunophenotypic similarities of these two tumors [23]. More work is needed to explain the differences in behavior of these two tumors and to determine whether they are distinct biologic entities.

Prognosis and Clinical Management

Complete surgical excision is required as syringomatous tumor has a tendency to recur if incompletely excised. There is a single case report of a syringomatous tumor of the nipple and "micrometastatic cells" in the sentinel lymph node. The images from the report demonstrate only isolated tumor cells in the lymph node; however, no mention is made of a prior CNB [27].

Nipple-Invasive Primary Carcinomas

Invasive carcinomas arising from ducts within the nipple dermis are rare (less than 1%). The term nipple-invasive primary carcinomas has recently been coined in an attempt to separate these lesions from those arising in the breast parenchyma or the epidermis of the nipple. These tumors are distinct from Paget disease with invasion into the skin [28]. Of 14 patients in a single study, the clinical presentation was as a nipple mass, with skin thickening, nipple crust, erythema, and pruritis. Importantly, 71% of these patients showed no mammographic abnormality. The histologic type of these carcinomas is similar to others in the breast, being approximately 50% ductal carcinoma of no special type, 21% lobular carcinoma, and 29% mixed ductal and lobular carcinomas. Given the limited data, little is known about the behavior of this lesion.

Lesions that Involve the Skin

The skin of the nipple may be affected by dermatologic conditions, such as eczema, psoriasis, dermatitis, and cutaneous malignancies, as well as lesions specific to the nipple-areolar complex such as nevoid hyperkeratosis. These entities will not be discussed in this chapter but should be considered in the differential diagnosis of Paget disease due to similarities in clinical presentation.

Paget Disease of the Nipple

Paget disease is the rare occurrence of adenocarcinoma in the squamous epithelium of the nipple. It is present in approximately 1–4% of breast cancer patients. In a small minority of patients (5–15%), no underlying DCIS or invasive carcinoma is identified [29].

Gross and Radiologic Features

Paget disease typically presents as erythema, ulceration, and scaling of the nipple-areolar complex that may be painful or itchy and mimics eczema. Rarely, pigmented plaques may be seen. Some patients may present with bloody nipple discharge.

Skin biopsies of Paget disease may have an erythematous or eczematous surface; excision specimens will similarly show erythema of the skin with or without associated eczematous changes and ulceration. Imaging studies in patients with Paget disease may reveal skin thickening on mammography and enhancement of the nipple on magnetic resonance imaging [30]; however, mammographic studies may be normal in up to 80% of patients [8, 28]. Therefore, even in the absence of imaging findings in the skin, if there is a clinical suspicion of Paget disease, careful radiologic examination to exclude an underlying invasive carcinoma is indicated.

Microscopic Features

Microscopically, large cells with abundant clear or amphophilic cytoplasm and high-grade nuclei with prominent nucleoli may be seen either in a single-cell pattern, in nests, or in glands most commonly located within the basal portion of the epidermis and ascending to the epidermal surface (pagetoid spread) (Figs. 19.13 and 19.14). The skin appendages may also be involved. Mitoses may be seen. Rarely, the tumor cells may be pigmented (Fig. 19.15) [31]. Secondary Paget disease is the occurrence of direct extension into the skin from an underlying carcinoma (without intraductal spread) (Fig. 19.16). Rarely, the converse pattern may be seen where there is invasion into the superficial dermis from intraepidermal Paget disease (i.e., "invasive Paget disease") (Fig. 19.17). Cases of invasive Paget disease are often accompanied by a lymphoplasmacytic infiltrate at the dermoepidermal junction, which is a clue to the possibility of invasion. The invasive component is usually quite small, either microinvasive or less than 5 mm (i.e., T1mi or T1a, respectively) [32, 33]. This contrasts with, and facilitates distinction from, cases of secondary Paget disease which are much larger tumors that invade directly into the overlying epidermis, as noted above [32, 33].

Differential Diagnosis

The histologic differential diagnosis principally includes malignant melanoma, squamous cell carcinoma, and Toker cell hyperplasia. Cutaneous sebaceous carcinoma should also be considered due to histologic similarities; however, this entity is very rare in the nipple. Toker cells are clear cells with small nuclei present within the epidermis of the nipple (Fig. 19.18). Typically, they are present singly, but

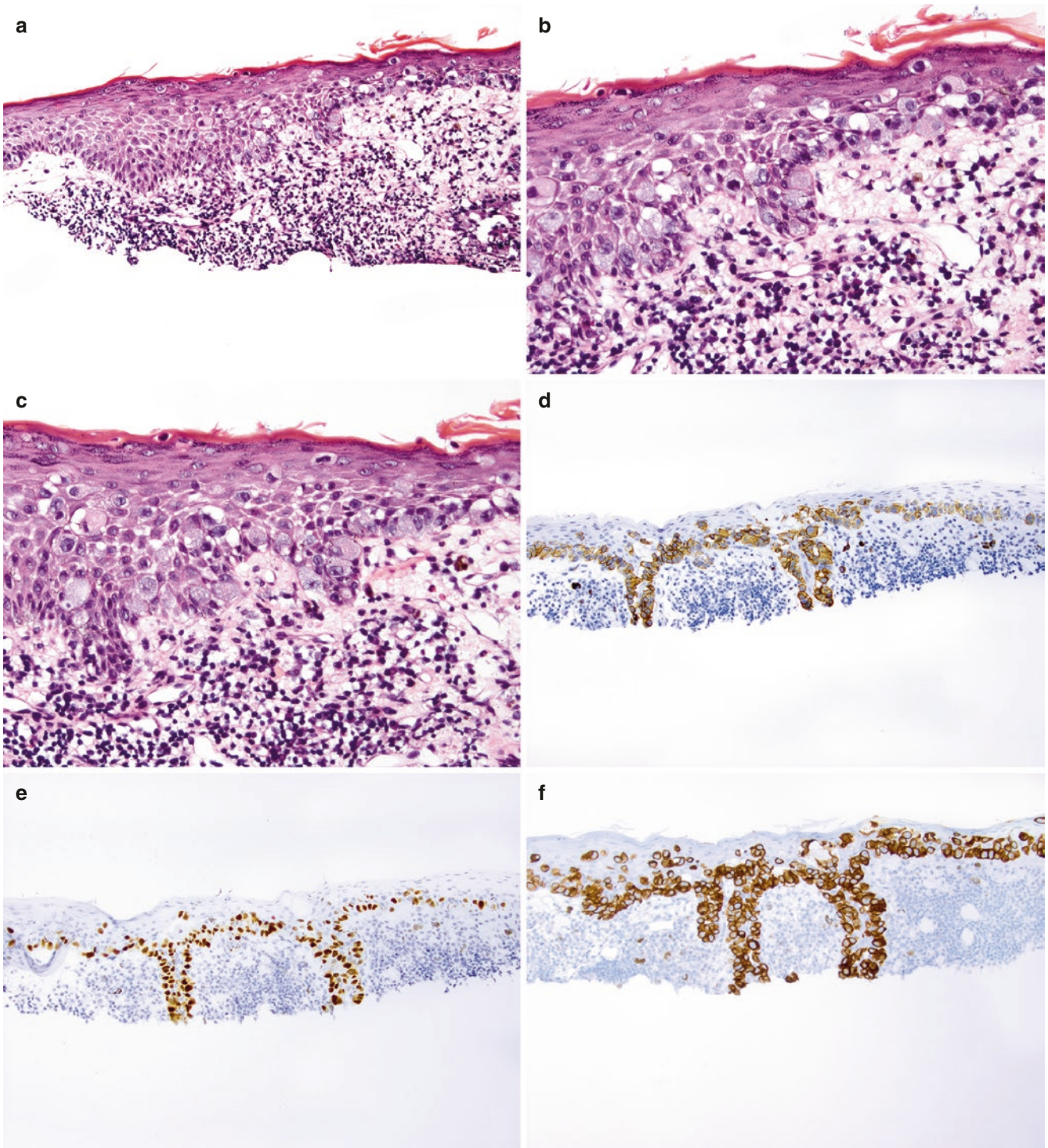

Fig. 19.13 Paget disease of the nipple. (**a**) In this low-power view of a shave biopsy of the nipple, large atypical glandular-appearing epithelial cells can be seen percolating along the basal layer of the epidermis. (**b**) Additional views show some upward (pagetoid) spread of the malignant cells. (**c**) On higher power magnification, the nuclear pleomorphism can be appreciated. (**d**) HER2 immunostain highlights the malignant epithelial cells. (**e**) An ER stain is positive in this case of Paget disease. (**f**) CK7 stain decorates the tumor cells, highlighting the extent of involvement of the nipple epidermis by Paget disease

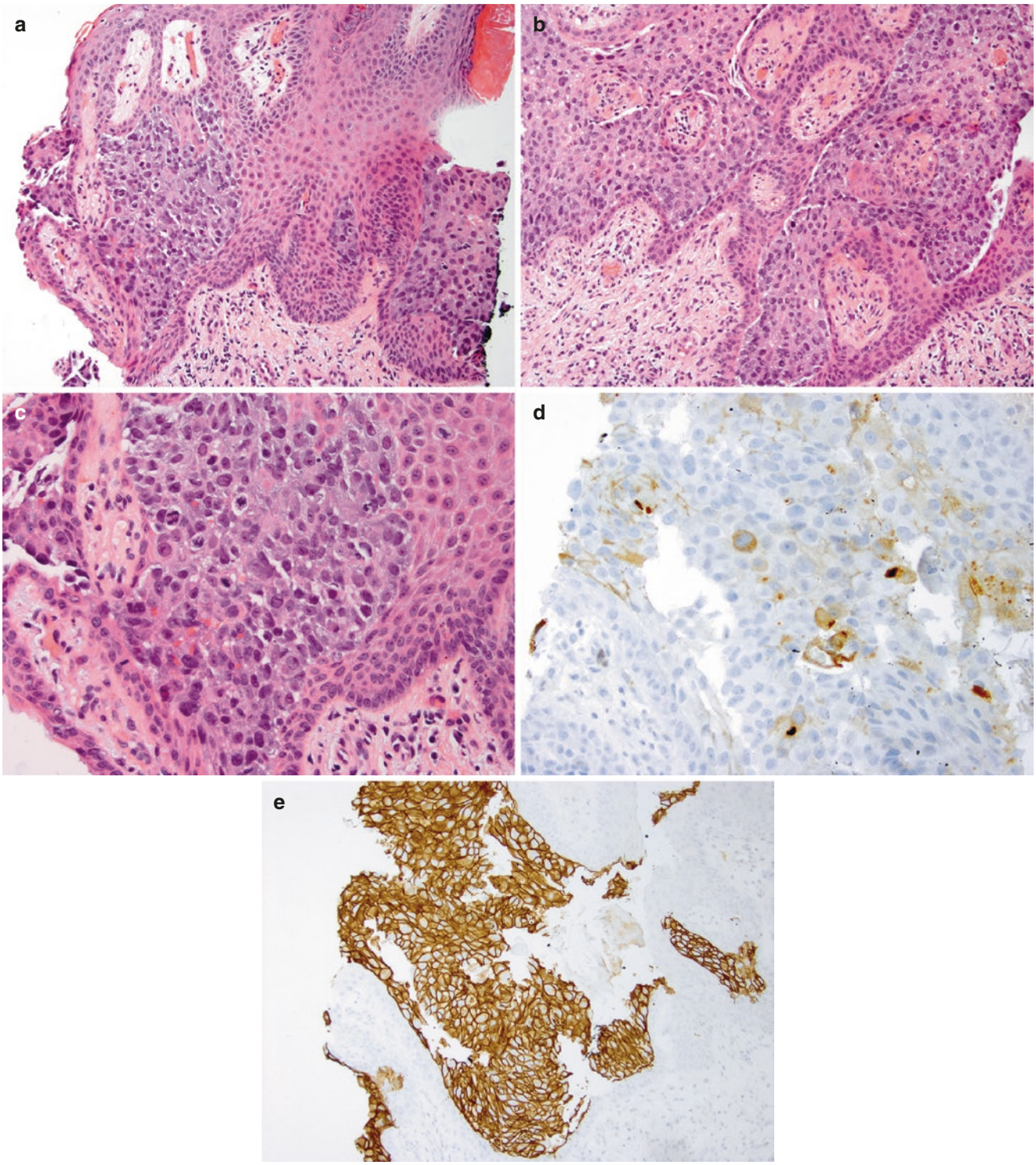

Fig. 19.14 Paget disease of the nipple. (**a**) This punch biopsy of the nipple reveals sheets of atypical epithelial cells involving the epidermis of the nipple. Mucin vacuoles can be appreciated in some cells. (**b**) In some fields, the distinction from the background squamous cells is subtle. (**c**) However, there is marked cytologic atypia and a brisk mitotic rate. (**d**) The atypical cells are gross cystic disease fluid protein-15 positive and (**e**) HER2 positive, confirming the diagnosis of Paget disease

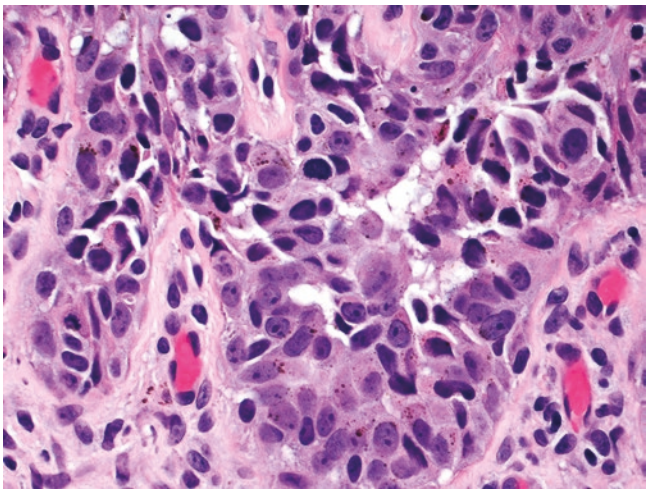

Fig. 19.15 Pigmented Paget disease. This high-power view displays brown pigment deposits in the cytoplasm of the tumor cells, mimicking melanoma both clinically and histologically. Immunohistochemical analysis is essential to differentiate pigmented Paget disease and melanoma

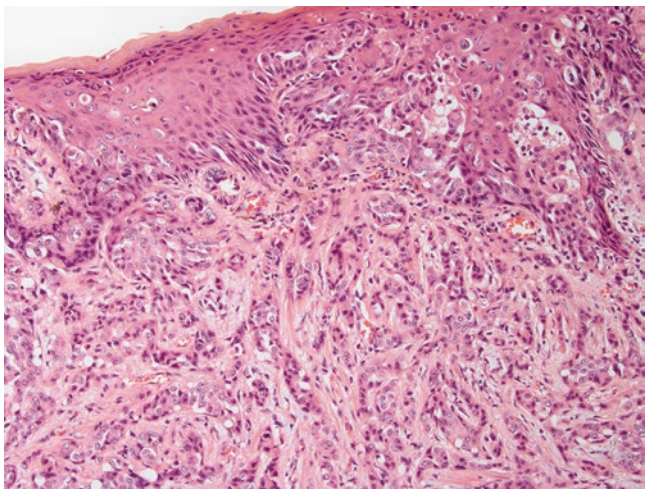

Fig. 19.16 Secondary Paget disease. This example of secondary Paget disease demonstrates secondary invasion of the epidermis of the nipple by a large underlying invasive carcinoma

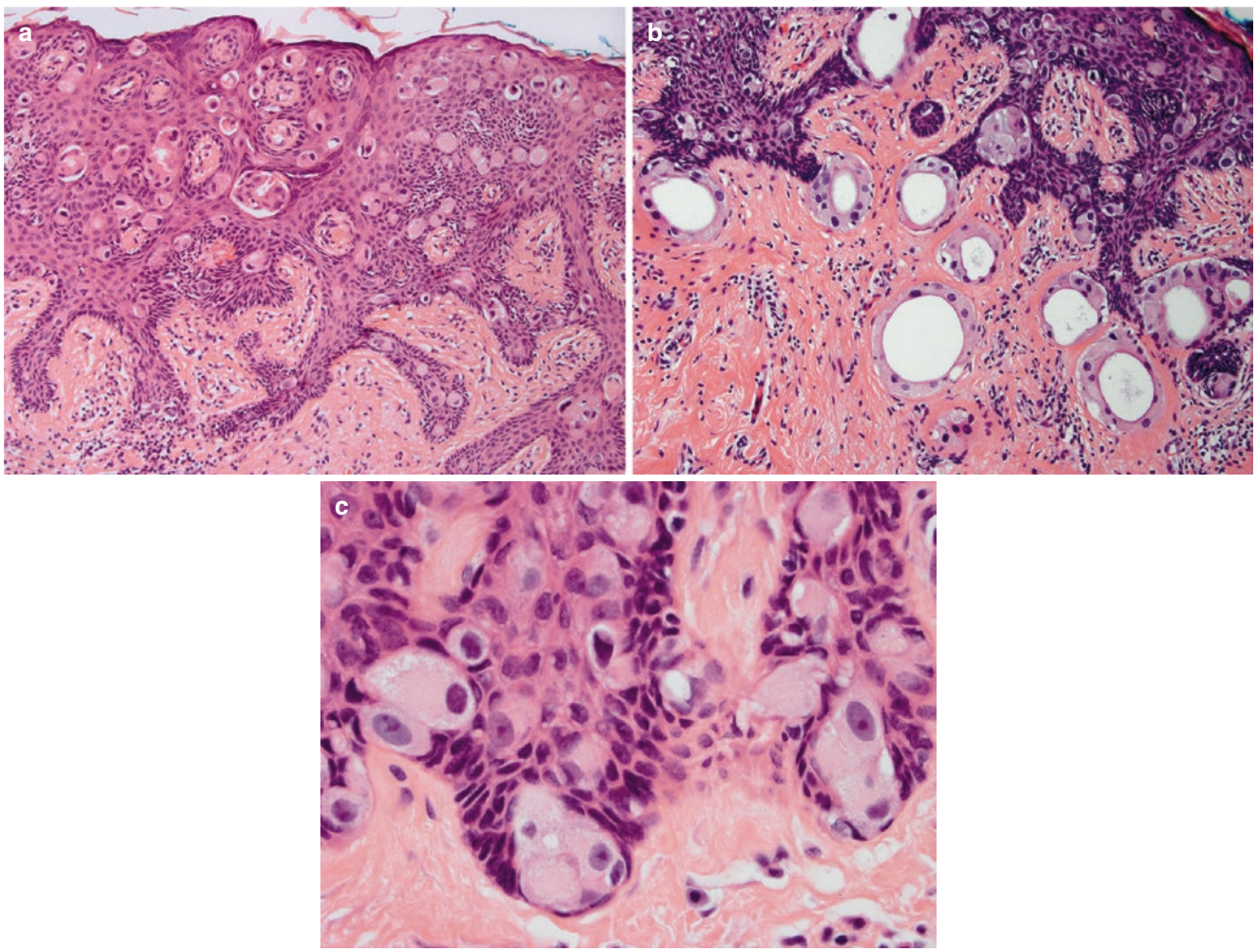

Fig. 19.17 Invasive Paget disease of the nipple. (**a**) In this intermediate-power view from a section of the nipple, large atypical glandular-appearing epithelial cells can be seen percolating throughout the epidermis (pagetoid spread). (**b**) Additional views reveal areas of gland formation within the epidermis as well as apparent invasion into the superficial dermis (invasive Paget disease). (**c**) On highest power, the malignant nature of the Paget cells is readily appreciated; the cells are large with abundant amphophilic cytoplasm, large nuclei, and prominent nucleoli

they may form nests or even glands mimicking Paget disease. Malignant melanoma, squamous cell carcinoma, and sebaceous carcinoma rarely involve the nipple; however, the number of reports is so few that accurate data on incidence are not available (Fig. 19.19). To further delineate Paget cells from others in the differential diagnosis, immunohistochemistry is often employed. In Paget disease, the tumor cells classically show strong staining with CK7 and epithelial membrane antigen (EMA). Almost all cases of Paget disease are HER2 positive; most cases will have an underlying high-nuclear-grade DCIS or invasive carcinoma that is similarly HER2 positive. Staining with ER and progesterone receptor (PR) in the tumor cells of Paget disease is variable. The cells are nonreactive for the melanocytic markers HMB-45 and Melan-A/MART1; note that S100 protein may be positive in Paget disease. Malignant melanoma is negative for keratins and breast biomarkers and positive for S100 protein, HMB45, and Melan-A/MART1. Squamous cell carcinoma may be positive for EMA but is negative for CK7 and breast and melanoma markers. Expression of p63 in malignant cells is a useful positive marker for squamous cell carcinoma in situ. Cutaneous sebaceous carcinoma displays tumor cells with clear to-vacuolated cytoplasm and stains for p63, EMA, and adipophilin and is negative for CK7 and CEA. Toker cells express CK7 and EMA and may be either positive or negative for ER, HER2, and S100 protein. GCDFP-15 is negative in Toker cells. A mucicarmine stain is also of value in separating the malignant entities; Paget (and Toker) cells contain mucicarmine. The other malignant entities in the differential diagnosis lack mucin [34].

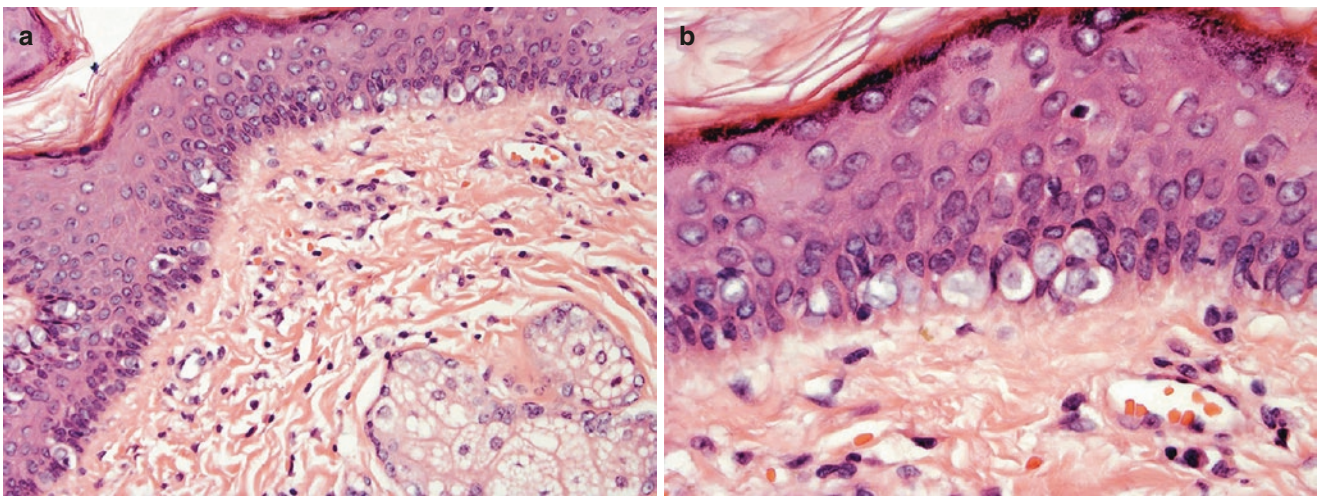

Fig. 19.18 Toker cells. (**a**) On intermediate power, cells with round nuclei and clear cytoplasm can be seen percolating along the basal layer of the nipple epidermis. Note the absence of pagetoid spread. (**b**) At higher power, the relatively bland nature of the nuclei of the Toker cells is better appreciated

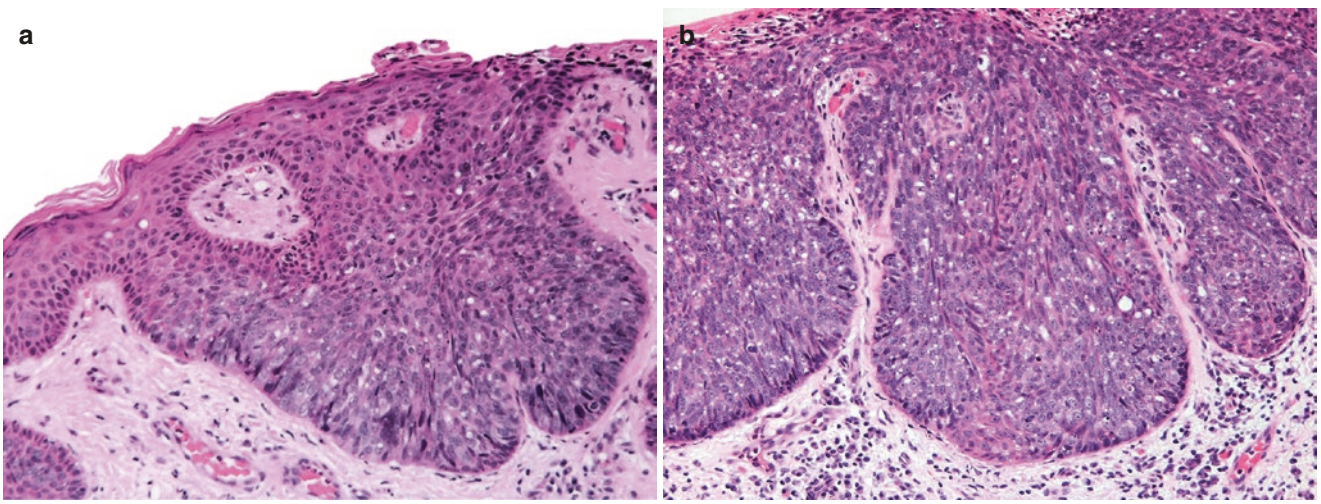

Fig. 19.19 Sebaceous carcinoma in situ of the nipple. (**a**) These low- and (**b**) intermediate-power images show highly atypical epithelial cells with clear cytoplasmic vacuoles replacing the epidermis. The tumor cells displayed membranous pattern staining with adipophilin, supporting the diagnosis

Pathogenesis: Histopathology and Biology

Paget disease is believed to arise from the spread of tumor cells up the nipple ducts into the epidermis from an underlying adenocarcinoma. In rare cases in which an underlying carcinoma is not identified, origin from keratinocytes at the squamocolumnar junction or from Toker cells has been postulated as the cell of origin [35, 36].

Prognosis and Clinical Management

The treatment and prognosis of Paget disease are determined by the underlying carcinoma. Treatment options, therefore, include wide local excision with radiation therapy, and mastectomy, depending on the disease extent and the patient preference. Examination of sentinel lymph nodes is usually indicated as metastases have been reported.

Conclusion

Lesions of the nipple are unusual and are rarely sampled by CNB, but issues of small sample size apply because skin punch biopsies or limited incisional biopsies are often performed instead; as such, it is critical that diagnostic consideration is given to all the possible benign lesions of the nipple before rendering a malignant diagnosis at this site. Furthermore, if immunohistochemistry is utilized, considerable care is required with interpretation, particularly of myoepithelial cell markers, as unexpected staining patterns are characteristic of some benign nipple lesions.

References

1. Zuska JJ, Crile G, Ayres WW. Fistulas of lactiferous ducts. Am J Surg. 1951;8:312–7.
2. Crile G Jr, Chatty EM. Squamous metaplasia of lactiferous ducts. Arch Surg. 1971;102(5):533–4. https://doi.org/10.1001/archsurg.1971.01350050099029.
3. Lo G, Dessauvagie B, Sterrett G, Bourke AG. Squamous metaplasia of lactiferous ducts (SMOLD). Clin Radiol. 2012;67(11):e42–6.
4. Furlong AJ, al-Nakib L, Knox WF, Parry A, Bundred NJ. Periductal inflammation and cigarette smoke. J Am Coll Surg. 1994;179(4):417–20.
5. Goyal A, Mansel RE, Young HL, Douglas-Jones A. Metastatic cutaneous Crohn's disease of the nipple: report of a case. Dis Colon Rectum. 2006;49(1):132–4.
6. Tourasse C, Coulon A, Denier JF. Radio-histological correlations of subtle sonography images. Diagn Interv Imaging. 2014;95(2):181–95.
7. Ferris-James DM, Iuanow E, Mehta TS, Shaheen RM, Slanetz PJ. Imaging approaches to diagnosis and management of common ductal abnormalities. Radiographic. 2012;32(4):1009–30.
8. Da Costa D, Taddese A, Cure ML, Gerson D, Poppiti R Jr, Esserman LE. Common and unusual diseases of the nipple-areolar complex. Radiographics. 2007;27(Suppl 1):S65–77.
9. Rahal RM, de Freitas-Junior R, Carlos da Cunha L, Moreira MA, Rosa VD, Conde DM. Mammary duct ectasia: an overview. Breast J. 2011;17(6):694–5.
10. Rahal RM, de Freitas-Junior R, Paulinelli RR. Risk factors for duct ectasia. Breast J. 2005;11(4):262–5.
11. Dixon JM. Mammary duct ectasia—periductal mastitis complex. Br J Surg. 1996;83(7):1017–9.
12. Dixon JM, Ravisekar O, Chetty U, Anderson TJ. Periductal mastitis and duct ectasia: different conditions with different aetiologies. Br J Surg. 1996;83(6):820–2.
13. Bonito M, Cantile M, Collina F, et al. Adenoma of the nipple: a clinicopathological report of 13 cases. Oncol Lett. 2014;7(6):1839–42.
14. Tsushimi T, Enoki T, Takemoto Y, et al. Adenoma of the nipple, focusing on the contrast-enhanced magnetic resonance imaging findings: report of a case. Surg Today. 2011;41(8):1138–41.
15. Jones MW, Tavassoli FA. Coexistence of nipple duct adenoma and breast carcinoma: a clinicopathologic study of five cases and review of the literature. Mod Pathol. 1995;8(6):633–6.
16. Salemis NS. Florid papillomatosis of the nipple: a rare presentation and review of the literature. Breast Dis. 2015;35(2):153–6.
17. Rosen PP. Subareolar sclerosing duct hyperplasia of the breast. Cancer. 1987;59(11):1927–30.
18. Tresserra F, Monzóna M, Grases PJ. Hiperplasia ductal esclerosante subareolar de la mama: presentación de ocho casos (subareolar sclerosing ductal hyperplasia of the breast: report of eight cases). Rev Senol Patol Mam. 2003;16:31–4.
19. Cheng E, D'Alfonso TM, Arafah M, Marrero Rolon R, Ginter PS, Hoda SA. Subareolar Sclerosing Ductal Hyperplasia. Int J Surg Pathol. 2017;25(1):4–11. https://doi.org/10.1177/1066896916677288. Epub 2016 Nov 10
20. Rosen PP. Syringomatous adenoma of the nipple. Am J Surg Pathol. 1983;7(8):739–45.
21. WHO Classification of Tumours of the Breast. 5th ed. Lyon: IARC Press; 2019.
22. AlSharif S, Tremblay F, Omeroglu A, Altinel G, Sun S, Mesurolle B. Infiltrating syringomatous adenoma of the nipple: sonographic and mammographic features with pathologic correlation. J Clin Ultrasound. 2014;42(7):427–9.
23. Boecker W, Stenman G, Loening T, et al. Differentiation and histogenesis of syringomatous tumour of the nipple and low-grade adenosquamous carcinoma: evidence for a common origin. Histopathology. 2014;65(1):9–23.
24. Jones MW, Norris HJ, Snyder RC. Infiltrating syringomatous adenoma of the nipple. A clinical and pathological study of 11 cases. Am J Surg Pathol. 1989;13(3):197–201.
25. Ku J, Bennett RD, Chong KD, Bennett IC. Syringomatous adenoma of the nipple. Breast. 2004;13(5):412–5.
26. Boecker W, Junkers T, Reusch M, et al. Origin and differentiation of breast nipple syringoma. Sci Rep. 2012;2:226.
27. Chang CK, Jacobs IA, Calilao G, Salti GI. Metastatic infiltrating syringomatous adenoma of the breast. Arch Pathol Lab Med. 2003;127(3):e155–6.
28. Sanders MA, Brock JE, Harrison BT, et al. Nipple-invasive primary carcinomas: clinical, imaging, and pathologic features of breast carcinomas originating in the nipple. Arch Pathol Lab Med. 2018;142(5):598–605.
29. Chen CY, Sun LM, Anderson BO. Paget disease of the breast: changing patterns of incidence, clinical presentation, and treatment in the U.S. Cancer. 2006;107(7):1448–58.
30. Frei KA, Bonel HM, Pelte MF, Hylton NM, Kinkel K. Paget disease of the breast: findings at magnetic resonance imaging and histopathologic correlation. Investig Radiol. 2005;40(6):363–7.
31. Tang X, Umemura S, Kumaki N, et al. A case report of pigmented mammary Paget's disease mimicking nevus of the nipple. Breast Cancer. 2014;21(3):370–4.
32. Ozerdem U, Swistel A, Antonio LB, Hoda SA. Invasive Paget disease of the nipple: a brief review of the literature and report of the first case with axillary nodal metastases. Int J Surg Pathol. 2014;22(6):566–9.

33. Sanders MA, Dominici L, Denison C, Golshan M, Wiecorek T, Lester SC. Paget disease of the breast with invasion from nipple skin into the dermis: an unusual type of skin invasion not associated with an adverse outcome. Arch Pathol Lab Med. 2013;137(1):72–6.
34. Kuan SF, Montag AG, Hart J, Krausz T, Recant W. Differential expression of mucin genes in mammary and extramammary Paget's disease. Am J Surg Pathol. 2001;25(12):1469–77.
35. Yao DX, Hoda SA, Chiu A, Ying L, Rosen PP. Intraepidermal cytokeratin 7 immunoreactive cells in the non-neoplastic nipple may represent interepithelial extension of lactiferous duct cells. Histopathology. 2002;40(3):230–6.
36. Mai KT, Yazdi HM, Perkins DG. Mammary Paget's disease: evidence of diverse origin of the disease with a subgroup of Paget's disease developing from the superficial portion of lactiferous duct and a discontinuous pattern of tumor spread. Pathol Int. 1999;49(11):956–61.

Lymphoid and Hematopoietic Tumors of the Breast

20

Julia Turbiner Geyer

Overview

Hematopoietic neoplasms of the breast are very uncommon. Non-Hodgkin lymphoma of the breast is the most frequently encountered disease subtype and accounts for approximately 2% of extranodal non-Hodgkin lymphoma and for less than 1% of all non-Hodgkin lymphomas [1–6]. Most cases represent secondary breast involvement by disseminated lymphoma. Primary lymphoma of the breast constitutes 0.4–0.5% of all malignant breast lesions [2–4, 7–9].

Lymphoid infiltrates occurring in the breast have traditionally posed a significant clinical and histopathologic dilemma. The difficulty in making a correct diagnosis is compounded by small tissue size available with the use of a core needle biopsy (CNB). Factors that historically contributed to diagnostic error and inaccurate prognostication include difficulties inherent in the histopathologic evaluation of extranodal lymphoid proliferations, particularly those predominantly composed of small lymphocytes [10–12]; lack of histopathologic criteria to recognize the existence of extranodal small lymphocytic lymphomas, mantle cell lymphomas, and extranodal marginal zone lymphomas [11]; lack of a large clinical series of patients whose lesions were diagnosed and categorized according to an acceptable standard histopathologic classification and who were systematically evaluated using modern staging practices; and finally lack of access to immunologic and molecular biologic techniques capable of delineating lymphoid cell subpopulations and determining their monoclonal or polyclonal nature.

The diagnostic dilemma posed by extranodal lymphoid infiltrates has been partially resolved by immunophenotypic analysis of their constituent lymphoid subpopulations [13]. Immunophenotypic analysis is capable of determining the immunologic polyclonality or monoclonality of B-lymphocytes and thus infers on the benign or malignant nature of lymphoid proliferations that cannot be deciphered morphologically [14]. The inclusion of these immunologic criteria in the evaluation of extranodal lymphoid infiltrates substantially altered many of the traditional beliefs concerning these lymphoid proliferations. In particular, widespread use of immunophenotypic analysis clarified that most extranodal diffuse monomorphic small lymphoid cell infiltrates are, in fact, monoclonal B-cell proliferations [13]. Nonetheless, in certain circumstances, immunophenotypic analysis may also be limited in its ability to prognosticate reliably for patients who have extranodal lymphoid proliferations [12, 15]. An additional breakthrough consisted of the discovery that the antigen recognition molecules of B and T cells, immunoglobulin, and T-cell receptors, respectively, were encoded by genetic loci that undergo somatic recombination to become functionally active in mature lymphocytes [16–18]. Clonal rearrangements of the immunoglobulin and T-cell receptor genes have proved to be accurate and objective molecular genetic markers of the lineage and clonality of B and T cells [14]. The demonstration of clonal immunoglobulin and T-cell receptor gene rearrangements by polymerase chain reaction (PCR) analysis has been used successfully to determine the lineage and clonality of lymphoproliferative disorders and has become an important adjunct in the diagnosis, classification, and investigation of lymphoid neoplasia. This approach is capable of determining the presence of clonal B- and T-cell populations that are not detectable by morphologic examination or by immunophenotypic analysis [19–21]. PCR and cytogenetic analysis including fluorescent in situ hybridization (FISH) are also capable of detecting chromosomal translocations, and structural alterations of proto-oncogenes and tumor suppressor genes.

Two important developments have contributed significantly to the understanding of lymphoid neoplasia, especially the extranodal lymphoid lesions. The first is the recognition of mucosa-associated lymphoid tissue (MALT)

J. T. Geyer (✉)
Department of Pathology and Laboratory Medicine, Weill Cornell Medicine, New York, NY, USA
e-mail: jut9021@med.cornell.edu

© The Author(s), under exclusive license to Springer Nature Switzerland AG 2022

S. J. Shin et al. (eds.), *A Comprehensive Guide to Core Needle Biopsies of the Breast*,
https://doi.org/10.1007/978-3-031-05532-4_20

and the special characteristics of MALT and malignant lymphomas that arise within MALT [22]. The second is the creation of the World Health Organization (WHO) classification of tumors of hematopoietic and lymphoid tissues, most recently updated in 2017—the most widely used and the only standard lymphoma classification for nodal and extranodal lymphomas [23, 24]. In this fashion, the terminology used in this chapter corresponds exclusively to that of the WHO classification. Thus, the term "pseudolymphoma" liberally used in the older literature pertaining to lymphoid proliferations of the breast is generally considered to be confusing and imprecise and is no longer acceptable as a diagnostic category [25].

Modern study of lymphoma is based on the correlative multiparametric clinical, morphologic, immunophenotypic, cytogenetic, and molecular genetic analysis far surpassing what was historically attainable by light microscopic examination alone. Image-guided CNB is the standard initial method of tissue sampling for breast lesions [26]. In this respect, CNB has several limitations in the definite diagnosis of hematopoietic neoplasms. Lack of adequate material may preclude performance of all the necessary studies for complete assessment and prognostication of the lymphoid neoplasms. Hematopoietic neoplasms involving the breast are often clinically indistinguishable from other breast tumors, and due to rarity of the primary breast lymphoma, the diagnosis is almost never suspected clinically. Thus, CNBs are typically fixed in formalin precluding immunophenotypic evaluation of the lymphoid infiltrate by flow cytometry and cytogenetic analysis. Other limitations of CNB in the diagnosis of breast lymphoma include loss of architectural patterns as seen with light microscopy, difficulty in distinguishing reactive lymphoid hyperplasia from low-grade lymphoma, and inability to fully subclassify low-grade and occasionally large-cell lymphomas. False-negative results may be due to sampling error, which becomes especially relevant in cases of classical Hodgkin's lymphoma and high-grade transformation of low-grade B-cell lymphoma. Lastly, small samples may be subject to various technical alterations, such as cell smudging and crush artifact. Thus, depending on the institutional experience, breast CNB is diagnostic in 50–80% of patients with primary breast lymphoma, while the remaining patients require a follow-up excisional biopsy [5, 26, 27]. In a large cohort reported by Caon and colleagues, the yield of breast CNB diagnosis was significantly higher with aggressive lymphoma (65% diagnosed by CNB) compared with indolent lymphoma (only 38% diagnosed by CNB) [27]. A more recent study by Bicchierai et al. confirmed that CNB may be an effective method of assessment for primary breast lymphoma, especially in cases of diffuse large B-cell lymphoma (DLBCL), which is its most common subtype [28].

Primary Lymphoma of the Breast

Overview

The most widely used definition of primary breast lymphoma was advocated by Wiseman and Liao as follows: primary breast lymphoma is a unilateral or bilateral breast lymphoma with close spatial relationship of lymphoma to the breast parenchyma and no evidence of systemic disease after staging in a patient without prior history of lymphoma [6] (Fig. 20.1). Cases of primary breast lymphoma include those with the involvement of ipsilateral axillary lymph nodes [6]. Other authorities accept presence of regional disease involvement (supraclavicular and internal mammary lymph nodes) as part of primary breast lymphoma [29]. Talwalkar and colleagues slightly modified these criteria specifically for breast CNB cases with limited material to include lymphomas where breast tissue was not identified microscopically but radiologic studies showed evidence of breast involvement [5, 30].

Primary breast lymphoma presents almost exclusively in women, although rare cases of male breast involvement have also been described [31–34]. Several recent reviews of epidemiological features of primary breast lymphoma in the USA based on the Surveillance, Epidemiology, and End Results (SEER) database have demonstrated a steady increase in its overall incidence over the past four decades [35–37]. In particular, the incidence continues to increase for younger women (<50 years old) and for two specific sub-

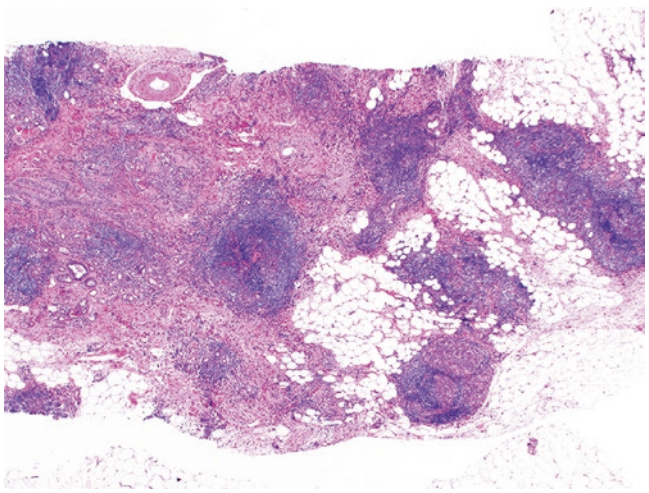

Fig. 20.1 This 54-year-old woman presented with right breast enhancing area. CNB yielded the diagnosis of extranodal marginal zone lymphoma. The atypical lymphoid infiltrate has a periductal growth pattern, consistent with primary breast lymphoma pattern. (Photomicrograph courtesy of Dr. Timothy D'Alfonso, Memorial Sloan Kettering Cancer Center, New York, with permission)

types of lymphoma (marginal zone lymphoma and anaplastic large-cell lymphoma) [37]. Patient's age ranges from 17 to 95 years with most patients presenting in fourth to sixth decades of life. Median age in Western patients appears to be greater than that in Asian patients (60–70 years old versus 50–60 years old) [27, 29, 35, 38–47]. Clinically, primary breast lymphoma tends to present as a painless breast mass, typically with no evidence of constitutional symptoms [29]. Right-breast involvement is slightly more common than left-breast involvement [27, 44, 48, 49]. Bilateral disease is present in approximately 10% of patients [27, 49, 50]. Cutaneous manifestations are very rare. Approximately 70% of patients have stage I disease at diagnosis, while the remaining patients have evidence of regional lymph node involvement (stage II) [27, 29, 49].

There are reports of primary breast lymphoma presenting in patients with a history of breast carcinoma or concurrently with breast cancer (up to 12% of patients per Genco and colleagues) [51–53]. However, among the concurrent cases, the majority of breast lymphoma was secondary (systemic) and an incidental finding. The possible association may need to be explored in larger studies.

The most common type of primary breast lymphoma is DLBCL, which constitutes 56–85% of cases, depending on the series [5, 29, 40, 49, 51, 54–56]. Overall, approximately 60% of all cases of primary breast lymphoma correspond to DLBCL. The majority of the remaining cases represent extranodal marginal zone lymphoma (MALT lymphoma, 10–30%) and follicular lymphoma (FL, 10–20%) [5, 29, 40, 49, 51, 54–56].

Gross and Radiologic Features

Up to 20% of patients are initially diagnosed with the use of screening mammogram [48, 57, 58]. The most common finding is a solitary oval-shaped lesion with irregular borders and high density [59]. No microcalcifications are typically seen. Although no radiographic findings are pathognomonic of lymphoma, large size of the mass (>4 cm) and absence of calcifications and architectural distortion in the surrounding breast tissue were suggested to differentiate lymphoma from carcinoma [58]. Ultrasound and magnetic resonance imaging (MRI) findings are nonspecific. Occasionally, primary breast lymphoma presents radiographically with multiple lesions or as a diffuse enlargement of one or both breasts [30, 58, 60]. There is no association between radiologic findings and different subtypes of lymphoma. Overall, multiple studies have shown that the imaging features of primary breast lymphoma overlap with those of breast carcinoma [56, 61].

Macroscopically, primary breast lymphoma lesions measure on average 4–5 cm, although there are reports of much larger tumors [29]. Thus, on average, breast lymphomas are larger than breast carcinomas. Approximately half of the patients with DLBCL have bulky disease; hence, this diagnosis should be considered when the breast mass measures more than 4–5 cm. This finding appears to be associated with worse prognosis [39, 50, 62, 63].

Microscopic Features and Immunohistochemical Workup

Diffuse Large B-Cell Lymphoma

DLBCL is the most common subtype of lymphoma in general and the most common primary lymphoma of the breast. DLBCL is a heterogeneous disease in terms of morphology, genetics, and biologic behavior. It frequently represents transformation of a less aggressive low-grade B-cell lymphoma. Several described cases of primary breast DLBCL had a component of marginal zone lymphoma, consistent with high-grade transformation. However, a large sample is typically needed to document this type of pathologic process, and it would be unusual to definitely ascertain this diagnosis on a small CNB [49, 64]. Since immunosuppression is an important risk factor, DLBCL is the most common lymphoma in patients with HIV, history of transplant, or primary immunodeficiency.

Morphologically, DLBCL is characterized by sheets of large lymphoid cells (Figs. 20.2 and 20.3). Neoplastic cells frequently surround and infiltrate the benign breast lobules and ducts (Figs. 20.4 and 20.5). Tumor cell morphology is very variable and includes cells with centroblastic morphology (round nuclei, several small nucleoli, and scant cytoplasm Fig. 20.6), immunoblastic morphology (round nuclei, one large central nucleolus, and moderate basophilic cyto-

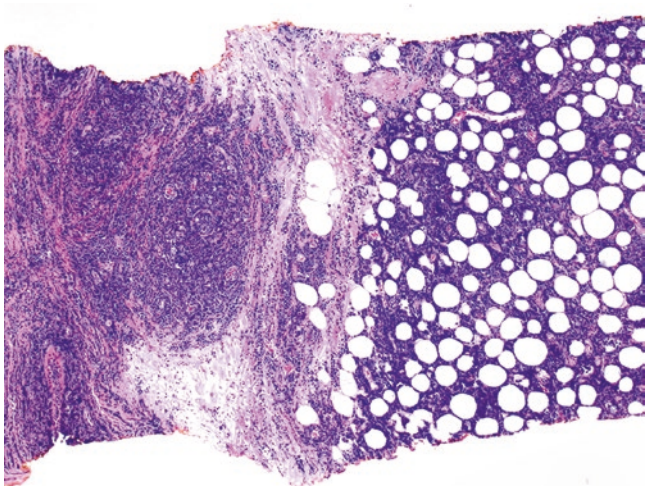

Fig. 20.2 Diffuse large B-cell lymphoma. Diffuse proliferation of large atypical lymphoid cells infiltrating fat and acinar breast tissue

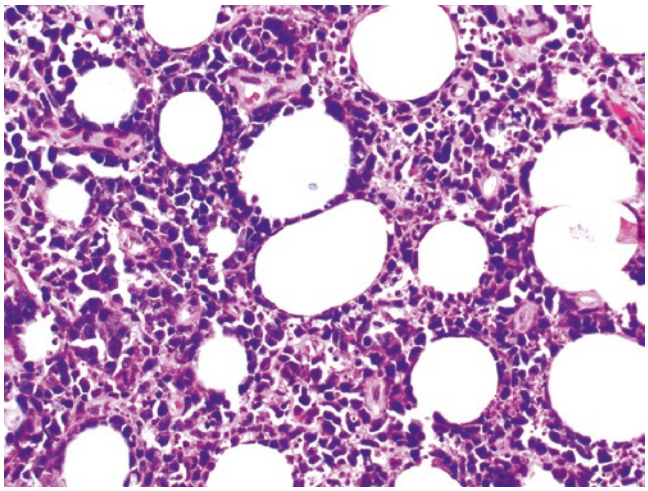

Fig. 20.3 Diffuse large B-cell lymphoma. The large atypical lymphoid cells display vesicular chromatin, occasional prominent nucleoli, and scanty to variable amount of cytoplasm. Numerous mitotic figures and apoptotic debris are identified. Prominent fat rimming and perivascular cuffing are present

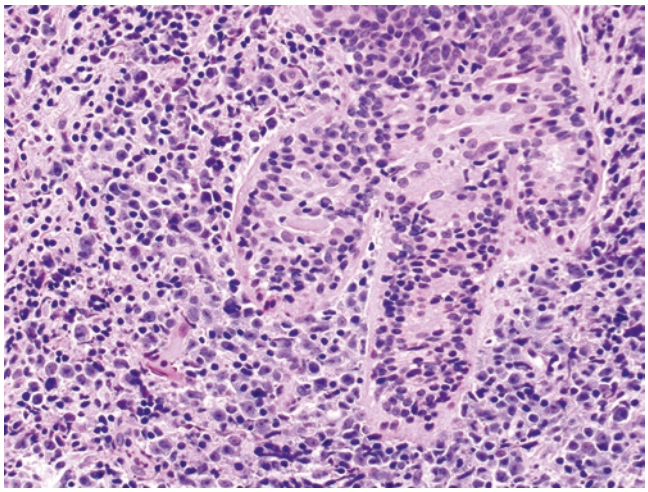

Fig. 20.4 Diffuse large B-cell lymphoma. Large neoplastic cells surround and infiltrate the benign breast lobular structures

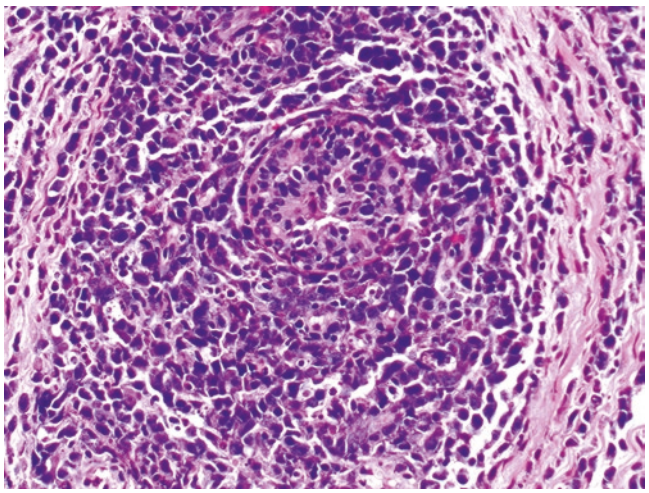

Fig. 20.5 Diffuse large B-cell lymphoma. Neoplastic lymphoid cells infiltrate the breast terminal duct unit

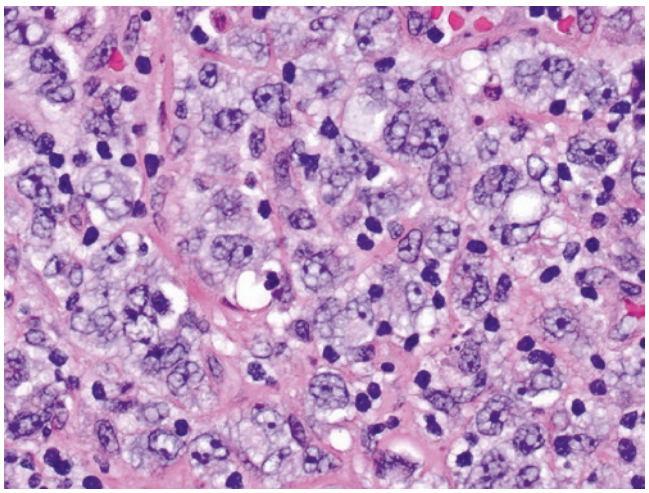

Fig. 20.6 Diffuse large B-cell lymphoma cells with centroblastic morphology

plasm Fig. 20.7), and anaplastic morphology (bizarre, multilobulated nuclei Fig. 20.8) [65]. Most primary breast DLBCL cases are of centroblastic type [5, 66]. Since DLBCL is an aggressive high-grade neoplasm, numerous mitoses, apoptotic debris, and necrosis are common findings. DLBCL is the most likely lymphoma morphologically misdiagnosed as breast carcinoma, especially the poorly differentiated lobular carcinoma that infiltrates as single cells that can closely resemble large lymphocytes. Thus, large-cell lymphoma should be considered in the differential diagnosis for breast malignancies with a dyscohesive pattern of infiltration when carcinoma in situ is absent, particularly in the absence of receptor expression [26] (see section on "Differential Diagnosis" below).

There have been recent reports of rare cases of Epstein-Barr virus (EBV)-positive DLBCL adjacent to macrotextured breast implants, which could meet the WHO criteria for either DLBCL associated with chronic inflammation or fibrin-associated DLBCL [67, 68]. All cases shared common pathological features consisting of sheets, clusters, and ribbons of large pleomorphic $CD30^+$ EBV-infected B cells, with EBV-encoded RNA (EBER) expression in virtually all lymphoma cells. The neoplastic cells were confined to the fibrous implant capsule, and all patients had a very indolent clinical course.

Three cases of primary breast intravascular large B-cell lymphoma have been described; curiously, two of them coexisted with a synchronous ductal carcinoma [52, 53, 69].

Immunohistochemistry/immunohistochemical (IHC) staining is necessary to confirm the diagnosis and distinguish DLBCL from breast carcinoma. Estrogen receptor α, estro-

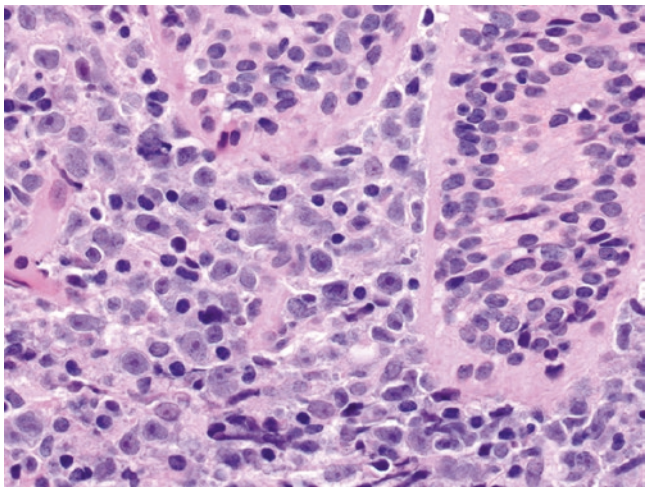

Fig. 20.7 Diffuse large B-cell lymphoma with immunoblastic morphology

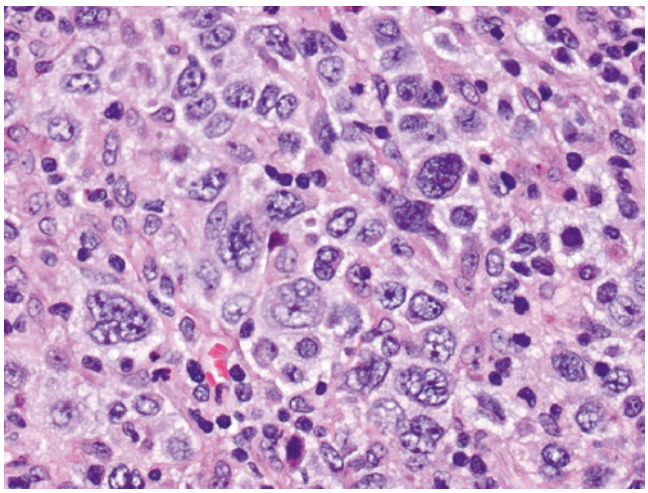

Fig. 20.8 Diffuse large B-cell lymphoma with anaplastic morphology

gen receptor β, and androgen receptors are not significantly expressed by IHC in breast lymphoma [26]. Tumor cells express B-cell antigens CD20, PAX5, and CD79a. Some cases have aberrant expression of CD5 [64]. The neoplastic B cells have limited expression of CD10, but Bcl-2, Bcl-6, and Mum-1 are expressed in the majority of cases. Seminal studies using gene expression profiling classified cases of DLBCL into two major groups: germinal center type (superior outcome) and activated B-cell type (poor prognosis) [70]. Hans algorithm (CD10, Bcl-6, Mum-1) [71] or Choi algorithm (CD10, Bcl-6, Mum-1, GCET, FoxP1) [72] is used in many laboratories as a substitute for molecular classification of DLBCL. Based on the Hans algorithm, results have been varied across institutions, with some reporting that cases of primary breast DLBCL have predominantly a non-germinal center immunophenotype [5, 48, 64, 73], while others showed that the majority were of germinal center origin [74, 75]. Proliferative fraction with Ki67 immunostain is high at >60% of all neoplastic cells [5, 64]. Flow cytometry may be attempted if fresh tissue is available for testing; however, the yield is not always high as this technique may be insensitive to the presence of large tumor cells.

If there is no fresh tissue for a complete cytogenetic analysis, paraffin-embedded unstained slides may be used for FISH analysis. Presence of *c-MYC* translocation is an important independent risk factor for poor outcome. Cases with *c-MYC* translocation should be tested for a concurrent *IgH-BCL2* translocation and *BCL6* break to exclude a double-hit lymphoma, which is characterized by dismal prognosis and poor response to conventional chemotherapy.

In cases with diagnostic uncertainty, paraffin-embedded unstained slides may be used for PCR analysis. Presence of a monoclonal *IgH* gene rearrangement confirms the diagnosis of B-cell lymphoma.

Finally, genetic sequencing studies have identified a high frequency of *PIM1*, *MYD88*, and *CD79B* gene mutations, similar to other extranodal DLBCLs, including primary central nervous system DLBCL and primary testicular DLBCL [74–76]. These findings indicate NFkB as the main pathway targeted for mutations in the pathogenesis of the primary breast DLBCL and suggest targeted therapeutic opportunities for this type of lymphoma.

Extranodal Marginal Zone Lymphoma (MALT Lymphoma)

Primary MALT lymphoma of the breast is frequently associated with a patient's personal history of systemic autoimmune disease. Histologic features of MALT lymphoma in the breast appear similar to what is seen in the other sites. MALT lymphoma is a low-grade lymphoma that morphologically emulates normal MALT as exemplified by Peyer's patches in the terminal ileum [22]. This may be a challenging diagnosis on a small CNB, and a multimodality approach with immunohistology and PCR clonality testing is typically required to distinguish MALT lymphoma from reactive chronic inflammatory infiltrates in the breast (see section on "Differential Diagnosis" below). MALT lymphomas are characterized by the presence of small neoplastic lymphoid cells distributed in a marginal zone pattern around reactive follicles and frequently attenuated rims of mantle zone lymphocytes [77] (Fig. 20.9). The neoplastic cells may infiltrate into the follicles (follicular colonization, Fig. 20.10). Tumor cells may also infiltrate and invade the breast acini and ducts to form lymphoepithelial lesions [77], although well-formed lymphoepithelial lesions are not as common in breast MALT lymphoma as in MALT lymphoma located in other sites of the body. Tumor cells are composed of monocytoid B cells (also called marginal zone B cells)

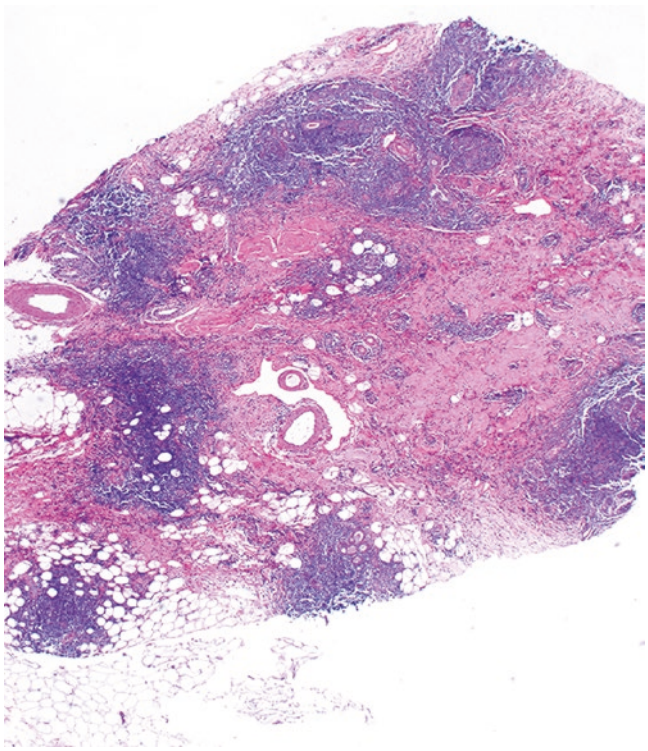

Fig. 20.9 MALT lymphoma. Breast parenchyma with a multifocal dense atypical lymphoid infiltrate. (Photomicrograph courtesy of Dr. Timothy D'Alfonso, Memorial Sloan Kettering Cancer Center, New York, with permission)

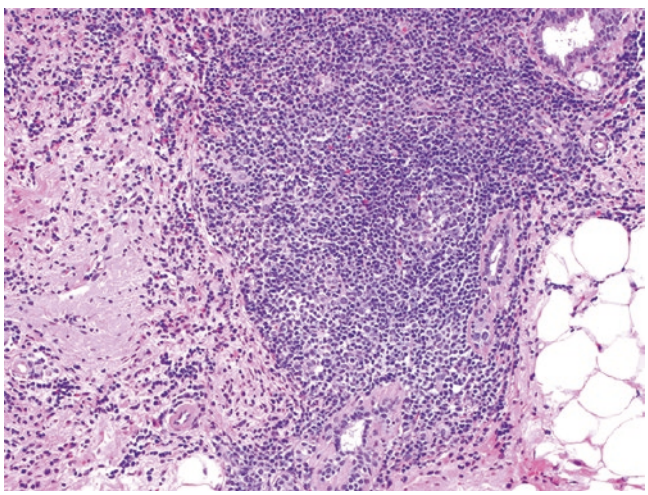

Fig. 20.10 MALT lymphoma. Neoplastic small lymphoid cells infiltrate and disrupt a reactive germinal center. (Photomicrograph courtesy of Dr. Timothy D'Alfonso, Memorial Sloan Kettering Cancer Center, New York, with permission)

with abundant pale cytoplasm, admixed with plasma cells and scattered immunoblasts (Figs. 20.11 and 20.12). Prominent plasma cell differentiation may be seen. A small subset of breast MALT lymphomas may be associated with amyloid deposition.

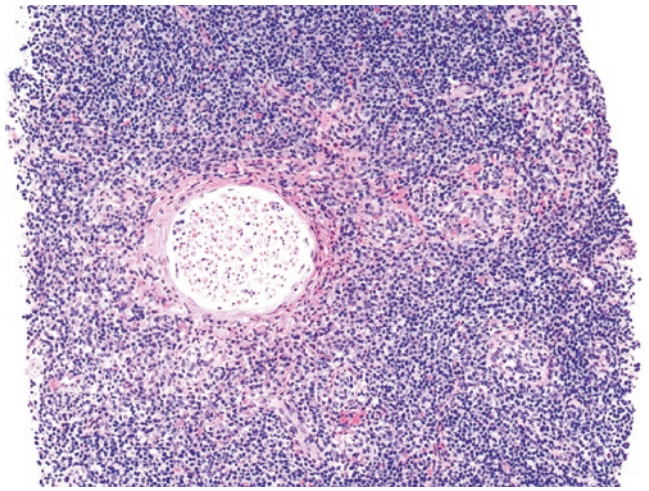

Fig. 20.11 MALT lymphoma. Dense atypical lymphoid infiltrate with a perineural distribution and a prominent component of monocytoid cells with abundant pale cytoplasm

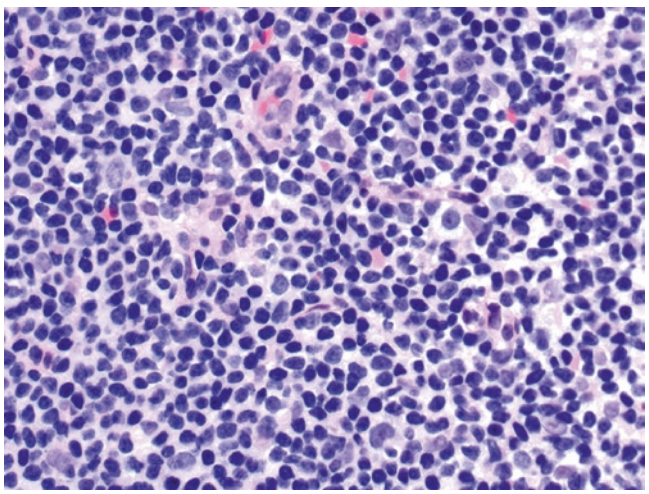

Fig. 20.12 MALT lymphoma. The neoplastic lymphoid infiltrate is composed of a mixture of small mature lymphocytes, monocytoid cells, plasma cells, and rare large transformed lymphocytes (immunoblasts)

IHC staining reveals that CD20-positive B cells are a predominant cell population. Tumor cells have aberrant expression of T-cell markers CD43 (in ~50% of the cases) and BCL2 (in most cases). Neoplastic cells are negative for CD5, CD10, Bcl-6, CD23, and cyclin D1. CD21 and CD23 antibodies are used to highlight the expanded and colonized follicular dendritic cell meshworks. Plasma cells express monotypic immunoglobulin light chain in cases with plasmacytic differentiation [78].

FISH analysis may demonstrate evidence of trisomy 3, 7, or 18 or translocations involving *BCL10* and *MALT1* genes. PCR testing for the presence of *IgH* gene rearrangement is very helpful and may be necessary in ambiguous cases, where the differential diagnosis is with reactive lymphoid hyperplasia.

Follicular Lymphoma

Similar to the primary MALT lymphoma of the breast, primary FL of the breast is very rare. In a large cohort of breast lymphoma studied by Talwalkar and colleagues, FL was the third most common type of lymphoma with 14% of the cases; however, all cases represented secondary breast involvement in patients with a history of disseminated disease [5]. Rare cases of primary breast FL in male patients and bilateral breast involvement have been described [31, 42]. Outcome appears less favorable than in primary breast MALT lymphoma or nodal based FL [42].

Morphologically, FL is characterized by the presence of lymphoid follicles (Figs. 20.13 and 20.14), which appear homogeneous in size and shape and consist of a mixture of small cleaved lymphocytes (centrocytes) and large lymphoid cells with round nuclei and several small nucleoli (centroblasts Fig. 20.15). Grading of FL may be difficult on CNBs and is not required if the tissue sample is small.

Immunophenotypic workup demonstrates that the neoplastic lymphoid cells are positive for B-cell antigens (Fig. 20.16a, b). Tumor cells typically coexpress Bcl-2, Bcl-6, and CD10 (Fig. 20.16c, d). CD21 and CD23 highlight the follicular dendritic cell meshworks. Ki67 proliferative fraction typically correlates with grading (<20% of the tumor cells in low-grade FL and > 20% in high-grade FL).

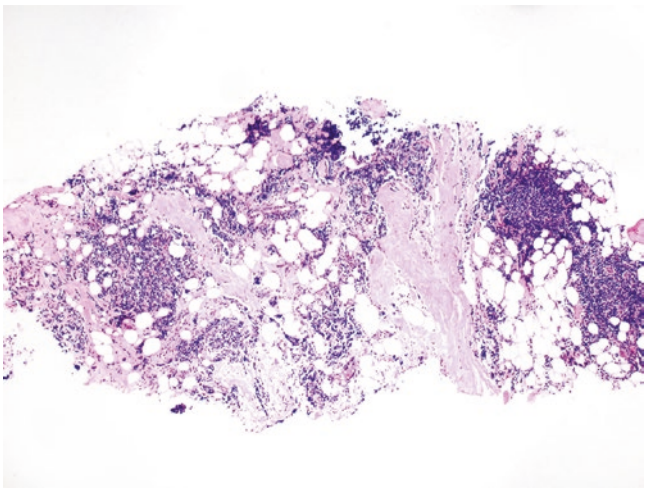

Fig. 20.13 Follicular lymphoma. Low power demonstrates follicular pattern (*right side*) and diffuse pattern (*left side*) of follicular lymphoma infiltration

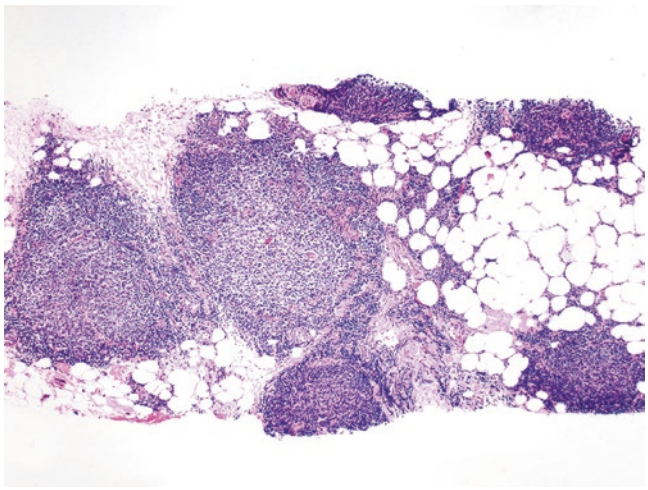

Fig. 20.14 Follicular lymphoma with closely packed lymphoid follicles. Neoplastic follicles have a homogeneous appearance and do not contain tingible body macrophages

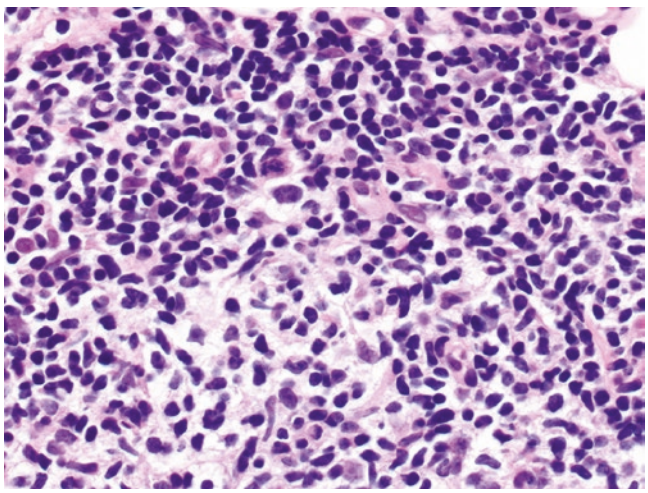

Fig. 20.15 Follicular lymphoma. High-power examination demonstrates presence of centrocytes and centroblasts

Paraffin-embedded unstained slides may be submitted for FISH analysis. *BCL2/IGH* gene rearrangement is present in up to 90% of low-grade FL, while *BCL6* gene rearrangement is present in 5–15% of the cases. By PCR, a monoclonal *IGH* gene rearrangement is seen in approximately 80% of the cases.

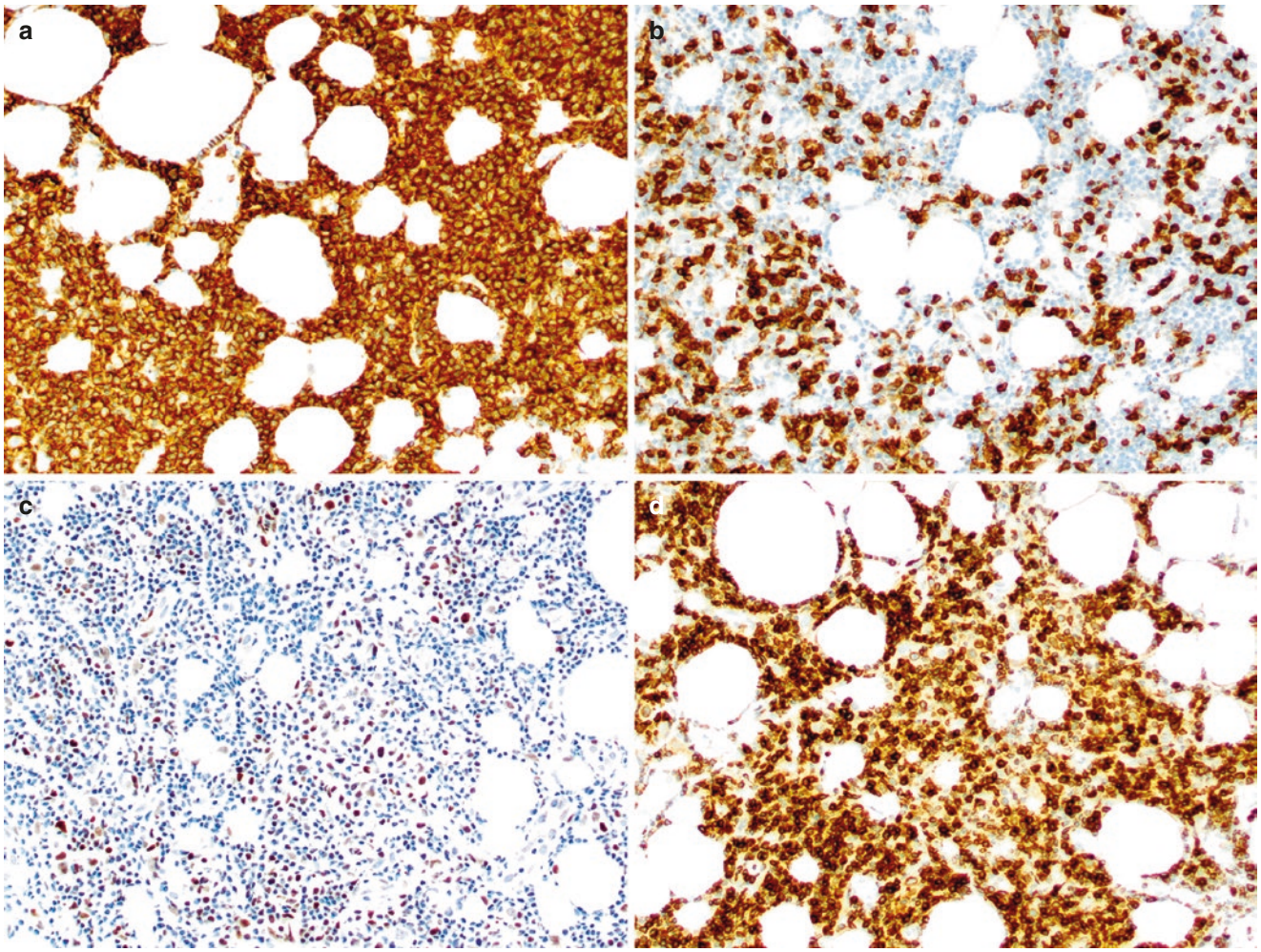

Fig. 20.16 Follicular lymphoma. IHC staining demonstrates that the majority of the lymphoid cells correspond to CD20-positive B-lymphocytes (**a**). CD3 stains numerous admixed T-lymphocytes (**b**). BCL-6 is positive in the neoplastic B cells (**c**). BCL2 is aberrantly expressed by the neoplastic B-lymphocytes (**d**)

Burkitt Lymphoma

Three distinct clinical forms of Burkitt lymphoma (BL) are recognized: endemic (African), sporadic, and immunodeficiency associated. Endemic BL represents 30–50% of all childhood cancer in equatorial Africa. Sporadic BL is one of the most common pediatric lymphomas in the USA and Europe. It also presents in young and middle-aged adults and has a male predominance. Immunodeficiency-associated variant is primarily seen in persons with HIV infection, who tend to have a high CD4 count and no evidence of opportunistic infections. BL is typically extranodal. The most common sites of involvement are the jaw, distal ileum, stomach, kidney, testis, and ovary. Primary breast BL is very rare and is typically of endemic type. Primary breast BL affects younger women and is often associated with pregnancy or lactation [79]. Most patients present with diffuse bilateral breast swelling [80–82]. BL is an extremely aggressive but also a highly curable lymphoma when treated with intensive chemotherapy.

Morphologically, there is a diffuse infiltrate of monotonous medium-sized lymphoid cells with numerous mitoses and frequent necrosis. Abundant apoptotic debris and scattered tingible body macrophages create a "starry-sky" appearance (Figs. 20.17 and 20.18).

Immunohistochemical workup demonstrates that the neoplastic lymphocytes express B-cell antigens and are positive for CD10 and Bcl-6 (Fig. 20.19a). Tumor cells do not express Bcl-2 or TdT. Ki67 proliferation rate is close to 100% (Fig. 20.19b). In situ hybridization for EBV-encoded RNA (EBER) is strongly and diffusely positive in virtually all endemic (African) cases and in a large subset of sporadic and immunodeficiency-associated cases.

FISH analysis can be performed to confirm the presence of *MYC* gene rearrangement (chromosome 8q24) in >90% of the cases.

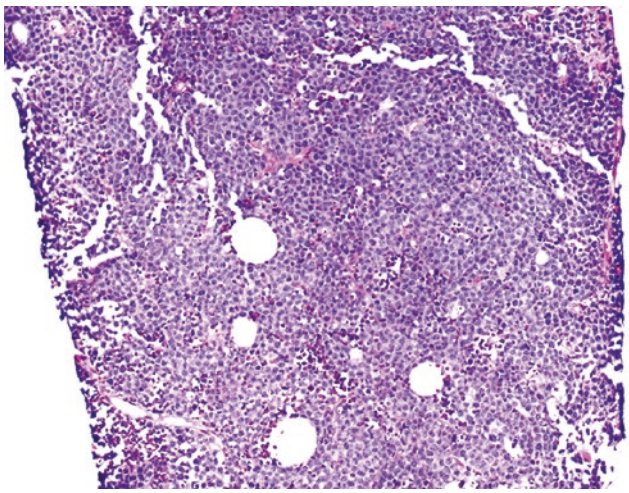

Fig. 20.17 Burkitt lymphoma. Diffuse infiltrate of monotonous lymphoid cells with abundant apoptotic debris

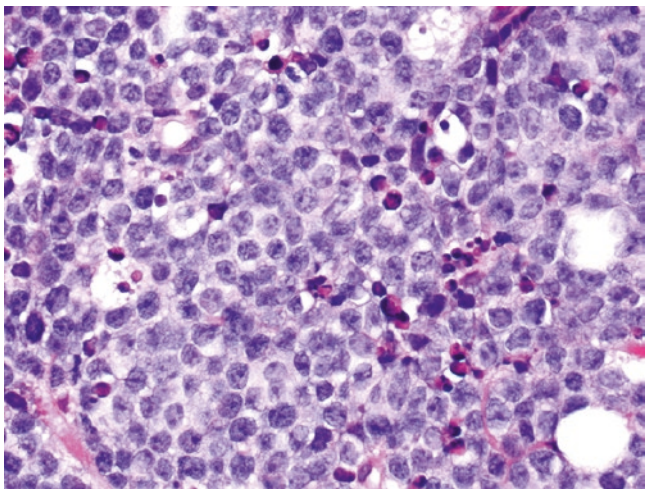

Fig. 20.18 Burkitt lymphoma. High-power magnification highlights a monotonous proliferation of medium-sized lymphoid cells

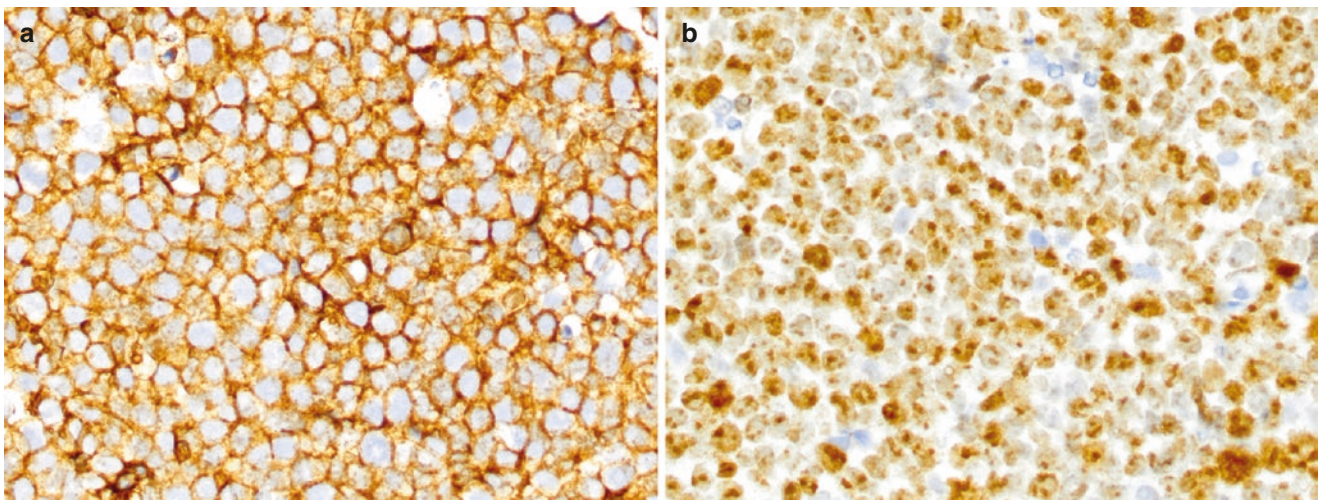

Fig. 20.19 Burkitt lymphoma. Neoplastic lymphocytes express CD20 (**a**). IHC stain for Ki67 highlights virtually every tumor cell with a proliferation rate close to 100% (**b**)

Breast Implant-Associated Anaplastic Large-Cell Lymphoma

As opposed to the overall predominance of B-cell lymphoma in the breast, anaplastic large-cell lymphoma (ALCL) predominates in women with implants performed for both cosmetic and reconstructive indications [29]. In the largest series to date of 60 women reported by Miranda and colleagues, approximately two-thirds of patients presented with a serous effusion adjacent to the implant, while the rest had a discrete mass detected by radiologic analysis or gross macroscopic examination [83]. The median time from implant insertion was 9 years [83]. Both saline and textured silicone implants have been associated with ALCL.

The diagnosis is typically obtained via cytologic examination of the seroma fluid or histologic review of the capsulectomy specimen. Occasionally, CNB is performed in patients with a discrete mass [84]. The vast majority of patients have an excellent prognosis with implant removal alone; thus, some authors advocate the term "CD30-positive T-cell lymphoproliferative disorder associated with a breast implant" [83–86]. The diagnosis of ALCL could be reserved for patients with a tumor mass or advanced-stage disease who are most likely to require aggressive therapy [83, 84]. However, the updated 2017 WHO classification currently recommends including all cases under the rubric of BI-ALCL, as a provisional entity [24].

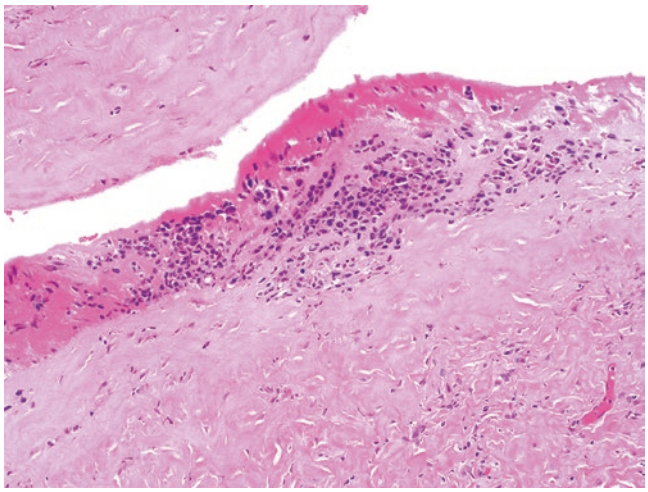

Fig. 20.20 Anaplastic large-cell lymphoma. Focal aggregates of neoplastic cells are lining the fibrous capsule. (Photomicrograph courtesy of Dr. Timothy D'Alfonso, Memorial Sloan Kettering Cancer Center, New York, with permission)

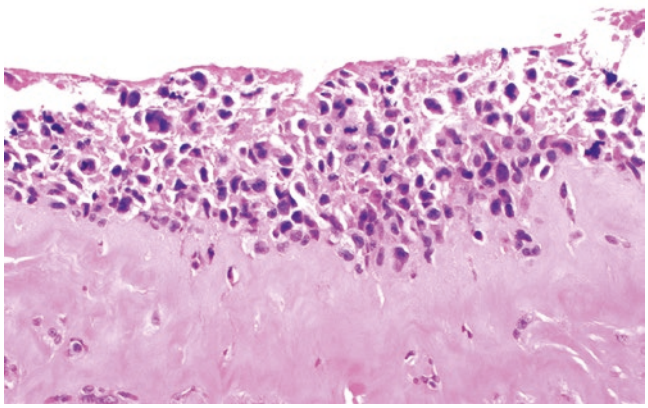

Fig. 20.21 Anaplastic large-cell lymphoma. Tumor cells are large in size, atypical, and pleomorphic with a variably abundant eosinophilic cytoplasm. (Photomicrograph courtesy of Dr. Timothy D'Alfonso, Memorial Sloan Kettering Cancer Center, New York, with permission)

Histologic examination reveals small clusters of neoplastic cells floating within fibrinoid effusion material or lining the fibrous capsule in the majority of the cases (Fig. 20.20). Tumor cells are large in size, atypical, and pleomorphic with a variably abundant eosinophilic cytoplasm (Figs. 20.21 and 20.22). Frequently, these cells are associated with a mixed inflammatory infiltrate composed of small lymphocytes, histiocytes, plasma cells, and scattered eosinophils [84, 85, 87, 88]. Refractile silicone particles may be present [87, 88]. In other cases, a distinct mass of tumor cells within the thickness of the capsule or beyond the capsule is found. There is no invasion of the adjacent breast tissue. Necrosis and/or sclerosis are frequently seen. Mitotic figures are typically conspicuous.

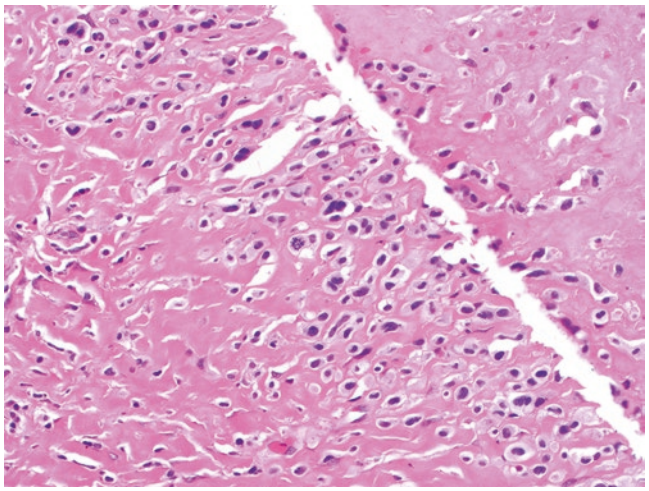

Fig. 20.22 Anaplastic large-cell lymphoma. In some cases, the majority of the cells have pale cytoplasm and centrally located nucleus referred to as "fried-egg appearance." Conspicuous mitotic figures are a common feature. (Photomicrograph courtesy of Dr. Timothy D'Alfonso, Memorial Sloan Kettering Cancer Center, New York, with permission)

With IHC, the neoplastic cells are positive for CD45, have variable expression of T-cell antigens, and are strongly positive for CD30 (Fig. 20.23a–c). EMA and cytotoxic antigens TIA-1 and granzyme B are frequently expressed (Fig. 20.23d). All tumors examined to date have been negative for ALK1 protein. PCR demonstrates evidence of T-cell receptor gamma-chain gene rearrangement in up to 97% of the cases [83].

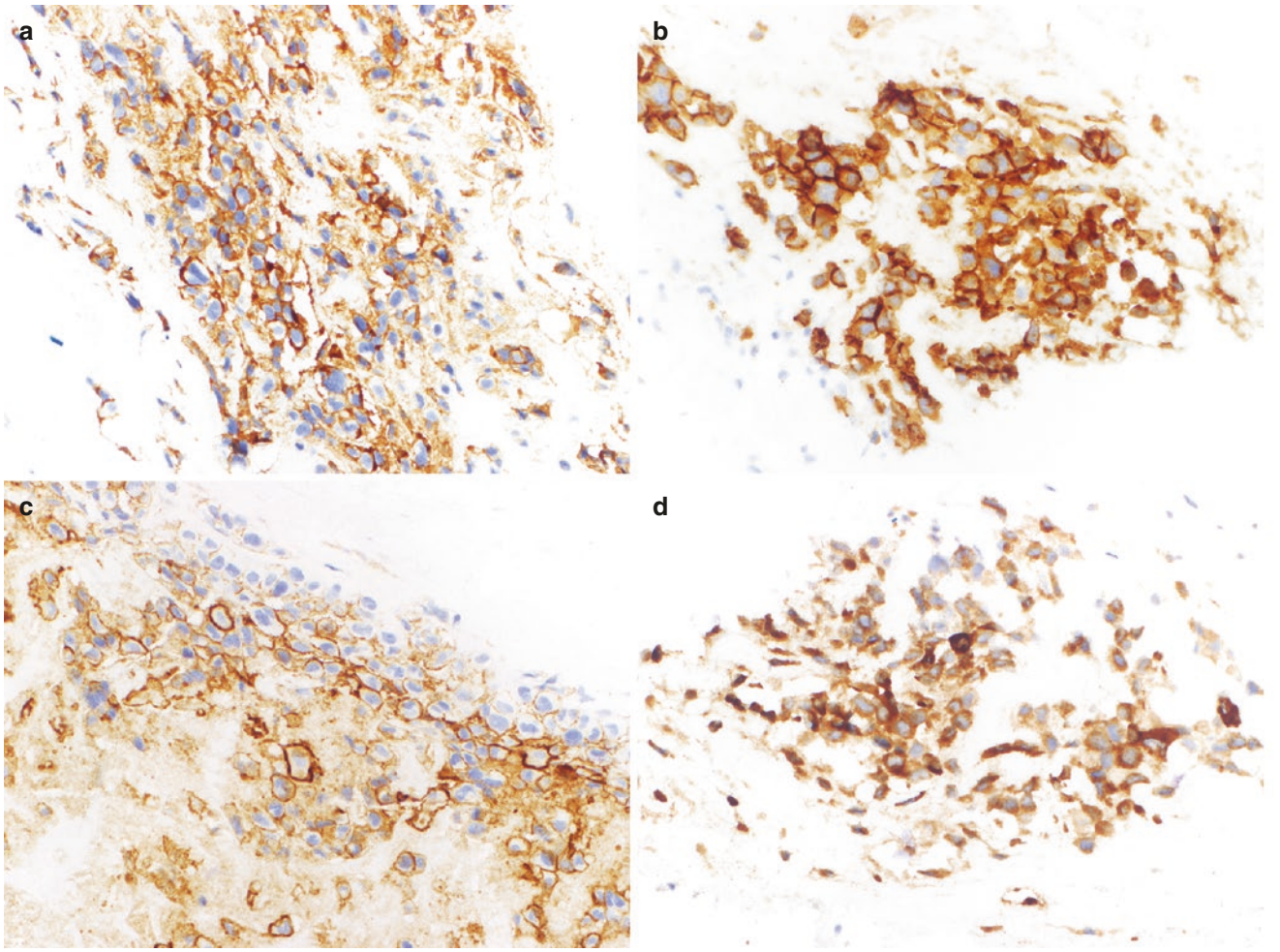

Fig. 20.23 Anaplastic large-cell lymphoma. Neoplastic cells express CD45 (**a**), strong diffuse CD30 (**b**), T-cell antigen CD43 (**c**), and EMA (**d**). (Photomicrograph courtesy of Dr. Timothy D'Alfonso, Weill Cornell Medical College, New York, with permission)

Other Rare Types of Primary Breast Lymphoma

T-cell lymphoma of the breast (with the exception of breast implant-associated ALCL) frequently disseminates, requires aggressive therapy, and has a worse prognosis than B-cell lymphoma of the breast. Based on a database of all reported cases of primary breast lymphoma, T-cell lymphoma represents approximately 7% of the cases [40]. Reported cases include peripheral T-cell lymphoma (PTCL, NOS); ALCL, ALK positive; adult T-cell leukemia/lymphoma (ATLL); and subcutaneous panniculitis-like T-cell lymphoma [4, 5, 89–91]. With careful staging, the majority of T-cell lymphomas of the breast appear to represent secondary breast involvement [5, 91, 92]. The typical clinical presentation is one or multiple painless breast masses, similar to breast B-cell lymphoma and breast carcinoma.

Occasional cases of B- and T-lymphoblastic lymphoma have been reported [5, 93]. In a study by Talwalkar and colleagues, six of seven cases were B-ALL and one case was T-ALL [5]. After staging, only one patient had truly localized disease [5]. Clinical presentation is that of a discrete mass or as bilateral diffuse breast involvement. Tumor cells demonstrate a diffuse infiltration of the breast parenchyma, typically in single-file pattern, reminiscent of lobular carcinoma [5].

Primary classical Hodgkin's lymphoma of breast is very rare as it usually represents direct extension from axillary or mediastinal lymph nodes and is part of regional or systemic disease [5, 40].

Differential Diagnosis

Clinically, the main differential diagnosis is with breast carcinoma, since lymphoma is very rarely suspected prior to biopsy. Microscopically, these tumors can also mimic primary carcinoma of the breast, especially in CNB specimens with limited material. Since DLBCL is the most frequent lymphoma of the breast, the distinction between DLBCL and poorly differentiated or lobular breast carcinoma is the most common dilemma in clinical practice (Fig. 20.24). Histologic features suggestive of lymphoma involvement include absence of in situ carcinoma, frequent individual karyorrhectic cells, lymphoepithelial lesions, and cellular dyscohesiveness. On the contrary, a cohesive growth pattern, lumen formation, or presence of intracellular mucin favor carcinoma. The neoplastic cells in DLBCL are, on average, significantly smaller in size than epithelial cells. Finally, a limited panel of IHC stains is necessary to confirm the diagnosis in challenging cases. Immunophenotypic profile of these malignancies is vastly different, since DLBCL cells are negative with cytokeratin stains and express CD45 and B-cell antigens CD20 and PAX5 (Fig. 20.25).

The distinction between a low-grade B-cell lymphoma and a reactive lymphoid infiltrate can be challenging on a small CNB, since the degree of architectural effacement cannot be reliably assessed. In particular, lymphocytic mastopathy (diabetic mastopathy) is a benign breast condition characterized by dense fibrosis, lobular atrophy, and presence of periductal and perivascular aggregates of small lymphocytes [94]. Reactive lymphoid follicles may be present. Rare cases have lymphoepithelial lesions. This condition is present in young to middle-aged women and is frequently associated with diabetes mellitus and other autoimmune disorders. Patients present with a breast mass, clinically and radiologically mimicking a primary breast neoplasm [94, 95]. The differential diagnosis is further complicated by the fact that unlike most benign lymphoid inflammatory lesions, lymphocytic mastopathy is characterized by a predominance of B cells with typically only rare scattered admixed T-lymphocytes. Additional IHC workup is necessary in these cases. Neoplastic B-lymphocytes may show aberrant expression of T-cell antigen CD43. Cases of MALT lymphoma frequently have plasmacytic differentiation, with increased number of plasma cells and evidence of immunoglobulin light-chain restriction. In addition, presence of epithelioid fibroblasts (large activated stromal cells with mild cytologic atypia) is described as a characteristic finding of diabetic mastopathy and may help in the differential diagnosis [94]. However, it should be noted that some cases cannot be reliably diagnosed based on the CNB [95]. Excisional biopsy should be recommended in cases where a low-grade B-cell lymphoma cannot be excluded.

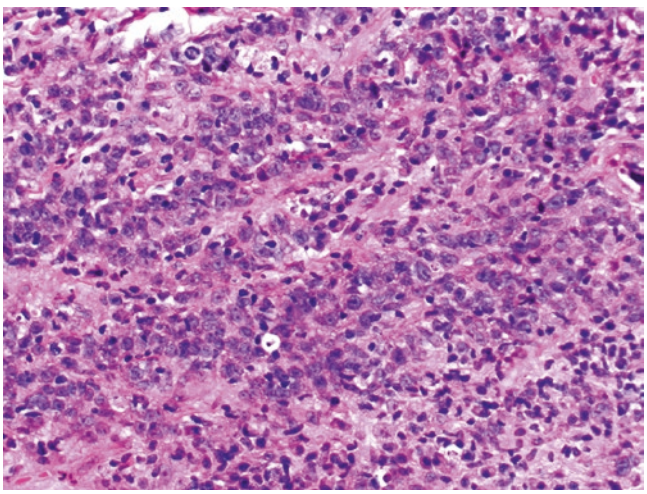

Fig. 20.24 Poorly differentiated carcinoma of the breast composed of sheets of dyscohesive neoplastic cells, reminiscent of large-cell lymphoma

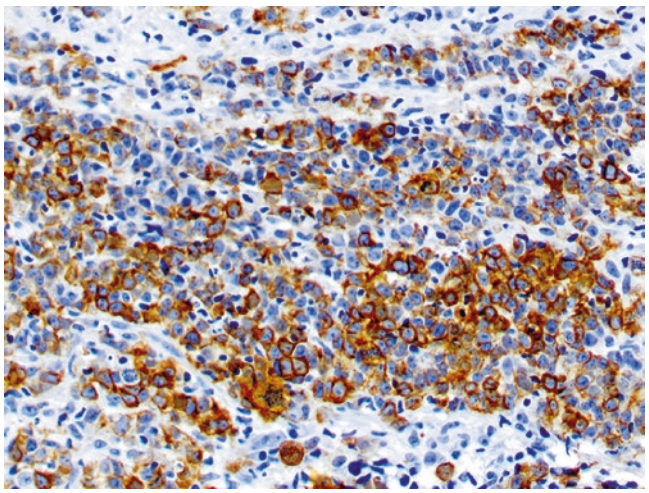

Fig. 20.25 Immunohistochemical stain for cytokeratin demonstrates the epithelial origin of this poorly differentiated neoplasm

MALT lymphoma and FL are the second and third most common lymphomas of the breast, respectively. Distinction between these two entities may be difficult, especially on the CNB. Cases of MALT lymphoma with prominent follicular colonization may appear virtually indistinguishable from FL. On the other hand, cases of FL may have marginal zone differentiation with numerous monocytoid B cells surrounding the neoplastic follicles. Both FL and MALT lymphoma are characterized by small lymphocytes with centrocyte-like morphology. FL contains admixed centroblasts, while MALT lymphoma may also have admixed large activated B cells. Therefore, an extensive IHC panel is

required in order to distinguish between these two entities. In particular, tumor cells in FL express germinal center markers CD10 and Bcl-6, while neoplastic cells in MALT lymphoma do not express germinal center antigens. FISH analysis demonstrates evidence of translocation t(14;18) in up to 90% of low-grade FL, while MALT lymphoma cases can have trisomy 3, 7, and 18 and translocations involving *BCL10* and *MALT1* genes in a small subset of cases. There are cases where a precise diagnosis cannot be rendered after a careful examination and diagnosis of "low-grade B-cell lymphoma" is warranted.

Occasionally, lymphoma may arise in an intramammary or axillary lymph node and not in the breast parenchyma. Knowledge of the precise biopsy site is very important to rule out biopsy of the axillary tail. Radiographically, benign intramammary lymph nodes are characterized by well-circumscribed borders, lobulation, and central radiolucency (fatty replacement). Intramammary nodes are considered abnormal on mammogram if they are enlarged, have an irregular border, show increased density, or lose the fatty hilum [96]. Microscopically, presence of fibrous capsule or patent sinuses filled with histiocytes points towards a lymph node, while presence of benign breast epithelium is diagnostic of primary breast parenchymal location.

Pathogenesis

The vast majority of primary breast lymphoma is present in female patients, including occasional case reports of lymphoma diagnosis coinciding with pregnancy and lactation [4, 5, 97, 98]. Thus, there may be a role for estrogen stimulation in lymphoma pathogenesis. Teras and colleagues have reported that unopposed use of estrogen hormone replacement therapy has been associated with a 29% increased risk of DLBCL and FL in a large cohort of 67,000 postmenopausal women [99]. Estrogen receptor beta (ERβ) is found on lymphoma cell lines, and ERβ-selective agonists have shown activity against lymphoma cells both in vivo and in vitro [100–102]. However, overall, the incidence rates of non-Hodgkin's lymphoma are lower for women than for men, and several epidemiological studies found no relationship between hormone replacement therapy or contraceptive use and non-Hodgkin's lymphoma. On the contrary, exogenous estrogens may have a protective effect in women [103–105].

In addition, prevalence of primary breast lymphoma appears increased in patients with autoimmune disease [2–4, 60]. MALT lymphoma in the breast has a particularly strong association with various autoimmune conditions, including Sjögren syndrome, rheumatoid arthritis, and inflammatory bowel disease.

Treatment and Prognosis

Primary breast DLBCL patients exhibit better outcome compared with lymph node-based DLBCL [36, 37]. Inferior outcome in patients with primary DLBCL of the breast has been associated with stage II disease (vs. stage I) [27, 39], poor performance status at presentation [57], tumor size of more than 4–5 cm [39, 50, 62, 63], and high microvascular density [106]. Some series have found that bilateral DLBCL has more aggressive behavior [49, 107]. Primary breast DLBCL appears to have extranodal tropism at relapse, where up to 44% of the patients experience ipsilateral or contralateral breast relapse [39, 46, 49]. Other extranodal sites frequently associated with relapse include bone marrow, lung or pleura, skin, and CNS [39, 46, 49, 108]. In particular, compared to patients with nodal based DLBCL, patients with breast DLBCL appear to have a predilection for CNS involvement, with many authorities advocating for CNS prophylaxis in these patients [29].

Treatment of primary breast lymphomas follows treatment recommendations for lymphomas of the same stage and histology in other locations. Mastectomy does not improve survival or risk of recurrence and should be avoided [29, 40]. Chemotherapy is the cornerstone of therapy. The choice of chemotherapy regimen is based upon histologic subtype, disease extent, and individual patient's performance status [29]. For patients with DLBCL, the combination of chemotherapy and consolidation radiotherapy to the ipsilateral breast appears to improve overall survival, compared to chemotherapy alone [38, 49].

Secondary Lymphoma of the Breast

Secondary breast lymphoma is defined as the presence of systemic lymphoma with concurrent or subsequent involvement of the breast [29]. It includes cases of treated lymphoma that relapses in the breast, as well as cases of breast lymphoma that appears as part of disseminated disease based on staging procedures. Secondary lymphoma is the most common secondary neoplasm in the breast [109]. Studies have shown different proportion of primary to secondary breast lymphoma, probably depending on the institution characteristics [5, 92, 109]. Patients with secondary lymphoma have a wide range of lymphoma types, with DLBCL and FL being the most common lymphoma types, similar to patients with primary lymphoma. FL appears to be much more common in the disseminated lymphoma group, compared to the localized lymphoma group [5]. A large subset of patients present with multifocal breast involvement [5, 109]. Patients with secondary DLBCL appear to have inferior disease-free survival compared to patients with primary breast DLBCL [27, 92].

The majority of patients with FL and Hodgkin lymphoma and virtually all patients with mantle cell lymphoma, chronic lymphocytic leukemia/small lymphocytic lymphoma, T-cell

lymphoma (with the exception of breast implant-associated ALCL), and lymphoblastic lymphoma have disseminated disease [5].

Other Rare Malignant Hematopoietic Disorders of the Breast

Myeloid Sarcoma (Granulocytic Sarcoma)

Myeloid sarcoma occurs in patients who have acute myeloid leukemia, as a sign of impending blast crisis in chronic myelogenous leukemia or leukemic transformation in patients who have myelodysplastic disorders, or as a forerunner of acute myeloid leukemia in nonleukemic patients. Leukemic infiltration of the breast is much more common in patients with advanced disseminated acute leukemia and is unusual as the initial presentation; thus, access to pertinent clinical history is paramount in making the correct diagnosis in these cases [110–112]. A study of 41 patients with extramedullary tumors after hematopoietic stem cell transplantation showed that the breast was the third most commonly involved site, following skin/soft tissue and central nervous system [113]. In 93% of the patients, myeloid sarcoma was the sole site of relapse [113].

Myeloid sarcoma of the breast usually presents as single or multiple masses with evidence of rapid growth and frequent necrosis [114]. Based on breast imaging, it may be difficult to differentiate from carcinoma [114].

Microscopically, neoplastic cells are dyscohesive and infiltrate normal breast parenchymal tissue as sheets of cells or cords of single cells, reminiscent of lobular carcinoma of the breast [110–112] (Fig. 20.26). Intraepithelial extension may be present and should not be confused with carcinoma in situ [110]. Most cases contain primitive-appearing blasts with round, ovoid, or reniform nuclei with finely stippled chromatin and one or two small nucleoli (Fig. 20.27). Other cases are characterized by a proliferation of myelomonocytic or monoblastic cells [115, 116]. Thus, with conventional light microscopy, the morphologic features can be misdiagnosed as carcinoma, DLBCL, lymphoblastic lymphoma, or BL [116] (Fig. 20.28).

Immunohistochemical staining is necessary to confirm the diagnosis. CD68/KP1 is the most commonly expressed marker (100% of cases), followed by myeloperoxidase,

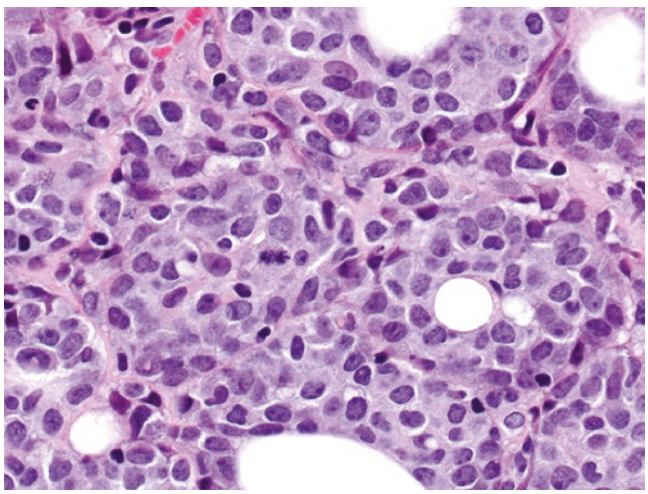

Fig. 20.27 Myeloid sarcoma. The neoplastic cells form small aggregates and have fine chromatin, occasionally prominent nucleoli, and moderate amount of pale cytoplasm

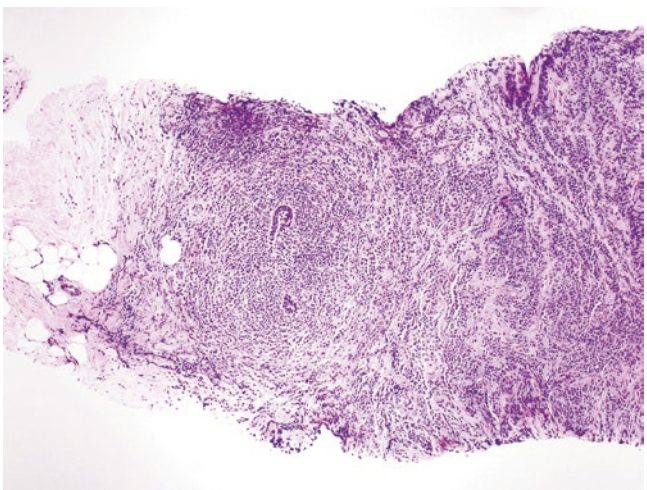

Fig. 20.26 Myeloid sarcoma. The neoplastic cells are dyscohesive and infiltrate the breast parenchymal tissue as sheets and cords of single cells

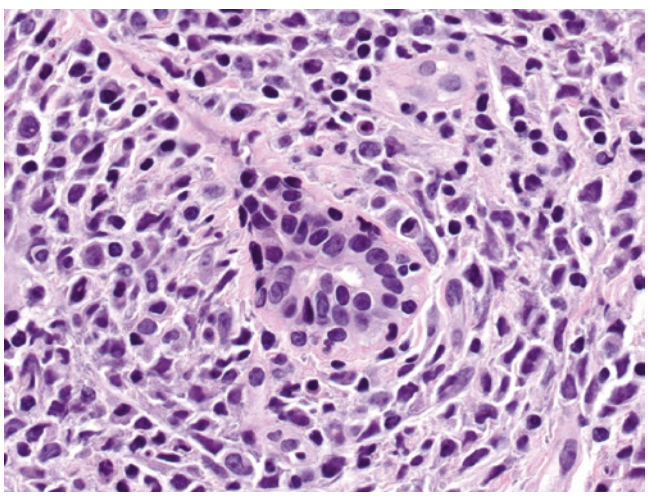

Fig. 20.28 Myeloid sarcoma. Primitive-appearing tumor cells infiltrate into the breast duct

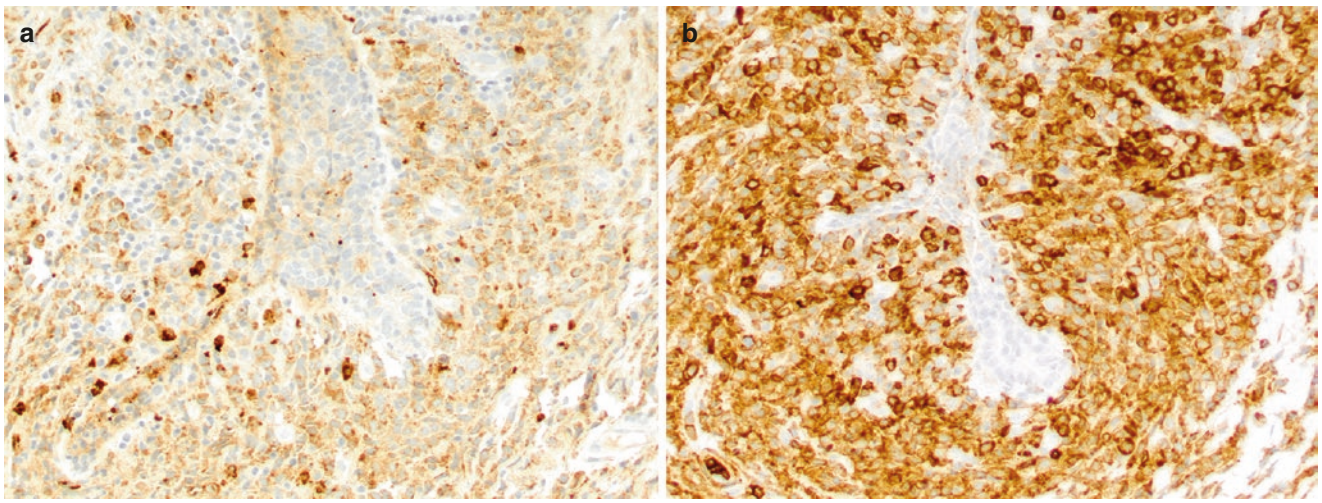

Fig. 20.29 Myeloid sarcoma. IHC staining demonstrates that the neoplastic cells express myeloid antigen lysozyme (**a**) and pan-hematopoietic marker CD45 (**b**)

CD117, CD99, lysozyme, CD34, TdT, and CD56 [116] (Fig. 20.29a). Approximately 90% of myeloid sarcoma cases express CD45 (Fig. 20.29b). Rare cases positive for CD30 have been reported [115, 116].

If tissue is available, FISH analysis may be very informative, since up to 50% of the cases have chromosomal abnormalities, including monosomy 7, trisomy 8, MLL gene rearrangement, inv.(16), t(8;21) translocation, and other abnormalities common in myeloid disorders [115, 116].

Histiocytic Sarcoma

Histiocytic sarcoma is a rare malignant neoplasm derived from tissue macrophages. It occurs predominantly in extranodal sites of older individuals [117, 118]. Patients typically present with a solitary mass [118].

Microscopically, there is a diffuse dyscohesive proliferation of large cells (Fig. 20.30). Tumor cell morphology is very heterogeneous and includes round, oval, and spindle-shaped cells with moderate-to-abundant eosinophilic cytoplasm and oval, folded, or multilobulated nuclei (Fig. 20.31). Cells with prominent nucleoli and multinucleated cells may be seen. Tumor cells have mild-to-marked atypia, and some cells with anaplastic morphology have been reported. Occasionally, neoplastic cells may be obscured by a significant polymorphous inflammatory infiltrate, including many neutrophils. Morphologic differential diagnosis includes poorly differentiated carcinoma and large-cell lymphoma.

Immunohistochemical staining is mandatory to make the diagnosis [117]. Neoplastic cells are negative for cytokeratins and express CD45 and histiocytic markers CD68, CD163, lysozyme, and CD4 [117, 118] (Fig. 20.32a, b).

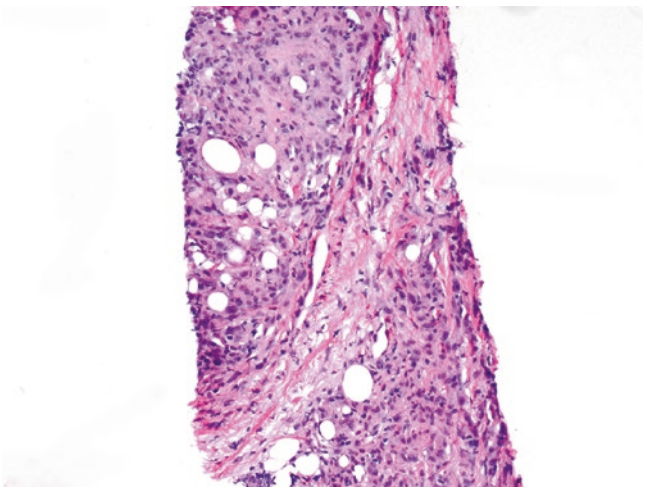

Fig. 20.30 Histiocytic sarcoma. Breast CNB with a diffuse infiltrate by cells with irregular nuclei and abundant eosinophilic cytoplasm

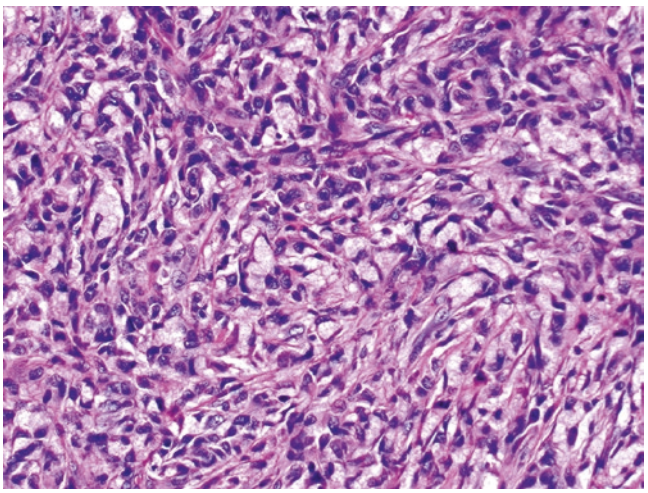

Fig. 20.31 Histiocytic sarcoma. Higher magnification shows atypical spindle-shaped cells with admixed foamy macrophages

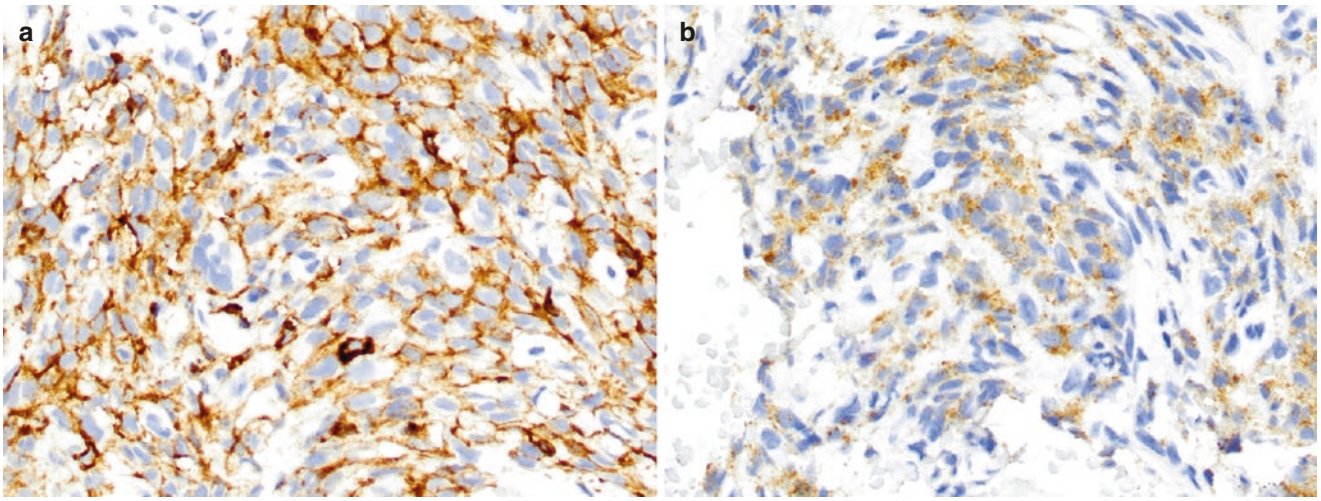

Fig. 20.32 Histiocytic sarcoma. IHC staining shows that the neoplastic cells are positive for CD45 (**a**) and histiocytic marker CD68 (**b**)

Plasma Cell Neoplasm

Plasma cell neoplasms of the breast include isolated extraosseous plasmacytoma (~15% of cases) or systemic manifestations of known plasma cell myeloma (~85% of cases), typically in patients with advanced, relapsed, or refractory disease [119]. Patients with extraosseous plasmacytoma have no clinical features of plasma cell myeloma. Therefore, clinical correlation and knowledge of the patient's prior history are necessary to confidently differentiate between these two possibilities.

Morphologic features include a diffuse proliferation of plasma cells (Fig. 20.33a). Patients with isolated plasmacytoma typically have small and mature-appearing plasma cells (Fig. 20.33b), while patients with advanced myeloma may occasionally show markedly atypical plasma cell morphology with large size, prominent nucleoli, irregular nuclear contours, and scant cytoplasm [24]. These cases may be mistaken for poorly differentiated carcinoma or sarcoma.

With IHC staining, the plasma cells express CD138 (Fig. 20.33c) and Mum-1 and show evidence of light-chain restriction (Fig. 20.33d). CD45 expression is usually present but may be weak or negative. Plasma cells do not express mature B-cell markers CD20 or PAX5 and may have aberrant expression of CD56 or cyclin D1 [24].

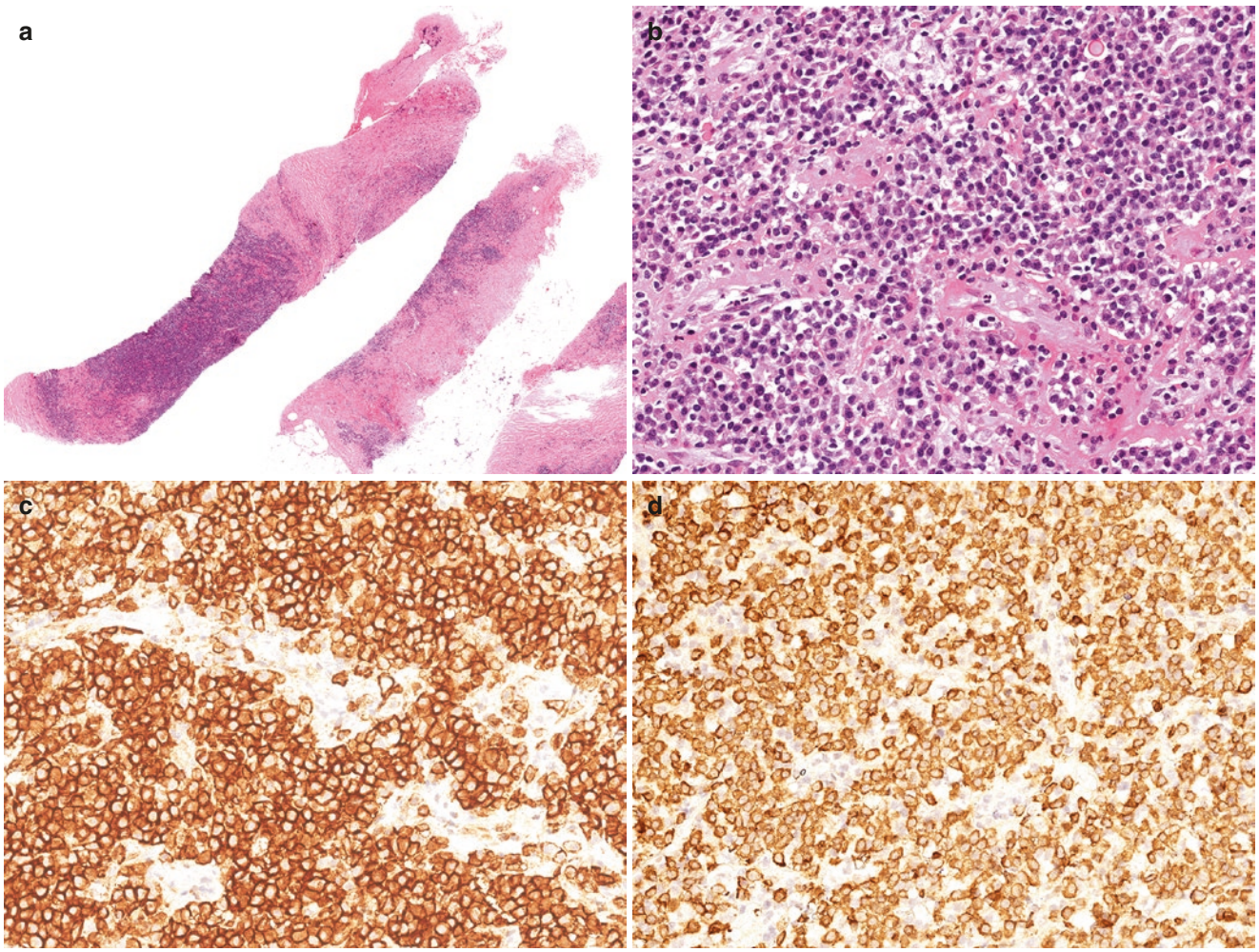

Fig. 20.33 Plasmacytoma. (**a**) Breast CNB with a patchy infiltrate by atypical cells that displace the normal breast epithelial structures. (**b**) Higher magnification shows sheets of small, mature-appearing plasma cells. Note the occasional Russell bodies. (**c**) Tumor cells are strongly positive for CD138. (**d**) In situ hybridization for kappa immunoglobulin light chain highlights virtually all the neoplastic cells, confirming a clonal plasma cell process. (Images courtesy of Dr. Kwun Wen, Department of Pathology, UCSF)

References

1. Brogi E, Harris NL. Lymphomas of the breast: pathology and clinical behavior. Semin Oncol. 1999;26(3):357–64.
2. Domchek SM, Hecht JL, Fleming MD, Pinkus GS, Canellos GP. Lymphomas of the breast: primary and secondary involvement. Cancer. 2002;94(1):6–13.
3. Farinha P, Andre S, Cabecadas J, Soares J. High frequency of MALT lymphoma in a series of 14 cases of primary breast lymphoma. Appl Immunohistochem Mol Morphol. 2002;10(2):115–20.
4. Hugh JC, Jackson FI, Hanson J, Poppema S. Primary breast lymphoma. An immunohistologic study of 20 new cases. Cancer. 1990;66(12):2602–11.
5. Talwalkar SS, Miranda RN, Valbuena JR, Routbort MJ, Martin AW, Medeiros LJ. Lymphomas involving the breast: a study of 106 cases comparing localized and disseminated neoplasms. Am J Surg Pathol. 2008;32(9):1299–309.
6. Wiseman C, Liao KT. Primary lymphoma of the breast. Cancer. 1972;29(6):1705–12.
7. Barista I, Baltali E, Tekuzman G, et al. Primary breast lymphomas—a retrospective analysis of twelve cases. Acta Oncol. 2000;39(2):135–9.
8. Giardini R, Piccolo C, Rilke F. Primary non-Hodgkin's lymphomas of the female breast. Cancer. 1992;69(3):725–35.
9. Julen O, Dellacasa I, Pelte MF, et al. Primary breast lymphomas. Rare Tumors. 2009;1(1):e14.
10. Knowles DM. The extranodal lymphoid infiltrate: a diagnostic dilemma. Semin Diagn Pathol. 1985;2(3):147–51.
11. Burke JS. Histologic criteria for distinguishing between benign and malignant extranodal lymphoid infiltrates. Semin Diagn Pathol. 1985;2(3):152–62.
12. Knowles DM, Jakobiec FA. Cell marker analysis of extranodal lymphoid infiltrates: to what extent does the determination of mono- or polyclonality resolve the diagnostic dilemma of malignant lymphoma v pseudolymphoma in an extranodal site? Semin Diagn Pathol. 1985;2(3):163–8.
13. Knowles DM, Halper JP, Jakobiec FA. The immunologic characterization of 40 extranodal lymphoid infiltrates: usefulness in

distinguishing between benign pseudolymphoma and malignant lymphoma. Cancer. 1982;49(11):2321–35.
14. Knowles DM. Immunophenotypic and immunogenotypic approaches useful in distinguishing benign and malignant lymphoid proliferations. Semin Oncol. 1993;20(6):583–610.
15. Knowles DM, Jakobiec FA, McNally L, Burke JS. Lymphoid hyperplasia and malignant lymphoma occurring in the ocular adnexa (orbit, conjunctiva, and eyelids): a prospective multiparametric analysis of 108 cases during 1977 to 1987. Hum Pathol. 1990;21(9):959–73.
16. Seidman JG, Leder P. The arrangement and rearrangement of antibody genes. Nature. 1978;276(5690):790–5.
17. Tonegawa S. Somatic generation of antibody diversity. Nature. 1983;302(5909):575–81.
18. Yanagi Y, Yoshikai Y, Leggett K, Clark SP, Aleksander I, Mak TW. A human T cell-specific cDNA clone encodes a protein having extensive homology to immunoglobulin chains. Nature. 1984;308(5955):145–9.
19. Pelicci PG, Knowles DM, Arlin ZA, et al. Multiple monoclonal B cell expansions and c-myc oncogene rearrangements in acquired immune deficiency syndrome-related lymphoproliferative disorders. Implications for lymphomagenesis. J Exp Med. 1986;164(6):2049–60.
20. Neri A, Jakobiec FA, Pelicci PG, Dalla-Favera R, Knowles DM. Immunoglobulin and T cell receptor beta chain gene rearrangement analysis of ocular adnexal lymphoid neoplasms: clinical and biologic implications. Blood. 1987;70(5):1519–29.
21. Knowles DM, Athan E, Ubriaco A, et al. Extranodal noncutaneous lymphoid hyperplasias represent a continuous spectrum of B-cell neoplasia: demonstration by molecular genetic analysis. Blood. 1989;73(6):1635–45.
22. Isaacson PG, Norton AJ. Extranodal lymphomas. Edinburgh: Churchill Livingstone; 1994.
23. Harris NL, Jaffe ES, Stein H, et al. A revised European-American classification of lymphoid neoplasms: a proposal from the International Lymphoma Study Group. Blood. 1994;84(5):1361–92.
24. Swerdlow S, Campo E, Harris NL, Jaffe ES, Pileri SA, Stein H, Thiele J. WHO classification of tumours of haematopoietic and lymphoid tissues. In: Bosman FT, Lakhani SR, Ohgaki H, editors. World Health Organization classification of tumours. Revised 4th ed. Lyon: IARC; 2017.
25. Kurtin PJ. How do you distinguish benign from malignant extranodal small B-cell proliferations? Am J Clin Pathol. 1999;111(1 Suppl 1):S119–25.
26. Guilbert MC, Hornick JL, Chikarmane SA, Lester SC. Hematologic malignancies of the breast: a contemporary series investigating incidence, presentation, accuracy of diagnosis on core needle biopsy, and hormone receptor expression. Breast Cancer (Auckl). 2019;13:1178223419830982. https://doi.org/10.1177/1178223419830982. PMID: 30814841
27. Caon J, Wai ES, Hart J, et al. Treatment and outcomes of primary breast lymphoma. Clin Breast Cancer. 2012;12(6):412–9.
28. Bicchierai G, Rigacci L, Miele V, Meattini I, De Benedetto D, Selvi V, Bianchi S, Livi L, Nori J. Role of core needle biopsy in primary breast lymphoma. Radiol Med. 2017;122(9):651–5. https://doi.org/10.1007/s11547-017-0773-3. Epub 2017 May 16. PMID: 28510806
29. Cheah CY, Campbell BA, Seymour JF. Primary breast lymphoma. Cancer Treat Rev. 2014;40(8):900–8.
30. Talwalkar SS, Valbuena JR, Abruzzo LV, et al. MALT1 gene rearrangements and NF-kappaB activation involving p65 and p50 are absent or rare in primary MALT lymphomas of the breast. Mod Pathol. 2006;19(11):1402–8.
31. Jung SP, Han KM, Kim SJ, Nam SJ, Bae JW, Lee JE. Primary follicular lymphoma in a male breast: a case report. Cancer Res Treat. 2014;46(1):104–7.
32. Mpallas G, Simatos G, Tasidou A, et al. Primary breast lymphoma in a male patient. Breast. 2004;13(5):436–8.
33. Rathod J, Taori K, Disawal A, et al. A rare case of male primary breast lymphoma. J Breast Cancer. 2011;14(4):333–6.
34. Lokesh K, Sathyanarayanan V, Lakshmaiah K, et al. Primary breast lymphoma in males-a report of two cases with a review of the literature. Ecancermedicalscience. 2013;7:347.
35. Peng F, Li J, Mu S, Cai L, Fan F, Qin Y, Ai L, Hu Y. Epidemiological features of primary breast lymphoma patients and development of a nomogram to predict survival. Breast. 2021;57:49–61. https://doi.org/10.1016/j.breast.2021.03.006. Epub 17. PMID: 33774459; PMCID: PMC8027901
36. Jia Y, Sun C, Liu Z, Wang W, Zhou X. Primary breast diffuse large B-cell lymphoma: a population-based study from 1975 to 2014. Oncotarget. 2017;9(3):3956–67.
37. Thomas A, Link BK, Altekruse S, Romitti PA, Schroeder MC. Primary breast lymphoma in the United States: 1975-2013. J Natl Cancer Inst. 2017;109(6):djw294.
38. Aviles A, Delgado S, Nambo MJ, Neri N, Murillo E, Cleto S. Primary breast lymphoma: results of a controlled clinical trial. Oncology. 2005;69(3):256–60.
39. Jeanneret-Sozzi W, Taghian A, Epelbaum R, et al. Primary breast lymphoma: patient profile, outcome and prognostic factors. A multicentre rare cancer network study. BMC Cancer. 2008;8:86.
40. Jennings WC, Baker RS, Murray SS, et al. Primary breast lymphoma: the role of mastectomy and the importance of lymph node status. Ann Surg. 2007;245(5):784–9.
41. Jung SP, Kim M, Han KM, et al. Primary breast lymphoma: a single institution's experience. J Korean Surg Soc. 2013;84(5):267–72.
42. Martinelli G, Ryan G, Seymour JF, et al. Primary follicular and marginal-zone lymphoma of the breast: clinical features, prognostic factors and outcome: a study by the International Extranodal Lymphoma Study Group. Ann Oncol. 2009;20(12):1993–9.
43. Ou CW, Shih LY, Wang PN, et al. Primary breast lymphoma: a single-institute experience in Taiwan. Biom J. 2014;37(5):321–5.
44. Seker M, Bilici A, Ustaalioglu BO, et al. Clinicopathologic features of the nine patients with primary diffuse large B cell lymphoma of the breast. Arch Gynecol Obstet. 2011;284(2):405–9.
45. Shao YB, Sun XF, He YN, Liu CJ, Liu H. Clinicopathological features of thirty patients with primary breast lymphoma and review of the literature. Med Oncol. 2015;32(2):448.
46. Yhim HY, Kang HJ, Choi YH, et al. Clinical outcomes and prognostic factors in patients with breast diffuse large B cell lymphoma; Consortium for Improving Survival of Lymphoma (CISL) study. BMC Cancer. 2010;10:321.
47. Zhang T, Zhao H, Cui Z, Xu H, Liu X, Wu Y, Li Y, Sun S, Wang P, Wang Y, Shi X. A multicentre retrospective study of primary breast diffuse large B-cell and high-grade B-cell lymphoma treatment strategies and survival. Hematology. 2020;25(1):203–10. https://doi.org/10.1080/16078454.2020.1769419.
48. Hosein PJ, Maragulia JC, Salzberg MP, et al. A multicentre study of primary breast diffuse large B-cell lymphoma in the rituximab era. Br J Haematol. 2014;165(3):358–63.
49. Ryan G, Martinelli G, Kuper-Hommel M, et al. Primary diffuse large B-cell lymphoma of the breast: prognostic factors and outcomes of a study by the International Extranodal Lymphoma Study Group. Ann Oncol. 2008;19(2):233–41.
50. Fukuhara S, Watanabe T, Munakata W, et al. Bulky disease has an impact on outcomes in primary diffuse large B-cell lymphoma of the breast: a retrospective analysis at a single institution. Eur J Haematol. 2011;87(5):434–40.
51. Genco IS, Gur H, Hajiyeva S. Lymphoma of the breast: a clinicopathologic analysis of 51 cases with a specific emphasis on patients with a history of breast carcinoma. Breast J. 2021;

52. Ho CW, Mantoo S, Lim CH, Wong CY. Synchronous invasive ductal carcinoma and intravascular large B-cell lymphoma of the breast: a case report and review of the literature. World J Surg Oncol. 2014;12:88.
53. Alakeel F, Lee E, Baird-Howell M, Easley S. Synchronous ductal carcinoma in situ and intravascular large B-cell lymphoma of the breast. Appl Immunohistochem Mol Morphol. 2019;27(9):e91–2.
54. Franco Pérez F, Lavernia J, Aguiar-Bujanda D, Miramón J, Gumá J, Álvarez R, Gómez-Codina J, Arroyo FG, Llanos M, Marin M, Alfaro J, Quero C, Delgado M, Nogales E, Menarguez F, Martinez N, Torrente M, Royuela A, Abreu D, Provencio M. Primary breast lymphoma: analysis of 55 cases of the spanish lymphoma oncology group. Clin Lymphoma Myeloma Leuk. 2017;17(3):186–91.
55. Kewan T, Covut F, Ahmed R, Haddad A, Daw H. Clinical characteristics and outcomes of primary breast lymphoma: the cleveland clinic experience. Cureus. 2020;12(6):e8611.
56. Picasso R, Tagliafico A, Calabrese M, Martinoli C, Pistoia F, Rossi A, Zaottini F, Derchi L. Primary and secondary breast lymphoma: focus on epidemiology and imaging features. Pathol Oncol Res. 2020;26(3):1483–8.
57. Ganjoo K, Advani R, Mariappan MR, McMillan A, Horning S. Non-Hodgkin lymphoma of the breast. Cancer. 2007;110(1):25–30.
58. Sabate JM, Gomez A, Torrubia S, et al. Lymphoma of the breast: clinical and radiologic features with pathologic correlation in 28 patients. Breast J. 2002;8(5):294–304.
59. Lyou CY, Yang SK, Choe DH, Lee BH, Kim KH. Mammographic and sonographic findings of primary breast lymphoma. Clin Imaging. 2007;31(4):234–8.
60. Fruchart C, Denoux Y, Chasle J, et al. High grade primary breast lymphoma: is it a different clinical entity? Breast Cancer Res Treat. 2005;93(3):191–8.
61. Raj SD, Shurafa M, Shah Z, Raj KM, Fishman MDC, Dialani VM. Primary and secondary breast lymphoma: clinical, pathologic, and multimodality imaging review. Radiographics. 2019;39(3):610–25.
62. Niitsu N, Okamoto M, Nakamine H, Hirano M. Clinicopathologic features and treatment outcome of primary breast diffuse large B-cell lymphoma. Leuk Res. 2008;32(12):1837–41.
63. Takahashi H, Sakai R, Sakuma T, Matsumura A, Miyashita K, Ishii Y, Nakajima Y, Numata A, Hattori Y, Miyazaki T, Hashimoto C, Koharazawa H, Takemura S, Taguchi J, Fujimaki K, Fujita H, Nakajima H. Comparison of clinical features between primary and secondary breast diffuse large B cell lymphoma: a yokohama cooperative study group for hematology multicenter retrospective study. Indian J Hematol Blood Transfus. 2021;37(1):60–6.
64. Yoshida S, Nakamura N, Sasaki Y, et al. Primary breast diffuse large B-cell lymphoma shows a non-germinal center B-cell phenotype. Mod Pathol. 2005;18(3):398–405.
65. De Paepe P, Achten R, Verhoef G, et al. Large cleaved and immunoblastic lymphoma may represent two distinct clinicopathologic entities within the group of diffuse large B-cell lymphomas. J Clin Oncol. 2005;23(28):7060–8.
66. Ribrag V, Bibeau F, El Weshi A, et al. Primary breast lymphoma: a report of 20 cases. Br J Haematol. 2001;115(2):253–6.
67. Mescam L, Camus V, Schiano JM, Adélaïde J, Picquenot JM, Guille A, Bannier M, Ruminy P, Viailly PJ, Jardin F, Bouabdallah R, Brenot-Rossi I, Bohers E, Robe C, Laurent C, Birnbaum D, Wotherspoon A, Gaulard P, Xerri L. EBV+ diffuse large B-cell lymphoma associated with chronic inflammation expands the spectrum of breast implant-related lymphomas. Blood. 2020;135(22):2004–9.
68. Khoo C, McTigue C, Hunter-Smith DJ, Walker P. EBV positive fibrin/chronic inflammation associated diffuse large B-cell lymphoma: an incidental finding associated with a breast implant. Pathology. 2021;53(5):673–5.
69. Monteiro M, Duarte I, Cabecadas J, Orvalho ML. Intravascular large B-cell lymphoma of the breast. Breast. 2005;14(1):75–8.
70. Alizadeh AA, Eisen MB, Davis RE, et al. Distinct types of diffuse large B-cell lymphoma identified by gene expression profiling. Nature. 2000;403(6769):503–11.
71. Hans CP, Weisenburger DD, Greiner TC, et al. Confirmation of the molecular classification of diffuse large B-cell lymphoma by immunohistochemistry using a tissue microarray. Blood. 2004;103(1):275–82.
72. Choi WW, Weisenburger DD, Greiner TC, et al. A new immunostain algorithm classifies diffuse large B-cell lymphoma into molecular subtypes with high accuracy. Clin Cancer Res. 2009;15(17):5494–502.
73. Aviles A, Neri N, Nambo MJ. The role of genotype in 104 cases of diffuse large B-cell lymphoma primary of breast. Am J Clin Oncol. 2012;35(2):126–9.
74. Franco F, González-Rincón J, Lavernia J, García JF, Martín P, Bellas C, Piris MA, Pedrosa L, Miramón J, Gómez-Codina J, Rodríguez-Abreu D, Machado I, Illueca C, Alfaro J, Provencio M, Sánchez-Beato M. Mutational profile of primary breast diffuse large B-cell lymphoma. Oncotarget. 2017;8(61):102888–97.
75. Taniguchi K, Katsuyoshi T, Chuang S, Miyata-Takata T, Sato Y, Satou A, Hashimoto Y, Tamura M, Nagakita K, Ohnishi N, Noujima-Harada M, Tabata T, Kikuti YY, et al. Frequent MYD88 L265P and CD79B mutations in primary breast diffuse large b-cell lymphoma. Am J Surg Pathol. 2016;40:324–34.
76. Cao XX, Li J, Cai H, Zhang W, Duan MH, Zhou DB. Patients with primary breast and primary female genital tract diffuse large B cell lymphoma have a high frequency of MYD88 and CD79B mutations. Ann Hematol. 2017;
77. Isaacson PG. Gastrointestinal lymphoma. Hum Pathol. 1994;25(10):1020–9.
78. Molina TJ, Lin P, Swerdlow SH, Cook JR. Marginal zone lymphomas with plasmacytic differentiation and related disorders. Am J Clin Pathol. 2011;136(2):211–25.
79. Horowitz NA, Benyamini N, Wohlfart K, Brenner B, Avivi I. Reproductive organ involvement in non-Hodgkin lymphoma during pregnancy: a systematic review. Lancet Oncol. 2013;14(7):e275–82.
80. Janbabai G, Kayedimajd S, Alian S, Naghshvar F, Rashidi M, Farazmandfar T. Bilateral breast swelling in a 23-year-old woman with Burkitt lymphoma. J Res Med Sci. 2012;17(12):1188–91.
81. Negahban S, Ahmadi N, Oryan A, et al. Primary bilateral Burkitt lymphoma of the lactating breast: a case report and review of the literature. Mol Diagn Ther. 2010;14(4):243–50.
82. Lingohr P, Eidt S, Rheinwalt KP. A 12-year-old girl presenting with bilateral gigantic Burkitt's lymphoma of the breast. Arch Gynecol Obstet. 2009;279(5):743–6.
83. Miranda RN, Aladily TN, Prince HM, et al. Breast implant-associated anaplastic large-cell lymphoma: long-term follow-up of 60 patients. J Clin Oncol. 2014;32(2):114–20.
84. Aladily TN, Medeiros LJ, Amin MB, et al. Anaplastic large cell lymphoma associated with breast implants: a report of 13 cases. Am J Surg Pathol. 2012;36(7):1000–8.
85. Fritzsche FR, Pahl S, Petersen I, et al. Anaplastic large-cell non-Hodgkin's lymphoma of the breast in periprosthetic localisation 32 years after treatment for primary breast cancer—a case report. Virchows Arch. 2006;449(5):561–4.
86. Roden AC, Macon WR, Keeney GL, Myers JL, Feldman AL, Dogan A. Seroma-associated primary anaplastic large-cell lymphoma adjacent to breast implants: an indolent T-cell lymphoproliferative disorder. Mod Pathol. 2008;21(4):455–63.
87. Farkash EA, Ferry JA, Harris NL, et al. Rare lymphoid malignancies of the breast: a report of two cases illustrating potential diagnostic pitfalls. J Hematop. 2009;2(4):237–44.

88. Sahoo S, Rosen PP, Feddersen RM, Viswanatha DS, Clark DA, Chadburn A. Anaplastic large cell lymphoma arising in a silicone breast implant capsule: a case report and review of the literature. Arch Pathol Lab Med. 2003;127(3):e115–8.
89. Muroya D, Toh U, Iwakuma N, et al. Primary breast peripheral T-cell lymphoma not otherwise specified: report of a case. Surg Today. 2015;45(1):115–20.
90. Mattia AR, Ferry JA, Harris NL. Breast lymphoma. A B-cell spectrum including the low grade B-cell lymphoma of mucosa associated lymphoid tissue. Am J Surg Pathol. 1993;17(6):574–87.
91. Gualco G, Chioato L, Harrington WJ Jr, Weiss LM, Bacchi CE. Primary and secondary T-cell lymphomas of the breast: clinico-pathologic features of 11 cases. Appl Immunohistochem Mol Morphol. 2009;17(4):301–6.
92. Lin YC, Tsai CH, Wu JS, et al. Clinicopathologic features and treatment outcome of non-Hodgkin lymphoma of the breast—a review of 42 primary and secondary cases in Taiwanese patients. Leuk Lymphoma. 2009;50(6):918–24.
93. Arber DA, Simpson JF, Weiss LM, Rappaport H. Non-Hodgkin's lymphoma involving the breast. Am J Surg Pathol. 1994;18(3):288–95.
94. Ely KA, Tse G, Simpson JF, Clarfeld R, Page DL. Diabetic mastopathy. A clinicopathologic review. Am J Clin Pathol. 2000;113(4):541–5.
95. Oba M, Sasaki M, Ii T, et al. A case of lymphocytic mastopathy requiring differential diagnosis from primary breast lymphoma. Breast Cancer. 2009;16(2):141–6.
96. Zack JR, Trevisan SG, Gupta M. Primary breast lymphoma originating in a benign intramammary lymph node. AJR Am J Roentgenol. 2001;177(1):177–8.
97. Antoniou SA, Antoniou GA, Makridis C, Spyrou A, Malkotsi T. Bilateral primary breast lymphoma masquerading as lactating mastitis. Eur J Obstet Gynecol Reprod Biol. 2010;152(1):111–2.
98. Kirkpatrick AW, Bailey DJ, Weizel HA. Bilateral primary breast lymphoma in pregnancy: a case report and literature review. Can J Surg. 1996;39(4):333–5.
99. Teras LR, Patel AV, Hildebrand JS, Gapstur SM. Postmenopausal unopposed estrogen and estrogen plus progestin use and risk of non-Hodgkin lymphoma in the American Cancer Society Cancer Prevention Study-II Cohort. Leuk Lymphoma. 2013;54(4):720–5.
100. Yakimchuk K, Hasni MS, Guan J, Chao MP, Sander B, Okret S. Inhibition of lymphoma vascularization and dissemination by estrogen receptor beta agonists. Blood. 2014;123(13):2054–61.
101. Yakimchuk K, Iravani M, Hasni MS, et al. Effect of ligand-activated estrogen receptor beta on lymphoma growth in vitro and in vivo. Leukemia. 2011;25(7):1103–10.
102. Yakimchuk K, Jondal M, Okret S. Estrogen receptor alpha and beta in the normal immune system and in lymphoid malignancies. Mol Cell Endocrinol. 2013;375(1–2):121–9.
103. Kane EV, Bernstein L, Bracci PM, et al. Postmenopausal hormone therapy and non-Hodgkin lymphoma: a pooled analysis of InterLymph case-control studies. Ann Oncol. 2013;24(2):433–41. https://doi.org/10.1093/annonc/mds340.
104. Deli T, Orosz M, Jakab A. Hormone replacement therapy in cancer survivors - review of the literature. Pathol Oncol Res. 2020;26(1):63–78. https://doi.org/10.1007/s12253-018-00569-x.
105. Nelson RA, Levine AM, Bernstein L. Reproductive factors and risk of intermediate- or high-grade B-Cell non-Hodgkin's lymphoma in women. J Clin Oncol. 2001;19(5):1381–7.
106. Zhao S, Zhang QY, Ma WJ, et al. Analysis of 31 cases of primary breast lymphoma: the effect of nodal involvement and microvascular density. Clin Lymphoma Myeloma Leuk. 2011;11(1):33–7.
107. Guo HY, Zhao XM, Li J, Hu XC. Primary non-Hodgkin's lymphoma of the breast: eight-year follow-up experience. Int J Hematol. 2008;87(5):491–7.
108. Wong WW, Schild SE, Halyard MY, Schomberg PJ. Primary non-Hodgkin lymphoma of the breast: the Mayo Clinic experience. J Surg Oncol. 2002;80(1):19–25. discussion 26
109. Gualco G, Bacchi CE. B-cell and T-cell lymphomas of the breast: clinical—pathological features of 53 cases. Int J Surg Pathol. 2008;16(4):407–13.
110. Lin Y, Govindan R, Hess JL. Malignant hematopoietic breast tumors. Am J Clin Pathol. 1997;107(2):177–86.
111. Stewart RL, Dell CM, Samayoa L. Myeloid sarcoma of the breast misdiagnosed as poorly differentiated mammary carcinoma with lobular features. Breast J. 2015;21(2):192–3.
112. Nalwa A, Nath D, Suri V, Jamaluddin MA, Srivastava A. Myeloid sarcoma of the breast in an aleukemic patient: a rare entity in an uncommon location. Malays J Pathol. 2015;37(1):63–6.
113. Huang Q, Reddi D, Chu P, Snyder DS, Weisenburger DD. Clinical and pathologic analysis of extramedullary tumors after hematopoietic stem cell transplantation. Hum Pathol. 2014;45(12):2404–10.
114. Delporte F, Voorhoopf LJ, Lodewyck T, De Paepe P. Primary granulocytic sarcoma of the breast: a case report and review of the literature. Eur J Gynaecol Oncol. 2011;32(4):435–8.
115. Campidelli C, Agostinelli C, Stitson R, Pileri SA. Myeloid sarcoma: extramedullary manifestation of myeloid disorders. Am J Clin Pathol. 2009;132(3):426–37.
116. Pileri SA, Ascani S, Cox MC, et al. Myeloid sarcoma: clinicopathologic, phenotypic and cytogenetic analysis of 92 adult patients. Leukemia. 2007;21(2):340–50.
117. Pileri SA, Grogan TM, Harris NL, et al. Tumours of histiocytes and accessory dendritic cells: an immunohistochemical approach to classification from the International Lymphoma Study Group based on 61 cases. Histopathology. 2002;41(1):1–29.
118. Dalia S, Jaglal M, Chervenick P, Cualing H, Sokol L. Clinicopathologic characteristics and outcomes of histiocytic and dendritic cell neoplasms: the moffitt cancer center experience over the last twenty five years. Cancers (Basel). 2014;6(4):2275–95.
119. Surov A, Holzhausen HJ, Ruschke K, Arnold D, Spielmann RP. Breast plasmacytoma. Acta Radiol. 2010;51(5):498–504.

21 Special Clinical Settings: Tumors Arising in Pregnancy, Pregnancy-Like (Pseudolactational) Proliferations, Breast Carcinoma in the Pre-neoadjuvant Chemotherapy Setting, Recurrent Breast Carcinoma, and Inflammatory Breast Carcinoma

Paula S. Ginter and Timothy M. D'Alfonso

Tumors During Pregnancy

Histopathologic and Physiologic Changes in the Pregnant or Lactating Breast

During pregnancy and lactation, glands and lobules increase in number as well as in their overall epithelial surface area compared to those in the nulliparous breast (Fig. 21.1). Secretory changes of epithelial cells include vacuolization and expansion of cytoplasm, enlarged nuclei with nucleoli, and pink luminal secretions. In contrast, myoepithelial cells investing these glands are inconspicuous. While stroma involutes, vascularity is increased during pregnancy. In the first trimester, these changes are predominately due to the effects of estrogen, and in the second and third trimesters, the changes are driven by progesterone [1]. Prolactin induces lactation in epithelial cells of the lobules, and milk ejection occurs when myoepithelial cells contract due to the influence of oxytocin [2, 3]. Upon cessation of lactation, the breast gradually undergoes involution over the next several months.

P. S. Ginter
Department of Pathology and Laboratory Medicine, Weill Cornell Medicine, New York, NY, USA
e-mail: psg9003@med.cornell.edu

T. M. D'Alfonso (✉)
Department of Pathology, Memorial Sloan Kettering Cancer Center, New York, NY, USA
e-mail: dalfonst@mskcc.org

© The Author(s), under exclusive license to Springer Nature Switzerland AG 2022
S. J. Shin et al. (eds.), *A Comprehensive Guide to Core Needle Biopsies of the Breast*,
https://doi.org/10.1007/978-3-031-05532-4_21

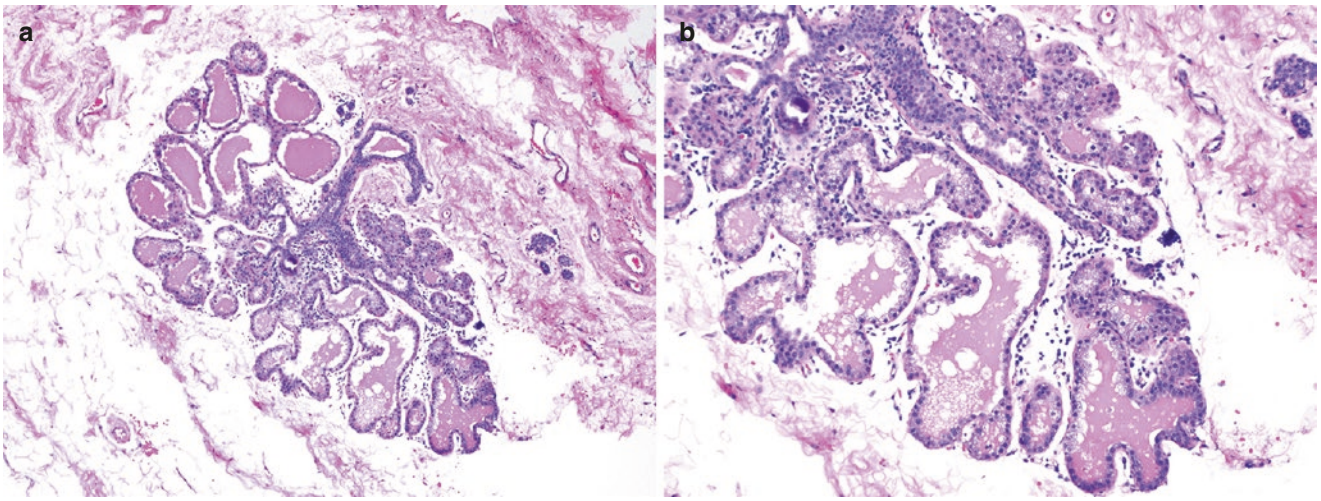

Fig. 21.1 Lobular hyperplasia in pregnancy. (**a**) Enlarged lobule with acinar dilation and focal calcifications. (**b**) Acini are lined by epithelial cells with vacuolated cytoplasm, and eosinophilic sections fill the lumina

Management of Breast Conditions in the Pregnant Patient

Breast lesions in pregnancy are most frequently detected as palpable masses, as routine radiologic screening is not performed on most patients during this period. Physical examination of these patients is also challenging due to the increased cellularity of the breast during pregnancy.

Radiologic Imaging and Biopsy

As most pregnant or lactating patients present due to palpable masses, radiologic evaluation of these patients can be challenging [1, 4]. Mammography is generally safe during pregnancy and lactation; however, decisions regarding screening must weigh considerations of underlying risk factors [1]. Overall, mammographic screening is recommended in pregnant and lactating patients with average risk who are 40 years of age or older and for younger intermediate and high-risk women [1].

Ultrasound is the first-line modality in the workup of a palpable breast mass in a pregnant or lactating patient. All pregnant patients with a dominant palpable breast mass that persists for 2 weeks or longer should be evaluated with a targeted ultrasound examination [4]. Unique advantages of ultrasound include both safety due to lack of ionizing radiation and high sensitivity in the detection of pregnancy-associated breast cancer. The utility of ultrasound in detecting malignant lesions in pregnancy-associated breast carcinomas has been well established, with studies reporting high sensitivity and negative predictive value [4]. While not used as a first-line modality, mammography is a useful adjunct to ultrasound and should be used if ultrasound does not demonstrate a correlate for a palpable mass. Following a suspicious ultrasound finding or after a new diagnosis of breast cancer is established, mammography should be performed to evaluate the extent of disease and the presence of suspicious calcifications [1, 5, 6].

US-guided core needle biopsy (CNB) is recommended as the method of choice to obtain tissue for pathologic diagnosis. While fine needle aspiration biopsy has been reported to be successful in distinguishing benign breast masses of pregnancy, pregnancy-related cellular atypia can lead to false-positive diagnosis of breast carcinoma in these samples [7]. Additionally, marked cytological atypia on fine needle aspiration specimens may necessitate surgical biopsy and further delay the diagnosis of carcinoma [7]. Therefore, ultrasound-guided CNB is ideal for not only maximizing diagnostic accuracy but also providing material for additional studies, including hormone receptor and HER2 evaluation should malignancy be detected.

The main issue regarding the use of magnetic resonance imaging (MRI) in pregnant patients is related to concerns of gadolinium-induced fetal toxicity. At this time, dynamic contrast-enhanced MRI (DCE-MRI) is not recommended in pregnant patients [1, 5].

Surgery

Surgical management requires a multidisciplinary approach and must take into consideration both the benefit for the mother and risk for the fetus. Tissue-diagnosed malignancies may be treated surgically; however, excision of most benign lesions ought to be performed postpartum in order to minimize fetal exposure to anesthesia. Each case requires an individualized approach incorporating a number of factors such as the stage of disease, patient preferences, and gestational age of the fetus.

Chemotherapy

Chemotherapy is only recommended after the first trimester of pregnancy [8], and anthracycline-based regimens have been most frequently utilized in this clinical setting. As an alternative choice, taxane-based therapies are also employed for those who are found to be unresponsive to anthracyclines or its use is contraindicated.

Benign Tumors During Pregnancy

While conceivably all benign tumors that arise in the non-pregnant patient can develop in the pregnant and lactating patient (Fig. 21.2), by far the most common benign tumor in the latter population is the lactating adenoma. Other benign tumors are discussed in other chapters, and lactating adenoma will be discussed here.

Lactating Adenoma

Overview

Lactating adenoma is the most common cause of a breast mass in pregnant or postpartum women accounting for 70% of CNBs in this patient population [9, 10]. Typically, it presents as a painless mass that becomes evident late in pregnancy (third trimester) or during the postpartum period. Occasionally, they may be bilateral or multifocal in nature. Lactating adenomas may also develop in ectopic breast tissue along the milk line, which extends from the axilla to the vulva [11]. They are often palpable, mobile lesions that may undergo rapid growth and can become large in size [12]. Large (>5 cm) lactating adenomas have a predilection to undergo infarction, which can lead to breast tenderness and pain. As such, recent onset of discomfort in a painless tumor is suggestive of infarction in these patients [13, 14].

Gross and Radiologic Features

By mammography, lactating adenomas are most frequently well circumscribed but rarely show obscured borders or appear as an asymmetric mass [15]. Lactating adenomas are oval, sharply circumscribed, hypoechoic masses which are parallel to the skin surface on ultrasound [16] (Fig. 21.3a). Grossly, these are gray-tan to yellow, well-circumscribed masses with firm to rubbery texture.

Microscopic Features

The epithelial cells of the lactating adenoma demonstrate physiological changes normally seen during lactation

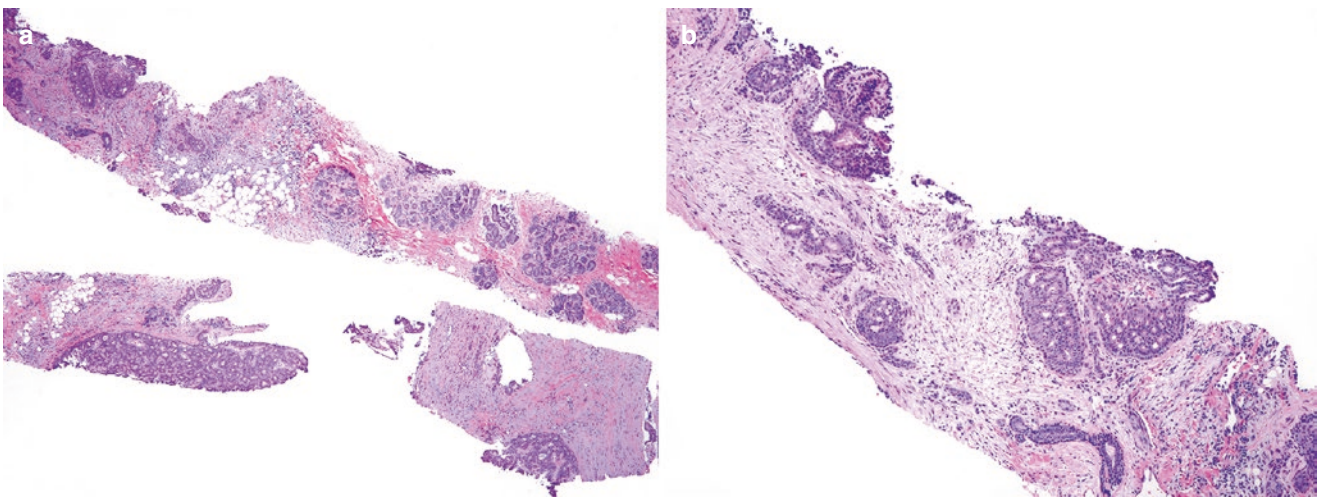

Fig. 21.2 Papilloma in pregnancy. (**a**) Core biopsy of a mass in a pregnant woman shows portion of a sclerosing papilloma. (**b**) Secretory change is not present in the lesional glands and only in the adjacent uninvolved lobules

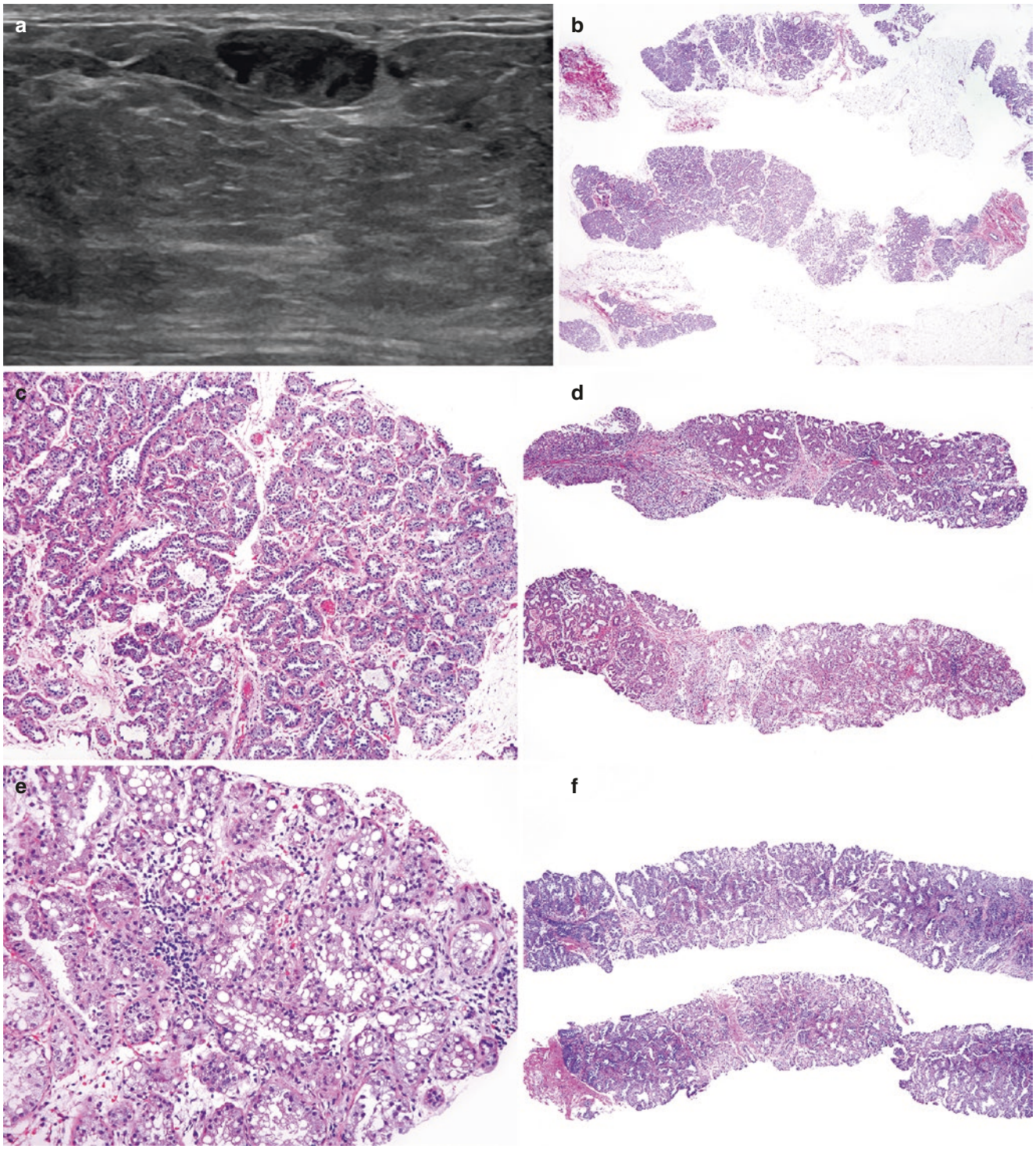

Fig. 21.3 Lactating adenoma. (**a**) Ultrasound shows a homogeneous well-circumscribed mass. *Courtesy of Dr. Michele B. Drotman, with permission*. (**b**) CNB from a mass lesion in a pregnant woman reveals a circumscribed lesion composed of closely arranged enlarged and hyperplastic lobules separated by thin fibrous septa and adipose tissue. (**c**) The glandular epithelium has finely vacuolated cytoplasm. (**d**) CNB from a mass lesion in another pregnant woman demonstrates a proliferation composed of tightly packed, enlarged, and hyperplastic lobules. (**e**) The glandular cells have hyperchromatic nuclei and vacuolated cytoplasm. (**f**) CNB from a mass in a third pregnant woman shows hyperplastic lobules with luminal dilatation. (**g**) The lining epithelium is hyperplastic and vacuolated

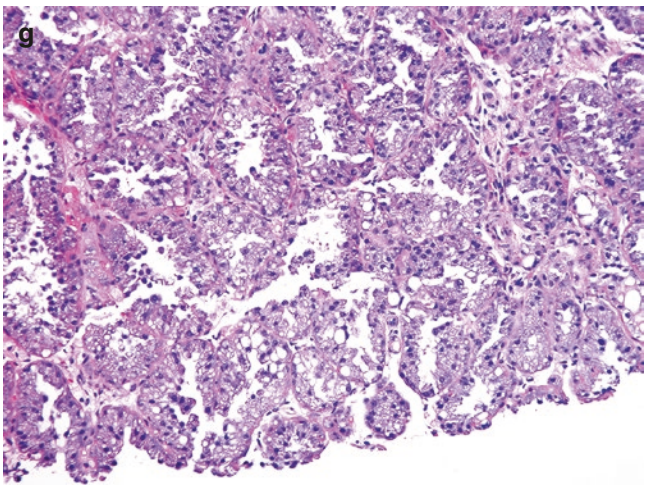

Fig. 21.3 (continued)

(described above) and retain much of their lactating activity (especially protein secretion).

Histologically, lactating adenomas are sharply demarcated nodules composed of closely arranged, enlarged, and hyperplastic lobules with spare intervening delicate connective tissue. Secretory changes such as the presence of cytoplasmic vacuoles as well as luminal eosinophilic secretions are prominent [11, 13, 17] (Figs. 21.3b–g and 21.4). No atypical mitotic figures or cytologic atypia is seen.

Differential Diagnosis

The differential diagnosis includes tubular adenoma, fibroadenoma with lactational change, and secretory carcinoma. Tubular adenoma is a benign, well-circumscribed tumor composed of a compact proliferation of round-to-oval glands surrounded by a scant stroma. Luminal secretions can be appreciated to a limited extent in these tumors, thus exhibiting resemblance to lactating adenomas. However, other secretory features such as cytoplasmic vacuolization are lacking. In general, lactating adenomas and tubular adenomas share morphologic and clinical similarities, and due to the overlapping histologic features, it is sometimes difficult to distinguish between these entities, particularly in limited samples of CNBs (Fig. 21.5).

Fibroadenoma harboring varying extents of lactational change or hyperplasia can also occur in pregnant women (Fig. 21.6). These can be distinguished from lactating adenoma based on the presence of a more prominent stromal component between the intervening glands. Similar to tubular adenomas, the distinction may not be critical for management decisions. Additionally, fibroadenoma with pregnancy-like change can be seen in the nonpregnant, nonlactating breast (Fig. 21.7).

Secretory carcinoma is low on the differential diagnosis as it only superficially resembles lactating adenomas due to their common secretory features. Secretory carcinoma is composed of pale neoplastic cells with amphophilic-to-eosinophilic vacuolated cytoplasm and low-grade nuclei. The infiltrative growth pattern and absence of investing myoepithelium distinguish this carcinoma from lactating adenoma (Fig. 21.8). Even in limited CNB material, the presence of myoepithelial cells around the lesional glands can be confirmed by immunohistochemical (IHC) stains, and it can easily distinguish lactating adenoma from secretory carcinoma [11, 17].

Immunohistochemical Workup

IHC staining with myoepithelial markers such as p63 and smooth muscle heavy-chain myosin (SMM) shows intact myoepithelial cells surrounding the glands of a lactating adenoma, whereas they are absent in secretory carcinoma. Furthermore, immunostains may be useful to highlight the architecture of infarcted lactating adenomas (Fig. 21.4c, e). IHC is of little value in distinguishing lactating adenoma from tubular adenoma or fibroadenoma with lactational change, which is purely a morphologic distinction.

Pathogenesis

The underlying pathogenesis of lactating adenomas is still questionable. Slavin et al. proposed that lactating adenomas represent nodules of physiologic lobular proliferation, which are more prominent than the adjacent breast tissue and resemble focal exaggerated physiological hyperplasia [14]. Interestingly, the current edition of the World Health Organization (WHO) does not recommend using "nodular lactational hyperplasia" [10]. It has also been hypothesized that lactating adenomas arise in preexisting tubular adenomas [17, 18]. In a study by Hertel et al., a subset of postpartum patients with tubular adenomas were observed to present with a breast lump during pregnancy, supporting the association of tubular adenomas with pregnancy [17]. It remains unclear whether lactating adenoma is an entirely separate entity or is a result of hyperplastic physiologic changes within a preexisting lesion. Molecular studies have failed to demonstrate *MED 12* exon 2 mutations that are frequently seen in fibroadenomas [19].

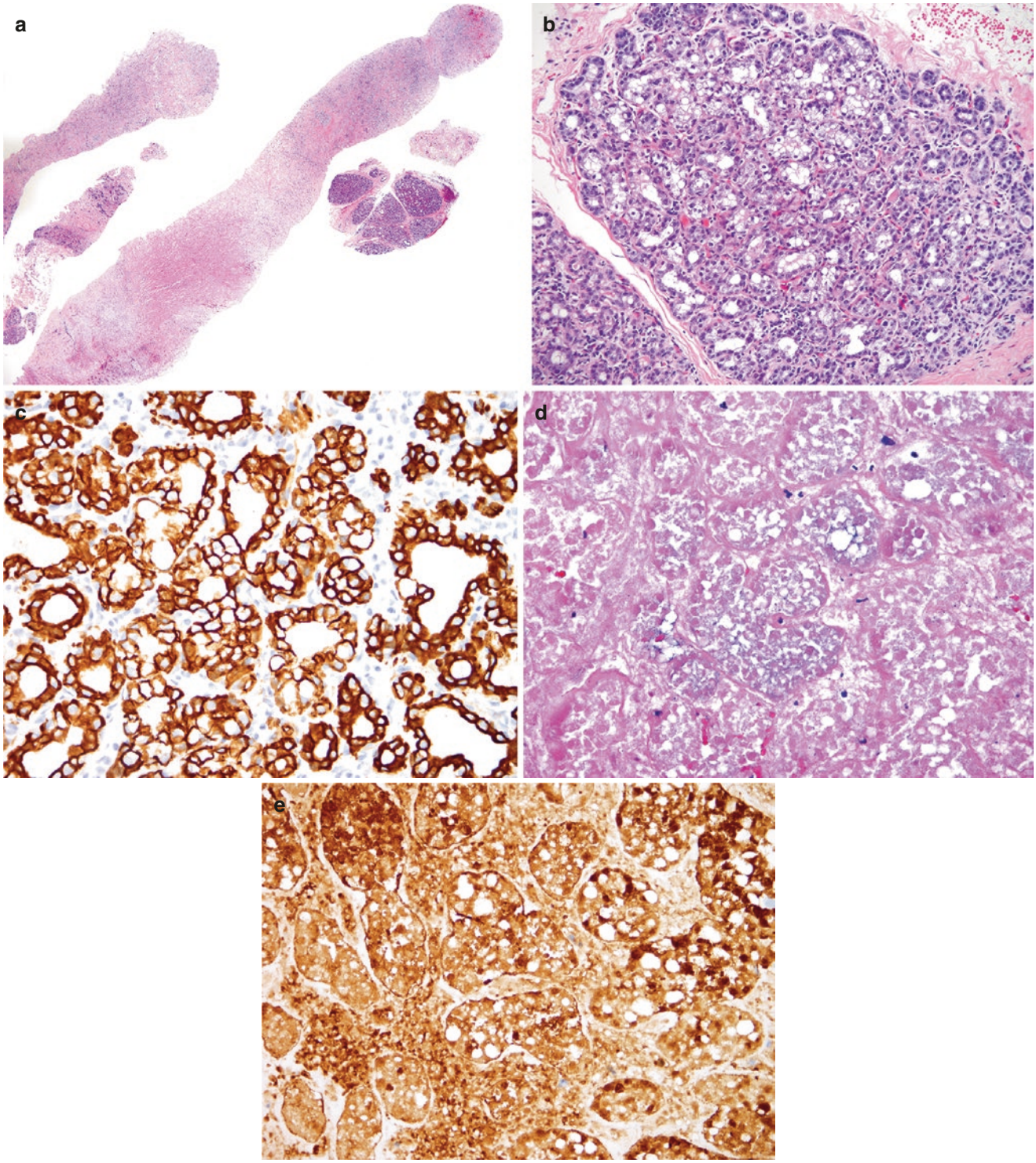

Fig. 21.4 Infarcted lactating adenoma. (**a**) CNB of a mass lesion in a pregnant woman shows a largely necrotic mass. Surrounding viable tissue shows enlarged, hyperplastic lobules indicative of her pregnancy. (**b**) Lobular epithelium shows vacuolated cytoplasm with eosinophilic luminal secretions. (**c**) The acinar structure of the lobule is outlined by pancytokeratin immunostain. (**d**, **e**) The acinar structure of the infarcted tumor can be appreciated histologically and is further highlighted by pancytokeratin immunostain albeit muddy due to leakage into surrounding tissue

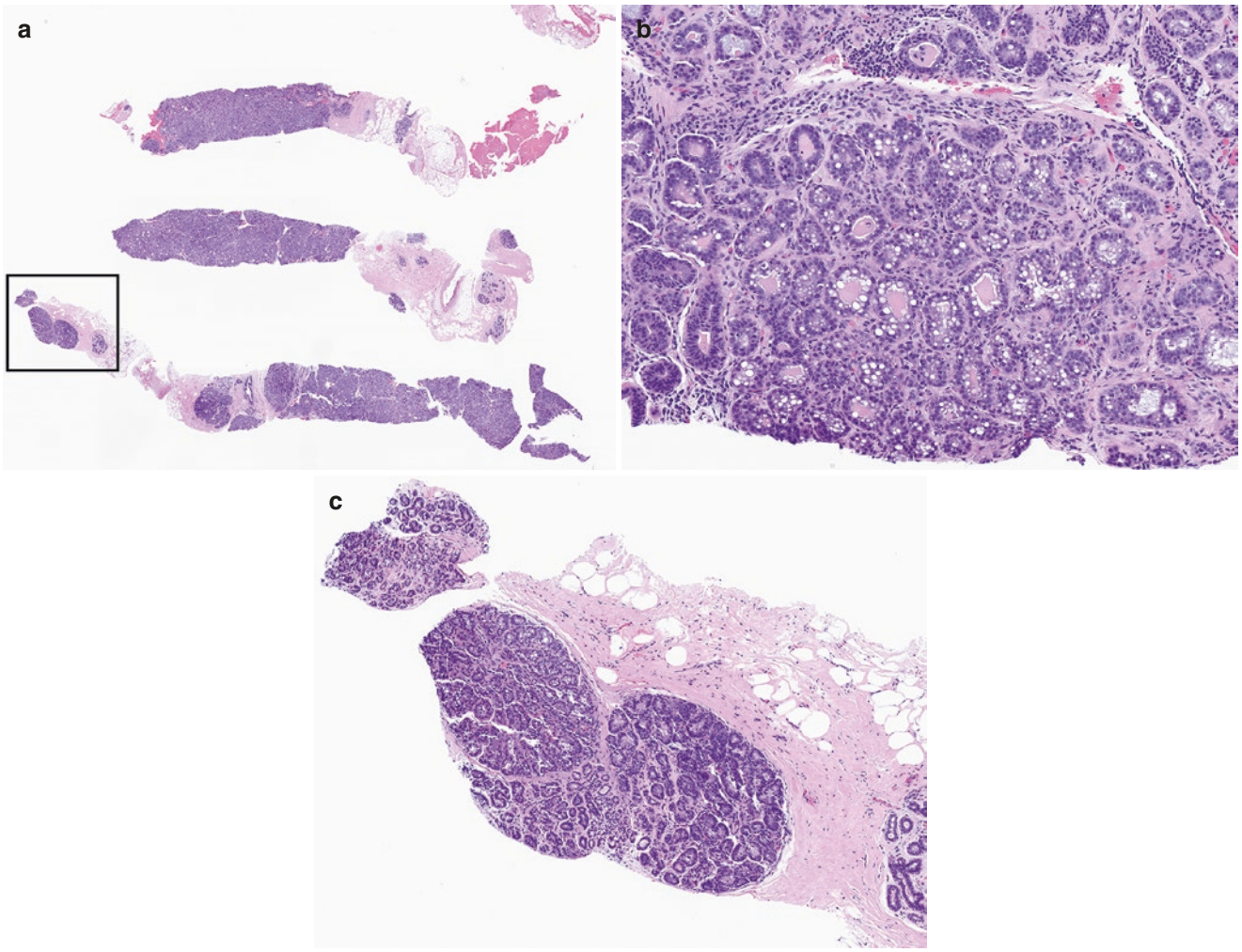

Fig. 21.5 Lactating adenoma resembling tubular adenoma in early pregnancy. (**a**) Low power of a CNB of a breast mass in a patient 13 weeks pregnant shows a well-circumscribed lesion composed of a dense proliferation of glands, which resembles a tubular adenoma. (**b**) Higher magnification shows that the dense glands exhibit vacuolated cytoplasm and luminal secretions. (**c**) Higher power view of area in *box* from (**a**) highlights the lactational change in the uninvolved breast lobules

Treatment and Prognosis

Surgical excision is not required for lactating adenoma, in the absence clinicoradiologic and pathologic discordance. In cases where surgical excision is performed, enucleation is recommended as there is a low risk of recurrence. Breastfeeding may be resumed after surgery. While bromocriptine, a dopamine agonist, can be used to shrink the tumor, it suppresses lactation. The benefits of tumor shrinkage must be weighed against the cessation of lactation [10, 12, 14].

Lactating adenoma does not represent a risk factor for developing breast carcinoma; however, rare cases of coexisting carcinoma and lactating adenoma, as well as subsequent carcinoma in the vicinity of a previously diagnosed lactating adenoma, have been reported [17, 20].

Lactating adenomas have been shown to express high amounts of the prolactin receptor and, together with progesterone, might be responsible for the rare initiation of carcinogenesis in these tumors [21, 22]. While the possibility of malignant transformation of lactating adenomas is still uncertain, case reports of women with lactating adenomas developing malignancies raise probable concern, and accordingly close clinical follow-up in these patients is recommended [17, 20].

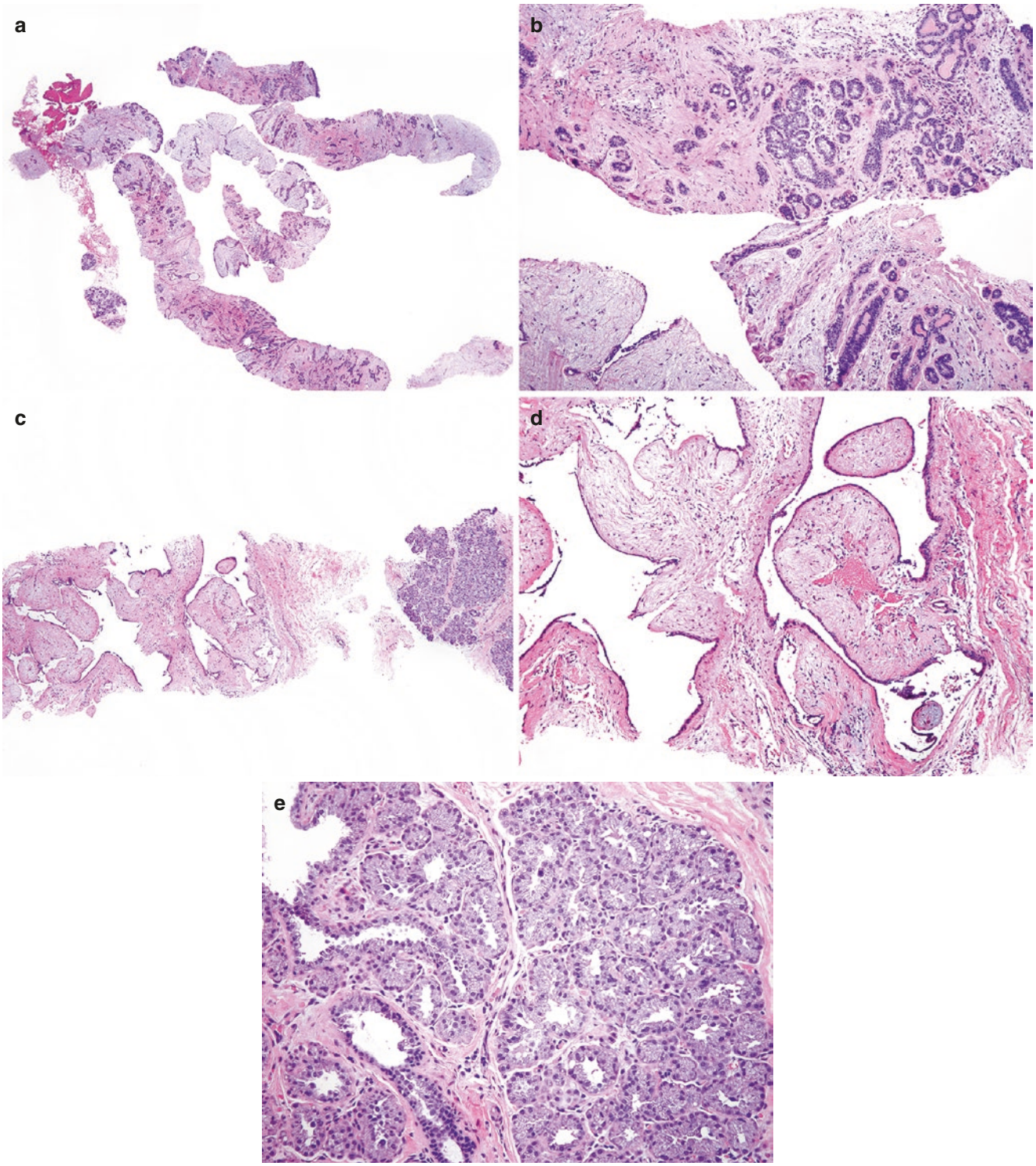

Fig. 21.6 Fibroadenoma in pregnancy. (**a**) CNB of a breast mass in a pregnant woman shows a fibroadenoma with homogeneous stroma and evenly distributed glandular elements. (**b**) Some glands within the tumor show secretory epithelial changes such as vacuolated cytoplasm and luminal secretions. (**c**) CNB of a breast mass in another pregnant woman shows a well-circumscribed fibroadenoma and surrounding breast tissue with secretory epithelial changes. (**d**) The tumoral stroma is paucicellular with intracanalicular growth leading to compression of ducts. (**e**) The uninvolved breast lobules show secretory changes such as notable cytoplasmic vacuolation

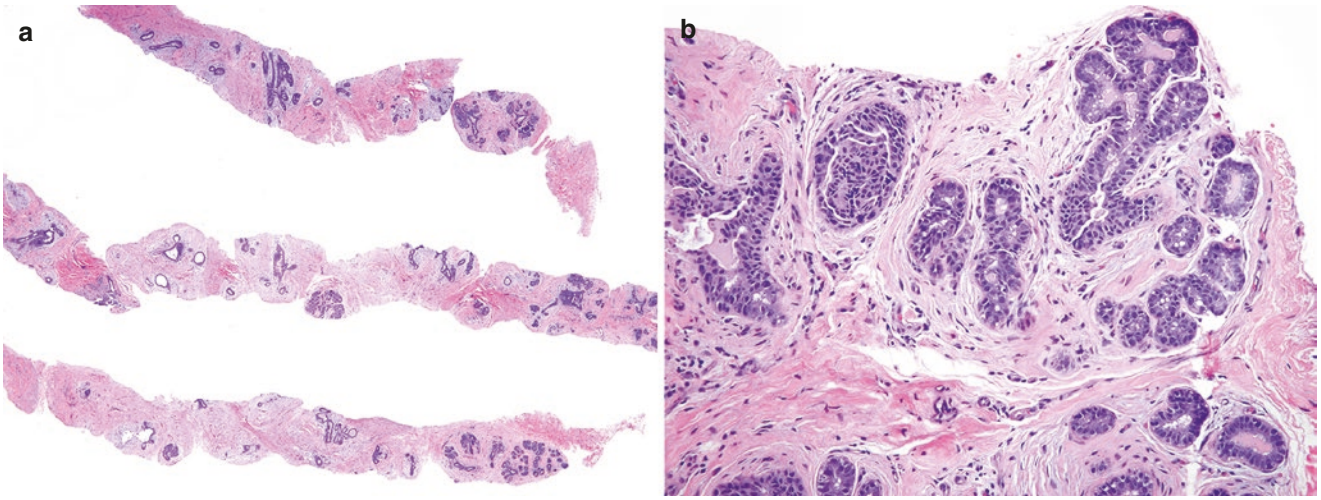

Fig. 21.7 Fibroadenoma with pregnancy-like change. (**a**) CNB of a breast mass from a nonpregnant woman shows a fibroadenoma with an even distribution of glands and stroma. (**b**) Some lesional glands show finely vacuolated cytoplasm with eosinophilic luminal secretions characteristic of pregnancy-like change

Pregnancy-Associated Breast Carcinomas

Overview

Pregnancy-associated breast cancer (PABC) is defined as any cancer that occurs during pregnancy or during the lactation period within 1 year of childbirth [23]. Generally, there is a transient increased risk of developing breast carcinoma during pregnancy and the postpartum period, followed by a long-lasting protective period [24]. While cervical carcinoma used to be the most common malignancy encountered in pregnant women, breast carcinoma is now the most common malignancy of pregnancy, due to decreasing incidence of cervical cancer [25–27]. PABC occurs in the range of 1 in 3000 to 10,000 pregnancies and is the most common cause of cancer-related death in the pregnant and lactating patients [23, 28, 29]. The mean age at diagnosis based on current studies is estimated to be between 32 and 34 years [4, 30]. In women younger than 45 years of age, the incidence of PABC varies from 2.6 to 14% [30, 31].

There is frequently a delay in diagnosis of PABC (2–15 months) leading to a 2.5-fold higher risk of diagnosis at an advanced stage [32–34]. Aside from a palpable breast mass, other presenting signs and symptoms include unilateral breast enlargement with skin redness and thickening, ulcers, nipple retraction, and nipple discharge [35]. Instances of "milk rejection," where an infant refuses to nurse from the affected breast, have also been reported [36].

The role of hormones in breast cancer development and regulation of breast cancer cell growth is very complex, and during pregnancy high concentrations of estrogen, progesterone, and prolactin are produced for lactation. Estrogen and progesterone have long been known to play a vital role in breast cancer. Recent evidence suggests that prolactin too has a role in human breast cancer [21].

Gross and Radiologic Features

PABC most commonly presents as a painless, palpable mass and is rarely associated with calcifications [4]. As previously mentioned, ultrasound is the modality of choice to evaluate breast masses in pregnant patients (Fig. 21.9). Grossly, the tumors are tan/white in color with irregular borders and may demonstrate a central (necrotic) cavitation.

Microscopic Features

Overall, there is no difference in the histologic types of breast carcinomas observed in PABC compared to non-PABC, with the most prevalent type being invasive breast carcinoma of no special type (IBC-NST) [37]. Other special types of carcinoma, including invasive lobular carcinoma, occur in low frequency or as case reports [37–40]. Histologically, PABC most frequently is poorly differentiated [23] (Fig. 21.9b, g, h). These tumors characteristically show syncytial growth pattern with high nuclear grade [23, 41]. The associated ductal carcinoma in situ (DCIS) tends to be extensive and high grade [41, 42]. Additionally, these tumors are associated with other aggressive clinicopathologic features including larger size, higher rates of lymphovascular invasion and axillary lymph node metastasis, and higher proportions of inflammatory carcinoma [4, 23, 41–43] (Fig. 21.9c, d, g–i). In general, PABCs are known to be of higher grade and more poorly differentiated compared to those arising in older women [41, 42].

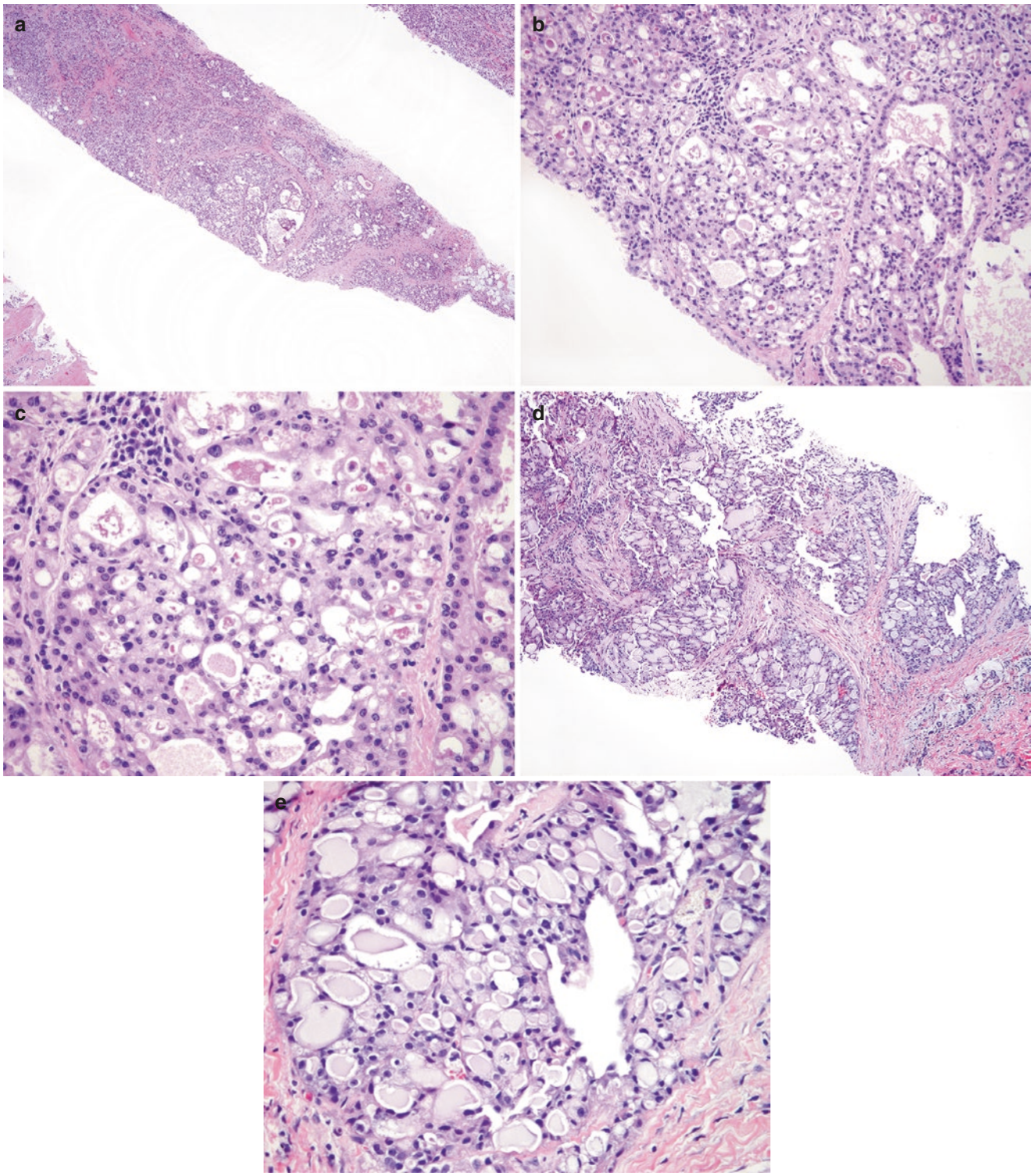

Fig. 21.8 Secretory carcinoma. (**a**) CNB of a mass shows an invasive carcinoma with solid and microcystic architecture associated with stromal fibrosis. (**b**, **c**) The microcysts are lined by tumor cells, which are finely vacuolated with pale-to-pink cytoplasm and eosinophilic luminal secretions. (**d**) CNB of another breast mass shows invasive carcinoma with a predominately microcystic architecture. (**e**) The neoplastic cells have amphophilic cytoplasm, and dense luminal secretions are present

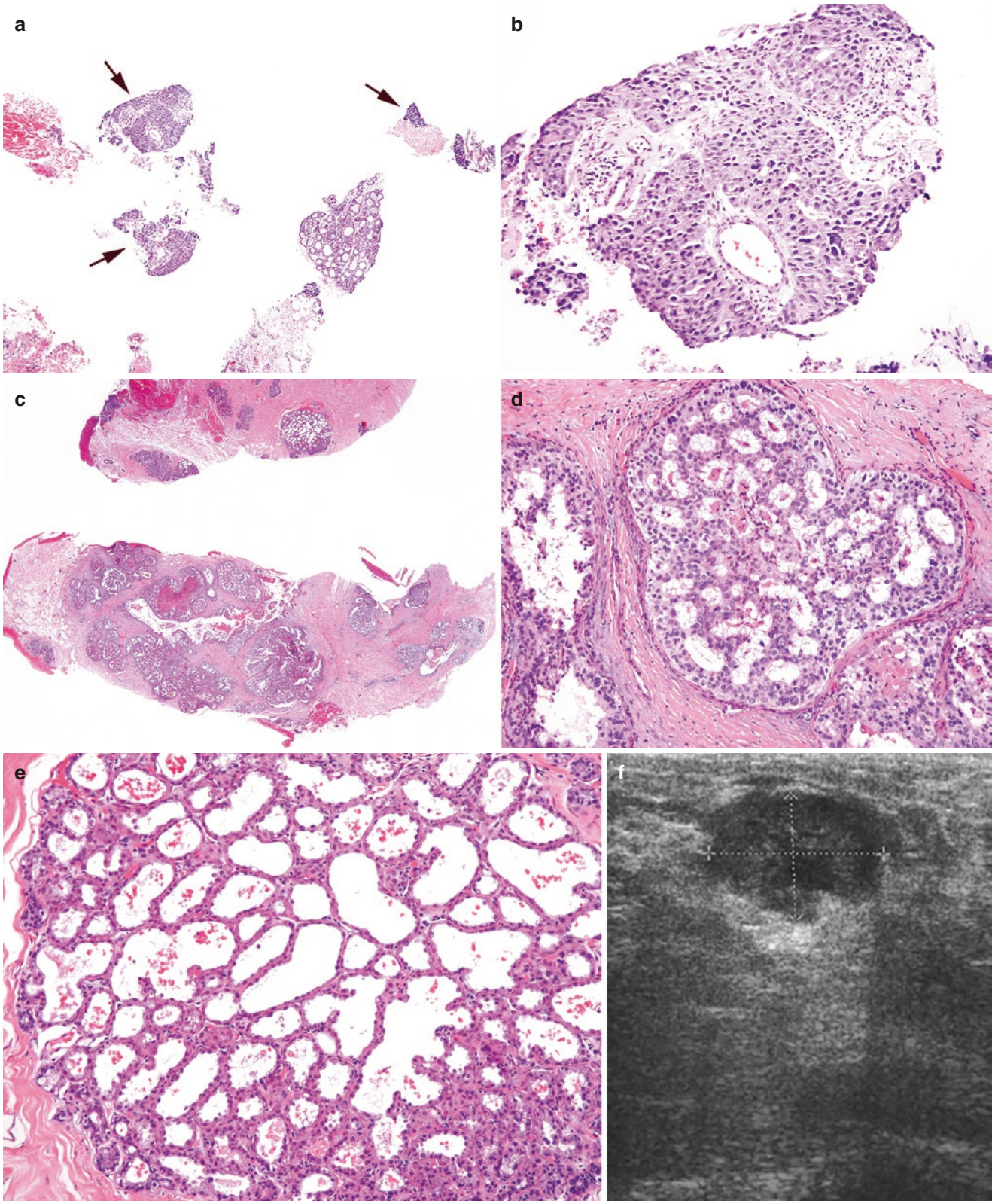

Fig. 21.9 Carcinoma in pregnancy. (**a**) CNB of a mass in a pregnant woman shows scant tissue fragments of invasive carcinoma associated with necrosis (*arrows*). Uninvolved lobules with secretory change are also present. (**b**) The invasive carcinoma is poorly differentiated. (**c**) CNB of a mass in another pregnant woman shows cribriform and micropapillary ductal carcinoma in situ (DCIS). Secretory changes are present in the surrounding lobules. (**d**) DCIS shows intermediate-to-high nuclear grade and is associated with necrosis. (**e**) Surrounding lobular glands with dilated acini lined by vacuolated epithelium indicative of pregnancy are present. (**f**) Ultrasound of the mass from (**a**) shows a hypoechoic mass with irregular borders and posterior acoustic shadowing. *Courtesy of Dr. Carolyn S. Eisen, with permission*. (**g**, **h**) CNB of a mass in another pregnant woman shows poorly differentiated invasive carcinoma. (**i**) CNB of an abnormal ipsilateral lymph node shows morphologically similar metastatic carcinoma involving a lymph node

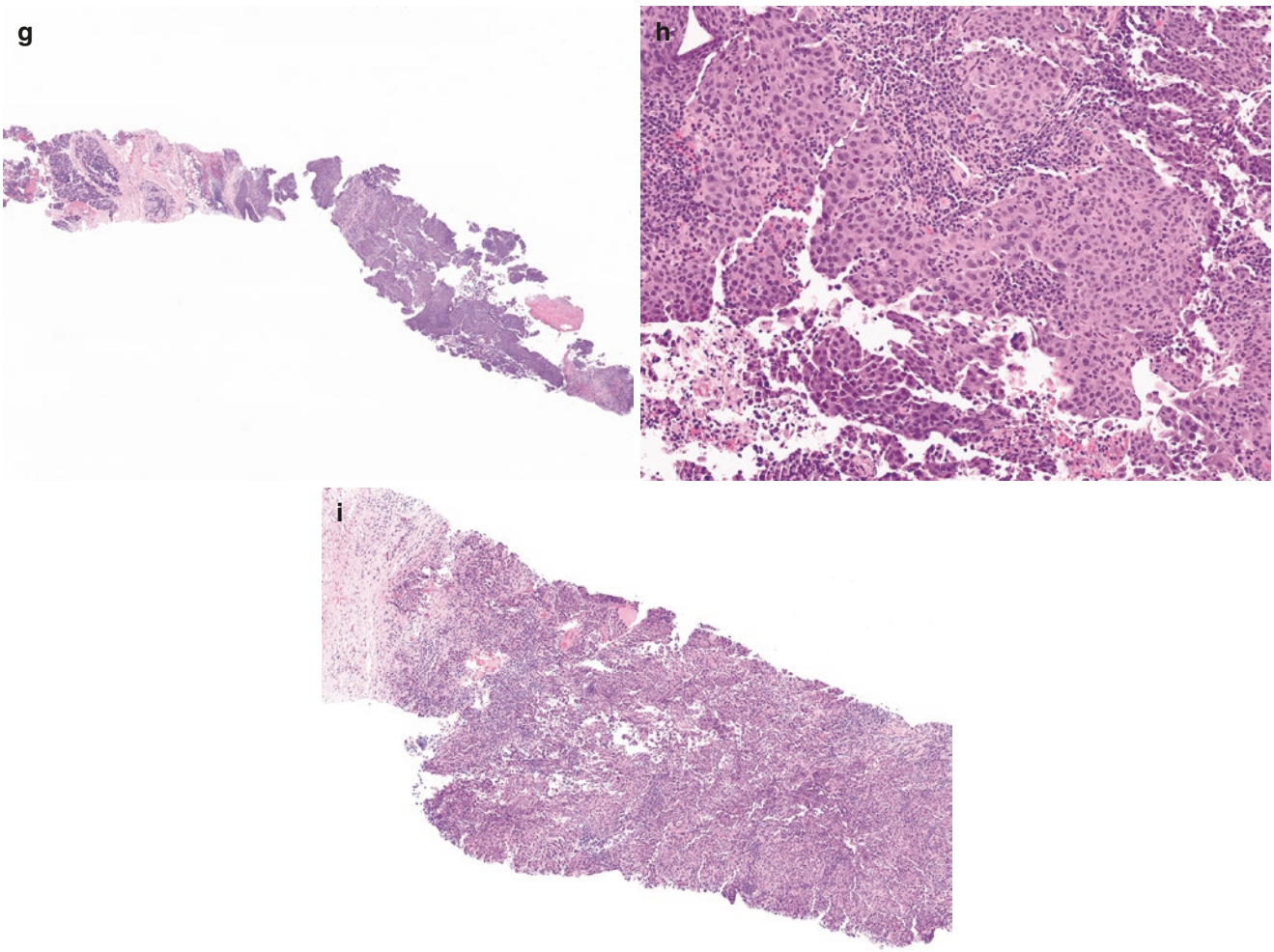

Fig. 21.9 (continued)

Immunohistochemical Workup

Standard approach of confirming the presence of invasive and/or in situ carcinoma using myoepithelial markers can be applied to cases arising in pregnant patients.

Biomarker Evaluation

As with all breast carcinomas, evaluation of biomarker expression is required for treatment decisions. Due to their poorly differentiated nature, these carcinomas tend to be estrogen receptor (ER) negative and progesterone receptor (PR) negative [42]. Occasionally, the breast glandular tissue of pregnant women is nonreactive (or very weakly reactive) for these hormone receptors, and it is critical to ensure the use of an alternative (external) positive control in these cases. In CNBs, this may be routinely required as adjacent normal breast tissue may be absent in limited samples.

Data regarding differences in ER, PR, and HER2 status in PABC compared to non-PABC is conflicting [41, 44, 45]. No significant difference in the Ki-67 proliferation rate or frequency of p53 positivity has been found in patients with PABC compared with age-matched nonpregnant control subjects [41].

Molecular Subtypes

In PABC, triple-negative (basal-like) and luminal B molecular subtypes predominate [42, 46]. In a study evaluating hot spot somatic mutations and evaluating transcriptomic profiling, approximately 30% of PABCs were basal-like, but no differences between PABC and non-PABC were observed [47]. Enriched pathways included the G protein-coupled receptor pathway and the serotonin receptor pathway [47].

Treatment and Prognosis

The treatment of PABCs requires a multidisciplinary approach and active communication among the patient, obstetrician, surgeon, and medical and radiation oncologists [48]. Both mastectomy and breast-conserving surgery (BCS) are acceptable surgical options for PABC [49]. However, if PABC is detected in the first trimester, mastectomy is the standard for local treatment in patients who choose to continue their pregnancy, as adjuvant radiation therapy would be delayed. In cases where definitive breast surgery is performed, delayed reconstruction is preferred to decrease anesthesia exposure to the fetus. Tissue expander insertion appears to ensure a short operative time and is not associated with considerable morbidity to the patient or the fetus [50]. Therefore, it can be considered in the multidisciplinary management of PABC. While axillary lymph node dissection has historically been the standard due to rates of axillary lymph node involvement >50% at diagnosis, the increasing number of node-negative PABC cases has allowed for increasing utilization of sentinel lymph node biopsy, which is considered safe in this setting [30, 37, 51, 52]. Systemic treatment for PABC is based on evidence-based practice in nonpregnant patients, except for considerations regarding contraindications during pregnancy. While adjuvant treatment is more commonly used, data regarding neoadjuvant treatment in PABC is increasing [53–56]. In the neoadjuvant setting, and only after the first trimester, anthracyclines in combination with cyclophosphamide, fluorouracil, or taxanes are used to treat PABC, while hormonal and anti-HER2 agents are avoided due to risk of malformation or oligohydramnios [57, 58].

While conflicting data exist regarding the prognosis of these patients, disease-free and overall survival rates of patients with PABC have been found to be lower when compared to matched controls among molecular subtypes [42, 59, 60]. The mortality increase was most pronounced in the subgroup of women diagnosed shortly after delivery [59]. Metastasis to distant organs such as brain and rare sites of metastasis such as placenta have been reported [61, 62].

Tumor-infiltrating lymphocytes (TILs) remain an emerging predictive factor for breast cancer patients, and TILs appear to be less prevalent in PABC. One study found that the mean stromal TILs in pregnant and nonpregnant young breast cancer patients were 2.9% versus 17.8%, respectively [63]. Furthermore, only 2.3% of pregnant patients had tumors with >50% TILs [63]. The low prevalence could reflect the state of low host immunity associated with pregnancy and therefore may not be as informative in this subset of patients. Further studies are needed to validate these findings.

Pregnancy-Like (Pseudolactational) Proliferations

Pregnancy-Like Change and Pregnancy-Like Hyperplasia

Overview

Pregnancy-like (pseudolactational) change or hyperplasia represents a combination of both secretory and involutional alterations of lobules in the nonpregnant, non-lactating breast [64]. The vast majority of cases have been reported in females, but one with atypia was recently described in a male [65]. Historically, the vast majority of instances have been incidentally discovered and clinically inapparent. However, the widespread practice of screening mammography has brought this lesion to clinical attention through its occasional association with microcalcifications. Rarely, they have been reported to present as a mass [66]. Causative roles by hormonal, antipsychotic, and antihypertensive medications have been reported in some patients; however, a definitive relationship has not been established to date [64].

Gross and Radiologic Features

Most examples are clinically silent unless they are seen secondarily involving a lesion that comes to clinical attention (i.e., fibroadenoma with lactational-like change). More recently, they have been mammographically evident due to the association with/formation of calcifications. These microcalcifications are generally interpreted to have benign features by radiologic criteria; however, they are occasionally biopsied for further evaluation. There are no gross features associated with this histologic finding.

Microscopic Features

The histologic features are identical to those seen in the pregnant or lactating breast (described above) and can be seen as partial or complete involvement of one or more lobules. Needless to say, obtaining accurate clinical history of current pregnancy or lactation is paramount.

Pregnancy-like change is recognized as one or more lobules consisting of ectatic glands lined by a single layer of epithelial cells with secretory features. Exaggerated apical snouts imparting a hobnail appearance with nuclear protrusion into the glandular lumina are typical. Nuclear "atypia" seen as nuclear enlargement and hyperchromasia is characteristic; however, mitoses are absent. The glandular lumina may be empty or partially filled with pink thin secretions (Fig. 21.10). In contrast, *pregnancy-like hyperplasia* is a term reserved for instances where the secretory cells become proliferative with piling and tufting within a given lobular

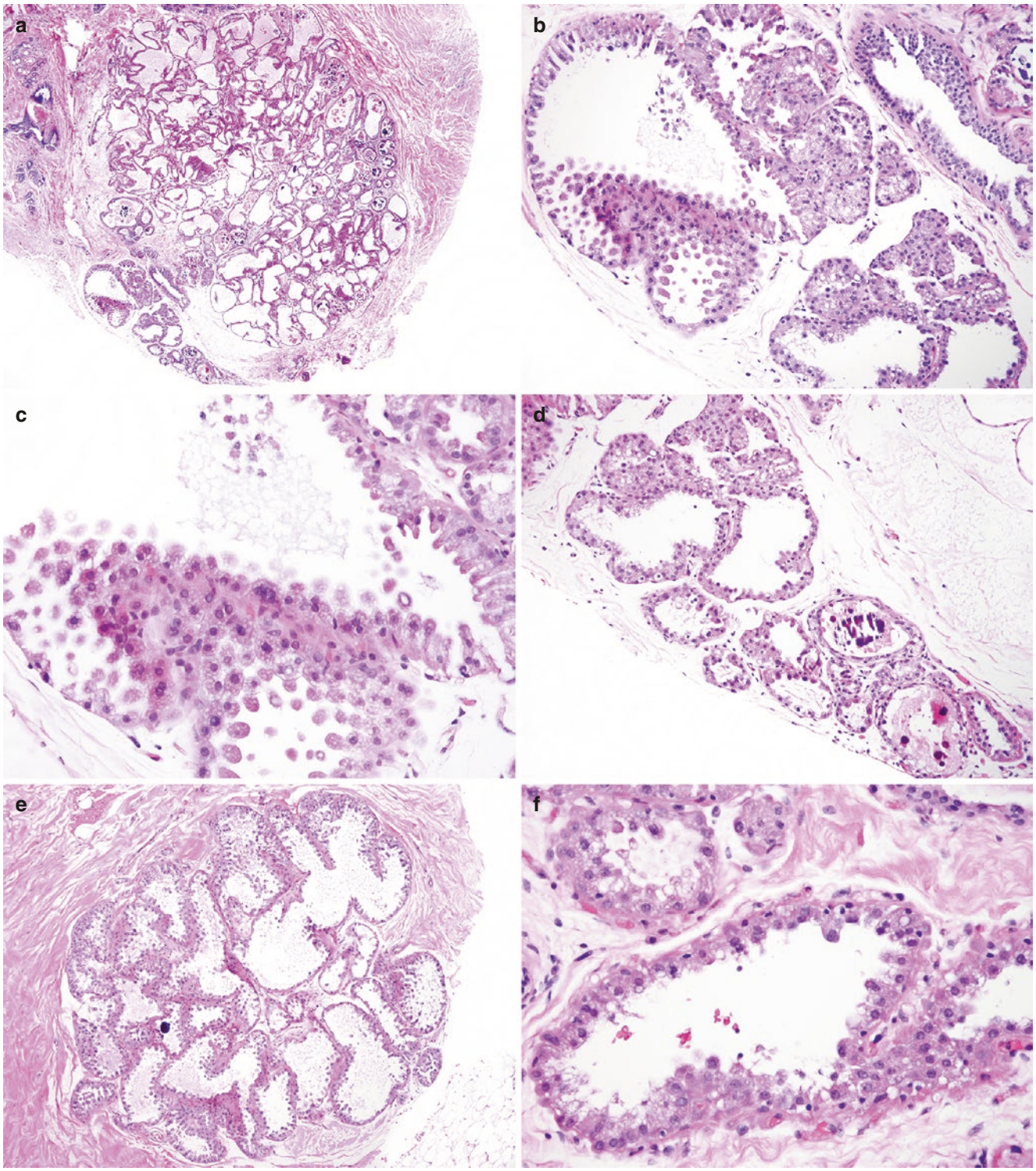

Fig. 21.10 Pregnancy-like change. (**a**) At low power, a cystically enlarged terminal duct lobular unit is present. (**b**, **c**) Higher power views show characteristic nuclear protrusion into the lumina, vacuolated cytoplasm, and associated calcifications. Additionally, pregnancy-like hyperplasia is seen in **b**. (**d**) Note that the epithelial lining of these ectatic lobular glands is single layered and contains luminal calcifications. (**e**–**h**) and (**i**, **j**) are two other examples of pregnancy-like change with similar histologic findings

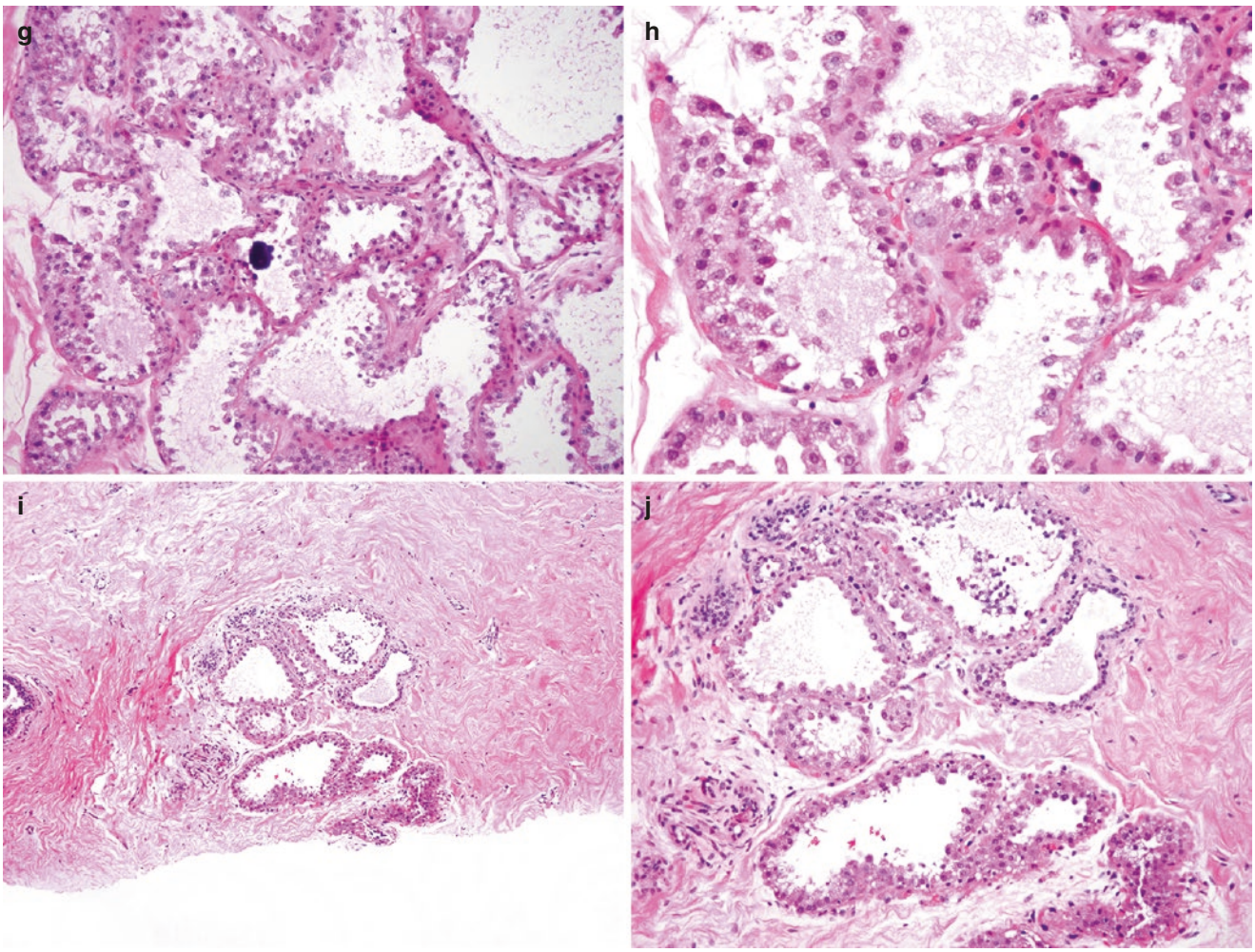

Fig. 21.10 (continued)

gland. This, in turn, leads to crowding and filling of the luminal spaces (Fig. 21.10b).

Calcifications associated with pregnancy-like lesions are often laminated with unevenly spaced concentric rings (psammomatous-like) and, in some cases, resemble the ossifying-type calcifications associated with columnar cell lesions (Fig. 21.11). However, there is no pathognomonic appearance of calcifications specifically associated with pregnancy-like proliferations [67].

Differential Diagnosis for Pregnancy-Like Change

The entities that may morphologically mimic pregnancy-like change include atypical pregnancy-like change, atypical cystic apocrine metaplasia, columnar cell lesions including flat epithelial atypia, lobules with radiation therapy-related atypia, and high-grade micropapillary DCIS (clinging type) extending into lobules.

Atypical cystic apocrine metaplasia is not particularly common as atypical apocrine change is often seen in the context of adenosis (i.e., atypical apocrine adenosis); however, if associated with calcifications (calcium oxalate crystals), an example could be the target of a CNB. The epithelial cells comprising atypical cystic apocrine metaplasia would show lightly apocrine-to-clear cytoplasm and more prominent nucleoli. A rare mitosis would further support the diagnosis. Secretory features would be absent (Fig. 21.12).

Columnar cell change or flat epithelial atypia (columnar cell change with cytologic atypia; FEA) can be confused with pregnancy-like change due to their common lobulocentric distribution and overlapping cytologic features. In columnar cell/FEA lesions, secretory changes are distinctly absent with the exception of luminal secretions that can be eosinophilic (or less commonly, basophilic) in color. Furthermore, the calcifications associated with both columnar cell/FEA and pregnancy-like lesions can be similar in appearance including psammomatous and ossifying forms. Please see images of the spectrum of columnar cell lesions in Chapter 8 for more information.

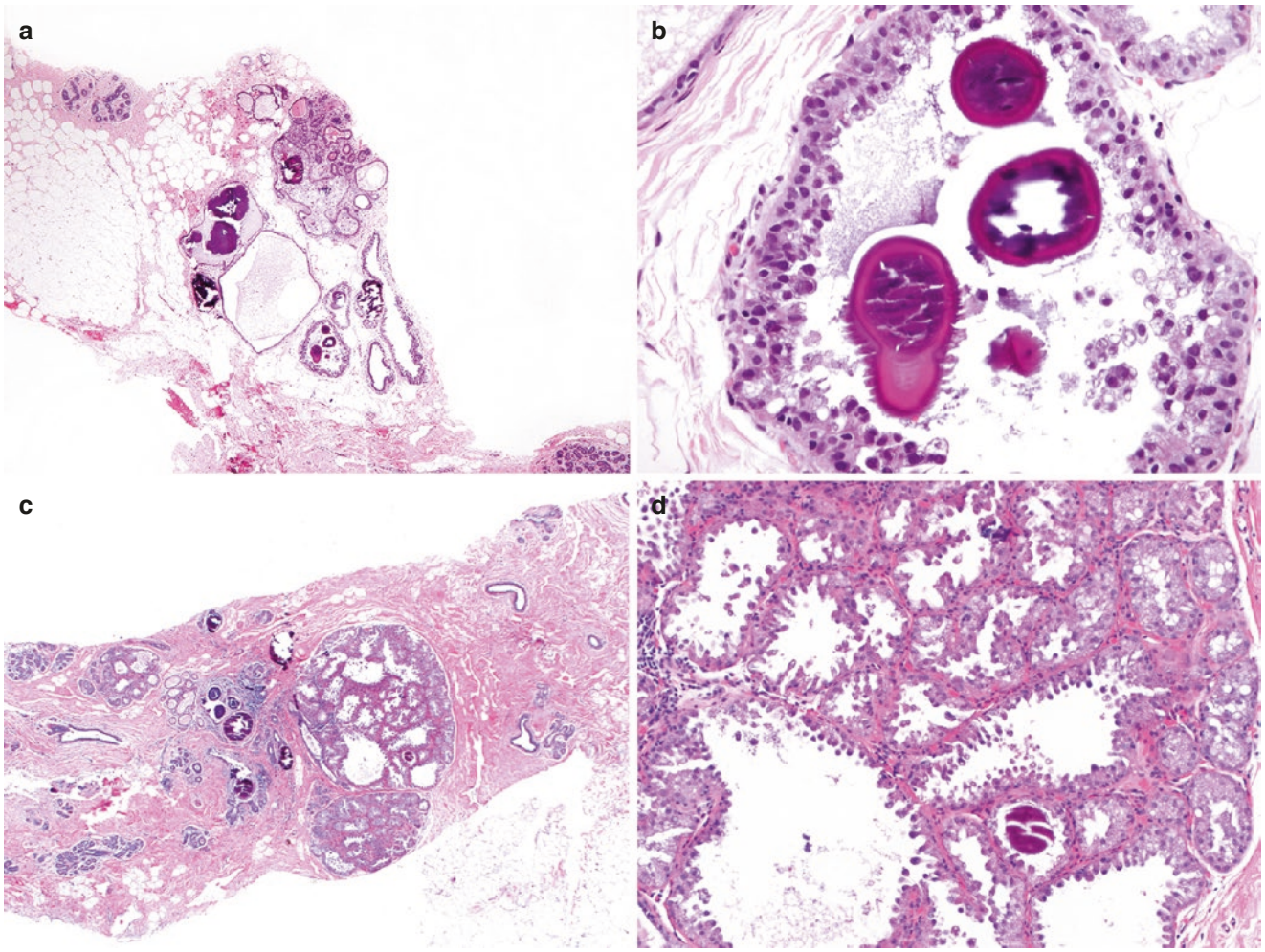

Fig. 21.11 Laminated calcifications in pregnancy-like proliferations. (**a**) CNB performed for calcifications shows a focus of pregnancy-like hyperplasia associated with calcifications. (**b**) Within the dilated acini lined by hyperplastic vacuolated cells are calcifying laminated sections. Focal atypical pregnancy-like hyperplasia can be seen. (**c**) Another CNB targeted for calcifications shows pregnancy-like change and focal pregnancy-like hyperplasia as the primary diagnosis. (**d**) Higher power view shows a partially fractured laminated calcification

If the lesion represents a lobule exhibiting radiation therapy-related atypia, in addition to obtaining relevant clinical history, the CNB sample may also show remote biopsy-site changes in the form of scar or stromal calcifications, common findings in biopsies performed to exclude recurrent carcinoma. Previously irradiated mammary glands may develop luminal calcifications but, importantly, lack secretory changes including luminal secretions (Fig. 21.13).

Micropapillary DCIS with high nuclear grade is commonly associated with calcifications and can show clear-cell features. In small samplings targeted for calcifications, this "clinging-type" DCIS may be difficult to recognize particularly if seen predominantly/exclusively as lobular involvement, thus bearing superficial resemblance to pregnancy-like change. Fortunately, the marked difference in nuclear grade makes their distinction easier on closer inspection (Fig. 21.14).

By far, the most difficult (and most common) distinction to be made is pregnancy-like change from its atypical form (atypical pregnancy-like change) (Fig. 21.15). Fortunately, in practice, atypical pregnancy-like change typically does not occur in isolation, and invariably, there are foci of adjacent atypical pregnancy-like hyperplasia which are diagnostically easier to identify (discussed below).

Differential Diagnosis for Pregnancy-Like Hyperplasia

In cases of pregnancy-like hyperplasia, the main considerations in the differential diagnosis are atypical pregnancy-like hyperplasia and, less so, atypical ductal hyperplasia. While pregnancy-like hyperplasia can be quite proliferative in appearance, the nuclear and cytoplasmic features of individual epithelial cells remain benign appearing. Lesional mitoses are not characteristic, and if one is found, the possi-

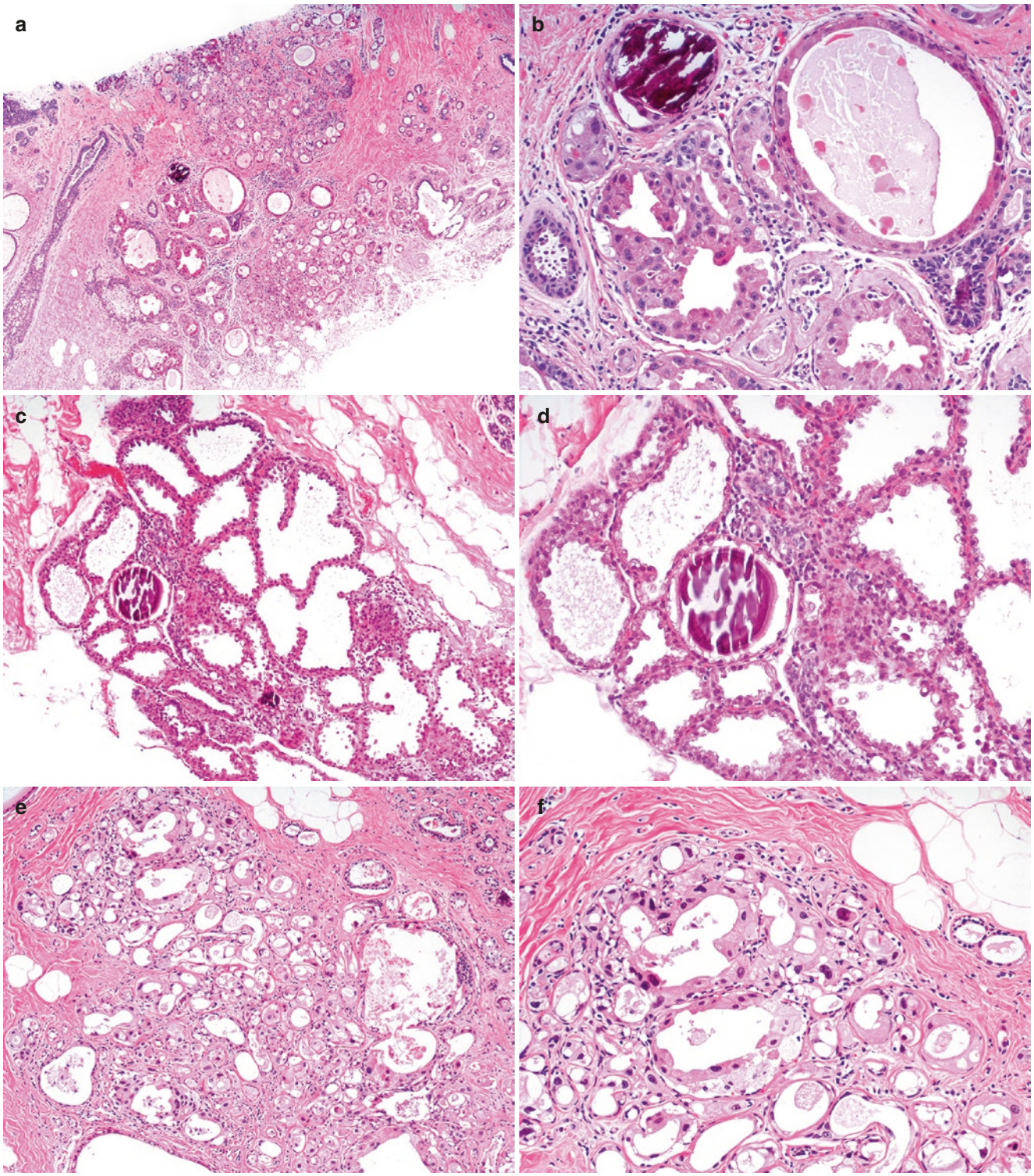

Fig. 21.12 Cystic apocrine adenosis versus pregnancy-like change. (**a**) At low power, a cystically dilated focus of adenosis is associated with calcifications. At scanning magnification, the differential diagnosis may include apocrine adenosis versus pregnancy-like change. (**b**) High magnification of this focus shows typical apocrine cytomorphology of the lesional cells with round nuclei with prominent nucleoli and eosinophilic cytoplasm. Calcifications which lack lamellations are present. (**c**) Cystically dilated lobule with calcifications lined by eosinophilic-to-clear epithelial cells suggests pregnancy-like change. (**d**) On higher magnification, the cells clearly demonstrate cytoplasmic vacuolization and lamellated luminal calcifications characteristic of pregnancy-like change. (**e**) Cystically dilated focus of adenosis lined by eosinophilic-to-clear cells with nuclear enlargement. At scanning magnification, the differential diagnosis may include atypical apocrine adenosis versus atypical pregnancy-like change. (**f**) High magnification shows that the glands are lined by eosinophilic-to-clear cytoplasm with round nuclei. Cytoplasmic vacuoles and luminal secretions typical of pregnancy-like change are absent. Based on the presence of cytologic atypia, a diagnosis of atypical apocrine adenosis is appropriate

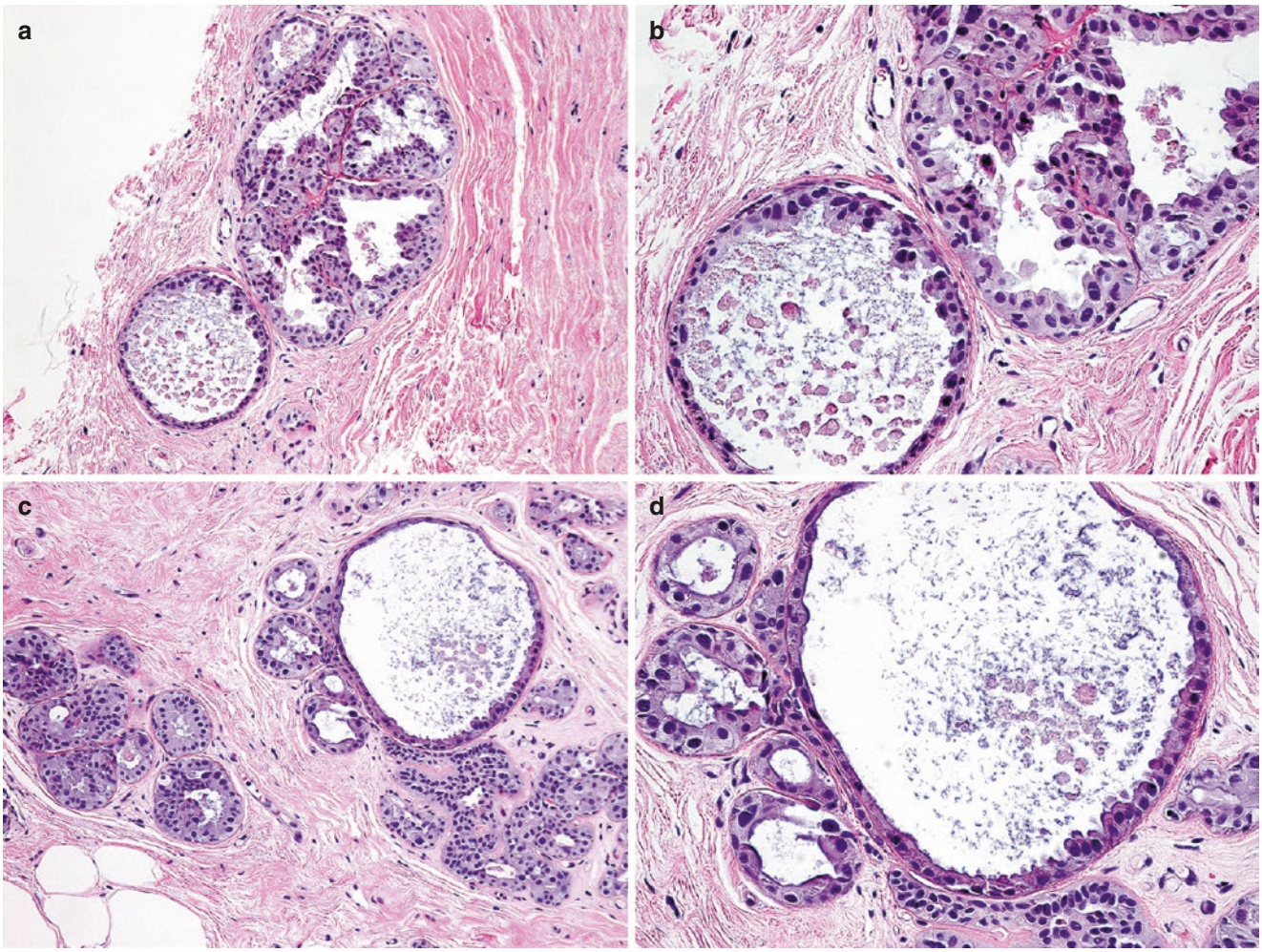

Fig. 21.13 Radiation therapy-related atypia of a lobule. (**a**–**d**) Two separate areas (**a**, **c**) of the same case showing partly cystic lobules with typical cytologic changes secondary to prior radiation therapy. This can resemble atypical pregnancy-like change; however, secretory traits are notably absent. Also, note the absence of luminal secretions

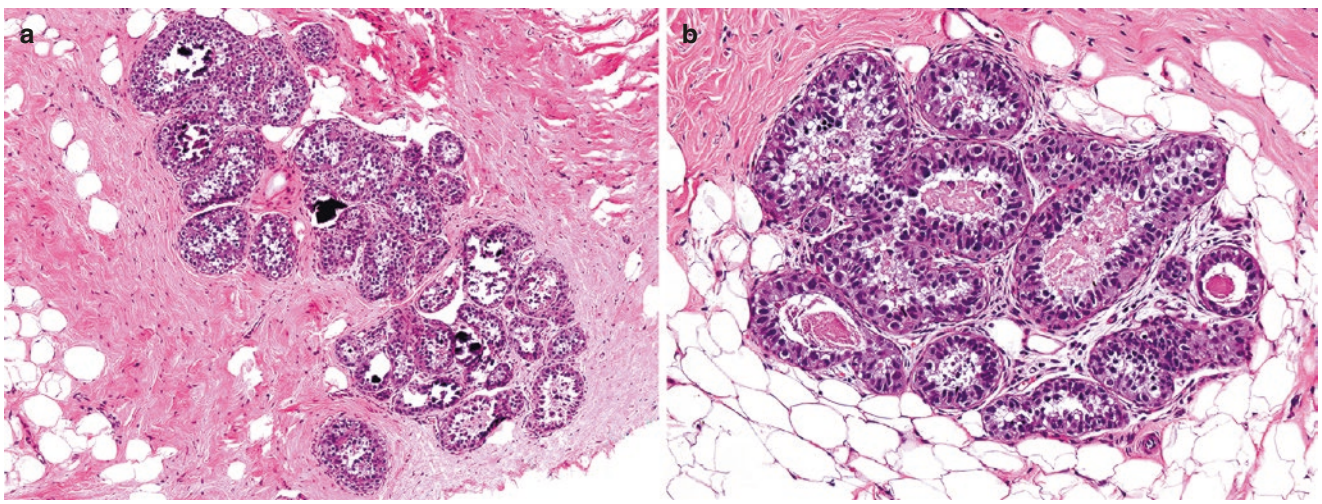

Fig. 21.14 Lobular involvement by clinging-type micropapillary ductal carcinoma in situ, high grade. (**a**, **b**) On first pass, the features are reminiscent of pregnancy-like change due to its lobular involvement and association with calcifications. However, higher magnification reveals overtly malignant nuclear features and luminal necrosis; features not seen in pregnancy-like change

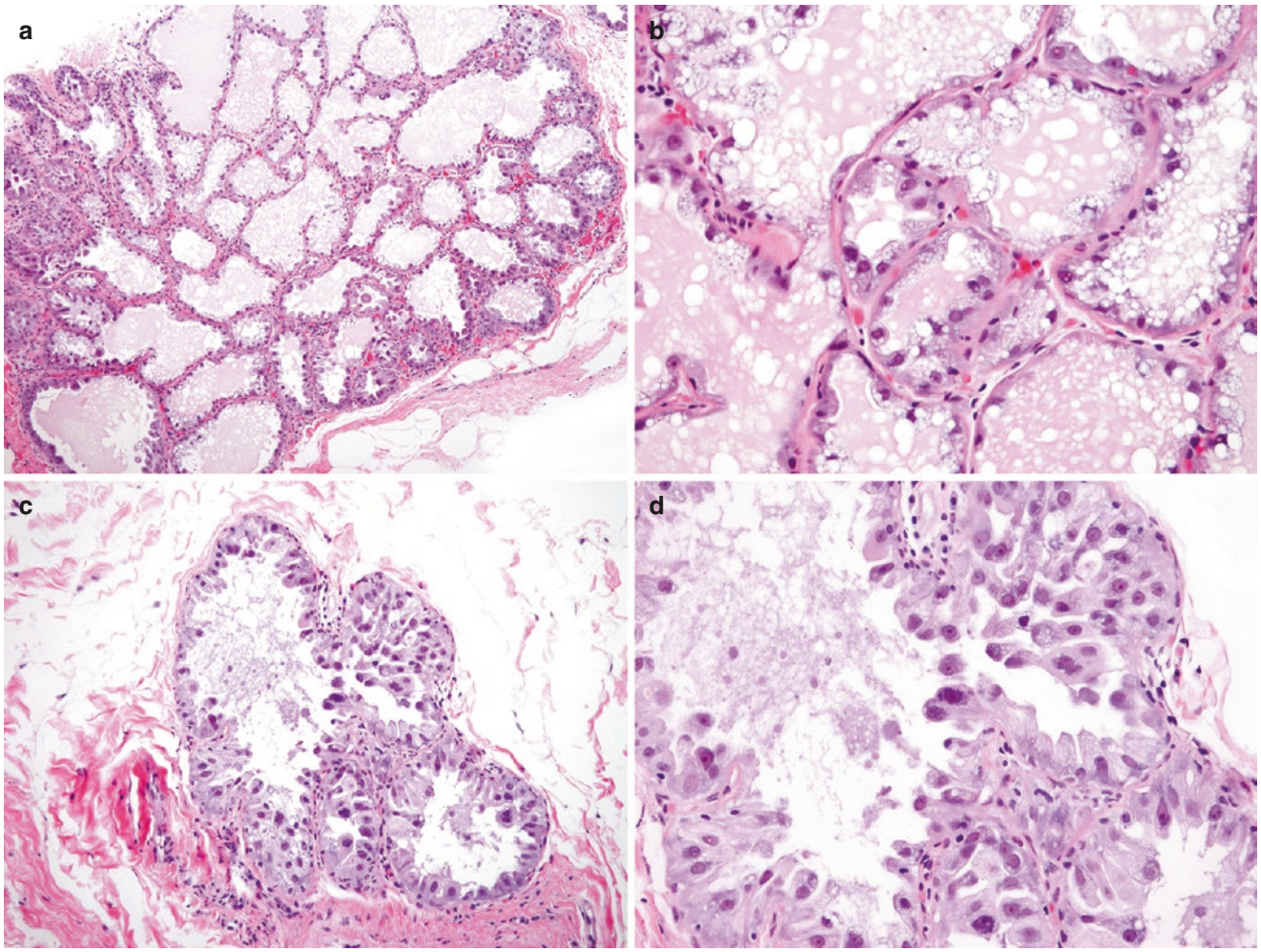

Fig. 21.15 Atypical pregnancy-like change. (**a**–**d**) An example of atypical pregnancy-like change coexisting with usual pregnancy-like change in the same lobule. (**b**) In the former, the cells show increase in nuclear-to-cytoplasmic ratio, nuclear hyperchromasia, enlargement and prominent nucleoli, and a relative decrease in vacuolated cytoplasm. (**c**, **d**) Some atypical areas are hyperplastic and would be better classified as atypical pregnancy-like hyperplasia. Occasional mitoses can be seen in these cases (not shown)

bility of the atypical form should be strongly entertained. The salient features of epithelial atypia in atypical pregnancy-like hyperplasia are nuclear pleomorphism, nuclear hyperchromasia, prominent nucleoli, increase in nuclear-to-cytoplasmic ratio secondary to loss of vacuolated cytoplasm, and lesional mitoses (Fig. 21.15c, d). The epithelial hyperplasia is characteristically micropapillary but can appear "clinging" (flat micropapillary) in focal areas. In cases of marked nuclear pleomorphism, discerning atypical pregnancy-like hyperplasia from micropapillary DCIS can be very difficult. Luminal calcifications are morphologically identical in both usual and atypical forms of pregnancy-like hyperplasia and therefore not discriminatory.

Occasionally, atypical pregnancy-like hyperplasia can be seen coexisting and merging with cystic hypersecretory change or cystic hypersecretory hyperplasia (Fig. 21.16). In situ carcinoma can focally arise in one or both components of these histologically combined lesions (Fig. 21.17). It is important to be cognizant of this histologically combined lesion in the CNB setting because not infrequently, atypia of one or both components can be seen in either the CNB or the subsequent excisional biopsy specimens [66, 68, 69]. This tendency is frequent enough that excisional biopsy is recommended in any instance of finding this combined lesion in CNB samples, even if both components are benign [68].

Discerning pregnancy-like hyperplasia from atypical ductal hyperplasia is less problematic as the latter exhibits various growth patterns and lacks secretory features.

Immunohistochemistry

In particularly challenging cases, immunostains for ER can be performed which would be strongly and diffusely positive in columnar cell lesions and heterogeneously positive in pregnancy-like proliferations.

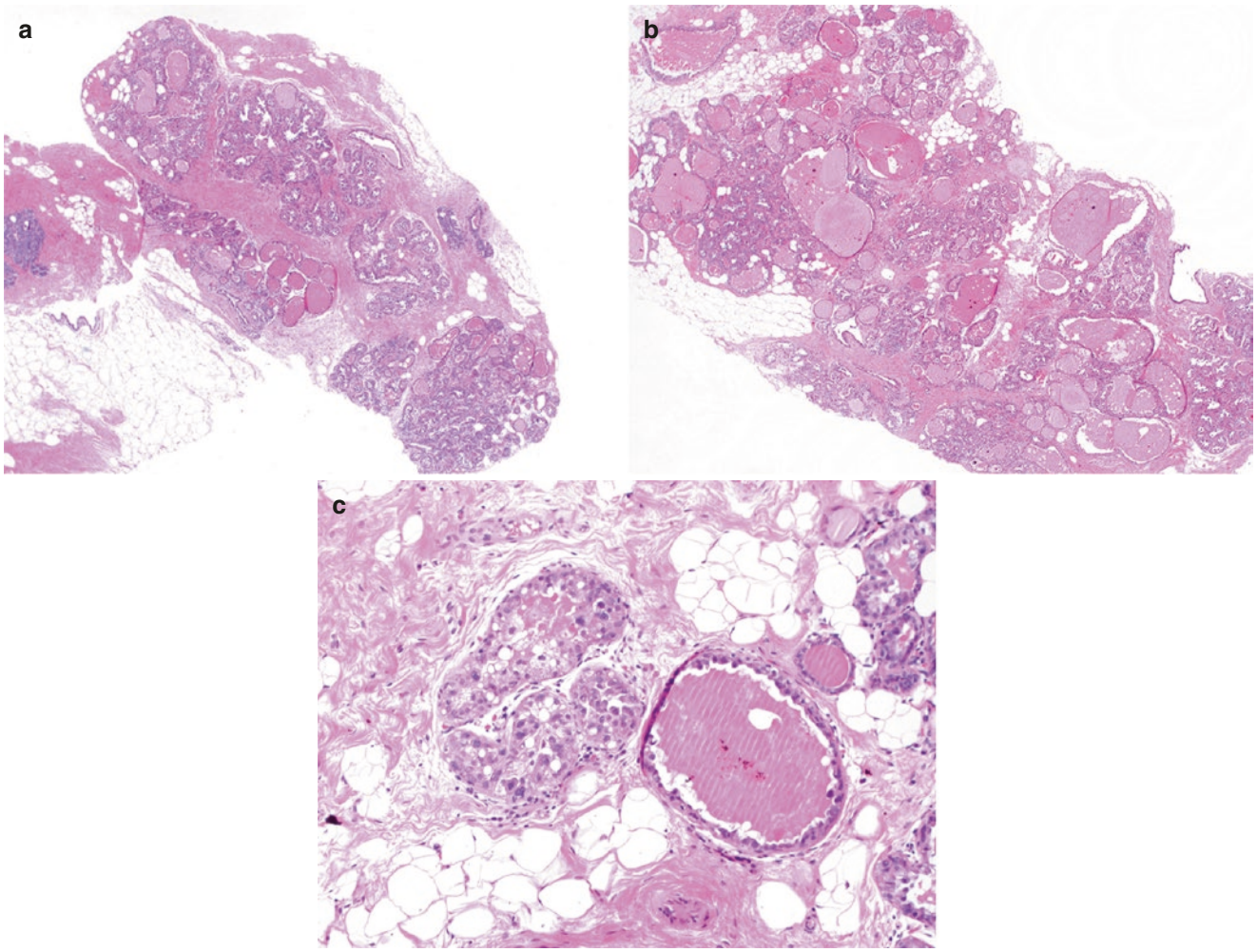

Fig. 21.16 Pregnancy-like hyperplasia and cystic hypersecretory hyperplasia. (**a**, **b**) CNB shows this histologically combined lesion. (**c**) Some glands show hyperplastic vacuolated cells filling the glandular lumen characteristic of pregnancy-like hyperplasia, and other glands are cystically dilated with dense eosinophilic secretions, which show retraction and linear cracks characteristic of cystic hypersecretory hyperplasia. In this example, pregnancy-like hyperplasia is atypical

Pathogenesis and Biologic Behavior

The pathogenesis of pregnancy-like proliferations in the nonpregnant, non-lactating breast remains unclear, but most observers would agree that it may be in part related to changes in hormonal levels. Moreover, the mechanism by which rare cases develop into carcinoma is even more elusive, and to date, only a single case of in situ carcinoma arising in atypical pregnancy-like hyperplasia has been reported [68]. No invasive carcinomas have been described to arise in this setting. However, instances of coexisting pregnancy-like and cystic hypersecretory proliferations have been reported to give rise to rare instances of invasive carcinoma [68, 69].

Treatment and Prognosis

Patients found to have pregnancy-like change or pregnancy-like hyperplasia as a primary diagnosis in a CNB targeted for microcalcifications experience a benign clinical course. No increased risk for developing breast carcinoma has been found thus far in these patients.

Atypical pregnancy-like change/hyperplasia identified in a CNB should be further managed by surgical excision to exclude invasive and/or in situ carcinoma that can rarely arise in these lesions. The possible benefit of chemoprevention of these patients is unknown. Biomarker expression (ER, PR) is variable in these lesions.

Carcinoma arising in a background of atypical pregnancy-like change/hyperplasia is characteristically micropapillary in type with high nuclear grade and presents along a morphologic continuum with atypical pregnancy-like changes. Therefore, the actual extent of DCIS is difficult to ascertain due to its sporadic distribution and histologic merging with atypical hyperplasia similar to some cases of micropapillary DCIS outside of this setting. Morphologically, the micropapillary DCIS retains little if any secretory features and out of

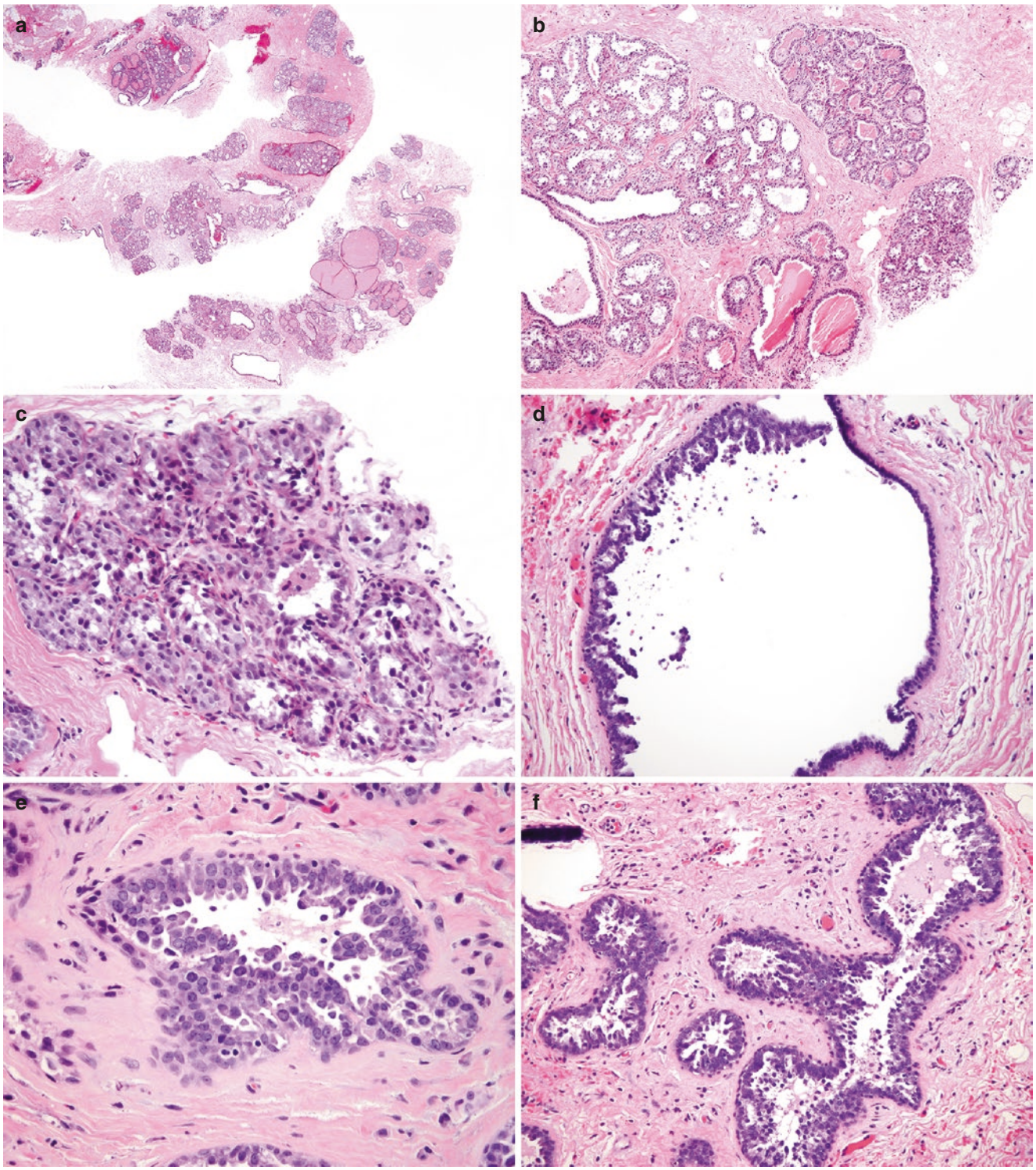

Fig. 21.17 Atypical pregnancy-like hyperplasia/cystic hypersecretory hyperplasia associated with cystic hypersecretory carcinoma. (**a**) CNB shows a histologically combined lesion. (**b**) Glands contain retracted and cracked secretion typical of cystic hypersecretory hyperplasia. (**c**) Cytologic atypia is present in pregnancy-like hyperplasia including increase in nuclear-to-cytoplasmic ratio, nuclear hyperchromasia, and decreased vacuolization of the cytoplasm. (**d**–**f**) Subsequent excisional biopsy showed intraductal cystic hypersecretory carcinoma with micropapillary architecture

context would be classified as conventional micropapillary DCIS. Currently, these patients should be treated in a similar fashion to patients with other forms of DCIS.

If atypical pregnancy-like hyperplasia is part of a combined lesion with usual or atypical cystic hypersecretory proliferation, then the carcinoma arising in this background tends to be cystic hypersecretory in type. An in-depth discussion of cystic hypersecretory carcinoma can be found in Chapter 13.

Breast Carcinoma in the Pre-neoadjuvant Chemotherapy Setting

Overview

Neoadjuvant chemotherapy (NACT) is a standard of care commonly used to treat locally advanced breast cancer and is also more widely being used in patients with early breast cancer. The use of NACT can not only mitigate the need for aggressive surgical procedures (i.e., mastectomy and/or axillary dissection) [70–72] but also monitor response and tailor treatments [73, 74]. As such, not only should patients with large tumors (≥5.0 cm) be considered for NACT, but some patients with smaller and surgically operable tumors can also benefit [70, 75].

Evaluation and Reporting of the Pre-neoadjuvant Chemotherapy Core Biopsy Specimen

In the neoadjuvant setting, pretreatment evaluation of breast cancer is important to later accurately assess the degree of pathologic response [75–77]. This is routinely performed on CNB samples where an unequivocal diagnosis of invasive carcinoma is established. Morphologic features such as histologic type, tumor grade, lymphovascular invasion, associated DCIS, and/or presence of necrosis should be included in the pathology report in order to compare with the post-chemotherapy response.

At a minimum, hormone receptors (ER, PR) and HER2 should be assessed on the CNB material prior to therapy [78]. Additionally, pathologists should be skeptical of histologic-immunophenotypic discordances, particularly for TNBC. Some low-grade special types of TNBC (i.e., adenoid cystic carcinoma, acinic cell carcinoma) are unlikely to respond to NACT (and may not require adjuvant systemic therapy). As such, histologic subtyping of TNBC should not be neglected in CNB material, and if there is suspicion of one of these special tumor types, it should be communicated with the treating clinician. Assessment of proliferation (by Ki-67) can be a useful predictive marker in pre-NACT CNB specimens [79]. While not required in routine practice, there are circumstances in which programmed cell death ligand 1 (PD-L1) status and assessment of TILs may be used to predict the response to NACT and can be provided upon request. Given the heterogeneity of PD-L1 testing platforms, antibody clones, and reporting systems, when PD-L1 testing is requested communication between the treating clinician and pathologist is of utmost importance to ensure that both the appropriate PD-L1 clone and reporting system are used.

Evaluation of the Sentinel/Axillary Lymph Nodes (Pre-neoadjuvant Chemotherapy)

While there was initial concern that NACT may modify lymphatic drainage patterns and that heterogeneous treatment response in axillary lymph nodes may lead to high false-negative rates for sentinel lymph node (SLN) biopsy, studies have now established the reliability of SLN biopsy following NACT [80–82]. Additionally, studies have demonstrated that the presence of residual disease in the breast and axilla is a better predictor of local regional recurrence than the pre-NACT stage [83]. As such, assessment of axillary lymph nodes prior to NACT should be performed using CNB or fine needle aspiration and SLN biopsy ought to be performed following completion of NACT. Details of the pathologic examination of the SLN biopsy performed following NACT are beyond the scope of this chapter.

Predictive Factors for Response to Neoadjuvant Chemotherapy Assessed in the Core Biopsy Sample

The molecular subtype of a given tumor has been found to be predictive of the degree of tumor response to NACT and can be estimated by IHC evaluation of the CNB sample for ER, PR, HER2, and Ki-67. In a study that evaluated the NACT response to outcome among breast cancer molecular subtypes, tumors of basal-like (triple negative) and HER2+/ER− subtypes were found to be more sensitive to anthracycline-based NACT than luminal (A and B) breast cancers [84]. While more chemosensitive, tumors of the basal-like and HER2+/ER− subtypes demonstrate lower distant disease-free and overall survival compared to those of luminal subtypes [84–86]. Moreover, a high Ki-67 index and hormone receptor-negative status were important predictors of pathologic complete response (pCR) [87].

Some studies have shown that the histologic type of the tumor is predictive of tumor response to NACT. Invasive lobular carcinomas (ILC) tend to have lower pCR in comparison to invasive ductal carcinomas (IDCs) [88]. The factors that contribute to lower response rate in ILCs are not

clearly understood but may partly be attributed to enrichment of hormone receptor-positive/HER2-negative status, non-histological grade 3 tumors, and luminal A molecular subtype in ILCs when compared to IDC [88, 89]. Younger age and negative hormone receptor status were found to independently predict pCR in ILCs [88].

While some studies have demonstrated that PD-L1 status predicts response to NACT in combination with certain immunotherapies, PD-L1 is not necessary to predict response to immunotherapy in all circumstances [90–92]. Studies have shown that TILs predict pCR in all breast cancer subtypes [93].

Evaluation and Reporting of the Neoadjuvant Chemotherapy-Treated Excisional Specimen

Evaluation and reporting of the NACT-treated mastectomy (or excisional) specimen and axillary lymph nodes are performed routinely in order to assess the degree of chemotherapy response. The categories of NACT-related pathologic response include complete response (pCR) (where there is no evidence of residual tumor), partial response (residual tumor identified with chemotherapy-related changes), no response (no change in size of tumor with minimal therapy-related changes), and progression of disease. These have been based on pre/post-chemotherapy assessment of radiologic and pathological measurements [94]. It has been found that in some examples, the in situ carcinoma and presence of lymphovascular invasion are relatively resistant when compared to invasive carcinoma involving the stroma. As this book is focused on CNB specimens, this discussion will be brief and is by no means inclusive of all the aspects required to fully and accurately assess the post-NACT specimens.

Assessment of the post-NACT specimen relies on correlation with the pre-NACT clinical and imaging findings. At the time of CNB, a clip should be placed, in order to assist with identification and assessment of the tumor bed. An international working group of breast experts have provided recommendations on standard pathologic assessment of breast specimens following neoadjuvant therapy, which include a multidisciplinary approach, incorporation of radiology, photography, or diagrams of the sliced specimen to map the tissue sections, and this requires reconciliation of macroscopic and microscopic findings [95]. Quantification of residual cancer burden and definition of pCR are based on current AJCC guidelines as well as the Residual Cancer Burden system [95–98]. When residual disease is present and the prior CNB is available, the change of tumor cellularity can be provided and is expressed in terms of percentage from what was assessed in the prior CNB sample. If present, residual tumor shows different patterns of distribution. If there is a marked treatment response, residual tumor may be seen only as scattered single or small clusters of tumor cells. Other cases may show residual tumor in the form of exclusively in situ carcinoma or lymphatic tumor emboli. Depending on the various classification schemes available to use, it is important to be aware that some consider cases of residual in situ carcinoma to represent pCR while others do not. Further, the presence of lymphovascular invasion as the only residual form of tumor is not addressed in certain classification models (Miller-Payne and Sataloff systems) [94]. Further details of the pathologic examination of the NACT-treated specimens are beyond the scope of this chapter. Illustrative examples of NACT in CNB and subsequent excision are seen in Figs. 21.18, 21.19, 21.20, 21.21, 21.22, 21.23, and 21.24.

Recurrent Breast Carcinoma

Overview

Locoregional recurrence (LRR) after breast-conserving therapy is a well-known independent risk factor associated with unfavorable long-term outcome [99]. LRR also varies according to breast cancer subtypes and clinicopathological features. Histologic factors such as tumor size >2.0 cm, triple negativity (ER−/PR−/HER2−), presence of lymphovascular invasion, and lymph node positivity are associated with increased risk for LRR [100, 101]. Breast cancer subtype, in particular, should be taken into account when considering local control, and more aggressive local treatment may be considered in this subset of patients [102, 103].

Clinical Presentation and Workup

When a patient with a prior history of breast carcinoma and treatment (surgical +/− radiation) comes to medical attention with a breast abnormality, the possibility of recurrent breast carcinoma must be excluded. In this setting, breast carcinoma may represent either a recurrent cancer or a new primary cancer. True recurrence is defined as regrowth of the disease at the site of the initial carcinoma, while a new primary is distinct from the index tumor in histology and location [104].

New mammographically detected calcifications at the site of the prior lumpectomy bed are always considered suspicious and usually categorized as Breast Imaging-Reporting and Data System (BI-RADS) 4. A majority of these findings can be subsequently targeted by CNB [105].

Once the CNB sample shows carcinoma, the challenge is to discern local recurrence from a new primary (provided

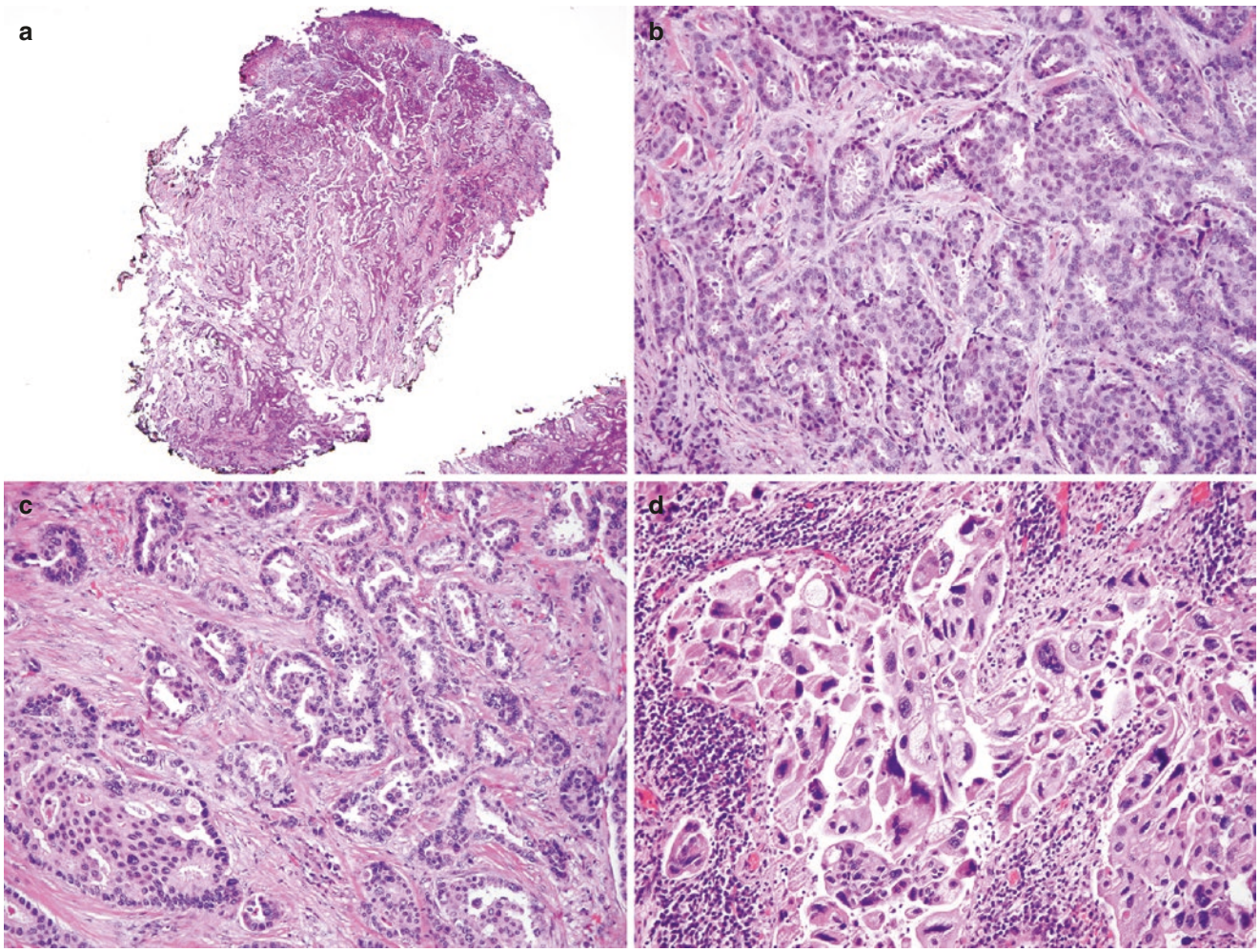

Fig. 21.18 NACT-related change in carcinoma. (**a**) Pre-NACT CNB shows a moderately differentiated IDC. (**b**) Tumor cells demonstrate nuclear grade 2. (**c**) Post-NACT residual carcinoma shows some areas of tumor with similar nuclear grade. There is focal evidence of therapy-induced change with some clusters transitioning to higher nuclear grade (*lower left*). (**d**) Post-NACT residual carcinoma shows marked therapy-induced change with tumor cells exhibiting overt nuclear grade 3

that the biopsy yields malignancy). In patients treated with adjuvant radiation, radiation-related atypia must be considered. It is imperative to ascertain the location of the prior breast cancer in cases of prior breast conservation as the finding of carcinoma in this area would suggest local recurrence over a new primary. In patients initially treated for invasive carcinoma, approximately 80% of cases will recur as invasive carcinoma and the remaining cases will recur as DCIS. In patients initially treated for DCIS, approximately half recur as invasive carcinoma while the rest as DCIS [106].

The workup of all CNB samples excluding recurrent carcinoma and/or radiotherapy-related atypia must include morphologic comparison with the patient's prior breast carcinoma; this is not performed routinely due to the logistic difficulty in obtaining these slides despite the clinical ramifications of misdiagnosis in this setting. Illustrative examples of recurrent carcinomas with morphologic comparison to patients' previous breast carcinomas are shown in Figs. 21.25, 21.26, 21.27, 21.28, 21.29, 21.30, 21.31, 21.32, 21.33, 21.34, and 21.35.

A new primary is favored over recurrent cancer if the site of the tumor is away from the location of the prior breast carcinoma. In postmastectomy patients, identifying coexisting in situ carcinoma can suggest a new breast cancer where residual breast tissue may be present. Morphologic dissimilarity with the patient's prior breast carcinoma would be further evidence if not confirmatory of a new primary. In both instances of local recurrence and new primary, biomarker evaluation (i.e., ER, PR, and HER2 as applicable) should be performed on the CNB material. While biomarker status can

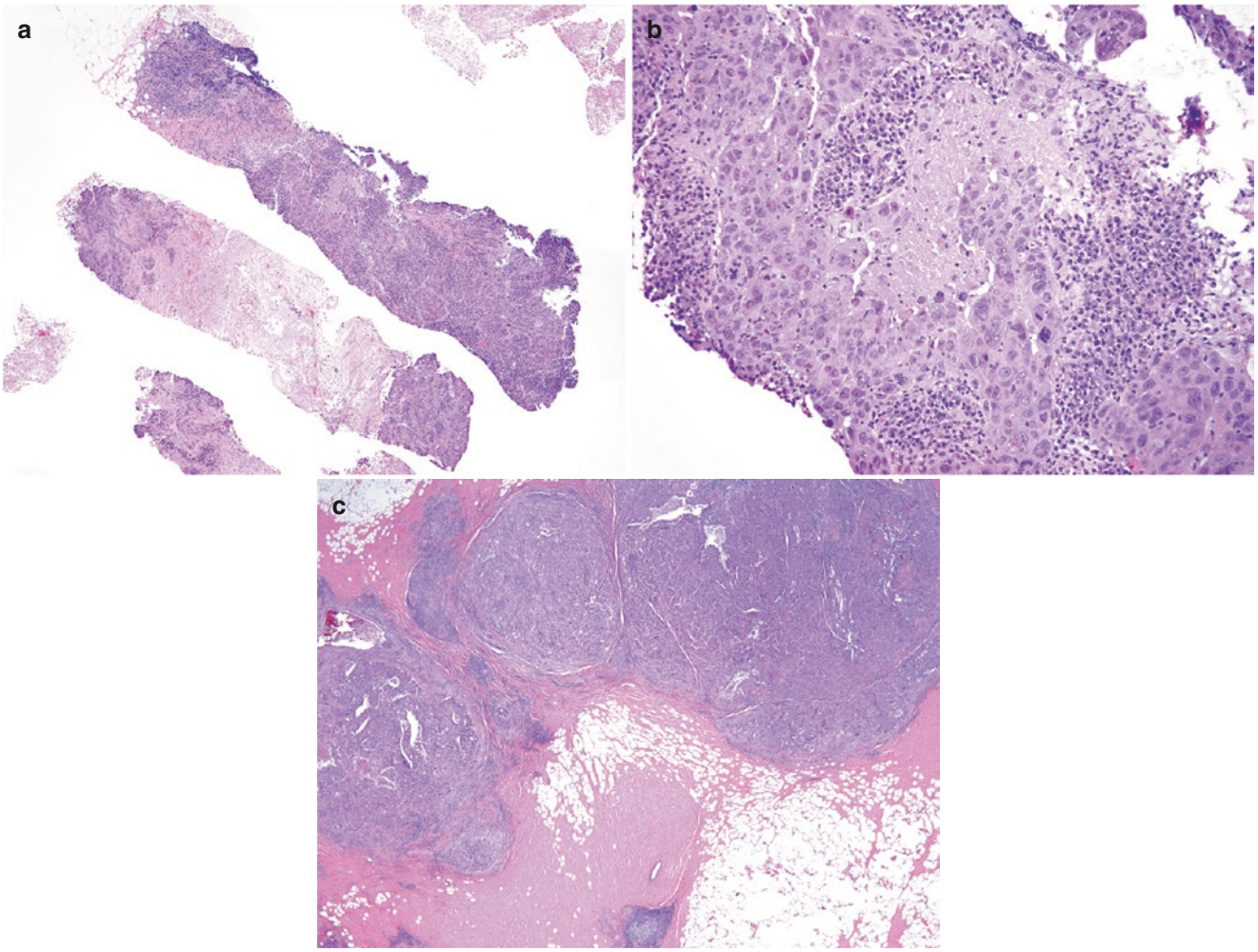

Fig. 21.19 NACT-treated carcinoma exhibiting partial response. (**a**) Pre-NACT CNB shows IDC with extensive necrosis involving multiple tissue cores. (**b**) The carcinoma is poorly differentiated with an associated lymphocytic infiltrate. (**c**) Post-NACT excisional biopsy specimen shows minimal evidence of response in the carcinoma, which is seen here as significant residual tumor burden within the tumor bed. Tumor cellularity is decreased by ~5% in comparison to the CNB

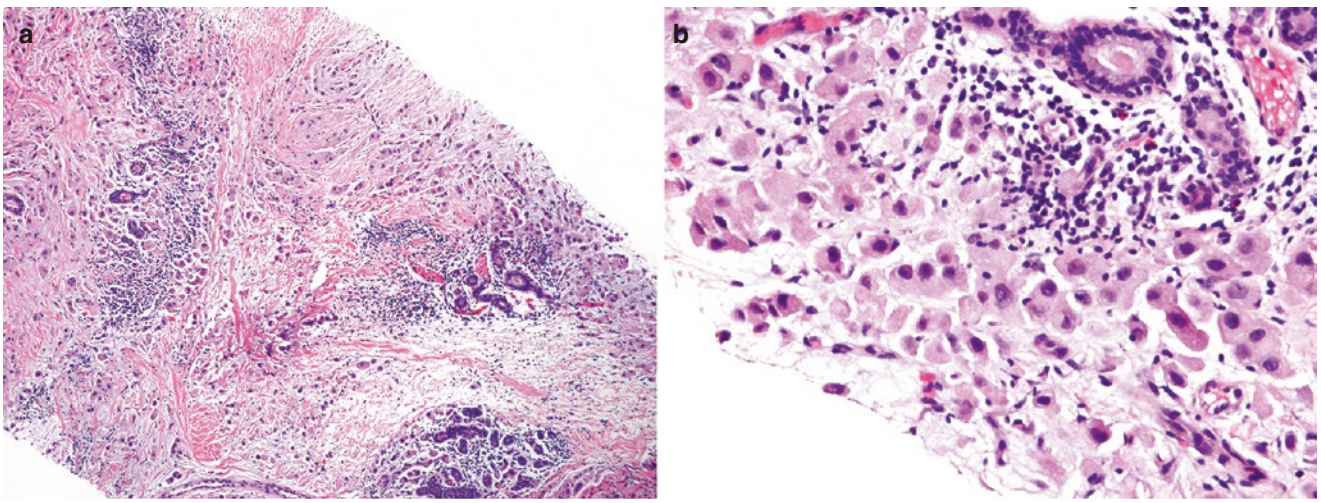

Fig. 21.20 NACT-treated carcinoma simulating macrophages. (**a**) Pre-NACT CNB shows ILC. (**b**) The carcinoma cells show apocrine traits with abundant vacuolated cytoplasm resembling histiocytes. (**c**) Histiocytoid-appearing cells with foamy clear-to-pink cytoplasm are present in a fibrotic tumor bed in the post-NACT specimen. (**d**, **e**) The cells are positive for pancytokeratin (AE1/AE3) and negative for CD68, confirming the presence of residual carcinoma (i.e., partial response)

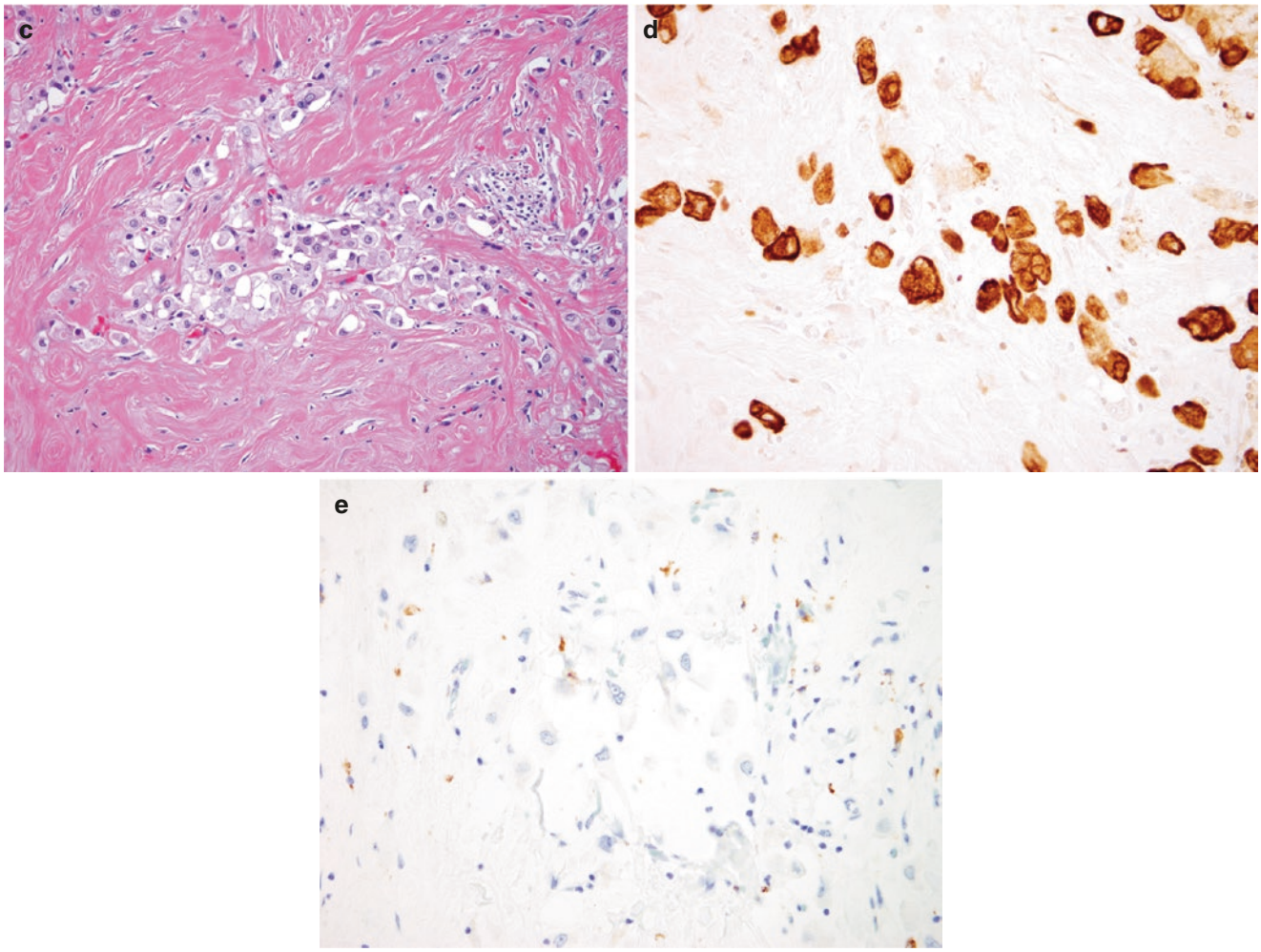

Fig. 21.20 (continued)

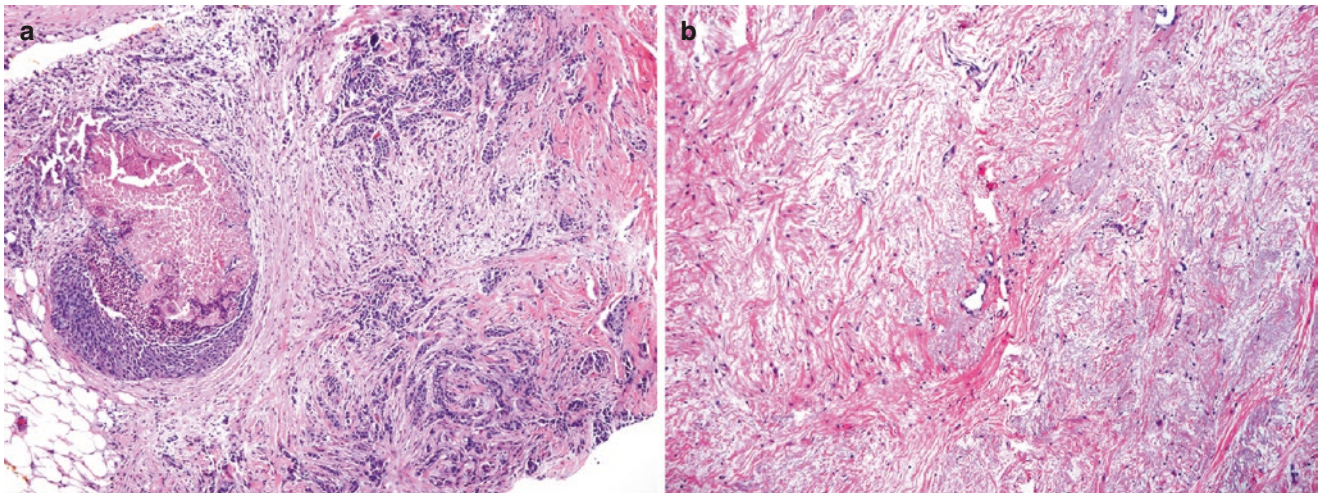

Fig. 21.21 Two examples of NACT-treated carcinoma with pCR. (**a**) Pre-NACT CNB shows poorly differentiated IDC and high-grade DCIS. (**b**) Post-NACT excisional biopsy shows an elastotic tumor bed with no residual carcinoma. (**c**) Pre-NACT CNB shows moderately differentiated IDC. (**d**) Post-NACT excisional biopsy shows tumor bed with myxoid change and focal chronic inflammation. No residual carcinoma is present

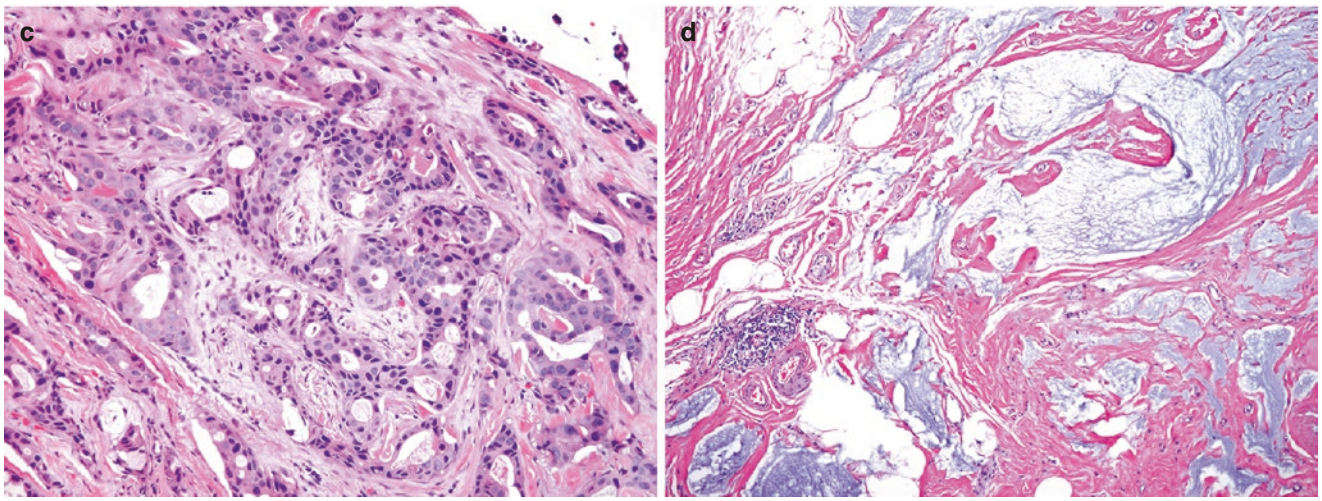

Fig. 21.21 (continued)

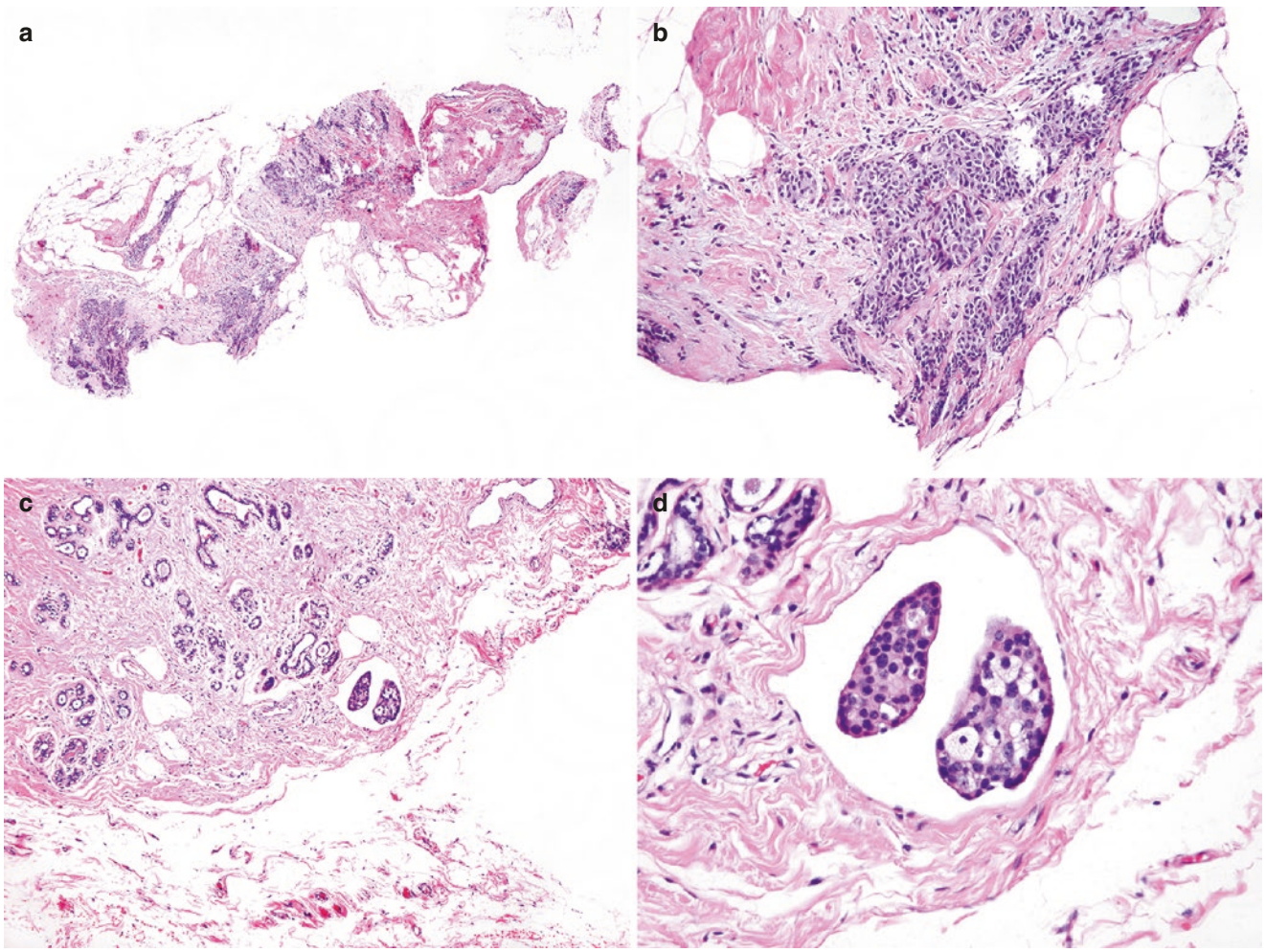

Fig. 21.22 NACT-treated carcinoma consisting of only lymphatic tumor emboli. (**a**) Pre-NACT CNB shows IDC. (**b**) The invasive carcinoma is moderately differentiated. (**c**) Post-NACT excisional biopsy specimen shows only residual carcinoma in lymphatic channels. (**d**) The tumor emboli present in an endothelial lined lymphatic channel are morphologically similar to the invasive carcinoma seen in the initial CNB

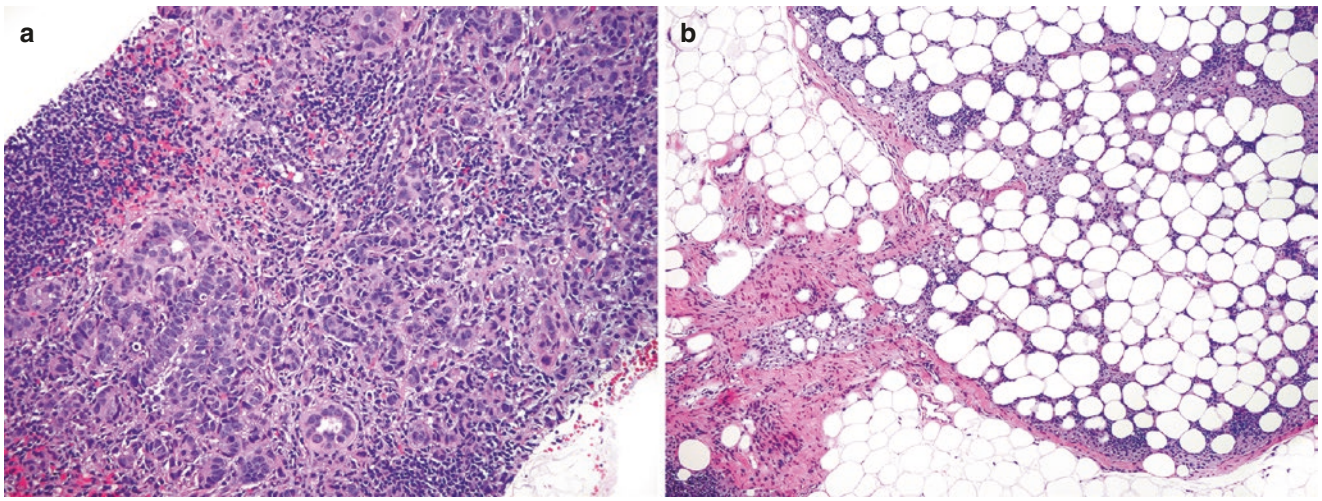

Fig. 21.23 pCR to NACT in an axillary lymph node. (**a**) Pre-NACT axillary CNB shows metastatic carcinoma involving portions of a lymph node. (**b**) Excised lymph node after NACT shows evidence of tumor regression with foamy macrophages and fibrous scarring. No residual metastatic carcinoma is present

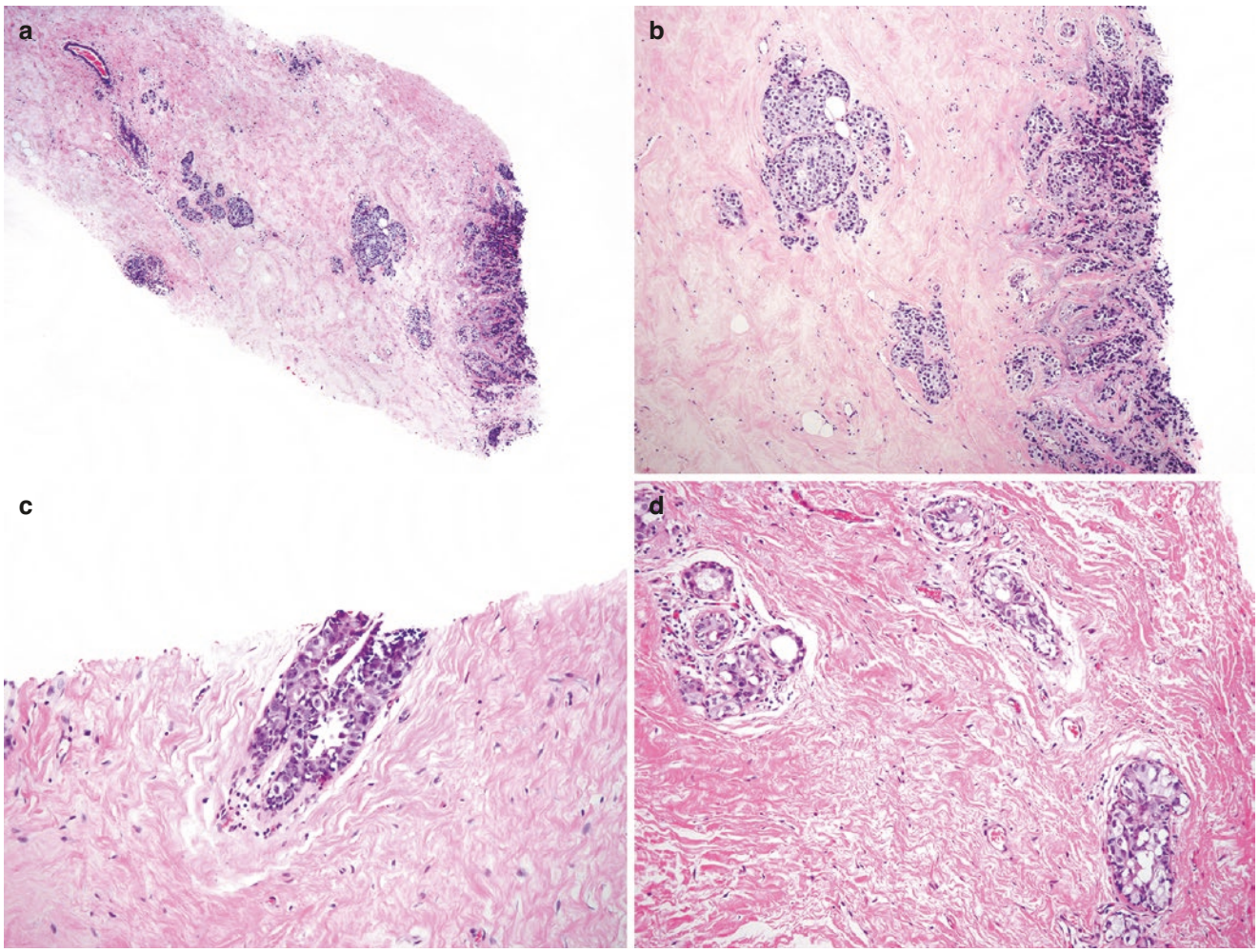

Fig. 21.24 NACT-treated carcinoma with residual DCIS. (**a**) Pre-NACT CNB shows invasive and in situ ductal carcinoma. (**b**) Invasive carcinoma is poorly differentiated, and DCIS extends into lobules. (**c**, **d**) Scattered ducts lined by atypical cells highly suspicious for residual DCIS. The differential diagnosis included therapy-related atypia. (**e**) DCIS is confirmed by the presence of HER2 overexpression similar to 3+ staining of the pre-NACT tumor (not shown), while adjacent benign glands are completely negative (not shown)

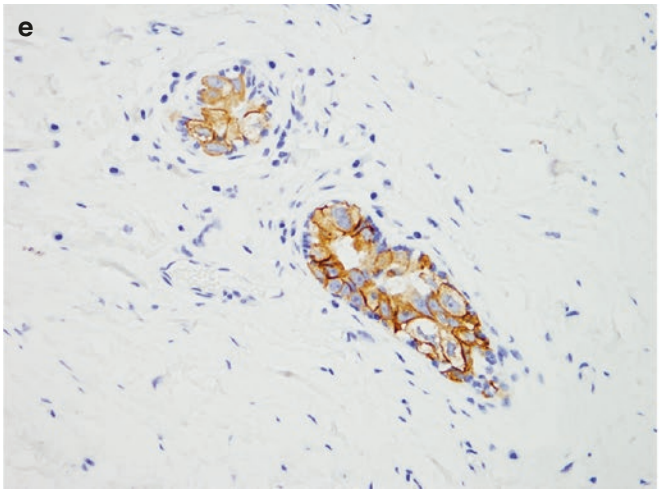

Fig. 21.24 (continued)

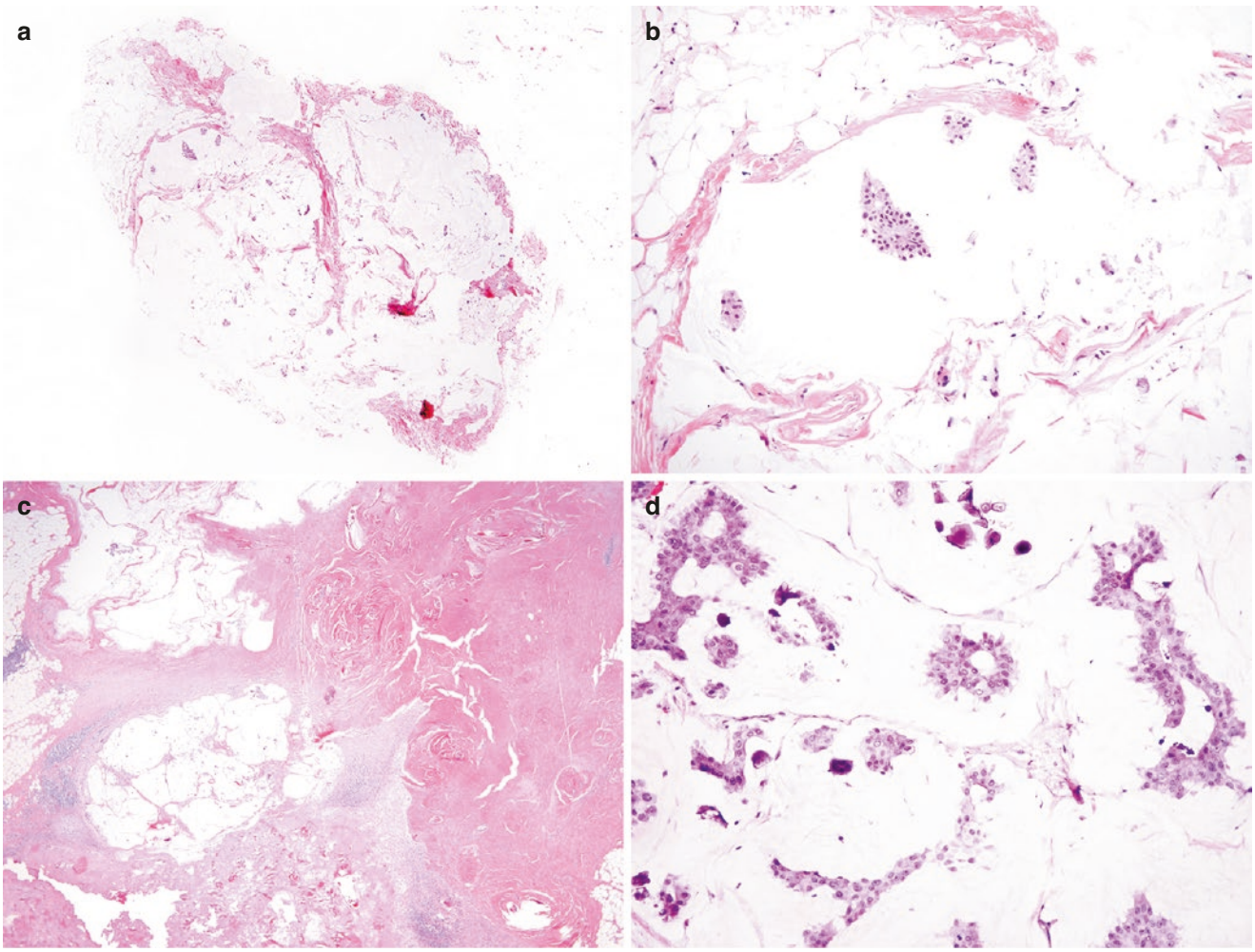

Fig. 21.25 Recurrent invasive mucinous carcinoma. (**a**) CNB performed for a breast mass shows clusters of recurrent invasive carcinoma present in pools of mucin. (**b**) Tumor clusters demonstrate intermediate nuclear grade. (**c**) Excisional biopsy shows dense fibrous tissue (i.e., scar) from the prior surgical procedure adjacent to the recurrent carcinoma. (**d**, **e**) Comparison to the index tumor shows a morphologically similar invasive mucinous carcinoma and mucin-producing micropapillary DCIS

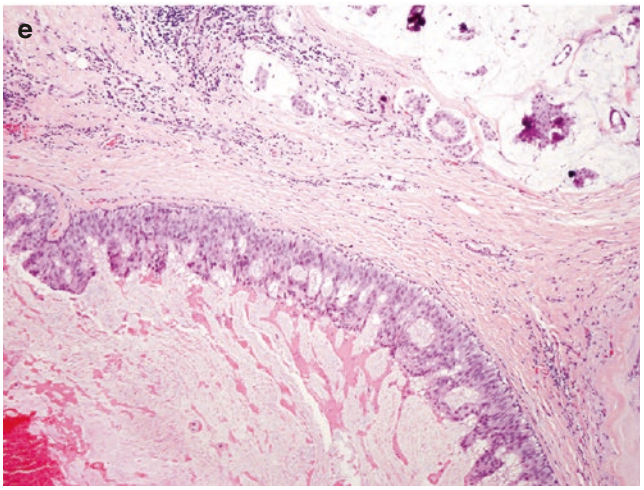

Fig. 21.25 (continued)

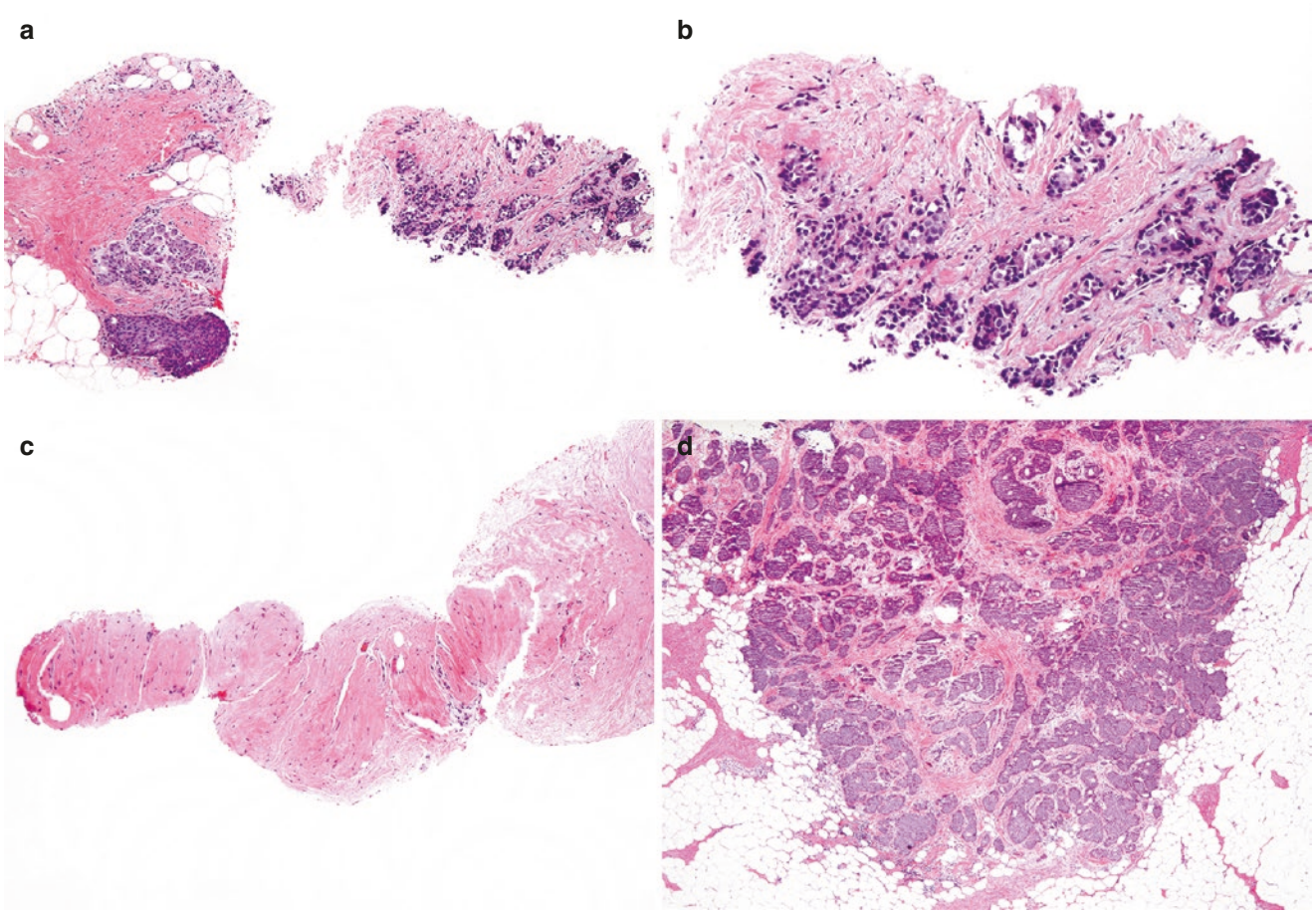

Fig. 21.26 Recurrent invasive carcinoma and scar in a CNB sample. (**a**) CNB performed for a breast mass shows recurrent IDC and DCIS. (**b**) The invasive carcinoma is moderately differentiated. (**c**) Other tissue cores show portions of dense fibrous tissue (i.e., scar) indicative of a remote biopsy site. (**d**) Comparison to the index carcinoma shows morphologically similar IDC

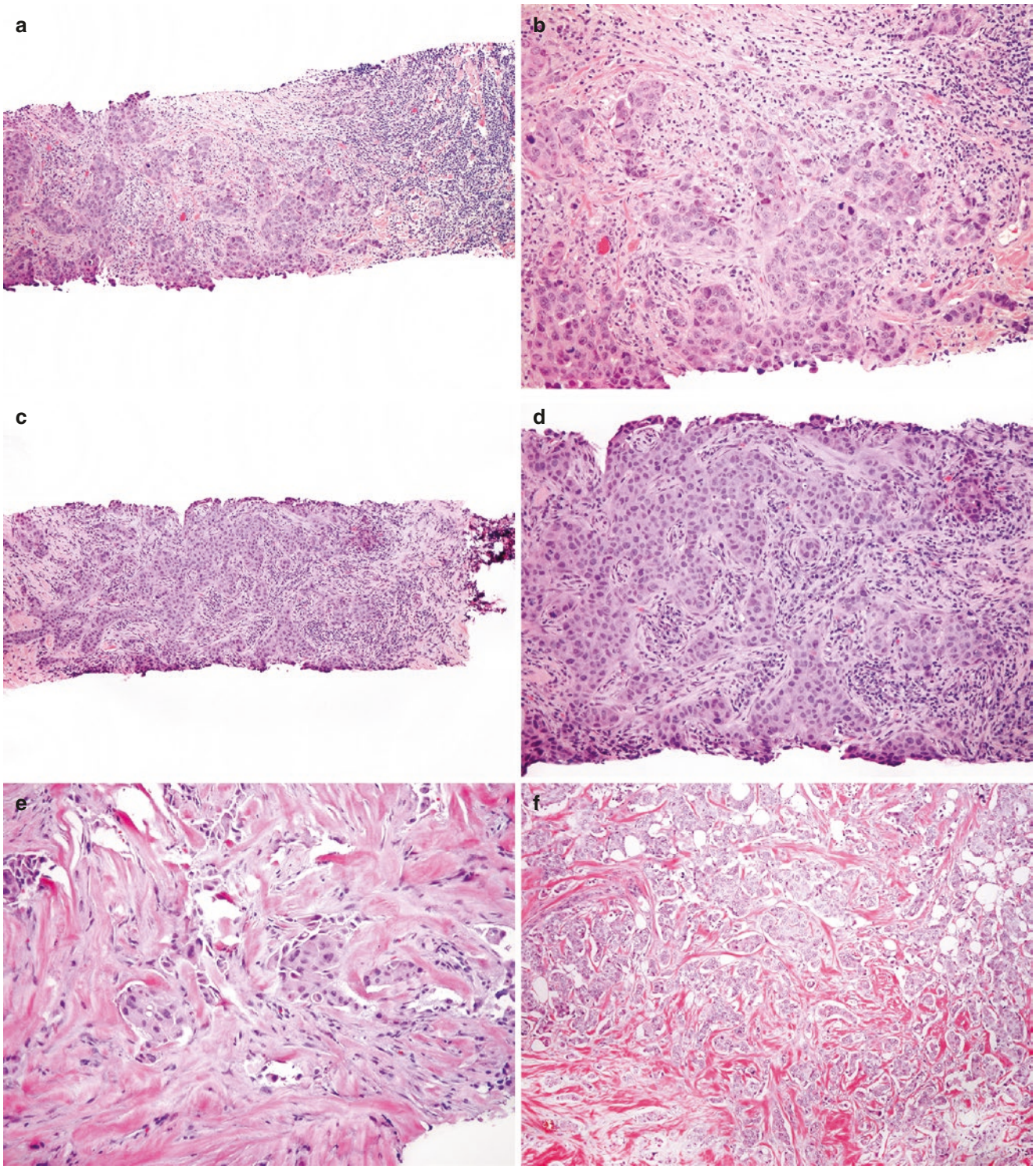

Fig. 21.27 Recurrent carcinomas with similar accompanying findings. (**a**) CNB performed for a breast mass shows recurrent IDC associated with a brisk lymphocytic infiltrate. (**b**) The invasive carcinoma is poorly differentiated. (**c**) CNB of initial invasive carcinoma with similar lymphocytic infiltrate. (**d**) The carcinoma is morphologically indistinguishable from the recurrent carcinoma. (**e**) Another core biopsy performed for a breast mass shows recurrent IDC associated with a fibrosclerotic stroma. (**f**) Comparison with the index carcinoma shows similar morphology of the invasive carcinoma and its distinctive associated fibrosclerotic stroma

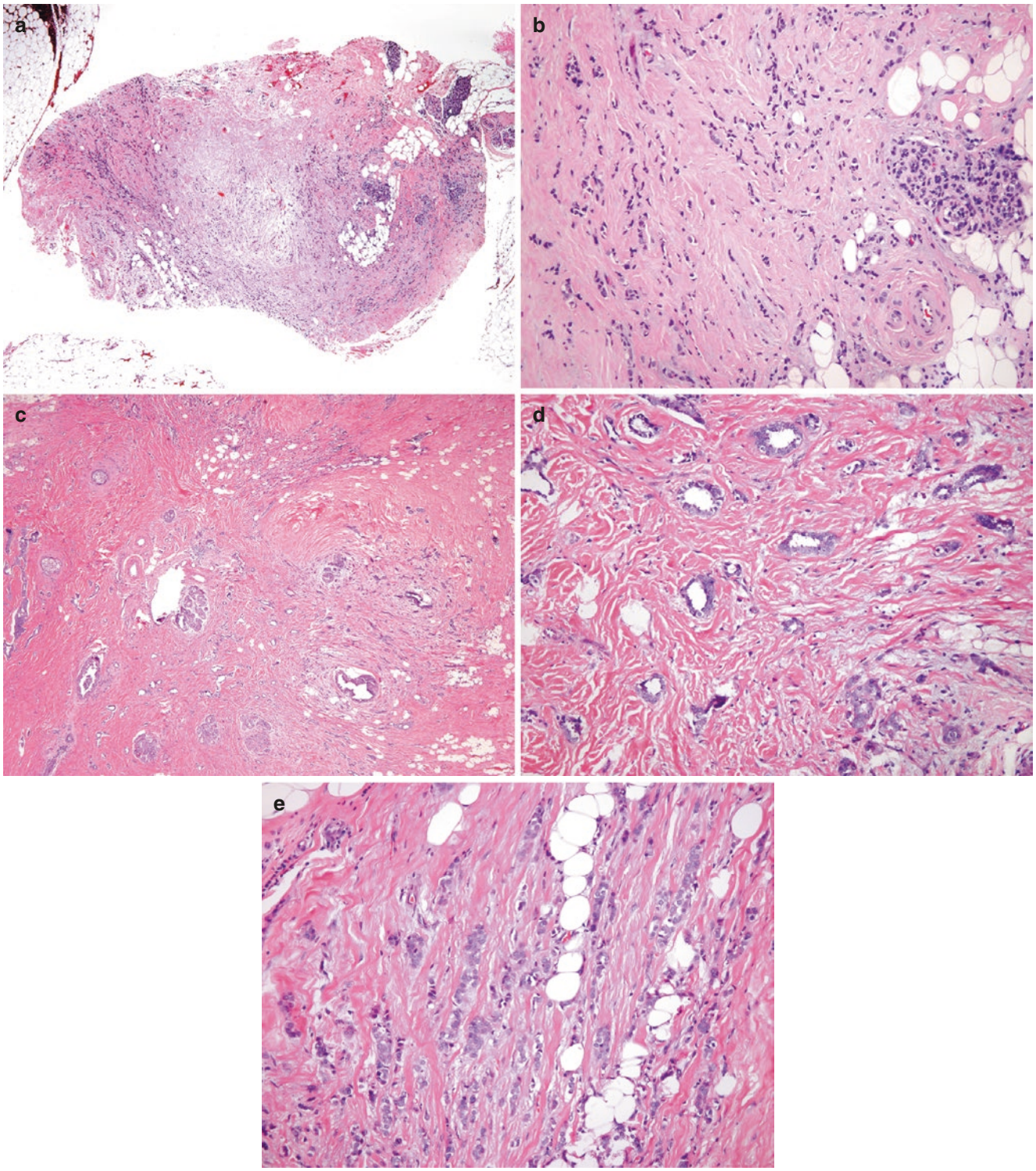

Fig. 21.28 Recurrent ILC in a patient with two index carcinomas. (**a**) CNB performed for a mass shows recurrent ILC. (**b**) The invasive carcinoma is classic type with low nuclear grade. The surrounding breast tissue shows radiation-induced lobular atrophy. Radiation-induced myointimal thickening is noted in adjacent vessels (*lower right*). (**c**) Excision of index tumor shows a mixed IDC (*lower right*) and ILC (*upper left*). (**d**) The IDC is well differentiated. Low-grade DCIS was also present (not shown). (**e**) The ILC is classic type with similar morphology to the recurrence. Classic-type lobular carcinoma in situ was also present (not shown)

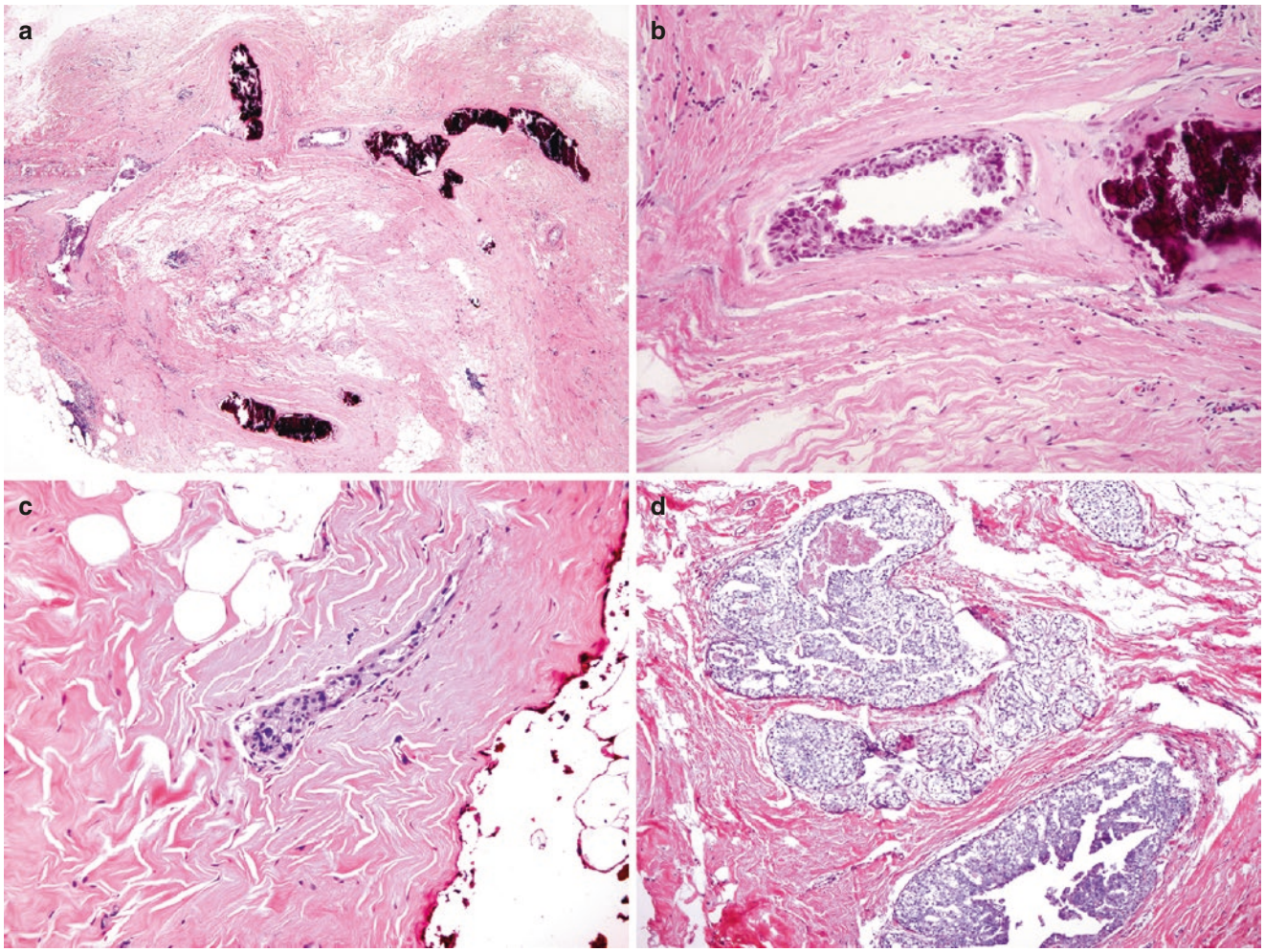

Fig. 21.29 Recurrent DCIS detected by calcifications. (**a**) CNB performed for calcifications shows calcifications within ducts involved by micropapillary DCIS. (**b**) DCIS shows intermediate nuclear grade and is associated with coarse calcifications. (**c**) Radiation-induced epithelial changes typified by cytoplasmic vacuolization, nuclear enlargement, and marked nuclear pleomorphism are present in the surrounding benign mammary glands morphologically distinct from recurrent DCIS. (**d**) The initial DCIS in this excisional biopsy demonstrates morphologic similarity to the recurrent tumor

either be further confirmatory of a recurrence or suggest evidence of a new primary, carcinomas are known to demonstrate tumoral heterogeneity and biomarker status may infrequently change in recurrent carcinoma [107]. Nevertheless, biomarker status should be confirmed to ensure that patients are receiving the most effective treatment, as well as providing useful information on prognosis [108, 109]. Please see Chapter 22 for more information about prognostic and predictive factors in breast cancer.

In a radiated breast, it is essential to differentiate local recurrence versus radiation-related atypia, which can be very challenging, especially when recurrent DCIS is suspected. In radiation-related change, benign epithelial cells are often noted lining scattered terminal duct lobular units. Typically, radiation-related atypia is nonuniform in the affected ducts, and the size of the cells can vary dramatically even within the same glandular structure. It is important to note that enlarged cells demonstrate cytomegaly, rather than nucleomegaly with preserved nuclear-to-cytoplasmic ratios. These findings are in keeping with a non-clonal, nonneoplastic process, which can be differentiated from either a recurrent or a new primary carcinoma. Impressive nuclear pleomorphism and hyperchromatic nuclei are typical. In some instances, the cells can have vacuolated and eosinophilic cytoplasm. Importantly, there are no mitotic figures or epithelial proliferation (Fig. 21.33b). In some instances, radiation-related atypia in apocrine proliferations may be confused with flat-micropapillary (clinging)-type DCIS; however,

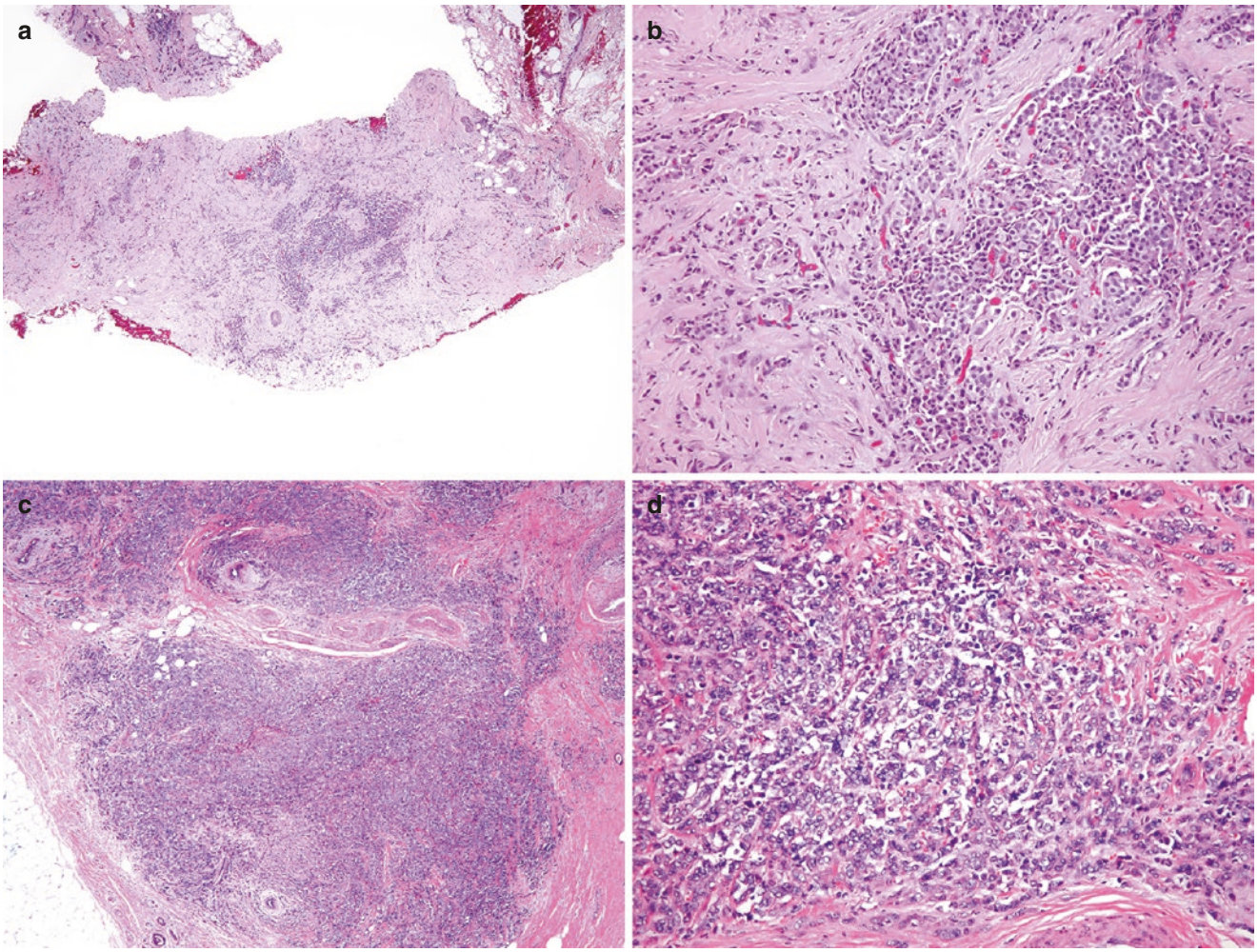

Fig. 21.30 Recurrent ILC. (**a**) CNB performed for a breast mass shows recurrent ILC. (**b**) The invasive carcinoma is classic type with focally solid growth pattern and intermediate nuclear grade. (**c**) The index ILC with solid growth is seen in this excisional biopsy. (**d**) The invasive carcinoma shares similar morphology with the recurrent carcinoma

with careful inspection, this diagnostic pitfall can be avoided (Fig. 21.36). Finally, benign ducts with or without epithelial proliferations that show apocrine features are more susceptible to severe therapy-induced atypical changes and may be confused with recurrent carcinoma. As such, morphologic comparison with the patient's prior breast carcinoma, particularly if reported to bear apocrine traits, is of utmost importance (Fig. 21.37).

Treatment and Prognosis

Differentiating new primary breast carcinomas from local disease recurrences is important in forming therapeutic decisions and chemoprevention strategies [104, 110]. The treatment of patients with (ipsilateral) recurrent breast carcinoma or new primary depends on clinical circumstances. Recurrent breast carcinoma typically undergoes multimodality treatment including surgery (mastectomy) with or without hormonal/chemotherapy, whereas those found to have a new primary are treated based on additional variables such as hormone receptor and HER2 status.

Patients with a new primary were found to have significantly lower rates of metastasis than patients with LRR but alternatively more likely to develop contralateral breast carcinomas [110]. Patients classified as having a new primary had more favorable overall and distant disease-free survival rates than those with tumor recurrence [110].

Inflammatory Breast Carcinoma

Overview

Inflammatory breast carcinoma (IBC) is a clinicopathological entity characterized by diffuse erythema and edema (*peau d'orange*) involving more than one-third of breast skin

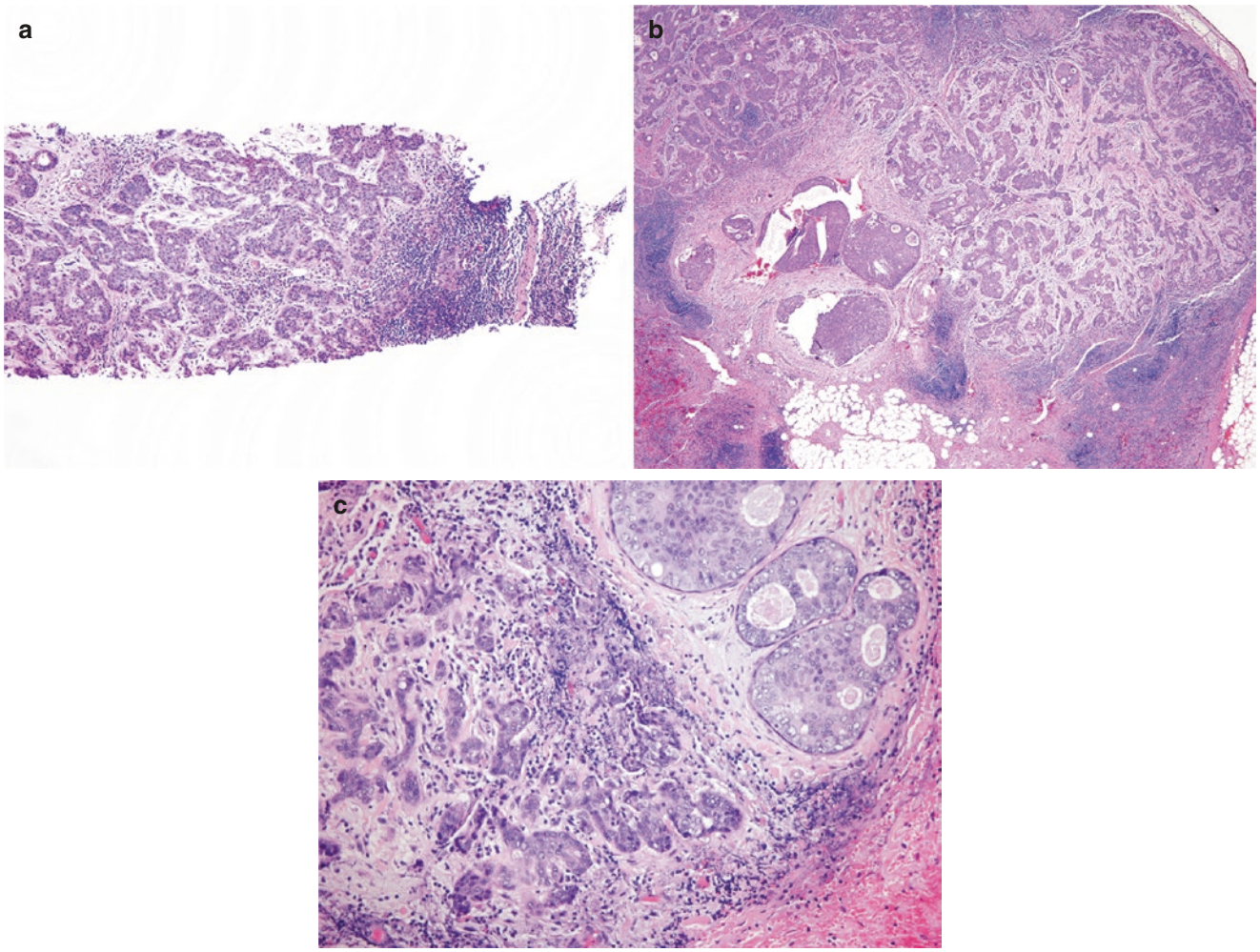

Fig. 21.31 Locoregional recurrence manifesting in an axillary lymph node. (**a**) CNB performed for an axillary mass shows recurrent metastatic carcinoma involving portions of a lymph node. (**b**) Subsequent lymph node dissection shows metastatic carcinoma almost entirely replacing a lymph node. (**c**) The initial IDC and associated DCIS were morphologically similar to the tumor recurrence in the lymph node

[111]. IBC is the most aggressive form of breast cancer and accounts for 1–6% of all breast cancers [112, 113]. This disease disproportionately affects younger and African-American women [112, 113]. It is important to recognize that IBC is primarily a clinical diagnosis and, as such, is classified as cT4d per the AJCC staging criteria [98]. Clinically, these patients experience tenderness and skin induration overlying a rapidly enlarging breast [111, 114]. In approximately 30% of patients, no palpable mass is evident [115]. Histologically, IBC is characterized by dermal lymphatic invasion by tumor emboli (Fig. 21.38). Because presence of these emboli may not be detected in small skin punch biopsy specimens, pathologic confirmation of tumor emboli in dermal lymphatics is not required to assign a clinical diagnosis of IBC, provided that a tissue diagnosis of invasive carcinoma has been established [98].

True to its aggressive biologic nature, IBC is characterized by its rapid time to progression, high proportion of local and distant metastases present at diagnosis, and lower overall survival despite the use of multimodality therapy [114]. Locally advanced invasive carcinoma that presents in the setting of patients who neglected their disease does not equate to IBC, and therefore, rapid onset (i.e., skin changes that present for no more than 6 months) is critical in the designation of IBC. The current epidemiologic and molecular evidence suggests that IBC may represent a distinct disease entity [114, 116–118].

Gross and Radiologic Features

Mammography may show skin thickening with no detectable mass, a breast mass, or sometimes an area of calcification [114]. Ultrasonography can be used to target masses for

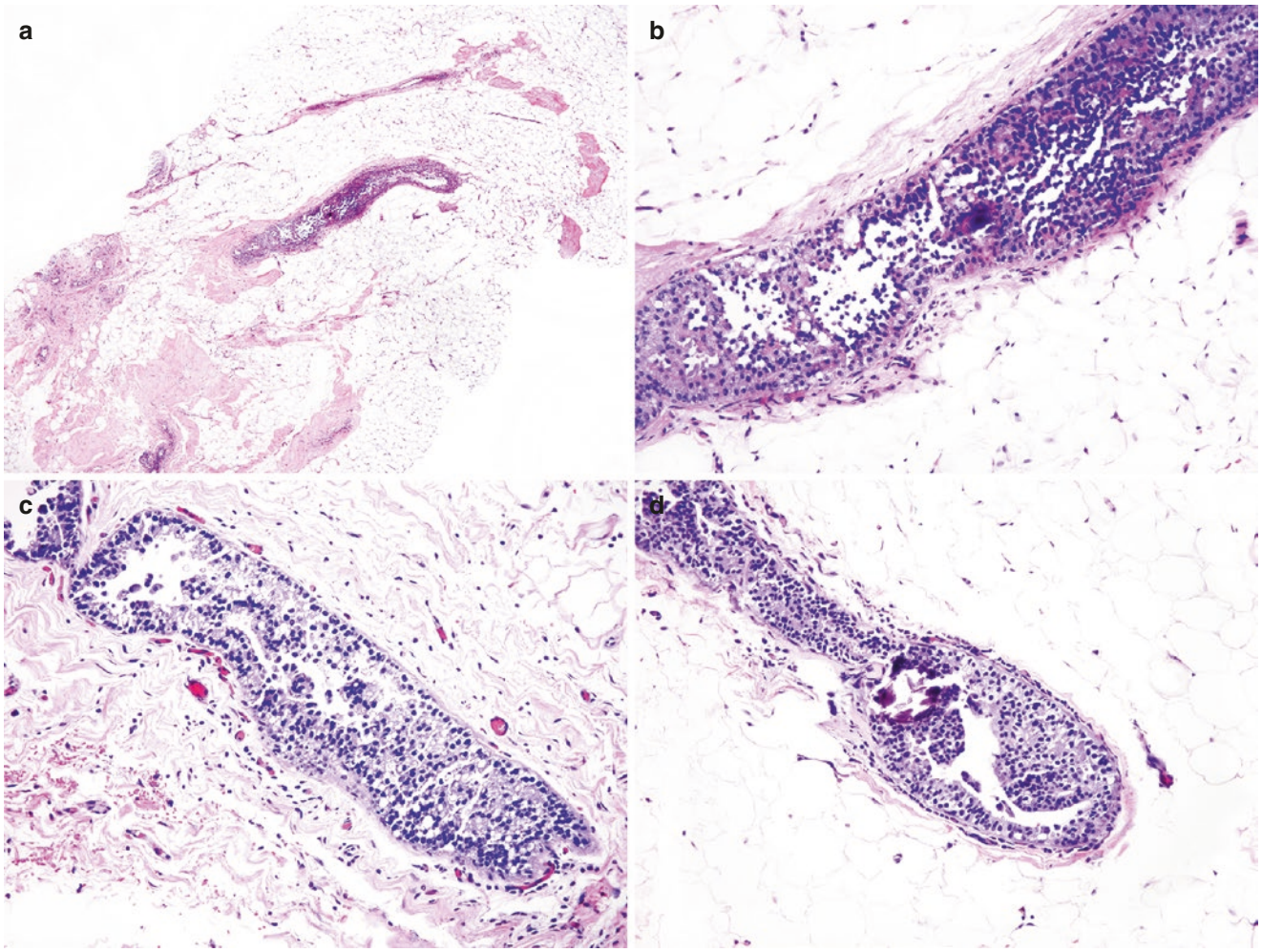

Fig. 21.32 Importance of morphologic comparison in suspected recurrence. (**a**) CNB performed for calcifications shows distended ducts filled with a ductal proliferation. (**b**) The proliferating cells show low-grade cytologic atypia. Calcifications are present. The differential diagnosis included atypical ductal hyperplasia versus low-grade DCIS. (**c**) Comparison of this patient's prior carcinoma shows a morphologically similar proliferation, confirming recurrent DCIS in the CNB seen in Figure (**a**). (**d**) Calcifications are also present in the index DCIS

CNB [114]. Compared to ultrasonography, MRI is somewhat more sensitive. Most commonly, MRI will demonstrate multiple, small, heterogeneously enhancing nodules along with diffuse skin thickening [119]. The skin changes seen secondary to lymphedema are caused by tumor emboli in the dermal lymphatic spaces and therefore not seen histologically.

Microscopic Features

A biopsy is required to establish a diagnosis to demonstrate the underlying invasive carcinoma either in the breast tissue or in dermal lymphatics [114]. Typically, sampling is in the form of a skin punch biopsy rather than a CNB (Fig. 21.39). It is important to be aware that the presence of lymphatic tumor emboli can be very focal and sporadic in distribution. As such, it is prudent to routinely obtain multiple (>5) H&E levels of the specimen as foci of tumor in lymphatics can appear (and disappear) as one evaluates deeper tissue sections. In some instances, the adjunctive use of cytokeratin stains may be helpful in the identification of these small tumor clusters. Histologically, the tumor present in the lymphovascular spaces can mimic dermal involvement of invasive or in situ tumor surrounded by artifactual clearing. While most IBCs are grade 3, a small minority are grade 1 tumors [120, 121]. Generally, IBC of no special type but lobular and other special type carcinomas have been reported [122]. Despite the propensity of invasive micropapillary carcinoma to be associated with lymphovascular invasion, this subtype is not overrepresented in IBC.

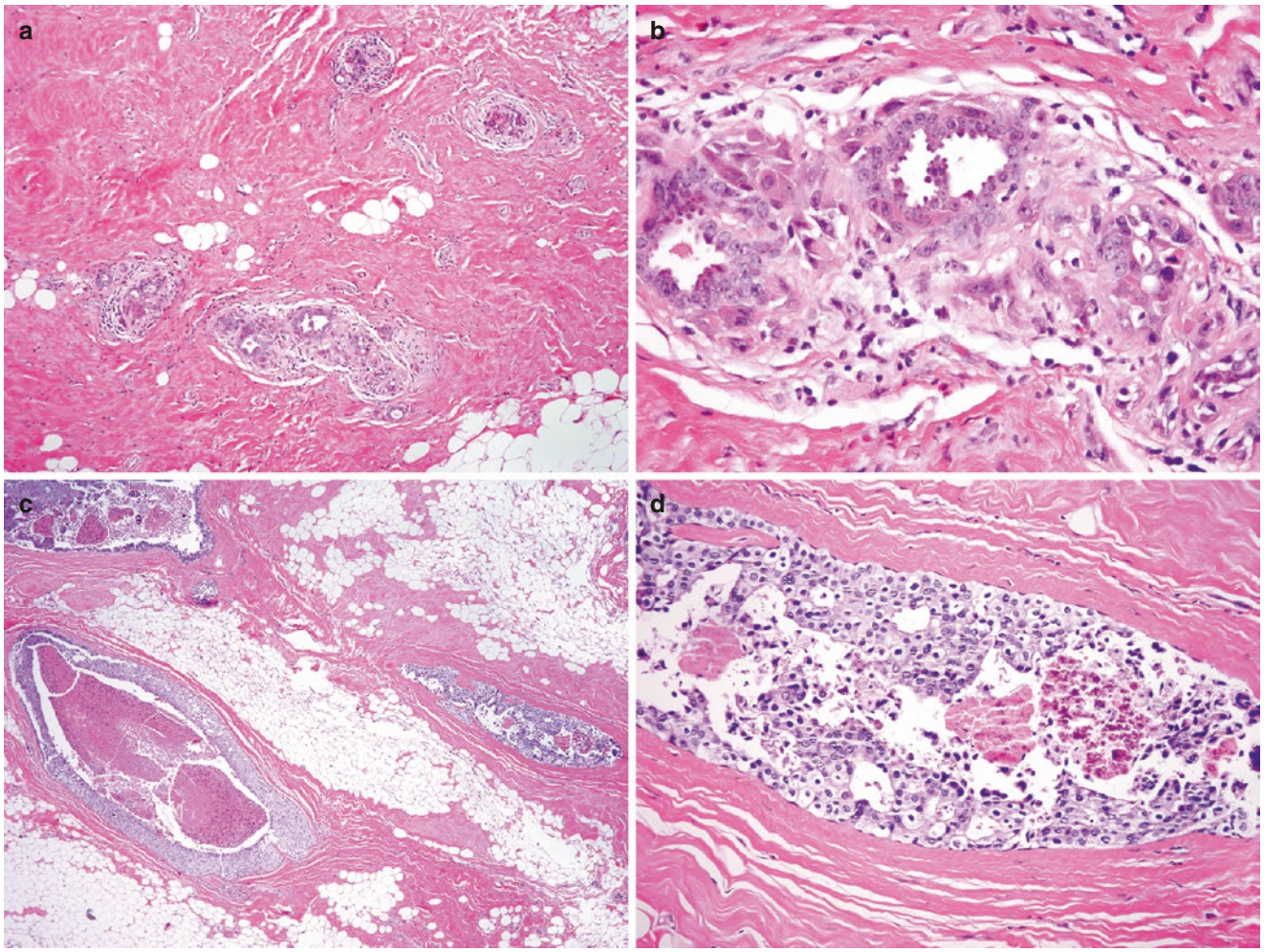

Fig. 21.33 Radiation-induced epithelial atypia versus recurrent DCIS. (**a**) CNB performed for a mass shows cytologically atypical epithelial cells lining scattered terminal ducts. The surrounding breast tissue showed dense fibrosis (i.e., scar), which may explain the mass lesion detected by imaging. (**b**) Higher magnification of these altered ducts shows evidence of squamous metaplasia and rare apoptotic cells. (**c**) Review of this patient's prior material shows solid and micropapillary DCIS associated with extensive central necrosis. (**d**) Cells comprising DCIS demonstrate clear-cell features and are morphologically distinct from the foci seen in the CNB. A diagnosis of radiation-induced epithelial atypia was rendered

Differential Diagnosis and Immunohistochemical Workup

The differential diagnosis includes dermal lymphatic tumor emboli versus invasive or in situ carcinoma with retraction. Angiolymphatic markers such as CD34, CD31, ERG, and D2–40 can be used to further delineate the tumor within dermal lymphatics (Fig. 21.40). Myoepithelial markers such as p63, SMM, and calponin can be used in conjunction with angiolymphatic markers to concurrently rule in or exclude that these tumor foci represent in situ or invasive carcinoma. Dermatologic malignancies should also be considered. An in-depth discussion of this differential can be found in Chapter 25.

Pathologic Reporting in a Biopsy Sample

Once the presence of dermal lymphatic tumor emboli is confirmed, ER, PR, and HER2 status should be performed and reported similarly as it is for invasive carcinoma [114, 123].

It should be emphasized that inflammatory carcinoma is not a pathologic diagnosis and requires clinicopathologic correlation. In the absence of the appropriate clinical setting, the presence of tumor in dermal lymphatics alone does not equate to a diagnosis of IBC. The term "inflammatory carcinoma" should not be used as a pathologic diagnosis in pathology reports.

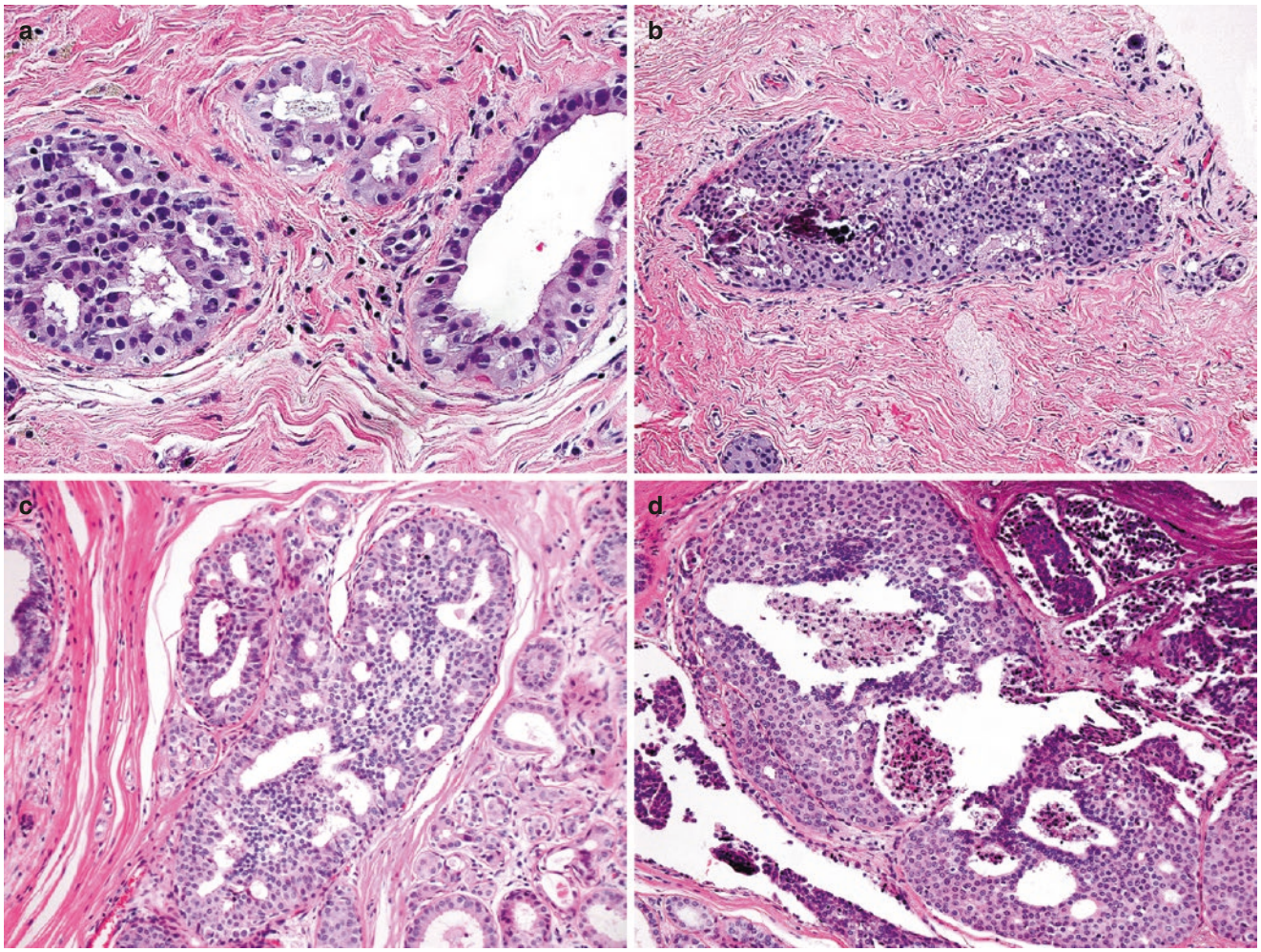

Fig. 21.34 A diagnostically difficult case of proliferative changes, possibly atypical ductal hyperplasia, with postradiation atypia versus recurrent DCIS. (**a**, **b**) A generous core biopsy reveals many foci, some proliferative, exhibiting radiation therapy-related atypia with the exception of this rare focus, which raised concern for recurrent DCIS. (**c**, **d**) Images of this patient's prior DCIS where some morphologic resemblance can be seen when compared to the atypical focus in Figures (**a**) and (**b**). A definitive diagnosis was not rendered in this case primarily due to the exceedingly limited extent of the lesion, and re-biopsy to evaluate additional material was recommended

Pathogenesis

The aggressive tumor biology of IBC is poorly understood and inconclusive. The high propensity of invasive breast carcinoma cells to invade lymphatic channels makes inflammatory breast cancer a distinct entity with unique pathogenesis. The current literature suggests that intralymphatic tumor cells strongly express E-cadherin, which might play a critical role in the malignant progression and metastasis of IBC [124]. Increased angiogenesis and lymphangiogenesis in IBC have been confirmed by histologic and molecular studies assessing endothelial cell proliferation [114, 118]. Patients with IBC also express higher levels of vascular endothelial growth factor D (VEGF- D), which is important in angiogenesis and lymphangiogenesis [125]. Additionally, it is proposed that a vasculogenic phenotype, in which tumor cells, rather than endothelial cells, form blood vessels, explains the metastatic route of IBC and why it is so clinically aggressive [126–128]. IBCs have been shown to have relatively high levels of tumor-associated macrophages (TAMs) and release high levels of inflammatory cytokines which may promote tumor progression [129]. The role of inflammation in the pathogenesis of IBC has yet to be fully elucidated. Recent studies have shown that IBC demonstrates heterogeneity in biomarker status with a mix of hormone receptor-positive, HER2-negative (39%); hormone receptor-positive, HER2-positive (16.5%); HER2-positive, hormone receptor-negative (18.9%); or triple-negative (25.6%) carcinomas [130]. However, it is important to note

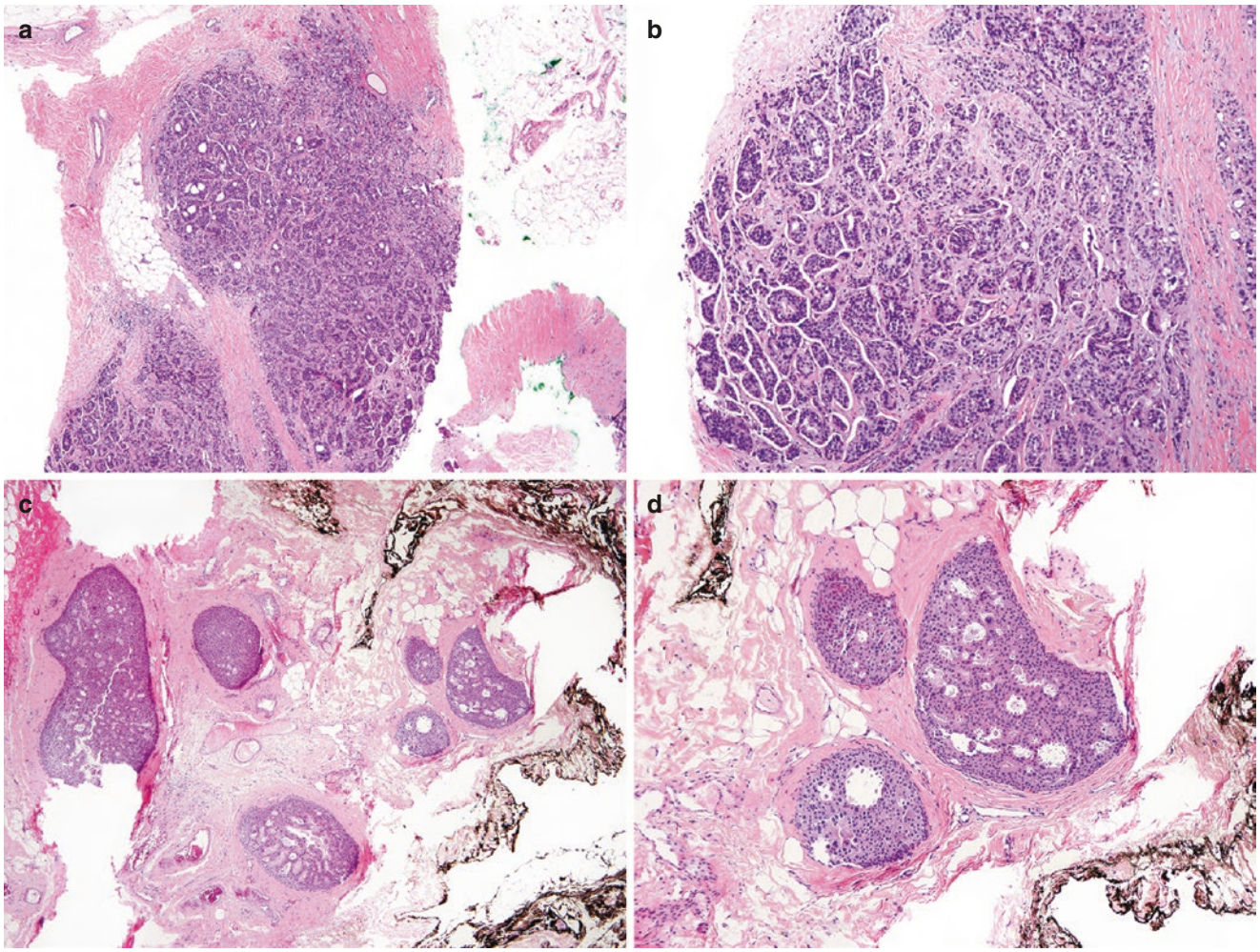

Fig. 21.35 Recurrent invasive carcinoma following index DCIS. (**a**, **b**) CNB performed for a breast mass shows recurrent IDC. Other tissue cores show dense stromal fibrosis (i.e., scar) (*lower right*). The recurrent carcinoma is moderately differentiated. (**c**) Excision of the index tumor showed only micropapillary and cribriform DCIS. (**d**) The cells comprising the DCIS bear resemblance to those of recurrent invasive carcinoma

that compared to non-IBC, the more aggressive, ER-negative phenotypes do predominate [114]. Similar to biomarker status, all molecular subtypes are represented in IBC; however, basal-like and HER2+ subtypes predominate [122] [123, 131]. Molecular testing has failed to demonstrate unique mutational patterns in IBC; however, frequent alterations in the HER/PI3K/mTOR pathway are seen [132]. Due to the marked heterogeneity of IBC, future collaborative studies will have to include more IBC cases to contribute to a more comprehensive understanding of IBC and provide new diagnostic and predictive factors for IBC, as well as for potential therapeutic targets.

Treatment and Prognosis

Despite multidisciplinary treatment with chemotherapy, radiation, and surgery, IBC still carries a poor prognosis, with a 5-year survival rate of about 30%, with no significant change in prognosis over the past 30 years [116]. In general, HER2-positive cases have the best survival, likely reflecting the efficacy of anti-HER2-targeted treatments [130, 133, 134], while hormone receptor-positive tumors are associated with worse outcome [130, 135]. Despite aggressive treatments, the worse survival is seen in patients with triple-negative IBC [133]. Furthermore, triple-negative IBC is associated with poorer survival compared to those with non-

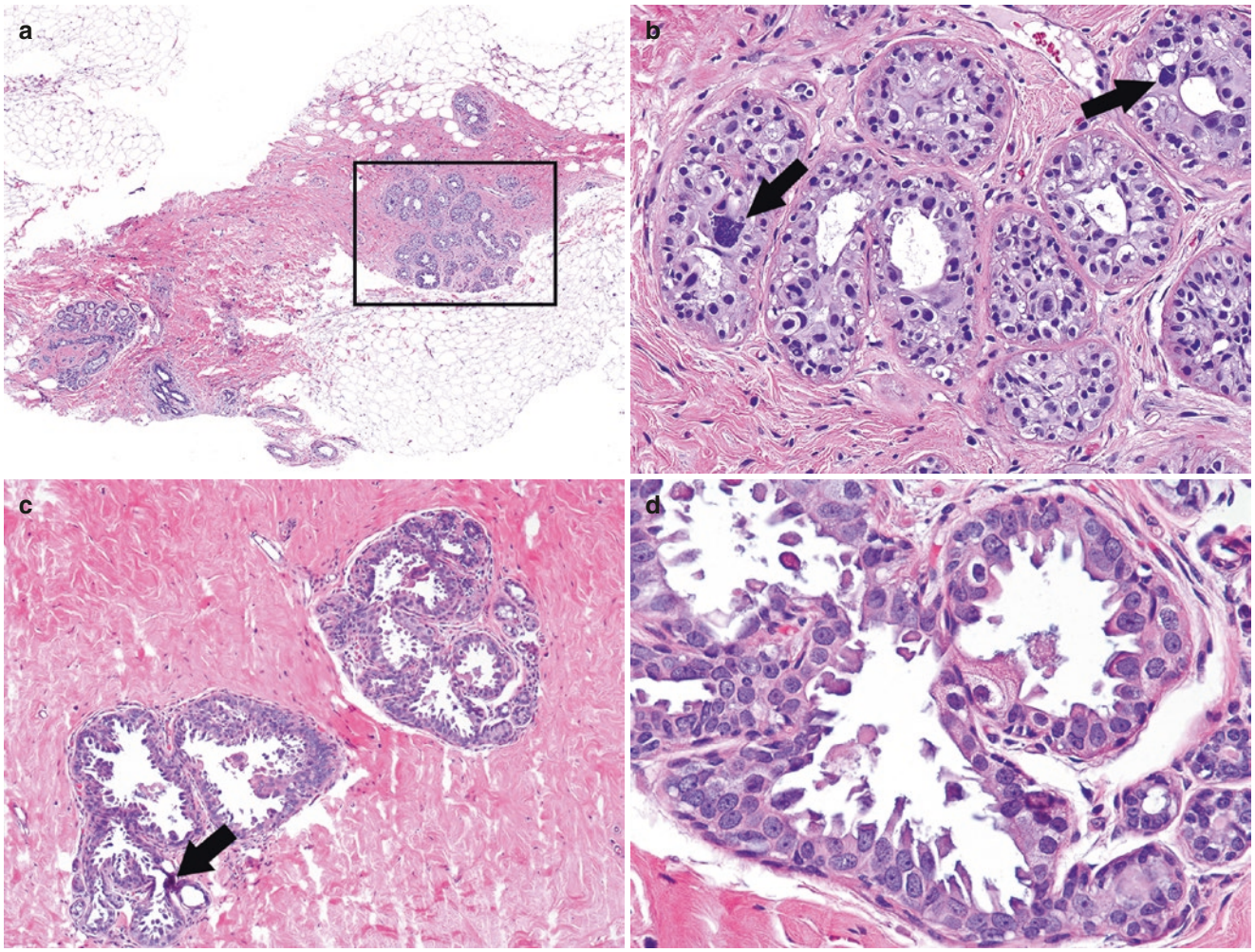

Fig. 21.36 Radiation-related change compared to flat-micropapillary (clinging) DCIS. (**a**) CNB performed for calcifications shows a slightly enlarged terminal duct lobular unit. (**b**) Higher power view of area in *box* from (**a**) shows the cells with apocrine morphology lining the acini. Nonuniform, scattered enlarged cells with hyperchromatic nuclei and smudged chromatin are present. Cytoplasmic vacuolization is evident in many cells. (**c**) Different CNB performed for calcifications shows a flat and micropapillary epithelial proliferation lining dilated ducts. Calcifications are identified within the involved ducts (arrow). (**d**) The neoplastic cells lining the ducts are uniform with increased nuclear-to-cytoplasmic ratio and small nucleoli, consistent with flat-micropapillary DCIS

inflammatory presentation [136]. Angiogenesis has been shown to be a valuable target for the therapy for patients with inflammatory carcinoma with a dual effect on both tumor cells and endothelial cells [114]. Furthermore, the role of microenvironmental factors such as inflammation may provide an avenue for novel treatments in IBC. Given frequent alterations in the HER/PI3K/mTOR pathway, some IBCs may benefit from therapies targeting these pathways. While much effort has been made to understand the pathogenesis of IBC which may allow for a more personalized approach to treat these patients, there is still much to be elucidated about IBC before more effective treatments can be developed.

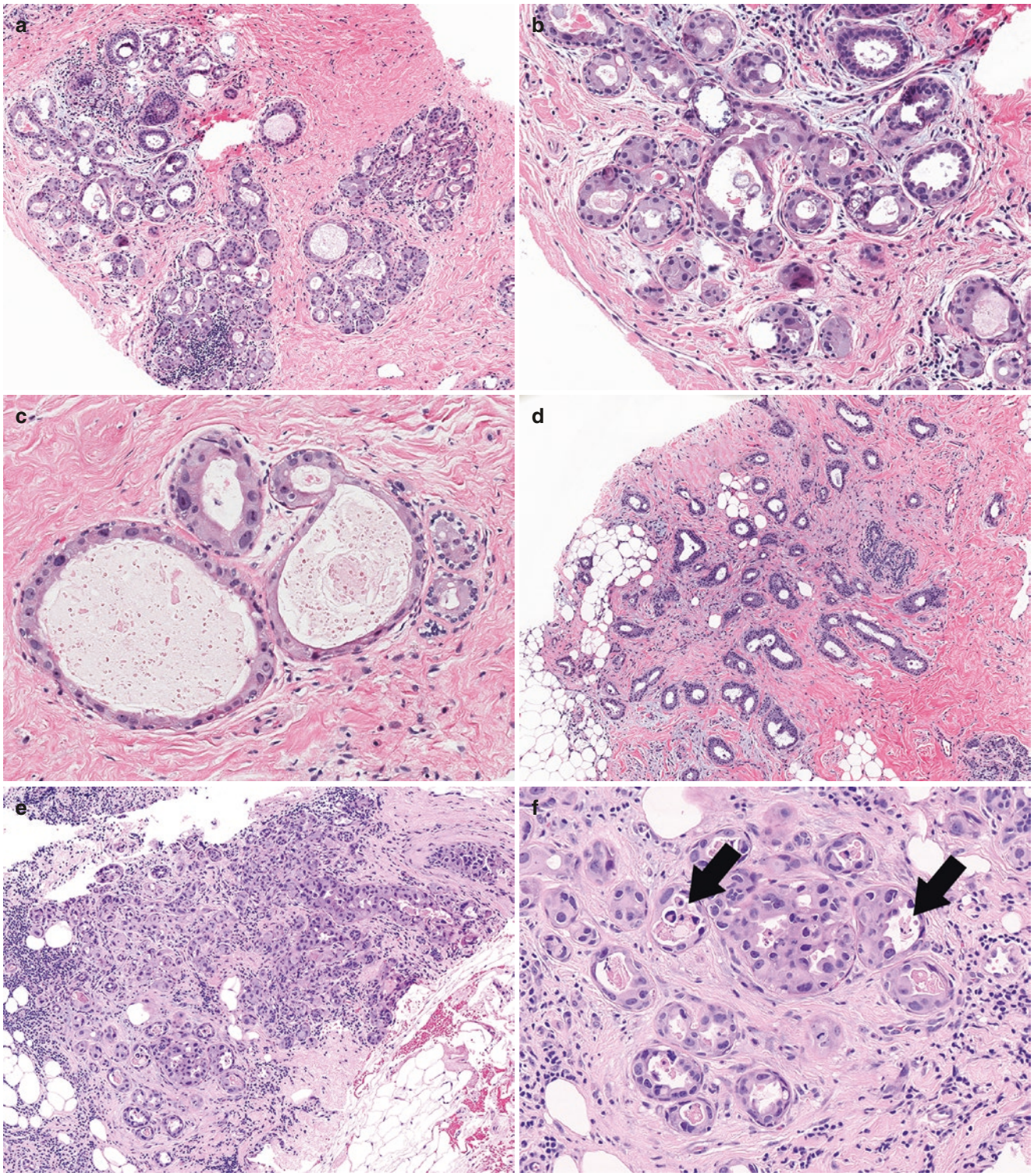

Fig. 21.37 Examples highlighting the importance of morphologic comparison in lesions with apocrine features following radiation therapy. (**a**) CNB performed for calcifications shows terminal duct lobular unit lined by prominent eosinophilic epithelial cells. (**b, c**) The acini are lined by a single layer of apocrine cells. Scattered, enlarged cells with hyperchromatic nuclei are present. (**d**) Comparison to the patient's prior invasive well-differentiated carcinoma lacking apocrine morphology confirmed the changes in Figures (a, b, c) representing radiation-related atypia. (**e**) Different CNB performed for calcifications shows terminal duct lobular units and surrounding glands with a flat and micropapillary epithelial proliferation with eosinophilic cytoplasm. (**f**) On higher magnification, the lining cells demonstrate uniform cytologic atypia, and apoptotic luminal debris is noted (arrows). (**g**) The patient's prior DCIS shows similar morphology and also extends into terminal duct lobular units, confirming recurrent DCIS in the CNB seen in Figures (**e, f**)

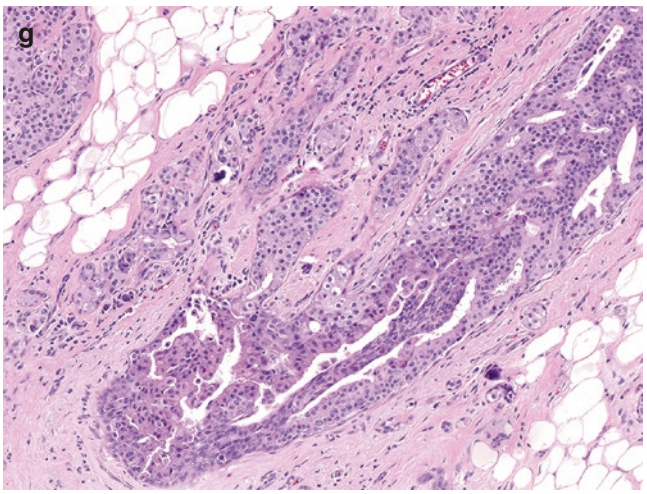

Fig. 21.37 (continued)

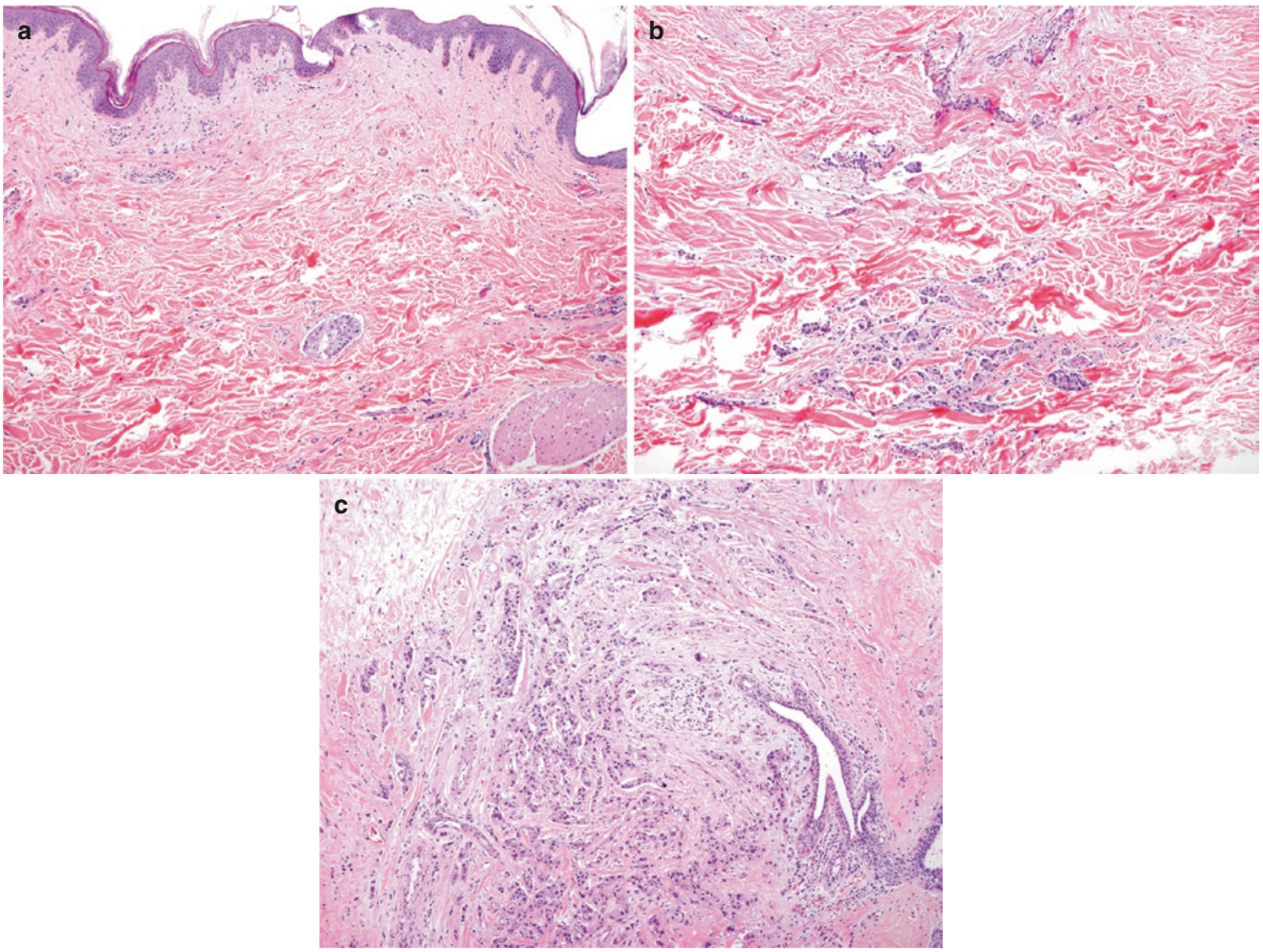

Fig. 21.38 Inflammatory carcinoma. (**a**) Punch biopsy for skin erythema reveals a cluster of carcinoma cells in a lymphatic channel. (**b**, **c**) Subsequent excision shows IDC present in the dermis (**b**) and underlying breast parenchyma (**c**)

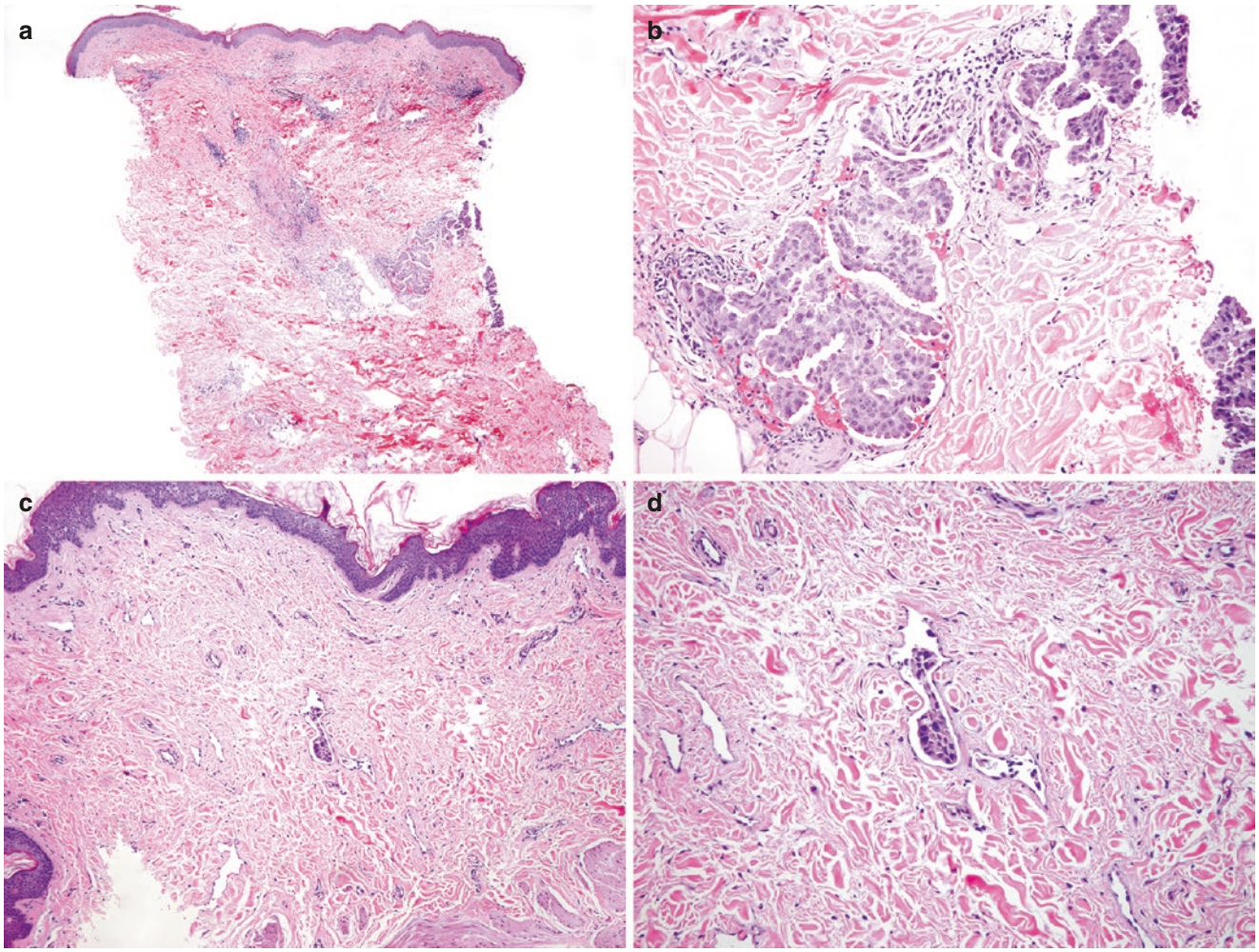

Fig. 21.39 Inflammatory carcinoma, two examples. (**a**) Punch biopsy of clinically erythematous breast skin shows clusters of carcinoma cells within vascular channels in the reticular dermis. (**b**) Tumor emboli are surrounded by red blood cells in the vascular channel. (**c**) Punch biopsy for skin erythema from another case shows a carcinomatous embolus with a lymphatic channel. (**d**) The lymphatic channel is lined by flat-to-plump endothelial cells

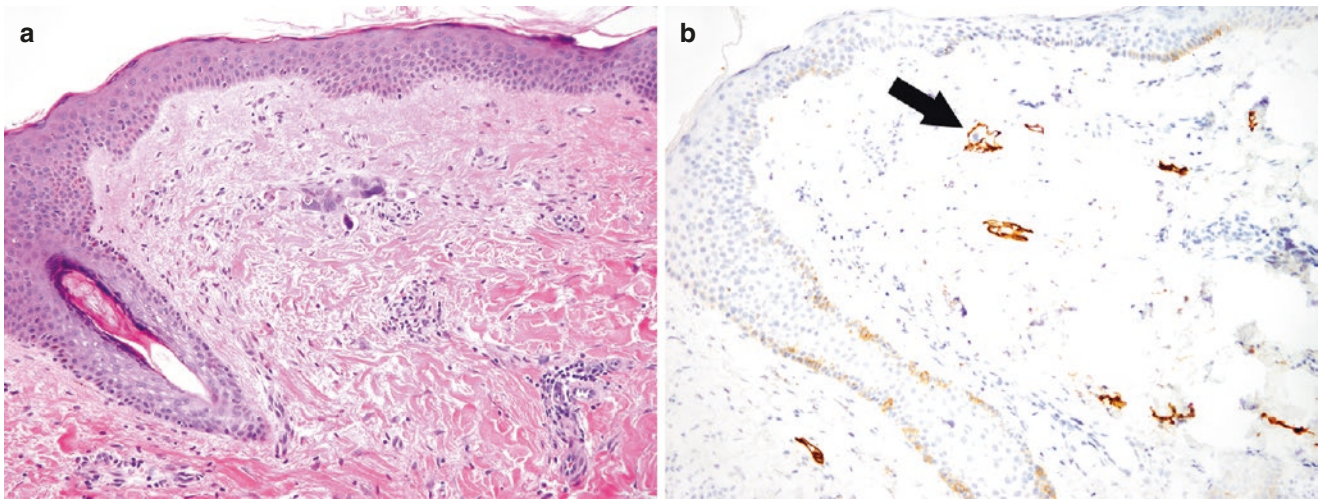

Fig. 21.40 Inflammatory carcinoma. (**a**) Cluster of tumor cells present within a space in the dermis. (**b**) A D2–40 immunostain confirms that the space is a lymphatic channel despite its markedly diminished size in this deeper section used for staining (*arrow*)

References

1. Kieturakis AJ, Wahab RA, Vijapura C, Mahoney MC. Current recommendations for breast imaging of the pregnant and lactating patient. AJR Am J Roentgenol. 2021;216(6):1462–75.
2. Neville MC, Morton J, Umemura S. Lactogenesis. The transition from pregnancy to lactation. Pediatr Clin N Am 2001;48(1):35–52.
3. Shiu RP, Friesen HG. Mechanism of action of prolactin in the control of mammary gland function. Annu Rev Physiol. 1980;42:83–96.
4. Vashi R, Hooley R, Butler R, Geisel J, Philpotts L. Breast imaging of the pregnant and lactating patient: imaging modalities and pregnancy-associated breast cancer. AJR Am J Roentgenol. 2013;200(2):321–8.
5. Expert Panel on Breast I, diFlorio-Alexander RM, Slanetz PJ, Moy L, Baron P, Didwania AD, et al. ACR Appropriateness Criteria((R)) Breast Imaging of Pregnant and Lactating Women. J Am Coll Radiol. 2018;15(11S):S263–S75.
6. Sabate JM, Clotet M, Torrubia S, Gomez A, Guerrero R, de las Heras P, et al. Radiologic evaluation of breast disorders related to pregnancy and lactation. Radiographics. 2007;27(Suppl 1):S101–24.
7. Novotny DB, Maygarden SJ, Shermer RW, Frable WJ. Fine needle aspiration of benign and malignant breast masses associated with pregnancy. Acta Cytol. 1991;35(6):676–86.
8. Cardonick E, Usmani A, Ghaffar S. Perinatal outcomes of a pregnancy complicated by cancer, including neonatal follow-up after in utero exposure to chemotherapy: results of an international registry. Am J Clin Oncol. 2010;33(3):221–8.
9. Baker TP, Lenert JT, Parker J, Kemp B, Kushwaha A, Evans G, et al. Lactating adenoma: a diagnosis of exclusion. Breast J. 2001;7(5):354–7.
10. World Health Organization Classification of Tumours: Breast Tumours. 5th ed. Board WCoTE, editor. Lyon: International Agency for Research on Cancer; 2019.
11. O'Hara MF, Page DL. Adenomas of the breast and ectopic breast under lactational influences. Hum Pathol. 1985;16(7):707–12.
12. Reeves ME, Tabuenca A. Lactating adenoma presenting as a giant breast mass. Surgery. 2000;127(5):586–8.
13. Behrndt VS, Barbakoff D, Askin FB, Brem RF. Infarcted lactating adenoma presenting as a rapidly enlarging breast mass. AJR Am J Roentgenol. 1999;173(4):933–5.
14. Slavin JL, Billson VR, Ostor AG. Nodular breast lesions during pregnancy and lactation. Histopathology. 1993;22(5):481–5.
15. Yu JH, Kim MJ, Cho H, Liu HJ, Han SJ, Ahn TG. Breast diseases during pregnancy and lactation. Obstet Gynecol Sci. 2013;56(3):143–59.
16. Vashi R, Hooley R, Butler R, Geisel J, Philpotts L. Breast imaging of the pregnant and lactating patient: physiologic changes and common benign entities. AJR Am J Roentgenol. 2013;200(2):329–36.
17. Hertel BF, Zaloudek C, Kempson RL. Breast adenomas. Cancer. 1976;37(6):2891–905.
18. Hill RP, Miller FN Jr. Adenomas of the breast with case report of carcinomatous transformation in an adenoma. Cancer. 1954;7(2):318–24.
19. Volckmar AL, Leichsenring J, Flechtenmacher C, Pfarr N, Siebolts U, Kirchner M, et al. Tubular, lactating, and ductal adenomas are devoid of MED12 Exon2 mutations, and ductal adenomas show recurrent mutations in GNAS and the PI3K-AKT pathway. Genes Chromosomes Cancer. 2017;56(1):11–7.
20. Saglam A, Can B. Coexistence of lactating adenoma and invasive ductal adenocarcinoma of the breast in a pregnant woman. J Clin Pathol. 2005;58(1):87–9.
21. Gill S, Peston D, Vonderhaar BK, Shousha S. Expression of prolactin receptors in normal, benign, and malignant breast tissue: an immunohistological study. J Clin Pathol. 2001;54(12):956–60.
22. Saglam O, Tavassoli FA. Expression of hormone receptors, cell regulatory and myoepithelial cell markers in lactating breast and associated carcinomas. Breast J. 2012;18(4):380–2.
23. Rovera F, Frattini F, Coglitore A, Marelli M, Rausei S, Dionigi G, et al. Breast cancer in pregnancy. Breast J. 2010;16(Suppl 1):S22–5.
24. Froehlich K, Schmidt A, Heger JI, Al-Kawlani B, Aberl CA, Jeschke U, et al. Breast cancer, placenta and pregnancy. Eur J Cancer. 2019;115:68–78.
25. Amant F, Loibl S, Neven P, Van Calsteren K. Breast cancer in pregnancy. Lancet. 2012;379(9815):570–9.
26. Loibl S, von Minckwitz G, Gwyn K, Ellis P, Blohmer JU, Schlegelberger B, et al. Breast carcinoma during pregnancy. International recommendations from an expert meeting. Cancer. 2006;106(2):237–46.
27. Van Calsteren K, Heyns L, De Smet F, Van Eycken L, Gziri MM, Van Gemert W, et al. Cancer during pregnancy: an analysis of 215 patients emphasizing the obstetrical and the neonatal outcomes. J Clin Oncol. 2010;28(4):683–9.
28. Loibl S. New Therapeutic Options for Breast Cancer during Pregnancy. Breast Care (Basel). 2008;3(3):171–6.
29. Loibl S. Adjuvant therapy in patients with breast cancer during pregnancy. Cancer Treat Res. 2009;151:317–28.
30. Genin AS, Lesieur B, Gligorov J, Antoine M, Selleret L, Rouzier R. Pregnancy-associated breast cancers: do they differ from other breast cancers in young women? Breast. 2012;21(4):550–5.
31. Andersson TM, Johansson ALV, Hsieh CC, Cnattingius S, Lambe M. Increasing incidence of pregnancy-associated breast cancer in Sweden. Obstet Gynecol. 2009;114(3):568–72.
32. Ishida T, Yokoe T, Kasumi F, Sakamoto G, Makita M, Tominaga T, et al. Clinicopathologic characteristics and prognosis of breast cancer patients associated with pregnancy and lactation: analysis of case-control study in Japan. Jpn J Cancer Res. 1992;83(11):1143–9.
33. Woo JC, Yu T, Hurd TC. Breast cancer in pregnancy: a literature review. Arch Surg. 2003;138(1):91–8. discussion 9
34. Zemlickis D, Lishner M, Degendorfer P, Panzarella T, Burke B, Sutcliffe SB, et al. Maternal and fetal outcome after breast cancer in pregnancy. Am J Obstet Gynecol. 1992;166(3):781–7.
35. Al-Amri AM. Clinical presentation and causes of the delayed diagnosis of breast cancer in patients with pregnancy associated breast cancer. J Fam Community Med. 2015;22(2):96–100.
36. Goldsmith HS. Milk-rejection sign of breast cancer. Am J Surg. 1974;127(3):280–1.
37. Bonnier P, Romain S, Dilhuydy JM, Bonichon F, Julien JP, Charpin C, et al. Influence of pregnancy on the outcome of breast cancer: a case-control study. Societe Francaise de Senologie et de Pathologie Mammaire Study Group. Int J Cancer. 1997;72(5):720–7.
38. Jach R, Piskorz T, Przeszlakowski D, Huras H, Pitynski K, Kolodziejski L, et al. Solid papillary carcinoma of the breast with neuroendocrine features in a pregnant woman: a case report. Neuro Endocrinol Lett. 2011;32(4):405–7.
39. Popovska S, Damianova P, Tomov S, Dineva T, Ivanov I. Case of encapsulated solid papillary carcinoma with triple-negative and basal-like phenotype occurred in pregnant woman with review of the literature. Akush Ginekol (Sofiia). 2015;54(2):50–6.
40. Bae SY, Jung SP, Jung ES, Park SM, Lee SK, Yu JH, et al. Clinical characteristics and prognosis of pregnancy-associated breast cancer: poor survival of luminal B subtype. Oncology. 2018;95(3):163–9.
41. Middleton LP, Amin M, Gwyn K, Theriault R, Sahin A. Breast carcinoma in pregnant women: assessment of clinicopathologic and immunohistochemical features. Cancer. 2003;98(5):1055–60.
42. Madaras L, Kovacs KA, Szasz AM, Kenessey I, Tokes AM, Szekely B, et al. Clinicopathological features and prognosis of pregnancy associated breast cancer - a matched case control study. Pathol Oncol Res. 2014;20(3):581–90.

43. Michieletto S, Saibene T, Evangelista L, Barbazza F, Grigoletto R, Rossi G, et al. Preliminary monocentric results of biological characteristics of pregnancy associated breast cancer. Breast. 2014;23(1):19–25.
44. Marikakis N, Yiangou C, Agrawal A. Hormone receptor expression in pregnancy-associated breast cancer: a systematic review of the literature. Eur J Surg Oncol. 2018;44(6):913.
45. Johansson ALV, Andersson TM, Hsieh CC, Jirstrom K, Cnattingius S, Fredriksson I, et al. Tumor characteristics and prognosis in women with pregnancy-associated breast cancer. Int J Cancer. 2018;142(7):1343–54.
46. Azim HA Jr, Botteri E, Renne G, Dell'orto P, Rotmensz N, Gentilini O, et al. The biological features and prognosis of breast cancer diagnosed during pregnancy: a case-control study. Acta Oncol. 2012;51(5):653–61.
47. Azim HA Jr, Brohee S, Peccatori FA, Desmedt C, Loi S, Lambrechts D, et al. Biology of breast cancer during pregnancy using genomic profiling. Endocr Relat Cancer. 2014;21(4):545–54.
48. Rosenkranz KM, Lucci A. Surgical treatment of pregnancy associated breast cancer. Breast Dis. 2005;23:87–93.
49. Rodriguez AO, Chew H, Cress R, Xing G, McElvy S, Danielsen B, et al. Evidence of poorer survival in pregnancy-associated breast cancer. Obstet Gynecol. 2008;112(1):71–8.
50. Lohsiriwat V, Peccatori FA, Martella S, Azim HA Jr, Sarno MA, Galimberti V, et al. Immediate breast reconstruction with expander in pregnant breast cancer patients. Breast. 2013;22(5):657–60.
51. Wang B, Yang Y, Jiang Z, Zhao J, Mao Y, Liu J, et al. Clinicopathological characteristics, diagnosis, and prognosis of pregnancy-associated breast cancer. Thorac Cancer. 2019;10(5):1060–8.
52. Zhang R, Liu X, Huang W, Shao B, Yan Y, Liang X, et al. Clinicopathological features and prognosis of patients with pregnancy-associated breast cancer: a matched case control study. Asia Pac J Clin Oncol. 2021;17(4):396–402.
53. Potluri V, Lewis D, Burton GV. Chemotherapy with taxanes in breast cancer during pregnancy: case report and review of the literature. Clin Breast Cancer. 2006;7(2):167–70.
54. Gadducci A, Cosio S, Fanucchi A, Nardini V, Roncella M, Conte PF, et al. Chemotherapy with epirubicin and paclitaxel for breast cancer during pregnancy: case report and review of the literature. Anticancer Res. 2003;23(6D):5225–9.
55. Cardonick E, Bhat A, Gilmandyar D, Somer R. Maternal and fetal outcomes of taxane chemotherapy in breast and ovarian cancer during pregnancy: case series and review of the literature. Ann Oncol. 2012;23(12):3016–23.
56. Cardonick E, Dougherty R, Grana G, Gilmandyar D, Ghaffar S, Usmani A. Breast cancer during pregnancy: maternal and fetal outcomes. Cancer J. 2010;16(1):76–82.
57. Beale JM, Tuohy J, McDowell SJ. Herceptin (trastuzumab) therapy in a twin pregnancy with associated oligohydramnios. Am J Obstet Gynecol. 2009;201(1):e13–4.
58. Berger JC, Clericuzio CL. Pierre Robin sequence associated with first trimester fetal tamoxifen exposure. Am J Med Genet A. 2008;146A(16):2141–4.
59. Azim HA Jr, Santoro L, Russell-Edu W, Pentheroudakis G, Pavlidis N, Peccatori FA. Prognosis of pregnancy-associated breast cancer: a meta-analysis of 30 studies. Cancer Treat Rev. 2012;38(7):834–42.
60. Raphael J, Trudeau ME, Chan K. Outcome of patients with pregnancy during or after breast cancer: a review of the recent literature. Curr Oncol. 2015;22(Suppl 1):S8–S18.
61. Gupta S, Jain P, McDunn S. Breast cancer with brain metastases in pregnancy. J Community Support Oncol. 2014;12(10):378–80.
62. Vetter G, Zimmermann F, Bruder E, Schulzke S, Hosli I, Vetter M. Aggressive Breast Cancer during Pregnancy with a Rare Form of Metastasis in the Maternal Placenta. Geburtshilfe Frauenheilkd. 2014;74(6):579–82.
63. Azim HA Jr, Vingiani A, Peccatori F, Viale G, Loi S, Pruneri G. Tumour infiltrating lymphocytes (TILs) in breast cancer during pregnancy. Breast. 2015;24(3):290–3.
64. Tavassoli FA, Yeh IT. Lactational and clear cell changes of the breast in nonlactating, nonpregnant women. Am J Clin Pathol. 1987;87(1):23–9.
65. Popnikolov NK, Yan J, Mendez AB, Imagawa WT. Pregnancy-like hyperplasia with focal atypia arising within a gynecomastic male breast: a case report. Clin Breast Cancer. 2015;15(2):e171–5.
66. Shin SJ, Rosen PP. Pregnancy-like (pseudolactational) hyperplasia: a primary diagnosis in mammographically detected lesions of the breast and its relationship to cystic hypersecretory hyperplasia. Am J Surg Pathol. 2000;24(12):1670–4.
67. Koktener A, Cakir B, Akin K, Kosehan D, Bayrak R, Yenidunya S. Pregnancy-like (pseudolactational) hyperplasia: uncommon cause of microcalcifications and mass in two cases. JBR-BTR. 2013;96(1):25–6.
68. Shin SJ, Rosen PP. Carcinoma arising from preexisting pregnancy-like and cystic hypersecretory hyperplasia lesions of the breast: a clinicopathologic study of 9 patients. Am J Surg Pathol. 2004;28(6):789–93.
69. Takeuchi T, Tsuzuki H, Numoto S, Furihata M. Coexistence of pregnancy-like and cystic hypersecretory hyperplasia with invasive lobular carcinoma. Onkologie. 2011;34(8–9):448–50.
70. Mieog JS, van der Hage JA, van de Velde CJ. Neoadjuvant chemotherapy for operable breast cancer. Br J Surg. 2007;94(10):1189–200.
71. Burstein HJ, Curigliano G, Loibl S, Dubsky P, Gnant M, Poortmans P, et al. Estimating the benefits of therapy for early-stage breast cancer: the St. Gallen International Consensus Guidelines for the primary therapy of early breast cancer 2019. Ann Oncol. 2019;30(10):1541–57.
72. Fisher B, Bryant J, Wolmark N, Mamounas E, Brown A, Fisher ER, et al. Effect of preoperative chemotherapy on the outcome of women with operable breast cancer. J Clin Oncol. 1998;16(8):2672–85.
73. Masuda N, Lee SJ, Ohtani S, Im YH, Lee ES, Yokota I, et al. Adjuvant capecitabine for breast cancer after preoperative chemotherapy. N Engl J Med. 2017;376(22):2147–59.
74. von Minckwitz G, Huang CS, Mano MS, Loibl S, Mamounas EP, Untch M, et al. Trastuzumab emtansine for residual invasive HER2-positive breast cancer. N Engl J Med. 2019;380(7):617–28.
75. Tanis E, van de Velde CJ, Bartelink H, van de Vijver MJ, Putter H, van der Hage JA. Locoregional recurrence after breast-conserving therapy remains an independent prognostic factor even after an event free interval of 10 years in early stage breast cancer. Eur J Cancer. 2012;48(12):1751–6.
76. Mathew J, Asgeirsson KS, Cheung KL, Chan S, Dahda A, Robertson JF. Neoadjuvant chemotherapy for locally advanced breast cancer: a review of the literature and future directions. Eur J Surg Oncol. 2009;35(2):113–22.
77. von Minckwitz G, Untch M, Blohmer JU, Costa SD, Eidtmann H, Fasching PA, et al. Definition and impact of pathologic complete response on prognosis after neoadjuvant chemotherapy in various intrinsic breast cancer subtypes. J Clin Oncol. 2012;30(15):1796–804.
78. Moon HG, Im SA, Han W, Oh DY, Han SW, Keam B, et al. Estrogen receptor status confers a distinct pattern of response to neoadjuvant chemotherapy: implications for optimal durations of therapy: distinct patterns of response according to ER expression. Breast Cancer Res Treat. 2012;134(3):1133–40.
79. Chen X, He C, Han D, Zhou M, Wang Q, Tian J, et al. The predictive value of Ki-67 before neoadjuvant chemotherapy for breast

cancer: a systematic review and meta-analysis. Future Oncol. 2017;13(9):843–57.
80. Boughey JC, Suman VJ, Mittendorf EA, Ahrendt GM, Wilke LG, Taback B, et al. Sentinel lymph node surgery after neoadjuvant chemotherapy in patients with node-positive breast cancer: the ACOSOG Z1071 (Alliance) clinical trial. JAMA. 2013;310(14):1455–61.
81. Breslin TM, Cohen L, Sahin A, Fleming JB, Kuerer HM, Newman LA, et al. Sentinel lymph node biopsy is accurate after neoadjuvant chemotherapy for breast cancer. J Clin Oncol. 2000;18(20):3480–6.
82. Mamounas EP, Brown A, Anderson S, Smith R, Julian T, Miller B, et al. Sentinel node biopsy after neoadjuvant chemotherapy in breast cancer: results from National Surgical Adjuvant Breast and Bowel Project Protocol B-27. J Clin Oncol. 2005;23(12):2694–702.
83. Mamounas EP, Anderson SJ, Dignam JJ, Bear HD, Julian TB, Geyer CE Jr, et al. Predictors of locoregional recurrence after neoadjuvant chemotherapy: results from combined analysis of National Surgical Adjuvant Breast and Bowel Project B-18 and B-27. J Clin Oncol. 2012;30(32):3960–6.
84. Carey LA, Dees EC, Sawyer L, Gatti L, Moore DT, Collichio F, et al. The triple negative paradox: primary tumor chemosensitivity of breast cancer subtypes. Clin Cancer Res. 2007;13(8):2329–34.
85. Petit T, Wilt M, Velten M, Rodier JF, Fricker JP, Dufour P, et al. Semi-quantitative evaluation of estrogen receptor expression is a strong predictive factor of pathological complete response after anthracycline-based neo-adjuvant chemotherapy in hormonal-sensitive breast cancer. Breast Cancer Res Treat. 2010;124(2):387–91.
86. Sanchez-Munoz A, Plata-Fernandez Y, Fernandez M, Jaen-Morago A, Fernandez-Navarro M, de la Torre-Cabrera C, et al. Tumor histological subtyping determined by hormone receptors and HER2 status defines different pathological complete response and outcome to dose-dense neoadjuvant chemotherapy in breast cancer patients. Clin Transl Oncol. 2014;16(6):548–54.
87. Yoo C, Ahn JH, Jung KH, Kim SB, Kim HH, Shin HJ, et al. Impact of immunohistochemistry-based molecular subtype on chemosensitivity and survival in patients with breast cancer following neoadjuvant chemotherapy. J Breast Cancer. 2012;15(2):203–10.
88. Loibl S, Volz C, Mau C, Blohmer JU, Costa SD, Eidtmann H, et al. Response and prognosis after neoadjuvant chemotherapy in 1,051 patients with infiltrating lobular breast carcinoma. Breast Cancer Res Treat. 2014;144(1):153–62.
89. Lips EH, et al. Breast Cancer. Res Treat 2012. PMID 22961065.
90. Schmid P, Cortes J, Pusztai L, McArthur H, Kummel S, Bergh J, et al. Pembrolizumab for early triple-negative breast cancer. N Engl J Med. 2020;382(9):810–21.
91. Schmid P, Park Y-H, Muñoz-Couselo E, Kim S-B, Sohn J, Im S-A, et al. Pembrolizumab (pembro) + chemotherapy (chemo) as neoadjuvant treatment for triple negative breast cancer (TNBC): preliminary results from KEYNOTE-173. J Clin Oncol. 2017;35(15_suppl):556.
92. Schmid P, Salgado R, Park YH, Munoz-Couselo E, Kim SB, Sohn J, et al. Pembrolizumab plus chemotherapy as neoadjuvant treatment of high-risk, early-stage triple-negative breast cancer: results from the phase 1b open-label, multicohort KEYNOTE-173 study. Ann Oncol. 2020;31(5):569–81.
93. Denkert C, von Minckwitz G, Darb-Esfahani S, Lederer B, Heppner BI, Weber KE, et al. Tumour-infiltrating lymphocytes and prognosis in different subtypes of breast cancer: a pooled analysis of 3771 patients treated with neoadjuvant therapy. Lancet Oncol. 2018;19(1):40–50.
94. Sahoo S, Lester SC. Pathology of breast carcinomas after neoadjuvant chemotherapy: an overview with recommendations on specimen processing and reporting. Arch Pathol Lab Med. 2009;133(4):633–42.
95. Bossuyt V, Provenzano E, Symmans WF, Boughey JC, Coles C, Curigliano G, et al. Recommendations for standardized pathological characterization of residual disease for neoadjuvant clinical trials of breast cancer by the BIG-NABCG collaboration. Ann Oncol. 2015;26(7):1280–91.
96. Provenzano E, Bossuyt V, Viale G, Cameron D, Badve S, Denkert C, et al. Standardization of pathologic evaluation and reporting of postneoadjuvant specimens in clinical trials of breast cancer: recommendations from an international working group. Mod Pathol. 2015;28(9):1185–201.
97. Symmans WF, Peintinger F, Hatzis C, Rajan R, Kuerer H, Valero V, et al. Measurement of residual breast cancer burden to predict survival after neoadjuvant chemotherapy. J Clin Oncol. 2007;25(28):4414–22.
98. Amin MB, American Joint Committee on Cancer. American Cancer Society. AJCC cancer staging manual. Eight edition/editor-in-chief, Mahul B. Amin, Stephen B. Edge; Donna M. Gress; Laura R. Meyer. ed. Chicago IL: American Joint Committee on Cancer, Springer; 2017. xvii, 1024.
99. Haffty BG, Fischer D, Beinfield M, McKhann C. Prognosis following local recurrence in the conservatively treated breast cancer patient. Int J Radiat Oncol Biol Phys. 1991;21(2):293–8.
100. Jagsi R, Raad RA, Goldberg S, Sullivan T, Michaelson J, Powell SN, et al. Locoregional recurrence rates and prognostic factors for failure in node-negative patients treated with mastectomy: implications for postmastectomy radiation. Int J Radiat Oncol Biol Phys. 2005;62(4):1035–9.
101. Li S, Yu KD, Fan L, Hou YF, Shao ZM. Predicting breast cancer recurrence following breast-conserving therapy: a single-institution analysis consisting of 764 Chinese breast cancer cases. Ann Surg Oncol. 2011;18(9):2492–9.
102. Kneubil MC, Brollo J, Botteri E, Curigliano G, Rotmensz N, Goldhirsch A, et al. Breast cancer subtype approximations and loco-regional recurrence after immediate breast reconstruction. Eur J Surg Oncol. 2013;39(3):260–5.
103. Lowery AJ, Kell MR, Glynn RW, Kerin MJ, Sweeney KJ. Locoregional recurrence after breast cancer surgery: a systematic review by receptor phenotype. Breast Cancer Res Treat. 2012;133(3):831–41.
104. Panet-Raymond V, Truong PT, McDonald RE, Alexander C, Ross L, Ryhorchuk A, et al. True recurrence versus new primary: an analysis of ipsilateral breast tumor recurrences after breast-conserving therapy. Int J Radiat Oncol Biol Phys. 2011;81(2):409–17.
105. Krishnamurthy R, Whitman GJ, Stelling CB, Kushwaha AC. Mammographic findings after breast conservation therapy. Radiographics. 1999;19 Spec No:S53–62; quiz S262-3
106. Huston TL, Simmons RM. Locally recurrent breast cancer after conservation therapy. Am J Surg. 2005;189(2):229–35.
107. Jabbour MN, Massad CY, Boulos FI. Variability in hormone and growth factor receptor expression in primary versus recurrent, metastatic, and post-neoadjuvant breast carcinoma. Breast Cancer Res Treat. 2012;135(1):29–37.
108. Nishimura R, Osako T, Okumura Y, Tashima R, Toyozumi Y, Arima N. Changes in the ER, PgR, HER2, p53 and Ki-67 biological markers between primary and recurrent breast cancer: discordance rates and prognosis. World J Surg Oncol. 2011;9:131.
109. Soomro R, Beg MA, ur Rahman SS. Discordance of biomarker status in recurrent breast cancer. J Pak Med Assoc. 2014;64(2):163–5.
110. Huang E, Buchholz TA, Meric F, Krishnamurthy S, Mirza NQ, Ames FC, et al. Classifying local disease recurrences after breast conservation therapy based on location and histology: new primary tumors have more favorable outcomes than true local disease recurrences. Cancer. 2002;95(10):2059–67.
111. Walshe JM, Swain SM. Clinical aspects of inflammatory breast cancer. Breast Dis. 2005;22:35–44.

112. Dawood S, Lei X, Dent R, Gupta S, Sirohi B, Cortes J, et al. Survival of women with inflammatory breast cancer: a large population-based study. Ann Oncol. 2014;25(6):1143–51.
113. Hance KW, Anderson WF, Devesa SS, Young HA, Levine PH. Trends in inflammatory breast carcinoma incidence and survival: the surveillance, epidemiology, and end results program at the National Cancer Institute. J Natl Cancer Inst. 2005;97(13):966–75.
114. van Uden DJ, van Laarhoven HW, Westenberg AH, de Wilt JH, Blanken-Peeters CF. Inflammatory breast cancer: an overview. Crit Rev Oncol Hematol. 2015;93(2):116–26.
115. Molckovsky A, Fitzgerald B, Freedman O, Heisey R, Clemons M. Approach to inflammatory breast cancer. Can Fam Physician. 2009;55(1):25–31.
116. Gomez R, Ossa CA, Montoya ME, Echeverri C, Angel G, Ascuntar J, et al. Impact of immunohistochemistry-based molecular subtype on chemosensitivity and survival in Hispanic breast cancer patients following neoadjuvant chemotherapy. Ecancermedicalscience. 2015;9:562.
117. Gueth U, Wight E, Schoetzau A, Langer I, Dieterich H, Rochlitz C, et al. Non-inflammatory skin involvement in breast cancer, histologically proven but without the clinical and histological T4 category features. J Surg Oncol. 2007;95(4):291–7.
118. Vermeulen PB, van Golen KL, Dirix LY. Angiogenesis, lymphangiogenesis, growth pattern, and tumor emboli in inflammatory breast cancer: a review of the current knowledge. Cancer. 2010;116(11 Suppl):2748–54.
119. Le-Petross HT, Cristofanilli M, Carkaci S, Krishnamurthy S, Jackson EF, Harrell RK, et al. MRI features of inflammatory breast cancer. AJR Am J Roentgenol. 2011;197(4):W769–76.
120. Akay CL, Ueno NT, Chisholm GB, Hortobagyi GN, Woodward WA, Alvarez RH, et al. Primary tumor resection as a component of multimodality treatment may improve local control and survival in patients with stage IV inflammatory breast cancer. Cancer. 2014;120(9):1319–28.
121. Manfrin E, Remo A, Pancione M, Cannizzaro C, Falsirollo F, Pollini GP, et al. Comparison between invasive breast cancer with extensive peritumoral vascular invasion and inflammatory breast carcinoma: a clinicopathologic study of 161 cases. Am J Clin Pathol. 2014;142(3):299–306.
122. Van Laere SJ, Ueno NT, Finetti P, Vermeulen P, Lucci A, Robertson FM, et al. Uncovering the molecular secrets of inflammatory breast cancer biology: an integrated analysis of three distinct affymetrix gene expression datasets. Clin Cancer Res. 2013;19(17):4685–96.
123. Zell JA, Tsang WY, Taylor TH, Mehta RS, Anton-Culver H. Prognostic impact of human epidermal growth factor-like receptor 2 and hormone receptor status in inflammatory breast cancer (IBC): analysis of 2,014 IBC patient cases from the California Cancer Registry. Breast Cancer Res. 2009;11(1):R9.
124. Kleer CG, van Golen KL, Braun T, Merajver SD. Persistent E-cadherin expression in inflammatory breast cancer. Mod Pathol. 2001;14(5):458–64.
125. Levine PH, Portera CC, Hoffman HJ, Yang SX, Takikita M, Duong QN, et al. Evaluation of lymphangiogenic factors, vascular endothelial growth factor D and E-cadherin in distinguishing inflammatory from locally advanced breast cancer. Clin Breast Cancer. 2012;12(4):232–9.
126. Colpaert CG, Vermeulen PB, Benoy I, Soubry A, van Roy F, van Beest P, et al. Inflammatory breast cancer shows angiogenesis with high endothelial proliferation rate and strong E-cadherin expression. Br J Cancer. 2003;88(5):718–25.
127. Dome B, Hendrix MJ, Paku S, Tovari J, Timar J. Alternative vascularization mechanisms in cancer: pathology and therapeutic implications. Am J Pathol. 2007;170(1):1–15.
128. Shirakawa K, Furuhata S, Watanabe I, Hayase H, Shimizu A, Ikarashi Y, et al. Induction of vasculogenesis in breast cancer models. Br J Cancer. 2002;87(12):1454–61.
129. Morrow RJ, Etemadi N, Yeo B, Ernst M. Challenging a misnomer? The role of inflammatory pathways in inflammatory breast cancer. Mediat Inflamm. 2017;2017:4754827.
130. Liu J, Chen K, Jiang W, Mao K, Li S, Kim MJ, et al. Chemotherapy response and survival of inflammatory breast cancer by hormone receptor- and HER2-defined molecular subtypes approximation: an analysis from the National Cancer Database. J Cancer Res Clin Oncol. 2017;143(1):161–8.
131. Bertucci F, Finetti P, Birnbaum D, Viens P. Gene expression profiling of inflammatory breast cancer. Cancer. 2010;116(11 Suppl):2783–93.
132. Ross JS, Ali SM, Wang K, Khaira D, Palma NA, Chmielecki J, et al. Comprehensive genomic profiling of inflammatory breast cancer cases reveals a high frequency of clinically relevant genomic alterations. Breast Cancer Res Treat. 2015;154(1):155–62.
133. Boudin L, Goncalves A, Sfumato P, Sabatier R, Bertucci F, Tarpin C, et al. Prognostic impact of hormone receptor- and HER2-defined subtypes in inflammatory breast cancer treated with high-dose chemotherapy: a retrospective study. J Cancer. 2016;7(14):2077–84.
134. Diessner J, Van Ewijk R, Weiss CR, Janni W, Wischnewsky MB, Kreienberg R, et al. Identifying the impact of inflammatory breast cancer on survival: a retrospective multi-center cohort study. Arch Gynecol Obstet. 2015;292(3):655–64.
135. Masuda H, Brewer TM, Liu DD, Iwamoto T, Shen Y, Hsu L, et al. Long-term treatment efficacy in primary inflammatory breast cancer by hormonal receptor- and HER2-defined subtypes. Ann Oncol. 2014;25(2):384–91.
136. Biswas T, Efird JT, Prasad S, James SE, Walker PR, Zagar TM. Inflammatory TNBC breast cancer: demography and clinical outcome in a large cohort of patients with TNBC. Clin Breast Cancer. 2016;16(3):212–6.

Current Standard Clinical Predictive Markers

22

Kimberly H. Allison

Introduction

In medicine, a prognostic factor or marker is generally considered to be a factor or marker that imparts some information regarding the disease course and probable behavior of a given disease [1]. In the original usage of the term, in times when therapies were nonexistent to rather limited, this future behavior of the disease was accepted to be the behavior or outcome *if the disease was left untreated*. With significant advances in multimodality therapy, the term has come to incorporate the clinical standard of care for the given stage of disease, including surgery, radiation, and chemotherapy in the case of breast cancer; some have defined prognostic markers as markers that help clinicians determine *which* patients to treat systemically (based on tumor characteristics that predict stage and, therefore, outcome) [2].

While a prognostic marker may on a basic level "predict" clinical outcome, accurate use of the term "predictive marker" is usually reserved for a marker or test that specifically predicts response to a given therapy, most commonly, a particular chemotherapeutic drug. In the current age of personalized or "precision" medicine emphasizing highly targeted clinical treatment, the standard biomarkers in breast cancer (hormone receptors and HER2) are actually both prognostic and predictive. Hormone receptor-negative cancers have a worse prognosis without treatment (prognostic marker), and in addition, a positive estrogen receptor (ER) test predicts potential benefit from treatment with hormone-targeted therapies like tamoxifen and aromatase inhibitors (predictive marker) [3–6]. HER2-positive breast cancers also have a worse prognosis without treatment (prognostic marker), and a positive HER2 test predicts potential benefit from HER2-targeted drugs (predictive marker) [7–10]. These critical and now standard predictive tests therefore help establish which patients need additional treatment and which specific targeted treatments they are candidates for. This chapter reviews the performance, interpretation, pitfalls, and guideline recommendations of these important predictive tests in breast cancer.

Since these predictive tests are so critical to breast cancer treatment planning, practicing pathologists should make every effort to ensure that their laboratories operate within well-accepted clinical testing guidelines and procedures; for most laboratories in the United States, participation in a laboratory accreditation program, such as that offered by the College of American Pathologists, serves to accomplish this goal. Pathologists signing out predictive tests should be familiar with the most recent CAP/ASCO testing guidelines for hormone receptors and HER2 testing [11–14]. Even if these tests are sent out to another laboratory, they should be correlated with the original pathology when reporting outside results, and efforts should be made to resolve any unusual or discordant results [15]. A general familiarity with how clinical treatment guidelines (such as the NCCN breast cancer treatment guidelines) incorporate the results of these tests into treatment algorithms is also recommended [16, 17].

In many respects, core needle biopsies are an ideal specimen on which to test and report predictive and prognostic markers in breast cancer. Biological tissue, its composite elements such as genes and proteins, and the resultant diagnostic and predictive tests to which they are subjected remain sensitive to a number of pre-analytic handling and processing factors, such as cold ischemia time, delay in tissue fixation, type and duration of fixation, type of processing, and various post-processing manipulations [18–25]. Core needle biopsies tend to be relatively small, are routinely placed

K. H. Allison (✉)
Department of Pathology, Stanford University School of Medicine, Stanford, CA, USA
e-mail: allisonk@stanford.edu

© The Author(s), under exclusive license to Springer Nature Switzerland AG 2022

S. J. Shin et al. (eds.), *A Comprehensive Guide to Core Needle Biopsies of the Breast*,
https://doi.org/10.1007/978-3-031-05532-4_22

essentially immediately in neutral-buffered formalin (some institutions may choose to radiograph cores to separate those cores with calcifications and those without, but this generally adds only a minimum delay of minutes to fixation), and fix well in a relatively short amount of time. In contrast to variably sized and variably thick surgical excision breast tissue, core needle biopsies tend to be more homogeneous in their extent of routine formalin fixation and can be fixed faster. This chapter covers the specifics of predictive testing in newly diagnosed breast cancers as well as briefly reviews testing in the metastatic/recurrent setting.

Biomarker Testing in Specific Clinical Scenarios

Biomarker testing in breast cancer can depend on the specific clinical scenario. These principles are summarized in Table 22.1. In the setting of a newly diagnosed invasive breast cancer, since treatment options and pathways are typically determined by hormone receptor [estrogen and progesterone receptors (PR)] and HER2 test results, multiple testing and treatment guidelines recommended that these markers are performed up front on the initial core needle biopsy sam-

Table 22.1 Summary of recommended breast cancer testing on core biopsies in specific clinical scenarios

Clinical scenario	Recommendation	Purpose
New diagnosis of DCIS	ER testing by IHC PR is optional (not predictive)	To predict potential benefit from hormonal therapies for prevention of local recurrence and risk reduction
New diagnosis of primary invasive breast cancer	ER and PR testing by IHC	ER ≥1% predicts potential benefit from endocrine therapies to prevent systemic or local recurrence and risk reduction. ER is also prognostic PR is primarily prognostic (see text)
	HER2 testing by IHC and/or ISH	HER2 positive results predict benefit from targeted HER2 therapies (usually with chemotherapy) HER2 is also prognostic.
	Ki67 by IHC is optional	The percentage Ki67-positive cells offers a measure of the proliferative rate, which should correlate with other findings and can be a prognostic measure (see text). It is also FDA approved to help identify patients with ER+, HER2- cancers with other high risk features that may benefit from additional risk reduction with ademaciclib (Ki 67 > or = to 20% using MIB-1 antibody on Dako Omnis platform).
ER+, HER2−, early-stage breast cancer when chemotherapy is being considered	Oncologist can consider ordering panel-based prognostic or predictive gene signatures such as: Oncotype DX® MammaPrint® Prosigna® EndoPredict®	Oncotype DX can be used to predict potential benefit of adding chemotherapy to endocrine therapy in lymph node-negative patients. It is prognostic in lymph node-positive patients. MammaPrint, Prosigna, and EndoPredict are currently validated as prognostic (can be used to identify higher risk patients) but not validated as predictive of chemo benefit.
ER+ early-stage disease, when considering the duration of endocrine therapy	Breast Cancer Index™ gene expression signature-based ratio of *HOXB13:IL17BR*	Predictive of benefit of extending endocrine therapy from 5 to 10 years
Residual disease post-neoadjuvant	Retesting ER/PR and HER2 is optional	Additional treatment decisions can be made based on original disease ER/PR/HER2 testing but posttreatment status may be informative if new targets are identified.
Newly metastatic breast cancer	Retest ER/PR and HER2	Metastatic progression may change ER/PR/HER2 status. HER2 IHC 1+ or 2+ (ISH negative) metastatic patients may be eligible for antibody drug conjugate treatment targeting lower levels of HER2 expression.
	BRCA1/2 germline testing recommended	*BRCA1/2* germline mutations predict response to PARP inhibitors
	If ER+, consider *PIK3CA* mutation testing by PCR or NGS (tumor or ctDNA)	*PIK3CA* mutation predicts benefit from an alpelisib–fulvestrant combination
	If ER/PR/HER2 negative, consider PD-L1 testing by IHC (22C3 antibody)	Combined positive score >10% using the 22C3 antibody predicts benefit from adding pembrolizumab
	Can consider MSI/MMR and/or TMB testing	MSI-high/deficient MMR and/or TMB-high predicts benefit from adding pembrolizumab (uncommon)
	Can consider NTRK testing by FISH (especially if secretory type)	NTRK gene fusions predict benefit from tropomyosin kinase receptor inhibitors (very rare)
	Consider comprehensive genomic profiling	Can help identify potential targeted therapy options

NGS next-generation sequencing, *MSI* microsatellite instability, *MMR* mismatch repair, *TMB* tumor mutation burden

ple of an invasive breast cancer [7–10, 16, 17]. Proliferation markers, such as Ki67 by IHC, are also often performed on the same core biopsy sample as an adjunct to grading and as a measure of how fast a cancer may be growing. Higher Ki67 indices are associated with more aggressive behavior, shorter times to recurrence/progression, and more frequent response to neoadjuvant chemotherapy or neoadjuvant endocrine therapy [26–30]. A decrease in Ki67 after neoadjuvant treatment is also associated with better outcomes [31, 32]. Recently, the FDA approved using Ki67 to help identify the highest risk patients with ER+/HER2- lymph node positive breast cancer that may benefit from adding CDK 4/6 inhibitor, abemaciclib, to treatment regimens [33]. A threshold of > or = to Ki67 of 20% was approved as the clinically relevant threshold for this purpose, although this threshold was prognostic rather than predictive of treatment benefit in the clinical trial (monarchE) and other features (grade 3, size > 5 cm) can also be used for this purpose. In addition, efforts are still ongoing to better standardize reproducible scoring systems for Ki67 [30, 34–36]. In the setting of multiple synchronous cancers, consideration should be given to testing each separate invasive cancer or to testing the biomarker status of the largest or highest grade cancer of each different histology. Newly diagnosed ductal carcinoma in situ should also be tested for estrogen receptor expression by IHC to determine if preventative hormonal therapies could prevent a local recurrence (see below for details) [11, 12]. Routine hormone receptor testing in lobular carcinoma in situ (including pleomorphic lobular carcinoma in situ) is not currently required since endocrine therapies can be used for risk reduction in this setting without the biomarker results (given the relative rarity of ER negativity in classic LCIS).

Although a core needle biopsy sample is ideal in terms of early treatment planning and pre-analytical tissue preservation aspects, there are some limitations that should be considered. Core biopsy samples can suffer from artifacts such as crush that can confound IHC interpretation, have limited amount of cancer present, or may not be representative of the status of the entire cancer (when heterogeneity is present). When these issues are a consideration, the test can be repeated on (or sometimes deferred to) a larger (but well-fixed) surgical sample. Repeat testing on a surgical sample should also be considered with unusual or discordant initial results (these will be reviewed below). Some tests, such as PCR-based (e.g., Oncotype DX) or next-generation sequencing (typically only used in the metastatic setting), need ample tissue to have robust results. Although there may be enough tissue in a core biopsy sample for these tests, the surgical sample typically provides more tissue for testing that does not involve in situ visualization of results.

Clinicians may be interested in the marker status of residual cancer after neoadjuvant treatment in surgical samples. Patients with residual disease in posttreatment surgical specimens may be candidates for additional targeted therapies based on either the pre- or the posttreatment status of specific biomarkers. This is the case for HER2-positive breast cancers, where it is now standard to offer additional HER2-targeted therapy with novel antibody-drug conjugates such as TDM-1 if there is residual cancer after initial neoadjuvant treatment [37].

Lastly, any newly metastatic or recurrent breast cancer should be tested for relevant biomarkers [16, 17]. All newly metastatic breast cancers should be characterized with ER/PR and HER2 testing to identify potential therapies and treatment pathways, since these markers can change with metastatic progression and offer new targeted therapy options [38, 39]. Recently, metastatic patients with low levels of HER2 expression by IHC (1+ or 2+ and negative for gene amplification) also became eligible for treatment with a new HER2 targeted antibody drug conjugate (trastuzumab deruxtecan), making the difference between HER2 IHC 0 vs 1+ or 2+ potentially relevant clinically in the metastatic setting [40]. However, as of the publication of this chapter, the specific threshold of IHC 0 vs 1+ HER2 has not been tested clinically. The eligibility and testing criteria for novel antibody drug conjugates using lower levels of HER2 expression for chemotherapy delivery are likely to continue to evolve. Other predictive markers beyond ER and HER2 are now recommended in specific metastatic breast cancer settings as well. BRCA1/2 germline mutation status is recommended by the NCCN as a test predictive of potential benefit from PARP inhibitor therapies in any metastatic patient [41, 42]. Recently, PARP inhibitors were also shown to improve invasive and distant disease-free survival in early-stage but high-risk HER2-negative cancer patients that have BRCA1/2 germline mutations, so the therapeutic indications for genomic testing may be expanding [43]. For metastatic ER-positive breast cancers, PIK3CA mutation testing (either in tumor or in ctDNA) can be considered since it is predictive of benefit from an alpelisib–fulvestrant combination to inhibit the PI3K and ER pathways [44]. And for metastatic triple-negative breast cancers, PD-L1 testing is also an option to predict benefit from specific immunotherapies like pembrolizumab [45, 46]. Although uncommon in breast cancers, MSI-H/dMMR or TMB-H test results on the cancer can also make a metastatic breast cancer patient a candidate for immunotherapy [47]. With progression after initial treatment, some medical oncologists will consider ordering comprehensive genomic profiling to determine if there are any unique targets present with therapeutic options. Rarely, a NTRK mutation is identified (especially in the uncommon secretory carcinoma) that is also targetable [48].

Hormone Receptors

Breast tissue is physiologically responsive to estrogen and normally expresses estrogen and progesterone receptors at relatively low levels (Fig. 22.1). The majority of breast cancers likewise express estrogen and progesterone receptors, albeit at

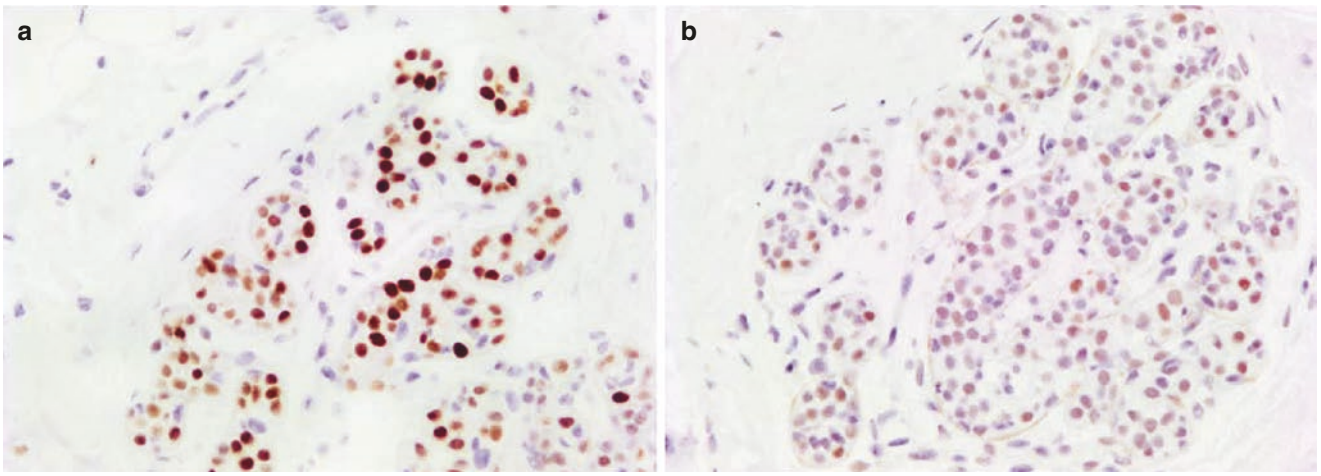

Fig. 22.1 Estrogen receptor (**a**) and progesterone receptor (**b**) expression in normal adult female breast tissue

much higher levels. Although it is usually not necessary, this increased estrogen and progesterone receptor expression may be helpful in diagnosis, such as in the setting of a low-grade intraductal proliferation raising the differential diagnosis of usual ductal hyperplasia and either atypical ductal hyperplasia or low-grade ductal carcinoma in situ. In these cases, atypical ductal hyperplasia and ductal carcinoma in situ typically exhibit strong, diffuse, and nearly complete estrogen receptor expression; in contrast, estrogen receptor expression in usual ductal hyperplasia is weak, patchy, and present in only a small percentage of cells. More important than its potential diagnostic utility, however, is the predictive value of hormone receptors in both in situ and invasive breast cancer.

Generally speaking, hormone receptor-expressing breast cancers tend to be of lower nuclear and overall grade than hormone receptor-negative cancers (although a spectrum of low- to high-grade ER-positive cancers do exist). Consequently, the majority of hormone receptor-expressing breast cancers tend to be slower growing and more indolent. Estrogen receptor testing's predictive value was first established in the 1970s' tamoxifen clinical trials, which used non-immunohistochemical (IHC) methods such as ligand-binding assay to determine the ER status of fresh tissue samples. Cases that were ER or PR positive were associated with a significantly better prognosis and showed benefit from hormone-targeted therapies like tamoxifen [3–6]. However, these methods have now been replaced by the standard IHC-based ER testing because of all the advantages offered by this method. ER testing by IHC can be performed even on small samples of tissue and offers direct visualization of what lesion is being scored. Therefore, current CAP/ASCO hormone receptor testing guidelines for breast cancer recommend hormone receptor testing only by IHC when used to predict potential benefit from endocrine therapies [11, 12, 49].

A summary of recommendations for hormone receptor testing in breast cancers is shown in Table 22.2. The threshold for a positive result is set quite low (at 1% of cancer cell staining by IHC) to include as many patients as possible that might benefit from the relatively low-risk hormonal therapies available (although not without side effects) [11, 50]. Even for the lowest levels of ER expression (10–19 fmol by ligand-binding assay, which correlates with 1–10% protein expression by IHC), the limited evidence available points to a one-third reduction in recurrences with 5 years of tamoxifen, even though many of these cancers have other characteristics more similar to ER-negative cancers [3, 6, 51–62]. However, recognizing this gray zone, the update also created the *ER low positive* reporting category for cases with 1–10% ER staining, which is to be reported with a comment that acknowledges the limitations of the data on cancers with low positive ER.

Progesterone receptor (PR) has more of a prognostic role in ER-positive breast cancers, with a predictive value that is not well established [63]. Although there is some evidence that ER-negative, PR-positive breast cancers exist (and possibly have some potential of benefit from endocrine therapy), some believe that this scenario should only occur in the setting of a false-negative ER result since PR is downstream of ER in the hormone pathway [64–70]. Low or negative PR results in an ER-positive breast cancer may be an indication of a potentially blunted response to hormone therapies due to pathway dysregulation; however, since these patients still have potential benefit from these therapies based on the ER-positive status alone, hormone therapy is still offered.

Overall, approximately 70–85% of invasive breast carcinomas have hormone receptor expression; however, different patient populations and geographic variation exist. Laboratories should closely monitor their percentages of estrogen receptor-negative breast cancers; if the percentage for all breast cancers is more than 30%, investigation into possible moderating pre-analytic, analytic, and post-analytic causes should be made.

Interpretation

Estrogen and progesterone receptor staining should be evaluated by a qualified pathologist to ensure that the invasive

Table 22.2 Summary of current recommendations for hormone receptor testing in breast cancer [11, 12, 50]

Issue	Recommendation	Comments
Sample to test	Core biopsies are preferred for testing if they are representative of the cancer (grade and type) at resection	See text for discussion about when to repeat on a surgical specimen Not recommended to use unstained slides cut more than 6 weeks prior to testing
Optimal tissue handling requirements	Time from tissue acquisition to fixation should be as short as possible	Cold ischemia time, fixative type, and time placed in formalin must be recorded
	Fix in 10% neutral buffered formalin for 6–72 h	
Scoring/interpretation	Score the percent of cancer cells with nuclear staining	A sample may be deemed "uninterpretable" if inadequate due to severe artifacts, insufficient cancer, controls fail, etc. Correlate with histology and be aware of unusual/discordant results and attempt to resolve or explain atypical findings
	Samples with 1–100% of cancer nuclei positive for ER or PgR are interpreted as positive	
	Samples with 0% or <1% are interpreted as negative	
	Have an SOP stating the steps the laboratory takes to confirm or adjudicate ER results for cases with weak stain intensity or 0–10% of cell staining (examples: review of controls, second pathologist reviews)	
Reporting	An interpretation as negative or positive should be included in the report If 1–10% of cancer cells stain, the sample should be reported as **ER low positive** with a recommended comment	See Table 22.3 for recommended report comments
	Reports should include the percent cells staining (0–100%) and intensity (0–3+)	
	The status of internal controls should be reported for cases with 0–10% staining. If no internal controls are present, an additional repot comment is recommended	
Controls	External controls should be run with each batch of testing	Tonsil is an ideal control for low ER-positive results and should be negative for PR staining
	There should be routine evaluation of external and any internal controls present	
	Optimal external controls are on slide (ideally) and should include multiple tissues, including ones with expected strong staining, lower limit of detection levels, and negative controls	
Initial test validation with revalidation as needed for significant changes to testing	Initial test validation is required prior to reporting clinical samples Revalidation should occur with a significant change to test system	Follow specific CAP recommendations on IHC validation of predictive IHC assays
Ongoing quality assurance, proficiency testing, and laboratory accreditation	There should be ongoing quality control measures, competency assessment of pathologists, external proficiency testing, and accreditation requirements met	

cancer is being scored to standards. CAP recommends that the pathologists interpreting breast cancer ER/PR stains for predictive purposes undergo assessment, such as participation in proficiency testing, to ensure the accuracy and reproducibility of these tests by all interpreters. In some settings, computer-based image-assisted semiautomated scoring may be performed, but these results must always be visually confirmed by a pathologist.

The steps to scoring an ER stain should begin with a quick check that the sample is adequate for testing, external and internal stains worked appropriately, and pre-analytic variables (fixative type, time to fixation, time in fixation) are documented and reviewed. If there are issues with this initial quality control, steps should be taken to address them since they may invalidate results. Next, the percent of cells with nuclear staining (of any intensity) for ER and PR should be assessed as the percentage of overall cancer cell staining (Fig. 22.2). The intensity of nuclear staining (ranging from 0 to 3+) should also be evaluated and reported, but only the percentage is used in the overall interpretation as positive or negative (Fig. 22.3). Cancers with ≥1% of cells expressing ER are considered positive per CAP/ASCO guidelines, and patients with these results are considered candidates for hormone therapies. Invasive cancers with 1–10% of cells staining are reported as ER low positive with the recommended comment (see Table 22.3). Cytoplasmic staining in the absence of nuclear expression should not be counted as a positive result. Although most often ER is uniformly expressed, it can be heterogeneous, and uncommonly distinct separate populations can be present with different histologic features (Fig. 22.4).

The 2020 ASCO/CAP guideline update also recognized that cases with <10% or weak ER staining may need additional steps to confirm the results and recommended that labs set up their own standard operating procedures (such as review of controls, having a second pathologist confirm results, or use digital-aided interpretation) to confirm or adjudicate these results [6]. An external control should always be evaluated (with appropriately positive and negative tissues), and internal controls should also stain as

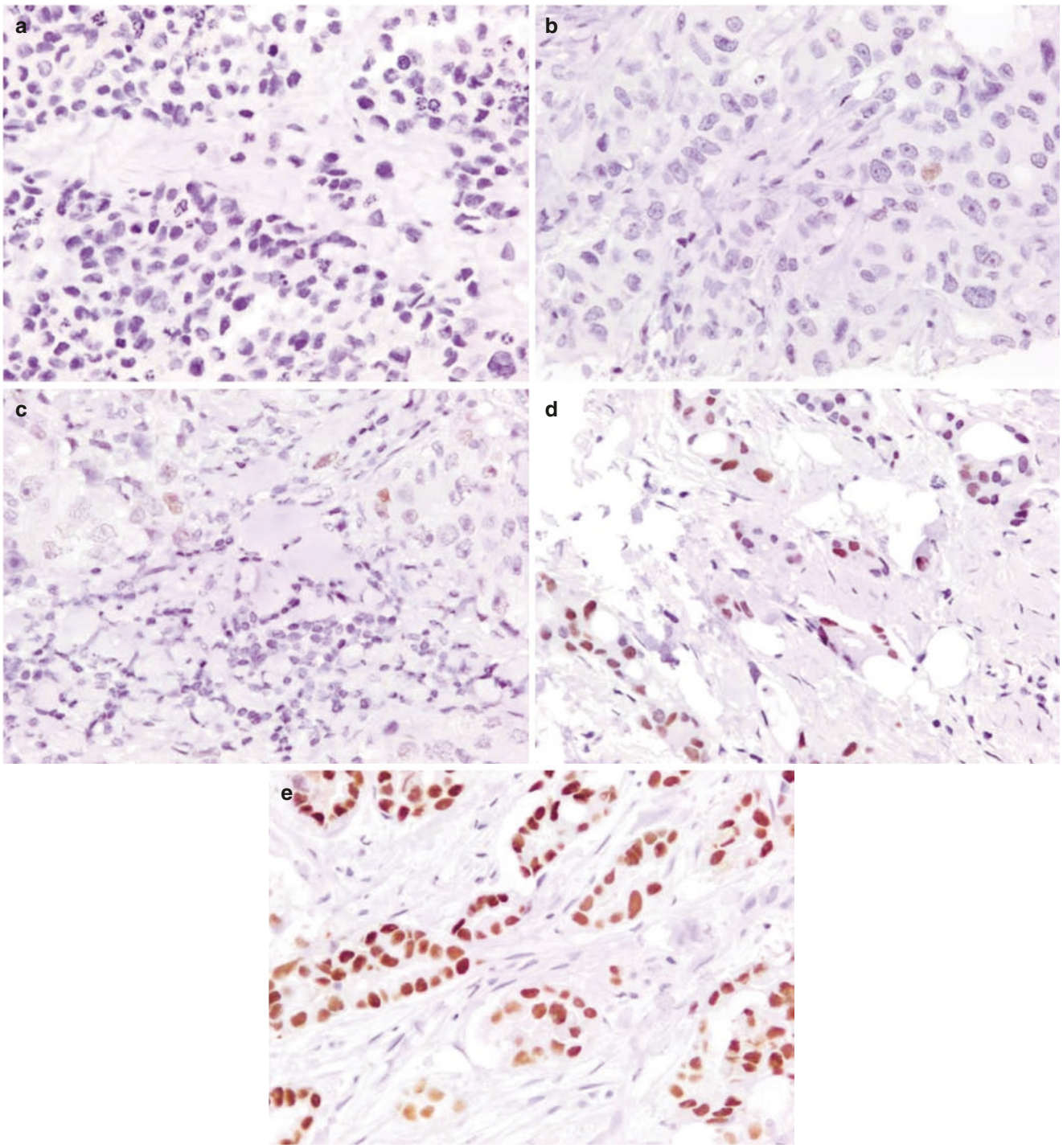

Fig. 22.2 Illustration of sample percentages of cells reactive to estrogen receptor antibody: (**a**) 0 (no cells staining); (**b**) 1% (approximately 90–100 tumor cells are present, only one of which shows nuclear expression); (**c**) 5–10% (approximately 40 tumor cells are present in the field, of which 3–4 are positive); (**d**) 70–80% (approximately 70 tumor cells are shown, of which 50–55 show nuclear expression); and (**e**) 100% (every tumor cell present in the field shows moderate-to-strong nuclear expression)

expected when present (Fig. 22.5). The ideal external control would be on the slide, typically as a tissue microarray, with a variety of expected results including tissue with strong staining, lower limit of detection levels, and negative controls. Tonsil is an ideal control for low ER-positive results and should be negative for PR staining (Fig. 22.6).

Correlation with histology is also critically important to recognize false-negative ER results or issues with the other histologic parameters reported. Nottingham grade 1 cancers, classic lobular carcinomas, tubular carcinomas, cribriform carcinomas, and mucinous carcinomas almost always express estrogen and progesterone receptors; repeat testing

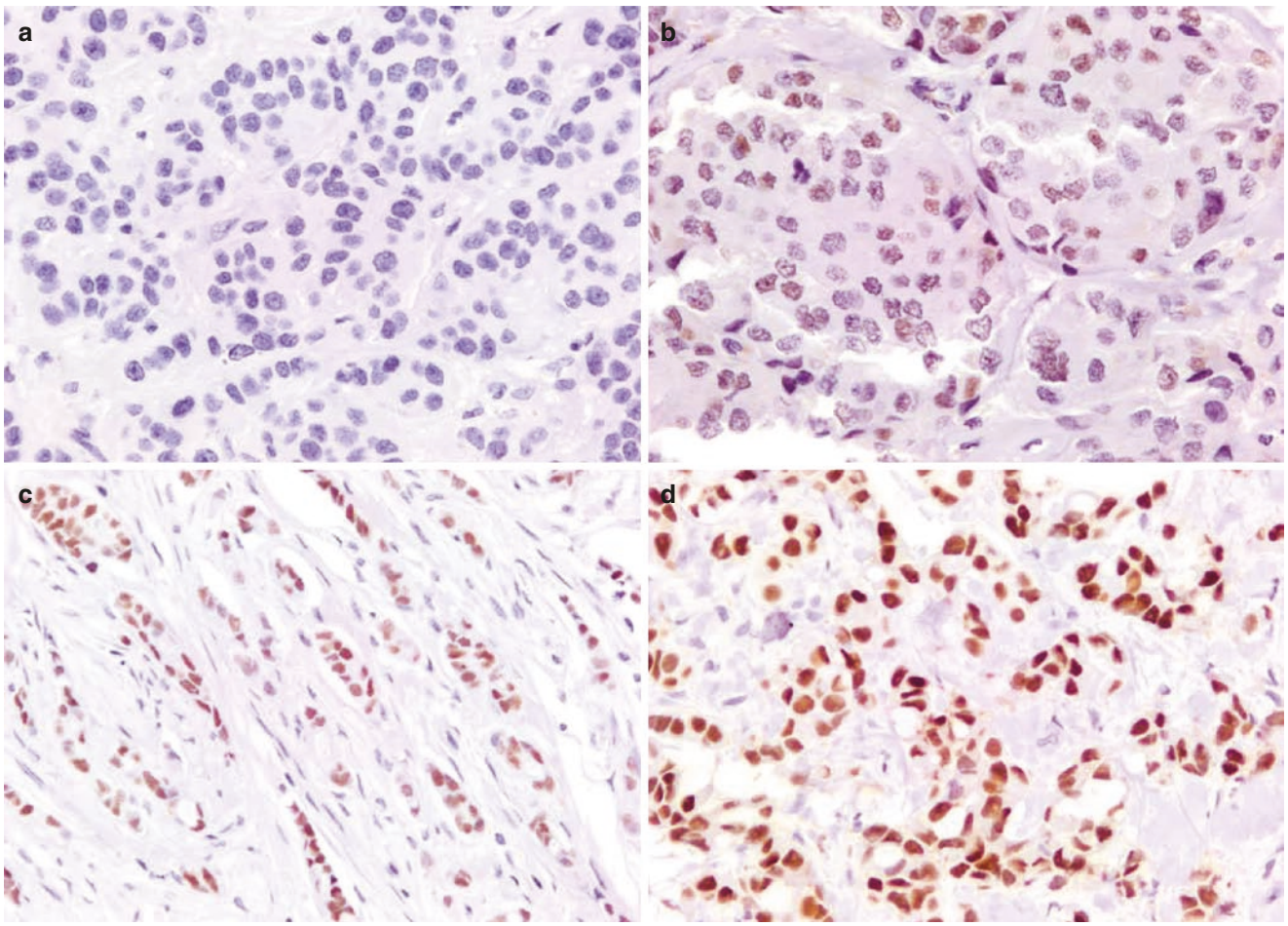

Fig. 22.3 Range of estrogen receptor staining intensity: (**a**) 0, negative; (**b**) weak (1+); (**c**) moderate (2+); (**d**) strong (3+)

Table 22.3 Recommended report comments for specific hormone receptor testing scenarios

Scenario	Recommended report comment
1–10% of cancer cells ER positive (low positive)	The cancer in this sample has a low level (1–10%) of ER expression by IHC. There are limited data on the overall benefit of endocrine therapies for patients with low-level (1–10%) ER expression, but they currently suggest possible benefit, so patients are considered eligible for endocrine treatment. There are data that suggest that invasive cancers with these results are heterogeneous in both behavior and biology and often have gene expression profiles more similar to ER-negative cancers
Negative (0 or <1%) or low positive (1–10%) and no internal positive controls present but external controls stain	No internal controls are present, but external controls are appropriately positive. If needed, testing another specimen that contains internal controls may be warranted for confirmation of ER status

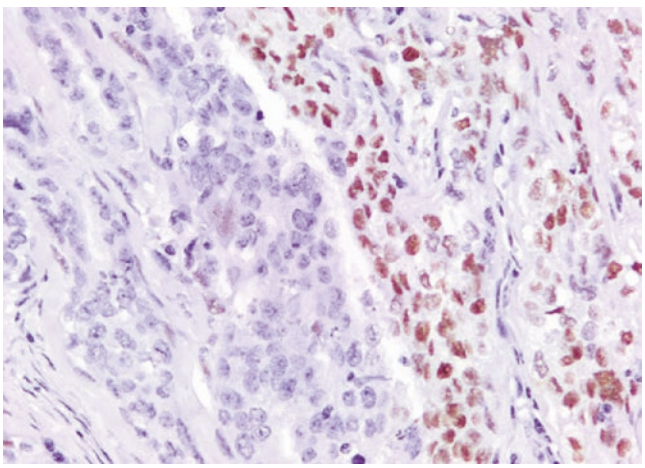

Fig. 22.4 Unusual estrogen receptor expression (patchy, heterogeneous, and in distinct populations) in a breast carcinoma

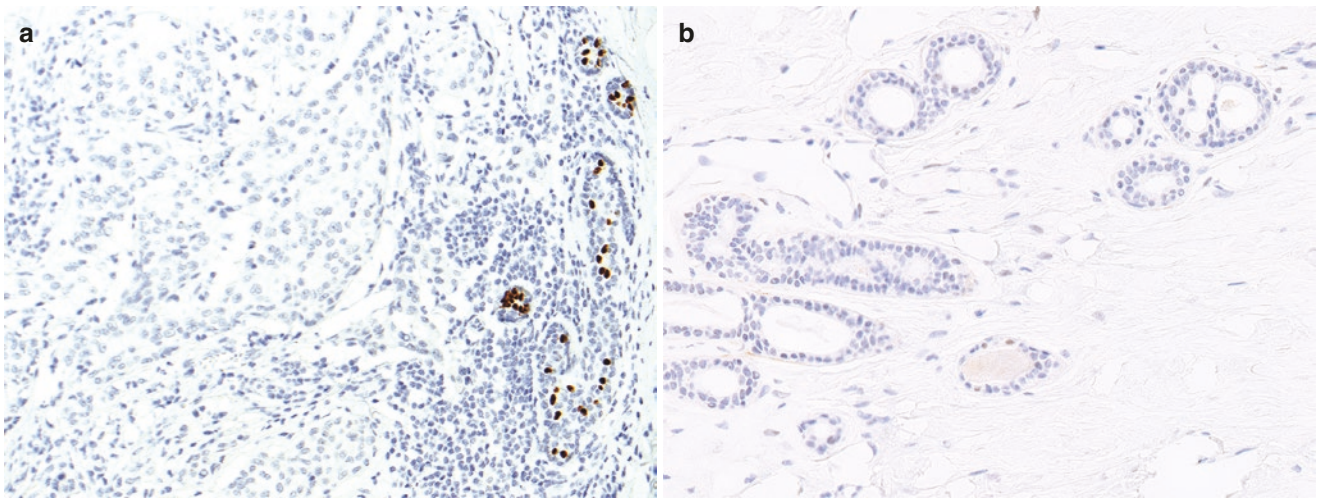

Fig. 22.5 Quality control in ER staining of breast carcinoma (**a**) Example of an ER-negative (0%) high-grade invasive cancer with adjacent positive normal internal controls. The positive internal control helps ensure that the stain worked on the slide and the negative cancer result is valid. (**b**) Normal breast tissue lacking ER staining, which indicates that the stain likely failed. Review of factors that may have affected staining, and repeat testing should occur before interpreting results in cancer tissue when normal internal controls fail to appropriately stain

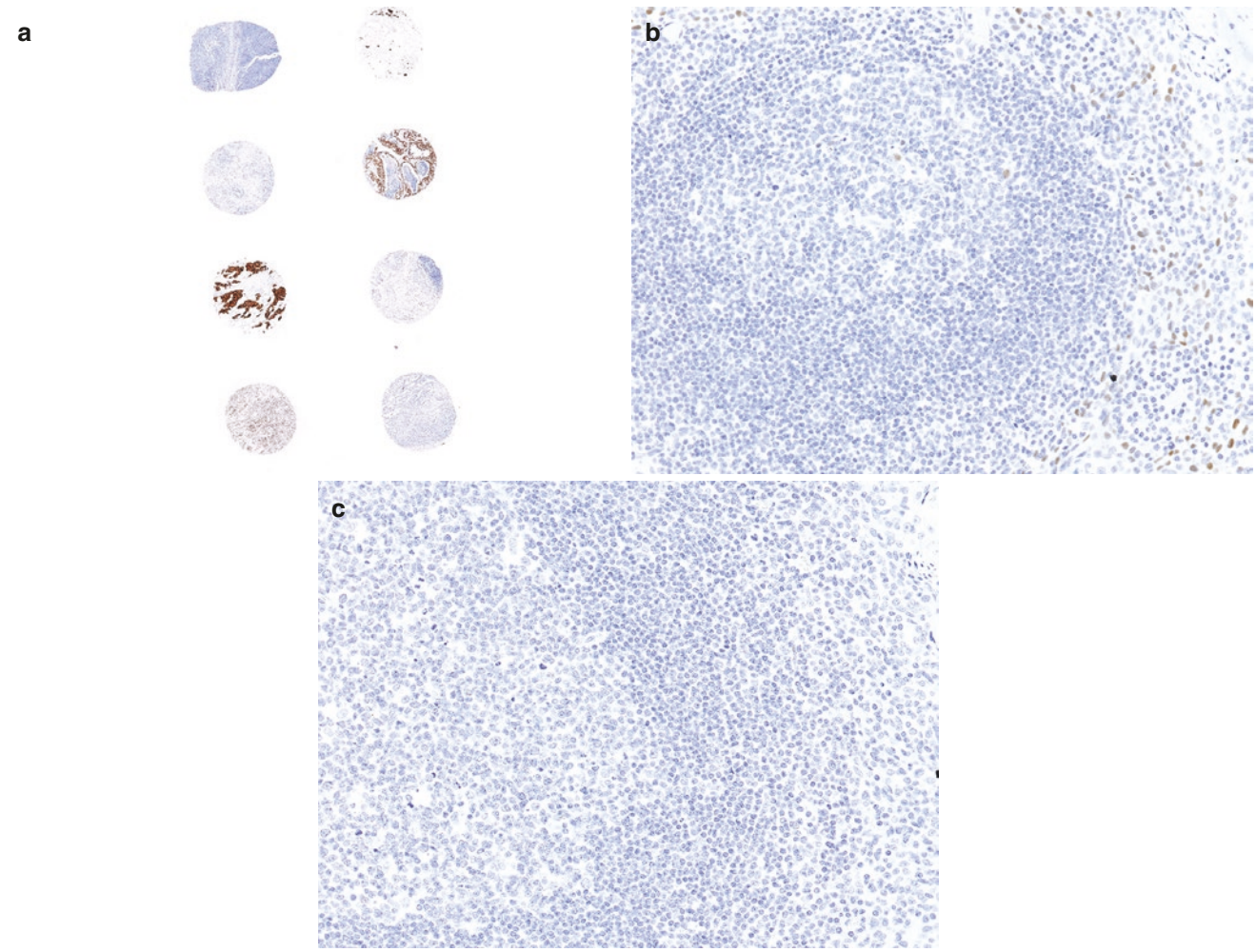

Fig. 22.6 Ideal external controls in ER/PR staining of breast carcinoma. (**a**) Ideal external controls for ER and PR include on-slide controls (such as a tissue microarray as shown) with a variety of expected results (including strong positive, negative, and lower limit of detection-level samples). (**b**) Tonsil is a useful low positive ER control and should stain dispersed germinal center cells and cells in the squamous epithelium. (**c**) There should be no PR staining of tonsil, making it a useful negative control

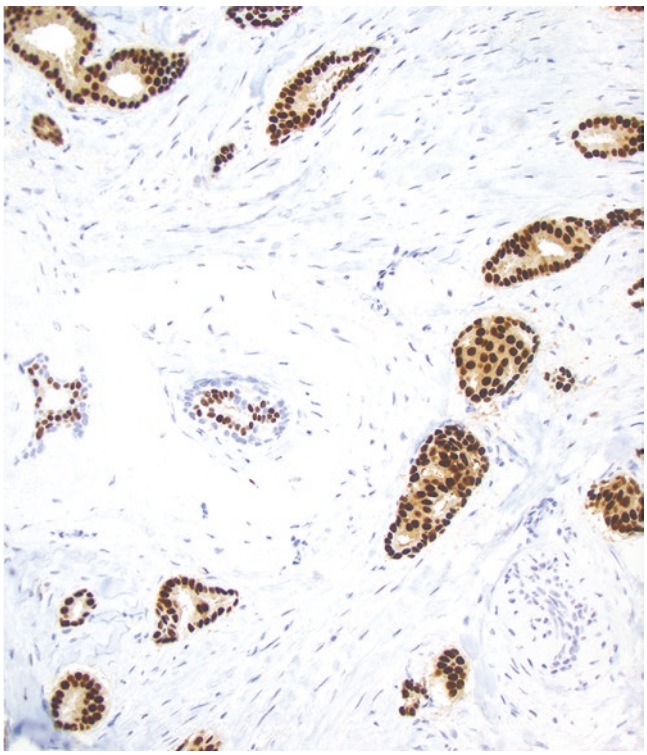

Fig. 22.7 A Nottingham grade 1 invasive ductal carcinoma with >95% of cells with 3+ intense nuclear staining. These results are as expected for a typical grade 1 cancer as well as for classic lobular cancers, tubular carcinoma, cribriform carcinoma, and mucinous carcinomas. Note that the internal controls are also positive but not as uniformly as the ER-driven breast cancer

should be performed and/or cautionary notes should be reported if these tumors fail to express estrogen receptors by immunohistochemistry (Fig. 22.7). Conversely, other special histologic types such as metaplastic carcinomas, adenoid cystic carcinomas, and secretory carcinomas should typically lack hormone receptor expression.

Progesterone receptor expression typically mirrors estrogen receptor expression, often both in intensity and percentage of cell staining, but demonstrates more frequent heterogeneity in expression. ER-negative, PR-positive cancers are rare, and the clinical relevance of these results is not clear since PR is downstream of ER in the hormone-driven pathway. If this occurs, consideration of false-negative ER results, false-positive PR results (check that expected external negative controls such as tonsil are negative), and correlation with other features should occur.

As alluded to in the Introduction, core needle biopsies of breast cancer present an ideal specimen for early predictive marker testing, unless for some reason the amount of tumor is so small that such testing would compromise accurate pathologic diagnosis. Any unexpected, ambiguous, or discrepant results (and negative results, if applicable) can be repeated or confirmed when a larger specimen is obtained, if necessary (except in the setting of neoadjuvant therapy).

Androgen Receptor

Androgen receptor immunohistochemical expression has shown recent promise as a predictive marker in breast cancer in the setting of "triple-negative" (estrogen and progesterone receptor negative and HER2 negative) breast cancer [71, 72] (Fig. 22.8). To date, there are no accepted testing guidelines for androgen receptor testing; laboratories that perform the testing most frequently apply ASCO/CAP criteria for estrogen and progesterone receptor testing in the absence of formal criteria.

Limitations and Pitfalls

If an accredited laboratory meets ASCO/CAP validation criteria and follows the ASCO/CAP guidelines, pitfalls in and limitations to hormone receptor testing are generally rare. The pathologist should ensure that they (or their imaging analysis system) are scoring the appropriate cancer cells and not background lymphocytes or stroma that may stain with ER (Fig. 22.9). To adequately evaluate for weakly positive tumors, microscopic (or computer image) evaluation should be conducted on medium to high magnification, rather than scanning magnification (Fig. 22.10). Many core needle biopsies of breast cancers will fortuitously contain normal breast tissue, allowing for confirmation of positive internal control of antibody expression in addition to routine positive external control expression. As discussed above, it may be helpful in cases with 0–10% ER to ask a second pathologist to confirm the finding, which can be a component of the laboratory-specific standard operating procedure recommended by ASCO/CAP for these cases. Repeat staining on larger specimens or subsequent tissue in the setting of negative hormone expression in a core needle biopsy can also be warranted. In the metastatic setting, non-formalin fixatives or decalcification can cause false-negative results, and if the stain is not validated in this setting, results need to be reported with disclaimers that negative results may be invalid.

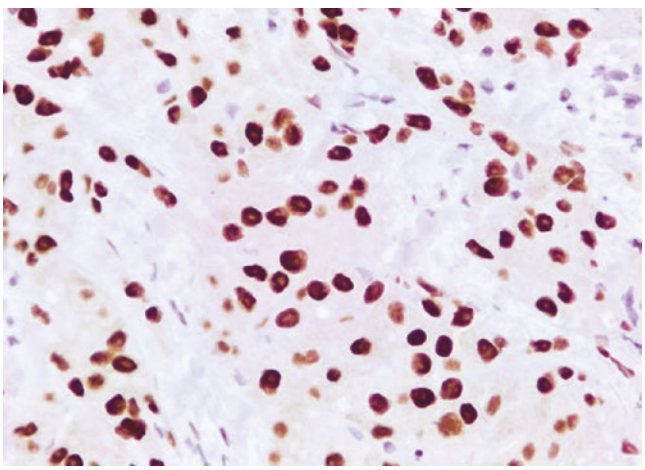

Fig. 22.8 This case shows strong androgen receptor expression in a poorly differentiated triple-negative invasive breast cancer

HER2

The discovery and therapeutic targeting of the HER2 (human epidermal growth factor receptor 2) molecule were a breakthrough in the treatment of one of the most aggressive forms of breast cancer. HER2 is a member of a family of growth factor receptors that regulate normal cell proliferation, development, and survival. While HER2 is expressed at low levels in normal breast ductal cells, approximately 10–15% of breast cancers significantly overexpress HER2 as a consequence of amplification of the HER2 gene on chromosome 17.

HER2 is also both a prognostic and predictive factor in breast cancer. HER2 protein overexpression can result in the promotion of more aggressive cancer biology and worse prognosis. In addition to being prognostic, HER2 is a powerful predictive factor as it is used to select which patients might benefit from HER2-targeted therapies in combination with chemotherapy [73–78]. The discovery and advent of targeted anti-HER2 therapy were all the more impactful because HER2-overexpressing tumors typically fail to express hormone receptors, leaving standard cytotoxic chemotherapy as the only treatment option up until the age of anti-HER2 therapy. However, HER2-targeted agents are currently still given only in combination with chemotherapy.

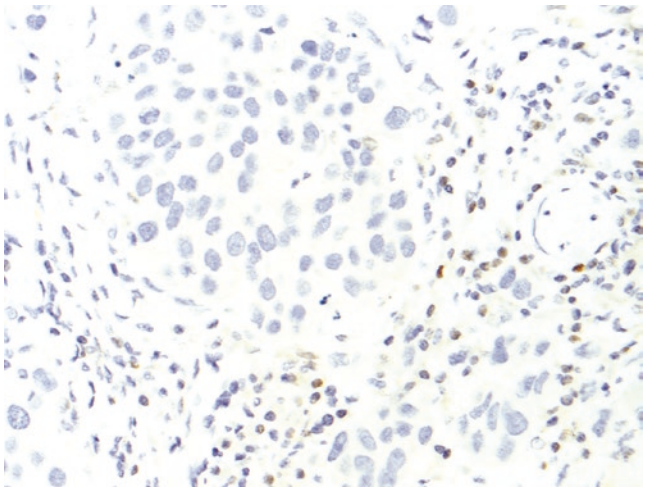

Fig. 22.9 An ER stain of a high-grade invasive cancer with abundant associated tumor-infiltrating lymphocytes. The larger invasive cancer cells are negative for ER staining, and the associated lymphocytes are expressing ER. Care should be taken that only the appropriate cancer cells are scored

The first HER2-targeted drug to be approved in the adjuvant setting in 2006 was the humanized monoclonal antibody, trastuzumab, which is believed to bind HER2 and block downstream signaling pathways [79]. With the expansion of HER2 antibody-directed therapeutic agents available, options for higher risk HER2-positive cancers today include dual blockage with two HER2 antibody therapies neoadjuvantly and treatment with novel HER2 antibody-drug conjugates (such as TDM-1) when there is residual disease post-neoadjuvant treatment [37, 76, 77]. Recently, HER2 antibody-drug conjugates are also being used in the metastatic setting on cancers that are HER2 negative but have low levels of HER2 protein expression (IHC 1+ or 2+, ISH negative).

HER2 testing in breast cancer can be performed by immunohistochemistry (evaluating expression at the protein level) and/or in situ hybridization (evaluating amplification at the gene level). Examples of positive and negative results by both IHC and FISH are shown in Fig. 22.11. If there is an IHC equivocal result (2+ staining), the case is referred for in situ hybridization (either in-house or at a reference laboratory). Figure 22.12 shows the typical testing algorithm if IHC is performed first. In the vast majority of cases, positive

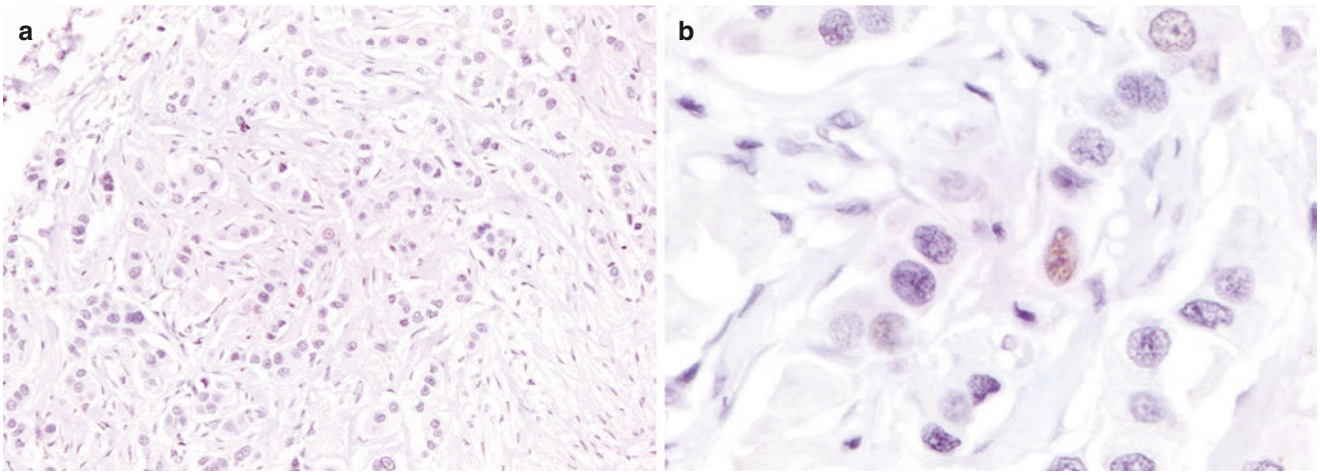

Fig. 22.10 Weak estrogen receptor expression at scanning (**a**) and high magnifications (**b**). Reviewing such cases at scanning magnification without higher magnification examination is a pitfall, causing potential under-recognition of estrogen receptor reactivity

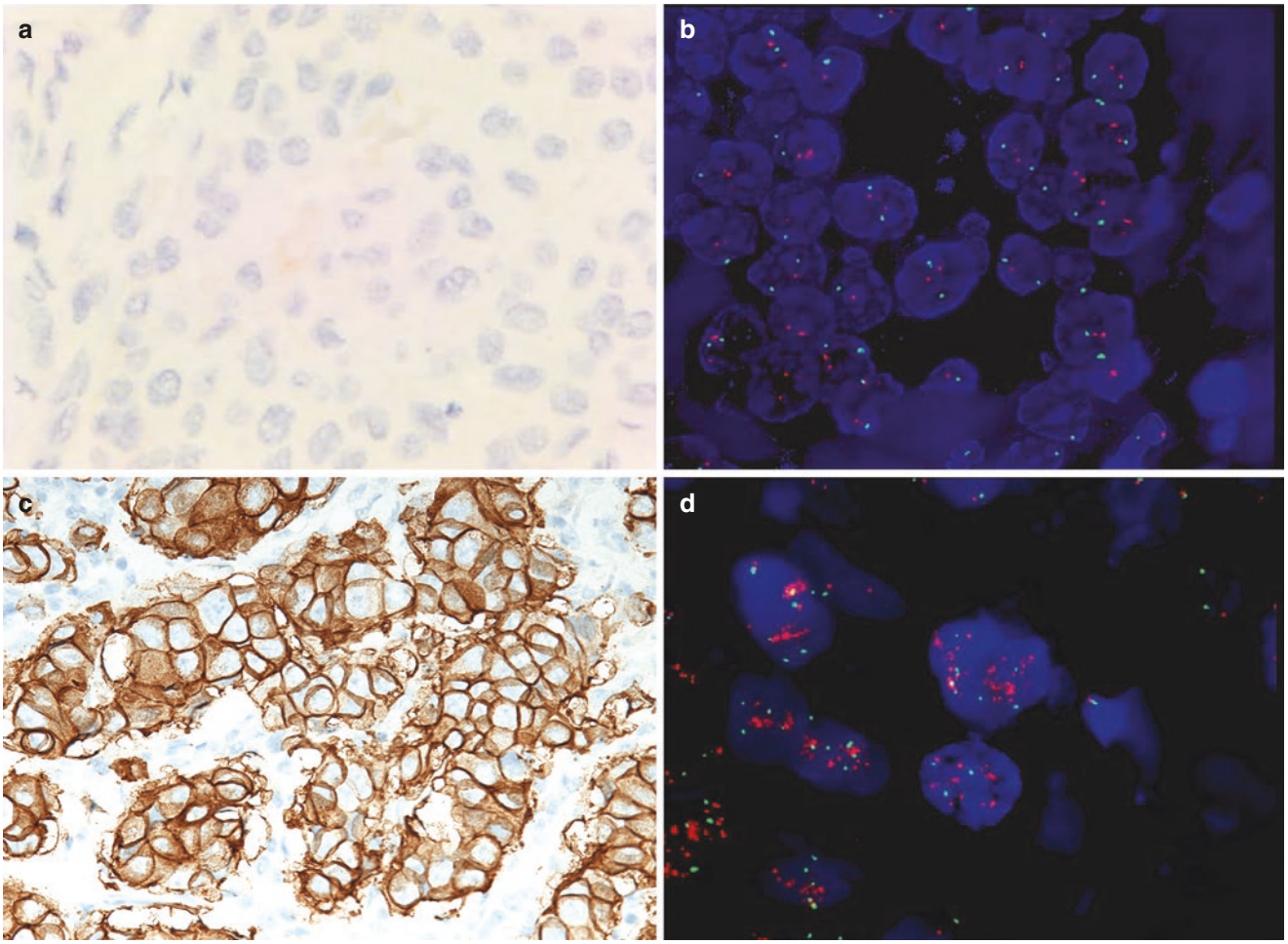

Fig. 22.11 Straightforward, concordant positive and negative HER2 results by both immunohistochemistry and fluorescence in situ hybridization. (**a**, **b**) HER2-negative carcinoma with no membranous staining on IHC (**a**) and the normal two red HER2 gene probe signals (and two green CEP17 control signals) per cell; (**c**, **d**) HER2-positive carcinoma. The brown membranous staining is strong in intensity and circumferential on the IHC stain (**c**), and the red-labeled HER2 gene probe on FISH (**d**) shows that many copies are present per cell (control CEP17 probe is green). When IHC is 2+ equivocal, reflex to in situ hybridization testing should be performed

and negative results by both methods are concordant. Despite older literature that may suggest otherwise, with the publication and widespread adoption of ASCO/CAP HER2 testing guidelines, "local" (potentially smaller laboratories at the site of originating diagnosis) and "central" (usually larger, high-volume testing laboratories) concordance is also present in the majority of cases [80, 81]. Furthermore, concordance between HER2 testing results on core needle biopsy and excisional tissue since the ASCO/CAP guidelines has repeatedly been shown to be very high, such that mandatory repeat testing of tumors (even high-grade tumors) previously HER2 negative on core needle biopsy is no longer considered a mandate and only needs to be considered if there was a limited initial sample, artifacts, and unusual or inconclusive results [82, 83].

Pathologists must determine, based on their available resources, budgets, experience, and qualifications, whether and how breast cancers will be tested for HER2 within their laboratory. The prevalence and familiarity with immunohistochemistry, as well as its relatively inexpensive operating costs and no need for specialized equipment, make HER2 immunohistochemistry a popular testing modality. Laboratories that successfully operate fluorescence in situ hybridization (FISH) tend to easily adopt HER2 FISH testing into their workflow; FISH testing certainly requires additional technical expertise and more specialized and expensive equipment such as fluorescence microscopes. More recently, in situ hybridization can be detected chromogenically or by using silver-enhanced detection (chromogenic in situ hybridization, or CISH, and silver-enhanced in situ hybridization, or SISH), such that fluorescence microscopy is not needed (Fig. 22.13). However, this method is not without its own pitfalls [84]. When the results of these methods are in doubt, IHC and FISH testing should be performed for confirmation of this critical test.

HER2 test results should also be correlated with the original histology, even when using a reference laboratory for

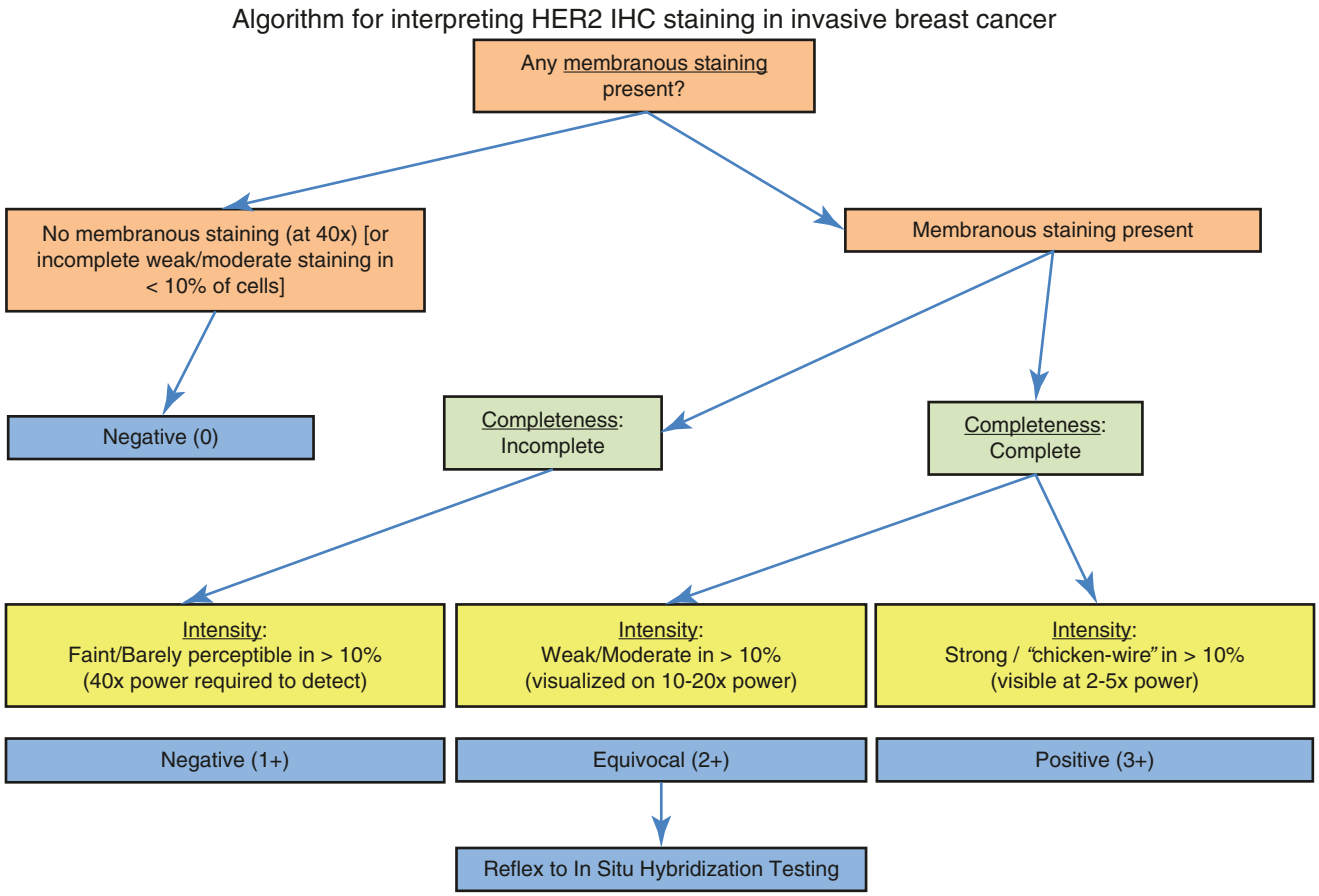

Fig. 22.12 HER2 test interpretation algorithm by IHC. First evaluate for membranous staining. If absent at high power (40×), the IHC is interpreted as negative (0). If there is membranous staining present but it is incomplete and faint/barely perceptible (need to evaluate at 40× to detect), then the stain is interpreted as negative (1+). If there is circumferential membranous staining in >10% of cells but it is weak to moderate in intensity (seen at 10–20×), the stain is interpreted as equivocal (2+), and reflex in situ hybridization testing needs to be performed for final overall HER2 results. If there is strong/intense (visible at 2–5×) circumferential staining, the stain is interpreted as positive (3+). Note that unusual staining patterns do exist that are not covered in this flowchart, such as incomplete but moderate-to-intense staining (which can occur in micropapillary carcinomas)—which should be interpreted as 2+ and reflexed to in situ hybridization testing. Cases with clustered populations with different results are another unusual scenario (see text)

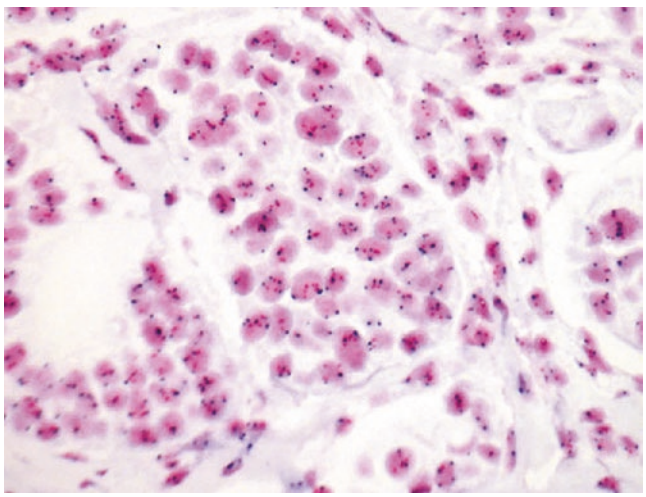

Fig. 22.13 HER2 chromogenic in situ hybridization (HER2-positive case). Evaluation requires high-magnification review. Red/pink signals are HER2; blue signals are CEP17

HER2 testing. For example, it is very unusual for a low-grade invasive carcinoma of any histologic type as well as the favorable histologic types such as tubular, mucinous, or adenoid cystic carcinomas to be HER2 positive. In addition, grade 1 invasive ductal or lobular carcinomas are typically not HER2 positive. If this occurs, additional workup should be performed to ensure the accuracy of both HER2 and other pathologic parameters. The typical HER2-positive cancer is intermediate to high grade, often with abundant eosinophilic cytoplasm or apocrine cytology, and demonstrates a high proliferation index (generally 20% or higher). HER2-positive cancers commonly present in younger patients and often with associated high-grade DCIS. However, these features are not considered specific for HER2 positivity, and as such, a HER2-negative case with these characteristics is not necessarily an unexpected or discordant result.

As with hormone receptor testing, ASCO/CAP have released clinical guidelines applying to HER2 testing in

breast cancer with updates to the original 2007 HER2 testing guideline in both 2013 and 2018 [7, 8, 10, 13, 14, 85, 86]. Many of the recommendations regarding pre-analytic factors impacting testing are identical for hormone receptors and HER2. Most laboratories performed HER2 by IHC as an initial screening test, with reflex to in situ hybridization testing only if the results are 2+ equivocal. However, some laboratories perform either in situ hybridization up front with IHC as a reflex only if there are unusual group results. Lastly, a growing minority of laboratories routinely perform both IHC and ISH testing on all cases. The HER2 testing practice will determine the frequency of some of the less common HER2 result scenarios (such as ISH Groups 2–4 and heterogeneous cases, which will be described below) [87]. Reporting comments are recommended to clarify issues with these unusual HER2 ISH result categories, so clinicians and patients can better understand when the HER2 status is nonstandard (see below).

CAP requires proof of initial validation of any new HER2 test with a previously clinically validated test. Ideally, concordance between IHC and ISH assays should be >95%. Ongoing concordance monitoring should be part of quality assurance. In addition, performing periodic trend analysis can be helpful to ensure that the percentage of HER2-positive cases are within the range of what is expected for the population being tested. Regional differences in the percentage of HER2-positive cancers have been reported, and it can be helpful to compare laboratories with similar population characteristics to one another [88, 89]. In addition, proficiency testing should be ongoing (at least twice/year) with at least 90% performance on graded challenges.

HER2 Testing by Immunohistochemistry

HER2 immunohistochemistry can be routinely incorporated into pathology practice, as most medium- to large-sized and even small laboratories and hospitals already perform immunohistochemistry on a daily basis for diagnosis. Most clinical, CAP-accredited laboratories that perform immunohistochemistry in this day and age use automated staining platforms and commercially available antibodies, which inherently contributes to a significant amount of standardization, reproducibility, and reliability to the testing. In the 2018 update of the CAP/ASCO HER2 testing guidelines, a greater emphasis on using IHC to guide interpretation and testing of unusual ISH categories was recommended [13, 14].

Interpretation

HER2 immunohistochemical stain interpretation requires an evaluation of the completeness (circumferential completeness) and intensity of membrane staining of tumor cells (Table 22.4; Fig. 22.14). Examples of the range of IHC results are shown in Fig. 22.14. Cases interpreted as equivocal or 2+ by immunohistochemical staining must be tested by an alternate method, the most commonly used of which is in situ hybridization. Overinterpretation of stain intensity is one of the most common causes of discordance between HER2 immunohistochemistry (positive) and in situ hybridization (negative) [90, 91]. Positive (3+) cases should show thickness and intensity of circumferential membrane staining to the point that the cell membranes stand out like "chicken wire." Careful medium- to high-magnification examination may be necessary to determine the completeness or incompleteness of circumferential staining in what

Table 22.4 HER2 IHC and ISH interpretation and reporting guidelines (2018 ASCO/CAP)

IHC	Positive	Circumferential membrane staining that is complete, intense, and in >10% of tumor cells
	Equivocal	Weak-to-moderate complete membrane staining observed in >10% of tumor cells
	Negative	Incomplete membrane staining that is faint/barely perceptible and in >10% of tumor cells (1+)
		No staining is observed or membrane staining that is incomplete and is faint/barely perceptible and in ≤10% of tumor cells (0)
In situ hybridization (dual probe)	Positive	HER2/CEP17 ratio ≥2.0 and average HER2 copy number ≥4.0 signals/cell (**Group 1**)
	Positive (based on IHC and ISH results, see comment)	HER2/CEP17 ratio ≥2.0 and average HER2 copy number <4.0 signals/cell (**Group 2**) **and concurrent IHC 3+**
		HER2/CEP17 ratio <2.0 and average HER2 copy number ≥6.0 signals/cell (**Group 3**) **and concurrent IHC 2+ or 3+**
		HER2/CEP17 ratio <2.0 and average HER2 copy number ≥4.0 and <6.0 signals/cell (**Group 4**) **and concurrent IHC 3+**
	Negative (based on IHC and ISH results, see comment)	HER2/CEP17 ratio ≥2.0 and average HER2 copy number <4.0 signals/cell (**Group 2**) **and concurrent IHC 0–1+ or 2+**
		HER2/CEP17 ratio <2.0 and average HER2 copy number ≥6.0 signals/cell (**Group 3**) **and concurrent IHC 0–1+**
		HER2/CEP17 ratio <2.0 and average HER2 copy number ≥4.0 and <6.0 signals/cell (**Group 4**) **and concurrent IHC 0–1+ or 2+**
	Negative	HER2/CEP17 ratio <2.0 and average HER2 copy number <4.0 signals/cell (**Group 5**)

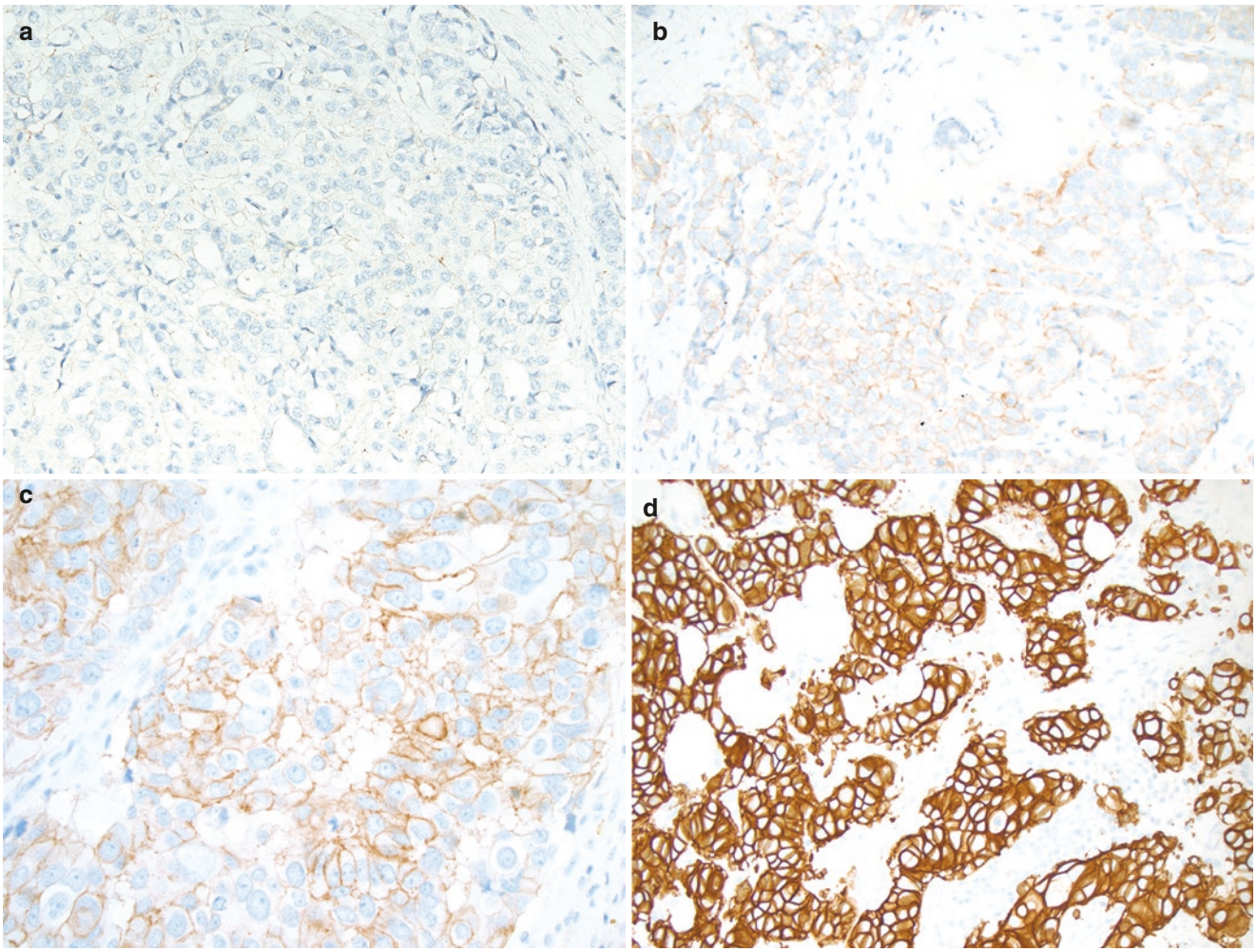

Fig. 22.14 Range of HER2 immunohistochemistry: (**a**) Negative (0) HER2 stain; (**b**) negative (1+) stain (faint, incomplete staining in more than 10% of tumor cells); (**c**) equivocal (2+) stain (incomplete, moderate staining in greater than 10% of cells); (**d**) positive (3+) (strong, complete, circumferential staining in virtually all cells). To call a case 3+ staining, the intensity of stain should be easily seen on low power. If there is any doubt about the intensity being strong enough (compared to positive controls), the stain should be interpreted as 2+ and reflexed to in situ hybridization testing. For Group 2–4 comments see Table 22.5

proportion of cells in less intensely staining cases (determine HER2 1+ vs. 2+).

The comparison of stain intensity with negative (0–1+) and positive (3+) controls should serve as a reference for intensity measures. The following is another handy guide when using a 10× ocular: staining noted with a 2–5× objective can be considered strong 3+ intensity, staining detected using a 10–20× objective can be considered weak-moderate (1–2+), and staining detected only on 40× magnification can be considered faint/barely perceptible.

Limitations and Pitfalls

Perhaps the greatest challenge in HER2 immunohistochemistry is subjectivity in assessing the intensity of staining, which is rather unique in immunohistochemistry to HER2 testing. More so than with hormone receptors, HER2 immunohistochemistry may be subject to edge staining artifact on core needle biopsy due to the relatively thin cores of tissue; this type of staining is typically less intense, less circumferential, and more patchy than true protein overexpression and should not be included in the overall interpretation of the

stain. Crush artifact can cause disruption of the cell membranes and should not be overinterpreted (Fig. 22.15) (when severe, the stain can be interpreted as insufficient due to artifact and reflexed to in situ hybridization testing). It should be remembered that if artifacts are severe or other pre-analytical or analytical issues are present, the test can be interpreted as insufficient with deferral to in situ hybridization testing. Cytoplasmic staining can also occur and obscure the intensity of membrane staining. These cases should also be interpreted as IHC equivocal (2+) with subsequent reflex testing (Fig. 22.16). In the metastatic setting, accurate identification of patients with low levels of HER2 protein expression will remain a challenge since this test is not optimized for this purpose. Since currently patients with HER2 IHC 0 results are not eligible for treatment with some of the newer HER2 antibody-drug conjugates that have activity in cancers with as low as IHC 1+ expression (ex. trastuzumab-deruxtecan), attempts should be made to ensure proper pre-analytic parameters and reproducible interpretation of 0 vs 1+ IHC results in this setting.

Interpreters should be aware of unusual staining patterns. Incomplete but moderate-to-strong membranous staining can occur in micropapillary cancers and should be considered 2+ equivocal with reflex to in situ hybridization testing since some of these cases can be gene amplified (Fig. 22.17). Discordant results with histology (e.g., a grade 1 cancer with 3+ HER2 staining) should also be further evaluated prior to reporting a final result [91]. Again, if there is any doubt about the results, reflex in situ hybridization should be performed. Rarely (<3% of cases), HER2 staining will reveal distant clustered cell populations with different HER2 results. These cases are considered HER2 heterogeneous. If one population is 3+ positive by IHC, the percentage of the overall population of invasive cancer in the sample should be reported: for example, "heterogeneous for HER2 overexpression with 50% of the sample 3+ positive." The IHC status of the second population should also be reported, and if equivocal, in situ hybridization testing can be considered. Per guidelines,

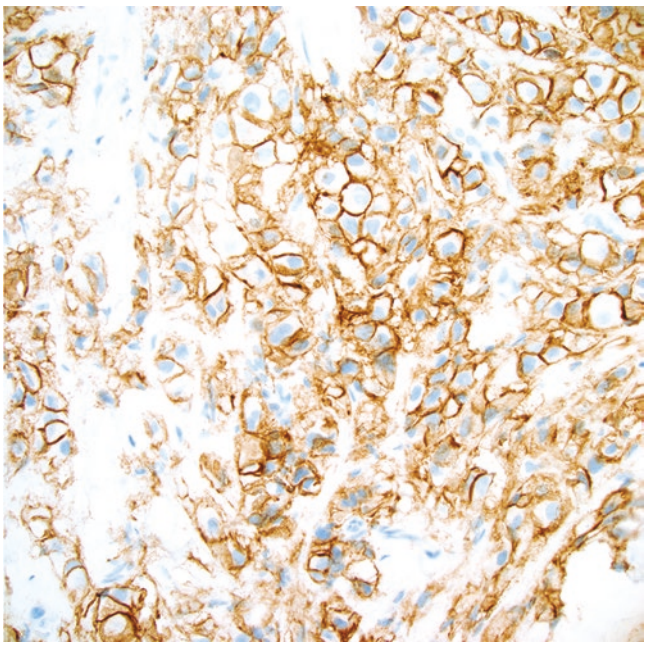

Fig. 22.15 Crush artifact-disrupting membranous HER2 staining. Areas with crush artifact should be avoided in the interpretation of the HER2 stain. If there are not areas with well-preserved cell membranes, the stain may be interpreted as insufficient due to crush artifact, and reflex testing by in situ hybridization should occur (or testing by IHC of another sample without crush artifact)

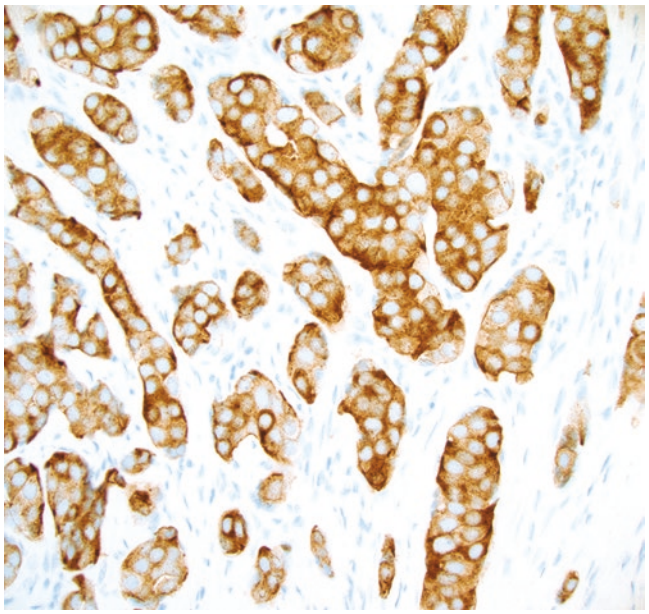

Fig. 22.16 Granular cytoplasmic staining is obscuring the evaluation of the membrane staining for HER2. This case should be interpreted as IHC equivocal (2+) and reflexed to in situ hybridization testing

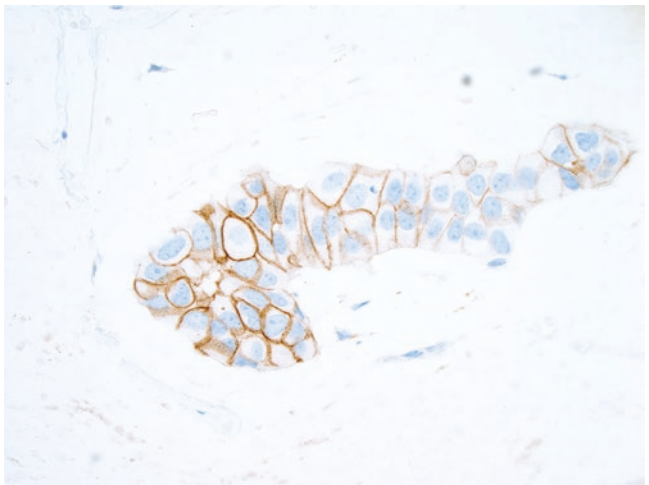

Fig. 22.17 Incomplete moderate-intensity basal-lateral HER2 IHC staining is present in this micropapillary carcinoma. This is an uncommon staining pattern to be aware of and should be interpreted as equivocal (2+) since some of these cases are positive for HER2 gene amplification

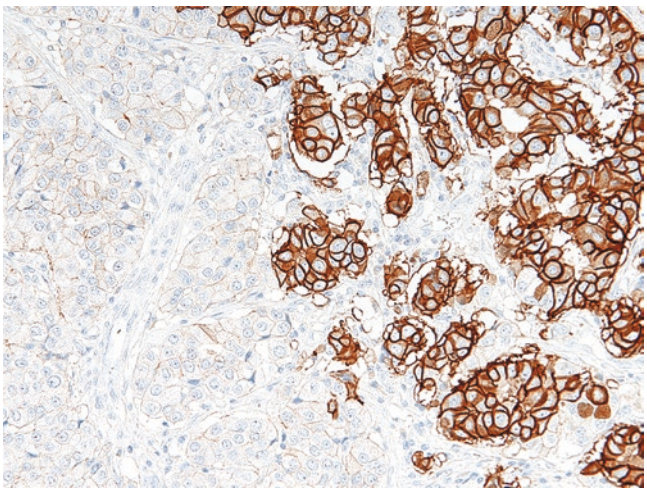

Fig. 22.18 A case with heterogenous HER2 protein expression. Distinct separate, clustered populations are present, with 3+ positive staining on the right and 1+ negative staining on the left of the image

if the 3+ population is >10% of the overall population of cancer cells, then the sample is considered HER2 positive and the patient is eligible for HER2-targeted therapy. If the positive population is <10% in the sample tested, there should be consideration for testing additional samples to see if the population increases. There is limited data on the clinical outcomes of HER2 heterogeneous cases because of their rarity, but because they are not uniformly HER2 driven, they may not respond the same as a typical uniformly positive case. If in situ hybridization is to be performed on a heterogeneous case, care should be taken to indicate to the cytogenetics lab the specific areas with different IHC results to be counted and resulted in the final report (Fig. 22.18).

HER2 Testing by In Situ Hybridization

HER2 in situ hybridization usually requires a longer incubation period and increased technical, equipment, and/or personnel resources as compared to HER2 immunohistochemistry. A fluorescent-labeled DNA probe to the HER2 gene as well as a control centromeric probe (CEP17) are used in the standard dual-probe FISH assays. The number of HER2 signals per cell and the CEP17 probe are reported as a HER2:CEP17 ratio as well as the absolute HER2 and CEP17 per cell counts and the results are reported as HER2 positive or negative based on guideline recommendations (see below).

A critical first step for FISH testing is to have a pathologist identify which area of the slide to score such that only the invasive carcinoma is scored. The presence of large areas of in situ carcinoma or other findings can confound results if this is not done carefully. Only invasive carcinoma should be scored. The areas with invasion on the slide are scanned at low power under the fluorescence microscope to get an overview of the findings and to identify if there is more than one population of cells with variable numbers of signals/cell. Per the CAP/ASCO HER2 testing guidelines, the pathologist must perform this review prior to counting of the slide or, alternatively, IHC can be used as the pathologist's screening method to identify any areas of protein overexpression that should be counted specifically [7]. If present in >10% of the overall cell population, these clustered foci of amplified cells are counted separately from the rest of the invasive cancer cell population. Clustered heterogeneity is rare, estimated to occur in less than 1% of cases; however, it is important to rule out [87, 92, 93]. Most cases have more uniform findings.

After scanning the slide, at least two areas are counted at high power (oil immersion) for a total of minimum 20 cells (at least 10 cells from each area counted). The individual cell counts are recorded, but in contrast to some FISH assays in which any detectable abnormality counts as a positive result, HER2 FISH results are reported as a cell population average. The criteria for positive, negative, and equivocal results by FISH testing have changed slightly between the 2007, 2013, and 2018 updates to the HER2 ASCO/CAP guidelines [7, 13, 86]. The most current 2018 HER2 FISH interpretation criteria are shown in Table 22.4. Reported results should include the overall HER2:CEP17 ratio, the mean HER2 signals/cell, and the mean CEP17 signals/cell.

There are five groups of possible results by in situ hybridization as per the 2018 CAP/ASCO HER2 testing guidelines update. The majority of cases will fall in the Group 5 category with a ratio <2.0 and <4.0 mean HER2 signals/cell. These are straightforward negative results and can be reported as such without additional workup. Similarly, Group 1 results with a ratio >2.0 and >4.0 mean HER2 signals/cell are typically straightforward HER2-positive results. However, cases with initial in situ hybridization results in Groups 2–4 require additional workup, beginning with correlation with HER2 results by IHC. These results should be performed on the same sample/tissue block and ideally by the same laboratory if they perform IHC. The IHC results are then used to aid in the overall interpretation of the case as HER2 positive or negative (see below for specific interpretations for each group). If the IHC is 2+ (equivocal), the in situ hybridization test should be evaluated by a second observer, blinded to the previous ISH results, and at least 20 additional cells should be counted. The areas with the strongest IHC staining should be included in this count. If including this new count in the overall ISH results changes the result group, this new category is used for the final result.

The 2018 guidelines update also recommends including a comment in the report when a Group 2–4 final result is negative based on IHC results. This comment should reflect that clinical correlation with other patient factors, including pathologic features of the patient's cancer (such as ER expression and grade) as well as test results from other specimens, may be used when selecting appropriate treatments.

Table 22.5 Recommended standardized comments for HER2 dual probe in situ hybridization Groups 2–4

HER2 ISH result group	Comment
Group 2 (HER2/CEP17 ratio ≥2.0 and average HER2 copy number <4.0 signals/cell)	This case has an unusual Group 2 HER2 result. Final ISH results were based on concurrent review of IHC, with recounting of the ISH test by a second reviewer if IHC is 2+ (per 2018 CAP/ASCO update recommendations). Evidence is limited on the efficacy of HER2-targeted therapy in the small subset of cases with HER2/CEP17 ratio ≥2.0 and an average HER2 copy number <4.0/cell. In the first generation of adjuvant trastuzumab trials, patients in this subgroup who were randomized to the trastuzumab arm did not appear to derive an improvement in disease-free or overall survival, but there were too few such cases to draw definitive conclusions. IHC expression for HER2 should be used to complement ISH and define HER2 status. If IHC result is not 3+ positive, it is recommended that the specimen be considered HER2 negative because of the low HER2 copy number by ISH and lack of protein overexpression.
Group 3 (HER2/CEP17 ratio <2.0 and average HER2 copy number ≥6.0 signals/cell)	This case has an unusual Group 3 HER2 result. Final ISH results were based on concurrent review of IHC, with recounting of the ISH test by a second reviewer if IHC is 2+ (per 2018 CAP/ASCO update recommendations). There are insufficient data on the efficacy of HER2-targeted therapy in cases with HER2 ratio <2.0 in the absence of protein overexpression because such patients were not eligible for the first generation of adjuvant trastuzumab clinical trials. When concurrent IHC results are negative (0–1+), it is recommended that the specimen be considered HER2 negative.
Group 4 (HER2/CEP17 ratio <2.0 and average HER2 copy number ≥4.0 and <6.0 signals/cell)	This case has an unusual Group 4 HER2 result. Final ISH results were based on concurrent review of IHC, with recounting of the ISH test by a second reviewer if IHC is 2+ (per 2018 CAP/ASCO update recommendations). It is uncertain whether patients with ≥4.0 and <6.0 average HER2 signals/cell and HER2/CEP17 ratio <2.0 benefit from HER2-targeted therapy in the absence of protein overexpression (IHC 3+). If the specimen test result is close to the ISH ratio threshold for positive, there is a high likelihood that repeat testing will result in different results by chance alone. Therefore, when IHC results are not 3+ positive, it is recommended that the sample be considered HER2 negative without additional testing on the same specimen.

The standardized comments are listed in Table 22.5. If the case is particularly challenging, consultation with a breast pathology specialist or reference laboratory with expertise in challenging HER2 ISH testing may be helpful. While the use of alternative probes may be a part of a consultative workup, they are not recommended as a required component of standard practice in the workup of these ISH cases.

Limitations and Pitfalls

While HER2 testing in breast cancers is straightforward in the majority of cases, the less common in situ hybridization groups can create added complexity to testing and interpretation. In addition, cases close to a result category threshold can be expected to have variability between samples, observers, and labs. Cases with low-level HER2 amplification (ratio >2.0 but only 4.0–5.9 mean HER2 signals/cell) are also a challenge to interpret when they occur in the setting of a negative IHC result [87, 94]. A multidisciplinary discussion can be helpful when treatment decisions are challenging. HER2 testing guidelines will also continue to evolve as additional evidence helps clarify which patients may benefit most from treatment.

Molecular Subtyping

A separate Chap. 23 in this book discusses the newest evolving molecular technologies and tests in breast cancer to date, but a brief mention of "molecular subtyping" as popularized by landmark gene expression array studies is warranted at this point [95]. Terms and clinical categories such as "luminal A," "luminal B," "HER2," and "basal/triple negative" have rapidly become routine clinical and pathologic (and even patient) language that succinctly bins cancers into clinically convenient and relevant groups. While these subtypes were originally applied to gene expression data obtained from hierarchical studies of fresh frozen tumor RNA, the pathology and clinical communities alike quickly generalized and adapted them to cancer subgroups characterized by widely available and standardized immunohistochemistry and/or in situ hybridization clinical tests alone (Table 22.6) [96].

Proliferation

Proliferation has almost always been an integral component of breast cancer, given its intimate role in grading tumors and its obvious biologic importance as a driver of tumor behavior. Histologic tumor grading is founded in H&E examination for mitotic figures over a given tumor surface area; this routine pathologic practice has generally high interobserver reproducibility. With the advent and widespread use of immunohistochemistry, utilizing Ki67 (MIB1) and other antibodies that detect dividing cells became a popular practice. The routine addition of Ki67 immunohistochemistry to hormone receptor and HER2 testing in breast cancer is felt by many to be a cost-effective, simple mechanism to readily provide enhanced clinical information that is a close surrogate to molecular subtype. Because ER-negative/HER2-positive, and ER-negative/HER2-negative cancers are highly proliferative (30–100% Ki67 proliferative rates), these cancers are more rapidly growing and are more often treated with chemotherapies. But ER-positive cancers have a wider range of proliferation rates, with highly proliferative forms

Table 22.6 Molecular subtypes approximated by immunohistochemical phenotypes

Molecular subtype	Immunophenotype	Comments
Luminal A	ER positive, HER2 negative, Ki67 low	Quality control for Ki67 and thresholds for determining luminal subtype not fully established
Luminal B HER2 negative	ER positive, HER2 negative, Ki67 high	Quality control for Ki67 and thresholds for determining luminal subtype not fully established
Luminal B HER2 positive	ER positive, HER2 positive	
HER2 non-luminal	ER negative, HER2 positive	
Basal-like	ER negative, PR negative, HER2 negative	Please see the chapter for discussion on rare ER-negative, PR-positive carcinomas; for the purpose of this approximation, such tumors should probably be considered of luminal subtype

correlated with more aggressive behavior but the majority having proliferative rates below 20%.

There are associations between Ki67 expression levels and both prognosis and prediction—specifically in hormone receptor-positive breast cancer. Most studies show that among hormone receptor-positive cancers, the higher the Ki67, the worse the long-term survival but the higher the likelihood of pathologic complete response to neoadjuvant chemotherapy. One challenge is that, unlike ER or HER2, the expression of Ki67 is not bimodal, and there is no natural threshold to define "high" or "low" Ki67 status. Different studies have used different definitions of high Ki67, which makes interpretation of the literature challenging. A threshold of 15% has been used for helping to discriminate between cases likely to correlate with the more aggressive "luminal B" molecular subtype (>15% Ki67) vs. the less aggressive "luminal A" subtype (<15% Ki67). However, this threshold has not been validated for the purposes of predicting response to chemotherapy. Panel-based gene expression assays that are largely proliferation driven, such as the 21-gene recurrence score (Oncotype DX, see below) have been more extensively validated for this purpose in ER-positive breast cancers. Recently, a threshold of Ki67 > or = to 20% was approved to identify high risk lymph node positive, ER positive, HER2 negative breast cancer patients that might benefit from the addition of CDK 5/6 inhibitor, abemaciclib, to treatment regimens [33]. While in the clinical trial patients with all Ki67 values had some benefit from treatment, the 20% threshold was prognostic of worse outcomes, so it was approved as a companion diagnostic to identify the highest risk group (using the MIB-1 antibody on the Dako Omin platform).

Interobserver and interlaboratory variability in Ki67 assessment has prevented its widespread adoption as a prognostic marker in breast cancer. In the past decade, the International Ki67 in Breast Cancer Working Group has attempted to standardize Ki67 testing [30, 97–99]. The group recently reported that expression levels of Ki67 <5% or >30% can be reliably reported, but levels between those thresholds are unreliable [30]. It appears that Ki67 IHC results are most reproducible at the extreme ends of the spectrum (e.g., Ki67 <5% or >30%). Therefore, Ki67 results should be interpreted in the context of other variables including age, grade, extent of ER positivity, size, and nodal status.

In the neoadjuvant endocrine therapy clinical trial setting, Ki67 has been used to guide adjuvant systemic therapy recommendations for postmenopausal women. In one trial, patients whose tumors had Ki67 expression levels were <10% prior to any systemic therapy or that decreased to <10% after 2 weeks of neoadjuvant aromatase inhibitor therapy had a lower 5-year breast cancer recurrence risk than those with >10% Ki67 expression level at baseline, and patients with no decrease in Ki67 expression level with treatment had the highest recurrence rates [31].

Given the reported challenges with quantification of Ki67 expression levels around critical thresholds, the use of Ki67 expression levels to guide care in the neoadjuvant setting remains controversial. However, when better validated multigene assays are not available, Ki67 expression in conjunction with other clinical and pathologic parameters may guide decisions on adjuvant systemic therapy and prognosis after neo-endocrine therapy and may serve as a cross-check and additional data point to the "pathologic picture" of an individual breast cancer.

Interpretation

Ki67 is a nuclear stain that will have variable intensities that may depend on cell cycle state and pre-analytical and analytical assay parameters. Different scoring methods have been recommended, including scoring to include "hot spots" at the leading edge of a cancer vs. "global" average scoring over the entire sample (similar to ER scoring). The most recent International Ki67 Working Group guideline recommends using an online scoring app that scores 100 nuclei and a "weighted global score" as the most analytically valid method (but not the only method) [30]. The Ki67 pharm-Dx kit for the abemaciclib indication also recommends using a global score to determine if a sample is > or = to 20%. Of note, digital image analysis Ki67 scores also had variability across scanners and analysis systems, but the variability was similar to pathologist-based scoring. Examples of Ki67 stains are shown in Fig. 22.19.

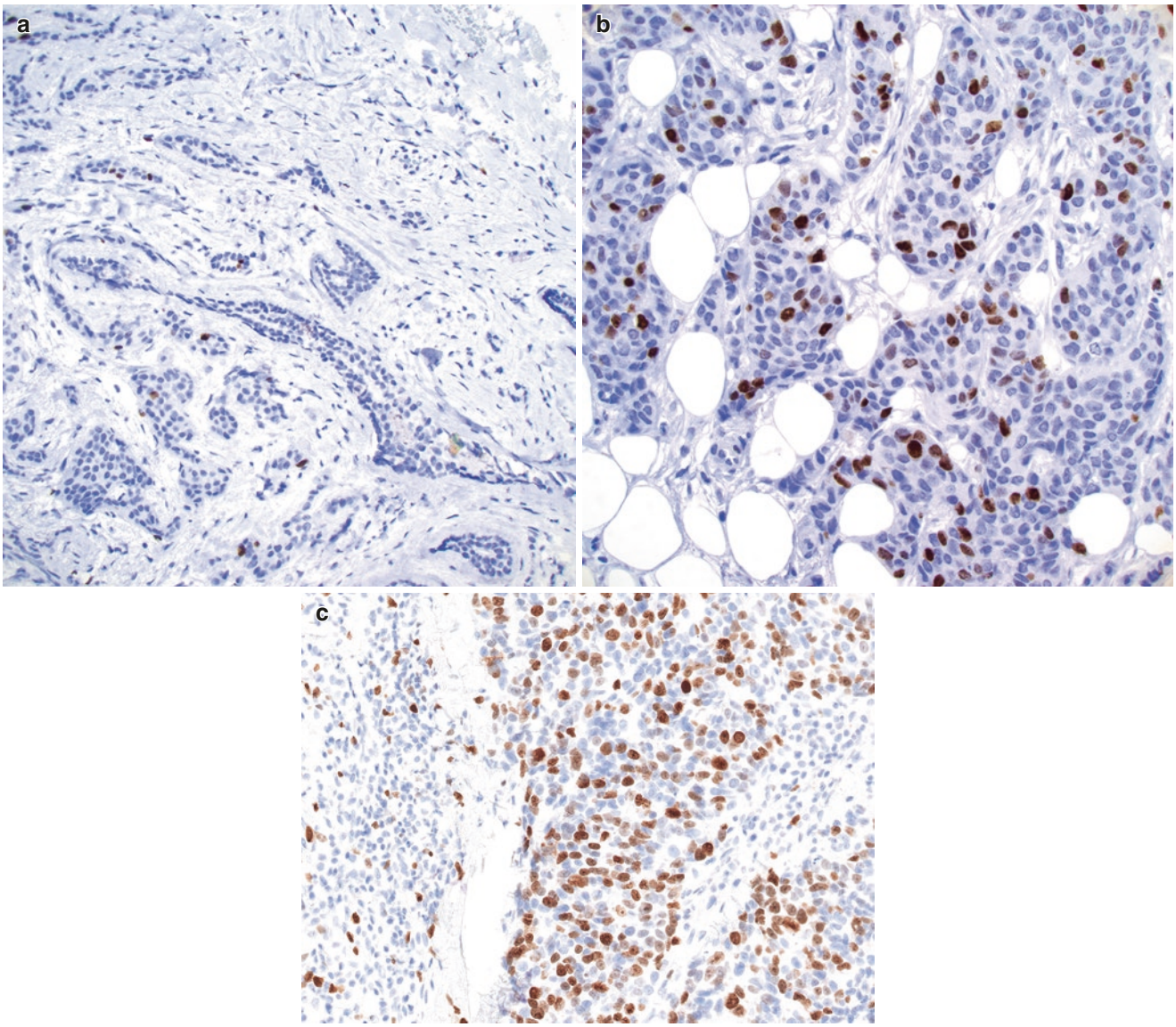

Fig. 22.19 Ki67 nuclear staining examples. (**a**) A low-grade invasive ductal carcinoma with a Ki67 proliferative rate of <5%. (**b**) An intermediate-grade invasive ductal carcinoma with a Ki67 proliferative rate of 25–30%. (**c**) A high-grade invasive ductal carcinoma with a Ki67 proliferative rate >50%. Note that proliferating-associated tumor-infiltrating lymphocytes will also stain with Ki67 and should not be included in the score

Limitations and Pitfalls

In the setting of a tumor with a significant number of tumor-infiltrating lymphocytes, many of which will be proliferating, interpretation of Ki67 can be challenging. A careful consideration of nuclear size may be helpful in avoiding overestimation of the proliferative rate. Side-by-side H&E and Ki67 comparisons can likewise be helpful in resolving discrepancies in mitotic rate seen by H&E staining and mitotic activity counted by Ki67 labeling. In some cases close to relevant thresholds, counting positive vs. negative cells or using automated image analysis may be a useful aid.

References

1. Aftimos PG, Barthelemy P, Awada A. Molecular biology in medical oncology: diagnosis, prognosis, and precision medicine. Discov Med. 2014;17(92):81–91.
2. van de Vijver MJ. Molecular tests as prognostic factors in breast cancer. Virchows Arch. 2014;464(3):283–91.
3. Harvey JM, Clark GM, Osborne CK, Allred DC. Estrogen receptor status by immunohistochemistry is superior to the ligand-binding assay for predicting response to adjuvant endocrine therapy in breast cancer. J Clin Oncol. 1999;17(5):1474–81.
4. Mohsin SK, Weiss H, Havighurst T, et al. Progesterone receptor by immunohistochemistry and clinical outcome in breast cancer: a validation study. Mod Pathol. 2004;17(12):1545–54.

5. Elledge RM, Green S, Pugh R, et al. Estrogen receptor (ER) and progesterone receptor (PgR), by ligand-binding assay compared with ER, PgR and pS2, by immuno-histochemistry in predicting response to tamoxifen in metastatic breast cancer: a Southwest Oncology Group Study. Int J Cancer. 2000;89(2):111–7.
6. Early Breast Cancer Trialists' Collaborative Group, Davies C, Godwin J, et al. Relevance of breast cancer hormone receptors and other factors to the efficacy of adjuvant tamoxifen: patient-level meta-analysis of randomised trials. Lancet. 2011;378(9793):771–84.
7. Wolff AC, Hammond ME, Hicks DG, et al. Recommendations for human epidermal growth factor receptor 2 testing in breast cancer: American Society of Clinical Oncology/College of American Pathologists clinical practice guideline update. J Clin Oncol. 2013;31(31):3997–4013.
8. Wolff AC, Hammond ME, Schwartz JN, et al. American Society of Clinical Oncology/College of American Pathologists guideline recommendations for human epidermal growth factor receptor 2 testing in breast cancer. J Clin Oncol. 2007;25(1):118–45.
9. Ballinger TJ, Sanders ME, Abramson VG. Current HER2 testing recommendations and clinical relevance as a predictor of response to targeted therapy. Clin Breast Cancer. 2015;15(3):171–80.
10. Wolff AC, Hammond MEH, Allison KH, Harvey BE, McShane LM, Dowsett M. HER2 testing in breast cancer: American Society of Clinical Oncology/College of American Pathologists clinical practice guideline focused update summary. J Oncol Pract. 2018;14(7):437–41.
11. Allison KH, Hammond MEH, Dowsett M, et al. Estrogen and progesterone receptor testing in breast cancer: ASCO/CAP guideline update. J Clin Oncol. 2020;38(12):1346–66.
12. Allison KH, Hammond MEH, Dowsett M, et al. Estrogen and progesterone receptor testing in breast cancer: American Society of Clinical Oncology/College of American Pathologists guideline update. Arch Pathol Lab Med. 2020;144(5):545–63.
13. Wolff AC, Hammond MEH, Allison KH, et al. Human epidermal growth factor receptor 2 testing in breast cancer: American Society of Clinical Oncology/College of American Pathologists clinical practice guideline focused update. J Clin Oncol. 2018;36(20):2105–22.
14. Wolff AC, Hammond MEH, Allison KH, et al. Human epidermal growth factor receptor 2 testing in breast cancer: American Society of Clinical Oncology/College of American Pathologists clinical practice guideline focused update. Arch Pathol Lab Med. 2018;142(11):1364–82.
15. Allison KH. Prognostic and predictive parameters in breast pathology: a pathologist's primer. Mod Pathol. 2021;34(Suppl 1):94–106.
16. Andre F, Ismaila N, Henry NL, et al. Use of biomarkers to guide decisions on adjuvant systemic therapy for women with early-stage invasive breast cancer: ASCO clinical practice guideline update-integration of results from TAILORx. J Clin Oncol. 2019;37(22):1956–64.
17. Telli ML, Gradishar WJ, Ward JH. NCCN guidelines updates: breast cancer. J Natl Compr Cancer Netw. 2019;17(5.5):552–5.
18. Apple S, Pucci R, Lowe AC, Shintaku I, Shapourifar-Tehrani S, Moatamed N. The effect of delay in fixation, different fixatives, and duration of fixation in estrogen and progesterone receptor results in breast carcinoma. Am J Clin Pathol. 2011;135(4):592–8.
19. Goldstein NS, Ferkowicz M, Odish E, Mani A, Hastah F. Minimum formalin fixation time for consistent estrogen receptor immunohistochemical staining of invasive breast carcinoma. Am J Clin Pathol. 2003;120(1):86–92.
20. Khoury T. Delay to formalin fixation (cold ischemia time) effect on breast cancer molecules. Am J Clin Pathol. 2018;149(4):275–92.
21. Khoury T, Liu Q, Liu S. Delay to formalin fixation effect on HER2 test in breast cancer by dual-color silver-enhanced in situ hybridization (Dual-ISH). Appl Immunohistochem Mol Morphol. 2014;22(9):688–95.
22. Khoury T. Delay to formalin fixation alters morphology and immunohistochemistry for breast carcinoma. Appl Immunohistochem Mol Morphol. 2012;20(6):531–42.
23. Qiu J, Kulkarni S, Chandrasekhar R, et al. Effect of delayed formalin fixation on estrogen and progesterone receptors in breast cancer: a study of three different clones. Am J Clin Pathol. 2010;134(5):813–9.
24. Khoury T, Sait S, Hwang H, et al. Delay to formalin fixation effect on breast biomarkers. Mod Pathol. 2009;22(11):1457–67.
25. Loi S, Symmans WF, Bartlett JM, et al. Proposals for uniform collection of biospecimens from neoadjuvant breast cancer clinical trials: timing and specimen types. Lancet Oncol. 2011;12(12):1162–8.
26. Sheri A, Dowsett M. Developments in Ki67 and other biomarkers for treatment decision making in breast cancer. Ann Oncol. 2012;23(Suppl 10):x219–27.
27. Robertson S, Acs B, Lippert M, Hartman J. Prognostic potential of automated Ki67 evaluation in breast cancer: different hot spot definitions versus true global score. Breast Cancer Res Treat. 2020;183(1):161–75.
28. Gallardo A, Garcia-Valdecasas B, Murata P, et al. Inverse relationship between Ki67 and survival in early luminal breast cancer: confirmation in a multivariate analysis. Breast Cancer Res Treat. 2018;167(1):31–7.
29. Ahmed ST, Ahmed AM, Musa DH, Sulayvani FK, Al-Khyatt M, Pity IS. Proliferative Index (Ki67) for prediction in breast duct carcinomas. Asian Pac J Cancer Prev. 2018;19(4):955–9.
30. Nielsen TO, Leung SCY, Rimm DL, et al. Assessment of Ki67 in breast cancer: updated recommendations from the international Ki67 in Breast Cancer Working Group. J Natl Cancer Inst. 2021;113(7):808–19.
31. Smith I, Robertson J, Kilburn L, et al. Long-term outcome and prognostic value of Ki67 after perioperative endocrine therapy in postmenopausal women with hormone-sensitive early breast cancer (POETIC): an open-label, multicentre, parallel-group, randomised, phase 3 trial. Lancet Oncol. 2020;21(11):1443–54.
32. Tokuda E, Horimoto Y, Arakawa A, et al. Differences in Ki67 expressions between pre- and post-neoadjuvant chemotherapy specimens might predict early recurrence of breast cancer. Hum Pathol. 2017;63:40–5.
33. Harbeck N, Rastogi P, Martin M, et al. Adjuvant abemaciclib combined with endocrine therapy for high-risk early breast cancer: Updated efficacy and Ki-67 analysis from the monarchE study. Ann Oncol. 2021;32:1571–81.
34. Leung SCY, Nielsen TO, Zabaglo LA, et al. Analytical validation of a standardised scoring protocol for Ki67 immunohistochemistry on breast cancer excision whole sections: an international multicentre collaboration. Histopathology. 2019;75(2):225–35.
35. Acs B, Pelekanou V, Bai Y, et al. Ki67 reproducibility using digital image analysis: an inter-platform and inter-operator study. Lab Investig. 2019;99(1):107–17.
36. Rimm DL, Leung SCY, McShane LM, et al. An international multicenter study to evaluate reproducibility of automated scoring for assessment of Ki67 in breast cancer. Mod Pathol. 2019;32(1):59–69.
37. von Minckwitz G, Huang CS, Mano MS, et al. Trastuzumab emtansine for residual invasive HER2-positive breast cancer. N Engl J Med. 2019;380(7):617–28.
38. Niikura N, Ueno NT. Change in HER2 status during breast tumor progression. Cancer Biomark. 2012;12(6):251–5.
39. Niikura N, Ueno NT. Biomarker discordance during tumor progression. Cancer Biomark. 2012;12(6):205–6.
40. Modi S, Jacot W, Yamashita T, et al. DESTINY-Breast04 Trial Investigators. Trastuzumab deruxtecan in previously treated HER2-low advanced breast cancer. N Engl J Med. 2022;387(1):9–20. https://doi.org/10.1056/NEJMoa2203690.

41. Robson M, Im SA, Senkus E, et al. Olaparib for metastatic breast cancer in patients with a germline BRCA mutation. N Engl J Med. 2017;377(6):523–33.
42. Litton JK, Rugo HS, Ettl J, et al. Talazoparib in patients with advanced breast cancer and a germline BRCA mutation. N Engl J Med. 2018;379(8):753–63.
43. Tutt ANJ, Garber JE, Kaufman B, et al. Adjuvant olaparib for patients with BRCA1- or BRCA2-mutated breast cancer. N Engl J Med. 2021;384(25):2394–405.
44. Andre F, Ciruelos E, Rubovszky G, et al. Alpelisib for PIK3CA-mutated, hormone receptor-positive advanced breast cancer. N Engl J Med. 2019;380(20):1929–40.
45. Schmid P, Adams S, Rugo HS, et al. Atezolizumab and nab-paclitaxel in advanced triple-negative breast cancer. N Engl J Med. 2018;379(22):2108–21.
46. Cortes J, Cescon DW, Rugo HS, et al. Pembrolizumab plus chemotherapy versus placebo plus chemotherapy for previously untreated locally recurrent inoperable or metastatic triple-negative breast cancer (KEYNOTE-355): a randomised, placebo-controlled, double-blind, phase 3 clinical trial. Lancet. 2020;396(10265):1817–28.
47. Le DT, Durham JN, Smith KN, et al. Mismatch repair deficiency predicts response of solid tumors to PD-1 blockade. Science. 2017;357(6349):409–13.
48. Drilon A, Laetsch TW, Kummar S, et al. Efficacy of larotrectinib in TRK fusion-positive cancers in adults and children. N Engl J Med. 2018;378(8):731–9.
49. Hammond ME, Hayes DF, Dowsett M, et al. American Society of Clinical Oncology/College of American Pathologists guideline recommendations for immunohistochemical testing of estrogen and progesterone receptors in breast cancer (unabridged version). Arch Pathol Lab Med. 2010;134(7):e48–72.
50. Hammond ME, Hayes DF, Dowsett M, et al. American Society of Clinical Oncology/College of American Pathologists guideline recommendations for immunohistochemical testing of estrogen and progesterone receptors in breast cancer. Arch Pathol Lab Med. 2010;134(6):907–22.
51. Yi M, Huo L, Koenig KB, et al. Which threshold for ER positivity? A retrospective study based on 9639 patients. Ann Oncol. 2014;25(5):1004–11.
52. Bouchard-Fortier A, Provencher L, Blanchette C, Diorio C. Prognostic and predictive value of low estrogen receptor expression in breast cancer. Curr Oncol. 2017;24(2):e106–14.
53. Khoshnoud MR, Lofdahl B, Fohlin H, et al. Immunohistochemistry compared to cytosol assays for determination of estrogen receptor and prediction of the long-term effect of adjuvant tamoxifen. Breast Cancer Res Treat. 2011;126(2):421–30.
54. Badve SS, Baehner FL, Gray RP, et al. Estrogen- and progesterone-receptor status in ECOG 2197: comparison of immunohistochemistry by local and central laboratories and quantitative reverse transcription polymerase chain reaction by central laboratory. J Clin Oncol. 2008;26(15):2473–81.
55. Fisher ER, Anderson S, Dean S, et al. Solving the dilemma of the immunohistochemical and other methods used for scoring estrogen receptor and progesterone receptor in patients with invasive breast carcinoma. Cancer. 2005;103(1):164–73.
56. Molino A, Micciolo R, Turazza M, et al. Prognostic significance of estrogen receptors in 405 primary breast cancers: a comparison of immunohistochemical and biochemical methods. Breast Cancer Res Treat. 1997;45(3):241–9.
57. Raghav KP, Hernandez-Aya LF, Lei X, et al. Impact of low estrogen/progesterone receptor expression on survival outcomes in breast cancers previously classified as triple negative breast cancers. Cancer. 2012;118(6):1498–506.
58. Honma N, Horii R, Iwase T, et al. Proportion of estrogen or progesterone receptor expressing cells in breast cancers and response to endocrine therapy. Breast. 2014;23(6):754–62.
59. Chen T, Zhang N, Moran MS, Su P, Haffty BG, Yang Q. Borderline ER-positive primary breast cancer gains no significant survival benefit from endocrine therapy: a systematic review and meta-analysis. Clin Breast Cancer. 2018;18(1):1–8.
60. Balduzzi A, Bagnardi V, Rotmensz N, et al. Survival outcomes in breast cancer patients with low estrogen/progesterone receptor expression. Clin Breast Cancer. 2014;14(4):258–64.
61. Gloyeske NC, Dabbs DJ, Bhargava R. Low ER+ breast cancer: Is this a distinct group? Am J Clin Pathol. 2014;141(5):697–701.
62. Deyarmin B, Kane JL, Valente AL, et al. Effect of ASCO/CAP guidelines for determining ER status on molecular subtype. Ann Surg Oncol. 2013;20(1):87–93.
63. Kurozumi S, Matsumoto H, Hayashi Y, et al. Power of PgR expression as a prognostic factor for ER-positive/HER2-negative breast cancer patients at intermediate risk classified by the Ki67 labeling index. BMC Cancer. 2017;17(1):354.
64. Regan MM, Francis PA, Pagani O, et al. Absolute benefit of adjuvant endocrine therapies for premenopausal women with hormone receptor-positive, human epidermal growth factor receptor 2-negative early breast cancer: TEXT and SOFT trials. J Clin Oncol. 2016;34(19):2221–31.
65. Albert JM, Gonzalez-Angulo AM, Guray M, et al. Patients with only 1 positive hormone receptor have increased locoregional recurrence compared with patients with estrogen receptor-positive progesterone receptor-positive disease in very early stage breast cancer. Cancer. 2011;117(8):1595–601.
66. Ahn SG, Yoon CI, Lee JH, et al. Low PR in ER(+)/HER2(−) breast cancer: high rates of TP53 mutation and high SUV. Endocr Relat Cancer. 2019;26(2):177–85.
67. Cuzick J, Dowsett M, Pineda S, et al. Prognostic value of a combined estrogen receptor, progesterone receptor, Ki-67, and human epidermal growth factor receptor 2 immunohistochemical score and comparison with the Genomic Health recurrence score in early breast cancer. J Clin Oncol. 2011;29(32):4273–8.
68. Dowsett M, Smith IE. Presurgical progesterone in early breast cancer: so much for so little? J Clin Oncol. 2011;29(21):2839–41.
69. Dowsett M, Allred C, Knox J, et al. Relationship between quantitative estrogen and progesterone receptor expression and human epidermal growth factor receptor 2 (HER-2) status with recurrence in the Arimidex, Tamoxifen, Alone or in Combination trial. J Clin Oncol. 2008;26(7):1059–65.
70. Prat A, Cheang MC, Martin M, et al. Prognostic significance of progesterone receptor-positive tumor cells within immunohistochemically defined luminal A breast cancer. J Clin Oncol. 2013;31(2):203–9.
71. Yuan Y, Lee JS, Yost SE, et al. A phase II clinical trial of pembrolizumab and enobosarm in patients with androgen receptor-positive metastatic triple-negative breast cancer. Oncologist. 2021;26(2):99–e217.
72. Anestis A, Zoi I, Papavassiliou AG, Karamouzis MV. Androgen receptor in breast cancer-clinical and preclinical research insights. Molecules. 2020;25(2):358.
73. Slamon DJ, Leyland-Jones B, Shak S, et al. Use of chemotherapy plus a monoclonal antibody against HER2 for metastatic breast cancer that overexpresses HER2. N Engl J Med. 2001;344(11):783–92.
74. Goldhirsch A, Gelber RD, Piccart-Gebhart MJ, et al. 2 years versus 1 year of adjuvant trastuzumab for HER2-positive breast cancer (HERA): an open-label, randomised controlled trial. Lancet. 2013;382(9897):1021–8.
75. Perez EA, Romond EH, Suman VJ, et al. Four-year follow-up of trastuzumab plus adjuvant chemotherapy for operable human epidermal growth factor receptor 2-positive breast cancer: joint analysis of data from NCCTG N9831 and NSABP B-31. J Clin Oncol. 2011;29(25):3366–73.
76. Swain SM, Kim SB, Cortes J, et al. Pertuzumab, trastuzumab, and docetaxel for HER2-positive metastatic breast cancer (CLEOPATRA study): overall survival results from a randomised,

double-blind, placebo-controlled, phase 3 study. Lancet Oncol. 2013;14(6):461–71.
77. Baselga J, Bradbury I, Eidtmann H, et al. Lapatinib with trastuzumab for HER2-positive early breast cancer (NeoALTTO): a randomised, open-label, multicentre, phase 3 trial. Lancet. 2012;379(9816):633–40.
78. Verma S, Miles D, Gianni L, et al. Trastuzumab emtansine for HER2-positive advanced breast cancer. N Engl J Med. 2012;367(19):1783–91.
79. Molina MA, Codony-Servat J, Albanell J, Rojo F, Arribas J, Baselga J. Trastuzumab (herceptin), a humanized anti-Her2 receptor monoclonal antibody, inhibits basal and activated Her2 ectodomain cleavage in breast cancer cells. Cancer Res. 2001;61(12):4744–9.
80. Ekholm M, Grabau D, Bendahl PO, et al. Highly reproducible results of breast cancer biomarkers when analysed in accordance with national guidelines - a Swedish survey with central re-assessment. Acta Oncol. 2015;54(7):1040–8.
81. Middleton LP, Price KM, Puig P, et al. Implementation of American Society of Clinical Oncology/College of American Pathologists HER2 guideline recommendations in a tertiary care facility increases HER2 immunohistochemistry and fluorescence in situ hybridization concordance and decreases the number of inconclusive cases. Arch Pathol Lab Med. 2009;133(5):775–80.
82. Rakha EA, Pigera M, Shaaban A, et al. National guidelines and level of evidence: comments on some of the new recommendations in the American Society of Clinical Oncology and the College of American Pathologists human epidermal growth factor receptor 2 guidelines for breast cancer. J Clin Oncol. 2015;33(11):1301–2.
83. Wolff AC, Hammond ME, Hicks DG, et al. Reply to E.A. Rakha et al. J Clin Oncol. 2015;33(11):1302–4.
84. Troxell M, Sibley RK, West RB, Bean GR, Allison KH. HER2 dual in situ hybridization: correlations and cautions. Arch Pathol Lab Med. 2020;144(12):1525–34.
85. Wolff AC, Hammond ME, Hicks DG, et al. Recommendations for human epidermal growth factor receptor 2 testing in breast cancer: American Society of Clinical Oncology/College of American Pathologists clinical practice guideline update. Arch Pathol Lab Med. 2014;138(2):241–56.
86. Wolff AC, Hammond ME, Schwartz JN, et al. American Society of Clinical Oncology/College of American Pathologists guideline recommendations for human epidermal growth factor receptor 2 testing in breast cancer. Arch Pathol Lab Med. 2007;131(1):18–43.
87. Ballard M, Jalikis F, Krings G, et al. 'Non-classical' HER2 FISH results in breast cancer: a multi-institutional study. Mod Pathol. 2017;30(2):227–35.
88. Ruschoff J, Lebeau A, Kreipe H, et al. Assessing HER2 testing quality in breast cancer: variables that influence HER2 positivity rate from a large, multicenter, observational study in Germany. Mod Pathol. 2017;30(2):217–26.
89. Lin CYC, Carneal EE, Lichtensztajn DY, Gomez SL, Clarke CA, Jensen KC, Kurian AW, Allison KH. Regional variability in percent of breast cancers reported as positive for HER2 in California: implications of patient demographics on laboratory benchmarks. Am J Clin Pathol. 2017;148(3):199–207.
90. Grimm EE, Schmidt RA, Swanson PE, Dintzis SM, Allison KH. Achieving 95% cross-methodological concordance in HER2 testing: causes and implications of discordant cases. Am J Clin Pathol. 2010;134(2):284–92.
91. Allison KH. Ancillary prognostic and predictive testing in breast cancer: focus on discordant, unusual, and borderline results. Surg Pathol Clin. 2018;11(1):147–76.
92. Starczynski J, Atkey N, Connelly Y, et al. HER2 gene amplification in breast cancer: a rogues' gallery of challenging diagnostic cases: UKNEQAS interpretation guidelines and research recommendations. Am J Clin Pathol. 2012;137(4):595–605.
93. Lee HJ, Seo AN, Kim EJ, et al. HER2 heterogeneity affects trastuzumab responses and survival in patients with HER2-positive metastatic breast cancer. Am J Clin Pathol. 2014;142(6):755–66.
94. Press MF, Villalobos I, Santiago A, et al. Assessing the New American Society of Clinical Oncology/College of American Pathologists guidelines for HER2 testing by fluorescence in situ hybridization: experience of an academic consultation practice. Arch Pathol Lab Med. 2016;140(11):1250–8.
95. Perou CM, Sorlie T, Eisen MB, et al. Molecular portraits of human breast tumours. Nature. 2000;406(6797):747–52.
96. Ward S, Scope A, Rafia R, et al. Gene expression profiling and expanded immunohistochemistry tests to guide the use of adjuvant chemotherapy in breast cancer management: a systematic review and cost-effectiveness analysis. Health Technol Assess. 2013;17(44):1–302.
97. Dowsett M, Nielsen TO, A'Hern R, et al. Assessment of Ki67 in breast cancer: recommendations from the International Ki67 in Breast Cancer Working Group. J Natl Cancer Inst. 2011;103(22):1656–64.
98. Polley MY, Leung SC, Gao D, et al. An international study to increase concordance in Ki67 scoring. Mod Pathol. 2015;28(6):778–86.
99. Polley MY, Leung SC, McShane LM, et al. An international Ki67 reproducibility study. J Natl Cancer Inst. 2013;105(24):1897–906.

Future Role of Molecular Profiling in Small Breast Samples and Personalised Medicine

23

Samuel Y. F. Foong, Peter T. Simpson, Margaret C. Cummings, and Sunil R. Lakhani

Introduction

The ongoing quest for an increasingly detailed understanding of the precise mechanisms of cancer evolution to provide better prognostic and predictive biomarkers and more specific therapeutic targets has underpinned major technological advances in recent years in the fields of cancer genomics, transcriptomics and proteomics. As these advances become more accessible to clinical practice and the role of targeted therapeutics becomes established, progressively more molecular information will be required from progressively smaller amounts of tissue, such as core biopsies, in the patient management pathway (Fig. 23.1). Here, we will discuss the evolving landscape of molecular profiling that may be applied to core biopsies of breast tissue. Key scenarios where comprehensive molecular information derived from core biopsies will become important include predicting the progression of in situ disease; predicting the likelihood of local recurrence or metastatic disease after definitive primary treatment; determining therapy and monitoring the response to therapy in the neoadjuvant setting; and determining appropriate targeted therapy for patients who have relapsed on conventional therapy or developed metastatic disease.

S. Y. F. Foong · M. C. Cummings · S. R. Lakhani
UQ Centre for Clinical Research, Faculty of Medicine, The University of Queensland, Brisbane, QLD, Australia

Pathology Queensland, The Royal Brisbane and Women's Hospital, Brisbane, QLD, Australia
e-mail: Samuel.Foong@health.qld.gov.au; m.cummings@uq.edu.au; s.lakhani@uq.edu.au

P. T. Simpson (✉)
UQ Centre for Clinical Research, Faculty of Medicine, The University of Queensland, Brisbane, QLD, Australia
e-mail: p.simpson@uq.edu.au

Genomics for Personalised Medicine

The concept of basing targeted therapy on the results of genomic analysis is now an enormous field of research and a major consideration with clinical trial design. This is because cancer, as a genetic disease [1], is largely driven by the accumulation of mutations that affect pathways important in tumourigenesis, particularly cell growth and survival. There have been significant technological developments in recent years in the field of cancer genomics that allow the comprehensive characterisation of the mutational landscape of tumours and an understanding of how specific gene mutations or more global patterns of mutations relate to tumour behaviour and therefore prognosis and treatment.

There are a range of types of somatic mutations that occur in cancer genomes: copy number alterations (amplifications and deletions); single-nucleotide variations, including substitutions and small insertions and deletions; and structural variants, for example, duplications, inversions, deletions, intra- and inter-chromosomal rearrangements or translocations. Many of these alterations probably play no or only a minor role in tumour behaviour and are thus referred to as passenger mutations. A small proportion affect what are considered to be cancer genes, and these alterations are the major drivers of tumourigenesis. Excitingly from a therapeutic angle, there are an increasing number of drugs in clinical trials or which are already approved for use, which can target these molecular alterations, including amplified oncogenes, mutated protein kinases or genes rearranged by translocations.

One important goal in personalised therapy is the identification of precise actionable genomic alterations in an individual's tumour that can be specifically targeted. Established examples of this approach include targeting the *ERBB2* gene amplification (leading to HER2 overexpression and activation), which has been a major therapeutic success for affected breast cancer patients. The *BRAF* V600E mutation frequently occurs in a range of malignancies including melanoma, thy-

© The Author(s), under exclusive license to Springer Nature Switzerland AG 2022
S. J. Shin et al. (eds.), *A Comprehensive Guide to Core Needle Biopsies of the Breast*,
https://doi.org/10.1007/978-3-031-05532-4_23

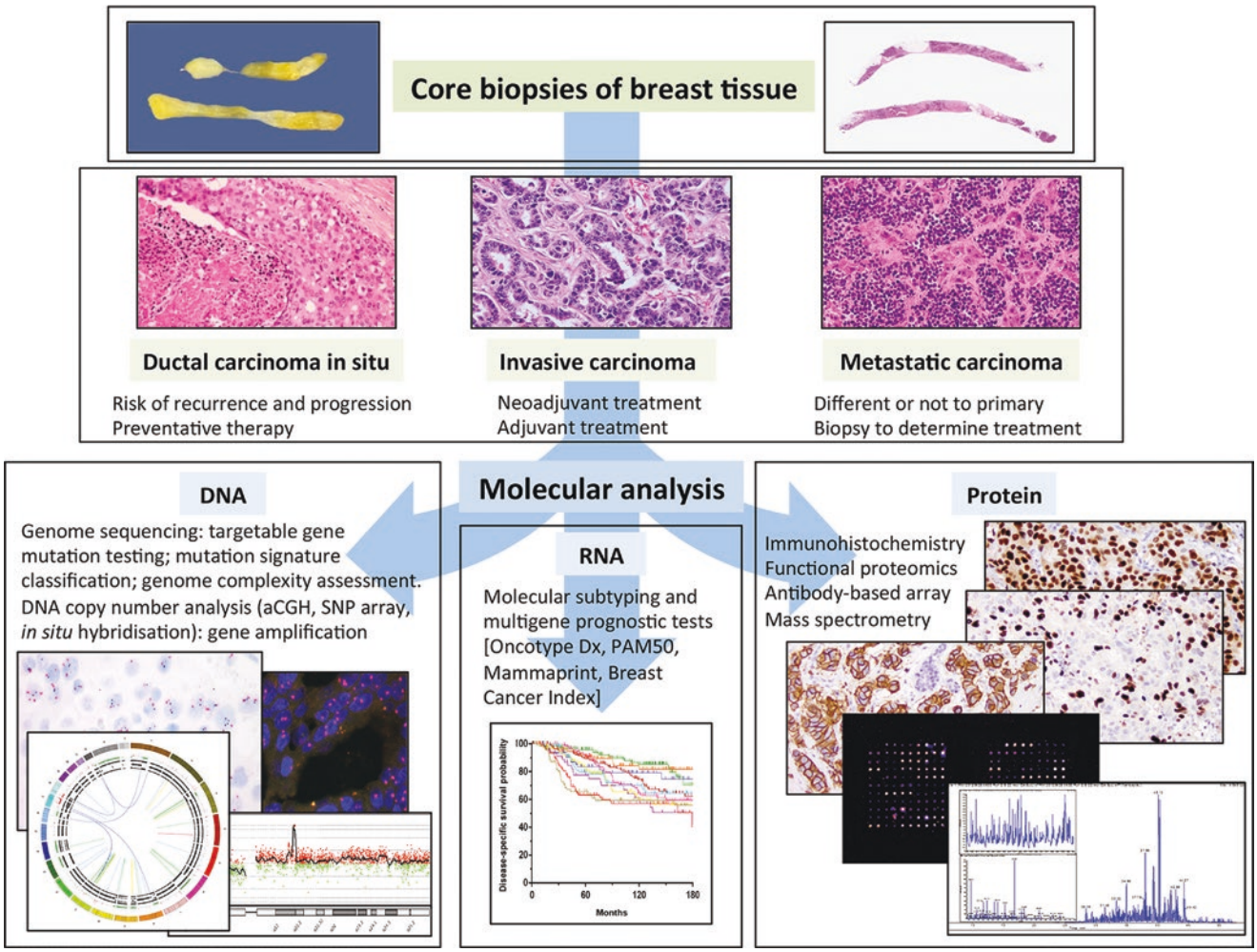

Fig. 23.1 The application of molecular testing to core biopsies for guiding patient management. Core biopsy sampling of breast tissue aids in the management of patients with in situ disease, invasive disease or metastatic dissemination. Multiple applications are or will become available for molecular testing of these small tissue samples, some of which are highlighted. DNA section pictures: fluorescence in situ hybridisation for a chromosome 1 probe, chromogenic in situ hybridisation for dual-HER2–CEP17 probes; array comparative genomic hybridisation (aCGH) plot showing HER2 amplification; and circus plot from whole-genome sequencing showing structural rearrangements. RNA section picture: survival curves of a modified analysis of integrated molecular clusters. Protein section pictures: immunohistochemistry for ER, Ki-67 and HER2; an antibody array; and tandem mass spectrometry spectrum

roid and colon cancer [2] and can be targeted using inhibitors such as vemurafenib. Molecular analysis of large numbers of tumours from initiatives such as The Cancer Genome Atlas (TCGA) and the International Cancer Genome Consortium (ICGC) has shown that known targets in one particular cancer type can be shared across different cancer types, albeit at different frequencies. This suggests the potential translation and implementation of molecular testing protocols and therapeutic strategies established in one cancer type to another, representing cross-cancer therapeutics. For example, subgroups of pancreatic, lung and gastric carcinomas appear to be driven by *ERBB2* amplification, suggesting potential benefit from already established trastuzumab therapy extending beyond the management of those with HER2-positive breast cancer.

A second important goal is to characterise the genome architecture, giving an overview of the extent and type of genome alterations of an individual tumour, as this broader picture may serve as a useful prognostic biomarker or indicator of the processes of DNA damage. This in turn may provide insight into the tumour's aetiology and behaviour and perhaps also the choice of therapy.

What possibilities are there for genomic investigations to identify mutations or, more specifically, actionable cancer genes, particularly in small biopsy material? Protocols currently available in pathology laboratories include in situ hybridisation, as used to detect *ERBB2* amplification, and mutation testing, for example, for *EGFR* in lung cancer and *BRAF* in melanoma and colon cancer. Such testing is restricted to known biomarkers or therapeutic targets and so

will not detect other potentially targetable alterations for which established drugs may already be being used in other cancer types.

Significant improvements in the design of genomic assays now enable complex and high-yielding genomic data to be obtained from smaller and smaller samples. We will briefly cover applications of DNA copy number profiling and various sequencing approaches (targeted gene panel sequencing, whole-exome and whole-genome sequencing) that are playing an important role in understanding breast cancer aetiology and impacting patient management. First, there is whole-genome copy number profiling using an array-based format, for example, comparative genomic hybridisation or single-nucleotide polymorphism (SNP) arrays. These techniques have evolved from more traditional, low-resolution cytogenetic techniques to be able to profile several million data points per tumour. Although structural chromosomal rearrangements or nucleotide resolution alterations (substitutions or indels) cannot be captured, very focal or large copy number alterations (such as deletions, gains and amplifications) can be characterised. These assays can therefore identify specific alterations with therapeutic potential (e.g. amplification of *ERBB2*/HER2, *FGFR1*, *PI3KCA*) and stratify tumours based on the type or extent of genome instability. Breast cancer genomes are quite heterogeneous, ranging from relatively few copy number alterations (simple) to complex genomes with multiple gains and losses distributed throughout the genome (complex sawtooth) to the presence of complex chromosomal rearrangements involving focal amplifications (complex firestorms) [3]. These firestorms often occur at sites of known oncogenes (such as *ERBB2*, *MYC*, *FGFR1*, *CCND1*) and so likely have an impact on tumour behaviour. Indeed, the development of a computational tool (the 'complex arm aberration index'; CAAI) to objectively score tumours based on the presence of these complex and focal alterations showed that they were associated with poor patient outcome [4, 5]. In a study of 1950 breast cancers, 43% of cases were deemed CAAI positive, and patients with these tumours had a higher mortality rate than those scored as CAAI negative. Additionally, the CAAI score enhanced prognostic discrimination when combined with the 21-gene and 70-gene prognostic gene expression signatures (discussed below) [5]. Tumours with numerous point mutations, chromosomal structural rearrangements and copy number changes may have homologous recombination (HR) DNA damage repair deficiency. These tumours are associated, in particular, with *BRCA1/2* germline mutations but may also occur in sporadic breast cancers. This is of clinical importance, as tumours with HR deficiency and/or *BRCA1/2* mutations may be more sensitive to platinum-based chemotherapy and poly(ADP-ribose) polymerase (PARP) inhibitors [6, 7]. The homologous recombination deficiency (HRD) score was designed by Telli et al. [6] to quantify genomic instability as a marker of HR deficiency. It used SNP arrays to identify large-scale genomic aberrations. It measures the sums of three markers of structural aberrations to achieve this. These are loss of heterozygosity (LOH), telomeric allelic imbalance (TAI) and large-scale state transitions (LST). This assay can be applied in the research setting to classify the HR status of tumours, from various sources of genomic data, including next-generation sequencing (NGS) data, and so is applicable to the analysis of small biopsy samples. It is also available as a NGS-based diagnostic tool, the Myriad myChoice test, for both identifying mutations in *BRCA1* and *BRCA2* and defining the HR status in ovarian cancer for selecting PARP inhibitors as a potential targeted therapeutic option [8].

The most comprehensive approach for genomic analysis is whole-genome sequencing, where the entire genome, both coding genes and non-coding regions, is analysed. This is an extremely powerful application for characterising, in an unbiased manner, the overall mutational landscape of a tumour, simultaneously capturing copy number alterations, single-nucleotide variations and structural variants. There is already evolving evidence that links the extent, type or pattern of alterations with both the aetiology of disease and tumour behaviour. For example, the vast numbers of so-called passenger mutations serve as a telltale imprint or mutation signature of the underlying mutational processes that contribute to the somatic mutation burden. Conspicuous examples are the mutation profiles associated with exposure to specific exogenous mutagens, such as those found in cigarette smoke or those induced by ultraviolet light, reflecting the aetiology of lung and skin cancer, respectively [9–11]. As mentioned above, regarding the pattern of copy number alterations associated with HR deficiency, there is a series of mutation signatures, seen most commonly in breast, ovarian and pancreatic cancer, which correlate with defects in *BRCA1* and *BRCA2* genes and hence compromised HR-mediated DNA repair [12]. These signatures involve specific patterns of substitutions, indels and rearrangements, and overall tumours have complex and highly rearranged or unstable genomes [13–15].

HRDetect is a tool that further expands on the HRD score using the above mutational signatures from whole-genome sequencing data to predict the HR status of a tumour [13]. HRDetect showed superior sensitivity when compared to HRD score and other methods for assessing HRD status. This tool exhibited 98.7% sensitivity in a cohort of 560 individuals, which, in addition to 22 germline *BRCA1/2* carriers, allowed the identification of a further 22 tumours with somatic loss of *BRCA1/2* and 47 tumours with functional deficiency without a known mutational cause, therefore increasing the proportion of patients who may benefit from a PARP inhibitor from 1–5% to 22%.

These genomic characteristics provide direct evidence of a specific genetic or functional deficiency that can be exploited therapeutically through showing susceptibility to specific types of DNA-damaging therapeutics (e.g. platinum-based chemotherapy) or PARP inhibitors [16–19].

Whole-genome sequencing is now entering into standard clinical care for some diseases where this unbiased assessment of the genome is required. Some programs (e.g. the Cambridge Personalised Breast Cancer Programme) are starting to apply whole-genome sequencing in the context of breast cancer management, to make use of the power to detect somatic mutations as well as mutation signatures to help in treatment decision-making. The high costs, the amount of DNA required for testing and the considerable bioinformatics support needed for both analysing and interpreting the complex data that is generated are all becoming more feasible in the clinic. However, simpler sequencing or genomic assays are being applied to small samples as a surrogate test for classifying tumour genomes to facilitate treatment selection or for identifying direct actionable target mutations.

There are already options for more targeted NGS approaches that are relevant to clinical practice. These methods are capable of capturing single-nucleotide variations and small insertions and deletions (indels), and the data can be used to interpret DNA copy number changes, to enable the delineation of gene amplifications (e.g. *ERBB2*) and global patterns of DNA copy number changes, such as seen in HR deficiency. This approach involves either exome sequencing, which interrogates the whole coding sequence of the genome for somatic mutations, or sequencing of focused panels of cancer genes [20, 21]. The latter approach has had considerable attention, where multiple targeted gene panels are beginning to help guide targeted treatment selection since the cost, the complexity of the data obtained and the time frames involved are more realistic for day-to-day practice. This method is also very applicable to core biopsies and fine needle aspirates [22, 23]. The fact that only a fraction of the genome is sequenced, up to 500 genes compared with approximately 20,000 genes, means that it is also possible to achieve a greater ‘depth’ of sequencing coverage. That is, each nucleotide can be sequenced many more times than can be done with exome or whole-genome sequencing. This not only provides great reliability of the data obtained but also enables samples that may not be suitable for molecular profiling due to low tumour cellularity to be sequenced. Furthermore, there is less reliance on the requirement for a normal DNA counterpart, which is used to ascertain which variants are somatically acquired mutations rather than germline variations.

To illustrate the applicability of this technique, targeted sequencing of a well-curated panel of 182 cancer genes in DNA derived from needle core biopsies of 33 primary and 18 metastatic breast cancers demonstrated that 84% of cases contained mutations in potentially ‘actionable’ target genes, including *PIK3CA*, *CCNE1*, *CCND1*, *FGFR1*, *FGFR2 and ERBB2* [22]. Sequencing the same gene panel in a larger cohort of primary and metastatic breast tumours demonstrated that somatic mutations in codons 537 and 538 of the *ESR1* gene were found in 12% of metastases from ER-positive primary disease and in 20% of patients who received at least seven different types of treatment [21]. These mutations were not identified in ER-negative tumours or ER-positive primary tumours or treatment-naive metastases, indicating that these mutations were selected for as a mechanism of resistance to endocrine therapy [21]. More recently, similar findings have been confirmed with a more select panel of 108 genes and a larger cohort of 322 patients, which showed that 74% of patients carried an actionable mutation, most commonly *PIK3CA* [24]. Some centres are already offering this approach to patients whose tumours have been refractory to conventional first-line therapies.

Clinically and commercially available comprehensive genomic profiling assays that are already in use include MSK-IMPACT, FoundationOne CDx, OncoPanel and Oncomine. MSK-IMPACT is a hybridisation capture-based NGS panel capable of detecting protein-coding mutations, copy number alterations and selected promoter mutations in up to 410 cancer-associated genes developed at Memorial Sloan Kettering Cancer Center and is available for use in patients in that facility for research and clinical purposes. Ten thousand advanced or metastatic tumours were sequenced, and 37% were found to have clinically relevant alterations and were subsequently matched to clinical trials [25]. A large cohort study was performed on 1918 biopsied breast cancers sequenced using the MSK-IMPACT platform [26]. They found that mutations in 32 genes were significantly more common in metastases than primary tumours. This gives an insight into selective therapeutic pressure from systemic treatment and resistance. Twenty-two percent of post-hormonal therapy for ER-positive, HER2-negative tumours had mutations in MAPK effectors, *MYC* or other transcription factors. These were mutually exclusive with *ESR1* mutations. Most commonly, activating *ERBB2* mutations or loss-of-function *NF1* mutations were present in these endocrine-resistant tumours. Findings like these suggest that there may be a use for targeted therapies depending on the independent mutations involved in endocrine resistance gained in advanced breast cancer. These include aromatase inhibitors for *ESR1* mutations, HER2 kinase inhibitors for *ERBB2* mutations, EGFR inhibitors and ERK inhibitors for loss-of-function *NF1* mutations.

FoundationOne CDx is a commercially available NGS panel test which analyses 324 genes, as well as genomic signatures including microsatellite instability and tumour mutational burden. It was used in the PREDICT study, where 347

patients with solid advanced cancers from multiple-organ systems including breast were biopsied [27]. A matching score was devised to provide the best treatment based on the number of aberrations. Eighty-seven patients were treated with a matched therapy and 93 were not. It was found that the matched group had a longer median progression-free survival (4.0 vs. 3.0 months). OncoPanel is another NGS assay which detects cancer-related genomic aberrations in 282 genes developed jointly at the Dana-Farber Cancer Institute and Brigham and Women's Hospital. A recent study used OncoPanel to sequence and compare de novo and recurrent metastatic breast cancers [28]. Their findings indicated that there may be genomic differences in mutations found between the two settings. This suggested that there may be intrinsic mechanisms of resistance developed in recurrent metastatic breast cancer that need to be overcome in future treatments. The number of research papers in this field is growing, and use of these as clinical tools may become more widespread in the near future.

SAFIR01/UNICANCER was a prospective multicentre trial undertaken to try to investigate the possibility of providing personalised targeted therapy applicable to the individual tumour's genomic abnormalities, in patients with metastatic breast cancer. Array comparative genomic hybridisation (aCGH) to identify focal amplifications and Sanger sequencing for hotspot mutations in *PI3KCA* and *AKT* were used. Amplifications in the region of *PIK3CA* and *FGFR1* genes were identified in 25% and 12% of patients, respectively, and a few patients showed *ERBB2* amplification in the metastatic tumour who previously had *ERBB2*-negative primary disease [29]. Targeted therapies were suggested for 55 patients (13%), and of 43 patients where this was implemented, 4 (9%) showed an objective response, while 9 patients (21%) had disease that remained stable for 4 months [29]. The seemingly low proportion may reflect substantial pretreatment of the group, but also the difficulty in identifying the appropriate drug target [29, 30]. For instance, although amplification in the region of 8p12 is detected, there are several candidate oncogenes co-located to this chromosomal region, and so targeting FGFR1 may not always be appropriate.

MOSCATO 01 was a monocentric prospective clinical trial which was aimed to investigate progression-free survival of targeted therapies [31]. Molecular portraits were obtained for 843 patients on fresh-frozen core biopsies of which 411 had actionable mutations identified. High-throughput genomic analyses were used with aCGH, targeted sequencing, RNA-seq analysis and whole-exome sequencing used depending on tumour cellularity. The most frequent targetable alterations present were *PIK3CA*, *ERBB2*, *PTEN*, *FGFR1*, *EGFR* and *NOTCH1/2/3/4* mutations. One hundred and ninety-nine patients were treated with targeted therapies. Progression-free survival on a targeted therapy was improved in 33% of patients with objective responses present in 11%. These results showed more positive results than previous trials, possibly due to the use of newer generation targeted therapies.

These approaches highlight the importance of integrating genomic profiling of core needle biopsy material into prospective clinical trial design, not only to help understand tumour biology in response to specific therapies but also to help identify molecular alterations suitable for targeted therapies in the setting of tumour recurrence or advanced, metastatic disease. Ongoing clinical trials involve investigating newly targetable alterations in metastatic tumours, for instance, MEK inhibitors to treat *NF1* mutations. However, currently there is limited evidence of an objective response in these cases [32]. Further steps would include validation of clinical utility in randomised trials to determine which patients could benefit from these tests.

Gene Expression Profiling

When a gene is transcriptionally activated, complementary messenger RNA (mRNA) is produced, forming the template for synthesis of the relevant protein. While there is not a direct correlation between levels of mRNA and those of the corresponding protein, relative mRNA transcript abundance enables inferences to be made concerning the phenotype of the cell or tumour being assessed. Gene expression analysis ranges from evaluating the expression of a single gene using PCR-based techniques to whole-genome analyses by sequencing-based strategies (RNA-seq), giving an unbiased readout of essentially all RNA transcripts that are produced, capturing splice variants of genes and non-protein-coding transcripts, such as microRNAs, which can play an important role in transcriptional regulation.

Expression profiling has been used to stratify breast cancers into different prognostic subgroups both in the research setting and in clinical practice. This has included comparing gene expression profiles from biopsies taken before chemotherapy with those taken afterwards to assess the response to treatment [33]. Mathematical formula derived from microarray data uses the expression levels of a specific set of genes from a tumour to predict prognosis or response to therapy, for example, the commercially available Oncotype DX Breast Cancer Assay. This measures the expression of 21 genes by real-time PCR to generate a recurrence score for predicting the benefit of chemotherapy and the likelihood of recurrence. This assay is currently being used in clinical practice [34, 35].

Gene expression profiling has also been used to develop molecular taxonomies to subtype tumours into clinically meaningful categories, which can provide both prognostic and therapeutic information. This class discovery approach

was used to develop the now well-recognised intrinsic molecular subtypes [36], which, as well as having a significant impact on breast cancer research, now play an important role in clinical decision-making [37]. These so-called intrinsic molecular subtypes of breast cancer are luminal A, luminal B, HER2-enriched, basal-like and normal breast-like [36, 38]. Luminal A and B subtypes are oestrogen receptor (ER) positive, while the basal-like, HER2 and normal breast-like subtypes are ER negative. Luminal A tumours are defined by being both ER and progesterone receptor (PR) positive and HER2 negative together with a low Ki-67 proliferation index. The tumours are of low histological grade and have the best prognosis of the various subtypes. Luminal B tumours are ER positive, are either positive or negative for PR and are either HER2 positive or show a high Ki-67 proliferation index [37, 39]. Luminal B tumours have a higher histological grade compared with the luminal A subtype, and patients with luminal B cancers may derive benefit from more aggressive therapy [40]. Luminal or ER-positive tumours of course represent a spectrum of diseases and most likely encompass multiple molecular subtypes with differing levels of hormone receptor activation, involving the interplay between ER, PR and androgen receptor (AR), as well as HER2 expression and expression of cell proliferation genes [41].

HER2-positive breast cancers are frequently of high histological grade and are associated with a worse prognosis compared with the luminal subtypes. These tumours were once considered a single disease driven by HER2 oncogenic activity, and indeed most of the tumours classified as the HER2-enriched molecular subtype are generally positive for HER2 (gene amplification/protein overexpression) and negative for hormone receptors. However, as with luminal tumours, this subgroup has recognised biological and clinical diversity. Some tumours overlap with luminal B tumours, being both HER2 and ER positive; some tumours identified clinically as HER2 positive by immunohistochemistry or in situ hybridisation could be classified as either luminal or basal-like by expression profiling; and similarly, some tumours classified as HER2 enriched may test negative for HER2 clinically but still express genes associated with or regulated by HER2.

The basal-like subtype is predominantly ER, PR and HER2 negative (triple negative) and is also associated with a poor outcome. Histologically, these tumours most usually have high-grade nuclei, a syncytial pattern of growth with pushing borders and a peripheral cuff of lymphocytes, and expression of basal/myoepithelial markers [42–44]. Basal-like carcinomas are associated with the poorest survival of all the subtypes but do not always show consistent behaviour. If patients do survive 5 years, their long-term outlook is very favourable [42]; indeed around half the patients show a very good response to treatment. This may in part be accounted for by the fact that some special histological subtypes, such as adenoid cystic and secretory carcinomas, are basal-like and are associated with good outcomes. However, discounting these special types, a study of histological grade 3, invasive carcinoma no special type (NST) also found that there were disparate outcomes for patients, with around half of patients having a good long-term prognosis [42]. Using a compilation of gene expression profiling data sets, Lehmann et al. identified seven molecular subtypes of triple-negative carcinomas [45, 46]. These subgroups exhibited different biological features, including the extent of lymphoid cell infiltration or mesenchymal features, and importantly, significant differences in both the response to chemotherapy and clinical outcomes were observed. The claudin-low molecular subtype is also associated with the basal-like subtype, with tumours likely to be triple-negative invasive carcinoma NST with a high frequency of metaplastic features and medullary pattern [47]. This subtype is poorly understood, and a recent study of the claudin-low molecular subtype using the METABRIC cohort has suggested that claudin-low should be considered a separate phenotype [48]. Molecular apocrine tumours are ER negative and AR positive [49, 50].

Gene Expression-Based Clinical Tools

There are several molecular tests currently in clinical practice that can be used to indicate prognosis for patients with breast cancer, and these have been developed using gene expression profiling data [51, 52]. In fact, many of these tests have been specifically optimised to work with formalin-fixed, paraffin-embedded (FFPE) surgical samples and core biopsy samples given the large pathology repositories containing FFPE material and the increasing importance of core biopsies in patient management. Information from these tests is used in conjunction with traditional clinicopathological parameters to predict the likelihood of disease progression or recurrence. The main features and clinical applicability of key multigene signatures (the 21-gene recurrence score Oncotype DX®, MammaPrint®, the breast cancer index, PAM50 and AIMS) will be described. In the latest eighth edition of the American Joint Committee on Cancer (AJCC) Staging Manual, the Oncotype DX score was included in the pathological prognostic staging for T1-2N0M0, ER-positive, HER2-negative tumours [53, 54].

Testing with Oncotype DX® is performed in a centralised laboratory and uses reverse transcription PCR. A final 'recurrence score' is derived, and this is based on the expression of 21 genes (16 cancer genes and 5 reference genes) using RNA extracted from FFPE tissues [55]. It serves as a prognostic indicator for patients with ER-positive, lymph node-negative breast cancer although it can also be used for those with up to three positive lymph nodes, who are treated with adjuvant

endocrine therapy. The likelihood of benefit from chemotherapy can be provided. A mathematical formula is used to predict the risk of distant relapse at 10 years. Importantly, for its application to core biopsies, it has been used in the neoadjuvant setting. In clinical trials, no patients with a recurrence score of less than 25 showed a complete response to treatment [34, 56, 57]. Based on that evidence, in the most recent American Society of Clinical Oncology (ASCO) clinical practice guideline update, Oncotype DX may be used to guide treatment for hormone receptor-positive, axillary lymph node-negative breast cancer [58]. The ASCO did not find sufficient evidence as yet for the clinical utility of any other multigene expression-based tools.

MammaPrint® is employed to assess the transcription of 70 genes and is used for patients with stage I or II, lymph node-negative breast cancer [59]. FFPE samples can be used. A score is provided indicating either a low or a high risk of developing distant metastases at 5 years. While given FDA approval in 2007 as a prognostic test, it was initially not shown to be predictive of chemotherapy benefit [60, 61]. However, recent findings from the MINDACT prospective, randomised trial demonstrated a rationale to exclude chemotherapy in the low-risk group [62]. Out of a total of 1550 patients at high clinical risk and low genomic risk, there was only a small difference in 5-year survival without distant metastasis between the group that received chemotherapy and the group that did not. The rate was 95.8% vs. 95.0%, respectively. The PROMIS trial found that when using the MammaPrint risk groups, 33.6% of physicians have changed their treatment decisions [63].

The breast cancer index (BCI; Biotheranostics) is a dual molecular assay developed from two complementary gene signatures that were combined to provide greater prognostic utility. The first is a two-gene expression ratio (HOXB13:IL17BR(H/I)), related to oestrogen receptor signalling, which is used to predict the clinical benefit from tamoxifen [64] or extended letrozole treatment [65]. The second assay represents a five gene molecular grade index (MGI) that recapitulates histological grade [66]. It highlights how important genes associated with proliferation are in gene expression signatures [40, 67, 68]. The combined BCI helps clinicians predict the risk of both early and late recurrence and the likely benefit to be gained from extended endocrine therapy for patients with ER-positive, lymph node-negative breast cancer. Patients are stratified into groups showing a low, intermediate or high risk of recurrence. The low and intermediate groups have a similar risk of recurrence in the first 5 years (2.6%), while for years 5–10, the intermediate- and high-risk groups display a similar risk (13.4%) [65].

The PAM50 signature is used to measure the expression levels of 50 genes in a breast tumour sample enabling it to be classified according to how closely it aligns to one of the four key intrinsic molecular subtypes [35, 69–71]. PAM50 is a quantitative reverse transcriptase PCR (qRT-PCR) assay or is available commercially as the NanoString's Prosigna™ Breast Cancer Prognostic Gene Signature Assay, and it can be applied to RNA extracted from FFPE tissue [70]. A risk of recurrence (ROR) score is generated using an algorithm, which includes the tumour's gene signature, tumour size, number of involved lymph nodes and its proliferative index. The ROR score is expressed on a scale of 0–100, indicating the probability of disease recurrence within 10 years. Similar to Oncotype DX® and the BCI, the ROR score stratifies patients into low-, intermediate- and high-risk groups. The PAM50 intrinsic subtype classification was held superior to a six-marker immunohistochemical panel (ER, PR, HER2, Ki-67, CK5/6, EGFR; see below) for both prognosis and prediction of benefit from adjuvant tamoxifen [72]. In the 5–10-year period after diagnosis and 5 years of endocrine treatment for node-negative patients, the PAM50 ROR score was a stronger predictor of late distant recurrences than standard clinicopathological variables [73]. This may assist in deciding whether to offer patients prolonged endocrine therapy or not. The ability to discriminate between luminal tumours in the neoadjuvant setting may also be useful. Using the PAM50 method to determine intrinsic subtypes and risk of relapse scores, the effects of neoadjuvant treatment with anastrozole for patients with ER-positive tumours were investigated, particularly with respect to a decline in the Ki-67 proliferation index on treatment. In the initial treatment phase, luminal A and B tumours showed a similar response; however, in the longer term, Ki-67 remained higher in the luminal B tumours, consistent with a less favourable long-term outlook [74]. Long-term follow-up over 16.6 years has shown that the PAM50 ROR has strong prognostic significance. A study of 653 tumours with long-term follow-up data showed that 53.7% of patients deemed low risk had an excellent breast cancer-specific survival at 15 years (96.3%) compared to patients in the intermediate-risk group [75]. This outperformed Ki-67 and grade used as prognostic factors in multivariate analysis.

The PAM50 method of assigning a tumour to a particular intrinsic subtype is partly determined relative to the tumours of other patients across the panel, thus with a potential for bias. The recently described absolute intrinsic molecular subtyping (AIMS) is similar to some extent to the PAM50 classifier but does not depend on having a comparable normalising data set. Instead, assignment of a tumour to an intrinsic molecular subtype is based on the expression levels of subtype-specific genes relative to levels of other genes within individual samples [76, 77].

EndoPredict (EP) is an eight-gene RNA-based multigene score used to predict the likelihood of distant recurrence in patients with early-stage, ER-positive, HER2-negative tumours [78]. The EP score is combined with clinical risk

factors, tumour size and nodal status to give a more comprehensive EPclin score. A modified EPclin score (mEPclin) can also independently predict the risk of distant recurrence after neoadjuvant chemotherapy [79].

A comparison of 774 postmenopausal women with ER-positive, HER2-negative cancer using six different prognostic signatures was made by Sestak et al. [80]. The signatures used were the Oncotype DX recurrence score, PAM50-based Prosigna ROR, BCI, EPclin, Clinical Treatment Score and 4-marker immunohistochemical score (IHC4, see below). The findings showed that for lymph node-negative cancer, the ROR followed by BCI and EPclin provided the most prognostic information, significantly more than that by Clinical Treatment Score, Oncotype DX and IHC4. There was less information provided by all tests for patients with 1–3 positive lymph nodes. Previously, the ROR has already been shown to be more discriminating in stratifying patients than the Oncotype DX recurrence score [69].

The multigene expression assays mentioned above have mostly been validated for use in low-grade, ER-positive, HER2-negative, node-negative breast cancers. Looking forward, the OPTIMA trial is underway to validate the predictive utility of the Oncotype DX recurrence score and PAM50 ROR in ER-positive, HER2-negative breast cancers with 1–9 involved lymph nodes [81].

Proteomics

The most comprehensive evaluation of patients with breast cancer comes from assessing a combination of the clinical, pathological and biological characteristics of the disease process. The biological behaviour of the tumour is a critical component. Assessment of the tumour genome for mutations and mRNA profiling provides a wealth of information about potential therapeutic targets and prognostic or predictive gene signatures. However, a possibly more significant level of biological information comes from the proteome and the functional end result of the various DNA alterations and mRNA levels that are present. Both the composition of the proteins expressed and their activity play a major role in controlling cell and tissue function. The majority of biomarkers used in clinical practice are proteins, and proteins also comprise the specific targets for many of the small-molecule inhibitors.

The most practicable method of breast cancer subtyping beyond traditional morphology is through immunophenotyping with scoring of the proteins ER, PR and HER2 (along with in situ hybridisation testing). The applicability of immunohistochemistry to small biopsies is well established. The clinical importance of these markers for classification and predicting prognosis is well known (and reviewed in [82]). Adjunct immunohistochemical assessment of the expression of the basal/myoepithelial markers cytokeratins 5/6 and 14 and EGFR and the proliferation marker Ki-67 adds particular value to ER, PR and HER2 testing by helping to classify tumours into surrogate molecular subtypes, and hence is important for molecular subtyping in clinical trials as the IHC4 test (ER, PR, HER2, Ki-67) [83] or with the addition of the basal markers EGFR and CK5/6 [71, 83–85]. Combining the score with clinical parameters (IHC4 + C score) may improve decision-making with respect to using adjuvant chemotherapy to provide similar prognostic information to that given by the 21-gene recurrence score [83, 86–90]. The St. Gallen International Breast Cancer Conference expert panel concluded that the IHC4 method of classification was adequate to help guide the selection of therapeutic regimens [37], but without central testing, quality assurance validation would acquire greater significance [91]. Importantly, Liu and colleagues performed the IHC4 test on 108 paired core needle biopsies and whole sections to assess the score's validity on core biopsy [92]. They showed high concordance, suggesting that the IHC4 can be used on adequately sampled core needle biopsies.

Ki-67 expression as an independent biomarker in the neoadjuvant setting has been investigated in numerous clinical trials with recently published results. These included POETIC for letrozole, PALLET for letrozole with and without palbociclib and ACOSOG Z1031A for aromatase inhibitors (AI) with or without a switch to chemotherapy [93–95]. POETIC showed that a low Ki-67 before and after neoadjuvant treatment was associated with a favourable outcome on standard endocrine therapy compared to a high Ki-67. ACOSOG Z1031A used the Ki-67-based preoperative endocrine prognostic index (PEPI), which included other prognostic variables to examine the risk of relapse and switched neoadjuvant chemotherapy if Ki-67 was greater than 10%. They showed that a higher score was associated with a higher risk of relapse and that chemotherapy efficacy was lower than expected in AI-resistant tumours. PALLET used the Ki-67 proliferation score to measure treatment response to letrozole versus letrozole plus palbociclib. They found a significant difference in the post-treatment Ki-67 reduction with letrozole plus palbociclib of −4.1% compared to letrozole alone of −2.2% in 190 patients. However, there was no difference in clinical response rate over 14 weeks. These findings are promising but indicate that the optimal therapy for ER-positive, AI-resistant tumours needs to be further investigated.

While the ER, PR or HER2 status may be predictive of treatment response, they do not demonstrate if the protein is functionally active. Measuring whether a specific target or its downstream signalling pathway is active may be a better predictive measure of whether a particular targeted therapy will be of benefit, thereby reducing potential de novo treatment resistance. In the setting of endocrine therapy, for example,

the complex interplay between ER, PR, other hormone receptors and their splice variants (e.g. AR or ERbeta) and the co-factors or pioneer factors, such as GATA3 and FOXA1, in regulating oestrogen signalling suggests that measuring ER and PR levels alone may not be the best method for determining the effectiveness of endocrine therapy [96]. Increasing information from molecular studies highlights, for example, that GATA3 and FOXA1 are both mutated in primary breast carcinoma and *ESR1alpha* mutations or ER and PR downregulation is detected in metastatic disease following endocrine therapy, suggesting that these alterations may affect treatment response or mediate resistance [21, 97, 98]. The combination of biomarker expression and mutation status of these genes (and others, e.g. *ERBB2*) or an assessment of functional oestrogen signalling may therefore become an important determinant of whether endocrine therapy will be effective or not.

HER2 status is a strong predictor of response to trastuzumab or similar therapies; however, a significant proportion of patients with HER2-positive tumours do not respond to treatment or develop resistance over time. There are likely to be a number of reasons for this. A functional readout of HER2 activation may be a better predictor of response than assessing whether the gene is amplified or the semi-quantitative assessment of HER2 overexpression provided by the HercepTest. VeraTag™ technology (Monogram Biosciences) has been developed to quantitatively measure protein levels in FFPE tissue sections and can be applied to large biopsy samples. The assay uses two antibodies to the protein(s) of interest, and the quantitation comes from the release of fluorescent tags from the antibodies when they are in close proximity. The HERmark assay uses this technology to quantitatively measure the total HER2 protein and the presence of HER2 homodimers [99]. In an early demonstration of the usefulness of HERmark, Lipton et al. showed that metastatic breast cancer patients with FISH-positive (*HER2*-amplified) breast cancer but with low levels of total HER2 protein had a lesser benefit from trastuzumab than patients whose tumours were FISH positive and with high level of HER2 protein [100]. In the neoadjuvant setting, increasing HER2 levels were associated with improved response to trastuzumab or combination of trastuzumab and lapatinib [101]. Assays are available to measure other proteins in the HER family, including heterodimers between HER2 and HER3, which may indicate active HER2 signalling in the absence of HER2 clinically positive disease (i.e. in situ hybridisation positive or IHC 3+ positive), thus potentially extending the utility of HER2-targeted therapy. HER2 and HER2-related biomarker expression measured by the HERmark assay has been shown to be predictive of improved response to lapatinib plus capecitabine in HER2-positive breast cancer refractory to trastuzumab [102, 103]. This shows the potential of protein expression-based assays to be used as a tool to direct therapeutics in the future.

There are a number of biomarker discovery proteomic platforms available for research that are being utilised to analyse breast cancer cohorts [104] including in the context of clinical trial samples [105]. The reverse-phase protein array (RPPA) [106] is a high-throughput dot blot assay, in which protein extracted from multiple tumour samples is spotted onto a membrane support. Multiple replicate membranes are produced, which are probed using a series of antibodies of interest. An alternative approach is to immobilise a large number of high-quality antibodies to the solid support and hybridise to this a protein extract from a tumour sample. Both approaches are scalable giving the opportunity for the high-throughput analysis of targeted groups of proteins, including phosphorylated (activated) proteins in large sample cohorts. Both techniques are also applicable to FFPE and fresh-frozen material and have been demonstrated to be effective in analysing small samples from FNAs, core biopsies or tumours enriched by laser capture microdissection [104].

Proteomic analysis of tumour samples by RPPA or other methods may become critical in clinical practice when evaluating whether specific signalling pathways are activated or not, prior to the selection of the most appropriate targeted therapy. Materials obtained from core needle biopsies lend themselves very well to this approach. It has been shown that certain proteins are prone to become dephosphorylated during tissue-processing time (from the time of initial ischaemia to the time of tissue fixation); hence, the use of biopsy material for proteomics is perhaps preferred to that of surgical samples [106–108]. Maintaining surgical tissue in a cold environment prior to fixation also improved the detection of certain antigens [107]. The use of laser capture microdissection to prepare the protein extract may also improve the sensitivity of these methods by reducing tissue sample complexity.

These proteomic techniques have been used for tumour classification and biomarker discovery and to investigate the activation status of specific signalling pathways as a way of understanding tumour biology and identifying therapeutic targets. Gonzales-Angulo et al. demonstrated, from an initial analysis of 146 antibodies in 712 breast tumours, that ten protein biomarkers could stratify the tumours into six molecular subgroups that were associated with defined clinical outcomes, and in a validation series of 132 FNA biopsies, these biomarkers predicted complete pathological response to neoadjuvant taxane and anthracycline-taxane-based systemic therapy [109]. TCGA complemented their genomic and transcriptomic analysis of breast cancers with RPPA proteomic profiling of 403 tumours and demonstrated that this could recapitulate the intrinsic molecular subtyping

derived through gene expression profiling. This enabled certain signalling pathways to be evaluated across subtypes. For instance, the PI3K pathway was activated most prominently in basal-like and HER2-enriched subtypes, despite the high frequency of *PI3KCA* mutations in luminal tumours. Alongside HER2 protein activation in the HER2-enriched subgroup were high expression and activation of EGFR. Similar to findings using the HERmark assay, evidence of HER2 phosphorylation and activation of the HER signal transduction cascade (including phosphorylation of EGFR and HER3) was observed in tumours classified as clinically negative for HER2 (i.e. ISH and IHC negative) [105], indicating that some patients may benefit from HER2-HER3-targeted therapy despite this not being indicated by HER2 levels alone. This information was obtained through investigating the HER2 signalling network in fresh-frozen and FFPE core biopsies or surgical material using RPPA, as part of the I-SPY clinical trial. Proteomic profiling of TCGA breast cancers was expanded in the TCGA Pan-Cancer Breast and Gynaecological effort [110]. Two thousand five hundred and seventy-nine tumours from breast, ovary, cervix and uterus were analysed using RPPA. It revealed five main clusters with potential therapeutic targets. These included two clusters that had high levels of hormone receptors and one cluster with high levels of immune markers. These could be paired with hormone therapies and immunotherapies, respectively. They also found that around half of the basal breast cancers clustered with HER2 and luminal B cancers, which suggested similarities not previously seen in transcriptomic analyses. The basal-like, triple-negative subtype has been shown to be heterogeneous in terms of clinical outcomes and molecular characteristics, and this heterogeneity can be seen at the proteomic level. An analysis of high-grade breast cancers using antibody-based arrays showed that there were at least two subgroups of triple-negative tumours, one of which showed high level of deregulation of multiple kinases and their phosphorylated counterparts, including ERK5, which may render the tumour cells sensitive to ERK5 inhibitors [111].

The assays discussed above have enabled the targeted investigation of specific proteins or signalling pathways of interest. They are cost effective, and provided that there is robust quality control, such analysis has the potential to be clinically informative with respect to selection of targeted therapeutics.

Alternative options exist for unbiased proteome profiling (akin to RNA-seq or whole-genome sequencing) using mass spectrometry, which through recent technological advances can now routinely identify and quantify several thousand proteins per sample. Proteins extracted from tissue or fluid are digested into their peptide components, separated by liquid chromatography and then analysed by mass spectrometry. Complex bioinformatics are required to deconvolute peptide mass peaks for the identification of total protein levels and protein modifications, such as phosphorylation and ubiquitylation, enabling the discovery of peptide signatures or biomarkers predictive of disease type or progression, and very importantly the study of functional pathways in disease [112]. Surface-enhanced laser desorption/ionisation time-of-flight (SELDI-TOF) mass spectrometry and matrix-assisted laser desorption/ionisation imaging mass spectrometry (MALDI-IMS) have been applied to breast cancer samples in this context. MALDI-IMS has been developed to assist in the analysis of proteomics across tissue sections, thus providing a spatial relationship between peptide abundance and tumour morphology, and hence a direct comparison between normal, carcinoma in situ and invasive carcinoma, or to assess intratumour heterogeneity. This can be applied to snap-frozen and FFPE tumour tissue and so in principle could be applied to small biopsy samples [104, 113]. Previous methods of mass spectrometry protein profiling required large inputs of important material, therefore not being practical in a clinical diagnostic setting. Recently, the microscale proteogenomic approach was developed, requiring frozen tissue five times smaller than the requirement from the Clinical Proteomic Tumour Analysis Consortium [114, 115]. Using this approach and in numerous other mass spectrometry studies, it has been shown that there may be heterogeneity between intrinsic subgroups and also ambiguity of HER2 amplification and expression [115, 116]. This was seen in both the pretreatment and neoadjuvant tumour settings. Therefore, there is potential for these techniques to utilise small biopsies to guide therapy in treatment-resistant HER2-positive breast cancer clones.

Ductal Carcinoma In Situ (DCIS)

A diagnosis of DCIS on core biopsy is an indication for surgical excision with clear margins, with subsequent adjuvant radiotherapy and sometimes, more recently, addition of endocrine therapy. A mastectomy may be undertaken if there is extensive disease or if adequate margins are difficult to achieve. However, some patients are potentially being overtreated for a disease that may follow only an indolent course. Consequently, much of the research into DCIS has focussed on trying to identify markers predictive of progression to invasive disease. Both clinicopathological characteristics and molecular profiling can be used for risk determination.

Several prospective clinical trials have been established to try to evaluate the clinical outcomes for women with DCIS after active surveillance rather than surgery and radiotherapy. The trials include LORIS (UK, NCT02766881) [117], LORD (The Netherlands, NCT02402607) [118] and COMET (USA, NCT02926911) [119]. Each trial has different and specific enrollment criteria. The requirements for LORIS

include asymptomatic women, who have a vacuum-assisted diagnosis of low- or intermediate-grade DCIS, with a low mitotic rate and no necrosis, and for each case, there is central histopathological review [120]. To be eligible for the LORD study, the women must be greater than 45 years of age, be asymptomatic and have screen-detected pure low-grade DCIS. The COMET trial, which compares operative treatment to monitoring and endocrine treatment, requires the women to be greater than 40 years and have newly diagnosed hormone receptor-positive, HER2-negative low- or intermediate-grade DCIS. Both the LORIS and LORD trials have been converted to registry trials because of low accrual rates, but the COMET trial continues to prospectively compare active surveillance to traditional treatment for women with low-risk disease. A not insignificant challenge with these trials is that it would be difficult to amalgamate the data already accrued, because the inclusion criteria are quite stringent [121]. The reliance on nuclear grade as an inclusion criterion is also potentially difficult because the assignment of grade in DCIS is associated with considerable interobserver variability [122, 123].

Various studies have evaluated patients with DCIS who underwent surgical management, but who would have been eligible for one or other of the active surveillance trials. Rates of invasive cancer detected in the resection specimens have ranged between 6% and 24% indicating the likelihood of at least some patients in the active surveillance arms having occult invasive disease [124].

Using a variety of assay-based and sequencing technologies, many studies have compared the genetic profile of DCIS with that of invasive carcinoma, within individual patients, trying to identify genetic biomarkers that might underlie disease progression [125]. Rane et al. could find no significant differences between the number and types of CNAs identified within DCIS and invasive disease in a meta-analysis of 26 studies, highlighting the difficulties of such an approach [126].

Molecular profiling has also been used to try to guide the management of patients with DCIS. For example, whole-exome sequencing has been utilised to try to characterise the progression from (non-low-grade) DCIS to invasive carcinoma, NST [127]. Both DCIS and invasive disease were shown to be genetically heterogeneous with a variety of evolutionary pathways followed in the progression to invasive disease. In only 28% of cases was clonal selection demonstrated, and these cases also showed higher levels of intralesional genetic heterogeneity than cases without clonal selection.

Molecular profiling of DCIS has contributed relatively more to an understanding of the biology of DCIS than it has to current clinical management. The PAM (Prosigna®) 50-gene signature, which has been used to classify invasive breast carcinoma into five intrinsic subtypes (luminal A, luminal B, HER2 enriched, basal-like and normal-like) [128], has also been utilised in the investigation of DCIS. For example, Lesurf et al. demonstrated substantial differences between the intrinsic subtypes of DCIS, supporting a distinct evolutionary course of disease progression, however, thought to reflect changes specific to the microenvironment, rather than to the individual DCIS cells [129].

Gil Del Alcazar was able to identify immune regulators that could shape tumour evolution, particularly the levels of activated CD8-positive T cells, which might be useful to predict which cases of DCIS may progress to invasion. Additionally, increased expression of immune checkpoint proteins, including PD-L1 and CTLA4, was associated with disease progression [130].

In an attempt to better quantify the risk of recurrence associated with DCIS, the Oncotype DX Breast Cancer Assay for DCIS, also known as the DCIS Score™, was developed and was launched by Genomic Health in 2011 [131–134]. Using FFPE tissue from an excision specimen or core biopsy, the expression levels of 12 genes (7 cancer-related genes and 5 reference genes) are calculated. The seven cancer-related genes are Ki-67, STK15, survivin, cyclin B1, MYBL2, PR and GSTM1. An algorithm is then used to calculate whether a woman who has already had surgery (but not radiation) for DCIS is likely to have the cancer recur either as in situ or invasive disease over the next 10 years. This information is presented in the form of two graphs, one for overall recurrence and the other for invasive recurrence. The scores are 1–39 low risk, 40–54 medium risk and 55 or greater high risk [132, 133].

The DCIS Score™ was validated using patient samples from the Eastern Cooperative Oncology Group Trial (ECOG E5194). This was a prospective, clinical trial that evaluated the rate of subsequent ipsilateral breast events in patients who had DCIS that was treated with local surgical excision but no radiation. Patients in that validation study had a maximum size of 25 mm for low- or intermediate-grade DCIS and 10 mm for high-grade DCIS [135]. A minimum clearance margin of 3 mm was required, although the majority had 10 mm margin. In this validation study, the 10-year risk of developing an ipsilateral breast event was 10.6%, 26.7% and 25.9%, respectively, for low-, intermediate- and high-grade disease, while for an invasive event, the risks were 3.7%, 12.3% and 19.2%. On multivariate analysis, tumour size, menopausal status and DCIS Score™ were each associated with a risk of recurrence.

A more recently developed biological signature to aid in predicting recurrence risk in patients with DCIS and also the potential benefit from radiotherapy is the DCISionRT (PreludeDx™) assay [136]. Scores for seven immunohistochemical markers (PR, HER2, Ki-67, Cox-2, FOXA1, p16/INK4A and SIAH2) are combined with four clinicopathological parameters (patient age, palpability, tumour size and

surgical margin status) of the DCIS. For patients treated with surgery alone, a group of women with an 8% risk of an ipsilateral recurrence at 10 years, and a 10% total breast event at 10 years in a validation study, were identified [137]. However, neither of these tools are likely to guide treatment when utilising a core biopsy alone because of the need to know the pathological features of the case such as lesion size, grade and width of excision margins.

Sentinel Lymph Node Biopsies: OSNA

Assessment of the sentinel lymph node is the initial procedure for investigating the nodal status for breast cancer patients who are clinically node negative, with the sentinel node being the first node likely to be involved by metastatic disease. It can be assessed as part of the routine surgical specimen, or intraoperatively, by frozen section or imprint cytology. The one-step nucleic acid amplification (OSNA) assay, an intraoperative molecular analysis of sentinel lymph nodes, can also be used. OSNA uses rapid nucleic acid amplification technology, which detects and quantifies the copy numbers of cytokeratin 19 mRNA, and this correlates with the size of the metastatic focus, if present. The lymph node is reported as negative or having either a micrometastasis or a macrometastasis. Several studies have shown that it is a good predictor of axillary lymph node status with high levels of sensitivity and specificity [138–141]. The method is slowly replacing conventional methods of intraoperative assessment of the node. All of the lymph node is submitted for processing, thus reducing false-negative results and second-time surgery, with associated cost reduction; however, there is no tissue remaining for morphological assessment. By examining the entire lymph node, as opposed to 2 mm slices, macrometastases can also be identified which would otherwise be falsely judged as micrometastases.

More recently, there have been multiple studies investigating the quantification of sentinel node tumour load using OSNA, in order to attempt to predict whether non-sentinel axillary nodes are involved with tumour [142, 143]. This would reduce the need for unnecessary axillary lymph node dissection and the related complications of such a radical procedure. These studies quantify total tumour load by the amount of cytokeratin 19 mRNA copy numbers present in positive sentinel lymph nodes (copies/μL).

OSNA has been shown to be significantly more sensitive for detecting micrometastases than traditional histology in sentinel lymph nodes. A study of 148 prospective patients and 123 retrospective patients compared the findings of sentinel nodes examined by conventional histology and OSNA [144]. They found that 11.4% of the lymph nodes had micrometastases detected by histology compared to 25% by OSNA. Other findings were comparable. Despite this increased rate of detection, the number of patients treated with axillary dissection was the same between patients examined with histology and OSNA. This is largely attributed to current axillary treatment guidelines becoming more conservative.

The B-CLOSER-II study aimed to investigate the viability of OSNA in axillary staging [145]. They found that histologically examined tissue sections significantly underestimated the presence of lymph node metastases. However, in the patients whose staging would have changed based on molecular methods of detection, prognosis did not. The use of molecular detection of metastases in sentinel lymph node biopsy and axillary staging is becoming more commonly used. Future investigations may help elucidate appropriate quantifiable cut-offs to aid decisions in clinical practice.

Practical Considerations for the Molecular Analysis of Small Tissue Biopsies

Core biopsies are used worldwide for the preoperative diagnosis of breast cancers and are regarded as highly accurate in confirming malignancy [146, 147]. Because of the small amount of material available, there are practical limitations to consider when using these samples for molecular analysis especially as morphological assessment and biomarker analysis generally also have to be undertaken. The choice of molecular testing therefore must be carefully made to suit the needs of the clinical situation, and this may mean gene sequencing, gene expression assays or proteomics. In most circumstances, the use of focused panels of genes or proteins means that relatively less tissue may be needed.

Although biopsies may be snap frozen in liquid nitrogen and stored at ultra-low temperatures (−80 to −140 °C), providing high-quality material for molecular analysis, most are processed as FFPE tissue. This is the best method for morphological assessment and is an excellent means of archiving tissue; however, this may damage nucleic acids and cause cross-linking between DNA and proteins. Formalin penetrates tissue at a rate of 1 mm per hour [148]. Under- or overfixation in formalin can interfere with later retrieval of DNA, RNA or protein. The degradation that occurs may continue in paraffin blocks [149, 150], which may partly explain why DNA extracted from older paraffin blocks can be of lesser quality compared with that from newer blocks. Given this limitation, it is an important prerequisite in developing clinically relevant molecular tests to ensure that they are applicable to FFPE samples. However, because core biopsies are very small and can be rapidly fixed after being obtained from the patient, the quality of the DNA, RNA and protein is generally better than that derived from surgical specimens that undergo FFPE processing. This is particularly pertinent to

the proteomic analysis of certain antigens, as described above.

Decalcification agents may be needed for the processing of biopsies derived from bony metastases, and these agents often contain strong acids that incidentally degrade nucleic acids. Nucleic acids derived from bone biopsies decalcified with EDTA or formic acid are generally of better quantity and quality [151, 152].

Substantial data exists to show that primary tumours exhibit morphological and molecular intratumoural heterogeneity, as do metastatic deposits compared to the primary tumour from which they arose. In considering the analysis of key biomarkers, it is clear that ER, PR and HER2 can all be heterogenous within a primary tumour and the expression of each can change during progression to metastatic disease [97]. These changes in tumour cell characteristics occur during tumour growth and progression due to selective pressures on tumour cells as they grow and interact with their microenvironment and as they respond to therapeutic interventions. A key aspect of this is the clonal evolution of tumour genomes, driven by the accumulation of DNA mutations. As new mutations occur, some confer further selective advantages to the cells and hence lead to the development of subclonal populations with differing biological potential [153]. This phenomenon was highlighted in great detail by recent massively parallel sequencing studies, which elegantly analysed multiple regions of a primary tumour or primary tumours and their matched metastatic deposits [154–160], and perhaps more simply by the detection of *ESR1* mutations in metastases (and liquid biopsies) following endocrine therapy as a mechanism of treatment resistance [21]. The scale of intratumour heterogeneity has been demonstrated in similar studies analysing preinvasive lesions, suggesting that much of the heterogeneity observed in invasive tumours is already existing in neoplastic cells growing within the confines of the ductal structures [154, 156]. Genome sequencing studies have shown that metastatic and post-treatment tumours acquire numerous potentially actionable mutations. These include those involving the genes *ERBB2*, *NF1*, *EGFR*, *KRAS*, *MYC*, *CTCF*, *FOXA1* and *TBX3*, among others [26, 161]. Of these, activating *ERBB2* mutations and *NF1* loss-of-function mutations were found to be more than twice as common in endocrine-resistant tumours and represent important mediators, with *ESR1* mutations, of endocrine treatment resistance. Recently, mutations inactivating the SWI-SNF and JAK2-STAT3 pathways involved in tumour progression were found in significant numbers of metastatic tumours, which have not been seen in earlier studies of primary breast cancer. Other studies have shown that alterations in *AKT1*, *BRCA2*, *CHEK2*, *ESR1*, *FGFR1*, *KMT2C*, *NCOR1*, *PIK3CA* and *TSC2* were significantly enriched in the metastatic population compared to primary breast cancer [24]. This biological phenomenon is therefore an important clinical consideration when assessing small biopsies for morphology, immunohistochemistry and molecular testing, as to whether the biopsy captures the clonal heterogeneity of the primary tumour or not and further whether treatment of metastatic disease should be based on the characteristics of the primary tumour. Biopsies of metastatic deposits have not been routinely performed; however, the National Comprehensive Cancer Network now recommends the biopsy of metastatic foci, especially when they represent the first recurrence of disease and particularly if the ER, PR or HER2 status was unknown or was originally negative [162]. Immunohistochemical analysis and molecular testing on metastatic biopsies would then better inform the most appropriate therapeutic approach to be taken [163].

As well as heterogeneity between tumour cells, a biopsy sample also includes a mixture of normal cells including fibroblasts, inflammatory cells, blood vessels and normal epithelial cells. These cells are considered contamination in many molecular assays, introducing noise to the mRNA species or proteins being analysed or reducing the sensitivity of detecting DNA alterations in the tumour. Clinically useful molecular tests must be sufficiently robust to be able to tolerate at least a degree of this type of contamination. Targeted sequencing of cancer gene panels can tolerate contamination by normal cells owing to the high depth of sequencing coverage obtained, and so in the guidelines for preparing samples for sending to central labs for testing, the maximum tolerated level of contamination by normal cells is defined (e.g. 20% tumour cell content) to enable evidence-based conclusions to be made for each assay. This is certainly the case for proteomic profiling, where reducing the complexity of the analyte has been shown to be very beneficial in biomarker discovery. Tumour cell enrichment is entirely feasible prior to molecular analysis, and this can be achieved by needle dissection or laser capture microdissection of the tissue section to obtain a more pure population of tumour cells. However, laser capture microdissection technology is expensive to establish and can be a time-consuming process.

The 'Liquid Biopsy'

Sampling of the blood of cancer patients is becoming an important mechanism for aiding clinical management. This 'liquid biopsy' provides a relatively non-invasive approach to measure a number of parameters, some of which are already performed routinely for the detection or monitoring of disease (e.g. PSA, CA125 tumour biomarkers) and others, such as circulating tumour cells (CTCs), circulating tumour DNA (ctDNA) and cell-free DNA (cfDNA), hold great promise for monitoring disease progression [164].

CTCs are tumour epithelial cells identified in the lymphovascular system and, when they are detected in bone marrow

biopsies, are referred to as disseminated tumour cells (DTC) [165]. It is easier to obtain a sample from the circulation compared with the bone marrow, making the assessment of CTCs a preferred mode of testing. Given the generally very small number of CTCs compared with millions of blood cells in the background, detection can be difficult and requires special enrichment and detection strategies [166]. CTC enrichment uses both physical and biological characteristics of the tumour cells to distinguish them from background blood cells. The CellSearch system is one of the more widely used CTC detection methods. CTCs are identified by labelling the blood sample with a fluorescent stain for cytokeratins (CK) and one for common leukocyte antigen (CD45) that detects lymphoid cells. A nuclear dye (DAPI) is also added. CTC-positive cells are CK positive, CD45 negative and DAPI positive [167]. Multiple meta-analyses using the CellSearch CTC quantitation method found that the CTC count was an independent prognostic factor for progression-free and overall patient survival in a mixed and neoadjuvant-treated population [168–170]. The EPISPOT (EPithelial ImmunoSPOT) assay was introduced to detect living CTCs to reduce the possibility of detecting apoptotic or non-viable tumour cells [171]. The limited volume of blood that can be obtained from patients is an issue. Saucedo-Zeni and colleagues devised a method using a functionalised and structured Seldinger medical wire that isolates CTCs [172]. The wire is inserted into a peripheral vein and left in situ for 30 min. Patients with early-stage, non-metastatic disease had detectable CTCs while healthy normal controls did not.

Molecular analysis of CTCs or indeed of cfDNA can also be helpful in detecting their presence, which may be of prognostic significance. A recent study by Magbanua et al. examined plasma samples from 84 high-risk early breast cancer patients undergoing neoadjuvant treatment [173]. Samples were taken prior to treatment, during treatment and prior to surgery. They used a multiplex PCR amplification followed by ultra-deep sequencing to detect specific tumour-related mutations, increasing accuracy with high sensitivity. They found that lack of ctDNA clearance was a significant predictor of poor response and metastatic recurrence. Conversely, clearance of ctDNA was associated with improved survival. In the NeoALTTO Phase III trial, the presence of ctDNA was also investigated in *HER2*-amplified breast cancer. They found that detection of ctDNA before neoadjuvant anti-HER2 therapies was associated with a worse treatment response [174]. CTCs could also be potentially useful in identifying specific characteristics of breast tumour cells that have metastasised, such as identifying phenotypes that are either resistant or sensitive to targeted therapy, and this information can be added to treatment algorithms for the oncologist [175]. As described above, the HER2 status of breast tumours can change during disease progression, where patients who initially had a HER2-negative primary disease develop HER2-positive recurrent disease (or vice versa). This may occur due to sampling of a heterogeneous primary tumour or due to the selection of *HER2*-amplified tumour cell clones as a mechanism of treatment resistance. The detection of HER2-positive CTCs would therefore allow for the early administration of HER2-targeted therapy. A randomised controlled trial of 642 patients used the CellSearch system with FITC-labelled anti-HER2 antibodies to assess the HER2 status of CTCs [176]. Programmed death-ligand 1 (PD-L1) has been investigated as a possible CTC biomarker using the same system [177]. The IMpassion130 study has shown that PD-L1 expression in tumour-infiltrating immune cells in the setting of triple-negative breast cancer is a highly reliable predictor of response to immune checkpoint inhibitors [178]. Epithelial-mesenchymal transition (EMT) is a theorised process of neoplastic epithelial cells gaining a mesenchymal phenotype, therefore aiding metastatic spread in advanced cancers. Stemness of cancer cells is another process which may be involved with this and other mechanisms of malignant and metastatic potential. Elevated aldehyde dehydrogenase (ALDH1) has been thought to be associated with increased stemness. TWIST, a transcription factor among others, has been proposed as a biomarker for EMT. Using an immunofluorescence assay, elevated expression of ALDH1 and TWIST in breast cancer patients showed potential as a biomarker of metastatic cancer in liquid biopsy [179].

Cell-free or circulating tumour DNA (cfDNA or ctDNA) can also be used as a biomarker of tumour recurrence. cfDNA, obtained from the plasma fraction of the blood sample, is released from cells as they die and can therefore be derived from any cell in the body. Logically, some cfDNA comes from tumour cells as confirmed by the ability to detect somatic mutations (e.g. gene mutations or translocations) from this component of the blood. It is not possible to determine whether this is from the primary tumour site, CTCs or metastatic site; nevertheless, there is growing evidence to show that the detection of mutations in cfDNA can identify the development of treatment-resistant tumour clones before they become clinically apparent [180–184] and also identify mutations which reflect mechanisms of treatment resistance (e.g. *ESR1* mutations [185]) or targetable mutations (e.g. *HER2* amplification or *PI3KCA* mutations [186–188]). Molecular techniques to analyse cfDNA have been used in multiple clinical trials (BOLERO-2, SoFEA, EFECT, PALOMA-3) to detect *ESR1* mutations and shown to predict inferior progression-free survival (PFS) and overall survival (OS) despite treatment [189–191]. This may be utilised to guide future clinical management. cfDNA has also been used to detect *PIK3CA* mutations and subsequently prolonged PFS with treatment with a PI3K and ER inhibitor [192–194]. The recent ESO-ESMO guidelines for advanced breast cancer (ABC 5) consensus

include the use of ctDNA for the diagnosis of *PIK3CA* mutations for the subsequent commencement of treatment on alpelisib, a CDK4/6 inhibitor [195]. Currently, the generally accepted evidence does not yet show validity for any other use of CTCs or cfDNA in clinical practice as per a joint review by the American Society of Clinical Oncology (ASCO) and the College of American Pathologists (CAP) [196]. However, it is acknowledged that frequent re-evaluation of the literature is required. However, there is current evidence and expert consensus that CTC enumeration should be used to stratify stage IV metastatic breast cancers. There is hope therefore that the genomic analysis of liquid biopsies holds great promise as a relatively easy mechanism to monitor response to treatment and disease progression and may even further determine treatment options.

Summary

Current practice relies heavily on a combination of morphology, immunohistochemistry and in situ hybridisation for a limited number of biomarkers to guide management practices. There have been tremendous advances in molecular technology in recent years, and these have made very valuable contributions to our understanding of cancer biology and are beginning to make a significant impact on our perceptions of patient management. The application of these new technologies to small, FFPE biopsies is imperative given the drive to implement clinical trials of precision medicine (neoadjuvant based and in the metastatic setting) based on the molecular features of tumours. Several challenges are being overcome as tests become implemented as companion diagnostics, including developing centralised testing for new molecular assays and data analysis; evidence-based, standardised guidelines for cut-offs; developing reporting guidelines for clinicians to interpret the molecular data and then implement a recommended treatment plan; delivering data in a clinically relevant time period; and balancing costs of the assay with those of implementing therapeutic recommendations.

A number of molecular options have been discussed, including genomics, transcriptomics and proteomics (Fig. 23.1), and so deciding on the most valuable and appropriate test to apply to such samples requires consideration since the cost and small amount of tissue clearly limit the amount of molecular profiling that can currently be undertaken. This will clearly be context dependent relative to the trial design, but it may not be long before several targeted molecular assays will be available to work in combination to provide a molecular classification (e.g. PAM50), a mutation profile (e.g. of targeted, actionable cancer genes) and a functional protein readout (e.g. by immunohistochemistry or targeted proteomics) to aid personalised patient management.

Acknowledgements We thank Fares Al Ejeh, Nic Waddell, Sriganesh Srihari and Rachael Murray for provision of images used in Fig. 23.1.

References

1. Stratton MR, Campbell PJ, Futreal PA. The cancer genome. Nature. 2009;458(7239):719–24.
2. Holderfield M, Deuker MM, McCormick F, McMahon M. Targeting RAF kinases for cancer therapy: BRAF-mutated melanoma and beyond. Nat Rev Cancer. 2014;14(7):455–67.
3. Hicks J, Krasnitz A, Lakshmi B, Navin NE, Riggs M, Leibu E, et al. Novel patterns of genome rearrangement and their association with survival in breast cancer. Genome Res. 2006;16(12):1465–79.
4. Russnes HG, Vollan HKM, Lingjaerde OC, Krasnitz A, Lundin P, Naume B, et al. Genomic architecture characterizes tumor progression paths and fate in breast cancer patients. Sci Transl Med. 2010;2(38):38ra47.
5. Vollan HK, Rueda OM, Chin SF, Curtis C, Turashvili G, Shah S, et al. A tumor DNA complex aberration index is an independent predictor of survival in breast and ovarian cancer. Mol Oncol. 2015;9(1):115–27.
6. Telli ML, Timms KM, Reid J, Hennessy B, Mills GB, Jensen KC, et al. Homologous recombination deficiency (HRD) score predicts response to platinum-containing neoadjuvant chemotherapy in patients with triple-negative breast cancer. Clin Cancer Res. 2016;22(15):3764–73.
7. Tutt A, Tovey H, Cheang MCU, Kernaghan S, Kilburn L, Gazinska P, et al. Carboplatin in BRCA1/2-mutated and triple-negative breast cancer BRCAness subgroups: the TNT Trial. Nat Med. 2018;24(5):628–37.
8. Timms KM, Mills GB, Perry M, Gutin A, Lanchbury J, Brown R. Comparison of genomic instability test scores used for predicting PARP activity in ovarian cancer. J Clin Oncol. 2020;38(15_Suppl):1586.
9. Alexandrov LB, Kim J, Haradhvala NJ, Huang MN, Tian Ng AW, Wu Y, et al. The repertoire of mutational signatures in human cancer. Nature. 2020;578(7793):94–101.
10. Alexandrov LB, Nik-Zainal S, Wedge DC, Aparicio SA, Behjati S, Biankin AV, et al. Signatures of mutational processes in human cancer. Nature. 2013;500(7463):415–21.
11. Alexandrov LB, Stratton MR. Mutational signatures: the patterns of somatic mutations hidden in cancer genomes. Curr Opin Genet Dev. 2014;24:52–60.
12. Zamborszky J, Szikriszt B, Gervai JZ, Pipek O, Poti A, Krzystanek M, et al. Loss of BRCA1 or BRCA2 markedly increases the rate of base substitution mutagenesis and has distinct effects on genomic deletions. Oncogene. 2017;36(6):746–55.
13. Davies H, Glodzik D, Morganella S, Yates LR, Staaf J, Zou X, et al. HRDetect is a predictor of BRCA1 and BRCA2 deficiency based on mutational signatures. Nat Med. 2017;23(4):517–25.
14. Nik-Zainal S, Davies H, Staaf J, Ramakrishna M, Glodzik D, Zou X, et al. Landscape of somatic mutations in 560 breast cancer whole-genome sequences. Nature. 2016;534(7605):47–54.
15. Nones K, Johnson J, Newell F, Patch AM, Thorne H, Kazakoff SH, et al. Whole-genome sequencing reveals clinically relevant insights into the aetiology of familial breast cancers. Ann Oncol. 2019;30(7):1071–9.
16. Lord CJ, Tutt AN, Ashworth A. Synthetic lethality and cancer therapy: lessons learned from the development of PARP inhibitors. Annu Rev Med. 2015;66:455–70.
17. Chopra N, Tovey H, Pearson A, Cutts R, Toms C, Proszek P, et al. Homologous recombination DNA repair deficiency and PARP inhibition activity in primary triple negative breast cancer. Nat Commun. 2020;11(1):2662.

18. Denkert C, Liedtke C, Tutt A, von Minckwitz G. Molecular alterations in triple-negative breast cancer-the road to new treatment strategies. Lancet. 2017;389(10087):2430–42.
19. Waks AG, Winer EP. Breast cancer treatment: a review. JAMA. 2019;321(3):288–300.
20. Frampton GM, Fichtenholtz A, Otto GA, Wang K, Downing SR, He J, et al. Development and validation of a clinical cancer genomic profiling test based on massively parallel DNA sequencing. Nat Biotechnol. 2013;31(11):1023–31.
21. Jeselsohn R, Yelensky R, Buchwalter G, Frampton G, Meric-Bernstam F, Gonzalez-Angulo AM, et al. Emergence of constitutively active estrogen receptor-alpha mutations in pretreated advanced estrogen receptor-positive breast cancer. Clin Cancer Res. 2014;20(7):1757–67.
22. Vasan N, Yelensky R, Wang K, Moulder S, Dzimitrowicz H, Avritscher R, et al. A targeted next-generation sequencing assay detects a high frequency of therapeutically targetable alterations in primary and metastatic breast cancers: implications for clinical practice. Oncologist. 2014;19(5):453–8.
23. Young G, Wang K, He J, Otto G, Hawryluk M, Zwirco Z, et al. Clinical next-generation sequencing successfully applied to fine-needle aspirations of pulmonary and pancreatic neoplasms. Cancer Cytopathol. 2013;121(12):688–94.
24. van Geelen CT, Savas P, Teo ZL, Luen SJ, Weng CF, Ko YA, et al. Clinical implications of prospective genomic profiling of metastatic breast cancer patients. Breast Cancer Res. 2020;22(1):91.
25. Zehir A, Benayed R, Shah RH, Syed A, Middha S, Kim HR, et al. Mutational landscape of metastatic cancer revealed from prospective clinical sequencing of 10,000 patients. Nat Med. 2017;23(6):703–13.
26. Razavi P, Chang MT, Xu G, Bandlamudi C, Ross DS, Vasan N, et al. The genomic landscape of endocrine-resistant advanced breast cancers. Cancer Cell. 2018;34(3):427–38.e6.
27. Schwaederle M, Parker BA, Schwab RB, Daniels GA, Piccioni DE, Kesari S, et al. Precision oncology: the UC San Diego Moores Cancer Center PREDICT experience. Mol Cancer Ther. 2016;15(4):743–52.
28. Garrido-Castro AC, Spurr LF, Hughes ME, Li YY, Cherniack AD, Kumari P, et al. Genomic characterization of de novo metastatic breast cancer. Clin Cancer Res. 2020;27(4):1105–18.
29. Andre F, Bachelot T, Commo F, Campone M, Arnedos M, Dieras V, et al. Comparative genomic hybridisation array and DNA sequencing to direct treatment of metastatic breast cancer: a multicentre, prospective trial (SAFIR01/UNICANCER). Lancet Oncol. 2014;15(3):267–74.
30. Swanton C. SAFIR01: steps towards precision treatment in breast cancer. Lancet Oncol. 2014;15(3):242–3.
31. Massard C, Michiels S, Ferte C, Le Deley MC, Lacroix L, Hollebecque A, et al. High-throughput genomics and clinical outcome in hard-to-treat advanced cancers: results of the MOSCATO 01 trial. Cancer Discov. 2017;7(6):586–95.
32. Bertucci F, Ng CKY, Patsouris A, Droin N, Piscuoglio S, Carbuccia N, et al. Genomic characterization of metastatic breast cancers. Nature. 2019;569(7757):560–4.
33. Koike Folgueira MA, Brentani H, Carraro DM, De Camargo Barros Filho M, Hirata Katayama ML, Santana de Abreu AP, et al. Gene expression profile of residual breast cancer after doxorubicin and cyclophosphamide neoadjuvant chemotherapy. Oncol Rep. 2009;22(4):805–13.
34. Albain KS, Barlow WE, Shak S, Hortobagyi GN, Livingston RB, Yeh IT, et al. Prognostic and predictive value of the 21-gene recurrence score assay in postmenopausal women with node-positive, oestrogen-receptor-positive breast cancer on chemotherapy: a retrospective analysis of a randomised trial. Lancet Oncol. 2010;11(1):55–65.
35. Dowsett M, Cuzick J, Wale C, Forbes J, Mallon EA, Salter J, et al. Prediction of risk of distant recurrence using the 21-gene recurrence score in node-negative and node-positive postmenopausal patients with breast cancer treated with anastrozole or tamoxifen: a TransATAC study. J Clin Oncol. 2010;28(11):1829–34.
36. Perou CM, Sorlie T, Eisen MB, van de Rijn M, Jeffrey SS, Rees CA, et al. Molecular portraits of human breast tumours. Nature. 2000;406(6797):747–52.
37. Goldhirsch A, Winer EP, Coates AS, Gelber RD, Piccart-Gebhart M, Thurlimann B, et al. Personalizing the treatment of women with early breast cancer: highlights of the St Gallen International Expert Consensus on the Primary Therapy of Early Breast Cancer 2013. Ann Oncol. 2013;24(9):2206–23.
38. Sorlie T, Perou CM, Tibshirani R, Aas T, Geisler S, Johnsen H, et al. Gene expression patterns of breast carcinomas distinguish tumor subclasses with clinical implications. Proc Natl Acad Sci U S A. 2001;98(19):10869–74.
39. Cheang MC, Chia SK, Voduc D, Gao D, Leung S, Snider J, et al. Ki67 index, HER2 status, and prognosis of patients with luminal B breast cancer. J Natl Cancer Inst. 2009;101(10):736–50.
40. Desmedt C, Haibe-Kains B, Wirapati P, Buyse M, Larsimont D, Bontempi G, et al. Biological processes associated with breast cancer clinical outcome depend on the molecular subtypes. Clin Cancer Res. 2008;14(16):5158–65.
41. Guedj M, Marisa L, de Reynies A, Orsetti B, Schiappa R, Bibeau F, et al. A refined molecular taxonomy of breast cancer. Oncogene. 2012;31(9):1196–206.
42. Fulford LG, Reis-Filho JS, Ryder K, Jones C, Gillett CE, Hanby A, et al. Basal-like grade III invasive ductal carcinoma of the breast: patterns of metastasis and long-term survival. Breast Cancer Res. 2007;9(1):R4.
43. Kreike B, van Kouwenhove M, Horlings H, Weigelt B, Peterse H, Bartelink H, et al. Gene expression profiling and histopathological characterization of triple-negative/basal-like breast carcinomas. Breast Cancer Res. 2007;9(5):R65.
44. Putti TC, El-Rehim DM, Rakha EA, Paish CE, Lee AH, Pinder SE, et al. Estrogen receptor-negative breast carcinomas: a review of morphology and immunophenotypical analysis. Mod Pathol. 2005;18(1):26–35.
45. Lehmann BD, Bauer JA, Chen X, Sanders ME, Chakravarthy AB, Shyr Y, et al. Identification of human triple-negative breast cancer subtypes and preclinical models for selection of targeted therapies. J Clin Invest. 2011;121(7):2750–67.
46. Masuda H, Baggerly KA, Wang Y, Zhang Y, Gonzalez-Angulo AM, Meric-Bernstam F, et al. Differential response to neoadjuvant chemotherapy among 7 triple-negative breast cancer molecular subtypes. Clin Cancer Res. 2013;19(19):5533–40.
47. Prat A, Parker JS, Karginova O, Fan C, Livasy C, Herschkowitz JI, et al. Phenotypic and molecular characterization of the claudin-low intrinsic subtype of breast cancer. Breast Cancer Res. 2010;12(5):R68.
48. Fougner C, Bergholtz H, Norum JH, Sorlie T. Re-definition of claudin-low as a breast cancer phenotype. Nat Commun. 2020;11(1):1787.
49. Farmer P, Bonnefoi H, Becette V, Tubiana-Hulin M, Fumoleau P, Larsimont D, et al. Identification of molecular apocrine breast tumours by microarray analysis. Oncogene. 2005;24(29):4660–71.
50. Lehmann-Che J, Hamy AS, Porcher R, Barritault M, Bouhidel F, Habuellelah H, et al. Molecular apocrine breast cancers are aggressive estrogen receptor negative tumors overexpressing either HER2 or GCDFP15. Breast Cancer Res. 2013;15(3):R37.
51. van de Vijver MJ. Molecular tests as prognostic factors in breast cancer. Virchows Archiv. 2014;464(3):283–91.
52. Zelnak AB, O'Regan RM. Genomic subtypes in choosing adjuvant therapy for breast cancer. Oncology (Williston Park). 2013;27(3):204–10.

53. Giuliano AE, Edge SB, Hortobagyi GN. Eighth Edition of the AJCC cancer staging manual: breast cancer. Ann Surg Oncol. 2018;25(7):1783–5.
54. https://cancerstaging.org/references-tools/deskreferences/Pages/Breast-Cancer-Staging.aspx.
55. Paik S, Shak S, Tang G, Kim C, Baker J, Cronin M, et al. A multigene assay to predict recurrence of tamoxifen-treated, node-negative breast cancer. N Engl J Med. 2004;351(27):2817–26.
56. Chang JC, Makris A, Gutierrez MC, Hilsenbeck SG, Hackett JR, Jeong J, et al. Gene expression patterns in formalin-fixed, paraffin-embedded core biopsies predict docetaxel chemosensitivity in breast cancer patients. Breast Cancer Res Treat. 2008;108(2):233–40.
57. Gianni L, Zambetti M, Clark K, Baker J, Cronin M, Wu J, et al. Gene expression profiles in paraffin-embedded core biopsy tissue predict response to chemotherapy in women with locally advanced breast cancer. J Clin Oncol. 2005;23(29):7265–77.
58. Andre F, Ismaila N, Henry NL, Somerfield MR, Bast RC, Barlow W, et al. Use of biomarkers to guide decisions on adjuvant systemic therapy for women with early-stage invasive breast cancer: ASCO clinical practice guideline update-integration of results from TAILORx. J Clin Oncol. 2019;37(22):1956–64.
59. van de Vijver MJ, He YD, van't Veer LJ, Dai H, Hart AA, Voskuil DW, et al. A gene-expression signature as a predictor of survival in breast cancer. N Engl J Med. 2002;347(25):1999–2009.
60. Buyse M, Loi S, van't Veer L, Viale G, Delorenzi M, Glas AM, et al. Validation and clinical utility of a 70-gene prognostic signature for women with node-negative breast cancer. J Natl Cancer Inst. 2006;98(17):1183–92.
61. Knauer M, Mook S, Rutgers EJ, Bender RA, Hauptmann M, van de Vijver MJ, et al. The predictive value of the 70-gene signature for adjuvant chemotherapy in early breast cancer. Breast Cancer Res Treat. 2010;120(3):655–61.
62. Cardoso F, van't Veer LJ, Bogaerts J, Slaets L, Viale G, Delaloge S, et al. 70-Gene signature as an aid to treatment decisions in early-stage breast cancer. N Engl J Med. 2016;375(8):717–29.
63. Tsai M, Lo S, Audeh W, Qamar R, Budway R, Levine E, et al. Association of 70-gene signature assay findings with physicians' treatment guidance for patients with early breast cancer classified as intermediate risk by the 21-gene assay. JAMA Oncol. 2018;4(1):e173470.
64. Ma XJ, Wang Z, Ryan PD, Isakoff SJ, Barmettler A, Fuller A, et al. A two-gene expression ratio predicts clinical outcome in breast cancer patients treated with tamoxifen. Cancer Cell. 2004;5(6):607–16.
65. Sgroi DC, Carney E, Zarrella E, Steffel L, Binns SN, Finkelstein DM, et al. Prediction of late disease recurrence and extended adjuvant letrozole benefit by the HOXB13/IL17BR biomarker. J Natl Cancer Inst. 2013;105(14):1036–42.
66. Ma XJ, Salunga R, Dahiya S, Wang W, Carney E, Durbecq V, et al. A five-gene molecular grade index and HOXB13:IL17BR are complementary prognostic factors in early stage breast cancer. Clin Cancer Res. 2008;14(9):2601–8.
67. Desmedt C, Sotiriou C. Proliferation: the most prominent predictor of clinical outcome in breast cancer. Cell Cycle. 2006;5(19):2198–202.
68. Sotiriou C, Wirapati P, Loi S, Harris A, Fox S, Smeds J, et al. Gene expression profiling in breast cancer: understanding the molecular basis of histologic grade to improve prognosis. J Natl Cancer Inst. 2006;98(4):262–72.
69. Dowsett M, Sestak I, Lopez-Knowles E, Sidhu K, Dunbier AK, Cowens JW, et al. Comparison of PAM50 risk of recurrence score with oncotype DX and IHC4 for predicting risk of distant recurrence after endocrine therapy. J Clin Oncol. 2013;31(22):2783–90.
70. Nielsen T, Wallden B, Schaper C, Ferree S, Liu S, Gao D, et al. Analytical validation of the PAM50-based Prosigna Breast Cancer Prognostic Gene Signature Assay and nCounter Analysis System using formalin-fixed paraffin-embedded breast tumor specimens. BMC Cancer. 2014;14:177.
71. Nielsen TO, Parker JS, Leung S, Voduc D, Ebbert M, Vickery T, et al. A comparison of PAM50 intrinsic subtyping with immunohistochemistry and clinical prognostic factors in tamoxifen-treated estrogen receptor-positive breast cancer. Clin Cancer Res. 2010;16(21):5222–32.
72. Chia SK, Bramwell VH, Tu D, Shepherd LE, Jiang S, Vickery T, et al. A 50-gene intrinsic subtype classifier for prognosis and prediction of benefit from adjuvant tamoxifen. Clin Cancer Res. 2012;18(16):4465–72.
73. Sestak I, Cuzick J, Dowsett M, Lopez-Knowles E, Filipits M, Dubsky P, et al. Prediction of late distant recurrence after 5 years of endocrine treatment: a combined analysis of patients from the Austrian breast and colorectal cancer study group 8 and arimidex, tamoxifen alone or in combination randomized trials using the PAM50 risk of recurrence score. J Clin Oncol. 2015;33(8):916–22.
74. Dunbier AK, Anderson H, Ghazoui Z, Salter J, Parker JS, Perou CM, et al. Association between breast cancer subtypes and response to neoadjuvant anastrozole. Steroids. 2011;76(8):736–40.
75. Ohnstad HO, Borgen E, Falk RS, Lien TG, Aaserud M, Sveli MAT, et al. Prognostic value of PAM50 and risk of recurrence score in patients with early-stage breast cancer with long-term follow-up. Breast Cancer Res. 2017;19(1):120.
76. Paquet ER, Hallett MT. Absolute assignment of breast cancer intrinsic molecular subtype. J Natl Cancer Inst. 2015;107(1):357.
77. Staaf J, Ringner M. Making breast cancer molecular subtypes robust? J Natl Cancer Inst. 2015;107(1):386.
78. Filipits M, Rudas M, Jakesz R, Dubsky P, Fitzal F, Singer CF, et al. A new molecular predictor of distant recurrence in ER-positive, HER2-negative breast cancer adds independent information to conventional clinical risk factors. Clin Cancer Res. 2011;17(18):6012–20.
79. Loibl S, Weber K, Huober J, Krappmann K, Marme F, Schem C, et al. Risk assessment after neoadjuvant chemotherapy in luminal breast cancer using a clinicomolecular predictor. Clin Cancer Res. 2018;24(14):3358–65.
80. Sestak I, Buus R, Cuzick J, Dubsky P, Kronenwett R, Denkert C, et al. Comparison of the performance of 6 prognostic signatures for estrogen receptor-positive breast cancer: a secondary analysis of a randomized clinical trial. JAMA Oncol. 2018;4(4):545–53.
81. Stein RC, Dunn JA, Bartlett JM, Campbell AF, Marshall A, Hall P, et al. OPTIMA prelim: a randomised feasibility study of personalised care in the treatment of women with early breast cancer. Health Technol Assess. 2016;20(10):xxiii–xxix, 1–201.
82. Rakha EA, Reis-Filho JS, Ellis IO. Combinatorial biomarker expression in breast cancer. Breast Cancer Res Treat. 2010;120(2):293–308.
83. Cuzick J, Dowsett M, Pineda S, Wale C, Salter J, Quinn E, et al. Prognostic value of a combined estrogen receptor, progesterone receptor, Ki-67, and human epidermal growth factor receptor 2 immunohistochemical score and comparison with the Genomic Health recurrence score in early breast cancer. J Clin Oncol. 2011;29(32):4273–8.
84. Blows FM, Driver KE, Schmidt MK, Broeks A, van Leeuwen FE, Wesseling J, et al. Subtyping of breast cancer by immunohistochemistry to investigate a relationship between subtype and short and long term survival: a collaborative analysis of data for 10,159 cases from 12 studies. PLoS Med. 2010;7(5):e1000279.
85. Cheang MC, Voduc D, Bajdik C, Leung S, McKinney S, Chia SK, et al. Basal-like breast cancer defined by five biomarkers has superior prognostic value than triple-negative phenotype. Clin Cancer Res. 2008;14(5):1368–76.
86. Barton S, Zabaglo L, A'Hern R, Turner N, Ferguson T, O'Neill S, et al. Assessment of the contribution of the IHC4+C score to deci-

sion making in clinical practice in early breast cancer. Br J Cancer. 2012;106(11):1760–5.
87. Jin L, Chen K, Tan C, Li J, Luo J, Yang Y, et al. Prognostic value of modified IHC4 score in patients with estrogen receptor-positive metastatic breast cancer. Oncologist. 2020;25(8):e1170–e80.
88. Lakhanpal R, Sestak I, Shadbolt B, Bennett GM, Brown M, Phillips T, et al. IHC4 score plus clinical treatment score predicts locoregional recurrence in early breast cancer. Breast (Edinburgh, Scotland). 2016;29:147–52.
89. Sheri A, Smith IE, Hills M, Jones RL, Johnston SR, Dowsett M. Relationship between IHC4 score and response to neo-adjuvant chemotherapy in estrogen receptor-positive breast cancer. Breast Cancer Res Treat. 2017;164(2):395–400.
90. Tan W, Luo W, Jia W, Liang G, Xie X, Zheng W, et al. A combination of Nottingham prognostic index and IHC4 score predicts pathological complete response of neoadjuvant chemotherapy in estrogen receptor positive breast cancer. Oncotarget. 2016;7(52):87312–22.
91. Harbeck N, Sotlar K, Wuerstlein R, Doisneau-Sixou S. Molecular and protein markers for clinical decision making in breast cancer: today and tomorrow. Cancer Treat Rev. 2014;40(3):434–44.
92. Liu M, Tang SX, Tsang JYS, Shi YJ, Ni YB, Law BKB, et al. Core needle biopsy as an alternative to whole section in IHC4 score assessment for breast cancer prognostication. J Clin Pathol. 2018;71(12):1084–9.
93. Ellis MJ, Suman VJ, Hoog J, Goncalves R, Sanati S, Creighton CJ, et al. Ki67 proliferation index as a tool for chemotherapy decisions during and after neoadjuvant aromatase inhibitor treatment of breast cancer: results from the American College of Surgeons Oncology Group Z1031 Trial (Alliance). J Clin Oncol. 2017;35(10):1061–9.
94. Johnston S, Puhalla S, Wheatley D, Ring A, Barry P, Holcombe C, et al. Randomized phase II study evaluating palbociclib in addition to letrozole as neoadjuvant therapy in estrogen receptor-positive early breast cancer: PALLET trial. J Clin Oncol. 2019;37(3):178–89.
95. Smith I, Robertson J, Kilburn L, Wilcox M, Evans A, Holcombe C, et al. Long-term outcome and prognostic value of Ki67 after perioperative endocrine therapy in postmenopausal women with hormone-sensitive early breast cancer (POETIC): an open-label, multicentre, parallel-group, randomised, phase 3 trial. Lancet Oncol. 2020;21(11):1443–54.
96. Ross-Innes CS, Stark R, Teschendorff AE, Holmes KA, Ali HR, Dunning MJ, et al. Differential oestrogen receptor binding is associated with clinical outcome in breast cancer. Nature. 2012;481(7381):389–93.
97. Cummings MC, Simpson PT, Reid LE, Jayanthan J, Skerman J, Song S, et al. Metastatic progression of breast cancer: insights from 50 years of autopsies. J Pathol. 2014;232(1):23–31.
98. Cancer Genome Atlas Network. Comprehensive molecular portraits of human breast tumours. Nature. 2012;490(7418):61–70.
99. Shi Y, Huang W, Tan Y, Jin X, Dua R, Penuel E, et al. A novel proximity assay for the detection of proteins and protein complexes: quantitation of HER1 and HER2 total protein expression and homodimerization in formalin-fixed, paraffin-embedded cell lines and breast cancer tissue. Diagn Mol Pathol. 2009;18(1):11–21.
100. Lipton A, Kostler WJ, Leitzel K, Ali SM, Sperinde J, Weidler J, et al. Quantitative HER2 protein levels predict outcome in fluorescence in situ hybridization-positive patients with metastatic breast cancer treated with trastuzumab. Cancer. 2010;116(22):5168–78.
101. Scaltriti M, Nuciforo P, Bradbury I, Sperinde J, Agbor-Tarh D, Campbell C, et al. High HER2 expression correlates with response to the combination of lapatinib and trastuzumab. Clin Cancer Res. 2015;21(3):569–76.
102. Duchnowska R, Sperinde J, Czartoryska-Arlukowicz B, Mysliwiec P, Winslow J, Radecka B, et al. Predictive value of quantitative HER2, HER3 and p95HER2 levels in HER2-positive advanced breast cancer patients treated with lapatinib following progression on trastuzumab. Oncotarget. 2017;8(61):104149–59.
103. Nishimura R, Toh U, Tanaka M, Saimura M, Okumura Y, Saito T, et al. Role of HER2-related biomarkers (HER2, p95HER2, HER3, PTEN, and PIK3CA) in the efficacy of lapatinib plus capecitabine in HER2-positive advanced breast cancer refractory to trastuzumab. Oncology. 2017;93(1):51–61.
104. Gromov P, Moreira JM, Gromova I. Proteomic analysis of tissue samples in translational breast cancer research. Expert Rev Proteomics. 2014;11(3):285–302.
105. Wulfkuhle JD, Berg D, Wolff C, Langer R, Tran K, Illi J, et al. Molecular analysis of HER2 signaling in human breast cancer by functional protein pathway activation mapping. Clin Cancer Res. 2012;18(23):6426–35.
106. Sonntag J, Schluter K, Bernhardt S, Korf U. Subtyping of breast cancer using reverse phase protein arrays. Expert Rev Proteomics. 2014;11(6):757–70.
107. Gundisch S, Annaratone L, Beese C, Drecol E, Marchio C, Quaglino E, et al. Critical roles of specimen type and temperature before and during fixation in the detection of phosphoproteins in breast cancer tissues. Lab Invest. 2015;95:561–71.
108. Meric-Bernstam F, Akcakanat A, Chen H, Sahin A, Tarco E, Carkaci S, et al. Influence of biospecimen variables on proteomic biomarkers in breast cancer. Clin Cancer Res. 2014;20(14):3870–83.
109. Gonzalez-Angulo AM, Hennessy BT, Meric-Bernstam F, Sahin A, Liu W, Ju Z, et al. Functional proteomics can define prognosis and predict pathologic complete response in patients with breast cancer. Clin Proteomics. 2011;8(1):11.
110. Berger AC, Korkut A, Kanchi RS, Hegde AM, Lenoir W, Liu W, et al. A comprehensive pan-cancer molecular study of gynecologic and breast cancers. Cancer Cell. 2018;33(4):690–705.e9.
111. Al-Ejeh F, Miranda M, Shi W, Simpson PT, Song S, Vargas AC, et al. Kinome profiling reveals breast cancer heterogeneity and identifies targeted therapeutic opportunities for triple negative breast cancer. Oncotarget. 2014;5(10):3145–58.
112. Kolch W, Pitt A. Functional proteomics to dissect tyrosine kinase signalling pathways in cancer. Nat Rev Cancer. 2010;10(9):618–29.
113. Casadonte R, Caprioli RM. Proteomic analysis of formalin-fixed paraffin-embedded tissue by MALDI imaging mass spectrometry. Nat Protoc. 2011;6(11):1695–709.
114. Mertins P, Mani DR, Ruggles KV, Gillette MA, Clauser KR, Wang P, et al. Proteogenomics connects somatic mutations to signalling in breast cancer. Nature. 2016;534(7605):55–62.
115. Satpathy S, Jaehnig EJ, Krug K, Kim BJ, Saltzman AB, Chan DW, et al. Microscaled proteogenomic methods for precision oncology. Nat Commun. 2020;11(1):532.
116. Tyanova S, Albrechtsen R, Kronqvist P, Cox J, Mann M, Geiger T. Proteomic maps of breast cancer subtypes. Nat Commun. 2016;7:10259.
117. Francis A, Thomas J, Fallowfield L, Wallis M, Bartlett JM, Brookes C, et al. Addressing overtreatment of screen detected DCIS; the LORIS trial. Eur J Cancer. 2015;51(16):2296–303.
118. Elshof LE, Tryfonidis K, Slaets L, van Leeuwen-Stok AE, Skinner VP, Dif N, et al. Feasibility of a prospective, randomised, open-label, international multicentre, phase III, non-inferiority trial to assess the safety of active surveillance for low risk ductal carcinoma in situ - The LORD study. Eur J Cancer. 2015;51(12):1497–510.
119. Hwang ES, Hyslop T, Lynch T, Frank E, Pinto D, Basila D, et al. The COMET (Comparison of Operative versus Monitoring and Endocrine Therapy) trial: a phase III randomised controlled clinical trial for low-risk ductal carcinoma in situ (DCIS). BMJ Open. 2019;9(3):e026797.
120. Rea D, Francis A, Wallis M, Thomas J, Bartlett J, Bowden S, et al. Confusion over differences in registration and randomization

criteria for the LORIS (Low-Risk DCIS) trial. Ann Surg Oncol. 2017;24(Suppl 3):566–7.
121. Van Bockstal MR, Agahozo MC, Koppert LB, van Deurzen CHM. A retrospective alternative for active surveillance trials for ductal carcinoma in situ of the breast. Int J Cancer. 2020;146(5):1189–97.
122. Sneige N, Lagios MD, Schwarting R, Colburn W, Atkinson E, Weber D, et al. Interobserver reproducibility of the Lagios nuclear grading system for ductal carcinoma in situ. Hum Pathol. 1999;30(3):257–62.
123. van Dooijeweert C, van Diest PJ, Willems SM, Kuijpers C, Overbeek LIH, Deckers IAG. Significant inter- and intra-laboratory variation in grading of ductal carcinoma in situ of the breast: a nationwide study of 4901 patients in the Netherlands. Breast Cancer Res Treat. 2019;174(2):479–88.
124. Schnitt SJ. Diagnosis of ductal carcinoma in situ in an era of de-escalation of therapy. Mod Pathol. 2021;34(Suppl 1):1–7.
125. Shee K, Muller KE, Marotti J, Miller TW, Wells WA, Tsongalis GJ. Ductal carcinoma in situ biomarkers in a precision medicine era: current and future molecular-based testing. Am J Pathol. 2019;189(5):956–65.
126. Rane SU, Mirza H, Grigoriadis A, Pinder SE. Selection and evolution in the genomic landscape of copy number alterations in ductal carcinoma in situ (DCIS) and its progression to invasive carcinoma of ductal/no special type: a meta-analysis. Breast Cancer Res Treat. 2015;153(1):101–21.
127. Pareja F, Brown DN, Lee JY, Da Cruz Paula A, Selenica P, Bi R, et al. Whole-exome sequencing analysis of the progression from non-low-grade ductal carcinoma in situ to invasive ductal carcinoma. Clin Cancer Res. 2020;26(14):3682–93.
128. Prat A, Parker JS, Fan C, Perou CM. PAM50 assay and the three-gene model for identifying the major and clinically relevant molecular subtypes of breast cancer. Breast Cancer Res Treat. 2012;135(1):301–6.
129. Lesurf R, Aure MR, Mork HH, Vitelli V, Oslo Breast Cancer Research Consortium, Lundgren S, et al. Molecular features of subtype-specific progression from ductal carcinoma in situ to invasive breast cancer. Cell Rep. 2016;16(4):1166–79.
130. Gil Del Alcazar CR, Huh SJ, Ekram MB, Trinh A, Liu LL, Beca F, et al. Immune escape in breast cancer during in situ to invasive carcinoma transition. Cancer Discov. 2017;7(10):1098–115.
131. Marshall E. Breast cancer. Dare to do less. Science. 2014;343(6178):1454–6.
132. Printz C. New method to predict DCIS recurrence. Cancer. 2013;119(22):3899.
133. Solin LJ, Gray R, Baehner FL, Butler SM, Hughes LL, Yoshizawa C, et al. A multigene expression assay to predict local recurrence risk for ductal carcinoma in situ of the breast. J Natl Cancer Inst. 2013;105(10):701–10.
134. Wood WC, Alvarado M, Buchholz DJ, Hyams D, Hwang S, Manders J, et al. The current clinical value of the DCIS Score. Oncology (Williston Park). 2014;28(Suppl 2):C2, 1–8, C3.
135. Hughes LL, Wang M, Page DL, Gray R, Solin LJ, Davidson NE, et al. Local excision alone without irradiation for ductal carcinoma in situ of the breast: a trial of the Eastern Cooperative Oncology Group. J Clin Oncol. 2009;27(32):5319–24.
136. Bremer T, Whitworth PW, Patel R, Savala J, Barry T, Lyle S, et al. A biological signature for breast ductal carcinoma in situ to predict radiotherapy benefit and assess recurrence risk. Clin Cancer Res. 2018;24(23):5895–901.
137. Weinmann S, Leo MC, Francisco M, Jenkins CL, Barry T, Leesman G, et al. Validation of a ductal carcinoma in situ biomarker profile for risk of recurrence after breast-conserving surgery with and without radiotherapy. Clin Cancer Res. 2020;26(15):4054–63.
138. Bettington M, Lakhani SR, Ung OA. Is the one-step nucleic acid amplification assay better for intra-operative assessment of breast sentinel nodes? ANZ J Surg. 2014;84(10):725–9.
139. Pathmanathan N, Renthawa J, French JR, Edstrom-Elder E, Hall G, Mahajan H, et al. Intraoperative sentinel lymph node assessment in breast cancer: a comparison of rapid diagnostic method based on CK19 mRNA expression and imprint cytology. ANZ J Surg. 2014;84(10):730–4.
140. Tamaki Y. One-step nucleic acid amplification assay (OSNA) for sentinel lymph node biopsy. Breast Cancer (Tokyo, Japan). 2015;22(3):230–4.
141. Shi F, Liang Z, Zhang Q, Wang C, Liu X. The performance of one-step nucleic acid amplification assay for intraoperative detection of sentinel lymph node macrometastasis in breast cancer: an updated meta-analysis. Breast (Edinburgh, Scotland). 2018;39:39–45.
142. Fougo JL, Amendoeira I, Brito MJ, Correia AP, Goncalves A, Honavar M, et al. Sentinel node total tumour load as a predictive factor for non-sentinel node status in early breast cancer patients - the porttle study. Surg Oncol. 2020;32:108–14.
143. Pena KB, Kepa A, Cochs A, Riu F, Parada D, Guma J. Total tumor load of mRNA cytokeratin 19 in the sentinel lymph node as a predictive value of axillary lymphadenectomy in patients with neoadjuvant breast cancer. Genes (Basel). 2021;12(1):77.
144. Hintzen KFH, de Rooij L, Schouten N, van Bastelaar J, Corvers SAJ, Janssen A, et al. Molecular analysis of sentinel lymph nodes in patients with breast cancer using one-step nucleic acid amplification (OSNA): does not lead to overtreatment in the current era of de-escalating axillary management. Surg Oncol. 2020;35:224–8.
145. Sansano I, Vieites B, Sancho de Salas M, Garcia C, Amendoeira I, Bernet L, et al. Axillary staging based on molecular analysis: results of the B-CLOSER-II study. Pathol Res Pract. 2020;216(11):153197.
146. Denley H, Pinder SE, Elston CW, Lee AH, Ellis IO. Preoperative assessment of prognostic factors in breast cancer. J Clin Pathol. 2001;54(1):20–4.
147. Verkooijen HM, Peeters PH, Buskens E, Koot VC, Borel Rinkes IH, Mali WP, et al. Diagnostic accuracy of large-core needle biopsy for nonpalpable breast disease: a meta-analysis. Br J Cancer. 2000;82(5):1017–21.
148. Fox CH, Johnson FB, Whiting J, Roller PP. Formaldehyde fixation. J Histochem Cytochem. 1985;33(8):845–53.
149. Cronin M, Pho M, Dutta D, Stephans JC, Shak S, Kiefer MC, et al. Measurement of gene expression in archival paraffin-embedded tissues: development and performance of a 92-gene reverse transcriptase-polymerase chain reaction assay. Am J Pathol. 2004;164(1):35–42.
150. Hewitt SM, Lewis FA, Cao Y, Conrad RC, Cronin M, Danenberg KD, et al. Tissue handling and specimen preparation in surgical pathology: issues concerning the recovery of nucleic acids from formalin-fixed, paraffin-embedded tissue. Arch Pathol Lab Med. 2008;132(12):1929–35.
151. Belluoccio D, Rowley L, Little CB, Bateman JF. Maintaining mRNA integrity during decalcification of mineralized tissues. PLoS One. 2013;8(3):e58154.
152. Singh VM, Salunga RC, Huang VJ, Tran Y, Erlander M, Plumlee P, et al. Analysis of the effect of various decalcification agents on the quantity and quality of nucleic acid (DNA and RNA) recovered from bone biopsies. Ann Diagn Pathol. 2013;17(4):322–6.
153. Yates LR, Campbell PJ. Evolution of the cancer genome. Nat Rev Genet. 2012;13(11):795–806.
154. Casasent AK, Schalck A, Gao R, Sei E, Long A, Pangburn W, et al. Multiclonal invasion in breast tumors identified by topographic single cell sequencing. Cell. 2018;172(1–2):205–17.e12.
155. Desmedt C, Fumagalli D, Pietri E, Zoppoli G, Brown D, Nik-Zainal S, et al. Uncovering the genomic heterogeneity of multifocal breast cancer. J Pathol. 2015;236(4):457–66.

156. Weng Z, Spies N, Zhu SX, Newburger DE, Kashef-Haghighi D, Batzoglou S, et al. Cell-lineage heterogeneity and driver mutation recurrence in pre-invasive breast neoplasia. Genome Med. 2015;7(1):28.
157. Yates LR, Gerstung M, Knappskog S, Desmedt C, Gundem G, Van Loo P, et al. Subclonal diversification of primary breast cancer revealed by multiregion sequencing. Nat Med. 2015;21(7):751–9.
158. Yates LR, Knappskog S, Wedge D, Farmery JHR, Gonzalez S, Martincorena I, et al. Genomic evolution of breast cancer metastasis and relapse. Cancer Cell. 2017;32(2):169–84.e7.
159. Gerlinger M, Rowan AJ, Horswell S, Math M, Larkin J, Endesfelder D, et al. Intratumor heterogeneity and branched evolution revealed by multiregion sequencing. N Engl J Med. 2012;366(10):883–92.
160. Wang Y, Waters J, Leung ML, Unruh A, Roh W, Shi X, et al. Clonal evolution in breast cancer revealed by single nucleus genome sequencing. Nature. 2014;512(7513):155–60.
161. Pearson A, Proszek P, Pascual J, Fribbens C, Shamsher MK, Kingston B, et al. Inactivating NF1 mutations are enriched in advanced breast cancer and contribute to endocrine therapy resistance. Clin Cancer Res. 2020;26(3):608–22.
162. National Comprehensive Cancer Network. Clinical practice guidelines in oncology: breast cancer Version 6; 2020.
163. Andre F, Vicier C, Delaloge S. The horizon of precision medicine in breast cancer: fragmentation, alliance, or reunification? American Society of Clinical Oncology educational book. ASCO American Society of Clinical Oncology Meeting. 2014;e5–10.
164. Ignatiadis M, Dawson SJ. Circulating tumor cells and circulating tumor DNA for precision medicine: dream or reality? Ann Oncol. 2014;25(12):2304–13.
165. Pantel K, Alix-Panabieres C. Bone marrow as a reservoir for disseminated tumor cells: a special source for liquid biopsy in cancer patients. Bonekey Rep. 2014;3:584.
166. Alix-Panabieres C, Schwarzenbach H, Pantel K. Circulating tumor cells and circulating tumor DNA. Annu Rev Med. 2012;63:199–215.
167. Pantel K, Alix-Panabières C. Detection methods of circulating tumor cells. J Thorac Dis. 2012;4(5):446–7.
168. Bidard FC, Michiels S, Riethdorf S, Mueller V, Esserman LJ, Lucci A, et al. Circulating tumor cells in breast cancer patients treated by neoadjuvant chemotherapy: a meta-analysis. J Natl Cancer Inst. 2018;110(6):560–7.
169. Bidard FC, Peeters DJ, Fehm T, Nole F, Gisbert-Criado R, Mavroudis D, et al. Clinical validity of circulating tumour cells in patients with metastatic breast cancer: a pooled analysis of individual patient data. Lancet Oncol. 2014;15(4):406–14.
170. Ye Z, Wang C, Wan S, Mu Z, Zhang Z, Abu-Khalaf MM, et al. Association of clinical outcomes in metastatic breast cancer patients with circulating tumour cell and circulating cell-free DNA. Eur J Cancer. 2019;106:133–43.
171. Alix-Panabieres C. EPISPOT assay: detection of viable DTCs/CTCs in solid tumor patients. Recent Results Cancer Res. 2012;195:69–76.
172. Saucedo-Zeni N, Mewes S, Niestroj R, Gasiorowski L, Murawa D, Nowaczyk P, et al. A novel method for the in vivo isolation of circulating tumor cells from peripheral blood of cancer patients using a functionalized and structured medical wire. Int J Oncol. 2012;41(4):1241–50.
173. Magbanua MJM, Swigart LB, Wu HT, Hirst GL, Yau C, Wolf DM, et al. Circulating tumor DNA in neoadjuvant-treated breast cancer reflects response and survival. Ann Oncol. 2020;32(2):229–39.
174. Rothe F, Silva MJ, Venet D, Campbell C, Bradburry I, Rouas G, et al. Circulating tumor DNA in HER2-amplified breast cancer: a translational research substudy of the NeoALTTO phase III trial. Clin Cancer Res. 2019;25(12):3581–8.
175. Rossi G, Ignatiadis M. Promises and pitfalls of using liquid biopsy for precision medicine. Cancer Res. 2019;79(11):2798–804.
176. Jaeger BAS, Neugebauer J, Andergassen U, Melcher C, Schochter F, Mouarrawy D, et al. The HER2 phenotype of circulating tumor cells in HER2-positive early breast cancer: a translational research project of a prospective randomized phase III trial. PLoS One. 2017;12(6):e0173593.
177. Mazel M, Jacot W, Pantel K, Bartkowiak K, Topart D, Cayrefourcq L, et al. Frequent expression of PD-L1 on circulating breast cancer cells. Mol Oncol. 2015;9(9):1773–82.
178. Schmid P, Rugo HS, Adams S, Schneeweiss A, Barrios CH, Iwata H, et al. Atezolizumab plus nab-paclitaxel as first-line treatment for unresectable, locally advanced or metastatic triple-negative breast cancer (IMpassion130): updated efficacy results from a randomised, double-blind, placebo-controlled, phase 3 trial. Lancet Oncol. 2020;21(1):44–59.
179. Papadaki MA, Kallergi G, Zafeiriou Z, Manouras L, Theodoropoulos PA, Mavroudis D, et al. Co-expression of putative stemness and epithelial-to-mesenchymal transition markers on single circulating tumour cells from patients with early and metastatic breast cancer. BMC Cancer. 2014;14:651.
180. Bettegowda C, Sausen M, Leary RJ, Kinde I, Wang Y, Agrawal N, et al. Detection of circulating tumor DNA in early- and late-stage human malignancies. Sci Transl Med. 2014;6(224):224ra24.
181. Cohen JD, Li L, Wang Y, Thoburn C, Afsari B, Danilova L, et al. Detection and localization of surgically resectable cancers with a multi-analyte blood test. Science (New York, NY). 2018;359(6378):926–30.
182. Dawson SJ, Tsui DW, Murtaza M, Biggs H, Rueda OM, Chin SF, et al. Analysis of circulating tumor DNA to monitor metastatic breast cancer. N Engl J Med. 2013;368(13):1199–209.
183. Leary RJ, Kinde I, Diehl F, Schmidt K, Clouser C, Duncan C, et al. Development of personalized tumor biomarkers using massively parallel sequencing. Sci Transl Med. 2010;2(20):20ra14.
184. Phallen J, Sausen M, Adleff V, Leal A, Hruban C, White J, et al. Direct detection of early-stage cancers using circulating tumor DNA. Sci Transl Med. 2017;9(403):eaan2415.
185. Sefrioui D, Perdrix A, Sarafan-Vasseur N, Dolfus C, Dujon A, Picquenot JM, et al. Short report: Monitoring ESR1 mutations by circulating tumor DNA in aromatase inhibitor resistant metastatic breast cancer. Int J Cancer. 2015;137(10):2513–9.
186. Gevensleben H, Garcia-Murillas I, Graeser MK, Schiavon G, Osin P, Parton M, et al. Noninvasive detection of HER2 amplification with plasma DNA digital PCR. Clin Cancer Res. 2013;19(12):3276–84.
187. Ma CX, Bose R, Gao F, Freedman RA, Telli ML, Kimmick G, et al. Neratinib efficacy and circulating tumor DNA detection of HER2 mutations in HER2 nonamplified metastatic breast cancer. Clin Cancer Res. 2017;23(19):5687–95.
188. Romero A, Acosta-Eyzaguirre D, Sanz J, Moreno F, Serrano G, Diaz-Rubio E, et al. Identification of E545k mutation in plasma from a PIK3CA wild-type metastatic breast cancer patient by array-based digital polymerase chain reaction: circulating-free DNA a powerful tool for biomarker testing in advance disease. Transl Res. 2015;166(6):783–7.
189. Chandarlapaty S, Chen D, He W, Sung P, Samoila A, You D, et al. Prevalence of ESR1 mutations in cell-free DNA and outcomes in metastatic breast cancer: a secondary analysis of the BOLERO-2 clinical trial. JAMA Oncol. 2016;2(10):1310–5.
190. O'Leary B, Cutts RJ, Liu Y, Hrebien S, Huang X, Fenwick K, et al. The genetic landscape and clonal evolution of breast cancer resistance to palbociclib plus fulvestrant in the PALOMA-3 trial. Cancer Discov. 2018;8(11):1390–403.
191. Turner NC, Swift C, Kilburn L, Fribbens C, Beaney M, Garcia-Murillas I, et al. ESR1 mutations and overall survival on fulvestrant versus exemestane in advanced hormone receptor-positive

breast cancer: a combined analysis of the phase III SoFEA and EFECT trials. Clin Cancer Res. 2020;26(19):5172–7.
192. Juric D, Andre F, Singer C, Sohn J, Campone M, Loibl S, et al. Abstract P4-10-04: Clinical outcomes of alpelisib in hormone receptor-positive, human epidermal growth factor receptor-2-negative advanced breast cancer by next-generation sequencing-detected PIK3CA alteration status and phosphatase and tensin homolog loss: biomarker analysis from the SOLAR-1 study. 2020;P4-10 p.
193. Juric D, Ciruelos E, Rubovszky G, Campone M, Loibl S, Rugo HS, et al. Abstract GS3-08: Alpelisib + fulvestrant for advanced breast cancer: subgroup analyses from the phase III SOLAR-1 trial. Cancer Res. 2019;79:GS3–08.
194. Rugo HS, Mayer I, Conte P, Loibl S, Campone M, Juric D, et al. Abstract CT142: Prevalence of PIK3CA mutations in patients with hormone receptor-positive, human epidermal growth factor-2-negative advanced breast cancer from the SOLAR-1 trial. Cancer Res. 2019;79(13 Suppl):CT142. https://doi.org/10.1158/1538-7445.SABCS18-CT142.
195. Cardoso F, Paluch-Shimon S, Senkus E, Curigliano G, Aapro MS, Andre F, et al. 5th ESO-ESMO international consensus guidelines for advanced breast cancer (ABC 5). Ann Oncol. 2020;31(12):1623–49.
196. Merker JD, Oxnard GR, Compton C, Diehn M, Hurley P, Lazar AJ, et al. Circulating tumor DNA analysis in patients with cancer: American Society of Clinical Oncology and College of American Pathologists Joint Review. Arch Pathol Lab Med. 2018;142(10):1242–53.

Metastases to the Breast

24

Ashley Cimino-Mathews, Emily B. Ambinder, Pedram Argani, and Marissa J. White

Overview

Metastases to the breast are rare, found in 0.08% of suspicious breast lesions and 0.17% of breast malignancies, yet correct identification of a neoplasm as a *metastasis* is imperative for patient treatment planning and appropriate prognostication [1]. However, this can pose a diagnostic challenge not only due to the rarity of metastases to the breast in comparison to the incidence of primary breast carcinoma, but also due to the lack of clinical history that may accompany a patient's pathologic specimen. In addition, although the majority of patients with metastases to the breast have a known cancer history, with up to 77% of patients having known active metastatic disease [2–4], a significant subset present with no known cancer history. The breast is the first site of metastatic disease in 11–31% of patients [2–5]. Although certain histologic features may suggest that a neoplasm in the breast is not primary to the breast, a clinical workup and a targeted immunohistochemical panel are often necessary to reach the correct diagnosis. Metastases to the breast may be diagnosed on core needle biopsy (CNB) or on fine needle aspiration [6, 7], and it is imperative that the correct diagnosis be made to prevent unnecessary surgery (such as mastectomy).

A. Cimino-Mathews (✉) · P. Argani
Departments of Pathology and Oncology, The Johns Hopkins Hospital, Baltimore, MD, USA
e-mail: acimino@jhmi.edu; pargani@jhmi.edu

E. B. Ambinder
The Russell H. Morgan Department of Radiology and Radiologic Science, The Johns Hopkins Hospital, Baltimore, MD, USA
e-mail: emcinto8@jhmi.edu

M. J. White
Department of Pathology, The Johns Hopkins Hospital, Baltimore, MD, USA
e-mail: mwhite44@jhmi.edu

Hematopoietic neoplasms are the most common extramammary neoplasm to involve the breast, but these are discussed separately in Chap. 20. In clinical series, non-hematopoietic, solid-organ metastases to the breast comprise approximately 0.2–1.2% of breast neoplasms [2, 5, 8, 9], with a higher frequency in postmortem studies [10]. In adults, carcinomas as a group comprise the majority of solid-organ metastases to the breast, followed by melanoma and sarcoma [2, 4, 11]. However, melanoma is the single most common solid-organ neoplasm to involve the breast [2–4, 11–13], and the most common carcinoma types to involve the breast are pulmonary [2, 11] and ovarian [4]. In certain populations, the frequency of metastases to the breast varies; for instance, in a Korean study, the most common extramammary source of metastases to the breast was the stomach [14], likely reflecting the high prevalence of gastric adenocarcinoma in this population. Among sarcomas, leiomyosarcoma is the most common to metastasize to the adult breast [4].

Metastases to the breast are more common in women than in men [2–5]. However, in one single-institution series containing 13 male patients, similar to women, the most common metastases to the breast were melanoma and lung carcinoma [4], followed by renal cell carcinoma, Merkel cell carcinoma, prostate carcinoma, and papillary thyroid carcinoma. In the pediatric population, metastatic neoplasms to the breast outnumber primary breast malignancies, with metastatic rhabdomyosarcoma being the most common breast neoplasm in children and adolescents [15, 16].

Gross and Radiologic Features of Metastases to the Breast

The majority of metastases to the breast are detected by physical exam [3], with approximately 14% detected on imaging alone. Most metastases are unilateral, solitary masses in the breast parenchyma, but 8–25% present as bilat-

© The Author(s), under exclusive license to Springer Nature Switzerland AG 2022
S. J. Shin et al. (eds.), *A Comprehensive Guide to Core Needle Biopsies of the Breast*,
https://doi.org/10.1007/978-3-031-05532-4_24

eral or multifocal breast masses [2–4], and a smaller subset present as solitary axillary masses.

There are no radiographic features that are diagnostic of a metastasis to the breast, and the radiographic findings can overlap with those of either benign lesions or primary breast carcinoma. Imaging findings on mammography and ultrasound for metastatic carcinoma, melanoma, and sarcoma to the breast are presented in Fig. 24.1a–h. Metastases to the breast may be seen on imaging performed as part of an evaluation for a breast palpable mass (Fig. 24.1a–d), as a new "incidental finding" on

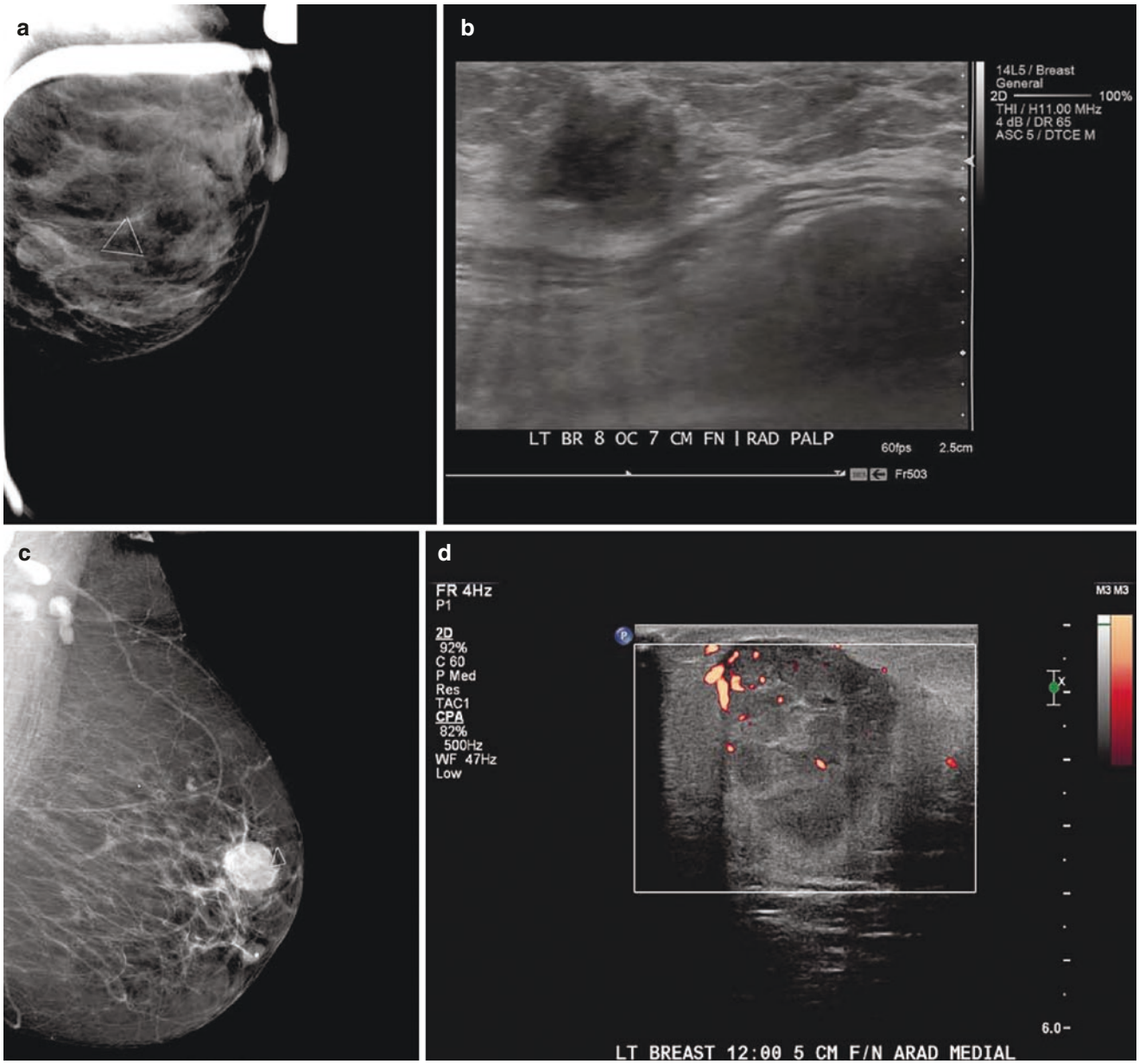

Fig. 24.1 Mammography and ultrasound correlates of biopsy-confirmed metastatic carcinoma, melanoma, and sarcoma to the breast. (**a**, **b**) Metastatic ovarian carcinoma: A 48-year-old female with a known ovarian carcinoma presented with a palpable left-breast mass. Digital mammographic views show heterogeneously dense breast tissue with no visible mass (triangle at palpable area of concern), but ultrasound shows an irregular mass with angulated margins and a heterogeneous hypoechoic pattern. (**c**, **d**) Metastatic lung carcinoma: A 66-year-old female with a known history of lung carcinoma presented with a palpable left-breast mass. Digital mammographic views show mainly fat density and a dense, round mass with circumscribed and indistinct margins and no associated calcifications. Ultrasound shows a vascular irregular mass with angular margins. The echo pattern is heterogeneous with an irregular anechoic central portion, echogenic areas, and an overall hypoechoic mass. There is posterior acoustic enhancement. This pattern of metastatic lesion is consistent with hematogenous spread of tumor. (**e**, **f**) Metastatic melanoma: A 42-year-old female with a history of melanoma had a screening mammogram that revealed a subtle equal-density round mass with circumscribed margins and no associated calcifications, which on ultrasound is hypoechoic, round, and circumscribed with no posterior sound change. (**g**, **h**) Metastatic leiomyosarcoma: A 67-year-old female with a known history of leiomyosarcoma had a screening mammogram that revealed primarily fat density tissue with a high-density oval circumscribed mass with no associated calcifications, which on ultrasound is parallel, oval, circumscribed, hypoechoic, and avascular with no posterior sound change

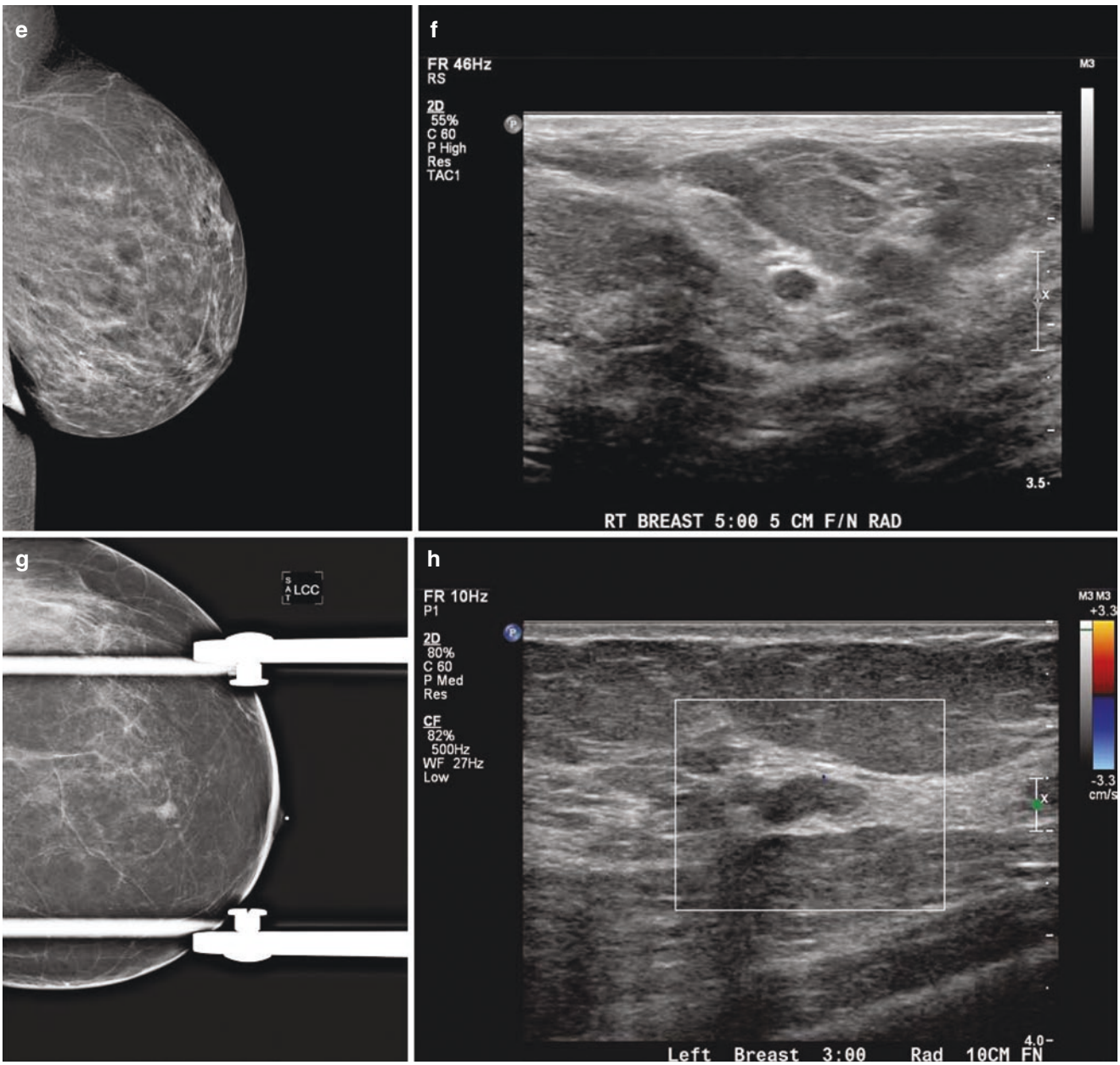

Fig. 24.1 (continued)

screening mammography (Fig. 24.1e–h), or as part of a staging workup for known metastatic disease (Fig. 24.2). Metastases to the breast have a wide range of radiographic characteristics; some may only be visible on ultrasound and not on the corresponding mammogram (Fig. 24.1a, b), whereas others are visible on both mammogram and ultrasound (Fig. 24.1c–h).

Metastases to the breast usually present as one or multiple circumscribed masses without corresponding microcalcifications (Fig. 24.1) [13, 17]. Because they often have circumscribed margins, metastases can be mistaken for benign masses. Microcalcifications in metastases to the breast are almost exclusively reported in metastatic gynecologic serous carcinomas [4, 5] and rarely with gastrointestinal, thyroid, or other primaries [14]. These mammographic features contrast with those of primary breast carcinomas, which are typically spiculated, irregular masses, often with associated microcalcifications (Fig. 24.3). More overlap of imaging findings occurs between metastatic lesions and primary breast cancers when the metastases to the breast involve the breast lymphatics. In this setting, the findings resemble inflammatory breast cancer, including adenopathy as well as breast skin and trabecular thickening.

The most common ultrasound features of metastases to the breast are the presence of one or multiple vascular, homoge-

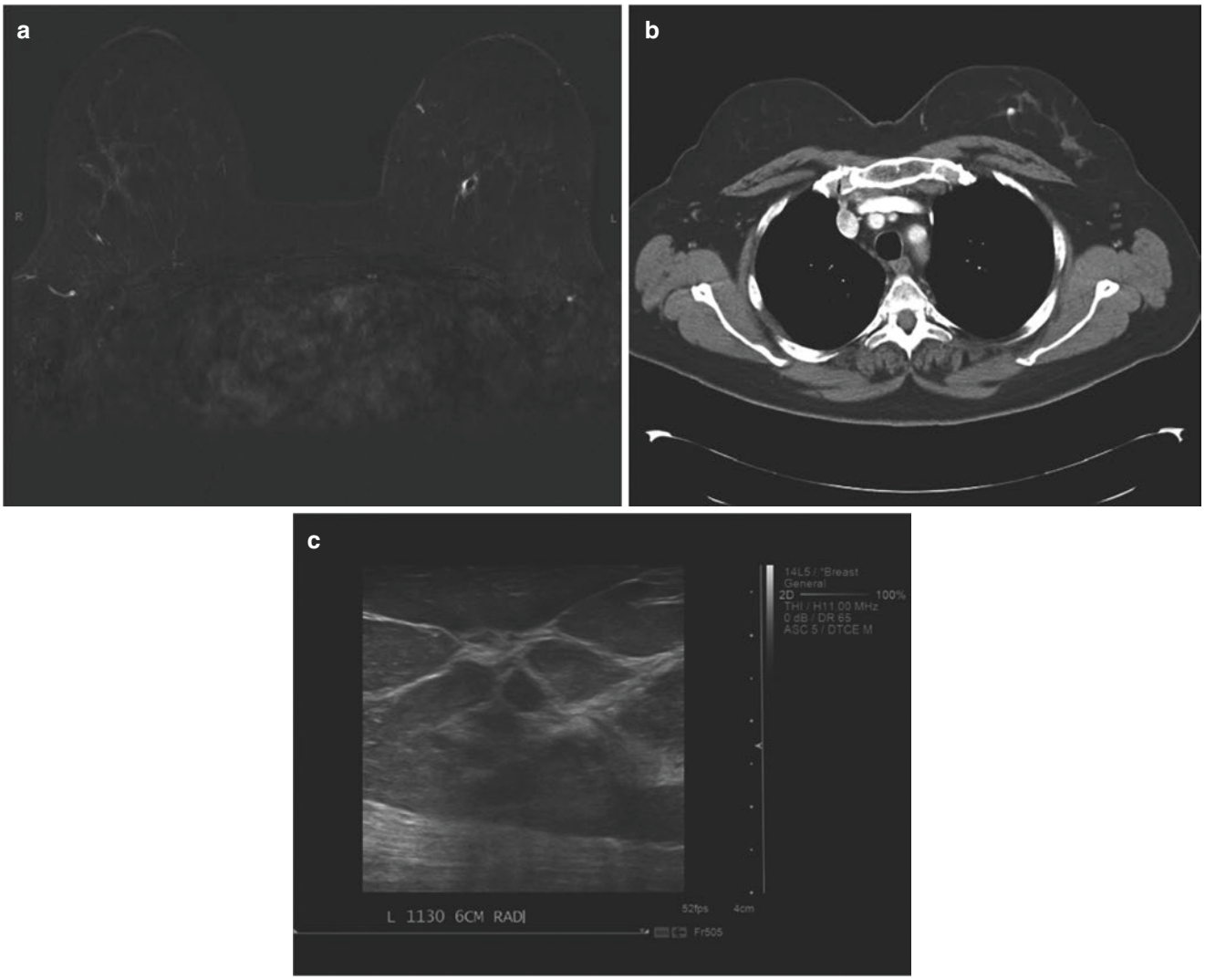

Fig. 24.2 Metastatic renal cell carcinoma to the breast detected on a staging workup. (**a**) A 54-year-old female with known renal cell carcinoma without known metastatic disease underwent a staging computed tomography scan that showed an enhancing round circumscribed mass in the inner left breast. There was no corresponding mammographic correlate (not shown). (**b**) Contrast-subtracted T1 fat-saturated axial breast MRI image shows the signal void artifact from the biopsy clip and a surrounding enhancing irregular mass with irregular margins. (**c**) Ultrasound shows a vascular isoechoic round mass with microlobulated margins and no posterior sound change at a middle depth in the breast

neously hypoechoic, oval or round masses with microlobulated or circumscribed margins and no posterior sound change (Figs. 24.1 and 24.3) [13, 17–19]. In contrast, primary breast carcinomas often show spiculated margins (Fig. 24.3) with posterior acoustic shadowing. However, heterogeneous echotexture is not uncommon in metastatic lesions, and rarely some may be anechoic. The lack of spiculation and irregularity is likely related to the lack of desmoplastic reaction in most metastatic lesions [4, 14]. Magnetic resonance imaging (MRI) and computer tomography scans are not commonly performed to assess metastases to the breast, as the lesions are typically biopsied when palpable or seen on mammography or ultrasound. However, MRI typically shows masses to be isointense to breast tissue on T1 and T2 with marked rapid enhancement (Fig. 24.2), similar characteristics to primary breast cancer. Melanoma is distinct in that it may be hyperintense on T1 due to the paramagnetic properties of melanin in the lesions [20].

If the lesions are bilateral, round, and circumscribed, they can be misinterpreted to be benign, with a differential diagnosis that includes cysts, fibroadenomas, and pseudoangiomatous stromal hyperplasia. Patient's history and comparison to prior exams are particularly important in these cases.

There is no single gross pathologic feature that is diagnostic of metastases to the breast. However, metastases to the breast are often firm, oval to round, single, well circumscribed, and sharply demarcated from the adjacent breast parenchyma [2, 4, 8]. These gross features would not be appreciated at the time of CNB evaluation.

Microscopic Features

Approximately 30% of metastases to the breast show no specific histologic features to distinguish them from primary breast carcinomas [5]. However, metastases to the breast often lack desmoplasia, microcalcifications, and an in situ component [4, 5], which are features commonly seen in primary breast carcinomas. Metastases to the breast frequently do not display evidence of lymphovascular invasion [4, 5]. However, when lymphovascular invasion is present, metastases to the breast may mimic ductal carcinoma in situ by distending lymphovascular spaces, which often creates a solid and micropapillary growth pattern [21]. One case of metastatic cancer (pancreatic endocrine neoplasm) colonizing duct epithelium to mimic ductal carcinoma in situ has been reported [22]. The presence of certain histologic findings may alert the pathologist to the possibility of a metastasis, such as estrogen receptor (ER) negativity in an otherwise well-differ-

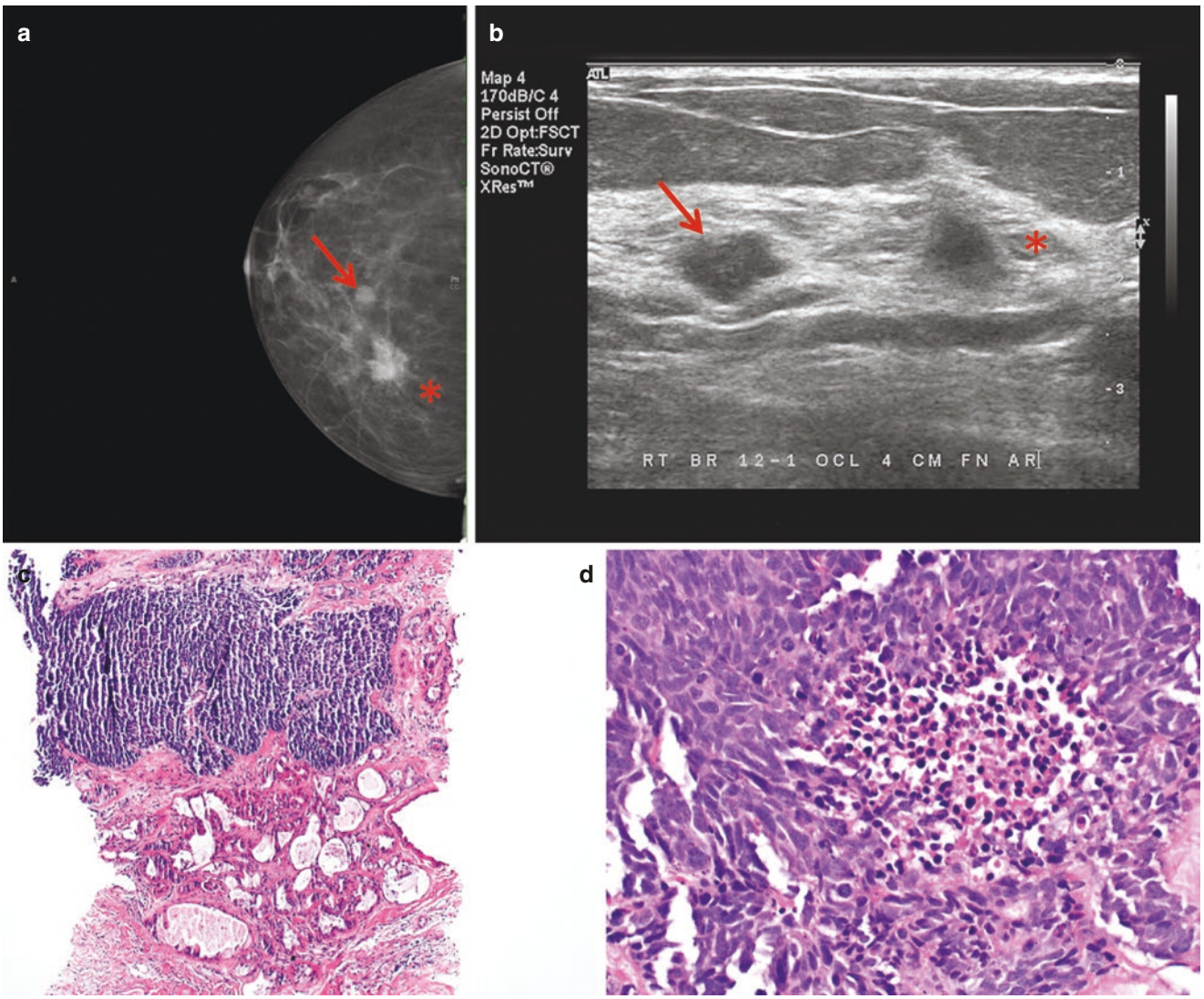

Fig. 24.3 Metastatic pulmonary small-cell carcinoma to the breast with an adjacent primary invasive ductal carcinoma. A 66-year-old woman with known pulmonary small-cell carcinoma was found to have two ipsilateral breast masses on screening mammography. (**a**) Digital mammogram shows scattered areas of fibroglandular density, with a high-density oval circumscribed mass (arrow) and an adjacent high-density irregular spiculated mass (asterisk). There are no calcifications associated with either mass. (**b**) Corresponding ultrasound shows both masses. One is hypoechoic oval with microlobulated margins (arrow), and the other is hypoechoic irregular with irregular margins (asterisk). These two appearances show the differences that are typical between a metastatic lesion (arrow) and a primary breast cancer (asterisk). (**c–e**) CNB of the oval mass (arrow) reveals atypical, infiltrating cells with hyperchromatic and angulated nuclei, no stromal desmoplasia, abundant mitoses, and necrosis. The cells are negative for ER by immunohistochemistry. These features are histologically characteristic of small-cell carcinoma. (**f–h**) In contrast, CNB of the irregular mass (asterisk) reveals a gland-forming adenocarcinoma, with low nuclear grade, associated stromal desmoplasia, and strong ER positivity by immunohistochemistry, characteristic of primary invasive ductal carcinoma

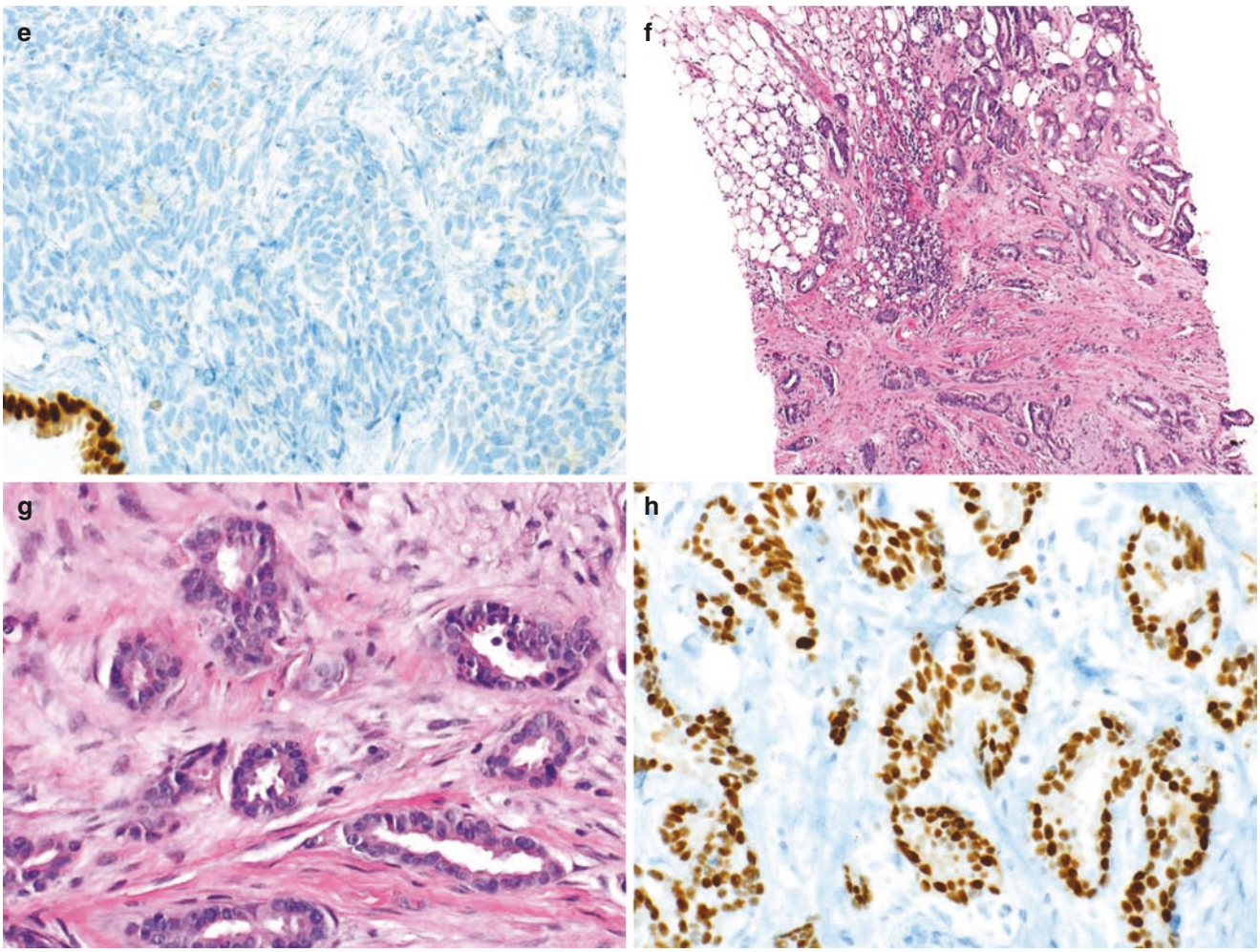

Fig. 24.3 (continued)

entiated adenocarcinoma (suggestive of pulmonary or gastrointestinal adenocarcinoma), or the presence of melanin pigment in a poorly differentiated epithelioid neoplasm (suggestive of melanoma). Immunostains are helpful and often necessary in distinguishing a primary carcinoma from a metastatic lesion, particularly in the case of an unknown primary. In one series, immunostains were used in 45% of lesions and most frequently included ER, progesterone receptor (PR), cytokeratin (CK) AE1/AE3, S100 protein, and thyroid transcription factor 1 (TTF1) [4]. The microscopic features, differential diagnoses, and immunohistochemical workup of specific metastatic entities will be discussed here.

Breast-Specific Markers

In addition to a thorough clinical history, immunohistochemistry is often key in distinguishing a primary breast carcinoma from a metastatic neoplasm involving the breast. No one single immunostain is entirely sensitive or specific for a given entity; thus, employing a selective panel of immunostains is necessary [9]. Breast carcinomas are typically immunoreactive for CK7 and negative for CK20 [23]. Gross cystic disease fluid protein-15 (GCDFP-15) and mammaglobin are traditional markers that are used to support a primary breast origin; overall, mammaglobin is reportedly more sensitive [24–26] but less specific [25, 26] for breast carcinoma than GCDFP-15. However, most triple-negative breast carcinomas are negative for both mammaglobin and GCDFP-15 [24, 27, 28], which limits the utility of these immunostains in the context of an ER-negative carcinoma. Immunohistochemistry for GATA3 has proven to be at least equally sensitive for breast carcinoma as mammaglobin and GCDFP-15 [29], and it has the added benefit of labeling 43% of triple-negative breast carcinomas [30]. SOX10 is an immunostain that was traditionally used to label neural crest-derived neoplasms such as nerve sheath tumors and melanomas [31], but it also labels the myoepithelial cells and neoplasms of the salivary gland and breast [32–35], including 66% of primary triple-negative breast carcinomas [32] and 57% of metastatic triple-negative

breast carcinomas [36]. Combined use of GATA3 and SOX10 immunohistochemistry can identify the majority of triple-negative breast carcinomas [37, 38]. Approximately half of all breast carcinomas are also immunoreactive for S100 protein [39], which like SOX10 is a potential diagnostic pitfall in the differential diagnosis of breast carcinoma and melanoma. Additional site-specific immunomarkers will be discussed in detail in the following sections.

Specific Entities

Hematopoietic Neoplasms

Hematopoietic neoplasms are the most common extramammary neoplasm to involve the breast, and they are discussed in depth separately (Chap. 20). Secondary involvement of the breast is generally a manifestation of systemic disease. Briefly, these hematopoietic neoplasms include diffuse large B cell lymphomas [40] (Fig. 24.4), acute leukemias/myeloid sarcomas [41] (Fig. 24.5), and myelomas [10, 42] (Fig. 24.6). Diffuse large B cell lymphoma is characterized by sheets of dyscohesive cells with high nuclear-to-cytoplasmic ratio that are immunoreactive for B cell markers such as CD20 (Fig. 24.4). Acute myeloid leukemias/myeloid sarcoma in the breast may resemble small round blue cell tumors with hyperchromatic, molded, and irregular nuclei and are often immunoreactive for immature cell or blast markers CD34 and c-kit/CD117 (Fig. 24.5). Plasma cell myeloma comprises sheets of plasma cells with eccentric nuclei, "clock-face" chromatin, and perinuclear pale zone (hof) representing the Golgi apparatus, and these are immunoreactive for plasma cell markers such as CD38, CD138, and MUM1 (Fig. 24.6). The differential diagnosis of hematopoietic neoplasms includes other small round blue cell tumors (such as rhabdomyosarcoma), melanoma, small-cell carcinoma, and poorly differentiated breast carcinoma.

Metastatic Melanoma

Microscopic Features

Melanoma is the single most common non-hematopoietic neoplasm to metastasize to the breast and has frequently been reported in case series [12, 13, 43–46]. The histologic features in the metastases can vary as widely as in the primary melanoma; the lesional cells may be spindle or epithelioid, and melanotic or amelanotic. Classically, melanoma is characterized by epithelioid, plasmacytoid cells with cherry red nucleoli, intranuclear inclusions, multiple mitotic figures, and intracytoplasmic melanin pigment (Fig. 24.7a–c).

Differential Diagnosis

The differential diagnosis of metastatic melanoma includes primary breast carcinoma, metastatic carcinoma, hematopoietic neoplasms such as lymphoma, and rarely primary cutaneous melanoma of the breast that is centered in the epidermis and dermis [47]. The presence of intracytoplasmic melanin pigment strongly suggests melanoma, although melanin pigment can be seen in other histologic contexts such as melanotic nerve sheath tumors.

Immunohistochemical Workup

Metastatic melanoma will be negative for CK, which will help distinguish it from primary ductal carcinoma or metastatic carcinoma involving the breast. Immunostains that support a diagnosis of metastatic melanoma when positive include HMB45, Melan-A, microphthalmia transcription factor, S100 protein, and SOX10 [48, 49] (Fig. 24.7d–f). However, caution should be used in interpreting S100 protein

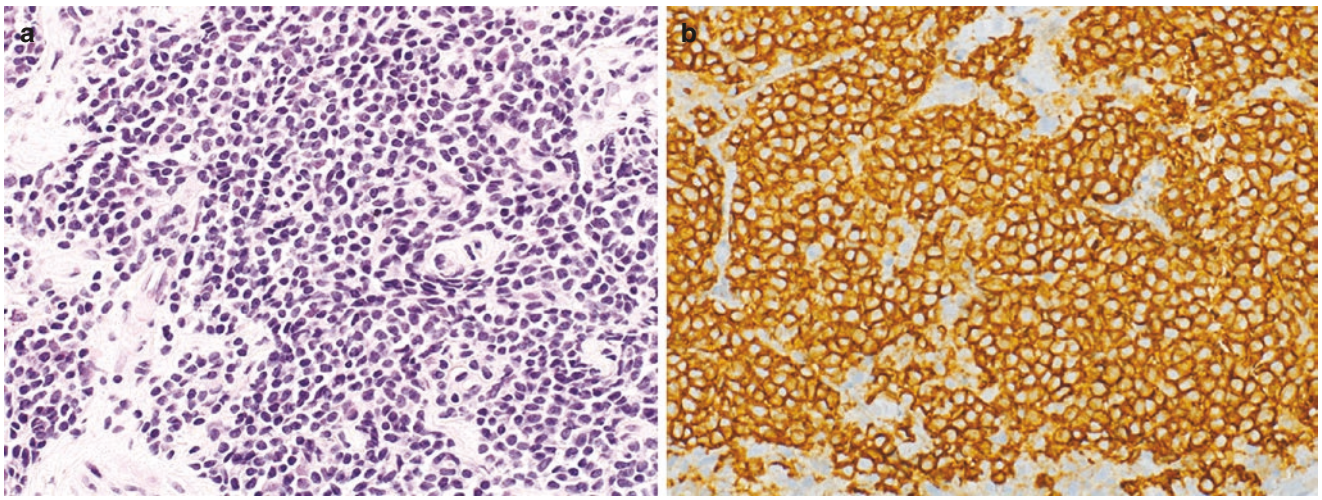

Fig. 24.4 Diffuse large B cell lymphoma involving the breast. (**a**) The tumor shows sheets of loosely cohesive cells with high nuclear-to-cytoplasmic ratio. The cells dissect the breast collagen. (**b**) An immunostain for CD20 is diffusely positive

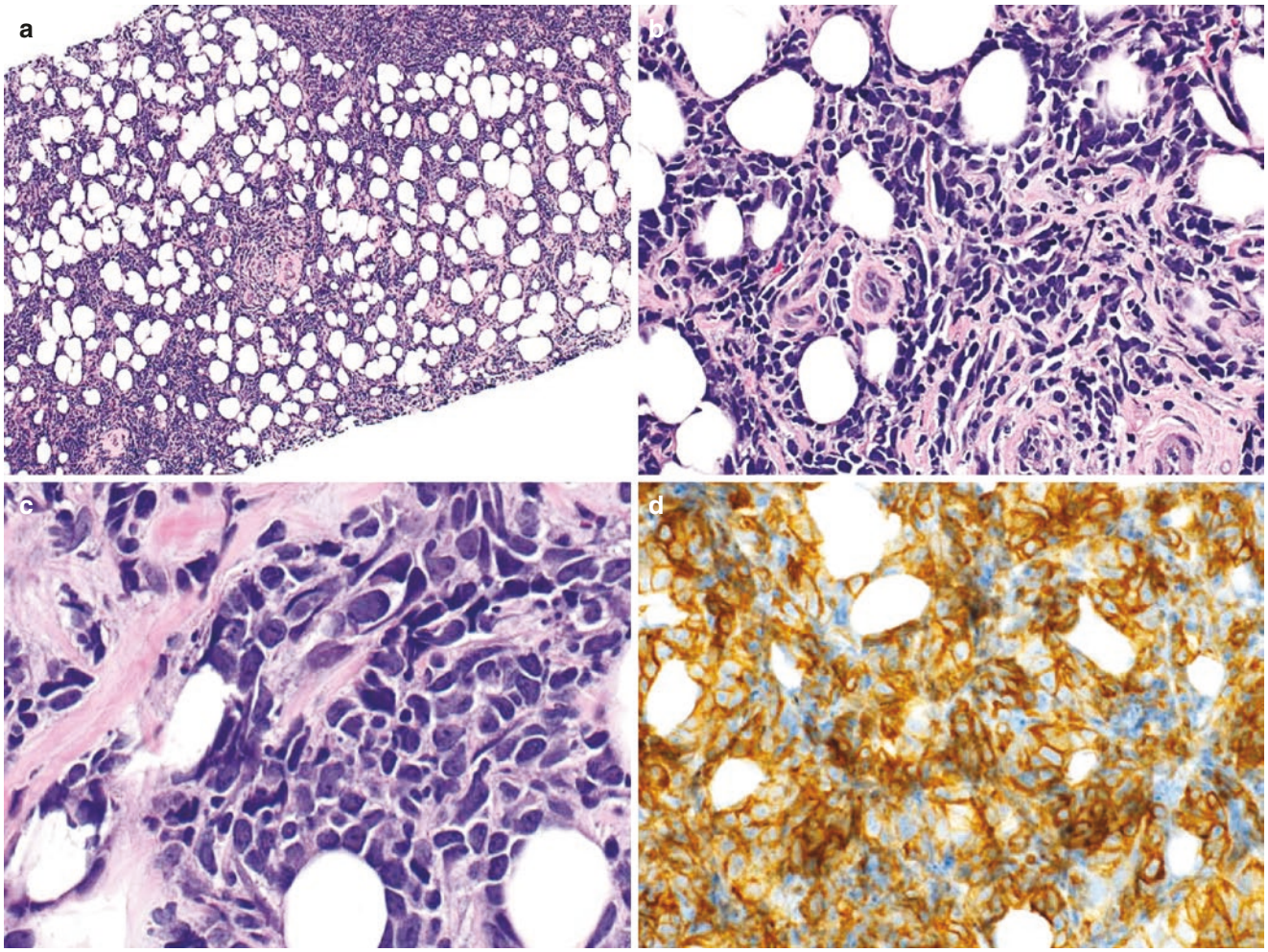

Fig. 24.5 Myeloid sarcoma involving the breast. (**a**–**c**) The CNB reveals sheets of small round blue cells infiltrating the breast adipose tissue and around benign lobules. The lesional cells have hyperchromatic, angulated nuclei, and high nuclear-to-cytoplasmic ratio. (**d**) An immunostain for c-kit/CD117 is diffusely positive

and SOX10 labeling in neoplasms in the breast or axilla, particularly on CNB, as both S100 protein [39] and SOX10 [32–34, 36] can be positive in primary or metastatic ductal carcinoma. SOX10, in particular, primarily labels ductal carcinomas that are triple negative for ER, PR, and human epidermal growth factor 2 [32]. Thus, an ER-, SOX10+, and S100 protein+ neoplasm in the breast may be either metastatic melanoma or primary ductal carcinoma, and additional site-specific markers such as CKs for carcinoma and HMB45 for melanoma should be employed in this setting.

Metastatic Carcinomas and Epithelial Neoplasms

Pulmonary Adenocarcinoma

Microscopic Features

The lung is the most common primary site of a carcinoma metastatic to the breast, although this includes all lung carcinomas including adenocarcinoma, squamous cell carcinoma, and small-cell carcinoma. Multiple reports of metastatic lung adenocarcinoma to the breast have been described [50–52]. Histologically, metastatic pulmonary adenocarcinomas to the breast are composed of either well- or poorly differentiated glands with variable intracytoplasmic mucin production (Fig. 24.8a–c). The glands are typically irregular and angulated with minimal desmoplastic stromal response and no associated in situ component. In addition to or in lieu of stromal invasion, metastatic pulmonary adenocarcinoma to the breast may also involve the breast and dermal lymphovascular spaces (Fig. 24.9). Microcalcifications rarely accompany metastatic carcinomas to the breast aside from metastatic high-grade papillary serous carcinomas, and microcalcifications detected on breast imaging are more likely to be associated with breast lesions than the metastasis. In one example of metastatic pulmonary adenocarcinoma to the breast intravascular spaces, microcalcifications were detected on screening mammography but were all associated with benign breast lobules and not the incidentally discovered carcinoma (Fig. 24.9).

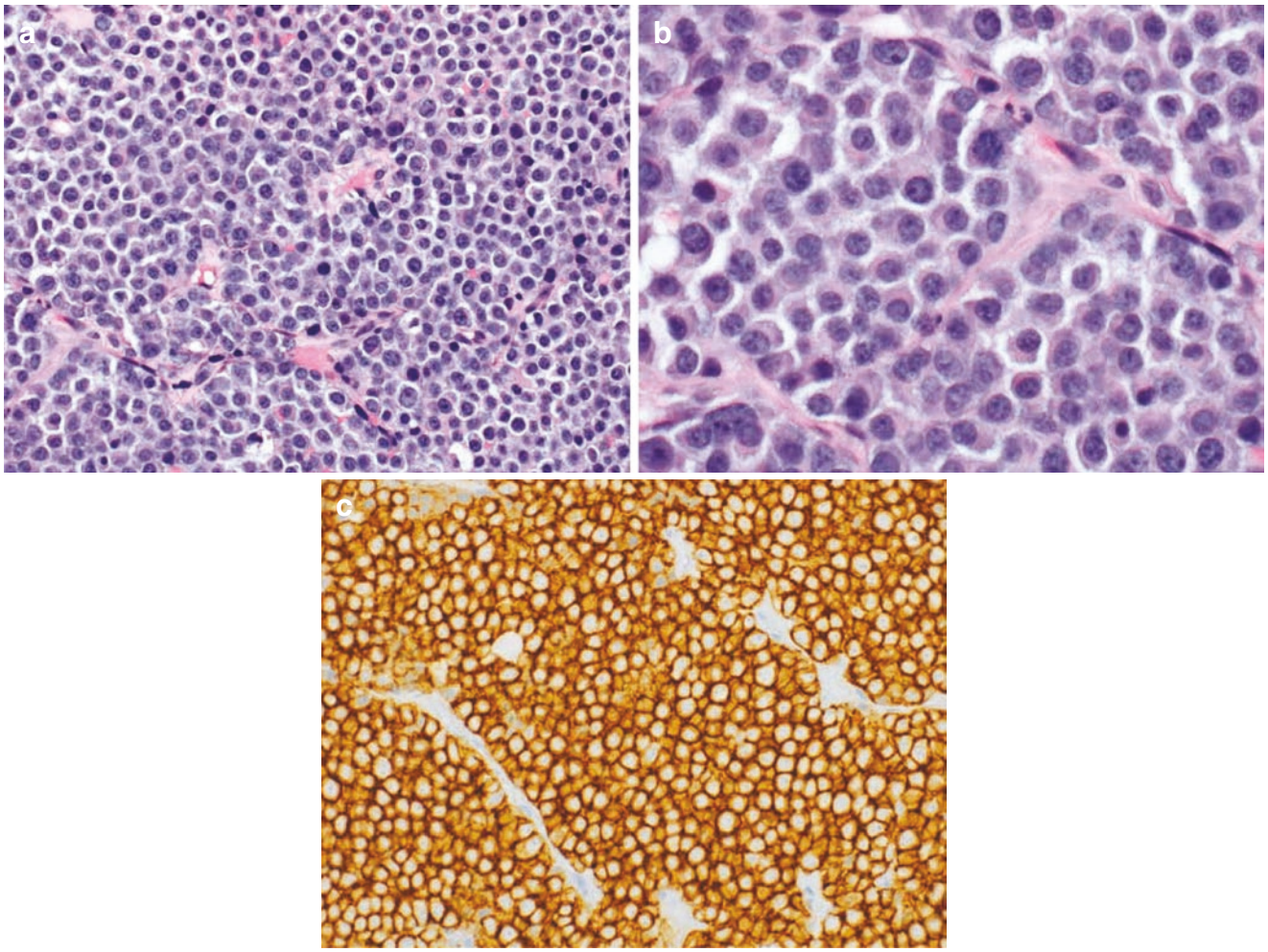

Fig. 24.6 Plasma cell myeloma involving the breast. (**a**, **b**) The lesion consists of sheets of loosely cohesive plasmacytoid cells with eccentrically located nuclei, speckled or "clockface" chromatin, and pale perinuclear cytoplasmic clearing. (**c**) An immunostain for CD138 is diffusely positive

Differential Diagnosis

The main differential diagnosis of metastatic lung adenocarcinoma to the breast and the main diagnostic pitfall are a primary low-grade ductal adenocarcinoma of the breast; however, metastases from other primary sites such as the gastrointestinal tract should also be entertained. The absence of a ductal carcinoma in situ component as well as ER negativity in a low-grade, well-differentiated carcinoma in the breast should raise suspicion that the lesion may be a metastasis from a non-mammary site.

Immunohistochemical Workup

Like primary breast ductal carcinoma, metastatic lung adenocarcinoma is typically immunoreactive for CK7 and negative for CK20. Immunostains that support a diagnosis of metastatic lung adenocarcinoma when positive include TTF1 and Napsin-A (Figs. 24.8d, e and 24.9d). Metastatic thyroid carcinomas would also be immunoreactive for TTF1, but they are typically also positive for thyroglobulin and PAX8 and negative for Napsin-A. The majority of lung adenocarcinomas are negative for breast-specific markers including GCDFP-15, mammaglobin, GATA3, ER, and PR. However, primary lung adenocarcinomas can show focal labeling for GCDFP-15 [53], GATA3 [54], and ER [53] (Fig. 24.8f, g), and thus caution should be used in interpreting these immunostains in isolation without an accompanying TTF1. Only approximately 2% of primary breast cancers label for TTF1 [55]. Knowledge of patient history of an antecedent or synchronous primary lung carcinoma and the immunoprofile of the primary lesion can also be helpful in these circumstances.

Pulmonary Squamous Cell Carcinoma

Microscopic Features

Metastatic squamous cell carcinoma to the breast can be well or poorly differentiated [56, 57]. When better differentiated, the squamous carcinoma will display cohesive nests of epithelial cells with keratin whorls, single-cell keratinization or mummification, and intracytoplasmic bridges illustrative of squamous differentiation (Fig. 24.10a–d).

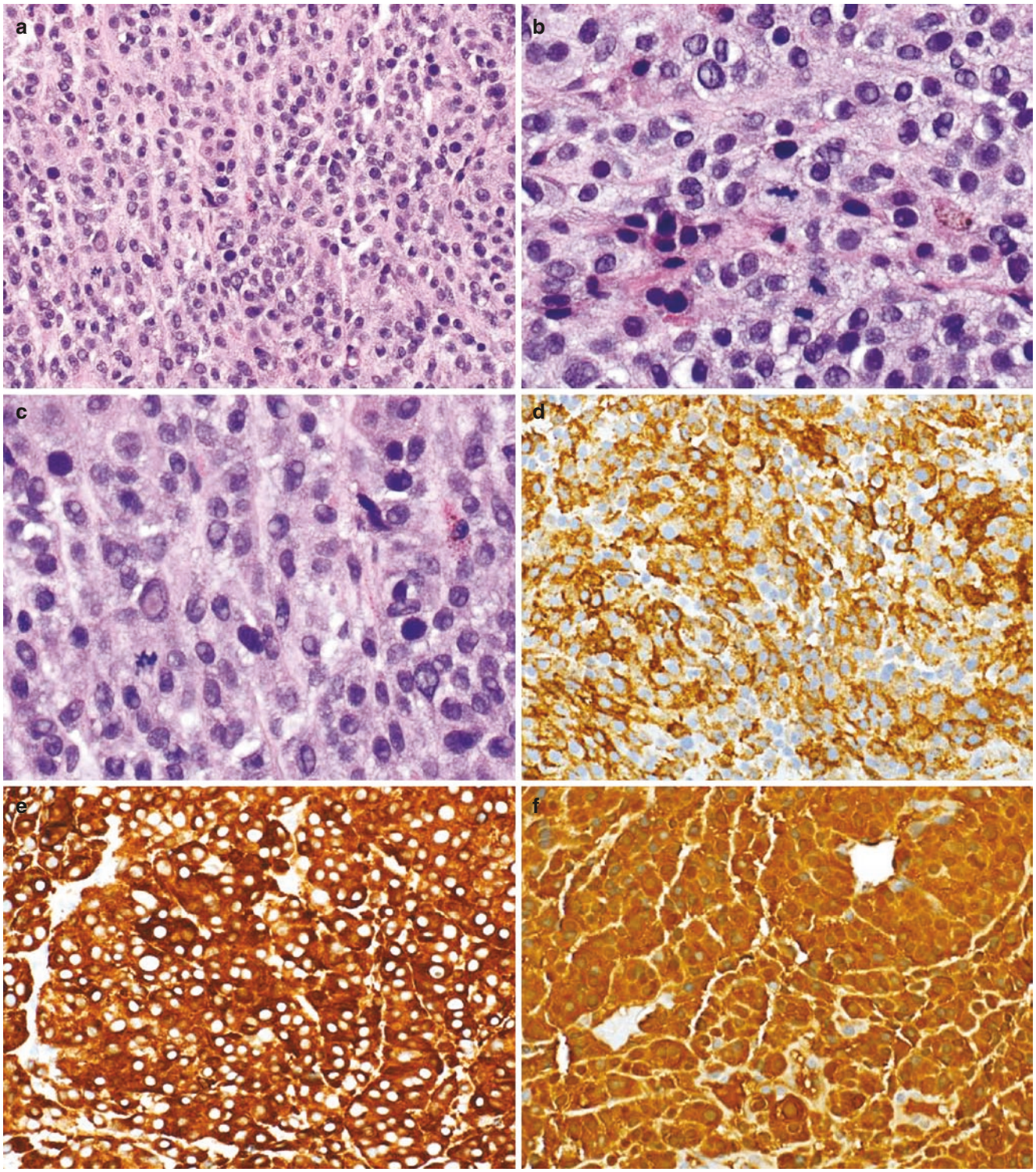

Fig. 24.7 Metastatic melanoma to the breast. (**a**–**c**) The CNB reveals sheets of epithelioid and plasmacytoid cells with frequent mitotic figures and intracytoplasmic melanin. Immunostains for (**d**) HMB45, (**e**) Melan-A, and (**f**) S100 protein are diffusely positive, whereas a cytokeratin immunostain is negative (not shown)

Differential Diagnosis

The differential diagnosis of a squamous cell carcinoma involving the breast includes primary breast carcinoma, extension from an overlying cutaneous squamous cell carcinoma, and metastasis from a non-mammary site such as lung, head and neck, bladder, or anogenital. The presence of

an associated conventional invasive or in situ ductal carcinoma component would favor classification as a primary breast carcinoma, although these features may not be present on a limited CNB sampling. When a large squamous cell carcinoma of the breast involves the overlying skin, it can often be impossible to distinguish secondary skin involvement by a breast carcinoma or deep extension of a skin primary. Knowledge of a clinical history and tumor morphology of a prior primary lung squamous cell carcinoma (Fig. 24.10e, f) may be necessary to make the diagnosis of a metastasis to the breast.

Immunohistochemical Workup

Immunostains are rarely necessary to support squamous differentiation in well-differentiated carcinomas with obvious keratinization, but immunostains may be needed to support a diagnosis of carcinoma in an otherwise poorly differentiated neoplasm. Squamous cell carcinomas of any site will typically have an overlapping if not identical immunohistochemical profile. Immunostains that support squamous differentiation when positive include CK5/6, p63, and p40 (Fig. 24.10f). Squamous cell carcinomas of the lung are negative for TTF1 and Napsin-A. Squamous cell carcinomas of the lung and breast are both immunoreactive for GATA3 [30, 54]; thus, immunolabeling for GATA3 does not distinguish the site of origin in this context. In fact, there are no site-specific immunostains for squamous cell carcinomas, aside from the use of immunohistochemistry for p16 and associated in situ hybridization for high-risk human papillomavirus (HPV) to distinguish HPV-related squamous cell carcinomas. HPV-related squamous cell carcinomas are typically of head and neck or anogenital origin.

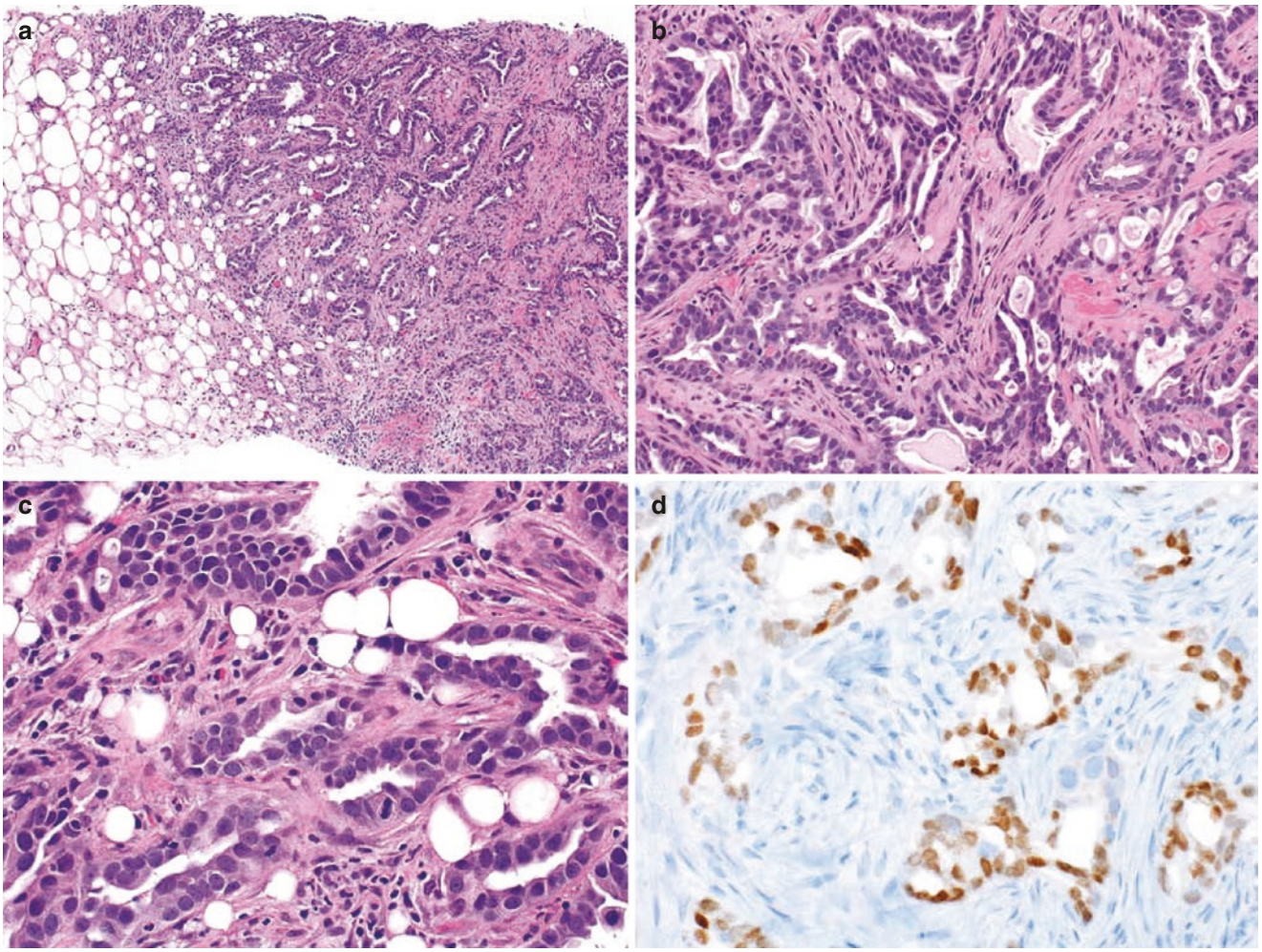

Fig. 24.8 Metastatic pulmonary adenocarcinoma to the breast. (**a**–**c**) The CNB of the breast mass in a patient with a known history of primary lung adenocarcinoma shows irregular, angulated glands that infiltrate the breast fibrous and adipose tissue with minimal desmoplastic response, frequent mitotic figures, and intracytoplasmic mucin vacuoles. Immunostains for (**d**) TTF1 and (**e**) Napsin-A are positive, supporting metastatic pulmonary adenocarcinoma. Immunostains for (**f**) GATA3 and (**g**) ER are also focally positive in the metastatic lung carcinoma, which is a potential diagnostic pitfall as these markers are traditionally used to support primary breast origin

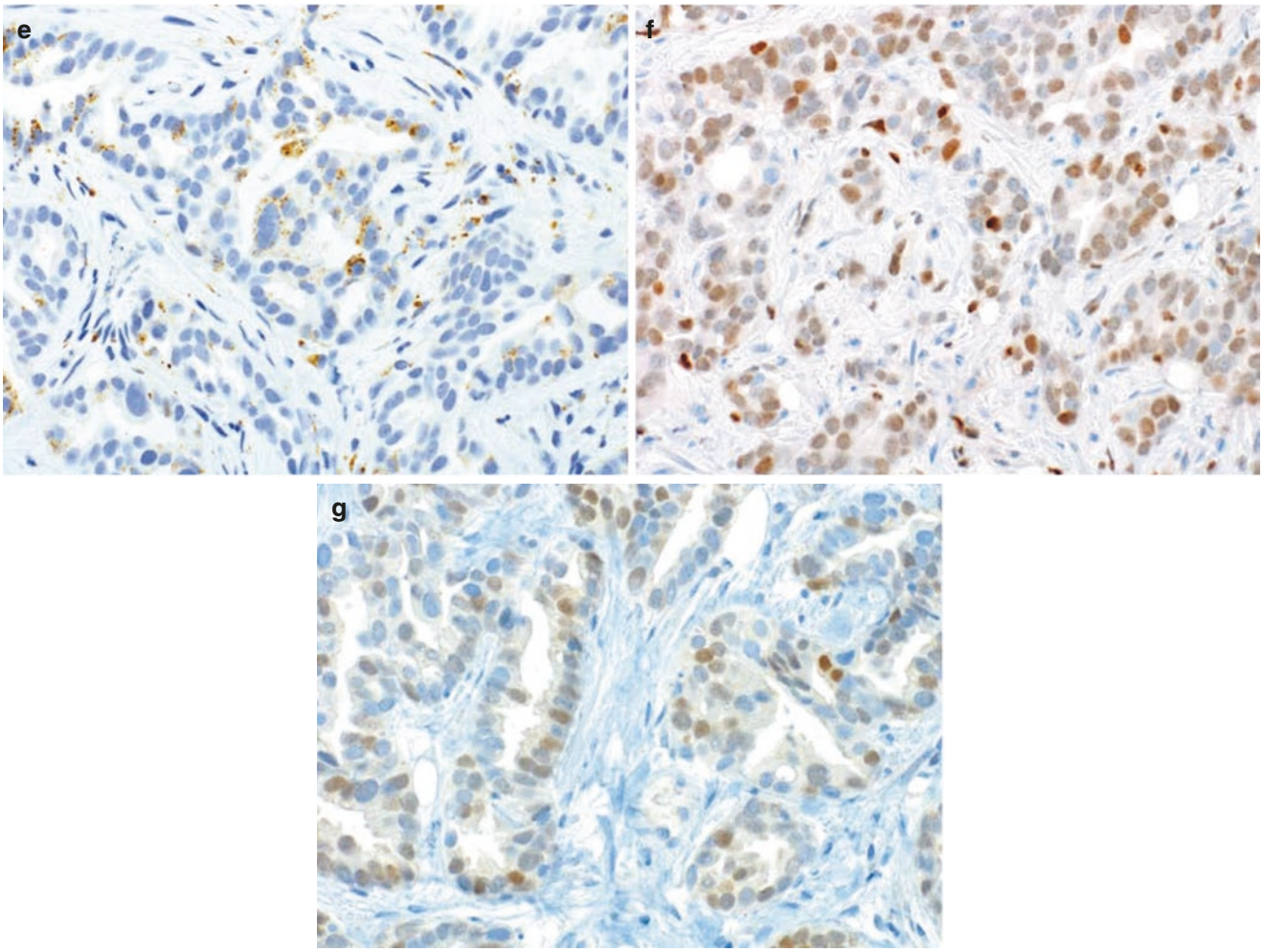

Fig. 24.8 (continued)

Pulmonary Small-Cell Carcinoma

Microscopic Features

The diagnosis of small-cell carcinoma is made on the basis of the histologic features of the carcinoma, including the presence of highly atypical cells with high nuclear-to-cytoplasmic ratio, hyperchromatic and homogeneous nuclei, nuclear molding, a high mitotic rate, and necrosis (Figs. 24.3 and 24.11).

Differential Diagnosis

The main differential diagnoses of metastatic pulmonary small-cell carcinoma to the breast [12, 58] are primary triple-negative ductal carcinoma and metastatic non-pulmonary small-cell carcinoma. Primary triple-negative ductal carcinomas may display features that morphologically resemble small-cell carcinoma, such as "basaloid features" including high nuclear grade, high nuclear-to-cytoplasmic ratio, abundant mitotic figures, and necrosis. These primary breast carcinomas frequently lack an in situ carcinoma component. Rarer entities in the differential diagnosis include other small round blue cell tumors such as Merkel cell carcinoma, rhabdomyosarcoma, and primary breast small-cell carcinoma, which is uncommon [59]. Small-cell carcinomas are more likely in the adult patient population, whereas rhabdomyosarcomas are more likely in the pediatric patient population.

Immunohistochemical Workup

Immunostains may be useful in supporting the histologic impression of small-cell carcinoma and in excluding other entities in the differential diagnosis. Small-cell carcinomas of any origin share overlapping immunohistochemical profiles. Immunostains and features that support a diagnosis of small-cell carcinoma include labeling with markers of neuroendocrine differentiation such as synaptophysin, chromogranin, insulinoma-associated protein 1 (INSM1), and CD56; a high Ki67 proliferation index; immunolabeling with TTF1; and perinuclear dot-like CK labeling. Notably, TTF1 labeling can be seen in small-cell carcinomas of any primary site and is not specific to pulmonary small-cell carcinomas [60]. TTF1 labeling is also seen in pulmonary ade-

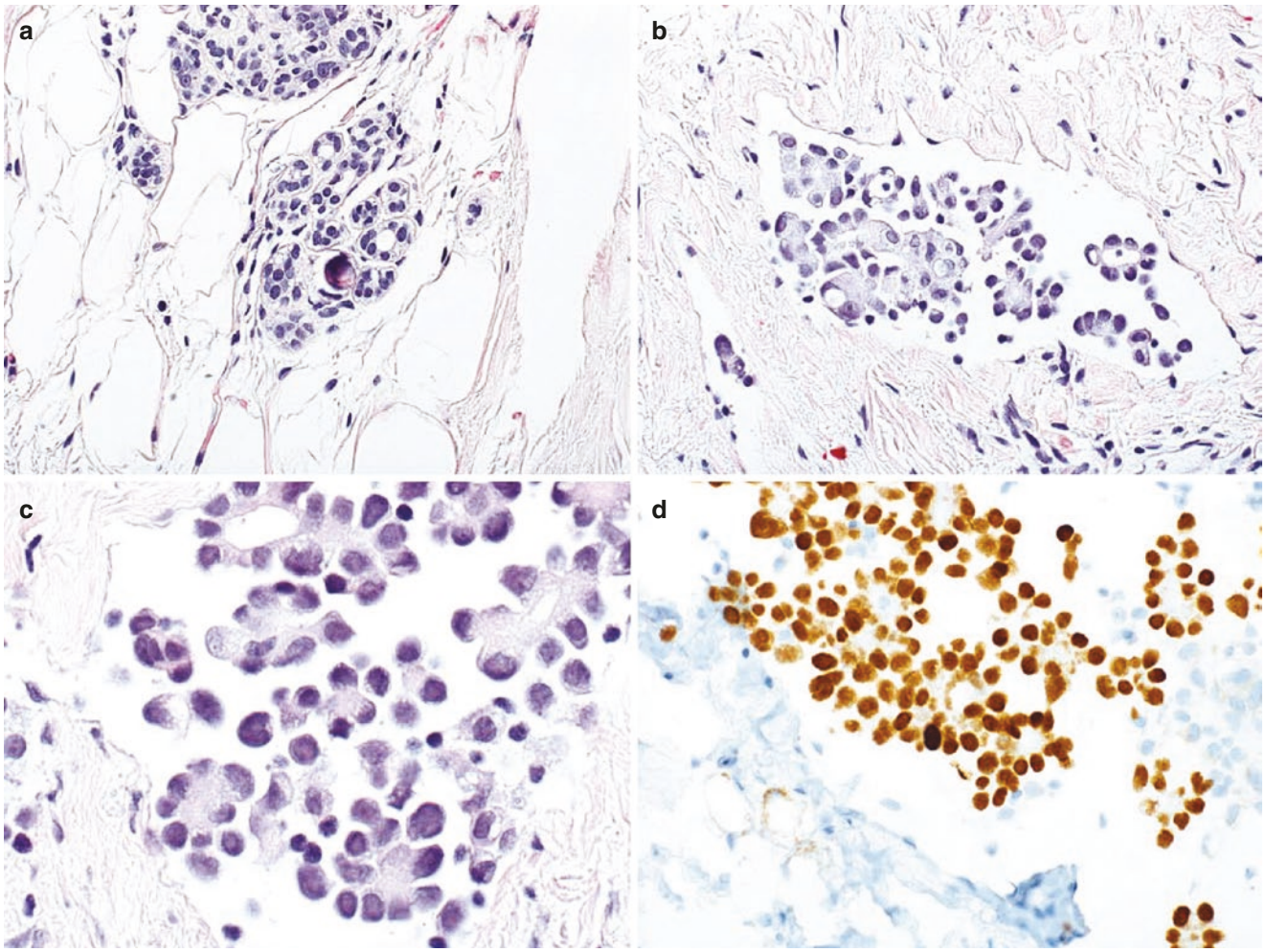

Fig. 24.9 Metastatic pulmonary adenocarcinoma to the breast lymphovascular spaces. (**a**) Routine screening mammography in a patient with a history of lung adenocarcinoma detected radiographically indeterminant microcalcifications, which on CNB were all associated with benign breast lobules. (**b**, **c**) The adjacent breast parenchyma showed extensive lymphovascular space involvement by an adenocarcinoma with micropapillary features. (**d**) An immunostain for TTF1 is positive, supporting diagnosis of metastatic pulmonary adenocarcinoma

nocarcinomas and in thyroid carcinomas, but small-cell carcinomas are negative for Napsin-A (unlike pulmonary adenocarcinoma) and PAX8 and thyroglobulin (unlike well-differentiated thyroid carcinomas).

In distinguishing metastatic small-cell carcinoma from primary high-grade ductal carcinoma of the breast, immunoreactivity for breast-specific markers such as ER, PR, HER2, GCDFP-15, mammaglobin, GATA3, or SOX10 may help support a primary breast origin. However, high-grade ductal carcinomas are often negative for many or all breast-specific markers. One additional marker with potential utility is CK5/6, as this is positive in a subset of breast ductal carcinoma with "basal" differentiation but is negative in pulmonary small-cell carcinomas [61]. Among the remaining entities in the differential diagnosis, Merkel cell carcinoma will display immunoreactivity for CK20 (perinuclear dot-like labeling) and neurofilament in addition to the neuroendocrine marker labeling, and rhabdomyosarcoma will display labeling for markers of skeletal muscle differentiation such as myogenin and desmin.

Ovarian Carcinoma

Microscopic Features

High-grade serous carcinoma of tubal/ovarian origin is the most common ovarian neoplasm to involve the breast, and multiple series have been reported [12, 62–64]. Microscopically, high-grade serous carcinoma is characterized by nests of cells with solid, glandular, papillary, or micropapillary growth pattern; nuclear hyperchromasia; and frequent mitoses (Fig. 24.12a–c). Serous carcinoma may be accompanied by psammomatous calcifications, and it is the only type of metastasis to the breast reported to have associated microcalcifications on imaging and histopathology [4, 5, 14].

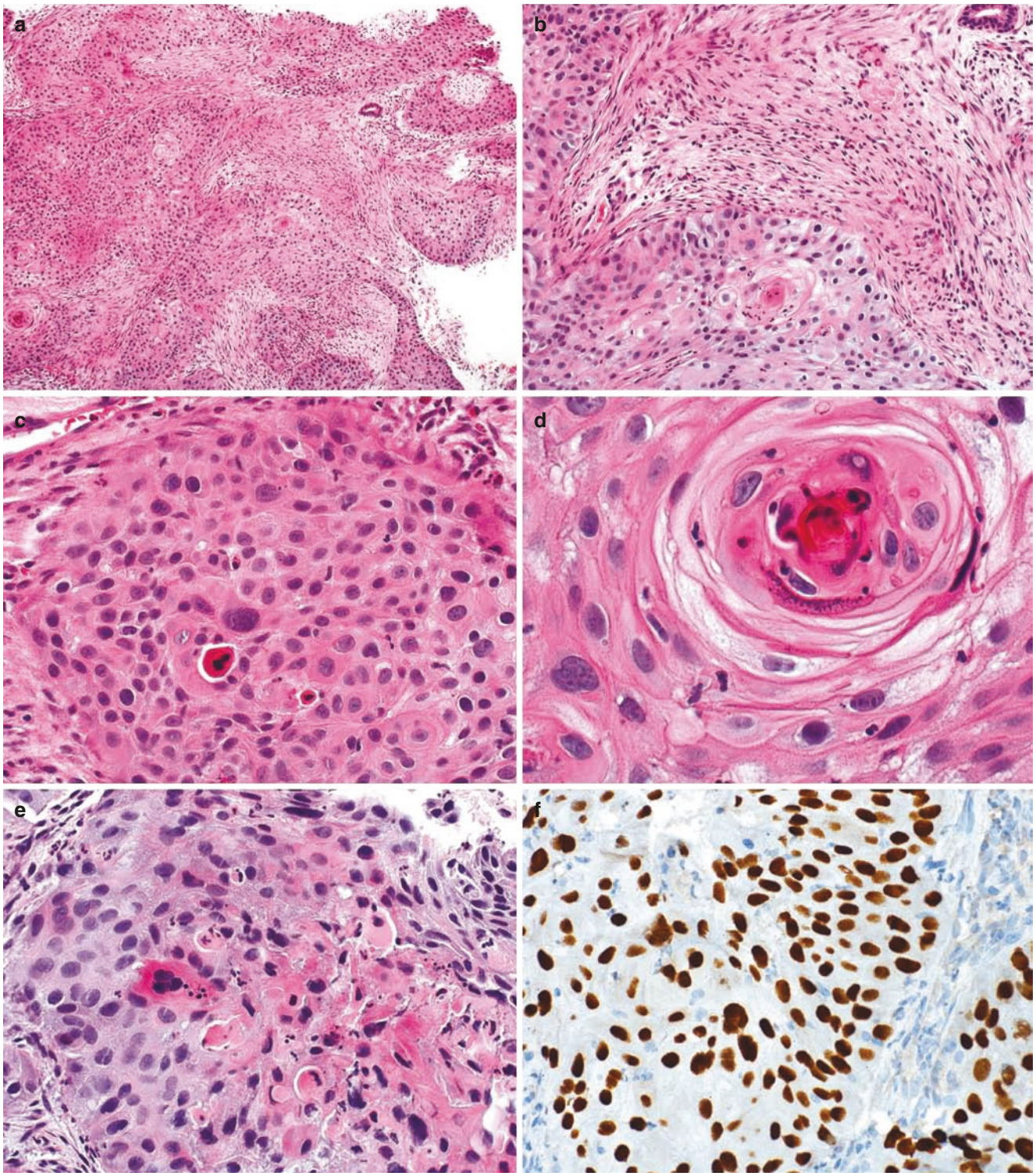

Fig. 24.10 Metastatic pulmonary squamous cell carcinoma to the breast compared with the patient's previously known primary pulmonary carcinoma. (**a**–**d**) CNB of a breast mass reveals an infiltrating nested carcinoma with obvious single-cell keratinization, intracellular bridges, and keratin whorls, consistent with a squamous cell carcinoma. (**e**, **f**) Comparison of the breast mass with the patient's previously known primary pulmonary squamous cell carcinoma shows similar morphologic features of single-cell keratinization and was diffusely positive for p40 and negative for TTF1 (not shown)

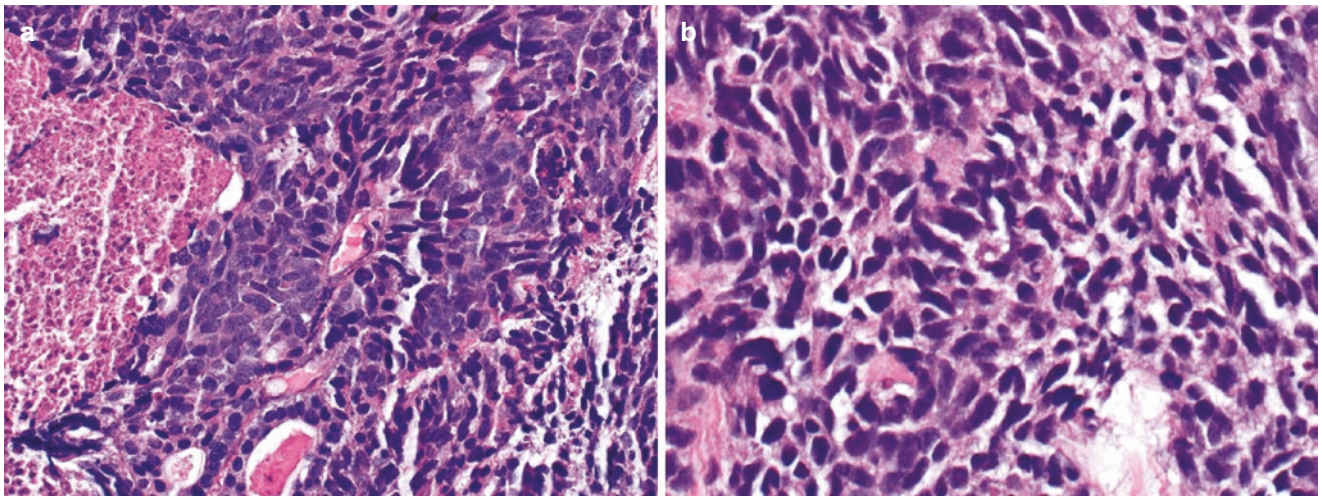

Fig. 24.11 Metastatic pulmonary small-cell carcinoma to the breast. (**a**, **b**) The neoplasm in the breast consists of high-grade cells with high nuclear-to-cytoplasmic ratio, nuclear hyperchromasia and molding, stippled chromatin, necrosis, and numerous mitotic figures

Differential Diagnosis

Histologically, it may be impossible to distinguish metastatic serous carcinoma from primary micropapillary breast carcinoma in the absence of an associated in situ component. Serous carcinomas of peritoneal origin will have the same morphology and immunoprofile as serous carcinomas of tubal/ovarian origin. The differential diagnosis of metastatic serous carcinoma in the breast also includes metastases from other adenocarcinomas with micropapillary growth pattern, such as the lung [65]. A clinical history is essential in these circumstances.

Immunohistochemical Workup

A targeted immunopanel is necessary to differentiate metastatic papillary serous carcinoma from primary breast carcinoma, as both lesions are typically positive for CK7, ER, and PR and negative for CK20. The most useful immunostains in this differential are PAX8, WT1, GCDFP-15, and mammaglobin (Fig. 24.12d–f). PAX8 labels carcinomas of the gynecologic tract, including serous carcinoma, and is typically negative in breast carcinomas [66–68], although PAX8 specificity varies with the antibody clone [69]. WT1 also labels serous carcinoma and is typically strong and diffuse [70]; however, labeling has been reported in a subset of primary breast carcinomas [71], including primary micropapillary and mucinous carcinomas, which can be confused with metastases. Hence, PAX8 is superior to WT1 in this setting. Serous carcinomas are typically considered negative for GCDFP-15 [66], but rare GCDFP-15 labeling has been reported [53]. Immunolabeling for other site-specific markers, such as TTF1 for lung or thyroid, can also aid in the differential.

Endometrial Carcinoma

Microscopic Features

In addition to carcinomas of the tubal/ovarian origin, gynecologic primary carcinomas of the endometrium can also metastasize to the breast. Endometrial carcinomas may be of a variety of subtypes, including endometrioid, serous, and clear cell or may display overlapping features. Endometrioid endometrial carcinomas are characterized by varying degrees of glandular and solid components with high nuclear grade and at times squamous differentiation (Fig. 24.13a, b).

Differential Diagnosis

The differential diagnosis of metastatic endometrial carcinoma to the breast includes primary invasive ductal carcinoma and metastatic carcinoma from other non-mammary sites, such as lung or gastrointestinal tract. If the carcinoma is predominantly solid pattern with focal keratinization, primary or metastatic squamous cell carcinoma may also be in the differential. The low-power impression of solid nests of carcinoma cells with a loosely cohesive center may mimic ductal carcinoma in situ with micropapillary architecture (Fig. 24.13a, b). However, immunostains for myoepithelial cells (such as p63 and smooth muscle myosin heavy chain) will be negative around the invasive foci. As in all cases of metastases to the breast, a complete clinical history is imperative.

Immunohistochemical Workup

Like primary breast carcinomas and high-grade serous carcinomas of tubal/ovarian origin, endometrial adenocarcinomas are also immunoreactive for CK7 and negative for CK20. As in the previous differential, the most useful immunostains in

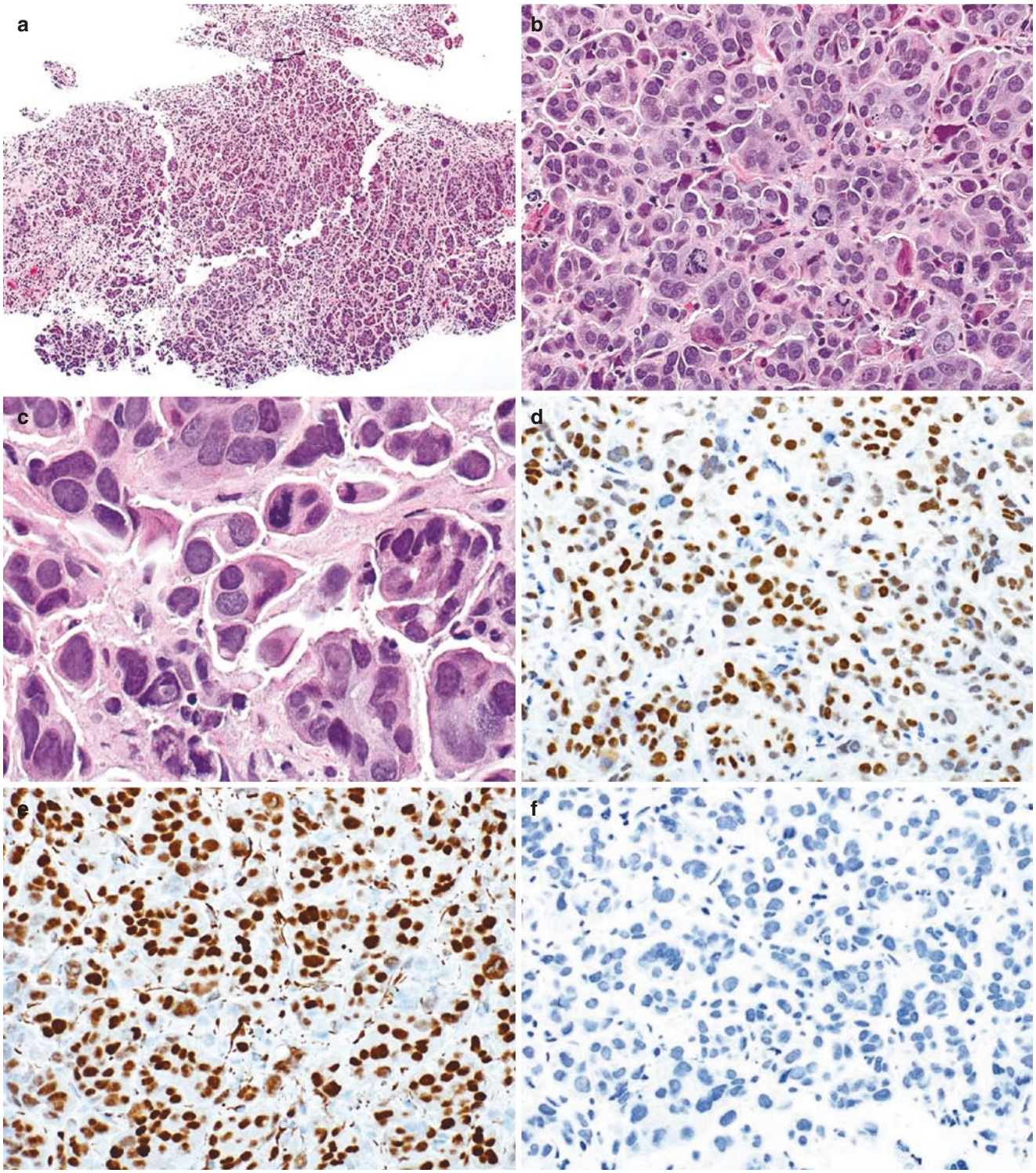

Fig. 24.12 Metastatic high-grade papillary serous carcinoma of tubal/ovarian origin to the breast. (**a**–**c**) The breast CNB reveals an invasive high-grade carcinoma with micropapillary architecture, numerous mitotic figures, and nuclear atypia. Immunostains show the carcinoma to be positive for (**d**) PAX8 and (**e**) WT1 and to be negative for (**f**) mammaglobin

this differential are PAX8 and GCDFP-15 (Fig. 24.13c, d). Endometrioid endometrial carcinomas are immunoreactive for PAX8 [67, 68], with only rare labeling for GCDFP-15 [53]. In contrast to papillary serous carcinomas of tubal/ovarian origin, endometrioid endometrial carcinomas are negative for WT1 [70].

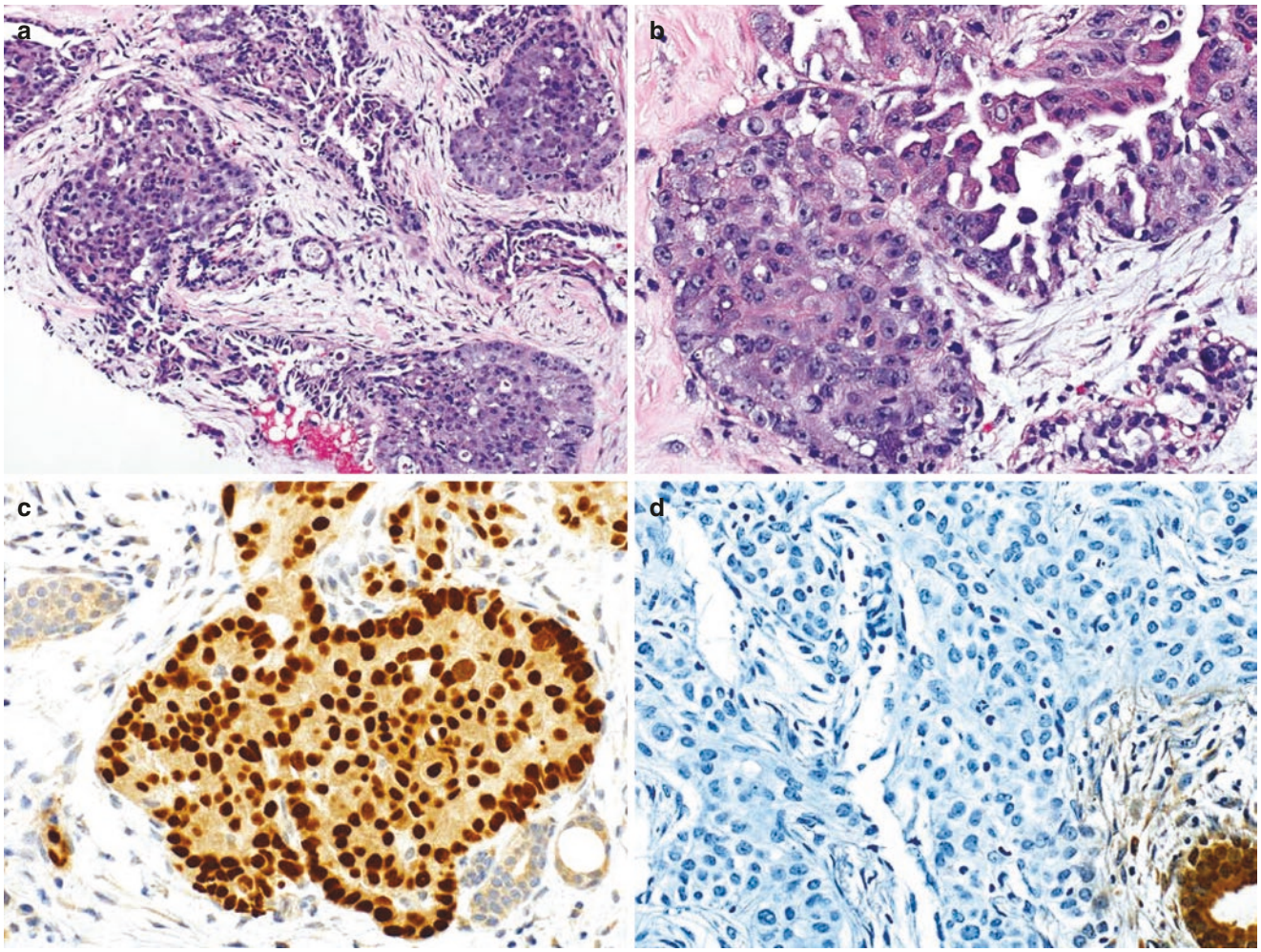

Fig. 24.13 Metastatic endometrioid endometrial carcinoma to the breast. (**a**, **b**) The breast CNB reveals solid and irregular nests of atypical epithelial cells with a focally loosely cohesive, micropapillary architecture and squamous features. The nests infiltrate around benign breast lobules. Immunostains show the carcinoma to be positive for (**c**) PAX8 and negative for (**d**) GCDFP-15

Renal Cell Carcinoma

Microscopic Features

Numerous case reports describe metastatic renal cell carcinoma involving the breast [2, 12, 72, 73], and clear-cell renal cell carcinoma is the most common subtype to metastasize to the breast. Clear-cell renal cell carcinoma is histologically characterized by nested cells with clear cytoplasm, atypical nuclei with irregular nuclear contours and variably prominent nucleoli, and a delicate capillary vasculature (Fig. 24.14).

Differential Diagnosis

The distinctive morphology of clear-cell renal cell carcinoma alone is often diagnostic of a metastasis in the setting of a known primary renal neoplasm. However, clear-cell renal cell carcinoma is known to metastasize after long disease-free intervals and to present as metastatic disease; thus, a metastatic renal cell carcinoma may involve the breast with a remote history of a primary lesion that is not provided to the pathologist or with no known primary lesion [74]. In this clinical context, making the diagnosis of metastatic renal cell carcinoma can be challenging. The differential diagnosis of metastatic clear-cell renal cell carcinoma to the breast includes primary breast carcinomas that have clear-cell features (such as glycogen-rich carcinoma, metaplastic carcinoma, and secretory carcinoma), cutaneous breast lesions with clear cytoplasm such as clear-cell hidradenoma, and metastases from other carcinomas with clear-cell features (such as parathyroid carcinoma or salivary myoepithelial carcinoma).

Immunohistochemical Workup

The morphology of clear-cell renal cell carcinoma is often characteristic and, coupled with a clinical history of a renal mass, may be enough to support the diagnosis of metastatic renal cell carcinoma. However, in the absence of a clinical

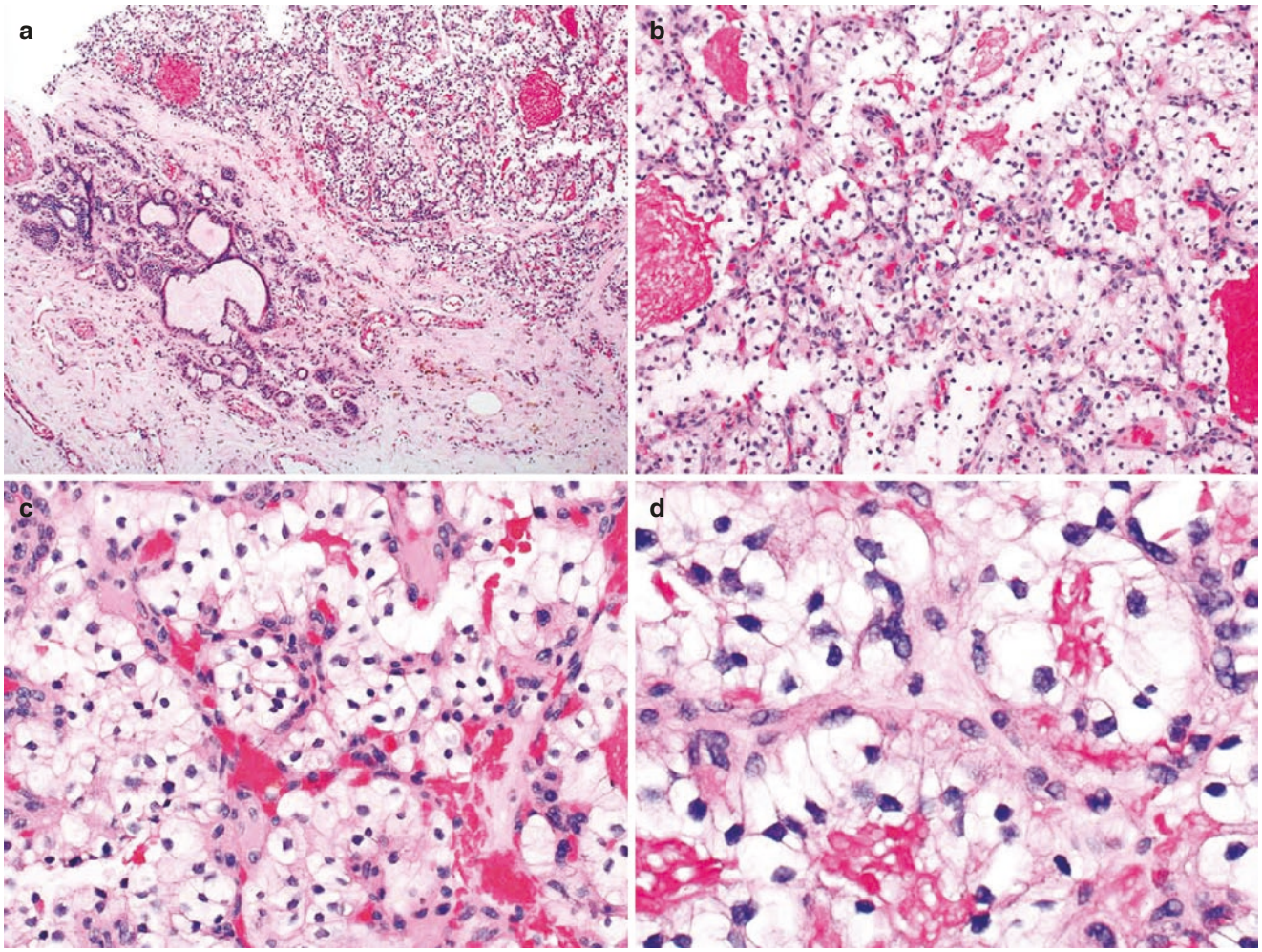

Fig. 24.14 Metastatic clear-cell renal cell carcinoma to the breast. (**a**–**d**) The breast CNB reveals nests of cells with abundant clear cytoplasm, irregular nuclei with focally prominent nucleoli, and a delicate capillary vasculature

history, immunostains may be used to support the diagnosis. Immunostains that support a diagnosis of clear-cell renal cell carcinoma when positive are PAX8, renal cell carcinoma antigen, CD10, and carbonic anhydrase IX. Renal cell carcinomas are negative for breast-specific markers such as GCDFP-15 [53].

Well-Differentiated Neuroendocrine Tumor/Carcinoid Tumor

Microscopic Features

Neuroendocrine neoplasms of the lung, gastrointestinal tract, and pancreas can metastasize to the breast [5, 12] and can mimic primary breast carcinoma. Histologically, well-differentiated neuroendocrine neoplasms (e.g., carcinoid tumors) consist of epithelial cells arranged in nests, trabeculae, or pseudo-rosettes and are characterized by eosinophilic-to-amphophilic, granular cytoplasm, and a "salt-and-pepper," speckled chromatin pattern (Fig. 24.15a, b). Nests of cells with a cribriform appearance may mimic ductal carcinoma in situ by myoepithelial cell markers (such as p63 and smooth muscle myosin heavy chain) that will be lost around the invasive foci.

Differential Diagnosis

The primary differential diagnosis of metastatic well-differentiated neuroendocrine tumor to the breast is primary breast neuroendocrine tumor [75]. Primary breast carcinomas can be entirely neuroendocrine or display focal neuroendocrine differentiation, and distinguishing between a primary breast carcinoma and a metastatic well-differentiated neuroendocrine tumor has different prognostic and therapeutic implications. Clinical history may be essential in these circumstances, and where possible, comparing the breast lesion with the known primary can be very useful (Fig. 24.15f).

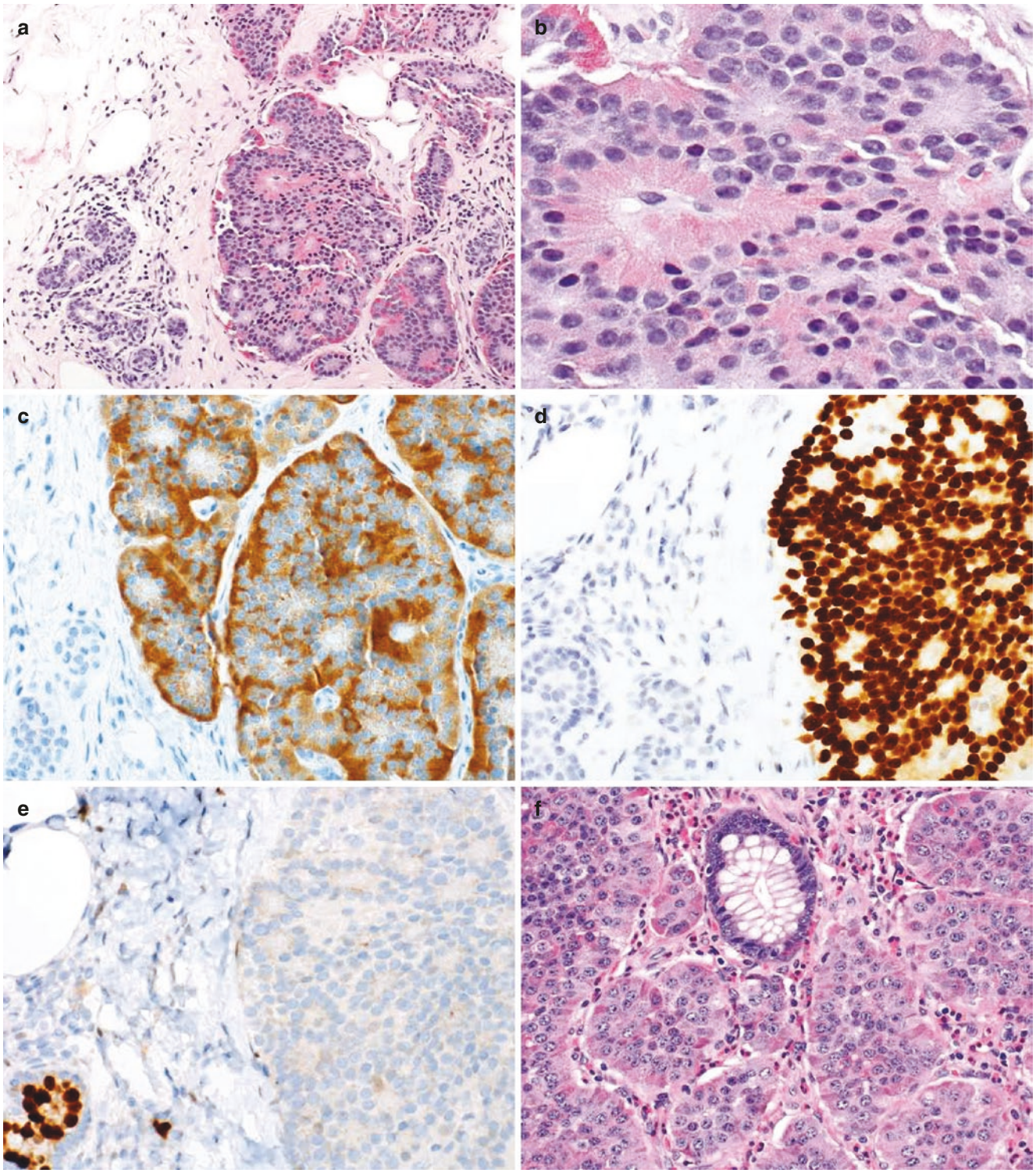

Fig. 24.15 Metastatic gastrointestinal well-differentiated neuroendocrine tumor to the breast. (**a**, **b**) The breast CNB reveals nests of cells with pseudo-rosette formation, pink granular cytoplasm, and a speckled chromatin pattern. Immunostains show the neoplasm to be positive for (**c**) synaptophysin and (**d**) CDX2 and to be negative for (**e**) ER, supporting the classification as metastatic gastrointestinal well-differentiated neuroendocrine tumor. (**f**) Comparison with the patient's known ileal primary shows identical tumor morphology

Immunohistochemical Workup

Metastatic well-differentiated neuroendocrine tumors often retain the immunoprofile of their site of origin. A useful immunopanel in differentiating between a primary and metastatic neuroendocrine neoplasm includes CK7, CK20, TTF1, CDX2, and ER (Fig. 24.15c–e). All well-differentiated neu-

roendocrine tumors regardless of site will be immunoreactive for neuroendocrine markers, such as synaptophysin, chromogranin, INSM1, and CD56. CK7 and CK20 can aid to differentiate neoplasms that originate from above or below the diaphragm, such that pulmonary carcinoid tumors are typically $CK7^{+}/CK20^{-}$, upper gastrointestinal tract well-differentiated neuroendocrine tumors are variably $CK7^{+/-}/CK20^{+/-}$, and lower gastrointestinal tract well-differentiated neuroendocrine tumors are typically $CK7^{-}/CK20^{+}$. TTF1 positivity suggests pulmonary origin [60]; CDX2 positivity suggests gastrointestinal origin [76]; and ER positivity suggests breast origin [77].

Prostate Carcinoma

Microscopic Features

Prostate carcinoma is the most common primary neoplasm in males, followed by lung carcinoma [78]. However, in the limited series in the literature, metastatic melanoma is the most common metastatic neoplasm to the male breast as in the female breast [4], followed by metastatic lung carcinoma as the second most common neoplasm. Metastatic prostate carcinoma has been reported in the literature [4, 5, 11], and it poses a diagnostic dilemma as it can morphologically mimic primary male breast carcinoma with its cribriform and papillary architecture. Metastatic prostatic adenocarcinoma can have variable morphologic growth patterns depending upon the primary Gleason grade, and these include acinar, papillary (Fig. 24.16a–d), and solid sheets of cells. The cells are characterized by amphophilic cytoplasm and prominent nucleoli (Fig. 24.16a–d).

Differential Diagnosis

The differential diagnosis of metastatic prostate carcinoma to the breast includes primary breast carcinoma and metastatic carcinoma of another site, such as lung or gastrointestinal tract. The distinction is critical, as the prognosis and treatment of metastatic prostate carcinoma and primary breast carcinoma are vastly different.

Immunohistochemical Workup

Immunostains, in addition to a thorough clinical history, are critical in identifying metastatic prostate carcinoma to the breast. A useful immunopanel includes prostate-specific antigen (PSA), P501S, NKX3.1 (Fig. 24.16e–g), and breast-specific markers including GCDFP-15 and ER (Fig. 24.16h). Prostate carcinoma is immunoreactive for PSA, P501S, and NKX3.1, which are useful in the metastatic setting. It is important to employ a panel of immunomarkers, as any one alone is not sufficient. For instance, PSA labeling has been reported in primary male breast carcinoma [79–81]. In addition, although NKX3.1 immunolabeling is primarily used in surgical pathology to support a diagnosis of prostate carcinoma, NKX3.1 labeling is reported in a small subset of primary breast carcinomas, most commonly in lobular carcinomas [82, 83]. Thus, NKX3.1 labeling should only be employed as part of a broad immunopanel in this setting.

Other Rare Carcinomas

Microscopic Features, Differential Diagnosis, and Immunohistochemical Workup

Metastases to the breast are reported from other primary carcinoma sites throughout the body in single-institution series and numerous case reports. These additional primary sites include, but are not limited to, the stomach [2, 14], gastroesophageal junction [5, 84], colorectum (Fig. 24.17) [85–88], liver [14], oral cavity or pharynx [4, 10], cervix (Fig. 24.18) [2], bladder (Fig. 24.19) [2, 4], thyroid (Figs. 24.20 and 24.21) [4, 11, 12], thymus [14, 89], salivary gland [4], and placenta (gestational trophoblastic disease/choriocarcinoma) (Fig. 24.22) [90].

Metastatic adenocarcinoma from any site can display well- or poorly differentiated glands with varying degrees of mucin production, and as discussed above, clinical history and a targeted immunopanel are often necessary to make the correct diagnosis. Metastatic colorectal adenocarcinoma will typically be immunoreactive for CK20 (Fig. 24.17c) and CDX2. Metastatic cervical carcinomas may be squamous or glandular (Fig. 24.18a, b). Cervical adenocarcinomas can be ER positive, which can mimic primary breast carcinomas. However, the majority of cervical neoplasms are driven by high-risk HPV integration, and detection of HPV infection by diffuse immunoreactivity for p16 (a surrogate marker for HPV infection) or by positive viral in situ hybridization studies can be helpful (Fig. 24.18c, d). Carcinomas of the anogenital region and head and neck may also be HPV related. Mucinous adenocarcinomas may arise from any organ, including the bladder (Fig. 24.19a–c), gastrointestinal tract, pancreas, ovary, or lung, and metastatic mucinous adenocarcinoma to the breast may mimic a primary mucinous (colloid) carcinoma. Mucinous adenocarcinomas of any site can show intestinal differentiation; thus, immunoreactivity for CDX2 does not point to a specific site of origin. However, immunoreactivity for CK20 and ER negativity suggests a non-breast primary (Fig. 24.19d).

Different types of thyroid carcinoma can metastasize to the breast. Well-differentiated follicular thyroid carcinoma displays uniformly sized follicles with pink intraluminal secretions (Fig. 24.20) and is immunoreactive for TTF1, thyroglobulin, and PAX8. Medullary thyroid carcinoma is a neuroendocrine neoplasm with characteristic finely stippled chromatin and amphophilic cytoplasm (Fig. 24.21) and is immunoreactive for neuroendocrine markers (such as synaptophysin), TTF1, CEA, and calcitonin and may be accompanied by amyloid production.

Choriocarcinoma is the most aggressive gestational trophoblastic disease and can metastasize to the breast

(Fig. 24.22). Choriocarcinoma is characteristically composed of a mixture of multinucleated syncytiotrophoblasts with mononuclear cytotrophoblasts and is immunoreactive for β-hCG and Mel-CAM (CD146). Of note, however, trophoblastic tumors including choriocarcinomas also label for GATA3 [91], which is a potential diagnostic pitfall in the differential diagnosis of primary breast carcinoma.

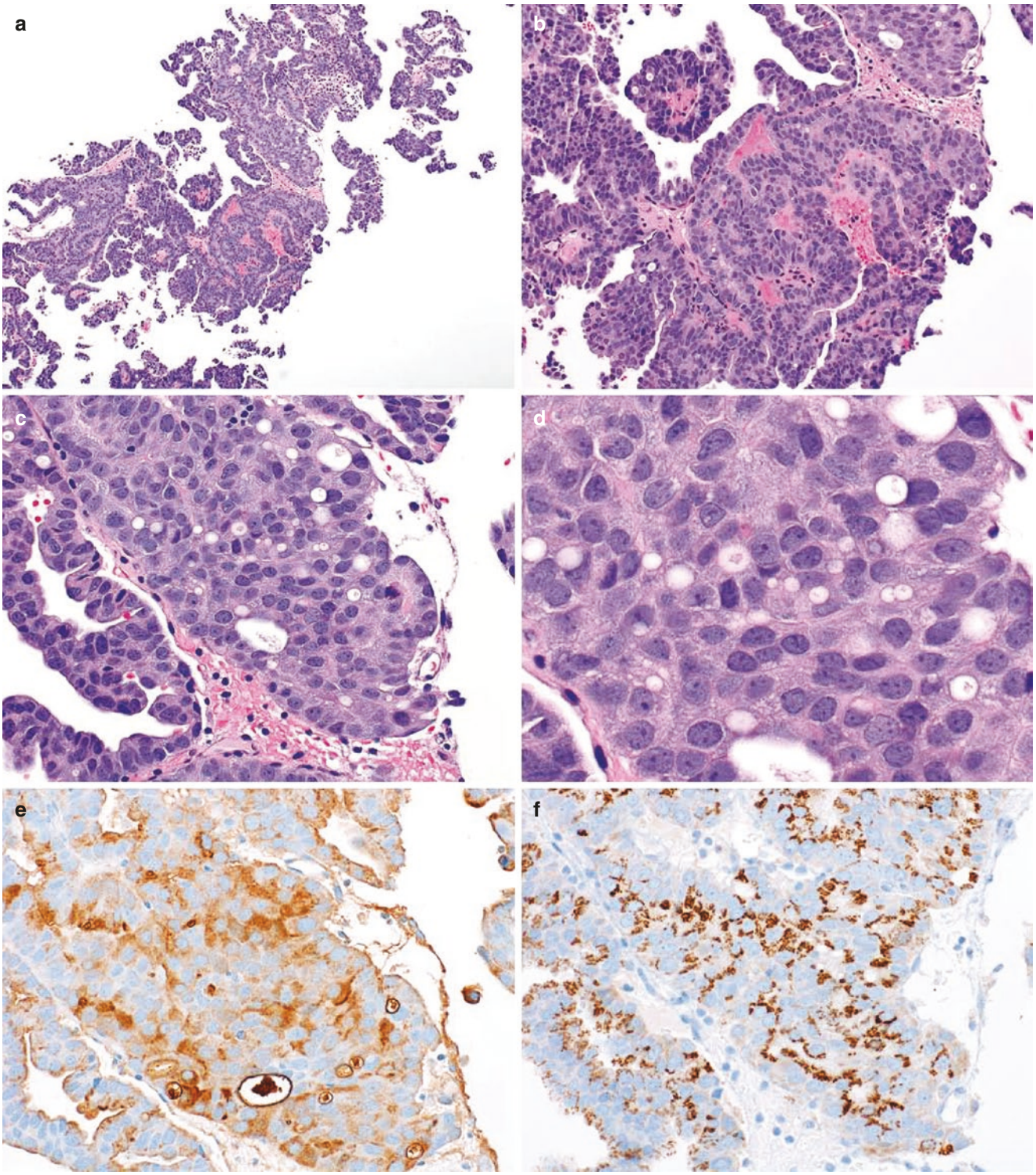

Fig. 24.16 Metastatic prostatic adenocarcinoma to the male breast. (**a**–**d**) CNB of a mass in a male breast reveals a papillary adenocarcinoma with amphophilic cytoplasm, intracytoplasmic vacuoles, and nuclear atypia including prominent nucleoli. Immunostains show the carcinoma to be immunoreactive for (**e**) PSA, (**f**) P501S in a characteristic granular pattern, and (**g**) NKX3.1 and to be negative for (**h**) ER

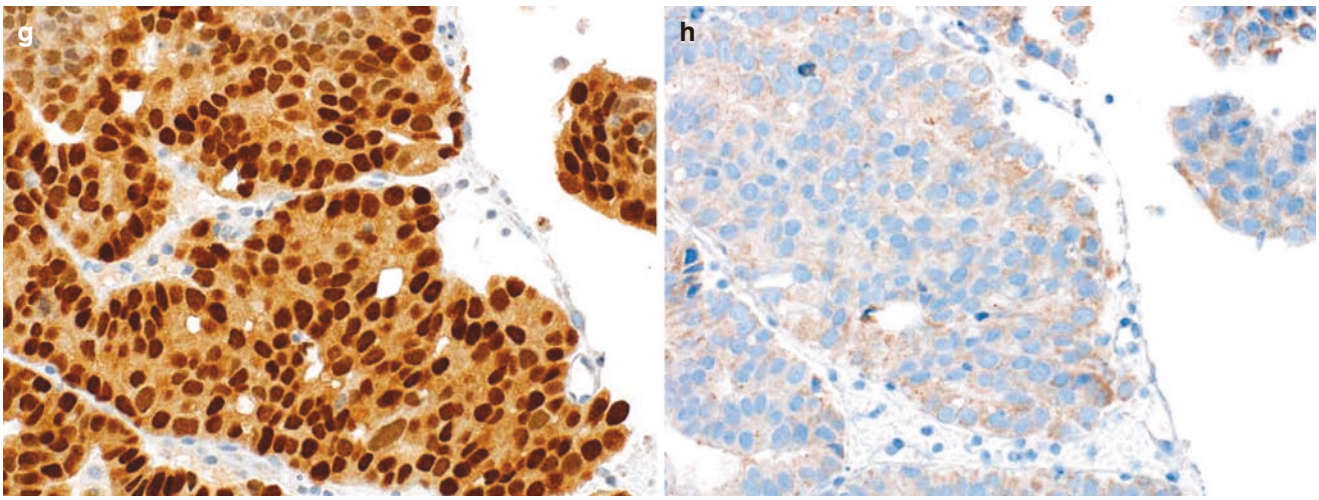

Fig. 24.16 (continued)

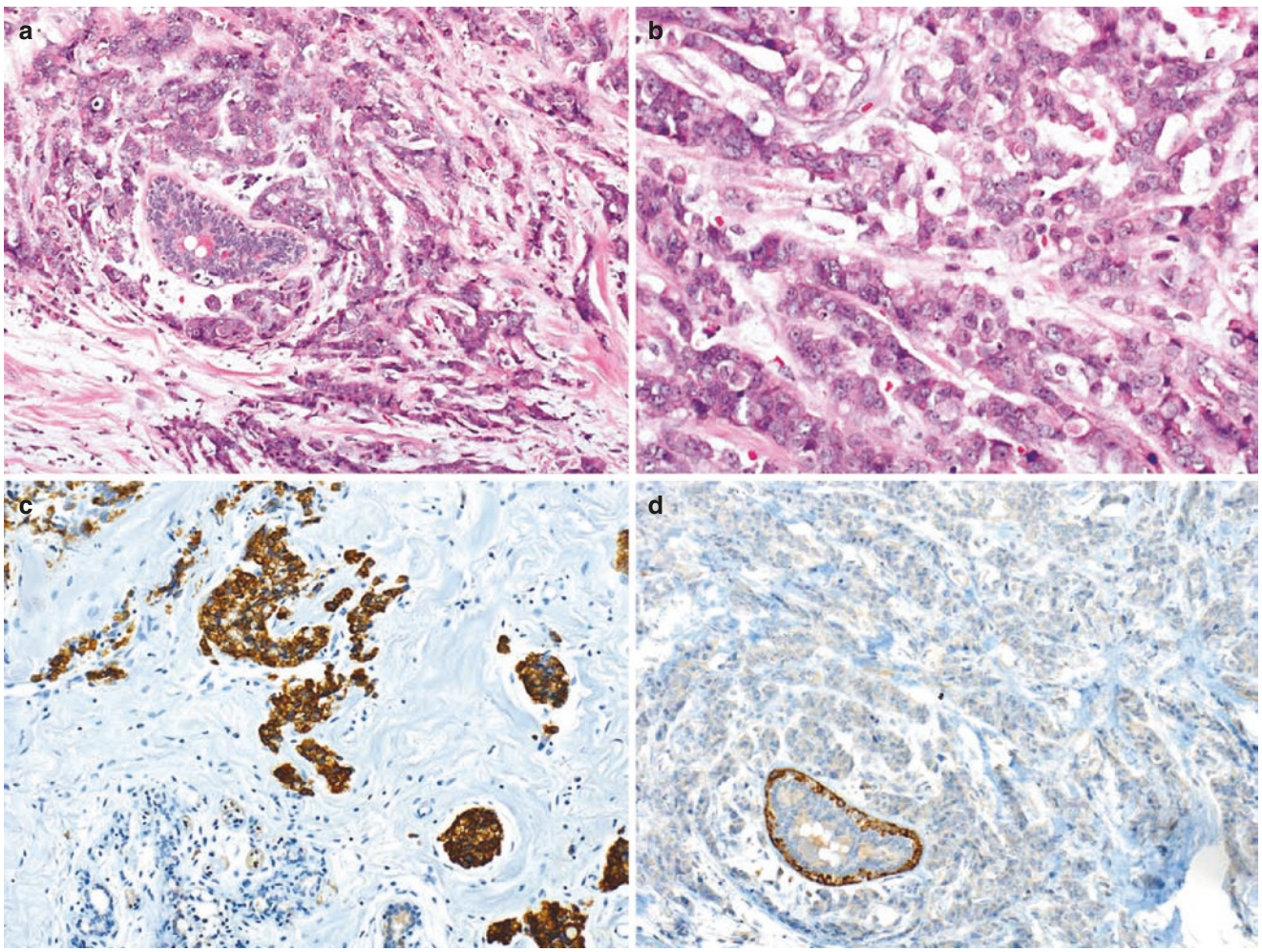

Fig. 24.17 Metastatic colonic adenocarcinoma to the breast. (**a**, **b**) The CNB reveals cords of cells with nuclear atypia, abundant mitotic figures, and minimal gland formation that infiltrate around benign breast lobules. The carcinoma is immunoreactive for (**c**) CK20. An immunostain for (**d**) smooth muscle myosin heavy chain (SMMHC) shows lack of myoepithelial cells around the invasive component and no in situ carcinoma component

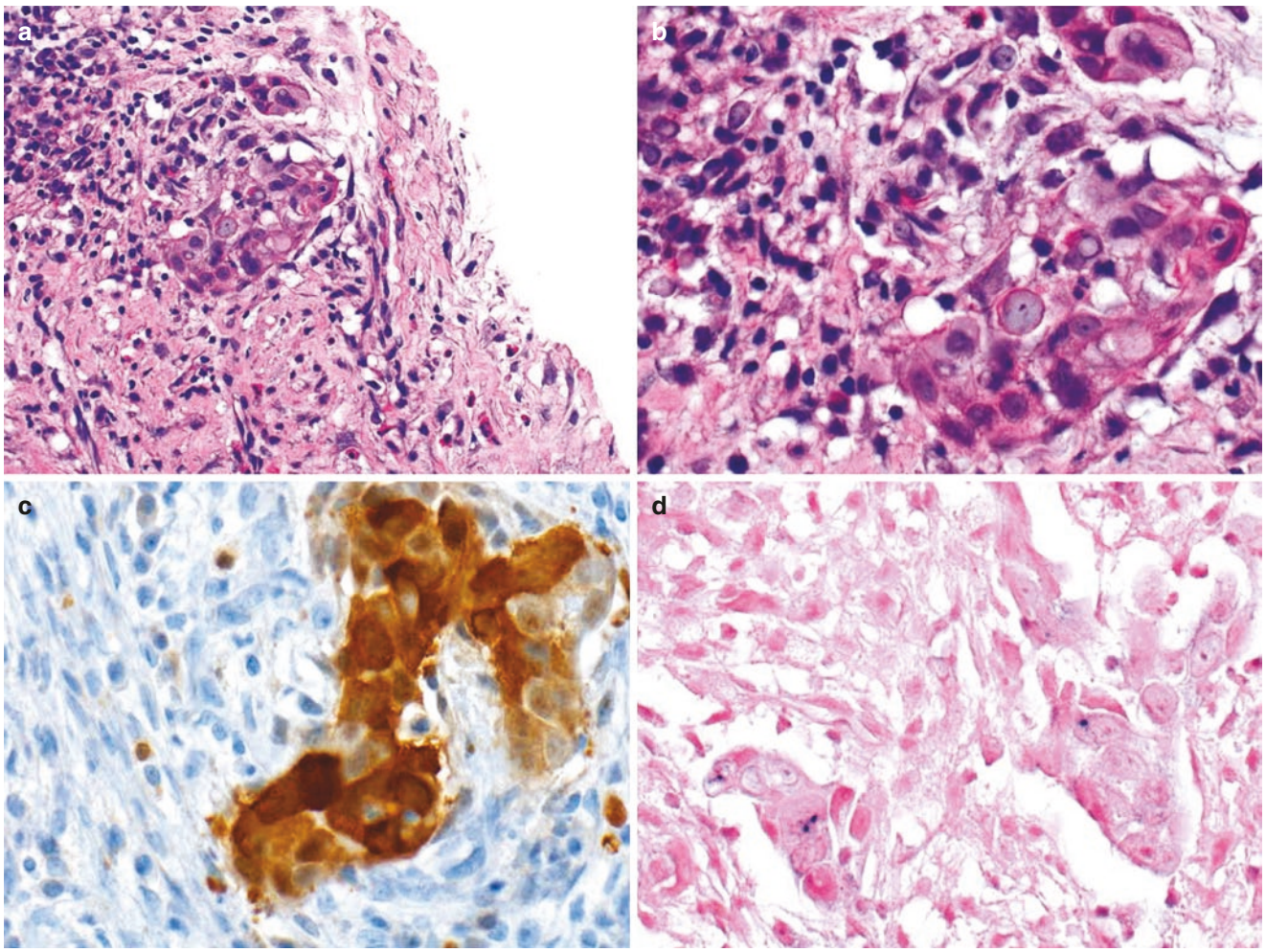

Fig. 24.18 Metastatic cervical adenocarcinoma to the breast. (**a**, **b**) The breast CNB shows small nests of atypical cells with hyperchromatic nuclei, pale pink cytoplasm, and intracytoplasmic vacuoles suggestive of mucin. The carcinoma is (**c**) strongly and diffusely positive for p16 by immunohistochemistry and is (**d**) positive for high-risk HPV by in situ hybridization

Metastatic Sarcomas

Leiomyosarcoma

Microscopic Features

Metastatic leiomyosarcoma to the breast has been described both in series [4] and case reports [92, 93], and uterine leiomyosarcoma is the most common sarcoma to metastasize to the adult breast [4]. Leiomyosarcoma is characterized by intersecting fascicles of atypical spindle cells with blunt-ended nuclei, nuclear hyperchromasia, and a typically brisk mitotic rate (Fig. 24.23a–d).

Differential Diagnosis

Primary and metastatic sarcomas in the breast are rare, and the differential diagnosis of any malignant spindle sarcomatoid neoplasm must include spindle cell metaplastic carcinoma and malignant phyllodes tumor, both of which are more common than pure breast sarcomas. The presence of an associated conventional invasive or in situ breast carcinoma suggests a metaplastic carcinoma, whereas the presence of a leaflike epithelial component suggests a phyllodes tumor. However, in some cases, these diagnostic clues (such as a conventional invasive component or leaflike architecture) may not be present on the CNB due to limited sampling of a larger and heterogeneous lesion. As always, knowledge of the patient's clinical history may be essential in identifying a breast lesion as a metastasis to the breast.

Immunohistochemical Workup

The morphology of leiomyosarcomas, including the fascicular growth and blunt-ended nuclei, suggests smooth muscle differentiation. By immunohistochemistry, the cells label for markers of smooth muscle differentiation such as caldesmon, desmin, and actin (Fig. 24.23e, f). Leiomyosarcomas

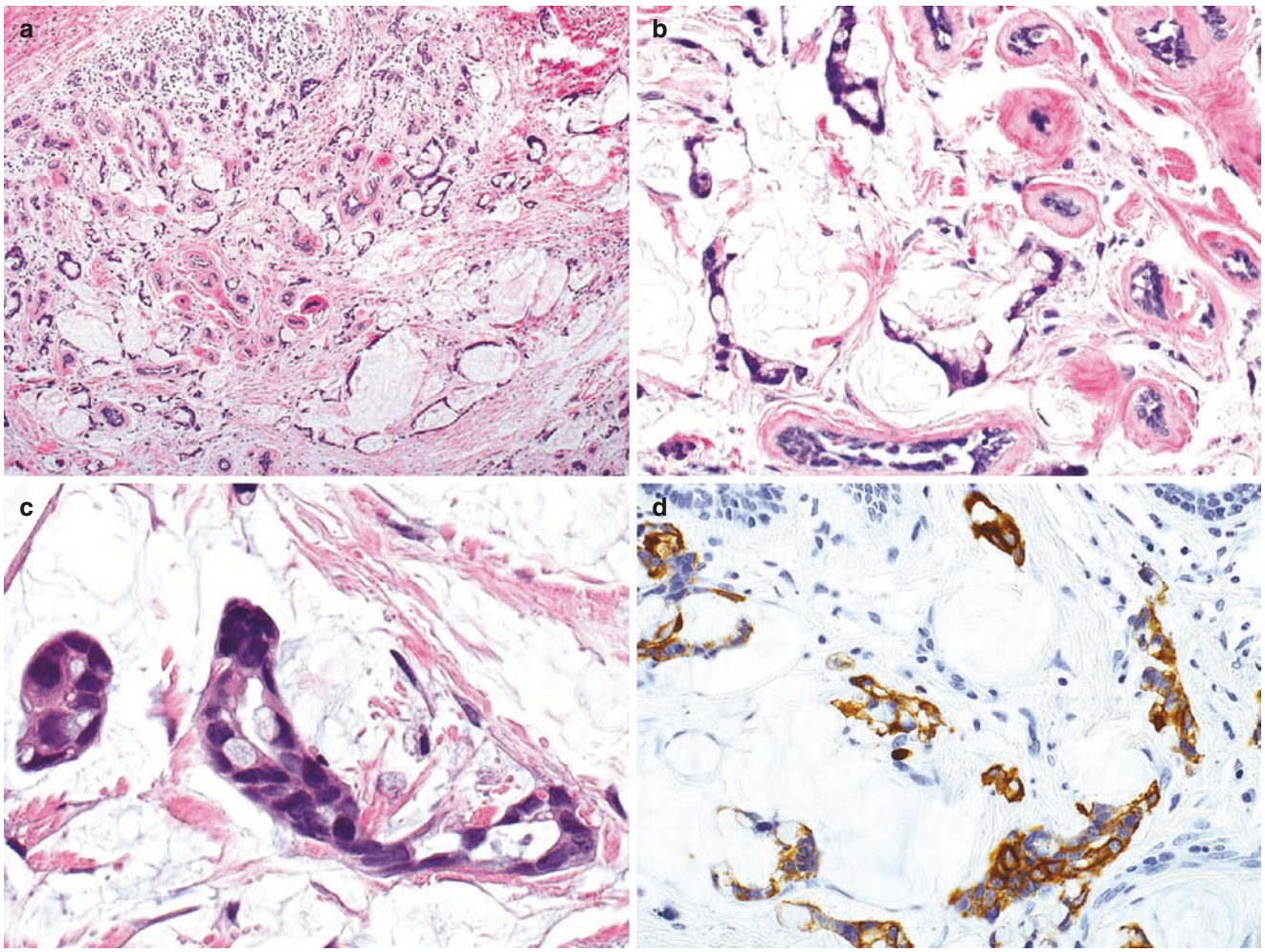

Fig. 24.19 Metastatic mucinous bladder adenocarcinoma to the breast. (**a**–**c**) The breast CNB reveals atypical glands floating in pools of extravasated mucin. This morphology could be consistent with a primary mucinous (colloid) carcinoma of the breast. However, this carcinoma is immunoreactive for (**d**) CK20 and is negative for CK7 (not shown), supporting classification as a metastasis to the breast

may exhibit focal CK labeling, as well as ER positivity, a feature particularly seen in uterine or retroperitoneal leiomyosarcomas in females.

Alveolar Rhabdomyosarcoma

Microscopic Features

Metastases are the most common malignant neoplasm in the breast in the pediatric/adolescent population [15, 16], and rhabdomyosarcoma is the most common primary lesion to metastasize to the breast. Rhabdomyosarcomas are also the most common pediatric sarcoma and may be of several types, most commonly alveolar or embryonal. Alveolar rhabdomyosarcomas are small round blue cell tumors characterized by nests of highly atypical cells with a "loosely cohesive" center, morphologically resembling pulmonary alveoli (Fig. 24.24). The cells have high nuclear-to-cytoplasmic ratios, variably eosinophilic cytoplasm, and hyperchromatic nuclei. Embryonal rhabdomyosarcomas comprise round-to-spindle cells with variably abundant eosinophilic cytoplasm and are more likely to exhibit cytoplasmic cross striations than alveolar rhabdomyosarcomas. Nearly all reported examples of rhabdomyosarcoma metastatic to the breast are of alveolar type [94].

Differential Diagnosis

The differential diagnosis of rhabdomyosarcoma includes other small round blue cell tumors including lymphoma, Ewing sarcoma, desmoplastic small round cell tumor, Wilms' tumor, neuroblastoma, and small-cell osteosarcomas and chondrosarcomas. Other tumors in the differential which are more common in adult patients would include primary invasive lobular carcinoma, metastatic small-cell carcinoma, and Merkel cell carcinoma. The differential diagnosis of a neoplasm exhibiting skeletal muscle differentiation also includes primary spindle cell metaplastic carcinoma, malignant peripheral nerve sheath tumor with skeletal muscle dif-

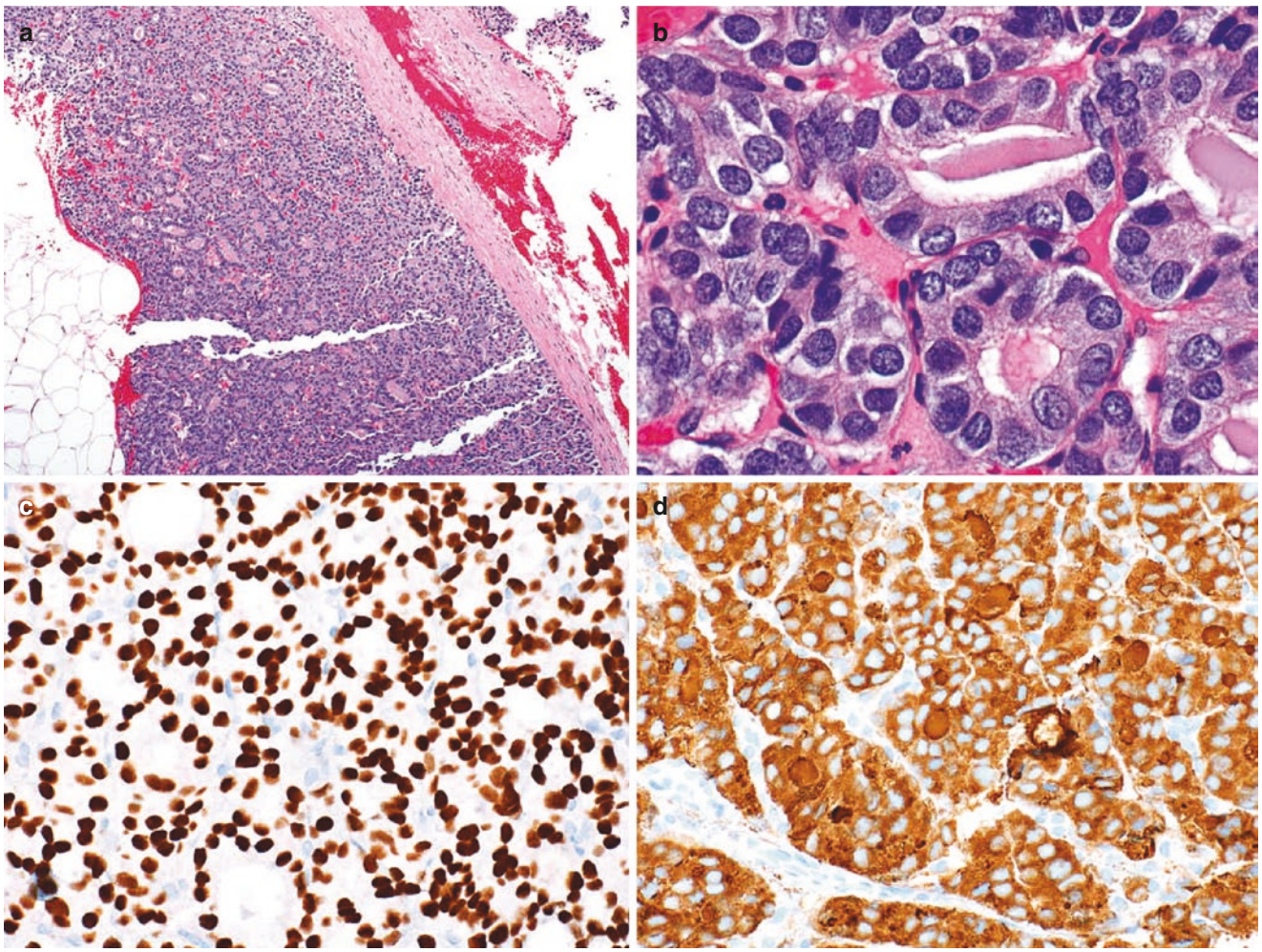

Fig. 24.20 Metastatic well-differentiated follicular thyroid carcinoma to the breast. (**a**, **b**) The breast CNB reveals a thinly encapsulated, well-circumscribed mass that comprises uniformly sized cuboidal cells and intraluminal pink secretions. The cells are immunoreactive for (**c**) TTF1 and (**d**) thyroglobulin

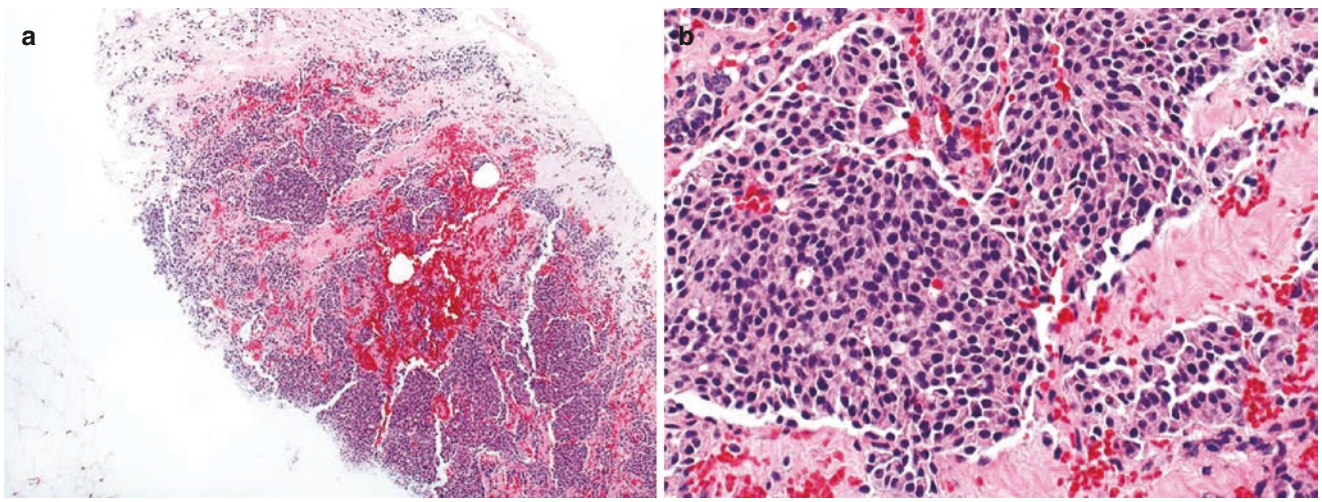

Fig. 24.21 Metastatic medullary thyroid carcinoma to the breast. (**a**, **b**) The breast CNB shows nests and sheets of monotonous cells with amphophilic cytoplasm, homogeneous and stippled chromatin, and extracellular matrix material consistent with amyloid

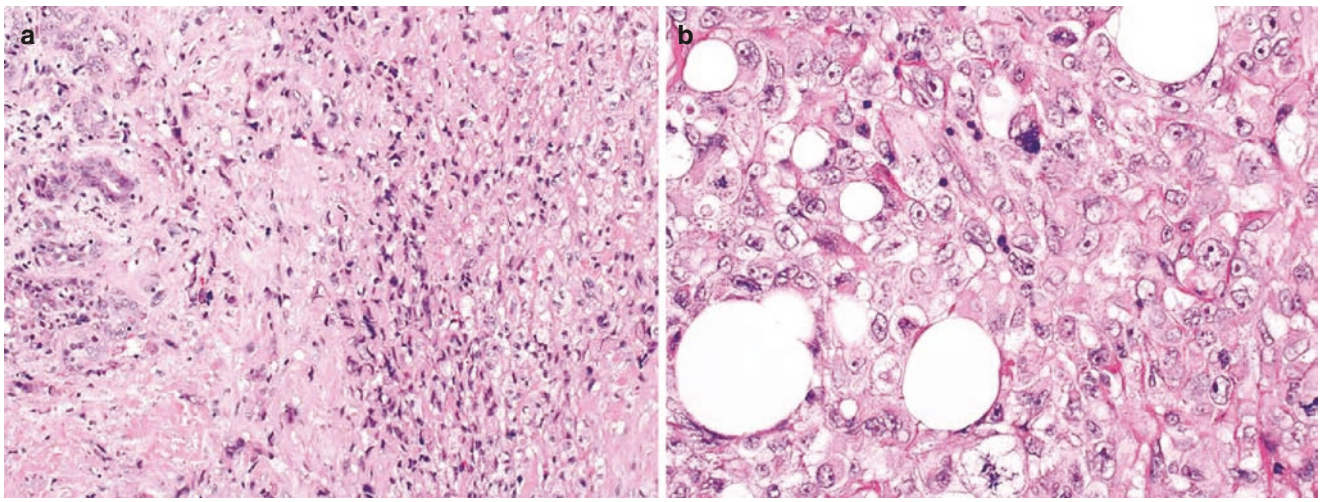

Fig. 24.22 Metastatic choriocarcinoma to the breast. (**a**, **b**) The CNB of a breast mass in a patient with a known placental choriocarcinoma shows sheets of admixed multinucleated syncytiotrophoblasts and mononuclear cytotrophoblasts that irregularly infiltrate around the breast lobules and into the breast adipose tissue. The cells are immunoreactive for β-hCG and GATA3 (not shown)

ferentiation (triton tumor), and a malignant phyllodes tumor with malignant heterologous elements. As in all cases, a clinical history is essential.

Immunohistochemical Workup

Rhabdomyosarcomas display skeletal muscle differentiation and thus are variably immunoreactive for myogenin and desmin. In addition, alveolar rhabdomyosarcomas are translocation tumors, and most display a translocation involving *PAX3-FKHR/FOXO1* or *PAX7-FKHR/FOXO1* partners [t(2;13) and t(1;13), respectively]. In the evaluation of a primitive neoplasm of unknown origin, a broad immunopanel including the following markers should be considered: CD45 and CD43 (hematopoietic); desmin, myogenin, and myoglobin (skeletal muscle); CD99 (suggestive but not diagnostic of Ewing sarcoma); WT1 (desmoplastic small round cell tumor and Wilms' tumor); synaptophysin, chromogranin, and INSM1 (neuroendocrine differentiation); and CKs.

Other Rare Sarcomas

Microscopic Features, Differential Diagnosis, and Immunohistochemical Workup

In addition to leiomyosarcoma and rhabdomyosarcomas, other sarcomas have been reported to metastasize to the breast. In one single-institution series [4], the sarcomas included Ewing sarcoma, pleomorphic undifferentiated sarcoma, synovial sarcoma, angiosarcoma, dendritic cell sarcoma, and myofibrosarcoma. A metastatic lesion should be considered in any neoplasm involving the breast with unusual morphologic or immunophenotypic features. A case of a metastatic central nervous system hemangiopericytoma to the breast illustrates one such example (Fig. 24.25a–c). Radiographically, the lesion is well circumscribed and centered deep within the breast parenchyma. The breast CNB reveals a well-circumscribed mass that comprises short spindle cells with a vaguely storiform architecture, pale pink cytoplasm, and numerous mitotic figures. The cells label for CD34 and BCL2 (Fig. 24.25d, e), but are negative for ER, actin, desmin, S100 protein, and all CKs. The immunohistochemistry and histologic pattern raise the possibility of a dermatofibrosarcoma protuberans, but the lesion does not involve the skin and is not infiltrative. The differential diagnosis includes other primary breast lesions such as spindle cell metaplastic carcinoma, malignant phyllodes tumor, and myofibroblastoma. Subsequently, the surgeon revealed that the patient had a history of a central nervous system hemangiopericytoma, which was morphologically identical to the lesion in the breast (Fig. 24.25f). This again illustrates the importance of reconciling the radiographic, morphologic, and immunophenotypic features of a lesion and of having a thorough clinical history.

Pathogenesis, Prognosis, and Review of the Literature

Non-hematopoietic, solid-organ metastases to the breast account for approximately 0.2–1.2% of breast neoplasms [2, 5, 8], with a higher frequency detected at autopsy [10]. The majority of patients with metastases to the breast have a known cancer history, and involvement of the breast often

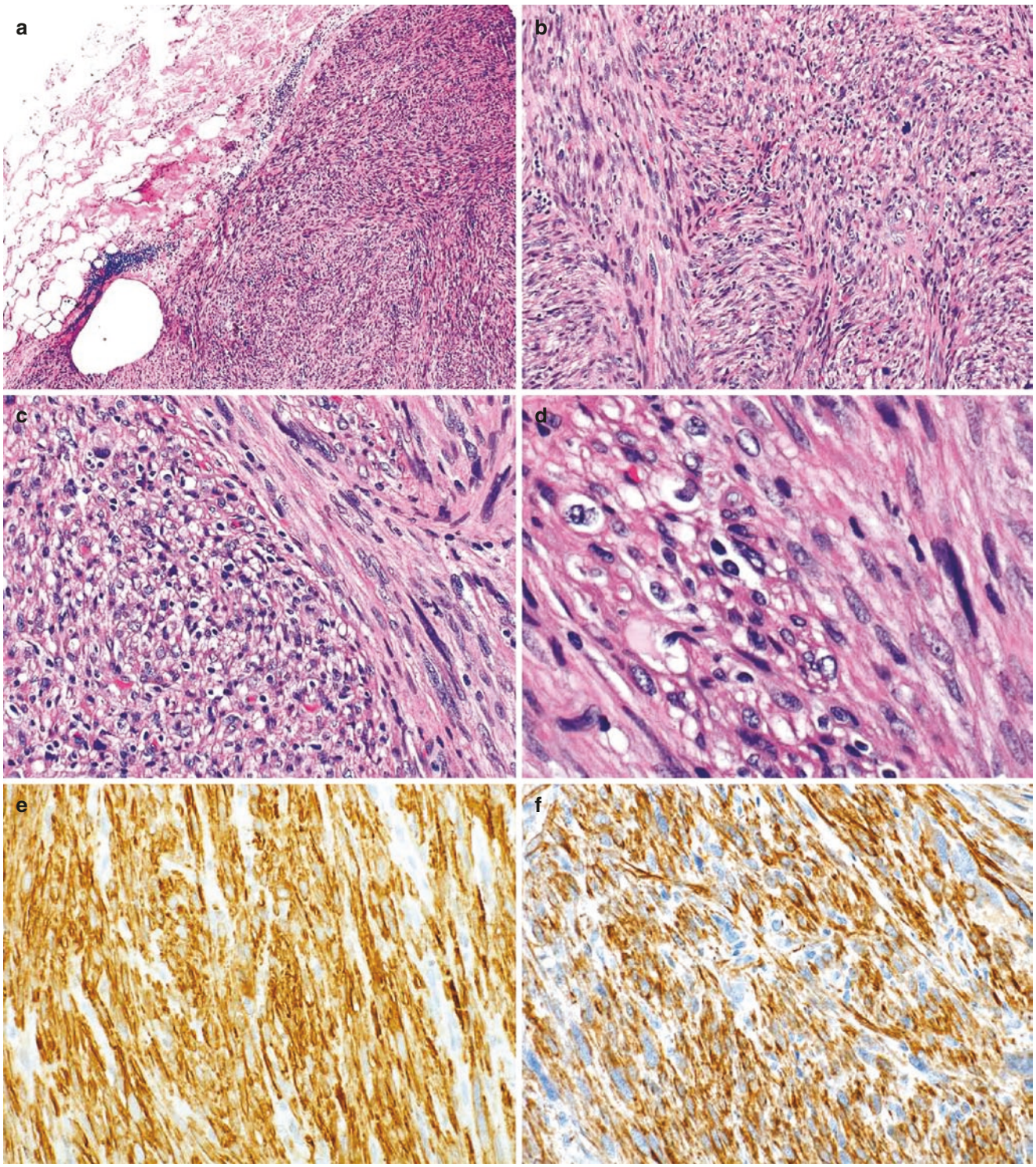

Fig. 24.23 Metastatic leiomyosarcoma to the breast. (**a**–**d**) The breast CNB reveals a well-circumscribed, solid, and homogeneously cellular mass that comprises intersecting fascicles of atypical spindle cells with hyperchromatic, blunt-ended nuclei and numerous mitotic figures. The neoplasm is immunoreactive for (**e**) caldesmon and (**f**) desmin

portends widespread systemic disease with poor outcome. The reported patient median survival after diagnosis of metastases to the breast is 10–15 months [3, 4]. Identification of a lesion as metastatic to the breast is imperative, both to avoid unnecessary therapy such as mastectomy and to guide prognosis.

In one series of metastases to the breast, a pathologic diagnostic error occurred on CNB in 12% of cases [4]. The major-

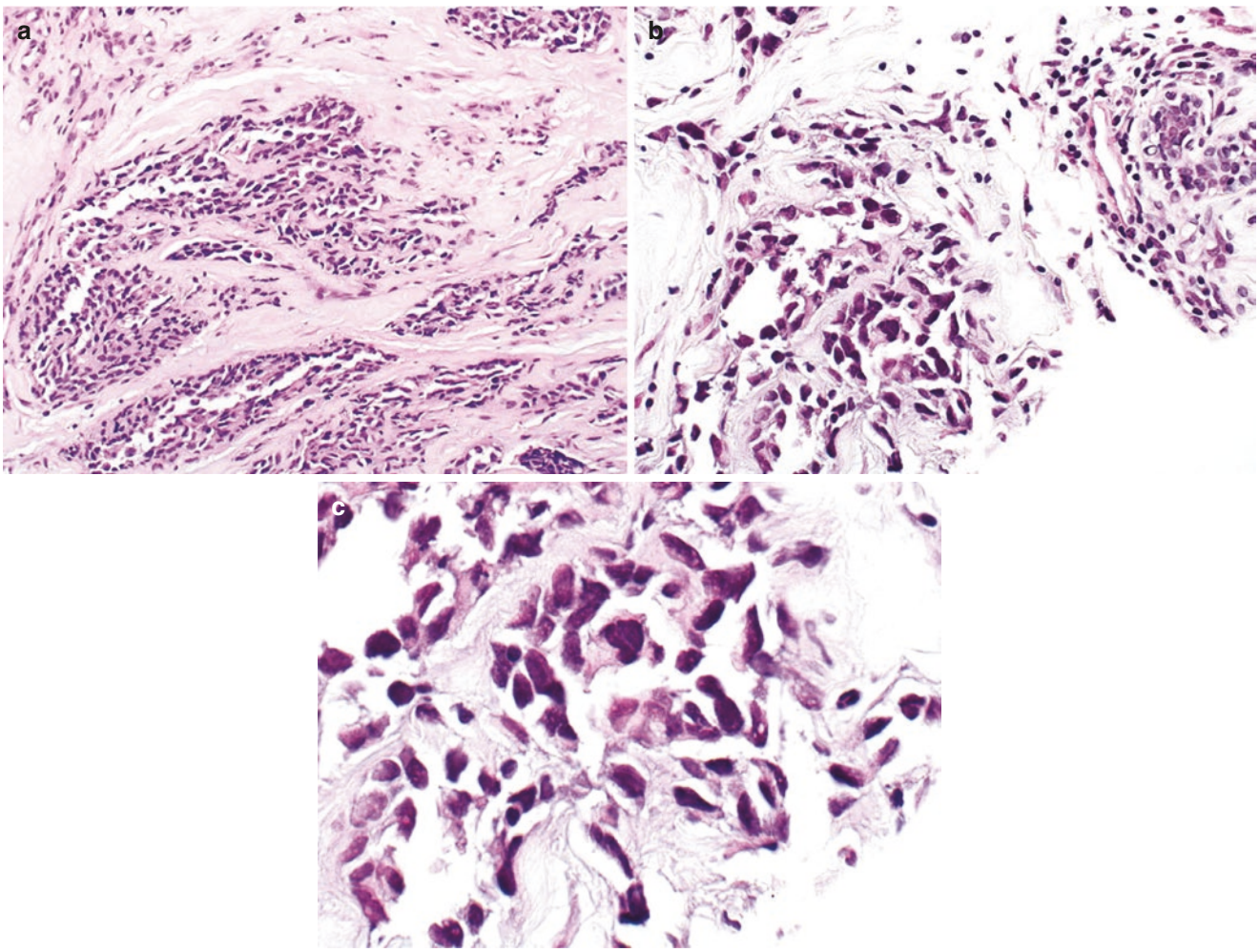

Fig. 24.24 Metastatic alveolar rhabdomyosarcoma to the breast in a pediatric patient. (**a**–**c**) The CNB of the breast mass reveals loosely cohesive nests of small round blue cells separated by delicate fibrous septa. The cells display high nuclear-to-cytoplasmic ratio, nuclear hyperchromasia, and focally eosinophilic cytoplasm

ity (60%) of these were papillary serous carcinomas, where the overlapping morphologic and immunophenotypic features shared with primary breast carcinoma led to a misdiagnosis, followed by melanoma and lung carcinoma. The majority of these diagnostic errors occurred due to a failure of communication of a known cancer history to the pathologist by the treating team; however, a subset also occurred because the primary lesion was not clinically known at the time of breast biopsy. These findings underscore both the importance of communication of clinical history and the importance of the pathologist having a reasonable index of suspicion to work up a case for possible metastasis if certain unusual histologic features are present to suggest a metastasis. These features include ER negativity in a well-differentiated adenocarcinoma (suggestive of pulmonary or gastrointestinal adenocarcinoma), psammomatous calcifications in an adenocarcinoma with micropapillary features (suggestive of high-grade serous carcinoma), and melanin pigment in a high-grade epithelioid neoplasm (suggestive of melanoma).

In summary, although rare, metastases to the breast present a diagnostic challenge due to the overlapping morphologic features with primary breast carcinoma. Although certain histologic features may suggest that a lesion is not a primary breast neoplasm, the clinical history, a clinical workup, and a targeted immunohistochemical panel are often necessary to reach the correct diagnosis.

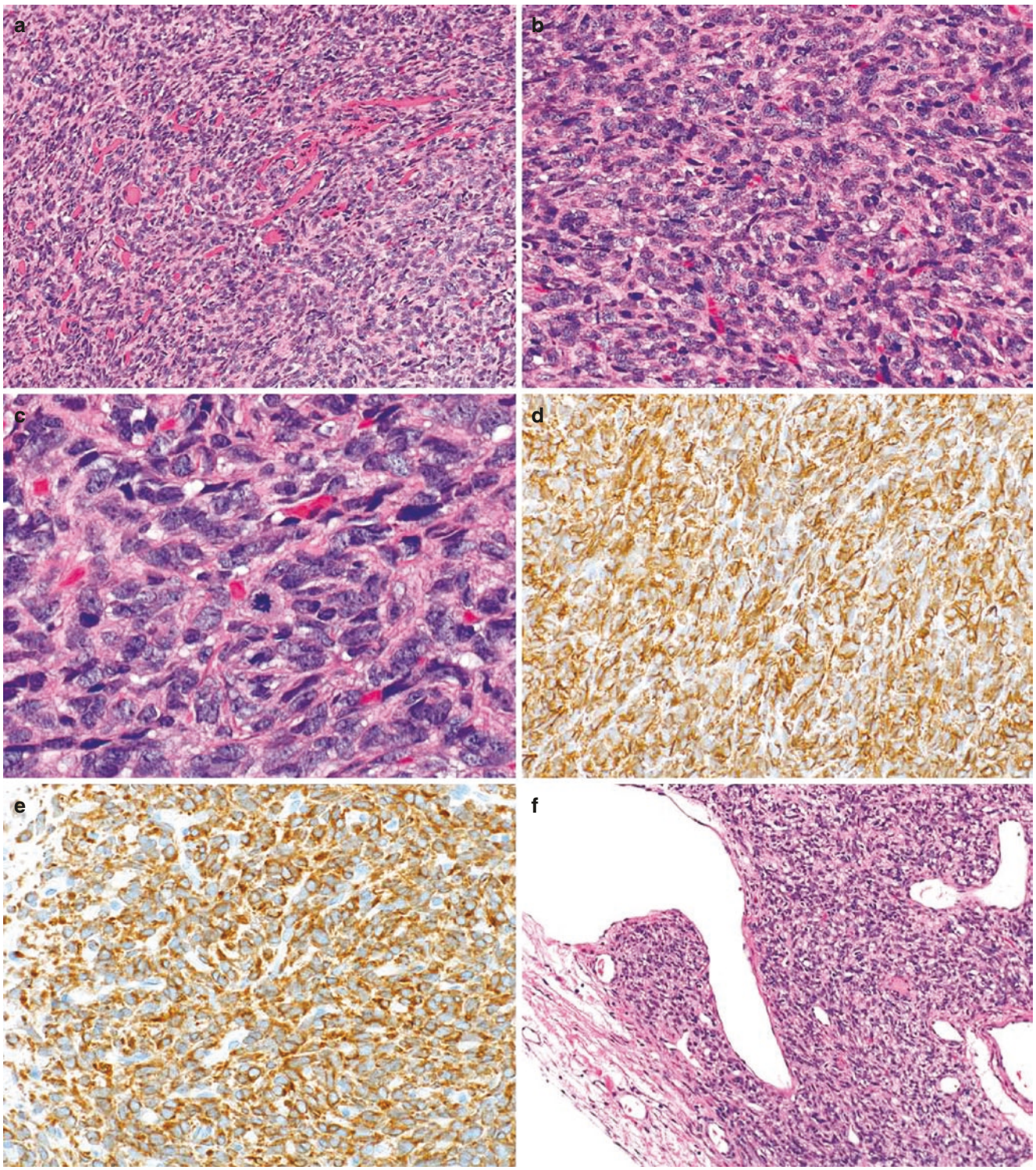

Fig. 24.25 Metastatic hemangiopericytoma of the central nervous system to the breast. (**a**–**c**) CNB of a deep-seated, well-circumscribed breast mass revealed sheets of short spindle cells with a vaguely storiform architecture, delicate vasculature, and abundant mitotic figures. The cells were diffusely immunoreactive for (**d**) CD34 and (**e**) BCL2 and negative for cytokeratins, actin, desmin, ER, and S100 protein (not shown). (**f**) Comparison with the patient's primary central nervous system hemangiopericytoma revealed identical morphologic features

References

1. Picasso R, Pistoia F, Zaottini F, Sanguinetti S, Calabrese M, Martinoli C, Derchi L. Breast metastases: updates on epidemiology and radiologic findings. Cureus. 2020;12(12):e12258. https://doi.org/10.7759/cureus.12258.
2. Hajdu SI, Urban JA. Cancers metastatic to the breast. Cancer. 1972;29(6):1691–6. Epub 1972/06/01
3. Williams SA, Ehlers RA II, Hunt KK, Yi M, Kuerer HM, Singletary SE, et al. Metastases to the breast from nonbreast solid neoplasms: presentation and determinants of survival. Cancer. 2007;110(4):731–7. Epub 2007/06/22
4. DeLair DF, Corben AD, Catalano JP, Vallejo CE, Brogi E, Tan LK. Non-mammary metastases to the breast and axilla: a study of 85 cases. Mod Pathol. 2013;26(3):343–9. Epub 2012/11/24
5. Lee AH. The histological diagnosis of metastases to the breast from extramammary malignancies. J Clin Pathol. 2007;60(12):1333–41. Epub 2007/11/29
6. Silverman JF, Feldman PS, Covell JL, Frable WJ. Fine needle aspiration cytology of neoplasms metastatic to the breast. Acta Cytol. 1987;31(3):291–300. Epub 1987/05/01
7. Shukla R, Pooja B, Radhika S, Nijhawan R, Rajwanshi A. Fine-needle aspiration cytology of extramammary neoplasms metastatic to the breast. Diagn Cytopathol. 2005;32(4):193–7. Epub 2005/03/09
8. Alvarado Cabrero I, Carrera Alvarez M, Perez Montiel D, Tavassoli FA. Metastases to the breast. Eur J Surg Oncol. 2003;29(10):854–5. Epub 2003/11/20
9. Lee AHS, Hodi Z, Soomro I, Sovani V, Abbas A, Rakha E, Ellis IO. Histological clues to the diagnosis of metastasis to the breast from extramammary malignancies. Histopathology. 2020;77(2):303–13. https://doi.org/10.1111/his.14141. Epub 2020 Jul 23
10. Georgiannos SN, Chin J, Goode AW, Sheaff M. Secondary neoplasms of the breast: a survey of the 20th Century. Cancer. 2001;92(9):2259–66. Epub 2001/12/18
11. Alva S, Shetty-Alva N. An update of tumor metastasis to the breast data. Arch Surg (Chicago: 1960). 1999;134(4):450. Epub 1999/04/13
12. Vaughan A, Dietz JR, Moley JF, Debenedetti MK, Aft RL, Gillanders WE, et al. Metastatic disease to the breast: the Washington University experience. World J Surg Oncol. 2007;5:74. Epub 2007/07/07
13. Noguera J, Martinez-Miravete P, Idoate F, Diaz L, Pina L, Zornoza G, et al. Metastases to the breast: a review of 33 cases. Australas Radiol. 2007;51(2):133–8. Epub 2007/04/11
14. Lee SK, Kim WW, Kim SH, Hur SM, Kim S, Choi JH, et al. Characteristics of metastasis in the breast from extramammary malignancies. J Surg Oncol. 2010;101(2):137–40. Epub 2010/01/19
15. Rogers DA, Lobe TE, Rao BN, Fleming ID, Schropp KP, Pratt AS, et al. Breast malignancy in children. J Pediatr Surg. 1994;29(1):48–51. Epub 1994/01/01
16. Pettinato G, Manivel JC, Kelly DR, Wold LE, Dehner LP. Lesions of the breast in children exclusive of typical fibroadenoma and gynecomastia. A clinicopathologic study of 113 cases. Pathol Annu. 1989;24(Pt 2):296–328. Epub 1989/01/01
17. Surov A, Fiedler E, Holzhausen HJ, Ruschke K, Schmoll HJ, Spielmann RP. Metastases to the breast from non-mammary malignancies: primary tumors, prevalence, clinical signs, and radiological features. Acad Radiol. 2011;18(5):565–74. Epub 2011/03/12
18. Mun SH, Ko EY, Han BK, Shin JH, Kim SJ, Cho EY. Breast metastases from extramammary malignancies: typical and atypical ultrasound features. Korean J Radiol. 2014;15(1):20–8. Epub 2014/02/06
19. Sippo DA, Kulkarni K, Carlo PD, Lee B, Eisner D, Cimino-Mathews A, Harvey SC. Metastatic disease to the breast from extramammary malignancies: a multimodality pictorial review. Curr Probl Diagn Radiol. 2016;45(3):225–32. https://doi.org/10.1067/j.cpradiol.2015.07.001. Epub 2015 Jul 4
20. Marx HF, Colletti PM, Raval JK, Boswell WD Jr, Zee CS. Magnetic resonance imaging features in melanoma. Magn Reson Imaging. 1990;8(3):223–9. Epub 1990/01/01
21. Gupta D, Merino MI, Farhood A, Middleton LP. Metastases to breast simulating ductal carcinoma in situ: report of two cases and review of the literature. Ann Diagn Pathol. 2001;5(1):15–20. Epub 2001/02/15
22. Judson K, Argani P. Intraductal spread by metastatic islet cell tumor (well-differentiated pancreatic endocrine neoplasm) involving the breast of a child, mimicking a primary mammary carcinoma. Am J Surg Pathol. 2006;30(7):912–8. Epub 2006/07/05
23. Tot T. Cytokeratins 20 and 7 as biomarkers: usefulness in discriminating primary from metastatic adenocarcinoma. Eur J Cancer (Oxford, England: 1990). 2002;38(6):758–63. Epub 2002/04/09
24. Luo MH, Huang YH, Ni YB, Tsang JY, Chan SK, Shao MM, et al. Expression of mammaglobin and gross cystic disease fluid protein-15 in breast carcinomas. Hum Pathol. 2013;44(7):1241–50. Epub 2013/01/22
25. Bhargava R, Beriwal S, Dabbs DJ. Mammaglobin vs GCDFP-15: an immunohistologic validation survey for sensitivity and specificity. Am J Clin Pathol. 2007;127(1):103–13. Epub 2006/12/06
26. Conner JR, Hornick JL. Metastatic carcinoma of unknown primary: diagnostic approach using immunohistochemistry. Adv Anat Pathol. 2015;22:149–67.
27. Lewis GH, Subhawong AP, Nassar H, Vang R, Illei PB, Park BH, et al. Relationship between molecular subtype of invasive breast carcinoma and expression of gross cystic disease fluid protein 15 and mammaglobin. Am J Clin Pathol. 2011;135(4):587–91. Epub 2011/03/18
28. Asch-Kendrick R, Cimino-Mathews A. The role of GATA3 in breast carcinomas: a review. Hum Pathol. 2016;48:37–47.
29. Wendroth SM, Mentrikoski MJ, Wick MR. GATA3 expression in morphologic subtypes of breast carcinoma: a comparison with gross cystic disease fluid protein 15 and mammaglobin. Ann Diagn Pathol. 2015;19(1):6–9. Epub 2014/12/30
30. Cimino-Mathews A, Subhawong AP, Illei PB, Sharma R, Halushka MK, Vang R, et al. GATA3 expression in breast carcinoma: utility in triple-negative, sarcomatoid, and metastatic carcinomas. Hum Pathol. 2013;44(7):1341–9. Epub 2013/02/05
31. Nonaka D, Chiriboga L, Rubin BP. Sox10: a pan-schwannian and melanocytic marker. Am J Surg Pathol. 2008;32(9):1291–8. Epub 2008/07/19
32. Cimino-Mathews A, Subhawong AP, Elwood H, Warzecha HN, Sharma R, Park BH, et al. Neural crest transcription factor Sox10 is preferentially expressed in triple-negative and metaplastic breast carcinomas. Hum Pathol. 2013;44(6):959–65. Epub 2012/12/25
33. Tacha D, Qi W, Ra S, Bremer R, Yu C, Chu J, et al. A newly developed mouse monoclonal SOX10 antibody is a highly sensitive and specific marker for malignant melanoma, including spindle cell and desmoplastic melanomas. Arch Pathol Lab Med. 2014;139(4):530–6. Epub 2014/12/02
34. Mohamed A, Gonzalez RS, Lawson D, Wang J, Cohen C. SOX10 expression in malignant melanoma, carcinoma, and normal tissues. Appl Immunohistochem Mol Morphol. 2013;21(6):506–10. Epub 2012/12/01
35. Miettinen M, McCue PA, Sarlomo-Rikala M, Biernat W, Czapiewski P, Kopczynski J, et al. Sox10-a marker for not only schwannian and melanocytic neoplasms but also myoepithelial cell tumors of soft tissue: a systematic analysis of 5134 tumors. Am J Surg Pathol. 2015;39(6):826–35. Epub 2015/02/28

36. Nelson ER, Sharma R, Argani P, Cimino-Mathews A. Utility of Sox10 labeling in metastatic breast carcinomas. Hum Pathol. 2017;67:205–10.
37. Qazi MS, McGregor SM. Combined use of SOX10 and GATA3 in mammary carcinoma. Pathol Res Pract. 2020;216:152801.
38. Tozbikian GH, Zynger DL. A combination of GATA3 and SOX10 is useful for the diagnosis of metastatic triple-negative breast cancer. Hum Pathol. 2019;85:221–7.
39. Dwarakanath S, Lee AK, Delellis RA, Silverman ML, Frasca L, Wolfe HJ. S-100 protein positivity in breast carcinomas: a potential pitfall in diagnostic immunohistochemistry. Hum Pathol. 1987;18(11):1144–8. Epub 1987/11/01
40. Topalovski M, Crisan D, Mattson JC. Lymphoma of the breast. A clinicopathologic study of primary and secondary cases. Arch Pathol Lab Med. 1999;123(12):1208–18. Epub 1999/12/03
41. Basara I, Orguc S. Giant breast involvement in acute lymphoblastic leukemia: MRI findings. J Breast Cancer. 2012;15(2):258–60. Epub 2012/07/19
42. De Chiara A, Losito S, Terracciano L, Di Giacomo R, Iaccarino G, Rubolotta MR. Primary plasmacytoma of the breast. Arch Pathol Lab Med. 2001;125(8):1078–80. Epub 2001/07/28
43. Cangiarella J, Symmans WF, Cohen JM, Goldenberg A, Shapiro RL, Waisman J. Malignant melanoma metastatic to the breast: a report of seven cases diagnosed by fine-needle aspiration cytology. Cancer. 1998;84(3):160–2. Epub 1998/07/25
44. Ravdel L, Robinson WA, Lewis K, Gonzalez R. Metastatic melanoma in the breast: a report of 27 cases. J Surg Oncol. 2006;94(2):101–4. Epub 2006/07/19
45. Arora R, Robinson WA. Breast metastases from malignant melanoma. J Surg Oncol. 1992;50(1):27–9. Epub 1992/05/01
46. Loffeld A, Marsden JR. Management of melanoma metastasis to the breast: case series and review of the literature. Br J Dermatol. 2005;152(6):1206–10. Epub 2005/06/14
47. Papachristou DN, Kinne DW, Rosen PP, Ashikari R, Fortner JG. Cutaneous melanoma of the breast. Surgery. 1979;85(3):322–8. Epub 1979/03/01
48. Miettinen M, Fernandez M, Franssila K, Gatalica Z, Lasota J, Sarlomo-Rikala M. Microphthalmia transcription factor in the immunohistochemical diagnosis of metastatic melanoma: comparison with four other melanoma markers. Am J Surg Pathol. 2001;25(2):205–11. Epub 2001/02/15
49. Jennings C, Kim J. Identification of nodal metastases in melanoma using sox-10. Am J Dermatopathol. 2011;33(5):474–82. Epub 2011/05/10
50. Sanguinetti A, Puma F, Lucchini R, Santoprete S, Cirocchi R, Corsi A, et al. Breast metastasis from a pulmonary adenocarcinoma: case report and review of the literature. Oncol Lett. 2013;5(1):328–32. Epub 2012/12/21
51. Ji FF, Gao P, Wang JG, Zhao J, Zhao P. Contralateral breast metastasis from pulmonary adenocarcinoma: two cases report and literature review. J Thorac Dis. 2012;4(4):384–9. Epub 2012/08/31
52. Masmoudi A, Mathieu MC, Soria JC. Breast metastasis from lung adenocarcinoma: a case report. Anticancer Res. 2003;23(2C):1825–6. Epub 2003/06/25
53. Dennis JL, Hvidsten TR, Wit EC, Komorowski J, Bell AK, Downie I, et al. Markers of adenocarcinoma characteristic of the site of origin: development of a diagnostic algorithm. Clin Cancer Res. 2005;11(10):3766–72. Epub 2005/05/18
54. Miettinen M, McCue PA, Sarlomo-Rikala M, Rys J, Czapiewski P, Wazny K, et al. GATA3: a multispecific but potentially useful marker in surgical pathology: a systematic analysis of 2500 epithelial and nonepithelial tumors. Am J Surg Pathol. 2014;38(1):13–22. Epub 2013/10/23
55. Robens J, Goldstein L, Gown AM, Schnitt SJ. Thyroid transcription factor-1 expression in breast carcinomas. Am J Surg Pathol. 2010;34(12):1881–5. Epub 2010/11/26
56. Hsu W, Sheen-Chen SM, Wang JL, Huang CC, Ko SF. Squamous cell lung carcinoma metastatic to the breast. Anticancer Res. 2008;28(2B):1299–301. Epub 2008/05/29
57. Genc B, Solak A, Sahin N, Gulsen A. Metastasis to the male breast from squamous cell lung carcinoma. Case Rep Oncol Med. 2013;2013:593970. Epub 2013/09/03
58. Luh SP, Kuo C, Tsao TC. Breast metastasis from small cell lung carcinoma. J Zhejiang Univ Sci B. 2008;9(1):39–43. Epub 2008/01/16
59. Shin SJ, DeLellis RA, Ying L, Rosen PP. Small cell carcinoma of the breast: a clinicopathologic and immunohistochemical study of nine patients. Am J Surg Pathol. 2000;24(9):1231–8. Epub 2000/09/08
60. Agoff SN, Lamps LW, Philip AT, Amin MB, Schmidt RA, True LD, et al. Thyroid transcription factor-1 is expressed in extrapulmonary small cell carcinomas but not in other extrapulmonary neuroendocrine tumors. Mod Pathol. 2000;13(3):238–42. Epub 2000/04/11
61. Zhang C, Schmidt LA, Hatanaka K, Thomas D, Lagstein A, Myers JL. Evaluation of napsin A, TTF-1, p63, p40, and CK5/6 immunohistochemical stains in pulmonary neuroendocrine tumors. Am J Clin Pathol. 2014;142(3):320–4. Epub 2014/08/16
62. Recine MA, Deavers MT, Middleton LP, Silva EG, Malpica A. Serous carcinoma of the ovary and peritoneum with metastases to the breast and axillary lymph nodes: a potential pitfall. Am J Surg Pathol. 2004;28(12):1646–51. Epub 2004/12/04
63. Klein RL, Brown AR, Gomez-Castro CM, Chambers SK, Cragun JM, Grasso-Lebeau L, et al. Ovarian cancer metastatic to the breast presenting as inflammatory breast cancer: a case report and literature review. J Cancer. 2010;1:27–31. Epub 2010/09/16
64. Yamasaki H, Saw D, Zdanowitz J, Faltz LL. Ovarian carcinoma metastasis to the breast case report and review of the literature. Am J Surg Pathol. 1993;17(2):193–7. Epub 1993/02/01
65. Maounis N, Chorti M, Legaki S, Ellina E, Emmanouilidou A, Demonakou M, et al. Metastasis to the breast from an adenocarcinoma of the lung with extensive micropapillary component: a case report and review of the literature. Diagn Pathol. 2010;5:82. Epub 2010/12/21
66. Tornos C, Soslow R, Chen S, Akram M, Hummer AJ, Abu-Rustum N, et al. Expression of WT1, CA 125, and GCDFP-15 as useful markers in the differential diagnosis of primary ovarian carcinomas versus metastatic breast cancer to the ovary. Am J Surg Pathol. 2005;29(11):1482–9. Epub 2005/10/15
67. Laury AR, Perets R, Piao H, Krane JF, Barletta JA, French C, et al. A comprehensive analysis of PAX8 expression in human epithelial tumors. Am J Surg Pathol. 2011;35(6):816–26. Epub 2011/05/10
68. Nonaka D, Chiriboga L, Soslow RA. Expression of pax8 as a useful marker in distinguishing ovarian carcinomas from mammary carcinomas. Am J Surg Pathol. 2008;32(10):1566–71. Epub 2008/08/30
69. Kilgore MR, Bosch DE, Adamson KH, Swanson PE, Dintzis SM, Rendi MH. Unexpected PAX8 immunoreactivity in metastatic high-grade breast cancer. Appl Immunohistochem Mol Morphol. 2019;27:637–43.
70. Acs G, Pasha T, Zhang PJ. WT1 is differentially expressed in serous, endometrioid, clear cell, and mucinous carcinomas of the peritoneum, fallopian tube, ovary, and endometrium. Int J Gynecol Pathol. 2004;23(2):110–8. Epub 2004/04/16
71. Domfeh AB, Carley AL, Striebel JM, Karabakhtsian RG, Florea AV, McManus K, et al. WT1 immunoreactivity in breast carcinoma: selective expression in pure and mixed mucinous subtypes. Mod Pathol. 2008;21(10):1217–23. Epub 2008/05/13
72. Falco G, Buggi F, Sanna PA, Dubini A, Folli S. Breast metastases from a Renal Cell Carcinoma. A case report and review of the literature. Int J Surg Case Rep. 2014;5(4):193–5. Epub 2014/03/19
73. Alzaraa A, Vodovnik A, Montgomery H, Saeed M, Sharma N. Breast metastasis from a renal cell cancer. World J Surg Oncol. 2007;5:25. Epub 2007/03/06

74. McLauglin SA, Thiel DD, Smith SL, Wehle MJ, Menke DM. Solitary breast mass as initial presentation of clinically silent metastatic renal cell carcinoma. Breast (Edinburgh, Scotland). 2006;15(3):427–9. Epub 2005/11/18
75. Rakha EA, Reis-Filho JS, Wu Y. Neuroendocrine tumor. In: WHO Classification of Tumours Editorial Board, editor. Breast tumours, WHO classification of tumours series, vol. 2. 5th ed. Lyon, France: International Agency for Research on Cancer; 2019. p. 156–8.
76. Werling RW, Yaziji H, Bacchi CE, Gown AM. CDX2, a highly sensitive and specific marker of adenocarcinomas of intestinal origin: an immunohistochemical survey of 476 primary and metastatic carcinomas. Am J Surg Pathol. 2003;27(3):303–10. Epub 2003/02/27
77. Sapino A, Righi L, Cassoni P, Papotti M, Pietribiasi F, Bussolati G. Expression of the neuroendocrine phenotype in carcinomas of the breast. Semin Diagn Pathol. 2000;17(2):127–37. Epub 2000/06/06
78. Siegel RL, Miller KD, Jemal A. Cancer statistics, 2020. CA Cancer J Clin. 2020;70(1):7–30. https://doi.org/10.3322/caac.21590. Epub 2020 Jan 8
79. Kidwai N, Gong Y, Sun X, Deshpande CG, Yeldandi AV, Rao MS, et al. Expression of androgen receptor and prostate-specific antigen in male breast carcinoma. Breast Cancer Res. 2004;6(1):R18–23. Epub 2003/12/19
80. Carder PJ, Speirs V, Ramsdale J, Lansdown MR. Expression of prostate specific antigen in male breast cancer. J Clin Pathol. 2005;58(1):69–71. Epub 2004/12/30
81. Kraus TS, Cohen C, Siddiqui MT. Prostate-specific antigen and hormone receptor expression in male and female breast carcinoma. Diagn Pathol. 2010;5:63. Epub 2010/09/25
82. Gurel B, Ali TZ, Montgomery EA, Begum S, Hicks J, Goggins M, et al. NKX3.1 as a marker of prostatic origin in metastatic tumors. Am J Surg Pathol. 2010;34(8):1097–105. Epub 2010/07/01
83. Asch-Kendrick RJ, Samols MA, Lilo MT, Subhawong AP, Sharma R, Illei PB, et al. NKX3.1 is expressed in ER-positive and AR-positive primary breast carcinomas. J Clin Pathol. 2014;67(9):768–71. Epub 2014/12/17
84. Jena S, Bhattacharya S, Gupta A, Roy S, Sinha NK. Breast metastasis from esophagogastric junction cancer: a case report. Case Rep Surg. 2014;2014:489427. Epub 2014/07/12
85. Ho YY, Lee WK. Metastasis to the breast from an adenocarcinoma of the colon. J Clin Ultrasound. 2009;37(4):239–41. Epub 2008/05/08
86. Ahmad A, Baiden-Amissah K, Oyegade A, Absar M, Swainson K, Titi S. Primary sigmoid adenocarcinoma metastasis to the breast in a 28-year-old female: a case study and a review of literature. Korean J Pathol. 2014;48(1):58–61. Epub 2014/03/15
87. Shackelford RE, Allam-Nandyala P, Bui MM, Kiluk JV, Esposito NN. Primary colorectal adenocarcinoma metastatic to the breast: case report and review of nineteen cases. Case Rep Med. 2011;2011:738413. Epub 2011/07/09
88. Mihai R, Christie-Brown J, Bristol J. Breast metastases from colorectal carcinoma. Breast (Edinburgh, Scotland). 2004;13(2):155–8. Epub 2004/03/17
89. Kim SM, Ko EY, Han BK, Shin JH, Kang SS, Nam SJ, et al. Metastatic thymoma of the breast. Korean J Radiol. 2008;9(1):80–3. Epub 2008/02/07
90. Kalra N, Ojili V, Gulati M, Prasad GR, Vaiphei K, Suri S. Metastatic choriocarcinoma to the breast: appearance on mammography and Doppler sonography. Am J Roentgenol. 2005;184(3 Suppl):S53–5. Epub 2005/02/25
91. Banet N, Gown AM, Shih Ie M, Kay Li Q, Roden RB, Nucci MR, et al. GATA-3 expression in trophoblastic tissues: an immunohistochemical study of 445 cases, including diagnostic utility. Am J Surg Pathol. 2015;39(1):101–8. Epub 2014/09/05
92. Lin CH, Yeh CN, Chen MF. Breast metastasis from uterine leiomyosarcoma: a case report. Archiv Gynecol Obstet. 2003;267(4):233–5. Epub 2003/02/20
93. Hsiao HH, Liu YC, Hou MF, Lin SF. Uterine leiomyosarcoma metastasis to the breast. Eur J Gynaecol Oncol. 2008;29(2):191–2. Epub 2008/05/08
94. D'Angelo P, Carli M, Ferrari A, Manzitti C, Mura R, Miglionico L, et al. Breast metastases in children and adolescents with rhabdomyosarcoma: experience of the Italian Soft Tissue Sarcoma Committee. Pediatr Blood Cancer. 2010;55(7):1306–9. Epub 2010/08/24

Dermatologic Mimickers of Breast Lesions Arising in the Breast Skin, Subcutis, or Axilla

25

Garrett Desman, Lurmag Y. Orta, and Sandra J. Shin

General Clinical and Radiologic Considerations

The breast is composed of multiple anatomic regions with distinct histologic compartments that harbor specific disease processes. Placed over the pectoralis muscles as a deep boundary, the breast is present within the anterior and posterior fascia of the chest. It extends to the axilla without a defined boundary. The skin extensively covers the breast and sends fibrous bands from the dermis to form the ligaments of Cooper, providing parenchymal support. Subcutaneous fat separates the skin from the underlying breast parenchyma. The skin of the axilla contains hair follicles, eccrine sweat glands, and large concentrations of apocrine sweat glands. Finally, the nipple-areolar complex, in which skin and breast tissue are in close proximity, contains the major lactiferous ducts, eccrine and apocrine sweat glands, cutaneous sebaceous glands, modified mammary sebaceous glands (Montgomery's glands), and sensory nerve endings [1–3].

Due to this complex regional microanatomy, the surgical pathologist must be careful when receiving a specimen labeled "breast mass," as it may represent tissue from the breast parenchyma, subcutaneous tissue, or skin. For a variety of reasons, including increased awareness of early breast cancer detection, medicolegal implications, and unique patient anatomy, lesions arising in the chest area of a female will be most likely be designated as "breast." In contrast, for male patients, a breast lesion will most likely be described as "chest." A complete clinical history and description of the lesion might be necessary for the proper identification of the anatomic region and subsequent differential diagnosis.

Since the skin overlying the breast measures only 0.5–2 mm in thickness, cutaneous mass lesions may occasionally be clinically misinterpreted as superficial breast tumors on imaging studies. This may result in the improper use of a core needle biopsy (CNB) instead of a shave or punch biopsy and potentially further limit the pathologist's ability to establish the correct diagnosis. The radiographic findings of skin and its associated lesions via mammography, ultrasound, and magnetic resonance imaging (MRI) have been reviewed elsewhere [2–4] and therefore will only be briefly summarized here. Skin overlying the breast normally reveals a symmetric thin enhancement by mammography and MRI and presents as an echogenic layer by ultrasound. Commonly encountered benign cutaneous lesions, such as epidermoid cysts and lipomas, often present as palpable masses on the breast or axilla or may be first diagnosed at screening mammography, where they will appear as isodense circumscribed masses or fat densities (Fig. 25.1a). In most instances, a benign diagnosis can be favored by radiographic appearance and the lesion can be followed clinically or conservatively removed. In other instances, the decision to further evaluate pathologically by way of CNB is made. These biopsies are received with a clinical history of the breast mass and can be a diagnostic pitfall to the unwary (Figs. 25.2 and 25.3).

Targeted ultrasound is the preferred modality for evaluating palpable breast masses, especially superficial lesions, since it can determine whether the mass is arising within the dermis or subcutaneous tissue. The use of a high-frequency transducer and advanced sonographic techniques will

G. Desman
Department of Pathology, Icahn School of Medicine at Mount Sinai, New York, NY, USA

Department of Dermatology, Icahn School of Medicine at Mount Sinai, New York, NY, USA

Dermatopathology Division, Optum Care, New Hyde Park, NY, USA
e-mail: garrett.desman@mountsinai.org

L. Y. Orta
Integrated Pathology Services, Trujillo Alto, Puerto Rico

Hospital Auxilio Mutuo, San Juan, Puerto Rico

S. J. Shin (✉)
Department of Pathology and Laboratory Medicine, Albany Medical College, Albany, NY, USA
e-mail: shins1@amc.edu

© The Author(s), under exclusive license to Springer Nature Switzerland AG 2022
S. J. Shin et al. (eds.), *A Comprehensive Guide to Core Needle Biopsies of the Breast*,
https://doi.org/10.1007/978-3-031-05532-4_25

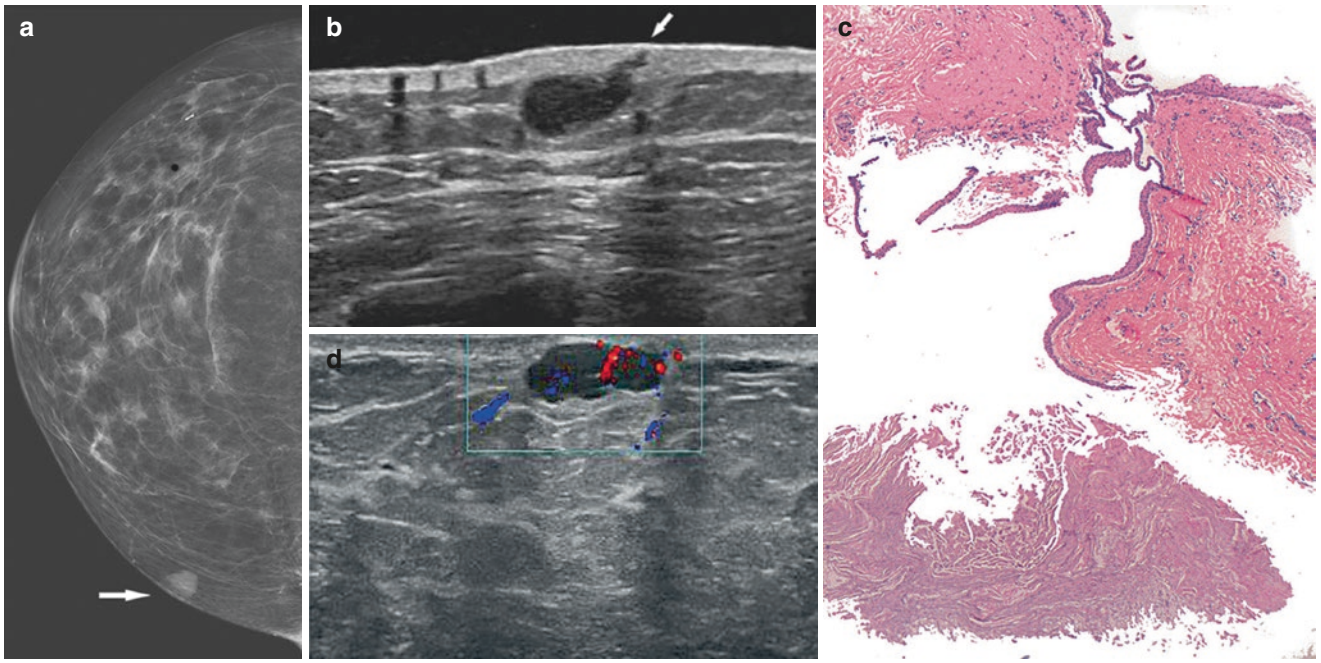

Fig. 25.1 Radiographic presentation of an epidermal inclusion cyst. (**a**) Screening mammography shows a round isodense mass in craniocaudal compression (CC view) (arrow). (**b**) Ultrasound demonstrates a well-circumscribed anechoic lesion with circumscribed borders that connects with the skin through a tract (arrow). (**c**) CNB revealed an epidermal inclusion cyst. (**d**) Ultrasound imaging of a subdermal circumscribed oval mass with sound transmission, with features similar to those in **b**. However, color Doppler evaluation shows internal vascularity. Ultrasound-guided biopsy confirmed the lesion as an invasive ductal carcinoma. ((**a**, **b**, **d**) Courtesy of Dr. Mayra Maldonado Durán, University of Puerto Rico, Medical Sciences Campus, with permission)

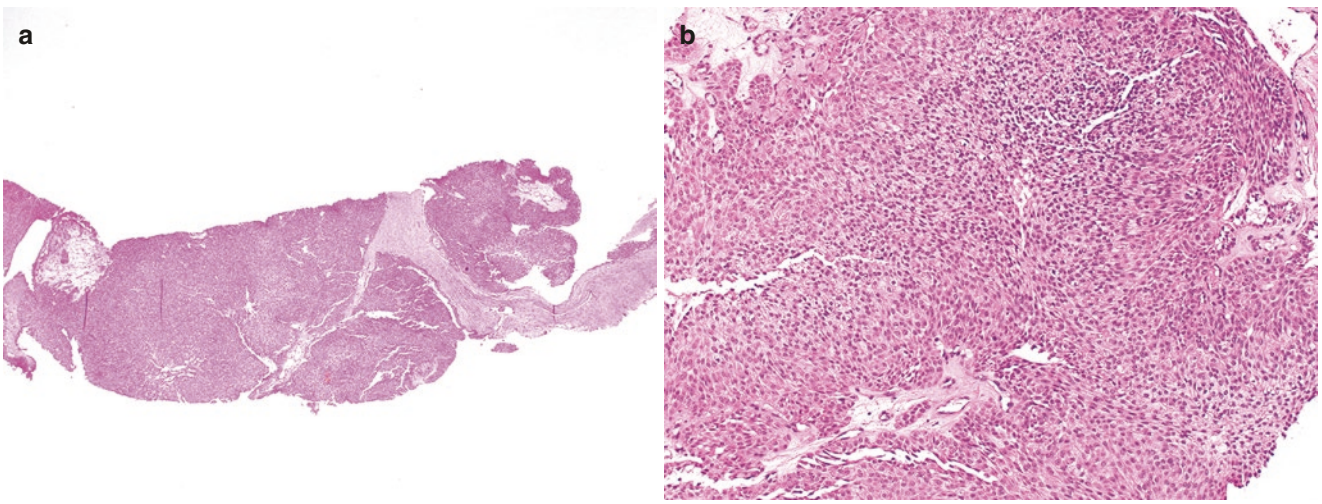

Fig. 25.2 Hidradenoma presenting as a breast mass. (**a**) CNB shows portions of a solid papillary tumor; (**b**) higher magnification shows a monotonous population of cells; (**c**) excisional biopsy demonstrates a benign tumor seated in the dermis and subcutis with no epidermal connection; (**d**) higher magnification shows the tumor to be composed of round to polygonal shaped cells with amphophilic cytoplasm and shows ductal differentiation with perfectly punched-out holes. (**e**) Areas of hyalinized stroma can be mistaken for fibrovascular cores of solid papillary proliferations in the breast. (**f**) Strong diffuse immunoreactivity for CK5/6 and (**g**) p63 further supports the diagnosis of hidradenoma. (Courtesy of Dr. Tiffany Chen, Department of Pathology and Laboratory Medicine, Albany Medical College)

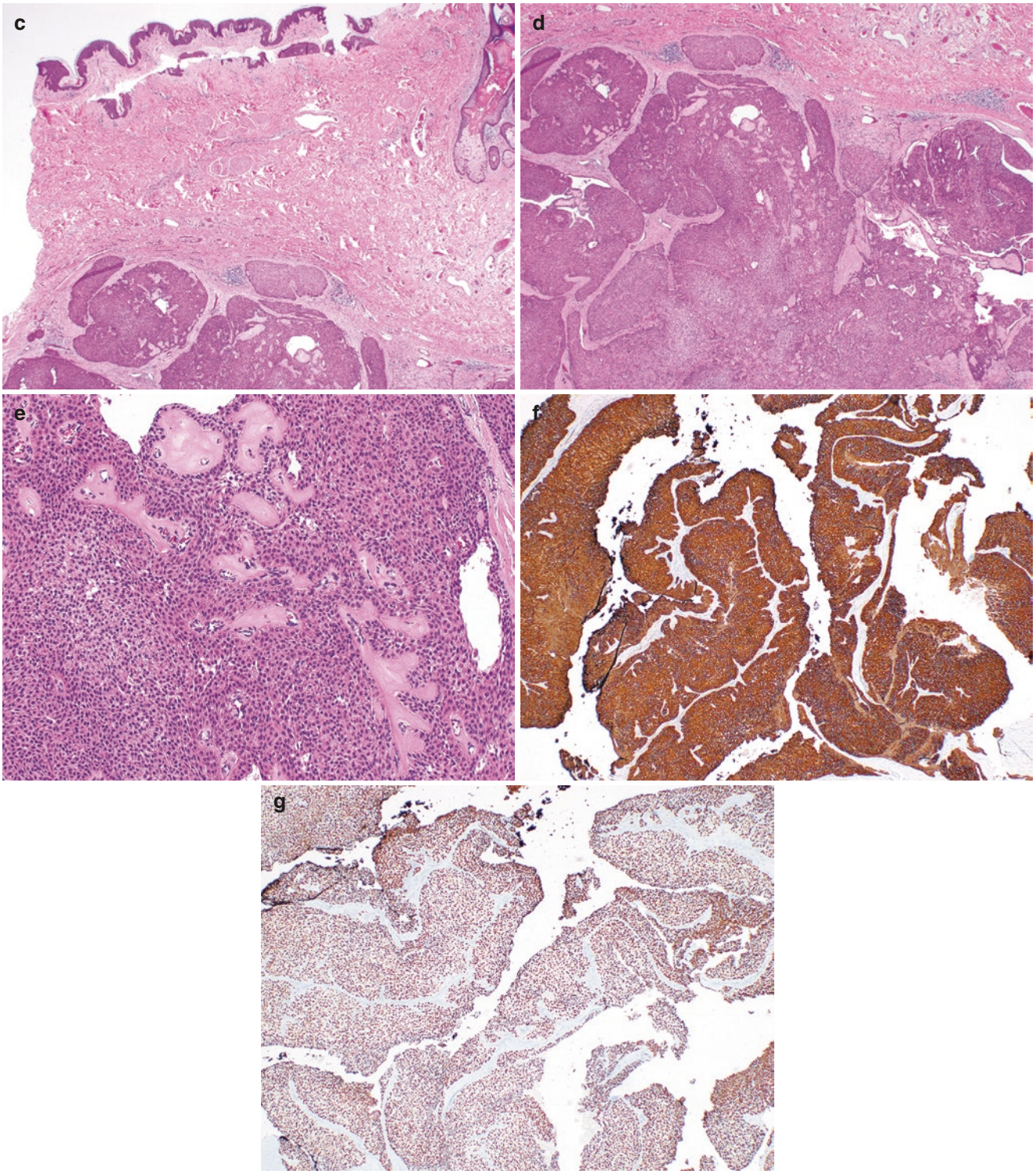

Fig. 25.2 (continued)

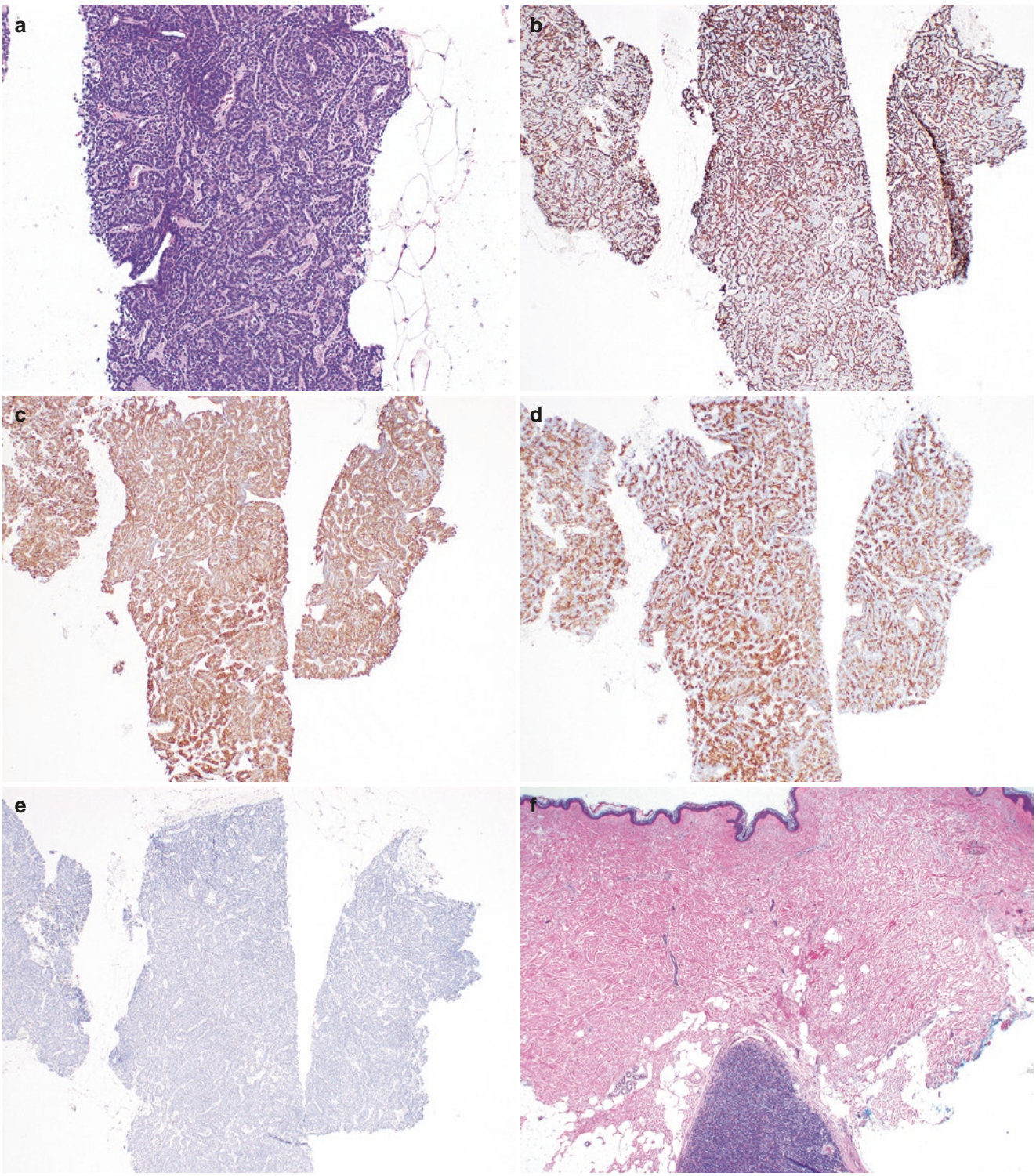

Fig. 25.3 Spiradenoma presenting as a breast mass. (**a**) Initial CNB performed shows critical features including biphasic cell population, hyaline, and ducts when architecture is not evident. Immunohistochemical workup demonstrated lesional cells to be positive for (**b**) p63, (**c**) CK7, and (**d**) CD117 and negative for (**e**) estrogen receptor. (**f**) Excisional biopsy shows a benign neoplasm of sweat gland origin seated in the dermis and subcutis with no epidermal connection and (**g**) found to be well-circumscribed and well-encapsulated nodule. (**h**) Higher magnification shows with biphasic cellular basaloid proliferation of smaller peripheral cells and larger central cells, with (**i**) a background of hyalinized stroma, scattered lymphocytes, and ductal formation. (Courtesy of Dr. Karl Robstad, Department of Pathology and Laboratory Medicine, Albany Medical College)

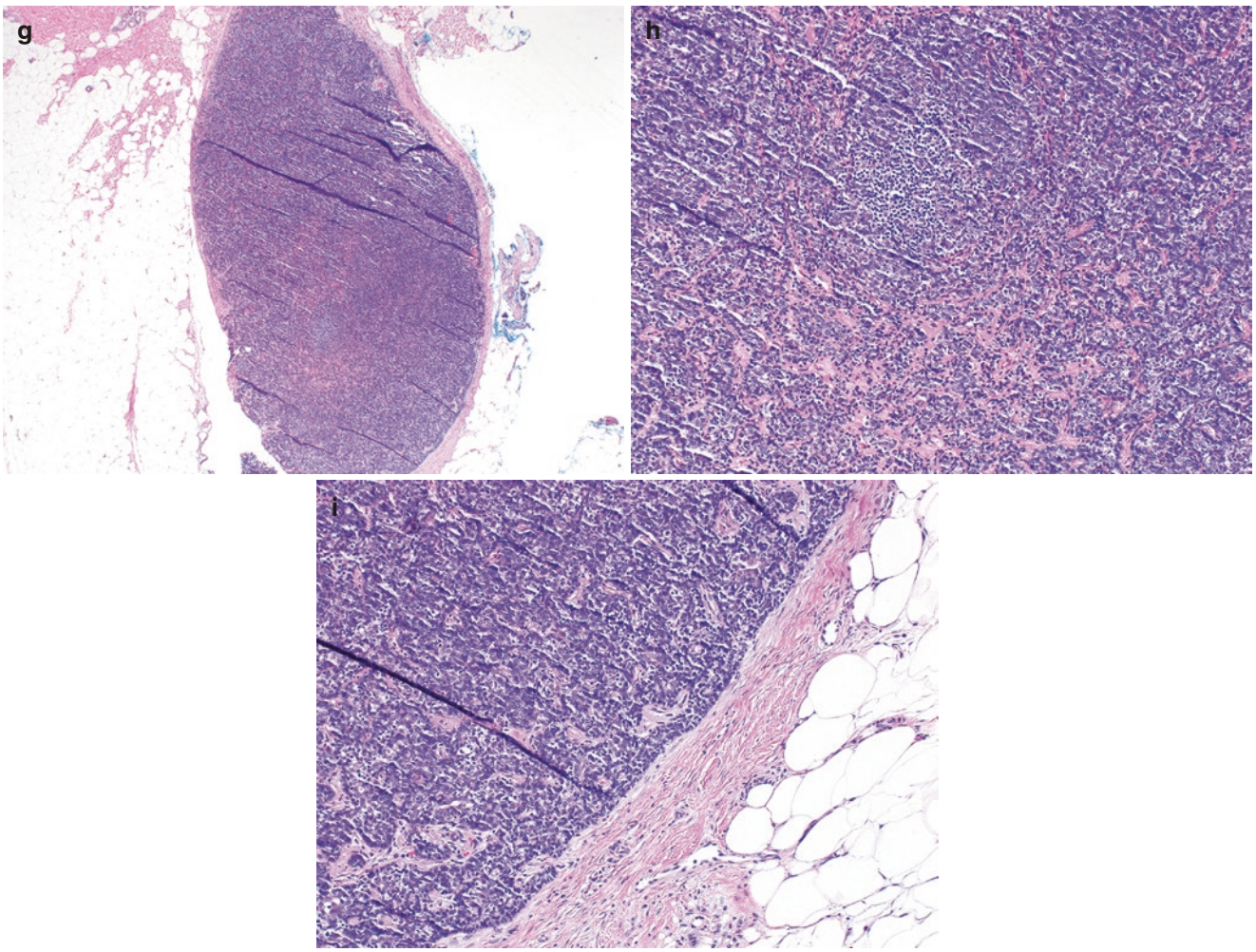

Fig. 25.3 (continued)

improve visualization. Benign cutaneous lesions demonstrate a varied appearance ranging from well-circumscribed to ill-defined lesions (usually corresponding to inflammation surrounding a ruptured cyst) and from hyperechoic to anechoic (Fig. 25.1b). Rarely, cutaneous lesions may appear hypoechoic. As breast carcinomas are usually hypoechoic lesions, other sonographic indications of malignancy, such as internal vascularity, need to be ascertained (Fig. 25.1d).

MRI is of limited utility in the visualization of superficial breast lesions. However, it may demonstrate asymmetric enhancement caused by radiation, postsurgical changes, or other inflammatory changes, such as those related to systemic disease. Physical examination and clinical history are required to definitively categorize the nature of these lesions. For example, psoriasiform and eczematous dermatitis of the nipple may be clinically confused with mammary Paget disease (Fig. 25.4). Benign epidermal lesions such as seborrheic keratosis and fibroepithelial polyps can also mimic a breast mass by MRI or mammography.

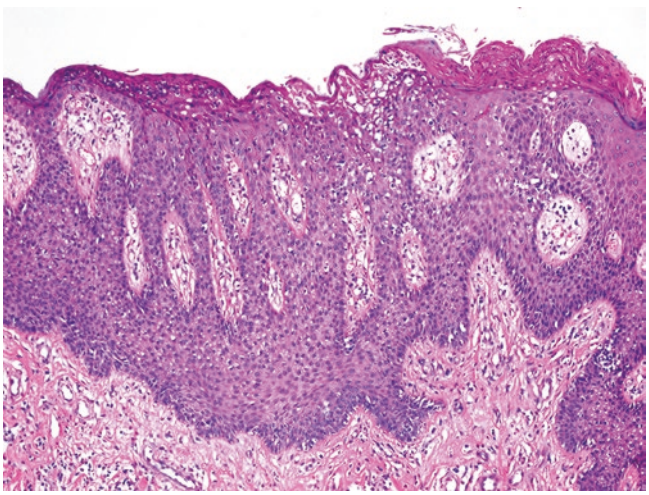

Fig. 25.4 Eczematous dermatitis of the nipple clinically diagnosed as Paget disease of the breast in a patient with a contralateral breast carcinoma. Regular acanthosis (hyperplasia) with hypogranulosis and thick neutrophilic parakeratosis are noted

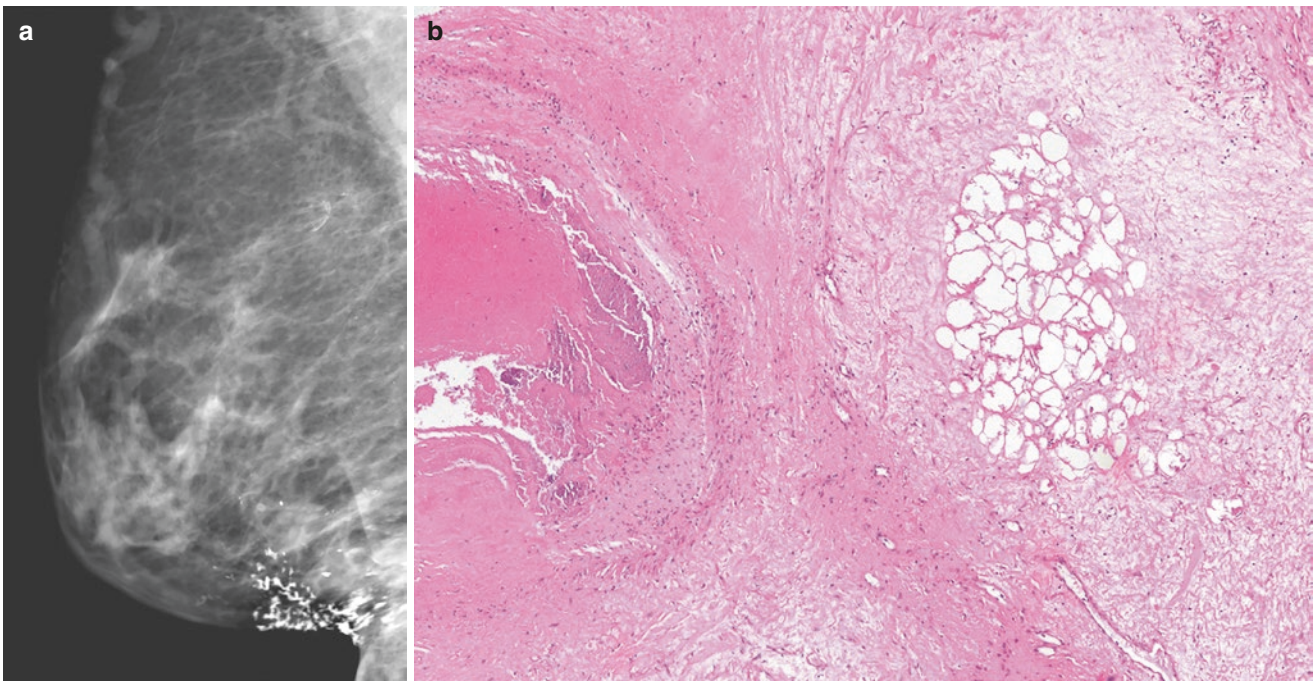

Fig. 25.5 Lupus mastitis. (**a**) Screening mammography of a 42-year-old female with a history of systemic lupus erythematosus shows an area of superficial coarse calcifications (Courtesy of Dr. Mayra Maldonado Durán, University of Puerto Rico, Medical Sciences Campus, with permission). (**b**) CNB revealed a necrotizing vasculitis with adjacent hyaline fat necrosis

A common mimicker of a mass-forming breast lesion with variable MRI detection includes fat necrosis, which may be secondary to trauma (direct insult such as a seat-belt injury) or procedure related. Histologic features of these reactive changes are described in Chap. 4.

In the region of the nipple-areolar complex, ultrasound and MRI are the best modalities to visualize mass lesions. As there are no specific clinical findings that distinguish skin from breast processes limited to this area, a biopsy is indicated for any mass lesion arising within this location. Of note, the nipple itself may be confused with a breast mass by mammography or MRI if the breast is not positioned correctly or if there is nipple inversion.

Mammographic calcifications seen superficially in the breast can correspond to skin lesions such as calcified cysts, hair follicle calcifications, vascular calcifications, or systemic disease (Fig. 25.5). The calcifications are described as round and lucent centered, close to the periphery of the skin. Advanced mammographic techniques have been described to help elucidate the location of the calcifications as projecting to the skin or to the breast parenchyma (Fig. 25.6).

At the other end of the spectrum, a breast lesion may be mistaken for a cutaneous lesion, leading to a small shave biopsy of the skin. Consider the case of a male patient presenting with a "chest mass." The referring physician could consider this a primary skin tumor and perform a shave biopsy of skin, when in fact a breast carcinoma extending into the skin is the correct diagnosis. Additionally, metastatic lesions to the skin, including breast, can clinically present as dermatitis, usually undergoing biopsy after a clinically diagnosed eczematous rash fails to respond to topical therapy [5].

Algorithmic Approach to Establish a Differential Diagnosis

Based on imaging and clinical findings, a decision of whether or not to perform a biopsy will be made. Depending on operator experience, core needle biopsies of the breast and axilla may contain epidermis, dermis, and subcutaneous fat along with breast parenchyma. In general, axillary samples consist mostly of adipose tissue with possible scattered adnexal structures. A collection of large clusters of apocrine sweat glands favors an axillary location. The additional presence of mammary lobules may indicate ectopic breast tissue or sampling of the axillary tail. A punch or shave biopsy of nipple-areolar skin will contain epidermis, dermis, and possibly subcutaneous fat. A unique finding of nipple skin is the presence of numerous dermal smooth muscle bundles and lactiferous ducts. For lesions of the nipple or the axilla, a table noting the most common cutaneous and mammary lesions present in each location is provided (Table 25.1).

Due to intrinsic limitations of biopsy sample size, many specimens will not contain the histologic landmarks needed

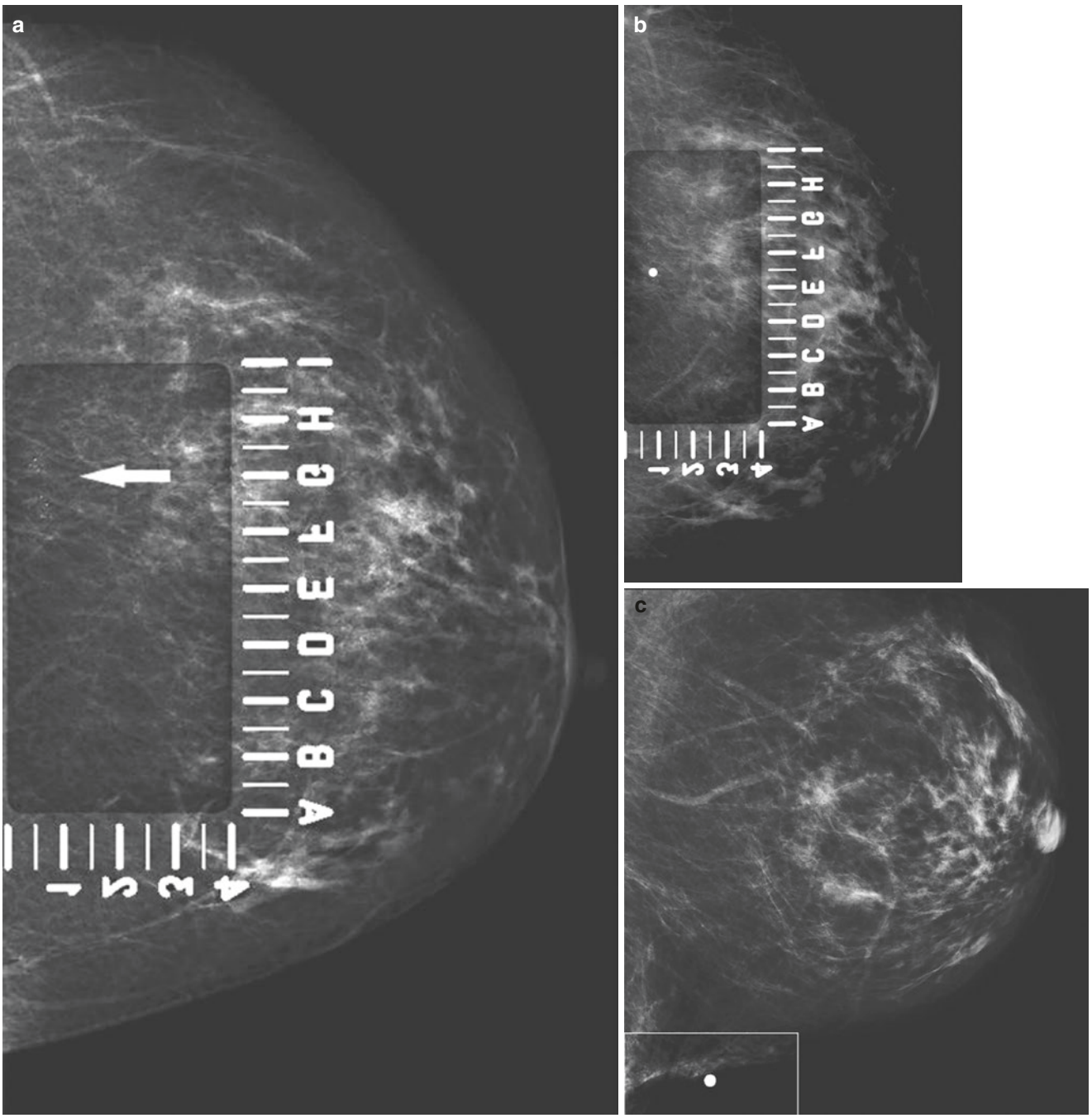

Fig. 25.6 Mammographic calcifications presenting in the skin. (**a**) Screening mammography of a 69-year-old female. Faint round calcifications are observed (arrow) in CC view with alphanumeric grid. (**b**) After placement of a skin marker, a second image is taken to confirm that the marker was correctly placed over the calcifications. (**c**) A tangential view shows the dermal localization of the calcifications ((**c**) and insert). (Courtesy of Dr. Mayra Maldonado Durán, University of Puerto Rico, Medical Sciences Campus, with permission)

to precisely establish the anatomic location without clinical information. A multidisciplinary approach with close communication with the referring physician is of the utmost importance in arriving at the proper diagnosis. The correct classification of a lesion as primary cutaneous versus primary mammary is imperative for proper management. With some notable exceptions, such as malignant melanoma and Merkel cell carcinoma, primary cutaneous neoplasms may be managed by surgical excision with adequate margins sufficient for locoregional control. However, primary breast neoplasms require a multidisciplinary approach with consideration of surgical procedure (i.e., lumpectomy vs. mastectomy), adequate margins, possible axillary staging, and potential neoadjuvant therapy.

Table 25.1 Differential diagnosis based on location

Location	Cutaneous differential diagnosis	Mammary differential diagnosis
Nipple	Nipple adenoma	Nipple adenoma, syringomatous tumor, well-differentiated ductal carcinoma
	Sebaceous carcinoma	Ductal carcinoma in situ, comedo type, invasive ductal carcinoma
	Leiomyoma	Myoid hamartoma, myofibroblastoma with myoid differentiation
	Leiomyosarcoma	Spindle cell metaplastic carcinoma
Axilla	Apocrine nevus, apocrine hidrocystoma, tubular apocrine adenoma	Apocrine metaplasia and apocrine cysts
	Eccrine nevus	Mammary lobules with apocrine or clear-cell metaplasia
	Syringoma	Tubular carcinoma, low-grade adenosquamous carcinoma
	Syringocystadenoma papilliferum	Sclerosing adenosis, intraductal papilloma, invasive ductal carcinoma
	Ductopapillary apocrine carcinoma	Invasive ductal carcinoma, ductal carcinoma in situ

Once the precise anatomic region of the lesion is confirmed, an attempt should be made at establishing whether the lesion is centered in the epidermis, dermis, subcutaneous tissue, or breast parenchyma. An algorithmic approach can be helpful when evaluating these lesions (Fig. 25.7). In CNBs of the breast or axilla, the presence of epidermis or dermal adnexal adjacent to the lesion indicates a cutaneous location. Primary cutaneous neoplasms will often have a connection to the epidermis, which will frequently contain an in situ component (i.e., squamous cell carcinoma, melanoma). These important features may not be present in the limited sampling of a CNB; therefore, additional deeper levels or a request for additional sampling may be necessary to establish this connection. Evidence of an adjacent benign sweat gland neoplasm may be present for some sweat gland carcinomas. The presence of mammary lobules adjacent to the lesion indicates a breast parenchymal location. Mammary neoplasms will often entrap or be surrounded by benign breast parenchyma. An associated component of in situ ductal or lobular carcinoma indicates primary mammary origin. A superficial shave or punch biopsy of skin containing an underlying breast carcinoma will most likely not contain these mammary epithelial elements, and therefore additional sampling might be necessary to establish a correct diagnosis. As a general statement, many cutaneous adnexal neoplasms

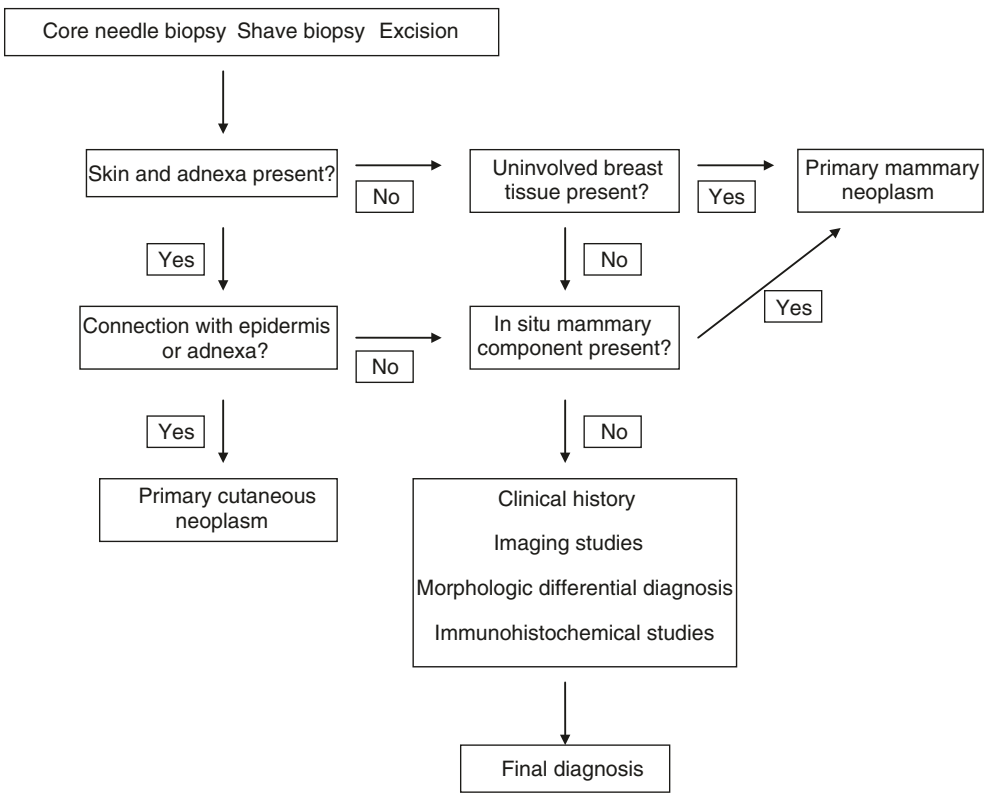

Fig. 25.7 Algorithm approach for evaluating cutaneous versus mammary origin

retain their basal/myoepithelial layer, as it is part of the neoplastic process, whereas invasive mammary neoplasms will only consist of one cell layer. A notable exception is ductal carcinoma in situ (DCIS), which by definition retains the myoepithelial layer.

A serious potential diagnostic pitfall involves the misinterpretation of benignity versus malignancy in CNBs that only sample the center of a tumor mass. Many benign cutaneous adnexal tumors will exhibit a reassuring well-circumscribed nodular growth pattern at low power. However, they may contain central areas with marked desmoplastic stroma. This stromal deposition can greatly distort the epithelial component and impart a pseudoinvasive appearance under high magnification. Tumors that are notorious for this phenomenon include poroma, hidradenoma, chondroid syringoma, and trichilemmoma (Fig. 25.8).

Immunohistochemical Workup

Once a differential diagnosis has been established, immunohistochemistry/immunohistochemical (IHC) stains can provide additional evidence to support a diagnosis. Although no individual marker can universally differentiate between primary cutaneous and mammary origin, when multiple markers are used in combination with histomorphology, a specific diagnosis can be favored. For organizational purposes, we have separated the panels of IHC stains into epithelial and spindle cell categories. Most of the published work in this area has been aimed at differentiating primary cutaneous sweat gland neoplasms from metastatic carcinoma to the skin, with only a few specifically looking at primary or metastatic breast carcinoma. In addition, malignant sweat gland neoplasms are not only rare, but can occasionally exhibit

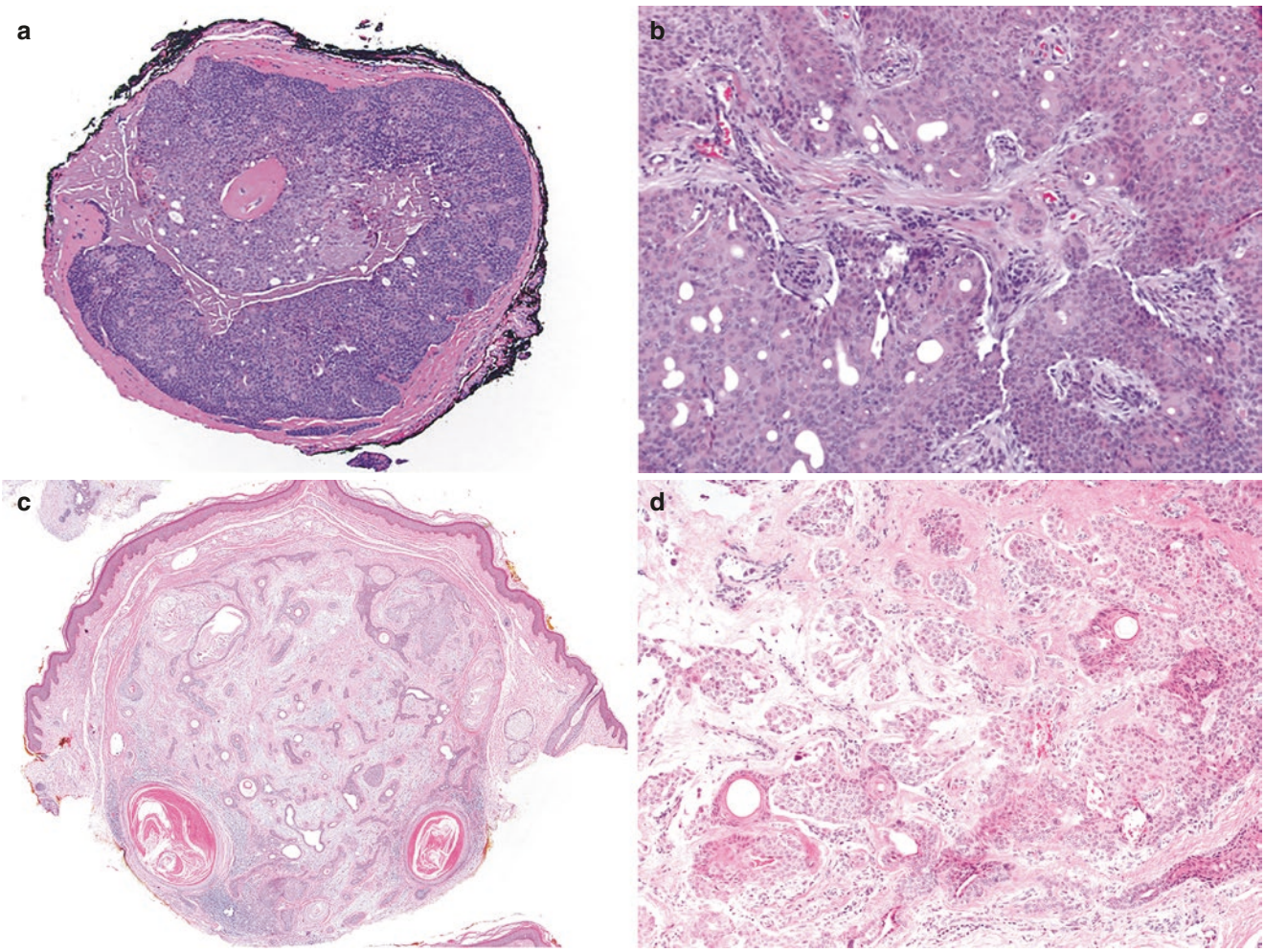

Fig. 25.8 Pseudoinvasive growth patterns attributed to central desmoplastic stroma. (**a**) Eccrine poroma, exhibiting a well-circumscribed nodular appearance at low power. (**b**) The center of the lesion shows a focal desmoplastic stroma that distorts the epithelium and imparts a pseudoinvasive pattern of growth. (**c**) Low-power image of a chondroid syringoma with a well-circumscribed nodular configuration. (**d**) The central region may exhibit dense collagenous stroma, which may distort the epithelial structures and impart a pseudoinvasive pattern of growth. ((**a**), (**b**) Reproduced from Desman GT, Ozerdem U, Shin SJ. Neighboring look-a-likes: Distinguishing between breast and dermatologic lesions. Adv Anat Pathol. 2014;21:228–247, with permission of Wolters-Kluwer Health)

morphologic plasticity with multiple lines of differentiation (i.e., apocrine, eccrine, sebaceous, follicular). Moreover, as expected from shared embryogenesis, tumors with cutaneous and mammary differentiation share similar IHC profiles. For these reasons, arriving at a definitive panel has proven difficult.

Epithelial Neoplasms

Markers commonly used to evaluate mammary origin are also positive in sweat gland neoplasms. Cytokeratins (CK) 7 and 20 show the same pattern of expression in both types of tumors, namely, CK7 positive and CK20 negative [5–7]. Mammaglobin has a relatively high specificity for breast origin; however, it lacks sensitivity. It can be helpful in evaluating cutaneous eccrine carcinomas, as it is reported to be negative in most series, with only one (5%) [8] or two (18.5%) cases showing weak positivity [9]. In contrast, expression of mammaglobin is noted in 57% of cutaneous apocrine sweat gland neoplasms [10]. As it can be negative in as high as 48% of mammary carcinomas [11], its utility in the differential diagnosis of these lesions is limited. Gross cystic disease fluid protein-15 (GCDFP-15) is usually negative in cutaneous eccrine sweat gland neoplasms [5, 9, 12] but is strongly and diffusely positive in cutaneous apocrine sweat gland neoplasms [7, 12, 13]. In the breast, the sensitivity of GCDFP-15 is lower than mammaglobin, as it is positive in only 26% of cases [11, 14]. GATA3 is a more sensitive marker for breast carcinoma than mammaglobin or GCDFP-15, showing expression in the vast majority of breast carcinomas of all subtypes [15–17]. Sweat gland neoplasms of eccrine differentiation are usually negative, while those with apocrine differentiation are positive [8, 10, 18]. Cutaneous epithelial neoplasms show varied expression of GATA3 [17]. Estrogen (ER) and progesterone receptors (PR) are variably expressed in cutaneous sweat gland neoplasms [7, 10, 12, 13, 19–21], similar to mammary neoplasms [11, 14]. HER2 is typically negative in cutaneous sweat gland neoplasms, with some exceptions. For example, primary cutaneous apocrine carcinomas can show 1+ or 2+ expression by IHC but will lack amplification by fluorescence in situ hybridization (FISH) [10, 12, 13, 21]. Androgen receptor (AR) is negative in most cutaneous eccrine carcinomas [9, 20] but is positive in cutaneous apocrine carcinomas [7, 10, 13, 18, 20] and positive in up to 80% of mammary carcinomas of all types [22].

The markers p63 and CK5/6 have been extensively studied in this setting. It is important to consider the intensity of staining as well as their pattern of expression when establishing a definitive origin. Most cutaneous folliculosebaceous and sweat gland neoplasms will show strong nuclear and cytoplasmic positivity for both p63 and CK5/6, respectively [5, 6, 8, 9, 13, 18, 23–26]. One exception that will be discussed later is cutaneous apocrine carcinomas, which are typically negative for p63 and variably express CK5/6. In contrast, invasive ductal carcinomas only show rare co-expression of these markers [5, 6, 9, 10, 13, 27–29], typically in basal-like carcinomas, which as a group constitute a minority of all breast cancers [28]. Therefore, most invasive ductal carcinomas will show no expression of p63 (Fig. 25.9a, b) [5, 6, 8, 9, 13, 18, 23, 24, 26, 27, 30, 31]. When they are positive for p63, they usually show focal cytoplasmic or weak nuclear expression [5, 10, 24, 30, 31], though rare cases can show strong nuclear positivity [27, 28]. CK5/6 expression is more varied, ranging from negative staining to strong positivity in up to 12% of cases of ductal carcinoma [5, 6, 8–10, 13, 25, 27, 28, 32]. In DCIS, p63 [28, 30] and CK5/6 [28, 32] are usually negative in the neoplastic component, although both markers are positive in the peripheral myoepithelial cells. Finally, spindle cell metaplastic carcinomas deserve special consideration, as they can represent a diagnostic pitfall if a diagnosis is based solely on IHC in a limited sample. As these tumors can also express p63 and CK5/6 [29–31, 33], evaluation of other specific cytokeratins, such as 34βE12, can assist in the differential diagnosis. However, these stains may not be positive in some cases or in limited samples. Therefore, a positive cytokeratin stain is helpful in establishing the diagnosis, but do not exclude it if negative.

Diagnostic pitfalls exist when evaluating p63 staining, as the pattern of expression within tumor cells is different among various tumors. In many tubular sweat gland neoplasms, p63 positivity is limited to the basal cells and not the luminal cells (Fig. 25.9c, d) [23, 24]. This finding should not be confused with the staining pattern of DCIS, which will also show peripheral positivity of p63 in the myoepithelial layer. Many solid primary cutaneous tumors, such as squamous cell carcinoma, basal cell carcinoma, poroma, porocarcinoma, hidradenoma, and hidradenocarcinoma, will demonstrate a diffuse pattern of staining for p63 (Fig. 25.9e, f). As there are rare cases of invasive ductal carcinomas that are positive for p63, one must be careful in the interpretation of this IHC stain and should correlate the findings with the histomorphology of the lesion.

Recently, the p40 antibody has been described as a more specific marker of basal cells and squamous epithelium, as it only recognizes the ΔNp63 isoform of p63 [34]. The few studies that have investigated the expression of this marker in cutaneous and mammary tumors confirm that p40 is more specific, although less sensitive, than p63 [18, 30, 33, 35–37] for cutaneous derivation. In one study comparing adnexal tumors with cutaneous metastasis, 80% of adnexal tumors showed positivity for p40, compared to absent expression in metastatic breast carcinomas, even when 7% were positive for p63 [18]. The expression of monoclonal and polyclonal

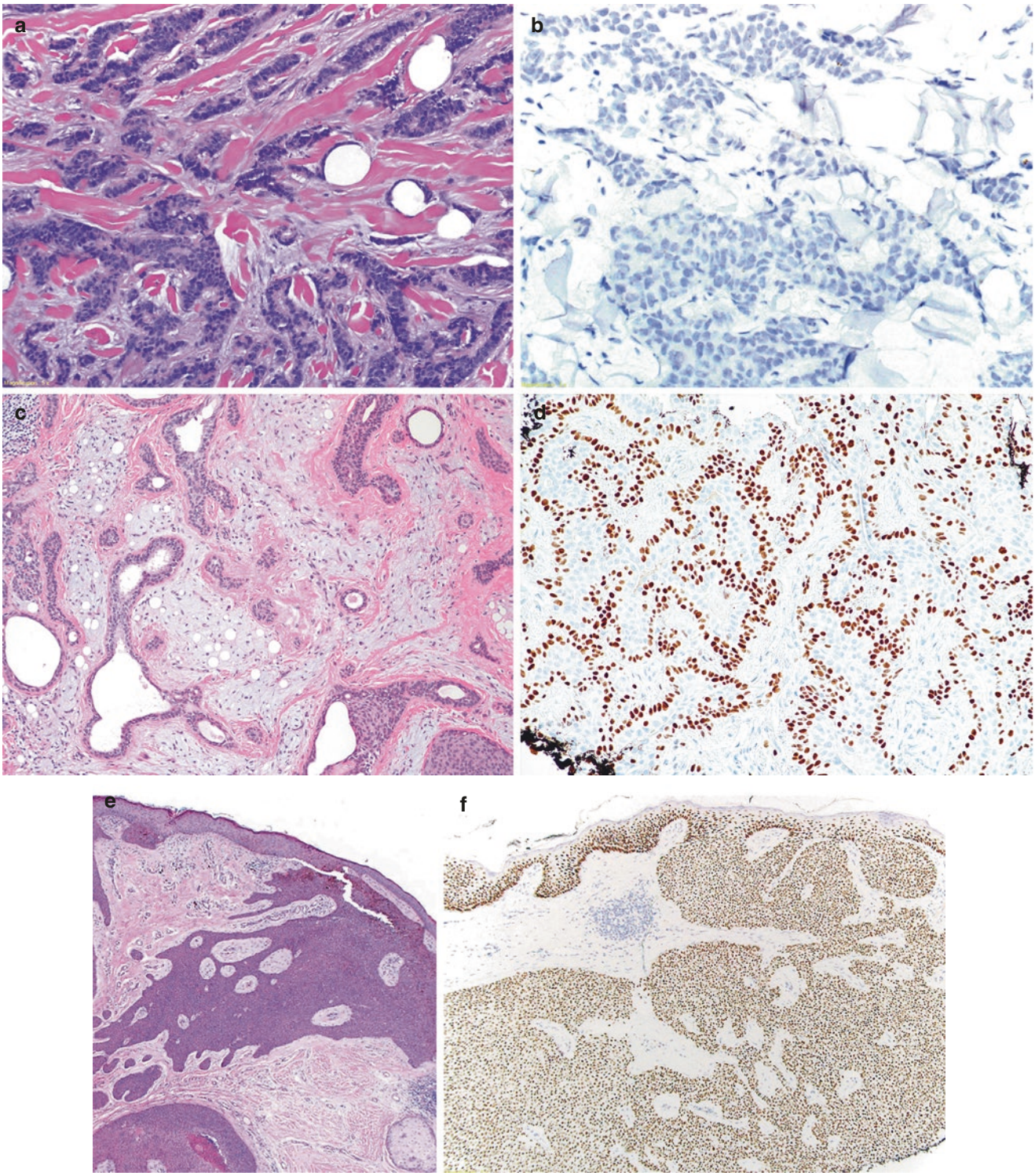

Fig. 25.9 Immunohistochemical staining patterns of p63. (**a**) Invasive ductal mammary carcinoma, (**b**) showing absent p63 staining. (**c**) Chondroid syringoma, (**d**) showing nuclear staining within the outer basal layer and negative inner secretory layer. (**e**) Eccrine poroma, (**f**) with strong diffuse nuclear staining, including the epidermal keratinocytes

p40 antibodies in breast lesions was investigated, showing that polyclonal p40 is more specific and can be positive in 1.9% of invasive ductal carcinomas [30]. Regarding metaplastic carcinomas, p40 expression is also more specific than p63 in evaluating the stroma and epithelial component but not as sensitive and therefore did not prove to show a diag-

nostic advantage when evaluating these tumors [30, 33, 38]. More studies are needed to evaluate the utility of this marker in the differential diagnosis of these lesions.

D2-40 is a marker that detects podoplanin. Podoplanin is more commonly known for its labeling of lymphatic endothelium, but it is also expressed in the basal layer of the epidermis and hair follicles, as well as in sebaceous glands [39, 40]. Cutaneous sweat gland neoplasms show varied expression and are positive in up to 91% of cases, while mammary carcinomas are typically negative [8, 23, 26, 40].

Apocrine sweat gland carcinomas deserve special consideration. These aggressive lesions are rare, but problematic, as they share a similar IHC profile and histomorphology with mammary apocrine and ductal carcinomas and can often present in the axilla and skin of the breast [7, 10, 13, 21]. Cutaneous apocrine carcinomas are CK7, mammaglobin, GCDFP-15, GATA3, EMA, S100 protein, and CD117 positive [7, 8, 10, 13, 18]. In rare cases [8, 26], both p63 and D2-40 may show a basal pattern of expression [10, 13, 18]. CK5/6 is more likely to be positive and shows strong diffuse expression [10, 13]. Compared specifically with mammary apocrine carcinomas, cutaneous apocrine tumors are more likely to express CK5/6, ER, PR, and AR and to be negative for HER2 [7, 10, 13, 18, 20]. In contrast, mammary apocrine carcinomas usually only express AR and are classified as either basal (triple negative) or HER2 type (ER/PR negative, HER2 positive) [20, 22]. Adipophilin, an adipose differentiation-related protein presumably involved in tumor upregulation, has been reported to show focal weak positivity in 36% of cutaneous apocrine carcinomas versus strong positivity in 88% of mammary apocrine carcinomas [10]. Ultimately, location and clinical history remain the best criteria for determining the site of origin.

Other markers have been studied in limited cases. PAX5 is positive (nuclear staining) in some malignant cutaneous sweat gland neoplasms, while negative in mammary neoplasms [9, 41]. B72.3 and calretinin show opposite patterns of expression in cutaneous sweat gland ($B72.3^{-}$/$calretinin^{+}$) and mammary ductal carcinomas ($B72.3^{+}$/$calretinin^{-}$) [5]. BerEP4 is positive in some cutaneous sweat gland and mammary neoplasms [5]. The most common antigens used and their patterns of expression are summarized in Table 25.2.

Table 25.2 Common immunohistochemical markers used in the differential diagnosis of cutaneous and mammary neoplasms

Marker	Cutaneous	Mammary
p63	Strong nuclear staining in eccrine and epithelial neoplasms	Weakly positive staining in basal-like carcinoma
	Basal staining in some malignant eccrine neoplasms and apocrine neoplasms	Positive in stromal cells and epithelial components of metaplastic carcinomas
		Positive (rarely) in stromal cells of phyllodes tumors
CK5/6	Strong cytoplasmic staining in eccrine, apocrine, and epithelial neoplasms	Positive in basal-like carcinomas and metaplastic carcinomas
Cytokeratins (other)	CK7+/CK20− sweat gland	CK7+/CK20−, rarely CK20+
	CK7−/CK20− sebaceous neoplasms and epithelial neoplasms	
	CK7−/CK20+ Merkel cell carcinoma	
D2-40	Positive in eccrine and epithelial neoplasms (except basal cell carcinomas)	Negative
	Basal staining in apocrine neoplasms	
	Negative to weakly positive in sebaceous neoplasms	
GCDFP-15	Negative in eccrine neoplasms	Positive in up to 26% of cases
	Strongly positive in apocrine neoplasms	
	Negative in epithelial neoplasms	
Mammaglobin	Low expression in eccrine neoplasms	Positive in up to 52% of cases
	Variable expression in apocrine neoplasms, similar to that in mammary neoplasms	
	Negative in epithelial neoplasms	
GATA3	Negative in eccrine neoplasms	Positive in the majority of cases of all subtypes
	Variable in adenoid cystic carcinoma	
	Positive in apocrine and epithelial neoplasms	
ER and PR	Variable expression in eccrine and sebaceous neoplasms	Variable expression
	Apocrine neoplasms more likely ER+/PR+	Apocrine carcinomas more commonly ER−/PR−
HER2	Negative	Variable expression
	Apocrine neoplasms rarely 1+ or 2+, but negative by FISH	
AR	Negative in eccrine neoplasms	Positive in up to 80% of cases
	Variable expression in apocrine neoplasms	
	Positive in sebaceous neoplasms	

Spindle Cell Tumors

Spindle cell lesions of the breast can be divided into three groups: pure spindle cell lesions with atypical cytomorphology, pure spindle cell lesions with bland cytomorphology, and mixed spindle cell and epithelioid cell proliferations [42]. Some of these spindle cell lesions must be differentiated from cutaneous neoplasms. When evaluating these lesions, the IHC panel performed should be selected based on the differential diagnosis (Table 25.3).

Histopathological Differential Diagnosis

If the lesion is still suspected of being primary cutaneous over mammary, consider the following differential diagnoses organized into categories based on the architectural pattern of growth (Table 25.4). For the purposes of providing an organized comprehensive review of the histopathologic and IHC features of primary cutaneous tumors that have been reported to arise within the vicinity of the breast, we have listed the following diagnostic entities into categories based on lines of cellular differentiation.

Table 25.3 Immunohistochemical profile of selected cutaneous and mammary spindle cell lesions

Morphology	Cutaneous	Mammary
Spindle cell lesions with atypical cytomorphology	***Melanoma***	***Metaplastic carcinoma***
	Pos: HMB45, Melan-A, S100 protein, SOX10, MITF	Pos: cytokeratin (CK34βE12, CK5/6)
	Neg: cytokeratin	Neg: CD34
	Desmoplastic melanoma	Var: p63, p40, GATA3, SMA, β-catenin*
	Pos: S100 protein, SOX10	***Phyllodes tumor (stroma)***
	Neg: Melan-A, HMB45, MITF	Pos: CD34, BCL2
	Squamous cell carcinoma, spindle	Var: cytokeratin, β-catenin, p63, p40
	Pos: p63, CK5/6, D2-40	
	Neg: CK7, EMA, CEA	
	Atypical fibroxanthoma	
	Pos: CD10, CD99, calponin, vimentin, α_1-antitrypsin, α_1-antichymotrypsin	
	Neg: cytokeratin, S100 protein	
	Leiomyosarcoma	
	Pos: muscle-specific actin, SMA, desmin	
	Neg: CD34, S100 protein	
	Var: cytokeratin	
Spindle cell lesions with bland cytomorphology	***Dermatofibroma***	***Metaplastic carcinoma, fibromatosis-like***
	Pos: factor XIIIa, D2-40, stromelysin	Pos: cytokeratin (CK34βE12, CK5/6)
	Neg: CD34, desmin, cytokeratin	Neg: CD34
	Var: SMA	Var: p63, SMA, β-catenin*
	Dermatofibrosarcoma protuberans	***Fibromatosis***
	Pos: CD34	Pos: β-catenin*
	Neg: cytokeratin, factor XIIIa, D2-40, S100 protein, desmin, SMA, CD117, stromelysin	Neg: CD34, cytokeratin, ER, PR, BCL2, factor XIIIa, D2-40
	Dermatomyofibroma	Var: actin, desmin
	Pos: SMA, vimentin	***Myofibroblastoma***
	Neg: desmin, CD34, factor XIIIa	Pos: CD34, desmin, SMA, CD99, bcl-2, vimentin, ER
	Leiomyoma	Neg: S100 protein, EMA, β-catenin, cytokeratin
	Pos: actin, SMA, desmin	Var: SMA, desmin, ER, PR
	Neg: CD34, S100 protein	***Pseudoangiomatous stromal hyperplasia***
	Var: cytokeratin	Pos: CD34, BCL2, CD99, PR > ER, Var: SMA, desmin

Pos positive, *Neg* negative, *Var* variable
*Positive β-catenin defined by aberrant nuclear expression

Table 25.4 Differential diagnosis of cutaneous mimics of mammary neoplasms based on histological pattern

Histological pattern	Cutaneous differential diagnosis	Mammary differential diagnosis
Ductal–tubular	Syringoma	Tubular carcinoma
	Chondroid syringoma	Invasive ductal carcinoma
	Squamoid eccrine adenocarcinoma	Low-grade adenosquamous carcinoma
	Microcystic adnexal carcinoma	Nipple adenoma
Solid	Squamous cell carcinoma	Invasive ductal carcinoma
	Sebaceoma	Metaplastic carcinoma
	Sebaceous carcinoma	Ductal carcinoma in situ, solid type
	Eccrine poroma	Mammary adenoid cystic carcinoma
	Eccrine porocarcinoma	Solid papillary carcinoma
	Melanoma	
Central "comedo-like" tumor necrosis	Basal cell carcinoma	Ductal carcinoma in situ, comedo type
	Cutaneous apocrine carcinoma	
	Sebaceous carcinoma	
	Hidradenocarcinoma	
	Merkel cell carcinoma	
Apocrine	Cutaneous apocrine carcinoma	Mammary apocrine carcinoma
	Apocrine hidrocystoma	Ductal carcinoma in situ
	Apocrine nevus	Invasive ductal carcinoma
	Tubular apocrine adenoma	Apocrine metaplasia
		Apocrine cysts
Cribriform	Eccrine cylindroma	Cribriform carcinoma
	Ductal apocrine carcinoma	Mammary adenoid cystic carcinoma
	Adenoid cystic carcinoma	Ductal carcinoma in situ, cribriform type
		Mammary cylindroma
Papillary/cystic	Syringocystadenoma papilliferum	Papillary carcinoma
	Tubular apocrine adenoma	Intraductal papilloma
	Papillary eccrine adenoma	
	Ductopapillary apocrine carcinoma	
	Apocrine cystadenoma	
	Apocrine hidrocystoma	
Mucinous	Cutaneous mucinous carcinoma	Mammary mucinous carcinoma
Spindle, atypical	Melanoma	Metaplastic carcinoma, spindle cell type
	Spindle squamous cell carcinoma	Phyllodes tumor
	Sarcoma	
Spindle, bland	Dermatofibroma	Metaplastic carcinoma, fibromatosis-like
	Dermatofibrosarcoma protuberans	Fibromatosis
	Scar	Myofibroblastoma
	Keloid	Pseudoangiomatous stromal hyperplasia
	Dermatomyofibroma	Biopsy site
Fibroepithelial	Fibroepithelioma of Pinkus	Fibroadenoma
	Syringofibroadenoma	Benign phyllodes tumor
Small blue round cells	Merkel cell carcinoma	Mammary small-cell carcinoma
	Cylindroma	Invasive ductal carcinoma
	Spiradenoma	
Biphasic tumors	Chondroid syringoma	Metaplastic carcinoma, matrix producing
	Trichoblastoma	Mammary pleomorphic adenoma
Pagetoid spread	Extramammary Paget disease (i.e., axilla)	Mammary Paget disease
	Squamous cell carcinoma in situ	
	Melanoma in situ	
	Sebaceous carcinoma	
Clear cells	Clear-cell syringoma	Invasive lobular carcinoma
	Cutaneous signet ring cell adenocarcinoma	Invasive ductal carcinoma with clear-cell features
	Clear-cell squamous cell carcinoma	
	Clear-cell hidradenoma	
	Clear-cell hidradenocarcinoma	
	Sebaceoma	
	Sebaceous carcinoma	

Pseudoneoplastic Lesions of Sweat Glands

On rare occasion, hamartomatous and reactive sweat gland proliferations may mimic neoplastic disease. This may pose a significant diagnostic dilemma when limited clinical history is provided. These lesions are typically located in the axilla and may be bilateral.

Eccrine Nevus (Hamartoma)

Also referred to as "nevus sudoriferous," this rare hamartoma is characterized by an increase in size and/or number of eccrine coils. Occasionally, the eccrine coils may be surrounded by abundant mucin, in which case they are referred to as "mucinous eccrine nevus" (Fig. 25.10a) [43]. These lesions present during early childhood or adolescence as solitary, linear, or grouped papules, nodules, and plaques, frequently with a tan-brown discoloration [43–45]. The most common location is the upper extremity, but axillary lesions have been reported. Localized hyperhidrosis (often unilateral) is a common finding and may be the only clinically appreciable finding [46]. Bilateral lesions have been reported.

Mammary Differential Diagnosis Mammary lobules can sometimes show clear-cell, lactational, or apocrine changes but will preserve a lobular arrangement not present in hamartomatous lesions (Fig. 25.10b). Fibrocystic changes of the breast are more likely to show a mix of hyperplastic ductal epithelial elements and can be associated with calcifications.

Apocrine Nevus (Hamartoma)

A rare hamartoma is characterized by an excess of normal mature apocrine sweat glands within the deep dermis and often extending into the subcutaneous fat (Fig. 25.11a) [47]. The most common clinical presentation is axillary swelling, but hyperhidrosis is typically not a feature. Lesions present at birth or during early adulthood and may be bilateral. A case of apocrine carcinoma arising in association with an apocrine nevus in an elderly patient has been reported [48]. An occasional association with syringocystadenoma papilliferum has been noted.

Mammary Differential Diagnosis Apocrine metaplasia and apocrine cysts (Fig. 25.11b). Apocrine metaplasia in the breast is usually accompanied by other fibrocystic changes. Apocrine cysts are usually markedly dilated and can contain calcium oxalate and calcium phosphate calcifications. In an axillary location, the presence of these changes may represent ectopic breast tissue. The presence of dermis favors cutaneous apocrine sweat glands.

Reactive Lesions/Syringometaplasias

Histopathologic features similar to eccrine and apocrine nevi have been reported in areas adjacent to neoplasms (squamous cell carcinoma, basal cell carcinoma, malignant melanoma), as well as chronic inflammatory conditions with scarring, such as scarring alopecia and infection [49]. Various medications, including nonsteroidal anti-inflammatory drugs and chemotherapeutic drugs (doxorubicin, tamoxifen), are associ-

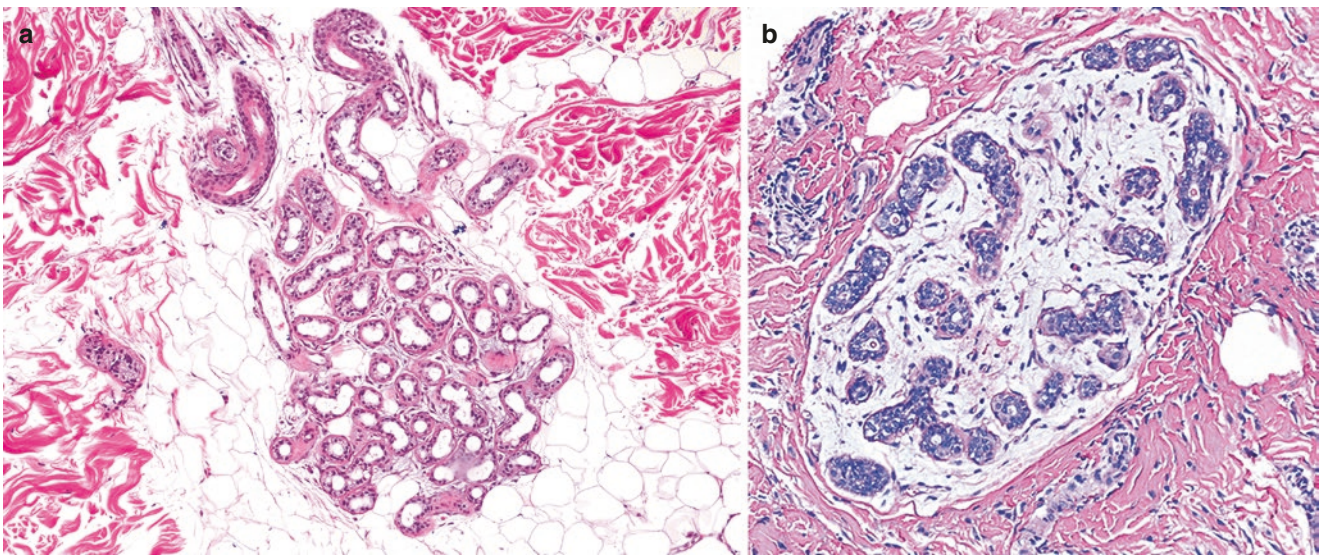

Fig. 25.10 Mucinous eccrine nevus. (**a**) There are numerous benign eccrine ducts and secretory coils surrounded by increased amounts of dermal mucin. (**b**) Mammary lobules with surrounding myxoid stroma and preservation of lobular arrangement

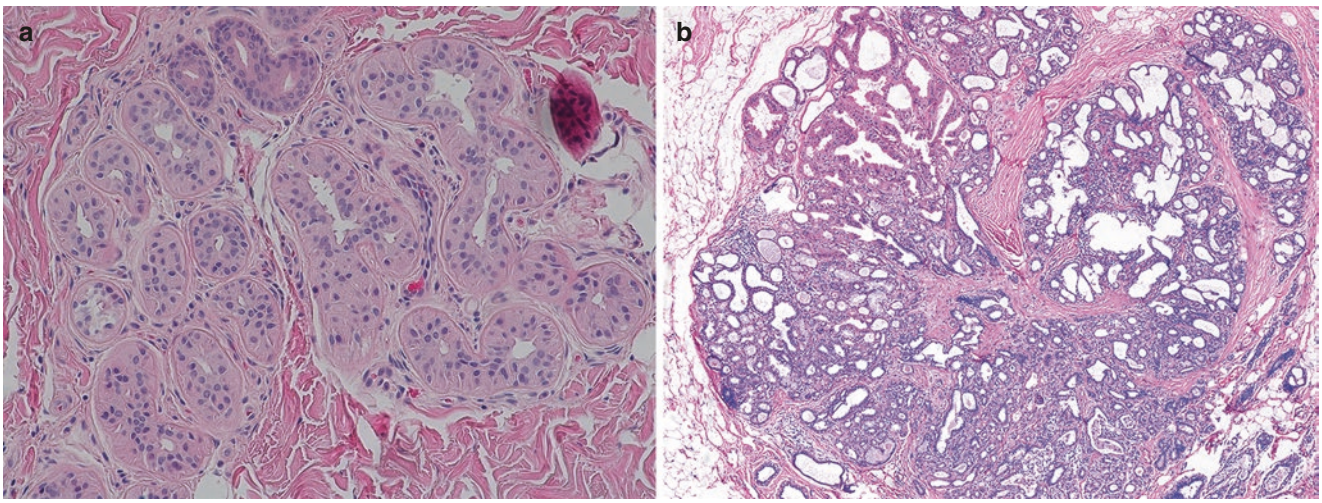

Fig. 25.11 Apocrine nevus. (**a**) Numerous glands lined by columnar cells with eosinophilic cytoplasm and decapitation secretion. (**b**) Apocrine metaplasia and fibrocystic changes. Note preserved lobular arrangement

ated with multifocal and bilateral lesions. These drug-associated lesions exhibit syringoma-like features, occasional squamous metaplasia of the sweat ducts, and mucin-producing glandular cells [50–52]. Similar lesions have been reported in association with chronic radiation dermatitis. Idiopathic cases are rare but have been documented [53].

Mammary Differential Diagnosis Mammary lobules can rarely show squamous metaplasia in luminal epithelial cells, which can also occur in instances of ductal hyperplasia.

Tumors of the Surface Epithelium

Basal Cell Carcinoma

Basal cell carcinoma shows a strong association with chronic UV light exposure, but can essentially arise anywhere on the body, including the breast and axilla [54]. Clinically, these tumors may present as red pearly papules or indurated plaques with telangiectasias. It is generally recommended to subclassify basal cell carcinomas based on their dominant growth pattern, namely, superficial, nodular, infiltrative, micronodular, desmoplastic, and metatypical, with the latter four representing the more aggressive variants [55]. Although distant metastasis is extremely rare, the more aggressive variants are at increased risk of locally infiltrative disease, commonly invading into the deeper aspects of the dermis or subcutis and with frequent perineural invasion [56]. The metatypical type of basal cell carcinoma, sometimes referred to as basosquamous carcinoma, has mixed basal and squamous differentiation and has a risk for metastatic spread similar to that of primary cutaneous squamous cell carcinoma [57]. Regardless of type, basal cell carcinoma is characterized by nests or infiltrative cords of basaloid cells with frequent mitoses and single-cell necrosis. The most characteristic features distinguishing basal cell carcinoma from other basaloid (follicular) tumors are peripheral palisading of tumor nuclei, tumor-stromal retraction artifact, scattered necrotic tumor cells, and accumulations of dermal mucin within the tumor and retraction cleft. Occasionally, the nodular pattern of basal cell carcinoma may contain large central areas of tumor necrosis, mimicking mammary ductal carcinoma in situ with comedo necrosis (Fig. 25.12a). The desmoplastic (morpheaform) growth pattern frequently lacks obvious retraction artifact and dermal mucin, as the tumor is tightly compressed within dense collagenous stroma. Therefore, this pattern of basal cell carcinoma can most likely mimic a breast carcinoma on CNB (Fig. 25.12b).

Mammary Differential Diagnosis Invasive ductal carcinoma and DCIS, comedo type (Fig. 25.12c, d): IHC stains can be helpful in some cases. Basal cell carcinomas express keratins associated with follicular epithelium of the hair bulge, namely, BerEP4. Other positive markers include BCL2, p53, CK5/6, and p63 [25, 58–63]. Basal cell carcinoma is negative or weakly positive for D2-40 [23, 64] and negative for CK7, EMA, and PAX5 [41, 64]. Negativity for CK7 and EMA best discerns basal cell carcinomas from invasive and in situ ductal carcinomas. Morphology, including basal cell palisading, as well as presence of a connection with the epidermis are clues to the appropriate diagnosis.

Fibroepithelioma of Pinkus

Fibroepithelioma of Pinkus is a less common variant of basal cell carcinoma that most frequently arises on the trunk and

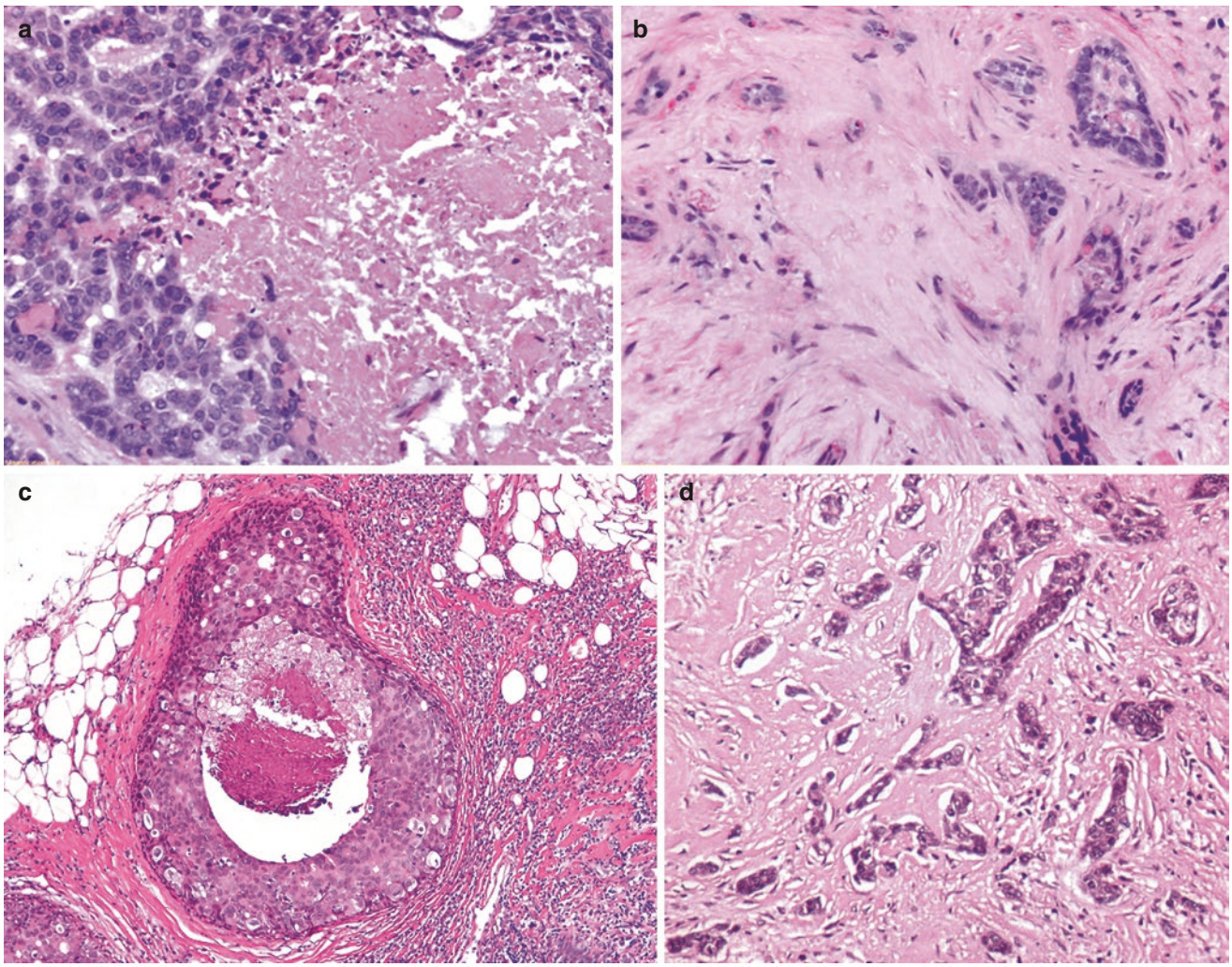

Fig. 25.12 Basal cell carcinoma. (**a**) Nodular basal cell carcinoma showing a tumor nodule with central comedo-like necrosis. The tumor cells are basaloid with retraction artifact and dermal mucin. (**b**) Desmoplastic basal cell carcinoma with infiltrative cords and nests of basaloid cells embedded within a dense sclerotic stroma. Note the absence of tumor-stromal retraction artifact and mucin. (**c**) Ductal carcinoma in situ, comedo type. (**d**) Invasive ductal carcinoma

thigh; however, cases involving the breast and nipple have been reported [65, 66]. Clinically, the tumors most often resemble a skin tag (fibroepithelial polyp). Multiple firm indurated nodular plaques may develop in sites treated with prior radiation. Histopathologically, the tumor is characterized by two to three layers of basaloid epithelial cells arranged in anastomosing strands that descend from the epidermis (Fig. 25.13a). Unlike conventional basal cell carcinoma, the tumor is biphasic with a compartmentalized peritumoral spindle cell stroma. These tumors characteristically lack the stromal retraction artifact and dermal mucin but frequently exhibit single-cell necrosis and are therefore considered malignant [67]. Ductular elements are absent. Tumor cells positively express BerEP4 and AR, similar to other forms of basal cell carcinoma. Ki-67 shows a low proliferation index, and p53 expression is weak. CK20 staining reveals retention of intratumoral Merkel cells analogous to trichoblastoma and trichoepithelioma [68], a feature not present in conventional basal cell carcinoma.

Mammary Differential Diagnosis Fibroepithelial lesions of the breast, such as fibroadenoma and phyllodes tumor (Fig. 25.13b): The intracanalicular variant of fibroadenoma closely resembles this lesion. Neither single-cell necrosis nor easily found mitoses should be present in a fibroadenoma. In both phyllodes tumors and fibroadenomas, the glandular component will be positive for CK7 and ER, a feature not present in a fibroepithelioma of Pinkus.

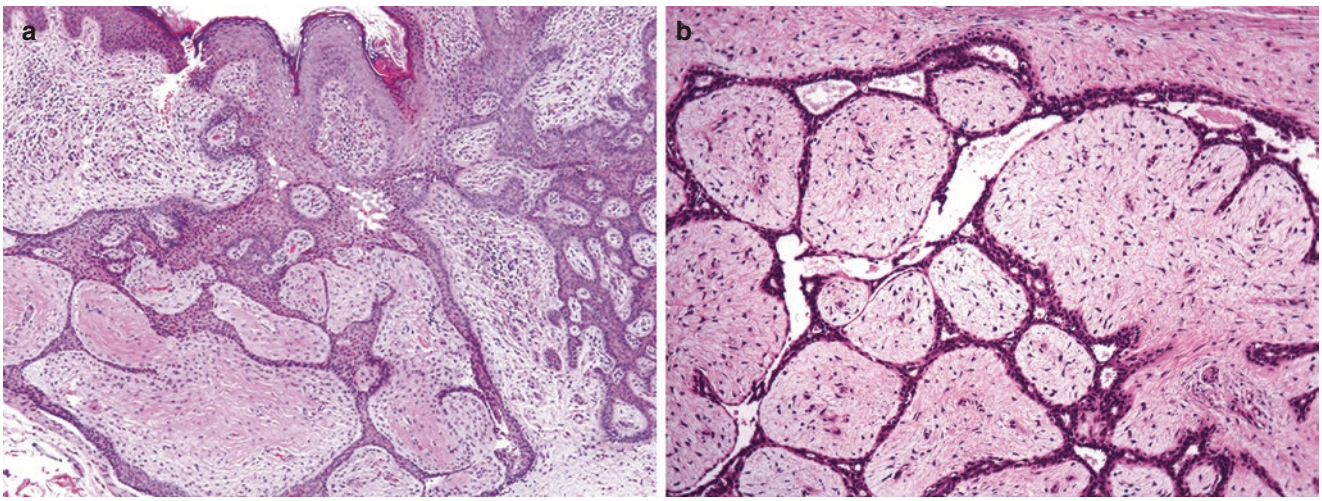

Fig. 25.13 Fibroepithelioma of Pinkus. (**a**) There is a reticular (lacelike) proliferation of anastomosing basaloid cords admixed with a spindle cell stroma. Note the peripheral palisading of the basal nuclei. (**b**) Benign phyllodes tumor with intracanalicular pattern

Squamous Cell Carcinoma

Primary cutaneous squamous cell carcinoma (SCC) is associated with chronic UVB exposure and less commonly with HPV infection [69]. Clinically, tumors present as an indurated slow-growing plaque or nodule with occasional ulceration. Although these tumors are locally aggressive, the overall 5-year metastasis rate is 5.2%, though the risk is much higher for tumors arising on the ear and lip (11% and 13.7%, respectively) [70]. Features associated with an aggressive clinical course include tumor diameter greater than 2 cm, tumor depth greater than 0.4 cm, neurotropism, clinical immunosuppression, and tumors arising within chronic ulcers or sites of prior radiation. Non-keratinizing (poorly differentiated) tumors generally have a worse prognosis than keratinizing (well-differentiated) tumors.

The features of squamous cell carcinoma vary depending on the degree of differentiation. Keratinizing (well-differentiated) tumors are characterized by infiltrating cords and nests of large epithelioid cells containing abundant eosinophilic cytoplasm, intercellular bridges, mitoses, and mild nuclear pleomorphism. Non-keratinizing (poorly differentiated) tumors may be difficult to distinguish from adenocarcinomas and are generally composed of cells with basophilic-to-amphophilic cytoplasm. Clear-cell variants that contain large amounts of clear glycogenated cytoplasm may mimic mucinous signet ring adenocarcinoma or lumen-like structures (Fig. 25.14a). Acantholysis and individual necrotic or apoptotic cells scattered throughout the tumor may be mistaken for luminal structures. The presence of intercellular bridges may be the only recognizable feature revealing squamous derivation. Poorly differentiated squamous carcinomas may occasionally exhibit a sarcomatoid spindle cell pattern resembling scars or other spindle cell tumors. IHC staining for cytokeratin is essential in identifying the true origin of these tumors (Fig. 25.14b, c).

The vast majority of invasive tumors arise in association with an epidermal in situ carcinoma component and therefore would rarely be mistaken for mammary carcinoma on shave or punch biopsies. However, a CNB will likely not contain fragments of epidermis to make this observation. As a general rule, dermal or subcutaneous nodules of SCC without an in situ component or connection with the overlying epidermal surface must be considered possible metastases. It is worth mentioning that a few special types may arise as invasive SCC without an overlying in situ component or connection with the epidermal surface. Follicular SCC (trichilemmal carcinoma) is a rare variant of cutaneous SCC that most commonly arises in the head and neck region but may arise at essentially any location. As the name implies, these tumors arise from the follicular outer root sheath epithelium and form nodules of invasive carcinoma in the dermis without epidermal connection. Tumor connection with a hair follicle may not be readily apparent and may require multiple deeper sections [71]. Invasive SCC arising within an epidermoid (epidermal inclusion) cyst will also lack a connection with the epidermal surface and an overlying in situ component [72]. Lastly, invasive tumors arising in a background of lichen simplex chronicus or lichen sclerosus will frequently exhibit an invasive growth pattern extending downward from the epidermis without an overlying in situ carcinoma component [73].

Squamous cell carcinomas positively express CK 34βE12, D2-40, CK5/6, and p63 [23, 25, 27, 40, 64] and are generally negative for CK7, AR, and PAX5 [41, 64]. It is worth mentioning that up to 25% of poorly differentiated SCC may

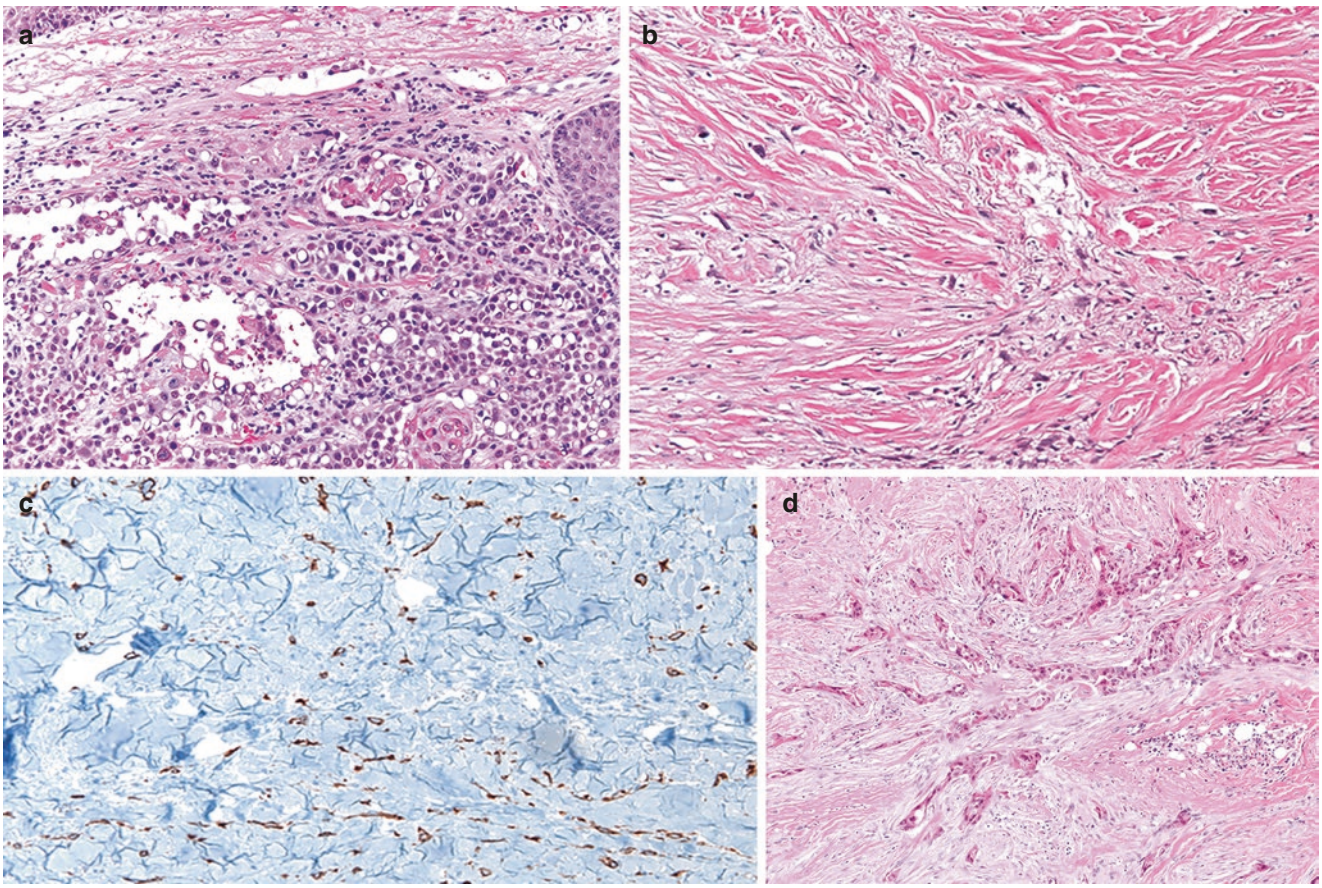

Fig. 25.14 Primary cutaneous squamous cell carcinoma (SCC). (**a**) Clear-cell variant of SCC. There are numerous infiltrating lobules and cords of squamous epithelium containing abundant clear cytoplasm. Additionally, large foci of acantholysis are present. Focal squamous eddy formation supports squamous differentiation. (**b**) Spindle cell squamous cell carcinoma. There are nondescript spindle cells embedded within a dense collagenous stroma. (**c**) IHC staining with CK5/6 reveals positive staining, confirming squamous cell carcinoma. (**d**) Metaplastic mammary carcinoma with squamous differentiation

exhibit focal staining for CK7 [74]. Acantholytic spaces and necrotic/apoptotic foci will be negative for EMA and CEA.

Mammary Differential Diagnosis Primary SCC of the breast, metaplastic carcinoma with squamous differentiation, and invasive ductal carcinoma (poorly differentiated): Since primary mammary squamous cell carcinomas will show an identical histopathology and phenotype to its cutaneous counterpart, the diagnosis should rely on clinical and radiological findings. A careful search for a spindle component is necessary to rule out a metaplastic carcinoma with squamous differentiation (Fig. 25.14d), which will also show positivity for p63 and possibly also CK5/6 [30, 31, 35, 75]. If the differential diagnosis is with a poorly differentiated ductal carcinoma, then the same considerations for p63 and CK5/6 positivity should apply as described in the previous sections. The marker p16 can be positive in both cutaneous SCC [76] and basal-like breast carcinoma [77].

Hair Follicle Neoplasms

Trichoblastoma

Trichoblastoma is a biphasic follicular neoplasm composed of basaloid germinative follicular epithelium and condensed perifollicular stroma reminiscent of the primitive hair papilla. These tumors may arise in any location where the skin contains hair follicles. Clinically, these tumors present as nonspecific nodules with occasional pigmentation [78, 79]. Rare giant forms have been reported. The tumors typically arise within the deep dermis or subcutis and are characterized by sheets, clusters, and anastomosing cords of basaloid epithelium surrounded by a condensed cellular stroma (Fig. 25.15a, b). Focal hair differentiation is usually identified by the masses of basaloid cells that are indented by the stroma, recapitulating the hair bulb. Occasionally, the tumor may be colonized by benign dendritic melanocytes and the basaloid

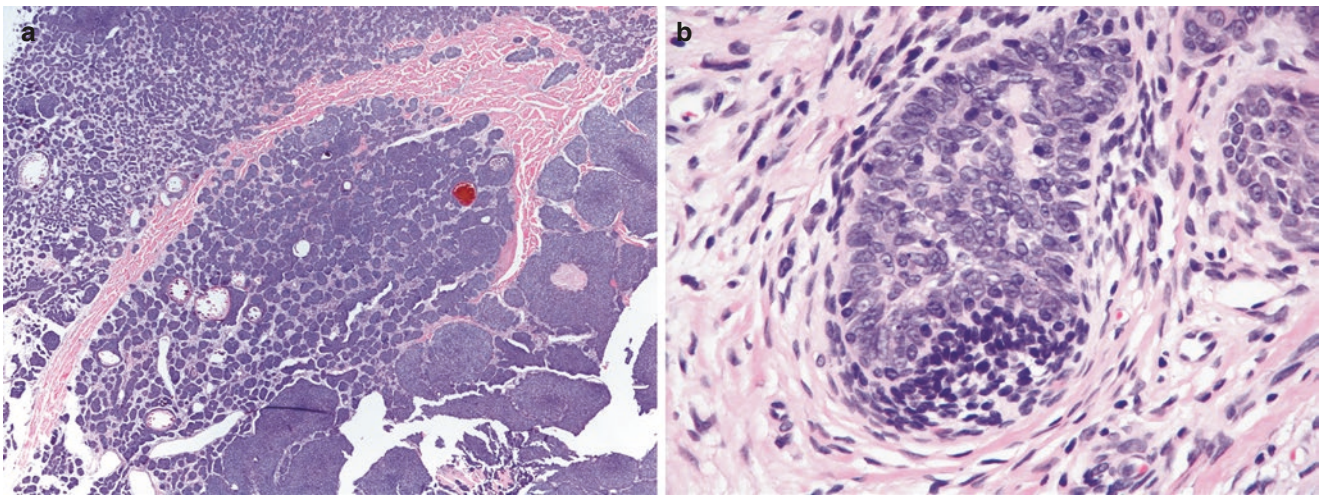

Fig. 25.15 Trichoblastoma. (**a**) Deep dermal nodular mass composed of numerous small basaloid nests. These nests trail off to the periphery of the tumor mass. (**b**) Note how the cellular stroma indents the basaloid epithelial clusters

cells may contain melanin pigment [80]. Trichoblastomas are positive for follicular markers, such as BerEP4, and diffusely express p63. Similar to basal cell carcinoma, these tumors express BCL2; however, unlike basal cell carcinoma, the peritumoral stromal cells are positive for CD10.

Mammary Differential Diagnosis Invasive ductal carcinoma: Follicular neoplasms will have peripheral palisading, a feature not present in breast carcinomas. Immunohistochemical stains for p63 and BCL2 are less likely to be diffusely positive in invasive ductal carcinomas.

Benign and Malignant Sebaceous Neoplasms

Sebaceous Adenoma and Sebaceoma

Benign sebaceous neoplasms are composed of both basaloid germinative cells and clear sebocytes. They are classified as sebaceous adenomas or sebaceomas based on the proportions of these separate components. Sebaceous adenomas are composed of lobules of sebocytes surrounded by two or more peripheral layers of germinative cells, yet this basaloid component accounts for less than 50% of the total cell population (Fig. 25.16) [81]. They rarely arise within close proximity of the breast parenchyma and characteristically connect with the overlying epidermis, and therefore are generally not considered a histopathologic mimic of breast carcinoma. In contrast, sebaceoma most commonly arises on the head and neck, but involvement of the chest has been documented. The lesion was first described by Troy and Ackerman as a distinct neoplastic entity separate from sebaceous adenoma, basal cell carcinoma with sebaceous differentiation, and sebaceous carcinoma [82]. They

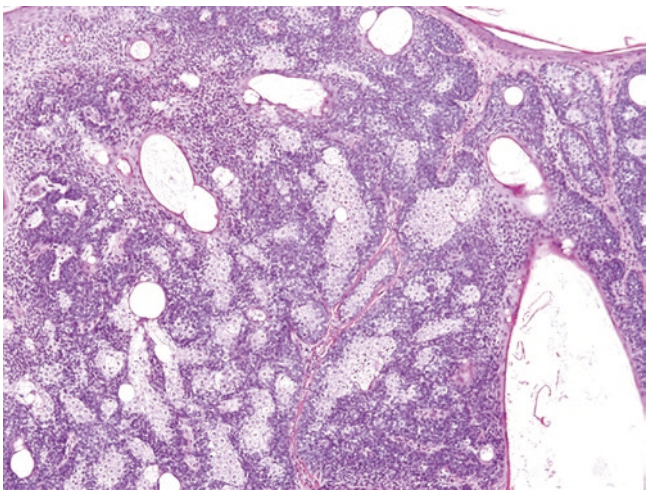

Fig. 25.16 Sebaceous adenoma. There are irregular lobules of basaloid cells and clear sebocytes. The basaloid component is located at the periphery of the lobules and accounts for less than 50% of the tumor cells

present more commonly in females in their sixth to ninth decades as yellow- to skin-colored nodules. An association with microsatellite instability and Muir-Torre syndrome has been described [83–85]. Microscopically, sebaceomas are characterized by disorganized lobules composed of mixtures of sebocyte clusters and germinative cells in excess of 50% of the total cell population (Fig. 25.17a). Although usually confined to the dermis, tumors may occasionally extend into the subcutaneous fat. Unlike basal cell carcinoma, peripheral palisading of nuclei and stromal retraction artifact are absent. The rippled pattern of sebaceoma shows a reticulated growth pattern where aligned tumor cell nuclei simulate the Verocay bodies of schwannomas or carcinoid tumors [86]. Immunohistochemistry

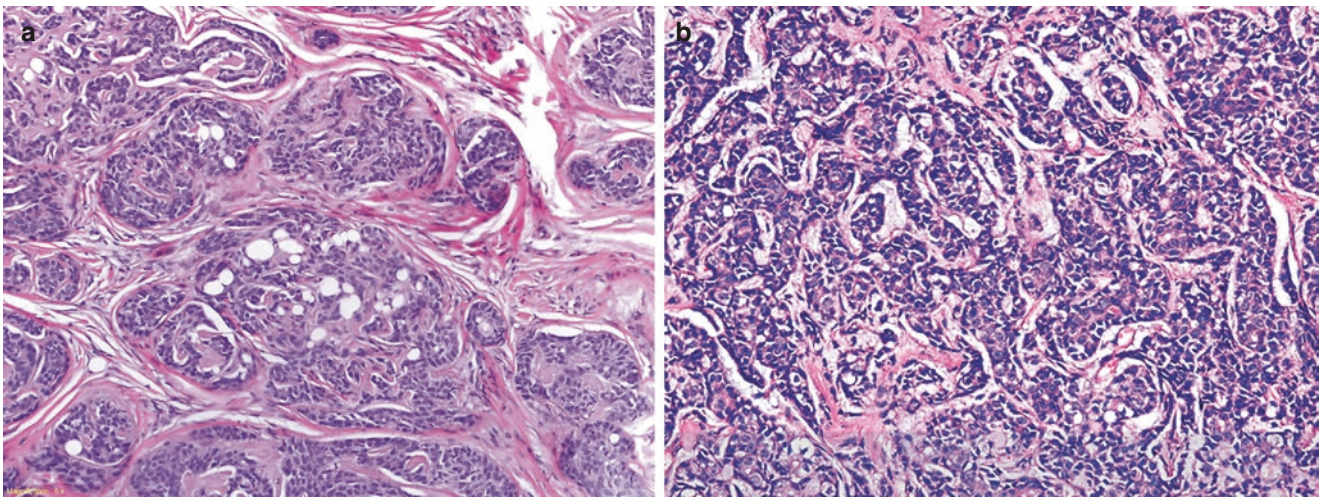

Fig. 25.17 Sebaceoma, rippled pattern. (**a**) A reticulated growth pattern of basaloid cells with focal sebocyte differentiation embedded in a densely hyalinized stroma (Reproduced from Desman GT, Ozerdem U, Shin SJ. Neighboring look-a-likes: Distinguishing between breast and dermatologic lesions. Adv Anat Pathol. 2014;21:228–247, with permission of Wolters-Kluwer Health). (**b**) Adenoid cystic carcinoma of the breast. Area showing trabeculae with a biphasic population embedded in a hyalinized stroma. Features more typical of adenoid cystic carcinoma were present (not shown)

shows positive expression for p63, D2-40, and EMA, as well as variable staining for CK7. Tumor cells are characteristically negative for BerEP4 [59, 87–89].

Mammary Differential Diagnosis Invasive ductal carcinoma and adenoid cystic carcinoma of the breast: Invasive ductal carcinoma does not typically show sebocyte-type cells or malignant cells embedded within collagenized stroma. Immunohistochemical stains for p63 and D2-40 can be helpful, as they will be positive in sebaceous neoplasms and negative in the majority of breast carcinomas. Adenoid cystic carcinoma can show this type of basement membrane-like deposition but will not show sebocyte-type cells (Fig. 25.17b). Although these tumors are also positive for p63, a panel showing positive CK7 and CD117, variable GATA3 and ER, and negative D2-40 is helpful in establishing the diagnosis.

Extraocular Sebaceous Carcinoma

Sebaceous carcinomas are traditionally divided into ocular and extraocular types; however, their biological behavior appears to be similar, with a risk of 30–40% for local recurrence, 25–35% for distant metastasis, and 10–20% for death from disease. Extraocular sebaceous carcinomas are less common than the ocular type and typically present as a painful or rapidly growing ulcerated nodule on the trunk, genitalia, or extremities [90–93]. Breast and nipple lesions are well documented in the literature [94, 95]. Extraocular tumors are more commonly associated with microsatellite instability and Muir-Torre syndrome [83–85]. The tumors exhibit a heterogeneous morphology, including closely arranged aggregates of infiltrative lobules composed of polygonal cells with mixed basaloid and clear cytomorphology (Fig. 25.18a). Well-differentiated tumors contain larger concentrations of vacuolated clear cells with hyperchromatic nuclei and occasional mitoses. Poorly differentiated tumors contain greater concentrations of amphophilic-to-basophilic cells with marked nuclear pleomorphism, prominent nucleoli, and numerous mitoses. Central comedo-like tumor necrosis is a common feature (Fig. 25.18b). Sebaceous carcinomas commonly colonize the overlying epidermis and may mimic mammary or extramammary Paget's disease. Currently, no individual immunohistochemical stain is specific for sebaceous differentiation. In general, these tumors are characteristically negative for the common markers expressed in other sweat gland tumors and visceral malignancies such as CK7, CK20, CEA, S100 protein, GCDFP-15, CA-125, and CA-19. However, they are positive for p63, CK5/6, and EMA with variable BerEP4 expression [6, 64, 88, 96, 97]. ER, PR, and AR are present in the majority of sebaceous gland neoplasms and in benign sebaceous glands [64, 98]. HER2 expression has been reported [99]. D2-40 shows negative-to-weak expression in a diffuse pattern that increases with poor differentiation. In contrast, sebaceous adenomas show basal expression of D2-40 [39, 40, 64].

Mammary Differential Diagnosis Invasive ductal carcinoma, DCIS, comedo type (Fig. 25.18c), and Paget disease of the breast: The presence of clear cells in poorly

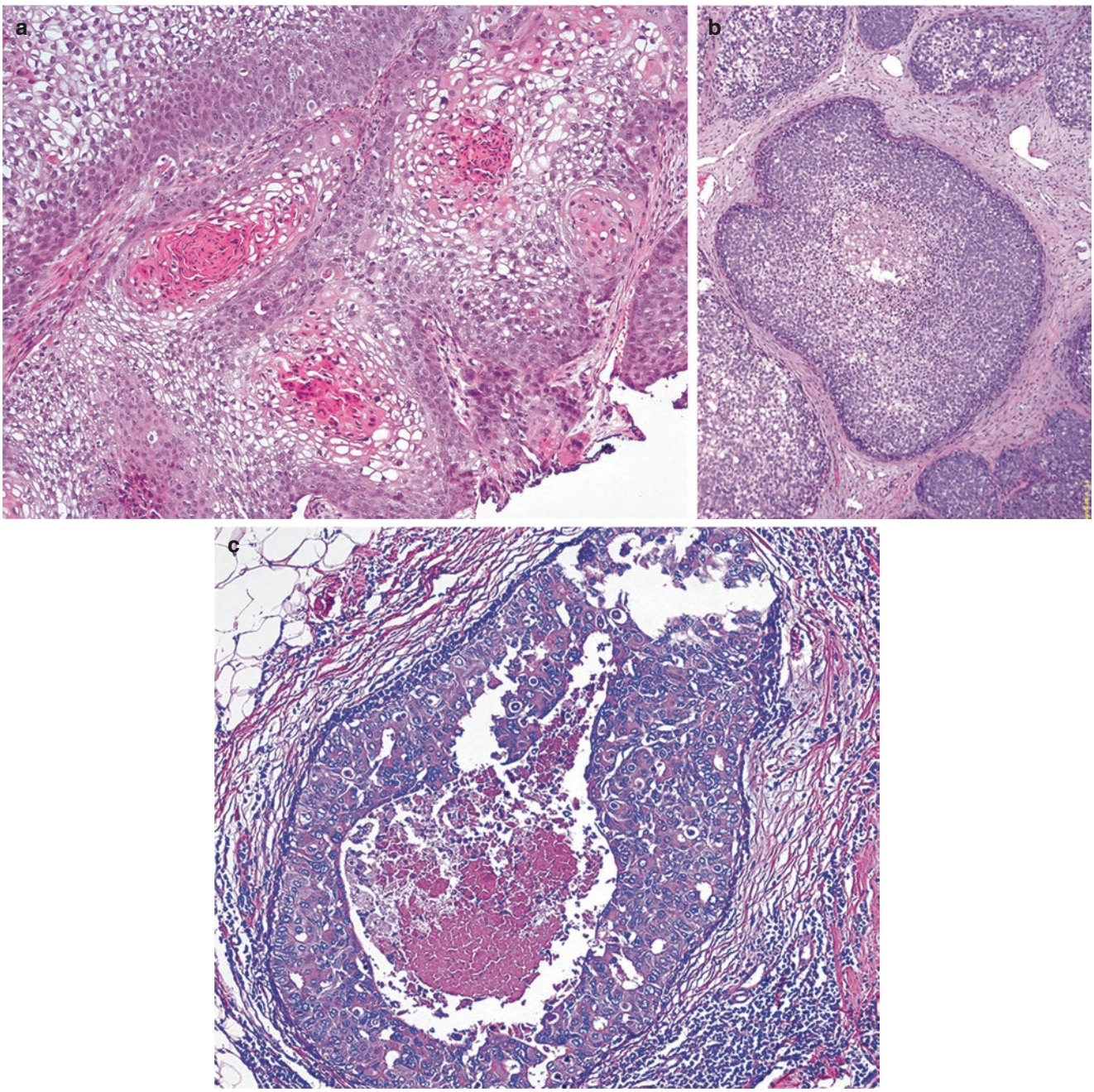

Fig. 25.18 Extraocular sebaceous carcinoma. (**a**) Closely aggregated lobules containing mixtures of basaloid and clear cells with marked nuclear pleomorphism. (**b**) Malignant lobule of sebaceous carcinoma containing central comedo-like necrosis (Reproduced from Desman GT, Ozerdem U, Shin SJ. Neighboring look-a-likes: Distinguishing between breast and dermatologic lesions. Adv Anat Pathol. 2014;21:228–247, with permission of Wolters-Kluwer Health). (**c**) Ductal carcinoma in situ, comedo type

differentiated ductal carcinomas (e.g., invasive breast carcinoma, lipid-rich carcinoma pattern, or glycogen-rich clear-cell carcinoma pattern) is rare but can occur. Invasive apocrine ductal carcinomas can also assume a clear appearance in some instances. Adjacent areas more typical for ductal carcinoma should be present. An in situ component can be helpful in establishing mammary origin if dealing with an example morphologically similar to invasive ductal carcinoma. Extraocular sebaceous carcinomas are negative for CK7 and CK20 and show strong positivity for p63 and CK5/6 and weak expression of D2-40. In contrast, mammary carcinomas are negative for D2-40, with negative or weak expression for p63 and CK5/6. Paget disease of the breast is positive for CK7 and

in the vast majority of cases also HER2 positive, while sebaceous carcinomas are negative for both in almost all cases.

Benign and Malignant Apocrine Neoplasms

Apocrine Hidrocystoma and Cystadenoma

Apocrine hidrocystomas present as skin-colored to bluish, translucent papules or nodules. These lesions most commonly arise on the face; however, axillary involvement has been documented [100]. These lesions are characterized by cystic dilatations of apocrine sweat ducts with variable epithelial hyperplasia (Fig. 25.19). Lesions with micropapillary intraluminal hyperplasia are referred to as cystadenomas [101]. The epithelial lining is composed of one to two layers of cuboidal-to-columnar cells with apical decapitation secretion (snouts) [102]. Cystadenomas frequently exhibit micropapillary projections into the cyst lumen. A feature of apocrine origin is the presence of hemosiderin granules admixed with the apocrine cells (Fig. 25.20a, b).

Mammary Differential Diagnosis Apocrine cysts (Fig. 25.20c): The presence of nearby mammary lobules or other fibrocystic changes will suggest a breast parenchymal location or ectopic breast tissue in the axilla.

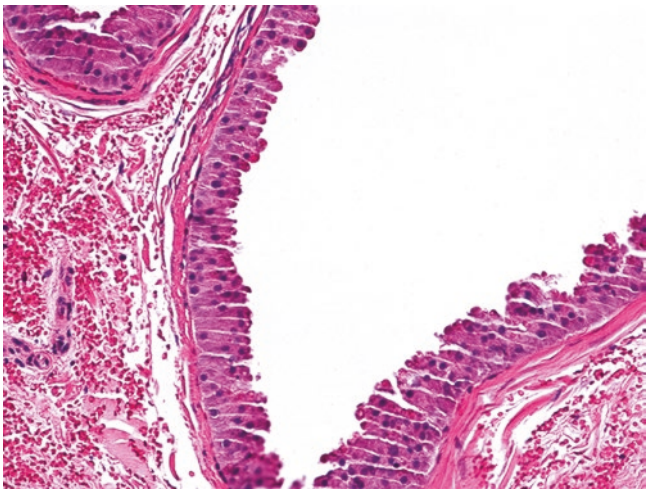

Fig. 25.19 Apocrine hidrocystoma. Dilated cystic space lined by a flattened layer of cuboidal epithelium exhibiting decapitation secretion

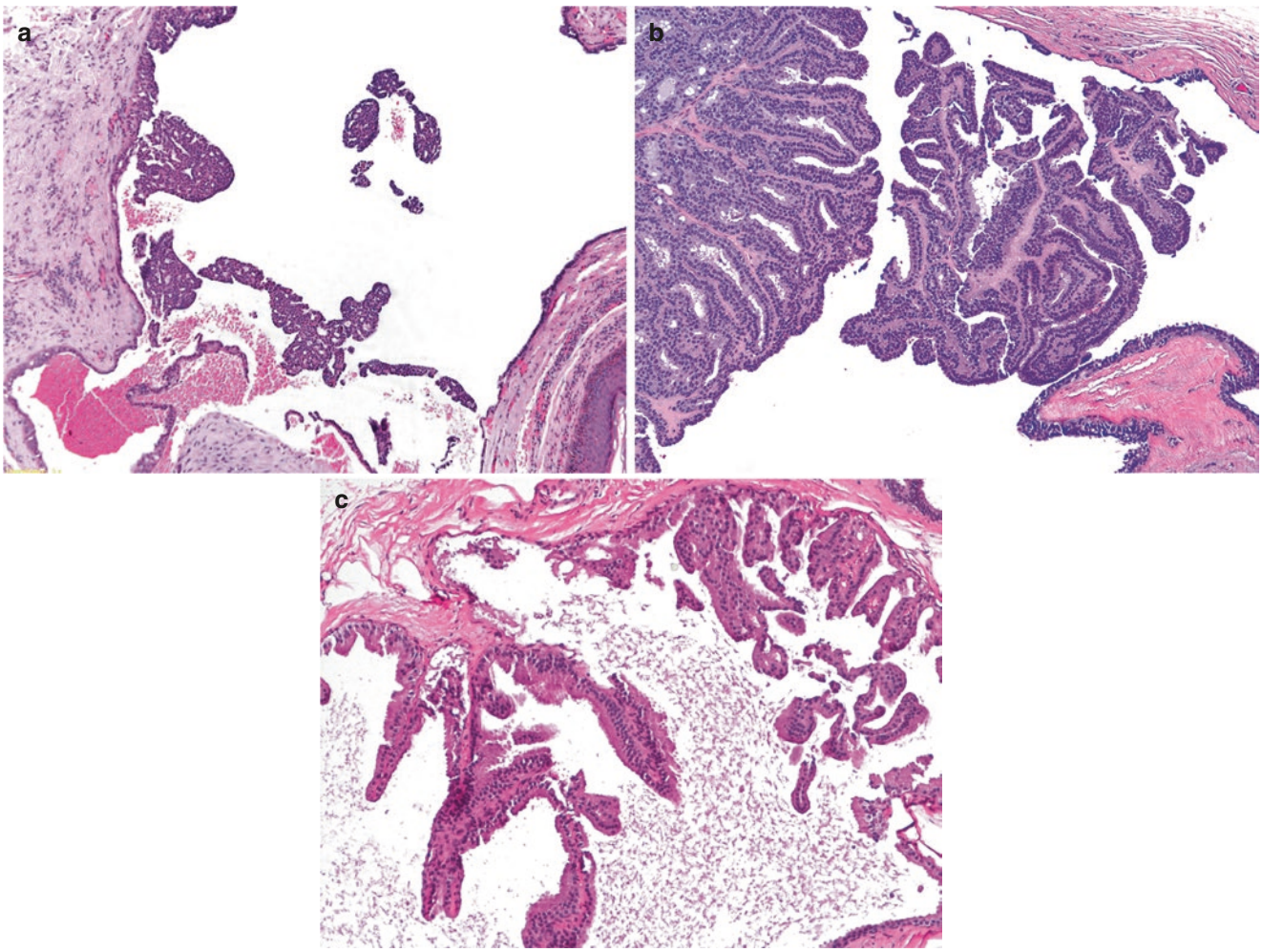

Fig. 25.20 Apocrine cystadenoma. (**a**) Large cystic cavity lined by micropapillary proliferative apocrine epithelium exhibiting numerous decapitation "snouts." (**b**) Some lesions contain papillary structures with true fibrovascular cores. (**c**) Apocrine cyst of the breast

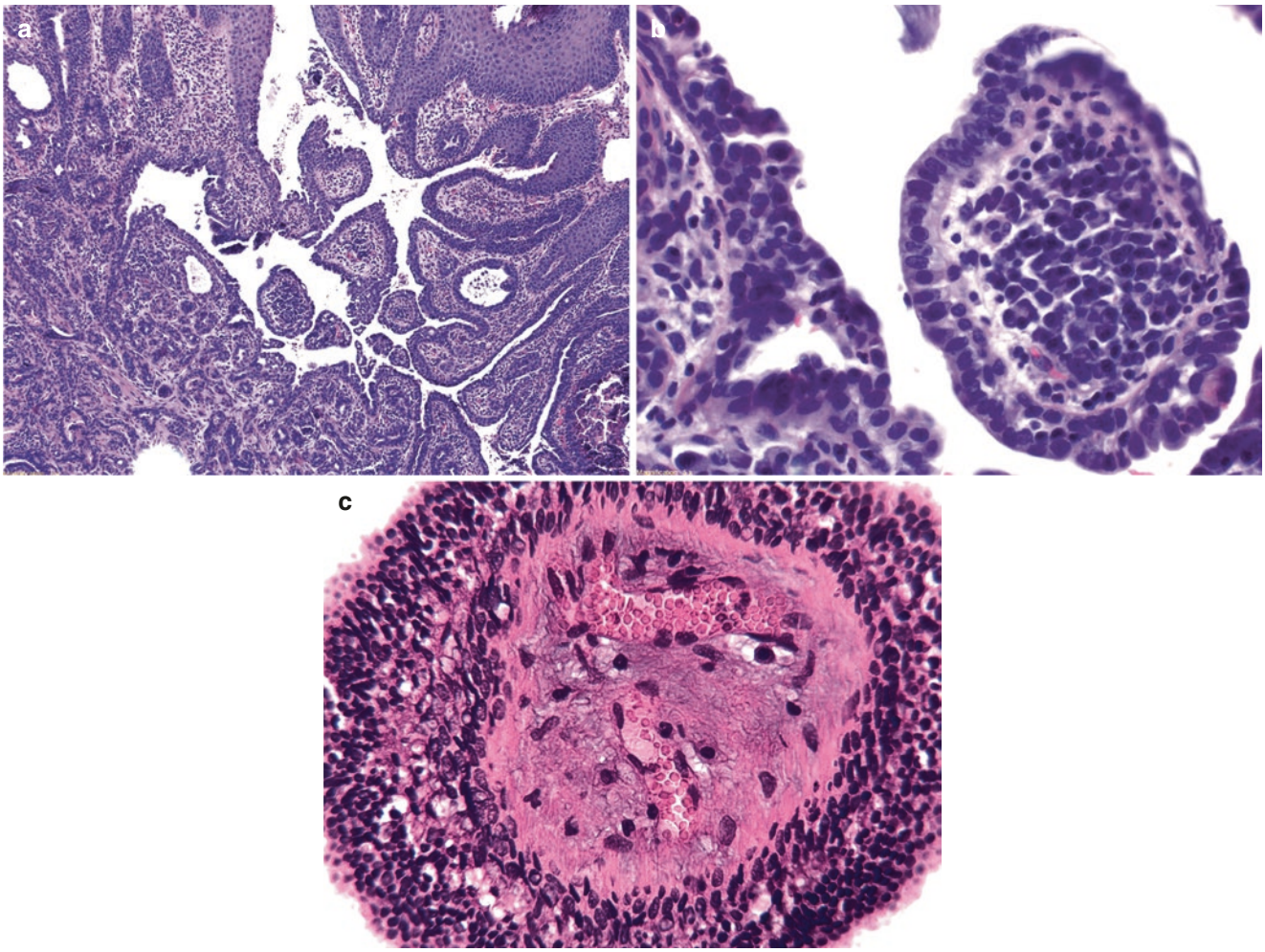

Fig. 25.21 Syringocystadenoma papilliferum. (**a**) Numerous tubules extend downward from the epidermis into a cystic cavity containing papillary structures. The epithelial lining is of cuboidal-to-columnar cells with eosinophilic cytoplasm. (**b**) Note the numerous plasma cells within the papillary stroma. (**c**) Fibrovascular core of an intraductal papilloma

Syringocystadenoma Papilliferum

Syringocystadenoma papilliferum most commonly arises on the scalp in association with a nevus sebaceus of Jadassohn; however, numerous sporadic tumors arising in the breast and axilla have been reported [103, 104]. Rarely, an extracranial linear or agminated configuration may be encountered [105, 106]. They present as skin-colored papules or nodules that contain a central dell. Sections show ductal or tubular structures that extend downward from the epidermis and end in a cystic dilatation that contains papillary structures (Fig. 25.21a). The tubules, cyst, and papillary structures are lined by cuboidal-to-low columnar glandular cells that often exhibit apical decapitation secretion (snouts). The fibrovascular cores contain numerous plasma cells (Fig. 25.21b).

Mammary Differential Diagnosis As this lesion shows different components, the differential diagnosis depends on the area sampled. The tubular area is reminiscent of sclerosing adenosis or a well-differentiated ductal carcinoma. Stains for p63 and S100 protein might prove helpful in making the distinction as both should show circumferential staining in the former and absence of staining in the latter, both of which are distinct from syringocystadenoma papilliferum. The papillary component is similar to that seen in an intraductal papilloma, although plasma cells are not a component of the fibrovascular core in the latter (Fig. 25.21c). Location in the epidermis and presence of dilated breast ducts are important clues for the diagnosis.

Nipple Adenoma

Also known as erosive adenomatosis or florid papillomatosis of the nipple, this tumor clinically presents as an ill-defined mass centered under the nipple-areolar complex in middle-aged to elderly females. There is frequent distortion of the

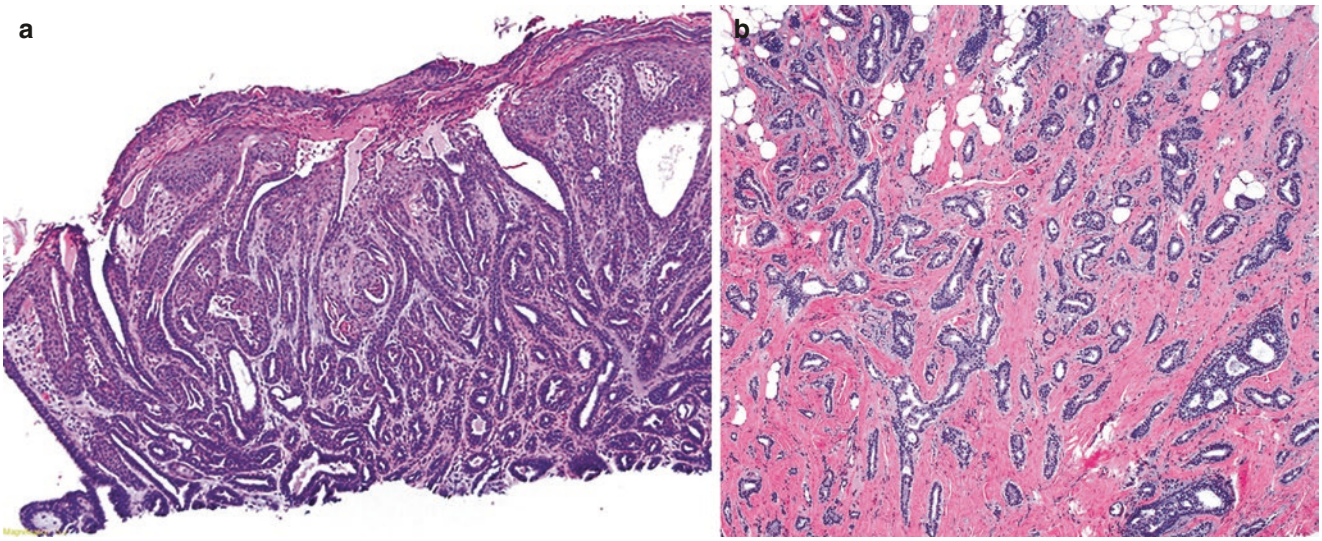

Fig. 25.22 Erosive adenomatosis of the nipple. (**a**) Extending downward from an eroded epidermis are numerous elongated tubules (Reproduced with permission from McGraw Hill Education; Barnhill's Dermatopathology Challenge, by Garrett T. Desman and Raymond L Barnhill). (**b**) Well-differentiated invasive ductal carcinoma

nipple. The surrounding nipple skin may be associated with eczematous dermatitis, clinically resembling mammary Paget disease. Microscopically, a vaguely nodular proliferation of small glands centered on large lactiferous ducts connects with the overlying nipple skin (Fig. 25.22a). The glandular structures may dissect in between smooth muscle bundles in the nipple skin, mimicking invasion. The glandular lining is composed of two cell layers: myoepithelial cells with pale cytoplasm and apical cells with eosinophilic cytoplasm and frequent apocrine snouts [107].

Mammary Differential Diagnosis In a limited tissue sample, morphologic features of nipple adenoma can resemble well-differentiated invasive ductal carcinoma and tubular carcinoma (Fig. 25.22b). The ductal structures in these invasive neoplasms will have a single layer of cells, with absent peripheral (myoepithelial) positivity for p63, in contrast with adenosis with varying degrees of sclerosis in a nipple adenoma. Please see Chap. 19 for more information about nipple adenoma.

Chondroid Syringoma

Chondroid syringoma (mixed tumor of the skin) is a benign biphasic glandular and stromal neoplasm that most commonly arises on the head and neck as a nondescript dermal or subcutaneous nodule; however, cases involving the breast and axilla are well documented [108–110]. Chondroid syringoma is the prototype for the frequent biphasic nature of benign cutaneous adnexal neoplasms, in which the tumor stem cells undergo divergent differentiation into dissimilar tissue types [111]. Histopathologically, the tumor is characterized by a well-circumscribed dermal or subcutaneous nodule composed of benign epithelial cords, nests, and tubuloalveolar structures embedded in a variable stromal matrix of cartilaginous, fibroblastoid, myoid, myoepithelial, lipoid, or even osteogenic appearance (Fig. 25.23a–c). The epithelial component may exhibit apocrine, eccrine, sebaceous, pilar, mucinous, clear cell, spindle cell, or simple glandular differentiation [112, 113]. Variable mixtures of these elements may be present within a single tumor. Apocrine-type epithelial differentiation is most common. The tubuloalveolar structures are believed to recapitulate secretory coil differentiation and are lined by two layers of cells: basolateral myoepithelial cells and apical cuboidal-to-low columnar secretory cells with frequent apocrine "snouts." One combination of elements may especially resemble sclerosing adenosis or invasive carcinoma of the breast: dense hyalinized stroma with compressed tubuloalveolar structures (Fig. 25.23d) [114]. Since the central portions of the tumor may exhibit sharp angular epithelial structures due to compression by the tumoral stroma, the partial sampling via CNB may reveal an epithelial-stromal pattern suggesting invasive carcinoma. The overall features reassuring of benignity are the well-circumscribed tumor growth combined with the absence of nuclear pleomorphism, mitoses, and necrosis. Occasionally, these tumors may contain small trailing elements beyond the tumor capsule or foci with enhanced cytologic atypia, usually of the myoepithelial cells. These tumors are referred to as atypical mixed tumors; however, they display a benign clinical course [115].

Immunohistochemistry will frequently reveal the apical epithelial cell layer to express CK AE1/AE3, EMA, CEA,

GCDFP-15, CD117, CK7, and androgen receptor, whereas the myoepithelial layer will express p63, vimentin, S100 protein, and sometimes SMA. The stromal cells are vimentin and S100 protein positive. Typically, there is no immunoreactivity for mammaglobin, ER, PR, or CK20 [116–118].

Mammary Differential Diagnosis Sclerosing adenosis and invasive ductal carcinoma (described above) and, if the stromal matrix of chondroid syringoma is particularly cartilaginous, then pleomorphic adenoma (mixed tumor), invasive mucinous carcinoma, and matrix-producing metaplastic carcinoma should be considered (Fig. 25.23e–g). Benign mixed tumors will show similar morphology regardless of the site of origin. Clinical and radiological correlation is necessary for definitive diagnosis. Metaplastic carcinomas of the matrix-producing type and invasive mucinous carcinoma can be difficult to exclude particularly in a limited sampling when an invasive growth pattern is not obvious. Cytomorphologically, both types of carcinomas can exhibit low nuclear grade similar to chondroid syringoma. Mucinous carcinomas are typically ER positive, which is distinctive from chondroid syringoma, but this is not always true of metaplastic carcinomas. However, diffuse p63 immunoreactivity if seen in a metaplastic carcinoma can be helpful as it may appear different from the distribution seen in chondroid syringomas. Confirming the location of the tumor is key.

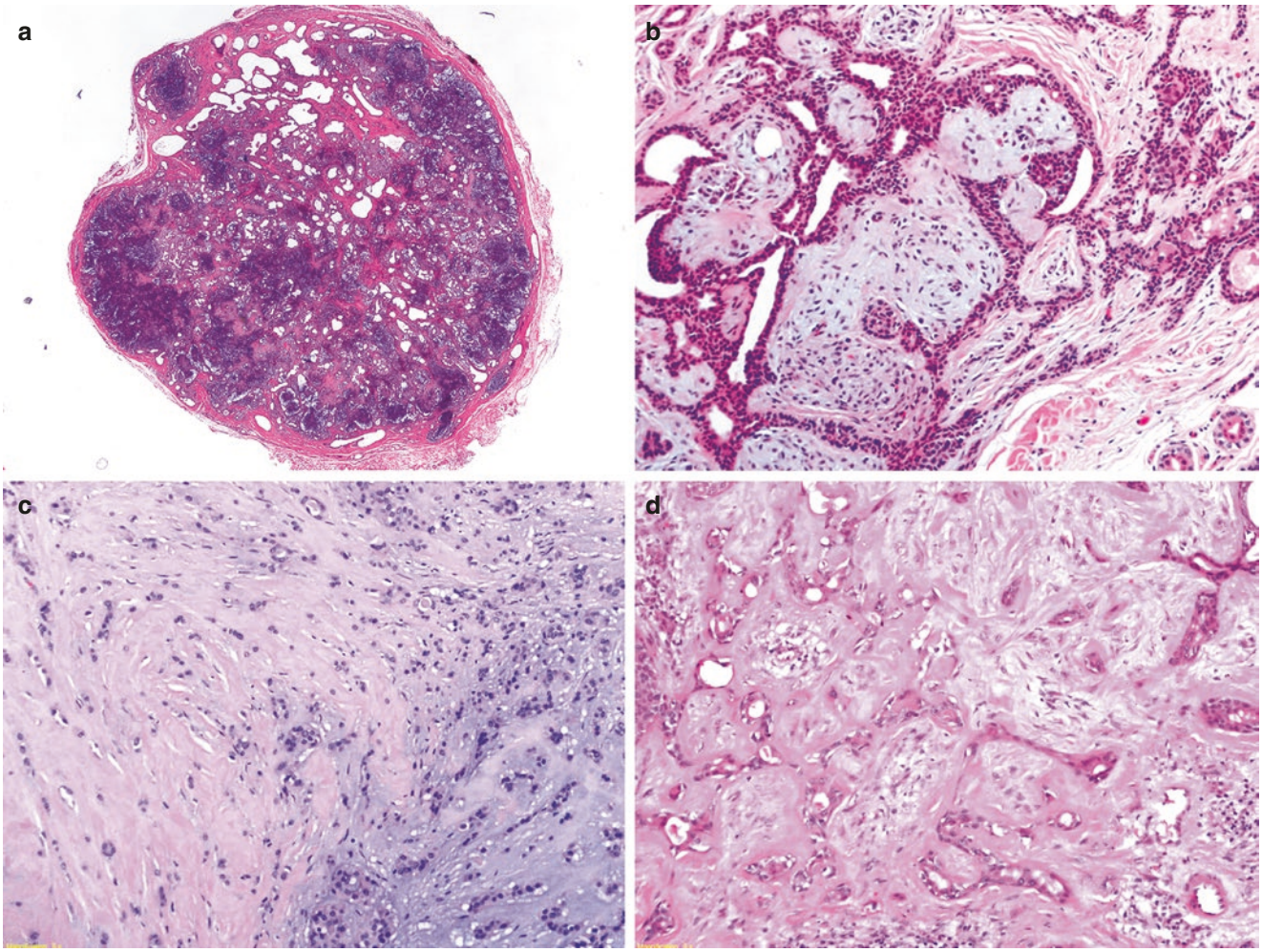

Fig. 25.23 Chondroid syringoma. (**a**) A low-power image reveals a well-circumscribed tumor mass. (**b**) On high power, a relatively heterogeneous composition of epithelial and stromal elements is evident. There are tubuloalveolar structures lined by a two-cell layer and a surrounding loose chondromyxoid stroma. (**c**) Chondroid stroma containing scattered solitary plasmacytoid-appearing myoepithelial cells. (**d**) Central hyalinized focus in which the glandular elements are compressed in between thick collagen, resembling sclerosing adenosis of the breast. (**e**) Pleomorphic adenoma (mixed tumor) of the breast. (**f**) Invasive mucinous carcinoma. (**g**) Matrix-producing metaplastic carcinoma

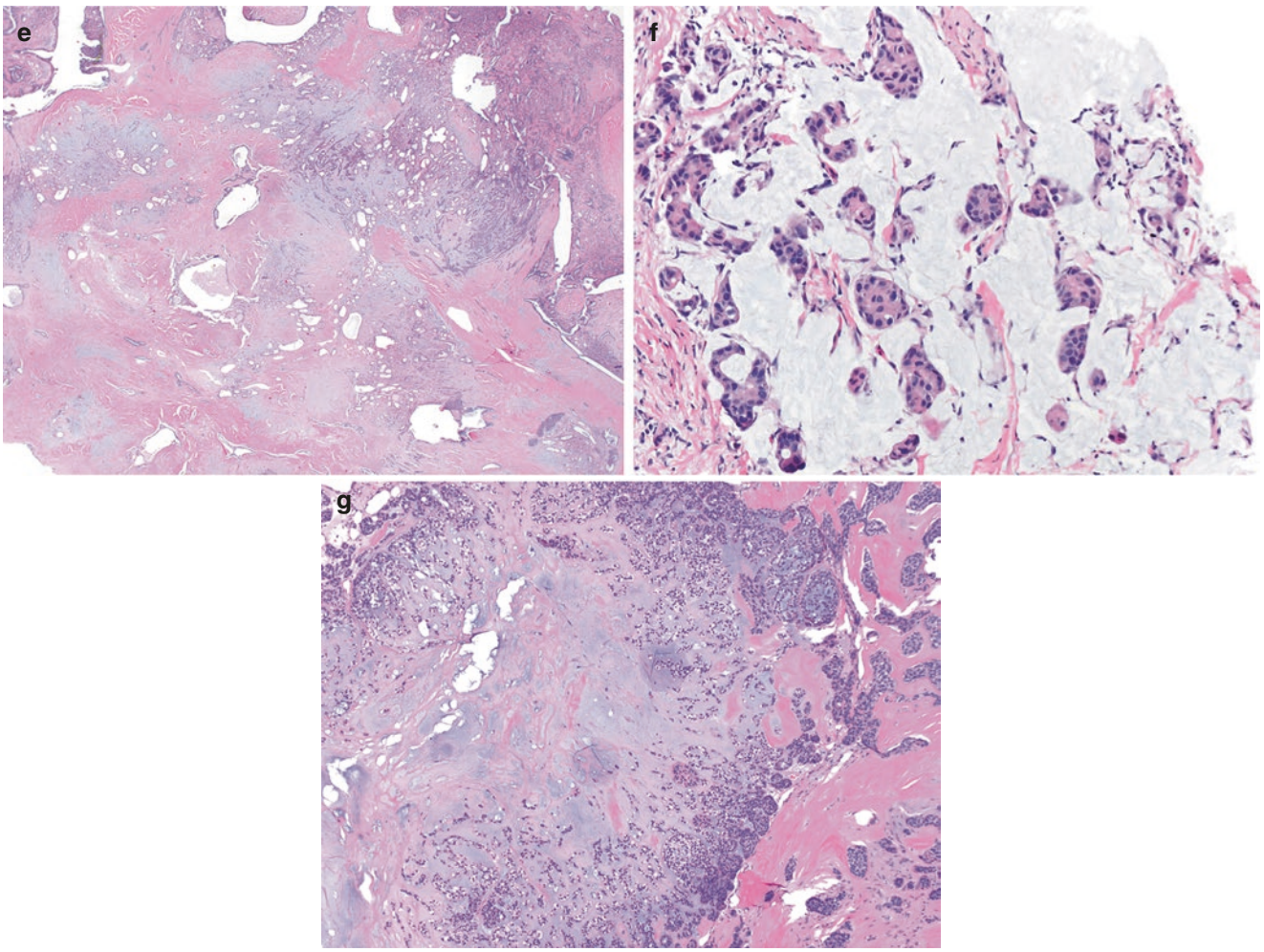

Fig. 25.23 (continued)

Sweat Gland Adenomas (Tubular Apocrine Adenoma Versus Papillary Eccrine Adenoma)

Papillary eccrine adenoma is a rare dome-shaped nodule or plaque that occurs almost exclusively on the extremities. Additionally, these tumors are more common in African American females. Microscopic features include the presence of well-circumscribed aggregates of dilated ductular structures within the dermis that are lined by uniform polygonal basaloid cells. This lining is proliferative with intraluminal micropapillary structures that have no fibrovascular cores [119]. Connection with the overlying epidermis via colonization of the eccrine duct or through neoplastic duct-like structures may be occasionally identified. By definition, apocrine differentiation with decapitation secretion is not present. Similar to other primary cutaneous eccrine tumors, immunohistochemistry will reveal basal layer staining for p63, distinguishing these lesions from mammary carcinoma.

A similar, yet malignant counterpart is referred to as aggressive digital papillary eccrine adenocarcinoma. It occurs almost exclusively on the distal extremities, typically the fingers and toes. The ducts exhibit an invasive growth pattern, tumor cell necrosis, and numerous mitoses [120]. Historically, a more morphologically banal tumor without necrosis and robust mitotic activity was known as aggressive digital papillary eccrine adenoma, but clinical follow-up studies have revealed similar malignant behavior. Therefore, they have been consolidated into the aggressive digital papillary eccrine adenocarcinoma category. The histopathologic features of both lesions may resemble invasive papillary carcinoma of the breast, but because these tumors do not arise within the breast or axilla, they are not included in our list of mammary carcinoma mimics. However, the equivalent lesion with apocrine differentiation, referred to as tubular apocrine adenoma or tubulopapillary adenoma, has been well documented in the axilla.

Tubular apocrine adenomas frequently arise within preexisting nevus sebaceous or syringocystadenoma papilliferum. Malignant degeneration into apocrine carcinoma has been reported [121]. Rare cases of mixed apocrine and eccrine dif-

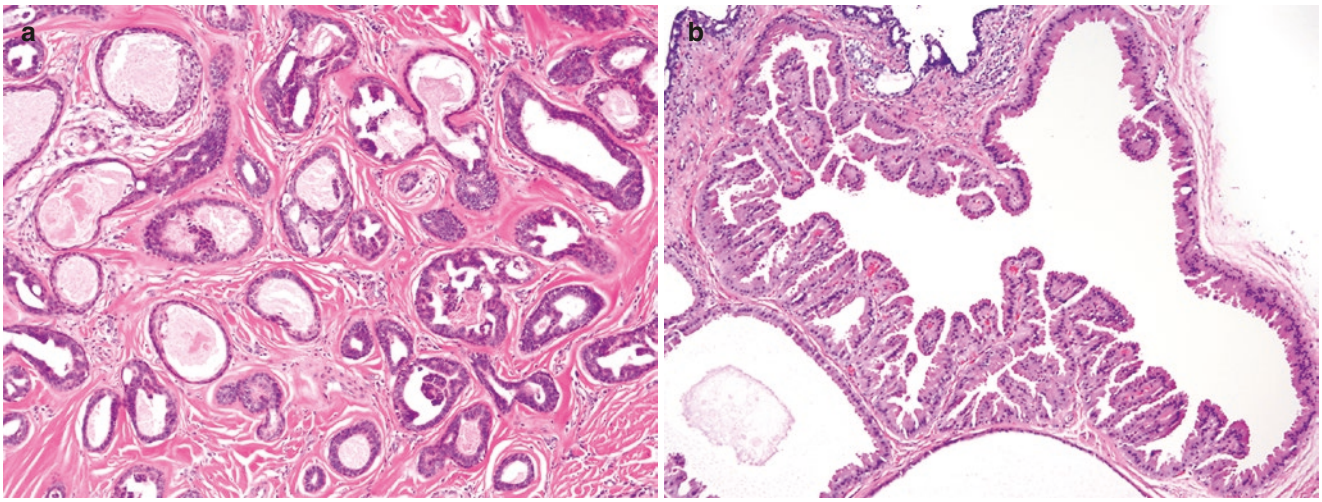

Fig. 25.24 Tubular apocrine adenoma. (**a**) Numerous dilated ductular structures lined by hyperplastic apocrine epithelium in a micropapillary configuration (Reproduced from Desman GT, Ozerdem U, Shin SJ. Neighboring look-a-likes: Distinguishing between breast and dermatologic lesions. Adv Anat Pathol. 2014;21:228–247, with permission of Wolters-Kluwer Health). (**b**) Cystic apocrine papillary hyperplasia of the breast

ferentiation have been documented [122]. The tumor may also connect with the epidermal surface via columns of cells that superficially resemble the normal sweat duct. Ductal spaces in these structures may contain luminal eosinophilic cuticles. The cytologic features are benign (Fig. 25.24a).

Mammary Differential Diagnosis Cystic apocrine papillary hyperplasia and apocrine cysts (Fig. 25.24b): Morphologic features are very similar to tubular apocrine adenomas. Location within the axilla requires evaluation of adjacent tissue for the presence of mammary lobules that will identify ectopic breast tissue in the axillary tail. Potential for recurrence of the cutaneous tumor underscores the importance of a thorough evaluation of these lesions.

Apocrine Adenocarcinomas

Apocrine adenocarcinomas are rare, with most reported cases involving the axilla and occasionally the chest and nipple [123, 124]. Other locations include the scalp, eyelid, ear, anogenital region, and wrist. These tumors typically present as solitary or multiple slow-growing nodules or plaques, which frequently ulcerate. There is a wide age range and no predilection for race or gender. Some tumors have been reported to be present for 30 years before diagnosis, suggesting an origin within a preexisting benign tumor [125]. Moreover, rare cases of bilateral axillary adenocarcinoma associated with apocrine nevi have been reported, as well as carcinomas arising within tubular apocrine adenomas and syringocystadenoma papilliferum [7, 126]. Metastatic intralymphatic cutaneous spread similar to that of inflammatory breast carcinoma has also been described [127].

Apocrine carcinomas characteristically exhibit morphologic plasticity, often revealing foci with varying patterns of growth and cytomorphology, making the distinction of primary cutaneous carcinoma versus cutaneous metastasis extremely difficult. For practical purposes, there are five types of apocrine adenocarcinoma. Two forms have reproducible histopathology that may be confidently diagnosed as primary cutaneous malignancies: ductopapillary apocrine carcinoma (DPAC) and the apocrine type of mammary or extramammary Paget's disease. The other three forms closely mimic metastatic mammary adenocarcinoma: ductal apocrine adenocarcinoma (DAA), primary cutaneous mucinous carcinoma, and primary cutaneous signet ring cell carcinoma.

Ductopapillary Apocrine Adenocarcinoma

Ductopapillary apocrine adenocarcinoma (DPAC) is morphologically similar to aggressive digital papillary eccrine adenocarcinoma. Unlike its eccrine counterpart, these tumors most frequently arise within the eyelids, axilla, and genitoperineal region. It is characterized by infiltrative tubules and true papillary structures with fibrovascular cores. Perineural and intravascular invasion are common. The tumor cells contain eosinophilic cytoplasm, with or without apical decapitation "snouts." Cytologic atypia is usually obvious with frequent mitoses and necrotic tumor cells. Regional lymph node involvement and subsequent distant metastasis are seen

in approximately 40% of cases [128]. Prussian blue histochemical stain will reveal intracytoplasmic iron deposition in 40–50% of cases, establishing apocrine differentiation [129]. Immunohistochemical stains reveal strong and diffuse expression of GCDFP-15. As mentioned previously, unlike most primary cutaneous tumors, the tumor cells of apocrine adenocarcinoma are frequently negative for p63.

Mammary Differential Diagnosis Invasive ductal carcinoma, papillary carcinoma, and DCIS: Differentiating between these lesions might not be possible on histologic grounds.

Ductal Apocrine Adenocarcinoma

Ductal apocrine adenocarcinoma shows randomly oriented infiltrative nests and cords with or without luminal structures. The luminal structures may be solid or have a cribriform arrangement. Occasional micropapillary structures may be present, but the tumor lacks true fibrovascular cores. Invasion into the subcutis with perineural and lymphovascular invasion is common. The tumor cells contain eosinophilic cytoplasm and decapitation secretion, consistent with apocrine differentiation. Marked cytologic atypia, mitotic activity, and spontaneous tumor cell necrosis are constant findings. The clinical, histochemical, and IHC features are identical to ductopapillary apocrine carcinoma (DPAC). In fact, the only distinguishing feature from DPAC is a more solid growth pattern and the absence of luminal papillary structures (Fig. 25.25a–c) [123, 128].

Mammary Differential Diagnosis Invasive ductal carcinoma and DCIS, solid and cribriform type (Fig. 25.25d, e): Clinical evaluation of the location of the lesion is necessary for the diagnosis. Immunostaining with p63 should be used with caution: DCIS will show peripheral positivity, while a primary cutaneous apocrine adenocarcinoma should be negative throughout.

Primary Cutaneous Mucinous Carcinoma

Primary cutaneous mucinous carcinoma most commonly occurs in the head and neck; however, cases arising in the axilla, chest wall, and breast are well documented. These tumors typically present as slightly discolored nodules that occasionally have a soft consistency. A high rate of local recurrence but relatively low rate of regional lymph node metastasis is reported [130]. The tumor is characterized by large extracellular pools of epithelial mucin in the dermis that dissect through the tissue and contain irregular nests and small clusters of amphophilic polygonal cells with oval nuclei and small nucleoli (Fig. 25.26a). Mitoses and perineural and lymphovascular invasion are rare. These tumors most commonly arise de novo without an associated benign counterpart but may have a connection with the overlying epidermis, providing evidence of primary cutaneous derivation. The pools of mucin stain with mucicarmine, colloidal iron, Alcian blue, and PAS with diastase. Immunohistochemistry will reveal positive expression of CK7, GCDFP-15, ER, and PR and may express p63 and CK5/6 [6, 24, 131–133]. Similar to mucinous carcinomas of the breast, cutaneous mucinous carcinoma may show neuroendocrine differentiation with expression of synaptophysin and chromogranin [134].

Mammary Differential Diagnosis Mucinous carcinoma of the breast (Fig. 25.26b). The presence of an in situ ductal component or epidermis connection will reveal the origin of the lesion as mammary or cutaneous, respectively. Immunohistochemical panel will be similar for both sites as described above, though primary cutaneous mucinous carcinomas are more likely to express p63 and CK5/6.

Benign and Malignant Eccrine Tumors

Syringoma

Syringoma is a benign proliferation of eccrine ducts that may present as a localized or generalized form. Whether they represent a hamartomatous versus neoplastic process remains to be determined. The localized form presents as symmetric clustered small white-yellow papules on the upper face (i.e., lower eyelids), axilla, and genitalia. Solitary lesions also exist, in which case complete excision is required to rule out microcystic adnexal carcinoma. The generalized and eruptive forms most commonly present on the chest, neck, and forearms [135]. Familial inheritance has been documented for some cases. Histopathologically, they are characterized by small, comma-shaped tubules or cords embedded within a collagenous stroma. The tubules are lined by two or more layers of polygonal or flattened cells containing clear-to-eosinophilic cytoplasm and monomorphic nuclei without nucleoli (Fig. 25.27a). The tubules are internally lined by a bright eosinophilic cuticle and frequently contain eosinophilic-to-amphophilic secretions. Distinguishing features from microcystic adnexal carcinoma are the absence of mitoses or infiltrative growth [136]. A clear-cell variant with enlarged cells that contain clear glycogen-rich cytoplasm is associated with diabetes (Fig. 25.27b) [137]. Immunohistochemistry will reveal antigen expression similar to that of normal eccrine ducts: EMA and p63 in peripheral cells, CK10 in intermediate cells, and CK5/6, CK19, and CEA in luminal cells [138]. Expression of ER and PR is consistently negative [139].

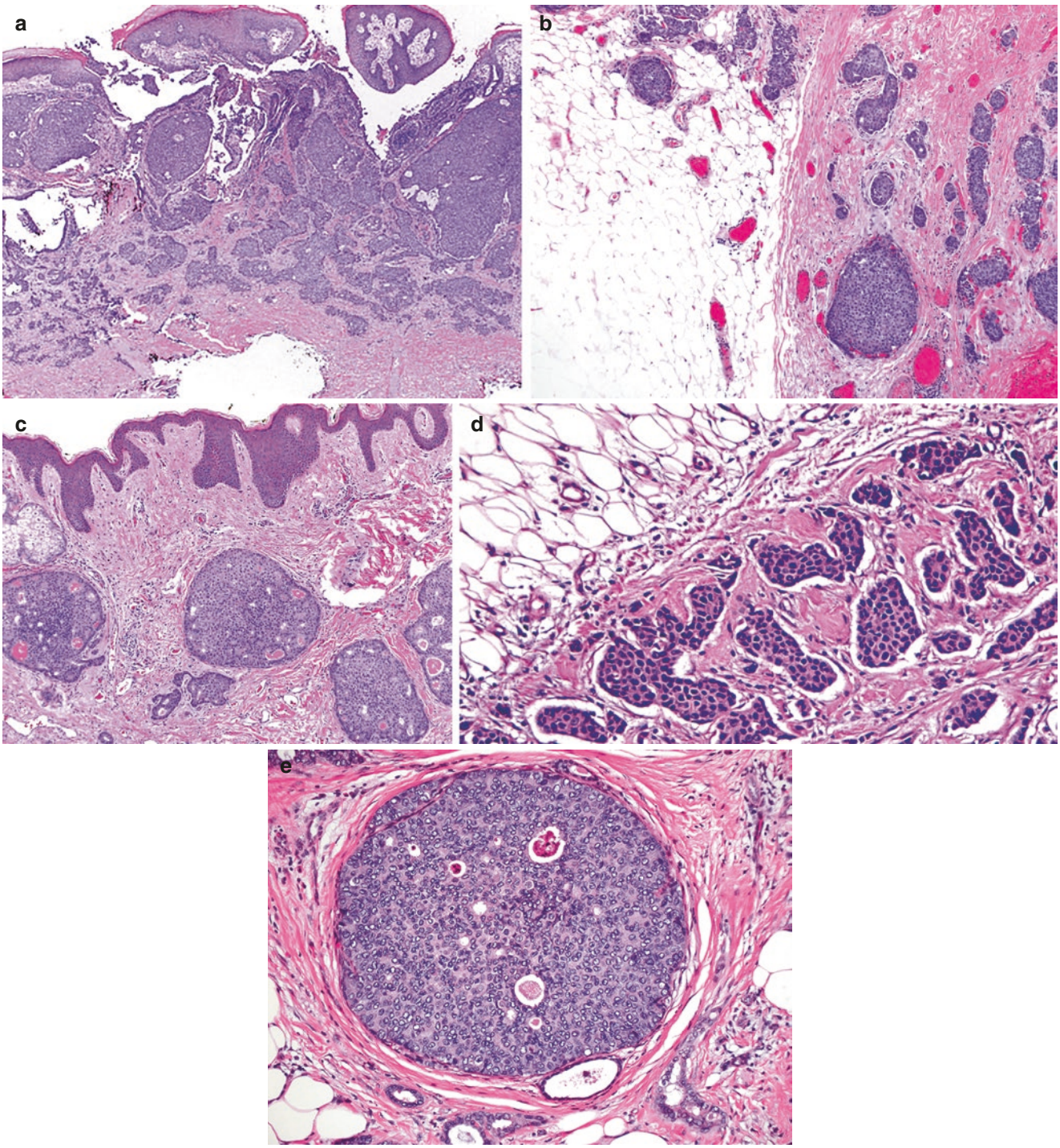

Fig. 25.25 Ductal apocrine adenocarcinoma arising in association with a syringocystadenoma papilliferum. (**a**) Numerous solid and cribriform nests composed of malignant amphophilic cells are present invading into the deep dermis. (**b**) Note the subtle angularity of the nests and extension into the fat, indicative of an invasive growth pattern (Reproduced with permission from McGraw Hill Education; Barnhill's Dermatopathology Challenge, by Garrett T. Desman and Raymond L. Barnhill). (**c**) Cribriform nests of ductal apocrine carcinoma (Reproduced from Desman GT, Ozerdem U, Shin SJ. Neighboring look-a-likes: Distinguishing between breast and dermatologic lesions. Adv Anat Pathol. 2014;21:228–247, with permission of Wolters-Kluwer Health). (**d**) Invasive ductal carcinoma of the breast invading into fat. (**e**) Ductal carcinoma in situ with intermediate nuclear grade and minimal necrosis

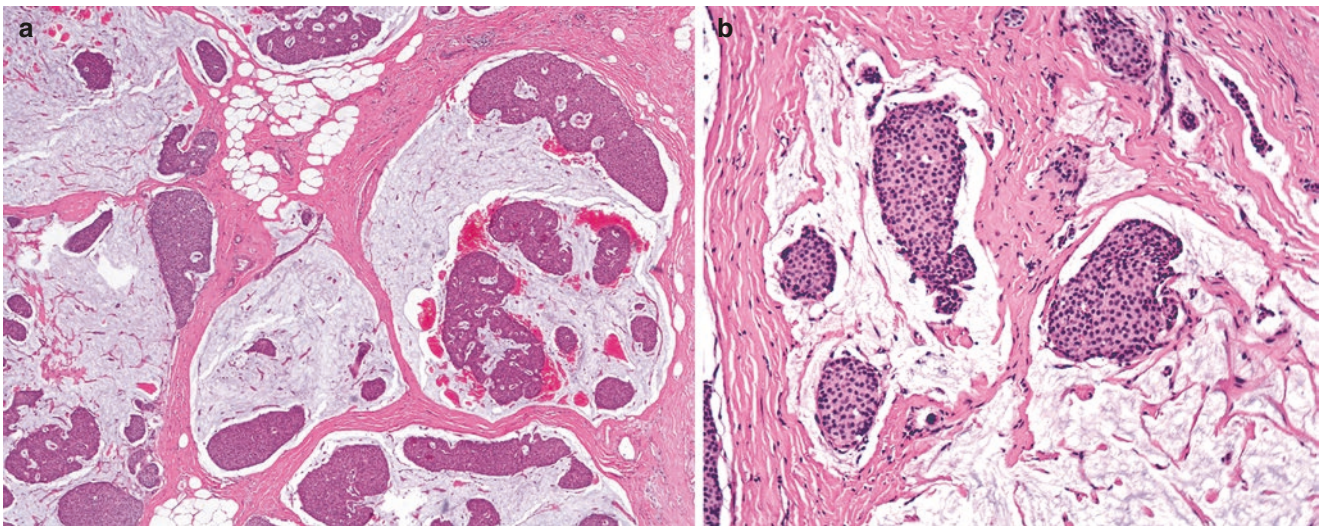

Fig. 25.26 Primary cutaneous mucinous carcinoma. (**a**) Infiltrative pools of mucin contain small clusters of epithelial cells. The epithelial cells are relatively monomorphous with eosinophilic cytoplasm and focal luminal structures. (**b**) Mucinous carcinoma of the breast

Mammary Differential Diagnosis Syringomatous tumor, well-differentiated invasive ductal carcinoma, and low-grade adenosquamous carcinoma: Syringomatous tumor shows similar morphology, but it is located in the nipple (Fig. 25.27c). A well-differentiated invasive ductal carcinoma or tubular carcinoma will show loss of myoepithelial cells with p63 staining, is typically ER positive, and, in some cases, will have an adjacent in situ component (Fig. 25.27d). Low-grade adenosquamous carcinoma shows a peripheral lymphocytic response and an infiltrative pattern with variable positivity for p63 (Fig. 25.27e).

Eccrine Poroma

The designation eccrine poroma encompasses benign neoplasms of eccrine sweat duct differentiation, which are then classified based on their location. When the lesion arises at the point where the sweat duct enters the epidermis, or acrosyringium, they are referred to as hidroacanthoma simplex. In contrast, tumors that arise within the dermal duct are referred to as dermal duct tumor. When both intraepidermal and dermal tumor nodules are present, they are referred to simply as poroma (Fig. 25.28a) [140]. Clinically, the tumor presents as a brownish raised friable papule or plaque with sharp demarcation or as a peripheral moatlike change on skin that has a high concentration of sweat glands. The soles of the feet are most commonly affected; however, cases involving the chest and breast have been documented [141, 142]. Some cases have been associated with chronic radiation dermatitis [143]. The histopathologic features of hidroacanthoma simplex include intraepidermal "lakes" of compact, monotonous polygonal cells with bland nuclei and small amounts of amphophilic cytoplasm, resembling "mosaic tiles." Peripheral palisading of the nuclei is not a feature. Small punched-out duct-like structures are randomly dispersed throughout the tumor (Fig. 25.28b). Mitoses are rare [144]. Dermal duct tumors have a similar cytomorphology with large lobules containing duct-like structures in the dermis. The surrounding stroma is fibrovascular. IHC stains reveal the tumor cells to express CK7 and p63 with EMA and CEA highlighting the duct-like foci [145, 146].

Mammary Differential Diagnosis If the tissue sample is very limited, DCIS with either solid or solid papillary growth patterns could be considered (Fig. 25.28c). It should be noted that in an example of solid papillary carcinoma, peripheral immunoreactivity for p63 may be absent, which is usually retained in other forms of DCIS. Fortunately, eccrine poromas will be diffusely positive for p63. Connection with the epidermis favors a cutaneous tumor.

Eccrine Porocarcinoma

Eccrine porocarcinoma is one of the more common malignant sweat gland tumors. There is a higher incidence in the elderly. Although it may occur essentially anywhere, eccrine sweat glands are highly concentrated, and common locations include the distal extremities, head and neck, and trunk [147]. Lesions arising in breast skin have been reported, some of which have arisen in the setting of chronic radiation dermatitis or lymphedema after lymph node dissection. The tumor presents as rapidly enlarging verrucous plaques or nodules that may ulcerate. An aggressive behavior is described, with local recurrence, lymph node involvement, and distant metastasis reported in 17%, 19%, and 11% of cases, respectively. Due to these worrisome findings, some authors have advo-

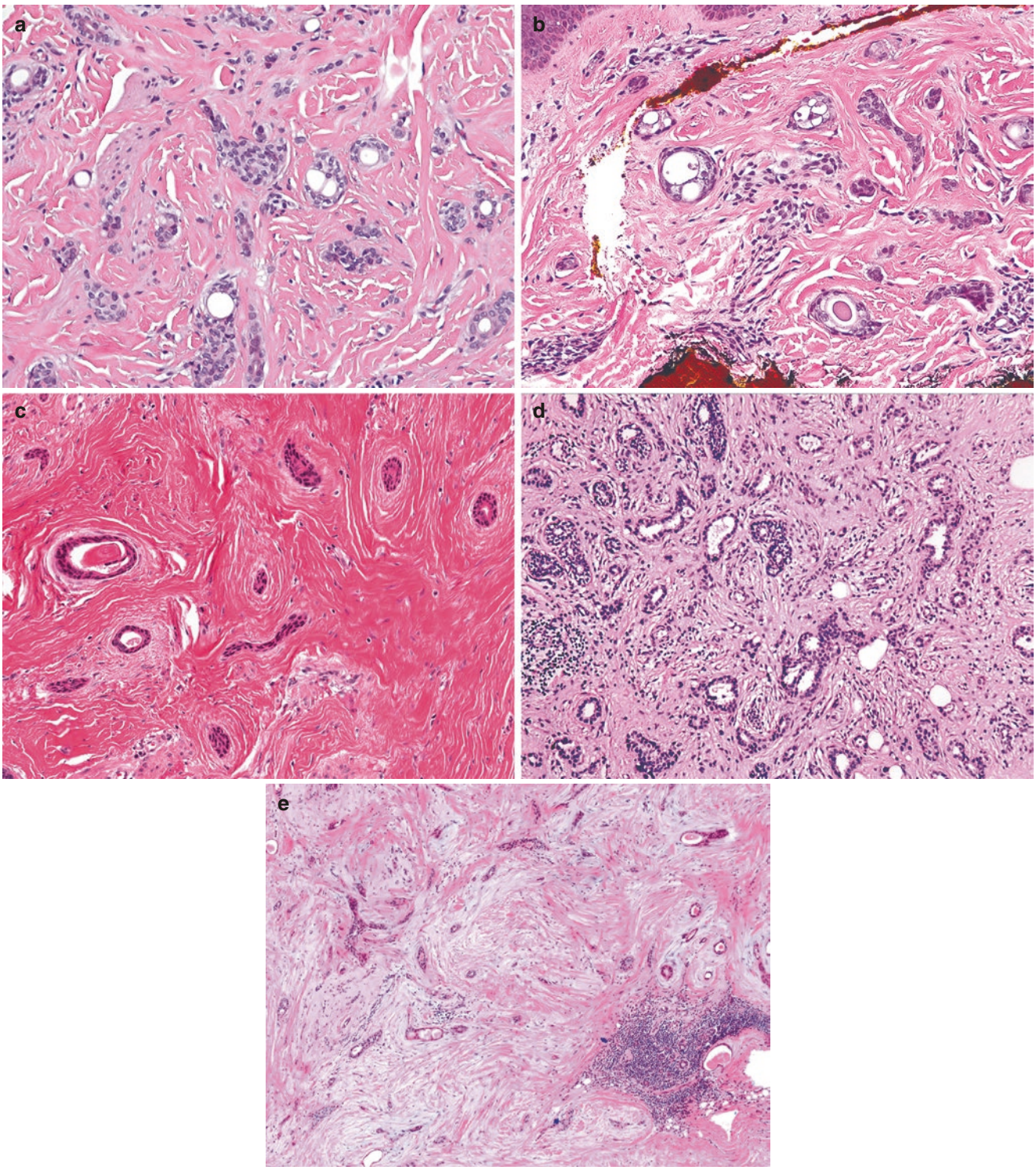

Fig. 25.27 Syringoma. (**a**) Duct-like structures embedded within collagenous stroma and lined by two or more layers of flattened cells, internal eosinophilic cuticular lining, and amphophilic secretions. (**b**) Clear-cell variant of syringoma, containing cells with abundant clear glycogenated cytoplasm. (**c**) Syringomatous tumor. (**d**) Tubular carcinoma of the breast. (**e**) Low-grade adenosquamous carcinoma of the breast

cated sentinel lymph node biopsy. Although these tumors may arise de novo, they most commonly arise within preexisting poromas. Similar to eccrine poroma, these tumors may arise anywhere within the eccrine duct and hence may connect to the epidermal surface (referred to as malignant hidroacanthoma simplex), be confined to the dermis (malignant dermal duct tumor), or both (porocarcinoma). These malignant counterparts exhibit an infiltrative growth pattern, peripheral desmoplastic stroma, tumor cell necrosis, nuclear pleomorphism, numerous mitoses, and frequent perineural and lymphovascular invasion (Fig. 25.29a). They more frequently exhibit enhanced squamous differentiation compared

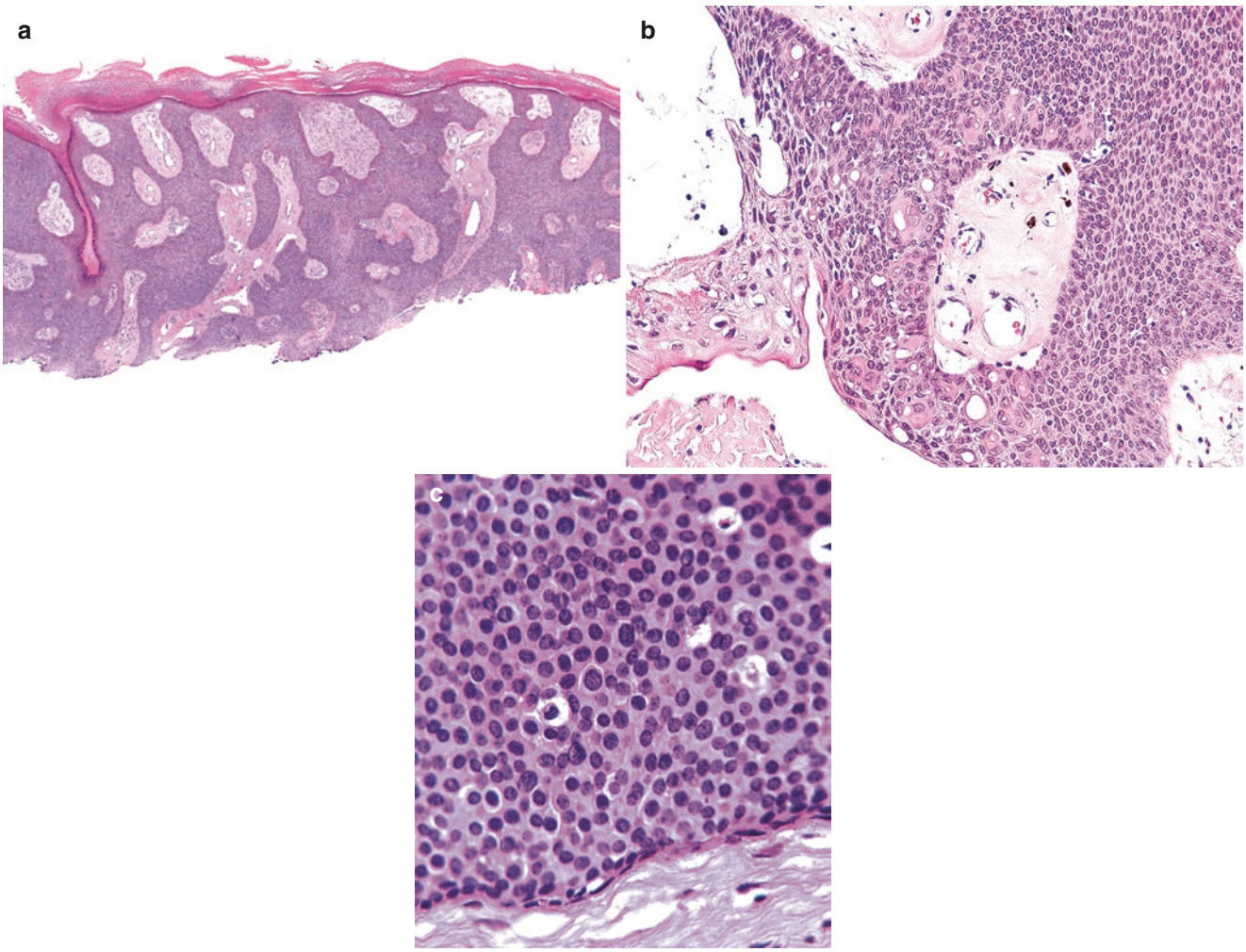

Fig. 25.28 Eccrine poroma. (**a**) Low-power view revealing a large irregularly shaped lobule in the dermis composed of squamoid cells. (**b**) Embedded within the tumor lobules are numerous ductules. (**c**) Solid papillary carcinoma

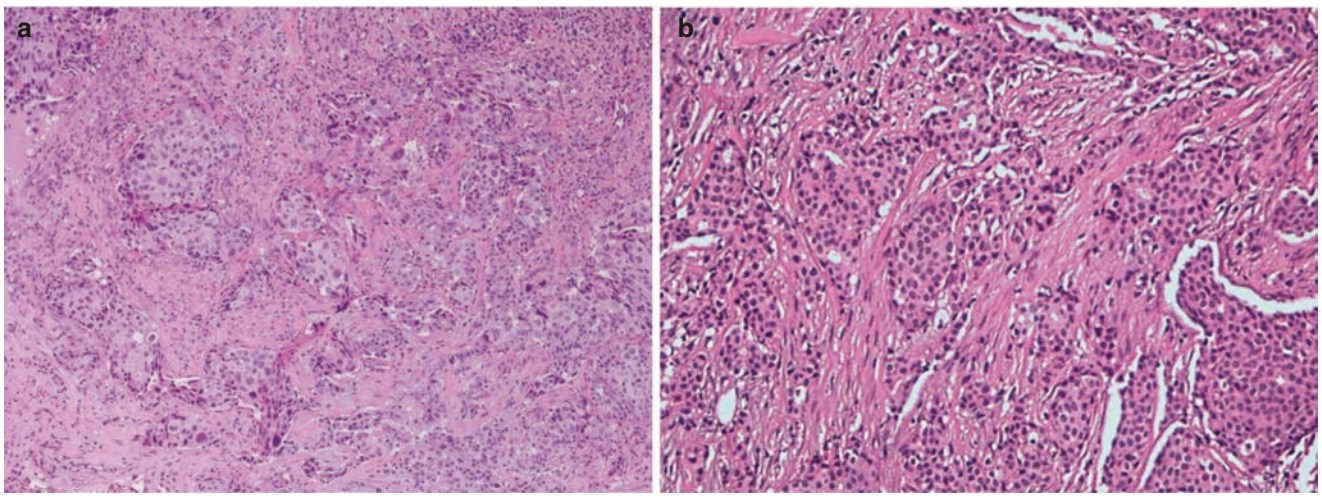

Fig. 25.29 Eccrine porocarcinoma. (**a**) Note the infiltrating nests and lobules with acantholysis and luminal structures. The cells exhibit eosinophilic cytoplasm, nuclear pleomorphism, and numerous mitoses. (**b**) Invasive ductal carcinoma

to benign poromas (unpublished observation, GTD). Luminal structures are scattered within nests and lobules of tumor cells, which is the most reliable feature distinguishing these tumors from SCC. IHC stains will reveal the tumor cells to express CK7, EMA, and CEA, with preferential staining of the luminal structures [74, 148].

Mammary Differential Diagnosis Invasive ductal carcinoma (Fig. 25.29b): Morphology can be very similar, especially in limited biopsy samples. The presence of DCIS favors a mammary primary. Preexisting poroma and diffuse strong positivity for p63 suggest a porocarcinoma.

Eccrine Syringofibroadenoma

Eccrine syringofibroadenoma is a rare tumor that presents as a nondescript solitary hyperkeratotic nodule on the extremities; however, we have personally encountered a case involving the nipple (unpublished observation GD). Histopathologically, the tumor exhibits features more reminiscent of eccrine poroma than syringoma. Multiple elongated thin anastomosing epithelial cords extending downward from the epidermis and encased in an inflammatory cell-rich fibrovascular stroma characterize the tumor. The cords contain ductular lumens lined by an eosinophilic cuticle (Fig. 25.30a, b) [149, 150].

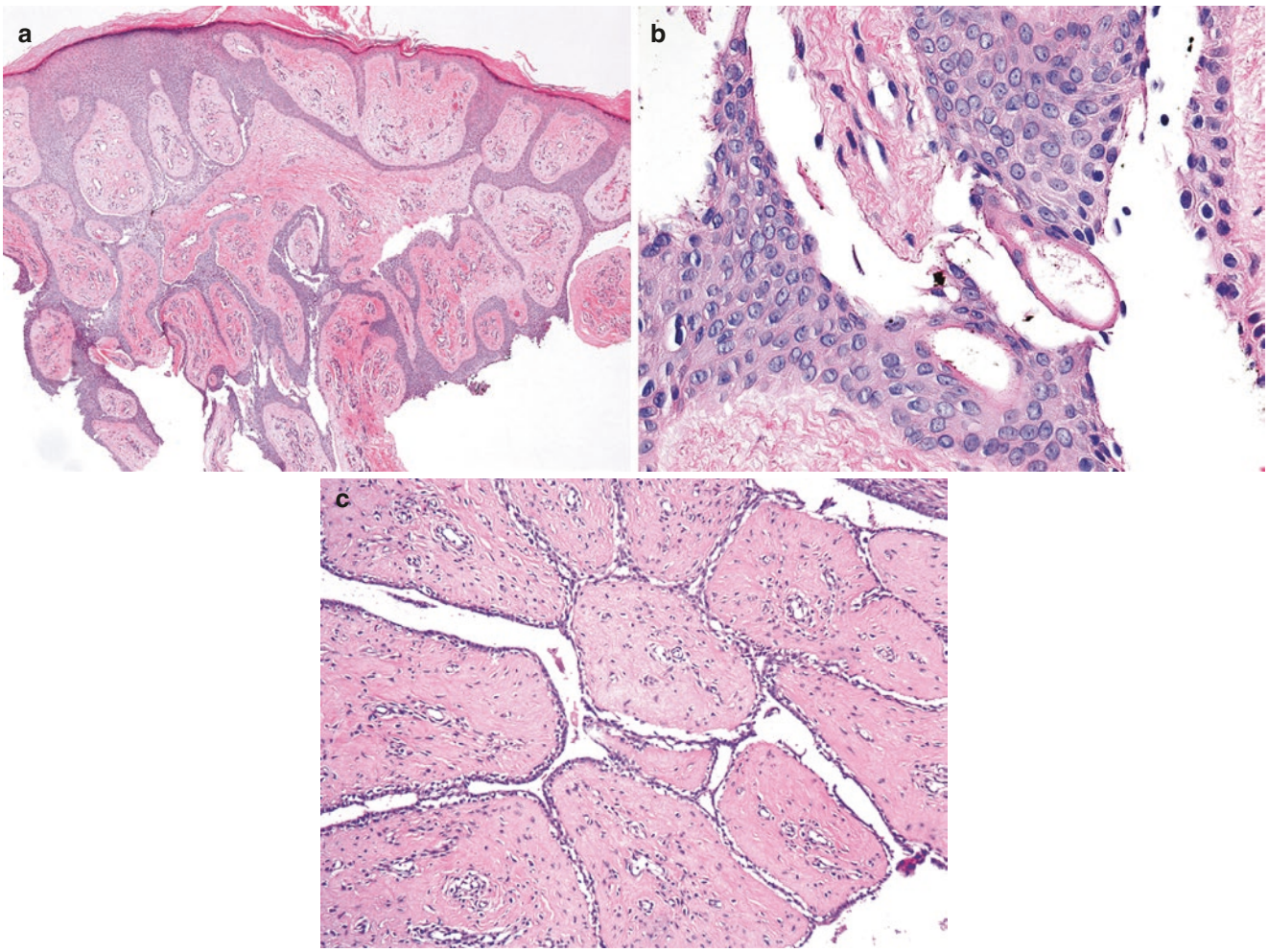

Fig. 25.30 Syringofibroadenoma. (**a**) Numerous thin anastomosing cords of basaloid cells extend downward from an ulcerated epidermal surface. The cords are surrounded by an inflammatory cell-rich fibrovascular stroma. (**b**) On high magnification, the tumor strands contain ductular lumens lined by an eosinophilic cuticle. (**c**) Fibroadenoma

Mammary Differential Diagnosis Fibroepithelial lesions. An intracanalicular fibroadenoma might resemble this lesion on a CNB if the epidermis is not sampled (Fig. 25.30c). Lack of a stromal component, as well as an adjacent inflammatory infiltrate, is suggestive of a syringofibroadenoma.

Eccrine Cylindroma

Eccrine cylindroma is a benign eccrine neoplasm that most commonly presents as a solitary nodule on the face, head, and neck of young adults. Multiple tumors are associated with Ancell-Spiegler syndrome, an autosomal dominant syndrome mapped to the *CYLD1* gene on chromosome 16q12-13 [151, 152]. A rare form arising in the breast parenchyma is morphologically and immunohistochemically identical to its cutaneous counterpart [153]. The tumor is characterized by angular nests that are molded to one another in a "jigsaw puzzle" configuration (Fig. 25.31a). The nests are surrounded by dense eosinophilic basement membrane material, a most helpful finding when evaluating limited sampling of a CNB. Globules of this material are frequently scattered within the nests, which stain bright pink with PAS stain with diastase. The nests are composed of two cell populations: compact basaloid cells and polygonal cells with amphophilic cytoplasm. Nucleoli are inconspicuous, and mitotic activity is rare. Retraction artifact between the tumor and stroma is absent. Small buds of tumor trailing off from the main lesion are common and should not be interpreted as malignant transformation. IHC staining will reveal the basaloid cells to express p63 and the amphophilic cells to express CK7. The tumor cells are consistently negative for ER, PR, and HER2 [154].

Mammary Differential Diagnosis Adenoid cystic carcinoma of the breast (Fig. 25.31b): Tumor nests can range from solid to cribriform and often contain basement membrane-like material. An infiltrative pattern, cytologic atypia, mitoses, and expression of CD117 distinguish this tumor from a cylindroma. Note that collagenous spherulosis demonstrates basement membrane-like deposition. The cutaneous and mammary forms of cylindroma are morphologically indistinguishable, but the lesion is extremely rare in the breast.

Eccrine Spiradenoma

Eccrine spiradenoma is a benign neoplasm most commonly arising on the ventral surfaces of the upper body of young adults that presents as a solitary skin-colored or bluish painful nodule [155]. There is substantial histopathological and IHC overlap with eccrine cylindroma. Features present in spiradenoma include the presence of tubuloalveolar structures (Fig. 25.32a) and intratumoral vascular spaces that may become dilated and filled with lymphatic fluid. Additionally, the tumor nests are permeated by mature lymphocytes [156] (Fig. 25.32b) but lack the "jigsaw puzzle" configuration of cylindroma.

Mammary Differential Diagnosis Ductal carcinoma in situ: Note that microluminal structures can be present in ductal carcinoma in situ, which are morphologically similar to the tubuloalveolar structures present in a spiradenoma. Peripheral p63 expression and nuclear atypia are distinguishing features.

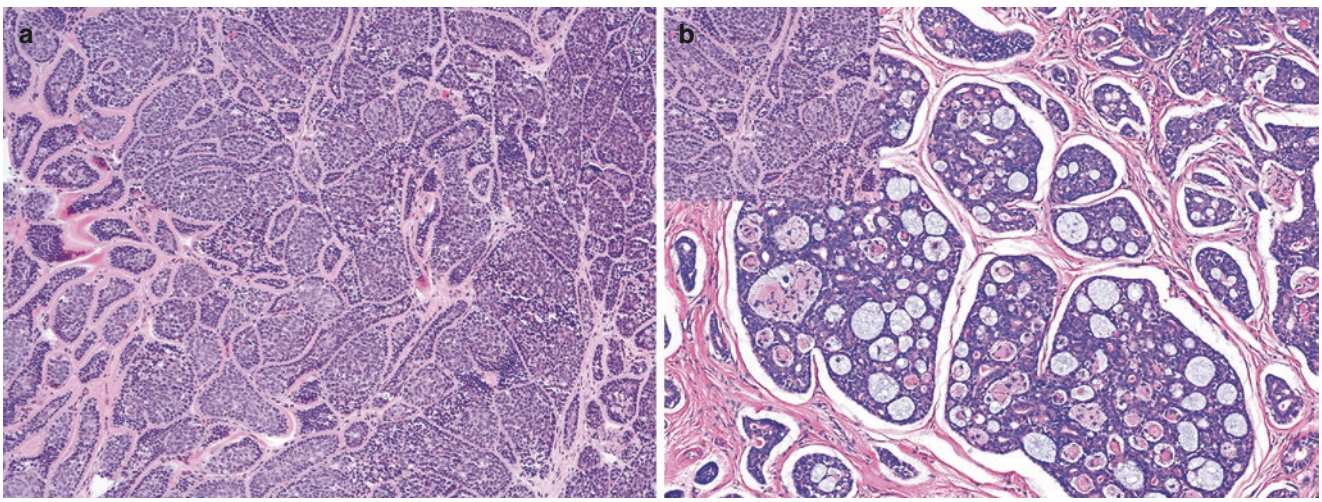

Fig. 25.31 Cylindroma. (**a**) Basaloid lobules molded against one another in a "jigsaw puzzle" configuration. The lobules are encased by a band of dense eosinophilic hyalinized stroma. (**b**) Adenoid cystic carcinoma of the breast

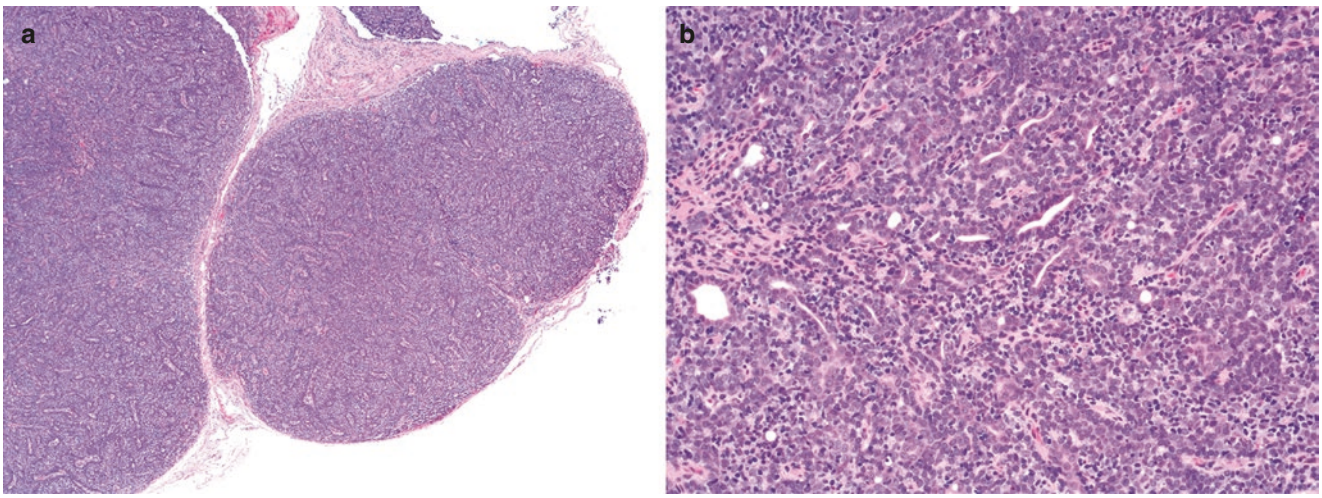

Fig. 25.32 Eccrine spiradenoma. (**a**) Well-circumscribed basophilic nodule in the dermis. (**b**) The tumor is composed of amphophilic glandular cells infiltrated by numerous lymphocytes

Eccrine Hidradenoma

Hidradenoma (acrospiroma) is a benign tumor most frequently presenting as a solitary nodule or cystic lesion at essentially any location. Although the pathogenesis is uncertain, most cases exhibit eccrine differentiation [157]. Rare cases with apocrine, squamous, and mucinous differentiation have been reported [158–160]. Approximately 50% of cases harbor the chromosomal translocation t(11:19) with *CRTC1-MAML2* fusion gene, particularly the clear-cell variant. An additional subset of tumors may exhibit the chromosomal translocation t(6:22). Rare cases arising within the breast parenchyma with a t(11:19) translocation have been reported [161]. This raises the question of whether hidradenomas have a counterpart in the breast, specifically mucoepidermoid carcinoma, which has been found to demonstrate similar morphologic and genetic features (see Chap. 12). The tumor is characterized by well-circumscribed nodules surrounded by fibrovascular or hyalinized stroma. Although they are occasionally connected to the overlying epidermis, they are usually centered in the deep dermis and sometimes the subcutis. The tumor nodules are predominantly solid, but areas with duct-like structures or cystic spaces may be present (Fig. 25.33a). The nodules are composed of a biphasic cellular population: round or polygonal cells with amphophilic cytoplasm containing vesicular nuclei, nuclear grooves and conspicuous nucleoli, and clear cells containing eccentric small hyperchromatic nuclei. The dominant cell type determines the designation of "nodular" versus "clear-cell" hidradenoma (Fig. 25.33b) [162–164]. Occasionally, the center of the tumor nodules may contain a densely hyalinized stroma, resulting in angular arrangements of the tumor lobules, thus imparting a "pseudoinvasive" growth pattern (Fig. 25.33c). Small nests may trail away from the main tumor nodule; however, this feature does not equate to hidradenocarcinoma (Fig. 25.33d). Mitoses are rare. Although local recurrence is rare, tumors that exhibit budding or irregular peripheral cords, focal nuclear pleomorphism, and increased mitoses (1–2 per 10 high-power fields) should be re-excised to exclude well-differentiated hidradenocarcinoma, which most commonly arises within benign precursor tumors [165]. IHC stains reveal the tumor cells to express p63 and CK AE1/AE3 with luminal staining for EMA and CEA. A PAS stain will highlight the clear cells, consistent with glycogen accumulation.

Mammary Differential Diagnosis Invasive or in situ ductal carcinoma with apocrine or clear-cell features (Fig. 25.33e). Mitoses are not easily found within the usual hidradenoma. Diffuse positivity for p63 in hidradenoma is a helpful distinguishing feature.

Hidradenocarcinoma

Hidradenocarcinoma is a rare eccrine neoplasm that predominantly arises on the face and extremities; however, lesions of the chest wall and breast have been reported [166]. The tumor can arise de novo or as malignant transformation from a preexisting benign hidradenoma. In contrast with their benign counterparts, the chromosomal translocation t(11:19), but not t(6:22), has been reported [167]. A high rate of local recurrence as well as mortality is described. As expected, the tumor is similar to hidradenoma but exhibits enhanced cytologic atypia, an infiltrative growth pattern, tumor necrosis, and high mitotic rate. Central comedo necrosis has been documented (Fig. 25.34a). Cytologic atypia may range from mild to anaplastic [168]. IHC will reveal tumor cell expres-

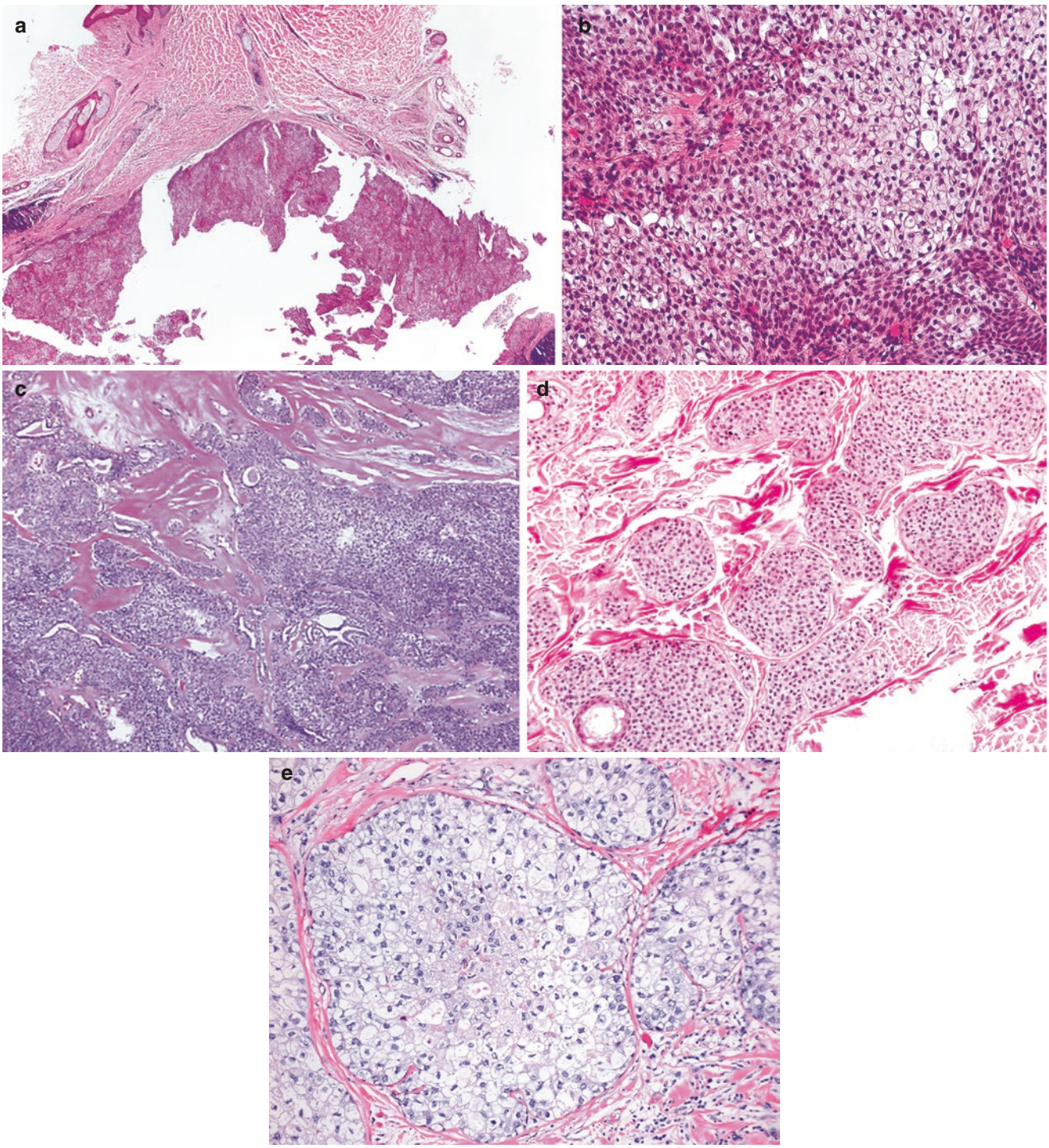

Fig. 25.33 Nodular and clear-cell hidradenoma (acrospiroma). (**a**) Well-circumscribed nodule composed of monomorphic cells with amphophilic cytoplasm surrounded by a condensed collagenous stroma. (**b**) High-power view of the tumor cells containing clear cytoplasm. (**c**) Occasionally, centralized dense hyalinized stroma may result in architectural disorganization of the tumor cells, creating a "pseudoinvasive" growth pattern (Reproduced from Desman GT, Ozerdem U, Shin SJ. Neighboring look-a-likes: Distinguishing between breast and dermatologic lesions. Adv Anat Pathol. 2014;21:228–247, with permission of Wolters-Kluwer Health). (**d**) This pattern mimics a ductal carcinoma in situ, solid type. (**e**) Ductal carcinoma in situ with clear-cell features

sion for CK AE1/AE3, CK5, CK7, p53, p63, CEA (focal), androgen receptor, EGFR, ER, MUC5AC, and strong/diffuse membranous staining for HER2 [169]. Ki-67 staining of greater than 10% of tumor nuclei warrants classification as adenocarcinoma. Although IHC staining for HER2 is frequently positive, amplification of the oncogene as demon-

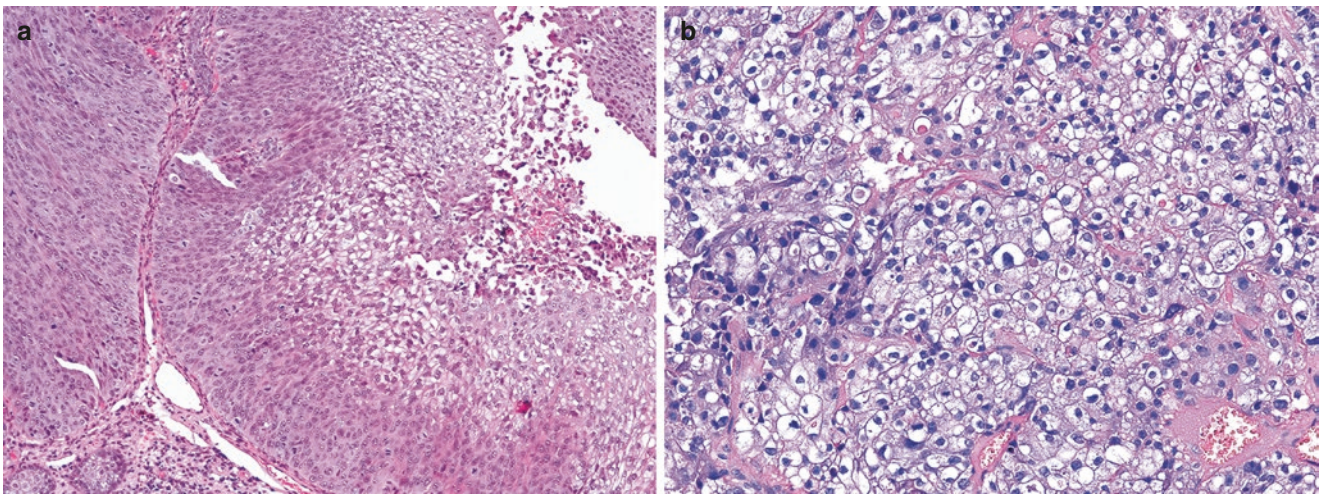

Fig. 25.34 Clear hidradenocarcinoma. (**a**) Marked cytologic atypia, numerous mitoses, and central comedo-like necrosis. (**b**) Invasive ductal carcinoma with clear-cell features

strated by FISH is rare, suggesting a limited therapeutic importance [166].

Mammary Differential Diagnosis Depending on the sampled area of tumor, invasive ductal carcinoma with clear-cell features (Fig. 25.34b) and DCIS, comedo type, should be considered. Immunostains p63 and CK5/6 can be helpful, as hidradenocarcinoma should be diffusely positive for both markers.

Microcystic Adnexal Carcinoma

Microcystic adnexal carcinoma (MAC), also referred to as sclerosing sweat duct (syringomatous) carcinoma, is a locally aggressive adnexal carcinoma with both sweat duct and follicular differentiation. These tumors involve the skin of the head (i.e., nasolabial and periorbital regions) and may rarely involve the axilla and breast [170]. An association with prior radiation therapy, as well as increased incidence in females, has been described [171]. A slow-growing, flesh-colored, hard plaque or nodule with an occasional central dell characterizes the tumor. Painful nodules may indicate perineural invasion. The margins are typically difficult to delineate by palpation. Although local recurrence is common after wide excision, distant metastasis is extremely rare [172]. Histopathologically, the superficial portions of the tumor are similar to syringoma, as it shows round cystic and comma-shaped structures embedded within fibrous stroma (Fig. 25.35a). Unlike syringoma, the cells frequently have a slight basaloid quality with rare mitoses and necrotic cells. The cystic structures may contain either keratinous or amphophilic secretions. The most important diagnostic feature is that as the tumor cells become more invasive as they descend into the deep dermis and subcutaneous fat, even involving skeletal muscle, tiny cell clusters and cords with focal lumen formation characterize these deep foci (Fig. 25.35b). Perineural invasion is common. Immunohistochemistry reveals basal cell expression of p63, CK5/6 (Fig. 25.35c), and D2-40 and luminal cell expression of EMA and CEA [23, 24, 114]. Rarely, the tumor cells may also express CK15 and BerEP4. Ki-67 will reveal a low mitotic index [173, 174]. GCDFP-15 and mammaglobin are negative [9].

Mammary Differential Diagnosis Syringomatous tumor and low-grade adenosquamous carcinoma. Syringomatous tumor commonly arises in the nipple and shows a less infiltrative growth pattern as well as bland cytologic features with the absence of mitoses and necrosis (Fig. 25.27c). Low-grade adenosquamous carcinoma commonly arises deeper within the breast parenchyma and lacks perineural invasion (Fig. 25.35d). Immunostains are not helpful, as both lesions can show p63 and CK5/6 positivity [175, 176].

Squamoid Eccrine Ductal Carcinoma

Squamoid eccrine ductal carcinoma is an extremely rare tumor arising as a solitary nodule in elderly adults. These tumors most commonly arise on the extremities, head and neck area, and occasionally the trunk [177]. Local recurrence is common; however, distant metastasis or death from disease has not been reported. Microscopically, these tumors are characterized by poorly demarcated and infiltrative cords extending into the deep dermis and subcutaneous tissue. The tumor may connect with the overlying epidermis or hair fol-

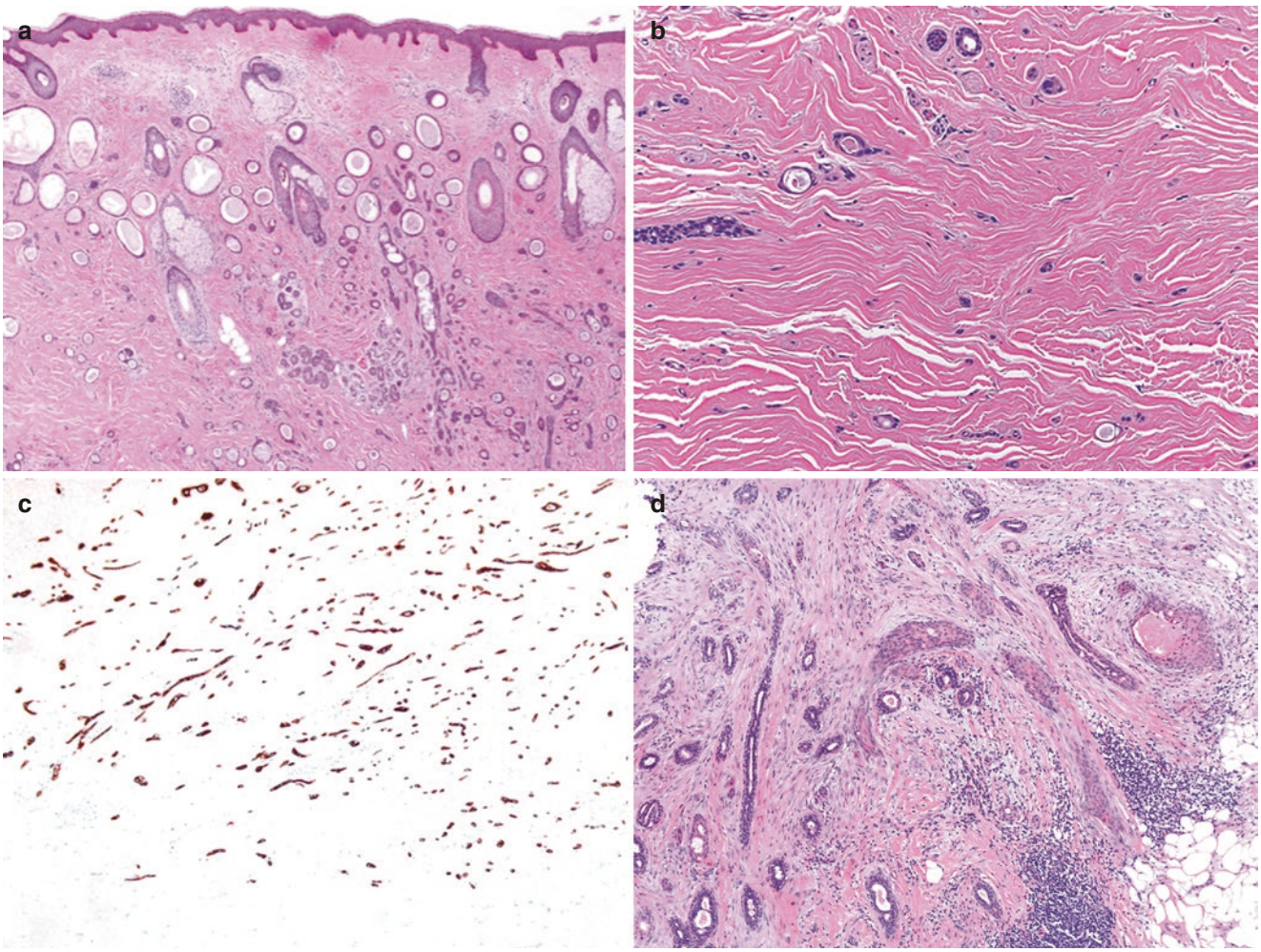

Fig. 25.35 Microcystic adnexal carcinoma. (**a**) Note the round cystic structures embedded within fibrous stroma. At this level of the epidermis, the distinction between benign syringoma and MAC is not possible. (**b**) Deeper aspect of the tumor where the tubules become smaller and convert into cords and small clusters as they descend into the dermis. (**c**) The tumor cells express CK5/6, which is sometimes helpful in margin assessment. (**d**) Low-grade adenosquamous carcinoma of the breast. ((**b**) Reproduced from Desman GT, Ozerdem U, Shin SJ. Neighboring look-a-likes: Distinguishing between breast and dermatologic lesions. Adv Anat Pathol. 2014;21:228–247, with permission of Wolters-Kluwer Health)

licles. The cells of the superficial portion of the tumor exhibit extensive squamous differentiation with squamous eddies, horn cysts, and ductal structures (Fig. 25.36). The deeper portion shows an infiltrative pattern characterized by small cords containing cuticle-lined luminal structures and intracytoplasmic vacuoles, reminiscent of microcystic adnexal carcinoma. Mitoses and perineural invasion are common, but lymphovascular invasion is rare. IHC staining reveals the tumor cells to express p63 and CK5/6 and luminal expression of CEA and EMA, confirming sweat duct differentiation [178].

Mammary Differential Diagnosis SCC of the breast and metaplastic carcinoma with squamous differentiation: Clinical correlation is necessary for the diagnosis. In small biopsy samples, the distinction might not be possible.

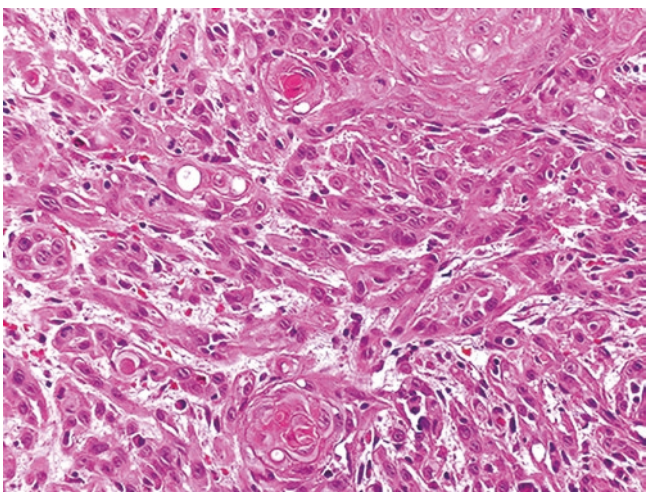

Fig. 25.36 Squamoid eccrine ductal carcinoma. Infiltrate cords of squamous cells with squamous eddies and small luminal structures

Adenoid Cystic Carcinoma of the Skin

Primary cutaneous adenoid cystic carcinoma (AdCC) is an extremely rare neoplasm most commonly arising on the scalp or chest. Lesions present as a slow-growing yet locally aggressive nodule or plaque. Equivalent lesions are found in other organ systems, such as the salivary glands, breast, respiratory tract, and genitourinary tract [179, 180]. Unlike salivary gland tumors, primary cutaneous tumors have a lower recurrence rate of 50% and rarely metastasize. Histopathologically, these tumors are characterized by clusters of basaloid cells arranged as tubules, elongated cribriform nests, solid nests, or cords within the dermis or subcutis without epidermal attachment. The tumor cells are believed to be of eccrine derivation and lack peripheral nuclear palisading and stromal retraction artifact. Although malignant, mitoses are rare. The cribriform pattern is the most common and diagnostically distinctive. The nests are surrounded by PAS-D-positive basement membrane material with small globules scattered within the nests. In addition to true luminal spaces, pseudoluminal spaces filled with hyaluronic acid (dermal mucin) will stain with Alcian blue or colloidal iron. The reported immunophenotype is positive expression of p63, p40, CK5/6, CK7, CD117, variable mammaglobin, GATA3, ER, PR, and S100 protein, and negative GCDFP-15, CK20, D2-40, and calretinin [6, 18, 26, 40, 181–187]. Variable true luminal staining for EMA, CEA, and SMA has been reported [186].

Mammary Differential Diagnosis Adenoid cystic carcinoma of the breast (Fig. 25.37): The morphology and immunophenotype are similar in all locations. Clinical and radiologic confirmation of the tumor location is paramount.

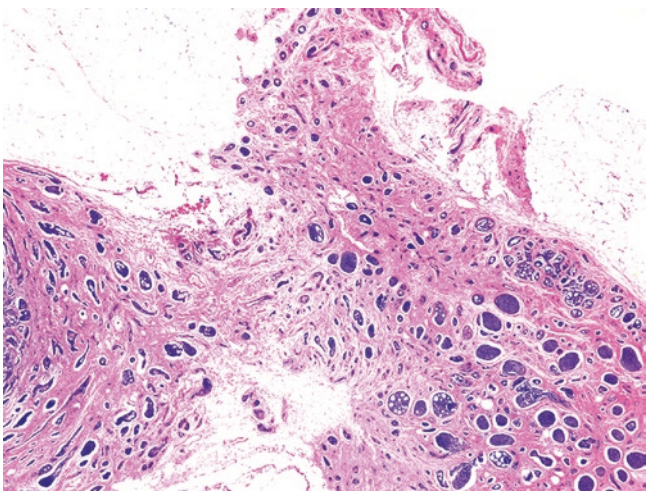

Fig. 25.37 Adenoid cystic carcinoma of the breast. Nests of basaloid cells with a solid or cribriform pattern

Eccrine Adenocarcinomas that Histologically Simulate Metastatic Tumors

While some eccrine carcinomas may resemble and arise within preexisting benign eccrine neoplasms, others do not have a benign counterpart and show a generic carcinoma histomorphology. In the latter scenario, the distinction from visceral metastasis may be impossible. In general, these de novo eccrine carcinomas most commonly arise on the head and neck as well as the extremities. The only two de novo eccrine adenocarcinomas with distinctive histomorphology that have been reported to arise within the breast or axilla are ductal eccrine adenocarcinoma (DEA) and primary cutaneous signet ring cell carcinoma. Primary cutaneous signet ring cell carcinoma is extremely rare.

Ductal Eccrine Adenocarcinoma

Ductal eccrine adenocarcinoma (DEA) is perhaps the most common of the de novo eccrine carcinomas. Several cases involving the breast have been reported [188]. They present as a solitary, slow-growing mass that may be present for months to years before clinical detection. Despite this, they exhibit an aggressive clinical course, with a relatively high rate of local recurrence (70%), distant metastasis (50%), and disease-related mortality (70%) [189]. The tumor is characterized by infiltrative solid nests, cords, or tubules composed of atypical basaloid polygonal cells embedded within a desmoplastic stroma (Fig. 25.38a). Involvement of eccrine ducts and colonization of the overlying epidermis have been reported, which is a helpful finding in distinguishing these tumors from metastatic disease. Tumor cells frequently contain small intracytoplasmic vacuoles. Necrotic tumor cells and numerous mitoses are usually present. The squamoid eccrine ductal carcinoma variant shows areas of squamous differentiation that resemble SCC; however, the tumor demonstrates a markedly improved clinical outcome [190]. IHC stains will reveal the tumor cells to express EMA, cytokeratin, p63 (Fig. 25.38b), luminal CEA, and variable expression of ER, PR, HER2, S100 protein, and GCDFP-15 [12, 191, 192].

Mammary Differential Diagnosis Invasive ductal carcinoma, poorly differentiated (Fig. 25.38c): Morphologic features are virtually identical. IHC stain for p63 might be helpful, but note that basal-like breast carcinomas may show some positivity. When evaluating skin lesions, note that metastatic breast carcinoma typically presents as rapidly enlarging crops of multiple nodules [193].

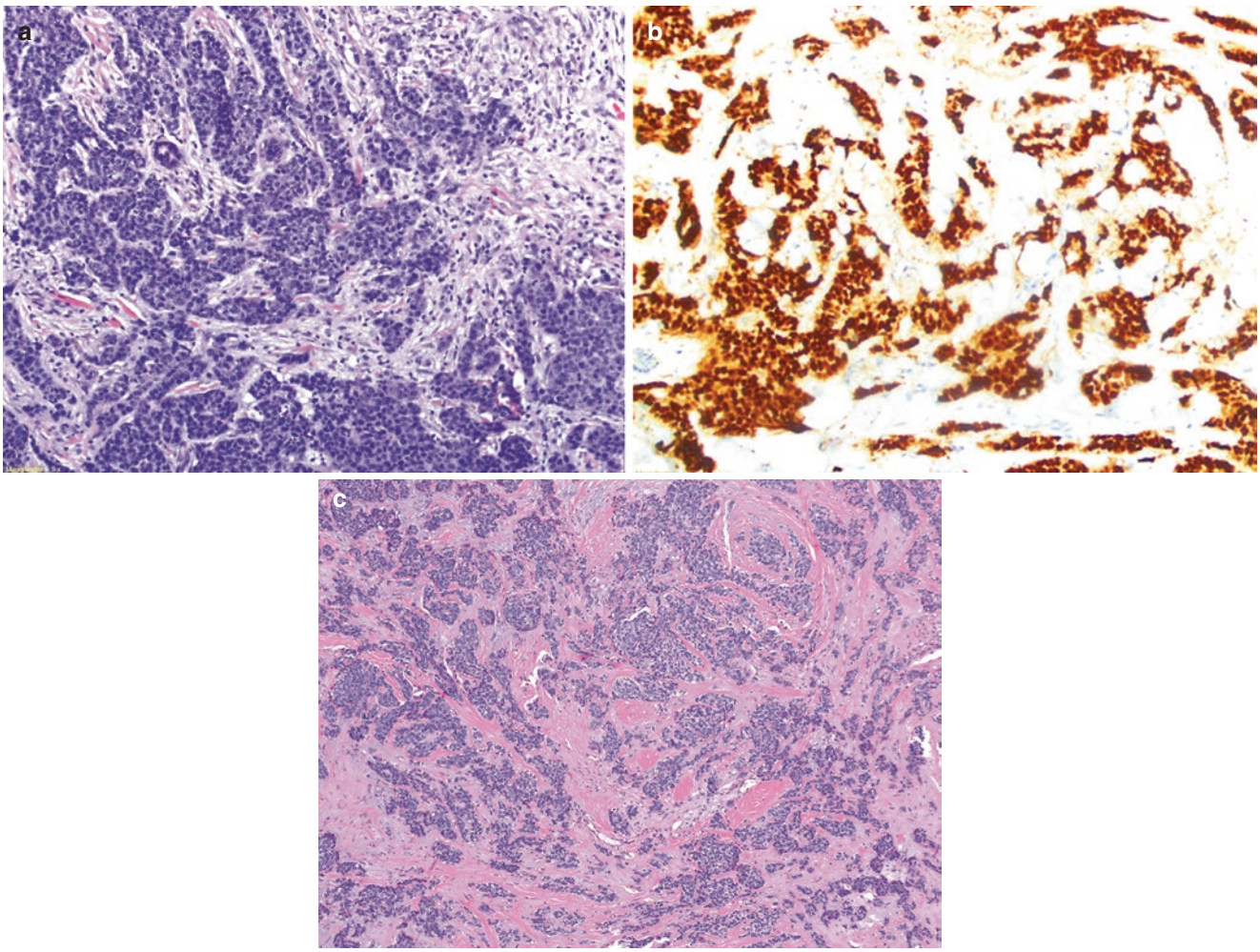

Fig. 25.38 Ductal eccrine adenocarcinoma. (**a**) Invasive nests and cords of basaloid cells embedded within a desmoplastic stroma. Note the focus forming a duct-like structure (upper left). (**b**) IHC stain for p63 reveals strong nuclear staining. (**c**) Invasive ductal carcinoma, poorly differentiated

Extramammary Paget Disease

Extramammary Paget disease can present in the skin of the breast as a manifestation of a cutaneous apocrine carcinoma and should be evaluated in the differential diagnosis of Paget disease of the nipple. Please see Chap. 19 for more information of this entity.

Paget Disease of the Skin, Apocrine Type

Extramammary Paget disease typically involves the vulva, perianal region, scrotum, and occasionally the penis [194]. The pathogenesis of extramammary Paget disease remains controversial, but a classification into primary and secondary forms has been proposed. In primary extramammary Paget disease, there is no association with an underlying adenocarcinoma. Some authors propose that the malignant cells originate within the epidermis by the proliferation of primitive native stem cells with the potential for glandular differentiation [195]. However, since the malignant cells exhibit features of apocrine differentiation, other authors argue in favor of an origin from cutaneous apocrine cells [196–198]. In secondary extramammary Paget disease, the lesion is most commonly attributed to epidermotropic metastasis of colorectal or urothelial carcinomas [199, 200]. Rarely mentioned in the literature is the fact that many primary cutaneous malignant adnexal neoplasms may seed epidermotropic metastases to the skin. Apocrine carcinomas are the most common tumors of origin; however, sebaceous and eccrine carcinomas have also been reported to manifest as Paget disease [201, 202].

Clinically, both extramammary and mammary forms of Paget disease present as red and eczematous scaling lesions on the involved areas of skin. The most common location for sweat carcinoma-associated Paget disease is the axilla [203].

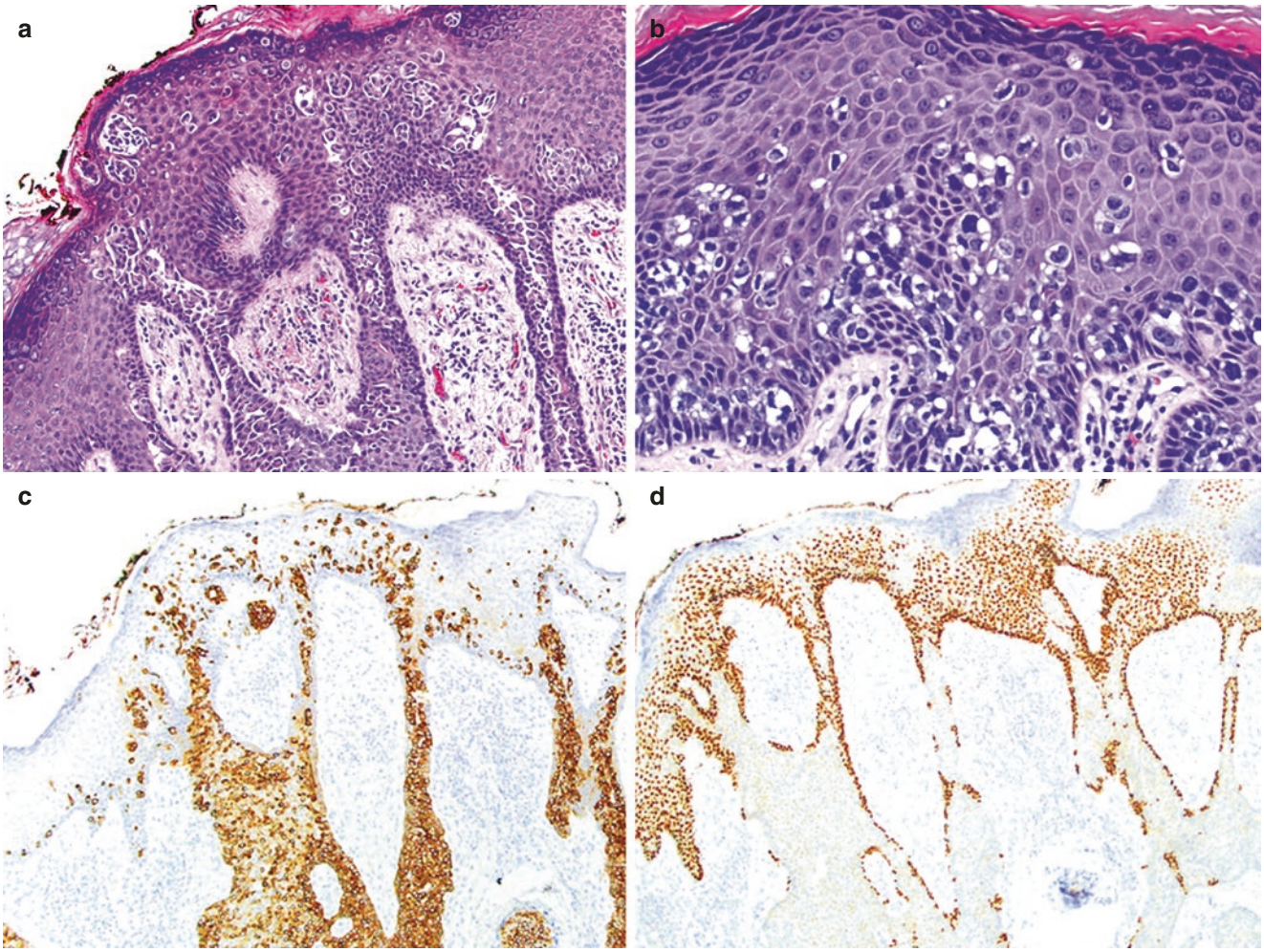

Fig. 25.39 Ductal apocrine adenocarcinoma with overlying Paget disease. (**a**) Malignant cells colonize the sweat ducts and infiltrate the epidermis in a scattered "buckshot" distribution. (**b**) The malignant epithelioid cells are scattered throughout the epidermis with a distinct cytomorphology from the adjacent keratinocytes. (**c**) CK7 is strongly and diffusely positive in the tumor cells. (**d**) The epidermal keratinocytes and peripheral cells of the sweat ducts express p63, but the tumor cells are negative. ((**a**–**d**) Reproduced with permission from McGraw Hill Education; Barnhill's Dermatopathology Challenge, by Garrett T. Desman and Raymond L. Barnhill)

The histopathologic features for both types include the presence of scattered large epithelioid cells arranged in the epidermis in a "buckshot" distribution (Fig. 25.39a). The cells are dispersed singly or in small clusters, have pale amphophilic and vacuolated cytoplasm, and contain eccentrically placed nuclei with vesicular chromatin (Fig. 25.39b). The overlying epidermis is frequently acanthotic with overlying hyperkeratosis. The histochemical stains PAS, mucicarmine, and Alcian blue will usually highlight intracytoplasmic mucin. IHC stains reveal the tumor cells of primary extramammary and mammary Paget disease to express AE1/AE3, CK7, Cam 5.2, and EMA (Fig. 25.39c). Staining for CEA is variable. GCDFP-15 is usually positive in primary extramammary and mammary Paget disease but negative in secondary disease [204–210]. The forms of Paget disease with apocrine differentiation (mammary, primary extramammary, and apocrine carcinoma associated) are typically negative for p63 expression (Fig. 25.39d). Additionally, the majority of these cases are also negative for PR and ER but positive for AR and HER2 [211–216].

Mammary Differential Diagnosis When evaluating a skin shave biopsy of the nipple with Paget disease, clinical and radiological correlation is necessary to exclude a visceral malignancy and identify a mammary primary.

Neuroendocrine Tumors

Merkel Cell Carcinoma

Merkel cell carcinoma (cutaneous neuroendocrine carcinoma) is an uncommon tumor that arises in chronically

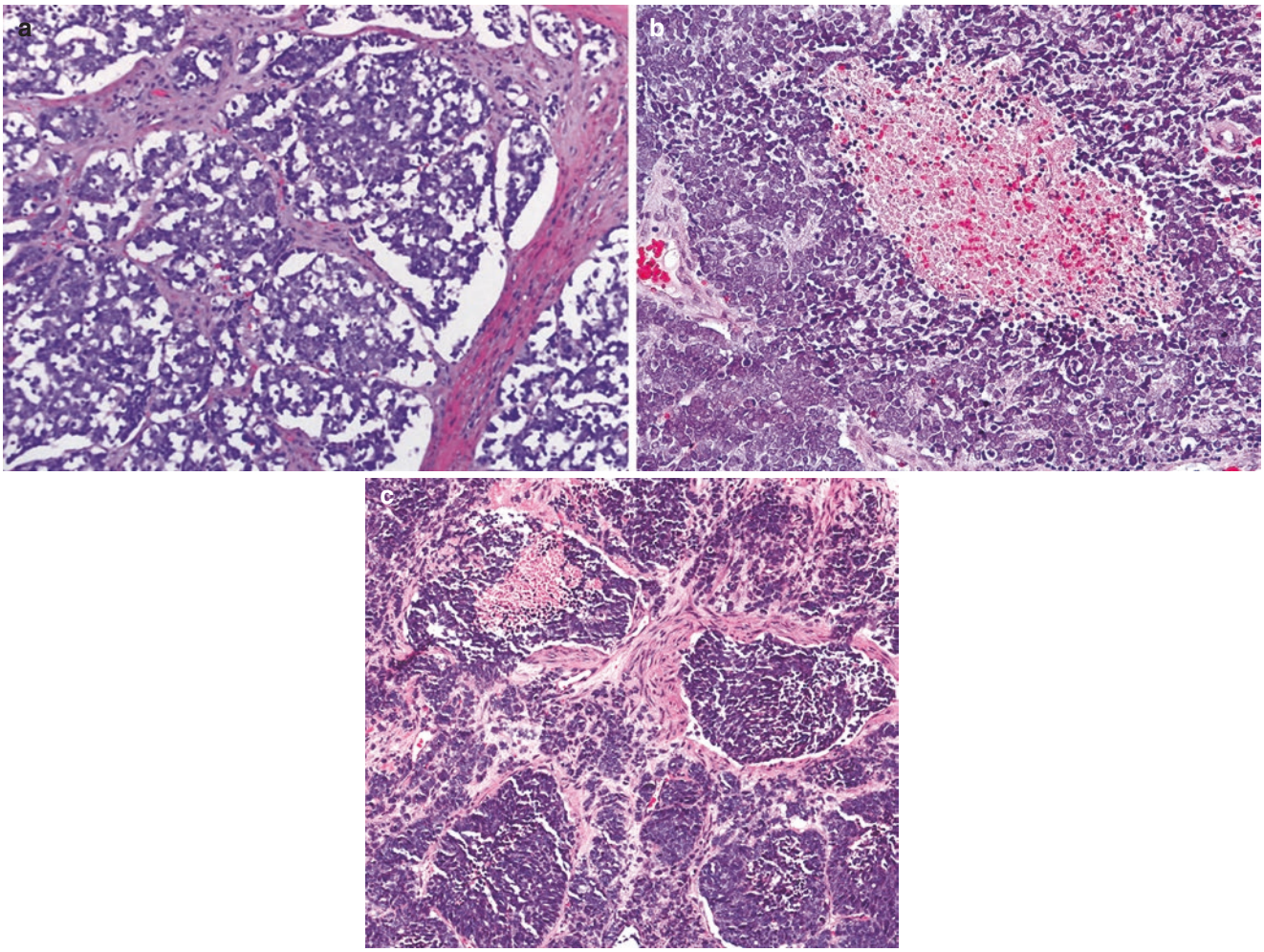

Fig. 25.40 Merkel cell carcinoma. (**a**) Dyscohesive nodular aggregate of basophilic cells with fine granular chromatin and nuclear molding. (**b**) Central focus of tumor cell necrosis. (**c**) Mammary small-cell carcinoma. (Reproduced from Desman GT, Ozerdem U, Shin SJ. Neighboring look-a-likes: Distinguishing between breast and dermatologic lesions. Adv Anat Pathol. 2014;21:228–247, with permission of Wolters-Kluwer Health)

sun-damaged skin. They present in elderly Caucasian patients as a firm raised painless nodule that usually measures 2 cm or less in diameter and slowly increases in size. The head, neck, and extremities are the most common sites, but any location may be affected [217]. Ulceration is uncommon. They are highly aggressive, with a local recurrence rate of approximately 40% and a 5-year survival rate for stage I disease of only 81%. Wide local excision combined with adjuvant radiotherapy may improve locoregional control of the disease, as well as relapse-free survival. Sentinel lymph node biopsy is now recommended due to the high incidence of lymph node metastasis. Evaluation of sentinel lymph nodes with IHC stains for CK20 and Cam5.2 greatly increases diagnostic sensitivity. The precise pathogenesis is unknown; however, there is a higher incidence in patients with chronic UV radiation exposure and immunosuppression [218]. Recently, the presence of Merkel cell polyomavirus (MCV) has been found in a significant subset of these tumors [219]. Of note, although JC and SV40 polyomaviruses have been reported in a minority of breast carcinomas [220, 221], MCV has yet to be reliably demonstrated in breast carcinomas [222, 223].

Microscopically, the tumor is characterized by dermal nodules composed of basophilic cells with vesicular nuclei containing small nucleoli. Nuclear molding, crush artifact, individual tumor cell necrosis, and numerous mitoses are common (Fig. 25.40a, b). Growth patterns include nodular and trabecular, the latter showing dissecting tumor cells in between collagen bundles. Intraepidermal colonization of tumor cells may be seen in up to 10% of cases. Merkel cell carcinoma shows a characteristic Cam5.2 and CK20 dot-like positivity, as well as positivity with neuroendocrine markers (neuron-specific enolase (NSE), chromogranin, synaptophysin, and CD56), variable p63 positivity [224], and negative

GATA3, vimentin, and S100 protein. Rare cases may express CK7 and TTF-1, complicating the distinction from a metastatic small-cell carcinoma of the lung [225].

Mammary Differential Diagnosis Mammary small-cell carcinoma (Fig. 25.40c) shares an immunophenotype similar to small-cell carcinomas at other locations, including positive Cam5.2, CK7, TTF-1, synaptophysin, chromogranin, CD56, and BCL2 and negative CK20. They are usually positive for ER and PR and negative for HER2 [226, 227]. Of note, primary lung small-cell carcinomas are negative for CK7. However, clinical exclusion of other primary sites is necessary for the diagnosis.

Other types of mammary carcinoma, such as solid papillary carcinomas and mucinous carcinomas, can express neuroendocrine markers. However, mammary neoplasms do not express CK20 [11]. Of note, PAX5 and PAX8 are strongly positive in a majority of Merkel cell carcinomas [41, 228], but they are negative in breast carcinomas, with few exceptions [41, 229, 230]. Correlation of histomorphology with clinical and radiographic findings is essential.

Melanocytic Proliferations

Melanocytic proliferations of benign, atypical, and malignant types can occur within the skin of the breast. It is beyond the scope of this chapter to describe all the different entities, but a few general concepts will be discussed that could represent potential diagnostic pitfalls in selected cases. Although most of these entities will present clinically as a pigmented skin lesion, suffice it to say that even partially sampled benign melanocytic nevi by core needle biopsy could potentially resemble mammary carcinoma (Fig. 25.41a). In general, melanocytic proliferations (benign and malignant) are the

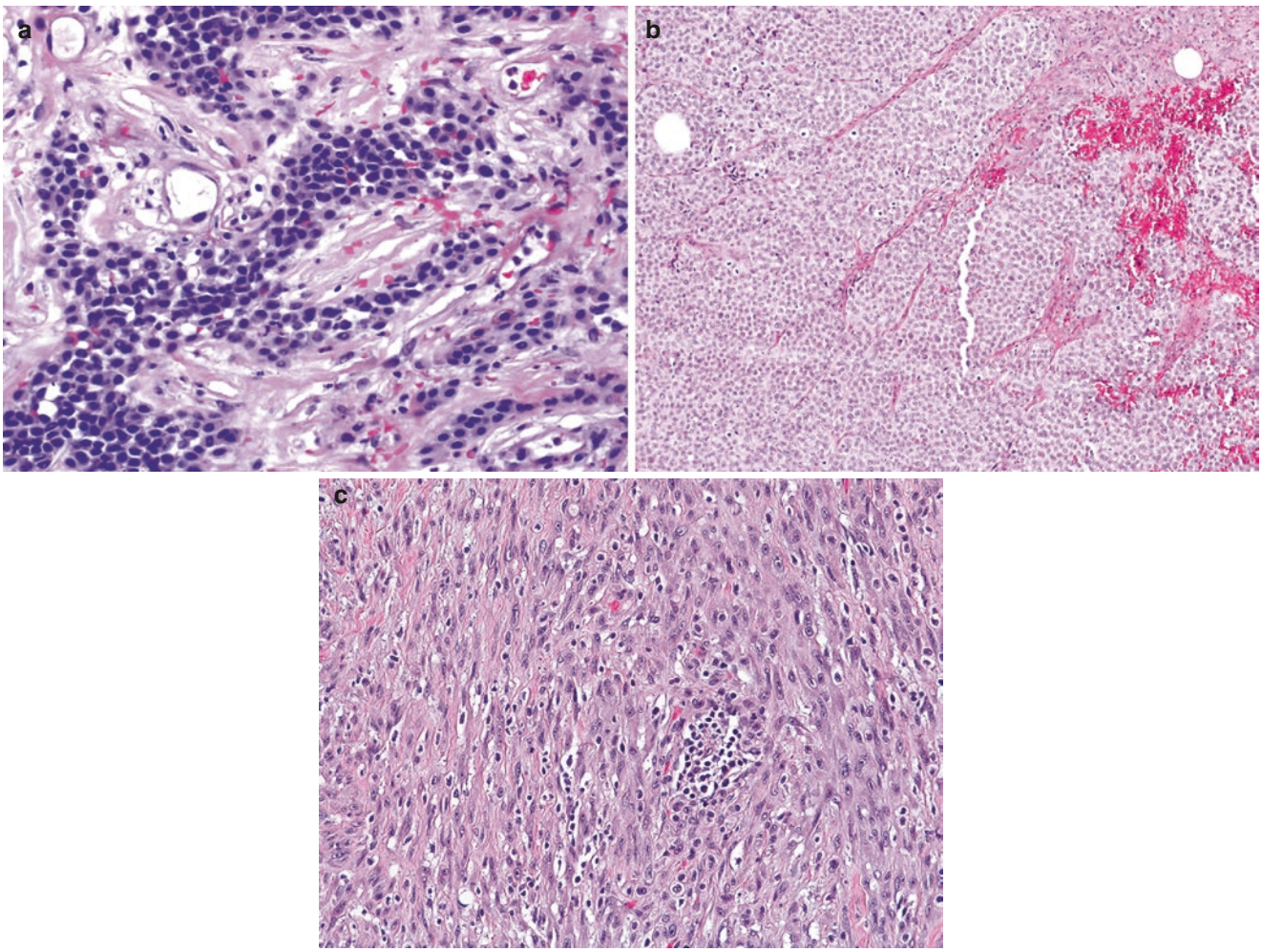

Fig. 25.41 Melanocytic proliferations. (**a**) Benign intradermal melanocytic nevus with loosely arranged nests of epithelioid cells with intercellular retraction spaces. Close inspection reveals rare cells containing melanin pigment. (**b**) Nodular melanoma with expansive sheets and lobules of epithelioid cells. Numerous mitoses and necrotic tumor cells are present. (**c**) Desmoplastic melanoma characterized by scattered spindle cells embedded within a dense sclerotic stroma

only tumors that produce melanin pigment, which can be highlighted with a Fontana-Masson stain. Malignant melanoma is known as "the great histopathologic mimic," since it may manifest a wide range of histomorphologic features. In cases with limited sampling, the presence of dermal mitotic activity and cytologic atypia are the most specific features of melanoma (Fig. 25.41b). The most common type of melanoma that arises in the breast is the superficial spreading type. IHC staining will label the tumor cells with Melan-A/Mart-1, S100 protein, SOX10, HMB45, and MITF. Chronically, sun-damaged skin, such as the "V" area of the neck and chest, may develop lentiginous melanomas (lentigo maligna) and rarely desmoplastic melanomas [231, 232].

Desmoplastic melanomas are spindle cell melanomas with locally aggressive behavior and decreased metastatic potential compared to conventional melanoma (Fig. 25.41c). In excision specimens, in situ lentigo maligna may be present overlying this type of melanoma. Unlike conventional melanoma, desmoplastic melanoma is typically negative for Melan-A/Mart-1, HMB45, and MITF and only positive for S100 protein and SOX10 [233, 234].

Mesenchymal Tumors

Mesenchymal tumors are composed of varying proportions of spindle cells and extracellular matrix. The spindle cells may be monomorphic or pleomorphic, while the matrix may range from a composition rich in collagen (i.e., fibroma or collagenoma) to rich in hyaluronic acid (i.e., myxomas). Occasionally, the mesenchymal cells may exhibit an epithelioid cytomorphology. Histomorphology is most helpful in establishing benignity versus malignancy in these lesions. IHC staining also assists in establishing the various lines of cellular differentiation.

Fibrohistiocytic Tumors

Dermatofibroma

Dermatofibroma, also referred to as benign fibrous histiocytoma, most frequently presents as a firm papule on the extremities or trunk of middle-aged women [235]. Since these tumors frequently arise in association with trauma, there is debate as to whether or not they represent true neoplasms. Microscopically, these tumors are characterized by an ill-defined dermal proliferation of spindled cells that may extend into the subcutaneous fat. The uniform cells are arranged in a storiform pattern and may be admixed with focal foamy macrophages, dilated vessels, and scattered hemosiderin pigment. Despite the name, these tumors are not composed of fibroblasts but rather dermal dendritic cells. The most specific feature is found at the periphery of the tumors, where these cells wrap their dendritic processes around collagen bundles (collagen wrapping) (Fig. 25.42a). The cellular infiltrate may focally abut the subcutaneous fat, but true invasion into the subcutis should not be present. Uncommon variants include cellular fibrous histiocytoma, epithelioid fibrous histiocytoma, and atypical fibrous histiocytoma (dermatofibroma with monster cells). IHC stains will reveal positive tumor expression of factor XIIIa, D2-40, and stromelysin. Occasionally, SMA expression may be seen. There is no staining for CD34 or desmin [236, 237]. Additionally, the dendritic cells of dermatofibroma do not express ER, PR, or p63 (unpublished observation, GTD).

Mammary Differential Diagnosis Fibromatosis (Fig. 25.42b), fibromatosis-like spindle cell metaplastic carcinoma, myofibroblastoma (cellular or collagenized/fibrous variant), and pseudoangiomatous stromal hyperplasia (PASH): These entities share a similar morphology with dermatofibroma. Immunohistochemical stains are helpful in establishing the diagnosis. Fibromatosis is positive for

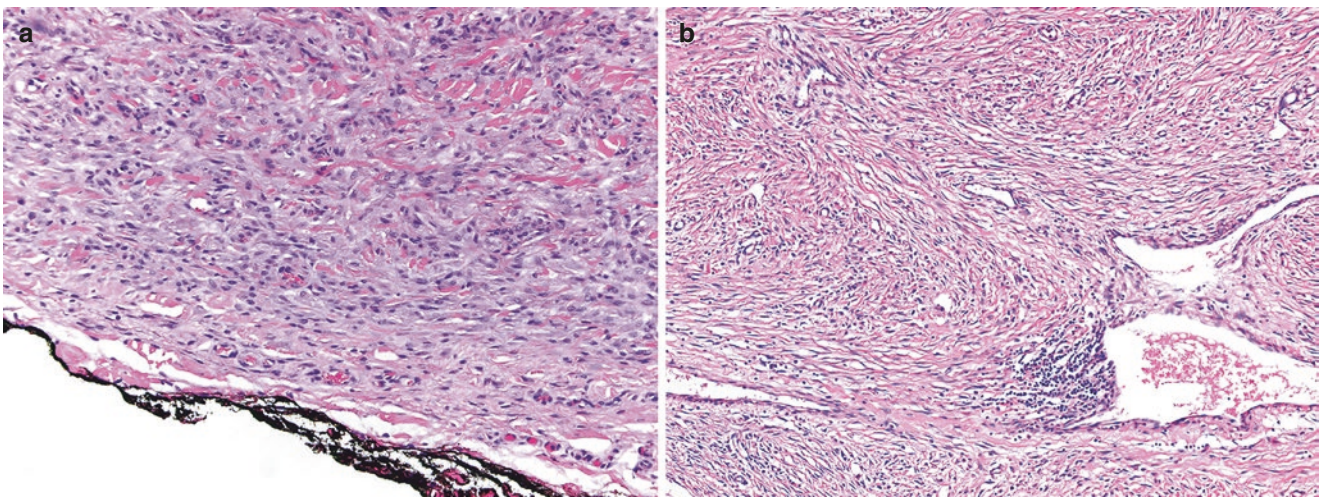

Fig. 25.42 (**a**) Dermatofibroma. The dermis contains a spindle cell proliferation with concomitant dermal sclerosis. The cells assume a vaguely whorled pattern within the dermis, and the cytoplasmic processes wrap around collagen bundles at the peripheral edge. (**b**) Fibromatosis of the breast

nuclear β-catenin and negative for factor XIIIa and D2-40. Fibromatosis-like spindle cell metaplastic carcinoma is immunoreactive for cytokeratins (e.g., CK 34βE12) and p63. Variable positivity for SMA and nuclear β-catenin staining can also be seen in these tumors. Myofibroblastoma is positive for CD34, desmin, CD99, ER, and SMA and negative for cytokeratin. PASH is positive for CD34 and variably immunoreactive for ER or PR.

Atypical Fibroxanthoma

Atypical fibroxanthoma is strongly associated with chronic UV light exposure and most commonly occurs on the head and neck; however, cases involving the chest have been described. Despite a seemingly malignant histopathology, atypical fibroxanthoma has little—if any—potential for distant metastasis when strict diagnostic criteria are applied [238]. Microscopically, these tumors exhibit relative symmetry and are well circumscribed at scanning magnification. Although the bulk of the tumor is located in the dermis, very superficial extension into subcutaneous fat may be seen. Intraepidermal involvement is absent, and a grenz zone is typically present. The presence of intraepidermal malignant cells should raise suspicion for either a desmoplastic/spindle cell melanoma or a pleomorphic/spindle cell SCC. The tumor cells are commonly arranged in a storiform pattern and consist of highly pleomorphic spindled and epithelioid forms with marked hyperchromasia, irregular nuclear outlines, and prominent nucleoli. Frequent bizarre multinucleated tumor giant cells and numerous mitoses with atypical forms are characteristics (Fig. 25.43). Inflammatory cells, including lipidized cells, are frequently seen within the tumor. The histopathological features that allow confident classification as an indolent atypical fibroxanthoma (compared to pleomorphic sarcoma, melanoma, or spindle cell SCC) are confinement to the dermis, absent tumor necrosis, and absent vascular invasion. If these strict criteria are followed, atypical fibroxanthoma may be regarded as benign neoplasms cured by simple excision [239, 240]. However, these essential parameters may be potentially absent in the limited sampling of a CNB, and therefore a complete excision is recommended for definitive diagnostic assessment.

By definition, atypical fibroxanthoma is negative for cytokeratin and S100 protein, excluding SCC and melanoma, respectively. Nonspecific markers that are commonly expressed include vimentin, α_1-antitrypsin, and α_1-antichymotrypsin. More specific markers include CD10, CD99, and calponin. Deeply invasive tumors raise the possibility of pleomorphic sarcomas including leiomyosarcoma (SMA+, desmin+), pleomorphic liposarcoma (S100 protein+), malignant peripheral nerve sheath tumor (CD56+, PGP9.5+, S100 protein+/), and pleomorphic rhabdomyosarcoma (myoglobin+, MyoD1+, SMA+, desmin+).

Mammary Differential Diagnosis Spindle cell metaplastic carcinoma: Findings including infiltrative growth, presence of in situ ductal component or admixed invasive ductal carcinoma, and expression of cytokeratins and p63 favor a metaplastic carcinoma.

Fibroblastic Tumors

Keloid

Keloids are common reactive lesions composed of exuberant scar tissue. They most commonly arise after trauma; however, spontaneous lesions may form on the chest. They typically present as well-circumscribed raised plaques and nodules that slowly enlarge over time [241]. The nodule is composed of thick hyalinized collagen bundles surrounded by scattered fibroblasts (Fig. 25.44).

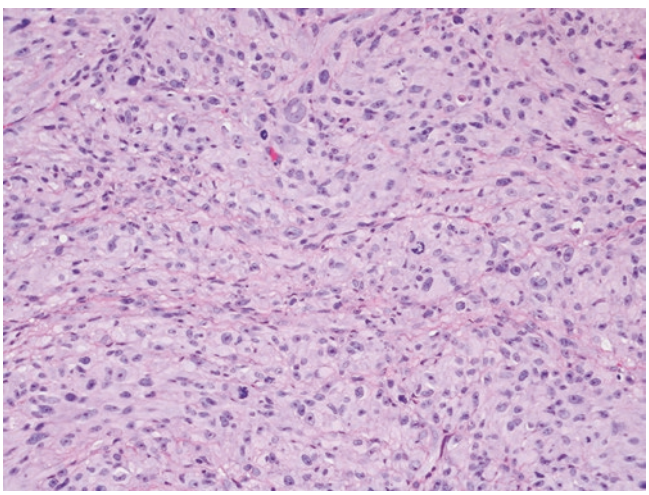

Fig. 25.43 Atypical fibroxanthoma. Mixed spindled and epithelioid cellular infiltrate with numerous mitoses and multinucleated giant cells

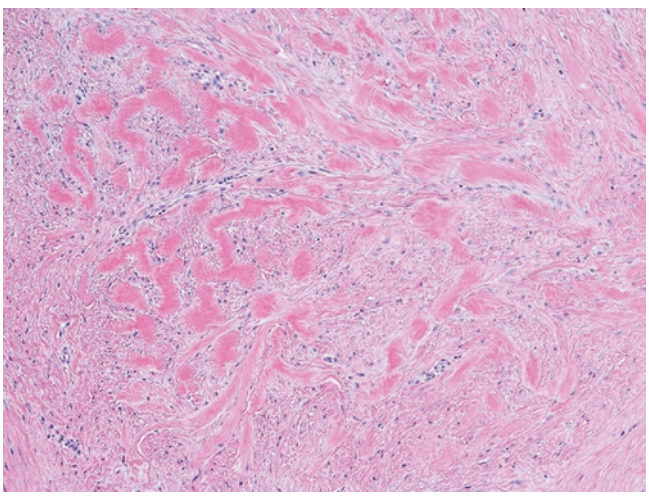

Fig. 25.44 Keloid. Thick, closely packed, hyalinized collagen fibers arranged in a nodular fashion

Mammary Differential Diagnosis Fibromatosis, fibromatosis-like spindle cell metaplastic carcinoma, myofibroblastoma (collagenized/fibrous and infiltrative variants), and scar: Morphology can be very similar between these lesions, especially in limited samples. Prior history of trauma or surgical procedure must be elicited. An IHC panel including cytokeratins, p63, β-catenin, CD34, and ER (discussed previously under dermatofibroma) will be helpful in establishing a diagnosis.

Storiform Collagenoma

Storiform collagenoma (sclerotic fibroma) is a benign fibroblastic tumor that most commonly arises on the trunk and proximal extremities but potentially may arise at any site. Tumors present as a solitary skin-colored nodule measuring less than 1 cm in diameter. Simple excision is curative. Multiple lesions are associated with Cowden's disease (multiple hamartoma and neoplasia syndrome). The well-circumscribed dermal nodules are composed of hypocellular hyalinized collagen bundles that are separated by storiform clefts containing rare spindle-shaped fibroblasts (Fig. 25.45a) [242]. Rare cellular and pleomorphic forms have also been described. IHC staining will reveal the tumor cells to be CD34 and CD99 positive [243].

Mammary Differential Diagnosis Fibromatosis, fibromatosis-like spindle cell metaplastic carcinoma (Fig. 25.45b), myofibroblastoma (collagenized and infiltrative variants), fibroepithelial lesions with pseudoangiomatous stromal hyperplasia (PASH), stroma (Fig. 25.45c), and scar: A storiform collagenoma is more hypocellular and shows a storiform pattern, compared with the mammary lesions listed above. In addition, the mammary lesions may show components more typical for each lesion. However, limited sampling can obscure these subtle differences. An immunohistochemical panel as described in the section discussing dermatofibroma can assist in the evaluation of these lesions.

Dermatofibrosarcoma Protuberans

Dermatofibrosarcoma protuberans is a locally aggressive fibroblastic malignancy that most commonly arises on the upper back of middle-aged patients; however, involvement

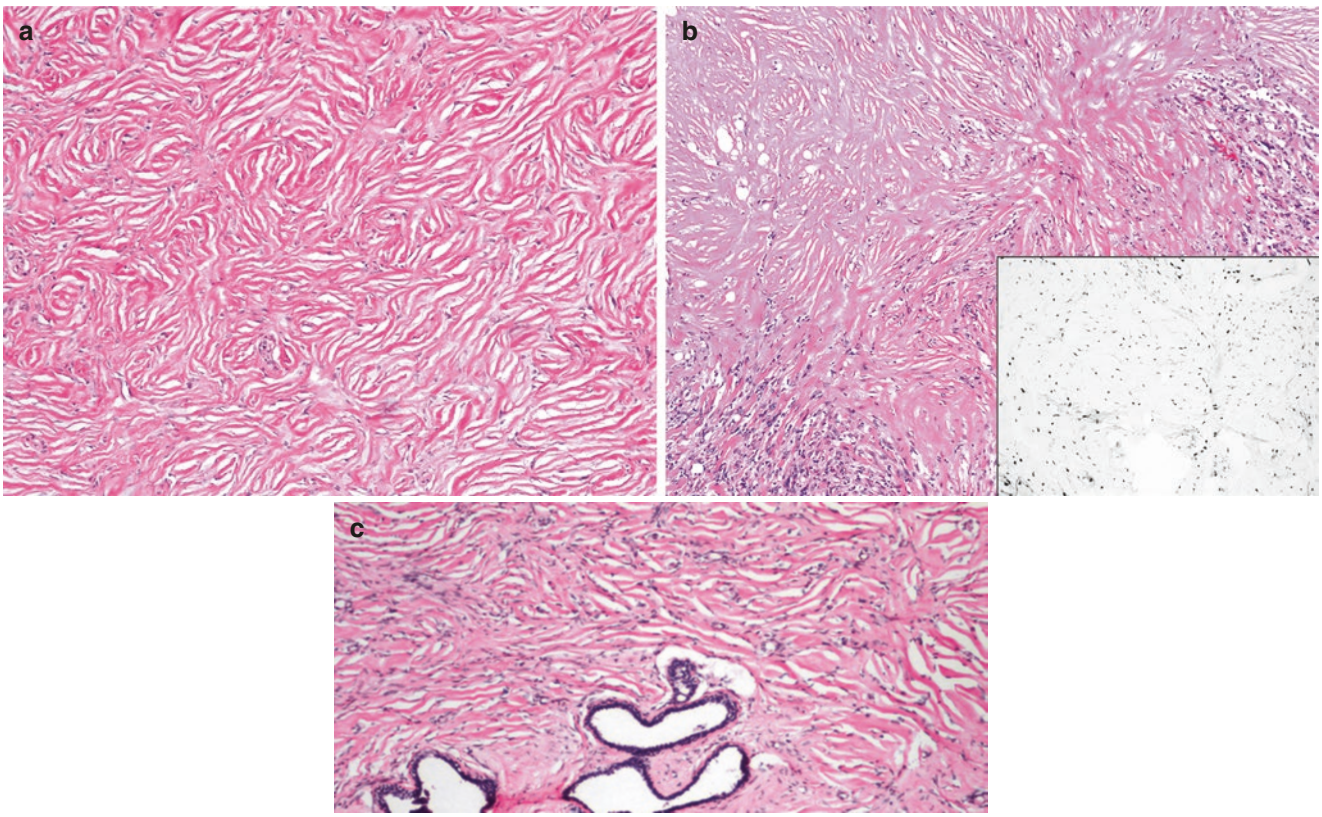

Fig. 25.45 Storiform collagenoma. (**a**) Dense sclerotic stroma admixed with numerous slit-like spaces, which contain fibroblasts arranged in a storiform pattern. (**b**) Fibromatosis-like metaplastic carcinoma with diffuse immunoreactivity for p63 (inset). (**c**) Borderline phyllodes tumor showing areas of collagenization

of the breast has been well documented [244, 245]. These tumors may occasionally arise at sites of previous trauma such as scars, injection sites, and infection [246]. Rapid growth during pregnancy has been reported [247]. Clinically, these tumors present as a slow-growing firm indurated plaque with ill-defined palpable borders. Occasional nodularity may occur in later stages. Although the local recurrence rate is relatively high (20–50%), distant metastasis is extremely rare. Removal via Mohs micrographic surgery has been shown to have lower recurrence rates than wide excision [248]. These tumors exhibit chromosomal translocations for t(17;22), creating a specific gene fusion of *COL1A1* and *PDGFB* [249]. Microscopically, these tumors are characterized by a deep dermal spindle cell proliferation with a storiform and fascicular pattern of growth (Fig. 25.46a). Vertical infiltration into the subcutis with entrapment of adipocytes is a characteristic (Fig. 25.46b). Mitotic activity is typically low, usually not exceeding five per ten high-power fields. IHC staining shows positive expression of CD34 but negative expression of factor XIIIa, S100 protein, desmin, SMA, CD117, stromelysin, and D2-40 [237, 250–253].

Mammary Differential Diagnosis Spindle cell metaplastic carcinoma, myofibroblastoma (cellular variant), and fibromatosis: IHC can be helpful. Spindle cell metaplastic carcinoma (Fig. 25.46c) is positive for cytokeratins (e.g., 34βE12), p63, and also sometimes SMA and β-catenin. Myofibroblastoma is positive for CD34, ER, desmin, CD99, and SMA and negative for cytokeratins. Fibromatosis is positive for nuclear β-catenin and negative for factor XIIIa and D2-40.

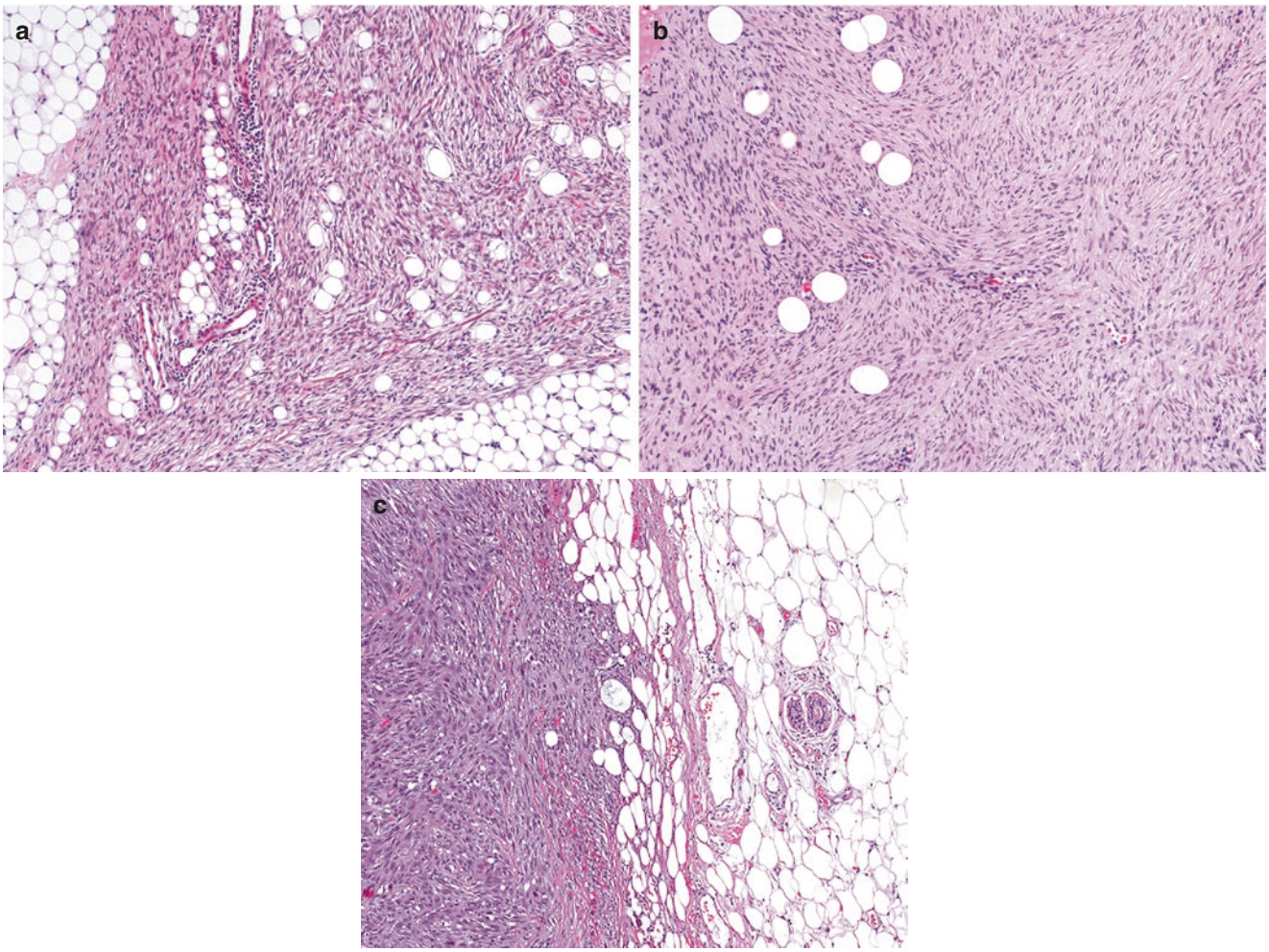

Fig. 25.46 Dermatofibrosarcoma protuberans. (**a**) Storiform and fascicular proliferation of spindle cells infiltrating the subcutis. (**b**) The spindle cells invade and entrap fat. (**c**) Spindle cell metaplastic carcinoma. ((**a**), (**c**) Reproduced from Desman GT, Ozerdem U, Shin SJ. Neighboring look-a-likes: Distinguishing between breast and dermatologic lesions. Adv Anat Pathol. 2014;21:228–247, with permission of Wolters-Kluwer Health)

Myofibroblastic Tumors

Dermatomyofibroma

Dermatomyofibroma classically presents as a plaque on the trunk or upper limb girdle of female patients. The tumors are characterized by an ill-defined proliferation of bland spindle-shaped cells, arranged in horizontal parallel fascicles that spare adjacent adnexal structures (Fig. 25.47a). IHC staining will reveal the tumor cells to be positive for SMA and vimentin but negative for desmin, CD34, factor XIIIa, and ER [254, 255].

Mammary Differential Diagnosis Myofibroblastoma and fibromatosis: Myofibroblastoma can show a similar histology, but the spindle cells do not follow a parallel arrangement and will be positive for CD34, ER, and desmin (Fig. 25.47b). Fibromatosis shows long interlacing bundles of spindle cells and collagen. It is immunoreactive for nuclear β-catenin and negative for factor XIIIa and D2-40.

Smooth Muscle Tumors

Smooth Muscle Hamartoma (Becker's Nevus)

Becker's nevus represents an uncommon cutaneous hamartoma frequently found on the chest and upper extremity. It presents clinically as hyperpigmented lesions associated with hypertrichosis. While leiomyomas tend to form a single mass, smooth muscle hamartomas are composed of discrete bundles that are surrounded by ordered collagen. The smooth muscle bundles of hamartomas are not associated with regional hair follicles [256].

Mammary Differential Diagnosis Myoid hamartoma, myofibroblastoma of leiomyomatous variant, mammary leiomyoma, and myoid metaplasia: Myoid hamartoma shows interlacing bundles of myoid cells admixed with glandular and stromal components. Sclerosing adenosis or fibrocystic changes will be present at the periphery of the lesion (Fig. 25.48). Myoid metaplasia will involve an otherwise unremarkable lobule. Cutaneous smooth muscle hamartomas arise within the dermis and will have adjacent adnexal structures. Leiomyomatous myofibroblastoma will most likely have at least a minor component of admixed adipocytes within its tumor. Mammary leiomyomas are not invested in collagen as a rule.

Accessory nipples may arise anywhere along the milk line, which runs vertically on either side from the mid axilla, through the nipple of the normal breast, and ends inferiorly at the medial groin. Multiple symmetrical lesions can be present. Histopathologically, these lesions are identical to smooth muscle hamartoma and require clinical correlation for diagnostic distinction.

Cutaneous Leiomyomas

Cutaneous leiomyomas can be separated into those that arise in the skin (pilar and nipple), those associated with the external genitalia (vulva and scrotum), and those associated with vessels (angioleiomyoma). Pilar and nipple leiomyomas have no gender preference, generally arise in early adulthood, and present as painful firm reddish-brown papules or nodules confined to the dermis. While solitary dermal leiomyomas usually do not recur, patients with multiple dermal leiomyomas often experience recurrence (50%) and develop

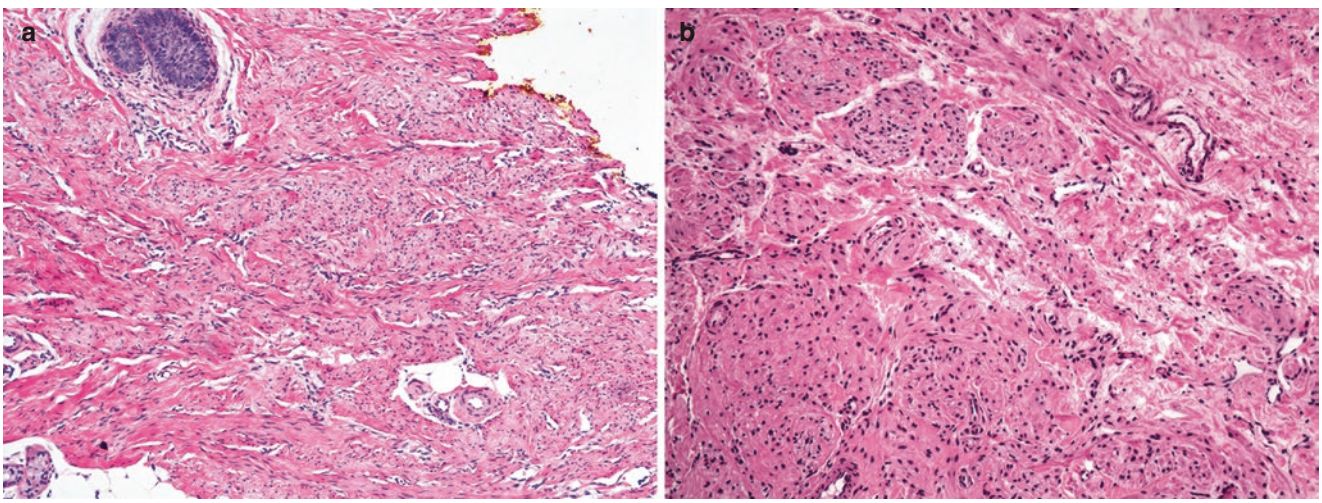

Fig. 25.47 Dermatomyofibroma. (**a**) Parallel fascicles of spindle cells with abundant eosinophilic cytoplasm. (**b**) Myofibroblastoma, leiomyomatous variant

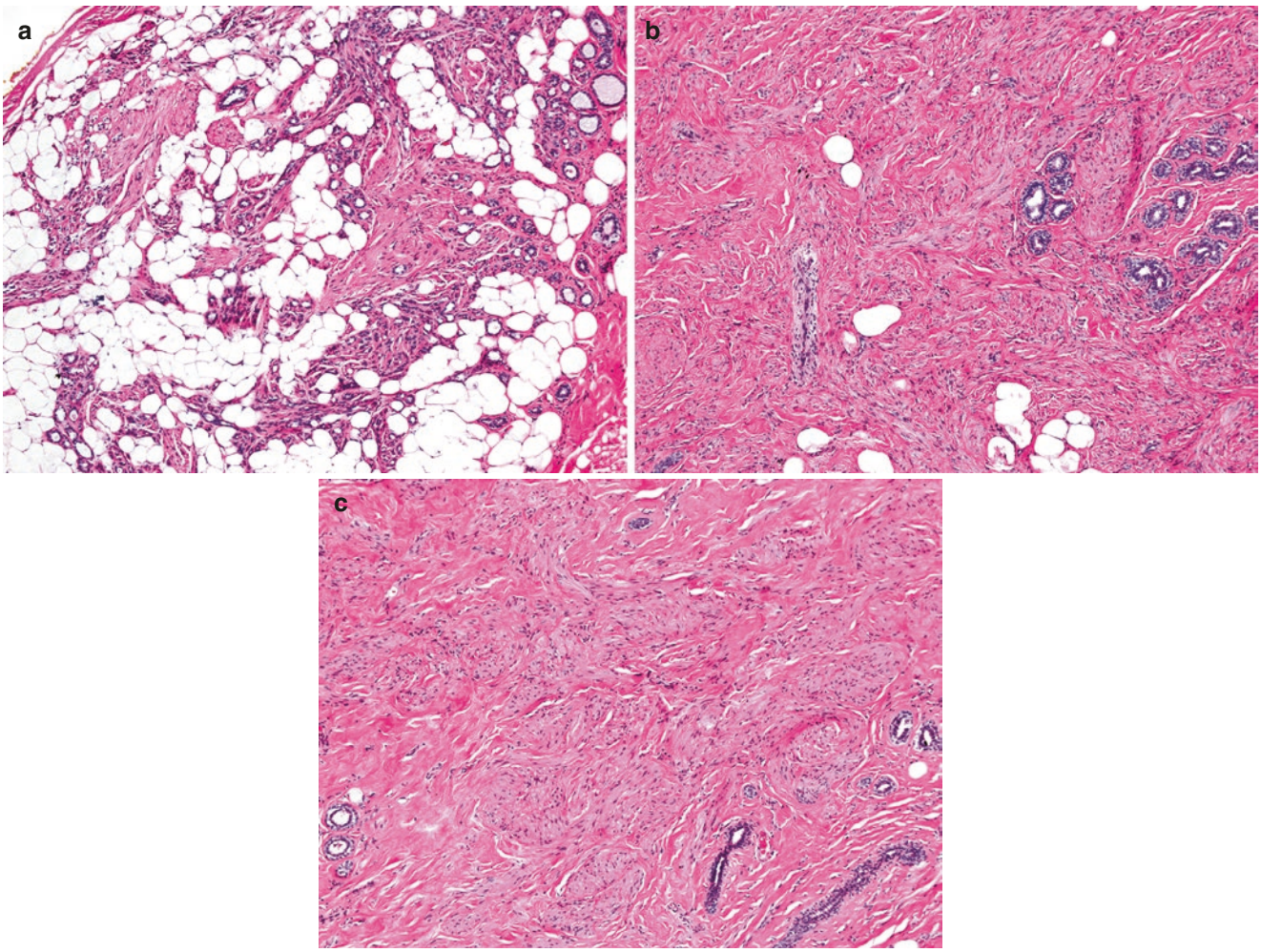

Fig. 25.48 Myoid hamartoma of the breast (**a**–**c**)

subsequent lesions. Microscopically, these tumors are characterized by a spindle cell proliferation with a fascicular growth pattern, admixed with variable amounts of collagen that is arranged randomly throughout the dermis or occasionally subcutaneous tissue [257]. They are unencapsulated and infiltrative, commonly involving adjacent hair follicles and sweat glands. The tumor cells classically contain elongated nuclei with round or blunt ends and abundant eosinophilic cytoplasm. Mitotic figures are extremely rare or absent (Fig. 25.49a, b).

Angioleiomyomas are well-circumscribed subcutaneous nodules presenting in adults as painful solitary masses. There is higher incidence in women. While they mainly arise on the lower extremities, cases involving the chest may occur. These lesions are benign and uncommonly recur. The tumors exhibit a nodular concentric array of spindle cells extending outward from muscular vessels. Mitotic figures are extremely rare or absent [258].

Mammary Differential Diagnosis Same as for smooth muscle hamartoma (see above).

Cutaneous Leiomyosarcomas

Cutaneous leiomyosarcomas are most common on the proximal extremities, especially the lower extremity. Cases involving the nipple are rare but well documented in the literature. It is generally believed that dermal tumors arise from erector pili muscle or nipple smooth muscle, while subcutaneous tumors arise from blood vessels. The prognosis is highly dependent on the size and anatomic compartment. In general, tumors smaller than 5 cm in diameter have a much better prognosis. Although dermal tumors have a significant local recurrence rate (40%), distant metastasis is extremely rare. For these reasons, many favor a diagnosis of "atypical leiomyomatous tumor" for these dermal-confined tumors. In

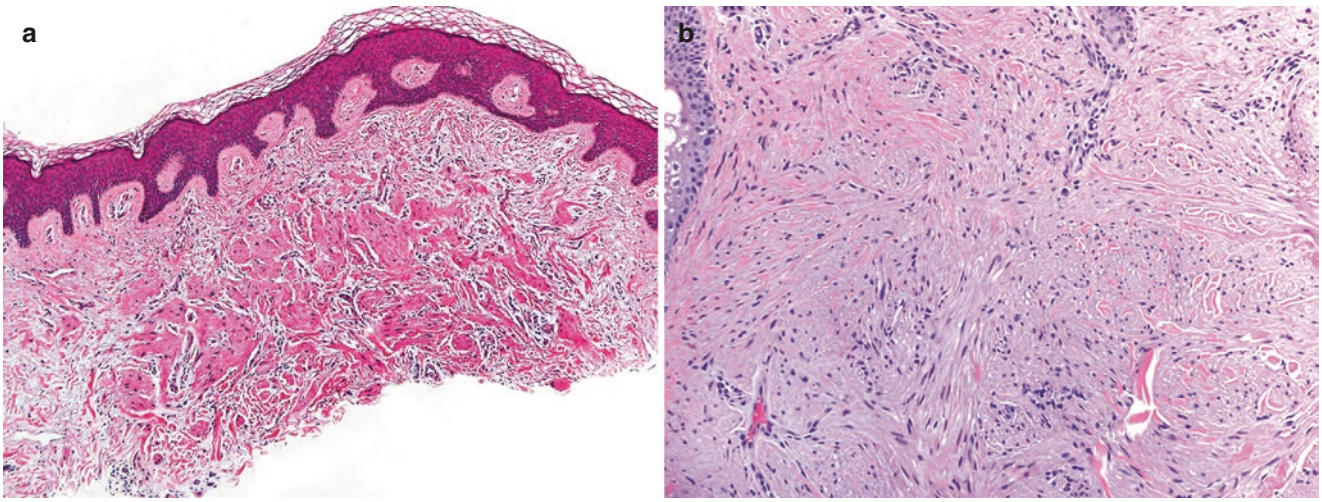

Fig. 25.49 Nipple leiomyoma. (**a**) Numerous disorganized fascicles of smooth muscle dissecting between collagen bundles. (**b**) The spindle cells are monomorphous with absent mitotic activity

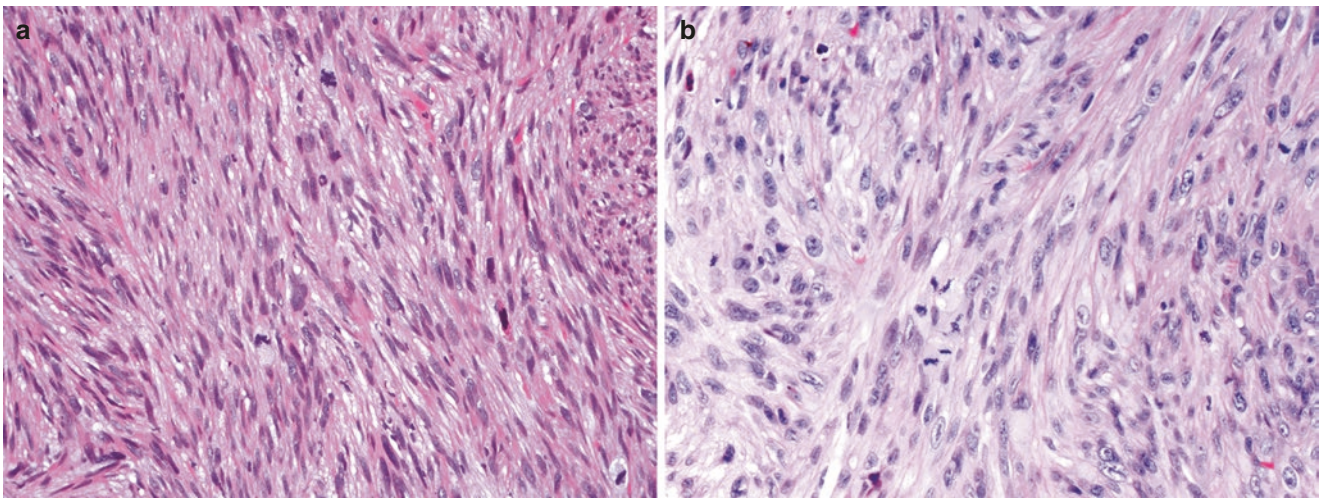

Fig. 25.50 Cutaneous leiomyosarcoma. (**a**) Fascicles of highly pleomorphic spindle cells with abundant eosinophilic cytoplasm and elongated nuclei with blunted ends. (**b**) Well-differentiated smooth muscle tumor with numerous mitoses, consistent with malignancy

contrast, subcutaneous tumors should be referred to and treated as sarcoma, since these lesions metastasize in up to 50% of cases. For subcutaneous leiomyosarcomas, aneuploidy may be an additional unfavorable prognostic feature [259, 260].

As occasional cytologic atypia, infiltrative growth pattern, and lack of circumscription can be present in leiomyomas [261], additional features must be evaluated to confidently diagnose malignancy. The most specific features of malignancy are mitotic rate (>1 mitoses per 10 high-power fields [40×]) and tumor necrosis (Fig. 25.50a, b). As a general rule, positive Ki-67 nuclear staining in greater than 10% of tumor cells should be considered sufficient evidence of malignancy. IHC stains will reveal the tumor cells to express markers associated with smooth muscle differentiation, namely, positive SMA, desmin, and caldesmon [262].

Mammary Differential Diagnosis Myofibroblastoma of leiomyomatous variant, mammary leiomyosarcoma, primary breast sarcoma including leiomyosarcoma or as part of a malignant phyllodes tumor, and metastatic sarcoma: On a limited core or punch biopsy, the distinction among these possibilities may not be possible. Clinical and radiologic correlation is paramount.

Nerve Sheath Tumors

Benign cutaneous nerve sheath tumors include neurofibroma, schwannoma, and neuroma. While the former two entities may arise essentially anywhere, neuromas occur almost exclusively on the face. A breast parenchymal presentation is very rare. Malignant nerve sheath tumors are rare in superficial locations as well as in the breast parenchyma. Although these tumors are easily identified in punch, shave, and excision specimens, diagnostic difficulties may arise in small specimens obtained via core needle biopsy. Morphology with adjunct immunohistochemistry for neural markers (SOX10, S100 protein, neuron-specific enolase, CD57, EMA, GFAP) will assist in the assessment of these tumors.

References

1. Hoda SA. Chapter 1: Anatomy and physiologic morphology. In: Rosen PP, editor. Breast pathology. 4th ed. Philadelphia: Lippincott Williams & Wilkins; 2014. p. 1–26.
2. Kalli S, Freer PE, Rafferty EA. Lesions of the skin and superficial tissue at breast MR imaging. Radiographics. 2010;30:1891–913.
3. Nicholson BT, Harvey JA, Cohen MA. Nipple-areolar complex: normal anatomy and benign and malignant processes. Radiographics. 2009;29:509–23.
4. Giess CS, Raza S, Birdwell RL. Distinguishing breast skin lesions from superficial breast parenchymal lesions: diagnostic criteria, imaging characteristics, and pitfalls. Radiographics. 2011;31:1959–72.
5. Sariya D, Ruth K, Adams-McDonnell R, et al. Clinicopathologic correlation of cutaneous metastases: experience from a cancer center. Arch Dermatol. 2007;143:613–20.
6. Qureshi HS, Ormsby AH, Lee MW, et al. The diagnostic utility of p63, CK5/6, CK 7, and CK 20 in distinguishing primary cutaneous adnexal neoplasms from metastatic carcinomas. J Cutan Pathol. 2004;31:145–52.
7. Robson A, Lazar AJF, Nagi JB, et al. Primary cutaneous apocrine carcinoma: a clinico-pathologic analysis of 24 cases. Am J Surg Pathol. 2008;32(5):682–90.
8. Mentrikoski M, Wick MR. Immunohistochemical distinction of primary sweat gland carcinoma and metastatic breast carcinoma. Can it always be accomplished reliably? Am J Clin Pathol. 2015;143:430–6.
9. Rollins-Raval M, Chivukula M, Tseng GC, et al. An immunohistochemical panel to differentiate metastatic breast carcinoma to skin from primary sweat gland carcinomas with a review of the literature. Arch Pathol Lab Med. 2011;135:975–83.
10. Piris A, Peng Y, Boussahmain C, et al. Cutaneous and mammary apocrine carcinomas have different immunoprofiles. Hum Pathol. 2014;45(2):320–6.
11. Gloyeske NC, Woodard AH, Elishaev E, et al. Immunohistochemical profile of breast cancer with respect to estrogen receptor and HER2 status. Appl Immunohistochem Mol Morphol. 2015;23(3):202–8. https://doi.org/10.1097/PAI.0000000000000076.
12. Wick MR, Ockner DM, Mills SE, et al. Homologous carcinomas of the breasts, skin, and salivary glands. A histologic and immunohistochemical comparison of ductal mammary carcinoma, ductal sweat gland carcinoma, and salivary duct carcinoma. Am J Clin Pathol. 1998;109(1):75–84.
13. Fernandez-Flores A. Immunohistochemical and morphologic evaluation of primary cutaneous apocrine carcinomas and cutaneous metastases from ductal breast carcinoma. Romanian J Morphol Embryol. 2012;53(4):879–92.
14. Luo MH, Huang YH, Ni YB, et al. Expression of mammaglobin and gross cystic disease fluid protein-15 in breast carcinomas. Hum Pathol. 2013;44(7):1241–50.
15. Wendroth SM, Mentrikoski MJ, Wick MR. GATA3 expression in morphologic subtypes of breast carcinoma: a comparison with gross cystic disease fluid protein 15 and mammaglobin. Ann Diagn Pathol. 2015;19(1):6–9.
16. Krings G, Nystrom M, Mehdi I, et al. Diagnostic utility and sensitivities of GATA3 antibodies in triple-negative breast cancer. Hum Pathol. 2014;45(11):2225–32.
17. Mettinen M, McCue PA, Sarlomo-Rikala M, et al. GATA3: a multispecific but potentially useful marker in surgical pathology: a systematic analysis of 2500 epithelial and nonepithelial tumors. Am J Surg Pathol. 2014;38(1):13–22.
18. Lee JJ, Mochel MC, Piris A, et al. P40 exhibits better specificity than p63 in distinguishing primary skin adnexal carcinomas from cutaneous metastases. Hum Pathol. 2014;45(5):1078–83.
19. Busam KJ, Tan LK, Granter SR, et al. Epidermal growth factor, estrogen and progesterone receptor expression in primary sweat gland carcinomas ad primary and metastatic mammary carcinomas. Mod Pathol. 1999;12(8):786–93.
20. Bayer-Garner IB, Smoller B. Androgen receptors: a marker to increase sensitivity for identifying breast cancer in skin metastasis of unknown primary site. Mod Pathol. 2000;13(2):119–22.
21. Le LP, Dias-Santagata D, Pawlak AC, et al. Apocrine-eccrine carcinomas: molecular and immunohistochemical analyses. PLoS One. 2012;7(10):e47290.
22. Niemeier LA, Dabbs DJ, Beriwal S, et al. Androgen receptor in breast cancer: expression in estrogen receptor-positive tumors and in estrogen receptor-negative tumors with apocrine differentiation. Mod Pathol. 2010;23(2):205–12.
23. Plaza JA, Ortega PF, Stockman DL, et al. Value of p63 and podoplanin (D2-40) immunoreactivity in the distinction between primary cutaneous tumors and adenocarcinomas metastatic to the skin: a clinicopathologic and immunohistochemical study of 79 cases. J Cutan Pathol. 2010;37:403–10.
24. Ivan D, Diwan AH, Prieto VG. Expression of p63 in primary cutaneous adnexal neoplasms and adenocarcinoma metastatic to the skin. Mod Pathol. 2005;18:137–42.
25. Plumb SJ, Argenyi ZB, Stone MS, et al. Cytokeratin 5/6 immunostaining in cutaneous adnexal neoplasms and metastatic adenocarcinoma. Am J Dermatopathol. 2004;26(6):447–51.
26. Mahalingam M, Nguyen LP, Richards JE, et al. The diagnostic utility of immunohistochemistry in distinguishing primary skin adnexal carcinomas from metastatic adenocarcinoma to skin: an immunohistochemical reappraisal using cytokeratin 15, nestin, p63, D2-40, and calretinin. Mod Pathol. 2010;23(5):713–9.
27. Kaufmann O, Fietze E, Mengs J, et al. Value of p63 and cytokeratin 5/6 as immunohistochemical markers for the differential diagnosis of poorly differentiated and undifferentiated carcinomas. Am J Clin Pathol. 2001;116:823–30.
28. Reis-Filho JS, Simpson PT, Martins A, et al. Distribution of p63, cytokeratins 5/6 and cytokeratin 14 in 51 normal and 400 neoplastic human tissue samples using TARP-4 multi-tumor tissue microarray. Virchows Arch. 2003;443:122–32.
29. Carpenter PM, Wang-Rodriguez J, Chan OT, et al. Laminin 5 expression in metaplastic breast carcinomas. Am J Surg Pathol. 2008;32:345–53.
30. Kim SK, Jung WH, Koo JS. p40 (ΔNp63) expression in breast disease and its correlation with p63 immunohistochemistry. Int J Clin Exp Pathol. 2014;7(3):1032–41.
31. Koker MM, Kleer CG. p63 expression in breast cancer. A highly sensitive and specific marker of metaplastic carcinoma. Am J Surg Pathol. 2004;28:1506–12.

32. Ding Y, Ruan Q. The value of p63 and CK5/6 expression in the differential diagnosis of ductal lesions of breast. J Huazhong Univ Sci Technol Med Sci. 2006;26(4):405–7.
33. Cimino-Mathews A, Sharma R, Illei PB, et al. A subset of malignant phyllodes tumors express p63 and p40. A diagnostic pitfall in breast core needle biopsies. Am J Surg Pathol. 2014;38(12):1689–96.
34. Bishop JA, Teruya-Feldstein J, Westra WH, et al. p40 (ΔNp63) is superior to p63 for the diagnosis of pulmonary squamous cell carcinoma. Mod Pathol. 2012;25(3):405–15.
35. Alomari AK, Glusac EJ, McNiff JM. p40 is a more specific marker than p63 for cutaneous poorly differentiated squamous cell carcinoma. J Cutan Pathol. 2014;41(11):839–45.
36. Ha Lan TT, Chen SJ, Arps DP, et al. Expression of the p40 isoform of p63 has high specificity for cutaneous sarcomatoid squamous cell carcinoma. J Cutan Pathol. 2014;41(11):831–8.
37. Henderson SA, Torres-Cabala CA, Curry JL, et al. p40 is more specific than p63 for the distinction of atypical fibroxanthoma from other cutaneous spindle cell malignancies. Am J Surg Pathol. 2014;38(8):1102–10.
38. D'Alfonso TM, Ross DS, Liu YF, et al. Expression of p40 and laminin 332 in metaplastic spindle cell carcinoma of the breast compared with other malignant spindle cell tumors. J Clin Pathol. 2015;68(7):516–21. https://doi.org/10.1136/jclinpath-2015-202923.
39. Gomaa AHA, Yaar M, Bhawan J. Cutaneous immunoreactivity of D2-40 antibody beyond the lymphatics. Am J Dermatopathol. 2007;29(1):18–21.
40. Liang H, Wu H, Giorgadze TA, et al. Podoplanin is a highly sensitive and specific marker to distinguish primary skin adnexal carcinomas from adenocarcinomas metastatic to skin. Am J Surg Pathol. 2007;31(2):304–10.
41. Mhawech-Fauceglia P, Saxena R, Zhang S, et al. Pax-5 immunoexpression in various types of benign and malignant tumours: a high-throughput tissue microarray analysis. J Clin Pathol. 2007;60:709–14.
42. Varma S, Shin SJ. An algorithmic approach to spindle cell lesions of the breast. Adv Anat Pathol. 2013;20(2):95–109.
43. Lee WJ, Chang SE, Lee MW, et al. Bilateral mucinous eccrine nevus in an adult. J Dermatol. 2008;35:552–4.
44. Kawaoka JC, Gray J, Schappell D. Eccrine nevus. J Am Acad Dermatol. 2004;51:301–4.
45. Morris ES, Scheel MM, Lundquist KF, et al. Grouped papules on the arm of an infant. Eccrine nevus. Arch Dermatol. 2000;136:549–52.
46. Cunliffe WJ, Johnson CE, Williamson DM. Localized unilateral hyperhidrosis—a clinical and laboratory study. Br J Dermatol. 1972;86:374–8.
47. Misago N, Narisawa Y. Syringocystadenoma papilliferum with extensive apocrine nevus. J Dermatol. 2006;33:303–5.
48. Nishikawa Y, Tokusashi Y, Saito Y, et al. A case of adenocarcinoma associated with hamartomatous apocrine gland hyperplasia of both axillae. Am J Surg Pathol. 1994;18:832–6.
49. Mehregan AH. Proliferation of sweat ducts in certain diseases of the skin. Am J Dermatopathol. 1981;3:27–31.
50. Martorell-Calatayud A, Sanmartín O, Botella-Estrada R, et al. Chemotherapy-related bilateral dermatitis associated with eccrine squamous syringometaplasia: reappraisal of epidemiological, clinical, and pathological features. J Am Acad Dermatol. 2011;64(6):1092–103.
51. Gallo E, Llamas-Velasco M, Navarro R, et al. Eccrine squamous syringometaplasia secondary to cutaneous extravasation of docetaxel: report of three cases. J Cutan Pathol. 2013;40(3):326–9.
52. Teoh DC, Aw DC, Jaffar H, et al. Tamoxifen-induced eccrine squamous syringometaplasia. J Cutan Pathol. 2012;39:554–7.
53. Jerasutus S, Laohabhan K, Suvanprakorn P. Primary squamous syringometaplasia with no underlying malignancy. Int J Dermatol. 1999;38:375–6.
54. Miller DL, Weinstock MA. Nonmelanoma skin cancer in the United States: incidence. J Am Acad Dermatol. 1994;30:774–8.
55. Wade TR, Ackerman AB. The many faces of basal cell carcinoma. J Dermatol Surg Oncol. 1978;4:23–8.
56. Salasche SJ, Amonette RA. Morpheaform basal-cell epitheliomas. A study of subclinical extensions in a series of 51 cases. J Dermatol Surg Oncol. 1981;7:387–94.
57. Martin RC, Edwards MJ, Cawte TG, et al. Basosquamous carcinoma: analysis of prognostic factors influencing recurrence. Cancer. 2000;88:1365–9.
58. Poniecka AW, Alexis JB. An immunohistochemical study of basal cell carcinoma and trichoepithelioma. Am J Dermatopathol. 1999;21:332–6.
59. Fan YS, Carr RA, Sanders DS, et al. Characteristic Ber-EP4 and EMA expression in sebaceoma is immunohistochemically distinct from basal cell carcinoma. Histopathology. 2007;51:80–6.
60. Yu L, Galan A, McNiff JM. Caveats in BerEP4 staining to differentiate basal and squamous cell carcinoma. J Cutan Pathol. 2009;36:1074–6.
61. Crowson AN, Magro CM, Kadin ME, et al. Differential expression of the BCL2 oncogene in human basal cell carcinoma. Hum Pathol. 1996;27:355–9.
62. Yada K, Kashima K, Daa T, et al. Expression of CD10 in basal cell carcinoma. Am J Dermatopathol. 2004;26:463–71.
63. Auepemkiate S, Boonyaphiphat P, Thongsuksai P. p53 expression related to the aggressive infiltrative histopathological feature of basal cell carcinoma. Histopathology. 2002;40:568–73.
64. Yang HM, Cabral E, Dadras SS, Cassarino DS. Immunohistochemical expression of D2-40 in benign and malignant sebaceous tumors and comparison to basal and squamous cell carcinomas. Am J Dermatopathol. 2008;30(6):549–54.
65. Bryant J. Fibroepithelioma of Pinkus overlying breast cancer. Arch Dermatol. 1985;121(3):310.
66. Avci O, Pabuççuoğlu U, Koçdor MA, et al. Basal cell carcinoma of the nipple—an unusual location in a male patient. J Dtsch Dermatol Ges. 2008;6(2):130–2.
67. Katona TM, Ravis SM, Perkins SM, et al. Expression of androgen receptor by fibroepithelioma of Pinkus: evidence supporting classification as a basal cell carcinoma variant? Am J Dermatopathol. 2007;29:7–12.
68. Bowen AR, LeBoit PE. Fibroepithelioma of Pinkus is a fenestrated trichoblastoma. Am J Dermatopathol. 2005;27:149–54.
69. Preston DS, Stern RS. Nonmelanoma cancers of the skin. N Engl J Med. 1992;327:1649–62.
70. Rowe DE, Carroll RJ, Day CL Jr. Prognostic factors for local recurrence, metastasis, and survival rates in squamous cell carcinoma of the skin, ear, and lip. Implications for treatment modality selection. J Am Acad Dermatol. 1992;26:976–90.
71. Diaz-Cascajo C, Borghi S, Weyers W, et al. Follicular squamous cell carcinoma of the skin: a poorly recognized neoplasm arising from the wall of hair follicles. J Cutan Pathol. 2004;31:19–25.
72. Morritt AN, Tiffin N, Brotherston TM. Squamous cell carcinoma arising in epidermoid cysts: report of four cases and review of the literature. J Plast Reconstr Aesthet Surg. 2012;65:1267–9.
73. Taube JM, Badger J, Kong CS, et al. Differentiated (simplex) vulvar intraepithelial neoplasia: a case report and review of the literature. Am J Dermatopathol. 2011;33:e27–30.
74. Pulitzer M, Desman G, Busam K. CK7 expression in primary cutaneous squamous cell carcinoma. J Cutan Pathol. 2010;37(9):966–72.
75. Altaf FJ, Mokhtar GA, Emam E, et al. Metaplastic carcinoma of the breast: an immunohistochemical study. Diagn Pathol. 2014;9(1):139.

76. Doxtader EE, Katzenstein AL. The relationship between p16 expression and high-risk human papillomavirus infection in squamous cell carcinomas from sites other than uterine cervix: a study of 137 cases. Hum Pathol. 2012;43(3):327–32.
77. Subhawong AP, Subhawong T, Nassar H. Most basal-like breast carcinomas demonstrate the same Rb−/p16+ immunophenotype as the HPV-related poorly differentiated squamous cell carcinomas which they resemble morphologically. Am J Surg Pathol. 2009;33(2):163–75.
78. Headington JT. Tumors of the hair follicle: a review. Am J Pathol. 1976;85:480–505.
79. Rosen LB. A review and proposed new classification of benign acquired neoplasms with hair follicle differentiation. Am J Dermatopathol. 1990;12:496–516.
80. Aloi F, Tomasini C, Pippione M. Pigmented trichoblastoma. Am J Dermatopathol. 1992;14:345–9.
81. Brownstein MH, Shapiro L. The pilosebaceous tumors. Int J Dermatol. 1977;16:340–52.
82. Troy JL, Ackerman AB. Sebaceoma. A distinctive benign neoplasm of adnexal epithelium differentiating towards sebaceous cells. Am J Dermatopathol. 1984;6:7–13.
83. Burgdorf WHC, Pitha J, Fahmy A. Muir-Torre syndrome: histologic spectrum of sebaceous proliferations. Am J Dermatopathol. 1986;8:202–8.
84. Schwartz RA, Torre DP. The Muir-Torre syndrome: a 25-year retrospect. J Am Acad Dermatol. 1995;33:90–104.
85. Orta L, Klimstra DS, Qin J, et al. Towards identification of hereditary DNA mismatch repair deficiency: sebaceous neoplasm warrants routine immunohistochemical screening regardless of patient's age or other clinical characteristics. Am J Surg Pathol. 2009;33(6):934–44.
86. Kurokawa I, Nishimura K, Hakamada A, et al. Rippled-pattern sebaceoma with an immunohistochemical study of cytokeratins. J Eur Acad Dermatol Venereol. 2007;21:133–4.
87. Reis-Filho JS, Torio B, Albergaria A, et al. p63 expression in normal skin and usual cutaneous carcinomas. J Cutan Pathol. 2002;29(9):517–23.
88. Ansai S, Takeichi H, Arase S, et al. Sebaceous carcinoma: an immunohistochemical reappraisal. Am J Dermatopathol. 2011;33(6):579–87.
89. Ansai S, Arase S, Kawana S, et al. Immunohistochemical findings of sebaceous carcinoma and sebaceoma: retrieval of cytokeratin expression by a panel of anti-cytokeratin monoclonal antibodies. J Dermatol. 2011;38(10):951–8.
90. Wick MR, Goellner JR, Wolfe JT III, et al. Adnexal carcinomas of the skin. II. Extraocular sebaceous carcinomas. Cancer. 1985;56:1163–72.
91. Nelson BR, Hamlet KR, Gillard M, et al. Sebaceous carcinoma. J Am Acad Dermatol. 1995;33:1–15.
92. Dasgupta T, Wilson LD, Yu JB. A retrospective review of 1349 cases of sebaceous carcinoma. Cancer. 2009;115:158–65.
93. Wolfe JT III, Wick MR, Campbell RJ. Sebaceous carcinomas of the oculocutaneous adnexa and extraocular skin. In: Wick MR, editor. Pathology of unusual malignant cutaneous tumors. New York: Marcel Dekker; 1985. p. 77–106.
94. Murakami A, Kawachi K, Sasaki T, et al. Sebaceous carcinoma of the breast. Pathol Int. 2009;59(3):188–92.
95. Cibull TL, Thomas AB, Badve S, et al. Sebaceous carcinoma of the nipple. J Cutan Pathol. 2008;35(6):608–10.
96. Sramek B, Lisle A, Loy T. Immunohistochemistry in ocular carcinomas. J Cutan Pathol. 2008;35:641–6.
97. Suster S. Clear cell tumors of the skin. Semin Diagn Pathol. 1996;13:40–59.
98. Kariya Y, Moriya T, Suzuki T, et al. Sex steroid hormone receptors in human skin appendage and its neoplasms. Endocr J. 2005;52(3):317–25.
99. Cho KJ, Khang SK, Koh JS, et al. Sebaceous carcinoma of the eyelids: frequent expression of c-erbB-2 oncoprotein. J Korean Med Sci. 2000;15:545–50.
100. Obaidat NA, Ghazarian DM. Bilateral multiple axillary apocrine hidrocystomas associated with benign apocrine hyperplasia. J Clin Pathol. 2006;59(7):779.
101. Hassan MO, Khan MA, Kruse TV. Apocrine cystadenoma. Arch Dermatol. 1979;115:194–200.
102. Farina MC, Pique E, Olivares M, et al. Multiple hidrocystoma of the face: three cases. Clin Exp Dermatol. 1995;20:323–7.
103. Xu XL, Zhang GY, Zeng XS, et al. A case of zonal syringocystadenoma papilliferum of the axilla mimicking verruca vulgaris. Am J Dermatopathol. 2010;32(1):49–51.
104. Singh UR. Syringocystadenoma papilliferum mimicking breast carcinoma. Am J Dermatopathol. 2000;22(1):91.
105. Patterson JW, Straka BF, Wick MR. Linear syringocystadenoma papilliferum of the thigh. J Am Acad Dermatol. 2001;45:139–41.
106. Ogunrinade K, Blobstein SH, Desman GT. Agminated syringocystadenoma papilliferum: a new clinical presentation of a rare benign adnexal neoplasm. Dermatol Online J. 2013;19(8):19270.
107. Rosen PP, Caicco JA. Florid papillomatosis of the nipple: a study of 51 patients, including nine with mammary carcinoma. Am J Surg Pathol. 1986;10:87–101.
108. Kunikane H, Ishikura H, Yamaguchi J, et al. Chondroid syringoma (mixed tumor of the skin): a clinicopathologic study of 13 cases. Acta Pathol Jpn. 1987;37:615–25.
109. Hardisson D, Linares MD, Nistal M. Giant chondroid syringoma of the axilla. J Cutan Med Surg. 1998;3(2):115–7.
110. Djakovic A, Engel JB, Geisinger E, et al. Pleomorphic adenoma of the breast initially misdiagnosed as metaplastic carcinoma in preoperative stereotactic biopsy: a case report and review of the literature. Eur J Gynaecol Oncol. 2011;32(4):427–30.
111. Mills SE. Mixed tumor of the skin: a model of divergent differentiation. J Cutan Pathol. 1984;11:382–6.
112. Kazakov DV, Belousova IE, Bisceglia M, et al. Apocrine mixed tumor of the skin ('mixed tumor of the folliculosebaceous-apocrine complex'). Spectrum of differentiations and metaplastic changes in the epithelial, myoepithelial, and stromal components based on a histopathologic study of 244 cases. J Am Acad Dermatol. 2007;57:467–83.
113. Dominguez Iglesias F, Fresno Forcelledo F, Soler Sanchez T, et al. Chondroid syringoma: a histological and immunohistochemical study of 15 cases. Histopathology. 1990;17:311–7.
114. Mambo NC. Hyaline cells in a benign chondroid syringoma. Report of a case and findings by conventional and electron microscopy. Am J Dermatopathol. 1984;6:265–72.
115. Kazakov DV, Bisceglia M, Spagnolo DV, et al. Apocrine mixed tumors of the skin with architectural and/or cytologic atypia: a retrospective clinicopathologic study of 18 cases. Am J Surg Pathol. 2007;31:1094–102.
116. Mentzel T, Requena L, Kaddu S, et al. Cutaneous myoepithelial neoplasms: clinicopathologic and immunohistochemical study of 20 cases suggesting a continuous spectrum ranging from benign mixed tumor of the skin to cutaneous myoepithelioma and myoepithelial carcinoma. J Cutan Pathol. 2003;30:294–302.
117. Argenyi ZB, Balogh K, Goeken JA. Immunohistochemical characterization of chondroid syringomas. Am J Clin Pathol. 1988;90:662–9.
118. Hafezi-Bakhtiari S, Al-Habeeb A, Ghazarian D. Benign mixed tumor of the skin, hypercellular variant: a case report. J Cutan Pathol. 2010;37(9):e46–9.
119. Biernat W, Kordek R, Wozniak L. Papillary eccrine adenoma: a case of cutaneous sweat gland tumor with secretory and ductular differentiation. Pol J Pathol. 1994;45:319–22.

120. Frey J, Shimek C, Woodmansee C, et al. Aggressive digital papillary adenocarcinoma: a report of two diseases and review of the literature. J Am Acad Dermatol. 2009;60:331–9.
121. Bujas T, Pavić I, Lenicek T, et al. Axillary apocrine carcinoma associated with apocrine adenoma and apocrine gland hyperplasia. Acta Dermatovenerol Croat. 2007;15(3):148–51.
122. Tellechea O, Reis JP, Marques C, et al. Tubular apocrine adenoma with eccrine and apocrine immunophenotypes or papillary tubular adenoma? Am J Dermatopathol. 1995;17:499–505.
123. Chamberlain RS, Huber K, White JC, et al. Apocrine gland carcinoma of the axilla. Review of the literature and recommendations for treatment. Am J Clin Oncol. 1999;22:131–5.
124. Vandeweyer E, Hubert A, Renard N. Apocrine adenocarcinoma of the nipple: a case report. Acta Chir Belg. 2004;104:476–8.
125. Miyamoto T, Hagari Y, Inoue S, et al. Axillary apocrine carcinoma with benign apocrine tumours: a case report involving a pathological and immunohistochemical study and review of the literature. J Clin Pathol. 2005;58:757–61.
126. Kiyohara T, Kumakiri M, Kawami K, et al. Apocrine carcinoma of the vulva in a band-like arrangement with inflammatory and telangiectatic metastasis via local lymphatic channels. Int J Dermatol. 2003;42:71–4.
127. Warkel RL, Helwig EB. Apocrine gland adenoma and adenocarcinoma of the axilla. Arch Dermatol. 1978;114:198–203.
128. Paties C, Taccagni GL, Papotti M, et al. Apocrine carcinoma of the skin: a clinicopathologic, immunocytochemical, and ultrastructural study. Cancer. 1993;71:375–81.
129. Horn RCJR. Malignant papillary cystadenoma of sweat glands with metastases to the regional lymph nodes. Surgery. 1944;16:348–55.
130. Kazakov DV, Suster S, LeBoit PE, et al. Mucinous carcinoma of the skin, primary, and secondary: a clinicopathologic study of 63 cases with emphasis on the morphologic spectrum of primary cutaneous forms: homologies with mucinous lesions in the breast. Am J Surg Pathol. 2005;29(6):764–82.
131. Laco J, Simáková E, Svobodová J, et al. Recurrent mucinous carcinoma of skin mimicking primary mucinous carcinoma of parotid gland: a diagnostic pitfall. Cesk Patol. 2009;45(3):79–82.
132. Papalas JA, Proia AD. Primary mucinous carcinoma of the eyelid: a clinicopathologic and immunohistochemical study of 4 cases and an update on recurrence rates. Arch Ophthalmol. 2010;128(9):1160–5.
133. Levy G, Finkelstein A, McNiff JM. Immunohistochemical techniques to compare primary vs. metastatic mucinous carcinoma of the skin. J Cutan Pathol. 2010;37(4):411–5.
134. Rahilly MA, Beattie GJ, Lessells AM. Mucinous eccrine carcinoma of the vulva with neuroendocrine differentiation. Histopathology. 1995;27:82–6.
135. Ghanadan A, Khosravi M. Cutaneous syringoma: a clinicopathologic study of 34 new cases and review of the literature. Indian J Dermatol. 2013;58(4):326.
136. Henner MS, Shapiro PE, Ritter JH, et al. Solitary syringoma: a report of five cases and comparison with microcystic adnexal carcinoma. Am J Dermatopathol. 1995;17:465–70.
137. Furue M, Hori Y, Nakabayashi Y. Clear-cell syringoma: association with diabetes mellitus. Am J Dermatopathol. 1984;6:131–8.
138. Demirkesen C, Hoede N, Moll R. Epithelial markers and differentiation in adnexal neoplasms of the skin: an immunohistochemical study including individual cytokeratins. J Cutan Pathol. 1995;22(6):518–35.
139. Lee JH, Chang JY, Lee KH. Syringoma: a clinicopathologic and immunohistologic study and results of treatment. Yonsei Med J. 2007;48(1):35–40.
140. Kakinuma H, Miyamoto R, Iwasawa U, et al. Three subtypes of poroid neoplasia in a single lesion: eccrine poroma, hidroacanthoma simplex, and dermal duct tumor. Am J Dermatopathol. 1994;16:66–72.
141. Kircik L, Armus S, Kipping H, et al. Eccrine poroma in an unusual location. Cutis. 1994;54(3):183–4.
142. Azma A, Tawfik O, Casparian JM. Apocrine poroma of the breast. Breast J. 2001;7(3):195–8.
143. Sidro-Sarto M, Guimerá-Martin-Neda F, Perez-Robayna N, et al. Eccrine poroma arising in chronic radiation dermatitis. J Eur Acad Dermatol Venereol. 2008;22(12):1517–9.
144. Pylyser K, DeWolf-Peeters C, Marien K. The histology of eccrine poroma: a study of 14 cases. Dermatologica. 1983;167:243–9.
145. Tokura Y, Yoshikuni K, Teraki Y, et al. Immunohistochemically detectable duct-like structures in benign and malignant eccrine poromas: CEA and involucrin immunostaining. J Dermatol. 1989;16:133–41.
146. Takanashi M, Urabe A, Nakayama J, et al. Distribution of epithelial membrane antigen in eccrine poroma. Dermatologica. 1991;183:187–90.
147. Robson A, Greene J, Ansari N, et al. Eccrine porocarcinoma (malignant eccrine poroma): a clinicopathologic study of 69 cases. Am J Surg Pathol. 2001;25:710–20.
148. Guldhammer B, Norgaard T. The differential diagnosis of intraepidermal malignant lesions using immunohistochemistry. Am J Dermatopathol. 1986;8:295–301.
149. Kim JY, Kim YC, Lee ES. Solitary eccrine syringofibroadenoma with prominent plasma cell infiltration. J Dermatol. 2007;34:138–41.
150. de Viragh PA, Meylan R, Montaldi G, et al. Eccrine syringofibroadenoma. Report of clinical aspects and histology of two cases with review of the literature. Hautarzt. 1992;43:724–7.
151. Thomson SA, Rasmussen SA, Zhang J, et al. A new hereditary cylindromatosis family associated with CYLD1 on chromosome 16. Hum Genet. 1999;105:171–3.
152. Kazakov DV, Soukup R, Mukensnabl P, et al. Brooke-Spiegler syndrome: report of a case with combined lesions containing cylindromatous, spiradenomatous, trichoblastomatous, and sebaceous differentiation. Am J Dermatopathol. 2005;27:27–33.
153. Albores-Saavedra J, Heard SC, McLaren B, et al. Cylindroma (dermal analog tumor) of the breast: a comparison with cylindroma of the skin and adenoid cystic carcinoma of the breast. Am J Clin Pathol. 2005;123(6):866–73.
154. Mahmoud A, Hill DH, O'Sullivan MJ, et al. Cylindroma of the breast: a case report and review of the literature. Diagn Pathol. 2009;4:30.
155. Mambo NC. Eccrine spiradenomas: clinical and pathologic study of 49 tumors. J Cutan Pathol. 1983;10:312–20.
156. Lee MW, Kelly JW. Dermal cylindroma and eccrine spiradenoma. Australas J Dermatol. 1996;37:48–9.
157. Hashimoto K, Dibella RJ, Lever WF. Clear cell hidradenoma: histological, histochemical and electron microscopic studies. Arch Dermatol. 1967;96:18–38.
158. Angulo J, Jaqueti G, Kutzner H, et al. Squamous cell apocrine hidradenoma. J Cutan Pathol. 2007;34:801–3.
159. Goh SG, Carr R, Dayrit JF, et al. Mucinous hidradenoma: a report of three cases. J Cutan Pathol. 2007;34:497–502.
160. Kazakov DV, Kutzner H, Spagnolo DV, et al. Sebaceous differentiation in poroid neoplasms: report of 11 cases, including a case of metaplastic carcinoma associated with apocrine poroma (sarcomatoid apocrine porocarcinoma). Am J Dermatopathol. 2008;30:21–6.
161. Kazakov DV, Vanecek T, Belousova IE, et al. Skin-type hidradenoma of the breast parenchyma with t(11;19) translocation: hidradenoma of the breast. Am J Dermatopathol. 2007;29:457–61.
162. Laws RA, English JC III, Elston DM. Acrospiroma: a case report and review. Cutis. 1996;58:349–51.
163. Ohi Y, Umekita Y, Rai Y, et al. Clear cell hidradenoma of the breast: a case report with review of the literature. Breast Cancer. 2007;14(3):307–11.

164. Khurshid A, Yaqoob N, Devan HA, et al. Nuclear grooves in nodular hidradenoma: frequency and significance of an unrecognized histopathological feature. J Cutan Pathol. 2007;34:871–5.
165. Nazarian RM, Kapur P, Rakheja D, et al. Atypical and malignant hidradenomas: a histological and immunohistochemical study. Mod Pathol. 2009;22:600–10.
166. Nash JW, Barrett TL, Kies M, et al. Metastatic hidradenocarcinoma with demonstration of Her-2/neu gene amplification by fluorescence in situ hybridization: potential treatment implications. J Cutan Pathol. 2007;34(1):49–54.
167. Kazakov DV, Ivan D, Kutzner H, et al. Cutaneous hidradenocarcinoma: a clinicopathological, immunohistochemical, and molecular biologic study of 14 cases, including Her2/neu gene expression/amplification, TP53 gene mutation analysis, and t(11;19) translocation. Am J Dermatopathol. 2009;31:236–47.
168. Liapakis IE, Korkolis DP, Koutsoumbi A, et al. Malignant hidradenoma: a report of two cases and review of the literature. Anticancer Res. 2006;26:2217–20.
169. Souvatzidis P, Sbano P, Mandato F, et al. Malignant nodular hidradenoma of the skin: report of seven cases. J Eur Acad Dermatol Venereol. 2008;22:549–54.
170. Yavuzer R, Boyaci M, Sari A, et al. Microcystic adnexal carcinoma of the breast: a very rare breast skin tumor. Dermatol Surg. 2002;28:1092–4.
171. Antley CA, Carney M, Smoller BR. Microcystic adnexal carcinoma arising in the setting of previous radiation therapy. J Cutan Pathol. 1999;26:48–50.
172. Friedman PM, Friedman RH, Jiang B, et al. Microcystic adnexal carcinoma: collaborative series review and update. J Am Acad Dermatol. 1999;41:225–31.
173. Smith KJ, Williams J, Corbett D, et al. Microcystic adnexal carcinoma: an immunohistochemical study including markers of proliferation and apoptosis. Am J Surg Pathol. 2001;25:464–71.
174. Hoang MP, Dresser KA, Kapur P, et al. Microcystic adnexal carcinoma: an immunohistochemical approach. Mod Pathol. 2008;21:178–85.
175. Kawagushi K, Shin SJ. Immunohistochemical staining characteristics of low-grade adenosquamous carcinoma of the breast. Am J Surg Pathol. 2012;36:1009–20.
176. Geyer FC, Lambros MB, Natrajan R, et al. Genomic and immunohistochemical analysis of adenosquamous carcinoma of the breast. Mod Pathol. 2010;23:951–60.
177. Herrero J, Monteagudo C, Jorda E, et al. Squamoid eccrine ductal carcinoma. Histopathology. 1998;32:478–80.
178. Terushkin E, Leffell DJ, Futoryan T, et al. Squamoid eccrine ductal carcinoma: a case report and review of the literature. Am J Dermatopathol. 2010;32(3):287–92.
179. Wick MR, Swanson PE. Primary adenoid cystic carcinoma of the skin. Am J Dermatopathol. 1986;8:2–13.
180. Chang SE, Ahn SJ, Choi JH, et al. Primary adenoid cystic carcinoma of skin with lung metastasis. J Am Acad Dermatol. 1999;40:640–2.
181. Schwartz LE, Begum S, Westra WH, et al. GATA3 immunohistochemical expression in salivary gland neoplasms. Head Neck Pathol. 2013;7(4):311–5.
182. Kulkarni N, Pezzi CM, Greif JM, et al. Rare breast cancer: 933 adenoid cystic carcinomas from the National Cancer Data Base. Ann Surg Oncol. 2013;20(7):2236–41.
183. Reyes C, Jorda M, Gomez-Fernández C. Salivary gland-like tumors of the breast express basal-type immunohistochemical markers. Appl Immunohistochem Mol Morphol. 2013;21(4):283–6.
184. Projetti F, Lacroix-Triki M, Serrano E, et al. A comparative immunohistochemistry study of diagnostic tools in salivary gland tumors: usefulness of mammaglobin, gross cystic disease fluid protein 15, and p63 cytoplasmic staining for the diagnosis of mammary analog secretory carcinoma? J Oral Pathol Med. 2015;44(4):244–51. https://doi.org/10.1111/jop.12226.
185. Patel KR, Solomon IH, El-Mofty SK, et al. Mammaglobin and S-100 immunoreactivity in salivary gland carcinomas other than mammary analogue secretory carcinoma. Hum Pathol. 2013;44(11):2501–8.
186. Ramakrishnan R, Chaudhry IH, Ramdial P, et al. Primary cutaneous adenoid cystic carcinoma: a clinicopathologic and immunohistochemical study of 27 cases. Am J Surg Pathol. 2013;37(10):1603–11.
187. Rocas D, Asvesti C, Tsega A, et al. Primary adenoid cystic carcinoma of the skin metastatic to the lymph nodes: immunohistochemical study of a new case and literature review. Am J Dermatopathol. 2014;36(3):223–8.
188. Park BW, Kim SI, Lee KS, et al. Ductal eccrine carcinoma presenting as a Paget's disease-like lesion of the breast. Breast J. 2001;7(5):358–62.
189. Wick MR, Goellner JR, Wolfe JT, et al. Adnexal carcinomas of the skin. I. Eccrine carcinomas. Cancer. 1985;56:1147–62.
190. Wong TY, Suster S, Mihm MC Jr. Squamoid eccrine ductal carcinoma. Histopathology. 1997;30:288–93.
191. Urso C, Bondi R, Paglierani M, et al. Carcinomas of sweat glands: report of 60 cases. Arch Pathol Lab Med. 2001;125:498–505.
192. Swanson PE, Mazoujian G, Mills SE, et al. Immunoreactivity for estrogen receptor protein in sweat gland tumors. Am J Surg Pathol. 1991;15:835–41.
193. Brownstein MH, Helwig EB. Patterns of cutaneous metastasis. Arch Dermatol. 1972;105:862–8.
194. Lloyd J, Flanagan AM. Mammary and extramammary Paget's disease. J Clin Pathol. 2000;53:742–9.
195. Chaundary MA, Millis RR, Lane B, et al. Paget's disease of the nipple: a ten-year review including clinical, pathological, and immunohistochemical findings. Breast Cancer Res Treat. 1986;8:139–46.
196. Mazoujian G, Pinkus GS, Haagensen DE. Extramammary Paget's disease: evidence for an apocrine origin. Am J Surg Pathol. 1984;8:43–50.
197. Regauer S. Extramammary Paget's disease—a proliferation of adnexal origin? Histopathology. 2006;48:723–9.
198. Nadji M, Morales AR, Girtanner RE, et al. Paget's disease of the skin: a unifying concept of histogenesis. Cancer. 1982;50:2203–6.
199. Ojeda VJ, Heenen PJ, Watson SH. Paget's disease of the groin associated with adenocarcinoma of the urinary bladder. J Cutan Pathol. 1987;14:227–31.
200. Minicozzi A, Borzellino G, Momo R, et al. Perianal Paget's disease: presentation of six cases and literature review. Int J Color Dis. 2010;25(1):1–7.
201. Ansai S, Hashimoto H, Aoki T, et al. A histochemical and immunohistochemical study of extra-ocular sebaceous carcinoma. Histopathology. 1993;22(2):127–33.
202. Misago N, Toda S, Hikichi Y, et al. A unique case of extramammary Paget's disease. Derivation from eccrine porocarcinoma? Am J Dermatopathol. 1992;14(6):553–9.
203. Chiu CS, Yang CH, Chen CH. Extramammary Paget's disease of the unilateral axilla: a review of seven cases in a 20-year experience. Int J Dermatol. 2011;50(2):157–60.
204. Guarner J, Cohen C, Derose PB. Histogenesis of extramammary and mammary Paget's cells. Am J Dermatopathol. 1989;11:313–8.
205. Russell-Jones R, Spaull J, Gusterson B. The histogenesis of mammary and extramammary Paget's disease. Histopathology. 1989;14:409–16.
206. Lundquist K, Kohler S, Rouse RV. Intraepidermal cytokeratin 7 expression is not restricted to Paget's cells but it is also seen in Toker cells and Merkel cells. Am J Surg Pathol. 1999;23:212–9.

207. Fitzpatrick JE. The histologic diagnosis of intraepithelial pagetoid neoplasms. Clin Dermatol. 1991;9:255–9.
208. Helm KF, Goellner JR, Peters MS. Immunohistochemical stains in extramammary Paget's disease. Am J Dermatopathol. 1992;14:402–7.
209. Yoneda K. Immunohistochemical staining properties of keratin type intermediate filaments in mammary and extra-mammary Paget's disease. J Dermatol. 1989;16:47–53.
210. Reed W, Oppedal BR, Eeglarsen T. Immunohistology is valuable in distinguishing between Paget's disease, Bowen's disease and superficial spreading malignant melanoma. Histopathology. 1990;16:583–8.
211. Yanai H, Takahashi N, Omori M, Oda W, et al. Immunohistochemistry of p63 in primary and secondary vulvar Paget's disease. Pathol Int. 2008;58(10):648–51.
212. Díaz de León E, Carcangiu ML, Prieto VG, et al. Extramammary Paget's disease is characterized by the consistent lack of estrogen and progesterone receptors but frequently express androgen receptor. Am J Clin Pathol. 2000;113:572–5.
213. Horn LC, Purz S, Krumpe C, et al. COX-2 and Her-2/neu are overexpressed in Paget's disease of the vulva and the breast: results of a preliminary study. Arch Gynecol Obstet. 2008;277:135–8.
214. Liegl B, Horn LC, et al. Androgen receptors are frequently expressed in mammary and extramammary Paget's disease. Mod Pathol. 2005;18:1283–8.
215. Lammie GA, Barnes DM, Millis RR, et al. An immunohistochemical study of the presence of c-erbB-2 protein in Paget's disease of the nipple. Histopathology. 1989;15:505–14.
216. Tanskanen M, Jahkola T, Asko-Seljavaara S, et al. HER2 oncogene amplification in extramammary Paget's disease. Histopathology. 2003;42:575–9.
217. Alzaraa A, Thomas GD, Vodovnik A, et al. Merkel cell carcinoma in a male breast: a case report. Breast J. 2007;13(5):517–9.
218. Pulitzer MP, Amin BD, Busam KJ. Merkel cell carcinoma: review. Adv Anat Pathol. 2009;16(3):135–44.
219. Feng H, Shuda M, Chang Y, et al. Clonal integration of a polyomavirus in human Merkel cell carcinoma. Science. 2008;319:1096–100.
220. Hachana M, Trimeche M, Ziadi S, et al. Evidence for a role of the Simian Virus 40 in human breast carcinomas. Breast Cancer Res Treat. 2009;113:43–58.
221. Hachana M, Amara K, Ziadi S, et al. Investigation of human JC and BK polyomaviruses in breast carcinomas. Breast Cancer Res Treat. 2012;133(3):969–77.
222. Khan G, Philip PS, Naase M, et al. No evidence for the involvement of XMRV or MCV in the pathogenesis of breast cancer. Br J Cancer. 2012;106(6):1166–70.
223. Antonsson A, Bialasiewicz S, Rockett RJ, et al. Exploring the prevalence of ten polyomaviruses and two herpes viruses in breast cancer. PLoS One. 2012;7(8):e39842. https://doi.org/10.1371/journal.pone.0039842.
224. Stetsenko GY, Malekirad J, Paulson KG. p63 expression in Merkel cell carcinoma predicts poorer survival yet may have limited clinical utility. Am J Clin Pathol. 2013;140(6):838–84.
225. Daoud MA, Mete O, Al Habeeb A, et al. Neuroendocrine carcinoma of the skin—an updated review. Semin Diagn Pathol. 2013;30(3):234–44.
226. Christie M, Chin-Lenn L, Watts MM, et al. Primary small cell carcinoma of the breast with TTF-1 and neuroendocrine marker expressing carcinoma in situ. Int J Clin Exp Pathol. 2010;3(6):629–33.
227. Shin SJ, DeLellis RA, Ying L, et al. Small cell carcinoma of the breast: a clinicopathologic and immunohistochemical study of nine patients. Am J Surg Pathol. 2000;24(9):1231–8.
228. Sangoi AR, Cassarino DS. PAX-8 expression in primary and metastatic Merkel cell carcinoma: an immunohistochemical analysis. Am J Dermatopathol. 2013;35(4):448–51.
229. Nonaka D, Chiriboga L, Soslow RA. Expression of PAX8 as a useful marker in distinguishing ovarian carcinomas from mammary carcinomas. Am J Surg Pathol. 2008;32(10):1566–71.
230. Woodard AH, Yu J, Dabbs DJ, et al. NY-BR-1 and PAX8 immunoreactivity in breast, gynecologic tract, and other CK7+ carcinomas: potential use for determining site of origin. Am J Clin Pathol. 2011;136(3):428–35.
231. Augustsson A. Melanocytic nevi, melanoma and sun exposure. Acta Derm Venereol. 1991;166(Suppl):1–34.
232. Elder DE, Jucovy P, Tuthill RJ, et al. The classification of melanoma. Am J Dermatopathol. 1980;2:315–20.
233. Pawlik TM, Ross MI, Prieto VG, et al. Assessment of the role of sentinel lymph node biopsy for primary cutaneous desmoplastic melanoma. Cancer. 2006;106:900–6.
234. Quinn MJ, Crotty KA, Thompson JF, et al. Desmoplastic and desmoplastic neurotropic melanoma. Experience with 280 patients. Cancer. 1998;83:1128–35.
235. Gonzáles S, Duarte I. Benign fibrous histiocytoma of the skin. A morphologic study of 290 cases. Pathol Res Pract. 1982;172:379–91.
236. Cerio R, Spaull J, Wilson JE. Histiocytoma cutis: a tumor of dermal dendrocytes (dermal dendrocytoma). Br J Dermatol. 1989;120:197–206.
237. Bandarchi B, Ma L, Marginean C, et al. D2–40, a novel immunohistochemical marker in differentiating dermatofibroma from dermatofibrosarcoma protuberans. Mod Pathol. 2010;23:434–8.
238. Kuwano H, Hashimoto H, Enjoji M. Atypical fibroxanthoma distinguishable from spindle cell carcinoma in sarcoma-like skin lesions. A clinicopathologic and immunohistochemical study of 21 cases. Cancer. 1985;55(1):172–80.
239. Luzar B, Calonje E. Morphological and immunohistochemical characteristics of atypical fibroxanthoma with a special emphasis on potential diagnostic pitfalls: a review. J Cutan Pathol. 2010;7:301–9.
240. Ang GC, Roenigk RK, Otley CC, et al. More than 2 decades of treating atypical fibroxanthoma at Mayo Clinic: what we have learned from 91 patients? Dermatol Surg. 2009;5:765–72.
241. Datubo-Brown DD. Keloids: a review of the literature. Br J Plast Surg. 1990;43:70–7.
242. Requena L, Gutiérrez J, Sánchez YE. Multiple sclerotic fibromas of the skin—a cutaneous marker of Cowden's disease. J Cutan Pathol. 1991;19:346–51.
243. Mahmood MN, Salama ME, Chaffins M, et al. Solitary sclerotic fibroma of skin: a possible link with pleomorphic fibroma with immunophenotypic expression for O13 (CD99) and CD34. J Cutan Pathol. 2003;30:631–6.
244. Fletcher CDM, Evans BJ, Macartney JC, et al. Dermatofibrosarcoma protuberans: a clinicopathological and immunohistochemical study with a review of the literature. Histopathology. 1985;9:921–38.
245. Yeniay L, Unalp O, Sezak M, et al. Dermatofibrosarcoma protuberans of the breast. Breast J. 2012;18(5):493–4.
246. Green JJ, Heymann WR. Dermatofibrosarcoma protuberans occurring in a smallpox vaccination scar. J Am Acad Dermatol. 2003;48:S54–5.
247. Parlette LE, Smith CK, Germain LM, et al. Accelerated growth of dermatofibrosarcoma protuberans during pregnancy. J Am Acad Dermatol. 1999;41:778–83.
248. Wacker J, Khan-Durani B, Hartschuh W. Modified Mohs' micrographic surgery in the therapy of dermatofibrosarcoma protuberans: analysis of 22 patients. Ann Surg Oncol. 2004;11:438–44.
249. Sirvent N, Maire G, Pedeutour F. Genetics of dermatofibrosarcoma protuberans family of tumors: from ring chromosomes to tyrosine kinase inhibitor treatment. Genes Chromosomes Cancer. 2003;37:1–19.

250. Aiba S, Tabata N, Ishii H, et al. Dermatofibrosarcoma protuberans is a unique fibrohistiocytic tumour expressing CD34. Br J Dermatol. 1992;172:79–84.
251. Brathwaite C, Suster S. Dermatofibrosarcoma protuberans. A critical reappraisal of the role of immunohistochemical stains for diagnosis. Appl Immunohistochem. 1994;2:36–41.
252. Labonte S, Hanna W, Bandarchi-Chamkhaleh B. A study of CD117 expression in dermatofibrosarcoma protuberans and cellular dermatofibroma. J Cutan Pathol. 2007;34:857–60.
253. Cribier B, Noacco G, Peltre B, et al. Stromelysin 3 expression: a useful marker for the differential diagnosis dermatofibroma versus dermatofibrosarcoma protuberans. J Am Acad Dermatol. 2002;46:408–13.
254. Mentzel T, Kutzner H. Dermatomyofibroma: clinicopathological and immunohistochemical analysis of 56 cases and reappraisal of a rare and distinct cutaneous neoplasm. Am J Dermatopathol. 2009;31:44–9.
255. Ng WK, Cheung MF, Ma L. Dermatomyofibroma: further support of its myofibroblastic nature by electron microscopy. Histopathology. 1996;29:181–3.
256. Slipman N, Harrist T, Rhodes A. Congenital arrector pili hamartoma. A case and review of the spectrum of Becker's melanosis and pilar smooth muscle hamartoma. Arch Dermatol. 1985;211:1034–7.
257. Yokoyama R, Hashimoto H, Daimaru Y, et al. Superficial leiomyomas. A clinicopathologic study of 34 cases. Acta Pathol Jpn. 1987;37:1415–22.
258. Argenyi ZB, Piette WW, Goeken J. Cutaneous angiomyolipoma. Am J Dermatopathol. 1991;13:497–502.
259. Jensen ML, Jensen OM, Michalski W, et al. Intradermal and subcutaneous leiomyosarcoma: a clinicopathological and immunohistochemical study of 41 cases. J Cutan Pathol. 1996;23:458–63.
260. Pijpe J, Broers GH, Plaat BE, et al. The relation between histological, tumor-biological and clinical parameters in deep and superficial leiomyosarcoma and leiomyoma. Sarcoma. 2002;6:105–10.
261. Usmani N, Merchant W, Yung A. A case of cutaneous symplastic leiomyoma—a rare variant of cutaneous pilar leiomyoma. J Cutan Pathol. 2008;35:329–31.
262. Fox SB, Heryet A, Khong TY. Angioleiomyomas: an immunohistological study. Histopathology. 1990;16:495–6.

Index

A
Abscess
  clinical overview, 156
  differential diagnosis, 156
  microscopic features, 156
  pathogenesis, 156, 158
  prognosis, 158
  radiological features, 156
Accessory nipple, 759, 997
Acinic cell carcinoma, 504, 520, 522–524
Adenoid cystic carcinoma (AdCC), 436–437, 983, 988
  clinical management, 478, 481
  cribriform proliferations, 471, 480
  differential diagnosis of, 469, 471, 472, 479, 480
  grade I, 466
  grade II, 466
  grade III, 466
  gross and radiologic features, 463
  immunohistochemistry, 467–469, 472, 475–478, 480, 481
  incidence of, 463
  Ki-67 proliferative index, 472
  microscopic features, 463–467, 469–474
  morphologic features, 480
  pathogenesis and risk factors, 472–478, 481
  perineural invasion, 474
  prognosis, 463, 478, 481
  reticular architecture, 464
  SBR grading system, 466
  tubular component of, 471
  with high-grade transformation, 465
Adenolipomas, 254, 258
Adenomyoepithelioma (AME)
  AME-M, 246, 248
  differential diagnosis, 239, 241–243
  gross appearance, 238
  immunohistochemistry, 245, 246
  management, 246
  microscopic features, 239, 241–243
  molecular features, 246
  overview, 238
Adenosis
  apocrine adenosis, 174, 175
  clinical management and prognosis, 173, 174
  clinical, radiologic and gross features, 165
  differential diagnosis, 168–170
  immunohistochemical studies, 171
  microscopic features, 165–172, 174
  overview, 165
  pathogenesis, 171, 173
ADH-5 stain, 125
Adipophilin, 960
Alveolar rhabdomyosarcoma, 940–942, 944
American Joint Committee on Cancer (AJCC) Cancer Staging Manual, 411, 900
American Society of Clinical Oncology (ASCO), 421, 455, 909
Amyloid deposits, 149
Amyloidosis
  clinical findings, 149
  diagnosis, 149
  differential diagnosis, 150
  gross and radiologic findings, 149
  microscopic findings, 149, 150
  overview, 149
  pathogenesis, 149
  prognosis, 151
Anaplastic large cell lymphoma (ALCL), 813–815
Androgen receptor (AR), 881, 882, 958
Angioleiomyoma, 997, 998
Angiolipoma, 739, 747
Angiomatosis, 737, 738, 741
Angiosarcoma, 737, 744, 747
Anthracycline-taxane-based systemic therapy, 903
Anti-HER2 therapies, 908
Apocrine adenocarcinomas, 976
Apocrine adenosis, 174, 175
Apocrine carcinomas, 976, 989
Apocrine cystadenoma, 971
Apocrine cysts, 89, 976
Apocrine hidrocystoma, 971
Apocrine metaplasia, 89, 93, 341, 963
Apocrine nevus, 963, 964
Apocrine sweat gland carcinomas, 960
Architectural distortion, 8, 9
Atypical apocrine adenosis, 110
Atypical cystic apocrine metaplasia, 839
Atypical cystic hypersecretory, 365
Atypical ductal hyperplasia (ADH), 209, 216, 217, 376
  bilateral risk lesion, 376
  borderline with low-grade DCIS, 377
  diagnostic agreement rates, 376
  differential diagnosis, 377
  vs. FEA, 379–380
  gross and radiologic features, 377
  immunohistochemistry, 380
  microscopic features, 377
  outcomes, 383
  pathogenesis, 382
  patients with, 376
  vs. UDH, 378
Atypical fibroxanthoma, 994

© The Editor(s) (if applicable) and The Author(s), under exclusive license to Springer Nature Switzerland AG 2022

S. J. Shin et al. (eds.), *A Comprehensive Guide to Core Needle Biopsies of the Breast*,
https://doi.org/10.1007/978-3-031-05532-4

Atypical lobular hyperplasia (ALH), 615
clinical features, 618
differential diagnosis, 630, 633, 635–638
gross and radiologic features, 618, 619
immunohistochemistry, 628
microscopic features, 619, 621, 622
nomenclature and classification, 616, 617
pathogenesis, 640, 643, 644
prognosis and management, 646, 647, 649
Atypical pregnancy-like hyperplasia, 843
Atypical vascular lesion, 747, 754, 755

B
Bacterial infections, 159
Basal cell carcinoma, 964, 965
B-CLOSER-II study, 906
Becker's nevus, 997
Benign cutaneous lesions, 953
Benign cutaneous nerve sheath tumors, 1000
Benign masses, 760–767
Benign sebaceous neoplasms, 968
BerEP4, 960
Bio-absorbable carrier material (BCM), 23–24
Biodegradable carrier material (BCM), 34
Bioinformatics, 898, 904
Biomarker discovery, 907
Biomedical research, 2
Blastomycosis, 159
Blunt duct adenosis, 339
Borderline phyllodes tumor, 282
BRAF in melanoma and colon cancer, 896
Brandwein and Armed Forces Institute of Pathology (AFIP) methods, 496
Breast cancer genomes, 897
Breast cancer index (BCI, Biotheranostics), 901
Breast carcinoma
IBC
biopsy sample, pathologic report, 861
characteristics, 858, 859
differential diagnosis and immunohistochemical staining, 861, 867
gross and radiologic features, 859
microscopic features, 860, 867
pathogenesis, 862, 863
treatment and prognosis, 863, 864
NACT
biopsy specimen, 846
excisional specimen, 847–852
overview, 846
predictive factors for response, 846, 847
sentinel/axillary lymph nodes, 846
recurrent breast carcinoma
clinical presentation, 847, 848, 853–865
LRR, 847
treatment and prognosis, 858
Breast core needle biopsy program
benefits to
biomedical research, 2
medical care system, 2, 3
pathologists, 1, 2
patients, 1
radiologists, 1
surgeons, 2
bio-absorbable carrier material, 23–24
clips, 21, 22, 30
core correlation conference, 30
cryobiopsy, 20
fine needle aspiration, 19
free-hand ("tru-cut") CNBs, 21
imaging modalities
BI-RADS, 4, 5
magnetic resonance imaging, 16, 17
mammography, 4–6, 8–14
ultrasound, 14–16
intact, 21
localization device, 31
mastectomy
acute biopsy site changes, 34
biodegradable carrier material, 34
carcinomas with indeterminant size, 34
cautery/freezing artifact, 38
epithelial displacement, 35, 36
gross appearance, 32
healed core needle biopsy sites, 39
hemorrhage, 38
infarction, 37
reactive spindle cell nodule, 37
squamous cells, 36, 37
true needle track seeding, 36
missing cancers, 39–41
non-vacuum-assisted, 19, 20
pathologist, role of, 28, 29
radiologic/pathology correlation, 28
radiologist, role of, 29
recurrent cancers after
benign results, 42
prior core site, 41
site of needle track, 41–42
size of, 19
specimen processing
in pathology department, 26, 27
in radiology department, 24–26
specimen requisition form, 24
tissue changes, 27
specimen radiography of excisions, 31
types of, 18
vacuum-assisted, 20
very large, 20, 21
Breast Imaging-Reporting and Data System (BI-RADS), 4, 5, 332
Breast mass, 949
Breast metastasis, 782
Breast pathology (B-Path) study, 343
Breast-specific markers, 922–942
Breast tumors
children and adolescents
benign masses, 760–767
defined, 759
developing mammary gland, 759
developmental abnormalities, 759
malignant tumors, 771–772
mass-forming lesions, 759
non-neoplastic lesions, 760
secretory carcinoma, 769–771
males including adolescents
breast metastasis, 782
DCIS, 776–778
gynecomastia, 774, 776
invasive carcinoma, 778–782
supernumerary nipple, 760
Burkitt lymphoma (BL), 771, 812, 813

C
Calcifications, 9, 10, 86, 89–93
absent, 13, 14
distribution, 10
grouped, 10
linear distribution, 10
milk of calcium, 10, 12
number, 10, 12
over time, changes in, 11, 12
radiologic terms and pathologic correlation, 10
size, 10, 12
vascular, 10
Calcium oxalate crystals, 9, 10
The Cancer Genome Atlas (TCGA), 896
Capillary hemangioma, 737, 739
Carcinoma with apocrine differentiation
definition, 509
diagnostic criteria, 510
differential diagnosis, 518–520, 522–525
gene expression signatures, 509
gross and radiologic features, 510
immunohistochemistry
apocrine differentiation markers, 516–518
CEA positivity, 518
CK20 reactivity, 518
epithelial markers, 518
ER, PR, AR, and HER2 biomarkers, 512, 517
microscopic features, 510–513, 515, 516
pathogenesis and risk factors, 522, 524
prognosis and clinical management, 524–525
Cautery/freezing artifact, 27, 38
Cavernous hemangioma, 737, 740
Cell free or circulating tumour DNA (cfDNA or ctDNA), 907, 908
CellSearch CTC quantitation method, 908
Cellular fibroadenoma, 264
Central comedo-like tumor necrosis, 969
Central nervous system hemangiopericytoma, 942
Cholesterol granulomas, 138
Cholesteroloma, 138, 140
Chondroid syringoma (mixed tumor of the skin), 973, 974
Chondrolipomas, 254
Choriocarcinoma, 936
Circulating tumour cells (CTC), 907
Circulating tumour DNA (ctDNA), 907
CK5/6 staining, 375, 379, 960
Claudin-low molecular subtype, 900
Clinging carcinoma, 356
Clinical Proteomic Tumour Analysis Consortium, 904
Clips, 21, 22
Collagenous spherulosis (CS), 124, 437, 479, 480
College of American Pathologists (CAP) criteria, 455, 909
Columnar cell change (CCC), 331, 332
Columnar cell hyperplasia (CCH), 331, 332
Columnar cell lesions (CCLs)
blunt duct adenosis, 339
clinical and radiographic features, 331, 332
clinical management, 346, 347
columnar cell change, 331, 332
columnar cell hyperplasia, 331, 332
differential diagnosis, 341, 343, 344
FEA, 331, 339 (*see* Flat epithelial atypia)
immunohistochemical profile, 344, 345
microscopic features, 332, 333, 339, 341
pathogenesis, 345, 346
prognosis, 347, 348
Comedonecrosis, 138
COMET trial, 905
Complex fibroadenoma, 272
Complex hemangiomas, 737–738
Complex sclerosing lesions (CSLs), 178, 426–427
clinical management and prognosis, 183, 184
clinical, radiologic and gross features, 176
differential diagnosis, 179, 181
immunohistochemical work-up, 182
microscopic features, 176–181
overview, 175, 176
pathogenesis, 182, 183
Cooper ligaments, 714
Core biopsies, 906
Core correlation conference, 30
Core needle biopsy (CNB), 576, 949, 954
Cowden syndrome, 701
Cribriform DCIS, 371, 435–436
Crush artifact, 27
Cryobiopsy, 20
Cryptococcus, 159
Cryptorchidism, 779
Cutaneous adnexal neoplasms, 956
Cutaneous apocrine carcinomas, 960
Cutaneous epithelial neoplasms, 958
Cutaneous leiomyomas, 997
Cutaneous leiomyosarcoma, 998, 999
Cutaneous neoplasms, 955
Cutaneous sweat gland neoplasms, 960
Cylindroma, 983
Cystadenomas, 971
Cystically dominant lesions of breast, 80–83
Cystic apocrine adenosis, 841
Cystic apocrine papillary hyperplasia, 976
Cystic dilatation, 80
Cystic hypersecretory carcinoma, 357
Cystic hypersecretory hyperplasia (CHH), 89, 343
Cystic hypersecretory lesions (CHLs), 81, 89, 501, 592
core biopsy setting, 605
gross and radiologic features, 593
immunohistochemical work-up, 602
microscopic features, 593–596
pathogenesis, 604, 605
Cystic neutrophilic granulomatous mastitis, 140, 141, 143, 159
Cysticercosis, 160, 161
Cytokeratin (CK), 749, 908
Cytokeratin CK 7 and 20, 958
Cytokeratin 19 mRNA, 906
Cytologic atypia, 79

D
D2-40, 960
Decalcification agents, 907
Deepers, 98
Deeply basophilic calcifications, 89
Dermatofibroma, 716–718, 993, 994
Dermatofibrosarcoma protuberans (DFSP), 717, 995, 996
Dermatomyofibroma, 997
Desmoplastic melanomas, 993

Diabetic mastopathy
definition, 145
differential diagnosis, 147, 148
fine-needle aspiration cytology, 145
gross and radiologic features, 145
histologic changes, 145
inflammation, 146
microscopic and immunohistochemical features, 145
pathogenesis, 147, 148
prognosis, 148
stromal changes, 146
Diffuse dermal angiomatosis, 739, 742
Diffuse large B-cell lymphoma (DLBCL), 404, 453, 807–809, 923
Digital breast tomosynthesis (DBT), 4
DNA alterations in the tumour, 907
DNA copy number profiling, 897
DNA damage, 896, 898
DNA mutations, 907
Ductal apocrine adenocarcinoma (DAA), 976–978, 990
Ductal carcinoma in situ (DCIS), 100, 218, 331, 353, 578, 776–778, 790, 904–906, 957
vs. ADH, 351
gross and radiologic features, 353
high-grade, 353
low-grade, 353
immunohistochemistry, 374
incidence of, 353
microscopic features
cystic hypersecretory, 357
high-grade spectrum, 354
low-grade spectrum, 357
natural history study, 353
outcomes, 376
pathogenesis, 375
Ductal eccrine adenocarcinoma (DEA), 988
Duct ectasia, 156, 760
See also Mammary duct ectasia
Ductopapillary apocrine adenocarcinoma (DPAC), 976
Duct wall obliteration, 139

E

EBV-encoded RNA (EBER), 808
Eccrine adenocarcinomas, histologically simulate metastatic tumors, 988
Eccrine cylindroma, 983
Eccrine hidradenoma, 984
Eccrine nevus (Hamartoma), 963
Eccrine porocarcinoma, 979, 981, 982
Eccrine poroma, 979, 981
Eccrine spiradenoma, 983, 984
Eccrine syringofibroadenoma, 982
Eczematous dermatitis of the nipple, 953
EGFR inhibitors, 898
EGFR in lung cancer, 896
Elevated aldehyde dehydrogenase (ALDH1), 908
Encapsulated papillary carcinoma (EPC), 221, 227, 229
Endocrine therapy, 902
Endometrial carcinomas, 931, 932
EndoPredict (EP), 901
Eosinophilic luminal secretions, 86, 88
Epidermal inclusion cyst, 950
Epithelial displacement, 35, 36
Epithelial hyperplasia, 403
EPithelial ImmunoSPOT (EPISPOT) assay, 908
Epithelial membrane antigen (EMA), 658, 749
Epithelial mesenchymal transition (EMT, 908
Epithelial-myoepithelial tumors
AME
AME-M, 246, 248
differential diagnosis, 239, 241–243
gross appearance, 238
immunohistochemistry, 245, 246
management, 246
microscopic features, 239, 241–243
molecular features, 246
overview, 238
pleomorphic adenoma
differential diagnosis, 235–237
gross and radiographic features, 235
immunohistochemistry, 238
management, 238
microscopic features, 235–237
molecular features, 238
overview, 235
prognosis, 238
Epithelial neoplasms, 958–961
Epithelioid angiosarcoma, 453, 747
ERBB2 amplification, 896, 899
ERK inhibitors, 898
ERK5 inhibitors, 904
ER-negative (triple-negative) small glandular proliferations, 61, 63–66
Erosive adenomatosis, 972, 973
ER-positive small glandular proliferations, 49–51, 53, 55, 56, 58–61
ESO-ESMO guidelines for advanced breast cancer (ABC 5) consensus, 908
Estrogen receptor (ER), 210, 625, 656, 876, 958
Estrogen receptor-positive DCIS, 375
Ewing sarcoma, 942
Excluding concomitant microinvasive carcinoma, 102
Expression profiling, 899
Extensive mass-forming sclerosing adenosis, 402
Extramammary Paget disease, 989
Extraocular sebaceous carcinoma, 970

F

Fat necrosis
differential diagnosis, 134
gross and radiologic features, 131
histologic diagnosis, 131
microscopic features, 132, 134
overview, 131
palpable abnormality, 131
prognosis, 136
Fibroadenoma (FA), 760, 761, 763, 764, 829, 832, 833
clinical management and outcomes, 278, 279
clinical presentation, 259, 260
differential diagnosis, 270, 271, 273, 276
gross and radiologic features, 260
immunohistochemistry, 270
microscopic features, 260–273, 275
overview, 259, 260
pathogenesis, 277, 278
relative risk, 278
risk factors, 277, 278
Fibroblastic tumors, 994–996
Fibroepithelioma of Pinkus, 964–966
Fibrohistiocytic tumors, 993, 994
Fibromatosis, 71, 72, 713, 715, 993
Fibromatosis-like metaplastic carcinoma (FLMBC)

differential diagnosis, 534
immunohistochemistry, 534
microscopic features, 531–534
Fibromatosis-like pattern, 153
Fibrosis, 138
Fine needle aspiration (FNAs), 19
Flat epithelial atypia (FEA), 331, 332, 339
vs. columnar cell change, 338
definition, 333
diagnosis of, 331, 341, 343
differential diagnosis, 341, 342
flat growth pattern, 333
histologic features, 341
MIB-1 proliferation index, 344
nuclear-to-cytoplasmic ratio, 333
Rosen triad, 340
with atypical ductal hyperplasia, 339
with atypical lobular hyperplasia, 340
with focal architectural atypia, 338
with prominent cellular stratification, 337
Florid adenosis, 166, 168, 169
Florid papillomatosis of the nipple, 972
Florid phase gynecomastia, 775
Fluorescence in situ hybridization (FISH), 671, 779
Focus of enhancement, 17
Follicular lymphoma, 811, 812
FoundationOne CDx, 898
Free-hand (“tru-cut”) CNBs, 21
Fungal infections, 159

G
Galactocele, 760
GATA3, 958
Gauze artifact, 27
GCDFP-15 labeling, 931
GCDFP–15 + Mammaglobin multiplex immunostain, 128
Gene expression analysis, 899
Gene expression-based clinical tools, 900–902
Gene expression profiling, 899, 900
Gene molecular grade index (MGI), 901
Genome architecture, 896
Genome instability, 897
Genome sequencing studies, 907
Genomic assays, 897, 898
Genomic profiling of core needle biopsy material, 899
Genomics for personalised medicine, 895–899
Gil Del Alcazar, C.R., 905
Glycogen-rich clear cell carcinoma (GRCCC), 606, 607
Granular cell tumor, 147, 718–722
Granulocytic sarcoma, 818, 819
Granulomas, 144
Granulomatous inflammation, 140
Granulomatous lobular mastitis, 156
clinical and imaging features, 140
definition, 140
differential diagnosis, 141
gross and radiologic features, 141
histochemical stains, 142
microscopic features, 141
pathogenesis, 144
prognosis, 144
Gross cystic disease fluid protein-15 (GCDFP-15), 958
Gynecologic primary carcinomas of the endometrium, 931
Gynecomastia, 774, 776

H
Hair follicle neoplasms, 967–968
Hamartoma, 699–701, 963
Hamartomatous and reactive sweat gland proliferations, 963
Healed core needle biopsy sites, 39
Hemangioma, 747
Hematopoietic neoplasms, 806, 917, 923
Hematoxylin and eosin (H&E) levels, 97
Hemorrhage, 38
HER2-enriched molecular subtype, 900
Heterogeneous morphology calcifications, 11
Hibernomas, 696, 697
Hidradenocarcinoma, 984, 986
Hidradenoma (HA), 499, 950, 984
High-grade serous carcinoma of tubal/ovarian origin, 929
High-grade spectrum
differential diagnosis, 362
gross and radiologic features, 353
microscopic features, 354
Histiocytic sarcoma, 819, 820
Histoplasmosis, 159
Hormone receptor (HR), 655
differential diagnosis, 875
estrogen receptor, 876
interpretation, 876–881
progesterone receptor, 876
recommendations, 876, 877, 879
HRDetect, 897
HR-mediated DNA repair, 897
Human epidermal growth factor receptor 2 (HER2)
amplification and expression, 904
CAP, 885
discovery and therapeutic targeting, 882
FISH, 883
histology, 884
hormone receptor testing, 884
immunohistochemistry, 882, 883, 885
in situ hybridization, 885, 888, 889
interpretation, 884–886, 890
limitations, 886–889, 891
kinase inhibitors for *ERBB2* mutations, 898
molecular subtyping, 889, 890
positive breast cancers, 900
prevalence, 883
proliferation, 889–891
staining, 375
status, 903

I
IgG4-related sclerosing mastitis (IgG4-SM), 151
Immunoglobulin G4-related disease (IgG4-RD)
differential diagnosis, 151, 153
gross and radiologic features, 151
histomorphologic and immunhistochemical findings, 151
microscopic features, 151, 152
overview, 151
prognosis, 153
Immunohistochemistry/immunohistochemical (IHC) staining, 808, 957
Immunophenotypic analysis, 805
Immunostains, 928, 936
Incomplete/tangential sections, 102–106
Infarction, 37
Infectious mastitis, 155
Infiltrating epitheliosis (IE), 179, 488

Inflammatory breast carcinoma (IBC)
biopsy sample, pathologic report, 861
characteristics, 858, 859
differential diagnosis, 861, 867
gross and radiologic features, 859
immunohistochemical staining, 861, 867
microscopic features, 860, 867
pathogenesis, 862, 863
treatment and prognosis, 863, 864
Inflammatory myofibroblastic tumors (IMT), 154
differential diagnosis, 155
etiology, 153
gross and radiologic features, 153
immunohistochemistry, 154, 155
microscopic features, 153
overview, 153
prognosis, 155
Initial H&E sections and/or slides, 97–101
In situ ductal/lobular carcinoma, 956
Intact Breast Lesion Excision System (BLES™), 21
Intact core needle biopsy, 21
International Cancer Genome Consortium (ICGC), 896
International Immuno-Oncology Biomarker Working Group on Breast Cancer, 456
Intraductal papilloma
adenomyoepitheliomatous features, 206, 209
ADH, 209, 216, 217
apocrine metaplasia, 208, 212
cellular stroma, 209, 215
classification, 215
differential diagnosis, 210, 220
dilated/fibrotic duct, 206, 207
entrapped glands, 209, 216
examples, 206, 210
fibrovascular cores, 206, 208
florid usual ductal hyperplasia, 206, 211
gross and radiographic features, 206
hypereosinophilic coagulative necrosis, 208, 212
immunohistochemical features, 210, 220
low magnification, 206, 208
management, 213, 215
molecular analyses, 213
myoepithelial cells, 206, 209
overview and clinical presentation, 205
prognosis, 215
sclerosing papilloma, 208, 214
squamous metaplasia, 208, 213
tissue fragments, 206, 207
Intraductal proliferations
characteristics, 351
cytologic features, 351
diagnosis, 351
Intrinsic molecular subtypes of breast cancer, 900
Invasive breast carcinoma of no special type (IBC-NST)
chalky-white appearance, 393
core needle biopsy, 401
diagnosis of, 391
differential diagnosis, 401–405, 407–409
digital breast tomosynthesis (DBT), 393
histologic grading, 396, 398, 399
immunohistochemistry, 405, 406
magnetic resonance imaging (MRI), 392, 393
mammographic findings, 391, 392
microscopic features, 394
morphology of, 394, 395
pathogenesis, 406, 408, 410
prognosis, 410
Surveillance Epidemiology and End Results (SEER) data, 391
ultrasonography, 391
with lobular features, 396
with targetoid growth pattern, 395
Invasive breast carcinoma with medullary pattern
clinical presentation, 554
differential diagnosis, 558, 559
gross and radiologic features, 554
immunohistochemistry, 557, 558
microscopic features, 554–557
pathogenesis and risk factors, 558
prognosis and clinical management, 558, 560
Invasive breast carcinoma with osteoclast-like multinucleated giant cells, 607–609
Invasive carcinoma, 779
Invasive cribriform carcinoma (ICC)
differential diagnosis, 435–438
gross and radiologic features, 433
immunohistochemistry, 437–438
microscopic features, 433–435
prognosis, 438
Invasive ductal carcinoma (IDC), 454, 655, 846, 964
Invasive lobular carcinoma (ILC), 655, 846
differential diagnosis, 674, 677, 680
gross and radiologic features, 656, 657
histologic grading, 665
immunohistochemistry, 668–671, 673
incidence and clinical presentation, 655, 656
microscopic features, 657, 658, 660, 662, 663
pathogenesis, 681, 682
prognosis and clinical management, 682–684
tumor microenvironment, 667
Invasive mammary carcinoma with osteoclast-like giant cells, 437
Invasive micropapillary carcinoma, 581
differential diagnosis, 582, 583
gross and radiologic features, 581
immunohistochemical work-up, 583
microscopic features, 582
pathogenesis, 583
prognosis, 584
Invasive papillary carcinoma, 229

J

Juvenile breast carcinoma, 500
Juvenile fibroadenoma, 273
Juvenile papillomatosis, 83, 84, 765–767

K

Keloids, 994
Ki67 assessment, 890, 891
Ki67 expression, 902
Klinefelter's syndrome, 779

L

Lactating adenoma
cause of, 827
differential diagnosis, 829, 831–834
gross and radiologic features, 827, 828
immunohistochemical staining, 829
microscopic features, 827, 830
pathogenesis, 829
treatment and prognosis, 831

Lactational abscess, 157
Lactational (puerperal) mastitis, 156
Langhans giant cells, 144
Large-scale state transitions (LST), 897
Laser-capture microdissection technology, 907
Leiomyomas, 697–699
Leiomyomatous myofibroblastoma, 997
Leiomyosarcoma, 939
Lipomas, 691
Liquid biopsy, 907–909
Lobular carcinoma in situ (LCIS), 124, 210, 219, 615–617, 620–624, 629, 631, 635, 638–640, 642, 655
  atypical lobular hyperplasia, 619–621
  clinical features, 618
  differential diagnosis, 630, 631, 633, 635–638
  florid, 622, 624
  gross and radiologic features, 618, 619
  histopathologic features, 619
  immunohistochemistry, 625, 628, 629
  microscopic features, 619
  morphologic features, 635
  nomenclature and classification, 616, 617
  pathogenesis, 640, 643, 644
  pleomorphic, 621, 644
  prognosis and management, 645, 646, 649
Localized hyperhidrosis, 963
Locoregional recurrence (LRR), 847
Loss of heterozygosity (LOH), 897
Low-grade adenosquamous carcinoma (LGASC), 428, 431, 986
  diagnosis, 526
  differential diagnosis, 529, 530
  immunohistochemistry, 528–529
  microscopic features, 526–528
Low-grade angiosarcoma, 750
Low-grade DCIS, 345
Low-grade mucoepidermoid carcinoma, 504
Low-grade spectrum
  differential diagnosis, 370
  gross and radiologic features, 353
  microscopic features, 357
Luminal A tumours, 900
Luminal B tumours, 900
Luminal/ER-positive tumours, 900
Luminal secretions, 84–89
Lupus mastitis, 954
Lymphoid infiltrates, 805
Lymphoma, 147

M
Magnetic resonance imaging (MRI), 16, 691
  DCIS, 353
  focus of enhancement, 17
  mass-like enhancement, 17
  non-mass-enhancement, 17
Malignant adenomyoepithelioma (AME-M), 246, 248
Malignant melanoma, 955
Malignant spindle cell tumors, 79
Mammaglobin, 958
MammaPrint®, 901
Mammary angiosarcoma, 743
Mammary carcinoma, 131
Mammary duct ectasia
  clinical management, 790
  differential diagnosis, 138, 139, 790
  gross and radiologic features, 137, 790
  immunohistochemistry, 139
  microscopic features, 137, 138, 790, 791
  nipple discharge, 136
  overview, 136
  pathogenesis, 139, 790
  prognosis, 139, 790
  with intraepithelial histiocytes, 138
Mammary fibromatosis, 70, 71
Mammary hamartoma
  clinical presentation, 253
  differential diagnosis, 257
  gross and radiologic features, 253, 254
  immunohistochemistry, 254
  microscopic features, 254–256, 258, 259
  overview, 253
  pathogenesis, 257, 258
  recurrences, 259
  risk fators, 257, 258
Mammary lobules, 963
Mammary neoplasms, 956, 961, 962
Mammary small cell carcinoma, 992
Mammographic calcifications, 954, 955
Mammography
  architectural distortion, 8, 9
  calcifications, 9, 10
    absent, 13, 14
    distribution, 10
    grouped, 10
    linear distribution, 10
    milk of calcium, 10, 12
    number, 10, 12
    over time, changes in, 11, 12
    radiologic terms and pathologic correlation, 10
    size, 10, 12
    vascular, 10
  craniocaudal (CC) view, 4
  density, 8
  focal asymmetry, 9
  margin, 6, 7
  masses, 6
  medial–lateral (ML) or vertical view, 4, 5
  medial–lateral–oblique (MLO) view, 4
  size, 6
Mammosite®, 131
Marginal zone lymphoma (MALT Lymphoma), 809, 810
Mass-like enhancement, 17
Mastectomy
  acute biopsy site changes, 34
  biodegradable carrier material, 34
  carcinomas with indeterminant size, 34
  cautery/freezing artifact, 38
  epithelial displacement, 35, 36
  gross appearance, 32
  healed core needle biopsy sites, 39
  hemorrhage, 38
  infarction, 37
  reactive spindle cell nodule, 37
  squamous cells, 36, 37
  true needle track seeding, 36
Mastitis obliterans, 138
Matrix-assisted laser desorption/ionisation imaging mass spectrometry (MALDI-IMS), 142, 904
Medical care system, 2
Melanocytic proliferations, 992
Melanoma, 677, 923
Memorial Sloan Kettering Cancer Center, 898

Merkel cell carcinoma (cutaneous neuroendocrine carcinoma), 917, 929, 955, 990, 992
Merkel cell polyomavirus (MCV), 991
Mesenchymal tumors, 993
  angiolipoma
    differential diagnosis, 694
    immunohistochemical work-up, 695
    microscopic features, 694
    pathogenesis, 695–696
    prognosis and management, 696
    radiologic features, 693
  dermatofibroma, 716–718
  fibromatosis, 713, 715
  hamartomas, 699–701
  hibernomas, 696, 697
  leiomyomas, 697–699
  lipomas
    differential diagnosis, 693
    immunohistochemical work-up, 693
    microscopic features, 691
    pathogenesis, 693
    prognosis and management, 693
  myofibroblastomas, 703, 704, 706, 708
  neural derived tumors
    granular cell tumors, 718–722
    neurofibromas, 721, 722, 724
    primary sarcomas, 725–730
    schwannomas, 724, 725
  nodular mucinosis, 701–703
  non-epithelial components, 691
  PASH, 709–713
Messenger RNA (mRNA), 899, 902
METABRIC cohort, 900
Metaplastic carcinoma, 178
  clinical features, 526
  definition of, 525
  epithelial and sarcomatoid, 525
  fibromatosis-like metaplastic carcinoma (*see* Fibromatosis-like metaplastic carcinoma (FLMBC))
  gross and radiologic features, 526
  low-grade adenosquamous carcinoma (*see* Low-grade adenosquamous carcinoma (LGASC))
  morphologic features, 525
  patient age distribution, 526
  WHO classification, 525
Metaplastic carcinoma with heterologous mesenchymal differentiation
  differential diagnosis, 545, 550
  immunohistochemistry, 545, 549
  microscopic features, 544–547
Metastases to breast
  histologic features, 921
  imaging findings on mammography and ultrasound, 918
  lymphovascular invasion, 921
  mammography and ultrasound, 918
  microcalcifications, 919
  ultrasound features, 919
Metastatic adenocarcinoma, 936
Metastatic alveolar rhabdomyosarcoma, 773, 944
Metastatic cervical adenocarcinoma, 939
Metastatic choriocarcinoma to the breast, 942
Metastatic colonic adenocarcinoma, 938
Metastatic endometrioid endometrial carcinoma to the breast, 933
Metastatic hemangiopericytoma of the central nervous system, 945
Metastatic high-grade papillary serous carcinoma of tubal/ovarian origin, 932
Metastatic leiomyosarcoma, 939
Metastatic lesions to skin, 954
Metastatic malignant melanoma, 452
Metastatic medullary thyroid carcinoma, 941
Metastatic melanoma, 783, 923, 926
Metastatic mucinous bladder adenocarcinoma, 940
Metastatic pulmonary adenocarcinoma, 927, 929
Metastatic pulmonary small cell carcinoma to the breast, 921, 931
Metastatic pulmonary squamous cell carcinoma, 930
Metastatic renal cell carcinoma, 499, 920
Metastatic rhabdomyosarcoma, 917
Metastatic small cell carcinoma, 929
Metastatic squamous cell carcinoma, 925
Metastatic well-differentiated follicular thyroid carcinoma, 941
Metastatic well-differentiated neuroendocrine tumors, 935
MIB-1 proliferation index, 344
Microcystic adnexal carcinoma (MAC), 986, 987
Microglandular adenosis (MGA), 427–429
  clinical management and prognosis, 192
  clinical, radiologic and gross features, 184
  differential diagnosis, 187, 189–191
  immunohistochemical Work-up, 189
  microscopic features, 184–188
  overview, 184
  pathogenesis, 189, 191
Microinvasive carcinoma (MIC)
  definition, 411
  differential diagnosis, 413, 416–420
  gross and radiologic features, 411
  immunohistochemistry, 417
  microscopic features, 411–413, 415
  prognosis, 418, 421
Micropapillary DCIS, 840
Micropapillary intraluminal hyperplasia, 971
Mimicking primary breast carcinoma, 714
Mixed metaplastic carcinomas, 551–554
Moh's micrographic surgery, 996
Molecular analysis of CTCs, 908
Molecular analysis of small tissue biopsies, 906–907
Molecular apocrine tumours, 900
Molecular profiling, 905
Molecular testing to core biopsies for guiding patient management, 896
Montgomery's glands, 949
Morphological and molecular intratumoural heterogeneity, 907
MOSCATO 01, 899
MSK-IMPACT, 898
Mucinous carcinoma, 575, 974
  differential diagnosis, 578, 579
  microscopic features, 576, 577
  pathogenesis, 580
  prognosis, 581
Mucinous cystadenocarcinoma, 584
  differential diagnosis, 584
  gross and radiologic features, 584
  immunohistochemical work-up, 585
  microscopic features, 584
  pathogenesis, 586
  prognosis, 586
Mucinous eccrine nevus, 963
Mucocele-like lesion (MLL), 578
  clinical management and prognosis, 199–201
  clinical, radiologic and gross features, 192, 193
  differential diagnosis, 193, 195, 199, 200
  immunohistochemical work-up, 195
  microscopic features, 193–198
  overview, 192

pathogenesis, 196, 199
Mucoepidermoid carcinoma (MEC)
Brandwein and Armed Forces Institute of Pathology (AFIP) methods, 496
differential diagnosis
breast tumors with clear cell cytology, 499
ductal carcinoma in situ, 498
hidradenoma (HA), 499
metaplastic carcinoma, 499
metastatic renal cell carcinoma, 499
papillary lesions, 498
secretory carcinoma, 498, 499
simple cysts, 497
usual ductal hyperplasia, 498
gross and radiologic features, 490
immunohistochemistry, 496, 497
incidence, 489
microscopic features, 490–493, 495–497
pathogenesis, 500
physical examination, 490
prognosis and clinical management, 500
Mucosa-associated lymphoid tissue (MALT), 404, 805
Multi-gene expression assays, 902
Multinucleated stromal giant cells, 147
Multiplex diagnoses, in CNB samples, 108–118, 120, 121, 124, 125
Multiplex immunohistochemistry, 125–128
Myeloid sarcoma, 818, 819, 924
Myofibroblastic tumors, 997
Myofibroblastoma, 77, 703, 704, 706, 708, 942, 994
Myoid hamartoma, 254, 259, 998
Myriad myChoice test, 897
Myxoid FAs, 262
Myxoid/granulation-tissue type (fasciitis-like) pattern, 153

N
Nashville Breast Cohort, 347
National Comprehensive Cancer Network (NCCN), 347, 907
Necrotizing granulomas and abscesses, 159
Neoadjuvant chemotherapy (NACT)
biopsy specimen, 846
excisional specimen, 847–852
overview, 846
predictive factors for response, 846, 847
SLN, 846
NeoALTTO Phase III trial, 908
Nerve sheath tumors, 1000
Neuroendocrine neoplasm (NEN), 586, 934
differential diagnosis, 588
gross and radiologic features, 586
immunohistochemical work-up, 589
microscopic features, 588
pathogenesis, 589
prognosis, 590, 591
Neuroendocrine tumor/carcinoid tumor, 934–936
Neurofibromas, 721, 722, 724
Nevus sudiferous, 963
Next generation sequencing (NGS), 590, 897, 898
Nipple
adenoma
differential diagnosis, 793–795
gross and radiologic features, 792
microscopic features, 792–794
pathogenesis, 795
prognosis and clinical management, 795
erythematous rash, 787
lactiferous duct, 787–789
lactiferous sinuses, 787, 788
mammary duct ectasia, 787, 788
differential diagnosis, 790
gross and radiologic features, 790
microscopic features, 790, 791
pathogenesis, 790
prognosis and clinical management, 790
nipple-invasive primary carcinomas, 798
Paget disease
differential diagnosis, 798, 802
gross and radiologic features, 798
microscopic features, 798–801
occurrence, 798
pathogenesis, 803
prognosis and clinical management, 803
skin lesions, 798
SSDH
differential diagnosis, 796
gross and radiologic features, 795
history, 795
microscopic features, 795
pathogenesis, 796
prognosis and clinical management, 796
syringomatous tumor
differential diagnosis, 796
gross and radiologic features, 796
history, 796
microscopic features, 796, 797
pathogenesis, 796, 798
prognosis and clinical management, 798
Nipple adenoma, 972–973
differential diagnosis, 793–795
gross and radiologic features, 792
microscopic features, 792–794
pathogenesis, 795
prognosis and clinical management, 795
Nipple-invasive primary carcinomas, 798
Nipple leiomyoma, 999
NKX3.1 labeling, 936
Nodular and clear cell hidradenoma (acrospiroma), 985
Nodular mucinosis, 701–703
Non-hematopoietic, solid organ metastases, 942
Non-Hodgkin lymphoma, 805
Non-lactating breast abscess, 157
Non-mass enhancement (NME), 17
Non-necrotizing granulomatous mastitis, 140
Non-puerperal abscesses, 156
Non-vacuum-assisted core needle biopsy, 19, 20
Nottingham grading system, 396, 399
Nottingham Prognostic Index (NPI), 396
Nuclear atypia, 531
Nuclear pleomorphism, 398
Nucleic acid amplification technology, 906
Nurses' Health Study, 347

O
Obliteration of duct wall, 139
Ochrocytes, 138
Oestrogen signalling, 903
Oncotype DX Breast Cancer Assay, 899, 900, 905
One-step nucleic acid amplification (OSNA) assay, 906
OPTIMA trial, 902
Optimal chemotherapy, 782
Orchitis, 779
"Ossifying type" calcifications, 91
Ovarian carcinoma, 929–931

P
p40 antibody, 958, 959
p63, immunohistochemical staining patterns, 959
p120 +E-cadherin breast cocktail, 125
Paget's disease, 777
  apocrine type, 989–990
  differential diagnosis, 798, 802
  gross and radiologic features, 798
  microscopic features, 798–801
  occurrence, 798
  pathogenesis, 803
  prognosis and clinical management, 803
Palpable lipomas, 691
PAM50 method, 901, 905
Papillary carcinoma
  core needle biopsy, 233, 235
  EPC, 221, 227, 229
  gross and radiographic features, 221
  invasive papillary carcinoma, 229
  microscopic features, 221–223, 225, 226
  molecular features, 233
  overview, 220, 221
  papillary DCIS, 221
  SPC, 227, 229–231, 234
Papillary DCIS, 221, 373
Papillary eccrine adenoma, 975
Papillary endothelial hyperplasia, 738
Papillary lesion, 777
  intraductal papilloma
    adenomyoepitheliomatous features, 206, 209
    ADH, 209, 216, 217
    apocrine metaplasia, 208, 212
    cellular stroma, 209, 215
    classification, 215
    DCIS, 218
    differential diagnosis, 210, 220
    dilated/fibrotic duct, 206, 207
    entrapped glands, 209, 216
    examples, 206, 210
    fibrovascular cores, 206, 208
    florid usual ductal hyperplasia, 206, 211
    gross and radiographic features, 206
    hypereosinophilic coagulative necrosis, 208, 212
    immunohistochemical features, 210, 220
    LCIS, 210, 219
    low magnification, 206, 208
    management, 213, 215
    molecular analyses, 213
    myoepithelial cells, 206, 209
    overview and clinical presentation, 205
    prognosis, 215
    sclerosing papilloma, 208, 214
    squamous metaplasia, 208, 213
    tissue fragments, 206, 207
  overview, 205
  papillary carcinoma
    core needle biopsy, 233, 235
    EPC, 221, 227, 229
    gross and radiographic features, 221
    invasive papillary carcinoma, 229
    microscopic features, 221–223, 225, 226
    molecular features, 233
    overview, 220, 221
    papillary DCIS, 221
    SPC, 227, 229–231, 234
Papillary thyroid carcinoma, 917
Paraffin-embedded unstained slides, 809, 811
Parasitic infections, 160
Pattern-based evaluation
  calcifications, 86, 89–93
  cystically dominant lesions of breast, 80–83
  luminal secretions, 84–89
  small glandular proliferations
    ER-negative (triple-negative), 61, 63–66
    ER-positive, 49–51, 53, 55, 56, 58–61
  spindle cell proliferations, 67–69, 73, 75
  to core needle biopsies, 47–48
PAX5, 960
PCR-based techniques, 899
Periductal fibrosis, 790
Periductal mastitis, 156
Periductal stromal hyperplasia, 290
Periductal stromal sarcoma, 290
Periductal stromal tumor, 290
Perilobular capillary hemangiomas, 737
Perilobular hemangioma, 737, 738
Personalised therapy, 895
Phyllodes tumor (PTs)
  clinical presentation, 279, 280
  differential diagnosis, 308–312, 314, 315
  grading, 295, 297, 299–302, 304
  gross and radiologic features, 280
  histological features, 280–286, 288, 290–292, 295, 296, 298
  immunohistochemistry, 306, 307
  metastases and survival, 317
  molecular pathology, 316, 317
  overview, 279, 280
  pathogenesis, 316, 317
  recurrence, 302, 305, 306, 317
  risk factors, 316, 317
  treatment, 317, 318
PIK3CA, 898
PI3K pathway, 904
Plasma cell mastitis, 153
Plasma cell myeloma, 925
Plasma cell neoplasm, 820, 821
Pleomorphic adenoma (PA)
  differential diagnosis, 235–237
  gross and radiographic features, 235
  immunohistochemistry, 238
  management, 238
  microscopic features, 235–237
  molecular features, 238
  overview, 235
  prognosis, 238
Pleomorphic invasive lobular carcinoma, 511
Pleomorphic lobular carcinoma (PLCIS), 365
Podoplanin, 960
Polymerase chain reaction (PCR) analysis, 805
Poorly differentiated angiosarcomas, 745, 746
Post-radiation angiosarcoma, 743
PREDICT study, 898
Predictive marker
  androgen receptor, 881, 882
  biological tissue, 873
  biomarkers testing, 874, 875
  definition, 873
  HER2, 873
    CAP, 885
    discovery and therapeutic targeting, 882
    FISH, 883
    histology, 884
    hormone receptor testing, 884
    immunohistochemistry, 882, 883, 885

in situ hybridization, 885, 888, 889
interpretation, 884–886, 890
limitations, 886–889, 891
molecular subtyping, 889, 890
prevalence, 883
proliferation, 889–891
hormone receptors
differential diagnosis, 875
estrogen receptor, 876
interpretation, 876–881
progesterone receptor, 876
recommendations, 876, 877, 879
Pregnancy
clinical management
chemotherapy, 827
radiologic imaging and biopsy, 826
surgery, 827
histopathologic and physiologic changes, 825, 826
IBC
biopsy sample, pathologic report, 861
characteristics, 858, 859
differential diagnosis and immunohistochemical staining, 861, 867
gross and radiologic features, 859
microscopic features, 860, 867
pathogenesis, 862, 863
treatment and prognosis, 863, 864
lactating adenoma
cause of, 827
differential diagnosis, 829, 831–834
gross and radiologic features, 827, 828
immunohistochemical staining, 829
microscopic features, 827, 830
pathogenesis, 829
treatment and prognosis, 831
NACT, breast carcinoma
biopsy specimen, 846
excisional specimen, 847–852
overview, 846
predictive factors for response, 846, 847
sentinel/axillary lymph nodes, 846
PABC
biomarker evaluation, 836
definition, 833
gross and radiologic features, 833, 835
immunohistochemical staining, 836
microscopic features, 833
molecular subtypes, 836
treatment and prognosis, 837
papilloma, 827
pregnancy-like change and pregnancy-like hyperplasia
differential diagnosis, 839–845
gross and radiologic features, 837
history, 837
immunohistochemistry, 843
microscopic features, 837, 838, 840
pathogenesis, 844
treatment and prognosis, 844, 846
recurrent breast carcinoma
clinical presentation, 847, 848, 853–865
LRR, 847
treatment and prognosis, 858
Pregnancy-like (pseudolactational) hyperplasia (PLH), 343
Pregnancy-like (pseudolactational) proliferations
differential diagnosis, 839–845
gross and radiologic features, 837
history, 837
immunohistochemistry, 843
microscopic features, 837, 838, 840
pathogenesis, 844
treatment and prognosis, 844, 846
Pregnancy-related breast carcinomas (PABC)
biomarker evaluation, 836
definition, 833
gross and radiologic features, 833, 835
immunohistochemical staining, 836
microscopic features, 833
molecular subtypes, 836
treatment and prognosis, 837
Premature thelarche, 759
Primary and secondary angiosarcomas, 743
Primary breast cancer, 766
Primary breast lymphoma, 806
ALCL, 813–815
Burkitt lymphoma, 812, 813
definition, 806
differential diagnosis, 816, 817
DLBCL, 807–809
epidemiological features, 806, 807
follicular lymphoma, 811, 812
gross and radiologic features, 807
MALT lymphoma, 809, 810
pathogenesis, 817
patient history, 806
treatment and prognosis, 817
types of, 815
Primary cutaneous mucinous carcinoma, 977, 979
Primary cutaneous squamous cell carcinoma (SCC), 966, 967
Primary mammary angiosarcoma, 743
Primary mammary Hodgkin's disease, 772
Primary sarcomas, 725–730
Problems in Breast Pathology, 331
Progesterone receptor (PR), 876, 958
Programmed death-ligand 1 (PD-L1), 908
Prostate carcinoma, 917, 936
Proteomic analysis of tumour samples by RPPA, 903
Proteomic profiling, 907
Proteomics, 902–904
Psammomatous calcifications, 90, 944
Pseudoangiomatous stromal hyperplasia (PASH), 254, 691, 709–713, 747, 764–765, 993
Pseudoinvasive growth patterns, central desmoplastic stroma, 957
Pseudolumens, 464
Pseudolymphoma, 806
Pseudo-micropapillary structures, 28
Pseudoneoplastic lesions of sweat glands, 963–964
Pulmonary adenocarcinoma, 924–925
Pulmonary small cell carcinoma, 928–929
Pulmonary squamous cell carcinoma, 925–927

Q

Quantitative reverse transcriptase PCR (qRT-PCR) assay, 901

R

Radial scars (RS)
clinical management and prognosis, 183, 184
clinical, radiologic and gross features, 176
differential diagnosis, 179, 181
immunohistochemical work-up, 182
microscopic features, 176–181
overview, 175, 176
pathogenesis, 182, 183

Reactive lesions/syringometaplasias, 963–964
Reactive spindle cell nodule, 37
Reed-Sternberg cells, 772
Relative risk (RR), 278
Renal cell carcinoma, 933, 934
Reverse phase protein array (RPPA), 903
Rhabdomyosarcomas, 942
Risk of recurrence (ROR) score, 901
RNA-seq, 899
Rosai–Dorfman Disease, 135, 136, 141, 153
Rosen triad, 345

S
SAFIR01/UNICANCER, 899
Sarcoidosis
  differential diagnosis, 145
  gross and radiologic features, 144
  microscopic features, 144
  overview, 144
  prognosis, 145
Scarff-Bloom-Richardson (SBR) system, 396, 466, 496, 501
Schistosomiasis, 160
Schwannomas, 724, 725
Sclerosed micropapillomas, 768
Sclerosing adenosis, 53, 57, 111, 122
Sclerosing papilloma, 403
Sclerotic fibroma, 995
Sebaceoma, 969
Sebaceous adenoma, 968
Sebaceous carcinomas, 969
Secondary breast lymphoma
  definition, 817
  histiocytic sarcoma, 819, 820
  myeloid sarcoma, 818, 819
  plasma cell neoplasm, 820, 821
Secretory carcinoma, 769–771, 829, 834
  acinic cell carcinoma, 504
  carcinoma with apocrine differentiation, 508
  cystic hypersecretory lesions, 501
  gross and radiologic features, 501
  immunohistochemistry, 501, 505, 506
  lactational/lactational-like change, 501
  low-grade mucoepidermoid carcinoma, 504
  microscopic features, 501, 502, 504
  morphologic and immunophenotypic features, 500
  pathogenesis, 508, 509
  prognosis and clinical management, 509
  tall cell carcinoma with reversed polarity, 508
  usual ductal hyperplasia, 504
Sensory nerve endings, 949
Sentinel lymph node (SLN), 846
Sentinel lymph node biopsy (SLNB), 421, 767, 906
Small cell carcinomas, 928
Smooth muscle hamartoma, 997–1000
Smooth muscle heavy chain myosin (SMM), 829
Smooth muscle tumors, 997–1000
Solid papillary carcinoma (SPC), 227, 229–231, 234
Solid patterns, 371
Somatic mutations, 895
Sparganosis, 160
Spindle cell carcinomas
  differential diagnosis, 537, 539, 540
  immunohistochemistry, 534, 536
  microscopic features, 534–538
Spindle cell lesions of breast, 961
Spindle cell metaplastic carcinoma, 69
Spindle cell proliferations, 67–69, 73, 75
Spindled DCIS, 372
Spiradenoma, 952
Squamoid eccrine ductal carcinoma, 986, 987
Squamous cell carcinoma (SCC), 966
  differential diagnosis, 542, 543
  etiology of, 540
  immunohistochemistry, 542
  microscopic features, 540–542
Squamous cells, 36, 37
Squamous metaplasia of lactiferous ducts (SMOLD), 139
  differential diagnosis, 788, 789
  gross and radiologic features, 788
  histopathology and biology, 789
  history, 788
  microscopic features, 788–790
  prognosis and clinical management, 789
16S rRNA sequencing methods, 142
Storiform collagenoma, 995
Stromal calcifications, 100
Stromal fibrosis, 147
Subareolar abscess, 156, 158
Subareolar sclerosing duct hyperplasia (SSDH)
  differential diagnosis, 796
  gross and radiologic features, 795
  history, 795
  microscopic features, 795
  pathogenesis, 796
  prognosis and clinical management, 796
Subcutaneous fat, 949
Superficial shave/punch biopsy of skin, 956
Surface-enhanced laser desorption/ionisation time of flight (SELDI-TOF) mass spectrometry, 904
Sweat gland adenomas, 975–976
Sweat glands, pseudoneoplastic lesions, 963–964
Syringocystadenoma papilliferum, 972
Syringofibroadenoma, 982
Syringoma, 977, 979, 980
Syringomatous tumor
  differential diagnosis, 796
  gross and radiologic features, 796
  history, 796
  microscopic features, 796, 797
  of nipple-areolar region, 428
  pathogenesis, 796, 798
  prognosis and clinical management, 798

T
Talazoparib, 457
Tall cell carcinoma with reversed polarity (TCCRP), 508
  differential diagnosis
    cytologic features, 487
    immunohistochemical markers, 488
    immunolabeling, 488
    infiltrating epitheliosis (IE), 488
    metastatic papillary thyroid carcinoma, 488
  gross and radiologic features, 482
  histologic and molecular features, 481
  immunohistochemistry, 483, 484, 486–488
  microscopic features, 482–485
  pathogenesis and risk factors, 489
  prognosis and clinical management, 489
Targeted ultrasound, 949
Telomeric allelic imbalance (TAI), 897

Testicular injury, 779
3D mammography, 5
Trastuzamab plus chemotherapy, 782
Trichoblastoma, 967
Triple-negative breast cancer (TNBC), 189
  *BRCA*1/*BRCA*2 mutation carriers, 445
  clinicopathologic profile, 445
  core needle biopsy (CNB) procedure, 448
  definition, 445
  differential diagnosis, 451–455
  ER reporting, 455
  features of, 448, 450, 451
  gene expression profiling studies, 455
  gross and radiologic features, 445–446
  IHC markers, 448
  immunohistochemical analysis, 456
  microscopic features, 446, 448
  molecular profiling, 456
  multidisciplinary treatment, 455
  neoadjuvant chemotherapy, 456
  pathogenesis, 455
  pCR, 456
  phase II neoadjuvant trials, 456
  potential sensitivity, 456
  treatment and clinical trials, 455
  triple-negative paradox, 445
  tumor-infiltrating lymphocytes (TILs), 456
  with circumscribed tumor margin, 447
  with squamoid features, 450
  with tumor cells, 447–449
True needle track seeding, 36
Tuberculous granulomas, 159
Tuberculous mastitis, 159
Tubular adenoma, 275, 766, 829
Tubular adenosis and sclerosing adenosis, 427
Tubular apocrine adenoma, 976
Tubular carcinoma (TC), 333
  differential diagnosis, 426–431
  gross and radiologic features, 422
  immunohistochemistry, 430, 431
  microscopic features, 423–425
  pathogenesis, 430
  prognosis, 421, 432
  Rosen triad, 424, 426
  SEER data, 421
Tubular sweat gland neoplasms, 958
Tubulolobular carcinoma (TLC), 428–430, 663
Tumor-associated lymphoid proliferation (TALP), 490
Tumor associated macrophages (TAMs), 862
Tumor infiltrating lymphocytes (TILs), 837
Tumour cell enrichment, 907
Tumourigenesis, 895
TWIST, 908

U
Ultrasound, 14–16
Usual and atypical apocrine adenosis, 59
Usual and atypical cystic hypersecretory lesions, 83
Usual ductal hyperplasia (UDH), 383, 792
  differential diagnosis, 384
  gross and radiologic features, 383
  immunohistochemistry, 384
  microscopic features, 383
  outcomes, 385
  pathogenesis, 384

V
Vacuum-assisted core needle biopsy, 20
Vacuum-assisted excision (VAE), 39
Van Nuys prognostic index, 376
Vascular lesions
  angiosarcoma
    clinical and radiologic features, 743
    differential diagnosis, 747, 749
    epithelioid angiosarcoma, 747
    immunohistochemistry, 749–750
    microscopic features, 743–747
    molecular alterations, 749–750
    treatment and prognosis, 750–752
  atypical vascular lesions
    clinical and radiologic features, 752
    differential diagnosis, 753
    immunohistochemistry, 753
    microscopic features, 752–753
    treatment and prognosis, 753–754
  benign vascular lesions
    angiomatosis, 737
    differential diagnosis, 740–743
    immunohistochemical work up, 743
    microscopic features, 737–740
    treatment and prognosis, 743
Venous hemangioma, 738, 740
VeraTag™ technology, 903
Very large core needle biopsy, 20, 21

W
Well-differentiated angiosarcomas, 744
Well-differentiated IBC with tubule formation, 428
Whole genome sequencing, 897, 898
World Health Organization Classification of Breast Tumours, 331
WT1, 931

Z
Zuska's disease, 156, 788